# 41ª Reunião Anual Sociedade Brasileira de Química

## LIVRO DE RESUMOS

## CONSTRUINDO O AMANHÃ

de 21 a 24/05/2018

Foz do Iguaçu, PR

ISBN: 978-85-64099-21-0

Realização

Sociedade Brasileira de Química

Patrocínio

Royal Society of Chemistry; UK-BR Year of Science and Innovation; GREAT Britain & Northern Ireland; Agilent Technologies; BUCHI

Apoio

CAPES; UFPR; Paraná Governo do Estado Secretaria da Ciência, Tecnologia e Ensino Superior; Fundação Araucária Apoio ao Desenvolvimento Científico e Tecnológico do Paraná; OPCW; FAPESP; UTFPR; UEPG; Iguassu Convention & Visitors Bureau; Ministério da Educação; Brasil

# 41ª Reunião Anual da Sociedade Brasileira de Química

# LIVRO DE RESUMOS

ISBN: 978-85-64099-21-0

**Foz do Iguaçu, PR**
**21 a 24 de maio de 2018**

# DIRETORIA DA SBQ

| | |
|---|---|
| Presidente da SBQ | *Aldo José G. Zarbin* (UFPR) |
| Presidente Sucessor da SBQ | *Norberto Peporine Lopes* (FCFRP-USP) |
| Vice-Presidente da SBQ | *Marília Oliveira F. Goulart* (UFAL) |
| Secretária Geral da SBQ - Presidente da CO 41ª RASBQ | *Rossimiriam P. de Freitas* (UFMG) |
| Secretário Adjunto da SBQ | *Silvio do Desterro Cunha* (UFBA) |
| Tesoureiro da SBQ | *Andre Galembeck* (CETENE) |
| Tesoureiro Adjunto da SBQ | *Fernando de Carvalho da Silva* (UFF) |

# CONSELHO CONSULTIVO DA SBQ

*Adriano D. Andricopulo* (USP)
*Etelvino José H. Bechara* (UNIFESP-Diadema)
*Fernando Galembeck* (UNICAMP)
*Maria Domingues Vargas* (UFF)
*Ronaldo Aloise Pilli* (UNICAMP)
*Vanderlan da Silva Bolzani* (IQAr-UNESP)
*Vitor Francisco Ferreira* (UFF)

# CONSELHO FISCAL DA SBQ

*Glaura Goulart Silva (UFMG*
*Roberto de Barros Faria*
*Romeu Cardoso Rocha Filho*

SOCIEDADE BRASILEIRA DE QUÍMICA - SBQ
Av. Prof. Lineu Prestes, 748
Instituto de Química da USP, bloco 3 superior
Cidade Universitária, São Paulo - SP
fone (11) 3032-2299 – fax (11) 3814-3602
endereço eletrônico: diretoria@sbq.org.br
sítio da internet: http://www.sbq.org.br
*endereço postal:*
Caixa Postal 26.037, 05513-970 - São Paulo - SP

Copyright© 2018 Sociedade Brasileira de Química

Todas as informações dos resumos publicadas neste livro foram reproduzidas de cópias fornecidas pelos autores. O conteúdo dos resumos é de exclusiva responsabilidade de seus autores. A SBQ, seus diretores e funcionários, a comissão organizadora da 41ª RASBQ e seus assessores *ad hoc* não se responsabilizam por consequências decorrentes de uso de quaisquer dados, afirmações e opiniões inexatos (ou que conduzam a erros) publicados neste livro.

# COMISSÃO ORGANIZADORA DA 41ª RASBQ

*Rossimiriam P. de Freitas* (UFMG) - Secretária Geral da SBQ - Presidente da CO 41ª RASBQ
*Aldo José G. Zarbin* (UFPR) - Presidente da SBQ
*Andre Galembeck* (CETENE) - Tesoureiro da SBQ
*Dirce Maria Fernandes Campos* (SBQ) - Diretora Executiva da SBQ
*Stanislau Bogusz Junior* (IQSC-USP) - Divisão de Alimentos e Bebidas
*Sibele Berenice Castellã Pergher* (UFRN) - Divisão de Catálise
*Maria Valnice B. Zanoni* (IQAr-UNESP) - Divisão de Eletroquímica e Eletroanalítica
*Márlon Herbert F. B. Soares* (UFG) - Divisão de Ensino de Química
*Nelson H. Morgon* (UNICAMP) - Divisão de Físico-Química
*Carla Cristina S. Cavalheiro* (IQSC-USP) - Divisão de Fotoquímica
*Roberto Gomes de S. Berlinck* (IQSC-USP) - Divisão de Produtos Naturais
*Maria Cristina C. Gazotti* (UENF) - Divisão de Química Ambiental
*Clésia Cristina Nascentes* (UFMG) - Divisão de Química Analítica
*Célia Machado Ronconi* (UFF) - Divisão de Química de Materiais
*Shirley Nakagaki Bastos* (UFPR) - Divisão de Química Inorgânica
*Rafael Victorio Carvalho Guido* (USP) - Divisão de Química Medicinal
*Mauricio Moraes Victor (UFBA) - Divisão de Química Orgânica*

# COMISSÃO CIENTÍFICA DA 41ª RASBQ

*Rossimiriam P. de Freitas* (UFMG) - Secretária Geral da SBQ - Presidente da CO 41ª RASBQ
*Aldo José G. Zarbin* (UFPR) - Presidente da SBQ
*Norberto Peporine Lopes* (FCFRP-USP) - Presidente Sucessor da SBQ
*Marília Oliveira F. Goulart* (UFAL) - Vice-Presidente da SBQ
*Silvio do Desterro Cunha* (UFBA) - Secretário Adjunto da SBQ
*Andre Galembeck* (CETENE) - Tesoureiro da SBQ
*Fernando de Carvalho da Silva* (UFF) - Tesoureiro Adjunto da SBQ
*Adriano D. Andricopulo* (USP) - Conselho Consultivo da SBQ
*Etelvino José H. Bechara* (UNIFESP-Diadema) - Conselho Consultivo da SBQ
*Fernando Galembeck* (UNICAMP) - Conselho Consultivo da SBQ
*Maria Domingues Vargas* (UFF) - Conselho Consultivo da SBQ
*Ronaldo Aloise Pilli* (UNICAMP) - Conselho Consultivo da SBQ
*Vanderlan da Silva Bolzani* (IQAr-UNESP) - Conselho Consultivo da SBQ
*Vitor Francisco Ferreira* (UFF) - Conselho Consultivo da SBQ
*Stanislau Bogusz Junior* (IQSC-USP) - Divisão de Alimentos e Bebidas
*Sibele Berenice Castellã Pergher* (UFRN) - Divisão de Catálise
*Maria Valnice B. Zanoni* (IQAr-UNESP) - Divisão de Eletroquímica e Eletroanalítica
*Márlon Herbert F. B. Soares* (UFG) - Divisão de Ensino de Química
*Nelson H. Morgon* (UNICAMP) - Divisão de Físico-Química
*Carla Cristina S. Cavalheiro* (IQSC-USP) - Divisão de Fotoquímica
*Roberto Gomes de S. Berlinck* (IQSC-USP) - Divisão de Produtos Naturais
*Maria Cristina C. Gazotti* (UENF) - Divisão de Química Ambiental
*Clésia Cristina Nascentes* (UFMG) - Divisão de Química Analítica
*Célia Machado Ronconi* (UFF) - Divisão de Química de Materiais
*Shirley Nakagaki Bastos* (UFPR) - Divisão de Química Inorgânica
*Rafael Victorio Carvalho Guido* (USP) - Divisão de Química Medicinal
*Mauricio Moraes Victor* (UFBA) - Divisão de Química Orgânica

# COMISSÃO LOCAL DA 41ª RASBQ

*Elisa Orth* (UFPR) - Presidente da Comissão Local da 41ª RASBQ
*Andrelson Wellington Rinaldi* (UEM)
*Elizabeth Weinhardt de Oliveira Scheffer* (UEPG)
*Fernando Molin* (UTFPR)
*Jose Ricardo Cezar Salgado* (UNILA)
*Luiz Henrique Dall'Antonia* (UEL)
*Renata Mello Giona* (UTFPR)

# ASSESSORES *AD HOC*

Adalgisa R. de Andrade
Adão Aparecido Sabino
Aderson Zottis
Adolfo Horn Jr.
Adonay Rodrigues Loiola
Adriana dos Santos Lages
Adriana Nunes Correia
Aguinaldo Robinson de Souza
Alam Gustavo Trovó
Alcione Silva de Carvalho
Alfredo Luis M. L. Mateus
Aline Thais Bruni
Altair Benedito Moreira
Aluísio Marques da Fonseca
Alvaro José dos Santos Neto
Alzir Azevedo Batista
Amadeu Moura Bego
Ana Luiza de Quadros
Ana Maria Pires
Anamaria Dias Pereira Alexiou
André Luiz B. Formiga
Andre Luiz Meleiro Porto
André Mauricio de Oliveira
André Romero da Silva
Angelo de Fatima
Anita J. Marsaioli
Anna Maria Canavarro Benite
Anne Helene Fostier
Antonio Aprigio da Silva Curvelo
Antonio Carlos B. Burtoloso
Antonio Eduardo da Hora Machado
Antonio Jacinto Demuner
Antonio Rogério Fiorucci
Antonio Salvio Mangrich
Arnaldo Alves Cardoso
Arthur Eugen Kummerle
Artur de Jesus Motheo
Aurea Echevarria Aznar
Auro Atsushi Tanaka
Ayres Guimarães Dias
Bernardo Almeida Iglesias
Brenno Amaro da Silveira Neto
Bruna Possato
Bruno Amaral Meireles
Bruno Silva Leite
Bruno Szpoganicz
Caio Costa Oliveira
Camila Greff Passos
Camila Silveira da Silva
Carla Beatriz Grespan Bottoli
Carla Cristina S. Cavalheiro
Carla dos Santos Riccardi
Carlos Alberto Marques
Carlos Alberto Policiano de Almeida
Carlos Cezar da Silva
Carlos Kleber Zago de Andrade
Carlos Mauricio R. de Sant'Anna
Carlos Roque Duarte Correia
Carmem Lucia de Paiva e Silva Zanta
Carmen Silvia da Silva Sá
Carolina Horta Andrade
Cássia Curan Turci/Novos Talentos/CAPES
Cassiana Carolina Montagner
Cassius Vinicius Stevani
Catarina de Nigris Del Cistia
Cedric Stephan Graebin
Célia Machado Ronconi
Celio Pasquini
Celso Aparecido Bertran
Christiane Fernandes
Christiane Philippini F. Borges
Cinthia Maria Felicio
Cíntia Duarte de Freitas Milagre
Claudia Carvalhinho Windmoller
Claudia Longo
Claudia Moraes de Rezende
Claudio Luis Donnici
Claudio Roberto Machado Benite
Claudio Viegas Junior
Cleder Alexandre Somensi
Cleônia Roberta Melo Araújo
Clésia Cristina Nascentes
Cristina Wayne Nogueira
Daiane Einhardt Blank
Daniel Lázaro Gallindo Borges
Daniel Rodrigues Cardoso
Danielle Cangussu de C. Gomes
Danielle Caroline Schnitzler
Danielle Ferreira Dias
Danilo Gustavo Rodrigues Silva
David Rodrigues da Rocha
Dayse Carvalho da Silva Martins
Débora Gonçalves
Denis Pires de Lima
Denise Freitas Siqueira Petri
Denise Leal de Castro
Djenaine de Souza
Dulce Helena Siqueira Silva
Ednei Gilberto Primel
Edson Antonio Ticianelli
Edson Ferreira da Silva
Edson Minatti
Eduardo Borges de Melo
Eduardo José Nassar
Eduardo Mathias Richter
Eduardo Rigoti
Eduardo Rolim de Oliveira
Elaine Pavini Cintra
Elene Cristina Pereira Maia
Elisa Prestes Massena
Elisa Souza Orth
Elisabete Frollini
Elizabeth Igne Ferreira
Emerson Henrique de Faria
Emerson Schwingel Ribeiro
Emílio Carlos de Lucca Júnior
Emmanoel Vilaça Costa
Ercules Epaminondas de S. Teotonio
Erick Leite Bastos
Erico Marlon de Moraes Flores
Ernesto Schulz Lang
Etelvino José Henriques Bechara
Fabiano Severo Rodembusch
Fábio Peres Gonçalves
Fábio Rodrigo Piovezani Rocha
Fávero Reisdorfer Paula
Fernanda Andreia Rosa
Fernanda Irene Bombonato
Fernanda Vasconcelos de Almeida
Fernando Antonio S. Coelho
Fernando Aparecido Sigoli
Fernando Batista da Costa

Fernando Fabriz Sodré
Fernando Wypych
Floriano Paes Silva Junior
Francisco Adriano de Oliveira Carvalho
Francisco Eduardo Aragão Catunda Jr.
Francisco Manoel dos Santos Garrido
Frederico Silva Castelo Branco
Fritz Cavalcante Huguenin
Gabriela Ramos Hurtado
Geani Maria Ucoski
Gilson de Freitas Silva
Giovanna Machado
Giuliano Cesar Clososki
Glaura Goulart Silva
Gleison Antonio Casagrande
Grace Gosmann
Guilherme Andrade Marson
Guilherme Sippel Machado
Gustavo Claro Monteiro
Gustavo Fernandes S. Andrade
Gustavo Henrique Goulart Trossini
Gustavo Henrique Ribeiro Viana
Gustavo Pozza Silveira
Hamilton Varela
Hector Henrique Ferreira Koolen
Heitor Avelino de Abreu
Hélcio Silva dos Santos
Heloise de Oliveira Pastore
Herenilton Paulino Oliveira
Hilma Alessandra R. do Couto
Humberto Marcio S. Milagre
Ignez Caracelli
Iolanda da Cruz Vieira
Irlon Maciel Ferreira
Irwin Rose Alencar de Menezes
Ísis Kaminski Caetano
Isis Martins Figueiredo
Italo Odone Mazali
Ivo Jose Curcino Vieira
Ivo Milton Raimundo Jr.
Ivone Carvalho
Izaura Cirino Nogueira Diógenes
Jaqueline Nicolini
Jean Marcel Ribeiro Gallo
Jez Willian Batista Braga
João Batista Lopes Martins
João Marcos Madurro
João Paulo dos Santos Fernandes
Joaquim de Araujo Nobrega
Jonas Gruber
Jorge Luiz de Oliveira Domingos
Jorge Luiz Ribeiro de Melos
Jose Alves Dias
Jose Gildo de Lima
José Luis de Paula Barros Silva
Josef Wilhelm Baader
Josué Carinhanha Caldas Santos
Juliana Limana Malavolta
Juliano Alves Bonacin
Julio Cezar Pastre
Julio Santos Reboucas
Káthia Maria Honório
Katia Bernardo Gusmão
Kátia Cristina Molgero Westrup
Katia Jorge Ciuffi
Kelly Aparecida Dias de F. Castro
Kleber Thiago de Oliveira
Koiti Araki
Laudemir Carlos Varanda
Laura Oliveira Péres
Lauro Tatsuo Kubota
Leandro Ferreira Pedrosa
Leandro Soter de Mariz e Miranda
Letícia Malta Costa
Lídia Moreira Lima
Ligia Maria M. Valente
Lílian Sibelle Campos Bernardes
Lindiane Bieseki
Lourdes Campaner dos Santos
Lucia Helena Mascaro Sales
Luciana Gonzaga de Oliveira
Luciane Hiromi Akahoshi
Luciano Dornelles
Luciano Morais Lião
Luis Octávio Regasini
Luiz Antônio Soares Romeiro
Luiz Antonio Sodré Costa
Luiz Gonzaga de França Lopes
Luiz Henrique Dall`Antonia
Luiz Sidney Longo Junior
Luzineide Wanderley Tinoco
Magaly Girão Albuquerque
Magdalena Nascimento Rennó
Mara Elisa Fortes Braibante
Marcela Mohallem Oliveira
Marcelo Giordan Santos
Marcelo Gomes Speziali
Marcelo Henrique dos Santos
Marcelo Henrique Gehlen
Marcelo Martins de Sena
Marcelo Oliveira Santiago
Marcelo Santos Castilho
Márcia Cristina Bisinoti
Márcia Foster Mesko
Marcia Matiko Kondo
Marcio Eduardo Vidotti Miyata
Márcio Peres de Araujo
Marco Edilson Freire de Lima
Marco Tadeu Grassi
Marcos Fernando de Souza Teixeira
Maria Carolina Blassioli-Moraes
Maria Cecilia Bastos V. de Souza
Maria Cristina Canela Gazotti
Maria Cristina Forti
Maria Cristina Nonato
Maria das Graças A. Korn
Maria de Fatima Fontes Lelis
Maria do Carmo Hespanhol da Silva
Maria Domingues Vargas
Maria Eunice Ribeiro Marcondes
Maria Fatima das G. F. da Silva
Maria Fernanda D'Oliveira Pimentel
Maria Goretti de V. Silva
Maria Helena Roxo Beltran
Maria Ines Nogueira Camargo Harris
Maria Lúcia Arruda de Moura Campos
Maria Lucia Belem Pinheiro
Maria Luiza Miranda Rocco
Maria Valnice B. Zanoni
Mariele Iara Soares de Mello
Marília Oliveira Fonseca Goulart
Mario Geraldo de Carvalho
Mario Roberto Senger
Marisa Tsao
Márlon Herbert F. B. Soares
Mary Ann Foglio
Maurício Angel Vega-Teijido
Mauricio Frota Saraiva
Mauricio Silva dos Santos
Maurícius Selvero Pazinato
Mauro Bertotti
Mauro Coelho dos Santos
Mauro Korn
Michael Jackson Vieira da Silva
Miriam Verginia Lourenco
Nadja Paraense dos Santos
Nailton Monteiro do Nascimento Júnior
Nelilma Correia Romeiro
Nelson Henrique Morgon
Nelson Ramos Stradiotto
Nito Angelo Debacher
Nubia Boechat Andrade
Nyuara Araújo da Silva Mesquita
Odair Pastor Ferreira
Olga Soares do Rego Barros
Onofre Vargas Junior
Orlando Fatibello Filho
Ozelito Possidônio de Amarante Jr.
Pablo Machado
Patrícia Mendonça Pauletti
Paula Alvarez Abreu
Paulo Augusto Netz
Paulo Gustavo Barboni Dantas Nascimento
Paulo Olivi
Paulo Roberto de Oliveira
Pedro de Lima Neto
Pedro Gregório Vieira Aquino
Pedro Henrique Cury Camargo
Pedro Sérgio Fadini
Pedro Vitoriano de Oliveira
Pérola de Castro Vasconcellos

Rafael Stieler
Rafael Victorio Carvalho Guido
Raoni Schroeder Borges Gonçalves
Raphael Nagao de Sousa
Regina Aparecida Correia Gonçalves
Regina Celia Galvao Frem
Reinaldo Francisco Teófilo
Renata Barbosa de Oliveira
Renata Barbosa Lacerda
Renata Diniz
Renato Sanches Freire
Renato Zanella
Ricardo Jorgensen Cassella
Ricardo José Alves
Ricardo Queiroz Aucelio
Robert Alan Burrow
Roberta Tesch
Roberto Carlos Campos Martins
Roberto de Barros Faria
Roberto Gomes de Souza Berlinck
Roberto Parise Filho
Roberto Santana da Silva
Rodrigo Alejandro Abarza Muñoz
Rodrigo Luiz Oliveira R. Cunha
Romeu Cardozo Rocha Filho
Rose Maria Carlos
Rosebelly Nunes Marques
Roselena Faez
Rosely Aparecida Peralta
Rosemeire Brondi Alves
Rosivaldo dos Santos Borges
Salete Linhares Queiroz
Samuel Silva da Rocha Pita
Sandra Helena Pulcinelli
Sandra Regina Longhin
Sebastião da Cruz Silva
Sergio Antonio Spinola Machado
Sergio de Paula Machado
Shirley Nakagaki Bastos
Sibele Berenice Castella Pergher
Sidney José Lima Ribeiro
Sonia Maria Alves Jorge
Stanislau Bogusz Junior
Susana Inés Córdoba de Torresi
Telma Leda Gomes de Lemos
Thalita Grando Rauen
Thiago Augusto de Lima Burgo
Thiago Barcellos da Silva
Thiago Pereira Goulart
Timothy John Brocksom
Valdemar Lacerda Júnior
Valderi Luiz Dressler
Valeriano Antonio Corbellini
Vanessa Égea dos Anjos
Vanessa Gisele Pasqualotto Severino
Vânia Gomes Zuin
Vanusa Regina Lando
Vera Lucia Eifler Lima
Vera Regina L. Constantino
Victor Marcelo Deflon
Vladimir C. Gomes Heleno
Warley de Souza Borges
Wendel Andrade Alves
Wendell Karlos Tomazelli Coltro
Zeki Naal
Zenilda de Lourdes Cardeal

# EDITORIAL

A 41ª Reunião Anual da Sociedade Brasileira de Química (41ª RASBQ) será realizada este ano no estado do Paraná, no lindíssimo destino turístico de Foz do Iguaçu, no Rafain Palace & Convention Center. Pela primeira vez em 41 anos, estudantes, professores e pesquisadores da área de química e de áreas correlatas, de todos os cantos do país, além de convidados e participantes estrangeiros, se reunirão neste quadro incrível para celebrar o avanço da ciência na área. Após o sucesso do 46th World Chemistry Congress/40ª RASBQ em São Paulo, a expectativa é que recebamos um grande número de participantes na região Sul do país, onde a última RA foi realizada em 2011, em Florianópolis, no memorável Ano Internacional da Química.

O tema da RA será "Construindo o Amanhã", e propõe uma reflexão importante sobre a criação de novas condições para que o ambiente de ciência e tecnologia do Brasil volte a crescer e se firme como um eixo fundamental do desenvolvimento econômico do país. O tema central da RA será discutido, no simpósio de mesmo nome, por personalidades de destaque no meio político-acadêmico-científico-industrial. O simpósio pretende ser um espaço importante de reflexão sobre a temática, que além de ser de suma importância ao país, é de particular interesse à comunidade de professores, estudantes de todos os níveis (graduação, mestrado e doutorado), cientistas e simpatizantes da Química que usualmente comparecem às Reuniões Anuais da SBQ.

Uma das formas de atingir as finalidades pelas quais a SBQ se propõe é através da realização de parcerias com diferentes instituições coirmãs. Dentre estas instituições, a Royal Society of Chemistry (RSC) é uma das mais representativas, e vem sistematicamente trabalhando em parceria com a SBQ. Na nossa RA em Foz um *Memorandum of Understanding (MoU*) entre as duas Sociedades será renovado e, para celebrar a parceria e como **parte da programação** do **Ano Brasil-Reino Unido de Ciência e Inovação 2018-19,** a SBQ realizará uma sessão SBQ-RSC, que terá duas importantes conferências científicas e a cerimônia de assinatura do MoU entre o presidente da SBQ, Professor Aldo Zarbin e o imediate-past President da RSC, Professor Dominic Tildesley.

As sessões temáticas abordarão temas de grande relevância para a comunidade. Em uma delas, cientistas renomados na área discursarão sobre os recentes avanços obtidos pela academia em relação ao tema energia. Em outra temática a química "da célula ao reator" ganha força, mostrando a visão e contribuição de importantes pesquisadores ligados à exploração de biomoléculas para diferentes aplicações. A importância do debate sobre as mulheres na ciência será destacada com entusiasmo e alegria por brilhantes mulheres na temática sobre "Elas, as cientistas". Finalmente uma sessão temática envolvendo nomes da indústria debaterá como as novas tendências tecnológicas relacionadas à digitalização devem ser incorporadas na formação do profissional de química para atender as futuras demandas do setor industrial.

Grandes nomes da química contemporânea apresentarão resultados recentes de suas pesquisas: Francisco José Krug (conferencista de abertura!), Carlos Moyses Graca Araujo, Claudio D. Borsarelli, Fabrizio Adani, Frank Glorius, Galo Soler Illia, Hamilton Brandão Varela de Albuquerque, Joaquim de Araújo Nóbrega, Jonathan S. Lindsey, Joost N. H. Reek, Luiz Carlos Dias, Mônica Tallarico Pupo, Richard G. Weiss, Teodorico de Castro Ramalho e Wilmo Ernesto Francisco Junior são os nomes que acrescentarão história à nossa RA!

Durante a 41ª RASBQ, a SBQ realizará mais uma vez a sua já tradicional atividade para divulgação da ciência entre os mais jovens. Este ano o “SBQ na Escola” trará mais de 500 alunos das escolas públicas de Foz do Iguaçu e região para visitar a Reunião. A mostra, organizada pelo professor Alfredo Luis Mateus (UFMG) focará na interatividade dos alunos, que farão eles mesmos os experimentos em companhia dos monitores.

A programação da RA conta ainda com a realização de 7 workshops, 12 minicursos, 3 sessões de paineis, 18 sessões coordenadas, assembleias regionais e divisionais, sessão de homenagens, sessão de lançamento de livros, além da tradicional exposição de empresas apoiadoras. Trata-se de um espaço único para networking e aproveitamento do que de melhor a comunidade química sabe fazer. Cerca de 1700 pessoas estão inscritas no evento até o momento e muito mais gente passará pelo local!

Além do livro de programa em pdf, todas as informações sobre a RA estão disponíveis no aplicativo 41ª RASBQ, disponível para iOS (Apple Store) e para Android (Google Play) . A Reunião também estará presente nas redes sociais (facebook, twitter e instagram). Divulgue a nossa Sociedade!

A RA é resultado de um trabalho árduo, começado muito tempo antes da sua realização. A Comissão Organizadora, formada pelo presidente, pela secretária geral, tesoureiro, diretora executiva, diretores e diretoras das 13 divisões científicas da SBQ tem um longo caminho a percorrer até atingir o formato de reunião que sonhamos. Os desafios são muitos! Além disso, o trabalho da comissão local, dos avaliadores dos trabalhos e da hercúlea secretaria da SBQ em São Paulo são essenciais para que estejamos aqui hoje!

Apesar dos grandes desafios do momento atual, estamos todos felizes com a construção da 41ª RASBQ, pelo local da realização do evento, que é maravilhoso, pela expectativa das pessoas, que se mostram receptivas e felizes com o encontro, e pela oportunidade de mostrar que a Química e a ciência brasileira resistirão! Sabemos que é hora da nossa comunidade mostrar coesão e reação, fortalecendo ainda mais a sociedade que a representa. É hora de aparecer em peso na nossa RA e mostrar a que viemos!

Nos vemos em Foz!

Abraços,

*Rossimiriam Freitas*
*Secretária Geral da SBQ*
*Presidente da Comissão Organizadora da 41ª RASBQ*

# SUMÁRIO

## *Segunda-feira – 21 de maio*


9:00 Entrega de material ..... 11
10:00-17:00 Workshops ..... 11
19:00-19:30 Abertura da 41ª Reunião Anual da Sociedade Brasileira de Química ..... 12
19:30-20:30 Conferência de Abertura ..... 12
20:30-23:00 Coquetel de Abertura ..... 12


## *Terça-feira – 22 de maio*


08:00-10:00 Minicursos ..... 13
10:10-11:10 Conferências Convidadas ..... 14
11:15-12:15 Conferências Convidadas ..... 14
11:15-12:15 Conferência Empresa ..... 14
14:00-17:50 Sessões Coordenadas ..... 14
18:00-20:00 Sessão I de discussão de painéis ..... 20
20:00-21:00 Assembleias Regionais ..... 20
21:00-22:00 Sessão de Homenagens ..... 20


## *Quarta-feira – 23 de maio*


08:00-10:00 Minicursos ..... 21
10:10-12:10 Sessão RSC-SBQ ..... 21
14:00-15:50 Simpósio ..... 21
16:00-17:00 Conferências Convidadas ..... 21
17:00-18:00 Conferências Convidadas ..... 21
18:00-20:00 Sessão II de discussão de painéis ..... 22
18:00-20:00 Lançamento de Livros ..... 22
20:00-21:00 Assembleias Divisionais ..... 23
22:00 Festa ..... 23


## *Quinta-feira – 24 de maio*


08:00-10:00 Minicursos ..... 24
10:10-12:00 Sessões Temáticas ..... 24
13:00-15:00 Sessão III de discussão de painéis ..... 25
15:00-18:30 Sessões Coordenadas ..... 25
19:00 Assembleia Geral Ordinária da Sociedade Brasileira de Química ..... 32

# *Índice de Painéis*

AMB – Química Ambiental ..... 34
ANA – Química Analítica ..... 37
BEA – Química de Alimentos e Bebidas ..... 40
BIO – Química Biológica ..... 41
CAT – Catálise ..... 42
COL – Química de Superfícies e Colóides ..... 43
EDU – Ensino de Química ..... 44
ELE – Eletroquímica e Eletroanalítica ..... 46
EST – Química Estrutural ..... 49
FIS – Físico-Química ..... 49
FOT – Fotoquímica ..... 50
INO – Química Inorgânica ..... 51
MAT – Química de Materiais ..... 55
MED – Química Medicinal ..... 59
ORG – Química Orgânica ..... 62
QPN – Química de Produtos Naturais ..... 66
QVE – Química Verde ..... 71
TEC – Química Tecnológica ..... 72
TEO – Química Teórica ..... 72

***Índice de Autores*** ..... 73

***Índice de Palavras-chave*** ..... 94

# Segunda-feira – 21 de maio

**9:00** **Entrega de material**

**10:00-17:00** **Workshops**

**Avanços recentes na caracterização de materiais e compostos inorgânicos e suas aplicações analíticas e eletroanalíticas** (Sala A-1)
Coordenadoras: *Clésia Cristina Nascentes* (UFMG)
*Maria Valnice B. Zanoni* (IQAr-UNESP)
*Shirley Nakagaki Bastos* (UFPR)
*Palestrantes:* *Maria Luiza Rocco* (UFRJ)
*Beate Saegesser Santos* (UFPE)
*Érico Marlon de Moraes Flores* (UFSM)
*Carla Beatriz Grespan Bottoli* (UNICAMP)
*Wendel A. Alves* (UFABC)
*Luiz Henrique Dall'Antonia* (UEL)

**Academia e Indústria em busca da inovação tecnológica** (Sala A-2)
Coordenadoras: *Célia Machado Ronconi* (UFF)
*Sibele Berenice Castellã Pergher* (UFRN)
Palestrantes: *Glaura Goulart da Silva* (UFMG)
*Donato Aranda* (EQ-UFRJ)
*José Vitor Bomtempo* (EQ-UFRJ)
*Oswaldo L. Alves* (IQ-UNICAMP)
*Cláudio J. A. Mota* (IQ-UFRJ)
*Marcelo do Amaral* (Diretor da GlobalYeast)
*Roberto Werneck* (Braskem)

**Química Orgânica e Medicinal: da Academia até a Iniciativa Privada** (Sala A-3)
Coordenadores: *Mauricio Moraes Victor* (UFBA)
*Rafael Victorio Carvalho Guido* (USP)
Palestrantes: *Eliezer J. Barreiro* (ICB-UFRJ)
*Jairton Dupont* (IQ-UFRGS)
*Antônio E. G. Santana* (UFAL)
*Alessandra Mascarello* (Aché Laboratórios Farmacêuticos)
*Marcelo Saraiva* (Gilead/USA)
*Fábio Barros* (Instituto Vitanova)

**Como é o ensino de Química Ambiental e Educação Ambiental no Brasil?** (Sala C-1)
Coordenadores: *Maria Cristina C. Gazotti* (UENF)
*Márlon Herbert F. B. Soares* (UFG)
Palestrantes: *Nyuara Araújo da Silva Mesquita* (UFG)
*Elizabeth Weinhardt Scheffer* (UEPG)
*Renato S. Freire* (IQUSP)
*Andréa Horta Machado* (UFMG)
*Maria Lucia Arruda de Moura Campos* (FFCLRP-USP)

**XVI Workshop de Pós-Graduação em Química** (Sala C-2)
Coordenadoras*:* *Marília Oliveira F. Goulart* (UFAL)
*Maria Domingues Vargas* (UFF)
Palestrantes: *Aldo J.G. Zarbin* (UFPR)
*Rochel Montero Lago* (UFMG)
*Paulo Anselmo Ziani Suarez* (UnB)

*Evaldo Vilela (FAPEMIG)*
*Carolina Maria M. de Carvalho Andrade* (SENAI Inovação em Química)
*Fabricio Parreira* (CTF)
*Maria Domingues Vargas* (UFF)
*Adriano Monteiro* (UFRGS)
*Norberto Peporine Lopes* (FCFRP-USP)
*Marília Oliveira F. Goulart* (UFAL)
*Maysa Furlan* (IQAr-UNESP)
*Hélio Duarte* (UFMG)

**Integração das Secretarias Regionais da SBQ (Sala Paraná IV)**
Coordenador: *Silvio do Desterro Cunha* (UFBA, Secretário Adjunto SBQ)
Palestrantes: *Aldo J.G. Zarbin* (UFPR, Presidente SBQ)
*André Galembeck* (CETENE, Tesoureiro da SBQ)
*Norberto Peporine Lopes* (Presidente da SBQ gestão 2018-2020)
*Aluísio M. da Fonseca* (UNILAB, SBQ-Regional Ceará)
*Ana Paula Silveira Paim* (UFPE, SBQ-Regional Pernambuco)
*André Romero da Silva* (IFES, SBQ-Regional Espirito Santo)
*David Rodrigues da Rocha* (UFF, SBQ-Regional Rio de Janeiro)
*Elisa Souza Orth* (UFPR, SBQ-Regional Paraná)
*Flávio Colmati Jr* (UFG, SBQ-Regional Goiás)
*Hállen D. R. Calado* (UFMG, SBQ-Regional Minas Gerais)
*Humberto Marcio S. Milagre* (IQAr-UNESP, SBQ-Regional Interior Paulista Waldemar Saffioti)
*Isis Martins Figueiredo* (UFAL, SBQ-Regional Alagoas)
*João Batista Martins* (UnB, SBQ-Regional Distrito Federal)
*Julio Cezar Pastre* (UNICAMP, SBQ-Regional Campinas)
*Luiz Antônio M. Alves da Costa* (UFRR, SBQ-Regional Roraima)
*Patrícia Santana B. Marinho* (UFPA, SBQ-Regional Pará)
*Reinaldo Francisco Teófilo* (UFV, SBQ-Regional Viçosa)
*Rennan Geovanny Oliveira Araujo* (UFBA, SBQ-Regional Bahia)

**SBQ Jovem: para construir o amanhã** (Sala C-3)
Coordenadores*:* *Fernando de Carvalho da Silva* (UFF)
*Diogo Montes Vidal* (UFMG)
Palestrantes: *Aldo J.G. Zarbin* (UFPR)
*Eliezer J. Barreiro* (ICB-UFRJ)
*Guilherme Andrade Marson* (IQUSP)
*Paulo H. G. Zarbin* (UFPR)
*Rochel Montero Lago* (UFMG)
*Romeu Cardozo Rocha Filho* (UFSCar)
*Ruben Dario Sinisterra Millán* (UFMG)

**19:00-19:30** **Abertura da 41ª Reunião Anual da Sociedade Brasileira de Química**
(Expocenter IV)

**19:30-20:30** **Conferência de Abertura**
**"Uma visão crítica sobre a espectrometria de emissão óptica com plasma induzido por laser (LIBS)"**
**-** Francisco José Krug (CENA-USP)

**20:30-23:00** **Coquetel de Abertura (Expocenter III)**

**SBQ na Escola** (Expocenter III)
- *Manhã 1 - de 8:00 às 9:30*
- *Manhã 2 - de 9:45 às 11:15*
- *Noite - 19:30 - 21:00*

**08:00-10:00 Minicursos**

1. **A Quimica Inorgânica na saúde e recentes avanços em metalofármacos** (Sala A-1)
   *- Alzir Azevedo Batista* (UFSCar)

2. **Micropoluentes emergentes em águas urbanas** (Sala A-2)
   *- Fernando Fabriz Sodré* (UnB)

3. **As diferentes versões da termodinâmica fora do equilíbrio** (Sala A-3)
   *- Paulo Augusto Netz* (UFRGS)

4. **Marcadores fluorescentes e as bases moleculares da aplicação de fluorescência em sistemas biológicos** (Sala C-1)
   *- Erick Leite Bastos* (USP)

5. **Métodos espectroscópicos avançados aplicados ao estudo de materiais** (Sala C-2)
   *- Maria Luiza Rocco Duarte Pereira* (UFRJ)

6. **Microfluídica** (Sala C-3)
   *- Wendell Karlos Tomazelli Coltro* (UFG)

7. **Avanços em polímeros molecularmente impressos (MIP) aplicados em sensores e extração** (Sala D-1)
   *- César Ricardo Teixeira Tarley* (UEL)
   *- Maria Del Pilar Taboada Sotomayor* (IQAr-UNESP)

8. **Fundamentos de catálise assimétrica** (Sala D-2)
   *- Carlos Roque Duarte Correia* (UNICAMP)
   *- Caio Costa Oliveira* (UNICAMP)

9. **Planejamento de fármacos baseado na estrutura do receptor (SBDD) e do ligante (LDBB)** (Sala D-3)
   *- Gustavo Henrique Goulart Trossini* (USP)

10. **Tópicos de quimioinformática na pesquisa de produtos naturais** (Sala F-1)
    *- Fernando Batista da Costa* (FCFRP-USP)

11. **Laboratório de experiência empreendedora: primeiros passos para criar uma empresa de base tecnológica** (Sala F-2)
    *- Rochel Montero Lago (UFMG)*
    **Facilitadores:**
    *- Arthur Gabriel da Silva* (UFMG)
    *- Maria Paula Duarte de Oliveira* (UFMG)
    *- Priscila Maria Teixeira G. de Souza* (UFMG)

**12. Desmedicalizando o olhar sobre a escola: contribuições para atuação do educador químico** (Sala F-3)
*- Hélio da Silva Messeder Neto* (UFBA)

**10:10-11:10 Conferências Convidadas**

**Developing a biorefinery concept for *Arundo donax*** (Sala A-2)
*- Fabrizio Adani (Universidade de Milão, Milão)*

**On discovery in photocatalysis, hydrogenation and on-surface chemistry** (Sala C-2)
*- Frank Glorius (Universidade de Munster)*

**Dinâmica complexa em eletrocatálise** (Sala D-2)
*- Hamilton Brandão Varela de Albuquerque* (IQSC-USP)

**Reflexões e aprendizagens sobre espectrometria atômica** (Sala F-2)
*- Joaquim de Araújo Nóbrega* (UFSCar)

**11:15-12:15 Conferências Convidadas**

**Polyelectrolytes containing thymine pendant groups: a "Swiss Army knife" for preparation of supramolecular assemblies for biosensing, microencapsulation, and photosensitization** (Sala A-2)
*- Claudio D. Borsarelli* (Universidad Nacional de Santiago del Estero, Argentina)

**Molecular and polymeric hydro- and organo-gels. What are they and why are they important?** (Sala C-2)
*- Richard G. Weiss* (Georgetown University)

**Innovation and opportunities toward new molecules for the agrochemical industry: from theory to application** (Sala D-2)
*- Teodorico de Castro Ramalho* (UFLA)

**11:15-12:15 Conferência Empresa**

**Utilização de ICP-MS para atendimento das normas ambientais** (Sala F-2)
*- Rodolfo Lorençatto* (Agilent Technologies)

**14:00-17:50 Sessões Coordenadas**

**Química Ambiental - I** (Sala A-1)

| | |
|---|---|
| Coordenador: | *Renato Sanches Freire* (IQUSP) |
| 14:00 – 14:25 | "Assessment of contamination of Amazonian streams by domestic sewage using sterols"<br>*Giovana Anceski Bataglion* (UFAM) |
| 14:25 – 14:30 | *Discussão* |
| 14:30 – 14:45 | "Bixin incorporated over a porous membrane as a biosorbent to remove mercury (II) from aqueous matrices"<br>*Julia Condé Vieira* (UFMG) |
| 14:45 – 14:50 | *Discussão* |
| 14:50 – 15:05 | "Pigments' profile of the polyextremophile *D. radiodurans* under extreme conditions for biosignature's detection"<br>*Larissa Lopes Cavalcante* (IQUSP) |
| 15:05 – 15:10 | *Discussão* |

15:10 – 15:25 "Detection of *p*-aminophenol and sub-products formed during oxidative process in water and hair salon effluent"
*João Carlos de Souza* (UNESP-IQAr)
15:25 – 15:30 *Discussão*
15:30 – 15:45 "Metallothionein and reduced glutathione: metal exposure biomarkers in rough-toothed dolphins (*Steno bredanensis*)"
*Fernanda Sousa Monteiro* (PUC-RIO)
15:45 – 15:50 *Discussão*
15:50 – 16:10 *Intervalo*
16:10 – 16:35 "Fósforo: implicações na segurança hídrica e alimentar"
*Pedro Sérgio Fadini* (UFSCar)
16:35 – 16:40 *Discussão*
16:40 – 16:55 "Evaluation of the influence of the toll station construction in BR-040 in particulate matter concentrations"
*Karmel Beringui de Oliveira da Silva* (PUC-RIO)
16:55 – 17:00 *Discussão*
17:00 – 17:15 "Economia circular na agropecuária: ensaios iniciais para estabilização de resíduos orgânicos e produção de biogás"
*Cleder Alexandre Somensi* (IFC)
17:15 – 17:20 *Discussão*
17:20 – 17:45 "Atmospheric contaminants in the gas phase: assessment at low cost"
*Vania Palmeira Campos* (UFBA)
17:45 – 17:50 *Discussão e Encerramento*

**QUÍMICA ANALÍTICA - I** *(SALA A-2)*
Coordenadora: *Márcia Foster Mesko* (UFPEL)
14:00 – 14:25 "Contornando as dificuldades analíticas na determinação de $H_2S$ em fase gasosa"
*Arnaldo Alves Cardoso* (UNESP)
14:25 – 14:30 *Discussão*
14:30 – 14:45 "On-column preconcentration of phenolic compounds by sequential injection chromatography"
*Maria Soledad Moura S. Fernández Acevedo* (CENA-USP)
14:45 – 14:50 *Discussão*
14:50 – 15:05 "Detecção colorimétrica de $H_2O_2$ em amostras de leite utilizando dispositivos analíticos fabricados em papel"
*Bárbara Guerra de Souza Guinati* (UFG)
15:05 – 15:10 *Discussão*
15:10 – 15:25 "SS-FF-AAS as an alternative technique for elemental impurities determination in high purity graphite"
*Rafael Francisco dos Santos* (UFSM)
15:25 – 15:30 *Discussão*
15:30 – 15:45 "Microdispositivo em papel para pseudotitulação ácido-base baseado em medida da distância"
*Rafaela Ferreira de Oliveira* (UNEB)
15:45 – 15:50 *Discussão*
15:50 – 16:10 *Intervalo*
16:10 – 16:35 "Ordered predictors selection: new approaches for variable selection in multivariate calibration"
*Reinaldo Francisco Teófilo (UFV)*
16:35 – 16:40 *Discussão*
16:40 – 16:55 "Development and validation of quantitative NMR method for illegal pesticides"
*Luana Conte Crocoli* (UCS)

16:55 – 17:00 *Discussão*
17:00 – 17:15 "An on-line preconcentration system using ion-imprinted polymer for determination of bismuth in seawater employing atomic fluorescence spectrometry "
*Caio Silva Assis Felix* (UFBA)
17:15 – 17:20 *Discussão*
17:20 – 17:45 "LIBS como ferramenta analítica no estudo de fontes hidrotermais oceânicas"
*Ivo Milton Raimundo Jr* (UNICAMP)
17:45 – 17:50 *Discussão e Encerramento*

**Ensino de Química** (Sala F-1)
Coordenador: *Márlon Herbert F. B. Soares* (UFG)
14:00 – 14:25 "Socioeconomic profile of Brazilian chemistry students: an analysis of the ENADE reports"
*Dayse das Neves Moreira* (UFPB)
14:25 – 14:30 *Discussão*
14:30 – 14:45 "Factors that influence the rates of reactions: discussing concepts from experimental investigative activities"
*Eliana Aparecida Silicz Bueno* (UEL)
14:45 – 14:50 *Discussão*
14:50 – 15:05 "Chemistry teaching for deprived of liberty: challenges of teaching in a recovery center"
*Dhaniella Cristhina de Brito Oliveira* (UEPA)
15:05 – 15:10 *Discussão*
15:10 – 15:25 "A Arte como princípio formativo de pibidianos em Química"
*Camila Silveira da Silva* (UFPR)
15:25 – 15:30 *Discussão*
15:30 – 15:45 "Use of photography as didactic approach for teaching Chemistry at high school groups"
*Daniela Santos Anunciação* (UFAL)
15:45 – 15:50 *Discussão*
15:50 – 16:10 *Intervalo*
16:10 – 16:35 "The influence of "ear" validation process of teaching sequences on pre-service chemistry teacher preparation"
*Amadeu Moura Bego* (UNESP-IQAr)
16:35 – 16:40 *Discussão*
16:40 – 16:55 "Atividades experimentais investigativas: visões e propostas de Professores de Química do Ensino Médio"
*Luciane Hiromi Akahoshi* (IQUSP)
16:55 – 17:00 *Discussão*
17:00 – 17:15 "Use of experimental class and play activity in chemistry teaching: An experience in elementary education"
*Danielle Rodrigues Monteiro da Costa* (UEPA)
17:15 – 17:20 *Discussão*
17:20 – 17:45 "Desafios e possibilidades no ensino de ligações químicas no nível médio"
*Maurícius Selvero Pazinato* (UFRGS)
17:45 – 17:50 *Discussão e Encerramento*

**Química Inorgânica - I** (Sala C-1)
Coordenador: *Ercules Epaminondas S. Teotonio* (UFPB)
14:00 – 14:25 "Materiais lamelares/fibrosos naturais e sintéticos: características estruturais e aplicações"
*Fernando Wypych* (UFPR)

14:25 – 14:30 *Discussão*
14:30 – 14:45 “Complexos Fluorescentes de Lantânio-Espiropirano com Aplicações em Materiais Poliméricos”
*Izadora Fonseca Reis* (UNIFEI)
14:45 – 14:50 *Discussão*
14:50 – 15:05 “Síntese e avaliação da eficiência da 5,10,15,20-tetraquis(4-metiltiofenil) porfirina para terapia fotodinâmica”
*Matheus Henrique Ignacio Souto* (UFMG)
15:05 – 15:10 *Discussão*
15:10 – 15:25 “Compostos de η6-arenorutênio(II) com ligantes fenilazo e feniloxadiazo: estabilidade, cinética de substituição de ligantes e atividade citotóxica em modelo de glioma humano”
*Jaqueline Pazinato (*UFPR)
15:25 – 15:30 *Discussão*
15:30 – 15:45 “Oxidation catalysts based on ironporphyrin supported on diatomaceous earth”
*Marcus Vinicius do Prado* (UNIFRAN)
15:45 – 15:50 *Discussão*
15:50 – 16:10 *Intervalo*
16:10 – 16:35 “*Adsorption of sulfur containing molecules on the metallic substrates of the copper triad*”
*Izaura Cirino Nogueira Diogenes (UFC)*
16:35 – 16:40 *Discussão*
16:40 – 16:55 “Rigid bipodal ligand as molecular building block to construct new metal-organic frameworks*”*
*Catiúcia Rodrigues M. Oliveira Matos* (UFF)
16:55 – 17:00 *Discussão*
17:00 – 17:15 “Ruthenium(II) terpyridine complexes containing heteroaryl-2-imidazole ligands featuring catalytic activity for water oxidation”
*Luis Enrique Santa Cruz Huamaní* (UNICAMP)
17:15 – 17:20 *Discussão*
17:20 – 17:45 “Derivados porfirínicos: da avaliação fotofísica a aplicação em interação com biomoléculas”
*Bernardo Almeida Iglesias* (UFSM)
17:45 – 17:50 *Discussão e Encerramento*

**Química de Materiais - I** (Salas C-2 e 3)
Coordenadora: *Marian Rosaly Davolos* (UNESP-IQAr)
14:00 – 14:25 “Polysaccharides - A versatile feedstock to design novel materials”
*André Ricardo Fajardo* (UFPel)
14:25 – 14:30 *Discussão*
14:30 – 14:45 “Synthesis of donor-acceptor (D-A) hybrids based on functionalized thiophene-imides for high fluorescent material development”
*Marina de Ávila Costa* (UFMG)
14:45 – 14:50 *Discussão*
14:50 – 15:05 “Avaliação dos engaços de uva BRS Violeta e *Vitis labrusca* Isabel como potenciais precursores de carvão ativado para fins de adsorção”
*Indira Carolina Brito Pires* (IFPE)
15:05 – 15:10 *Discussão*
15:10 – 15:25 “A scalable new platform to produce all-carbon low-cost paper-based electrodes”
*João Paulo F. Bertacchi* (UNICAMP)
15:25 – 15:30 *Discussão*
15:30 – 15:45 “Synthesis and characterization of a conjugated metallopolymer complexed with terbium ions”
*Emerson Cortez Gallego Campos* (UFPR)

15:45 – 15:50 *Discussão*
15:50 – 16:10 *Intervalo*
16:10 – 16:35 "New efforts to design enhanced efficiency fertilizers from natural resources"
*Roselena Faez* (UFSCar)
16:35 – 16:40 *Discussão*
16:40 – 16:55 "From graphite to graphene: improving the Hummers method to produce high quality reduced graphene oxide (rGO)"
*Danilo Argentoni Nagahoka* (UPM)
16:55 – 17:00 *Discussão*
17:00 – 17:15 "Estudo de reações biocatalíticas envolvendo microrganismos funcionalizados com óxidos metálicos"
*Cristian Lins da Cruz Almeida* (UFBA)
17:15 – 17:20 *Discussão*
17:20 – 17:45 "Nanoparticles and nanocomposites for medical and environmental application"
*Koiti Araki* (IQUSP)
17:45 – 17:50 *Discussão e Encerramento*

**Química Medicinal/Química Biológica** (Sala D-1)
Coordenadora: *Carolina Horta Andrade* (UFG)
14:00 – 14:25 "Contribuição para a busca de novos antimaláricos"
*Núbia Boechat Andrade* (FIOCRUZ)
14:25 – 14:30 *Discussão*
14:30 – 14:45 "Evaluation of decoralin peptide identifies activity determinants and synthetic variants with *in vivo* activity"
*Marcelo Der Torossian Torres* (UFABC)
14:45 – 14:50 *Discussão*
14:50 – 15:05 "Molecular modeling of thiosemicarbazones, candidate dual inhibitors of snake venoms metalloproteases and pospholipases A2"
*Nathally Lima do Nascimento* (UFRRJ)
15:05 – 15:10 *Discussão*
15:10 – 15:25 "Evaluation of the interaction of β-carbolines derivatives with DNA by molecular fluorescence and correlation with antiproliferative activity"
*Marina de Magalhães Silva* (UFAL)
15:25 – 15:30 *Discussão*
15:30 – 15:45 "Evaluation of new inhibitors of homoserine dehydrogenase for the development of drugs against paracoccidioidomycosis"
*Andrew Matheus Frederico Rozada* (UEM)
15:45 – 15:50 *Discussão*
15:50 – 16:10 *Intervalo*
16:10 – 16:35 "Affinity-based screening assays in the search of enzyme ligands"
*Quezia Bezerra Cass* (UFSCar)
16:35 – 16:40 *Discussão*
16:40 – 16:55 Design of new analogs and investigation of SmTGR inhibition by fragments identified by X-ray crystallography"
*Lauro Ribeiro de Souza Neto* (FIOCRUZ)
16:55 – 17:00 *Discussão*
17:00 – 17:15 "ADMET and pharmacokinetic parameters of antitrypanosomal / antitumoral analogues of licarin A"
*Thiago Rahal Morais* (UNIFESP)
17:15 – 17:20 *Discussão*
17:20 – 17:45 "Medicinal chemistry approaches for neglected tropical diseases"
*Leonardo Luiz Gomes Ferreira* (IFSC-USP)
17:45 – 17:50 *Discussão e Encerramento*

**Química Orgânica - I** (Salas F-2 e 3)

Coordenadora: *Fernanda Andreia Rosa* (UEM)

14:00 – 14:25 "Captura e transformação de $CO_2$ em espaços confinados"
*Jairton Dupont* (UFRGS)

14:25 – 14:30 *Discussão*

14:30 – 14:45 "New chiral oxazolidine-dihydropyridines"
*Rebeca Garcia Moura* (IQUSP)

14:45 – 14:50 *Discussão*

14:50 – 15:05 "Efficient synthesis of N-phenethylarylthioamides by Kindler reaction"
*Paula Romanhi dos Santos (UFF)*

15:05 – 15:10 *Discussão*

15:10 – 15:25 A Practical synthesis of densely substituted 2*H*-furo[3,2-b]benzopyran-2-ones"
*Wilson Elias Rozo Nuñez* (UFBA)

15:25 – 15:30 *Discussão*

15:30 – 15:45 "Relationship between Hammett's parameters and in silico density functional with tandem mass ESI-CID fragmentation: Dihydropyridines as prototype"
*Paulo Roberto dos Santos* (UCS)

15:45 – 15:50 *Discussão*

15:50 – 16:10 *Intervalo*

16:10 – 16:35 "Síntese de derivados da curcumina ligados a carboidratos potencialmente bioativos"
*Carolina Passarelli Gonçalves* (UFABC)

16:35 – 16:40 *Discussão*

16:40 – 16:55 "Abordagens complementares nas sínteses totais de (+)- e (-)-bernumidina"
*Tamiris Reissa Cipriano da Silva* (UNIFESP)

16:55 – 17:00 *Discussão*

17:00 – 17:15 "Síntese de selenoésteres mediante rearranjo sigmatrópico entre selenoacetilenos e difenilsulfóxido catalisada por ácido tríflico"
*Lucas Loss Baldassari* (UFRGS)

17:15 – 17:20 *Discussão*

17:20 – 17:45 "Fluoração nucleofílica catalítica promovida por éteres coroa, criptantes e derivados hidroxilados"
*Josefredo Rodriguez Pliego Júnior* (UFSJ)

17:45 – 17:50 *Discussão e Encerramento*

**Química de Produtos Naturais - I** (Salas D-2 e 3)

Coordenador: *Roberto Gomes de Souza Berlinck* (IQSC-USP)

14:00 – 14:25 "Duguetinine, an isoquinoline-derived alkaloid with an unprecedented skeleton from the bark of *Duguetia surinamensis* (Annonaceae)"
*Emmanoel Vilaça Costa* (UFAM)

14:25 – 14:30 *Discussão*

14:30 – 14:45 "Chemical composition of bufonids toads from legal Amazonia"
*Jacqueline Kerkhoff* (UFMT)

14:45 – 14:50 *Discussão*

14:50 – 15:05 "Chemical, cytotoxic and antimalarial study of *Dipteryx lacunifera*"
*Leonardo Santos Alexandre* (UFPI)

15:05 – 15:10 *Discussão*

15:10 – 15:25 "Evaluation of synthetic Peptidomimetics as cathepsin K inhibitors"
*Taynara Lopes Silva* (UFSCar)

15:25 – 15:30 *Discussão*

15:30 – 15:45 "Dereplication study by HPLC-MS-MS and activity against *Leishmania chagasi* of the leaf extract of *Trichilia emarginata*"
*Flávia Pereira Dias Viegas* (UNIFAL)

15:45 – 15:50 *Discussão*
15:50 – 16:10 *Intervalo*
16:10 – 16:35 "Natural product chemistry as a tool for ensuring the efficacy and safety of the use of medicinal products prepared with medicinal plants"
*Esther Maria Ferreira Lucas* (CEFET-MG)
16:35 – 16:40 *Discussão*
16:40 – 16:55 "New steroidal saponins from *Solanum paniculatum* L. (Solanaceae) leaves"
*Alexander Bárbaro Valerino Díaz* (UNESP-IQAr)
16:55 – 17:00 *Discussão*
17:00 – 17:15 "Bergenin from *Peltophorum dubium*: isolation and cytotoxicity and antioxidant activities of its chemical derivatives"
*Oscar Caetano da Silva Neto* (UFBA)
17:15 – 17:20 *Discussão*
17:20 – 17:45 "Prospecção quimio-farmacológica de espécies brasileiras de Lauraceae - seleção de moléculas com ação antiparasitaria e antitumoral"
*João Henrique Ghilardi Lago* (UFABC)
17:45 – 17:50 *Discussão e Encerramento*

**18:00-20:00 Sessão I de discussão de painéis (Expocenter II)**
**Atenção:** os painéis deverão ser fixados no período das 11:30 às 13:30 e retirados a partir das 20:00 até 9:00 do dia seguinte.

| | |
|---|---|
| AMB-001 a AMB-035 | ANA-001 a ANA-032 |
| BEA-001 a BEA-008 | BIO-001 a BIO-007 |
| EDU-001 a EDU-022 | ELE-001 a ELE-021 |
| FIS-001 a FIS-015 | INO-001 a INO-035 |
| MAT-001 a MAT-044 | MED-001 a MED-024 |
| ORG-001 a ORG-038 | QPN-001 a QPN-045 |
| TEC-001 a FINAL | |

**20:00-21:00 Assembleias Regionais** (Sala a definir)

**21:00-22:00 Sessão de Homenagens** (Sala C-2)

**Medalha Simão Mathias**
- *Francisco José Krug* (CENA-USP)

**Prêmio SBQ de Inovação - Fernando Galembeck**
- *Jaime A. Rabi* (Microbiológica Química e Farmacêutica Ltda)

**JBCS Medal of Honor**
- *Richard G. Weiss* (Georgetown University)

**Prêmio Revista Virtual de Química**
- *Fabio Minoru Yamaji* (UFSCar)

**Prêmio PubliSBQ - Angelo da Cunha Pinto**
- *SciELO - Scientific Electronic Library Online*

# Quarta-feira – 23 de maio

**SBQ na Escola** (Expocenter III)
- *Manhã 1 - de 8:00 às 9:30*
- *Manhã 2 - de 9:45 às 11:15*
- *Noite - 19:30 - 21:00*

**08:00-10:00** **Minicursos**

**10:10-12:10** **Sessão RSC-SBQ** (Expo IV, espaço C)
- *Aldo José G. Zarbin* (UFPR)

- *Dominic Tildesley* (Imediate-past President da RSC)

- *Carlos Roque Duarte Correia* (UNICAMP)
"Noninnocent functional groups. enantioselective non-covalent substrate-directable heck and oxidative heck reactions: new paradigms and synthetic applications"

- *Mirella Di Lorenzo* (University of Bath)
"Screen printed fuel cell for self powered water quality monitoring"

**14:00-15:50** **Simpósio**

**Construindo o amanhã** (Expo IV, espaço C)
Coordenador: *Aldo José G. Zarbin* (UFPR)

Palestrantes: *Marcelo Marcos Morales* (Diretor de Instituição do CNPq)
*Ildeu Castro Moreira* (Presidente da SBPC)
*Paulo Coutinho* (Gerente do Instituto SENAI de Inovação)

**16:00-17:00** **Conferências Convidadas**

**Tetrapyrrole macrocycles – ancient molecules, brilliant future** (Sala A-2)
*- Jonathan S. Lindsey (North Carolina State University)*

**Learning with nature: chemical communication in microbial symbionts drives natural products discovery** (Sala C-2)
*- Mônica Tallarico Pupo* (FCFRP-USP)

**Química, arte e educação: soluções ou precipitações?** (Sala D-2)
*- Wilmo Ernesto Francisco Junior (UFAL)*

**17:00-18:00** **Conferências Convidadas**

**Materials design for energy harvesting and storage: insights from first-principles theory** (Sala A-2)
**-** *Carlos Moyses Graca Araujo (Uppsala University, Uppsala, Sweden)*

**Responsive and programmable hybrid materials obtained from self-assembly of nanobuiding blocks** (Sala C-2)
*- Galo Soler Illia (Instituto de Nanosistemas, Universidad Nacional de San Martín, Buenos Aires, Argentina)*

**Supramolecular approaches to control activity and selectivity in transition metal catalysis via the second coordination sphere** (Sala D-2)
- *Joost N. H. Reek* (University of Amsterdam)

**Programa de otimização de compostos líderes visando o desenvolvimento de candidatos clínicos em colaboração com a MMV e com a DNDi** (Sala F-2)
*- Luiz Carlos Dias (UNICAMP)*

**18:00-20:00** **Sessão II de discussão de painéis** (Expocenter II)
**Atenção:** os painéis deverão ser fixados no período das 11:30 às 13:30 e retirados a partir das 20:00 até 9:00 do dia seguinte.

| | |
|---|---|
| AMB-036 a AMB-070 | ANA-033 a ANA-064 |
| CAT-001 a CAT-017 | COL-001 a COL-005 |
| EDU-023 a EDU-045 | ELE-022 a ELE-042 |
| EST-001 a FINAL | FIS-016 a FIS-030 |
| FOT-001 a FOT-008 | INO-036 a INO-070 |
| MAT-045 a MAT-090 | MED-025 a MED-046 |
| ORG-039 a ORG-075 | QPN-046 a QPN-090 |

**18:00-20:00** **Lançamento de Livros (Expocenter II)**

Título: **"QUÍMICA – matéria, energia e transformações"**
Autores: *José Carlos de Azambuja Bianchi, Carlos Henrique Albrecht e Daltamir Justino Maia*
Editora: Editora do Brasil

Título: **"Fundamentos de Espectrometria e Aplicações"**
Autores: *Valdemar Lacerda Júnior (Editor) e Diversos Colaboradores*
Editora: Atheneu

Título: **"QUÍMICA ORGÂNICA – Estrutura e Propriedades de Compostos Orgânicos"**
Autores: *Paulo Marcos Donate (Editor do Volume), Arlene Conçalves Correa, Claudio Di Vitta, Flávio da Silva Emery, Giuliano Cesar Clososki, Luiz Alberto Beraldo de Moraes, Massami Yonashiro, Rosangela da Silva de Laurentiz*
Editora: Atheneu

Título: **"Estudos de Caso para o Ensino de Química 1"**
Autores: *Salete Linhares Queiroz e Erasmo Moisés dos Santos Silva*
Editora: CRV; Ano Edição: 2017

Título: **"Comunicação e Linguagem Científica: Guia para Estudantes de Química (2ª Edição)"**
Autores: *Salete Linhares Queiroz e Jane Raquel Silva de Oliveira*
Editora: Editora Átomo; Ano Edição: 2017

Título: **"Introdução à Modelagem Molecular para Química, Engenharia e Biomédicas: Fundamentos e Exercícios"**
Autor: *André Mauricio de Oliveira*
Editora: Appris

Título: **"Grandezas, Unidades e Símbolos em Físico-Química (Livro Verde)"**
*Tradução atualizada para o Português (nas variantes brasileira e portuguesa) da 3ª edição em Inglês, coordenada por Romeu C. Rocha-Filho e Rui Fausto*
Editora: Editora da SBQ - EditSBQ

**20:00-21:00** **Assembleias Divisionais**

Divisão de Catálise (Sala D-1)
Divisão de Eletroquímica e Eletroanalítica (Sala D-2)
Divisão de Ensino de Química (Sala D-3)
Divisão de Físico-química e Química Teórica (Sala F-1)
Divisão de Fotoquímica (Sala F-2)
Divisão de Produtos Naturais (Sala C-2)
Divisão de Química Ambiental (Sala C-3)
Divisão de Química Analítica (Sala A-1)
Divisão de Química de Materiais (Sala A-2)
Divisão de Química Inorgânica (Sala C-1)
Divisão de Química Medicinal (Sala F-3)
Divisão de Química Orgânica (Sala A-3)

**22:00** **Festa**

# Quinta-feira – 24 de maio

**SBQ na Escola** (Expocenter II)
- *Manhã 1 - de 8:00 às 9:30*
- *Manhã 2 - de 9:45 às 11:15*

**08:00-10:00 Minicursos**

**10:10-12:00 Sessões Temáticas**

**Energia: uma abordagem multidisciplinar** (Sala A-1)
Coordenadoras: *Shirley Nakagaki Bastos* (UFPR)
*Célia Machado Ronconi* (UFF)
*Clésia Cristina Nascentes* (UFMG)
*Maria Valnice B. Zanoni* (IQAr-UNESP)
Palestrantes: *Ana Flávia Nogueira* (UNICAMP)
"**Nanomaterials applied to solar energy conversion"**

*Marco Antônio Chaer do Nascimento* (UFRJ)
**"Células fotovoltaicas do tipo Gratzel"**

*Roberto Manuel Torresi* (USP)
**"O protagonismo da eletroquímica na disrupção tecnológica da distribuição, armazenamento e conversão de energia"**

**A química da vida: da célula ao reator** (Sala A-2)
Coordenadores: *Mauricio Moraes Victor* (UFBA)
*Rafael Victorio Carvalho Guido* (USP)
*Roberto Gomes de S. Berlinck* (IQSC-USP)
Palestrantes: *Rodrigo Octavio M. Alves de Souza* (UFRJ)
*Marin van Heel* (LNNano-CNPEM)
*Gregory Challis* (University of Warwick)

**Elas, as cientistas!** (Sala A-3)
Coordenadoras*: Elisa Orth* (UFPR)
*Rossimiriam P. de Freitas* (UFMG)

Palestrantes: *Yvonne Primerano Mascarenhas* (IFSC-USP)
"**Women in Science and Society**"

*Paulina Pavez* (Pontificia Univ. Católica de Chile)
"**Women and research in Chile**"

*Elisama Vieira dos Santos* (UFRN)
"**Women in Brazilian Science**"

**Os desafios na formação do profissional da química no âmbito da transformação digital: Química 4.0** (Sala C-2)
Coordenador: *Fernando Tibau* (Gerente de Inovação e Assuntos Regulatórios ABIQUIM)

Mesa Redonda*: Luiz Henrique Catalani* (IQUSP) – Moderador
*Reinaldo Spitzner Neto* (Diretor de Função Industrial da América Latina, SOLVAY) – Palestrante
*Alex Rodrigues* (Gerente de gestão estratégica, BRASKEM) - Palestrante

**13:00-15:00 Sessão III de discussão de painéis (Expocenter II)**

**Atenção:** os painéis deverão ser fixados no período das 09:30 às 11:30 e retirados a partir das 15:00 até às 19:00.

| | |
|---|---|
| AMB-071 a FINAL | ANA-065 a FINAL |
| BEA-009 a FINAL | BIO-008 a FINAL |
| CAT-018 a FINAL | COL-006 a FINAL |
| EDU-046 a FINAL | ELE-043 a FINAL |
| FIS-031 a FINAL | FOT-009 a FINAL |
| INO-071 a FINAL | MAT-091 a FINAL |
| MED-047 a FINAL | ORG-076 a FINAL |
| QPN-091 a FINAL | QVE-001 a FINAL |
| TEO-001 a FINAL | |

**15:00-18:30 Sessões Coordenadas**

**Química Ambiental - II** (Sala A-1)

Coordenadora: *Márcia Cristina Bisinoti* (UNESP)

15:00 – 15:25 "Importância dos compostos orgânicos voláteis para a química da atmosfera da região metropolitana de São Paulo"
*Adalgiza Fornaro* (IAG-USP)

15:25 – 15:30 *Discussão*

15:30 – 15:45 "Hidrocarbonetos policíclicos aromáticos (HPA) no material particulado (MP) do estado de Goiás"
*Dênia Kássia Aureliano Dal Castel (UFG)*

15:45 – 15:50 *Discussão*

15:50 – 16:05 "Influência da adição de matéria orgânica em interações matal nano-parículas"
*Daniele Frasson Vieira* (UNESP)

16:05 – 16:10 *Discussão*

16:10 – 16:25 "Evaluation of arsenic bioavailability in waste from cyanidation gold processing using sequential extraction schemes (SES)"
*Daniel Alves Barcelos* (UFRJ)

16:25 – 16:30 *Discussão*

16:30 – 16:45 "Development of a nanomaterial incorporated with bixin: a sustainable approach for dye removal from aqueous matrices"
*Junielly Tomaz Domingues* (UFMG)

16:45 – 16:50 *Discussão*

16:50 – 17:15 "UV-C/$H_2O_2$, microfiltration and reverse osmosis applied to remove emerging contaminants considering the potable reuse treatment of water"
*Cassiana Carolina Montagner (UNICAMP)*

17:15 – 17:20 *Discussão*

17:20 – 17:35 "Utilização da mistura de macrófitas aquáticas para tratamento de efluentes contendo corante"
*Rachel de Moraes Ferreira* (FIOCRUZ)

17:35 – 17:40 *Discussão*

17:40 – 17:55 "Influence of the iron source and pH on degradation of fipronil by photoFenton process"
*Oswaldo Gomes Junior* (UFU)

17:55 – 18:00 *Discussão*

18:00 – 18:25 “C lábil em solos do Paraná – correlações utilizando análise multivariada”
*Ísis Kaminski Caetano* (UNICENTRO)
18:25 – 18:30 *Discussão e Encerrament*

**Química Analítica - II** (Sala A-2)
Coordenador: *Josué Carinhanha Caldas Santos* (UFAL)
15:00 – 15:25 “Biopolímeros como adsorventes de espécies elementares e orgânicas para análises de águas por técnicas espectrométricas”
*Pedro Vitoriano de Oliveira* (IQUSP)
15:25 – 15:30 *Discussão*
<15:30 – 15:45 “Luminomagnetic core-shell nanoparticles for detection of metallic ions”
*Eliane Ayumi Namikuchi* (UNICAMP)
15:45 – 15:50 *Discussão*
15:50 – 16:05 “Polydiacetylene/triblock copolymer nanosensor for the detection of lidocaine in the presence of cocaine adulterants”
*Thaís Silva Soares* (UFV)
16:05 – 16:10 *Discussão*
16:10 – 16:25 “Development and validation of a LC-MS/MS method for analysis of fentanyl and its analogs in stamps”
*Jandyson Machado Santos* (UNICAMP)
16:25 – 16:30 *Discussão*
16:30 – 16:45 “Development and validation of a method to quantify acetaminophen in plasma from small rodents for the study of gastric emptying alterations”
*Monica Regina Pimentel Siqueira* (UERJ)
16:45 – 16:50 *Discussão*
16:50 – 17:15 “Versatile extraction phases: from sample preparation to direct injection techniques”
*Andréa Rodrigues Chaves (UFG)*
17:15 – 17:20 *Discussão*
17:20 – 17:35 “3D-printed platform for highly-reproducible handling of microvolumes and nanofluidic injection coupled to electrochemical detection”
*Dianderson Mendonça* (UFU)
17:35 – 17:40 *Discussão*
17:40 – 17:55 “Synthesis and application of molecularly impressed polymers for the extraction of caffeine from food and beverage samples”
*Fernanda Neves Feiteira* (UFF)
17:55 – 18:00 *Discussão*
18:00 – 18:25 “A experiência do Laboratório de Química Analítica Fundamental e Aplicada da UFF em amostras ambientais e de alimentos”
*Annibal Duarte Pereira Netto* (UFF)
18:25 – 18:30 *Discussão e Encerramento*

**Catálise** (Sala D-1)
Coordenador: *Dalmo Mandelli* (UFABC)
15:00 – 15:25 “Bimetallic nanoparticles for $H_2$ production: what is the true phase of the catalyst during reaction”
*Daniela Zanchet* (UNICAMP)
15:25 – 15:30 *Discussão*
15:30 – 15:45 “Cobalt(II) complexes of bidentate Schiff bases derived from cycloalkylamines as mediators in controlled radical polymerization of vinyl acetate”
*Yan Fraga da Silva* (UNESP)
15:45 – 15:50 *Discussão*

15:50 – 16:05 "Chemical modification of gum arabic for dephosphorylation reactions: hydroxamate-derived biocatalyst"
*Willian Hideki Takarada* (UFPR)
16:05 – 16:10 *Discussão*
16:10 – 16:25 "Use of Carboxyl Cellulose Metal Complexes in Heterogeneous Catalytic Systems to Promote Suzuki-Miyaura Coupling"
*Guilherme Bandeira Candido Martins* (UnB)
16:25 – 16:30 *Discussão*
16:30 – 16:45 "Novel fragrant aldehydes via hydroformylation of the bio renewable valencene"
*Gabriel Matos Vieira* (UFMG)
16:45 – 16:50 *Discussão*
16:50 – 17:15 "Solventless liquid phase conversion of glycerol with $CO_2$"
*Pedro Pablo Florez Rodriguez (UFAL)*
17:15 – 17:20 *Discussão*
17:20 – 17:35 "Heterogeneous acid catalysts based on sulfonated graphene like structures produced from bio-oil"
*Fabiane Carvalho Ballotin* (UFMG)
17:35 – 17:40 *Discussão*
*17:40 – 17:55* "Síntese de compostos de aroma catalisados por lipases através do reaproveitamento da borra de café"
*Regiane Késsias Sousa Lira* (UFRJ)
17:55 – 18:00 *Discussão*
18:00 – 18:25 "Pushing the boundaries of gold catalysis"
*Liane Marcia Rossi* (IQUSP)
18:25 – 18:30 *Discussão e Encerramento*

**Eletroquímica e Eletroanalítica** (Sala D-2)
Coordenador: *Nelson Ramos Stradiotto* (IQAr-UNESP)
15:00 – 15:25 "Why could the nature of surface facets lead to differences in the activity and stability of metal oxide-based electrochemical sensors?"
*Susana Inés Córdoba de Torresi (IQUSP)*
15:25 – 15:30 *Discussão*
15:30 – 15:45 "Development of an electrochemical lectin-based biosensor using a novel galectin-1-maltose binding protein fusion molecule"
*Pâmela Oliveira Martins Gomes* (FCFRP-USP)
15:45 – 15:50 *Discussão*
15:50 – 16:05 "Electrochemical sensor based on MIP grafted on multi-walled carbon nanotubes for 17-beta-estradiol determination"
*Fernanda Garcia de Almeida* (UEL)
16:05 – 16:10 *Discussão*
16:10 – 16:25 "Niobium as co-electrocatalyst for Pd in alkaline medium: improved selectivity and mechanism for ethanol electrooxidation reaction"
*Felipe de Moura Souza* (UFABC)
16:25 – 16:30 *Discussão*
16:30 – 16:45 "Influence of the electrode and chaotropicity of the electrolyte on the oscillatory behavior of the electrocatalytic oxidation of $SO_2$"
*Renan Lopes Munhos* (IQUSP)
16:45 – 16:50 *Discussão*
16:50 – 17:15 "Advances on batch-injection analysis: new materials for improved electrochemical detection and *on-site* applications"
*Rodrigo Alejandro Abarza Muñoz* (UFU)
17:15 – 17:20 *Discussão*

17:20 – 17:35 "Evaluation of sulfonamide-based anilines as a corrosion inhibitor for 1020 carbon steel "
*Vinícius Latgé Meira* (IFRJ)
17:35 – 17:40 *Discussão*
17:40 – 17:55 "Correlating surface growth of nanoporous gold with electrodeposition parameters to optimize amperometric sensing of nitrite"
*Josué Martins Gonçalves* (IQUSP)
17:55 – 18:00 *Discussão*
18:00 – 18:25 "Rational design of carbon material for nanomedicine applications"
*Zeki Naal* (FCFRP-USP)
18:25 – 18:30 *Discussão e Encerramento*

**Físico-Química/Química Teórica/Química de Superfícies e Colóides** (Sala D-3)
Coordenador: *Nelson Henrique Morgon (UNICAMP)*
15:00 – 15:25 "Chiromagnetic nanoparticles and gels"
*André Farias de Moura* (UFSCar)
15:25 – 15:30 *Discussão*
15:30 – 15:45 "Superhydrophobic self-cleaning surfaces and slippery lubricated ones effect upon inorganic scaling"
*Filipe Signorelli* (UNICAMP)
15:45 – 15:50 *Discussão*
15:50 – 16:05 "Surface modification of aseptic carton package for energy harvesting devices"
*Kelly Schneider Moreira* (UFSM)
16:05 – 16:10 *Discussão*
16:10 – 16:25 "Microbial habitability of Europa sustained by radioactive sources"
*Douglas Galante* (CNPEM)
16:25 – 16:30 *Discussão*
16:30 – 16:45 "Evaluation of the power conversion efficiencies of organic photovoltaic devices - theoretical investigation"
*Gabriela Martinez Miranda* (UFPR)
16:45 – 16:50 *Discussão*
16:50 – 17:15 "Structure–behavior study of "hybrid cyanine" phenolate dyes which exhibit inverted solvatochromism"
*Vanderlei Gageiro Machado (UFSC)*
17:15 – 17:20 *Discussão*
17:20 – 17:35 "The use of agro-industrial waste and *Moringa oleifera* leaves as antioxidants' sources for soy oil biodiesel"
*Marcia Gabriela Pianaro Valenga* (UNICENTRO)
17:35 – 17:40 *Discussão*
17:40 – 17:55 "Topological study of interactions between some inhibitors and ALK-5 using QTAIM methodology"
*Michell de Oliveira Almeida* (UFABC)
17:55 – 18:00 *Discussão*
18:00 – 18:25 "Interactions of biomolecules with cell membrane models probed by sum-frequency vibrational spectroscopy"
*Rafael de Oliveira Pedro* (IQSC-USP)
18:25 – 18:30 *Discussão e Encerramento*

**Fotoquímica** (Sala F-1)
Coordenador: *Antonio Eduardo da Hora Machado (UFU)*
15:00 – 15:25 "Nature-inspired fluorescent betalains"
*Erick Leite Bastos* (IQUSP)
15:25 – 15:30 *Discussão*

15:30 – 15:45 “Estudo da interação entre azul de metileno e curcumina para uso em terapia fotodinâmica combinada com antiangiogênica”
*Rodrigo Costa e Silva* (UFG)
15:45 – 15:50 *Discussão*
15:50 – 16:05 “Síntese e caracterização do complexo [Ru(phen)2(iso)]PF6”
*Beatriz Pachel* (UFSCar)
16:05 – 16:10 *Discussão*
16:10 – 16:25 “Photocatalyzed [2+2]-cycloaddition of 3-(2-oxo-2-phenylethylidene)-2-oxindole by ruthenium complexes”
*Rodolfo Inêz Teixeira* (UFRJ)
16:25 – 16:30 *Discussão*
16:30 – 16:45 “Synthesis and photophysical studies of new fluorescent N-acylhydrazone and semicarbazone-7-NEt2-coumarin dyes”
*Thiago Moreira Pereira* (UFRRJ)
16:45 – 16:50 *Discussão*
16:50 – 17:15 “Fotodegradação de diclofenaco de sódio e monitoramento de redução de toxicidade”
*Danilo Rodrigues de Souza (UFOB)*
17:15 – 17:20 *Discussão*
17:20 – 17:35 “Produção fotoquímica de $O_2$ e $H_2$ a partir da água usando um complexo triscarbonil de Mn(I) na ausência de oxidantes*”*
*Rafael Cavalieri Marchi* (UFSCar)
17:35 – 17:40 *Discussão*
17:40 – 17:55 “Amyloid beta monitoring through a Ru(II) Complex: Luminescent probe candidate for early diagnosis of Alzheimer’s disease”
*Mariana Pigozzi Cali* (UFSCar)
17:55 – 18:00 *Discussão*
18:00 – 18:25 “Photobleaching comportament of different phthalocyanines with a similar singlet oxygen quantum yield”
*André Romero da Silva* (IFES)
18:25 – 18:30 *Discussão e Encerramento*

**Química Inorgânica - II** (Sala C-1)
Coordenador: *André Luiz B. Formiga* (UNICAMP)
15:00 – 15:25 “Modificação de mesoporos de silica para aplicação em adsorção”
*Maria Helena de Araujo* (UFMG)
15:25 – 15:30 *Discussão*
15:30 – 15:45 “Synthesis and characterization of basic catalysts designed by calixarenes or silicas to take advantage of glycerol”
*Daniela Machado* (UNIFESP)
15:45 – 15:50 *Discussão*
15:50 – 16:05 “Novel binuclear chromium(III) complexes with potential application as building blocks in single molecule magnets synthesis”
*Bruno José Stoeberl* (UTFPR)
16:05 – 16:10 *Discussão*
16:10 – 16:25 “Iron (III) dinuclear metallacycle cavity as an effective ammonia storage system”
*Ingrid Fernandes Silva* (UFMG)
16:25 – 16:30 *Discussão*
16:30 – 16:45 “Synthesis, characterization and biological activity of complex nitrosyls”
*Iury Araújo Paz* (UFC)
16:45 – 16:50 *Discussão*

16:50 – 17:15 “Organic and inorganic amphiphiles as a basis for new antitumors, thin films and devices”
*Herbert Winnischofer (UFPR*)
17:15 – 17:20 *Discussão*
17:20 – 17:35 “Helical coordination polymer from manganese(II) 16-metallacrown-6 recognition of zwitterionic L-glutamate*”*
*Thomaz Arruda Wioppiold* (UFSM)
17:35 – 17:40 *Discussão*
17:40 – 17:55 “Investigation of the adduct between chlorite and chlorine dioxide by electronic spectroscopy”
*Gláucia Wanzeller Martins* (UFRJ)
17:55 – 18:00 *Discussão*
18:00 – 18:25 “Porfirinas de manganês: catalisadores versáteis para a oxidação de substratos orgânicos por vias mais sustentáveis”
*Gilson de Freitas Silva* (UFMG)
18:25 – 18:30 *Discussão e Encerramento*

**Química de Materiais - II** (Salas C-2 e 3)
Coordenador: *Patrícia Pommé Confessori Sartoratto* (UnB)
15:00 – 15:25 “Functionalization and nanocatalysis: the perfect match!”
*Elisa Souza Orth* (UFPR)
15:25 – 15:30 *Discussão*
15:30 – 15:45 “Novel conducting, biocompatible and biodegradable copolymer PEDOT-co-PLLA for biomedical applications”
*Aruã Clayton da Silva* (IQUSP)
15:45 – 15:50 *Discussão*
15:50 – 16:05 “Influence of different fuels in the combustion synthesis of copper vanadate and its application in photocatalysis”
*Luan Pereira Camargo* (UEL)
16:05 – 16:10 *Discussão*
16:10 – 16:25 “Rare earth oxide-based nanoparticles with application in photodynamic therapy for cancer”
*Bianca Almeida da Silva* (PUC-Rio)
16:25 – 16:30 *Discussão*
16:30 – 16:45 “Preparation of $BiVO_4$-decorated ZnO nanorods for oxygen evolution using photo-electrocatalysis”
*Rafael Mascarenhas de Almeida* (UFABC)
16:45 – 16:50 *Discussão*
16:50 – 17:15 “The size effect and hierarchical nanostructuring on semiconductor and metallic materials”
*Italo Odone Mazali* (UNICAMP)
17:15 – 17:20 *Discussão*
17:20 – 17:35 “Study of LCC and quitosane gel toxicity: parametrisation in arthropod test*”*
*Francisco Cardôso Figueiredo* (UFPI)
17:35 – 17:40 *Discussão*
17:40 – 17:55 “Photoluminescence and scintillation of $GdOCl:Eu^{3+}$ obtained from homogeneous precipitation method”
*Maike de Oliveira Krauser* (UNESP-IQAr)
17:55 – 18:00 *Discussão*
18:00 – 18:25 “Banana-shaped and ionic liquid crystals derived from *N*-heterocycles: Synthesis and mesomorphic characterization”
*Hugo A. Gallardo Olmedo* (UFSC)
18:25 – 18:30 *Discussão e Encerramento*

**Química Orgânica - II** (Sala -A-3)

Coordenador: *Cristiano Raminelli* (UNIFESP)

15:00 – 15:25 "On the synthesis of bioactive quinoidal molecules via C-H functionalization logic: A new frontier for potent trypanocidal quinones"
*Eufrânio Nunes da Silva Júnior* (UFMG)

15:25 – 15:30 *Discussão*

15:30 – 15:45 "Palladium-catalyzed arbonylative α-arylation of azlactones"
*Danielle Lobo Justo Pinheiro* (UFJF)

15:45 – 15:50 *Discussão*

15:50 – 16:05 "Reações de bromoaminociclização enantiosseletivas"
*Jullyane Emi Matsushima* (UNIFESP)

16:05 – 16:10 *Discussão*

16:10 – 16:25 "Laccase-catalyzed synthesis of dimers from 2,6-DMP: Optimization of TMBP synthesis and evaluation of its antioxidant action in biodiesel"
*Jeseka Gabriela Schirmann* (UEL)

16:25 – 16:30 *Discussão*

16:30 – 16:45 "Arylation of β-ketosulfoxonium ylides with arynes: a direct synthesis of pro-chiral ylides and mono-arylated ketones"
*Alexander Garay Talero* (IQSC-USP)

16:45 – 16:50 *Discussão*

16:50 – 17:15 "C-H functionalization. An efficient synthetic strategy for the synthesis of poly-aromatic fluorophores"
*Simon John Garden* (UFRJ)

17:15 – 17:20 *Discussão*

17:20 – 17:35 "Silver-catalyzed direct selenylation of indoles"
*Elise Ane Maluf Rios* (UFPR)

17:35 – 17:40 *Discussão*

17:40 – 17:55 "Continuous flow biocatalyzed process enhanced production of (r)-1,2-propanediol mediated by immobilized candida antarctica lipase B"
*Anderson Rodríguez Aguillón* (UFRJ)

17:55 – 18:00 *Discussão*

18:00 – 18:25 "Síntese total de produtos naturais bioativos"
*Julio Cezar Pastre* (UNICAMP)

18:25 – 18:30 Discussão e Encerramento

**Química de Produtos Naturais - II** (Salas F-2 e 3)

Coordenadora: *Eliane de Oliveira Silva* (UFBA)

15:00 – 15:25 "Espectrometria de massas sequencial e molecular networking para a desreplicação/descoberta de azafilonas do fungo *Penicillium sclerotigenum*"
*Hector Henrique Ferreira Koolen* (UEA)

15:25 – 15:30 *Discussão*

15:30 – 15:45 Antitrypanosomal activity and evaluation of the mechanism of action of acetogenins from the seeds of *Porcelia macrocarpa* (Annonaceae)"
*Emerson Alves de Oliveira* (UNIFESP)

15:45 – 15:50 *Discussão*

15:50 – 16:05 "Potencial antiproliferativo em células tumorais humanas do alcaloide 4-N-óxido-harmano isolado da espécie *Psychotria schlechtendaliana*"
*José Guilherme de Souza Corrêa* (UEM)

16:05 – 16:10 *Discussão*

16:10 – 16:25 "Butenolídeos com atividade anti-*Leishmania* isolados de *Nectandra oppositifolia* Ness & Mart (Lauraceae)"
*Geanne Alexsandra Alves Conserva* (UFABC)

16:25 – 16:30 *Discussão*

16:30 – 16:45 "Evaluation of the effect on the mitochondrial membrane potential in *L. amazonensis* caused by calealactone C isolated from *Calea pinnatifida*"
*Lhaís Araújo Caldas* (UNIFESP)
16:45 – 16:50 *Discussão*
16:50 – 17:15 "Molecular Networking como uma Estratégia de Desreplicação de *Hymenaea stigonocarpa* (Fabaceae)"
*Vanessa Gisele Pasqualloto Severino (UFG)*
17:15 – 17:20 *Discussão*
17:20 – 17:35 "Chemical composition and mineral content in monofloral bee pollen from *Elaeis guineensis"*
*Ayala Nara Pereira Gomes* (UFRPE)
17:35 – 17:40 *Discussão*
17:40 – 17:55 "Interações químicas de micro-organismos presentes no formigueiro das formigas cortadeiras: análise do metabolismo secundário do cocultivo do fungo mutualista, *Leucoagaricus gongylophorus*, com fungos negros"
*Alana Kelyene Pereira* (UFSCar)
17:55 – 18:00 *Discussão*
18:00 – 18:25 "*Citrus phytopathogens* battle: A nature's story of chemical warfare and survival"
*Taicia Pacheco Fill* (UNICAMP)
18:25 – 18:30 *Discussão e Encerramento*

**19:00** **Assembleia Geral Ordinária da Sociedade Brasileira de Química** (Expocenter IV)
Após o término da Assembleia, coquetel de Encerramento

# Expositores

**AGILENT Technologies Brasil Ltda.**
www.agilent.com

**BÜCHI Brasil Ltda.**
www.buchi.com/en/worldwide/brasil

**GVS do Brasil Ltda.**
www.gvs.com/

**MBRAUN Inc.**
www.mbraun.com

**METROHM Pensalab Instrumentação Analítica Ltda.**
www.metrohm.com.br/

**PENSALAB Equipamentos Industriais S.A.**
www.pensalab.com.br

**Royal Society of Chemistry, RSC**
www.rsc.org

**SIGMA-ALDRICH Brasil Ltda.**
www.sigmaaldrich.com/brazil.html

**Bruker do Brasil Com. Rep. de Prod. Cient.**
www.bruker.com

www.gov.uk/world/organisations/british-embassy-brazil.pt

**HORIBA Scientific**
www.horiba.com/br/scientific/

**Maxcrom Instrumentos Científicos Ltda.**
allcrom.com.br

**NOVA ANALÍTICA Imp. e Exp. Ltda.**
www.analiticaweb.com.br

**Quantum Design International - Latin America**
qd-latam.com

**SHIMADZU do Brasil Comércio Ltda.**
www.shimadzu.com.br

**Waters Comercial Ltda.**
www.waters.com/waters/home.htm

# AMB – Química Ambiental

**AMB-001** **Hidrocarbonetos policíclicos aromáticos (HPA) no material particulado (MP) do estado de Goiás.** Castel, D. K. A. D. (PG); Araújo, E. S. (TC); Melo, G. R. (TC); Urban, R. C. (PQ) UFG

**AMB-002** **Evaluation of the Influence of the toll station construction in BR-040 in particulate matter concentrations.** Silva, K. B. O. (PQ); Ribeiro, J. P.R. (IC); Dionisio, E. R. (PQ); Maia, L. F. P. G. (PQ); Gioda, A. (PQ) PUC-RIO

**AMB-003** **Concentration of aliphatic and polycyclic aromatic compounds in atmospheric samples collected around a petrochemical site at São Paulo, Brazil.** Caumo, S. (PG); Custódio, D. (PQ); Vicente, A. (PQ); Alves, C. (PQ); Vasconcellos, P. C. (PQ) IQUSP

**AMB-004** **Evaluation of lead exposure in cooperative recycling workers.** Regina, C. A. C. (PG); Furtado, D. Z. S. (PG); Naozuka, J. (PQ); Silva, H. D. T. (PQ); Bechara, E. J. H. (PQ); Assuncao, N. A. (PQ) UNIFESP-Diadema

**AMB-005** **Estudo das taxas de emissão de aldeídos provenientes de uma câmara de combustão com OEC sob excitação acústica.** Cavalcante, J. B. H. (IC); Pereira, A. R. B. (PQ); Santos, A. A. B. (PQ); dos Anjos, J. P. (PQ); Guarieiro, L. L. N. (PQ) SENAI CIMATEC

**AMB-006** **The impact of Tijuca Forest in the mitigation of CO2.** Silva, C. M. de (PQ); Souza, T. de C. (IC); Dantas, T. C. (IC); Silva, L. L. da (IC); Corrêa, S. M. (PQ); Arbilla, G. (PQ) UFRJ

**AMB-007** **Carbonyl Compounds in Tijuca Forest, the largest secondary urban rainforest in the world, and Rio de Janeiro urban area.** Braga, A. (PG); Siciliano, B. (PG); Dantas, G. (PG); Silva, C. M. de (PQ); Arbilla, G. (PQ) UFRJ

**AMB-008** **Hourly isoprene concentrations in an urban forest, São Paulo megacity.** Santos, T. C. (PG); Dominutti, P. A. (PQ); Nogueira, T. (PQ); Fornaro, A. (PQ) IAG-USP

**AMB-009** **Contaminants in the gas phase, in the atmosphere of the Todos os Santos Bay - Ba.** Santana, F. O. (PG); Barbosa, J. L. (PG); Brito, A. V. S. (IC); Campos, V. P. (PQ) UFBA

**AMB-010** **Characterization of the morphological and mineral composition of total suspended particles collected in an urban area by SEM-EDS.** Araujo, R. G. O. (PQ); Costa, S. S. L. (PQ); Alves, J. C. (FM); Ribeiro, V. S. (PG); Garcia, C. A. B. (PQ); da Rocha, G. O. (PQ) UFBA

**AMB-011** **Hidrocarbonetos policíclicos aromáticos em águas do complexo lagunar de Jacarepaguá, Rio de Janeiro, RJ.** Souza, T. M. (PG); Sobrinho, M. L. (PQ); Bernardes, M. C. (PQ); Pereira Netto, A. D. (PQ) UFF

**AMB-012** **Etanol, peróxido de hidrogênio e acetaldeído na atmosfera de Ribeirão Preto e São Paulo: cidades impactadas pelo uso de etanol combustível.** Scaramboni, C. (PG); Campos, M. L. A. M. (PQ) FFCLRP-USP

**AMB-013** **Use of moss bag technique, Sphagnum subsecundum as biofilter, for the monitoring of metals in the air in the city of Barreiras-BA.** Leite, O. D. (PQ); De Sá, C. F. (PG); Ogava, L. E. (PG); Da Guarda, L. D. C. (PG); Santos, J. L. O. (PQ); Torquato, A. S. (PQ); Flores, E. L. M. (PQ) UFOB

**AMB-014** **High uranium concentrations in the groundwater of the Rio de Janeiro State Mountainous Region.** Godoy, J. M. (PQ); Ferreira, P. R. (PQ); Souza, E. M. (PQ); Silva, L. I. (IC); Bittencourt, I. (IC); Fraifeld, F. (IC) PUC-RIO

**AMB-015** **Detection of p-aminophenol and sub-products formed during oxidative process in water and hair salon effluent.** Souza, J. C. (PG); Silva, B. F. (TC); Zanoni, M. V. B. (PQ) IQAr-UNESP

**AMB-016** **Quantification and statistical evaluation of metals and metalloids in water samples from Barra Longa after the rupture of the Fundão dam (Mariana).** Diniz, C. F. S. (PG); Nascentes, C. C. (PQ); Windmöller, C. C. (PQ) UFMG

**AMB-017** **Assessment of the risk of contamination of water resources by pesticides in the city of Petrolina - PE.** Oliveira, F. P. S. (IC); Nunes, J. T. L. (IC); Almeida, M. D. S. (PQ); Oliveira, A. H. B. (PQ); Melo, D. Q. (PQ); Vieira, G. A. B. (PQ) IF-Sertão Pernambucano

**AMB-018** **Optimization of large volume injection for determination of organophosphorus flame retardants in river water by GC-MS.** Cristale, J. (PQ); Fagnani, E. (PQ) FT-UNICAMP

**AMB-019** **Determinação da concentração de íons próximo a foz do rio Paraíba do Sul.** Nunes, C. R. de O. (TC); Menezes, G. da G. (IC); Borges, C. G. (TC); Araujo, T. M. de R. (PQ) IFF

**AMB-020** **Microextraction using RDSE and BAμE techniques as strategies for the determination of pesticides and emerging contaminants in environmental water samples by UHPLC-MS/MS.** Zanella, R. (PQ); Donato, F. F. (PQ); de Souza, M. P. (PG); Prestes, O. D. (PQ); Adaime, M. B. (PQ) UFSM

**AMB-021** **Análise por varredura de resíduos de agrotóxicos nas águas do Parque Indígena do Xingu.** Gonçalves, H. (IC); Cerqueira, T. (PG); Oliveira-Silva, D. (PQ) UNIFESP-Diadema

**AMB-022** **PAH baselines for riverine surficial sediments from Amazonian Coastal Zone.** Rodrigues, C. C. S. (PG); Ramos, B. S. (IC); Santos, E. (PG); Damasceno, F. D. (PQ) UFS

**AMB-023** **Assessment of contamination of amazonian streams by somestic sewage using sterols.** de Melo, M. G. (PG); de Lima, V. R. L. (IC); da Silva, B. A. (IC); Costa, G. de S. (IC); Val, A. L. (PQ); Koolen, H. H. F. (PQ); Bataglion, G. A. (PQ) UFAM

**AMB-024** **River basin barigui: determination of the drugs ibuprofen, ketoprofen and acetylsalicylic acid.** Silva, G. P. C. (IC); Filippe, T. C. (PG); Mayumi, L. (IC); Azevedo, J. C. R. (PQ); Monego, M. L. C. D. (PQ) UTFPR

**AMB-025** **Determination of biosorption capacity of microalgae biomass using the Boehm method.** Heidelmann, G. P. (IC); Roldão, T. M. (TC); Egler, S. G. (PQ); Giese, E. C. (PQ) CETEM

**AMB-026** **Evaluation of Arsenic bioavailability in waste from cyanidation Gold Processing using sequential extraction schemes (SES).** Barcelos, D. A. (PG); Pontes, F. V. M. (PQ); Silva, F. A. N. G. (PQ); Castilhos, Z. C. (PQ) UFRJ

**AMB-027** **Effects of chlorination on pesticides after drinking water treatment: residue analysis and acetylcholinesterase inhibition.** Costa, R. O. (PG); Barcellos, P. S. (PQ); Canela, M. C. (PQ) UENF

**AMB-028** **Especiação de cromo em águas naturais: estudos em Guarapuava, Santa Terezinha do Itaipu e Ponta Grossa, Paraná, Brasil.** Anjos dos, V. E. (PQ); De Andrade, J. K. (PG); De Andrade, C. K. (PG); Felsner, M. L. (PQ) UEPG

**AMB-029** **Human health risk assessment of metals and metalloids in superficial waters near different industrial sources in Juiz de Fora City, Brazil.** Soares, R. (PQ); Machado, W. T. V. (PQ); Campos, D. V. B. (PQ); Monteiro, M. I. C. (PQ); Freire, A. S. (PQ); Santelli, R. E. (PQ) UFF

**AMB-030** **Metals characterization in surface sediments of rivers in the Central Amazonian region.** Bisinoti, M. C. (PQ); Constantino, I. C. (PG); Teodoro, G. C. (IC); Paschoal, F. M. M. (PQ); Trindade, W. G. (PQ); Piovezan, C E (IC); Moreira, A B (PQ) IBILCE-UNESP

**AMB-031** **Monitoring of trace elements in sediments from the beaches next to the Doce River Estuary - ES/Brazil.** Cunha, T. (PG); Wyatt, N. L. P. (IC); Vieira, L. V. (PG); Krause, M. (PG); Brandão, G. P. (PQ); Albino, J. (PQ); Carneiro, M. T. W. D. (PQ) UFES

**AMB-032** **Evaluation of agrochemicals trifluralin, atrazine, alachlor and chlorpyrifos in soil samples from Arapongas - PR region.** Morro, F. G. (IC); Bernardelli, J. K. B. (PQ); Schnitzler, D. C. (PQ) UTFPR

**AMB-033** **Carbono oxidável com permanganato em solos do Paraná - horizontes dos solos e correlações com análise de macronutrinentes usando PCA.** Caetano, I. K. (PQ); Novacoski, E. J. (FM); Lustosa, L. H. (IC); Genú, A. M. (PQ); Lombardi, K. C. (PQ); Figueiredo Filho, A. (PQ); González-Borrero, P. P. (PQ) UNICENTRO

**AMB-034** **Adsorção individual e competitiva de chumbo em cinco solos de uma topossequência do cerrado brasileiro.** Sena, M. M. (PG); Busato, J. G. (PQ); Costa, A. C. S. (PQ); Sodré, F. F. (PQ) UnB

**AMB-035** **Utilização da estatística multivariada para a determinação dos parâmetros físicos e químicos mais relevantes do solo de trilha de Ubatuba-SP.** Jorge, M. C. O. (PQ); Guerra, A. J. T. (PQ); Mendonça, M. L. T. G. (FM); Cruz, R. P. (FM) UFRJ

**AMB-036** **Influência da adição de matéria orgânica em interações Metal-nanopartículas.** Vieira, D. F. (IC); Botero, W. G. (PQ); Oliveira, L. C. (PQ); Goveia, D. (PQ) UNESP-Itapeva

**AMB-037** **Avaliação da recuperação de potássio no vinhoto tratado por biorreator a membrana de duplo estágio (BRMAn).** Corrêa, L. B. M. (IC); Santos, L. V. S. (PQ); Guimarães, I. P. M. (IC); Barbosa, J. R. (IC) PUC-MG

**AMB-038** **CO2 capture by mixed matrix membranes with metal organic frameworks (MOF) of Al.** Abreu, T. P. (PG); Ferraz, H. C. (PQ); Moura, L. C. (PQ); Miranda, J. L. (PQ) UFRJ

**AMB-039** **Evaluation of the development of an acidophilic chemolithotrophic microorganism using meteoritic material as energy source.** Silva, G. G. (PG); Rodrigues, F. (PQ) IQUSP

**AMB-040** **Geração de microrganismos seletivos a partir da biomassa residual da casca do arroz para produção biocombustíveis.** Vieira, J. L. (IC); Silva, C. S. (PG); João, J. J. (PQ) UNISUL

**AMB-041** **Economia circular na agropecuária: ensaios iniciais para estabilização de resíduos orgânicos e produção de biogás.** Silva da, M. B. G. (IC); Domingues, M. P. P. (IC); Somensi, C. A (FM) IFC

**AMB-042** **Characterization of biomass produced in Algae Turf Scrubber (ATS®) system instaled in the Lago Dourado - Santa Cruz do Sul - RS.** Martini, F. A. (PG); Rubert, A. (IC); Souza, M. P. (PG); Kist, L. T. (PQ); Hoeltz, M. (PQ); Benitez, L.B. (PQ); Schneider, R. C. S. (PQ); Gressler, P. D. (PQ) UNISC

**AMB-043** **Utilização do babaço de cevada como adsorvente natural para a remoção do agrotóxico carbaril de solução aquosa.** Milhomem, K. P. (PG); Silva, T. F. (PG); Freitas, S. S. (PQ) UFG-Catalão

**AMB-044** **Development of a nanomaterial incorporated with bixin: a sustainable approach for dye removal from aqueous matrices.** Domingues, J. T. (PG); Rodrigues, G. D. (PQ); Orlando, R. M. (PQ); Millan, R. D. S. (PQ); Pinzón, A. D. G. (PG); Carvalho, P. L. G. (IC) UFMG

**AMB-045** **Application of Kraft lignin as alternative adsorbent for dyes and potential toxic metals.** Akiba, A. N. (PG); Silva, S. V. F. N. (PQ); Gaubeur, G. I. (PQ) UFABC

**AMB-046** **Development of nanostructured materials incorporated with bixin and extracting agents for metal removal from aqueous matrices.** Leite, D. S. (PG); Carvalho, P. L. G. (PG); Garcia, A. D. P. (PQ); Orlando, R. M. (PQ); Millán, R. D. S. (PQ); Rodrigues, G. D. (PQ) UFMG

**AMB-047** **Zeolites with different chemical and textural properties for metal removal.** Oliveira de, D. F. (PG); Neri, J. A. M. (IC); Ribeiro, J. A. A. (IC); Santos dos, F. S. (PQ); Pietre de, M. K. (PQ) UFF

**AMB-048** **UV-C/$H_2O_2$, microfiltration and reverse osmosis applied to remove emerging contaminants considering the potable reuse treatment of water.** Montagner, C. C. (PQ); Cochran, K. H. (PG); Fryer, B. (IC); Kimura-Hara, S. (PQ); Abdelraheem, W. (PG); Huang, Y (PG); Coffin, S. (PG); Schlenk, D. (PQ); Dionysiou, D. (PQ); Richardson, S. (PQ) SC. USA

**AMB-049** **Influence of the iron source and pH on degradation of fipronil by photo-Fenton process.** Gomes, O. (PG); Trovo, A. G. (PQ) UFU

**AMB-050** **Otimização multivariada de sistema UV/$H_2O_2$ para desinfecção de efluentes secundários.** Malvestiti, J. (PG); Diogo Junior, J.P. (PG); Dantas, R.F. (PQ) UNICAMP

**AMB-051** **Removal of azo dyes mixture by layered double hydroxides.** Lemes, L. O. (PG); Rosseto, R. (PQ) UEG

**AMB-052** **Síntese e caracterização de um novo polímero de coordenação fotocataliticamente ativo.** Manduca, B. (PG); Freire, R. S. (PQ) IQUSP

**AMB-053** **Adsorption of pharmaceuticals from aqueous solutions on FAU zeolite.** de Sousa, D. N. R. (PQ); Mozeto, A. A. (PQ); Fadini, P. S. (PQ) UFSCar

**AMB-054** **Degradation of Bisphenol A (BPA) by Trametes versicolor fungus.** Gracio, C. E. R. (IC); Bianchi, V. N. (IC); Montini, A. C. S. (IC); Silva, P. G. (PG); de Lima, E. C. (PQ) UFABC

**AMB-055** **Utilização do filtro de bagaço de cana de açúcar no tratamento simplificado de água.** Marcelo, L. R. (PQ); Almeida, V. P. (IC); Marcelo, C. R. (PQ); Arruda, V. M. (PQ) UEMG

**AMB-056** **Synthesis of polyurethane biocomposition used as adsorvent of yellow tartrazine food coloring.** França, I. A. (IC); Vollbrecht, C. P. (IC); Rizzato, T. M. (TC); Batistela, V. R. (PQ); Keller, M. (PQ) UEM

**AMB-057** **Phosphate adsorption by different clay minerals modified with lanthanum and iron for application in aquatic eutrophic environments.** Castro, L. F. (PG); Souza, W. F. L. (PQ); Teixeira, V. G. (PQ) INT

**AMB-058** **Sensitivity to the cadmium ion by a strain of Ensifer meliloti.** Morais, A. A. (IC); Leonel, T. F. (PG); Moretto, C. (PQ); Lemos, E. G. M. (PQ); Alves, L. M. C. (PQ); Saran, L. M. (PQ) FCAV-UNESP

**AMB-059** **Use of ultrasound to development of substrates for Saccharomyces cerevisiae.** Cordeiro, M. E. (IC); Nicolini, J. (PQ); Nicolini, K. P. (PQ) IFPR

**AMB-060** **Synthesis and characterization of pyroaurite-type material at room temperature employing bauxite residues from Amazon Region.** Nascimento, R. S. (PG); Costa, B. S. (IC); Figueira, B. A. M. (PQ); Silva, L. N. (PG); Telles, G. C. (PQ); Mercury, J. M. R. (PQ) UFOPA

**AMB-061** **Bixin incorporated over a porous membrane as a biosorbent to remove mercury (II) from aqueous matrices.** Vieira, J. C. (PG); Windmöller, C. C. (PQ); Rodrigues, G. D. (PQ); Orlando, R. M. (PQ) UFMG

**AMB-062** **Labilidade de íons ferro e manganês na presença de nano-sílica em diferentes valores de pH.** Goveia, D. (PQ); Vieira, D. F. (IC); Botero, W. G. (PQ); Oliveira, L. C. de (PQ) UNESP-Itapeva

**AMB-063** **Micropartículas poliméricas como um sistema carreador de nutrientes para plantas.** Chagas, J. O. (PG); Silva, G. A. (PQ); Lobo, F. A. (PQ) UFOP

**AMB-064** **Study of the partition of emerging contaminants employing aqueous two-phase systems as extraction technique.** Assis, R. C. (PG); Orlando, R. M. (PQ); Mageste, A. B. (PQ); Lemos, L. R. (PQ); Rodrigues, G. D. (PQ) UFMG

**AMB-065** **CHEMICAL WASTE MANAGEMENT IN TEACHING LABORATORIES: an activity proposal for academic community awareness.** Siqueira, L. D. F. (IC); Santos, J. M. S. R. (IC); Morais, K. C. (IC); Pereira, R. S. (IC); Paula, R. R. (IC); Mesquita, I. S. (TC); Teixeira, A. M. S. (PQ) IFRJ-Campus Duque de Caxias

**AMB-066** **Método alternativo para o descarte de resíduos de cobre e iodo.** Linhares, G. T. (IC); Vieira, B. L. M. (IC); Chinelate, B. M. (IC); Toledo, T. A. (TC); Barbosa, D. B. A. (FM) IF Sudeste MG

**AMB-067** **Chlorexidine behavior in chlorinated medium and occurrence of byproducts.** Colombo, R. (PQ); Carvalho, V. S. (IC) EACH-USP

**AMB-068** **Diagnóstico das condições sanitárias de residências localizadas às margens do Rio Sarapuí - Duque de Caxias, Rio de Janeiro.** Pereira, L. F. (IC); Santos, I. da S. P. (IC); Almeida, L. D. (IC); Sá, N. R. L. (TC); Marcelo, L. R. (PQ) IFRJ-Campus Duque de Caxias

**AMB-069** **Propriedades térmicas de blendas de ésteres metílicos e etílicos obtidos do óleo de Attalea phalerata (Arecaceae) e soja.** Silva, J. C. M. (PG); Nicolau, C. L. (PG); Coutinho, E. J. (IC); Klein, A. F. N. V. (PG); Simionatto, E. (PQ); Stropa, J. M. (PG); Oliveira, L. C. S. (PG) UEMS

**AMB-070** **Longitudinal variation of the energetic properties of clones Eucalyptus sp.** Santos dos, J. (IC); Silva, W. P. (PQ); Morais, S. A. (PG); Sá, V. A. (PQ); Accioly, J. E. S. (PQ) UFAL

**AMB-071** **Pigment's profile of the polyextremophile D. radiodurans under extreme conditions for biosignature's detection.** Cavalcante, L. L. (IC); Yamaguchi, L. F. (PQ); Paulino-Lima, I. G. (PQ); Rodrigues, F. (PQ) IQUSP

**AMB-072** **Evaluation of persistent toxic substances (PTS) in Brazilian coast fishes using exploratory chemometric methods.** Santos, I. C. (IC); Ferreira, V. B. (PQ); Figueiredo, E. R. (PG); Santos dos, G. R. (PG); Finco, F. D. B. A. (PQ); Lobo, F. A. (PQ); Torres, J. P. M. (PQ); Da Silva, G. A. (PQ) UFOP

**AMB-073** **Metallothionein and Reduced Glutathione: metal exposure biomarkers in rough-toothed dolphins (Steno bredanensis).** Monteiro, F. (PG); Moura, J. F. (PQ); Lemos, L. S. (PG); Moreira, I. (PQ); Saint'Pierre, T. D. (PQ); Kehrig, H. A. (PQ); Di Beneditto, A. P. M. (PQ); Siciliano, S. (PQ); Hauser-Davis, R. A. (PQ) PUC-RIO

**AMB-074** **Slow pyrolysis conditions applied to several types of lignocellulosic materials, industrial and domestic wastes - A review.** Romeiro, G. A. (PQ); Peixoto, B. S. (PG); Schroeder, P. (PG); Oliveira, P. C. O. (PG); Silva, R. V. S. (PQ); Figueiredo, M. K. K. (PQ); Veloso, M. C. C. (PQ); Bitencourt, G. F. (IC) UFF

**AMB-075** **Oxidative stability thermal properties study of esters formulated form Attalea speciosa oil.** Nicolau, C. L. (PG); Simionatto, E. (PQ); Costa, E. R. (PG); Louro, G. M. (PG); Silva, J. C. M (PG); Medeiros, T. A. (PG); Coutinho, E. J. (PG); Stropa, J. M. (PG) UEMS

**AMB-076** **Antibiotics colorimetric detection by stabilized silver nanosensors in water.** Moraes, L. D. (PG); Lopes, R. P. M. (PQ) UFV

**AMB-077** **Utilização da mistura de macrófitas aquáticas para tratamento de efluentes contendo corante.** Ferreira, R. M. F. (PG); Stapelfeldt, D. M. A. S. (PQ) UFRJ

**AMB-078** **Characterization of Sedimentary Humic Substances from White-water and black-water rivers.** Constantino, I. C.; Constantino, I. C (PG); Piovezan, C. E. (IC); Toschi, S. S. (IC); Bisinoti, M. C. (PQ); Moreira, A. B. (PQ) IBILCE-UNESP

**AMB-079** **Pesticides wastewater treatment by coagulation-flocculation: Evaluation and optimization of operational parameters.** Nossol, A. B. S. (PG); Santos, M. G. B. (IC); Trovó, A. G. (PQ) UFU

**AMB-080** **Atrazina e seus metabólitos em mananciais e águas de abastecimento público: sazonalidade e eficiência de remoção das ETA.** Silva, G. S. (IC); Montagner, C. C. (PQ) UNICAMP

**AMB-081** **Air quality biomonitoring of trace elements in Huancayo City, Peru using transplanted Tillandsia capillaris as bioindicators.** Andrade, V. P. (IC); De La Cruz, A. R. H. (PG); Calderon, E. R. D. (PQ); Aunque, R. F. O. (IC); De La Cruz, J. K. H. (IC); Gioda, A. (PQ) PUC-RIO

# *ANA – Química Analítica*

**ANA-001** **Stability of pesticides in green pepper samples stored at different temperatures.** Libardi, V. M (PG); Heleno, F. F. (PQ); Queiroz, M. E. L. R. (PQ); Neves, A. A. (PQ); Oliveira, A. F. (PQ) UFV

**ANA-002** **Development and optimization of analytical method for determination the antihypertensive drugs.** Ferreira, A. D. (PG); Weinert, P. L. (PQ) UEPG

**ANA-003** **Separation investigation of elaidic and vaccenic trans fatty acids isomers by CZE-UV.** Amorim, T. L. (PG); Oliveira, M. A. L. (PQ) UFJF

**ANA-004** **Synthesis and application of molecularly impressed polymers for the extraction of caffeine from food and beverage samples.** Feiteira, F. N. (PG); Francisco, J. E. (PG); da Silva, W. A. (PG); Pacheco, W. F. (PQ); Pereira Netto, A. D. (PQ) UFF

**ANA-005** **Síntese e caracterização de polímeros fluorescentes com núcleo de sílica para aplicação em cromatografia em camada delgada.** Ierick, I. F. (IC); Pupin, R. R. (PG); Monteiro, G. C. (PQ); Bolzani, V. S. (PQ); Sotomayor, M. P. T. (PQ) IQAr-UNESP

**ANA-006** **Determinação do teor de docetaxel em medicamentos injetáveis por HPLC-DAD.** Figueiredo, N.G. (PQ); Martins, V.G. (FM); Chiapetta, S.C. (PQ) INT

**ANA-007** **Development and optimization of chromatographic method for determination of hypolipidemic drugs in pharmaceutical formulations.** Golembiouski, C. (PG); Weinert, P. L. (PQ) UEPG

**ANA-008** **Otimização de metodologia para análise de cocaína em cédulas de real.** Mariano Junior, D. R. (PG); Alves, D. da P. (IC); Almeida, V. G. K. (PQ) UFRRJ

**ANA-009** **Development of a low-consuming solvent extraction for determination of 36 multiclass pesticides in atmospheric particulate matter (PM2.5).** Nascimento, M. M. (PG); da Rocha, G. O. (PQ); de Andrade, J. B. (PQ) UFBA

**ANA-010** **Influence of sample preparation in the determination of phenolic compounds in mate tea beverages by UPLC-MS.** Iop, G. D. (PG); Mendes, A. L. G. (PG); Codevilla, C. F. (PG); Barin, J. S. (PQ); Duarte, F. A. (PQ); Mello, P. A. (PQ) UFSM

**ANA-011** **Método bioanalítico para quantificação de Doxiciclina em plasma canino: aplicação em estudos de farmacocinética.** Lima, I. P. (PG); Ferreira, T. P. (TC); Magalhães, V. S. (TC); Scott, F. B. (PQ); Cid, Y. P. (PQ) UFRRJ

**ANA-012** **Determinação de pesticidas organoclorados na bacia hidrográfica do rio de Ondas, oeste da Bahia, por CG-MS.** do Rego, E. L. (PG); da Silva, J. D. S. (PG); Nakamura, T. C. (PG); Almeida, P. V. B. (PG); Pinto, C. O. (IC); Souza, R. C. (PG); de Souza, J. R. (PQ); Santos, J. V. da S. (PQ) UFOB

**ANA-013** **Desenvolvimento de método para análise de catecolaminas e metabólitos em urina por CL-EMAR.** Roiffé, R. R. (PG); Sardela, V. F. (PQ); de la Cruz, M. N. S. (PQ); Souza, K. R. (PQ); Nacif, J. E. (IC); Aquino Neto, F. R. (PQ) UFRJ

**ANA-014** **Characterization of 18 organochlorine pesticides in samples of coconut water in natura using CG-MS.** Nakamura, T. C. (PG); Rego, E. L. (PG); Brito, P. V. N. (PG); Silva, J. D. S. (PQ) UFOB

**ANA-015** **Development and validation of a method to quantify acetaminophen in plasma from small rodents for the study of gastric emptying alterations.** Siqueira, M.R.P. (PG); Moreira, D. de L. (PQ); Paumgartten, F.J.R. (PQ); Santos, R. dos (PG); Rosa, L. C. da (PG) ENSP

**ANA-016** **On-column preconcentration of phenolic compounds by sequential injection chromatography.** Acevedo, M. S. M. S. F. (PG); Gama, M. R. (PQ); Rocha, F. R. P. (PQ) CENA-USP

**ANA-017** **Development and validation of a LC-MS/MS method for analysis of fentanyl and its analogs in stamps.** Santos, J. M. (PQ); Morais, D. R. (PQ); Barbosa, L. M. (PG); Costa, J. L. (PQ); Eberlin, M. N. (PQ) UNICAMP

**ANA-018** **Evaluation of a chromatographic method for the determination of phenolic acids and methylxanthins in teA.** Azevedo, R. S. A. (PG); Teixeira, B. S. (TC); Santos, W. N. D. (PQ); Sauthier, M. C. S. (PG); Santana, M. V. A. (PQ); Santana, D. A. (PQ) UNEB

**ANA-019** **QuEChERS-SPE method for determination of endocrine disrupting compounds in harbor sediment.** Suagaura, L.E. (PG); Marchi, M. R. R. (PQ) IQAr-UNESP

**ANA-020** **A direct Mass Spectrometry method for determination of biomarkers in plasma samples.** Fernandes, A R (PG); Mendes, T P P (PG); Vaz, B G (PQ); Chaves, A R (PQ) UFG

**ANA-021** **Determinação dos aditivos presentes em cigarros e produtos derivados do tabaco por Espectrometria de Massas de Alta Resolução (nano-ESI-Orbitrap).** Guedes, J. S. (TC); Figueiredo, N. G. (PQ); Chiapetta, S. C. (PQ) INT

**ANA-022** **Berenil as a groove binding mode probe for DNA interaction process evaluation.** Silva, E. S. (IC); Lima, A. D. S. (IC); Figueiredo, I. M. (PQ); Santos, J. C. C. (PQ) UFAL

**ANA-023** **Fluorescent nanoprobes based on CdTe quantum dots for bioanalytical applications: determination of cationic protein.** Costa, K. R. (IC); Santos, J. C. C. (PQ) UFAL

**ANA-024** **Determination of the total polyphenol content in wines and grape juice by spectrofluorimetry and comparison with the Folin-Ciocalteu method.** E Souza, S.B. (IC); Oliveira, A.C.S. (IC); Donagemma, R.A. (PQ); Marques, F.F.C. (PQ) UFF

**ANA-025** **Chemiluminescent flow system for the determination of complexation capacity in opacity solutions: an automatic procedure.** Lima, M.J.A (PG); Reis, B.F (PQ); Kamogawa, M.Y (PQ) CENA-USP

**ANA-026** **Desenvolvimento de uma cela de fluxo para detecção de quimiluminescência empregando fotodiodo com detector.** Marinho, O.R (PG); Lima, M.J.A. (PG); Reis, B. F. (PQ) CENA-USP

**ANA-027** **Wetting film liquid-liquid microextraction in a sequential injection system for spectrofluorimetric determination of bisphenol A in tap waters.** Soares, S. S. (PG); Nascimento, N. F. C. (PG); Rocha, R. P. R. F. (PQ) CENA-USP

**ANA-028** **Procedimento limpo baseado em análises em fluxo para extração on-line de propoxur em amostras de carne.** Bragaia, G. P. (IC); Melchert, W. R. (PQ) ESALQ-USP

**ANA-029** **Real-Time Monitoring of Mono-, Di-, Triglycerides and FAME Composition by Low-Field 1H NMR and NIR Spectroscopy During Transesterification Reaction of Vegetable Oils.** Galvan, D. (PG); Aguiar, L. M. (PG); Rohwedder, J. J. R. (PQ); Borsato, D. (PQ); Killner, M. H. M. (PQ) UEL

**ANA-030** **Determination of lipid bioactive compounds in yellow, brown and black mustard seeds.** Nicacio, A. E. (PG); Rodrigues, C. A. (PG); Visentainer, J. V. (PQ); Maldaner, L. (PQ) UEM

**ANA-031** **Development and validation of quantitative NMR method for illegal pesticides.** Crocoli, L.C. (PG); Ortiz, R.S. (PQ); Moura, S. (PQ) UCS

**ANA-032** **Polydiacetylene/triblock copolymer nanosensor for the detection of lidocaine in the presence of cocaine adulterants.** Soares, T. S. (IC); Chagas, F. O. (PG); Patrício, P. R. (PQ); Maldaner, A. O. (PQ); da Silva, L. H. M. (PQ); Hespanhol, M. C. (PQ) UFV

**ANA-033** **Novel analytical method using reversed-phase dispersive liquid-liquid microextraction for determination of metallic contaminants in edible vegetable oils.** Flores, E. L. M. (PQ); Beato, M. O. (IC); Leite, O. D. (PQ); Canan, C. (PQ); Picoloto, R. S. (PQ); Ferreira, A. H. (PG) UTFPR

**ANA-034** **Development of method for direct multi-elemental analysis of whisky using total reflection X-ray fluorescence.** Gama, E. M. (PG); Matos, R. P. (PQ); Nascentes, C. C. (PQ); Rodrigues, G. D. (PQ) UFMG

**ANA-035** **Determination of bioavailability of nutrients in soil by extraction procedures and total reflection X-ray fluorescence.** Matos, R. P. (FM); Gama, E. M. (PG); Windmöller, C. C. (PQ); Nascentes, C. C. (PQ) UFMG

**ANA-036** **Application of fluorescence of X-rays (EDXRF) in atmospheric biomonitoring using tree bark.** Bitencourt Oliveira, L. (PQ); Teles de Oliveira, M. (IC); de Oliveira Almeida, C. M. (IC); Soares de Araújo, L. S. (IC); Lopes Coriolano, D. (PQ); Rodrigues Gomes, M. R. (PQ) IFS

**ANA-037** **Fast determination of metals using direct analysis of deodorants by inductively coupled plasma optical emission spectrometry.** Costa, W. K. O. C. (PG); Silva, C. S. (PQ); Fiqueiredo, J. F. D. (PQ); Nóbrega, J. A. (PQ); Paim, A. P. S. (PQ) UFSCar

**ANA-038** **Evaluation of a method for the decomposition of spent fluorescent lamps for the determination of rare earth elements.** Ferreira, E. M. (IC); Pontes, F. V. M. (PQ); Paulino, J. F. (PQ); Carneiro, M. C. (PQ) UFRJ

**ANA-039** **Silica functionalized with 2,6-pyridinedicarboxylic acid for selective preconcentration of Rare Earth elements traces before ICP-MS analysis.** Artiushenko, O. (PG); Sandoval, W. (PG); D. Saint'Pierre, T. (PQ); Zaitsev, V. (PQ) PUC-RIO

**ANA-040** **Determination of Cu, Ni, Pb and V in Brazilian gasoline by GF AAS using the technique of Extraction Induced by Microemulsion Breaking.** Vinhal, J.O. (PQ); Cassella, R.J. (PQ) UFF

**ANA-041** **An on-line preconcentration system using ion-imprinted polymer for determination of bismuth in seawater employing atomic fluorescence spectrometry.** Costa Ferreira, S. L. (PQ); Carvalho Andrade, H. M. (PQ); Assis Felix, C. S. (PG); Silva, D. G. (PG) UFBA

**ANA-042** **Microextração induzida por quebra de emulsão (MIEB) para determinação de metais em amostras de óleo diesel.** Fernandes, A. (PG); Dutra, A.J.B. (PQ); Cassella, R.J. (PQ) UFF

**ANA-043** **SS-FF-AAS AS an alternative technique for elemental impurities determination in high purity graphite.** Santos, R. F. (PG); Carvalho, G. S. (PG); Silva, F. A. (IC); Picoloto, R. S. (PQ); Bizzi, C. A. (PQ); Flores, E. M. M. (PQ) UFSM

**ANA-044** **Nickel and Vanadium Determination in Diesel Oil by ICP-OES after Reverse-Phase Dispersive Liquid-Liquid Microextraction.** Delpino, I. S. (PG); Druzian, G. T. (PG); Santos, R. F. (PG); Bolzan, R. C. (PQ); Flores, E. L. M. (PQ); Picoloto, R. S. (PQ) UFSM

**ANA-045** **Online Preconcentration of Sb(III) using $SiO_2/Al_2O_3/SnO_2$ Ternary Oxide Coupled with HGAAS.** Tarley, C.R.T. (PQ); de Almeida, F.G. (PG); Ribeiro, E.S. (PQ); de Oliveira, L. L.G. (PG); Orlandin, G. (IC) UEL

**ANA-046** **Evaluation of the analytical performance of a solid phase magnetic extraction method for $Pb^{2+}$ determination.** Alves, V. N (PQ); Silva, C. A. S (PG) UFG-Catalão

**ANA-047** **Determinação de Cr e Pb em óleo de peixe rico em ômega-3 por GF AAS utilizando a extração induzida por quebra de emulsão.** Arruda, T. F. (PG); Cassella, R. J. (PQ); Lepri, F. G. (PQ) UFF

**ANA-048** **Aplicação de ácido diluído em digestão assistida por micro-ondas para determinação multielementar em variedades de mosto de uva.** Santos, V. de S. (PG); Korn, M. das G. A. (PQ); Santos, W. P. C. (PQ) UFBA

**ANA-049** **Precipitação homogênea de $Al(OH)_3$ assistida por micro-ondas para separação de metais em salmouras.** Batista, K. S. (IC); Santos, E. B. G. N. (PG); Junior, L. P. (PG); Korn, M. (PQ) UNEB

**ANA-050** **Feasibility of microwave-induced combustion for honey decomposition and further indirect determination of Cl and S by ion chromatography.** Balbinot, F. P. (IC); Rondan, F. S. (PG); Pereira, R. M. (PG); Bielemann, N. J. (IC); Scaglioni, P. T. (PQ); Mesko, M. F. (PQ) UFPel

**ANA-051** **Development of a green and efficient method for determination of iodine in mineral dietary supplements.** Bielemann, N. J. (IC); Pereira, R. M. (PG); Mello, J. E. (PG); Brum, J. R. (IC); Novo, D. L. R. (PG); Mesko, M. F. (PQ) UFPel

**ANA-052** **Can the digestion of carbon nanotubes using diluted acid be a feasible approach?.** Krzyzaniak, S.R. (PG); Pereira, L.S.F. (PG); Bitencourt, G.R. (IC); Bizzi, C.A. (PQ); Flores, E.M.M. (PQ); Mello, P.A. (PQ) UFSM

**ANA-053** **Luminomagnetic core-shell nanoparticles for detection of metallic ions.** Namikuchi, E. A. (PG); Mazali, I. O. (PQ); Raimundo Jr, I. M. (PQ) UNICAMP

**ANA-054** **Feasibility of miniaturazed system for light crude oil microwave-assisted digestion.** Seeger, T. S. (PG); Dalla Vecchia, P. (PG); Pereira, L. S. F. (PQ); Mello, P. A. (PQ); Flores, E. M. M. (PQ); Duarte, F. A. (PQ) UFSM

**ANA-055** **Avaliação do processo de difusão de BTEX em sistemas de amostragem passiva com membranas semipermeáveis utilizando acetonitrila como fase receptora.** Martins, T. G. (PG); Cassella, R. J. (PQ) UFF

**ANA-056** **Multiple Response for Determination of BTEX in Water Samples Produced Using Semipermeable Membranes for Passive Sampling.** Robaina, N. F. (PQ); Cruz, G. F. B. (PG); Cassella, R. J. (PQ) UFF

**ANA-057** **Corn stalks study (Zea mays L.) as adsorbent of the Chromium (VI) Oxyanion present in aqueous solution.** Rocha, R. C. N. (IC); Oliveira, K.T. DOS. S. DE (IC); Caldas, L. A. (PG); Ribeiro Filho, W. A. (PQ) FATECPG-CEETEPS

**ANA-058** **Comparative study between activated charcoal, coffee grounds and fish scales as adsorbents for Congo Red dye present in aqueous solution.** Bier, C. C. (IC); Rocha, R. C. N. (IC); Santos, C. S. (IC); Garcia, M. N. U. (IC); Caldas, L. A. (PG); Palanch, M. F. (PQ); Ribeiro Filho, W. A. (PQ) FATECPG-CEETEPS

**ANA-059** **Study on the formation and stabilization of the derived free radical from the N-(4-methoxyphenyl)-p-phenylenediamine. Reactivity to phenolics.** Oliveira, L. B. (IC); Moya, H. D. (PQ) FMABC

**ANA-060** **DISTRIBUTION OF CRUDE OIL SARA FRACTIONS IN SOIL: AN ONSHORE SPILL SIMULATION.** Castiblanco, J. E. (PG); Santos, J. M. (PQ); Wisniewski, A. (PQ) UFS

**ANA-061** **Soil texture classification by Mid-infrared spectroscopy (MIR).** Morais, P. A. O. (PG); Souza, D. M. (PG); Madari, B. E. (PQ); Carvalho, M. T. M. (PQ) Embrapa Arroz e Feijão

**ANA-062** **Microdispositivo em papel para pseudotitulação ácido-base baseado em medida da distância.** Oliveira, R. F. de (PG); Silva, P. J. C. (PG); Korn, M. (PQ) UNEB

**ANA-063** **Synthesis of chitosan films for the quantification of Indigotine in candy samples by digital image analysis.** Coreixas de Sá, C.S. (PG); Felippe Pacheco, F. P. (PQ) UFF

**ANA-064** **Construção e avaliação de um colorimetro portátil para análise do teor de acido acético em vinagre empregando sistema FIA.** Costa, N. C. (PG); Almeida, G. A. (IC); Bueno, M. C. (IC); Luccas, P. O. (PQ); Lima, G. F. (PQ); Wisniewski, C. (PQ) UNIFAL

**ANA-065** **3D-printed platform for highly-reproducible handling of microvolumes and nanofluidic injection coupled to electrochemical detection.** Mendonça, D. M. H. (PG); Rocha, D.P. (PG); Dutra, G. S. V. (IC); Cardoso, R. M. (PG); Batista, A. D (PQ); Richter, E. M. (PQ); Munoz, R. A. A. (PQ) UFU

**ANA-066** **Use of external electrolysis to improve electrophoretic separations of sugars on glass microfluidic devices.** Duarte-Junior, G. F. (PG); Lobo-Junior, E. O. (PG); Medeiros Junior, I. (PQ); da Silva, J. A. F. (PQ); do Lago, C. L. (PQ); Coltro, W. K. T. (PQ) UFG

**ANA-067** **Detecção colorimétrica de $H_2O_2$ em amostras de leite utilizando dispositivos analíticos fabricados em papel.** Guinati, B. G. S. (IC); Cardoso, T. M. G. (PG); Coltro, W. K. T. (PQ) UFG

**ANA-068** **Contactless conductivity detection of bacteria in droplets using 3D printed microfluidic device.** Duarte, L. C. (PG); Figueredo, F. (PG); Ribeiro, L. E. B. (PG); Cortón, E. (PQ); Coltro, W. K. T. (PQ) UFG

**ANA-069** **Application of full factorial 23 design for optimization of glycerolysis reaction.** Carvalho, R. C. (PG); Dias, G. P. (IC); Souza, C. G. (PQ); Andrade, D. F (PQ); Pontes, F. V. M. (PQ); d'Avila, L. A. (PQ) UFRJ

**ANA-070** **Robustness evaluation of analytical procedure for the determination of residual solvent in [11C]-PK11195 using fractional factorial design.** Costa, C. L. S. (TC); Vieira, E. G. (IC); Ramos, D. P. (IC); Almeida, F. A. F. (PG); Silva, J. B. (PQ) CDTN

**ANA-071** **Evaluation of the compatibility between scale inhibitor and matrices with different calcium concentrations based on experimental design.** Gonçalves, A. D. (PQ); Machado, A. B. (PG); Dos Santos, E. C. M. (PG); Barbosa, J. R. (IC); Dáas, A. (IC); Damasceno, R. N. (PQ); Rocha, A. A. (PQ) UFF

**ANA-072** **Traceability of adulteration in acai pulp (Euterp Oleracea) by means data fusion strategy.** Oliveira, A. S. (IC); Araújo, A. (IC); Marinho, W. (IC); Pinto, Licarion (PG); Gomes, A. A. (PQ) UNIFESSPA

**ANA-073** **Influence of the stationary phase on the chemical profile of saturated and aromatic hydrocarbons of a medium density petroleum.** Ferreira, P. S. (IC); Rodrigues, E. A. (PG); Luz, D. A. (PG); Santos, R. P. (PQ); Filgueiras, P. R. (PQ); Kuster, R. M. (PQ) UFES

**ANA-074** **Characterization of lipid profiles from coconut (Cocos nucifer Linn) oil of different varieties using ESI-MS and chemometrics.** Bottoli, C. B. G. (PQ); Ferreira, J. A. (PQ); Ferreira, J. M. S. (PQ); Santos, J. M. (PQ); Breitkreitz, M. C. (PQ); Eberlin, M. N. (PQ); Lins, P. M. (PQ) UNICAMP

**ANA-075** **Multivariate Classification of Perfumes by Ion Analysis and Ethanol Content.** Andrade, F. B. C. (IC); Nunes, J. T. L. (IC); Fonseca, A. S. (IC); Gomes, C. L. (PQ); Vieira, G. A. B. (PQ); Melo, D. Q. (PQ) IF-Sertão Pernambucano

**ANA-076** **Ordered Predictors Selection: New Approaches for Variable Selection in Multivariate Calibration.** Roque, J. V. (PG); Peternelli, L. A. (PQ); Teófilo, R. F. (PQ) UFV

**ANA-077** **Determination of glufosinate, glyphosate and AMPA in soybean oil and wine by liquid chromatography coupled with tandem mass spectrometry.** Chiarello, M. (PG); Roméro-Gonzalez, R. (PQ); Moura, S. (PQ) UAL

**ANA-078** **Near infra-red espectroscopy and chemometrics: potential for coffee quality control.** Ayala, A. H. (IC); Nixdorf, S. L. (PQ); Madeira, T. B. (PG); Lopes, C.T. (IC); Alves, D. P. (IC); Almeida, M. B. (PG); Silva, M. P. (IC); Watanabe, L. S. (PG) UEL

**ANA-079** **Multivariate Analysis of Perfumes by Ultraviolet Spectrophotometry.** Nunes, J. T. L. (IC); Andrade, F. B. C. (IC); Fonseca, A. S. (IC); Gomes, C. L. (PQ); Melo, D. Q. (PQ) IF-Sertão Pernambucano

**ANA-080** **Standardization of urinary tract infection diagnosis by ATR/PLS-DA.** Souza, P. B. (IC); Corbellini, V. A. (IC) UNISC

**ANA-081** **Characterization of the mineral composition of Oiti (Licania tomentosa) employing multivariate analysis.** Silva, E.F.R. (PG); Santos, B.R.S. (PG); Brandão, G.C. (PQ); dos Santos, W.P.C. (PQ); Silva, M.V.L. (PQ); dos Santos, A.M.P. (PQ); dos Santos, W.N.L. (PQ) UNEB

**ANA-082** **Use of webcam in flow analysis to phosphorus determination in soil extract.** Severo, E. A. (IC); Santos, J. L. O. (PQ); Bazzi, C. (PQ); Kamogawa, M. Y. (PQ); Flores, E. L. M. (PQ); Leite, O. D. (PQ) UTFPR

**ANA-083** **Estudo da Eficiência de decomposição nítrica da matéria orgânica de amiláceos em frascos fechados irradiados por micro-ondas.** Silva, W. N. (IC); Peralva, V.N. (PG); Santos, L.R. (PG); Santos, D.C.M.B. (PQ); Korn, M.G.A. (PQ); Korn, M (PQ) UNEB

**ANA-084** **Desenvolvimento de um sistema on-line de extração magnética em fase sólida para determinação de Cd por FAAS.** Rocha, P. S. M. (PG); Cassella, R. J. (PQ) UFF

**ANA-085** **Metals analysis by ICP-OES in samples of colonial wines produced in Palotina-PR.** Friedrich, L. C. (PQ); Gomes, A. K. S. (IC); Souza, D. G. (IC); Schneider, L. A. E. (IC); Lenz, G. F. (TC); Bautitz, I. R. (PQ); Milinsk, M. C. (PQ) UFPR

**ANA-086** **Estudo da composição química cuticular de formigas da espécie Odontomachus bauri expostas a diferentes temperaturas.** Duarte, B. F. (PG); Michelutti, K. B. (PG); Antonialli-Junior, W. A. (PQ); Cardoso, C. A. L. (PQ) UEMS

**ANA-087** **Desenvolvimento de metodologia para quantificação de TBHQ, BHT e alfatocoferol utilizando CLAE-DAD em amostras de biodiesel com avaliação do período de indução por Rancimat.** Vargas, T. S. (IC); Azevedo, R. S. (IC); Chiapetta, S. C. (PQ) INT

**ANA-088** **Vantagens e desvantagens da quantificação de terc-butilhidroquinona (TBHQ) em biodiesel utilizando bomba peristáltica e bomba de alta eficiência.** Chiapetta, S. C. (PQ); Vargas, T. S. (IC); Gomes, I. S. (IC) INT

**ANA-089** **Estudo de estabilidade de açúcares em tabaco de cigarros comerciais.** Rodrigues, M. N. (TC); Guedes, J. S. (TC); Chiapetta, S. C. (PQ) INT

**ANA-090** **Observações críticas sobre a quantificação de glifosato pelo método colorimétrico do "púrpura de Ruhemann".** Tomaso, L. P. S. (IC); Hottes, E. (PG); Cardoso, C. M. (PQ); Herbst, M. H. (PQ) UFRRJ

**ANA-091** **Síntese, caracterização e avaliação de um polímero de impressão molecular para quantificação seletiva de corante têxtil ácido violeta 19 visando aplicação em amostras ambientais.** Luna, M.A. (PG); Khan, S. (PQ); Picasso, G. (PQ); Sotomayor, M.D.P.T. (PQ) IQAr-UNESP

**ANA-092** **Ion chromatography as an alternative for simultaneous determination of citrate and phosphate in anticoagulant solutions of blood bags.** Cruz, G. C. S. (PG); Venâncio, L. F. (TC); Fust, A. M. B. S. (TC); Vale, R. F. D. (TC); Silva, F. S. Q. (PQ); Feitoza-Silva, M. (PQ) FIOCRUZ

**ANA-093** **Evaluation of techniques for analysis of plasticants in blood bags.** Carvalho, C.M.de (PG); Fust, A.M.B.S. (TC); Vale, R.F.D. (TC); Venâncio, L.F. (TC); Albert, A. L. M. (PQ); Leandro, K. C. (PQ); Feitoza-Silva, M. (PQ) FIOCRUZ

**ANA-094** **REGULATORY IMPACT FROM THE ANALYTICAL ADEQUACY IN THE QUALITY CONTROL OF BLOOD BAGS.** Vale, R. F. D. (TC); Fust, A. M. B. S. (TC); Venâncio, L. F. (TC); Leandro, K. C. (PQ) FIOCRUZ

**ANA-095** **Aplicação de aerogel de grafeno como fase extratora na determinação on-line de $Cd^{2+}$ com detecção por FAAS.** Lima, G. C. (PG); Mendonça, L. F. M. (IC); Rodrigues, L. C. (IC); Figueiredo, E. C. (PQ); Luccas, P. O. (PQ); Martins, G. F. L. (PQ) UNIFAL

# *BEA – Química de Alimentos e Bebidas*

**BEA-001** **Difratometric and thermogravimetric study of commercial coconut flour.** Porcu, O. M. (PQ); Lima de, V. A. (PQ); Anaisse, F. J. (PQ) UTFPR

**BEA-002** **Chemometrics evaluation of oxidative degradation of the Brazilian extra virgin olive oil produced from the varietal Maria da Fé.** Gonçalves, T. R. (PG); Gonçalves, R. P. (PG); Rosa, L. N. (PG); Graeff, F. (IC); Domingues, H. P. (IC); Leite, O. D. (PQ); Torquato, A. S. (PQ); Março, P. H. (PQ); Valderrama, P. (PQ); Matsushita, M. (PQ) UEM

**BEA-003** **Enrichment of gluten-free bread with avocado pulp (Persea Americana Mill).** Santos, M. R. (IC); Souza, A. H. P. (PQ); Steinmacher, N. C. (PQ); Zimmer, F. C. (PG); Lovera, D. C. V. (PG); Rodrigues, A. C. (PQ) UTFPR

**BEA-004** **Efeito da esterilização por irradiação gama na camomila [Chamomilla recutita (L.) Rauschert].** Peres, R. L. (PQ); Garcia, H. (IC); Quinhones, R. (PQ) IF Baiano - Campus Teixeira de Freitas

**BEA-005** **One-Shot, Fast and Green Determination of the Alcoholic Content of Wines Using Thermal Infrared Enthalpimetry.** Oliveira, A. S. (PG); Tischer, B (PQ); Duarte, F. A. (PQ); Helfer, G. A. (PQ); Costa, A. B. (PQ); Barin, J. S. (PQ) UFSM

**BEA-006** **Intercalation of vitamin L and adsolubilization of vanillin in lamellar hydroxide salts for obtention of multifunctional food supplements.** Zanotelli, N. C. (IC); Maruyama, S. A. (FM); Cursino, A. C. T. (PQ) UTFPR

**BEA-007** **Determinação de compostos fenólicos em vinhos comerciais por UPLC-UV.** Alves, D.P (IC); Ayala, A.H.F (IC); Lopes, C.T (IC); Valente, L.J (IC); Silva, M.P.A (IC); Ishikawa, R.L (IC); Almeida, M.B (PG); Madeira, T.B (PG); Nixdorf, S.L (PQ) UEL

**BEA-008** **Avaliação do perfil de ácidos graxos de amostras de óleo de coco comercializados em Belo Horizonte/MG.** Ferraz, B. S. R. (IC); Porto, B. L. S. (PQ); Botelho, B. G. (PQ) UFMG

**BEA-009** **Composição fenólica de extratos de resíduos industriais de amora-preta e seriguela por UPLC-PDA.** Mazalli, A. V. G. (PG); Lopes, C. T. (IC); Sena, D. H. S. (IC); Almeida, M. B. (PG); Madeira, T. B. (PG); Nixdorf, S. L. (PQ) UEL

**BEA-010** **Spectrophotometric method for quantification of antioxidant capacity of tropical fruits based on the formation of Fe(II)/2,2'-bipyridyl complex.** Bortolozi, G. G. (IC); Moya, H. D. (PQ) FMABC

**BEA-011** **Caracterização de pesticidas em leite humano.** Souza, R. C. (PG); Nakamura, T. C. (PG); Brito, P. V. N. (PG); Portella, R. B. (PQ); Santos, J. V. (PQ); Domingos, J. D. S. (PQ) UFOB

**BEA-012** **Quantification of the antioxidant activity of the fruits using the colored free radical derived from N-(4-methoxyphenyl)-p-phenylenediamine.** Youssef, K. (IC); Moya, H. D. (PQ) FMABC

**BEA-013** **Determination of 16 carbonyl compounds in mineral water.** Melo Cardozo, I. M (PG); P. dos Anjos, J (PQ); B. de Andrade, J (PQ) UFBA

**BEA-014** **Oxidative stability study of edible vegetable oils using near-infrared emission spectroscopy.** Andrade, D. C. (TC); Vieira, F. S. (PG); Pasquini, C. (PQ) UNICAMP

**BEA-015** **Caracterização dos constituintes da cagaita empregando-se a PS-MS.** Barrett Reina, L. Del C. (PQ); Souza, A. G. (PQ); Silva, M. R. (PG); Freitas, L. G. (IC); Araújo, R. L. B. (PQ); Lacerda, I. C. A. (PQ); Augusti, R. (PQ); Melo, J. O. F. (PQ) UFMG

**BEA-016** **Bromine and iodine determination in different legumes by ICP-MS after decomposition by microwave-induced combustion.** Rondan, F. S. (PG); Coelho Junior, G. S. (PG); Henn, A. S. (PG); Brum, J. R. (IC); Scaglioni, P. T. (PQ); Mesko, M. F. (PQ) UFPel

**BEA-017** **Production and impregnation of starch aerogels using supercritical $CO_2$.** Villegas, M. E (PG); Oliveira, A. L (PQ); Bazito, R. (PQ); Vidinha, P. (PQ) IQUSP

**BEA-018** **Analysis of antioxidant capacity of peels, pulp and seed of Brazilian native fruits.** Zeraik, M. L. (PQ); Silva, G. L. (PG); Russo, H. M. (PG); E. F., Queiroz (PQ); Cuendet, M. (PQ); Wolfender, J. L. (PQ); Bolzani, V. S. (PQ) UEL

**BEA-019** **Determinação de compostos fenólicos em cervejas artesanais brasileiras usando HPLC-DAD.** Silva, M. C. (IC); Anjos, J. P. (PQ); Guarieiro, L. L. N. (PQ); Machado, B. A. (PQ) SENAI CIMATEC

**BEA-020** **Determinação de $Fe^{2+}$ em cervejas especiais por espectrofotometria UV-vis após extração por ponto nuvem.** Santos, R. R. (IC); Gama, E.M. (PG); Costa, L.M. (PQ) UFMG

# *BIO – Química Biológica*

**BIO-001** **Effects of hesperetin, from citrus fruits, on proteinases isolated from Bothrops asper snake venom.** dos Santos, R. V. (PG); Grillo, G. R. (IC); de Oliveira, H. F. M. (IC); Peroni, L. A. (PQ); Volpe, P. L. O. (PQ); Tasic, L. (PQ) UNICAMP

**BIO-002** **Leshimanicidal activity of extracts of endophytic fungi from Apidosperma excelsum.** Carvalho, J. M. (PG); Santos, L. A. (IC); Silva, J. V. S. (PG); Dolabela, M. F. (PQ); Marinho, P. S. B. (PQ); Marinho, A. M. R. (PQ) UFPA

**BIO-003** **A direct assay for measuring the activity of phosphoenolpyruvate carboxykinase (PEPCK) by liquid chromatography-tandem mass spectrometry.** Amaral, B. S. (PG); Souza de, D. H. F. (PQ); Cass, Q. B. (PQ) UFSCar

**BIO-004** **Peak-fraction at-line screening assay of kallikrein inhibition for complex matrices by LC-MS/MS.** Cardoso, C. L. (PQ); Sonsen, G. W. (PQ); Kool, J (PQ) VU.NL

**BIO-005** **Interaction of thimerosal with hemoglobin causes alteration of structure and loss of oxygen binding capacity.** Silva, M. M.; Dantas, M.D. A. (PG); S. Filho, R. C. (PG); Leite, A. C. R. (PQ); Santos, J. C. C. (PQ); Figueiredo, I. M. (PQ) UFAL

**BIO-006** **Synthesis and evaluation of the antibacterial properties of colloidal silver nanoparticles for application in cosmetics industry.** Santos, A. G. C. (IC) Newton

**BIO-007** **Naftoquinone derivatives: in vitro photo protective activity and interaction studies with tyrosinase and DNA.** Guimaraes, A. S. (PG); Nunes, C. da silva (PG); Santos, R. R. F. (PG); Cardoso, S. H. (PQ); Figueiredo, I. M. (PQ); Santos, J. C. C. (PQ) UFAL

**BIO-008** **Avaliação do líquido celomático de minhoca na atividade inibitória de fungos do gênero Fusarium.** Kuhn, D. (PG); da Rosa, P. D. (PG); Goldani, L.Z. (PQ); de Freitas, E. M. (PQ); Ethur, E.M. (PQ); Hoehne, L. (PQ) UNIVATES

**BIO-009** **Computer-aided prediction and cytotoxicity evaluation of bis-hydrazones as novel anticancer agents.** Donnici, C. L. (PQ); Ávila-Costa, M. (PG); Lopes, J. C. D. (PQ); Goulart, M. O. F. (PQ); Xavier, J. A. (PG); Kadooca, L. N. (IC); Furst, C. G. (IC) UFMG

**BIO-010** **Evaluation of decoralin peptide identifies activity determinants and synthetic variants with *in vivo* activity.** Torres, M. D. T. (PG); de la Fuente-Nunez, C. (PQ); Lu, T. K. (PQ); Oliveira Jr, V. X. (PQ) UFABC

**BIO-011** **Ensaios antioxidantes com extratos das raízes de Clusia grandiflora Spligt. e Platonia insignis Mart. (Clusiaceae).** Fernandes, W. B. C. (IC); Araújo, R. N. M. (PG); Ripardo Filho, H. S. (PQ); Silva, L. P. S. (PQ); Lopes Junior, M. L. (PG); Guilhon, G. M. S. P. (PQ); Santos, L. S. (PQ) UFPA

**BIO-012** **Evaluation of new inhibitors of homoserine dehydrogenase for the development of drugs against paracoccidioidomycosis.** Bagatin, M. C (PG); Rozada, A. M. F. (PG); Rodrigues, F. A. V. (PG); Kioshima, E. S. (PQ); Seixas, F. A. V. (PQ); Gauze, G. F. (PQ) UEM

**BIO-013** **Temperature effect upon kinetic of dissociation/aggregation of the Glossoscolex paulistus hemoglobin.** Da Silva, R. P. (IC); Nascimento, E. D. (PG); Simões, Y. S. (IC); Carvalho, F. A. O. (PQ) UNIFESSPA

**BIO-014** **Atividade antimicrobiana e reação de biotransformação de chalconas promovidas pelo fungo endofítico Glomerella cingulata.** Lopes Junior, M. L. (PG); Araújo, R. N. M. (PG); Ripardo Filho, H. S. (PQ); Ribeiro, W. S. (PG); Corrêa, M. J. C. (PQ); Guilhon, G. M. S. P. (PQ); Santos, L. S. (PQ) UFPA

# *CAT – Catálise*

**CAT-001** **Preparation and characterization of catalysts based on nickel niobate modified with Mg, Ca or Sr for hydrogen production.** Sousa, J. L. S. (IC); Lima de, S. P. (PG); Carvalho, L. S. (PG); Ruiz, D. (PG); Martins, A. R. (PG) IFBA

**CAT-002** **Hidroformilação de álcoois provenientes da bio-massa (1R)-(-)mirtenol e (1R)-(-)nopol catalisada por complexo de ródio.** Delolo, F. G. (PG); de Oliveira, K. C. (PQ); dos Santos, E. N. (PQ); Gusevskaya, E. V. (PQ) UFMG

**CAT-003** **Hydrolysis of soybean oil over solid acid catalysts.** Crisóstomo, C. A. B.; Soares, R. R.

**CAT-004** **Study of the photocatalytic capacity of the Black Mud for the degradation of the molecules of methylene blue and hydroxybenzene (phenol).** Lourenço, V. S. (IC); Asencios, Y. J. O. (PQ); Boto, S. M. (PQ) FATECPG-CEETEPS

**CAT-005** **Production of carbon nanostructured materials by CVD method using supported catalysts: Study of two different carbon precursor gases.** Silva, A. P. (IC); Lelo, R. V. (PG); Guerreiro, M. C. (PQ); Mezalira, D. Z. (PQ) UFSC

**CAT-006** **Green oxidation of etanol, acetol and other primary alcohols by $FeCl_3/H_2O_2$ in aqueous medium.** Mandelli, D. (PQ); Shul'pin, G.B. (PQ); Carvalho, W. A. (PQ); Araújo, M. L. (PG) UFABC

**CAT-007** **Unveiling the structural and electronic properties of the B-$Nb_2O_5$ surfaces and their interaction with $H_2O$ and $H_2O_2$.** De Abreu, H. A. (PQ); Diniz, R. (PQ); Duarte, H. A. (PQ); Soares Jr., A. L. (PQ); Quintão, M. C. (IC); Pinto, M. B. (PG) UFMG

**CAT-008** **Síntese de compostos de aroma catalisados por lipases através do reaproveitamento da borra de café.** Lira, R. K. S. (PG); Itabaiana, I. Jr. (PQ); Gomes, S. F. (PQ) UFRJ

**CAT-009** **Heterogeneous acid catalysts based on sulfonated graphene like structures produced from bio-oil.** Ballotin, F.C. (PG); Perdigão, L.T. (IC); Resende, M.V.B. (IC); da Silva, M.J. (PQ); Teixeira, A. P. C. (PQ); Lago, R.M. (PQ) UFV

**CAT-010** **Statistical study of the oxidation reaction of benzyl alcohol in the absence of base with silica-supported gold nanoparticles.** Giertyas, C.J. (PG); de Melo, L.N. (PG); da Silva, E.C. (PQ); de Almeida, R.M. (PQ); Meneghetti, M.R. (PQ); Bortoluzzi, J.H. (PQ) UFAL

**CAT-011** **GO/$(CdS)_x/(ZnO)_y$ bifunctional photocatalyst for ecotreatment of tannery sludge wastewaters with simultaneous generation of hydrogen.** Souza, E. A. (PG); Araújo, R. J. (PG); Silva, L. A. (PQ) UFBA

**CAT-012** **Influence of the $CeO_2$ support nano-morphology on Gold nanoparticles activity for photooxidation reactions.** Teixeira, I. F. (PQ); Geonmonond, R. S. (PG); Rocha, G. F. S. R. (IC); Tsang, E. (PQ); Camargo, P. H. C. (PQ) IQUSP

**CAT-013** **Chemical modification of gum arabic for dephosphorylation reactions: hydroxamate-derived biocatalyst.** Takarada, W. H. (IC); Ferreira, J. G. L. (PG); Orth, E. S. (PQ); Riegel-Vidotti, I. C. (PQ) UFPR

**CAT-014** **Ethanol steam reforming catalyzed by supported Rh nanoparticles: investigating the effect of the nature of the oxides supports.** Rodrigues, T. S. (PQ); e Silva, F. A. (IC); Candido, E. G. (IC); Bergamaschi, V. S. (PQ); Linardi, M. (PQ); Fonseca, F. C. (PQ) IPEN

**CAT-015** **Synthesis of mixed oxide supported niobium catalysts and their applications in reactions with primary amine.** Granato, A. S. (PG); Carvalho, G. S. G. (PQ); Amarante, G. W. (PQ) UFJF

**CAT-016** **Pushing the boundaries of gold catalysis.** Rossi, L. M. (PQ); Fiorio, J. L. (PG); Gonçalves, R. V. (PQ); Teixeira-Neto, E. (PQ); Lopez, N (PQ) IQUSP

**CAT-017** **Ir-Fe bimetallic catalysts for glycerol hydrogenolysis.** Pamphile-Adrian, A. J. (PQ); Florez-Rodriguez, P. P. (PQ); Passos, F. B. (PQ) UFF

**CAT-018** **Novel fragrant aldehydes via hydroformylation of the bio renewable valencene.** Vieira, G. M. (PG); de Paulo, R. S. (IC); dos Santos, E. N. (PQ); Gusevskaya, E. V. (PQ) UFMG

**CAT-019** **Hydrodeoxygenation (HDO) of lignin-derived model compounds at low temperature using perovskites.** Shetty, M. (PG); Zanchet, D. (PQ); Green, W.H. (PQ); Roman-Leshkov, Y. (PQ) IQ-UNICAMP

**CAT-020** **Use of carboxyl cellulose metal complexes in heterogeneous catalytic systems to promote Suzuki-Miyaura coupling.** Martins, G. B. C. (PG); dos Santos, M. R. (PG); Rodrigues, M. V. R. (IC); Sucupira, R. R. (IC); Meneghetti, L. (IC); Monteiro, A. L. (PQ); Suarez, P. A. Z. (PQ) UnB

**CAT-021** **Synthesis of ethanol from the reduction of carbon dioxide under supercritical conditions.** Rozendo, J. D. (PG); Gothe, M. L. (PG); Bazito, R. C (PQ); Rossi, L. M. (PQ); Vidinha, P. (PQ) IQUSP

**CAT-022** **Propylsulfonic acid anchored on mesoporous SBA-15 as heterogeneous catalyst for esterification of fatty acids.** Moreira, A.F.S. (PG); Brito, T.C. (IC); Vieira, J.S.C. (PQ); Mota, C.J.A., (PQ); Lachter, E.R. (PQ) UFRJ

**CAT-023** **Estudo introdutório sobre conversão catalítica de $CO_2$ a hidrocarbonetos utilizando um rejeito industrial a base de Fe como catalisador.** Mombrini, L. M. (IC); Miranda, J. L. (PQ); Ferreira, H. B. P. (PQ) IFRJ - Campus Nilópolis

**CAT-024** **Ruthenium(II) complexes of Schiff base derived from cycloalkylamines as pre-catalysts for ROMP and ATRP.** Cruz, T. R. (IC); Afonso, B. A. (PG); Goi, B. E. (PQ); Carvalho-Jr, V. P. (PQ) FCT-UNESP-Câmpus de Presidente Prudente

**CAT-025** **Use of biomasses from Acrocomia aculeata in the synthesis of activated charcoal and its use in the purification of crude glycerol.** Freitas, M. S. (PG); Barbosa, S. L. (PQ); Lima, C. D. (PQ); Aguiar, L. P. (IC); Rocha, A. S. (IC); Borges, C. B. (IC); Almeida, V. R. G. (IC) UFVJM

**CAT-026** **Microwave-assisted organic synthesis versus conventional heating. A comparative study for polyols condensation with ketones at heterogeneous catalysis $SiO_2$-$SO_3H$ under free solvent.** Almeida, M. A. R. (IC); Lage, G. L. C. (PG); Oliveira, P. M. (PQ); Barbosa, S. L. (PQ) UFVJM

**CAT-027** **M/$SiO_2$ (M = Co or Ni) nanoparticles prepared by magnetron sputtering deposition method for $CO_2$ valorization by reverse water gas shift reaction.** Galhardo, T. S. (PQ); Gonçalves, R. V. (PQ); Rossi, L. M. (PQ) IQUSP

**CAT-028** **Easily accessible ROMP and ATRP catalysts based on dimethyl sulfoxide ruthenium(II) complexes bearing N-heterocyclic carbene ligands.** Gois, P. D. S. (PG); Idehara, A. H. S. (PG); Goi, B. E. (PQ); Carvalho-Jr, V. P. (PQ) FCT-UNESP-Câmpus de Presidente Prudente

**CAT-029** **Cobalt(II) complexes of bidentate Schiff bases derived from cycloalkylamines as mediators in controlled radical polymerization of vinyl acetate.** Silva, Y. F. (PG); Carvalho-Jr, V. P. (PQ); Goi, B. E. (PQ) FCT-UNESP-Câmpus de Presidente Prudente

**CAT-030** **Mn(II) and Fe(II) complexes of bidentate Schiff base as mediators for Organometallic Mediate Radical Polymerization (OMRP) of Vinyl Acetate.** Hashimoto, P. K. (PG); Goi, B. E. (PQ); Carvalho-Jr, V. P. (PQ) FCT-UNESP-Câmpus de Presidente Prudente

**CAT-031** **Reaction of alkaline metals Li+, Na+ and K+ with serpentinite to form different solid basic catalysts.** Da Paz, G. M. (PG); Vieira, S. S. (PG); Bertoli, A. C. (PG); Ballotin, F. C. (PG); De Moura, E. M. (PQ); Teixeira, A. P. C. (PQ); Carmignano, O. (PG); Sebastião, R. C. O. (PQ); Lago, R. M. (PQ) UFMG

**CAT-032** **Heterogeneous catalysts based on Pd supported in mesoporous silica for selective hydrogenation: influence of the ionic liquid on the catalytic properties.** Araujo, M.H. (PQ); Haun, U. G. (PG); Teixeira, A. P. C. (PQ) UFMG

**CAT-033** **Glycerol conversion in presence of $CO_2$: solvent absence in semi-batch reactor.** Florez-Rodriguez, P. P. (PQ); Pamphile-Adrián, A. J. (PQ); Passos, F. B. (PQ) UFF

**CAT-034** **Preparation of Poly(lactic acid) blends by heterogenous catalysis using supported 12-tungstophosphoric acid.** Paiva, M. F. (IC); Chafran, L. S. (PQ); Dias, J. A. (PQ); Dias, S. C. L. (PQ) UnB

**CAT-035** **Mesoporous structures for catalytic pyrolysis of plastic waste.** Parente, T. P. (PG); Marques, M. F. V. (PQ) UFRJ

**CAT-036** **Hybrid catalysis in carbon dioxide valorization.** Gothe, M.L. (PG); Barone, M. (IC); Marques, L. (IC); Caricatti, V. (IC); Bazito, R.C. (PQ); Rossi, L.M. (PQ); Vidinha, P. (PQ) IQUSP

**CAT-037** **Estudo do uso de rejeitos industriais como catalisadores na degradação de corantes industriais por processo fenton.** Ferreira, A. C. L. N. (IC); Ferreira, H. B. P. (PQ); Ribeiro, R. P. (PQ) IFRJ - Campus Nilópolis

**CAT-038** **Development of new materials from industrial waste and biomass for application in catalysis.** Fonseca, M. E. (PG); Mambrini, R. V. (PQ) CEFET-MG

**CAT-039** **Esterification of FFA in Soybean oil with acid zeolite catalyst for biodiesel production.** Dal Pozzo, D. M. (PG); Costa, M. B. (PQ); Zanatta, E. R. (PQ) UTFPR

# *COL – Química de Superfícies e Colóides*

**COL-001** **Influence of an alternate magnetic field on the cellulase activity immobilized in magnetic nanoparticles.** Rocha, C. O. (PG); Lucena, G. N. (PG); Jafelici Jr, M. (PQ); Marques, R. F. C. (PQ) IQAr-UNESP

**COL-002** **Adsorption of sodium dodecylbenzenesulfonate (SDBS) and dodecylpyridinium chloride (DPC) onto modified mesoporous silica-coated magnetite.** Dorigon, L. (IC); Frota, J.P.R.A. (IC); Andriolli, C.R. (IC); Bail, A. (PQ); Giona, R.M. (PG) UTFPR

**COL-003** **Synthesis and characterization of magnetic mesoporous silica nanoparticles for Ba2+ removal from aqueous media.** Reolon, C. M. M. (IC); Bail, A. (PQ); Giona, R. M. (PQ); Tondo, D. W. (PQ) UTFPR

**COL-004** **Superhydrophobic self-cleaning surfaces and slippery lubricated ones effect upon inorganic scaling.** Signorelli, F. (PG); Sousa, M. F. B. (PQ); Bertran, C. A. (PQ) UNICAMP

**COL-005** **Formation of polymer - hexadecylpyridinium chloride complexes using different structures of poly(vinyl alcohol).** Andrade, J. M. B. (IC); Santos, G. H. F. (IC); Agudelo, A. J. P. (PG); da Silva, L. H. M. (PQ); Ferreira, G. M. D. (PQ) UFLA

**COL-006** **Spectrophotometric and tensiometric investigation of the interaction between Norbixin and surfactants in aqueous medium.** Penido, J. A. (PG); Carvalho, I. M. (IC); Junqueira, C. M. (PQ); Virtuoso, L. S. (PQ); Mageste, A. B. (PQ) UFOP

**COL-007** **Magnetic composite nanoparticles for hyperthermia and drug delivery to treat cancer.** Perecin, C. J. (PG); Tirich, B. M. (IC); Cerize, N. N. P. (PQ); Varanda, L. C. (PQ) IQSC-USP

**COL-008** **Effect of the formation and dissociation of hydrate on the stability of an W/O emulsion.** Rodrigues, R. K. R. (PQ); Naccache, M. F. N. (PQ); de Souza Mendes, P. R. S. M. (PQ) PUC-RIO

**COL-009** **Avaliação citotóxica de pirazolina com actividade anticâncer em nanocapsulas de carboximetil-hexanoil quitosana.** Rengifo, A.F.C (PG); Stefanes, N.M (PG); Mendes, C. (PG); Toigo, J. (IC); Nunes, R. J. (PQ); Silva, M. C.S (PQ); Parize, A. L. (PQ); Minatti, E. (PQ) UFSC

**COL-010** **Síntese de nanopartículas de prata com alto desempenho em espectroscopia SERS no infravermelho próximo.** Belgo, H. C. (IC); Sant'Ana, A. C. (PQ) UFJF

**COL-011** **Liquid-liquid equilibria of aqueous two-phase systems (ATPS) containing triton-X100 and choline chloride at different temperatures.** Silva, S. J. B. (PG); Ferreira, A. L. G. (IC); Penido, J. A. (PG); Mageste, A. B. (PQ); Ferreira, G. M. D. (PQ) UFOP

**COL-012** **Adsorption of fluoride by magnetic Li-Al layered double hydroxide.** Meira, A. C. R. (PG); Kreutz, J. C. (PG); Bail, A. (PQ); Giona, R. M. (PQ) UTFPR

**COL-013** **Variation of the electrokinetic parameters of colloidal systems.** Cottet, L.; Almeida, C. A. P.; Pochapski, D. J. (IC) UNICENTRO

# *EDU – Ensino de Química*

**EDU-001** **Balanceamento de equações químicas utilizando o feltro como ferramenta de ensino na Semana Nacional de Ciência e Tecnologia 2017.** Santos, P. V. (IC); Junior, A. C. (IC); Silva, M. B. (IC); Santos, J. C. (IC); Silva, M. G. A. (PQ) UFAL

**EDU-002** **A inserção da Química Ambiental na Educação Básica utilizando a experimentação como estratégia pedagógica.** Almeida, L. D. (IC); Pereira, L. F. (IC); Santos, I. S. P. (IC); Vieira, C. D. (IC); Almeida, G. B. (IC); Marcelo, L. R. (PQ) IFRJ-Campus Duque de Caxias

**EDU-003** **Feira de negócios como espaço não-formal para o ensino técnico em química.** Machado, M. C. (PQ) FIEC

**EDU-004** **A Arte como princípio formativo de pibidianos em Química.** SILVA, C. S. (PQ) UFPR

**EDU-005** **Investigando o conhecimento dos conceitos mistura, substância, átomo e elemento em uma Olimpíada de Química.** Maruyama, J. A. (FM); Carvalho, F. F. (IC); Ferreira, K. C. (IC); Rocha, C. O. (PG); Marques, R. F. C. (PQ) IQAr-UNESP

**EDU-006** **Use of experimental class and play activity in chemistry teaching: An experience in elementary education.** Oliveira, J. M. D. (IC); Costa da, D. R. M. (PQ); Lopes, B. H. S. (IC); Batista, J. C. (IC); Neres, M. E. S. (IC); Sousa, N. M. (IC); Silva, S. R. (IC) UEPA

**EDU-007** **Uma nova metodologia para o registro e análise da interação de estudantes com representações tridimensionais de moléculas.** Ayres, C. (PG); Consoli, R. A. (IC); Cicuto, C. A. T. (PQ); da Cruz, G. N. (FM); Marson, G. A. (PQ) IQUSP

**EDU-008** **Uso de jogos didáticos: desafios e superações na visão de uma professora de química.** Santos, S. S. (FM); Moreira, B. C. T. (PQ); Varjão, T. A. (PQ) UNEB

**EDU-009** **The influence of ``EAR'' validation process of teaching sequences on pre-service chemistry teacher preparation.** Bego, A. M. (PQ); Giordan, M. (PQ) IQAr-UNESP

**EDU-010** **Compreensão textual de graduandos em química: tema biodiesel em foco.** Cabral, P. F. O. (PG); Queiroz, S. L. (PQ) IQSC-USP

**EDU-011** **Atribuição de nota: moeda de troca para frequência dos acadêmicos na monitoria de Química Inorgânica?.** Corsi, W. L. (IC); Stevanato, A. (PQ) UTFPR

**EDU-012** **Assessment of construction of knowledge in Covalent Bond in high school through the philosophical zones.** Pazinato, M. S. (PQ); Braibante, M. E. F. (PQ); Miranda, A. C. G. (PG) UFRGS

**EDU-013** **Factors that influence the rates of reactions: discussing concepts from experimental investigative activities.** Bueno, E. A. S. (PQ); Tavares, F. S. C. (FM); Arrigo, V. (PG); Broietti, F. C. D. (PQ) UEL

**EDU-014** **Estudo de caso da disciplina 'Química Aplicada à Engenharia': processo corrosivo em portões metálicos em São Miguel-RN.** Dias, S. S. (PQ); Chaves, F. A. (IC); Ramos, J. E. T. (PQ) UFERSA

**EDU-015** **Utilização de Normas Técnicas de produtos no ensino de Química.** Oliveira, T. S. A. (IC); Nunes, R. C. (PQ) IFF

**EDU-016** **Um exemplo da aplicação de séries em aulas de Físico-Química: dedução da equação de Ramette.** Pietezak, D. F. (IC); Meier, M. M. (PQ); Santana, L. H. (PQ) UDESC

**EDU-017** **Texto didático interativo no contexto da atmosfera terrestre com aportes da geometria e polaridade de moléculas.** Santos, L. P. (IC); Moreira, B. C. T. (PQ); Santana, D. A. (PQ) UNEB

**EDU-018** **The approach of the principles of Green Chemistry by means of ludic activities in the formation of chemistry professionals.** Costa, M. C. S. (PG); Soares, M. H. F. B. (PQ); Mesquita, N. A. S. (PQ) UFG

**EDU-019** **Destilaria: An innovative board game to improve the organic chemistry learning.** MARTINS, M. F. (IC); AVERSA, T. M. (PQ) IFRJ-Campus Duque de Caxias

**EDU-020** **Uso de simuladores no estudo dos estados físicos da matéria e do modelo cinético molecular.** FURLANI, J. M. S. (PQ); CANDIDO, L. V. (IC); OLIVEIRA, M. B (IC) UNIFEI

**EDU-021** **Territórios analíticos: Uma abordagem dinâmica para o equilíbrio de complexação.** Avelino, D. O. S.; Alves, G. F. S.; Santos, D. J. S.; Lira, P. H. A.; Félix, A. M. A.; Santos Alves, G. F. (IC) UFAL

**EDU-022** **Leite em "mama" África e a lei 10639/03 no ensino de química.** S. Neto, M.; Silva, J. P (PG); Faustino, G. A. A (IC); Alvino, A. C. B. (PG); Santos, M. A (PG); Santos, V. L (PQ); Camargo, M. R (PQ); Vargas, R. N (PQ); Bastos, M. A (PG); Moura, A. R (IC); Lima, G. L. M (IC); Oliveira, L. A (IC); Fernandes, F. S (IC); Silva, A. G (IC); Benite, C. R. M (PQ); Benite, A. M. C (PQ) UFG

**EDU-023** **Teaching Chemistry: an interface between the teaching of chemical bonds and alternative materials.** FEIJÓ, G.S. (IC); MORAES, A.C. (IC); SILVA, M.D.B. (PQ); REIS, A.S. (PQ) UEPA

**EDU-024** **Estruturas educacionais virtuais (EEV) por meio de modelos físicos (MF).** Fonseca, A. M. (PQ); Oliveira de, S. J. (IC); Santos, F. K. O. (IC); Martins, E. S. (PG); Sousa de, L. M. (PG); Colares, R. P. (PQ); Seco, M. A. (IC) UNILAB

**EDU-025** **Production of a two-dimensional tactile Water Treatment Station for students with visual impairment.** Santos, L. S. (IC); Oliveira, M. S. (IC); Cid, T. P. (IC); Rocha, A. C. S. (IC); Penco, V. S. N. (PQ); Estevão, A. P. S. S. (PQ); Silva, A. C. (PQ) IBC

**EDU-026** **Low cost molecular models production with digital modeling and fabrication.** Mateus, A. L. (PQ) UFMG

**EDU-027** **3D model of Chemistry for assembly of molecules accessible to all and low cost.** Candido, Geovany (TC); Duarte, E A (PQ); Maia, D J (PQ) IFSP

**EDU-028** **Universidade e Sociedade - o que a Universidade Pública pode Oferecer aos Estudantes - Eletroquímica ao Alcance de toda Sociedade.** Castione, R. C. M. S. (FM); Vicinguera, M.L.F. (FM); Oliva, A. D. (FM); Salgado, J. R. C. (PQ) UNILA

**EDU-029** **Chemical Kinetics on the tip fingers: an Assistive Technology Resource for Blind and Low Vision Students.** Oliveira, M. S. (IC); Santos, L. S. (IC); Cid, T. P. (IC); Rocha, A. C. S. (IC); Penco, V. S. N. (PQ); Estevão, A. P. S. S. (PQ); Silva, A. C. (PQ) IBC

**EDU-030** **Scientific articles: a tool for teaching enviromental chemistry in technical enviromental course.** Cruz, R. P. (FM); Mendonça, M. L. T. G. (FM); Sarmento, J. P. (IC); Mesquita, L. M. (TC); Silva, I. O. (IC); Lima, T. R. Q. (IC) UFRRJ

**EDU-031** **Use of photography as didactic approach for teaching Chemistry at high school groups.** Anunciação, D. S. (PQ); Queiroz, S. F. (IC); Ferreira Júnior, J. C. (PQ) UFAL

**EDU-032** **An Educational Game for the Heat Conceptual Profile Mapping.** Leite, M. A. S. (PG); Mesquita, N. A. S. (PQ); Soares, M. H. F. B. (PQ) UFG

**EDU-033** **Microplastics and Superheroes - Learning through a Playful Activity.** Almerindo, G. I. (PQ); Ehrhardt, A. (PQ); Nalepa, K. T. (IC); Bona, T. F. (IC); Brandellero, M. V. (IC); Fischer, A. C. K. (IC); Costódio, P. F. S. (PQ); Furlanetto, L. (PQ) UNIVALI

**EDU-034** **O uso do vídeo no ensino e na aprendizagem de habilidades laboratoriais técnicas.** Alvim, T.R. (PQ); Batista, G.F. (IC) CEFET-MG

**EDU-035** **Kit para experimentos de eletroquímica, produzido com condutores flexíveis de grafite laminado sobre celulose.** Santos, J. (PG); Abreu Filho, P. (PQ); Batista, B. (PQ); Galembeck, F. (PQ) UNICAMP

**EDU-036** **Produção de biodiesel a partir de óleo de azeite (Olea europae) como proposta de contextualização no ensino de química.** Oliveira, S. J. (IC); Fonseca, A. M. (PQ); Carmo, M. (IC); Colares, R. P. (PQ); Martins, V. E. P. (PQ); Silva, B. A. E. (IC) UNILAB

**EDU-037** **Visão dos discentes a respeito de jogos analógicos e digitais no ensino de química.** Beltrame, A. C. F. (IC); Stevanato, A. (PQ); Zapateiro, G. A. (IC); MORAES, M. P. (IC); Santos, D. P. (IC); Poli, C. T. (FM) UTFPR

**EDU-038** **Representação Social de graduandos de Química sobre "Experimentação".** Receputi, C. C. (PG); Pereira, T. M. (PG); Vogel, M. (PQ); Rezende, D. B. (PQ) IQUSP

**EDU-039** **Atividades Experimentais Investigativas: Visões e Propostas de Professores de Química do Ensino Médio.** Akahoshi, L. H. (PQ); Marcondes, M. E. R. (PQ); Souza, F. L. (PQ); Ayres-Pereira, T. I. (PG) IQUSP

**EDU-040** **Valuable Obstacle as a challenge to the development of the professional knowledge of a Chemistry teacher.** PENA, G. B. O (PG); MESQUITA, N. A. S (PQ) UFG

**EDU-041** **O ensino da química na concepção dos estudantes de Licenciatura em Educação do Campo-CNM/UFMA.** Marcelo, C. R. (PQ) UFMA

**EDU-042** **Chemistry teaching for deprived of liberty: challenges of teaching in a recovery center.** Oliveira, D. C. B. (IC); Santos, R. A. (IC); Silva, L. O. (PQ) UEPA

**EDU-043** **Chemistry teaching perceptions of students from Territorial Center of Professional Education from Vitória da Conquista/BA.** Novaes, A. B. S. V. (IC); Silva, S. A. (IC); Santos, S. A. (FM) IFBA

**EDU-044** **Perfil formativo dos professores de Química do Instituto Federal de Educação, Ciência e Tecnologia de Goiás.** Ferreira, V. S. (IC); Mesquita, N. A. (PQ) IFG

**EDU-045** **Socioeconomic Profile of Brazilian Chemistry Students: An Analysis of the Enade Reports.** Moreira, D. N. (PQ); Geglio, P. C. (PQ) UFPB

**EDU-046** **A Supervisor narration on the history of a PIBID-Chemistry subproject and the construction of teacher professionalism.** Pereira, T. M. (PG); Receputi, C. C. (PG); Vogel, M. (PQ); Rezende, D. B. (PQ) IQUSP

**EDU-047** **Incentivo, estímulo, e as ações que levam um aluno do ensino fundamental a se tornar um pesquisador. Uma parceria universidade/escola pública.** Castione, R. C. M. S. (FM); Salgado, J. R. C. (PQ); Bet, M. A. (IC) Colégio Estadual Professor Flávio Warken

**EDU-048** **Synthesis of alpha-Lapachol, beta-lapachone and hydroxy-hydrolapachol from lapachol (demolition timber): A Research Module for the Organic Chemistry Laboratory.** Oliveira, M. D. A. (PG); Costa, J. M. S. (IC); Andrade, T. J. A. S. (PQ); Costa Júnior, J. S. (PQ) IFPI

**EDU-049** **Experimento de fotocatálise para aula prática de físico química utilizando resíduo de laboratório.** Castro, L. M. F. (PG); Santos, T. S. (IC); Cavalcante, L. A. (IC); Souza, M. O. G. (PQ) UNEB

**EDU-050** **Microwave reactions: a green alternative to laboratory classes.** SILVA, G. A. L. (IC); SILVA, B. B. (IC); ALMEIDA, Q. A. R. (PQ) IFRJ-Campus Duque de Caxias

**EDU-051** **Investigação de parâmetros da cromatografia em camada delgada para avaliação preliminar da qualidade de biodiesel.** Lourencetti, C. (PQ) IFSP-Matão

**EDU-052** **Experiments and interactive tools to stimulate the learning of fundamental concepts of chemistry.** Pedrozo, E. C. (PQ); Santos, D. M. D. (IC); Nascimento, B. N. (IC); Moura, L. C. M. (IC) EEL-USP

**EDU-053** **Auto-discharge of a cell: experimental proposal from a continuous professional development courses about applied electrochemistry.** Goes, L. F. (PG); Albuquerque, G. Z. Q. (IC); Vairolette, Lucas (IC); Santos, A. H. (TC); Fernandez, C. (PQ); Agostinho, S. M. L. (PQ) IQUSP

**EDU-054** **Determination of the Iron(III)-Thiocyanate Reaction Equilibrium Constant using digital images.** Mendonça, P.X (IC); Ledesma, C.M (PG); Borges, E.M (PQ) FURB

**EDU-055** **Extraction of caffeine from tea in experimental classes of organic chemistry: comparative study.** Quintino, M. P. (PQ); Bastos, T. L. (IC); Arantes, G. C. V. (IC) PUC-GO

**EDU-056** **Algumas estratégias para ensino de química no Ensino Médio Técnico.** Cunha, E. M. S. (IC); Melo, J. C. S. (IC); Couto, G. G. (FM) IFMS

**EDU-057** **As contribuições da pedagogia de teatro na formação de professores.** Feliciano, J. M. O. (IC); Alves, V. A. (PQ); Siqueira, M. C. (PQ) UFTM

**EDU-058** **Study of the contribution of augmented reality for the teaching of organic chemistry in high school.** Silva, C. C. (FM); Almeida, S. H. (PG) IFG

**EDU-059** **Química no recreio, uma nova forma de ensinar a eletroquímica aos alunos do Ensino Médio.** Pasin, R. O. (IC); Silva, C. R. (IC); Castione, R. C. M. S. (FM); Carmona, J. L. C. (IC); Dutra, R. (IC); Estimable, R. (IC); Rodrigues, A. T. G. (IC); Ortiz, F. J. A. (IC); Junior, M. G. O. (IC); Salgado, J. R. C. (PQ) Colégio Estadual Professor Flávio Warken

**EDU-060** **Cozinha científica: motivando e promovendo o ensino de química.** Colares, R. P. (PQ); Santos, R. M. (IC); Fonseca, A. M. (PQ); Sousa, M. B. (PQ); Oliveira, S. J. (PG); Souza, M. C. M. (PQ); Menezes, E. A. (PQ); Barros, M. S. P. (PG) UNILAB

**EDU-061** **Atividade experimental de eletroquímica: contribuição ao processo ensino-aprendizagem.** Diniz, B.P. (PG); Brito, E.C.P. (IC); Madalena, L.S. (IC); Silva, L.A. (PQ); Alves, V.A. (PQ) UFTM

**EDU-062** **QUÍMICA LÚDICA: a arte de aprender brincando.** Fonseca, A. S. (IC); Rodrigues, N. M. C. (IC); Almeida, M. D. S. (PQ); Anjos, D. S. C. (PQ) IF-Sertão Pernambucano

**EDU-063** **O ensino de química: um olhar sobre as metodologias empregadas aos alunos surdos.** Santos, D. C. P. (PG); Meireles, G. K. Q. (FM); Fonseca, K. C. J. L. (PQ) FBCT

**EDU-064** **Chemical Circuit - a Pratical Experience of PET on Alexander Grahan Bell Public School.** Siqueira, C. T. (IC); Cassa, S. G. S. (IC); Pessoa, T. C. C. (IC); Pinheiro, A. F. (IC); Silva, A. N. (IC); Souza, A. T. (IC); Cunha, B. S. (IC); Cassini, G. C. (IC); Costa, I. S. (IC); Santos, J. B. (IC); Pereira, M. F. (IC); Costa, P. R. A. (IC); Santos, A. P. B. (PQ); Crespo, L. T. C. (PQ) IFRJ-Campus Duque de Caxias

**EDU-065** **Jogo da Veeelha Estequiometria - abordagem interdisciplinar para o ensino envolvendo conteúdos químicos e matemáticos.** Bastos, C. S. (IC); Moreira, B. C. T. (PQ) UNEB

**EDU-066** **Estudo de casos: uma análise de aplicação do método.**

Rodrigues, N. M. C. (IC); Fonseca, A. S. (IC); Vieira, G. A. B. (PQ) IF Sertão Pernambucano - Campus Petrolina

# *ELE – Eletroquímica e Eletroanalítica*

**ELE-001** **Determination of fenitrothion in food samples by using single-wall carbon nanohorns and zein thin film.** Itkes, M. P. M. (IC); Oliveira, G. G. (PQ); Fatibelo-Filho, O. (PQ); Janegitz, B.C. (PQ) UFSCar-Campus de Araras

**ELE-002** **Evaluation of Triazoles Compounds as a corrosion inhibitor for 1020 carbon steel.** Godoy, A. A. (IC); Lougon, D. J. F. (IC); Teixeira, S. F. (IC); Cotrim, B. A. (FM); Resende, G. O. (FM); Souza, F. C. (FM) IFRJ

**ELE-003** **Correlating surface growth of nanoporous gold with electrodeposition parameters to optimize amperometric sensing of nitrite.** Kumar, A. (PQ); Gonçalves, J. M. (PQ); Sukeri, A. (PQ); Koiti, A. (PQ); Bertotti, M. (PQ) IQUSP

**ELE-004** **A sample drop cell based on gold microelectrodes obtained from split electronic chips.** Pedrotti, J. J. P. (PQ); Oliveira, W. V. O. (IC); Higino, G. S. H. (PG); Trevisan, J. T. T. (IC) UPM

**ELE-005** **Carbon supported hybrids nanostructures PtSn with $CeO_2$ nanorods for Direct Ethanol Fuel Cells.** Gentil, T. C. (PG); Parreira, L. S. (PQ); Souza, F. M. (PG); Pinheiro, V. S. (PG); Nandenha, J. (PQ); Neto, A. O. (PQ); Santos, M. C. (PQ) UFABC

**ELE-006** **Improving the electrochemical response of furosemide by drop casting chemically reduced graphene oxide onto glassy carbon electrodes.** Vasconcelos, S. C. (IC); Rodrigues, E. M. (IC); da Silva, F. D. (PG); Semaan, F. S. (PQ); Dornellas, R. M. (PQ) UFF

**ELE-007** **A novel thin film Sn3O4 supported titanium ($Sn_3O_4$/Ti) successfully applied in the photoelectrocatalytic degradation of Acid Yellow 17 under visible light.** Huda, A. (PG); Torquato, L. D. M. (PQ); Suman, P. H. (PQ); Handoko, C. T. (PQ); Gulo, F (PQ); Zanoni, M. V. B. (PQ); Orlandi, M. O. (PQ) IQAr-UNESP

**ELE-008** **O uso de filmes nanoporosos de Au na fabricação de microssensores eletroquímicos para a detecção de peróxido de hidrogênio.** Carvalho Junior, E. J. (IC); Hernández Saravia, L. P. (PG); Catota Saénz, H. S. (IC); Bertotti, M. (PQ) IQUSP

**ELE-009** **Evaluation of adsorption behavior of fibronectin protein onto PEDOT-co-PDLLA thin films supported on Au electrodes by QCM-D.** Araujo Silva, R. (PQ); de Torresi, S. I. C. (PQ) IQUSP

**ELE-010** **Direct detection of BHA in food samples using oil/water interface electrochemistry as main tool.** Alcantara, A. C. (PG); de Godoi, K. T. S. (PG); Suffedini, H. B. (PQ) UFABC

**ELE-011** **Synthesis and characterization of cerium nanoparticles supported in graphene nanosheets.**

Lima, T. S. (PG); Paz, E. C. (PG); Santos, M. C. (PQ); Codognoto, L. (PQ) UNIFESP-Diadema

**ELE-012** **Development of electrochemical paper-based analytical device for detection of Pseudomonas aeruginosa in water and saliva samples.** Silva, R. F. (IC); de Araujo, W. R. (PQ) IQUSP

**ELE-013** **Flow injection analysis of furosemide in pharmaceutical formulations using electrochemically reduced graphene oxide modified electrode.** Ataide, V. N. de (PG); Gonçalves, J. M. (PG); Mendes, L. F. (PG); Araujo, W.R. de (PQ); Araki, K. (PQ); Paixão, T. R. L. C. da (PQ) IQUSP

**ELE-014** **$H_2O_2$ detection in alkaline medium by Batch Injection Analysis using Prussian blue/carbon nanotubes/reduced graphene oxide film.** Silva, S. C. (IC); Nossol, E. (PQ); Cardoso, R. M. (PG); Richter, E. M. (PQ); Munoz, R. A. A. (PQ) UFU

**ELE-015** **Influence of the electrode and chaotropicity of the electrolyte on the oscillatory behavior of the electrocatalytic oxidation of SO2.** Dourado, A. H. B. (PG); Munhos, R. L. (PG); Varela, H. (PQ); Torresi, S. I. C. (PQ); Arenz, M. (PQ) IQUSP

**ELE-016** **Effect of iron concentration on degradation of Orange II azo dye by electro-Fenton and UVC Photoelectro-Fenton.** Paz, E. C. (PG); Pinheiro, V. S. (PG); Aveiro, L. R. (PG); Santos, M. C. (PQ) UFABC

**ELE-017** **Silk fibroin based impedance biosensor using interdigitated array microelectrode.** Costa, M. F. (PG); Cipriano, T. (PQ); Rojas, J. E. U. (PG); Peroni, L. A. (PQ); Christoffolete, M. A. (PQ); Benvenho, A. R. V. (PQ); Guha, S. (PQ); Alves, W. A. (PQ) UFABC

**ELE-018** **Modeling of poly(Vinylidene Fluoride) by molecular dynamics simulations.** Da Silva, R. C. (IC); Silva, F. C. A. (PG); Costa, L. T. (PQ) UFF

**ELE-019** **Electrodeposition of Prussian Blue/Carbon Nanotubes Composites at a Liquid-Liquid Interface.** Husmann, S. (PG); Booth, S. G. (PG); Dryfe, R. A. W. (PG); Zarbin, A. J. G. (PQ) UFPR

**ELE-020** **Sensor eletroquímico à base de polieletrólito para a determinação de prometazina.** Oliveira, R. C. (IC); Sousa, C. P. (PQ); Lima-Neto, P. (PQ); Correia, A. N. (PQ) UFC

**ELE-021** **Use of $TiO_2$ nanotubes electrodes decorated with silver nanoparticle/nanocubes for enhanced $CO_2$ photoelectroreduction.** Perini, J. A. L. (PQ); Christovam, L. M. (PG); Torquato, L. D. M (PQ); Ribeiro, S. J. L. (PQ); Zanoni, M. V. B. (PQ) IQAr-UNESP

**ELE-022** **Electrochemical study and quantification of anesthetic xylazine in urine and pharmaceutical formulations.**

de Araujo, W. R. (PQ); Mendes, L. F. (PG); Silva, A. R. S. (IC); Bacil, R. P. (PG); Paixão, T. R. L. C. (PQ); Angnes, L. (PQ) IQUSP

**ELE-023** **Determination of fructose in fruit juices using an electrode modified with reduced graphene oxide and molecularly imprinted polymer poly(phenylboronic acid).** Moreira, L. F. P. P. (IC); Buffon, E. (PG); Sá, A. C. (PQ); Stradiotto, N. R. (PQ) IQAr-UNESP

**ELE-024** **Development of electroanalytical sensors based on electropolymeric films and molecular imprinting technology.** Teixeira, W. S. R. (PG); Silva, M. K. L. (PG); Gruber, Jonas (PQ); Cesarino, I. (PQ); Megid, J. (PQ) IBB-UNESP

**ELE-025** **Evaluation of sulfonamide-based anilines as a corrosion inhibitor for 1020 carbon steel.** Godoy, A. A. (IC); Lougon, D. J. F. (IC); Teixeira, S. F. (IC); Meira, V. N. (IC); Santiago, V. S. (FM); Souza, F. C. (FM) IFRJ

**ELE-026** **Platinum surface oxidation in the presence of different alcohols.** Roquetto, J. M. (IC); Santiago, P. V. B. (PG); Angelucci, C. A. (PQ); Souza-Garcia, J. (PQ) UFABC

**ELE-027** **Electrochemical oxidation of the Sunset Yellow in acidic medium using boron-doped diamond anode (BDD).** Neves, C. G. (IC); da Silva, L. A. L. (PG); Carvalho, A. E. (PQ); Barros, W. R. P. (PQ) UFGD

**ELE-028** **Desenvolvimento de eletrodos de grafite para detecção eletroquímica em substrato de papel.** Rocha, D. S. (IC); Duarte, L. C. (PG); Dias, A. A. (PG); Santana, M. H. P. (PQ); Coltro, W. K. T. (PQ) UFG

**ELE-029** **TiO2 nanotubes modified with ZIF-8 used for $CO_2$ capture and photoelectroreduction.** Cardoso, J. C (PQ); Stulp, S. (PQ); Brito, J.F (PG); Flor, J. B. (PQ); Frem, R. C. G (PQ); Zanoni, M. V. B (PQ) IQAr-UNESP

**ELE-030** **Gold Leaf: from gilding to the fabrication of AuNP-modified electrochemical sensor.** Ameku, W. A. A. (PG); Santos, M. S. F. S. (PQ); Gutz, I. G. R. G. (PQ); Paixão, T. R. L. C. P. (PQ) IQUSP

**ELE-031** **Niobium as co-electrocatalyst for Pd in alkaline medium: improved selectivity and mechanism for ethanol electrooxidation reaction.** Souza, F. M. (PG); Parreira, L. S. (PQ); Oliveira, V. H. A. (IC); Pinheiro, V. S. (PG); Batista, B. L. (PQ); Nandenha, J. (PQ); Neto, A. O. (PQ); Santos, M. C. (PQ) UFABC

**ELE-032** **Comportamento voltamétrico de um análogo sulfonil-hidrazona do nitrofural com potencial atividade antichagásica.** Almeida, L. S. (IC); Chiavassa, L. D. (PG); Gatti, F. M. (PG); Trossini, G. H. G. (PQ); La Scalea, M. A. (PQ) UNIFESP-Diadema

**ELE-033** **Inner- or outer-sphere. We should still learn about heterogeneous electronic transfer.** Chaves, B. P. (IC); Cavallieri, M. C. (IC); Beruski, O. B. (PQ); Cabral, M. F. (FM) IFRJ

**ELE-034** **Modeling the electroreduction of hydrogen peroxide in alkaline media.** Rodrigues Pinto, M. R. (PG); Miranda, R. C. C. (PG); da Silva, K. N. (PG); Sitta, E. (PQ); Nagao, R. (PQ) UNICAMP

**ELE-035** **Amperometric and voltammetric determination of tibolone in pharmaceutical and saliva samples.** da Silva, W. P. (PG); da Rocha, R. G. (PG); Muñoz, R. A. A. (PQ); Richter, E. M. (PQ) UFU

**ELE-036** **QCM-D and ATR-FTIR studies applied to the understanding of LCysteine adsorption: how can viscoelastic changes be explained?.** Dourado, A. H. B. (PG); Silva, R. A. (PQ); Torresi, R. M. (PQ); Arenz, Matthias (PQ); Córdoba de Torresi, S. I. (PQ) IQUSP

**ELE-037** **Application of the carioca bean (Phaseolus vulgaris L.) for the electroanalytical detection of phenol using graphite- $SiO_2$-$TiO_2$ electrode.** Mihos, F. C. S. S. (PG); Guedes, P. H. C. (IC); Ribeiro, E. S. (PQ); Silva, M. L. C. (PQ); Salgado, A. M. (PQ) UFRJ

**ELE-038** **Electrocatalytic activity of niquel hexacyanoferrate supported on reduced graphene oxide for electrooxidation reaction Glycerol.** Rodrigues, I. A. (PQ); Viégas, D.S.S. (PG); Silva, L. M.S. (PG); Marques, A.L.B. (PQ) UFMA

**ELE-039** **Development of an enzymatic cascade immobilized on modified nafion to produce an efficient ethanol/$O_2$ biofuel cell.** Franco, J. H. (PQ); De Andrade, A. R. (PQ) FFCLRP-USP

**ELE-040** **Voltammetric Behavior Study of Nitrofurazone at Multi-wall Carbon Nanotube-Modified Glassy Carbon Electrode in Aqueous Media.** Brito, C.L. (PG) FCF-USP

**ELE-041** **Platinum nanoparticles supported on carbon-based materials as electrocatalysts for methanol oxidation reaction.** Giareta, R. (IC); Pasin, R. O. (IC); Salgado, J. R. C. (PQ) UNILA

**ELE-042** **Eletrodeposição e caracterização da liga NiFe com 20 e 30% de substituição do Ni no banho de watts.** Tavares, I. L. M. (IC); Cunha, A. C. C. (IC); Medeiros, F. C. (IC); Silva, P. S. G. (PQ) UFCG

**ELE-043** **Nanoporous Gold Microelectrode as Scanning Electrochemical Microscopy (SECM) Probe for the Study of Dopamine Diffusion.** Selva, J. S. G. (PG); Sáenz, H. S. C. (IC); Saravia, L. H. (PG); Sukeri, Anandhakumar (PQ); Montero, P. J. E. (PQ); Bertotti, M. (PQ) IQUSP

**ELE-044** **Performance and caracterization a new electrochemical sensor based on $Fe_3O_4$/MWCNT-O to detection Metribuzin Herbicide.** Silva da, L. A. L. (PG); Corazza, M. Z. (PQ); Carvalho, A. E. (PQ) UFGD

**ELE-045** **Voltammetric study of nitrofurazone in ionic liquids by using a carbon fiber microelectrode.** Chiavassa, L.D. (PG); Camilo, F.F. (PQ); La-Scalea, M.A. (PQ) UNIFESP-Diadema

**ELE-046** **Fabrication of a disposable electrochemical paper-based device for cortisol quantification.** Mendes, L. F. (PG); Araujo, W. R. (PQ); Paixão, T. R. L. C. (PQ) IQUSP

**ELE-047** **Electrochemical sensor based on MIP grafted on multi-walled carbon nanotubes for 17beta-estradiol determination.** Marques, G. L. (IC); Dos Santos, D. M. (PQ); Almeida, F. G. (IC); Rocha, L. R. (PG); Tarley, C. R. T. (PQ) UEL

**ELE-048** **Development of an electrochemical lectin-based biosensor using a novel Galectin-1-Maltose Binding Protein fusion molecule.** Gomes, P. O. M. (PG); De Leo, T. C. (PG); Batistuti, M. R. (PQ); Dias-Baruffi, M. (PQ); Naal, Z. (PQ) FFCLRP-USP

**ELE-049** **Submicro quantification of N-acetylcysteine by electrochemically-driven homogeneous catalysis, on boron-doped diamond electrodes.** Goulart, M.O.F. (PQ); Santos, A.C.F. (PG); Moura, F.A. (PQ); Luz, R.C. (PQ); Kubota, L.T. (PQ); Damos, F.S. (PQ) UFAL

**ELE-050** **Electrochemical biosensor based on botryosphaeran as a novel biomaterial for laccase immobilization.** Mattos, G. J. (IC); Dekker, A. M. B. (PQ); Dekker, R. F. H. (PQ); Camargo, P. H. C. (PQ); Barbosa, E. C. M. (PG); Sartori, E. R (PQ) UEL

**ELE-051** **Complex Dynamic during the oscillatory electro-oxidation of glucose on platinum.** Ferreira, G. C. A. (PG); Varela, H. (PQ) IQSC-USP

**ELE-052** **Carbon nanotube/reduced graphene oxide nanocomposite formed at interfacial method: Properties and potential electroanalytical applications.** Rocha, D. P. (PG); Castro, S. V. F. (PG); Silva, M. N. T. (PG); Cardoso, R. M. (PG); Tormin, T. F. (PG); Richter, E. M. (PQ); Nossol, Edson (PQ); Munoz, R. A. A (PQ) UFU

**ELE-053** **Desenvolvimento e caracterização de um sensor fotoeletroquímico nanoestruturado utilizando $BiVO_4$.** Araujo, M. S. (IC); Galvão, J.C.R. (PG); Dall'Antonia, L.H (PQ); Tarley, C.R.T. (PQ); Matos, R. (PQ); Medeiros, R.A. (PQ) UEL

**ELE-054** **Electrochemical bistability induced by surface area changes.** Rospendowiski, J. (IC); Rodrigues, M. (PG); Nagao, R. (PQ) UNICAMP

**ELE-055** **Nanostructed Nickel Hydroxide Electrodes by Electrodeposition.** Cerqueira, G (IC); Colombo, R. N. P. (PG); Torresi, S. I. C. (PQ) IQUSP

**ELE-056** **Electrochemical study of carbon nanotube@polyaniline hybrid for application in active solar cell layer.** Ferreira, L. L. (PG); Fengler, T. A. L. (IC); Calado, H. D. R. (PQ) UFMG

**ELE-057** **Enzymatic biosensor based on tyrosinase and gold nanostructures for Bisphenol A determination.** Silva, J. A.; Lavayen, V. G.; Inroga, F. A. D. (PG) UFRGS

**ELE-058** **Performance of the LiFePO4 in supercapatteries.** Ortega, P. F. R. (PQ); Santos, G. O. (IC); Silva, G. G. (PQ); Blanco, C. (PQ); Santamaría, R. (PQ); Lavall, R. L. (PQ) UFMG

**ELE-059** **Eletrodeposição de prata usando líquido iônico [$HMIM^+$][$HSO_4^-$].** Sousa, N. G. (IC); Sousa, C. P. (PQ); Eguiluz, K. I. B. (PQ); Salazar-Banda, G. R. (PQ); Correia, A. N. (PQ); Lima-Neto, P. (PQ) UFC

**ELE-060** **MBP-Gal-1 chimeric protein immobilization onto GCE functionalized by electrochemical reduction of pyridinium diazonium derivative.** Gomes, M. F. (PG); Gomes, P. O. M. (PG); Silva, W. R. (TC); Batistuti, M. R. (PQ); Donate, P. M. (PQ); Naal, Z. (PQ) FFCLRP-USP

**ELE-061** **Electrochemical SERS of Flavin on a Gold Surface.** Jaimes, R.F.V.V.J. (PQ); Salcedo, W.J.S. (PQ); Corio, P.C. (PQ) IQUSP

**ELE-062** **Carbon nanofibers modified screen-printed electrode for copper analysis in bioethanol by anodic stripping voltammetry.**

Azevedo, V. H. R. (IC); Da Silva, J. L. (PQ); Stradiotto, N. R. (PQ) IQAr-UNESP

# *EST – Química Estrutural*

**EST-001** **In Situ Preparation of a complex salt formed by the anionic metallacycle $[Co_2(H_2mpba)_3]_{2-}$ stabilized by the [Co(tppz)2] 2+ complex.** Mariano, L. S. (IC); Do Pim, W. D. (PQ); Doriguetto, A. C. (PQ); Rosa, I. M. L. (PQ); Ribeiro, M. A. (PQ); Stumpf, H. O. (PQ); Marinho, M. V. (PQ) UNIFAL

# *FIS – Físico-Química*

**FIS-001** **Estudo de modelagem molecular, em compostos híbridos de Nor-β-lapachona com chalconas, na investigação do tratamento do câncer.** LIRA, P. H. A. (IC); Malta, V. R. S. (PQ); Silva, S. W. D. (PQ); da Silva, J. R. N. (IC) UFAL

**FIS-002** **Secondary ion emission from water ice induced by mev cf fission fragments and its applicability in astrochemistry.** Santos, J. de C. (IC); Andrade, D. P. P. (PQ); da Silveira, E. F. (PQ); Baptista, Leonardo (PQ); Boechat-Roberty, H. M. (PQ) UFRJ

**FIS-003** **A Study of the Influence of Debris on the Adsorption Capacity of Functionalized Multi-Walled Carbon Nanotubes.** Amaral, T. M. (IC); Santos, G. O. (IC); Pires, N. J. (PQ); Castro, V. G. (PQ); Silva, G.G. (PQ); Lavall, R. L. (PQ); Ortega, P. F. R. (PQ) CEFET-MG

**FIS-004** **Impact of water concentration on the electro-oxidation of methanol on platinum.** Romano, R. L. (IC); Previdello, B. A. F. (PQ); Varela, H. (PQ) IQSC-USP

**FIS-005** **A homemade device colorimeter foron quantitative and qualitative analysis of organophosphates.** Nascimento, L. L. Q. (IC); Baptista, V.S. (PG); Souza, E.O. (PQ) UFPR

**FIS-006** **Colorimetric detection of glyphosate via an aromatic derivative.** Hellinger, H.R. (IC); Silva, S. V. (PG); Orth, E. S. (PQ) UFPR

**FIS-007** **2D, 3D and 4D QSAR studies relating flavanoid inhibitor activity in alpha estrogen receptors.** Barcelos, V. H. T. (IC); Borges de Melo, E. (PQ); Martins, J. P. A. (PQ) UFMG

**FIS-008** **Study of the influence of NaY zeolite particle size on CO adsorption: analysis by infrared spectroscopy with fourier transform.** Viana, A.; Neto, P. R. C.; Rizzo-Domingues, R. C. P.; Kich Severo, I. (IC) UTFPR

**FIS-009** **Amides as nucleophiles in dephosphorylation processes: reactivity favored by tautomerism.** Fernandes, J. M. (IC); Campos, R. B. (PQ) UTFPR

**FIS-010** **Stereochemical studies of Dansylglycine bound to protein Human Serum Albumin.** de Souza, A. R. (PQ); Boza, I. A. F. (PG); Ximenes, V. F. (PQ); Morgon, N. H. (PQ) UNESP-Bauru

**FIS-011** **Reverse solvatochromism of iminophenolate dyes comprised of 5-nitrofuran-2-yl or 5-nitrothiophen-2-yl as electron acceptor.** Melo, C. E. A. (PG); Nicoleti, C. R. (PQ); Rezende, M. C. (PQ); Bortoluzzi, A. J. (PQ); Heying, R. S. (PG); Oliboni, R. S. (PQ); Caramori, G. F. (PQ); Machado, V. G. (PQ) UFSC

**FIS-012** **4-Aminoantipyrine abatement from water by electrochemical advanced oxidation processes and study of its complex with Fe(III).** Silva, L. M. (PG); Gozzi, F. (PQ); Sirés, I. (PQ); Brillas, E. (PQ); Oliveira, S. C. (PQ); Machulek Jr., A. (PQ) UFMS

**FIS-013** **Physical Chemical properties and vibrational analysis of Reline, a choline chloride based DES, and dimethyl sulfoxide mixtures.** Triolo, A.; Andanson, J. M.; Husson, P.; Avila, J. N. L. IQUSP

**FIS-014** **Spontaneous electrostatic charging during phase transition at solid-gas and liquid-gas interfaces.** Burgo, T. A. L. (PQ); Moreira, K. S. (IC); Galembeck, F. (PQ) UFSM

**FIS-015** **Effect of temperature on the liquid-liquid equilibrium of the ternary system water + pluronic10R5 + ammonium thiosulfate.** Fontoura, B.M. (PG); Chagas, F.O. (PG); Vargas, S.J.R (PG); da Silva, L.H.M (PQ); Hespanhol, M.C (PQ) UFV

**FIS-016** **Probing the biophysical interactions of chitosan derivatives with cell membrane models using Sum-Frequency Generation Spectroscopy.** De Oliveira Pedro, R. (PQ); Miranda, P. B. (PQ) IFSC-USP

**FIS-017** **Excess of vibrational density of states and relaxation processes studies on glass forming ionic liquids.** Lima, T.A. (PQ); Li, Z. (PG); Zhang, Y. (PQ); Ribeiro, M. C. C. (PQ) IQUSP

**FIS-018** **Synthesis $Ag/Nb_2O_5$ nanoestructures for the visible light photocatalytic degradation of the methylene blue dye.** Jambo, R. B. A. (IC); Santos, P. B. (PG); Andrade, G. F. S. (PQ) UFJF

**FIS-019** **Mechanistic study between the pesticide methyl-parathion and imidazole: unusual selective attack at the aliphatic carbon.** Silva, V. B. (PG); Nunes, M. C. (PQ); Nascimento, L. L. Q. (IC); Oliveira, A. R. M. (PQ); Orth, E. S. (PQ) UFPR

**FIS-020** **Descoloração e degradação do corante reativo Remazol Preto B por oxidação com $H_2O_2$/NaOH.** Mora, A. (IC); Floriani, H. L. (IC); Mittersteiner, M. (PG); De Jesus, P. C. (PQ) FURB

**FIS-021** **Phase inversion behavior of poly(ethylene glycol) + NaOH + water aqueous two-phase systems (ATPSs): Effect of polymer molar mass.** Penido, J. A. (PG); Gonçalves, G. R. S. (IC); Carvalho, I. M. (IC); Mageste, A. B. (PQ); Ferreira, G. M. D. (PQ) UFOP

**FIS-022** **Use of surfactants as selective modulators in the partition in aqueous two-phase systems: An alternative for speciation of dyes.** Penido, J.A. (PG); Martins, P.L. (IC); Ferreira, G.M.D. (PQ); Mageste, A.B. (PQ) UFOP

**FIS-023** **Análise de dopagens substitucionais com V e N na superfície de $TiO_2$ através do método DFT-GGA.** Da Silva, G. O. (PG); Politi, J. R. S. (PQ); Martins, J. B. L. (PQ) UnB

**FIS-024** **The effect of acetone and sulfuric acid concentrations on sequential oscillations in a modified Belousov-Zhabotinsky reaction.** Chern, M. S. (PG); Faria, R. B. (PQ) UFRJ

**FIS-025** **The use of agro-industrial waste and Moringa oleifera leaves as antioxidants sources for soy oil biodiesel.** Valenga, M. G. P. (PG); Boschen, N. L. (PG); Rodrigues, P. R. P. (PQ); Maia, G. A. R. (PQ) UNICENTRO

**FIS-026** **Study of the behavior of the methyl orange (MOR) dye in binary mixtures using amphiprotic solvents.** Sant'Ana, A. C. (IC); Dangui, A. Z. (IC); Nicolini, K. P. (PQ); Nicolini, J. (PQ) IFPR

**FIS-027** **Effect of inhibitors and a bad solvent on a Brazilian crude oil: kinetics of asphaltene adsorption on gold surfaces of QCM electrode.** Balestrin, L. B. S. (PG); Bertran, C. A. (PQ); Cardoso, M. B. (PQ); Loh, W. (PQ) UNICAMP

**FIS-028** **Estudo comparativo da eficiência de adsorção de diferentes classes de corantes texteis empregando residuo industrial.** Miguel, T. (IC); Schmitz, F. (PG); Barcellos, I.O. (PQ) FURB

**FIS-029** **Solubilidade de timina (THY) em água do mar artificial para estudos de química prebiótica.** Carvalho, D. A. (IC); Silva, A. C. (PG); Carneiro, C. E. A. (PQ) UFOB

**FIS-030** **Análise físico-química e determinação de metais tóxicos presentes na manipueira.** Melo, I. K. L. (IC); Tavares, M. C. (PG); Cavalcanti, J. C. M. (PQ); Júnior, J. G. S. (PQ); Botero, W. G. (PQ); Del Colle, V. (PQ) UFAL

**FIS-031** **Surface modification of aseptic carton package for energy harvesting devices.** Moreira, K. S. (IC); Burgo, T. A. L. (PQ) UFSM

**FIS-032** **Raman spectroscopy applied to the restoration and conservation of cellulose-supported work of art.** Campos, P. S. (IC); Castro, A. A. N. (PQ); Sant'Ana, A. C (PQ) UFJF

**FIS-033** **Influência da relação molar óleo de macaúba / metanol na produção de biodiesel em um reator de leito fixo.** Aguiar, F. C. L. (PG); Silva, F. M. (PQ); Suarez, P. A. Z. (PQ); Cunha, M. F. (IC) UnB

**FIS-034** **New Approach For Calculation Of Enthalpy Of Formation From Computational Thermochemistry.** Batistela, V. R. (PQ); Sene, A. P. (IC); Dias, A. O. (PG); Vanzin, D. (PG); Ueno, L. T. (PQ) UEM

**FIS-035** **Computer simulations of chiromagnetic nanoparticles.** Santos, U. S. (PG); Yeom, J. (PQ); Kotov, N. A. (PQ); de Moura, A. F. (PQ) UFSCar

**FIS-036** **Microbial habitability of Europa sustained by radioactive sources.** Thiago, A. (PG); de Avellar, M. G. B. (PQ); Rodrigues, F. (PQ); Galante, D. (PQ) CNPEM

**FIS-037** **Effect of macromolecule hydrophobicity on liquid-liquid equilibrium of aqueous two-phase system composed of (NH4)2S2O3.** Chagas, F. O. (PG); Fontoura, B. M. (PG); Vargas, S. J. R. (PG); da Silva, L. H. M. (PQ); Hespanhol, M. C. (PQ) UFV

**FIS-038** **Síntese e caracterização do monômero di-hidrogenofosfato de 10-metacriloxidecil (10-MDP).** Furtado, P. R. P. (IC); Meier, M. M. (PQ); Castro, N (PG); Gariani, R. G. (PQ) UDESC

**FIS-039** **Encapsulação de monômero metacrílico: caracterização do complexo de inclusão e do polímero formado.**

Savanhago, R. M. (IC); Meier, M. M. (PQ) UDESC

# *FOT – Fotoquímica*

**FOT-001** **The photodegradation behavior of two indium phthalocyanines and its influence on the photohaemolysis of human red blood cells.** Silva da, A. R. (PQ); Silva da, L. C. D. (IC); Rocha, S. L. (IC) IFES-Campus Aracruz

**FOT-002** **Synthesis and characterization of tetraporphyrins dispersed in peptide based low molecular weight gelators.** Vassiliades, S. V. (PG); Pinheiro, M. V. B. (PQ); Krambrock, K. (PQ); Giutinni, F. (PQ); Alves, W. A. (PQ) UFABC

**FOT-003** **Produção fotoquímica de $O_2$ e $H_2$ a partir da água usando um complexo triscarbonil de Mn(I) na ausência de oxidantes.** Marchi, R. C. (PG); Carlos, R. M. (PQ) UFSCar

**FOT-004** **Photocatalytic treatment of wastewater from cassava processing by using NiO/Ni/$TiO_2$ composites.** SANTOS, K. S. (PG); LOPES, P. A. L. (PG); SILVA, L. A. (PQ) UFBA

**FOT-005** **Amyloid Beta Monitoring Through a Ru(II) Complex: Luminescent Probe Candidate for Early Diagnosis of Alzheimer's Disease.** Cali, M. P. (PG); Carlos, R. M. (PG) UFSCar

**FOT-006** **A study of the photophysical and solvatochromic properties of naphtho[2,3-b]benzofuran-6,11-diones.** Teixeira, R. I. (PG); Tonin, M. D. (PG); de Lucas, N. C. (PQ); Garden, S. J. (PQ) UFRJ

**FOT-007** **Photocatalyzed [2+2]-cycloaddition of 3-(2-oxo-2-phenylethylidene)-2-oxindole by ruthenium complexes.** Teixeira, R. I. (PG); Garden, S. J. (PQ); de Lucas, N. C. (PQ) UFRJ

**FOT-008** **Synthesis and photophysical studies of new fluorescent N-acylhydrazone and semicarbazone-7-$NEt_2$-coumarin dyes.** Pereira, T. M. (PG); Miranda, F. S. (PQ); Kummerle, A. E. (PQ) UFRRJ

**FOT-009** **Estudo por fotólise por pulso de laser da reatividade do triplete de dimetoxi-xantonas frente a doadores de energia, elétron e hidrogênio.** Ferreira, R. C. (PG); de Almeida, V. G. (IC); de Oliveira, C. H. C. S. (PG); Machado, A. E. H. (PQ); Cesarin-Sobrinho, D. (PQ); Netto-Ferreira, J. C. (PQ) UFRRJ

**FOT-010** **Photodegradation of sodium diclofenac and toxicity monitoring.** Lima, L. S. (IC); Galdino, M. M. (IC); Souza, D. R. (PQ) UFOB

**FOT-011** **Estudo da interação entre azul de metileno e curcumina para uso em terapia fotodinâmica combinada com antiangiogênica.** Silva, R. C. (PG); Neri, C. R. (TC); Serra, O. A. (PQ); Iamamoto, Y. (PQ); Buzzá, H. H. (PQ); Borissevitch, I. E. (PQ); Gonçalves, P. J. (PQ) UFG

**FOT-012** **Síntese e avaliação fotofísica preliminar de benzimidazóis bifenílicos.** Araujo, N. S. de (PG); Rocha, T. C. da (IC); Villar, J. D. F. (PQ); Miranda, F. da S. (PQ) IME

**FOT-013** **Preparation and characterization of fibroin hydrogels for potential application in photodynamic therapy.** Ulloa, J.E (PG); Giuntini, F (PQ); Alves, W (PQ) UFABC

**FOT-014** **Síntese e caracterização do complexo $[Ru(phen)_2(iso)]PF_6$.** Pachel, B. (IC); Marchi, R.C. (PG); Silva, D. F. (PQ); Fernandes, J. B. (PQ); Silva, M. F. G. F. (PQ); Carlos, R. M. (PQ) UFSCar

**FOT-015** **Nature-inspired fluorescent betalains.** Bastos, E. L. (PQ) IQUSP

**FOT-016** **Development of topical formulation containing methylene blue for photodynamic therapy.** Costa, L. A. G. (IC); Pereira, H. K. M. (IC); Fontes, A. (PQ); Falcão, J. S. A. (PQ); Santos, B. S. (PQ) UFPE

# *INO – Química Inorgânica*

**INO-001** **Degradação do antibiótico levofloxacino catalisada por porfirinas de manganês.** Lage, A. L. A. (PG); Silva da, M. A. N. (TC); Martins, D. C. S. (PQ) UFMG

**INO-002** **trans-$[Ru(NH_3)_4(pyS)X]$ complexes: syntheses, characterization and self-assembled monolayer on gold.** Azevedo, I. A. L. (IC); Paulo, T. de F. (PQ); Castro de, C. B. (PG); Diógenes, I. C. N. (PQ) UFC

**INO-003** **Stability study of the complex ion $[Cu(opba\text{-}dCl)]^{2-}$ in function of pH.** Souza, D. O. (IC); Pedroso, E. F. (PQ); Dutra, R. C. Q. (PQ) CEFET-MG

**INO-004** **Indirect Detection of HO• Radical Produced by a Copper Complex under Electrolysis Conditions: Ascorbic Acid as Redox Probe.** Dibo, V. S. (IC); Abreu, D. S. (PG); Ramos, A. I. B. (PG); Nascimento, O. R. (PQ); Diógenes, I. C. N. (PQ) UFC

**INO-005** **Síntese e comportamento catalítico de porfirinas de Mn(III) na formação de carbonatos cíclicos utilizando $CO_2$ e epóxidos.** Milani, J. L. S. (PQ); Meireles, A. M. (PG); Bezerra, W. A. (IC); Martins, D. C. S. (PQ); Chagas, R. P. (PQ); Cangussu, D. (PQ) UFG

**INO-006** **Energy transfer in trivalent europium diphenylphosphinate matrix associated with a\β-diketone ligand.** Lazzarini, A. B. (IC); Castro de, P. R. (IC); Bim, L. F. B. (PG); Cebim, M. A. (PQ) IQAr-UNESP

**INO-007** **Helical Coordination Polymer from Manganese(II) 16-Metallacrown-6 Recognition of Zwitterionic L-Glutamate.** Wioppiold, T. A. (PG); Abram, U. (PQ); Lang, E. S. (PQ) UFSM

**INO-008** **Luminescent lanthanide MOFs based on ligand 4,4',4''-((benzene-1,3,5-triyltris(methylene))tris(oxy))tribenzoate ligand: syntheses, structures and photophysical properties.** Petiot, L. (PG); Mazali, I. O. (PQ); Sigoli, F. A. (PQ) UNICAMP

**INO-009** **Synthesis, characterization and antitumor activity of a 2,5-diketopiperazine copper coordination compound.** Silva da, F. F. (PQ); Silva Neto da, J. F. (PQ); Jimenez, G. C. (PQ); Souza de, D. M. B. (PQ); Falcão, E. H. L. (PQ); Alves Jr., S. (PQ) UFPB

**INO-010** **Particularities of trivalent europium luminescence in a pure phenylphosphinate matrix.** Bim, L. F. B.; Cebim, M. A.; Teotônio, G. L. E. (IC) IQAr-UNESP

**INO-011** **Derivado de 1,3,4-oxadiazol como ligante em compostos beta-dicetonados de Gadolínio.** Scapolan, M. I. X. (IC); Adati, R. D. (PQ); Westphal, E. (PQ) UTFPR

**INO-012** **Chemosensor based on HABA for detection of $F^-$, $CH_3COO^-$ and $PO_4^{3-}$ anions.** Santos, C. H. (IC); Bagatin, I. A. (PQ) UNIFESP-Diadema

**INO-013** **Ruthenium(II) terpyridine complexes containing heteroaryl-2-imidazole ligands featuring catalytic activity for water oxidation.** Huamaní, L. E. S. C. (PG); Guerra, R. B. (PG); Bibi, N. (PG); Formiga, A. L. B. (PQ) IQ-UNICAMP

**INO-014** **Chemical fixation of carbon dioxide to cyclic carbonates catalyzed by zinc(II) complexes bearing 1,2-disubstituted-benzimidazole ligands.** das Chagas, R. P. (PQ); Milani, J. L. S. (PQ); Cangussu, D. (PQ); Vilela, G. A. (IC); Bezerra, W. D. (IC) UFG

**INO-015** **Propriedades fotoluminescentes do $CeO_2$ dopado com Cobalto.** Tavares, M. S. (IC); Ferreira, G. B. (PQ); Siqueira Júnior, J. M. (PQ) UFF

**INO-016** **Amphiphilic complexes of terbium(III) and gadolinium(III) nanostructured micelles: synthesis, cytotoxic and apoptotic activities in tumor cells and MRI applications.** Silva, S. R. (PQ); Islam, A. (PG); Duarte, E. C. (IC); Dittz, D. (PQ); Colnago, L. A. (PQ); Paiva, F. F. (PQ); Lopes, M. T. P. (PQ); Frezard, F. (PQ); Demicheli, C. P. (PQ) UFRR

**INO-017** **Titanium films by sol-gel process doped $Yb^{3+}$ and $Er^{3+}$ :thermal treatment effect.** Baldini, D. C. (PG); Faria, E. H. (PQ); Ciuffi, K. J. (PQ); Rocha, L. A. (PQ); Nassar, E. J. (PQ) UNIFRAN

**INO-018** **Oxidação de cicloexano por PhIO ou $PhI(OAc)_2$ em solventes da Química Verde catalisada por uma Mn-porfirina.** Malheiros, R. O. (IC); Guimarães, A. S. (PG); Meireles, A. M. (PG); Lage, A. L. A. (PG); Silva, G. F. (PQ) UFMG

**INO-019** **Synthesis, chemical characterization and DNA interaction study of a new valproate zinc (II) ternary complex.** dos Santos, P. R. (PG); Smiderle, F. (IC); Back, D. F. (PQ); Pich, C. T. (PQ); Moura, S. (PQ) UCS

**INO-020** **Synthesis, characterization and LB films construction of a ruthenium complex with a new methyl 9-hydroxyphenalene-5-carboxylate ligand.** Winnischofer, H. (PQ); Godoy, I. M. W. (PG); Westphal, E. (PQ) UFPR

**INO-021** **Chemical behavior of chloridotetrakis(ibuprofenato)diruthenium(II,III).** Hayashi, M. (IC); Rehman, H. U. (PG); Silva, D. O. (PQ) IQUSP

**INO-022** **Synthesis of magnetic composites by combustion method: Materials for photodegradation of methylene blue.** Ferreira, M. G. (IC); Garrido, F. M. S. (PQ); Medeiros, M. E. (PQ) UFRJ

**INO-023** **Otimização da síntese de um complexo de cobalto(III) através de síntese em fluxo.** Pacheco, C. M. (IC); Mello, M.V.P. (PG); Lanznaster, M. (PQ) UFF

**INO-024** **Coumarin-N-acylhydrazone ligands and their Ru(II) complexes: structure, characterization and antimicrobial activity.** Almeida, P. S. V. B. (PG); Pereira, T. M. (PG); Guedes, G. P. (PQ); Kummerle, A. E. (PQ); Oliveira, L. L. (PQ); Neves, A. P. (PQ) UFRRJ

**INO-025** **Synthesis, crystal structure and magnetic properties of a luminescent Europium(III) complex containing oxamate as a ligand.** Vaz, R. C. A.; Esteves, I. O.; Oliveira, W. X. C.; Pedroso, E. F.; Pereira, C. L. M.; Viana, T. K. F. P. (IC) UFMG

**INO-026** **Síntese, estrutura cristalina e caracterização vibracional de um ligante pirazólico funcionalizado e um novo complexo de Coll.** Dias, I. M. (PG); Soares, I. C. (PG); Junior, H. C. S. (PG); Ferreira, G. B. (PQ); Guedes, G. P. (PQ) UFRRJ

**INO-027** **Rigid bipodal ligand as molecular building block to construct new metal-organic frameworks.** Matos, C. R. M. O. (PG); Ronconi, C. M. (PQ) UFF

**INO-028** **Iron(III) complexes with tridentate Schiff bases derived from diaminomaleonitrile: synthesis and characterization.** Döring, T. H. (IC); Dockal, E. R. (PQ); da Cruz Jr, J. W. (PQ) UFSC

**INO-029** **Oxamate-based Cobalt(II) Complex and dpss: assembling of the $[Co(H_2O)_6][Co_2(H_2mpba)_3]\}\cdot 2$,2-dpss$\cdot 2H_2O$ complex in the solid.** Campos, N. R. (PG); do Pim, W. D. (PQ); Doriguetto, A. C. (PQ); Valdo, A. K. S. M. (PG); Martins, F. T. (PQ); Stumpf, H. O. (PQ); Marinho, M. V. (PQ) UNIFAL

**INO-030** **Síntese e caracterização do novo complexo metálico estrôncio com ligante 1-10-fenantrolina.** Calisto, G. C. M. (IC); Silva, S. R. (PQ) UFRR

**INO-031** **Investigation of photodynamic efficiency of new porphyrin derivative.** Gomes, A. (PG); Marques, J. A. (PQ); Borges, C. P. F. (PQ) UEPG

**INO-032** **Síntese e avaliação da eficiência da 5,10,15,20-tetraquis(4-metiltiofenil)porfirina para terapia fotodinâmica.** Ignácio, M. H. (IC); Dias, F. S. (IC); Martins, D. C. S. (PQ) UFMG

**INO-033** **Properties and photocatalytic activity of $BiVO_4$ nanoflowers decorated with AuNP synthesized under conventional and microwave heating.** Hirata, F. T. H. (IC); Souza, J. S. (PQ); Corio, P. (PQ) IQUSP

**INO-034** **Citotoxicidade de complexos de Ru(II) com diferentes tipos de isomeria.** Campos, V. N. S.; Leite, C. M.; Oliveira, K. M.; SILVA, T. E. M.; Honorato, J.; Corrêa, R. S.; Otero, D. M.; Batista, A. A. UFMA

**INO-035** **Identification of molecular species in solution by theoretical calculations: how far can we trust the models?.** Madureira, J. (PQ); Lucchetti, P. (IC); Moreira, G. M. (IC) UFF

**INO-036** **Synthesis, characterization, cytotoxic and anti-M. tuberculosis activity of novel platinum(II) complexes.** Lima, M. F. (IC); Oliveira, L. P. (PG); Carneiro, Z. A. (PQ); Ribeiro, C. M. (PQ); Paixão, D. A. (PQ); Pivatto, M. (PQ); Souza, M. V. N. (PQ); Teixeira, L. R. S. (PQ); Albuquerque, S. (PQ); Pavan, F. R. (PQ); Guerra, W. (PQ) UFU

**INO-037** **Synthesis and characterization of gadolinium coordination compounds containing different classes of ligands.** Oliveira, D. H. (IC); Westphal, E. (PQ); Adati, R. D. (PQ) UTFPR

**INO-038** **Reactions of organic and inorganic tellurium derivatives with 2,6-dipicolinoyl-bis(N,N-diethylthiourea).** Santos dos, S. S. (PQ); Nhuyen, H. H. (PQ); Lang, E. S. (PQ); Abram, U. (PQ) FU-Berlin

**INO-039** **Aromatic Beta-diamide and beta-monoketo-monoamide as promising ligands for Eu(III) and Tb(III) complexes with high luminescence.** Correa, L. A.; Donnici, C. L. (PQ); Araujo, M. H. (PQ); Borges, A. S. B. (PQ); Scarpari, S. L. (PQ); Ribeiro, S. J. L. (PQ) UFMG

**INO-040** **Synthesis and characterization of thiosemicarbazones and their coordination compounds.** Costa, V. A. (IC); Mota, F. D. (IC); Lima, M. A. (PG); Rocha, F. V. (PQ) UFSCar

**INO-041** **Novel binuclear chromium(III) complexes with potential application as building blocks in single molecule magnets synthesis.** Reis, D. M. (PQ); Stoeberl, B. J. (IC); Santana, F. S. (PG); Giese, S. O. (PQ); Hughes, D. L (PQ); Soares, J. F. (PQ) UTFPR

**INO-042** **Surface immobilization of carboxymethylated cashew gum (Anacardium Occidentale L.) on FeCo magnetic nanoparticles.** Oliveira, M. K. S. (PG); Costa, L. A. (IC); Silva, M. A. S. (PQ); Richter, A. R. (PG); Paula, R. C. M. (PQ); Diógenes, I. C. N. (PQ) UFC

**INO-043** **Lowering water oxidation overpotential of a mononuclear ruthenium(II) complex bearing ionizable imidazole moieties.** Guerra, R. B. (PG); Huamaní, L. E. S. C. (PG); Bibi, N. (PG); Formiga, A. L. B. (PQ) IQ-UNICAMP

**INO-044** **Application of gold mining sludge in the preparation of materials for photo degradation of methylene blue.** Ferreira, M. G. (IC); Grigorovski Júnior, J. M. A. (IC); Garrido, F. M. S. (PG); Medeiros, M. E. (PQ); Silva, F. A. N. G. (PQ); Silva, V. P. R. (PG); Castilho, Z. C. (PQ) UFRJ

**INO-045** **Investigation of the adduct between chlorite and chlorine dioxide by electronic spectroscopy.** Martins, G. W. (PG); Faria, R. B (PQ) UFRJ

**INO-046** **Dinuclear platinum(II) complex with oxadiazol adamantane.** Silva, J. T. (IC); Querino, A. L. de A. (TC); Diniz, R. (PQ); Silva, H. (PQ) UFMG

**INO-047** **Estudo da coordenação dos ligantes 4-cloro e 4-nitro-benzaldeído-tiosemicarbazona derivados do R-(+)-limoneno com cobre(II).** Santos, B. R. (IC); Beltrame, A. C. F. (IC); Stocco, A. F. (IC); Stevanato, A. (PQ); Vandresen, F. (PQ) UTFPR

**INO-048** **Estudo teórico da inclusão de complexos de platina (II) não covalentes em beta-ciclodextrinas.** Candido, J. M. B. (IC); Paixão, N. M. (PG); Costa, L. A. S. (PQ) UFJF

**INO-049** **DNA/BSA binding properties of metallo-tetrakis(1-naphtyl)porphyrins: the metal central ion effect.** Silveira da, C. H. (PG); Garoforo, E. (IC); Iglesias, B. A. (PQ) UFSM

**INO-050** **Identificação de ácido acetilsalicílico em formulações farmacêuticas sólidas por espectroscopia de infravermelho.** Alhadas, R. D. (IC); Vieira, B. L. M. (IC); Toledo, T. A. (TC); Barbosa, D. B. A. (FM) IF Sudeste MG

**INO-051** **The effect of the temperature on Brilliant Green dye bleaching catalyzed by zinc hydroxide nitrate.** Rocha, M. G. (IC); Ucoski, G. M. (PQ); Nakagaki, S. (PQ); Machado, G. S. (PQ) UFPR

**INO-052** **Study of crylene acid ligand coordinated to lanthanide compound.** Cardoso, L. P. (IC); Dias, M. R. G. (PG); Pilissão, C. (PQ); Adati, R. D. (PQ) UTFPR

**INO-053** **Co(II) benzimidazoles complexes: Synthesis, characterization and catalytic studies to chemical fixation of CO2 in cyclic carbonates.** Milani, J. L. S. (PQ); Cangussu, D. (PQ); das Chagas, R. P. (PQ); Vilela, G. A. (IC); Valdo, A. K. S. M. (PG); Terra, F. (PQ) UFG

**INO-054** **Organically modified Urea-sepiolite to application in caffeine removal.** da Silva, E. (PG); Saltarelli, M. (PQ); de Faria, E. H (PQ); Nassar, E. J. (PQ); Ciuffi, K. J. (PQ) UNIFRAN

**INO-055** **Lanthanide complex as potential nitric oxide luminescent probe.** Cabral, F. M. (PG); Brito Júnior, G. A. (PQ); Mazali, I. O. (PQ); Sigoli, F. A. (PQ) IQ-UNICAMP

**INO-056** **Iron (II) oxalate as precursor of magnetic composites for dye adsorption.** Aldighieri Grigorovski Júnior, J. M. (IC); Garrido, F. M. S. (PQ); Medeiros, M. E. (PQ) UFRJ

**INO-057** **Synthesis of a new copper (II) complex with Benzoylpyridylthiourea: Characterization by X-ray diffraction.** Santos, J. R. N. (IC); Quintino, M. P. (PQ); Sabino, J. R. (PQ) PUC-GO

**INO-058** **Síntese e caracterização química dos complexos de Sb(III) e Bi(III) com ligante bidentado para atuação como agentes leishmanicidas.** Lopes, D. S. (IC); Silva, S. R. (PQ) UFRR

**INO-059** **Spectroscopy and electrochemical studies of phenanthroline derivatives $Cu^{2+}$, $Pd^{2+}$ and $Ru^{3+}$ complexes.** Barbosa, R. S. (IC); Bagatin, I. A. (PQ) UNIFESP-Diadema

**INO-060** **Complexos binucleares de Fe(III)/Cu(II) e Co(III)/Cu(II) contendo bases de Schiff tetradentadas: síntese e caracterização.** de França, I. V. (IC); Dockal, E. R. (PQ); da Cruz Jr, J. W. (PQ) UFSC

**INO-061** **Síntese, caracterização vibracional e estruturas cristalinas de dois novos polímeros de coordenação contendo um ligante pirazólico.** Soares, I. C. (PG); Brito, H. A. (IC); Dias, I. M. (PQ); Junior, H. C. S. (PG); Ferreira, G. B. (PQ); Guedes, G. P. (PQ) UFRRJ

**INO-062** **Layered double hydroxides and acetylsalicylic acid: reactivity and desorption studies.** Oliveira, I. N. (PG); Silva, K. K. S. (IC); Morais, C. C. (PG); Rosseto, R. (PQ) UEG

**INO-063** **Synthesis, spectroscopy of copper(II) catechol complexes.** Correa, C.P. (IC); Chinelate, B.M. (IC); Martins, G. S. (IC); Toledo, T.A. (PQ); Barbosa, D.B.A. (PQ) IF Sudeste MG- Juiz de Fora

**INO-064** **Spectroscopic studies of Copper I and II complexes by DFT calculations.** Oliveira, H. F. S. (PG); SIlveira, R. G. (PQ); Rocha, F. V. (PQ) UFSCar

**INO-065** **Synthesis and characterization of $Cu_2O$ Thin Films for Photoelectrochemical (PEC) applications.** Coli, J. F. C. (IC); Gonçalves, C. B. (PG); Zapata, M. (PQ); Doriguetto, A. C. (PQ) UNIFAL

**INO-066** **Papaína incorporada em sílica mesoporosa ordenada.** Losito, D. W. (IC); Corazza, F. G. (PG); Lopes, P. S. (PQ); Martins, T. S. (PQ) UNIFESP-Diadema

**INO-067** **Síntese, caracterização e atividade eletrocatalítica frente à RRO de um novo complexo de níquel (II).** Diniz, M.M. (IC); Moura, F.S. (PG); Petizero, T.D. (PG); Casellato, A. (PQ); Medeiros, M.E. (PQ); Garrido, F.M.S. (PQ) UFRJ

**INO-068** **Reactivity studies on a cobalt(III) complex towards the development of catechol-based bioreductive prodrugs.** da Silva, A. F. M (PG); Gómez, J. A. G. (PQ); Lanznaster, M. (PQ) UFF

**INO-069** **Exploring DNA binding and cleavage, Topo I inhibition, and cytotoxic activity of two new Cu(II) compounds containing 4-aminoantipyrine.** Souza, I. P. (PG); Machado, B. P. (IC); Carvalho, A. B. (PG); Binatti, I (PQ); Kellett, A. (PQ); Pereira-Maia, E. C. (PQ); Silva-Caldeira, P. P. (PQ) CEFET-MG

**INO-070** **Synthesis and characterization of Copper Metal-Organic Frameworks for adsorption of Phenol.** Carvalho, A. N. (IC); Ribeiro, G. (PQ) UNIFEI

**INO-071** **Porfirinas de manganês imobilizadas em partículas magnéticas: catalisadores heterogeneizados para degradação do ciprofloxacino.** Marciano, A. C. (IC); Lage, A. L. A. (PG); Vieira, S. S. (PQ); Araújo, M. H. (PQ); Martins, D. C. S. (PQ) UFMG

**INO-072** **Determination of Point of Zero Charge of Super Fine Fibrous Peat.** Szpoganicz, B. P. (PG); Meurer, L. (IC); Probst, L. F. D. (PQ); Szpoganicz, B. (PQ) UFSC

**INO-073** **Palladium complexes with oxadiazol and thiazolidine-adamantane ligands: the influence of heterocycle in Pd-S bond.** Silva, J. T. (IC); Alvarenga, G. M. (IC); Silva, H. (PQ) UFMG

**INO-074** **Diphenylphosphine/Ru(II) complexes with antitumor activity: interactions with DNA and with HSA.** Guedes, A. P. M. (PG); Grawe, G. F. (PG); Leite, C. M. (PG); Silveira-Lacerda, E. P. (PQ); Silva, T. E. M. (IC); Batista, A. A. (PQ) UFSCar

**INO-075** **Pd (II) complexes as potential inhibitors of Topoisomerase II.** Lima, M. A. (PG); Deflon, V. M. (PQ); Rocha, F. V. (PQ) UFSCar

**INO-076** **Experimental and theoretical characterization of Sn(IV), Sb(III) and Bi(III) Xanthate.** Silva da, V. H. M. (IC); Ferreira, G. B. (PQ) UFF

**INO-077** **Spin crossover tuning through ligand design: Magnetic measurements, Mössbauer and crystal structures of two isomeric Fe(II) complexes with 2-aryl-imidazole ligands.** Bibi, N. (PG); Huamaní, L. E. S. C. (PG); Guerra, R. B. (PG); Oliveira, A. A. (PG); Berón, F. (PQ); Paesano Júnior, A. (PQ); Formiga, A. L. B. (PQ) UNICAMP

**INO-078** **Synthesis and structural characterization of multinuclear palladium(II) arylchalcogenolates compounds.** Fagundes, N. V. (IC); Cechin, C. N. (PG); Tirloni, B. (PQ); Lang, E. S. (PQ) UFSM

**INO-079** **Degradação do antibiótico norfloxacino por $H_2O_2$ e $KHSO_5$, catalisada por porfirinas de manganês halogenadas.** Meireles, A. M. (PG); Idemori, Y. M. (PQ); Martins, D. C. S. (PQ) UFMG

**INO-080** **Synthesis and Characterization of basic catalysts designed by Calixarenes or Silicas to take advantage of Glycerol.** Machado, D. (PG); Gomes, E. L. (PQ); Bagatin, I. A. (PQ) UNIFESP-Diadema

**INO-081** **Synthesis and analysis of a novel dinuclear bis(oxamate) type complex using $[Co_2(H_2mpba)_3]_2$. mesocate as building block.** Simosono, C. A. (IC); Campos, N. R. (PG); Pim, W. D. (PQ); Doriguetto, A. C. (PQ); Valdo, A. K. S. M. (PG); Martins, F. T. (PQ); Stumpf, H. O. (PQ); Marinho, M. V. (PQ) UNIFAL

**INO-082** **Complexos fluorescentes de Lantânio-Espiropirano com aplicações em materiais poliméricos.** Reis, I. F. (PG); De Sousa, F. B. (PQ) UNIFEI

**INO-083** **Studies of chromium (VI) adsorption in Eucalyptus grandis bark.** Alexiou, A. D. P. (PQ); Godim, A. S. (IC); Romoff, P. (PQ) UPM

**INO-084** **Synthesis and characterization of new Zn(II) complexes designed as prototypes for chemotherapeutic treatment of bacterial infections.** Arruda, H. J. (PG); Vitório, F. (PG); Neves, A. P. (PQ); Kummerle, A. E. (PQ) UFRRJ

**INO-085** **Investigation on formation of highly luminescent\β-Diketone-Ln(III)-edta water-soluble complexes.** Teotonio, E. E. S. (PQ); Silva, H. M. (PG); Faustino, W. M. (PQ); Brito, H. F. (PQ); Malta, O. L. (PQ); Felinto, M. C. F. C. (PQ) UFPB

**INO-086** **Perylene-derived calix[4]arenes with potential application in luminescent systems.** Oliveira, G. M. (IC); Bagatin, I. A. (PQ) UNIFESP-Diadema

**INO-087** **Complexos de Fe(II), Mn(II) e Zn(II) derivados de um ligante do tipo oxamato funcionalizado: síntese e caracterização.** Maciel, J. W. O. (PG); Kalinke, L. H. G. (PG); Valdo, A. K. S. M. (PG); Martins, F. T. (PQ); Gomes, D. C. C. (PQ) UFG

**INO-088** **Synthesis, characterization and biological activity of complex nitrosyls.** Paz, I. A. (PG); Lopes, L. G. F. (PQ); Nascimento, N. R. F. (PQ); Silva, C. D. S. (PQ); Sousa, E. H. S. (PQ) UFC

**INO-089** **Bright Orange-Red Emission in a New Heteroleptic CuI complex Based on Phosphine/Pyrazoline Ligands.** Favarin, L. R. V. (PG); Laranjeira, G. B. (PG); Teixeira, C. F. A. (PG); Lima, L. M. (IC); Pinto, L. M. C. (PQ); Bezerra, L. (PG); Júnior, A. M. (PQ); Duarte, A. P. (PQ); Pizzuti, L. (PQ); Back, D. F (PQ); Maia, G. (PQ); Casagrande, G. A. (PQ) UFMS

**INO-090** **Investigação de um complexo cobalto(III)-4-cloroacetoacetato de etila como possível plataforma biorredutível para liberação de fármacos.** Mello, M. V. P. (PG); Gomez, J. A. G. (PQ); Lanznaster, M. (PQ) UFF

**INO-091** **Sínteses de decavanadatos contendo complexos de cobalto(II), cobre(II) e níquel(II).** Leme, L. B. P. (IC); Missina, J. M. (PG); Postal, K. (PG); Franco, M. P. (PG); Santana, F. S. (TC); Hughes, D. L. (PQ); Soares, J. F. (PQ); Nunes, G. G. (PQ) UFPR

**INO-092** **Synthesis and characterization of $Fe_3O_4$@$SiO_2$ core-shell magnetic nanoparticles.** Ribas, V.C. (IC); Lavayen, V. (PQ); Arguello, J. (PQ) UFRGS

**INO-093** **Visible-light photocatalytic response of titanate nanotubes (TiNT) - polyheptazine (HPZ) hybrid.** Almeida, V. A. (IC); Souza, J. S. (PQ) UFABC

**INO-094** **Glifosato como ligante frente ao chumbo divalente.** Hottes, E. (PG); Hottes, S. (IC); Herbst, M. H. (PQ) UFRRJ

**INO-095** **Effects of new ruthenium amphiphile compounds on peptides aggregation.** Soares, B. M. (PG); Winnischofer, H. (PQ); Pazinato, J. (PG); Westphal, E. (PG); Cavalieri, F. (PQ); Alves, W. A. (PQ) UFABC

**INO-096** **Electrocatalytic activity of water oxidation by coordination polymer Co-pentacyanidoferrate(II).** Pires, B. M. (PG); Strohauer, S (PG); Formiga, A. L. B. (PQ); Bonacin, J. A. (PQ) UNICAMP

**INO-097** **Iron (III) dinuclear metallacycle cavity as an effective ammonia storage system.** Silva, I. F. (PG); Teixeira, I. F. (PG); Barros, W. P. (PQ); Pinheiro, C. B. (PQ); Teixeira, A. P. C. (PQ); Stumpf, H. O. (PQ) UFMG

**INO-098** **Oxidation catalysts based on ironporphyrin supported on diatomaceous earth.** do Prado, M.V. (PG); Ciuffi, K. J. (PQ) UNIFRAN

**INO-099** **Compostos de\η6-arenorutênio(II) com ligantes fenilazo e feniloxadiazo: estabilidade, cinética de substituição de ligantes e atividade citotóxica em modelo de glioma humano.** Pazinato, J. (PG); Cesca, E. C. (PG); Winnischofer, H. (PQ); Westphal, E. (PQ); Gallardo, H. (PQ); Winnischofer, S.M.B. (PQ) UFPR

**INO-100** **Complexos de Cu (I) que incorporam trifenilfosfina e aciltioureias: avaliação de suas propriedades citotóxicas.** Leite, C. M (PG); Castellano, E. E (PQ); Batista, A. A (PQ) UFSCar

**INO-101** **Outstanding Optical Properties from Partial Substitution of Pb by Sn in Cs-Pb-Sn-Br Nanocrystals.** Vitoreti, A. B. F. (PG); Agouram, S. (PQ); de la Fuente, M. S. (PQ); Muñoz-Sanjosé, V. (PQ); Schiavon, M. A. (PQ); Mora-Seró, I. (PQ) UJI

**INO-102** **Aplicação de palygorskita organofilizada na remoção de glifosato em efluente aquoso.** Napoli Barbato, C.N.B. (PQ); Viana Rodrigues, P. V. R. (IC); Bertolino, L. C. B. (PQ); Arruda Nogueira Gomes da Silva, F. A. N. G. S. (PQ); Schwenck Brandão, V. S. B. (PQ) IFRJ

# *MAT – Química de Materiais*

**MAT-001** **Temperature Induced Optical Changes in Type II Metallopolymer based in Fluorene-Terpyridine Europium Complex.** Turchetti, D. A. (PQ); Santana, A. J. (PG); Duarte, L. G. T. A. (PG); Domingues, R. A. (PQ); Atvars, T. D. Z. (PQ); Akcelrud, L. C. (PQ) UFPR

**MAT-002** **Síntese de Filmes de Nanopartículas de Ouro e Polímero Luminescente em Substrato de Sílica para Aplicação em Sensores Óticos.** Klimpovuz, C. R. (IC); Silva, H. V. C. (IC); Turchetti, D. A. (PG); Akcelrud, L. C. (PQ); Oliveira, M. M. (PQ) UTFPR

**MAT-003** **Thermal processing optimization to obtain composites for controlled release of fertilizer.** Chiaregato, C. G. (IC); Faez, R. (PQ) UFSCar-Campus de Araras

**MAT-004** **Efeito da temperatura na molhabilidade de fibras de blendas de Ecovio®/PNIPAAm eletrofiadas.** Pascoalino, L. A. (IC); Muniz, E. C. (PQ); Curti, P. S. (PQ) UTFPR

**MAT-005** **Electrochemical vs Chemical: The most efficient synthesis method for a new ternary nanocomposite GO/WO3NW/PAni.** Aquino, C. B. (PG); Nagaoka, D. A. (PG); Cândido, E. G. (IC); Machado, M.M. (PQ); Camargo, P. H. C. (PQ); Domingues, S. H. (PQ) UPM

**MAT-006** **Synthesis and characterization of superparamagnetic iron oxide nanoparticles covered with methylene blue and hypericin molecules.** Toledo, V. H. (IC); Haddad, P. S. (PQ); Ribeiro, M. S. (PQ); Yoshimura, T. M. (PG); Toledo, S. P. (PG) UNIFESP-Diadema

**MAT-007** **Cerium (IV) hydrogenphosphate as an intercalation matrix for Pd(II).** Duarte, J. P. P. (IC); Rocha, L. D. S. (PG); Souza, R. M. (PQ); Medeiros, M. E. (PQ); Malta, L. F. B. (PQ) UFRJ

**MAT-008** **Preparation of graphene oxide (GO) membranes with potential application in water desalination.** Barros, M. F. (IC); Sousa, S. C. B. (IC); Tecchio, C. M. (TC); Fernandes, L. S. (IC); Martins, I. V. (IC); Vasconcelos, C. K. B. (PQ); Viana, M. M. (PQ) UFMG

**MAT-009** **Three-dimensional graphene nanofilters for heavy metal ions removal from water: a combined experimental and theoretical study.** Lino, B. (IC); Ximenes, V. (IC); Reis, G.R.L. (IC); Bordin, J.R. (PQ); Matos, C.F. (PQ) UNIPAMPA

**MAT-010** **Er3+ and Yb3+ up conversion on oxide matrix obtained by non-hydrolytic sol-gel.** Granito, C. J. (IC); de Andrade, F. H. P. (IC); Ferreira, M. F. (IC); Baldini, D. C. (PG); de Faria, E. H. (PQ); Ciuffi, K. J. (PQ); Rocha, L. A. (PQ); Nassar, E. J. (PQ) UNIFRAN

**MAT-011** **Swelling behavior of gelatin/dextran hydrogel crosslinked by Diels- Alder click chemistry.** Piazza, R. D. (PG); Brandt, J. V. (PG); Marques, R. F. C. (PQ); Jafelicci Jr, M. (PQ) IQAr-UNESP

**MAT-012** **Effect of functionalization of porous silica as nanoreactor for preparation of fluorescent Carbon Dots.** Mikhraliieva, A. (PG); Motta, H. B. (IC); Zaitsev, V. (FM) PUC-RIO

**MAT-013** **Utilização da técnica de reels e do método DFT para a obtenção do GAP dos copolímeros PFO-DBT e PSiF-DBT.** Santos, V. F. (IC); Machado, S. P. (PQ); Rocco, M. L. M. (PQ) UFRJ

**MAT-014** **Development of active SERS platform via self-assembly monolayers of AuNRs.** Bär, J. (PG); Barros, A. (PQ); Camargo, D. H. S. (PG); Oliveira, L. H. (PQ); Falsetti, L. O. Z. (IC); Sigoli, F. A. (PQ); Santos, D. P. (PQ); Bufon, C. C. B. (PQ); Mazali, I. O. (PQ) IQ-UNICAMP

**MAT-015** **Pseudocapacitors from crumpled graphene balls/mixed transition metal oxides composites.** Nonaka, L. H. (IC); Barce, E. T. (IC); Souza, V. H. R. (PQ) UFGD

**MAT-016** **Obtenção de fibras a partir da blenda polimérica de PCL e PBAT para liberação de sulfadiazina de prata.** Hardt, J. C. (PG); Dragunski, D. C. (PQ); Caetano, J. (PQ); Rosenberger, A. G. (PG) UNIOESTE

**MAT-017** **Porous ceramic based on phlogopite from the polymeric sponge method.** Filho, F. M. (PQ); Procópio, A. M. S. (PG); Silva, M. C. (PQ) UNIFEI

**MAT-018** **Influence of different fuels in the combustion synthesis of copper vanadate and its application in photocatalysis.** Camargo, L. P. (IC); Lucilha, A. C. (PQ); Dall'Antonia, L. H. (PQ) UEL

**MAT-019** **Synthesis of Nickel Molybdates - a comparative study of co-precipitation and sol-gel method.** Silva da, M. V. (PG); Siqueira, K. P. F. (PQ) UFOP

**MAT-020** **Structure determination of NVP-AS co-crystal at different temperatures.** Costa, R. N. (PG); Siedler, S. (PG); Cardoso, S. G. (PQ); Linck, Y. G (PQ); Reviglio, L. (PG); Monti, G. A. (PQ); Carvalho, A. M. G. (PQ); Resende, J. A. L. C. (PQ); Rocha, H. V. A (PQ); Cuffini, S. L. (PQ) UNIFESP-SJC

**MAT-021** **Coating of organosilicon thin films protecting polypropylene against photodegradation.** Freitas, A. S. M. (PG); Fernandes, F. O. (IC); Rangel, E. C. (PQ); Cruz, N. C. (PQ); Delgado-Silva, A. O. (PQ); Waldman, W. R. (PQ) UFSCar

**MAT-022** **Incorporation of carbon SWNT in polymer blends based on Nylon 66 and Silk Fibroin for application in engineering materials.** Souza, L. M. (PG); Scremin, F. R. (PQ); Bittencourt, P. R. S. (PQ) UTFPR

**MAT-023** **Spray-dried materials components ratio evaluation by TGA.** França, D. (PG); Faez, R. (PQ) UFSCar-Campus de Araras

**MAT-024** **Synthesis of Donor-Acceptor (D-A) hybrids based on functionalized thiophene-imides for high fluorescent material development.** Costa, A. M. (PG); Donnici, L. C. (PQ) UFMG

**MAT-025** **Study of the adsorption of tannic acid by clay modified with polyethylenimine.** Henriques, R.R. (PG); Celestino, G.G. (IC); Shiguihara, A.L. (PQ); Constantino, V.R.L. (PQ); Soares, B.G. (PQ); Amim Jr., J. (PQ) UFRJ

**MAT-026** **Kinetics of adsorption of methylene blue dye in mesoporous silica encapsulated magnetite nanoparticles.** Silva, R. M. A. (IC); Rodrigues, L. S. (IC); Silva, J. A. D. (PQ) IFF

**MAT-027** **Nanogold on porous glass as a passive sampler for monitoring of gaseous elemental mercury in artisanal gold mining.** Santos, E. B. (PQ); Moher, P. (PQ); Ferlin, S. (IC); Fostier, A. H. (PQ); Mazali, I. O. (PQ); Telmer, K. (PQ); Brolo, A. G. (PQ) UNIFESP-SJC

**MAT-028** **Novel conducting, biocompatible and biodegradable copolymer PEDOT-co-PLLA for biomedical applications.** Da Silva, A. C. (PG); Semeano, A. T. S. (PG); Ulrich, A. H. (PQ); Higgins, M. J. (PQ); Torresi, S. I. C. (PQ) UOW

**MAT-029** **Polythiophene/Au and polythiophene/Au/CNTs nanocomposite thin films to organic solar cell application.** Inagaki, C. S. (PG); Neves, M. F. F. (PG); Lima, L. F. (PG); Oliveira, M. M. (PQ); Roman, L. S. (PQ); Zarbin, A. J. G. (PQ) UFPR

**MAT-030** **A new route for preparing multi-oxide nanocomposites of nanoparticles-decorated nanotubes.** Dias, C. S. B. (PQ); Garcia, F. (PQ); Mazali, I. O. (PQ); Cardoso, M. B. (PQ); Souza e Silva, J. M. S. (PQ) LNLS

**MAT-031** **Extracellular matrix digestion products for tissue engineering.** Lobato, G. M. M. (PG); Catalani, L. H (PQ); Winck, F. V. (PQ) IQUSP

**MAT-032** **Fast and efficient graphene oxide (GO) reduction by using a lab-made UV photoreactor.** Iorio, E.I.C. (IC); Sousa, N.C.O.S. (PG); Pedrotti, J.J.P. (PQ) UPM

**MAT-033** **Estudo de reações biocatalíticas envolvendo microrganismos funcionalizados com óxidos metálicos.** Almeida, C. L. da C. (PG); Maciel, V. M. B. (PG); Santana, D. A. de (PQ); Santos, R. M. G. dos (PQ); Santos, M. M. dos (PQ) UFBA

**MAT-034** **Photoluminescence and scintillation of GdOCl:Eu3+ obtained from homogeneous precipitation method.** Krauser, M. O. (PG); Davolos, M. R. (PQ); Cebim, M. A. (PQ) IQAr-UNESP

**MAT-035** **Preparação de catalisadores de óxido de ferro a partir do minério de ferro.** Santos, J.R.L (IC); Mendes, A.P.S. (IC); Martins, A.R. (PQ); Lima, S.P. (PQ); Rangel, M.C. (PQ) IFBA

**MAT-036** **Synthesis and characterization of chitosan-based nanocarriers for siRNA release.** Martins, G. O. (PG); Junior, A. M. M. (PG); Lima, A. M. F. (PQ); Petrônio, M. S. (PQ); Tiera, V. A. O. (PQ); Tiera, M. J. (PQ) IBILCE-UNESP

**MAT-037** **Study of dye-modified Ag/$TiO_2$ nanocomposites for application in photocatalysis.** Almeida, G. C. (IC); Mohallen, N. D. S. (PQ); Viana, M. M. (PQ) UFMG

**MAT-038** **Anti-scaling performance of a textured copper-based Slippery Liquid-Infused Porous Surface (SLIPS).** Diniz, G.A. (IC); Sofiatti, E. (IC); Sousa, M. F. B. (PQ); Bertran, C. A. (PQ) IQ-UNICAMP

**MAT-039** **Síntese e caracterização de um novo candidato a sistema veiculador de fármaco empregando-se nanopartículas magnéticas e pilar[n]arenos.** Fernandes, T. S. (PG); Santos, E. C. S (PG); Madriaga, V. G. C. (IC); Barroco, C. V. (IC); Nascimento, V. (PQ); Ronconi, C. M. (PQ) UFF

**MAT-040** **Quantification and separation of rare earth elements from fluorescent lamp phosphors and synthesis of luminescent nanoparticles.** Alonso Freitas, G. A. F. (IC); Huaman De La Cruz, A. R. H. L. C. (PG); Padilla-Chavarría, H. I. P. C. (PG); Gioda, A. G. (PQ); Dillenburg Saint'Pierre, T. D. S. (PQ); Kai, J. K. (PQ) PUC-RIO

**MAT-041** **Study of the interactions between carboxymethylcellulose and ethylenediamine for synthesis of nanoparticles.** Britto, D. (PQ); Tostes, B. de V. A. (IC); Duarte, D. S. (IC); Pires, I. C. B. (IC) Embrapa Semiárido

**MAT-042** **Thermal stability of the Green Coffee Cake as a response to the water vapor blast process for the production of high value materials.** Brito, E. B. (PG); Pimenta, L. T. G. (IC); Barbosa, S. C. (PQ); Marques, M. F. V. (PQ) UFRJ

**MAT-043** **Efficient amine functionalization of carbon nanotubes with triethylenetetramine through microwave assisted reaction for applications in nanofluids.** Silveira, T. G. O. (IC); Monteiro, V. E. M. M. (IC); Silva, A. P. (IC); Nuncira, J. A. V. (PG); Caliman, V. (PQ); Silva, G. G. (PQ) UFMG

**MAT-044** **Activated material obtained from shale by-products for sulfur removal of fuel oil.** Mangrich, A. S. (PQ); Drabecki, A. B. A. (PG); Schultz, J. (PQ) UFPR

**MAT-045** **Core-shell nanofibers as drug carriers for transdermal delivery of drugs with antimalarial activity.** Rebouças, L. O. (PG); Catalani, L. H. (PQ); Immich, A. P. S. (PQ) IQUSP

**MAT-046** **Copolymers used as additives for fuels.** Muniz, A. S. (PQ); Ferraz, F. A. (PQ); Oliveira, A. R. S. (PQ); César-Oliveira, M. A. F. (PQ) UFPR

**MAT-047** **Hierarchical structured materials formed by combination of zeolite crystals and bacterial cellulose fibers.** Bessa, R. A. (PG); Castro, A. L. P. (IC); Pereira, A. L. S. (PG); Rosa, M. F. (PQ); Loiola, A. R. (PQ) UFC

**MAT-048** **Irreversible low-temperature dehydration of H+-exchanged titanate nanostructures.** Leite, M. M. (PQ); Vichi, F. M. (PQ) IQUSP

**MAT-049** **Graphene Oxide functionalized with (3-Aminopropyl) triethoxysilane and its applications in composites.** Serodre, T. (PG); Resende, V. G. (PQ); Santos, A. P. (PQ); Furtado, C. A. (PQ) CDTN

**MAT-050** **Colloidal stability of silica nanoparticles during bioconjugation reactions with a silylated amyloidogenic peptide.** Decandio, C.C (PG); Liberato, M.S. (PQ); Cardoso, M.B (PQ); Alves, W.A. (PQ) UFABC

**MAT-051** **Polyethylene glycol conjugation to amyloidogenic peptide via click reaction.** Pereira, W. S. G. (PG); Domakoski, A. C. (PG); Vassiliades, S. V. (PG); Cavalieri, F. (PQ); Alves, W. A. (PQ) UFABC

**MAT-052** **Influence of reagents concentrations during synthesis for silver nanoparticles stability.** Novais de Abreu, A. (IC); Silva, G. (IC); Damasceno, D. (PQ); Casanova Coltro, M.C.R. (PQ) IFG

**MAT-053** **Hydrophobic and Electrostatic Effects of Chitosan Derivatives on the Antifungal Activity against Aspergillus flavus.** Amoroso, H. C. (IC); Lima, A. M. F. (PQ); Tiera, M. J. (PQ); Assis, O. B. G. (PQ); Tiera, V. A. O. (PQ) IBILCE-UNESP

**MAT-054** **Preparação e caracterização de filmes de zeína contendo pontos quânticos de ZnO.** Schmitz, F. (PG); da Silva, A. L. E. P. (IC); Vidotti, I. C. R. (PQ); Zimmermann, L. M. (PQ) FURB

**MAT-055** **Chitosan/waste coffee grounds composite: An efficient and eco-friendly adsorbent for removal of pharmaceuticals contaminants from water.** Lessa, E.F. (PG); Nunes, M.L. (IC); Fajardo, A.R. (PQ) UFPel

**MAT-056** **Synthesis and characterization of a conjugated metallopolymer complexed with terbium ions.** Campos, E. C. G. (PG); Zanlorenzi, C. (PQ); Turchetti, D. A. (PQ); Akcelrud, L. C. (PQ) UFPR

**MAT-057** **Optimization of the Ni/Al layered double hydroxide synthesis by factorial design.** Rocha, L. D. S. (PG); Nascimento, L. A. (IC); Correa, B. G. (IC); Santos, R. V. (PG); Senra, J. D. (PQ); Malta, L. F. B. (PQ) UFRJ

**MAT-058** **Avaliação dos engaços de uva BRS Violeta e *Vitis labrusca* Isabel como potenciais precursores de carvão ativado para fins de adsorção.** Pires, I. C. B. (IC); Costa, K. B. S. (PQ); Anjos, D. S. C. dos A. (PQ); Tostes, B. de V. A. (IC) IF Sertão Pernambucano - Campus Petrolina

**MAT-059** **A photodispositive based on reduced graphene oxide modified with polyethylenimine to deliver amphotericin B.** Vitorino, L. S. (IC); Bessa, I. A. A. (IC); Custódio, T. (PG); Santos, E. C. S. (PG); Ronconi, C. M. (PQ) UFF

**MAT-060** **Desenvolvimento de nanocompósito argila aniônica/carvão hidrotérmico para uso como adsorvente multifuncional.** Albano, R. L. B. S. (PG); Ferreira, O. P. (PQ) UFC

**MAT-061** **Oleylamine-mediated synthesis of unusual 4H (hcp)/fcc phase in gold nanorods.** Moares, D. A. (PG); Souza Jr., J. B. (PG); Mogili, V. (PQ); Ferreira, F. F. (PQ); Varanda, L. C. (PQ) IQSC-USP

**MAT-062** **45S5 Bioglass Scaffold to repair bone tissue damages.** de Oliveira Silva, M. (PG); Bertran, C. A. (PQ) UNICAMP

**MAT-063** **Síntese de nanopartículas de sílica MCM-48 funcionalizadas com difenilssilano para adsorção de BTEX.** Garcia Osorio, D. S. (PG); Nogueira, H. P. (PG); Araki, K. (PQ) IQUSP

**MAT-064** **Relation between porosity, particle size and adsorption efficiency of methyl methacrylate-based crosslinked polymer resins.** Martins, M. F. (IC); Silva, C. M. F. (PQ); Lucas, E. F. (PQ); Almeida, Q. A. R. (PQ); Aversa, T. M. (PQ) UFRJ

**MAT-065** **Atividade antimicrobiana e caracterização de filmes de amido de mandioca/quitosana reforçados com fibras de cana-de-açúcar.** Franco, P. C. I. (PG); Faria, M. L. (PQ); Bilck, A. P. (PQ); Menegon, E. A. S. (PQ) FEMA

**MAT-066** **Controlled delivery fertilizer: from agro-residues to agribusiness.** Faez, R. (PQ); Hsieh, Y.L. (PQ) UC Davis

**MAT-067** **Glycerol oleate reaction with citric acid to produce solid and liquid products for different applications.** Mendonça, F. G. (PG); Menezes, I. R. S. (IC); Fonseca, P. X. (IC); Gomes, M. S. (PG); Santos, M. R. D. (IC); Salviano, A. B. (PG); Martins, P. S. (PQ); Lago, R. M. (PQ) UFMG

**MAT-068** **Peptide-graphene composite material in the development of energy storage devices.** Cipriano, T. C. (PQ); Torresi, R. M. (PQ) IQUSP

**MAT-069** **Preparation and use of porous $TiO_2$ in adsorption and photocatalytic degradationof organic dyes in water.** Vieira, K. C. (IC); Stumpf, H. O. (PQ); Pim, W. D. do (PQ) CEFET-MG

**MAT-070** **Photoluminescence and scintillation of $Gd_2O_2S$:Y,Lu,Eu spherical particles.** Requena, G. F. (IC); Moralles, V. A. (PG); Krauser, M. O. (PG); Cebim, M. A. (PQ); Davolos, M. R. (PQ) IQAr-UNESP

**MAT-071** **Study of LCC and quitosana gel toxicity: parametrisation in arthropod test.** FIGUEIREDO, F. C. (FM); SANTOS, S.T (PG); LIMA JUNIOR, R.O. (PQ); FERREIRA, N. S. (IC); SANTOS JUNIOR, J.S (PQ) UFPI

**MAT-072** **Two routes comparison for silver and gold nanoparticles deposition on silica substrate for future application in optic sensors.** Pereira, A. F. (PG); Oliveira, M. M. (PQ) UTFPR

**MAT-073** **Polyaniline against black phosphorus degradation: a long-term stability study.** Fonsaca, J. E. S. (PG); Domingues, S. H. (PQ); Orth, E. S. (PQ); Zarbin, A. J. G. (PQ) UFPR

**MAT-074** **Adsorption of metformin hydrocloride by ecovio® solution in electrospinning and activated carbon.** Meira, A. C. R. (PG); Módenes, A. N. (PQ); Dragunski, D. C. (PQ); Bittencourt, P. R. S. (PQ) UNIOESTE

**MAT-075** **Investigation of the structural and optical properties of cobalt molybdate - A possible temperature indicator.** Costa, R. K. S. (PG); Teles, S. C. (IC); Siqueira, K. P. F. (PQ) UFOP

**MAT-076** **Electrical conductive films of reduced graphene oxide and polyaniline prepared from a solid gel.** Martins, V. H. N. (IC); Souza, V. H. R. (PQ) UFGD

**MAT-077** **Biopolymeric films of diethylaminoethyl-chitosan derivatives: potential application as antimicrobial coatings.** Cunha, O. M. (PG); Tiera, M. J. (PQ); Lima, A. M. F. (PQ); Assis, O. B. G. (PQ); Tiera, V. A. O. (PQ) IBILCE-UNESP

**MAT-078** **Tri-ureasil hybrid gel as biofilm forming for controlled release of cubebin.** Jesus, N. A. M. (PG); Silva, M. L. A. (PQ); Cunha, W. (PQ); Tavares, D. C. (PQ); Furtado, R. A. (PG); Molina, E. F. (PQ) UNIFRAN

**MAT-079** **Structure-property relations of chiral polyfluorene derivatives.** Baev, A.; Prasad, P. N.; Zanlorenzi, C. (PQ); Nowacki, B. (PQ); Akcelrud, L. (PQ) UFPR

**MAT-080** **Hydrophobic papers based on cellulose coated with recycled polystyrene.** Maturi, F. E.; Barud, H. S.; Silva, R. R.; Ribeiro, S. J. L.; Cardoso, M. B.; Cebrian, A. V. S. (IC) IQAr-UNESP

**MAT-081** **Accelerated aging study on rheological properties of synthetic bitumens.** Souza, R. S. (PG); Visconte, L. L. (PQ); Costa, V. G. (PQ) INT

**MAT-082** **Gold Electrodeposition on Porous Polymeric Templates for Raman Spectroscopy.** Colombo, R. N. P. (PG); Moreira, R. V. (PG); Faria, D. L. A. (PQ); Torresi, S. I. C. (PQ) IQUSP

**MAT-083** **Dye-sensitized solar cells based on TiO2 nanoparticles.** Amparo, S. Z. S. (IC); Almeida, G. C. (IC); Lage, A. L. A. (PG); Martins, D.C. da. S. (PQ); Mohallem, N. D. S. (PQ); Viana, M. M. (PQ) UFMG

**MAT-086** **Corrosive process study at a central of water treatment and distribution in Potiretama - CE rural area.** Ramos, J. E. T. (PQ); Dias, S. S. (PQ); Moura, R. A. (IC) UFERSA

**MAT-087** **Nanoencapsulação do extrato do fruto de *Guazuma ulmifolia* Lam. utilizando poli (ácido lático-co-ácido glicólico).** Zafred, A. F. D (IC); Santos, M. N. G. (PG); Terezan, A.P. (PQ); Silva, J.R (PQ); Azevedo, R. B. (PQ); Kato, L. (PQ); Oliveira, C. M. A. (PQ); Rabelo, D. (PQ); Sartoratto, P. P. C. (PQ) UFG

**MAT-088** **Synthesis of a luminescent hybrid of silica and Iridium complex for biomarker application.** Mutti, A. M. G. (PG); Santos, J. A. O. (PG); Canisares, F. S. M. (PG); Pires, A. M. (PQ); Lima, S. A. M. (PQ) FCT-UNESP-Câmpus de Presidente Prudente

**MAT-089** **Simultaneous oxygen and temperature ratiometric optical probes based on an europium(III) complex and anthracene covalently bounded to pdms.** Gálico, D. A. (PG); Mazali, I. O. (PQ); Sigoli, F. A. (PQ) UNICAMP

**MAT-090** **Synthesis, characterization and photophysical properties of a fluorene-benzothiadiazole / fluorene-terpyridine block copolymer.** Turchetti, D. A.; Akcelrud, L. C.; Santana, A. J. (PG) UFPR

**MAT-091** **Study of the Association of Few-walled Carbon Nanotubes with the Semiconductor Complex Bu4N[Ni(dmit)2].** Rodrigues, M. K. (IC); Lara, L. R. S (PQ); Mambrini, R. V. (PQ); do Pim, W. D (PQ); Stumpf, H. O. (PQ) UFMG

**MAT-092** **A scalable new platform to produce all-carbon low-cost paper-based electrodes.** Bertacchi, J. P. F. (PG); Galembeck, F. (PQ) UNICAMP

**MAT-093** **Development of materials based on calcium polyphosphate/alginate for bone cement applications.** Monte, J. P. (IC); Silva, G. B. A. (IC); Falcão, J. S. A. (PQ); Santos, B. S. (PQ) UFPE

**MAT-094** **Preparation and characterization of ashes from cassava and sugarcane bagasse wastes.** Oliveira, A. V. B. (IC); Silva, T. M. R. (TC); Fávaro, S. L. (PQ); Batistela, V. R. (PQ) UEM

**MAT-095** **Synthesis and characterization of AuPd and AuPt bimetallic nanoparticles for biointegration with microorganisms.** Santana, S. M. F. (PG); Bispo, V. M. (PG); Geris, R. (PQ); Malta, M. (PQ) UFBA

**MAT-096** **Conjugated polymer to gold nanoparticles passivation. Synthesis, characterization and photophysics interpretation.** Silva, H. V. C. (IC); Klimpovuz, C. R. (IC); Turchetti, D. A. (PQ); Oliveira, M.M. (PQ); Akcelrud, L. C. (PQ) UFPR

**MAT-097** **Intensified Raman spectrum of 4-MBA on nonstoichiometric $CeO_2$.** Reinaldo, A. C. (IC); Silva, I. C. (PG); Sigoli, F. A. (PQ); Mazali, I. O. (PQ) UNICAMP

**MAT-098** **Hidrogéis nanoestruturados contendo nanowhiskers de celulose para liberação tópica de fármaco.** Melo, B.C. (IC); Rodrigues, F.H.A. (PQ) UVA

**MAT-099** **Reutilização de sílica gel contaminada com compostos orgânicos na síntese de vidros silicatos.** Gomes, I. F. (IC); Silva, C. F. (PG); Pedrosa, L. F. (PQ); Ribeiro, G. (PQ); Ribeiro, S. (PQ); Souza, M. L. (PQ); Silva, L. (PQ); Ferreira, E. A. (PQ) UFF

**MAT-100** **Electronic structure, morphology and charge transport of GO-PEDOT:PSS blends for organic photovoltaics.** Holakoei, S. (PG); Lima, L.F. (PG); Borges, B.G.A.L. (PQ); de Matos, C.F. (PQ); Zarbin, A.J.G. (PQ); Roman, L.S. Roman (PQ); Turci, C.C. (PQ); Rocco, M.L.M. (PQ) UFRJ

**MAT-101** **Rare earth oxide-based nanoparticles with application in photodynamic therapy for cancer.** Silva, B. A. (PG); Padilla-Chavarría, H. I. (PG); Zaitsev, V. (PQ); Mendivelso, E. A. C. (PQ); Alves, L. A. (PQ); Xing, Y. (PQ); Kai, J. (PQ) PUC-RIO

**MAT-102** **Photoelectrochemical degradation of methylene blue dye on $Ti/TiO_2$ nanotubes electrode.** González-Moya, J. R. (PQ); Santos, I. M. (IC); Machado, G. (PQ) CETENE

**MAT-103** **UV-Shielding and enhanced thermal stability of poly(vinyl alcohol)/graphene composites.** Carvalho, R. D. E. (PG); Carvalho, R. H. (IC); Silva, V. R. (PQ); Ferreira, M. P. (PQ); Santos, A. P. (PQ); Furtado, C. A. (PQ) CDTN

**MAT-104** **From graphite to graphene: improving the Hummers method to produce high quality reduced graphene oxide (rGO).** Nagaoka, D. A. (PQ); Domingues, S. H. (PQ) UPM

**MAT-105** **Unraveling the differences in the activity and stability of non-enzymatic electrochemical sensors by controlling surface facets.** da Silva, A.G.M. (PQ); Pastrián, F.A.C. (PG); Dourado, A.H.B. (PG); Batista, A.P.L. (PQ); de Oliveira-Filho, A.G.S. (PQ); Camargo, P.H.C. (PQ); de Torresi, S.I.C. (PQ) IQUSP

**MAT-106** **Sínteses de cristais líquidos iônicos e estudo de suas propriedades mesomórficas.** Ovalle, S. (PG); Westphal, E. (PQ); Gallardo, H. (PQ) UFSC

**MAT-107** **Uso do Poliestireno expandido no aumento da hidrofobicidade em isoladores elétricos cerâmicos usados em linhas de transmissão.** Ferreira, R. G. (IC); Souza, D. O. (IC); Calado, C. R. (PQ) CEFET-MG

**MAT-108** **Thin films of ternary nanocomposites between carbon nanotubes, Prussian blue and polyaniline.** Schmidt, A. (PG); Husmann, S. (PG); Zarbin, A. J. G. (PQ) UFPR

**MAT-109** **Aqueous dispersions of carbon nanotubes without passivation or functionalization.** Damasceno, J. P. V. (PG); Zarbin, A. J. G. (PQ) UFPR

**MAT-110** **Characterization of the Pani/$MoO_3$ hybrid for ethanol electrooxidation.** Ratuchne, F.; Antoniazzi, C.; Danczuck, M.; Castro, E. G. (PQ) UNICENTRO

**MAT-111** **Charcoal and activated carbon from yeast biomass residues.** Melo, V. F.; Modesto, H.; Komatsu, J. S.; Carvalho, W. A.; Labuto, G.; Santos, M. S. (IC) UNIFESP-Diadema

**MAT-112** **Effect of glass powder as reinforcing filler in the production of recycled polypropylene composites.** Costa, I. S. (IC); Almeida, L. A. (IC); Junior, J. C. J. (PQ); Silva, A. L. N. (PQ); Nasser, R. O. (PQ); Aversa, T. M. (PQ) IFRJ-Campus Duque de Caxias

**MAT-113** **Functionalization of fungal cells with transition metal oxides for the development of biomimetic hybrid structures.** Bispo, V. M. (PG); Geris, R. (PQ); Malta, M. (PQ) UFBA

**MAT-114** **Frontier micro/mesoporous silica obtained by the hydrolysis of TEOS in pressurized aqueous CO2.** Winkler, M. E. G. (PG); Kunita, M. H. (PQ); Muniz, E. C. (PQ); Rubira, A. F. (PQ) UEM

**MAT-115** **Mixed matrix membranes Synthesis with MIL-101(Cr) for gas separation.** Santos, G.H.G. (PG) UFRJ

**MAT-116** **Removal of Cu2+ ions from aqueous solutions using starch-g-poly(acrylic acid)/rice husk ash: adsorption kinetics.** Melo, B. C. (IC); Rocha, A. J. R. (IC); Cardoso, V. A. (IC); Magalhães, C. E. C. (PQ); Rodrigues, F. H. A (PQ) UVA

**MAT-117** **Evaluation of silicone rubber hydrophobicity after different periods of accelerated photo-ageing.** Munaro, A. P. (PG); Salum, A. S. (PQ); Richart, F. S. (PQ); Silva, F. I. C. (PQ); Molinari, J. (TC); Munaro, M. (PQ); Akcelrud, Leni (PQ) UFPR

**MAT-118** **Comparison of Hybrid Conjugates Containing Amyloidogenic Peptides and Gold Nanoparticles.** Pelin, J. N. B. D. (PG); Alves, W. A. (PQ) UFABC

**MAT-119** **Isolation of cellulose and cellulignin from sugarcane bagasse by green chemical treatments.** Messa, L. L. (PG); Faez, R. (PQ) UFSCar-Campus de Araras

**MAT-120** **Preparation of BiVO4-decorated ZnO nanorods for oxygen evolution using photo-electrocatalysis.** Almeida, R. M. (PG); Freitas, A. L. M. (PG); Souza, J. S. (PQ); Souza, F. L. (PQ); Alves, W. A. (PQ) UFABC

**MAT-121** **Importance of corrosion resistence of the cannula test in control quality of hypodermic needles.** Carvalho, C. M. (PG); Vale, R. F. D. (TC); Fust, A. M. B. S. (TC); Venâncio, L. F. (TC); Leandro, K. C. (PQ); Gemal, A. L. (PQ); Silva, F. S. Q. (PQ); Feitoza-Silva, M. (PQ) FIOCRUZ

**MAT-122** **Proposed regulatory change in view of the silicone quantification test in hypodermic syringes.** Alves, C. S. (PG); Vale, R. F. D. (TC); Fust, A. M. B. S. (TC); Venâncio, L. F. (TC); Leandro, K. C. (PQ); Feitoza-Silva, M. (PQ) FIOCRUZ

**MAT-123** **Electrochemical application of all-chemically synthesized graphene/iron oxide composites.** dos Santos, J. (IC); Lopes, L. C. (PG); Zarbin, A. J. G. (PQ) UFPR

**MAT-124** **Activity of immobilized porcine pancreatic lipase into mesoporous silica SBA-15 in transesterification reactions.** Rocha, I. N. d. S. (IC); Silva, J. A. D. (PQ) IFF

**MAT-125** **Thin films of nanocomposites between graphene and nickel hexacyanoferrate nanoparticles applied in energy storage.** Neiva, E. G. C. (PQ); Zarbin, A. J. G. (PQ) UFPR

**MAT-126** **Ag2WO4 polymorphs: selective synthesis and characterization.** Alvarez-Roca, R. (PQ); Lemos, P. S. (PG); Longo, E. (PQ) UFSCar

## *MED – Química Medicinal*

**MED-001** **Serine protease from Bothrops asper snake venom and its inhibition in the presence of hesperitin.** Grillo, G. R. (IC); dos Santos, R. V. (PG); Tasic, L. (PQ) UNICAMP

**MED-002** **Discovery of new Plasmodium cGMP-dependent protein kinase inhibitors with antiplasmodial and transmission blocking activities.** Cassiano, G. C. (PQ); Tomaz, K. C. P. (PG); Lima, M. N. N. (PG); Neves, B. J. (PQ); Tavella, T. A. (PG); Mottin, M. (PQ); Braga, R. C. (PQ); Calit, J. (IC); Cravo, P. V. L. (PQ); Bargieri, D. Y. (PQ); Andrade, C. H. (PQ); Costa, F. T. M. (PQ) UNICAMP

**MED-003** **Synthesis, acute toxicity, antioxidant and antinociceptive activity of new sulfonamides derived from carvacrol.** Oliveira, A.S. (PQ); Brighente, I. M. C. (PQ); Nunes, R. J. (PQ); Yunes, R. A. (PQ); Nucci-Martins, C. (PG); Santos, A. R. S. (PQ) UFSC

**MED-004** **Structure-activity relationships for a series of benzimidazole derivatives as cruzain inhibitors.** Ferreira, L. L. G. (PQ); Pauli, I. (PQ); de Souza, M. L. (PQ); Oliva, G. (PQ); Ferreira, R. S. (PQ); Dessoy, M. A. (PQ); Slafer, B. W. (PQ); Dias, L. C. (PQ); Andricopulo, A. D. (PQ) IFSC-USP

**MED-005** **Identificação de novos candidatos a agentes antitumorais.** Martins, C.T. (IC); Silva, E.M.G. (IC); Magalhães, L.G. (PG); Mass, E.B. (PG); Russowsky, D. (PQ); Andricopulo, A.D. (PQ) IFSC-USP

**MED-006** **Screening of the MMV pathogen box on *Schistosoma mansoni* juvenile worms for antischistosomal drug discovery.** Neto, J. M. R. (PG); Valente, W. C. G. (TC); Chino, M. E. T. A. (TC); Chaves, E. F. C. L. (TC); Santos, M. K. S. (IC); Schirato, G. V. (PQ); Santos, A. L. (PQ); Dantas, R. F. (PQ); Senger, M. R. (PQ); Júnior, F. P. S. (PQ) FIOCRUZ

**MED-007** **ADME-T and pharmacokinetic parameters of antitrypanosomal / antitumoral analogues of licarin A.** Morais, T. R. (PG); Fernandes, J. P. S. (PQ); Sartorelli, P. (PQ); Tempone, A. G. (PQ); Girola, N. (PG); Fortuna, A. C. B. (PQ); Falcão, A. C. (PQ); Lago, J. H. G. (PQ) UC

**MED-008** **A new 3-nitro-1,2,4-triazole derivative is more potent and selective than benznidazole against Trypanosoma cruzi.** Castelo-Branco, F. S. (PQ); França, R. R. F. (PG); Menozzi, C. A. C. (PG); Baptista, M. S. (IC); Sales-Júnior, P. A. (PQ); Murta, S. M. F. (PQ); Romanha, A. J. (PQ); Pinto, A. C. (PQ); Boechat, N. (PQ) FIOCRUZ

**MED-009** **Analysis of the biological activity of antidiabetic compounds using CoMFA models.** Pantaleão, S. Q. (PG); Lima, A. N. (PQ); Philot, E. A. (PQ); Scott, A. L. (PQ); Honorio, K. M. (PQ) UFABC

**MED-010** **Design, synthesis and anti-plasmodium falciparum activity of novel bis-trifluoromethylquinolines derivatives.** Gandi, M. O. (IC); Carvalho, A. S. (PQ); Mendonça, J. S. (PQ); Krettlie, A. U. (PQ); Boechat, N. (PQ) FIOCRUZ

**MED-011** **Construction and validation of 3D chemical similarity models of triclosan.** Fernandes, P. O. (IC); Franco, I. D. (IC); Maltarollo, V. G. (PQ) UFMG

**MED-012** **Planejamento, síntese e avaliação biológica de novos derivados carbohidrazonamidas candidatos a protótipos tripanocidas.** do Nascimento, M. S. S. (PG); Teixeira, R. L. (IC); Barbosa, J. M. C. (IC); Salomão, K. (PQ); de Castro, S. L. (PQ); Carvalho, S. A. (PQ); da Silva, E. F. (PQ); Fraga, C. A. M. (PQ) FIOCRUZ

**MED-013** **Interaction models of the protein Phosphoethanolamine Methyltransferase from Haemonchus contortus relating drugs and lignans through molecular docking.** Féboli, A. (PG); Borges, A. (PG); Laurentiz, R. S. (PQ) FEIS-UNESP

**MED-014** **Plasmonic photothermal cancer therapy with reduced graphene oxide core/shell nanocomposites.** Turcheniuk, K.; Dumych, T.; Bilyuy, R.; Nazarkovskyi, M.; Zaitsev, V. (PQ) PUC-RIO

**MED-015** **Blind docking and Semi-Empirical Studies of\β-Tubulin Inhibitors.** Fokoue, H. H. F. (PQ); Carneiro, T. R. C (PQ); Barreiro, E. J. B. (PQ); Lima, L. M. L. (PQ); Sant'Anna, C. M. R. S. (PQ) UFRJ

**MED-016** **Drug Design based on vouacapanic derivative with antileukemic activity.** Lobato, C. C. (PG); Borges, R. S. (PQ); Silva, C. H. T. P. (PQ); Santos, C. B. R. (PQ) UNIFAP

**MED-017** **Sirtinol analogues design and molecular docking in the search for *Trypanosoma cruzi* Sirtuin 2 inhibitors.** Fornari Pereira, E. (PG); Trossini, G. H. G. (PQ); Ferraz, W. (IC); Ferreira, G. M. (PG) FCF-USP

**MED-018** **Estudos visando a síntese e avaliação farmacológica de compostos heterocíclicos candidatos a protótipos de fármacos inovadores para o tratamento da doença de Alzheimer.** Gontijo, V. S. (PQ); Rosa, M. C. (IC); Castro, N. G. (PQ); Viegas, C. V. (PQ) UNIFAL

**MED-019** **Synthesis, cytotoxicity and in vitro evaluation of antileishmanial activity of benzoylguanidines.** Silva, K. M. S. (PG); Fabris, M. (PG); Brito, T. O. (PG); Macedo Jr., F. C. (PQ); Bortoleti, B. T. S. (PG); Pavanelli, W. R. (PQ); Costa, I. C. (PQ); Bispo, M. L. F. (PQ) UEL

**MED-020** **Antibacterial activity of new 2-amino-1,4-naphtoquinones.** Silva da, C. C. (PG); Paiva, R. O. (PQ); Costa da, G. L. (PQ); Echevarria, A. (PQ) UFRRJ

**MED-021** **Theoretical Investigation of thiosemicarbazones and dialkylphosphorylhydrazones as Proposed Serine Proteases Inhibitors.** Mendes, B. H. M. (IC); Sant'Anna, C. M. R. (PQ) UFRRJ

**MED-022** **Synthesis and cytotoxicity activity of new analogs of Santacruzamate A.** Andrade, S. N. (PG); Seckler, D. E. L. (IC); Freitas, T. R. (PG); Nunes, R. R. (PG); Evangelista, F. C. G. (PG); Humberto, J. L. (PQ); Sabino, A. P. (PQ); Taranto, A. G. (PQ); Varotti, F. P. (PQ); Hilário, F. F. (PQ) UFSJ

**MED-023** **Risk Assessment for synthetic cannabinoids: an application in criminal science.** Castro, C. J. (FM); Rodrigues, R. C. (PG); Melo, M. E. (PQ); Bruni, B. A. (PQ) FFCLRP-USP

**MED-024** **Drug Discovery applied to Agrobusiness: prediction of Riphicephalus microplus Acetylcholinesterases isoforms, an important target in the development of carrapaticides.** Estrela, I. O. (IC); Freitas, H. F. (PQ); Pita, S. S. R. (PQ) UFBA

**MED-025** **Synthesis and biological evaluation of the coumarins derivatives as potential inhibitors of the production of the *Pseudomonas aeruginosa* Virulence factor pyocyanin.** Maciel, C. A. O. (IC); Froes, T. Q. (PG); Forezi, L. S. M. (PQ); Cardoso, M. F. C. (PQ); Costa, D. C. S (PG); Ferreira, V. F. (PQ); Silva, F. C. (PQ); Castilho, M. S. (PQ) UFBA

**MED-026** **Design of new analogs and investigation of SmTGR inhibition by fragments identified by X-ray crystallography.** Souza-Neto, L. R (PG); Silva-Jr, F. P. (PQ); Dantas, R. F. (PQ) FIOCRUZ

**MED-027** **Development of a protocol for the virtual screening of a series of small-molecules ligands of the tubulin colchicine binding site.** Palomino-Salcedo, D. L. (PG); Magalhães, L. G. (PG); Oliva, G. (PQ); Andricopulo, A. D. (PQ) IFSC-USP

**MED-028** **Study of the molecular interactions between DPP-IV and some inhibitors used for the treatment of type II diabetes mellitus.** Martins, M. C. M. R. (PG); Pantaleão, S. Q. (PG); Honório, K. M. (PQ) UFABC

**MED-029** **Chemoinformatics strategies for a series of antichagasic compounds.** Medeiros, A. R. (IC); Ferreira, L. L. G. (PQ); Braga, R. C. (PQ); Andricopulo, A. D. (PQ) IFSC-USP

**MED-030** **New pyrazolopyrimidines as Inhibitor of *L. amazonensis* Arginase.** Pinheiro, L. C. S. (PQ); Feitosa, L. M. (PG); Silveira, F. F. (PG); Ferreira, M. L. G. (PQ); Souza, D. L. (IC); Hoelz, L. V. B. (PQ); Come, J. A. A. S. S. (PG); Silva, E. R. (PQ); Boechat, N. (PQ) FIOCRUZ

**MED-031** **Multivariate QSAR study of Modafinil derivatives with molecular descriptors derivated from SMILES notations and free softwares.** de Melo, E. B. (PQ); Bruni, A. T. (PQ) FFCLRP-USP

**MED-032** **Thiosemicarbazones indole-based derivatives: Anticancer activity and Docking Studies towards topoisomerase inhibition.** Couto, T. R. (PQ); Silva, L. A. (IC); Rodrigues, L. M. S. (IC); Aguiar, E. C. (PQ); Oliveira, J. F. (PQ); Lima, T. S. (PG); Pedrosa, S. C. B. L. (PQ); Lima, M. C. A. (PQ) UFRPE

**MED-033** **Molecular modeling studies upon the hybrid prophylactic agent between 7-methoxytacrine (7-MEOTA) and 4-pyridinealdoxime (4-PA) with different spacer lengths.** Silva, J. A. V. (PG); Nepovimova, E. (PQ); Ramalho, T. C. (PQ); Kuca, K. (PQ); França, T. C. C. (PQ) IME

**MED-034** **3'-Hydroxychalcones against multidrug-resistant Mycobacterium tuberculosis: Design using Topliss' method, synthesis and bioassay.** Assis, L. R. (PG); Rodrigues, L. O. (PG); Campos, D. L. (PG); Ribeiro, C. M. (PG); Silva, I. C. (PQ); Pavan, F. R. (PQ); Regasini, L. O. (PQ) IBILCE-UNESP

**MED-035** **Sulfation of the ß-1,3;1,6-D-glucan botryosphaeran and evaluation of its derivatives against herpes and dengue viruses.** Sacchelli, B. A. L. (PG); Bernardes, T. M. (IC); Barbosa-Dekker, A. M. (PQ); Galhardi, L. C. F. (PQ); Linhares, R. E. C. (PQ); Orsato, A. (PQ) UEL

**MED-036** **Synthesis, antileishmanial activity and protease inhibition of benzoxazoles derivatives.** Folquitto, L. R. S. (PG); Nogueira, P. F. (IC); Espuri, P. F. (PG); Gontijo, V. S. (PQ); Souza, T. B. (PQ); Marques, M. J. (PQ); Carvalho, D. T. (PQ); Júdice, W. A. S. (PQ); Dias, D. F. (PQ) UNIFAL

**MED-037** **Synthesis of thiosemicarbazide derivatives with antimicrobial activity.** Lima, MLL (IC); Ximenes, RM (PQ); Sena, KXFR (PQ); Albuquerque, JFC (PQ) UFPE

**MED-038** **Pharmacokinetic and Docking studies of Thiazolidinedione derivatives inhibitors of Trypanothione Reductase of Trypanosoma cruzi (TcTR).** Peralva, C. M. S. (IC); Metwally, K. (PQ); Pita, S. S. (PQ) UFBA

**MED-039** **Discovery of marinoquinolines as potent and fast-acting *Plasmodium falciparum* inhibitors with *in vivo* activity.** Aguiar, A. C. C. (PQ); Panciera, M. (PQ); dos Santos, E. F. S. (PG); Singh, M. K. (PG); Garcia, M. L. (PG); de Souza, G. E. (PG); Nakabashi, M (PQ); Garcia, C. R. S. (PQ); Oliva, G. (PQ); Correia, C. R. D. (PQ); Guido, R. V. C. (PQ) IFSC-USP

**MED-040** **Molecular modeling of thiosemicarbazones, candidateDual inhibitors of snake venoms metalloproteases and Pospholipases A2.** Nascimento, N. L. (IC); Cistia, C. D. N. (PG); Kürmmerle, A. E. (PQ); Sant'Anna, C. M. R. (PQ) UFRRJ

**MED-041** **Chalcones synthesis by Claisen-Schmidt condensation and evaluation of larvicidal activity in *Aedes aegypti*.** Barreiros, A. L. B. S.; Souza, G. B. (PG); Alves, P. B. (PQ); Barreiros, B. S. B. (PQ); Barreiros, M. L. (PQ); Cavalcante, S. C. H. (PQ); Brito, T. B. (PG); Costa, E. V. (PQ) UFS

**MED-042** **Evaluation of the interaction of\ß-carbolines derivatives with DNA by molecular fluorescence and correlation with antiproliferative activity.** Silva, M. M. (PG); Pereira, K. T. O. (PG); Barbosa, V. A. (PQ); Sarragiotto, M. H. (PQ); Santos, J. C. C. (PQ); Figueiredo, I. M. (PQ) UFAL

**MED-043** **H2S-Donating monastrol: A new calcium channel modulator.** Braga, T. C. (PG); Soares, K. V. (IC); Jesus, I. C. G. (PG); Guatimosim, S. (PQ); Fátima, A. (PQ) UFMG

**MED-044** **Molecular modeling studies of the nicotinic acetylcholine receptor (nAChR)\α7: Validation and analysis of bioactive compounds.** Frediani, N. F (PG); Batista, V. S (PG); Nascimento-Júnior, N. M (PQ) IQAr-UNESP

**MED-045** **In vitro Screening of chalcones against urease activity.** Severino, R. P. (PQ); Rosa, T. F. (IC); Mendes, L. C. (IC); Lima, R. S. (PG); De Castro, M. R. C. (PG); Bernardes, A. (PG); Perez, C. N. (PQ); De Sousa, L. R. F. (PQ) UFG-Catalão

**MED-046** **Biochemical characterization of new *Schistosoma mansoni* aspartic proteases inhibitors identified by virtual screening.** Gomes, B. F. (IC); Senger, M. R. (PQ); Neves, B. J. (PG); Owens, R. (PQ); Furnham, N. (PQ); Andrade, C. H. (PQ); Silva-Junior, F. P. (PQ) FIOCRUZ

**MED-047** **In vitro inhibition of Helicobacter pylori, interaction studies and molecular docking of lichen natural products with jack bean urease.** Nunes, C. S. (PG); Maciel, T. M. S. (PG); Lage, T. C. A. (PG); Mota, Y. C. C. (PG); Masia, C. (PG); Fátima, A. (PQ); Fernandes, S. A. (PQ); Modolo, L. (PQ); Sisto, F. (PQ); Santos, J. C. C. (PQ); Figueiredo, I. M. (PQ) UFAL

**MED-048** **Caracterização de novos agentes perturbadores de microtúbulos com propriedades anticâncer.** Silva, E. M. G. (IC); Martins, C. T. (IC); Magalhães, L. G. (PG); Mass, E. B. (PG); Russowsky, D. (PQ); Andricopulo, A. D. (PQ) IFSC-USP

**MED-049** **Construction and validation of QSAR models for thiazole derivatives with antifungal activity.** Teixeira, I. N. S. (PG); Maltarollo, V. G. (PQ); Oliveira, R. B. (PQ) UFMG

**MED-050** **Biotransformation of taxifolin by Beauveria bassiana ATCC 7159.** Werworn, L. F. M. (IC); Nascimento, S. L. F. (IC); Sinhorin, A. P. (PQ); de Oliveira, V. (PQ); Pazini, F. (PQ) UFMT

**MED-051** **Antitumor Activity of Mesoionic Salts in Osteosarcoma.** Sousa-Pereira, D. (PG); Barbosa, L. D. (PG); Frauches-Santos, C. (PG); Cruz, V. (IC); Leal, A. C. (PQ); Cavalcanti, A. S. (PQ); Echevarria, A. (PQ) UFRRJ

**MED-052** **Synthesis and antileishmanial activity of novel\ß-carboline-1,3,5-triazine hybrids.** Barea, P. (PG); Barbosa, V. A. (PQ); Leoncio, M. S. (IC); de Paula, J. C. (PG); da Costa, W. F. (PQ); Nakamura, C. V. (PQ); Sarragiotto, M. H. (PQ) UEM

**MED-053** **Development of new potential Mycobacterium tuberculosis enoyl-ACP reductase inhibitors.** Maia, F. L. (IC); Gonçalves, R. S. (PQ); Albuquerque, M. G. (PQ); Lima, C. H. (PQ); Oliveira, L. N. (PG); Castro, J. C. (IC); Mathias, L. S. (IC) UFRJ

**MED-054** **Planejamento, síntese e avaliação biológica de novos derivados 4-nitroimidazólicos candidatos a agentes tripanocidas.** Alcântara, G. P. (PG); Barbosa, J. M. C. (IC); Salomão, K. (PQ); de Castro, S. L. (PQ); Carvalho, S. A. (PQ); da Silva, E. F. (PQ); Fraga, C. A. M. (PQ) FIOCRUZ

**MED-055** **Docking studies of alkaloids from *Prosopis juliflora* against Acetylcholinesterase 1 of *Riphicephalus microplus* (RmAChE1).** Pita, S. S. R. (PQ); Branco, A. (PQ); Lima, H. G. (PG); Batatinha, M. J. M. (PQ); Freitas, H. F. (PQ) UFBA

**MED-056** **Molecular modeling and prediction toxicity studies of organozinc metallodrugs candidate to anticancer agents.** Santos, P. R. (PG); Fernandes, M. S. (IC); Oliveira, A. F. (PG); Paula, F. R. (PQ); Melo, E. B. (PQ); Machado, P. (PQ); Silva, S. M. (PQ) UNIPAMPA

**MED-057** **Construction and Validation of HQSAR models for cell permeability, human intestinal absorption and oral bioavailability.** Almeida, I. A. (IC); Maltarollo, V. G. (PQ) UFMG

**MED-058** **Antiglycation activity of new derivatives of lipoic acid.** Torres, N. M. P. O. (PG); Batista, A. C. S. (IC); Fernandes, P. O. (IC); Silva, R. A. (IC); Xavier, J. A. (PG); Goulart, M. O. F. (PQ); Alves, R. B. (PQ); Freitas, R. P (PQ) UFMG

**MED-059** **In vitro leishmanicidal activity of dihydroquinoline lactones.** Laurentiz, R. S. (PQ); Pissurno, A. P. R. (PG); Magalhães, L. G. (PQ) FEIS-UNESP

**MED-060** **Simplificação molecular como estratégia para descoberta e otimização de candidatos a fármacos antituberculose.** Borsoi, A. F. (IC); Pissinate, K. (PQ); Bizarro, C. V. (PQ); Basso, L. A. (PQ); Machado, P. (PQ) PUC-RS

**MED-061** **Síntese e avaliação farmacológica de acilhidrazonas como protótipos de fármacos multialvos para o tratamento da doença de Alzheimer.** Santos, D. C. (IC); Nogueira, T. L. C. (IC); Quimas, J. V. F. (IC); Henriques, R. R. (PG); Lopes Jr., M. A. A. (PG); Carvalho, L. L. (PQ); Romeiro, N. C. (PQ); Silva, L. L. (PQ); Souza, A. L. F. (PQ) UFRJ

**MED-062** **Estudos computacionais utilizados na procura de potenciais inibidores da enzima arilalkilamina N-acetiltransferase do mosquito Aedes Aegypti.** Dantzger, D. R. C. (IC); Scotti, L. (PQ); Scotti, M. T. (PQ); Ishiki, H. M. (PQ) UNOESTE

**MED-063** **Molecular modeling studies of the nicotinic acetylcholine receptor (nAChRs)\α4β2: Validation and analysis of bioactive compounds.** Batista, V. S. (PG); Nascimento-Júnior, N. M. (PQ) IQAr-UNESP

**MED-064** **Síntese e avaliação farmacológica de derivados de dihidropirimidinonas inibidores duais MPO/AChE para o tratamento da Doença de Alzheimer.** Souza, A. L. F.; Oliveira, T. C. C. (PG); Quimas, J. V. F. (IC); Nogueira, T. L C. (IC); Bastos, J. M. D. (IC); Romeiro, N. C. (PQ); Silva, L. L. (PQ); Ferreira Souza, A. L. (PQ) UFRJ

**MED-065** **Molecular modeling studies of the Penicillium Camembertti Lipase (PCL) enzyme: Docking and validation of bioactive compounds.** Ribeiro, T. R. (PG); Batista, V. S. (PG); Nascimento-Júnior, N. M. (PQ) IQAr-UNESP

**MED-066** **Structure-activity methods applied to NPS amphetamines e cathinones in order to predict risk assessment.** Melo de, E. B. (PQ); Pinke Rodrigues, C. H. (PG); Martins, J. P. A. (PQ); Bruni, A. T. (PQ) FFCLRP-USP

**MED-067** **Novel azido and glucuronamide-based nucleosides of potential therapeutic interest.** Pereira, R. G.; Jorda, R.; Reznicková, E.; Krystof, V.; Csuk, R.; Oliva, G.; Xavier, N. M.; Loesche, A.; Mesquita, N. N.

## *ORG – Química Orgânica*

**ORG-001** **?-hydroxy(amino)amides: enzymatic catalysis via nitrile hydratases and ketoreductases.** Tordato, E. A. (PG); Machado, L. H. C. (IC); Milagre, C. D. F. (PQ) IQAr-UNESP

**ORG-002** **Relevance of kinetic data of cellulose acylation to the synthesis of cellulose mixed esters.** Bioni, T. A. (PG); El Seoud, O. A. (PQ) IQUSP

**ORG-003** **Quantificação de ésteres metílicos por análise termogravimétrica aplicando parâmetros cinéticos.** Costa, M. B. (PQ); Thomas, N. (PG); Dal Pozzo, D. M. (PG); Gato, F. (PG); Scremin, F. R. (PQ) UTFPR

**ORG-004** **Synthesis of Carboxyl-functionalized ionic liquids from cyclic anhydrides.** Cassol, T. M. (PG); Berton, G. H. (IC); Souza, T. J. (PG); Junior, S. A. (PQ) UTFPR

**ORG-005** **Mechanochemical the synthesis of enaminones.** Evangelista, E. S. (PG); Cunha, S. (PQ) UFBA

**ORG-006** **Pentacyclic triterpenes and the cytotoxic potential of *Vochysia divergens* Pohl stem extract.** Pimenta, L. P. (PG); Pedroso, R. C. N. (PG); Souza, W. P. (PG); Valerino-Diaz, A. B. (PG); Santos dos, L. C. (PQ); Soares, M. A. (PQ); Tavares, D. C. (PQ); Silva, M. L. A. (PQ); Cunha, W. R. (PQ); Pauletti, P. M. (PQ); Januário, A. H. (PQ) UNIFRAN

**ORG-007** **Use of Trichloroisocyanuric Acid for the Conversion of Amides to Amines via Hofmann Degradation.** Bastos, G. A. (IC); de Mattos, M. C. S. (PQ) UFRJ

**ORG-008** **New chiral oxazolidine-dihydropyridines.** Moura, R. G. (PG); Palma, D. Y. R. (IC); Di Vitta, C. (PQ); Marzorati, L (PQ) IQUSP

**ORG-009** **Substituent effect evaluation on spectroscopic properties of Schiff bases derived from diaminomaleonitrile and salicylaldehydes.** Mello, L. S. (PG); Dockal, E. R. (PQ); Cruz Júnior, J. W. (PQ) UFSCar

**ORG-010** **Synthesis and characterization of non-symmetric dimeric ionic liquid crystals derived from 1,3,4-oxadiazole heterocycle.** Kutz, M. S. (IC); Molin, F. (PQ) UTFPR

**ORG-011** **Chemical composition of essential oil from inflorescences from male and female specimens of Baccharis punctulata DC.** Oliveira de, M. S. (IC); Ascari, J. (PQ); Nunes, D. S. (PQ); Scharf, D. R. (PQ); Simionatto, E. L. (PQ); Heiden, G. (PQ) UTFPR

**ORG-012** **Synthesis and theoretical studies of the rotational barrier of 2,4,6-Trifenetil-1,3,5-triazine.** Del Cistia, C. D. N. (PQ); Barbosa, I. R. (IC); Echevarria, A. (PQ); Sant'Anna, C. M. R. (PQ) UFRRJ

**ORG-013** **A study of extraction of natural products from renewable sources: naringin from grapefruit peels and hesperidin from orange peels.** Cortez, M. V. M. (IC); Nunes, A. V. J. (IC); França, E. L. (PG); Sakukuma, M. C. K. (PG); David, J. M. (PQ); Victor, M. M. (PQ) UFBA

**ORG-014** **Solvent effect on the conformational preference of some 1,3-disubstituted acyclic compounds by 1H NMR.** Karas, L. J. (PG); Batista, R. B. (PG); Viesser, R. V. (PG); Tormena, C. F. (PQ); Rittner Neto, R. (PQ); de Oliveira, P. R. (PQ) UTFPR

**ORG-015** **Three-component synthesis of arylidene-succinimides via *in situ* wittig reaction.** Barretto, F. A. (PG); Cunha, S. D. (PQ) UFBA

**ORG-016** **A new multicomponent synthesis of pyrimido[4,5-b]quinolinetetraones.** Santana, L. L. B. (PQ); Dourado, G. A. A. (PG); Cunha, S. (PQ) UFBA

**ORG-017** **Síntese de 2,5-dicloro-3,6-bis[(quinolon-6-il)amino]-1,4-benzoquinonas com potencial atividade antipriônica.** Costa, A. R. P. (IC); Silva, R. C. (PG); Batalha, P. N. (PQ); Boechat, F. C. S, (PQ); Souza, M. C. B. V. (PQ) UFF

**ORG-018** **Síntese e aplicação de organocatalisadores bifuncionais em reações de Michael estereosseletivas envolvendo nitrociano-compostos.** Soares, P. M. A. (PG); Vinhato, E. (PQ); Rodrigues, A. (PQ) UNIFESP-Diadema

**ORG-019** **Palladium-Catalyzed Carbonylative alfa-Arylation of Azlactones.** Pinheiro, D. L. J. (PG); Nielsen, D. U. (PQ); Amarante, G. W. (PQ); Skrydstrup, T. (PQ) AU-DK

**ORG-020** **Abordagens complementares nas sínteses totais de (+)- e (-)-bernumidina.** Corrêa, B. K. (PG); Silva, T. R. C. (PG); Raminelli, C. (PQ) UNIFESP-Diadema

**ORG-021** **Synthesis of New Schiff Bases (N-Aryl)Phosphoramidic. Possible Microbiocidal.** De Macedo, W. P. (PQ); Lousa, P. H. F. (PG) UEG

**ORG-022** **Synthesis and biological screening of tetrazolyl-4-oxoquinolines as antitumor agents.** Oliveira, P. H. R.; Souza, M. C. B. V.; Boechat, F. C. S.; Fernandes, P. D.; Tolentino, N. M. C.; Vale, T. M. (IC) UFF

**ORG-023** **Enantioselective Heck-Matsuda Reaction on Dihydrofurans: Synthesis of Isobenzofuranones and Isochromanones.** de Lucca Jr., E. C. (PQ); Kattela, S. (PQ); Correia, C. R. D. (PQ) IQ-UNICAMP

**ORG-024** **Syntheses of sulfides via wittig reaction using thiosulfonates.** Moura, I. M. R. (IC); Silva, A. T. (PG); Menezes, P. H. (PQ) UFPE

**ORG-025** **Síntese de cristais líquidos liotrópicos e sua aplicação como meio de alinhamento para obtenção de parâmetros anisotrópicos em RMN.** Silva, D.G.B (PG); Hallwass, F (PQ); Navarro-Vázquez, A (PQ) UFPE

**ORG-026** **Synthesis and photophysical investigation of new quinoline derivatives.** Pastrello, B. (PG); Dos Santos, G. C. (PG); Silva-Filho, L. C. (PQ); Ximenes, V. F. (PQ) UNESP-Bauru

**ORG-027** **Síntese de oxazolidinonas via reação de cloroaminociclização promovidas por sais de Pd(II).** Papa, B. L. (PG); Vinhato, E. (PQ); Rodrigues, A. (PQ) UNIFESP-Diadema

**ORG-028** **Synthesis of isocoumarins and 3,4-dihydroisocoumarins for antiproliferative activity.** Santos, L. S. (PG); Chapadeiro, R. T. (IC); de Freitas, R. P. (PQ); Alves, R. B. (PQ) UFMG

**ORG-029** **Direct sequential C-H iodination/organoyl-thiolation of quinonoid deactivated systems: A new frontier for potent trypanocidal quinones.** Jardim, G. A. M. (PG); Oliveira, W. X. C. (PQ); de Freitas, R. P. (PQ); Menna-Barreto, R. F. S. (PQ); Silva, T. L. (PQ); Goulart, M. O. F. (PQ); da Silva Júnior, E. N. (PQ) UFMG

**ORG-030** **Enantioselective Heck−Matsuda arylation of the non-activated cyclopentene.** Chorro, T. H. D. (IC); Polo, E. C. (PQ); Correia, C. R. D. (PQ) UNICAMP

**ORG-031** **Strong conformational preference of cis-2-fluoro- and cis-2-chlorocyclohexylamine measured by DNMR.** Basso, E. A. (PQ); Francisco, C. B. (PG); Fernandes, C. S. (PG); Melo, U. Z. (PG); Paschoalino, V. T. (IC) UEM

**ORG-032** **Resolução cinética de derivados de 1-feniletanol mediadas por Lipase B de *Candida antarctica* imobilizada em batelada e fluxo contínuo.** de Melo, L. S. (IC); Junior, J. C. C. da S. (IC); Felner, P. P. (IC); de Souza, L. C. (IC); Aguillón, A. R. (PQ); Leão, R. A. C. (PQ); Miranda, L. S. M. (PQ); de Souza, R. O. M. A. (PQ) UFRJ

**ORG-033** **Estudos visando às sínteses totais de (R)- e (S)-nuciferina.** Perecim, G. P. (PG); Rivero, E. A. I. (IC); Silva, D. O. (PQ); Raminelli, C. (PQ) UNIFESP-Diadema

**ORG-034** **Síntese de Selenoésteres mediante rearranjo sigmatrópico entre selenoacetilenos e difenilsulfóxido catalisada por ácido tríflico.** Baldassari, L. L. (PG); Mantovani, A. C. (PQ); Maulide, N. (PQ); Lüdtke, D. S. (PQ) UFRGS

**ORG-035** **Heterociclo quinoxalina aplicado à preparação de cristais líquidos: síntese, mesomorfismo e propriedades físicas.** Aguiar, L. O. (PG); Souza, S.P. (IC); Vieira, A. V (PQ) UFBA

**ORG-036** **Síntese de N-ftalimidas derivados do Eugenol e avaliação da sensibilidade de cepas de Candida Albicans frente à estes compostos.** Santana, K. S (IC); Silva, C. M (TC); Marçal, L. L (PQ) IFRJ - Campus Nilópolis

**ORG-037** **Zinc-promoted, L-proline catalyzed allylation of aromatic aldehydes with allyl bromide in aqueous medium.** Silva, R. A. (PQ); Souza, F. A. M. (IC); Couto, T. R. (PQ) UFRPE

**ORG-038** **Arylation of\β-ketosulfoxonium ylides with arynes: a direct synthesis of pro-chiral ylides and mono-arylated ketones.** Talero, A. G. (PG); Martins, B. S. (PQ); Burtoloso, A. C. B. (PQ) IQSC-USP

**ORG-039** **Continuous flow enzymatic kinect resolution of benzylic alcohols: development of a low-cost homemade bioreactor.** Januário, G. O.; Milagre, H.M. S. (PQ) IQAr-UNESP

**ORG-040** **Estudo da oxidação catalisada por Lacase de amidas derivadas da tiramina.** Aguiar de, V. M. (PG); Miranda, L. S. M. (PQ); Gonçalves, R. S. B. (PQ); Silva, R. E. (IC) UFRJ

**ORG-041** **Estudo sintético da delta-decalactona e derivados.** Costa, M. B. (PQ); Paula de, E. L. (PG); Feliciano, A. S. (IC) UEG

**ORG-042** **Solvent-free synthesis of a-acylated b-thioenaminones.** Matos, J. S. (PG); Cunha, S. D. (PQ) UFBA

**ORG-043** **Síntese e caracterização de novos derivados piperazínicos, análogos ao SQ109: Potenciais agentes antituberculose.** Saraiva, M. F. (PQ); Reis, D. B. (PG) UNIFEI

**ORG-044** **Synthesis of new inhibitors of cathepsin K with potential use in osteoporosis therapy.** Gontijo, T. B. (PG); Silva Júnior, E. N. (PQ); Freitas, R. P. (PQ) UFMG

**ORG-045** **Synthesis of new compounds based on Lawsone via a multi-component reaction.** Cardoso, M. F. C. (PQ); Forezi, L. M. (PQ); Gil, C. C. (IC); Santos, T. S. (IC); De Paula, G. R. (PQ); Teixeira, L. A. (PQ); Silva, F. C. (PQ); Ferreira, V. F. (PQ) UFF

**ORG-046** **Continuous flow biocatalyzed process enhanced production of (R)-1,2-propanediol mediated by Immobilized Candida Antarctica Lipase B.** Aguillón, A. R. (PG); Câmara, D. N. (IC); Souza de, S. P. (PQ); Leão, R. A. C. (PQ); Miranda, L. S. M. (PQ); Souza de, R. O. M. A. (PQ) UFRJ

**ORG-047** **Synthesis and condensation of amides derivatives from nonsteroidal anti-inflammatory drugs (NSAIDs) in "environmentally friendly" conditions.** Santos, D. C. (PG); Ponquio, F. P. (IC); Reis, A. K. C. A. (PQ) UNIFESP-Diadema

**ORG-048** **Catalyst-free synthesis of pyridazinones from 3-hydroxy-indole-2-ones.** Santos, G. A. (PG); Cunha, S. D. (PQ) UFBA

**ORG-049** **Dynamic kinetic resolution of amines with nickel catalysts supported on mixed oxides of lanthanum and alkaline earth metals.** Silva, L. A. (IC); Lima, S.M (PQ); Siqueira, F.A (PQ); Fernandes, T. N. C. (IC) UNIFESP-Diadema

**ORG-050** **Synthesis of Novel N-heterocycles from Biomass-derived Building Block Dimethyl Itaconate.** Santos, G. J. S. R. (IC); Ludwig, F. P. (PG); Bastos, A. V. (PG); Bareño, V. D. O. (PG); Silva, S. M. (PQ); Flores, A. F. C. (PQ); Flores, D. C. (PQ) FURG

**ORG-051** **Resolução cinética dinâmica da (±)-1-feniletilamina catalisada por níquel suportado em óxidos mistos de metais lantanídeos.** Fernandes, T. N. C. (IC); Silva, L. A. (IC); Lima, S. M. (PQ); Siqueira, F. A. (PQ) UNIFESP-Diadema

**ORG-052** **Synthesis and leishmanicidal activity of eugenol triazolic derivatives.** Teixeira, R. R. (PQ); Gazolla, P. A. R. (PG); Lima, W. P. (PQ); Borsodi, M. P. G (IC); Bergmann, B. R. (PQ); da Silva, A. M. (PQ) UFV

**ORG-053** **Mechanochemical chlorination of acetamides via chemometric optimization.** Araújo, D. M. (PG); Cunha, S. (PQ) UFBA

**ORG-054** **Synthesis of indol sulfoxides and sulfones as broad spectrum antibacterials against the ESKAPE pathogens.** Silveira, G. P. (PQ); Silva, E. E. (PG) UFRGS

**ORG-055** **Emprego de partículas magnéticas modificadas com cálix[4]arenos como catalisadores heterogêneos para síntese de xantenonas.** Souza, G. C. (IC); Zacchi, C. H. C. (PG); Fátima de, A. (PQ); Araújo de, M. H. (PQ) UFMG

**ORG-056** **Synthesis of quinolinyl lactones.** Pissurno, A. P. R. (PG); Laurentiz, R. S. (PQ) FEIS-UNESP

**ORG-057** **Use of humic substances as a biostimulant in Solanum lycopersicum.** Oliveira, D. C. B (IC); Orlando, B. H. S. L. (IC); Pereira, G. M. (PQ) UEPA

**ORG-058** **Efficient Synthesis of N-phenethylarylthioamides by Kindler Reaction.** Romanhi, P. (IC); Pontes, T. S. (IC); Proença, G. S. (IC); Oliveira, C. J. (IC); Viegas, P. R. (IC); Castro, B.G. (IC); Machado, L. A. (PG); Souza, M. C. (PQ); Pedrosa, L. F. (PQ) UFF

**ORG-059** **Synthesis and luminescent properties of new naphthoquinoline lactones derivatives.** Santos, F. A. (PG); Laurentiz, R. S. (PQ) FEIS-UNESP

**ORG-060** **Estudo de derivados pirazólicos como inibidores de corrosão.** Maia, C.E.B. (PG); Romeiro, G.A. (PQ); Velloso, M.C.C. (PQ); Silva, G.C. (IC); Ferro, M.V. (IC) UFF

**ORG-061** **Synthesis of new bis-1,2,3-triazoles derivatives containing carboxylic acid groups: potential inhibitors of osteoclastogenesis.** Reis, W. J. (PG); Freitas, R. P. (PQ); Alves, R. B. (PQ) UFMG

**ORG-062** **Oxone-mediated direct alpha-hydroxylation of beta-dicarbonyl compounds.** Marques, M. V. (TC); Peterle, M. M. (PG); Sá, M. M. (PQ) UFSC

**ORG-063** **Dienone-amide produced by the bioluminescent mushroom Neonothopanus gardneri.** Oliveira, M. D. D. A. (PG); Andrade, T. J. A. S. (PQ); Silva, D. H. S. (PQ); Stevani, C. V. (PQ); Junior, J. S. C. (PQ); Cito, A. M. G. L. (PQ) UFPI

**ORG-064** **Synthesis of polycatenar photoisomerizable liquid crystals based on an expanded acylhydrazone core.** Oliveira, W. A. (IC); Westphal, E. (PQ) UTFPR

**ORG-065** **Laccase-catalyzed synthesis of dimers from 2,6-DMP: Optimization of TMBP synthesis and evaluation of its antioxidant action in biodiesel.** Schirmann, J. G. (PG); Dekker, R. F. H. (PQ); Borsato, D. (PQ); Barbosa-Dekker, A. M. (PQ) UEL

**ORG-066** **Síntese e Estudo de Cristais Líquidos Assimétricos Derivados do Heterocíclico 2,1,3-benzotiadiazol.** de Jesus, E. C. (IC); Silva, T. O. B. (IC); Silva, E. R. (PG); Vieira, A. A. (PQ) UFBA

**ORG-067** **Cleaving paraoxon with hydroxylamine: ammonium oxide isomer favors a frontside attack mechanism.** LIMA, M. F. (PQ); da Cruz, P. A. U. (IC); Fernandes, M. E. C. (PG); Polaquini, C. R. (PG); Miguel, E. L. M. (PG); Pliego Jr., J. R. (PQ); Scorsin, L. (PG); de Oliveira, B. S. (IC); Nome, F. (PQ) IBILCE-UNESP

**ORG-068** **Study of sulfamide and its N,N'-diindolyl derivative as anion carriers.** Freitas, M. P. (PQ); Mendonça, J. G. P. (PG); Cormanich, R. A. (PQ); Fernandes, S. A. (PQ) UFLA

**ORG-069** **Synthesis of aryl-amides derived from L-cysteine - potential double inhibitors of HIV1-PR and renin.** Serralbo, A. S. (IC); Reis, A. K. C. A. (PQ); Longo Jr., L. S. (PQ) UNIFESP-Diadema

**ORG-070** **Selective functionalization of N-heterocyclic substrates using the TMPLi/ZnCl2 system.** Nishimura, R. H. V. (PG); Murie, V. E. (PG); Clososki, G. C. (PQ) FCFRP-USP

**ORG-071** **Pirrol-2,3-diona: Intermediário-chave para Acessar 4-(2-amino-2-oxoacetil)-5-aril-N-arilpirazóis Regiosseletivamente.** SILVA da, M. J. V. (PG); RIBEIRO, G. M. (PG); ROSA, F. A. (PQ) UEM

**ORG-072** **Synthesis, X-Ray Structure of new complex with Paddle-Wheel SBUs.** Silva, M.C (IC); Salzer, G. (IC); Barbosa, D.B.A (PQ); Toledo, T.A (PQ); Barbosa, E.P (PQ) IF Sudeste MG

**ORG-073** **Relationship between Hammett's parameters and in silicodensity functional with tandem mass ESI-CID fragmentation:Dihydropyridines as prototypes.** Dos Santos, P.R. (PG); Pereira, C.M.P. (PQ); de Paula, F.R. (PQ); Moura, S. (PQ) UCS

**ORG-074** **Synthesis of 5-aminotetrazoles from thioureas using trichloroisocyanuric (TCCA).** Lima da Silva, T.L.S. (PQ); Christine Dutra da Silva, A. C.Dutra S. (IC) UFRJ

**ORG-075** **A multidimensional liquid chromatography method for monitoring on flow the activity of PNP-Mt immobilized enzyme.** Castro, A. C. (IC); Moraes, M. C. (PQ); Martinelli, L. K. B. (PQ); Santos, D. S. (PQ); Basso, L. A. (PQ) UFF

**ORG-076** **Bidirectional synthesis of symmetric bis-benzoxazines by Mannich reaction of eugenol and diamines.** Mattos, R. R. (PG); Cunha, S. D. (PQ) UFBA

**ORG-077** **Multicomponent synthesis of 5-aminotetrazoles and bistetrazoles promoted by bismuth nitrate pentahydrate.** Jesus de, I. S. (PG); Cunha, S. D. (PQ) UFBA

**ORG-078** **Aplicação de carbodiimidas na síntese de anestésicos locais.** Bezerra, M. A. M. (PG); Pimentel, J. V. P. (IC); Miranda, L. S. M. (PQ); Souza, R. O. M. A. (PQ) UFRJ

**ORG-079** **Assignment of the relative and absolute stereochemistry of two novel epoxides using NMR and DFT-GIAO calculations.** Demuner, A. J. (PQ); Alvarenga, E. S. (PQ); Viana, V. M. (IC); Moraes, F. C. (PG) UFV

**ORG-080** **Rare Earth Triflate-Catalyzed Gröebke-Blackburn-Bienaymé reaction under microwave heating to access imidazo[2,1-b] thiazoles.** Longo Jr., L. S. (PQ); Anjos, N. S. (IC); Fiorentino, E. S. C. (IC) UNIFESP-Diadema

**ORG-081** **Systematic studies toward iodocyclization of (Z)-thiobutenynes using water as solvent: Ecofriendly synthesis of 3-Iodothiophenes.** Carvalho, D. B. (PG); Andrade, C. B. (PG); Soares, O. (PG); Shiguemoto, C. Y. K. (PQ); Baroni, A.C. M. (PQ) UFMS

**ORG-082** **Síntese de cristais líquidos iônicos derivados do núcleo tristriazolotriazina.** Dutra, B. N. (IC); Molin, F. (PQ) UTFPR

**ORG-083** **An 8-step approach for the total synthesis of (−)-pleocarpanone.** Novaes, L. F. T. (PG); Pastre, J. C. (PQ) UNICAMP

**ORG-084** **Preparation of magnetic particles modified with calixarenes and evaluation as catalyst in Biginelli reaction.** Zacchi, C. H. C. (PG); Vieira, S. S. (PQ); Ardisson, J. D. (PQ); de Fátima, A. (PQ); Araujo, M. H. (PQ) UFMG

**ORG-085** **Síntese de aciclonucleosídoes fosfonatos quinolônicos, ANPs, possíveis compostos anti-CHIKV.** Faro, L. V. (PQ); Boechat, F. C. S. (PQ); Souza de, M. C. (PQ); Paixão, I. C. N. P. (PQ); Souza de, M. C. B. V. (PQ) UFF

**ORG-086** **Síntese de sílicas ativas: avaliação da matriz e de adsorção de boro.** Couto, M.T. (PQ); Cassella, R.J. (PQ); Souza, J.M. (PG); Silva, D.A. (TC); Rodrigues, J.E.F.C (TC) IFRJ

**ORG-087** **Síntese de quinolonas conjugadas a triazóis e investigação de sua atividade leishmanicida.** Oliveira, V. G. (PG); Regufe, P. F. (IC); Lima, M. F. O. (IC); Faiões, V. S. (PQ); Pacheco, J. S. (PG); Boechat, F. C. S. (PQ); Torres-Santos, C. (PQ); Silva, F. C. (PQ); Souza, M. C. B. V. (PQ) UFF

**ORG-088** **Synthesis of 4-quinolone-porphyrin conjugates as potential photosensitizers.** Sagrillo, F. S. (PG); Gomes, A. T. P. (PQ); de Souza, A. G. (IC); Costa, A. R. P. (IC); Boechat, F. C. S. (PQ); de Souza, M. C. B. V. (PQ); Neves, M. G. P. M. S. (PQ); Cavaleiro, J. A. S. (PQ) UA-Portugal

**ORG-089** **Chemical characterization of pyriproxifene by chromatography (HPLC-PDA and CG-MS).** Alves, P. S. (PG); Costa, J. M. S. (IC); Oliveira, M. D. A. (PG); Andrade, T. J. A. S. (PQ); Costa Júnior, J. S. (PQ) UESPI

**ORG-090** **Optimization of the solvent mixture for extraction of phenolic compounds with antioxidant activity from Byrsonima basiloba Juss.** Roberto, T. C. (IC); Scaramboni, B (PG); dos Santos, C. (PQ) UNESP-FCL-Assis

**ORG-091** **Synthesis of 2-aminothiazoles using\α-bromoketones and thiourea in PEG-400.** Matos, G. F. (PG); Ferreira, A. S. (PG); Chagas, R. P. (PQ); Barros, O. S. R. (PQ) UFG

**ORG-092** **Regiospecific synthesis and antitumor evaluation of thioethers derived from Juglone.** Gomes, C.B.S.M.R. (PG); Moreira, C.S. (PG); Forezi, L.S.M. (PQ); Cordeiro, P.S. (IC); do Nascimento, V. (PQ); Montenegro, R.C. (PQ); Ferreira, V.F. (PQ); da Rocha, D.R. (PQ) UFF

**ORG-093** **Theoretical insights on the racemization of azlactone rings.** de Castro, P. P. (PG); Batista, G. M. F. (IC); dos Santos, H. F. (PQ); Amarante, G. W. (PQ) UFJF

**ORG-094** **Desenvolvimento de novos biocatalisadores imobilizados contendo lipases para a produção do carbonato de glicerila em batelada e fluxo contínuo.** Nascimento, M.A. (PG); Gotardo, L.E. (IC); Raul, L. (IC); Leão, R.A.C. (PQ); Junior, I.I. (PQ); Souza, R.O.M.A. (PQ) UFRJ

**ORG-095** **Reações de bromoaminociclização enantiosseletivas.** Matsushima, J. E. (IC); Rodrigues, A. (PQ) UNIFESP-Diadema

**ORG-096** **Synthesis of analytical standards of 25I-NBOMe and 25I-NBOH for forensic purposes.** Queiroz, M. P. (IC); de Barros, W. A. (PG); Neto, L. S. (PQ); Nascentes, C. C. (PQ); de Fátima, A. (PQ) UFMG

**ORG-097** **Synthesis and antifungal evaluation of alpha amino acids.** Araújo, A. F. (FM); Ferreira, A. P. (IC); Lima, P. S. V. (PG); Souza, H. D. S. (PG); Silva, D. F. (PG); Lima, E. O. (PQ); Filho, P. F. A. (PQ); Oliveira, R. F. (PG); Huang, M. N. (PG); Neris, A. M. (PG) UFPB

**ORG-098** **Expanding the redox-relay strategy: accessing carbonylated compounds from alkenyl silyl and methyl ethers by heck arylations.** Esteves, H. (PG); Menezes da Silva, V. H. (PQ); Correia, C. R. D. (PQ) UNICAMP

**ORG-099** **Silver-Catalyzed Direct Selenylation of Indoles.** Rios, E. A. M. (PG); Rampon, D. da S. (PQ) UFPR

**ORG-100** **Push-pull systems: A very useful building blocks for the preparation of biological active heterocycles.** Bitencourt, J. (PG); Passarelli, C. (PQ); Costa, J.M. de F. (PG); Almeida, M. (PQ); Pedroso, N. (IC); de Lima, Ednilza (IC); da Silva, J. (IC); Quincoces, J. (PQ) UNIAN

**ORG-101** **Sand-Starch mixtures as stationary phases: Low-cost Columm Chromatography for dyes purification in Organic Chemistry class.** Costa Cerqueira, B. C. C. (IC); De Paula, R. D. P. (PQ) UFRB

**ORG-102** **Unequivocal structural assignments of three cardanol - derived: an experimental and theoretical approach.** Barbosa, LRB (PG); Lacerda Junior, VLJ (PQ); Beatriz, AB (PQ); Neto, ACN (PQ) UFES

**ORG-103** **Synthesis of new nitroxides modified with disulfide functionality to be used as spin label.** Batista, A. C. S. (IC); Santos, F. S. (PG); Freitas, R. P. (PQ) UFMG

**ORG-104** **A Practical Synthesis of densely substituted 2H-furo[3,2-b]benzopyran-2-ones.** Rozo Nuñez, W.E. (PG); Cunha, S. (PQ) UFBA

**ORG-105** **Síntese de um novo ligante quiral do tipo sanduíche cobaltoceno-imidazolina.** Vinhato, E (PQ); Souza, I. A. (IC) UNIFESP-Diadema

**ORG-106** **Novel 4-arylaminoquinoline-3-carbonitriles as Inhibitors of HIV-1 reverse transcriptase.** Bernardino, A. M. R. (PQ); Melo, B. C. L. (PG); Polillo, G. (PG); Pereira, H. S. (PQ); Paixão, I. C. P. (PQ); Ribeiro, M. S. (PG); Borges, J. C. (FM) UFF

**ORG-107** **Síntese de Dihidropirimidinonas e avaliação de interação com o ssDNA.** Schmoeller, L.A. (IC); Gariani, R. A. (PQ); Xavier, F. R. (PQ); Wodtke, F. (PG) UDESC

**ORG-108** **Synthesis of carbohydrate-linked pentadienone derivative with antitumor properties.** Passarelli, C. (PQ); Michalik, D. (PQ); Costa, J.M. de F. (PG); Almeida, M. (PQ); Maria, D.A. (PQ); Ribeiro, A.O. (PQ); Vogel, C. (PQ); Quincoces, J. (PQ) Rostock Universität

**ORG-109** **Production of biodiesel with homogeneous and heterogeneous catalysts by microwave in ethanol.** Costa, P. R. A da (IC); Cassa, S. G. S. (IC); Aversa, T. M. (PQ); Almeida, Q. A. R. de (PQ) IFRJ-Campus Duque de Caxias

**ORG-110** **Síntese, caracterização e avaliação das atividades citotóxica e antiacetilcolinesterase de chalconas.** Farias, I.F. (PG); Lemos, T. L. G. (PQ); Nascimento, P.G.G. (PG); Mesquita, B.M. (PG); Silva, R.A.C. (PQ); Oliveira, I.R. (PQ); Trevisan, M.T.S. (PQ); Rocha, D.D. (PQ); Filho, M.O.M. (PQ) UFC

**ORG-111** **Biocatalytic Promiscuity: Use of lipases as catalyst on Henry reaction.** Durigon, M. C. S. (IC); Dias, M. R. G. (PG); Krieger, N. (PQ); Couto, G. H. (PQ); Pilissão, C. (PQ) UTFPR

# *QPN – Química de Produtos Naturais*

**QPN-001** **Composição química e atividade biológica do óleo essencial da semente de Schinus molle.** Valente, V. M. M. (PQ); Morais, N. K. (IC); Valente, P. M. (PG) UFV-Campus de Rio Paranaíba

**QPN-002** **Antifungal activity of the essential oil of *Campomanesia macrobracteolata* and *Protium* sp. against Thielaviopsis paradoxa.** Santos dos, K. R. (PG); Dutra, J. P. (PG); Luber, J (PG); Kitagawa, R. R. (PQ); Borges, W. S. (PQ) UFES

**QPN-003** **Variabilidade composicional em óleo essencial de flores de *Caesalpinia pulcherrima* (L.) SW.** Catunda Jr., F. E. A. (PQ); Azevedo, A. M. A. (PG); Sá Jr., E. P. (PG); Carvalho, M. G. (PQ); Araújo, T. F. (PQ) UNINTA

**QPN-004** **Chemical composition and antimicrobial activity of essential oil obtained from two species of the Lauraceae family.** Coutinho, E. J. (IC); Costa, É. R. (PG); Louro, G. M. (PG); Nicolau, C. L. (PG); Silva, J. C. M. (PG); Filho, C.C.S. (IC); Fernandes, S.S.L. (PG); Cabral, M.R.P. (PG); Simionatto, E. (PQ) UEMS

**QPN-005** **Chemical composition of leaves and fruits essential oils from Schinus terebinthifolius genders cultivated at Ceara-Brazil.** Rodrigues, T. H. S. (PQ); Dias, F. M. F. (IC); Azevedo, F. R. P. (IC); Silva, P. T. (IC); Santos, H. S. (PQ); Bandeira, P. N. (PQ) UVA

**QPN-006** **Chemical composition and antimicrobial activity of essencial oil Psidium Myrtoides O. Berg.** Dias, R. F. C.; DIAS, R. F. C. (PG); Aquino, F. J. T. (PQ); Morais, S. A. L. (PQ); Nascimento, E. A. (PQ); Oliveira, A. (PQ); Cunha, L. C. S. (PQ); Ambrosio, M. A. L. V. (PQ); Martins, C. H. G. (PQ); Souza, J. M. (IC) UFU

**QPN-007** **Avaliação da ação fotoprotetora do extrato aquoso de *Campomanesia adamantium*.** Gaiola, L. (IC); Catalan, T. B. S. (PG); Cardoso, C. A. L. (PQ) UEMS

**QPN-008** **Antimicrobial activity of the essential oil of leaves of Banisteriopsis malifolia (Ness\& Martius) B. Gates.** Chang, R. (PQ); Martins, V. E. X. (PG); Silingardi, H. M. T. (PQ); Nascimento, E. A. (PQ); Cunha, L. C. S. (PQ); Martins, C. H. G. (PQ); Ambrósio, M. A. L. V. (PQ); Garcia, L. A. (IC); Morais, S. A. L. (PQ); Aquino, F. J. T. (PQ) UFU

**QPN-009** **Chemical composition of essential oils of seven Piper species (Piperaceae) from Marambaia Island, Mangaratiba, RJ (Brazil).** Ramos, Y.J. (PG); Moreira, D.L. (PQ) FIOCRUZ

**QPN-010** **Extraction of the essential oil from the leaves of Piper hispidinervum using supercritical CO2.** Simionatto, E. L. (PQ); Scharf, D. R. (PQ); Wientage, G. H. (IC); Klinkowski, B. H. (IC); Salamoni, J. (IC); Cardozo Filho, L. (PQ) FURB

**QPN-011** **The influence of abiotic factors on the production of essential oils of Eugenia uniflora.** Santos, R. O.; Pioker, F. C.; Imbernon, R. A. L.; Sannomiya, M. (PQ) EACH-USP

**QPN-012** **Chemical study of flowers from two species of Croton visited by bees: velame (*Croton heliotropiifolius* Kunth) and marmeleiro (Croton sonderianus Muell. Arg.).** Pereira Cabrera, P.C. (PG); Guade da Silva, G.S. (PG); Amorim Camara, A.C. (PQ); Sarmento Silva, S.S. (PQ) UFRPE

**QPN-013** **Chemical composition of the volatile oil from two Xylopia species from the State of Pará, Brazil.** Cascaes, M. M. (PQ); Andrade, E. H. A. (PQ); Sousa, E. M. (IC); Nascimento, L. D (PG); Guilhon, G. M. S. P. (PQ); Anjos, T. O. (IC); Pereira, S. F. M. (IC); Oliveira, J. (PQ) MPEG

**QPN-014** **Chemical Composition and biological activities of the essential oil from leaves of *Bauhinia cheilantha* Bong. Steud.** Silva, A. M. A. (PG); da Silva, H. C. (IC); Monteiro, A. O. (PG); Santiago, G. M. P. (PQ); Alves, P. B. (PQ); Militão, G. C. G. (PQ) UFC

**QPN-015** **Multivariate analysis of chemical composition and theoretical study on muscarinic receptors of essential oils from medicinal plants.** ROCHA, G.N.S.A.O. (IC); SILVA, L.O.B. (PQ); VILAR, F.C.R. (PQ); CAMELO, M.L.V. (PQ); LORENZO, V.P. (PQ) IF-Sertão Pernambucano

**QPN-016** **Chemical composition and biological activity of essential oil of species Nectandra lanceolata (Lauraceae).** Costa, É. R (PG); Simionatto, E (PQ); Coutinho, E. J (IC); Louro, G. M (PG); Nicolau, C. L (PG); Silva, J. C. M (PG) UEMS

**QPN-017** **Identificação do composto antifúngico no óleo essencial das folhas de *Callistemon viminalis*.** Valente, P. M. (PG); Valente, V. M. M. (PQ); lima, J. A. M. (IC) UFV-Campus de Rio Paranaíba

**QPN-018** **Antimicrobial activity of essential oils of *Psidium salutare* var. sericeum e mucronatum (Myrtaceae) against *Candida albicans*.** Ethur, E. M. (PQ); Bona, C. M. (IC); Buhl, B. (IC); Scheibel, T. (IC); Kauffmann, C. (PQ); Hoehne, L. (PQ); Freitas, E. M. (PQ); Marchi, M. I. (PQ) UNIVATES

**QPN-019** **Flavonoids of in situ and in vitro culture from *Lomatozona artemisiifolia* Baker leaves.** Wakui, V. G. (PG); Moreira, M. P. (PG); Terezan, A. P. (PG); Sibov, S. T. (PG); Lopes, F. J. F. (PQ); Oliveira de, C. M. A. (PQ); Kato, L. (PQ) UFG

**QPN-020** ***Pterodon pubescens* Benth. (Sucupira) ethanol extract mouthwash pharmaceutical forms.** Alves, N. (IC); Figueiredo, M. C. (PG); Foglio, M. A. (PQ) UNICAMP

**QPN-021** **Isolation in alginate microcapsules of the pathogen Tritrichomonas foetus, to evaluate the tricomonicidal activity of plant extracts.** Ramirez, M. R. (PQ); Oyhenart, J. A. (PQ) UFRGS

**QPN-022** **Estudo químico de três espécies de Chamaecrista Moench nativas do Nordeste do Brasil.** Almeida, M. T. (IC); Lima, D. R. (PG); Vasconcelos, M. G. (PQ) UFC

**QPN-023** **Comparative study of drying methods of Vitis labrusca grape peels: greenhouse or Oshibana?.** Carra, J. B. (PG); Matos, R. L. N. (PG); Novelli, A. P. (IC); Casagrande, R. (PQ); Georgetti, S. R. (PQ); Arakawa, N. S. (PQ); Baracat, M. M. (PQ) UEL

**QPN-024** **Ethnopharmacology of medicinal plants of the Cerrado Region (Goiás, Brazil).** Oliveira, Y. F. (IC); Gomides, N. A. M. T. P. (PG); Severino, V. G. P. (PQ) UFG

**QPN-025** **Phytochemical prospection and phytotoxic effect of plant species Luehea candicans stem bunch.** Camara, M. B. P. (PG); Cantanhede Filho, A. J. (PQ); Carneiro, F. J. C. (PQ); Dias, E. J. S. (PG); Pereira, S. G. (PQ); Marques, G. E. C. (PQ) IFMA

**QPN-026** **Oxidative evaluation of blends of soy oil, chia oil and coconut oil in biodiesel.** Pedraça, P. (IC); Silva, M. A. (IC); Souza de, M. L. (IC); Atala, A. P. (TC); Ávila, M. C. (IC); Fraga, I. M. (PQ); Souza, D. A. (PQ) IFMT

**QPN-027** **Atividade antiproliferativa de frações ricas em biflavonoides de espécies de Ouratea, Ochnaceae.** Fidelis, Q. C. (PQ); Perdomo, R. T. (PQ); Teixeira, J. V. S. (IC); Carvalho, M. G. (PQ) UFRRJ

**QPN-028** **Phenolic composition of a propolis type from Ceará-Brazil: study of different extraction techniques.** Frota, V. M. (IC); Dias, F. M. F. (IC); Santos, H. S. (PQ); Rodrigues, T. H. S. (PQ); Bandeira, P. N. (PQ); Vale, J. P. C (PQ) UVA

**QPN-029** **Evaluation of Syntetic Peptidomimetics as Cathepsin K Inhibitors.** Silva, T. L. (PG); Santos, D. A. (PG); Brömme, D. (PQ); Correia, A. G. (PQ); Vieira, P. C. (PQ) UFSCar

**QPN-030** **Extraction of species Mimosa Tenuiflora (Willd.) front of different ethanolic concentrations and temperature.** Morais, S. A. (PQ); Santos dos, J. (IC); Balliano, T. L. (PQ); Soletti, J. I. (PQ) UFAL

**QPN-031** **Chemical characterization and study of the antibacterial activities of the extract of the palm tree *Acrocomia aculeata* (Jacq) Lodd ex Mart.** Oliveira, A. I. T. (PG); Costa, R. F. (PG); Silva, J. F. M. (PQ); Pimenta, R. S. (PQ); Mahmoud, T. S. (PQ); Nascimento, G. N. L. (PQ); Morais, P. B. (PQ) UFT

**QPN-032** **Dereplication Study by HPLC-MS-MS and activity against *Leishmania chagasi* of the leaf extract of Trichilia emarginata.** Viegas, F. P. D. (PG); Espuri, P. F. (PG); Amaral, J. G. (PG); Marques, M. J. (PQ); Lopes, N. P (PQ); Soares, M. G. (PQ) UNIFAL

**QPN-033** **Avaliação da composição química, toxicidade, atividades antioxidante e antimicrobiana de extratos das folhas de *Doliocarpus dentatus*.** Almeida, T. A. F. (IC); Marcorini, L. F. B. (PQ); Cardoso, C. A. L (PQ) UEMS

**QPN-034** **Nutritional value, physicochemical and rheological parameters of pulp and by-products of buriti fruit (*Mauritia flexuosa*) after lyophilization.** Freire, J. A. P. (PQ); Araújo, R. O. (IC); Aquino, J. S. (PG); Campos, A. R. N. (PG); Viana, V. G. F. (PQ); Costa Júnior, J. S. (PQ); Moura, A. K. S. (PG); Citó, A. M. G. L. (PQ); Medeiros, S. R. A. (PG); Lima, A. C. S. (PQ); Oliveira, M. D.A. (PG); Ferreira, P. M. P. (PQ) IFPI

**QPN-035** **Avaliação fitoquímica da espécie vegetal Manilkara Subsericea (Mart.) Dubard.** Riehl, C. A. S.; Silva, A. A.; Gutierrez, E. D. P. M. (PG) UERJ

**QPN-036** **Avaliação da atividade antioxidante e viabilidade celular de extratos do fruto de *Guazuma ulmifolia* Lam. (mutamba).** dos Santos, M. N. G. (PG); Terezan, A. P. (PQ); da Silva, J. R. (PQ); de Azevedo, R. B. (PQ); Rabelo, D. (PQ); Kato, L. (PQ); de Oliveira, C. M. A. (PQ); Sartoratto, P. P. C. (PQ) UnB

**QPN-037** **Phytotoxic evaluation of agroindustrial vinasse residue in relation to *Lactuca sativa* and *Ipomoea purpurea*.** Luz, D. A (PG); Ferreira, P. S (IC); Simas, N. K (PQ); Gomes, A. C. C (PQ); Kuster, R. M (PQ) UFES

**QPN-038** **Evaluation of three methodologies to optimization of phycobiliprotein extraction in aqueous fraction of *Arthrospira platensis*.** Cavalcanti, L. P. A. N. (PG); Teixeira, C. M. L. L. (PQ); Martins, R. C. C. (PQ) INT

**QPN-039** **Chemical composition and biological activities of the leaves and stem of *Macrolobium rigidum* R.S. Cowan (Leguminosae).** Nascimento, B. O. (PG); David, J. M. (PQ); Santos, P. A. (PG); Araújo Neto, J.F. (PG); David, J. P. (PQ) UFBA

**QPN-040** **Identification of alkaloids from the stem bunch of the plant species *Annona tomentosa* R. E. Fr. (Araticum-bravo).** Pinheiro, A. A. (IC); Camara, M. B. P. (PG); Santos, J. R. J. (PQ); Rocha, C. Q. (PQ); Dias, G. O. C. (PQ) UFMA

**QPN-041** **Ocorrência de flavonoides e outros compostos fenólicos em folhas de *Casearia arborea* (Salicaceae).** Santos, A.L. (PG); Ferreira, M.J.P. (PQ); Soares, M.G. (PQ); Lago, J.H.G. (PQ); Sartorelli, P. (PQ) UNIFESP-Diadema

**QPN-042** **Evaluation of monoamine oxidase inhibitory potential of Erythrina verna alkaloids using zebrafish model.** Rambo, D. F. (PG); Biegelmeyer, R. (PQ); Toson, N. S. B (IC); Henriques, A. T. (PQ) UFRGS

**QPN-043** **Composição química e atividade antiparasitária in vitro de Nectandra barbellata Coe-Teixeira (Lauraceae).** Londero, V. S. (PG); Antar, G. M. (PG); Baitello, J. B. (PQ); Costa-Silva, T. A. (PG); Tempone, A. G. (PQ); Lago, J. H. G. (PQ) UNIFESP-Diadema

**QPN-044** **Chemical composition of cuticular waxes of Bignonieae species (Bignoniaceae).** Carvalho, J. C. S (PG); Lohmann, L. G. (PQ); Ferreira, M. J. P. (PQ) IB-USP

**QPN-045** **Evaluation of acaricidal activity of extracts of *Spilanthes acmella* (Jambu) against *Tetranychus urticae* and isolation of spilanthol.** Arrospide, T. M. (IC); Liesen, A. P. (PQ); da Camara, C. A. G. (PQ); Moraes, M. M. (PQ); Silva, M .M. (PG) UFRPE

**QPN-046** **Chemical study of Myrcia sylvatica (G. Meyer) DC. leaves.** Duarte, B. H. S.; Cascaes, M. M.; Guilhon, G. M. S. P.; Andrade, E. H. A.; Santos, L. S.; Delgado, J. P. S. (PG) UFPA

**QPN-047** **Method for isolation of flavonoids from *Solanum paludosum* with activity on the enzyme human topoisomerase II-alpha.** Oliveira, A.V.T. (IC); Silva, A.F.F. (IC); Silva, G.R (PQ); Camara, C.A. (PQ); Silva, T.M.S (PQ) UFRPE

**QPN-048** **Antichemotactic activity of Verbena montevidensis and brasoside.** Vestena, A. S. (PG); Soares, K. D. (PG); von Poser, G. L. (PQ); Zuanazzi, J. A. S. (PQ); Bordignon, S. A. L. (PQ); Apel, M. A. (PQ) UFRGS

**QPN-049** **Phytochemical screening of dried leaves of *Calea pinnatifida* (R. Br.) Less.** Amorim, J. M. (IC); Gama, R. M. (PQ); Armando Júnior, J. (PQ) FMABC

**QPN-050** **Avaliação in vitro da atividade antifúngica e prospecção fitoquímica da *Lafoensia pacari* (Mangaba Brava).** Santos, A.K.M. (IC); Carneiro, F.J.C. (PQ); Fonseca, A.S. (IC); Dias, E.J.S. (PG); Câmara, M.B.P. (PG); Cardoso, D.V.V. (PQ) IFMA

**QPN-051** **Semi-high resolution\α-glucosidase and PTP1B inhibition profiling for investigation of antidiabetic constituents in Picramnia bahiensis.** Gimenes, L. (PG); da Silva, M.F.G.F (PQ); Vieira, P.C. (PQ); Fernandes, J.B (PQ); Staerk, D. (PQ) KU

**QPN-052** **Estudo químico do extrato acetato da casca do fruto da *Pithecoctenium crucigerum* Gentry (Bignoniaceae).** Picro, K. G. (PG); Costa, M. B. (PQ); Pereira, E. T. V. (PG); Forim, M. R. (PQ) UEG

**QPN-053** **Prospecção fitoquímica e atividade antifúngica da espécie vegetal *Humiria balsamifera* (Mirim).** Marques, J. C. (IC); Câmara, M. B. P. (PG); Marques, G. E. C. (PQ); Filho, A. J. C. (PQ); Moraes, F. C. (PQ); Melo, A. L. M. (IC); Dias, E. J. S. (PG) IFMA

**QPN-054** **Atividade antioxidante por HPTLC-DPPH dos extratos de folhas, caule e raiz de *Pleonotoma jasminifolia* Kunth Miers. (Bignoniaceae).** Rodrigues, C. N. (IC); Rocha, W.C. (PQ); Yamaguchi, K. K. Lima (PQ) UFAM

**QPN-055** **Obtenção de álcoois através de bioreduções de carbonilados utilizando células íntegras de *Phaseolus lunatus* (feijão-fava).** Pereira, A. K. L. S. (PQ); Moraes, M. I. (PG); Saraiva, E. S. (PG); Vieira, E. C. (PQ); Bezerra, F. S. (PQ); Machado, L. L. (PQ); Nunes, F. M. (PQ); Lemos, T. L. G. (PQ) UFPI

**QPN-056** **SistematX, an online web-based cheminformatics tool for data management of secondary metabolites.** Scotti, M. T. (PQ); Herrera-Acevedo, C. (PG); Branquinho, T. O. (PQ); Costa, R. P. O. (IC); Santos, S. Y. K. O. (PG); Rodrigues, R. P. (PQ); Scotti, L. (PQ); Da-Costa, F. B. (PQ) UFPB

**QPN-057** **Antimicrobial activity of the lichen Usnea steineri and isolated compounds against phytopathogens.** Cintra, L. S. (PG); Sampaio, D. F. G. (IC); Vasconcelos, M. A. L. (TC); Tozatti, M. G. (PQ); Januário, A. H. (PQ); Pauletti, P. M. (PQ); Silva, M. L. A. (PQ); Martins, C. H. G. (PQ); Cunha, W. R. (PQ) UNIFRAN

**QPN-058** **In vitro cytotoxic potential of the crude extract of fungi derived from ascidians *Didemnum perlucidum* and *Botrylloides giganteum*.** Kellner Filho, L. C. (PG); Pimenta, L. P. (PG); Pedroso, R. C. N. (PG); Assis, R. N. A. (IC); Dos Anjos, E. O. (IC); Cosme, W. Z. (TC); Siqueira, K. A. (PG); Soares, M. A. (PQ); Tavares, D. C. (PQ); Januario, A. H. (PQ) UNIFRAN

**QPN-059** **Selective biotransformation of coumarins by *Cunninghamella elegans*.** Nascimento, J. S. (PG); Conceição, J. C. S. (PG); Nuñez, W. E. R. (PG); Cunha, S. (PQ); Silva, E. O. (PQ) UFBA

**QPN-060** **Dereplication of azaphilones from the Amazonian endophytic fungus *Penicillium sclerotium* by LC-QTOF-MS/MS and molecular networking.** Santiago, P. A. L. (PG); Guimarães, D. R. (IC); Souza, M. P. (PG); Angolini, C. F. F. (PQ); da Silva, F. M. A. (PQ); Costa, E. V. (PQ); de Souza, A. Q. L. (PQ); de Souza, A. D. L. (PQ); Koolen, H. H. F. (PQ) UEA

**QPN-061** **Ion mobility spectrometry combined with ultra-performance liquid chromatography/mass spectrometry for the study of natural products.** Carnevale Neto, F. (PQ); Egan, J. M. (PG); McFarlane, J. (PG); Costa-Lotufo, L. V. (PQ); Lopes, N. P. (PQ); Linington, R. G. (PQ) SFU

**QPN-062** **The role of secondary metabolites in structuring benthic communities in seaweeds of sandstone reefs on the coast of Pernambuco (Brazil).** Rosa Filho, J.S. (PQ); Alves, R.V.A. (IC); Rebouças, P.H.L. (IC); Silva, F.F. (PQ); Santana, A.L.B.D. (PQ); Carvalho, T.L. (IC); Nascimentov, V.M.S. (IC); Nascimento, M.S. (PQ) UFPE

**QPN-063** **Bioprospecting anticancer metabolites from Microsphaeropsis arundinis, an endophytic fungi from Paepalanthus planifolius.** Botero, W. B. (PG); Amorim, M. R. (PG); Polesi, M. C. (TC); Carlos, I. Z. (PQ); Santos, L. C. (PQ) IQAr-UNESP

**QPN-064** **Compounds identified by CG-MS in mycelium from Cercospora brachiata fungi.** Felisbino, J. K. R. P. (PG); Vieira, B. S. (PQ); Silva, N. A. (PG); Oliveira, A. (PQ); Sousa, R. M. F. (PQ) UFU

**QPN-065** **Chemical study of Aspergillus sp. (FSF06), a soil fungus from the forest of the Serra de Carajás.** Watanabe, L. A. (PG); Rocha, A. S. (IC); Souza, M. G. S (PG); Santos, A. S (PQ); Feitosa, A. O. (PG); Carvalho, J. M. (PG); Marinho, A. M. R. (PQ); Marinho, P. S. B. (PQ) UFPA

**QPN-066** **Chemical prospection of Humicola fuscoatra, an endophyte of marine red alga Asparagopsis taxiformis.** Mendonça, I. C. (PG); Honório, A. E. (PG); Medina, R. P. (PQ); Silva, D. H. S. (PQ) IQAr-UNESP

**QPN-067** **Metabolic production analysis of Hypoxylon investiens, an endophytic fungus isolated from the marine red algae Asparagopsis taxiformis.** Rufino, V. H. L. (PQ); Medina, R. P. (PG); Silva, D. H. S. (PQ) IQAr-UNESP

**QPN-068** **Doxycycline biodegradation by symbiotic bacteria from Diabrotica speciosa (Coleoptera: Chrysomelidae).** Madera, K.S.M. (IC); Durango, L.G.C. (PG); Lima, E.M. (PG); Martínez, O.C. (PQ); Forim, M.R. (PQ) UFSCar

**QPN-069** **A Novel Strategy for Heterologous Production of the Depsipeptide Ionophore Valinomycin.** Sigrist, R. (PG); Paulo, B. S. (PG); de Oliveira, L. G. (PQ) IQ-UNICAMP

**QPN-070** **Interações químicas de micro-organismos presentes no formigueiro das formigas cortadeiras: análise do metabolismo secundário do cocultivo do fungo mutualista, Leucoagaricus gongylophorus, com fungos negros.** Pereira, A. K. (PG); Zandonai, D. P. (PG); Pimenta, E. F. (PQ); Pagnocca, F. C. (PQ); Silva, M. F. G. F. (PQ); Forim, M. R. (PQ); Vieira, P. C. (PQ); Fernandes, J. B. (PQ) UFSCar

**QPN-071** **Potencial fitotóxico do extrato e da citocalasina H produzidos pelo fungo endofítico Diaporthe anacardii.** Romano, J R (IC); Biasetto, C R (PQ); Bolzani, V. S. (PQ); Araujo, A R (PQ) IQAr-UNESP

**QPN-072** **Bioreduções de aldeídos e cetonas utilizando Cucurbita moschata (abóbora) como biocatalisador para a produção de álcoois.** Nunes, F. M. (PQ); Moraes, M. I. (PG); Saraiva, E. S. (PG); Vieira, E. C. (PQ); Bezerra, F. S. (PQ); Machado, L. L. (PQ); Lemos, T. L. G. (PQ); Pereira, A. K. L. S. (PQ) UFPI

**QPN-073** **Synthesis of artesunic acid and dihydroartemisinin acetate and studies of *in vitro* activity against Schistosoma mansoni, BH strain.** Boaventura Jr., S. (PQ); Oliveira, R.N. (PQ); Corrêa, S.A.P. (PG); Allegretti, S.M. (PQ); Garcia, V.L. (PQ) UNICAMP

**QPN-074** **Bergenin from Peltophorum dubium: isolation and cytotoxicity and antioxidant activities of its chemical derivatives.** Silva Neto, O. C. (PG); Santos, P. A. (PG); Teodoro, M. T. F. (PG); Pinto, L. S. (PG); David, J. M. (PQ); David, J. P. (PQ) UFBA

**QPN-075** **Metabolomic analyses of Strongylodon macrobotrys (Leguminosae) and molluscicidal activity on Achatina fulica.** Pimenta, L. P. S. (PQ); Souza, B. A. (PG); Melo, N. O. (IC); Costa, F. M. P. (IC); Filho, J. D. S (PQ); Machado, A. R. T. (PQ) UFMG

**QPN-076** **Psychotria vellosiana Benth: A cyclotide-rich species.** Pinto, M. E. F. (PQ); Ciili, E. M. (PQ); Bolzani, V. S. (PQ) IQAr-UNESP

**QPN-077** **Ácidos aristoloquicos em chás de espécies de Aristolochia.** Silva, T (PQ); Pinto, A. C. M. (IC); Nascimento, I. R (PQ); Lopes, L. M. X. (PQ) IQAr-UNESP

**QPN-078** **Chemical composition of bufonids toads from Legal Amazonia.** Kerkhoff, J. (PG); Souza, E. B. R. (PG); Vasconcelos, L. G. (PG); Rodrigues, D. J. (PQ); Dall'Oglio, E. L. (PQ); Sinhorin, A. P. (PQ) UFMT

**QPN-079** **The citrus defense in response to phytopathogen Xylella fastidiosa.** Soares, M. S (PQ); Amaral, J. C (PG); da Silva, D. F (PG); da Silva, M. M (PG); da Silva, M. F. das G. F. (PQ); Fernandes, J. B. (PQ); de Souza, A. A. (PQ) UFSCar

**QPN-080** **Chemical composition and antiradicalar activity of pollen bee from *Melipona mandaçaia* Smith (Hymenoptera: Apidae).** Monteiro, A. L. B. (PG); Neto, J. F. (PQ); Silva, E. M. S. (PQ); Correia, R. C. (PQ); Camara, C. A. (PQ); Silva, T. M. S. (PQ) UFRPE

**QPN-081** **Analysis of geopropolis from the stingless bee Melipona subnitida (jandaira) by UHPLC-QTOF-MS/MS.** Souza, H. J. S. (IC); Cabrera, S. P. (PG); Silva, E. M. S. (PQ); Camara, C. A. (PQ); Silva, T. M. S. (PQ) UFRPE

**QPN-082** **Chemical composition and antioxidant potential of honey bee of abelha branca(Frieseomelitta doederleini).** Santisteban, M.R. (PG); Neto, F.J (PQ); Silva, S.M.E (PQ); Correia, C.R (PQ); Camara, A.C (PQ); Silva, S.M.T (PQ) UFPE

**QPN-083** **(Z)-octadec-9-enolide, a kairomone isolated from the Mediterranean flour moth (Anagasta kuehniella) frass.** Melo, D. J. (PG); Favaris, A. P. (PG); Vidal, D. M. (PQ); Bento, J. M. S. (PQ); Zarbin, P. H. G. (PQ) UFPR

**QPN-084** **Amino-naphthoquinones and isatins of *Salinispora arenicola*, a bacterium recovered from the marine sediments of St. Peter and St. Paul, Brazil.** Silva, A. B. (PG); Silveira, E. R. (PQ); Wilke, D. V. (PQ); Costa-Lotufo, L. V. (PQ); Torres, M. C. M. (PQ); Pessoa, O. D. L. (PQ) UFC

**QPN-085** **Avaliação da atividade anti-Trypanossoma. cruzi de alcaloides identificados em *Duguetia lanceolata*.** Dantas, E. P. (PG); Caldas, L. A. (PG); Lago, J. H. G. (PQ); Soares, M. G. (PQ); Tempone, A. G. (PQ); Sartorelli, P. (PQ) UNIFESP-Diadema

**QPN-086** **Dereplication strategies for discovering cytotoxic compounds from *Swinglea glutinosa* (Rutaceae).** Carvalho, A.C. (PG); Ribeiro, A.I (PG); Silva, M.F.G.F. (PQ); Medeiros, L.S. (PQ); Veiga, T.A.M. (PQ) UNIFESP-Diadema

**QPN-087** **Duguetinine, an isoquinoline-derived alkaloid with an unprecedented skeleton from the bark of *Duguetia surinamensis* (Annonaceae).** De Oliveira, R. N. (PG); Da Silva, F. M. A. (PQ); Baliza, I. R. S. (IC); Bomfim, L. M. (IC); Soares, M. B. P. (PQ); Bezerra, D. P. (PQ); Almeida, J. R. G. S. (PQ); Koolen, H. H. F. (PQ); Costa, E. V. (PQ) UFAM

**QPN-088** **Chemical, Cytotoxic and Antimalarial Study of Dipteryx lacunifera.** Alexandre, L. S. (IC); Chaves, M. H. (PQ); Vieira Junior, G. M. (PQ) UFPI

**QPN-089** **Elaboration of spectral library on HPLC-DAD and identification of chemical constituents in *Dipteryx lacunifera*.** Gomes, J. P. S. (IC); Chaves, M. H. (PQ); Vieira Junior, G. M. (PQ) UFPI

**QPN-090** **Phytochemical study of polar phases from *Richterago campestris* (Asteraceae).** Farinella, V. F. (PG); Tamayose, C. I. (PG); Roque, N. (PQ); Ferreira, M. J. P. (PQ) IB-USP

**QPN-091** **Chemodiversity of exudates from foliar surfaces of *Richterago discoidea* (Asteraceae).** Tamayose, C. I. (PG); Roque, N. (PQ); Ferreira, M. J. P. (PQ) IQUSP

**QPN-092** **Chemical characterization of antidiabetic active ethanolic extract from *Jatropha aethiopica* (Euphorbiaceae) leaves.** Gamiotea-Turro, D. (PG); Valerino-Diaz, A. B. (PG); Ortiz-Nuñez, Y. (PQ); Rinaldo, D. (PQ); Bosqueiro, J. R. (PQ); Camaforte, N. A. P. (PQ); dos Santos, L. C. (PQ) IQAr-UNESP

**QPN-093** **Acyl-glycosyl flavone from *Glandularia selloi* (Verbenaceae).** Vestena, A. S. (PG); von Poser, G. L. (PQ); Vignoli-Silva, M. (PQ); Castro-Gamboa, I. (PQ); Zuanazzi, J. A. S. (PQ) UFRGS

**QPN-094** **Phenolic compounds isolated from *Renealmia nicolaioides* rhizomes.** Gevú, K. V. (PG); Silva, I. G. (PG); Lima, H. R. P. (PQ); da Cunha, M. (PQ); de Carvalho, M. G. (PQ) UFRRJ

**QPN-095** **Identificação de ácido elágico e derivados das folhas de *Terminalia actinophylla* por ESI-ITMS.** Sousa, R. P. (PG); Araújo, B. Q. (PQ); Vieira Júnior, G. M. (PQ); Chaves, M. H. (PQ) UFPI

**QPN-096** **Genotoxic and mutagenic assessment of neolignans isolated from Nectandra leucantha on human melanoma cells.** Sousa, F. S. (PG); Nunes, E. A. (PG); Grecco, S. S. (PQ); Conserva, G. A. (PG); Cerchiaro, G. (PQ); Lago, J. H. G. (PQ) UFABC

**QPN-097** **Atividade antifúngica de quinoides isolados de *Pentacalia desiderabilis* (Vell.) Cuatrec. (Asteraceae).** Gomes, K. S. (PG); Murakami, C. (PG); Young, M. C. M. (PQ); Antar, G. M. (PQ); Ferreira, M. J. P. (PG); Sartorelli, P. (PQ); Lago, J. H. G. (PQ) UFABC

**QPN-098** **Butenolídeos com atividade anti-Leishmania isolados de *Nectandra oppositifolia* Ness & Mart (Lauraceae).** Conserva, G. A. A. (PG); Costa-Silva, T. A. (PG); Tempone, A. G. (PQ); Antar, G. M. (PG); Lago, J. H. G. (PQ) UFABC

**QPN-099** **Biological activities and identification of compounds of *Cordiera sessilis* Vell. (Kuntze).** UFU

**QPN-100** **Constituintes químicos isolados das partes aéreas de *Serissa foetida* (Rubiaceae).** Sebold, S.B.S (PG); Côrrea, J.G.S. (IC); Avincola, A.S. (PG); Pomini, A.M. (PQ); Santin, S.M.O (PQ) UEM

**QPN-101** **New steroidal saponins from Solanum paniculatum L. (Solanaceae) leaves.** Valerino-Diaz, A. B. (PG); Gamiotea-Turro, D. (PG); Zanatta, A. C. (PG); Vilegas, W. (PQ); dos Santos, L. C. (PQ) IQAr-UNESP

**QPN-102** **Influence of the decoction time in the extraction of the bioactive terpenes of white sucupira`s seeds (Pterodon emarginatus) in alcoholic beverages.** Oliveira, J.B. (IC); Ferreira, B.L. (IC); Machado, A. M. R. (PQ); Lucas, E.M.F. (PQ) CEFET-MG

**QPN-103** **Triterpenoides do caule de Tocoyena hispidula Standl.** Sousa, E. A. (PG); Rosa, A. P. A. (IC); Vieira-Júnior, G. M. (PQ); Chaves, M. H. (PQ) UFPI

**QPN-104** **Identification of bufadienolides and cytotoxic activity of *Rhinella jimi* venom.** Monção Filho, E. S. (PG); Chaves, M. H. (PQ); Sousa, R. P. (PG); Araújo, B. Q. (PQ); Ferreira, P. M. P. (PQ); Fonseca, M. G. (PQ); Pessoa, C. (PQ); Lima, D. J. B. (PQ); Vieira Júnior, G. M. (PQ) UFPI

**QPN-105** **Estudo fitoquímico e atividadefotoprotetora dos galhos de Platonia Insignis Mart. (Clusiaceae).** Aragão da Silva, A.G (IC); Moreira, R.A (IC); Freitas, Sâmya D.L (PQ); de Sousa, Renato P. (PG); Chaves, Mariana H. Chaves (PQ) UFPI

**QPN-106** **Clerodane and other terpenoids from Croton sacaquinha Croizat leaves.** Silva, E. S.; Sacramento, B. S.; Duarte, B. H. S.; Delgado, J. P. S.; Guilhon, G. M. S. P.; Santos, L. S.; Andrade, E. H. A. UFPA

**QPN-107** **Isoprenoides das folhas de Ephedranthus pisocarpus R. E. Fries.** Chaves, M. C. (PQ); Veras, M. D. A. (PG); Vieira Júnior, G. M. (PQ); Freitas, S. D. L. (PQ); Araújo, B. Q. (PQ) UFPI

**QPN-108** **Triterpenoides, Esteroides e ácidos graxos dos frutos de *Senna acuruensis* Benth.** Silva, L. F. F. (PG); Santiago, R. F. (IC); Vieira Júnior, G. M. (PG); Chaves, M. H. (PG) UFPI

**QPN-109** **Isolamento e caracterização de metabólitos secundários da fração hexânica da espécie vegetal *Machaerium brasiliense* Vogel (Fabaceae).** Silva, J.F. (IC); Peixoto, M.A. (PG); Jasper, J.O. (IC); Ximenez, G.R. (PG); Pastorini, L.H. (PQ); Pomini, A.M. (PQ); Santin, M.O. (PQ) UEM

**QPN-110** **Anti-inflammatory activity of friedelanes from *Maytenus robusta* branches.** Sousa, G. F. (PQ); Aguilar, M. G. (PG); Dias, D. F. (PQ); Moreira, M. E. C. (PQ); Vieira Filho, S. A (PQ); Duarte, L. P. (PQ) UFMG

**QPN-111** **Triterpenoides de Luehea divaricata Mart.\& Zucc.** SANTOS, L.F (PG); CHAVES, M.H (PQ); VIEIRA-JÚNIOR, G.M (PQ) UFPI

**QPN-112** **Estudo fitoquímico do extrato hexânico de galhos de Tontelea micrantha: isolamento do novo triterpeno friedelan-1,3,21-triona.** Ferreira, F. L. (PG); Silva, L. S.M. (IC); Duarte, L. P. (PQ); Vieira-Filho, S. A. (PQ); Pimenta, L. P. S. (PQ); Simões, M. O. M. (PQ) UFMG

**QPN-113** **Sesquiterpenos, diterpenos, p-cumaratos de alquenila e flavonóide das partes aéreas de *Baccharis retusa* (Asteraceae).** Barcellos, A.F. (PG); Ueno, A.K. (PQ); Grecco, S.S. (PQ); Sartorelli, P. (PQ); Guadagnin, R.C. (PQ); Romoff, P. (PQ); Ferreira, M.J.P. (PQ); Tcacenco, C.M. (PQ); Lago, J.H.G. (PQ) UFABC

**QPN-114** **Antitrypanosomal activity and evaluation of the mechanism of action of acetogenins from the seeds of *Porcelia macrocarpa* (Annonaceae).** Oliveira, E. A. (PG); Sartorelli, P. (PQ); Young, M. C. M. (PQ); Murakami, C. (PQ); Soares, M. G. (PQ); Tempone, A. G. (PQ); Costa-Silva, T. A. (PQ); Lago, J. H. G. (PQ) UNIFESP-Diadema

**QPN-115** **Potencial antiproliferativo em células tumorais humanas do alcaloide 4-N-óxido-harmano isolado da espécie *Psychotria schlechtendaliana*.** Corrêa, J. G. S. (IC); Peixoto, M. A. (PG); Moura, V. M. (PQ); Carvalho, J. E. (PQ); Ruiz, A. L. T. G. (PQ); Meurer, E. C. (PQ); Pomini, A. M. (PQ); Santin, S. M. O. (PQ) UEM

**QPN-116** **Evaluation of the effect on the mitochondrial membrane potential in *L. amazonensis* caused by Calealactone C isolated from Calea pinnatifida.** Caldas, L. A. (PG); Yoshinaga, M. L. (IC); Ferreira, M. J. P. (PQ); Lago, J. H. G. (PQ); Passero, L. F. D. (PQ); Sartorelli, P. (PQ) UNIFESP-Diadema

**QPN-117** **A bioguided study of the *Tabernaemontana catharinensis*: the indole alkaloids in focus.** Rosales, P.F. (PG); Cusin, Y.T. (IC); Canci, B.T. (PG); Roesch-Ely, M (PQ); Gower, A.C.E. (PQ); Silva, S.M. (PQ) UCS

**QPN-118** **Chemical composition and mineral content in monofloral bee pollen from *Elaeis guineensis*.** Gomes, A. N. P. (PG); Silva, G. R. (PQ); Santos, F. A. R. (PQ); Alves, R. F. (PQ); Camara, C. A. (PQ); Silva, T. M. S. (PQ) UFRPE

**QPN-119** **Untargeted metabolomics analysis of Asteraceae species, targeting glucose-uptake enhancing metabolites in C2C12 cells.** Jaiyesimi, O. A. (PG); Sampaio, I. H. (PG); Alberici, L. C. (FM); Vargas-Rechia, C. G. (FM); Gobbo-Neto, L. (FM) FCFRP-USP

**QPN-120** **Estudo fitoquímico do extrato hexânico das folhas de *Maytenus quadrangulata* (Celastraceae).** Aguilar, M. G. (PG); Sousa, G. F. (PQ); Duarte, L. P. (PQ); Filho, S. A. V. (PQ); Simões, M. O. M. (PQ) UFMG

**QPN-121** **Investigação das substâncias presentes nas frações apolares do extrato de uma amostra de própolis verde.** Pires, L. O. (PG); Castro, R. N. (PQ) UFRRJ

**QPN-122** **Copaifera reticulata and the antibacterial activity of the acidic diterpenes.** Rezende, C.R (PQ); Santos, D.G. (PG); Uekane, T. (PQ); Castro, V.S. (PG); Comte Junior, C.A. (PQ) UFRJ

**QPN-123** **Purification of bioactive natural Products by centrifugal partition chromatography (CPC).** Mandova, T.; Audo, G.; Michel, S.; Grougnet, R. Faculty of Pharmacy Paris Descartes

**QPN-124** **Citrus phytopathogens battle: A nature's story of chemical warfare and survival.** Costa, J. H.; Wassano, C. I.; Angolini, C. F. F.; Eberlin, M. N.; Fill, T. P. UNICAMP

**QPN-125** **Orbitides from Jatropha mollissima and their Synthetic Analogues as Inhibitors of Butyrylcholinesterase.** Ramalho, S. D.; Sanches, P. R. S.; Cilli, E. M.; Cardoso, C. L.; Bolzani, V. S.; Pinto, M. E. F.; Lima de, J. L.

# *QVE – Química Verde*

**QVE-001** **Greem synthesis of Ag nanoparticles using quercetin flavonoid: Synthesis and characterization by UV/VIS and FTIR techniques.** Rodrigues, D. R. F. (IC); Silva, V. I. (IC); Soares, J. J. (TC); Denardin, E. L. G. (PQ) UNIPAMPA

**QVE-002** **Deep eutectic solvents as functional additives for Starch-based films.** Maia, R. A. (IC); Araújo, A. C. L. (IC); Andrade, I. M. G. (IC); França, V. F. (IC); Morais, W. S. (PG); Costa, T. S. (TC); Moreira, D. N. (PQ) UFPB

**QVE-003** **Síntese de biodiesel metílico e de biodiesel etílico a partir do óleo de algodão.** Reolon, D. (IC); Lazarotto, G. (IC); Lencina Filho, P. S. D. (IC); Schneid, C. C. (PQ); Osti, R. Z. (PQ); Shimamoto, G. G (PQ); Tubino, M. (PQ); Silveira, E. L. C. (PQ) UFMT

**QVE-004** **Sustainable catalysts for organophosphate degradation: rice husk functionalization with hydroxamic acid groups.** Ferreira, J. G. L. (PG); Takarada, W. H. (IC); Orth, E. S. (PQ) UFPR

**QVE-005** **Recuperação de solventes orgânicos. Alternativa sustentável já praticada na UFRGS.** Dias, B.C. (IC); Leseux, E.J. (IC); Schwarz, F.W. (PG); Oliveira, G.V. (TC); Dias, S.L.P. (PQ); de Oliveira, E.R. (PQ) UFRGS

**QVE-006** **Development of starch-based films using a biofriendly ionic liquid as plasticizer.** Araújo, A. C. L. (IC); Costa, T. S. (TC); Sousa, A. S. B. (PG); Silva, S. M. (PQ); Moreira, D. N. (PQ) UFPB

**QVE-007** **Effect of deep eutectic solvents on the heating profile of sonicated organic solvents.** França, V. F. (IC); Maia, R. A (IC); Andrade, I. M. G. (IC); Morais, W.S. (PG); Costa, T.S. (TC); Moreira, D.N. (PQ) UFPB

**QVE-008** **How green additives affect the water heating profile under ultrasound irradiation: a methodological study.** Andrade, I. M. G. (IC); Maia, R. A. (IC); França, V.F. (IC); Morais, W.S. (PG); Costa, T.S. (TC); Moreira, D.N. (PQ) UFPB

**QVE-009** **Synthesis of esters and ketals from levulinic acid and alcohols obtained by heterogeneous catalysis with a sulfonic acid resin.** Behenck, L. S. (PG); Paula, F. H. M. (PG); Teixeira, A. T. (IC); Almeida, L. M. P. (IC); Lachter, E. R. (PQ) UFRJ

**QVE-010** **A Green Chemistry approach: pectin extraction of the pinion pell for use in synthesis of silver nanoparticles.** Schram, M. (IC); Takata, N. H. (PQ); Castro, E. G. (PQ) UNICENTRO

**QVE-011** **A renewable catalyst for a renewable chemical: gram scale conversion of furfural to furfuryl alcohol by carrots (Daucus carota).** Yamamoto, D.Y (IC); Filho, R.E.O (PG); Capeletto, M.G (PG); Omori, A.T (PQ) UFABC

**QVE-012** **Avaliação do uso de óleo vegetal de Crambe (Crambe abyssinica Hochst) como fluído isolante para transformadores elétricos.** Reis, A. C. C. S. (PG); Guedes, C. L. B. (PQ) UEL

**QVE-013** **Chemical waste treatment: importance of the academic community awareness about responsible disposal.** Morais, K.C. (IC); Paula, R.R. (IC); Pereira, R.S. (IC); Santos, J.M.S.R. (IC); Siqueira, L.D.F. (IC); Mesquita, I.S. (TC); Teixeira, A.M.S. (PQ) IFRJ-Campus Duque de Caxias

# TEC – Química Tecnológica

**TEC-001** **The chemical data science by scientific and technological knowledge in big data of the antiretrovirals patents.** Magalhães, J. L. (PQ); Mendes, F. M. L. (PQ); Antunes, A. M. S. (PQ); Hartz, Z. (PQ) FIOCRUZ

**TEC-002** **Niobium oxide and calcium oxide catalyzing the transesterification reaction of Acrocomia aculeate and Orbinya martiana oils.** Cubides-Román, D. C. (PQ); Constantino, A. F. (PG); Araújo de, M. C. (IC); Santos dos, R. B. (PQ); Neto, A. C. (PQ); Lacerda Jr., V. (PQ) UFES

**TEC-003** **Incorporation of benzimidazoles and benzothiazoles to urea: Preparations and effects on ammonia loss from urea.** Oliveira, B. G. F. (PG); de Fátima, A. (PQ); Cantarutti, R. B. (PQ) UFMG

**TEC-004** **Optimization of the transesterification reaction of soy oil catalyzed by sodium ethyleneglycoxide.** Santos, S. J. (IC); De Oliveira, M. K. (IC); Renner, R. E. (IC); Espíndola, G. C. (PG); Fontoura, L. A. M. (PQ); De Souza, G. (PQ); Priebe, G. P. S. (PQ) CIENTEC

**TEC-005** **Determination of physicochemical properties of biodiesel and blends using low-field NMR and multivariate calibration.** Constantino, A. F. (PG); Román, D. C. C. (PG); Santos, R. B. (PQ); Neto, A. C. (PQ); Barbosa, L. L. (PQ); Filgueiras, P. R. (PQ); Júnior, V. L. (PQ) UFES

**TEC-006** **Evaluation of sodium glyceroxide as catalyst in the oils and fats transesterification reaction.** Santos, S. J. (IC); Claro, M. N. (IC); Da Silva, J. A. (IC); Renner, R. E. (IC); De Castro, E. M. S. (IC); Fontoura, L. A. M. (PQ); De Souza, G. (PQ); Priebe, G. P. S. (PQ) CIENTEC

**TEC-007** **Effect of acetic acid on the pyrolytic sugar yield during fast pyrolysis from several biomasses type.** David, G. F. (PQ); Perez, V. H. (PQ); Fernandes, S. A. (PQ); Justo, O. R. (PQ); Lacerda Jr, V. (PQ) UFES

**TEC-008** **Colorimetric paper indicator associated with smarthphone for formaldehyde detection in milk based and personal care products.** Martins, G. B. C. (PG); Sucupira, R. R. (PG); Suarez, P. A. Z. (PQ) UnB

**TEC-009** **Ultrasound-assisted demineralization of sugar cane straw with hydrogen peroxide as pre-treatment for biofuel production.** Giacobe, K.; Silva, C. M.; Santos, D.; Flores, E. M. M.; Bizzi, C. A.; Motta, G. V. (PG) UFSM

**TEC-010** **Extraction and characterization of passion fruit and guava oils from industrial residual seeds and their application as biofuels.** Montenegro, M. A. (IC); Iha, O. K. (PG); Martins, G. B. C. (PG); Ehlert, E. (IC); Sucupira, R. R. (IC); Suarez, P. A. Z. (PQ) UnB

**TEC-011** **Continuous ethanol production in an ideal mixing reactor.** Silva, S, S, B, (IC); Armoa, M. H. (PQ); Meyer, W. R. (PQ) FATEC

# TEO – Química Teórica

**TEO-001** **Merging two coarse-grained force fields: Extension of the ELBA force field for dipeptides and lipopeptides through SIRAH force field.** de Souza, R. M. (PG); Dias, L. G. (PQ) FFCLRP-USP

**TEO-002** **Bonding Dissociation Energy of M-NO bonding on [Ru(L1)L2NO]n complexes.** Silva, S C (PQ); Santos, F B (IC) UFMT

**TEO-003** **Directional search algorithm for electrochemical oscillating time-series in a multidimensional parameter space.** Nagao, R.; Miranda, R. C. C. (PG) UNICAMP

**TEO-004** **Evaluation of the power conversion efficiencies of organic photovoltaic devices - theoretical investigation.** Miranda, G. M. (PG); Zanlorenzi, C. (PQ); Akcelrud, L. (PQ) UFPR

**TEO-005** **Conformational analysis of chalcone 1-(4-nitrophenyl)-2-propen-3-(4-hydroxy-3-methoxyphenyl)-1-one.** Guaringue, R. P (IC); Rozada, T. C. (PQ); Fiorin, B. C. (PQ) UEPG

**TEO-006** **Theoretical Study of Structural and Thermodynamic Properties for Ibuprofen Synthesis Mechanism.** Morgon, N. H. (PQ); Lima, L. V. C. (PG) IQ-UNICAMP

**TEO-007** **Análise computacional dos isômeros do Espiropirano e suas possibilidades de formar complexos de cobalto(II).** Furlani, C. S. (IC); Reis, I. F. (PG); Lopes, J. F. (PQ) UNIFEI

**TEO-008** **In silico methods applied in forensic science: simulated NMR spectra of new amphetamine- and cathinone-derived psychoactive substances.** Assis, V. O.; Fernandes, J.; Dias, G.; Bruni, A. T.; Pinke Rodrigues, C. H. (IC) FFCLRP-USP

**TEO-009** **Quantum mechanical molecular dynamics of liquid water - SCC-DFTB method reparametrized.** Lourenço, M. P. (PQ); Dos Santos, E. C. (PG); Pettersson, L. G. M. (PQ); Duarte, H. A. (PQ) UFMG

**TEO-010** **Topological study of interactions between some inhibitors and ALK-5 using QTAIM methodology.** Almeida, M. O. (PG); Faria, S. H. D. M. (PG); Honório, K. M. (PQ) UFABC

**TEO-011** **LC-wPBE: an appropriate DFT functional for a reliable description of transition energies in phthalocyanines.** Silva, L. H. F. (IC); Caixeta, B. P. (PG); Machado, A. E. H. (PQ) UFU

**TEO-012** **Inhibition mechanism of monoamine oxidase b by propargylamines: molecular docking and quantum-chemical approaches.** Cunha da, E. F. F. (PQ); Ramalho, T. C. (PQ) UFLA

**TEO-013** **Free energy profile of alkyl mesylate fluorination with CsF promoted by BACCA in tert-butanol solvent.** Pliego, J. R. (PQ) UFSJ

**TEO-014** **Computational evaluation of the effectiveness of Cu and Pt catalysts in the first steps of ethanol reforming.** Tormena, M. M. L. (PG); Pontes, R. M. (PQ) UEM

**Área:** AMB **Inscrição:** 00753

# Hidrocarbonetos policíclicos aromáticos (HPA) no material particulado (MP) do estado de Goiás

**Dênia Kássia A. Dal Castel (PG),[1] Ernando S. Araújo (TC),[2] Giselle R. de Melo (TC),[2] Roberta Cerasi Urban (PQ)[1,3*]**

**denia_castel@hotmail.com; roberta.urban@ufscar.br***

*[1]Instituto de Química, UFG; [2]SECIMA; [3] Departamento de Química, UFSCar*

Palavras Chave: *HPA, MP, Goiás.*

## Highlights

Polycyclic aromatic hydrocarbons (PAH) in particulate matter (PM) of Goiás State.

PAH were quantified in PM of Goiás State.
Carcinogenic compounds in the PM were higher than the limit set by WHO.

## Resumo/Abstract

Há mais de 100 diferentes HPA na atmosfera, sendo 16 deles considerados prioritários (USEPA), pois possuem características mutagênicas e/ou carcinogênicas.[1] O objetivo deste estudo foi quantificar HPA no MP de Goiás, e identificar suas fontes e implicações na saúde.

A soma das concentrações dos 24 HPA analisados nas amostras de MP de Goiânia variaram de 35,9 a 82,7 ng.m$^{-3}$ (48,4±13,6 ng.m$^{-3}$; n=10; Figura 1). Embora não tenham sido observadas diferenças significativas entre as concentrações dos HPA nos períodos seco e chuvoso, os maiores valores do índice benzo(a)pireno equivalente (BaPE) foram obtidos nos meses mais secos do ano (Figura 2).

A soma das concentrações de HPA nas amostras de Anápolis foram maiores e mais variáveis, 32,5 a 92,9 ng.m$^{-3}$ (61,7±20,2 ng.m$^{-3}$; n=10; Figura 1). Isto pode ser devido à proximidade entre o amostrador e uma rodovia. Neste sítio também não foram observadas variações sazonais nas concentrações de HPA, porém, diferente do observado em Goiânia, o valor do BaPE recomendado pela OMS foi ultrapassado (Figura 2).

O HPA mais abundante em ambos os sítios foi o fenantreno, que é proveniente de emissões por queima de combustíveis fósseis e incineração de resíduos.[1] Razões de diagnóstico serão calculadas para avaliar a possível fonte de emissão.

Neste trabalho também serão discutidas as possíveis causas das variações sazonais e anuais nas concentrações de HPA. Dados meteorológicos e comparações com outros sítios amostrais também serão incluídos.

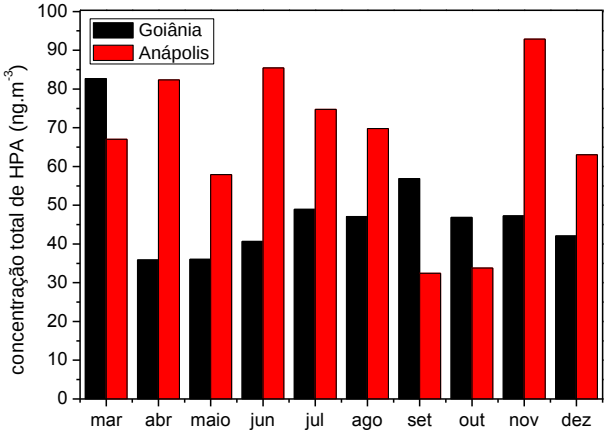


Figura 1. Concentrações totais de HPA no MP coletado em Goiânia e Anápolis.

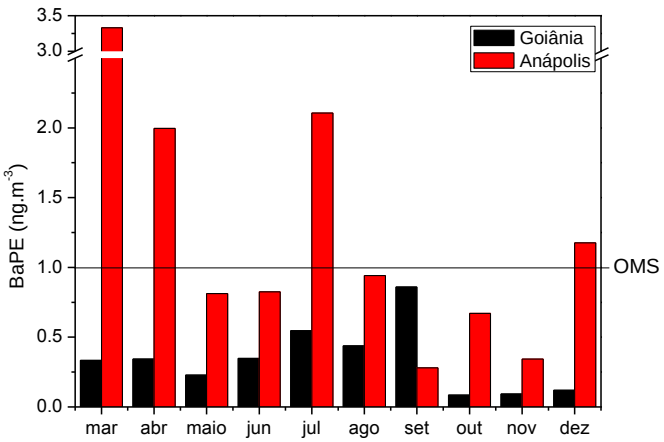


Figura 2. Índice BaPE calculado para as amostras coletadas em Goiânia e Anápolis.

[1]Dat, N.-D.; Chang, M.B. *Sci. Total Environ.* **2017**, *609*, 682.

**Área: AMB** **Inscrição: 01255**

# Evaluation of the Influence of the Toll Station Construction in BR-040 in Particulate Matter Concentrations

**Karmel Beringui O. Silva (PG)[1*], João Pedro R. Ribeiro (IC),[1] Enrique R. Dionisio (PQ),[1] Luiz Francisco P. G. Maia (PQ)[2] e Adriana Gioda (PQ),[1]**

**karmelberingui@gmail.com;**

[1]*Departament of Chemistry, PUC-Rio*
[2]*Departament of Meteorology, UFRJ*

*Keywords: PTS, Monitoring, Atmospheric Pollution*

## Highlights

Impact of works on the PTS levels.
Analysis of the metal content in particulate matter by ICP-MS

## Abstract

Highways cause considerable environmental impact due to the emissions generated by mobile sources, [1]. Works in roads contribute to additional impact in a region. Total suspended particles (TSP) are pollutants that can indicate the influence of these activities.[2] In June 2013, a new track on the BR-040, between Rio de Janeiro, RJ, and Juiz de Fora, MG, began to be built. Part of the works crosses the Parque Nacional da Serra dos Órgãos (PARNASO), an environmental preservation area. In order to evaluate air pollution, TSP samples were collected in 5 highway points near to the toll works and PARNASO, from 2014 to 2016.

The annual means of PTS and the sampling sites sampled are shown in Figures 1 and 2.

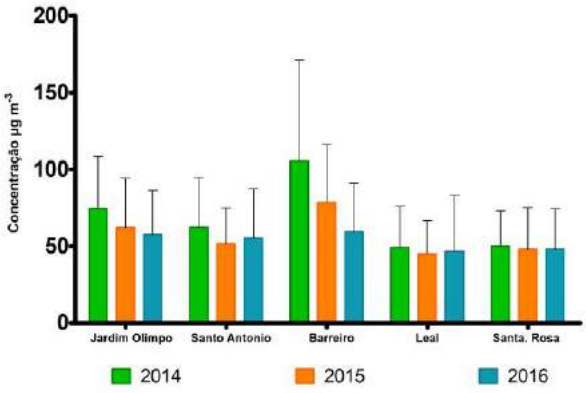


Figure 1 - Annual means of TSP

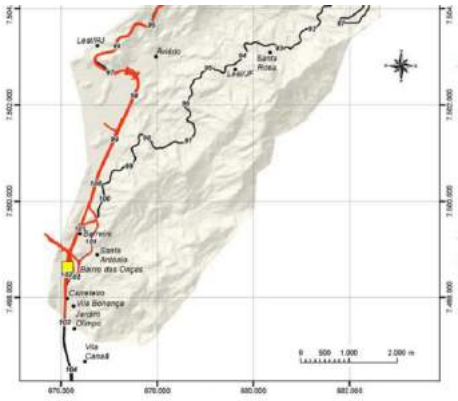

Figure 2 - Localization of sampling sites

The sampling sites Jardim Olimpo, Santo Antônio and Barreiro presented higher annual average concentrations, close to the CONAMA's limit (80 especially in 2014, when the toll was inaugurated. These sites are located very close to the toll, therefore the works contributed to the TSP levels. On the other hand, the sampling sites far from the toll (Leal and Santa Rosa) had little influence of the works and the PTS levels remained constant in the evaluated years. Preliminary results of metals in the TSP samples revealed high concentrations for Pb, Mn, V, Ni and Ti in the sampling sites close to the toll. These metals are related to vehicular emissions and the resuspension of soil dust.

[1] Pant, Pallavi, and Roy M. Harrison. *Atmospheric Environment* 2013, 77, 78-97.
[2] Joseph, Joshy, R. S. Patil, and S. K. Gupta. *Environmental monitoring and assessment* 2009, 159.1, 85-98.
[3] http://www.concer.com.br/Investimentos/NovaSubidadaSerra.aspx Acesso em 15 de janeiro as 10:18
[4] _____ CONAMA Resolution No 3, de June 28th, 1990.

**Área: AMB**
*(Inserir a sigla da seção científica para qual o resumo será submetido. Ex: ORG, BEA, CAT)*

**Inscrição:01424**
*(Inserir o número de inscrição do autor que fez a submissão)*

# Concentration of aliphatic and polycyclic aromatic compounds in atmospheric samples collected around a petrochemical site at São Paulo, Brazil.

**Sofia Caumo (PG)[1], Danilo Custódio (PQ)[2], Ana Vicente (PQ)[2], Célia Alves (PQ)[2], Pérola Vasconcellos Vasconcellos (PQ)[1*]**

sofia.caumo@usp.br

*[1]Institute of Chemistry – University of São Paulo - São Paulo, Brazil; [2]Department of Environment – University of Aveiro - Aveiro, Portugal.*

Key words: *Atmospheric particulate matter, Organic pollutants, Hopanes, n-Alkanes, PAH, Air quality*

## Highlights

Composition of atmospheric particulate matter •Industrial activities influencing air quality •Hopanes presented in crude and engine lubricating oil •The BaPEq indicates carcinogenic and mutagenic potential risks to human health.

## Abstract

Some of organic compounds emitted during incomplete combustion have adverse impacts on human health. *N*-alkanes and polycyclic aromatic hydrocarbons were abundantly emitted by fossil fuel combustion. The hopanes were presented in crude oil and engine lubricating oil.

Particulate matter samples and gaseous samples were collected simultaneously in 2015 at a site next to a petrochemical site located in Santo André city, metropolitan area of São Paulo. Samples were analyzed for elemental and organic carbon (EC and OC), hopanes, n-alkanes and polycyclic aromatic hydrocarbons (PAH). The range for total suspended particle (TSP) varied from 26 to 99 μg $m^{-3}$. One day before the sampling, it was reported a burning inside the petrochemical industry that probably it was affected the sample composition. Fifteen hopanes were identify in all the samples. The hopane with high concentration was C29αβ (2.2 ng $m^{-3}$) in PM and C27-Ts (1.6 ng $m^{-3}$) in PUF. The sum of isomers was greater for 17α(H), 21β(H) these results indicate that the hopanes were emitted by the petroleum completely mature (Alves et al., 2016).

The series of *n*-alkanes comprising between $C_{11}$ and $C_{35}$ were identify in all the samples. $C_{11}$ (40 ng $m^{-3}$) was predominant for PM and $C_{19}$ (105 ng $m^{-3}$) was majority for PUF. For the both phases, the compounds less than $C_{25}$ presented high concentration; petroleum residues commonly range between $C_{15}$ and $C_{26}$. For total *n*-alkanes concentration were 263 ng $m^{-3}$ and 453 ng $m^{-3}$ for PM and PUF, respectively. The carbon preferential index (CPI), a parameter to indicate a major contribution of petroleum residues in the samples, was 1.6 and 1.3 for PM and PUF, respectively. *N*-alkanes with influence of petroleum emissions present the CPI ~ 1 (Simoniet, 1984).

Fifteen PAH were quantify in this study. The PAH with low molecular weight were predominant in PUF, while high molecular weight were majority in PM phase. Phenanthrene presented the highest concentration (1.5 ng $m^{-3}$) in PUF and benzo(b)fluorantene was dominant (1.2 ng $m^{-3}$) in PM.

**Área: AMB**
*(Inserir a sigla da seção científica para qual o resumo será submetido. Ex: ORG, BEA, CAT)*

**Inscrição: 01310**
*(Inserir o número de inscrição do autor que fez a submissão)*

# Evaluation of Lead Exposure in Cooperative Recycling Workers

**Carlos Alberto Conde Regina(PG)[1], Danielle Zildeana Sousa Furtado(PG)[1], Juliana Naozuka(PQ)[1], Heron Dominguez Torres Silva(PQ)[1], Etelvino José Henriques Bechara(PQ)[2] and Nilson Antonio Assuncao(PQ)[1]***

**nilson.assuncao@gmail.com;**

*[1]Department of Chemistry, Institute of Environmental, Chemical and Pharmaceutical Sciences, Federal University of São Paulo, Diadema, São Paulo, Brazil; [2]Department of Chemistry. Institute of Chemistry, University of São Paulo, Sao Paulo, Brazil.*

Keywords: *LEAD CONTAMINATION, COOPERATIVE COLLECTORS, ELECTRONIC WASTE, RECYCLABLE MATERIALS, SOCIAL BEHAVIOUR.*

## Highlights

- Lead found in nails is correlated with aggressive tendencies;
- A socio-behavioural questionnaire was applied to evaluated workers;
- E-waste is the most common source of lead found in recycling cooperatives;
- Chemometric tools revealed behavioral changes related to lead levels.

## Resumo/Abstract

we report the presence and levels of lead (Pb) in electronic waste collected by recycling cooperatives, and in the collectors' fingernails working at the metropolitan city of São Paulo. Impacts of the metal exposure on the behavioural health of the collectors due to their chronic contact with lead and incorrect handling of electronic waste were verified. Lead (Pb) was determined in soils and in fingernails of collectors and cooperative employees. The analyses in cooperatives were conducted using Handheld X-ray Fluorescent (XRF) equipment, and the fingernails were analysed in a laboratory by graphite furnace atomic absorption spectrometry (GF AAS). A socio-behavioural questionnaire was applied to these workers to check if, in some way, the presence of lead in these workplaces interfered in their everyday behaviour. Exploratory and multivariate analyzes were applied to the data with the intention of checking convergence of behavioral variables and establish a regression model for correlation of behavioral parameters with lead levels. Concentrations of lead in situ were found to range from 10 to 10,000 ppm in routine places of such workers, and levels of 11,170-241,000 ppm were detected in electronic materials incorrectly stored on the field. In fingernails, lead amounts were found to range from (0.12 ± 0.04) to (94.13 ± 6.02) ppm. The methodology applied to evaluate the workers' behaviour displayed 40% with anxiety performance and depression, 38% with aggressive habits, 68% suffering from internalizing problems and 52% externalizing problems.

**[FAPESP, FINEP and CAPES]**

**Área: AMB** **Inscrição: 01298**

# Estudo das taxas de emissão de aldeídos provenientes de uma câmara de combustão com OEC sob excitação acústica

**Julia B. H. Cavalcante (IC),[1]* Astério R. B. Pereira (PQ),[1] Alex A. B. Santos (PQ),[1] Jeancarlo P. dos Anjos (PQ),[1,2] Lílian L. N. Guarieiro (PQ),[1,2]**

**jbhcavalcante@gmail.com**

*[1]Centro Universitário SENAI CIMATEC; [2]INCT de Energia e Ambiente, UFBA.*

Palavras Chave: *Aldeídos, Emissão, OEC, Excitação Acústica, Câmara de Combustão.*

## Highlights

Study of the emission rates of aldehydes from a combustion chamber with OEC under acoustic excitation.
* Formaldehyde showed no significant trend using the OEC technique;
* Acetaldehyde were reduced according to the equivalence ratio, but were increased with the presence of acoustic excitation.

## Resumo/Abstract

Os queimadores industriais são responsáveis por grandes impactos ambientais por se tratar de um equipamento de grande emissão de poluentes de compostos, destacando-se as emissões de compostos carbonílicos (CC). Dentre os CC emitidos, o formaldeído e acetaldeído têm relevância já que desempenham importante função na formação do ozônio e oxidantes fotoquímicos na atmosfera, além de serem considerados como carcinogênicos[1,2]. A técnica de Combustão Enriquecida por Oxigênio (OEC), ao ser estudada em queimadores, apresenta na literatura resultados com menor volume de gases de exaustão e, consequentemente, redução nas emissões de poluentes[3,4]. A técnica de combustão pulsante também apresenta uma diminuição nas emissões de poluentes gasosos de oxidação parcial e particulados[1]. Porém, estas duas técnicas ainda não foram estudadas concomitantemente na análise de emissão de aldeídos. Visto isso, o objetivo deste trabalho foi analisar as emissões de formaldeído e acetaldeído proveniente da queima de gás natural na câmara de combustão de modo a entender o efeito do teor de oxigênio e variação de amplitude sobre as taxas de emissão destes compostos. As análises dos CC foram realizadas utilizando cromatografia líquida de alta eficiência. As coletas seguiram o planejamento apresentado na Tabela 1. As análises demonstraram que as emissões de acetaldeído foram reduzidas conforme a razão de equivalência, porém foram aumentadas com a presença de excitação acústica (Fig. 1). O formaldeído não apresentou nenhuma tendência significativa.

**Tab. 1.** Planejamento experimental.

| Amostra | Razão de Equivalência | Amplitude (v) | Enriquecimento com O2 (%) |
|---|---|---|---|
| EXP1 | 1,3 | 0 | 21 |
| EXP2 | 1,3 | 5,3 | 21 |
| EXP3 | 1,3 | 5,3 | 30 |
| EXP4 | 1,3 | 0 | 30 |
| EXP5 | 0,7 | 0 | 21 |
| EXP6 | 0,7 | 5,3 | 21 |
| EXP7 | 0,7 | 5,3 | 30 |
| EXP8 | 0,7 | 0 | 30 |
| EXP9 | 1 | 2,65 | 25 |

**Fig. 1.** Resultado da Razão de formaldeído e acetaldeído

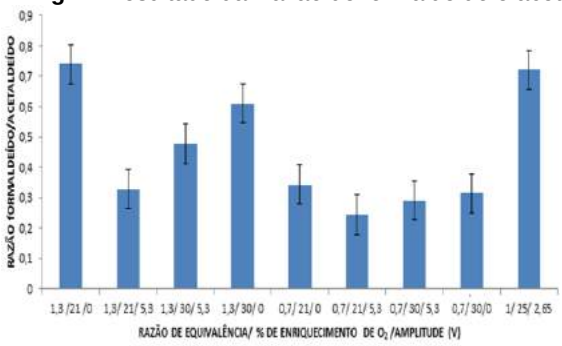


[1] PEREIRA, A. *et al*. Desenvolvimento de protótipo experimental para o estudo da correlação da OEC e excitação acústica em chamas confinadas de gás natural. In: CONGRESSO NACIONAL DE ENGENHARIA MECÂNICA, 9., 2016, Ceará.

[2] GUARIEIRO, L. *et al*. Acetaldehyde and formaldehyde concentrations from sites impacted by heavy-duty diesel vehicles and their correlation with the fuel composition: Diesel and diesel/biodiesel blends. **Fuel.** v.92. p. 258-263, 2012.

[3] BAUKAL JR. C. **Oxygen-Enhanced Combustion**. Nova Iorque: CRC Press, 1998.

[4] SANTOS, Alex A. B. et al. Avaliação das Taxas de Emissão de Formaldeído e Acetaldeído em Chamas de Gás Natural Confinado com OEC. **Revista Virtual de Química.** v.8. p. 1181-1191, 2016**.**

**Área: AMB** **Inscrição:_1044_____**
*(Inserir o número de inscrição do autor que fez a submissão)*

# The impact of Tijuca Forest in the mitigation of $CO_2$.

**Cleyton M. da Silva (PQ),[1,2]* Thainá de C. e Souza (IC),[3] Taisa C. Dantas (IC),[3] Luane L. da Silva (IC)[2], Sergio M. Corrêa (PQ),[3] Graciela Arbilla (PQ).[1]**

**martins.cleyton@gmail.com**

*[1]Instituto de Química UFRJ; [2]Universidade Veiga de Almeida, Campus Maracanã; [3]Faculdade de Tecnologia UERJ*
Key words: *Greenhouse Gases*, *Global Warming*, *Anthropocene, Great Aceleration, $CO_2$ mitigation.*

## Highlights

Tijuca Forest is surrounded by the city. $CO_2$ concentrations suggest that the forest acts as a carbon sink. Compacted forests, mainly re-forested areas, seem important in the process of carbon capture.

## Resumo/Abstract

Mankind's growing influence on the environment has raised exponentially during the past three decades leading to a substantial change in the Earth system and supporting the concept of Anthropocene.[1] The increasing concentrations of greenhouse gases (GHG), the processes leading to $CO_2$ capture and the mitigation of GHG concentrations to control global warming, are of high concern. In this study, the concentrations of $CO_2$, $CH_4$ and $N_2O$ were determined in several locations of Tijuca Forest (Figure 1) and compared with concentrations in the non-vegetated areas of the city of Rio de Janeiro. Tijuca Forest, with 39,51 $km^2$, is the largest secondary urban rainforest in the world and represents a source of leisure, clean water and air, contributing to the regulation of climate.

GHG were determined using the method implemented and described by Silva *et al.*[2] $CO_2$, $CH_4$ and $N_2O$, within the forest, were in the range of 389-419 ppmv, 1,61-1,76 ppmv and 318-335 ppbv, respectively. $CH_4$ and $N_2O$ determined concentrations are in the same range of values reported worldwide. $CO_2$ levels within the forest were similar to those determined in the Botanical Garden of Rio de Janeiro (357-412 ppm) and several residential and commercial districts (411-413 ppm). $CO_2$ levels in Rio de Janeiro (both in the forest and in the urbanized area) were >10% lower than those determined in another Brazilian cities (531-542 ppm in winter and 407-441 ppm in summer).[3] These results suggest the important role of the forest in the process of carbon capture.

Figure 1. sampling locations within Tijuca Forest.

References

1. Crutzen, P. J.; Stoermer, E. F. *Global Change Newsletter* **2000**, *41*, 17.
2. Silva, C. M.; Corrêa, S. M.; Arbilla, G. *Journal of the Brazilian Chemical Society* **2016**, *27*, 778.
3. Moreira Júnior, D.P.; Silva, C. M.; Bueno, C.; Corrêa, S. M.; Arbilla, G. *Revista Virtual de Química* **2017**, *9*, 2032.

**Área: AMB** **Inscrição:_1040_____**
*(Inserir o número de inscrição do autor que fez a submissão)*

# Carbonyl Compounds in Tijuca Forest, the largest secondary urban rainforest in the world, and Rio de Janeiro urban area.

**André Braga (PG),[1] Bruno Siciliano (PG),[2] Guilherme Dantas (PG),[2] Cleyton M. da Silva (PQ),[1,2] Graciela Arbilla (PQ).[2]***

**gracielaiq@gmail.com**

[1]*Universidade Veiga de Almeida, Campus Maracanã;* [2]*Instituto de Química UFRJ*
Palavras Chave: *Carbonyl Compounds*, *Pollution Mitigation*, *Urban Forest, Land-use, Reforestation.*

## Highlights

Tijuca Forest is a protected area surrounded by the city of Rio de Janeiro. Carbonyl compounds concentrations suggest that the forest acts as a sink for pollutants. Anthropogenic emissions impact the forest.

## Resumo/Abstract

Atmospheric concentrations of carbonyl compounds (CC) were determined in Tijuca Forest, the largest secondary urban tropical forest in the world, and in a commercial and residential district of the city of Rio de Janeiro (Tijuca). A total of 40 samples was collected using C18 resin cartridges, coated with 2,4-dinitrophenylhydrazine, and analysed by high performance liquid chromatography (HPLC) with a diode array UV-Vis detector, as described in TO11A Method.[1] Within Tijuca Forest, formaldehyde (F) and acetaldehyde (A) levels were in the range of <detection limit – 2,76 and <detection limit – 3,25 μg $m^{-3}$, respectively. In the urban non-vegetated area, values were in the range of of 1,15 – 6,88 and 1,22 – 4,22 μg $m^{-3}$, respectively. Mean values are presented in Table 1.

**Table 1**. Mean concentrations values for formaldehyde, acetaldehyde and total CC (in μg $m^{-3}$)

| | Formaldehyde (F) | Acetaldehyde (A) | F/A ratio |
|---|---|---|---|
| Tijuca Forest, N=24 | 0,97±1,01 | 0,93±1,06 | 1,04 |
| Tijuca (Saens Peña Square), N=16 | 3,09±1,61 | 2,78±0,91 | 1,11 |

Distance between Tijuca Forest and Saens Peña Square is approximately 10 km. Concentrations were not correlated with solar radiation. Also F/A ratios are similar for the three locations and literature values for downtown in Rio de Janeiro.[2] These results indicate that biogenic emissions of CC are low in comparison to anthropogenic emissions and the CC determined within the forest are mainly due to transport for the city. The lower values determined in Tijuca Forest suggest that the forest is a sink of atmospheric pollutants and reinforce the importance of compacted forested areas, mainly secondary forest and re-forested areas in the improvement of urban air quality.

References:
1. *Compendium Method TO-11A. Determination of Formaldehyde in Ambient Air Using Adsorbent Cartridge Followed by High Performance Liquid Chromatography (HPLC)*. EPA-625/R-96/010b. US Environmental Protection Agency, Cincinnati, OH, **1997**.
2. Corrêa, S. M.; Arbilla, G.; Martins, E. M.; Quitério, S. L.; Guimarães, C. de S.; Gatti, L. V. *Atmospheric Environment*, **2010**, *44*, 2302.

**Área: AMB** **Inscrição: 01032**

# Hourly isoprene concentrations in an urban forest, São Paulo megacity

**Tailine C. Santos (PG)[1], Pamela A. Domonitti (PQ)[1,2], Thiago Nogueira (PQ)[1], Adalgiza Fornaro* (PQ)[1]**

**adalgiza.fornaro@iag.usp.br**

*[1]Departamento de Ciências Atmosféricas, IAG-USP, São Paulo; [2]Laboratoire de Météorologie Physique LaMP- CNRS, UBP, France*

Key words: Atmospheric Chemistry, Biogenic Hydrocarbons, Air Pollution, Monoterpenes, Urban Forest, Online GCFID.

## Highlights

In urban environment, green areas have usually been associated with several benefits.
Trees, emitting isoprene contribute for the ozone and secondary organic aerosol production.
Isoprene react with $O_3$.

## Resumo/Abstract

Isoprene is the most abundant HC produced by vegetation, but is also produced by anthropogenic processes, as fuel burning. Their biogenic emissions are controlled by photossynthetically active radiation (PAR) and air temperature (Guenther et al., 1995; Finlayson-Pitts and Pitts, 1999). São Paulo megacity (MASP) has presented serious air pollution problems, mainly ozone and fine particulate matter. This study aims to evaluate the isoprene in an urban forest in MASP.

The sampling site was located inside the University of São Paulo (USP), in the western region of MASP, it is a little green-park (~7.5 $km^2$), with traffic along the day, and surrounded by important roads with intense traffic of vehicles. Isoprene was measured by an on-line TD-CG-FID Perkin Elmer system from 2012 to 2015, reaching 5789 samples hourly.

The isoprene maximum mixing ratios was observed in summer (average 1.19 ppbv), presenting the hourly variability characteristic from biogenic emissions with maximums from 9 am to 4 pm, but not in the other seasons (Fig. 1a). The isoprene decreasing in the presence of ozone (Fig. 1b), is explained by the reactions between them. It was also possible to observe that isoprene presented different profile from NOx and NO, being the isoprene concentrations increasing continuously after 10 am (Fig. 1 b), indicating different sources.

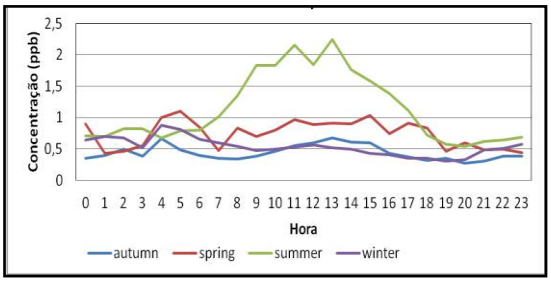


a

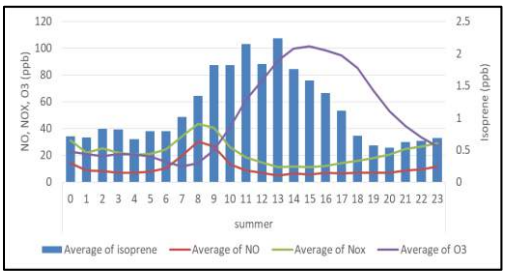


b

**Figure 1.** Hourly profile of isoprene mixing ratios compared among seasons (a) and also with ozone, NO and NOx (b).

These results showed the conditions complexity controlling the atmospheric isoprene concentrations in the urban forest, including seasonality, sources, meteorological conditions and pollutants.

Finlayson-Pitts, B.J.; Pitts, J.N, Chemistry of the Upper and Lower Atmosphere: Theory, Experiments, and Applications, 1999.

Guenther et al., J. Geophys. Res., 100, 8873–8892, 1995.

**Área: AMB** **Inscrição:00970**

# Contaminants in the gas phase, in the atmosphere of the Todos os Santos Bay - Ba.

**Franciele O. Santana (PG)*, Juliana L. Barbosa (PG), Anne V. S. de Brito (IC), Vânia P. Campos (PQ)**

**vpalmeiracampos@gmail.com; francieleufba@hotmail.com**

*Instituto de Química, Departamento de Química Analítica - Universidade Federal da Bahia - UFBA*

Keywords: *Atmospheric Contaminants, Passive Sampling, Todos os Santos Bay*

## Highlights

Air quality assessment at low cost.
Atmospheric pollutants in the Todos os Santos Bay.
Benzene and formaldehyde exceeding recommended values.

## Abstract

Air pollution is a concern due to well-established adverse effects on human health. It was considered in 2015 by the World Health Organization to be responsible for 6.4 million deaths worldwide. The Todos os Santos Bay, the largest on the Brazilian coast, with 1,052 km$^2$, is perhaps the largest receptor of the atmospheric pollutant load of the anthropic activities in the Recôncavo of Bahia, which comprises the lands around it, where there are important sources of urban and industrial emissions. This work evaluated, in 5 points, concentrations of 16 contaminants/pollutants in the atmosphere of the Todos os Santos Bay, using passive sampling. At each sampling point, *AnaliseAr* kits were used (www.analisear.com.br) in partnership with *INCT-E&A*, with measurements in triplicate, per 10-days exposure period. The mean value of the five sample points (Table 1) was found as 1.15 µg m$^{-3}$ for benzene, a volatile organic pollutant considered carcinogenic, exceeds the annual average value limited in 2012 by Canadian Air Quality Criteria (0.45 µg m$^{-3}$), which aims to protect the health of populations, with the highest value (1.7 µg m$^{-3}$) obtained in Madre de Deus. The average concentration of formaldehyde (3.4 µg m$^{-3}$) is in the limit indicated in 2014 by the Texas Environmental Quality Commission, USA (3.3 µg m$^{-3}$). The concentration levels of the other contaminants measured were found to be normal.

**Table 1 - Atmospheric contaminants/pollutants concentrations (µg m$^{-3}$). Todos os Santos Bay (April/2016)**

| Site | Convencional | | | Nitrogenated | | | | Carbonyls | | Carboxylics | | Volatile Organic Compounds | | | | |
|---|---|---|---|---|---|---|---|---|---|---|---|---|---|---|---|---|
| | $SO_2$ | $NO_2$ | $O_3$ | $HNO_3$ | $NH_3$ | NO | NOx | $CH_3COH$ | HCOH | $CH_3COOH$ | HCOOH | Benzeno | Tolueno | Etil-benzeno | o-Xileno | m,p-Xileno |
| Madre de Deus | 2.73 ± 0.23 | 6.66 ± 0.15 | 17.2 ± 1.4 | 1.66 ± 0.48 | < 1.1 - | 0.310 ± 0.21 | 6.71 ± 0.39 | 2.15 ± 0.40 | 2.78 ± 0.93 | 1.45 ± 0.33 | 1.21 ± 0.030 | 1.72 ± 0.040 | 2.71 ± 0.060 | 1.05 ± 0.010 | 0.900 ± 0.030 | 1.70 ± 0.070 |
| São Francisco do Conde | 8.24 ± 0.11 | 8,00 ± 1.1 | 6.99 ± 0.12 | 0.710 ± 0.15 | 1.23 ± 0.080 | 0.66 ± 0.06 | 8.41 ± 0.22 | 2.42 ± 0.31 | 3.23 ± 0.53 | 1.64 ± 0.14 | 1.26 ± 0.060 | 0.95 ± 0.040 | 2.01 ± 0.25 | 0.920 ± 0.15 | 0.875 ± 0.15 | 1.44 ± 0.050 |
| Salvador | 1.12 ± 0.17 | 10.71 ± 0.70 | 6.88 ± 0.15 | < 0.28 - | 1.71 ± 0.50 | 1.01 ± 0.11 | 11.9 ± 0.39 | 3.22 ± 0.53 | 4.93 ± 0.46 | 2.59 ± 0.66 | 7.71 ± 0.020 | 0.87 ± 0.030 | 1.43 ± 0.060 | 0.678 ± 0.040 | 0.802 ± 0.030 | 1.35 ± 0.23 |
| Itaparica | 2.51 ± 0.03 | 7.41 ± 0.37 | 1.09 ± 0.010 | < 0.28 - | < 1.1 - | 1.03 ± 0.71 | 8.68 ± 0.090 | 4.40 ± 0.54 | 3.00 ± 0.90 | 2.90 ± 0.60 | 2.12 ± 0.060 | 1.30 ± 0.030 | 1.24 ± 0.25 | 0.678 ± 0.04 | 0.877 ± 0.050 | 0.616 ± 0.050 |
| Salinas das Margaridas | 4.29 ± 0.53 | 5.47 ± 0.27 | 6.92 ± 0.050 | < 0.28 - | < 1.1 - | 0.463 ± 0.19 | 6.12 ± 0.45 | 4.73 ± 1.1 | 2.37 ± 1.1 | 5.33 ± 0.84 | 1.49 ± 0.060 | 0.92 ± 0.070 | 1.20 ± 0.19 | 0.732 ± 0.060 | 0.757 ± 0.080 | 0.700 ± 0.040 |
| **MEAN** | **3.78** | **7.65** | **7.82** | **0.560** | **0.940** | **0.700** | **8.37** | **3.38** | **3.26** | **2.79** | **2.76** | **1.15** | **1.72** | **0.810** | **0.840** | **1.16** |
| CONAMA 003/90 | 40 /80 | 100 | 160 | | | | | | | | | | | | | |
| Guidelines | 55 [b] 20 [c] | 55 [b] 200/h | 40 [b] 120/8 h | 35 [b] | 100 [b] | | 30 [c] | 90 [d] | 3.3 e 15d.1 100/30 min | | | 20 [b] | 0.45 b 5 c; 1.7 e.2 | 260/week | | |

**a:** CONAMA 003/90. **b:** OME. Ontario Ministry of the Environment. Ambient Air Quality Criteria (AAQCs), 2012. **c:** EC-Directive 2008/50/EC of the European Parliament and of the Council of 21 May 2008 on ambient air quality and cleaner air for Europe. **d:** USA. Texas Commission on Environmental Quality, 2014. **e:** World Health Organization. Air Quality Guidelines for Europe. 2nd Ed, 2000. **1:** For short or long exposure, respectively **2:** Associated with the risk of leukemia: 1 / 100.000.

**Área: AMB** **Inscrição: 00700**

# Characterization of the morphological and mineral composition of total suspended particles collected in an urban area by SEM-EDS

**Rennan Geovanny O. Araujo (PQ),[1*] Silvânio Silvério L. Costa (PQ),[2] Jeferson C. Alves (FM),[2] Vaniele S. Ribeiro (PG),[1,3] Carlos Alexandre B. Garcia (PQ),[2] Gisele O. da Rocha (PQ).[1]**

**E-mails: rgoa01@terra.com.br* and silvanioslc@yahoo.com.br**

*[1]Instituto de Química, Campus Ondina, UFBA, Salvador/BA; [2]Núcleo de Petróleo e Gás, Campus São Cristóvão, UFS, São Cristóvão/SE; [3]Instituto Federal Baiano, Campus Guanambi, Guanambi/BA.*

Keywords: Total suspended particles, Urban area, Trace elements, Morphological, Mineral composition.

## Highlights

Variability of total suspended particles (TSP) concentration through a shift (intra-day) and temporal (inter-month) evaluation. Determination of the morphological and chemical composition of particles by SEM-EDS.

## Resumo/Abstract

Coastal urban centers are been affected by atmospheric emissions mainly from vehicle traffic, but also from natural sources, such as marine aerosols. Therefore, knowledge about the main sources of emission, periods with higher emission flux, as well as the morphology and chemical composition of the particles are opportune. Simultaneous sampling of total suspended particles (TSP) were performed in three shifts of eight hours each one, throughout 24 hours periods, with considerable variability between shifts (intra-day) and time (inter-month) (Figure 1). The TSP samples were collected in urban area of São Cristóvão city, Sergipe State, Brazil. Particles of biogenic origin (pollen), which act as carriers of secondary aerosols, were identified, even as particles of geological origin, from the soil resuspension, and especially soot particles from burning fossil fuels, through analysis by scanning electron microscopy and energy dispersive X-ray spectrometry (SEM-EDS) (Figure 2). Analysis by EDS showed mainly particles from earth's crust (Al, Si, Fe, K, Ca, Mg) and particles rich in carbon (soot). The characterization proved to be an important tool for identification of probable emission sources, collaborating to design strategies for control and prevention of air pollution in urban centers.

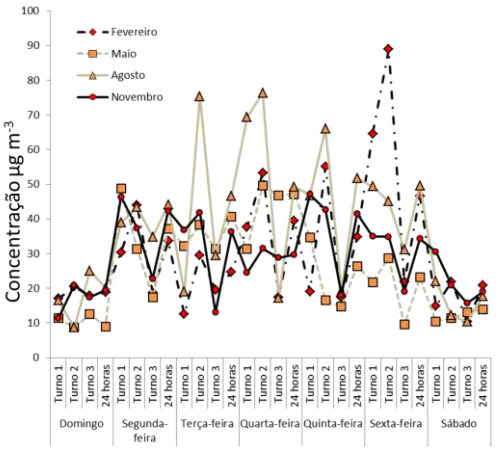


**Figure 1.** Concentration of TSP in the air, with sampling in 24 h periods and in fractionation.

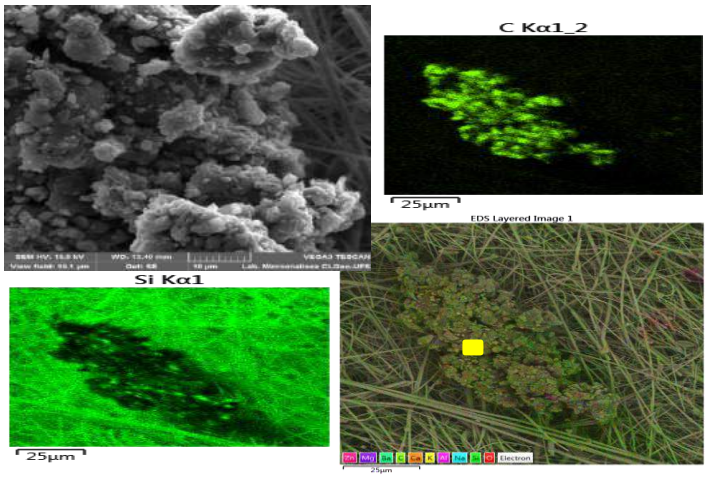


**Figure 2.** Micrograph and EDS analysis of a coarse particle cluster of soot in TSP with mapping.

[1]Sachdeva, K. & Attri, A. K. *Atmospheric Environment*, 42, 1025-1034, 2008.

[2]Chithra, V. S. & Nagendra, S. M. S. *Atmospheric Environment*, 77, 579-587, 2013.

[3]Alves, D. D.; Osório, D. M. M.; Rodrigues, M. A. S.; Illi, J. C.; Bianchin, L.; Benvenuti, T. *Brasilian Journal of Biology*, 75, 43-52, 2015a.

**Área: AMB** **Inscrição: 00558**

# Hidrocarbonetos policíclicos aromáticos em águas do complexo lagunar de Jacarepaguá, Rio de Janeiro, RJ

**Thallis M. Souza (PG),[1] Rodrigo L. Sobrinho (PQ),[2] Marcelo C. Bernardes (PQ),[2] Annibal D. Pereira Netto (PQ),[1,3]***

**annibal@vm.uff.br**

*[1]Programa de Pós-graduação em Química, Instituto de Química, UFF, Niterói, RJ; [2]Departamento de Geoquímica, IQ, UFF; [3]Departamento de Química Analítica, IQ, UFF*

Palavras Chave: HPAs, Águas superficiais, Monitoramento, Poluição ambiental

## Highlights

Determination of polycyclic aromatic hydrocarbons (PAHs) in water from the Jacarepaguá lagoon system, Rio de Janeiro, Brazil. Highest PAH concentrations were found during the dry season. PAH concentrations were lower in the lagoons than rivers.

## Resumo/Abstract

As principais fontes dos hidrocarbonetos policíclicos aromáticos (HPAs) são a emissão veicular e industrial, de forma que, em áreas urbanas, os ambientes aquáticos são diretamente impactados por drenagem superficial e deposição atmosférica[1]. O objetivo deste trabalho foi determinar as concentrações de 18 HPAs, (os 16 prioritários da EPA, além de benzo(e)pireno e perileno), nas águas do complexo lagunar de Jacarepaguá, na cidade do Rio de Janeiro. Foram realizadas três coletas, nos meses de março, junho e novembro de 2017. Amostras de água não filtradas foram extraídas com hexano (4 etapas) usando metodologia previamente desenvolvida e validada, após adição de solução contendo seis padrões internos perdeuterados.[2] Os extratos de cada amostra foram combinados e concentrados em evaporador rotativo a 40°C com troca de solvente para tolueno, obtendo-se uma solução final de 1,0 mL. HPAs foram determinados nestes extratos por cromatografia a gás de alta resolução com detecção por espectrometria de massas (HRGC-MS) e monitoramento d os respectivos íons de peso molecular de cada HPA (Tabela 1). Curvas analíticas entre 0,25 e 50 μg $L^{-1}$ foram preparadas com bons coeficientes de correlação linear. As concentrações totais dos HPAs foram maiores no período com menor deposição pluviométrica (novembro), (Figura 1). Em média, os rios que deságuam no complexo lagunar apresentaram concentrações maiores devido à drenagem superficial. Além de HPAs, outras classes de substâncias estão sendo avaliadas naquele complexo lagunar para avaliar o impacto antrópico nas águas da região.

Tabela 1. Condições usadas na determinação dos HPAs.

| HRGC-MS | |
|---|---|
| Coluna | DB17-MS (30 m x 0,25 mm x 0,25 μm) |
| Injeção | Modo *splitless* |
| T injetor | 350 °C |
| Rampa de Aquecimento | 60°C (1 min)<br>60-230°C a 40°C $min^{-1}$ (1 min)<br>230-260°C a 4°C $min^{-1}$ (1 min)<br>260-310°C a 4,5°C $min^{-1}$ (1 min)<br>310°C (2 min) |
| Gás de arraste | He a 1,0 mL $min^{-1}$ |
| T interface | 310°C |

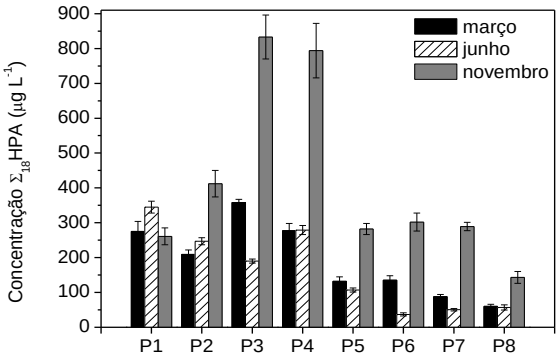


Figura 1. Concentração total de HPAs (μg $L^{-1}$) em rios (P1 a P4) e lagoas (P5 a P8) do complexo lagunar de Jacarepaguá, Rio de Janeiro.

[1]Franco CFJ, Resende MF, Furtado LA, Brasil TF, Eberlin MN, Pereira Netto AD, Science of the Total Environment, 599-600 (2017) 303.
[2]Brum DM, Pereira Netto, Journal of Hazardous Materials, 165 (2009) 447.

**Agradecimentos**: CNPq, FAPERJ

**Área: AMB** **Inscrição: 00135**

# Etanol, peróxido de hidrogênio e acetaldeído na atmosfera de Ribeirão Preto e São Paulo: cidades impactadas pelo uso de etanol combustível

**Caroline Scaramboni[1] (PG)*; M. Lúcia A. M. Campos[1] (PQ)**

**carolinesc@usp.br; lcampos@ffclrp.usp.br**

*[1]Departamento de Química, Faculdade de Filosofia, Ciências e Letras de Ribeirão Preto, USP*

Palavras Chave: emissões veiculares, cana-de-açúcar, fotoquímica, políticas públicas

## Highlights

Atmospheric ethanol, hydrogen peroxide and acetaldehyde in Ribeirão Preto and São Paulo: cities impacted by ethanol fuel.
Atmospheric levels of ethanol in Brazil were ~21 times higher than USA. São Paulo and Ribeirão Preto had similar ethanol concentrations, despite the large difference in the vehicular fleet. $H_2O_2$ may have an important role in atmospheric oxidation of ethanol to acetaldehyde.

## Introdução

A atmosfera brasileira é especialmente rica em espécies orgânicas oxigenadas voláteis devido ao elevado uso de etanol como combustível, principalmente em grandes centros urbanos. A participação do $H_2O_2$ na oxidação de álcoois, com consequente produção de aldeídos de elevada toxicidade, ainda é pouco conhecida. Considerando a futura produção de etanol de segunda geração em larga escala no Brasil, e o aumento mundial do uso desse combustível, nosso objetivo é avaliar o impacto das emissões de etanol no consumo e produção de $H_2O_2$ na atmosfera.

## Metodologia

As amostras de fase gasosa foram coletadas utilizando o método de coleta do condensado[1] em Ribeirão Preto (RP) e São Paulo (SP), de outubro/2016 a julho/2017. A determinação de $H_2O_2$ foi realizada por fluorescência[2] e de etanol e acetaldeído por GC-FID[3].

## Resultados e discussões

A concentração atmosférica média de etanol deste trabalho foi cerca de 21 vezes maior que a média relatada em Wilmington (EUA)[4], reflexo do elevado uso de etanol combustível no Brasil. Apesar da frota veicular de SP ser ~16 vezes maior que a de RP, as concentrações médias de etanol em ambas as cidades foram próximas (Tabela 1).

*Tabela 1. Concentrações atmosféricas médias (ppbv)*

| Espécie | RP (n=19) | SP (n=10) |
|---|---|---|
| $H_2O_2$ | 2,10 ± 1,46 | 1,29 ± 0,62 |
| Etanol | 15,0 ± 6,6 | 22,0 ± 9,4 |
| Acetaldeído | 16,3 ± 6,0 | 14,4 ± 5,4 |

Além das emissões veiculares, as emissões evaporativas das usinas de açúcar e álcool da região podem justificar a concentração relativamente elevada de etanol na atmosfera de RP. A menor concentração média de $H_2O_2$ em SP pode ser resultante de uma maior quantidade de contaminantes atmosféricos, como $SO_2$ e $NO_x$, que podem consumir $H_2O_2$ ou competir por seus radicais precursores[2]. A análise diurna das concentrações atmosféricas em Ribeirão Preto mostrou uma conversão de etanol a acetaldeído de acordo com a radiação solar, que pode ter sido, pelo menos parcialmente, mediada pela produção fotoquímica de $H_2O_2$ (Figura 1).

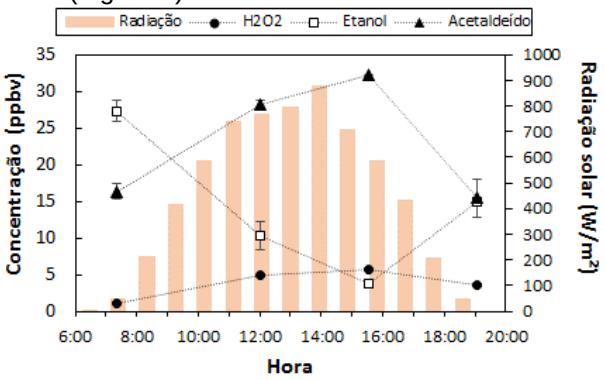


Figura 1 – Concentrações de $H_2O_2$, etanol e acetaldeído na fase gasosa e radiação solar em função do período do dia em Ribeirão Preto.

## Conclusão

O $H_2O_2$ pode ser um importante oxidante de etanol a acetaldeído em fase gasosa. Este estudo traz subsídios que auxiliam na compreensão de como as políticas públicas para uso de etanol podem impactar a atmosfera, sua capacidade oxidativa e a saúde humana.

## Agradecimentos

À FAPESP e ao CNPq.

## Referências

[1]FARMER, J.C.; DAWSON, G.A. **Journal of Geophysical Research**, 87, 8931–8942, 1982.
[2]SCARAMBONI, C. et al. **Atmospheric Environment** 176, 201–208, 2018.
[3]GIUBBINA, F.F. et al. **Analytical Methods**, 9, 2915–2922, 2017.
[4]AVERY, G.B. et al. **Chemosphere**, 144, 360–365, 2016.

**Área: AMB** **Inscrição: 046**

# Use of moss bag technique, Sphagnum subsecundum as biofilter, for the monitoring of metals in the air in the city of Barreiras-BA

**Oldair D. Leite (PQ),[1,2] Cleiçon F. De Sá (PG),[2*] Luci E. Ogava (PG),[2] Leandro D. C. Da Guarda (PG),[3] Jorge L. O. Santos (PQ),[4] Jose D. S. da Silva (PQ),[2] Alex S. Torquato (PQ),[1] Eder L.M. Flores (PQ),[1]**

**oldair.leite@gmail.com; cleiconfelix@yahoo.com.br**

*[1]Departamento de Química, Universidade Tecnológica Federal do Paraná, UTFPR, campus Medianeira; [2] Universidade Federal do Oeste da Bahia, UFOB, campus Barreiras; [3]Universidade Federal do Oeste da Bahia, UFOB, campus Luís E. Magalhaes; [4]Universidade Federal do Oeste da Bahia, UFOB, campus Bom Jesus da Lapa*

Palavras Chave: *Heavy metals; Atmospheric deposition, Sphagnum subsecundum,*

## Highlights

- Moss bag technique was tested in an urban area of city Barreiras-Ba;
- The species Sphagnum subsecundum was used as a biofilter for the accumulation of metals;
- Two sampling campaigns covering the rainy and dry period lasting 45 days each were employed;
- Of the thirteen metals analyzed, Fe and K reached values of determination higher than the values normally analyzed for these elements in the atmosphere

## Resumo/Abstract

Mosses (bryophytes) have been recognized as the most effective type of organisms for biomonitoring of air quality, because it shows a significant tendency to accumulate and retain pollutants. The biomonitoring techniques appear to be particularly useful in areas industrial and/or urban to examine deposition patterns and to recognize pollution point sources. In this work we used moss Sphagnum subsecundum as an active biofilter, using the Moss bag technique, for the monitoring of metals in the air in the urban perimeter of the city of Barreiras-BA. The field experiments were carried out in two sampling campaigns covering the rainy and dry period lasting 45 days each. The material collected in the post-exposure was analyzed in the laboratory employing the techniques of absorption spectrometry and flame atomic emission (F-AAS and GF-AAS) for the determination of thirteen species of metals (Cu, Cd, Pb, Cr, Fe, Ni, Co, Zn, Mg, Mn, K, Na e Li) accumulated in the moss samples. The results showed that most of the studied metals (Cu, Cd, Pb, Cr, Ni, Co, Zn, Mg, Mn, Na and Li) did not present worrying atmospheric contamination indexes. On the other hand, the metals Fe and K reached values of determination superior to the minimum values stipulated for these elements in the atmosphere. The moss Sphagnum subsecundum presented a useful alternative to estimate particles and toxic elements in the air.

**Área: AMB____** *(Inserir a sigla da seção científica para qual o resumo será submetido. Ex: ORG, BEA, CAT)*

**Inscrição: 01390** *(Inserir o número de inscrição do autor que fez a submissão)*

# HIGH URANIUM CONCENTRATIONS IN THE GROUNDWATER OF THE RIO DE JANEIRO STATE MOUNTAINOUS REGION

**José M. Godoy[1] (PQ), Paulo R. Ferreira[2] (PQ), Elder M. de Souza[2] (PQ), Larisse I. da Silva[1] (IC), Isabela Bittencourt[1] (IC), Felipe Fraifeld[3] (IC)**

**jmgodoy@puc-rio.br**

*[1]Departamento de Química, PUC-RIO; [2]Instituto de Radioproteção e Dosimetria, CNEN, [1]Departamento de Engenharia Civil e Ambiental, PUC-RIO*

Palavras Chave: *Uranium, Brazil, Groundwater, Natural Radioactivity, Rio de Janeiro.*

## Highlights

- Very high uranium concentration in groundwater was observed
- $^{222}Rn$ and $^{210}Pb$ content are also issues of concern
- Public water supply affected by natural radionuclides
- Mandatory uranium and $^{222}Rn$ determination suggested

## Resumo/Abstract

Unexpectedly high uranium concentrations, up to 930 µg $L^{-1}$, contrasting with the Brazilian maximum allowed concentration of 30 µg $L^{-1}$, were observed in groundwater samples from the mountainous region near Rio de Janeiro City, the so-called *"Região Serrana"* of Rio de Janeiro, approximately 60 km from the city. The region is characterized by an intense amount of tourist activities and water-related industries, such as mineral water and breweries, that can be severely impacted by these findings. In addition, the water supplies of small communities of this region are partially or entirely based on groundwater sources. Uranium contaminations were observed in 5 of the 16 counties of this region. Based on the data, this study attempted to define where the probability of obtaining uranium-contaminated groundwater is high. In addition, high $^{222}Rn$ concentrations were verified, with levels reaching 1570 Bq $L^{-1}$. Furthermore, a maximum level of 4.6 Bq $L^{-1}$ $^{210}Pb$ was also measured, which WHO guidance level is 0.10 Bq $L^{-1}$. Based on the present findings, it is suggested that any artesian well deeper than 80 meters in this region should be tested for uranium and $^{222}Rn$.

Fig. 1: Occurrences of high uranium concentrations in groundwater in the mountainous region around Rio de Janeiro City (red dots indicate uranium concentrations higher than 30 µg $L^{-1}$, Brazilian maximum allowed value, and yellow markers indicate uranium concentrations between 15 and 30 µg $L^{-1}$)

**Área: AMB** **Inscrição: 01311**

# Detection of *p*-aminophenol and sub-products formed during oxidative process in water and hair salon effluent

**João Carlos de Souza (PG),[1] Bianca Ferreira da Silva (TC),[1] Maria Valnice Boldrin Zanoni (PQ),[1]**

**souza_jc33@yahoo.com.br; mvboldrin@gmail.com**

*[1]Universidade Estadual Paulista (UNESP), Chemistry Institute, Department of Analytical Chemistry, Araraquara-SP-Brazil*

Palavras Chave: *P-Aminophenol, Permanent hair dyes, Precursors. Hair salon effluents, Water*

## Highlights

Harmful products were formed during the oxidation of *p*-aminophenol in alkaline and oxidative medium.
The sub-products formed during *p*-aminophenol oxidation are found in hair salon effluent.
*P*-Aminophenol were detected in samples of surface water and tap water.

## Resumo/Abstract

Permanent hair dyeing is a popular process adopted by millions of people in the the world. Complex oxidative reactions are involved between precursor agents (aromatic amines) and couplers (phenolic compounds) in oxidizing alkaline medium inside the hair strand[1]. As result of these reactions colorful compounds are formed known as the proper hair dye. Simultaneously the reaction can also produce polynuclear by-products recognized for its high toxicity and mutagenic properties[1]. Thus, effluents from beauty salons can produce many contaminants that are commonly discarded in the sewer, contaminating water supply source, when the conventional sewage treatment system are not efficiently to treat this type of waste. The aim of this work is the investigation of the detection of *p*-aminophenol (PAF) a precursor of permanent hair dyeing and its oxidative sub-products formed in alkaline condition. In order to monitor its occurrence in hairdressing salon effluents collected after to receive wastewater from dyeing hair process, as well as to quantify the content of PAF in samples of surface water and tap water after treatment process in the drinking water plant.

The effect of hydrogen peroxide at PAF was monitored by spectrophotometry UV-Vis and infrared spectrometry PAF in 0.1 mol $L^{-1}$ ammonium buffer at pH 8.0. The intermediates and by-products generated during the polymerization side reaction of PAF were analyzed using mass spectrometry and hydrogen nuclear magnetic resonance spectroscopy. Previous extraction was used by thin layer chromatography and a mixture of chloroform, ethyl acetate and methanol in the ratio of 6:2:1 (v/v), respectively as the mobile phase. Quantitative analysis were carried out using high performance liquid chromatography with diode array detector for samples collected from surface water, tap water and hairdressing salon effluent.

Under oxidizing alkaline medium, currently used in dyeing process it was observed a polymerization mechanism of PAF, forming the semi-quinoneimine radical as intermediate. Further oxidation generates the quinoneimine, which reacts subsequently with original PAF forming dimers, trimer and tetramer, respectively. The mass spectra obtained for the sample of hair salon effluents confirmed the presence of PAF and its reaction products as subproducts formed during the hair dyeing process. For the determination of PAF, analytical curve was constructed Area = $51914C_{(PAF)}$ – 100.2 ($R^2$ = 0.9994), with linearity to 300.0 mg $L^{-1}$. Limits of detection and quantification were de 0.01 e 0.05 mg $L^{-1}$, respectively. The recuperation of method was 97.4% and the relative standard deviation intra and interday were 3.6 and 6.8%, respectively.

The residual concentrations of PAF in surface water, tap water and hairdressing salon effluent samples were $1{,}0x10^{-2}$ mg $L^{-1}$, $5{,}78x10^{-3}$ mg $L^{-1}$ and $3{,}4x10^{-2}$ mg $L^{-1}$ of PAF, respectively. Therefore, the results obtained indicate that PAF is oxidized in peroxide medium commonly used in hair dyeing process without coupler presence and can forms many by-products identified by mass spectra and hydrogen nuclear magnetic resonance spectroscopy. Both, original PAF and their sub-products are found in hairdressing salon effluent. Taking into account, that PAF is considered highly toxic compounds when discarded in common sewage, and not properly treated could contaminate drinking and non-drinking water sources. The method proposed is able to detect the PAF and also their polynuclear by-products.

**Acknowledgements:** IQ/UNESP and Fapesp (Process n° 2015/12998-1).
**References:** [1]OLIVEIRA, R. A. G. et al. Quím. Nova, v. 37, n. 6, p. 1037-1046, 2014.

**Área: AMB** **Inscrição: 01256**

# Quantification and statistical evaluation of metals and metalloids in water samples from Barra Longa after the rupture of the Fundão dam (Mariana)

**Caroline F. S. Diniz (PG),[1]* Clésia C. Nascentes (PQ),[1] Cláudia C. Windmöller (PQ),[1]**

**claucw@qui.ufmg.br; cfsaldanha@gmail.com**

[1]*Departamento de Química, UFMG*

*Keywords: Fundão Dam, Doce river basin, Metals, Water, ICP-MS*

## Highlights

Quantification and statistical evaluation of metals and metalloids in water samples from Barra Longa after the rupture of the Fundão dam (Mariana)
Determination of metals and metalloids in water samples from wells, ponds and river by ICP-MS
Samples of well water from Barra Longa showed concentrations of Fe and Ni above the maximum values allowed for drinking water.
Pre-consumption water treatment proved to be efficient for metal removal.

## Abstract

In November 2015, the disruption of an iron ore tailings dam located in the Doce river basin caused the largest environmental disaster ever occurred in Brazil and one of the largest in the world, releasing tons of mud that until today cause changes in the composition of the water. The objective of this work was to determine the total concentrations of metals and metalloids in the waters of Barra Longa, a district close to where the disaster occurred and to discuss the data using statistical methods. A total of 15 water samples were collected and the total concentrations of Ag, Al, As, Ba, Be, Cd, Co, Cr, Cu, Fe, Hg, Ni, Pb, Sb, Se, Ta, U and V were determined in well waters and Fe, Al and Cu dissolved in pond and river waters by inductively coupled plasma mass spectrometry (ICP-MS). Four well water samples, which are consumed without any treatment, showed Fe concentrations well above the Maximum Permissible Values (MPV) by Portaria nº2921 do Ministério da Saúde and 1 sample presented Ni concentration 3 times above. Statistical analysis using HCA showed two groups, one of well water samples (group A) similar due to the higher concentrations of Cr (0.598 to 3.224 $\mu g.L^{-1}$) and other group (group B) with the other samples. The samples that underwent treatment were grouped due to the lower contents of Fe, showing the importance of the treatment in the removal of the metals.

## References

PORTARIA N° 2.914, DE 12 DE DEZEMBRO DE 2011 Disponível em: <http://bvsms.saude.gov.br/bvs/saudelegis/gm/2011/prt2914_12_12_2011.html>.

IGAM.**RELATÓRIO TÉCNICO** 2017 <http://www.igam.mg.gov.br/images/stories/2015_ARQUIVOS/QUALIDADE_RIO_DOCE/Relatorio_Qualidade_17novCompleto.pdf>

CONAMA. **Resolução CONAMA N° 357/2005**Conselho Nacional do Meio Ambiente-Ministério do Meio Ambiente, , 2005

## Acknowledgments

CNPQ, FAPEMIG and INCT-ACQUA

**Área: AMB** **Inscrição: 01200**

# Assessment of the risk of contamination of water resources by pesticides in the city of Petrolina - PE

**Fernanda P. da S. Oliveira (IC)*, [1] Jonas T. L. Nunes (IC),[1] Mônica D. de S. Almeida (PQ), [1] André H. B. de Oliveira (PQ), [1] Diego de Q. Melo (PQ),[1] Gizelle A. B. Vieira (PQ). [1*]**

**f.paulaoliveira1991@gmail.com; gizelle.angela@ifsertao-pe.edu.br**

[1]*Instituto Federal de Educação, Ciência e Tecnologia do Sertão Pernambucano, Campus Petrolina*

Palavras Chave: Inventário, Agrotóxicos, Meio Ambiente

## Highlights

A risk analysis of contamination of water resources was carried out in Petrolina - PE. 103 agrochemicals were verified, 63 active principles, some of them potential environmental contaminants.

## Resumo/Abstract

A cidade de Petrolina - PE está situada na região do Vale do Submédio do Rio São Francisco, o qual é protagonista na produção de insumos agrícolas, sendo o principal pólo exportador de fruticultura do Nordeste, o que a credencia como consumidora em potencial de agrotóxicos. Nesse contexto, o trabalho teve como objetivo estimar o impacto ecológico causado pelo uso de agrotóxicos através da elaboração de um inventário de princípios ativos e risco de contaminação química. Os dados de pesticidas comercializados na região para as culturas predominantes, manga e uva, foram obtidos na Agência de Defesa e Fiscalização Agropecuária de Pernambuco (ADAGRO), para o primeiro semestre de 2016. Foi verificado o uso de 103 agrotóxicos, sendo 63 princípios ativos. Foi analisado o potencial de contaminação em águas superficiais (método de Goss), associado ao sedimento (método de Goss) e em água subterrânea (índice GUS e critérios da Environmental Protection Agency – EPA), através das propriedades físico-químicas destes princípios ativos consultadas na IUPAC FOOTPRINT. Os resultados foram que 11,11% dos princípios ativos são altos potenciais contaminantes associados aos sedimentos, 19,05% dissolvidos em água superficial e 15,87% contaminantes de água subterrânea (**Tabela 1**).

**Tabela 01** – Indicação de princípios ativos a serem monitorados por conferirem alto potencial de risco aos recursos hídricos

| |
|---|
| **Princípios ativos com alto potencial de contaminação associado ao sedimento – Método Goss** |
| Lambda-cialotrina, paraquate, dicloreto de paraquate, buprofezina, tiabendazol, cloridrato de formentanato, difenoconazol. |
| **Princípios ativos com alto potencial de contaminação dissolvido em água superficial – Método Goss** |
| Azoxystrobina, boscalid, ciproconazol, zoxamida, fosetil, tetraconazol, imidacloropride, tiamethoxam, diuron, tiabendazol. flutriafol, paclobutrazol |
| **Princípios ativos com alto potencial de contaminação de águas subterrâneas – Índice GUS e critérios EPA** |
| Azoxistrobina, Zoxamida, Piraclostrobina, Imidacloprido, Tiamethoxam, Diuron, paraquate, Dicloreto de paraquate, tebuconazole, ciproconazol |

Goss, D.W. (1992) **Screening procedure for soils and pesticides for potential water quality impacts.** Weed Technology, v. 6, n. 3, p. 701-708.

Gustafson, D.I. (1989) **Groundwater Ubiquity Score: a simple method for assessing pesticide leachability**. Environmental Toxicology and Chemistry, v. 8, n. 4, p. 339-357.

**Área: AMB** **Inscrição: 01136**

# Optimization of large volume injection for determination of organophosphorus flame retardants in river water by GC-MS

**Joyce Cristale (PQ),* Enelton Fagnani (PQ).**

**joycecristale@gmail.com**

*Faculdade de Tecnologia, UNICAMP*

Palavras Chave: *Organophosphorus Flame Retardants, River Water, GC-MS, Multivariate Optimization.*

## Highlights

A large volume injection method for GC-MS was developed
The instrumental conditions were optimized using a multivariate approach
The method was feasible for determination of ten OPFRs in river water

## Resumo/Abstract

Contamination of surface water by organophosphorus flame retardants (OPFRs) is of concern due their persistency and toxic properties. The main sources of OPFRs to the aquatic environment are industrial and domestic effluents since these substances are not efficiently removed in wastewater treatment plants. Analytical methods for determination of OPFRs at trace concentrations in river water are necessary for monitoring studies that aim to evaluate the risks to the aquatic environment. In this study, an analytical method was developed for determination of ten OPFRs in river water extracts by large volume injection and gas chromatography coupled to mass spectrometry. The conditions of the programmed temperature vaporization injector were optimized using a multivariate experimental design. Two full factorial experiments were performed in order to optimize the solvent evaporation and the transferring of the analytes to the chromatographic column. Among the factors evaluated only the gas purge flow and the purge time were significant on the instrumental response. These factors were further optimized using a central composite experiment. The optimized conditions were presented at Table 1. The developed method allowed the determination of all the OPFRs in river water extracts at levels of environmental relevance.

**Table1** – Optimized large volume injection conditions

| | |
|---|---|
| Injection volume | 9 µL |
| Evaporation temperature | 40 °C |
| Injection speed | 100 µL $s^{-1}$ |
| Gas purge flow | 10 mL $min^{-1}$ |
| Purge time | 0,25 min |
| Transferring temperature | 280 °C |
| Heating rate | 3 $^{o}C$ $seg^{-1}$ |
| Splitless time | 5 min |
| Column isotherm | 6 min |

**Área: AMB** **Inscrição:01125**

# Determinação da concentração de íons próximo a foz do rio Paraíba do Sul

**Carolina R. de O. Nunes (TM), Gabriel da G. Menezes (IC), Charles G. Borges (TM), Thiago M. de R. Araújo (PQ).***

**carolina.nunes@iff.edu.br; taraujo@iff.edu.br**

*Laboratório de Monitoramento das Águas da Foz do Rio Paraíba do Sul, LabFoz, Polo de Inovação Campos dos Goytacazes, IF Fluminense/RJ.*

Palavras Chave: *Foz, Cromatografia Iônica, Íons, Salinidade, Rio Paraíba do Sul.*

## Highlights

Ions concentration nearby Paraíba do Sul river mouth.
Paraíba river flow has been decreasing in its mouth. This work showed that, even close to the encounter river/sea, during a river flood period, there is low concentration of ions in the river water.

## Resumo/Abstract

Nas últimas décadas, a vazão do rio Paraíba do Sul em sua foz vem diminuindo drasticamente. Principalmente, devido a construções de barragens e transposições. Só a do rio Guandu desloca cerca de dois terços do seu volume para abastecer a região metropolitana do Rio de Janeiro e há, ainda, a transposição, em construção, que fará a interligação das bacias do Cantareira e do Paraíba. Essa diminuição na vazão vem trazendo graves problemas a São João da Barra/RJ, dentre eles: o avanço do mar sobre seu território e a dificuldade, em algumas épocas do ano, em se captar água doce para tratamento e distribuição à população. Nesse contexto, o presente trabalho determinou a condutividade e a concentração de alguns íons em amostras de água do Paraíba coletadas em quatro pontos (Figura 1) próximos a sua foz visando avaliar o avanço da água do mar sobre o rio.

As coletas foram realizadas a 2,00 metros de profundidade no dia 29/11/2017, período de cheia, em maré baixa e alta. A análise dos íons foi feita por cromatografia iônica, em triplicata, após validação do método, e os resultados encontram-se nas Figuras 2 e 3.

Figura 1: Pontos de coleta de amostras de água do rio Paraíba do Sul.

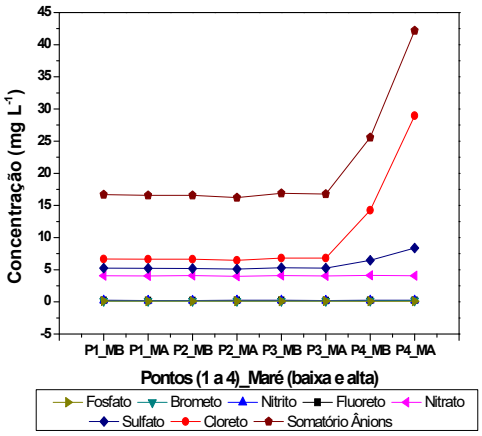


Figura 2: Concentração dos ânions.

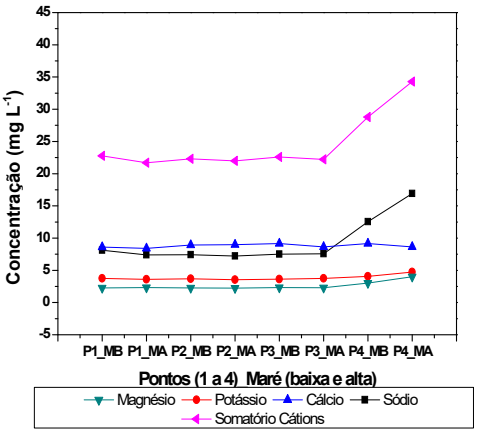


Figura 3: Concentração dos cátions.

Analisando-as, observa-se que somente no ponto 4 houve influência do mar na composição iônica da água do rio. Porém, mesmo nesse ponto, nas condições avaliadas neste estudo, o somatório das massas dos principais cátions e ânions existentes no mesmo não passou de 80,0 mg $L^{-1}$, o que indica baixa salinidade.

**Área: AMB** **Inscrição: 00956**

# Microextraction using RDSE and BAμE techniques as strategies for the determination of pesticides and emerging contaminants in environmental water samples by UHPLC-MS/MS

**Renato Zanella (PQ)*, Filipe F. Donato (PQ), Maiara P. de Souza (PG), Osmar D. Prestes (PQ), Martha B. Adaime (PQ)**

**renato.zanella@ufsm.br**

[1]*Departamento de Química, LARP-UFSM, Santa Maria - RS, Brazil*

Keywords: *Pesticides, Water, Sample preparation, RDSE, BAμE, UHPLC–MS/MS.*

## Highlights

New methods using microextraction devices were presented. Validation provided good results for 62 pesticides by RDSE and 13 emerging contaminants by BAμE. Small amount of sorbent and solvent required.

## Resumo/Abstract

The excessive use of pesticides and emerging contaminants result in human health and environmental problems, especially regarding to water resources. In this work, the viability of simple and sensitive microextraction devices for multiresidue determination in water samples is highlighted. The rotating disk sorptive extraction (RDSE)[1] technique was used for the development and validation of a method for the determination of 62 pesticide residues in surface water by ultra-high-performance liquid chromatography tandem mass spectrometry (UHPLC–MS/MS). A small amount (20 mg) of the polymeric sorbent Oasis® HLB was used for extraction. The RDSE method presented limit of detection from 0.015 to 0.03 μg $L^{-1}$, with recoveries from 70.1 to 119.9% and RSD <20%. The application to river water samples indicated residues of atrazine, azoxystrobin, clomazone, difenoconazole, epoxiconazole, propoxur, simazine and tebuconazole from 0.06 to 0.35 μg $L^{-1}$.

With the bar adsorptive microextraction (BAμE)[2] technique, an efficient method was established and validated for the determination of 13 emerging contaminants, representative of pharmaceuticals, hormones, plasticizers and flame retardants, in water by UHPLC-MS/MS. Different coating phases and others parameters were optimized by a central composite design. The sorbent Oasis® HLB presented the best performance with recoveries from 74 to 118% and RSD <19%. Method detection limits from 0.012 to 0.6 μg $L^{-1}$ were obtained. Real surface and drinking water samples presented bisphenol A (0.08 to 0.665 μg $L^{-1}$) and paracetamol (0.104 to 4.2 μg $L^{-1}$).

References

1. F. F. Donato, N. M. G. Bandeira, G. C. dos Santos, O. D. Prestes, M. B. Adaime, R. Zanella. Evaluation of the rotating disk sorptive extraction technique with polymeric sorbent for multiresidue determination of pesticides in water by ultra-high-performance liquid chromatography–tandem mass spectrometry. J. Chromatogr. A 1516 (2017) 54-63.

2. M. P. de Souza, T. M. Rizzetti, J. Z. Francesquett, O. D. Prestes and R. Zanella. Bar adsorptive microextraction (BAmE) with a polymeric sorbent for the determination of emerging contaminants in water samples by ultra-high performance liquid chromatography with tandem mass spectrometry. Anal. Methods 2018. https://doi.org/10.1039/c7ay02792c.

[CNPq, CAPES, UFSM]

**Área: AMB** **Inscrição: 824**

# Análise por varredura de resíduos de agrotóxicos nas águas do Parque Indígena do Xingu

**Heloisa Gonçalves (IC), Tiago Cerqueira (PG), Diogo Oliveira-Silva (PQ).***

**heloisa.goncalves@unifesp.br; dosilva@unifesp.br**

*Grupo de Bio-orgânica e Bioanalítica - GBB, Departamento de Química*
*Instituto de Ciências Ambientais, Químicas e Farmacêuticas, UNIFESP – Campus Diadema*

Palavras Chave: Fitossanitários, Praguicidas, DLLME, LC-MS/MS

## Highlights

**Screening of pesticide residues in water from Xingu Indigenous Park.** The agrochemical overuse around the Xingu Indigenous Park is an environmental mandatory issue. Analyses of water samples by LC-ESI-MS/MS yielded consistent evidences of pesticide contamination.

## Resumo/Abstract

O adensamento da agricultura extensiva próxima ao Parque Indígena do Xingu (PIX) tem causado preocupação aos líderes das mais de 14 etnias dessa região. O uso desmedido de defensivos agrícolas tem comprometido a qualidade da água nas bacias do Alto Xingu. O PIX é um protagonista ambiental e não existem relatos sobre o monitoramento de agrotóxicos ou a indicação de metodologias específicas para esta finalidade. Este trabalho tem como objetivo iniciar o monitoramento de resíduos de agrotóxicos no PIX por meio da análise de varredura destas substâncias em amostras de água coletadas na região do Alto Xingu. O estudo teve início com o levantamento dos cultivos de maior ocorrência, juntamente com uma estimativa dos princípios ativos indicados e populares na região. A metodologia contemplou 53 substâncias, entre princípios ativos e produtos de degradação e transformação, seguindo as etapas do fluxograma abaixo:

Método Analítico está resumido na tabela a seguir:

| | |
|---|---|
| **Sistema Analítico** | **UHPLC Nexera-X2 e LCMS-8060 (Shimadzu)** |
| **Coluna Cromatográfica** | **Restek Ultra AQ C18 (100 x 2 mm, 3 um)** |
| **Fase Móvel (gradiente)** | **A: formiato de amônio 20 mmol/L<br>B: acetonitrila** |
| **Vazão** | **0,5 mL/min** |
| **Parâmetro de Detecção** | **Monitoramento de Reações Selecionadas (SRM)** |

A detecção foi realizada com duas transições de íons precursor/produto. Para garantir a confiabilidade da metodologia de *screening*, inserimos amostras-controle de bentozona, clorpirifós, fenaminfós, imazaquim e malation. Todos os 5 padrões resultaram precisão e exatidão adequadas. Todas as amostras apresentaram atrazina e 74% destas continham o seu produto de transformação desisopropil-atrasina. Carboxim e azoxistrobina apareceram em 87% e 67% das amostras (respectivamente). Também apareceram sinais de carbendazim, fipronil, haloxifope e pendimetalina. A análise quantitativa das substâncias detectadas está em andamento para que sejam obtidos os resultados confirmatórios.

Agradecimentos:

**Área: AMB** **Inscrição: 00801**

# PAH baselines for riverine surficial sediments from Amazonian Coastal Zone

**Camila C.S. Rodrigues (PG),[1*] Brunalisa S. Ramos (IC),[2] Ewerton Santos (PG),[2] Flaviana C. Damasceno (PQ).[2]**

**flavydamasceno@yahoo.com.br; santos.camilac@gmail.com**

*[1]Departamento de Geociências, UFPA; [2]Departamento de Química, UFS*

Palavras Chave: *Polycyclic aromatic hydrocarbons, Sediment quality guidelines, Diagnostic ratios, Baselines, Amazonic aquatic systems.*

## Highlights

*Sources, distribution and ecological risk of 16 priority PAH in sediments samples were determined.*
*GC/MS method was utilized to PAH identification and quantification.*
*The aim of this study was to evaluate baselines for PAH in the Amazonian Coastal Zone.*
*PAH total concentration were generally low compared to highly urbanized and industrialized areas.*
*Naphthalene was the most representative PAH and it may be from a biogenic source.*
*Pyrogenic PAH predominated in the studied area, mainly by grass, wood and coal combustion.*
*Emissions from local sources are main PAH origin for the amazonic aquatic systems.*
*The ecological risk assessment did not indicate possible negative effects to the local biota.*
*The presented data can be assumed as baselines for PAH in the Amazonian Coastal Zone.*

## Resumo/Abstract

The distribution, sources and ecological risk assessment of 16 polycyclic aromatic hydrocarbons (PAH) in surface sediments from 3 aquatic bodies (Guajará Bay, Guamá River and Amazon River Estuary) from the Amazonian coastal zone (Northern Brazil) (Figure 1) were determined. The aim of this study was to suggest baselines for PAH in the presented area. Baseline levels are considered an important tool in environmental management. PAH were identified and quantified by GC/MS. The total PAH concentration ranged from 18.6 to 46.9 ng $g^{-1}$ dw (mean value 29.3 ng $g^{-1}$ dw), which were generally low compared to other coastal zones in Brazil and around the world. The upper 95% confidence interval on the mean was 2.9 ng $g^{-1}$ for total PAH. Naphthalene was the most representative PAH in sediment samples (38% of the total PAH concentration). The presence of this PAH in natural forests can be associated to a biogenic origin as termite nests because they product Naphthalene as a part of their defensive system. Termites are common in the studied area. PAH diagnostic ratios showed that pyrogenic PAH (mainly caused by grass, wood and coal combustion) from local emissions were predominant in the surface sediments. The ecological risk assessment indicated that non-negative effects in this area are expected. Based on all the results obtained with a multiple tools and statistical analysis done, the presented data can be assumed as baselines for PAH in the Amazonian Coastal Zone.

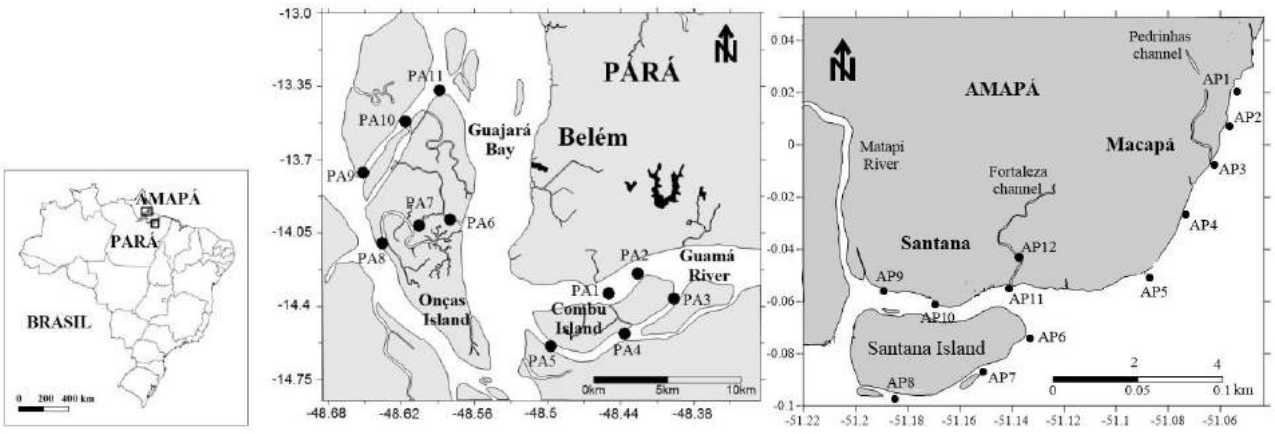


**Figure 1** The studied area and sampling sites location.

**Área: AMB** **Inscrição: 00651**

# Assessment of Contamination of Amazonian Streams by Domestic Sewage using Sterols

**Moacir G. de Melo (PG),[1] Valéria R. L. de Lima (IC),[1] Brina A. da Silva (IC),[1] Gilcllys de S. Costa (IC),[1] Adalberto L. Val (PQ),[2] Hector H.F. Koolen (PQ),[3] Giovana A. Bataglion (PQ).[1]***

**giovanabataglion@ufam.edu.com**

*[1]Chemistry Department, UFAM; [2]National Institute of Amazon Research (INPA); [3]University of Amazonas State (UEA)*

Key Words:*(Pollution; Coprostanol; LC-MS/MS; Igarapés; Manaus).*

## Highlights

Sterols have been quantified in sediments from three streams crossing the city of Manaus (Amazonas, Brazil). These urban streams are highly impacted by domestic sewage.

## Resumo/Abstract

Sterols are used as indicators of current and past ecosystem health and the relative contributions of aquatic vs. terrestrial sources of organic matter (OM) and natural vs. anthropogenic input. In particular, coprostanol, which is a stanol from the conversion of cholesterol by reducing bacteria in the digestive track, allows the assessment of domestic sewage in an environment. This study aimed to quantify sterols in sediments of three important streams of Manaus, a city of 2 million people in the middle of the Amazon forest. Samples of surface sediment were collected in Mindu, Quarenta, and Tarumã-Açu streams. The samples were frozen, freeze-dried, extracted with dichloromethane and methanol and, then, analyzed by LC-MS/MS using atmospheric pressure chemical ionization source in the positive ion mode and selective reaction monitoring. Chromatographic separation was performed on a C18 column using methanol as the mobile phase. The relative proportions of sterols in the samples from the three studied streams are shown in the figure below.

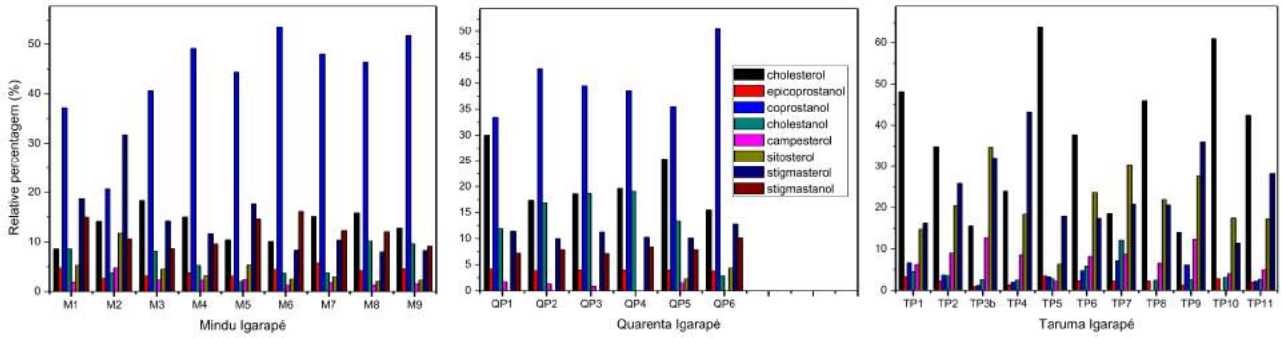


Coprostanol was found in high concentrations and high proportions in all samples collected in the Mindu stream that crosses many heavily populated districts of the city, and also in the Quarenta stream that crosses the Industrial District of Manaus. The sediments of the Tarumã-Açu stream also presented coprostanol; however, concentrations and proportions were much lower in this stream, which crosses poorly populated districts. These results indicate a marked contamination of urban streams by domestic sewage.

**Área: AMB** **Inscrição: 00705**

# River basin barigui: determination of the drugs ibuprofen, ketoprofen and acetylsalicylic acid.

**Gesieli Prado Cardoso da Silva (IC),[1*] Luana Mayumi (IC),[1] Tais Cristina Filippe (PG),[1] Júlio César Rodrigues de Azevedo (PQ),[1] Maurici Luzia Charnevski Del Monego (PQ)[1] .**

**gesieli@alunos.utfpr.edu.br;**

[1]*Departamento Acadêmico de Química e Biologia, UTFPR;*

Keywords: *(Drugs , Emerging contaminants, Barigui River, Ibuprofen, Ketoprofen, Acetylsalicylic acid).*

## Highlights

The present work analyzed the drugs ibuprofen, ketoprofen and ASA present in the Barigui river basin. The data confirms the anthropic interference in this river, due the disordered population growth.

## Abstract

Drugs classified as emerging pollutants have been studied by the scientific community. The high consumption of chemical compounds by the population causes threats in the development in aquatic environments, due to the toxicity that these compounds possess. The main route of contamination of the contaminated rivers with drugs is the irregular discharge of sewage network and the low effluent treatment efficiencies. The Barigui River Basin has an area of 279 km², passing in three municipalities: Almirante Tamandaré, Curitiba and Araucária, the increase in population brings as a consequence a compromise in water quality. The present work aims to determine the presence of the emerging contaminants in the Barigui River Basin, where four points were sampled. The collected water samples were extracted in solid phase (SAI) and later analyzed by high performance liquid chromatography (HPLC). Three contaminants, ibuprofen, ketoprofen and acetylsalicylic acid were analyzed. Ibuprofen was detected at the four collection points, reaching concentrations of 0.29 $\mu g.L^{-1}$ in the second and fourth collections of the river. It was possible to quantify the concentration of cetroprofen only in the first two points, maximum of 0.021 $\mu g.L^{-1}$ for the second sampling. In the analysis of acetylsalicylic acid, it was possible to quantify only the fourth point of the collection with a concentration of 1.29 $\mu g.L^{-1}$. Through the analysis of these drugs, the presence of anthropic activity in the Barigui River Basin is confirmed, where it is related to disordered population growth.

**Área: AMB** **Inscrição: 00469**

# Determination of biosorption capacity of microalgae biomass using the Boehm method

**Gisele P. Heidelmann (IC),[1] Tamine M. Roldão (TC),[1] Sílvia G. Egler (PQ),[1] Ellen C. Giese (PQ),[1]***

**egiese@cetem.gov.br**

[1]*Center for Mineral Technology (CETEM), 21941 908, Rio de Janeiro, Brazil*
Key words: *biosorption; microalgae; Boehm titration; lanthanide*

## Highlights

• Biosorption can be considered as a “green technology” solution for aqueous recovery environment.
• The biosorption capacity of two microalgae biomasses surfaces using Boehm method was investigated aiming lanthanide recovery.

## Abstract

Many algae biomass has been successfully employed for treating metals and dyes from contaminated effluents. Microalgae have been described as a potential biosorbent for the treatment of industrial dilute aqueous solutions containing lanthanides. This study aims to assess the potential for biosorption of *Chlorella vulgaris* and *Ankistrodesmus falcatus* through a prior characterization of its surfaces using Boehm titration. Biosorption depends on the protonation or deprotonation of the functional groups on the surface of the biosorbent. The Boehm method is a technique that allowed characterizing the acid and basic sites of the different adsorbent materials in base to selective neutralization. The values found evidence that the biomass presents acidic and basic groups, which is fundamental to the biosorptive process. In the quantification of basic groups, the biomass of *C. vulgaris* showed a larger number of groups, being this 1654.36 $mEq.g^{-1}$, while the *A. falcatus* biomass contained 734.52 $mEq.g^{-1}$. The results indicated that the surface of both biomasses has a higher number of basic groups than of acidic groups. The lactonic groups were not detected by the methodology used, only phenolic groups and carboxylic acids in similar amounts for both *C. vulgaris* and *A. falcatus*. The carboxyl groups were found in a higher proportion (54 $mEq.g^{-1}$) about the phenolic groups (14 $mEq.g^{-1}$). These results showed a good capacity and efficiency of biosorption of both microalgae biomasses for the ions $Ln^{3+}$, which can improve lanthanides recovery strategies using biotechnological processes.

**Área: AMB** **Inscrição: 00456**

# Evaluation of Arsenic bioavailability in waste from cyanidation Gold Processing using sequential extraction schemes (SES)

**Daniel Alves Barcelos (PG),[1*] Fernanda Veronesi M. Pontes (PQ),[1] Fernanda Arruda N. G. da Silva (PQ),[1] Zuleica Carmen Castilhos (PQ),[2]**

**danielbarcelos@gmail.com**

*[1]Instituto de Química, UFRJ; [2]Centro de Tecnologia Mineral CETEM/RJ*

Palavras Chave: *Arsênio, Ouro, Cianetação, Extração Sequencial, Meio Ambiente.*

## Highlights

Cyanidation waste is deposited at dam. Arsenic is a toxic and carcinogenic element, our results showed that it is available for contamination of the environment.

## Resumo/Abstract

Non-free Gold ores is frequently associated with minerals rich in Arsenic, such as arsenopyrite. The waste from Gold mining processing from the flotation and cynidation stages. The dams are a potentially source of environmental contamination, because many hazard elements are present, especially Arsenic. The study of characterization is essential, once that many natural processes can interfere at the stability and mobility of these elements. Sequential Extraction Schemes (SES) is a method where it is possible to evaluate the characteristic of bioavailability which the element of interest is associated. Marin SES[1] uses reagents to extract transition metals from four phases, classified from the easiest, available with just an exchange of pH, named Exchangeable, until the metals associated with the crystal structure, named residual. This research studied the waste from Cyanidation process in order to evaluate Arsenic forms potentially available to the environment. Marin SES evaluated the amount of each one of the schemes. The extractions were analyzed by Inductive Couple Plasma Optical Emission Spectrometry (ICP-OES) technique (Table 1), the average total digestion concentration for As is 413 $\pm$ 4 mg $Kg^{-1}$. The sum from fractions was 405 $\pm$ 15 mg $Kg^{-1}$. The Arsenic was released in the order residual>organic matter>bound to Fe/Mn oxides>exchangeable (Figure 1). This result shows that Arsenic is a potential source of contamination from this tailing sample.

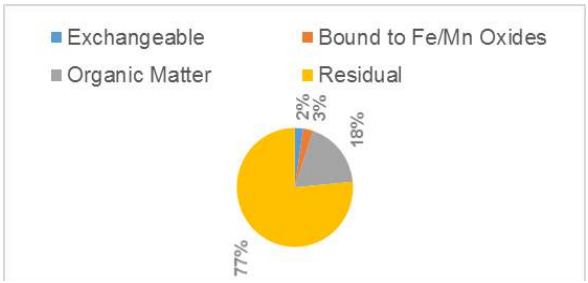


Figure 1. Percentage Extracted from each fraction by Marin SES

Table 1. Operation parameters of ICP-OES

| | | | |
|---|---|---|---|
| Generator power (W) | 1.100 | Nebulizer Glass | concentric |
| Spray chamber | Cyclonic | Integration time (s) | 0.5 |
| Plasma gas flow (L $min^{-1}$) | 12 | Analysis mode | Gauss |
| Nebulization gas flow (mL $min^{-1}$) | 0.91 | Integration time (s) | 0.5 |
| Nebulization pressure (bar) | 2.5 | Pump rate (rpm) | 20 |
| Sheath gas flow (L $min^{-1}$) | 0.2 | Emission lines (nm) | As (189.042); As (193.759) |

[1] MARIN et. al. Analytica Chimica Acta 342 (1997) 91-112.

**Área: __AMB_____** *(Inserir a sigla da seção científica para qual o resumo será submetido. Ex: ORG, BEA, CAT)*

**Inscrição:__0299___** *(Inserir o número de inscrição do autor que fez a submissão)*

# Effects of chlorination on pesticides after drinking water treatment: residue analysis and acetylcholinesterase inhibition.

**Rafael de Oliveira Costa (PG),[1,2] Polyana Soares Barcellos[1] (PG), Maria Cristina Canela (PQ)[1]**

**mccanela@gmail.com; rcostaiff@gmail.com**

*[1]Grupo de Pesquisa em Química Ambiental, Universidade Estadual do Norte Fluminense Darcy Ribeiro; [2] Instituto Federal Fluminense Campus Quissamã*

Key word: water treatment, pesticides, chlorination, byproducts, acetylcholinesterase.

## Highlights

There is a reduction in the concentration of the pesticides after chlorination step, however, were generated byproducts which caused a higher acetylcholinesterase inhibition.

## Resumo/Abstract

Pesticides can cause damage to aquatic environments or even contaminate drinking water[1]. Therefore, the complete removal of these contaminants in water treatment systems is cause for concern. In this perspective, the objective of this work is to investigate whether conventional water treatment can remove atrazine, ametrine, malathion and chlorpyrifos and what the effect of chlorination step on the residues in the activity of the enzyme acetylcholinesterase. A test solution containing these pesticides was subjected to coagulation, flocculation and decantation steps using the Jar test equipment, followed by filtration and chlorination (5 ppm chlorine). It was observed that conventional treatment after filtration was not able to remove these pesticides efficiently, and the organophosphates (malathion and chlorpyrifos) were removed in percentage greater than the triazines (atrazine and ametrine) (Table 1). After chlorination there was an increase in pesticide reduction. However, the by-products of malaoxon and ametrine-sulfoxide (Figure 1) were generated, which caused a greater inhibition of acetylcholinesterase (Table 2). The results showed that additional steps are required in the conventional treatment to remove these persistent contaminants, especially prior to the chlorination step, since the by-products generated were more toxic than the initial ones.

**Table 1.** Average percentage of removal of pesticides

| *Pesticides* | *% Removal after filtration* | *% Removal after chlorination* |
|---|---|---|
| Atrazine | 10.79 ± 0.58 | 16.72 ± 1.02 |
| Ametryn | 14.76 ± 0.29 | 87.71 ± 0.53 |
| Malathion | 62.21 ± 0.01 | 73.21 ± 0.15 |
| Chlorpyrifos | 43.75 ± 0.89 | 62.94 ± 0.77 |

**Table 2**. Acetylcholinesterase inhibition (AChE)

| *sample* | *% AChE* inhibition |
|---|---|
| Control | 100.00 ± 1.68 |
| Chlorine | 99.58 ± 1.09 |
| After filtration | 96.34 ± 1.06 |
| After chrlorination | 50.84 ± 2.11 |

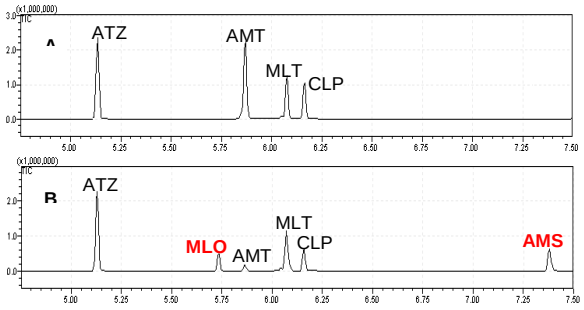


**Figure 1**. Chromatogram GC-MS Scan. A – After filtration B – After chlorination. ATZ- Atrazine/AMT-Ametrine/ MLT-Malathion/CLP-Chlorpyrifos/MLO-Malaoxon/AMS-Ametrine-sulfoxide.

**Acknowledgment:** INCTAA and CAPES.

[1] SIVAGAMI, K.; Krishna, R. R.; SWAMINATHAN, T. Photo catalytic degradation of pesticides in immobilized bead photo reactor under solar irradiation. Solar Energy, v.103, p. 488-493, 2014.

**Área: AMB** **Inscrição: 00258**

# Especiação de Cromo em Águas Naturais: Estudos em Guarapuava, Santa Terezinha do Itaipu e Ponta Grossa, Paraná, Brasil

**Vanessa Egéa dos Anjos (PQ),[1] Jucimara Kulek de Andrade (PG),[1] Camila Kulek de Andrade (PG),[2] Maria Lurdes Felsner (PQ),[2].**

**venajos@uepg.br ou vanessaegea.quim@gmail.com**

*[1]Departamento de Química, UEPG; [2]Departamento de Química, UNICENTRO*

Palavras Chave: especiação química, metal traço, Cr(III), Cr(VI), águas superficiais.

## Highlights

Chromium Speciation in Natural Waters: Studies in Guarapuava, Santa Terezinha do Itaipu, and Ponta Grossa, Paraná, Brazil. Ultrasound-Assisted Emulsification Microextraction was used. Parameters of water quality were analyzed.

## Resumo/Abstract

Em águas naturais é amplamente conhecido que a dinâmica, o comportamento, e toxicidade de metais traço é dependente das suas formas e espécies, de sua especiação química. O Cr(VI) é a espécie mais solúvel, móvel, e biodisponível. Essa espécie é considerada carcinogênica, enquanto, que o Cr(III) é a um espécie essencial no organismo humano. Devido as diferenças de toxicidade e o amplo uso de cromo em diversas atividades humanas, é de amplo interesse a avaliação da especiação de Cr em águas naturais. O objetivo do trabalho vem sendo estudar a presença de espécies de cromo em água naturais localizadas em diferentes regiões do Estado do Paraná, Brasil. Para tal, um procedimento simples foi implantado e validado para o estudo da especiação de cromo empregando a Microextração por Emulsificação Assistida por Ultrassom (UAEME) e Espectrometria de Absorção Atômica. Avaliou-se os teores de Cr(total), Cr particulado (CrPart), Cr(III) e Cr(VI) dissolvidos em amostras coletadas em Guarapuava (Rio das Pedras, Jordão e São Francisco), Ponta Grossa (Rio Verde, São Jorge e Pintangui) e Santa Terezinha do Itaipu (Rio Paraná). As concentrações totais de Cr foram baixas, compatíveis com ambientes não contaminados, e variaram entre 0,32 e 0,72 µg $L^{-1}$. O Cr dissolvido foi a fração majoritariamente para as amostras, indicando maior mobilidade e possível biodisponibilidade. Na fração dissolvida, o Cr(VI) foi predominante, como esperado, por se tratar de águas oxigenadas. O teor de Cr(III) variou entre 0,02 a 0,16 µg $L^{-1}$.

**Área: AMB** **Inscrição: 00114**

# Human health risk assessment of metals and metalloids in superficial waters near different industrial sources in Juiz de Fora City, Brazil

**Ricardo Soares (PQ),[1]* Wilson Machado(PQ),[2] David V. B. Campos(PQ),[3] Maria Inês C. Monteiro(PQ),[4] Aline S. Freire(PQ),[5] Ricardo E. Santelli(PQ).[5]**
**ricardosoaresuff@gmail.com**

*[1]State Environmental Institute, INEA; [2]Department of Geochemistry, UFF; [3]EMBRAPA Solos; [4]Mineral Technology Center; [5]Department of Analytical Chemistry, UFRJ*

Key words: Carcinogenic Risk, Metal pollution, Hazard quotient, Public Health.

## Highlights

- The risk to human health for potentially toxic elements has been assessed.
- Water Ingestion pathway contributed more for risk.
- People exposed to waters of Paraibuna River are at risk.

## Resumo/Abstract

The concentration of 11 metals and metalloids in surface waters near a tannery and a zinc smelter in Juiz de Fora City were investigated, and the human health risk posed to local residents via ingestion and dermal contact was evaluated. Concentrations of some elements (B, Cd, Cu, Mn and Zn) in Paraibuna River water were above the drinking water quality guidelines from the Brazilian National Council of Environment (Figure 1), as well as observed by Soares et al.[1] The findings of this study indicate potential health risks to the adults and children due to chronic exposure to contaminated superficial waters in the study area. Estimations of non-carcinogenic health risk for surface water revealed that mean hazard index (HI) values derived from the 11 elements for combined pathways (*i.e.*, ingestion and dermal contact) were >1.0 for children and adults. The point 4 exceeds in more 11 times the maximum HI for children and 3 times for adults, mainly due cadmium contribution. The estimated risk mainly associated to the ingestion pathway. Total cancer risk (TCR) related to Paraibuna River water exceeded the acceptable limit of $1 \times 10^{-6}$ for children and adults. Overall, the population exposed to Paraibuna River water remained at carcinogenic and non-carcinogenic health threat and the risk was higher for children.

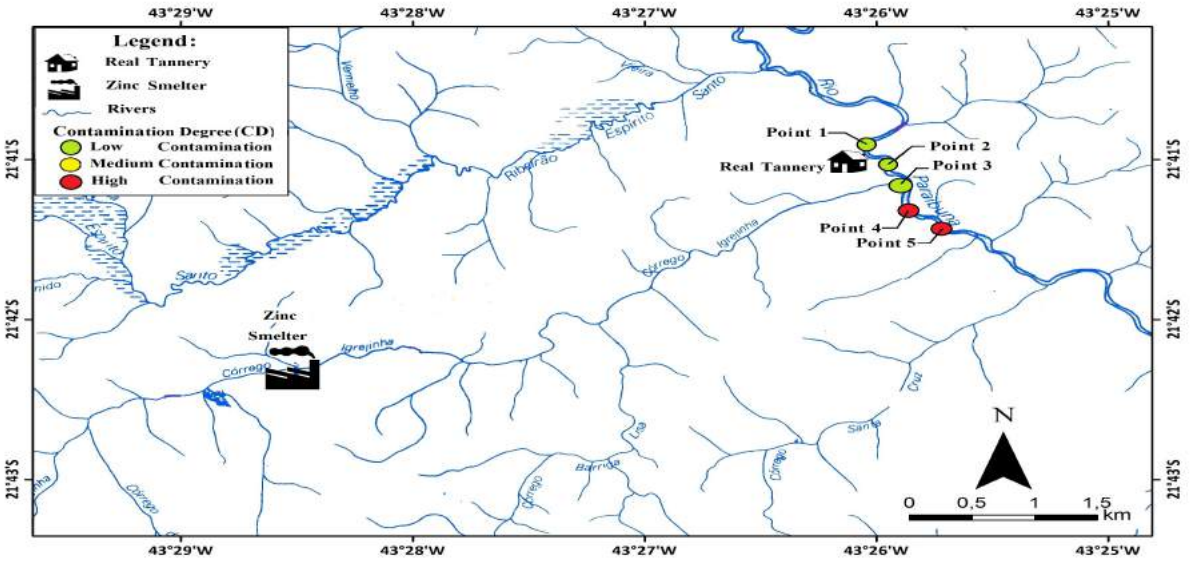


Figure 1. Contamination degree on superficial waters of Paraibuna River.

References:
Soares, R.; Machado, W.; Campos, D.; Monteiro, M.; Santelli, R. Rev. Virtual Quím., 2016, 8, 2105-2122.

**Área: AMB**
*(Inserir a sigla da seção científica para qual o resumo será submetido. Ex: ORG, BEA, CAT)*

**Inscrição:208**
*(Inserir o número de inscrição do autor que fez a submissão)*

# Metals characterization in surface sediments of rivers in the Central Amazonian region

**Márcia C. Bisinoti (PQ),[1] Isabela C. Constantino (PG),[1*] Grazielly C. Teodoro (IC),[1] Fabiana M. M. Paschoal (PQ), Wanderson G. Trindade (PQ), [2]Carlos E. Piovezan (IC),[1] Altair B. Moreira (PQ),[1]**

**bisinoti@ibilce.unesp.br; isabela.carreira@gmail.com**

[1]*Instituto de Biociências, Letras e Ciências Exatas, UNESP- Campus de São José do Rio Preto*
[2]*Instituto de Ciência Exatas e Tecnologia - UFAM, Campus de Itacoatiara-AM.*

Palavras Chave: *Amazonian, Sediment, Metal, Assessment.*

## Highlights

Surface sediments from Amazon region around Itacoatiara city were characterized;
Metals Al, Cu, Zn, Pb, Ni, Fe, Cr e Cd were determined by FAAS and GFAAS;
Levels observed for metal in surface sediments were considered safety maintenance of aquatic organisms;

## Abstract

The evaluation of sediment quality is a relevant tool in environmental studies, being a dynamic processes influenced by weathering, soil runoff, atmospheric precipitation[1,2]. Amazon is one of the most relevant biome of the world, but due to its great extension area, almost there are not researches in the region of Itacoatiara, the third most populous city in the state. A total of 8 superficial sediments were collected, being 3 in White water rivers (WW)(Amazonas 1 and 2, Madeira), and others 5 samples in Black water rivers (BW) (Anebá, Carú 1 and 2, Urubu 1, 2 and 3), during the dry season. Sediments were collected using a Ekman-Birge grab according the protocols of sampling and preservation recommended (CETESB, 2011).[4] Al, Cu, Zn, Pb, Ni, Fe, Cr e Cd were quantified by Flame or Graphite Furnace Atomic Absorption Spectrometer (240AA and 280Z, Varian) (USEPA, 1996). [5]Metals were related to the guidelines of the Canadian Council of Ministers of the Environment as showed in Table 1.[6] For all the sediments the results were below concentrations to Probable Effects Level (PEL) and Threshold Effects Levels (TEL), except for Cu. Overall, metal concentrations in sediments from WW samples (Madeira, Amazonas 1 and 2) were bigger than sediments from BW. Despite these rivers getnearestfromurbanareas, metals determination allowed to infer that all sediments sampled had values within the limits of the insurance for the maintenance of aquatic life in Central Amazonian.

**Table 1 -** Metals content (Pb, Cr, Ni, Al, Fe, Cu and Zn) in surface sediments from Itacoatiara region.

| | Pb mg kg$^{-1}$ | Cr mg kg$^{-1}$ | Ni mg kg$^{-1}$ | Al g kg$^{-1}$ | Fe mg g kg$^{-1}$ | Cu mg kg$^{-1}$ | Zn mg kg$^{-1}$ |
|---|---|---|---|---|---|---|---|
| **Amazonas 1** | 9.5 | 19 | 11 | 14 | 1.1 | 13 | 24 |
| **Amazonas 2** | 28 | 28 | 15 | 22 | 1.4 | 26 | 40 |
| **Madeira** | 15 | 28 | 17 | 132 | 2.0 | 27 | 50 |
| **Carú 1** | 20 | 20 | < 6.0 | 45 | 1.4 | < 11 | 11.7 |
| **Carú 2** | 0.2 | 2.2 | < 0.02 | 1.2 | 0.05 | < 2 | 0.6 |
| **Anebá** | 21 | 23 | 9 | 57 | 1.5 | 16 | 9.7 |
| **Urubu 1** | 11 | 22 | 9.7 | 18 | 1.3 | 14 | 31 |
| **Urubu 2** | 2.5 | 2.8 | < 1.7 | 2.1 | 0.7 | < 21 | 3.3 |
| **Urubu 3** | 1.6 | 1.4 | < 0.5 | 0.6 | 0.1 | < 0,9 | 1.2 |
| **TEL** | 35 | 37 | * | * | * | 36 | 123 |
| **PEL** | 91 | 90 | * | * | * | 197 | 315 |

(*) not determined

## References

[1]BLASCO, J.; SÁENZ, V.; GÓMEZ-PARRA, A. *Science of the Total Environment*, 247, 189-199, 2000.
[2]SANTOS-ECHEANDIA, J. et al. *Marine Chemistry*, 117, 77-87, 2009.
[3]MURCHA, A.P; VASCONCELOS M.T.S; BORDALO, A.A. *Environmental Pollution*, 121, 169–180, 2003.
[4]CETESB. Brandão, C. J. et al. (Org.). São Paulo: CETESB; Brasília: ANA, 2011.
[5]USEPA - Method 3050B - Acid digestion of sediments, sludges, and soils. Ohio, 1996.
[6]CCME- Canadian Sediment Quality Guidelines for the Protection of Aquatic Life: Sumary tables. Winnipeg, 2002.

**Acknowledgements:** To financial support granted from FAPESP(Project nº2015/22954-1) and CNPq.

**Área: AMB** **Inscrição: 00042**

# Monitoring of trace elements in sediments from the beaches next to the Doce River Estuary – ES/Brazil

**Tiago Cunha (PG),[1*] Nathália L. P. Wyatt (IC),[1] Luiza V. Vieira (PG),[1] Maiara Krause (PG),[1] Geisamanda P. Brandão (PQ),[1] Jacqueline Albino (PQ),[2] Maria Tereza W. D. Carneiro[1](PQ),[1]**

**mariacarneiro@hotmail.com; cunha.tiagopereira@gmail.com**

*[1]Departamento de Química, Universidade Federal do Espírito Santo; [2]Departamento de Oceanografia e Ecologia, Universidade Federal do Espírito Santo.*

Palavras Chave: *Monitoring, Trace elements, Beach, Sediment.*

## Highlights

Trace elements determination in sediments. Evaluation of the beaches next to Doce River estuary after Samarco dam collapse. Regência beach showed higher values than Comboios and Riacho beaches.

## Resumo/Abstract

The region of the mouth of Doce river deserves special attention, because it is of great ecological importance due to animals threatened with extinction and to be a biological reserve area. The objective of this work was the determination of Co, Cr, Cu, Mn, Ni, Pb and V in sediments samples from the beaches next to Doce river estuary (Regencia, Comboios and Barra do Riacho). The samples were collected in October 2016 and June 2017 from face, berm and restinga points of each beach. The methodology adopted to samples was US EPA 3051A with subsequent by ICP-MS analysis. The results showed high levels of trace elements in the sediments from Regencia beach, nearer site of the Rio Doce Estuary. The principal components analysis was applied and showed separation in the data of the Regencia beach (Figure 1). Although the metals concentrations are below the reference values stablished by environmental legislations,[1,2] this coastal region deserves attention. The higher concentrations near to the Doce river may indicate that the Regencia beach is impacted by the collapse of a dam in Minas Gerais.

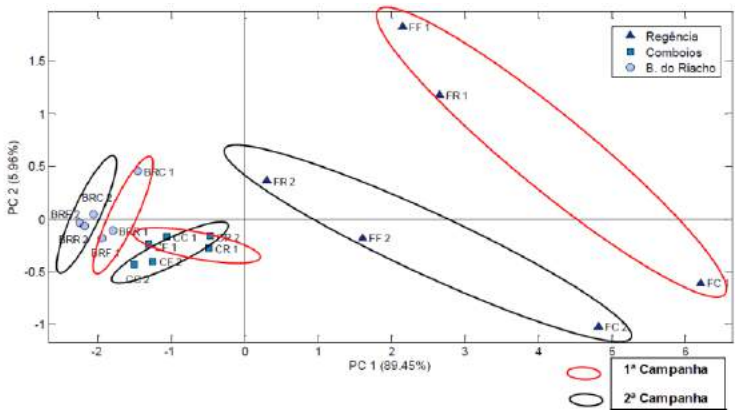


Figure 1: Score plot obtained from trace elements concentration values in sediments from the beaches next to the Doce River Estuary.

[1] CCME (Canadian Council of Ministers of the Environment). 1995. Protocol for the derivation of Canadian sediment quality guidelines for the protection of aquatic life.
[2] CONSELHO NACIONAL DO MEIO AMBIENTE – CONAMA. Resolução nº 420, de 28 de dezembro de 2009.

**Área: AMB** **Inscrição: 01397**

# Evaluation of agrochemicals trifluralin, atrazine, alachlor and chlorpyrifos in soil samples from Arapongas - PR region.

**Fernanda Gonçalves Morro (IC),[1] Jossy K. Brasil Bernardelli (PQ),[1*] Danielle C. Schnitzler (PQ),[1]**

**fernandamorro@alunos.utfpr.edu.br; jossybrasil@hotmail.com**

*[1]Department Academic of Chemistry and Biology, UTFPR*

Keywords*: Agrochemicals, Soil contamination, gas chromatography, mass detector.*

## Highlights

The presence of agrochemicals in soil samples is indicative of environmental contamination.
The analyzed samples presented concentration of agrochemicals lower than the limit of quantification (LQ).

## Resumo/Abstract

In order to evaluate the presence of agrochemicals, trifluralin, atrazine, alachlor and chlorpyrifos, six soil samples were collected at 3 different points, at the surface and at 20 cm depth using a Dutch auger. These points are located in Arapongas, in the Paraná state, in this region, there is a suspicion of contamination of the environmental matrices with agrochemicals, due to the presence of agricultural areas and an agrochemical factory.
The analytical method was developed and validated (LQ of 1.70, 1.98, 1.95 and 1.80 ng $g^{-1}$ for Trifluralin, atrazine, alachlor and chlorpyrifos, respectively, linear range of 5 to 100 ppb, recovery between 70 and 110% relative standard deviation of less than 12%) and consisted of sample extraction and analysis by GC-MS/MS (Agilent, model 7890/7000). The method was precise and accurate. Five grams of the samples were extracted with 20 mL of ethyl acetate on an ultrasound for 45 minutes and a frequency of 40 kHz. Thereafter, filtration, cleanup, and evaporation of the solvent were performed in a rotary evaporator. Compounds were reconstituted in 1 mL of ethyl acetate and filtered through a 0.22 µm PVDF membrane. Despite the indications of contamination of environmental matrices by agrochemicals, due to the use in agriculture and the production and storage by an installed factory near the collection points, the results obtained show that, for all the samples, the four compounds analyzed had a concentration below LQ.

**Área: AMB** **Inscrição: 01360**

# Carbono oxidável com permanganato em solos do Paraná – horizontes dos solos e correlações com análise de macronutrinentes usando PCA.

**Ísis K. Caetano*** **(PQ),[1] Ezequiel J. Novacoski (FM),[2] Laura H. Lustosa (IC), [3] Aline Marques Genú (PQ), [4] Katia Cylene Lombardi (PQ),[5] Afonso Figueiredo Filho[5] (PQ). Pedro P. Gonzáles-Borrero (PQ)[2]**

**isiskc@hotmail.com**

*[1]Departamento de Química, UNICENTRO; [2]Departamento de Física UNICENTRO; [3] Departamento de Química, UTFPR, Curitiba – PR, [4]Departamento de Agronomia UNICENTRO – Guarapuava – PR e [5]Departamento de Engenharia Florestal – UNICENTRO - Irati – PR.*

Palavras Chave soil organic matter, :C labil, soil management, C sequestration, Oxisoil, greenhouse effect.

## Highlights

Permanganate Oxidizable Carbon and macronutrients analysis in Paraná soils – soils horizons and correlations using PCA
The reforestation Dystrudepts soils have more C labil than Oxisols. The C lábil have inverse correlations with clay content and pH. PCA differentiated surfaces of the subsurfaces soil.

## Resumo/Abstract

As mudanças no C oxidável por permanganato[1] (carbono lábil) podem indicar variações na qualidade do solo[2]. A diferença entre o C total e o oxidável fornece o C que pode ser capturado pelo solo e que ajuda a minimizar o efeito estufa.. A determinação dos macronutrientes[3] (Ca, Mg, K, P), Al, Al + $H^+$, pH, argila, silte, C, H, N e C oxidável com permanganato de potássio[2] foram correlacionados utilizando a análise de componentes principais (PCA). O Cambisolo háplico Ta distrófico típico, Latossolo amarelo distrófico típico (ambos com Floresta Ombrófila Mista) e Cambissolo háplico alítico típico (com plantio de *Araucária angustifólia*) contiveram mais C lábil do que os Latossolos bruno (com cultivo de milho 5 anos –plantio direto e com mata natural), Latossolo vermelho distrófico típico , Cambissolo háplico alítico típico e Cambissolo Háplico Ta distrófico lépitico ( com Floresta Ombrófila Mista), então os últimos sequestram mais C. Como esperado, os horizontes A têm mais C lábil do que os Horizontes B. A PCA correlacionou a matéria orgânica lábil rica em N e a não rica em N para a separação dos horizontes do solo. O pH, teor de argila e N foram inversamente correlacionados ao teor de C lábil, outras análises (Figura 1a) foram positivamente correlacionadas. O PCA diferenciou horizontes A do B de solos. Esses resultados são importantes para avaliar o seqüestro de C e sensibilidade ao manejo do solo dos Cambissolos em Latossolos.

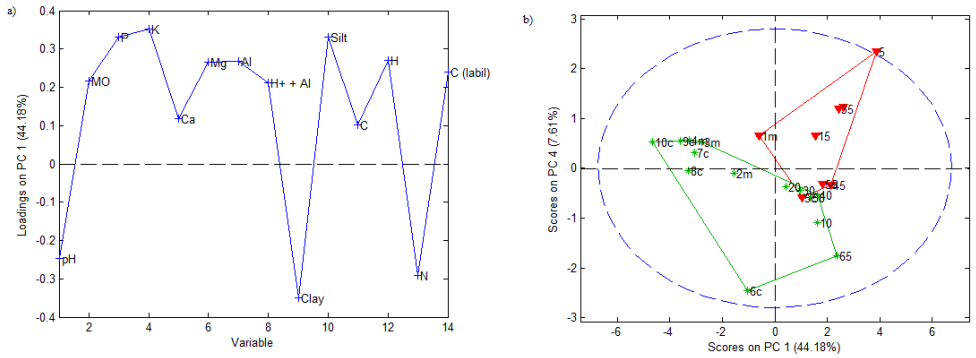


Figura 1 – PCA das analises físicas e químicas do solo e C oxidável com permanganato de potássio (C lábil) – 22 amostras de solo: a) pesos and b) escores

[1] Weil R. R. et al. 2012. *Soil Sci. Soc. Am. J*. 76, 494.
[2] Weil, R. R. et al. *2003. Am. J. of Alt. Agric*. 18,3.
[3] Brasil, Ministério da Agricultura. 1997. *Manual de métodos de análise de solos*. Rio de Janeiro – RJ. EMBRAPA.

**Área: AMB** **Inscrição: 01352**

# Adsorção individual e competitiva de chumbo em cinco solos de uma topossequência do cerrado brasileiro.

**Milenna Milhomem Sena (PG),[1] Jader Galba Busato (PQ),[2] Antonio Carlos Saraiva da Costa (PQ),[3] Fernando Fabriz Sodré (PQ)[1*]**

**ffsodre@unb.br**

*[1]Instituto de Química, UnB; [2]Faculdade de Agronomia e Medicina Veterinária, UnB; [3]Departamento de Agronomia, UEM.*

Palavras Chave: *Chumbo, Adsorção competitiva, Solos, Freundlich.*

## Highlights

Individual and competitive adsorption of lead in four soils from the Brazilian Cerrado. For all soils, sorption capacity decreases in competitive systems containing copper. In the organosol, this decrease was limited to the higher affinity of copper to organic binding sites.

## Resumo/Abstract

O comportamento e a disponibilidade de metais em solos são governados por inúmeros processos atuantes em grupos funcionais orgânicos e inorgânicos. Uma das maneiras de se investigar o comportamento destas espécies consiste na obtenção de isotermas de adsorção cujos com a consequente ajuste dos dados empíricos empregando-se diferentes modelos. Este trabalho buscou avaliar a adsorção de chumbo em solos de uma toposoquencia do cerrado, bem como o efeito competitivo da adsorção do chumbo em sistemas contendo cobre. Foram selecionados cinco solos, sendo dois Latossolos Vermelhos (LV1 e LV2), um Latossolo Vermelho-Amarelo (LVA), um Gleissolo (G) e um Organossolo (O). Os experimentos de adsrção consistiram na transferência de 0,1 g de solo previamente homogeneizado para tubos de ensaio seguido da adição de solução de 0,002 mol/L de $CaCl_2.2H_2O$ enriquecida com 0, 10, 20, 30, 40, 60, 80 e 100 mg/L de $Pb^{2+}$. Sistemas competitivos foram preparados de maneira idêntica, porém em soluções também contendo 80 mg/L de $Cu^{2+}$. As suspensões foram agitadas por 24h, centrifugadas (2000 rpm, 15 min) e a concentração de $Pb^{2+}$ foi determinada no sobrenadante ($C$) por espectrometria de emissão atômica com plasma de micro-ondas. Isotermas de adsorção foram construídas tendo-se a quantidade adsorvida ($\theta$) avaliada em função de $C$, sendo os dados então ajustados pelo modelo de Freundlich ($\theta = K_f C^{1/n}$) que melhor descreve o fenômeno adsortivo em superfícies heterogêneas. A Tabela abaixo mostra os valores obtidos para os parâmetros $K_f$, relacionado à capacidade adsortiva, e $n$ que indica a heterogeneidade das superfícies.

| Solos | Sistema individual | | | Sistema competitivo | | |
|---|---|---|---|---|---|---|
| | $K_f$(mg g$^{-1}$) | $n$ | $r^2$ | $K_f$(mg g$^{-1}$) | $n$ | $r^2$ |
| LV1 | 0,96 | 2,50 | 0,9974 | 0,29 | 1,99 | 0,9902 |
| LV2 | 0,83 | 2,41 | 0,9904 | 0,28 | 1,95 | 0,9839 |
| LVA | 0,36 | 1,90 | 0,9964 | 0,11 | 2,03 | 0,9949 |
| G | 1,37 | 2,61 | 0,9941 | 0,54 | 1,98 | 0,9920 |
| O | 2,49 | 2,56 | 0,9929 | 1,24 | 2,31 | 0,9824 |

Para ambos os sistemas, individuais e competitivos, o ajuste pelo modelo de Freundlich foi significativo ($R^2$>0,98). A capacidade adsortiva do chumbo foi superior para os solos localizados na base da topossequência (O e G), provavelmente em função das quantidades mais elevadas de matéria orgânica e argilominerais do tipo 2:1. Este comportamento foi evidenciado tanto nos sistemas individuais quanto nos competitivos. Para todos os solos observou-se redução da capacidade adsortiva do chumbo sob competição com o cobre. A redução no valor de $K_f$ foi maior nos solos mais intemperizados, ou seja, localizados no topo da toposequencia. A menor redução, de cerca de 50%, foi observada para o Organossolo que contém níveis mais elevados dew carbono orgânico, evidenciando assim uma maior competição com o cobre que exibe elevada afinidade a grupos funcionais orgânicos.

**Área: AMB** **Inscrição: 00565**

# Utilização da estatística multivariada para a determinação dos parâmetros físicos e químicos mais relevantes do solo de trilha de Ubatuba-SP

**Maria do Carmo Oliveira Jorge (PQ),[1]* Antônio José Teixeira Guerra (PQ),[1] Maria Lucia T. G. Mendonça (FM), [2] Rosana Petinatti da Cruz (FM)[3] .**

**maria.mendonca@ifrj.edu.br; orofila@gmail.com**

*[1]Departamento de Geografia UFRJ; [2]IFRJ – Campus Maracanã ; [3]UFRRJ- CTUR*

Palavras Chave: *Solo; Análise físico-química; Estatística multivariada*

## Highlights

Análises físico-química de solos de Ubatuba - SP como ferramenta para um turismo sustentável.

## Resumo/Abstract

Determination of the most relevant physical and chemical parameters of soil samples of tracks for sustainable tourism, using multivariate statistics.

## Introdução

O turismo é considerado uma importante atividade com um papel significativo no desenvolvimento econômico, social e cultural em diversas localidades, com um lado antagônico. Quando realizado de forma planejada e consciente, é possível se associar a geração de emprego e renda, com a conservação da cultura, da identidade regional e do ambiente. Por outro lado, quando é realizado sem planejamento, os impactos negativos ao ambiente podem ser inúmeros (BUARQUE, 2002). Este trabalho teve o objetivo de avaliar o solo de trilhas, empregando uma metodologia com análises de densidade real e aparente, porosidade, pH, granulometria e matéria orgânica e os elementos químicos, os quais foram determinados por espectrometria de fluorescência de Raios-X (FRX) e espectrometria de difração de Raios-X (DRX), no Laboratório de Geomorfologia, da Universidade de Wolverhampton, Inglaterra. Foram 19 pontos de coletas, com duplicatas de amostras de solo de talude, ao longo das trilhas: Sítio Lama Mole, Sítio Recanto da Paz, Sete Praias, Quilombo e Cachoeira Água Branca, situadas em Ubatuba-SP. Com os resultados obtidos foram efetuadas as análises estatísticas de modo multivariado: matriz de correlação e análise fatorial (*FA-Factorial Analysis*) utilizando o *software* Statistica 6.0, com a intenção de reduzir o número de variáveis, mas com a perda mínima de informações.

## Resultados e Discussão

O primeiro procedimento empregado foi de padronizar os dados para que o fator escala não influenciasse em nenhuma variável. Na matriz de correlação [R], foi constatando que apenas o pH não encontrava-se correlacionado com nenhum outro parâmetro; a matéria orgânica, apenas com a porosidade, densidade aparente e real e a argila; os óxidos encontravam-se bastante correlacionados, sendo o $Na_2O$ e o $K_2O$ com 12 parâmetros; os elementos químicos que se apresentavam mais correlacionados foram o Pb, Re, Th e Nb (12 parâmetros) todas as correlação foram superiores a p › 0,5. Para a análise fatorial, empregou-se o procedimento de rotação ortogonal, utilizando o método Varimax, obtendo uma porcentagem acumulada da variância total dos dados originais de 80,29%, determinando três fatores F1, F2 e F3. No primeiro (F1), $Na_2O$, $Fe_2O_3$, $Al_2O_3$(-), $P_2O_5$, $SiO_2$, Ti, Mn, Zn, Br, Rb e Re com pesos de 0,71 a 0,98, fatores quando apresentam pesos altos, são indicativos de variáveis determinantes para qualificar as amostras de solo. No segundo (F2), as variáveis foram: MgO, $SO_3$, CaO, Ga, Sr, Y, Zr, Nb, Te, Nd e Th; no terceiro (F3), as variáveis forma somente densidade aparente e argila. O primeiro grupo (F1) é um indicativo da estrutura do solo, o segundo grupo (F2) é um indicativo das propriedades magnéticas do solo e o terceiro (F3) é um indicativo da possibilidade da deterioração do solo (intemperismo), sendo dois parâmetros relacionados.

## Conclusões

A técnica estatística multivariada utilizada, análise fatorial (*FA-Factorial Analysis*), reduziu o número de 31 variáveis analisadas para 11 parâmetros significativos para a definição da qualidade do solo. Acarretando uma economia no custo e no tempo de análise.

[1]BUARQUE, S.C. Construindo do desenvolvimento local sustentável. Rio de Janeiro: Garamond, 180 p.2002 .

**Área: AMB** **Inscrição: 01178**

# Influência da adição de matéria orgânica em interações Metal-nanopartículas

**Daniele Frasson Vieira* (IC)[1], Wander Gustavo Botero (PQ)[2], Luciana Camargo de Oliveira(PQ)[3], Danielle Goveia (PQ)[1]**

**daniele.frasson@grad.itapeva.unesp.br**

[1]*Universidade Estadual Paulista "Júlio de Mesquita Filho" - UNESP, Campus Experimental de Itapeva, Itapeva-SP.*
[2] *Universidade Federal de Alagoas, Campus de Arapiraca, Arapiraca-Al.*
[3]*Universidade Federal de São Carlos, Campus de Sorocaba, Sorocaba - SP.*

Palavras Chave: *íons metálicos, sistemas aquáticos, nanomaterial.*

## Highlights

Influence of the addition of organic matter in metal-nanoparticle interactions. Metal released after addition of Humic Substances in M-nano interactions. Essential metals are available in the environment. Toxic metals are potentiated.

## Resumo/Abstract

A nanotecnologia é um dos principais focos das atividades de pesquisa e seu desenvolvimento tem sido apontado como uma nova revolução tecnológica. Dadas as suas características, estudar suas interações químicas, seu ciclo e destino é fundamental uma vez que existe possível risco de contaminação ambiental. Em águas naturais, apenas uma parcela de metais está presente em sua forma livre enquanto a maior parte está complexada com material inorgânico ou orgânico (Substâncias Húmicas Aquáticas). Nosso foco será estudar a influência das nanopartículas descartadas em sistemas aquáticos extremamente complexos, verificando como a inserção de matéria orgânica na forma de substâncias húmicas aquáticas afetarão as interações Metal-nano.

Foram preparadas soluções de contendo íons Fe e Mn (2,0 $mgL^{-1}$) e nanopartícula de sílica LUDOX LS30 (800$\mu$L). Em seguida foram submetidas a um sistema de ultrafiltração com uma membrana de porosidade de 1kDa. Determinou-se o metal livre. Adicionou-se às soluções as Substâncias Húmicas Aquáticas. As determinações dos metais foi feita por espectrômetro de absorção atômica com atomização por chama. A Tabela 7 apresenta os resultados inicialmente e após 24 horas da adição de SHA.

**Tabela 7.** Concentração de metal complexado e livre antes e depois de 24 horas da adição das SHA.

| **Nanopartículas + Metais** | | | **Nanopartículas + Metais + SHA** | | |
|---|---|---|---|---|---|
| | Metal complexado | Metal livre | | Metal complexado | Metal livre |
| Fe-nano | 34,3 % | 65,7% | Fe-nano/Fe-SHA | 2,0% | 98,0% |
| Mn-nano | 30,1% | 69,9% | Mn-nano/Mn-SHA | 11,3% | 88,7% |

Os resultados apresentaram valores elevados de metal livre para os dois metais estudados. Em estudos anteriores verificou-se que interações SH-metal são mais fortes, os metais não são disponibilizados ao adicionar nanopartículas ao sistema. Neste caso as nanopartículas apresentam inicialmente baixa interação com os metais estudados. Com a adição das Substâncias Húmicas, estas podem estar protegendo os sítios das nanopartículas, e vice-versa, liberando os metais em solução. Quando o íon está inicialmente interagindo com a nano-sílica, observamos que o metal lábil é liberado para o ambiente. Esta característica pode ser interessante quando estudamos o metal essencial, porém, pode ser crítica se olharmos para os não essenciais, potencialmente tóxicos.

Agradecimentos à FUNDUNESP, CNPQ (458875/2014-7) e FAPESP (2016/23728-8) pelo auxílio financeiro e FAPESP (2015/ 21232-2) pela bolsa concedida.

**Área: AMB** **Inscrição:00363**

# Avaliação da recuperação de potássio no vinhoto tratado por biorreator a membrana de duplo estágio (BRMAn).

**Luana B. M. Corrêa (IC)[1*], Inês P. M. Guimarães (IC) [1], Jessica R. Barbosa (IC) [1], Lucilaine V. S. Santos(PQ) [1,2]**

**luanabmcorrea@gmail.com**

*[1] Departamento de Engenharia Química (PUC/MG); Departamento de Engenharia Sanitária e Ambiental (UFMG)[1],[2].*
Palavras Chave:*Vinhoto, Potássio, Precipitação, Biorreator a membrana, Recuperação de nutrientes.*

## Highlights

Evaluation of potassium recovery in vinasse treated by a two-stage anaerobic membrane bioreactor. Brazil has acid soil and needs to use fertilizers to make it productive. The production of potassium fertilizer is limited to only one mine, and it is not enough to supply the national demand. The vinasse is an effluent rich in potassium and can be an alternative for getting this nutrient.

## Resumo/Abstract

O Brasil é um país de solos majoritariamente ácidos, fato que justifica a utilização de grandes quantidades de fertilizantes, compostos por micro e macronutrientes, dentre eles, o potássio. A produção nacional de potássio fertilizante é condicionada somente à usina de Taquari-Vassouras, em Sergipe, a qual não atende à demanda exigida pelo país, fazendo com que gastos extras sejam gerados com importações para o devido suprimento.

Figura 1- Fluxograma metodológico

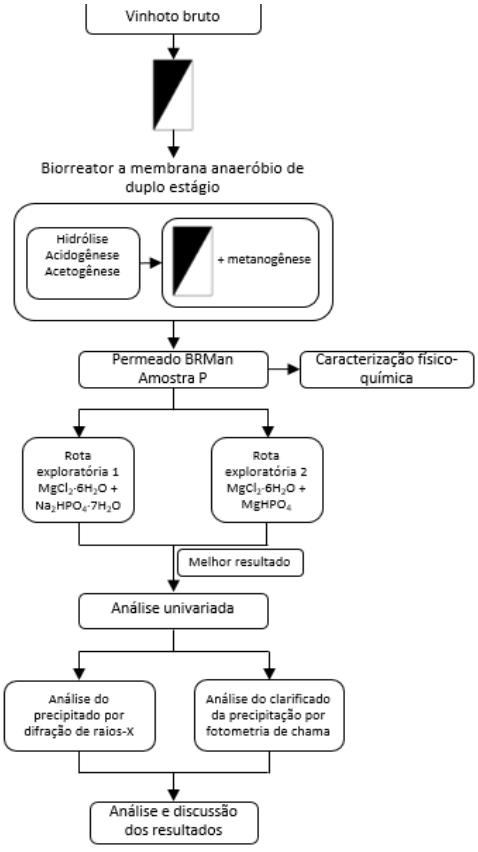


Na busca por fontes alternativas do nutriente, o vinhoto – resíduo da destilação fracionada do mosto fermentado de cana-de-açúcar – é uma potencial opção para obtenção deste mineral, pois em sua complexa composição estão presentes, em especial, sais de potássio. Apesar de já ser utilizado como fertilizante a aplicação descontrolada do vinhoto sobre os solos pode causar a desertificação do local, justificando a necessidade de pré-tratamento. Portanto, o presente trabalho avaliou a recuperação de potássio através de sua precipitação no efluente vinhoto tratado biologicamente por biorreator a membrana de duplo estágio. As etapas metodologicas são apresentadas na Figura 1. Após 30 minutos do inicio da precipitação química observou-se a formação de cristais que, de acordo com os testes realizados por difração de raios-X, Figura 2, eram compostos pelos seguintes minerais: Newberyta, Catita e Fosfato de Magnésio e Potássio.

Figura 2 – Resultado da Fluorescência de Raios X

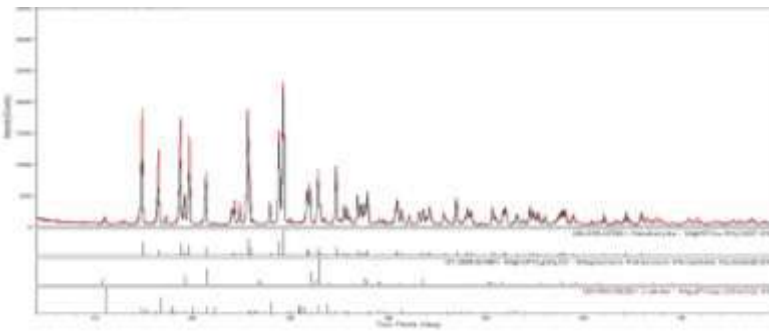

O efluente, após precipitação, foi analisado por fotometria de chama que indicou 55% de remoção de potássio. Assim, demonstrou-se que a precipitação química é uma técnica viável para obtenção de potássio através de efluentes, a exemplo do vinhoto.

**Área: AMB** **Inscrição: 00429**

# $CO_2$ capture by mixed matrix membranes with metal organic frameworks (MOF) of Al

**Tatiana P. Abreu[1] (PG), Helen C. Ferraz[2] (PQ), Luiza C. Moura[1] (PQ), Jussara L. Miranda[1]* (PQ)**

**tatiana.abreu26@gmail.com; jussara@iq.ufrj.br**

*[1]Instituto de Química, UFRJ. [2]Programa de Engenharia Química, COPPE, UFRJ.*

Keywords: *Metal Organic Frameworks, $CO_2$ Capture, Polymer Membranes, Mixed Matrix Membranes*

## Highlights

Mixed matrix membranes were obtained with the dispersion of MOFs in polymers in order to increase the permeability and selectivity to $CO_2$ and cheapen its capture and separation process.

## Resumo/Abstract

The anthropogenic emission of carbon dioxide is one of the main causes of the increase of the greenhouse effect and global warming. In order to selectively capture this gas, in this work, mixed matrix membranes were synthesized with dispersed MOF MIL-53 (Al). The synthesis of MIL-53 (Al) was performed by the hydrothermal method and its activation done according to Bezverkhyy[1]. MIL-53 (Al) was analyzed by X-ray diffraction (Fig. 1), FTIR, thermogravimetric analysis and $CO_2$ and $CH_4$ sorption, The methodology of mixed membrane matrix synthesis (MMM) was done using modifications of Musselman I.[2] and Ferraz H.[3] MMM were analyzed by Scanning Electron Microscopy (Fig. 2), FTIR, XRD, permeability and selectivity analyses.

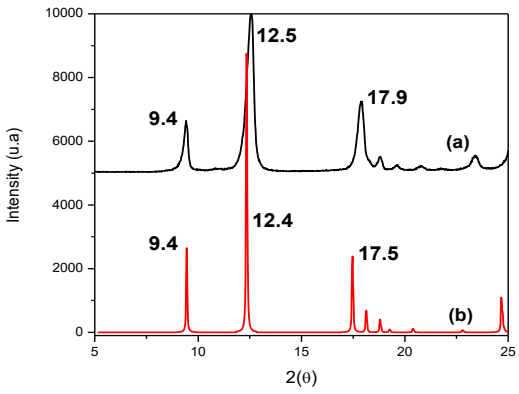


Figure 1. XRD of (a) MIL-53(Al) activated and (b) literature[1].

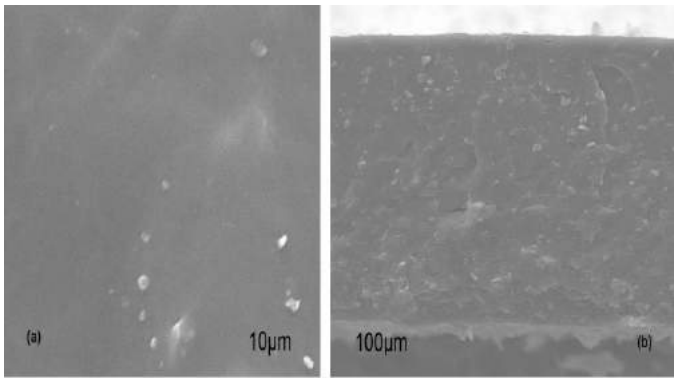


Figure 2. SEM front (a) and side (b) of MMM.

The activated MIL-53 (Al) showed good crystallinity, with the characteristic peaks at 9.4º, 12.5º and 17.9º of the reported XRD (Fig. 1). The thermogravimetric analysis showed that MIL-53 (Al) presented a high thermal stability, decomposing at 833 K. $CO_2$ adsorption analyses showed up to 14 mmol $CO_2$/g at 10 bar and 22 mmol $CO_2$/g at 30 bar. SEM of mixed matrix membrane (fig.2) showed a good dispersion of the MOF in the polymer. It can then be concluded that MIL-53 (Al) was obtained, as well as a good MMM. $CO_2$ and $CH_4$ permeability and selectivity analyses are in progress.

1.BEZVERKHYY,I; et.al.. Microporous and Mesoporous Materials, 2014.
2.MUSSELMAN,I; et.al.;. Microporous and Mesoporous Materials, 2014.
3.FERRAZ,H.;MIRANDA J.; Separation and Purification Technology, 2018.

**Área: _AMB_** *(Inserir a sigla da seção científica para qual o resumo será submetido. Ex: ORG, BEA, CAT)*

**Inscrição: _01406_** *(Inserir o número de inscrição do autor que fez a submissão)*

# Evaluation of the development of an acidophilic chemolithotrophic microorganism using meteoritic material as energy source

**Gabriel G. Silva (PG),[1]* Fabio Rodrigues (PQ)[1]**

**g_goncalves_silva@hotmail.com**

[1]*Instituto de Química, USP*

Palavras Chave: *Acidithiobacillus ferrooxidans, meteorite, astrobiology, biosignature.*

## Highlights

Iron oxidation and mineral formation during interaction between organisms and simulated meteoritical material was monitored. Meteorites are explored as a novel source of energy for microorganisms on oligotrophic conditions.

## Resumo/Abstract

*Acidithiobacillus ferrooxidans* is an acidophilic chemolithotrophic microorganism that oxidizes iron or sulfur to obtain energy. When using iron as an energy source, $Fe^{2+}$ ions in solution are oxidized to $Fe^{3+}$ with release of electrons. These electrons provide the necessary energy for oxidative phosphorylation in order to allow the production of ATP from ADP. Under optimum conditions for organism development, the $Fe^{3+}$ generated is precipitated initially in form of the metastable mineral Schwertmannite - $Fe_8^{3+}O_8(OH)_{8-2x}(SO_4)_x \cdot nH_2O$, where x = 0.5 to 2 and n = 13 to 17 - which eventually becomes the mineral Jarosite - $XFe_3^{3+}(SO_4)_2(OH)_6$, where x = $K^+$, $NH_4^+$, or $H_3O^+$. Besides being abundant on our planet, iron can be found as natural metallic alloys and in different mineral species distributed over various bodies of the Solar System. Meteorites are presented as a good alternative for laboratorial study of these bodies since they represent rocks from different places of the Solar System. Cultures of *Acidithiobacillus ferrooxidans* were grown in simulated meteorite media, while the ability to oxidize iron in these conditions was monitored. The change in pH trend showed the moment that precipitates' formation begun and their compositions were studied. Within astrobiology, the results evaluate potential use of meteoritical material as source of nutrients and energy for organisms in space or during the formation of life on Earth and to provide information on how these interactions could generate biosignatures.

**Área: AMB** **Inscrição: 01101**

# Geração de microrganismos seletivos a partir da biomassa residual da casca do arroz para produção biocombustíveis

**José Luiz Vieira (IC)*, Cíntia Souza da Silva (PG), Jair Juarez João (PQ).**
**jair.joao@unisul.br; jlvieira1994@uol.com.br**

*Departamento de Ciências Ambientais, Universidade do Sul de Santa Catarina, UNISUL, Tubarão, SC.*
Palavras Chave: *Casca de arroz, Biomassa residual, Biocombustíveis, Microrganismos, Açúcares redutores.*

## Highlights

**Generation of selective microorganisms from the residual biomass of the rice husk for the production of biofuels.** Rice husk is a rich source of microbiological diversity that makes them able of producing highly efficient microorganisms for the production of reducing sugars and transformed into bioalcohol.

## Resumo/Abstract

A casca do arroz, devido às suas propriedades e composição química, pode ser utilizada como fonte de nutriente para o desenvolvimento de microrganismos seletivos que podem gerar enzimas lignocelulósicas e produzir biocombustíveis. Inicialmente foi realizado o pré-tratamento da casca do arroz, onde foi observado uma diminuição da concentração de hemicelulose devido ao aumento na concentração de açúcares redutores (pentoses) e de lignina **Figura 1b**). O pré-tratamento da casca do arroz permitiu a remoção de parte da lignina e hemicelulose da estrutura da biomassa e, com isso, foi possível obter as enzimas a partir dos microrganismos gerados. É importante ressaltar que a biomassa da casca do arroz é uma fonte rica de diversidade microbiológica que os torna capazes de produzir microrganismos altamente eficientes para produção de açúcares redutores (**Figura 1a**). Os resultados mostraram que as enzimas obtidas são capazes de hidrolisar a estrutura lignocelulósica da casca do arroz, produzindo concentrações significativas de açúcares redutores no meio, com valor máximo de 4 $g.L^{-1}$ em aproximadamente 3 horas. Após este período ocorre uma estabilização na produção dos açúcares, que foi confirmado com testes com DNS. Com os resultados obtidos, pode-se concluir que os microrganismos presentes no inoculo obtido a partir da casca de arroz são capazes de produzir enzimas celulósicas capazes de realizar a hidrólise da casca do arroz para produção de açúcares redutores que posteriormente podem ser transformados em bioálcool.

**Figura 01: (a)** Fluxograma da metodologia utilizada; **(b)** Cinética de formação de açúcares.

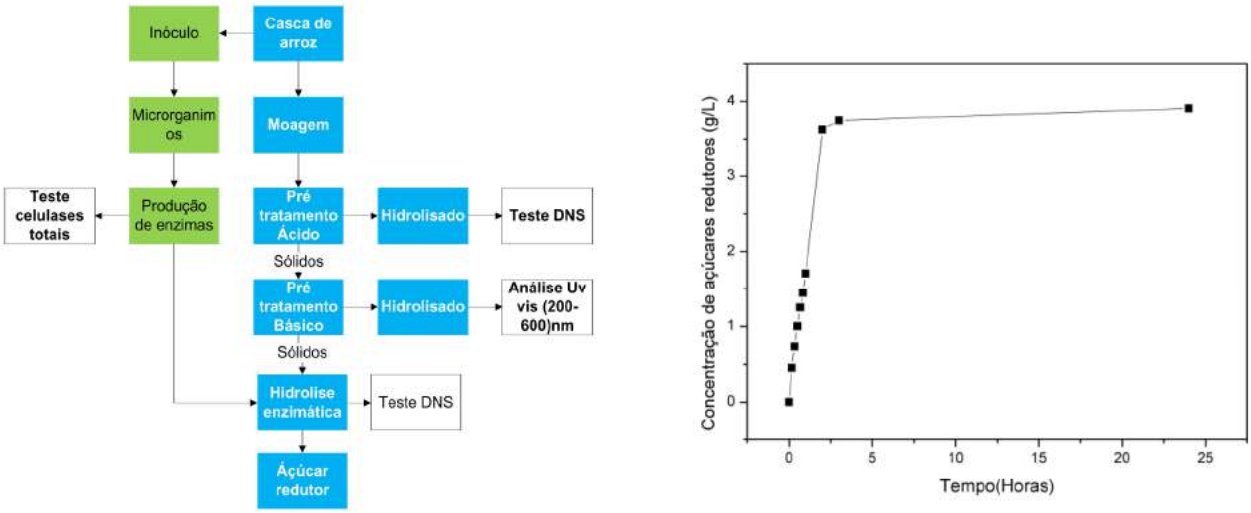


[1] DEMAIN, A.L.; DAVIES, J. E. Manual of Industrial Microbiology and Biotechnology. Second Edition, ASM Press, Washington, D.C., **1999**, 830P

**Agradecimentos:** À UNISUL e a CNPQ.

**Área:** AMB **Inscrição:** 00197

# Economia Circular na Agropecuária: Ensaios Iniciais para Estabilização de Resíduos Orgânicos e Produção de Biogás

**Marina Bêz Gório da Silva*** **(IC),[1] Maria Paula Pedão Domingues (IC),[1] Cleder Alexandre Somensi (FM),[1]**

**cleder.somensi@ifc.edu.br; bezgoriomarina@gmail.com**

*[1] UEA Gestão de Resíduos, Laboratório de Química Analítica e Ambiental - Instituto Federal Catarinense – Campus Araquari – IFC Araquari*

Palavras Chave: Economia Circular; Biogás; Bioenergia; Estabilização de Dejetos Animais

## Highlights

Circular Economy in Agricultural Activity: Initial Tests for Stabilization of Organic Residues and Biogas Production
- Optimization of Biogas Production by Anaerobic Digestion of Animal Manure;
- Agricultural Activity in Closed Cycle
- Treatment and Valorization of Waste.

## Resumo

A Agricultura Catarinense é caracterizada principalmente por pequenas propriedades que diversificam atividades agropecuárias, facilitando a visão cíclica da produção de alimentos e eliminação de resíduos, favorecendo processos de valorização/reciclagem, cerne do conceito de economia circular[1]. Este trabalho objetivou o tratamento/estabilização de dejetos suínos (DS), bovinos (DB) e restos de alimentos (RA), além da produção de biogás/biofertilizantes. Dois biodigestores modelo batelada (170 L para resíduos/biogás e 50 L para o chorume) foram inoculados com (1) 75% DS e 25% RA e (2) 50% DS, 25% DB e 25% RA (V:V). $NH_3$ e $H_2S$ foram mensurados colorimetricamente, $CO_2$ e $CH_4$ volumetricamente. No material sólido foram mensurados[2]: pH, umidade, e COT/NKT. Todas as análises foram realizadas após 45 dias de tratamento:

| Biodigestor / Parâmetro | $CH_4$ (%) | $CO_2$ (%) | $NH_3$ (ppmV) | $H_2S$ (ppmV) | pH | Umidade (%) | Relação C/N |
|---|---|---|---|---|---|---|---|
| **1** | 87 | 12 | 50 | 20 | 7,2 | 65 | 32,3 |
| **2** | 79 | 20 | 160 | 28 | 8,3 | 65 | 43,0 |

**Quadro 1.** Concentração dos gases e parâmetros físico-químicos do material sólido após 45 dias.

O biodigestor 1 foi mais eficiente devido a melhor relação C/N, possivelmente ocasionada pela ausência de DB. Menores concentrações de $NH_3$ no tratamento 1 também contribuem pois a amônia inibe a produção de metano. Após 45 dias os resíduos não estavam estabilizados, necessitando maior tempo de tratamento. Cada biodigestor produziu cerca de 3 L de chorume, que deverá ter o seu potencial fertilizante analisado, mesmo que seja necessário o beneficiamento (*e.g.*, precipitação da estruvita). Os tratamentos realizados demonstram que a mistura de DS/DB com RA é potencialmente viável para produção de biogás de boa qualidade e reciclagem/valorização dos resíduos, fomentando relações viáveis entre a sustentabilidade ambiental e crescimento econômico, conforme preceitos da economia circular.

1) Sauve, S.; Bernard, S.; Sloan, P. Environmental sciences, sustainable development and circular economy: Alternative concepts for transdisciplinary research. Environ. Dev. 2016, 17, 48–56;
2) EMBRAPA - Manual de Análises Químicas de Solos, Plantas e Fertilizantes, 2ª edição, EMBRAPA: Brasília, 2009, 627.

**Área: AMB** **Inscrição: 01237**

# Characterization of biomass produced in Algae Turf Scrubber (ATS®) system instaled in the Lago Dourado – Santa Cruz do Sul - RS.

**Felipe Augusto Martini (PG),[1]* Aline Rubert (IC),[2] Maiara Priscilla de Souza (PG),[1] Lourdes Teresinha Kist (PQ),[1-2] Michele Hoeltz (PQ),[1-3] Lisianne Brittes Benitez (PQ), [1-3] Rosana de Cassia de Souza Schneider(PQ),[1-2] Pablo Diego Gressler.[1]**

**rosana@unisc.br; felipeamartini@gmail.com**

*[1]Programa de Pós-graduação em Tecnologia Ambiental, UNISC; [2]Departamento de Química e Física, UNISC; [3] Departamento de Biologia e Farmácia, UNISC.*

Palavras Chave: *ATS, Biomass, Periphyton, Bioremediation, Algae Turf Scrubber.*

## Highlights

Algae turf scrubber to promote natural water treatment.
Periphyton as biomass to developed bioproducts.
N and P sequestration of water.
ATS application to bioremediation and biomass production.

## Resumo/Abstract

Eutrophication is recognized as one of the most important water quality problems today, and there is a strong need to develop strategies that reduce nutrient loading in water. The aim of this study was to characterize the periphytic biomass produced in the Algae Turf Scrubber (ATS®) system used to promote the treatment of eutrophic waters. The system was drained from the freshwater reservoir for human supply in the Santa Cruz do Sul city (Lago Dourado). A pilot-scale ATS® system (0.9 m wide, 5 m long, 1.0% inclination) was constructed which received continuous flow of approximately 2 L $min^{-1}$ of pumped water from Lago Dourado, during 7 months. On average, the system produced 1.33 - 7.64 g $m^2$ $d^{-1}$ of periphytic biomass (dry weight). The analysis were performed based on the methods of the National Renewable Energy Laboratory (NREL) - USA. The lipid phase of the biomass was extracted by Bligh Dyer method, transesterified with $BF_3$-methanol and analyzed by Gas Chromatography with Mass Spectrometry Detector and pigments were extracted with acetone. The collected periphyton contained a mean composition of fixed carbon 27.97%, protein 17.81%, lipids 5.90% (fatty acids: saturated (53.72%) and unsaturated (45.59%), pigments 0.25% and carbohydrate 50 to 55%. The results indicated that the use of ATS® systems being used as an effective means of treatment of eutrophic waters, also produces periphytic biomass that can be used with potential market value, mainly due to the content of proteins and carbohydrates.

A

B

Figure 1. A) ATS installed in the Lago Dourado; B) Periphytic biomass produced.

**Área: AMB** **Inscrição: 00821**

# Utilização do babaço de cevada como adsorvente natural para a remoção do agrotóxico carbaril de solução aquosa

**Thiago Felipe Silva (PG),[1] Karoline Pinto Milhomem (PG),[1*] Silvia de Sousa Freitas (PQ).[1]**

**thfelipesilva005@gmail.com; karolpms@gmail.com**

[1]*Unidade Acadêmica Especial de Química, UFG - Regional Catalão*

Palavras Chave: *Adsorção, Adsorvente Natural, Carbaril, HPLC, Cevada*

## Highlights

Use of barley bagasse as a natural adsorbent for the removal of the pesticide carbaryl from aqueous solution. The results of this study showed that this natural material can be used as an effective and alternative adsorbent to removal of carbaryl from aqueous solution.

## Resumo/Abstract

Este estudo avalia o uso de babaço de cevada como adsorvente para remoção de carbaril de solução contaminada. Nos experimentos o bagaço de cevada, previamente tratado com álcool etílico, foi submetido a ensaios de adsorção utilizando 200 mg do material e 10 mL de amostra de água fortificada com carbaril (1,0 $mgL^{-1}$). O tempo de contato variou entre 1 e 120 min. Após cada ensaio a solução filtrada foi analisada em um HPLC equipado com detector UV (coluna e pré-coluna C18, eluição: acetonitrila/água, 50:50 (v/v), fluxo 1 $mLmin^{-1}$, λ = 280 nm). Os limites de quantificação (LQ) e detecção (LD) foram 0,1 e 0,01 $mgL^{-1}$. A quantidade de carbaril removida pelo material foi avaliada pela comparação da concentração inicial da solução ($C_{inicial}$) com a concentração após o tratamento com o adsorvente ($C_{final}$).

A concentração de carbaril diminuiu significativamente (52%) nos 10 primeiros minutos de contato (**Figura 1**). Entre 90 e 120 minutos, a concentração manteve-se constante (variação < 2%), com remoção de 68%. A cinética de adsorção foi avaliada utilizando diferentes modelos teóricos. Os modelos de pseudo-segunda ordem e Avrami proporcionaram melhor ajuste (**Figura 2**).

Os resultados mostram que a utilização do bagaço de cevada como adsorvente alternativo promoveu a remoção de até 68% de carbaril da solução após 90 min de contato. O estudo cinético mostrou que o processo pode apresentar mais que um mecanismo de adsorção, sendo dependente da superfície de adsorção e da concentração do composto.

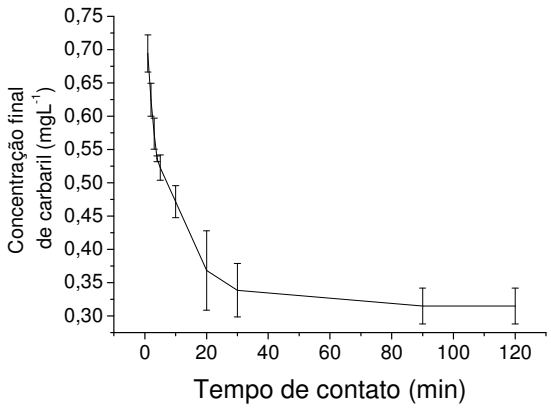


**Figura 1-** Concentração final de carbaril na solução em função do tempo de contato.

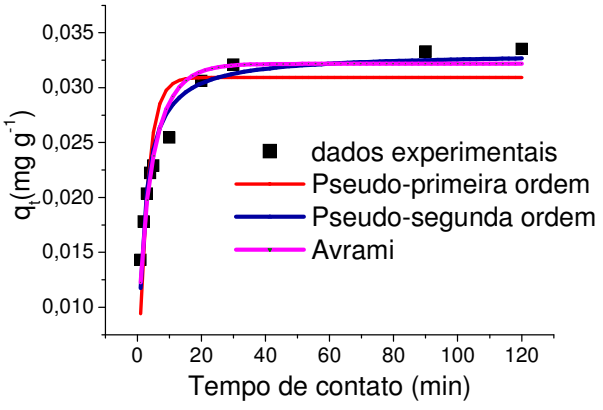


**Figura 2**- Modelos cinéticos não-lineares (pseudo-primeira ordem, pseudo-segunda ordem e Avrami ) para a adsorção do carbaril pelo bagaço de cevada

**(CNPq)**

**Área: AMB** **Inscrição: 00769**

# Development of a nanomaterial incorporated with bixin: a sustainable approach for dye removal from aqueous matrices

**Junielly T. Domingues (PG),[1*]Guilherme D. Rodrigues (PQ),[1]Ricardo M. Orlando (PQ),[1]Rubén D. S. Millan (PQ),[2]Ana Délia G. Pinzón (PG),[2]Pablo Luis G. Carvalho (IC).**

**juniellytomaz@gmail.com**

*[1]LaSAV - Laboratório de Soluções Analíticas Verdes, Departamento de Química, UFMG; [2]LEMB – Laboratório de encapsulamento molecular e biomateriais, Departamento de Química, UFMG.*

*Keywords: Adsorption, Nanofibers, Brilliant green, Methylene blue, Bixin, Effluent.*

## Highlights

Bixin was used as a non-toxic precursor to be incorporated into nanofibers;
The nanomaterial was applied as an adsorbent for dyes removal in real samples;
The nanofibers are a promising adsorbent.

## Abstract

An environmentally safe technology was developed for the removal of brilliant green (VB) and methylene blue (AM) dyes from aqueous samples. A new nanostructured adsorbent material composed of polycaprolactone polymer (8.00% w/v) and bixin (0.00800% w/v) was manufactured using an electrospinning technical. The best sorption conditions were obtained evaluating the following parameters: deposition time of nanofibers on the support; area of adsorbent; temperature during the adsorption experiments; pH of the reactive medium; adsorption kinect and adsorption isotherm. The highest removal percentage of dyes at the concentration of 20.0 mg $kg^{-1}$ was obtained in pH = 6.00 at room temperature (25.0ºC) applying the material with nanofibers deposited for 80 minutes with 6.76 $cm^2$ area. The adsorption kinect observed was fast (Figure 1A), reaching the adsorption equilibrium in 2 hours of analyte contact with the adsorbent and the kinect model that best adjusted to the experimental data was pseudo-second order model. The dyes sorption showed to be influenced by the presence of some salts ($Na_2SO_4$, NaCl, $NaNO_3$, $NH_4Cl$ e $CaCl_2$) suggesting the process occurs by ion exchange mechanism. The material was also applied for AM and VB removal in matrices receiving the raw textile effluent (Figure 1B) and in fish-breeding and shrimp-breeding water (%$E_{máx}$ of 75 and 90% to AM and VB). With this result, the material proved to be a promising and green adsorbent.

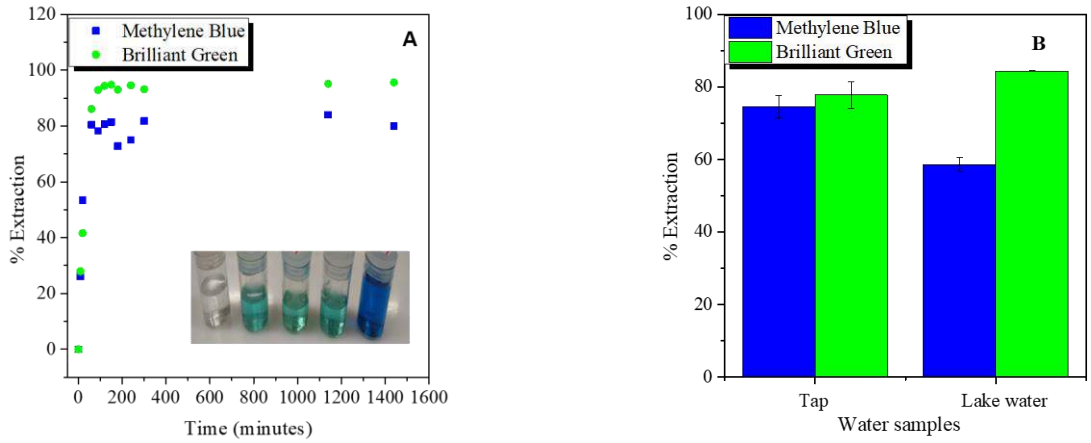


**Figure 1.** (A) Adsorption kinetics study of adsorption test with the bright green dye in matrices of secondary receptors of textile effluents and (B) result of the application in matrices receiving the raw textile effluent.

Acknowledgment: Fapemig, Capes e CNPQ.

**Área: AMB** **Inscrição:00412**

# Application of Kraft lignin as alternative adsorbent for dyes and potential toxic metals

**Naomi Akiba[1] (PG), Vinícius F. N. Silva[2] (PQ), Ivanise Gaubeur [1]* (PQ)**

**naomi.akiba@ufabc.edu.br; ivanise.gaubeur@ufabc.edu.br**

*[1]Centro de Ciências Naturais e Humanas - UFABC; [2]Pesquisa, Desenvolvimento e Inovação - Suzano Papel e Celulose*

Keywords: *Chelant agent, Adsorption, Dye, Metal, Effluent.*

## Highlights

- Alternative solid substrate for remotion of metals and dyes from contaminated effluent
- Low cost material and eco-friendly adsorbents

## Abstract

Recently, human activities have contributed to environmental pollution, such as wastewater contamination by heavy metals and dyes. Therefore, it is necessary to treat effluent before its discharge into the environment. Among numerous technologies, the adsorption process is a promising alternative by its operability, economical feasibility, wide availability and simplicity of design. Lignin is a natural polymer containing diverse functional groups and it is useful as an inexpensive adsorbent material with low toxicity. The aim of the present study is to investigate the adsorption of single metal ions or dye aqueous solutions on Kraft lignin, which was obtained from a paper mill provided by Suzano Pulp and Paper Company. Parameters that affect the adsorption process, such as pH, contact time, initial metals/dyes concentration, and adsorbent dose were optimized. By using a microtube with the addition of 30 mg of Kraft lignin to 1.5 mL of one metal solution (Au, Co, Cu, Cr, Ni, Pb, Pd e Zn) or dye solution (Reactive Blue 19, Reactive Blue 21), pH was adjusted to pH 7.0 and were stirred at 25 ºC for 12 hours (metals) or 4 hours (dyes). After, the solution was separated and the metals/dyes concentration was determined. Figure 1 shows the percentage of the analytes removal in the optimized condition. The amount of metals and dyes adsorbed was higher than 75% and 92%, respectively. These results show how promising is the use Kraft lignin for real effluent samples application. In addition to experimental data were applied isotherm and kinetic models.

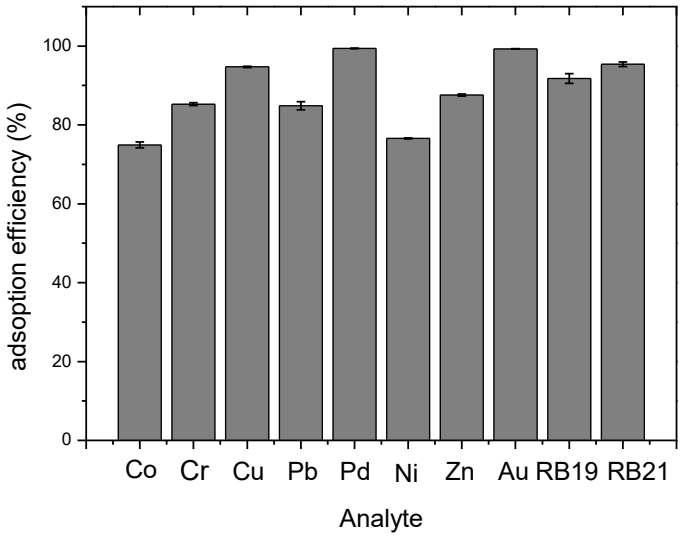


*Figure 1: Percentage adsorption efficiency of metal/dye on Kraft lignin. Initial metal concentration ($Au^{3+}$, $Co^{2+}$, $Cu^{2+}$, $Cr^{3+}$, $Ni^{2+}$, $Pb^{2+}$, $Pd^{2+}$ e $Zn^{2+}$) was 10 mg.$L^{-1}$, initial dye concentration (RB19, RB 21) was 2x$10^{-4}$ mol.$L^{-1}$, pH 7.0, adsorbent dose was 0.03 g at 25ºC, and contact time 12 and 4 hours for metals and dye, respectively.*

**Área: AMB** **Inscrição: 293**

# Development of nanostructured materials incorporated with bixin and extracting agents for metal removal from aqueous matrices

**Daniela da Silveira Leite (PG),[1*]Pablo Luiz Gutierrez Carvalho (PG),[1]Ana Delia Pinzón García (PQ),[2] Ricardo Mathias Orlando (PQ),[2]Rubén Dario Sinisterra Millán (PQ),[2] Guilherme Dias Rodrigues (PQ).[1]**

**danielasilveiraleite@gmail.com;**

*[1]LASaV – Laboratório de Soluções Analíticas Verdes, [1,2]Departamento de Química, DQ/ICEx-UFMG*

Key words:*bixin, nanofibers, electro-spining, metal removal, Rio Doce basin.*

## Highlights

Green Chemistry approach for metal removal from aqueous matrices
Metal removal using nanomaterials
Association of bixin and extraction agents for metals removal

## Resumo/Abstract

The Rio Doce basin in the southeastern Brazil, located on the states of Minas Gerais and Espírito Santo, suffered of one of the greatest environmental disasters in history. The disruption of the Fundão tailings dam in 2015 triggered a spill of a large volume of mining waste in the river. In this context, a new nanostructured materials composed by the polymer polycaprolactone nanofibers incorporated with bixin and common extracting agents were studied in metal recovery process. The materials were created by utilizing the electro-spinning technique, where thesorbentwas incorporated on both sides of an iron mesh surface. The goal of this project was to optimize the following parameters: pH; concentration of bixin and different extracting agents (1-(2-pyridyl-azo)-2-naphthol (PAN) and 1-nitroso-2-naphthol(1N2N)); deposition time of nanofibers; kinetics of metal removal and adsorption isotherm, in order to reach high metal percentage removal (%R) from aqueous matrices. The best conditions for iron removal were using a nanofiber incorporated with bixin and PAN, with 20 minutes of deposition time, at pH=6, in which %R equals to (81.5±0.9)% was achieved (Fig.1). In the kinetic studies, an adsorption plateau with %R=72.3% was reached at 240 minutes of contact between the solution and the nanofiber (Fig.2). In addition,the nanofibers were also evaluated for the recovery of aluminum and manganese, in which high values of adsoption were not observed, demonstrating a selectivity of this material for iron recovery.

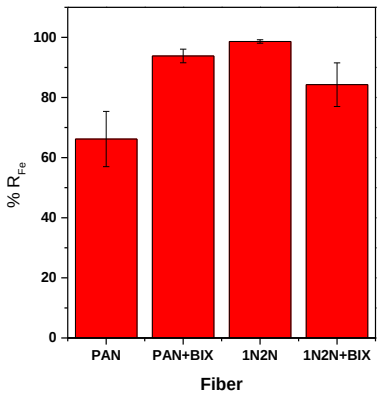


**Figure 1.**Using of different extracting agents types incorporated into nanofibers by associated or not to bixin (BIX)

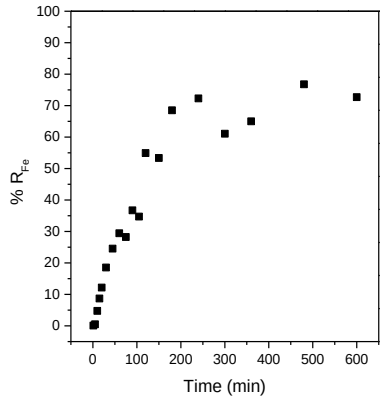


**Figure 2.** Kinect behavior of iron adsorption in nanofibers formed by BIX and PAN.

**(PPG Química/UFMG, FAPEMIG, CAPES, CNPq)**

**Área: AMB** **Inscrição: 00025**

# Zeolites with different chemical and textural properties for metal removal

**Danielle F. de Oliveira (PG)[1], Jefferson A. M. Neri (IC)[1], Jonas A. A. Ribeiro (IC)[2], Fabiana S. dos Santos (PQ)[2], Mendelssolm K. Pietre (PQ)[1*]. Email: mkpietre@yahoo.com.br**

*[1]Departamento de Química-ICEx, UFF-Aterrado-Volta Redonda-RJ; [2]Departamento de Engenharia de Agronegócios-UFF-EEIMVR-Vila Santa Cecília -Volta Redonda-RJ.*

Keywords: β-Zeolite, Exfoliation, Ferrierite, Ion Exchange, lead, zinc.

## Highlights

- Zeolites with different chemical and textural properties were synthesized for $Zn^{2+}$ and $Pb^{2+}$ ions removal.
- The removal of these metals at a considerable extent may be attained.
- β-zeolite displayed the better performance due its higher aluminum content and surface area
- Kinetic data indicates that the chemical interaction is the rate-limiting step.
- β-zeolite displayed good performance in reusability testing.

## Abstract

In this study β-zeolite, ferrierite and partially delaminated PREFER (designated as PREFER DEL) zeolites with several chemical and textural properties were synthesized for the removal of zinc and lead ions metals from their solutions [1]. The X-ray diffraction profile of the PREFER, ferrierite and β-Zeolite samples indicated that those phases were successfully obtained with non-detectable impurities (Fig 1A and inset Fig 1A). The PREFER DEL solid shows a structural disorder through peak broadening and low intensity. The $Zn^{2+}$ uptake results showed that for 50 mg of all adsorbents there was an equilibrium uptake within 5 min. A considerable increase in the $Zn^{2+}$ uptake percentage with adsorbent dosage is observed only for β-Zeolite (Fig 1B, not shown for PREFER derivatives). It was found a decrease in $Pb^{2+}$ ions removal with increasing adsorbent mass for all adsorbents (shown only for β-Zeolite, Fig 1C). The increase in zeolite mass results in a decrease in the pH from 5.5 to 4.2, respectively. In low pH values, the Pb (II) uptake percentage significantly decreases. The improved performance of β-zeolite when compared with PREFER derived adsorbents may be explained in terms of (i) a higher density of Al related sites, which is responsible for the ion exchange event, (ii) higher surface area and external surface area in comparison to PREFER derivatives (not shown), iii) to it wider pore system dimensions in relation to ferrierite, that allows a greater density and availability of ion adsorption active sites.

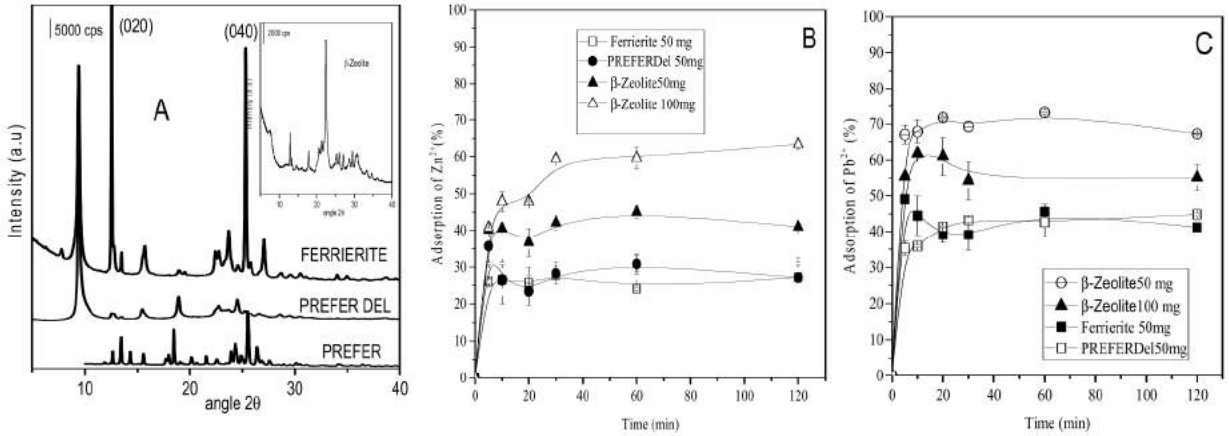


**Figure 1:** XRD (A) and uptake of zinc (B) and lead (C) in function of contact time and zeolite mass (optimum pH=5.5).

## Acknowledgments/ References

The authors acknowledge the FAPERJ, CAPES and Water Science and Technology for the publication of the paper.

[1] Oliveira D. S. *et al.* Synthesis of zeolites with different chemical and textural properties for metal ions removal from aqueous solutions. *Water science and technology*, 2017, **76 (12),** 3441-3451.

**Área: AMB** **Inscrição: 00082**

# UV-C/$H_2O_2$, microfiltration and reverse osmosis applied to remove emerging contaminants considering the potable reuse treatment of water

**Cassiana C. Montagner (PQ),[1,2*] Kristin H. Cochran (PG),[2] Benjamin Fryer (IC),[2] Susana Kimura-Hara (PQ),[3] Wael Abdelraheem (PG),[4] Ying Huang (PG),[4] Scott Coffin (PG),[5] Daniel Schlenk (PQ),[5] Dionysios Dionysiou (PQ),[4] Susan D. Richardson (PQ)[2]**

**montagner@iqm.unicamp.br**

*[1]University of Campinas (LQA-IQ-UNICAMP), Campinas, SP, Brazil; [2]University of South Carolina, Columbia, SC, USA; [3]University of Calgary, Calgary, AB, Canada; [4]University of Cincinnati, Cincinnati, OH, USA; [5]University of California-Riverside, Riverside, CA, USA*

Palavras Chave: Reuse of water, WWTP, Drinking water, LC-MS/MS, DBP, Emerging contaminants

## Highlights

Potable reuse of water and the risks to get water safer. Advanced oxidation technologies brings efficient tools to remove emerging contaminants from WWTP effluent. The transformation products and disinfection by-products formed during the treatment of water must to be considering in the risk evaluation to human health.

## Resumo/Abstract

The United Nations Environment Program and the World Health Organization classifies as essential and urgent knowledge of the sources, transformations and fate of emerging contaminants in the environment due unequivocal evidence about numerous observed effects to wild populations, as well as possible damages observed in humans. These are thousands of chemicals that are present in the environment and may cause risks to the intended uses of water. The prioritization of these substances is essential to the beginning of the regulatory process, whether for prevention or control of input. In addition, potable reuse of wastewater is becoming more common as populations increase and freshwater resources become more scarce. Producing safe drinking water from treated wastewater is challenging due to the presence of contaminants that are not completely removed in conventional wastewater treatment and due to transformation products that can be formed with advanced oxidation technologies (AOTs) that are used in potable reuse treatments. These contaminants can be harmful for human and ecological health. In 2013, two Science Advisory panels determined two lists of priority emerging contaminants to be monitored in aquatic ecosystems and human potable water reuse. These compounds were determined based on toxicity, persistence through wastewater treatment, and environmental water concentrations. This project have investigated the removal and/or transformation of 21 of these priority emerging contaminants from US through UV-C/$H_2O_2$, microfiltration and reverse osmosis in three samplings from Full-Scale Advanced Wastewater Treatment Plant (Orange County GWRS) in order to make indirect potable reuse of wastewater safer. Ultra performance liquid chromatography-tandem mass spectrometry (UPLC-MS/MS) was used to quantify bisphenol A, ρ-nonylphenol, bis (2-ethylhexylphthlate), butylbenzyl phthlate, perfluorooctanoic acid (PFOA), perfluorooctane sulfonate (PFOS), diclofenac, ibuprofen, erythromycin, triclosan, 17α-ethinylestradiol, 17β-estradiol, estrone and chlorpyrifos. Gas chromatography mass spectrometry (GC-MS/MS) was used to quantify permethrin, galaxolide (HCCB), polybrominated diphenyl ether (PBDE)-47, polybrominated diphenyl ether (PBDE)-99, bifenthrin and N-nitrosodimethyl-amine (NDMA). Transformation products, disinfection by-products (DBPs), and unknown compounds are being identified via high resolution-time-of-flight GC(TOF)MS/MS and UPLC(Q-TOF)MS/MS. Some compounds were not removed even after UV treatment. The results brings a critical conclusion about the efficiency of treatment of water considering the risks involving the presence of many different contaminants in the environment even in the trace levels.

**Área: AMB** **Inscrição:00964**

# Influence of the iron source and pH on degradation of fipronil by photo-Fenton process

**Oswaldo Gomes Junior (PG),[1*] Alam G. Trovó (PQ)[1]**

**oswaldogjr2015@gmail.com**

[1]*Instituto de Química, Universidade Federal de Uberlândia, MG, Brasil.*

Keywords: *Advanced Oxidation Process, Iron complexes, Near-neutral conditions, Pesticides.*

## Highlights

FIP was efficiently degraded at pH 2.5;
Best results of FIP degradation were at pH 2.5 using 1:1 Fe/Cit and 1:3 Fe/Ox;
Improvement in FIP degradation was seen at pH 6.0 using 1:3 Fe/Cit and 1:6 Fe/Ox.

## Abstract

This work describes the degradation of the insecticide fipronil (FIP) by photo-Fenton process using different iron sources ($Fe^{2+}$, $Fe^{3+}$ and $Fe^{3+}$-citrate and $Fe^{3+}$-oxalate, named FeCit and FeOx, respectively) at initial pH values of 2.5 and 6.0. The best results at initial pH 2.5 were achieved using 32 µmol $L^{-1}$ FeCit or FeOx at molar iron/organic ligand ratios of 1:1 and 1:3 respectively, when the FIP concentration reached values below the quantification limit of the HPLC (< 0.066 mg $L^{-1}$) after 10 and 20 min of treatment, respectively (Figure 1a). However, at initial pH 6.0 improvements in the results (37% and 54% for FeCit, and 23% for FeOx) were achieved by using an excess of citrate (32 and 64 µmol $L^{-1}$) and oxalate (96 µmol $L^{-1}$) ligands resulting in molar iron/organic ligand ratios to 1:2 and 1:3 (Fe/Cit) and 1:6 (Fe/Ox), respectively (Figure 1b). These results pointed out the possibility of using the photo-Fenton process at near-neutral conditions, avoiding the main disadvatage of the photo-Fenton treatment: the need to use a pH between 2.5 and 3.0.

**Figure 1.** Influence of the (a) iron source at initial pH 2.5 and (b) replacement of organic ligands during the treatment at initial pH 6.0 on FIP degradation by photo-Fenton process. Initial conditions: [FIP] = 1 mg $L^{-1}$; [iron] = 32 µmol $L^{-1}$ and [$H_2O_2$] = 23 mg $L^{-1}$.

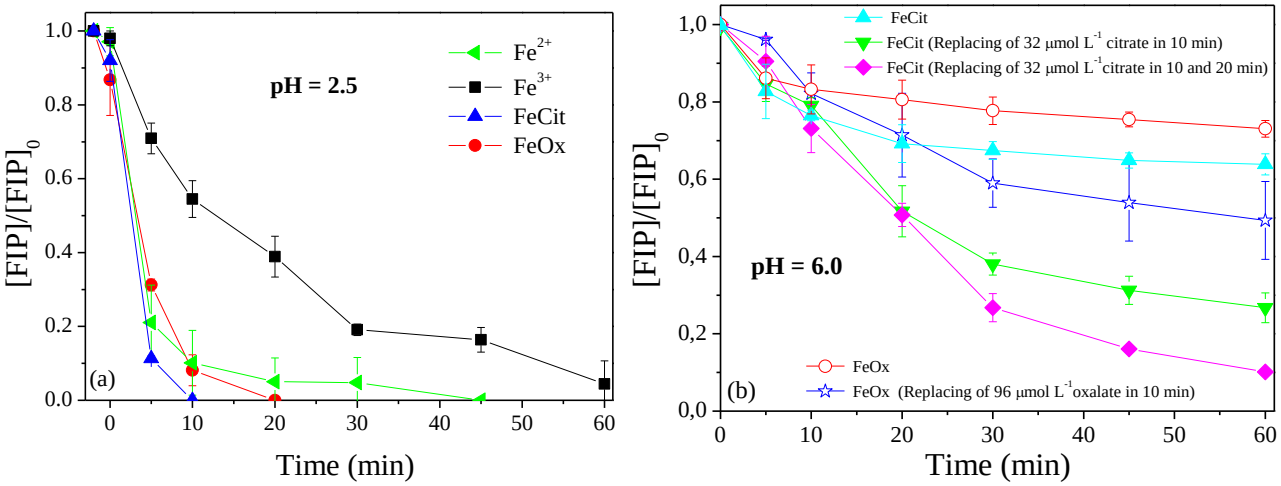

**Área: AMB** **Inscrição: 01128**

# Otimização multivariada de sistema UV/$H_2O_2$ para desinfecção de efluentes secundários

**Jacqueline A. Malvestiti (PG), José Paulo Diogo Júnior (PG), Renato Falcão Dantas (PQ)***

**renatofalcaod@ft.unicamp.br; jacque.edf@gmail.com**

*Faculdade de Tecnologia,Universidade Estadual de Campinas, Paschoal Marmo 1888, Limeira SP.*

Palavras Chave: *Desinfecção, UV/$H_2O_2$, Delineamento Composto Central; Matriz Doehlert.*

## Highlights

Multivariate optimization of UV/$H_2O_2$ system for secondary effluent disinfection

-Optimization of AOP disinfection through dye removal was proved to be efficient.
-DM was more efficient than CCD due to the less quantity of experiments

## Resumo/Abstract

A otimização experimental de UV/$H_2O_2$ para a desinfecção de efluentes secundários urbanos foi realizada por meio de delineamento experimental utilizando a reação do radical hidroxila (HO*), que neste caso foi indiretamente representado pela remoção do corante azul de metileno. Foram utilizadas duas classes de planejamento experimental, a matriz Doehlert e o delineamento composto central. As variáveis mais importantes para o processo foram: concentração de peróxido de hidrogênio, taxa de volume iluminado/volume total do reator e fluxo de recirculação da bomba. As duas abordagens diferentes permitiram estabelecer o significado de cada variável e quantificar as correlações entre elas. A classe experimental Matriz Doehlert foi mais eficiente na otimização do sistema, já que ele usou um número menor de experimentos e obteve resultados semelhantes, quando comparado ao delineamento composto central. Após a otimização, a eficiência de desinfecção dos sistemas foi testada com os indicadores microbiológicos, *Escherichia coli* e coliformes totais, utilizando a condição otimizada e a pior condição, anteriormente obtida com a remoção do corante azul de metileno como resposta. No final de 30 minutos de tratamento, a eficiência de inativação em condições ótimas foi muito alta, permitindo uma desinfecção eficiente, bem como a produção de um efluente com qualidade para reutilização de acordo com legislações específicas, enquanto que nas piores condições, a taxa de inativação dos indicadores microbiológicos não atingiu padrões para reutilização. Esses resultados confirmam a eficiência da otimização de processos oxidativos avançados para uma desinfecção confiável de efluentes municipais.

**Área: AMB** **Inscrição: 1238**

# Removal of azo dyes mixture by layered double hydroxides

**Lorrany Oliveira Lemes (PG), Renato Rosseto (PQ)***

**lorranny.lemes@hotmail.com; renato.rosseto@ueg.br**

*Campus Anápolis de Ciências Exatas e Tecnológicas, BR 153 Km 98, Universidade Estadual de Goiás.*

Palavras Chave: Azo dyes; Anionic clays; Wastewater treatment.

## Highlights

Textile industries consume large amount of water. Textile effluents are difficult to be treated and the search for new adsorbents, such as layered double hydroxides (LDHs), is encouraged.

## Abstract

The aim of this work was the evaluation of removal capacity of azo dyes mixture (methyl orange, Congo red and remazol black-b) by Zn/Al and Mg/Al calcined LDHs, to establish relationships among charge and molecular weight of azo dyes, and adsorptive abilities of LDHs. The LDHs synthesized were characterized by X-ray diffraction, atomic absorption, thermogravimetry, and scanned electron microscopy, and the removal kinetics of azo dyes were performed in different experimental conditions, monitored by UV-vis spectroscopy and HPLC analysis. The Zn/Al LDH showed much better ability to remove individual dye compared to Mg/Al LDH, independently of the employed conditions. However for dyes mixture, Mg/Al LDH exhibited better performance, showing removal efficiency higher than 95% and overall adsorption capacity around 870 mg $g^{-1}$ within 4 h (Table 1).

Table1. Azo dyes kinetic parameters data at room temperature and near-neutral pH.

| **Time** | **Removal capacity (%)** | | | | | | | |
|---|---|---|---|---|---|---|---|---|
| | **[MO]** | | **[CR]** | | **[RB]** | | **[AM + CR + RB] mixture** | |
| | Zn/Al LDH | Mg/Al LDH | Zn/Al LDH | Mg/Al LDH | Zn/Al LDH | Mg/Al LDH | Zn/Al LDH | Mg/Al LDH |
| 1 | 91,2 | 22,0 | 91,5 | 27,6 | 93,0 | 18,7 | 62,1 | 27,9 |
| 4 | 98,5 | 34,4 | 98,5 | 56,3 | 94,9 | 27,8 | 92,5 | 96,5 |

[MO]: methyl orange; [CR]: Congo red; [RB]: remazol black-b. Initial individual dye concentration: 30 mg $L^{-1}$. Initial dyes mixture concentration: 90 mg $L^{-1}$ (30 mg/dye in 1 L water solution).

The adsorption results indicate that the kinetics for individual dyes followed same removal patterns, and thermogravimetric and X-ray diffraction analysis of saturated LDH/dye suggest that the interactions between LDHs and dyes occur essentially on inorganic matrix surface. The obtained results give us insights on the structure-property relationship of these materials for removal of environmental contaminants. Details of the synthesis, characterization, removal kinetic studies and relationships/explanation between dye structures/charges and LDHs will be presented.

The authors acknowledge to the Programa de Bolsa de Incentivo à Pesquisa e Produção Científica (PROBIP/UEG), Universidade Estadual de Goiás/Pró-Projetos/Programas, PrP/UEG (Pró-Eventos/UEG), CAPES and FAPEG for sponsorships.

**Área: __AMB_____** **Inscrição: 01110**
*(Inserir a sigla da seção científica para qual o resumo será submetido. Ex: ORG, BEA, CAT)* *(Inserir o número de inscrição do autor que fez a submissão)*

# Síntese e caracterização de um novo polímero de coordenação fotocataliticamente ativo

**Bruno Manduca (PG) e Renato S. Freire (PQ)**

**rsfreire@iq.usp.br**

*Instituto de Química, USP*

Palavras Chave: *Fotocatálise Heterogênea, Polímeros de Coordenação, Química Ambiental, Materiais catalíticos, degradação de poluentes*

## Highlights

A new coordination polymer formed by $Ni^{2+}$ and BTC was synthesized and characterized. It has shown photocatalytic activity toward the discoloration of a Remazol RN dye solution under visible light.

## Resumo/Abstract

Fotocatálise heterogênea consiste na ativação de um semicondutor sólido por absorção de radiação eletromagnética.[1,2] A maior parte dos fotocatalisadores heterogêneos são inorgânicos, porém, recentemente, materiais híbridos têm mostrado resultados interessantes.[3] Polímeros de coordenação (PC) são materiais formados por íons metálicos, ou clusters, conectados por ligantes orgânicos.[4] Alguns desses materiais apresentaram características de semicondutor, o que estimulou a pesquisa em aplicações fotocatalíticas.[3,4] Neste trabalho está descrito um novo PC com atividade fotocatalítica. O material é formado por $Ni^{2+}$ como íon metálico e ácido benzeno-1,3,5-tricarboxílico (BTC) como ligante orgânico. O composto foi obtido por síntese solvotérmica. Soluções contendo $Ni(NO_3)_2 \cdot 6H_2O$ e BTC 1:1 em DMF foram aquecidas a 160 ºC por 24 horas em reatores pressurizados. O produto formado foi filtrado, lavado com metanol e seco em rotaevaporador. A caracterização foi realizada por DRX, espectroscopia de refletância difusa, análise de adsorção de $N_2$, infravermelho e MEV. A atividade fotocatalítica foi avaliada pela descoloração de uma solução do corante Azul Brilhante de Remazol RN. Foi utilizado 1 mg do fotocatalisador para cada mililitro de solução do corante. A suspensão ficou sob agitação magnética em um reator de temperatura controlada (18 ºC), e $O_{2(g)}$ foi borbulhado no sistema a uma taxa de 3 $cm^3.min^{-1}$. Como fonte de radiação foi utilizada uma lâmpada de xenônio, sendo a radiação UV filtrada por uma camisa de vidro. Os resultados mostram uma redução de 52% da concentração do corante após 310 minutos. Os resultados obtidos mostram que o material sintetizado tem potencial para ser usado como fotocatalisador.

1 R. Andreozzi, R; Caprio, V.; Insola, A.; Marotta, *Catal. Today*, 1999, **53**, 51–59.
2 A. Mills, R. H. Davies and D. Worsley, *Chem. Soc. Rev.*, 1982, **22**, 417–425.
3 H. Zhang, G. Liu, L. Shi, H. Liu, T. Wang and J. Ye, *Nano Energy*, 2016, **22**, 149–168.
4 M. a. Nasalevich, M. van der Veen, F. Kapteijn and J. Gascon, *CrystEngComm*, 2014, **16**, 4919.

**Área: AMB** **Inscrição: 01355**

# Adsorption of pharmaceuticals from aqueous solutions on FAU zeolite

**Diana Nara Ribeiro de Sousa (PG),[1*] Antonio Aparecido Mozeto (PQ),[1] Pedro Sérgio Fadini (PQ)[1].**

**dnrsousa@yahoo.com.br; psfadini@ufscar.br**

*[1]Laboratório de Biogeoquímica Ambiental-LBGqA, Departamento de Química, UFSCar.*

Palavras Chave: *Pharmaceuticals, Adsorption, Zeolite, Efficiency.*

## Highlights

Fast and effective removal of pharmaceuticals in aqueous medium by FAU zeolite;
pH-dependent adsorption of pharmaceuticals by FAU zeolite;
Adsorption of pharmaceuticals at environmental relevant concentration;
High adsorption of pharmaceuticals from a wastewater sample onto FAU zeolite.

## Abstract

Pharmaceuticals and other emerging contaminants has been become contaminants of environmental concern in the last decades and the studies about options aiming their removal or reduction in the environment has been growing in the field of environmental chemistry. In this study, the performance of a commercial Faujasite (FAU) zeolite was evaluated for the removal of pharmaceuticals of different classes, including atenolol, carbamazepine, ibuprofen and diclofenac, from aqueous solutions. The adsorption experiments were conducted in batch mode in a series of 50 mL glass bottles containing 30 mL of ultrapure water spiked with an initial 100 µg $L^{-1}$ concentration of the individual pharmaceuticals. After equilibration time, the remaining pharmaceutical concentrations in the aqueous solutions were determined by HPLC-ESI-MS/MS analyses. Use of a small adsorbent dosage (0.005 to 1 g $L^{-1}$) resulted in fast pharmaceutical adsorption with removal efficiency higher than 60% at the first 15 min, and the fitting of the experimental data followed pseudo-second order kinetics. The removals of carbamazepine, diclofenac and ibuprofen were highly pH-dependent, with high removal percentages observed at acidic medium (pH 2-4) and low removal in basic (pH 8-10) conditions. The Freundlich isotherm model provided the best fits to the adsorption data, and the adsorption mechanisms appeared to involve both electrostatic and hydrophobic interactions. Results in a wastewater effluent sample showed removals values above 60% for atenolol and carbamazepine, pointing to FAU zeolite as an excellent candidate for the removal of contaminants of emerging concern, such as pharmaceuticals.

*The authors are grateful to the São Paulo State Research Foundation (FAPESP, grant #2014/21871-2) for financial support to the first author, in the form of a postdoctoral fellowship and to Zeolyst International for the donation of zeolite.*

**Área: AMB** **Inscrição: 01289**

# Degradation of Bisphenol A (BPA) by *Trametes versicolor* fungus

**Carlos E. R. Gracio (IC),[1*] Viviane N. Bianchi (IC),[1] Andressa C. S. Montini (IC),[1] Patrícia G. Silva (PG),[1] Elizabete C. de Lima (PQ),[1]**

**carlos.gracio@aluno.ufabc.edu.br**

[1]*Centro de Ciênicas Naturais e Humanas, UFABC*

Key words: Biorremediation, Emerging Pollutants, Bisphenol A, Trametes versicolor, Laccase.

## Highlights

*Trametes versicolor* specie was grown in MEA 2% for 7 days, and inoculated in enriched medium for 7 and 14 days. BPA pattern was added after the fungal incubation. Lacase activity assays were performed, and degradation was evaluated in HPLC analysis. BPA concentration in treatment systems decreased due to the enzymatic activity.

## Resumo/Abstract

Emerging concern pollutants are substances commonly found in small concentrations in the environment, and despite this fact, they have the potential of causing serious damages to both animals and human health. There are several compounds that fit into this classification, and Bisphenol A (BPA) is one of them. Although it has low affinity to endocrine receptors, some researches indicate that there are a plenty of paths in which it can induce an estrogenic response of the body, being in some cases equivalent to that of estriol. In this study, *Trametes versicolor* fungus was purchased from the Algae, Cyanobacteria and Fungi Culture Collection of the Botany Institute (CCIBt) and maintained on Malt Extract Agar medium (MEA) 2%, at 4ºC. BPA, Sigma-Aldrich brand, was solubilized in acetonitrile (ACN) to a concentration of $1gL^{-1}$. The cultures were incubated as shown in image 1. The fungal inoculum was grown in petri dish with MEA 2%, at 28ºC. 10 discs (5mm) of grown mycelium were inoculated in Erlenmeyer flasks containing 100 ml of enriched medium (EM), and incubated for 7 and 14 days at 28° C. After the incubation time, Treatment systems (TR) and Abiotic Control systems (CA) received 100µL of the BPA solution, Biotic Control with acetonitrile systems (CBX) received 100µL of ACN and biotic controls (CB) did not receive any. For the monitoring of compound degradation and enzymatic activity, 4 ml aliquots were withdrawn from each flask at 0h, 24 h and 48 h after the pattern addition. The withdrawn TR and CA aliquots were analyzed on the Agilent Infinity 1220 chromatograph (HPLC) with diode array detector (DAD). Laccase activity was analyzed following the methodology described by Bourbonnais and Paice (1988). For 7 days incubation flasks, laccase activity showed to be greater on CB's (maximum 14,1369 $UL^{-1}$) and smaller on TR ones (maximum 3,0379 $UL^{-1}$); however, for 14 days of incubation, TR's showed greater laccase activity (maximum 92,6988 $UL^{-1}$). As a conclusion, the addition of ACN on culture medium did not interfere on enzymatic activity. BPA concentration had a higher decrease on TR flasks than CA ones, due to the activity of the low-specific enzymes, such as laccase. In most of 14 days flasks, BPA peak was not detected in the chromatogram, and this fact was attributed to the efficiency of the high activity of laccases in degrading this compound, corroborating what previous studies had already observed.

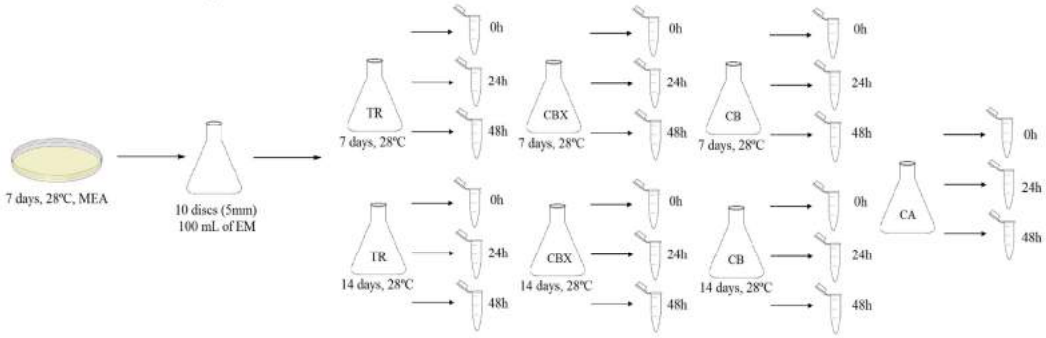


Image 1: Methodology used for inoculum and culture conditions.

**Área: AMB** **Inscrição: 01210**

# Utilização do filtro de bagaço de cana de açúcar no tratamento simplificado de água

**Luciana R. Marcelo (PQ),*[1] Vanessa P. Almeida (IC),[2] Cristiana R. Marcelo (PQ),[3] Viviane M. Arruda (PQ).[2]**

**luciana.marcelo@ifrj.edu.br; luciana.marcelo@ifrj.edu.br**

*[1]Instituto Federal de Educação, Ciência e Tecnologia (IFRJ) - Campus Duque de Caxias; [2]Depto. de Ciências Exatas e da Terra, UEMG - Campus Ubá; [3] Coordenação de Licenciatura em Educação do Campo, UFMA - Campus Bacabal.*

Palavras Chave: *População rural, Água para consumo humano, Biossorvente.*

## Highlights

Use of the sugar cane bagasse filter in the simplified water treatment

In the rural area the collected water is consumed directly, without treatment
Sugar cane bagasse can be used as a biosorbent
The bagasse filter is capable of retaining chemicals, improving water quality

## Resumo/Abstract

Na área rural, a maioria da população não tem acesso à rede de distribuição de água potável. A água é coletada em poços e nascentes e consumida diretamente, sem qualquer tratamento. Assim, o desenvolvimento de técnicas práticas e viáveis para o tratamento de água consumida em comunidades rurais torna-se necessário. O presente estudo tem como objetivo avaliar a eficiência de um sistema de tratamento simplificado, o Filtro de Biossorvente. Para isso preparou-se uma solução a partir de reagentes químicos denominada de solução fortificada e a mesma foi passada pelo filtro contendo o biossorvente de bagaço de cana-de-açúcar. A amostra fortificada e a amostra filtrada foram caracterizadas a partir dos seguintes parâmetros: pH, turbidez, sólidos totais, cloreto, dureza total, nitrato, fósforo total e ferro total. Os resultados encontrados para os parâmetros analisados na amostra de água antes e após a filtração estão apresentados na Tabela 1. Após o tratamento, exceto para o pH e fósforo total, verifica-se que os valores diminuíram de modo a se tornarem aceitáveis para o consumo humano. O tratamento provocou um ligeiro aumento da turbidez, porém seu valor se manteve dentro do permitido pela legislação. Os resultados confirmaram a eficácia do biossorvente de cana de açúcar. Desta forma, o filtro mostrou-se um tratamento simples e promissor para o tratamento de água nas áreas rurais.

**Tabela 1**. Valores para os parâmetros físico-químicos das amostras de água antes e após o tratamento

| Parâmetro | Solução Fortificada | | VMP* |
|---|---|---|---|
| | Antes | Após | |
| pH | 4,48 | 5,56 | 6,0 – 9,0 |
| Turbidez (UNT) | 1,48 | 1,67 | 5 |
| Sólidos Totais (mg $L^{-1}$) | 1540,00±48,08 | 53,00±1,41 | 1000 |
| Cloreto (mg $Cl^{-}$ $L^{-1}$) | 477,45±7,28 | 134,61±7,29 | 250 |
| Dureza Total (mg $CaCO_3$ $L^{-1}$) | 726,00±5,19 | 282,00±10,39 | 500 |
| Nitrato (mg N $L^{-1}$) | 24,82±0,035 | 5,48±0,32 | 10 |
| Fósforo Total (mg P $L^{-1}$) | 0,85±0,0015 | 0,14±0,020 | 0,025 |
| Ferro Total (mg Fe $L^{-1}$) | 2,46±0,0058 | 0,043±0,0032 | 0,3 |

*VMP – Valor Máximo Permitido pela Portaria nº 2.914/2011 do Ministério da Saúde.

BRASIL. Leis, decretos, etc. Portaria nº 2.914 do Ministério da Saúde, 12 de Dezembro de 2011. **Diário Oficial da União**, Brasília (DF), 2011.

**Área: AMB**
*(Inserir a sigla da seção científica para qual o resumo será submetido. Ex: ORG, BEA, CAT)*

**Inscrição: 01400**
*(Inserir o número de inscrição do autor que fez a submissão)*

# SYNTHESIS OF POLYURETHANE BIOCOMPOSITION USED AS ADSORVENT OF YELLOW TARTRAZINE FOOD COLORING

**Izabelle Alves de Castro França (IC)[1], Chrislayne Pais Vollbrecht (IC)[1], Tânia Mara Rizzato (TC)[1], Vagner Roberto Batistela (PQ)[1], Milena Keller Bulla (PQ)[1*].**

**izabelleacf@hotmail.com; mbullakeller@gmail.com**

[1]*Department of Technology, UEM.*

Key words: *Polyurethane foams, Banana peels, Residues, Adsorption.*

## Highlights

- Banana peels (*Musa Cavendishi*) were milled, sifted and dried, obtaining the banana peel flour that was used in the synthesis of polyurethane foams.
- The synthetic polyol used in the synthesis of polyurethane foams was partially replaced by the residue of the banana peels.
- The highest adsorption of yellow Tartrazine food coloring was obtained in 60 min for the polyurethane foam with the banana peel flour and 120 min for the polyurethane foam without the flour.
- The biocomposite with the banana peel flour had 99.7% yellow Tartrazine food coloring adsorption in pH 3 in 120 min.

## Abstract

In this work, a synthetic polyol, used in the synthesis of polyurethanes, was partially replaced by an agroindustrial residue and its adsorbent capacity was tested. Polyurethane foams were synthesized without residue (EPU) and with residue from banana peels (*Musa Cavendishi*) (ECB). The peels were subjected to grinding, sieving and oven drying, obtaining a flour. For the EPU synthesis, the polyethylene glycol (PEG 1500) was melted, polydimethylsiloxane and glycerol were added and mixed. In another container, it was merged 4,4-methylene diphenyldiisocyanate plus a catalyst and everything was added to the mixture containing PEG 1500, being stirred until the foam growth. For the synthesis of ECB the same procedure was performed, however replacing 10% of PEG 1500 by the residue. The foams were characterized by FTIR, TG and MEV. The influence of pH and kinetics on the adsorption of the Tartrazine E102 (AT) by the foams was evaluated.The highest adsorption was found at pH 3.0 for both, for EPU the adsorption was 99.7% of food coloring and for ECB it was 87.3%. The kinetic study was performed at pH 3.0 and 6.0. In both values the highest amount of adsorbed food coloring was obtained in the time of 120 min for EPU and 60 min for ECB.The model that best represented the kinetic data was the pseudo-second order model. The biocomposite with residue of the banana peels made the synthesis of the foam more sustainable and presented good adsorption capacity.

**Área: AMB**
*(Inserir a sigla da seção científica para qual o resumo será submetido. Ex: ORG, BEA, CAT)*

**Inscrição: 00736**
*(Inserir o número de inscrição do autor que fez a submissão)*

# Phosphate adsorption by different clay minerals modified with lanthanum and iron for application in aquatic eutrophic environments

**Laís Ferreira de Castro[1,2 *] (PG), Weber F. L. de Souza[1] (PQ), Viviane Gomes Teixeira [2] (PQ)**
***lais.castro@int.gov.br**

[1] *Instituto Nacional de Tecnologia, Divisão de Química Analítica, Av. Venezuela, 82, Rio de Janeiro, RJ.*
[2] *Universidade Federal do Rio de Janeiro, Instituto de Química, Av. Athos da Silveira Ramos, 149, Rio de Janeiro, RJ.*

Palavras Chave: Phosphate, Clay minerals, Adsorption, Eutrophication.

## Highlights

The phosphate adsorption by the clay minerals was directly related to the percentage of lanthanum.
The materials were selective for phosphate adsorption in the presence of $Cl^-$, $NO_3^-$ and $SO_4^{2-}$ anions.

## Resumo/Abstract

Excessive supply of phosphorus in aquatic environments from urban areas, mainly from domestic and industrial sewage leads to eutrophication. Modified clay minerals have been explored for remediation of eutrophic areas because of the better adsorption properties and functions of these materials[1]. The objective of this work was the modification of two smectites clays with lanthanum and iron aiming their application in the removal of phosphate in aquatic eutrophic environments. The materials Bent and PetBent were modified as described in Table 1 and characterized by X-ray diffraction, X-ray fluorescence, physical adsorption of $N_2$ and scanning electron microscopy. The degree of lanthanum and iron incorporation in the clays was dependent on their pore diameter but the chemical composition of the materials governed the adsorption capacity for phosphate. The adsorption of phosphate by the clay minerals was directly related to the percentage of incorporated lanthanum. Adsorption and kinetic models were evaluated, being better described by Lagmuir model and pseudo-second order, respectively. The materials were selective for phosphate adsorption in the presence of $Cl^-$, $NO_3^-$ and $SO_4^{2-}$ anions. In addition the most promising material was evaluated in the laboratory with a sample of real water from the Jacarepaguá Lagoon (Brazil). The water characteristics were: suspended particulate material: 93.25±2.47 $mg.L^{-1}$; $Cl^-$: 2.68±0.3 $g.L^{-1}$; $SO_4^{2-}$: 383.85±4.45 $mg.L^{-1}$; $NO_3^-$: 5.37±0.08 $mg.L^{-1}$; $PO_4^{3-}$ inorganic: 0.41±0.01 $mg.L^{-1}$. The modified clay adsorbed the amount of 69.84 mg $PO_4^{3-}$/g from the water, which represents 86% of adsorption yield, remaining only 0.06 $mg.L^{-1}$ of inorganic phosphate in solution.

**Table 1**
Modification and chemical composition of clay minerals.

| | | **Bent** [a] | La1Bent | La2Bent | LaFeBent | **PetBent** [b] | La2PetBent |
|---|---|---|---|---|---|---|---|
| Modification | $[La^{3+}]$ | - | 0.05 $mol.L^{-1}$ | 0.4 $mol.L^{-1}$ | 0.2 $mol.L^{-1}$ | - | 0.4 $mol.L^{-1}$ |
| | $[Fe^{3+}]$ | - | - | - | 0.1 $mol.L^{-1}$ | - | - |
| Chemicalcomposition (wt%) | $SiO_2$ | 67.0 | 67.4 | 65.2 | 68.2 | 68.0 | 69.4 |
| | $Al_2O_3$ | 22.8 | 23.0 | 22.9 | 21.5 | 17.5 | 17.6 |
| | $Fe_2O_3$ | 3.9 | 3.8 | 3.7 | 4.7 | 8.1 | 7.7 |
| | $La_2O_3$ | 0.0 | 2.3 | 4.0 | 2.2 | 0.0 | 2.6 |
| | MgO | 2.6 | 2.3 | 2.1 | 2.3 | 2.3 | 1.7 |
| | $Na_2O$ | 1.3 | 0.3 | 0.9 | 0.4 | 1.1 | 0.0 |
| | CaO | 1.3 | 0.3 | 0.6 | 0.2 | 1.0 | 0.0 |
| | $K_2O$ | 0.3 | 0.3 | 0.3 | 0.4 | 0.8 | 0.8 |
| Specific surface area ($m^2.g^{-1}$) [c] | | 31 | 39 | 35 | 40 | 103 | 116 |
| Desorption average pore diameter (Å) [d] | | 100 | 74 | 69 | 69 | 60 | 59 |

a: Standard clay Sigma-Aldrich; b: Pet litter line named Peepcat Benonite União Nordeste Ind. and Com. Ltda (Boa Vista, PB, Brazil); c: BET method; d: BJH method.

[1] Zhu, R.; *et al.*, Appl. Clay Sci. **2016**, 123, 239.

**Área: AMB** **Inscrição: 00497**

# Sensitivity to the cadmium ion by a strain of *Ensifer meliloti*

**Aline Aparecida Morais (IC)[1], Tatiane Fernanda Leonel(PG)[1], Cristiane Moretto (PQ)[1], Eliana Gertrudes de Macedo Lemos (PQ)[1], Lucia Maria Carareto Alves (PQ)[1], Luciana Maria Saran (PQ)[1,*]**

**lmsaran@fcav.unesp.br**

[1]*Departamento de Tecnologia, Faculdade de Ciências Agrárias e Veterinárias (FCAV), Universidade Estadual Paulista (UNESP), campus de Jaboticabal, SP, Brasil*

Keywords: *Living Cells, Rhizobia, Bioaccumulation, Potentially Toxic Metals, Bioremediation.*

## Highlights

Living cells of *Ensifer meliloti* may bioaccumulate $Cd^{2+}$.
*Ensifer meliloti* has 0.010 mmol $L^{-1}$ of $Cd^{2+}$ as the minimum inhibitory concentration.
*Ensifer meliloti* can be grown in up to 0.025 mmol $L^{-1}$ of $Cd^{2+}$.

## Abstract

Studies have addressed the immobilization of potentially toxic metals in aqueous solution by various microorganisms (algae, fungi and bacteria)[1]. Rhizobia are bacteria not pathogenic and do not produce secondary metabolites that cause damage to animals and plants. These bacteria stand out for the high production of biopolymers such as exopolysaccharides (EPS) and polyhydroxybutyrate (PHB), involved in the natural protection of cells, such as in the action of potentially toxic metals during the process of bioaccumulation[2]. These characteristics reveal great potential of rhizobia in bioremediation processes. In view of the above, the sensitivity to the cadmium ion ($Cd^{2+}$) of a rhizobia strain, *Ensifer meliloti* (LBMP-C02), was studied in order to evaluate its potential for the bioaccumulation of this metal ion. The strain LBMP-C02, grown in nutrient broth medium containing 0 (control), 0.010, 0.025, 0.050, 0.075, 0.100 and 0.200 mmol $L^{-1}$ of $Cd^{2+}$ presented cell growth sensitivity at concentrations above 0.010 mmol $L^{-1}$. The number of cells was not altered until 0.025 mmol $L^{-1}$ of $Cd^{2+}$ (Figure 1), which could be confirmed by bacterial growth in petri dishes and determination of colony forming units (CFU). The minimal inhibitory concentration (MIC) of $Cd^{2+}$, as $CaCl_2.H_2O$, for strain LBMP-C02 corresponds to 0.010 mmol $L^{-1}$ (Figure 2). Micrographs resulting from the analysis of the rhizobia cells by transmission electron microscopy revealed that they have the capacity to retain $Cd^{2+}$ inside them and produce biopolymers under the conditions in which they were evaluated.

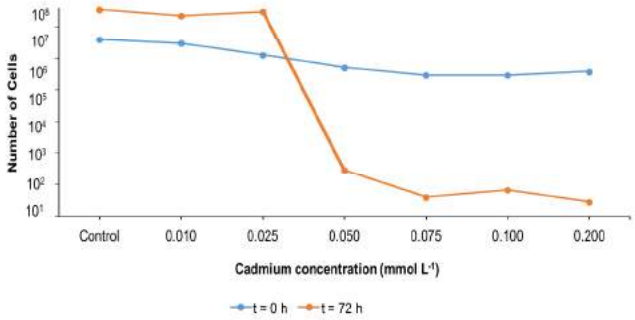


**Figure 1.** Cell growth of the *Ensifer meliloti* strain (LBMP-C02) in nutrient broth for 72 h at 30 °C and 150 rpm: control (without $Cd^{2+}$) and 0.010, 0.025, 0.050, 0.075, 0.100 and 0.200 mmol $L^{-1}$ of $Cd^{2+}$. Readings performed in Neubauer chamber.

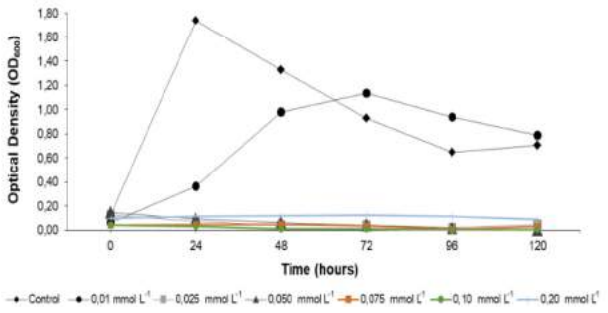


**Figure 2.** Cell growth curve ($OD_{600}$ as a function of time) of the *Ensifer meliloti* strain (LBMP-C02) in nutrient broth medium: control (without $Cd^{2+}$) and in 0.010, 0.025, 0.050, 0.075, 0.100 and 0.200 mmol $L^{-1}$ of $Cd^{2+}$, maintained up to 120 h under 150 rpm stirring at 30 °C.

## References

[1]Hansda, A.; Kumar, V.; Anshumali. *World Journal of Microbiology and Biotechnology*, **2016**, *32*(10), 170.

[2]Castellane, T.C.L.; Persona, M.R.; Campanharo, J.C.; Lemos, E.G.M. *International Journal of Biological Macromolecules*. **2015**, *74*, 515.

## Acknowledgments

The authors thank Research Support Foundation of the State of São Paulo (FAPESP) by the scholarship of scientific research awarded (FAPESP process n. 2017/03146-7)

**Área: AMB** **Inscrição: 00112**

# Use of ultrasound to development of substrates for *Saccharomyces cerevisiae*

**Marcelo Eduardo Cordeiro (IC),[1] Jaqueline Nicolini (PQ)[1], Keller Paulo Nicolini (PQ).[1*]**

**keller.nicolini@ifpr.edu.br;**

[1]*Colegiado de Química – IFPR, Campus Palmas*

Palavras Chave: hydrothermal treatment, biomass, DRUV, inhibitory concentration.

## Highlights

Temperature and ultrasound are strategies for the substrates development.
DRUV spectroscopy and the band gap energy of substrates are associated with the inhibitory concentration of *S. cerevisiae*.

## Resumo/Abstract

Ultrasonic treatment (UT) favors the enzymatic attack on plant materials[1] and influences the biological activity.[2] This study aims to develop substrates for *Saccharomyces cerevisiae* from the hydrothermal treatment (HT) and UT of the biomass of *Pinus* spp. The biomass undergo HT for 3 hours: (a) 450 °C and UT for 0 (BAP450-0), 10 (BAP450-10), 80 (BAP450-80) and 100 min (BAP450-100); (b) 550 °C and TU for 0 (BAP550-0), 10 (BAP550-10), 80 (BAP550-80) and 100 min (BAP550-100); and (c) 650 °C and TU for 0 (BAP650-0), 10 (BAP650-10), 80 (BAP650-80) and 100 min (BAP650-100). The inhibitory concentration for *Saccharomyces cerevisiae* ($IC_{30}$) was evaluated.

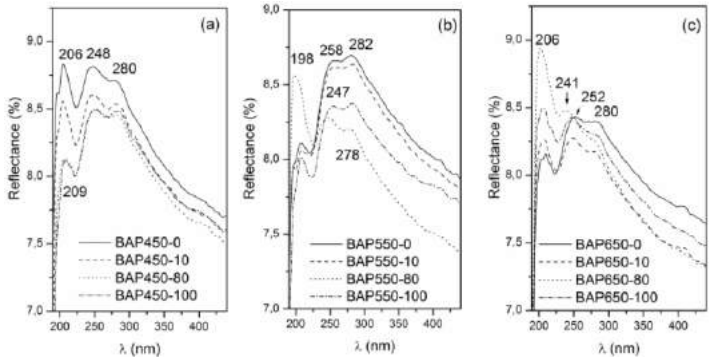


**Figure 1.** DRUV spectra: (a) BAP450-0, BAP450-10, BAP450-80 e BAP450-100; (b) BAP550-0, BAP550-10, BAP550-80 e BAP550-100; e (c) BAP650-0, BAP650-10, BAP650-80 e BAP650-100

**Table 1**. Band gap energy (E), ratio between wavelengths $\lambda_{200/280}$ and inhibitory concentration $IC_{30}$

| Sample | E (eV) | $\lambda_{200/280}$ | $IC_{30}$ (ppm) |
|---|---|---|---|
| BAP450-0 | 3.20 | 0.993 | > 50000 |
| BAP450-10 | 2.98 | 0.987 | 19188 |
| BAP450-80 | 3.16 | 0.946 | 32128 |
| BAP450-100 | 3.28 | 0.917 | > 50000 |
| BAP550-0 | 2.95 | 0.916 | > 50000 |
| BAP550-10 | 2.94 | 0.910 | > 50000 |
| BAP550-80 | 3.30 | 1.028 | > 50000 |
| BAP550-100 | 3.43 | 0.924 | > 50000 |
| BAP650-0 | 3.37 | 0.953 | > 50000 |
| BAP550-10 | 3.26 | 1.004 | 445 |
| BAP550-80 | 3.44 | 1.082 | 713 |
| BAP550-100 | 3.48 | 1.011 | > 50000 |

The lower $IC_{30}$ at 450 °C (BA450-10) was observed (Table 1) for the ratio $\lambda_{206/248} \approx 1$ and at 650 °C (BAP650-10) for $\lambda_{200/250}$ and $\lambda_{250/280} > 1$ ratios. HT samples at 450 °C have lower band intensity at 200, 250 and 280 nm at higher UT times (Figure 1). The samples with UT at 550 and 650 °C have higher reflectance bands in the region of 200 nm after 80 min of UT and lower band gap energies associated with lower $IC_{30}$. The HT for 100 min generates the most promising materials to be used as substrates for the eukaryotic model *Saccharomyces cerevisiae*.

References:

[1] Klein JM, et al., *International Journal of Biological Macromolecules*, 2018.
[2] Bhangu SK, et al., *Green Chemistry*, 2018.

**Área: AMB**
*(Inserir a sigla da seção científica para qual o resumo será submetido. Ex: ORG, BEA, CAT)*

**Inscrição: 00460**
*(Inserir o número de inscrição do autor que fez a submissão)*

# Synthesis and characterization of pyroaurite-type material at room temperature employing bauxite residues from Amazon Region

**Renata de Sousa Nascimento (PG),[1*] Bianca Soares Costa (IC),[1] Bruno A. M. Figueira (PQ),[1] Liliane N. Silva (PG),[2] Grazi C. Telles (PQ),[3] José Manuel R. Mercury (PQ)[4].**

**bruno.figueira@pq.cnpq.br, renataasnascimento22@gmail.com;**

*[1]Programa de Pós Graduação em Sociedade, Ambiente e Qualidade de Vida, UFOPA; [2]Programa de Pós Graduação em Geociências, UFPA; [3]Departamento de Física, UFPA; [4]Departamento de Química, IFMA.*
Palavras Chave: *Residues, Bauxite, Amazon, Synthesis, Layered Double Hydroxides, Pyroaurite.*

## Highlights

- The chemical and mineralogical of bauxite residues from Amazon Region was investigated to convert them into layered double hydroxide.
- A facile method for fabricating pyroaurite-type material at room temperature has been presented.
- It could be concluded that bauxite residues are an interesting low cost starting material for synthesis of lamellar material.

## Resumo/Abstract

The synthesis of hydrotalcite-type material from bauxite residues from Juruti mine (Pará State, northern Brazil) is presented. The residues and the final product were characterized by X-Ray Diffraction (XRD), Thermogravimetric analysis and Scanning Electron Microscopy (SEM). According to the results obtained, although residues have been employed as starting material, pure hydrotalcite could be synthesized with rhombohedral (R3-m) structure-like and 7,82 Å interlayer spacing. The unit cell parameters were obtained as a=3.130(7)Å, c=23.47(6)Å, as well as size crystal (31 nm) by Scherrer Equation. The thermal behavior of hydrotalcite could be divided into four main decomposition steps (TG-DTA curves) related to the loss of interlamellar water, decomposition of OH- groups and collapse of the hydrotalcite structure. The material exhibited morphology in the form of plates and small agglomerates around 10 μm.

**Área: AMB** **Inscrição:00254**

# Bixin incorporated over a porous membrane as a biosorbent to remove mercury (II) from aqueous matrices

**Júlia Condé Vieira(PG)*[1],Cláudia Carvalhinho Windmöller (PQ)[1], Guilherme Dias Rodrigues(PQ)[1];Ricardo Mathias Orlando (PQ)[1].**

***juliacondev@hotmail.com**

[1]*Departamento de Química, UFMG, Belo Horizonte, Minas Gerais, Brasil.*

Palavras Chave: *Mercury, Sorption; Metal removal; Bixin; Biosorbent system; Inorganic contaminants.*

## Highlights

A bixin film was used to remove mercury from aqueous samples.
Bixin was incorporated on cellulose membranes by drop coating.
Adsorption parameters were evaluated to study bixin mercury removal capacity.

## Resumo/Abstract

Mercury is a highly toxic metal listed among the ten chemical elements that cause major public health concerns according to World Health Organization[1]. Therefore new materials have been developed in order to remove mercury from aqueous systems effectively and selectively[2-4]. Bixin, an apocarotenoid extracted from *urucum* seeds (*Bixa orellana*), can be a promising alternative as a biosorbent for removal environmental contaminants. For the present work, bixin solutions were incorporated into cellulose membranes by drop coating technique in order to stabilize and fix the compound. The membranes containing the thin film of the apocarotenoid were left in contact with standard solutions of Hg (II) under stirring. The contact time, temperature, pH, salt concentration and ionic strength of the analyte solutions were the parameters evaluated in this work. The direct mercury analyzer (DMA 80, Milestone) was used to determine the total mercury content in the final solutions. In basic pH the mercury adsorption occurred more efficiently presenting 91% of removal. Even at slightly acidic pH the removal was approximately 70%. Saline solutions (X-Y %, m/v, sodium chloride concentrations) did not significantly affect mercury sorption. At temperatures of 20ºC and 25ºC the mercury removal was higher than 80%. Based on these previous results it is possible to conclude that bixin incorporated into the membranes is a potential sorbent for the removal of mercury II and can be tested in filters for aqueous purification.

[1] WHO. *World Health Organization.* Available in: <http://www.who.int/mediacentre/factsheets/fs361/en/>.
[2]Hernández, P. B.; Morales, G. R.; Silva, M. T. R;Romo, M. R.; Sevilla, E. R.; Schulz, J. M. E.;Gomez, J. J. *Chemosphere, 167 (2017) 314-312*.
[3] Sinha, A.; Pant, K. K.; Khare, S. K. *International Biodeterioration & Biodegradation, 71 (2012) 1-8.*
[4] Saman, N.; Johari, K.; Tien, S. S.; Mat, H.*Clean – Soil, Air, Water, 42, (2013) 1541-1548.*

Acknowledgments:

**Área: AMB** **Inscrição: 00829**

# Labilidade de íons Ferro e Manganês na presença de nano-sílica em diferentes valores de pH

**Danielle Goveia* (PQ)[1], Daniele Frasson Vieira (IC)[1], Wander Gustavo Botero (PQ)[2], Luciana Camargo de Oliveira(PQ)[3]**

**danielle@itapeva.unesp.br**

[1]*Universidade Estadual Paulista "Júlio de Mesquita Filho" - UNESP, Campus Experimental de Itapeva, Itapeva-SP.*
[2] *Universidade Federal de Alagoas, Campus de Arapiraca, Arapiraca-Al.*
[3]*Universidade Federal de São Carlos, Campus de Sorocaba, Sorocaba - SP.*

Palavras Chave: *Metais, Sistemas aquáticos, nanopartículas.*

## Highlights

Lability of iron and manganese ions in the presence of nano silica at different pH values. Nanosilica were added to M-humic complexes. Iron labile at pH 3.5, 5.5 and 7.5. Manganese labile at pH 3.5.

## Resumo/Abstract

Íons metálicos em sistemas aquáticos formam complexos com matéria orgânica ou inorgânica, podendo ser considerados desta forma lábeis ou inertes. Nanomateriais estão emergindo como objeto de pesquisa em todos os campos da química e invariavelmente tem como destino o ambiente. Busca-se verificar a labilidade de íons metálicos originalmente complexados à matéria orgânica, após adição de nano-sílica, em diferentes pHs.

Para verificar se modificações nas condições do ambiente irão afetar o comportamento dos íons metálicos. Foram preparadas soluções contendo os íons Fe e Mn, material húmico e o pH foi ajustado. As soluções foram ultrafiltradas, onde o filtrado contém os metais livres. Adicionou-se a nanopartícula de sílica LUDOX LS30 (8 nm) e foram coletadas alíquotas de tempos em tempos. A determinação dos metais foi feita por espectrômetro de absorção atômica. As Figuras 1 e 2 apresentam, respectivamente, a concentração de Fe livre e Mn livre em três diferentes pHs: 3,5; 5,5 e 7,5.

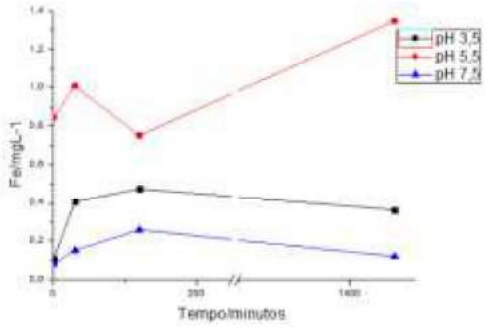


**Figure 1**. Fe livre determinado após adição de nanopartícula em pHs diferentes

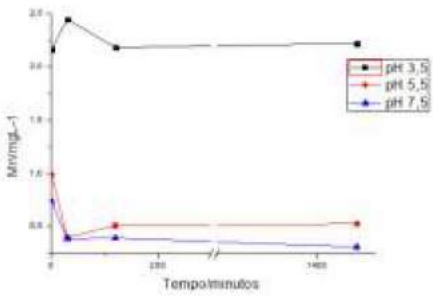


**Figure 2**. Mn livre determinado após adição de nanopartícula em pHs diferentes

O estudo com o ferro apresentou resultados divergentes, a maior concentração de íons livre foi encontrada em pH 5,5. Provavelmente formaram hidroxocomplexos em pH 7,5, explicando valores baixos de Ferro livre nesta condição. Para o manganês, há pequenas alterações até 120 minutos, em seguida estabelece o equilíbrio até completar 24 horas. Em pH mais baixo (3,5) apresentou maior concentração de metal livre, ou seja, menor interação do manganês com os ligantes. Os resultados indicam que a adição das nanopartículas aumenta a concentração do metal livre, ou seja, está disponibilizando o metal lábil para o sistema, em todos os pHs estudados para Ferro, e em pH 3,5 para Manganês. Os resultados obtidos até o momento apresentaram ser promissores em relação ao impacto das nanopartículas no ambiente indicando que o pH do meio interferem no comportamento e na disponibilidade dos metais no ambiente.

Agradecimentos à FUNDUNESP, CNPQ (458875/2014-7) e FAPESP (2016/23728-8) pelo auxílio financeiro e FAPESP (2015/ 21232-2) pela bolsa concedida.

**Área: AMB**
*(Inserir a sigla da seção científica para qual o resumo será submetido. Ex: ORG, BEA, CAT)*

**Inscrição: 00626**
*(Inserir o número de inscrição do autor que fez a submissão)*

# Micropartículas poliméricas como um sistema carreador de nutrientes para plantas

**Júnior Olair Chagas (PG),[1]* Gilmare Antônia da Silva (PQ),[1] Fabiana Aparecida Lobo (PQ).[1]**

**fabiana@iceb.ufop.br; chagasojunior@gmail.com***

[1]*Departamento de Química, UFOP.*

Palavras Chave: *Liberação controlada, Micropartículas, Nutrientes.*

## Highlights

Polymeric microparticles as a plant nutrient carrier system.
A new microencapsulated fertilizer with NPK was developed.
Multivariate experimental designs and the desirability function were used to obtain the optimal encapsulation condition.

## Resumo/Abstract

Devido aos problemas das técnicas tradicionais de fertilização, propôs-se o desenvolvimento de micropartículas[1] de poli(ε-caprolactona) (PLC) e poliglicerol (PLG) carreadoras de NPK (nitrogênio, fósforo e potássio). A síntese das partículas foi feita pelo método de nanoprecipitação[1] e estudou-se sistematicamente as variáveis que influenciam a taxa de associação (%EE) de NPK por meio de planejamentos experimentais multivariados[2]. As cinco variáveis estudadas foram massa de PLC, massa de PLG, volume de clorofórmio, volume de água na fase orgânica e concentração da solução de álcool polivinílico (PVA). Por meio do planejamento fracionário $2^{5-1}$ com triplicata no ponto central[2] foi possível identificar que as cinco variáveis foram significativas, e para a otimização aplicou-se o planejamento composto central e a função de desejabilidade. A condição ótima foi 100 mg de PLC; 825 mg de PLG; 9,25 mL de clorofórmio; 3,00 mL de água e 0,9% m/v para o PVA. Os resultados mostraram partículas com diâmetro entre 5 a 60 µm e %EE de 94,23% para nitrogênio; 99,80% para fósforo e 65,00% para potássio. A degradação das partículas foi avaliada em 90 dias e não houve variação de pH, tamanho e %EE, indicando que durante este período as micropartículas foram estáveis. Os perfis de liberação, baseados na Lei de Fick, foram similares e mostraram que houve liberação lenta, contínua e prolongada de NPK.

[1]de Melo NFS, *et al.,* Química Nova, 33, 2010, 65.
[2]Teófilo RF, *et al.,* Química Nova, 29, 2006, 338.

[**CAPES, CNPq; FAPEMIG; PROPP/UFOP**]

**Área: AMB** **Inscrição:** 00212

# Study of the partition of emerging contaminants employing aqueous two-phase systems as extraction technique

**Roberta C. de Assis (PG),[1*] Ricardo M. Orlando (PQ),[2] Aparecida B. Mageste (PQ),[3] Leandro R. de Lemos (PQ),[4] Guilherme D. Rodrigues(PQ),[1]**

**robertaconde@ufmg.br**

*[1]LaSaV - Laboratório de Soluções Analíticas Verdes, Departamento de Química, DQ/ICEX, UFMG; [2] Departamento de Química, DQ/ICEX, UFMG, [3]Departamento de Química, DQUI/ICEB, UFOP; [4]Departamento de Química, DEQUI, UFVJM.*

Keywords: *Aqueous Two-Phase Systems, Emerging Contaminants, Drugs, Partition Coefficient.*

## Highlights

Drugs classified as emerging contaminants;
Partition of the drugs in aqueous two-phase system;
Determination of antibiotics and anti-inflammatory by UV-Vis spectrophotometer.

## Abstract

The wide use of synthetic products in industries, agriculture and for personal use has caused a great concern about the persistence of these compounds in the environment[1]. As examples of these compounds classified as emerging contaminants (EC) are the drugs, with antibiotics and anti-inflammatory being the most cited. The extraction technique aqueous two-phase systems (ATPS) was employed for the partition of the drugs. These systems are formed by top phase (TP) and bottom phase (BP), and are composed mainly of water and non-toxic reagents. The objective of this work was to study the partition coefficient ($K = A_{TP}/A_{BP}$) of ibuprofen, paracetamol, ciprofloxacin and norfloxacin in ATPS. Aiming the best extraction conditions, the following parameters was optimized: pH, nature of the polymer and the ATPS-forming electrolyte, the tie-line length (TLL), and temperature. The higher *K* results of the drugs are shown in Figures 1 and 2. The ATPS composed of L35+$Na_2SO_4$, at pH=2, at a temperature of 40°C and TLL=46.77%w/w presented the best partition conditions for ciprofloxacin and norfloxacin, and ATPS formed by L35+$MgSO_4$, pH=6, TLL=45.52%w/w, and temperature equal to 40°C and 10° C, presented best results for ibuprofen and paracetamol, respectively. Therefore, ATPS under the conditions chosen for each drug class is an effective and environmentally friendly extraction technique.

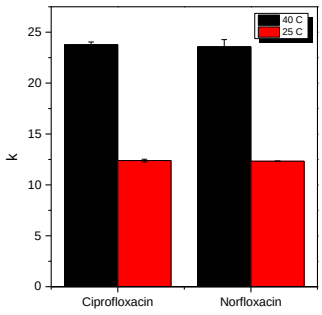


**Figure 1.** Partition coefficient of the drugs Ciprofloxacin and Norfloxacin in ATPS L35+$Na_2SO_4$, pH= 2, TLL = 46.77% w/w.

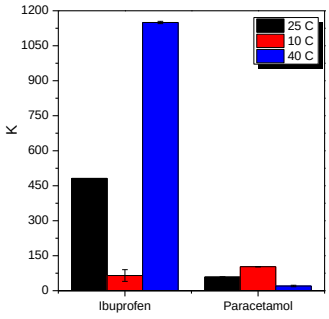


**Figure 2.** Partition coefficient of the drugs Ibuprofen and Paracetamol in ATPS L35+$MgSO_4$, pH = 6, TLL = 45.52% w/w.

[1]Stuart, M., et al., 2012.Science of the Total Environment. 416, 1-21.

[PPG-DQ/UFMG, CAPES, CNPq, FAPEMIG]

**Área: AMB** **Inscrição: 01171**

# CHEMICAL WASTE MANAGEMENT IN TEACHING LABORATORIES: an activity proposal for academic community awareness

**Letícia D. F. de Siqueira (IC)[1], João Marcos S. R. dos Santos (IC)[1], Karolynne C. Morais (IC)[1], Ray de S. Pereira (IC)[1], Rafaela R. de Paula (IC)[1], Iago S. Mesquita (TM)[1], Aline M. S. Teixeira (PQ)[1*]**

**lcdayane49@gmail.com; rosendo.joaom@gmail.com; aline.santos@ifrj.edu.br**

[1]*Instituto Federal de Educação, Ciência e Tecnologia do Rio de Janeiro – IFRJ Campus Duque de Caxias*

Keywords: Chemical Waste, Sustainability, Teaching Laboratory, Academic Community Awareness.

## Highlights

Management of materials considered useless after some kind of chemical process. Science and technological week. Awareness of the academic community about chemical waste management.

## Resumo/Abstract

Given the large amount of chemical waste stored in the teaching laboratories of the IFRJ Campus Duque de Caxias, emerged the need to manage and treat the chemical waste, according to 357 and 420 CONAMA resolutions[1,2]. These resolutions set waste disposal parameters for fresh and underground water respectively, most commonly polluted by companies and residents in general. During the VIII Science and Technological Week, an activity was presented with the aim to evaluate the public knowledge on the disposal, treatment and storage of chemical wastes. Furthermore, was emphasized the difference between waste and tailings, in order to classify the different types of waste according to 358 CONAMA[3] and 10004 ABNT NBR[4]. The activity was geared at the academic community (students, teachers from different areas and other employees) of the IFRJ Campus Duque de Caxias and 48 visitors participated. Questionnaires were applied before and after the presentations in order to diagnose the knowledge of the academic community about the theme and to evaluate the effects of the project, Figure 1. The questionnaires replies showed that 70% of visitors were able to define precisely what a chemical residue is. The activity followed the ideals of 5R's sustainability, aiming at the awareness and engagement the reuse of natural resources, as well as promoting the reduction of waste generated.

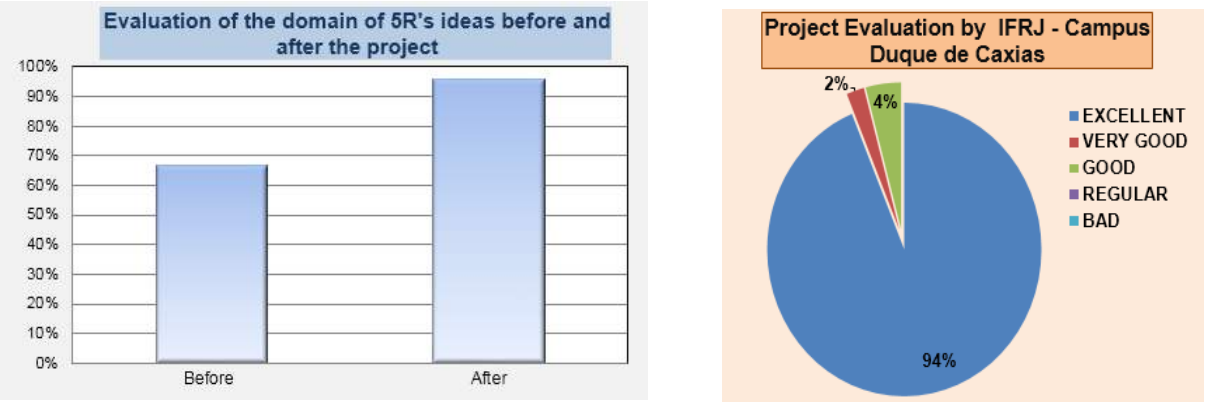


(a) (b)

**Figure 1.** Some Results about the effects of the project: (a) domain about 5R's ideas; (b) evaluation by IFRJ

## REFERENCES

[1] <http://www.mma.gov.br/port/conama/legiabre.cfm?codlegi=459>. Acesso em: 28 de Janeiro de 2018.
[2] <http://www.mma.gov.br/port/conama/legiabre.cfm?codlegi=620>. Acesso em: 28 de Janeiro de 2018.
[3] <http://www.mma.gov.br/port/conama/legiabre.cfm?codlegi=462>. Acesso em: 28 de Janeiro de 2018.
[4] ASSOCIAÇÃO BRASILEIRA DE NORMAS TÉCNICAS (ABNT). Resíduos Sólidos − Classificação. Norma Técnica NBR 10004. Rio de Janeiro: ABNT, 2004.

**Área: AMB** **Inscrição: 00597**

# Método alternativo para o descarte de resíduos de cobre e iodo

**Gabriela T. Linhares (IC),[1] Bruna L. M. Vieira (IC)*,[1] Bruna M. Chinelate (IC),[1] Tatiana A. Toledo (TM), Denise B. A. Barbosa (FM)[1].**

***brunalmvieira@gmail.com; tatiana.alves@ifsudestemg.edu.br**

[1]*Laboratório de Pesquisa e Experimento em Nanociência, Instituto Federal de Ciência e Tecnologia do Sudeste de Minas Gerais – Campus Juiz de Fora*

Palavras Chave: tratamento resíduo, resíduos, cobre, iodo

## Highlights

Alternative method for the disposal of copper and iodine residues - treatment of KI tailings, using the treatment discard product and recovery of CuSO4, in order to minimize the volume of the material to be sent to the final destination.

## Resumo/Abstract

A conscientização para o destino adequado de resíduos químicos, associado a uma gestão ambiental eficiente, contribuem para minimizar possíveis impactos negativos para a saúde e para o ecossistema, uma vez que o descarte inadequado potencializa a contaminação do solo e de mananciais[1,3,4].

O objetivo desse trabalho foi tratar rejeitos de iodeto de potássio oxidados reaproveitando o resíduo final do tratamento de rejeito sulfato de cobre, pela perspectiva dos 3Rs da sustentabilidade[1].

Método empregado:

Após tratamento e recuperação de $CuSO_4$, ainda existiam resíduos a serem descartados. E com o rejeito de KI, observou-se uma alternativa interessante de tratamento do composto já deteriorado. Destaca-se também que o reaproveitamento do resíduo de $CuSO_4$ propicia a economia/redução do consumo de novos reagentes, validando a política dos 3Rs[1].

Equação[2] de formação dos precipitados 1 e 2:

Equação 1 – Formação do iodeto de cobre (I):

$$4I^- + 2Cu^{2+} \rightarrow 2CuI\downarrow + I_2$$

$$I_2 + S_2O_3^{2-} \rightarrow 2I^- + S_4O_6^{2-}$$

É importante salientar que com o tratamento desses resíduos reduziu-se o volume para ser armazenado, facilitando o descarte adequado. Além disso, ressalta-se a contribuição econômica e ambiental desse trabalho, uma vez que se limitou a utilização de novos reagentes e não foi eliminado para o meio ambiente íons potencialmente prejudiciais.

Referências:

[1]Anais do IV SINGEP – Ações para minimizar a produção de resíduos nas aulas práticas de química em laboratórios de uma instituição de ensino superior. São Paulo/SP. 08 a 10 novembro 2015. [2]BASSETT, J.; DENNEY, R. C; JEFFERY. G. H.E; MENDHAN, J. *Análise Inorgânica Quantitativa de Vogel*. 4ª ed. Rio de Janeiro, Ed. Guanabara Dois, 1981. 690p. [3]DEL PIERO, P.B., *et al*. Tratamento de resíduos de cobre, prata e níquel provenientes de aulas práticas. 48 CBQ, Rio de Janeiro, 2008. [4]GAUZA, O.R.; BASSTTI, F.J.; BARBOSA, V.M. Alternativas Ecoeficientes no Gerenciamento de Resíduos Sólidos em

**Área: AMB** **Inscrição: 00945**

# Chlorexidine behavior in chlorinated medium and occurrence of byproducts

**Renata Colombo (PQ)*; Viviane S. Carvalho (IC).**

**renatacolomb@gmail.com**

*Escola de Artes, Ciências e Humanidades, Universidade de São Paulo, 03828-000, São Paulo, SP, Brasil.*

Palavras Chave: Clorexidina, Micropoluentes, Oxidação, Cloração, Águas.

## Highlights

The chlorhexidine biocide is a micropollutant of the aquatic system
Chlorhexidine is reactive in the presence of chlorine
Chloramine is a class of byproducts formed in waters by the chlorination of chlorhexidine

## Resumo/Abstract

Chlorhexidine is the active principle of antiseptic products with antifungal and bactericidal action used in large scale for different applications (human, veterinary and general cleaning). The increasing use and disposal of these products has resulted in the contamination of several environmental compartments by chlorexidine, including waters of springs and aquifers. Data on the behavior and safety of this micropollutant, as well as their derivatives, on the environment and human health are still scarce. Regulatory agencies in Brazil and in the world have required studies that may support more specific and safe regulations. In this study chlorhexidine was investigated in chlorinated medium to verify its behavior and to detect plausible derivatives to be formed in chlorinated aquatic environments (focusing on water supply). This molecule will be subjected to conditions of pH (6-9), light (presence/absence), temperature (20 to 40°C) and chlorine concentration (0.2 to 5.0 $mgL^{-1}$) usually present in the natural environment and/or applied during the treatment and distribution of water supply. Analytical methodology using liquid chromatography coupled to mass spectrometry will be developed to monitor the target molecule and identify their derivatives. Under the different conditions studied, forty-one derivatives were detected. Some of them were formed under different conditions and others formed specifically in a given condition. These compounds were formed from oxidation, fragmentation and / or chlorination of the chlorhexidine molecule generating analogues of several organic classes including chloramine, class of organic compounds with proven toxicological activity.

**Área: AMB** **Inscrição: 01262**

# Diagnóstico das condições sanitárias de residências localizadas às margens do Rio Sarapuí - Duque de Caxias, Rio de Janeiro

**Larissa F. Pereira (IC),[1*] Isabella da S. P. dos Santos(IC),[1] Lucas D. de Almeida (IC),[1] Nick R. L. de Sá (TM),[1] Luciana R. Marcelo(PQ),[1]**

**larissafpereira24@gmail.com**

[1]*Instituto Federal de Educação, Ciência e Tecnologia do Rio de Janeiro- Campus Duque de Caxias*

Palavras Chave: *Condições sanitárias, Rios, Poluição, Doenças, Qualidade da água*.

## Highlights

Diagnosis of sanitary conditions of residences located on the banks of the Sarapuí river- Duque de Caxias, Rio de Janeiro.
The datas of sanitary conditions were collected by questionnaires applied to residents living on the banks of the Sarapuí River, in Duque de Caxias. The study corroborate the lack of public policies.

## Resumo/Abstract

O município de Duque de Caxias (RJ) apresenta como principal fonte de abastecimento de água o Rio Sarapuí. O crescimento populacional e políticas públicas ineficazes acarretaram em urbanização não planejada resultando sérios danos ambientais, entre eles o comprometimento da qualidade de seus recursos hídricos. Este trabalho apresenta dados preliminares do projeto sobre análise da qualidade da água do rio Sarapuí. Os dados foram coletados por questionários aplicados aos moradores residentes nas margens do rio Sarapuí. O objetivo dessa etapa foi realizar um levantamento das condições sanitárias da área estudada, além das informações subsidiar a escolha dos pontos de coleta de água para análises futuras. Das 26 moradias visitadas, 57,69% são contempladas pelo sistema de abastecimento público, porém há relatos de baixa qualidade e falta de água. Dos entrevistados, 30,77% possuem abastecimento de água clandestino e 75,00% desses relatam doenças atribuídas ao contato com o rio. A maioria (69,23%) alega não utilizar a água do rio para nenhum fim, mas há relatos do uso para fins recreativos. Cerca de 42,31% afirmam que suas casas já foram alagadas e 76,92% que não há rede pública de esgoto que os atendam, sendo este despejado no rio. Além das informações fornecidas pelos entrevistados, verificou-se in loco uma piora expressiva na poluição e a presença de ratos, moscas e mosquitos. Os dados obtidos corroboram a falta de políticas públicas ao longo do tempo e, principalmente, nos últimos anos em que pararam as drenagens.

**Área: AMB** **Inscrição: 00962**

# Propriedades térmicas de blendas de ésteres metílicos e etílicos obtidos do óleo de *Attalea phalerata* (Arecaceae) e soja.

**Jaqueline Cândido M. da Silva (PG),[1] Cleber L. Nicolau (PG),[1]Érica R. Costa (PG),[1] Eduardo J. Coutinho (IC),[2]Aline F. N. Volpini Klein (PG),[1] Euclésio Simionatto (PQ)[1], Jusinei M. Stropa (PG)[3], Lincoln C. Silva de Oliveira (PG)[3].**

**jaquecandido18@gmail.com**

*[1] Programa de Pós-Graduação em Recursos Naturais da Universidade Estadual de Mato Grosso do Sul, UEMS; [2]Curso de Química,UEMS; [3]Instituto de Química Universidade Federal do Mato Grosso do sul, UFMS.*

Palavras Chave: *Biocombustíveis, estabilidade térmica, óleos vegetais.*

## Highlights

Thermal properties of methyl and ethyl ester blends obtained from *Attalea phalerata* (Arecaceae) and soybean oil.. In this work esters were synthesized from *Attalea phalerata* (Bacuri) and mixtures of esters (blends) of bacuri oil with soybean oil were analyzed and their thermal stability was analyzed.

## Resumo/Abstract

**Introdução:** O biodiesel é um combustível biodegradável, obtido a partir de fontes renováveis, como óleos vegetais e gorduras animais. O Brasil possui uma grande diversidade de espécies de oleaginosas que podem ser utilizadas na produção do biocombustível[1, 2]. Baseado nesse contexto a espécie *Attalea phalerata* (Bacuri), encontrada no MS foi estudada neste trabalho visando avaliar o teor de óleo das amêndoas, caracterização química e o comportamento térmico por TG/DTG e DSC de blendas de seus ésteres com os ésteres provenientes do óleo de soja. **Resultados e Discussão:** Os teores de ésteres das amostras puras e blendas foram superiores a 96,5%, estando de acordo com os parâmetros estabelecidos pela ANP (Agência Nacional do Petróleo, Gás Natural e Combustível). Através da análise térmica (TG /DTG, foi possível observar a estabilidade dos ésteres puros e blendas, como mostra a Tabela 1. Na tabela 2 são apresentadas as temperaturas de cristalização dos ésteres puros de soja, bacuri e blendas. Observou-se o efeito positivo dos ésteres de bacuri, os quais provocaram um decréscimo na temperatura de cristalização das blendas. **Conclusão:** Os ésteres provenientes da transesterificação do óleo de bacuri apresentam uma composição predominantemente saturada (63%)**.** Os principais ésteres são os derivados do ácido láurico (30,7%), mirístico (12,0%) e oleico (30,5%). Esta composição com predomínio de ésteres saturados afeta o comportamento térmico das blendas com ésteres de óleo de soja.

Tabela 1: Temperatura de início de degradação dos ésteres puros de bacuri (100%) e das blendas de ésteres bacuri/soja (TG/DTG).

| Amostras | Temperatura (ºC) |
|---|---|
| Éster metílico | 64,4 |
| Éster metílico 10% | 99 |
| Éster metílico 50% | 73,5 |
| Éster etílico | 65,6 |
| Éster etílico 10% | 101 |
| Éster etílico 50% | 79,2 |

Tabela 2: Pontos de cristalização (°C) de ésteres metílicos e etílicos (puros e blendas) obtidos a partir de óleos de soja e bacuri por DSC.

| Amostras | Éster etílico | Éster metílico |
|---|---|---|
| Ésteres de soja | -3,7 | -2,8 |
| Ésteres de bacuri | -5,8 | -3,9 |
| Ésteres 10% | -4,6 | -2,7 |
| Ésteres 50% | -5,6 | -3,5 |

**Referências:** [1]SANTOS, A. P.; PINTO, A. Biodiesel: Uma alternativa de combustível limpo. **Química Nova na Escola,** v.31, n.1, 2009.
[2]ANGELO, C. P.; CÉSAR, Z.; FERNANDO, G.; JAILSON B. de A.; PAULO, C. V. Chemistry without borders. **Quím. Nova**. vol. 35, n.10. São Paulo, 2012.
**Agradecimentos:** UEMS, PGRN,CAPES.

**Área: AMB** **Inscrição: 00156**

# Longitudinal variation of the energetic properties of clones *Eucalyptus sp.*

**Jaqueline dos Santos (IC),[1] Wislania P. Silva (PQ),[1*] Samara A. Morais (PG),[2] Vânia A. Sá (PQ),[3] José E. A. Souza (PQ).[2]**

**Jaqueline.dos.santos.ufal@gmail.com;** wislania@yahoo.com.br

*[1]Centro de Tecnologia – CTEC, UFAL; [2]Instituto de Química e Biotecnologia, UFAL; [3]Centro de Ciências Agrárias – CECA, UFAL.*

Keywords: *eucalyptus urograndis, characterization, biomass, renewable energy.*

## Highlights

Aiming at the energetic potential of the Eucalyptus species, the work aims to evaluate the energetic properties of the species varying the length of the clone.

## Resumo/Abstract

The species of the genus Eucalyptus present an excellent potential for wood production due to its high productivity, diversity, adaptability and numerous applications. The Eucalyptus planting is, therefore, a solution to enable the production of wood and meet the needs of society on a sustainable basis.

An important use of this species is for the generation of energy, from its direct burning in the form of firewood or its conversion into by-products of greater energetic value, such as charcoal. For these purposes, calorific value and moisture content are some of the main properties that determine the energy potential of wood, according to Brito & Barrichelo (1978).

Thus, the objective of this work was to evaluate the longitudinal (base-top) behavior of the energetic properties of E. urophylla hybrids with E. grandis. The upper calorific power (PCS) and moisture content (U) of the wood (wet mass basis) were determined, following the specifications of NBR 8290 (ABNT, 1984). For this, 5-year-old specimens were collected from Teotônio Vilela municipality in the State of Alagoas, and five discs corresponding to 0%, 25%, 50%, 75% and 100% of the commercial height of the trunk were used.

Figure 1 - Longitudinal variation of PCS for *Eucalyptus sp.*

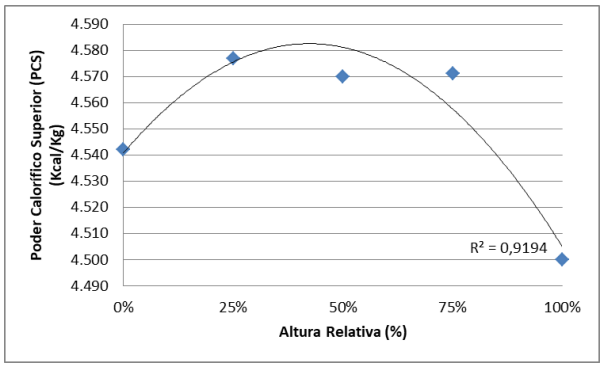


Figure 2 - Longitudinal variation of moisture content for *Eucalyptus sp*.

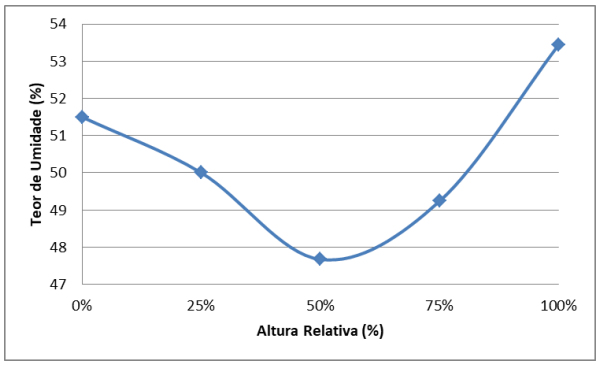


It is noted with Figures 1 and 2 that the properties are related, because the lower moisture content makes the wood with the PCS larger. It is concluded that the average wood height (50%) has a better result. Above this height, wood becomes unviable for power generation.

**Área: AMB** **Inscrição: 01052**

# PIGMENTS' PROFILE OF THE POLYEXTREMOPHILE *D. RADIODURANS* UNDER EXTREME CONDITIONS FOR BIOSIGNATURE'S DETECTION.

**Larissa L. Cavalcante (IC)[1*], Lydia F. Yamaguchi (PQ)[1], Ivan G. Paulino-Lima (PQ)[2] and Fabio Rodrigues (PQ)[1].**

**larissa.cavalcante@usp.br**

*[1]Department of Fundamental Chemistry - Institute of Chemistry - University of São Paulo (Av. Prof. Lineu Prestes, 748, São Paulo/SP, Brazil, 05508-000); [2]Universities Space Research Association - NASA Ames Research Center (Mail Stop 239-20, Bldg N239 Rm 377 , P.O. Box 1, Moffett Field, CA, USA, 94035-0001).*

Palavras Chave: *Carotenoids, Pigments, Astrobiology, Metabolomic, Biosignatures, Mars*.

## Highlights

The profile of carotenoids from cultures of bacteria *D. radiodurans* exposed to extreme conditions such as UV radiation and oxidative stress, simulating Martian conditions, were studied using HPLC.

## Resumo/Abstract

The polyextremophile bacteria *Deinococcus radiodurans* is widely studied due to its high resistance to different forms of environmental stress, induced by dissecation, ultraviolet radiation and ionization radiation, thus being a model organism for Astrobiology related studies, such as on the search for life on other planets. One of its several strategies of protection against radiation is the production of pigments, which protects not only against UV-radiation, but also against oxidative stress. There are more than 10 different carotenoids in this microorganism, being deinoxanthin the carotenoid in major concentration in *D. radiodurans*. Due to its participation in protecting bacteria exposed to oxidative environments and with high UV-radiation incidence, these carotenoids have been suggested as biosignatures, i.e., indicatives of biological activities, in missions searching for life in Mars and, in the near future, in other planets and moons [1,2]. In this work, the profile of carotenoids (both in higher and lower concentrations) from a standard culture (cultivation in mild environmental conditions) and in samples exposed to extreme conditions [3] such as UV radiation and oxidative stress, simulating Martian conditions, were studied using liquid chromatography. The changes on the carotenoid profile, related to the metabolic response due to the simulated extraterrestrial conditions were analyzed, aiming to refine our knowledge of its potential as biosignature for the search of life beyond Earth.

**References:** [1] Tian, B. et al. (2007) *Biochemica et Biophysica Acta*. [2] Krisko, A. and Radman, M. (2013) *Cold Spring Harb Perspect Biol*. [3] Lipton, M.S. et al. (2002) *PNAS*.

**Área: AMB** **Inscrição: 00384**

# Evaluation of persistent toxic substances (PTS) in Brazilian coast fishes using exploratory chemometric methods

**Ingrid C. Santos (IC),[1]* Verona B. Ferreira (PQ),[2] Eliana R. Figueiredo (PG),[3] Grazielle R. dos Santos (PG),[4] Fernanda D. B. A. Finco (PQ),[5] Fabiana A. Lobo (PQ),[6] João P. M. Torres, (PQ),[2] Gilmare A. da Silva (PQ).[6]**

**gilmare@iceb.ufop.br; ingridcouto13.02@gmail.com**

*[1]Department of Pharmacy, UFOP; [2]Carlos Chagas Filho Institute of Biophysics, UFRJ; [3]Postgraduate Program in Chemistry, UFOP; [4]Postgraduate Program in Environmental Engineering, UFOP; [5]Food Engineering Course, UFT; [6]Department of Chemistry, UFOP.*

Keywords*: PTS, Brazilian Coast Fishes, GC-MS, Multivariate Exploratory Analysis, Kohonen Neural Network.*

## Highlights

Persistent toxic substances (PTS) have high persistence and dispersion in the environment.
Evaluation of PTS in fishes of the Brazilian coast by means of chemometric methods of exploratory analysis.

## Resumo/Abstract

Persistent toxic substances are highly dispersed and have the potential to bioaccumulate in the environment. However, little is known about the behavior and final destination of these substances. Faced with this, this study determined, through biomarkers on the Brazilian coast and using exploratory chemometric methods, the presence of PTS highlighted in meetings of the United Nations Environmental Program (UNEP) held in Brazil, Chile and Peru from 2000 to 2002. The presence of HCB, α-HCH, β-HCH, γ-HCH, δ-HCH, heptachlor, cis-heptachlor epoxide, trans-heptachlor epoxide, Aldrin, Isodrin, Dieldrin, Endrin, Oxyclordane, cis-chlordane, trans-chlordane, α-endosulfan, β-endosulfan, o,p'-DDE, p,p'-DDE, o,p'-DDD, p,p'-DDD, o,p'-DDT, p,p'-DDT, t,t'-DDT, Methoxychlor and Mirex was investigated in samples of true-sardines, corvina and mullet, sampled in Guanabara's Bay - RJ (Suruí, Gradim and Barreto) from January to December 2015. The samples were extracted and then analyzed by gas chromatography with mass spectrometry with a solution of PCB 103 and 198 (surrogate)[1]. Using the neural network of Kohonen[2] and PCA[3], investigating the relationships between the samples and variables, the analyzed data showed that all organochlorines had a particular occurrence for each sample, except for the p,p'-DDE and t,t'-DDT that presented simultaneous occurrences. Methoxychlor revealed higher concentrations than the other compounds and t,t'-DDT had the higher frequency. However, data on the estimation of the toxicological risk of OCP ingestion through the fish from Guanabara Bay state that this consumption does not pose a risk to human health.

[1]Botaro, D. et al. Food and Chemical Toxicology, 49 (9): 2125, 2011.
[2]Kohonen, T. Self-organization and associative memory. 3 ed; Springer Verlag: Berlin, 1989.
[3]Brereton, R. G. Chemometrics: Data analysis for the laboratory and chemical plant. John Wiley & Sons Inc: Chinchester, 2003.

**Acknowledgements: CAPES, CNPq; FAPEMIG; PROPP/UFOP; UFOP**

**Área: AMB** **Inscrição: 00105**

# Metallothionein and Reduced Glutathione: metal exposure biomarkers in rough-toothed dolphins (*Steno bredanensis*)

**Fernanda Monteiro (PG)[1], Jailson F. Moura (PQ)[2], Leila S. Lemos (PG)[3], Isabel Moreira (PQ)[1], Tatiana D. Saint'Pierre (PQ)[1], Helena A. Kehrig (PQ)[5], Ana Paula M. Di Beneditto (PQ)[5], Salvatore Siciliano (PQ)[4], Rachel A. Hauser-Davis* (PQ)[6]**

**fsmonteiro@outlook.com.br; rachel.hauser.davis@gmail.com**

*1Departamento de Química, PUC-Rio, RJ, Brasil*

*2Systems Ecology Group, Leibniz Center for Tropical Marine Ecology, Bremen, Germany*

*3Escola Nacional de Saúde Pública, Fiocruz, RJ, Brasil*

*4Instituto Oswaldo Cruz, Fiocruz, RJ, Brasil*

*5Laboratório de Ciências Ambientais, UENF, Campos dos Goytacazes, RJ, Brasil*

*6Centro de Estudos do Trabalhador e Ecologia Humana, Escola Nacional de Saúde Pública, Fiocruz, RJ, Brasil*

*Key words: Dolphins; Oxidative Stress; Metal exposure; Metallothionein; GSH.*

## Highlights

MT and GSH were determined in *S. bredanensis*
Both were induced, signifying metal exposure, detoxification and oxidative stress
MT has no anti-oxidant role, as no correlations were found for MT x GSH

## Abstract

Dolphins are distinctive ocean health sentinel species, as they are apex predators[1]. The rough-toothed dolphin (*Steno bredanensis*) is under frequent human-related pressure along its pantropical distribution, known to feed on large carnivorous fish, such as cutlassfish, and usually presenting alarming organic pollutant (e.g. PCBs)[2] and non-essential elemental (e.g. Hg)[3] loads. However, its metal detoxifying pathways have not yet been elucidated. Metallothionein (MT) and Reduced Glutathione (GSH), a metal exposure and oxidative stress biomarker, were determined in *S. bredanensis* kidney (n=3), liver (n=7) and muscle (n=10). MT was purified by thermal extraction and GSH was extracted with a phosphate buffer. Both were spectrophotometrically determined at 412 nm after Ellman's reaction. MT did not differ among tissues (ANOVA, $p>0.05$), while GSH was higher in liver (ANOVA, $p<0.05$). High MT levels indicate metal-exposure and detoxification, while GSH levels indicate oxidative stress. No GSH x MT correlations (Spearman's test) were observed. Thus, MT seems to play no anti-oxidant role, since this is the main GSH function, and is only implicated in metal detoxification. This study increases baseline knowledge on the MT-detoxifying pathway and oxidative stress in this species. Future steps shall include total and subcellular elemental load determinations, as well as further statistical analyses.

[1]De Moura, J.F., *et al.* **Reviews of Environmental Contamination and Toxicology**, 228, p. 1-29, 2014.
[2]Lavandier R., *et al.* **Marine Pollution Bulletin**, 99, p.1-7, 2015.
[3]Lemos, L., *et al.* **Ecotoxicology and Environmental Safety**, 97, p.166-175, 2013.

**Área: AMB** *(Inserir a sigla da seção científica para qual o resumo será submetido. Ex: ORG, BEA, CAT)*

**Inscrição: 00911** *(Inserir o número de inscrição do autor que fez a submissão)*

# Slow pyrolysis conditions applied to several types of lignocellulosic materials, industrial and domestic wastes – A review

**Gilberto A. Romeiro(PQ),[1] Bruno S. Peixoto (PG),[1] Priscila Schroeder (PG),[1] Pamella C. O. Oliveira (PG),[1] Raquel V.S. Silva (PQ),[1] Monique K.K. Figueiredo (PQ),[1] Marcia C.C. Veloso (PQ),[1]** Gustavo F. Bitencourt (IC)[1]

**gilbertoromeiro@ig.com.br**

[1]*Universidade Federal Fluminense, Instituto de Química, Programa de Pós-Graduação em Química, Outeiro de São João Batista, Valonguinho, Centro, Niterói, RJ, Brazil, CEP: 24210-150;* [2]*Universidade Federal do Rio de Janeiro, Instituto de Química, Ilha do Fundão, Rio de Janeiro, RJ, Brazil, CEP: 21941-909;* [3]*Instituto Federal de Educação Ciência e Tecnologia, Campus Nilópolis, Centro, RJ, Brazil, CEP: 26530-060*

**Keywords**: *Slow pyrolysis, Oil, Char, Biomass, Domestic and Industrial wastes*

## Highlights

Biomasses, domestics and industrial wastes were submitted to slow pyrolysis conditions
Char, oil, gas and water fraction were isolated and studied

## Resumo/Abstract

This paper describes two groups of samples, Group I - Lignocellulosics and Group II – Industrial and Domestics Wastes, studied upon slow pyrolysis conditions by Romeiro's research group (Figure 1). Group I include agricultural, forest and aquatic biomasses and the Group II include sludges, industrial blends, urban wastes, health wastes and electronic wastes. These materials were submitted to slow pyrolysis at the temperature of 400 °C, under a $N_2$ atmosphere during two hours. The products obtained were oil, char, gas and an aqueous fraction. The characterizations of the products were achieved using several analytical methods to stablish some of their chemical and physicochemical properties. Here, we focus the yields and calorific values to evaluate the possibility of the applicability of the oil and char. More than forty raw materials were analyzed by these slow pyrolysis conditions.

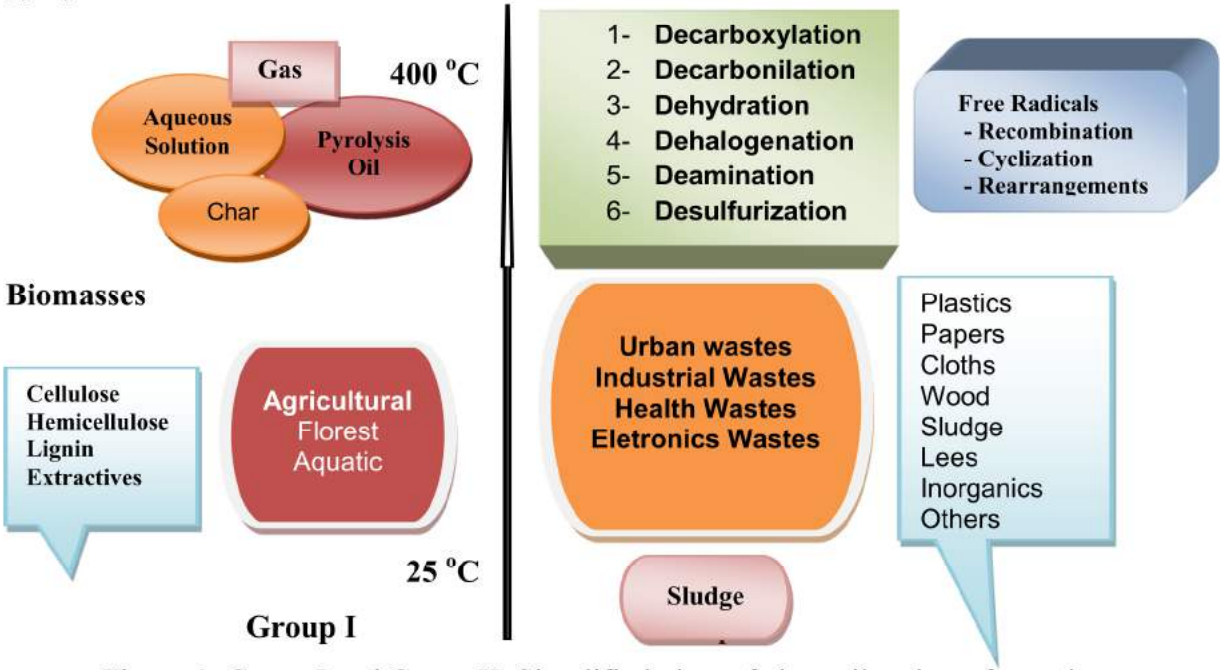


Figure.1: Group I and Group II. Simplified view of char, oil and gas formation.

**Área: AMB** **Inscrição: 00961**

# Oxidative stability thermal properties study of esters formulated form *Attalea speciosa* oil

**Cleber L. Nicolau (PG),[1*] Euclésio Simioatto (PQ),[1] Érica R. Costa (PG),[1] Gabriela M. Louro (PG),[1] Jaqueline C. M. da Silva (PG),[1] Tiziana A. Medeiros (PG),[1] Eduardo J. Coutinho (IC),[3] Jusinei M. Stropa,[2]**

**cleber.langalaitte@hotmail.com**

*[1]Programa de Pós-graduação em Recursos Naturais, UEMS; [2]Instituto de Química, UFMS, [3]Curso de Química, UEMS.*

Palavras Chave: *babaçu, cromatografia gasosa, Rancimat, análise térmica*

## Highlights

Blends were prepared in different proportions. The chemical profile was determined by gas chromatography. The thermo-oxidative stability was evaluated by Rancimat and thermal analysis (TG/DTG) and the crystallization point by DSC.

## Resumo/Abstract

**Introdução:** Para minimizar o uso da soja para produção de biodiesel novas fontes de oleaginosas vem sendo estudadas,[1] uma delas é a *A. speciosa* (Arecaceae), palmeira adaptada ao clima brasileiro e rica em ácidos graxos saturados, que possuem melhores propriedades para produção de biodiesel.[2] Preparou-se misturas (Soja/Babaçu) nas proporções de 90:10, 80:20, 70:30, 60:40 e 50:50 m/m para investigar mudanças nas propriedades físico-químicas, com a adição de ésteres de babaçu. **Resultados:** As blendas apresentaram teores altos de ésteres (>96,5%). A composição do biodiesel de babaçu é predominantemente de ésteres saturados (>80%), sendo os majoritários o ácido láurico, oleico e místico. Em contraste o perfil químico da soja, mostrou-se predominantemente insaturado, sendo os ésteres majoritários, o linoleico, oleico e palmítico, mais susceptíveis a termo-oxidação. As análises de Rancimat mostraram que com o aumento dos teores de ésteres de babaçu nas misturas o tempo de indução aumentou (6,13 h), devido a maior resistência dos ésteres saturados. Os testes de análise térmica mostraram que o biodiesel de babaçu metílico é estável até 49,6 °C e o etílico até 53,7 °C. O ponto de cristalização (DSC) apresentou temperaturas inferiores a -9,0 °C (Tabela 1 e 2). **Conclusão:** De forma geral com o aumento dos ésteres do babaçu nas misturas obteve-se melhores propriedades nas blendas elevando a estabilidade termo-oxidativa. Os ésteres do óleo de babaçu mostraram desempenho satisfatório para seu uso em regiões de baixas temperaturas, em relação ao ponto de cristalização.

**Tabela 1:** Propriedades das blendas metílicas preparadas com ésteres de óleo de soja/babaçu.

| Blendas | S90/B10 | S80/B20 | S70/B30 | S60/B40 | S50/B50 |
|---|---|---|---|---|---|
| Teor ésteres saturados (%) | 17,55 | 27,93 | 33,54 | 50,19 | 51,94 |
| Teor ésteres insat. (%) | 78,75 | 69,09 | 63,57 | 48,60 | 45,27 |
| Teor em ésteres (%) | 99,30 | 97,03 | 97,12 | 98,80 | 97,22 |
| Tempo indução (horas) | 3,27 | 4,44 | 4,61 | 4,96 | 6,13 |
| Temp. Onset (ºC) | 157,40 | 150,20 | 141,70 | 112,50 | 109,0 |
| Temp. cistalização (ºC) | -3,80 | -4,92 | -5,25 | -6,36 | -6,73 |

**Tabela 2:** Propriedades das blendas etílicas preparadas com ésteres de óleo de soja/babaçu.

| Blendas | S90/B10 | S80/B20 | S70/B30 | S60/B40 | S50/B50 |
|---|---|---|---|---|---|
| Teor ésteres saturados (%) | 21,65 | 27,84 | 34,73 | 41,50 | 47,72 |
| Teor ésteres insat. (%) | 74,94 | 68,92 | 62,26 | 55,79 | 48,90 |
| Teor em ésteres (%) | 96,59 | 96,76 | 96,99 | 97,29 | 96,61 |
| Tempo indução (horas) | 2,75 | 3,24 | 4,25 | 4,97 | 5,07 |
| Temp. Onset (ºC) | 159,70 | 154,20 | 143,50 | 135,20 | 120,70 |
| Temp. cistalização (ºC) | -5,24 | -6,32 | -7,61 | -8,04 | -9,12 |

1. Kareem, S.O.; Falokum, E.I.; Balogun, S.A.; Akinloye, O.A.; Omeike, S.O. *Egyptian Journal of Petroleum.* 2017, 26, 635-642.
2. Paiva, E.J.M.; Silva, M.L.C.P.; Barbosa, J.C.S.; Oliveira, P.C.; Castro, H.F.; Giordani, D.S. *Ultrason. Sonochem.* 2013**,** 20*,* 833-838.

**Área: AMB** **Inscrição: 00979**

# Antibiotics colorimetric detection by stabilized silver nanosensors in water.

**Luiza Dumont de M. Moraes (PG),[1*] Renata Pereira L. Moreira (PQ),[2]**
**dumontluiza@gmail.com*** *[1,2]Departamento de Química, UFV*

*Palavras Chave: Nanossensores, Antibióticos, Química ambiental, Absorção plasmônica.*

## Abstract

This work evaluates the capacity of detection of fluoroquinolones in water by silver nanosensors stabilized with glutathione, which demonstrates a selectivity between β-lactams and fluoroquinolones.

## Introdução

Os antibióticos são uma classe de poluentes emergentes que podem ser encontrados em diversos compartimentos do meio ambiente, principalmente a água, devido à sua solubilidade e grande consumo que são usados. A preocupação quanto à emissão de antibióticos na natureza se deve ao alto risco de desenvolvimento de resistência antimicrobiana por parte desses microorganismos. As fluoroquinolonas são a segunda geração de antibióticos quinolônicos, as quais apresentam agentes bactericidas de amplo espectro e de geral uso clínico. Apesar de já existirem muitos métodos de detecção e tratamento desses compostos na literatura[1], há uma necessidade de desenvolvimento de métodos que sejam rápidos, seletivos, de fácil manuseio e baratos, tanto no uso dos reagentes como nos equipamentos. Deste modo, o objetivo deste trabalho é desenvolver um método semi-quantitativo para determinação de fluoroquinolonas em água, utilizando a prata coloidal como um nanossensor colorimétrico.

## Resultados e Discussão

A primeira etapa do trabalho consistiu na síntese das nanopartículas de Ag (NPs Ag) com borohidreto de sódio. A solução apresenta uma coloração amarela, sendo observada uma banda na região do visível (Figura 1). Na presença das fluoroquinolonas, o pico característico das NPs Ag (403 nm) é deslocado para 528 nm, onde se observa uma coloração rósea. Na presença de antibióticos beta-lactâmicos esse efeito não foi observado, garantindo a seletividade do método. É relatado na literatura que agentes estabilizantes, que contenham enxofre em sua estrutura, são capazes de influenciar no efeito de ressonância plasmônica das NPs Ag [2]. Dessa forma, utilizou-se a glutationa (um tripeptídeo) como agente estabilizante das NPs Ag. De acordo com a Figura 2, existe uma relação não linear, mas bem comportada, entre absorbância e concentração de ciprofloxacina, na presença de GSH (528 nm). Para melhor visualizar esse efeito, construiu-se um gráfico da absorbância e concentração de ciprofloxacina, com e sem GSH.

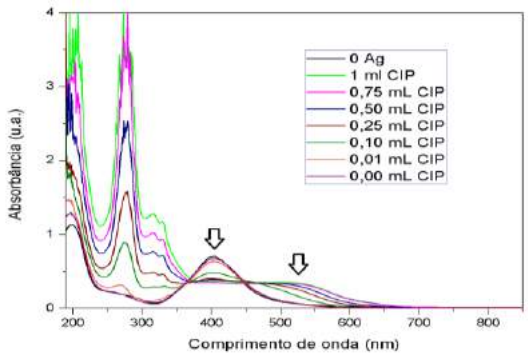


Fig. 1. NPs de Ag estabilizadas com GSH na presença de presença de ciprofloxacina.

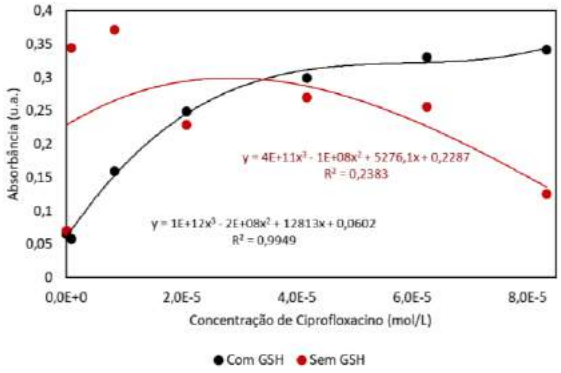


Fig. 2. Comportamento das NPs Ag na presença de ciprofloxacina, com e sem estabilizante GSH.

## Conclusão

Pode-se concluir que a presença do estabilizante GSH foi fundamental para garantir uma maior estabilidade das NPs Ag, o que proporcionou uma relação entre concentração do fármaco e resposta do detector.
As próximas etapas consistem na validação do método semi-quantitativo.

## Agradecimentos

CNPq, FAPEMIG, CAPES e UFV

[1]YIN, S. N. et al. **Talanta**, v. 174, n. March, p. 14–20, 2017.
[2]WANG, C. et al. **Sensors & Actuators: B. Chemical**, v. 238, p. 1136–1143, 2017

**Área: AMB** **Inscrição: 01015**

# Utilização da mistura de macrófitas aquáticas para tratamento de efluentes contendo corante

**Rachel de M. Ferreira[1](PG); Danielle M. A. Stapelfeldt[2](PQ).**

**rachelmoraes@hotmail.com.br; E daniara2@yahoo.com.br**

*[1]Escola Nacional de Saúde Pública, Fundação Oswaldo Cruz – Rio de Janeiro R. Leopoldo Bulhões, 1480 - Manguinhos, Rio de Janeiro - RJ, CEP 21041-210*

*[2] Universidade Federal do Rio de Janeiro – Campus Macaé. Rua Aloísio da Silva Gomes, 50, Granja dos Cavaleiros, Macaé, Rio de Janeiro, CEP 27930-560*.

Palavras Chave: *Adsorção, Biomassa, Corante.*

## Highlights

Use of mixture of aquatic macrophytes for the treatment of dye-containing effluents.
The combination of the surface characteristics of the biosorbents *Salvinia* sp and *Pistia stratiotes* when mixed may provide an increase in adsorption yield with the crystal violet dye.

## Resumo/Abstract

O rápido crescimento de novas tecnologias nos últimos anos aumentou consideravelmente a comercialização de produtos cada vez mais modernos e coloridos, que por sua vez vem aumentando a demanda de efluentes contendo corantes. Uma das alternativas tem sido o uso de macrófitas aquáticas secas e moídas como materiais adsorventes não convencionais para a remoção de corantes, ganhando forte credibilidade nos últimos anos por apresentar um bom desempenho[1].

Este estudo tem como objetivo investigar a capacidade de adsorção da mistura das macrófitas *Salvinia sp.* e *Pistia stratiotes* para soluções aquosas contendo corante violeta cristal. Secas ao sol após lavagem, as macrófitas foram trituradas. Os testes de adsorção foram realizados com a mistura das macrófitas (MS) e com a Salvinia in natura (SSP) para fins de comparação.

Os testes de adsorção foram feitos em batelada, e os parâmetros avaliados foram variação da concentração inicial, da temperatura, pH e tempo de contato. A concentração final do corante foi verificada pela leitura UV-Visível.

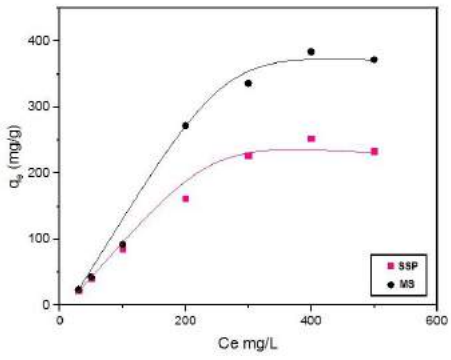


**Figura 1:** Isoterma de adsorção da SSP e da MS

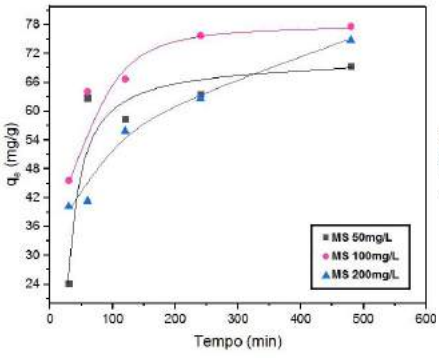


**Figura 2:** Cinética de adsorção da MS

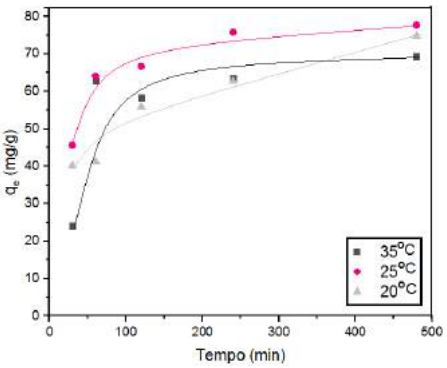


**Figura 3:** Cinética de adsorção da MS com variação da temperatura

A SSP teve $q_{max}$ de 255mg/g, e a MS 370 mg/g para a solução de violeta cristal com concentração de 400mg/L, o que indica uma adsorção de 92,5%. Nos testes de cinética ocorreu uma adsorção rápida, nos primeiros 60 min. Enquanto que nos testes de variação da temperatura, os cálculos para obtenção dos dados termodinâmicos em que constatou-se que as biomassas têm leve caráter endotérmico, sendo necessário adquirir pouca energia do sistema para que a adsorção ocorra. Dessa forma pode-se concluir que a combinação da característica das superfícies dos biossorventes *Salvinia* sp e *Pistia stratiotes* quando misturados pode proporcionar um aumento de sítios ativos, aumentando o rendimento de adsorção com o corante violeta cristal.

Referência:

[1] Schneider, I. A. H., Biossorção de metais pesados com biomassa de macrófitos aquáticos. Tese apresentada ao Programa de Pós-Graduação em Engenharia Metalúrgica e dos Materiais da Universidade Federal do Rio Grande do Sul, 1995.

**Área: AMB**
*(Inserir a sigla da seção científica para qual o resumo será submetido. Ex: ORG, BEA, CAT)*

**Inscrição:_209___**
*(Inserir o número de inscrição do autor que fez a submissão)*

# Characterization of Sedimentary Humic Substances from white-water and black-water rivers.

**Isabela C. Constantino[1], Carlos E. Piovezan[1], Stefani S. Toschi[1], Márcia C. Bisinoti[1], Altair B. Moreira[1*].**

*[1]Instituto de Biociências, Letras e Ciências Exatas, UNESP- Campus de São José do Rio Preto-SP.*
**altair@ibilce.unesp.br*

Palavras Chave: matéria orgânica, sedimentos, caracterização, Amazônia.

## Highlights

- Sedimentary humic substances (SHS) were extracted from Amazonian rivers.
- Humic material from white-water and black-water rivers were characterized by $SUVA_{254}$ and Infrared spectroscopy.
- SHS from black-water rivers presented higher $SUVA_{254}$ than SHS extracted from white-water.
- Infrared spectra showed similar bands for all samples, but SHS from black-waters had more oxygenated content and strong bond in 1600 $cm^{-1}$ (C=C, probably aromatic rings).
- SHS extracted from black-water seems more aromatic than SHS extracted from white-water rivers.

## Resumo

As substâncias húmicas de sedimentos (SHS), são de grande importância na biogeoquímica de compostos orgânicos ou inorgânicos. Para as espécies metálicas, as SH atuam na especiação e influenciam a biodisponibilidade (complexação). As SH não apresentam estrutura definida e a sua caracterização empregando técnicas espectroscópicas clássicas, como Infravermelho e Absorção molecular por Fluorescência e UV-Vis. permite inferir sobre características da sua estrutura química. Portanto, objetivou-se caracterizar as SHS de rios de águas brancas (AgB) e pretas (AgP), da região de Itacoatiara e Maués-AM, visando contribuir para o conhecimento das propriedades dessas SHS para futuros experimentos de interação com outras espécies. Sedimentos superficiais foram amostrados em 5 rios de AgP: e em 2 rios AgB. SHS foram extraídas segundo Sociedade Internacional de Substâncias Húmicas (IHSS). $SUVA_{254}$ foi determinado utilizando espectrofotômetro UV-Vis (2600, Shimadzu, Japão) (5 mg $L^{-1}$ de carbono orgânico dissolvido, pH 8, $NaHCO_3$ 0,05 mol $L^{-1}$).[1,2,3] Espectros de Infravermelho foram obtidos com varredura de 4000 a 400 $cm^{-1}$ (Spectrum Two UATR, PerkinElmer). SHS AgP apresentaram maiores $SUVA_{254}$, atribuído a estruturas mais aromáticas comparado às SHS AgB.[1] Nos espectros de Infravermelho verificaram-se bandas em 1200 $cm^{-1}$ (presença de ácidos carboxílicos) mais intensas para SHS AgP. Todas amostras apresentaram banda em 1070 $cm^{-1}$ (vibração C-O de estruturas alifáticas), porém foram mais intensas para SHS AgB.[4] Observaram-se bandas de vibração de C=O e C=C (1700 e 1600 $cm^{-1}$, respectivamente) para todas SHS, sendo as de C=C mais intensas em SH AgP.

**Acknowledgements:** To financial support granted from FAPESP (Project nº2015/22954-1) and CNPq.

**References**

[1] HELMS, J.R. et al. *Limnol. Oceanogr.*2008, 53, 955–969.
[2] WEISHAAR,J.L. et al. *Environ. Sci. Tech*. 2003, 37, 4702-4708.
[3] RODRÍGUEZ, F. J.; NÚÑEZ, L. A. *Water Environ J*, 2011, 25,163–170.
[4] DERRIEN, M. et al. *Environ Sci Pollut Res*. 2017, 24, 16933-16945.

**Área: AMB** **Inscrição: 01005**

# Pesticides wastewater treatment by coagulation-flocculation: Evaluation and optimization of operational parameters

**Arlene B. S. Nossol (PG),*[1] Maria G. B. Santos (IC),[1] Alam G. Trovó (PQ).[1]**

**arlenebs@hotmail.com**

[1]*Institute of Chemistry, Universidade Federal de Uberlândia - UFU*

Keywords: *Aluminum, Color, Industrial effluents, Iron*, *Physical-chemical treatment, Turbidity.*

## Highlights

The best results of turbidity and color removal were obtained using $Fe(NO_3)_3$ salt;
99% removal efficiencies using 8 mmol $L^{-1}$ $Fe(NO_3)_3$ as coagulant.

## Abstract

Effluents from the pesticide industry have a high toxicity associated with its high organic load, elevated levels of turbidity, suspended solids and color. The effluent used contains the pesticides ametrine, atrazine, imidacloprid and tebuthiuron, provided by a pesticide factory. The coagulation-flocculation-decantation processes were evaluated as an alternative of wastewater treatment. First, the influence of the coagulant ion ($Fe(NO_3)_3$ and $Al(NO_3)_3$) and concentration (ranging from 2 to 32 mmol $L^{-1}$) was evaluated in natural pH (4.9). The best results in terms of turbidity and color removal were obtained using $Fe(NO_3)_3$ and high concentrations of this salt were requested to reach almost complete color and turbidity removal (Figure 1). After this treatment, the pH decreases between 3.8 and 2.1 for the different concentrations of $Fe^{3+}$ due the hydrolysis reactions mediated by $Fe^{3+}$. Second, in order to reduce the solubility of this ion and increase the efficiency of the process, the pH was adjusted to 4.0 and new analyses were performed. Under these conditions, the use of 8 mmol $L^{-1}$ $Fe(NO_3)_3$ resulted in 99% color and turbidity removal. In addition, a partial removal of the pesticides (between 43 and 78%) and 20% of total organic carbon was reached. However, no significant removal on toxicity was obtained, since the $EC_{50}$ changed from 0.4 to 4.5 (% v/v), being extremely toxic. The coupling with photo-Fenton process is being evaluated as an additional stage to the effective treatment of this type of effluent.

**Figure 1.** Influence of the coagulation ion and concentration on color and turbidity removal.

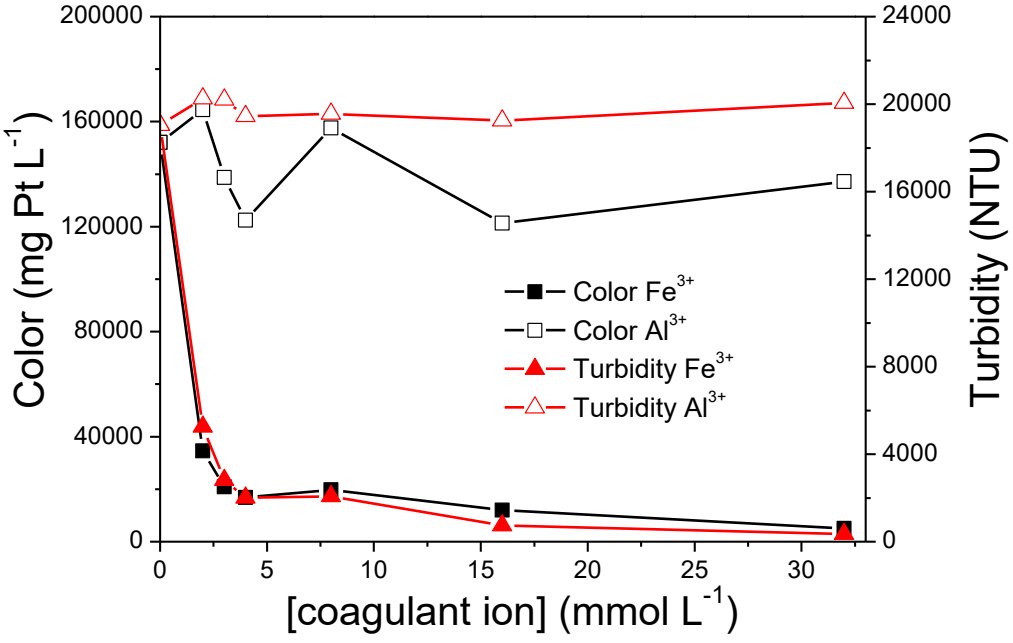

**Área: AMB** **Inscrição: 48202**

# Atrazina e seus metabólitos em mananciais e águas de abastecimento público: sazonalidade e eficiência de remoção das ETA

**Giulia S. Silva (IC), Cassiana C. Montagner (PQ)**

**giuliasilvadasilva@gmail.com; montagner@iqm.unicamp.br**

*Laboratório de Química Ambiental, Departamento de Química Analítica, Instituto de Química, UNICAMP*

Palavras Chave: *Atrazina, DIA, DEA, 2-Hidroxi-atrazina*, *estação de tratamento de água*

## Highlights

Atrazine and its metabolites in source and drinking waters: seasonality and efficiency of removal by DWTP. Efficiency of removal of atrazine and its degradation products (DIA, DEA and 2-hidroxy-atrazine) by conventional DWTP that supplies water to 1.1 million people in Campinas (SP, Brazil) was evaluated during a year.

## Resumo/Abstract

O projeto tem como objetivo estudar a presença de atrazina (ATZ) e de seus principais produtos degradação, deetilatrazina (DEA), deisopropilatrazina (DIA) e 2-hidroxiatrazina (OHATZ), em mananciais e águas de abastecimento público a fim de verificar a eficiência de remoção pelas Estações de Tratamento de Água (ETA) convencionais ao longo de um período sazonal completo. O estudo está sendo realizado na ETA 3 e 4 e na ETA Capivari (SANASA) localizadas na cidade de Campinas (SP), as quais captam água dos rios Atibaia e Capivari, respectivamente e, juntas abastecem cerca de um milhão de habitantes. A atrazina é um dos herbicidas da família das triazinas mais utilizados no Brasil. Resíduos desses compostos têm sido encontrados no ambiente em concentrações da ordem de nanogramas por litro as quais podem estar relacionadas a efeitos adversos oriundos da exposição crônica de animais e seres humanos. Nesse trabalho foi desenvolvido e validado um método analítico empregando extração em fase sólida e cromatografia liquida acoplada à espectrometria de massas (LC-MS/MS) para a determinação simultânea da atrazina e seus metabólitos com limites de detecção entre 5 e 47 ng $L^{-1}$, recuperações entre 80 e 112 % para uma concentração de 500 ng $L^{-1}$ dos analitos em uma amostra sintética preparada em água ultrapura. O efeito de matriz não foi considerado significativo, exceto para o OHATZ que apresentou um aumento de 40 % no sinal analítico para ambas matrizes. A eficiência de remoção bem como a concentração dos contaminantes variaram significativamente com a sazonalidade. A Figura 1 expõe os resultados obtidos nos primeiros meses do estudo sazonal (entre setembro e dezembro) para a atrazina e 2-hidroxiatrazina, os demais compostos apresentaram-se abaixo dos limites de detecção nessas amostras.

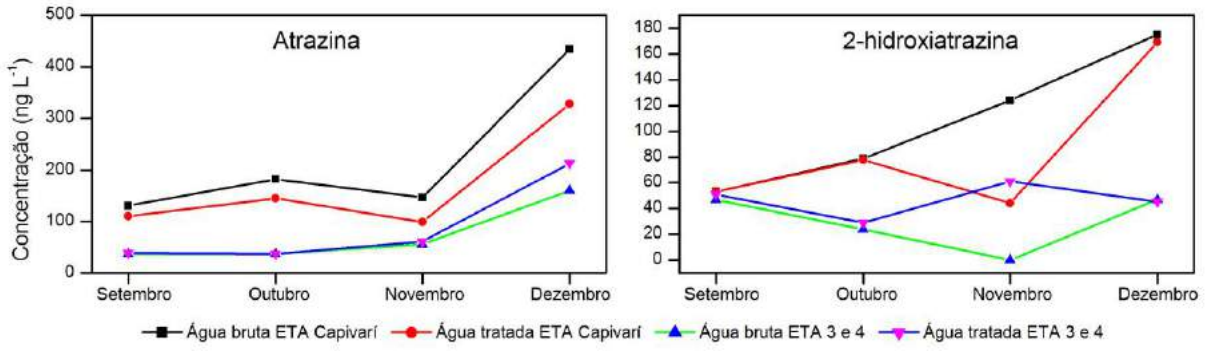


Figura 1- Concentração de Atrazina e 2-hidroxiatrazina no período de setembro a dezembro.

**Área: AMB** **Inscrição:** 1294

# Air quality biomonitoring of trace elements in Huancayo City, Peru using transplanted *Tillandsia capillaris* as bioindicators

**Vinicius D.P. Andrade (IC),[1] Alex R. H. De La Cruz (PG),[1*] Enrique R. D. Calderon (PQ),[1] Rodolfo F. O. Aunque (IC),[2] Jusber K. H. De La Cruz (IC),[3] Adriana Gioda (PQ) [1].**

**viniciuspaiva1993@hotmail.com; alebut2@hotmail.com**

*[1]Department of Chemistry, PUC-Rio; [2]Department of Chemical Engineering UNCP; [3]Department of Investigation UNCP*

Palavras Chave: *Biomonitoring, trace metals, Peruvian Andes, air pollution.*

## Highlights

Biomonitoring of toxic metals;
High concentrations of Pb, although this element was restricted as gasoline component since 2009;
Spatial distribution of trace elements were mapped in the study area.

## Resumo/Abstract

Huancayo is a Peruvian city whose development has caused an increase in vehicular fleet, urban growth and agriculture activities. This rapid and disorderly growth has resulted in environmental problems, such as deterioration of the air quality. *Tillandsia capillaris* is a perennial and endemic species of the Peruvian Andes, resistant to hydric stress and usually found grow on trees, walls, rocks, cables, and electric poles. This species is useful as biomonitor of the air quality. The purpose of the study was to investigate the content of some toxic metals in transplanted specimens of *T. capillaris* after three months of exposure in three sites with different contamination levels. Table 1 shows the average concentrations of toxic metals determined by ICP-MS.

Table 1. Average concentrations in µg g-1 ± standard deviation of toxic metals in three sites of the metropolitan area of Huancayo, Peru

| Sites | Zn | Pb | Sb | As | Cd |
|---|---|---|---|---|---|
| Chupaca (urban-agricultural) | 77.50±12.30 | 37.23±17.2 | 3.87±1.77 | 8.17±3.56 | 0.26±0.12 |
| Huancayo (urban) | 59.24±23.22 | 28.81±18.3 | 2.91±1.89 | 6.42±2.78 | 0.25±0.10 |
| Hualhuas (urban-agricultural) | 31.75±21.12 | 10.23±5.23 | 1.06±0.56 | 5.94±3.44 | 0.34±0.19 |
| control site (unpolluted site) | 18.02±5.23 | 7.34±3.44 | 0.49±0.23 | 4.47±3.22 | 0.14±0.11 |

Higher concentration values of Zn and Pb was measured in Chupaca. The concentrations are influenced by heavy traffic and intense agricultural activities. Elements such as Cd and As showed elevated concentrations in areas where agricultural activities are predominant (Chupaca and Hualhuas). *T. capillaris* showed to be a suitable biomonitor, since the results in each site reflect the local pollution sources. Accumulation of Zn, Pb, and Sb can be related to vehicular sources (soil resuspension and car's wear), while As and Cd to the intense use of agrochemical (pesticides, fertilizer and herbicides) by farmers.

**Área: ANA** **Inscrição: 00310**

# Stability of pesticides in green pepper samples stored at different temperatures

**Vitor M. Libardi (PG),[1]* Fernanda F. Heleno (PQ),[1] Maria Eliana L. R. de Queiroz (PQ),[1] Antônio A. Neves (PQ),[1] André F. de Oliveira (PQ).[1]**

**vitorlibardi@gmail.com**

[1]*Chemistry Departament, UFV*

Keywords: *residue analysis, SLE/LTP, chromatography*

## Highlights

Stability of 4 pesticides in pepper stored at different temperatures was studied. Extracts of pesticides were analyzed by GC-ECD. Storage temperature influenced the stability of the compounds.

## Resumo/Abstract

Green pepper has one of the highest index of irregularities according to the Brazilian Monitoring Program for Pesticides Residues in Food.[1] A major challenge in the extraction and analysis of pesticide residues is the stability of these residues in the matrix, since their concentrations may change by the time and storage temperature.[2] In this study, the stability of the pesticides azoxystrobin, chlorothalonil, diphenoconazole and iprodione was evaluated in processed green pepper samples stored at 4°C and -20°C. Pesticide-free green pepper were crushed, fortified with known concentrations and stored. Weekly, these samples and control samples were submitted to the solid-liquid extraction with low-temperature partitioning, and analyzed by gas chromatography with electron capture detector. The data were statistically evaluated using the post-hoc Tukey test (95%). Regardless of temperature, the stability of the pesticides was generally low in the green pepper samples. Only diphenoconazole at -20 ° C and iprodione at 4 ° C were stable for 7 and 35 days, respectively. The results showed that the active principles can have different responses in function of the storage temperature, and the extraction step must be done right after the pepper harvest in order to guarantee the result quality.

[1] ANVISA. *Programa de análise de resíduos de agrotóxicos em alimentos (PARA): Relatório das análises de amostras monitoradas no período de 2013 a 2015*. (Agência Nacional de Vigilância Sanitária, 2016).

[2] Kocourek, V., Hajslová, J., Holadová, K., Poutska, J. Stability of pesticides in plant extracts used as calibrants in the gás chromatographic analysis of residues. *Journal of Chromatography A* **800**, 297-304 (1998).

Acknowledgments: The authors thank Capes, FAPEMIG, CNPq and UFV for their support.

**Área: ANA** **Inscrição: 00454**

# Development and optimization of analytical method for determination the antihypertensive drugs

**Amanda D. Ferreira*** **(PG),[1] Patricia L. Weinert (PQ).[1]**

**amandaquimdias@gmail.com;**

[1]*Departamento de Química, Universidade Estadual de Ponta Grossa;*

Palavras Chave:*Losartano potássica, Hidrocloritiazida, planejamento, CLAE*

## Highlights

The chromatographic method for determination of the hydrochlorothiazide and losartan was develop and optimized by experimental design. The method was applied for the analysis of the drug samples.

## Abstract

The Losartan potassium (LOS) is a drug used in the treatment of hypertensive patients[1]. It is sold in Brazil commercially associated with Hydrochlorothiazide (HCTZ), and, according to ANVISA[1], LOS is among the best selling drugs in the country. The development of analytical methods which are simple, fast, selective and sensitive is importante to ensure not only the quality of the products, as well as detect the counterfeiting and/or adulteration of drugs. In this context it is proposed the development, optimization and validation of reversed phase HPLC method, isocratic, with UV detection for the determination of LOS and HCTZ in pharmaceutical formulations. The optimization of the chromatographic conditions was performed using Central Composite experimental design. Figure 1 shows the response surface methodology obtained in the optimization studies of the variables flow rate and temperature of the column. Using the optimized conditions: C18 column with temperature of 40 °C, mobile phase consisting of water: acetonitrile (50:50) and flow rate 0.60 mL $min^{-1}$, symmetrical peaks with optimal resolution were obtained Figure 2. Analytical curves were constructed in the concentration range of 0.5 to 3.0 µg $mL^{-1}$ (r = 0.9999) for LOS and 5.0 to 30 µg $mL^{-1}$ (r = 0.9996) for HCTZ. The method was applied on commercial samples with recovery rates between 96.0 - 103.0%. The validation, considering the merit parameters recommended by ANVISA, allowed to verify that the proposed method is safe and reliable.

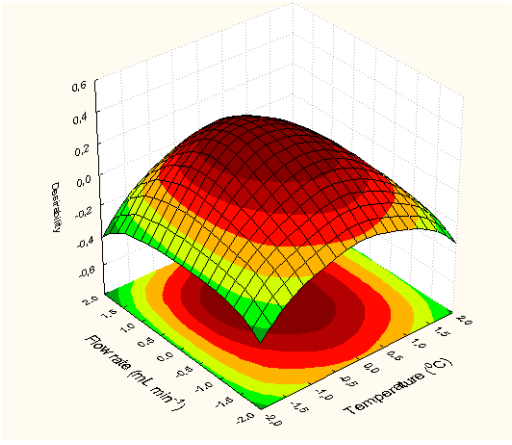


**Figure 1.** Response surface composite central experimental design for LOS and HCTZ

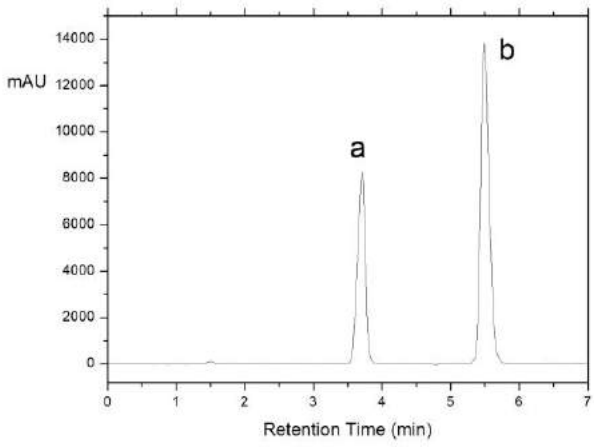


**Figure 2.** Chromatogram peak for a) LOS and b) HCTZ

[1] Farmacopeia Brasileira. 5º Ed. Brasilia: Agência Nacional de Vigilância Sanitária, **2010**.

**Área: ANA** **Inscrição: 00653**

# Separation investigation of elaidic and vaccenic trans fatty acids isomers by CZE-UV

**Tatiane Lima Amorim (PG) [1*], Marcone Augusto Leal de Oliveira (PQ)[1]**

**tatianelamorim@gmail.com**

*[1]Chemistry Department, UFJF*

Palavras Chave: *Trans Fatty Acids, Capillary Zone Electrophoresis, Elaidic Acid, Vaccenic Acid*

## Highlights

New promising fast method for simultaneous separation of elaidic and vaccenic fatty acids isomers by CZE-UV with simple sample pretreatment. Screening analysis as an alternative method to the classical GC-FID.

## Abstract

The separation of elaidic and vaccenic fatty acids is of great importance for food industry and regulation agencies since one has deleterious and other beneficial effects to human health. New methods capable of determine these fatty acids with reliability and rapidity are needed and capillary electrophoresis can be very useful as an alternative to the classical GC-FID method, which requires a long time to carry out analysis, long specific columns, as well the derivatization of analytes. This initial study signals the potential employment of capillary electrophoresis for the simultaneous determination of elaidic and vaccenic trans fatty acids isomers in food samples, as evidenced in Figure 1. It can be observed that CZE-UV detection employing a background electrolyte composed by a tetraborate buffer (pH=9), Brij 35, methanol and acetonitrile was promising for the partial separation of fatty acids standard rapidly. New efforts need to be carried out in order to achieve total baseline separation of these compounds and validate the method.

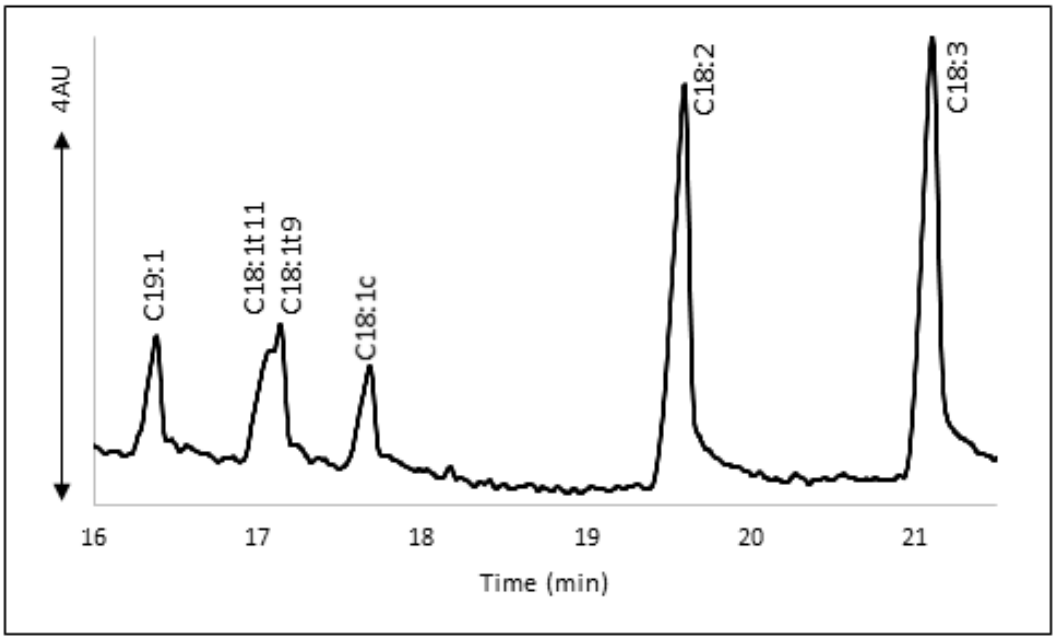


Figure 1 – Partial separation of C18:1 t11 and C18:1 t9 by CZE-UV in a standard mix of fatty acids using C19:1 as an internal standard. Electrophoretic conditions: hydrodynamic injection of 25 mbar for 5.0 s, positive voltage of 24 kV, cartridge temperature maintained at 27 ºC, TSP capillary of 68.5 cm total length (75 µm of internal diameter) and detection at 200 nm (peak width >0.025 min; 0.5 s response time; 10 Hz).

Acknowledgments: CAPES, CNPq, FAPEMIG, Rede Mineira de Química and UFJF for Financial Support

**Área: ANA** **Inscrição: 00657**

# Synthesis and application of molecularly impressed polymers for the extraction of caffeine from food and beverage samples

**Fernanda N. Feiteira[1*] (PG), Janaína E. Francisco[1] (PG), Wanderson A. da Silva[1] (PG), Annibal D. Pereira Netto[1] (PQ), Wagner F. Pacheco[1] (PQ)**
**fnfeiteira@id.uff.br**
[1] *Departamento de Química Analítica, Universidade Federal Fluminense (UFF), Niterói/RJ, Brazil*

Keywords: *molecularly impressed polymers, caffeine, sample preparation.*

## Highlights

• Caffeine MIP were synthesized and characterized, showing better sorptive capacity than the non impressed polymers.
• The Caffeine MIP were efficient in selectively extracting the analyte from food and beverage samples.

## Resumo/Abstract

For the last decades Molecularly Impressed Polymers (MIP) have been a tendency for analyte separation from complex matrices, allowing to achieve adequate selectivity, as a function of their molecular recognition characteristics, and sensibility, due to the possibilities of analyte pre concentration they offer. This work intends to apply MIP to selectively extract caffeine, in order to make such a pre treatment able to eliminate interferences present in food and beverage samples.

The molecularly impressed and control (non impressed, NIP) polymers synthesized in this work were prepared based on the method proposed by Theodoridis and Manesiotis[1] and Farrington *et al*[2]. The synthesized polymers were washed in Soxhlet apparatus for 6 hours with a methanol/water 9:1 v $v^{-1}$ mixture, dried, inserted in cartridges and evaluated as solid phases for solid phase extraction (MIP-SPE).

The MIP-SPE method was conducted by conditioning the cartridges with 4,00 mL acetonitrile, adding 1,00 mL of 25,0 mg $L^{-1}$ aqueous caffeine solution, washing with sodium phosphate buffer 50 mmol $L^{-1}$ at pH 10,6 and eluting the analyte with 1,00 mL acetonitrile. The collected fractions were spectrophotometrically and chromatographically analyzed. Under these conditions, the analytical parameters of merit shown in Table 1 were obtained.

By the study of possible interferents, it was found that other xanthines, such as theophylline and theobromine, did affect the quantification of the analyte. For that reason, samples that did not contain other xanthines, such as soft drinks or coffee powder, could be simply spectrophotometrically analyzed. Samples containing other xanthines, as energy drinks, chocolate powder and black tea leaves needed also chromatographic separation previously to quantification. The results of some of these quantifications and their respective recovery tests are shown in Table 2, revealing the accuracy and applicability of the method. It is valid to emphasize that even for the samples that were quantified by HPLC the use of MIP became indispensable for the elimination of interferences.

Table 1. Analytical parameters of merit.

| **Parameter** | | |
|---|---|---|
| Typical analytical curve | Abs = 1,267 [caf, mg $L^{-1}$] – 0,1327 | |
| $r^2$ | 0,9995 | |
| LOD | 0,0565 mg $L^{-1}$ | |
| LOQ | 0,188 mg $L^{-1}$ | |
| Accuracy | MIP<br>104 ± 8,3% | NIP<br>109 ± 8,7% |
| Cartridge reuse | MIP<br>3 cicles | NIP<br>2 cicles |
| Sorption capacity | MIP<br>> 43,7 mg $g^{-1}$ | NIP<br>8,01 mg $g^{-1}$ |

Table 2. Samples quantification and recovery tests.

| **Sample** | **Caffeine content** (n = 3) | **Recovery test** (n = 3) |
|---|---|---|
| Soft drink | 114,5 ± 21,2 mg $L^{-1}$ | 95,4 ± 0,2 % |
| Coffee powder | 19,2 ± 1,0 mg $g^{-1}$ | 97,6 ± 3,6 % |
| Energy drink | 381,4 ± 7,5 mg $L^{-1}$ | 92,6 ± 2,6 % |
| Chocolate powder | 0,268 ± 0,009 mg $g^{-1}$ | 101 ± 1 % |
| Black tea leaves | 15,6 ± 0,8 mg $g^{-1}$ | 101 ± 2 % |

[1] Theodoridis, G.; Manesiotis, P. *J. Chromatogr. A.* **2003**, 948, 163.
[2] Farrington, K.; Magner, E.; Regan, F. *Anal. Chim. Acta*. **2006**, 566, 60.

**Área: ANA** **Inscrição: 00660**

# Síntese e caracterização de polímeros fluorescentes com núcleo de sílica para aplicação em cromatografia em camada delgada.

**Isabela F. Ierick (IC),[1*] Rafael R. Pupin (PG),[2] Gustavo C. Monteiro (PQ),[3] Vanderlan S. Bolzani (PQ),[4] Maria del Pilar T. Sotomayor (PQ).[5]**

**isabela.ierick@outlook.com**

[1]*Instituto de Química, UNESP - Univ Estadual Paulista, Araraquara, São Paulo, Brasil, 14800-060*

Palavras Chave: *Polímeros fluorescentes, Cromatografia em camada delgada.*

## Highlights

Synthesis and characterization of fluorescente polymers with silica core for application in thin layer chromatography.

- Silica nanoparticles as nucleus for polymer provide an increase in the recognition performance of the polymer.
- Chromatography makes it easy to separate compounds.

## Resumo/Abstract

Diversos polímeros são eficazes quando se trata de selecionar moléculas distintas, permitindo assim, a associação com a técnica de cromatografia em camada delgada (CCD), que possui vantagens como simplicidade e baixo custo. Portanto, o objetivo do trabalho é a síntese e otimização de polímeros fluorescentes visando sua aplicação em CCD, para a separação de compostos orgânicos.

A obtenção destes polímeros, foi realizada a partir da síntese do análogo estrutural da fluoresceína utilizando uma reação de substituição nucleofílica, em meio básico, levando a obtenção do produto dialilfluoresceína, caracterizado por espectroscopia de ressonância magnética nuclear (RMN).

As próximas etapas deste estudo foram a obtenção das nanopartículas de sílica e a síntese do polímero. As nanopartículas foram sintetizadas através da hidrolise do tetraetil ortossilicato (TEOS) e as mesmas foram modificadas com 3-(trimetoxissilil)propil metacrilato (MPS). Já a polimerização foi realizada utilizando etilenoglicoldimatacrilato (monômero estrutural), ácido acrílico (monômero funcional) e azobisisobutironitrila (iniciador radicalar) como exibido pelo Esquema 1; seguido pela caracterização por espectroscopia de infravermelho.

Visando a aplicação do polímero obtido em CCD, a próxima etapa do trabalho consistiu na limpeza e ativação do vidro para posterior imobilização do polímero sintetizado. Para tanto, as placas de vidro (40 mm x 20 mm) foram previamente limpas em solução de NaOH 2,0 mol $L^{-1}$ e HCl 0,5 mol $L^{-1}$, respectivamente. A ativação das superfícies com grupos silanóis foi realizada colocando as placas em contato com solução de $H_2O_2$:$H_2SO_4$ (7:3 v/v) por uma hora.

As sínteses foram realizadas com sucesso como mostrado nas caracterizações, o que permitirá a futura aplicação dos polímeros fluorescentes.

**Esquema 1** – Síntese do polímero contendo núcleo de Sílica.

**Área: ANA**
*(Inserir a sigla da seção científica para qual o resumo será submetido. Ex: ORG, BEA, CAT)*

**Inscrição: 00719**
*(Inserir o número de inscrição do autor que fez a submissão)*

# Determinação do teor de docetaxel em medicamentos injetáveis por HPLC-DAD

**Natália G. de Figueiredo (PQ),[1] Vivianne G. Martins (TM),[1] Simone C. Chiapetta (PQ),[1]**

**natalia.figueiredo@int.gov.br;**

[1] *Instituto Nacional de Tecnologia, Av. Venezuela, 82, Saúde, Rio de Janeiro- RJ.*

Palavras Chave: *docetaxel, antineoplásico, HPLC-DAD.*

## Highlights

Determination of docetaxel by HPLC-DAD in injection formulations. This work describes the use of a chromatographic method to evaluate if docetaxel injection samples are in agreement with the quality standards determined in official guides such as USP Pharmacopeia.

## Resumo/Abstract

Docetaxel é um agente antineoplásico amplamente utilizado no Brasil para o tratamento de câncer de mama.[1] Drogas antineoplásicas apresentam índice terapêutico restrito, ou seja, pequenas variações nas doses administradas podem expor os pacientes a tratamentos ineficazes ou maior toxicidade desses agentes[2]. O objetivo desse trabalho foi avaliar o teor do antineoplásico docetaxel em medicamentos injetáveis por HPLC-DAD. Foram utilizadas amostras frasco-ampola de 1 mL e 4 mL em concentrações 20 $mg.mL^{-1}$ diluídas 100 x em solução de acetonitrila, ácido acético e água (1:0,1:1, v/v). As análises foram realizadas de acordo com o descrito na farmacopeia americana[3], por HPLC utilizando coluna $C_{18}$ e fase móvel constituída por gradiente binário de acetonitrila e água. O comprimento de onda utilizado foi $\lambda$ 232 nm. A análise do padrão (Figura 1) resultou em tempo de retenção para o docetaxel de 8,6 min e linearidade na faixa de 0,05 a 0,35 $mg.mL^{-1}$ ($r^2$ = 1, n=3). A concentração de docetaxel nas amostras variou entre 18,1 $mg.mL^{-1}$ a 23,6 $mg.mL^{-1}$ com desvios padrões relativos inferiores a 1% (n=6). O teor de docetaxel em medicamentos injetáveis deve variar entre 90 e 110% (18 a 22 $mg.mL^{-1}$) do declarado pelo fabricante[3]. Nossos resultados demonstraram que algumas das amostras apresentaram teor superior ao recomendado. Não foram detectados, no entanto, picos referentes a produtos de degradação e/ou impurezas de síntese nas amostras analisadas.

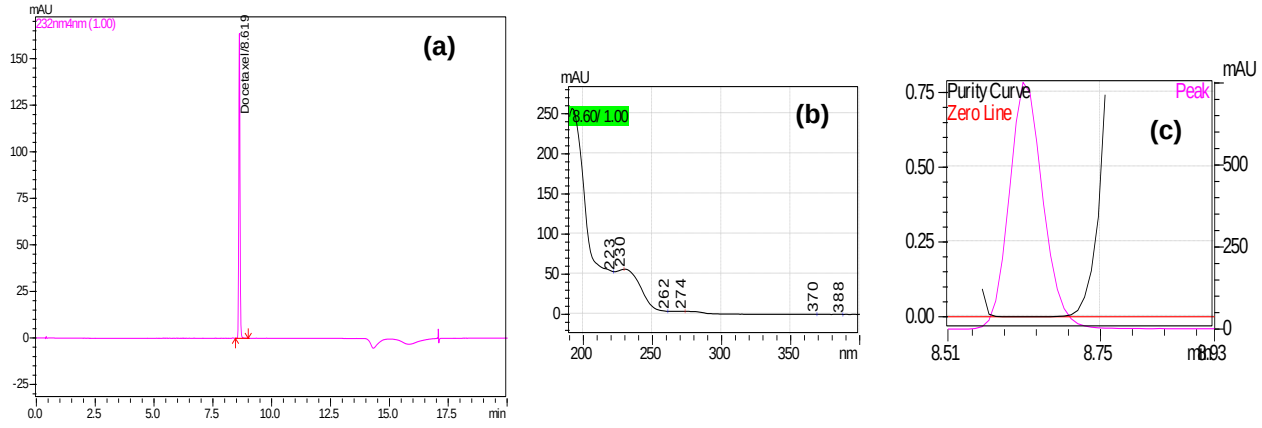


**Figura 1.** (a) Análise do Padrão de Docetaxel (tempo de retenção 8,6 min) por HPLC-DAD em $\lambda_{máx.}$ 232 nm, (b) Espectro de Absorção do docetaxel em 8,6 min na faixa 190 nm - 400 nm, (c) Gráfico de pureza de pico para o docetaxel em 8,6 min

[1]Acta Paul Enferm. 2016; 29, p.397
[2]J Pharm Biomed Anal, 2009, 49, p.1213
[3]United States Pharmacopeia, 2012

**Área: ANA** **Inscrição: 00825**

# Development and optimization of chromatographic method for determination of hypolipidemic drugs in pharmaceutical formulations

**Caroline Golembiouski (PG)[1]; Patrícia Los Weinert (PQ)[2].**

**golembiouski1@gmail.com; patilos@yahoo.com.br**

[1,2]*Departamento de Química – UEPG, CEP 84030-900, Ponta Grossa/PR*

Key words: *Simvastatin, ciprofibrate, HPLC, experimental design*

## Highlights

The determination was performed using HPLC with UV detection. The experimental conditions were optimized through experimental design. The method was applied for the analysis of the drug samples.

## Resumo/Abstract

Currently the number of people who develop hypercholesterolemia is raising (increase in blood LDL-cholesterol levels) increasing the use of drugs in treatment of patients who have this pathology. The most used hypolipidemics agents in treatment are fibric acid derivatives and statins[1]. In this work we propose the development of a methodology from simultaneous determination and quantification the ciprofibrate and simvastatin in pharmaceuticals formulations using the HPLC technique with detection UV. The methodology of HPLC in reverse phase and isocratic elution with mobile phase constituted of acetonitrile: methanol: water (50:30:20). The experimental conditions were optimized through experimental design. With the optimized conditions, it can be verified that there was an optimal separation of the drugs according to Figure 1.

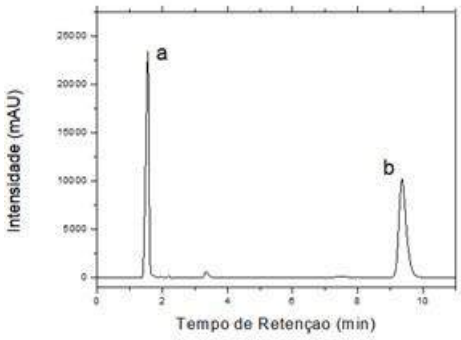


**Figura 1.** Chromatogram of the mixture of drugs in the concentration 5 $\mu gmL^{-1}$**.** (a) ciprofibrate (retention time, 1,56 min) and (b) simvastatin (retention time, 9,36 min)

Analytical curves from the standard solution of ciprofibrate and simvastatin in the concentration range of 0,5 – 10 $\mu gmL^{-1}$ were obtained with excellent linear correlation (r = 0,9999). The proposed method was applied in drugs determination in commercial samples with recovery rates ranging from 97 to 103 %. The validation considering the parameters of merit recommended by ANVISA allowed to verify that the proposed method is safe and reliable, being possible to use the HPLC technique with UV detection for the determination of ciprofibrate and simvastatin in pharmaceutical formulations.

## Bibliographic references

[1] National Cholesterol Education Program. National Heart, Lung, and Blood Institute. National Institutes of Health. **"Detection, Evaluation, and Treatment of High Blood Cholesterol in Adults (Adult Treatment Panel III)"** NIH Publication No. 01-3670, May 2001

**Área: ANA** **Inscrição:00830**

# Otimização de metodologia para análise de cocaína em cédulas de real

**Durval R. Mariano Junior** ***(PG),[1] Diego da P. Alves (IC),[2] Vanessa G. K. Almeida (PQ).[1]**

**durvalmariano@gmail.com**

*[1]PPGQ, UFRRJ; [2]Instituto de Agronomia, UFRRJ*

Palavras Chave: *Cocaína, Cédulas, Extração, Ultrassom, HPLC.*

## Highlights

Optimization of methodology for analysis of cocaine in banknotes
Banknotes may contain cocaine. For its quantification, this work presents a method of cocaine analysis using HPLC and ultrasonic bath for extraction.

## Resumo/Abstract

O cloridrato de cocaína, uma das formas de apresentação da cocaína, é o sal da cocaína altamente solúvel em água, o que faz com que sua administração possa ser por via nasal, aspirando-se o pó, ou endovenoso. É um pó branco, inodoro, sendo de alto valor no mercado por ser um produto de refino caro, incentivando a adulteração. O papel moeda está contaminado com cocaína, devido ao seu uso como ferramenta no consumo da droga e ao manuseio dos traficantes. Muitos usuários utilizam as cédulas para inalar o pó, formando um canudo. Por esse motivo, é importante determinar a presença de traços dessa droga nas notas, como uma evidência forense na tentativa de relacionar o usuário e a droga. Neste trabalho são apresentados estudos sobre a extração de cocaína de cédulas coletadas no município de Seropédica, Rio de Janeiro, resultando numa taxa de recuperação de até 95% utilizando ácido acético diluído em banho ultrassom, como mostrado na Figura 1. Foram avaliados também as melhores condições de análise para a cocaína em HPLC, e utilizou-se ácido acético 0,01% e acetonitrila 80:20 como fase móvel, na temperatura de 60ºC e fluxo 1 mL/min, em 230 nm. A Figura 2 apresenta o cromatograma de um padrão de cocaína nessas condições analíticas. O método apresenta linearidade entre 1 mg/L e 100 mg/L, com limites de detecção e quantificação de 0,3 mg/L e 1,0 mg/L, respectivamente.

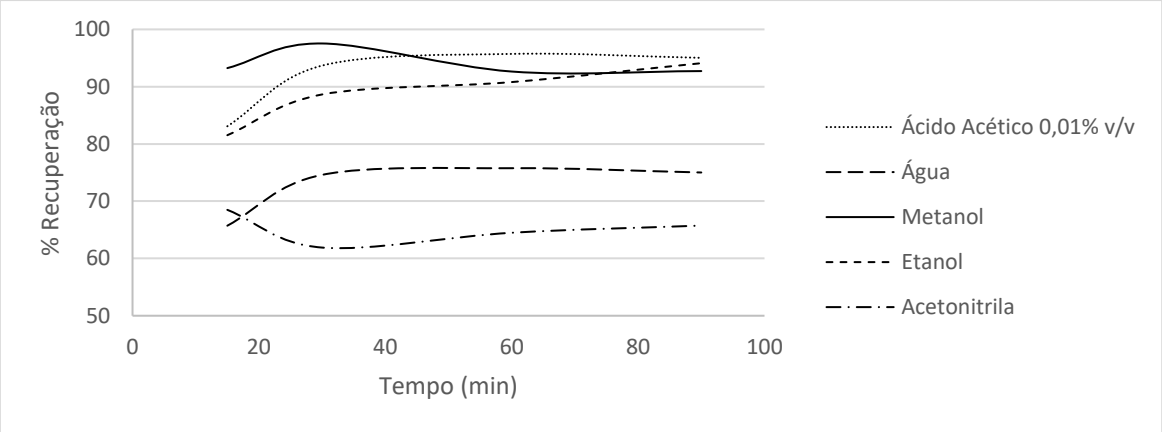


*Figura 1: Percentual e perfil de recuperação da cocaína em diferentes solventes*

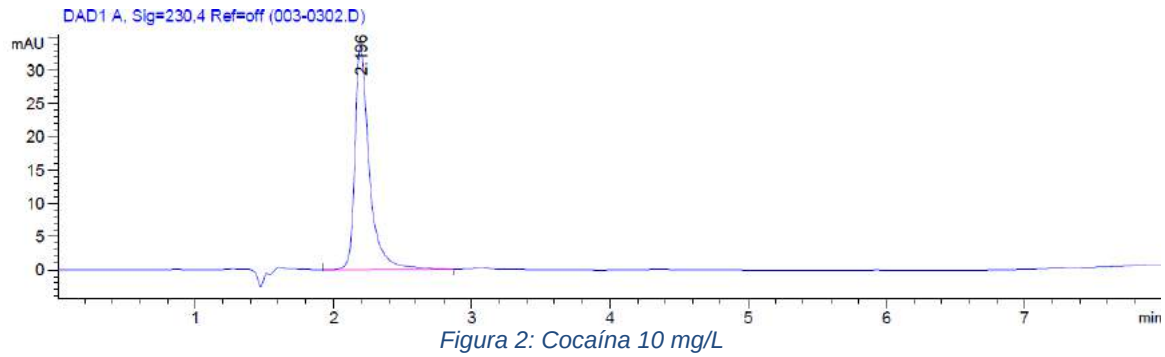


*Figura 2: Cocaína 10 mg/L*

**Área: ANA** **Inscrição: 00833**
*(Inserir o número de inscrição do autor que fez a submissão)*

# Development of a low-consuming solvent extraction for determination of 36 multiclass pesticides in atmospheric particulate matter (PM2.5)

**Madson M. Nascimento (PG)[1], Gisele O. Da Rocha (PQ)[1], Jailson B. de Andrade(PQ)[1],**

**madchemis89@gmail.com**

*[1]Departamento de Química Geral e Inorgânica, Instituto de Química, UFBA;*
*Palavras Chave: Miniaturized extraction, Multiclass pesticides, GC-MS, PM2.5*

## Highlights

A fast and environmental friendly extraction procedure was successfully developed. The GC-MS conditions and sample extraction procedure were optimized. A central composite design was applied in the optimization of ultrasound assisted-extraction conditions. The developed procedure was validated and applied in real PM2.5 samples.

## Resumo/Abstract

In the present study, a fast, miniaturized and low-consuming solvent extraction procedure has been developed for the simultaneous determination of 36 multiclass pesticides in PM2.5 samples. After optimization of GC-MS conditions, all compounds were separated within 20 min of runtime (Figure 1).

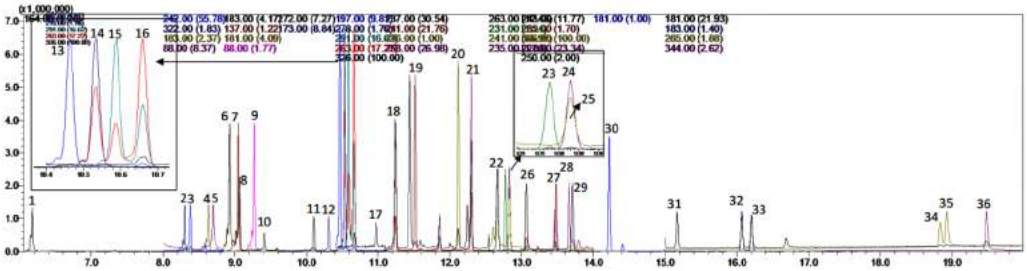

Figure 1. GC-MS chromatogram of 36 multiclass pesticides in SIM mode.

The composition of extracting solvent also was optimized and 500 µL of a binary mixture composed by 70 % of acetonitrile and 30 % of ethyl acetate was chosen. A central composite design was applied for ultrasound-assisted-extraction optimization. The optimal conditions led to an extraction time of 17 minutes at 39 °C of temperature (Figure 2), extracting efficiently particle masses as low as 321 µg of PM2.5. The matrix effect was also evaluated. The recoveries ranged from 72.1 % (endrin aldehyde) to 120% (sulfotep) with RSD ≤ 20 % for most pesticides. After validation, the method was applied in the determination of multiclass pesticides in 12 PM2.5 samples collected in the Baía de Todos os Santos region, Salvador, Bahia-Brazil. 25 pesticides were successfully identified and quantified, among them organophosphates prohibited by European Union and banned organochlorine. The average concentration considering the total volume of air sampled ranged from 0.88 pg $m^{-3}$ to 255 pg $m^{-3}$ for aldrin and endrin aldehyde, respectively. Malathion, chlorpyrifos, 4,4'-DDE, endrin aldehyde, λ-cyhalothrin and permethrin were detected with frequencies above 50%.

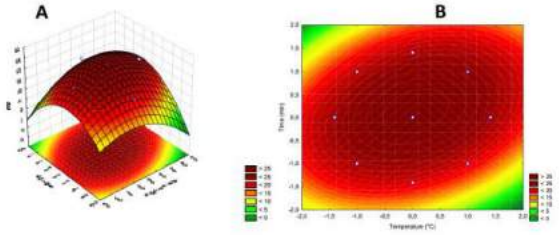


Figure 2. Response surface (A) and contour graph (B).

**Área: ANA** **Inscrição: 00897**

# Influence of sample preparation in the determination of phenolic compounds in mate tea beverages by UPLC-MS

**Gabrielle D. Iop (PG),[1] Ana L. G. Mendes (PG),[1] Cristiane F. Codevilla (PG),[2] Juliano S. Barin (PQ),[2] Fábio A. Duarte (PQ),[1] Paola A. Mello (PQ),[1]***

**gabrielle.iop@gmail.com; paola.mello@ufsm.br**

*[1] Departamento de Química, UFSM; [2]Departamento de Tecnologia e Ciência dos Alimentos, UFSM*

Palavras Chave: *Sample preparation, Phenolic compounds, Mate tea beverages, Liquid chromatography, Mass spectrometry, Folin-Ciocalteau method*

## Highlights

Evaluation of sample preparation methods to extract phenolic compounds in mate tea beverages was performed;
Influence of temperature, ultrasound and pH in species conversion was investigated.

## Abstract

Phenolic compounds are important components of many plants, food and beverages. These compounds are essential to human diet and are associated to prevention of diseases due to their bioactive functions. The determination is commonly performed by Folin-Ciocalteau method (spectrophotometry), which is used to determine the total phenolic content.[1] Nowadays, speciation of phenolic compounds is becoming increasingly required, once the total content may not allow the complete understanding in this issue. The aim of this work was to evaluate the influence of sample preparation methods and conditions to extract phenolic compounds in mate tea beverages. Determination of phenolic compounds was performed by ultra performance liquid chromatography mass spectrometry (UPLC-MS; Xevo G2 qTOF, Waters, USA). An analytical method for separation and identification was developed and validated for this purpose. With regard to the sample preparation, infusion, ultrasound-assisted extraction, conventional extraction and solid-phase extraction were evaluated for three types of mate tea beverages. It was obtained a higher concentration of chlorogenic acid for all sample preparation methods and samples, as well as their isomers. By the use of an infusion method, a higher total phenolic content was extracted in comparison to other methods. Interconversion of the species was not observed at several sample preparation conditions. The developed method was suitable to perform the speciation analysis of phenolic compounds in mate tea beverages thus contributing to the studies with regard to its nutritional aspects.

1. Angelo, P. M. and Jorge, N. Rer. Inst. Adolfo Lutz, 2007, 66, 1.
2. Puig, M. C., Ayala, H. G. and Lacorte, S. Curr. Anal. Chem., 2012, 8, 436.

**Área: ANA** **Inscrição: 00944**

# Método bioanalítico para quantificação de Doxiciclina em plasma canino: aplicação em estudos de farmacocinética

**Isabela P. Lima (PG),[1*] Thais P. Ferreira (TC),[2] Viviane de S. Magalhães (TC),[2] Fábio B. Scott (PQ),[2] Yara P. Cid (PQ),[3]**

**isabeladlima@gmail.com**

*[1]Departamento de Química, ICE, UFRRJ; [2]Departamento de Parasitologia Animal, IV, UFRRJ; [3]Departamento de Ciências Farmacêuticas, ICBS, UFRRJ*

Palavras Chave: *Doxiciclina, Plasma canino, Preparo de amostras, CLAE.*

## Highlights

Bioanalytical method for quantification of Doxycycline in canine plasma: application in pharmacokinetic studies. Development and validation of bioanalytical method by HPLC/UV for application in comparative pharmacokinetics study of oral doxycycline formulations in dogs.

## Resumo

A preocupação com a saúde de animais domésticos é responsável pelo crescimento e especialização das indústrias veterinárias[1]. Dentre as doenças causadas por parasitas, a mais frequente é a Erliquiose Canina, transmitida pela picada do *Rhipicephalus sanguineus*.

A Erliquiose Canina é frequentemente tratada com Doxiciclina, antibiótico amplamente usado na medicina veterinária e humana, com diferentes metodologias para sua quantificação, principalmente em plasma humano[2]. Em plasma canino existem poucas metodologias por CLAE-UV[3], sendo mais utilizados os métodos microbiológicos.

Neste trabalho realizou-se o desenvolvimento e validação de um método bioanalítico por CLAE-UV a partir da comparação de diferentes técnicas de extração: extração líquido-líquido (ELL); extração em fase sólida (EFS) e extração líquido-líquido com partição em baixa temperatura (ELL/PBT). A separação cromatográfica foi feita em coluna C18, fase móvel acetonitrila/água (pH = 2,5) (80:20 v/v) com fluxo gradiente (0,8-1,0 mL/min) e comprimento de onda de 357 nm. Na extração foram avaliados seletividade, precisão e exatidão, os resultados apresentados para ELL/PBT foram (CV <15%) e (EPR ±15%) para precisão e exatidão. O método foi validado segundo critérios da Anvisa. A linearidade estabelecida encontra-se entre 0,5-10 µg/mL. O método foi aplicado para monitorar concentrações plasmáticas após administração oral de doxiciclina em cães, verificando-se similaridade nos perfis plasmáticos das duas formulações testadas.

[1] Broom, D.M.; Molento, C.F.M., **2004**, vol 9 (2)p. 1–11.
[2] Axisa, B. et al., **2000**, vol 744 (2) p. 359-365.
[3] Bidgood, T.L.; Papich, M.G, **2003**, vol 64 (8) p. 1040-1046.

**Área: ANA** **Inscrição:00960**

# Determinação de pesticidas organoclorados na bacia hidrográfica do rio de Ondas, oeste da Bahia, por CG-MS

**Enoc Lima do Rego (PG),[1*] José Domingos S. da Silva (PQ),[2] Thamilin C. Nakamura (PG),[2] Paula Valéria B. Almeida (PG),[2] Caroline O. Pinto (IC),[2] Raiane C. Souza (PG)[2], Jurandir R. de Souza (PQ)[1], João V. da S. Santos (PQ)[3].**

**jvquimico@yahoo.com.br; el.enoc.lima@gmail.com**

*[1]Instituto de Química, UnB; [2]Centro de Ciências Exatas e Tecnológicas, UFOB; [3] Campus Uruçuca, IF baiano*

Palavras Chave: *Agricultura, agrodefensivos, água, abastecimento público*

## Highlights

Determination of organochlorine pesticides in the water shed of the Ondas river, western Bahia, by CG-MS. Where does the "poison" go? Concentrations of pesticides in samples of river water above that allowed for human consumption. Agricultural expansion and water quality.

## Resumo/Abstract

Os pesticidas contém substâncias que devido as suas propriedades químicas, possuem efeitos letais para determinados seres vivos, incluindo o homem, sendo utilizado, principalmente, no extermínio de pragas. A região oeste da Bahia, caracteriza-se pela produção de *commodities* agrícolas (soja, milho e algodão), gerando um uso intensivo de agrodefensivos para reduzir as perdas nas safras. Desta forma, o objetivo deste trabalho foi determinar as concentrações de pesticidas nas águas do rio de Ondas. Para o estudo foi utilizada cromatografia gasosa com espectrômetria de massas. As amostras foram coletadas em 10 pontos distintos ao longo do rio (montante a foz). As amostras foram submetidas a extração liquido/liquido e quantificadas por GC-MS. A Figura 1 apresenta os pesticidas organoclorados investigados e os seus níveis nos respectivos pontos.

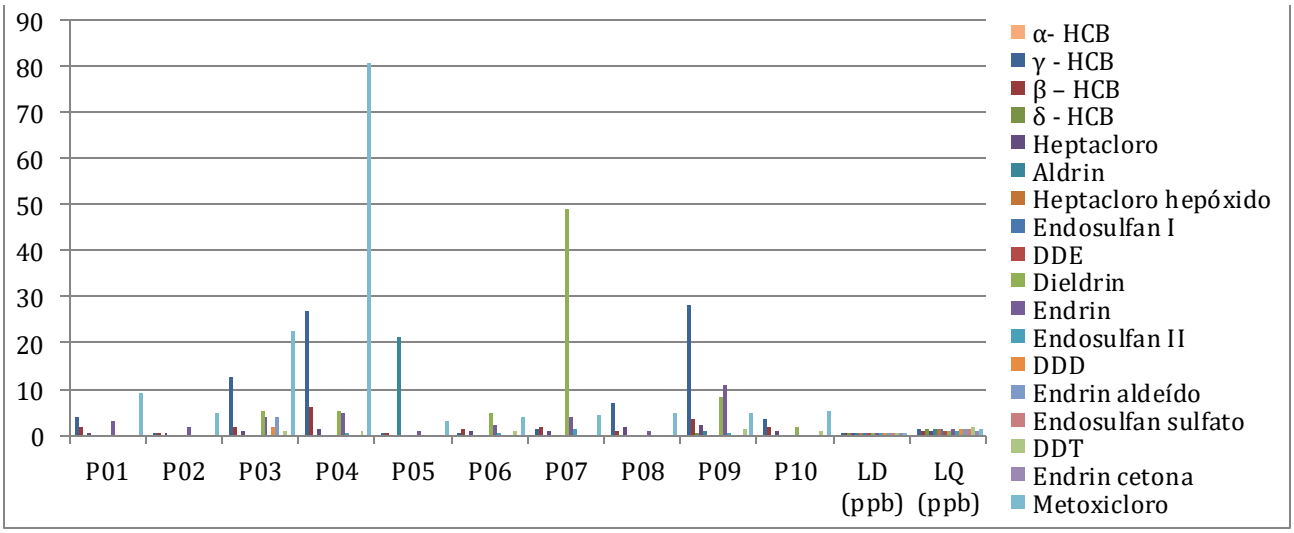


Figura 1: Níveis de pesticidas organoclorados ao longo do rio de Ondas.

Em todas as amostras foram identificados a presença γ-HCB, β–HCB e metoxicloro com concentrações variando entre 0,33 e 28,19, 0,56 e 5,96, 2,92 e 80,78 µg/L, respectivamente. As concentrações obtidas de DDT, DDD, dieldrin, endrin, aldrin, endosulfan, heptacloro e metoxicloro em todos os pontos identificados foram acima dos valores máximos estabelecidos pelo CONAMA 357/2005 para o consumo humano (0,005 µg/L para Aldrin + Dieldrin, 0,002 µg/L para DDT e DDD, 0,056 µg/L para Endossulfan, 0,004 µg/L para Endrin, 0,01 µg/L para Heptacloro epóxido + Heptacloro e 0,03 µg/L para Metoxicloro). Sendo assim, observa-se que há indícios de fontes contaminadoras na região da bacia hidrográfica do rio de Ondas, podendo afetar as populações ribeirinhas e a qualidade da água do abastecimento público das cidades.

**Área: ANA** **Inscrição: 00996**

# Desenvolvimento de método para análise de catecolaminas e metabólitos em urina por CL-EMAR

**Rafaela R. Roiffé (PG),[1]* Vinícius F. Sardela (PQ),[2] Márcia N. S. de la Cruz (PQ),[2] Kátia R. de Souza (PQ),[1] João E. Nacif (IC),[2] Francisco R. Aquino Neto (PQ).[2]**

**raroiffe@hotmail.com**

[1]*Instituto Militar de Engenharia, IME;* [2]*Universidade Federal do Rio de Janeiro - Instituto de Química, UFRJ-IQ.*

Palavras Chave: Catecolaminas, Metabólitos, Fluido Biológico, Desenvolvimento De Método, Cromatografia Líquida, Espectrometria De Massas.

## Highlights

Method development for analysis of catecholamines and metabolites in urine by LC-HRMS. Development of a screening method for urine analysis. Analysis of the catecholamines and metabolites in biologic fluid by Liquid Chromatography-High Resolution Mass Spectrometry.

## Resumo/Abstract

Alterações nos níveis catecolaminérgicos endógenos podem ser originadas pelo desenvolvimento de determinadas patologias, como Parkinson e Alzheimer, ou ainda devido a administração intencional de alguma catecolamina, o que neste caso, quando associado ao esporte, pode gerar um resultado analítico adverso (*doping*). Portanto, o objetivo deste estudo é desenvolver um método de análise por cromatografia líquida acoplada à espectrometria de massas de alta resolução (CL-EMAR) que permita separar, identificar e quantificar as catecolaminas e seus metabólitos de modo a auxiliar no controle de dopagem e no diagnóstico de patologias. O desenvolvimento do método consistiu no pré-tratamento de amostras, previamente fortificadas com as catecolaminas de interesse, através de uma extração em fase sólida da urina previamente hidrolisada com uma solução de β-glicuronidase. A etapa de reconcentração do eluato foi realizada com a combinação da mistura de fase móvel e parte da urina *in natura*. As amostras foram então introduzidas no cromatógrafo líquido e analisadas por espectrometria de massas em dois modos de ionização: positivo e negativo. A seletividade do procedimento foi avaliada com diferentes proporções de lavagem da coluna de extração e a proporção metanol:água 60:40 foi a mais indicada. O rendimento da extração dos analitos também foi avaliado e todos apresentaram valores adequados. A tabela 1 apresenta os resultados obtidos a partir das análises utilizando a coluna amida.

Tabela 1. Resultados obtidos na análise utilizando a coluna amida como, tempo de retenção ($t_R$), razão massa/carga (*m/z*) encontrada e modo de ionização das catecolaminas e metabólitos disponíveis.

| Catecolamina/Metabólito | $t_R$ | *m/z* encontrada | Modo de ionização |
|---|---|---|---|
| Dopamina | 7,84 | 154,08629 | Positivo |
| Noradrenalina | 13,81 | 168,06586 | Negativo |
| Adrenalina | 10,68 | 182,08185 | Negativo |
| Metanefrina | 4,60 | 180,10188 | Positivo |
| Normetanefrina | 10,73 | 166,08638 | Positivo |
| Ácido Homovalínico | 1,41 | 181,04997 | Negativo |
| Ácido 4-hidroxi-3-metoximandélico | 1,60 | 197,04515 | Negativo |
| Ácido 3,4 -dihidroximandélico | 1,38 | 183,02911 | Negativo |
| Acido 3,4-hidroxifenilacetico | 1,38 | 167,03442 | Negativo |
| Cloridrato de 3-metoxitiramina | 4,19 | 168,10196 | Positivo |

Eisenhofer, G.; Kopin, I. J.; Goldstein, D. S. Catecholamine Metabolism: A Contemporary View with Implications for Physiology and Medicine. Pharmacological Reviewrs, 2004, 56, 331-349.

WADA, World Anti-Doping Agency. The World Anti-Doping Code International Standard, Prohibited List January 2017. Montreal, Canada, 2017, 01-09.

**Área: ANA** **Inscrição: 01184**

# Characterization of 18 organochlorine pesticides in samples of coconut water *in natura* using CG-MS

**Thamilin Costa Nakamura (PG),[1*] Enoc Lima do Rego (PG),[2] Paula Valéria Nunes Brito (PG),[1] José Domingos Santos da Silva (PQ).[1]**

**thamilintcn@hotmail.com**

*[1]Programa de Pós-Graduação em Química Pura e Aplicada, UFOB, CCET; [2]Instituto de Química, UnB.*

Palavras Chave: *Extração líquido-líquido, Micro-ondas doméstico, Pesticidas, Água de coco, Cromatografia gasosa.*

## Highlights

Since 2008, Brazil has been the world's largest consumer of pesticides. Bahia is the seventh largest consumer of pesticides in the Brazilian's states. Contamination by pesticides of foods consumed *in natura*. Use of low sample volume and solvent for pesticide determination in coconut water *in natura*. Use of microwaves as a method of drying the sample.

## Abstract

The mesoregion of the extreme west of Bahia has become the main agricultural frontier of the state, where these activities are based on a model of management with intense use of pesticides to increase productivity, in this context the present study aimed to determine 18 organochlorine pesticides, prohibited by Brazilian's legislation, in coconuts water from two plantations located in the municipality of Barreiras, which distribute the product to local commerce. A simple and fast method extraction of the pesticides was developed, evaluating different parameters such as type and proportion of solvent, time and stirring speed of the sample with the solvent, and time and power of drying in the domestic microwave. Better results were obtained by using 10 mL of sample to 0.5 mL of extractive solvent (hexane: toluene 7:3), under magnetic stirring for 30 minutes and microwave drying at low power, with cooling intervals. Mean recoveries were 82.2% to 107.7%, except Endolsufan II that recovered was 62.2 %. To characterize the pesticides, gas chromatography with coupled mass spectrometry (CG-MS) was used. Limits of detection (LOD) ranged from 0.15 to 0.54 μg $L^{-1}$ and quantification (LOQ) ranged from 0.5 to 1.81 μg $L^{-1}$ for α-BHC and DDT, respectively. Analytical procedures were applied to 10 samples of coconut water *in natura*, yielding the results set forth in Table 1.

Table 1. Concentration of organochlorine pesticides in samples of coconut water *in natura*.

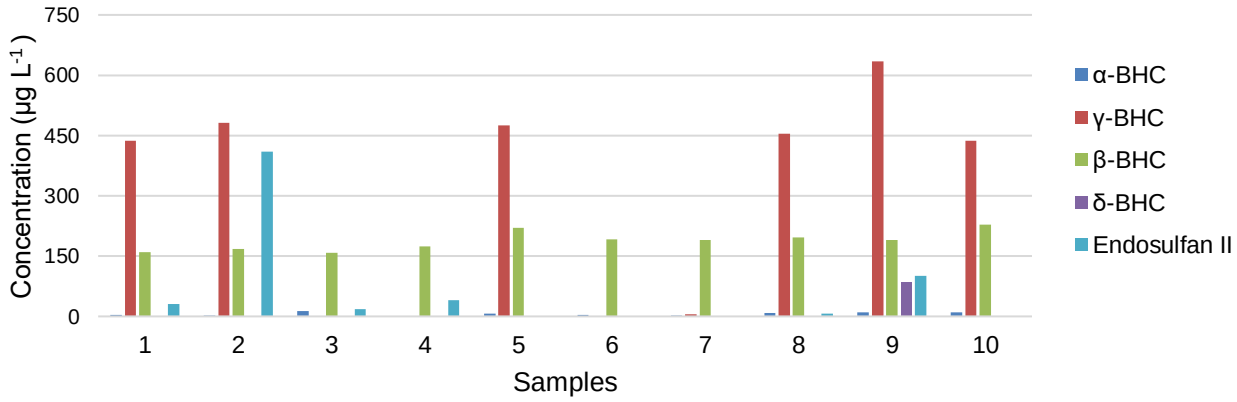


In the samples, 7 species were identified, of which 2 were in concentrations below the LOQ, standing out the γ-BHC and β-BHC that presented concentrations superior to 430 μg $L^{-1}$ and 158.77 μg $L^{-1}$, respectively.

**Área: ANA** **Inscrição: 01185**

# Development and validation of a method to quantify acetaminophen in plasma from small rodents for the study of gastric emptying alterations.

**Monica Regina Pimentel Siqueira (PG)[1,2*], Davyson de Lima Moreira (PQ)[1,2,3], Francisco José Roma Paumgartten (PQ)[1], Rafael dos Santos (PG)[1,2], Lorenna Carvalho da Rosa (PG),[1,2].**

**monicarpsiqueira@gmail.com;**

*[1]Escola Nacional de Saúde Pública, FIOCRUZ; [2]Programa de Pós-Graduação em Biologia Vegetal da Universidade do Estado do Rio de Janeiro, UERJ); 3 Departamento de Produtos Naturais, Instituto de Tecnologia em Fármacos, FIOCRUZ.*

Keywords: *(Gastric emptying, HPLC-DAD-UV, Acetaminophen, DBA/2 mice, Swiss mice, Wistar rats).*

## Highlights

Acetaminophen quantification by HPLC-DAD-UV; Acetaminophen plasma levels as gastric emptying marker;

## Resumo/Abstract

Factors that affect drugs plasma levels, and consequently their kinetics, such as diet, diseases and pregnancy, can influence the safety and efficacy of treatments. Depending on whether gastric emptying is physiologic, accelerated or retarded and on the place where drug absorption takes place (stomach or intestines) drug absorption can be modified. Acetaminophen, an analgesic and antipyretic drug, is absorbed almost exclusively in the intestine and the rate of its absorption depends on the time of gastric emptying. Therefore, investigations on the gastric emptying rate can be done indirectly by measuring acetaminophen blood plasma levels. The aim of this work was to develop and validate a methodology for the analysis of acetaminophen on plasma sample from small rodents (mice and rats) to infer about gastric emptying of testing drugs/ preparations such as new synthetic compounds or phytomedicines. The methodology used was High Performance Liquid Chromatography coupled to Diode-Array Detector and visualization on Ultraviolet range (HPLC-DAD-UV), using a Shimadzu Nexera equipment. In this study, DBA/2 mice, Swiss mice and Wistar rats were oral treated with 50 $mg.kg^{-1}$ of saline acetaminophen solution alone or in combination with metoclopramide or morphine sulfate (10 $mg.kg^{-1}$), previously administered by sub-cutaneous route. Acetaminophen analysis method development and validation in blood plasma were in accordance with recommendation of the Brazilian National Health Surveillance Agency (Resolution 899/93). The extraction of acetaminophen from blood plasm (only 50 µL) was procedure with protein precipitation, subsequent supernatant recovery and directly analysis by HPLC-DAD-UV. Acetaminophen recovery rates with this methodology were above 90%. Best analysis parameters to analyze acetaminophen were achieved with silica-modified ACE® 5 C18 column (250 mm x 4.6 mm id, 5 µm particle size); mobile phase composed of acidified ultrapure water (pH 3.0) and HPLC grade acetonitrile in the ratio of 80:20; flow rate at 1.0 $mL.min^{-1}$; oven temperature of 50° C. The developed and validated method showed to be selective for analysis of acetaminophen in plasma is short time (6 minutes, including differentiating it from morphine and metoclopramide retention time), as well as being linear, accurate, precise and robustness. The detection and quantification limits were 30 $ng.mL^{-1}$ and 45 $ng.mL^{-1}$, respectively. The test chosen for the study of gastric emptying was adequate to detect both acceleration (metoclopramide) and retard (morphine) of drug absorption using acetaminophen as marker. This developed test is great for pre-clinical studies of synthetic or natural compounds/ extracts since it is fast, employs low amount of plasma blood sample and spends low amounts of acetonitrile in the mobile phase.

**Área: ANA** **Inscrição: 01219**

# On-column preconcentration of phenolic compounds by sequential injection chromatography

**Maria Soledad M. S. F. Acevedo (PG)*, Mariana R. Gama (PQ), Fábio R. P. Rocha (PQ).**

***msoledad@usp.br**

*Centro de Energia Nuclear na Agricultura, Universidade de São Paulo.*
*Keywords: Chromatography; In-line concentration; Fused core columns.*

## Highlights

Analyte retention at the head of a chromatographic column was exploited for on-column preconcentration. High enrichment factors without hindering separation capability or sample throughput.

## Abstract

Phenolic compounds are secondary metabolites of plants involved in defense against chemical and biological attacks. They are also highly important constituents of food, mainly fruits, vegetables, and beverages, such as tea and wine, because of the benefits to human health (e.g. antioxidant, antimicrobial, and anticancer properties). As phenolic compounds are generally found at low concentrations in food, analyte preconcentration is often needed for analytical determination. This work proposes the on-column preconcentration of phenolic compounds in SIC by exploiting analyte retention at the head of a C18 fused core packed column (Supelco Ascentis Express, 2.7 µm, 30 x 4.6 mm i.d.). The on-column preconcentrantion involved aspiration of water as carrier, followed by the sample aliquot to a holding coil. The sample zone was then directed to the chromatographic column and, because of the low eluent strength, the analytes were effectively accumulated at the head of the column. Then, the mobile phase (acetonitrile and water, 35:65 v/v, with pH adjusted to 2.5) eluted the analytes for spectrophotometric detection at 254 nm. The approach was successful, without peak broadening or significant changes in retention times with the increase of the sample volume (Figure 1). Figure 2 shows the linear relation between the peak height and the sample volume, thus increasing the detectability of the analytes. For example, a preconcentration factor of 13 was estimated for kaempferol with 750 µL of sample. The proposed procedure can be extended for preconcentration of different analytes, after optimization of both stationary and mobile phases.

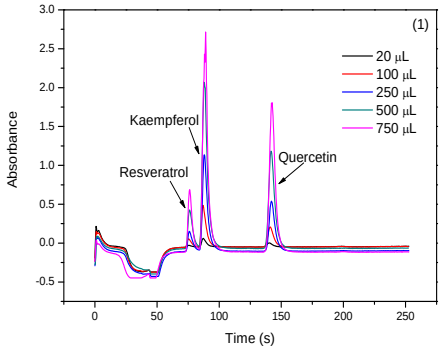


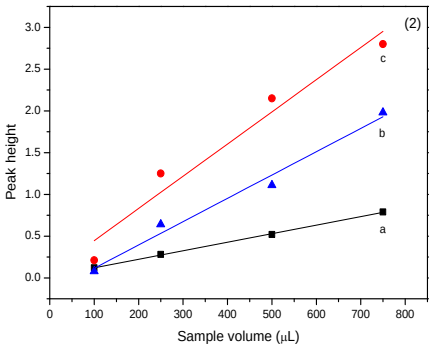


Figure 1. Chromatograms of the phenolic compounds (3 mg $L^{-1}$ each) with increasing sample volumes.

Figure 2. Increase of the peak height with the sample volume. a, b, and c correspond to resveratrol, quercetin, and kaempferol, respectively.

The authors acknowledge the financial support from FAPESP, CAPES, and CNPq.

**Área: ANA** **Inscrição: 01234**

# Development and validation of a LC-MS/MS method for analysis of fentanyl and its analogs in stamps

**Jandyson Machado Santos (PQ),[1*] Damila Rodrigues de Morais (PQ),[1] Lilian de Melo Barbosa (PG),[2,3] José Luiz da Costa (PQ),[4] Marcos Nogueira Eberlin,[1] (PQ)**

***jandyson.machado@gmail.com**

*[1]Insituto de Química, UNICAMP; [2]Polícia Técnico-Científica do Estado de São Paulo, SPTC; [3]Universidade de São Paulo-Campus Ribeirão Preto, USP; [4]Faculdade de Ciências Farmacêuticas, UNICAMP.*

Keywords: *Fentanyl, Stamps, Mass Spectrometry, LC-MS/MS and Method validation.*

## Highlights

- The first LC-MS/MS method to quantify of fentanyl and its analogs in stamp samples
- The LC-MS/MS method developed may be applied in routine forensic cases

## Resumo/Abstract

Fentanyl is a synthetic opioid, 50-100 times stronger than morphine. These powerful effects are also observed in the fentanyl analogues, which presents similar chemical structure. The human consume of these molecules may produce psychoactive effects have been associated with cases of deaths worldwide. The goal of this work was the development and validation of a method based on LC-MS/MS to quantify fentanyl, acetylfentanyl, acetyl-norfentanyl, acrylfentanyl, carfentanyl, furanylfentanyl, tiofentanyl and valerylfentanyl in samples of stamps. The LC-MS/MS method was developed using a Force Biphenyl column (1.8 µm and 50 x 2.1 mm) with a specific temperature program in a LCMS-8040 (Shimadzu, Kyoto, Japan) coupled with electrospray ionization, using the multiple reaction monitoring (MRM) mode, totaling 4 min for each run (Figure 1). Fentanyl-d5 was used as internal standard and the validation was based on international guidelines for illicit drug analysis. The method was also found to be linear from 1 to 100 ng/mL for all eight compounds. The imprecisions (intraday and interday %RSD) and accuracy bias (%) were satisfactory at both quality control concentrations, with no more than 10% of RSD. The recovery rates were found between 94-105%. In the real stamps samples analysis, we have quantified 0.58-2.17 mg/blotter of furanylfentanyl. In the best of our acknowledgment, we have developed the first LC-MS/MS method to analyze fentanyl analogs with application in real samples of stamps collected in São Paulo-SP, Brazil.

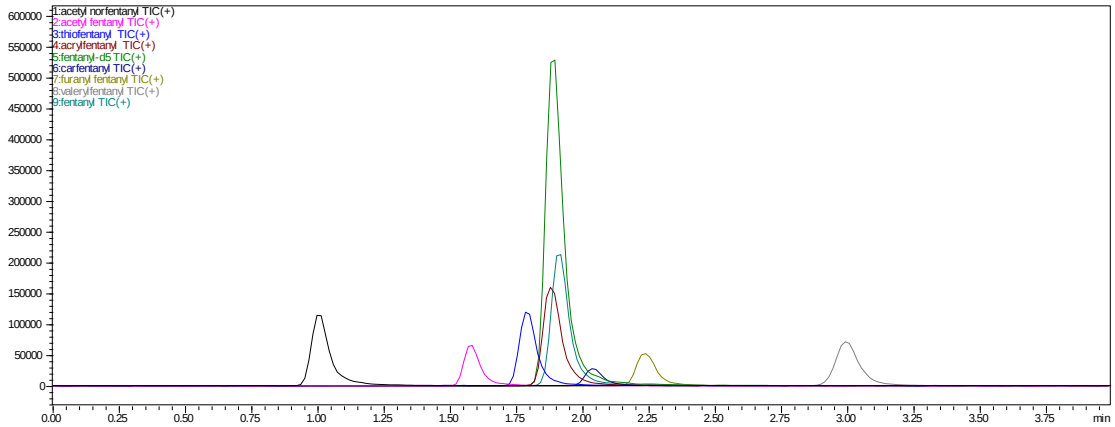


**Figure 1.** LC-MS/MS method in full scan mode for fentanyl, fentanyl-d5, acetylfentanyl, acetyl-norfentanyl, acrylfentanyl, carfentanyl, furanylfentanyl, tiofentanyl and valerylfentanyl in the concentration of 0.6 ng $mL^{-1}$.

**Área: ANA** **Inscrição:01354**

# EVALUATION OF A CHROMATOGRAPHIC METHOD FOR THE DETERMINATION OF PHENOLIC ACIDS AND METHYLXANTHINS IN TEA

**Ravena S. A. Azevedo (PG) ,[1] Bianca S. Teixeira (TM),[2] Maria Celeste S. Sauthier (PG),[3,4] Marta Valéria A. Santana (PQ),[1] Walter Nei L. dos Santos (PQ), [1,3] Débora de Andrade Santana (PQ).[1]***

**deboradeandradesantana@gmail.com**

*[1]Departamento de Ciências Exatas e da Terra UNEB; [2] Departamento de Química IFBA; [3]Departamento de Química UFBA; 4Departamento de Química IFBaiano*

Palavras Chave: HPLC; phenolic acids; methylxanthines; Camellia sinensis *(máximo 6, separadas por vírgula, primeiras letras em maiúscula, arial 9, itálico).*

## Highlights

Presents the development of a method for analysis of bioactive compounds
The univariate study was used for the optimization of factors affecting the chromatographic separation
The efficiency-related and validation parameters were evaluated

## Resumo/Abstract

Teas are play a very important role in the control of diseases mainly due to the presence of polyphenols and alkaloids present, associated with beneficial effects in relation to the central nervous system, anti-inflammatory and antioxidant action. [1] This study deals with the development of a separation and quantification method by high performance liquid chromatography with a diode array detector (HPLC- DAD), for the determination of six phenolic acids (gallic, trans-cinnamic, caffeic, ferulic and p-coumaric acids) and two methylxanthines (caffeine, theobromine) in tea (*Camellia Sinensis*) samples.
Widely used in the evaluation of chromatographic separation, univariate optimization consists in the study of each variable (gradient, temperature and flow) in isolation. A univariate study was used for the optimization of factors affecting the chromatographic separation: gradient, flow and temperature of the oven. Changes in gradient conditions were evaluated using the parameters: retention time (Rt), retention factor (K), separation factor (α), resolution (Rs), and number of theoretical plates (N).[2]
The method was validated in terms of linearity, limits of detection and quantification, precision (repeatability and intermediate precision), accuracy (recovery), matrix effects and process efficiency. [2]

**Table 1 -** Separation assessment parameters.

| Compound | Rt | K | α | N | Rs | *Regression equation[a]* | *Correlation coefficient* | *LOD[b] (mg L$^{-1}$)* | *LOQ[c] (mg L$^{-1}$)* | *Precisions[d] (% RSD)* | | *Recovery (%)[e] (n = 9)* |
|---|---|---|---|---|---|---|---|---|---|---|---|---|
| | | | | | | | | | | Intraday (n = 9) | Interday (n = 9 | |
| gallic acid | 4.395 | 1.53 | 1.72 | 12224.85 | 9.94 | y = 18226x + 19420 | 0.9915 | 0.12 | 0.37 | 4.42 | 10.09 | 86.83 |
| theobromine | 6.309 | 2.64 | 1.12 | 12468.79 | 1.83 | y = 11149x - 1479.2 | 0.9921 | 0.47 | 1.41 | 4.08 | 8.47 | 98.97 |
| chlorogenic acid | 6.856 | 2.95 | 1.09 | 5405.60 | 1.50 | y = 55469x - 1988.5 | 0.9922 | 0.10 | 0.29 | 4.43 | 12.32 | 88.45 |
| caffeic acid | 7.312 | 3.22 | 1.11 | 15622.86 | 2.91 | y = 160619x - 8164.2 | 0.9972 | 0.07 | 0.21 | 5.43 | 11.56 | 103.70 |
| caffeine | 7.946 | 3.58 | 1.03 | 24757.93 | 1.15 | y = 99893x + 3762.3 | 0.9933 | 0.09 | 0.27 | 1.10 | 8.03 | 95.09 |
| p-coumaric acid | 8.155 | 3.70 | 1.03 | 41565.02 | 1.16 | y = 98612x - 3838.1 | 0.9928 | 0.09 | 0.28 | 1.50 | 1.72 | 83.14 |
| ferulic acid | 8.366 | 3.82 | 1.28 | 26908.86 | 9.31 | y = 60244x + 1643.2 | 0.9962 | 0.10 | 0.30 | 4.06 | 12.79 | 75.87 |
| transcinnamic acid | 10.218 | 4.89 | 1.28* | 44386.24 | 9.31* | y = 156487x - 3081.9 | 0.9950 | 0.08 | 0.23 | 3.24 | 13.80 | 76.57 |

* Values for the previous peak. a Expresses the detection response (peak area mAU) x concentration of phenolic compound (in mg L$^{-1}$). b Limit of detection, the lowest analyte concentration that produces a response detectable above the noise level of the system. c Limit of quantification, the lowest level of analyte that can be precisely measured. d Average of relative standard deviation for three different measures, expressed as %. e Average of recoveries at three spike levels (0.5, 1.0 and 2.0 mg L$^{-1}$).

The Chromatographic separation optimized, showing good resolution, selectivity and sensitivity in the simultaneous determination of 8 compounds studied and the detection by DAD was adequate, showing low limits of detection

References

1 Hall, S., Desbrow, B., Anoopkumar-Dukie, S., Davey, A. K., Arora, D., McDermott, C., & Grant, G. D. (2015). Food Research International, 76, 626-636.
2 LANÇAS, F. M. Cromatografia Líquida Moderna. São Carlos: Ed. Átomo, 2009.

**Área: ANA**
*(Inserir a sigla da seção científica para qual o resumo será submetido. Ex: ORG, BEA, CAT)*

**Inscrição:01381**
*(Inserir o número de inscrição do autor que fez a submissão)*

# QuEChERS-SPE method for determination of endocrine disrupting compounds in harbor sediment

**Lucy Elaine Sugauara(PG)[1], Mary Rosa Rodrigues de Marchi(PQ)[1],**

lucy_sugauara@yahoo.com.br maryrmarchi@gmail.com,

[1]*Departamento de Química Analítica UNESP Araraquara*

Palavras Chave: EDCs, Quechers, SPE, HPLC-FLD

## Highlights

- Simple method for hormones determination on harbor sediment is presented
- LOD ranged 2- 5 ng $g^{-1}$, LOQ was 20 ng $g^{-1}$ , recovery 64-114% (CV <16%), for spiked samples in five concentrations
- Harbor sediments from Baixada Santista presented E3 as more abundant hormone and E2 and EE2 are close to the LOQ

## Resumo/Abstract

Endocrine disrupting compounds (EDCs), including synthetic and natural hormones, are commonly found in aquatic systems mainly as result of wastewater treatment discharges where they can reach all compartments due to the broad range of physicochemical properties. Studies focousing EDCs occurrence in natural water are more abundant than on sediments (river or sea), however for ecotoxicological studies are very important the EDcs determination in both environmental compartments to evaluate the marine biota exposition. The analytical challenge is to determine EDCs at very low concentrations in high complexicity matrices, as sea harbor sediments. In this work we present a method coupling QuEChERS and SPE for hormones (17β estradiol -E2, 17α ethinylestradiol -EE2 and estriol -E3) determination in harbor sediment. Quantification was carried out by HPLC with fluorescence detector. On figure 1 we show all extraction process.

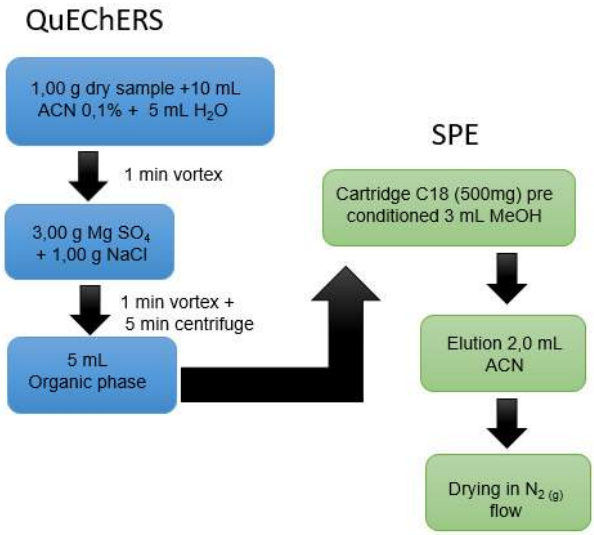


Figure 1: Extraction by QuEChERS and SPE clean up

Recovery on spiked samples (five concentrations ranged 20-200 ng $g^{-1}$) were between 64 and 114%, CV<16%, LOD for E3, E2 and EE2 was 5.4, 2.6 and 3.8 ng $g^{-1}$ , respectively, while the LOQ was 20.0 ng $g^{-1}$, for all studied hormones. For harbor sediment from Baixada Santista (São Paulo State, Brazil), we observed high concentration E3 in all samples (n=14) (21 to 177 ng $g^{-1}$), E2 was below the LOQ and EE2 was very close to LOQ.

**Área: ANA** **Inscrição: 00318**

# A direct Mass Spectrometry method for determination of biomarkers in plasma samples

**Aline Rosa Fernandes (PG)[1*] , Thais Pontes Pereira Mendes (PQ)[1], Boniek Gontijo Vaz (PQ)[1] , Andréa Rodrigues Chaves (PQ)[1],**

**andrea_chaves@ufg.br; arosfernandes@gmail.com**

[1]*Instituto de Química, Universidade Federal de Goiás, Goiânia .*

Palavras Chave: Biomarkers, Catecholamines, RAM, PSI-MS.

## Highlights

A direct Mass Spectrometry method for determination of biomarker in plasma samples
The RAM-PSI-MS method was developed and allowed the analysis of dopamine, norepinephrine and epinephrine in complex samples, without any previous treatment, exhibiting accuracy and precision for ppb levels.

## Abstract

The dopamine, norepinephrine and, epinephrine are polar and hydrophilic molecules classified as catecholamines.[1] Determination of these biomarkers in biological samples present significant challenges to mass spectrometry method due to common suppression, poor sensitivity at residual levels and a narrow dynamic linear range. Here we modified the paper surface with restricted access material (RAM) and applied this as paper spray ionization (PSI) ambient source for MS. The developed coated paper was submitted to catecholamines in plasma sample determination. The RAM material have a hydrophilic barrier enables the small molecules to permeate through the hydrophobic part, while at the same time it excludes the macromolecules (by physical or chemical means, or a combination of both), which minimizes the adsorption of matrix proteins. [2]

The RAM coated paper was evaluated to protein exclusion, and showed efficiency of 99% that was verified by Bradford test. The RAM-PSI-MS developed method was linear in range of 10 to 1000 ppb with $R^2$ > 0,999. The LOQ and LOD were found in ppb levels (LOQ <5,4 ppb e LOD's <1,8 ppb). Precision and accuracy showed coefficients of variation and relative errors less than 5.8%. Recovery test results ranged between 96 and 99% (Table 1). The RAM-PSI-MS developed method analytical performance was compared to traditional paper substrate and ESI. The proposed methodology showed significant improvement on LOQ and method linearity values, showing a promising alternative for direct determination of these compounds in biological matrices by MS without derivatization or pretreatment of samples.

Table-1. Accuracy, intra-day precision and recovery obtained for dopamine and epinephrine in plasma samples after RAM-PSI-MS analysis.

| | Concentration (ppb) | Intra-day precision (%) | Accuracy (%) | Recovery (%) |
|---|---|---|---|---|
| **Dopamine** | 10 | 5.1 | 9.6 | 96 |
| | 600 | 2.6 | 1.6 | 97 |
| | 1000 | 1.7 | 1.7 | 99 |
| **Epinephrine** | 10 | 5.8 | 1.9 | 98 |
| | 600 | 1.2 | 0.1 | 98 |

1. Mendes et al., *Analytical Methods* 9 (**2017**) 6117.
2. Chaves et al., Journal of Chromatography A, 1218 (2011) 3376.

**Área: ANA** **Inscrição: 00603**

# Determinação dos aditivos presentes em cigarros e produtos derivados do tabaco por Espectrometria de Massas de Alta Resolução (nano-ESI-Orbitrap)

**Jéssica de S. Guedes (TC),[1] Natália G. de Figueiredo (PQ),[1] Simone C. Chiapetta (PQ),[1]**

jessica.siqueira@int.gov.br; guedesjessica@outlook.com

[1]*Laboratório de Tabaco e Derivados, Divisão de Química Analítica, Instituto Nacional de Tecnologia (INT)*

Palavras Chave: Tabaco, Cigarros, Aditivos, Flavorizantes, Aromatizantes.

## Highlights

Determination of additives present in cigarettes and tobacco products by High resolution mass spectrometry (nano-ESI-Orbitrap).
Twenty main flavoring additives were investigated in different types of cigarettes marketed in Brazil and all samples showed positive results for at least seven additives which increase health risk for smokers.

## Resumo/Abstract

Nas duas últimas décadas, as empresas de tabaco aumentaram os investimentos sobre a inclusão de aditivos nas formulações de cigarros, a fim de aumentar a prática tabagista e a iniciação do público jovem. Nesse contexto, tendo em vista o impacto dessas modificações na saúde dos usuários, a Anvisa publicou a RDC nº 14 de 2012, que dispõe, entre outras coisas, sobre a restrição do uso de aditivos nos produtos fumígenos derivados do tabaco. Apesar disso, o uso desses compostos ainda é permitido no Brasil por força de liminar concedida à Confederação Nacional da Indústria (CNI), tornando necessário avaliar os aditivos presentes nesses produtos. Assim sendo, este trabalho tem como objetivo principal comparar através de espectrometria de massas de alta resolução em modo negativo e positivo por infusão direta baseada em chip com fonte de ionização nanoelectronspray (nano-ESI-Orbitrap) a presença dos 20 principais aditivos de cigarros comercializados no Brasil, determinando seu *fingerprint*. Para tanto, extrações metanólicas foram realizadas em cigarros macerados de diversas marcas e, em seguida, empregou-se tratamentos estatísticos para avaliar a diferença entre os grupos examinados. Como resultado foi possível observar que todos os cigarros comerciais analisados apresentaram muitos dos aditivos inquiridos. Sendo esse número superior em cigarros flavorizados e com menor quantidade de nicotina e alcatrão. Vale destacar, que não foi observado na literatura trabalhos com anterioridade sobre a análise comparativa dos perfis de massas em cigarros comercializados no mercado brasileiro, indicando a sua necessidade de estudo.

**Área: ANA** **Inscrição: 00344**

# Berenil as a groove binding mode a probe a for DNA a interaction a process a evaluation

**Eduardo S. a Silva**[1*] a (IC), [a] **Alef D. a S. a Lima**[1] a (IC), a **Isis M. a Figueiredo a (PQ)**[1], a **Josué C. a C. a Santos a (PQ)**[1] a

eduardosampaio1994@gmail.com; a leflimaeq@gmail.com

*Instituto de Química e Biotecnologia, Universidade Federal de Alagoas.*

Palavras Chave: Berenil, DNA interaction, connection mode, *groove*, probe, molecular fluorescence

## Highlights

Berenil binds selectively to DNA by groove without fluorescence emission, thus, was explored as an alternative probe to avoid spectral interference, commonly observed in commercially available probes

## Resumo

Avaliar o modo de ligação ao DNA é um importante parâmetro para a compreensão do mecanismo de ação e desenvolvimento de fármacos seletivos a este alvo. Uma das formas para avaliar o modo de ligação ao DNA baseia-se em estudos de competição do composto de interesse com sondas fluorescentes *off-on*, as quais não apresentam fluorescência livres, contudo emitem na presença do DNA. Neste trabalho, utilizamos como sondas modelo o DAPI ($\lambda_{em}$ 420-540 nm), Hoeschst ($\lambda_{em}$ 410-500 nm) e Tioflavina T ($\lambda_{em}$ 400-500 nm). Quando o composto avaliado não emite fluorescência (livre ou ligado ao DNA) ou emite em uma faixa espectral com 540 < $\lambda_{máx}$ < 400 nm a utilização das sondas comerciais é uma estratégia indicada. Contudo, caso o composto emita de 400-550 nm a utilização destas sondas é inadequada devido a interferências espectrais. Desta forma, a utilização do berenil (BE, Fig. 1) torna-se uma estratégia atraente para avaliação e seu uso como sonda de marcação ainda não foi explorado, uma vez que não apresenta fluorescência livre ou ligado ao DNA. Neste trabalho, avaliamos a influência da proporção composto/DNA (1:5; 1:10 e 1:20) e da força iônica (NaCl 0; 25; 50 e 100 mM) em relação a capacidade do BE em deslocar as sondas comerciais utilizando $K_{SV}$ (constante de Stern-Volmer) para parâmetro de avaliação (Tabela 1). Em todos os sistemas avaliados o BE mostrou-se eficiente como sonda de marcação deslocando as sondas comerciais independente da salinidade do meio.

**Fig. a 1. a** Estrutura do Berenil**.**

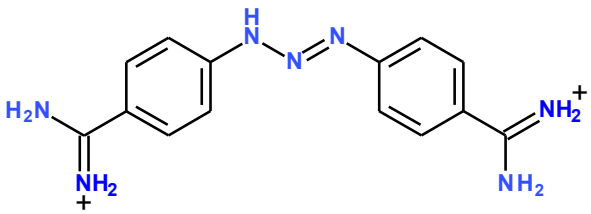


**Tabela a 1**. Dados calculados para a constante de Stern-Volmer ($K_{SV}$). A proporção sonda:DNA foi 1:10.

| Sonda | $K_{SV}$ (×10⁶ a M⁻¹) | |
|---|---|---|
| | **Sem a NaCl** | **Com a NaCl a (100 a mM)** |
| Hoechst | 8,80 ± 0,74 | 1,64 ± 0,11 |
| DAPI | 1,05 ± 0,08 | 0,20 ± 0,02 |
| Tioflavina T | 0,90 ± 0,02 | 0,19 ± 0,01 |

**Área: ANA** **Inscrição: 502**

# Fluorescent nanoprobes based on CdTe quantum dots for bioanalytical applications: determination of cationic protein

**Karolayne Rocha da Costa (IC)* e Josué Carinhanha C. Santos (PQ)**

karolaynerocha97@gmail.com

*Instituto de Química e Biotecnologia, Universidade Federal de Alagoas*

Palavras chave: *Pontos quântico, proteínas catiônicas, protamina, nanosondas fluorescentes*

## Highlights

Synthesis and characterization of nanofluorescent CdTe quantum dot functionalized with mercaptosuccinic acid with different diameters for determination of protamine (rich in arginine and lysine).

## Resumo/Abstract

Quantum dots (QD) são nanopartículas formadas por semicondutores cuja característica principal é sua alta fluorescência, sendo utilizados como sondas fluorescentes em sistemas variados.[1] Visando a determinação de proteínas catiônicas projetamos *quantum dots* de CdTe funcionalizados com ácido mercaptosuccínico ($pK_{a1}$ = 3,30 e $pK_{a2}$ = 4,60). Este ligante foi selecionado pois em pH > 5 a superfície do QD encontra-se preferencialmente com carga negativa e a interação com a proteína é favorecida. Portanto, os QDs produzidos foram aplicados na determinação de protamina, a qual é utilizada na purificação de DNA e neutralização do efeito da heparina.[2] O tempo de síntese foi o primeiro parâmetro avaliado para produção das nanosondas fluorescentes (Tabela 1). O método se baseia na supressão da fluorescência do QD (carga negativa) na presença da protamina (proteína catiônica), devido a formação de agregados do nanomaterial (Figura 1). A influência do pH foi avaliada de 5-11, tendo maior sensibilidade para $QD_{60}$ em pH 5. A melhor performance do método foi alcançada com tampão succinato a 25 mM e concentração do $QD_{60}$ fixada em 0,25 µM. A força iônica do meio não exerceu influência na sensibilidade até 50 mM (NaCl). O $QD_{60}$ foi fotoestável por até 2 h com exposição continua de radiação. A faixa linear foi de 0,25 a 2 mg $L^{-1}$ (50 a 400 nM) com limite de detecção de 0,08 mg $L^{-1}$ (16 nM). O método foi aplicado em amostras de protamina com recuperações superiores a 90%.

**Tabela 1.** Parâmetros dos QD sintetizados em função do tempo de síntese.

| Código | tempo (min) | $\lambda_{absorção}$ (nm) | $\lambda_{emissão}$ (nm) | diâmetro (nm) | $C_{QD}$ (µM) |
|---|---|---|---|---|---|
| $QD_{30}$ | 30 | 490 | 518 | 2,04 | 33,1 |
| $QD_{60}$ | 60 | 500 | 525 | 2,34 | 17,4 |
| $QD_{90}$ | 90 | 533 | 550 | 3,03 | 10,5 |

**Figura 1.** Princípio do método proposto.

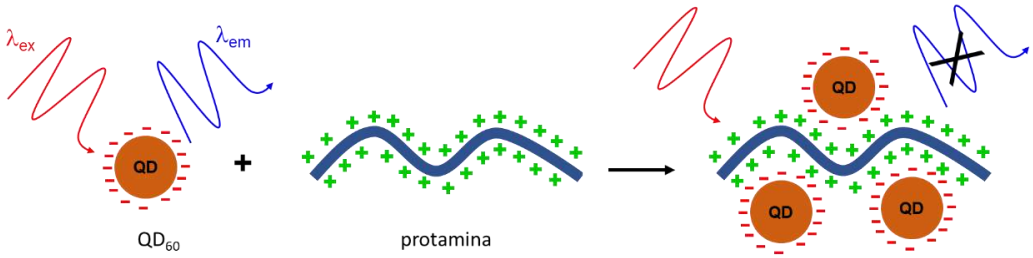


[1]CARVALHO, M. S. et al. *J. Braz. Chem. Soc.* 2017, 28(7) 1167-1176.
[2]ZHANG, Z. et al. *Analytical Biochemistry*, 2015, 478, 90–95.

**Área:** *ANA* **Inscrição:** 00907

# Determination of the total polyphenol content in wines and grape juice by spectrofluorimetry and comparison with the Folin-Ciocalteu method

**Stefanie Baldasso e Souza (IC),[1]* Ana Christina S. de Oliveira (IC),[1] Raquel A. Donagemma (PQ),[1] Flávia F. de Carvalho Marques (PQ).[1]**

**flaviamarques@id.uff.br; stefaniebaldasso@id.uff.br**

[1]*Departamento de Química Analítica, UFF*

Palavras Chave: *Total polyphenol, Gallic acid, Spectrofluorimetry, Folin-Ciocalteu method, Wine, Grape juice*

## Highlights

Phenolic compounds in wines and grape juice bring benefits to health.
Development of a new spectrofluorimetric method to polyphenol content determination and comparison with the Folin-Ciocalteu method.

## Resumo/Abstract

Wines and grape juice have antioxidant substances represented by the phenolic compounds in their composition, which are directly related to health benefits.[1] This work aimed the development of a spectrofluorimetric method (FM) to the determination of total polyphenol content (TPC) in wines and grape juice and its comparison with the Folin-Ciocalteu method (FCM). All studies were done in equivalent of gallic acid (mgGA $L^{-1}$) and the best condition achieved to the FM was: dilution of GA or sample in water:Britton-Robinson buffer (pH 8.5) 1:1 %v/v. To the FCM it was necessary to perform a colorimetric reaction with the Folin reagent before measurements. The analytical parameters of merit are in Table 1. Samples were analyzed by both methods (Table 2; Fig.1). The discrepancy between the results is due to some substances, such as ascorbic acid and carbohydrates, that interfere with the FCM.[2] The FCM is time-consuming, has experimental limitations and the need for complementary technique to remove interferers. The FM has faster response, as there is no sample preparation or derivatization reaction. Interference studies and separation techniques (HPLC-Fluo and CE-UV) are being carried out for comparison and better elucidation of the results.[3] As far as we know, this is the first FM for the determination of TPC in wines and grape juice and its comparison with the FCM.

**Table 1:** Analytical parameters of merit

| Parameters | Spectrofluorimetric method | Folin-Ciocalteau method |
|---|---|---|
| Linear range (mgEGA $L^{-1}$) | 0.01 – 0.2 | 0.2 – 2.4 |
| Regression line ($R^2 > 0.99$) | $y = 3035.3x + 13.2$[a] | $y = 0.1010x + 0.0097$[b] |
| Limit of detection (mgEGA $L^{-1}$) | 0.0029 | 0.048 |
| Limit of quantification (mgEGA $L^{-1}$) | 0.0097 | 0.16 |
| Recovery (n = 5) | 97-102% | 95-105% |
| Repeatability (RSD%, n = 9)[c] | < 3.62% | < 4.99% |
| Intermediary precision (RSD%, n = 18; 2 days) | < 4.49% | < 10.64% |

[a]y = fluorescence intensity (a.u.); x = mgEGA $L^{-1}$; [b]y = absorbance (a.u.); x = mgEAG $L^{-1}$;[c] RSD = Relative Standard Deviation

**Table 2:** Determination of total polyphenol content

| | Spectrofluorimetric method | Folin-Ciocalteau method |
|---|---|---|
| Red wine (n = 10) | 88 to 412 mgEGA $L^{-1}$ | 1389 to 3869 mgEGA $L^{-1}$ |
| Grape juice (n = 5) | 85 to 324 mgEGA $L^{-1}$ | 1274 to 3697 mgEGA $L^{-1}$ |

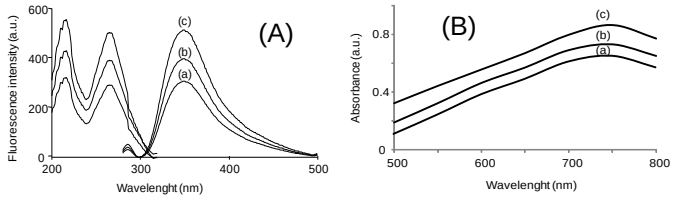


**Figure 1**: (A) Fluorescence spectra (FM) performed in a 10 nm passing spectral band and $\lambda_{exc}/\lambda_{em}$= 280/360 nm; (B) UV spectrum (FCM) of: (a) GA standard solution, (b) grape juice (dilution of 1:1000 v/v) and (c) red wine sample (dilution of 1:2000 v/v).

[1] LEEUW, R. *et al*. *J Food Compost Anal,* 36(1–2), 40–50, 2014.
[2] EVERETTE, J. D. *et al. J Agric Food Chem*, 58, 8139-8144, 2010.
[3] PADILHA, C.V.S. *et al*. *Food Chem*, 228, 106-115, 2017.

**Área: ANA** **Inscrição: 01059**

# Chemiluminescent flow system for the determination of complexation capacity in opacity solutions: an automatic procedure

**Manoel de Jesus de Aquino Lima (PG),[1] Boaventura Freire dos Reis (PQ),[1] Marcos Yassuo Kamogawa (PQ),[2*]**

**aquinolima@usp.br; kamogawa@usp.br**

*[1]Centro de Energia Nuclear na Agricultura, CENA-USP; [2]Escola Superior de Agricultura Luiz de Queiroz, ESALQ-USP*

Palavras Chave: *Complexation capacity, Chemiluminescent, Flow analysis, Arduino*

## Highlights

A flow batch and multicommutation automatic chemiluminescent system;
Determination of the complexation capacity in aqueous media with high opacity;
Complexation capacity of milk and humic substance.

## Resumo/Abstract

Uma dificuldade em titulações colorimétricas é a identificação do ponto final em soluções/suspensões que apresentam uma forte coloração, impossibilitando o uso de indicadores convencionais. Com o objetivo de estabelecer novas estratégias para determinações mais robustas e eficientes nestes meios, é apresentado um sistema titulométrico com ponto final quimiluminescente para soluções com alta opacidade.[1] O procedimento é baseado na estratégia de busca binária aliada aos métodos em fluxo (multicomutação em fluxo e flow-batch) com detecção quimiluminescente. O sistema é baseado no efeito catalítico do cobre na reação de oxidação do luminol por peróxido de hidrogênio. O cobre iônico, não complexado pelas substâncias húmicas ou pelas proteínas do leite, catalisa a reação peroxido/luminol. O controle dos processos de acionamento dos dispositivos dosadores de fluídos e a aquisição dos sinais gerados pelo sistema de detecção, foram realizados por um Arduino Due (Figura 1).

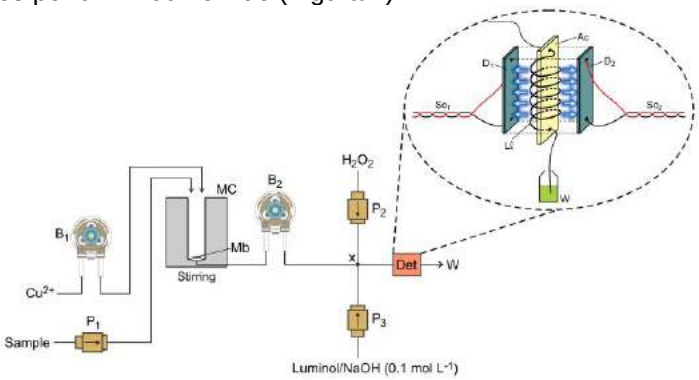


Figura 1. Módulo de análise flow-batch para determinação da capacidade complexante.

Em condições otimizadas, o sistema foi capaz de determinar a capacidade complexante em soluções coloridas dopadas com DDTC e EDTA. A recuperação analítica dos complexantes modelo em leite (diluído 10 vezes) e leonardita (400 mg $L^{-1}$) foi de 114 ± 4 e 102 ± 2, respectivamente.

Referências:
1. F. Kenny, R. B. Kurtz. Anal. Chem. 24 (1952) 1218.

Agradecimentos: CNPq (165478/2015-2) e FAPESP (2011/23498-9)

**Área: ANA** **Inscrição: 01078**

# Desenvolvimento de uma cela de fluxo para detecção de quimiluminescência empregando fotodiodo com detector

**Oziel R. Marinho (PG),[1*] Manoel de Jesus de Aquino Lima (PG),[2] Boaventura F. Reis (PQ).[2]**

**student.quimica@gmail.com; reis@cena.usp.br**

*[1]Universidade Federal de São Carlos, UFSCar; [2] Centro de Energia de Energia Nuclear na Agricultura, CENA - USP*

*Palavras Chave: Quimiluminescência, Análises em fluxo, Multicomutação em análise em fluxo, Instrumentação e automação.*

## Highlights

Development of a flow cell for chemiluminescence detection using photodiodes as detector

A flow cell with a new design for the detection of chemiluminescence.
A cost effective multicommuted flow analysis setup for the detection of chemiluminecense.
An environmental friendly flow system for the detection of chemiluminescence.

## Resumo/Abstract

Metodologias analíticas baseadas em quimiluminescência tem como atrativo alta sensibilidade, empregando equipamento de detecção de baixo custo. A emissão de radiação em reações quimiluminescente, assemelha-se a um *flash*. Em vista disso, o emprego de sistemas automáticos (por exemplo, análise em fluxo) para sua detecção é essencial. A cela de fluxo é o elemento principal, pois a reação deve ocorrer dentro dela. Celas de fluxo com canais na forma de serpentina ou em espiral são as mais usadas. Neste trabalho, apresentamos uma cela de fluxo para detecção de quimiluminescência com geometria ainda não utilizada. A cela foi moldada com um tubo de vidro com entradas de fluidos frontais, para melhorar a mistura. A reação de oxidação do luminol ocorre dentro da cela. Nas extremidades, foram encaixados guias de onda, os quais coletam parte da radiação emitida e transportam para os fotodetectores. A viabilidade foi averiguada usando a reação de oxidação do luminol com hipoclorito de sódio em meio alcalino e um módulo de análise baseado no processo de multicomutação em análise em fluxo, usando mini-bombas solenoide para propulsão de fluídos. O controle do módulo de análise e a aquisição de dados foram realizadas empregando o microcotrolador Arduino Due. A detecção fotométrica foi realizada usando dois fotodiodos e um amplificador operacional, configurado como somador de sinal. Os testes com soluções de hipoclorito mostraram resposta linear a partir da concentração de 1 mmol$L^{-1}$, usando um volume de amostra de 80 µL por determinação.

Agradecimentos: CNPq, CAPES, FAPESP, INCTAA e FAPEAM.

**Área: ANA** **Inscrição: 01131**

# Wetting film liquid-liquid microextraction in a sequential injection system for spectrofluorimetric determination of bisphenol A in tap waters

**Samara Soares (PG), Carina de Fátima Nascimento* (PG), Fábio R. P. Rocha (PQ).**

**soaressamara@usp.br; cfnascimento@cena.usp.br**

*Centro de Energia Nuclear na Agricultura, Universidade de São Paulo*

*Keywords: Flow analysis, Liquid-phase microextraction, Emerging pollutants, Bisphenol A, 1-Octanol*

## Highlights

A simple strategy for liquid-liquid microextraction of bisphenol A. High enrichment factor with only 30 µL of the extractor solvent. Analytical determination based on the native fluorescence of the analyte.

## Resumo/Abstract

Bisphenol A (BPA) shows estrogenic effects for humans and concentrations in the µg $L^{-1}$ range have been found in tap waters of some countries, including Brazil, thus requiring fast and reliable procedures for its monitoring. A flow-based liquid-liquid microextraction procedure was developed for separation and preconcentration of BPA, aiming at the determination based on its native fluorescence, which significantly increases in organic media. Extraction was carried out in a sequential injection system (Figure 1) by means of a film of the extractor (1-octanol) reproductively formed on the walls of a hydrophobic tube (wetting film approach), followed by elution of the extract with ethanol. An enrichment factor of 15.5 was achieved with only 1.5 mL of sample and 30 µL of 1-octanol. The consumptive index of 0.097 mL and concentration efficiency of 2.6 $min^{-1}$ indicate that the proposed approach is highly efficient for analyte preconcentration. A linear response was observed from 5.0 to 100 µg $L^{-1}$ with a detection limit of 1.8 µg $L^{-1}$, sampling rate of 10 $h^{-1}$ and coefficient of variation of 2.3% (n = 10). Recoveries of BPA spiked to tap water samples were in the range 96-108%. The procedure was successfully applied to tap water samples (BPA concentrations within 6.7 and 13.4 µg $L^{-1}$) and the results agreed with those obtained by the HPLC reference method at the 95% confidence level. Because analyte derivatization and the use of toxic solvents are avoided, the proposed procedure is a more environmental friendly alternative for BPA determination.

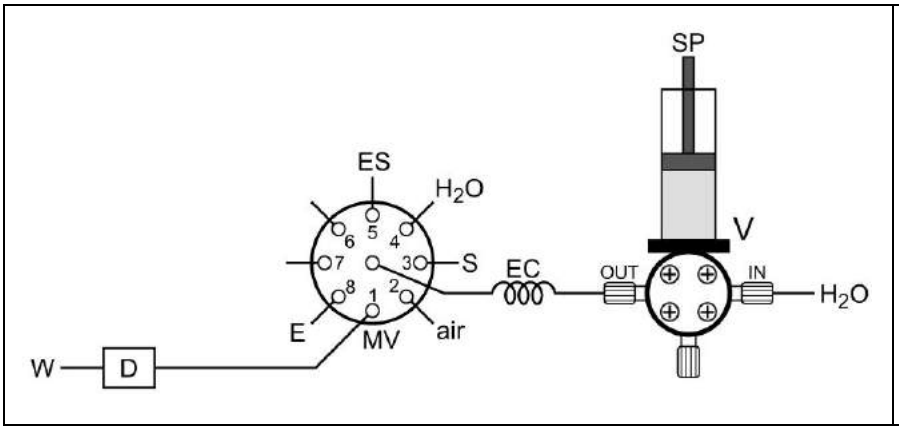


**Figure 1.** Flow diagram of the SIA system for wetting film liquid-liquid microextraction. S: sample; E: ethanol; ES: extractor solvent (1-octanol); EC: extraction coil; W: waste vessel; SP: syringe pump; MV: multiposition valve; V: three-way solenoid valve; D: Spectrofluorometer equipped with a quartz flow cuvette.

The authors thank FAPESP, CAPES, and CNPq for the fellowships and financial support.

**Área: ANA** **Inscrição: 01199**

# Procedimento limpo baseado em análises em fluxo para extração on-line de propoxur em amostras de carne

**Gabriel Pereira Bragaia (IC), Wanessa R. Melchert (PQ). gabrielbragaia@usp.br**

*Escola Superior de Agricultura "Luiz de Queiroz" - ESALQ /USP – Av. Pádua Dias, 11; Piracicaba/SP*

Palavras Chave*: Propoxur, On-line extraction, Flow injection analysis, Cloud point, Spectrophotometry, Clean chemistry.*

## Highlights

A clean flow-based procedure for on-line extraction of propoxur in meat samples

A simple, fast, greener and inexpensive procedure;
Clean on-line extraction of propoxur in flow injection analysis;
Minimization of reagent consumption and residue generation.

## Resumo/Abstract

O propoxur (2-isopropoxifenil-N-metilcarbamato) é utilizado em animais de corte e leiteros no controle de pulgas e moscas que pode permanecer no tecido muscular mesmo após o abate. Procedimentos de extração de propoxur da carne bovina são morosos e utilizam grandes volumes de solventes orgânicos (25-200 mL de acetona ou acetonitrila por extração). O presente trabalho visa desenvolver um procedimento limpo para extração on-line de propoxur. Para tanto, foi utilizado um sistema de análises em fluxo e pré-concentração em ponto nuvem para a quantificação do propoxur. Amostras de carne bovina moídas (*ca.* 0,4000 g) foram acondicionadas dentro de colunas (ponteiras de micropipetas) sob agitação constante. Após percolação da solução extratora (água, vazão 1,1 mL $min^{-1}$), 5 mL do extraído foram recolhidos em tubo tipo falcon e a pré-concentração em ponto nuvem foi realizada com 0,5 mL de p-aminofenol 6,9x$10^{-3}$ mol $L^{-1}$, 150 µL de NaOH 0,25 mol $L^{-1}$ e 1 mL de Triton X-114 7%. A mistura foi aquecida (40 °C por 15 minutos) e a separação das fases foi acelerada por centrifugação (15 minutos). A fase aquosa foi removida por aspiração e a fase rica em surfactante foi diluída a 600 µL de etanol. As medidas espectrofotométricas foram realizadas em 637 nm. Estudos de adição e recuperação foram realizados com adição de 2,0x$10^{-5}$ ou 3,0x$10^{-5}$ mol $L^{-1}$ de propoxur e recuperações foram obtidas entre 79-93%, demonstrando as potencialidades aos preceitos da química limpa.

**Área: ____ANA_____** **Inscrição: 01213**
*(Inserir o número de inscrição do autor que fez a submissão)*

# Real-Time Monitoring of Mono-, Di-, Triglycerides and FAME Composition by Low-Field $^1$H NMR and NIR Spectroscopy During Transesterification Reaction of Vegetable Oils

**Diego Galvan (PG),[1]* Leticia Magalhães de Aguiar (PG),[1] Jarbas J. R. Rohwedder (PQ),[2] Dionisio Borsato (PQ),[1] Mario Henrique M. Killner (PQ).[1]**

**diegogalvann@hotmail.com.**

[1]*Departamento de Química, Universidade Estadual de Londrina (UEL);*
[2]*Departamento de Química, Universidade Estadual de Campinas (UNICAMP).*

Keywords: *Nuclear magnetic resonance, Near infrared spectroscopy, Partial least squares, Diglycerides, Monoglycerides, Mobile compact $^1$H NMR.*

## Highlights

A new approach-based on LF-$^1$H NMR and NIR spectral data offers several advantages for online monitoring of major and minor compounds composition during the transesterification reaction to produce biodiesel.

## Abstract

Nowadays, most of the biodiesel commercialized in the world is produced by the transesterification reaction of vegetable oils with methanol and basic catalysis. Understanding the reaction kinetics and controlling its optimum progress are crucial concerns to improve the final quality of the fuel and to reduce the production costs. In this work, LF-$^1$H NMR (43 MHz) and NIR spectroscopic techniques were applied to directly quantify, by different chemometric calibration models (PLS), the molar percentage of triglycerides (TG), diglycerides (DG), monoglycerides (MG) and fatty acids methyl esters (FAME) present in the reaction medium. For this purpose, High Field-$^1$H NMR (400 MHz) was applied as a reference methodology to build the PLS models with LF-$^1$H NMR and NIR. Fig. 1 shows all the composition profile of major and minor compounds, determined by HF-$^1$H NMR, as reactions proceeds. This data was then used as Y reference matrix to build the PLS calibration models applying LF-$^1$H NMR and NIR spectral data as X matrix. Most of the relative errors found for the determination of major and minor compounds by the PLS models were lower than 10% when applied to validation samples. In this way, these 2 simple methodologies (LF-$^1$H NMR and NIR) could be equally applied to monitor the transesterification of vegetable oils to produce biodiesel. The key advantage of these techniques when compared to more stablished ones (HF-$^1$H NMR and Chromatographic techniques) is that the measurements are simple, fast and no sample preparation is required.

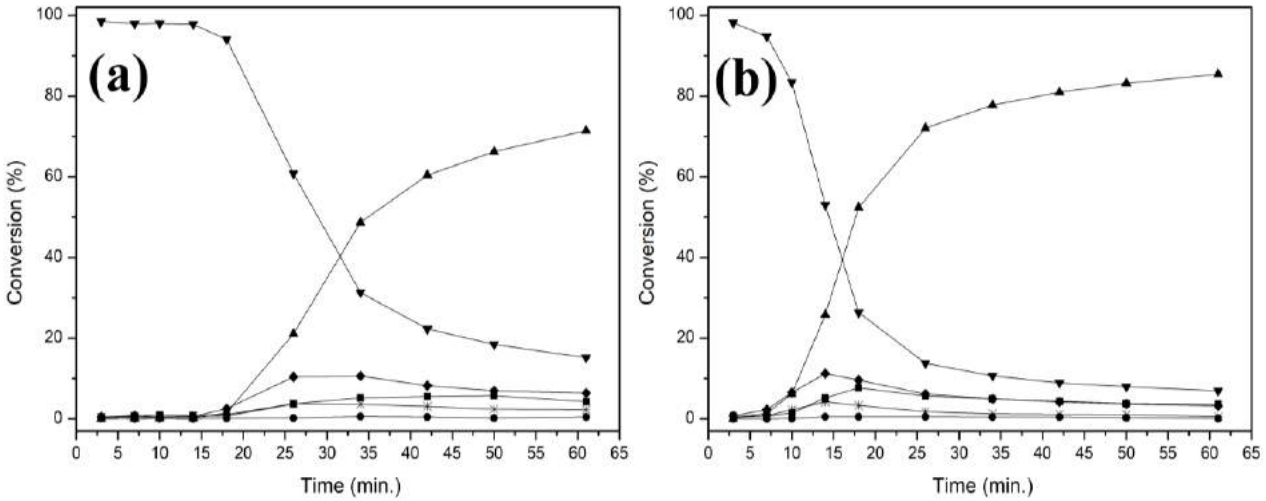


**Figure 1** – Kinetic profile of transesterification reactions obtained by HF-$^1$H NMR using 0.50% **(a)** and 0.75% **(b)** of NaOH (m/m). Where: ▼ TG, ♦ 1,3–DG, ❊ 1,2–DG, ● 2–MG, ■ 1–MG, ▲ FAME.

**Área: ANA** **Inscrição:00392**

# Determination of lipid bioactive compounds in yellow, brown and black mustard seeds

**Antonio Eduardo Nicácio (PG),[1] Carina Alexandra Rodrigues (PG),[1] Jesuí Vergílio Visentainer (PQ),[1] Liane Maldaner (PQ)[1]**

**eduardo.nica@gmail.com**

[1]*Departamento de Química da Universidade Estadual de Maringá*

Palavras Chave: *Tocopherols, Phytosterols, Fatty acids, Carotenoids, Mustard seeds.*

## Highlights

- Polyunsaturated fatty acids, γ-tocopherol, campesterol, and β-sitosterol were found in mustard seeds.
- Mustard seeds presented low total carotenoids content.

## Resumo/Abstract

Mustard seeds, traditionally used as temper and seasoning due to its pungency and bitterness, are also a good source of edible oil, containing different bioactive compounds, such as, fatty acids, phytosterols, tocopherols and carotenoids. These lipid bioactive compounds have been correlated to health beneficial effects preventing and combating chronic diseases in regular dietary intakes. In this work, three different species of mustard seeds (*Brassica alba, Brassica juncea and Brassica nigra*) were investigated aiming the determination of the fatty acid composition, phytosterols (campsterol, stigmasterol, β-sitosterol), tocopherols (α-, δ-, γ-, tocopherol) and total carotenoids content in the respectively oil extracts. Phytosterols and tocopherols were determined by ultrasound-assisted saponification coupled with gas chromatography-flame ionization detector (GC-FID) and carotenoids were determined by ultraviolet-visible spectrophotometry (UV-Vis). Black and brown mustard seeds showed similar fatty acids composition, and in all the mustard seeds, the polyunsaturated fatty acids were found in higher amounts than saturate fatty acids. Among the phytosterols and tocopherols analyzed, only γ-tocopherol, campesterol, and β-sitosterol were found in the three species of mustard seeds evaluated. Furthermore, the three mustard seeds presented low total carotenoids content.

**Área: ANA** **Inscrição: 00629**

# Development and validation of quantitative NMR method for illegal pesticides

**Luana C. Crocoli (PG),[1*] Rafael S. Ortiz (PQ),[2] Sidnei Moura (PQ),[1]**

**lccrocoli@ucs.br**

*[1]Laboratory of Biotechnology of Natural and Synthetic Products - University of Caxias do Sul, RS, Brazil;*
*[2] Rio Grande do Sul Technical and Scientifical Division, Brazilian Federal Police, Porto Alegre, Rio Grande do Sul, Brazil.*

Keywords: *Smuggling, Pesticides, qNMR, Validation*

## Highlights

Brazil is a large consumed of legal or illegal pesticides; qNMR: simple, fast and non-destructive methodologies; efficient and safe analytical methods to elucidate the composition of formulated products.

## Resumo/Abstract

Since the 1950s, the consumption of agrochemicals has increase disorderly in Brazil. In this way, the smuggling of these products has also increased exponentially. According to the Brazilian's Federal Police report, in 2016 the increase of pesticides smuggling was aroud 188% in relation to 2015[1]. However, smuggled agrochemicals showed characteristics unknown from the chemical, physical and biological point of view. Thus, these products should be characterize. The qNMR is a simple, fast and non-destructive methodology that allows a simultaneous qualification and quantification of various substances (target and non-target)[2]. Therefore, the objective of the present work is to develop and validate a quantitative method by $^1$H NMR for analysis of smuggled agrochemicals seized by the Federal Police. The validation was performer according to ABNT NBR 14029: 2016 and the Association of Official Analytical Chemists (AOAC) using standards of azoxystrobin, imidacloprid, λ-cyhalothrin, tebuconazole and thiamethoxam, which were determinate simultaneously. All analyzes were performed on a Fourier300 Bruker NMR equipment, using $CDCl_3$ as solvent. To verify the method viability, there were tested 08 commercial samples as well as 02 products seized. The mean validation results are show in Table 1.

Table 1: Average results of the validation parameters evaluated

| | Selectivity (ppm) | Linearity ($R^2$) | LOD ($mg.L^{-1}$) | LOQ ($mg.L^{-1}$) | Precision (%) | Recovery (%) |
|---|---|---|---|---|---|---|
| Azoxystrobin | 3.77 | 0.9999 | 89.19 | 269.12 | 2.351 | 101.75 |
| Imidacloprid | 4.56 | 0.9998 | 106.02 | 321.89 | 1.019 | 99.35 |
| λ-Cyhalothrin | 1.23 | 0.9976 | 86.34 | 260.35 | 2.525 | 97.79 |
| Tebuconazole | 1.04 | 0.9993 | 80.12 | 244.74 | 1.822 | 98.63 |
| Thiamethoxam | 3.06 | 0.9994 | 79.33 | 235.61 | 1.705 | 100.34 |

About analyzes of the commercial pesticides, all showed the amount of active principle specified by the manufacturer. However, the smuggled products presented difference ranging 20-26% less than the concentration specified. Thus, the method developed is applicable to identify the active principles of commercial pesticides as well as to differentiate between those seized.

Acknowledgement:
UCS, Capes, INCT Forense 465450/2014-8 for support research

References:

1. Brazil. Federal Revenue. Customs Balance 2016. (2016). Available at: http://idg.receita.fazenda.gov.br/dados/resultados/aduana. (Accessed: 3rd October 2017)
2. Malz, F. & Jancke, H. Validation of quantitative NMR. J. Pharm. Biomed. Anal. 38, 813–823 (2005).

**Área: ANA** **Inscrição: 00667**

# Polydiacetylene/triblock copolymer nanosensor for the detection of lidocaine in the presence of cocaine adulterants

**Thaís S. Soares (IC)[1], Francielle O. Chagas (PG)[1], Pamela R. Patrício (PQ)[1], Adriano O. Maldaner (PQ)[3], Luís H. M. da Silva (PQ)[1], Maria C. Hespanhol (PQ)[1,2]**

**tha.soares09@gmail.com**

*[1]Grupo de Química Verde Coloidal e Macromolecular (QUIVECOM), [2]Grupo de Análises e Educação para a Sustentabilidade (GAES), Instituto Nacional de Ciências e Tecnologias Analíticas Avançadas (INCTAA), Departamento de Química, Centro de Ciências Exatas e Tecnológicas, Universidade Federal de Viçosa – MG. [3]Instituto Nacional de Criminalística, Polícia Federal, Brasília-DF*

Key-word: Optical nanosensor, Cocaine, Colorimetric transition, Adulterants, Forensic chemistry.

## Highlights

New optical nanossensor for detection adulterant cocaine. Intermolecular interaction between PCDA nanostructures and lidocaine. PCDA/L64 nanostructures showed efficient discrimination between lidocaine and other adulterants.

## Abstract

Cocaine is one of the main psychostimulant substances used worldwide[1], its use causes a variety of toxic effects that can be intensified by the adulteration of the drug with substances like lidocaine. Determining the main compounds added to the drug is essential to formulate restriction actions on the sale of these products. Polydiacetylenes (PDAs) are alternating double and triple bond polymers, formed from diacetylene monomers in an addition reaction induced by ultraviolet radiation[2]. Changes in their optical and electronic properties have motivated researchers to use PDAs as sensors of a diverse nature. This work presents application of optical nanosensor (ON) of PDA made of 10,12-pentacosadiynoic acid (PCDA) monomers self-assembled in a amphiphilic mid formed by aqueous solution of triblock copolymer (L64) for detection of lidocaine adulterant. Fig. 1 shows that the nanosensor does not present color change from blue to red for benzocaine (BZ), caffeine (CF), diltiazen (DT), phenacetin (FN), hydroxyzine (HD), levamisole (LV), and procaine (PR) adulterants. However, in the presence of the lidocaine (LD) occurs change in the color from blue to red. Fig.2 shows the color transition when the sensor is in contact with the lidocaine pure and in the presence of others cocaine adulterants. Even in the presence of adulterants separately or even all together (AP) the sensitivity of the sensor to the lidocaine is not affected.

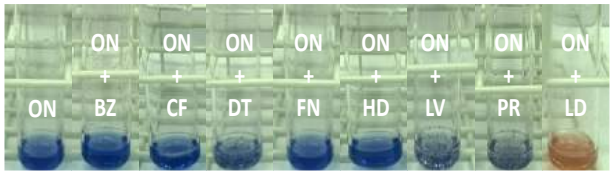


**Fig.1** Color appearance of optical nanosensor in the presence of the adulterants distinct

**Fig.2** Color appearance of optical nanosensor in the presence of the adulterants distinct + lidocaine

References
[1]GOSTIC, T; KLEMENC, S; STEFANE, B. Forensic Science International, Slovênia, 187 (2009).
[2]OKADA, S.; PENG, S.; SPEVAK, W.; CHARYCH, D Acc. Chem. 229 (1998).

Acknowledgements: CAPES/Ciência Forense, INCTAA, FAPEMIG, and CNPq

**Área: ANA** **Inscrição: 00088**

# Novel analytical method using reversed-phase dispersive liquid-liquid microextraction for determination of metallic contaminants in edible vegetable oils.

**Eder L. M. Flores (PQ)[1], Murilo O. Beato (IC)[1], Oldair D. Leite (PQ)[1], Cristiane Canan (PQ)[2], Rochele S. Picoloto (PQ)[3], Aline H. Ferreira (PG)[4*].**

**eder@utfpr.edu.br; alinehespanhol@hotmail.com.**

*[1]Departamento de Química, UTFPR - Campus Medianeira; [2]Departamento de Tecnologia de Alimentos, UTFPR - Campus Medianeira; [3]Departamento de Química, UFSM; [4]Programa de Pós-graduação em Processos Químicos e Biotecnológicos, UTFPR – Campus Toledo.*

Palavras Chave: *sample preparation, microextraction, metallic contaminants, edible oil.*

## Highlights

- Novel analytical method using reversed-phase liquid-liquid dispersive microextraction (RP-DLLME);
- Determination of metallic contaminants (Cu, Ni and Mn) in vegetable oils.

## Resumo/Abstract

In this work, a method based on reversed-phase dispersive liquid-liquid microextraction (RP-DLLME) as sample preparation for the extraction and pre-concentration of Cu, Mn and Ni in edible vegetable oils (chia, flaxseed, sesame, safflower and canola) was developed. For the proposed sample preparation method, a solvents mixture of n-propanol (dispersant, 700 µL) and 1.0 mol $L^{-1}$ $HNO_3$ (extractant, 300 µL) was injected into the sample (10.0 g) preheated to 80 °C. After flasks were centrifuged (10 min at 5600 g), the sample phase was partially withdrawn using a pipette, and the aqueous phase was transferred to volumetric flask and volume was completed to 5.0 mL, for further elemental determination by F AAS. Some parameters, such as type and volume of dispersive and extraction solutions and $HNO_3$ concentration (extraction solution), were evaluated. During the optimization of RP-DLLME, samples of chia oil were spiked with Conostan® S21+K oil standard. Analytes determination was performed by F AAS using external calibration with aqueous reference solutions. The accuracy was evaluated by recovery tests, which ranged from 92 to 100%, with relative standard deviation lower than 4% for all analytes. Then, the proposed method was applied for various samples of vegetable edible oils. Thus, comparing to conventional methods for metallic contaminants determination in edible oils, RP-DLLME combined to F AAS can be considered simple, low cost, low consumption of reagents and provides LOQs significantly below the limits established by Brazilian legislation for these elements in biodiesel.

**Acknowledgements**

The authors are grateful to Conselho Nacional de Desenvolvimento Científico e Tecnológico (CNPq), Coordenação de Aperfeiçoamento de Pessoal de Nível Superior (CAPES), and Fundação Araucária de Apoio ao Desenvolvimento Científico e Tecnológico do Estado do Paraná for supporting this work.

**Área: ANA** **Inscrição: 00368**

# Development of method for direct multi-elemental analysis of whisky using total reflection X-ray fluorescence

**Ednilton M. Gama (PG),[1,2] Roberta P. Matos (PQ),[2] Clésia C. Nascentes (PQ),[1] Guilherme D. Rodrigues (PQ)[1].**

**ednilton.gama@ifnmg.gov.br**

[1] *Department of Chemistry, Federal University of Minas Gerais, 31270-901Belo Horizonte, MG, Brazil*
[2]*Federal Institute of North of Minas Gerais, - IFNMG Campus Almenara, Brazil*

Keywords: *TXRF, whisky, inorganic constituents, alcoholic beverage.*

## Highlights

TXRF was applied to quantify 15 analytes in whiskys.

No sample preparation was required.

The proposed method is simple and fast.

LOQ obtained are adequate to determine Pb and As according Brazilian legisltation

## Abstract

This work describes a method for direct analysis to quantify S, Cl, K, Ca, Ti, V, Mn, Fe, , Cu, Zn, As, Br, , Rb, Ba and Pb in whiskys by total reflection X-ray fluorescence (TXRF). In the optimization step were evaluated the influence of reading time (100, 250, 500 and 1000 s), internal standard-IS (Ga, Y, Ge) and IS concentration (1 and 10 mg $L^{-1}$) using Johnnie Walker Red Label whisky spiked with contaminants indicated in Brazilian legislation[1] (200 µg $L^{-1}$ Pb and 100 µg $L^{-1}$ As). Samples with and without spike were analyzed directly and in the optimized conditions the recoveries and relative standard deviations (RSD%) found for Pb and As were 98% and 3% and 102 % and 2%, respectively. The method was applied to 23 whisky samples of three differents brands. The concentration ranges (mg $L^{-1}$) for the studied analytes were: S (0.9 – 1.5); Cl (0.02 - 2); K (0.7 - 7); Ca (0.26 - 15); Ti (0.01 – 2.3); V (<LD – 0.1); Mn (0.003 – 0.16); Fe (0.2 - 5.4); Cu (0.04 - 0.9); Zn (0.01 – 0.2); As (<LD - 0.01); Br (0.003 – 0.01); Rb (<LD – 0.01); Ba (<LD – 9.4) and Pb (<LD - 0.2). Most of the whisky samples had As and Pb concentrations below of the established by Brazilian legislation[1]. The developed method is simple, fast, consumes few reagents and allows multi-elemental determination.

**Acknowledgements:** IFNMG, FAPEMIG, CNPq and PPGQ-UFMG.

**References:**

**1** ANVISA - National Agency for Sanitary Vigilance. RESOLUTION - RDC No. 42 of 29 August 2013. It has about MERCOSUR Technical Regulation on Maximum Contaminant Inorganic Chemicals in Food. DOU Brazil. Brasilia, 30 August 2013. Section 1, p.34-35.

**Área: ANA** **Inscrição: 00369**

# Determination of bioavailability of nutrients in soil by extraction procedures and total reflection X-ray fluorescence

**Roberta P. Matos (FM)[1*], Ednilton M. Gama (PG)[1,2], Cláudia C. Windmöller (PQ)[2], Clésia C. Nascentes (PQ)[2]**

*[1]Federal Institute of North of Minas Gerais – IFNMG, Campus Almenara; [2]Department of Chemistry, UFMG*

***e-mail: roberta.matos@ifnmg.edu.br**

Keywords: *TXRF, Bioavailability, Nutrients, Soil, Single Extractions*

## Highlights

TXFR and single extraction were used to determine the bioavailability of Ca, S, Cu, Mn, Zn and Fe in soils.

The bioavailability depends of the soil characteristics.

The method is simple and fast.

## Abstract

In this work the bioavailability of Ca, S, Cu, Mn, Zn and Fe in soil fractions was determined. The A and B horizons of three soils (Red-Yellow Latosol, Red Latosol and Argisol) were analyzed. Total reflection X-rayfluorescence (TXRF) and three extractants (ultrapure water, phosphate buffer (0.1 mol $L^{-1}$ - pH 7.0) and NaOH 0.1 mol $L^{-1)1}$ were employed. The parallel single extraction procedures were adapted from the sequential extraction method[1,2]. For analyte quantification by TXRF, 1.0 mg $L^{-1}$ Ga was used as internal standard and data acquisition time was 1000 s. Total content of nutrients was determined by inductively coupled plasma mass spectrometry (ICP-MS) after *aqua regia* digestion. The total concentrations (mg $kg^{-1}$) of analytes were: Ca (100.0 to 200.0), S (200.0 to 400.0), Cu (0.80 to 2.58), Mn (22.0 to 74.0), Zn (6.20 to 20.90) and Fe (1.81 to 49.60 %). The concentration ranges (%) of nutrients in soil fractions are shown in Table 1. The most bioavailable nutrients were Ca and S. In general, Red Latosol presented higher bioavailability of nutrients. The proposed method to assess bioavailability is simple, multilemental and inexpensive.

**Table 1.** Concentration ranges (%) of Ca, S, Cu, Mn, Zn and Fe in soil fractions.

| | Elements | | | | | |
|---|---|---|---|---|---|---|
| Fractions | Ca | S | Cu | Mn | Zn | Fe |
| Water-soluble (%) | 4.42 -11.90 | 0.01 - 4.52 | 0.33 - 1.68 | 0.22 - 1.46 | 1.02 - 4.03 | 0.01 - 0.08 |
| Exchangeable (%) (Phosphate buffer) | 8.49 -37.01 | 11.73 - 30.60 | 2.67 - 9.43 | 0.25 - 2.06 | 0.68 - 13.73 | 0.02 - 0.18 |
| Organic matter-bound (%) (NaOH 0.1 mol $L^{-1}$) | 1.10 -14.35 | 17.80 - 49.17 | 8.62 - 26.87 | 0.01 - 2.86 | 1.26 - 7.46 | 0.06 - 8.26 |

**Acknowledgements:**
IFNMG, DQ-UFMG, CNPq, FAPEMIG

**References:**
1 Tolu J, Thiry Y, Bueno M, Jolivet, C, Potin-Gautier M, Hecho IL. Science of the Total Environmental, 479-480 (2014) 93-101.
2 Wang J, Li H, Li Y, Yu J, Yang L, Feng F, Chen Z, Biol. Trace Elem. Res., 156 (2013) 367-375.

**Área: ANA** **Inscrição: 00377**

# APPLICATION OF FLUORESCENCE OF X-RAYS (EDXRF) IN ATMOSPHERIC BIOMONITORING USING TREE BARK

**Manoel T. de Oliveira (TM),[1] Carla M. de O. Almeida (TM),[1] Lucas S. S. de Araújo (IC),[2] Luciana B. Oliveira (PQ),[1]* Diego L. Coriolano (PQ),[1] Márcio R. R. Gomes (PQ).[3]**

**fmanuel2009.2010@hotmail.com; luciana.bitencourt.ifs@gmail.com**

*[1]Instituto Federal de Sergipe, campus Lagarto, IFS; [2] Instituto Federal de Sergipe, campus Socorro, IFS; [3]Instituto Federal de Alagoas, campus Penedo, IFAL*

Key words: *EDXRF, Bark tree, Atmospheric Biomonitoring, Pollution.*

## Highlights

In this study, biomonitoring with tree bark as an instrument to measure atmospheric pollution was based on the investigation of the concentrations of Fe, V, Cr, Mn, Co, Ni, Cu, Zn, Mg, P, S, Cl, K, Ca, Al, Cd and Ba, from a residential area, after the closure of the activities of a cement production industry.

## Resumo/Abstract

Biomonitoring is an alternative technique that uses living organisms to check for changes in the environment caused by water, air and soil pollution. Based on atmospheric emissions located in the region of Estiva, Nossa Senhora do Socorro, Brasil (where there is a portland cement industry, whose activities were closed about a year ago), the objective of this work was to collect samples of tree bark to verify the spatial variability of some chemical elements present in the area. The results obtained from the chemical analyzes can be used to make decisions regarding raw materials used in the processes such as cement production, review of procedures and measures in relation to the protection of the environment and human health. For the analytical control of the samples, the concentrations of the elements Fe, V, Cr, Mn, Co, Ni, Cu, Zn, Mg, P, S, Cl, K, Ca, Al, Cd and Ba were investigated. In order to control the analytical quality, for precision and accuracy, replicates of the reference materials NIST 1515 and NIST 1573, were analyzed by means of Energy Dispersion X-Ray Fluorescence Spectrometry (EDXRF), characterized as one of the techniques the most important multielemental analyzes for the evaluation of natural ecosystems, mainly because it allows the determination of elemental chemical compositions of samples from different matrices with high precision and accuracy, added to the relative ease of sample preparation, avoiding contamination of the same.

Tabela 1: Comparison between certified values and actual samples determined using EDXRF.

| Element | NIST1515 | NIST1573 | A0 | A1 | A2 | A3 | A4 | A5 | A6 | A7 | A8 | A9 |
|---|---|---|---|---|---|---|---|---|---|---|---|---|
| Fe (ppm) | 344.551 | 364.767 | 439.222 | 531.844 | 477.039 | 455.474 | 542.190 | 610.241 | 639.143 | 477.984 | 664.063 | 430.644 |
| V (ppm) | 0.761 | 0.781 | 0.879 | 1.051 | 1.024 | 0.965 | 1.249 | 1.071 | 1.395 | 1.044 | 1.421 | 0.907 |
| Cr (ppm) | 1.881 | 1.882 | 1.870 | 1.856 | 1.856 | 1.861 | 1.847 | 1.777 | 1.858 | 1.873 | 1.868 | 1.873 |
| Mn (ppm) | 87.162 | 223.613 | 36.421 | 124.579 | 19.207 | 34.214 | 70.518 | 72.681 | 56.635 | 57.983 | 44.199 | 46.766 |
| Co (ppm) | 0.554 | 0.513 | 0.674 | 0.770 | 0.697 | 0.683 | 0.728 | 0.831 | 0.837 | 0.684 | 0.843 | 0.635 |
| Ni (ppm) | 1.571 | 1.544 | 1.545 | 1.558 | 1.556 | 1.564 | 1.555 | 1.620 | 1.546 | 1.554 | 1.557 | 1.571 |
| Cu (ppm) | 5.162 | 4.682 | 5.991 | 7.097 | 5.846 | 6.671 | 6.673 | 6.756 | 6.315 | 5.980 | 6.027 | 5.847 |
| Zn (ppm) | 26.155 | 27.415 | 29.778 | 31.425 | 30.848 | 31.565 | 43.264 | 37.488 | 34.436 | 45.692 | 34.155 | 28.593 |
| Mg (%) | 0.214 | 1.010 | 0.072 | 0.038 | 0.168 | 0.138 | 0.116 | 0.139 | 0.131 | 0.096 | 0.183 | 0.115 |
| P (%) | 0.138 | 0.180 | 0.049 | 0.094 | 0.087 | 0.093 | 0.111 | 0.075 | 0.085 | 0.123 | 0.113 | 0.050 |
| S (%) | 0.130 | 0.812 | 0.038 | 0.138 | 0.123 | 0.120 | 0.104 | 0.141 | 0.167 | 0.125 | 0.248 | 0.019 |
| Cl (ppm) | 451.428 | 5.631.487 | 455.780 | 144.473 | 198.916 | 359.117 | 325.050 | 433.729 | 284.207 | 293.925 | 157.106 | 1.255.700 |
| K (%) | 2.132 | 2.458 | 0.318 | 0.493 | 0.297 | 0.267 | 0.436 | 0.250 | 0.282 | 0.336 | 0.299 | 0.283 |
| Ca (%) | 1.645 | 4.448 | 1.164 | 1.359 | 4.707 | 3.612 | 2.199 | 1.870 | 3110 | 3.172 | 3.393 | 0.858 |
| Al (ppm) | 305.982 | 562.015 | 389.920 | 603.897 | 581.286 | 560.119 | 1094311 | 739.407 | 1127855 | 743.377 | 1.388.372 | 409.181 |
| Cd (ppm) | 1.554 | 1.649 | 1.580 | 1.544 | 1.788 | 1.650 | 1.773 | 1.535 | 1673 | 1.569 | 1.834 | 1.668 |
| Ba (ppm) | 67.068 | 56.142 | 28.881 | ND | ND | ND | ND | ND | ND | ND | ND | 0.857 |

References: MAIOLI, O. L. G., *et al*, **Parâmetros bioquímicos foliares das espécies *Licania tomentosa* (BENTH.) e *Bauhinia forficata* para avaliação da qualidade do ar.** Quim. Nova, Vol. 31, No. 8, 1925-1932, 2008

**Área: ANA** **Inscrição:_00414_____**
*(Inserir o número de inscrição do autor que fez a submissão)*

# Fast determination of metals using direct analysis of deodorants by inductively coupled plasma optical emission spectrometry

**Wiviane Kássia O. C. da Costa (PG)[1*], Caroline S. da Silva (PQ)[2], José Fernando D. Fiqueiredo (PQ)[3], Joaquim A. Nóbrega (PQ)[2], Ana Paula S. Paim (PQ)[1]**

**anaspaim@ufpe.br; wianecosta@yahoo.com.br**

*[1]Departament of Chemistry Fundamental, UFPE; [2]Departament of Chemistry, UFSCar; [3] Academic Unit of Cabo de Santo Agostinho,· UFRPE*

Keywords: Deodorants, Metals, Direct analysis, Particle size, ICP OES, Cosmetics

## Highlights

Development of a simple and precise procedure based on direct analysis.
Fast determination of fifteen analytes in deodorants by ICP OES.
Simple analytical procedure for routine analysis of deodorants.

## Resumo/Abstract

Cosmetics, as deodorants and antiperspirants, nowadays, are considered indispensable in the daily lives of people.[1] The concentrations of components in their formulation and the presence of metals may affect human health.[2] The multielemental capability of ICP OES has aroused interest in its application for elemental analysis of deodorants. Direct analysis is an efficient alternative for determination of trace elements, reducing risks of losses and contamination, use of reagents and residual generation, contributing to the principles of green chemistry.[3] In this context, this work aimed the development of a simple and fast procedure using dilute-and-shoot strategy for determination of Al, As, Ba, Cd, Cu, Fe, Mg, Mn, Ni, Pb, Sc, Ti, V, Zn and Zr in nine deodorants samples by ICP OES. The sample preparation was carried out by diluting 1 mL of deodorant sample in 1% (v $v^{-1}$) $HNO_3$ and the final volume was 10.0 mL. The accuracy of the analytical procedure was evaluated using addition and recovery experiments, and recoveries ranged from 80 to 119%. The limits of detection varied from 0.001 to 0.76 mg $kg^{-1}$. The maximum concentrations found (mg $kg^{-1}$) were: Al (0.01 to 7.0%), Mg (0.005 to 1.44), Fe (1.0), Mn (0.1), Ti (1.02), V (0.33), Zn (255) and Zr (0.5), showing wide variation depending on the sample type. The developed procedure was adequate for determining these analytes in routine analysis presenting high sample throughput and demonstrated the feasibility of direct analysis measurements after simple dilution step.

**Acknowledgements:** The authors are grateful to support provided by INCTAA (CNPq and FAPESP) and to Analítica – Thermo Scientific.

### References

[1]B. Hall, S. Tozer, B. Safford, M. Coroama, W. Steiling, M. C. Leneveu-Duchemin, C. Mcnamara, M. Gibney, European consumer exposure to cosmetic products, a framework for conducting population exposure assessments, Food Chem. Toxicol. 45 (2007) 2097-2108.

[2]K.G. Mcgrath, An easier age of breast cancer diagnosis related to more frequent, use of antiperspirants/deodorants and underarm shaving, Eur. J. Cancer Prev. 12 (2003) 1479-1580.

[3]S. Armenta, S. Garrigues, M. De La Guardia, Green Analytical Chemistry, Trends Anal. Chem. 27 (2008) 497-511.

**Área: ANA** **Inscrição: 00519**

# Evaluation of a method for the decomposition of spent fluorescent lamps for the determination of rare earth elements

**Evelyn Muguet Ferreira (IC)[1*], Fernanda Veronesi Marinho Pontes (PQ)[1], Jéssica Frontino Paulino (PQ)[1], Manuel Castro Carneiro (PQ)[2]**

**muguet.evelyn@gmail.com***

*[1]Departamento de Química Analítica, UFRJ; [2]Centro de Tecnologia Mineral, CETEM*

Palavras Chave: *Rare earth elements, spent fluorescent lamps, HPA-S.*

## Highlights

Two decomposition systems were compared for determination of REEs in powdered spent fluorescent lamps. High pressure asher system is faster and requires lower amounts of sample and reagents.

## Resumo/Abstract

Rare earth elements (REEs) are regarded as being critical chemical elements. One of the most important applications of REEs is the production of luminescent materials (phosphors)[1]. Spent fluorescent lamps (SFL) are considered as source of yttrium and europium[1]. The aim of this study was to compare of decomposition methods, using a closed pressurized system (HPA-S) (method A) and a classical method using hot plate (method B) followed by quantification of REEs by the inductively coupled plasma mass spectrometry (ICP-MS). The method A consisted in the addition of HCl and $HNO_3$ to 0.2 g of powdered SFL, and heating of system up to 200°C during 30 min, using a ramp of 6.7°C $min^{-1}$, followed heating up to 320°C and a dwell time of 30 min. The method B consisted in addition of HCl, $HClO_4$ and HF to 1 g of powdered SFL and heating on a hot plate until dryness for about 8 h. Similar REEs concentrations for Y, La, Eu, Gd and Tb (Table 1) were obtained in both methods (n=3; test-t 95% confidence level). The proposed method (A) presented good repeatability with RDS ≤ 9%. HPA-S method presented several advantages when compared to the classical method: lower contamination, faster and requires lower amounts of sample and reagents. A certified reference material (NCS DC 86309 – rare earth mineral) was used for evaluation the method accuracy.

Table 1. Analytical results for determination of REEs in powdered spent fluorescent lamps obtained by methods A and B (n=3).

| Element | Method A<br>µg $g^{-1}$ | Method B<br>µg $g^{-1}$ |
|---|---|---|
| Y | 22451 ± 354 | 25623 ± 466 |
| La | 2021 ± 35 | 2117 ± 31 |
| Eu | 1471 ± 28 | 1643 ± 15 |
| Gd | 239 ± 6 | 276 ± 1 |
| Tb | 1064 ± 14 | 842 ± 12 |

Method A - closed-pressurized (HPA-S) system/ICP-MS; Method B classical method using hot plate/ICP-MS

[1]TUNSU *et al*. Hydrometallurgy, 156 (2015), 239-258.

**Área: ANA** **Inscrição: 00616**

# Silica functionalized with 2,6-pyridinedicarboxylic acid for selective preconcentration of Rare Earth elements traces before ICP-MS analysis

**Olena Artiushenko (PG),[1] Wendy Sandoval (PG),[1] Tatiana D. Saint'Pierre (PQ),[1] Volodymyr Zaitsev (PQ).[1]***

**helen.artiushenko@gmail.com; vnzaitsev@gmail.com**

[1]*Departamento de Química, PUC-RIO;*

Palavras Chave: silica based adsorbent, 2,6-pyridinedicarboxylic acid, solid phase extraction, preconcentration, separation, REE.

## Highlights

Silica based adsorbent with immobilized 2,6-pyridinedicarboxylic acid. Adsorption of 17 lanthanide ions simultaneously. Reversible desorption and ICP-MS analysis of lanthanides in the presence of Ba, Fe and Cu ions.

## Resumo/Abstract

There are several methods for pre-concentration of Rare Earth elements (REE) before their ICP-MS determination. Most of them based on metal adsorption on solid support with further analysis of eluate. Major problem of such approach is low selectivity of the adsorbent and slow kinetic of adsorption/desorption process. Since REE can be found in groundwater or minerals in trace amount, the adsorbents must demonstrate high selectivity towards these elements. In addition, such adsorbents shall be able to separate REE from $Ba^{2+}$ ions commonly presented in solution as macro component, since ICP-MS analysis of $Nd^{3+}$, $Gd^{3+}$, $Sm^{3+}$, and $Eu^{3+}$ ions is limited on single quadrupole ICP-MS because of serious polyatomic interferences with barium matrix (such as $BaO^{+}$ and $BaOH^{+}$). To improve the adsorbent selectivity towards REE we proposed to use new adsorbent with covalently immobilized fragments of 2,6-pyridinedicarboxylic acid (PdCA). To ensure high kinetic characteristics of the adsorption/desorption process PdCA was immobilized on silica gel ($SiO_2$) with high surface area and large pore size. $SiO_2$-PdCA was characterized by elemental analysis, FT-IR and XPS. The concentration of surface immobilized groups ($C_L$ = 0.3 mmol/g) was determined from several independent methods, including titration, CHN elemental analysis and TGA. The adsorption properties of $SiO_2$-PdCA were investigated in static conditions for 17 different REE in a mixture, in large excess of $Ba^{2+}$ and some key heavy metal ions in the pH range 2-6. $SiO_2$-PdCA demonstrates reversible adsorption and very high kinetic characteristics. Complete adsorption/desorption process was observed for 10 min. The adsorbent demonstrated high capacity (200 µg/g for $Eu^{3+}$ ions) and strong affinity towards all REE. $SiO_2$-PdCA quantitatively adsorbs most of REE from solution with pH>2 containing 20 µg $L^{-1}$ of metals (see picture below). $Ba^{2+}$ ions has no influence on REE adsorption until pH>3.5-4. The adsorbent provide high recovery (>95%) of all REE in presence of 500-fold of $Ba^{2+}$ ions at pH=3.0. Ions of $Fe^{3+}$ and $Cu^{2+}$ in 1600-fold caused little or no interference on the determination of REE with recovery >80%.
After adsorption of $Eu^{3+}$ and $Tb^{3+}$ ions, $SiO_2$-PdCA demonstrates strong red and green luminescent and can be used as luminescent probes for monitoring of $Eu^{3+}$ and $Tb^{3+}$ ions in solution.

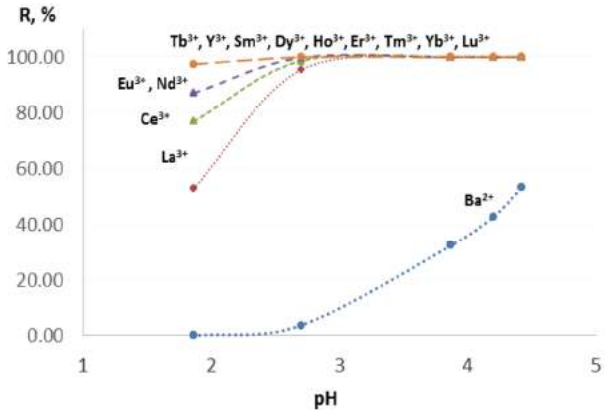


**Figure 1.** Adsorption of REE and $Ba^{2+}$ on $SiO_2$-PdCA.

**Área: ANA** **Inscrição: 00799**

# Determination of Cu, Ni, Pb and V in Brazilian gasoline by GF AAS using the technique of Extraction Induced by Microemulsion Breaking

**Jonas O. Vinhal (PQ),[1*] Ricardo J. Cassella (PQ).[1]**

**jbvinhal@hotmail.com**

[1]*Programa de Pós-Graduação em Química, Universidade Federal Fluminense, Outeiro de São João Batista s/n, Centro, Niterói, RJ, 24020-141, Brazil.*

Palavras Chave: *Extraction, Microemulsion, Gasoline, Metals, GF AAS.*

## Highlights

Extraction/preconcentration of Cu, Ni, Pb and V from Brazilian gasoline.
New technique to extract and determine metals in fuels.
Formation and breaking of microemulsions gasoline:alcohol:aqueous acid.

## Abstract

The presence of metals in gasoline can generate several problems in internal parts of automotive vehicles[1]. The new technique Extraction Induced by Microemulsion Breaking (EIMB) was recently proposed for determination of Hg in Brazilian commercial gasoline samples[2]. The aim of this work was to optimize this technique to extract, preconcentrate and determine Cu, Ni, Pb and V in Brazilian gasoline samples by GF AAS. First study revealed propan-1-ol for Ni, Pb and V and isopropanol for Cu, as the best dispersant agent for microemulsion formation. The optimum ratio sample:alcohol obtained was 92:7 with a total volume of microemulsion of 5 mL. In these experiments, 0.05 mL of $HNO_3$ solution was used to achieve the analyte extraction. The volume of water added to break the microemulsions was always 0.15 mL. In study of type and concentration of acid, the results (Fig. 1) revealed an increase on analytical signal with concentration of HCl and $HNO_3$ until 25% (v/v). The influence of the volume of water and $HNO_3$ solution to break the microemulsion revealed (Fig. 2) no significant differences between water and acid. Analysis shown different signals for each analized metal with different volumes to break. The chosen volumes used in microemulsion breaking were 0.2 mL of water for Cu, Pb and V, and 0.4 mL of $HNO_3$ 25% (v/v) for Ni.

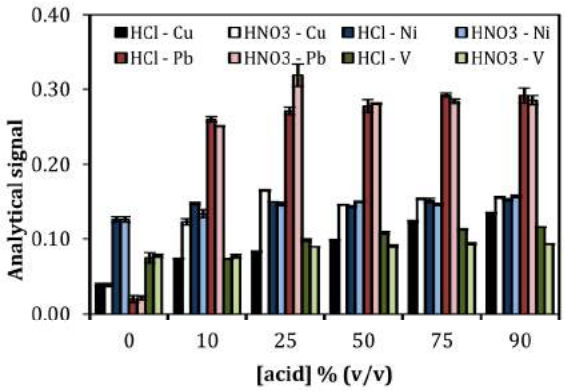


**Fig. 1.** Influence of type and [acid]

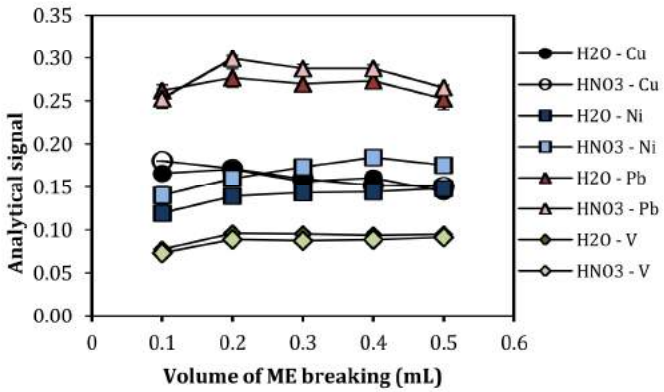


**Fig. 2.** Influence of type and volume on ME breaking

For the next steps, will be evaluated the application of the method in different gasoline samples and determine analytical parameters.

**Acknowledgments:** CNPq, CAPES, FAPERJ

[1] Heneghan, S.P.; Zabarnick, S. Fuel **1994**, 73, 35.
[2] Vicentino, P.O.; Cassella, R.J. Talanta **2017**, 162, 249.

**Área: ANA** **Inscrição: 00892**

# An on-line preconcentration system using ion-imprinted polymer for determination of bismuth in seawater employing atomic fluorescence spectrometry

**Sergio L. C. Ferreira(PQ)[1,2]; Heloysa M. C. Andrade (PQ)[1,2]; Caio S. A. Felix (PG)[1,2]; Darllen G. Silva (PG)[1,2].**
slcf@ufba.br
[1] *Universidade Federal da Bahia, Instituto de Química, Programa de Pós-Graduação em Química, Campus Ondina, 40170-115, Salvador, Bahia, Brazil*
[2] Instituto Nacional de Ciência e Tecnologia de Energia e Ambiente, UFBA, *40170-115, Salvador, Bahia, Brazil*

*Keywords: Bismuth; Seawater; ion-imprinted polymer; Box-Behnken design; AFS.*

## Highlights

An on-line preconcentration system using ion-imprinted polymer for determination of bismuth in seawater by by atomic fluorescence spectrometry was proposed.

## Resumo/Abstract

This work proposes an on-line preconcentration system using ion-imprinted polymer (IIP) for determination of bismuth in seawater employing atomic fluorescence spectrometry (AFS). The polymer was synthesized using 2- (5-bromo-2-pyridylazo) -5-diethylaminophenol (Br-PADAP) for complex formation, ethylene glycol dimethacrylate (EGDMA) as cross-linking reagent, methacrylic acid (AMA) reagent employed as the functional monomer and 2,2-azobisisobutyronitrile utilized as the radical initiator. The polymer was characterized employing the Fourier transform infrared spectroscopy (FTIR), and scanning electron microscopy (SEM).

The determination of bismuth was performed employing hydride generation atomic fluorescence spectrometry (HG AFS) and the experimental conditions were optimized using a Box Behnken design involving the factors sample pH, eluent concentration and sodium tetrahydroborate concentration. So, using the optimized conditions the system allows the determination of bismuth with limits of detection and quantification of 26 and 88 ng $L^{-1}$ and a preconcentration factor of 19.8.

The system proposed was applied for the determination of bismuth in four seawater samples collected in Salvador City, Bahia State Brazil. The concentrations obtained varied from 0.38 to 0.45 µg $L^{-1}$. The accuracy was evaluated by addition/recovery test. The recoveries found varied from 92 to 101%.

[CAPES, CNPq, FAPESB].

**Área: ANA** **Inscrição: ID00940**

# Microextração induzida por quebra de emulsão (MIEB) para determinação de metais em amostras de óleo diesel.

**Aline Fernandes (PG) [1*], Achilles J.B. Dutra (PQ) [2], Ricardo J. Cassella (PQ) [1]**

**linefernandes@uol.com.br**

*[1] Universidade Federal Fluminense, Departamento de Química Analítica, Niterói, RJ, Brasil; [2] Universidade Federal do Rio de Janeiro, Departamento de Engenharia Metalúrgica e de Materiais, COPPE, Rio de Janeiro, Brasil.*

Palavras Chave: *EIEB, microextração, emulsão, diesel, chumbo, cobre, níquel.*

## Highlights

Microextraction induced by emulsion breaking (MIEB) for determination of metals in diesel oil samples.

Microextraction has as differential the easy manipulation of the extractant phase and the fact that it does not need the use of organic solvents even for analysis of petroleum derivatives.

## Resumo/Abstract

O desenvolvimento do método MIEB foi realizado inicialmente com o preparo de uma emulsão com 1,5 mL de óleo diesel e 0,5 mL do extratante, composto de surfactante Triton X 114 em meio ácido ($HNO_3$). A quebra da emulsão foi realizada em banho maria a 80ºC por 10 min. As determinações de Pb, Cu e Ni foram realizadas por espectrometria de absorção atômica com forno de grafite (GF AAS) em equipamento Varian AA240Z com corretor de fundo baseado no efeito Zeeman. As temperaturas ótimas utilizadas no GF AAS foram: 1100ºC (Cu e Pb) e 1300ºC (Ni) para pirólise e 1900ºC (Pb), 2200ºC (Cu) 2500ºC (Ni) para atomização. Para a otimização da microextração foram avaliados os parâmetros mostrados na **Tabela 1**. A melhor condição encontrada durante os estudos foi: 1,5 mL da amostra de óleo diesel, 300 µL de extratante (contendo Triton X 114 2,5 % m / v em $HNO_3$ 50 % v /v), agitação manual vigorosa e quebra da emulsão em banho-maria a 80 ºC por 10 min. As quantificações dos elementos foram realizadas com curva analítica aquosa e por adição de analito de 0 a 75 $\mu g.L^{-1}$, com recuperações entre 84 e 99%. A miniaturização da técnica de extração induzida por quebra de emulsão apresentou um ótimo resultado com a vantagem da utilização de quantidades mínimas de reagentes no processo.

**Tabela 1**: Parâmetros avaliados para o desenvolvimento da MIEB:

| Parâmetros estudados | Faixa estudada |
|---|---|
| Volume da fase extratora | 100 a 500 µL |
| Concentração de $HNO_3$ e HCl | 5 a 60% v / v |
| Concentração de HCl | 5 a 60% v / v |
| Concentração do surfactante Triton X 114 | 2,5 a 10% m / v |
| Tempo de agitação mecânica | 0, 30, 60 e 120 min |

**Área: ANA** **Inscrição:** *943*

# SS-FF-AAS AS AN ALTERNATIVE TECHNIQUE FOR ELEMENTAL IMPURITIES DETERMINATION IN HIGH PURITY GRAPHITE

**Rafael F. Santos (PG), Gabriel S. Carvalho (PG), Felipe A. Silva (IC), Rochele S. Picoloto (PQ), Cezar A. Bizzi (PQ), Érico M. M. Flores (PQ).**

**rfsantos88@gmail.com; c_bizzi@yahoo.com.br**

*Departamento de Química, Universidade Federal de Santa Maria - UFSM*

Palavras Chave: *High Purity Graphite, Trace Analysis, Solid Sampling Flame Furnace Atomic Absorption Spectrometry, Solid Sampling.*

## Highlights

The proposed SS-FF-AAS system was suitable for the determination of Cu at trace levels (μg $g^{-1}$) in high purity graphite. The system allowed analysis of solid sample, with high sensitivity and low LOD.

## Resumo/Abstract

The solid sampling flame furnace atomic absorption spectrometry (SS-FF-AAS) system was proposed for the determination of Cu in high purity graphite without a previous sample preparation step. A homemade quartz tube, with two perpendicular tubes, (T-shaped tubes) were positioned above the burner of the flame atomic absorption spectrometer. Graphite samples were pressed as a pellet, positioned inside the quartz T-tube (Fig 1A and 1B) and reached up to the T-connection (above the burner). In this part, with high temperature and in the presence of controlled $O_2$-flow, sample burns and the products were transferred to the upper slit tube, where the atomization and absorption process occurs.

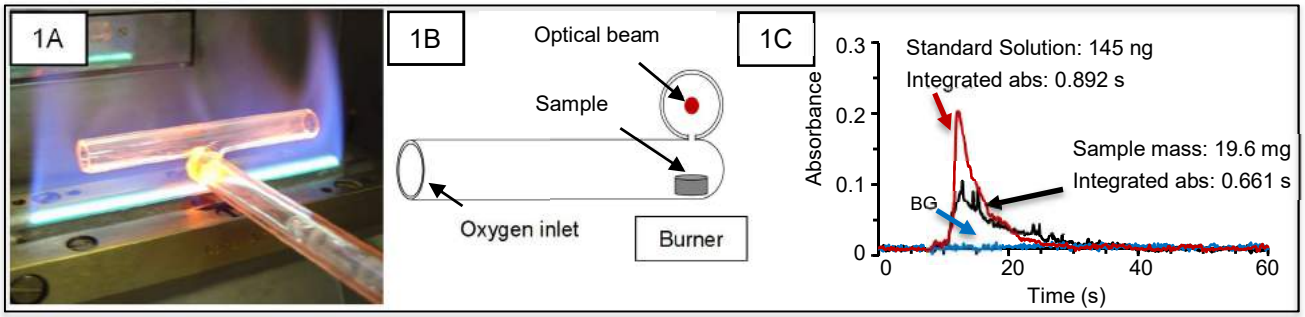


Figure 1. Solid Sampling Flame Furnace Atomic Absorption Spectrometry system (SS-FF-AAS).1A) quartz tube above the burner of the F AAS equipment; 1B) schematic side view of the system; 1C) analytical signal (324.8 nm)

The flame stoichiometry and oxygen flow-rate were evaluated to allow calibration using aqueous reference solutions which was added directly on the cleaned graphite carrier (free from Cu). During determination step, no mass influence was observed from 7 to 75 mg of sample. The transient analytical signal was integrated for 60 s (Fig 1C). The accuracy was evaluated by Cu determination using ICP-MS with previous step of sample digestion. The agreement was higher than 94% for all samples and no statistical difference was observed (ANOVA, 95%). The proposed SS-FF-AAS was considered suitable for Cu determination at trace levels in graphite powder, presenting high sensibility (characteristic mass: 720 pg) and low limits of detection (0.3 μg $g^{-1}$).

**Área: ANA** **Inscrição: 00988**

# Nickel and Vanadium Determination in Diesel Oil by ICP-OES after Reverse-Phase Dispersive Liquid-Liquid Microextraction

**Isabela S. Delpino (PG),[1] Gabriel T. Druzian (PG),[2] Rafael F. Santos (PG),[2] Rodrigo C. Bolzan (PQ),[2] Eder L. M. Flores (PQ),[1] Rochele S. Picoloto (PQ),[2*]**

*rspicoloto@gmail.com*

*[1]Departamento de Química, Universidade Tecnológica Federal do Paraná (UTFPR-MD), [2]Departamento de Química, Universidade Federal de Santa Maria (UFSM);*

Palavras Chave: Reverse-phase dispersive liquid-liquid microextraction; Diesel oil analysis; Impurities; Trace analysis; Inductively coupled plasma optical emission.

## Highlights

- ✓ A simple, rapid and high sensitive method for Ni and V determination by ICP-OES was developed.
- ✓ Onlydiluted acids solution were used and no sample digestion was required before analytes determination.

## Resumo/Abstract

A simple, rapid and high sensitive method for Ni and V extraction in diesel oil based on the reverse-phase dispersive liquid-liquid microextraction (RP-DLLME) and further determination by inductively coupled plasma optical emission (ICP-OES) was developed. For RP-DLLME method optimization, extraction solvent concentration, ratio between dispersive and extraction solvents, temperature, sample mass and influence of the use of ultrasound were investigated. The RP-DLLME method was performed by addition of 2 mL of a solution containing 1.5 mol $L^{-1}$ $HNO_3$ solution mixed with isopropyl alcohol, used as extraction and dispersive solvents, respectively. After, extracts were centrifuged to phases separation. No influence of sample mass was observed and up to 10 g of diesel oil were used for RP-DLLME method. Accuracy evaluation was performed by comparison of results obtained after microwave-assisted wet digestion and by recovery tests. Quantitative results were obtained by both accuracy studies performed. Relative standard deviations lower than 7% were obtained. With the proposed method was possible to use high sample mass and low volume of reagents obtaining negligible blank values and consequently low limit of quantification (0.112 and 0.302 for Ni and V, respectively). The proposed method presented many advantages, such as low time is required for sample preparation step, use of high sample mass, reduced volumes of reagents and greener solvents, minimizing the generation of toxic laboratory residues and making RP-DLLME method well suitable for routine ultra-trace determination of inorganic contaminants in diesel oil.

**Área: ANA** **Inscrição: 01225**

# Online Preconcentration of Sb(III) using $SiO_2/Al_2O_3/SnO_2$ Ternary Oxide Coupled with HGAAS

**César R.T. Tarley (PQ),[1,2*] Fernanda Garcia de Almeida (PG)[1], Emerson Schwingel Ribeiro (PQ)[2], Leandro L.G. de Oliveira (PG), [1]Guilherme Orlandin (IC).[1]**

**tarley@uel.br**

*[1]Departamento de Química, UEL; [2]Instituto Nacional de Ciência e Tecnologia (INCT) de Bioanalítica, UNICAMP; Instituto de Química [3]*

*Key words: Antimony, HGAAS, FIA, Ternary Oxide.*

## Highlights

Online preconcentration of Sb(III) was investigated by HG AAS using $SiO_2/Al_2O_3/SnO_2$ Ternary Oxide for the coupled with HG AAS. The robustness for Sb(III) sorption was attested in under wide pH range

## Resumo/Abstract

The oxide ternary was previously synthesized and characterized as phase extractor for online preconcentration of $Pb^{2+}$ by FAAS.[1] In this work, studies are been performed with the aim to develop an analytical method using a ternary oxide coupled to Hydride Generation Atomic Absorption Spectrometry (HG AAS) for antimony determination. Chosen conditions for pH study of $Sb^{3+}$ were: HCl 1.5 mol $L^{-1}$, $NaBH_4$ 3.0% (m/v) in NaOH 0.5% (m/v) and 20.0 µg $L^{-1}$ of Sb(III). Online FIA-HG AAS system parameters were: 0.8, 2.5 e 6.20 mL $min^{-1}$ for borohydride, hydrochloric acid and preconcentration flow rate, respectively. The material (50.0mg) was packed into a column and coupled online to commutator injector. Sample was aspirated and after 3.15 minutes the injector was shifted to injection position and antimony retained was eluted by the HCl towards the hydride generation. Then, Sb(III) is easily reduced to stibine ($SbH_3$) with borohydride at acid medium. From the results obtained higher intensity was observed at pH 3.5. Above that, a slight decrease was realized and the intensity remains up to pH 7.5. Therefore, no influence from Sb(III) preconcentration was detected from pH 2.5 to 7.5. In the pH range of 2.0 – 11.0, Sb(III) should form a neutral complex $Sb(OH)_3$.[2] The surface offers oxygen for hydrogen bonds with $Sb(OH)_3$, but the excess of $OH^-$ competes with the surface, which explain the low preconcentration at higher pH value (pH 9.0).[3]

1.Tarley, C. R. T.; Scheel, G. L.; Ribeiro, E. S; Zappielo, C. D.; Suquila, F. A. C.. Journal Braz. Chem. Soc., (2018), 1-12.
2.Smith, R. M.; Martell, A. E. Critical Stability Constants; Inorganic Complexes, Plenum Press: New York, v.4, 1976.
3.Buschmann, J.; Sigg, L. Environmental Science technol. 38 (2004), 4535-4541.

**Área: ANA** **Inscrição: 01246**

# Evaluation of the analytical performance of a solid phase magnetic extraction method for $Pb^{2+}$determination

**Vanessa N. Alves (PQ),[1] Carolina A. de S. Silva* (PG).[1]**

vanessanalves@gmail.com; carolsousa1@yahoo.com.br

[1] *Universidade Federal de Goiás, Unidade Acadêmica Especial de Química, Catalão-GO, Brasil, 75704-020*

Palavras Chave: Magnetic Nanoparticles, *Magnetic Solid phase extraction (MSPE), Adsorption.*

## Highlights

Magnetic Solid phase extraction (MSPE) with magnetic particles (MPs) as adsorbents is an interesting alternative to the conventional SPE, since the pre-treatment of the sample is greatly simplified;
Phase separation can be quickly and easily performed by applying an external magnetic field;
The synthesis of MPs is easy and low-cost;
High pre factors are obtained.

## Resumo/Abstract

Considering the relevant daily exposure and danger of lead ions, the development of methodologies capable of determining this ion at low concentrations in different matrices becomes essential[1]. Several spectroscopic techniques allow this detection, however, due to sensitivity-related problems, a preconcentration step can be made necessary. Magnetic solid phase magnetic extraction (MSPE) is a preconcentration technique based on the use of magnetic particles such as adsorbentes[2]. Iron oxide nanoparticles ($Fe_3O_4$) are promising and, in this work, have been synthesized by the coprecipitation method, characterized and applied as an adsorber for $Pb^{2+}$ ions by MSPE and detection by FAAS. 3.0 mg of $Fe_3O_4$ were maintained under vortex agitation for 4 minutes with $Pb^{2+}$ solutions [1 mg $L^{-1}$] and pH 9.0. Subsequently, magnetic separation and elution was carried out by the addition of 0.5 mL of $HNO_3$ 0.5 mol $L^{-1}$ for 2 minutes. After a new magnetic separation, the supernatant was analyzed by FAAS. The synthesized material was characterized by X-ray diffraction (Figure 1), observing that adsorption does not cause displacement in diffraction spikes, indicating that the material maintains its crystallographic structure and magnetism after adsorption.

**Figura 1**: X-Ray Diffractogram for $Fe_3O_4$ before and after

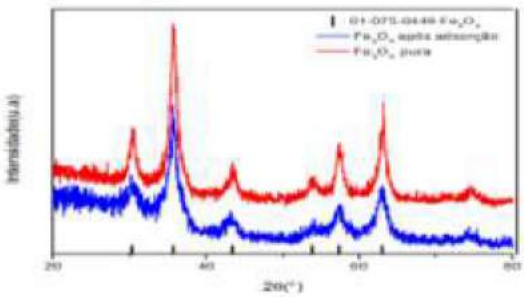

The detection and quantification limits obtained of 5.44 and 16.4 µg $L^{-1}$ respectively, R.S.D(%) of 4% and a preconcentration factor of 135 were obtained. indicating that the magnetite nanoparticles behave as a promising material in the development of a new methodology for determining $Pb^{2+}$ ions.

[1]Marinovich, M.; Boraso, M, S.; Testai, E.; Galli, C,L, Regulatory Toxicology and Pharmacology, 69, 2014, 416.

[2]Kumari, M.; Pittman, JR.; Mohan, D., Heavy metals [chromium (VI) and lead (II)] removal from water using mesoporous magnetite ($Fe_3O_4$) nanospheres. Journal of Colloid and Interface Science, 442, 2015, 132.

Acknowledgements: FAPEG, CNPq, CAPES e UAEQ – UFG/RC

**Área: ANA** **Inscrição: 01434**
*(Inserir o número de inscrição do autor que fez a submissão)*

# Determinação de Cr e Pb em óleo de peixe rico em ômega-3 por GF AAS utilizando a extração induzida por quebra de emulsão.

**Thais F. Arruda (PG)[1]*, Ricardo J. Cassella (PQ)[1], Fábio Grandis Lepri (PQ)[1]**

**fabio_grandis@id.uff.br; thais.faustinoo@gmail.com**

[1]*Programa de Pós-Graduação em Química, UFF.*

Palavras Chave: *Metais, Óleo de peixe, Ômega-3, Extração induzida por quebra de emulsão.*

## Highlights

Determination of Cr and Pb in fish oil rich in ômega-3 by GF AAS using the extraction induced by emulsion breaking.
Method development. Chromium and Pb determination by GF AAS in fish oil rich in ômega-3. Sample preparation using extraction induced by emulsion breaking.

## Resumo/Abstract

Os óleos de peixe são fontes fonte do ácido eicosapentaenóico (EPA) e o ácido docosaexaenóico (DHA), ambos presentes no ômega-3. O EPA relaciona-se com a proteção da saúde cardiovascular, e o DHA é considerado fundamental para o desenvolvimento do cérebro e sistema visual. A presença de metais nestes óleos pode trazer características negativas em termos de toxicidade, estabilidade e prazo de validade do produto final. Portanto, a determinação de metais em óleos de peixe ricos ômega-3 torna-se importante, sob diversos aspectos.O presente trabalho apresenta o estudo do preparo de amostra utilizando a extração induzida por quebra de emulsão (EIEB), para determinação de Cr e Pb por GF AAS em amostras de óleo de peixe encapsuladas, rico em ômega-3. Os melhores resultados foram obtidos com a emulsificação de 2 mL de amostra e 1 mL de solução extratora contendo 10% m/v em Triton X-100 e 1,07 mol $L^{-1}$ em $HNO_3$, após agitação manual por 5 min a emulsão formada foi então quebrada por aquecimento a 90 ºC durante 30 min. A concentração de Cr e Pb no extrato aquoso foi determinada utilizando calibração com padrões aquosos. O método foi aplicado a cinco amostras de óleo de peixe encapsulado, comercialmente disponíveis na cidade de Niterói - RJ. A exatidão do método foi avaliada com testes de recuperação em dois níveis de concentração utilizando padrões organometálicos para a fortificação, e os resultados obtidos situaram-se dentro da faixa aceitável, entre 80 - 120%.

**Área: ANA** **Inscrição: 01342**

# Aplicação de ácido diluído em digestão assistida por micro-ondas para determinação multielementar em variedades de mosto de uva

**Vanessa de S. Santos (PG)[1]*, Maria das Graças A. Korn (PQ)[1], Wagna Piler C. dos Santos (PQ)[2].**

**vanessa_quimic@hotmail.com**

*[1]Grupo de Pesquisa em Química Analítica, Instituto de Química, Universidade Federal da Bahia, Campus Universitário de Ondina, Salvador; [2]Departamento de Química, Instituto Federal de Educação, Ciência e Tecnologia da Bahia.*

Palavras Chave: *Mosto de Uva, Ácido diluído, Análise Multivariada, Submédio São Francisco.*

## Highlights

APPLICATION OF DILUTED ACID MICROWAVE ASSISTED DIGESTION FOR MULTIELEMENT DETERMINATION IN GRAPE MUST VARIETIES. Principal Component Analysis (PCA) was applied to establish profiles of different types of grapes produced in Petrolina/PE. The determination of Cu, Fe, Zn, Mn, Sb, Se and As was performed using inductively coupled plasma optical emission spectrometry (ICP OES) after diluted acid microwave assisted digestion.

## Resumo/Abstract

Neste trabalho aplicou-se digestão assistida por micro-ondas com ácido diluído em 25 amostras de mosto de uva (*Moscato, Melhorada, Arra-15 e Scarlotta*) cultivadas em Petrolina/PE, localizada no Vale Submédio São Francisco, para determinação de Cu, Fe, Zn, Mn, Sb, Se e As por espectrometria de emissão atômica com plasma indutivamente acoplado (ICP OES). O uso de ácido diluído reduz a concentração final de ácido residual e evita o desgaste dos componentes de equipamentos. O método analítico utilizado apresentou recuperações dentro da faixa recomendada, entre 80 e 119%, e os valores de LOQ variaram de 0,008 mg $L^{-1}$ para Sb a 0,101mg $L^{-1}$ para As. Análise de Componentes Principais (PCA) foi aplicada nos resultados com o intuito de avaliar as principais influências das variáveis no perfil dos diferentes tipos de uvas. A Figura 1 e 2 mostram a separação de três grupos ao longo das duas componentes principais que sintetizaram uma variância acumulada em torno de 70,9%. As espécies químicas que influenciam o primeiro grupo no eixo PC1 (valores positivos) são Se, As e Sb. Ao longo do eixo positivo de PC2 as variáveis que mais contribuem no segundo grupo são Cu, Zn e Fe. Já o Mn influência no terceiro agrupamento, que apresenta valores negativos em PC2 e PC1.

Figura 1. Gráfico de scores das amostras: Uva Itália Moscato (▲), Uva Itália Melhorada (●), Uva Arra-15 (♦) e Uva Scarlotta (■)

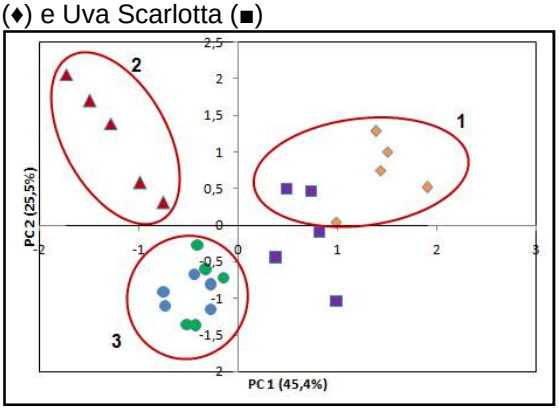


Figura 2. Comportamento das variáveis.

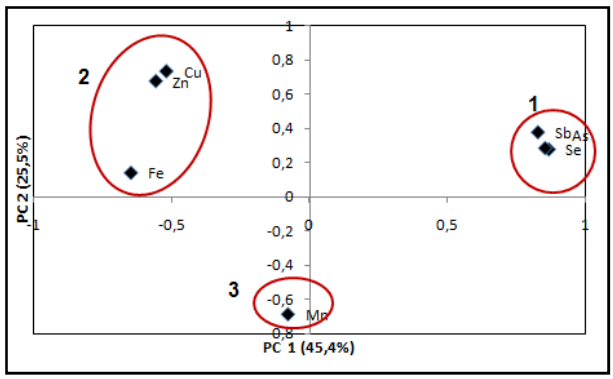

**Área: ANA** **Inscrição: 676**

# PRECIPITAÇÃO HOMOGÊNEA DE $Al(OH)_3$ ASSISTIDA POR MICRO-ONDAS PARA SEPARAÇÃO DE METAIS EM SALMOURAS

**Kerolaine S. Batista (IC),[1] Eduardo B.G.N. Santos (PG),[2,3] Lidio P. Junior (PG),[1] Mauro Korn (PQ).[1]***

**kerolainebatista1@gmail.com; mkorn@uneb.br**

*[1]Departamento de Ciências Exatas e da Terra, UNEB; [2]Instituto de Química, UFBA; [3]Campus Catu, IFBAIANO*

Palavras Chave: *Precipitação homogênea, Micro-ondas, Salmoura, Separação. Determinação de metais.*

## Highlights

Homogeneous precipitation of $Al(OH)_3$ assisted by microwave radiation for metal's separation from brine

The homogeneous precipitation of aluminum hydroxide was carried out by different heating conditions leading to proper characteristics of precipitate to make easier species separation.

## Resumo/Abstract

A aplicabilidade da precipitação de hidróxido de alumínio a partir de solução homogênea assistida por micro-ondas foi investigada para criar alternativa para determinações de elementos em amostras com altas concentrações de NaCl. Contrariamente ao que ocorre nas precipitações convencionais, a precipitação homogênea produz cristais mais puros e densos e que se aglomeram rapidamente, facilitando sua separação física do sobrenadante. Assim, solução de ureia contendo íons $Al^{3+}$ foi adicionada às amostras de salmoura (reais e sintéticas) e irradiada com micro-ondas por 60 s, garantindo a nucleação e crescimento do precipitado em múltiplos pontos da solução onde a temperatura foi suficiente para decompor a ureia e elevar localmente o pH, diferentemente do que ocorre com aquecimento condutivo. Em seguida a mistura bifásica foi centrifugada e o sólido foi separado e lavado. Os teores de Ba, Cu, P, Cd, Cr, Fe e Pb foram determinados por espectrometria de emissão ótica após dissolução do precipitado com solução de ácido diluído. As quantidades determinadas para os diferentes metais foram comparadas com os valores nas amostras sintéticas, indicando remoção quantitativa de diversos metais. Os resultados mostraram que o precipitado produzido sob irradiação micro-ondas removia rápida e eficientemente os metais da solução salina junto ao precipitado de $Al(OH)_3$, livre da influência dos íons sódio. O procedimento foi aplicado para a determinação de concomitantes em amostras de sal grosso e flor de sal.

**Área: ANA** **Inscrição: 00743**

# Feasibility of microwave-induced combustion for honey decomposition and further indirect determination of Cl and S by ion chromatography

**Fernanda Pitt Balbinot (IC) [1], Filipe Soares Rondan (PG) [1], Rodrigo Mendes Pereira (PG) [1], Natália Jorge Bielemann (IC) [1], Priscila Tessmer Scaglioni (PQ) [1], Márcia Foster Mesko (PQ) [1] *.**

**priscilascaglioni@gmail.com; *marcia.mesko@pq.cnpq.br**

[1]*Centro de Ciências Químicas, Farmacêuticas e de Alimentos, UFPel.*

Palavras Chave: *Honey, Chlorine, Sulfur, Microwave-Induced Combustion, Ion Chromatography.*

## Highlights

High honey mass (900 mg) was decomposed by MIC.
Using the proposed method suitable solutions for further determination by IC were obtained.
The proposed method provides a high throughput.

## Abstract

A method for indirect determination of Cl and S in honey by ion chromatography (IC) with conductivity detection, after decomposition by microwave-induced combustion (MIC) was developed. For this, it was necessary to use microcrystalline cellulose as combustion aid and polyethylene film for sample wrapping. Ultrapure water and ammonium hydroxide solutions (25, 50 or 100 mmol $L^{-1}$) were evaluated as absorbing solution. No statistical differences (ANOVA/Tukey test, confidence level of 95%) were observed among the results for all evaluated absorbing solutions. Thus, water was selected for further studies and recoveries from 94 to 109% were obtained for both analytes. The limits of quantification were of 25 mg $kg^{-1}$ for Cl and 20 mg $kg^{-1}$ for S. The concentration of Cl was 170 mg $kg^{-1}$ and for S was below 20 mg $kg^{-1}$ in the analyzed sample. The main advantages of the proposed method are the high sample mass that can be decomposed and the possibility to use water as absorbing solution. Besides, will be evaluated other parameters during the sample preparation with aim to obtain lower detection limits for S considering the high blank values when microcrystalline cellulose was used as combustion aid. Posteriorly the proposed method will be applied to honeys from different origins.

**Área: ANA** **Inscrição: 00746**

# Development of a green and efficient method for determination of iodine in mineral dietary supplements

**Natália J. Bielemann (IC), Rodrigo M. Pereira (PG), Julia E. Mello (PG), Janaína R. Brum (IC), Diogo L.R. Novo (PG), Márcia F. Mesko (PQ).***

**natbielemann@gmail.com; marcia.mesko@pq.cnpq.br**

*Centro de Ciências Químicas, Farmacêuticas e de Alimentos, Universidade Federal de Pelotas, Pelotas, RS, Brazil.*

Keywords: *Iodine, Mineral Dietary Supplements, IC, MIC*

## Highlights

Dietary supplements were efficiently digested by MIC for further iodine determination by IC. The proposed method presents suitable accuracy and precision. Iodine was absorbed using a diluted solution.

## Resumo/Abstract

In this work, an analytical method for iodine determination in mineral dietary supplements was developed. Microwave–induced combustion (MIC) was evaluated as sample preparation method and iodine was determined by ion chromatography (IC). It was possible to decompose up to 800 mg of supplement using 20 bar of oxygen and 6 mL of a diluted alkaline solution (200 mmol $L^{-1}$ $NH_4OH$). Accuracy was evaluated by analyte recovery tests using standard solution, and the recoveries ranged from 94 to 106%. Relative standard deviations (RSDs) were always lower than 9% and the limit of detection was 2.2 µg $g^{-1}$. The proposed method was applied for the analysis of dietary supplements of variety brands containing different dosages of iodine (from 100 to 1250 µg $g^{-1}$, according to the manufacturers). Iodine concentrations for all analyzed samples presented statistical differences (Student's *t*-test, 95% of confidence level, n=10) within values reported by manufacturers, when 30 tablets/capsules were homogenized and analyzed by the proposed method. An additional study was performed based on the uniformity dosage units assessment of the United States Pharmacopeia. In this evaluation, the tablets/capsules were digested individually and the RSDs were up to 42%, which demonstrate possible problems on the uniformity dosage units and the importance of the dietary supplements quality control. The proposed method presents a high throughput, a suitable accuracy and precision and allows the use of diluted solutions according to green chemistry.

**Área: ANA** **Inscrição: 00896**

# Can the digestion of carbon nanotubes using diluted acid be a feasible approach?

**Sindy R. Krzyzaniak (PG),[1] Letícia S. F. Pereira (PG),[1] Gustavo R. Bitencourt (IC),[1] Cezar A. Bizzi (PQ),[1] Erico M. M. Flores (PQ),[1] Paola A. Mello (PQ),[1*]**

**sindykrzyzaniak@gmail.com; paola.mello@ufsm.br**

*[1] Departamento de Química, UFSM;*

Palavras Chave: *Carbon nanotubes, Inorganic contaminants, Sample preparation, ICP-MS, ICP-OES*

## Highlights

CNT digestion for elemental determination by ICP-based techniques was explored.
Several tools of sample preparation (diluted acids, auxiliary reagent and UV lamps) were evaluated.

## Abstract

Carbon nanotubes (CNTs) represent an important class of nanomaterials with attractive use due to their physical, chemical, electrical and mechanical properties. This nanomaterial can be obtained by different processes using metallic catalyst (the most common are Co, Fe, La, Ni or their combinations). Even using a purification step, metals can be present in the final material at relatively high levels, affecting the properties of CNTs.[2,3] To determine these contaminants, sample preparation using wet acid digestion for elemental determination by plasma-based techniques is the most common approach. However, hard conditions of pressure and temperature with concentrated acids are required. Based on the recent developments in sample preparation, alternative approaches are proposed in this work. Microwave-assisted wet digestion (MAWD) is studied for further determination of metals by ICP-based techniques (ICP-MS and ICP-OES). Suitable conditions, such as irradiation time (30 to 65 min), CNT mass (25 to 175 mg), the volume (6 and 15 mL) and the concentration of the digestion solution (0.5, 1, 3 and 14 mol $L^{-1}$ $HNO_3$), the influence of the air flow-rate on digestion temperature, the microwave power, the use of UV lamps and the use of oxygen and $H_2O_2$ as auxiliary reagents were evaluated. The accuracy was evaluated by comparison of the results with those obtained using neutron activation analysis (NAA) and also by high resolution continuum source graphite furnace atomic absorption spectrometry with direct solid sampling (DSS-HR-CS-GF AAS).

[1] Dresselhaus M.S, *et al*. Science of Fullerenes and Carbon Nanotubes, Academic Press, San Diego, 1996.
[2] MacKenzie, K, *et al*. Separation and Purification Technology 2009, 66, 209-222.
[3] Stefano, J. S, *et al*. Electrochimica Acta 2017, 20, 80-89.

**Área: ANA** **Inscrição: 01130**

# Luminomagnetic core-shell nanoparticles for detection of metallic ions

**Eliane A. Namikuchi (PG), [1]Italo O. Mazali (PQ), [1]Ivo M. Raimundo Junior (PQ) [1*]**

**ayuminamikuchi@gmail.com, ivo@iqm.unicamp.br**

*[1]Institute of Chemistry – University of Campinas (UNICAMP), Brazil.*

*Keywords: PEG-assisted solvothermal method, Stöber method, Microemulsion-assisted, Luminomagnetic nanoparticles, Cupper ions.*

## Highlights

Synthesis of luminomagnetic core-shell nanoparticles with uniform size distribution, spherical morphology for detection of $Cu^{2+}$ ions. Proposing a new pathway in the exploration of these nanoparticles.

## Abstract

In this work, luminomagnetic core-shell nanoparticles of $Fe_3O_4$@$SiO_2$@RhB@$SiO_2$ were prepared aimed their application as nanosensor for $Cu^{2+}$. For this purpose, the size of magnetic core (MNps) and thickness of $SiO_2$ shell were modulated and their influence on the luminescent properties were investigated. PEG-assisted solvothermal method was used to prepare the MNps. PEG 4000, PEG 8000 and PEG 20000 were used as surfactants in the solvothermal method, producing MNPs of 145, 107 and 97 nm, respectively. The modified Stöber method was used to deposit the silica on the MNPs. Two different concentrations of TEOS, $Fe_3O_4$ and $NH_4OH$ were used, following the ratios of reagents described in the literature[1]. These coatings were named as FeSi4K_100, FeSi4K_50, FeSi8K_100, FeSi8K_50, FeSi20K_100 and FeSi20K_50. The effect of dilution was verified and TEM analysis showed silica coated nanoparticles with relative uniform size distribution. $Fe_3O_4$@$SiO_2$ nanoparticles exhibited suitable magnetic response, facilitating their separation from reaction media. Rhodamine B (RhB), a fluorescent complexing agent and enable to response to $Cu^{2+}$, was deposited on core-shell nanoparticles via modified microemulsion-assisted[2]. Diluted nanoparticles dispersions showed a fluorescent emission band characteristic around 572 nm under excitation at 495 nm. Experiments with $Cu^{2+}$ (fluorescence quenching) were carried out with FeSi4K_100, FeSi8K_100 and FeSi20K_100 functionalized with RhB, showing changes in the emission band.

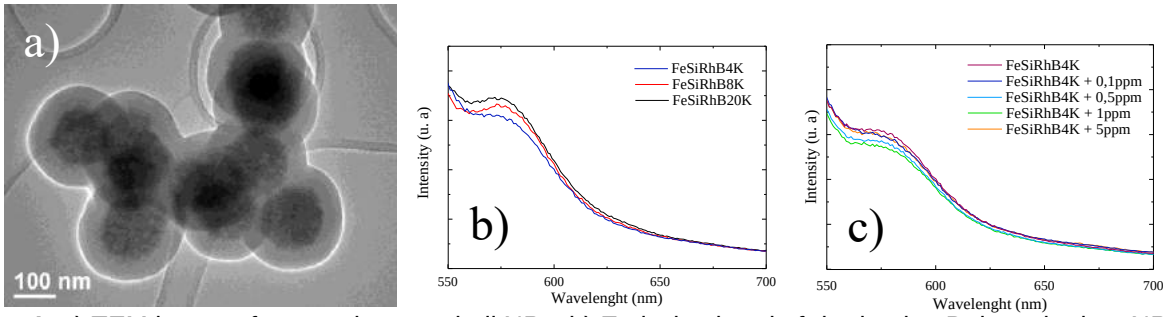


**Figure 1**. a) TEM image of magnetic core-shell NPs; b) Emission band of rhodamine B deposited on NPs and c) FeSiRhB4K NPs in the presence of Cu(II).

References:

[1] Y.H. Deng *et al. Colloids Surf. A* , 262 (2005) 87.
[2] C.G.S. Souza, W. Beck Jr., L.C. Varanda, *J Nanopart Res*, 15 (2013) 1545.

Acknowledgement: INCTAA, CNPq, FAPESP.

**Área: ANA** **Inscrição: 01239**

# Feasibility of miniaturazed system for light crude oil microwave-assisted digestion

**Tássia S. Seeger (PG), Paula Dalla Vecchia (PG), Letícia S. F. Pereira (PQ), Paola A. Mello (PQ), Érico M. M. Flores (PQ), Fábio A. Duarte (PQ).***

**tassiaseeger@gmail.com; fabioand@gmail.com**

*Departamento de Química, UFSM*

Palavras Chave: Crude oil, Sample preparation, Microwave-assisted digestion.

## Highlights

Parameters for crude oil digestion using miniaturized system were evaluated.
Several element were determined in crude oil.
Suitable limits of detection were achieved even using low sample amount.

## Resumo/Abstract

Crude oil may contain several elements with variable concentration, but some metals such as Fe, Ni and V have been known for causing problems during the refining process. Generally, a sample preparation method is required previously to the metals determination in crude oil to avoid matrix effects. In conventional digestion methods, a high sample mass is required, but in some cases low amounts are available. Therefore, the development of alternative and simple methods of sample preparation for crude oil is an important task for routine analysis. In this work, the microwave-assisted digestion (MAD) using miniaturized system was proposed for crude oil digestion. The miniaturized system was composed by three quartz microsampling inserts (3 mL each vessel) placed in a PTFE rack. About 25 mg of crude oil were weighed directly into the micro vessels followed by addition of 100 µL of concentrated $HNO_3$. This system was inserted into a vessel (containing 6 mL concentrated $HNO_3$) and submitted to microwave irradiation. Some parameters such as digestion solution ($HNO_3$ or $HNO_3$ + $H_2O_2$) and its volume were evaluated. The proposed method provides limits of detection of 0.47, 0.25 and 0.17 µg $g^{-1}$ for Fe, Ni and V, respectively, after determination by ICP-OES. For accuracy evaluation, results were compared with those obtained after conventional MAD and determination by, with agreement ranging from 90 to 98%.

1 J.H. Gary, G.E. Handwerk, Petroleum Refining: Technology and Economics, 4 ed. Marcel Dekker, 2001.
2 J.G. Speight, Handbook of Petroleum Analysis, John Wiley and Sons, 2001.
3 P.A. Mello, J.S.F. Pereira, M.F. Mesko, J.S. Barin, E.M.M. Flores, Anal. Chim. Acta 746 (2012) 15-36.

**Área: _ANA_____ Inscrição:___01177___**

# Avaliação do processo de difusão de BTEX em sistemas de amostragem passiva com membranas semipermeáveis utilizando acetonitrila como fase receptora.

**Tayene G. Martins (PG),[1*] Ricardo J. Cassella (PQ).[1]**

**tayene.quimica@yahoo.com.br**

[1]*Programa de Pós-Graduação em Química, Universidade Federal Fluminense, Outeiro de São João Batista s/n, Centro, Niterói, RJ, 24020-141, Brazil.*

Palavras Chave: *BTEX, Sistemas de amostragem passiva, Membranas semipermeáveis.*

## Highlights

Evaluation of the BTEX diffusion process in passive sampling systems with semipermeable membranes using acetonitrile as receptor phase.
BTEX diffusion using passive samplers.
Evaluation of interference between BTEX.

## Resumo

O crescimento populacional e da frota de veículos, são alguns dos fatores que contribuem para um aumento nas taxas de emissões de poluentes atmosféricos, dentre eles BTEX (benzeno, tolueno, etilbenzeno e xileno)[1]. A exposição da população a esses poluentes pode aumentar a probabilidade de adquirirem câncer ou outros danos a saúde[2]. A dificuldade no controle e fiscalização dessas emissões corroboram para que hajam mais estudos que controlem os poluentes do ar. Assim sendo, foi realizado um estudo qualitativo para avaliar a transferência de BTEX utilizando um amostrador passivo com fase aceptora líquida. Tal estudo foi realizado utilizando-se garrafa transparente com volume de 1 L (sistema fechado) contendo: papel de filtro, onde foram adicionados volumes conhecidos de padrão 1000 $mg.L^{-1}$ de cada analito (10, 20, 30 e 50 µL), e o dispositivo de membrana semipermeável (DMSP) com 3 ml de acetonitrila em seu interior. Os resultados obtidos indicam que processo de transferência de BTEX mostrou-se constante para xilenos e etilbenzeno, a medida que se aumentava o volume dos mesmos no meio, porém, o mesmo não foi observado para benzeno e tolueno, como apresentado na figura 1. Sendo assim, foram realizados estudos individuais para avaliar possíveis interferências em benzeno e tolueno. Os resultados obtidos comprovam que há uma queda de aproximadamente 70% no processo de transferência de benzeno e tolueno em contato com qualquer volume de xilenos e etilbenzeno no meio.

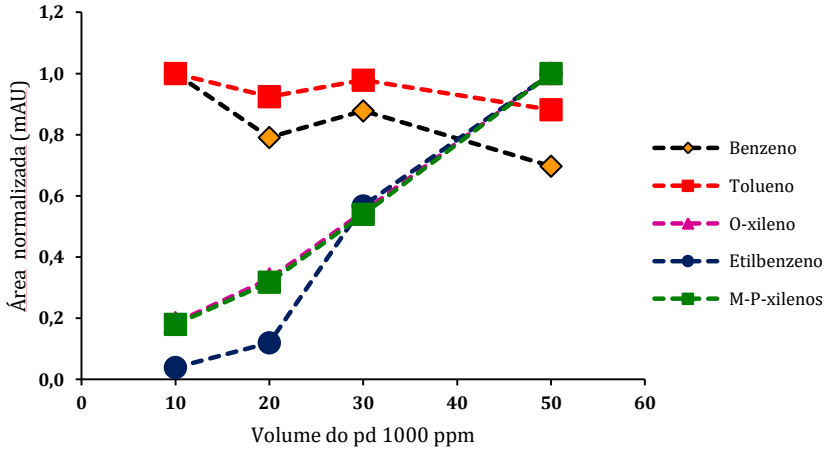


**Fig. 1.** Constância no processo de transferência de BTEX.

**Agradecimentos:** CNPq, CAPES, FAPERJ

[1] Ferreira S.L.; Santos A.M.; Souza, G.R.; Polito, W.L.; Módolo, D.L. Química Nova, 31, **2008**, 539.
[2] United States Environmental Protection Agency (US-EPA).

**Área: ANA** **Inscrição: 00912**

# Multiple Response for Determination of BTEX in Water Samples Produced Using Semipermeable Membranes for Passive Sampling

**Nicolle F. Robaina (PQ),[1*] Graziela F. B. Cruz (PG),[2] Ricardo J. Cassella (PQ).[2.]**

**nfrobaina@hotmail.com**

*[1]Departamento de Polícia Técnico-Científica, Polícia Civil Estado do Rio de Janeiro; [2]Departamento de Química Analítica, Universidade Federal Fluminense (Niterói, RJ).*

Palavras Chave: *Planejamento experimental multivariado, BTEX, Amostrador passivo, Membranas semipermeáveis, Água produzida.*

## Highlights

Aqueous samples with high salinity. Preparation of the sample based on the separation of the analyte. Doehlert matrix with two variables. Attractive method for estimation of BTEX concentration.

## Resumo/Abstract

Supersaline waters are complex samples that require the use of sample preparation based on analyte separation. In the oil industry it is common to co-produce huge volumes of water with high salinity containing inorganic and organic substances (such as benzene, toluene, ethylbenzene and xylenes - BTEX), which may present a risk to aquatic life. The objective of this work is to use low-density polyethylene semipermeable membrane devices (SPMD) to monitor the presence of BTEX by high performance liquid chromatography with ultraviolet detection in samples of produced water using multivariate experimental planning based on the Doehlert matrix with two variables in the quantification stage. The use of the Doehlert matrix was proposed due to previous studies that demonstrated the transfer rates alteration of the analytes in supersaline enviroment and the possibility of these variables interaction. The previously optimized procedure consists of a closed system containing 50 mL of aqueous solution of the analytes/sample and a SPMD filled with 3 mL of acetonitrile as the acceptor phase immersed in the solution for 4h. The multivariate study model was obtained using the analytes concentration (0,25 – 0,75 mg $L^{-1}$) and the salinity (15 – 150 ‰) as variables according to the experiments indicated by Doehlert matrix. The developed methodology was applied in real samples and the accuracy was obtained by recovery tests with good results which makes the method attractive for estimating the BTEX concentration in samples of produced waters.

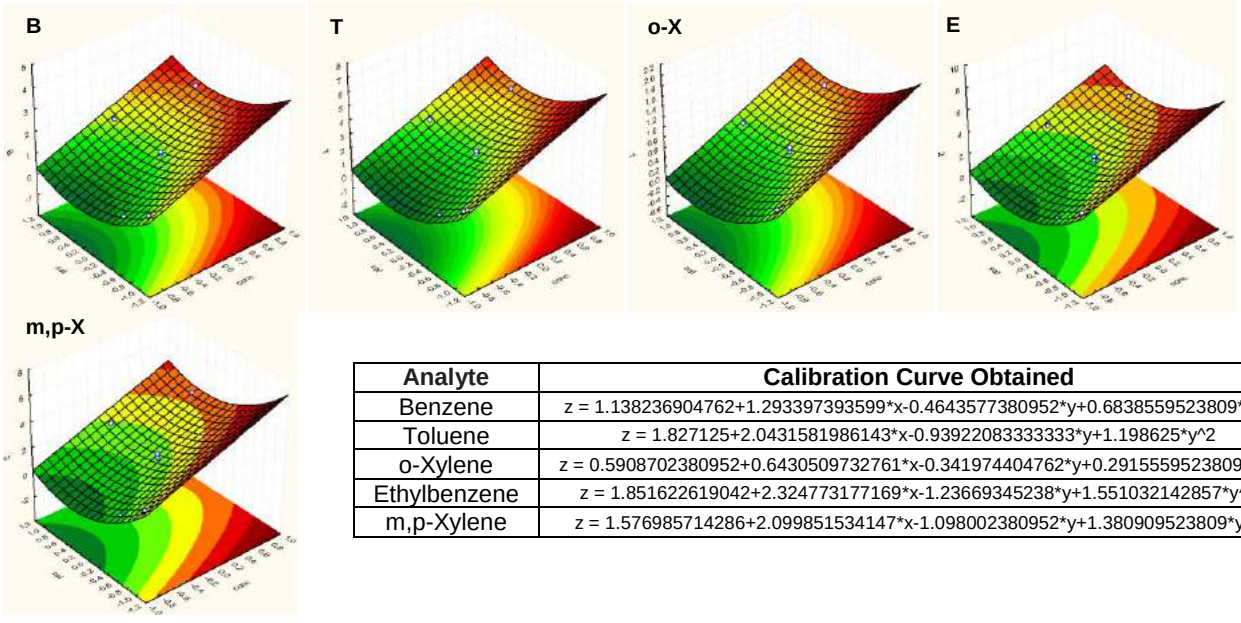


| Analyte | Calibration Curve Obtained |
|---|---|
| Benzene | z = 1.138236904762+1.293397393599*x-0.4643577380952*y+0.6838559523809*y^2 |
| Toluene | z = 1.827125+2.0431581986143*x-0.93922083333333*y+1.198625*y^2 |
| o-Xylene | z = 0.5908702380952+0.6430509732761*x-0.341974404762*y+0.2915559523809*y^2 |
| Ethylbenzene | z = 1.851622619042+2.324773177169*x-1.23669345238*y+1.551032142857*y^2 |
| m,p-Xylene | z = 1.576985714286+2.099851534147*x-1.098002380952*y+1.380909523809*y^2 |

**Área: ANA** **Inscrição: 00493**

# Corn stalks study (*Zea mays* L.) as adsorbent of the Chromium (VI) Oxyanion present in aqueous solution

**Ketheleen Tânia dos Santos de Oliveira (IC),[1] Raphaela Cristina Nascimento Rocha (IC),[1] Lhaís Araújo Caldas (PG),[2] Waldemar Alves Ribeiro Filho (PQ).[1]***

**rafacond_22@hotmail.com; warff@hotmail.com**

*[1] Faculdade de Tecnologia de Praia Grande – Centro Paula Souza; [2] Universidade Federal de São Paulo – UNIFESP.*

*Keywords*: *Adsorption isotherms, Biosorption, Chromium (VI), Corn stalks (Zea Mays L.), UV-Visible Spectrophotometry.*

## Highlights

Finding cheap materials from waste sources, such as bagasse, lumps, bark, straw and seeds, is an alternative to remove Chromium (VI) present in aqueous solution through adsorption techniques.

## Abstract

Corn stalks is the residue generated after corn (*Zea mays* L.) is threshed and presents adsorptive properties and water decontamination capacity.[1] In this study, assays varying the granulometry (50, 100 and 200 mesh), pH (2 to 10), agitation time (30 and 60 minutes) and chromium (VI) concentration (0.25 to 2.0 mg $L^{-1}$) were performed to verify the best adsorption conditions of this heavy metal. UV-Visible Spectrophotometry method was used to determine the presence of Chromium (VI) in aqueous solution in the form of oxyanions.[2] The biomass was dried crushed and subsequently grinding and separated using a mechanical sieve. The results showed that adsorbent particles of 100 mesh, aqueous solution of chromium (VI) with pH 6.0 and contact time of 30 minutes, are acceptable conditions to carry out the adsorption isotherm construction tests. The percentage of removal was greater than 84% (Figure 1). The Freundlich and Langmuir isotherms did not show good results and a nonlinear model allowed a better evaluation of the experimental curve (Figure 2).

**Figure 1 - Percentage of Removal as a function of initial concentration.**

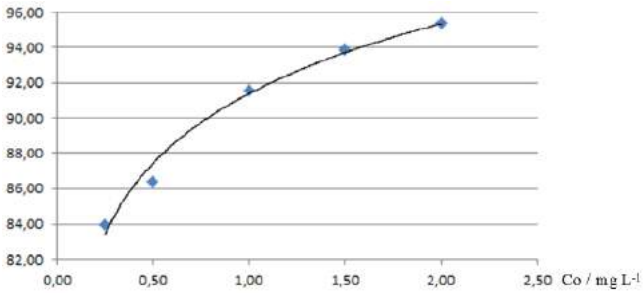


Source: performed research, 2017.

**Figure 2 – Isotherm. Non-linear model. Amount of adsorbed Chromium (VI) (Qeq) vs concentration of chromium (VI) in equilibrium (Ceq).**

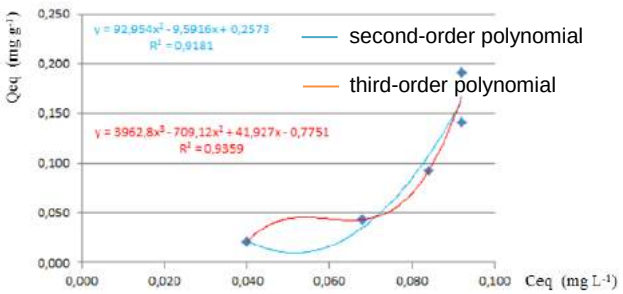


Source: performed research, 2017.

[Fixed conditions: $m_{adsorbent}$ = 1,00 g (100 mesh); pH = 6,0; V = 100 ml; $t_{contact}$ = 30 min; T = (25 ± 1)ºC]

The convex shape of the curve indicates an unfavorable isotherm due to the low removal capacity at low concentrations. The Sips linearized isotherm was also constructed and it was possible to calculate the maximum adsorption capacity (*Qmax* = 0.198 mg $g^{-1}$), the Sips constant ($K_S$ = 15.055 L $mg^{-1}$), the Gibbs Free Energy ($\Delta G^o$ = – 6.72 kJ $mol^{-1}$) and the parameter value that measures the degree of heterogeneity (n = 0.18). Finally, we conclude that this is an exergonic adsorption physical process (25°C) and as Brunauer can be classified as Type III or according to Giles class S and subgroup 1. [3]

### References

[1] NEVES, H. J. P.; NEVES, R. P.; da ROCHA, O. R. S. (**2015**) *Estudo da capacidade adsortiva de produtos naturais para tratamento de efluente por adsorção.* In: Anais do Congresso Brasileiro de Gestão Ambiental e Sustentabilidade - Vol. 3: Congestas, pp.633-637.

[2] CARNEIRO, M. C.; JÚNIOR, S. de S. H.; MONTEIRO, M. I. C.; SILVA, L. I. D. da S.; NETO, A. A. (**2007**) *Especiação de Cromo usando Método Espectrofotométrico e Análise Multicomponente.* In: Anais do Congresso do Centro de Tecnologia Mineral, CETEM.

[3] NASCIMENTO, R. F.; LIMA, A. C. A. L.; VIDAL, C. B.; MELO, D. Q. M.; RAULINO, G. S. C. (**2014**) *Adsorção: aspectos teóricos e aplicações ambientais.* Fortaleza: Imprensa Universitária.

**Área: ANA** **Inscrição: 00387**

# Comparative study between activated charcoal, *coffee grounds* and *fish scales* as adsorbents for Congo Red dye present in aqueous solution.

**Caroline Carvalho Bier (IC),[1] Raphaela Cristina Nascimento Rocha (IC),[1] Caíque Simão Santos (IC),[2] Matheus Naoto Ueyhara Garcia (IC),[2] Lhaís Araújo Caldas (PG),[3] Maria Fernada Palanch (PQ),[2] Waldemar Alves Ribeiro Filho (PQ).[1,2] ***

**carolcbier@gmail.com; warff@hotmail.com**

*[1] Faculdade de Tecnologia de Praia Grande – Centro Paula Souza; [2] Centro Universitário Monte Serrat – UNIMONTE; [3] Universidade Federal de São Paulo – UNIFESP.*

*Keywords*: *Adsorption, Coffee grounds, Fish scales, Congo Red, UV-Visible Spectrophotometry.*

## Highlights

The use of adsorbents such as *coffee grounds* and *fish scales* may be an alternative to remove Congo Red dye present in aqueous solution.

## Abstract

Activated Carbon is a form of pure carbon of great porosity that shows remarkable adsorptive properties attributed to its surface area, among them, the removal of impurities dissolved in solution.[1] Solid residues known as *coffee grounds* are the result of the industrial production of soluble coffee (*Coffea arabica* L.).[2] Tainha (*Mugil brasiliensis*) is a much consumed fish in Brazil and has scales firm and porous structure.[3] In this study, dry activated carbon had yours adsorptive properties compared to *coffee grounds* and *fish scales*. The two biomass was dried crushed and subsequently grinding and separated using a mechanical sieve. The biomasses were tested "*in nature*" and treated with NaOH (aq) 0.1 mole $L^{-1}$ for the removal of dye. UV-Visible Spectrophotometry method was used to determine the presence of Congo Red dye initially present in aqueous solution at the concentration of 1.0 mg/L.[4] After the analyzes were calculated the amount of adsorbed dye ($Q_{eq}$) and the percentage of the Congo Red removed from the solution (%$R$). Table 1 presents the results including the Congo Red concentration after treatment with the adsorbents ($C_{eq}$). In it the conditions under which the tests were performed are also presented.

**Table 1 - Percentage of removal and amount of adsorbed Congo Red dye (Qeq).**

| Adsorbents | Equilibrium concentration ($C_{eq}$ / mg $L^{-1}$) | Amount of adsorbed dye ($Q_{eq}$ / mg $g^{-1}$) | Percentage removed (%$R$) |
|---|---|---|---|
| Activated Carbon | 0.108 ± 0.031 | 0.089 ± 0.003 | 89.20 ± 3.11 |
| *Coffee grounds* | 0.197 ± 0.035 | 0.081 ± 0.004 | 80.35 ± 3.46 |
| *Fish scales* | 0.130 ± 0.028 | 0.087 ± 0.003 | 87.00 ± 2.83 |

[Fixed conditions: $m_{adsorbent}$ = 1.00 g (100 mesh); pH = 6.0; V = 100 ml; $t_{contact}$ = 30 min; T = (25 ± 1)ºC]

Source: performed research, 2017.

The results with the *fish scales* were better than those obtained with the *coffee grounds* and the two biomasses approached the values obtained with activated charcoal. The research will continue with tests varying the conditions of analysis and the construction of the isotherms of adsorption.

## References

[1] BANSAL, Roop Chand and GOYAL Meenakshi. *Activated Carbon Adsorption.* New York, CRC Press – Taylor & Francis Group, **2005**.

[2] SOARES, Larissa de Souza; MORIS, Virgínia Aparecida da Silva; YAMAJI, Fábio Minoru e PAIVA, Jane Maria Faulstich de. *Utilização de Resíduos de Borra de Café e Serragem na Moldagem de Briquetes e Avaliação de Propriedades.* Revista Matéria (Rio J.) [online]. **2015**, vol.20, n.2, pp.550-560.

[3] VIEIRA, Maria de Fátima Pereira. *Determinação de Ba, Cd, Cr, Cu, Ni, Pb, Sn e Zn em Tainha (Mugil brasiliensis) nos estuários potiguares.* Tese (Doutorado) – Universidade Federal do Rio Grande do Norte. Natal, **2007**.

[4] SKOOG, Douglas A.; CROUCH, Stanley R. & HOLLER, F James. *Princípios de análise instrumental.* Editora Artmed, 6ª ED., **2009**.

**Área: ANA** **Inscrição: 00624**

# Study on the formation and stabilization of the derived free radical from the N-(4-methoxyphenyl)-p-phenylenediamine. Reactivity to phenolics.

**Lucas B. Oliveira (IC), Horacio D. Moya (PQ)[1]*.**

**lucasbelini@outlook.com; horacio.moya@fmabc.br**

*[1] Faculdade de Medicina da Fundação do ABC – CEPES (Centro de Estudos, Pesquisa, Prevenção e Tratamento em Saúde) – CEP – 09060-650 – Santo André – SP – Brazil.*

Key words: *N-(4-methoxyphenyl)-p-phenylenediamine, MPPD$^{\bullet+}$, Free radical, Phenolic acids, Spectrophotometry*

## Highlights

N-(4-methoxyphenyl)-p-phenylenediamine (MPPD) is an amine used as indicator in the complexometric titration but under certain conditions gives the free radical MPPD$^{\bullet+}$ which reacts with antioxidants.

## Abstract

MPPD, also known as variamine blue[1], was oxidized by $Fe^{3+}$ and $S_2O_8^{2-}$ (solutions) and $MnO_2$ and $Co(OH)_3$ (powder) in acid medium giving the corresponding purple free radical ($\lambda_{max}$ 569 nm) (Eq. 1). All oxidants used were effective. Excess of $MnO_2$ and $Co(OH)_3$ need to be centrifuged. $S_2O_8^{2-}$ shows a higher % decrease in the $A_{569nm}$ *vs*. time, hence $Fe^{3+}$ was chosen.

$$\text{MPPD} + \text{Oxidant} \xrightarrow{H+} \text{Reducing} + \text{MPPD}^{\bullet+} \qquad \textbf{(1)}$$

At 7.0 ≤ pH ≤ 12 the MPPD$^{\bullet+}$ seems not to be formed. At (6.0 ≤ pH ≤ 7.0) MPPD$^{\bullet+}$ is formed but disappears after 30 minutes. At (3.0 ≤ pH ≤ 5.0) there was a maximum [MPPD$^{\bullet+}$] but pH 4.0 (acetate buffer) was chosen because it showed the smallest decrease in [MPPD$^{\bullet+}$] after 30 min. Two water-soluble solvents were tested. Ethanol and 1,4-dioxane promoted sharp decrease in the $A_{569nm}$ *vs*. time. Finally, the method of continuous variations showed that the reaction stoichiometry is 2 [$Fe^{3+}$]: 1 [MPPD] but a 5-fold [MPPD] excess should be used to increase the stability of MPPD$^{\bullet+}$ for analytical applications.

Table I shows the reactivity of MPPD$^{\bullet+}$ (represented by $AA_{EC}$) to some phenolic acids (Eq. 2). $AA_{EC}$ values were found dividing the "slope" of the analytical curve of phenolic acids by the "slope" of AA (ascorbic acid) analytical curve. As can be seen, $AA_{EC}$ varies according to the number and also the position of -OH (Fig. 1).

$$\text{MPPD}^{\bullet+} + \text{Phenolic acid} \rightarrow \text{MPPD} + \text{Phenolic acid}_{\text{oxidized}} \qquad \textbf{(2)}$$

Table I - Reactivity of MPPD$^{\bullet+}$ to some phenolic acids

| Phenolic acid | PHG | $R_1$ | $R_2$ | $R_3$ | $R_4$ | $R_5$ | FW | LR×$10^6$ | $AA_{EC}$ |
|---|---|---|---|---|---|---|---|---|---|
| Phenol | 1 | H | H | H | H | H | 94.11 | 2000-10000 | 0.001 |
| *p*-Coumaric acid | 1 | H | H | CH=CH-COOH | H | H | 164.16 | 100-500 | 0.046 |
| Resorcinol | 2 | H | OH | H | H | H | 110.00 | 100-500 | 0.047 |
| *o*-Pyrocatechol | 2 | OH | H | H | H | H | 100.10 | 100-300 | 0.100 |
| Gallic acid | 3 | OH | H | COOH | H | OH | 170.12 | 10-50 | 0.470 |
| Pirogalic acid | 3 | OH | OH | H | H | OH | 126.11 | 1-5 | 3.90 |
| Ascorbic acid | - | - | - | - | - | - | 176.13 | 10-30 | 1.00 |

PHG = phenolic hydroxyl group; FW = Formula weight; LR = linear range (mol $L^{-1}$) and $AA_{EC}$ = ascorbic acid equivalent capacity

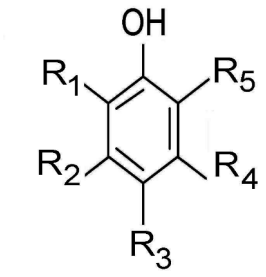


Figure 1

1] Pankratov, A. N.; Mushtakova, S. P. *Journal of Analytical Chemistry* (2000), 55 (8), 715-718.

**Área:** ANA **Inscrição: 00702**

# DISTRIBUTION OF CRUDE OIL SARA FRACTIONS IN SOIL: AN ONSHORE SPILL SIMULATION

**Julian Eduardo Ballén Castiblanco (PG),[1*] Jandyson Machado Santos (PQ),[2] Alberto Wisniewski Jr (PQ),[1]**

**julianbc@outlook.com**

*[1]Departamento de Química, UFS; [2]Insituto de Química, UNICAMP.*

Keywords: *(Crude oils, Spill, SARA, Gas chromatography, Mass spectrometry).*

## Highlights

- Chemical composition changes of crude oil fractions (saturate, aromatics and resins) in contact with soil;
- Investigation by Orbitrap-MS of the resins fraction of crude oils in a spill simulation.

## Resumo/Abstract

Contamination of terrestrial environments by oil spills is a recurrent fact in the world, which creates biological risks to the humans´ and ecosystems´ health. The studies about oil spill aim to evaluate the toxicity and changes in the chemical composition of soils and waters, in a field of potential interest to the scientific community. In this context, the present work evaluated the changes in the chemical composition of crude oil fractions after the simulation of a spill in soil with emphasis on a temporal investigation. Samples of oils from the Sergipe-Alagoas basin and soil from the rural area of São Cristóvão-SE were used. The simulation was performed with a 40:1 (*m/m*) mixture of soil/oil with direct influence of a 60 Hz lamp. The aliquots were taken from the system at times of 1, 12, 24, 36 and 72 hours, then were extracted with toluene and submitted to SARA fractionation and GC-FID analysis. Preliminary SARA gravimetric data (Table 1) showed that the saturated fraction decreased from 57.8% to 40.1%, while the GC-FID chromatographic profiles were similar, when compared the 72 hours oil and the initial crude oil. The aromatic fraction showed a slight increase and the resins remained constant through the exposure time (from 1 to 72 hours) but decreased when compared with the initial crude oil. Recent analysis by Orbitrap-MS have shown that the mass spectrum profile changes throughout the oil exposure process to the soil.

**Table 1.** Gravimetric percentages of SARA fractionation

| | Exposure time (hours) | | | | | |
|---|---|---|---|---|---|---|
| **Fractions* (%)** | **Crude oil** | **1** | **12** | **24** | **36** | **72** |
| Saturate | 57.8 ± 1.7 | 44.5 ± 1.5 | 43.3 ± 0.6 | 43.1 ± 0.8 | 40.3 ± 1.1 | 40.1 ± 1.8 |
| Aromatic | 13.7 ± 3.9 | 12.6 ± 2.3 | 13.1 ± 1.8 | 14.0 ± 1.8 | 15.0 ± 0.9 | 15.4 ± 0.4 |
| Resins | 17.4 ± 0.3 | 11.1 ± 0.9 | 11.1 ± 0.6 | 11.1 ± 1.1 | 11.4 ± 0.2 | 11.4 ± 1.0 |

**N = 2 (95% confidence interval)*

**Área: ANA** **Inscrição: 00916**

# Soil texture classification by Mid-infrared spectroscopy (MIR)

**Pedro A.O. Morais (PG),[1*] Diego M. Souza (PQ),[1] Beata E. Madari (PQ),[2] Márcia T.M Carvalho (PQ).[2]**

**pedro_augusto_04@hotmail.com**

*[1]Instituto de Química, UFG; [2]Embrapa Arroz e Feijão*

Palavras Chave: Classificação Textural, Método da Pipeta, MIR, Química Verde, LS-SVM.

## Highlights

- Textural classification is usually determined based on analysis by the Pipette method;
- This study proposes the classification of soil texture by MIR, a more operational and clean method.

## Resumo

A classificação textural do solo é um parâmetro de fertilidade determinado de acordo com as proporções das partículas físicas, areia, silte e argila (Gee e Bauder, 1986), Figura 1.

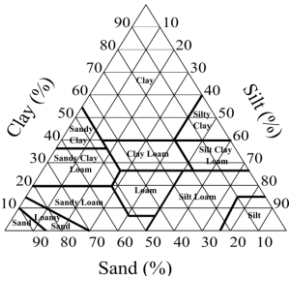


**Figura 1** – Diagrama triangular utilizado na classificação textural.

A quantificação dessas partículas é geralmente realizada pelo método da Pipeta. Este método, embora seja simples, apresenta baixa produtividade e gera um volume considerável de resíduo. Diante disso, metodologias verdes e de maiores rendimentos em análise de solo vêm se destacando. Nessa direção, o objetivo deste trabalho é propor uma metodologia de classificação textural através de MIR e do método de calibração multivariado máquinas de vetores de suporte por mínimos quadrados (LS-SVM). Para isso, um total de 1083 amostras de solo de diversas regiões do Brasil foi analisado utilizando o método da Pipeta. Em seguida, espectros de MIR foram obtidos de cada amostra. Após a subdivisão das amostras entre calibração e validação utilizando o algoritmo Kennard-Stone (Kennard e Stone, 1969), utilizou-se a ferramenta LS-SVM para classificar as amostras do conjunto de validação em 12 grupos texturais. As classificações texturais determinadas pelo LS-SVM foram comparadas com as obtidas pelo método da Pipeta. Obteve-se uma taxa de acerto de 81%.

A classificação textural por MIR além de ser um método não destrutível, apresenta alta produtividade de ensaio, e também um baixo impacto ambiental em relação à metodologia de referência.

## Agradecimentos

UFG CAPES CNPq

[1] Gee, G. W., & Bauder, J. W. Particle-size analysis. Methods of soil analysis: Part 1 - Physical and mineralogical methods, 383-411, 1986.
[2] Kennard, R. W.; Stone, L. A. Tecnometrics. 1969, 11, 137.

**Área: ANA** **Inscrição: 00812**

# Microdispositivo em papel para pseudotitulação ácido-base baseado em medida da distância

**[1]Rafaela F. de Oliveira (PG),[1] Paula J.C. Silva (PG),[1] Mauro Korn (PQ).[1*]**

**rafaelaferoliver@hotmail.com; mkorn@uneb.br**

*[1]Departamento de Ciências Exatas e da Terra, UNEB*

Palavras Chave: *Miniaturização, Microdispositivos em papel, Pseudotitulação, Concentração ácida*

## Highlights

Paper microdevice for acid-base pseudotitration based on distance measurement.

The proposed microdevice for determination of acid concentration was produced layer-by-layer
Acid concentration in sample solution is determined by analytical curve as in pseudo-titration methods

## Resumo/Abstract

Um microdispositvo em papel foi desenvolvido explorando a técnica de colagem de camada sobre camada. Assim, uma tira seca de papel quantitativo (3,7 x 50 mm) previamente tratada com solução centimolar de NaOH era fixada com cola e sensibilizante sobre folha de acetato cristal e exposta à radiação UV. A cola atuava como barreira hidrofóbica e definia o canal fluídico sobre o papel. Esse dispositivo foi empregado para determinar concentrações de soluções ácidas (entre 2 e 12 mmol.$L^{-1}$), explorando características inerentes às titulações de neutralização com indicação visual do ponto final. 40 µL da amostra (ácido) era adicionada numa das extremidades do canal microfluídico e era deixada em repouso para fluir por capilaridade. Após *ca.* 10 min, o dispositivo estava seco e então era inserido o indicador (vermelho de metila) com pincel sobre todo o canal e esse adquiria coloração vermelha (zona ácida) e amarela (zona alcalina). Finalmente, com o auxílio de uma régua era medida a distância entre o ponto de aplicação da amostra e o ponto em que era observada a transição de cor (vermelho para amarelo). Para a determinação da concentração da solução ácida era traçada uma curva de calibração (concentração x distância). Esses microdispositivos, apesar de não serem reutilizáveis, podem ser armazenados embalados por até 3 dias. Também foi observado que o indicador poderia ser aplicado até 24 h após feita a adição da amostra, sem comprometimento dos resultados, facilitando seu uso em monitorações *outdoor*.

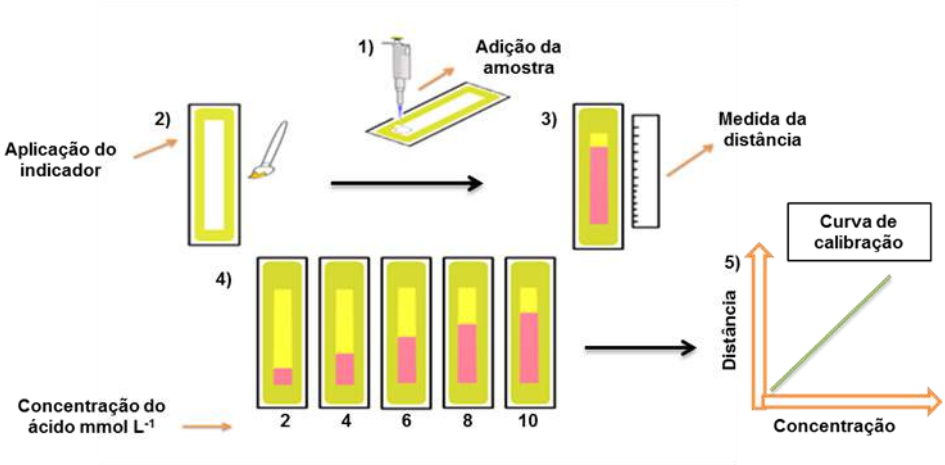

**Área: ANA** **Inscrição: 00991**

# Synthesis of chitosan films for the quantification of Indigotine in candy samples by digital image analysis

**Igor Coreixas (PG),[1] Wagner F. Pacheco (PQ),[2]**
**igorcoreixas@gmail.com; wfpacheco@id.uff.br**

[1] *Departamento de Química Analítica, Universidade Federal Fluminense (UFF), Niterói/RJ, Brazil*

Keywords: *Digital image analysis, Chitosan films, Indigotine, Adsorption, Candy*

## Highlights

•The technique of digital image analysis of the adsorbed chitosan film showed a good linearity in the concentration's interval of 0,1 mg.L$^{-1}$ to 10mg.L$^{-1}$ of indigotine.
•The spike curve had statistically the same inclination coefficient as the standard curve, corroborating the absence of matrix effect in candy samples.

## Resumo/Abstract

Chitosan is a linear polysaccharide derived from the deacetylation of Chitin, which is the second most abundant polysaccharide found naturally, it's present mainly in the exoskeleton of crustaceans[1]. Due to some characteristics such as biodegradability, non-toxicity, high abundance, surface area and especially high adsorption, chitosan films are a great alternative for the removal of food dyes. Therefore, the aim of this work is to evaluate the making and usage of chitosan films for the adsorption of Indigotine as well as the quantification of this dye by digital image analysis.

The chitosan films were prepared by the casting method proposed by *Nga et al*[2]. Some parameters were studied such as surface area, pH, adsorption time, dye concentrations and buffer to evaluate the optimum parameters. The analytical signal was obtained by sticking the films on a paper and scanning it with a flatbed scanner to obtain the digital image. Hence, the image was treated using the software *ImageJ* in terms of RGB pixel frequency.

This study showed that the analytical signal is higher when decreasing the surface area of the film. The best pH was 7,5 which is ideal for food samples, as sorption time increases it also increases the signal and it reaches an equilibrium in 90 min. The buffer phosphate/citric acid 0,1M was used. Lastly, a calibration curve and spiking curve were made, and it had nearly the same inclination coefficient, both with a reasonable good linearity as shown below.

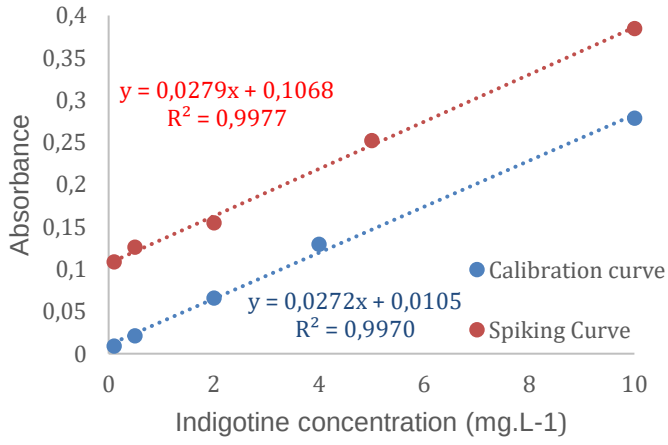


Image 1: Calibration curve and spiking curve

Image 2: Digital image of the calibration curve (0,1-10mg.L$^{-1}$)

References:

1. Rinaudo,M. *Prog. Polym. Sci.* 31 (2006) 603-632.
2. Nga, N.K; Chinh, H.D.; Hong, P.T.T.; Huy, T.Q.; *J. Polym. Environ.* (2017), 25:146-155.

**Área: ANA** **Inscrição: 00188**

# Construção e avaliação de um colorimetro portátil para análise do teor de acido acético em vinagre empregando sistema FIA.

***Nathália Carvalho Costa* (PG),[1*] Gizele Aparecida de Almeida (IC),[2] Mariele Chagas Bueno (IC),[3] Pedro Orival Luccas (PQ),[1] Giovana de Fatima Lima (PQ),[2] Célio Wisniewski (PQ)[3]**

**nathyquimica08@yahoo.com.br**

[1]*Departamento de Ciências Exatas, Instituto de Química, UNIFAL*

Palavras Chave:*(óleo vegetal, titulação ácido-base, automação, FIA).*

## Highlights

Continuous flow analysis system for determination of acetic acid in vinegar samples. Gravity-driven flow injection analysis. Portable photocolorimeter

## Resumo/Abstract

Embora a literatura reporte diferentes procedimentos para fins de determinação de acido acético em vinagre, grande parte baseada em titulação convencional e potenciométrica. Neste trabalho propõe o desenvolvimento de um sistema de análise em fluxo (FIA) impulsionado por gravidade e acoplado a um colorímetro portátil desenvolvido em laboratório para determinação desse índice visando minimizar custo e melhorar resultado analitico. O colorimetro contém diodo emissor (LED-RGB), fotodiodo como sensor, cubeta em acrílico com passo ótico 2 cm, LEDs e fotodiodos acoplados na cubeta sem necessidade de janelas, conversor analógico digital de uma placa arduino uno® e programa desenvolvido Visual Basic® para aquisição de dados. Fatores: alça de amostragem (AA), reator (R), vazão dos reagentes (V) e concentração da base (CB) foram otimizados de maneira multivariada usando planejamento fatorial $2^4$ os resultados são apresentados no Diagrama de Pareto abaixo. Assim condições de análise foram: CB 0,001 mol.$L^{-1}$, AA 300 cm (1,5 mL), R 100 cm; V 1,8 ml/min. O sistema apresentou faixa linear 3,55x$10^{-4}$ g $L^{-1}$ a 1,10 g $L^{-1}$. y=9,69038+87,8137; frequência analítica de 30 leituras/h, precisão 0,58% e 1,2% para HCl 0,005 e 0,01 mol.$L^{-1}$, respectivamente. Limites de detecção e quantificação 1,02x$10^{-3}$ e 3,37x$10^{-3}$ g$L^{-1}$ respectivamente. A metodologia otimizada foi aplicada em amostras de vinagre de maçã e alho. A tabela 1 apresenta os resultados obtidos, nota-se boa concordância e viabilidade entre os métodos. O equipamento é de baixo custo (~100 reais), rápido e desempenho analítico satisfatório em precisão e exatidão.

**Tabela 1:** resultados obtidos experimentalmente com amostra de vinagre de maçã e alho.

| *Amostra* | *Sistema FIA (%)* | *MétodoPadrão(%)* | *Erro %* |
|---|---|---|---|
| Vinagre de maçã | 6,87±0,08 | 6,59 | -0,04 |
| Vinagre de alho | 4,21±0,15 | 4,58 | -7,9 |

FERREIRA, S. L. C.; SANTOS, W. N. L.; QUINTELLA, C. M.; NETO, B. B.; SENDRA, J. M. B. Doehlert matrix: a chemometric tool for analytical chemistry—review, Talanta 63 (2004) 1061–1067, 2004.

TROJANOWICZ, M.; KOŁACIŃSKA, K. Recent advances in flow injection analysis. The Royal Society of Chemistry, 141, 2085–2139, 2016.

**Área: ANA** **Inscrição: 00682**
*(Inserir o número de inscrição do autor que fez a submissão)*

# 3D-printed platform for highly-reproducible handling of microvolumes and nanofluidic injection coupled to electrochemical detection

**Dianderson M. H. Mendonça (PG)*,[1] Diego P. Rocha (PG),[1] Gustavo S. V. Dutra (IC),[1] Rafael M. Cardoso (PG), Alex D. Batista (PQ),[1] Eduardo M. Richter (PQ),[1] Rodrigo A. A. Munoz[1] (PQ).**

**dianderson.mendonca@gmail.com;**

[1]*Departamento de Química, Universidade Federal de Uberlândia*

Palavras Chave: *Automated system, Mechanized system, Microfluidic, Nanofluidic*

## Highlights

Portable, low-cost and mechanized analytical system constructed using 3D-printing technology.

Demonstration of the proposed system with electrochemical detectors for antioxidant and forensic analyses.

## Resumo/Abstract

Automated or mechanized systems are a worldwide trend in the last years. The reduction of demand for qualified professionals and greater agility are some of the main advantages of these systems. In industry and laboratories the annulment of analyst error is demanded, and in this context, this work presents a mechanized system fabricated using 3D-printing technology, capable of manipulating microvolumes and performing nanofluidic injections on different electrochemical sensing platforms. Stepper motors, microcontroller (Arduino), Lead Screw, electronics components, syringe and 3D-printed structural components were used to construct this analytical system. The electrochemical system was composed of portable potentiostat, 3D-printed electrochemical cell and different electrodes evaluated to demonstrate the wide range of applications. This system was applied for: 1) the determination of total antioxidant capacity based on the monitoring of DPPH radical by amperometric detection on glassy-carbon electrode; and 2) determination of common adulterants in seized cocaine samples using screen-printed electrodes. The proposed analytical system enabled the preparation of standard solutions based on the dilution of a stock solution in electrolyte in mechanized manner. Handling of microliter aliquots was very precise (RSD<1%). Moreover, controlled injections of 500 nL of standard or sample solutions can be performed over the working electrodes in a highly-reproducible way (current RSD<2%). Compared with flow-injection and batch-injection analysis, this mechanized analytical system is more reproducible, faster, and enables programmed obtaining of calibration curve and nanoliter injections of samples for real-time electrochemical monitoring.

Acknowledgements: FAPEMIG, CAPES, CNPq, IQUFU.

**Área:** ANA **Inscrição:** 00742

# Use of external electrolysis to improve electrophoretic separations of sugars on glass microfluidic devices

**Gerson F. Duarte-Junior (PG),[1]* Eulício O. Lobo-Júnior (PG),[1] Iris Medeiros Junior (PQ),[2] José A. Fracassi da Silva (PQ),[3] Claudimir L. do Lago (PQ),[4] and Wendell K. T. Coltro (PQ)[1].**

***gduartejr16@gmail.com**

*[1]Instituto de Química, UFG; [2]Centro de Pesquisas e Desenvolvimento Leopoldo Américo Miguez de Melo, Petrobrás; [3]Instituto de Química, Unicamp; [4]Instituto de Química, USP.*

Palavras Chave: Carbohydrates, Microchip, Electrophoresis

## Highlights

Separated electrolysis system was implemented in microfluidic systems.
Separation of five sugars was achieved in less than 300 s.
Stability on migration time as improves on separation parameters was reached.

## Resumo/Abstract

In electrophoresis, applying high voltage on electrolytes with high conductivity and ionic strength can lead to a variation in terms of migration times due to the electrolysis phenomena. This effect can compromise the separation reproducibility and repeatability. Herein, we propose the adaptation of a scheme to minimize the electrolysis in microfluidic systems. The proof-of-concept was tested on the separation of five sugars, including sucrose (SUC), Lactose (LAC) galactose (GAL), glucose (GLU) and Fructose (FRU), using a high pH electrolyte to promote the ionization of sugars. A commercial microchip electrophoresis system model ER455 Quad MCE System ( eDAQ pty, Austrália) and a glass microchip (T85100C4D, Micronit, Netherlands) with 90 mm long was employed to perform the separations. Separated electrolysis system was made by applying the voltage in four 1.5 mL polypropylene tubes connected to microfluidic platform reservoirs by a saline bridge made with Tygon tubes (0.4 mm i.d.). Firstly, an electrolyte composed by NaOH (75 mmol/L) was used to promote the separation of SUC, GLU and FRU (Fig. 1A). A variation on migration time and co-migration between FRU and GLU were observed. In the 7th run, it was observed that SUC peak disappeared indicating that it was neutral and co-migrating with EOF marker (water). Trisodium phosphate (15mmol/L) was added to insert a buffering effect and increase the ionic strength, improving the separation between FRU and GLU. The improvement on the performance allowed the addition and separation of LAC and GAL to the previous mixture (Fig. 1B). However, the problem remained unaltered. To minimize the electrolysis, the separated electrolysis system was implemented reaching now the complete separation of the five sugars and improved stability and repeatability (Fig. 1C). With the external reservoirs, the variation in terms of migration times was reduced from 4% to less than 1%. Also, the separation efficiency was increased from c.a. 14,000-29,000 plates/m to ca. of 45,000-70,000 plates/m for the five sugars. In summary, we propose for the first time the electrophoretic separation of five sugars in a microfluidic system. This was achieved due to the use of additional reservoirs for external electrolysis that ensured stability on migration times and resolution working with a high conductive and ionic strength electrolyte. Moreover, external electrolysis provided enhanced separation efficiency.

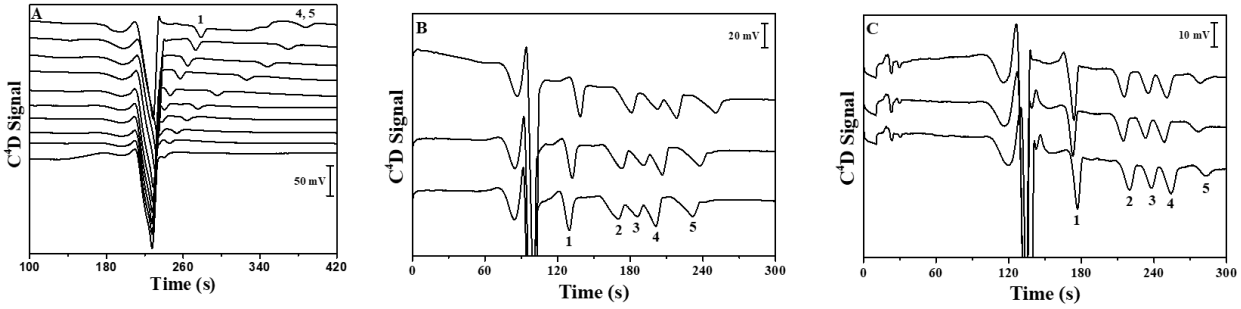


***Figure1.*** *(A) Electropherograms for a sequence of ten runs for a separation of (1) SUC, (4) GLU and (5) FRU (5 mmol/L each) in MCE, showing the decrease of time of migration for sugars. (B and C) Electropherograms obtained for separation of (1) SUC, (2) LAC, (3) GAL, (4) GLU and (5) FRU with the addition of trisodium phosphate 15 mmol/L to the electrolyte. In (B), the separation was performed without external electrolysis system, while in (B) it was used. Samples were electrokinetically injected by applying 1kV during 10 s and separated by 2.4 kV. Electrolyte: NaOH 75 mmol/L and Detection: 200 kHz and 100 Vpeak-to-peak.*

**Área: ANA** **Inscrição: 01154**

# Detecção colorimétrica de $H_2O_2$ em amostras de leite utilizando dispositivos analíticos fabricados em papel

**Bárbara Guerra de Souza Guinati (IC)[1*], Thiago Miguel Garcia Cardoso (PG)[1], Wendell Karlos Tomazelli Coltro (PQ)[1]**

**barbaraguinati@hotmail.com; wendell@ufg.br**

*[1]Laboratório de Microfluídica e Eletroforese, Instituto de Química, Universidade Federal de Goiás, Goiânia, GO, Brasil*

Palavras Chave: *Detecção colorimétrica, dispositivos analíticos, química forense, controle de qualidade de leite.*

## Highlights

Colorimetric detection of $H_2O_2$ in milk samples using paper-based analytical devices.
Two different colorimetric methods were performed to identify $H_2O_2$ in milk samples using paper-based devices. The proposed methods reached LD of 324 µM and 14,5 µM.

## Resumo/Abstract

Os dispositivos analíticos a base de papel (PADs) são ferramentas alternativas de uso no *point-of-care*, pois são dispositivos de fácil fabricação, custo quase zero e requerem instrumentação mínima para utilização em campo. Estas plataformas analíticas de baixo custo podem ser utilizadas em vários métodos de análise, viabilizando o seu uso no monitoramento de qualidade de produtos comerciais, como por exemplo, o leite.
A adição de peróxido de hidrogênio ($H_2O_2$) no leite tem como objetivo diminuir a quantidade de microrganismos, porém, no Brasil o seu uso é proibido seguindo-se o Regulamento do Ministério da Agricultura, que considera fraudado, adulterado ou falsificado o leite que contenha substâncias conservadoras. Neste sentido, este trabalho apresenta o uso de PADs para detecção de $H_2O_2$ em amostras de leite via detecção colorimétrica. Os dispositivos foram fabricados utilizando a técnica de impressão a cera desenvolvida por Carrilho e colaboradores (Analitical Chemistry, 2009, 81, 7091-7095) em que a geometria escolhida foi a de spot test. As análises foram realizadas utilizando dois métodos colorimétricos.
No primeiro método, utilizou-se KI como reagente cromógeno e obteve-se uma faixa linear entre 1,0 e 6,0 mM (Figura 1A e 1B). Enquanto que no segundo método, obteve-se uma faixa linear de 0,2 a 1,0 mM, como mostra a Figura 1C e 1D, empregando-se uma mistura de 2-4-aminoantipirina (4-AAP) e 3,5-dicloro-2-hidroxibenzeno sulfonato (DHBS) como reagentes cromógenos na presença de peroxidase para catalisar a reação. Os LDs encontrados demonstram a potencialidade do dispositivo para o controle de qualidade de leite com geração zero de resíduo. Estudos eletroquímicos estão sendo realizados a fim de se acoplar ambas as técnicas de análise em um dispositivo único para detecção desse analito em amostras de leite.

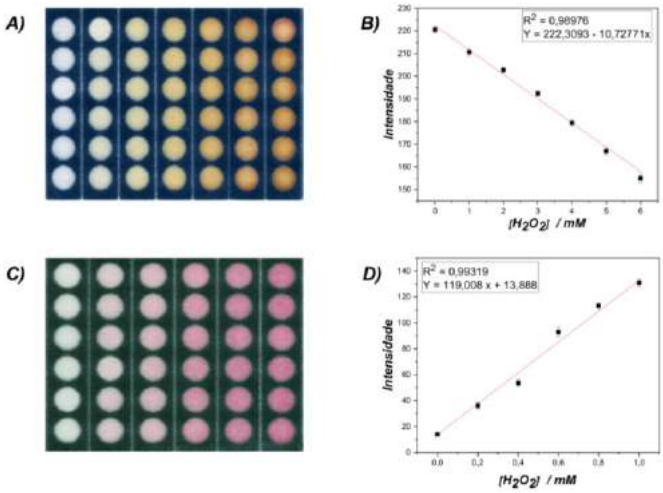


Figura 1: Dispositivos utilizados e curvas analíticas obtida para detecção de $H_2O_2$. A e B refere-se ao método de detecção com iodeto de potássio, o limite de detecção (LD) para este método foi de 324 µM. Bem como C e D refere-se ao método para detecção utilizando 4-AAP/DHBS e peroxidase, o qual apresentou um LD igual a 14,5 µM. O canal de cor utilizado para as análises foram RGB e Magenta, respectivamente.

**Área: ANA** **Inscrição: 01161**

# Contactless conductivity detection of bacteria in droplets using 3D printed microfluidic device

**Lucas C. Duarte (PG)[1], Federico Figueredo (PG)[2], Luiz E. B. Ribeiro (PG)[1], Eduardo Cortón (PQ)[2] and Wendell K. T. Coltro (PQ)[1]**

**lucascd@outlook.com**

*[1]Instituto de Química, UFG; [2]Departamento de Química Biológica e IQUIBICEN´ −CONICET, UBA*

Keywords: 3D printing, Microfluidics devices, Bacteria detection, Droplets, Contacless detection, Printed electrodes.

## Highlights

Microfluidic device with integrated electrodes manufactured entirely by 3D printing;
Detection of bacteria in droplets generated in microfluidic channels by contactless conductometric detection.

## Resumo/Abstract

Electrochemical detection has been widely explored in microbiology grow monitoring due to its flexibility and compatibility with microfluidic systems. However, traditional methods of manufacturing microfluidic systems require specialized and costly instrumentation, as well as laborious steps such as sealing. In this way, 3D printing has become an alternative manufacturing method for analytical microdevices because it allows automated, single-stage and low-cost fabrication. In this sense, this work presents an electrochemical approach to monitor and quantify bacteria cells in microdroplets by means of contactless conductometric detection $C^4D$ system. The microdevice was manufactured using 3D printer with fused deposition modeling (FDM) technology containing integrated electrodes consisting of polylactic acid (PLA) doped with carbon nanotubes. The droplets containing E. coli were generated by pumping the bacterial sample as the dispersed phase in microchannel I, while the continuous phase (mixture of oil and 1% Span 80) was pump in microchannel II, shown in Figure 1A. Through the statistical method of Poisson it was possible to estimate bacteria quantity per drop referring to the injected bacterial density. In this way, the $C^4D$ signal intensity value was plotted against the logarithm of the number of bacteria found per drop, which can be seen in Figure 1B. A linear profile was found between the second and last four points of the curve with $r^2 = 0.9864$, a satisfactory response to the proposed detection system showing its high potency to be used in the cell count on microfluidic devices.

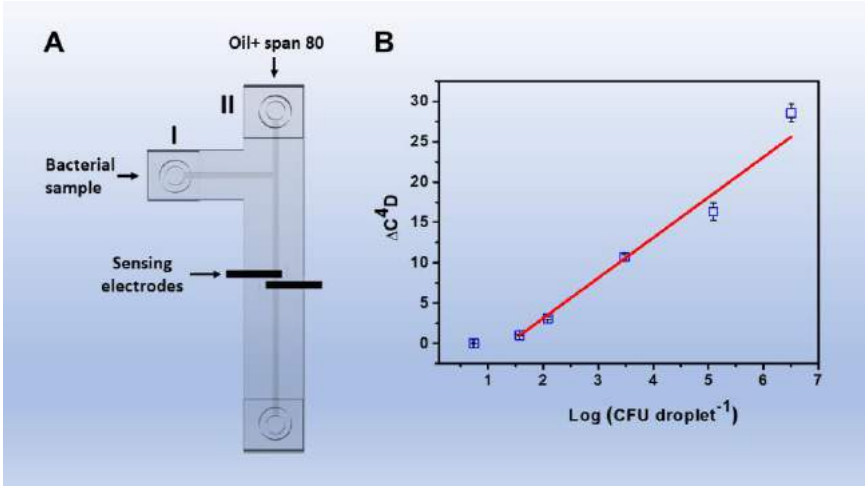


**Figure 1**: In (A) Schematic representation showing the microdevice 3D printing containing the microchannels in T-junction format and the pair of integrated electrodes. The bacterial sample and the oil mixture were injected into channels I and II, respectively. In (B) correlation between the signal obtained by $C^4D$ and number of bacteria estimated by droplet.

**Área: ANA** **Inscrição: 00240**

# Application of full factorial $2^3$ design for optimization of glycerolysis reaction.

**Renato Carneiro de Carvalho (PG),[1*] Gabriella Pinho Dias (IC),[2] Cristiane Gimenes de Souza (PQ),[2] Débora França de Andrade (PQ),[1] Fernanda Veronesi Marinho Pontes (PQ),[1] Luiz Antonio d'Avila (PQ)[2]**

**debora.franca.andrade@gmail.com; *rc-carvalho@hotmail.com.br**

*[1]Instituto de Química, UFRJ; [2]Laboratório de Combustíveis e Derivados de Petróleo, Escola de Química, UFRJ.*

Palavras Chave: *Glycerolysis, Factorial design, Monoacylglycerols, Diacylglycerols*

## Highlights

Application of full factorial $2^3$ design for optimization of glycerolysis reaction. Monoacylglycerols and diacylglycerols standards production.

## Resumo/Abstract

Biodiesel is an established renewable source in the world and necessity of monitoring its quality becomes an important issue. Constituents can be analyzed by chromatographic techniques, using standards of monoacylglycerols (MAG), diacylglycerols (DAG) and triacylglycerols (TAG), which have a high acquisition cost due to its purity. Although, it is possible to synthesize significant volumes of MAG and DAG in order to obtain such standards in laboratory scale by glycerolysis reaction, which consists of the esterification of TAG in the presence of catalysts such as $Ca(OH)_2$ and NaOH. This work aims to use a full factorial design approach ($2^3$) with triplicate of central point – totalizing 11 experiments - to optimize glycerolysis reaction. The following variables were studied: (i) temperature (180°C and 230°C), (ii) reaction time (30 min and 60 min) and (iii) molar ratio glycerol/oil (2: 1 and 3: 1). The HPLC analyses were carried out according to the procedure described by ANDRADE, 2011[1]. Effect of variables on MAG and DAG yield in glycolysis reaction are given in the Table 1. The Highest yields of DAG (53.67%) and MAG (46.20%) were obtained in the experiments 4 and 6, respectively. Estimation of coefficients of the model showed that variables of temperature and molar ratio have greater response influence. The temperature influences positively in the response, whereas the molar ratio influences negatively.

**Table 1: Full Factorial $2^3$ Design with triplicate of central point (CP).**

| Experimental Matrix | | | | | |
|---|---|---|---|---|---|
| **Exp** | **T (ºC)** | **t (min)** | **Molar Ratio** | **MAG (%)** | **DAG (%)** |
| **1** | 180 | 30 | 2:1 | 32.33 | 52.99 |
| **2** | 230 | 30 | 2:1 | 41.09 | 48.15 |
| **3** | 180 | 60 | 2:1 | 37.41 | 37.11 |
| **4** | 230 | 60 | 2:1 | 33.90 | 53.67 |
| **5** | 180 | 30 | 3:1 | 7.19 | 8.74 |
| **6** | 230 | 30 | 3:1 | 46.20 | 46.50 |
| **7** | 180 | 60 | 3:1 | 6.79 | 10.96 |
| **8** | 230 | 60 | 3:1 | 40.40 | 49.02 |
| **CP1** | 205 | 45 | 2.5:1 | 42.56 | 48.85 |
| **CP2** | 205 | 45 | 2.5:1 | 44.52 | 42.99 |
| **CP3** | 205 | 45 | 2.5:1 | 38.05 | 47.40 |

Andrade, D. F.; Mazzei, J. L.; d'Avila, L. A. Separation of Acylglycerols from Biodiesel by High Performance Liquid Chromatography and Solid-phase Extraction. *Rev. Virtual Quim*. **2011**, *3*(6), 452–466.

**Área: ANA** **Inscrição: 00346**

# Robustness evaluation of analytical procedure for the determination of residual solvent in [11C]-PK11195 using fractional factorial design

**Cassiano L. S. Costa (TC),[1*] Elias G. Vieira (IC),[1] Daleska P. Ramos (IC),[1] Fernanda A. F. Almeida (PG),[1] Juliana B. Silva (PQ).[1]**

**clsc@cdtn.br; cassianolino@yahoo.com.br**

[1]*Serviço de Radiofármacos, Centro de Desenvolvimento da Tecnologia Nuclear, Comissão Nacional de Energia Nuclear*

Palavras Chave: *Procedure validation, Chemometrics, GC-FID, Organic solvents, Radiopharmaceutical.*

## Highlights

$2_{IV}^{(6-2)}$ fractional factorial design was used to robustness test of chromatographic method. Six variables and four responses were studied. The result indicated the sample injection as a critical step.

## Abstract

Carbon-11 labeled (Fig.1) N-butan-2-yl-1-(2-chlorophenyl)-N-methylisoquinoline-3-carboxamide ([11C]PK11195) is used as a positron emission tomography (PET) radiopharmaceutical for neuroinflammatory imaging.[1] During the production process of [11C]PK11195 organic solvents (acetone, ethanol, acetonitrile and dimethyl sulfoxide) can be used and their complete removal in the final product is practically impossible, which can cause toxic effects if above acceptable concentration limits. A quality control in radiopharmaceuticals is needed to ensure patient safety and meet regulatory expectations.[2] The procedure applied to control residual solvents must be validated. Robustness is a parameter that has been evaluated in validation studies, which has been defined as the capacity of an analytical procedure to produce unbiased results in the presence of small changes in the experimental conditions.[3] This work aimed to robustness evaluation of analytical procedure based on gas chromatography (GC-FID) for the determination of residual solvent in [11C]-PK11195 using $2_{IV}^{(6-2)}$ fractional factorial design. Six variables were studied: carrier gas flow (mL/min), time held at initial temperature (min), temperature gradient (°C/min), injection split rate, injection type (automatic or manual) and initial temperature (°C). Four types of response were monitored: time of analysis, resolution between the ethanol and acetonitrile peaks, retention time and concentration. The $2_{IV}^{(6-2)}$ fractional factorial design was an appropriate chemometric tool, because it allowed determining the significance of all main effects without confounding between them. The results indicated that the procedure presents restrictions related to the injection type; in this way, special attention should be given to this step.

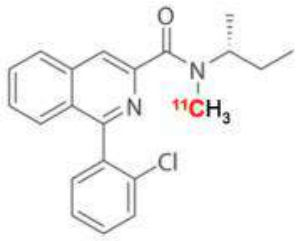


Fig. 1 - Structural formula of [11C]PK11195 [4]

**Acknowledgements:**
UPPR, CNEN, FAPEMIG, CNPq.

**References:**

1. P. Luoto et al. Molecular imaging and biology (2010) 12:435-442
2. M. Tankiewicz et al. Trends in Analytical Chemistry 80 (2016) 328–344
3. S. L. C. Ferreira et al. Microchemical Journal 131 (2017) 163–169
4. https://bme.ucdavis.edu/cmgi/available-radiotracers/

**Área: ___ANA_____ Inscrição:__01107__**

# Evaluation of the compatibility between scale inhibitor and matrices with different calcium concentrations based on experimental design

**Aline D. Gonçalves (PQ),[1*] Alice B. Machado (PG),[1] Eliza C. M. dos Santos (PG),[1] Joseane R. Barbosa (IC),[1] Andressa Dáas (IC),[1] Raimundo N. Damasceno (PQ),[1] Anderson A. Rocha (PQ).[1]**

**aline_gi@yahoo.com.br**

[1]Núcleo de Estudos em Biomassa e Gerenciamento de Água (NAB), R. Edmundo March, S/N, Gragoatá, Niterói, RJ, 24210-310, Brasil.

Keywords: Scale Inhibitor, Compatibility, Experimental design.

## Highlights

Formation waters in pre-salt fields.
Evaluation of the scale inhibitor/saline matrix compatibility.
Verification of $Ca^{2+}$ and NaCl concentrations influence over the inhibitor combatibility based on Doehlert design.

## Abstract

The oil production scenario in the pre-salt fields poses challenges for the oil industry. The chemical composition of the water associated to the produced oil differs from the traditional fields, and may represent a restriction to the application of some scale inhibitors (SI). In this way, the evaluation of the compatibility between SI and the matrix in which it will be used is very important for guaranteeing the flow of oil[1]. The combination of two or more factors may result in behavioral diagrams of the SI, identifying compatibility/incompatibility bands with the medium[2]. In this context, this work aims to verify the compatibility of SI (II52) using Doehlert design, for three variables: II52, $Ca^{2+}$ and NaCl concentrations. The response was given in terms of the turbidity of the solutions, and the measurements performed on a HACH model 2100AN turbidimeter. The Pareto Diagram (Figure 1) shows that the concentrations of calcium and sodium chloride, as well as the interaction between these factors, are the most significant effects on the response variable (turbidity). The estimated coefficients show a tendency of turbidity increase directly proportional to the factors. The desirability function of the STATISTICA software allowed to obtain the optimum values of the investigated parameters (Table 1). These values indicate the highest compatibility condition checked. It is concluded that the application of the Doehlert design was efficient in identifying the factors that influence the response, besides allowing to identify an optimal condition of compatibility.

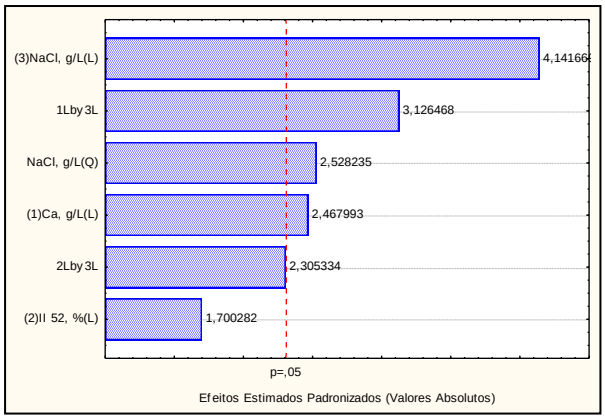


Figure 1: Pareto Diagram with the most significant effects for turbidity.

Table 1: Investigated parameters and their respective optimized values.

| Parameters | Optimized values |
|---|---|
| [Ca], g $L^{-1}$ | 15 |
| [II 52], % | 2,55 |
| [NaCl], g $L^{-1}$ | 150 |

**Acknowledgments:** PETROBRAS

[1] Goodwin, N.J. SPE 154934, Aberdeen, UK, 2012.
[2] Rabaioli, M.R.; Lockhart, T.P. J. Pet. Sci. Eng. 15, 1996, 115.

**Área: ANA** **Inscrição:00189**

# Traceability of adulteration in acai pulp (*Euterp Oleracea*) by means data fusion strategy

**Alan S. Oliveira (IC)[1], Alisson Araújo (IC)[1], Weverton Marinho (IC)[1], Licarion Pinto[2], Adriano A. Gomes (PQ)[1,3].**

**adrianogmes@gmail.com; alanoliveiraq7@hotmail.com**

*[1]Faculdade de Química/ICE, Unifesspa; [2]Departamento de Química/UFPB, [3]Departamento de Química Inorgânica/IQ UFRGS*

*Keywords: adulteration, food, digital images, infrared, chemometrics.*

## Highlights

Detection of adulteration in acai pulp. Digital images and FTIR-ATR combined by data fusion approaches. Food traceability accessed by means of chemometrics tools.

## Abstract

Acai (*Euterpe Olerace*) is a typical fruit of the amazon region, which has reached the national and international market due to its characteristics of taste and chemical composition[1]. However, contrary to its popularity, recent cases of acai adulteration have been showing the necessity for the development of analytical methodologies for the quality control of this product. In addition, there are several adulteration processes and changes used to avoid surveillance; this often lead to failure when only one type of instrumental analytical technique is used. The combined use of data recorded by different sources, an approach known as data fusion, may be a useful alternative in the field of food authenticity[2]. In this work, the use of data fusion at low-level based on digital image (DI) and infrared spectra recorded by attenuated total reflectance (FTIR-ATR) it has been investigated. Sixty samples of fresh acai pulp were purchased at markets in the city of Marabá, State of Pará. The samples were properly preserved until the time of analysis. Adulterated samples were generated by the addition of wheat and cassava. Additional amounts of adulterants were not sufficient to promote change in taste or color perceptible in a trivial way. Digital images were acquired in a homemade system to provide a lightness adjustment (see Figure 1A). FTIR-ATR spectra were recorded in an Agilent Cary 630 FTIR spectrometer in the range of 4000 to 650 $cm^{-1}$, with a resolution of 4 $cm^{-1}$. Fused data were analyzed by PCA decomposition, and the results are displayed in terms of score plot (see Figure 1B, on top PC1 x PC2 and PC2 x PC3 bellow). As can be seen, the samples are grouped according to type. The distance between the center of each cluster was higher than those obtained using the data recorded in each instrument individually. In addition, a classification of an independent tests set carried out by PLS-DA showed the following correct classification rates 78%, 98% and 100% for DI, FTIR-ATR and fused data respectively. This shows that there is a synergism between the data.

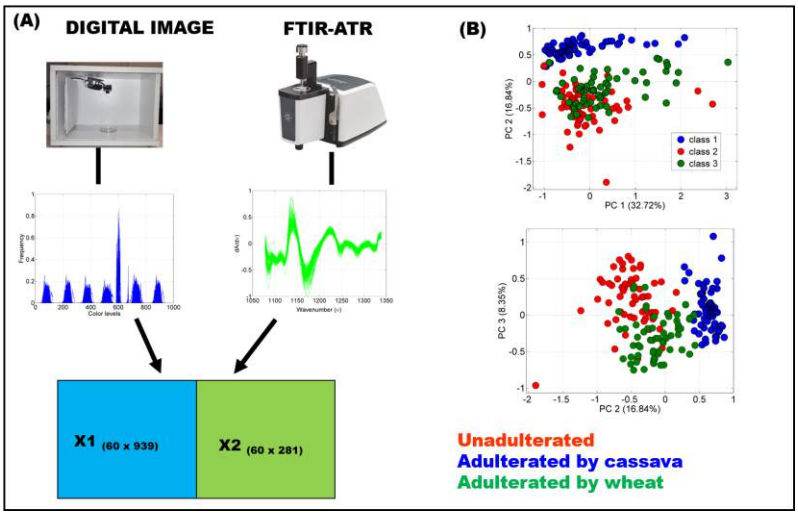


**Figure 1**: (A) Data fusion scheme and results of the exploratory analysis by PCA.

References

[1] Borras, E., at al, *Anal. Chim. Acta* 891 (2015) 1–14.
[2] Yamaguchi, K. K. L., et al, *Food Chem*. 179 (2015) 137–151.

**Área: ____ANA____ Inscrição:____00701___**

# Influence of the stationary phase on the chemical profile of saturated and aromatic hydrocarbons of a medium density petroleum

**Polianna S. Ferreira (IC)[2*], Erica A. Rodrigues (PG)[1], Dandara A. Luz (PG)[1], Roberto P. Santos (PQ)[2], Paulo R. Filgueiras (PQ)[1], Ricardo M. Kuster (PQ)[1]**

**polianna_silva@hotmail.com**

[1]*Federal University of Espírito Santo (UFES) - LABPETRO, Av. Fernando Ferrari, 514, 29075-910, Vitória–ES, Brasil.*

[2]*Federal Institute of Education,Science and Technology of Espírito Santo, Campus Vila Velha, Avenida Ministro Salgado Filho, 1000, 29106-010, Bairro Soteco, Vila Velha-ES, Brasil.*

Keywords: *PCA, Petroleum, GC-MS, Chemometrics, SAP.*

## Highlights

Verification of the qualitative differences in the saturated and aromatic profile of a petroleum prepared by the SAP method using two distinct stationary phases (silica gel and alumina).

## Resumo/Abstract

This work aimed to separate (SAP) a médium-density petroleum sample using two diferente stationary phases (sílica gel or alumina) as well as evaluate qualitative diferences between sílica and alumina fractions using GC-MS and chemometrics. Chromatographic data generates by GC-MS, for both saturated and aromatic fractions were used to make a PCA model, in order to find diferences between results obtained with sílica or alumina. Most of the explained variance occurred in the first two main components, and only the pre-treatment centered on the mean and the derivative presented values above 90% for the sum of PC1 and PC2, as shown in the scores graphic below.

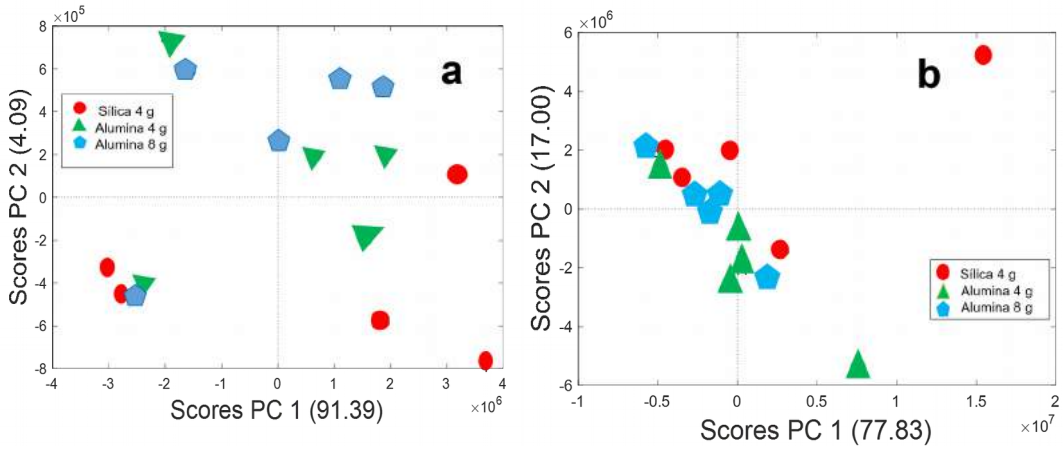


Figure 1: Graphic of scores PC1 X PC2 of the saturated fractions (a); and aromatics (b) both centered on the mean.

By the PCA method used to observe possible differences in the fractionation of petroleum with distinct stationary phases there was no great discrimination of the data, thus, both silica gel and alumina provided similar chromatographic separations for the saturated and aromatic fractions of petroleum.However, it was observed in the analysis of the graphic of scores that the aromatic fraction had a tendency to group the fractions obtained, which did not occur for the saturated fraction, where the tendency was to separate.

Speight (1991), Aleme (2011), Riazi (2005)

**Área: ANA** **Inscrição:00923**

# Characterization of lipid profiles from coconut (*Cocos nucifera* Linn.) oil of different varieties using ESI-MS and chemometrics

**Carla Beatriz Grespan Bottoli (PQ),[1] Jordana Alves Ferreira (PQ),[1]* Joana Maria Santos Ferreira (PQ),[2] Jandyson Machado Santos (PQ),[1] Marcia Cristina Breitkreitz (PQ),[1] Marcos Nogueira Eberlin (PQ),[1] Paulo Manoel Lins (PQ).[3]**

**carlab@iqm.unicamp.br; jordanaalvesferreira@gmail.com**

[1]*Institute of Chemistry, University of Campinas, POB 6154, 13083-970 Campinas, SP, Brazil*; [2]*Department of Agricultural Engineering, Embrapa Tabuleiros Costeiros, Av. Beira Mar, n° 3250, 49025-040 Aracaju, SE, Brazil*; [3]*Sococo Agroindústria da Amazônia, POB 015, 68450-000, Moju, Pará, Brazil*

Palavras Chave: Coconut oil, *Cocos nucifera* Linn., lipid, ESI-MS, ICA, PCA

## Highlights

This study evaluated the lipid profiles from coconut oils of different coconut palm varieties using ESI-MS analysis, associated with chemometric tools such as PCA and ICA.

## Resumo/Abstract

Coconut (*Cocos nucifera* Linn.) is one of the most important oil crops in tropical regions. The oil from coconut palm is extracted from the endocarp of dried and desiccated nuts. The size and weight of the nuts and the copra yield of coconut varies accordingly to the varieties such as Dwarf, Tall and Hybrids. In order to evaluate the lipid profiles of coconut oils, the endocarp of three dry coconut fruits of the same plant from 15 cultivars was crushed, ground and homogenized using an industrial blender. The resulting coconut milk was extracted with distilled hot water, collected in glass flasks and placed in the oven for 20 hours at 70 °C. In addition, one oil sample processed on the industrial scale also was collected. For ESI-MS analysis, the samples were prepared from a solution of 1 µL of the coconut oil (CO) in 1 mL of methanol. The CO were analyzed using the HCT Ultra spectrometer from Bruker Daltonik coupled with an electrospray ionization source by direct infusion of the sample solutions. The data set was evaluated by multivariate methods of Principal Component Analysis (PCA) and Independent Component analysis (ICA). This study shows that a simple analysis by ESI-MS coupled to a chemometric approach was able to differentiate the coconut varieties/cultivars according to the lipid profile, showing that different varieties may produce oils with lower or higher abundance of lipidic compounds, as shown Figure 1.

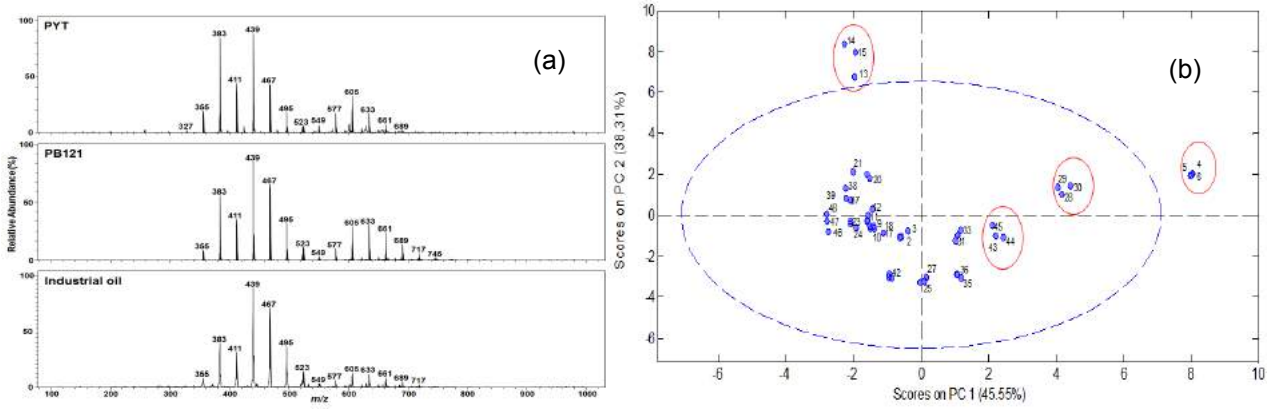


**Figure 1:** (a) ESI(+)-MS for the some samples of the coconut oils; (b) PCA

**Área: ANA** **Inscrição: 01180**

# Multivariate Classification of Perfumes by Ion Analysis and Ethanol Content

**Felipe B. C. Andrade (IC),[1] Jonas T. L. Nunes (IC),[1] Alexandra S. Fonseca (IC),[1] Clerton L. Gomes (PQ),[2] Gizelle A. B. Vieira(PQ),[1] Diego de Quadros Melo (PQ)*.[1]**

**felipebrunnocaetano@gmail.com; diego.quadros@ifsertao-pe.edu.br**

*[1] Instituto Federal de Educação, Ciência e Tecnologia do Sertão Pernambucano , IF-SERTÃO; [2] Instituto Federal de Educação, Ciência e Tecnologia do Ceará, IFCE*

Palavras Chave: *Perfumes, Cromatografia gasosa, analise de componentes principais*

## Highlights

Chemometrics was effective for distinguishing the original perfumes from false
The fake perfume had low levels of ethanol and high levels of chloride compared to the original product

## Resumo/Abstract

Nos últimos anos a comercialização de perfumes falsificados vêm aumentando em diversas partes do mundo causando risco a saúde da população, pois podem ser encontrados alguns constituintes que podem ser tóxicos.. O objetivo foi realizar um estudo comparativo entre produtos originais e falsos investigando o teor de etanol, por cromatografia gasosa, os cátions sódio, potássio e ânion cloreto por cromatografia de íons, juntamente com ferramentas quimiométricas, PCA e LDA. Observou-se que nos perfumes falsos, em geral, os cátions estavam presentes em concentrações moderadamente elevadas, quando em comparação com o perfume original, como pode ser observado no gráfico de box-plot de $Na^+$ e de $K^+$ na figura 1. Este teor de cloreto pode ser devido a qualidade e/ou quantidade da água empregada na fabricação do perfume. Na análise de etanol em perfumes, observou-se que os perfumes originais apresentaram concentrações mais elevadas do que os falsos. Na figura 2, a PCA explica 96,74% do conjunto de dados, sendo PC1(60,08%), PC2 (22,82%) e PC3 (12,84%). Os perfumes falsos encontram-se agrupados devido a um menor teor de etanol e maior concentração de cloreto, demonstrando não ter um controle de qualidade, como o esperado.

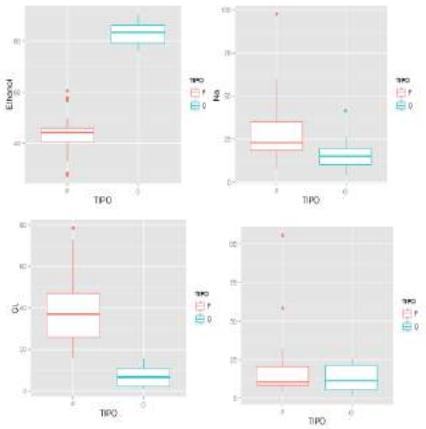


Figura 1 Gráfico Box-plot para análise de íons e etanol

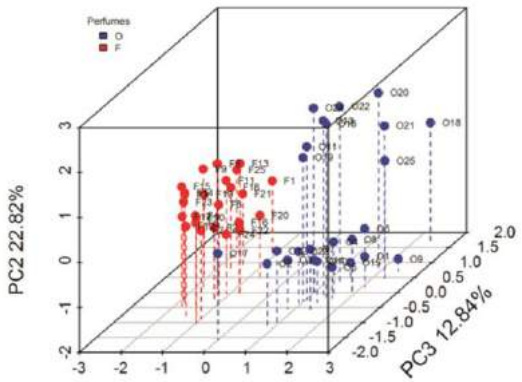


Fig. 2 PCA íons e etanol.

GOMES, C. L., **Classificação Multivariada de Perfumes e Analise de Fragrâncias Alégernas.** Fortaleza, CE; 2015.

**Área: ANA** **Inscrição: 00124**

# Ordered Predictors Selection: New Approaches for Variable Selection in Multivariate Calibration

**Jussara V. Roque (PG)[1]*, Luiz A. Peternelli (PQ)[2], Reinaldo F. Teófilo (PQ)[1]**

***jussararoque@gmail.com; rteofilo@gmail.com**

*[1]Department of Chemistry, Universidade Federal de Viçosa, [2]Department of Statistic, Universidade Federal de Viçosa*

Key words: Variable Selection, Ordered Predictors Selection, Partial Least Squares.

## Highlights

New approaches of ordered predictors selection (OPS), a variable selection method, were developed; Comparison between new approaches and other three methods of variable selection was performed.

## Abstract

The ordered predictors selection (OPS)[1] is a variable selection method based on obtaining an informative vector that contains information about the location of the best independent variables for prediction. In this work, three new OPS approaches are proposed and applied: (1) *AutoOPS*, where is chosen automatically the vector that selecting the set of variables with the best prediction capability; (2) *FeedOPS*, wherein the pre-selected variables return to a new selection until obtain the best set of variables and (3) *iOPS*, where the OPS is applied at variable independent intervals.

Multivariate calibration models using partial least squares (PLS) regression were built applying the old OPS version (OPS1.0), new approaches of OPS (OPS2.0) and other three algorithms of variable selection: genetic algorithm[2] (GA), successive projections algorithm[4] (SPA) and recursive weighted partial least squares[3] (RPLS).

A Raman spectroscopy dataset[5] was used in this study. This dataset and additional information about it are available at http://www.models.ku.dk/datasets. The property analyzed was the iodine value, which ranged from 52 to 60 g $I_2$/100g fat. The calibration and prediction sets were separated into 75 and 30 samples respectively. 5667 variables were used. The homemade OPS algorithms were written, tested and applied in Matlab R2017b.

Statistical parameters of models are shown in Table 1. RMSEP values and relative error (%) are shown in Fig. 1. A Tukey test was applied to the *RMSEP* values with 95% confidence level.

**Table 1** – Statistical parameters of full and variable selection models.

| | *nVars* | *RMSECV* | $R_{CV}$ | *RMSEP* | $R_P$ |
|---|---|---|---|---|---|
| **Full*** | 5667 | 2.16 | 0.76 | 2.05[a] | 0.88 |
| **OPS1.0*** | 180 | 2.07 | 0.78 | 1.97[b] | 0.90 |
| **OPS2.0*** | 395 | 2.04 | 0.79 | 1.80[d] | 0.91 |
| **GA*** | 2450 | 2.15 | 0.76 | 1.94[c] | 0.89 |
| **SPA*** | 566 | 2.12 | 0.77 | 1.97[b] | 0.91 |
| **RPLS*** | 5648 | 2.16 | 0.76 | 2.05[a] | 0.88 |

*Models were built using 2 latent variables. *nVars*: number of variables; *RMSECV*: root mean square error of cross-validation; $R_{CV}$: correlation coefficient of cross-validation; *RMSEP*: root mean square error of prediction; $R_P$: correlation coefficient of prediction.

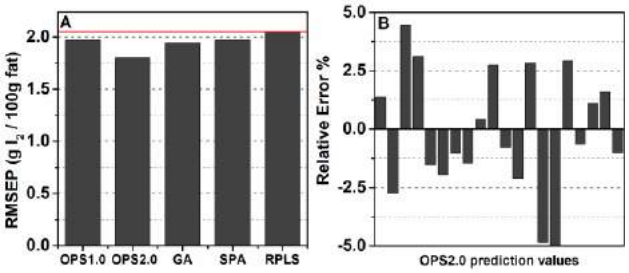


**Fig. 1** – (A) *RMSEP* values of variable selection models (bar) and full model (red line). (B) Relative error of prediction.

These results indicated that the OPS2.0 was able to improve statistical parameters regarding the other methods investigated in this work, providing substantially better predictions. For other different data sets, OPS2.0 has also shown better performance.

Acknowledgments: FAPEMIG and UFV.

References:

(1) Teófilo, R. F.; Martins, J. P. A.; Ferreira, M. M. C. *J. Chemom.* **2009**, *23* (1), 32–48.
(2) Leardi, R.; Lupiáñez González, A. *Chemom. Intell. Lab. Syst.* **1998**, *41* (2), 195–207.
(3) Rinnan, Å.; Andersson, M.; Ridder, C.; Engelsen, S. B. *J. Chemom.* **2014**, *28* (5), 439–447.
(4) de Araújo Gomes, A.; et al. *Microchem. J.* **2013**, *110* (Supplement C), 202–208.
(5) Lyndgaard, L. B.; Sørensen, K. M.; van den Berg, F.; Engelsen, S. B. *J. Raman Spectrosc.* **2012**, *43* (4), 482–489.

**Área: ANA** **Inscrição:00270**

# Determination of gluphosinate, glyphosate and AMPA in soybean oil and wine by liquid chromatography coupled with tandem mass spectrometry.

**Marilda Chiarello (PG)[1,2*], Roberto Roméro-Gonzales (PQ)[1], Sidnei Moura e Silva (PQ)[2]**

**mchiarello@ucs.br**

*[1]Chemistry and Physics department, group of analytical chemical investigation of contaminants, UAL/Spain; [2]Laboratory of Biotechnology of Natural and Synthetic Products (LBIOP), UCS/Brazil.*

*Key words: Glyphosate, Wine, Soybean oil, UHPLC-MS/MS.*

## Highlights

A rapid, sensitive and specific UHPLC-MS/MS method has been developed for the quantification of glyphosate, gluphosinate and aminomethylphosphonic acid (AMPA) in oil soybean and wine white.

## Resumo/Abstract

A fast method, without derivatization, has been developed for the monitoring of glyphosate, its metabolite AMPA and gluphosinate residues in white wine and soybean oil, using the QuPPE method[1] for the extraction of the compounds. Analytical determination of the target compounds has been performed by ultra-high performance liquid chromatography coupled to mass spectrometry (UHPLC-MS/MS). The method was developed and validated according to SANTE guideline.[2] For the extraction, QuPPE[1] modified method was used. The MS/MS detection was carried out by MRM mode, monitoring the fragmentation of *m/z* 180→94.8 and 180→84.9 for gluphosinate, *m/z* 168→150 and 168→63.1 for glyphosate, 110→78.9 and 110→63.0 for AMPA, showing in Figure 1 the extracted ion chromatograms for both compounds.

The developed analytical method for the determination of herbicides in soybean oil and wine was adequate for soybean. Shown in the table below.

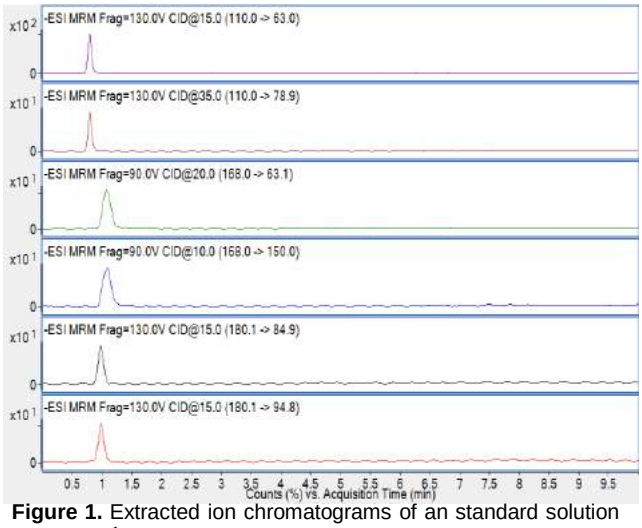


**Figure 1.** Extracted ion chromatograms of an standard solution of 50 µg $L^{-1}$ of gluphosinate, glyphosate and AMPA.

**Table 1**: Pesticide parameters: Recovery and precision.

| Herbicides | Matrix | Recovery (%) (n=5) (µg $kg^{-1}$) | | Inter-day precision RSD % (n = 3) (µg $kg^{-1}$) | | LOQ |
|---|---|---|---|---|---|---|
| | | 10 | 100 | 10 | 100 | |
| Glyphosate | Soy oil | 105 | 116 | 6.5 | 12.4 | 10 |
| | Wine | 70 | 74 | 18.0 | 9.4 | 10 |
| AMPA | Soy oil | 102 | 98 | 11.2 | 4.3 | 5 |
| | Wine | 73 | 94 | 20.0 | 14.3 | 10 |
| Glufosinate | Soy oil | 98 | 96 | 11.2 | 4.3 | 10 |
| | Wine | 68 | 78 | 19.8 | 18.3 | 10 |

The method proved to be adequate for the analysis of herbicide residues in soybean oil, but for wine it is necessary to carry out further tests to achieve accurate results. In the studied samples, no residues were found of the compounds under study, but it is important to monitor them, mainly due to the high consumption of soybean oil.

**Acknowledgment**

À University of Almería (UAL), University of Caxias do Sul (UCS), Coordination for the Improvement of Higher Level Personnel (CAPES - PSDE).

[1]Anastassiades, M.; Kolberg D.I.; Benkenstein, A.; Eichhorn, E.; Zechmann, S.; Mack, D.; Wildgrube, C.; Sigalov, I.; Dörk, D.; Barth, A.; *EURL-SRM*, Version 9.3. **2013**.

**[2] SANTE/EU/11945/2015. *Legal Deposit*, *11945*, 1–42. Retrieved from https://ec.europa.eu/food/sites/food/files/plant/docs/pesticides_mrl_guidelines_wrkdoc_11945.pdf.**

**Área:** ANA. **Inscrição:** 47818

# NEAR INFRA-RED ESPECTROSCOPY AND CHEMOMETRICS: POTENTIAL FOR COFFEE QUALITY CONTROL

**Ana H.F. Ayala (IC),[1] Danieli Paulani Alves (IC),[1] CarolineTeixeira Lopes (IC)[1], Mayara Portieri A. da Silva (IC)[1], Thiago B. Madeira (PG)[1], Mariana Botholazzi Almeida (PG)[1], Lycio Shinji Watanabe (PG)[1], Suzana Lucy Nixdorf (PQ)[1] *.**

**a_heloayala@hotmail.com; snixdorf@uel.br***

*[1]Departamento de Química-UEL.*

Key Words: *Sensorial analysis; NIR; Coffee quality control; Adulterants; Defects.*

## Highlights

The potential NIR with chemometrics for coffee quality control; Comparation between the sensorial analysis and the NIR.

## Abstract

Aiming to add objectivity to the quality control of roasted and ground coffee, done conventionally by sensorial analysis, we investigated the potential of using the near-infrared spectroscopy (NIR) combined with chemometrics. As a good quality profile, coffees awarded at sensory contest were analyzed, being 41 of raw and 52 of roasted coffee. In addition to these samples, we got some adulterants as wheat, soybeans, rye, corn, and we select black beans as defective grains. All samples were roasted, milled, sieved to 22 mesh and their moisture determined by halogen lamp thermocouple at 105 °C for 7 min. On average the samples presented 6% of moisture. After these, trigonelline and caffeine content were determined by primary technique using liquid chromatography with diode array detection (HPLC-DAD). To create a database for each type of sample all NIR spectra were acquired from 400 to 2400 nm using 2.5 g of sample directly in a spinning quartz cell. Thus, multivariate calibration was performed for moisture, trigonelline and caffeine, with NIR spectra processed using PLS, PCR and PCA. Experimental results for moisture and caffeine differed in less than 5% ($p < 0.05$) considering predictive models compared to the values measured by primary methods, while the error was less than 10% ($p < 0.1$) for trigonelline. In conclusion, NIR spectra were able to distinguish the raw and roasted coffee of the adulterants and black beans studied, splitting them into groups, endorsing the assessments made by the sensory analysis.

**Área: ANA** **Inscrição:01147**

# Multivariate Analysis of Perfumes by Ultraviolet Spectrophotometry

**Jonas T. L. Nunes (IC),[1] Felipe B. C. A. (IC),[1] Alexandra S. Fonseca (IC),[1] Clerton L. Gomes (PQ),[2] Diego de Quadros Melo (PQ).[1]***

**jonastadeu7@gmail.com; diego.quadros@ifsertao-pe.edu.br**

*[1] Instituto Federal de Educação, Ciência e Tecnologia do Sertão Pernambucano , IF-SERTÃO; [2] Instituto Federal de Educação, Ciência e Tecnologia do Ceará, IFCE*

Palavras Chave: *Perfumes, Fragrâncias alérgenas, Cromatografia gasosa*

## Highlights

Chemometrics was effective for distinguishing the original perfumes from false
UV spectrophotometry can be used to differentiate original perfumes from counterfeit ones

## Resumo/Abstract

O mercado de cosméticos é considerado muito promissor, principalmente no Brasil, que é considerado um grande produtor, consumidor e distribuidor de cosméticos. Em vista disso, os perfumes se tornam alvo potencial para falsificações. Logo, esta pratica leva à redução dos custos pela evasão de impostos, rendas e empregos, além de gerar riscos a saúde. Neste contexto, estudos recentes têm investigado perfumes falsificados usando várias técnicas analíticas. No caso apresentado, o estudo enfoca a classificação de perfumes, destacando o uso da espectrofotometria UV, uma técnica rápida e de baixo custo, utilizando a aplicabilidade de técnicas estatísticas quimiométricas. A análise dos espectos UV dos perfumes originais, figura 1a, e falsos, figura 1b, pode se observar que os perfumes originais apresentam um perfil espectral bem distinto do perfume falsificado. Os perfumes originais por apresentarem maior quantidade de fragrância absorvem mais que os perfumes falsificados. O estudo PCA resultou em componentes principais que explicam 92,8% do conjunto de dados, figura 2. Esta ilustra o suficiente para observar um agrupamento das amostras, sendo as vermelhas os perfumes falsos.

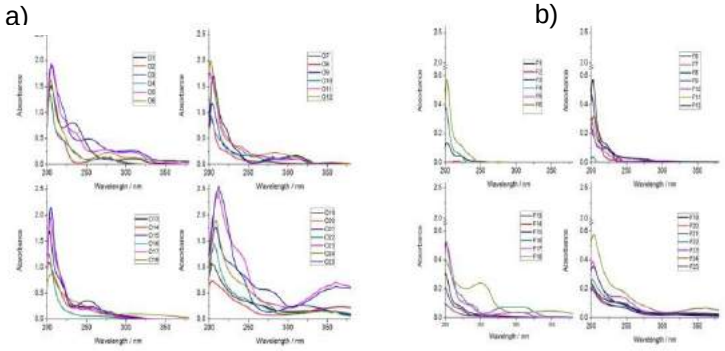


Figura 1. Os espectros de UV dos perfumes a)originais b) falsos

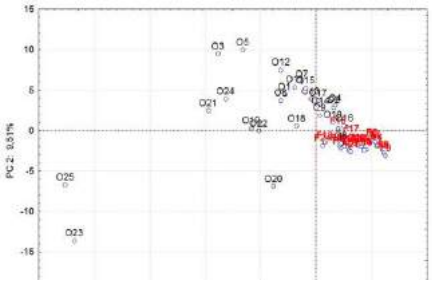

Figura 2. Pca dos dados UV perfumes

A análise linear discriminante, através do método Stepwise identificou que apenas a variável V203 possui o melhor poder discriminatório. Assim, chegou-se ao modelo: Z = -3,270 + 3,661 x V203 (Equação 1). Valores de Z maiores que 1,105 a classificação do perfume será original, caso seja menor, será falso. A espectroscopia UV combinada com quimiometria mostrou ser eficaz para distinguir os perfumes originais de falsos.

**Área: ANA** **Inscrição:** 328797

# Standardization of urinary tract infection diagnosis by ATR-FTIR/PLS-DA

**Priscilla B. Souza (IC),[1] Valeriano A. Corbellini (PQ).[1]***

**valer@unisc.br; valer@unisc.br**

[1]*Departamento de Química e Física, UNISC;*

Palavras Chave: *ATR, PLS-DA, clinical chemistry, urinary tract infection*

## Highlights

A fast ATR-FTIR method without reagents and sample pretreatment for UTI detection
PLS-DA provides the construction of classification model of UTI on urine samples of high quality

## Resumo/Abstract

Introduction: The UTI diagnosis includes positivity for leukocyte esterase, nitrite, Gram staining, and urine culture (UC, reference method). UC can take 24h (bacteria) to 48h (*Candida* spp.) forcing the clinician to prescribe early antibiotic therapy, sometimes unnecessary. Therefore, it would be more practical to make this result faster. In this context, we proposed the elaboration of a predictive model of UTI using infrared spectroscopy (FTIR) and chemometrics aiming the substitution of the UC.

Material and methods: Urine samples (n=232) were analyzed by UC (1 µL, CLED agar, 37ºC, 48h). Samples were classified as UTI(+) when have presented ≥ $1.10^5$ colony-forming unit (CFU/mL). FTIR analysis was carried out by Attenuated Total Reflectance (ATR, 8 scans, 4000-650 $cm^{-1}$) using dehydrated urine films (50 µL on 35 $mm^2$ aluminum surfaces) in triplicates. Spectral dataset was normalized by amplitude, the average spectrum of each sample was calculated, and the average ATR-FTIR spectra dataset (Figure 1) was analyzed by PLS-DA with preprocessing (2nd derivative, 5 points, two orthogonal signal correction components) in calibration step (training samples, leave-one-out cross-validation, LOO-CV) and external validation step (test samples, EVS, 2:1).

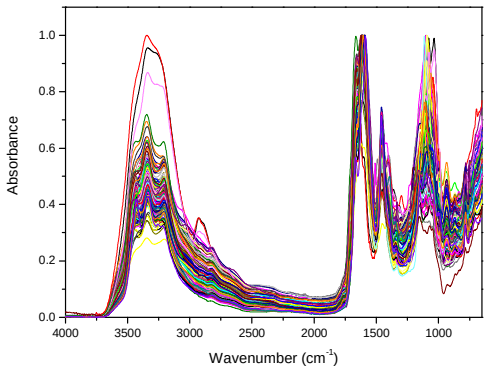


Figure 1 – ATR-FTIR spectra dataset from 232 urine samples.

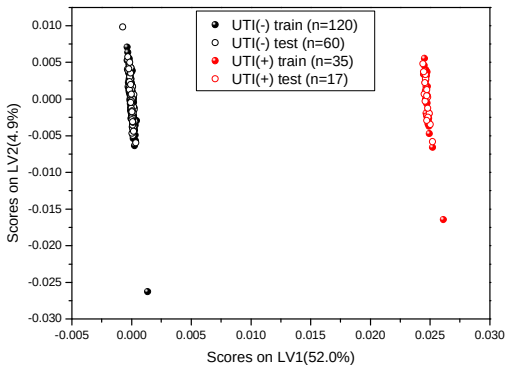


Figure 2 – Scores plot for the first two latent variables (LV) of PLS-DA model of negative and positive urine samples to UTI.

Results: The PLS-DA model (2 LV) presented RMSECV= 0.0046 (UTI(-)), 0.0042 (UTI(+)), respectively, $R^2$ greater than 0.999, and high discrimination for both classes (Figure 2). Standard errors of prediction were similar in EVS with 100% of sensibility, specificity and accuracy. Results show that ATR/PLS-DA regression models can substitute UC for UTI diagnosis.

**Área: ANA** **Inscrição: 01361**
*(Inserir o número de inscrição do autor que fez a submissão)*

# Characterization of the mineral composition of Oiti (*Licania tomentosa*) employing multivariate analysis

**Emmanuelle F. Requião Silva (PG),[1]* Bruna Rosa da S. Santos (PG),[1] Geovani C. Brandão (PQ),[2] Wagna P. C. dos Santos (PQ),[3] Mariângela V. Lopes Silva (PQ),[2] Ana Maria P. dos Santos (PQ),[1] Walter Nei L. dos Santos (PQ).[1,2]**

**waltrs8@gmail.com; emmanuellerequião@gmail.com**

*[1]Universidade Federal da Bahia, UFBA; [2]Universidade do Estado da Bahia, UNEB; [3]Instituto Federal de Educação, Ciência e Tecnologia da Bahia, IFBA*

Palavras Chave: *Oiti fruit, Mineral composition, PCA, HCA.*

## Highlights

The mineral composition of oiti pulp was evaluated.
Multivariate analysis was applied to evaluate the analytical data.
The fruit can be added in the human diet as a potential source of nutrients.

## Abstract

In this work, it was performed an evaluation of the mineral composition of oiti (*Licania tomentosa*) [1] samples collected from different localities in City of Salvador, Bahia, Brazil, employing multivariate analysis techniques. The samples were digested with $HNO_3$ and $H_2O_2$ in microwaves oven and analyzed by inductively coupled plasma optical emission spectrometry (ICP OES). Principal component analysis (PCA) and hierarchical cluster analysis (HCA) were used to separate and classify the samples. A data matrix was generated using the samples as objects and the concentrations of the elements as variables. Auto-scaling was used as method of pre-processing the data. By analyzing the scores and loadings plots for the first two PC's (Figs 1a and 1b), it was observed that the oiti pulp samples formed two groups: DJ, BON, EVB, PIT and NAZ, showing high correlations for Ca and Mg; and CVI, COM, GRA, PER, STI and OND, with high correlations for Cu, K, Mn, P and Zn. This result was confirmed by applying HCA to data. The differences observed between the two groups can be attributed to the radical system of the plant and soil (water content, pH and microbiological activity) that influence on absorption and distribution of the ions in the different parts of plant. From PCA and HCA, it was possible to classify the oiti samples collected in City of Salvador. According to the results, this fruit can be recommended as a nutritional supplement in the human diet.

**Figure 1**: Evaluation of the mineral composition of oiti fruit by PCA: **(a)** score plot and **(b)** loadings plot.

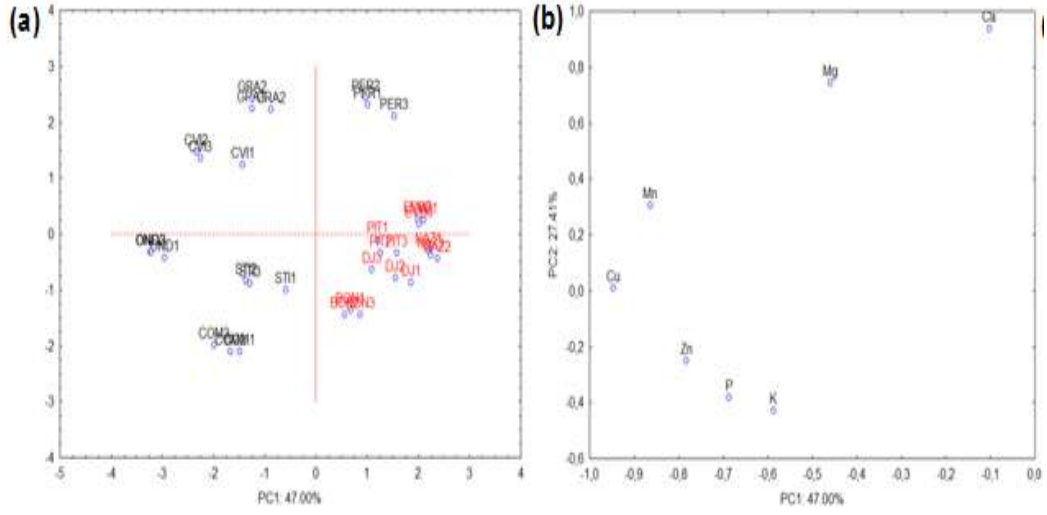


1) F. C. Sousa, E. P. Sousa, L. M. M. Silva, J. J. A. Martins, J. P. Gomes, A. P. T. Rocha. Rev. Educ. Agríc. Super. 26 (2011) 108-112.

**Área:ANA**
*(Inserir a sigla da seção científica para qual o resumo será submetido. Ex: ORG, BEA, CAT)*

**Inscrição:00894**
*(Inserir o número de inscrição do autor que fez a submissão)*

# Use of webcam in flow analysis to phosphorus determination in soil extract.

**Eduarda A. Severo (IC),[1] Jorge L. O. Santos (PQ),[2] Claudio Bazzi (PQ),[3] Marcos Y. Kamogawa (PQ),[4] Eder L.M. Flores (PQ),[1] Oldair D. Leite (PQ)[1*].**

*[1]Departamento de Química, Universidade Tecnológica Federal do Paraná, UTFPR, campus Medianeira; [2]Centro Multidisciplinar do campus de Bom Jesus da Lapa, Universidade Federal do Oeste da Bahia, UFOB; [3]Departamento de Química, Universidade Tecnológica Federal do Paraná, UTFPR, campus Medianeira; [4]Esalq/Departamento de Ciências Exatas, Universidade de São Paulo, USP.*

**eduardaaguitasevero@gmail.com; oldair.leite@gmail.com**

Keywords: *Webcam, Flow analysis, Video digital, Transient signal, Phosphorus.*

## Highlights

- digital image in analytical chemistry;
- Webcam detection in flow analysis;
- phosphorus in soil extract;

## Resumo/Abstract

Knowing the level of available P in farmland is very important to manage the phosphorus supply by soils. Consequently, the accurate determination of phosphorus species in soils is essential. Use of the webcam presents a high potential for analysis in the visible region of the electromagnetic spectrum, and the proposed strategy constitutes itself in a promising alternative to traditional absorbance measurements relying on conventional equipment. In this work, a chemistry analysis system employing webcam as detector was applied to determine $PO_4^{3-}$ amounts in soil (Mehlich-I extract), by using procedure based on blue molybdenum method (AOAC, 1995) adapted to the flow system. The typical transient signal inherent to the flow system was obtained using a digital video and quantified by the ImageJ, freeware software. The dynamical concentration range for phosphorus determination were 0.5 - 4.0 mg $L^{-1}$ P-$PO_4^{3-}$, with R.S.D < 5%. Limit of detection and analytical frequencies was 0.08 mg $L^{-1}$, and 52 $h^{-1}$, respectively. The results obtained in the analyzes with the proposed system were in agreement with those obtained using spectrophotometric detection at a 95% confidence level. The use of the flow system associated with webcam detection (digital images) was shown to be a promising alternative for traditional absorbance measurements using conventional equipment in the determination of phosphorus in soil samples.

Reference

AOAC. Official methods of analysis of AOAC international., 16a ed. Cap. 2 e 3. CUNNIFF P. (Ed.). Arlington. AOAC International, p. 984, 1995.

**Área: ANA** **Inscrição: 675**

# Estudo da eficiência de decomposição nítrica da matéria orgânica de amiláceos em frascos fechados irradiados por micro-ondas

**Williane N. Silva (IC),[1] Vanessa N. Peralva (PG),[1] Leilane R. Santos (PG),[2] Daniele C.M.B. dos Santos (PQ),[2] Maria G.A. Korn (PQ),[2] Mauro Korn (PQ).[1*]**

**willianensilva@gmail.com; mkorn@uneb.br**

*[1]Departamento de Ciências Exatas e da Terra, UNEB; [2]Instituto de Química, UFBA*

Palavras Chave: *Micro-ondas, Digestão nítrica, Matriz orgânica, Amiláceos, Ácido diluído.*

## Highlights

Evaluation of nitric digestion efficiency of organic matter of starchy samples in closed vessels exposed to microwave irradiation
- Dissolved organic carbon efficiency was monitored by mean and standard deviation
- Influence of diverse parameters on organic matrix decomposition were systematically evaluated

## Resumo/Abstract

Amostras de alimentos amiláceos como amido de milho e as farinhas de trigo e de tapioca foram submetidas em triplicata e sem tratamento prévio a diferentes condições de digestão com soluções diluídas de $HNO_3$ em frascos fechados e sob irradiação de micro-ondas até pressão de 20 bar, sendo monitorado no digerido o teor de carbono orgânico dissolvido (COD) pelo sinal correspondente à emissão a 193,027 nm. Os ensaios foram realizados com *ca.* 250 mg da amostra e variando o programa de aquecimento em termos da temperatura máxima (160 – 210 $^oC$), do período nesta temperatura (de 2 a 25 min), além da concentração ácida (de 1 a 14 mol $L^{-1}$). Inicialmente, era observado o aspecto visual dos digeridos e apenas aqueles que não tinham partículas suspensas eram encaminhados para determinação de COD em ICP OES. A curva analítica para carbono foi construída a partir da diluição de solução de ácido cítrico sendo a concentração máxima em carbono igual a 2000 mg $L^{-1}$. Os valores de COD foram multiplicados por 2,5 para a expressão dos resultados em massa de $CH_2O$, pois as amostras eram majoritariamente constituídas por carboidratos. Foi observado que o aumento da fração decomposta de $CH_2O$ ocorreu com o aumento concomitante da concentração ácida e da temperatura máxima de digestão com a consequente diminuição da incerteza em até duas ordens de grandeza. O período de aquecimento em temperatura máxima se mostrou mais importante para a decomposição de amostras dos alimentos avaliados com partículas mais grossas. Para as amostras de farinha avaliadas o menor percentual de COD (2,1±0,6) pôde ser obtido após 10 min de irradiação (rampa de aquecimento da temperatura ambiente até 210 $^oC$ em 6 min e patamar a 210 $^oC$ por 4 min), empregando solução de $HNO_3$ 7 mol $L^{-1}$.

**Área: __ANA_____ Inscrição:__00397____**

# Desenvolvimento de um sistema on-line de extração magnética em fase sólida para determinação de Cd por FAAS.

**Pamela S. M. Rocha (PG),[1*] Ricardo J. Cassella (PQ).[1]**

***ps.spamer@gmail.com**

[1]*Universidade Federal Fluminense, Departamento de Química Analítica, Outeiro de São João Batista s/n, Niterói - RJ.*

Palavras Chave:*(Preparo de amostra, Pré-concentração, Nanopartícula magnética).*

## Highlights

Development of an on-line system of solid phase magnetic extraction for determination of Cd by FAAS. Magnetic nanoparticles for selective solid phase extraction and pre-concentration of Cd. Automated sample treatment for further determination of Cd by FAAS.

## Resumo

O uso de nanopartículas magnéticas funcionalizadas (NPMF) como sorvente para extração magnética em fase sólida (MSPE) confere à técnica de preparo de amostra uma alta seletividade e sensibilidade tornando-a bastante promissora na determinação de analitos em matrizes complexas. No entanto, erros relacionados a contaminação e a perda de analitos podem ser observados devido à alta manipulação das amostras. Uma alternativa para reduzir tais problemas é o uso da Análise por Injeção em Fluxo (FIA) que oferece vantagens como baixo consumo de reagentes e diminuição dos erros analíticos. Diante dos fatos expostos, o presente projeto propõe o desenvolvimento de uma metodologia analítica para determinação de Cd após extração magnética em fase sólida em linha utilizando nanopartículas de magnetita ($Fe_3O_4$) funcionalizada com L-glutamina como sorvente seletivo para Cd. O trabalho foi realizado nas seguintes etapas: síntese e caracterização por Microscopia Eletrônica de Varredura e Difração de Raio-X das NPMF's; montagem do sistema FIA (Figura 1) e estudo dos parâmetros físicos e químicos do sistema (Tabela 1). Todos os testes analíticos foram realizados em solução aquosa. A síntese da NPMF foi realizada em três etapas: síntese do núcleo de magnetita, recobrimento com 3-cloropropil-trimetóxisilano e por fim a funcionalização com L-glutamina. O fator de pré-concentração obtido demonstrou um aumento de cerca de sete vezes quando comparadas as curvas analíticas com e sem o sistema de pré-concentração, indicando que a metodologia desenvolvida foi eficiente para pré-concentrar Cd em solução aquosa.

Tabela 1: Principais variáveis estudadas no sistema desenvolvido.

| Parâmetro estudado | Faixa de estudo | Condição ideal |
|---|---|---|
| pH da dispersão da NPMF | 2,0 - 12,0 | 11,0 |
| Concentração do tampão Britton-Robinson (M) | 0,0025 - 0,010 | 0,0075 |
| Massa de NPM na dispersão aquosa (mg $mL^{-1}$) | 0,020 - 0,40 | 0,20 |
| Concentração do eluente HCl (M) | 1,0 - 6,0 | 4,0 |
| Vazão da solução de Cd (mL $min^{-1}$) | 2,20 - 4,80 | 4,80 |
| Vazão da dispersão de NPM (mL $min^{-1}$) | 2,20 - 4,80 | 2,20 |
| Vazão do eluente HCl (mL $min^{-1}$) | 2,80 - 8,00 | 8,00 |

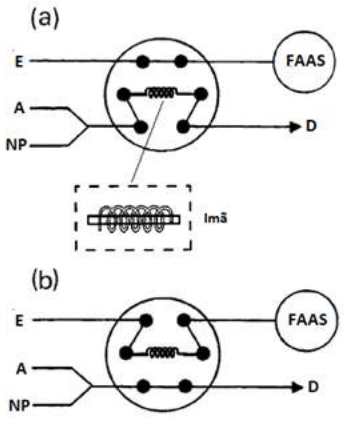


Figura 1: Sistema FIA. (a) Extração. (b) Eluição. E - Eluente; A - amostra; NP - dispersão da NPMF; D - descarte; FAAS - detector.

AGRADECIMENTOS: CAPES, FAPERJ e CNPQ.

**Área: ANA** **Inscrição: 00184**

# Metals determination by ICP-OES in samples of colonial wines produced in Palotina-PR

**Leidi Cecilia Friedrich (PQ)*, Ana Karoliny S. Gomes (IC), Douglas G. Souza (IC), Louize A. E. Schneider (IC), Guilherme F. Lenz (TC), Ivonete R. Bautitz (PQ) and Maria Cristina Milinsk (PQ).**

***leidif@ufpr.br**

*Universidade Federal do Paraná – Setor Palotina, Departamento de Engenharias e Exatas, Rua Pioneiro 2153 – CEP 85950-000, Palotina, PR.*

Palavras Chave: *Wines, Metals, Inductively Coupled Plasma Atomic Emission Spectrometry (ICP-OES) and Quality.*

## Highlights

Metals analysis by Inductively Coupled Plasma Atomic Emission Spectrometry (ICP-OES) in samples of colonial wines produced in Palotina-PR. The data obtained show the importance of determining the concentration of metals in wines produced in Palotina, in order to improve the quality of these products.

## Resumo/Abstract

The analysis by ICP-OES stands out for its linearity range, low limit of detection and quantification, sensitivity and fast response. Were collected 36 samples, 10 white wines (B01 to B10) and 16 red wines (T01 to T16), all the samples were analysed in triplicate. Determination of metals were performed at 20°C according to the described by the Adolfo Lutz Institute[1], under the following conditions: axial view, RF power 1150 watt with nebulizing gas flow 0.70 mL/min and auxiliary gas flow 0.5 mL/min. The results are showed at Tables 1 and 2.

Table 1: Results of metals determination in white wines (mg/L) with standard deviation.

| | Al | Ca | Fe | K | Mg | Mn | Na | P | Zn |
|---|---|---|---|---|---|---|---|---|---|
| **B01** | 0,894 ±0,170 | 70,080 ±0,800 | 0,987 ±0,004 | 789,500 ±8,333 | 54,945 ±0,089 | 1,118 ±0,003 | 15,497 ±0,464 | 60,298 ±0,311 | 0,741 ±0,005 |
| **B02** | 0,584 ±0,43 | 77,913 ±1,011 | 0,103 ±0,007 | 958,500 ±4,333 | 55,262 ±0,100 | 1,428 ±0,014 | 8,283 ±0,122 | 65,548 ±0,222 | 0,234 ±0,003 |
| **B03** | 0,461 ±0,016 | 83,913 ±0,378 | 1,850 ±0,046 | 1080,667 ±2,444 | 51,795 ±0,211 | 1,462 ±0,002 | 39,547 ±0,178 | 57,332 ±0,111 | 0,312 ±0,009 |
| **B04** | 1,282 ±0,08 | 73,447 ±0,389 | 2,704 ±0,015 | 1072,500 ±3,667 | 56,662 ±0,167 | 1,210 ±0,005 | 7,245 ±0,087 | 83,282 ±0,278 | 0,376 ±0,001 |
| **B05** | 0,864 ±0,023 | 72,513 ±0,744 | 0,965 ±0,07 | 1060,500 ±7,000 | 74,262 ±0,100 | 1,267 ±0,003 | 0,643 ±0,331 | 70,898 ±0,611 | 1,502 ±0,015 |
| **B06** | 1,631 ±0,058 | 82,313 ±0,622 | 2,226 ±0,021 | 1060,833 ±9,111 | 73,595 ±0,189 | 1,962 ±0,007 | 21,583 ±0,514 | 92,982 ±0,278 | 1,425 ±0,015 |
| **B07** | 1,624 ±0,037 | 74,697 ±0,211 | 2,091 ±0,109 | 1066,833 ±4,556 | 63,828 ±0,189 | 1,428 ±0,006 | 13,985 ±0,173 | 102,782 ±0,111 | 3,907 ±0,083 |
| **B08** | 0,326 ±0,021 | 75,080 ±0,833 | 1,658 ±0,019 | 922,333 ±2,778 | 59,762 ±0,267 | 4,064 ±0,021 | 4,602 ±0,189 | 62,315 ±0,167 | 0,554 ±0,002 |
| **B09** | 0,551 ±0,028 | 73,297 ±0,722 | 1,369 ±0,100 | 943,667 ±2,444 | 61,095 ±0,344 | 4,343 ±0,031 | 5,118 ±0,119 | 74,815 ±0,100 | 2,169 ±0,036 |
| **B10** | ND[1] | 64,463 ±0,522 | 0,162 ±0,003 | 1100,833 ±5,111 | 51,428 ±0,456 | 1,246 ±0,006 | 1,050 ±0,217 | 70,348 ±0,656 | 0,312 ±0,003 |

ND[1]: No detected

Table 2: Results of metals determination in red wines (mg/L) with standard deviation.

| | Al | Ca | Fe | K | Mg | Mn | Na | P | Zn |
|---|---|---|---|---|---|---|---|---|---|
| **T01** | 0,786 ±0,026 | 101,213 ±0,378 | 2,027 ±0,013 | 804,667 ±1,889 | 75,612 ±0,367 | 1,780 ±0,007 | 12,727 ±0,128 | 83,115 ±0,133 | 0,577 ±0,001 |
| **T02** | 0,249 ±0,023 | 74,863 ±0,289 | 0,378 ±0,007 | 979,167 ±0,778 | 73,562 ±0,233 | 4,832 ±0,028 | 2,000 ±0,020 | 46,998 ±0,278 | 0,452 ±0,002 |
| **T03** | 0,586 ±0,024 | 80,930 ±0,333 | 2,128 ±0,003 | 806,167 ±4,556 | 72,262 ±0,433 | 1,365 ±0,004 | 12,815 ±0,353 | 48,015 ±0,167 | 0,755 ±0,004 |
| **T04** | 0,384 ±0,017 | 84,230 ±0,867 | 0,780 ±0,011 | 1103,833 ±5,444 | 85,428 ±0,344 | 0,813 ±0,003 | ND[1] | 114,748 ±0,411 | 0,671 ±0,003 |
| **T05** | 0,647 ±0,014 | 80,730 ±0,233 | 1,444 ±0,008 | 1118,167 ±3,111 | 86,895 ±0,322 | 0,541 ±0,001 | 9,442 ±0,089 | 127,115 ±0,433 | 1,718 ±0,006 |
| **T06** | 0,056 ±0,027 | 91,247 ±0,578 | 1,304 ±0,003 | 938,000 ±1,333 | 77,095 ±0,256 | 3,956 ±0,012 | 4,133 ±0,013 | 65,632 ±0,356 | 0,498 ±0,002 |
| **T07** | 0,063 ±0,013 | 96,347 ±0,844 | ND[1] | 1015,667 ±5,889 | 65,495 ±0,289 | 1,151 ±0,003 | 0,160 ±0,250 | 66,298 ±0,111 | 0,419 ±0,003 |
| **T08** | 0,156 ±0,032 | 78,547 ±1,144 | 0,910 ±0,006 | 1008,167 ±6,556 | 77,478 ±0,278 | 4,615 ±0,013 | 8,687 ±0,329 | 103,165 ±0,133 | 0,487 ±0,000 |
| **T09** | 0,246 ±0,036 | 84,113 ±0,144 | 1,567 ±0,08 | 890,667 ±2,444 | 76,595 ±0,389 | 1,402 ±0,002 | ND[1] | 74,065 ±0,233 | 0,356 ±0,009 |
| **T10** | 0,592 ±0,041 | 78,980 ±0,700 | 1,058 ±0,008 | 1102,500 ±4,000 | 66,478 ±0,178 | 1,672 ±0,006 | 1,883 ±0,076 | 71,948 ±0,222 | 0,468 ±0,005 |
| **T11** | 0,922 ±0,052 | 80,847 ±1,144 | 0,718 ±0,017 | 949,000 ±2,000 | 69,812 ±0,233 | 3,999 ±0,025 | 9,272 ±0,182 | 37,998 ±0,144 | 0,568 ±0,013 |
| **T12** | 1,249 ±0,020 | 95,747 ±0,244 | 2,338 ±0,005 | 1039,667 ±1,778 | 69,912 ±0,500 | 1,805 ±0,006 | 8,387 ±0,119 | 70,365 ±0,067 | 1,072 ±0,009 |
| **T13** | 0,969 ±0,030 | 70,730 ±0,633 | 1,126 ±0,009 | 1182,333 ±5,111 | 77,828 ±0,189 | 2,069 ±0,007 | 2,285 ±0,190 | 116,848 ±0,378 | 0,626 ±0,003 |
| **T14** | 0,334 ±0,007 | 102,880 ±1,033 | 3,447 ±0,046 | 1030,500 ±3,667 | 80,712 ±0,200 | 1,701 ±0,006 | 2,278 ±0,129 | 105,482 ±0,122 | 2,981 ±0,245 |
| **T15** | 0,252 ±0,024 | 93,180 ±1,067 | 12,450 ±0,040 | 914,500 ±3,000 | 77,312 ±0,067 | 2,957 ±0,015 | 5,800 ±0,083 | 64,215 ±0,133 | 0,653 ±0,004 |
| **T16** | 0,244 ±0,020 | 87,805 ±0,225 | 0,845 ±0,016 | 917,500 ±3,000 | 71,637 ±0,175 | 2,281 ±0,005 | 2,853 ±0,048 | 75,215 ±0,150 | 4,344 ±0,006 |

ND[1]: No detected

About thirty metals were detected and quantified, being the ones with the highest concentration and essential: Al, Ca, Fe, K, Mg, Mn, Na, P and Zn. The red wines had higher concentrations of the metals Ca, Fe, Mg and Na when compared to the white wines. These values can be related to the type of soil, fertilization and production process. The parameters analyzed show the importance of evaluating the wines produced in the city of Palotina in order to improve the quality of these products. And the data obtained show the importance of determining the concentration of metals in wines to guarantee quality of these wines.

[1]Zenebon, O.; Pascuet, N.S.; Tiglea, P. Métodos físico-químicos para análise de alimentos Instituto Adolfo Lutz, São Paulo (2008).

**Área: ANA** **Inscrição: 00679**

# Estudo da composição química cuticular de formigas da espécie *Odontomachus bauri* expostas a diferentes temperaturas

**Bianca F. Duarte (PG),[1] Kamylla B. Michelutti (PG),[2] William F. Antonialli-Junior(PQ),[2] Claudia A. L. Cardoso (PQ).[1]**

**biancaferreira@hotmail.com**

*[1]Centro de Estudos em Recursos Naturais, Laboratório de Análise Instrumental, UEMS; [2]Centro de Estudos em Recursos Naturais-Laboratório de ecologia comportamental (LABECO), UEMS*

Palavras Chave: Comprimento de cadeia, Alcanos, Hidrocarbonetos cuticulares, Cromatografia

## Highlights

Study of the cuticular chemical composition of ants of the species *Odontomachus bauri* exposed to different temperatures. *Odontomachus bauri* presented alteration in the cuticular composition when exposed to different temperatures. Reduction of the compounds with smaller length under high temperatures.

## Resumo/Abstract

O estudo dos compostos químicos presentes na cutícula de diversos insetos tem chamado atenção de muitos pesquisadores. Por atuar primariamente como uma barreira contra dessecação[1], sua análise pode indicar a capacidade de reajuste ou não de insetos a diferentes variações ambientais. O objetivo deste estudo foi avaliar alterações no perfil químico cuticular de *O. bauri* quando submetidas a diferentes temperaturas empregando cromatografia gasosa acoplada a espectrometria de massas. Para cada temperatura foram utilizadas 10 formigas. As temperaturas de 10ºC a 35ºC apresentam maiores teores de alcanos lineares (Figura 1). A partir de 35ºC há um aumento no teor dos alcanos ramificados, sendo que em 40ºC esta classe apresenta maior percentagem. Em relação ao teste de sobrevivência, todas as formigas sobreviveram nas temperaturas de 10ºC a 30ºC, em 35ºC ocorreu 97% de sobrevivência e em 40ºC houve 100% de mortalidade. Em temperaturas mais elevadas um aumento de compostos ramificados foi evidenciado, acompanhado de uma diminuição na concentração de alcanos lineares. Os alcanos lineares atuam como uma barreira de proteção a perca de água[1], justificando a maior concentração de alcanos lineares nas temperaturas de 25ºC e 30ºC, as quais estão na faixa em que a espécie costuma forragear.

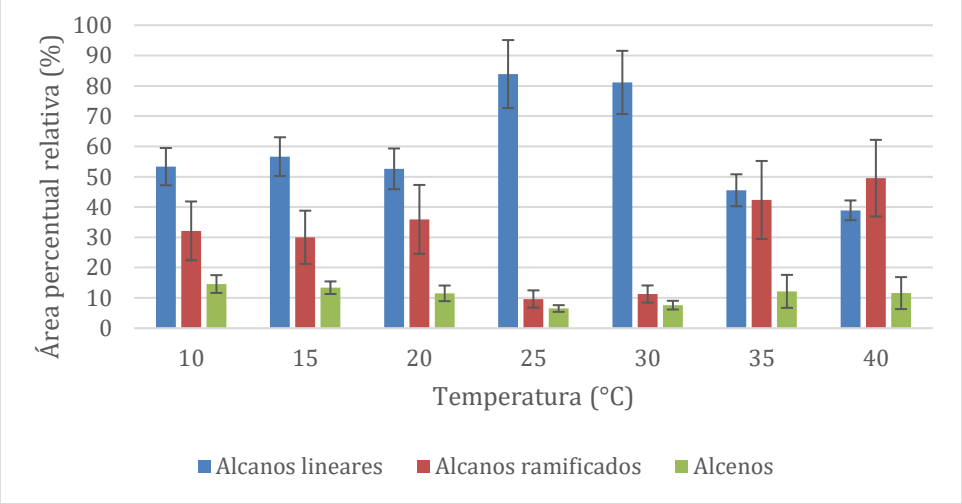


**Figura 1**- Percentagem das classes de compostos presentes na cutícula de forrageadoras de *O. bauri* submetidas a diferentes temperaturas.

[1]BLOMQUIST, Gary J.; BAGNÈRES, Anne-Geneviève (Ed.). Insect hydrocarbons: biology, biochemistry, and chemical ecology. Cambridge University Press, 2010.



Classificação da informação: Uso Interno

**Área: ANA** **Inscrição:** 00968

# Desenvolvimento de metodologia para quantificação de TBHQ, BHT e alfatocoferol utilizando CLAE-DAD em amostras de biodiesel com avaliação do período de indução por Rancimat.

**Tayná S. Vargas (IC),[1*] Raul S. de Azevedo, Simone C. Chiapetta (PQ).[1]**

**tayna.vargas@int.gov.br**

[1]*Divisão de Química Analítica, Instituto Nacional de Tecnologia, INT, Rio de Janeiro.*

Palavras Chave: *Biodiesel, Antioxidantes, ANP.*

## Highlights

This work developed a new methodology to determine TBHQ, BHT e Alphatocoferol in high performance liquid cromotography (HPLC) in a single run.

## Resumo/Abstract

Os antioxidantes sintéticos e naturais são usados como aditivos no biodiesel para prevenir ou retardar o processo de oxidação dos ácidos graxos. Após estar conforme com todos os requisitos exigidos pela ANP (Agência Nacional do Petróleo, Gás Natural e Biocombustíveis), o mesmo pode ser comercializado ou misturado ao diesel. Os sintéticos mais utilizados no país são o BHT e o TBHQ, sendo o alfatocoferol um antioxidante natural. De modo a assegurar a qualidade do biocombustível ao longo da cadeia de produção, venda e utilização, a ANP nº 45 estabelece que vinte e quatro parâmetros devem ser verificados para conseguir a certificação[1]. A metodologia desenvolvida neste trabalho teve por objetivo quantificar alfatocoferol, BHT e TBHQ (Fig. 1) em uma corrida única, além de verificar através do Rancimat se a estabilidade oxidativa (período de indução) da amostra se encontra dentro do valor mínimo exigido pela norma vigente. Foram comparadas amostras recém-produzidas e posteriormente envelhecidas no Rancimat, de acordo com a EN 14112. Não foi encontrada a presença de alfatocoferol na amostra, devido à sua evaporação durante a transesterificação do biodiesel, nem a presença de BHT, tendo sido o TBHQ o único quantificado, sendo este o mais utilizado pela indústria (Fig. 2). A amostra envelhecida não apresentou o TBHQ, devido a degradação do mesmo no Rancimat (Fig. 3) e o período de indução encontrado foi 8,28h, estando conforme a norma, que exige no mínimo 8h. A concentração da amostra foi 20,22 mg.L$^{-1}$ e RSD ± 0,41.

| | |
|---|---|
| Fase móvel (%): | (100% ACN):(ACN:MeOH 50:50 v/v):(Ác. Acético 5%) |
| Vazão (mL.min$^{-1}$): | gradiente (figura abaixo) |
| Comprimento de onda: | 290 |
| Coluna: | Zorbax SB-C18 |
| Tempo de corrida (min): | 25 |
| Volume de injeção (µL): | 10 |
| Tipo de injeção: | Automática |

Tabela 1. Parâmetros utilizados na metodologia otimizada.

| tempo (min) | %B | %C | %D | Fluxo (mL.min) |
|---|---|---|---|---|
| 0 | 0.0 | 90.0 | 10.0 | 1.0 |
| 7.50 | 0.0 | 90.0 | 10.0 | 1.0 |
| 8.00 | 100.0 | 0.0 | 0.0 | 1.0 |
| 20.00 | 100.0 | 0.0 | 0.0 | 1.0 |
| 21.00 | 0.0 | 90.0 | 10.0 | 1.0 |
| 25.00 | 0.0 | 90.0 | 10.0 | 1.0 |

Tabela 2. Gradiente utilizado para a metodologia otimizada.

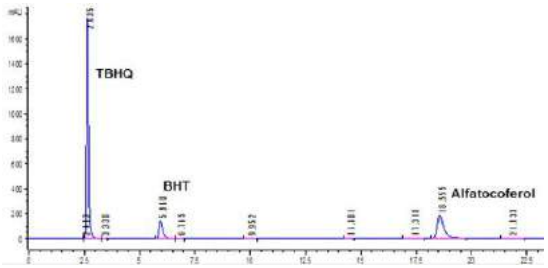


Figura 1. Perfil cromatográfico do mix contendo 1000 mg.L$^{-1}$ de TBHQ, BHT e Alfatocoferol.

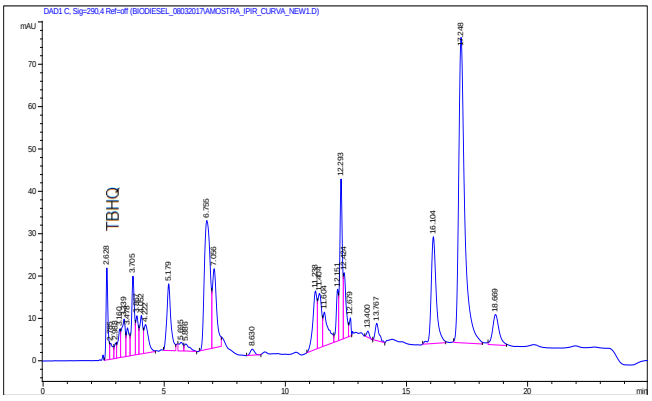


Figura 2. Cromatograma da amostra de B100 contendo TBHQ.

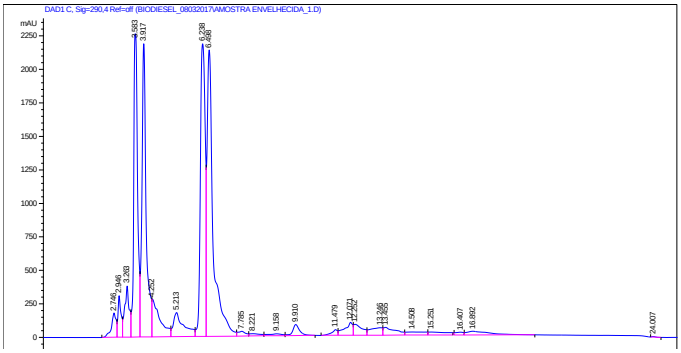

Figura 3. Cromatograma da amostra de B100 envelhecida de acordo com a metodologia EN 14112.

**Área: ANA** **Inscrição:** 00718

# Vantagens e desvantagens da quantificação de terc-butilhidroquinona (TBHQ) em biodiesel utilizando bomba peristáltica e bomba de alta eficiência.

**Simone C. Chiapetta[1*] (PQ), Tayná S. Vargas[1] (IC), Isabella S. Gomes[1] (IC).**

**simone.chiapetta@int.gov.br**

[1]*Divisão de Química Analítica, Instituto Nacional de Tecnologia, INT, Rio de Janeiro.*

Palavras Chave: *Biodiesel, Antioxidantes, TBHQ, ANP.*

## Highlights

This work compares the TBHQ's determination in biodiesel samples marketed in the country using two equipaments with differents pumps.

## Resumo/Abstract

O terc-butilhidroquinona (TBHQ) é o antioxidante sintético mais utilizado como aditivo no biodiesel para prevenir ou retardar o processo de oxidação do mesmo.[1] A utilização do biodiesel fora das especificações referentes à oxidação pode causar a corrosão de metais e borrachas, além da formação de depósitos e entupimento de filtros nos motores a diesel. O preparo de amostra e curva analítica foram os mesmos para ambos os equipamentos. Os parâmetros utilizados são apresentados nas Tabelas 1, 2 e 3 e os perfis cromatográficos são apresentados nas Figuras 1 e 2. O cromatógrafo com bomba de alta eficiência apresentou menor tempo de corrida, economizando 1h e 25 min, também utilizou uma quantidade menor de solventes, sendo mais economicamente viável e apresentou desvio padrão relativo baixo e dez vezes menor que o desvio do cromatógrafo com bomba peristáltica, sendo então mais sensível e mais indicado para a determinação de TBHQ em biodiesel, de acordo com os resultados apresentados na tabela 4.

| Fase móvel (%): | (100% ACN):(ACN:MeOH 50:50 v/v):(Ác. Acético 5%) |
|---|---|
| Vazão (mL.min$^{-1}$): | gradiente (figura abaixo) |
| Comprimento de onda: | 290 |
| Coluna: | Zorbax SB-C18 |
| Tempo de corrida (min): | 25 |
| Volume de injeção (µL): | 10 |
| Tipo de injeção: | Automática |

Tabela 1: Parâmetros utilizados no cromatógrafo líquido com bomba de alta eficiência.

| **Fase móvel (%)** | 90:10 (ACN:MeOH):Ác. Acético 5% |
|---|---|
| **Vazão (mL.min-1)** | 0.6 |
| **Comprimento de onda (nm)** | 290 |
| **Coluna** | Zorbax SB - C18 |
| **Tempo de análise (min)** | 30 |
| **Volume de injeção (µL)** | 20 |
| **Injeção** | Manual |

Tabela 2. Parâmetros utilizados no cromatógrafo líquido com bomba peristáltica.

| tempo (min) | %B | %C | %D | Fluxo (mL.min$^{-1}$) |
|---|---|---|---|---|
| 0 | 0.0 | 90.0 | 10.0 | 1.0 |
| 7.50 | 0.0 | 90.0 | 10.0 | 1.0 |
| 8.00 | 100.0 | 0.0 | 0.0 | 1.0 |
| 20.00 | 100.0 | 0.0 | 0.0 | 1.0 |
| 21.00 | 0.0 | 90.0 | 10.0 | 1.0 |
| 25.00 | 0.0 | 90.0 | 10.0 | 1.0 |

Tabela 3. Gradiente utilizado para análise em bomba de alta eficiência.

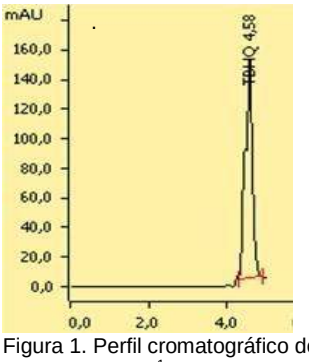


Figura 1. Perfil cromatográfico do TBHQ (40 mg.L$^{-1}$) em bomba peristáltica.

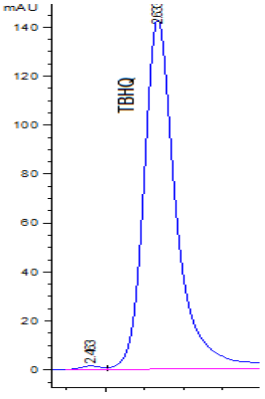


Figura 2. Perfil cromatográfico do TBHQ (40 mg.L$^{-1}$) em bomba de alta eficiência.

**Concentração de TBHQ na amostra (mg.L$^{-1}$) ± DPR (n=3)**

| Cromatógrafo liquido de alta eficiência | Cromatógrafo liquido com bomba peristáltica |
|---|---|
| 20,22 ± 0,41 | 18,32 ± 4,079 |

Tabela 4. Resultados obtidos para comparação dos dois cromatógrafos.

1 - *FOOS INGREDIENTS BRASIL*, 2009. **Dossiê antioxidantes**. Disponível em: < http://www.revista-fi.com/materias/83.pdf> nº 6, p. 17 e 18.

**Área: ANA** **Inscrição: 00725**

# Estudo de estabilidade de açúcares em tabaco de cigarros comerciais

**Mariani D. N. Rodrigues (TC),[1*] Jessica D. S. Guedes (TC),[1] Simone Carvalho Chiapetta (PQ),[1].**

**mariani.neves@int.org.br**

[1]*Divisão de Química analítica, Instituto Nacional de Tecnologia - INT.*

Palavras Chave: *Tabaco, Açúcares, Degradação, Estudo de estabilidade*.

## Highlights

Stability study of sugars in tobacco of commercial cigarette
In the process of making cigarettes there is a loss of the sugars present in the leaves of the tobacco resulting in a bitter product. To compensate for this loss, sugars are added to the tobacco in order to turn the cigarette into a product more pleasant, making it more attractive for children and teenagers. However, with the pyrolysis of sugars there is the formation of carcinogenic substances. This work aims to evaluate the possible degradation of sugars present in commercial cigarettes due to temperature and humidity variations that may occur during storage in sales outlets.

## Resumo/Abstract

A indústria tabagista adiciona açúcares no processo de fabricação de cigarros devido à perda que ocorre naturalmente durante a etapa de secagem das folhas (cura). Esta adição resulta em um produto final mais palatável, promovendo assim uma maior adesão do público infanto-juvenil. Durante a queima do cigarro ocorre a pirólise desses açúcares com formação de substâncias carcinogênicas[1]. Frente a isto, surge a necessidade do monitoramento do teor de açúcares presentes em cigarros comerciais (Glicose, Sacarose e Frutose). Este trabalho tem como foco um estudo de estabilidade, avaliando variações de temperatura e umidade que podem levar a degradação dos açúcares nos cigarros comerciais, passíveis de ocorrer durante a estocagem nos pontos de venda, prejudicando assim o monitoramento desses compostos, visto que atualmente não há uma legislação que define o valor máximo desse aditivo ao cigarro. As condições avaliadas foram: (1) norma ABNT NBR ISO 3402/2007: 22°C e 60% de umidade, (2) estocagem em refrigeração: 06°C e 60% de umidade, e (3) alta temperatura: 40°C e 21% de umidade, as amostras foram condicionadas por 48 horas antes da extração. Foram pesadas 500mg de cada amostra, extraídas em 10 mL de água tipo 2 e filtradas em filtro 0,22 µm. Os extratos aquosos foram analisados em cromatógrafo líquido de alta eficiência, acoplado a detector evaporativo com espalhamento de luz (UPLC-ELSD). Foram avaliadas as três condições, destacando a atmosfera para condicionamento de 22°C e 60% de umidade, apresentando resultados mais lineares, tendo um $R^2 \geq 0,9$ podendo ser observado na Figura 1.

Tabela 1: Condições instrumentais de injeção em UPLC-ELSD

| | |
|---|---|
| **Fase móvel** | **Acetonitrila : água milli-q 80:20%; 0,2% Trietilamina Acetonitrila : água milli-q 30:70%; 0,2% Trietilamina** |
| **Coluna Cromatográfica** | **Acquity UPLC BEH Amide (50 mm x 2.1 mm x 1.7 µm)** |
| **Volume de injeção** | **0,5 µL** |
| **Vazão** | **0,17 a 0,25 mL min-1** |
| **Tempo de análise** | **4 min** |
| **Temperatura da coluna** | **85ºC** |
| **Temp. do Drift Tube** | **40 ºC** |
| **Pressão do gás (N2)** | **40 psi** |

Figura 1: Curva de adição padrão a matriz de tabaco

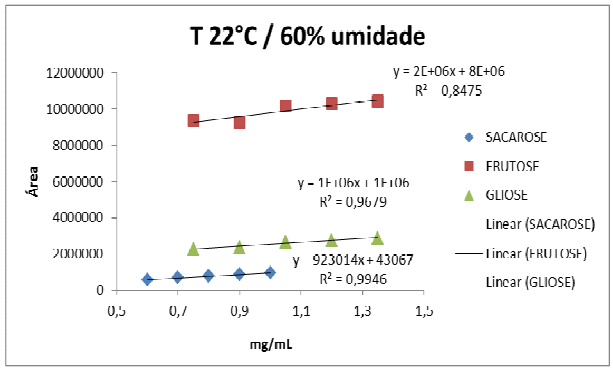


[1] - ANVISA. AGÊNCIA NACIONAL DE VIGILÂNCIA SANITÁRIA. Resolução da Diretoria Colegiada - RDC nº 14, de 15 de Março de 2012.

**Área: ANA** **Inscrição: 00826**

# Observações críticas sobre a quantificação de glifosato pelo método colorimétrico do "púrpura de Ruhemann".

**Luiz Phelipe de Souza Tomaso (IC), Emanoel Hottes (PG)*, Cristiane M. Cardoso (PQ) Marcelo H. Herbst (PQ).**

**phelipe.tomaso@gmail.com; emanoelhottes@yahoo.com.br**

*Departamento de Química, UFRRJ.*

Palavras Chave: *Glifosato, método colorimétrico, quantificação.*

## Highlights

The quantification of free glyphosate in aqueous solutions using Ruhemann colorimetric method was critically investigated. The results obtained shown that quantification of glyphosate using that method is sensible either to the temperature and reagents concentration, being a complex alternative of analysis.

## Resumo/Abstract

O método colorimétrico de Ruhemann é tradicionalmente utilizado na quantificação de aminoácidos e também glifosato, devido à analogia estrutural entre tais moléculas. Dificuldades na quantificação do glifosato por tal método são encontradas devido às diferentes características do meio de onde se deseja analisar o herbicida e também fatores físicos [1]. Verificou-se que o método de Ruhemann apresenta resultados variáveis para uma mesma concentração de glifosato quando condições como tempo de reação, concentração de reagentes e modos de resfriamento são diferentes. Este trabalho tem como objetivo uma análise crítica do método, buscando uma padronização que possa traduzir confiavelmente a medida da concentração de glifosato em soluções aquosas oriundas de reações de intercalação e/ou de complexação. O ensaio realizou-se com alterações na metodologia descrita em literatura [1]. Em tubos de ensaio adicionou-se 1mL de solução de glifosato em diferentes concentrações, 1 mL de ninhidrina e 1 mL de $Na_2MoO_4$, ambos 0,5 %. A solução formada foi aquecida por 4 minutos e resfriada de duas formas: em temperatura ambiente e em banho de gelo. Observou-se que para soluções com concentrações de glifosato na faixa entre 0,1 e 0,2 mg/mL o resfriamento em temperatura ambiente não alterou significativamente os resultados e a reprodutibilidade. Já para concentrações na faixa 0,2 a 1 mg/ml o processo de resfriamento em banho de gelo apresentou-se mais satisfatório. Por meio da análise dos resultados, pode-se concluir que o método não se mostra uniforme para toda a faixa de concentrações analisada, sendo necessário padronização prévia para se obter resultados confiáveis.

1 - Bhaskara, *et al*. Helvetica Chimica Acta. 89, 2006, 2686 – 2693.

**Área: ANA** **Inscrição: 00934**

# Síntese, caracterização e avaliação de um polímero de impressão molecular para quantificação seletiva de corante têxtil ácido violeta 19 visando aplicação em amostras ambientais

**Miguel Luna (PG)[1], Sabir Khan (PQ)[2], Gino Picasso (PQ)[1], Maria Del Pilar Taboada Sotomayor* (PQ)[2]**

**mpilar@iq.unesp.br**

*1. Facultad de Ciencias - Universidad Nacional de Ingenieria (UNI) - Lima - Peru*
*2.Instituto de Química, Universidade Estadual Paulista (UNESP)- Araraquara, SP-Brasil 14800-060*

Palavras Chave: *MIP, Acid violet 19, Environmental control*

## Highlights

"Synthesis, characterization and evaluation of a molecularly imprinted polymer for selective quantification of Acid violet 19 textile dye aim at application in environmental samples"

- Computational simulation application to an experimental synthesis.
- Good selectivity

## Resumo

Este trabalho tem como objetivo o desenvolvimento de um polímero de impressão molecular (MIP) seletivo para a determinação do corante violeta ácido 19 (VA19), da classe dos trifenilmetanos. O MIP e NIP (polimero analogo preparado sem template) foram sintetizados usando 1-vinilimidazol como monómero funcional, 2,2'-azo*bis*-(2-metilpropionitrilo) como iniciador radical. O monómero funcional foi previamente escolhido por simulação computacional usando o método semi-emprírico. Para caracterizar a eficiência do MIP foi avaliada a seletividade através das isotermas de adsorção, que se ajustaram ao modelo Langmuir-Freundlich (LF), usando CLAE. No ajuste matemático da isoterma com o modelo LF obtiveram-se os parâmetros de Qm de 8,6 mg $g^{-1}$ e cinética de segunda ordem ($K_1$ 2.5 x $10^{-4}$ $s^{-1}$). Para o estudo de seletividade (Figura 1) foram testados outros corantes trifenilmetanos, com estrutura análoga à do analito alvo. O polímero impresso MIP apresentou maior adsorção pelo VA19 - (100%) do que o NIP (66%), e do que pelas substancias análogas, Vermelho ácido 9 - BR9 (31%), Verde ácido 16 - AG16 (3,3%) e Verde básico 1 - BG1 (12%), o que confirma a eficiencia do polímero sintetizado.

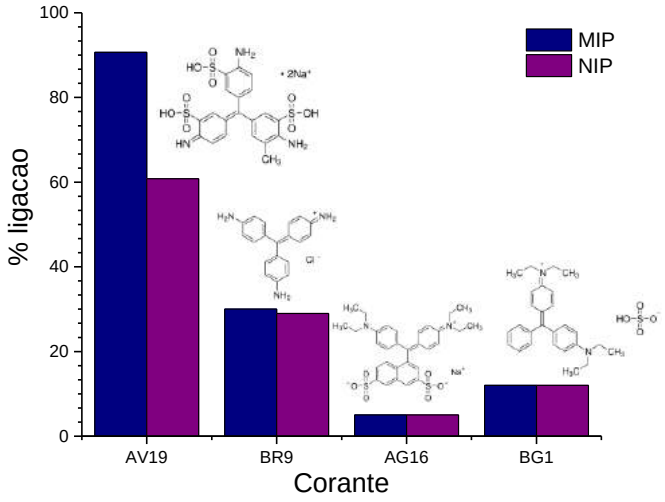


**Figura 1: Perfil da seletividade do MIP em relação ao NIP e outros corantes com estrutura análoga**

**Área: ANA** **Inscrição: 01092**

# Ion chromatography as an alternative for simultaneous determination of citrate and phosphate in anticoagulant solutions of blood bags

**Lilian de F. Venâncio (TC),[1] Anna Maria B. S. Fust (TC),[1] Renata de F. D. Vale (TC),[1] Filipe S. Q. da Silva (PQ),[2] Michele Feitoza-Silva (PQ),[1] Gleyce C. S. Cruz (PG).[1]***

**lilian.venancio@incqs.fiocruz.br; gleyce.cruz@incqs.fiocruz.br**

*[1]Departamento de Química, INCQS-FIOCRUZ; [2]Vice-Diretoria de Ensino e Pesquisa, INCQS-FIOCRUZ*

Palavras Chave: *Blood bags, Anticoagulant solution, Citrate, Phosphate, Ion chromatography*

## Highlights

Quality control of blood bags.
CLAE with ionic detection.
Simultaneous quantification of citrate and phosphate present in anticoagulant solutions of blood bags.

## Resumo/Abstract

Blood bags are risk III highly complex products designed to collect, store and transfer blood in an efficient and safe way. The national reference for the analysis of this product is the National Institute for Quality Control in Health (INCQS / FIOCRUZ), responsible for the analysis prior to-registration and control of these products. The objective of this study was to perform the optimization and validation of the analytical method for the simultaneous determination of total citrate and sodium acid phosphate monohydrate in anticoagulant solutions of blood bags by ionic comatography. For the optimization of the analytical methodology, the parameters of the proposed method were evaluated and the validation was carried out. The results showed variations of specific analytical conditions related to the mobile phase, temperature and analytical curve. Despite the different detection system, the comparison indicated similarity in the principle of analytical separation of the analytes. The results (selectivity / specificity, linearity, limit of detection, limit of quantification, precision and accuracy) indicated that the new method is reproducible. The study allowed to compare the analytical conditions and to present the relevant aspects of the implementation of the alternative method, mainly, for allowing the simultaneous determination of the analytes of interest. Additionally, it suggests new advances in the quality control of this product and reiterates INCQS participation in sanitary regulatory aspects, using reliable and reproducible analytical methodology under the analytical validation rules of the current legislation.

**Área: ANA** **Inscrição: 00770**

# Evaluation of techniques for analysis of plasticants in blood bags

**Anna Maria B. S. Fust (TC),[1] Renata de F. D. Vale (TC),[1] Lilian F. Venancio (TC),[1] Michele Feitoza-Silva, (PQ),[1] André L. M. Albert (PQ),[1] Kátia C. Leandro (PQ),[2] Carolina M. de Carvalho (PG).[1]***

**anna.fust@incqs.fiocruz.br; caroldemesquita@hotmail.com**

*[1]Departamento de Química, INCQS/FIOCRUZ; [2]Programa de Pós-graduação em Vigilância Sanitária, INCQS-FIOCRUZ*

Palavras Chave: *Blood bag, Plasticizers, Health Surveillance*

## Highlights

Plasticizers in plastic bags.
Evaluation of analytical techniques for DEHP.
HPLC-CAD as an analytical technique for plasticizers.

## Resumo/Abstract

Plastic blood bags are products that present a high risk associated with their use and are part of the Ministry of Health's blood and blood derivatives strategic program. Blood bags are made of plastified PVC with DEHP and should not release any substance above the limits specified in RDC nº 35/2014; however, plasticizers are not chemically bound to PVC and migration to the blood occurs during use of the medical device. In addition, the development of analytical methodologies for migration analysis is of paramount importance to assess patient exposure to plasticizers during the use of blood bags. This work aims to determine the plasticizer content (DEHP and DEHA) by spectrophotometric (pharmacopoeial) and chromatographic methods (CG-FID, HPLC-UV and HPLC-CAD). Plasticizer content determination was performed with three blood bag samples from three different batches and manufacturers. All the methods studied were linear in the studied concentration ranges and allowed the detection of DEHP. All samples were considered satisfactory in relation to the amount of extractable DEHP and the presence of DEHA in the analyzed samples was not detected. In the comparison of the methods by linearity, Mann-Whitney/Wilcoxon test indicated that there were no significant differences between the methods. The use of the HPLC-CAD technique for the determination of DEHP in blood bags is a technological innovation and an alternative for determination of DEHP in blood bags.

**Área: ANA** **Inscrição: 01119**

# REGULATORY IMPACT FROM THE ANALYTICAL ADEQUACY IN THE QUALITY CONTROL OF BLOOD BAGS

**Renata de F. D. Vale (TM),[1] Anna Maria B. S. Fust (TM), [1] Lilian de F. Venâncio (TM), [1] Katia Christina Leandro (PQ), [1] Michele Feitoza-Silva (PQ).[1*]**

**katia.leandro@incqs.fiocruz.br; michele.feitoza@incqs.fiocruz.br**

[1]*Department of Chemistry, National Institute of Quality Control in Health, FIOCRUZ*

Keywords: Regulation, Quality, *Boold bags*

## Highlights

Regulation of blood bags.
Quality control of blood bags.
Study of some methodologies.
Comparison of methodologies.
Determination of citrate and phosphate in blood bags simultaneous.

## Resumo/Abstract

The National Institute of Quality Control in Health (INCQS/Fiocruz) is a national reference institute in the quality control of blood bags. Currently the legislation that describes this control is the RDC n° 35/2014 that replaced the Administrative Rule n° 950/1998. The objectives of this study were to evaluate technical-scientific advances in the control of the substances present in the solutions and propose new methodologies to update the legislation. First, methodologies and techniques were compared. The second moment new studies were presented. In the comparison, it was observed a great advance in the methodologies, mainly regarding the conserve of the maintenance of the chromatographic columns, time of analyse and reproducibility of results. The methodologies were developed, optimized and validated searching efficiency, robustness and lower cost. Of the eleven methodologies, five were altered and discussed in this study. For further updating of legislation, the development of a methodology to determine the concentration of citrate and phosphate simultaneously, advances in studies related to pH, and evidence of two new methodologies for determination of the main contaminant (Hydroxymethylfurfural) are in progress. The present study presented the evolution in the parameters of product quality and highlighted the importance of INCQS as part of the National Surveillance System and the updating of regulatory issues.

**Área: ANA** **Inscrição: 01297**

# Aplicação de aerogel de grafeno como fase extratora na determinação *on-line* de $Cd^{2+}$ com detecção por FAAS

**Grazielle Cabral de Lima (PG),*[1] Luiz Felipe de Moura Mendonça (IC),[1] Larissa Castro Rodrigues (IC),[1] Giovana de Fátima Lima (PQ),[1] Pedro Orival Luccas (PQ),[1] Eduardo Costa de Figueiredo (PQ)[1].**

**graziunifal@yahoo.com.br***

[1]*Instituto de Química, Universidade Federal de Alfenas (UNIFAL-MG).*

Palavras Chave: *extração em fase sólida, aerogel de grafeno, cádmio, FAAS.*

## Highlights

Synthesis and application of graphene airgel as extraction phase in the on-line determination of $Cd^{2+}$ with detection by FAAS. Solid phase extraction; Graphene airgel as extractive material; Flow injection analysis; Multivariate optimization.

## Resumo/Abstract

Considerando a exposição humana e meio ambiente aos metais tóxicos, é inquestionável a necessidade de monitoramento e quantificação desses contaminantes. Contudo, pré-tratamentos que visam eliminar interferências e/ou melhorar a detectabilidade podem ser necessários. A extração em fase sólida é uma excelente alternativa sendo o aerogel de grafeno (GA) um forte candidato a adsorvente, principalmente devido a elevada porosidade, área superficial, resistência mecânica com redes 3D interligadas e um sistema de elétrons π deslocalizados que pode formar fortes interações hidrofóbicas. Nesse estudo avalia-se o potencial extrator do GA na pré-concentração *on-line* de $Cd^{2+}$ com sistema de análise em fluxo (FIA) e detecção por FAAS. O material foi sintetisado segundo P. Zang et al.[1]. Neste sistema, percola-se 20 mL de amostra pela minicoluna (150 mg de GA) com eluição em $HNO_3$ e detecção por FAAS. Os fatores pH amostra (pHa), vazão pré-concentração (VP), concentração tampão (CT) e eluente (CE) foram otimizados com planejamento fatorial $2^4$ (Figura 1) seguido de Matriz de Doehlert para os 3 fatores significativos (pHa, CT, CE), gerando as superfícies de resposta na Figura 1. Nas condições ótimas (CE=1,2 mol $L^{-1}$, CT=0,049 mol $L^{-1}$, pH = 5,13) o sistema apresentou: faixa linear de 5 a 300 µg $L^{-1}$ ($r^2$ = 0,9952); LD e LQ de 1,67 e 5,58 µg $L^{-1}$ respectivamente; fator de pré-concentração (17); índice de consumo (1,18 mL); frequência de amostragem (20 análises/hora); precisão de 5,5% ($Cd^{2+}$ 50 µg $L^{-1}$) e 2,24% ($Cd^{2+}$ 200 µg $L^{-1}$). Estudos futuros incluem interferentes, exatidão, aplicação em amostras ambiental e/ou alimentícia.

**Figura 1:** (a) Diagrama de Pareto; Superfícies de resposta: (a) pHxCT; (b) pHxCE e (c) CExCT.

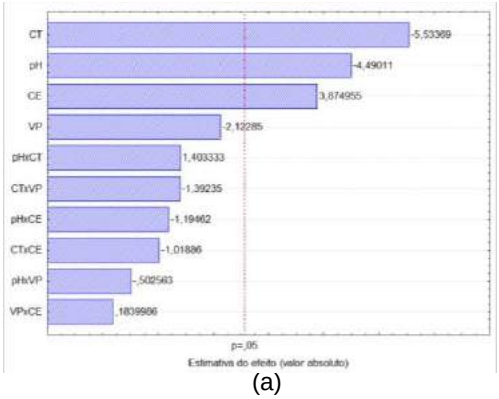


(a)

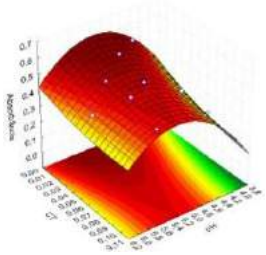

(b)

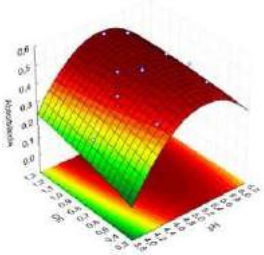

(c)

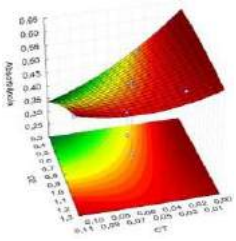

(d)

**Agradecimentos:**

Unifal-MG Universidade Federal de Alfenas

FAPEMIG

**Referência Bibliográfica:**

[1] P. Zang et al., Electrochimica Acta, v. 212, p. 171–178, 2016.

[2] Barros N. B. et al., 2a ed., Ed. Unicamp: Campinas, 2002

**Área: BEA** **Inscrição: 00048**

# DIFRATOMETRIC AND THERMOGRAVIMETRIC STUDY OF COMMERCIAL COCONUT FLOUR

**Ornella M Porcu* (PQ),[1] Vanderlei A de Lima (PQ),[2] Fauze J Anaisse (PQ),[3]**

**ornellamporcu@gmail.com**

*[1]Departamento de Química, UTFPR campus Medianeira e UTFPR campus Pato Branco PPGTP; [2]Departamento de Química UTFPR campus Pato Branco; [3]Departamento de Química UNICENTRO, Guarapuava/PR; Brasil.*

Palavras Chave: *(Fruit flour; Food analysis; X-ray analysis, Thermoanalytical profile).*

## Highlights

The great diversity of fruits in Brazil allowed their industrialization and transformation into flour as an alternative of consumption, representing a source of fiber and minerals. Fruit flours can be used as ingredient for new and healthier products, such as gluten free food or with reduced gluten content. In this study the commercial coconut flour (CO) was characterized. The thermoanalytical profile of commercial coconut flour showed high thermal stability probably due to its composition (high fiber content, minerals and moisture). The analysis of the X-ray diffraction for CO showed a high degree of cristallinity (classified as type V, formed by the crystallization of amylose with lipids). The technical quality demonstrated that the coconut flour can be an alternative ingredient to enrich food products, bakery products for example, making them healthier and more balanced.

## Resumo/Abstract

This work aimed to study X-ray diffraction application and the thermogravimetric characterization of commercial coconut flour. Three different batches of commercial coconut flour (CO) from Francisco Beltrão city - Parana state, were analyzed in this study. The diffractograms were obtained in X-Ray Diffractometer (D2 Phaser Bruker) source of CuKα radiation, 30 kV and 10 mA, with scan angle of 5º and 70º 2θ. The thermal analyzer STA 6000 (Perkin Elmer) characterized 10 mg mass of CO sample submitted in a heating from 50 to 600 ºC in a ratio of 10 ºC.min$^{-1}$ and nitrogen atmosphere in flow of 20 mL.min$^{-1}$. The software TA *Universal Analysis* was used to prepare data graphics. The X-Ray diffraction analysis enabled an attempt to assign crystallinity being classified CO as type V. The commercial coconut flour presented intense signals at the diffraction angles in 10.0, 16.0 and 20.0º. The thermoanalytical curve allowed the perception of a carbonized final residue (0.50 ± 0.05 %), which occurred at 600 $^{0}$C. In this stage there was an intense heat release with generation of metal oxides and mineral salts. This flour presented thermal stability until 250 ºC temperature and it can be heated until higher temperatures, close to 280 ºC. In this way, the commercial coconut flour can be indicated to be used as ingredient and fortification agent in food products.

**Área: BEA** **Inscrição:00049**

# Chemometrics evaluation of oxidative degradation of the Brazilian extra virgin olive oil produced from the varietal *Maria da Fé*.

**Thays R. Gonçalves (PG)[1], Rhayanna P. Gonçalves (PG)[2], Larissa N. Rosa (PG)[1], Francieli Greff (IC)[3], Hillary P. Domingues (IC)[3], Oldair D. Leite (PQ)[3], Alex S. Torquato (PQ)[3*], Paulo H. Março (PQ)[2], Patrícia Valderrama (PQ)[2], Makoto Matsushita (PQ)[1]**

alexstorquaro@utfpr.edu.br

*[1] Universidade Estadual de Maringá – UEM, [2] Universidade Tecnológica Federal do Paraná – UTFPR, campus Campo Mourão, [3] Universidade Tecnológica Federal do Paraná – UTFPR, campus Medianeira*

Keywords: *Chemometrics, Antioxidants, Oxidation products, Signal separation.*

## Highlights

- Rapid and green detection of the formation of oxidation products.
- Method proposed is faster than the conventional;
- Does not requires samples pretreatment nor reagents or solvents.

## Abstract

The olive oil is known for its resistance for the oxidative processes, being characterized as a stable oil due to their composition, which is rich in naturals antioxidants and its low concentration in polyunsaturated fatty acids. The production of extra virgin olive oil (EVOO) is concentrated in the Mediterranean areas, however, some countries have started the cultivation of olive trees, in Brazil, the manufacturing of olive oil is having been initiated. The varietal *Maria da Fé* was developed by The *Empresa de Pesquisa Agropecuária de Minas Gerais – Epamig*, in this study three samples of EVOO from this varietal was monitored over a period of twelve months, with the aim to observe the chemical changes during the storage time. Therefore, the samples evaluated by the ultraviolet-visible spectroscopy (UV-Vis) and the chemometric method of multivariate curve resolution with alternated least squares, MCR-ALS. A spectrum was collected at 0, 1, 3, 6 and, 12 months of storage. The results demonstrate the presence of two important compounds, the vegetable oils are rich in tocopherol, which is the main antioxidant present in the olive oil, during the storage time a concentration decrease is observed, while and the formation of oxidation products has a linear increase. The MCR-ALS has proven to be an effective tool for the monitoring thermal degradation, and provide information of oxidative processes, from spectral data, as a fast determination, without the use of reagents or solvents.

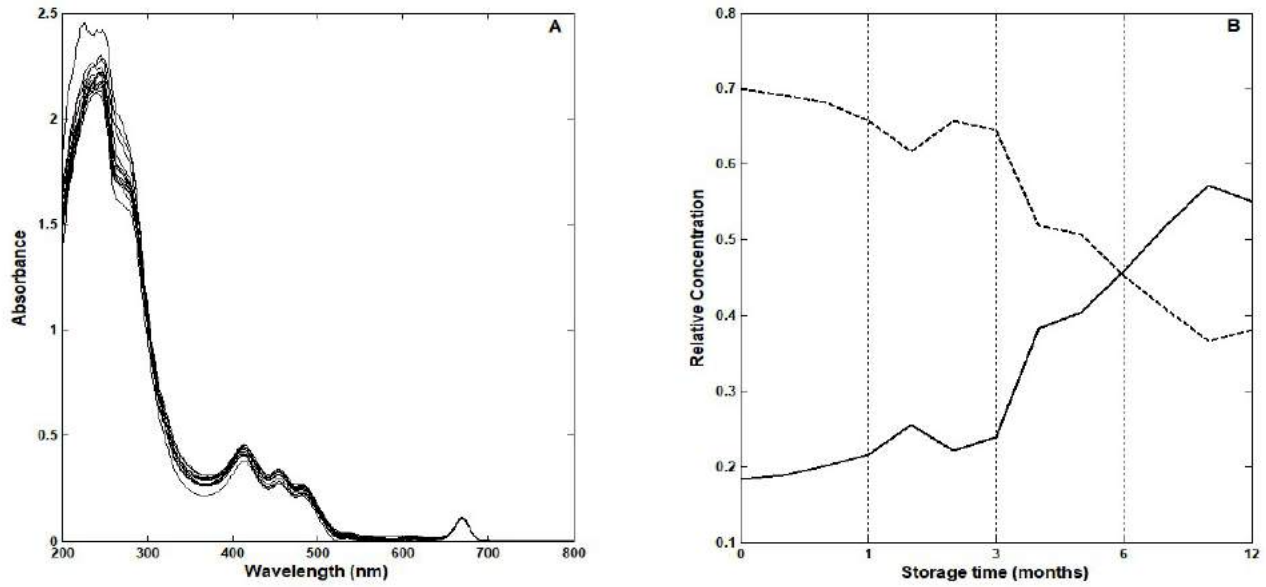


**Figure 1.** (A) UV-Vis spectra of EVOO produced from the varietal *Maria da Fé*. (B) Recovered relative concentration profile (**--**) antioxidants; (**–**) oxidation products.

**Área: BEA** **Inscrição: 00056**

# Enrichment of gluten-free bread with avocado pulp (*Persea Americana Mill)*

**Maristela Raupp dos Santos (IC),[1]* Aloisio H. P. de Souza (PQ),[2] Nadia C. Steinmacher (PQ),[3] Fernanda Caspers Zimmer (PG),[4] Daiany Cristina Vitorassi Lovera (PG),[3] Angela C. Rodrigues (PQ),[1]**

**angelac.utfpr@gmail.com; maristela_raupp@hotmail.com**

*[1]Departamento de Química, UTFPR; [2]Departamento de Alimentos, IFMS; [3]Departamento de Alimentos, UTFPR; [4]Departamento de Química, UEM.*

Palavras Chave: *Bread, Hydrocolloids, Planning of binary mixtures.*

## Highlights

Development of a gluten-free product. Bread enriched with fruit pulp. Increase in the levels of crude protein, ash, moisture and total lipids. Presence of mono and polyunsaturated fatty acids.

## Resumo/Abstract

Celiac disease affects the small intestine of genetically predisposed individuals. It is caused by the ingestion of gluten. Therefore, it is sought to develop gluten-free products that have nutritional value and characteristics acceptable by the consumer. This study aimed to enrich with fresh avocado pulp (*Persea americana Mill*), gluten-free bread formulations, pre-optimized with the HPMC hydrocolloid, through a binary mix design, varying the amounts of potato starch and avocado pulp, and identify the best formulation, having as parameter the responses specific volume and firmness of the crumb of the bread. The formulations containing higher concentrations of pulp showed higher levels of crude protein (4.2 to 4.5%), ashes (0.91 to 1.05%), moisture (29.5%) and total lipids (17.2% to 18.2%), consequently higher caloric value (369 to 372 Kcal 100 $g^{-1}$). However, the formulation with 0% avocado had higher carbohydrate contents (54.3%) when compared to the other trials. The major fatty acids identified in the formulations, in descending order, were alfalynolenic, linoleic, palmitic, stearic, palmitoleic and oleic acids. By means of the desirability function, the test of the centroid point (Table 1) of the mix planning (in the proportion 0.5: 0.5 avocado pulp and potato starch) was characterized as the best formulation (Figure 1), in which there was an increase in the value nutritional, when compared to bread without avocado pulp, and desirable conditions in the responses of volume and firmness.

**Table 1 – Ingredients used in the formulation of the centroid point**

| Ingredients | Mass (g) |
|---|---|
| Rice Flour | 75.40 |
| Potato Starch | 26.10 |
| Sweet Manioc Starch | 17.40 |
| Avocado Pulp* | 26.10 |
| Sugar | 30.00 |
| Salt (NaCl) | 1.50 |
| Olive Oil | 36.70 |
| Water | 27.80 |
| Eggs* | 50.00 |
| Instant Dry Yeast | 2.50 |

* Fresh

**Figure 1 - The best formulation containing avocado pulp**

**Área: ____BEA_____ Inscrição: 00071**

# EFEITO DA ESTERILIZAÇÃO POR IRRADIAÇÃO GAMA NA CAMOMILA [Chamomilla recutita (L.) Rauschert]

**Rodrigo Loreto Peres (PQ),[1*] Hemerson Garcia (IC),[2] Rogério Quinhones (PQ),[3]**

**rodrigo.peres@ifbaiano.edu.br**

*[1,3]Departamento de Agronomia, IFbaiano Campus Teixeira de Freitas - BA; [2]Departamento de Química UNIVALE*

Palavras Chave:*Chamomilla recutita, Radiação Gama, Contagem Microbiana*.

## Highlights

Effect of gamma irradiation sterilization in Chamomila recutita. The gamma radiation is used in food because it inactivates enzymes and increasing the storage time. The levels of irradiation were, 1 kGy, 3 kGy, 5 kGy, 20 kGy. A level of 2.049 KGy where the count reached levels suitable for consumption.

## Resumo/Abstract

The chamomila [*Chamomilla recutita(L). Rauschert*] is an aromatic species whose properties are of pharmacological and nutritional interest. The gamma radiation is used in food because it inactivates autocatalytic enzymes and decreases the levels of microorganisms, increasing the storage time. Different tests were performed in order to evaluate if there is difference in biological activity, level of contamination and chemical composition after irradiation of the plant material. A microbiological test was conducted to check some changes after the treatment with irradiation. The levels of irradiation were, 1 kGy, 3 kGy, 5 kGy, 20 kGy and the treatment has no control. The analysis performed showed that the contamination of the plant already had low levels of fungi in the control (13.83 CFU/ml) and the recommended is less than $10^2$ CFU/ml, but for bacteria the level was $8x10^3$ CFU/ml, above allowed (103 CFU/ml). We established a level of 2.049 KGy where the count reached levels suitable for consumption. The extraction methods used, maceration and Soxhlet, the latter method was more efficient in relation to the amount of mass.

Tabela 3 - Comparação dos resultados dos perfis cromatográficos, obtido por CG-MS para o extrato de *Chamomilla recutita* (L.) Rauschert macerada nos níveis de irradiação 1 KGy;3 KGy;5 KGy;20 KGy

| Nível de irradiação | N° de substâncias | RT inicial (min) | RT final (min) | N° de substâncias majoritárias | Σ das % das substâncias majoritárias |
|---|---|---|---|---|---|
| Controle | 79 | 10.31 | 46.96 | 12 | 84,6% |
| 1 KGy | 120 | 8.00 | 51.61 | 11 | 88,7% |
| 3 KGy | 119 | 39.27 | 52.59 | 17 | 71,7% |
| 5 KGy | 89 | 8.00 | 54.88 | 9 | 78,3% |
| 20 KGy | 87 | 10.33 | 51.56 | 11 | 85,0% |

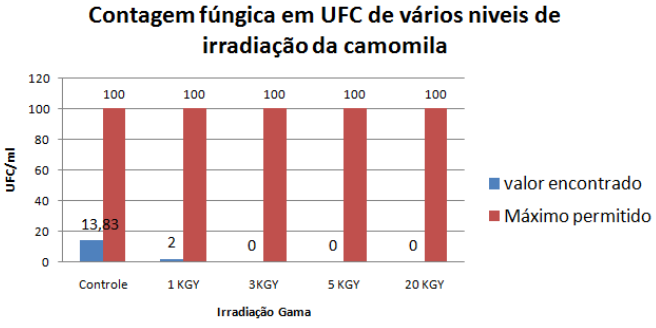


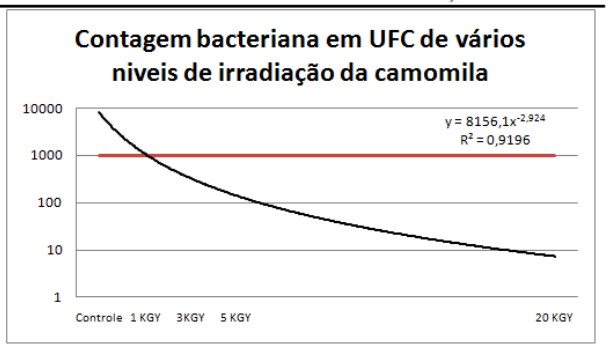


Referências Bibliográficas:**1-**Segurança e Trabalho. **Radiações Ionizantes: Aplicações e Cuidados.** Disponível em: <http://www.segurancaetrabalho.com.br/download/rad-ioniz-cuidados.pdf>. Acessado em 04/05/201; **2-**OLIVEIRA R.S. & COLAÇO W. Radiossensitividade Gama de Extrato de *Maytenus ilicifolia:* Desenvolvimento de Protocolo para Controle de Qualidade. **Latin American Journal of Pharmacy**.V.27,n.2,p 235-9,2008.

**Área: BEA** **Inscrição: 0113**

# One-Shot, Fast and Green Determination of the Alcoholic Content of Wines Using Thermal Infrared Enthalpimetry

**Alessandra S. Oliveira* (PG),[1] Bruna Tischer (PQ),[2] Fábio A. Duarte (PQ),[1] Gilson A. Helfer (PQ),[3] Adilson B. Costa (PQ),[3] Juliano S. Barin (PQ).[1]**

**juliano@ufsm.br; alessandra_stangherlin@hotmail.com**

*[1]Departamento de Tecnologia e Ciência dos Alimentos, UFSM; [2] Instituto de Ciência e Tecnologia de Alimentos, UFRGS; [2] Instituto de Ciência e Tecnologia de Alimentos, UFRGS; [3] Departamento de Biologia e Farmácia, UNISC*

Palavras Chave: *Alcoholic beverages, Wines, Thermal infrared, Enthalpimetry, Green chemistry, Calorimetry*.

## Highlights

Only one step is required for analysis. No sample preparation (e.g., dilution, distillation). Energy consumption is reduced and hundreds of measurements could be performed per hour. Easy adaption in laboratory.

## Resumo/Abstract

An innovative use of thermal infrared enthalpimetry[1] (TIE) is proposed for the determination of alcoholic content of wines. Notwithstanding the presence of ethanol in beverages, absolute ethanol was added directly to wines, and the temperature rise caused by the heat of dilution was monitored using an infrared camera. Hydroalcoholic solutions (from 3.0% to 18.0%, v/v, 1.2 mL) or samples were introduced in wells of a microplate followed by the addition of dried absolute ethanol (1.2 mL). A polytetrafluoroethylene covered magnetic stir bar (3.0 x 6.5 mm) was used for stirring. The temperature was monitored using an infrared camera (7.5-13.0 µm, E60 model, FLIR, USA). Blanks were analyzed using dried absolute ethanol. Afterwards, a least squares calibration curve was constructed using reference. The 24 microplate wells were used for reference solutions or samples in all experiments (n=24). A linear calibration curve was obtained from 3.0 to 18.0% (v/v) ethanol ($R^2$=0.9987). The results for ten samples of dry and sweet wines (red and white ones) showed agreement ranging from 98.2 to 104.0% with 942.06 and 969.12 methods of AOAC. Organic compounds (e.g., sugar) did not interfere in the determinations. The proposed method provided fast results, with a throughput of 480 samples per hour and negligible energy consumption (0.001 kWh). In addition, the consumption of reagents was reduced when compared with conventional method fulfilling green analytical chemistry requirements.

*[1] Barin et al., Anal. Chem., 87, 12065, 2015.*

**Área: BEA** **Inscription: 00155**

# Intercalation of vitamin L and adsolubilization of vanillin in lamellar hydroxide salts for obtention of multifunctional food supplements

**Natália C. Zanotelli (IC),[1*] Swami A. Maruyama (FM),[2] Ana C. T. Cursino (PQ).[1]**

**natalia.zanotelli@hotmail.com; anacursino@utfpr.edu.br**

*[1]Departamento de Química, UTFPR – Medianeira*
*2 SESI - Departamento Regional do Estado do Paraná.–SESI Araucária, Thomaz Coelho. CEP 83707-130 – Araucária – PR.*

Palavras Chave: *Layered hydroxide salt, Thermal stability, Nutraceutical properties, Controlled release*

## Highlights

Vanillin/vitamin L provides organoleptic/nutraceutical properties for layered hydroxide salts (LHS).
Vitamins/odorants are more resistant to thermal degradation after reactions with LHS.

## Abstract

Vitamin L (2-aminobenzoic acid) was intercalated inside sheets of layered hydroxide salts (LHS) with general formula of $M^{2+}(OH)_{2-x}(A^{n-})_{x/n}.zH_2O$, where $M^{2+}$ = $Zn^{2+}$ and A = vitamin-L, by coprecipitation method. The obtained compound was named HSL/2AB. Then, HSL/2AB-VN was synthesized by adsolubilizing vanillin (3-methoxy-4-hydroxybenzaldehyde) in the HSL/2AB surface. All the synthetic procedures cited above were simple and cheap. The X-ray diffraction patterns (Fig. 1-I) showed defined peaks and good crystallinity. The HSL/2AB compound showed a basal spacing of 13.6 Å, while after the reaction with vanillin such distance was increased to 14.02 Å (HSL/2AB-VN), confirming the adsolubilization. TGA assays (Fig. 1-II) were used to confirm the thermal stability improvement of intercalated vitamin-L. Decomposition of vanillin (in the free state (Fig. 1-IIb)) starts at 129 °C, and it is completely oxidized at 226 °C. After intercalation of vitamin-L (Fig. 1-IIc), the HSL/2AB decomposition starts at 397 °C. The increases of decomposition temperature and weight loss were also observed in HSL/2AB-VN, and the FTIR spectrum (not shown) of HSL/2AB-VN features characteristic bands of vitamin-L and vanillin, confirming intercalation/adsolubilization. It was observed that organic molecules (vitamins/odorants), when intercalated between LHS layers, are less volatile and more resistant to thermal degradation, which causes the aroma to remain in the LHS for a longer period of time due to slow release. Therefore, a multifunctional food additive was obtained, with organoleptic and nutraceutical properties, and with a thermal resistance suited for potential applications in the food industry.

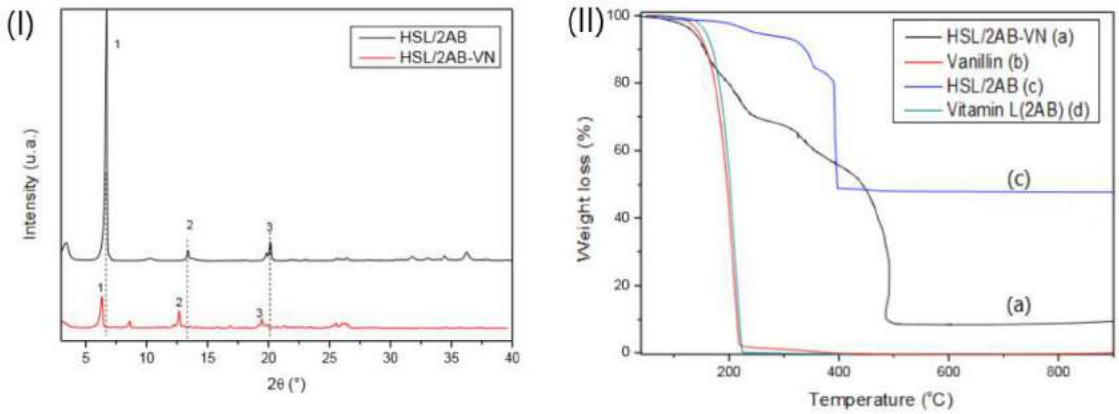


*Figura 1. X-ray diffraction patterns (I) and TGA curves (II): HSL/2AB (c) and HSL/2AB-VN (a).*

**Área: BEA** **Inscrição: 00295**

# Determinação de compostos fenólicos em vinhos comerciais por UPLC-UV

**Danieli Paulani Alves (IC)*,[1] Ana Heloisa F. Ayala (IC),[1] Caroline T. Lopes (IC),[1] Leticia J. Valente (IC),[1] Mayara P.A. da Silva (IC),[1] Rhye L. Ishikawa (IC),[1] Mariana B. Almeida (PG),[1] Tiago B. Madeira (PG),[1] Suzana L. Nixdorf (PQ).[1]**

[1]*Departamento de Química, UEL*

Palavras-Chave: *Cabernet Sauvignon, SPE, cromatografia.*

## Highlights

Determination of phenolic compounds in commercial wines by UPLC-UV. 16 phenolic compounds were evaluated. Commercial samples presented low values of most part of the compounds under study.

## Resumo/Abstract

Os compostos fenólicos estão amplamente distribuídos no reino vegetal e, apresentam basicamente um núcleo aromático. Vários destes compostos apresentam mais que um grupo hidroxila, o que altera sua reatividade. Entre as frutas, a uva é considerada uma das maiores fontes de compostos fenólicos e os principais fenólicos presentes são flavonoides (antocianinas, flavanols e flavonóis), os estilbenos (resveratrol), os ácidos fenólicos (derivados dos ácidos cinâmicos e benzoicos) e uma ampla variedade de taninos. Uma vez que as uvas tenham sido colhidas, a composição fenólica de seus derivados, como o vinho, torna-se dependente do processamento industrial. Desse modo, buscou-se avaliar a composição fenólica de 6 amostras de vinho comercial da variedade *Cabernet Sauvignon*. Os compostos fenólicos foram extraídos através de cartuchos C18. Empregou-se um método cromatográfico (Acquity UPLC, Waters) com detecção no UV á 270 nm. Foram avaliados 16 compostos sabidamente presentes no vinho. Dentre as amostras analisadas, apenas os compostos rutina (0,4 a 3,3 mg $L^{-1}$), ácido ferúlico ( 0,7 a 2,2 mg $L^{-1}$ ) e kaempferol (0,9 a 1,1 mg $L^{-1}$) foram encontrados dentro dos valores descritos na literatura para esta variedade. Não foi detectado ácido nicotínico em nenhuma amostras e apenas 4 amostras apresentaram ácido gálico (<0,3 mg $L^{-1}$). Os demais compostos como epicatequina, catequina, ácido gálico e quercetina foram encontrados em valores muito abaixo do esperado, o que pode indicar a baixa qualidade do produto final.

**Área: BEA** **Inscrição: 00319**

# Avaliação do perfil de ácidos graxos de amostras de óleo de coco comercializados em Belo Horizonte/MG

**Bruna S.R. Ferraz (IC)[1], Brenda L. S. Porto (PQ)[1], Bruno G. Botelho (PQ)[1*]**

**brunasrf.b@gmail.com; botelhobrunog@gmail.com**

[1]*Departamento de Química,UFMG;*

*Palavras Chave: Óleo de coco, GC-FID, ácidos graxos metil ésteres, cromatografia à gás*

## Highlights

Fatty acid profile of coconut oil samples sold at Belo Horizonte/MG

Fatty acid profiles of coconut samples sold in Belo Horizonte were analysed using GC-FID

Differences in the fatty acid profile were significant, even in samples from the same brand.

## Resumo/Abstract

O óleo de coco é um óleo vegetal produzido a partir da copra, “carne” do coco (*cocos nucifera L.*), ou do leite de coco. Diferente dos outros óleos vegetais, mais 80% do total de ácidos graxos do óleo de coco tem cadeia igual ou menor a 16 carbonos, e é por essa composição, rica em ácidos de graxos de cadeia média (principalmente ácido láurico), que o seu consumo vem sendo associado a bons hábitos alimentares[1]. Em função da atenção que vem sendo dada a este produto nos últimos anos, o objetivo deste trabalho foi avaliar o perfil lipídico de algumas amostras de óleo de coco comercializados em Belo Horizonte/MG. Quatro amostras de óleo de coco foram compradas no mercado comum de Belo Horizonte/MG, e armazenadas até análise em temperatura ambiente ao abrigo da luz. O teor de ácidos graxos foi determinado de acordo com o descrito por Porto e colaboradores (2016)[2], utilizando a transesterificação metanólica básica. Os ácidos graxos metil esteres foram identificados através da comparação dos tempos de retenção com um padrão (Supelco 37, mix de C4:0 a C22:6n3). Os resultados encontrados estão apresentados na figura 1. O perfil das amostras analisadas está condizente com o descrito pela literatura, o que pode indicar uma procedência destes óleos. Uma variação significativa nos teores de C12:0 foi verificado nos diferentes lotes da amostra A, o que pode indicar que estes lotes vieram de diferentes produtores ou regiões.

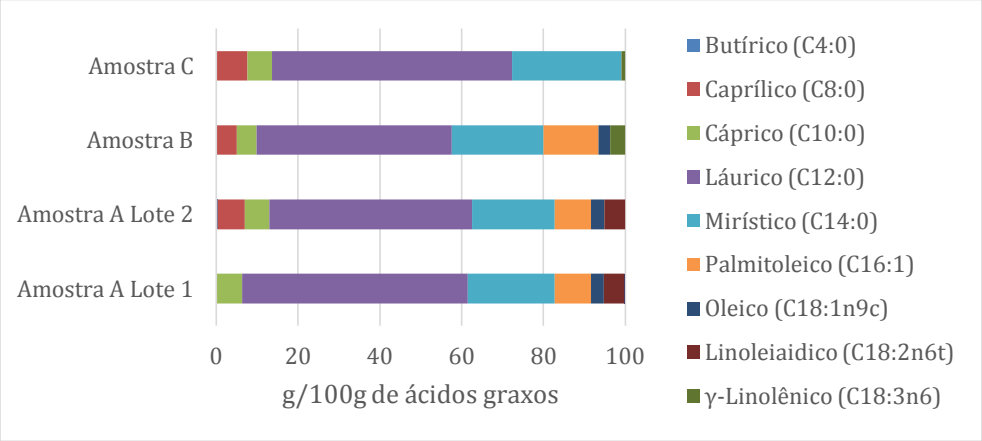


Figura 1 - Perfil de ácidos graxos das amostras de óleo de coco analisadas

[1] Kaunitz, H. *Ceylon Cocon. Q.***1973**, 23, 85-91

[2] Porto, B.L.S, et al. *Rev Inst Adolfo Lutz*. **2016**,75, 1694-1705

**Área: BEA** **Inscrição: 00335**

# Composição fenólica de extratos de resíduos industriais de amora-preta e seriguela por UPLC-PDA

**Caroline T. Lopes (IC),[1] Alexandre V. G. Mazalli (PG),[1,2*] Daniel H. S. Sena (IC),[2] Mariana B. Almeida (PG),[1] Tiago B. Madeira (PG),[1] Suzana L. Nixdorf (PQ)[1]**

**caroline.lopes.1@hotmail.com; ale_mazalli@hotmail.com**

[1]*Departamento de Química, UEL*
[2]*Departamento de Química, FEMA*

Palavras Chave: *frutas tropicais, cromatografia, extração por solvente*

## Highlights

Phenolic composition of industrial residues extract of blackberry and seriguela by UPLC-PDA. Phenolic compounds are related to the antioxidant activity. Tropical fruits can be considered an important source of phenolics compounds. Industrial residue of fruits are rich in bio compounds.

## Resumo/Abstract

A caracterização da composição fenólica em alimentos, principalmente das frutas tem sido de grande interesse devido à sua atividade antioxidante. Buscando minimizar o descarte incorreto e o acúmulo de resíduos industriais, surge a necessidade do estudo da composição química destas sobras, visando agregar valor a estes subprodutos. Dentre as frutas tropicais nativas de interesse industrial, foram selecionadas a amora-preta e a seriguela. As amostras de resíduos do processamento industrial de polpas, foram cedidas pela empresa Sítio do Belo Frutas Nativas, situado na cidade de São Paulo. O preparo das amostras foi realizado utilizando de 10,00 g do resíduo da fruta, contendo semente e casca e 100 mL do solvente extrator (água, metanol ou mistura binária dos mesmos). A solução final foi então filtrada em membrana 0,22 µm (PTFE) e analisada por cromatografia em sistema UHPLC (Acquity UPLC Waters) com detecção a 270 nm. Um total de 16 compostos foi monitorado em um intervalo de 13 minutos. Observou-se que o tipo de extração exerce influência significativa sobre a concentração final dos compostos fenólicos nos extratos. Dentre os compostos fenólicos presentes em ambas as frutas, pode-se destacar a ocorrência de elevadas concentrações de ácido ascórbico (45,13 mg/100 g) na seriguela, e de ácido caféico (45,66 mg/ 100 g) na amora-preta, obtidas a partir dos extratos metanólicos. Foi confirmado a presença de compostos bioativos com elevado potencial antioxidante nos resíduos das frutas, o que torna interessante o seu uso em novos produtos.

**Área: BEA** **Inscrição: 00532**

# Spectrophotometric method for quantification of antioxidant capacity of tropical fruits based on the formation of Fe(II)/2,2'-bipyridyl complex

**Gabrielli G. Bortolozi (IC), Horacio D. Moya (PQ).[1]***

**gabibortolozi@yahoo.com.br; horacio.moya@fmabc.br**

[1] *Faculdade de Medicina da Fundação do ABC – CEPES (Centro de Estudos, Pesquisa, Prevenção e Tratamento em Saúde) – CEP – 09060-650 – Santo André – SP*

Key words: *Antioxidant capacity, 2,2'-bipyridine, Fe(III), Tropical fruits, Spectrophotometry.*

## Highlights

Antioxidant compounds present in fruits reduce Fe(III) in the presence of 2,2'-bipyridyl forming the Fe(*bipy*)$_3^{2+}$ complex which is used to determine the antioxidant capacity of unconventional fruits.

## Abstract

The suggested method is based on the reduction of Fe(III) to Fe(II) by antioxidant compounds (acetate buffer; pH 4.6) containing 2,2'-bipyridine (*bipy*, Fig. 1) in aqueous solution. Absorbance values recorded at 521 nm characteristic of the orange-reddish Fe(*bipy*)$_3^{2+}$ complex formed were used to determine the TAC (expressed as equivalents of ascorbic acid) of ten unconventional Brazilian fruits. These TCA results were compared with those obtained with the free radical ABTS$^{\bullet+}$ reagent[2] and also with the Folin-Ciocalteu (FC) index. For the analyzed fruit samples (Table 1) the TAC values obtained with the proposed method (Fe(*bipy*)$_3^{2+}$) showed very correlation well with those obtained using the ABTS$^{\bullet+}$ ($r^2$ = 0.818) indicating that both methods can be used in the TAC quantification in this type of sample.

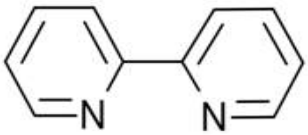

Figure 1

Table 1 - TAC values and Folin-Ciocalteu index for the fruits analyzed

| Brazilian name | Scientific name | ABTS$^{\bullet+}$ (a) | Fe(*bipy*)$_3^{2+}$ (b) | FC index (c) |
|---|---|---|---|---|
| Cajá Manga | *Spondias dulcis* | 334±25 | 18.6±1.60 | 0.287±0.015 |
| Canistel | *Pouteria campechiana* | 667±59 | 8.87±0.37 | 1.303±0.018 |
| Cupuaçu | *Theobroma grandiflorum* | 905±9 | 15.71±0.75 | 0.696±0.034 |
| Cruá | *Sicana odorifera* | 446±5 | 23.13±0.58 | 0.432±0.019 |
| Juá | *Physalis angulata* | 303±19 | 12.12±0.24 | 0.241±0.007 |
| Mangostim | *Garcinia mangostana* | 293±10 | 24.1±1.05 | 0.198±0.008 |
| Marola | *Annona crassiflora* | 3524±83 | 1.32±0.03 | 1.790±0.247 |
| Pitomba | *Talisia esculenta* | 677±12 | 14.1±0.96 | 0.412±0.060 |
| Sapoti | *Manilkara zapota* | 3322±1700 | 0.86±0.05 | 1.761±0.110 |
| Tamarindo | *Tamarindus indica* | 794±19 | 9.64±0.59 | 0.524±0.054 |

a = μM trolox/g fruit, b = g AA/g fruit, c = g Pirogallic acid/100 g fruit
The results are averages and standard deviation of triplicates

Both TAC values (Fe(*bipy*)$_3^{2+}$ and ABTS$^{\bullet+}$) also showed a positive correlation with the Folin-Ciocalteu index ($r^2$ = 0.818 and $r^2$ = 0.849, respectively) suggesting that the compounds oxidized by the Folin-Ciocalteu reagent[3] are responsible for the antioxidant capacity found in these samples. The suggested method is simple, easy to perform, reproducible and can be used in routine analysis because reagents are not expensive and equipment and materials are commonly available in most laboratories.

Financial support: PIBIC/ CNPq

1] Rufino, et al. *Comunicado Técnico da EMBRAPA* 128, 1-4, 2007.
2] Farmacopéia Brasileira. (4th ed.). Atheneu. São Paulo. Vol. 2, p.194; 2003.

**Área: BEA** **Inscrição: 00580**

# Caracterização de pesticidas em leite humano.

**Raiane C. Souza (PG),[2]* Thamillin C. Nakamura (PG),[1] Paula V. N. Brito (PG).[1] Roberto B. Portella (PQ),[2] João V. da S. Santos (PQ)[1,3] José D. S. da Silva (PQ),[1]**

**jose.silva@ufob.edu.br; rai_csouza@hotmail.com**

*[1]Programa de Pós-Graduação em Química Pura e Aplicada-UFOB; [2]Programa de Pós-Graduação em Ciências Ambientais-UFOB.[3] Campus Uruçuca, IF baiano.*

Palavras Chave: Pesticidas, alimentos, organoclorados, leite materno.

## Highlights

Characterization of pesticides in human milk.
Determination of 18 organochlorine pesticides in samples of human milk in the Western Region of Bahia.
The analyzed samples presented profiles of contamination by up to ten residues of organochlorine pesticides

## Resumo/Abstract

A agricultura contemporânea geralmente envolve o uso intenso de pesticidas sintéticos de diversas classes como herbicidas, fungicidas, entre outras. A aplicação destas espécies em campo é pouco eficiente, sendo menor que 10%, proporcionando a deriva destas espécies para a atmosfera, solo e corpos d'água. Assim, a frequente contaminação de compartimentos ambientais leva ao consumo de alimentos e derivados, de origem animal e vegetal, por residuos de pesticidas, podendo ocasionar a contaminação humana e desencadear uma série de complicações à saúde. Sendo assim, o objetivo deste trabalho foi avaliar a contaminação humana, caracterizando resíduos de 18 organoclorados (α,γ,β,δ–HCB, Heptacoro, Aldrin, Heptacloro hepóxido, EndosulfanI, DDE, Dieldrin, Endrin, EndosulfanII, DDD, Endrin aldeído, Endosulfan sulfato, DDT, Endrin cetona, Metoxicloro), em amostras de leite humano. O estudo foi realizado em 34 amostras coletadas na Região Oeste da Bahia. As analises foram feitas por CG-MS, e o método analítico apresentou as seguintes figuras de mérito: limites de detecção e quantificação (0,15-0,54 μg $L^{-1}$ e 0,5-1,54 μg $L^{-1}$); exatidão (69-120%); precisão (2,6-8,7%). O resultado demostrou que os resíduos de Metoxicloro, Dieldrin, δ–HCB e DDE foram as espécies que apresentaram as maiores frequências de detecção, 100,0%, 94,1%, 82,4% e 64,7%, respectivamente. O Metoxicloro (102,2 ng $mL^{-1}$), o Dieldrin (56,2 ng $mL^{-1}$) e o Endossulfan I (20,2 ng $mL^{-1}$) foram encontrados nas maiores concentrações médias Figura 1.

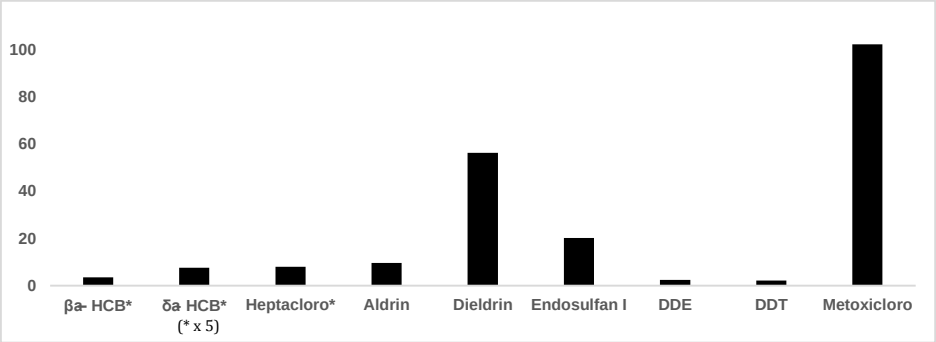


**Figura 1.** Concentração de pesticidas em amostras de leite humano (ng $mL^{-1}$).

As amostras apresentaram perfis de contaminação por até dez resíduos de pesticidas, os quais tem uso proibido no Brasil, o que mostra que ou há uso ilegal destes compostos ou sua persistência no meio ambiente é maior que descrito. A contaminação por pesticidas é preocupante, pois além de causar efeitos deletérios nas nutrizes, também podem provocar sérios danos aos lactantes, pois a exposição aguda pode ampliar estes efeitos.

**Área: BEA** **Inscrição: 00786**

# Quantification of the antioxidant activity of the fruits using the colored free radical derived from N-(4-methoxyphenyl)-p-phenylenediamine

**Karina Youssef (IC), Horacio D. Moya (PQ)[1]*.**

**karinayoussef@icloud.com; horacio.moya@fmabc.br**

*[1] Faculdade de Medicina da Fundação do ABC – CEPES (Centro de Estudos, Pesquisa, Prevenção e Tratamento em Saúde) – CEP – 09060-650 – Santo André – SP – Brazil.*

Key words: *Antioxidant activity, N-(4-methoxyphenyl)-p-phenylenediamine, Brazilian fruits, Spectrophotometry.*

## Highlights

The consumption of the free radical MPPD$^{\bullet+}$, derived from N-(4-methoxyphenyl)-p-phenylenediamine, was used in a new spectrophotometric procedure to quantify the antioxidant capacity of fruits.

## Abstract

N-(4-methoxyphenyl)-p-phenylenediamine (MPPD, Figure 1) has been used as a visual indicator in a complexometric titration of $Fe^{3+}$ with EDTA (pH 2, HCl). It was noted that the oxidation of MPPD by Fe(III) in an acetate buffer solution (pH 4) (Eq. 1) originate gave the purple free radical MPPD$^{\bullet+}$ ($\lambda_{max}$ 569 nm), which can react with antioxidant compounds (AOs). In the present study a procedure to determine the total antioxidant capacity (TAC) based on the extinction of the colored MPPD$^{\bullet+}$ by AOs present in the aqueous extracts of fruits (Eq. 2) was developed. Ascorbic acid, which also consumes the MPPD$^{\bullet+}$ radical and is biologically active in the fruits, was chosen to express the TAC values.

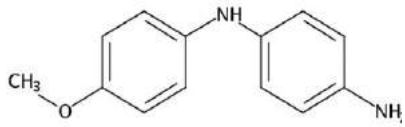


Figure 1

$$MPPD + 2\ Fe(III) \xrightarrow{H+} 2\ Fe(II) + MPPD^{\bullet+} \quad \textbf{(1)}$$

$$MPPD^{\bullet+} + AOs \rightarrow MPPD + AOs\ oxidized \quad \textbf{(2)}$$

The TAC values of six Brazilian tropical fruits obtained with the proposed method (MPPD$^{\bullet+}$) showed a good positive correlation ($r^2$ = 0.951) with the values obtained using the DPPH$^{\bullet+}$ reagent (EMBRAPA)[1], suggesting that both methods can be used in TAC quantification of fruits. As the sample was diluted 10 times (1.0 g pulp/10 mL water) and the absorbance measurements were performed at 569 nm, the proposed procedure was not subject to the color interference from the tested samples. The suggested procedure is simple, easy to perform and not use organic solvents, which makes it environmentally-friendly.

Table 1 - TAC values obtained with MPPD$^{\bullet+}$ and DPPH$^{\bullet+}$ methods for six fruits analyzed

| Brazilian name | Scientific name | MPPD$^{\bullet+}$ (a) | DPPH$^{\bullet+}$ (b) |
|---|---|---|---|
| Cajá Manga | *Spondias dulcis* | 2.71 ± 0.15 | 995 ± 37 |
| Canistel | *Pouteria campechiana* | 3.15 ± 0.075 | 498 ± 59 |
| Cruá | *Sicana odorifera* | 0.60 ± 0.031 | 2059 ± 43 |
| Jenipapo | *Genipa americana* | 1.91 ± 0.16 | 1190 ± 140 |
| Mangostim | *Garcinia mangostana* | 2.88 ± 0.23 | 907 ± 25 |
| Umbu | *Spondias tuberosa arruda* | 1.46 ± 0.082 | 1403 ± 57 |

a = g AA/g fruit , b = g fruit/ g DPPH. The results are averages and standard deviation of triplicates

Financial support: PIBIC - FMABC

1] Rufino, et al. Metodologia Científica: Determinação da Atividade Antioxidante Total em Frutas pela Captura do Radical Livre DPPH. Comunicado Técnico 127. Empresa Brasileira de Pesquisa Agropecuária, *EMBRAPA,* 127, 1-4, 2007.

**Área: BEA** **Inscrição: 00802**

# Determination of 16 Carbonyl Compounds in Mineral Water

**Ingrid Marcela M. Cardozo (PG),*[1,2] Jeancarlo P. dos Anjos[2,3,4] (PQ), Jailson B. de Andrade[1,2,3] (PQ).**

**Imarce24@gmail.com**

*[1]Instituto de Química, UFBA, 40170-290, Salvador-BA, Brasil; [2]Centro Interdisciplinar de Energia e Ambiente – CIEnAm, UFBA, Canela, 40110-040, Salvador-BA, Brasil; [3]INCT de Energia e Ambiente, UFBA, 40170-290 Salvador, BA, Brasil,* [4]Centro Universitário SENAI CIMATEC, 40170-010, Salvador, BA, Brasil.

***Keywords: Mineral Water, Carbonyl Compounds, UFLC.***

## Highlights

A new analytical methodology was developed to quantify 16 CC (C1-C6) in commercial fresh water, with or without gas using UFLC-MS. The concentrations determined were in the range of 0.01 to 3.50ppb.

## Abstract

Carbonyl compounds (CCs), like formaldehyde and acrolein, are recognized as highly toxic pollutants, especially when present in the air, food or beverages. (CCs) can be characterized and quantified by addition reactions with nucleophilic reagents. The most used reagent for characterization and quantification of CC is 2,4-dinitrophenylhydrazine (2,4-DNPH), forming the respective hydrazones (base de Schiff)[1] (Figure1).

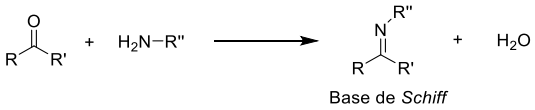


Figure 1. Formation of hydrazones from 2.4 DNPH.

The mineral water market is one of the fastest growing branches in the sector of non-alcoholic beverages. The water is exposed to contaminants from different sources and, for bottled water, the material by which the bottle or container is produced can be a source of contamination of different classes of substances such as carbonyl compound. On the other hand, the quality and origin of the carbon dioxide used in the gasification, can be sources of contamination by different classes of substances, such as CC. The main objective of the present work was to develop a new analytical methodology to quantify CC in samples of mineral water, carbonated or not, commercialized in the city of Salvador-BA.

The CC analyzes were performed using a Shimadzu Ultra Fast Liquid Chromatograph (Series 21398), equipped with a MS detector. For the analysis, a previous purification of the 2,4-DNPH (1 g) was performed through Liquid-Liquid Extraction using 120 mL of acetonitrile and 78 mL of water. Thus, a 2,4-DNPH solution with concentration of 0.5% was obtained. The CC were derivatized by reacting 100 mL of mineral water (acidified by addition of 5 drops of HCl) with 20 mL of 2,4-DNPH 0.5%, under sonication (20 min) and then passed throughout a C18 SEP PAK cartridge. The elution was done using 2 mL of Acetonitrile.

The hydrazones (Formaldehyde, Acetaldehyde, Acetone, Acrolein, Propionaldehyde, Crotonaldehyde, Metacroline, Isobutyraldehyde + Butyraldehyde, Benzaldehyde, Cyclohexanone, Valeraldehyde, Tolualdehyde + M-Tolualdehyde, Hexaldehyde, Heptanal) were separated in 16.5 min and 15 CC were quantified in the water samples studied.

Formaldehyde, acetaldehyde, acetone, valeraldehyde and benzaldehyde were found in all studied samples. The highest concentration determined was 3.50 ppb (acetaldehyde). For example, the concentration range determined for acrolein and formaldehyde were 0.01 ppb - 0.44 ppb and 0.44ppb– 1.23 ppb, respectively.

Comparing carbonated and non carbonated water, for most of the CC studied we observed no significant differences in the measured concentratations. Nevertheless, for acrolein, for example, the measured concentratios in carbonated water was, on average, 3.8 times higher than that measured in non carbonated waters.

The analytical methodology developed is comprehensive, precise, accurate and suitable for use in the studies o water quality.

[1]Azevedo, L.C; Reis, M.M; Motta, L. F; Rocha, G.O; Silva, L; De Andrade, J.B.. J. Agric. Food Chem. (2007) 55: 8670-8680.

**Área: BEA_____** *(Inserir a sigla da seção científica para qual o resumo será submetido. Ex: ORG, BEA, CAT)*

**Inscrição:00899_____** *(Inserir o número de inscrição do autor que fez a submissão)*

# Oxidative stability study of edible vegetable oils using near-infrared emission spectroscopy

**Diego C. Andrade (TC),[1*] Francisco S. Vieira (PG),[1] Celio Pasquini (PQ).[1]**

**diegoca@g.unicamp.br;**

[1]*Institute of Chemistry, State University of Campinas - UNICAMP;*

Key-words: *Near-Infrared, Spectroscopy, Induction-Time, Vegetable Oils*

## Highlights

Induction time determination of edible vegetable oils NIRES. Autoxidation and vegetable oils quality. Edible vegetable oils shelf life. Shelf life estimation by Arrhenius plot.

## Abstract

Lipids are important constituents of food, and their oxidative stability is related to the time required to detect significant amounts of a degradation product (Induction Time - IT), such as hydroperoxides (HP). A new technique for determining IT is based on near-infrared emission spectroscopy (NIRES) to detect HP. Compared to the standard Rancimat method, the technique has advantages such as wide working temperature range, low sample volume and rapid analysis.
In the present work a NIRES photometer was used to the study shelf life (SL) of soybean oil, submitted to domestic storage conditions. The determination of IT by NIRES was compared with the reference technique to detect conjugated dienes (CD). This work also proposed to study the correlation between the IT value for different types of edible oils and the concentration of pro-oxidative and antioxidant substances available in the literature. The possibility of estimating SL using Ahrrenius plot was also evaluated.
The use of NIRES photometer in the soybean oil SL study was efficient since it was possible to quantify the effect of the different storage forms on the IT. Moreover, it was observed that there was a correlation with the results obtained by the CD analysis (Figure 1). The correlation between the IT of different types of oils and their respective chemical composition and also the estimation of SL based on the Arrhenius plot should be done carefully.

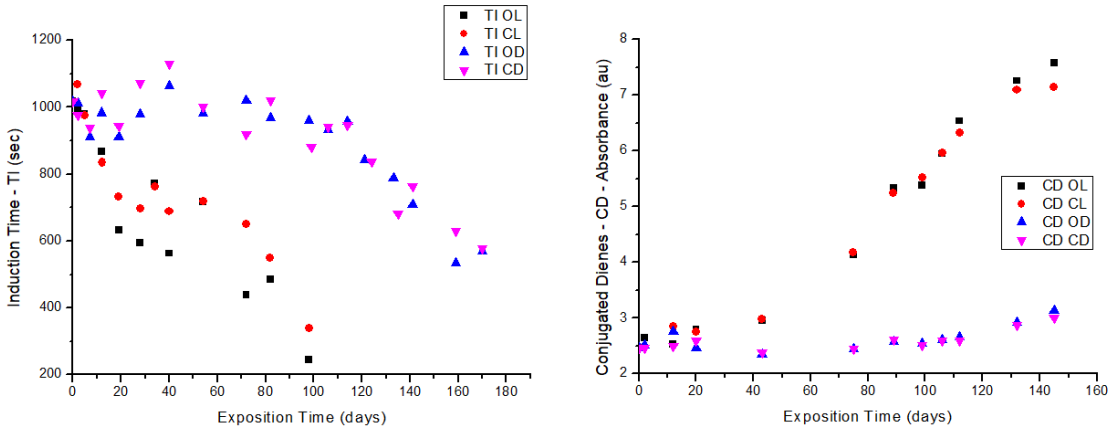


Figure 1: Comparison between induction time (IT) and conjugates dienes (CD) absorbance in a arbitrary scale; the left plot shows the IT results, and the right one shows the CD results. The sample name is related to type of analysis (IT – induction time by NIRES, CD – conjugated dienes absorbance) and the storage condition (OL – opened in light, CL – closed in light, OD – opened in dark, CD – closed in dark). The IT values show a constant fall tendency, more intense for the samples exposed to light. The CD values have a tendency of increase, more intense for the samples exposed to light.

Acknowledgements: INCTAA (CNPQ 573894/2008-6 FAPESP 2008/57808-1), EDUCORP (UNICAMP Corporative Education School)

**Área: BEA** **Inscrição: 00930**

# Caracterização dos constituintes da cagaita empregando-se a PS-MS

**Luisa Del C. Barrett Reina (PQ)[1], Amauri G. Souza (PQ)[2], Mauro R. Silva (PG)[3], Lucas G. Freitas (IC)[3], Raquel L. B. Araújo (PQ)[3], Inayara C. A. Lacerda (PQ)[3], Rodinei Augusti (PQ)[4], Júlio O. F. Melo (PQ)[2]*.**

**luisabarrett@gmail.com; onesiomelo@gmail.com**

*[1]Instituto de Ciências Naturais, Humanas e Sociais, Campus de Sinop, UFMT; [2]Departamento de Ciências Exatas e Biológica, UFSJ; [3]Departamento de Alimentos, UFMG; [4]Departamento de Química, UFMG.*

Palavras-Chave:*Compostos fixos, Paper spray, Espectrometria de massas, Eugenia dysenterica.*

## Highlights

Characterization of the constituents of cagaita using PS-MS. The fixed compounds of cagaita were evaluated by ambient ionization mass spectrometry. PS-MS allowed the identification of several compounds such as sugars, amino acids, anthocyanins and coumarins.

## Resumo/Abstract

A análise dos constituintes dos alimentos geralmente é realizada por métodos tradicionais como a Cromatografia Líquida de Alta Eficiência (HPLC) e/ou espectrometria de massas (HPLC-MS). No entanto, essas técnicas possuem algumas desvantagens por apresentarem várias etapas laboratoriosas. Nesse sentido, a espectrometria de massas com ionização por *paperspray* (PS-MS) têm proporcionado análises muito rápidas (poucos segundos) com preparo mínimo das amostras e de baixo custo.

As cagaitas foram coletadas na cidade de Paraopeba, Sete Lagoas e Prudente de Morais/MG. Após lavagem e sanitização das amostras, as sementes e as cascas dos frutos foram descartadas e as polpas armazenadas a -18 ºC até o momento da análise.

As análises foram realizadas segundo procedimento descrito por Bueno (2017), utilizando-se um espectrômetro de massas. A aquisição dos dados ocorreu no modo *FullScan* com faixa de massas de 50 a 600 m/z no modo positivo. Na Figura 1 está apresentado o diagrama do PS-MS. As substâncias identificadas nas cagaitas estão mostradas na Tabela 1.

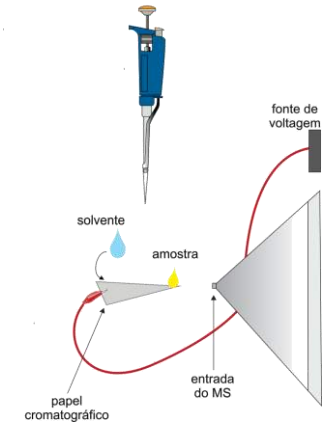


**Figura 1.** Diagrama da fonte de ionização PS-MS.

**Tabela 1.** Compostos identificados em cagaitas por PS-MS.

| Composto | *m/z* | ID | MS/MS |
|---|---|---|---|
| Colina | 104 | $[M+H]^+$ | 60 |
| *L*-arginina | 175 | $[M+H]^+$ | 60, 70, 129 |
| Citropten | 206 | $[M]^+$ | 121 |
| Hexoses | 381 | $[M+K]^+$ | - |
| Delfinidina-3-glicosídeo | 465 | $[M]^+$ | 303 |

A PS-MS permitiu a identificação de açúcares, aminoácidos, antocianinas e cumarinas. A identificação desses compostos foi realizada de acordo com seu perfil de fragmentação e pela comparação com dados da literatura. Portanto, a PS-MS mostrou-se eficiente e rápida (poucos segundos), uma vez que permitiu a identificação de várias classes de compostos da cagaita.

**Agradecimentos:** FAPMIG, FAPMAT, CNPq, UFSJ, UFMT e PRPQ/UFMG.

**Área: BEA** **Inscrição:00949**

# Bromine and iodine determination in different legumes by ICP-MS after decomposition by microwave-induced combustion

**Filipe Soares Rondan (PG),[1] Gilberto da Silva Coelho Junior (PG),[1] Alessandra Schneider Henn (PG),[2] Janaína do Rosário Brum (IC),[1] Priscila Tessmer Scaglioni (PQ),[1] Márcia Foster Mesko (PQ).[1]***

**fsrondan@gmail.com; *marcia.mesko@pq.cnpq.br**

[1]*Centro de Ciências Químicas, Farmacêuticas e de Alimentos, Universidade Federal de Pelotas, Pelotas – RS, Brazil;*
[2]*Departamento de Química, Universidade Federal de Santa Maria, Santa Maria – RS, Brazil.*

Palavras Chave: *Legumes, Bromine, Iodine, MIC, ICP-MS*

## Highlights

Legumes were efficiently digested by MIC allowing to determine Br and I by ICP-MS.
Bromine and iodine were absorbed using diluted solution.
Bromine and iodine were determined in a variety of legumes.

## Resumo/Abstract

In this study, a method for bromine and iodine determination in legumes by inductively coupled plasma mass spectrometry (ICP-MS) after digestion by microwave-induced combustion (MIC) was developed. Samples (up to 500 mg) were digested in closed system pressurized with 20 bar of oxygen (8 samples in less than 30 min). Ultrapure water and $NH_4OH$ solutions (25, 50 and 100 mmol $L^{-1}$) were evaluated as absorbing solution. Water and 25 mmol $L^{-1}$ $NH_4OH$ were not suitable for Br and I absorption, while 50 and 100 mmol $L^{-1}$ $NH_4OH$ did not presented statistical difference between the results for both analytes (ANOVA/Tukey test, confidence level of 95%). Recovery tests were performed using standards solution or a reference material of corn bran (NIST 8433) mixed with the sample. Recoveries from 98 to 108% were obtained for Br and I, using 50 mmol $L^{-1}$ $NH_4OH$. The relative standard deviations were up to 9 and 11% for Br and I, respectively. Limits of quantification of 0.03 for Br and 0.009 mg $kg^{-1}$ for I were obtained. The proposed method was applied to 7 samples of legumes (beans, lentils and soybeans) produced in Brazil. The results showed a wide variation for Br concentrations (0.423 to 2.49 mg $kg^{-1}$), whereas for I it was not observed (< 0.009 to 0.012 mg $kg^{-1}$). In this way, the proposed method is an excellent alternative for Br and I determination in legumes and presents several advantages for the routine analysis.

**Área: BEA**

**Inscrição: 00957**
*(Inserir o número de inscrição do autor que fez a submissão)*

# Production and impregnation of starch aerogels using supercritical CO2

**Maria Villegas (PG),[1,2] Alessandra L. Oliveira (PQ)[2], Reinaldo C. Bazito (PQ) [1], Pedro Vidinha (PQ).[1]***

**mariavillegas@usp.br; pvidinha@iq.usp.br**

[1] *Instituto de Química USP - Av. Prof. Lineu Prestes, 748 - Vila Universitária, São Paulo - SP, 05508-000.*
[2]*Facultade de Zootecnia e Engenheria de Alimentos USP - Av Duque de Caxias Norte, 225 – Pirassununga, São Paulo – SP, 13635-900*

Palavras Chave: *CO2 supercrítico, amido, aerogéis*

## Highlights

Straightforward method for drying aerogels
Impregnation of aerogels with ibuprofen

## Resumo/Abstract

The present work reports the development of a process to produce highly surface starch aerogels for the impregnation of green coffee oil. The strategy presented here is based on a novel method for drying hydrogels in supercritical carbon dioxide ($scCO_2$) without using alcogel traditional step. The drying step was performed using a mixture of $scCO_2$ and ethanol which was pumped through a high-pressure flow cell. The best drying conditions were achieved at 200 bar and 40°C using 2 mL/min of $CO_2$ with 5% of ethanol during 5 hours. The obtained materials exhibit a surface area of 96 $m^3/g$ which is in line with the best starch aerogel obtained through the traditional alcogel approach. These materials were further impregnated with ibuprofen in scCO2 in order to develop an integrated process between drying and impregnation.

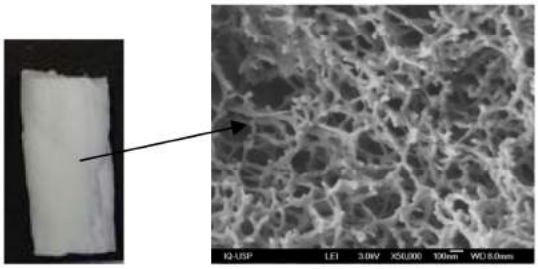

**Área: BEA** **Inscrição:** 01111

# Analysis of antioxidant capacity of peels, pulp and seed of Brazilian native fruits

**Maria Luiza Zeraik (PQ),[1]* Giselle Lopes Silva (PG),[1] Helena M. Russo (PG),[2] Emerson F. Queiroz (PQ),[3] Muriel Cuendet (PQ),[3] Jean-Luc Wolfender(PQ),[3] Vanderlan da Silva Bolzani (PQ)[2].**

**zeraikml@uel.br**

*[1]Departament of Chemistry, Londrina State University (UEL), 86051-990, Londrina, Paraná, Brazil; [2]NuBBE, Department of Organic Chemistry, Institute of Chemistry, São Paulo State University (UNESP), P. O. Box 355, 14800-900, Araraquara, São Paulo, Brazil; [3]School of Pharmaceutical Sciences, University of Geneva, 1211, Geneva 4, Switzerland.*

Keywords: *native fruits, antioxidant capacity, liquid chromatography*

## Highlights

Antioxidant activities of native fruit extracts were evaluated.
The extract of umbu displayed the highest antioxidant activity.
Bioactive fruit extracts can lead to the development of functional foods.

## Abstract

Tropical fruits represent a valuable source of bioactive compounds, and its consumption is increasing on national and international markets due to the growing recognition of its nutritional and therapeutic value [1]. Brazil is one of the largest fruit producers in the world, however, in most cases, the potential of these fruits remains unknown or poorly studied. Thus, the purpose of this study was to evaluate the antioxidant capacity of extracts of pitomba (*Talisa esculenta*, Sapindaceae), umbu (*Spondias tuberosa* Arr. Camara, Anacardiaceae), ciriguela (*Spondias Purpúrea* L., Anacardiaceae), pitanga (*Eugenia uniflora* L., Myrtaceae) and caju (*Anacardium occidentale*, Anacardiaceae) by DPPH, ABTS and ORAC methods. The peels, pulp and seed were analyzed separately after partition with hexane, dichlorometane and methanol. Methanolic extract of umbu pulp displayed the highest antioxidant activity in the DPPH (89%), ABTS (97%) and ORAC (64%) assays at 40 μg $mL^{-1}$, followed by methanolic extract of pitomba peels (71%, 99%, 61%), methanolic extract of caju seeds, (91%, 98%, 38%), methanolic extract of pitanga pulp (56%, 60%, 29%) and dichloromethane extract of ciriguela pulp (32%, 15%, 91%). The other extracts were considered inactive at 40 μg $mL^{-1}$ (<50% in all tests). The HPLC/UV analysis of these extracts showed the presence of high amount of flavonoids, which might be responsible for the antioxidant activity. Such type of studies may lead to the development of functional foods with valuable health benefits.

Reference: 1. Zeraik, M.L et al. (2011). Food Chem. 128: 259-265.

**Área: BEA** **Inscrição: 01150**

# DETERMINAÇÃO DE COMPOSTOS FENÓLICOS EM CERVEJAS ARTESANAIS BRASILEIRAS USANDO HPLC-DAD

**Marcelo C. Silva (IC)[1*], Jeancarlo P. dos Anjos (PQ)[1,2], Lilian L. N. Guarieiro (PQ)[1,2], Bruna A. Machado (PQ)[1]. jeancarlo.anjos@fieb.org.br; celo12br@hotmail.com**

*[1]Centro Universitário SENAI CIMATEC, 40170-010, Salvador, BA, Brasil;*
*[2]INCT de Energia e Ambiente, UFBA, 40170-290, Salvador, BA, Brasil*

Palavras Chave: *Compostos Fenólicos, Cerveja Artesanal, HPLC-DAD, Cromatografia.*

## Highlights

**Determination of phenolic compounds in Brazilian craft beers using HPLC-DAD**

A simple chromatographic method, with little prior manipulation of the samples, to determine the concentration of phenolic compounds in Brazilian craft beers;
The method showed good sensitivity with LOD ranging from 0.08 mg $L^{-1}$ to 0.83 mg $L^{-1}$, and LOQ from 0.26 mg/L to 2.77 mg/L;
Determination of nine phenolic compounds in Brazilian craft beers, highlighting the catechin (showed the highest concentrations) and formonetin (found in all samples).

## Resumo/Abstract

A cerveja é uma bebida difundida mundialmente e seu consumo é extremamente amplo e apreciado. A produção e o consumo de cerveja artesanal no Brasil têm crescido consideravelmente nos últimos anos. A necessidade de conhecer os compostos presentes na bebida é de alta relevância à qualidade da cerveja artesanal, tais como compostos fenólicos, que possuem conhecidas propriedades antioxidantes. Assim, este trabalho teve como objetivo determinar a concentração de compostos fenólicos em amostras de cervejas artesanais brasileiras, utilizando um método simples por HPLC-DAD. Foram analisados 9 compostos fenólicos em amostras (n= 6) de cervejas artesanais brasileiras adquiridas em estabelecimentos comerciais da cidade de Salvador-BA. As análises foram precedidas da desgaseificação das amostras, seguidas de filtragem (0,45 µm) e injetadas no HPLC-DAD. Foram obtidos LD variando de 0,08 mg/L a 0,83 mg/L e LQ de 0,26 mg/L a 2,77 mg/L, atestando a boa sensibilidade do método. A catequina apresentou maiores concentrações nas amostras analisadas (até 16,8 mg $L^{-1}$), seguida da epicatequina (até 3,56 mg $L^{-1}$) e ácido *trans*-ferúlico (até 2,18 mg $L^{-1}$) (Tabela 1). As amostras analisadas apresentaram compostos fenólicos e concentrações similares aos da literatura para análises de cervejas industriais.[1,2] Pode-se inferir que através de um método simples, com pouca manipulação prévia das amostras, foi possível determinar a presença de compostos fenólicos em amostras de cervejas artesanais brasileiras, em concentrações relativamente baixas.

Tabela 1 – Compostos fenólicos encontrados nas amostras de cervejas artesanais brasileiras*

| Compostos fenólicos | Curva analítica (mg $L^{-1}$) | LD (mg $L^{-1}$) | LQ (mg $L^{-1}$) | Faixa de concentração (mg $L^{-1}$) |
|---|---|---|---|---|
| catequina | 0,1 - 12,5 | 0,08 | 0,28 | ND – 16,8 |
| ácido caféico | 0,25 - 12,5 | 0,22 | 0,74 | ND – <LQ |
| epicatequina | 0,5 - 12,5 | 0,39 | 1,29 | ND – 3,56 |
| ácido p-cumárico | 0,1 - 10 | 0,08 | 0,27 | ND – 1,11 |
| rutina hidratada | 0,25 - 12,5 | 0,10 | 0,35 | 0,39 – 1,07 |
| ácido trans-ferúlico | 0,1 - 10 | 0,08 | 0,28 | <LQ – 2,18 |
| quercetina | 0,5 - 12,5 | 0,35 | 1,16 | <LQ** |
| kaempferol | 1,0 - 12,5 | 0,83 | 2,78 | ND – <LD |
| formonometina | 0,1 - 7,5 | 0,09 | 0,32 | 0,71 – 1,88 |

*ND = não detectado; <LD = menor que limite de detecção; <LQ = menor que limite de detecção; **<LQ em todas as amostras

1. RAMPAZZO, V. **Caracterização da composição fenólica e capacidade antioxidante de cervejas comerciais de diferentes processos de fermentação.** UTFPR, 2014.
2. MOURA-NUNES, N.; et al. **Food Chem.**, v. 199, p. 105-113, 2016.

**Área: BEA** **Inscrição: 01338**

# Determinação de $Fe^{2+}$ em cervejas especiais por espectrometria UV-vis após extração por ponto nuvem

**Raiane Reis Santos* (IC), Ednilton Moreira Gama (PG), Letícia Malta Costa (PQ)**

**lemalta41@gmail.com; raiane_reis@yahoo.com.br**

*LEAQUAA, Departamento de Química, ICEx, Universidade Federal de Minas Gerais, Av. Antônio Carlos, 6627, Pampulha, Belo Horizonte - MG, 31270-901*

Palavras Chave: *cerveja especial, ferro, especiação, ponto nuvem, UV-Vis.*

## Highlights

Determination of $Fe^{2+}$ in special beer by UV-vis spectrometry after cloud point extraction

- ✓ Cloud point extraction procedure directly in sample beer, without digestion step.
- ✓ It was possible to quantify $Fe^{2+}$ in special beer by UV-vis spectrometry.
- ✓ Figures of merit with adequate values.

## Resumo

Cerveja é a bebida obtida pela fermentação alcoólica do mosto cervejeiro oriundo do malte de cevada e água potável, por ação da levedura, com a adição de lúpulo (Decreto nº 2314, de 04 de junho de 2009, art. 36 a art. 50) [1]. É uma bebida de rápida absorção no organismo, porém provoca elevado efeito diurético, causado pelas resinas do lúpulo. Ela possui quantidades adequadas de componentes essenciais para o metabolismo humano como íons cálcio, ferro e fósforo, sendo considerada repositora de eletrólitos. O consumo moderado garante quantidades recomendadas de vitaminas do complexo B (riboflavina, niacina e piridoxina), além de ser uma fonte importante de selênio e folatos [2,3]. Associado a essas substâncias, seu consumo pode ser benéfico à saúde, quando em doses moderadas, devido à ação antioxidante e anti-inflamatória dos polifenóis do malte e principalmente do lúpulo. As propriedades antioxidante podem estar associadas à diminuição de riscos de doenças cardiovasculares [4]. Neste trabalho foi proposto um método de extração/pré-concentração de íons $Fe^{2+}$ por ponto nuvem, empregando-se Br-PADAP [2-(5-bromo-2-piridilazo)-5-di-etilaminofenol] como complexante, com posterior determinação por espectrofotometria de absorção molecular na região do ultravioleta-visível no comprimento de onda de 742 nm. Foram realizados testes para avaliar a influência dos íons $Fe^{+3}$ e da matriz etanólica da cerveja na formação do complexo $Fe(Br\text{-}PADAP)_2$. Os complexos apresentaram intensos sinais de absorbância, não sendo observadas interferências. O método apresentou linearidade satisfatória e limites de detecção e de quantificação de 32 e 98 µg $L^{-1}$, respectivamente. O método mostrou-se seletivo para a determinação de $Fe^{2+}$, sendo possível sua especiação pela adição de agente redutor ácido ascórbico. Após avaliação de algumas figuras de mérito, o método proposto foi aplicado em amostras de cervejas especiais adquiridas no comércio de Belo Horizonte. As concentrações de Fe total variaram de 0,32 a 1,13 mg $L^{-1}$ e de $Fe^{2+}$ de 0,32 a 1,06 mg $L^{-1}$. As concentrações de $Fe^{3+}$, obtidas pela subtração de Fe total e $Fe^{2+}$, variaram de 0 a 0,37 mg $L^{-1}$.

## Referências

1. Decreto nº 2314, de 04 de junho de 2009, art. 36 a art. 50, **Diário Oficial**, Brasília, 05 jun. 2009. Seção 1, p. 20. BRASIL, 2009.
2. BAMFORTH, C. **Beer: tap into the art and science of brewing**. Nova Iorque, Oxford University Press, 2009.
3. ROSA, N. A., AFONSO, J. C. A Química da Cerveja. **Química Nova Escola**, 37(2), 98, 2015.
4. ARRANZ, S., CHIVA-BLANCH, G., VALDERAS-MARTÍNEZ, P., MEDINA-REMÓN, A., LAMUELA-RAVENTÓS, R. M., & ESTRUCH, R. Wine, beer, alcohol and polyphenols on cardiovascular disease and cancer. **Nutrients**, 4(7), 759, 2012.

## Agradecimentos

CNPq, FAPEMIG

**Área: BIO** **Inscrição: 01425**

# Effects of hesperetin, from citrus fruits, on proteinases isolated from *Bothrops asper* snake venom

**Roney Vander dos Santos (PG),[1*] Giovanna Rivabem Grillo (IC),[1] Henrique Fonseca Monteiro de Oliveira (IC),[2] Luís Antônio Peroni (PQ),[3] Pedro Luis Onófrio Volpe (PQ),[1] Ljubica Tasic (PQ).[1]**

**roney.santos@iqm.unicamp.com**

*[1]Instituto de Química, UNICAMP; [2]Faculdade de Engenharia Mecânica, UNICAMP; [3]Rheabiotech LTDA*

Key words: *Snake venom, Proteinases, Hesperetin, Immunoglobulins.*

## Highlights

Interaction among inhibitor, such hesperetin and specific immunoglobulins, with the target enzymes isolated from *B. asper* snake venom were investigated applying spectroscopic and biochemical methods.

## Abstract

Hesperetin is a natural compound that can be obtained from hydrolysis, in the presence of acids, organic solvents and water, of the isolated hesperidin from citrus fruits. Thus, it is a low-cost compound with great potential as a drug as demonstrated by some recent studies. Snake venom glands are rich in proteolytic enzymes, such as metallo- and serine proteinases that contribute to the digestion of prey and affect various physiological functions. Antibodies are still the best option in snake envenoming but their use could be late as to prevent sequelae. Therefore, new drugs that can ameliorate snake venom effects just after accidents are jet to be discovered.

Our aims could be divided in three main streams: (1) to obtain hesperetin and isolate, purify and characterize proteinases from the *Bothrops asper* snake venom; (2) produce specific immunoglobulins for these protein targets and, finally, (3) investigate interactions among protein targets and hesperetin or immunoglobulins.

Snake venom proteinases were isolated and purified by chromatographic methods. All targets were biochemically and biophysically characterized using CD, fluorescence and MS techniques. Also, hesperetin was successfully obtained and characterized. Interaction studies showed that two from three target enzymes were inhibited in some extent in the presence of hesperetin and rabbit-antibodies showed a good sensitivity and specificity to target enzymes.

We would like to thank CAPES for scholarship, CNPq and FAPESP for the grants.

Reference: Vander dos Santos *et al.*, *Toxicon 143* (**2018**) 36-43.

**Área: BIO** **Inscrição: 01033**

# Leshimanicidal activity of extracts of endophytic fungi from *Apidosperma excelsum*

**Josiwander M. Carvalho (PG),[1] Layana A. dos Santos (IC),[1] João Victor S. Silva (PG),[2] Maria Fani Dolabela (PQ),[2] Patrícia S.B. Marinho (PQ),[1] Andrey M.R. Marinho (PQ).[1]***

**andrey@ufpa.br**

*[1]Programa de Pós-graduação em Química, UFPA; [2] Programa de Pós-graduação em Ciências Farmacêuticas, UFPA*

Key-words: leishmanicidal activity, endophytid fungi, *Apdosperma*

## Highlights

bioactive extracts of endophytes against leishmania amazonensis; chemical profile; the extracts showed very good activities AEC 11 $IC_{50}$ = 6.539 µg/mL and AEC 12 $IC_{50}$ = 3.820 µg/mL

## Resumo/Abstract

Leishmanioses are tropical disease caused by protozoan of *Leishmania* genus. These infect around 12 millions of people in 80 country in the World, and is estimated have 3 millions of new case per year.[1] Medicinal treatments available for leishmaniasis are based on pentavalent antimonial drugs, such as Pentostan® and Glucantime®, that are toxics and few effectives. In this way, the present work aimd evaluate the chemical profile and leshmanicidal activity of the extracts obtained of endophytic fungi from *Aspidosperma excelsum*, species of *Aspidosperma* genus has as important characteristic the production of indole alkaloids, the most monoterpenics, which have large variety of biological activities, among them leishmanicidal activity.[2] first of all, were isolated 26 fungi from host plant, which were cultivated on Petri dish containing PDA medium, and the microextracts were obtained conform Smedsgaad (1997)[3] method, after the chemical profile of 26 extracts were analyzed by high performance liquid chromatography in reverse phase, using C-18 column and DAD detector (HPLC-DAD), then 6 extracts were selected (with the codes AEC 02, AEC 08, AEC 09, AEC 11, AEC 12, AEC 14) because them showed in their UV spectra standards similar to the indole alkaloids. The leishmanicidal assay were carried out *in vitro* with promastigotes of *Leishmania amazonensis*, being the extracts with better results were AEC 11 $IC_{50}$ = 6.539 µg/mL and AEC 12 $IC_{50}$ = 3.820 µg/mL

**References**

1. Carvalho, J. M. **Dissertação de Mestrado**. Programa de Pós-Graduação em Química, UFPA, 2014.
2. Henrique, M. C.; Nunomura, S. M.; Pohlit, A. M. **Química Nova**, v.33, n.2, p.284-287, 2010.
3. Smedsgaad, J. **Journal of Chromatography A**, v.760, p. 264-270, 1997.

**Área: BIO** **Inscrição: 00879**

# A direct assay for measuring the activity of phosphoenolpyruvate carboxykinase (PEPCK) by liquid chromatography-tandem mass spectrometry

**Bruno S. Amaral (PG)[1], Dulce Helena F. de Souza (PQ)[1], Quezia B. Cass* (PQ)[1]**

**qbcass@gmail.com**

[1]*Departamento de Química, UFSCar, Rodovia Washington Luis s/n, km 235, Caixa postal 676, 13565-905, São Carlos/SP, Brasil.*

Palavras Chave: *PEPCK, LC-MS, Enzyme assays.*

## Highlights

Direct detection of PEPCK reaction product

## Abstract

Phosphoenolpyruvate carboxykinase (PEPCK) is a ubiquitous enzyme found in all known groups of organisms, acting in the reversible conversion of oxaloacetate (OAA) to phosphoenolpyruvate (PEP) and $CO_2$, in the presence of divalent metal ion, and dependent of ATP or GTP.[1]
Their catalytic activity is usually measured by coupled assays with malate or pyruvate kinase/lactate dehydrogenases as preferred second enzyme. Thus, the PEPCK reaction product is converted by the action of a NADH-dependent enzyme, wherein the catalytic reaction is followed by the decrease in the absorbance at 340 nm due to the consumption of NADH. The main drawback in coupled assays is that any interference in the activity of the second enzyme will affect the result of the first enzyme. In addition, in the case of PEPCK, NADH has been reported as inhibitor of some of these enzymes. [2] To overcome these problems, herein we report a direct assay to quantity PEP by liquid chromatography-tandem mass spectrometry (LC-MS). For that, PEPCK of *T. cruzi* was expressed as an active enzyme in *Escherichia coli* and purified by anionic exchanged chromatography. The enzymatic reactions were carried out (in a final volume of 100 μL) using 200 μM OAA and 240 μM ATP in 50 mM ammonium acetate buffer, pH 9.0, containing 1 mM DTT, 1 mM $MnCl_2$ (buffer A). The reaction was started by addition of the enzyme, incubated at 36 °C, and stopped after 10 min by addition of 100 μL MeOH, followed by centrifugation (4 ºC, 9300 g per 10 min) previously to the analysis of the supernatant. The used chromatographic conditions were Luna C18 (2) ® column (50 x 2,0 mm, 3 μM) with a 15 mM ammonium acetate buffer (pH 8.50): MeOH 1:1 (v/v) as mobile phase at a flow rate of 0.15 mL/min. The ionization and fragmentation conditions for the PEP were evaluated by infusion into the ion-trap mass spectrometer (IT-MS/MS Esquire 6000 Bruker) of a solution of 10 μg/mL PEP prepared in the mobile phase. The MS parameters optimized for the PEP ion $[M-H]^-$ 167 *m/z* with its ion fragment were: capillary voltage 2877 V; skimmer voltage: -15.0 V; nebulizer gas ($N_2$) 30 psi; dry gas ($N_2$) 8 L/min and source temperature 325 °C. The difficulty related to PEPCK's substrates and products are their higher hydrophilicity and poor retention in reverse-phase elution mode, which leads to coelution or low peak resolution. In spite of this, PEP was quantified in coelution with OAA by the differentiation obtained by the mass spectra data. The developed method was validated and all the significant figures were in accordance with the adopted criteria.[3] The developed method was used to monitor the purification of *T. cruzi* PEPCK as well as to determine all the kinetics parameters of the purified enzyme, in which *T. cruzi* PEPCK has shown a Michaelian kinetic behavior with $K_M$ constant value of 96,11 ± 3,99 μM to OAA as substrate and 275,10 ± 18,51 μM to ATP as substrate showing higher affinity for the first substrate. The direct method herein disclosed can be used for others PEPCKs.

[1]Trapani, S. et al. *J. Mol. Biol.* **2001**, 313, 1059-1072.
[2] Cymeryng, C. et al. *Mol. Biochem. Parasitol.* **1995**, 73, 91-101.
[3]Cassiano, N. M. et al. *Quim. Nova.* **2009**, 32, 1021-1030.

**Área: _BIO** **Inscrição:00324_____**

# Peak-fraction at-line screening assay of kallikrein inhibition for complex matrices by LC-MS/MS

**Carmen Lucia Cardoso*** **(PQ),[1,2] Govert W. Sonsen (PQ),[2] Jeroen Kool (PQ),[2]**

**ccardoso@ffclrp.usp.br**

*[1] Grupo de Cromatografia de Bioafinidade e Produtos Naturais -Departamento de Química - Faculdade de Filosofia, Ciências e Letras de Ribeirão Preto - Universidade de São Paulo, 14040-901, Ribeirão Preto - SP, Brasil; [2]Amsterdam Institute for Molecules Medicines and Systems, Division of BioAnalytical Chemistry, VU University Amsterdam, De Boelelaan 1083, 1081HV Amsterdam, The Netherlands*

Palavras Chave: At-line-bioassay, Kallikrein inhibitors, Complex matrices, Screening, nonofractionation

## Highlights

High–resolution fractionation strategies for identifying Kallikrein inhibitors.
Direct chemical characterization of inhibitors found

## Resumo/Abstrac

Screening of biological activities of compounds from complex matrices such as natural products is laborious, time consuming and costly. To overcome the drawbacks of traditional Bioassay-Guided Fractionation (BGF), herein we report an at-line screening assay based on nanofractionation. In this approach, many nanofractions per separation can be collected at very short time intervals for bioaffinity analysis [1] preserving the high resolution obtained during the chromatographic separation. Kallikrein (KLK)-related peptidases are targets for many crucial functions. In fact, it is now well-known that dysregulation of KLK activity can lead to certain pathophysiological conditions. Consequently, inhibition of the excessive proteolytic activity of KLKs by small synthetic or natural compounds might constitute a novel and challenging road under construction in cancer therapeutics. [2] KLK from porcine was selected as model enzyme for the new at-line inhibitor assay for complex matrices. In kinetic studies, pH, and buffer composition were optimized furnishing the following bioassay conditions: enzyme and substrate (100ng/ml, and 15uM, respectively), in 0.1M of Tris-HCl buffer, (pH 8.7), $\lambda_{excit}$ 380 $\lambda_{em}$= 460 nm. Leupeptin was used as standard inhibitor to validate the assay. Each point of the bioactivity profile represents the slope of the enzymatic activity in a corresponding well plate versus time. The baseline corresponds to the basal activity. In the presence of inhibitors, the basal activity is reduced resulting in negative peaks. As a proof of concept natural extracts that were active against KLK (in a solution assay) were submitted to the modulated assay. These results will be fully discussed at the presentation.

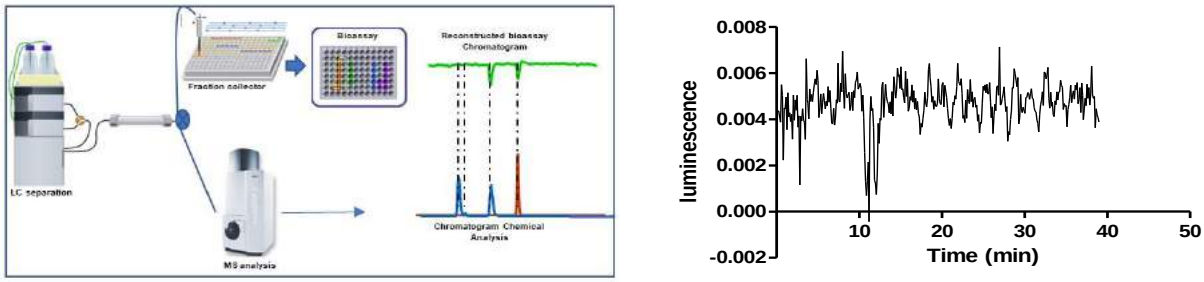


Fig 1. A) Schematic view of the nanofractionation LC-MS/MS setup: Briefly the method consists of injection of sample, LC separation, and eluate split (1:9) for parallel MS detection and at line nanofractionation in 384-well plates; freeze-drying of the nanofractionated plate; Pipetting of the bioassay, readout of the bioassay and correlation with the MS data. B) Kallikrein assay in the presence of the standard inhibitor leupeptin.

**Acknowledgments**
FAPESP, CAPES and AIMMS for the financial support and fellowship.

**References**

[1] Kool, J. et al. Anal. Chem. 83, 125-132 (2011). [2] Kalinska, M, et al. Biochimie 122 270-282, (2016).

**Área: BIO** **Inscrição: 00214**

# Interaction of thimerosal with hemoglobin causes alteration of structure and loss of oxygen binding capacity

**Marina M. Silva (PG),* Maria Dayanne A. Dantas (PG), Reginaldo Correia S. Filho (PG), Ana Catarina R. Leite (PQ), Josué C. C. Santos (PQ) and Isis M. Figueiredo (PQ).**

marinaquimicaufal@gmail.com

*Instituto de Química e Biotecnologia, IQB - UFAL.*

Palavras chave: Hemoglobin, thimerosal, interaction process, ethylmercury, spectroscopic techniques.

## Highlights

Hemoglobin interacts with thimerosal by electrostatic forces leading to conformational changes in the protein structure and decreasing of 52% in the $O_2$ binding capacity in physiologic conditions.

## Resumo/Abstract

Thimerosal (TH, Fig. 1a) is an organomercurial used as an antibacterial in vaccines. Recent studies have shown that $EtHg^+$ are absorbed by red blood cells and can bind to hemoglobin (Hb, Fig. 1b).[1] This protein is fundamental for the oxygen transport and is the major component of erythrocytes.[2] Due to human exposure to these species potentially toxic, we evaluate the interaction of TH with hemoglobin using spectroscopic techniques. Initially, a spectrofluorometric titration was performed exploring intrinsic Hb fluorescence. The increasing of TH concentration leaded to a gradual reduction of analytical signal, indicating that interaction process occurs. Table 1 shows that $K_b$ and $K_{sv}$ values decreased with temperature increasing, characteristic of static quenching mechanism. $K_b$ values indicates that the Hb-TH presents a moderate interaction and this interaction is stabilized by electrostatic interactions ($\Delta H < 0$ and $\Delta S > 0$). Synchronous fluorescence assay shown that polarity in the microenvironment near of Trp was more changed. These data corroborate with the results obtained by 3D fluorescence. The intermolecular distance between Hb-TM was less than 8 nm ($r^0$ = 2.63 nm) based on FRET studies. Finally, hemoglobin $O_2$ binding capacity decreased 52% comparing free Hb (38.05 ± 2.26 nmol $O_2$ / 10 nmol Hb) with Hb-TM (18.14 ± 0.34 nmol $O_2$ / 10 nmol Hb) at ratio 1:1. Finally, the loss $O_2$ binding capacity must be associated with the transfer of $EtHg^+$ from the TM to the free Cys residue in the Hb β-chain.

**Fig. 1.** a) Thimerosal and b) Hemoglobin structures in physiologic conditions.

**a)**

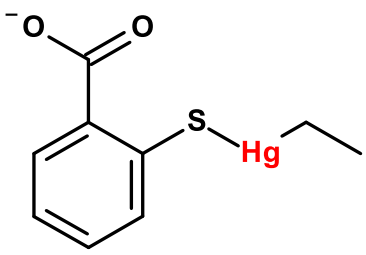


**b)**

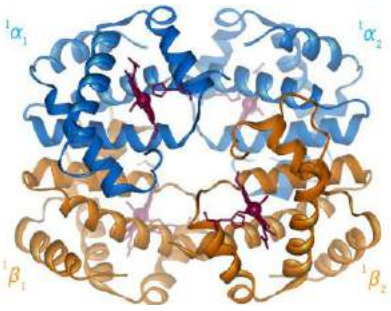

**Table 1.** Results obtained in the evaluation of Hb-TH interaction by molecular fluorescence.

| Temp. (K) | Stern-Volmer constant | | Binding parameters | | Thermodynamic parameters | | |
|---|---|---|---|---|---|---|---|
| | $K_{sv}$ ($10^4$ L mol$^{-1}$) | *f* | $K_b$ ($10^3$ L mol$^{-1}$) | *n* | ΔH (kJ mol$^{-1}$) | ΔS (J mol$^{-1}$) | ΔG (kJ mol$^{-1}$) |
| **296** | 1.24 ± 0.02 | 0.77 | 7.90 ± 0.02 | 0.96 | | | -22.1 |
| **303** | 1.16 ± 0.01 | 0.66 | 7.61 ± 0.04 | 1.01 | - 4.45 | + 59.72 | -22.5 |
| **310** | 0.60 ± 0.01 | 0.40 | 7.28 ± 0.01 | 1.36 | | | -22.9 |

[1] Gibson, M.A. *Metallomics*, 9, 2017, 1060.
[2] Wang, R. J. *J. Lumin.*, 144, 2013, 79.

**Área: BIO**
*(Inserir a sigla da seção científica para qual o resumo será submetido. Ex: ORG, BEA, CAT)*

**Inscrição: 01431**
*(Inserir o número de inscrição do autor que fez a submissão)*

# Synthesis and evaluation of the antibacterial properties of colloidal silver nanoparticles for application in cosmetics industry.

**Amanda G. C. Santos (IC),[1] Juliana A. de Sales (PQ)*, Valéria M. Godinho (PQ).**

**amandagabrielasantos@yahoo.com.br; juliana.sales@newtonpaiva.br**

[1]*Centro Universitário Newton Paiva; Unidade Buritis – Departamento de Engenharia Química.*

Palavras Chave: *Nanotechnology, Silver Nanoparticles, Escherichia coli, Klebisiella pneumae, antimicrobian activity*.

## Highlights

This paper presents the synthesis of silver nanoparticles (AgNP) by reduction and its antimicrobian activity against *E. coli* and *K. pneumae*. The best results using the AgNP were obtained to K. pnemae by using inhibition zone method.

## Resumo/Abstract

Há várias pesquisas que mostram que a prata em escala nanométrica exibe propriedade antimicrobiana. Há uma forte tendência na indústria de cosméticos a incorporação destas nanoestruturas nas embalagens de cosméticos a fim de auxiliar na preservação e aumento da vida útil do produto. Dessa forma, o objetivo do presente trabalho foi o de sintetizar nanopartículas de prata (AgNP), bem como avaliar a atividade microbiana das AgNP por meio de ensaios microbiológicos contra as bactérias *Escherichia coli e Klebsiella pneumae*. As AgNP foram obtidas pelo método da redução química, utilizando o citrato de sódio como agente redutor e a carboximetilcelulose com agente estabilizante. A partir dos espectros obtidos no UV-Vis, foi possível concluir que as nanopartículas obtidas apresentaram dimensões na faixa de 50 a 100 nm. Os ensaios microbiológicos foram realizados utilizando-se a técnica do halo de inibição. Foram utilizadas oito placas de Petri, previamente autoclavadas e preparadas com ágar nutriente. As placas foram divididas por uma marcação para que fazer um comparativo entre a inibição com hipoclorito de sódio (3,9 a 5,6% m/m). Os microorganismos foram colocados em uma solução salina a 0,85% m/v com auxílio de uma alça. A Figuras 1 mostra os resultados obtidos dos ensaios microbiológicos.

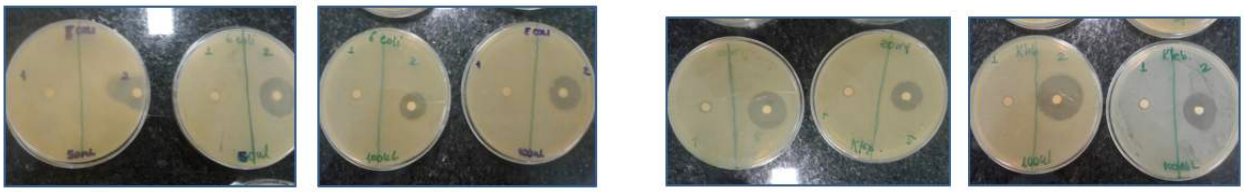

Figura 1 – Resultado do teste do halo de inibição da AgNP para colônias de *E. coli* (à esquerda) e colônias de *K. pneumae (à direita).* (1) refere-se a AgNP e (2) refere-se ao controle de hipoclorito de sódio.

Notou-se que a inibição foi perceptível, mas não significativa. Destaca-se como possível fator que pode ter afetado o resultado, a baixa concentração das AgNP na solução. Entretanto é possível concluir que as soluções coloidais de AgNP possuem eficácia para inibir o crescimento dos microoganismos, em especial para a K. pneumae que apresentou maior halo de inibição. Sendo assim, essas nanoestruturas devem apresentar grande interesse no segmento da indústria de cosméticos.

Referências :

FERNANDES, Patrícia Érica. Síntese, caracterização e ação antimicrobiana de nanopartículas de prata. 2014. 101 f. Tese.

ALMEIDA, Jean Carlos Bosquette de. Nanopartículas de prata: Síntese, Caracterização e Toxicidade a diferentes organismos. 2016. 104 f. Dissertação.

**Área: BIO** **Inscrição: 01235**

# Naftoquinone derivatives: *in vitro* photo protective activity and interaction studies with tyrosinase and DNA

**Ari S. Guimarães (PG)[1*], Camila da S. Nunes (PG)[1], Roberta R. F. Santos (PQ)[1], Silvia H. Cardoso (PQ)[2], Isis M. Figueiredo (PQ)[1] e Josué C. C. Santos (PQ)[1].**

ari.sguimaraes@gmail.com

[1]*Instituto de Química e Biotecnologia, Universidade Federal de Alagoas (UFAL)*
[2] *Núcleo de Ciências Exatas e da Terra, departamento de Química, nCEX-UFAL*

Key words: Naftoquinones, photoprotection, DNA interaction, docking molecular

## Highlights

Lapachol *N*-imino derivatives exhibited the highest SPF-UVB in agreement with molecular docking, also interacts with DNA *via groove*.

## Abstract

Melanoma is one of the most serious consequences of skin cancer where melanocytes proliferate actively with enhanced accumulation of melanin and tumor formation. The regulation of the tyrosinase level appear to contribute significantly to the enhanced synthesis and accumulation of melanin in melanocytes[1]. In this way, the synthesis, characterization, *in vitro* studies of UVB sun protection factor, molecular docking with tyrosinase and initial DNA-ligand interaction studies of *N*-iminonaphthoquinones were carried out. The compounds were synthesized by nucleophilic addition reaction to the C1 or C2 carbonyl carbon of the 1,4-naphthoquinone by the nitrogenated reagent[2]. The UVB sun protection factor (SPF-UVB) was determined using the Mansur et al. procedure[2], in which all the molecules tested presented SPF > 7 with relevant photoprotective activity. Lapachol *N*-imino (**1**) derivatives exhibited the highest SPF-UVB when compared with oxybenzophenone[3]. *N*-imino naphthoquinone (**2**) analogues demonstrate that the exchange of carbonyl by a nitrogen group potentiated the photoprotective activity in six-fold compared with starting quinone. The theoretical studies of the tyrosinase interaction with the most effective photo protector compounds showed that **1** had higher binding affinity (-8.0 kcal $mol^{-1}$), followed by **3** and **2** (-6.9 and -6.5 kcal $mol^{-1}$), respectively. These results have the same trend of the experimental data. However, in this first evaluation these compounds would be non-competitive inhibitors. Finally, in the competition assays with *Hoechst* probe **1** has interacted with DNA *via* groove, which may in future be exploited exploring DNA as a therapeutic target.

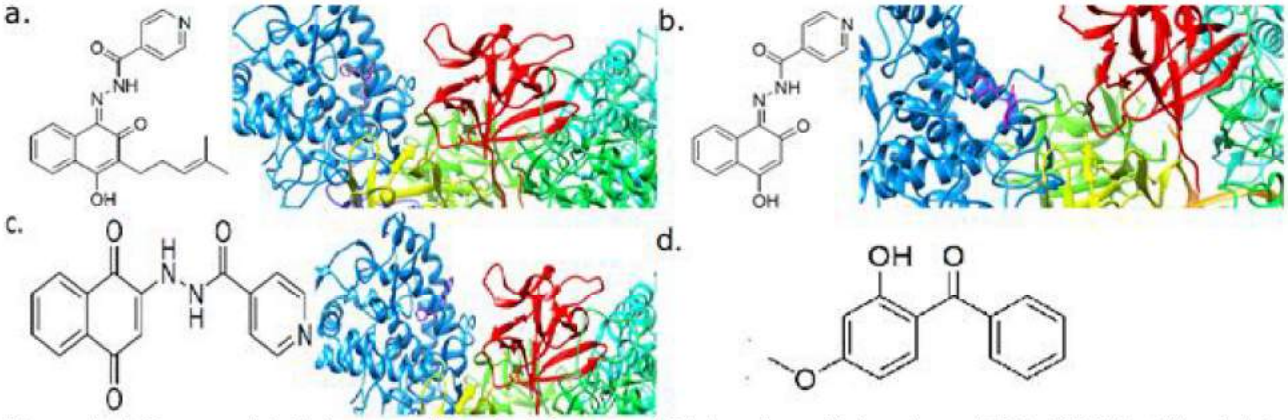


**Figura 1**. **a)** Compound **1** **b)** Compound **2** and **c)** Compound **3** interacting with tyrosinase (PDB: 2Y9X) by hidrophobics sites and H-bonds and **d)** oxybenzophenone;

[1] RAO, A. R., SINDHUJA, H. N., DHARMESH, S. M. *et al*, *J. Agric. Food Chem.* 61 (16), 3842–3851, 2013.
[2] ARAÚJO, C. R. M. et al. *Rev. Virtual Química* 6 (6),1702-1712, 2014.
[3] NASCIMENTO, L. F. et al. *Rev. Virtual Química* 6 (2), 190-223.2014.

**Área: _BIO_____** *(Inserir a sigla da seção científica para qual o resumo será submetido. Ex: ORG, BEA, CAT)*

**Inscrição: 00901____** *(Inserir o número de inscrição do autor que fez a submissão)*

# Avaliação do líquido celomático de minhoca na atividade inibitória de fungos do gênero *Fusarium.*

**Daniel Kuhn (PG),[1] Priscila Dallé da Rosa (PG), [2] Luciano Zubaran Goldani (PQ), [2] Elisete Maria de Freitas (PQ), [1] Eduardo Miranda Ethur (PQ), [1] Lucélia Hoehne (PG)[1]* luceliah@univates.br**

*[1] Universidade do Vale do Taquari - Univates. Programa de Pós-Graduação em Biotecnologia (PPGBiotec), Address: Rua Avelino Tallini, 171 sala 406-8 Bairro Universitário. Lajeado, RS, ZIP CODE: 95914-014 Brazil.*
*[2]Universidade Federal do Rio Grande do Sul, Programa de Pós-graduação em Ciências Médicas (PPGCM/UFRGS).Adress: Rua Ramiro Barcelos - 2400, 2° andar | Porto Alegre - RS - Brazil.*

Palavras Chave: *Eisenia andrei*, fluído biológico, atividade inibitória, fungos.

## Highlights

Use of the coelomic fluid *Eisenia andrei* in the inhibitory activity of fungi of the genus *Fusarium*.
Development of the methodology of extraction of coelomic fluid.
The bioproduct was not effective for the fungi tested.

## Resumo/Abstract

As minhocas desempenham um importante papel como decompositores, e além da participação no processo de vermicompostagem e regulação da biota do solo, há trabalhos que visam a utilização do líquido celomático da minhoca como inibidor de fungos (PLAVSIN et al., 2017), e purificação de peptídeos do líquido celomático com ação analgésica e anti-inflamatória. Dessa forma, o objetivo deste trabalho foi desenvolver metodologia para extração do líquido celomático e aplicação deste como inibidor de crescimento nos fungos do gênero *Fusarium*. Como metodologia, três testes foram feitos para a extração do líquido celomático: aquecimento (a 50 °C por 15 min), congelamento (0 °C por 15 min) e choque elétrico (pulsos de 10 em 10 s por 2 min) nas minhocas. Como melhor resultado, o líquido celomático foi extraído da minhoca através de indução de corrente elétrica pelo corpo da minhoca. Primeiramente, as minhocas adultas oriundas de minhocários construídos em laboratório no Tecnovates, foram coletas e então seu trato digestivo foi lavado, através de imersão em água destilada por um período de 6 horas. Posteriormente, foram transferidas para uma placa de petri esterilizada, onde foi adicionado 500 uL de solução de NaCl 0,1% por minhoca. Após, foi aplicada uma corrente elétrica de 9 V para estimular a liberação do líquido celomático. O líquido obtido foi filtrado em membrana 0,2 um e posteriormente armazenado em recipiente adequado em ultrafreezer, em temperatura inferior a -40° C. Para os testes usando o líquido celomático como inibidor de crescimento, quatro espécies isoladas do fungo *Fusarium* foram testados: *F. keratoplasticum*, *F. falciforme*, *F. oxysporum*, e *F. solani,* estes foram isolados de pacientes com onicomicose que foram ao Serviço de Dermatologia (Posto G) do Hospital Santa Clara do Complexo Hospitalar Santa Casa de Misericórdia de Porto Alegre. As análises de atividade antifúngica foram realizadas no laboratório Especial de Doenças Infecciosas (LEDI), no Hospital de Clínicas de Porto Alegre. Os testes feitos foram de acordo com a norma Norma M38-A-Método de Referência para Testes de Diluição em Caldo para a Determinação da Sensibilidade a Terapia Antifúngica dos Fungos Filamentosos. Como resultados, em nenhum dos fungos, o líquido celomático teve eficiência. Todos os fungos cresceram, comparando com os brancos feitos. Dessa forma, o líquido celomático não teve atividade inibitória nos fungos do gênero *Fusarium* testados. Testes posteriores serão feitos aplicando o bioproduto em outros fungos.

Referência:
PLAVSIN I., VELKI M., ECIMOVIC, S., VRANDECIC K., COSIC J.; *Inhibitory effect of earthworm coelomic fluid on growth of the plant parasitic fungus Fusarium oxysporum.* European Journal of Soil Biology, 78, 1-6, 2017.

**Área: _BIO_____ Inscrição: 00362 _____**

# Computer-aided Prediction and Cytotoxicity Evaluation of Bis-Hydrazones as Novel Anticancer Agents

**Claudio L. Donnici (PQ),[1]*Júlio C. D. Lopes (PQ),[1] Marina A. Costa (PG)[1], Carolina G. Furst (IC)[1], Luciana N. Kadooca (IC)[1], Marília O. F. Goulart (PQ),[2] Jadriane de Almeida Xavier (PG)[2].**

cdonnici@terra.com.br

[1]***LASELORG-QUIM-****Depto de Química,UFMG–BH- MG;* [2]*Instituto de Química e Biotecnologia- UFAL- Maceió- AL*

Kew-words: *Computer-Aided prediction, anticancer activity, cyclic voltammetry, bis-hydrazones.*

## Highlights

Strategic planning and computer-aided prediction were used for the synthesis of new bis-hydrazones, which show relevant cytotoxic activity, being promising anticancer agents

## Abstract

Among several possible novel bioactive compounds, hydrazones provide a rich platform for the design of novel bioactive compounds. They are easily synthesized and show a large variety of biological activities, such as antimicrobial, anti-tubercular and antitumor.[1] This work presents the theoretical studies concerning the design and biological activity prediction, the synthesis and antitumor activity of three (thio-)glycolic- and 3,3'-bis-thio-propanoic-bis-hydrazones(**3**), synthesized as described[2]. It was performed the prediction of pharmacological activity spectra by Activity-It system[3] with 2136 models built from PubChem/ADMET datasets. Several activities already reported for hydrazones were confirmed for our compounds, together with new putative activities against leukemia, trypanosoma and leishmania. The cytotoxic activity of hydrazones was evaluated *in vitro* (MTT,cell viability) against selected human cancer cell lines: colon (HCT116), leukemia(HL60), prostate(PC3), glioblastoma(SF-295) and breast(MX1). The derivatives**1** and **2** are the most potent anticancer agents with cytotoxic activity against all tested cell lines ($IC_{50}$µg/mL and CI 95%,respectively: 7.27-24.08 and 6.79-25.87), but **1** is less toxic (mouse fibroblast L929). The electrochemical studies of **1** and **2** were also performed by cyclic voltammetry in aprotic media (DMF/0.1M $Bu_4NPF_6$/glassy carbon) and **1** and **2** showed an electrochemical reduction mechanism related to the nitroaromatic function, with a self-protonation mechanism and oxidation on the thioether function.These substances are promising candidates as novel antitumoral agents for the treatment of cancer.

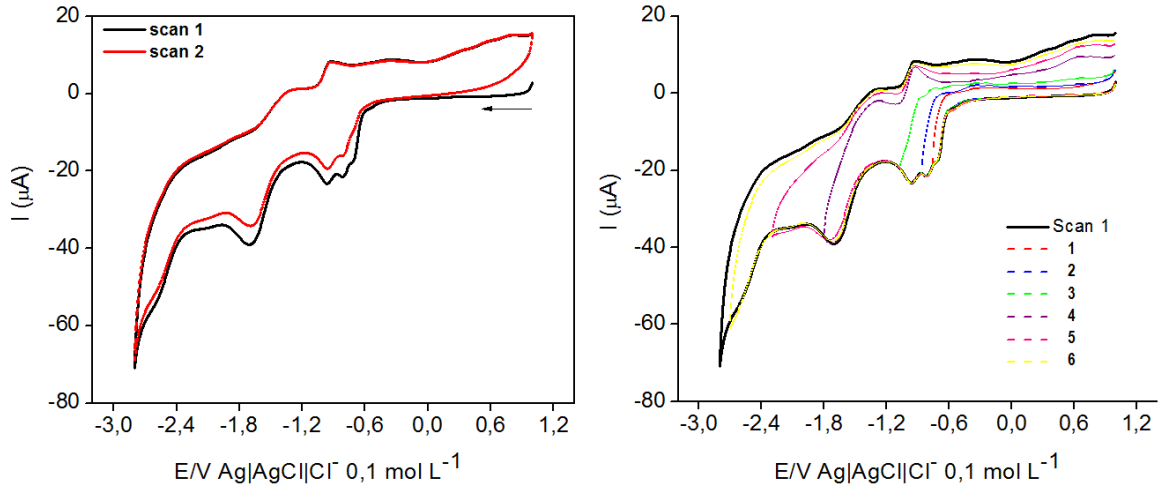


**Fig. 1.**Cyclic voltamogramms of hydrazone**1** in DMF/$TBAPF_6$ (0.1 mol $L^{-1}$) at glassy carbon electrode, scan rate: 100 mV $s^{-1}$

**ACKNOWLEDGMENTS:CNPQ,FAPEMIG(CEX-PPM0281-17)**

[1]S. Rollas, Ş. Güniz-Küçükgüzel, *Molecules* **2007**, *12*, 1910-1939

[2] Ávila-Costa, M.;Donnici,C.L. et al.,*Abstracts7th BrazMedChem2014, Campos do Jordão-SP, Brazil, 2014*

[3]NEQUIM–ChemoinformaticsGroup, Departamento de Química,UFMG,**2017**

**Área: BIO** **Inscrição:00261**

# Evaluation of Decoralin Peptide Identifies Activity Determinants and Synthetic Variants with *In Vivo* Activity

**Marcelo D.T. Torres (PG),[1-3] César de la Fuente-Nuñez (PQ),[2,3] Timothy K. Lu (PQ),[2,3] Vani X. Oliveira Jr (PQ),[1*]**

**marcelo.torres@ufabc.edu.br; vani.junior@ufabc.edu.br**

*[1]Centro de Ciências Naturais e Humanas, Universidade Federal do ABC; [2]Synthetic Biology Group, MIT Synthetic Biology Center; The Center for Microbiome Informatics and Therapeutics; Research Laboratory of Electronics, Department of Biological Engineering, and Department of Electrical Engineering and Computer Science, Massachusetts Institute of Technology; [3]Broad Institute, MIT and Harvard.*

Keywords: *Decoralin, Antimicrobial Peptides, SAR Studies, Physicochemical Features.*

## Highlights

- A physicochemical-guided screen to identify functional hotspots in decoralin AMP;
- Enabling peptide design to generate novel potent antibiotics with low toxicity and anti-infective *in vivo* activity.

## Abstract

AMPs constitute promising alternatives to conventional antibiotics for the treatment of drug-resistant infections, which are rapidly emerging as a global health challenge. However, our understanding of the structure-function relationships of AMPs is limited, and we are just beginning to rationally engineer these molecules in order to develop them as therapeutics. Here, we leverage a physicochemical-guided screen to identify specific functional hotspots in the wasp-derived AMP decoralin and enable peptide design. Peptides were synthesized, and tested against fungi, Gram-negative and Gram-positive bacteria, and human kidney cells. Conformational analyses were performed by Circular Dichroism in ten different media. The scarification skin infection mouse model used involved inducing a *P. aeruginosa* abscess and treating mice with a single dose of the selected peptides at 8 μmol $L^{-1}$. The Ala-scan screening was performed aiming to check the importance of amino acid side chains and hydrophilic/hydrophobic ratio of decoralin derivatives. After, we demonstrate that by tuning physicochemical parameters, such as net charge, helical fraction and hydrophobicity-related features, by substituting original residues by positively charged residues or symmetric aliphatic residues, it is possible to design synthetic peptides with enhanced nanomolar antimicrobial potency *in vitro* and anti-infective activity *in vivo*, and also low toxicity. We present a physicochemical-guided rational design strategy for identifying functional hotspots in a small cationic amphipathic natural peptide and for tuning structure-function to generate novel potent peptide antibiotics with low toxicity.

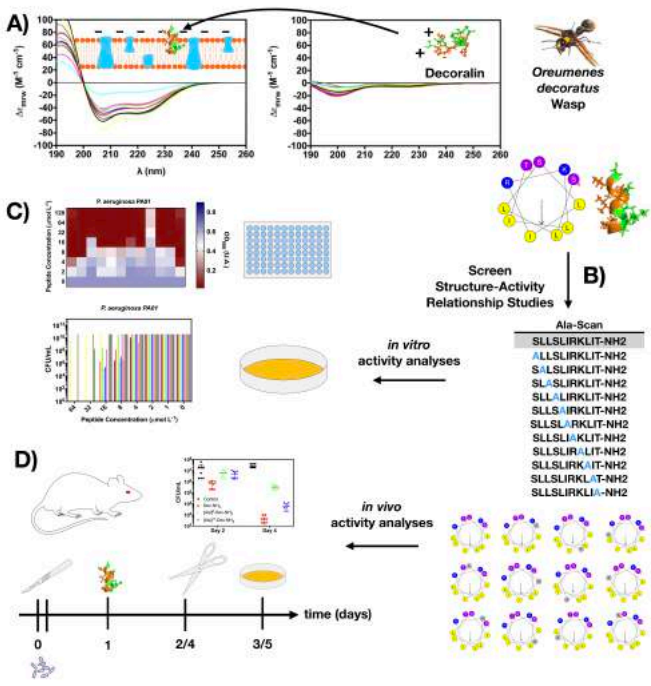


Figure 1. Schematic of the structure-function-guided exploration approach leveraged to generate peptide antibiotics.

**Área: BIO** **Inscrição: 01378**

# ENSAIOS ANTIOXIDANTES COM EXTRATOS DAS RAÍZES DE *CLUSIA GRANDIFLORA* SPLIGT. E *PLATONIA INSIGNIS* MART. (CLUSIACEAE)

**Wilson Bruno Conceição Fernandes (IC),[1] Railda Neyva Moreira Araújo (PG),[2] Haroldo da Silva Ripardo Filho (PQ),[1*] Luan Patrick Santos Silva (PQ),[1] Manoel Leão Lopes Júnior (PG),[2] Giselle Maria Skelding Pinheiro Guilhon (PQ),[2] Lourivaldo da Silva Santos (PQ).[2]**

**raildamoreira@hotmail.com; haroldo.filho@ifap.edu**

[1]*Instituto Federal de Educação Ciências e Tecnologia do Amapá – IFAP – Campus Laranjal do Jari;*
[2]*Programa de Pós-Graduação em Química, Universidade Federal do Pará – UFPA. Belém-PA*

Palavras Chave: *Platonia insignis, Clusia grandiflora, Clusiaceae, Bacuri, Cebola brava, DPPH.*

## Highlights

Antioxidant Tests With Extracts of the Roots of *Clusia grandiflora* Spligt. and *Platonia insignis* Mart. (Clusiaceae). Antioxidant tests by bioautography with extracts obtained from the roots of *Clusia grandiflora* and *Platonia insignis* (Clusiaceae), collected at the Jari Ecological Station.

## Resumo

Neste trabalho foi avaliado o potencial antioxidante dos extratos das raízes de *Clusia grandiflora* (cebola brava) e *Platonia insignis* (bacuri), coletadas na Estação Ecológica do Jari (ESEC-Jari), no Estado do Amapá. A atividade antioxidante foi avaliada pela técnica de bioautografia[1], em que os extratos foram aplicados na placa de CCD de sílica gel em três concentrações diferentes. A placa foi eluída no sistema de solventes $CH_2Cl_2$:$CH_3OH$ 5% e após secagem foi borrifada com solução de DPPH 0,66 mM. Após 40 minutos, a placa de CCD foi analisada e observou-se que ambos os extratos foram ativos em todas as concentrações testadas. A atividade foi evidenciada pela presença de colorações amarelas resultantes da reação das substâncias presentes nos extratos com o radical DPPH, que foi convertido em sua forma molecular (Figura 1). Os resultados revelam que *P. insignis* e *C. grandiflora* são espécies produtoras de compostos com atividade capturadora de radicais livres. Tal atividade se deve à composição das espécies da família Clusiaceae, uma das grandes produtoras de compostos antioxidantes, como as xantonas, cumarinas, flavonoides e outros compostos[2-4]. Os resultados revelam a necessidade da realização de estudos com os extratos envolvendo técnicas de separação e identificação, para determinar quais as substâncias responsáveis pela atividade observada.

Figura 1. Fotografia da cromatoplaca utilizada no teste antioxidante.

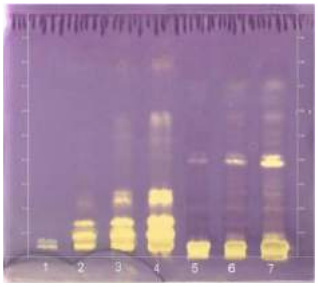


Fonte: JUNIOR LOPES, M. L., 2017

Legenda: (1) Ácido ascórbico, 500 ng; (2) Extrato de bacurí, 25 µg; (3) Extrato de bacurí, 50 µg; (4) Extrato de bacurí, 100 µg; (5) Extrato de cebola, 25 µg; (6) Extrato de cebola, 50 µg; (7) Extrato de cebola, 100 µg.

---

[1]CHOMA, I. M. E GRZELAK, E. M. **Bioautography Detection in Thin-Layer Chromatography**. Journal of Chromatography A, 1218 (19), 2684-2691, 2011.
[2]RIPARDO FILHO, H. S.; PACHECO, L. C.; ANDRADE,E. S.; CORREA, M. J. C.; ARAÚJO, R. N. M; GUILHON, G. M. S. P.; SILVA, J. K. R.; SANTOS, L. S. **Xanthones from the Roots of *Moutabea guianensis* Aubl.** Molecules, 20, 127-134, 2015.
[3]TRUEBA, G. B. **Los flavonoides: antioxidantes e prooxidantes**. Revista Invest Biomed, 22, 48-57, 2003.
[4]CORTEZ, D. A. G. et al. **Xanthones, triterpenes and a biphenyl from *Kielmeyera coriaceae*.** Phytochemistry, v. 47, n. 7, p. 1367-1374, 1998.

**Área: BIO** **Inscrição:00952**

# Evaluation of new inhibitors of homoserine dehydrogenase for the development of drugs against paracoccidioidomycosis

**Mariane C. Bagatin (PG),[1] Andrew M. F. Rozada (PG),[1] Franciele A. V. Rodrigues (PG),[2] Érika S. Kioshima (PQ),[2] Flávio A. V. Seixas (PQ).[3] Gisele de F. Gauze (PQ)[1*]**

**andrewrozada19@gmail.com; gfgbandoch@uem.br***

*[1]Department of Chemistry, UEM; [2]Department of Clinical Analysis and Biomedicine, UEM; [3]Department of Biochemistry, UEM.*

Keywords: *Virtual screening, Paracoccidoides brasiliensis, systemic mycoses, 4-methoxy-1-naphthalene, carboydrazides*

## Highlights

-*Virtual Screning* in the development of specific drugs for paracoccidioidomycosis
-Synthesis of new 4-methoxy-1-naphtoic acid derivatives
-*In vitro* antifungal tests against *P. brasiliensis* e *lutzii.*

## Abstract

Paracoccidioidomycosis (PCM) is a systemic mycosis, caused by the fungi *Paracoccidioides brasiliensis* or *lutzii*.[1] It mainly covers Latin America, especially Brazil, and despite presenting high rates of hospitalization and mortality, is a neglected disease with low visibility and few studies. It is treated with non-specific antifungal drugs such as Amphotericin B, sulfonamides and azole derivatives which have disadvantages, such as side effects, toxicity and long treatment periods. The enzyme homoserine dehydrogenase (HSD) is the first enzyme involved in the biosynthesis of methionine and threonine in the metabolic pathway of fungi and plants. As HSD is not found in humans, it's a promising target for the development of new drugs that exhibit specific antifungal activity and fewer side effects. Thus, in a previous study[2] HSD of *P. brasiliensis* was investigated through virtual screening, using a library with 187,841 compounds, and four was selected for *in vitro* tests. Two of these compounds presented good results and were used as leads for the development of a new synthetic series of analogous compounds (Scheme 1) that were obtained in good yields (47-90%). Derivatives **2** and **3** were active in the *in vitro* tests (Table 1) with highlight for carbohydrazide **3** with MIC from 8 to 32 μg $mL^{-1}$. Thus, these new prototypes may represent an option for the development of drugs against PCM and other systemic mycoses.

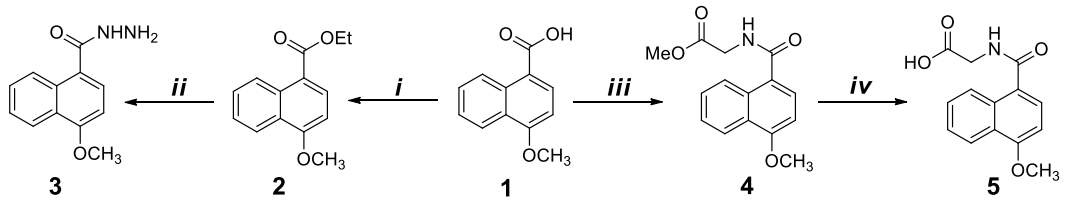


Reagents and conditions: ***i)*** $SOCl_2$ , EtOH, reflux, 12h; ***ii)*** $NH_2NH_2.H_2O$, reflux, 2h; ***iii)*** glycine methyl ester hydrochloride, Py, DMTMM, EtOH, r.t., 30min; ***iv)*** NaOH 2.5M, MeOH, r.t., 24h.

**Scheme 1**. Synthetic route of 4-methoxy-1-naphtoic acid derivatives

**Table 1**. MIC (μg $mL^{-1}$) against *Paracoccidioides* spp strains for compounds **2** and **3**

| Compound | *P. brasiliensis* | | | | *P. Lutzii* | | |
|---|---|---|---|---|---|---|---|
| | Pb18 | Mg14 | Mg15 | Mg16 | Pb01 | 8334 | ROSC |
| **2** | 64 | 64 | 128 | 8 | 64 | 64 | >512 |
| **3** | 16 | 32 | 8 | 8 | 32 | 16 | 32 |

**Acknowlegments**
CNPq, Fundação Araucária, PQU-UEM and ECO-DM

1. Wanke B. et al. *J. Bras. Pneumol*. 2009;35(12):1245-1249.
2. Bagatin M. C. et al.. *Antimicrob. Agents Chemother*. 2017;61(9):1-13.

**Área: BIO**
*(Inserir a sigla da seção científica para qual o resumo será submetido. Ex: ORG, BEA, CAT)*

**Inscrição: 00494**
*(Inserir o número de inscrição do autor que fez a submissão)*

# Temperature effect upon kinetic of dissociation/aggregation of the *Glossoscolex paulistus* hemoglobin

**[1] Regina P. da Silva (IC), [1] Evair D. Nascimento (PG), [1] Yago. S. Simões (IC), [1] Francisco A.O. Carvalho (PQ)**

**adriano.carvalho@unifesspa.edu.br;**

[1]*Faculdade de Química, do Instituto de Ciências Exatas, Unifesspa – Marabá, Pará - Brasil*

Palavras Chave: *EXTRACELLULAR HEMOGLOBIN, CHAOTROPIC AGENTS, KINETIC, OLIGOMERIC DISSOCIATION, AGREGATION.*

## Highlights

At 25 °C the chaotropic agents promotes the oligomeric dissociation process; The aggregation occurs only in the presence of guanidine; However, the protein dissociation inhibits the aggregation process.

## Resumo/Abstract

Extracellular hemoglobins are giant proteins, known as erythrocruorins, which are highly cooperative respiratory macromolecules found in mollusks and annelids [1]. *Glossoscolex paulistus* hemoglobin (HbGp) has a molecular mass of 3600 kDa, and its oligomeric structure is composed of heme containing globin-like chains (144 subunits) and additional polypeptide chains lacking a heme group (36 subunits), and named linkers [2,3]. In the current study, the dissociation and aggregation kinetic processes, in the presence of guanidine hydrochloride (GuHCl) and urea, at pH 7.0, as a function temperature were investigated. Up to 0.5 of GuHCl, at 25 °C, DLS data show that the hydrodynamic diameter, Dh, remains constant, as a function of time, suggesting that the HbGp is quite stable. In the presence of 1.2 mol/L of denaturant the kinetic constant is very small and subtle changes are noticed in the Dh values. However, the oligomeric dissociation process speed becomes very fast with the increase of chaotropic agent concentration, and, at 2.0 mol/L of GuHCl, the oxy-HbGp is fully dissociated after incubation for 3.0 h.

The speed constants at 42 °C are larger, as compared to the values at 25 °C, since the increase of temperature promotes the decrease of HbGp oligomeric stability. Moreover, the significant increase of Dh values, at 42 °C, is associated to the HbGp aggregation process. In the absence of GuHCl the aggregation starts after 11.0 h, while, in the presence of 0.8 mol/L of denaturant agent, the onset of the process occurs 2.5 h after the mixture, suggesting that low GuHCl concentration promotes the aggregation.

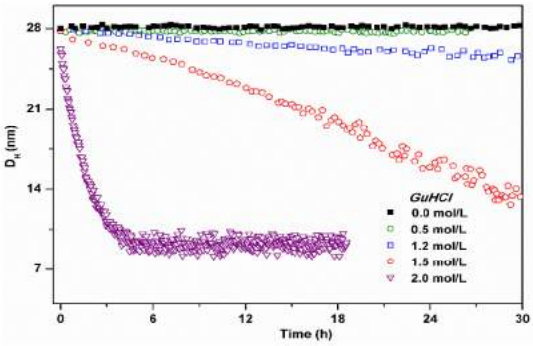


Fig.1: Kinetic curves of oxy-HbGp, 1.0 mg/mL, at pH 7.0, as a function of GuHCl concentration, at 25 ºC. The curves show the hydrodynamic diameter (Dh), as a function of time.

However, at 1.2 mol/L of GuHCl, the intense dissociation in shorter times (1.5 h) inhibits the formation of aggregates species in the solution and shifts the start of aggregation process to longer time around 5.5 h. Our study provides strong evidence that dissociation and aggregation kinetics of HbGp, in the presence of GuHCl, depend on the denaturant concentration and the medium temperature. The authors thank FAPESP and CNPq for partial financial support.

**References**

[1] Righi, G. (1971). *Arquivos de Zoologia S. Paulo 20*, v. 29, p. 1-95.

[2] Carvalho, F.A.O, et al. (2008). *Analytical Biochemistry*, v. 385, n. 2, p. 257-263.

[3] Bachega, J.F.R; et al. (2011). *Journal of Synchrotron Radiation*, v. 18, p. 24-28.

**Área: BIO** **Inscrição: 00296**

# Atividade antimicrobiana e reação de biotransformação de chalconas promovidas pelo fungo endofítico *Glomerella cingulata*

**Manoel L. Lopes Júnior (PQ),[1] Railda Neyva M. Araújo (PG),[1] Haroldo S. Ripardo Filho (PQ),[2] Williams S. Ribeiro (PG),[1] Marivaldo José C. Corrêa (PQ),[1] Giselle Maria S. P. Guilhon (PQ),[1] Lourivaldo S. Santos (PQ).[1*]**

**lsslouri@gmail.com**

[1]*Programa de Pós-Graduação em Química, Universidade Federal do Pará – UFPA. Belém-PA;*
[2]*Instituto Federal de Educação Ciências e Tecnologia do Amapá – IFAP – Campus Laranjal do Jari*

Palavras Chave: *Glomerella cingulata, Biotransformação, Chalconas, Diidrochalconas. Atividade antimicrobiana.*

## Highlights

Antimicrobial activity and biotransformation reaction of chalcones promoted by the endophytic fungus *Glomerella cingulata*. Isolation of the endophytic fungus from the leaves of *Virola surinamensis*. Chemoselective bioreduction of chalcones. Antimicrobial activity of chalcones and dihydrochalcones.

## Resumo/Abstract

Biotransformações são definidas como um conjunto de reações químicas catalisadas por enzimas, células ou tecidos de origem vegetal, microbiana ou animal.[1] O principal apelo para a uso de biotransformações em uma síntese é o controle estereo/regioquímico que pode ser obtido.[2] Neste trabalho, o fungo endofítico *Glomerella cingulata* isolado de folhas jovens de *Virola surinamensis* foi utilizado na reação de biotransformação das chalconas **1** e **2**. As reações de biotransformação (Esquema abaixo) foram realizadas usando meio modificado SDA (peptona de carne 10 g/L, D-glicose anidra 10 g/L e cloranfenicol 1,0 g/L) durante 10 dias, produzindo, respectivamente, os compostos **3** e **4**. A reação foi quimiosseletiva, onde somente a dupla ligação C=C da porção enona das chalconas foi reduzida. As duas substâncias biotransformadas foram testadas frente às bactérias *Escherichia coli* (ATCC 8739), *Staphylococcus aureus* (ATCC 25923), *Enterococcus feacalis* (ATCC 29212) e *Klebesia pneumonae* (ATCC 70063). Somente a diidrochalcona **3** apresentou atividade bacteriostática a 7,81 µg/mL frente à bactéria *Enterococcus feacalis*.

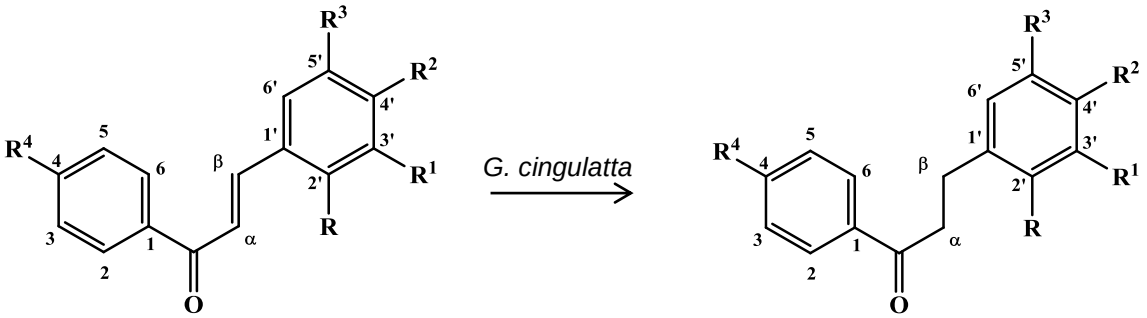


**1** $R^1$ = H; $R^2$ = OMe
**2** $R^1$ = OMe; $R^2$ = H

**3** $R^1$ = H; $R^2$ = OMe
**4** $R^1$ = OMe; $R^2$ = H

Referências

[1]GIRI, A.; DHINGRA, V.; GIRI, C. C.; SINGH, A.; WARD, O. P. E.; NARASU, M. L. *Biotechnology Advances*. v.19, p. 175-199, 2001.
[2]KEPPLER, A. F. Dissertação de Mestrado.123f. Universidade de São Paulo, São Paulo, 2005.

**Área: CAT** **Inscrição: 00099**

# Preparation and characterization of catalysts based on nickel niobate modified with Mg, Ca or Sr for hydrogen production

**João Lucas S. de Sousa (IC)[1], Simone P. de Lima (PQ)[2], Luciene S. Carvalho (PQ)[3], Doris Ruiz (PQ)[4], André R. Martins (PQ)[1]***

**andremartins@ifba.edu.br**

*[1]Instituto Federal da Bahia, Campus Porto Seguro, Porto Seguro, BA, Brazil; [2]Instituto Federal da Bahia, Campus Salvador, 40301-015, Salvador, BA, Brazil; [3]Instituto Federal da Bahia, Campus Camaçari, Camaçari, BA, Brazil; [4]Universidad de Concepción, Facultad de Ciencias Químicas, Concepción, Chile.*

*Keywords: Nickel Niobate, Niobium Oxide, Magnesium, Calcium, Strontium, Hydrogen.*

## Highlights

The addition of metals changes the structural properties of nickel niobate.
Ca addition promove reduce of nickel species.
Mg increases the Ni/niobia interaction, the specific area, and acidity of nickel niobate.

## Abstract

The Brazil is the world's largest producer of niobium, which among its many applications has been highlighted its use as a component of nickel catalysts used to obtain hydrogen from organic compounds such as methane and ethanol [1-3]. Based on these aspects, this work aimed to prepare and characterize catalysts based on nickel niobate (NiNb), modified with alkaline earth metals (Mg, Ca and Sr), to evaluate the effect of these dopants on the properties of the catalyst. The samples were prepared by coprecipitation method of the metallic precursors solutions, followed by dry and calcination at 800 °C. The obtained solids were characterized by X-ray diffraction (XRD), specific area measurement, scanning electron microscopy (SEM), temperature programmed reduction (TPR) and acidity measurement by ammonia temperature programmed desorption (TPD). Results showed that metals addition changed the structural properties of the solids, with the formation of nickel oxide and of niobates in all samples (Fig. 1), BET results showed low specific areas values (3-6 $m^2g^{-1}$) typical of niobium oxides. Magnesium effect was the most pronounced, since this one, apparently incorporated to the nickel niobate structure (Fig. 1), increased the metal/niobium oxide interaction, making it difficult to reduce nickel species, as showed in Fig. 2. On the other hand, its presence contributed to increasing the specific area (from 4 to 6 $m^2g^{-1}$) and the acidity (from 3 to 13 $\mu molg^{-1}$) of the nickel niobate.

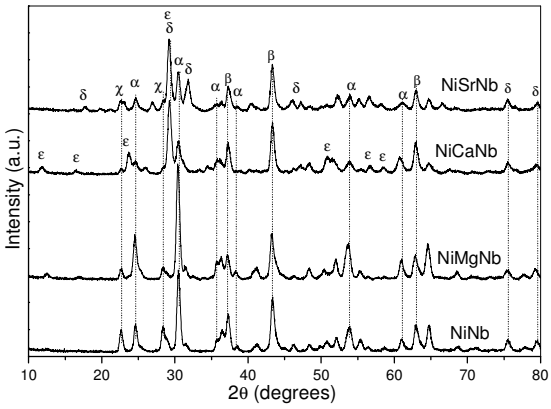


**Fig. 2** XRD profiles. Phases - α: $NiNb_2O_6$ (orthorhombic); β:NiO (cubic); χ: $Nb_{16,8}O_{42}$ (orthorhombic); δ: $Sr(NbO_3)_2$; ε: $CaNb_2O_6$ (orthorhombic).

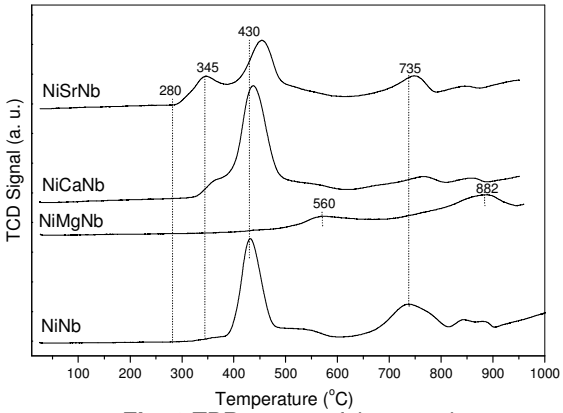


**Fig. 1** TPR curves of the samples.

### Acknowledgments

FAPESB and PRPGI/IFBA by the financial support. CBMM by the niobium oxide precursor.

### References

1. Nico, C., Monteiro, T. &Graça, M. P. F.,Prog. Mater. Sci. 80, 1–37 (2016).
2. Amjad, U.,Gonçalves Lenzi, G., Camargo Fernandes-Machado, N.R.&Specchia, S., Catal. Today 257, 122 (2015).
3. Sena, M. P., Sousa, J. L. S. de, Carvalho, L. S. & Martins, A. R. *in* 3, 2577–2582 (Anais da 68ª RASBPC, 2016).

**Área: CAT**
*(Inserir a sigla da seção científica para qual o resumo será submetido. Ex: ORG, BEA, CAT)*

**Inscrição:00213**
*(Inserir o número de inscrição do autor que fez a submissão)*

# Hidroformilação de álcoois provenientes da bio-massa (1R)-(-)mirtenol e (1R)-(-)nopol catalisada por complexo de ródio.

**Fábio Godoy Delolo (PG)[1], Kelley Cristina de Oliveira (PQ)[1], Eduardo Nicolau dos Santos (PQ)[1], Elena Vitalievna Gusevskaya (PQ)[1]***

**fabiodelolo@hotmail.com; elena@ufmg.br**

*[1]Departamento de Química, Universidade Federal de Minas Gerais; UFMG*

Palavras Chave: *Substratos trissubstituídos. Diastereoseletividade. Hemiacetalizaçao intramolecular. Solventes verdes. Fragrâncias.*

## Highlights

Hydroformylation of biomass-based alcohols (1R)-(-)myrtenol and (1R)-(-)nopol catalized by rhodium complex.
The diastereoselectivity is controlled by the steric difference between the two faces of the olefinic bonds.
The substrate coordination to rhodium preferably takes place on the face opposite to the isopropilene bridge
The system was active only in presence of phosphites, with the P/Rh ratio being crucial for selectivitiy.
Only the aldehyde derived from myrtenol undergoes an intramolecular hemiacetalization during the separation process.
The cyclic product shows an unexpected structure due to the epimerization process.
The polar solvents (alternative to toluene) were more efficient in terms of conversion and selectivity to the desired products.

## Resumo/Abstract

The hydroformylation of terpenes is a versatile route to aldehydes and their derivatives from bio-renewable feedstocks.The hydroformylation of (1R)-(-)myrtenol (**1a**) and (1R)-(-)nopol (**2a**), biomass-based hydroxyolefins containing trisubstituted endocyclyc C=C bonds, has been systematically studied using [Rh(μ-OMe)(1,5-cod)]$_2$ as the pre-catalyst (Scheme 1). The effects of the temperature, nature of phosphorus ligands, P/Rh molar ratio and solvent were studied aiming to develop a stable, active and selective catalytic system. As phosphorus auxiliary ligands were used $PPh_3$, $P(OPh)_3$ and tris(2,4-di-tert-butylphenyl) phosphite (TBDP). Both substrates gave corresponding hydroxyaldehydes derived from the rhodium interaction with the less substituted olefinic carbon: **1b** and **2b** with the best results being obtained in the presence of TBDP. Aldehyde **1b**, differently from **2b**, suffered a complete intramolecular hemiacetalization during the separation by column chromatography on silica gel 60 to give tetrahydrofuran compound **1c**. Only using purified and neutralized silica it was possible to isolate hydroxyaldehyde **1b** from the reaction solutions. The hydroformylation was seriously complicated by the concomitant isomerisation of both substrates, with the P/Rh ratio being a crucial factor for the improvement of selectivity for hydroformylation. The reactions can be also performed in eco-friendly: ethanol, 2-methyltetrahydrofuran and diethylcarbonate, as alternatives for rather toxic toluene. The processes developed in the present work represent a valuable route to novel fragrance aldehydes starting from bio-mass based substrates.

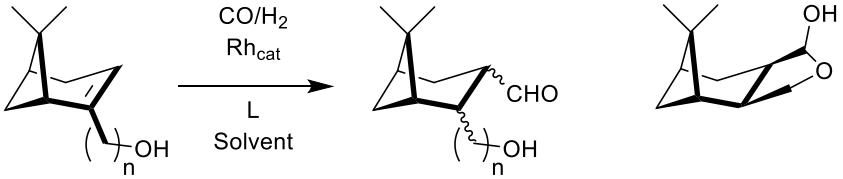


n = 1: **1a -** (1R)-(-)Myrtenol
n = 2: **2a -** (1R)-(-)Nopol

**1b-2b** **1c**

*Figure 1. Products of the Hydroformylation of (1R)-(-)myrtenol (1a) and 1(R)-(-)nopol (2a) respectively.*

[CNPq, CAPES, FAPEMIG, and INCT-Catálise]

**Área: CAT**
*(Inserir a sigla da seção científica para qual o resumo será submetido. Ex: ORG, BEA, CAT)*

**Inscrição: 00378**
*(Inserir o número de inscrição do autor que fez a submissão)*

# Hydrolysis of soybean oil over solid acid catalysts

**Camilo Aurélio Brandão Crisóstomo[1] (FM) e Ricardo Reis Soares[2,*] (PQ)**

**rrsoares@ufu.br**

*[1]Instituto de Química, UFU; [2]Faculdade de Engenharia Química, UFU*

*Soybean oil, hydrolysis, Solid acid catalysts, Kinetics, Isopropylamine-TPD.*

## Highlights

The catalytic hydrolysis of vegetable oils and fats is of great importance to the oleochemical industry in other to produce valuable as free fatty acids.
Solid acid materials such as γ-$Al_2O_3$ (G-250), niobium oxide ($Nb_2O_5$), niobium phosphate ($NbOPO_4$), ZSM-5 and β-zeolite can be used as catalysts.
The catalytic performances and their kinetics are fundamental for further industrial process design.

## Resumo/Abstract

The hydrolysis reaction to produce free fatty acids is of great importance to the oleochemical industry. The process is can performed thermally as a liquid-liquid (or gas-liquid) reaction or using a catalyst. The reaction proceeds in three stages (simultaneously), but with different rates. Initially, triacylglycerides (TG) are converted to diacylglycerides (DG) and free fatty acids (FFA), followed by monoacylglycerides (MG) and AGL and finally, AGL and glycerol. The present study evaluated the performance of solid acids as the γ-$Al_2O_3$ (G-250), niobium oxide ($Nb_2O_5$), niobium phosphate ($NbOPO_4$), ZSM-5 and β-zeolite in the hydrolysis reaction of degummed soybean oil. The textural properties (BET surface area, diameter and pore volume) were determined by $N_2$-physisorption and acidic sites were characterized by temperature programmed desorption of isopropyl amine (IPA-TPD). Typical reactions tests were performed in a 500 mL-stirrer batch reactor at 25 bar and 250 °C during 3h by using Oil/H2O/catalyst mass ratio of 50/50/10. The catalytic performances (TG conversions and MG and DG yields) of some catalysts are exhibited in the figures below. The best catalytic activity exhibited by the γ-$Al_2O_3$, which may be associated with its high specific area and the presence of strong Lewis acid sites.

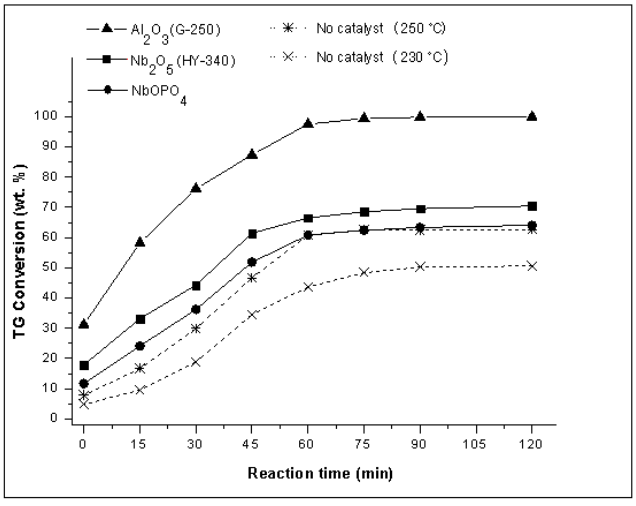


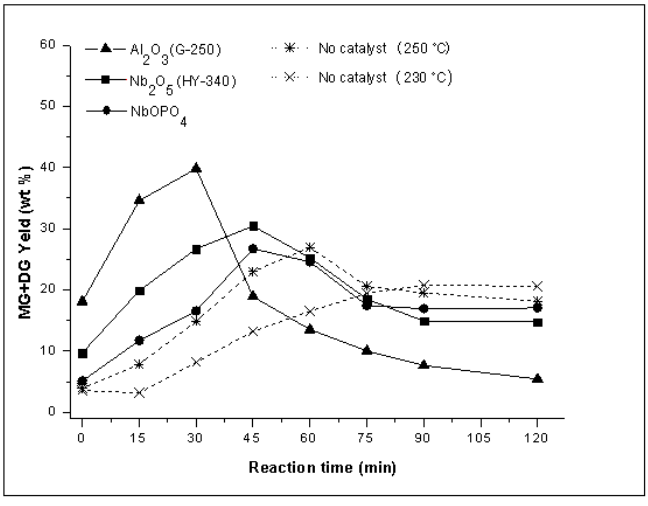


**Figures:** Triacylglycerides (TG) conversions and Mono and Diacylglycerides (MG+DG) Yields vs. TOS

**Área: CAT** **Inscrição: 00382**

# Study of the photocatalytic capacity of the Black Mud for the degradation of the molecules of methylene blue and hydroxybenzene (phenol).

**Vitória S. Lourenço (IC),[1] Sabrina M. Boto (PQ),[1] Yvan J. O. Asencios (PQ),[2*]**

**vitória.slourenco@outlook.com; yvanolortiga@gmail.com*.**

*[1]Faculdade de Tecnologia de Praia Grande - FATEC; [2] Instituto do Mar, Universidade Federal de São Paulo – Santos.*

*Keywords: Methylene Blue, Phenol, Heterogeneous Photocatalysis, Black Mud.*

## Highlights

Peruíbe's Black Mud can become a cheaper material to degrade different organic compounds, such as methylene blue and phenol.

## Abstract

The Black Mud (BM), found in the neighborhood of Rio Preto in Peruíbe / SP, is a porous material, with adsorbent properties and ion-exchange capacity[1], it has a mineralogical composition composed by mixtures of semiconductor oxides. All these characteristics are interesting for heterogeneous-photocatalysis. In this process, organic compounds can be degraded by the action of hydroxyl radicals generated from the interaction of a semiconductor with light[2]. The objective of this work was to use BM pure and doped with $TiO_2$, as photocatalysts to degrade phenol and methylene blue. The materials were characterized by X-ray Dispersive Energy Spectroscopy (EDX) and X-ray Diffraction (XRD). BM showed a predominant composition of quartz ($SiO_2$) and muscovite and a lower proportion of $Al_2O_3$, $Fe_2O_3$ and $TiO_2$. The catalytic tests were performed in a batch reactor, in a dark chamber with ventilation and exhaustion, in the presence of ultraviolet light (UV-C, 254 nm), varying the catalyst concentration, residence time and pH. Figures 1 and 2 present the results obtained for the kinetics of methylene blue and phenol.

**Figure 1 – Kinetics of methylene blue with BM (a)**

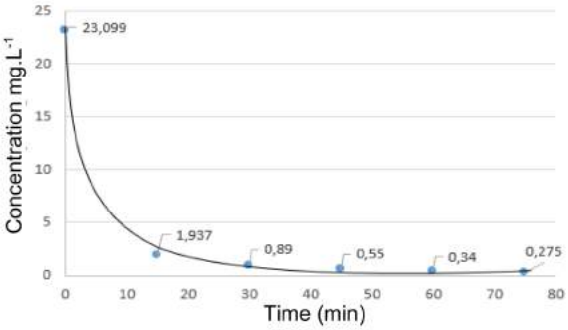


Source: performed research, 2017.

**Figure 2 – Kinetics of phenol with BM and $H_2O_2$ (b)**

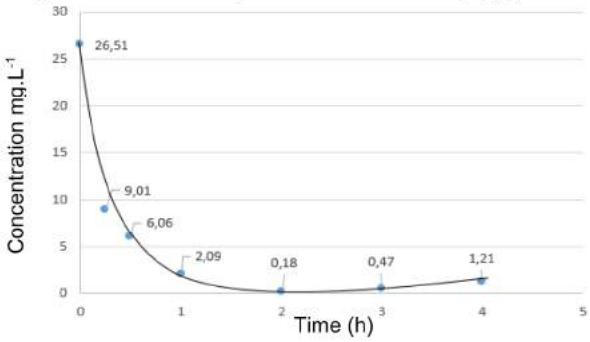


Source: performed research, 2017.

[Fixed conditions: [catalyst] = 1 g $L^{-1}$; pH (a) = 3,5; pH (b) = 5,0; T = (25 ± 1)ºC]

Based on the interpretation of the kinetic data we verified that the methylene blue molecule showed a fast adsorption reaching more than 90% of the dye removal. The results with the phenol molecule were not very positive, making it necessary to add $H_2O_2$ to increase the amount of radicals formed. This suggests a better efficiency of the BM for certain type of molecules to the detriment of others. Finally, the BM was shown a possible application in the photocatalysis by the presence of quartz, $TiO_2$ and its porous structure.

## References

[1] SILVA, P. S. C.; TORRECILHA, J. K.; GOUVEA, P. F. M.; MADUAR, M. F.; OLIVEIRA, S. M. B.; SCAPIN, M. A. Chemical and radiological characterization of Peruíbe Black Mud. Applied Clay Science, 2016.

[2] QUINJO, M. V.; MARCOS, F. C. F.; ASSAF, E. M.; ASENCIOS, Y. J. O. Uso de óxidos de nióbio e argila modificada com nióbio como fotocatalisadores na remoção de Rodamina B em meios aquosos. Universidade Federal de São Paulo. XXI Congresso Brasileira de Engenharia química, 2016.

[3] MANUAL 4 – AAP with distillation. Method 9065 phenolics (spectrophotometric), 1986.

**Área: CAT** **Inscrição: 00395**

# Production of carbon nanostructured materials by CVD method using supported catalysts: Study of two different carbon precursor gases

**Aellyngton Palandrani da Silva (IC),[1] Ricardo Velloso Lelo (PG),[2] Mário César Guerreiro (PQ),[3] Daniela Zambelli Mezalira (PQ).[2*]**

**daniela.z.m@ufsc.br**

*[1]Depto de Engenharia de Materiais, UFSC; [2]Depto de Química, UFSC; [3]Depto de Química, UFLA.*

Palavras Chave: Acetylene, Methane, Catalytic decomposition, Supported catalysts, Carbon nanostructure.

## Highlights

Synthesis of carbon nanostructured. Decomposition of acetylene and methane gases using supported catalysts. Characterization of carbonaceous materials obtained.

## Resumo/Abstract

Chemical Vapor Deposition (CVD) has been reported as a good method to synthesize carbon nanostructured materials.[1] The growth of carbon nanostructures by thermal CVD employs a carbon precursor molecule and a transition metal as a catalyst.[2] In the present study we examine the possibility to synthesize carbon nanostructured using supported catalysts. The catalysts consist of iron oxides doped with copper (MagSilCu2,5) or nickel (MagSilNi2,5) supported on amorphous silica and presented a good dispersion of metals.[3] Two carbon precursors were tested: acetylene and methane. CVD was carried out at atmospheric pressure, in a horizontal fixed-bed reactor at a temperature of 700 °C. The reactor consists of a quartz tube placed inside a horizontal high temperature furnace. Before the reaction, the active metal components were reduced by heating at 800 °C for 1 h in 1:1 $H_2/N_2$ at a flow rate of 40 mL $min^{-1}$. The carbonaceous materials obtained were characterized by thermogravimetric analysis (TGA) and Raman spectroscopy.

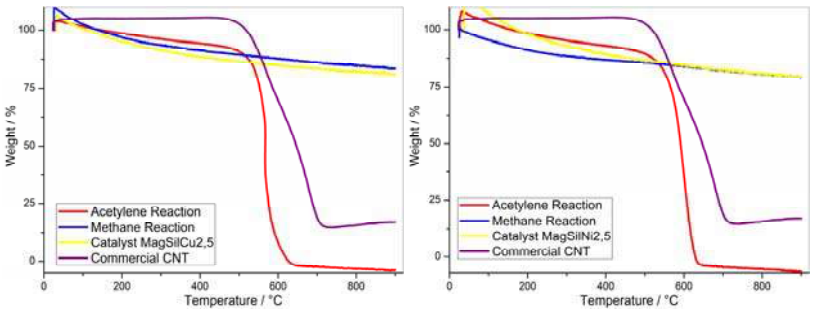


**Fig. 01:** TGA of commercial NTC (purple line) and the sample obtained by CVD using acetylene (red line) and methane (blue line) using (a) MagSilCu2,5 and (b) MagSilNi2,5 catalysts (yellow line).

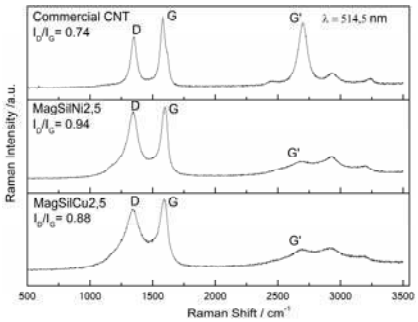


**Fig. 02:** Raman spectra of commercial NTC and materials obtained by CVD with acetylene gas using supported catalysts.

TGA (**Fig. 01**) shows that samples synthesized with methane gas presented no significant amount of carbonaceous material after synthesis. However, a good thermal stability of structured carbonaceous materials was observed with acetylene gas. The Raman spectra (**Fig. 02**) showed that the products of the reaction with acetylene gas have the CNTs characteristic bands (D, G and G'), comparing them to the commercial CNTs and the literature. $I_D/I_G$ ratio indicated that the carbon nanostructured for both samples presented lower degree of ordering and probably more defects than the commercial CNTs.

1 SHANOV, Vesselin et al. CVD growth, characterization and applications of carbon nanostructured materials. Surface & Coatings Technology, 2013, vol. 230, pp. 77–86.
2 VERISSIMO, Carla et al. Different carbon nanostructured materials obtained in catalytic chemical vapor deposition. J. Braz. Chem. Soc. [online]. 2006, vol.17, n.6, pp.1124-1132.
3 LELO, Ricardo Velloso; GUERREIRO, Mário César. Síntese de óxidos de ferro magnéticos dopados com cobre ou níquel suportados em sílica: uso como catalisadores redox. Dissertação de mestrado. Universidade Federal de Lavras. 2016.

**Área: CAT**
*(Inserir a sigla da seção científica para qual o resumo será submetido. Ex: ORG, BEA, CAT)*

**Inscrição: 396**
*(Inserir o número de inscrição do autor que fez a submissão)*

# Green oxidation of etanol, acetol and other primary alcohols by $FeCl_3/H_2O_2$ in aqueous medium

**Dalmo Mandelli (PQ)[1], Georgiya B.a Shul'pin (PQ)[2], Wagner A. Carvalho (PQ)[1], Marcos L. de Araújo (PG)[1]* dalmo.mandelli@gmail.com; m.dearaujo@hotmail.com**

*[1]Center of Natural and Human Sciences, UFABC, Brazil; [2]Institute of Chemical Physics, Russian Academy of Sciences, Russia*

Keywords: *Catalysis, Green Chemistry, Alcohol oxidation, Ethanol, $H_2O_2$, Aqueous medium*

## Highlights

Low cost and green oxidation of renewable ethanol in water is accomplished. Oxidation of acetol, that can be obtained from glycerol, was also performed under the same conditions.

## Resumo/Abstract

Alcohol oxidation is an essential reaction for organic synthesis, once it leads to the formation of products and intermediates of great industrial importance. Traditional oxidizing agents such as $KMnO_4$, $CrO_3$, PCC and others, present the drawback of generating a stoichiometric amount of metallic residues. Alternatively, the use of $H_2O_2$ as oxidizing agent is gaining importance, once it decomposes into $H_2O$ and $O_2$, two non-toxic residues. The need of a metallic catalyst for this kind of reaction has led to a search for efficient and low cost catalysts, such as iron, for example, which is highly versatile for the catalysis of several types of reactions. Thus, the primary alcohols methanol, ethanol and 1-propanol, as well as hydroxyacetone (acetol), were oxidized using $FeCl_3/H_2O_2$ in aqueous medium. In a typical reaction, it was used 0.5M of substrate, $H_2O_2$ and nitromethane (internal standard), 1mM of $FeCl_3$ and water up to 5mL in a jacketed glass reactor at 60°C. The reactions were monitored by gas chromatography. Among the studied substrates, ethanol, a renewable substrate, and acetol, that can be obtained from dehydration of glycerol, a biodiesel manufacture byproduct, generate more economic and environmental interest. Both form acetic acid and formic acid as oxidation products (0.084M of acetic acid and 0.022M of formic acid from ethanol oxidation and 0.19M of acetic acid and 0.23M of formic acid from acetol oxidation).

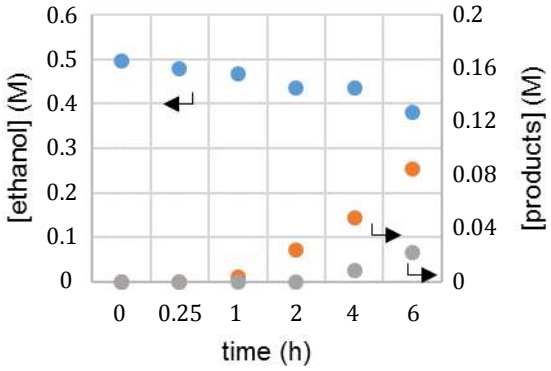


Figure 1: Concentration of ethanol (•), acetic acid (•) and formic acid (•) from etanol oxidation. Conditions: 0,5M acetol, nitromethane and $H_2O_2$, 1mM of $FeCl_3$, water up to 5mL, 60°C.

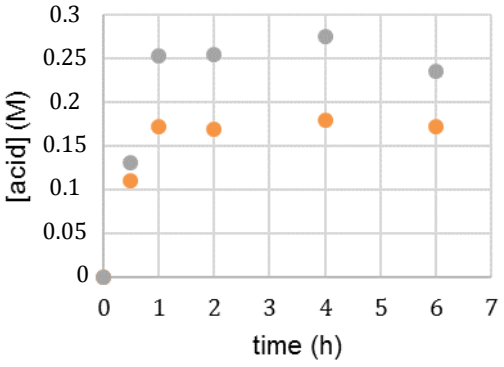


Figure 2: Concentration of acetic acid (•) and formic acid (•) from acetol oxidation. Conditions: 0,5M acetol, nitromethane and $H_2O_2$, 1mM of $FeCl_3$, water up to 5mL, 60°C.

Table1: Conversion for primary alcohols

| substrate | methanol | ethanol | 1-propanol |
|---|---|---|---|
| conversion (%) | 31 | 23 | 22 |

Conditions: 0,5M acetol, nitromethane and $H_2O_2$, 1mM of $FeCl_3$, water up to 5mL, 60°C.

**Área: CAT** **Inscrição: 00472**

# Unveiling the structural and electronic properties of the B-$Nb_2O_5$ surfaces and their interaction with $H_2O$ and $H_2O_2$

**Heitor Avelino De Abreu (PQ), Renata Diniz (PQ), Hélio Anderson Duarte (PQ), Antônio Lenito Soares Jr. (PQ), Matheus Campos Quintão (IC), Mirele Bastos Pinto (PG)**

**heitorabreu@ufmg.br**

*Departamento de Química – Instituto de Ciências Exatas, Universidade Federal de Minas Gerais (UFMG)*

Palavras Chave: *Niobia, DFT, Bader Analysis, $H_2O$ and $H_2O_2$ Adsorption.*

## Highlights

Niobia has been applied in several areas among others in heterogeneous catalysis.
Niobia presents high acidity and its Lewis acid sites are tolerant to water.
The interaction of $H_2O$ and $H_2O_2$ with the (001) surface of niobia was studied through computational methods.

## Resumo/Abstract

Niobium pentoxide ($Nb_2O_5$) also known as niobia has been applied in several areas among others in heterogeneous catalysis. This is due to both its high acidity (Brönted and Lewis acid sites) and its Lewis acid sites tolerant to water. The structure and morphology of these sites present tunable quantity and strength, however, little attention has been given to its polymorphic forms and reactivity. In this work, the surface properties of stoichiometric B phase (B-$Nb_2O_5$), including the cleavage surfaces, structural, energetic, electronic properties and chemical reactivity towards $H_2O$ and $H_2O_2$, by means of periodic density functional theory (DFT), have been studied. An initial investigation was carried out to determine cleavage surface of the B-$Nb_2O_5$. Our results show that the B-$Nb_2O_5$ (010)-2 surface (Figure 1) is the most stable (surface energy 0.52 J $m^{-2}$) of the surfaces studied. Projected density of state (PDOS) analysis showed that the niobium atoms is a Lewis acid site. When $H_2O$ was adsorbed on the (010)-2 surface, the molecular adsorption is the most stable, under Nb site. However, the results showed that both dissociative and molecular mechanisms must be present on the surface, although the dissociative one to a lesser extent. When $H_2O_2$ was adsorbed on the (010)-2 surface, the dissociative process is the most stable than molecular, and the hydrosuperoxo ($HO_2^-$) species is the most stable species.

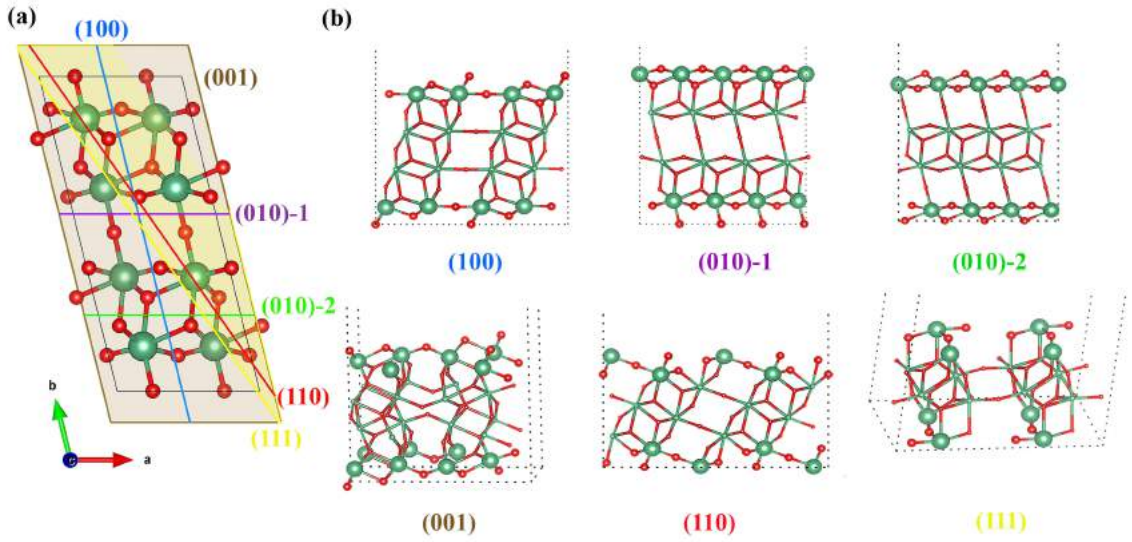


Figure 1. (a) Optimized structure of the B-$Nb_2O_5$ bulk, and the six different cleavage planes and (b) six different surfaces studied in the present work.

Acknowledgments: FAPEMIG, CNPq, CAPES and the National Institute of Science and Technology for Mineral Resources, Water and Biodiversity - INCT-ACQUA.

**Área: CAT** **Inscrição: 00507**

# Síntese de compostos de aroma catalisados por lipases através do reaproveitamento da borra de café

**Regiane Késsias Sousa Lira (PG),[1]* Ivaldo Itabaiana Júnior (PQ),[2] Selma Ferreira Gomes (PQ)[2].**

**regianekessias@eq.ufrj.br; ivaldo@eq.ufrj.br; selma@eq.ufrj.br**

*Escola de Química, [1]Programa de Tecnologia em Processos Químicos e Bioquímicos EQ/TPQB-UFRJ; [2]Departamento de Engenharia Bioquímica, EQ/DEB-UFRJ*

Palavras Chave: *Aromas, Borra de café, Lipases, Biocatálise.*

## Highlights

Synthesis of aroma compounds catalyzed by lipases through reuse of the coffee grounds. Effect of different polar and apolar solvents on the simple extraction of the lipid components of the coffee grounds. Selection of different lipases for the synthesis of aroma esters.

## Resumo/Abstract

Nos últimos anos, a demanda por produtos naturais aumentou em todo o mundo, e a investigação de novos métodos de produção de compostos de aroma natural atraíram a atenção da indústria química e alimentar[1]. Nesse cenário, a borra de café se torna uma matéria-prima interessante à produção de novos bioaromas devido sua abundância e por apresentar um aroma residual notável de grãos de café torrado[2]. As lipases (glicerol éster hidrolases, E.C. 3.1.1.3), destacam-se dentre as enzimas, com vasto potencial de aplicação na síntese de ésteres usados na indústria de aromas[3]. Este trabalho investiga a síntese de ésteres de aroma catalisada por lipases utilizando extratos lipídicos da borra de café. Os substratos lipídios da borra de café foram obtidos por extração com solventes de diferentes polaridades, analisados em CG-MS, sendo o hexano o solvente com maior rendimento, o metanol e etanol os únicos que extraíram a cafeína como componente majoritário. A análise em MEV-EDS (Figura 01) mostrou o efeito da polaridade dos solventes na variação das propriedades físicas da borra de café. Um *screening* de cinco lipases comerciais (*Amano Lipase AK e PS; Lipozyme RMIM e TLIM; Novozyme 435*) revelou maior atividade de esterificação à Novozyme 435 tanto pelo método de Lowry-Tinsley (Figura 02) como por CG-MS. A reação para a formação de ésteres de aroma utilizando os extratos lipídicos em solvente hexano catalisado pela lipase Novozyme 435 foi realizada em CG-MS, indicando a formação de diferentes ésteres (Figura 03).

**Figura 01** – Micrografia obtida por MEV das partículas de borra de café.
I – antes da extração

II – após a extração

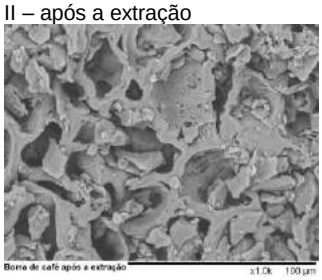


**Figura 02** - Atividade de esterificação das lipases do a) Ácido Oléico e b) Ácido palmítico, em n-heptano.

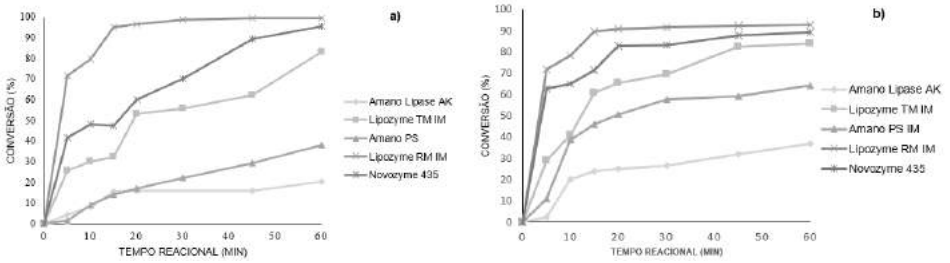


**Figura 03** – Cromatograma da reação de esterificação da borra de café por Novozyme 435 (Formação de ésteres de aroma). Razão molar substrato em heptano/etanol 1:1, temp. 30°C

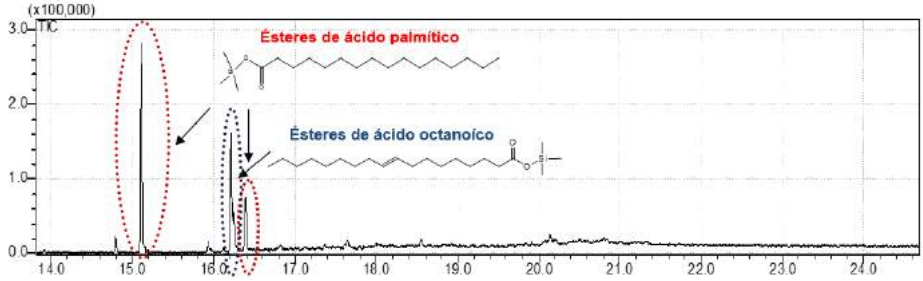


**Referências**: [1]SÁ, A. G. A. et al. A review on enzymatic synthesis of aromatic esters used as flavor ingredients for food, cosmetics and pharmaceuticals industries. ***Trends in Food Science and Technology***, v. 69, p. 95–105, 2017. [2]MUSSATTO, Solange I. et al. A study on chemical constituents and sugars extraction from spent coffee grounds. ***Carbohydrate Polymers***, v. 83, n. 2, p. 368 – 374, 2011. [3]STERGIOU, P. Y. et al. Advances in lipase-catalyzed esterification reactions. ***Biotechnology Advances***, v. 31, n. 8, p. 1846–1859, 2013.

**Área: CAT** **Inscrição: 00600**

# Heterogeneous acid catalysts based on sulfonated graphene like structures produced from bio-oil

**Fabiane Carvalho Ballotin (PG),[1*] Lucas Teodoro Perdigão (IC),[1] Marcus Vinícius B. Resende (IC),[1] Márcio José da Silva (PQ),[2] Ana Paula C. Teixeira (PQ),[1] Rochel Montero Lago (PQ).[1]**

**fabianeballotin@yahoo.com.br; fabianeballotin@yahoo.com.br**

*[1]Departamento de Química, UFMG; [2]Departamento de Química, UFV.*

Palavras Chave: *bio-oil, sulfonation, heterogeneous acid catalysts, esterification, biodiesel.*

## Highlights

Sulfonated graphene-like structure produced from bio-oil. Efficient heterogeneous acid catalyst for esterification of oleic acid.

## Abstract

In this work, bio-oil (BO) obtained from the flash pyrolysis of sugar cane straw was reacted with concentrated sulfuric acid (weight ratios $H_2SO_4$: BO of 1.8; 3.6; 9.2 and 18.4 at 120 °C for 2 h) to produce graphene-like structures containing -$SO_3H$ groups. RAMAN, FTIR, TG, potentiometric titrations and SEM suggests that the reaction of BO with $H_2SO_4$ starts with dehydration process, carbonization followed by sulfonation (Figure 1).

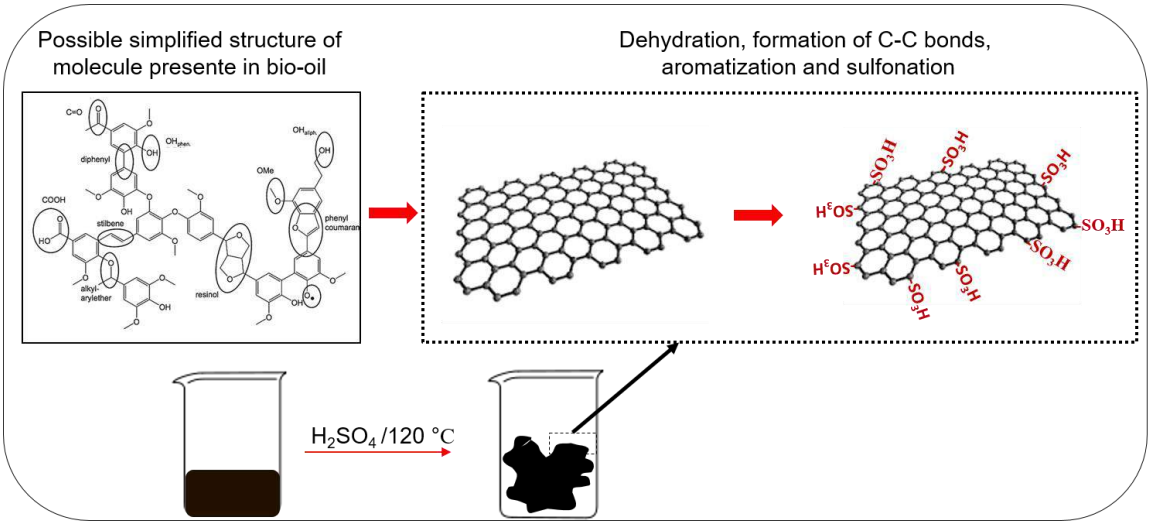


Figure 1. Scheme of dehydration, formation of C-C bonds, aromatization and sulfonation during the bio-oil reaction with $H_2SO_4$.

A very intense G band in the Raman spectra suggested the formation of graphene structures with very few defects. The acidity strength of catalysts was potentiometrically measured with n-butylamine titration. All the materials presented strong acid sites (Ei >300 mV). The amount of acid sites was 0.02, 0.11, 0.26 and 0.30 mmol.g$^{-1}$ for $BS_{1.8}$, $BS_{3.7}$, $BS_{9.2}$ and $BS_{18.4}$ samples, respectively. The esterification reactions of oleic acid with methanol were carried out at 100 °C during 3 h (oleic acid/methanol molar ratio 1:10, catalyst 7.5 %). Conversions of 90, 98, 100 and 100 %, were achieved, in the presence of $BS_{1.8}$, $BS_{3.7}$, $BS_{9.2}$ or $BS_{18.4}$, respectively. Thus, bio-oil sulfonation proved to be effective on carbonization and –$SO_3H$ groups' formation, producing acid sites with sufficient acidity to convert fatty acids to esters.

**Acknowledgements**
The authors thank CNPQ, CAPES and FAPEMIG.

**Area: CAT** **Registration: 00647**

# Statistical study of the oxidation reaction of benzyl alcohol in the absence of base with silica-supported gold nanoparticles.

**Cristian J. Giertyas (PG),[1]* Lucas N. Melo (PG),[1] Eid C. da Silva (PQ),[1,2] Rusiene M. de Almeida (PQ)[1], Mario R. Meneghetti (PQ),[1] Janaína H. Bortoluzzi (PQ),[1]**

**janaina.bortoluzzi@iqb.ufal.br; giertyascris@gmail.com**

[1]Group of Catalysis and Chemical Reactivity, Institute of Chemistry and Biotechnology, Federal University of Alagoas/ Maceió-AL / Brazil. (GCAR, IQB, UFAL) / INCT Catalysis; [2] *Center of Technology, UFAL.*

Keywords: *Alcohol oxidation, Benzyl alcohol, Factorial design, Gold nanocatalysts.*

## Highlights

Absence of base in oxidation reaction
Application of $2^3$ factorial design for evaluation of reaction variables
Oxidation of benzyl alcohol

## Abstract

Gold is known for its catalytic activity toward the oxidation reaction of alcohols in aqueous media. In this regard, the reaction can lead to the formation of different products depending on the parameters used (media pH, temperature, pressure and reaction time).[1] Currently, many studies have aimed the development of catalytic systems that could minimize environmental impacts, reducing or removing significant amounts of acids and bases in the process of conversion of alcohols. In the present work, a complete factorial design ($2^3$) was carried out for evaluation of the oxidation reaction of benzyl alcohol (BA) in the absence of base, assessing factors as reaction time (1-3h), temperature (120 – 150 °C) and amount of catalyst (50 – 200 mg). During factorial design, eight experiments were performed with duplicate of center point. Evaluation of the Pareto Chart (Fig. 1) showed that the assessed parameters did not significantly influence the conversion of BA. However, this data show that increasing temperature and reaction time together with decreasing amounts of catalyst can be applied in order to obtain higher conversions of BA. In the statistical study, conversions < 9% of BA were found, of which all reactions showed selectivity > 90% for benzaldehyde (BZ). It should be noted that the absence of base in the catalytic system remarkably leads to low conversions of BA.

***Figure 1: Pareto Chart obtained from $2^3$ factorial design***

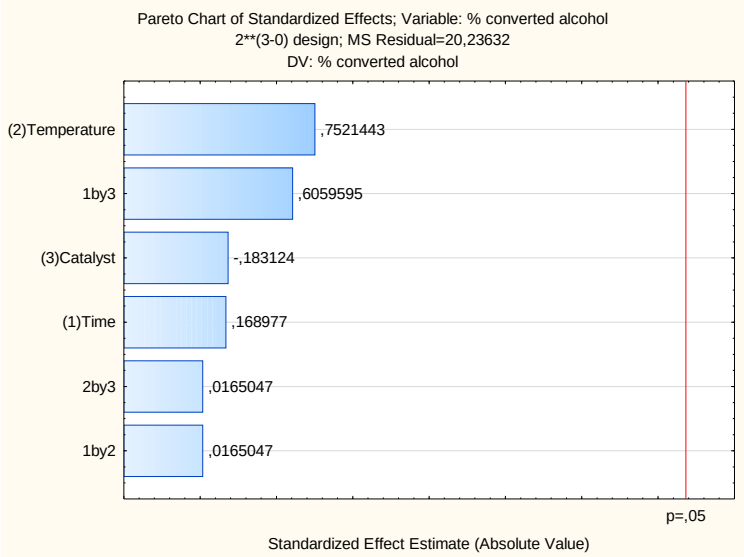


Source: StatSoft, Inc. (2011). STATISTICA (data analysis software system), version 10. www.statsoft.com.

[1] J. Hu, L. Chen, K. Zhu, A. Suchopar, R. Richards. Catalysis Today 122 (2007) 277–283

**Área: CAT** **Inscrição: 00673**

# GO/(CdS)x/(ZnO)y bifunctional photocatalyst for ecotreatment of tannery sludge wastewaters with simultaneous generation of hydrogen

**Elisson A. Souza (PG)[1]*, Rodrigo J. Araújo (PG)[1], Luciana A. Silva (PQ)[1,2]. elissons@ufba.br**

*[1]Instituto de Química; [2]INCT de Energia e Ambiente, Universidade Federal da Bahia, Campus de Ondina, CEP 40170-290, Salvador-BA.*

Keywords: *Photocatalysis, Energy recovery, Tannery sludge, Hydrogen, Graphene oxide.*

## Highlights

- (CdS)x/(ZnO)y composites are active as a photocatalyst to convert tannery waste into $H_2$ using solar power.
- Graphene oxide acts as an efficient co-catalyst in hydrogen generation.

## Abstract

The composition of the liming bath sludge from the hides treatment during tanning process to produce wet blue leather meets the necessary requirements to act as a good sacrificial agent in the photocatalytic hydrogen production, such as the presence of organic matter and high sulfide content. In general, the presence of sulfide ions, as well as other sacrificial agents, increases the hydrogen production rate due to suppression of charges recombination. In a previous work [1], we have used CdS as a photocatalyst and Pt as a co-catalyst in hydrogen production from tannery sludge wastewaters, at a rate of 294.38 μmol $g^{-1}_{cat}h^{-1}$, with simultaneous decrease of pollutant charge in this effluent. In the present work, we evaluate the composites (CdS)x/(ZnO)y as photocatalysts, in order to decrease cadmium content, and graphene oxide (GO) as a co-catalyst in the photocatalytic treatment of tannery sludge. Composites were prepared by Pechini method followed by ion exchange using $CdCl_2$ and $Zn(NO_3)_2.6H_2O$ as precursors in different Zn/Cd ratios (y/x). It was obtained a highly dispersed mixture of ZnO and $CdCl_2.H_2O$ (y/x=0.4). XRD analysis (Figure 1) associated with EDX elemental analysis confirm the (CdS)x/(ZnO)y formation after ion exchange. The photocatalytic tests were performed under argon atmosphere using 60 mg of the composite or pure CdS and GO 2% (w/w). The hydrogen production rate for GO/(CdS)x/(ZnO)y was 1578 μmol $g^{-1}_{cat}h^{-1}$ (Figure 2), which means an increase in photocatalytic activity compared to GO/CdS (4 times) and Pt/CdS (5 times).

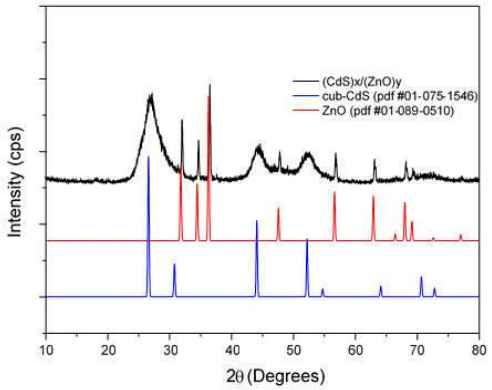


Figure 1. XRD patterns of the composite after ion exchange compared to ICSD standards.

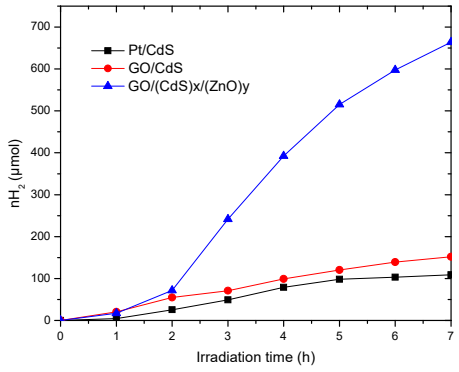


Figure 2. Hydrogen production from different photocatalysts under visible light irradiation (λ > 400 nm): Pt/CdS, GO/CdS and GO/(CdS)x/(ZnO)y.

[1] SOUZA, E. A.; SILVA, L. A.; Energy recovery from tannery sludge wastewaters through photocatalytic hydrogen production. J. Env. Chem. E., v. 4, p. 2114-2120, 2016.

**Área: CAT** **Inscrição: 00744**

# Influence of the $CeO_2$ support nano-morphology on Gold nanoparticles activity for photooxidation reactions

**Ivo F. Teixeira (PQ),[1] Rafael S. Geonmonond (PG),[1] Guilherme F. S. R. Rocha (IC),[1] Edman Tsang,[2] Pedro H. C. Camargo (PQ).[1]**

**ivo@iq.usp.br; camargo@iq.usp.br**

*[1]Departamento de Química Fundamental, Instituto de Química, Universidade de São Paulo, Av. Prof. Lineu Prestes, 748, 05508-000 São Paulo-SP, Brazil.*

*[2]Wolfson Catalysis Centre, Inorganic Chemistry Laboratory, Department of Chemistry, University of Oxford, Oxford, OX1 3QR UK*

Keywords: *$CeO_2$; Photooxidation; Photocatalysis; Gold; Nanoparticles; Plasmonic Catalysis.*

## Highlights

- Influence of the $CeO_2$ support morphology on the activity of gold nanoparticles (NPs) for photooxidation reactions;
- $CeO_2$ Nanocube/Au samples are more active for photooxidations;

## Resumo/Abstract

Herein, it was studied the influence of the $CeO_2$ support morphology on the activity of gold nanoparticles (NPs) for photooxidation reactions, especially benzyl alcohol oxidation and aniline oxidation into azobenzene. The $CeO_2$ was prepared as nanocubes and nanorods, following the synthesis well reported in the literature.[1] The nanocubes presented edges with dimension around 30 nm (**Fig 1.a,c**), while the nanorods around 100 nm of length and 10 nm of width (**Fig 1.b,d**). The Au NPs were synthesized separately following the method reported by Damato et al,[2] as expected the NPs were obtained as nanospheres with ~30 nm of diameter. After, the Au NPs were impregnated over the $CeO_2$ support by incipient wetness impregnation. Samples before and after the Au NPs deposition were fully characterized by scanning electron microscopy (SEM), transmission electron microscopy (TEM), X-Ray powder diffraction (XRD), UV-Vis and Raman spectroscopy.

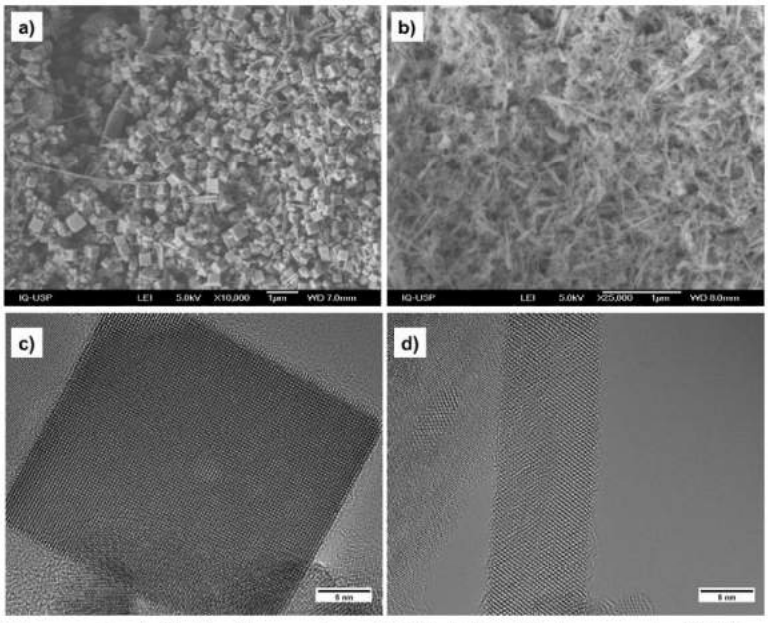


**Figure 1.** a) $CeO_2$ Nanocubes SEM; b) $CeO_2$ Nanorods SEM; c) HRTEM for $CeO_2$ Nanocubes and d) $CeO_2$ Nanorods.

Preliminary catalytic tests were performed in a glass reactor illuminated by a visible light loaded with 10 mg of sample, 10 mL of $H_2O$, 1 mmol of benzyl alcohol or aniline and pressurized with 8 bar of oxygen. Both samples presented activity for the photooxidation of benzyl alcohol, however, the nanocube samples showed higher conversion, with no significantly difference in the products selectivity, which may be related with the presence of more oxygen vacancies. More experiments are needed to confirm the differences in the samples activity for photooxidation reactions and better understand the influence of the $CeO_2$ support morphology for the photoreactions.

1. Si, R. & Flytzani-Stephanopoulos, M. Shape and Crystal-Plane Effects of Nanoscale Ceria on the Activity of Au-$CeO_2$ Catalysts for the Water – Gas Shift Reaction. *Angew. Chemie - Int. Ed.* **2,** 2884–2887 (2008).
2. Damato, T. C., De Oliveira, C. C. S., Ando, R. A. & Camargo, P. H. C. A facile approach to $TiO_2$ colloidal spheres decorated with Au nanoparticles displaying well-defined sizes and uniform dispersion. *Langmuir* **29,** 1642–1649 (2013).

*Acknowledgments: FAPESP, CNPq and CAPES are acknowledged for financial support.

**Área: CAT** **Inscrição: 00900**

# Chemical modification of gum arabic for dephosphorylation reactions: hydroxamate-derived biocatalyst

**Willian H. Takarada (IC),[1] José G. L. Ferreira (PG),[1] Elisa S. Orth (PQ),[1] Izabel C. Riegel-Vidotti (PQ)[1]**

**willianhideki@ufpr.com;**

*[1]Department of Chemistry, Universidade Federal do Paraná (UFPR), CP 19032, CEP 81531-980, Curitiba, PR, Brazil.*

Palavras Chave: *Gum Arabic, Detoxification, Biocatalyst, Organophosphates.*

## Highlights

A biocatalyst was developed by chemical modification of gum arabic with hydroxamic acid groups. The sample presented prominent catalytic activity in dephosphorylation reactions.

## Resumo/Abstract

Gum arabic (GA) is a complex polymer obtained from exudates of *Acacia* trees. It is a cheap product and highly employed in food and pharmaceutical industry. Moreover, GA presents considerable biocompatibility and previous studies revealed its potential in design of catalysts for detoxification reactions of organophosphates[1] (OP). Degradation of OP are of great interest but are difficult due its toxicity and stability, a reason why these compounds are employed as pesticides and chemical warfare agents. Herein, a sustainable catalyst for OP degradation was obtained by chemical modification of GA with hydroxamic acid groups (GAHDA). For that, the uronic groups on GA were functionalized with hydroxamic acid groups by 1-ethyl-3-(3-dimethylaminopropyl)carbodiimida (EDC) / *N*-hydroxysuccinimide (NHS) / hydroxylamine hydrochloride method[2], represented in Figure 1A. The samples obtained were characterized by Fourier-transform infrared spectroscopy, nuclear magnetic resonance and potentiometric titration proving the functionalization. Finally, GAHDA was evaluated as a catalyst with the model substrate diethyl 2,4-dinitrophenylphosphate (DEDNPP), resulting an increment almost $10^6$-fold compared to the spontaneous reaction. The results so far indicate an increasing in dephosphorylation reaction, as shown in Figure 1B, due to hydroxamic acid groups in GAHDA and the increment is between the highest reported in the literature. Thus, the catalyst allows several applications, such as chemical detoxification of OP and the development of sensors for these compounds.

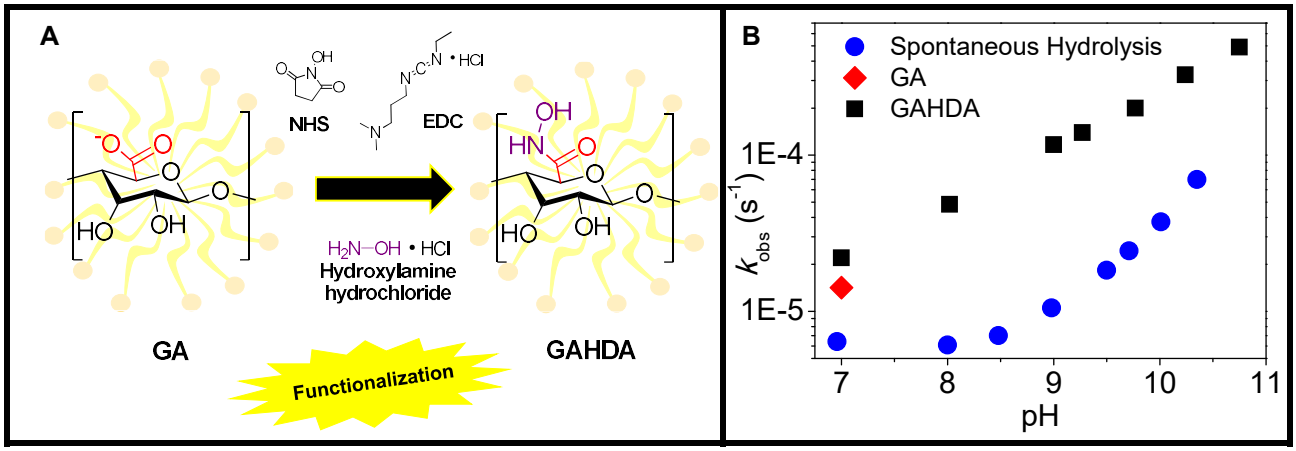


Figure 1. (A) Functionalization of GA with hydroxamic acid groups; (B) pH rate profile at 21ºC with DEDNPP

[1] J. G. Ferreira *et al.*, *Chemical Communications* **2015**, *51*, 6210-6213.
[2] R. K. Shervedani and M. Bagherzadeh, *Electrochimica Acta* **2008**, *53*, 6293-6303.

Authors acknowledge the Financial support from UFPR, CNPq, CAPES, FINEP, Fundação Araucária, LabRMN-DQUI and L'Oréal-UNESCO-ABC.

**Área: CAT** **Inscrição: 00921**

# Ethanol Steam Reforming Catalyzed by Supported Rh Nanoparticles: Investigating the Effect of the Nature of the Oxides Supports

**Thenner S. Rodrigues (PQ)[1]*, Felipe Anchieta e Silva (IC)[1], Eduardo G. Candido (IC)[1], Vanderlei S. Bergamaschi (PQ)[1], Marcelo Linardi (PQ)[1], Fabio Coral Fonseca (PQ)[1]**

**thenner07@yahoo.com.br***

[1]*Instituto de Pesquisas Energéticas e Nucleares, IPEN-CNEN, São Paulo/SP, 05508-000, Brazil*

Keywords: *Ethanol steam reforming, Effect of the support, Rhodium nanoparticles.*

## Highlights

Rh nanoparticles supported onto the surface of different commercial oxides.
Catalytic activities strongly affected by the nature of the oxide supports.
Production of hydrogen by ethanol steam reforming.

## Abstract

Rhodium, even presenting a great potential for many applications, remains little explored due to its very complicated stabilization in nanometric scale. However, its incorporation onto solid supports have shown as a promising alternative to overcome this limitation. We propose herein, the synthesis of Rh nanoparticles supported onto the surface of different commercial oxides ($SiO_2$, ZnO, $CeO_2$ and $Al_2O_3$) as catalyst with outstanding performances towards ethanol steam reforming aiming to systematically investigate the role played by the nature of the support towards the catalytic performances. The catalysts were obtained by a urea-assisted deposition method without any additional stabilizing or capping agent. Here, no modifications in the oxides structures and properties were observed after Rh incorporation, indicating the robustness of this strategy. The catalytic experiments (Figure 1), performed at 550 ºC and $H_2O$/EtOH molar ratio = 3, showed an strong dependence between activity, selectivity, and stability and the nature of the oxide support probably due the differences in the intrinsic properties of each metal oxide such as the magnitude of the metal-support interactions and specific surface areas. Here, the best results in terms of ethanol conversion and selectivity for hydrogen production were observed with Rh/$CeO_2$ catalyst, in agreement with their superior capability of oxygen storage and mobility at its surface, which is very attractive for applications towards gas-phase catalytic transformations with carbon-based compounds.

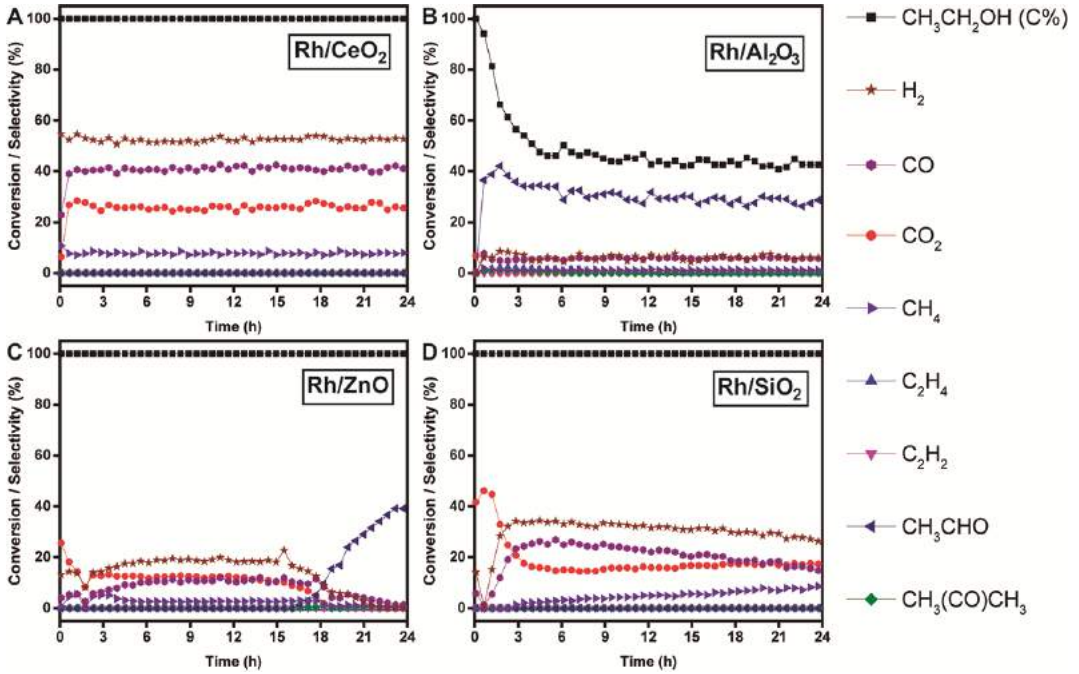


**Fig 1.** Catalytic performances of Rh supported catalysts towards ethanol steam reforming.

**Área: CAT** **Inscrição:00989**

# Synthesis of mixed oxide supported Niobium catalysts and their applications in reactions with primary amine

**Álisson S. Granato (PG),[1,2*] Gustavo Senra G. de Carvalho (PQ),[2] Giovanni W. Amarante (PQ)[2]**

**alissongranato@gmail.com**

*[1]Departamento de Farmácia, UFJF; [2]Departamento de Química, UFJF.*

Palavras Chave: *(heterogeneous catalysis, mixed oxides, niobium, amine oxidation, organic synthesis)*

## Highlights

Synthesis of supported niobium heterogeneous catalysts. Reactions with primary amine in the presence of hydrogen peroxide as oxidizing agent. Preparation of benzaldoxime and benzylhydroxylamine.

## Resumo/Abstract

A series of Niobium catalysts supported in mixed oxide, derived from Al/Zn/Mg in different proportions, were synthesized and characterized through IR, Raman, SSNMR and X-Ray crystallography and their catalytic activities for the oxidation of benzylamine were evaluated. The reactions were performed in the presence of $H_2O_2$, ranging from 2 to 8 equivalents, and 10% weight of catalyst in a chamber irradiated with violet light and at room temperature. The ratio of products was measured by $^1H$ and $^{13}C$ NMR spectra of the crude reaction mixture. The results indicated conversion rates up to 77%, leading to benzaldoxime with selectivity up to 74%.

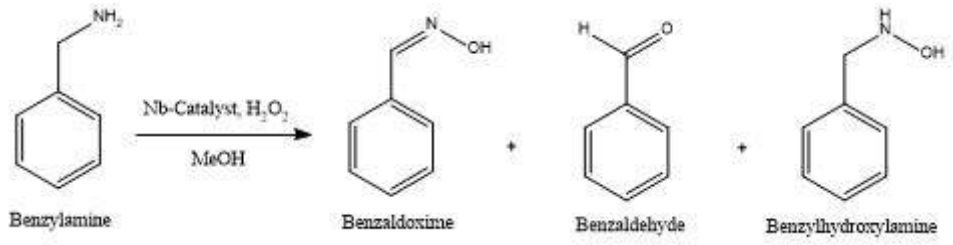


Fig. 01 - Products obtained by the reaction of benzylamine with Nb catalyst in the of presence hydrogen peroxide.

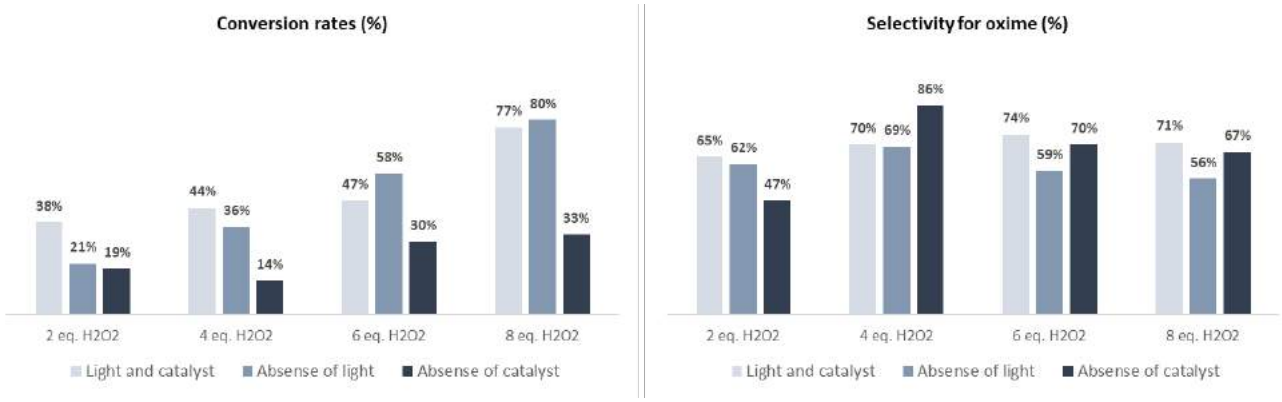


Fig. 02. - Conversion rates for the reaction of benzylamine in presence of catalyst increases with higher equivalents of $H_2O_2$. In absence of catalyst the conversion rates drop to levels similar to the reaction background. In absence of light a slightly decrease in selectivity for oxime was observed.

Acknowledgments: CAPES, CNPq, FAPEMIG and UFJF for financial support.

**Área: CAT** **Inscrição: 01000**

# Pushing the boundaries of gold catalysis

**Liane M. Rossi (PQ),[1]* Jhonatan L. Fiorio (PG),[1] Renato V. Gonçalves (PQ),[2] Erico Teixeira-Neto (PQ),[3] Nuria Lopez (PQ)[4]**

**lrossi@iq.usp.br**

*[1]Instituto de Química, USP; [2]Instituto de Física de São Carlos, USP; [3]LNNano, CNPEM; [4]ICIQ, The Barcelona Institute of Science and Technology.*

Keywords: *gold, nanoparticles, catalysis, hydrogenation, N-doped carbon.*

## Highlights

Au@N-doped carbon/$TiO_2$: a full-heterogeneous catalyst for selective hydrogenation of numerous structurally diverse alkynes and other compounds with reducible functional groups.

## Resumo/Abstract

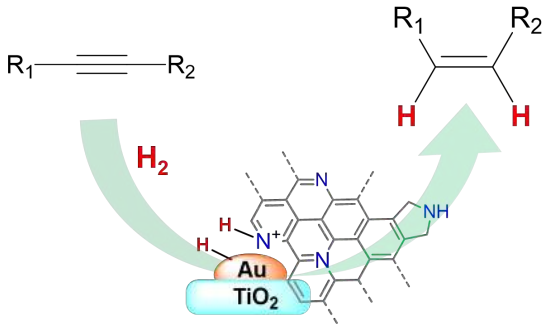


Gold has received much more attention as catalyst for selective oxidations than as a hydrogenation catalyst, mainly due to its limited capability to dissociate $H_2$. We have recently found a way to activate gold based on the adsorption of nitrogen-containing bases on gold surfaces [1]. The activation of $H_2$ was proposed to occur at the metal-ligand interface forming a tight ion pair induced by a frustrated Lewis pair (FLP) like structure, which was able to promote the heterolytic activation of $H_2$ and the H-transfer to alkynes. Here we present a new Au catalyst supported on N-doped carbon that exhibited excellent activity and selectivity for hydrogenations. The intriguing structure of the novel gold heterogeneous catalyst, which could be also understood as frustrated Lewis pairs (FLP) interface, enables the heterolytic activation of molecular hydrogen, boosting gold catalytic activity while avoiding addition of external ligands. The catalyst demonstrated ~100% conversion and >99% selectivity (95% isolated yield) for the benchmark hydrogenation of phenylacetylene **1a**. Notably, a gold catalyst prepared without addition of any ligand (Au/$TiO_2$) showed only 4% conversion of **1a**. Highly selective hydrogenation of numerous structurally diverse alkynes, epoxydes, nitro and aldehydes proceeded in moderate to excellent yield under mild conditions.

[1] J. L. Fiorio, N. López, L. M. Rossi, *ACS Catal.* **2017**, 7, 2973–2980.
Acknowledgements: This work was supported by FAPESP, CAPES and CNPq.

**Área: CAT** **Inscrição:01016**

# Ir-Fe bimetallic catalysts for glycerol hydrogenolysis

**Aracelis J. Pamphile-Adrian (PQ),[1]* Pedro Pablo Florez-Rodriguez (PQ),[1] Fabio Barboza Passos (PQ),[2]**

**aracelis.adrian@iqb.ufal.br**

*[1]Instituto de Química e Biotecnologia, Universidade Federal de Alagoas; [2]Departamento de Engenharia Química, Universidade Federal Fluminense*

Keywords: *Glycerol hydrogenolysis, Bimetallic catalysts, Iridium, Iron.*

## Highlights

Addition of Fe to Ir/γ-$Al_2O_3$ catalyst led to an increase in glycerol conversion.
Calcination process of bimetallic Ir-Fe catalysts was determinant for the activity and selectivity to 1,2-propanediol.

## Abstract

The effect of the addition of Fe to an Ir/γ-$Al_2O_3$ catalyst in different Fe/Ir molar ratios (0.5; 1.0 e 2.0) on the conversion and selectivity of the glycerol hydrogenolysis reaction was investigated. Additionally, the effect of the calcination of the catalysts was evaluated. The catalysts were prepared by incipient wetness impregnation of the Ir and Fe salts on the support and were characterized by textural analysis, DRX, TPR and XPS techniques.
The interaction between Ir and Fe was evidenced in the characterization of the catalysts. The addition of Fe to the Ir catalyst produced an increase in the activity, Table 1, however, this effect was observed only for non-calcined catalysts series. Fe monometallic catalysts presented a very low activity (0.1% of conversion). Calcined catalysts series did not present significant increase in glycerol conversion and selectivity to 1,2-PDO. The calcination process of the bimetallic catalysts may have led to the sintering of metals, leading to conversions and low reaction rates in comparison to the non-calcined bimetallic catalysts.
For non-calcined bimetallic catalysts, the conversion increased from 7 to 21.5% for $IrFe_2$/γ-$Al_2O_3$ and selectivity to 1,2-PDO remained high (90,1%). Contrary to what was observed with the Ir-Ni bimetallic catalysts in previous work [1], the reaction course could have been determined by structural effects rather than synergistic effects.

**Tabela 1.** Glycerol conversion and products selectivity in glycerol hydrogenolysis reaction on mono and bimetallic catalysts.

| | | | Selectivity (%) | | | |
|---|---|---|---|---|---|---|
| Catalyst* | Conversion (%) | $(-r_A)_0$ $(mol/s \cdot g_{cat})*10^{-7}$ | 1,2-PDO | 1,3-PDO | PrOH | Others |
| Fe_C | 0,1 | 0,1 | 0,0 | 0,0 | 72,8 | 27,2 |
| Ir_C | 5,9 | 2,2 | 89,9 | 1,3 | 5,4 | 3,5 |
| Ir | 6,6 | 1,2 | 39,9 | 6,5 | 48,5 | 5,2 |
| $IrFe_2$_C | 9,7 | 1,8 | 92,6 | 0,2 | 4,6 | 2,6 |
| $IrFe_2$ | 21,5 | 4,2 | 90,1 | 0,5 | 6,0 | 3,3 |
| $IrFe_{1,0}$_C | 6,7 | 1,2 | 87,8 | 0,2 | 5,9 | 5,7 |
| $IrFe_{1,0}$ | 15,0 | 2,9 | 83,9 | 1,5 | 11,8 | 2,7 |
| $IrFe_{0,5}$_C | 8,0 | 1,4 | 85,5 | 0,3 | 9,5 | 4,3 |
| $IrFe_{0,5}$ | 11,1 | 2,1 | 68,8 | 3,7 | 23,1 | 4,4 |

*Calcined catalysts are denoted as $IrFe_x$_C. Reaction conditions: 20 wt% glycerol solution; P=360 psi; T=200 °C; Ir/Gli=0,0014; $t_r$= 12 h; 500 RPM. 1,2-PDO=1,2-porpanediol; 1,3-PDO=1,2-propanediol; PrOH=Propanol. Others: Ethanol, Methanol, Acetone, Acetol.

[1] Pamphile-Adrián, A. J., et al. *Catalysis Today* 289, 302, 2017

**Área: CAT** **Inscrição: 01026**

# Novel fragrant aldehydes via hydroformylation of the bio renewable valencene

**Gabriel M. Vieira (PG),[1] Rodrigo S. de Paulo (IC),[1] Eduardo N. dos Santos (PQ),[1] Elena V. Gusevskaya (PQ).[1]**

**gabrielmatosvieira@yahoo.com.br; gabrielmatosvieira@yahoo.com.br**

*[1]Departamento de Química-ICEx, UFMG*

Keywords: *Hydroformylation*, *Rhodium Catalyst, Aldehyde, Terpene, Valencene*

## Highlights

Valencene, a bio renewable sesquiterpene, was hydroformylated to form new aldehydes. The choice of ligands and the reaction conditions allows obtaining selectively mono or dialdehydes.

## Resumo/Abstract

Terpenes are bio renewable feedstock especially useful for the fragrance industry[1]. Valencene (**1**) is a sesquiterpene extracted from valencia orange peel and it is an important precursor of fragrant compounds[2]. Although there are various studies in the functionalization of valencene via oxidation[3], to the best of our knowledge, its hydroformylation has never been reported.

In this work, the hydroformylation of **1** was studied using a rhodium(I) catalyst modified by phosphorus(III) ligands. The exocyclic double bond is readily hydroformylated to yield **2**, under mild condition. Under harsher conditions, the endocyclic double bond also reacts to produce **3**. However, under these conditions, the aldehyde group is partially reduced to alcohols (**4**).

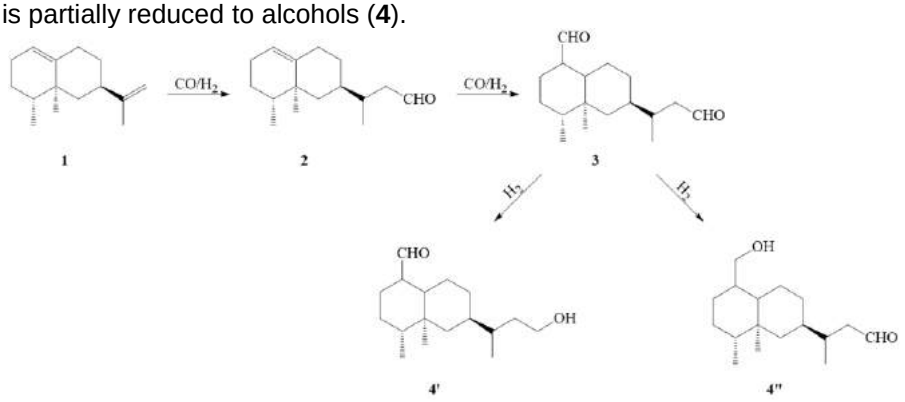


Figure 1 – Hydroformylation of valencene

With triphenylphosphine ($PPh_3$) as a promoter, **2** can be obtained selectively. Employing tris(2,4-di-tert-butylphenyl)phosphite (TBDP) instead, the catalyst activity increases. Nevertheless, with the latter ligand at higher temperatures, the formation of **4** is significant. The aldehydes obtained in this work, which have never been described in literature, have a great potential of being used as fragrances.

1. Sell, C. *The Chemistry of Fragrances: From Perfumer to Consumer*. Royal Society of Chemistry, **2006**.
2. Abreu, I. et al. *Journal of Food Science,* **2017**, *82*, 2805-2815.
3. Kolwek, J. et al. *Journal of Industrial Microbiology & Biotechnology*, **2017**, *45*, 89-101

**Área: ___CAT_____** *(Inserir a sigla da seção científica para qual o resumo será submetido. Ex: ORG, BEA, CAT)*

**Inscrição:_01094 _____** *(Inserir o número de inscrição do autor que fez a submissão)*

# Hydrodeoxygenation (HDO) of lignin-derived model compounds at low temperature using perovskites

**Manish Shetty (PG),[1] Daniela Zanchet (PQ),[1,2*] William H. Green (PQ),[1] Yuriy Roman-Leshkov (PQ).[1*]**

**daniela@iqm.unicamp.br; yroman@mit.edu**

*[1]Department of Chemical Engineering, MIT, USA; [2] Chemistry Institute, UNICAMP, Brazil.*

Keywords: Catalysis, Hydrodeoxygenation, Biomass, Perovskite, HDO.

## Highlights

Lignin-derived oxygenates were hydrodeoxygenated in vapor phase using $La_{0.8}Sr_{0.2}CoO_3$ catalyst. Selectivity toward C-O and C-C bond cleavage was tuned and correlated to the role played by metallic Co.

## Resumo/Abstract

Hydrodeoxygenation (HDO) is a common upgrading strategy for the production of renewable transportation fuels and chemicals from lignocellulosic biomass by using $H_2$ to selectively cleavage C-O bonds from the recalcitrant oxygenates found in bio-oil. Here, the perovskite lanthanum strontium cobaltite ($La_{0.8}Sr_{0.2}CoO_3$) was, for the first time, used as catalyst for vapor-phase conversion of lignin-derived oxygenates, anisole and guaiacol, being effective at low temperature (473-623 K) and hydrogen pressures ($P_{H2}$≤ 2 bar). In particular, selectivity toward C-O and C-C could be tuned: while C-O bond cleavage was achieved at lower temperatures and higher $P_{H2}$, higher temperature and lower $P_{H2}$ increased the selectivity toward C-C bond hydrogenolysis (Figure 1a,b). The complete set of results suggest that the hydrogenation/dehydrogenation mechanism plays an important role on perovskites, favoring the C-C bond hydrogenolysis pathway. In particular, the low selectivity towards hydrogenation products, i.e, cyclo-hexane from benzene and methoxycyclohexane from anisol, indicates that once they are formed they fast go to sequential hydrogenolysis. Characterization by X ray diffraction (XRD) and X ray photoelectron spectroscopy (XPS) (Figure 1c) showed that the appearance of metallic Co phase matches the change in selectivity. Comparison with the undoped perovskite, $LaCoO_3$ , and cobalt oxides, showed: 1) the crucial role played by oxygen vacancies and $Co^{2+}$in tuning the selectivity toward the HDO reaction, and 2) the importance of the peroviskte structure to stabilize the $Co^{2+}$ phase at higher temperatures and $P_{H2}$. This work was supported by BP. DZ acknowledges funding by FAPESP and CNPq.

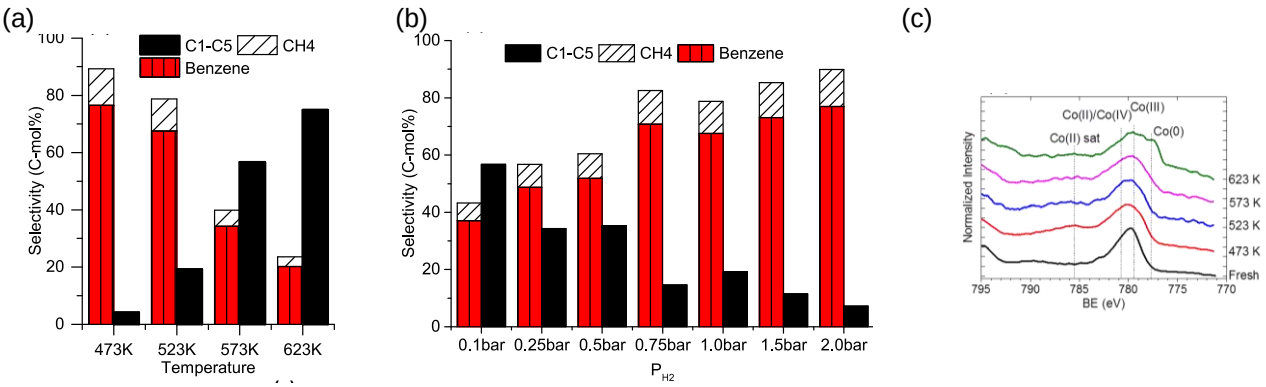


Figure 1. Conversion of anisole as a function of (a) temperature and (b) $P_{H2}$. (c) XPS spectra of post-reaction catalysts, reaction performed in the 473-623 K range. Reaction conditions: $P_{Anisole}$ = 0.0098 bar at all conditions. $P_{Total}$ = 1.013 bar at $PH_2$ ≤ 1 bar, else $P_{Total}$ ≈ $P_{H2}$. Nitrogen was used as a balance gas when $P_{H2}$ < 1.0 bar in (b).

**Área: CAT** **Inscrição: 01127**

# Use of Carboxyl Cellulose Metal Complexes in Heterogeneous Catalytic Systems to Promote Suzuki-Miyaura Coupling

**Guilherme B.C. Martins (PG),[1] Marcelo R. dos Santos (PG),[1] Marcus V.R. Rodrigues (IC),[1] Renata R. Sucupira (IC),[1] Luisa Meneghetti (IC),[1] Adriano L. Monteiro (PQ),[2] Paulo A. Z. Suarez (PQ).[1]***

**guilherme.martins@docente.unip.br; psuarez@unb.br**

*[1]INCT-CATÁLISE, Laboratório de Materiais e Combustíveis, Instituto de Química, Universidade de Brasília (IQ-UnB), Campus Universitário Darcy Ribeiro; [2]INCT-CATÁLISE, Laboratório de Catálise Molecular, Instituto de Química, Universidade Federal do Rio Grande do Sul (IQ-UFRGS).*

Palavras Chave: *Cellulose modification, TEMPO oxidation, Metal ligand, Coupling reactions, Carboxyl cellulose*

## Highlights

- Cellulose was modified by oxidation to generate carboxylate groups in its structure and was used as support for metals in coupling reactions
- Metals such as $Ni^{2+}$ and $Pd^{2+}$ using carboxylate cellulose as support had improved performances in Suzuki coupling reactions.
- Metal-Carboxylate cellulose reduce the occur of homocoupling when compared to the respective metal acetates as catalyst.
- Reactions had improved yields in presence of polar solvents such as water.

## Resumo/Abstract

Coupling reactions are one of the exponent of chemistry in the last years, which has contributed with several pharmaceuticals inputs. The mechanism and catalyst of Suzuki-Miyaura is well described in the literature. It is very important to study other variables in the reactions, and so to adequate it to the concepts of green and sustainable chemistry. This work shows the modification of microcrystalline cellulose by the selective oxidation of primary hydroxyl groups to carboxylate groups by a 2,2,6,6-tetramethylpiperidine-1-oxyl radical (TEMPO)-mediated system[1] and its application as a heterogeneous ligand by ionic exchange with catalytic metals ions such as palladium and nickel. Afterwards is described the application of the synthesized material as catalyst in Suzuki-Miyaura coupling reactions in different conditions. The carboxyl cellulose matrix shows to have superior catalytic results as a ligand for all coupling reactions as can be seen on Table 1. Can be also highlighted the affinity of the carboxyl cellulose ligand in polar solvents such as water and alcohols and its application in mild conditions, which shows the role of the cellulosic structure in such systems. The efficient and environmentally friendly methodology that was used contributes to the advancement of sustainable chemistry adding value to cellulose and indicating the role of macromolecules in coupling catalytic systems.

Table 1. Values of variation parameters in Suzuki coupling reactions

| Entry | Metal | Solvent | Temp. (°C) | Yield (%) | HC yield (%) |
|---|---|---|---|---|---|
| **1[a]** | Pd | DMF | 80 | 20 | <1 |
| **2[a]** | Pd | MeOH | 80 | 94 | <1 |
| **3[b]** | Ni | dioxane | 130 | 5 | <1 |
| **4[b]** | Ni | toluene | 130 | 40 | 5 |

[a] Reaction conditions: 0.5 mmol of bromobenzene, 0.7 mmol of 4-methoxyphenylboronic acid, 1.5 mmol of $K_2CO_3$, 0.5% of catalyst, 3 mL of solvent, 1 h of reaction under argon atmosphere; [b] reaction conditions: 1.0 mmol of 4-bromoanisole, 1.2 mmol of phenylboronic acid, 2.0 mmol of $K_2CO_3$, 1.0% of catalyst, 4.0 mol% of triphenylphosfine, 3 mL of solvent, at 130 °C, 24 h of reaction under argon atmosphere.

[1]Saito, T.; Kimura, S.; Nishiyama, Y.; Isogai, A.; Biomacromolecules 2007, 8, 2485.

**Área: CAT** **Inscrição: 01209**

# Synthesis of ethanol from the reduction of carbon dioxide under supercritical conditions

**Jennifer Dayana Rozendo (PG)[1], Maitê Lippel Gothe (PG) [1], Reinaldo C. Bazito (PQ) [1], Liane M. Rossi[1] (PQ), Pedro Vidinha (PQ) [1]**

**jennifer@iq.usp.br; pvidinha@iq.usp.br**

[1] *Instituto de Química USP - Av. Prof. Lineu Prestes, 748 - Vila Universitária, São Paulo - SP, 05508-000*

Palavras Chave:*($CO_2$, hydrogenation, reductive transformation, ethanol).*

## Highlights

- Homogenous catalysis in supercritical dioxide carbon reduction; using Iridium complexes;
- Synthesis of alcohols and acids from $CO_2$ hydrogenation;
- Formation of ethanol and formic acid at low temperature (313 K);
- Water effect over ethanol production.

## Abstract

The control of greenhouse gases emissions is one of mankind greatest challenges. Among the gases that cause greenhouse effect, $CO_2$ stands out. The use of fossil fuels is the main source of $CO_2$ production[1] and several strategies to consume $CO_2$ in the atmosphere are being studied. Among those strategies, the transformation of $CO_2$ into valuable products such as ethanol and acetic acid is one of the most important strategies to (re)use $CO_2$ [2]. The reduction of $CO_2$ to ethanol and/ or carboxylic acids is generally carried out at high pressure and temperature which the makes energetic balance unfavorable. Thus, different catalytic strategies must be developed in order to address this issue. The aim of present work is to develop a catalytic strategy that enables the reduction of $CO_2$ at mild temperatures. To accomplish this different Ir based catalysts were used to reduce $CO_2$ under supercritical conditions (250 bar, 313K) (Figure 1.a and 1.b). The obtained results show that the formation of ethanol can be correlated with % $H_2O$ (Figure 1.c.). Moreover, the type of catalyst produced an interesting effect on reaction selectivity. These preliminary results point to the fact that the water might play and important role on reaction mechanism. However, the $CO_2$ reduction mechanism is not fully understood. Therefore, these results also open an interesting starting point for elucidation of what reaction routes might take place.

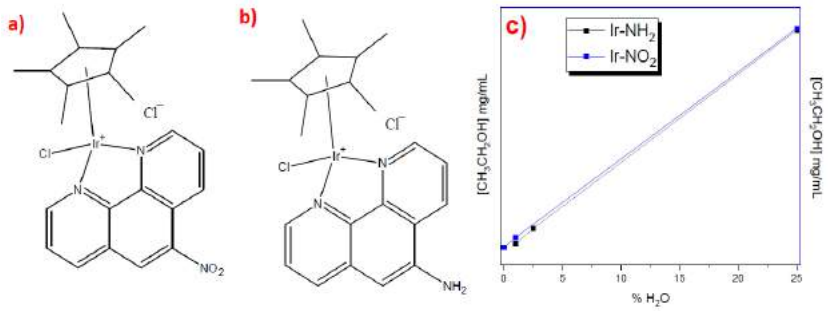


**Figure 1:** Ir-$NO_2$ a) and Ir-$NH_2$ catalysts b) used in the reduction of $CO_2$ to ethanol and c) the variation of ethanol concentration (mg / mL) versus% $H_2O$.

## References

[1] Z. He *et al.* Synthesis of higher alcohols from CO $_2$ hydrogenation over a PtRu/$Fe_2O$ $_3$ catalyst under supercritical condition. *Philos. Trans. R. Soc. A Math. Phys. Eng. Sci.*, vol. 373, no. 2057, p. 20150006, 2015.

[2] S. Wang, E. T. Schrunk, H. Mahajan, and and R. J. Farrauto. The Role of Ruthenium in $CO_2$ Capture and Catalytic Conversion to Fuel by Dual Function Materials (DFM). *Catalysts*, vol. 7, no. 3, p. 88, 2017.

**Área: CAT** **Inscrição: 01221**

# Propylsulfonic acid anchored on mesoporous SBA-15 as heterogeneous catalyst for esterification of fatty acids.

**Anderson F.S. Moreira (PG),[1] Thamires Collares de Brito (IC),[1] João Sebastião C. Vieira (PQ),[2] Cláudio J.A. Mota (PQ),[1,3*] Elizabeth R. Lachter (PQ).[1*]**

**lachter@iq.ufrj.br; afsm.ufrj@hotmail.com**

*[1]Instituto de Química, UFRJ;[2] Instituto Federal do Maranhão; [3]Escola de Química, UFRJ*

Palavras Chave: Esterification; Heterogeneous Catalysis; Pr-$SO_3H$-SBA-15; Fatty acids

## Highlights

This work aimed to use heterogeneous catalysis to convert fatty acids and free fatty acids present in vegetable oils into esters.
By using Pr-$SO_3H$-SBA-15 was possible to obtain conversion superior to 90% in the esterification reactions.

## Resumo/Abstract

In the esterification process for biodiesel production it's possible used a not refined raw material as vegetable oil with high amount of free fatty acids or fatty acids from refined vegetable oil [1, 2]. Propylsulfonic acid functionalized mesostructured silica (Pr-$SO_3H$-SBA-15) have been reported in the literature as acid catalyst for esterification of fatty acids [3]. The present work aimed to evaluate the catalytic activity of Pr-$SO_3H$-SBA-15 in the esterification of fatty acids with methanol present in vegetable oil (babaçu and pequi) and in the fatty acids residue of the soybean oil and babaçu refining industry. This catalyst was produced by the co-condensation method and characterized by textural properties, FTIR, CP/MAS NMR and thermal analysis. The vegetable oils babaçu and pequi were characterized in terms of acid value and were found about 2.36 and 2.32 mg KOH. g $oil^{-1}$, respectively. Some reaction variables such as: oil:methanol ratio, temperature, time and the amount of catalyst were evaluated. By using babaçu oil and pequi oil in an oil:methanol ratio of 1:8, 110ºC, 5,0% of catalyst for 120 minutes of reaction was achieved conversion of 94% and 86% into esters, respectively. In the esterification reaction of fatty acids residue of the soybean and babaçu oil were used oil:methanol ratio of 1:10, 120ºC, 15,0% of catalyst and 90 minutes of reaction and was achieved conversion up to 96%.This catalyst is effective for fatty acids esterification and can be reused without significant loss of the activity.

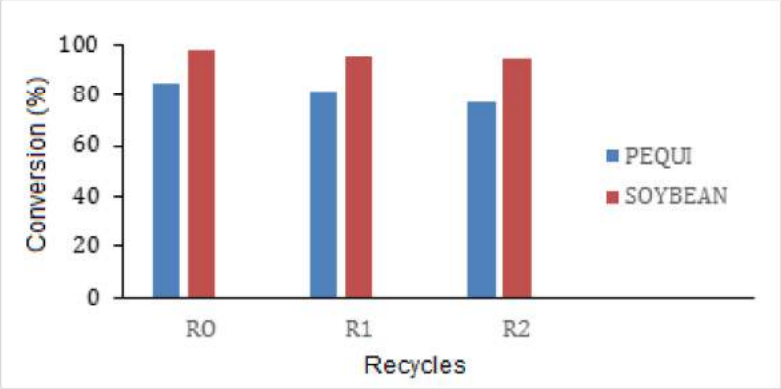


Figure 1. Reuse of the Pr-$SO_3H$-SBA-15 in the esterification of Pequi oil and Fatty acids from soybean oil. R0 = first reaction, R1 = first recycle, R2 = second recycle.

1. E. Lotero, Y. Liu, D.E. Lopez, K. Suwannakarn, D.A. Bruce, J.G. Goodwin J., Synthesis of biodiesel via acid catalysis, Ind. Eng. Chem. 44 (2005) 5353-5363.
2. V. M. Aguiar, A. L. F. Souza, F. S. Galdino, M. M. C. Silva, V. G.Teixeira, E. R. Lachter, Renewable Energy 114 (2017) 725-732.
3. J. A Melero, L. F. Bautista, J. Iglesias, G. Morales, R. Sánchez-Vázquez, K. Wilson, A. F Lee, Applied Catal, A, 488 (2014) 111-118.

**Área: CAT** **Inscrição: 01224**

# Estudo introdutório sobre conversão catalítica de $CO_2$ a hidrocarbonetos utilizando um rejeito industrial a base de Fe como catalisador

**Letícia Mombrini Marques (IC),[1*] Jussara Lopes de Miranda (PQ),[2] Heitor Breno Pereira Ferreira (PQ),[1]**

**leticia.mombrini@gmail.com**

[1] *Instituto Federal de Educação, Ciência e Tecnologia do Rio de Janeiro; Universidade Federal do Rio de Janeiro.*

Palavras Chave: Conversão de $CO_2$, Dióxido de carbono, Hidrocarbonetos.

## Highlights

An introductive study about $CO_2$ catalytic conversion into hydrocarbons using iron industrial waste as a catalyst.
A study in development. Catalytic conversion into hydrocarbons. Iron industrial waste as a catalyst. Satisfactory results for iron industrial waste.

## Resumo

Emissões do dióxido de carbono ($CO_2$), um dos principais gases causadores do agravamento do efeito estufa, cresce a cada ano segundo o IPCC. Com isso, cresce o interesse em se desenvolver processos de captura, armazenamento oceânico e conversão do $CO_2$[1].
O objetivo principal deste trabalho é a conversão catalítica do $CO_2$ em hidrocarbonetos utilizando um rejeito industrial como catalisador.
O catalisador utilizado é um rejeito industrial a base de ferro que ainda está em período de caracterização. A reação foi realizada utilizando 0,5 gramas do catalisador, previamente calcinado e peneirado, em uma unidade PID Eng&Tech, com reator de leito fixo, acoplada a cromatógrafo a gás, Shimadzu, com TCD e FID. Inicialmente, procedeu-se à redução em atmosfera de $H_2$ a uma temperatura de 400 °C. Na sequência, passou-se uma carga de $H_2$ e $CO_2$ nas proporções: 7,5 para 22,5; 15 para 15 e 10 para 20, em uma temperatura de 320 °C e 20 bar de pressão, analisando-se os efluentes, do reator, por cromatografia em fase gasosa. Além de CO, foram identificados diversos hidrocarbonetos, dentre eles: metano, etano, propano, butano e pentano. As olefinas leves, eteno e propeno, também foram observadas, representando um ótimo resultado visto que estas são insumos para a produção de plásticos. Os próximos passos serão testar o desenvolvimento do catalisador em diferentes pressões, temperaturas e vazões.
O catalisador utilizado se apresentou ativo para a conversão de $CO_2$ a hidrocarbonetos. Demonstrando resultados bastante satisfatórios para um rejeito industrial.

## Agradecimentos

Ao CNPq pela bolsa concedida e ao Instituto Federal de Educação, Ciência e Tecnologia do Rio de Janeiro/Campus Nilópolis.

[1] WANG, W.; WANG, S.; MA, X.; GONG, J.; Recent advances in catalytic hydrogenation of carbon dioxide, **Chemical Society Review**, v.40, p.3703, 2011.

**Área: CAT** **Inscrição: 01226**

# Ruthenium(II) complexes of Schiff base derived from cycloalkylamines as pre-catalysts for ROMP and ATRP

[1]**Thais Regina Cruz (IC)***, [1]**Maria Beatriz A. Afonso (PG)**, [1]**Beatriz E. Goi (PQ)**, [1]**Valdemiro P. Carvalho-Jr (PQ)**.

**thais_cruz43@hotmail.com**

*[1]Departamento de Química e Bioquímica, Faculdade de Ciências e Tecnologia, UNESP Universidade Estadual Paulista, CEP 19060-900, Presidente Prudente, SP, Brazil*

Palavras Chave*: Schiff base, Ruthenium complexes, ROMP, ATRP; Norbornene, Methyl methacrylate.*

## Highlights

Well-defined starting type Werner amine-ruthenium complexes were active in ATRP. Cyclic amines successfully behaved as ancillary ligands. Polymers in semi-quantitative yields were obtained.

## Resumo/Abstract

Ruthenium(II) complexes of Schiff base derived from cycloalkylamines (cycloalkyl = cyclopentyl (1a), cyclohexyl (**1b**), cycloheptyl (**1c**), and cyclooctyl) (**1d**) (Fig. 1) were synthesized: [RuCl(CyPen-Salen)$(PPh_3)_2$] (**2a**), [RuCl(CyHex-Salen)$(PPh_3)_2$] (**2b**), [RuCl(CyHep-Salen)$(PPh_3)_2$] (**2c**), and [RuCl(CyOct-Salen)$(PPh_3)_2$] (**2d**) (Fig. 2).

The Schiff base-Ru(II) complexes 2a-d were characterized by FTIR, UV-Vis, 1H-, 13C- and 31P-NMR, and cyclic voltammetry. The complexes 2a-d were evaluated as catalytic precursors for ROMP of norbornene (NBE) and for ATRP of methyl methacrylate (MMA). The syntheses of polynorbornene (polyNBE) via ROMP with complexes 2a-d as pre-catalysts were evaluated under different reaction conditions ([HCl]/[Ru], [EDA]/[Ru], [NBE]/[Ru], and temperature). The highest yields of polyNBE were obtained with [NBE]/[HCl]/[Ru] = 5000/25/1 molar ratio in the presence of 5 µL of EDA for 60 minutes at 50 °C. MMA polymerization via ATRP was conducted using the complexes 2a-d in the presence of ethyl-α-bromoisobutyrate (EBiB) as initiator. The catalytic tests were evaluated as a function of the reaction time using the initial molar ratio of [MMA]/[EBiB]/[Ru] = 1000/2/1 at 85 °C. The linear correlation of $ln([MMA]_0/[MMA])$ and time clearly indicates that the concentration of radicals remains constant during the polymerization and that the ATRP of MMA mediated by 2a-d proceeds in a controlled manner. Molecular weights increased linearly with conversion, however, the experimental molecular weights were higher than the theoretical ones.

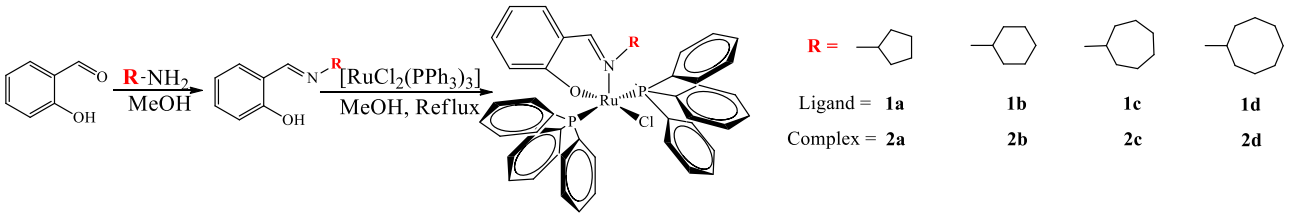


**Fig. 1:** Synthesis protocol of Schiff base 1a-d and their ruthenium complexes 2a-d.

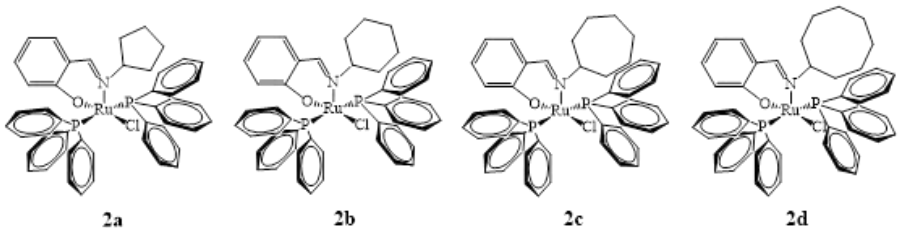


**Fig. 2:** Illustration of the Schiff base ruthenium(II) complexes (2a-d).

**Área: CAT**
*(Inserir a sigla da seção científica para qual o resumo será submetido. Ex: ORG, BEA, CAT)*

**Inscrição: 01232**
*(Inserir o número de inscrição do autor que fez a submissão)*

# Use of biomasses from *Acrocomia aculeata* in the synthesis of activated charcoal and its use in the purification of crude glycerol.

**Milton S. Freitas (PG),[1*] Sandro L. B. dos Santos (PQ),[2] Camila D. Lima (PQ),[3] Luíza P. Aguiar (IC),[4] Alessandro S. Rocha (IC),[4] Carina B. Borges (IC-Jr),[5] Vitor R. G. de Almeida (IC-Jr).[6]**

**freitas.milton@hotmail.com;**

*[1]Programa de Pós-Graduação em Ciências Farmacêuticas, UFVJM; [2]Departamento de Farmácia, UFVJM; Programa de Pós-Graduação em Biocombustíveis, UFVJM; [3] Instituo de Ciência e Tecnologia, UFVJM; [4] Departamento de Farmácia, UFVJM; [5]Colégio Tiradentes da Polícia Militar de Minas Gerais de Diamantina, CTPMMG; [6]Escola Estadual Professora Ayna Torres;*

Palavras Chave: *Purification, activated charcoal, crude glycerol, adsorption.*

## Highlights

This work uses macauba cake obtained as a residue from the extraction of vegetable oil in the production of activated charcoal for the purification of crude glycerol in order to obtain a high added value product.

## Resumo/Abstract

Activated carbon is a porous adsorbent with high surface area due to its adsorption capacity. It is applied in the removal of organic compounds from the water, as a support for catalysts, gas purification and has an affinity for a variety of organic products [1]. Lignocellulosic materials are important precursors for the production of activated carbon because of their abundance and low cost. Thus, in view of the expansion of biodiesel production by transesterification of triacylglycerides contained in vegetable oils, there is an increasing production of residual tarts and accumulation of this material. Therefore, macaúba cake (*Acrocomia aculeata*), Figure 1, was visualized as a precursor in the production of activated charcoal, Figure 2, aiming at the purification of crude glycerol obtained from the transesterification of triacylglycerides, obtaining a compound with high purity and higher added value. The process of extracting vegetable oil generates large amounts of biomass residues, which represent 500 g / kg of processed fruit. The developed medotology employs lesser amount of activated carbon compared to the data available in the literature, besides the adsorption process occurs at room temperature and without agitation. The purified glycerol, figure 3, has been used with reagent by our research group in the synthesis of ketals (potential additives for fuels and biofuels), monoacylglycerides (used in pharmaceutical and food industries) and the synthesis of polyhydroxy soaps.
The authors thank FAPEMIG and CNPq for their financial support.

**Figure 1. Macauba palm fruits.**

**Fonte: Portal macaúba.**

**Figure 2. Activated charcoal of macauba cake.**

**Figure 3. Left: crude glycerol . Right: purified glycerol.**

References

[1] S. Ismadji *et al*., Activated carbon from char obtained from vacuum pyrolysis of teak dust: structure development and characterization. Bioresource Tech. 96, 1364 (2005.)

**Área: CAT** **Inscrição: 01240**

# Microwave-assisted organic synthesis versus conventional heating. A comparative study for polyols condensation with ketones at heterogeneous catalysis $SiO_2$-$SO_3H$ under free solvent.

**Melina A. R. Almeida (IC),[1] Guilherme L.C. Lage (PG),[1] Patrícia M. Oliveira (PQ),[2] and Sandro L. Barbosa[1]**

**sandro.barbosa@ufvjm.edu.br**

*[1]Programa de Pós-graduação em Biocombustíveis, UFVJM; [2]Departamento de Química UFVJM)*

Palavras Chave: *Microwave-assisted, Conventional heating, Condensation, Heterogeneous catalysis, Free solvent.*

## Highlights

Synthesis of different ketals by polyols and ketones condensation, under conventional heating and microwave radiation, both at heterogeneous catalysis $SiO_2$-$SO_3H$. All of reactions were performed solvent-free conditions.

## Resumo/Abstract

Ketals are well-known compounds with interesting industrial and commercial applications in a number of fields, especially as surfactants and emulsifiers.[1i] In organic synthesis, ketals are useful intermediates that protect carbonyl groups of the more reactive ketones or hydroxyl groups of diols, when performing organic transformations.[2ii] This work describes the synthesis of different ketals by polyols and ketones condensation, under conventional heating and microwave radiation, both at heterogeneous catalysis $SiO_2$-$SO_3H$. All of reactions were performed solvent-free conditions. Preparation of ketals was used the corresponding polyols (ethylene glycol, neopentylglycol, trimethylolpropane and glycerol) with ketones (propanone, cyclohexanone, acetophenone, 1-*p*-tolylethanone and benzophenone). The reactions were performed under microwave heating results in ketals compounds were obtained in higher yields and shorter reaction times (2-8 min) *versus* conventional heating (2-12h). An example involves the preparation of the cyclohexanone ketal in 90% yield by conventional heating at reflux in for 2 hours, the same reaction was performed under low microwave irradiation power (360W), the temperature of the slurry did not exceed 73 $^oC$, and a 99.9% yield was obtained in only two minutes. However, these experimental conditions yielded only about 50% of the acetophenone ketal (microwave radiation), against 13% yield (12 hours reflux) at conventional heating. Interestingly, aromatics ketones they self did not give goods yields and many starting materials could be recovered.[3] The microwave-assisted heterogeneous catalysis reaction was able to reduce ketal chemical reaction times from hours to minutes; increased yields also to decrease side reactions and improve reproducibility.

The authors thank Fapemig and CNPq for financial support.

[1]CERÓN-CAMACHO, Ricardo et al. Microwave-assisted organic synthesis versus conventional heating. A comparative study for Fisher glycosidation of monosaccharides. **Comptes Rendus Chimie**, v. 16, n. 5, p. 427-432, 2013.

[2] WUTS, Peter GM; GREENE, Theodora W. **Greene's protective groups in organic synthesis**. John Wiley & Sons, 2006.

[3]BARBOSA, Sandro et.al. **Journal Brazilian Chemical Society**, 2018, accepted for publication.

**Área: CAT** **Inscrição: 01244**

# $M/SiO_2$ (M = Co or Ni) nanoparticles prepared by magnetron sputtering deposition method for $CO_2$ valorization by reverse water gas shift reaction

**Thalita S. Galhardo (PQ),[1]* Renato V. Gonçalves (PQ),[2] Liane M. Rossi (PQ).[1]**

**thalita@iq.usp.br**

*[1]Instituto de Química, USP; [2]Instituto de Física de São Carlos, USP*

Key words: *Co nanoparticles, Ni nanoparticles, magnetron sputtering deposition method, $CO_2$ valorization, reverse water gas shift.*

## Highlights

Co and Ni nanoparticles prepared by magnetron sputtering deposition (MSD) method were tested as catalysts in reverse water gas shift reaction for $CO_2$ valorization. 1.4%Ni/$SiO_2$ was the most active material, leading to 75% of $CO_2$ conversion.

## Abstract

In this work, magnetron sputtering deposition method was used to prepare very small Co and Ni nanoparticles supported on $SiO_2$ catalysts and applied to reverse water gas shift (RWGS) reaction for $CO_2$ valorization. The results obtained in the optimized reaction condition are presented in Figure 1. At this condition, Co nanoparticles reached a $CO_2$ conversion next to 60 and 50% at 800°C (for 0.4 and 0.5% of metal loading, respectively) and Ni nanoparticles reached $CO_2$ conversion near to 60 and 75% at 800°C (for 0.6 and 1.4% of metal loading, respectively). Co and Ni nanoparticles were tested in a reaction condition to study $CH_4$ formation with two consecutive cycles and it was observed that there is no $CH_4$ formation when Co nanoparticles are employed and for Ni nanoparticles $CH_4$ is formed just in the first cycle of reaction. The results suggest that Co and Ni materials prepared by magnetron sputtering deposition method are promising for $CO_2$ valorization by RWGS reaction. The authors gratefully acknowledge support of the RCGI – Research Centre for Gas Innovation, hosted by the University of São Paulo (USP) and sponsored by FAPESP – São Paulo Research Foundation (2014/50279-4) and Shell Brazil. The work was also supported by CNPq (Project 439389/2016-0 and Process 150623/2017-8).

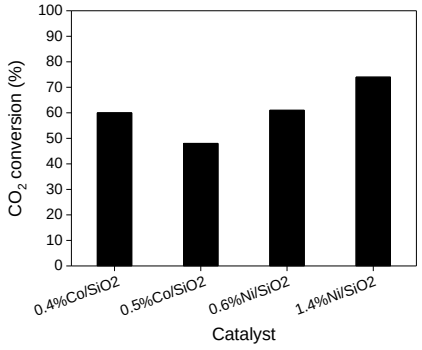


**Figure 1.** $CO_2$ conversion for Co and Ni catalysts at flow reactant mixture containing 2 vol.% $CO_2$ and 2 vol.% $H_2$ in Ar balance, at 800°C.

**Área: CAT**
*(Inserir a sigla da seção científica para qual o resumo será submetido. Ex: ORG, BEA, CAT)*

**Inscrição: 01301**
*(Inserir o número de inscrição do autor que fez a submissão)*

# Easily accessible ROMP and ATRP catalysts based on dimethyl sulfoxide ruthenium(II) complexes bearing N-heterocyclic carbene ligands

**Patrik D.S. Gois (PG),[1] André H.S. Idehara (PG),[1] Beatriz E. Goi (PQ),[1] Valdemiro P. Carvalho-Jr(PQ).[1]***

**patrikdione@gmail.com; valdemiro@fct.unesp.br**

*[1]Faculdade de Ciências e Tecnologia, UNESP Univ. Estadual Paulista, CEP 19060-900, Presidente Prudente, SP, Brazil*

Palavras Chave: *Ruthenium complexes, ROMP, ATRP, Norbornene, Methyl methacrylate.*

## Highlights

Novel DMSO ruthenium(II) complexes of NHCs derived from cycloalkylamines have been synthesized.
The complexes have been successfully employed as catalytic precursors for ROMP and ATRP reactions.

## Resumo/Abstract

Dimethyl sulfoxide ruthenium(II) complexes of N-heterocyclic carbenes derived from cycloalkylamines (cycloalkyl= cyclopentyl (**1a**), cyclohexyl (**1b**), cycloheptyl (**1c**), and cyclooctyl (**1d**)) were synthesized: $[RuCl_2(S\text{-}dmso)_2(IPent)]$ (**2a**), $[RuCl_2(S\text{-}dmso)_2(IHex)]$ (**2b**), $[RuCl_2(S\text{-}dmso)_2(IHept)]$ (**2c**), and $[RuCl_2(S\text{-}dmso)_2(IOct)]$ (**2d**). The imidazolium salts **1a**-**1d** were characterized by FTIR, UV–vis, and $^1H$ and $^{13}C$ NMR spectroscopy, while their respective dimethyl sulfoxide ruthenium(II) complexes (**2a**-**2d**) were characterized by elemental analysis, FTIR, UV–vis, $^1H$ and $^{13}C$ NMR, and cyclic voltammetry. The complexes **2a**-**2d** were evaluated as catalytic precursors for ROMP of norbornene (NBE) and for ATRP of methyl methacrylate (MMA). The polynorbornene (polyNBE) syntheses via ROMP using the complexes **2a**-**2d** as pre-catalysts were evaluated under reaction conditions of [EDA]/[Ru]=28, [NBE]/[Ru]=5000 at 50 °C as a function of time. The catalytic activity of complexes **2a**-**2d** in ROMP increased as the $CH_2$ group decrease in the cycloalkyl substituents, that means from **2d** to **2a**. Nucleophilic attack of the NBE at the Ru centre is disfavored by increasing the cycloalkyl group due to steric reasons, which explains the decrease of the yields values in the following order: **2d** < **2c** < **2b** < **2a**. MMA polymerization via ATRP was conducted using the complexes **2a**-**2d** in the presence of ethyl 2-bromoisobutyrate (EB*i*B) as the initiator. All tests were using the molar ratio [MMA]/[EB*i*B]/[Ru]=1000/2/1 and conducted at 85 °C. The linear correlation of $\ln([MMA]_0/[MMA])$ and time clearly indicates that the concentration of radicals remains constant during the polymerization and that the ATRP of MMA mediated by **2a**-**2d** proceeds in a controlled manner.

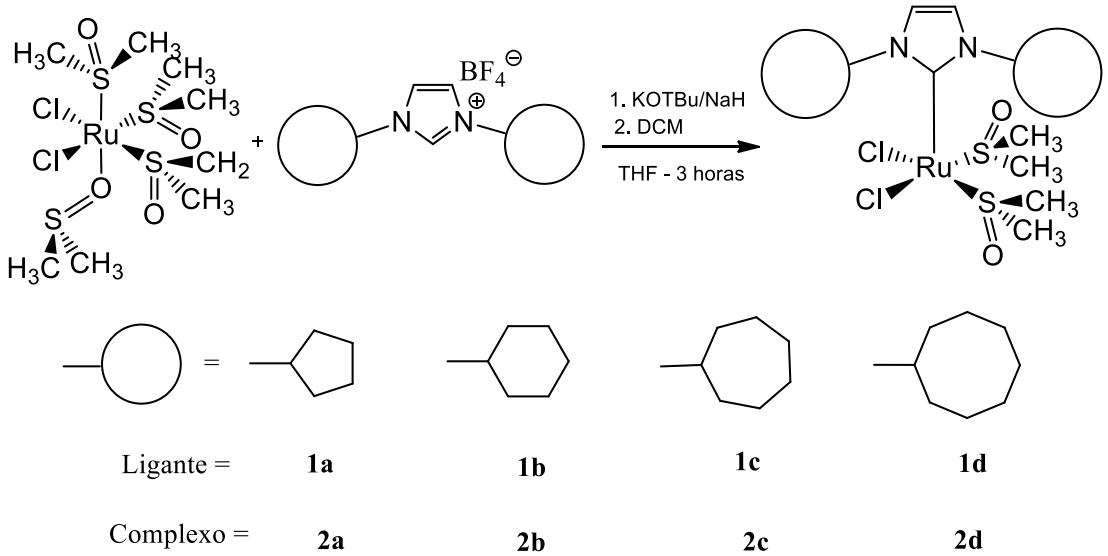

**Área: CAT** **Inscrição: 01308**

# Cobalt(II) complexes of bidentate Schiff bases derived from cycloalkylamines as mediators in controlled radical polymerization of vinyl acetate

**Yan F. Silva (PG), Valdemiro P. Carvalho-Jr (PQ) e Beatriz E. Goi (PQ)*.**

***beatriz_goi@fct.unesp.br**

*Faculdade de Ciências e Tecnologia, UNESP Universidade Estadual Paulista, CEP 19060-900, Presidente Prudente, SP, Brazil.*

Palavras Chave: *Schiff Base, Cobalt(II) Complexes, Polymerization, Vinyl Acetate CMRP*.

## Highlights

Cobalt(II) Schiff base complexes were successfully synthesized and characterized. Cobalt(II) Schiff base complexes were applied in CMRP of vinyl acetate. Schiff base as ancillary ligands can tune the reactivity of mediators in CMRP.

## Resumo/Abstract

A series of new cobalt(II) complexes of Schiff base derived from the salicylaldehyde and different cycloalkylamines (cycloalkyl = cyclopentyl-**1a**, cyclohexyl-**1b**, and cycloheptyl-**1c**) was synthesized: [Co(CyPen-Salicyl)$_2$] (**2a**), [Co(CyHex-Salicyl)$_2$] (**2b**), and [Co(CyHep-Salicyl)$_2$] (**2c**). The complexes **2a**-**2c** were used as controlling agents for the polymerization of vinyl acetate (VAc) initiated by AIBN, according to an organometallic-mediated radical polymerization (OMRP) mechanism. The VAc polymerization mediated by complexes **2a**-**2c** suggests that the level of control can be slightly tuned by the substitution of the cycloalkyl group on the Schiff base ligand. The complex **2b** showed the smaller discrepancy between observed and calculated molecular weight, and narrower molecular weight distribution.

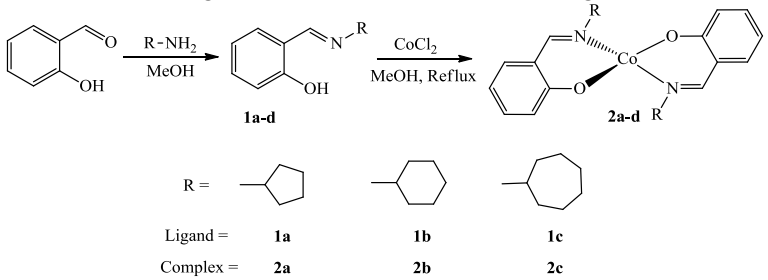


**Scheme 1.** Synthesis of ON donor Schiff bases **1a-c** and their cobalt(II) complexes **2a-c**.

The preliminary VAc polymerizations mediated by **2a**-**2c** as a function of time ([VAc]/[AIBN]/[Co] = 542/3.25/1 at 55 °C) were first order in monomer, as assessed by the linear dependence of ln([M]$_0$/[M]$_t$) versus time. The VAc polymerization mediated by **2a-2c** suggests that the level of control can be slightly tuned by the substitution of the cycloalkyl group on the Schiff base ligand. The difference in the reactivity of the complexes studied is directly related to the electronic characteristics of the Schiff base ligands, which are modulated by their substituents (cycloalkyl groups).

**Fig. 1.**

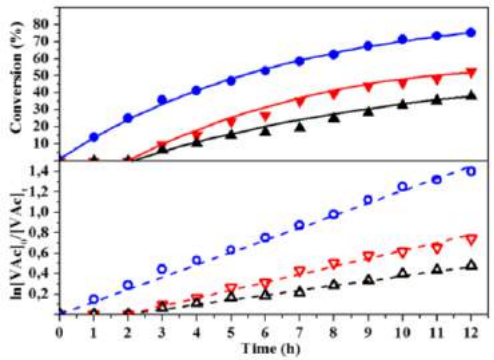


**Fig. 2.**

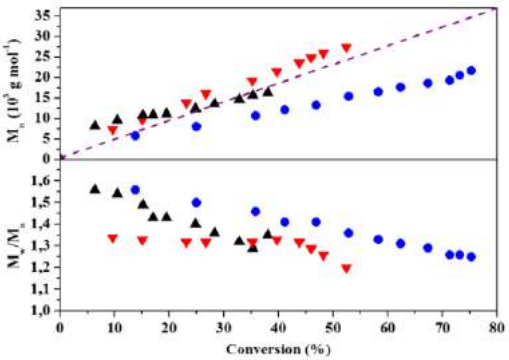


**Fig. 1.** Dependence of conversion and ln([VAc]$_0$/[VAc]) on the reaction time for CMRP of VAc with **2a** (▲), **2b** (▼) and **2c** (●); [VAc]/[AIBN]/[Co] = 542/3.25/1 with 20 µmol of complex in bulk at 55 ºC

**Fig. 2.** Dependence of $M_n$ and $M_w/M_n$ on the reaction time for CMRP of VAc with **2a** (▲), **2b** (▼) and **2c** (●); [VAc]/[AIBN]/[Co] = 542/3.25/1 with 20 µmol of complex in bulk at 55 ºC; $M_{n(theor)}$ (dash line).

**Área:** CAT **Inscrição:** 01309

# Mn(II) and Fe(II) complexes of bidentate Schiff Base as mediators for Organometallic Mediate Radical Polymerization (OMRP) of Vinyl Acetate

**Patrícia K. Hashimoto (PG),[1*] Beatriz Eleutério Goi (PQ),[2] Valdemiro P. Carvalho Jr.[3]**

**patriciakazuyo@gamil.com**

*Faculdade de Ciências e Tecnologia, UNESP Univ. Estadual Paulista, CEP 19060-900, Presidente Prudente, SP, Brazil*

Palavras Chave: *Schiff bases, Mn(II) and Fe(II) complexes, Radical polymerization,OMRP, Vynil acetate.*

## Highlights

Manganese(II) and Iron(II) complexes of Schiff base were successfully synthesized and characterized.
Manganese(II) and Iron(II) complexes of Schiff base were applied in OMRP of vinyl acetate.

## Resumo/Abstract

In the last decades, controlled radical polymerization (CRP) has become very important, since it facilitates the synthesis of macromolecules of specific architectures with excellent control over the chemical and physical properties. Here, this study describes the synthesis and characterization of a series of novel manganese(II) and iron(II) complexes of Schiff base derived from the salicylaldehyde and different cycloalkylamines (cycloalkyl = cyclopentyl-1a, cyclohexyl-1b, cycloheptyl-1c, and cyclooctyl-1d) (Scheme 1). The $Mn^{II}$ and $Fe^{II}$ complexes of Schiff base were prepared in good yields from the metallation of the corresponding ligands 1a-1d with $MnCl_2$ and $FeCl_2$, respectively, by stirring and heating under reflux. The complexes were characterized by elemental analyses, FTIR, UV-vis, electron paramagnetic resonance spectroscopy, cyclic voltammetry, and computational methods. The $Mn^{II}$ and $Fe^{II}$ complexes were applied as controlling agents for the polymerization of vinyl acetate (VAc) initiated by AIBN, according to an organometallic-mediated radical polymerization (OMRP) mechanism. The influences of the Schiff base ligand structure, focusing the steric hindrance at the manganese and iron center, were assessed by modification of the cycloalkyl substituents. Different conditions of reaction time, concentrations of VAc and AIBN as initiator were investigated. The VAc polymerization mediated by theses complexes suggests that the level of control can be slightly tuned by the substitution of the cycloalkyl group on the Schiff base ligand and the metal center.

**Scheme 1.** Synthesis of ON donor Schiff bases **1a-1d** and their manganese(II) and iron(II) complexes..

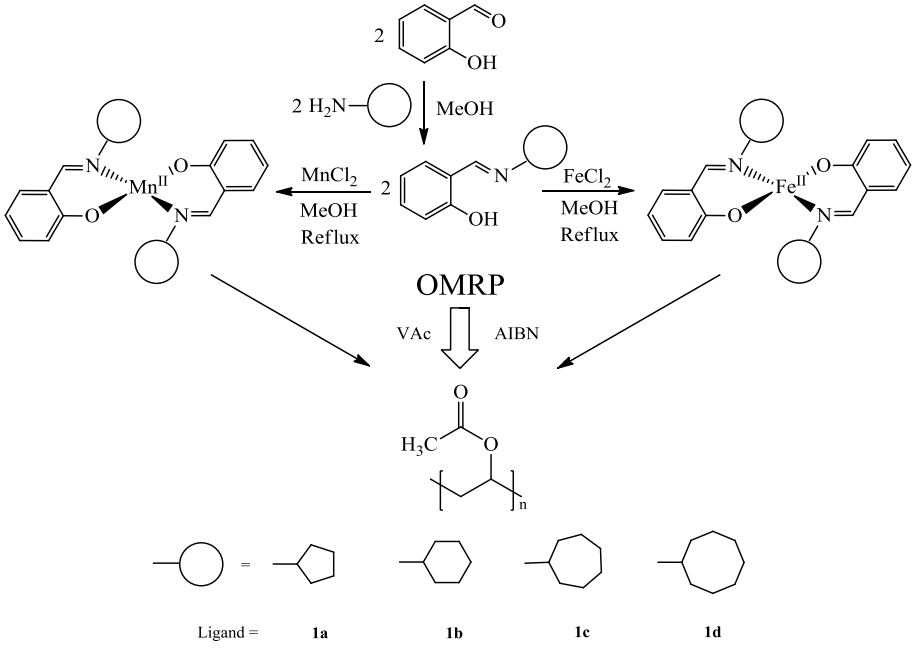

**Área: CAT** **Inscrição:** 01318

# Reaction of alkaline metals $Li^+$, $Na^+$ and $K^+$ with serpentinite to form different solid basic catalysts

**Gilvan M. Paz (PG)[1,2]*, Sara S. Vieira (PG)[1], Alexandre C. Bertoli (PG)[1], Fabiane C. Ballotin (PG)[1], Edmilson M. de Moura (PQ)[3], Ana Paula C. Teixeira (PQ)[2], Ottávio Carmignano (PG)[4], Rita C. O. Sebastião (PQ)[2], Rochel M. Lago (PQ)[2]**

**gilvan@ifpi.edu.br**

*[1]Departamento de Química, UFMG; [2] Departamento de Ensino, IFPI; [3]Departamento de Química, UFPI; [4]Doutorado Inovação, UFMG*

Palavras Chave:*(serpentinite, impregnation, metals alcalines íons, new phases, synthesis).*

## Highlights

Serpentinite $Mg_3Si_2O_5(OH)_4$ reacts with $Li^+$, $Na^+$ and $K^+$ to form new magnesium silicates hydrated phases. These phases $Li_4SiO_4$, $Na_2Mg_2Si_2O_7$ and $K_2MgSiO_4$ show great potential as basic catalysts

## Abstract

Serpentinite minerals (composed of antigorite, chrysotile and lizardite) has proved to be a versatile material for different applications. They have a molecular formula $Mg_3Si_2O_5(OH)_4$ and its structure consists of octahedral ($MgO_6$) sheets rich in magnesium bound to silicon-rich tetrahedral sheets ($SiO_4$), in a ratio of 1: 1. The layers have spacings of about 0.72 nm, which allows impregnation/intercalation with different ions to obtain new phases. In this work, serpentinite was impregnated with lithium, sodium and potassium ions (20%) and thermally treated in air at 700 ° C for the synthesis of potential heterogeneous basic catalysts. X-ray diffraction (XRD), IR, Raman, SEM, TG, BET results showed, the impregnation of serpentinite with the different alkali metal ions has led to the formation of new phases. $Li_4SiO_4$ and MgO, with lithium ions, $Na_2Mg_2Si_2O_7$ and MgO with sodium ions and $K_2MgSiO_4$ with potassium ion. The different phases, Figure 1, formed from the impregnation of the serpentinite with alkali metal ions showed very promising results as catalysts for the transesterification to produce biodiesel. These structures open the possibility to obtain new materials, with possible applications of technological and / or environmental interest.

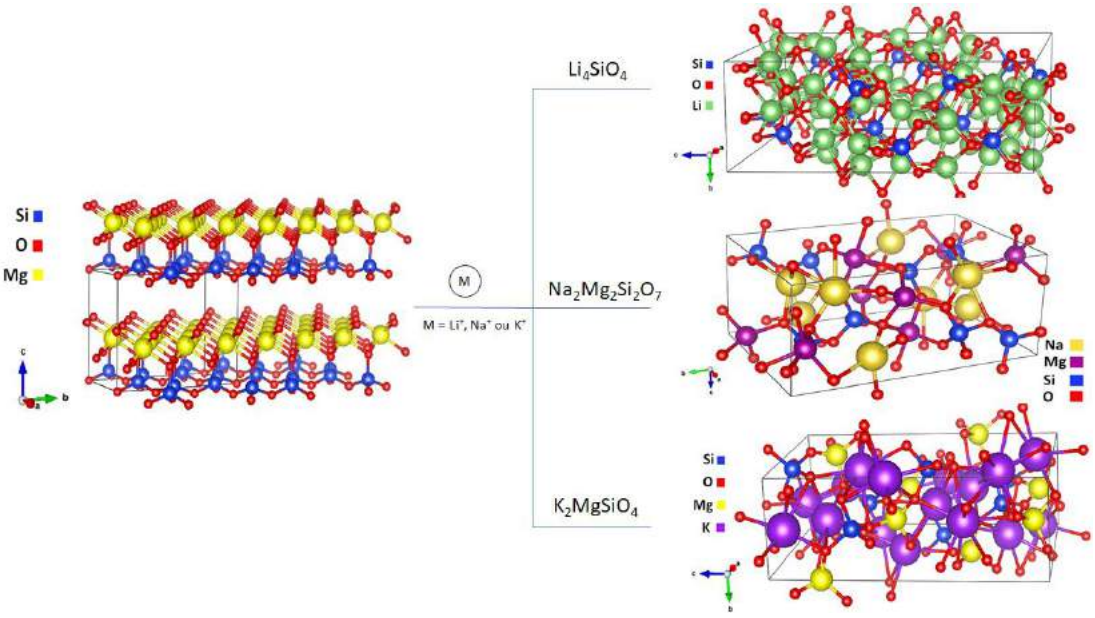


**Figure 1:** Representation of the three-dimensional structure of the arrangement of the atoms in $Li_4SiO_4$, $Na_2Mg_2Si_2O_7$ e $K_2MgSiO_4$

**Área: CAT**

**Inscrição: 01392**
*(Inserir o número de inscrição do autor que fez a submissão)*

# Heterogeneous catalysts based on Pd supported in mesoporous silica for selective hydrogenation: influence of the ionic liquid on the catalytic properties

**Maria Helena Araujo (PQ),Ully Gomes Haun (PG),*Ana Paula C. Teixeira (PQ).**

**maria.araujo@pq.cnpq.br; ully.gomes@hotmail.com***

*Departamento de Química, Universidade Federal de Minas Gerais (UFMG).*

Key Words: *Ionic Liquid, Mesoporous Silica, Supported Ionic Liquid, Heterogeneous Catalysis, Selective Hydrogenation.*

## Highlights

-One-pot synthesis of mesoporous support using ionic liquid (IL) as a template and functionalizer.
-Layer-effect of IL on heterogeneous catalyst lead to good metallic dispersion and high selectivity.

## Abstract

In this work the ionic liquid 1-metyl-3-decyl-imidazolium bromide was used as structural template and functionalizer of mesoporous silica (180 $m^2g^{-1}$), that showed predominantly spherical morphology. This material was used as support for palladium nanoparticles, without removal of the IL from the structure. For the comparison, Pd nanoparticles were also supported on silica after removal of the IL. It was observed that the IL reduced the metallic clusters formation on support surface (**Figure 1**).After calcination, high surface area (901 $m^2g^{-1}$), mesopore volume (0.71$cm^3g^{-1}$) and presence of micropores were observed. However the Pd nanoparticles were less dispersed in this material. The catalytic results showed different performance due the presence of IL on the structure. The catalyst without IL reached high 1,5-cyclooctadiene (1,5-COD)conversion rates, but with lower selectivity (60%). This was associated with cyclooctene (COE) consumption after total conversion of the substrate. On the other hand, the IL-containing catalyst showed high but slower conversion, due to the difficult access of 1,5-COD in the active sites, caused by the presence of IL (**Figure 2**). In addition, the IL molecules in the support showed a layer effect on the surface of the catalyst, similar to that obtained by the SCILL (Supported Catalyst with Ionic Liquid Layer) method. This avoided COE adsorption on the active sites because of its lower solubility in the IL, causing a repelling effect of their molecules for the solvent phase, leading to greater catalyst selectivity (93%).

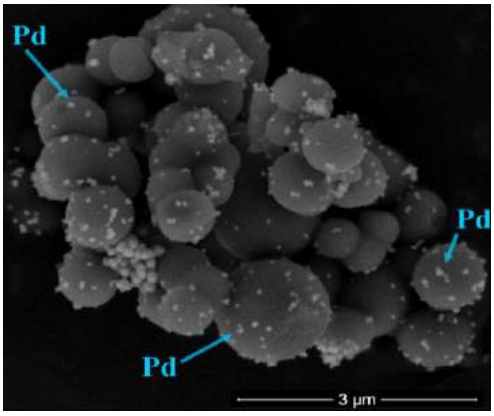


**Figure 1**. SEM image of microspheres of supported catalyst containing ionic liquid.

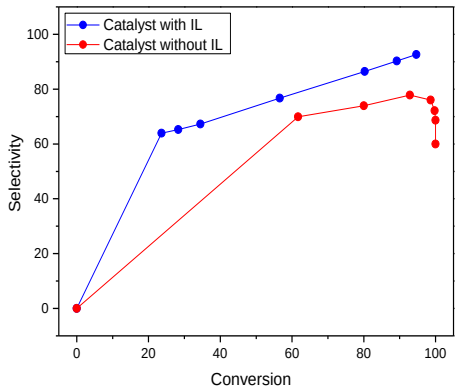


**Figure 2.** Graphic of *conversion* X *selectivity* for the catalysts with and without IL in the support

**Acknowledgments:** FAPEMIG, CAPES, CNPq and INCT-MIDAS

**Área: CAT** **Inscrição: 01019**

# Glycerol conversion in presence of $CO_2$: solvent absence in semi-batch reactor.

**Pedro P. Florez-Rodriguez**[*1](PQ), **Aracelis J. Pamphile-Adrián**[1](PQ), **Fabio B. Passos**[2](PQ)

**pedrorodriguez@iqb.ufal.br**

[1]*Instituto de Química e Biotecnologia, UFAL;* [2]*Departamento de Engenharia Química e de Petróleo, UFF.*

Key words: *Glycerol, Carbon dioxide, Epoxides, Semi-batch reactor.*

## Highlights

γ-$Al_2O_3$ supported Ni and Co catalysts are active in glycerol conversion in presence of $CO_2$, Ni being the most stable catalyst.
The use of semi-batch reactor increased the selectivity of the reaction.

## Abstract

Glycerol conversion with $CO_2$ in liquid phase in a semi-batch system was investigated. γ-$Al_2O_3$ supported catalysts with 13 wt% Ni, Co, Cr and Zn content were prepared, and a reduction-passivation process was performed. Passivated catalysts were characterized by XRD, TPR, BET and XPS techniques. TPR profiles showed that 65% of total Ni content and 39% of total Co content, was reduced; which was not observed for Zn and Cr catalysts. This fact was confirmed by XRD analysis, where the presence of Ni and Co metallic phases was observed, for Ni and Co catalysts, respectively, while diffractograms of Cr and Zn catalysts presented $Cr_2O_4$ and $ZnAl_2O_4$ peaks, respectively. Thus, it is observed that reduction-passivation process was efficient.
Ni catalyst presented a higher activity and selectivity, with 38% of glycerol conversion, while Co catalyst presented a conversion of 14% with deactivation after 100 min of reaction (Figure 1). Zn and Co presented a very low activity. Semi-batch system remarkably improved gas and liquid phases selectivity above 250 °C during 6 h, when compared to batch system, studied in previous work [1]. In the presence of Ni and Co catalysts, were obtained the same products: $H_2O$, 1,2-Diformyloxypropane, 2-(ethoxymethyl)oxirane, 2-propoxymethyl-oxirano, pinacolone and acetol, representing 50 and 70% of total yield, respectively. Recycle reactions performed with Ni catalyst presented a decreased of 50%, approximately, from408 to 206 g of converted glycerol per gram of $Ni^0$, after 3 h of recycle reaction.

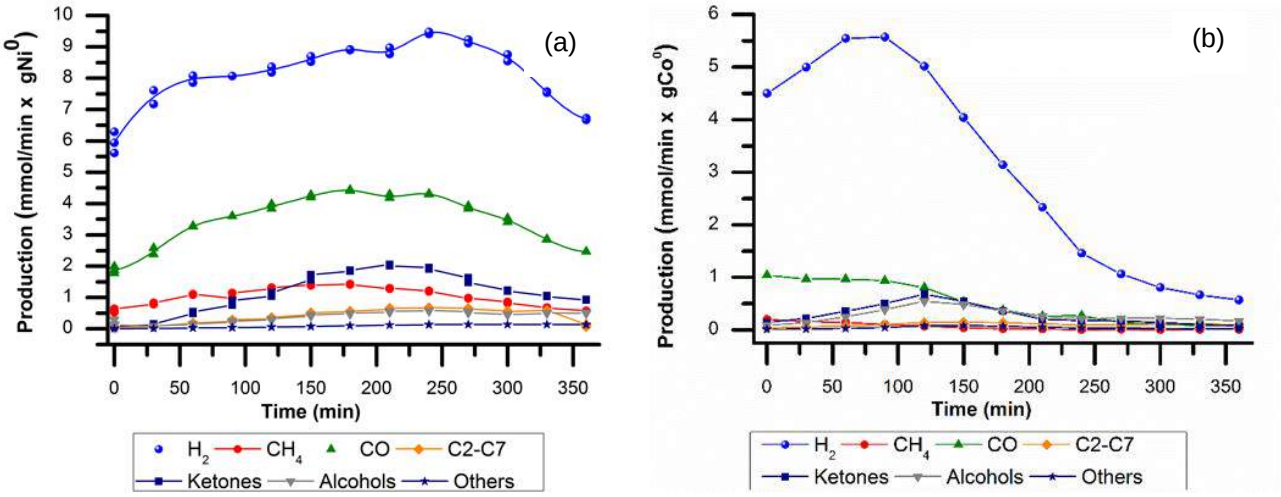


Fig. 1 Gas phase production for: (a) Ni(EG)RP and (b) Co(EG)RP catalyst in the semi-batch system in the presence of $CO_2$. Reaction conditions: T = 250 °C, $V_{CO2}$= 150 mL/min, $m_{catalyst}$= 1 and 3 g, $m_{glycerol}$ = 150 g, 1300 rpm, P = 70-80 psig, $t_{reaction}$= 6 h.

[1] P.P. Florez-Rodriguez et. al, Catalysis Today, 237, 38-46, **2014**.

**Área: CAT** **Inscrição: 00183**

# Preparation of Poly(lactic acid) blends by heterogenous catalysis using supported 12-tungstophosphoric acid

**Mateus F. Paiva[1*] (IC), Liana S. Chafran[2] (PQ), José A. Dias[1] (PQ), Sílvia C. L. Dias[1] (PQ)**

**freitas-paiva@hotmail.com**

*[1]Universidade de Brasília, Campus Darcy Ribeiro - Asa Norte, Instituto de Química, Laboratório de Catálise (A1-62/21), Brasília-DF, 70910-900, Brazil; [2]Union of the Central Plateau, FACIPLAC, Brasília-DF, 72445-020, Brazil.*

Keywords: *Supported heteropolyacid, Acidity, Blends of poly(lactic acid), Poly(lactic acid).*

## Highlights

Supported 12-tungstophosphoric acid materials results in enantioselective polymerization of D,L-lactic acid; Acidity is a key property to relate structure-activity of impregnated catalysts.

## Resumo/Abstract

Preparation of poly(lactic acid) (PLA) by catalytic reactions is a prominent research area for application of this material at the industrial scale. Considered a green polymer, the main challenge in its synthesis includes producing an economical material with high level of enantioselective isomer and low level of contaminants. Supported $H_3PW_{12}O_{40}$ ($H_3PW$) are important catalysts for several processes, especially those that takes place non-polar solvents, which eliminate any leaching concerns of these materials. This work addresses the polymerization of a racemic mixture of D,L-lactic acid, which resulted blends of PLLA and PDLA via heterogeneous catalysis using supported 12-tungstophosphoric acid on activated carbon (C), silica ($SiO_2$) and alumina ($Al_2O_3$). These catalysts were characterized by multiple techniques to confirm the integrity of the Keggin anion, as well as acidity as the key property to relate structure-activity. Evidence of the structure was proven by $^{31}P$ MAS NMR spectroscopy (Figure 1), which is correlated to the highest possible acidity of these materials (Table 1). Optimal conditions (20 wt. % $H_3PW$/Support calcined at 400 ºC; 0.1 wt. % of the catalyst relative to D,L-lactic acid; temperature of 180 ºC and 15 h reaction time) were developed to prepare blends of PLA with up to 95% of enantiomeric excess for poly(L-lactic acid). The average molar mass ($M_w$) of the formed PLA was up to approximately 17,700 Daltons, and this molar mass was well correlated to the acidity of the catalysts, as revealed by the different blank tests.

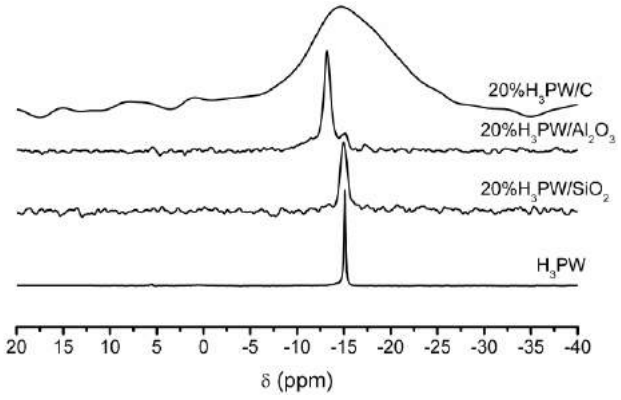


**Figure 1.** $^{31}P$ MAS NMR spectra of $H_3PW$ and supported materials (20%), calcined at 400 °C.

**Table 1.** Calculated enthalpy ($-\Delta H_1$), amount ($n_1$) of the strongest sites obtained by microcalorimetry of pyridine adsorption on the supported catalysts and enantiomeric excess (ee) of D,L-lactic acid in the polymers obtained from each catalyst.

| Catalyst | $-\Delta H_1$[a] (kJ mol$^{-1}$) | $n_1$ (mmol g$^{-1}$) | ee (%) |
|---|---|---|---|
| 20%$H_3PW$/C | 91 | 0.12 | 85 |
| 20%$H_3PW/SiO_2$ | 110 | 0.09 | 83 |
| 20%$H_3PW/Al_2O_3$ | 97 | 0.14 | 95 |

[a] The enthalpy measured in this work is an average of the first additions of pyridine (limiting reagent) in the titration. The standard deviation is ±2 kJ mol$^{-1}$ in all cases.

**Área: CAT** **Inscrição: 00246**

# Mesoporous Structures for Catalytic Pyrolysis of Plastic Waste

**Taihana P. Paula (PG)[1*], Maria de Fátima V. Marques (PQ)[1]**

**taihana.parente@ima.ufrj.br; fmarques@ima.ufrj.br**

*Instituto de Macromoléculas Professora Eloisa Mano, UFRJ.*

Keywords: *Chemical recycling, plastic waste, pyrolysis, catalyst, mesoporous structures, zeolites.*

## Highlights

Chemical recycling of plastics by catalytic pyrolysis using zeolites with mesoporous structures.
Influence of catalysts on the thermal degradation temperature of post-consumer plastics.

## Abstract

Waste plastics commodities have heterogeneous composition, variable and inherent structural complexity, and cannot be exclusively recovered by mechanical reprocess. An alternative to recycling these materials is conversion of plastic waste to products of high added value through pyrolysis. The thermocatalytic method provides greater selectivity, resulting in narrow fraction of molecules with appropriate molar mass that can be used directly as fuel oils[1,2]. Larger pores allow greater access of the polymer chains to more internal acid sites, which increases the catalytic activity and decrease the catalyst deactivation. The mesoporous mordenite was synthesized by soft template hydrothermal routes using cationic surfactant by means of moist (MOR 200) and dry syntheses (MOR DRY). Mesoporous ZSM-5 was synthesized by the hydrothermal method using structure-directing agent. The synthesized samples showed characteristic peaks of mordenite and ZSM-5, confirming the formation of the desired crystal structure (Figure 1). Total density of acid sites (Table 1) and distribution of these sites were determined by temperature-programmed desorption of ammonia ($NH_3$-TPD) (Figure 2). Mordenite has higher ratio of stronger/weak sites than ZSM-5, however, it has a more homogeneous distribution of acid forces.

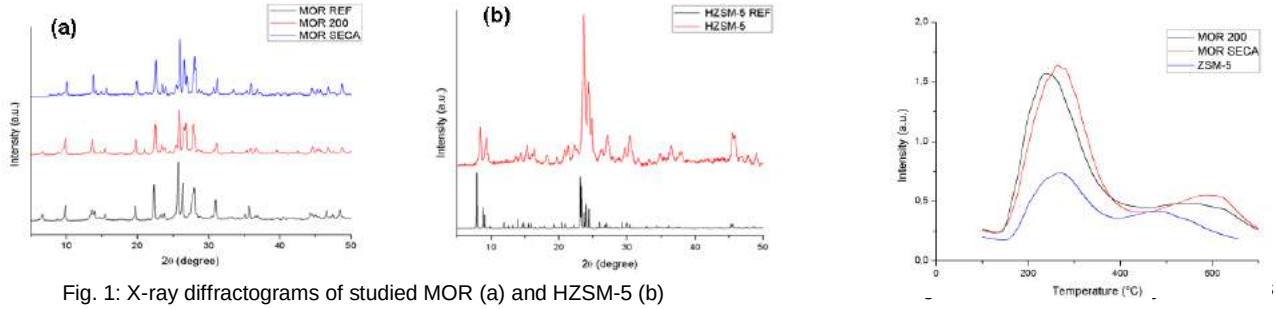


Fig. 1: X-ray diffractograms of studied MOR (a) and HZSM-5 (b)

Two plastic waste mixtures were prepared according to Abisplast (2016). The components of these blends are polyethylene (58.5%), polypropylene (31.6%) and polystyrene (9.9%). The MP mixture corresponds to the mixture of post-consumer plastics that are useful for mechanical recycling, while the MF mixture corresponds to that of non-usable plastic wastes directed to the landfills. These materials were extruded with each catalyst (10% m/m) and evaluated in thermogravimetric analysis (Table 2). The results show that all the evaluated catalysts were able to decrease the degradation temperatures of both plastics mixtures, especially ZSM-5 zeolite.

Table 1: Density of acid sites

| Sample | Acidity (μmol $NH_3$/g) |
|---|---|
| MOR 200 | 2178 |
| MOR DRY | 2093 |
| ZSM-5 | 1215 |

Table 2. Data obtained from the TGA

| Samples | $T_{onset}$ (°C) | $T_{10\%}$ (°C) | $T_{50\%}$ (°C) | $T_{max}$ (°C) | Residue (%) |
|---|---|---|---|---|---|
| MP | 432,1 | 421,5 | 453,5 | 459,4 | 0,89 |
| MP+MOR 200 | 425,3 | 415,7 | 448,6 | 453,7 | 9,10 |
| MP+MOR DRY | 423,0 | 411,2 | 449,3 | 456,4 | 8,90 |
| MP+ZSM-5 | 385,7 | 383,7 | 410,9 | 406,7 | 13,72 |
| MF | 432,0 | 390,5 | 457,3 | 464,1 | 11,27 |
| MF+MOR 200 | 424,4 | 379,8 | 453,9 | 461,7 | 16,05 |
| MF+MOR DRY | 425,3 | 390,0 | 454,6 | 463,1 | 12,88 |
| MF+ZSM-5 | 411,5 | 345,5 | 445,1 | 461,6 | 11,59 |

[1] MIANDAD, R.; BARAKAT, M. A.; ABURIAZAIZA, A. S.; REHAN, M.; NIZAMI, A. S. *Process Safety and Environmental Protection*, v. 102, p. 822-838, **2016**.
[2] SHARUDDIN, S. D. A.; ABNISA, F.; DAUD, W. M. A. W.; AROUA, M. K. *Energy Conversion and Management*, v. 115, p. 308-326, **2016**.

**Área: CAT** **Inscrição: 00925**

# *Hybrid catalysis in carbon dioxide valorization*

**Maitê L. Gothe (PG),[1] Matheus Barone (IC),[1] Lucas Marques (IC),[1] Vitor Caricatti (IC)[1], Reinaldo Bazito (PQ)[1], Liane Rossi (PQ)[1], Pedro Vidinha (PQ).[1]***

**maite.gothe@usp.br; pvidinha@iq.usp.br**

[1]*Instituto de Química, USP;*

Palavras Chave: *Catálise híbrida, Valorização de CO2, Imobilização de enzima, Regeneração de NADH.*

## Highlights

Biocatalytic reduction of CO2
Regeneration of NADH using hydrogen gas and homogeneous catalysis

## Resumo/Abstract

Carbon dioxide, generally viewed as pollutant, has recently started being considered a building block molecule in green synthesis. In order to produce valuable chemicals from carbon dioxide, strategies based on hybrid catalysis and simulation of biological processes were devised and integrated. A method of immobilization was optimized to support an enzyme, alcohol dehydrogenase, on magnetic nanoparticles, making them easily recoverable and active. The enzymatic cofactor NADH was successfully regenerated from NAD+, with either formate anion or molecular hydrogen as hydride donor, using an organometallic catalyst based on Iridium, $[Ir(\eta^5\text{-}C_5Me_5)phenNO_2Cl]^+Cl^-$.

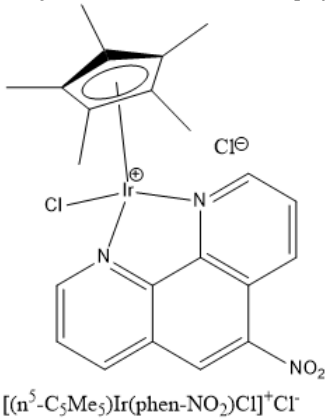


$[(\eta^5\text{-}C_5Me_5)Ir(phen\text{-}NO_2)Cl]^+Cl^-$

$NAD^+ + HCOO^- \rightarrow NADH + CO_2$ - TOF 52,7 $h^{-1}$

$NAD^+ + H_2 \rightarrow NADH + H^+$ - TOF 8,6 $h^{-1}$

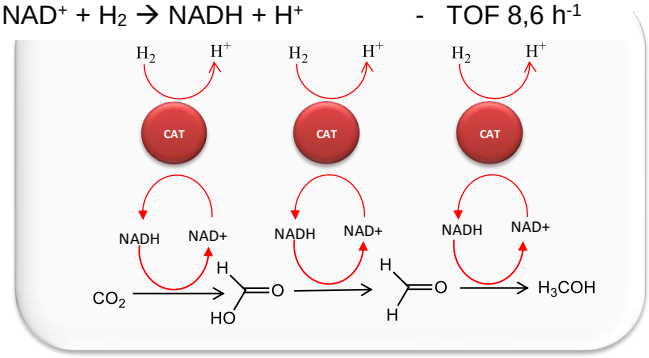


The Turn-Over-Frequency (TOF) of the immobilized enzyme and that of the catalytic regeneration of NADH was similar, with the generation of NADH being slightly faster than its consumption, which is ideal for integrating both on the same system. Using formate anion as the hydride source, TOF for the conversion of $NAD^+$ into NADH was 274 mmol $NADH.h^{-1}.g\ Ir^{-1}$, while the conversion of acetaldehyde into ethanol with ADH immobilized in magnetic nanoparticles, consuming NADH, was 45 mmol $NADH.h^{-1}.g\ ADH^{-1}$.

Efficiency of the integration of both steps was evaluated by the formation of ethanol from acetaldehyde, $NAD^+$, formate anion, immobilized ADH and iridium catalyst. Ethanol was quantified by GC-FID using acetonitrile as internal standard, showing a TOF of 58 mmol $Etanol.h^{-1}.g\ ADH^{-1}$.

Currently, the enzymatic activity under hydrogen gas as hydride donor, as well as the immobilization of the remaining enzymes of the dehydrogenation cascade: formaldehyde dehydrogenase and formate dehydrogenase, is being studied, in order to convert carbon dioxide into methanol with a reusable, bio-inspired catalytic system.

In summary, our results suggest the development of a promising biocatalytic system for the conversion of $CO_2$ to methanol.

**Área: CAT** **Inscrição: 01260**

# Estudo do uso de rejeitos industriais como catalisadores na degradação de corantes industriais usando o processo fenton

**Ana C. L. N. Ferreira (TM)[1*], Renato P. Ribeiro (PQ)[1], Heitor B. P. Ferreira (PQ)[1] anaclaralnf@outlook.com;**

*[1]Instituto Federal de Educação, Ciência e Tecnologia do Rio de Janeiro – IFRJ. Rua Delio Menezes Porto, 1045, 26530-060. Centro, Nilópolis.*

*Palavras Chave: Degradação, Azul De Metileno, Reação Fenton, Reação Fotofenton, Catálise Heterogênea.*

## Highlights

Study of the use of industrial wastes as catalyzers in industrial dyes degradation using the fenton process. Industrial wastes as catalyzers. Methylene blue degradation. Fenton and photo-fenton reactions. Sustainable dye degradation. Temperature in fenton reactions.

## Introdução

Os corantes industriais têm capacidade de interferir negativamente no meio ambiente devido, por exemplo, à sua decomposição em meio aquático. Para diminuir a concentração destes corantes, tem-se dado importância aos Processos Oxidativos Avançados (POA), principalmente à reação Fenton. Neste trabalho, o foco foi verificar a remoção do corante azul de metileno por reações Fenton e Fotofenton, utilizando como catalisadores rejeitos industriais.

## Resultados e Discussão

Na etapa inicial deste estudo foram feitas reações fenton em temperatura ambiente utilizando, em cada uma delas, os diferentes catalisadores propostos. A eficiência do processo é apresentada no gráfico 1. Os catalisadores tiveram eficiência de remoção variando entre 9% e 33%. Com os dois catalisadores mais efetivos (CAT 3 e CAT 7), prosseguiram-se as análises utilizando temperatura na reação fenton. A segunda etapa, realizada em 40°C, mostrou semelhança quanto à eficiência. Visando valores mais satisfatórios, foi realizada a terceira etapa, em 60°C. Nesta, houve expressivo aumento na eficiência do processo, tendo a remoção sido quase total. Na última fase do estudo, foi realizada a reação fotofenton. O catalisador CAT 7 se comportou de maneira esperada, tendo eficiência superior à primeira etapa e inferior à terceira (com uso de temperatura). O catalisador CAT 3 não apresentou distinção de resultados, exceto com relação à terceira etapa. Os resultados conseguintes à primeira etapa são apresentados na tabela 1.

**Gráfico 1.** Eficiência de remoção em temperatura ambiente

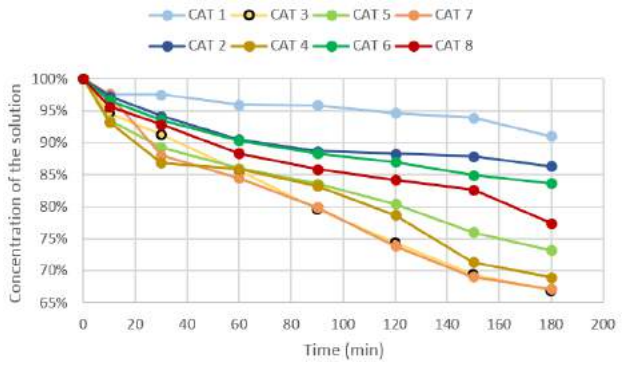


**Tabela 1.** Eficiência de remoção em condições não-ambientes

| Catalisador | Eficiência de remoção | | |
|---|---|---|---|
| | 40°C | 60°C | Fotofenton |
| CAT 3 | 32% | 93% | 33% |
| CAT 7 | 33% | 95% | 62% |

## Conclusão

O uso de rejeitos industriais como catalisadores mostrou-se viável neste estudo, de modo que a remoção foi quase completa em uma das condições.

**Área: CAT** **Inscrição: 01421**

# Development of new materials from industrial waste and biomass for application in catalysis

**Mariana Erculano da Fonseca (PG),[1]* Raquel Vieira Mambrini (PQ).[1]**

**kellmambrini@gmail.com**

[1]*Departamento de Química, Centro Federal de Educação Tecnológica de Minas Gerais – CEFET-MG*

Palavras Chave*: Biomass, industrial waste, Catalysis, electric arc furnace dust*

## Highlights

Biomass of papaya peel was used as catalytic support for an electric arc furnace dust. The materials were characterized and used in removal of petroleum contaminants with good removal results.

## Resumo/Abstract

Electric arc furnace (EAF) dust is a waste generated in the steelmaking process through the electric arc furnace and is classified as hazardous waste. It is estimated that 15 kg to 20 kg of electric arc furnace are generated for each ton of steel produced. EAF dust has a high cost of proper management and it is necessary to develop new technologies for its reuse.

In this work biomass (B) of papaya peel (dried at 100 ºC, without previous treatment) was used as catalytic support for electric arc furnace dust (EAF). Wet impregnated in proportions of 5%, 9%, and 13% were done and the materials were named according to the impregnated content. The materials were characterized by X-ray diffraction and thermogravimetric analysis (Figure 1), which confirmed the insertion of EAF in the surface of biomass by the impregnation process.

Figure 1. X-ray diffraction and TG curves to materials

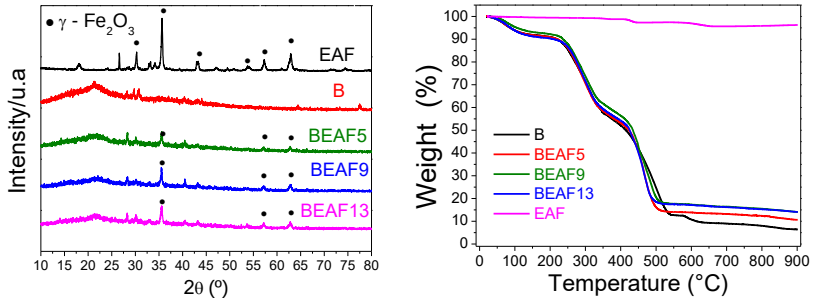


Figure 2. Total Removal of quinoline and dibenzothiophene in the presence of materials

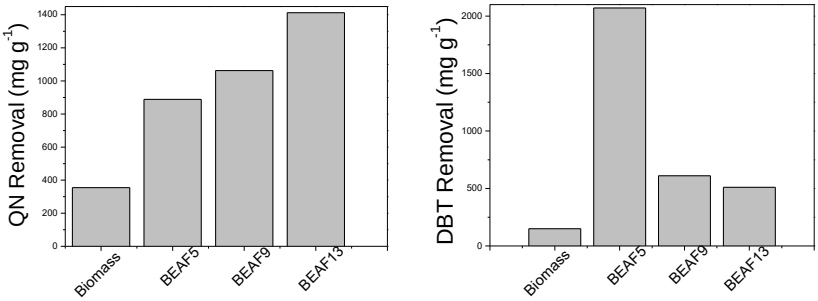


Then, the materials were applied in quinoline (QN) and dibenzothiophene (DBT) removal, petroleum contaminants, with removal capacity of the materials reaching values up to 1.412 mg $g^{-1}$ of QN removal and 2.070 mg $g^{-1}$ of DBT removal (Figure 2).

Thus, it is concluded that the use of biomass of papaya peel as catalytic support has proved to be a cheap and promising possibility for environmental remediation, presenting good results for the removal of petroleum contaminants. In addition, the materials impregnated with EAF showed excellent results, above those described in the literature.

**Acknowledgments:** FAPEMIG, Rede Mineira de Química, and Cefet-MG.

**Área: _CAT_____** *(Inserir a sigla da seção científica para qual o resumo será submetido. Ex: ORG, BEA, CAT)*

**Inscrição:_01097_____** *(Inserir o número de inscrição do autor que fez a submissão)*

# Esterification of FFA in Soybean oil with acid zeolite catalyst for biodiesel production

**Daniel M. Dal Pozzo (PG),[1*] Michelle B. Costa (PQ),[1] Elciane R. Zanatta (PQ)[1]**

**danielpozzo@utfpr.edu.br**

[1]*Laboratório de Análise Térmica e Espectroscopia de Materiais e Biocombustíveis, Universidade Tecnológica Federal do Paraná, Medianeira (UTFPR-Câmpus Medianeira), Avenida Brasil, 4232 - Parque Independência CEP: 85884-000, Medianeira - Paraná, Brasil.*

Keywords: *Fatty acids, Pre-treatment, Sustainability.*

## Highlights

The H-Beta zeolite can be applied in a sustainable pre-treatment of esterification of FFA (Free Fatty Acids) for biodiesel production. Full conversion was obtained after 6 h reaction time. Low quality feedstocks with high content of FFA can be pre-treated with BEA zeolite catalyst. The zeolite is a selective and high active catalyst for esterification. The easy separation of the catalyst, catalytic activity and the possibility of reuse in new reactional cycles make interest the application of H-Beta for biodiesel production.

## Resumo/Abstract

The use of waste cooking oils is interesting for the production of biodiesel, however, the presence of FFA results in some problems when alkaline transesterification is performed. In this context, low quality feedstocks with high content of FFA can be also pre-treated before this process for the removal FFA. The catalytic activity of zeolite Beta was evaluated for the esterification reaction pre-treatment. Beta zeolite (Si/Al = 19) was purchased from *Zeolyst International* and used in the protonic form. As a model reaction to evaluate the catalytic activity of the H-Beta zeolite, a mixture of oleic acid and soybean oil with methanol was esterified. Reactions were performed in different temperatures, catalyst amounts and excess of alcohol, aiming to optimize the conversion of free fatty acids. The results obtained are shown in Figure 1.

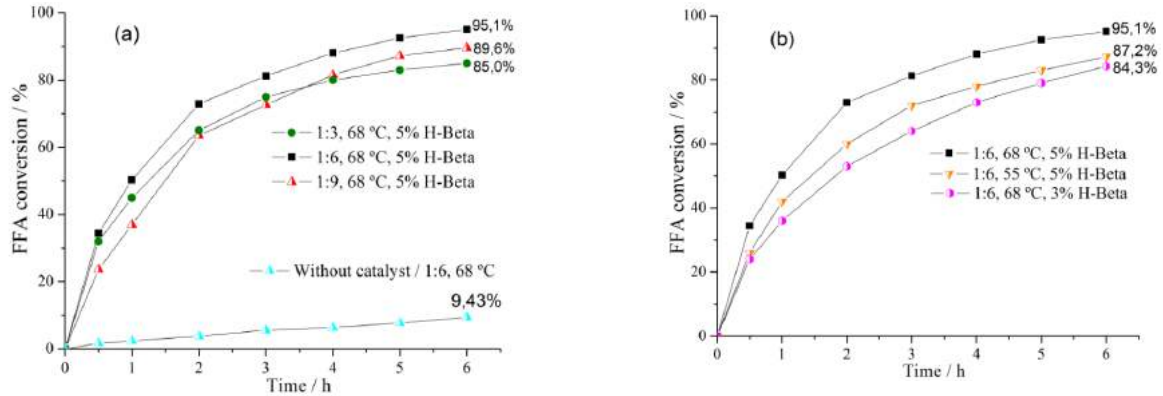


Fig 1. a). Fatty Acid: alcohol molar ratio effect. b). Temperature and amount of catalyst effect.

The selectivity of reagent was observed. The H-Beta zeolite was active in the esterification of FFA. Conversions to methyl esters above 95% were obtained. The pore size of H-Beta zeolite (6,6 x 6,7 and 5,6 x 5,6 Å) was determinant for the reactions, allowing only the esterification of the oleic acid. The increase in temperature favored the reaction, as well as the amount of catalyst. The most favorable molar ratio for the esterification pre-treatment was 1:6, Oleic Acid:Methanol. The optimized condition resulted in a conversion of 95.1% after 6 h of reaction with a molar ratio of 1:6 and a temperature of 68 °C, allowing the reduction of the content of FFA to a negligible level, so that the production can continue by alkaline transesterification. These facts, together with the easy separation and recovery of this zeolite, make this material an efficient catalyst for a pretreatment of esterification of low quality feedstocks with high FFA content for a sustainable biodiesel production.

**Área: COL** **Inscrição: 1254**

# Influence of an alternate magnetic field on the cellulase activity immobilized in magnetic nanoparticles

**Caroline Oliveira da Rocha (PG),[1*] Guilherme Nunes Lucena (PG),[1] Miguel Jafelici Junior (PQ),[1] Rodrigo Fernando Costa Marques (PQ).[1]**

**carolnine@iq.unesp.br**

*[1]Physic-Chemistry department, Institute of Chemistry, UNESP Araraquara*

Palavras Chave: *Magnetic nanoparticles. Cellulase immobilization. Second generation ethanol. Magnetic reactors.*

## Highlights

Evaluating activity of cellulase immobilized on magnetic supports and use of reactors with alternating magnetic field to application in biocatalysis in the production of second generation ethanol.

## Resumo/Abstract

Lignocellulosic biomass is a heterogeneous material composed of lignin, hemicellulose, and cellulose. The ability to convert cellulose components of material to fermentable sugars for production of biofuels depends on access of enzyme to substrate protected by lignin. In this work, commercial cellulase was immobilized on superparamagnetic nanoparticles (SP) functionalized with amine groups (SP-APTS) for use in second generation ethanol. Cellulose immobilization on magnetic nanoparticles (SP-APTS-CEL), in order to prolong enzymatic activity in several cycles in industrial processes. The preparation of stable enzymes immobilized on magnetic nanoparticles for recovery and reuse is done using a combination of nanoparticle aggregates and cross-linked enzymes (MCLEAs). The cross-links are formed with the addition of crosslinking agent (glutaraldehyde-GA). The advantages of the immobilized enzymes relative to the free enzymes arise from their greater stability and ease of separation for microscopic agitation using alternating magnetic field, which entails significant savings in the overall cost of the process. The superparamagnetic nanoparticles phase was demonstrated for X-Ray Diffraction (DRX). The cellulase immobilization was verified for Scanning Electron Microscopy (SEM) and bands of amine groups (1454 $cm^{-1}$) for Infrared Spectral Range (FT-IR). The free and immobilized cellulase activity was used GHOSE protocol and it has been proven activity for filter paper unit (FPU) and cellobiase for High Performance Liquid Chromatography (HPLC). The cellulase immobilized with magnetic nanoparticles is an innovative study that will provide the production of second generation ethanol in large scale with reduced costs and operating time.

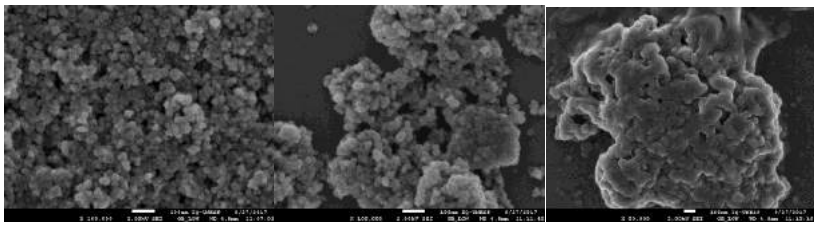

**Fig. 1:** SEM a) NP b) NP-APTS and c) NP-APTS-CEL.

| Sample | Abs. | FPU (U/mL) |
|---|---|---|
| Free cellulase | 0,085 | 7,18 |
| Immobilized cellulase | 0,244 | 3,24 |

Table 1: Activity Filter Paper Unit (FPU)

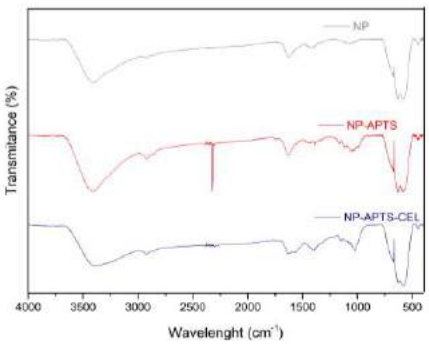


Fig. 2: FT-IR: NP, NP-APTS and NP-APTS-CEL.

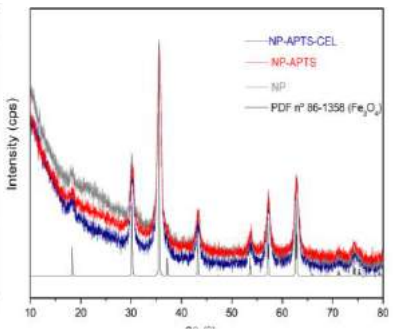


Fig. 3: DRX of samples compared with standard magnetite PDF nº 86-1358 ($Fe_3O_4$).

| Diluition (x) | [glicose] (y) (mg/mL) |
|---|---|
| 1 | 0,0814 |
| 0,5 | 0,04215 |
| 0,33 | 0,0354 |

Table 2: Activity cellobiase for (HPLC).

**Área: COL** **Inscrição: 00889**

# Adsorption of sodium dodecylbenzenesulfonate (SDBS) and dodecylpyridinium chloride (DPC) onto modified mesoporous silica-coated magnetite

**Larissa Dorigon (IC)[1], Juan Pablo R. A. Frota (IC)[1], Cristian R. Andriolli (IC)[1], Alesandro Bail (PQ)[2], Renata Mello Giona (PQ)[1*].**

**cristianrafaelandriolli@gmail.com; renatam@utfpr.edu.br**

*[1]LAMAFI, Departamento de Química, UTFPR – Medianeira; [2]LAQMATS, UTFPR - Apucarana*

Keywords: *Magnetite, Mesoporous-silica, Surfactant, Physisorption, Hydrophobicity.*

## Highlights

A core-shell structure formed by silica-coated magnetite was synthesized. CTAB incomplete monolayer allowed hydrophobic interaction with the SDBS and DPC molecules.

## Resumo/Abstract

Silica-coated magnetite (Mag-Sil) was prepared by the co-precipitation method using sodium metasilicate under an inert atmosphere and a fine pH control.[1,2] Mag-Sil was modified by cetyltrimethylammonium bromide (CTAB) adsorption with the purpose of decreasing the hydrophilicity of the silica surface, in order to study its interaction with SDBS and DPC surfactants. The synthesized materials were characterized by XRD, nitrogen physisorption analysis, TGA, FTIR and TEM. Kinetic experiments revealed an instantaneous physisorption of both DPC and SDBS on Mag-Sil-CTAB associated with their high accessibility to the adsorption sites. The physisorption data were fitted by Langmuir and Freundlich isotherm models (Figure 1) and the equilibrium parameters obtained are shown in Table 1. The maximum adsorption capacities found suggests that hydrophobic (tail-to-tail) interaction has a key role in the adsorption process (Figure 2) and surfactant uptake occurs based on four-region model[3], that takes place when, depending on surfactant concentration, hydrophobic interaction prevails and the formation of aggregates or admicelles is expected (Scheme 1).

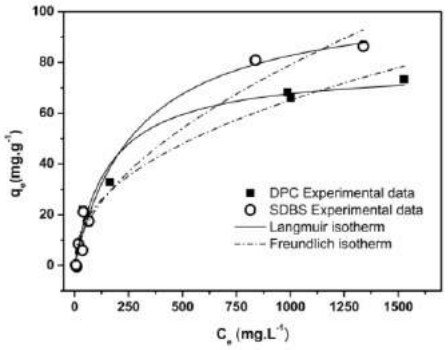


Fig 1. Isotherms for SDBS and DPC adsorption on Mag-Sil-CTAB. Experimental conditions: $[Surfactant]_{initial}$ 1x10$^{-5}$-1x10$^{-2}$ mol.L$^{-1}$; weight of adsorbent: 35 mg; T: 30°C; volume of solution: 5 mL.

Table 1. Equilibrium parameters obtained by Langmuir and Freundlich isotherm models to surfactant uptake on Mag-Sil-CTAB

| | **Langmuir model** | | | **Freundlich model** | | |
|---|---|---|---|---|---|---|
| | $q_e = \frac{bq_{max}C_e}{1+bC_e}$ | | | $q_e = K_F C_e^{1/n}$ | | |
| | $q_{max}$ (mg.g$^{-1}$) | b (L.mg$^{-1}$) | $R^2$ | $K_F$ (mg.g$^{-1}$(L.mg$^{-1}$)$^{1/n}$) | n | $R^2$ |
| SDBS | 106.66 | 0.0035 | 0.982 | 1.780 | 1.821 | 0.961 |
| DPC | 78.39 | 0.0063 | 0.984 | 3.075 | 2.263 | 0,967 |

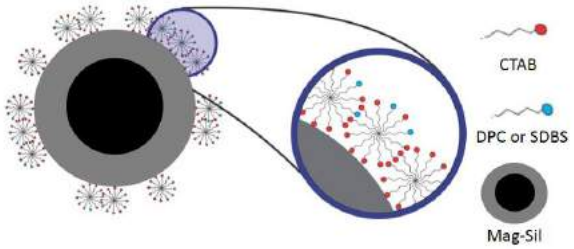


Scheme 1

## References

[1]DORIGON, L. *et al*. **Applied Surface Science**. v. 420, p. 954-962, 2017.
[2]WANG, J. *et al*. **J. Colloid Interf. Sci**. v. 349, p. 293-299, 2010.
[3] Tyrode, E. *et al*. **J. Am. Chem. Soc**. v. 130, p. 17434-17445, 2008.

The authors would like to thank SANEPAR, Fundação Araucária and Universidade Tecnológica Federal do Paraná.

**Área: COL** **Inscrição:00058**

# Synthesis and characterization of magnetic mesoporous silica nanoparticles for $Ba^{2+}$ removal from aqueous media

**Caroline M. M. Reolon (IC)[1]*, Alessandro Bail (PQ)[2], Renata M. Giona (PQ)[1], Daniel W. Tondo (PQ)[1]**

**danielw@utfpr.edu.br**

*[1]LAMAFI, UTFPR – Medianeira; [2]LAQMATS, UTFPR - Apucarana*

Key words: *Adsorption, Barium, Core-shell, Nanoparticles*

## Highlights

Core-shell nanoparticles were prepared and characterized. The material was tested on $Ba^{2+}$adsorption from aqueous solutions. The adsorbent showed great potential for waste water treatment for $Ba^{2+}$ removal.

## Resumo/Abstract

According to the World Health Organization[1], the maximum limit of barium in drinking water is 0,7 $mg.L^{-1}$. Magnetic nanoparticles are potential candidates for removing $Ba^{2+}$ ions due to their high adsorption capacity, easy separation for magnetic field and low cost synthesis[2]. In this work, we have synthesized magnetic mesoporous silica nanoparticles ($Fe_3O_4$@$SiO_2$), using previously described methodology[2]. The material was characterized by FTIR, TGA, DRX, and TEM, which enhanced images are showed in figure 1. The left image shows magnetite spherical particles having an average diameter of 7,5 nm, while the right image shows bigger aggregates with 13,8 nm, due to the magnetite´s coated process with silica. For $Ba^{2+}$ removal, it was performed experiments using 5 mL of 5 ppm of barium solutions in contact with 100 mg of $Fe_3O_4$@$SiO_2$ for 5, 15, 30, 60, 90 and 120 minutes. The barium concentration was then determined by UV-vis spectroscopy following the formation of the complex between the $Ba^{2+}$ and sulfonazo III ion at $\lambda$ = 580 nm (Figure 2). The linearized model of pseudo-second order for kinetic adsorption[3] can be described by equation 1:

$$\frac{T}{Q_T} = \frac{1}{K_2 . Q_e^2} + \frac{1}{Q_e} . T \qquad \text{(equation 1)}$$

where $Q_T$ e $Qe$ are the amounts of adsorbate adsorbed per gram of the adsorbent ($mg.g^{-1}$) at time "$T$" and at equilibrium respectively. $K_2$ is the pseudo-second order rate constant ($g.mg^{-1}.min^{-1}$), and can be obtained from the slope of the graph of figure 3, which showed a correlation coefficient $R^2$ = 0,99937

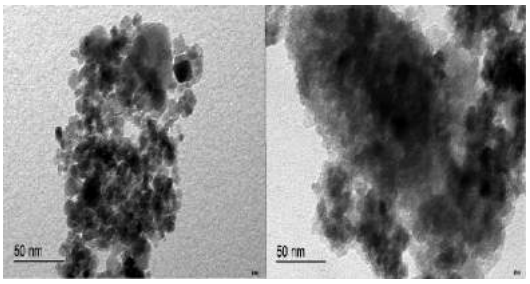


**Figure 1**. TEM of solids $Fe_3O_4$ (left) and $Fe_3O_4$@$SiO_2$ (right)

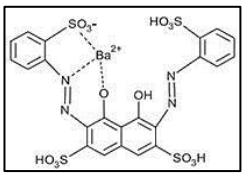


**Figure 2**. Complex formed between the ions $Ba^{2+}$ and sulfonazo III

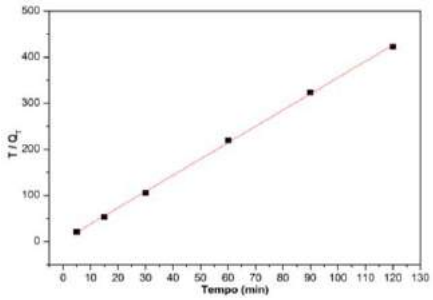


**Figure 3**. Second-order kinetic model for adsorption of $Ba^{2+}$

Agradecimentos:

FUNDAÇÃO ARAUCÁRIA
Apoio ao Desenvolvimento Científico e Tecnológico do Paraná

SANEPAR

UTFPR
UNIVERSIDADE TECNOLÓGICA FEDERAL DO PARANÁ

Referências:

[1]WHO; *World Health Organization,* **2011**, 178.
[2]Wang, J.; Zheng, S.; Shao, Y.; Liu, J.; Xu, Z.; Zhu, D. J.; *Journal of Colloid and Interfaces Science*, **2010**, 293
[3]HO. Y. S.; McKAY, G.; *Process Biochemistry*, 34, p. 451-465. (1999).

**Área: COL** **Inscrição:00543**

# Superhydrophobic self-cleaning surfaces and slippery lubricated ones effect upon inorganic scaling.

**Filipe Signorelli (PG),[1*] Maria F.B. Sousa (PQ),[1] Celso A. Bertran (PQ).[1]**

**filipe.signorelli@iqm.unicamp.br**

[1]*Functional Materials and Interfaces Laboratory, Institute of Chemistry, University of Campinas (UNICAMP)*

Palavras Chave: *superhydrophobic surface, slippery surface, anti-scaling, anti-fouling, polyaniline.*

## Highlights

Electropolymerized polyaniline acts like a good model to assess both superhydrophobic and slippery surfaces.
Superhydrophobic surfaces cannot prevent scaling while slippery surfaces can prevent it efficiently.

## Resumo/Abstract

Several industrial processes involving a medium rich in carbonates and sulfates suffer from inorganic scaling onto its facilities, which can result in severe damage to equipment, production and the environment.

Nucleation and growth inhibitors are often used to minimize or prevent scaling. Nonetheless, such procedures require constant refill of inhibitor compounds, which means higher costs and higher environment impact. An alternative method to avoid scaling would be prevent the salts from adhering to the surface, and, for that, surface modifications aiming to create low adhesion and low wettability could be employed.

Barthlott and Neinhuis[1] unveiled the Lotus Effect, by which the path to superhydrophobic self-cleaning surfaces development was open. Wong *et al*.[2] stepped forward mimicking *Nepenthes* pitcher plant slippery lubricated surface, which presented omniphobic behavior. Both surface phenomena seem to be eligible to act like scaling preventers avoiding adhesion of precipitates, thus, they were tested at this work.

Polyaniline was electropolymerized by galvanostatic method onto stainless steel, leading to hierarchical structures which were chemically modified with perfluorinated thiol to lower their surface energy. Then, the surfaces were characterized as superhydrophobic self-cleaning by contact angles measurements. Slippery surfaces were built by a lubrication of the abovementioned superhydrophobic surfaces with perfluorinated oil. Both surfaces were assessed after immersion at controlled inorganic scaling environment. Results showed that superhydrophobic self-cleaning surfaces not only fail to stand its properties as also increases the inorganic scaling formation, while lubricated slippery one superbly prevents it (Figure 1).

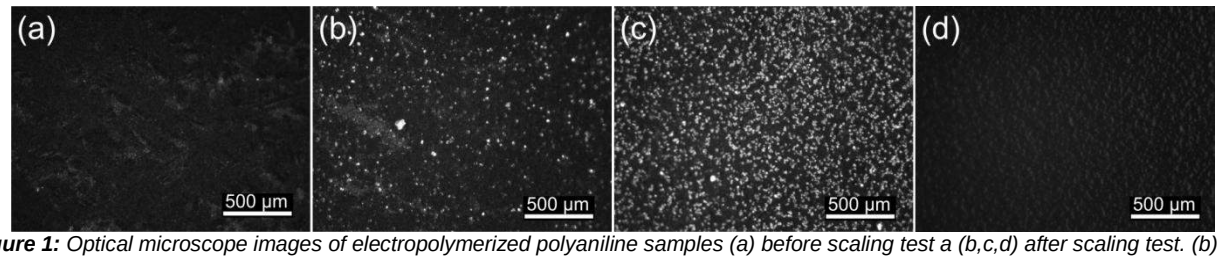


***Figure 1:*** *Optical microscope images of electropolymerized polyaniline samples (a) before scaling test a (b,c,d) after scaling test. (b) Non-modified, (c) modified with perfluorodecanethiol and (d) modified with perfluorinated thiol and oil. The scaling can be seen as bright dots.*

References:

1 – Barthlott, W.; Neinhuis, C. **1997**, *Planta*, 202, 1-8.
2 – Wong, T. S. *et al*. **2011**, *Nature*, 477, 443-447.

**Área: COL** **Inscrição: 00302**

# Formation of polymer – hexadecylpyridinium chloride complexes using different structures of poly(vinyl alcohol)

**Júlia Maria Bruno de Andrade (IC),[1] Gabriel Henrique Fávero Santos (IC),[1] Álvaro Javier Patiño Agudelo (PG),[2] Luis Henrique Mendes da Silva (PQ),[2] Guilherme Max Dias Ferreira (PQ).[1]***

**julia.andrade@engenharia.ufla.br; guilherme.ferreira@dqi.ufla.br**

*[1]Departamento de Química, Universidade Federal de Lavras; [2]Grupo de Química Verde Coloidal e Macromolecular, Departamento de Química, Universidade Federal de Viçosa*

Keywords: poly(vinyl alcohol), cationic surfactant, molecular aggregation, calorimetry.

## Highlights

- Poly(vinyl alcohol) interacted with the hexadecylpyridinium chloride surfactant;
- Presence of carboxylic groups in the polymer structure favored the complex formation;
- The aggregation process was endothermic.

## Resumo/Abstract

Poly(vinyl alcohol) (PVA), a strategic biodegradable and biocompatible polymer, can interact with surfactants to provide desirable properties in several applications, such as in cosmetics formulation. Here, the interaction process between hexadecylpyridinium chloride (C16PyCl) surfactant and different structures of PVA were investigated using conductivity, turbidimetry, and isothermal titration calorimetry (ITC). Figure 1 shows the results obtained for the titration of C16PyCl into water with or without PVA (hydroxylated, PVOH, or carboxylated, PVCOOH).

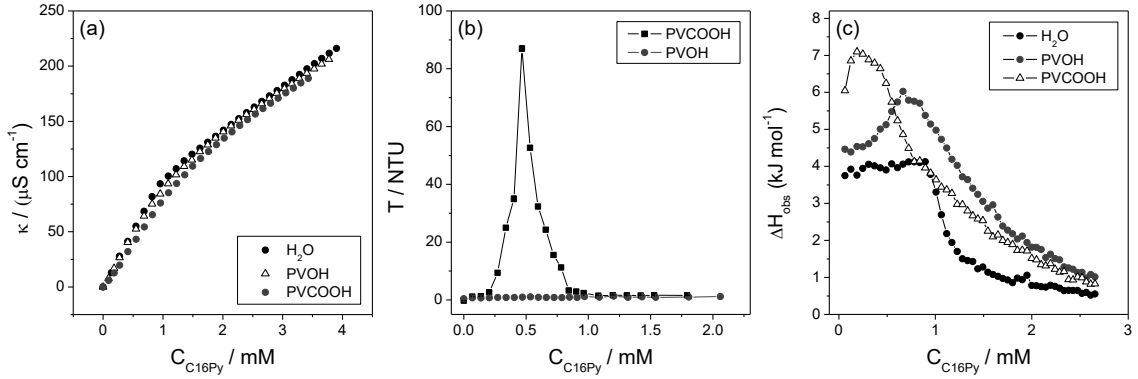


Figure 1. (a) Conductimetric, (b) turbidimetric, and (c) calorimetric curves for titration of C16Py into 0.20% m/m PVA aqueous solutions.

The critical micellar concentration (cmc) of the C16PyCl was (1.03 ± 0.03) mmol $L^{-1}$ (Figure 1a). In the presence of PVOH, the surfactant interacted with the polymer, and the critical aggregation concentration (cac) was (0.8 ± 0.1) mmol $L^{-1}$. In PVCOOH solution, the aggregation process was observed at concentrations smaller than 0.1 mM, indicating a more favorable interaction between the C16PyCl and the carboxylated PVA. This result came from the more intense electrostatic interactions between the surfactant (positively charged) and the PVCOOH, more negatively charged than the PVOH. The formation of $C16Py^{+}$-$PVCOO^{-}$ complexes was accompanied by phase separation due the formation of a precipitate that was dissolved at higher surfactant concentration (Figure 1b). Interestingly, for both polymers, ITC results (Figure 1C) showed that the $\Delta H_{obs}$ values were lower when PVA was not present into the calorimetric cell, indicating that the polymer-surfactant interaction was endothermic, and suggesting the incorporation of the PVA in the surfactant aggregate.

**Acknowledgments:** FAPEMIG, CAPES, CNPq, INCTAA.

**Área: COL** **Inscrição: 00165**

# Spectrophotometric and tensiometric investigation of the interaction between Norbixin and surfactants in aqueous medium

**Jussara Alves Penido (PG),[1] Isabela de Melo Carvalho (IC),[1] Cristina Mazeu Junqueira (PQ),[2] Luciano Sindra Virtuoso (PQ),[2] Aparecida Barbosa Mageste (PQ).[1*]**

**isabelameloc@gmail.com; aparecida@iceb.ufop.br.**

*[1] Chemistry Department, UFOP, Minas Gerais, Brazil. [2] Chemistry Department, UNIFAL, Minas Gerais, Brazil.*

*Keyword: Norbixin, CTAB, SDS, Surfactant, Dye-surfactant aggregates*

## Highlights

- Surfactant-Norbixin interaction was studied.
- Norbixin interacted with cationic surfactant forming different aggregates.
- The formation of the aggregates was driven by electrostatic interaction.

## Abstract

Dyes and surfactants are important compounds of the chemical industry. The combination of these chemicals in solution to form aggregates is strategic in several applications. Therefore, the investigation of the dye-surfactant interaction is of relevance fundamental. Here, the interaction between the natural dye Norbixin and the dodecyltrimethylammonium bromide (CTAB) and sodium dodecyl sulfate (SDS) surfactants was investigated using UV-vis spectroscopy (Figure 1a) and tensiometry (Figure 1b). In region I (CTAB < $2x10^{-5}$ mol $kg^{-1}$), the Norbixin surface tension values are lower than pure CTAB and absorption value decreased. These indicate the formation of hydrophobic ion-par that concentrates at interface. In the end of region I (at $2x10^{-5}$ mol $kg^{-1}$ of CTAB), the absorption value decreased and a new band appear at 366 nm, indicating dye dimerization process. In the region II ($2x10^{-5}$ < CTAB < $2x10^{-4}$ mol $kg^{-1}$), the turbidity was observed and surface tension increase. These suggest the dimers dye form solid Norbixin-rich aggregates, which are solubilized with increasing CTAB concentration. In the region III ($2x10^{-4}$ < CTAB < $8.9x10^{-4}$ mol $kg^{-1}$), the surface tension decrease, and maximum wavelength value of dye solution shifts, indicating the Norbixin-rich micelle formation. In the region IV (CTAB > $8.9x10^{-4}$ mol $kg^{-1}$), surface tension curves to CTAB on water and on Norbixin overlap and remains constant, and there is an increase on absorption values. These suggest the formation of CTAB-Norbixin mixed micelle. Interaction between Norbixin and SDS was not observed.

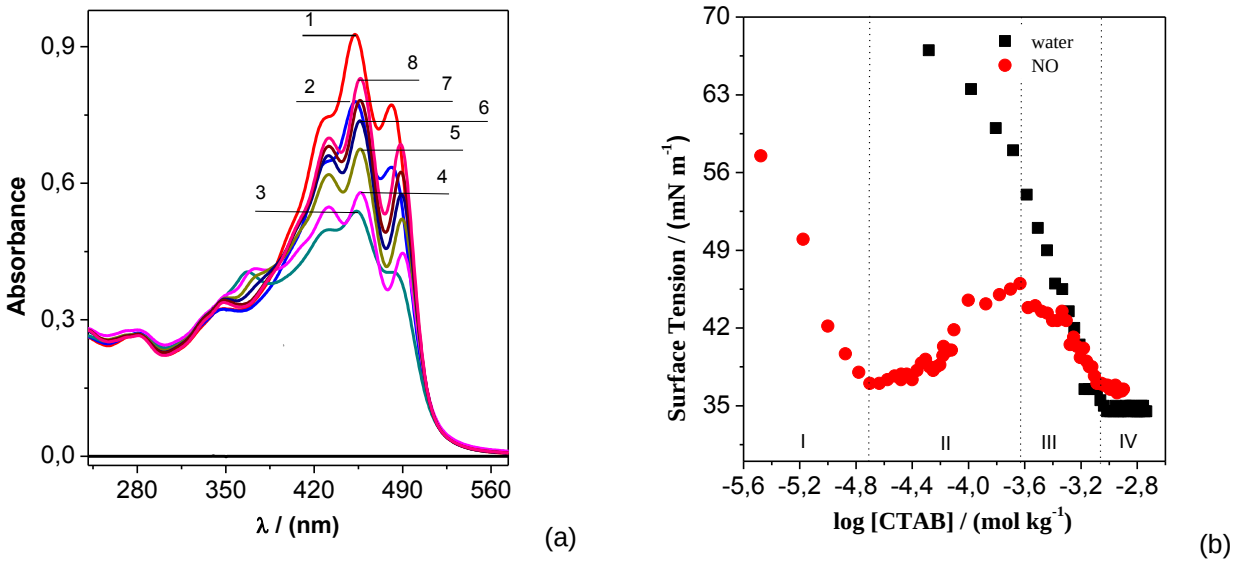


**Figure 1**. (a) Absorption spectra of 0.05% (m/v) norbixin in the presence of CTAB concentrations of (1) 0 mol $kg^{-1}$, (2) 1 x $10^{-5}$ mol $kg^{-1}$, (3) 2 x $10^{-5}$ mol $kg^{-1}$, (4) 2 x $10^{-4}$ mol $kg^{-1}$, (5) 4 x $10^{-4}$ mol $kg^{-1}$, (6) 6 x $10^{-4}$ mol $kg^{-1}$, (7) 8 x $10^{-4}$ mol $kg^{-1}$ and (8) 1 x $10^{-3}$ mol $kg^{-1}$. (b) Changes in surface tension according to the concentration of CTAB in water and 0.05% (m/v) norbixin, at 25°C.

**Área: COL** *(Inserir a sigla da seção científica para qual o resumo será submetido. Ex: ORG, BEA, CAT)*

**Inscrição: 01436** *(Inserir o número de inscrição do autor que fez a submissão)*

# Magnetic composite nanoparticles for hyperthermia and drug delivery to treat cancer

**Caio J. Perecin (PG),[1]* Beatriz M. Tirich (IC),[1] Natalia N. P. Cerize (PQ),[2] Laudemir C. Varanda (PQ).[1]**

**caio.perecin@usp.br**

*[1]Instituto de Química de São Carlos, IQSC-USP; [2]Instituto de Pesquisas Tecnológicas, IPT*

Palavras Chave: Nanoparticles, Magnetite, Polydopamine, Magnetic Hyperthermia, Cancer.

## Highlights

Magnetite nanoparticles coated with polydopamine can perform magnetic hyperthermia while being able to carry drugs to specific sites, in order to treat cancer in an effective and selective manner.

## Abstract

The application of magnetic hyperthermia treatment for cancer demands high efficiency to produce heat, given by biocompatible materials, synthesized via low-cost routes, with high colloidal stability. Magnetite nanoparticles present both biocompatibility and capacity to yield large amount of heat under alternate magnetic fields. Aqueous synthesis routes of magnetite are usually cheaper, but do not provide enough morphological control compared to thermal decomposition. In this work, we propose a low cost aqueous synthesis route by reduction-precipitation with nearly monodisperse spherical nanoparticles and size appropriate for high hyperthermic efficiency. The colloidal stability is enhanced by a polydopamine coating through mussel-inspired surface chemistry, which gives a hydrophilic surface that can be used to encapsulate drugs and release in low pH regions, as generally observed at tumor tissues. Results from transmission electron microscopy, X-ray diffraction, Fourier-transform infrared spectroscopy, dynamic light scattering and zeta potential indicate that the material presents magnetic nanoparticles of magnetite about 12 nm in size coated with polydopamine, resulting in a hydrodynamic diameter near 100 nm and zeta potential around -30 mV at physiological pH. Hyperthermia tests using a magnetic field of 25 mT amplitude and 100 kHz frequency gave heating rates close to 1°C/minute at nanoparticles concentration of 6 $gL^{-1}$, which shows the potential of the material to kill cancer cells. Further work will focus on loading drugs and performing controlled release, as well as on adding molecules onto the nanoparticle surface that could allow effective targeted therapy to cancer.

Figure 1 – Heating rate of a sample of magnetite coated with polydopamine suspended in water with concentration of 6 $gL^{-1}$, submitted to an alternate magnetic field that was turned on and off as indicated in the picture.

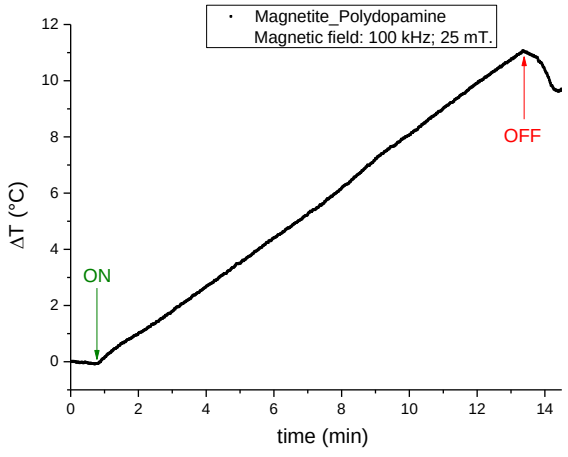

**Área: COL** **Inscrição: 01066**

# Effect of the formation and dissociation of hydrate on the stability of an W/O emulsion

**Roberta K Rodrigues (PQ),[1] Mônica F. Naccache (PQ),[1] Paulo R. de Souza Mendes (PQ)[1]**

**rkamei@esp.puc-rio.br; naccache@puc-rio.br; pmendes@puc-rio.br**

*[1]Departamento de Engenharia Mecânica, Pontifícia Universidade Católica-RJ, Rua Marquês de São Vicente 225, Rio de Janeiro-RJ, 22451-900.*

Palavras Chave: Hydrate, Emulsion Stability, Cyclopentane

## Highlights

The formation of hydrate was induced in laboratory at ambient pressure.
The effect of hydrate formation and dissociation on the stability of a water-in-oil emulsion was studied.

## Resumo/Abstract

The present work describes the study carried out from the formation of cyclopentane hydrates. The structure of the cyclopentane hydrate is similar to the structure formed by natural gas hydrate [1], however cyclopentane hydrate can be formed at environmental pressure [1]. Hydrate formation was induced in emulsions formed by water, mineral oil, the surfactant dioctadecyldimethylammonium chloride and cyclopentane. The stability of the emulsion when the formation of the hydrate is induced was verified. The experiments were carried out in a rheometer in which the viscosity was measured, while the stress was kept constant. The formation of hydrate as well as the destabilization of the emulsion was verified from changes in the viscosity of the system. Preliminary results showed that cyclopentane hydrate formation can reduce the stability of the emulsion. This verification is consistent with the results obtained by Lachance et al. [2], i.e. the coalescence of water droplets in crude oil after formation of hydrate. Figure 1 shows a scheme of the hydrate formation on the surface of the droplets of an emulsion, causing the aggregation between them, and the consequent coalescence of the emulsion.

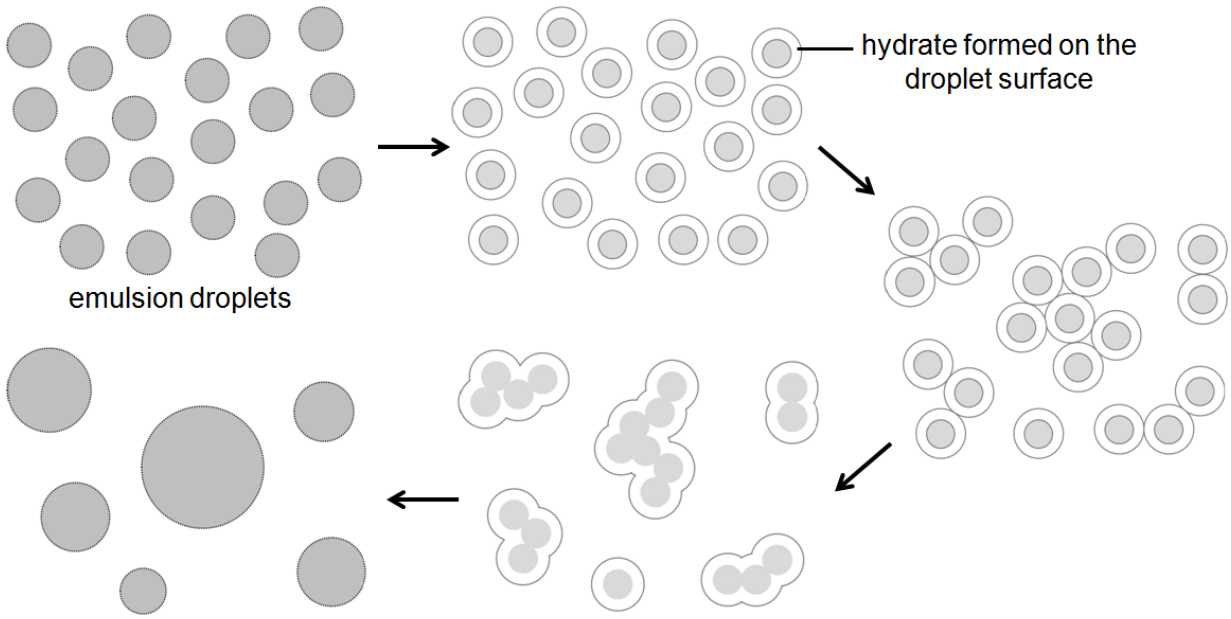


Figure 1. Representative scheme of hydrate forming on the surface of the droplets of an emulsion, inducing the approximation between them and, consequently, the coalescence.

[1] M. Nakajima, R. Ohmura, Y. H. Mori, Industrial & Engineering Chemistry Research 47 (2008) 8933.
[2] J. W. Lachance, E. D. Sloan, C. A. Koh, Chemical Engineering Science 63 (2008) 3942.

**Área: COL** **Inscrição: 00815**

# Avaliação citotóxica de pirazolina com actividade anticâncer em nanocapsulas de carboximetil-hexanoil quitosana

**Andrés F.C. Rengifo (PG)[1], Natália M. Stefanes (PG)[2], Cassiana Mendes (PG)[1], Jessica Toigo (IC)[1], Ricardo. J. Nunes (PQ)[1], Maria C.S Silva (PQ)[2], Alexandre L. Parize (PQ)[1*], Edson Minatti (PQ)[1].**

**achamorro14@gmail.com; alexandre.parize@ufsc.br**

*[1]Departamento de Química, UFSC; [2]Departamento de Análises Clínicas, UFSC.*

Palavras Chave: *Nanocapsulas, Quitosana, Pirazolina, Câncer.*

## Highlights

Cytotoxic evaluation of pyrazoline with anticancer activity on carboxymethyl-hexanoyl chitosan nanocapsules. Nanocapsules, chitosan, encapsulation of pyrazoline, high cytotoxicity.

## Resumo/Abstract

No tratamento contra a leucemia e câncer de pele, a quimioterapia é a alternativa médica mais aplicada. Porém, os fármacos utilizados são altamente tóxicos contra o organismo, causando danos colaterais. Uma alternativa, são as pirazolinas derivadas de flavonóides. No entanto, a alta hidrofobicidade destes compostos limitam sua aplicação. Nanocápsulas de quitosana são uma alternativa para carregar e internalizar em células compostos altamente hidrofóbicos. Assim, neste trabalho foi sintetizado o biopolimero carboximetil-hexanoil-quitosana (ONCHC) e utilizado para formar nanocápsulas por autoagregação com dodecil sulfato de sódio (ONCHC-SDS). Estas foram utilizadas para encapsular a pirazolina H3TM04 (1-(5-(naftaleno-2-il)-3-(3,4,5-trimetoxifenil)-4,5-dihidro-1H-pirazol-1-il)etanona) e avaliar sua citotoxicidade frente células de leucemia e de pele.

O biopolimero foi sintetizado pelo método aminação redutiva baseado no estudo publicado por Kun-Ho Liu e colaboradores(1). O $H^1$ RMN foi determinado que o polímero modificado apresenta um grau de acetilação e de substituição dos grupos hexanoil de 25,8% e 51,60% respectivamente. Por espalhamento de luz dinâmico foi determinado que as nanocápsulas de ONCHC – SDS sem o composto ativo apresentaram um raio hidrodinâmico de 93,5 nm e 118,1 nm com a pirazolina encapsulada. O sistema numa concentração de 1 mg $mL^{-1}$ tem uma eficiência de encapsulação de 96,8 ± 0,1 %, mostrando que é eficiente na encapsulação de pirazolinas hidrofóbicas. A citotoxicidade do composto livre e encapsulado na nanocápsula de ONCHC/SDS foi avaliada em células de leucemia Jurkat e K-562, como também para células de pele B16F10. A tabela 1 mostra as concentrações de inibitória media $IC_{50}$ para 24 horas de encubação.

Tabela 1. Valores de IC50 da pirazolina H3tm04 nas células de leucemia e pele.

| Composto | Jurkat | K-562 | B16F10 |
|---|---|---|---|
| Livre | 32,05 ± 1,06 | 30,77 ± 0,59 | 98,72 ± 1,60 |
| Encapsulado | 19,32 ± 1,01 | 31,78 ± 2,64 | 28,81 ± 1,82 |

Os Resultados mostram que a nanocápsula favorecem a internalização nas células diminuído os valores de $IC_{50}$, especialmente para células de pele.

[1] *Macromolecules* **2008**, *41*, 6511-6516

**Área: COL**

**Inscrição: 00692**
*(Inserir o número de inscrição do autor que fez a submissão)*

# Síntese de nanopartículas de prata com alto desempenho em espectroscopia SERS no infravermelho próximo

**Hugo C. Belgo (IC), *Antônio C. Sant'Ana(PQ)**

**hugo_camarano@hotmail.com; antonio.sant@ufjf.edu.br**

[1]*Departamento de Química, UFJF;*

Palavras Chave: *Raman effect, Surface plasmon, UV-VIS-NIR spectroscopy.*

## Highlights

Synthesis of silver nanoparticles with high performance in SERS spectroscopy in the near infrared.
The domain of the surface chemistry of the silver nanoparticles for controlling of the adsorption.
The SERS investigation of biomolecules adsorption for conceiving biodevices.

## Resumo/Abstract

Surface-enhanced Raman scattering (SERS) spectroscopy is an outstanding technology for understanding the adsorption mechanism involving organic analytes interacting with the surfaces of coinage metals. In this workUV-VIS-NIR spectroscopic was used to verify the size distributions of the silvernanoplates(AgNP) synthesized under different conditions.These syntheses based on successive oxidation and reduction of the metal,by using sodium borohydride and hydrogen peroxide, allow stabilizing AgNP with dimensions around 80-200 nm. The size control was important for the presence of resonance between the localized surface plasmon absorption and the exciting radiations with wavelength in the red and near infrared regions. The final passivated surface, obtained in the end of the syntheses, allow stabilizing the suspension, but precludes the adsorption of the analytes without treatment of the metallic surface. The SERS spectra were obtained after centrifugation followed by the resuspension of the precipitate with borohydride aqueous solution.

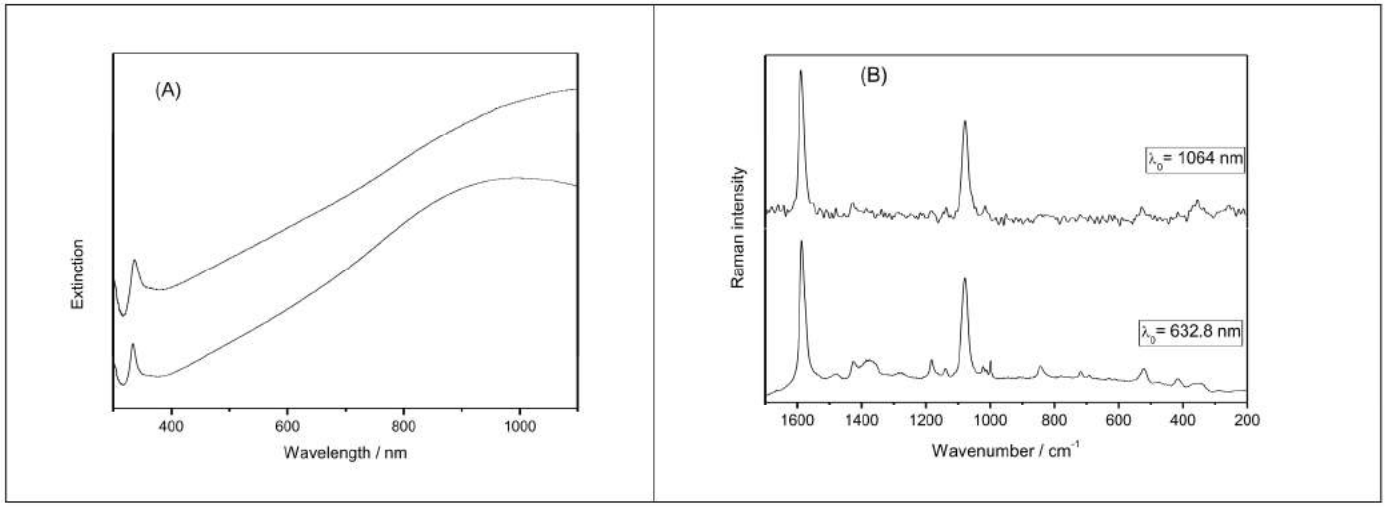


Figure 1: UV-VIS-NIR spectra of two different AgNP suspension (A) and SERS spectra of mercaptobenzoic acid on thin film surface by using 632.8 nm laser line and on AgNP aqueous suspension by using 1064 nm excitation.

The high SERS response of mercaptobenzoic acid allows its use as probe molecule for optimizing the SERS signal of the substrate. Figure 1 shows the UV-VIS-NIR spectra of two distinct syntheses of AgNPs, with localized surface plasmon resonance in the red and infrared region, and the SERS spectra of the probe molecule by using two different exciting radiations.

**Área: COL** **Inscrição: 00313**

# Liquid-liquid equilibria of aqueous two-phase systems (ATPS) containing triton-X100 and choline chloride at different temperatures

**Silvia Juliana Barros e Silva (PG), Alana Luiza Gonçalves Ferreira (IC), Jussara Alves Penido (PG), Aparecida Barbosa Mageste (PQ), Gabriel Max Dias Ferreira (PQ)***

**silviajbarros@gmail.com; gabrielmdf@yahoo.com.br**

*Chemistry Department, UFOP, Minas Gerais, Brazil*

Keywords: *Aqueous two-phase systems, Phase diagrams, Triton-X100, Choline Chloride.*

## Highlights

- ATPSs containing triton-X100 and choline chloride were studied;
- Phase diagrams were obtained at different temperatures;
- Binodal curves exhibited an unusual shape;
- Binodal region increased with the temperature increase.

## Resumo/Abstract

The use of aqueous two-phase systems (ATPSs) in processes of extraction and purification of strategic solutes such as proteins, metal ions, and nanomaterials have provided an important advance in the development of green separation technologies. In this research field, the discovery and the study of new ATPSs, especially those formed by nontoxic components, is a very important issue. In this work, a new ATPS formed by triton-X100 (TX-100), choline chloride (CC), and water was studied, and its phase diagrams were experimentally obtained at different temperatures (298.15 - 328.15 K). The concentrations of TX-100 and $H_2O$ were determined in each phase of the system using UV-vis spectroscopy and gravimetric analyses, respectively. The CC content in both phases was determined by mass balance. Interestingly, the shape of the binodal curves (Figure 1) was distinct from those reported for triton-based ATPSs described in the literature [1]. Moreover, the increase in the temperature of the system promoted an increase in the biphasic region (Figure 2), indicating an endothermic phase-separation process. All systems evaluated presented a top phase enriched with CC and a bottom phase enriched with TX-100, showing the segregation between these two components. Studies on the effect of hydrophilic chain length of triton on the ATPSs properties are under investigation in our laboratory. These new ATPSs are strategic for the extraction of biomolecules due to the biocompatibility of their components.

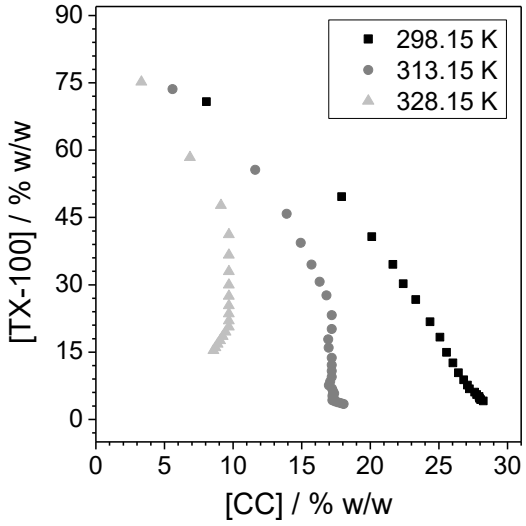


Figure 1. Binodal curves for TX-100 / CC / $H_2O$ ATPS at different temperatures. Curves were obtained by turbidimetric titration.

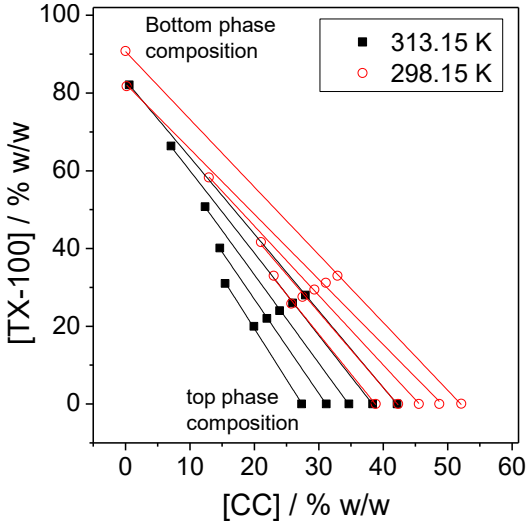


**Figure 2.** Phase diagrams for the TX-100 / CC / $H_2O$ ATPS at 298.15 and 313.15 K.

**References: [1]** A. Salabat, M.R. Far, S.T. Moghadam, *J. Solution Chem.* 40 (2011) 61-66.

**Área: COL** **Inscrição: 00055**

# Adsorption of fluoride by magnetic Li-Al layered double hydroxide

**Ana C. R. Meira (PG),[1] Juliana C. Kreutz (PG),[1] Alesandro Bail (PQ),[2] Renata M. Giona (PQ)[1*]**

**renatam@utfpr.edu.br**

*[1]LAMAFI, Departamento de Química, UTFPR – Medianeira; [2]LAQMATS, UTFPR - Apucarana*

Keywords: *Adsorption, LDH, Magnetite, Fluoride ion.*

## Highlights

A $Fe_3O_4$@LDH-Li/Al structure was synthesized. Results showed the LDH was effective in the fluoride ion uptake from aqueous solution. Fluoride adsorption data were fitted by Langmuir isotherm model.

## Resumo/Abstract

The use of adsorbents to uptake hazardous ions from water and wastewater has attracted the attention of researchers due to their high effectiveness.[1] Magnetite-containing materials possess interesting magnetic properties and the layered double hydroxides (LDHs) are known to be excellent ion exchangers. Core@shell structures, such as $Fe_3O_4$@LDH-Li/Al, possess the advantage of combining physico-chemical properties of two different materials.[2]

The magnetic LDH was evaluated in the fluoride ion ($F^-$) uptaken from water. Despite its comprehensive use for dental health, depending on its concentration, $F^-$ ion is considered highly toxic and may cause dental fluorosis. According to the Ministerial Decree # 2914/2011, the maximum limit of fluoride ion in the water is 1.5 mg/L.[3]

The magnetic material was prepared by a simple synthetic route and characterized by XRD and FTIR. Then, it was evaluated in batch experiments for the fluoride ion uptaken from water. The fluoride adsorption better fitted the pseudo-second order kinetics model with $k_2$ of 10.73 $g.mg^{-1}.min^{-1}$. The adsorption data were fitted by Langmuir (Eq. 1) and Freundlich (Eq. 2) isotherm models (Table 1) and the maximum adsorption capacity was 5.58 $mg.g^{-1}$ (Figure 1).

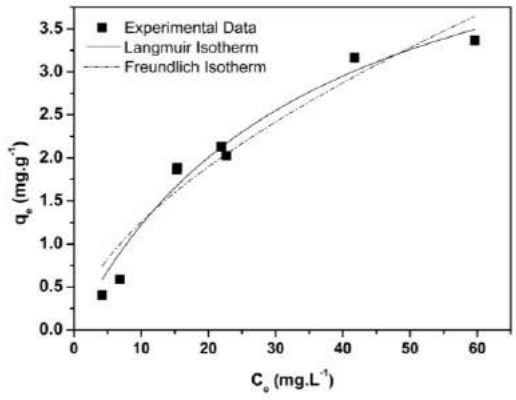


Fig. 1. Isotherms for $F^-$ adsorption on magnétic LDH. Experimental conditions: $[F^-]_{initial}$ 3-100 $mg.L^{-1}$; weight of adsorbent: 35 mg; T: 30°C; volume of solution: 5 mL.

Table 1. Equilibrium parameters obtained by Langmuir and Freundlich isotherm models to $F^-$ adsoption on $Fe_3O_4$@LDH-Li/Al.

| Langmuir model | | | Freundlich model | | |
|---|---|---|---|---|---|
| $q_{max}$ ($mg.g^{-1}$) | b ($L.mg^{-1}$) | $R^2$ | $K_F$ ($mg.g^{-1}(L.mg^{-1})^{1/n}$) | n | $R^2$ |
| 5.584 | 0.028 | 0.9593 | 0.317 | 1.674 | 0.9156 |

$$q_e = \frac{bq_{max}C_e}{1+bC_e} \quad (1) \qquad q_e = K_F C_e^{1/n} \quad (2)$$

## References

[1]DORIGON, L. et al. **Applied Surface Science**. v. 420, p. 954-962, 2017.
[2]SONG, H. et al. **Transactions of Nonferrous Metals Society of China**, v. 23, p. 3337-3345, 2013.
[3] BRASIL (2011). Ministério da Saúde. www.saude.gov.br. Disponível em: http://bvsms.saude.gov.br/bvs/saudelegis /gm/2011/prt2914_12_12_2011.html

The authors would like to thank SANEPAR, Fundação Araucária and Universidade Tecnológica Federal do Paraná.

**Área: _COL__ Inscrição:_00741_____**

# Variation of the electrokinetic parameters of colloidal systems

**Daniel José Pochapski (IC) [1]*, Leila Cottet (PG) [2], Carlos Alberto Policiano Almeida (PQ) [1]**

**danieljosepochapski@hotmail.com**

*[1]Departamento de Química, UNICENTRO; [2]Departamento de Química UFSC*

Key Words: *Electric Double Layer (EDL), Electrophoretic Mobility, Zeta Potential, Hydrodynamic Size*

## Highlights

A charge distribution model around the particles was proposed.

Zeta potential (ζ-potential) and hydrodynamic size (H-Size) of montmorillonite clay were studied at different temperatures and pHs.

The effect of the concentration of monovalent, bivalent and trivalent electrolytes on ζ -potential was discussed.

The influence of particle concentration on ζ -potential was studied at different temperatures.

## Resumo/Abstract

In this work, the surface charge of the particles, one of the most important properties of colloidal systems, was studied. The control of this parameter is the fundamental key to the stability of these systems. According to DLVO theory (Derjaguin & Landau, 1941; Verwey & Overbeek, 1948), high values of ζ-potential (±30mV) ensure greater electrostatic repulsion between particles, avoiding aggregation due to the attraction forces of van der Waals.

The electrokinetic properties of montmorillonite clay (MC) were determined at different pHs, temperatures and electrolytes. The MC presented negative values of the ζ-potential in the range of pH 2-12 and 10-60 °C of temperature. High values of ζ-potential (-27-45mV), without isoelectric points, are characteristic of MC. The surface electric charge originates from the isomorphic substitutions of $Al^{+3}$ for $Mg^{+2}$ and/or $Fe^{+2}$ in the octahedral sites and $Si^{+4}$ for $Al^{+3}$ in the tetrahedral sites of MC.

The presence of electrolyte in the medium decreases the magnitude of the ζ -potential due to the compression of the EDL. If the dispersed ion is the potential determining ion (PDI), ζ-potential value will be controlled by the concentration of the PDI.

Furthermore, the behavior of H-Size of particles, in different conditions, was studied and compared with Transmission Electron Microscope (TEM) analyzes. A charge distribution model around MC particles has been proposed.

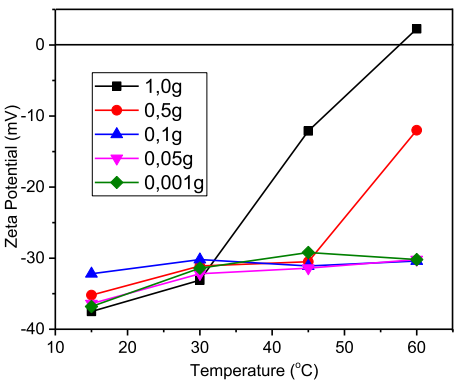


**Fig 1-** Variation of ζ-potential with temperature at different particle concentrations.

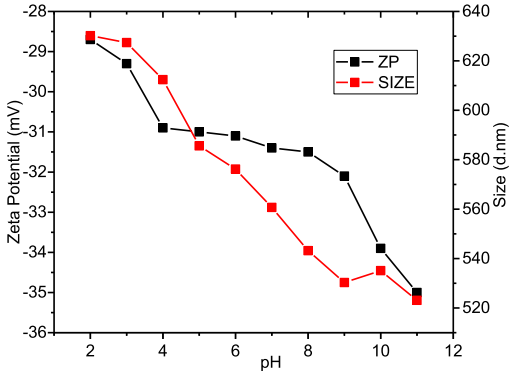


**Fig 2-** ζ-potential and H-Size versus pH.

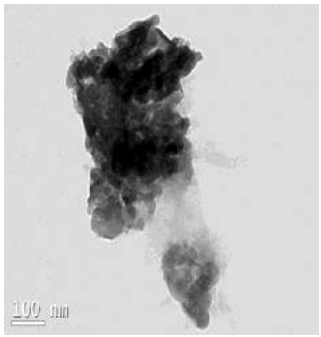

**Fig 3-** TEM of MC particles.

**Área: EDU** **Inscrição: 00054**

# Balanceamento de equações químicas utilizando o feltro como ferramenta de ensino na Semana Nacional de Ciência e Tecnologia 2017

**Pedro Vitor dos Santos (IC),[1] Ailton Coelho Junior (IC),[1] Mariana Barboza da Silva (IC),[1] Josenice Conceição dos Santos (IC)[1], Monique Gabriella Angelo da Silva (PQ)[1*].**

**vitor.pedro96@hotmail.com; monique.silva@iqb.ufal.br**

[1]*Instituto de Química e Biotecnologia, UFAL*

Palavras Chave: *Show de Química, Feltro, Balanceamento, Material Didático.*

## Highlights

Balancing chemical equations by using felt as teaching tool in the National Science and Technology Week 2017.

The use of felt frame during the presentation of the Chemistry Show to spread the theme "The Mathematics is in Everything" with public in the cities of state of the Alagoas, Brazil. The result was to provide an effective tool for attempts at balancing the equations and discussing the importance of mathematics to chemistry.

## Resumo

Em 2017, a Usina Ciência da Universidade Federal de Alagoas (UC-UFAL) auxiliou a difundir o tema "A Matemática está em Tudo" da Semana Nacional de Ciência e Tecnologia (SNCT) através dos Shows de Química (SQ) apresentados nas cidades de Batalha, Belo Monte e Palestina em Alagoas. O SQ da UC-UFAL consiste em experimentos que retomam os conteúdos de química do Ensino Médio e discutem situações de processos químicos do nosso cotidiano. Para introduzir o tema abordado, foi confeccionado, com feltro e EVA, um quadro com as equações das reações de dupla troca entre KI e $Pb(NO_3)_2$ e da decomposição de $H_2O_2$, que são apresentadas no Show, sem os índices e os coeficientes. A tarefa dos expectadores era balancear as equações aderindo os números em EVA no quadro de feltro enquanto eram apresentados os experimentos das respectivas equações. Após o término do preenchimento do quadro, foi feita uma discussão de outras formas que a matemática está inclusa na química. O quadro em feltro foi um grande facilitador, pois proporcionou aos expectadores retirar e colocar os números novamente com facilidade quando erravam e fazer as tentativas do balanceamento até acertarem. Segundo Sousa (p.13, 2007) o uso de recursos didáticos pode tornar a construção da aprendizagem mais ativa, em razão de, esquematizar e concretizar os conceitos e as ideias vistos em sala de aula. É preocupado com melhoria da educação que o SQ da UC-UFAL disponibiliza inúmeros recursos todos os anos na SNCT.

Figura 1. Discussão do quadro de feltro durante a apresentação.

SOUSA, Salete Eduardo de. O Uso de Recursos Didáticos no Ensino Escolar. Disponível em: <http://www.dma.ufv.br/downloads/MAT%20103/2015-II/slides/Rec%20Didaticos%20-%20MAT%20103%20-%202015-II.pdf> Acesso em: 2 fev 2018.

**Área: EDU** **Inscrição: 01208**

# A inserção da Química Ambiental na Educação Básica utilizando a experimentação como estratégia pedagógica

**Lucas D. Almeida (IC),*[1] Larissa F. Pereira (IC),[2] Isabella S. P. Santos (IC),[1] Camille D. Vieira (IC),[1] Gabriella B. Almeida (IC),[2] Luciana R. Marcelo (PQ),[1].**

**lucas.domingues.almeida@outlook.com.br; lucas.domingues.almeida@outlook.com.br**

[1]*Instituto Federal de Educação, Ciência e Tecnologia (IFRJ) - Campus Duque de Caxias*
Palavras Chave: *Ensino de Química, Química Ambiental, Experimentação, Formação Docente.*

## Highlights

The inclusion of environmental chemistry in basic education using experimentation as a pedagogical strategy.

The environmental as a cross-cutting theme
The relationship between chemistry and environmental issues
The use of experimentation in the dissemination of science and teacher education

## Resumo/Abstract

Os documentos curriculares oficiais sugerem que conceitos químicos podem ser relacionados com questões ambientais e esta relação pode promover a contextualização e a interdisciplinaridade. Embora existam incentivos para a implementação dessa temática nas escolas, a sua abordagem de forma crítica, transformadora e emancipatória é um desafio. O objetivo desse trabalho é relatar as experiências vivenciadas pelos alunos do curso de Licenciatura em Química (LQ) do IFRJ - Duque de Caxias na atividade *Mostra de Experimentos de Química Ambiental*. A mostra ocorreu no campus do IFRJ Duque de Caxias em duas edições. A primeira teve como público alvo os alunos e professores do ensino fundamental e médio de duas escolas públicas localizas próximas ao campus. Já na segunda, participaram os alunos do ensino médio dos cursos técnicos integrados do IFRJ. Realizamos os seguintes experimentos: Será que a chuva é ácida?; A densidade de líquidos e os desastres ambientais; Na água que você bebe tem ferro?; Mini estação: compreenda o tratamento de água; Desastre de Mariana: entenda a erosão hídrica. A mostra faz parte da disciplina optativa do curso da LQ Métodos Laboratoriais de Análise de Água e Solo. A partir das observações realizadas durante o evento e dos relatos dos sujeitos envolvidos verificamos os seguintes impactos gerados a partir desta ação: estimulação dos alunos da educação básica para o ensino de química; formação docente dos licenciandos; integração entre o instituto e a educação básica; contribuição com a missão extensionista do instituto.

**Figura 1**. Demonstração de um dos experimentos da Mostra de Química Ambiental (à esquerda) e Mini estação utilizada em um dos experimentos (à direita)

**Área: EDU** **Inscrição: 01263**

# Feira de negócios como espaço não-formal para o ensino técnico em química

**Marcos C. Machado (PQ).[1]***

**marcosiq@gmail.com**

[1]*Fundação Indaiatubana de Educação e Cultura, FIEC*

Palavras Chave: *Ensino técnico, Espaço não-formal.*

## Highlights

Business fair as non-formal space for technical education in chemistry. Integration of program content and future professional practice. Technical students researching about laboratory equipment and its uses. Socio-interactionist learning perspective.

## Resumo

Dentre os desafios do ensino técnico em química está a necessidade de integrar os conteúdos programáticos às práticas profissionais, notadamente àquelas voltadas para a utilização de técnicas e equipamentos de laboratório, todavia, por questões de custo e infraestrutura tal prática é dificultada, indicando a necessidade de buscar alternativas para o ensino, como os espaços não-formais de educação. Tais espaços são caracterizados como aqueles em que as atividades aprendizagem ocorrem externamente à instituição de ensino, desde que as atividades possuam um objetivo e sejam devidamente orientadas. Objetivou-se neste a integração citada através de uma atividade em uma feira de negócios do setor de química analítica como parte integrante da disciplina de análise instrumental. Para tal, os alunos do curso técnico foram divididos em grupos, e a cada grupo foram distribuídos um conjunto de equipamentos que deveriam ser encontrados na feira, sendo necessário elencar um conjunto de características como valor, condições de operação, possibilidade de automação, consumíveis utilizados em conjunto e aplicabilidades comuns, sendo que tais dados deveriam ser expostos à classe em um momento posterior. Através da observação dos alunos na feira, constatou-se que houveram poucas situações em que não ocorreu diálogo com os responsáveis dos estandes, sendo necessária a intervenção do professor. Dentro de uma perspectiva sócio-interacionista avaliou-se positivamente a atividade uma vez que os alunos inseriram-se em contextos de futura atuação profissional, assim como possibilitou maior aproveitamento dos conteúdos em classe de aula.

**Área: EDU** **Inscrição: 00393**

# A Arte como princípio formativo de pibidianos em Química

**Camila Silveira da Silva (PQ)**[1]

**camila@quimica.ufpr.br**

[1]*Universidade Federal do Paraná/Departamento de Química/Bolsista PIBID-CAPES*

Palavras-chave: Formação de Professores, PIBID, Ciência e Arte.

## Highlights

Art as formative principle of pibidians in Chemistry. Analysis of the formative potential of a Sarau (Science and Art) for undergraduate students.

## Resumo

O Programa Institucional de Bolsas de Iniciação à Docência (PIBID) tem se caracterizado como um modelo formativo que leva em conta as principais demandas pedagógicas contemporâneas, possibilitando e estimulando a construção de saberes docentes complexos e integradores. No contexto de um Subprojeto de Química, de uma Universidade Pública Federal, uma ação de destaque tem sido a organização e a participação em um Sarau cuja temática é Ciência e Arte. No presente trabalho, analisamos o potencial formativo desse Sarau para os licenciandos em Química. Na perspectiva da pesquisa qualitativa participante, nesse recorte, tomamos como dados as reflexões escritas desses sujeitos - participantes do Subprojeto, registradas no relatório do segundo semestre de 2017 que continha dados e comentários sobre todas as atividades desenvolvidas ao longo do período (incluindo o Sarau). A quantidade de menções ao Evento foi bastante expressiva, com relatos extensos e emocionantes contemplando multidisciplinaridade, contextualização, interpretação, ressignificação de conceitos científicos, trabalho colaborativo, ludicidade, olhar investigativo, criticidade, criatividade, movimentação corporal, expressão, comunicação de ideias e construção da identidade profissional. No Quadro 1 encontram-se excertos de tais registros, de acordo com o tipo de participação do pibidiano. Todos participaram do processo de elaboração do Sarau. Outros, além disso, atuaram como artistas no palco performando canções do disco *Quanta*, de Gilberto Gil.

**Quadro 1:** Excertos de registros escritos dos pibidianos de acordo o tipo de participação no Sarau.

| Tipo de Participação | Excertos de registros escritos |
|---|---|
| Atuação no Palco | "*foi lindo* [...]*, um momento muito magnífico pra mim, foi a primeira vez em que subi em um palco, pensei que ficaria muito nervosa com o público, até porque meus pais e minha irmã foram me ver, mas pelo contrário, fiquei muito tranquila com a apresentação, pois nós ensaiamos dois dias por semana de agosto até o dia do sarau*". **(R2_2017_Dúbnio*)**. "*Algumas das impressões que tive desse evento foram muito fortes. Relacionar a Ciência com a Arte de forma tão íntima é muito emocionante* [...] *Além disso, isso serve muito como fonte de inspiração para futuras atividades que podem ser desenvolvidas em sala de aula e aplicando isso na nossa vida profissional grandes mudanças na forma de ensino podem ser geradas*" **(R2_2017_Boro*)**. |
| Atuação fora do Palco | "*Passamos o dia realizando a decoração do espaço. Foi um dia de muito trabalho e bastante cansativo, mas quando chegou o fim da tarde o espaço estava lindo.* [...] *Eu optei por não participar de apresentações culturais, mas apesar de estar do lado de fora fiquei observando as apresentações, que foram lindas e emocionantes*" **(R2_2017_Prata*)**. "*A atividade de confecção de móbiles foi como uma terapia para mim, sendo um momento agradabilíssimo e que a conversa e a interação entre o grupo fluiu muito bem* [...] *O sarau teve apresentações muito lindas e a participação expressiva de pessoas do Departamento de Química*" **(R2_2017_Tântalo*)**. |

*nomes fictícios para preservar a identidade dos pibidianos participantes da pesquisa.

Analisando o potencial do Sarau, consideramos que a Arte tem se constituído como uma dimensão formativa importante dos pibidianos em Química com destaque para a construção de conhecimentos, de si e da docência, a partir da articulação da linguagem científica com a artística.

**Área: EDU** **Inscrição: 654**

# Investigando o conhecimento dos conceitos Mistura, substância, átomo e elemento em uma Olimpíada de Química.

**José Antonio Maruyama (FM)[1,2,3], Francine Ferreira de Carvalho (IC)[2], Karen Chibana Ferreira (IC)[2], Caroline Oliveira Rocha (PG)[2], Rodrigo Fernando C. Marques (PQ)[2].**

**jamaruyama@ifsp.edu.br**

*[1]Colégio Dom Bosco COC/Guariba/SP; [2]Centro de Ciências de Araraquara, UNESP; [3]Instituto Federal de Ciência e Tecnologia de São Paulo, campus Matão/IFSP/MTO*

Palavras Chave: Substâncias, Elementos, Átomos, Mistura, Olimpíada de Química, Conceitos.

## Highlights

Investigating the knowledge of concepts Mixture, substance, atom and element in a Chemistry Olympiad. The work investigates the understanding of simple concepts of Chemistry by students of the second year of high school in the public network, through a Chemistry Olympiad held in the city of Araraquara.

## Resumo/Abstract

O trabalho analisa uma Olimpíada de Química (OIQ) realizada pelo Instituto de Química da Unesp na cidade de Araraquara junto aos alunos do 2ª ano do Ensino Médio das escolas estaduais da referida cidade. Todas as escolas estaduais participaram da OIQ, sendo um total de 1145 respostas. Um dos objetivos da OIQ é investigar as dificuldades dos alunos e, posteriormente, auxiliar os professores a solucionar/melhorar tais problemas. Este trabalho analisa o desempenho dos alunos em uma das questões que envolveu os conceitos de átomos, elementos, moléculas e substâncias, figura 1. Ao analisar as respostas nota-se que menos de um quinto dos alunos acertaram a resposta (18,52%), figura 2, o que permite afirmar que a grande maioria deles não consegue distinguir/definir os conceitos de átomo, elemento, molécula, composto e substância, uma vez que a maioria deles, 32,75% confunde os termos “mistura” e “compostos”. A soma das porcentagens das duas alternativas mais assinaladas indica que a maioria deles apenas substituiu a palavra “misturinha” por mistura e “coisa” por substância, reforçando a deficiência nos conceitos já citados. Essa troca de conceitos mostra que a maioria dos estudantes confunde uma substância com um elemento químico. Essa confusão ocasiona problemas futuros para o entendimento de conceitos como transformações da matéria e propriedades das substâncias, dentre outros. Essa análise preliminar indica a importância do entendimento de conceitos tidos como simples, porém, caso não ocorra, ocasionará problemas piores e consequentemente o não gosto pela disciplina de Química.

**1.** (FUVEST 2012) Na obra **O poço do Visconde**, de Monteiro Lobato, há o seguinte diálogo entre o Visconde de Sabugosa e a boneca Emília:

- Senhora Emília, explique -me o que é hidrocarboneto . A atrapalhadeira não se atrapalhou e respondeu:

- São misturinhas de uma coisa chamada hidrogênio com outra coisa chamada carbono. Os carocinhos de um se ligam aos carocinhos de outro.

Nesse trecho, a personagem Emília usa o vocabulário informal que a caracteriza. Buscando-se uma terminologia mais adequada ao vocabulário utilizado em Química, devem-se substituir as expressões "misturinhas", "coisa" e "carocinhos", respectivamente, por:

A. compostos, íon, moléculas.
B. misturas, substância, moléculas.
C. misturas, substância, átomos.
D. substâncias compostas, molécula, íons.
E. compostos, elemento, átomos.

**Figura 1:** Uma das questões aplicadas aos alunos do 2º ano do Ensino Médio.

| Texto da alternativa | TOTAL | Porcentagem |
|---|---|---|
| A. Compostos, íons, moléculas | 120 | 10,48 |
| B. misturas, substância, moléculas | 375 | 32,75 |
| C. misturas, substância, átomos | 255 | 22,27 |
| D. substâncias compostas, molécula, íons | 183 | 15,98 |
| E. compostos, elemento, átomos | 212 | 18,52 |
| Total | 1145 | 100,00 |

Figura 2: Tabela com o número total das alternativas escolhidas e respectivas porcentagens.

**Área: EDU**
*(Inserir a sigla da seção científica para qual o resumo será submetido. Ex: ORG, BEA, CAT)*

**Inscrição:00043**
*(Inserir o número de inscrição do autor que fez a submissão)*

# Use of experimental class and play activity in chemistry teaching: An experience in elementary education

**Danielle R. M. da Costa (PQ), [1*]João M. D. Oliveira, [1] Brenda H. S. Lopes (IC),[1] Johnathan da C. B (IC),[1] Mayra E. S. Neres (IC),[1] Nayara M. de Sousa (IC),[1] Shirlei R. da S (IC)[1] danymont@uepa.br; marcosdichtl@hotmail.com**

[1]University of the State of Pará (UEPA). Course of natural sciences-Chemistry, Marabá, Pará, Brazil

Keywords: Acids and Bases, Experimental practice, Play activity.

## Highlights

Currently there is a focus of researchers (FOLLMAN, 2013, MORAN, 2015, ASSIS, 2011) in the area of methodological research to promote the teaching of chemistry, be it fundamental and / or medium, from experimental classes and play material. For Lôbo (2012), the proposal of experimental activities is important in teaching and understanding of chemistry, as well as experimental procedures can increase students' motivation. Almeida et al (2013) states that the practice of play activity ensures that the game provides fun and pleasure tied to the educational function, favoring the teaching and learning process.

## Abstract

The process of teaching and learning that occurs in schools is through traditional methods, where the organization of the room and the silence of the students show that they are absorbing content. Researchers report in the literature (LIMA, 2006; MORAN, 2015) that this type of teaching is insignificant when compared to the results obtained from innovative methodologies. The objective was to analyze the potential of different methodological approaches in chemistry teaching. The research was carried out in a primary school class of a public school, where experimental classes were given that addressed the topic about acids and bases in everyday life, and at another time, a playful game similar to "battle naval. From the collected data, it is possible to affirm that the students had the opportunity for the first time to experience educational methodologies different from the traditional ones. According to Assis (2011), the experimental classes serve as a strategy that helps the teacher to retake the content taught and the approach to play activity, according to Silva et al (2007), children are independent to determine their attitudes and that nature play effectively in the teaching and learning process. Therefore, the use of the experimental class in the science laboratory and the realization of a playful activity in the classroom, give the students a dynamic experience, which allowed them to stimulate creativity and effective participation in the classroom.

**References**

ALMEIDA, C. M. M; LOPES, T. C; ROSSANO, A. D. O lúdico como prática pedagógica no ensino de ciências: jogo didático sobre o sistema esquelético. Atas do IX Encontro Nacional de Pesquisa em Educação em Ciências – IX ENPEC, 2013.

ASSIS, M. S. Experimentação como estratégia didática para o ensino de química na educação de jovens e adultos, 2011.

LÔBO, S. F. O TRABALHO EXPERIMENTAL NO ENSINO DE QUÍMICA. **Química Nova**, Vol. 35, No. 2, p. 430-434, 2012.

FOLLMAN, R. M; LORENZ, P. G. O LÚDICO NO PROCESSO DE APRENDIZAGEM. **Salão do Conhecimento**, v. 1, n. 01, 2013.

LIMA, K. E. C; VASCONCELOS, S.D. Analise da metodologia de ciências nas escolas da rede municipal de recife. **Pesquisa em Síntese**, V. 14, n, 52, p. 397-412. Rio de Janeiro, 2006.

M0RAN. J. Mudando a educação com metodologias ativas. **Educação e Cidadania**, v.II. Ponta Grossa, 2015.

SILVA, A. M. T; METTRAU, M. B; BARRETO, M. S. L. O lúdico no processo de ensino-aprendizagem das ciências. **Revista Brasileira de Estudos Pedagógicos**, v. 88, n. 220, 2008.

**Área: EDU** **Inscrição: 01344**
*(Inserir o número de inscrição do autor que fez a submissão)*

# Uma nova metodologia para o registro e análise da interação de estudantes com representações tridimensionais de moléculas

**Claudia Ayres (PG)[1], Rodrigo A. Consoli (IC)[1], Camila A. T. Cicutto (PQ)[2], Gustavo N. da Cruz (FM)[3] Guilherme A. Marson (PQ)[1]***

***gamarson@iq.usp.br**

*[1]Insituto de Química - Depto de Química Fundamental, USP São Paulo – SP; [2]Lic. Educ. no Campo – UNIPAMPA, Campus D. Pedrito – RS; [3]Instituto Silvio Passareli, São Paulo – SP.*

Palavras Chave: Modelos *Moleculares, Habilidades Visuoespaciais, Visualização, Tecnol. da Inf. e do Conhecimento*

## Highlights

**A novell methodology for recording and analyzing the interaction process of students with tri-dimensional representations of molecules.**
The method allows quantitative and qualitative studies from large cohorts. Results (*n*=50) suggest that interactivity supplant visuo-rotation skills differences. Colors act as important visual clues.

## Resumo/Abstract

Comumente, estudos sobre visualização de moléculas baseiam-se em duas abordagens: i-tomar dados semi-quantitativos gerais de muitos indivíduos, ii – tomar dados qualitativos específicos com pequenos grupos. Propomos uma metodologia de registro e análise das interações de estudantes com modelos moleculares tridimensionais interativos que pode contemplar as duas abordagens. Parte-se de um problema: *manipule o modelo interativo de uma molécula até que o considere igual ao modelo estático da mesma molécula*. No processo, registra-se a curva da diferença de orientação entre os modelos *versus* o tempo (Figura abaixo). Além do tempo de resolução (tRes) e da precisão, registra-se a posição da molécula a cada movimento do estudante. Foram realizadas tomadas de dados com 50 estudantes (17 de cursinho popular e 33 graduandos em química), por meio de um instrumento incluindo os seguintes testes: interpretação de representações estáticas, rotação mental (PV-ROT), daltonissmo, esforço mental, e a aplicação da ferramenta com as versões colorida (CPK) e cinza do modelo bola-bastão da molécula da batracotoxina. A análise hierárquica de grupos dos dados indica 3 perfis distintos: A (*n*=15, tRes colorido= 18s, tRes cinza=27s); B (*n*=20, tRes colorido=23s, tRes cinza=36s), e C (*n*=15, tRes colorido=27s, tRes cinza=40s). A baixa correlação de Pearson (-0,36) entre PV-ROT e tRes sugere que o fato dos modelos serem interativos permite superar diferenças individuais na habilidade de rotação, sobretudonos grupos B e C. Átomos coloridos parecem ser referências visuais importantes para estudantes de C. Não se observou diferenças significativas de gênero.

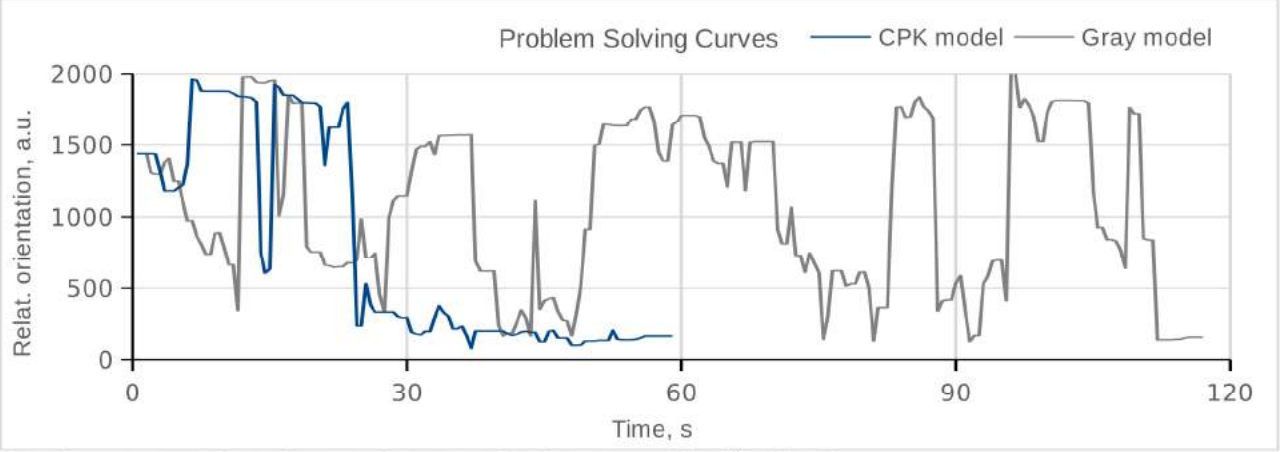


SUPORTE FINANCEIRO FAPESP – REDOXOMA Proc. 2013/07937-8.

**Área: EDU** **Inscrição: 00757**

# USO DE JOGOS DIDÁTICOS: DESAFIOS E SUPERAÇÕES NA VISÃO DE UMA PROFESSORA DE QUÍMICA

**Tatiana do A. Varjão (PQ)[1], Bárbara C. T. Moreira (PQ)[1], Suzana S. Santos (FM)[2*].**

**tvarjao@uneb.br; suzie.santos1226@gmail.com**

*[1]Departamento de Ciências Exatas e da Terra, UNEB; [2]Colégio Estadual Thales de Azevedo*

Palavras Chave: *Formação de professores, Jogo didático, Pibid.*

## Highlights

Use of didactic games: challenges and overcomes in the vision of a chemistry teacher. Presents the experience of a supervising teacher of Pibid in the production of games. Concluded that the University/Basic Education partnership favored the teaching-learning process in diverse points.

## Resumo/Abstract

Apresenta-se a experiência de uma professora supervisora (PS) do Pibid-Química/UNEB na elaboração e aplicação de jogos didáticos (JD), os desafios enfrentados e os reflexos em sua prática. Coletou-se relatos, orais e escritos, examinando-os com base na Análise Textual Discursiva, buscando capturar elementos essenciais para identificar e discutir pontos de dificuldades e o processo de reelaboração da prática da PS. No transcorrer da investigação, observou-se que houve integração das experiências das professoras da Universidade com a da PS, em um movimento que facilitou o emergir dos significados subjetivos dos discursos, estabelecendo-se uma interpretação simultânea, dando conta dos objetos vivido e analisado. Dentre outros pontos, a PS destacou que há fatores limitantes para o uso de JD pelos professores da Educação Básica (EB), enfatizando o tempo despendido para a sua construção e a falta de embasamentos teórico-metodológicos dos aspectos pedagógicos e de experiências lúdicas durante a formação acadêmica desses profissionais. Isto exige dedicação à apropriação das bases teóricas, necessárias à construção dos jogos, de acordo com as necessidades de cada turma. Na análise dos relatos da PS, pode-se perceber indícios da reelaboração de sua prática, como reflexo da experiência propiciada pelo Pibid, a qual concretiza sem dúvida a relação Universidade/EB, a partir de algumas iniciativas explanadas. Assim, concluiu-se que a parceria Universidade/EB foi profícua à conduta reflexiva da PS e que o uso de JD foi laborioso, mas prazeroso e educativo, favorecendo o processo ensino-aprendizagem em aspectos diversos.

**Área: EDU**
*(Inserir a sigla da seção científica para qual o resumo será submetido. Ex: ORG, BEA, CAT)*

**Inscrição: 00122**
*(Inserir o número de inscrição do autor que fez a submissão)*

# THE INFLUENCE OF "EAR" VALIDATION PROCESS OF TEACHING SEQUENCES ON PRE-SERVICE CHEMISTRY TEACHER PREPARATION

**Amadeu Moura Bego (PQ)[1*], Marcelo Giordan (PQ)[2].**

**amadeu@ig.unesp.br**

*[1] São Paulo State University (UNESP), Institute of Chemistry, Araraquara, Brazil; [2] University of São Paulo (USP), Faculty of Education, São Paulo, Brazil.*

Palavras Chave: *Teaching Sequences, Pre-service Teacher Preparation, Topological Model of Teaching, PIBID.*

## Highlights

What is the influence of the EAR validation process of Teaching Sequences, based on Topological Model of Teaching, on the quality of didactic-pedagogical planning of pre-service chemistry teachers?

## Resumo/Abstract

The teacher training, in the scope of the practical rationality model, must enable a rational-practical and grounded knowhow to act in intrinsically complex teaching situations. We support that the didactic-pedagogical planning based on the research and the school objective reality, materialized on structured teaching plans, can be a fundamental element in pre-service chemistry teacher preparation. Giordan developed a model based on the sociocultural perspective to support the elaboration of Teaching Sequences (TS), which is named Topological Model of Teaching, and is based on the Theory of Mediated Action. This paper aims to investigate the influence of the EAR (elaboration, application and redesigning) validation process of TS on the quality of didactic-pedagogical planning of pre-service chemistry teachers. This is a qualitative documentary research that used two different versions of chemistry TS produced by pre-service chemistry teachers in the context of the Institutional Program of Scholarship for Teaching Initiation (PIBID) developed in the Institute of Chemistry of UNESP, Araraquara, São Paulo, Brazil. The data showed significant advances in the TS redesigned that became more cohesive with the problematization, fulfilling the role of structuring element throughout all didactic activities. This increase can be attributed to the assessment process of TS from different perspectives, inserted in this virtuous cycle of EAR movement, which is fundamental to relate the disciplinary contents to pedagogical theories, approximating the theoretical planning and concrete professional practice, as well as developing an investigative attitude about the didactical activities.

**Área: EDU** **Inscrição: 00308**

# Compreensão textual de graduandos em química: tema biodiesel em foco

**Patrícia Fernanda de Oliveira Cabral (PG),[1*] Salete Linhares Queiroz (PQ).[2]**

**salete@iqsc.usp.br; petycabral@gmail.com**

*[1] Programa de Pós-Graduação Interunidades em Ensino de Ciências, Instituto de Física, USP; [2] Instituto de Química de São Carlos, USP*

Palavras Chave: *Horizontes de leitura, Artigos científicos, Biodiesel.*

## Highlights

Textual comprehension among undergraduate chemistry students: theme biodiesel in focus. This paper describes the use of primary research articles in a scientific communication course. The main goal is to demonstrate how the students can understand and benefit from using it.

## Resumo/Abstract

Diversos trabalhos destacam a importância da compreensão de artigos originais de pesquisa (AOP) para a formação de graduandos em química. Assim, no presente trabalho investigamos uma atividade didática, desencadeada a partir da leitura de artigos dessa natureza (tema biodiesel), para a posterior produção de *slides* que deram suporte à elaboração de exposições orais (EO), por grupos de alunos matriculados em disciplina de comunicação científica. Analisamos os *slides* de acordo com os horizontes de compreensão textual (MARCUSCHI, 2008), com o intuito de responder ao questionamento: os componentes dos *slides* elaborados pelos alunos fornecem indícios da compreensão dos mesmos com relação aos AOP? Para uma das EO foram produzidos 20 *slides* como material de apoio (Figura 1).

Figure 1 - Horizontes de compreensão textual**.**

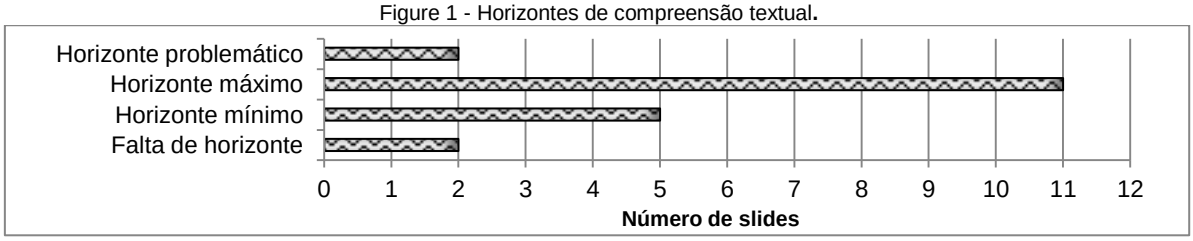


O horizonte máximo foi o mais expressivo, visto que foi evidenciada a produção de sentidos por meio da sumarização de informações presentes no texto e/ou a adição de informações.
O horizonte mínimo foi identificado em *slides* que trataram de operações de paráfrase. O horizonte problemático em *slides* que trataram da inserção de informações equivocadas à EO. A falta de horizonte foi identificada e denotou a cópia de gráficos do AOP, não caracterizando a compreensão do mesmo. A análise dos *slides* indica que houve o entendimento significativo em relação ao AOP: foram mantidas as suas ideias centrais, sem que se perdesse de vista a base informacional estabelecida pelos autores.

MARCUSCHI, L. A. Produção textual, análise de gêneros e compreensão. Parábola Editorial, 2008.

**Área: EDU** **Inscrição: 00239**

# Atribuição de nota: moeda de troca para frequência dos acadêmicos na monitoria de Química Inorgânica?

**Alessandra Stevanato (PQ)[1*], Waleska L. Corsi (IC)[2]**

**stevanato@utfpr.edu.br; waleskacorsi@hotmail.com**

*[1]Departamento de Química, UTFPR - Câmpus Londrina; [2]Departamento de Engenharia de Materiais, UTFPR - Câmpus Londrina.*

Palavras Chave: *Ensino superior, Monitoria, Química inorgânica*.

## Highlights

Assignment of note: currency of exchange for attendance of academics in the monitoring of Inorganic Chemistry? The monitoring project is important in student learning. An analysis of the passing rate and the number of the appointments higher than the grading encourages students to attend frequently.

## Resumo

A facilidade de acesso ao ensino superior da maioria dos estudantes, expôs um nível de formação básico heterogêneo em relação à aprendizagem. O baixo conhecimento e as dificuldades de compreensão dos conteúdos mais complexos abordados nas disciplinas do ensino superior levam a um grande percentual de estudantes desperiodizados[1]. Para auxiliar neste quesito, o projeto de monitoria é uma ferramenta importante de ensino dos acadêmicos, assim foi ofertada monitoria de Química Inorgânica aos alunos de graduação de Engenharia de Materiais e Licenciatura em Química da UTFPR - Londrina, de 2016 a 2017. Em 2016 atribuiu-se 0,1 ponto na média àqueles que frequentassem a monitoria e resolvessem listas de exercícios correspondentes aos conteúdos trabalhados nos horários de atendimentos, em 2017 não houve atribuição de notas. No primeiro e segundo semestres de 2016 foram realizados respectivamente, 182 e 138 atendimentos, enquanto que nos mesmos períodos de 2017 houveram 54 e 30 atendimentos, respectivamente. Estes dados inferem o comparecimento as monitorias relacionado a atribuição de nota ao final do semestre, no entanto, observou-se que a frequência nos horários da monitoria, refletiram de maneira direta no número de acadêmicos aprovados, como apresentado nas Tabelas 1 e 2. Ref.: [1] FERNANDES, D. M. S.; SALDANHA, G. C. B. Dificuldades de Aprendizagem no Nível Superior: estudo de caso com graduandos de licenciatura em química. In: Encontro Nacional de Licenciaturas, 5, 2014. Natal. Anais...Natal: EDUFRN, 2014, p. 1-12. Disponível em: http://enalic2014.com.br/anais/anexos/7704.pdf. Acesso em: 15 ago. 2015.

Tabela 1. Dados obtidos dos acadêmicos do Curso de Licenciatura em Química no período de 2016 a 2017.

| Semestres | Licenciatura em Química | | | |
|---|---|---|---|---|
| | Nº alunos matriculados | Nº desistências | Nº aprovações | % aprovação |
| 2016-1 | 10 | 0 | 8 | 80 |
| 2016-2 | 22 | 0 | 12 | 55 |
| 2017-1 | 14 | 0 | 6 | 43 |
| 2017-2 | 14 | 3 | 5 | 45 |

Tabela 2. Dados obtidos dos acadêmicos do Curso de Engenharia de Materiais no período de 2016 a 2017.

| Semestres | Engenharia de Materiais | | | |
|---|---|---|---|---|
| | Nº alunos matriculados | Nº desistências | Nº aprovações | % aprovação |
| 2016-1 | 45 | 3 | 20 | 49 |
| 2016-2 | 48 | 0 | 17 | 35 |
| 2017-1 | 47 | 5 | 18 | 43 |
| 2017-2 | 48 | 1 | 10 | 21 |

**Área: EDU** **Inscrição: 01163**

# Assessment of construction of knowledge in Covalent Bond in high school through the philosophical zones

**Maurícius S. Pazinato (PQ),[1*] Mara E. F. Braibante (PQ),[2] Ana Carolina G. Miranda (PG).[2]**

***mauriciuspazinato@gmail.com**

[1]*Departamento de Química Orgânica, Instituto de Química, Universidade Federal do Rio Grande do Sul.*
[2]*Programa de Pós-Graduação em Educação em Ciências: Química da Vida e Saúde, Universidade Federal de Santa Maria.*

Keywords: *Chemical bonds, Epistemological obstacles, Teaching and learning.*

## Highlights

The conceptual evolution in Covalent Bond was made possible by the understanding of the structure of matter and the concept of electronegativity, which are essential for understanding this topic.

## Resumo/Abstract

During the study of the topic of covalent bond, high school students are faced with a number of obstacles to learning. Some research indicates that it is common among them the thought that the electrons are equally shared in all covalent bonds and that this type of chemical bond is weak or ruptured in physical transformations[1]. The conceptual evolution implies in overcoming of epistemological obstacles and the knowledge progresses philosophically from realism to empiricism and these to rationalism[2]. The objective of this study is to assessment the conceptual evolution of 29 students of the 1st year high school about covalent bond, along a Teaching-Learning Sequence (TLS). The TLS lasted six classes and was elaborated from problematic situations, modeling and experimental activities, as well as moments of discussion and re-elaboration of the models. The data were collected through questionnaires applied before, during and after the TLS and analyzed based on the philosophical zones of Bachelard (Table 1).

**Table 1.** Characterization of philosophical zones.

| Realistic | Empiricist | Rationalist |
|---|---|---|
| Expressions loaded with common sense and observable facts of everyday life. | Derive from observation and application of general and automatic rules. | Explanations based on theoretical models and various relationships with other concepts. |

**Figure 1.** Results by zone and reserach phase

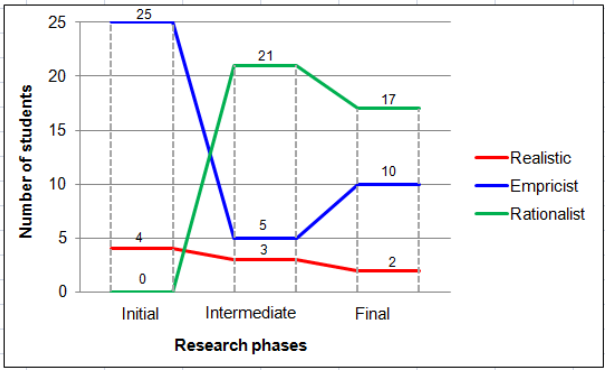


It is observed in Figure 1 that, after participation in the SEA, rationalist conceptions arose and became the majority, while the frequency of other zones decreased. The advanceis obtained is attributed to the understanding of the structure of matter and the concept of electronegativity, which allowed the perception of how the formation of the covalent bond occurs.

[1]Fernandes, L. S; Campos, A. **RBPEC**, v. 12, n. 2, 2012.
[2]Bachelard, G. **A filosofia do não**: Filosofia do Novo Espírito Científico. 2009.

**Área: EDU** **Inscrição: 00325**

# Factors that influence the rates of reactions: discussing concepts from experimental investigative activities

**Eliana Ap. S. Bueno (PQ),[1] Flávia da S. C. Tavares (FM),[2*] Viviane Arrigo (PG),[1] Fabiele C. D. Broietti (PQ).[1]**

**silicz@uel.br; flavia4334@hotmail.com.**

*[1] Chemistry Department, State University of Londrina; [2] State Secretariat for Education of Paraná*

Key words: investigative experiments, Chemical Kinetics; Chemistry Education.

## Highlights

Investigative experimental activities and the active participation of students; Rates of reactions depending on the circumstances of the reaction system; Construction of explanations for the observed phenomena.

## Abstract

Experimentation in the Chemistry Education, elaborated and developed with an investigative character, enables the active participation of students in (re) elaboration of the concepts, with a view to solving a problem situation(1). In this study, we report results of experimental activities of investigative nature, proposed for students of the High School, during the study of Chemical Kinetics. Our goal was to analyze the understanding of students about the influence of some factors on the occurrence rate of reactions depending on the circumstances of the reaction system. At the end of the activities, they were asked to answer the following questions: *1-What happened to the effervescent tablets when they were placed in hot water and ice water? 2-Why did the steel sponge oxidize (rust) faster than the nail although both were placed in 0.2 mol.L$^{-1}$ $CuSO_4$ solution. 3-What is the influence of the concentration of the solutions on the nail oxidation process? 4-What happened when potassium iodide was added to hydrogen peroxide? 5-What is the function of potassium iodide?* The methodological procedures of content analysis (2) allowed us to analyze and interpret the answers provided by the students, a movement that originated the Table 1:

**Table 1: Analysis of student responses**

| Questions | number of established categories | Discussion of the responses |
|---|---|---|
| 1 | 6 | Most students mentioned that the increase in temperature causes a faster dissolution of the effervescent tablet, however, they did not relate the phenomenon observed to the increase of the kinetic energy of the reactant molecules. |
| 2 | 4 | Although they assert that the steel sponge undergoes oxidation with greater rate than the nail, most of them did not explain that the larger the exposure surface of the iron to the environment the greater the amount of oxygen incorporated, which causes a greater interaction between the reagents. |
| 3 | 4 | Most reported that the solution concentration value is directly proportional to the fastness of the nail oxidation, since only in four responses did the concentration increase be associated with the increase in the number of reagent molecules. |
| 4 | 5 | The students recognized that the potassium iodide has the function of accelerating the reaction, acting as a catalyst, but only one of them related the action of the catalyst to the decrease of the activation energy |

Based on the analyzes, we verified that the experiments were important for the students to understand the influence of some factors on the speed of the reactions, since they could observe macroscopically the occurrence of the phenomena. However, we realize that there are still some limitations to be overcome when working with experimental activities, especially regarding the inherent actions of this type of activity, since students have to investigate the phenomenon observed, to propose hypotheses; perform tests and construct plausible explanations for their occurrence supported by scientific theories.

[1]SUART R. C.; MARCONDES, M. E. R. A manifestação de habilidades cognitivas em atividades experimentais investigativas no ensino médio de química. *Ciência & Cognição*, v.14, n.1, p. 50-74, 2009.
[2]MORAES, R. Análise de conteúdo*. Revista Educação,* v.22, n.37, p. 7-32, 1999.

**Área: _EDU_____ Inscrição:__00069_____**

# Estudoa dea casoa daa disciplinaa ‘Químicaa Aplicadaa àa Engenharia’:a processo corrosivo em portões metálicos em São Miguel-RN

**Sanderlir S. Dias (PQ),[1,*] Francisco A. Chaves (IC),[2] Josy E. T. Ramos (PQ),[1]**

**sanderlir.dias@ufersa.edu.br**

*[1]Departamento de Exatas e Naturais, CMPF, UFERSA [2]Discente, Engenharia Civil, CMPF, UFERSA*

Palavras Chave: Corrosão, Portões, Ensino-aprendizagem, Contextualização.

## Highlights

Case study of the discipline 'Applied Chemistry to Engineering': corrosive process in metallic gates in São Miguel-RN. In the discipline is approached the theme 'Corrosion'. Students should present an object or site or monument, identifying the material, the corrosive medium and protective measures.

## Resumo/Abstract

O tema ‘Corrosão’ está inserido no conteúdo programático da disciplina ‘Química Aplicada à Engenharia” que faz parte da grade curricular do Curso de Bacharelado em Ciência e Tecnologia da Universidade Federal Rural do Semi-Árido no Município de Pau dos Ferros-RN. Quando esse tema é abordado, uma parte da avaliação consiste em analisar um objeto/local/monumento que esteja com indícios de processos corrosivos, avaliar qual o meio corrosivo e propor formas de prevenção, construindo assim o chamado ‘triângulo da corrosão’. Surgem vários objetos de estudos interessantes, rendendo boas discussões nas apresentações dos trabalhos de campo. Os discentes apresentam uma elevada participação e alguns encontram motivação/inspiração para elaborar projetos de término de curso. Um desses trabalhos, especificamente, avaliou o processo corrosivo em portões metálicos no Município de São Miguel-RN, utilizando registros fotográficos ao longo de dois meses e meio. A atmosfera de São Miguel-RN pode ser considerada pouco agressiva, visto que a cidade é pouco industrializada. Foi encontrado, por se tratar de portões expostos ao meio atmosférico, a corrosão de morfologia uniforme como a forma mais presente. Entretanto, não foi a única, pois outros fatores também atuaram sobre estes, como esforços mecânicos. Mostrou-se o comparativo de portões com/sem pintura expostos as mesmas condições, enfatizando que a pintura é uma ótima proteção e é viável devido ao seu custo benefício. Trabalhos como o exposto tem contribuído para melhorar o ensino-aprendizagem por meio da contextualização e de exemplos do cotidiano.

**Área: EDU** **Inscrição: 01251**

# Utilização de Normas Técnicas de produtos no ensino de Química

**Thabata de S. A. Oliveira (IC),[1*] Renata C. Nunes (PQ).[1]**

**thabata.araujo96@gmail.com; nunesrenatac@gmail.com**

[1] *Instituto Federal de Educação, Ciência e Tecnologia Fluminense – campus Cabo Frio*

Palavras Chave: *Normas Técnicas, Educação Ambiental, Experimentação, Consumo*

## Highlights

The use of products' Technical Standards in Chemistry teaching

Experimental activities were developed based on technical standards of PET bottles and safety matches. These activities allow for interdisciplinary discussions and products quality awareness.

## Resumo/Abstract

Apesar de muito se referir a uma crise ambiental, o que se percebe é uma crise de valores, cujas consequências, em última instância, periclitam o meio ambiente (GOMES, 2006, p. 20). Um recurso para converter esse quadro é a Educação Ambiental que, no ensino de Química, pode ser estabelecida através da experimentação.

A utilização de normas técnicas seria um instigante meio de fazer essa conexão; seu conteúdo, referente a padrões e testes estabelecidos para avaliar a conformidade de produtos, propicia a elaboração de experimentos e a discussão sobre segurança e qualidade, fazendo com que os discentes reflitam sobre seus hábitos de consumo.

Mais da metade dos alunos entrevistados para essa pesquisa não possuem conhecimento sobre a regulamentação de produtos, mas gostariam de aprender a respeito. Formularam-se atividades experimentais baseadas na ABNT NBR 15395, concernente a garrafas PET e na ABNT NBR 13725, relativa a fósforos de segurança. A adaptação dos ensaios descritos nas mesmas possibilitou, inicialmente, a composição de oito procedimentos experimentais. Aqueles relacionados à NBR 15395, como o teste de resistência ao impacto na queda livre, permitem a abordagem de polímeros, enquanto os ligados a NBR 13725, como o registro da extensão do palito que a chama percorre e o tempo que esta permanece acesa, propiciam a contextualização histórica e o tratamento de reações de combustão. É importante salientar que esses são experimentos de baixo custo que, além da aproximação de diversos outros conteúdos, suscitam a interdisciplinaridade.

## Referências

ASSOCIAÇÃO BRASILEIRA DE NORMAS TÉCNICAS. **NBR 13725**: Fósforos de segurança — Métodos de ensaio. Rio de Janeiro, 2014. 5 p.

ASSOCIAÇÃO BRASILEIRA DE NORMAS TÉCNICAS. **NBR 15395**: Garrafa soprada de PET para refrigerantes e águas — Requisitos e métodos de ensaio. Rio de Janeiro, 2006. 10 p.

GOMES, D. V. Educação para o consumo ético e sustentável. **Revista Eletrônica do Mestrado em Educação Ambiental,** Rio Grande, v. 16, p.18-31, jan. 2006. Disponível em: <https://www.seer.furg.br/remea/article/view/2778>. Acesso em: 24 jan. 2018.

**Área: EDU** **Inscrição: 01041**

# Um exemplo da aplicação de séries em aulas de Físico-Química: dedução da equação de Ramette

**Daniel F. Pietezak*** **(IC), Márcia M. Meier[1](PQ),[1]Luís H. de Santana(PQ)[2]**

**Danielfpj98@gmail.com;**

*[1]Departamento de Química,Universidade do Estado de Santa Catarina (UDESC, Joinville/SC); [2]Departamento de Matemática,Universidade do Estado de Santa Catarina (UDESC, Joinville/SC)*

Palavras-Chave: *Ramette, Ensino, Matemática, Cálculo, Séries, Equilíbrio Químico*

## Highlights

An example of series application in physical chemistry lectures: Working out Ramette's Equation.
Working out Ramette´s equation, using reverse series method, in experimental physical chemistry lectures, gave an opportunity to link abstract mathematics with chemical knowledge offered in undergraduated course in Chemistry.

## Resumo/Abstract

Observam-se dificuldades de alguns alunos de graduação de Licenciatura em Química da UDESC em transpor os conceitos e notações matemáticas abstratas ao contexto químico. Frequentemente a não compreensão das etapas de dedução de determinadas equações é um bloqueio para compreender a importância da equação em contextos químicos. Analisando a literatura, constatou-se que a dedução da equação de Ramette, utilizada para determinar a constante de equilíbrio (K) da reação de formação do complexo $[Fe(OH_2)_5(SCN)]^{2+}$, é apresentada parcialmente - carecendo de demonstração da etapa final. Com o objetivo de transpor o conhecimento matemático abstrato a uma aplicação química, este trabalho apresenta o uso do Método de Reversão de Séries (MRS) para deduzir a equação de Ramette.
Partindo-se da equação rearranjada (Cobb & Love, 1998) (1) e renomeando seus termos têm-se a equação (2), onde $C_f = [Fe^{3+}]+[FeSCN^{2+}]$; $C_s = [SCN^-]+[FeSCN^{2+}]$; A é absorbância, a é coeficiente de absortividade molar, b é caminho óptico e K é a constante de equilíbrio. Para se utilizar o MRS em (2), faz-se uso de (3), obtendo-se a equação (4). Desconsideramos o segundo e os demais termos da série, pois tendem a zero, obtendo-se (5). Após isso, realizam-se algumas operações matemáticas para se chegar finalmente em (6).

$$C_f C_s = \left(C_f + C_s + \frac{1}{K}\right)\left(\frac{A}{ab}\right) - 1\left(\frac{A}{ab}\right)^2 \quad (1)$$

$$\frac{A}{ab} = \frac{(C_f C_s)}{(C_f + C_s + \frac{1}{K})} + \frac{(C_f C_s)^2}{(C_f + C_s + \frac{1}{K})} + \ldots \quad (4)$$

$$y = a_1 x + a_2 x^2, C_f C_s = y; C_f + C_s + \frac{1}{K} = a_1; \frac{A}{ab} = x; -1 = a_2 \quad (2)$$

$$\frac{A}{ab} = \frac{C_f C_s}{(C_f + C_s + \frac{1}{K})} \quad (5)$$

$$x = A_1 y + A_2 y^2 \quad (3)$$

$$\frac{CfCs}{A} = \frac{C_f + C_s}{ab} + \frac{1}{Kab} \quad (6)$$

o coeficiente angular é $(Cf + Cs)$ e o coeficiente linear é $\frac{1}{Kab}$.

Observou-se que a dedução completa da equação de Ramette criou um contexto para fortalecer e aprofundar conceitos matemáticos nas aulas de laboratório de Físico-Química e contribui dando significado às aulas de cálculo.

**Área: EDU** **Inscrição: 000760**

# Texto didático interativo no contexto da atmosfera terrestre com aportes da geometria e polaridade de moléculas

**Bárbara C. T. Moreira (PQ)[1], Larissa P. dos Santos (IC)[1]*, Débora de A. Santana (PQ)[1]**

bmoreira@uneb.br; larisapassos@gmail.com
[1]*Departamento de Ciências Exatas e da Terra- Universidade do Estado da Bahia (UNEB)*

Palavras Chave: *Material didático, Geometria molecular, Polaridade, Atmosfera, Leitura*.

## Highlights

Interactive didactic text in the context of the terrestrial atmosphere with focus on geometry and polarity of molecules. The didactic material was developed to help students understand the importance of studying the geometries of molecules in the understanding of atmospheric phenomena at different levels of education.

## Resumo/Abstract

Este trabalho apresenta as etapas do processo de construção de um material didático (MD) elaborado para auxiliar a compreensão dos estudantes sobre a importância do estudo das geometrias e polaridades de moléculas no entendimento de fenômenos da atmosfera, em diferentes níveis de ensino. O MD é constituído de um texto que apresenta ilustrações e um personagem que interage com o leitor para a explicação da geometria e polaridade de algumas moléculas que compõem os gases de estufa, bem como a explicação da absorção da radiação na região do infravermelho por essas moléculas e as consequências frente aos conceitos estudados. O texto ilustrado e interativo seguiu as temáticas sugeridas pelos Parâmetros Curriculares Nacionais (PCNs) com o objetivo de possibilitar as discussões e a formação de pensamentos críticos a partir da reflexão do contexto social apresentado. Foi produzido a partir do embasamento de notícias veiculadas sobre questões ambientais, estabelecendo correlações que contribuem para o ensino e aprendizagem da geometria e polaridade das moléculas. O MD foi aplicado em turmas de ensino superior e médio, compreendendo cinco aplicações: na Universidade do Estado da Bahia e nos Colégios Estaduais Governador Roberto Santos e Thales de Azevedo, Salvador/BA. Através da análise das aplicações, das respostas obtidas, das conclusões elaboradas pelos estudantes e do questionário de avaliação do MD, pode-se concluir que o mesmo se mostrou eficiente para os objetivos propostos.

Figura 01: Primeira folha textual do MD.

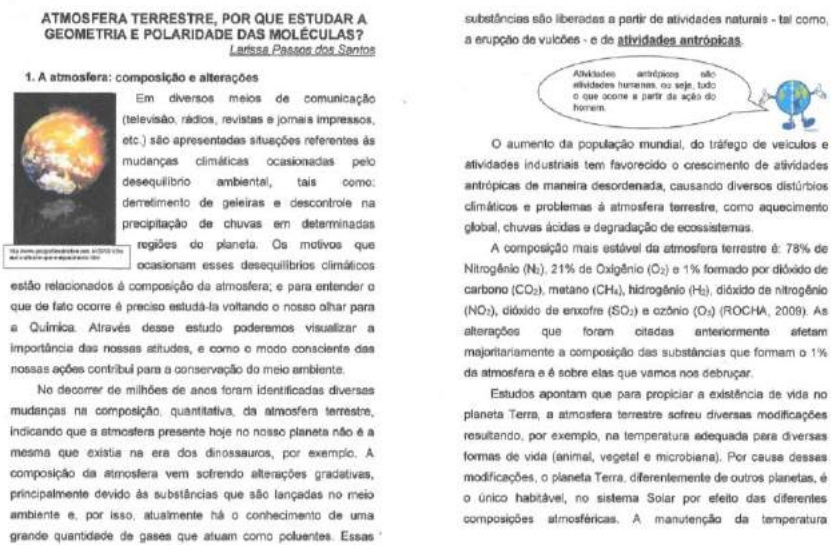

ATMOSFERA TERRESTRE, POR QUE ESTUDAR A GEOMETRIA E POLARIDADE DAS MOLÉCULAS?

Larissa Passos dos Santos

1. A atmosfera: composição e alterações

Em diversos meios de comunicação (televisão, rádios, revistas e jornais impressos, etc.) são apresentadas situações referentes às mudanças climáticas ocasionadas pelo desequilíbrio ambiental, tais como: derretimento de geleiras e descontrole na precipitação de chuvas em determinadas regiões do planeta. Os motivos que ocasionam esses desequilíbrios climáticos estão relacionados à composição da atmosfera; e para entender o que de fato ocorre é preciso estudá-la voltando o nosso olhar para a Química. Através desse estudo poderemos visualizar a importância das nossas atitudes, e como o modo consciente das nossas ações contribui para a conservação do meio ambiente.

No decorrer de milhões de anos foram identificadas diversas mudanças na composição, quantitativa, da atmosfera terrestre, indicando que a atmosfera presente hoje no nosso planeta não é a mesma que existia na era dos dinossauros, por exemplo. A composição da atmosfera vem sofrendo alterações gradativas, principalmente devido às substâncias que são lançadas no meio ambiente e, por isso, atualmente há o conhecimento de uma grande quantidade de gases que atuam como poluentes. Essas substâncias são liberadas a partir de atividades naturais - tal como, a erupção de vulcões - e de atividades antrópicas.

Atividades antrópicas são atividades humanas, ou seja, tudo o que ocorre a partir da ação do homem.

O aumento da população mundial, do tráfego de veículos e atividades industriais tem favorecido o crescimento de atividades antrópicas de maneira desordenada, causando diversos distúrbios climáticos e problemas à atmosfera terrestre, como aquecimento global, chuvas ácidas e degradação de ecossistemas.

A composição mais estável da atmosfera terrestre é: 78% de Nitrogênio ($N_2$), 21% de Oxigênio ($O_2$) e 1% formado por dióxido de carbono ($CO_2$), metano ($CH_4$), hidrogênio ($H_2$), dióxido de nitrogênio ($NO_2$), dióxido de enxofre ($SO_2$) e ozônio ($O_3$) (ROCHA, 2009). As alterações que foram citadas anteriormente afetam majoritariamente a composição das substâncias que formam o 1% da atmosfera e é sobre elas que vamos nos debruçar.

Estudos apontam que para propiciar a existência de vida no planeta Terra, a atmosfera terrestre sofreu diversas modificações resultando, por exemplo, na temperatura adequada para diversas formas de vida (animal, vegetal e microbiana). Por cause desses modificações, o planeta Terra, diferentemente de outros planetas, é o único habitável, no sistema Solar por efeito das diferentes composições atmosféricas. A manutenção da temperatura

Fonte: Elaboração própria, 2016.

**Área: EDU** **Inscrição: 00272**

# The approach of the principles of Green Chemistry by means of ludic activities in the formation of chemistry professionals

**Mariangela C. S. Costa (PG),[1] Márlon H. F. B. Soares (PQ), Nyuara A. S. Mesquita (PQ)**

**nyuara@ufg.br**

*Laboratório de Educação Química e Atividades Lúdicas (LEQUAL/IQ-UFG)*

Kaywords: *Chemical Jury, Ludic Activity, Appropriation of Concepts.*

## Highlights

Discussing Green Chemistry in the formation of chemistrians is important in the environmental context and this discussion can be done through a Chemical Jury that is configured as a ludic activity.

## Resumo/Abstract

Desde a década de 1990, com diretrizes para inserção da discussão ambiental na formação de químicos, muitos aspectos sobre as relações entre a Química e o contexto ambiental passaram a ser incorporados aos currículos dos cursos. Nesse recorte, a Química Verde (QV) e seus Princípios se constituem como abordagens importantes para a formação. No âmbito de uma pesquisa de mestrado, realizou-se um Júri Químico envolvendo os 12 Princípios da QV na perspectiva de discutir as questões ambientais por meio de uma atividade lúdica. A investigação se caracterizou como uma pesquisa-ação tendo como fases a identificação das situações iniciais, projeção das ações, realização das atividades previstas e avaliação dos resultados. Foram disponibilizados textos de apoio para subsidiar os alunos em suas argumentações. As atividades planejadas foram desenvolvidas durante seis aulas do curso de graduação em Química da UFG, Regional Goiânia, na disciplina de Química Ambiental, ofertada para alunos de licenciatura e bacharelado. A turma foi dividida nos grupos de composição do Júri: advogados de defesa e acusação, testemunhas, jurados, representantes dos envolvidos. A situação fictícia envolvia uma indústria farmacêutica que estava poluindo o rio que abastecia a cidade vizinha. Toda a abordagem envolveu questões químicas e, principalmente, os princípios da QV. Na análise das gravações transcritas, pode-se perceber a apropriação de conceitos relacionados à QV na construção das argumentações tanto de defesa quanto de acusação. Alguns recortes de falas, de trechos de diferentes diálogos, são apresentados nas seguintes figuras.

AA2 – *É eu gostaria, eu gostaria de saber já que vocês são a empresa de Química Verde que estão consultando a QuímicoLab, é se vocês também estão atentos as outras questões de Química Verde que estão nessa empresa como por exemplo, a utilização de energia renovável, uso dos solventes, e reagentes tóxicos que foram detectados nos resíduos.*

TD1 – *Não, eu estou dizendo que nós estamos implantando uma política Verde na nossa empresa para tentar minimizar os resíduos gerados por ela, isso que eu estou dizendo.*

TD2 – *O uso de catalisadores, o uso de solventes diferentes que vão gerar menos resíduos e menos produtos indesejados.*

AD1 – *Então a gente quer dizer que estamos tentando novos financiamentos para poder, através de projetos socioambientais em parcerias, novas parcerias com universidades, para conseguir essa verba e investir em solventes diferentes, catalisadores para que a energia de ativação das reações que a gente gera na nossa empresa diminua gerando assim menos resíduos como forma de minimizar esses danos que vem sendo causados.*

**Área: EDU**
*(Inserir a sigla da seção científica para qual o resumo será submetido. Ex: ORG, BEA, CAT)*

**Inscrição: 00639**
*(Inserir o número de inscrição do autor que fez a submissão)*

# *Destilaria:* An innovative board game to improve the organic chemistry learning

**Maximiliano de Freitas Martins (IC)[1]*, Thiago Muza Aversa (PQ)[1]**

**maxfmartins@gmail.com**

[1] *Federal Institute of Education, Science and Technology of Rio de Janeiro, IFRJ*

Keywords: *board game; organic chemistry; ludic learning; IUPAC nomenclature; laboratory glassware*

## Highlights

Educational games may improve the teaching-learning process.
Introductory topics in Organic Chemistry used to be impactant for the students.
An innovative dual board game may turn Organic Chemistry more attractive.

## Abstract

Chemistry educational games could be characterized as an effective strategy to stimulate learning-resistant students by proposing an enjoyable form of teaching, differentiating from the traditional methodologies[1] instigating the development of new abilities due to interaction with the other students and the teacher. Specifically in organic chemistry, the writing of the nomenclature of organic compounds, e.g, due to the amount of rules and details established by IUPAC and the employed methodology, result in demotivation of students, impacting on the subsequent learning of related subjects[2]. Within this context, we sought the development of an innovative ludic game that would allow a differentiated teaching approach making the learning encouraging and enjoyable, capable of arousing the interest and curiosity of students corroborating the teaching-learning process. Thereby, a vertical board which simulates a fractional distillation system was designed to be supported by a horizontal board, where three sets of cards involving questions and tasks to be performed would create the interaction between the boards. The next stage will apply this project in high school and undergraduate classes to evaluate the game dynamic.

[1] SOARES, M. H. F. B. Jogos e atividades lúdicas no ensino de química: uma discussão teórica necessária para novos avanços. **Revista Debates em Ensino de Química**, v. 2, n. 2, p. 5-13, 2016.

[2] FERREIRA, M.; DEL PINO, J. C. Estratégias para o ensino de química orgânica no nível médio: uma proposta curricular. **Acta Scientiae**, v. 11, n. 1, p. 101-118, 2009.

**Área: EDU** **Inscrição: 01012**

# Uso de simuladores no estudo dos estados físicos da matéria e do modelo cinético molecular

**Juliana Maria Sampaio Furlani (PQ),[1*] Lavínia Vitória Candido (IC),[2] Mariana Borges de Oliveira (IC),[2].**

**jufurlani@unifei.edu.br;**

*[1] Instituto de Física e Química, Unifei; [2]Escola Estadual Barão do Rio Branco.*

Palavras Chave: *modelagem, simulação computacional, modos de representação, modelo cinético-molecular.*

## Use of simulators in the study of the physical states of matter and the molecular kinetic model

Modelling and argumentation about physical states of matter and its constitution. Use of simulators to aid the comprehension of experimental situations and proposal of models. Study of the molecular kinetic model.

## Resumo/Abstract

A aprendizagem por modelagem pode "favorecer tanto a compreensão de ideias científicas quanto um entendimento mais amplo sobre a própria ciência"[1]. Ao entrar em contato com diferentes modos de representação (gráficos, modelos matemáticos, computacionais, concretos), enriquecem-se as relações entre a situação experimental e a proposição dos modelos.

Nesta pesquisa, participaram 11 estudantes do 2º ano do Ensino Médio de uma escola pública de Itajubá/MG, após assinatura de um Termo de Consentimento Livre e Esclarecido. A atividade didática[2] foi realizada em dois dias, com duração total de seis horas e pode ser entendida na Figura 1.

**Figura 1 – Etapas da atividade didática**

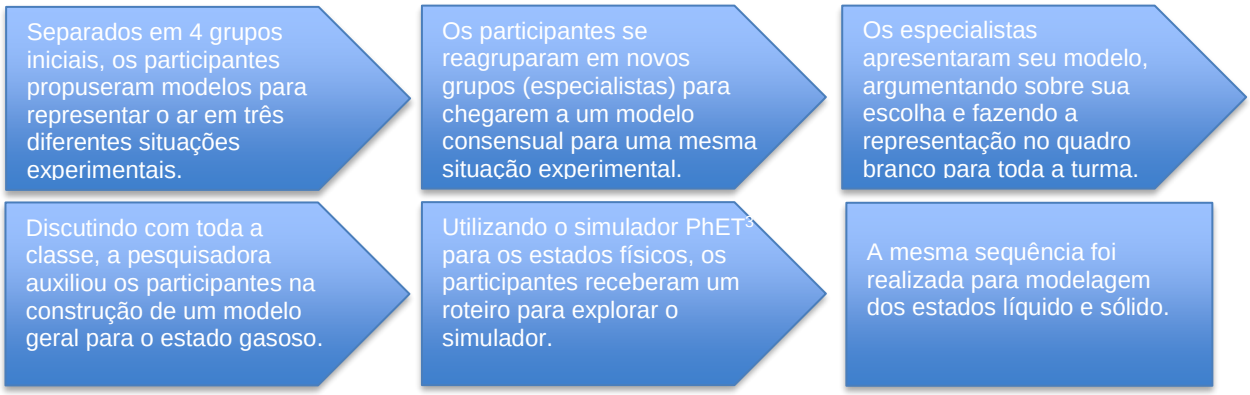


Metodologicamente, aplicaram-se um pré e um pós-teste, contendo nove questões, mas neste trabalho apenas duas serão discutidas.

Quando questionados sobre o que entendiam sobre modelo, nove participantes associaram a ideia de modelo ao mundo da moda "*modelo de passarela*", "*desfile*", "*pessoa magra e alta*". Já no pós-teste, nenhum dos respondentes apresentou novamente as ideias iniciais relativas a modelo associada ao mundo da moda. Porém, eles também não conseguiram elaborar um conceito próximo ao discutido durante a pesquisa, que modelos são representações parciais de uma entidade e podem ser modificados. Quando questionados se *"O uso de vários tipos de representação (imagens, gráficos, vídeos, simulação, maquetes etc) facilita o estudo da Química*", os participantes unanimemente concordaram com a afirmação.

Concluiu-se que os diferentes modos de representação, desenvolvidos a partir de atividades de modelagem e com uso da argumentação, favoreceram uma percepção mais dinâmica da ciência pelos participantes e contribuíram no aprendizado dos conceitos propostos.

### Referências

1 - JUSTI, Rosária, Relações entre argumentação e modelagem no contexto da ciência e do ensino de ciência. **Ensaio** Pesquisa em Educação em Ciências, vol. 17, 2015, pp. 31-48.

2 - MORTIMER, E. F. e MACHADO, A. H. **Química**. v. 1. 2ª Edição. Editora Ática, São Paulo, 2016.

3 - https://phet.colorado.edu/pt_BR/ Acesso em 02/02/2018.

4 - JUSTI, Rosária. Modelos e modelagem no ensino de química: um olhar sobre aspectos essenciais pouco discutidos. In: SANTOS, W. P. S e MALDANER, O. A. (Org) **Ensino de Química em Foco**. Ijuí, Editora Unijuí, 2011.

**Agradecimentos:** Ao Instituto de Física e Química da Unifei pelo transporte e pelo uso do Laboratório de Ensino de Química; à FAPEMIG, agradecemos pelas bolsas de estudo.

**Área:** *EDU*

**Inscrição: 00227**
*(Inserir o número de inscrição do autor que fez a submissão)*

# Territórios analíticos: Uma abordagem dinâmica para o equilíbrio de complexação

**Daniela S. Anunciação (PQ),[1*] Débora O. da S. Avelino (IC),[1] Gleybhson F. dos S. Alves (IC),[1] Débora J. S. Santos (IC),[1] Paulo H. A. Lira (IC),[1] Alice M. A. Félix (IC).[1]**

**daniela.anunciacao@iqb.ufal.br**

[1]*Instituto de Química e Biotecnologia UFAL.*
Palavras Chave: *Jogos didáticos, Química Analítica, Equilíbrio*, *Complexação*.

## Highlights

Analytical territories: A dynamic approach for complexation equilibrium
The application of educational games is a promising tool of evaluation and self-evaluation of the student performance along a subject as they can interact better in the classroom groups.

## Resumo

O desenvolvimento de jogos didáticos tem sido explorado com sucesso no Ensino de Química como estratégia de construção de conteúdos de difícil abordagem e entendimento por parte dos estudantes.[1] O presente trabalho teve como objetivo elaborar e aplicar um jogo envolvendo "equilíbrio de complexação" numa turma de Química Analítica da UFAL. O mapa de Alagoas foi dividido em 6 territórios (conceitos fundamentais, reações, expressões matemáticas, exemplos/compostos, conceitos avançados e aplicações) cujo domínio representa a compreensão do conteúdo. Com o auxílio de um dado, o jogador que obtivesse o maior número iniciaria a partida. Cada jogador teve uma carta-objetivo com indicação de cartas-pergunta a responder (n = 6), sendo que todos os jogadores teriam que responder no mínimo um conceito fundamental e um avançado. O resultado do jogo era estratificado de modo que pudesse haver mais de um vencedor e mantivesse o interesse dos jogadores ativos no jogo. A elaboração do jogo pelos estudantes já aprovados na disciplina permitiu uma consolidação dos conteúdos já apreendidos e lhes proporcionou assumirem postura de avaliadores/orientadores durante a execução do jogo, conferindo a oportunidade de prática docente na qualidade de licenciandos. Quanto aos jogadores da turma em curso, foi claro o melhor desempenho dos mesmos no semestre, bem como a possibilidade de diagnóstico e auto-avaliação quanto ao próprio desempenho na disciplina. Ademais, para uma disciplina que possui bastante rejeição no curso, a abordagem lúdica e interativa despertou nos estudantes mais interesse na construção dos conteúdos.

Figura 1. Composição do jogo "Territórios Analíticos – Equilíbrio de Complexação".

[1]ROMANO, C. G.; CARVALHO, A. L.; MATTANA, I. D.; CHAVES, M. R. M.; ANTONIASSI, B. Perfil Químico: Um Jogo para o Ensino da Tabela Periódica. Revista Virtual de Química, vol 9, n. 3, p. 1235 - 1244, jun 2017

**Área: EDU** **Inscrição: 256**

# Leite em "*mama*" África e a lei 10639/03 no ensino de química.

**Juvan P. da Silva (PG)[1], Gustavo A. A. Faustino (IC)[1], Antonio C. B. Alvino (PG)[1], Marciano A. dos Santos (PG)[1], Vander L. dos Santos (PG)[1], Morgana A. Bastos (FM)[1], Arcanjo R. Moura (IC)[1], Marysson J. R. Camargo (PG)[1], Regina N. Vargas (PG)[1], Geisa L. M. Lima (IC)[1], Lalesla L. Oliveira (IC)[1], Fernada S. Fernandes (IC)[1], Mariana S. Neto (IC)[1], Alyny O. Silva (IC)[1], Claudio R. M. Benite (PQ)[1], Anna M. C. Benite* (PQ).[1]* juvan.quimica.ufg@gmail.com; * Anna@ufg.br**

[1] Laboratório de Pesquisas em Educação Química e Inclusão (LPEQI), Universidade Federal de Goiás.

Palavras Chave: Leite, África, Lei 10639, ensino de química.

## Highlights

Milk in "mother" Africa and law 10639/03 in the teaching of chemistry. Milk production in Africa. Chemical reactions with milk. Addition of foreign substances to milk. Determination of starch, boric acid and salicylate anion in milk. Epistemic displacement of the curriculum.

## Resumo/Abstract

Apresentam-se resultados de uma Intervenção Pedagógica na qual se buscou discutir química através de reações com o leite e história da produção leiteira africana, com vistas ao cumprimento da lei 10.639/03 no ensino superior. Foram sujeitos dessa investigação (SI): 12 alunos de Engenharia de uma IES de Goiás, da disciplina de química geral prática. A imagem abaixo mostra alguns discursos produzidos.

Imagem/quadro 1: Alguns discursos produzidos na IP.

| Turno | SI | Discurso |
|---|---|---|
| 44 | A6 | [...] a gente estuda pegando o ponto de vista europeu, [...] surge primeiro a agricultura, e depois o pastoreio, e do pastoreio, o leite e a própria carne. Mas no estudo falou que na África, elas (as comunidades) inicialmente eram sedentárias, a pratica comum de usar o pastoreio, apesar de não ter o registro do uso da carne eles acharam registro de consumo do leite [...] |
| 63 | A9 | [...] foram extraídas 81 amostras de cerâmica para passar por diversas técnicas de análise por presença de gordura, e destas 29 passou por análise cromatografia gasosa, infravermelho e espectrometria de massas onde 18 apresentaram evidências e gorduras de origem animal, e 11 tinha perfil de lipídios providos da mistura de gordura animal e vegetal. |
| 36 | A6 | [...] o amido vem sendo utilizado na fraude do leite, já que como esse composto possui baixo custo, ele está sendo adicionado de forma fraudulenta com o objetivo de aumentar o volume e o peso do alimento. No caso de leite fluido, ele pode ser usado com finalidade de disfarçar a adição de água, pois corrige a densidade original do leite. |
| 34 | A5 | Bem, com o amido dissolvido, observamos que ao adicionar gotas da solução de lugol ocorre a formação de uma coloração azul escuro. Este azul é o produto da reação entre o íon triiodeto e o amido, formando um complexo que possui esta coloração característica. E aí tem a ionização do iodo, que rege com o iodeto formando o $I^{3-}$e reage com o amido formando o complexo. $I_2 + I^- \rightleftharpoons I_3^-$ $I_3^-$ + amido ⇌ complexo azul |

Diversas técnicas analíticas têm sido usadas para recontar a história dos povos africanos e seus legados nas ciências[1]. Nos turnos **T.44** e **T.63,** A6 e A9 discutem a produção de leite em África como maneira de mostrar uma visão não totalmente eurocêntrica de ciências. Ensaios qualitativos que permitem a detecção de substâncias estranha ao leite foram realizados[2]. No **T.36** A6 argumenta o porquê de se fraudar o leite com o amido. No **T.34**, A5 discorre sobre os aspectos fenomenológicos, teórico e representacional do conhecimento químico[3] a partir da reação entre o amido adicionado ao leite e o iodo presente na solução de lugol. Por fim, foi avaliado se existe ou não autoria nos textos produzidos pelos alunos/as após aulas práticas nas confecções de relatórios e preparação/apresentação de seminários. Nossos resultados mostram como o professor do ensino superior de ciências, em especial o de química, pode a partir de elementos diaspóricos da África, contextualizar conceitos químicos, fazer um deslocamento epistêmico do currículo e tecer representatividades sobre quem se é, e para quem se ensina.

[1] ISKANDER, Z. A Arqueologia da África e suas técnicas **–** Processos de datação. In: KI-ZERBO, Joseph. **História geral da África, I:** Metodologia e pré-história da África. Brasília: UNESCO, 2010.

[2] LISBOA, J.C. F.; BOSSOLANI, M. Experiências Lácteas. **Química nova na escola. n. 6**, 1997.

[3] MORTIMER Eduardo Fleury; MACHADO Andréa Horta; ROMANELLI Lilavate Izapovitz. A proposta curricular de química do estado de Minas Gerias: Fundamentos e pressupostos. **QUÍMICA NOVA**, São Paulo, v. 23, n.2, p. 273-283, 2000.

**Área: EDU** **Inscrição: 00981**

# Teaching Chemistry: an interface between the teaching of chemical bonds and alternative materials.

**Abraão C. Moraes[1] (IC), Gabriel da S. Feijó[1*] (IC), Maria Dulcimar de B. Silva[1] (PQ), André S. dos Reis[1] (PQ).**

**gabrielfeijo1@hotmail.com**

*[1]Universidade do Estado do Pará. Email: abraaocm001@gmail.com, gabrielfeijo1@hotmail.com, mariadulcimar@gmail.com, andre.reis@uepa.br.*

Palavras Chave: *Materiais alternativos, Ligações Químicas, Ensino de Química.*

## Highlights

The importance of using alternative materials as an educational tool for the teaching of chemical bonds. An effective and economical proposal.

## Resumo/Abstract

Este trabalho foi realizado com estudantes de graduação de Ciências Naturais - Química da Universidade do Estado do Pará (UEPA) a fim investigar e divulgar a importância do uso de materiais alternativos como ferramenta didática para o ensino de ligações químicas. O estudo contou, primeiramente, com um questionário que visou realizar um levantamento para sondagem dos conhecimentos prévios dos estudantes de graduação em relação ao emprego de recursos didáticos utilizando materiais alternativos no ensino de Química. Posteriormente, houve uma expositiva sobre ligações químicas a partir da análise cristalográfica do mineral petalita. Logo após, os estudantes participaram de uma oficina que lhes propôs a confecção da estrutura cristalina da petalita com palitos de churrasco e massinhas de modelar. Seguidamente, foi aplicado outro questionário com a finalidade de verificar a avaliação dos estudantesquanto à metodologia aplicada na oficina para a melhoria no ensino de Química. Os resultados expressam que maioria dos estudantes não possuía conhecimento a respeito do uso de materiais alternativos como recurso didático, como pode ser visto na resposta do aluno "**B**": "*não conheço muito sobre esse assunto"*, contudo, na avaliação seguinte, verificou-se resultados satisfatórios quanto a metodologia utilizada. O aluno "**B**" avaliou da seguinte forma "*é interessante, a fim de levar o ensino também para a pratica, e não ficar apenas no campo da teoria*". Por tanto, nota-se que a utilização de materiais alternativos contribuem para o ensino de Química de maneira significativa e econômica.

**Área: EDU**

**Inscrição: 00410**
*(Inserir o número de inscrição do autor que fez a submissão)*

# ESTRUTURAS EDUCACIONAIS VIRTUAIS (EEV) POR MEIO DE MODELOS FÍSICOS (MF)

**Aluísio M. da Fonseca (PQ),[1,*] Sara J. de Oliveira (IC),[1] Francisco K. de O. Santos (IC),[2] Elcimar S. Martins (PQ),[1] Luana M. de Sousa (IC),[1] Regilany P. Colares (PQ),[2] Maiuca A. Seco (IC)[2]**

**aluisiomf@unilab.edu.br; regilany@unilab.edu.br**

*[1]Mestrado Acadêmico em Sociobiodiversidade e Tecnologias Sustentáveis (MASTS), UNILAB; [2]Instituto de Ciências Exatas e da Natureza, UNILAB;*

Palavras Chave:*(modelos físicos, realidade aumentada, hologramas).*

## Highlights

Title: Virtual Educational Structures (VEE) through Physical Models (FM)
The physical models as teaching tools in scientific education. Motivating the classroom through alternative experiences with virtual learning objects. The handwriting to holography using molecular structures.

## Resumo/Abstract

O grau de motivação e interesse pela ciência precisa ser estimulado através de práticas contextualizadas, onde sua inserção deve ser adequada, com o intuito de fazer-se compreender por meio das inter-relações entre teoria e prática, minimizando assim, as dificuldades para alcançar uma aprendizagem significativa.[1] Portanto, o uso de modelos físicos (MF) tem crescido muito nos últimos anos para que o abstracismo e a complexidade sejam sanadas e que se compreenda conceitos relacionados a estruturas moleculares.[2,3] As TIC's, que são ferramentas educacionais que sincronizam o interesse e a motivação do discentes, podem transcender e gerar novos espaços virtuais. Um dos métodos foi a conversão de estruturas planares em modelos físicos (MF), onde as estruturas são feitas por meio de aplicativos livres como o chemdraw, chemsketch, chemwindow e chemlab lite. E desta forma a conectividade para a formação de modelos físicos virtuais (MFV) tanto em realidade aumentada (RA) como a realidade mista (RM) por meio do augmentaty author e outros aplicativos de 3D, Figura 1. É possível também gerar estruturas químicas projetáveis em ambientes 3D, gerando vídeos holográficos, por meio do chemdraw e powerpoint. Com todos esses recursos foi possível se criar um ambiente virtual voltado para que todos possam apreciar as moléculas de um modo mais lúdico, os módulos interativos de Química (MinQ's). Com isso, a prática apresentou-se como uma proposta viável para docentes, incentivando os alunos a desenvolver o gosto pelos conceitos relacionados a ligações químicas e estereoquímica.

**Figura 1**. Representações de modelos físicos e virtuais

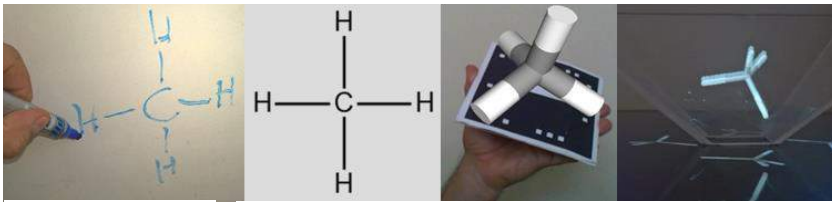


estrutura plana escrita | estrutura planar | RA de um modelo 3D (stick) | holografia de um modelo 3D (stick)

## Referências

[1]PEREIRA, T.A; TARCIA, R.M.L; SIGULEM, D. Uso das tecnologias de informação e comunicação (TIC) na educação superior. Disponível em: http://www.abed.org.br/hotsite/20-ciaed/pt/anais/pdf/225.pdf. 09 Out. 2015.
[2]AZUMA, R. (1997) "A Survey of Augmented Reality", Presence: Teleoperators and Virtual Environments, v .6, n.4, August, p. 355-385.
[3]BROWN, T.L.; LEMAY JR, H.E.; BURSTEN, B.E. e BURDGE, J.R., Química: A ciência Central, 9. ed., São Paulo: Pearson Education, 2005.

**Área: EDU** **Inscrição: 00787**

# Production of a two-dimensional tactile Water Treatment Station for students with visual impairment

**Larissa S. Santos (IC),[1] Matheus S. Oliveira (IC),[1] Thamiris P. Cid (IC),[1] Anne Caroline S. Rocha (IC),[1] Vanessa S. N. Penco (PQ),[1] Ana Paula S. S. Estevão (PQ)[1], Aires C. Silva (PQ).[2]***

**larissassds@gmail.com; airessilva@ibc.gov.br**

*[1]Instituto Federal de Educação, Ciência e Tecnologia do Rio de Janeiro (IFRJ) – Campus Duque de Caxias; [2]Instituto Benjamin Constant – Urca – Rio de Janeiro.*

Keywords: *Chemistry teaching, Visual impairment, Inclusive education.*

## Highlights

Didactic material for the visually impaired. Production of a water treatment station to contextualize the teaching of mixture separation processes. Braille, different textures and colors were used.

## Abstract

Inclusive Education is based on the rights to education, equal opportunities and participation in society. Despite the existence of policies for inclusive education, the education system mainly serves students considered ideal. This fact can be explained due to the difficulty faced by some teachers in applying different strategies in Teaching Chemistry for the visually impaired. Therefore, to contextualize the teaching of mixture separation processes, the present work presents in a simple way the production of a Water Treatment Station (WTS) adapted for blind and low vision people. The main idea of the Water Treatment Station is to present how treated water reaches our homes through different separation processes. For students with low vision, the material was enlarged in size 42x30cm and it was also used specialized type font (APHont). The material received adequate colors and contrasts to allow a better visualization, as can be seen in Figure 1, left. In the adaptation of WTS, Figure 1 (right), for blind students, several types of textures were used, such as lines, paper, sand, sandpaper, crafts foam, so that they could perceive the difference of the processes through the touch, Braille System was also used. The material was evaluated, and approved, by blind students during the interdisciplinary fair held in the Instituto Benjamin Constant occurred in June/2017 with the water theme. The most interesting thing was to notice blind students using the material to show to other blind participants of the event.

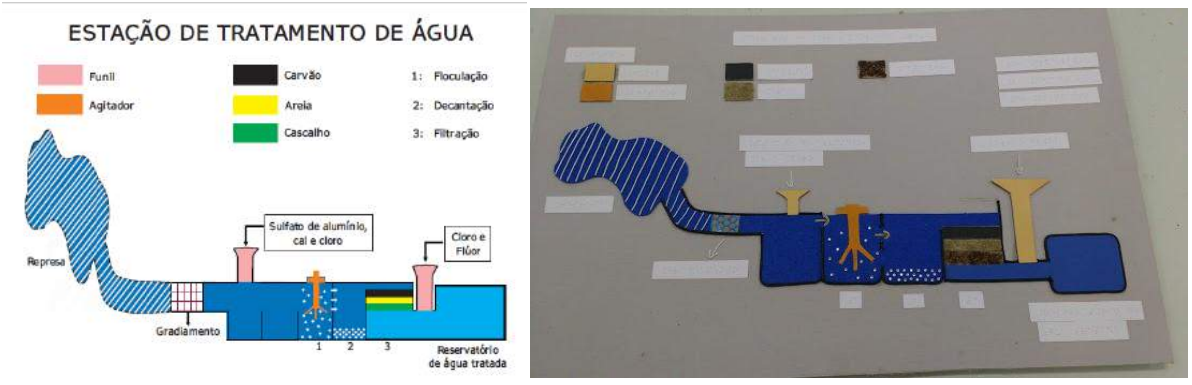


Figure 1. Water Treatment Station. Left: for low vision students, Right: for blind people.

**Área: EDU** **Inscrição: 01072**

# Low cost molecular models production with digital modeling and fabrication

**Alfredo Luis Mateus (PQ)**[1].

**almateus@gmail.com**

[1] *Colégio Técnico (COLTEC), Universidade Federal de Minas Gerais*

Palavras Chave:*Molecular Models, STEM, Maker Culture, Makerspace.*

## Highlights

A low cost molecular model is proposed using digital fabrication tools (3D printing and laser cutting). We present a viable alternative that uses a makerspace to build the "atoms" and regular plastic straws as the "bonds".

## Resumo/Abstract

Digital fabrication tools like 3D printing and computer controlled laser cutting are new and exciting ways to create classroom resources. These technologies are not accessible to teachers due to the high cost of the machines and the need for computer design software (3D and 2D). Makerspaces are a way to have access to these machines at a reasonable cost. We used SENAI´s Laboratório Aberto makerspace in Belo Horizonte for the production of molecular models for classroom use.

Our first option was to use a 3D printer and to create the 3D file in a free, easy to use, online software called BlocksCAD. Two "atom" models were printed (Figure 1), one a 120 degree connector for the making of a fullerene model (type 1), and the other a tetrahedral connector to represent a carbon atom in other molecules (type 2). Only one of each of the two models was printed for testing (R$ 15).

A second alternative was tested to lower the cost of the model, using a laser cut machine and 3 mm MDF board. The 2D contour file for cutting was made in an illustration software. One 60 x 90 cm board costs around R$10 and allows for the cutting of at least 450 type 1 or 300 type 2 connectors (Figure 2). A fullerene model with 60 atoms connected by plastic straws is shown in Figure 3. The fullerene model costs less than R$10 (US$3) to make.

Figure 1: 3D printed models

Figure 2: Laser cut models

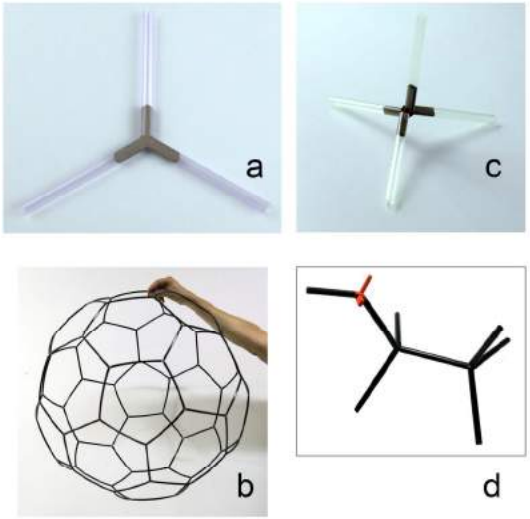


Figure 3: a) trigonal conector; b) fullerene model, c) tetrahedral connector, d) ethanol model

**Área: EDU** **Inscrição:328267**

# 3D model of Chemistry for assembly of molecules accessible to all and low cost

**Geovany Candido (TM),[1] Edson A. Duarte (FM),[1] Daltamir J. Maia* (FM),[1]**

**daltamir.maia@gmail.com**

[1]*Instituto Federal de Educação, Ciência e Tecnologia, IFSP – Campus Campinas.*

*Keywords: Molecular modeling kit, Braille, 3D printer, accessibility.*

## Highlights

*Assembly of molecules through atomic models made in a 3D printer, aimed at attending all students, including visually impaired. The atoms are printed with the atomic symbol also in Braille to facilitate the perception of the visually impaired.*

## Resumo

Este projeto visa desenvolver um kit de química orgânica/inorgânica, modelo 3D de montagem de moléculas, que seja acessível a todos os estudantes, inclusive àqueles com deficiência visual; e que seja de baixo custo. O protótipo foi obtido através de uma impressora 3D, na qual os principais elementos formadores das moléculas orgânicas (C, H, O e N), em um primeiro momento, foram impressos respeitando o número de ligações químicas que o mesmo pode fazer. Estes átomos tiveram seus símbolos químicos representados em braile para que estudantes com deficiência visual também possa fazer uso do mesmo.

Os átomos foram impressos respeitando a tendência dos kits disponíveis no mercado, na qual átomos de carbono são pretos, de oxigênio são vermelhos, de nitrogênio são azuis e de hidrogênio são brancos. Os átomos foram projetados através do programa de modelamento SolidsWorks, obedecendo a proporção de tamanho entre eles. O modelo atômico possui uma área plana com o símbolo do elemento químico em braile para que o mesmo possa ser identificado pelo estudante com deficiência visual.

Kits de modelos moleculares são ferramentas que ajudam muito no entendimento de muitos aspectos relacionados à química, tais como composição molecular e geometria das moléculas. A percepção através de um modelo mecânico auxilia muito no aprendizado do estudante.

A figura abaixo mostra os átomos confeccionados e possíveis moléculas montadas através dele.

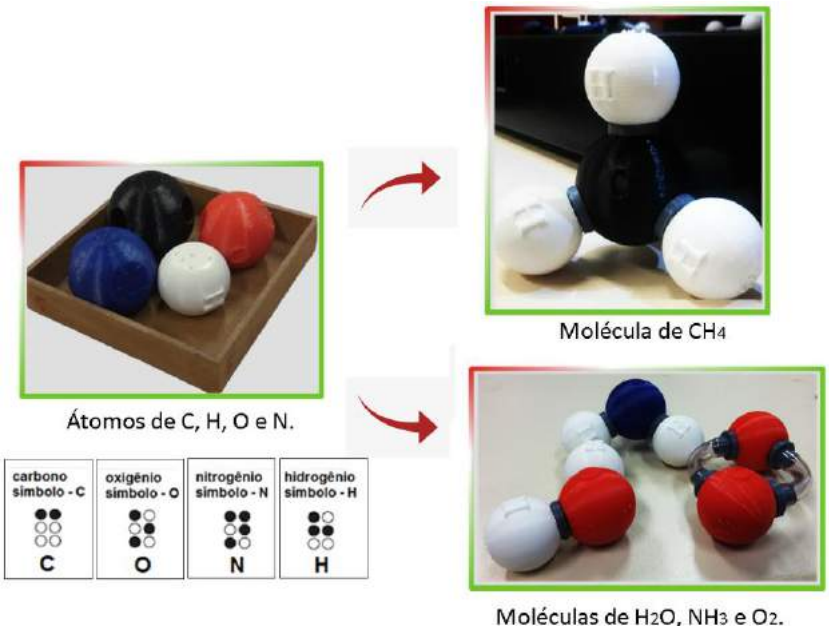

**Área: EDU** **Inscrição: 00201**

# Universidade e Sociedade - o que a Universidade Pública pode Oferecer aos Estudantes - Eletroquímica ao Alcance de toda Sociedade

**Regiane C.M.S. Castione (FM)[1], Maria Lucia F. Vicinguera (FM)[2], Alexandra D. Oliva (FM)[3] e José Ricardo C. Salgado (PQ) [4,*]**

***jose.salgado@unila.edu.br**

*[1]Colégio Estadual Prof. Flávio Warken – E.F.M.P.; [2]Colégio Estadual Bartolomeu Mitre – E.F.M.; [3]Colégio Estadual Dom Pedro II – E.F.M.; [4]UNILA, Universidade Federal da Integração Latino-Americana, CEP.: 85867-970, Foz do Iguaçu, PR, Brasil*

Palavras Chave: *Ensino, Escola, Pilhas, Baterias, Eletroquímica.*

## Highlights

Public University and Society, Electrochemistry, Batteries, Electrolysis, Chemistry at home, day-to-day chemistry.

## Resumo

Este trabalho tem como objetivo interagir os alunos e professores das Escolas Estaduais públicas de Foz do Iguaçu-PR com os alunos e professores da Universidade Federal da Integração Latino Americana (UNILA). Esta interação se concentrou basicamente em atividades de experiências de química, especificamente de eletroquímica, para os alunos do ensino fundamental e médio. Os alunos bolsistas de diferentes cursos da UNILA preparavam roteiros experimentais previamente de eletroquímica e posteriormente demostravam em laboratório e salas de aulas das Escolas. Entre 2016 e 2017 participaram três escolas, Colégio Estadual Prof. Flávio Warken, Bartolomeu Mitre e Dom Pedro II. Foram mais de 15 experimentos realizados de baixo custo e materiais que são utilizados em casa e apresentados semanalmente. O objetivo das atividades é buscar atenção dos alunos e estimularem a capacidade de conhecer, entender e aprimorar os conhecimentos apreendidos em sala de aula ou que irão estudar nos semestres seguintes. Como hoje em dia a maioria dos alunos possuem aparelho de celular e este possui uma bateria. A ideia é mostrar como ocorre uma reação química nestas baterias, como por exemplo, uma reação de oxidação e redução, materiais e reagentes, esquemas e as equações químicas envolvidas. Foram também exibidos os componentes da formação de baterias e pilhas através de quadros montados pelos próprios alunos.

**Área: EDU** **Inscrição: 00797**

# Chemical Kinetics on the tip fingers: an Assistive Technology Resource for Blind and Low Vision Students

**Matheus S. Oliveira (IC),[1] Larissa S. Santos (IC),[1] Thamiris P. Cid (IC),[1] Anne Caroline S. Rocha (IC),[1] Vanessa S. N. Penco (PQ),[1] Ana Paula S. S. Estevão (PQ)[1], Aires C. Silva (PQ).[2]***

**matheussilva330@gmail.com; airessilva@ibc.gov.br**

*[1]Instituto Federal de Educação, Ciência e Tecnologia do Rio de Janeiro (IFRJ) – Campus Duque de Caxias; [2]Instituto Benjamin Constant – Urca – Rio de Janeiro.*

Keywords: *Didactic material, Chemistry teaching, Visual impairment, Inclusive education.*

## Highlights

Didactic materials were prepared for blind and low vision students. For the blind, the material was transcribed in braille. For the low vision, the focus was on the type font, colors and contrasts.

## Abstract

The discipline of Chemistry helps the student to become a more critical citizen. Since chemical concepts are present in every day-to-day process, this training should be encompassed in the education of all students in the basic education system, providing equal learning for students with or without disabilities. Teachers have faced many challenges so that the student's teaching-learning process is achieved with regard to the teaching of Chemistry for the visually impaired. The lack of adequate materials is an example. Therefore, the present work addresses the issue of inclusion of visually impaired people in classrooms in regular schools, based on the adaptation of a didactic material prepared for high school students addressing the subject of Chemical Kinetics. In order to fulfill the proposed objective, the creation of the material followed the steps: writing the textual part, transcription, texturing of figures, revision, printing, and avaliation. After its creation, it was evaluated by blind reviewers of the Instituto Benjamin Constant (IBC) and by five students (three blind and two low vision) of regular schools so that it can be checked for its efficiency and applicability, being approved for national replication through thermoforming process and registration in IBC. The Figure 1 shows one page as an example, the picture in the left contains two different colors for the better visualization of low vision students and the image in the right shows the same page texturized with bottons (reactants) and stickers (products).

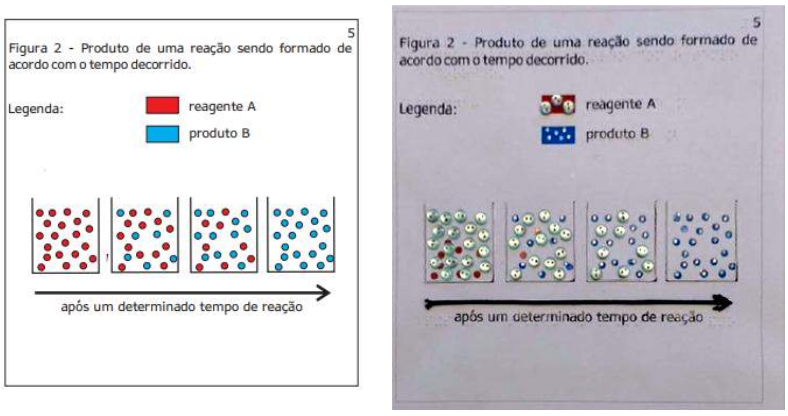


Figure 1. Product of a reaction being formed according to the elapsed time. Left: for low vision students, Right: for blind people.

**Área: EDU** **Inscrição: 00529**

# SCIENTIFIC ARTICLES: A TOOL FOR TEACHING ENVIROMENTAL CHEMISTRY IN TECHNICAL ENVIROMENTAL COURSE

**Rosana Petinatti da Cruz (FM),[1]* Maria Lucia T. G. Mendonça (FM),[2] Juliana Petinatti Sarmento (IC),[3] Luiza Magalhães Mesquita (TM),[1] Isabella Oliveira da Silva (IC),[1] Thayssa R. Quintialiano Lima (IC).[1]**

**rosanapetinatti@gmail.com; rosanapetinatti@gmail.com**

*[1]UFRRJ- CTUR; [2]IFRJ – Campus Maracanã; [3]UERJ – Campus Maracanã*

Key Words: *Scientific Articles, Motivation, Education.*

## Highlights

Presentation of scientific articles which generated motivation and improvement in Environmental Chemistry.

## Abstract

The goal of the work was to motivate the students of technical course in learning Environmental Chemistry from articles published in scientific journals recognized by the academic community. The teacher selected several articles that were directed to groups of students and they prepared a presentation for the class explaining or performing experiments related to the content of the article. It was concluded that the work generated several debates on various contents related to Environmental Chemistry, bringing an approach with academic subjects distant from the student's daily life and broadening his scientific knowledge.

## Introduction

The study was carried out at the Technical College of UFRRJ, with students from the 2nd and 3rd year of the Technical Environmental Course. The teacher analyzed several articles of the journal "Química Nova" observing that they could be worked by high school's students and could be tools for a better use of the discipline. The students were separated into groups, and made presentations or experiment on the content.

## Results and Debate

The first group worked with the article by Otenio et al (2008) that approached alternative treatments for human consumption water, students realized that the use of aluminum sulfate in conventional treatment can leads to mental illness. The article of Silva et al (2008) promoted a discussion about alternatives for air quality improvement and the quality of the complete burning of gasoline, by replacing ethanol with certain ethers. The scientific paper by Silva et al (2012) elaborates alternatives ways to determinate the concentration of $CO_2$, the students tried to reproduce the experiment proposed in the paper and they were impressed with the simplicity of the experiment. Vidotti and Rollemberg (2004) discusses the variety of algae in aquatic environments, so the students could observe the importance of algae, concepts of bioremediation and bioaccumulation. The scientific article by Godoi et al (2003) on the environmental contamination by organotin compounds led to discussions about the concentration of these pollutants as well as curiosity about the method used to determine the concentration of those pollutants, in result, subjects, such as cromatography, could be approached and explained. The Brazilian energy matrix was discussed through the article by Vichi and Mansor (2009), where the student observed that the use of fossil fuels has caused environmental damage, due to global warming, and also discussed the possibility of finite fossil resources by verifying the importance of alternatives renewable energy sources.

## Conclusion

It was concluded that the work provoked several discussions about topics of Environmental Chemistry. These debates led the students to approach academic subjects that at first seemed very difficult and gradually were demystified, improving their formation.

Otenio, M. H; Panchoni, L. C; Cruz, G.C.A.; Ravanhani, C. Avaliação em escala laboratorial da utilização do processo eletrolítico no tratamento de água. **Química. Nova**, v. 31, n. 3, p. 508-513, 2008.

Silva, R; Menezes, E.W; Cataluña, R. Rendimento térmico e emissões de contaminantes atmosféricos de gasolinas formuladas com etanol, mtbe e taee. **Química. Nova**, v. 31, n. 5, p. 980-984, 2008

Silva, R; Santos, F.S; Pires, M. Uso de materiais recicláveis na determinação gravimétrica de $CO_2$ no ar ambiente e tratamento dos resíduos de laboratório gerados. **Química. Nova**, v. 35, n. 10, p.2067-2071, 2012

Vidotti, E.C; Rollemberg, M.C.E. Algas: da economia nos ambientes aquáticos à bioremediação e à química analítica. **Química. Nova**, v. 27, n. 1, p. 139-145, 2004

Godoi, A.F.L; Favoreto. R; Silva, M.S. Contaminação ambiental por compostos organoestânicos. **Química. Nova**, v. 26, n. 5, p. 708-716, 2003

Vichi, F.M; Mansor, MTC. Energia, meio ambiente: o Brasil no contexto mundial. **Química. Nova**, v. 32, n. 3, p 757-767, 2009

**Área:** *EDU* **Inscrição:** 00739

# Emprego da fotografia como abordagem didática para o Ensino de Química em turmas do nível médio

**Daniela S. Anunciação (PQ),[1*] Stella Freitas de Queiroz (IC),[1] Jésu C. Ferreira Júnior (PQ),[2]**

**daniela.anunciacao@iqb.ufal.br**

*[1]Instituto de Química e Biotecnologia, Universidade Federal de Alagoas – UFAL; [2]Instituto Federal de Alagoas - IFAL*
Palavras Chave: *Ensino de Química, TICs, Didática, Fotografias*.

## Highlights

Use of photography as didactic approach for teaching Chemistry at high school groups.
The possibility of relating Chemistry to everyday life through the student's view provides a better performance in the classroom in a qualitative and quantitative way.

## Resumo

As Tecnologias de Informação e Comunicação têm sido excelentes ferramentas direcionadoras no processo de ensino-aprendizagem, a exemplo de aparelhos celulares e câmeras digitais[1,2]. O presente trabalho teve como objetivo explorar fotografias como abordagem didática para o ensino de Química. Foram selecionadas duas turmas de Nível Médio (1º e 3º ano) do Instituto Federal de Alagoas às quais solicitou-se que cada estudante fotografasse algum objeto que lhes remetesse à Química e associasse uma palavra e uma frase de própria autoria. A partir de uma lista de conteúdos contemplados por cada foto o estudante selecionou um e elaborou conceito referenciado com palavras-chave que constituíram um minidicionário ilustrado. As fotos, respectivas frases e os conceitos foram explanados em uma exposição fotográfica intitulada “A Química através dos meus olhos” . Os estudantes expositores foram avaliados por docentes do IFAL e os três primeiros classificados foram premiados tendo como critério originalidade, postura, clareza e domínio do conteúdo. A acessibilidade aos instrumentos empregados proporcionou a aplicação dessa metodologia com consequente envolvimento dos estudantes estimulando assim a interação com a equipe executora do trabalho. As fotografias obtidas evidenciaram seus conhecimentos prévios acerca da Química e a intervenção pedagógica possibilitou maior compreensão dos conteúdos envolvidos nas imagens. A despeito da carência de estudos que relacionem fotografia ao ensino de Química, os resultados observados qualitativa e quantitativamente apontam para melhor desempenho dos estudantes e possibilidade de se explorar a fotografia como recuso didático no processo de ensino-aprendizagem nessa área.

Figura 1. Fluxograma aplicado à abordagem (a), exposição fotográfica “A Química através dos meus olhos” (b) e foto vencedora da exposição (c).

[1]ARAÚJO, Cristina Maria de Souza. **O uso das TICS no processo educativo: exigências do desenvolvimento profissional docente.** Lisboa, 2017, 205 p. Dissertação (Mestrado em Ciências da Educação) – Programa de Pós-Graduação em Educação, ESEAG.
[2]CAMPANHOLI, Julie A. M. **O uso da fotografia na prática docente.** Revista Pandora, n. 49, p. 40-49, São Paulo: Mackenzie, 2012. ISSN: 2175-3318.

**Área: ED**
*(Inserir a sigla da seção científica para qual o resumo será submetido. Ex: ORG, BEA, CAT)*

**Inscrição: 000154**
*(Inserir o número de inscrição do autor que fez a submissão)*

# An Educational Game for the Heat Conceptual Profile Mapping

**Maria Aparecida da Silva Leite* (PG), Nyuara Araújo da Silva Mesquita e Márlon Herbert Flora Barbosa Soares (PQ).**

**marlon@ufg.br**

*Laboratório de Educação Química e Atividades Lúdicas - Instituto de Química - Universidade Federal de Goiás.*

Palavras Chave:*(chemistry teaching; conceptual profile; educational game.*

## Highlights

We present a fun way to map the heat conceptual profile among students of Adult and Youth Education using an educational multi-level question and answers game.

## Resumo/Abstract

The conceptual profile establishes that a concept can be dispersed and that anyone can have different ways of understanding reality in their different concepts. The profile is compost by several zones that correspond to a way of thinking. The conceptual profile of heat, for example, presents the realistic, animistic, substantialist, empirical and rationalist zones. From this, we propose an educational game as a way of mapping these zones of the conceptual profile of heat. The Trilha Termoquímica game (Figure 1) was applied in classes of EJA of a public school in Goiânia city. We observed that in the initial phases of the game that works initial definition of heat the students responded within the realistic zone (heat as sensation). In the intermediate stages on endothermic and exothermic processes and heat units, the students responded in the animist (heat as living), substantiist (heat as inert substance) and empirical (heat as temperature) zones. In the final stages the students answered the questions within the rationalist zone (heat as energy resulting from the temperature difference), making possible the teaching of thermochemistry in the game. The game was able to map the zones of the conceptual profile, considering the free expression of the students, besides teaching the content and entertaining. Using this activity we know the conceptions that were placed in the center of the class and avoid conflicts when faced with scientific concepts.

Figure 1 – Game Images.

**Área:EDU** **Inscrição:00849**

# Microplastics and Superheroes – Learning through a Playful Activity

**Gizelle I. Almerindo (PQ),* Anelise Ehrhardt (PQ), Katlyn T. Nalepa (IC), Tainara F. de Bona (IC), Marianna V. Brandellero (IC), Ana C. K. Fischer (IC), Patrícia F. S. Costódio (PQ), Lourdes Furlanetto (PQ).**

**gizelle.almerindo@univali.br**

[1]*Engenharia Química, UNIVALI*

Keywords: *Chemistry Education, Microplastics, Plastic marine pollution, Superheros.*

## Highlights

Awareness of microplastics in the oceans. Importance of "Life on the Water" - Sustainable Development Goals (SDGs). Recognition and Collection of microplastics on Atalaia Beach/Itajaí City/ Santa Catarina State/Brazil. Drawings and histories created with microplastics. Microplastic superheroes. Dissemination and Popularization of Chemistry. Plastics' properties and superheroes' powers.

## Resumo/Abstract

The introduction of plastic wastes into the marine environment is a grown concern in the recent decades. Specifically, the presence of plastic fragments - called microplastics - represents the most relevant impacts onto marine environment, such as food suppression of biota.[1] In order to contribute to one of the Sustainable Development Goals (SDGs) - "Life on the Water", the University Extension Program "Divulgation and Popularization of Chemistry in the Fulltime Education Center Green Valley" led by the Chemical Engineering Department of UNIVALI (Universidade do Vale do Itajaí) accomplished an approach on microplastics with a group of twelve children (10 to 14 years old). After a brief explanation how these solid residues reached the coastal area, they were asked to recognize and collect microplastics in the sands of Atalaia Beach, a local beach located in Itajaí City/ Santa Catarina State/Brazil, during 20 minutes. Having previously known that children were fond of superheroes, they form teams of 2~3 students in order to develop a story creating a character and designing it with microplastics. There was much excitement and interaction in the book-cover illustration and in the story writing. Among the different stories, were created the "Super-Plastic-Cat", the "Plastic Fairy" and the "Plastic Super Man", which owned super-powers on the whiskers to collect microplastics, to transform microplastics into toys and to fight against a trash man.
Figure 1. Collection of microplastics at the beach and superheroes' drawings created with microplastics.

[1]XANTHOS, D.; WALKER, T. R. International policies to reduce plastic marine pollution from single-use plastics (plastic bags and microbeads): A review. **Marine Pollution Bulletin**. v. 118, p. 17-26, fev. 2017

**Área: EDU** **Inscrição: 00281**

# O uso do vídeo no ensino e na aprendizagem de habilidades laboratoriais técnicas.

**Gabriel F. Batista (IC),[1] Terezinha R. Alvim (PQ).[1*]**

**gabrielbatistadf2@hotmail.com; talvim@cefetmg.br**

*[1]Departamento de Química, CEFET-MG.*

Palavras Chave: Vídeo, Habilidade técnica, Aprendizagem, Laboratório escolar.

## Highlights

**The application of the video as a learning tool to enhance laboratorial skills.** The lab classes were recorded, and the tapes were exhibited to the students, as a method to improving their lab skills. The use of video has shown to be effective in improving the technical skills.

## Resumo/Abstract

A aquisição e o aprimoramento de habilidades laboratoriais são essenciais para técnicos em química. Visando este aprimoramento, pesquisas buscam novas metodologias que melhorem e auxiliem o processo de aprendizado técnico. Uma de destaque é a incorporação de ferramentas tecnológicas nas aulas[1]. Esta pesquisa tem como objetivo estudar a influência do uso do vídeo na performance técnica dos alunos. Foram gravadas três aulas e uma prova prática de uma turma de laboratório de Química Analítica Quantitativa. Os vídeos foram exibidos para os alunos na aula posterior à gravação, distribuindo-se *checklists* para os alunos preencherem conforme sua performance técnica. Para avaliar o desempenho dos alunos, os vídeos foram assistidos pelos pesquisadores, com foco individual na performance de cada aluno, e foi desenvolvida uma avaliação de escala global contendo onze tópicos, agrupados em três grupos, montagem do sistema (MS), preparo da amostra (PA) e técnica de titulação (TT), com notas variando de um a cinco. Foram realizadas entrevistas com quatro dos nove alunos estudados, visando validar o método. Observou-se que o desempenho da turma no grupo de maior interesse, TT, apresentou uma melhoria gradual à cada semana, como apresentado na **Tabela 1**.

**Tabela 1:** Avaliação média semanal da turma para a técnica de titulação.

| | Semana 1 | Semana 2 | Semana 3 | Semana 4* |
|---|---|---|---|---|
| **Pontuação Média** | 4,02 | 4.60 | 4,63 | 4,71 |

* A prova foi realizada na semana 4

Todos os alunos entrevistados afirmaram que o uso do vídeo influenciou diretamente o desenvolvimento de suas habilidades laboratoriais, permitindo-lhes observar com precisão seus erros e corrigi-los.

**Referências**

[1]WANG, C.Y. et al. *Educational Technology & Society*, 17, 2, 2014.

**Agradecimentos**

FAPEMIG e CEFET-MG.

**Área: EDU** **Inscrição: 00669**

# Kit para experimentos de eletroquímica, produzido com condutores flexíveis de grafite laminado sobre celulose.

**Jeferson dos Santos[1]* (PG)*, Pompeu A. Filho[1] (PQ), Bruno Batista[1] (PQ), Fernando Galembeck[1] (PQ)**

**jeferson.santos@iqm.unicamp.br**

[1]*Instituto de Química, Universidade Estadual de Campinas – UNICAMP, Campinas/SP.*

Palavras Chave: *Kit didático, eletroquímica, grafite laminado, eletrônica flexível.*

## Highlights

Electrochemical kits, produced with flexible conductors of graphite laminated on cellulose
A kit to test the conductivity of materials and solutions. Used to assemble galvanic cells, fuel cells, electrolysis and metal deposition. Inexpensive, portable and safe. Requires small test samples.

## Resumo

Os kits de laboratório para ensinar eletricidade e eletroquímica são muitas vezes caros e são frequentemente alimentados pela rede elétrica, o que gera riscos pessoais para professores e estudantes e riscos patrimoniais, para a escola. Este trabalho descreve um novo kit para experimentos de eletroquímica, que utiliza partes feitas com uma nova tecnologia de laminação de grafite sobre celulose [1,2]. Estes novos materiais são seguros, de baixo custo e podem ser descartados corretamente, sem dificuldades. O kit foi utilizado para avaliar o caráter condutor ou isolante de sólidos, óleos, água, soluções ácidas, básicas e salinas, em aulas sobre ligações químicas e condução eletrolítica, observando-se a intensidade de um LED inserido em série com a amostra (figura 1a). A alimentação é feita com uma pilha de 3V, ou ainda por fontes DC ou carregadores de celular, que são dispositivos baratos e de fácil reposição. Conceitos sobre eletrólise (figura 1b), pilhas (figura 1c), deposição de metais e células de combustível podem ser abordados utilizando a mesma plataforma, com pequenas alterações na configuração dos componentes. O kit foi usado por alunos de ensino médio e graduação mostrando-se útil no estudo dos conceitos abordados. Além de utilizar pequenas quantidades de amostras, o kit não apresenta risco de choque elétrico, suas partes podem ser livremente manuseadas pelos alunos, é barato e facilmente transportável, podendo ser usado em sala de aula ou mesmo em casa, além do laboratório.

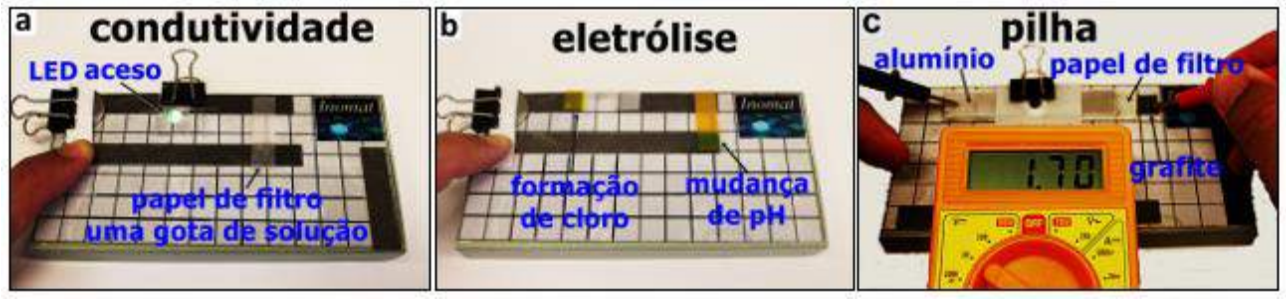


Figura 1: Kit de eletroquímica usado em: (a) teste de condutividade de solução aquosa de HCl 0,1 mol/L (b) eletrólise de solução aquosa de NaCl 0,1 mol/L (c) pilha galvânica formada de filme laminado de grafite (cátodo), papel de filtro com NaCl (0,1mol/L) e ânodo de alumínio.

Agradecimentos
Ao Inomat (INCT via programa CNPq (465452/2014-0) e Fapesp (2014/50906-9)). Fapesp Proc 2016/02386-1.

Bibliografia:
[1] – Ferreira, E.S. et al. Graphite exfoliation in cellulose solutions. Nanoscale, Cambridge, v. 9, 10219-10226, 2017.
[2] - Ferreira, E.S.; Galembeck, F. Processo de obtenção de dispersões aquosas estáveis de grafeno, grafite e carbono amorfo, isento de tensoativos e utilizando celulose como dispersante. BR 102015026420, 18 out. 2015, 09 mai. 2017.

**Área: EDU**

**Inscrição: 00834**
*(Inserir o número de inscrição do autor que fez a submissão)*

# PRODUÇÃO DE BIODIESEL A PARTIR DE ÓLEO DE AZEITE (*Olea europae*) COMO PROPOSTA DE CONTEXTUALIZAÇÃO NO ENSINO DE QUÍMICA

**Sara Jane de Oliveira (IC),[1] Margareta do Carmo (IC),[2] Victor Emanuel Pessoa Martins (PQ),[1] Brunna Angelica Evarista da Silva (IC),[1] Regilany Paulo Colares (PQ), [2]Aluísio Marques da Fonseca (PQ),[1,*]**

**saraquimica@hotmail.com; aluisiomf@unilab.edu.br**

*[1]Mestrado Acadêmico em Sociobiodiversidade e Tecnologias Sustentáveis (MASTS), UNILAB; [2]Instituto de Ciências Exatas e da Natureza, UNILAB;*

Palavras Chave: *(Biodiesel, óleo de azeite, energia renovável, transesterificação).*

## Highlights

Title: Production of Biodiesel from Olive Oil (*Olea europae*) as proposal of contextualization in teaching chemistry
Motivating the classroom through alternative experiments The use of biomass in energy interest oils, adding value to trial with concepts of environmental education, economics and organic synthesis.

## Resumo/Abstract

O biodiesel é um combustível renovável, produzido por uma reação de transesterificação utilizando acilglicerol e álcoois de cadeias curtas na presença de um catalisador[1]. Diante da variedade de matérias primas para a produção de biodiesel o óleo de azeite tem uma boa disponibilidade, o mesmo funciona também como alternativa para a redução das emissões de gases poluentes. A motivação e interesse dos alunos pela Química deve ser estimulado através de atividades práticas contextualizadas, cabendo ao professor a tarefa de prepará-los e aplicá-las adequadamente, a fim de ajudar os alunos a aprender por meio do estabelecimento de inter-relações entre teoria e prática[2]. A prática foi aplicada em forma de oficina para alunos da rede estadual de ensino, residentes no município de Redenção – CE, no laboratório de Química da UNILAB. A produção do biodiesel começa a partir de uma reação de transesterificação utilizando o reagente metóxido de potássio (KOH), dissolvido com metanol ($CH_3OH$), aquecido em um banho maria, direcionado para o funil de separação e adicionado HCl 0,5% para separar as fases orgânicas. Após a separação da solução NaCl, adicionou-se água destilada e agitou-se, esperou-se a separação das fases e recolheu-se a água destilada para medir o PH. Após o término da oficina os alunos responderam a um questionário, observado no gráfico 1. Este trabalho propõe a obtenção de biodiesel a partir de óleo de azeite (*Olea europae*) como proposta de experimentação, contextualização e reflexão do ensino de química.

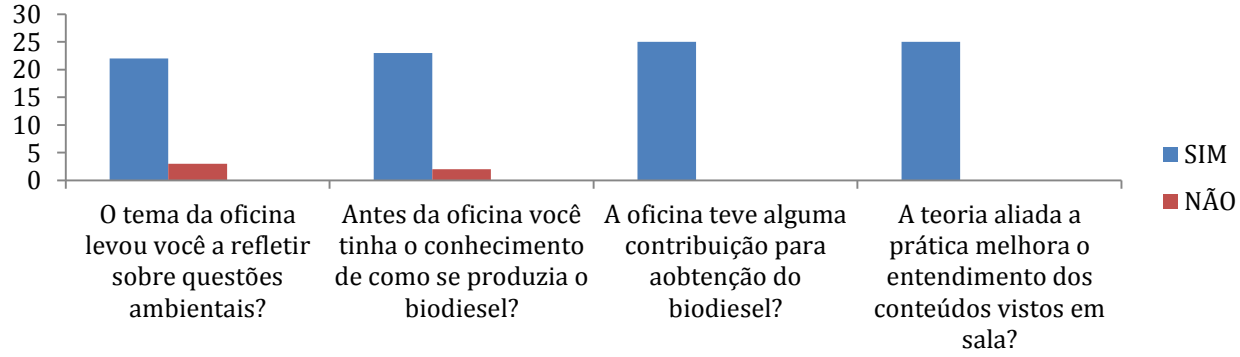


Gráfico 1.

REFERÊNCIAS

[1] MURPHY, M. J.; KETOLA, H. N. & RAJ, P. K. Summary and assessment of the safety, health, environmental and system risks of alternatives fuels. Helena: U. S. Department of Transportation Federal Transit Administration, 1995. 28 p.

[2] SALVADEGO, W. N.; C. LABURÚ, Carlos Eduardo. Uma análise das relações do saber profissional do professor do ensino médio com a atividade experimental no ensino de química. Química nova na Escola. V. 31, n.3, p.216-223, 2009.

**Área: EDU** **Inscrição: 00241**

# Visão dos discentes a respeito de jogos analógicos e digitais no ensino de química

**Ariane C. F. Beltrame (IC)[1]*, Gean A. Zapateiro (IC)[1], Marlon P. Moraes(IC)[1], Daniela P. Santos (IC)[1], Alessandra Stevanato (PQ)[1], Celita T. Poli (FM)[2].**

**ariane_beltrame@hotmail.com**

[1] *Universidade Tecnológica Federal do Paraná (UTFPR) – Câmpus Londrina Avenida dos Pioneiros, 3131 CEP 86036-370 Londrina – PR.*
[2] *Colégio Estadual Marcelino Champagnat – Rua São Salvador, 998 CEP 86026-480 Londrina – PR.*

Palavras Chave: *Jogo Analógico, Jogo Digital, Ensino de Química, Ensino e aprendizagem.*

## Highlights

Students' view of analog and digital games in chemistry teaching. Comparative analysis of analog and virtual games as educational tools in the teaching and learning process. Student opinion and data collection by means of a diagnostic questionnaire.

## Resumo

Os jogos didáticos permitem ao aluno "o desenvolvimento de competências no âmbito da comunicação, das relações interpessoais, da liderança e do trabalho em equipe, utilizando estas em um contexto formativo" [1]. Assim, esse trabalho tem por objetivo analisar a visão de alunos do ensino médio a respeito de duas categorias de jogos educacionais como ferramentas de aprendizagem. Para isso, foi desenvolvida uma aula sobre ácidos e bases aplicando essas diferentes abordagens de jogos (analógico e digital), em seguida questionou-se aos alunos: *Qual(is) ferramenta(s) utilizadas você considera mais interessante no processo de ensino e aprendizagem? O jogo analógico ou jogo digital? Explique.* As respostas foram analisadas e 64,3% dos alunos afirmaram que o analógico foi mais relevante, cerca de 7,1% afirmaram que o digital contribuiu mais para a evolução do conhecimento químico e 28,6% disseram que a união das duas ferramentas fazem com que os estudantes aprendam com maior facilidade. A Tabela 1 apresenta algumas falas que justificam esses percentuais. A utilização de jogos educacionais no contexto escolar desperta a interação dos alunos, o trabalho em equipe e o desenvolvimento de habilidades cognitivas que favorecem a construção do conhecimento. Assim, do ponto de vista dos alunos o jogo analógico foi mais relevante, pois contribuiu para o desenvolvimento de muitas dessas habilidades citadas.

Tabela 1. Justificativa dos licenciandos acerca da utilização dos jogos analógico e digital no ensino de ácidos e bases.

| ***Pergunta*** | ***Jogo Analógico*** | ***Jogo Digital*** | ***Ambos*** |
|---|---|---|---|
| *Qual(is) ferramenta(s) utilizadas você considera mais interessante no processo de ensino e aprendizagem? O jogo analógico (twister Químico) ou jogo digital? Explique.* | *''O analógico pois é mais interativo e estimula a vontade de responder as perguntas e ganhar. Além disso a dinâmica é muito divertida o que faz com que saiamos da passividade e tenhamos vontade e alegria para aprender'.'* | *''O jogo digital é mais legal, pois não precisamos nos expor a dinâmicas em grupos, podemos jogar sozinhos e assim os alunos ficam menos intimidados a errarem'.'* | *''O jogo analógico foi mais divertido, enquanto o digital facilitou a aprendizagem, assim concluo que ambos foram primordiais para a evolução do conhecimento científico*'.' |

Referências:
[1] BRASIL, Ministério da Educação. Secretaria da Educação Básica. **Orientações curriculares para o ensino médio**: Ciências da Natureza, Matemática e suas Tecnologias. v. 2. Brasília: MEC/SEB, 2006.

| Área: EDU | Inscrição: 00163 |
|---|---|

# Representação Social de graduandos de Química sobre "Experimentação"

**Caian C. Receputi (PG)[1], Thaiara M. Pereira (PG)[1], Marcos Vogel (PQ)[2] e Daisy B. Rezende (PQ)[1,3]**

**caian.receputi@usp.br; dbrezend@iq.usp.br**

*[1]USP, Programa de Pós-Graduação Interunidades em Ensino de Ciências, São Paulo; [2]Universidade Federal do Espírito Santo, Centro de Ciências Exatas, Naturais e da Saúde, Departamento de Química e Física, Alegre, ES; [3]USP, Instituto de Química, Departamento de Química Fundamental, São Paulo, SP.*

Palavras Chave: *Representação Social; Núcleo Central; Estudantes de Química; Experimentação*

## Highlights

Social Representation of Chemistry undergraduate students concerning "Experimentation": The unveiled Social Representation´s Central Core indicates that these students comprehension about "Experimentation" attains to its empirical character regardless of their specific track.

## Resumo/Abstract

Este trabalho apresenta os termos do Núcleo Central (**NC**) da Representação Social (**RS**)[1] de estudantes de Química da USP sobre "Experimentação", obtidos pela análise das informações de um questionário de livre associação a esse termo indutor aplicado, em 2017/2, a 58 sujeitos (Tabela 1). O **NC** orienta a organização e a significação da **RS**, enquanto seu sistema periférico a protege.[2] A análise dessas informações baseou-se em trabalhos anteriores de nosso grupo de pesquisa[3] obtendo-se os resultados mostrados no Quadro 1. O conjunto dos termos do **NC** e do sistema periférico da **RS** indica que a visão desses graduandos sobre "Experimentação" remete à perspectiva de comprovação empírica dos dados, de comprovação da hipótese sobre um fenômeno observado, corroborando dados da literatura.[4]

Tabela 1: Caracterização dos Sujeitos participantes da pesquisa.

| Curso | Ano de Curso | | | | | | Sujeitos[a] | |
|---|---|---|---|---|---|---|---|---|
| | 1º | 2º | 3º | 4º | 5º | 6º | | Total |
| **Bacharelado** | 13 | 07 | 04 | | 01 | | 25 | 33 |
| **Bacharelado e Licenciatura** | | 03 | 02 | 01 | 03 | 02 | 11 | 15 |
| **Licenciatura** | 02 | 02 | 02 | 02 | 01 | | 9 | 10 |

a. Alguns sujeitos não responderam indicando o tempo de curso

| **NC** | **Primeira periferia** |
|---|---|
| Ciência; experimento; laboratório; prática; teste | erro; estudo; hipótese |
| **Zona de Contraste** | **Segunda periferia** |
| aprendizado; curiosidade; dados; investigação; método; Química; resultado; tentativa; estar | análise; conhecimento; descoberta; novidade; observação; planejamento; relatório |

Quadro 1: Quadro paradigmático para a RS de experimentação pelos alunos de graduação do IQUSP.

Concepções de subgrupos minoritários ou de indivíduos, como *Aprendizado,* estão expressas na zona de contraste. Conclui-se haver sujeitos para os quais o termo "Experimentação" vincula-se também ao processo pedagógico.

1. MOSCOVICI, S. **Representações Sociais**. 5. ed. Petrópolis, RJ: Vozes, 2007, 302 p.
2. ABRIC, J-C. Las Representaciones Sociales: Aspectos Teóricos. In: ABRIC, J.-C. (Ed.). **Prácticas sociales y representaciones**. México, D.F.: Cultura Libre, 11-32, 2001.
3. Grupo de Pesquisa em Linguagem no Ensino de Química; VOGEL, M. Tese. Programa de Pós-Graduação Interunidades em Ensino de Ciências, USP, SP. 2016, 216 p.
4. ADORNI, D.S; AMARAL, N.S; ROCHA-FILHO, O. P; SILVA-JUNÍOR, A. J. Concepções de alunos do Ensino Médio sobre as aulas práticas de química. In: **Anais** XII Congresso Nacional de Educação – EDUCERE, Paraná, 2267-2676, 2015.

*C.C.R agradece à CAPES pela bolsa de Mestrado concedida.*

**Área: __EDU__** *(Inserir a sigla da seção científica para qual o resumo será submetido. Ex: ORG, BEA, CAT)*

**Inscrição: __00280__** *(Inserir o número de inscrição do autor que fez a submissão)*

# Atividades Experimentais Investigativas: Visões e Propostas de Professores de Química do Ensino Médio

**Luciane Hiromi Akahoshi (PQ),[1] Maria Eunice Ribeiro Marcondes (PQ),[1] Fabio Luiz de Souza (PQ),[1] Terezinha Iolanda Ayres-Pereira (PG)[1].**

**luhoshi@iq.usp.br**

*[1]GEPEQ – Instituto de Química da Universidade de São Paulo*

Palavras Chave: *Atividades Experimentais Investigativas, Formação Continuada, Ensino Investigativo, Experimentação no Ensino de Química, Ensino de Química, Formação de Professores.*

## Highlights

Inquiry-based experimental activities: understanding and proposals of High school chemistry teachers
We investigate the beliefs of a group of high school chemistry teachers about teaching with classroom experiments
We also investigate how chemistry teachers design inquiry-based experimental activities

## Resumo/Abstract

A experimentação no ensino de Química é uma estratégia considerada importante por professores. Mas para contribuir para a aprendizagem dos estudantes, é preciso promover a formação de conceitos e a aquisição de habilidades de pensamento mais complexas.
Assim, os experimentos deveriam apresentar situações problemáticas, dando-lhes características de um ensino investigativo.
Em nosso trabalho, investigamos as ideias apresentadas por 25 professores de Química sobre o papel da experimentação em um curso de formação que objetivou planejar atividades experimentais investigativas. Nesta pesquisa, analisou-se a resposta individual dada a dois instrumentos (início/fim) e as propostas de atividades investigativas elaboradas por grupos de professores.
Nos instrumentos, analisou-se a seleção feita pelos professores das 5 afirmações mais relevantes de 21 propostas sobre os objetivos do ensino experimental. Elas foram categorizadas como visão: simplista (VS: 2 afirmações) – experimento ilustra teorias e motiva participação do aluno; empirista (VE: 7 afirmações) – experimento prova ou nega teorias e estudante aprende técnicas experimentais; pedagógica (VP: 12 afirmações) – experimento propicia a participação dos estudantes na elaboração de hipóteses, controle e previsão de fenômenos, desenvolvendo a argumentação e a compreensão dos fenômenos observados.
"Motivar o aluno" (VS) foi escolhido como um dos objetivos mais relevantes, outras afirmações selecionadas estavam relacionadas a VP (quadro). Percebe-se que os professores passaram a valorizar mais os aspectos sociais (trabalho em grupo e autonomia do aluno), além dos cognitivos. Os planejamentos tangenciam um ensino investigativo, porém há dificuldade em propor o levantamento de hipóteses com os alunos.

| Afirmações consideradas mais relevantes | Início (nº prof.) | Fim (nº prof.) |
|---|---|---|
| motivar aluno (VS) | 15 | 14 |
| aprender por meio da prática conceitos científico (VP) | 11 | 9 |
| desenvolver o raciocínio (VP) | 12 | 10 |
| desenvolver a capacidade de trabalhar em grupo (VP) | 9 | 13 |
| desenvolver a autonomia do aluno (VP) | 9 | 13 |
| analisar dados para obter conclusões (VP) | 4 | 8 |
| propor hipóteses para solucionar problemas sugeridos (VP) | 5 | 10 |

**Área: EDU** **Inscrição:00683**

# Valuable Obstacle as a challenge to the development of the professional knowledge of a Chemistry teacher

**Graziele B.O. Pena (PG),[1] Nyuara A.S. Mesquita (PQ),[2]**

**grazieleborges@hotmail.com**

*[1]Intituto de Ciências Exatas e da Terra – UFMT/CUA; [2]Instituto de Química – Programa de Pós Graduação em Química UFG/Goiânia*

Keywords: professional knowledge in teaching, *epistemological obstacle, Chemistry teachers, teaching formation*

## Highlights

The conceptions of graduates in Chemistry have been investigated, since they can constitute obstacles of an epistemological nature to the development of the professional knowledge when assigning different values to the formative knowledge.

## Resumo/Abstract

One of the concepts of the bachelardian epistemology is that of an epistemological obstacle that is related to aspects that cause stagnation in the act of knowing.[1] Porlán *et al.* [2-4] use the concept of epistemological obstacle proposed by Bachelard for the field of didactics of Science and extended its meaning to the case of Science teachers related to the process of development of professional knowledge in teaching. In this sense, this work sought to discuss the characterization of an epistemological obstacle, titled valuable, identified in the conception of Chemistry Graduates. The research was carried out with sixteen Graduates in Chemistry. Interviews were carried out and questionnaires were applied. From the process of categorization, which occurred through the organization of units of analysis, which had some coherence, the category named "Valuable Obstacle" emerged, which highlighted a conception of distinct values attribution to the same Science depending on how it is taught.

Picture 1. Fluxogram which representes one of the stages of categorization of the process of *Discursive Textual Analysis.*

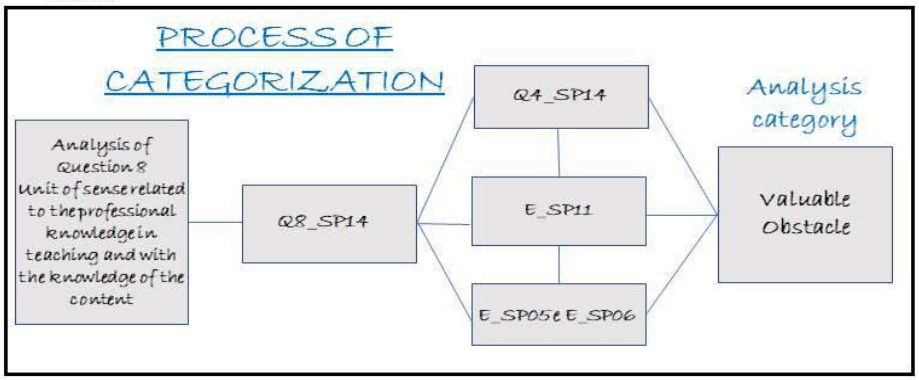


Picture 2. Opinion of a person of research SP11 during the interview

***E_SP11:*** Student´s learning is much worth than the traditional teaching. Even if he/she asimilates less.

This conception is constituted as an obstacle because it implicates the process of development of the professional knowledge, once it blocks the future Chemistry teacher to understand the importance of the transformation of the Chemistry content facing the simple transmission of the content.

[1]PORLÁN, R. et al. *Enseñanza de las Ciencias*, 28, 1, 31-46, 2010.
[2]PORLÁN, R.; RIVERO, A.; MARTÍN, P. *Enseñanza de las Ciencias*. 15, 2, 155-171, 1997.
[3]PORLÁN, R.; RIVERO, A.; MARTÍN, P. *Enseñanza de las Ciencias.* 16, 2, 271-288, 1998.
[4]BACHELARD, G. Trad. ABREU, E. S. RJ. Editora Contraponto, 1996, 316 p.

**Área: ___EDU_____ Inscrição: __01328_____**

# O ensino da química na concepção dos estudantes de Licenciatura em Educação do Campo-CNM/UFMA

**Cristiana R. Marcelo,[1] (PQ).**

**cristiana.resende@ufma.br**

*[1]Coordenação da Licenciatura em Educação do Campo, UFMA-Campus Bacabal.*

Palavras Chave:*(ensino de química, educação do campo).*

## Highlights

**Chemistry teaching in the conception of undergraduate students in Rural Education-CNM/UFMA**. This work describe the conceptions of undergraduate students in Rural Education-CNM/UFMA about chemistry teaching. It possible see that students recognize the chemistry as an important science for their lives. Many say that chemistry is a science that helps in understanding the formulation of medicament, food composition and natural phenomena, however they find it difficult to understand.

## Resumo/Abstract

A UFMA oferta o curso de Licenciatura em Educação do Campo (Ledoc) em duas ênfases: Ciências Agrárias (CA) e Ciências da Natureza e Matemática (CNM). O alunado da Ledoc é composto por sujeitos que possuem algum vínculo com o campo, sendo oriundos basicamente das distintas regiões do estado do Maranhão e com diferentes vivências escolares. O presente trabalho objetivou investigar, por meio de questionário semiestruturado, as concepções dos estudantes ingressantes na Ledoc-CNM/UFMA quanto ao ensino da química. Dos 40 alunos pesquisados, cerca de 90% declaram que conseguem observar a presença da química em certas situações do seu cotidiano, reconhecendo que é uma ciência importante em suas vidas. A maioria dos alunos indicaram os “medicamentos”, os “alimentos” e a própria “natureza” como exemplos da importância da química. A associação da química a esses elementos do cotidiano se deve, provavelmente, ao modo de vida do povo do campo, uma vez que lidam diretamente com a produção de alimentos; utilizam medicamentos e/ou plantas medicinais como agentes químicos para tratar suas enfermidades; e estão em contato constante com o ambiente natural, o que os tornam possíveis temas geradores. Outro aspecto identificado foi que grande parte dos entrevistados (80%) afirmaram que a química é uma disciplina de difícil compreensão, atribuindo essa problemática a diversos fatores, tais como a falta de contextualização para associar as teorias às vivências do seu dia a dia; a grande quantidade de informações, inclusive bastante complexas, já que são muitas teorias, fórmulas, símbolos e cálculos envolvidos e com pouco significado para os alunos; o pouco contato com a disciplina no percurso escolar, o que gera a falta dos conhecimentos prévios necessários para incorporar os novos conceitos; dentre outras questões. Além disso, foi possível verificar o consenso dos alunos quanto à necessidade de qualificação docente, com formação de professores capazes de elaborar estratégias metodológicas que favoreçam o processo de ensino-aprendizagem e que considerem as especificidades dos alunos do campo. Diante das observações aqui explanadas, pode-se inferir que, para os alunos da Ledoc-CNM/UFMA, o ensino da química é importante, embora pouco eficiente, ainda mais quando se trata de escolas do campo, onde a alfabetização científica praticamente não se faz presente, e quando se faz nem sempre considera os princípios da Educação do Campo[1]. Assim, pensar no “Construir o Amanhã” é, além de buscar novos avanços científicos, reconhecer e valorizar os conhecimentos populares produzidos e promover formação humana-científica-cidadã que considere os diferentes aspectos históricos, sociais, culturais e econômicos que compõem a nossa sociedade.

**Referências Bibliográficas**

BRASIL. **Decreto n° 7.352, de 04 de novembro de 2010.** Brasília: 2010.

**Área: Edu** **Inscrição: 00268**

# Chemistry teaching for deprived of liberty: challenges of teaching in a recovery center.

**Dhaniella C. de B. Oliveira (IC),[1] Renata A. Santos (IC),[2] Luely O. da Silva (PQ),[3]**

**dhaniella.admm@gmail.com**

*[1]Graduating degree in Natural Sciences-Chemistry (UEPA); [2]Graduating degree in Natural Sciences-Chemistry (UEPA); [3]Department of Natural Sciences (UEPA)*

Palavras Chave: *Chemistry, Deprived of liberty, Teaching performance*

## Highlights

What challenges do chemistry teachers in prisons face? The objective was to analyze the challenges reported by a professional from recovery center in the State of Pará.

## Abstract

By the Federal Decree n. 7626 it was established that the brazilian States should draw up their State Eduacation Plans in Prisons. We know, however, that this process is slow and that some brazilian States, including the one in the present research, do not yet have such plans. Thus, the teaching performance in prison establishes in an intuitive way through the absence of a basis to guide the educational practice. Figure 1 illustrates a research methodology and Figure 2 presents some reports from the chemistry teacher investigation.

Figure 1.: Methodology

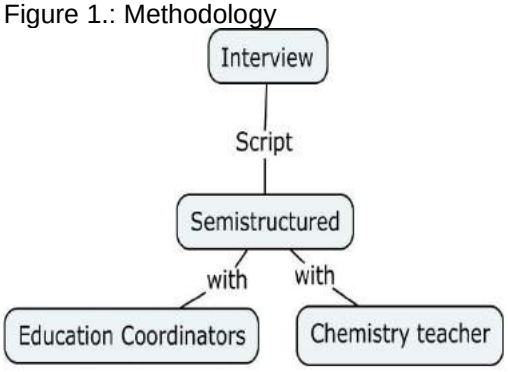


Graf. 1: Challenges of teaching

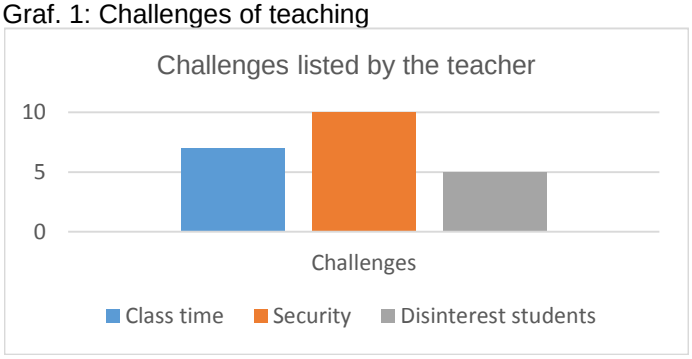


Figura 2.: Teacher reports

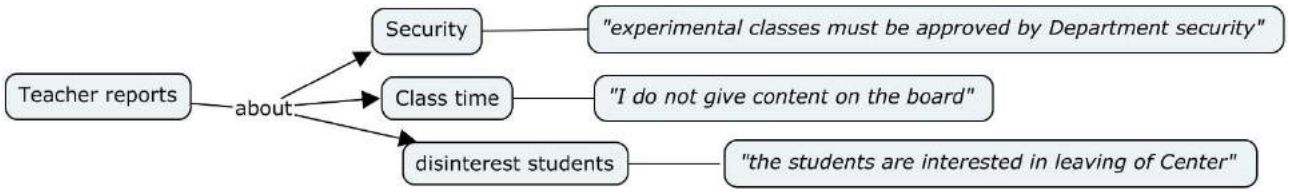


Coordination of education related to the capacities of 30 to 35 minutes each, and how the experimental experiences can carry risks depending on the material used and because of this are avoided. In the present research, it is possible to identify the weakness in prison education at the locus of research and the necessary specific training for teachers on the provision of education in the prisons area, leading to the emergence of challenges in which it is believed that, based on the elaboration of a State Plan of Prison Education that as presented by Silva and Moreira (2006) such challenges could be overcome, since the teacher would already act in prison education by creating specific didactics for their practices in these places.

REFERENCES

BRASIL. Decreto nº 7.626, de 24 de novembro de 2011. Disponível em: < http://www.planalto.gov.br/ccivil_03/_ato2011-2014/2011/decreto/d7626.htm > Acesso em: 7 de Jan/2018

SILVA, Roberto da; MOREIRA, Fábio Aparecido. Objetivos educacionais e objetivos da reabilitação penal: o diálogo possível. IN: Dossiê Questões Penitenciárias. Revista Sociologia Jurídica. n.03. Julho/Dezembro de 2006

**Área: EDU** **Inscrição: 00098**

# Chemistry teaching perceptions of students from Territorial Center of Professional Education from Vitória da Conquista/BA.

**Ana Beatriz S. V. Novaes[1*] (IC), Saulo A. Silva[1] (IC), Shaiala A. Santos[2] (FM).**

**química.ananovaes@gmail.com, amaral.sas@gmail.com, shaiaquino@hotmail.com**

*[1]Chemistry department, IFBA, Vitória da Conquista Campus; [2]Territorial Center of Professional Education of Vitória da Conquista/BA*

Keywords: Chemistry Teaching, Technical Course

## Highlights

This paper analyzes the students' perception of the two-year chemistry classes in the integrated technical course compared to regular high school's three years.

## Abstract

The proposal of the current Brazilian technical education, in its different configurations, is guided by two basic principles: integration and articulation[1]. In this context, the articulation works promoting a better use of the available workload so that there is simultaneously integration between work, science and culture. The Chemistry teaching, included in the three years of secondary education, is restricted to only two in integrated technical education[2]. Therefore, this study aims to analyze the students perception of this articulation, through the application of a questionnaire directed to the students and the analysis of the course plan and pedagogical project of the institution. To obtain the data, a questionnaire was applied to students from the first to fourth grade of the edification technical course of the Territorial Center for Professional Education, Vitória da Conquista / BA campus. It was observed, through the analysis of students opinions, a conflict between pedagogy and politics[3], in which the curricular change, according to the students perception, generates a disadvantage in relation to the students of the regular high school.

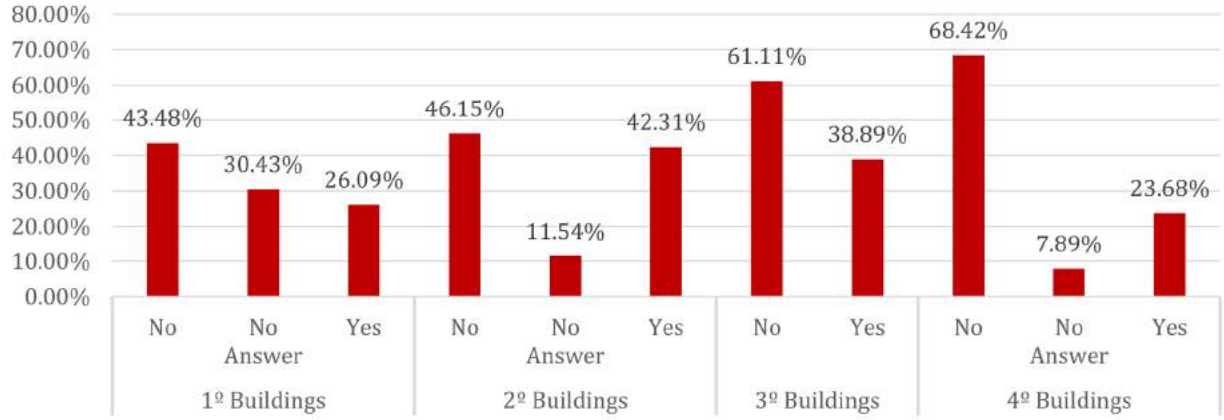


Graphic 1 – Approval of two-year chemistry teaching model

[1]CNE/CEB. Resolução 6/2012. Diário Oficial da União, Brasília, 21 de setembro de 2012, seção 1, p. 22
[2]CETEP/VCA. Projeto Político Pedagógico
[3]CASTRO, Mad'Ana D. R; MACHADO, Maria M; VITORETTI; Jacqueline M. B. Educação integrada e PROEJA: Educação Integrada e PROEJA: diálogos possíveis. *Educação & Realidade,* vol. 35, no. 1, 2010, pp. 151-166. Editorial Universidade Federal do Rio Grande do Sul.

**Área: EDU** **Inscrição: 00150**

# Perfil formativo dos professores de Química do Instituto Federal de Educação, Ciência e Tecnologia de Goiás

**[1,2]Vinicius Sousa Ferreira (IC),[2] Nyuara Mesquita (PQ)**

**Viniciusquimica.12@gmail.com; nyuara2006@gmail.com**

*[1]Instituto Federal de Goiás-Câmpus Formosa - IFG*
*[2]Universidade Federal de Goiás – Instituto de Química – UFG – IQ-NUPEC - LEQUAL*
Palavras Chave: *licenciatura, ensino de química, LDB*

## Highlights

In surveying the initial training of the IFG teachers, it identifies with about 40% of the documents are not licensed, which may compromise an update of these in the middle of teaching.

## Resumo/Abstract

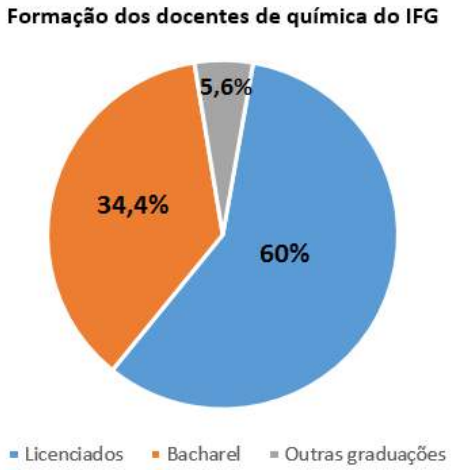


A LDB explicita que a formação para atuar na educação básica é de licenciatura plena.[1] Os Institutos Federais (IF) são de extrema importância para uma educação básica de qualidade nesse cenário e possuem docentes qualificados, a maioria com mestrado e doutorado, o que possibilita a melhoria do ensino em nível médio e superior.[2] Entretanto, nem todos docentes são licenciados. Em vista disso, o objetivo do presente trabalho foi realizar o levantamento da formação dos docentes que atuam como professores de Ensino Médio Técnico Integrado (EMTI) nos IF em Goiás (IFG) a fim de identificar e analisar distorções em relação à LDB. Foram analisados os currículos de 90 professores docentes da área de Química dos 14 campus do IFG. Desses 90, 54 possuem o curso de licenciatura em química, 31 possuem bacharelado e 5 possuem outras graduações relacionadas à química, como farmácia, agronomia e engenharia química. Os docentes, quando contratados, também atuam no EMTI. Embora estes cursos do IF tenham disciplinas profissionalizantes de caráter específico, a LDB determina a licenciatura para o exercício do magistério em todas as etapas da educação básica. A falta da licenciatura pode comprometer a qualidade do ensino de Química considerando-se importantes aspectos relacionados aos conhecimentos didáticos, como reconhecimento de obstáculos epistemológicos e entendimento do processo avaliativo, dentre outros, que corroboram com uma formação docente que torne a abordagem de conteúdos efetiva para o processo ensino e aprendizagem.

1. BRASIL. 1996. Lei nº 9.394, de 20 de dezembro de 1996. Estabelece as diretrizes e bases da educação nacional. Brasília. Disponível em: *Acesso em 30 de janeiro de 2018.*
2. BRASIL. 2008a. Lei nº 11.892, de 29 de dezembro de 2008. Institui a Rede Federal de Educação Profissional, Científica e Tecnológica, cria os Institutos Federais de Educação, Ciência e Tecnologia, e dá outras providências. Brasília. *Acesso em: 30 de janeiro de 2018.*

**Agradecimento**s: IFG, UFG.

**Área: EDU** **Inscrição: 191**

# Socioeconomic Profile of Brazilian Chemistry Students: An Analysis of the Enade Reports

**Dayse das Neves Moreira (PQ),[1] Paulo César Geglio (PQ)[2]**

**daysemoreira@cca.ufpb.br**

*[1]Departamento de Química e Física, UFPB; [2]Departamento de Fundamentação da Educação, UFPB*

Keywords: *Chemistry student; Socioeconomic profile, Enade reports.*

## Highlights

Expansion higher education in Brazil. The change of the chemistry students profile was studied. Increase in the afro- and afro-caucasian descendants in the higher education.

## Resumo/Abstract

In the last two decades, a significant increase in the number of vacancies in higher education was achieved, driven by the expansion of private initiative and by the presence of public power in this sector. A greater part of the population has accessed to this educational segment, especially those with lower income.[1] Therefore, a change in the population of this school level can be expected. In this context, we present herein a study about the profile of undergraduate students of chemistry in Brazil in the last decade. The database for this research was the Brazilian Exam of Students Performance reports (Enade) from 2005 to 2014 period[2] and the data about gender and social-economic variables to trace their profile were selected. Considering the range 18 to 24 years as the great age to be on higher education, we observed an increase from 40.2% to 49.7%. Female students have also demonstrated a percentage grow of almost 10%. In this same context, an increase of afro-descendent students was attained, reaching more than 50% from the total amount of students, which is a result from the opportunities enlargement of the higher education. The family income and financial situation data show that a great part of these students have low salaries (until 3 salaries) and must contribute to the family maintenance. In fact, a process towards the study democratization is occurring in the higher education, allowing that disadvantaged persons achieve the higher education level.

**Table 1**. Selected data from the Brazilian Exam of Students Performance (Enade) reports.

| Enade | Age | | | Gender | | Ethnicity | | |
|---|---|---|---|---|---|---|---|---|
| **Year** | < 24 years | 25 to 29 years | Above 30 years | Male | Female | Caucasian | Afro-caucasian descendant | Afro-descendant |
| **2005** | 40.2% | - | - | 48.3% | 51.7% | 65.9% | 25.0% | 6.2% |
| **2008** | 62.7% | 22.6% | 14.7 | 45.7% | 54.3% | 62.3% | 27.4% | 7.4% |
| **2011** | 47.9% | 32.6% | 19.5 | 43.8% | 56.2% | 61.9% | 28.5% | 7.2% |
| **2014** | 49.7% | 25.0% | 25.3 | 40.4% | 59.6% | 43.4% | 43.0% | 11.6% |

[1]Ristoff, D. Vinte e Um Anos de Educação Superior. Expansão e Democratização. Cadernos do GEA, Rio de Janeiro, n.9, **2013**.
[2]Ristoff, D. O novo perfil do campus brasileiro: uma análise do perfil socioeconômico do estudante de graduação. *Avaliação* **2014**, *19*, 723.

**Área: EDU** **Inscrição: 00167**

# A Supervisor narration on the history of a PIBID-Chemistry subproject and the construction of teacher professionalism

**Thaiara M. Pereira (PG)[1], Caian C. Receputi (PG)[1], Marcos Vogel (PQ)[2], Daisy B. Rezende (PQ)[1,3]**

**thaiara.mp@usp.br; dbrezend@iq.usp.br**

*[1]Programa de Pós-Graduação Interunidades em Ensino de Ciências da Universidade de São Paulo; [2]Departamento de Química Fundamental, Instituto de Química da Universidade de São Paulo, São Paulo; [3] Centro de Ciências Exatas, Naturais e da Saúde, Universidade Federal do Espírito Santo, Alegre.*

*Keyword*: *Oral History; Teacher Education; PIBID-Chemistry; Chemistry Undergraduation.*

## Highlights

The results concerning PIBID´s role in initial teacher education show the subproject´s actions are pivotal to the identification of the undergraduates with both the course and as a social group.

## Abstract

PIBID encourages the University-School partnership to improve the initial teacher education through various actions, including those activities developed in the High-school context that leads the undergraduates to formative experiences. Aiming at understand by the importance of this program to the initial chemistry teacher education (ICTE), we investigated a PIBID-Chemistry subproject according to the precepts of Oral History.[1] This approach allows the interviewees, through the narration of their experiences, to contribute to a better understanding of the research topic: in this work, a subproject of Chemistry teacher formation and its nuances for the training of the future teachers. The analysis of the transcribed material, inspired by the concepts of Content Analysis,[2] led to the construction of five categories, of which three were selected to be presented (Table 1).

| Categories | Categories definition | Interview excerts |
|---|---|---|
| **ICTE students** | Students view on the importance of PIBID for their education, as reported by the supervisor interviewed | ✓ They [undergraduates] feel much more supported. And thus, they also think that a matured decision related to become a teacher is favored.<br>✓ What PIBID brought to them [undergraduates], too, is a possibility of identification: 'we are a group of ICTE students´. |
| **ICTE** | Conceptions of the supervisor on teacher education in Chemistry | ✓ We are focused on the scholarship holder: I am forming a future teacher. So, the more opportunities I give for this ICTE student experience the teaching reality, the better teacher I'm gonna form, I believe.<br>✓ We have this practice of holding joint meetings with the secondary school teachers, the university staff, and undergraduate fellows that participate of the project. |
| **Característic** | Organization of the subproject and its influence on the development of activities | ✓ We've reached the understanding we've got to focus into ensuring a better future teacher formation, by valorizing the undergraduate formative experiences that help the blossoming of a good teacher. |

Table 1 – Categories and demonstrative excerts.

In the subproject investigated, the different activities allow the undergraduates to experience the school environment from different perspectives. The collective project planning building was performed across the years under the supervisor encouragement, to accomplish the ICTE students needs. In this sense, the referred subproject can be understood as a dynamic formative space, which leads to the reinforcement of the actions that the group participants recognize as essential to enhancing the formation of the teacher students and other actors. The analysis of the interview shows that the fact that the undergraduate students identifying themselves as future teachers is a positive result of the actions implemented along the subproject duration.

### References

1. MEYHI, J. C. S. B. Manual de história oral. 5ª ed. São Paulo: Edições Loyola, 2005.
2. BARDIN, L**. Análise de conteúdo**. 4ª ed., Lisboa, Portugal: Edições 70, 2009.

TMP acknowledges CAPES for the scholarship.

**Área: EDU** **Inscrição: 00440**

# Incentivo, estímulo e as ações que levam um aluno do ensino fundamental a se tornar um pesquisador. Uma parceria Universidade/Escola Pública

**Regiane C.M.S. Castione (FM)[1,*], Maria Luiza Bet (IC)[1] e José Ricardo C. Salgado (PQ)[2]**

***regianecastione@gmail.com, jose.salgado@unila.edu.br**

*[1]Colégio Estadual Prof. Flávio Warken - E.F.M.P.; [2]UNILA, Universidade Federal da Integração Latino-Americana, CEP.: 85867-970, Foz do Iguaçu, PR, Brasil*

Palavras Chave: *Ensino, Escola, Pilhas, Solo, Eletroquímica, Meio Ambiente.*

## Highlights

Incentive, encouragement and actions that lead a student to be researcher. Federal University / Public School partnership. Batteries, Electrochemistry, Environment.

## Resumo/Abstract

As atividades experimentais de eletroquímica desenvolvidas na "*Química no recreio*" no Colégio Estadual Prof. Flávio Warken em parceria com o projeto da Unila "*Universidade e Sociedade - O que a universidade pública pode oferecer aos estudantes - Eletroquímica ao alcance de toda sociedade*" forneceram estímulo para alguns alunos do ensino fundamental realizarem atividades para a "Feira de Ciências - 5ª Feira Tecnocultural". Um dos trabalhos que se destacou, é de uma aluna do 8 ano que se interessou em desenvolver um experimento para mostrar os danos que causam a saúde humana e ao meio ambiente o descarte inadequado de pilhas e baterias no solo. O experimento foi feito em uma caixa de madeira, devidamente isolada onde o espaço foi dividido em três partes. Em duas partes, foi colocada uma pilha comum e em outra uma pilha alcalina. No centro foram colocadas minhocas. Após seis meses de ensaios, foram feitas análise de difratometria de raios X para analisar a composição do solo de possíveis metais presentes. Em todo o momento, a aluna acompanha todas as atividades, inclusive com registros em diário de bordo e fotos. O estímulo dado e o método investigativo proposto, incentiva o aluno a continuar o projeto, buscar mais literatura sobre o tema e além de tudo aprender fazendo. O papel da escola e da universidade são fundamentais para oportunizar uma nova forma de aprender indo além dos limites dos "muros da escola".

Figura 1. Demonstração na 5ª Feira Tecnocultural - 2017.

**Área: *EDU*** **Inscrição: 00780**

# Synthesis of α-Lapachol, β-lapachone and hydroxy-hydrolapachol from lapachol (demolition timber): A Research Module for the Organic Chemistry Laboratory

**Maria D. A. Oliveira[1] (PG), Josiane M. S. Costa (IC)[2], Teresinha J. A. S. Andrade[3] (PQ), Joaquim S. Costa Júnior[2,*] (FM).**

**josianemarciel@outlook.com; jquimjr@gmail.com***

[1]*Federal University of Piauí, Department of Chemistry, Campus Ministro Petrônio Portela, Teresina, Piauí, Brazil.*
[2] *Federal Institute of Piauí, Department of Chemistry, Campus Central, Praça da Liberdade, Teresina, Piauí, Brazil.*
[3]*Federal Institute of Maranhão, Department of Chemistry, Campus São Raimundo das Mangabeiras, Maranhão, Brazil.*

**Keywords:** naphthoquinones; Laboratory Instruction; LCMS MS; Organic Chemistry; Synthesis; Demolition timber.

## Highlights

Synthesis of α-Lapachol, β-lapachone and hydroxy-hydrolapachol from lapachol (demolition timber): A Research Module for the Organic Chemistry Laboratory. Naphthoquinone derivatives. Naphthoquinones are obtained in high yields. Project-Oriented Laboratory Course.

## Resumo/Abstract

This work describes one of the projects developed in the discipline of Experimental Organic Chemistry which deals with the synthesis of lapachol derivatives in acid-base media, α-Lapachol, β-lapachone and hydroxy-hydrolapachol, with a common multistep sequence starting from lapachol. Students undertake, in a two week independent project, the synthesis of a lapachol derivatives from demolition timber, comprising instructor-guided tasks such as literature search, planning, critical discussion, observation, and results interpretation. In this project, in addition to searching and using information found in primary and secondary sources, students learn to design the methodology the acid-base concepts in organic chemistry, bearing in mind safety and environmental concerns. The synthesis of the substances was confirmed confirme by electrospray ionization mass spectrometry analysis, in the positive mode. The mass spectrum of β-lapachone showed peak of the protonated molecule in m/z 243 $[M+H]^+$ and showed ions fragments in m/z 243; 221; 196; 158; 159; 181; and melting point m.p: 152-156 °C. The α-lapachone presented the protonated molecule in m/z 243 $[M+H]^+$ and presented the following fragments íons m/z 242; 227; 209; 199; 181, with melting point m.p. 118-120 °C. The mass spectrum of Hydroxy-hydrolapachol showed the protonated molecule in m / z 243 $[M + H]^+$ and showed the following ions fragments m/z 242; 227; 209; 187; 196; 183; and a melting point. m.p. 123-126 °C. All the resulting analyzes were compatible with the fragmentation proposals found in the literature[1]. Several important laboratory techniques, such as TLC, melting point and recrystallization, are emphasized. Spectrometric methods, including LCMS–MS and HPLC, are used to identify the final product as well as the intermediates. Since each step of the procedure involves two or thre hours, parts of this experiment can be interspersed with other laboratory activities.

[1]SOUZA, M. A. A.; et al. Atividade biológica do lapachol e de alguns derivados sobre o desenvolvimento fúngico e em germinação de sementes. **Quím. Nova**, São Paulo , v. 31, n. 7, p. 1670-1672, 2008.

**Área: EDU** **Inscrição: 00835**

# Experimento de fotocatálise para aula prática de físico química utilizando resíduo de laboratório

**Lucas M. F. de Castro (PG),[1] Thayane S. dos Santos (IC)[1], Lucas A. Cavalcante (IC), Marluce O. G. Souza (PQ).[1]* lmalone12@hotmail.com; mosouza@uneb.br**

*[1]Departamento de Ciências Exatas e da Terra – Campus I Universidade do Estado da Bahia – UNEB*

Palavras Chave: *Fotocatálise, resíduo, corante, prática, cinética, ambiental*

## Highlights

Photocatalysis experiment for physical chemistry practical class using laboratory waste
Comparison of photocatalysis and photolysis results: Effect of the catalyst.
Students demonstrated understanding of photocatalysis, associating physical chemistry with environmental aspects.

## Resumo/Abstract

A necessidade de atualização na formação de químicos, acompanhando os avanços da ciência e tecnologia, com proposta de popularização e contextualização, é um incentivo para que se investigue experimentos que contemplem as vertentes da química, em diversos processos, incluindo aspectos ambientais. Nesse contexto foi elaborado, e aplicado a quatro grupos de três discentes cada, em duas aulas práticas de físico-química, um experimento de fotocatálise heterogênea com abordagens de cinética e tratamento de efluentes. Os experimentos de fotocatálise e fotólise (irradiação sem o semicondutor) foram conduzidos em um reator fabricado artesanalmente, a 30 °C, utilizando uma solução de cristal de violeta - CV (100 mg $L^{-1}$), ou resíduo do laboratório (contendo CV), e dióxido de titânio. Inicialmente o sistema permaneceu no escuro (agitação por 20 min). Em seguida, a lâmpada foi ligada coletando-se alíquotas (entre 0 e 60 minutos) e analisando em um espectrofotômetro UV-VIS. Os resultados foram debatidos com os discentes em seminários, aplicando também um questionário, sendo abordado principalmente: efeito do fotocatalisador na cinética comparando os testes de fotocatálise e fotólise; diferença entre a velocidade de descoloração da solução do CV e do resíduo (figura 1), analisando o efeito da composição, além dos distintos valores das constantes de velocidade, obtidos construindo-se gráficos de ln(C/Co) versus tempo. A eficiência do processo no tratamento de efluente também foi explorada nas discussões. De um modo geral, os discentes demonstraram compreensão dos parâmetros cinéticos, associando também aspectos ambientais, evidenciando o potencial da proposta.

Figura 1 – Descoloração do CV e do resíduo

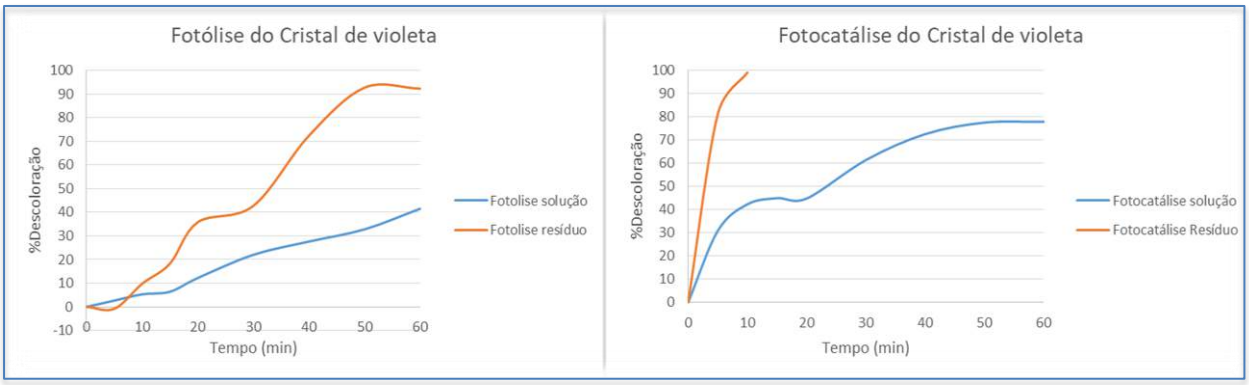

**Área: EDU**
*(Inserir a sigla da seção científica para qual o resumo será submetido. Ex: ORG, BEA, CAT)*

**Inscrição: 00822**
*(Inserir o número de inscrição do autor que fez a submissão)*

# MICROWAVE REACTIONS: A GREEN ALTERNATIVE TO LABORATORY CLASSES

**Geovani Aristeu L. Silva (IC)[1] ; Bianca Bassetti e Silva (IC)[1]; Queli Aparecida R. de Almeida (PQ)[1*]**

**geovaniaristeu@hotmail.com; queli.passos@ifrj.edu.br**

[1] Federal Institute of Science and Technology of Rio de Janeiro , IFRJ - Duque de Caxias

Keywords: *Green Chemistry, Environment, Experimental Chemistry, Environmental Education, Microwave*

## Highlights

Green Chemistry in lab classes;
Improvement of synthetic methodologies;
Using of the microwave as a search for energy efficiency;
Technological future linked to environmental issues.

## Resumo/Abstract

A new chemical conduct for the improvement of techniques and methodologies that generate the least amount of waste becomes more necessary. The Green Chemistry has as definition the creation, development and application of chemical processes in order to reduce the use of harmful substances[1]. In current work, reactions of condensation, isomerization, alcohols oxidation with the Clayfen (K-10 / $Fe(NO_3)_3$) and Claycop (K-10 /$Cu(NO_3)_2$) systems[2], multicomponent reactions and drugs synthesis in microwave were developed with the principles of green chemistry, reducing reaction time, increasing yield and promoting reactions without the use of volatile and harmful solvents. Two examples of the reactions tested and their results are shown in schemes 1 and 2 below.

*Isomerization of trans-Dichlorobis-(ethylenediamine)-cobalt(III) chloride:*

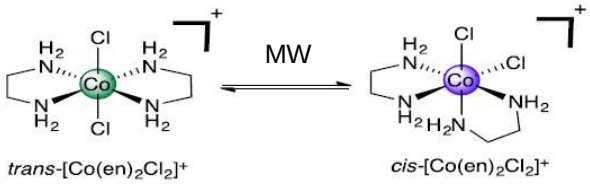


**Green solution**[3] **Pink solution – 15s MW - Irradiation**

**Scheme 1:** Isomerization reaction

*Synthesis of 7-hydroxy-4-methyl coumarin:*

**Scheme 2:** Synthesis of coumarin in microwave, using K-10 Montmorillonite

The use of experimental classes with the principles of Green Chemistry is of extreme importance, sensitizing the future professionals to the relations of the technological and scientific future with environmental issues.

**References:**

1- Anastas, P.; Eghbali, N., Green Chemistry: Principles and Practice. **Chem. Soc. Rev.** 2010, 39.
2- Varma, R.S.; Dahiya, R. **Tetrahedron Lett.**1997, 38.
3- Moura, Aline O. *et al.* **Quím. Nova**, 2006, 29; Marin, G.P. *et al.* West Chester University, Pennsylvania, EUA.

**Acknowledgements:** CNPq, IFRJ

**Área: EDU** **Inscrição: 00285**

# Investigação de parâmetros da cromatografia em camada delgada para avaliação preliminar da qualidade de biodiesel

**Carolina Lourencetti (PQ)**

**carollourencetti@ifsp.edu.br**

*Instituto Federal de Educação, Ciência e Tecnologia de São Paulo, Câmpus Matão.*

Palavras Chave: *Experimentação, Biodiesel, Cromatografia em camada fina.*

## Highlights

Investigation of thin layer chromatography parameters for preliminary evaluation of biodiesel quality. Experiment to compare mobile phase (polar/non-polar) and revelation ($I_2$ vapor/$KMnO_4$ sol) for biodiesel, oil and glycerin. Students were able to transpose their knowledge into a new problem situation.

## Resumo/Abstract

Este trabalho apresenta uma proposta de aula experimental para alunos de graduação dos cursos de Química ou Tecnologia em Biocombustíveis que objetiva despertar o graduando para o aprender investigando, relacionando aspectos teóricos e discutindo as melhores condições experimentais para acompanhar a reação de transesterificação durante a produção de biodiesel empregando a técnica cromatografia em camada delgada (CCD)[1], evitando assim o método tradicional com a execução da prática com as condições experimentais já definidas. A sequência didática proposta foi organizada em cinco etapas: 1) levantamento de conhecimentos prévios sobre a reação de transesterificação e propriedades de seus produtos e coprodutos, interações intermoleculares e suas relações com a técnica CCD, 2) debate sobre os parâmetros de qualidade do biodiesel e técnicas para determiná-los[2], 3) experimentação para avaliar melhores condições para separação (fases móvel polar e apolar) e identificação dos produtos e coprodutos da reação de transesterificação (revelação com vapor de iodo ou solução de $KMnO_4$)[3], 4) interpretação dos resultados e 5) sistematização de conceitos, definindo as melhores condições para analisar uma amostra desconhecida para identificar a presença de biodiesel, óleo e/ou glicerina. Além da participação ativa dos alunos durante a aula prática, foi possível observar indícios de apropriação de conceitos/conhecimentos discutidos ao analisar os relatórios elaborados. A necessidade da comparação das diferentes condições testadas fez com que os alunos buscassem justificativas teóricas para explicar o observado (Figura 1), viabilizando aos mesmos a possiblidade de transpor seus conhecimentos em uma nova situação-problema[4].

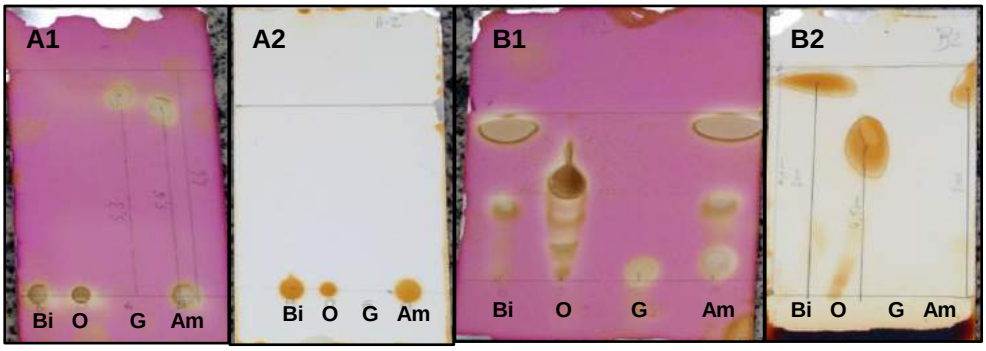


Figura 1. Placas cromatográficas de alumínio contendo sílica como fase estacionária. **A1** - melhor condição para identificar glicerina. **B1** e **B2** - condições possíveis para identificar biodiesel e óleo.

Fase móvel: **A** (metanol:água (1:1, v/v) e **B** (hexano:éter etílico (4:2, v/v) e 1 gota de ácido acético glacial. Revelação: **1** (solução $KMnO_4$ (0,5%, m/v) em NaOH (1 mol $L^{-1}$) e **2** (vapor $I_2$). Aplicação: Bi: 250 μL de padrão de biodiesel de soja B100 e 1 mL de acetona; O: 0,5 mL de óleo de soja e 1 mL de éter etílico; G: 20 μL de glicerina, 250 μL de água destilada e 1 mL de acetona; Am: amostra fornecida ao grupo contendo 250 μL de padrão de biodiesel de soja B100, 20 μL de glicerina e 1 mL de acetona.

[1] PAVIA, D. L. Química orgânica experimental: técnicas de escala pequena. 2. ed. Porto Alegre: Bookman, 2009.
[2] ANP. Resolução Nº 45, de 25 de agosto de 2014.
[3] Oliveira, D. M. et al. Quim. Nova. 2013. v. 36, 734-737. Bansal, K. et al. Fuel. 2008. v. 87, 3369-3372.
[4] Kassaboehmer, A. C.; Hartwig, D. R.; Ferreira, L. H. Contém Química 2: pensar, fazer e aprender pelo método investigativo. São Carlos: Pedro & João Editores, 2015.

**Área: EDU** **Inscrição: 01156**

# Experiments and interactive tools to stimulate the learning of fundamental concepts of chemistry

**Eliane C. Pedrozo (PQ),[1*] Dennyer M.D. Santos (IC),[1] Matheus B. Nascimento (IC),[1] Stela L.C. Moura (IC).[1]**

**ecpedrozo@usp.br**

*[1]Department of Chemical Engineering, USP – Lorena/SP;*

Keywords: *small experiments, interactive tools, classroom, general chemistry.*

## Highlights

This project tackled the planning of experiments and interactive tools that can be applied in the classroom. In this way, the project presents alternatives to make learning process more interesting.

## Abstract

In general, in the undergraduate courses that offer the content of the subjects of theoretical and experimental general chemistry it is not possible to relate the theory that is seen in the classroom and its application in the laboratory at the same time. Students have difficulty in relating theory to practice even when the contents coincide. Most of the concepts taught in theory are not applied in the laboratory, so these concepts are presented in an abstract way for the student in the classroom. Topics that present only theoretical lessons do not stimulate students. Students do not understand the importance of only theoretical content in their professional training.

One of the alternatives to reduce these problems was to apply small experiments and other interactive tools in classroom to observe the impact of this approach on chemistry students I and II. The topics studied were Atomic Structure, Periodic Table, Chemical Bonds, Molecular Geometry, Intermolecular Forces, Solutions, Gases, Chemical Kinetics, Thermodynamics, Chemical Equilibrium and Electrochemistry. At the end of the course, the final evaluations of the students who received this approach were compared with the final assessments of previous students (2012-2017). Questions on the topic presented were applied to the students at the end of the classes and at the end of the course to evaluate the importance of this methodology in their own learning. After its application, the teacher observed a greater motivation and interest of the students.

| | |
|---|---|
| **General Chemistry I and II classes** | 13 |
| **Number of students** | 640 |
| **Performance statistics (by class and type of methodology)** | 1. Approved; 2. disapproved by frequency; 3. disapproved by grade; 4. disapproved by frequency and grade; 5. cancellation of registration; 6. average grade; 7. distribution of number of students per grade |
| **Methodologies** | exercises in the classroom, exercises for note, theoretical work, extraclasses or monitoring, experiments in the classroom and interactive tools |
| **Questionnaires answered by students** | 1. after each class; 2. at the end of the course |

Table: Data used for statistical analysis

Figure: Ilustrative examples of experiments and interactive tools used in the classroom.

**Área: EDU** **Inscrição:00632**

# Auto-discharge of a cell: experimental proposal from a continuous professional development courses about applied electrochemistry

**Luciane F. de Goes (PG),[1*] Gabriela Z. Q. Albuquerque (IC),[2] Lucas Vairolette (FM),[3] Armando Henrique dos Santos (TC),[4] Carmen Fernandez (PQ),[1,4] Silvia M. L. Agostinho (PQ).[4]**

**luciane@iq.usp.com; smlagost@iq.usp.com**

*[1]Programa de Pós-Graduação Interunidades em Ensino de Ciências da Universidade de São Paulo; [2]Instituto Federal de Ciência Tecnologia e Educação de São Paulo; [3]Grupo Fênix de Educação; [4]Instituto de Química da Universidade de São Paulo.*

Keywords: *Electrochemistry, galvanic cell, salt bridge, auto-discharge, teacher training.*

## Highlights

High school teachers present difficulties in electrochemistry. Electrochemistry courses were given. Evaluations showed progress. Galvanic cells are proposed to understand the auto-discharge.

## Abstract

Continuous professional development (CPD) courses for high school teachers have shown that they have difficulties in explaining basic concepts of electrochemistry[1,2,3]. In an applied Electrochemistry course (40 hours in five days) the movement of ions, the function of the saline bridge and the galvanic cell auto-discharge were approached from experimentation. Two galvanic cells were constructed: 1) Zn(s)|$H_2SO_4$ 0,5 mol.$L^{-1}$| C(grafite) e 2) Zn(s)|NaCl 0,5 mol.$L^{-1}$||$CuSO_4$ 0,5 mol.$L^{-1}$| C(grafite)[4] and questions were proposed followed by discussion. The twenty-one participating teachers were evaluated before and after the course in order to verify their progress. Figure 1 shows an improvement of correct answers. However, the wrong answers number is still high. An experiment is proposed in this paper to better approach these concepts. In addition to cell 1, it is suggested the construction of the cell Zn(s)|$ZnSO_4$ 0,5 mol.$L^{-1}$||$H_2SO_4$ 0,5mol.$L^{-1}$ |$H_2$|C(grafite) in which a 1 mol.$L^{-1}$ KCl salt bridge is placed between the half-cells. It is suggested also the use of Daniell cell with and without saline bridge. The experiment allows to compare the two galvanic cells, identical when considering its electromotive force (fem), and to verify the role of the saline bridge in eliminating the auto-discharge. It is possible to discuss the transport of ions and electrons, fem, current and power in an electrochemical circuit. From the applied Electrochemistry course it was possible to conclude that these concepts need to be emphasized in CPD courses for high school teachers.

**What is the function of the salt bridge in a galvanic cell?**

a) attract the ions in solution

b) accelerate the reaction

c) ensure that one of the half cells is positive and one negative

d) maintain the electrical neutrality in the two half-cells by the supply of ions separate the oxidation and reduction semi-reactions in different compartments

e) separate the oxidation and reduction semi-reactions in different compartments

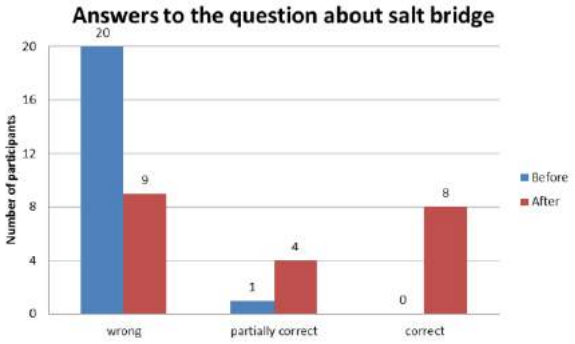


Figure 1. Saline bridge question and participants answers

## Acknowledgements

The authors are grateful to the teachers who participated on this research, to the financial support, Grants #2013/07937-8 and #2014/14356-4, São Paulo Research Foundation (FAPESP) and to the Program Encontro USP-Escola / Pró-Reitoria de Cultura e Extensão da Universidade São Paulo.

References

[1]GOES, L. F.; VAIROLETTE, L.; ALBUQUERQUE, G. Z. C.; BLOISI, G.; FERNANDEZ, C.; AGOSTINHO, S. M. L. Reflexos de um curso de formação contínua em Eletroquímica em um grupo de professores do Ensino Médio. In: 39ª Reunião Anual da Sociedade Brasileira de Química, 2016, Goiânia. Anais da 39ª RASBQ, 2016. v. 1. p. 1-1.
[2]ALBUQUERQUE, G. Z. C.; VAIROLETTE, L.; ROCHA, F.; GOES, L. F.; FERNANDEZ, C.; AGOSTINHO, S. M. L. Difficulties of chemistry teachers in the representation of chemical transformations in aqueous medium. In: 46° World Chemistry Congress/ 40° Reunião Anual da Sociedade Brasileira de Química/ IUPAC 49° General Assembly, 2017, São Paulo. 40ª RASBQ. São Paulo, 2017. v. 1. p. 1-1.
[3]GOES, L. F.; FERNANDEZ, C.; AGOSTINHO, S. M. L. Concepções e dificuldades de um grupo de professores de química sobre conceitos fundamentais de eletroquímica. In: XVIII Encontro Nacional de Ensino de Química, 2016, Florianópolis. Anais do XVIII Encontro Nacional de Ensino de Química, 2016.
[4]BESSLER, K. E., NEDER, A. de V. F. Química em tubos de ensaio: uma abordagem para principiantes. São Paulo: Blucher. 2011.

**Área: EDU**
*(Inserir a sigla da seção científica para qual o resumo será submetido. Ex: ORG, BEA, CAT)*

**Inscrição: 00877**
*(Inserir o número de inscrição do autor que fez a submissão)*

# Determination of the Iron(III)-Thiocyanate Reaction Equilibrium Constant using digital images

**Pamela Xavier Mendonça (IC),[1*] Cláudia Martins Ledesma (PG),[2] Endler Marcel Borges (PQ),[2]**

**marcelborgesb@gmail.com; pamela.xavier.mendoza@gmail.com**

*[1] Escola Técnica do Vale do Itajaí, ETEVI, Rua Antônio da Veiga, 140, Victor Konder, 89012-900 Blumenau-SC, Brasil; [2] Departamento de Química, Universidade Regional de Blumenau, FURB, Campus 1, Rua Antônio da Veiga, 140, Victor Konder, 89012-900 Blumenau-SC, Brasil.*

***45813***

Palavras Chave: *ImageJ; equilibrium constant; Iron thiocyanate; digital image.*

## Highlights

Determination of Equilibrium constant.
Quantitative analysis using digital images obtained with a flatbed scanner
Automated extraction of RGB values suing ImageJ1s plugin ReadPlate

## Resumo/Abstract

The reaction $Fe^{3+}$ + $CSN^-$ ⇆ $Fe(SCN)^{2+}$ is simple and easy to observe, because $Fe^{3+}$ has a slight yellow color, $CSN^-$ is colorless and $Fe(SCN)^{2+}$ are deep blood-red ($\lambda_{max}$ = 447 nm), the determination of equilibrium constant of this reaction is presented in many laboratory manuals. $Fe(SCN)^{2+}$ concentrations were determined using a calibration polt, then, the equilibrium constants were measured in mixtures of $Fe^{3+}$ and $SCN^-$. For the colorimetric determination of $Fe(SCN)^{2+}$ absorbance at 447 nm were measured in each solution. $Fe(SCN)^{2+}$ concentrations are also determined using digital images, where solutions were placed in a 96 micro-well plate and a digital image obtained using a flatbed scanner, R (red) values of each well were extracted simultaneously using ImageJ's plugin ReadPlate. In 2017, this laboratory experiment was carried out in *Universidade Regional de Blumenau* with chemical engineering, students. It was typically finished in approximately 150 mim with 15 students working in groups of three. The goal of this project was to develop a simple spectrophotometric method based on images obtained with a regular consumer-grade computer scanner. These results would then be compared to measurements from conventional spectroscopy using one-way ANOVA. Whether there is statistical evidence that the associated population means are significantly different. Using the Analysis ToolPak in Excel, within the confidence level of 95%, we found $F_{calculated}$ = 1.33 < $F_{critical}$ = 1.94 showing that results obtained with both methods were equivalent at a 95% confidence interval.

**Área: EDU** **Inscrição: 00947**

# Extraction of caffeine from tea in experimental classes of organic chemistry: comparative study

**Michelle Pereira Quintino (PQ),[1,2*] Tarso Leandro Bastos (IC),[1] Gabriel Costa Vieira Arantes (IC).[1]**

**quintino.michelle@gmail.com**

*[1]Escola de Ciências Exatas e da Computação, PUC Goiás; [2]Campus Itumbiara, UEG*

Key words: *Caffeine extraction, Organic chemistry, Experimental class*

## Highlights

Different procedures of caffeine extraction from instant black tea have been tested, for organic chemistry lessons, the aim is to find the faster and which gives the highest yield.

## Abstract

Caffeine is a stimulant derived from xanthine. Its extraction is a common procedure discussed on laboratory lessons for chemistry undergraduate students, especially in laboratory disciplines of organic chemistry. Instant black tea is one of the most used raw materials in laboratory classes about caffeine extraction, because of its high solubility in water.[1] This study aimed at optimizing the procedure of caffeine extraction from instant black tea, making it more time-saving for organic chemistry laboratory classes. Figure 2 shows the two methods used for the extraction of caffeine, after which, the product weight was obtained for calculating the yield. The caffeine was characterized by the murexide reaction (figure 1), placed in a heated porcelain capsule with 4 drops of $H_2O_2$ and 6 drops of HCl 6M. $NH_4OH$ 6M was added to the red residue that become violet. Table shows the extraction data. The Ext 06 presented the best yield, being indicated for a class of 100 minutes. For classes of 200 minutes you can reproduce Ext 04, which doesn't use 10 g of catalyst. Using the suggested methods, it is possible to perform reflux and caffeine extraction in one class only. Thus, the time required for extraction with other methods can be used to perform other extractions and analyzes during the same class.

Figure 1: Murexide reaction.

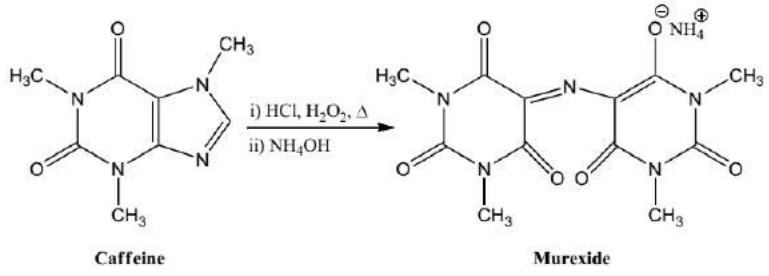


Table: Caffeine content extracted from tea.

| | Method | Time | Catalysis | Yield (%) |
|---|---|---|---|---|
| Ext 01 | 1 | 2 h | No | 0,3382 |
| Ext 02 | 1 | 4 h | No | 0,8390 |
| Ext 03 | 1 | 6 h | No | 0,9057 |
| Ext 04 | 2 | 1 h | No | 0,7960 |
| Ext 05 | 2 | 30 min | NaOH | 0,7762 |
| Ext 06 | 2 | 30 min | $Na_2CO_3$ | 1,9198 |
| Ext 07 | 2 | 30 min | $H_2SO_4$ | 1,3210 |

Figure 2: Tea extraction procedure.

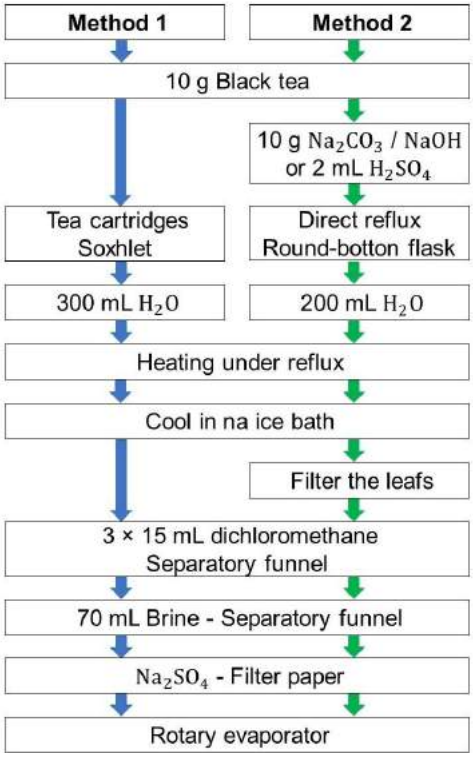


[1]BRENELLI, E. C. S. *Química Nova*, Vol. 26, Nº 1, 136-138, **2003.**

[2]LOPES, T. R. F.; JUNIOR, N. L. N. *Cenarium Pharmacêutico*, Ano 4, N° 4, **2011**.

**Área: ____EDU___ Inscrição:_00993___**

# Algumas estratégias para ensino de química no Ensino Médio Técnico

**Eduardo Matheus Silva Cunha(IC)[1], Jéssica Caroline Santos Melo(IC)[1], Giselle Giovanna do Couto(FM)[1*]**

**giselle.couto@ifms.edu.br**

[1]*Instituto Federal de Educação, Ciência e Tecnologia de Mato Grosso do Sul, Campus Naviraí.*

Palavras Chave: Jogos Lúdicos, Aulas experimentais, Jogos eletrônicos.

## Highlights

Some strategies for teaching chemistry for Technical High School
To make chemistry easy is necessary to use strategies for teaching.
Teacher needs to provide funny learning experiences such as games.
The students show great interest in these new learning methods.

## Resumo/Abstract

As atividades lúdicas foram executadas durante o primeiro ano do ensino médio técnico. Ao todo foram usadas quatro tipos de atividades e a escolha se deu devido às características teórico/prático dos conteúdos. As aulas que versavam sobre (i) misturas e separação de misturas, (ii) ácidos e bases e (iii) reações químicas foram feitas aulas experimental, pois o material pode ser encontrado em farmácias. As aulas experimentais formam uma ponte entre teoria e a vivência diária, pois permite observar os fenômenos do cotidiano, despertando o interesse em estudar e fornecendo uma aprendizagem diferenciada, além de colocar estudante em contato com vidrarias e equipamentos. Na opinião dos alunos a aula experimental podia ser usada com mais frequência. Para os conteúdos mais teóricos, tais como, modelo atômico e Tabela Periódica foram propostos a confecção de maquetes, sendo que os alunos pesquisaram os temas, estudaram sozinhos, montaram as maquetes e fizeram uma apresentação oral sobre os conteúdos estudados. O mais interessante da exposição das maquetes se deu com o comportamento dos alunos ouvintes, bem como a melhoria nas explicações e notas obtidas ao longo do ano. O uso da paródia foi para auxiliar na confecção do diagrama de Linus Pauling, que é usado na distribuição eletrônica. Nesse caso, foi possível ver que, mesmo depois de meses da execução da atividade os alunos lembraram a paródia e conseguiram montar o diagrama. Indicando que foi possível estimular a memória de longa duração, indicando uma aprendizagem significativa do conteúdo proposto. Para o conteúdo de nomenclatura de compostos inorgânicos foi efetuado três jogos lúdicos para auxiliar na memorização dos nomes e fórmulas dos compostos. Foram feitos três jogos diferentes, um da memória, um baralho e um dominó. Em todas as atividades as substâncias eram as mesmas e foram escolhidas devido à aplicação e uso diário. Os jogos serviram como instrumento facilitador de sociabilidade, pois os alunos participaram ativamente da atividade. Segundo alguns estudantes o interesse pela atividade cresceu durante a realização dos jogos. Este trabalho permitiu concluir que introduzir jogos lúdicos no cotidiano escolar é extremamente importante, pois desperta o interesse dos alunos em estudar, melhorando o rendimento acadêmico, a integralização da sala e relação entre estudante e professor.

**Área: EDU** **Inscrição: 47694**

# As contribuições da pedagogia de teatro na formação de professores

**Junfanlee Manoel O. Feliciano (IC),[1] Valéria A. Alves(PQ),[1] Mônica C. Siqueira Martines (PQ)[2]**

**junfanleemanoel@hotmail.com; valeria.alves@uftm.edu.br; monicasiqueiramartines@gmail.com**

*[1]Departamento de Química, UFTM; [2]Departamento de Matemática, UFTM.*

Palavras Chave: *Arte e ensino, Formação de professores.*

## Highlights

The contribution of theater pedagogy to teacher training.
The scope of the present work is to evaluate the impact of the project "*Show of Chemistry and Mathematics*" in the initial formation of basic education teachers; it intends to disseminate science.

## Resumo/Abstract

O trabalho aqui apresentado é resultado de uma pesquisa realizada com os graduandos participantes do Grupo Alquimistas S.A. da UFTM e tem como objetivo, avaliar a influência do projeto de Extensão Universitária *Show da Matemática e da Química* na formação inicial de professores. Avaliamos a influência da metodologia usada nas apresentações do tipo *Show*, nos licenciandos integrantes do grupo que apresentaram o referido *Show* nas escolas parceiras ao projeto. Foram 5 apresentações realizadas a alunos da educação básica na cidade de Uberaba-MG. Cada apresentação durou, em média, 50 minutos, com 4 experimentos de Matemática e 4 de Química. Os experimentos foram escolhidos pelas professoras da educação básica parceiras e, encenados por meio de teatro *Show*, que de acordo com Henriques *et al*. (2009), pode ser classificado como teatro de rua. A pesquisa amparou-se no paradigma quantitativo, acerca das contribuições do projeto no processo de formação de professores. Aplicou-se um questionário composto por 14 afirmativas aos 14 licenciandos, cujas respostas foram baseadas na *Escala Likert* de 5 pontos. O instrumento permitiu mensurar quão formativo foi o projeto para os participantes, bem como conhecer o grau de satisfação quanto ao seu funcionamento. Os resultados (Tabela 1) indicam que o projeto contribuiu para a formação acadêmica e inicial do professor, aumentando a sua motivação para a realização das suas atividades na UFTM; também se mostrou como uma alternativa viável para a formação continuada de professores da Educação Básica.

Tabela 1 - Afirmativas relacionadas à contribuição do projeto na formação inicial dos licenciandos participantes da equipe executora do projeto *Show da Matemática e da Química*. Legenda da *Escala Likert*: 1. Muito ruim/Nunca; 2. Ruim/Raramente; 3. Regular/Às vezes; 4. Bom/Frequentemente; 5. Muito bom/Sempre.

| Afirmativa | Respostas 1 e 2 | Respostas 4 e 5 | Resposta 3 |
|---|---|---|---|
| **1** - As atividades do projeto contribuem para a sua formação acadêmica. | 0 | 14 | 0 |
| **2** - Grau de satisfação com as 5 apresentações realizadas até o momento. | 0 | 13 | 1 |
| **3** - As atividades do projeto contribuem para melhorar a sua disciplina, organização, pontualidade, assiduidade, trabalho em equipe, desenvoltura para falar em público, criatividade e oralidade. | 0 | 13 | 1 |
| **4** - As atividades do projeto contribuem para despertar o interesse do Aluno da Educação Básica para as disciplinas Matemática e/ou Química. | 0 | 12 | 2 |
| **5** - As atividades do projeto contribuem para a formação inicial do Professor da Educação Básica. | 0 | 14 | 0 |
| **6** - As atividades do projeto contribuem para a formação continuada do Professor da Educação Básica. | 0 | 13 | 1 |
| **7** - As atividades do projeto contribuem para a formação continuada do Professor da Educação Superior. | 0 | 14 | 0 |
| **8** - As atividades do projeto apresentam potencial de inovação no processo de ensino na Educação Básica. | 0 | 14 | 0 |
| **9** - As atividades do projeto contribuem diminuir a evasão dos alunos da UFTM. | 2 | 7 | 5 |
| **10** - As atividades do projeto contribuem diminuir a retenção dos alunos da UFTM. | 2 | 5 | 7 |
| **11** - As atividades do projeto contribuem para incrementar conhecimentos técnico-científicos na área correlata à do seu curso de graduação na UFTM. | 0 | 13 | 1 |
| **12**- As atividades do projeto aumentam a sua motivação para o desenvolvimento das suas atividades na UFTM. | 0 | 13 | 1 |
| **13** - As atividades do projeto apresentam potencial interdisciplinar. | 0 | 13 | 1 |
| **14** - As atividades do projeto ajudam na divulgação dos cursos de graduação da UFTM para a comunidade externa. | 0 | 13 | 1 |

Henriques, Bruna; Marcelo, Madalena; Nunes, Manuel; Ferreira, Suse. Renascer da Arte: Os vários tipos de Teatro. 2009. Disponível em http://renascer-da-arte.blogspot.com.br/2009/04/os-varios-tipos-de-teatro.html. Acesso em: 08 mar 2018.

| Área: EDU | Inscrição: 00288 |
|---|---|

# STUDY OF THE CONTRIBUTION OF AUGMENTED REALITY FOR THE TEACHING OF ORGANIC CHEMISTRY IN HIGH SCHOOL

**Carlos Cézar da Silva (FM),[1] Sérgio Henrique de Almeida (PG)[1]**

**ccezas@gmail.com; shalmeida@gmail.com**

*[1]Departamento de Áreas Acadêmicas, IFG - Câmpus Jataí*

Palavras Chave:*(Tecnologhy, Augmented, Reality, Teaching, Chemistry).*

## Highlights

Augmented reality as innovative instructional resource.
Contributes to the teaching of Constitutional Isomeria.
Visualization of structural formulas in 3D dimension.

## Resumo/Abstract

This study analyzed the contributions of the Technology of Augmented Reality (RA)[1] in the teaching of Organic Chemistry, addressing Constitutional Isomeria for 18 students of the 3rd year of the Technical Courses Integrated to High School in IFG Campus Jataí. The Avogadro[2] application was used for three-dimensional object modeling (3D) and for the development of interactive RA activity, the FLARAS[3] creation tool, an application that facilitates the use of chemistry teachers. The research proposal was based on the perspective that if the student succeeded in the activity using the technology[4], this could be attested when he could express in writing the arguments in his answers pre-established by the researchers. In the data collection and subsequent content analysis, questionnaires were applied during and after the survey. The RA technology contributed to the teaching of chemistry, since when visualizing the structural formulas $C_3H_8O$, $C_4H_{10}O$ and $C_4H_8O$ and their different isomers in (3D) and real time, the majority of students were successful in the answers of the items on classification of chains / carbons , functional groups (Graph 1) and found greater difficulty in physical properties and reactivity, evidencing the need for greater commitment in teaching these subjects.

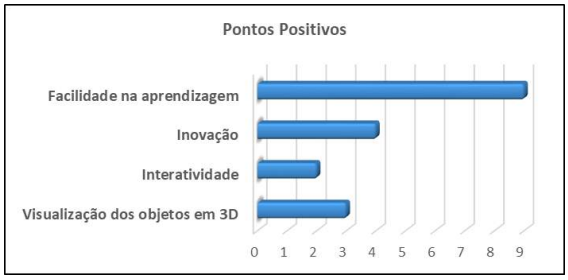


Gráfico 1 – Pontos positivos no estudo de isomeria utilizando RA na visão dos alunos

1. TORRES, F.; KIRNER, T.; KIRNER, C. **Uso da Realidade Aumentada no Ensino de Ciências**. Disponível em: <http://www.lbd.dcc.ufmg.br/colecoes/wrva/2012/ 0046.pdf>. Acesso em: 26 de jan. 2018.
2. MEDEIROS, A. C. S. et al. **AVOGADRO**: **Um recurso digital para a aprendizagem de modelos moleculares e ligações químicas.** In: III CONEDU - Congresso Nacional de Educação. 2016.
3. **FLARAS**. **Ferramenta de Autoria de Aplicações de Realidade Aumentada**. Disponível em: <http://ckirner.com/flaras2/>. Acesso em 10 set. 2016.
4. MORENO, E. L.; HEIDELMANN, Stephany P. **Recursos Instrucionais Inovadores para o Ensino de Química.** In: Revista Química Nova na Escola. Vol. 39 nº 01, p. 12-18, 2017.

**Área: EDU** **Inscrição: 00379**

# Química no Recreio, uma Nova Forma de Ensinar a Eletroquímica aos Alunos do Ensino Médio.

**Raul O. Pasin (IC)[*, 2], Cristiane R. Silva (IC)[1,2], Regiane C.M.S. Castione (FM)[1], João L.C. Carmona (IC)[2], Renato Dutra (IC)[2], Roland Estimable (IC)[2], Aline T.G. Rodrigues (IC)[2], Francisco J.A. Ortiz (IC)[2], Moacir G.O. Junior (IC)[2] e José Ricardo C. Salgado (PQ)[2]**

**pasinraul@gmail.com**

*[1]Colégio Estadual Prof. Flávio Warken - E.F.M.P.; [2]UNILA, Universidade Federal da Integração Latino-Americana, CEP.: 85867-970, Foz do Iguaçu, PR, Brasil*

Palavras Chave: *Ensino, Escola, Pilhas, Baterias, Eletroquímica.*

## Highlights

Chemistry in the Recreation, a New Way of Teaching Electrochemistry to High School Students, Batteries, Electrolysis, Chemistry at home, day-to-day chemistry.

## Resumo

As atividades de eletroquímica foram desenvolvidas no Colégio Estadual Professor Flávio Warken com o objetivo de estimular os alunos do ensino médio através de atividades experimentais durante o recreio (15 min.). Neste período os alunos da UNILA realizaram experimentos, fáceis de preparação e com relação ao cotidiano do aluno do ensino médio. O conteúdo de eletroquímica faz parte da ementa dos cursos de Licenciatura em Química e Engenharias e integra o projeto “Universidade e Sociedade - O que a universidade pública pode oferecer aos estudantes - Eletroquímica ao alcance de toda sociedade”. Através desta parceria, os alunos da UNILA desenvolveram experimentos e atividades capazes de estimular os alunos a compreenderem melhor a parte teórica da química e a sua aplicação tecnológica. Durante os períodos escolares foram desenvolvidos mais de 15 experimentos com materiais de baixo custo, fácil de realizar e utilizando de preferência materiais que se tem em casa. Entre eles citamos: pilha de batatas e de tomates, eletrólise da água e outros. Foram também exibidos os componentes das baterias e pilhas em formas de esquemas e cartazes. Os experimentos realizados despertaram interesse dos alunos, houveram questionamentos teóricos e práticos e os aspectos visuais prenderam a sua atenção motivando o interesse pela ciência, especialmente pela química. Além disto, das atividades realizadas, estimularam os alunos a participarem nas Feiras de Ciências da Escola e os experimentos com alimentos são os que mais despertaram a curiosidade deles.

Figura 1. Demonstração de uma pilha de batatas.

Figura 2. Demonstração de uma pilha de latinhas de alumínio.

**Área: EDU**
*(Inserir a sigla da seção científica para qual o resumo será submetido. Ex: ORG, BEA, CAT)*

**Inscrição: 13511**
*(Inserir o número de inscrição do autor que fez a submissão)*

# Cozinha científica: motivando e promovendo o ensino de química.

**Regilany P. Colares (PQ),[1*] Rayssa M. Santos (IC),[1] Aluísio M. Fonseca (PQ),[1] Márcia B. Sousa (PQ),[1] Sara J. Oliveira (PG),[1] Maria C. M. Souza(PQ), [1] Eveline A. Menezes (PQ) [1], Márcia S. P. Barros (PG) [1].**

**regilany@unilab.edu.br**

[1]Instituto de Ciências Exatas e da Natureza, UNILAB; [2]Mestrado Acadêmico em Sociobiodiversidade e Tecnologia Sustentável, UNILAB.

Palavras Chave: *Química no cotidiano, Aulas práticas, Fermentação, Interdisciplinaridade, Ensino de química.*

## Highlights

Scientific kitchen: motivating and promoting the teaching of chemistry. The kitchen environment is a scenario that can contribute to the process of teaching of chemistry.

## Resumo/Abstract

A Química é uma ciência muito presente em nossas vidas, mesmo assim, boa parte dos discentes tem dificuldade em relacioná-la com o seu cotidiano. Estudos apontam que as práticas de laboratório são ferramentas de ilustração e partes integrantes no aprendizado. [1] No entanto, na maioria das escolas do Brasil e dos países lusófonos inexistem condições de infraestrutura para a proposição de aulas experimentais. Dentro deste contexto, o presente trabalho objetiva mostrar aos alunos do curso de licenciatura em química, que é possível utilizar a cozinha das escolas como um laboratório de aulas práticas, buscando uma correlação entre os conteúdos abordados em sala e o seu dia-a-dia. O trabalho foi desenvolvido por meio de uma oficina em uma turma do 5º semestre (público-alvo) do curso de licenciatura em química da UNILAB-CE. O conteúdo trabalhado foi reações químicas, exemplificado através de processos reacionais que ocorrem durante a produção do pão, Figura 1. Após a oficina, foi aplicado um questionário baseado na *escala Likert* aos alunos, para sondar suas impressões e concepções sobre a proposta do trabalho. Dos trinta alunos presentes, 80% "*concordaram fortemente*" e 20% "*concordaram*" que é possível uma aula experimental mesmo sem um laboratório disponível. A avaliação positiva feita pelos discentes demonstra que a metodologia empregada na oficina foi adequada para a proposta. Assim, o ambiente da cozinha é um cenário que pode contribuir com o processo de ensino e aprendizagem das ciências, em especial da química.

**Figura 1. (a)** Grão de trigo. **(b)** Formação do glúten. **(c)** Fermentação pela *Saccharomyce cerevisiae*. **(d)** Modelagem do pão com cortes ou pestanas.

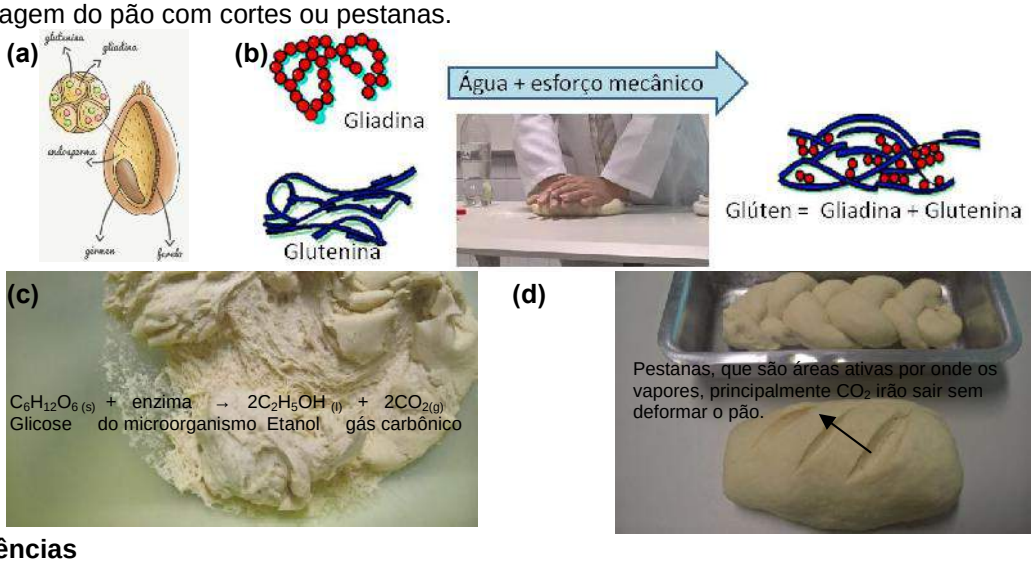


**Referências**

[1]CHASSOT, A. I. **Para que(m) é útil o ensino? Alternativas para um ensino (de Química) mais crítico**, Canoas: ULBRA, 1995.

**Área: EDU** **Inscrição: 00535**

# Atividade experimental de eletroquímica: contribuição ao processo ensino-aprendizagem

**Bruno P. Diniz (PG),[1*] ElenC. P. de Brito (IC),[2] Ludmila dos S. Madalena (IC),[2] Luís Antônio da Silva(PQ),[2] Valéria A. Alves(PQ).[2]**

**brunopereiradiniz@yahoo.com.br**

*[1]Programa de Mestrado Profissional em Química em Rede Nacional - PROFQUI, UFTM; [2]Departamento de Química, UFTM.*

Palavras Chave: *Experimento; aprendizagem.*

## Highlights

Experimental activity of electrochemistry: contribution to the teaching-learning process
The aim of this study was to investigate the contribution of learning to the use of experimental activities in chemistry teaching. The proposal consisted in the application of an evaluative questionnaire and experimental activity.

## Resumo/Abstract

A abordagem experimental na sala de aula está intimamente ligada à função pedagógica de auxiliar o aluno a explicitação, problematização, discussão, dando significação aos conceitos químicos.[1]O trabalho teve como objetivo investigar a contribuição na aprendizagem a partir da utilização de atividade experimental. A proposta consistiu na aplicação de questionário e atividade experimental no 2º semestre de 2017, com uma turma do 2º ano do Ensino Médio do Colégio Atenas (Patrocínio/MG). A atividade compreendeu uma aula de 50 minutos e foi realizada na sala de aula. Os alunos foram divididos em 5 grupos de 6 alunos, para montagem da Pilha de Daniell e observação do seu funcionamento (Figura 1).As soluções de sulfato de cobre e zinco, bem como a ponte salina, foram previamente preparadas. O questionáriocontinha 13 questões, sendo as 8 primeiras aplicadas antes e as 5 últimas pós-experimento. Ao responder o que a eletroquímica estuda, 92% dos alunos mencionaram que é a ciência que estuda interfaces carregadas eletricamente.As questões abordadas após o experimento demonstraram que os alunos perceberam a importância do conteúdo no seu cotidiano, e consideraram que o experimentofoi útil na elucidação dos conceitos relacionados ao tema eletroquímica que, segundo eles, é de difícil compreensão.Foi consenso que a atividades práticas potencializam as aulas teóricas. Conclui-se que a Pilha de Daniell, utilizada para ministrar conceitos básicos de eletroquímica,ajudou na fixação do conteúdo e no seu entendimento mais aprofundado.

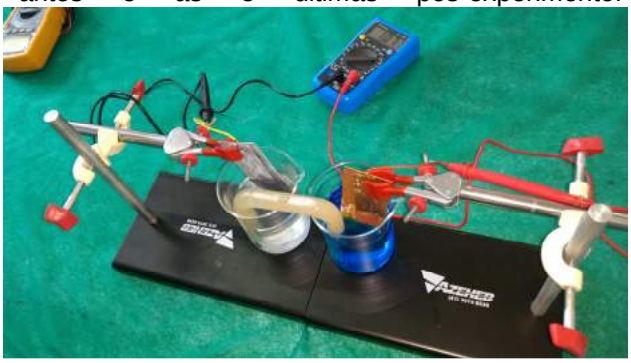

Figura 1 – Foto da atividade experimental realizada (Pilha de Daniell) em sala de aula comuma turma de alunos do 2º ano do Colégio Atenas (Patrocínio/MG).

[1]Nanni, R. A natureza do conhecimento científico e a experimentação no ensino de ciências. Revista Eletrônica de Ciências. 2004v. 26, p. 389-404.

Os autores agradecem o apoio financeirodo PROFQUI/CAPES.

**Área: EDU** **Inscrição:00619**

# QUÍMICA LÚDICA: A arte de aprender brincando

**Alexandra da S. Fonseca (IC)*,[1] Naiane Mª C. Rodrigues (IC),[1] Mônica D. de S. Almeida (PQ)[2], Débora S. C. dos Anjos (PQ).[2]**

**alexandra.fonsecaif@gmail.com**

*[1]Licencianda em Química, Campus Petrolina, IF Sertão-PE, Petrolina-PE; [2]Docente, Coordenação de Licenciatura em Química, Campus Petrolina, IF Sertão-PE, Petrolina-PE.*

*Palavras Chave: Contextualização, Ensino de Química, Kits didáticos, Jogos Educativos.*

## Highlights

Playful chemistry: the art of learning. The goal of the educational game is to improve the cognitive character through fun. The importance of games and interactions between students and teacher for the process are described.

## Resumo/Abstract

Segundo Soares (2013) aprender pode ser uma brincadeira, assim como na brincadeira pode-se aprender. O objetivo deste projeto consiste em promover o Ensino de Química através de jogos como forma de discutir e construir conceitos, aproximando o caráter lúdico à possibilidade de se aprimorar o desenvolvimento cognitivo. A pesquisa foi realizada em 4 escolas municipais e estaduais. Os jogos didáticos Dama Química, Pif-Paf inorgânico, Química legal e Perfil químico foram construídos e aplicados em 2 turmas do 9ºano (A e B), 1 turma do 1ºano e 1 turma do 2º ano (Fig.1).

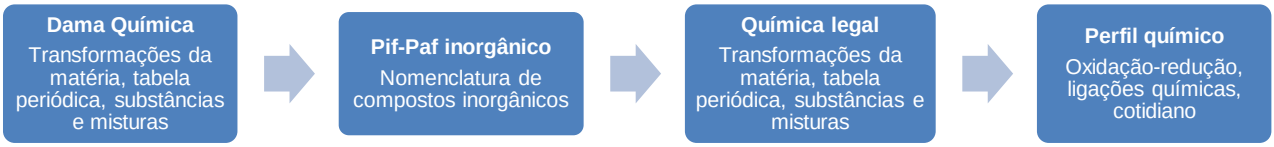


**Fig.1**: Jogos Didáticos e Conteúdos discutidos.

Aproximadamente 111 alunos participaram do projeto. 79% responderam que consideram química interessante. 54% citaram que jogos/dinâmicas facilitam a aprendizagem: *"mais interessante que fossem aulas dinâmicas, divertidas, que acontecesse competições".* A maioria (70%) respondeu que sentem dificuldades nos cálculos, fórmulas e em nomes difíceis. O trabalho em equipe consiste em uma estratégia motivadora da aprendizagem, sendo aprovada por 81%, representando uma ótima aceitação dos jogos aplicados (Fig.2). Quanto a importância de estudar química, 80% consideram importante pela ciência estar inserida em nosso cotidiano e no desenvolvimento do ser humano. Após aplicação dos jogos, os alunos relataram o quanto consideraram proveitosa a estratégia utilizada para o ensino-aprendizagem da química. Pode-se perceber a importância dos jogos e da interação aluno-professor e aluno-aluno na construção dos conceitos químicos de maneira prática, divertida e integradora.

**Fig.2:** Aplicação dos Jogos Didáticos.

**Referências:** Soares, M. Jogos Didáticos e Atividades Lúdicas para o Ensino de Química, 2013.

**Agradecimentos:** EMNSRA, EMJF, EEDAC e EEPAA, Prodocência/CAPES/IF Sertão-PE.

**Inscrição:** 00696

***Área: EDU***

# O ensino de química: um olhar sobre as metodologias empregadas aos alunos surdos

**Diellem C. P. dos Santos (PG),[1*] Grace K. Q. Meireles (FM),[2] Keyla C. de J. L. Fonseca[3] (PQ); *d2. cristina@hotmail.com**

*[1] Faculdade Brasileira de Ciências e Tecnologia e Universidad Nacional de Rosário, UNR; [2] Faculdade Brasileira de Ciências e Tecnologia e Universidade do Estado do Pará, UEPA; [3] Faculdade Brasileira de Ciências e Tecnologia.*

Palavras Chave: *Disciplina Química, Surdez e Atendimento Educacional Especializado.*

## Highlights

The Teaching of Chemistry: a look at methodologies employed for deaf students.
The Brazilian education for deaf people, in particular educational making of the teacher of Chemistry.

## Resumo/Abstract

A educação brasileira para surdos, em especial o fazer educativo dos professores de Ciências em particular, a Química, por não possuírem formação que lhes possibilite trabalhar com alunos com surdez, têm grandes dificuldades em lidar com a construção de conceitos científicos para esse grupo. A pesquisa de campo desenvolveu-se na E.E.E. F. M. Vilhena Alves e na escola E.E.F.M. Cristo Redentor, município de Belém/PA, tendo como público-alvo os profissionais do AEE e professores de química da rede regular. A pesquisa foi realizada nos meses de junho e agosto do ano de 2017 e para coleta de dados foi utilizado como instrumento um formulário composto por perguntas abertas e fechadas. Buscou-se conhecer as metodologias que os profissionais empregavam na ministração dos conteúdos específicos de química. Os resultados: os conteúdos que podem ser demonstrados na prática tornam mais fáceis a aprendizagem, como as reações químicas, pois algumas podem ser demonstradas, tendo a visão como o sentido facilitador. Entendeu-se ser o aluno protagonista desse processo, já que muito dos materiais pedagógicos utilizados eram adaptados e construídos pelo próprio aluno com surdez. Ou ainda, os colegas de classe que dominavam a LIBRAS auxiliavam na aprendizagem. Já o professor de Química fazia uso apenas de apostilas como metodologia de ensino. É importante conhecer as possibilidades metodológicas no que se refere ao ensino de Química para a educação de alunos com surdez, já que recentes investigações apontam para uma realidade de profunda exclusão desse grupo social.

Figura 1- E.E.E. F.M. Vilhena Alves

Figura 2: E.E.E.F.M Cristo Redentor

References

SOUSA, Sinval Fernandes de (et al.). Química Nova na Escola. Terminologias Químicas em Libras. Vol. 33, N° 1, Fevereiro 2011. Minas Gerais. Recebido em 04/05/2009, aceito em 07/10/2010.

REIS, Esilene dos Santos. O ensino de química para alunos surdos: desafios e práticas dos professores e interpretes no processo de ensino e aprendizagem de conceitos químicos traduzidos para libras. Fortaleza. 2015. Universidade Federal do Ceará. Disponível em: < http:// www.repositorio.ufc.br /bitstream/ riufc/13228/3/ 2015_dis_esreis2.pdf>. Acessado em: 02. Jun. 2017.

**Área: EDU** **Inscrição:48022**

# Circuito Químico – O Relato da Experiência do PET na Escola Estadual Alexander Graham Bell

**Cíntia Teles Siqueira (IC),[1]* Anne Elouise F. Souza (IC),[1] Amanda Feliz Pinheiro (IC),[1] Andressa Nascimento Silva (IC),[1] Andressa Teixeira de Souza (IC),[1] Beatriz Soares Cunha (IC),[1]Grazieli de Carvalho Cassini (IC),[1] Ian dos Santos Costa (IC),[1] Jéssica Barcelos dos Santos (IC),[1] Mateus de Fonseca Pereira (IC),[1] Pamela Roberta Alves da Costa (IC),[1] Sonara Gonçalves Silva Cassa (IC),[1] Thatiane Cotias C. Pessoa (IC),[1] Ana Paula Bernardo dos Santos (PQ)[1], Lívia Tenório C. Crespo (PQ)[1]**

**cintiasiqueiracts@gmail.com**

*[1]Instituto Federal de Educação, Ciência e Tecnologia do Rio de Janeiro – campus Duque de Caxias. Avenida República do Paraguai, 120, Sarapuí - Duque de Caxias.*

Palavras Chave*: Chemistry teaching, Experimentation, Chemical Circuit.*

## Highlights

Chemical Circuit – a Pratical Experience of PET on Alexander Grahan Bell Public School. Use of experiments in the chemistry teaching. Experiments realization with high school students of a public school.

## Resumo/Abstract

A utilização de experimentos no ensino de química promove uma aproximação da teoria vista na sala de aula com a realidade do aluno[1]. Apesar de existirem diversos experimentos fáceis de realizar em sala de aula e que utilizam materiais acessíveis, eles são pouco utilizados nas turmas de ensino médio de escolas públicas. Sabendo dessa carência, o grupo PET (Programa de Educação Tutorial) do IFRJ/CDUC, que trabalha com o desenvolvimento de ferramentas didáticas e atividades de extensão com foco na divulgação científica e na melhoria do ensino e aprendizagem de química, tem realizado ações em escolas públicas da redondeza. Este trabalho tem por objetivo relatar a realização de um circuito de experimentos de química na Escola Estadual Alexander Graham Bell pelo grupo PET.

Para a elaboração do circuito foram escolhidos alguns experimentos que contemplassem os conteúdos estudados em química, como modelo atômico, tipos de misturas e os processos de separação destas, acidez e basicidade, soluções eletrolíticas, densidade e interações intermoleculares. Durante cada circuito, de cerca de 90 minutos, os alunos, divididos em grupos de oito, percorreram todos os 10 experimentos propostos. Os mediadores explicavam o experimento e os conceitos químicos envolvidos e, posteriormente, os alunos realizavam cada um dos experimentos propostos. Foi possível perceber o entusiasmo deles durante o circuito, indagando os mediadores e querendo repetir os experimentos. Devido ao grande interesse demonstrado pelo corpo docente e discente da escola, a ação será repetida nesta e em outras escolas do município.

[1]Marcos F.S. **O Ensino de Química por Meio de Atividades Experimentais: A Realidade do Ensino nas Escolas**. Presidente Prudente, (...). Disponível em: <http://www.unesp.br/prograd/ENNEP/Trabalhos%20em%20pdf%20-20Encontro%20 de%20Ensino/T4.pdf> Acesso em 30 de fev.2018.

**Área: EDU** **Inscrição: 00882**

# Jogo da Veeelha Estequiometria – abordagem interdisciplinar para o ensino envolvendo conteúdos químicos e matemáticos

**Camila S. Bastos (IC)[1]*, Bárbara C. T. Moreira (PQ)[1].**

**camilaspecht@hotmail.com**

[1]*Departamento de Ciências Exatas e da Terra, UNEB.*

Palavras Chave: *Material didático, Jogo da velha, Estequiometria, Símbolos químicos.*

## Highlights

Stoichiometry tic tac toe – interdisciplinary approach to teaching involving chemical and mathematical content. This game aims to facilitate the learning by exploring the meanings of the symbols. Made with low cost materials. The applications evidenced their playfulness and the teaching potentiality.

## Resumo/Abstract

O Jogo da Veeelha Estequiometria (JVE) foi elaborado com o objetivo de facilitar a aprendizagem desse conteúdo, explorar os significados de símbolos químicos e propiciar ao estudante a interpretação dos cálculos envolvidos. Seguindo a dinâmica do jogo da velha, com o acréscimo de regras específicas, o JVE foi confeccionado com material de baixo custo e de fácil acesso - podendo ser reproduzido pelo professor, que o aplica sozinho, caso não possua auxílio; e apresenta versatilidade de uso, permitindo diferentes enfoques ao conteúdo. Foi aplicado em aulas de Química, em 7 turmas do 3º ano do ensino médio do Colégio Thales de Azevedo – SSA/BA. Cada turma foi dividida em 4 grupos aos quais foram entregues um kit contendo as peças do jogo, 2 folhas de respostas – a fim de que fossem anotados os cálculos realizados no decorrer do jogo – e questionários sobre o jogo. Estes instrumentos foram utilizados para avaliar os estudantes e o jogo. As observações durante as aplicações do JVE e o feedback dos estudantes evidenciaram a ludicidade e as potencialidades de ensino e revisão demonstrando que o jogo forneceu contribuições relevantes para o processo de ensino e aprendizagem do conteúdo. A abordagem dinâmica e interativa do JVE despertou a curiosidade dos estudantes pelo conhecimento, movidos pelo desejo de atingir o objetivo do jogo, pelo prazer obtido durante a realização da atividade, ou por permitir aos estudantes a execução de ações que os levam a refletir sobre suas ideias.

Figura 01. Tabuleiro e cartas Jogo da Veeelha Estequiometria

Fonte: Elaboração própria, 2016.

**Área: EDU** **Inscrição: 01204**

# Estudo de casos: uma análise de aplicação do método

**Naiane Maria C. Rodrigues (IC),[1] Alexandra da S. Fonseca (IC),[1] Gizelle Angela B. Vieira (PQ).** [1*]

**naianerodriguesif@gmail.com; gizelle.angela@ifsertao-pe.edu.br**

[1]*Instituto Federal de Educação, Ciência e Tecnologia do Sertão Pernambucano, IF-SERTÃO.*

Palavras Chave: *Metodologia ativa, Estudo de caso.*

## Highlights

Case study: an analysis of the application of the method. Study on the application of the Case Study method in High School that aimed to promote the development of skills in the teaching of chemistry.

## Resumo/Abstract

O método de Estudo de Casos tem como objetivo estimular o aluno a direcionar sua própria aprendizagem, com situações reais ou simuladas, e despertar tomadas de decisões para identificar e solucionar o problema (Sá e Queiroz, 2009). Assim, o presente trabalho utilizou o método de Estudo de Casos, como estratégia metodológica para que os alunos pudessem relacionar o conteúdo "lei dos gases" com acontecimentos diários, além de analisar a eficiência do método quando usado para introduzir e concluir o conteúdo. O trabalho foi aplicado em duas turmas do 2º ano do Ensino Médio de uma escola pública da cidade de Petrolina-PE, usando a sequência didática abaixo (Fluxograma 1). Através de observações realizadas durante o acompanhamento da aplicação dos 'casos' foi possível perceber, na turma do 2º ano B, que já havia estudado o conteúdo, soluções embasadas teoricamente. Entretanto, na turma do 2º ano A, os grupos chegaram a diferentes soluções, todas baseadas no senso comum, demonstrando falta de base teórica, já que o assunto estava sendo introduzido pelo método adotado. Estes tiveram dificuldades em listar termos ou frases relevantes, essenciais para solucioná-los. Fica evidente que o método é viável em ambas as situações, porque desenvolve diversas habilidades necessárias à compreensão do assunto abordado, mas é preciso sua familiarização para sanar as dificuldades de identificação do problema.

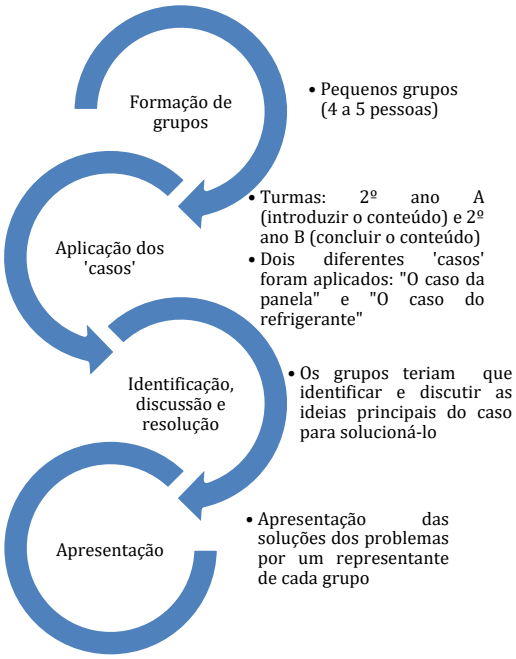


Fluxograma 1: Sequência didática.

REFERÊNCIAS: SÁ, L. P.; QUEIROZ, S. L. Estudo de casos no ensino de Química. 2ª ed. Campinas: Editora Átomo, 2009.

**Área: ELE** **Inscrição: 00811**

# Determination of fenitrothion in food samples by using single-wall carbon nanohorns and zein thin film

**Marina P. M. Itkes (IC)[1*], Geiser G. Oliveira (PQ)[2], Orlando Fatibelo-Filho (PQ)[2], Bruno C. Janegitz (PQ)[1]**

**marinapmitkes@gmail.com; brunocj@ufscar.br**

*[1]Departamento de Ciências da Natureza, Matemática e Educação, UFSCar-CCA; [2]Departamento de Química, UFSCar*

Keywords*: (Nanohorn, Zein, Fenitrothion, Sensors).*

## Highlights

In this work is proposed a modified electrochemical sensor within the single wall carbon nanohorns(SWCNH) as the conductive nanomaterial and zein(ZE) as support, to detect fenitrothion(FT) in fruit juice.

## Abstract

SWCNH are considered promising nanomaterials, since they have good electrical conduction [1]. It is known that ZE is a prolamine, used in the production of flexible and porous films [2]. FT is an insecticide widely used and toxic to many living beings, especially mammals, where its toxicological effect are severe, making its detection very important to ensure the safety and quality of foods [3,4]. In this work, a new electrochemical sensor was proposed using the modified GCE with SWCNH and ZE for the voltammetric determination of FT in food samples. The GCE was modified by casting technique, and, after total drying, the electrode was subjected to voltammetric measurements. Characterizations were performed by CV using the SWCNH-ZE/GCE and GCE. The comparison of the calculated electroactive areas showed that the modified electrode has an electroactive area 2.3 times superior than GCE. The AdSV was the electrochemical technique used to detect FT. It can be noted that both GCE and SWCNH-ZE/GCE presents the two characteristics peaks of FT, and five parameters were analyzed for AdSV optimization. The linear response was tested by using the AdSV and a linear behavior was observed, with linear range from 0.049 to 12.30 μmol $L^{-1}$ and LOD of $2{,}15\times10^{-7}$ mol $L^{-1}$. The detection of FT was performed in orange juice, and the results proved that the SWCNH-ZE/GCE can be applied in real samples. Therefore, the modified electrode is a new device and an interesting alternative for FT detection.

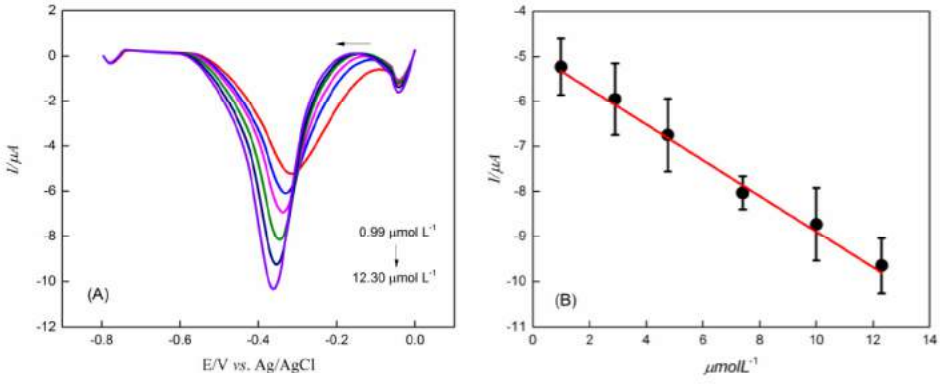


Fig.1: (A) AdSV voltammogram obtained from SWCSH-ZE/GCE in $9.90\times10^{-7}$, $2.90\times10^{-6}$, $4.70\times10^{-6}$, $7.40\times10^{-6}$, $1.00\times10^{-5}$ and $1.23\times10^{-5}$ mol $L^{-1}$ of FT in 0.1 mol $L^{-1}$ phosphate buffer (pH 3.0); $a$ = 0.165 V, $t$ = 0.10 s, $v$ = 0.03 $Vs^{-1}$ and adsorption time = 6.0 min. (B) Analytical curve.

[1] F. R. Baptista, S.A. Belhout, S. Giordani, S.J. Quinn, Chem. Soc. Rev. 44(2015) 4433-4453.
[2] L. A. Forato, D. de Britto, J.A. Scramin, L.A. Colnago, O.B.G. Assis, Polímeros23(2013) 42-48.
[3] C. Li, C. Wang, Y. Ma, Microchim. Acta 148(2004) 23- 27
[4] L. M. Ravelo-Pérez, J. Hernández-Borges, M. A. Rodríguez-Delgado, J. Chromatogr. 1211 (2008) 33–42

**Área: ELE** **Inscrição: 01290**

# Evaluation of Triazoles Compounds as a corrosion inhibitor for 1020 carbon steel

**Alexandre de Araújo Godoy[1] (TM), Dafne Júlia Ferreira Lougon[1] (TM), Sara Fagundes Teixeira[1] (TM), Bruno Almeida Cotrim[2] (FM), Gabriel Oliveira de Resende[2] (FM), Flávia Carvalho de Souza*[1] (FM)**

**flavia.souza@ifrj.edu.br**

[1]*Instituto Federal de Educação Ciência e Tecnologia do Rio de Janeiro – Campus São Gonçalo.*
[2] *Instituto Federal de Educação Ciência e Tecnologia do Rio de Janeiro – Campus Rio de Janeiro*

Palavras Chave: *triazoles, corrosion inhibitors, carbon steel.*

## Highlights

This work shows the synthesis of triazoles compounds and evaluate its inhibitor activities. These compounds were used in both weight loss and electrochemical tests and compared with commercial inhibitor.

## Abstract

Corrosion inhibitors are chemicals, which in certain conditions, eliminate or reduce the corrosive process of a material, preventing the development of reactions that promote corrosion. The use of these substances increases the useful life of industrial ducts and equipment, reducing operating costs and, thus, generating higher revenue for the company. The compounds 1,2,3-triazole have been studied as anticorrosive substances of metallic surfaces, being an economical alternative for the industry, since it has a relatively synthetic route (Figure 1).

**Fig. 1 - Structures of triazoles: 1,2,3-triazole**

[A] [B]

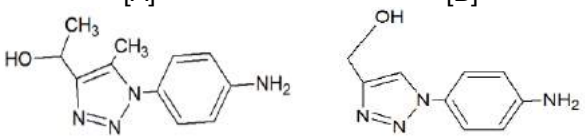


The synthesis of the triazoles shown in Fig. 1 was performed reacting p-nitroaniline with sodium nitrite in acidic medium and addition of sodium azide. To synthesize triazole A the organoazide intermediate reacted with acetylacetone in the presence of triethylamine (78% yield) and subsequent reduction with $NaBH_4$ / $CuSO_4$ (82%). The synthesis of compound b was carried out reacting the azide with propargylic alcohol and subsequent reduction with Zn / $NH_4Cl$ (68%) in aqueous solution.

For the inhibition efficiency study of the synthesized triazoles, gravimetric tests were performed over carbon steel 1020 pieces in a solution of 1.0 mol $L^{-1}$ HCl in the absence and presence of inhibitor, with time 24 hours immersion. These preliminary results are shown in Table 1. Electrochemical tests also performed with carbon steel in a solution of 1.0 mol $L^{-1}$ HCl in the absence and presence of inhibitor. Table 1 shows that the inhibitors studied showed efficiencies higher than the Commercial Inhibitor. The results obtained from electrochemical tests corroborate with gravimetric tests of weight loss.

**Table 1 - Inhibition efficiency by gravimetric test.**

| Conc. (mg $L^{-1}$) | Inhibitor A | | | Inhibitor B | | | Inhibitor Comercial | | |
|---|---|---|---|---|---|---|---|---|---|
| | $W_{corr}$ (g/cm²) | I.E. (%) | Error (%) | $W_{corr}$ (g/cm²) | I.E. (%) | Error (%) | $W_{corr}$ (g/cm²) | I.E. (%) | Error (%) |
| 0 | 0.0281 | - | - | 0.0281 | - | | 0.0281 | - | |
| 250 | 0.0012 | 95.8 | 0.7 | 0.0023 | 91.9 | 1.3 | 0.0078 | 72 | 1.9 |
| 500 | 0.0009 | 96.7 | 0.3 | 0.0019 | 93.4 | 0.3 | 0.0048 | 83 | 1.2 |
| 750 | 0.0013 | 95.5 | 5.5 | 0.0016 | 94.3 | 0.8 | 0.0048 | 83 | 0.9 |
| 1000 | 0.0005 | 98.2 | 0.3 | 0.0014 | 95.0 | 0.5 | 0.0045 | 84 | 0.7 |
| 1250 | 0.0002 | 99.2 | 0.3 | 0.0011 | 96.2 | 0.2 | 0.0030 | 89 | 1.1 |

## References

1. Kennedy, J.L., Oil and Gas Pipeline Fundamentals. 2nd ed. 1993: PennWell Books.
2. Torres, V.V., et al., Study of Thioureas Derivatives Synthesized from a Green Route as Corrosion Inhibitors for Mild Steel in HCl Solution. Corrosion Science, 2014. 79(0): p. 108-118.
3. Torres, V.V., et al., Inhibitory Action of Aqueous Coffee Ground Extracts on the Corrosion of Carbon Steel in HCl Solution. Corrosion Science, 2011. 53(7): p. 2385-2392.

**Área: ELE** **Inscrição:01387**

# Correlating surface growth of nanoporous gold with electrodeposition parameters to optimize amperometric sensing of nitrite

**Abhishek Kumar (PQ),[1]* Josué M. Gonçalves (PG),[1] Anandhakumar Sukeri (PQ),[1] Koiti Araki (PQ),[1] Mauro Bertotti(PQ).[1]**

**josuemartins@usp.br; abkumar@iq.usp.br**

*[1]Department of Fundamental Chemistry, Institute of Chemistry, University of São Paulo - USP*

Palavras Chave: *Nanoporous gold, Electrodeposition, sensor.*

## Highlights

The novelty of this work comes at first with the selection of DHBT assisted growth of NPG for generation of a new platform for nitrite analysis, with substantial improvement in analytical performance. Secondly, efforts have been made to interlink electrodeposition parameters, growth mechanism and electrocatalytic activity.

## Abstract

The electrochemical deposition of nanoporous gold (NPG) on a solid substrate has been an intensive area of research in recent years. Such facile technique offers a fine control over the growth and nucleation mechanism, which determines the grain size and the morphology of the deposited NPG, which in turn strongly influences its electrochemical activity[1]. Accordingly, a systematic study was performed in the present work to fabricate NPG modified gold electrodes using the Dynamic Hydrogen Bubble Template (DHBT) method[2], which were subsequently tested for the electrooxidation of nitrite. Two sets of experiments were carried out: a) NPG were electrodeposited at applied potentials of -1 V, -2 V, -3 V and -4 V at a fixed time of 100 s; and b) at constant applied potential of -4 V varying the deposition time (100 s, 200 s, 400 s and 600 s). NPG modified electrodes ware characterized using profilometry, SEM, XRD and EDXRF. The porous gold nanostructures electrodeposited on a solid gold substrate are strongly dependent on electrodeposition parameters, especially the applied potential and time of deposition, influencing the electrocatalytic activity towards nitrite oxidation. Based on results of surface characterization experiments, it was established that the film gets denser with more negative potential, while a more porous morphology was achieved, including nanodendrite formation, as the deposition time increased. Changes in the gold surface were correlated with different growth models and nucleation processes. Based on electrochemical and surface characterization studies, an NPG platform prepared at -4 V for 100 s was found to be the most suitable for electrochemical nitrite sensing applications because of a potential shift towards less positive potentials with enhanced sensitivity. The sensor was employed for amperometric detection of nitrite and sensitivity and limit of detection values were found to be 0.2 μA $\mu M^{-1}$ and 10 nM, respectively. The modified electrode exhibited good reproducibility and shelf-life stability in experiments carried out for a prolonged time (two months). Finally, the applicability of the proposed NPG modified electrode was successfully confirmed by measuring nitrite in real samples including processed meat and lake and tap water, whose results were validated by the spectrophotometric Griess method. To further understand the growth mechanism of NPG, electrodeposition on a single crystal gold substrate has been envisaged.

**Acknowledgment**
CNPq e Fapesp.

**References**

[1] N.D. Nikolić, K.I. Popov, L.J. Pavlović, M.G. Pavlović, **J. Electroanal. Chem.** 588 (2006) 88-98.
[2] A. Sukeri, M. Bertotti, **J. Electroanal. Chem**. 805 (2017) 18-23.

**Área: ELE**
*(Inserir a sigla da seção científica para qual o resumo será submetido. Ex: ORG, BEA, CAT)*

**Inscrição: 01366**
*(Inserir o número de inscrição do autor que fez a submissão)*

# A sample drop cell based on gold microelectrodes obtained from split electronic chips

**Welisson V. de Oliveira (IC), Jessica T. Trevisan (IC), Giane S. Higino (PG), Jairo J. Pedrotti (PQ)***

**welisson.oliveira@mackenzie.br; jpedrotti@mackenzie.br**

*MackGraphe – Graphene and Nanomaterials Research Center - Mackenzie Presbyterian University - Rua da Consolação, 896 – São Paulo, SP – CEP 01302-907.*

Keywords: electrochemical cell, miniaturization, gold microelectrodes, voltammetry.

## Highlights

- The micro electrochemical cell was fabricated from disposable electronic chips.
- The cell uses microvolume of 10 to 30 µL sample drops.
- The working microelectrodes can be used individually or in arrays.

## Abstract

The electrochemical devices offer attractive characteristics for field measurements, including low cost, portability and easily of miniaturization. In this work, a one drop batch cell was fabricated on a platform with 14 gold microelectrodes obtained from disposable electronic chips packaged by surface-mount device (SMD) technology [1]. Fig 1 depicts the design of electrochemical cell. The fourteen gold microelectrodes (AuMEs) are distributed in an almost circular shape on polymeric platform, as can be seen on Fig 1G. Four AuMEs were interconnected in parallel to work as auxiliary electrode. A micro Ag/AgCl reference electrode was positioned in the central circle of the microelectrodes to measure the potentials of the working electrodes [2]. Ten AuMEs can be individually or in parallel addressed to operate as working electrode. The cell uses microvolume of 10 to 30 µL sample drops. Fig. 2 shows typical cyclic voltammograms with sigmoidal shape obtained with two AuMEs with different concentrations of $[Fe(CN)_6]^{3-}$ in 0.10 mol $L^{-1}$ KCl by using sample drops of 30 µL. The good proportionality between the anodic limiting current and $[Fe(CN)_6]^{3-}$ concentration can be confirmed by calibration plot shown in the inset ($R^2$ = 0.998). The repeatability of five CVs of 5 mmol $L^{-1}$ $[Fe(CN)_6]^{3-}$ obtained with a sample drop shown an RSD = 2 % while for different sample drops a RSD = 3% was found.

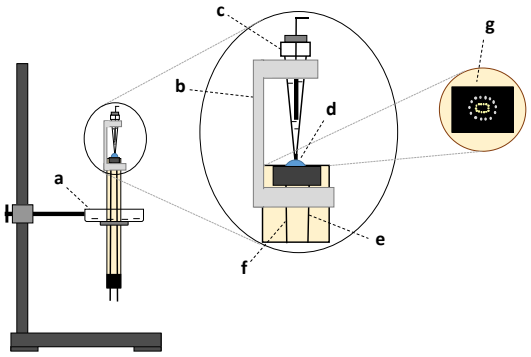


Fig. 1. Electrochemical cell. a) Waste solution collector; b) Silicon piece; c) Ag/AgCl reference electrode; d) drop sample; (e) Auxiliary electrode electric contact; f) Working electrode contact; g) Array of AuMEs (external dots).

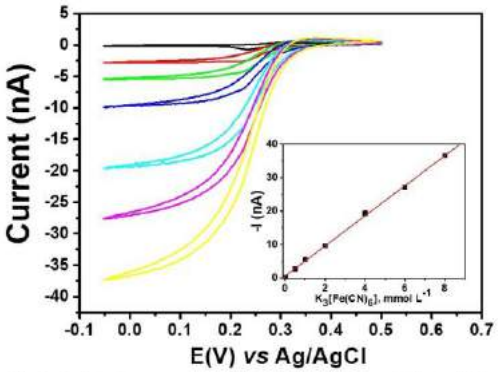


Fig. 2. Cyclic voltammograms of $[Fe(CN)_6]^{3-}$ solutions obtained with two AuMEs in 0.10 mol $L^{-1}$ KCl. $Fe(CN)_6]^{3-}$ concentration: 0.5 to 8.0 mol $L^{-1}$. Scan rate: 20 mV $s^{-1}$.

The cell set up is simple, inexpensive and easy to operate, which are very attractive for field measurements.

Acknowledgment: MACKPESQUISA

1. B.D. Pacheco, J. Valério, L. Angnes, J.J. Pedrotti, Anal. Chim. Acta 2011, 696, 53-58.
2. J.J. Pedrotti, L. Angnes, I.G.R. Gutz, Electroanalysis 1996, 8, 673-675.

**Área: ELE** **Inscrição: 01253**

# Carbon supported hybrids nanostructures PtSn with $CeO_2$ nanorods for Direct Ethanol Fuel Cells

**Tuani Carla Gentil (PG),[1] Luanna S. Parreira (PQ),[2] Felipe M. de Souza (PG),[1] Victor S. Pinheiro (PG),[1] Júlio Nandenha (PQ),[3] Almir O. Neto (PQ),[3] Mauro C. dos Santos (PQ),[1]*.**

**tuani.gentil@ufabc.edu.br; mauro.santos@ufabc.edu.br**

*[1]Centro de Ciências Naturais e Humanas, Universidade Federal do ABC, Rua Santa Adélia, 166, 09210-170 Santo André, SP, Brazil; [2]Instituto de Química, Universidade de São Paulo, Av. Prof. Lineu Prestes, 748, 05508-000 São Paulo, SP, Brazil. [3]Instituto de Pesquisas Energéticas e Nucleares (IPEN), CNEN/SP. Av. Prof. Lineu Prestes 2242, 05508-000, São Paulo - SP, Brazil.*

Keywords: *Fuel Cell, Platinum, Tin, Ceria, Ethanol.*

## Highlights

$Pt_3Sn_1$_20%NR/C can be an interesting alternative for DEFC considering the cost of the electrocatalyst.
The presence of $CeO_2$ nanorods improve the electrocatalytic activity for CO oxidation.

## Abstract

New energetic sources have been the focus of current researches, including on fuel cells. This device has as its operating principle the conversion of chemical energy into electrical energy, making possible the use of renewable energy sources [1]. In the fuel cells operation are applied nanostructured electrocatalysts capable of oxidizing organic molecules such as ethanol [2]. This work was carried out using PtSn-based electrocatalysts with ceria nanorods ($CeO_2$), synthesized by chemical reduction method via sodium borohydride [2], and supported on carbon Vulcan XC 72 (20% w/w). The synthesized materials have the following mass metal ratios: Pt/C; $Pt_3Sn_1$/ C and $Pt_3Sn_1$_20%NR/ C, with % of the $Pt_3Sn_1$ load replaced by ceria nanorods in the last nanomaterial, in order to reduce the costs of noble metals such as platinum. The evaluation of the activity for ethanol oxidation is given by polarization and power density curves, according to **Figure 1**. From the polarization curve it was observed that the $Pt_3Sn_1$_20%NR/ presented higher open circuit potential value (572 mV), and power density higher than the Pt/C composite material. The $Pt_3Sn_1$/C material presented a higher value of power density related to the others, but $Pt_3Sn_1$_20%NR/C generated a power density for ethanol oxidation relatively close to the best activity material, by the supply of oxygenated species improved the electrocatalytic activity for CO oxidation, making its application possible.

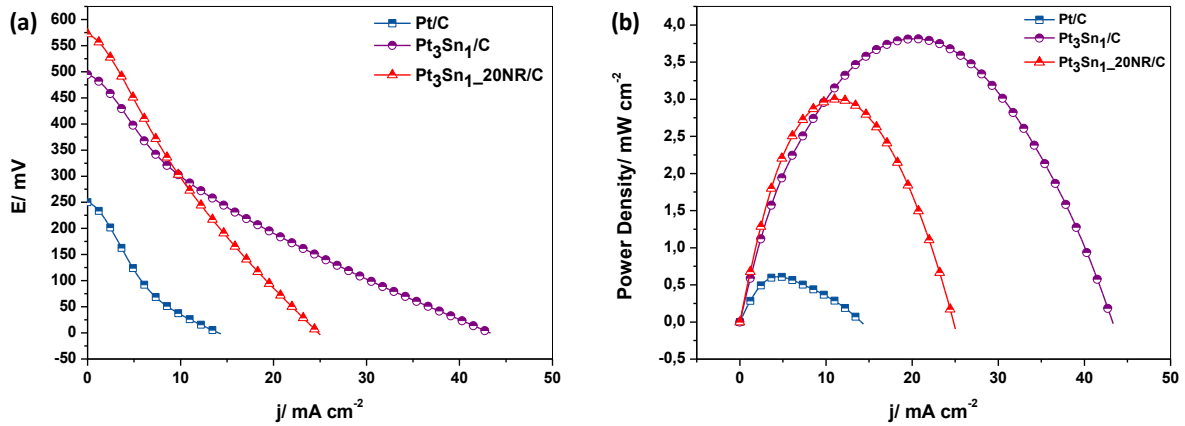


**Figure 1. (a)** Polarization and **(b)** Power density curves of a direct ethanol fuel cell, with an operating temperature of 80°C, 1 mL $min^{-1}$ flow of ethanol 2 mol $L^{-1}$ and 500 mL $min^{-1}$ oxygen flow, under a 2 bar pressure.

**Acknowledgements:** The authors are grateful to Fapesp (2015/10314-8, 2016/00819-8, 2017/21846-6) and the CEM-UFABC for the experimental support.

**References:** [1] R. Raza, *et al.*, *Renew. Sustain. Energy Rev.*, vol. 53, pp. 450–461, 2016.
[2] M. A. F. Akhairi, *et al.*, *International Journal of Hydrogen Energy*, v. 41, n. 7, p. 4214-4228, 2016.

**Área: _ELE_** **Inscrição: _01243_**

# Improving the electrochemical response of furosemide by drop casting chemically reduced graphene oxide onto glassy carbon electrodes

**Sancler C. Vasconcelos (IC), Eduardo M. Rodrigues (IC), Francisco D. da Silva (PG), Felipe S. Semaan (PQ), Rafael M. Dornellas (PQ)***

**rafaeldornellas@id.uff.br; sanclervasconcelos@id.uff.br**

[1]*Departamento de Química Analítica, Universidade Federal Fluminense, Outeiro de São João Batista, S/N, Centro, Niterói – RJ – Brasil.*

Palavras Chave: *CRGO, Furosemide, BIA, biological fluids, natural waters.*

## Highlights

Chemically reduced graphene oxide provided higher current signals for the determination of furosemide when compared to those in similar condition onto a bare electrode.

## Resumo/Abstract

Furosemide is a popularly used antihypertensive medicine due to its diuretic properties. It is also considered doping agent (since it can mask the use of others anabolic compounds), being almost entirely excreted in urine in its unaltered form (65-70%), leading to a highly possible occurrence in natural waters[1]. The objective of this work was to evaluate the possibility of using the glassy carbon electrode (GCE) modified with chemically reduced graphene oxide (CRGO) as a sensor for the furosemide amperometric determination using batch-injection analysis (BIA). Cyclic voltammograms were carried out under different acidic conditions (pH 3-9) using Britton-Robinson (BR) buffer. Other supporting electrolytes at the same optimum pH were also assessed such as phosphate and acetate buffers. At the best found condition, it could be observed an improvement on current signal intensity for furosemide using acetate buffer pH 5 with the GCE-CRGO (Fig. 1). Mass transport studies suggested a diffusional process, minimizing the need for mechanically stirring when using the BIA system. BIA parameters with amperometric detection were studied and optimized. Hydrodynamic voltammograms showed highest current intensity at +1.0 V. Repeatability study was performed by two different concentrations (1 and 10 µmol $L^{-1}$) leading to satisfactory relative standard deviations (DPR, lower than 5%). A linear range from 1 to 600 µmol $L^{-1}$, with good linearity ($R^2$> 0.99) was reached, being the limit of detection (LOD) calculated as 0.82 µmol $L^{-1}$. Possible application in biological fluids and natural waters will be evaluated.

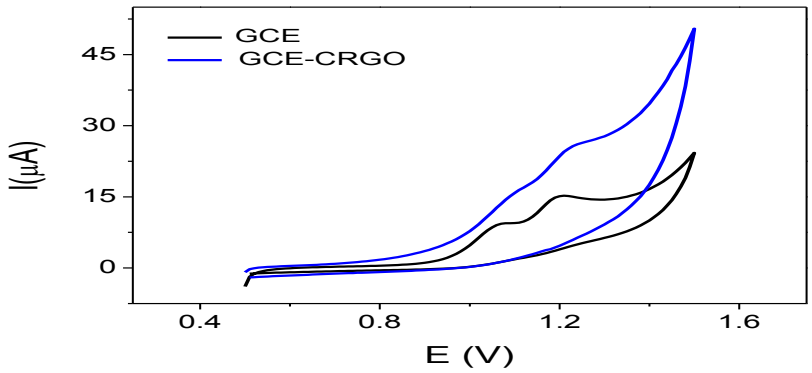


Figure 1: Cyclic voltammograms for furosemide 1 mmol $L^{-1}$ in GCE cleaned and modified with CRGO. Electrochemical parameters: electrolyte support buffer acetate 0.1 mol $L^{-1}$ pH 5, scanning speed: 50 mV $s^{-1}$ and step 5 mV.

[Acknowledgments: CNPq, FAPERJ, PROPPI-UFF and CAPES]

[1] B. C. Witjes, M. J. Ahsman, B. C. Van Der Nagel, Biomedical Chromatography, 24 (2010) 180.

**Área: ELE** **Inscrição:01142**

# A novel thin film $Sn_3O_4$ supported titanium ($Sn_3O_4$/Ti) successfully applied in the photoelectrocatalytic degradation of Acid Yellow 17 under visible light

**Adri Huda (PG),[1]* Lilian D. M. Torquato (PQ),[2] Pedro H. Suman (PQ),[2] Chanel T. Handoko (PQ),[1] Fakhili Gulo (PQ),[1] Maria Valnice Boldrin Zanoni (PQ)[2] and Marcelo O. Orlandi (PQ)[2].**

**liliantorquato@yahoo.com.br; adrihuda@student.pps.unsri.ac.id**

*[1]Departament of Environmental Science, Graduate Program, Sriwijaya University, Palembang-Indonesia; [2]Institute of Chemistry, São Paulo State University, Araraquara, São Paulo, Brazil.*

Keywords: *$Sn_3O_4$/Ti, microwave-assisted-hydrothermal, dye-degradation, photoelectrocatalysis, visible-light*

## Highlights

- The $Sn_3O_4$ nanostructure was successfully prepared by microwave-assisted hydrothermal method at mild conditions
- The material demonstrated high activity for dye degradation using visible radiation

## Resumo/Abstract

Photoelectrocatalysis is a powerful method resulting from the combination of heterogeneous photocatalysis and electrochemical techniques, in which a semiconductor is irradiated by light energy equal or greater than its band gap and simultaneously biased by a gradient potential. Within the numerous types of semiconductors used as photocatalysts, tin oxides with different forms (SnO, $SnO_2$ and $Sn_3O_4$), present wide-spread applications, because of its abundant availability and non-toxicity. The aim of this work was to perform the synthesis of a $Sn_3O_4$ ordered structure under mild operational conditions to further apply it in the photoelectrocatalytic degradation of a dye, taken Acid Yellow 17 as a model of textile dye treatment. The hierarchical form of $Sn_3O_4$, with the flower-like nanostructure (Fig. 1) with triclinic $Sn_3O_4$/Ti, was successfully prepared using microwave-assisted hydrothermal method at pH 6, in 150 °C. The as-prepared $Sn_3O_4$ was deposited in the titanium substrate using spin coating methods. The $Sn_3O_4$ /Ti nanostructure demonstrated high photocatalytic activity (Fig. 2) in the visible wavelength (λ>390 nm), calculated band gap of energy 2.4 eV by diffuse reflectance and presented optimally efficiency on degradation of 10 ppm solution of AY17 (pH 4) at low bias potential (0.5 V) after only 30 min of experiment (Fig. 3). Therefore, the flower-like nanostructured $Sn_3O_4$ proved to be efficient in the visible light driven photoelectrocatalytic degradation of AY17 dye, which represents an energy-saving option for its future treatment and removal of the environment.

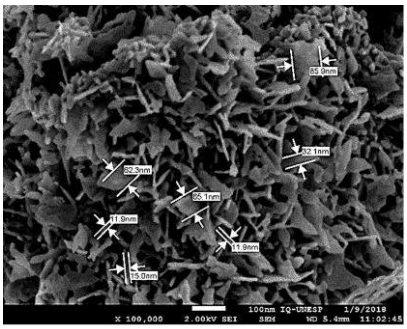

Fig. 1. SEM images of the $Sn_3O_4$ synthesized nanostructures

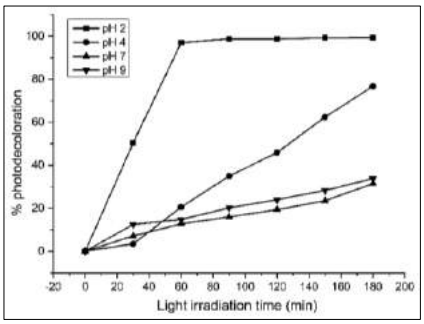


Fig. 2. Photocatalytic degradation of AY17 in different pH conditions

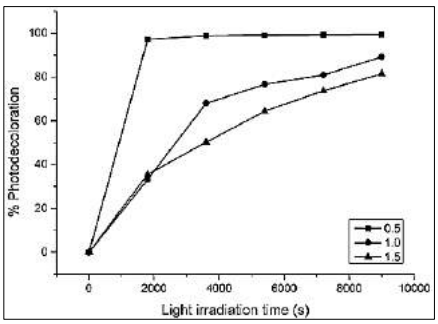


Fig. 3. Photoelectrocatalytic degradation of AY17 in different bias potentials

**Acknowledgements**

The authors are grateful to FAPESP (#2014/50945-1 and #2015/118109-4) and INCT-DATREN (#465571/2014-0) for support of this work and for the scholarship from CNPq (#150493/2017-7) of Lilian D. M. Torquato.

**Área: ELE** **Inscrição: 01014**

# O Uso de Filmes Nanoporosos de Au na Fabricação de Microssensores Eletroquímicos para a Detecção de Peróxido de Hidrogênio

**Eduardo J. C. Junior (IC),[1] Lucas P. H. Saravia (PG),[1] Henry S. C. Sáenz (IC),[2] Mauro Bertotti (PQ)[1]**

**eduardo.jose.carvalho@usp.br**

*[1]Departamento de Química Fundamental, IQ-USP, Av Prof. Lineu Prestes, 748 - São Paulo-SP, Brasil; [2]Departamento de Ciência dos Alimentos e Biotecnologia, Escola Politécnica Nacional (Equador)*

Palavras Chave:*Microeletrodos, Ouro, Nanoporos, Peróxido de Hidrogênio, Eletrocatálise.*

## Highlights

The Use of Nanoporous Gold Film in the Fabrication of Electrochemical Microsensors for Detection of Hydrogen Peroxide

The nanoporous gold film microelectrode showed remarkable electrocatalytic activity towards the cathodic reduction of $H_2O_2$ in terms of reducing the overpotential and increasing the sensitivity.

## Resumo

Um microeletrodo de ouro nanoporoso (NPG-µE) foi fabricado por voltametria cíclica aplicando-se potencial na faixa de 0,0 a 2,0 V a um microeletrodo de ouro (Au-µE) em solução de $H_2SO_4$ 0,5 mol $L^{-1}$ (velocidade de varredura = 0,02 V $s^{-1}$) [1]. Após a varredura, o Au-µE foi mantido a 2,0 V por 20 minutos para a formação de uma película de óxido de ouro na superfície, a qual foi posteriormente reduzida durante a varredura inversa, com formação de filme contendo nanoporos de ouro. O comportamento eletroquímico do NPG-µE foi testado em solução de $H_2SO_4$ 0,5 mol $L^{-1}$, observando-se aumento expressivo da área eletroquimicamente ativa em comparação com o microeletrodo de ouro, como se observa na Fig. 1A. O NPG-µE fabricado foi utilizado como sensor eletroquímico para a detecção de $H_2O_2$ em solução aquosa de PBS 0,1 mol $L^{-1}$. Conforme observa-se pela análise das curvas voltamétricas mostradas na Fig. 1B, o processo de redução catódica do $H_2O_2$ é facilitado ao se empregar o NPG-µE (deslocamento de ~0,50 V para potenciais menos negativos) e, adicionalmente, ocorre aumento da corrente. O NPG-µE será empregado como sensor de $H_2O_2$ em meio celular durante processos de stress oxidativo induzido.

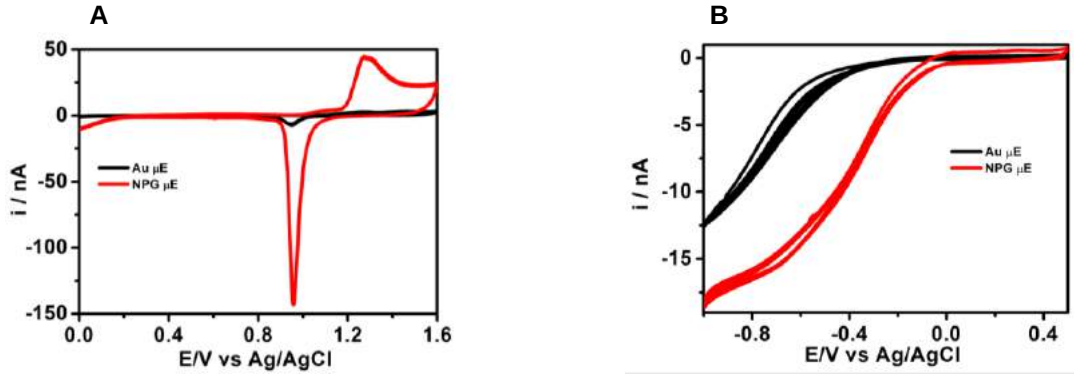


Fig.1 - Voltamogramas cíclicos registrados em soluções de $H_2SO_4$ 0,5 mol $L^{-1}$ (**A**) e $H_2O_2$ 1,0 mmol $L^{-1}$ + PBS 0,1 mol $L^{-1}$ **(B)** utilizando Au-µE (linha preta) e NPG-µE (linha vermelha); velocidade de varredura 0,1 V $s^{-1}$.

Referências:

[1] Anandhakumar Sukeri, Lucas P. H. Saravia and Mauro Bertotti. A facile electrochemical approach to fabricate a nanoporous gold film electrode and its electrocatalytic activity towards dissolved oxygen reduction. Phys. Chem. Chem. Phys., **17,** 28510–28514 (2015).

**Área: ELE** **Inscrição: 00972**

# Evaluation of adsorption behavior of fibronectin protein onto PEDOT-co-PDLLA thin films supported on Au electrodes by QCM-D.

**Rubens Araujo da Silva (PQ)[1,1], Susana Inés Córdoba de Torresi (PQ)[2,1]**

**[1] rubens.silva@usp.br; [2] storresi@iq.usp.br**

**[1]Departamento de Química Fundamental, USP**

Palavras Chave: *Electroactive polymer, conductive polymer, PEDOT, QCM-D, biocompatible polymer and biodegradable polymer.*

## Highlights

The PEDOT-co-PDLLA copolymer exhibits the electroactivity, biocompatibility and biodegradability properties, characteristics required by bio-clinic interest, especially if functionalized with protein fibronectin.

## Abstract

Functional surface coatings are a key option for many biomedical applications, from polymeric supports for tissue engineering to smart matrices for controlled drug delivery[1]. For this proposal, biocompatible and electroactive polymers are interesting since they allow the study of cell adhesion and proliferation processes, especially if functionalized with protein fibronectin[2]. Gold electrodes (AuE) were covered by spin coating with the copolymer. Topographic images of the thin films obtained by Atomic Force Microscopy confirm an uniform coating (Figure 1a). Figure 1b shows the cyclic voltammetry of the copolymer in 10mM DPBS buffer with a scanning rate of 10 $mV.s^{-1}$. Cyclic voltammetry when coupled with QCM-D shows resonance frequency and dissipation oscillations due to the oxidation and reduction events of the copolymer justified likely to charge compensation processes[3] (Figure c). This can best be visualized when the variation of the resonance frequency and dissipation are plotted versus the applied potential (Figure d). The resonance frequencies for the different overtone show maximum in 0.44 V and minimum in 0.5 V. These values show discrepancy with that observed in the cyclic voltammetry shown in Figure 1b. This can be explained by changes in the mechanical properties of the copolymer.

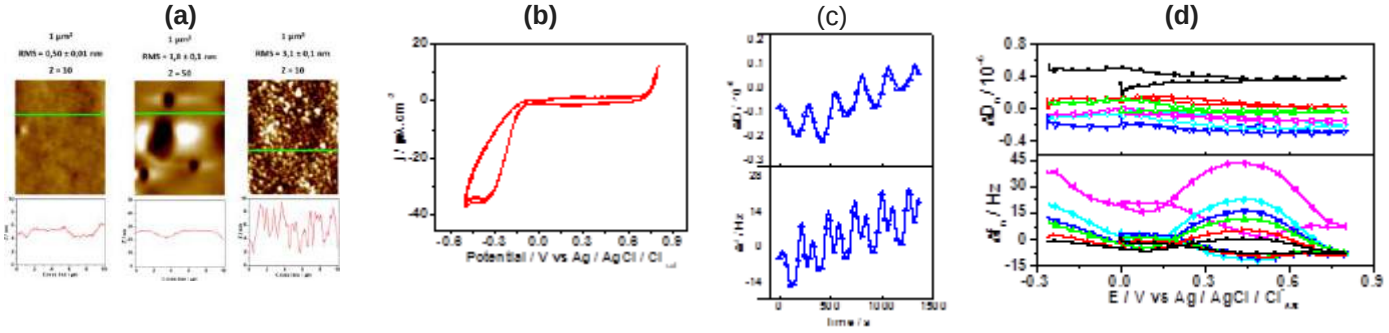


Figure 1: (a) Topographic images obtained by AFM of the surfaces of the native AuE, modified with PEDOT-co-PDLLA before and after the voltammetry cycle, respectively, (b) PEDOT-co-PDLLA cyclic voltammetry obtained in $10mV.s^{-1}$, (c) Frequency of resonance and dissipation as a function of time for the 9th overtone and (d) Frequency of resonance and dissipation as a function of the applied potential.

### References

**1** Merino, S.; Martín, C.; Kostarelos, K.; Prato, M.; Vázquez, E. *ACS nano*, *9*(5), 4686-4697, 2015.

**2** Gelmi, A.; Higgins, M. J.; Wallace, G. G. *Small*, *9*(3), 393-401, 2013.

**3** Corrêa, C. M.; de Torresi, S. I. C.; Benedetti, T. M.; Torresi, R. M. *Journal of Electroanalytical Chemistry*. https://doi.org/10.1016/j.jelechem.2017.11.016.

**Área: ELE** **Inscrição: 00873**

# Direct detection of BHA in food samples using oil/water interface electrochemistry as main tool.

**Alexandre Colen de Alcantara* (PG),[1] Keyla Teixeira Santos de Godoi (PG),[1] Hugo Barbosa Suffredini (PQ).[1]**

**keyla.tsnts@gmail.com; alexandre.colen@gmail.com; hugo.suffredini@ufabc.edu.br**

[1]*Centro de Ciências Naturais e Humanas (CCNH), UFABC – Santo André – São Paulo - Brazil.*

Keywords: Oil/water interface, food additives, *BDD electrode*

## Highlights

Oil-Water interface electrochemistry was used to promote the detection of BHA. It determination in food samples was carried out using a Boron-Doped Electrode without of pre-treatment steps.

## Abstract

Analysis of BHA (tert-butyl-4-hydroxyanisole), a very common food additive, is commonly carried out by chromatographic techniques [1-3]. On the other hand, the intention of this research is to promote a simple and effective detection of BHA using electrochemistry, since that can present lower cost and could be more effective than the conventional methodologies of analysis.

We describe here the direct detection of BHA using oil/water electrochemistry in conjunction with the square wave voltammetry (SWV) technique as main tools to promote this type of analysis. BHA determination was performed with a catodically pre-treated Boron-Doped Diamond (BDD) plate as working electrode, which was inserted directly at the interface, constituted by an oily solution of BHA and a conventional aqueous phase (Britton-Robinson buffer). Figure 1 shows a schematic representation of the electrochemical cell. The position of the BDD electrode at the interface must be carefully controlled, avoiding area differences.

Preliminary tests indicated that BHA oxidation is an irreversible process and the generated oxidation product is also electroactive. The partitioning of BHA reaches an equilibrium situation at around 15 minutes of contact between oil and aqueous phase.

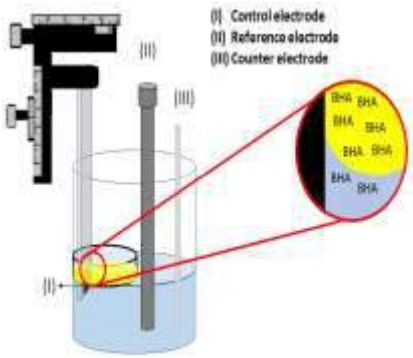


**Fig 1:** Scheme of cell assembly showing the position of BDD electrode.

All experiments were carried out by SWV. Figure 2 shows the electrochemical responses after completing the partitioning of BHA from oil to aqueous phase.

BHA concentrations were vary from 9,7 x $10^{-2}$ to 1,2 x $10^{-1}$ mol $L^{-1}$. In this experiment, a very good linearity was observed, with an $R^2$ of 0,98. It was possible to conclude that the methodology is feasible and the use of a catodically pre-treated BDD electrode can constitute a good choice to promote this type of study.

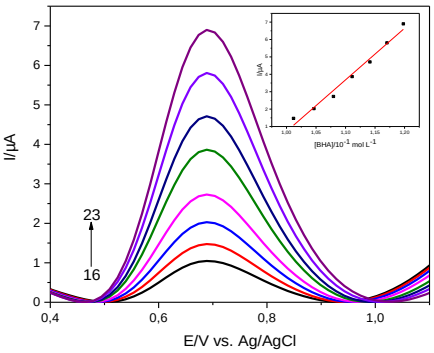


**Fig 2:** SWV studied varying the concentration from 9,7x$10^{-2}$ to 1,2x$10^{-1}$ mol $L^{-1}$. (f= 30Hz, a=0,09 mV e ΔEs= 0,015mV). Inset shows the obtained analytical curve.

## Referências

[1] Polônio, M.L.T. and F. Peres. Food additive intake and healthe effects: public health challenges in Brazil. Cad. Saúde Pública, 2009. 25(8): p. 1653-1666.

[2] International, Agency for Research on Cancer (IARC), butylated hydroxyanisole (BHA), Vol. 40, Lyon, France, 1986, p. 123.

[3] Maynart, M., R. Silva, and H. B. Suffredini. Electroanalysis, 2013. 25(6): p. 1541-1546.

**Área:** ELE *(Inserir a sigla da seção científica para qual o resumo será submetido. Ex: ORG, BEA, CAT)*

**Inscrição:** 00838 *(Inserir o número de inscrição do autor que fez a submissão)*

# Synthesis and characterization of cerium nanoparticles supported in graphene nanosheets.

**Thays S. Lima (PG),[1] Edson C. Paz (PG),[2] Mauro C.Santos (PQ),[2] Lúcia Codognoto (PQ).[1]**

**thays.lima@gmail.com**

*[1] Department of Chemistry, DQ-UNFESP,Rua prof. Artur Riedel, 275, Diadema, SP, 09972-270, Brazil.*
*[2]Universidade Federal do ABC (UFABC), Av. dos Estados, 5001 - Bangu, Santo André - SP*

Palavras Chave: Graphene nanosheets; Cerium nanostructured; Electrocatalytic activity; Oxigen reduction reaction.

## Highlights

Synthesis and characterization of cerium nanoparticles supported on graphene nanosheets

## Resumo/Abstract

In this work, we prepared 4% cerium nanoparticles supported on graphene nanosheets using the polymeric precursor method [1] to further investigate the electrocatalytic activity for $H_2O_2$ production from oxygen reduction reaction (ORR). Firstly, the electroactivity of graphene in the generation of $H_2O_2$ was analyzed. The measurements were performed using a rotating ring-disc electrode with a vitreous carbon disc (0.245 $cm^2$ ) and gold ring (0.1866 $cm^2$ ), efficiency factor: 0.28. For graphene nanosheets the $H_2O_2$ percentage was 86 % for two electrons transferred during ORR [2]. After the synthesis cerium nanoparticles supported in graphene nanosheets were characterized by scanning electron microscopy (SEM), energy dispersive spectroscopy (EDS) and X-ray diffraction analysis (XRD). Analysis using SEM Figure 1A shows the nanoparticles of cerium on the graphene sheet (region highlighted in the figure). Characterization by X-ray diffraction analysis showed the presence of the $CeO_2$ and $CeO_{2-x}$ phases in the cerium-based material as can be seen in Figure 1 B (insert) [3]. EDS showed the formation of the cerium nanoparticles on the graphene sheets. The results are promising for further application in the generation of $H_2O_2$, since using only graphene there is a high production of hydrogen peroxide, as cerium oxide is recognized as a good electrocatalyst for hydrogen peroxide production, the value of 86 % can be increased.

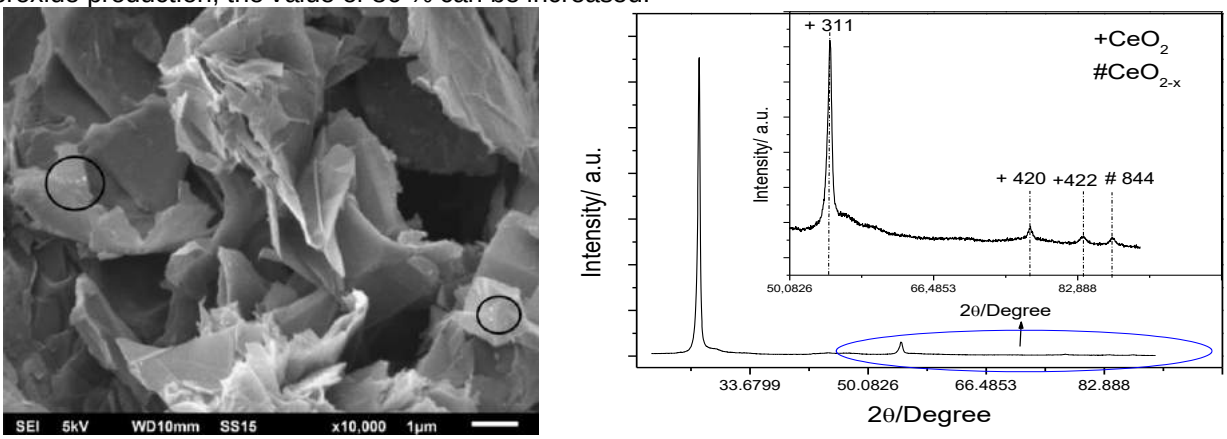


(A) (B)

Figure1: Characterization of cerium nanoparticles supported on graphene: A) SEM; B) XRD.

**Acknowledgments:**
UNIFESP, UFABC, CEM-UFABC, FAPESP (2017/21846-6) and Laboratório de Eletroquímica e Materiais Nanoestruturados (LEMN)-UFABC

**References**

*[1] M. H. M. T. Assumpção et al., Applied Catalysis A: General 411-412 (2012) 1-6.*
*[2] L. Demarconnay et al., Electrochimica Acta 49 (2004) 4513-4521.*
*[3]M. H. M. T. Assumpção et al., Applied Catalysis B: Environmental 142-143 (2013) 479-486*

**Área: ELE** **Inscrição: 00810**

# Development of electrochemical paper-based analytical device for detection of *Pseudomonas aeruginosa* in water and saliva samples

**Rafael Ferreira e Silva (IC),[1] William Reis de Araujo (PQ)[1*]**

**rafael8.silva@usp.br; *will.wra@usp.br**

[1]*Instituto de Química – USP, Av. Prof. Lineu Prestes, 748 – São Paulo – SP, Brazil.*

Keywords: *Pseudomonas aeruginosa, Bacterial infection, Paper-based analytical devices, Portable and disposable sensor.*

## Highlights

We present the development of portable electrochemical paper-based analytical sensor for detection of Bacterial infection*; Pseudomonas aeruginosa* was electrochemically monitored by the major metabolite, Pyocyanin.

## Abstract

*Pseudomonas aeruginosa* is a versatile and opportunistic human pathogen with an exceptional resistance to a wide range of antibiotics. Currently, it is one of the major human pathogens associated with serious illnesses – hospital-acquired infections.[1] Usually, the bacterial infection is detected by lab-based methods like culturing the microorganisms on agar plates followed by standard biochemical identifications (Polymerase Chain Reaction, imunoassays, etc)[2], that are laborious and time consuming. So, it is extremely relevant the development of portable, simple and rapid analytical tools to assist in the detection and monitoring of this kind of bacterial infection, especially in centers lacking laboratory infrastructure and with high clinical demand. In this work, we demonstrate the fabrication of portable electrochemical paper-based analytical device (ePAD) using two graphite leads and conductive silver ink as working, auxiliary and pseudo-reference electrode, respectively. The devices were fabricated in filter paper and patterned by wax-printing method. The monitoring of *P. aeruginosa* was conducted indirectly by Pyocyanin (PYO), a major metabolite used as key biomarker[3]. PYO is a redox active compound that exhibit two reversible electrochemical processes closed zero volts, providing a selective detection. The analytical method was performed using square wave voltammetry in 0.1 M phosphate buffer pH = 7.0 for clinical (simulated saliva) and water analyses. Our ePAD is simple, inexpensive and offer fast detection of bacterial infection caused by *P. aeruginosa* with suitable repeatability (~5%), and great sensitivity (nanomolar range). These analytical features allow indicate the potential use of this device to remote places or resource-limited settings.

**Acknowledgment**
CNPq, Capes e Fapesp.

**References**

1. A.Y. Peleg, D.C. Hooper, Hospital-Acquired Infections Due to Gram-Negative Bacteria, N. Engl. J. Med. 19 (2010) 1804–1813.
2. Law, J. W.-F., Ab Mutalib, N.-S., Chan, K.-G. & Lee, L.-H. Rapid methods for the detection of foodborne bacterial pathogens: principles, applications, advantages and limitations. *Front. Microbiol.* 5, 770 (2015).
3. S. Jayaseelan, D. Ramaswamy, S. Dharmaraj, Pyocyanin: Production, applications, challenges and new insights, World J. Microbiol. Biotechnol. 30 (2014) 1159–1168

**Área: ELE** **Inscrição: 00714**

# Flow injection analysis of furosemide in pharmaceutical formulations using electrochemically reduced graphene oxide modified electrode

**Vanessa N. de Ataide (PG),[1] Josué M. Gonçalves (PG),[1] Letícia F. Mendes (PG),[1] William R. de Araujo (PQ),[1] Koiti Araki (PQ),[1] Thiago R.L.C. da Paixão (PQ).[1]**

**vanneiva@usp.br; vanneiva@gmail.com**

[1]*Instituto de Química- USP*

Palavras Chave: *Electrochemically reduced graphene oxide, Modified electrode, Furosemide.*

## Highlights

We present a "green" approach to obtaining reduced graphene oxide (RGO) using electrochemical techniques. We characterize the RGO and the modified electrode by Raman spectroscopy, SEM, XPS, AFM, and EIS. The modified electrode was applied to electrochemical quantification of furosemide in pharmaceutical formulations.

## Resumo/Abstract

Graphene-based materials, such as reduced graphene oxide, have been widely used in electroanalysis due to their excellent electronic, thermal and mechanical properties[1]. The electrochemical reduction of graphene oxide (GO) was carried out on the surface of a glassy carbon electrode (GCE) using the cyclic voltammetry technique. Electrochemically reduced graphene oxide (ERGO) was characterized using Raman spectroscopy, SEM, XPS, AFM, and EIS technique. From the Raman spectra, the $I_D$ / $I_G$ ratio (disorder degree) was used and estimated as 0.98 and 1.15, respectively for GO and RGO, indicating that the electrochemical reduction promoted a structural disorganization that could be related to the reestablishment of the double carbon bonds present in the ERGO. The XPS data also confirm the reduction of GO to ERGO, where the ratio of the peak intensities of C1s and O1s can be used to determine the oxygen content in those graphene derivatives. For instance, the ratio was 2.35 for GO and 5.56 for ERGO material corroborating with the decrease of the concentration of oxygen groups in the carbon material. Rugosity was verified using square mean roughness (RMS) parameter obtained by AFM images and the values for unmodified GCE and ERGO surfaces were 14.20 and 19.96 nm, respectively. EIS measurements were also evaluated for bare and ERGO modified GCE, the values obtained for charge transfer resistance were 0.410 and 0.012 kΩ, respectively, indicating that the modified electrode provides a better electrochemical performance. The ERGO electrode was used as a sensor for furosemide (FUR) quantification, a diuretic drug for several treatments in human and veterinary medicine [2]. Flow injection analysis (FIA) with amperometric detection was used to quantify furosemide concentration in pharmaceutical formulations. Under the optimized conditions, the analytical parameters were 0.36 µmol $L^{-1}$ and 2.4% (n=13) to LOD and repeatability, respectively. Two pharmaceutical samples were analyzed and demonstrated a good correlation between the FUR concentrations found by our method with the labeled value.

**Acknowledgment**
CNPq, Capes e Fapesp.

**References**

[1]BASIRUN, W.J. et al. Solid-phase electrochemical reduction of graphene oxide films in alkaline solution. **Nanoscale Research Letters,** vol. 8, p. 397-405, 2013.
[2]RUIZ-ANGEL, M.J. et al. Analytical techniques for furosemide determination. **Separation & Purification Reviews**, vol. 35, p. 39-58, 2006.

**Área: ELE** **Inscrição: 00694**

# $H_2O_2$ detection in alkaline medium by Batch Injection Analysis using Prussian blue/carbon nanotubes/reduced graphene oxide film

**Samuel C. Silva (IC),[1] Rafael M. Cardoso (PG),[1] Eduardo M. Richter (PQ),[1] Rodrigo A. A. Munoz (PQ),[1] Edson Nossol (PQ).[1*]**

**samuelsilva73@gmail.com; enossol@ufu.br**

[1]*Institute of Chemistry, UFU*

Keywords: *Carbon structures, Prussian blue high stability, nanocomposite.*

## Highlights

Prussian blue/carbon/nanotube/reduced graphene oxide (PB/CNTs/rGO) nanocomposite presented high electrochemical stability.
The use of PB/CNTs/rGO film makes possible the detection of $H_2O_2$ at high values of pH.

## Abstract

The PB/CNTs/rGO film was synthetized by the interfacial method[1] from a 10 mmol $L^{-1}$ $K_3[Fe(CN)_6]$, 9 mmol $L^{-1}$ $FeSO_4$ and 17 mmol $L^{-1}$ sodium citrate aqueous solution and a dispersion containing 0.15 mg of MWCNT and 2.0 mg of rGO in toluene kept under magnetic stirring for 24 hours. The synthesis of Prussian blue is controlled by the addition of 100 µL nitric acid 14,5 mol $L^{-1}$. The interaction between the Prussian blue nanoparticles and the carbon structures enhanced electrochemical stability of the film, with no significant decay of current after application of 50 cycles. Figure 1-a shows cyclic voltammogram of PB/CNT/rGO evidencing the catalytic activity of the film to reduce $H_2O_2$. Figure 1-b presents the analytical curve obtained after successive injections of $H_2O_2$, highlighting that the nanocomposite film enabled the detection of $H_2O_2$ at high pH values, despite the limitations of using alkaline medium, as described in previous work in literature. [2] This method has great benefits such as repeated analysis using a small area of film. Additional studies are being done to analyze the effect of interferers and viability of others molecules that require high pH values to be detected.

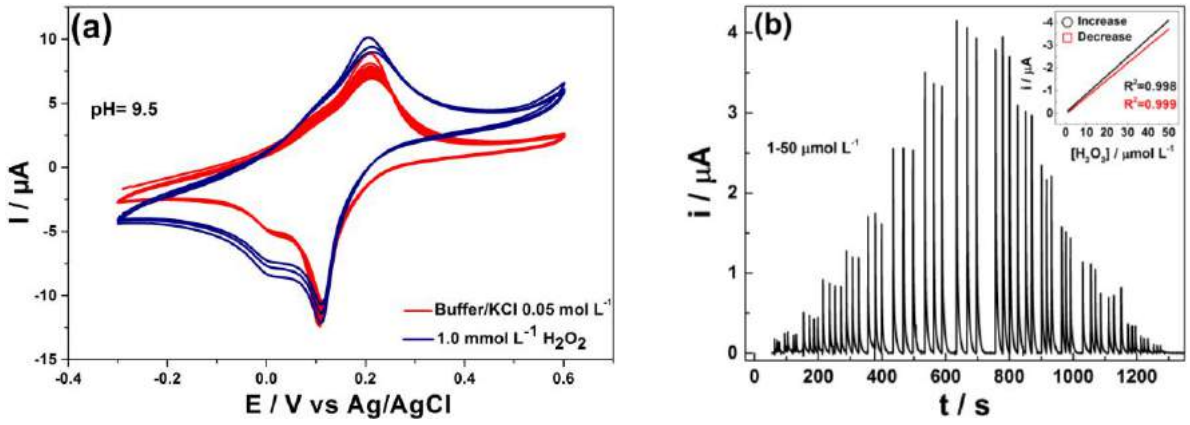


**Figure 1)** (a) Cyclic voltammogram of PB/rGO/CNTs in (—) absence and (—) presence of 1.0 mmol $L^{-1}$ $H_2O_2$. (b) Successive injections 1.0 to 50 µmol $L^{-1}$ of $H_2O_2$. Applied potential -0.1V. Injected volume: 75 µL. Inset: Obtained analytical curves with respective linear coefficients.

Acknowledgment
FAPEMIG, UFU, CNPq, CAPES, GMIT

References

1. *SALVATIERRA, R.V.; et al. Chem. Mater., v. 22, p. 5222, 2010.*
2. *RICCI, F. et al. . Biosensors and Bioelectronics, v. 18, n. 2, p. 165, 2003.*

**Área: ____ELE_____ Inscrição:___00615_____**

# Influence of the Electrode and Chaotropicity of the Electrolyte on the Oscillatory Behavior of the Electrocatalytic Oxidation of $SO_2$

**André H. B. Dourado[1] (PG),Renan L. Munhos[1] (PG), Hamilton Varela[2] (PQ), Susana I. Córdoba de Torresi[1]* (PQ), Matthias Arenz[3] (PQ).**

**rmunhos@iq.usp.br; storresi@iq.usp.br**

*1Instituto de Química, Departamento de Química Fundamental, USP; [2]Instituto de Química de São Carlos, USP; [3]Philosophisch-naturwissenschaftliche Fakultät, DepartementfürChemieundBiochemie, Universität Bern*

PalavrasChave:*$SO_2$ oxidation, $H_2$ generation, Oscillatory Behavior, Chatropicity dependence*

## Highlights

Oscillatory behavior dependent on the catalyst and electrolyte
Au in kosmotropic media does not oscillate
Au in chaotropic media oscillates

## Resumo/Abstract

The $SO_2$ is an atmospheric pollutant of high toxicity. But, it is possible mitigate the impact of this mortal gas: oxidizing the $SO_2$ to $H_2SO_4$, while the counter reaction is the production of $H_2$, $E_0$= 0.157 V. This process presents advantages over the traditional electrochemical method is water electrolysis, $E_0$= 1,23V. The use of $SO_2$ is too more environmental friendly than to produce $H_2$ by means of catalytic reform of organic compounds. To apply this system is necessary to utilize a metallic electrocatalyst. Cyclic voltametric studies show different profiles for Pt and Au and that current density for gold is one order of magnitude higher than platinum. Tests with different electrolytes showed that just for Au electrode in $ClO_4^-$, a chaotropic anion, current and potential oscillations were observed. Potential steps revealed that these oscillations were observed from 1.0V. When the electrolyte was $HSO_4^-$, a kosmotropic anion, it has presented only fluctuations in the current. The same behavior was observed for current steps, just for Au in chaotropic media and just when the electrode could reach potentials as positive as 1.00 V. Therefore, it can classify oscillatory behavior as a HNDR (hidden negative differential resistor).This implies the presence of at least, two catalytic poisons that block surface of electrode. The cleaning of the surface occurs with de oxygen evolution reaction. The mechanism of electroxidation of the sulfur dioxide is dependent of the material of the electrode and the chaotropicity of the anion in solution.

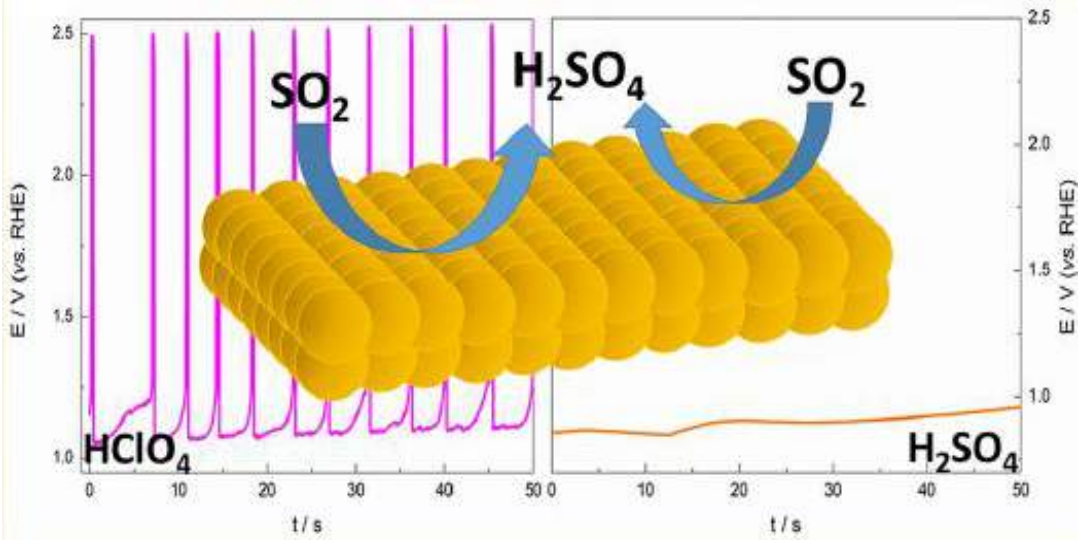

**Area:** ELE **Inscription:** 00550

# Effect of iron concentration on degradation of Orange II azo dye by electro-Fenton and UVC Photoelectro-Fenton

**Edson C. da Paz (PG),[1,2] Victor S. Pinheiro (PG),[1] Luci R. Aveiro (PG),[1] Mauro C. Santos (PQ).[1*]**

**edson.paz@ufabc.edu.br; mauro.santos@ufabc.edu.br**

*[1]Centro de Ciências Naturais e Humanas, UFABC; [2]Campus Açailândia, IFMA*

Keywords: *Orange II, Azo dye, $WO_{2.72}$/Vulcan XC72, Decolorization, Mineralization.*

## Highlights

The iron concentration strongly influenced the decolorization rather than mineralization
There is no significant difference in decolorization by PEF and EF.
Mineralization by PEF was superior to EF.

## Abstract

The degradation of 350 mL of 0.260 mM Orange II (OII) azo dye were studied by electro-Fenton (EF) and UVC photoelectro-Fenton (PEF). Comparative experiments were carried out by electrolysis of OII solution in 0.1 M $K_2SO_4$ under stiring with 0.25, 0.50 or 1.0 mM $Fe^{2+}$ at pH 3.0 and at 20 °C using a undivided reactor equipped with $WO_{2.72}$/Vulcan XC72 gas diffusion electrode, Pt sheet and Ag/AgCl as cathode, anode and reference electrodes, respectively [1][2]. The 100% dye decolorization by EF and PEF occurred after about 30, 40 and 105 minutes for electrolysis with 1.0, 0.5 and 0.25 mM $Fe^{2+}$, respectively (Fig. 1a). In addition, the EF and PEF with same $Fe^{2+}$ concentration showed similar color removal. This is due to the action of hydroxyl radicals ($^{\bullet}OH$) generated from water oxidation at the Pt anode surface and in the bulk from the Fenton's reaction between $Fe^{2+}$ and $H_2O_2$ produced at the cathode [2]. This last reaction is responsible for the faster decolorization with the highest $Fe^{2+}$ concentration. The PEF with 1.0 and 0.5 mM $Fe^{2+}$ were more efficient in OII mineralization showing 73 and 71% mineralization after 3 h of electrolysis, respectively (Fig. 1b). EF with 0.25 mM $Fe^{2+}$ had the worst performance mineralizing only 35% OII after 3 h. Different from decolorization, PEF mineralization was better than EF. This can be explained by the additional photolysis reactions of $Fe(OH)^{2+}$ species and Fe(III)-carboxylate complexes, which can not occur in EF [2].

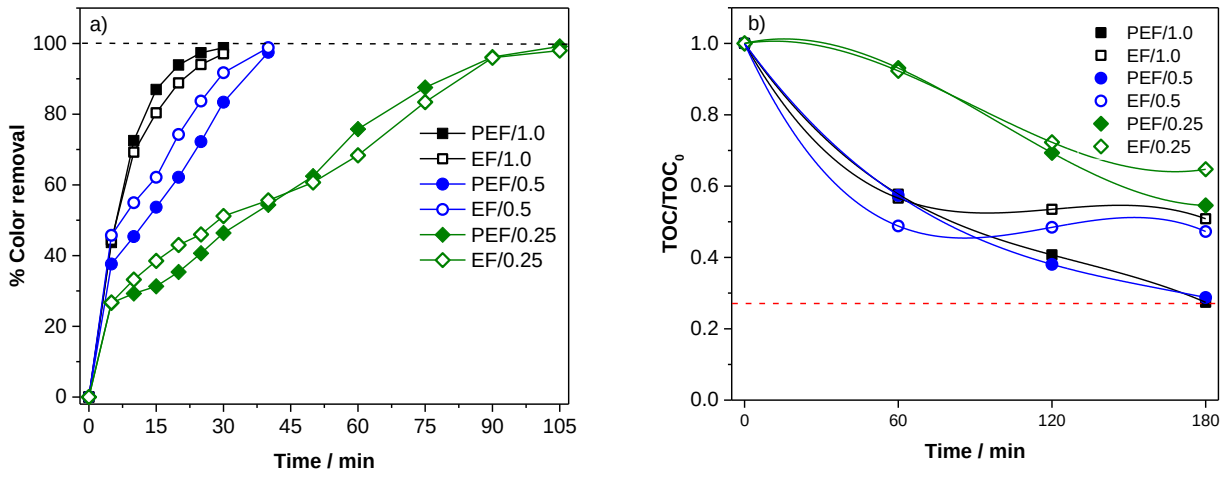


**Fig. 1.** Effect of iron concentration on (a) decolorization efficiency and (b) normalized TOC removal with electrolysis time for the photoelectro-Fenton (PEF) and electro-Fenton (EF) for the degradation of 350 mL of 0.260 mM Orange II solution.

**Acknowledgments:**
UFABC, CEM-UFABC, FAPESP (2017/21846-6), Laboratório de Engenharia e Controle Ambiental (LENCA)-UNIFESP and PROQUALIS – IFMA.

**References:**

[1] M. H. M. T. Assumpção et al., Applied Catalysis B: Environmental 142-143 (2013) 479-486.
[2] S. Garcia-Segura et al., Applied Catalysis B: Environmental 181 (2016) 681–691.

**Área: ELE** **Inscrição: 00513**

# Silk fibroin based impedance biosensor using interdigitated array microelectrode

**Mayra F. Costa (PG),[1] Thiago Cipriano (PQ),[1] Jose Eduardo U. Rojas (PG),[1] Luis A. Peroni (PQ),[2] Marcelo A. Christoffolete (PQ),[1] Adriano R. V. Benvenho (PQ),[1] Suchismita Guha (PQ),[3] Wendel A. Alves (PQ)[1]***

mayra.costa@ufabc.edu.br; wendel.alves@ufabc.edu.br

*[1]Center for Natural and Human Sciences Federal University of ABC 09210-580, Santo André, SP, Brazil; [2]Rheabiotech Company, 13.080-650, Campinas, SP, Brazil; [3]Department of Physics and Astronomy, University of Missouri, Columbia, MO 65211, USA*

Keywords: *Silk fibroin, biosensor, antigen-antibody interaction, impedance*

## Highlights

We demonstrate a novel detection platform based on silk fibroin films for antigen-antibody interaction using impedance spectroscopy. This work opens up a viable path towards low-cost fibroin-based immunosensors.

## Abstract

Silk fibroin, a protein polymer, has emerged as a potential biomaterial for sensing applications due to its biocompatibility, mechanical strength, and ease of chemical modification. By a suitable degumming process, silk fibroin was functionalized with a synthetic epitope specific to β-actin antigen**,** [$NH_2$]-DNGSGMCKAGFAGDDAPRA-[OH]**,** and applied as thin films onto interdigitated array microelectrode (Fig. 1). Using impedance spectroscopy, the antigen-antibody interaction was monitored as a function of the antibody concentration onto fibroin-antigen films. The biosensors were sensitive down to a few ng/ml of the antibody concentration. The detection mechanism takes advantage of the fibroin structure, a natural dielectric, providing insulation to the individual gold contacts. The antigen-antibody interaction results in a change of the relaxation frequency in the admittance spectrum with increasing antibody concentration. For a non-specific antibody there is no change in impedance with antibody concentration. Nyquist plots for the real and imaginary part of the impedance are modeled by an equivalent circuit comprising a resistor and constant phase elements (CPE). One of the CPE elements that describe the electrode-electrolyte interface capacitance becomes more resistive upon antibody-antigen binding. This same model was used with PSA *L. infantum* antigen*.* The epitope used was [$NH_2$]-CTSSAPVARAAGTGDFTEEQRTNTL-[OH], and the antigen-antibody interaction was also observed in the admittance spectrum.

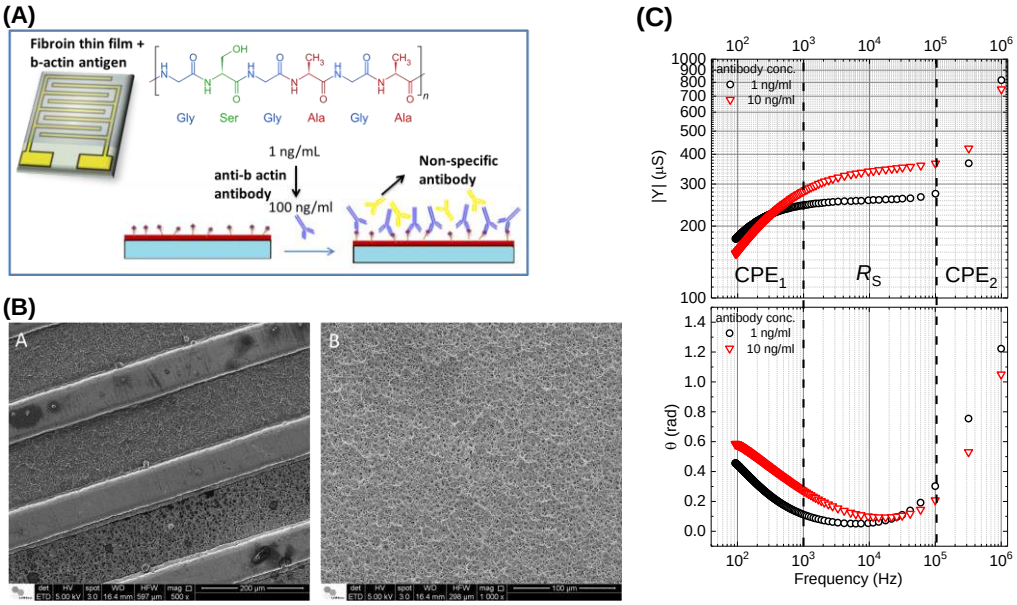


**Fig. 1-** Schematic of the fibroin-based impedance sensor for antigen-antibody interaction; (B) Images obtained from fibroin film deposited on the interdigitated electrode; (C) Admittance spectra for two different antibody concentrations showing the three frequency ranges where the different elements of the equivalent circuit dominate.

**Área: ELE**
*(Inserir a sigla da seção científica para qual o resumo será submetido. Ex: ORG, BEA, CAT)*

**Inscrição: 00437**
*(Inserir o número de inscrição do autor que fez a submissão)*

# Modeling of Polyvinylidene Fluoride (PVdF) by Molecular Dynamics Simulation

**Rodrigo Cardoso da Silva (IC),[1*], Flávia C. A. Silva (PQ),[3] Luciano T. Costa (PQ)[2]**

**rc_silva@id.uff.br; ltcosta@id.uff.br**

*[1]Departamento de Físico Química, Campus Valonguinho, Instituto de Química, UFF*
*Polímero, PVdF, Bateria, Lítio, Líquido, Iônico*

## Highlights

MD simulation studies of SPE provides information about ionic motion and the influence of the polymer structure on the transport processes, and is frequently used in studies of polymer electrolytes

## Resumo/Abstract.

Lithium rechargeable batteries are an alternative to the available options for sustainable and effective energy generation due to the high tension and numbers of charge and discharge cycles[1,2]. While searching for more efficient batteries, many studies have modified the polymeric matrix, in order to build safer electrochemical devices[3]. In this context, PVdF and PVdF-HFP copolymers stands out as good candidates for working as polymer matrix in solid polymer electrolyte (SPE)[4].

In this study, it was used GROMACS[5] package and Byutner et al.[6] force field for the computational simulations of pure PVdF. The same protocol was followed to validate the polymer model. *NPT* simulations (constant number of particles *N*, pressure *P* and temperature *T*), in 5 different temperatures (333, 373, 413, 453, 493K), were accomplished, with 5 ps and 1 ps as coupling time for pressure and temperature, respectively. Figure 1 presents density values in 5 different temperatures referenced above, comparing with the result obtained by Byutner and the experimental values presented by Zoller and Walsh[7]. With the validated model, the next steps include the characterization of the polymers' structure and then addition of ionic liquid for applications in lithium batteries prototype. We have calculated thermodynamics, structural and dynamics properties and will be able to give a better comprehension of the ion mobility, supporting possible future modifications and the way to improve polymer electrolyte efficiency based on PVdF.

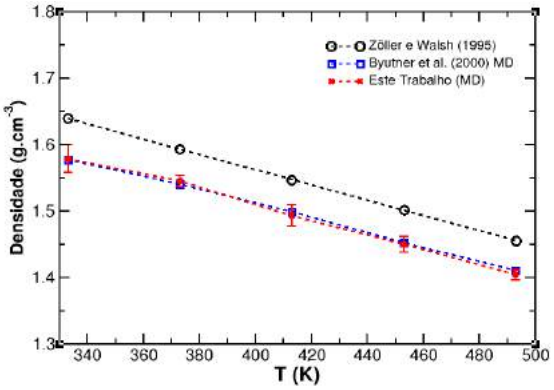


Figure 1. Density x Temperature for Byutner et al., this study and experimental values.

1. Girishkumar, G. *Chem. Phys.* **2010**, 2193–2203
2. Kuboki, T. *Journal of Power Sources,* **2005,** 766-769
3. Shin. J, *Journal of The Electrochemical Society,* **2000,** 978-983
4. Lewandowski, A. *Journal of Power Sources,* **2009,** 601-609
5. PRONK, S. et al. GROMACS 4.5: A high-throughput and highly parallel open source molecular simulation toolkit. Bioinformatics, v. 29, n. 7, p. 845–854, 2013.
6. Byutner, O.; Smith, G. Macr*omolecules.* **2000**, 33, 4264–4270.
7. Zoller, P.; Walsh, D. Standard Pressure–Volume–Temperature Data for Polymers, Technomic: Lancaster, **1995**

**Área: ELE** **Inscrição: 00399**

# Electrodeposition of Prussian Blue/Carbon Nanotubes Composites at a Liquid-Liquid Interface

**Samantha Husmann (PG),[1]* Samuel G Booth (PG),[2] Robert A. W. Dryfe (PQ),[2] Aldo J. G. Zarbin (PQ)[1]**

**samanthahus@gmail.com**

*[1]Grupo de Química de Materiais (GQM), Chemistry Department, UFPR (Curitiba, PR - Brasil); [2]Manchester Electrochemistry Research Group, School of Chemistry, University of Manchester (Manchester – UK)*

Palavras Chave: Liquid-liquid Interface, Prussian blue, Carbon nanotubes, Raman, ITIES

## Highlights

Prussian blue electrodeposition over a carbon nanotube film assembled at a liquid-liquid interface was monitored by in situ Raman spectroscopy.

## Resumo/Abstract

The interface between two immiscible liquids has long being used for the study of interfacial ion and electron transfer reactions or for the synthesis and assembly of materials. In this work, Prussian blue (PB - $Fe_4[Fe(CN)_6]_3$) was electrodeposited over a free-standing carbon nanotube (CNT) film assembled at a liquid-liquid (L/L) interface formed between water and 1,2-dichlorobenzene (Figure 1). With a four-electrode cell, the interface polarization was performed through both cyclic voltammetry and chronoamperometry. PB was formed by heterogeneous reaction using species in aqueous phase and iron from CNTs cavities, generating a stable CNT/PB composite. Aqueous phase of $K_3[Fe(CN)_6]$ showed to be unstable under applied conditions, decomposing during PB synthesis. However, $K_4[Fe(CN)_6]$ presented a more stable behavior thus suitable for composite preparation. The modification of the interface through electrodeposition was monitored by in situ Raman spectroelectrochemsitry. PB formation was confirmed by a shift and an increase of CN stretching modes due to iron coordination to nitrogen and arise of resonant Raman effect, as well as changes in CNT bands due modification of their walls by PB deposition and a p-doping due components interaction. The obtained CNT/PB composite formed at the biphasic system was stable and electrochemically active at the L/L interface, making it suitable for applications not only after transfer to a desired substrate but also in situ at the L/L interface itself.

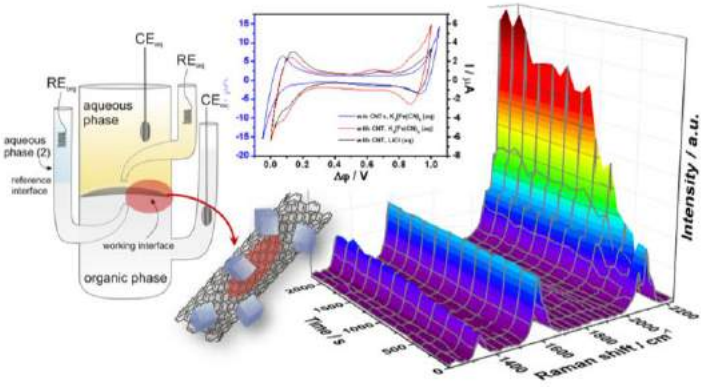


Figure 1: CNT/PB composite was prepared by deposition of PB over CNT thin film through L/L interface polarization and followed by in situ Raman spectroelectrochemistry.

**Área: ELE** **Inscrição: 00028**

# Sensor eletroquímico à base de polieletrólito para a determinação de prometazina

**Raíssa C. de Oliveira. (IC), Camila P. Sousa. (PQ), Pedro de Lima-Neto (PQ), Adriana N. Correia (PQ).**

**raissacostaufc@yahoo.com.br**

*Grupo de Eletroquímica e Corrosão, DQAFQ-UFC, Fortaleza-CE*

Palavras Chave: Eletroanalítica, Sensor, Prometazina, Polieletrólito, Polietilenoimina.

## Highlights

Electrochemical sensor based on polyelectrolyte for the promethazine determination
Promethazine can cause adverse effects in humans, such as endocrinal and reproductive alterations.
Carbon nanotubes and SWV were used to develop a methodology with detection limit of 0,23 µmol $L^{-1}$.

## Resumo

Prometazina (PMZ) que pertence ao grupo das fenotiazinas, é um fármaco utilizado por sua ação anti-histamínica, sedativa, antiemética e analgésica. Contudo, PMZ pode causar efeitos adversos, como alterações endócrinas, cardíacas e reprodutivas. Nesta perspectiva, torna-se premente o desenvolvimento de sensores com elevada sensibilidade. Assim, desenvolveu-se metodologia para detecção e quantificação de PMZ baseada na modificação de carbono vítreo (CV) por nanotubos de carbono com paredes múltiplas funcionalizados em mistura ácida por quatro horas (NTCPMF4h) e por polietilenoimina (PEI). Solução estoque de PMZ 1,0 × $10^{-3}$ mol $L^{-1}$ foi preparada por dissolução de massa apropriada em água ultrapura. Os voltamogramas de onda quadrada para CV/NTCPMF4h-PEI foram registrados para avaliar a resposta eletroquímica de PMZ 2,91×$10^{-5}$ mol $L^{-1}$ e os resultados apresentaram um pico de oxidação irreversível em 0,75 V (vs Ag/AgCl/$Cl^-_{KCl\ sat}$) em tampão Sörensen pH 2, $f$ = 90 $s^{-1}$, $a$ = 40 mV e $\Delta E_s$ = 2 mV (condições otimizadas). Na sequência, curvas analíticas foram construídas em triplicata e na Tabela 1 tem-se algumas figuras de mérito calculadas a partir desta metodologia. Estudos de recuperação foram realizados usando Fenergan® 25 mg, formulação farmacêutica disponível comercialmente na forma de comprimidos. Os valores calculados estão apresentados na Tabela 2.

**Tabela 1**. Figuras de mérito calculadas a partir da metodologia desenvolvida.

| Parâmetros | Valores |
|---|---|
| Região de linearidade / mol $L^{-1}$ | 8,91×$10^{-7}$ e 5,03×$10^{-6}$ |
| LD/mol $L^{-1}$ | 2,31 × $10^{-7}$ |
| LQ/mol $L^{-1}$ | 7,71 × $10^{-7}$ |
| Repetibilidade | 3,32 (n = 7) |
| Reprodutibilidade | 2,78 (n = 5) |

LD = limite de detecção, LQ = limite de quantificação

**Tabela 2.** Valores de recuperação e de %RSD

| Parâmetros | Fenergan® |
|---|---|
| $[PMZ]_{adicionada}$ (mol $L^{-1}$) | 8,91 × $10^{-7}$ |
| $[PMZ]_{encontrada}$ (mol $L^{-1}$) | 9,75 × $10^{-7}$ |
| Intervalo de confiança (%) | ± 5,05 × $10^{-8}$ |
| Recuperação (%) | 109,54 |
| RSD (%) | 4,57 |

RSD = desvio padrão relativo (do inglês *relative standard deviation*)

De acordo com os resultados obtidos, conclui-se que esta metodologia pode ser empregada na determinação de PMZ, devido à sua sensibilidade e seletividade.

**Área: ELE** **Inscrição: 01148**

# Use of $TiO_2$ nanotubes electrodes decorated with silver nanoparticle/nanocubes for enhanced $CO_2$ photoelectroreduction

**João Angelo de Lima Perini (PQ),[1*] Lívia M. Christovam (PG),[1] Lilian D. M. Torquato (PQ),[1] Sidney J. L. Ribeiro (PQ),[1] Maria Valnice Boldrin Zanoni (PQ).[1]**

**joaoperini@gmail.com**

[1]*Institute of Chemistry, São Paulo State University (UNESP), Araraquara, São Paulo, Brazil*

Palavras Chave: *$CO_2$ reduction, photoelectrocatalysis, methanol, nanostructure.*

## Highlights

Silver nanostruture was easier deposited over $TiO_2$ nanotubes and improves $CO_2$ reduction.
Good performance of Ti/$TiO_2$NT-Ag electrodes for methanol generation.

## Resumo/Abstract

$CO_2$ conversion to higher value-added compounds is a topic of great importance nowadays due to problems generated by the increase of its emission in the atmosphere. The present work aims to investigate the use of silver nanostructure as modifier of Ti/$TiO_2$ nanotubes (NT) electrode in the photoelectrocatalytic $CO_2$ reduction. Silver was deposited on the surface of Ti/$TiO_2$NT by different methods. (I) Ag nanoparticles (NP) was electrodeposited over Ti/$TiO_2$NT surface applying −0.70 V *vs* Ag|AgCl for 15 s in an electrochemical cell containing $AgNO_3$ (0.01 M) in $NaNO_3$ (0.1 M). (II) deposition of Ag nanocubes (NC) on Ti/$TiO_2$NT was carried out using dopamine (13 mM) as ligand in a tris-buffer (10 mM, pH 8.6). Ti/$TiO_2$NT electrode was maintained in a dopamine and silver NC solution for 8 h, respectively. The reduction of electrolyte solutions ($Na_2SO_4$, 0.1 M) saturated with $CO_2$ was drive in a photoelectrocatalytic reactor, using Ti/$TiO_2$NT-Ag as photocathode, irradiated with UV/Vis light for 1 h at −0.6 V potential. An electrode of DSA was used as a counter electrode and an Ag|AgCl as reference electrode. Generation of methanol was monitored by GC-FID after extraction using a solid-phase microextraction fiber. Methanol formation under Ti/$TiO_2$NT electrode was very small, achieving only 0.045 mM during one hour of reaction. On the other hand, with the deposition of silver NC or NP on the surface of Ti/$TiO_2$NT, the formation of methanol was enhanced 8.1 and 7.1 times, respectively **(Fig. 1)**. So, the modification of $TiO_2$NT with silver nanostructures is efficient for alcohol generation, once Ag acts as cocatalysts of $TiO_2$ semiconductor.

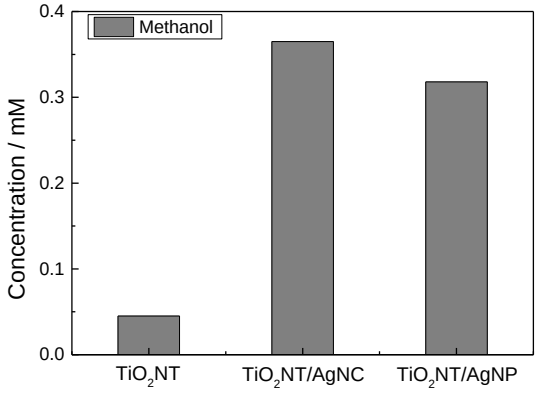


**Fig. 1.** Evaluation of products formed by photoelectrocatalytic $CO_2$ reduction in 0.1 M $Na_2SO_4$ and applying −0.6 V, using Ti/$TiO_2$NT, Ti/$TiO_2$NT-AgNC (silver nanocubes) and Ti/$TiO_2$NT-AgNP (silver nanoparticles).

**Acknowledgements**
The authors are grateful to FAPESP (#2014/50945-1 and #2015/118109-4) and INCT-DATREN (#465571/2014-0) for support of this work. João A. L. Perini received scholarship from FAPESP (#2016/18057-7) and Lilian D. M. Torquato received scholarship from CNPq (#150493/2017-7).

**Área: ELE** **Inscrição: 01088**

# Electrochemical study and quantification of anesthetic xylazine in urine and pharmaceutical formulations

**William R. de Araujo (PQ),*[1] Letícia F. Mendes (PG),[1] Ângela R.S. Silva (IC),[2] Raphael P. Bacil (PG),[1] Thiago R.L.C. Paixão(PQ)[1], Lúcio Angnes (PQ)[1]**

**william_reis_araujo@hotmail.com; *will.wra@usp.br**

*[1]Instituto de Química da USP, Departamento de Química Fundamental, IQUSP; [2] Centro de Matemática, Computação e Cognição, Universidade Federal do ABC- UFABC*

Keywords: *Electroanalysis, Electrochemical mechanism, Xylazine, Forensic application, Pharmaceutical formulations.*

## Highlights

Electrochemical detection of xylazine; Electro-oxidation study of xylazine; Potential use of paper-based analytical device for on-site analysis; Electroanalysis of drug-facilitated sexual assault.

## Abstract

Xylazine is marketed as a veterinary drug and used to sedative and analgesic purposes; being not approved to human use due several side effects [1]. Over the recent years, xylazine has emerged as a drug of abuse and associated as drug-facilitated sexual assaults [1]. Herein, we describe, for the first time, the electrochemical study and quantification method for xylazine using glassy carbon electrode. Xylazine exhibits at least two well-defined and pH-dependent oxidation processes and one reduction peak in the range of pH from 2.0 to 12.0. The simple and accurate quantification method was performed using Differential Pulse Voltammetry and under the optimized experimental conditions, a linear analytical curve was obtained for xylazine concentrations ranging from 0.5 to 256 μmol $L^{-1}$, with an estimated detection limit of 200 nmol $L^{-1}$. The proposed method was applied to determination of xylazine in pharmaceutical formulation, and for forensic scenario, a standard addition protocol in urine samples exhibits excellent recovery values in the range of 93 – 103%, demonstrating the potentiality for clinical analysis of xylazine intoxication. We also show the potential use of portable analytical device fabricated on paper platform coupled with graphite leads as an inexpensive electrode material for on-site analysis.

**Acknowledgment**

CNPq, CAPES and FAPESP.

**References:**

1. Hoffmann U., Meister C.M., Golle K., Zschiesche M.; Severe intoxication with the veterinary tranquilizer xylazine in humans. J. Anal. Toxicol., 25, (2001), 245–249.

2. Meyer, G.M.J. & Maurer, H.H.; Qualitative metabolism assessment and toxicological detection of xylazine, a veterinary tranquilizer and drug of abuse, in rat and human urine using GC–MS, LC–$MS^n$, and LC–HR-$MS^n$; Anal. Bioanal. Chem., 405, (2013), 9779–9789.

**Área: ELE** **Inscrição: 01428**

# Determination of fructose in fruit juices using an electrode modified with reduced graphene oxide and molecularly imprinted polymer poly(phenylboronic acid)

**Luiz Felipe Pompeu Prado Moreira (IC),[1] Edervaldo Buffon (PG),[1] Acelino Cardoso de Sá (PQ),[1] Nelson Ramos Stradiotto (PQ)[1-2]***

**nrstradi@gmail.com**

*[1]Department of Analytical Chemistry, Institute of Chemistry, São Paulo State University (UNESP), Araraquara, SP, Brazil; [2]School of Industrial Engineering Metallurgical Volta Redonda, Fluminense Federal University (UFF), Volta Redonda, RJ, Brasil.*

Keywords: *Electrochemical Sensor, Electrode Modified, Reduced Graphene Oxide, Molecularly Imprinted Polymer Fructose, Fruit Juices.*

## Highlights

Fruit juices are consumed in large scale by the world population; Fructose is the main sugar found in fruits; Control of the fructose concentration in fruit juices is of great interest; MIP sensor for determination of fructose.

## Abstract

Fruit juices are basically constituted by water, sugars, organic acids, lipids, proteins and minerals. Fructose is the sugar found in bigger quantity in these juices and is related to several diseases, such as diabetes, obesity and cardiovascular problems[1], being of fundamental importance the control of its concentration during the production process of these beverages. Thus, are necessary the development of simple, sensitive, selective and low cost analytical methodologies to determine such sugar in fruit juices. In this context, electrodes modified with reduced graphene oxide (RGO) and molecularly imprinted polymer (MIP) using phenylboronic acid (PBA) as functional monomer (FM) are a viable option for this purpose, since RGO and MIP provide the modified electrode a increase of sensitivity and selectivity respectively, when compared to unmodified electrodes. In addition, PBA has a high affinity for making covalent bonds between hydroxyl groups with sugars in general[2], being used for the development of several sensors for this class of compounds. Thus, the objective of this work was to develop a sensor based on a glassy carbon electrode (GCE) modified with RGO and MIP (using PBA as FM) for determination of fructose in fruit juices. Modification of the GCE with RGO was performed by applying a constant potential of 1.5 V for 500 seconds using an aqueous suspension of graphene oxide 0.50 mg $mL^{-1}$ in $Na_2SO_4$ 0.10 mol $L^{-1}$. For MIP electrosynthesis, the GCE-RGO electrode was immersed in a solution containing PBA $1.0x10^{-3}$ mol $L^{-1}$ and fructose $1.0x10^{-3}$ mol $L^{-1}$ (pH 8.0) and 35 consecutive voltammetric cycles were applied in a potential range of -0.2 to 1.2 V at a scan rate of 50 mV $s^{-1}$. For removal of the template, the electrode was inserted in an acetonitrile-acetic acid solution 5:1 (v:v) for 60 seconds under low stirring rates. For the rebinding studies, the sensor was inserted in different fructose solutions for 5 minutes under low stirring rates. GCE-RGO-MIP sensor was characterized by techniques: cyclic voltammetry, electrochemical impedance spectroscopy, scanning electron microscopy, and atomic force microscopy. Parameters that influence the performance of the GCE-RGO-MIP sensor were optimized and the responses obtained were measured by differential pulse voltammetry using the redox pair $[Fe(CN)_6]^{-3/-4}$. The developed sensor presented two analytical linear ranges, $1.0x10^{-14}$ to $1.0x10^{-13}$ mol $L^{-1}$ and $1.0x10^{-13}$ to $6.0x10^{-13}$ mol $L^{-1}$. The figures of merit, as limit of detection and limit of quantification were obtained using the first linear range as being $9.5x10^{-14}$ mol $L^{-1}$ and $3.2x10^{-14}$ mol $L^{-1}$ respectively. In addition, this sensor showed considerable inter-day and intra-day repeatability, with RSD values ≤ 5.0%. In the presence of potentially interfering molecules that are present in the fruit juices, the GCE-RGO-MIP sensor showed up selective for recognition of the fructose molecule. The method developed was successfully applied in the determination of fructose in grape, orange and apple juices. Average recoveries varied from 95% to 105% with RSDs between 2.0% and 4.5%, indicating that the developed method had good accuracy for the determination of fructose.

## References

[1] JOHNSON, R. J. et al. *The American journal of clinical nutrition*, v. 86, p. 899–906, 2007.
[2] AYTAÇ, S. et al. *Sensors and Actuators B: Chemical*, v. 160, p. 405–411, 2011.

## Acknowledgment

CAPES (Process: AUX/PE/PROEX/0486/2017), CNPq (Process: 162425/2015-5) and FAPESP (Process: 2014/23846-5 and 2017/23529-6).

**Área: ELE** **Inscrição: 01347**

# Development of electroanalytical sensors based on electropolymeric films and molecular imprinting technology

**Wanderson S. R. Teixeira (PG)*,[1] Martin K. L. da Silva (PG),[2] Jonas Gruber (PQ),[1] Ivana Cesarino (PQ),[2] Jane Megid (PQ) [3].**

**wandersonteixeira01@gmail.com**

*[1]Departamento de Química Fundamental, IQ-USP; [2]Departamento de Bioprocessos, FCA- UNESP Botucatu; [3]Departamente de Higiene Veterinária e Saúde Pública, FMVZ- UNESP Botucatu*

Key words: *Molecular imprinted polymer, molecular recognition, electropolymerization, electroanalytical sensor*

## Highlights

Nowadays, specific and tailor made solutions have been created and widely applied in many fields. In Chemistry, more specifically in Analytical Chemistry, it has not been different. The development of sensors/biosensors of ease preparation/assembly, low cost and specific to a given analyte/application (with analytical requirements, such as reliability, reproducibility, specificity, and fast answer) is desirable.
This work describes a general methodology to obtain electropolymerized thin films with imprinted molecular properties, which can be used as sensing material for development of specific and selective sensors.

## Abstract

Molecular imprinted polymers can be obtained by different methodologies, electropolymerization may be an efficient one due to its simple and fast synthesis and easy coupling with electrochemical techniques. Figure 1 shows the cyclic voltammograms (CVs) corresponding to the synthesis of molecular imprinted polymer (MIP) based on o-phenylenediamine (10.0 mmol/L) and pyrrole (5.0 mmol/L) monomers and ascorbic acid (10.0 mmol/L) as model template molecule in acetate buffer solution, pH 5. Non-imprinted polymer (NIP) was obtained in the same way, however, the template was not used. For both cases, the high oxidation currents suggest the formation of the polymeric film on the Glass Carbon (GC) electrode. Figure 2 shows the CVs corresponding to the electrochemical response of GC, GC-NIP and GC-MIP electrodes before and after extraction of the template, and after incubation in a template solution, using $K_3[Fe(CN)_6]$ as electrochemical probe. Template extraction is performed by CV in NaOH 0.1 mol/L. Small currents are observed for GC-NIP and GC-MIP before template extraction because the film hinders the diffusion of the probe from solution to the electroactive surface of the electrode. For GC-MIP after template extraction, the current increases remarkably due to the channels left in polymeric matrix by template molecules. After incubation in a solution containing ascorbic acid (5 mmol/L and 10 mmol/L), the template molecule rebinds to the polymer, which is evidenced by the decreasing currents.

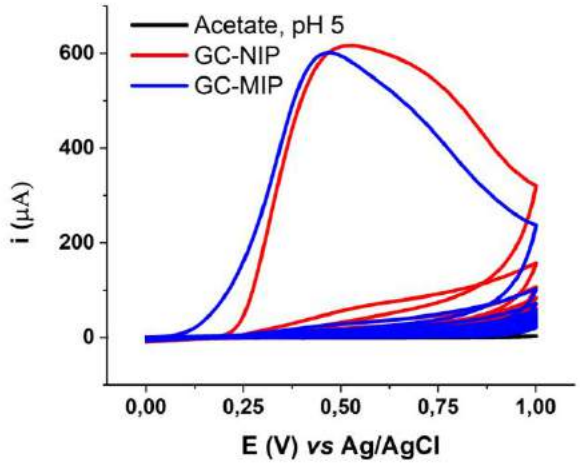


Figure 1: Cyclic Voltammetry- Synthesis of NIP and MIP in acetate solution 0,2 mol/L, pH 5.0 using o-phenylenediamine 10 mmol/L and Pyrrole 5 mmol/L, ascorbic acid 10 mmol/L as template.

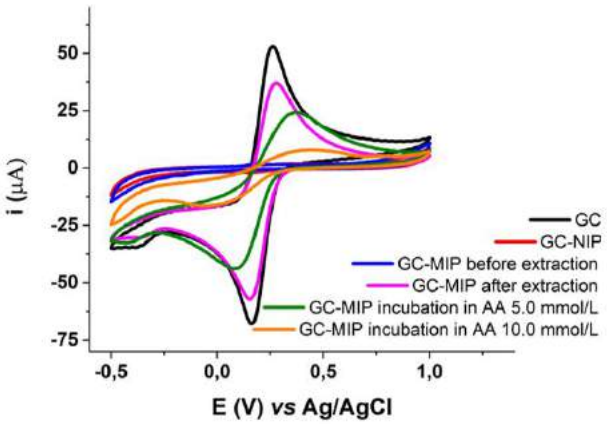


Figure 2: Cyclic Voltammetry- GC, GC-NIP, GC-MIP before extraction, GC-MIP after extraction, GC-MIP after incubation in ascorbic acid solution 5.0 and 10 mmol/L. Probe solution: $K_3[Fe(CN)_6]$ 5 mmol/L and KCl 0,1 mol/L.

**Área: ELE**
*(Inserir a sigla da seção científica para qual o resumo será submetido. Ex: ORG, BEA, CAT)*

**Inscrição: 01324**
*(Inserir o número de inscrição do autor que fez a submissão)*

# Evaluation of sulfonamide-based anilines as a corrosion inhibitor for 1020 carbon steel

**Alexandre de Araújo Godoy[1] (TM), Dafne Júlia Ferreira Lougon[1] (TM), Sara Fagundes Teixeira[1] (TM), Vinicius Latgé Meira[1] (TM), Vitor Sueth Santiago[1] (FM), Flávia Carvalho de Souza*[,1] (FM)**

**vnciuslmeira@gmail.com; flavia.souza@ifrj.edu.br**

[1]*Instituto Federal de Educação Ciência e Tecnologia do Rio de Janeiro – Campus São Gonçalo.*

Palavras Chave: *anilines, corrosion inhibitors, sulfonamides.*

## Highlights

This work shows the synthesis of three anilines containing the sulfonamide. These compounds were used in both weight loss and electrochemical tests, showing that 4-(piperidin-1-ylsulfonyl) aniline was considerate the best corrosion inhibitor.

## Abstract

Corrosion inhibitors are substances that, when prevent the development of corrosion reactions. The use of corrosion inhibitors aims to maintain the integrity of the metal components under severe corrosion conditions, which would lead to the failure or reduction of the operational cycle of equipment. Several synthetic and semisynthetic substances, as well as natural products, are being studied as corrosion inhibitors of metallic materials. The synthesized anilines [Fig. 1] are shown as promising corrosion inhibitors, both by the performance in the electrochemical tests and by the ease of synthesis on a laboratory scale.

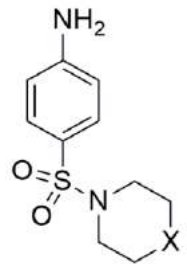


Fig. 1 - Molecular framework of the synthesized anilines. X= $CH_2$, *N*-$CH_3$ or *N*-Ph.

The synthesis of the anilines shown in Fig. 1 was performed with chlorosulfonation of commercial acetanilide (78% yield) which was subsequently reacted with excess of functionalized piperidine (yields of 60-80%). These solids were deprotected to provide the final products through an alkaline hydrolysis and the final product was isolated and characterized.

For the inhibition efficiency study of the synthesized anilines, gravimetric tests were performed over carbon steel 1020 pieces in a solution of 1.0 mol $L^{-1}$ HCl in the absence and presence of 250 mg $L^{-1}$ of inhibitor, with time 24 hours immersion. These preliminary results are shown in Table 1.

Table 1 - Inhibition efficiency by gravimetric test.

| Inhibitor | Weight loss (g/cm²) | I.E. (%) | Error (%) | C. R. (mm/year) |
|---|---|---|---|---|
| Blank | 0.09187 | - | - | 42.0 |
| An-$CH_2$ | 0.00205 | 98 | 1 | 0.9 |
| An-*N*$CH_3$ | 0.00391 | 96 | 1 | 1.8 |
| An-*N*Ph | 0.01919 | 79 | 4 | 8.8 |

The electrochemical assays shown in Table 2 and Fig 2, showed good efficiency (greater than 80%).
All three inhibitors showed a shift of OCP to less negative potentials, characterizing an anodic inhibitor behavior. The An-$CH_2$ inhibitor showed a higher inhibition efficiency, and a synthesis with high yield.

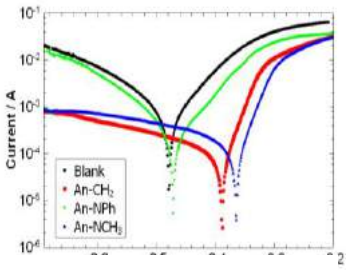


Fig. 2- Polarization curves

Table 2 - Inhibition efficiency by electrochemical tests.

| Inhibitor | $\beta_a$ (mv/dec) | $\beta_c$ (mv/dec) | OCP (mV) | $j_{corr}$ (mA) | I.E. (%) |
|---|---|---|---|---|---|
| Control | 0.09187 | - | - | 42.0 | - |
| An-$CH_2$ | 0.00205 | 98% | 1% | 0.9 | 89 |
| An-*N*$CH_3$ | 0.00391 | 96% | 1% | 1.8 | 84 |
| An-*N*Ph | 0.01919 | 79% | 4% | 8.8 | 81 |

## References

1. RAMACHANDRAN, Sunder *et al*. Langmuir, v. 12, n. 26, July 1996. p. 6419-6428.
2. BARBOSA, Maria Leticia *et al*. Eur J Med Chem, v. 44, n. 9, 2009. p. 3612-3620.

**Área: ELE** **Inscrição: 01288**

# Platinum surface oxidation in the presence of different alcohols

**Julia Maria Roquetto (IC)[1], Patrícia V. B. Santiago (PG)[1], Camilo Andrea Angelucci (PQ)[1], Janaina Souza-Garcia (PQ)[1*].**

**julia.roquetto@aluno.ufabc.edu.br; patricia.santiago@ufabc.edu.br; camilo.angelucci@ufabc.edu.br; janaina.garcia@ufabc.edu.br*.**

[1]*Center of Natural and Human Sciences, CCNH - UFABC;*

Palavras Chave: *alcohol oxidation, Pt surface oxidation, platinum, electrooxidation, oxides.*

## Highlights

The electrooxidation of different species on platinum electrode depends on the presence of OH species.
The competition between Pt and the organic species for OH can interfere in Pt oxidation.
The alcohol oxidation offset potential is inversely related to the surface oxidation extension.
Pt surface oxidation is affected by the presence of alcohols in solution.

## Resumo/Abstract

The oxidation of organic molecules on platinum electrodes is directly associated to the presence of OH species on the surface. However, this is the same species that is oxidized to PtO form. Since it is difficult to study the organic molecule oxidation and Pt surface oxidation at the same time, it has been assumed that in there is no chance in the surface oxidation process in the presence of organic molecules. However, considering that both reactions depend on the same species, it is reasonable to believe that a competition must take place. In this way, the goal of this work was to investigate if the Pt surface oxidation is influenced in the presence of different alcohols.

In order to analyze this theory, two different experiments were carried out in the absence and in the presence of different alcohols (methanol, ethanol, ethylene glycol, 1,2-propanediol, 1,3-propanediol and glycerol). The first one was carried out with a Pt polycrystalline electrode and Pt reduction charge was used to investigate the surface oxidation extension during the positive going sweep. In order to avoid the alcohol oxidation current in the negative going sweep, the experiment was carried out in low alcohol concentration ($10^{-2}$ molL$^{-1}$) and with different scan rates to the positive (50 mVs$^{-1}$) and negative (15 Vs$^{-1}$) sweeps. In the second experiment, the defects created on Pt(111) electrode after cycling in the absence and presence of alcohol ($10^{-1}$ molL$^{-1}$) were used to measure the surface oxidation.

Considering Pt(111) studies, it was observed that in the presence of alcohol molecules bigger than methanol, the formation of (110) defects is inhibited. The existence of vicinal hydroxyls seems to enhance this behavior. A relation between the end of alcohol oxidation (offset potential) and the disordering of the surface was observed. These results are in agreement with those obtained for Pt polycrystalline oxidation.

From these experiments, it was possible to observe that the offset of the alcohol oxidation is inversely related to the number of Pt atoms oxidized. The surface oxidation extension in the presence of alcohols follows the order: methanol > 1,3-propanediol > ethanol > 1,2-propanediol > ethylene glycol > glycerol.

**Área: ELE** **Inscrição: 01276**

# Electrochemical oxidation of the Sunset Yellow in acidic medium using boron-doped diamond anode (BDD)

**Camila G. Neves* (IC),[1] Leonardo A. L. da Silva (PG),[1] Adriana E. de Carvalho (PQ),[1] Willyam R. P. Barros (PQ).[1]**

**camilagarcianeves@gmail.com*; leonardoamaral8@gmail.com; adrianacarvalho@ufgd.edu.br; willyambarros@ufgd.edu.br.**

*[1] Universidade Federal da Grande Dourados, Rodovia Dourados – Itahum, Km 12 - Dourados – MS – Brasil.*

Keywords: *Sunset Yellow dye, electrochemical oxidation, BDD.*

## Highlights

The dye was degraded using boron-doped diamond anode (BDD) in the acidic medium;
The complete color removal of dye was maximal after 1.5 h of electrolysis;
The highest color removal was 98% at 20 mA.

## Resumo/Abstract

Sunset Yellow dye is widely studied due its various applications and is generally known for its great potential toxic mainly when used over concentration limits determined by legislation[1]. Studies reports several systems for the SY removal using oxidation electrochemical. In this case, BDD stands out as alternative for the complete oxidation of this compound[2]. This work shown electrochemical degradation of SY dye using BDD in acidic medium ($Na_2SO_4$ 0.5 mol $L^{-1}$; pH 3.0). The electrochemical system was a single compartment cell composed by BDD as work electrode, reference electrode (Ag/AgCl) and Pt wire as counter-electrode. To study of SY oxidation was applied 20 mA of current and small aliquots were collected in specific times. To study of color removal was used a UV-Vis spectroscopy Varian Cary 50. In order to verify the morphology aspects of deposition boron film on substrate that composes the electrode, were analyzed by optical microscopy. To verify electrochemical stability of the BDD, were performed chronoamperometry measurements before and after anodic studies. It was noted that the electrode remains stable and there was not changes toward to the low overpotential and high current density i.e., which shows that this anode is promising for SY oxidation. The color removal was 98% at 90 min. of electrolysis. The process kinetic was pseudo-first order, reaching apparent constant ($k_{app}$) value of ~ $1.0x10^{-2}$ $min^{-1}$. The results will optimize and discussed in terms of electrochemical/chemical mechanism.

[1] A. Yadav, A. Kumar, A. Tripathi, M. Das. **Toxicology. Letters,** 217 (2013) 197–204.
[2] A. C.-Rizo, S.G.-Granados, R. Salazar, J. M. P.-Hernández. **Separation and Purification Technology,** 172 (2017) 296–302.

**Área: ELE** **Inscrição: 01155**

# Desenvolvimento de eletrodos de grafite para detecção eletroquímica em substrato de papel

**Danielly S. Rocha (IC),[1*] Lucas C. Duarte (PG)[1], Anderson A. Dias (PG)[1], Mário H. P. Santana (PQ)[2], Wendell K. T. Coltro (PQ)[1]**

**daniellysr@outlook.com, wendell@ufg.br**

*[1]Laboratório de Microfluídica e Eletroforese, Instituto de Química, Universidade Federal de Goiás, Goiânia, GO, Brasil; [2]Unidade Técnico-Científica – Superintendência Regional da Polícia Federal em MG, Uberlândia, MG, Brasil*

Palavras Chave: Eletrodo de grafite, Boa noite cinderela, Detecção eletroquímica, Bebidas adulteradas, Química forense

## Highlights

Development of graphite electrodes for electrochemical detection on paper substrate
Development of the hand-drawn pencil electrodes (PDEs) made from sandpaper
Determination of midazolam maleate (good night Cinderella) by Square Wave Voltammetry (SWV)

## Resumo/Abstract

Os eletrodos de lápis desenhados à mão (*hand-drawn pencil electrodes*, PDEs) têm sido amplamente explorados em determinações eletroquímicas, pois apresentam baixo custo e simplicidade de fabricação, além de desempenho analítico semelhante aos eletrodos tradicionais. A eficiência na condutividade dos PDEs está diretamente relacionada ao papel selecionado e ao lápis utilizado. Nessa perspectiva, desenvolveu-se um PDE com potencial aplicação em análises forenses usando lixa de polimento como substrato de papel, grafite de lápis aquarelado 6B e tinta de prata. Os eletrodos foram fabricados pintando-se manualmente com lápis as áreas delimitadas do eletrodos auxiliar (EA) e de trabalho (ET) e posteriormente, o eletrodo de referência (ER) com tinta de prata (Figura 1A). Para a caracterização eletroquímica empregou-se o estudo do efeito da variação da velocidade de varredura da voltametria cíclica usando ferrocianeto de potássio 5 mmol $L^{-1}$ em KCl 0,5 mol $L^{-1}$ como sonda redox. A curva da corrente de pico em função da raiz quadrada da velocidade de varredura apresentou um comportamento linear de 10 a 40 $mVs^{-1}$ com $R^2$= 0,981 e $R^2$=0,996 referentes as correntes de pico anódica e catódica, respectivamente (Figura 1B). Este perfil linear indica que a transferência de massa das espécies eletroativas para a superfície do eletrodo é predominantemente controlada por difusão. Testes preliminares para a detecção de maleato de midazolam (vulgo "boa noite cinderela") apresentaram perfil linear na faixa de 50 a 1000 mg $L^{-1}$ com $R^2$=0,998 (Figura 1C) demostrando grande potencialidade de aplicação do eletrodo proposto em análises forenses.

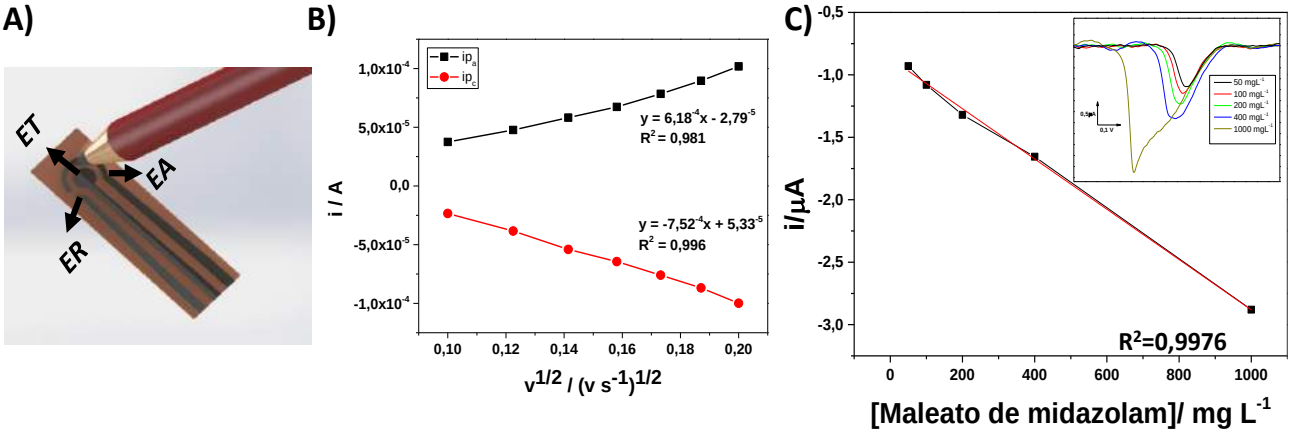


Figura 1. (A) *Layout* dos eletrodos e processo de pintura com lápis de grafite. (B) Variação da corrente de pico de oxidação e redução do eletrodo de grafite em função da raiz quadrada da velocidade de varredura mediante o estudo do efeito da variação da velocidade de varredura com ferrocianeto de potássio 5 mmol $L^{-1}$ em KCl 0,5 mol $L^{-1}$. (C) Curva de calibração do maleato de midazolam e voltamogramas de onda quadrada.

**Área: ELE**
*(Inserir a sigla da seção científica para qual o resumo será submetido. Ex: ORG, BEA, CAT)*

**Inscrição: 01082**
*(Inserir o número de inscrição do autor que fez a submissão)*

# $TiO_2$ nanotubes modified with ZIF-8 used for $CO_2$ capture and photoelectroreduction

**Juliano C. Cardoso (PQ)[1*], Simone. Stulp (PQ)[2], Juliana F. Brito (PG)[1], Jáder B. Flor (PQ)[1], Regina Frem (PQ)[1], Maria V. B. Zanoni (PQ)[1]**

**mvboldrin@gmail.com; jcarvalho82@gmail.com**

*[1] Universidade Estadual Paulista (Unesp), Instituto de Química, Araraquara; [2] UNIVATES, Lajeado - RS*

Palavras Chave: *Metal Organic Frameworks; Zeolite Imidazole Framework-8; Methanol; Ethanol; Photoelectrocatalysis.*

## • Highlights

Alcohols are obtained by photoelectrocatalytic reduction of $CO_2$ in aqueous solution
Light and bias potential at Ti/$TiO_2$NT-ZIF-8 improves reduction of $CO_2$

## Resumo/Abstract

This work describes, the decoration of Ti/$TiO_2$ nanotubes by nanoparticles of ZIF-8 (zeolite imidazole framework-8) grown using a layer-by-layer process. Morphological and crystallographic analyses showed that the $TiO_2$ nanotubes were coated with ZIF-8 nanoparticles around 50 nm in size. Curves of Iph vs. E showed that the incorporation of ZIF-8 at Ti/$TiO_2$ electrodes increased the photocurrent and that the values were dramatically increased in solution saturated with $CO_2$. The $CO_2$ adsorbed on the ZIF-8 formed stable carbamates, as demonstrated by spectroscopic and voltammetric assays. Photoelectrocatalytic reduction of $CO_2$ at Ti/$TiO_2$NT-ZIF-8 electrodes resulted in formation of up to 10 mmol $L^{-1}$ of ethanol and 0.7 mmol $L^{-1}$ of methanol in 0.1 mol $L^{-1}$ $Na_2SO_4$, at $E_{app}$ of +0.1 V, under UV-vis irradiation at room temperature. Our findings open up new applications of metal-organic frameworks (MOFs) in photoelectrocatalysis for the highly efficient preconcentration and conversion of $CO_2$ in aqueous media at ambient temperature.

Reference

[1] J.C. Cardoso; S. Stulp; J.F. de Brito; J.B.S. Flor; R.C.G. Frem; M.V.B. Zanoni. MOFs based on ZIF-8 deposited on $TiO_2$ nanotubes increase the surface adsorption of $CO_2$ and its photoelectrocatalytic reduction to alcohols in aqueous media, Appl. Catal. B Environ. 225 (2018). doi:10.1016/j.apcatb.2017.12.013.

Acknowledgements

The authors are grateful for the financial support provided by the Brazilian funding agencies:

- FAPESP (#2015/18109-4 and #2014/50945-1 INCT-DATREM);
- CNPq (#152274/2016-2, #465571/2014-0, and #446245/2014-3)
- CAPES.

**Área: ELE**
*(Inserir a sigla da seção científica para qual o resumo será submetido. Ex: ORG, BEA, CAT)*

**Inscrição: 01020**
*(Inserir o número de inscrição do autor que fez a submissão)*

# Gold Leaf: From Gilding to the Fabrication of AuNP-modified Electrochemical Sensor

**Wilson A. Ameku (PG),[1*] Mauro S. F. Santos (PQ),[1] Ivano G. R. Gutz (PQ),[1] Thiago R. L. C. Paixão (PQ).[1]**

**wilson.ameku@usp.br**

[1]*Department of Fundamental Chemistry, Institute of Chemistry, University of São Paulo*

Key Words: *AuNP; Graphite; Glucose; $H_2O_2$; Electrochemistry.*

## Highlights

A AuNP-modified graphite device was fabricated using ordinary materials such as graphite mine and gold leaf sheets often used in gilding crafts and modified electrode was applied to detect relevant biomolecules in clinical diagnosis, *e.g.* glucose and $H_2O_2$.

## Resumo/Abstract

Recently, the gold substrate received attention for its applicability in the electrocatalysis and electrochemistry fields. The high price of this noble metal has been fostered the development of cost-efficient method to fabricate gold-metal devices. As inexpensive source of gold metal the commercial available gold leaf sheets, commonly used in gilding crafts, have been reported as a good source to fabricate gold electrodes.[1] In this work the gold leaves were used as reagent to synthesize citrate-capped gold nanoparticles (AuNPs) which were employed to modified an ordinary graphite mine (AuNP/Gra) to fabricate an electrochemical sensor to detect relevant biomolecules in the clinical diagnosis field, such as glucose and $H_2O_2$.[2] The linear range and the limit of detection were 0.50 mM and 1.8-10.0 mM, respectively. The AuNPs were characterized through TEM micrograph, X-ray diffraction pattern and UV-vis spectroscopy, and then the morphology and nature of AuNP/Gra device were characterized by SEM micrograph, electrochemical impedance spectroscopy and cyclic voltammetry (CV)(Fig 1).The device advantages are its low-cost fabrication method, it can be easily modified with thiol compounds and its surface can be easily renewed scratching it in paper instead of alumina slurry pad.

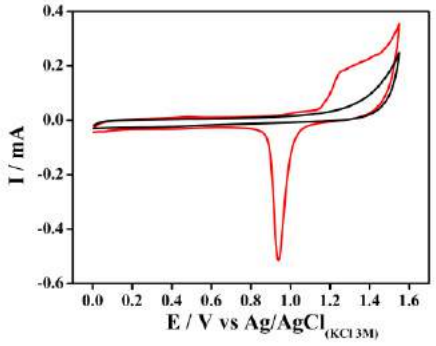


,

Fig 1: CV recorded with scan rate of 50mV $s^{-1}$ using graphite (black line) and AuNP/Gra (red line) device as working electrode in 0.50M $H_2SO_4$ solution.

**Reference**

(1) Santos, M. S. F.; Ameku, W. A.; Gutz, I. G. R.; Paixão, T. R. L. C. Gold Leaf: From Gilding to the Fabrication of Disposable, Wearable and Low-Cost Electrodes. *Talanta***2018**, *179*, 507–511.

(2) Ju, J.; Chen, W. In Situ Growth of Surfactant-Free Gold Nanoparticles on Nitrogen-Doped Graphene Quantum Dots for Electrochemical Detection of Hydrogen Peroxide in Biological Environments. *Anal. Chem.***2015**, *87* (3), 1903–1910.

**Área: ELE**
*(Inserir a sigla da seção científica para qual o resumo será submetido. Ex: ORG, BEA, CAT)*

**Inscrição: 00987**
*(Inserir o número de inscrição do autor que fez a submissão)*

# Niobium as co-electrocatalyst for Pd in Alkaline Medium: Improved Selectivity and Mechanism for Ethanol Electrooxidation Reaction

**Felipe M. Souza (PG),[1] Luanna S. Parreira (PQ),[2] Vitor. H. A. Oliveira (IC),[1] Victor. S. Pinheiro (PG),[1] Bruno L. Batista (PQ),[1] Julio Nandenha (PQ),[3] Almir O. Neto (PQ),[3] Mauro C. Santos (PQ).[1*]**

**felipe.moura@ufabc.edu.br; mauro.santos@ufabc.edu.br**

*[1]Centro de Ciências Naturais e Humanas, Universidade Federal do ABC, Rua Santa Adélia, 166, 09210-170 Santo André, SP, Brazil; [2]Instituto de Química, Universidade de São Paulo, Av. Prof. Lineu Prestes, 748, 05508-000 São Paulo, SP, Brazil. [3]Instituto de Pesquisas Energéticas e Nucleares (IPEN), CNEN/SP. Av. Prof. Lineu Prestes 2242, 05508-000, São Paulo - SP, Brazil.*

**Keywords:** *Direct ethanol fuel cell, Ethanol oxidation reaction, Palladium, Niobium.*

## Highlights

Pd/C with Nb nanoparticles shows highest current exchange density in Tafel plots. FTIR *ex situ* spectra indicated that $Pd_1Nb_1$/C displayed the minimum production of acetaldehyde.

## Resumo/Abstract

Direct ethanol fuel cells (DEFC) have been evaluated as a possible alternative source of sustainable energy, because it can reach high current densities with minimal pollutant production [1]. In this work, we report the synthesis of $Pd_xNb_y$/C binary electrocatalysts supported on Vulcan XC-72 carbon by the sol-gel method [2]. These synthesized electrocatalysts were physically characterized by DRX, EDS, ICP-MS, XPS and TEM. Their electrochemical activities (CV and CA) were evaluated as already reported by Souza [2]. Here, we reported new results from Tafel plots and FTIR *ex situ* experiments for ethanol oxidation reaction using those electrocatalysts.

**Figure 1**. Tafel plot of EOR from LSV using 1.0 mol $L^{-1}$ ethanol and 1.0 mol $L^{-1}$ KOH, at 1 mV $s^{-1}$ and room temperature.

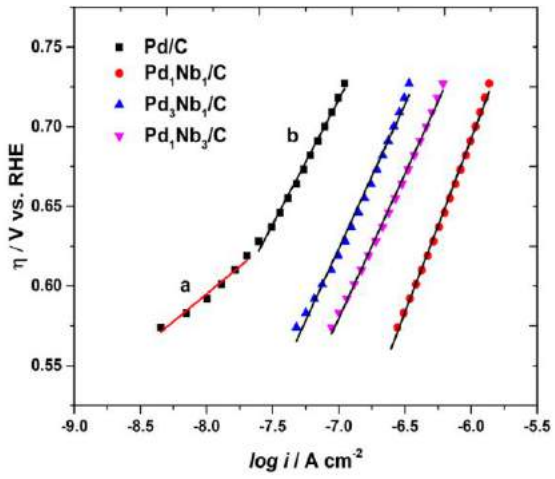


Pd/C electrocatalyst has the EOR governed by two determining steps since it showed two straight lines between 570 mV and 730mV, presenting also two different slopes (a and b, in Figure 1). Unlike the other electrocatalysts, with Nb in their chemical composition, that the EOR occurs by one determining step since there is just one slope. The exchange current densities (A $cm^{-2}$) were $2.3x10^{-17}$, $2.7x10^{-12}$, $6.6x10^{-10}$, $3.6x10^{-11}$ and $7.3x10^{-11}$ for Pd/C[a], Pd/C[b], $Pd_1Nb_1$/C, $Pd_3Nb_1$/C and $Pd_1Nb_3$/C, respectively. This shows that Nb increases the electron exchange rate at the analyte/electrode interface, improving the kinetics of the EOR reaction [3]. FTIR experiments strengthened the evidence that Nb modifies the Pd mechanism for EOR electrocatalysis to a mechanism that present almost no formation of acetaldehyde, avoiding the reaction $CH_3CH_2OH_{ads} + 2\,OH^-_{ads} \rightarrow CH_3CHO_{ads} + 2\,H_2O_{ads} + 2e^-$. The FTIR spectra showed that $Pd_1Nb_1$/C displays the highest production of $CO_2$ and the lowest production of acetaldehyde. Furthermore, the ADT experiments with ICP-MS analysis indicated that $Pd_1Nb_1$/C obtained the highest peak current density during 1000 cycles of the experiment, presenting the lowest Pd mass loss after the ADT.

**Acknowledgements:**
The authors are grateful to Fapesp (2015/10314-8, 2016/00819-8, 2017/21846-6), CNPq (406612/2013-7) and Capes for the scholarship. The authors are grateful to the CEM-UFABC for the experimental support.

**References:**

[1] Geraldes, A. N., *et al*. (2015). *Journal of Power Sources*, *275*, 189-199.
[2] Souza F. M., *et al*. (2017). *Journal of Solid State Electrochemistry*, 1-12.
[3] Bard, A. J., *et al*. *New York: wiley*, 1980.

**Área: ELE** **Inscrição: 00893**

# Comportamento voltamétrico de um análogo sulfonil-hidrazona do nitrofural com potencial atividade antichagásica

**Lígia Scandoglieri de Almeida (IC),[1] Luísa D. Chiavassa(PG),[1] Fernando M. Gatti (PG),[2] Gustavo H. G. Trossini (PQ),[2] Mauro Aquiles La Scalea (PQ),[1]**

**ligia.scan.7@gmail.com; malscalea@gmail.com**

*[1]Departamento de Química, UNIFESP - Diadema; [2]Departamento de Farmácia, USP –São Paulo*

Palavras chave: *nitroheteroclíclico, derivado sulfonil-hidrazônico, doença de Chagas, voltametria cíclica.*

## Highlights

**Voltametric behavior of a sulfonylhydrozone analogue of nitrofurazone with potential antichagasic activity.** The reduction mechanism of this nitro-heterocyclic derivative was studied by cyclic voltammetry in aqueous medium for being an antichagasic candidate, since the biological activity is related with charge transfer processes.

## Resumo

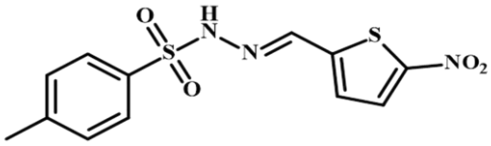

Figura 1. Fórmula estrutural do NTBS

Técnicas eletroquímicas apresentam-se como excelente alternativa para o estudo de fármacos que possuam como característica de ação biológica baseada em processos de transferência de carga, como compostos nitroheterocíclicos que apresentam potencial atividade antichagásica e sua redução eletroquímica leva à formação do nitro radical aniônico e o derivado hidroxílamínico, considerados os principais responsáveis pela atividade biológica. Realizou-se estudo por voltametria cíclica do comportamento eletroquímico de um derivado sulfonil-hidrazônico (Fig. 1, 4-metil-N-[(Z)-(5-nitro-2-tienil)metilenoamino]benzenosulfonamida, NTBS) análogo ao nitrofural, em meio aquoso, tendo carbono vítreo como eletrodo de trabalho (ECV), Ag/AgCl como referência e Pt como eletrodo auxiliar. Em pH = 4,0 observou-se a formação de um pico catódico irreversível com $Ec_{p1}$ = -0,396 V (Fig.2A), sendo deslocado no sentido negativo de potencial com aumento da velocidade de varredura ($\nu$), indicando sistema irreversível. Esse processo corresponde à redução do grupo nitro ($R\text{-}NO_2$) ao derivado hidroxilamínico (R-NHOH) com o envolvimento de quatro elétrons. A relação entre $Ip_1$ *vs* $\nu^{1/2}$ mostrou-se linear, indicando processo controlado por difusão e $Ep_1$ foi deslocado linearmente (Ep = -0,21 - 0,045 pH) para valores mais negativos de potencial com diminuição da acidez do meio, indicando a existência de etapa de protonação anterior ao processo de transferência de carga. Em meio alcalino a redução mostrou-se independente do pH e de forma similar ao nitrofural, observou-se a formação do par reversível $R\text{-}NO_2/R\text{-}NO_2^{\bullet -}$ (Fig. 2B e 2C), sendo $Ec_{p1}$=-0,577 V e $Ea_{p1}$=-0,468 V em pH=12.

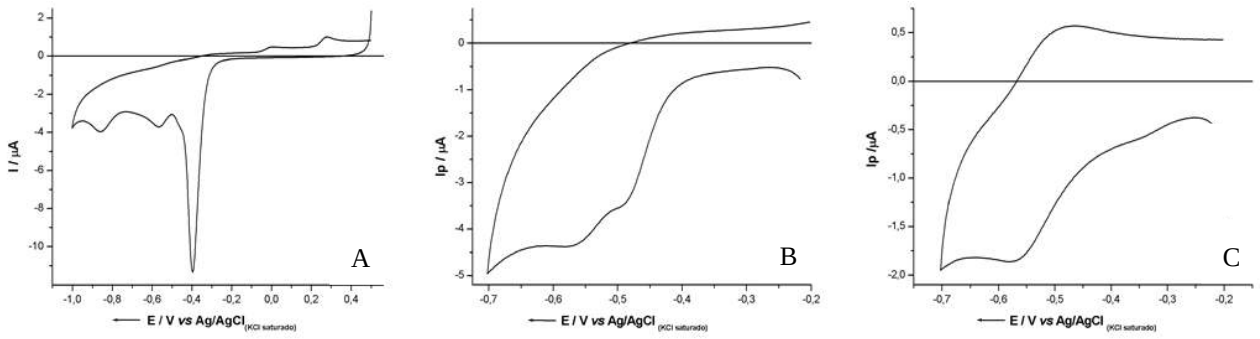


Figura 2. Voltamogramas cíclicos do NTBS a 0,1 V/s, [NTBS] = 1,0 x $10^{-4}$mol/L. (A) pH 4,0, $E_{inicial}$= 0,5 V; $E_{final}$= -1,0 V; (B) pH 8,0 e (C) pH 12,0, ambos com $E_{inicial}$= 0,2 V e $E_{final}$= -0,7 V.

**Área: ELE** **Inscrição: 00750**

# Inner- or outer-sphere. We should still learn about heterogeneous electronic transfer

**Bruna P. Chaves[1] (IC), Mariana Cavallieri[1] (IC), Otávio Beruski[2] (PQ), Murilo F. Cabral[1]* (FM)**

**brunapchaves@outlook.com; murilo.cabral@ifrj.edu.br**

*[1]Instituto Federal de Educação, Ciência e Tecnologia do Rio de Janeiro – Campus Rio de Janeiro, [2]Instituto de Pesquisas Energéticas e Nucleares*

Palavras Chave: *Electrochemical kinetics, carbon-based electrodes, melatonin, ferri/ferrocyanide.*

## Highlights

Redox couples are extensively used in order to characterize electrodic materials. In this way, basic electrochemical process are sometimes missed or just left behind to justify results that are not completely understood. It is shown how such data be analyzed taking into account what the results really show through.

## Resumo/Abstract

There are a lot of carbon-based electrodic materials and among those, pyrolytic and glassy carbon are extensively applied in several electrochemical studies. In order to figure out the advantages of carbon-based materials, researchers have used redox couples: compounds connected through reduction-oxidation reactions, where the couple can interact strongly or not with the material.

In this way, electrochemical processes are often missed or left behind when characterizing electrodic materials. It is reminded how one can make use of basic electrochemical theory in order to analyze and take into account what the data truly shows.

Figure 1 (a – d) shows the electrochemical behavior of ferro/ferricyanide (a) and melatonin (c) on pyrolytic carbon electrode. It can be observed that scan rate may change the apparent kinetics of the electrochemical process. At low scan rates the electronic transfer seems evidently nonlinear (cf. See Fig. 1(b)); however, in higher scan rate values such behavior changes. It is worth mentioning that such range of scan rates are widely used to characterize eletrodic materials.

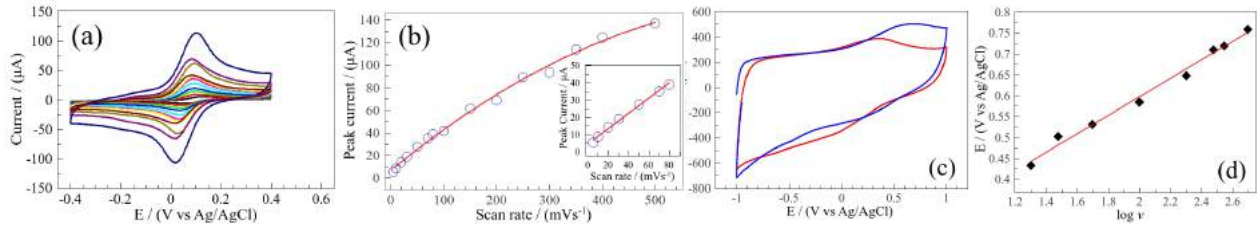


Figure 1. (a) Cyclic voltammograms obtained using a pyrolitic carbon electrode in a 1mM $K_4[Fe(CN)_6]$, 0.5 M $H_2SO_4$ solution. (b) Peak current of (a) as function of scan rate, showing $v \leq 80$ mV $s^{-1}$ as insert. (c) Cyclic voltammograms for pyrolitic carbon electrode in 0.1 M phosphate buffer solution (—), pH 6.82, and in presence of 3.23 mM melatonin (—). (d) Peak potential of (c) as function of the logarithm of scan rate.

On the other hand, the electrochemical profile of melatonin shows an oxidation peak at 0.65 V, while the relationship between the peak potential (at different scan rates) and log *v* reveals α = 0.12, according to Laviron's equation. Such slope value suggests a quasi-reversible process (cf. Fig. 1(d)), contrary to some works describing the process as irreversible.

Cyclic voltammetry and further treatment of the data have shown that full comprehension is not easy to reach. There are several factors that should be considered prior to determine the electronic transfer or mass transport properties of a redox couple, and therefore the properties of an electrodic material.

**Área: ELE** **Inscrição: 00712**

# Modeling the electroreduction of hydrogen peroxide in alkaline media

**Maria Rodrigues Pinto (PG),[1] Renan C. C. de Miranda (PG),[1] Kaline N. da Silva (PG),[2] Elton Sitta (PQ),[2] Raphael Nagao (PQ)[1,*]**

**maria.rodriguesp@hotmail.com; nagao@iqm.unicamp.br**

*[1]Institute of Chemistry – University of Campinas (UNICAMP); [2]Department of Chemistry – Federal University of São Carlos (UFSCAR)*

Key-words: *Nonlinear dynamics, Electroreduction, Oscillations*

## Highlights

A kinetic mechanism for the cation-dependent hydrogen peroxide reduction reaction catalyzed by platinum in alkaline media is proposed.

## Resumo/Abstract

Contrary to the hydrogen peroxide ($H_2O_2$) reduction reaction (HPRR) in acidic solutions, the kinetic mechanism in alkaline media is still unclear. In this study we propose, for the first time, a model to describe HPRR in alkaline media taking in account the effect of metallic cation ($C^+$) in the electrolyte. $H_2O_2$ is mainly found as deprotonated hydrogen peroxide ($HO_2^-$) due to alkaline media. The reduction process initiates by a dissociative adsorption (asterisks represent free active sites) of $HO_2^-$ (r1), that produces adsorbed oxygenated species ($OH_{ad}$ and $O_{ad}$). As they are unstable adsorbates it is assumed that, as soon as they are formed, $O_{ad}$ promptly reacts with water to form $OH_{ad}$ (r2) and $OH_{ad}$ is reduced to $OH^-$ (r3). Water, which is an abundant molecule, is constantly adsorbing (r5) and desorbing (r6) at the surface. The water reduction step (r7) promotes the formation of $H_{ad}$ that acts as a blocking agent for HPRR and generates $H_2$ (r9). The effectiveness for water reduction is correlated with noncovalent interactions between cation and adsorbed water (r10). As the coverage of $H_2O_{ad}$ is stabilized by $C^+$, the formation of $H_{ad}$ can be enhanced (r12), the poisoning effect induced by these interactions could result in a decrease of the faradaic current and the oscillatory frequency because of the formation of $H_{ad}$. To verify the coherency of the proposed mechanism numeric simulations of electrochemical kinetics of HPRR is being currently developed under conventional and oscillatory conditions.

$$2* + HO_2^- \xrightarrow{k_1} OH_{ad} + O_{ad} + e^- \quad \text{(r1)}$$

$$O_{ad} + H_2O + e^- \xrightarrow{k_2} OH_{ad} + OH^- \quad \text{(r2)}$$

$$OH_{ad} + e^- \xrightarrow{k_3} * + OH^- \quad \text{(r3)}$$

$$* + OH^- \xrightarrow{k_4} OH_{ad} + e^- \quad \text{(r4)}$$

$$* + H_2O \xrightarrow{k_5} H_2O_{ad} \quad \text{(r5)}$$

$$H_2O_{ad} \xrightarrow{k_6} * + H_2O \quad \text{(r6)}$$

$$H_2O_{ad} + e^- \xrightarrow{k_7} H_{ad} + OH^- \quad \text{(r7)}$$

$$H_{ad} + OH^- \xrightarrow{k_8} H_2O_{ad} + e^- \quad \text{(r8)}$$

$$2H_{ad} \xrightarrow{k_9} 2* + H_2 \quad \text{(r9)}$$

$$H_2O_{ad} + C^+ \xrightarrow{k_{10}} [H_2O_{ad} - C^+]_{ad} \quad \text{(r10)}$$

$$[H_2O_{ad} - C^+]_{ad} \xrightarrow{k_{11}} H_2O_{ad} + C^+ \quad \text{(r11)}$$

$$[H_2O_{ad} - C^+]_{ad} + e^- \xrightarrow{k_{12}} H_{ad} + OH^- + C^+ \quad \text{(r12)}$$

**Área: ELE** **Inscrição: 00681**

# Amperometric and voltammetric determination of tibolone in pharmaceutical and saliva samples

**Weberson P. da Silva (PG),[1]* Raquel G. da Rocha (PG),[1] Rodrigo A. A. Muñoz (PQ),[1] Eduardo M. Richter (PQ).[1]**

**webersonpereirasilva@gmail.com**

[1]*Instituto de Química, UFU;*

Palavras Chave: *Square-wave voltammetry, Tibolone, Steroids, Amperometric, Saliva.*

## Highlights

New electrochemical method for determination of Tibolone in saliva and pharmaceutical samples. The method showed good repeatability, recovery for proposed analysis, and lower detection limit.

## Resumo/Abstract

Tibolone (TIB) is a synthetic steroid used in the treatment of postmenopausal osteoporosis and for the treatment of climacteric symptoms.[1] TIB is one of the androgenic anabolic steroids banned by the World Anti-Doping Agency(WADA) [2], because it can alter athletes physical performance. This work presents the results obtained for determination of tibolone in pharmaceutical and saliva samples using SWV and BIA with amperometric detection. Boron doped diamond (BDD), platinum and $AgCl/KCl_{(sat)}$ were used as working, auxiliary and reference electrodes, respectively. The results showed that TIB presents an oxidation peak at +1.4 V using BDD with anodic activation and 0.1 mol $L^{-1}$ phosphate buffer (pH = 7.0) as supporting electrolyte (better results). Using the optimized parameters of SWV ($f$ = 40 $s^{-1}$; a = 60 mV; step potential = 4 mV) and amperometry (applied potential = +1,4 V; injection volume = 100 µL; dispensing rate = 213 µL $s^{-1}$), TIB showed good linearity between 1 - 110 µmol $L^{-1}$ (r = 0.999; Fig, 1A) and 1 - 140 µmol $L^{-1}$ (r = 0.998; Fig. 1B). Additionally, both techniques present good repeatability (DPR = 2.4 and 4.2 %, for SWV and amperometry, respectively).

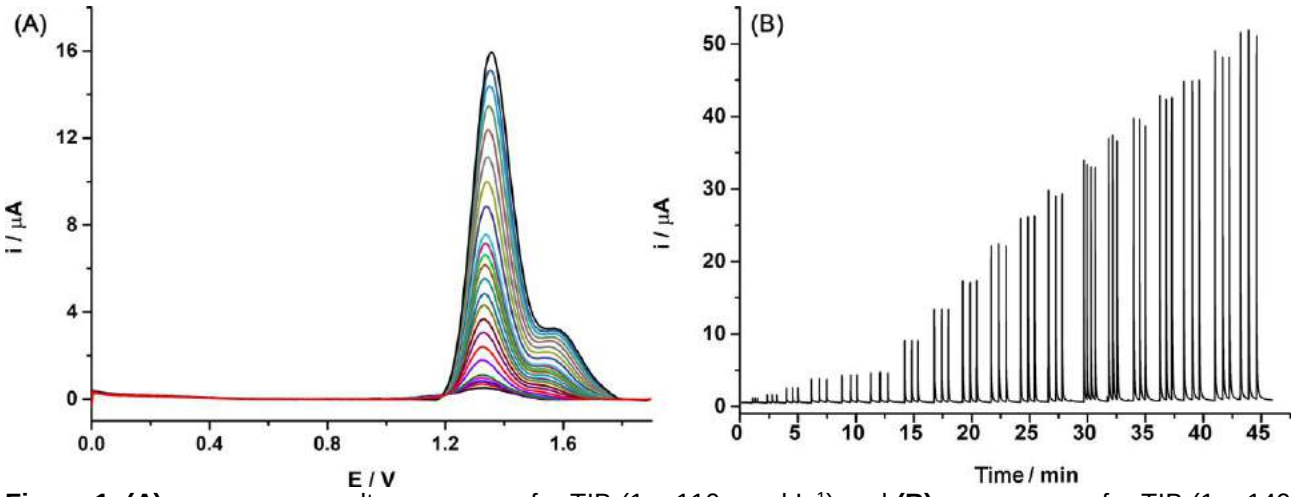


**Figure 1. (A)** square-wave voltammograms for TIB (1 – 110 µmol $L^{-1}$) and **(B)** amperogram for TIB (1 – 140 µmol $L^{-1}$).

Both techniques were successfully used for the determination of TIB in pharmaceutical samples. The performance of the methods for detection of TIB in saliva sample is under investigation.

References

[1]Modelska, K.; cummings, S. *J. Clin. Endocrinol. Metab*. **2002**, *87*, 16.
[2]Basaria, S. J. *Clin. Endocrinol. Metab*. **2010**, *95*, 1533.

**Área: _____ELE_____** *(Inserir a sigla da seção científica para qual o resumo será submetido. Ex: ORG, BEA, CAT)*

**Inscrição:___00621___** *(Inserir o número de inscrição do autor que fez a submissão)*

# QCM-D and ATR-FTIR studies applied to the understanding of L-Cysteine adsorption: how can viscoelastic changes be explained?

**André H. B. Dourado(PG),[1] Rubens A. Silva (PQ),[1] Roberto M. Torresi (PQ),[1] Matthias Arenz (PQ),[2] Susana I. Córdoba de Torresi (PQ).[1]***

**dourado@iq.usp.br; storresi@iq.usp.br**

[1]*Instituto de Química, USP;* [2]*Departament of Chemistry and Biochemistry, Universität Bern*

Palavras Chave: *L-Cysteine adsorption, QCM-D, ATR-FTIR, structure control,.*

## Highlights

High viscoelasticity of the adsorbed species, higher than proteins;
Structure and assembling verified by FTIR allowed the interpretation of high viscoelasticity;
Structure control of the adsorbates upon pH and potential.

## Resumo/Abstract

The occurrence of L-Cysteine (L-Cys) adsorption on metallic surfaces was widely studied. Even though, quantitative data about its kinetics are still few, meanly due to the viscoelasticity of the adsorbed film. In the present work QCM-D technique was used to study the kinetics of adsorption of L-Cys on Pt surfaces at different pHs. The viscoelasticity of the film is higher than for other proteins, like BSA. The kinetics analysis were done considering a Frumkin adsorption isotherm, showing the most favorable condition was pH 9 when thiolate is present, but the amine is protonated while the least favorable one is when it is full deprotonated (pH 14).

Since L-Cys is just a monomer, this high viscoelasticity observed was not expected, so to understand the origin of this behavior, it was necessary to use ATR-FTIR, in order to obtain structural molecular data of the species adsorbed. This approach corroborated observations obtained by QCM-D, and also allowed the verification of many simultaneous processes that cannot be separated by QCM-D. The conformation of the adsorbed species is very much dependent on the pH and the assembling follows a slower kinetics than the S-Pt bond formation. The different conformations observed as function of the pH allowed, also, an increase in anion adsorption and wettability justifying the high viscolasticity and its pH dependence.

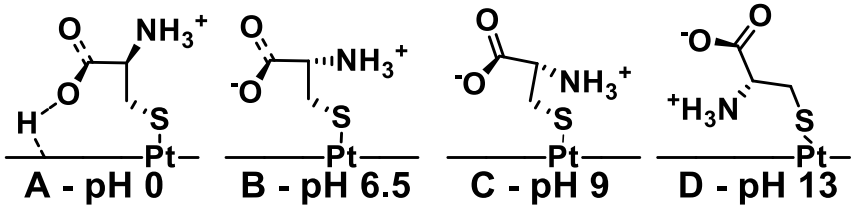


Proposed structures for L-Cys(ads) as function of the pH. Angles not preserved.

**Área: ELE** **Inscrição: 00578**

# Application of the *carioca* bean (*Phaseolus vulgaris* L.) for the electroanalytical detection of phenol using graphite- $SiO_2$-$TiO_2$ electrode

**Pedro Henrique C. Guedes (IC),[1] Francisca das C. S. S. Mihos (PG),*[1] Emerson S. Ribeiro (PQ),[2] Lívia Maria da C. Silva (PQ),[3] Andréa M. Salgado(PQ),[1]**

**pedrohenriq98@poli.ufrj.br; franciscamihos@gmail.com**

*[1]Escola de Química, Departamento de Engenharia Química, UFRJ; [2]Instituto de Química, UFRJ; [3]Departamento de Engenharia Agrícola e Meio Ambiente, UFF.*

Palavras Chave: *Feijão Carioca, Peroxidase, Detecção de Fenol, Eletrodo grafite-$SiO_2$-$TiO_2$, Biossensor, Voltametria*

## Highlights

The peroxidase (PO) extracted from the *carioca* bean was applied as a biological component in an amperometric biosensor. The enzyme was immobilized on the $SiO_2$-$TiO_2$ matrix and the electrode was formulated by the graphite- $SiO_2$-$TiO_2$ mixture, being able to detect phenol in the potential range from -0,2 to +0,3 eV *vs* Ag/AgCl , applying the adequate square wave voltammetry technique.

## Resumo

Conforme o CONAMA[1] o fenol e seus derivados são poluentes tóxicos que provocam danos ambientais. A legislação estabelece limite máximo de 0,5 $mgL^{-1}$, para lançamento em efluentes.Os biossensores são alternativas auxiliares para detecção desses poluentes devido ao uso de biomoléculas especificas, além de poderem ser miniatuzinados e transportados[2].**Objetivo:** o presente estudo tem por objetivo a detecção de fenol, utilizando para isso o extrato do feijão carioca contendo a enzima peroxidase. **Metodologia**: O extrato enzimático foi preparado a partir da homogeneização de 50,0 g do feijão e 150,0 mL de tampão fosfato pH 7,0, e precipitado com 40% de $(NH_4)_2SO_4$. Uma alíquota de 1,0 mL do extrato foi adicionada sobre 0,05 g do óxido de sílica-titânio pela adição de 100 µL de glutaraldeído 0,5%. O óxido foi sintetizado pelo método sol-gel[3,4] nas proporções de 70% de sílica e 30% de titânio. O sinal de corrente catódica foi obtido pela redução das quinonas, reduzidas na superfície do eletrodo. **Resultados e Discussão**: O teor proteico do extrato foi de 4,63±0,02 $mgmL^{-1}$ e atividade da PO de 2500 $UmL^{-1}$. A Figura 1 mostra aumento da densidade de corrente de redução das quinonas à medida que há o aumento na concentração de fenol (0,2 a 2,0 $mgL^{-1}$), o que demonstra a sensibilidade de resposta do biossensor frente a variação da concentração do composto em solução. A reação para formação de quinonas ocorre conforme Figura 2.**Conclusão**: A partir dos resultados obtidos pode-se inferir que o dispositivo desenvolvido é uma ferramenta viável para determinação de fenol, detectando concentrações abaixo do valor permitido pela legislação da CONAMA.Porém há ainda a necessidade de validação do método, pesquisas que se encontram em andamento do Lab. de Sensores Biológicos da UFRJ.

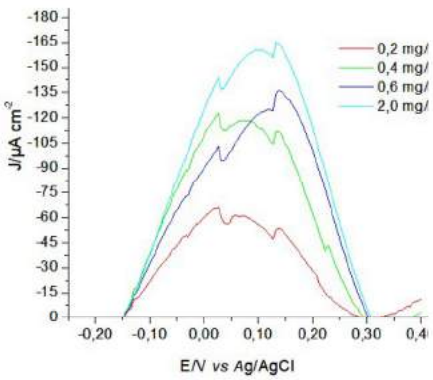


**Figura 1.** Picos de corrente catódica para soluções de fenol pH 7.0 em diferentes concentrações.

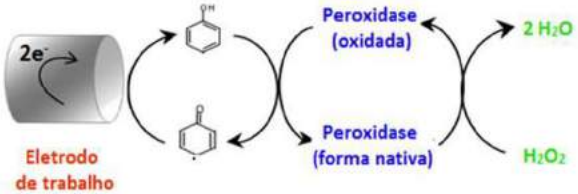


**Figura 2.** Ciclo catalítico da peroxidase.

## Referências:

**[1]** CONAMA, C. N. D. M. A. Resolução no 430, de 13 de Maio de 2011.

**[2]** DERKUS, B. Applying the miniaturization technologies for biosensor design. Biosensors and Bioelectronics, v. 79, p. 901–913, 2016.

**[3]** SANTOS, J. C. S. DOS et al. Importance of the Support Properties for Immobilization or Purification of Enzymes. Chem. Cat. Chem, v. 7, n. 16, p. 2413–2432, 17 ago. 2015.

**[4]** OLIVEIRA, S. SOUTHGATE DE. Protoporfirina-IX imobilizada sobre $SiO_2$-$TiO_2$ preparada pelo processo Sol-Gel: Síntese, Caracterização e Aplicação Fotoquímica.UFRJ, 295, 2012.

**Agradecimentos:**

**Área: ELE** **Inscrição: 00546**

# Electrocatalytic activity of niquel hexacyanoferrate supported on reduced graphene oxide for electrooxidation reaction Glycerol

**Isaide A. Rodrigues (PQ)[1], Deracilde S. Silva Viégas (PG)[2]*, Leila Maria S. da Silva (FM), Aldalea Lopes B. Marques (PQ)[2]**

**isaide.rodrigues@gmail.com; cindy.g.f@hotmail.com**

*[1]Departamento de Química, UFMA; [2]Departamento de Química de Tecnologia, UFMA.*

Palavras Chave:*(Glycerol, níquel Hexacyanoferrate, reduced graphene oxide).*

## Highlights

Vitreous carbon (VC) electrode chemically modified by a reduced graphene oxide supported nickel hexacianoferrate. Glycerol oxidation in a basic environment. Electrocatalytic activity evaluated by Cycilic Voltametry, cronoamperimetry and electrochemical impedance spectroscopy (EIS).

## Resumo/Abstract

The study of glycerol electrooxidation was evaluated over a vitreous carbon (VC) electrode chemically modified by a reduced graphene oxide supported nickel hexacianoferrate. We have characterized the prepared NiHCF/rGO electrode by means of X-ray diffraction (DRX), Energy-dispersive X-ray spectroscopy (EDX) and Scanning electron microscopy. The material electrocatalytic activity was evaluated by cyclic voltammetry, cronoamperometry and electrochemical impedance spectroscopy. Voltamograms registered at basic environments for the NiHCF/rGO electrode presented the formation of well defined redox peaks associated with the redox couple Ni(II)/Ni(III). These results show that the NiHCF/rGO electrode significantly enhances electrocatalytic activity for glycerol oxidation in comparison to the unmodified VC electrode. By using Laviron theory we were able to calculate, for the glycerol oxidation reaction, the charge transference speed constant ($k_s$) and the electron transference coefficient ($\alpha$) obtaining the values of 0,55 e 0,19 $s^{-1}$ respectively. The anodics currents increased with increasing concentrations of $OH^-$ and glycerol. By means of cronoamperometry we have determined glycerol diffusion coefficient ($D = 2,8 \times 10^{-4}$ $cm^2$ $s^{-1}$). The electrochemical impedance spectroscopy data show that the charge transference resistence decreases with an increase in glycerol concentration therefore demonstrating the efficiency of the NiHCF/rGO electrocatalyst for this reaction.

**Área: ELE**
*(Inserir a sigla da seção científica para qual o resumo será submetido. Ex: ORG, BEA, CAT)*

Inscrição: **00492**
*(Inserir o número de inscrição do autor que fez a submissão)*

# Development of an enzymatic cascade immobilized on modified nafion to produce an efficient ethanol/$O_2$ biofuel cell

**Jefferson Honorio Franco (PG),[*] e Adalgisa Rodrigues de Andrade (PQ).**

**jeffersonhfranco@gmail.com; ardandra@usp.br**

Departamento de Química, FFCLRP, Universidade de São Paulo, Ribeirão Preto, SP, Brazil

Palavras Chave: *Energia, Eletrocatálise, Etanol, Biocélulas a combustível enzimáticas.*

## Highlights

An enzymes cascade was obtained for ethanol bioelectrooxidation.

Quaternary ammonium bromide salt-treated Nafion membranes provide an ideal environment for enzyme immobilization.

CLAE-UV / RID technique has proved to be an important tool for identification of new compounds formed.

## Abstract

Biofuel cells are devices that use chemical reactions to produce energy employing biological catalysts (enzymes or micro-organisms), providing clean and renewable energy, moreover present great potential as alternative power sources for low-power electronic devices. Enzymatic biofuel cells have shown a great development, nevertheless, still necessary to increase the service life of the bio cell, the power densitie. This presentation focus is the preparation cascade of enzymatic bioanodes aiming the complete oxidation of ethanol through the immobilization of dehydrogenase enzymes at carbon support surface. Enzymatic immobilization at the bioanode was performed using tetrabutylammonium modified nafion membrane. The electrochemical experiments were carried out using an AUTOLAB potentiostat / galvanostat with a three-electrode standard cell. The cascade oxidation of ethanol was followed by electrolysis appling a cpnstant potential (0.600 V vc. Ag/AgCl) during 12 hours. The products obtained after 12 hours of electrolysis were analyzed by HPLC-UV / RID in Full-Scan mode. Ethanol / $O_2$ biofuel cells produced power densities of 29.5 μW $cm^{-2}$ with a single enzyme system, alcohol dehydrogenase (ADH), and 186.0 μW $cm^{-2}$ with a two enzyme system, alcohol dehydrogenase and aldehyde dehydrogenase (ADH and AldH) on the surface of the carbon paper electrode. This result indicates that bi-enzymatic system is able to further oxidize acetaldehyde (n=2) to acetate (n=4). The maximum current density for the bi-enzymatic system during chronoamperometry was also higher (1.22 mA/$cm^2$) compared to the system with only alcohol dehydrogenase (0.43 mA/$cm^2$). CLAE-UV / RID analytical technique was able to demonstrated that the two dehydrogenase enzymes system is able to electrochemically oxidize ethanol (40 mmol) on a carbon electrode by collecting ($2< n < 4$) electrons, acetaldehyde (n=2) (6.57 mmol) and acetic acid (n=4) (0.72 mmol). We concluded that the modified Nafion membranes with tetrabutylammonium bromide provide an ideal environment for enzymatic immobilization, Thus, the etanol / $O_2$ biofuel cell acts on the first two catabolic steps of ethanol oxidation.

## Acknowledgements

Financial support from CNPq (40.0712/2014-8), FAPESP (Grant # - 2017/20431-7)

**Área: ELE**
*(Inserir a sigla da seção científica para qual o resumo será submetido. Ex: ORG, BEA, CAT)*

**Inscrição:00433**
*(Inserir o número de inscrição do autor que fez a submissão)*

# Voltammetric Behavior Study of Nitrofurazone at Multi-wall Carbon Nanotube-Modified Glassy Carbon Electrode in Aqueous Media

**Charles de L. Brito (PG)[1*], Elizabeth I. Ferreira (PQ)[1], Mauro A. La-Scalea (PQ)[2].**

charles.brito@usp.br*

[1]*Departamento de Farmácia, FCF-USP;* [2]*Departamento de Química, UNIFESP-Diadema*

*Keywords*: *Electrochemical sensor, Carbon nanotubes, Chemical functionalization, Nitrofural, Voltammetry.*

## Highlights

Development of modified electrode using the functionalized carbon nanotubes on glassy carbon. A more sensitive sensor has been developed for the mechanistic studies of nitroheterocycle reduction.

## Abstract

Carbon nanotubes, NTs, have been greatly prominent due to their varied electronic properties, which allow the transduction of signals. The NTs chemical functionalization improves detection traits, eliminating interferences from commercial NTC. Based on the foregoing information, this work aims to evaluate the functionalization influence of carbon nanotubes on glassy carbon electrode by means of electrochemical reduction behavior of nitrofurazone applying cyclic voltammetry. All voltammograms were recorded by using an electrochemical cell with three electrodes: Ag/ACl, Pt and working electrode. Three kinds of working electrodes, functionalized carbon nanotube (GCE-NTC-F), carbon nanotube (GCE-NTC-N) and GCE without modification were evaluated. The chemical functionalization of carbon nanotubes was carried out in a mixture of sulfuric and nitric acids. Solvents such as $H_2O$, EtOH, MeOH, ACN, DMSO, DMF, 1,3-dioxolane were evaluated to get the best NTs dispersing agents. The 1,3-dioxolane solvent was shown to be the best, as it presented greater current signals, despite being nontoxic[1]. Table I and Figure 1 indicate the results.

**Tabela I.** Values of the reduction potentials and peak currents, nitrofurazone [0.1 mM] NTCs, 3 mg/mL

| Electrode | -Ep,c (V) pH 4.02 | -Ep,c (V) pH 7.41 | - Ip,c (A) pH 4.02 | - Ip,c (A) pH 7.41 |
|---|---|---|---|---|
| GCE-F | 0.332 | 0.445 | $2.64 \times 10^{-4}$ | $1.20 \times 10^{-4}$ |
| GCE-N | 0.323 | 0.425 | $3.12 \times 10^{-4}$ | $3.07 \times 10^{-4}$ |
| GCE | 0.345 | 0.423 | $1.16 \times 10^{-4}$ | $1.02 \times 10^{-5}$ |

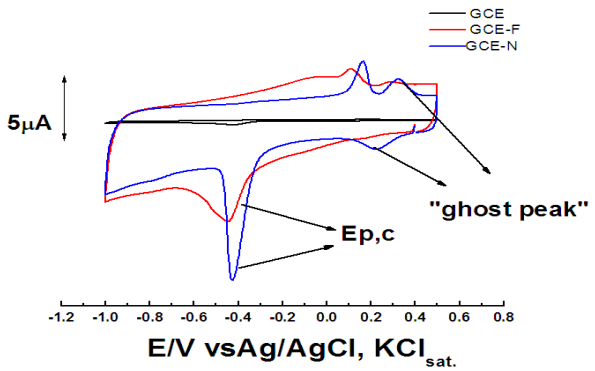


**Figure 1. Cyclic Voltammograms at pH 7.41.**

It can be observed that there are no significant differences among the potential values obtained. The current peak values of both modified electrodes at pH 4.02 are similar and, at pH 7.41, GCE-N presented the highest Ip,c value, indicating that the modification influences positively the electrochemical response of the hydroxylamine derivative formation from the nitrofurazone reduction. Moreover, the functionalization contributes actively to the elimination of the “ghost peaks”, which are irreproducible register by GCE-N.

[1]Squella, J.A.et al.; Electrochemistry Communications, 48,69,2014.

**Área: ELE** **Inscrição: 00374**

# Platinum nanoparticles supported on carbon-based materials as electrocatalysts for methanol oxidation reaction.

**Renan Giareta (IC), Raul O. Pasin (IC) e José Ricardo C. Salgado (PQ)**

**renan.giaretta@hotmail.com; jose.salgado@unila.edu.br**

*Universidade Federal da Integração Latino-Americana, CEP.: 85867-970, Foz do Iguaçu, PR, Brasil*

Palavras Chave: *Fuel cells; Electrochemistry; Electrocatalysis, Energy Conversion.*

## Highlights

Platinum and Nickel electrocatalysts based on carbon-based materials were analyzed with the aim of reducing costs and increase the efficiency of methanol oxidation reactions.

## Abstract

The high amount of gases emitted by burning fossil fuels has caused many environmental problems and is related to several diseases that significantly affect the quality of life of people. Therefore, new alternatives to energy generation that are not so aggressive to the environment are necessary. An alternative is the fuel cell which is an electrochemical energy conversion device that operates by means of oxidation, where hydrogen reacts with oxygen to form water and release electrons. The great advantage of this method is that it doesn't involve any combustion, which eliminates the problem of the emission of gases, and results in a relatively efficient energy and that doesn't generate any harmful emission. However, in order to operate efficiently, the use of an electrocatalyst is required. Most of these electrocatalysts are made of platinum, as it has shown great catalytic activity, but is too expensive and also contaminates rapidly by the absorption of carbon monoxide, which bind to the metal and inhibit its catalytic action. Five samples of platinum and nickel electrocatalysts supported on different carbon-based materials were investigated in alkaline and acidic solutions. The physical and electrochemical characterization of the electrocatalysts were performed by X-ray diffraction, cyclic voltammetry and chronoamperometry techniques. In the results by cyclic voltammetry, it was observed that in the methanol solution, the platinum metal in graphene shows good electrocatalytic properties for the oxidation of methanol.

Área: ELE Inscrição: 00182

# ELETRODEPOSIÇÃO E CARACTERIZAÇÃO DA LIGA NiFe COM 20 e 30% DE SUBSTITUIÇÃO DO Ni NO BANHO DE WATTS

**[1]Israel L. M. Tavares (IC), [2]Analice C. C. Cunha(IC), [3]Francisco C. M. Filho(IC), [4]Paulo S. G. Silva(PQ).**

**paulosgs@ufcg.edu.br; israellazaromt@gmail.com**

*1, 2, 3 e 4 - Universidade Federal de Campina Grande, Centro de Educação e Saúde, Unidade acadêmica de Biologia e Química, Curso de Licenciatura em Química*

Palavras Chave:*( Liga NiFe, modificação no banho de watts, eletrodeposição NiFe).*

## Resumo

A deposição de metais em uma liga constitui-se em unir propriedades distintas em um único material. As características químicas do metal Ni, às vezes não superam o fator econômico de utilizar este metal puro, dai a necessidade de unir as características do Ni com um metal menos nobre, como o Fe, formando a liga NiFe. Utilizou-se o banho de watts com substituição do sal de níquel (Ni) por um sal de Fe (ferro), resultando nos eletrólitos de NiFe(20) e NiFe(30). Os eletrólitos utilizaram sais simples. Para manutenção do pH, agindo também como complexante, utilizou-se o $H_3BO_4$ (ácido bórico). A composição das ligas correspondeu a um teor maior do metal Ni, que pode ser explicado devido maior concentração do seu sal no eletrólito. Os testes de corrosão em meio a NaCl 0,1M apresentaram um potencial mais positivo para liga NiFe(20), assim como a resistência a polarização, com valores muito próximo aos de Ni puro, dessa forma a liga NiFe(20), apresenta melhores condições para substituição e de menor custo ao Ni.

## Introdução

As ligas formadas por Ni e Fe vem sendo estudadas há varias décadas, elas são da classe ferromagnéticas e possuem alta performance e permeabilidade, possuindo importantes características metalúrgicas como, por exemplo, a resistência a corrosão. A eletrodeposição desta liga é considerada anômala, pelo fato do metal menos nobre (Fe) ser depositado preferencialmente ao metal mais nobre (Ni)[1]. O interesse nas ligas NiFe é explicado também pelo fato da liga adquirir características do Fe como: dureza elevada, alta força e a resistência à fadiga e ao desgaste, visando utilizá-la como memoria ferromagnética, dentre aplicações substituindo revestimentos mais caros. Procura-se dessa forma, produzir um revestimento constituído pelos metais Ni e Fe utilizando a técnica de eletrodeposição com adaptação no banho de watts, substituindo o Ni por Fe em 20% e 30% respectivamente, conferindo propriedades provenientes do Fe, mas mantendo características do Ni, produzindo um material economicamente mais viável a utilização como possível substituto para esse tipo de revestimento. Os eletrodepósitos foram obtidos por modificação do banho de watts, substituindo 20% ou 30% do $NiSO_4$ por $FeSO_4$, a 60°C, 73,33 mA/cm², 100 Coulomb e rotação de 60 RPM, sobre substrato de cobre de 4,5 cm². Foi caracterizado por MEV, EDX, PLP e EIE.

## Resultados e discussão

O eletrodepósito de NiFe(20) tem 89,9% m/m de Ni, morfologia granular com grãos de diferentes tamanhos, distribuídos uniformemente, os maiores grãos atribuídos aos 10,89% m/m de Fe no eletrodepósito obtido. No eletrodepósito de NiFe(30), com 24,59% m/m de Fe, tem distribuição granular irregular que pode induzir a formação de regiões de diferentes potencias, e facilitar o processo de corrosão. O maior teor de Ni na ligas NiFe(20) explica uma variação de 0,100V do valor de Ecorr comparado com NiFe(30) obtidos por PLP. Os arcos de impedância, obtidos por EIE para NiFe apresentaram valores menores em relação ao de Watts.

## Conclusões

A obtenção da liga NiFe foi satisfatória e mostra que o aumento do teor de Fe, a morfologia apresenta grãos maiores em tamanhos crescentes diretamente com o Fe. O potencial e a resistência à corrosão mostra-se inversamente ao teor de Fe. A liga NiFe(20) apresentou propriedades semelhantes ao Ni podendo substituí-lo a um menor custo.

## Referências

1 - SANTANA, A. I. C., Estudo Cinético da Eletrodeposição da Liga Ni-Fe em Soluções de Sulfato, 2010.
2 - CECCONELLO, E. L. S., Morfologia e Porosidade de Níquel Eletrodepositado em Cobre, 2006.

**Área: ___ELE_____ Inscrição:_00840_**

# Nanoporous Gold Microelectrode as Scanning Electrochemical Microscopy (SECM) Probe for the Study of Dopamine (DA) Diffusion

**Jéssica S. G. Selva (PG),[1] Henry S. C. Sáenz (IC),[2] Lucas H. Saravia (PG),[1] Anandhakumar Sukeri (PQ),[1] Patricio J. E. Montero (PQ),[3] Mauro Bertotti (PQ) [1]**

**jessica.soares.iq@usp.br**

*[1]Departamento de Química, IQ-USP; [2]Departamento de Ciência dos Alimentos e Biotecnologia, Escola Politécnica Nacional (Equador); [3]Centro de Investigação e Controle Ambiental, Escola Politécnica Nacional (Equador)*

Palavras Chave: *Dopamine,nanoporous gold.microelectrode,scanning electrochemical microscopy, SECM.*

## Highlights

A nanoporous gold microelectrode used as SECM probe for the detection of DA diffused through a membrane. Electrochemical images showed that NPG-µE is suitable for biosensing applications involving DA.

## Resumo/Abstract

A nanoporous gold microelectrode (NPG-µE) with enlarged electroactive surface area, high sensitivity and selectivity was fabricated for detection of DA. Aiming to demonstrate the applicability of this device, an electrochemical cell with two compartments separated by an impermeable membrane containing a micrometric hole in the middle was used to simulate the DA release (assuming like a living cell). Hence, the monitoring of DA diffusion through the membrane hole was performed using the NPG-µE as SECM probe as a proof-of-concept. The bottom compartment of the electrochemical cell was filled with a 20mmol $L^{-1}$ DA in 0.1 mol $L^{-1}$ PBS solution (pH 7), whereas the upper compartment contained only a 0.1 mol $L^{-1}$ PBS solution. The microelectrode was polarized at 0.25V and kept at a fixed height (20 µm) during the scanning along the xy plan of the membrane. The Fig.1 exhibits the optical image of the microelectrode near to the membrane hole and two SECM images regarding the DA diffusion. The expressive current increase shown in both images when the tip was moved close to the hole is a consequence of the transport of DA from the lower compartment to the upper one, producing a concentration gradient that can be visualized by the 3D image. These results suggest that the NPG-µE can be a suitable sensor platform for electrochemical detection of DA in microbiological environments.

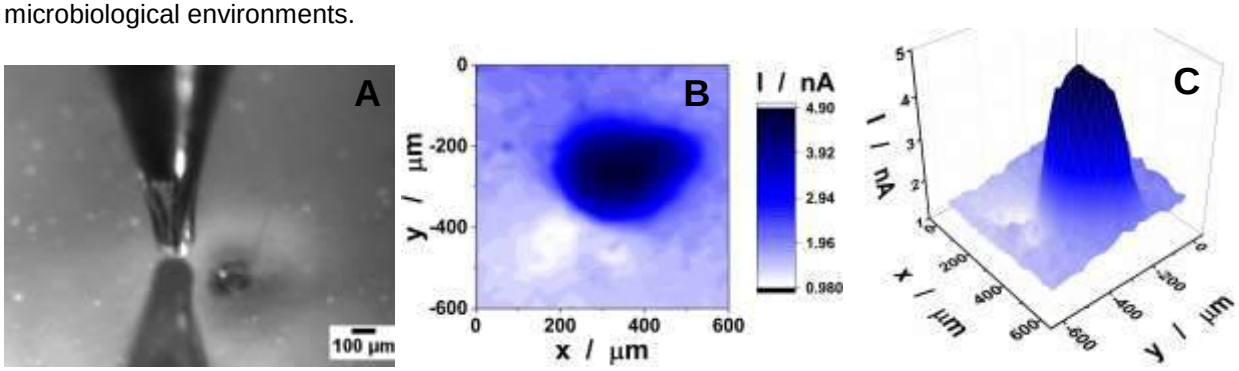


**Fig. 1 –** Optical image of NPG-µE and the membrane hole (**A**). Current map of the scanned area in 2D (**B**) and 3D (**C**). E = 0.25V. Pixel size = 25 x 25µm.

**Área: ELE** **Inscrição: 01275**

# Performance and caracterization a new electrochemical sensor based on $Fe_3O_4$/MWCNT-O to detection Metribuzin Herbicide

**Leonardo Amaral Lopes da Silva (PG)[1], Marcela Zanetti Corazza (PQ)[1], Adriana Evaristo de Carvalho (PQ)[1].**

**leonardoamaral8@gmail.com; marcelacorazza@ufgd.edu.br; adrianacarvalho@ufgd.edu.br**

[1] *Faculdade de Ciências Exatas e Tecnologia, Universidade Federal da Grande Dourados.*

Palavras Chave: *Magnetite, Carbon Nanotube, Adsorption, Metribuzin.*

## Highlights

- Here one new sensor is proposed to pesticides determination
- $Fe_3O_4$/MWCNT-O as modifield carbon paste electrode
- New material with better surface area than graphite

## Resumo/Abstract

Modifield electrodes can be used to improve some quality, like surface area, selectivity, or sensibility. In this context herer we propose a new sensor constructed of graphite powder and magnetic nanoparticles supported in oxided carbon nanotubes to used as sensor for pesticides determination. Our material werer characterized by FT-IR, TGA, BET, the morphology were analyzed by TEM and SEM. The electrochemical response towards standard probe potassium iron cyanide were analyzed using cyclic voltammetry and Electrochemical impedance spectroscope this techniques give us electrochemical active surface area, towards carbon paste electrode, our new propose sensor show a better signal. Athwart electrochemical impedance spectroscope were maked adjust to circuit and we calculate heterogeneous Kinect constant.

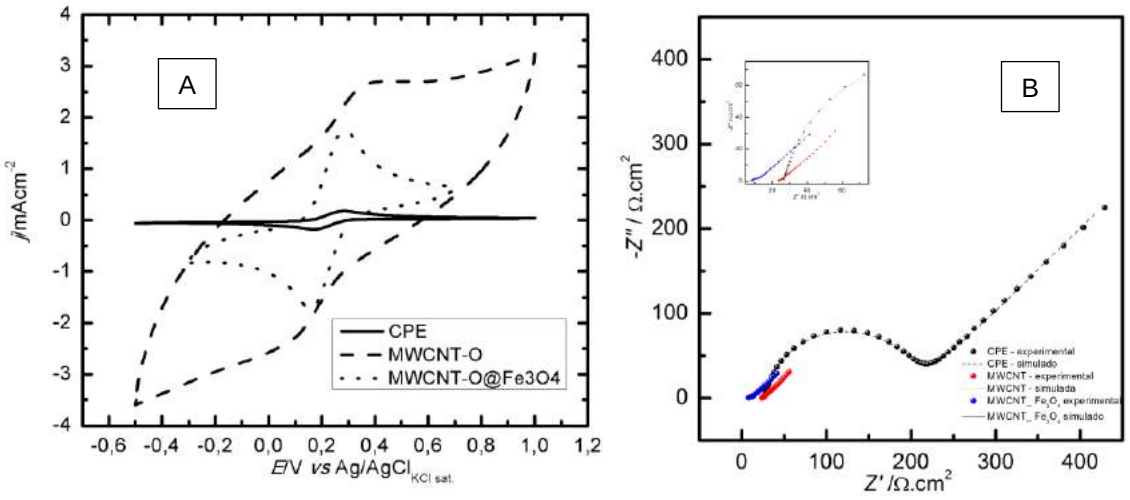


**A)** Cyclic voltamogran of thre electrodes testeds carbon paste electrode (curve line), carbon paste electrode modifield with mult walled carbon nanotubes oxided (dashe line) and modifiel electrode with final material, magnetic carbon nanotubes oxided (point line). **B)** Electrochemical impedance spectroscope of testeds electrodes and respective adjust fit simulations. Carbon paste electrode (black point), mult walled carbon nanotubes oxided (point red) and magnetic mult walled carbon nanotubes oxided (blue point).

**Área: ELE**

**Inscrição: 01215**
*(Inserir o número de inscrição do autor que fez a submissão)*

# Voltammetric study of nitrofurazone in ionic liquids by using a carbon fiber microelectrode

**Luísa D. Chiavassa[1]*(PG), Fernanda F. Camilo[1] (PQ), Mauro A. La Scalea[1](PQ)**

**luisadchiavassa@gmail.com; mauro.scalea@unifesp.br**

*[1]Departamento de Química, Instituto de Ciências Ambientais, Químicas e Farmacêuticas, Universidade Federal de São Paulo, Rua Prof. Artur Riedel.275, Diadema, SP 09972-270, Brasil*

Palavras Chave: *nitrofurazone, carbon fiber microelectrode, nitro-anion radical, ionic liquids,*

## Highlights

The nitrofurazone reduction was studied by cyclic and square-wave voltammetric techmiques. The nitro-anion radical formation was observed in ionic liquids having a carbon fiber as working microelectrode.

## Abstract

Nitrofurazone (NF) exhibits a broad spectrum of biological action and the understanding of its reduction mechanism in aqueous media has been widely studied. The NF reduction was studied by cyclic (CV) and square-wave (SWV) voltammetric techniques having a homemade carbon fiber microelectrode and employing three different ionic liquids: 1-Butyl-3-methylimidazolium bis(trifluoromethanesulfonyl)imide (BMImTf2N), 1-Ethyl-3-methylimidazolium bis(trifluoromethanesulfonyl)imide (EMImTf2N) and 1-Butyl-3-methylimidazolium tetrafluoroborate ($BMImBF_4$). The NF reduction behavior was similar for the three ionic liquids used, being a single cathodic peak (-0.623 V, -0.742 V and -0.760 V in $BMImBF_4$, $BMImTf_2N$ and $EMImTf_2N$, respectively) recorded by SWV. However, only the SW voltammograms obtained in $BMImBF_4$ and $BMImTf_2N$ showed that the net currents are composed by the forward and backward components, which indicates the existence of a reversible system (Figs. 1A and 1B). Similarly, this reversibility also could be observed by CV, since a reversible redox couple was recorded for the NF reduction in the same ionic liquids (Figs. 1C and 1D). From the frequency variation by SWV it was observed that the cathodic peak potential values were practically kept constant and that the net currents varied linearly with the frequency square-root, confirming a reversible system with adsorption of the reagent and product on the electrode surface. Based on this behavior, it was possible to calculate the number of electrons involved in the NF reduction in $BMImBF_4$ and $BMImTf_2N$, reaching values between 0.8 and 0. 9, indicating clearly a nitro-anion radical generation.

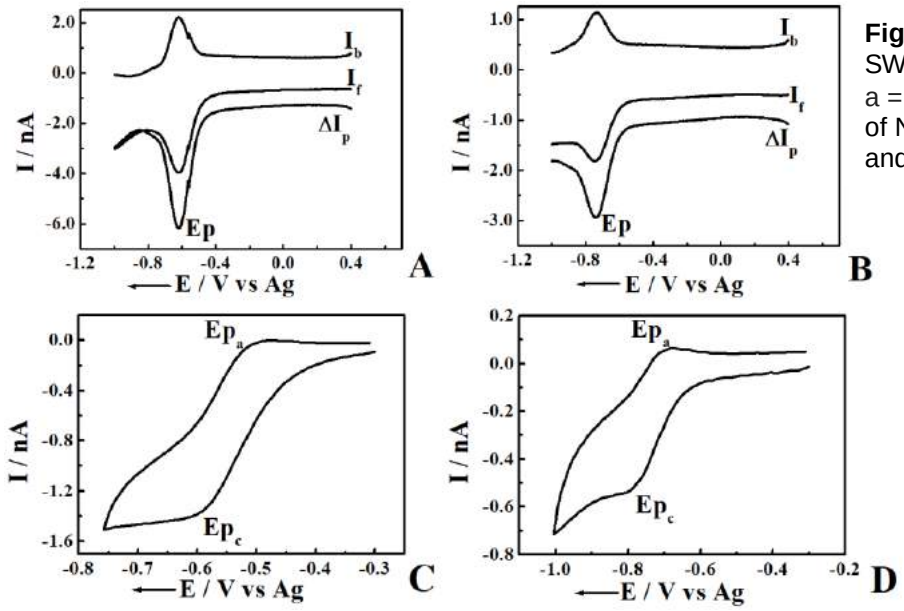


**Figure 1.**
SWV ($f$ = 100 Hz; ΔEs = 2 mV; a = 50 mV) and CV (ν = 500 mV/s) of NF 10 mmol $L^{-1}$ in $BMImBF_4$ (A;C) and $BMImTf_2N$ (B;D).

**Área: ELE** **Inscrição: 01039**

# Fabrication of a disposable electrochemical paper-based device for cortisol quantification

**Letícia. F. Mendes (PG)*[1], William R. de Araujo (PQ)[1] e Thiago R. L. C. Paixão (PQ)[1]**

***leticiafrancinemendes@yahoo.com.br; leticiafrancinemendes@yahoo.com.br**

[1] *Instituto de Química - USP, Av. Prof. Lineu Prestes, 748 – São Paulo – SP – Brazil.*

Keywords: *Cortisol, paper, disposable device.*

## Highlights

In this work we developed a disposable and low-cost paper-based device for cortisol detection using graphite leads as inexpensive working electrode material.

## Abstract

Cortisol is a steroid hormone, secreted by adrenal gland that plays an important role in physiological processes regulation such as inflammation, blood pressure and glucose levels. Therefore, in severe stress, there is a considerable high production of this hormone in human, which is why popularly it is called “stress-hormone”, indicating that cortisol could be a good biomarker to measure the stress level in biological fluids[1]. Hence, cortisol monitoring is important and new strategies have been developed to cortisol quantification, such as electrochemical techniques, due their facility and simplicity[2]. Additionally, paper-based devices have attracted great attention in analytical chemistry due their interesting advantages, such as low-cost, easy fabrication, operational simplicity, besides being disposable devices, where it is possible to use as portable platform for electrochemical measurements[3]. In this work, initially, a glassy carbon electrode was used to investigate electrochemical behavior of cortisol in a conventional electrochemical cell using 0.1M acetate buffer solution pH = 4.5 as electrolyte. In this case, cortisol exhibited an irreversible reduction process around -1.30 V versus $Ag/AgCl_{(KCl\ 3M)}$ using Square Wave Voltammetry (SWV) technique. However, reproducible measures were not attained due the strong adsorption effect, hindering the electrode surface renovation. Therefore, a disposable sensor was developed to circumvent this drawback in the cortisol sensing. We fabricate a low-cost paper-based device using a chromatography paper and wax printing technology. The pseudo-reference electrode was painted using conductive silver ink. After that, the printed paper was heated in a stove for 30 min at 80 ºC. Then graphite leads were used as working and counter electrodes. Electrochemical tests using SWV method were performed in 0.1M acetate buffer solution pH = 4.5 as electrolyte. It was observed that the cortisol reduction peak appears at approximately -1.50 V *vs* Ag. In addition, potassium ferricyanide was used as internal standard to correct lack of reproducibility associated with the fabrication process providing low standard deviations when the devices are single used. A linear range of 10 - 100 µmol $L^{-1}$ was achieved, showing a great potential of these devices for cortisol analysis.

**Acknowledgment**

CNPq, CAPES and FAPESP.

**References:**

1. A. KAUSHIK, A. Vasudev, S. K. Arya, S. K. Pasha, S. Bhansali. Biosens. Bioelectron. 53 (2014) 499-512.
2. J. Smajdor; R. Piech; M. Rumin; B. P. Bator. Electrochimica Acta 182, (2015) 67-72.
3. W. R. de Araujo, T. R. L. C. Paixão, Analyst 139 (2014) 2742–2747.

**Área: ELE** **Inscrição:01003**

# Electrochemical sensor based on MIP grafted on multi-walled carbon nanotubes for 17β-estradiol determination

**Gabriel L. Marques (IC),[1] Dayana M. dos Santos (PQ),[1] Fernanda G. de Almeida (IC),[1] Luana R. Rocha (PG) [1]; César R.T. Tarley (PQ).[1,2*]**

**fergarciaalmeida@gmail.com; tarley@uel.br**

*[1]Departament of Chemistry, State University of Londrina (UEL); [2]National Institute of Science and Technology of Bioanalytics (INCT), State University of Campinas (UNICAMP).*

Keywords: *Estrogens, Carbon nanotubes, MIPs, Cyclic voltammetry.*

## Highlights

Development of innovative electrochemical sensor based on multi-walled carbon nanotube and molecularly imprinted polymer. Optimization of electroanalytical parameters for 17β-estradiol determination.

## Resumo/Abstract

The 17β -estradiol (E2) is a natural estrogenic hormone of great relevance in physiological process and for the development of sexual female features.[1] For the determination of this compound in biological matrices, sensitive, cheap and low-cost methods have been developed, as electroanalytical techniques and the use of sensors.[2] Aiming the increase of sensor selectivity, the use of molecularly imprinted polymers (MIPs) is investigated[1]. However, MIPs have an insulating property, and their synthesis supported in a conducting material as multi-walled carbon nanotubes (MWCNT) can be an interesting alternative.[3] In this sense, the present work aims the development of a voltammetry sensor for the determination of E2, based on the modification of a bare glass carbon electrode (GCE) with the grafted MIP-MWCNT. Optimized voltammetric measurements were performed using the PalmSens potenciostat/galvanostat in cyclic voltametric mode with the parameters: potential: -1,0 to 1,0 V; step: 0,03 V; scan rate: 0,5 V/s; deposition time: 270 s at -1,5 V. Studies involving optimization of suspension and support electrolyte were developed. Results have been demonstrating higher anodic peak of estradiol compared with the GCE or oxidized MWCNT. For the suspension, the major peaks were obtained for concentration: MIP (2,0 mg)/ DHP (2,0 mg) in 2,0 mL of ethanol, where the support electrolyte with the best results was phosphate buffer in pH 7,0. Until now, the use of MIP-MWCNT electrodes presents a great potential in application of E2 quantification and further studies will be developed.

1. Florea, A.; Cristea, C.; Vocanson, F.; Săndulescu, R.; Renault, J. N. Electrochem. Commun. 2015, 59, 36.
2. Gorla, F. A.; Duarte, E. H.; Sartori, E. R.; Tarley, C.R.T. Microchem J. 2015, 124, 65.
3. Moretti, E. S.; Giarola, J.F.; Kuceki, M.; Prete, M.C.; Pereira, A.C.; Tarley, C.R.T. RSC Adv., 2016, 6, 28751

**Área: ELE** **Inscrição: 00985**

# Development of an electrochemical lectin-based biosensor using a novel Galectin-1-Maltose Binding Protein fusion molecule.

**Pâmela O. M. Gomes (PG),[1] Thaís Canassa De Leo (PG),[2] Marina Ribeiro Batistuti (PQ),[2] Marcelo Dias-Baruffi (PQ),[2] Zeki Naal (PQ)[2].**

pamelaomartins@usp.br

*[1]Faculty of Philosophy Sciences and Letters of Ribeirão Preto - University of São Paulo - Brazil; [2]School of Pharmaceutical Sciences of Ribeirão Preto - University of São Paulo - Brazil.*

Keywords: *Biosensors, MBP-Gal-1, PPB, Oriented Immobilization.*

## Highlights

Genetic engineering methodologies have been widely employed to develop biosensors which are designed through the oriented immobilization of a protein onto an appropriately chemically modified surface.

## Abstract

The development of new analytical devices is totally dependent on the integration of various areas such as biotechnology, chemical biology and genetic engineering. Such devices are essential for linking and elucidating chemical and biochemical processes by improving accuracy, sensitivity, and operational simplicity with low cost.[1] An extremely interesting strategy to promote integration between electrochemical techniques and genetic engineering is the employment of lectin-based biosensors for the detection and quantification of biomolecules. In this work, we described the production of a novel chimeric-lectin composed by Galectin-1 (Gal-1), a multifunctional β-galactoside-binding protein which is being constantly investigated because of its intriguing role in cancer[2], and Maltose Binding Protein (MBP). Also, the electrochemical behavior of (MBP-Gal-1) was reported using Cyclic Voltammetry (CV) and Electrochemical Impedance Spectroscopy (EIS). The soluble and homogenous preparation of MBP-Gal-1 was obtained by affinity chromatography on amylose resin and analyzed by SDS-PAGE, MALDI-TOF/TOF, Western-blot, and Dynamic Light Scattering (DLS). The pure MBP-Gal-1 presented molecular mass of 57,83 kDa. For EIS analyses, MBP-Gal-1 was immobilized onto bared gold electrodes and glassy carbon modified with a redox polymer, obtained from oxidation of N-(3-pyrrol-1-ylpropyl)-4,4'-bipyridine (PPB), which interacts with the MBP domain.[3] Preliminary data on EIS suggested that this system provided an oriented immobilization of MBP-Gal-1 chimeric protein onto PPB-modified surface. In addition, Gal-1 lectin activity was preserved and was confirmed through interaction with lactose. These results suggest that MBP-Gal-1 could be a promising lectin-based biosensor for electrochemical platform to evaluate the interactions between Gal-1 and different targets.

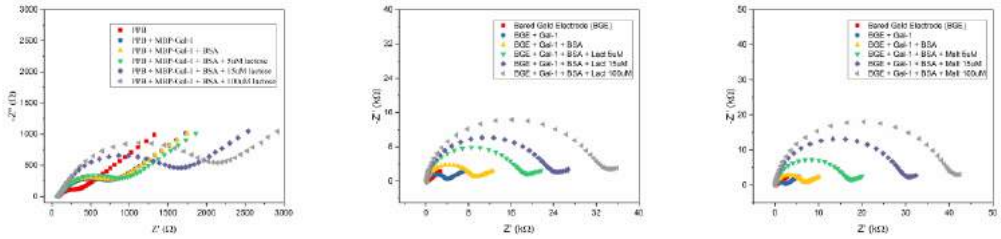

**Figure 1:** Nyquist plots obtained from characterization of different layers, using Gal-1 and MBP-Gal-1 fused protein.

## References

1. Pu, J. *et al.* Evolution of a split RNA polymerase as a versatile biosensor platform. *Nature Chem. Biology,* **13**, 432-440 (2017).
2. Park, Y. K. *et al.* Binding affinities of carbohydrate-conjugated chlorins for galectin-3. *Bull. Korean Chem. Soc.* **29,** 130-134 (2008).
3. Naal, Z. *et al.* Amperometric TNT biosensor based on the oriented immobilization of a nitroreductase maltose binding protein fusion. *Anal. Chem.* **74,** 140-148 (2002).

**Área: ELE**
*(Inserir a sigla da seção científica para qual o resumo será submetido. Ex: ORG, BEA, CAT)*

**Inscrição: 00954**
*(Inserir o número de inscrição do autor que fez a submissão)*

# Submicro quantification of N-acetylcysteine by electrochemically-driven homogeneous catalysis, on boron-doped diamond electrodes

**Marilia O.F. Goulart (PQ),[1] Ana Caroline F. Santos (PG),[1] Fabiana A. Moura (PQ),[1] Rita C.S. Luz (PQ),[2] Lauro T. Kubota (PQ),[3] Flavio S. Damos (PQ)[2]**

[1] *Universidade Federal de Alagoas, Av. Lourival Melo Mota s/n – Maceió- AL;* [2] *Universidade Federal do Maranhão-Avenida dos Portugueses s / n – São Luís –MA; UNICAMP, Campinas, SP, Brazil; INCT-Bioanalítica*

*Palavras Chave: Biothiols; electroanalysis, thiol/disulfide equilibrium; boron-doped diamond electrode;*

## Highlights

Use of boron-doped diamond for the electroanalysis of biothiols, simple and sensitive method in submicro levels

## Resumo/Abstract

Biologically relevant thiols (biothiols) are the most important systemic and intracellular endogenous antioxidants, useful in the fight against oxidative stress (OS). This work describes the development of a simple and ultrasensitive electrochemical method for the determination of N-acetylcysteine (NAC), on a boron doped diamond electrode (BDDE), based on an electrochemically-driven homogeneous catalysis, between lipoic acid ($LipS_2$) and NAC. $LipS_2$ suffers oxidation to the sulfoxide, at potentials around +0.85 V vs Ag/AgCl. The addition of NAC (not oxidized at this potential) causes the increase of the anodic current of $LipS_2$. Analytical parameters were obtained and redox mechanisms were proposed. The electrochemical response of NAC, in the presence of $LipS_2$ is strongly pH-dependent and favored in neutral pH, being 7 the best value, which facilitates the application and the study of this interaction in biological samples. Several analytical parameters of the method were optimized for NAC, and the analytical curves were built in the range of 1 up to 100 μmol $L^{-1}$, with a good correlation coefficient (0.993), with a submicrodetection limit of 93 nM. This method was successfully applied in pharmaceutical samples (capsules, syrup and suspension) containing NAC. The present study shows that the redox homogeneous reaction between the studied thiol and disulfide, on BDDE, is a promising analytical tool, which can be used for quantifying NAC in a simple, rapid, convenient, sensitive and low-cost way.

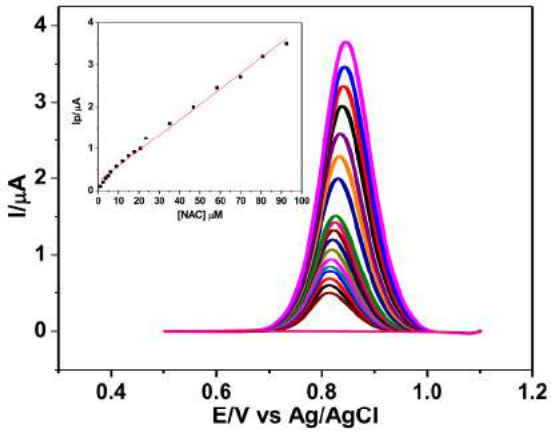


Figure 1. Differential pulse voltammograms with consecutive additions of NAC (NAC concentration from 1 μM up to 100 μM), pH 7 in 0.1 M McIlvaine buffer solution in presence of 5 μM $LipS_2$. The inset shows the analytical curve to NAC.

**Area:** ELE **Inscription:** 00762

# Electrochemical biosensor based on botryosphaeran as a novel biomaterial for laccase immobilization

**Gabriel Junquetti Mattos (IC)[1*], Aneli de Melo Barbosa-Dekker (PQ)[1], Robert F. H. Dekker (PQ)[2], Pedro Henrique Cury Camargo (PQ)[3], Eduardo César Melo Barbosa (PG)[3], Elen Romão Sartori (PQ)[1].**

**gabrieljunquetti@gmail.com**

*[1]Departamento de Química, Universidade Estadual de Londrina; [2]Universidade Tecnológica Federal do Paraná, Programa de Pós-Graduação em Engenharia Ambiental, Câmpus Londrina; [3]Universidade de São Paulo - Departamento de Química Fundamental do Instituto de Química – São Paulo.*

Keywords: *Laccase, botryosphaeran, electrochemical biosensors, nanostructured materials, phenolic compounds.*

## Highlights

A novel biosensor platform was developed using carbon electrode/AuNps.
Laccase from *Botryosphaeria rhodina* was immobilized on the exopolysaccharide, (1→3;1→6)-β-D-glucan.
Hydroquinone was determined in different sample types.

## Abstract

A new architecture for a novel biosensing platform is proposed using the exopolysaccharide, botryosphaeran (EPSB) and a crude laccase extract (CLE)[1] from the ascomyceteous fungus *Botryosphaeria rhodina* MAMB-05. Laccase was immobilized by physical adsorption on botryosphaeran using a carbon black paste electrode (CBPE) modified with gold nanoparticles (AuNps). The physicochemical characterization of the biosensor was performed by using transmission electron microscopy and electrochemical impedance spectroscopy. The performance of this novel biosensing platform was evaluated by choosing hydroquinone (HQ) as a typical model of a phenolic compound. Different sensors were prepared to evaluate the contribution of each modifier employed (Fig. 1). All electrodes showed better responses than the unmodified CBPE, and the highest analytical signal was obtained using the immobilized laccase on the CBPE-AuNps support. This could be attributable to the electrocatalytic properties of AuNps[2] associated with the stable immobilization mechanism proposed, by EPSB, that promotes a biocompatible microenvironment, since both biomaterials were produced by the same fungus, and the EPSB did not affect laccase activity. Experimental variables such as laccase concentration, the pH value and operational parameters of the electroanalytical technique were optimized. Using square-wave voltammetry, we observed a linear dependence of cathodic peak current and hydroquinone concentration in the range of 2.00 - 56.5 μmol $L^{-1}$ with a detection limit of 0.143 μmol $L^{-1}$ (Fig. 2). The proposed methodology was successfully applied in determining HQ in a dermatological cream, and in environmental and synthetic biological samples. Good selectivity was presented in the presence of other organic compounds, inorganic ions, and attests the potential application of this novel biosensing platform in complex matrices. The different aspects regarding the operational stability of this laccase-biosensor were evaluated, and showed good intra-day and inter-day repeatability, as well as long-storage stability.

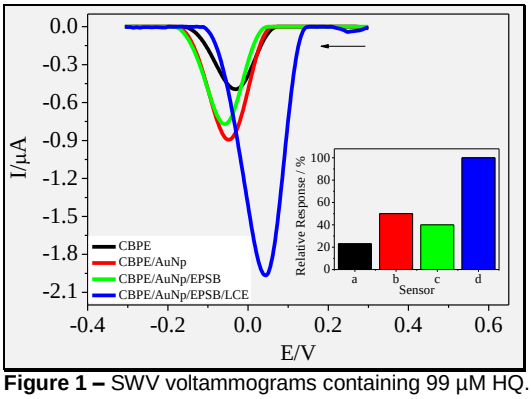


**Figure 1 –** SWV voltammograms containing 99 μM HQ. Insert graph: Relative response.

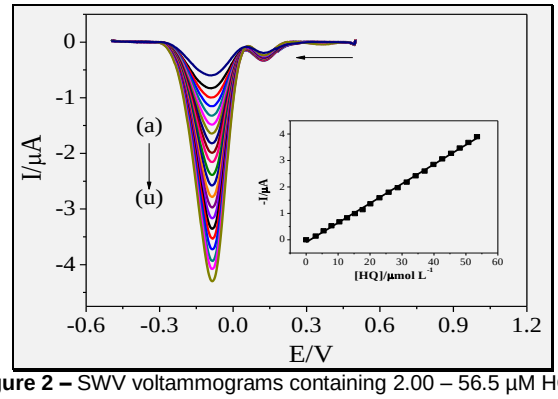


**Figure 2 –** SWV voltammograms containing 2.00 – 56.5 μM HQ. Insert graph: Analytical curve.

**References:**

[1] M. D. Cannatelli and A. J. Ragauskas, *Chem. Rec.*, 2017; [2] T. R. Silva and I. C. Vieira, *Analyst*, 2016.

**Área: ELE** **Inscrição: 717**

# Complex Dynamic during the oscillatory electro-oxidation of glucose on platinum

**Graziela C. A. Ferreira (PG), Hamilton Varela (PQ)***

**grazielacaferreira@gmail.com; hamiltonvarela@usp.br**

*Institute of Chemistry of São Carlos, University of São Paulo, PO Box 780, 13560-970, São Carlos-SP, Brazil*

*Keywords: Electrocatalysis, glucose, platinum oscillations.*

## Highlights

We have studied the emergence of oscillatory reaction rates during the electrocatalitic oxidation of glucose on platinum, in aqueous acidic and alkaline media.

## Abstract

Understanding mechanistic details of the electrocatalytic oxidation of glucose is important from both fundamental and applied perspectives. Glucose is an abundant and environmentally friendly carbohydrate and generate 24 electrons in its complete oxidation. The objective of this work was to investigate the catalytic activity of Pt towards the electro-oxidation of glucose, in acidic and alkaline medium, exploring the oscillatory kinetics and its implications in practical systems. The very rich oscillatory dynamics observed under galvanostatic regime has been characterized. High amplitude potential oscillations (0.5 to 0.9 V), Figure 1(a), were observed in acidic and alkaline media and the periodic oscillation between high and low potential values may represent a self-cleaning process for the catalytic surfaces. However, potential oscillations in acidic media are unstable, whereas in alkaline media are very stable and have long duration. This process allows the oxidation of strongly adsorbed intermediates at each potential oscillation cycle and increases the power density of practical conversion systems of chemical to electrical energy c.f. Figure 1(b).

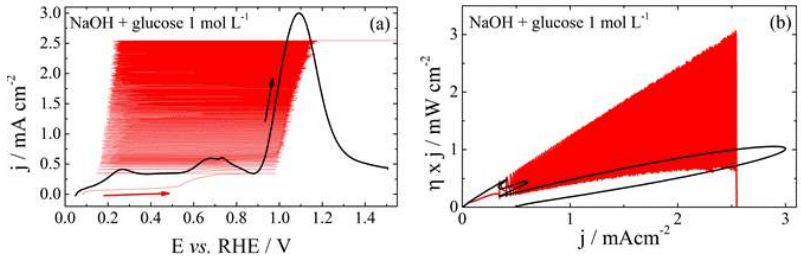


Figura 1: (a) Potentio (black)/galvanodynamic (red) sweeps, and (b) power density *vs.* current density curves, for oscillatory and regular regimes. Electrode: polycrystalline platinum; electrolyte: aqueous 0.5 mol $L^{-1}$ NaOH and 0.5 mol $L^{-1}$ $H_2SO_4$. dE/dt = 50 $mVs^{-1}$, and dI/dt = 0.1 μA $s^{-1}$.

Acknowledgments: The authors acknowledge FAPESP, Capes e CNPq.

**Área: ELE** **Inscrição: 00680**

# Carbon nanotube/reduced graphene oxide nanocomposite formed at interfacial method: Properties and potential electroanalytical applications

**Diego P. Rocha (PG)*,[1] Sílvia V. F. Castro (PG),[1] Murilo N. T. Silva (PG),[1] Rafael M. Cardoso (PG),[1] Thiago F. Tormin (PG),[1] Eduardo M. Richter (PQ),[1] Edson Nossol (PQ),[1] Rodrigo A. A. Munoz[1] (PQ).**

**diego_co2@hotmail.com;**

[1]*Instituto de Química, Universidade Federal de Uberlândia*

Palavras Chave: *Batch-injection analysis, Boron doped diamond, Catechol, Dopamine, Forensic, Trinitrotoluene*

## Highlights

New route to produce CNT/rGO nanocomposite thin films using the interfacial method.
Comparison of CNT-, rGO- and CNT/rGO-modified BDDE regarding to molecules of pharmaceutical and forensic interest.

## Resumo/Abstract

This work presents a new route to produce carbon nanotube/reduced graphene oxide (CNT/rGO) nanocomposites using the interfacial method to produce high-performance electroanalytical sensing. The nanocomposite thin-film is formed at the cyclohexane/water immiscible interface after stirring of a mixture of CNT and rGO in the biphasic solution and can be transferred to any planar substrate. As a proof-of-concept, the nanocomposite film was transferred to a boron-doped diamond electrode. Improved electrochemical sensing of molecules of pharmaceutical (phenolic compounds (dopamine and catechol)) and forensic interest (trinitrotoluene (TNT)) under stationary (cyclic voltammetry) and hydrodynamic (amperometry) conditions was verified in comparison with unmodified and modified surfaces with rGO and CNT using the same method. Electrochemical impedance spectroscopy also evidenced the faster electron transfer for a redox probe on the nanocomposite surface. Scanning electron microscopic images show the interaction of rGO with CNT and Raman spectra revealed the defect density. Amperometric and voltammetric detection of phenolic compounds and TNT, respectively, showed synergistic properties of CNT and rGO on the response of nanocomposite, which resulted in highly sensitive sensors with superior performance in comparison with electrochemical sensors based on CNT or rGO already reported (nanomolar detection limits for dopamine, catechol, and trinitrotoluene). Hence, this new protocol offers great promises to develop improved electrochemical sensors for a wide range of analytes, including pharmaceutical and forensic applications.

Acknowledgements: FAPEMIG, CAPES, CNPq, IQUFU.

**Área: ELE** **Inscrição: 00574**

# Desenvolvimento e caracterização de um sensor fotoeletroquímico nanoestruturado utilizando $BiVO_4$

**Mayara da Silva Araujo (IC),[1] Juliana Costa Rolim Galvão (PG),[2] LuizaHenriqueaDall'Antonia (PQ),[1] César Ricardo Teixeira Tarley (PQ),[2] Roberto de Matos (PQ), Roberta Antigo Medeiros (PQ).[1]* asmayara@uel.br; ramedeiros@uel.br**

[1]*Departamento de Química, UEL*

Palavras Chave: *Sensor Fotoeletroquímico, nanopartículas de $BiVO_4$, Fotocorrente, caracterização eletroquímica, efeito fotoeletrocatalítico*

## Highlights

Development and characterization of a nanostructured photoelectrochemical sensor using $BiVO_4$
Nanostructured $BiVO_4$ photoelectrochemical sensor
ITO modified with bismuth vanadate
Higher Photocurrent signals obtained with visible light irradiation
Photoelectrocatalytic effect of $BiVO_4$ nanoparticles

## Resumo/Abstract

O desenvolvimento de sensores fotoeletroquímicos tem crescido significativamente, bem como, seu uso no desenvolvimento de procedimentos analíticos aplicados nas mais diversas. A detecção fotoeletroquímica consiste na produção de fotocorrente através da incidência de radiação na superfície do eletrodo modificado com um material fotoativo. [1].

Para a construção do sensor fotoeletroquímico foi utilizando o óxido de índio dopado com estanho (ITO) o qual foi limpo por sonicação em etanol e em água deionizada. A superfície do ITO foi modificada pela adição de 11,0 µL de uma suspensão contendo o vanadato de bismuto- $BiVO_4$ (2,0 mg $mL^{-1}$) e o polieletrólito fosfato ácido de dihexadecil (DHP) (1,0 mg $mL^{-1}$), procedendo com um tempo de secagem de no mínimo de duas horas.

Na caracterização eletroquímica do sensor desenvolvido, utilizou-se a técnica amperométrica e uma solução contendo uma solução de $K_3[Fe(CN)_6$ 1,0 mmol $L^{-1}$. Com pode ser observado na Figura 1 a intensidade do sinal de fotocorrente para o ITO puro é desprezível quando comparado à intensidade do sinal obtido com o ITO-$BiVO_4$, tais resultados comprovam o efeito fotocatalítico das nanopartículas de $BiVO_4$, como descrito na literatura[2], há um aumento de 25 vezes na intensidade do sinal de corrente ao irradiar luz visível à superfície do eletrodo. Tais resultados indicam a viabilidade e a eficácia na utilização das nanopartículas de $BiVO_4$ na confecção deste sensor fotoeletroquímico.

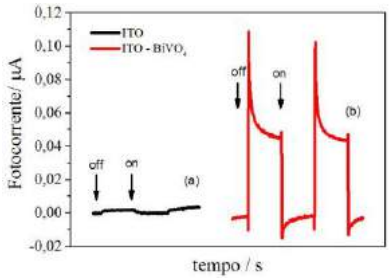


Figura 1. Amperogramas obtidos para ITO puro (linha preta) e ITO-$BIVO_4$ (linha vermelha), com irradiação (on) e sem irradiação (off) de luz visível.

Neste contexto, este sensor apresenta-se promissor para futuras aplicações no desenvolvimento de métodos eletroanaliticos.

[1] ZHANG, Chunjing; SI, Shihui; YANG, Zhengpeng. ***Biosens Bioelectron.*****,** 2015, 65, 115.
[2] SERAFIM, Jéssica Aparecida; AFONSO, Renata; LUCILHA, C., Adriana; OLIVEIRA, A., Lucas; SILVA, C., R., Paulo; SILVA, R., Marcelo; SARTORI, R., Elen; DALL´ANTONIA, H., Luiz.. ***Química Nova*****,** 2014, 37, 1158-1164.

**Área: ELE** **Inscrição: 00539**

# Electrochemical Bistability Induced by Surface Area Changes

**Júlia Rospendowiski (IC), Maria Rodrigues (PG), Raphael Nagao (PQ)***

**julia.rwk@gmail.com; nagao@iqm.unicamp.br**

*Institute of Chemistry – University of Campinas (UNICAMP)*

Keywords: *Electrodeposition, Nonlinear dynamics, Bistability.*

## Highlights

Electrodeposition of copper from acidic aqueous solutions is modified by the addition of small amounts of *o*-phenanthroline giving rise to bistability.

## Resumo/Abstract

Nanostructured metallic multilayers in the electrodeposition of copper can be spontaneously synthetized when the system is kept far from thermodynamic equilibrium. We have focused on the understanding of how blocking agents, mainly induced by strong adsorption, can tune the thickness of these self-organized layers, therefore, altering the total surface area. For this purpose, we perturbed the electrodeposition of copper under potentiostatic control with small amounts of *o*-phenanthroline (*phen*). Indeed, the addition of *phen* gives rise to a distinct current-potential profile. A negative differential resistance (NDR) and hysteresis are clearly observed in the cyclic voltammograms (Figure 1a-g). The appearance of the NDR is attributed to the adsorption of the reduced form of $[Cu(II)(o\text{-phen})_2]^{2+}$ complex in lower potentials which suppresses the copper electrodeposition. The hysteresis, in its turn, indicates that the system has two stable steady states (SSI and SSII) for the same set of controlling parameters, the so-called bistability (BS). By adding increasing values of external resistance ($R_{ext}$) between the working and reference electrodes, the hysteresis potential intervals become larger. We have monitored the bistability domain by mapping the bifurcation diagram $R_{ext}$ *vs.* E obtained from the experimental data (Figure 1h). Our results suggest that strong adsorption of copper complexes formed in the electrolyte can favor the appearance of bistability. This condition is important once it shows the presence of an autocatalytic process – a necessary step to generate electrochemical oscillations.

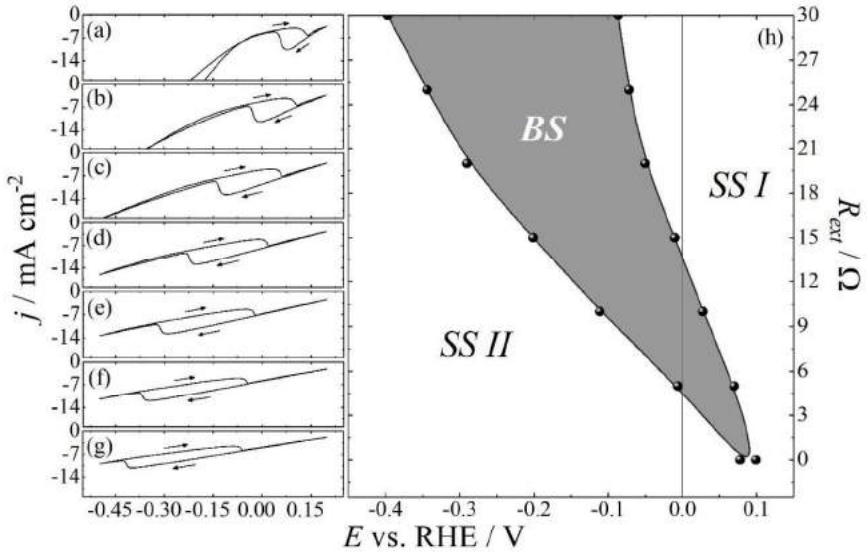


**Figure 1.** Cyclic voltammetry at d*E*/dt = 0.01 V $s^{-1}$ with different values of external resistances ($R_{ext}$) from (a) 0 to (g) 30 Ω, in steps of 5 Ω each. (h) Bifurcation diagram: $R_{ext}$ vs. E.

**Área: ELE** **Inscrição: 00489**

# Nanostructed Nickel Hydroxide Electrodes by Electrodeposition

**Gabrielle Cerqueira (IC),[1]* Rafael N. P. Colombo (PG),[1] Susana I. C. de Torresi (PQ).[1]**

**gabrielle.cerqueira.silva@usp.br**

[1] *Instituto de Química, USP.*

Keywords: *Nanostructure, Nickel Hydroxide, Nanocubes, Electrodeposition, Sensor, Nanoparticles.*

## Highlights

Nanocubic $Ni(OH)_2$ synthesized by the electrodeposition of Ni followed by electrochemical oxidation.
The material can be applied to selective non-enzymatic sensing.

## Abstract

Nickel hydroxide electrodes are highly researched[1] because it is versatility, being applied to electrochromism, non-enzymatic sensing and electrocatalysis.
Nanocubic $Ni(OH)_2$ is synthetized by electrodeposition of nickel on ITO (indium tin oxide) substrate, using a $NiSO_4$ and $NiCl_2$ solution. The conversion of Ni to $Ni(OH)_2$ was performed by cycling the ITO/Ni electrode in basic media.
Picture 1a shows the cyclic voltammogram of this conversion, emphasizing the change of the voltammograms by the number of cycles, Picture 1b presents the SEM image of the resulting material containing nanocubes of $Ni(OH)_2$ formed.
To verify the formation mechanism of the material, linear positive potential sweeps were made from 0V on steps of 0.1 V, Picture 1c presents the linear sweep of the first oxidation scan. And, the last Picture shows nanocubes formation at the region of 0.5 to 0.6 V, and the remaining amorphous structure of nickel.

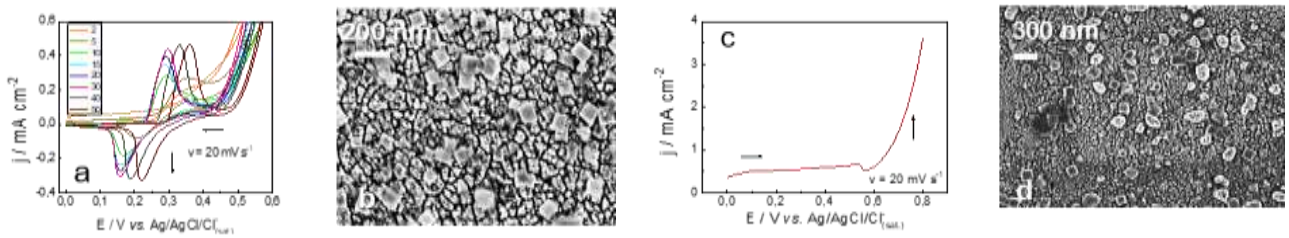


Picture 1 – a) Voltammetric cycling of ITO/Ni electrode, b) Electrode SEM after cycling, c) KOH linear potential sweep, d) SEM after Ni oxidation from 0.5 to 0.6 V.

The nanocubic $Ni(OH)_2$ is formed during the anodic voltammogram scan waves, and by increasing the number of cycles more Ni is converted to $Ni(OH)_2$ which would allow its application to non-enzymatic sensing on glucose solutions with preliminary results showing low response to common interferences, Picture 2.

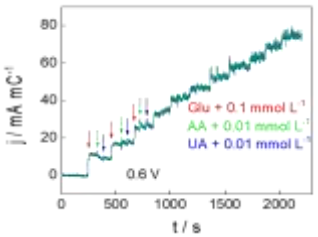


Picture 2 – Chronoamperogram of the electrode in presence of glucose, ascorbic and uric acids.

[1]Hall DS, *et al*, *R. Soc.*, 2015, A 471.

**Área:ELE**
*(Inserir a sigla da seção científica para qual o resumo será submetido. Ex: ORG, BEA, CAT)*

**Inscrição:** 00418
*(Inserir o número de inscrição do autor que fez a submissão)*

# Electrochemical study of carbon nanotube@polyaniline hybrid for application in active solar cell layer

**Luiza De L. Ferreira* (PG), Tcharles A. L. Fengler (IC), Hállen D. R. Calado (PQ)**

**luizadl@yahoo.com.br; hallendaniel@yahoo.com.br;**

*Departamento de Química, UFMG;*

Keyword: electrochemistry; cyclic voltammetry; impedance; carbon nanotube; polyaniline.

## Highlights

Electrochemical study of carbon nanotube@polyaniline hybrid for application in active solar cell. The hybrid solar cells are attractive for the energetic scenario by the lightness and low cost. The interconnected nanogrids formed by the insertion of MWCNT in the polymer matrix results in materials with better optoelectronic properties.

## Abstract

The carbon nanotube@polianiline hybrid (**MWCNT@TEPANI**) was synthesized in three steps: **MWCNT** oxidation; insertion of the amine tetraethylenepentamine - **TE**PA; polymerization of aniline - **PANI** (formic acid – HCOOH). The hybrid structure was confirmed by physico-chemical techniques, such as XPS and RAMAN. The electrochemical studies were conducted on a simple three-electrode cell (WE=Pt; CE=Pt; RE=Ag/Ag$^+$). The hybrid has better electrochemical properties (stability of the charge by cycling - Figure 2) and electrical (impendance study - Figure 3) compared to pure polymer (Figure 1).

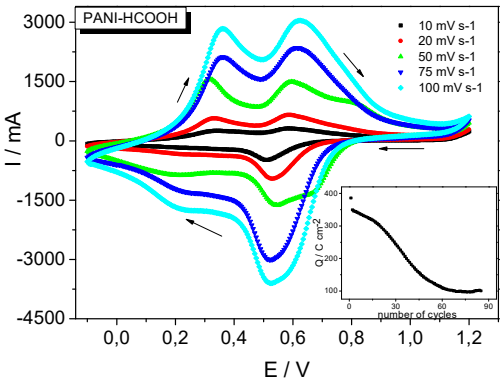


Figure 1: Cyclic voltammogram of PANI-HCOOH at different scan rates. Detail to the right: study of load loss by cycling.

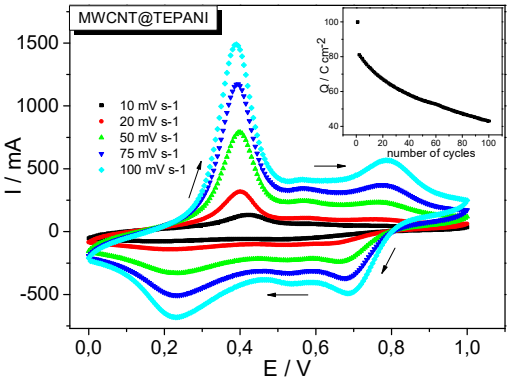


Figure 2: Cyclic voltammogram of MWCNT@TEPANI at different scan rates. Detail to the right: study of load loss by cycling.

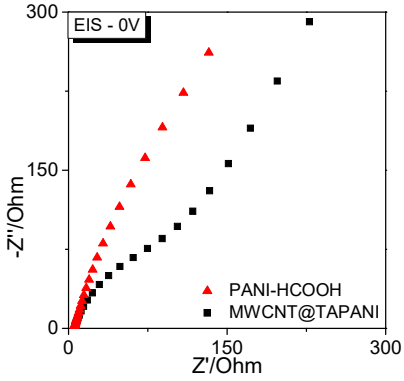


Figure 3: Electrochemical impedance spectroscopy for PANI and MWCNT@TEPANI.

Tabel 1: Electrochemical parameters for the polymers and the hybrid at 50 mV s$^{-1}$.

| | PANI | MWCNT@TEPANI |
|---|---|---|
| $E_{pa}$ / V | 0,59 | 0,40 |
| $E_{pc}$ / V | 0,55 | 0,22 |
| $I_{pa}$ / mA | 1,49 | 0,79 |
| $I_{pc}$ / mA | -1,63 | -0,33 |
| $E^{0'}$ / V | 0,57 | 0,31 |
| $E_{p/2}$ / V | 0,04 | 0,17 |
| η | 1,02 | 1,48 |

Acknowledgements: CNPq, FAPEMIG, CTNano.

**Área: _ELE_____ Inscrição:_00380_____**

# Enzymatic biosensor based on tyrosinase and gold nanostructures for Bisphenol A determination

**Filomeno A. D. Inroga (PG),[1] Jacqueline A. Silva (PQ),[1*] e Vladimir G. Lavayen (PQ)[1]**

**finroga@gmail.com; jacqueline.arguello@ufrgs.br**

*[1]Instituto de Química - UFRGS*

Palavras Chave: *Gold nanostructures, biosensor, BPA, cyclic voltammetry.*

## Highlights

Biosensor production based on tyrosinase. Gold nanoparticles electrodeposited on a screen-printed carbon electrode. Determination of optimum conditions, pH, preconcentration time, scan rate and calibration curve of BPA

## Resumo/Abstract

Gold nanostructures are versatile for a broad range of applications in various areas including catalysis, biomedicine, diagnostic and detection[1]. Their attractive characteristics such as high surface area, biocompatibility, high stability and potential of multifunctionality, make them suitable for the development of (bio)sensors[2]. In this work, we present the development and application of a tyrosinase-based biosensor for the detection of bisphenol A (BPA). Before enzyme immobilization, gold nanostructures were electrodeposited on a screen-printed carbon electrode (SPE) to improve the analytical performance of the biosensor. Leaf-shaped gold nanostructures resulted from the electrochemical reduction of tetrachloroauric acid ($HAuCl_4$) in a 0.1 mol $L^{-1}$ $Na_2SO_4$ aqueous solution through an applied potential of -0.6V for 600 s. The experiment was performed using a potentiostat/galvanostat Autolab PGSTAT128 (Ecochemie, Holland) interfaced to a computer and controlled by NOVA 2.1 software. The SEM image of the modified surface is depicted in Fig. 1a. For the enzyme immobilization, a solution containing 500 U of tyrosinase solution was dropped and left to dry. Nafion solution was also applied to prevent leaching of the enzyme into the solution. Cyclic voltammograms (CVs) were registered at different concentrations of BPA in 0.1 mol $L^{-1}$ phosphate buffer solution (pH=7.3) to evaluate the performance of the biosensor. The voltammograms exhibit a well-defined irreversible peak corresponding to BPA oxidation, see in Fig. 1b. For comparison, CVs were obtained using a modified SPE without the enzyme (shown in the inset of Fig. 1b`), a higher sensitivity it is observed in the presence of tyrosinase. The optimum conditions for the biosensor, pH, pre-concentration time and scan rate were studied, from which it was possible to construct a calibration curve of BPA Fig 1c., and LOD=0,93µmol/L.

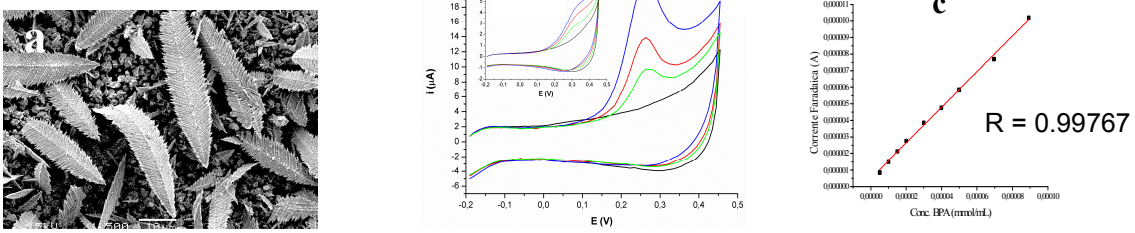


**Fig. 1. a**) Scanning electron micrograph (SEM) of the electrodeposited gold nanostructures; **b**) Cyclic voltammograms at different concentrations of BPA (0-30 µmol $L^{-1}$) using the biosensor; **b'**) Cyclic voltammograms obtained with the electrode without the enzyme e **c**) BPA analytical curve for the biosensor.

**References:** (1) S. Ashraf, B. Pelaz, P. Del Pino, M. Carril, A. Escudero, W. J. Parak, M. G. Soliman, Q. Zhang, C.Carrillo Carrion. Top. Curr. Chem. 370, 2016, 169-202.
(2) N. Sharma, G. Bhatt, P. Kothiyal. Indian J. Pharm. Biol. Res. 3(2), 2015, 13-27.

**Acknowledgments:** INCTBio, CNPq, PROPESQ-UFRGS and Calouste Gulbenkian Foundation.

**Área: ELE** **Inscrição: 00267**

# Performance of the $LiFePO_4$ in supercapatteries

**Paulo F. R. Ortega (PQ),[1,2] Guilherme O. Santos (IC),[2] Glaura G. Silva (PQ),[1] Clara Blanco (PQ),[3] Ricardo Santamaría (PQ),[3] Rodrigo L. Lavall (PQ),[1*]**

**Email: guielh@gmail.com; rodrigo.lavall@qui.ufmg.br**

*[1]Departamento de Química/ICEx, UFMG; [2]Departamento de Formação Geral, CEFET-MG/Campus IV; [3]Instituto Nacional del Carbón, INCAR/CSIC (Spain)*

Keywords: *($LiFePO_4$, Supercapatteries, Ionic liquid, Mesoporous carbon)*

## Highlights

The performance of the $LiFePO_4$ was investigated in supercapatteries;
Capacity data were compared with a standard ion-lithium cell;
Capacitive anode reduces the capacity of the $LiFePO_4$ at high currents.

## Abstract

Significant efforts have been devoted to finding new electrochemical storage devices capable of satisfying the high energy/power demands of electric cars.[1] In this context, it is desirable to find a device capable of combining the advantageous properties of batteries and supercapacitors in so-called supercapatteries (SCT).[2] SCT are devices that accumulate charge by means of different mechanisms: faradaic reactions in one electrode and electric double layer in the other. In this work, a SCT was assembled with a battery cathode ($LiFePO_4$), a mesoporous carbon as anode, and a mixture of Lithium bis(trifluoromethylsulfonyl)imide (LiTFSI) salt and the ionic liquid 1-Ethyl-3-methylimidazolium bis(trifluoromethylsulfonyl)imide (EMITFSI) as electrolyte. Here, the objective is to evaluate the performance of the $LiFePO_4$ in this SCT compared to a standard ion-lithium cell ($LiPF_6$ dissolved in ethylene carbonate/dimethyl carbonate (electrolyte); lithium metal (anode)).[3] The capacities are summarized in Table 1.

***Table 1.*** *Capacity values for $LiFePO_4$ at different C rates in SCT and in standard ion-lithium cell.*

| ***Current density / A $g^{-1}$*** | ***C rate*** | ***Capacity (mA h $g^{-1}$) (SCT)*** | ***Capacity (mA h $g^{-1}$) (standard ion-lithium cell)*** |
|---|---|---|---|
| *0.010* | *C/5* | *138.2* | *154.7* |
| *0.025* | *C/2* | *90.5* | *140.4* |
| *0.050* | *C* | *73.5* | *129.8* |
| *0.100* | *2C* | *51.0* | *114.9* |

At the lowest current densities, $LiFePO_4$ present similar capacities in both cells, and the SCT achieves a high energy density (43.3 W h $kg^{-1}$). However, the capacity is reduced at 2C by 63% in SCT and 74% in the battery. This effect shows the difficulty of $LiFePO_4$ in equalizing the kinetics of the electric double layer of the anode, reducing the energy density to 15.3 W h $kg^{-1}$ at $10^2$ W $kg^{-1}$. Based on these results, our group is dedicated to the synthesis of $LiFePO_4$ with morphologies more suitable for fast ionic insertion and to meet the demands of a SCT.

**Acknowledgements**

*CNPq, FAPEMIG, INCT de Nanomateriais de carbono, Rede Mineira de Química*

**References**

*[1]Energy Environ. Sci., 2012,5, 9363-9373*
*[2]Int. Mater. Rev., 2017, 62, 173-202*
*[3]J. Phys. Chem. C, 2018, 122, 1456−1465*

**Área: ELE** **Inscrição:00036**

# Eletrodeposição de prata usando líquido iônico [$HMIM^+$][$HSO_4^-$]

**Natalia Gomes Sousa (IC),[1] Camila P. Sousa (PQ),[1] Katlin I. B. Eguiluz (PQ),[2] Giancarlo R. Salazar-Banda (PG),[2] Adriana N. Correia (PQ),[1] Pedro de Lima-Neto (PQ).[1]**

**nataliagelcorr@gmail.com**

*[1]Grupo de Eletroquímica e Corrosão, DQAFQ-UFC, Fortaleza-CE; [2]Laboratório de Eletroquímica e Nanotecnologia-ITP/Programa de Pós-graduação em Engenharia de Processos, Universidade Tiradentes, Aracaju-SE*
Palavras Chave: *Eletrodeposição, Líquido iônico, Ouro, Prata.*

## Highlights

Electrodeposition of silver using ionic liquid [$HMIM^+$][$HSO_4^-$].
Morphological characterization of silver coatings was performed.
Morphology of silver coatings depends on the type of the electrodeposition mode.
Higher temperatures promoted more homogeneous coatings.

## Resumo/Abstract

Para atender a demanda atual por química sustentável, desenvolve-se revestimentos com menor custo-benefício, onde se obtenha material eletródico de elevada qualidade sem riscos ao ambiente. Nesse contexto, o uso de líquidos iônicos é essencial quando comparado a soluções aquosas, devido à sua baixa toxicidade e estabilidade em elevadas temperaturas. Neste trabalho, eletrodepósitos de prata foram obtidos usando $AgBF_4$ em hidrogenossulfato de 1-H-3-metilimidazol ([$HMIM^+$][$HSO_4^-$]) a 23, 35 e 45 ºC para avaliar o efeito da temperatura e do modo de eletrodeposição. Experimentos voltamétricos foram realizados utilizando disco de ouro como eletrodo de trabalho, pseudo-referência de fio de prata e placa de platina como eletrodo auxiliar. No modo potenciostático, os revestimentos foram obtidos em −0,04 V durante 60, 300 e 600 s; no modo galvanostático, aplicou-se 5, 15 e 30 mA $cm^{-2}$ para obtenção de revestimentos com espessura teórica de 10 μm. Nos dois modos de deposição observou-se que a morfologia do material eletrodepositado sofreu alteração (tabela abaixo). Potenciostaticamente com o aumento da temperatura e do tempo de deposição houve sobreposição do material inicialmente eletrodepositado em regiões isoladas da superfície, resultando em revestimento uniforme. Galvanostaticamente, houve formação dendrítica de prata a 23 ºC e 5 mA $cm^{-2}$; com o aumento da temperatura e da densidade de corrente para 45 ºC e 30 mA $cm^{-2}$, verificou-se agora, além de uniforme, a formação de filme compacto. Assim, conclui-se que a eletrodeposição de prata em [$HMIM^+$][$HSO4^-$] é influenciada pelo modo e pela temperatura de deposição.

**Tabela -** Imagens obtidas por microscopia eletrônica de varredura dos filmes de prata formados sobre ouro

| | **Modo Potenciostático** | | | **Modo Galvanostático** | |
|---|---|---|---|---|---|
| T. | 60 s | 600 s | 1μm | 5 mA $cm^{-2}$ | 30 mA $cm^{-2}$ |
| 23 ºC | 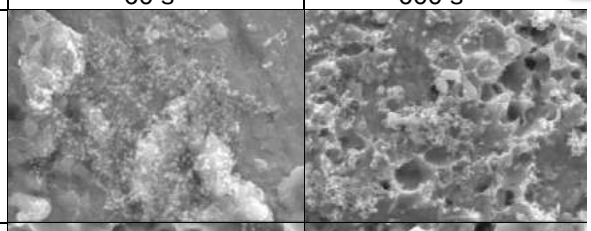 |  | | 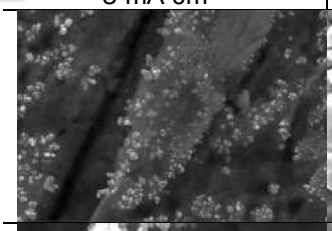 | 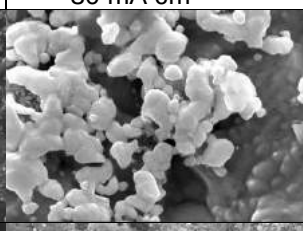 |
| 45 ºC | 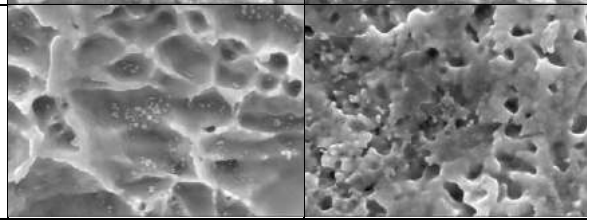 |  | | | |

**Área: ELE** **Inscrição: 00927**

# MBP-Gal-1 chimeric protein immobilization onto GCE functionalized by electrochemical reduction of pyridinium diazonium derivative

**Miquéias Ferreira Gomes (PG),[1] Pâmela Oliveira Martins Gomes (PG),[1] Wesley Romário da Silva (TC),[1] Marina Ribeiro Batistuti (PQ),[1] Paulo Marcos Donate (PQ).[1] Zeki Naal (PQ).[2]***

**miqueiasgomes@usp.br**

[1]Faculty of Philosophy Sciences and Letters of Ribeirão Preto - University of São Paulo - Brazil; [2]School of Pharmaceutical Sciences of Ribeirão Preto - University of São Paulo - Brazil.

Keywords: *Electrochemically Modified Electrode, Maltose Binding Protein, Galectin-1, Electrochemical Capacitance Spectroscopy*

## Highlights

This work shows results regarding the immobilization of Galectin-1 fused with maltose binding protein on pyridinium diazonium salt modified electrode film. Electrochemical Capacitance Spectroscopy (ECS) results suggest that protein maintained its activity after immobilization.

## Abstract

Galectin-1 (Gal-1) is a member of galectin family which have an important role in tumor progression and proliferation, angiogenesis, resistance to drugs and masking against recognition by the immune system[1]. Thus, there is a great interest in the development of biosensors which use Gal-1 as a biomarker for oncological conditions[2]. In this work, we investigated the oriented immobilization of the chimeric Gal-1 onto glassy carbon electrode (GCE) electrically modified by the pyridinium diazonium salt in situ generate from 1-(4-aminophenethyl)-[4,4'-bipyridin]-1-ium bromide (Fig. 1). The immobilization was performed using Maltose Binding Protein (MBP) as a fused protein to Gal-1 (MBP-Gal-1). The MBP domain exhibits good affinity by the nonquaternized nitrogen from pyridinium derivative film[3]. Electrochemical Capacitance Spectroscopy (ECS) results indicated that the MBP domain was important for the modified electrode interaction (Fig. 2). Immobilization time and the MBP-Gal-1 concentration were also relevant to the kinetics and the results suggested a monolayer saturation in 40 minutes of interaction, using 1 µmol $L^{-1}$ MBP-Gal-1 (Fig. 2 and 3 A). Lactose detection experiments indicated that Gal-1 activity was preserved after immobilization (Fig. 3 B). Therefore, the chimeric protein presented adequate orientation and maintained its activity after immobilization, indicating that the system is promising for the development of Gal-1 biosensor.

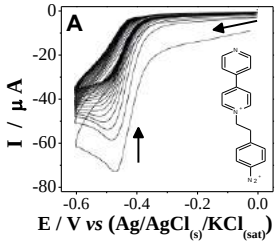


**Fig. 1:** Cyclic voltammograms of bare GCE in HCl 0.5 mol $L^{-1}$ containing 1 mmol $L^{-1}$ of diazonium salt. Scan rate 100 mV $s^{-1}$; 20 cycles.

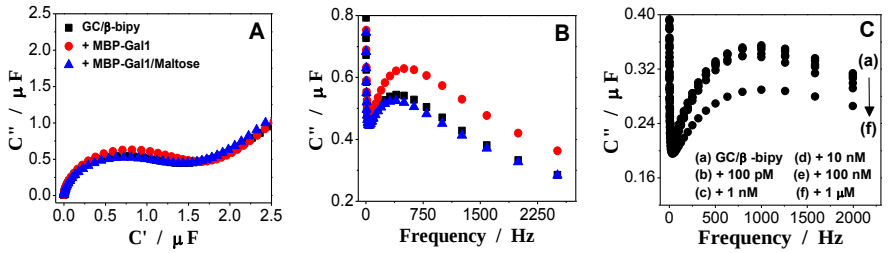


**Fig. 2: (A)** Capacitance Nyquist plots and Bode diagrams of the imaginary part of the complex capacitive for GC/β-Bipy electrode **(B)** after MBP-Gal-1 immobilization for 4 hours and **(C)** after 10 minutes of MBP-Gal-1 immobilization in different concentrations.

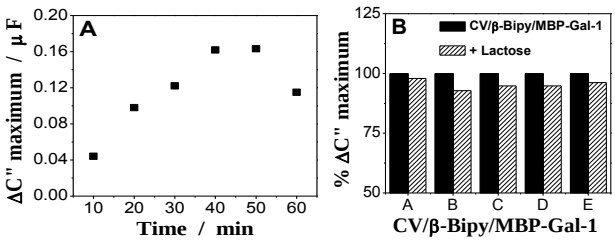


**Fig. 3: (A)** Maximum ΔC'' for different immobilization periods of MBP-Gal-1. **(B)** Percentage of ΔC'' after 5 µmol $L^{-1}$ lactose immobilization for 30 minutes on the different GC/β-Bipy/MBP-Gal-1 electrodes.

### Acknowledgments

FFCLRP/USP, FCFRP/USP, INCT Bionalítica and IFGoiano – Campus Urutaí.

### References

1. Bojarova, P., & Kren, V. (2016). *Biomaterials Science*, 1142–1160.
2. Chuang, C. H., Du, Y. C., Wu, T. F., Chen, C. H., Lee, D. H., Chen, S. M., Shaikh, M. O. (2016). *Biosensors and Bioelectronics*, *84*, 126–132.
3. Naal, Z., Park, J. H., Bernhard, S., Shapleigh, J. P., Batt, C. A., & Abruña, H. D. (2002). *Analytical Chemistry*, *74*(1), 140–148.

**Área: ELE___** **Inscrição:__01417__**

# Electrochemical SERS of Flavin on a Gold Surface

**Ruth F.V.V. Jaimes (PQ),[1] Walter J. Salcedo (PG),[2] Paola Corio (PQ),[1]**

**rfvillam@iq.usp.br; paola@iq.usp.br**

*[1]Departamento de Química, USP; [2]Departamento de microeletrônica EPUSP.*

Palavras Chave: In situ electrochemical surface enhanced Raman (SERS), Flavin adenine dinucleotide (FAD), Gold Surface.

## Highlights

The SERS of FAD shows a strong potential dependence in the non-Faradaic regions. A strong band near 1350 $cm^{-1}$ is assignable to the Flavin. The comparison of the SERS signals obtained in several redox states, and at several excitation wavelengths, allows the evolution of the electromagnetic, resonance Raman and charge-transfer mechanisms at the electrode surface.

## Resumo/Abstract

Surface-enhanced Raman scattering (SERS) spectroscopy has received a great deal of attention for its utility as a sensitive technique for chemical. Noble metal nanoparticles (NPS) (Au, Ag and Cu) are the most commonly used SERS substrates both in colloidal solutions and on solid surfaces[1]. They have advantages such as ease of formation and handling, and tunable size and shape dependent optical properties. Electrochemistry of redox enzymes is of current interest because of the potential application in bioelectronics and biosensors. Detailed information, that is, conformation, orientations, as well as active sites for adsorbates, is beyond the resolution of electrochemistry, while the technique of surface-enhanced Raman Spectroscopy (SERS) could provide molecular level information for the molecules at the interface. Small molecular cofactors (ligands) are essential for cells to perform numerous biological functions. To understand the mechanism by which these ligands effect protein function, is it important to identify ligand-binding and in the present work, we will report the results of studies on the interaction of Dinucleótido de Flavina e Adenina (FAD) on a gold electrode. In the solid FAD spectrum (Fig. 1 (a)) the strongest Raman signal as observed. Xiao et al.[2] have obtained the SERS spectra of FAD. Under positive polarization, the main characteristic of SERS for FAD is the appearance of peaks at 1353 $cm^{-1}$ ($\nu$CN, $\delta CH_3$), 1373 $cm^{-1}$ ($\nu$CN, $\nu$CC), $\delta CH_3$), 1449 $cm^{-1}$ ($\nu$CN), 1499 $cm^{-1}$ ($\nu$CN, $\nu$CC) e 1511 $cm^{-1}$ ($\nu$CN, $\nu$CO) and on a negatively charged electrode at 1499 $cm^{-1}$ ($\nu$CN, $\nu CH_3$), 1739 $cm^{-1}$ ($\nu$CN, $\nu$CC) e 1623 $cm^{-1}$ ($\nu$CN, $\nu$CO). In addition, a strong band near 1350 $cm^{-1}$ is assignable to the Flavin[3]. The SERS of FAD shows a strong potential dependence in the non-Faradaic regions. The comparison of the SERS signals obtained in several redox states, and at several excitation wavelengths, allows the evolution of the electromagnetic, resonance Raman and charge-transfer mechanisms at the electrode surface.

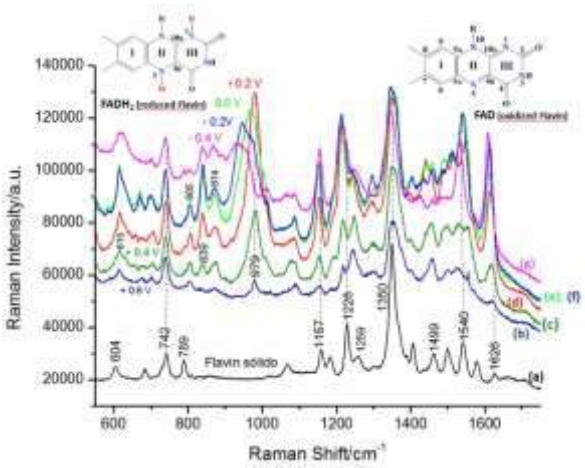


Figure 1. Raman spectra: (a) FAD solid; (b) and (g) SERS spectrum of $10^{-4}$ mol $dm^{-3}$ FAD on gold electrode in 0,1 mol $dm^{-3}$ KCL solution. The Raman and SERS spectra were acquired on Raman spectrometer microscope form Renishaw in Via model with an 50X objective to focus the laser beam on the sample and collect the scattered light. The spectra were excited by the 785nm line from an solid state laser. Raman spectroelectrochemistry was performed in a cell made of Teflon with a gold working electrode, a platinum wire as auxiliary electrode and Ag/AgCl as reference electrode and two different laser lines for excitation, 633 nm (He-Ne source, Renishaw RL6333) and 785 nm (solid state laser).

[1]Braun, SJ. Lee et al. J. Am. Chem. Soc 2007, 129,6378;
[2]Xiao, Y.J. et al. Langmuir, 1997,13,7068.

**Área: ELE** **Inscrição: 01411**

# Carbon nanofibers modified screen-printed electrode for copper analysis in bioethanol by anodic stripping voltammetry

**Victor H.R. Azevedo (IC),[1,2] José L. da Silva (PQ), [1,2*] Nelson R. Stradiotto (PQ). [1,2,3]**

**silva_jluiz@yahoo.com.br**

*[1]Department of Analytical Chemistry, Institute of Chemistry, UNESP, Araraquara, SP; [2]Bioenergy Research Institute, UNESP Araraquara, SP; [3]School of Industrial Engineering Metallurgical, UFF, Volta Redonda, RJ.*

Palavras Chave: *Copper determination, Carbon nanofibers, Screen-printed electrode, Bioethanol, Linear sweep anodic stripping voltammetry,*

## Highlights

Carbon nanofibers modified screen-printed electrode. Copper determination in bioethanol sample by anodic stripping voltammetry. High sensitivity, stability, precision and accuracy were obtained.

## Resumo/Abstract

Bioethanol is a renewable, clean and self-sustaining biofuel. Their use helps reduce emissions of gaseous pollutants into the atmosphere compared to fossil fuels. Current public policies require this biofuel to have a high degree of purity. Moreover, the presence of metals in high concentrations in their composition is detrimental to the engines, reducing their efficiency, in addition to being able to form undesirable residues.[1] Considering these assumptions into account and the need for metals quantification in bioethanol, carbon nanofibers (CNF) were selected as a modifier of carbon screen-printed electrode (SPE) due to their mechanical resistance and high sensitivity, which allows the development of resistant and efficient sensors. In this work was developed a carbon screen-printed electrode (SPE) modified with carbon nanofibers (CNF) for copper determination in bioethanol sample. The SPE was activated in a phosphate buffer (pH 7) solution containing KCl applying potentials from 0.0 to 2.0 V at 50 mV $s^{-1}$ by 10 voltammetric cycles. The nanofibers were immobilized on electrode surface through a suspension containing CNF, Nafion and ethanol. From the scanning electron microscopy images, it is possible to note a uniform distribution of the CNF and mean diameter of 93 ± 23 nm. Energy dispersive x-ray spectroscopy spectrum showed carbon, oxygen and fluorine peaks, indicating that the modification was successful. In the characterization by electrochemical impedance spectroscopy (frequency of 0.10 Hz to 100 kHz and potential 0.22 V) with 10 mM $Fe(CN)_6^{4-/3-}$ in 1.0 M KCl solution showed that the electron transfers resistance (Rct) of the CNF/SPE (Rct: 0 Ω) decreased in comparison with unmodified SPE (Rct: 704 Ω).The Raman spectrum presented two intense bands at ~ 1328 and ~ 1600 $cm^{-1}$, associated with band D and G, respectively, for the modified and unmodified surfaces. For analytical method develepment was investigated the copper eletrooxidation with linear sweep (LSASV), square wave (SWASV) and differential pulse anodic stripping voltammetry (DPASV). The LSASV ($3,4\times10^{-4}$ A) showed the best sensitivity compared to SWASV ($8,3\times10^{-5}$ A) and DPASV ($6,5\times10^{-5}$ A). Using the LSASV under optimized conditions, the analytical method was developed. Copper solutions were prepared in concentration range from $1.0\times10^{-8}$ to $1.0\times10^{-3}$ M.The analytical curve presented a linear range of $1.0\times10^{-7}$ to $1.0\times10^{-5}$ ($y = -3.6x + 5.5\times10^{-6}$) with detection limit of $5.0\times10^{-8}$ M, quantification limit of $1.5\times10^{-7}$ M, sensitivity of 3.6 A $mol^{-1}$ L and correlation coefficient of 0.996. The recovery study showed that the method has good accuracy and repeatability, with recovery of 101 ± 2 %. The copper concentration found in bioethanol sample by standard addition method was $1.1\times10^{-7}$ ± $2.5\times10^{-9}$ mol $L^{-1}$. In addition, the stability and reproducibility of the prepared modified electrode were investigated. The excellent long-term stability and reproducibility of the prepared CNF/SPE make them attractive as sensor. The results indicated that the analytical method proposed employing the modified electrode and LSASV presented better analytical performance. Moreover, the sensor has shown to be an excellent alternative for the copper determination in bioethanol samples.

**Acknowledgments**: CNPq (170176/2017-7), CAPES and FAPESP (2017/25329-6).

**References**: [1]Silva, J. J.; Paim, L. L. e Stradiotto, N. R. *Electroanalysis* **2014**, 26, 1794.

**Área: EST** **Inscrição: 00716**

# *In Situ* Preparation of a complex salt formed by the anionic metallacycle $[Co_2(H_2mpba)_3]^{2-}$ stabilized by the $[Co(tppz)_2]^{2+}$ complex.

**Ludmila dos S. Mariano (IC),[1]* Walace D. do Pim (PQ),[2] Antônio C. Doriguetto (PQ),[1] Iara M. L. Rosa (PQ),[1] Marcos A. Ribeiro (PQ),[3] Humberto O. Stumpf (PQ),[4] and Maria Vanda Marinho (PQ).[1*]**

***luudmariano@gmail.com; maria.marinho@unifal-mg.edu.br**

*[1]Instituto de Química, Universidade Federal de Alfenas, Campus Santa Clara, Alfenas, MG, 37130-001, Brazil;[2]Departamento de Química, Centro Federal de Educação Tecnológica de Minas Gerais, Belo Horizonte, MG, 30421-169, Brazil;[3]Departamento de Química, Universidade Federal do Espírito Santo, Vitória, ES, 29075-910, Brazil;[4]Departamento de Química, Universidade Federal de Minas Gerais, Campus Pampulha, Belo Horizonte, MG, 31270-901, Brazil.*

*Keywords: polymeric network, coordination chemistry, cobalt(II), oxamate.*

## Highlights

- Crystal engineering and molecular materials research fields are increasing;
- An unusual mesocate formed by the anionic metallacycle $[Co_2(H_2mpba)_3]^{2-}$ stabilized by the $[Co(tppz)_2]^{2+}$ cationic complex;
- 2,3,5,6-tetra-(2-pyridyl)pyrazine (tppz) as donor ligand.

## Abstract

Crystal engineering and molecular materials research fields have allowed the design of a wide variety of compounds useful to many different technological applications.[1] The combination of entities able to perform specific functions in a same crystal has been attempted in order to conceive new multifunctional molecular materials.[2] Trying to control the self-assembling process, which can be governed by a series of parameters,[1] we chose the bottom-up strategy for this work. Here, we describe the preparation of a new compound with formula $[Co(tppz)_2][Co_2(H_2mpba)_3]\cdot 6H_2O$ **(1)** and the characterization by IR, TG, powder X-ray diffraction (PXRD) and the structure determined by single crystals X-ray diffraction (SXRD). The elemental analysis (Table 1) is in agreement with the proposed formula $C_{78}H_{62}N_{18}Co_3O_{24}$.The IR and TG results indicate the presence of the organic ligands ($H_2mpba^{-2}$ and tppz) in the structure. The results were confirmed by SXRD and the data show three independent $Co^{II}$ ions, one coordinated to two tppz ligands with a tridentate chelate coordination mode and two $Co^{II}$ centers coordinated to three $H_2mpba^{2-}$ ligands in bridging coordination mode (see Figure 1).

**Table 1.** CHN data for $C_{35}N_6Co_3H_{48}O_{28}S_2$ **(1)**.

| **(1)** | % C | %H | %N |
|---|---|---|---|
| Experimental | 51.70 | 3.45 | 13.91 |
| Calculated | 49.90 | 3.40 | 13.88 |

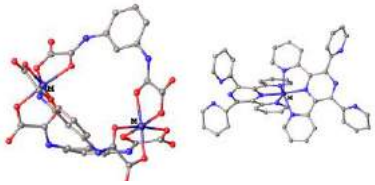

**Figure 1.** Molecular structure of **1**.

The mesocates are connected by intermolecular hydrogen bonds forming a one-dimensional supramolecular zig-zag chain along the [001] direction as shown in Figure 2. For our knowledge, it is the first example of oxamate-based complexes, in which, the mesocate formed by $[Co_2(H_2mpba)_3]^{2-}$ anionic metallacycle is stabilized by an another $[Co(tppz)_2]^{2+}$ cationic complex.

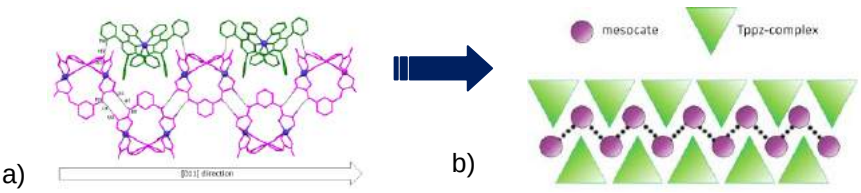


**Figure 2.** a) View (along axis *a*) of a supramolecular zig-zag (the mesocates are represented by purple molecules and the tppz are represented by green molecules); b) Packing illustration.

[1]Oliveira, W. X. C., *et al*., *Cryst.Grow.Des.*, **2015**,*15*,1325; [2]Aakeröy, C. B. *et al*., *Cryst.Eng.Comm*., **2010**, *12*, 22.

***Acknowledgments***

*PIBICT/Fapemig (Unifal-MG), Fapemig, CNPq, Capes, FINEP (ref.134/08), RMQ-MG.*

**Área: FIS** **Inscrição:** 00053

# Estudo de modelagem molecular, em compostos híbridos de Nor-β-lapachona com chalconas, na investigação do tratamento do câncer.

**Paulo Henrique Almeida Lira (IC),[1*] Valéria Rodrigues dos Santos Malta (PQ),[1] Sheyla Welma Duarte Silva (PQ)[1], Júlia Regina Nascimento da Silva (IC).[1]**

**Paulo.rick_66@hotmail.com; paulo.rick_66@hotmail.com**

[1]*Institudo de Química e Biotecnologia, UFAL*

Palavras Chave:*(câncer, naftoquinonas, propriedades físico-químicas).*

## Highlights

Molecular modeling study in hybrid compounds of Nor-β-lapachone with chalcones, in the investigation of cancer treatment. The research proposes structural alterations that increase the activity in naftoquinone compounds with chalcones, by the study QSAR / QSPR, being that the studied compounds report antitumor activity.

## Resumo/Abstract

Para o biênio 2016-2017, o INCA (Instituto Nacional do Câncer) já estimava a ocorrência de 600 mil novos casos de câncer dos mais diferentes tipos no Brasil[1]. Em virtude do grande número de casos e mortes, e ainda considerando a ineficiência e/ou efeitos colaterais de alguns medicamentos usados no tratamento do câncer, a busca por novas drogas que apresentem atividade antitumoral é de extrema importância para inibir o avanço dessa enfermidade. Portanto, o presente trabalho propõe alterações estruturais que aumentem a atividade em compostos naftoquinonicos com chalconas (Figura 1), tendo em vista que tal classe apresenta atividade antitumoral considerável para alguns tipos de linhagens como: HL-60 (leucemia promielocitica humana) e SF295 (Glioblastoma humano)[2]. Para realização dos cálculos das propriedades físico-químicas foi utilizado o programa HyperChem[3]. Os cálculos das propriedades eletrônicas em conjunto com os resultados estruturais, possibilitou uma análise das reatividades desses compostos. Dentre os derivados estudados, o composto **2** apresentou melhor caráter doador (HOMO = -8,535 eV) e o **1** melhor caráter receptor (LUMO = -1,549 eV). Para o momento dipolar (MD) notou-se que **1** apresentou menor valor, já o **3** reportou maior deslocamento. Observou-se nas relações QSAR/QSPR que a presença de um substituinte no anel aromático interferiu tanto nas propriedades como na atividade dos compostos. Constatando assim que a melhor atividade se dá com o anel aromático sem substituição, e que a inclusão de um substituinte, seja polar ou apolar, irá reduzir atividade antitumoral.

Figura 1. Compostos híbridos de Nor-β-lapachona com chalconas

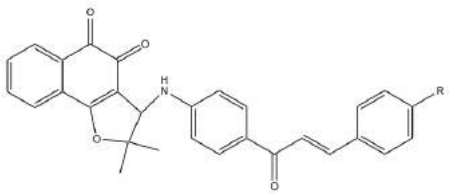

1: R= H; 2: R= OMe; 3: R=$CH(CH_3)_2$

Fonte: JARDIM, et al., 2015.

[1]Instituto Nacional do Câncer. Estimativa 2016: Incidência de Câncer no Brasil, Rio de Janeiro, 2015.
[2]JARDIM, G. A. M.; GUIMARAES, T.T.; PINTO, M. C. F. R.; CAVALCANTI, B.C.; FARIAS, K. M. DE; PESSOA, C.; GATTO, C. C.; NAIR, D.K.; NAMBOOTHIRI, I. N. N.; JUNIOR, E. N. S. Naphthoquinone-based chalcone hybrids and derivatives: synthesis and potent activity against cancer cell lines **Med. Chem. Commun**., v.6, 120, 2015.

**Área: FIS** **Inscrição: 00612**

# Secondary Ion Emission from Water Ice Induced by MeV Cf Fission Fragments and Its Applicability in Astrochemistry

**Julia de C. Santos (IC)*[1], Diana P. P. Andrade (PQ)[2], Enio F. da Silveira (PQ)[3], Leonardo Baptista (PQ)[4], Heloísa M. Boechat-Roberty (PQ)[2].**

**juliadcsantos@gmail.com**

*[1]Instituto de Química, UFRJ; [2]Observatório do Valongo, UFRJ; [3]Departamento de Física, PUC/RIO; [4]UERJ-Resende*

Palavras Chave: Astrochemistry, Mass spectrometry, Radio-astronomy, Secondary ion emission, Water radiolysis

## Highlights

In the present work, pure water ice was bombarded with Cf fission fragments (FF), at a temperature of 70K, simulating the radiolysis caused by cosmic rays impact in interstellar ices of different thicknesses. Time-of-flight mass spectra of positive secondary ions ejected from the ice were measured, providing the secondary ion yields for the species that dessorved to the gas phase. Theoretical calculations of frequencies for rotational transitions of the predominant secondary ions were made, aiming the radio-observation of those species in space.

## Resumo/Abstract

Secondary ion emission from vapor-deposited water ice has been investigated in exploring the influence of phase transitions on the desorption yield of $H_2O$ ions, particularly, the hydronium $H_3O^+$ and the cluster ions $(H_2O)_nH_3O^+$, with $1 \leq n \leq 10$. Because water amorphous ices are commonly found on interstellar grains and continuously bombarded by ionizing agents such as cosmic rays, electrons and photons, the production rate of secondary ions that desorb from the ice surface is of great relevance to the chemistry of interstellar environments. In the present work, time-of-flight mass spectra of positive secondary ions ejected from pure water ices of different thicknesses at 70K bombarded with Cf FF with energy around 65 MeV were measured. The sum of the yields of $H_3O^+$ and of the first cluster ion represents 35% of the positive ion yield (i.e., 0.05 ions/impact) and 16% of the total $H_2O$ molecular sputtering yield. The cluster ion yields of $(H_2O)_nH_3O^+$ ions with n = 0, 1 and 2 were predominant in the spectra, and therefore theoretical calculations of the rotational transition frequencies of those ions were made, aiming future radio-observation of these species in space environments. Non-identified rotational bands observed in stellar objects were searched in the literature and compared with the calculated radiofrequencies, resulting in fourteen candidate bands for the water clusters.

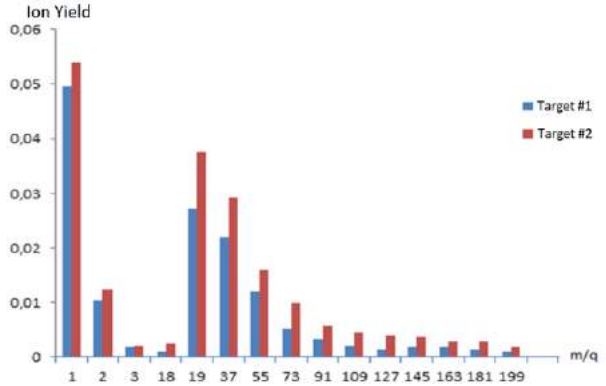


Figure 1: Histogram of the absolute secondary ion yields for each target.

| Transition $J^0$ -> $J^n$ | Frequency (GHz) |
|---|---|
| n = 0 | 18.47 |
| n = 3 | 69.51 , 71.00 , 74.40 |
| n = 4 | 83.02 , 84.97 , 85.26 , 86.82 , 88.47 |
| n = 5 | 102.48 , 104.96 , 106.25 , 107.17 |
| n = 7 | 142.47 |

Table 1: $(H_2O)H_3O^+$ candidate rotational bands and the respective frequencies.

**Área: FIS** **Inscrição: 00266**

# A Study of the Influence of Debris on the Adsorption Capacity of Functionalized Multi-Walled Carbon Nanotubes

**Talita K. M. Amaral (IC),[1] Guilherme O. Santos (IC),[1] Natal J. Pires (PQ),[1] Vinicius G. Castro (PQ),[2] Glaura G. Silva (PQ),[2] Rodrigo L. Lavall (PQ),[2] Paulo F. R. Ortega (PQ),[1]***

**talitamagalhaees@gmail.com; pauloortega@cefetmg.br**

*[1]Departamento de Formação Geral, CEFET-MG Campus IV; [2]Departamento de Química/ICEx, UFMG.*

Keywords: *(Carbon nanotubes, Acid oxidation, Debris, Adsorption, Methylene blue)*

## Highlights

Acid oxidation of CNT increases the adsorption of polar molecules;
This process generate oxidized fragments (*debris*) adhered to the CNT;
This study reveals the debris influence on the adsorption in CNT.

## Abstract

The functionalization of multi-walled carbon nanotubes (CNT) via acid oxidation is a relevant strategy to increase their adsorption capacity, especially for polar adsorbates. These treatments generate oxidized fragments (*debris*) adhered to the CNT, which is not removed by simple washing. Unfortunately, most of the papers do not mention any purification procedure for the removal of debris and therefore the adsorption data are inaccurate. Here, we study the effect of the debris on the adsorption of methylene blue (MB). Three CNT were used: pristine (p-CNT), oxidized (ox-CNT), and ox-CNTs after removal of debris (@-CNT). The procedures used to obtain ox-CNT and @-CNT were previously reported.[1,2]

Elemental analysis show that the acid oxidation increases the oxygen content from 0.15 (p-CNT) to 13.9% (ox-CNT). For @-CNT, this content was reduced to 7.7%. Deconvolution of the XPS data show that 13% of the oxygen of ox-CNT originates from carboxylic acids (-COOH) and 87% corresponds to alcohols, ethers and lactones, while @-CNT has only 3% of carboxylic groups. These differences in surface chemistry affect the adsorption as summarized in Table 1.

***Table 1.*** *Parameters of Langmuir adsorption isotherm model for MB adsorbed by the three CNT at different pHs and at 298.15 K.*

| *pH* | *Adsorbent* | *Maximum adsorption capacity (Qe) / mg g$^{-1}$* | *Langmuir constant ($K_L$)* | *$R^2$* |
|---|---|---|---|---|
| 3 | *p-CNT* | *85.98 ± 2.74* | *292.90 ± 4.87* | *0.99* |
| | *ox-CNT* | *111.98 ± 2.21* | *398.31 ± 3.11* | *0.99* |
| | *@-CNT* | *97.37 ± 1.87* | *298.70 ± 3.24* | *0.98* |
| 7 | *p-CNT* | *161.81 ± 0.97* | *331.73 ± 2.85* | *0.99* |
| | *ox-CNT* | *170.94 ± 1.63* | *344.51 ± 4.01* | *0.99* |
| | *@-CNT* | *177.63 ± 2.01* | *472.46 ± 3.98* | *0.98* |
| 9 | *p-CNT* | *174.83 ± 2.73* | *496.56 ± 4.02* | *0.98* |
| | *ox-CNT* | *188.68 ± 1.60* | *513.58 ± 3.98* | *0.98* |
| | *@-CNT* | *218.82 ± 1.49* | *830.09 ± 4.56* | *0.99* |

In neutral and basic medium, @-CNT has higher affinity ($K_L$) and $Q_e$ values than ox-CNT. This is due to the conversion of –COOH to carboxylates on the debris. This causes their desorption from CNT and a decrease in the MB adsorption on ox-CNT. Therefore, these data show how debris influences the adsorption of functionalized CNT, reducing by up to 38% depending on the pH.

**Acknowledgements**

*CNPq, FAPEMIG, INCT de Nanomateriais de carbono, Rede Mineira de Química*

**References**

*[1]P.F.R. Ortega, J.P.C. Trigueiro, M.R. Santos, A.M.L. Denadai, L.C.A. Oliveira, A.P.C. Teixeira, G.G. Silva, R.L. Lavall, Journal of Chemical and Engineering Data, 62 (2017) 729-737.*
*[2]R. Verdejo, S. Lamoriniere, B. Cottam, A. Bismarck, M. Shaffer, Chemical Communications, (2007) 513-515.*

**Área: FIS** **Inscrição: 00602**

# IMPACT OF WATER CONCENTRATION ON THE ELECTRO-OXIDATION OF METHANOL ON PLATINUM

**Rafael Luiz Romano (IC),* Bruno Alarcon Fernandes Previdello (PQ), Hamilton Varela (PQ).**

***rafaromanoluiz@gmail.com**

*Institute of Chemistry of São Carlos, University of São Paulo, USP.*

Keywords: *Electrocatalysis, Water Concentration, Methanol Electro-oxidation, Potential Oscillations, Polycrystalline Platinum, Phosphoric Acid.*

## Highlights

In this work, we investigate how the water concentration affects the methanol electro-oxidation on polycrystalline platinum. The study is carried under both conventional and oscillatory regimes.

## Resumo/Abstract

The electro-oxidation of small organic molecules on platinum commonly occurs via a mechanism that involves different reaction pathways and several steps of adsorption and desorption of species. Intrinsic features of this mechanism may result in dynamic instabilities. The electro-oxidation of methanol on platinum, in acidic media, occurs by a mechanism that, under constant current conditions, potential oscillations emerge spontaneously. The study of such oscillations provides mechanistic information which is, commonly, inaccessible under conventional regime. Variables such as temperature, alcohol concentration, supporting electrolyte identity and water concentration can affect not only the potential oscillation, but also the reaction kinetics. Thus, in this work we investigate how the water concentration affects the electro-oxidation of methanol on polycrystalline platinum, using phosphoric acid as supporting electrolyte. Particularly, we investigate the impact of water concentration on kinetic parameters, such as reaction order relative to water. Besides, we study how water concentration and temperature affect the oscillatory dynamics of the reaction. It was found that water concentration plays a key role in the reaction kinetics. The increase of water concentration results in a corresponding increasing in the oscillatory frequency.

References

[1] Camargo, A.P.M.; Previdello, B.A.F.; Varela, H., Gonzalez, E.R. **Electrochem. Commun.**, v. 12, p. 140-143, 2010.
[2] Okamoto, H.; Gojuki, T.; Okano, N.; Kuge, T.; Morita, M.; Maruyama, A.; Mukouyama, Y. **Electrochimica Acta**, v. 136, p. 385-395, 2014.
[3] Krausa, M.; Vielstich, W. **J. Electroanal. Chem.**, v. 399, p. 7-12, 1995.

**Área: FIS** **Inscrição:01022**

# A homemade colorimeter for quantitative and qualitative analysis of organophosphates

**Leonardo L. Q. Nascimento (IC),[1]* Valmir B. Silva (PG),[1] Elisa S. Orth (PQ).[1]**

**leonardolqn@gmail.com;** valmir-baptista@hotmail.com ; elisaorth@gmail.com

*[1]Departamento de Química, UFPR*

Key Words: *Colorimeter, dephosphorylation, organophosphates*

## Highlights

Low cost device to make simple detections of organophosphates, including kinetics of dephosphorylation. Testing it´s viability by comparing the results with a comercial spectrophotometer.

## Resumo/Abstract

Organophosphates are widely used as pesticides, and many of these may bring risks to the human health. Therefore, the knowledge of whether or not these compounds are being used in abusive amounts is important. There are many analytical methods that can provide determination of these compounds, such as NMR and UV-Vis spectroscopy, but these methods are not practical for practical, simples and fast field analysis. In this context, we built a homemade colorimeter for low cost analysis of organophosphates[2].

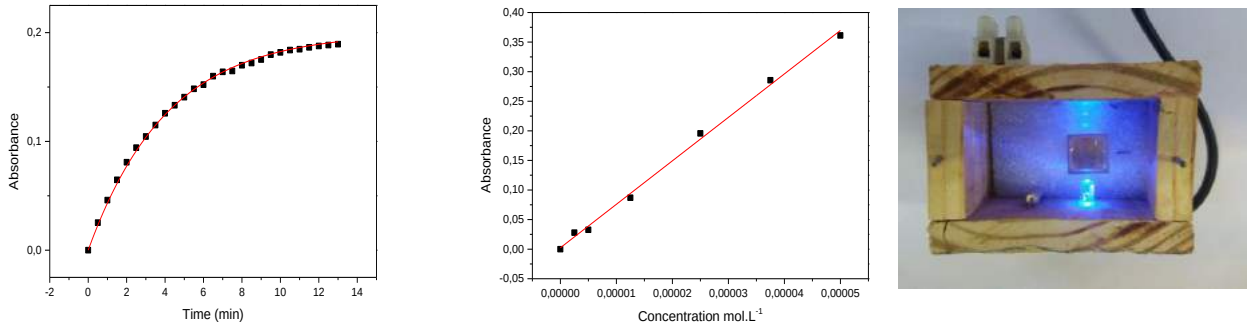


**A** **B** **C**

Figure 1: A and B Kinetic profile and calibration curve from the colorimeter C: colorimeter

The colorimeter (C) was built using two LEDs, one emitting light through a sample, and another LED detecting the light that passed. The second LED converts the light into potential energy, measured with a multimeter[1]. With this, it is possible to calculate the absorbance of the sample, which is the product of degradation of the studied pesticides(paraoxon and parathion). A calibration curve of the product has to be previously made, so the concentration can be determined.

To test it's quality, the alkalin hydrolysis of parathion was carried out on it to study the kinetics, and compare it with a comercial photometer.

The rate constant calculated by the colorimeter was 0,013 $cm^{-1}$, with the spectrophotometer was 0,012 $cm^{-1}$, meaning an error of 8,33%. The reactions were repeated several times, maintaining the results, now we aim to use catalysts to improve the process.

The colorimeter had decent results to evaluate the concentration, or to detect pesticides with colored hydrolysis products, being much more practical and cheaper (10,00US$) than the usual equipment.

Acknowledgments: UFPR, CAPES, CNPq, Fundação Araucária and L'Oréal-UNESCO-ABC

References:

[1]Jorge Delgado *et al J. Chem. Educ.*, **2014**, *91* (12), pp 2158–2162

[2]Valmir B. Silva; Elisa S. Orth *Quim. Nova*, **2017** Vol. 40, No. 2, 238-245

**Área: FIS** **Inscrição:** 00684

# Colorimetric detection of glyphosate via an aromatic derivative

**Renata Hellinger (IC),* Valmir B. Silva (PG), Elisa S. Orth (PQ)**

**hellinger.renata@gmail.com,**

*Departamento de química, UFPR.*

Palavras Chave: Organophosphate, Herbicide, UV-Vis Detection.

## Highlights

- Fast detection and quantification of glyphosate herbicide using a chemical reaction.
- Determination of reaction kinetics at different pH for the formation of colorimetric product.

## Abstract

Glyphosate (GFT) is an organophosphorus compound which belongs to the phosphonate group. It is used as an herbicide to kill weeds and annual grasses. However, GFT shows toxicity and has a carcinogenic potential in humans.[1] For this reason, it is important to develop easy, cheap and fast detection methods. An alternative is the use of derivative reactions. Herein, we propose a novel reaction of GFT with 1-Fluoro-2,4-dinitrobenzene (DNFB), which leads to a colored product, which can thereby be detected by UV-Vis spectroscopy. We evaluated the kinetics of the reaction, in order to understand and optimize the detection method. The experiments were performed under pseudo first order conditions (DNFB excess), in buffered media (pH 8 – 11) and controlled temperature (25°C). The reaction occurs with the nitrogen attack of GFT on the aromatic ring of DNFB, replacing the fluorine, forming a colored GFT derivative (GFTD) (Figure 1a) that absorbs in 400 nm, (Figure 1b). The kinetic profiles for pH 8 - 11 were obtained and at pH 9.5 the half-life time is 3,3 x $10^3$ minutes, as shown in Figure 1c. The reaction rate increases as the pH becomes more basic because nitrogen (p$K_{aH}$ 8.6) is converted in free base form. The reaction presented a yellow product, in reduced time and mild conditions. This method developed is innovator and can be used to detect and quantify real GFT samples in distribution centers and plantations. NMR and mass spectroscopy analysis are being carried.

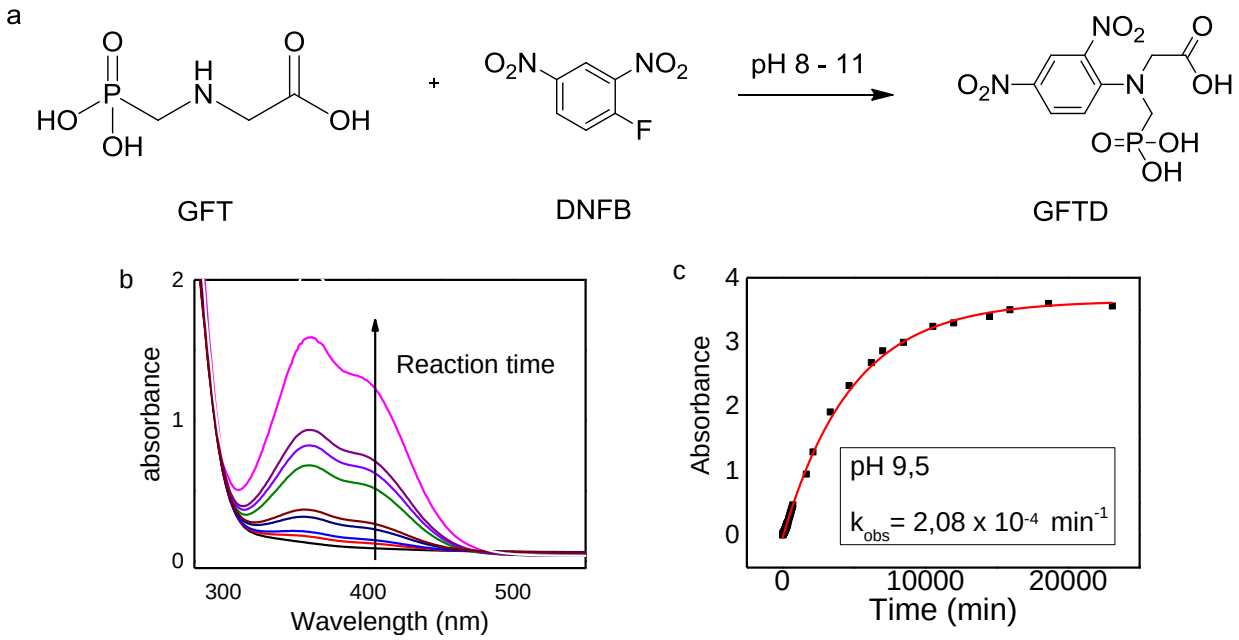


Figure 1 – (a) Reaction of GFT and DNFB. (b) Reaction UV-vis spectra and (c) Kinetics profile at pH 9,5

[1] A.H.C. Van Bruggen, Et al, *Sci. Total Environ*. **2018** , *616–617, 255-268*

Acknowledgments: UFPR, CAPES, CNPq, Fundação Araucária and L'Oréal-UNESCO-ABC

**Área: FIS** **Inscrição: 01065**

# 2D, 3D and 4D QSAR studies relating flavanoid inhibitor activity in alpha estrogen receptors

**Victor H.T. Barcelos (IC)[1], Eduardo Borges de Melo(PQ)[2], João Paulo Ataide Martins (PQ)[1].**

barcelosvictor@outlook.com; eduardo.b.de.melo@gmail.com; joaopauloam@ufmg.br

*[1]Departamento de Química, UFMG; [2] Laboratório de Química Medicinal e Ambiental Teórica (LQMAT), UNIOESTE, campus Cascavel, PR. .*

Palavras Chave: *Flavonoid, estrogen receptors, LQTA-QSAR, QSAR model.*

## Highlights

- SERSMs may be useful in the hormone replacement therapy;
- 2D, 3D and 4D-QSAR models based on 21 flavonoids were obtained;
- These will be analyzed related to interaction with α-estrogen receptors.

## Resumo/Abstract

With the discovery of the alpha-estrogen receptor, so-called selective estrogen receptor subtype modulators (SERSMs) may be even more selective, and therefore more efficient in hormone replacement causing less side effects associated to the development of breast and ovarian cancer. The present work aims at proposing 2D, 3D and 4D QSAR models based on 21 flavonoid compounds and derivatives relating the inhibitory activity in alpha estrogen receptors. Field descriptors were calculated with LQTAGrid program, while the 4D-QSAR descriptors with LQTA-QSAR methodology (includes the conformational variation in the model). The data set was split into a training (16 compounds) and test (5 compounds) sets. As a result of this work, a 2D model was obtained containing an electronic descriptor and other topological descriptors from the Dragon program. The models were obtained and validated using QSAR Modeling. The PLS models and statistical parameters obtained are shown below:

2D model: 10 molecular descriptors (MDs), 4 latent variables (LVs), R2= 0.970, Q2LOO= 0.710; R2pred= 0.686
3D model: 4 MDs, 4 LVs, R2= 0.917, Q2LOO= 0.807, R2pred= 0.703
4D model: 6 MDs, 1 LV, R2= 0.860. Q2LOO= 0.797, R2pred= 0.506

The models were validated regarding their robustness and chance correlation using leave-N-out and y-randomization tests, respectively, and all models passed in these tests. The descriptors selected in the three models will be analyzed for a future interpretation of the mechanism of action of these compounds in alpha estrogen receptors.

**Área: FIS_____ Inscrição:_00630_____**

# Study of the influence of NaY zeolite particle size on CO adsorption: analysis by infrared spectroscopy with fourier transform

**Ingrid Kich Severo (IC)[1], Andressa Viana (PG)[1], Pedro R. C. Neto(PQ)[1], Roberta C. P. Rizzo-Domingues (PQ)[1*].**

**ingrids@alunos.utfpr.edu.br; robertac@utfpr.edu.br**

[1]*Departamento Acadêmico de Química e Biologia, UTFPR*

Palavras Chave: *CO Adsorption, Zeolite Synthesis NaY, Characterization of materials.*

## Highlights

As a result of its possibility to monitor the perturbation of molecules in the adsorbed state, IR spectroscopy is a widely used technique for the study of these adsorption phenomena.
The adsorption measured in this work suggests that the NaY zeolite may be able to capture CO at room temperature.
It can be stated that zeolites of the NaY type are promising materials for use in processes of CO emission minimization.
It is concluded that adsorbents synthesized in different granulometries capture the CO gas as much as the industrial NaY.

## Resumo/Abstract

Air pollution and all the consequences it brings a huge matter of importance and concern. One of the processes to minimize the gases emission responsible for the greenhouse effect is the adsorption process. Zeolite is a microporous commercial adsorbent with crystalline structures formed by chains of tetrahedral rings of $SiO_4$ and $AlO_4$, linked by interstitial cations (Na, Ca, K, Ba, Sr) to give a porous structure, capable of accommodating most of the organic and inorganic molecules. The Y-type zeolite has a three-dimensional pore structure having a diameter of about 0.74 nm and the Si/Al ratio in the range of 1.0-1.5. In this work the zeolite NaY was synthesized at a temperature of 353.15K and a time of 24 hours in greenhouse. The adsorbents were pelletized, crushed and sieved, the pellets having a diameter of approximately 0.07 cm being used and thin, through the 0.06 cm sieve opening in the adsorption tests.The synthesized material and in commercial NaY were characterization with by means of textural analysis, scanning electron microscopy, X-ray diffraction. The adsorption tests were conducted with the adsorbents in the two sizes of pellets, being the influence of the particle size on the adsorption by the analysis of infrared spectroscopy (FTIR).In general, it can be stated that zeolites of the NaY type are promising materials for use in processes for minimizing the emission of carbon monoxide.

1. A. Corma, **Chemical Reviews.** v.95,p.559, 1995.
2. L. M. Kustov, V. B. Kazansky, S. Beran, L. Kubelková, P. Jirú, J. **The Journal of Physical Chemistry.** v. 91, p.5247, 1987.
3. W. E. Farneth, R. J. Gorte. **Chemical Reviews.** v. 95, p. 615, 1995.
4. A. Zecchina, C. Lamberti, S. Bordiga, **Catalysis Today** v. 41, p. 169, 1998.
5. I. Mirsojew, S. Ernst, J. Writkamp, H. Knözinger. **Catalysis. Letters**. v. 24, p.235, 1994.
6.WANG, Z. et al. **NaY zeolite membranes with high performance prepared by a variable-temperature synthesis**. Microporous and Mesoporous Materials, 2013.
7. MORALES-PACHECO, P. et al. **Synthesis and structural properties of zeolitic nanocrystals II: FAU- type zeolites**. Journal of Physical Chemistry C, v. 113, n. 6, p. 2247-2255, 2009.
8. SEVERANCE, M. et al. **Rapid crystallization of faujasitic zeolites: mechanism and application to zeolite membrane growth on polymer supports.** Langmuir : the ACS journal of surfaces and colloids, v. 30, n. 23, p. 6929, 2014.

**Área: FIS** **Inscrição: 00339**

# Amides as nucleophiles in dephosphorylation processes: reactivity favored by tautomerism.

**Juliano M. Fernandes[1](IC) and Renan B. Campos[1] (PQ).**

**jfernandes@alunos.utfpr.edu.br; renan@utfpr.edu.**

*1. Departamento Acadêmico de Química e Biologia, Universidade Tecnológica Federal do Paraná - UTFPR, CEP 81280-340, Curitiba-PR*

Keywords: *Amides*, *Tautomerism, Dephosphorylation reactions.*

## Highlights

Iminol tautomer of amides can act as a N-nucleophile in dephosphorylation. Hydrogen bonding/prototropic shift plays essential role lowering the activation barrier in the first step of the reaction.

## Abstract

Obsolete stocks of pesticides require sustainable methods of degradation.[1] Therefore, studies involving dephosphorylation processes of phosphate triesters — an important class of pesticides — have attracted great interest. We hypothesized that primary and secondary amides could represent candidates for this purpose, once its inherent tautomerization (*e.g.* formamide (**FMD**), Scheme 1) leads to a small formation ($K_{eq}=10^{-8}$)[2] of the iminol species. Consequently, iminol could act as a N-nucleophile towards phosphorus atom (Scheme 1) supported by a hydrogen bond during the nucleophilic substitution. In this study we have assessed the reactivity of **FMD**, thioacetamide (**TCM**), N-N-dimethylformamide (**NDMF**), **urea** and succinimide (**SCD**) with the phosphotriester diethyl 2-4-dinitrophenylphosphate (**DEDNPP**) in **DMSO**. Probably due to the electron withdrawing character — and the steric hindrance — of carbonyl group, no nucleophilic activity was observed for **SCD**. In contrast, **FMD** and **urea** presented interesting reactivity, showing experimental $k_N$ values of $1{,}3\times10^{-2}$ and $8{,}8\times10^{-4}$ $M^{-1}\,s^{-1}$, respectively. These values become $10^8$-fold larger considering only the concentration of the reactive tautomer (iminol; estimated in $10^{-6}$ %). Since no reactivity was detected by **NDMF** (which does not present tautomerism) and **TCM** (which tautomerizes to an iminothiol), two important evidences were verified for **FMD** and **urea**, respectively: (i) the reactivity is governed by tautomerism and (ii) OH hydrogen bonding plays an important role by lowering the activation barrier. *DFT* calculations at the B3LYP/6-31+g(d,p) level of theory have been performed for the reaction of **FMD(B)** with **DEDNPP**. Results suggest the nucleophilic attack by nitrogen lone pair occurs simultaneously to a prototropic shift ($TS_1$). A pentacoordinate intermediate ($INT_1$) is formed followed by a proposed intramolecular acid catalysis, which is still under investigation (Scheme 1).

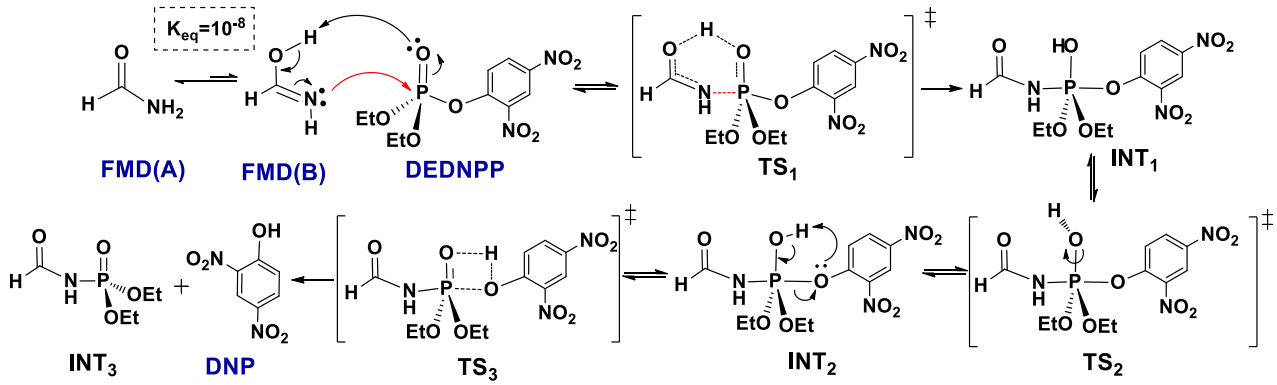


**Scheme 1**

## Acknowledgements

HPC-UTFPR, Grupo de Catálise e Cinética - UFPR and Tantillo Group.

**[1]** Kim, K., Tsay, O. G., Atwood, D. A. and Churchill, D. G. *Chem. Rev*., **2011**, 111, 9, 5345
**[2]** Fairlie, D. P., Woon, T. C., Wickramasinghe, W. A., & Willis, A. C., *Inorg. Chem*, **1994**, 33, 26, 6425

**Área: FIS**
*(Inserir a sigla da seção científica para qual o resumo será submetido. Ex: ORG, BEA, CAT)*

**Inscrição: 638**
*(Inserir o número de inscrição do autor que fez a submissão)*

# Stereochemical studies of Dansylglycine bound to protein Human Serum Albumin.

**Aguinaldo Robinson de Souza (PQ),[1] Izabelle Amorin Ferreira Boza (PG),[1*] Valdecir Farias Ximenes (PQ),[1] Nelson Henrique Morgon (PQ).[2]**

**arobinso@fc.unesp.br; izabelle.tif@gmail.com; vfximenes@fc.unesp.br; nhmorgon@gmail.com**

*[1]Departament of Chemistry, UNESP; [2]Departament of Physical Chemistry, UNICAMP*

Keywords: *Electronic Circular Dichroism, Isomer, Enantiomers, Density functional theory, Human serum albumin.*

## Highlights

Dansylglycine has a nitrogen atom as the center of chirality. Through experimental, ECD, and theoretical studies, TDDFT, we can infer that the *R* isomer of Dansylglycine is the configuration bound to the site 2 of the Human Serum Albumin protein.

## Resumo/Abstract

The Electronic Circular Dichroism (ECD) spectrum of Dansylglycine (DG) bound to Human Serum Albumin (HSA) was obtained at different solvents. In addition, Time Dependent Density Functional Theory (TDDFT) calculations was used to obtain information about the stereochemistry of this interaction. The ECD spectra was obtained with 1 nm step resolution, response time of 1 second and scanning speed of 50 nm/min. The TDDFT calculation was carried out using the CAM-B3LYP hybrid functional and the 6-311++G(2d,p) basis set including the solvation effects (SMD model). Figure 1 shows the experimental ECD spectrum of DG in the presence or absence of HAS, and a positive Cotton effect occurs with a maximum at 346 nm. This effect was only observed when both, HSA and DG were present.

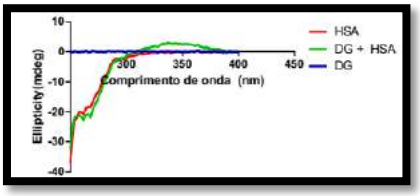


Figure 1. ECD of DG in the presence and absence of HSA.

Figure 2 shows the theoretical ECD spectrum of DG in water, as obtained using TDDFT level of calculation. It can be seen the maximum Cotton effect in the same region obtained experimentally.

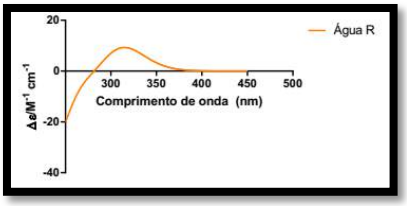


Figure 2. TDDFT of ECD in water.

The ECD signal of DG bound to HSA was attributed to its *R* configuration. DG does not have ECD signal in solution. However DG presents a positive Cotton effect when bound to HSA. The explanation for this phenomenon was attributed to the stacking of the *R* configuration of DG when complexed at site 2 of HSA.

FAPESP: 2016/20549-5, 2015/22338-9, 308480/2016-3, 2014/50926-0; CNPq: 302793/2016-0, 306975/2013-0, 440503/2014-0, GridUnesp.

**Área: FIS** **Inscrição: 01160**

# Reverse solvatochromism of iminophenolate dyes comprised of 5–nitrofuran–2–yl or 5–nitrothiophen–2–yl as electron acceptor

**Carlos E. A. de Melo (PG),[1] Celso R. Nicoleti (PQ),[1] Marcos C. Rezende (PQ),[2] Adailton J. Bortoluzzi (PQ),[1] Renata da S. Heying (PG),[1] Robson da S. Oliboni (PQ),[3] Giovanni F. Caramori (PQ),[1] Vanderlei G. Machado (PQ).[1*]**

**vanderlei.machado@ufsc.br**

*[1]Departamento de Química, UFSC; [2]Facultad de Química y Biología, Universidad de Santiago; [3] Centro de Ciências Químicas, Farmacêuticas e de Alimentos, UFPEL.*

Palavras-Chave*:* Solvatochromic dyes, Solvatochromic reversal, Solvatochromism, Solute–solvent interactions

## Highlights

Iminophenols with 5-nitrothiophen-2-yl or 5-nitrofuran-2-yl acceptor moieties in their molecular structures were synthesized. Their corresponding phenolates exhibited an inverted solvatochromism.

## Resumo/Abstract

Compounds **1a**-**8a**, with phenols as electron–donating groups and 5–nitrothiophen–2–yl or 5–nitrofuran–2–yl acceptor moieties in their molecular structures (**Figure 1A**), were synthesized and studied as probes of pure solvents polarities. Their corresponding phenolate dyes (**1b**-**8b**) were studied in 29 solvents with different polarities, which exhibit different colors (**Figure 1B**), confirming that the compounds are solvatochromic species. The solvatochromic bands in the vis region of the spectra are a result of π–π* electronic transitions, with an intramolecular CT from the electron–donor phenolate moiety towards the electron–acceptor 2–nitrothiophenyl or 2–nitrofuranyl moiety. **Figure 1C** shows a plot of the transition energies obtained as a function of the $E_T(30)$ solvent polarity values for dye **5b**, these being similar to those obtained for the other dyes. In all cases, a reverse solvatochromism was verified.

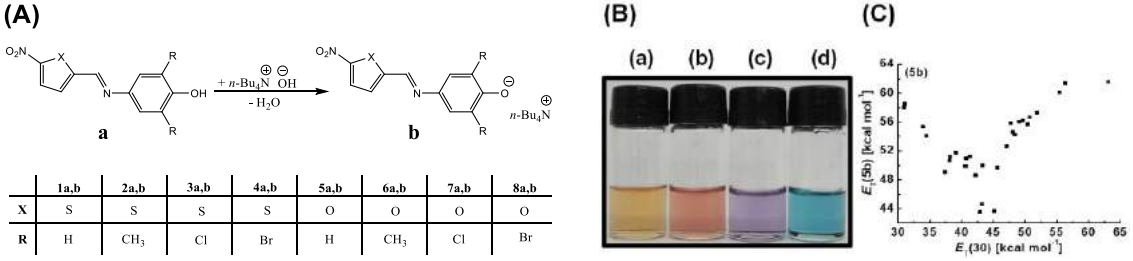


| | 1a,b | 2a,b | 3a,b | 4a,b | 5a,b | 6a,b | 7a,b | 8a,b |
|---|---|---|---|---|---|---|---|---|
| X | S | S | S | S | O | O | O | O |
| R | H | $CH_3$ | Cl | Br | H | $CH_3$ | Cl | Br |

**Figure 1. (A)** Compounds **1a–8a** and their deprotonation to generate **1b–8b**. **(B)** Solutions of the **5b** in **(a)** water, **(b)** methanol, **(c)** dimethoxyethane, and **(d)** acetone. **(C)** $E_T(30)$ value as a function of $E_T$(dye) for dye **5b**.

The crystalline structures of six compounds were obtained (**Figure 2A**). Nearly complete coplanarity between the phenolic ring and the nitro–substituted heterocyclic fragment was verified, with small dihedral angles between the two rings. The frontier molecular orbitals were analyzed for the protonated and deprotonated forms of the compounds (**Figure 2B**). The calculated geometries are in agreement with X–ray structures determined for the compounds and an increase in the electron delocalization occurs after their deprotonation. Data obtained using the Catalán multiparameter equation revealed that the medium acidity is responsible for hypsochromic shifts, while the solvent basicity, polarizability, and dipolarity contributed to bathochromic shifts of the solvatochromic band of these dyes. [CNPq, CAPES, FAPESC, FINEP, UFSC]

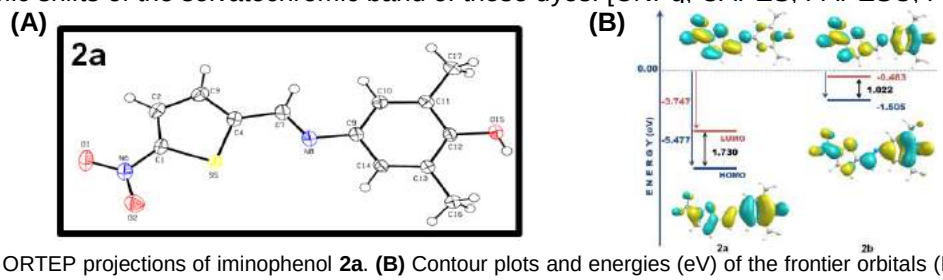


**Figure 2. (A)** ORTEP projections of iminophenol **2a**. **(B)** Contour plots and energies (eV) of the frontier orbitals (HOMO and LUMO) for **2a** and **2b**.

**Área: FIS** **Inscrição: 00560**

# 4-Aminoantipyrine abatement from water by electrochemical advanced oxidation processes and study of its complex with Fe(III)

**Lucas de Melo da Silva (PG)[1], Fábio Gozzi (PQ)[1], Ignasi Sirés (PQ)[2], Enric Brillas (PQ)[2], Silvio Cesar de Oliveira (PQ)[1], Amilcar Machulek Junior (PQ)[1]***

**machulekjr@gmail.com; lucas.melosilva@hotmail.com**

*[1]Institute of Chemistry, Federal University of Mato Grosso do Sul; [2]Laboratori d'Electroquímica dels Materials i del Medi Ambient, Departament de Química Física, Facultat de Química, Universitat de Barcelona*

***Keywords:*** 4-Aminoantipyrine; boron-doped diamond anode (BDD); electrochemical advanced oxidation processes; Fe(III)-4AA complex.

## Highlights

Electrochemical advanced oxidation processes (EAOPs) as a solution for water treatment

Total removal of 50 mg $L^{-1}$ 4-AA at pH 3.0 after 7.5 min at $j$ = 30 mA $cm^{-2}$ with $[Fe^{2+}]$ = 15 mg $L^{-1}$

Lower mineralization efficiency in the order: PEF-UVA > EF > EO-$H_2O_2$

Formation of 4-AA complex with Fe(III)

## Abstract

Electrochemical advanced oxidation processes (EAOPs) have been studied for the degradation of recalcitrant compounds based on the in situ generation of hydroxyl radicals ($^{\bullet}OH$, $E°$ = 2.8 V), capable of yielding the complete mineralization of parent pollutants. In the present study, electro-oxidation with electrogenerated $H_2O_2$ (EO-$H_2O_2$), electro-Fenton (EF) and photoelectro-Fenton (PEF) were employed to investigate the degradation and mineralization of 4-aminoantipyrine (4-AA), a metabolite of the dipyrone that is a persistent compound. In addition, the formation of a complex between Fe(III) and 4-AA was assessed spectrophotometrically. The assays were performed in an undivided glass cell. The anode was a BDD electrode of 3 $cm^2$ geometric area. An air-diffusion cathode with the same geometric area was made from a carbon-PTFE paste. The experiments were performed with [4-AA] = 50 mg $L^{-1}$ at pH 3 and $j$ = 30 mA $cm^{-2}$, comparing the performance of EO-$H_2O_2$, EF and PEF. A $Fe^{2+}$ concentration of 15 mg $L^{-1}$ was employed to catalyze the Fenton-based processes. In PEF, 95% 4-AA was degraded after 7.5 min, being much greater than EO-$H_2O_2$ (71%) and EF (76%), see Fig. 1a. Furthermore, EO-$H_2O_2$, EF and PEF showed 50%, 51% and 55% mineralization in 240 min, respectively (Fig. 1b). PEF process was more efficient due to the photoreduction of Fe(III) to Fe(II). The complex between Fe(III) and 4-AA was evidenced at a ratio 1:2, with a complexation constant $K$ = 6.2x$10^6$ $M^{-1}$, thus being considered a stable complex.

**Fig. 1.** (a) 4-AA degradation and (b) 4-AA mineralization.

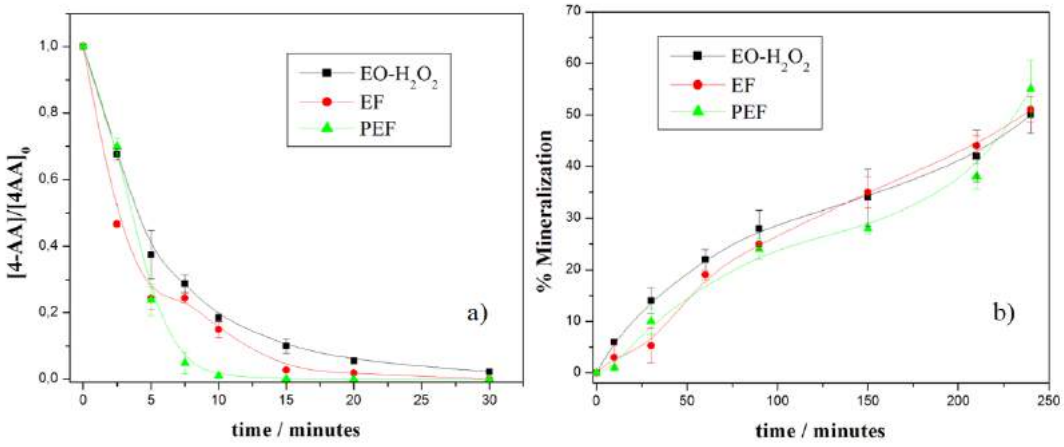

**Área: ___FIS_____** **Inscrição:_00990_____**

*(Inserir a sigla da seção científica para qual o resumo será submetido. Ex: ORG, BEA, CAT)*

*(Inserir o número de inscrição do autor que fez a submissão)*

# Physical Chemical properties and vibrational analysis of Reline, a Choline Chloride based DES, and Dimethyl Sulfoxide mixtures

**Jocasta N L Avila (PG),[1] Alessandro Triolo (PQ),[2] Jean-Michel Andanson (PQ)[3], Pascale Husson (PQ)[3]**

**jocasta@usp.br**

*[1]Laboratório de Espectroscopia Molecular (Lab. 411), Instituto de Química da Universidade de São Paulo, CEP 05508-000, São Paulo, SP, Brasil.*
*[2]Istituto Struttura della Materia, Consiglio Nazionale delle Ricerche Area della Ricerca Tor Vergata, Via Fosso del Cavaliere, 100 00133 Rome, Italy.*
*[3]CNRS, UMR 6296, Institut de Chimie de Clermont-Ferrand, BP 80026, F-63171 Aubière, France; Clermont Université, Université Blaise Pascal, Institut de Chimie de Clermont-Ferrand, BP 10448, F-63000.*

Palavras Chave: *DES, Reline, DMSO, green solvents.*

## Highlights

Volumetric properties and Walden´s rule together with Raman Spectra were used to clarify the intermolecular interactions and the ionic mobility in the Reline/DMSO mixtures.

## Abstract

Deep eutectic solvents (DES) has been discussed to replace the usual volatile ones in industries. They are cheap, non-toxic and biodegradable, however, high viscosities and limited thermal and chemical stabilities are the main disadvantages of these liquids. Thus, mixing known compounds, such as DMSO, to modulate their properties has been investigated to improve its application[1]. DMSO is an aprotic molecular solvent with enhanced capability of dissolving polar and apolar compounds, used in general as a versatile, low toxic solvent.[2]

The DES (Reline=Choline Chloride:Urea, 2:1) and all the mixtures, from $\chi_{DMSO}$=0.1 to $\chi_{DMSO}$=0.95, were prepared by weighting the components. The molar volume excess, $V^E$, is negative for all concentrations and the minimum at -2 $cm^3.mol^{-1}$ was found between $\chi_{DMSO}$=0.6 and $\chi_{DMSO}$=0.8 (Fig. 1A). This negative excess molar volume is due to strong attractive interactions and/or due the efficient packing of the components in the mixture. The Walden's rule, $\Lambda_m.\eta$=constant, reflects the mobility of ions moving independently in a viscous media determined by the frictional forces exerted by the medium and this quantity is approximately constant from pure DMSO to $\chi_{DMSO}$=0.8, increasing significantly from $\chi_{DMSO}$=0.8 to $\chi_{DMSO}$=0.1 (Fig 1A). The Raman spectra suggests a dissociation of DMSO molecules due the blue shift of C-S-C (Fig. 1B) mode and an interaction via SO group (Fig. 1C) with Reline, showing changes in the band shape of νSO and a new peak, $\nu_{int.}$, shifted to the red side of the spectra.

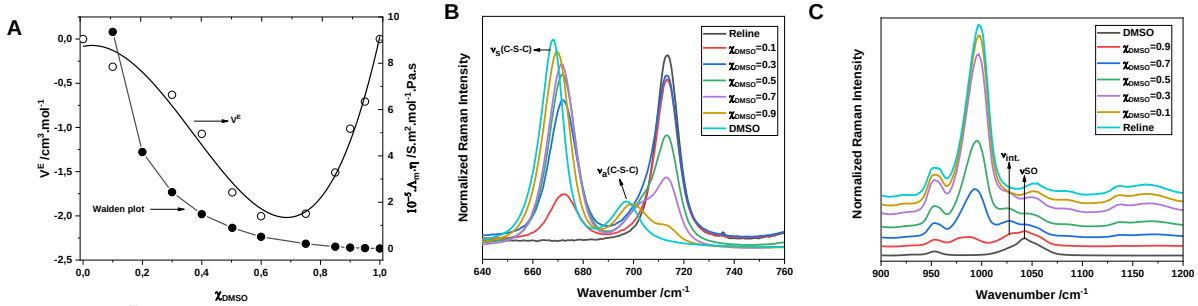


**Figura 1.** (A) $V^E$ and Walden's plot of Reline/DMSO mixtures. Raman spectra of (B) νSO and (C) ν(C-S-C) modes of DMSO.

## Acknowledgements

The authors would like to thanks Fapesp and Consiglio Nazionale delle Ricerche for the financial support.

[1] Smith, E. L.; Abbott, A. P.; Ryder, K. S. Chem. Rev. 2014,114, 11060-11082.
[2] Santos, N. C.; Figueira-Coelho, J.;Martins-Silva, J.; Saldanha, C. Biochem. Pharmacol. 2003, 65, 1035-1041.

**Área: FIS** **Inscrição: T0445**

# Spontaneous electrostatic charging during phase transition at solid-gas and liquid-gas interfaces

**Thiago A. L. Burgo (PQ),[1,2]* Kelly S. Moreira (IC)[2] F. Galembeck (PQ)[3]**

**thiago.burgo@ufsm.br**

*[1]Departamento de Física, UFSM; [2]Departamento de Química UFSM; [3]Instituto de Química, Unicamp*

Palavras Chave: electrostatic charging, phase transition, interfaces, vapor electricity, electric double layer.

## Highlights

Spontaneous electrostatic charging during phase transition at solid-gas and solid-liquid interfaces: Interfaces are important sites for charge accumulation; Non-electroneutral interfaces are spontaneously formed during phase transition; Electroneutrality is a controversial principle.

## Resumo/Abstract

The role of interfaces as important sites for electric charge accumulation is well established in solid-solid, liquid-liquid and liquid-solid systems. However, this is not the case for gas-liquid or gas-solid interfaces. As seen in the figure (left) below, water with excess charge is the outcome of many different events triggered by electric fields or by interfacial phenomena either liquid, solid or vapor, due to excess $H^+$ or $OH^-$ concentration. As interfaces are recognized sites for electrification, we used a very simple apparatus to measure the electrostatic charge during phase transition at liquid-gas and solid-gas interfaces. The experiment consists on recording the electrostatic charge of a water drop on polytetrafluoroethylene (PTFE) during evaporation. As shown in the figure (right) below, when a drop (NaCl 3%) is positioned on PTFE surface, a negative potential of – 6 V is build-up and remains stable for roughly 5 hours. Then, the negative potential starts to increase, passing through zero and reaching + 12 V. Finally, there is a slight decreasing on the potential, reaching a plateau when there is only NaCl crystal on PTFE. This equilibrium electrostatic potential is very stable and did not change even after 21 days of measurement.

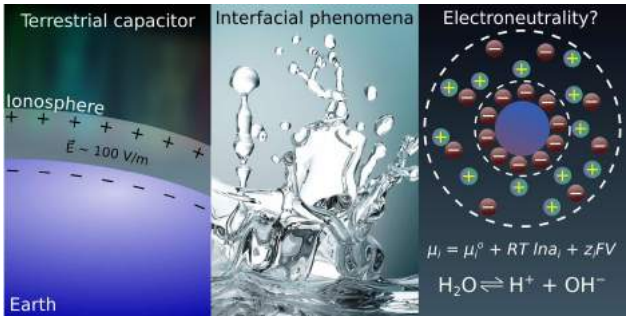


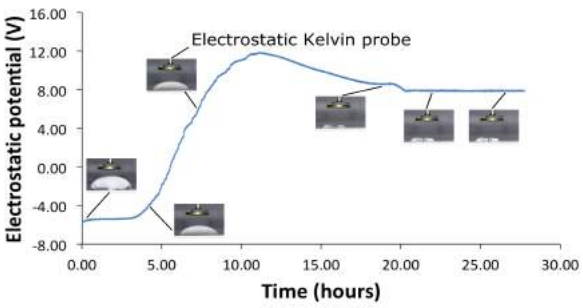


The present information leads to a particle charging mechanism based on charge partition at interfaces. This new understanding may contribute to progress in scavenging electrical energy from the atmosphere and must be particularly relevant for cloud formation and to understand regions of thunderstorm clouds.

**Área: FIS** **Inscrição: 00663**

# Effect of temperature on the liquid-liquid equilibrium of the ternary system water + pluronic10R5 + ammonium thiosulfate

**Beatriz M. Fontoura* (PG),[1] Francielle O. Chagas (PG),[1] Silvia J. R. Vargas,[1] Luís H. M. da Silva (PQ),[1] Maria C. Hespanhol (PQ).[1,2]**

**beatriz.fontoura@ufv.br**

*[1]Grupo de Química Verde Coloidal e Macromolecular (QUIVECOM), [2]Grupo de Análises e Educação para a Sustentabilidade (GAES), Instituto Nacional de Ciências e Tecnologias Analíticas Avançadas (INCTAA), Departamento de Química, Centro de Ciências Exatas e Tecnológicas, Universidade Federal de Viçosa – MG.*

Key-word: *Aqueous two-phase system, Phase diagram, Temperature, Pluronic10R5*, *Ammonium thiosulfate.*

## Highlights

Little information is available regarding copolymer pluronic10R5. In this work, the phase diagrams for pluronic10R5 + ammonium thiossulfate + water, were determined at three temperatures.

## Resumo/Abstract

Aqueous two-phase system (ATPS) have been investigated as alternative system for liquid-liquid extraction. Many ATPS phase diagrams for triblock copolymers (PPG-PPO-PPG) have been reported, but few information is available regarding liquid-liquid equilibrium data for inverted copolymers (PPO-PPG-PPO), denote pluronic10R5. Self-aggregated structures formed by triblock copolymers have range of applications, extending from the cosmetic field to the nanotechnology[1]. In the present work, the phase diagrams for pluronic10R5 + ammonium thiossulfate + $H_2O$ were experimentally determined at 283.2, 298.2, and 313.2 K. The statistic treatment was introduced by the gravimetric method[2]. The method is the following: initially a curve representing the binodal is obtained through a turbidimetric titration. A point is selected in the phase diagram, containing a certain concentration and the components required are weighed and mixed thoroughly. The tubes are left in thermostatic bath until complete separation of phase. Posteriorly, the bottom phase is collected and weighed. With the mathematical treatment the compositions of the top and bottom phases are obtained. The Fig. 1 shows that the increase in temperature enlarges the area of the phase diagram, indicating the enthalpic contribution to the formation of the biphasic system. This is indication that the phase-separation process is endothermic and is entropically directed as proposed by da Silva and Loh[3].

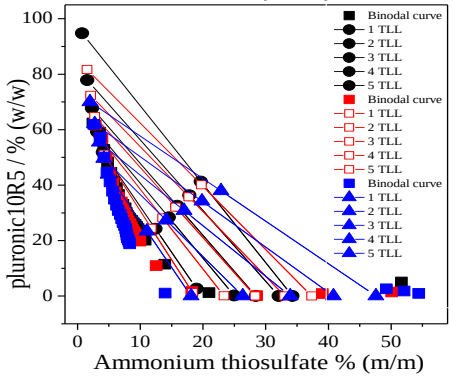


**Fig.1** Phase diagrams for pluronic10R5+ammonium thiosulfate + $H_2O$ at 283.2, 298.2, and 313.2 K.

References
[1] Seydel, C.,*Science*, 300 (2003) 80-81.
[2] Merchuk,C. et al, *J. Chromatogr. B*, 711 (1998) 285–*293.*
[3] *da Silva, Luís H. M.,Watson, Loh. J. Phys. Chem. B,* 104 *(*2000*),* 10069-10073

Acknowledgements: FAPEMIG, CNPq, INCTAA e CAPES

**Área: FIS** **Inscrição: 00331**

# Probing the biophysical interactions of chitosan derivatives with cell membrane models using Sum-Frequency Generation Spectroscopy

**Rafael de Oliveira Pedro (PQ)[1], Paulo Barbeitas Miranda (PQ)[1]***

**raolipe@alumni.usp.br; miranda@ifsc.usp.br**

[1]*Instituto de Física de São Carlos, Universidade de São Paulo, São Carlos, SP, Brasil.*

Keywords: *Chitosan, Langmuir monolayer, SFG spectroscopy, Phospholipids, DPPC, DPPG*

## Highlights

Interactions of chitosan with lipids in Langmuir monolayers were investigated; Chitosan promotes expansion on anionic DPPG; SFG spectra indicate the interaction mode of chitosan;

## Abstract

Chitosan, a biopolymer, has been used in many biological applications such as drug delivery, gene therapy, tissue engineering and antimicrobial systems. Although these applications have grown greatly in recent years, little is known about the modes of interaction at the molecular level of chitosan with biological membranes. Therefore, in this study we investigated the interactions of chitosan with lipids in Langmuir monolayers as model membranes using two chitosan samples: unmodified chitosan (CH) and positively charged chitosan functionalized with quaternary amino groups (CH-$P_{40}$). The anionic dipalmitoyl phosphatidylglycerol (DPPG) and zwitterionic dipalmitoyl phosphatidylcholine (DPPC) lipids were used as membrane models. The interactions at the air-water interface were assessed by surface pressure-area isotherms, Brewster angle microscopy and sum-frequency generation (SFG) spectroscopy. It was found that both samples had an insignificant effect on DPPC monolayers formed on PBS buffer containing the chitosans, but it noticeably affected DPPG monolayers. The SFG spectra showed a well-packed DPPC monolayer, with few gauche defects in the acyl chains probably due to the insertion of the chitosans, pushing laterally the lipid molecules. Oppositely, an increase in gauche defects was observed for DPPG. This can be explained by the uniform expansion of the film molecules due to the interaction between chitosan and DPPG anionic groups occurring underneath monolayer. Morphological changes from the BAM imaging confirmed the association of both samples into the film. The results obtained may be helpful in identifying the interaction mode of chitosan with phospholipids.

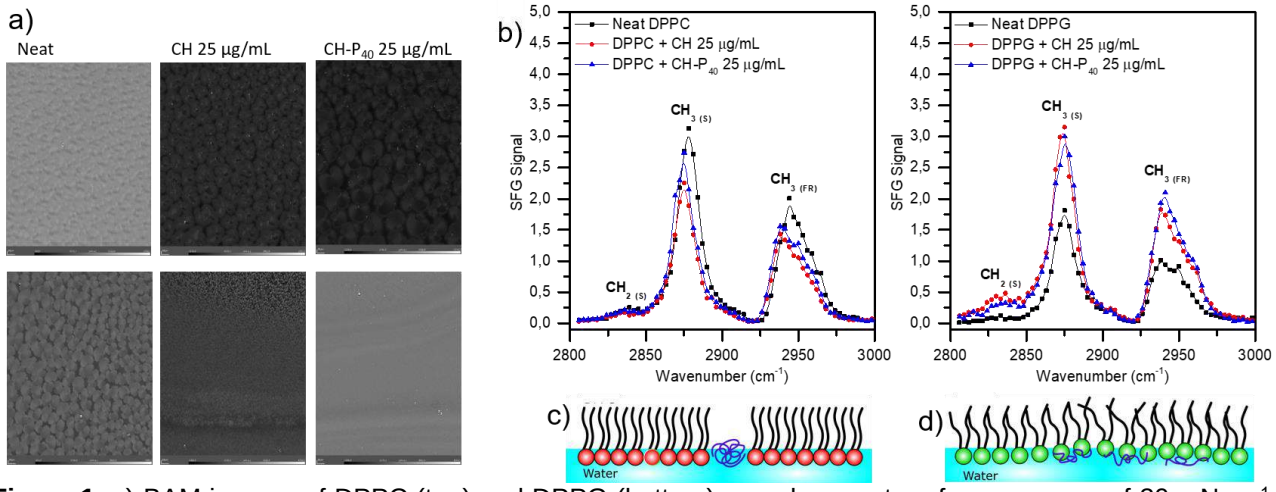


**Figure 1.** a) BAM images of DPPC (top) and DPPG (bottom) monolayers at surface pressure of 30 mN $m^{-1}$. b) SFG spectra using SSP polarization for the C–H stretching region of monolayers at 30 mN $m^{-1}$. Interaction mode of chitosan with c) DPPC and d) DPPG.

Acknowledgements
FAPESP (2017/03503-4), IFSC/USP, Grupo de Polímeros “Bernhard Gross”.

**Área: FIS**
*(Inserir a sigla da seção científica para qual o resumo será submetido. Ex: ORG, BEA, CAT)*

**Inscrição: 00360**
*(Inserir o número de inscrição do autor que fez a submissão)*

# Excess of vibrational density of states and relaxation processes studies on glass forming ionic liquids.

**Thamires A. Lima (PQ)[1], Zhixia Li (PG)[2], Yang Zhang (PQ)[2], Mauro C. C. Ribeiro (PQ)[1*].**

**thamires@iq.usp.br; mccribei@iq.usp.br**

*[1]Departamento de Química, USP*; *[2]Department of Nuclear, Plasma, and Radiological Engineering, UIUC*

*keywords: Raman Spectroscopy, Neutron Scattering, Glass Transition, Ionic Liquids, Boson Peak, Relaxation Processes.*

## Highlights

The boson peak behavior was studied by Raman and neutron spectroscopies at low temperatures.
Structural and thermal nature of $\alpha$ and $\beta$-relaxation processes of aliphatic ionic liquids has been revealed.

## Resumo/Abstract

Excess of vibrational density of states compared to Debye's prediction (e-VDoS) and relaxation processes for two ionic liquids (ILs) were investigated by means of Low Frequency Raman Spectroscopy, Quasielastic and Inelastic Neutron Scattering techniques (LFRS, QENS and INS) at different temperatures (180 K – 300 K) and wave vectors transfer (0.3 $A^{-1}$ – 2.0 $A^{-1}$), aiming to investigate the spatial heterogeneity dynamics contribution to the glass and melting transitions, and their relationship with the boson peak (BP). The samples, tributylmethylammonium bis(trifluoromethylsulfonyl)imide ($N_{1444}$TFSI) and trimethylbutylammonium bis(trifluoromethylsulfonyl) ($N_{1114}$TFSI) were studied under heating from the glass to the liquid state after an almost instantaneous cooling by 180 K. Both ILs experienced a cold crystallization. Figure 1 presents INS and LFRS data of $N_{1114}$TFSI at different states.

We used the Damped Harmonic Oscillator function to fit the BP obtained by INS. The BP parameters presented a good agreement with the log-normal function used to analyze the LFRS data. The BP intensity increases, and the BP energy decreases with the increasing of the temperature.

The Kohlrausch−Williams−Watts stretched exponential was used to probe the relaxation processes time. We obtained the $\alpha$ and $\beta$ relaxation times to the glassy, supercooled liquid and liquid states. The results were compared with previous structural analyses using X-ray diffraction and besides the diffusion process on the liquid state, our study correlates the relaxation processes with the spatial heterogeneity and provides direct evidence on the structural origins of the slow relaxations in ionic glass.

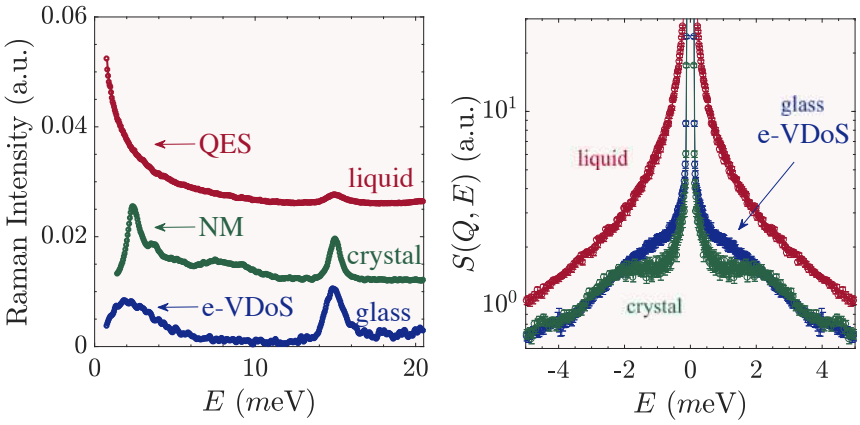


Figure 1: LFRS (left panel) and INS (right panel) data of $N_{1114}$TFSI at liquid (red curves), crystalline (green curves) and glassy (blue curves) states.

**Área: FIS**
*(Inserir a sigla da seção científica para qual o resumo será submetido. Ex: ORG, BEA, CAT)*

**Inscrição: 00381**
*(Inserir o número de inscrição do autor que fez a submissão)*

# Synthesis $Ag/Nb_2O_5$ nanoestructures for the visible light photocatalytic degradation of the methylene blue dye

**Raíssa B. A. Jambo (IC)[1], Patrícia B. Santos (PG)[1], Gustavo F. S. Andrade (PQ)[1]***

**gustavo.andrade@ufjf.edu.br.**

[1] *Laboratório de Nanoestruturas Plasmônicas, Centro de Estudos de Materiais, Departamento de Química, Universidade Federal de Juiz de Fora, 36036-900, Juiz de Fora, MG*

Palavras Chave:*(Processos Oxidativos Avançado, Fotocatálise Plasmônica, Pentóxido de Nióbio, Nanopartículas de Prata, Azul de Metileno).*

## Highlights

Synthesis of $Ag/Nb_2O_5$ nanostructures. Photodegradation of methylene blue using visible light catalyzed by the $Ag/Nb_2O_5$ nanostructures. Low loading of Ag nanoparticles relative to niobium pentoxide results in larger degradation process rate.

## Resumo/Abstract

$Ag/Nb_2O_5$ combined nanostructures were synthetized by association of metallic Ag nanoparticles and niobium pentoxide. Two catalysts were obtained with constant amount of Ag nanoparticles, but one containing 86 times less $Nb_2O_5$ (A) than the other (B). These catalysts were characterized by UV-Vis spectroscopy and X-Ray Diffraction and then they were applied on photodegradation of the dye methylene blue using white LED lamps as light source. First, the suspensions were kept in dark, overnight, to allow for the adsorption of the dye on the catalyst. Then, the suspensions were exposed to visible light for up to 24 hours. The reaction was monitored by means of UV-Vis and Raman/SERS spectroscopy, in order to observe the dye degradation and its modifications during the photodegradation process. Figure 1 present the absorption of the most intense electronic band of methylene blue as a function of time of degradation.

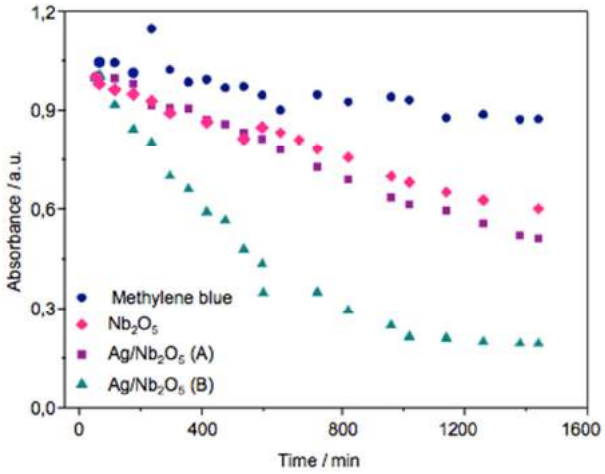


Figure 1. Absorbance of methylene blue as a function of visible light irradiation time for the indicated suspensions.

The catalyst (B) had 81% of degradation of the dye after 24 h, which was a larger amount than the degradation of the catalyst (A), which was 48%. The fitted first order rate constant was 215% larger for (B) relative to (A). From the above results, we may infer that silver nanoparticles in the higher loading studied, which is still a <5% loading, combined to $Nb_2O_5$ is efficient to increase at least twice the photodegradation rate of methylene blue under visible light excitation.

**Área: FIS** **Inscrição: 00422**

# Mechanistic study between the pesticide methyl-parathion and imidazole: unusual selective attack at the aliphatic carbon

**Valmir B. Silva (PG),* Marcelo C. Nunes (PG), Leonardo L. Q. Nascimento (IC), Alfredo R. M. de Oliveira (PQ), Elisa S. Orth (PQ)**

**valmir-baptista@hotmail.com;**

*Departamento de Química, UFPR;*

Palavras Chave: parathion, organophosphorus, imidazole.

## Highlights

- The pesticide methyl-parathion reacts by a peculiar mechanism with imidazole;
- Mechanistic investigation by kinetics, NMR and Mass Spectrometry

## Abstract

Methyl-parathion (PRT) is one of the sulphurated-organophosphorus agrochemicals used in several crops. It is very toxic to humans by the acetylcholinesterase deactivation and in 2016 was banned in Brazil. Imidazole (IMZ) is an organic molecule known to be important in a lot of biochemical process and to be a potent catalyst for P-O cleavage. – Herein, the reaction kinetics and mechanism of IMZ and PRT was studied by $^{31}$P NMR, UV-vis and mass spectrometry.

Results showed that in high pH values (>9) alkaline hydrolysis liberates 4-nitrophenolate ion is the predominant pathway, literature according.[1] However in neutral and weakly basic conditions the principal pathway is the imidazole attack at the aliphatic methyl carbons to produce 1-methyl imidazole and desmethyl-parathion (Figure 1). Thus, IMZ unusally attacks the aliphatic carbon which can be a new route towards the synthesis of methylated IMZ or even IMZ-derived ionic liquids. The IMZ attack at phosphoryl moiety is a disfavored pathway, probably due to sulfur effect that converts the phosphorus atom to a weak electrophile. Interestingly, the reaction of IMZ with the analogous pesticide Paraoxon (which instead of P=S has P=O), occurs exclusively on the phosphoryl group.[3].

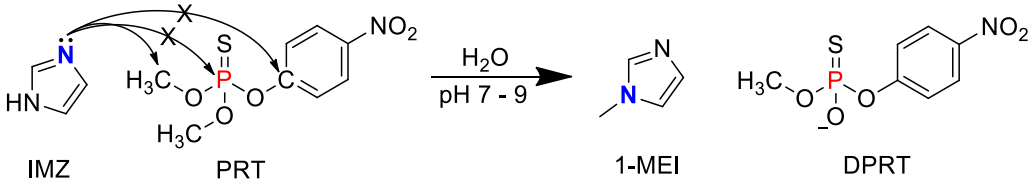


Figure 1 – Reaction of IMZ and PRT

The reaction has a potential to use in chemical detoxification and to comprehend interaction of imidazole moieties with various toxic agents. We evidence that slight changes in the organophosphate structure can greatly trend the mechanism, which directly affects the detoxication process pursued.

Acknowledgments: UFPR, CAPES, CNPq, Fundação Araucária and L'Oréal-UNESCO-ABC

References:

[1] Webpage http://portal.anvisa.gov.br/noticias/-/asset_publisher/FXrpx9qY7FbU/content/anvisa-determina-banimento-da-parationa-metilica-ingrediente-ativo-de-agrotoxico/219201/pop_up?_101_INSTANCE_FXrpx9qY7FbU_viewMode=print&_101_INSTANCE_FXrpx9qY7FbU_languageId=pt_BR Acessed in 16/01/2018.

[2] Liu, Y., Zhang, C., Liao, X. et al. **Environ. Sci. Pollut. Res.** (2015) 22, 19747.

[3] Orth E.S. et al. **J. Mol. Catal. A: Chem.** (2015) 403, 93.

**Área: *FIS*** **Inscrição: 00869**

# Descoloração e degradação do corante reativo Remazol Preto B por oxidação com $H_2O_2$/NaOH.

**Amanda Mora (IC),[1] Henrique Luís Floriani (IC),[1] Mateus Mittersteiner (PG),[2] Paulo Cesar de Jesus (PQ).[1]*. pcj@furb.br.**

*[1]Departamento de Química, Universidade Regional de Blumenau, FURB, Blumenau, SC; [2]Departamento de Química, UFSM, Santa Maria, RS.*

Palavras Chave: *Remazol Preto B, Descoloração, Degradação, Peróxido de hidrogênio, Oxidação, Cinética.*

## Highlights

**Decolorization and degradation of Remazol Black 5 reactive dye by oxidation with $H_2O_2$/NaOH.**
The influence of the dye concentration, $H_2O_2$ and temperature were evaluated. The highest decolorization efficiencie was observed at 60°C using $H_2O_2$ 30%(81%,120 min) and first-order kinetics behavior.

## Resumo/Abstract

Os corantes são utilizados nos mais diversos segmentos da indústria química, e são responsáveis pela alta carga orgânica e cor dos efluentes. O corante reativo Remazol Preto B (Black 5), muito empregado na indústria têxtil, apresentam difícil degradabilidade e se presente nas águas residuais, pode causar sérios danos à vida aquática e a saúde humana.[1] A fim de contribuir com estes estudos, neste trabalho foram avaliados os aspectos cinéticos da descoloração e degradação do corante Remazol Preto B (**Figura 1a**) através da oxidação química pelo uso da combinação de peróxido de hidrogênio e hidróxido de sódio ($H_2O_2$/NaOH). Foram avaliados a influência da concentração de corante (0,02g.L$^{-1}$, 0,03g.L$^{-1}$, 0,04g.L$^{-1}$), peróxido de hidrogênio (0,03%, 0,3%, 3%, 30%) e temperatura (30°C, 40°C, 50°C, 60°C) e hidróxido de sódio (1,0 mol.L$^{-1}$). Os experimentos foram realizados em um reator encamisado, conectado a um banho termostatizado, onde alíquotas foram retiradas em tempos pré-determinados, realizando-se a leitura de absorbância em 595 nm ($\lambda_{max}$ do corante). Observou-se que as curvas cinéticas obedeceram ao modelo cinético de primeira ordem ($k_{obs}$ 2,77x10$^{-3}$min$^{-1}$, 30°C a 1,71x10$^{-2}$min$^{-1}$, 60 °C). Em todos os estudos ocorreu a descoloração da solução de corante com eficiência variando de 29% a 30°C até 81% a 60°C ($r^2 \geq 0,98$). O melhor sistema foi com 0,03g.L$^{-1}$ de corante, $H_2O_2$ 30%/NaOH e temperature de 60°C com 81% de eficiência de descoloração da solução em 120 minutos de reação (**Figuras 1b e 1c**). Os parâmetros de ativação obtidos para $H_2O_2$ 30%/NaOH (60°C) foram: $E_a$ 59,9 kJ mol$^{-1}$($r^2$ 0,99), $\Delta H^{\#}$ 54,0 kJ mol$^{-1}$ ($r^2$ 0,98), $\Delta G^{\#}$ 13,2 kJ mol$^{-1}$ and $\Delta S^{\#}$ 102,1 J K$^{-1}$ mol$^{-1}$.

**Figura 1** - **(a)** Estrutura do corante reativo Remazol Preto B; **(b)** Descoloração de soluções do Remazol Preto B nas diferentes temperaturas: (■) 30°C, (●) 40°C, (▲) 50°C, (▼) 60°C; [corante] = 0,03g.L$^{-1}$, $H_2O_2$ 30%; **(c)** Decaimento da absorbância da solução do Remazol Preto B durante processo oxidativo via $H_2O_2$/NaOH (15 mL solução de corante 0,03 g.L$^{-1}$; 2,0 mL $H_2O_2$ 30%; 1,0 mL NaOH 1,0 mol.L$^{-1}$; 60°C).

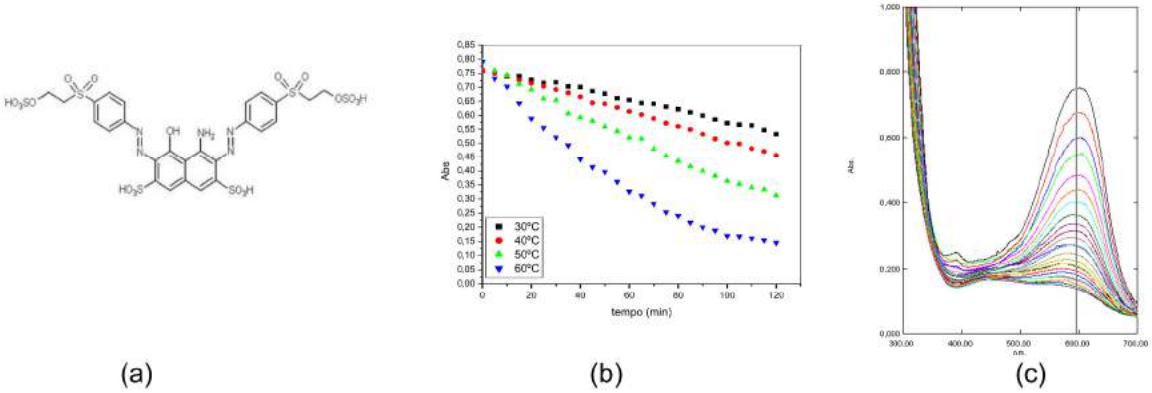


(a) (b) (c)

[1]Cardoso, F. N; et al. *Desalination*, **2011**, 269, 92-103.

*Agradecimentos: DQ-FURB, INCT Catálise.*

**Área: FIS** **Inscrição: 00164**

# Phase inversion behavior of poly(ethylene glycol) + NaOH + water aqueous two-phase systems (ATPSs): Effect of polymer molar mass

**Jussara Alves Penido (PG), Gessyca Rosa Silva Gonçalves (IC), Isabela de Melo Carvalho (IC), Aparecida Barbosa Mageste (PQ), Gabriel Max Dias Ferreira (PQ)***

**gessycarosa@yahoo.com.br; gabrielmdf@yahoo.com.br**

*Chemistry Department, UFOP, Minas Gerais, Brazil*

Keywords: *Aqueous two-phase systems, Phase diagrams, Triton-X100, Choline Chloride.*

## Highlights

- ATPSs containing poly(ethylene glycol) and NaOH presented phase inversion behavior;
- Higher temperatures and smaller global compositions favored the phase inversion behavior;
- Phase inversion behavior was dependent on the polymer molar mass.

## Abstract

In the last decades, the phase inversion behavior of aqueous two-phase systems (ATPSs) has been commonly reported for some systems. For instance, some ATPSs formed by poly(ethylene glycol) (PEG) and electrolyte, extensively employed in processes of separation and purification of strategic solutes, exhibit that behavior [1]. This unique phenomenon was proved to be dependent on the temperature and composition of the system, however the effect of the molar mass of the polymer was not discussed. Here, investigation was made of the effect of the PEG molar mass on the phase inversion behavior of ATPSs formed by PEG, sodium hydroxide, and water. For the experiments, PEGs of molar masses of 1500, 4000, 10000, and 20000 g $mol^{-1}$ were used to prepare the ATPSs in three different compositions. Each system was placed in a bath with controlled temperature (25-80 °C) and allowed to separate phase. A dye that concentrated in the PEG-enriched phase was used as probe to identify the temperature in which the phase inversion occurred. As a general result, inside the biphasic region, higher temperatures and smaller global compositions favored the formation of ATPSs in which the bottom phase was observed to be the PEG-enriched phase. This result was contrary to the feature described for the most of ATPSs, in which the PEG-enriched phase was the top phase [2]. The phase inversion behavior was caused by density changes in the phases, and it occurred in lower temperatures when the PEG molar mass increased (Fig. 1).

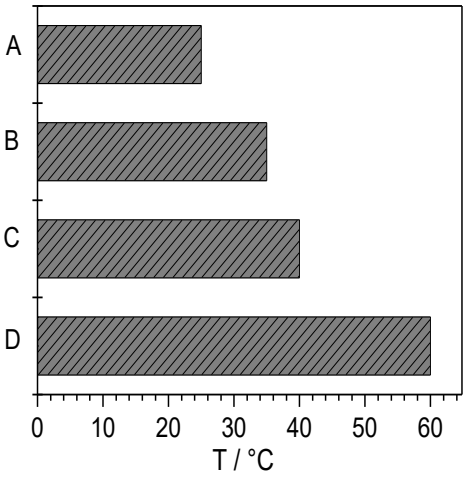


Figure 1. Effect of PEG molar mass on the temperature in which the phase inversion behavior occurs. A, B, C, and D refer to the ATPSs formed by PEG 20000, PEG 10000, PEG 4000, and PEG 1500, respectively.

References: [1] M.A. Eiteman, *J. Chromatogr. A* 668 (1994) 13-19; [2] M.T.Z. Moattar, P. Jafari, *Fluid Phase Equilib.* 337 (2013) 224-233.

**Área: FIS** **Inscrição: 00203**

# Use of surfactants as selective modulators in the partition in aqueous two-phase systems: An alternative for speciation of dyes

**Jussara Alves Penido (PG), Poliana Lima Martins (IC), Gabriel Max Dias Ferreira (PQ), Aparecida Barbosa Mageste (PQ)***

**jussarapenido@hotmail.com; aparecidamageste@gmail.com**

*Chemistry Department, UFOP, Minas Gerais, Brazil.*

Keywords: *Aqueous two-phase systems, Dyes, Surfactant, Interaction, Speciation.*

## Highlights

- Effect of surfactant on the partition of dyes in aqueous two-phase systems (ATPSs) was evaluated;
- The surfactant selectively affected the partition of anionic dye;
- Dyes were speciated using ATPSs.

## Abstract

The inappropriate disposal of effluents containing dyes in water bodies is one of the greatest environmental concerns in the last decades. An efficient alternative for the removal of those compounds from aqueous matrices is the use of aqueous two-phase systems (ATPSs). However, there are no investigation on the use of these systems for speciation of dyes. Here, we evaluated the use of ATPSs for the speciation of remazol yellow (RY) and methylene blue (MB) using the dodecyltrimethylammonium bromide (CTAB) surfactant as selective modulator in the partition. Experiments of individual partition of RY and MB were performed in the presence of different concentrations of CTAB in ATPSs formed by poly(ethylene glycol) (PEG), salt, and water. In the absence of CTAB, RY and MB partitioned to the top phase of the systems. However, in the presence of the surfactant, while the MB dye remained in the top phase, the RY dye was transferred to the bottom phase. This result was attributed to a specific interaction between the CTAB cationic surfactant and the RY anionic dye, and was highly dependent on the PEG molar mass (Figure 1a) and nature of salt (Figure 1b). Furthermore, when the CTAB concentration increased, the removal of RY to the bottom phase increased. From this finding, experiments of simultaneous partition of the dyes were performed in high CTAB concentration. In ATPSs formed by PEG 6000, $(NH_4)_2SO_4$, and water, 92.99% of the MB dye remained in the top phase, while 78.34% of RY dye was transferred to the bottom phase. This result showed the potential of ATPSs for the speciation among dyes of opposite charges.

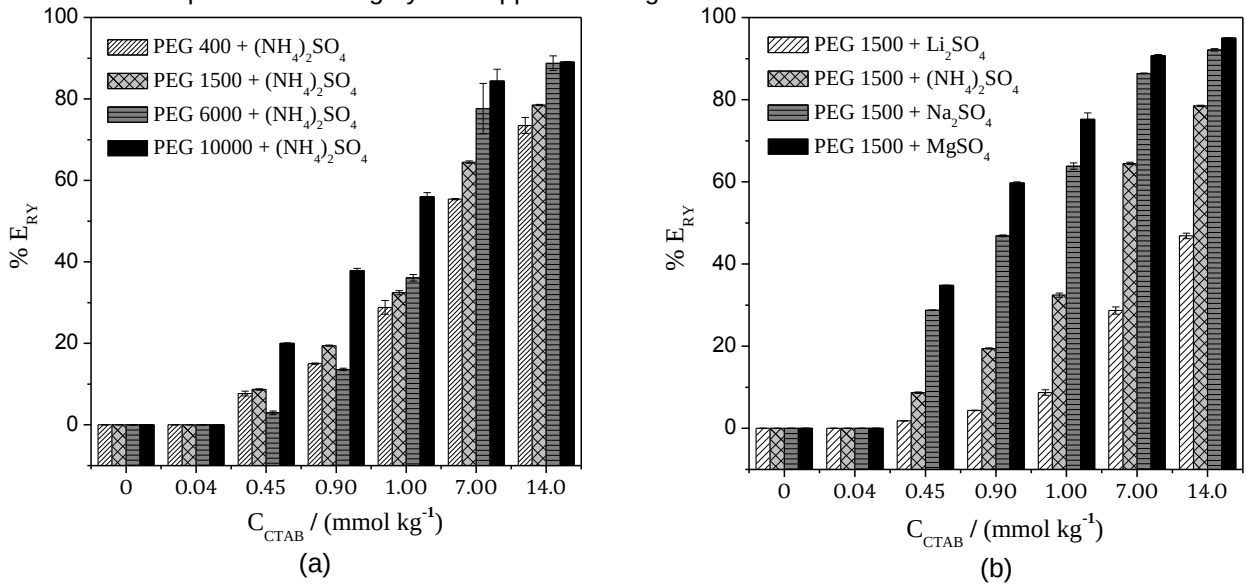


**Figure 1.** Effects of (a) PEG molar mass and (b) nature of the salt on the removal of RY to the bottom phase of the ATPSs formed by PEG + salt + water, at different concentrations of CTAB and 25°C.

**Área: FIS**
*(Inserir a sigla da seção científica para qual o resumo será submetido. Ex: ORG, BEA, CAT)*

**Inscrição: 00238**
*(Inserir o número de inscrição do autor que fez a submissão)*

# Análise de dopagens substitucionais com V e N na superfície de $TiO_2$ através do método DFT-GGA

**Gustavo Olinto da Silva (PG), José R. S. Politi (PQ), João B. L. Martins (PQ)***

**lopes@unb.br; gustavo_olinto@hotmail.com**

*Instituto de Química, UnB)*

Palavras Chave: GGA, TiO2, dopagem.

## Highlights

V and N substitutional dopant on $TiO_2$ surface using DFT-GGA method. $TiO_2$ is a widely used in photocalysis. We used plane wave DFT-GGA to study the substitutional V and N on $TiO_2$ surface. Monodiping and co-doping was studied.

## Resumo/Abstract

The titanium dioxide in the anatase form in the direction (101) is well known in the literature for its potential as a photocatalyst. However, this catalyst has some limitations in the photocatalytic process, because it is activated only by UV light and has a high recombination rate (e- / h +). Doping is one of the optimization strategies for photocatalysts.[1,2,3] In this work, the surface of titanium dioxide was doped in the outer layer, in order to determine the best position to do the replacement. This step was performed using the theoretical DFT-GGA method on plane wave basis, with the value of the supercell slab. Vanadium and nitrogen monodopants and a co-doping with nitrogen and vanadium were performed. The results observed in monodoping with vanadium showed that there was no significant difference (<0.002 eV) in a substitutional doping at the atoms contained in the same alignment, which was expected due to the symmetry of these points, and all atoms in this alignment are hexacoordinate. However, when comparing with other positions in the same layer the results show that the substitutional doping in the P1 position is the most stable when compared to the doping process performed at the P4, P5 and P6 positions. Monodoping with nitrogen showed that there was no significant difference (<0.01 eV) in a substitutional doping at the atoms contained in the same line. The largest difference between the doping of the same alignment is between the atoms P4 and P5 (-0.0095 eV). Another note to be highlighted is in relation to the coordinating number of positions. The doped surfaces in tricomposed positions presented a higher stability than the two-coordinate positions. Position P7 is the most stable when compared to the dopants at positions P5, P6 and P6. In the $V_{Ti}$-$N_O$ co-doping, the dopant structures bonded together are more stable than the unbound dopant structures. Between the positions P1 and P2, the position P1 presented the smallest energy of the slab.

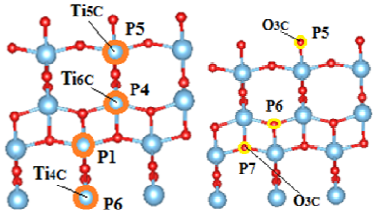


Figure 1 – Positions of doping process.

References

1- Na Phattalung, S.; Limpijumnong, S.; Yu, J. Appl. Catal. B Environ. 2017, 200, 1–9.

2- El Koura, Z.; Rossi, G.; Calizzi, M.; Amidani, L.; Pasquini, L.; Miotello, A.; Boscherini, F. Phys. Chem. Chem. Phys. 2018, 20 (1), 221–231.

3- Colmenares, J. C.; Xu, Y. From Fundamentals to Green Applications; 2016; Vol. 93.

**Área: FIS** **Inscrição:298**

# The effect of acetone and sulfuric acid concentrations on sequential oscillations in a modified Belousov-Zhabotinsky reaction.

**Michael S. Chern (PG), Roberto B. Faria (PQ)***

**michaelsunchern@hotmail.com; faria.ufrj@gmail.com**

*Instituto de Química, UFRJ*

Palavras Chave: *Oscillating reaction, Sequential oscillations, Induction period, Belousov-Zhabotinsky.*

## Highlights

The range of sulfuric acid and acetone concentrations for the appearance of sequential oscillations in a modified Belousov-Zhabotinsky were determined.

## Resumo/Abstract

Oscillatory reactions are reactions where it is possible to measure oscillations on the concentration of some reaction intermediates. The original Belousov-Zhabotinsky (BZ) reaction is composed of sulfuric acid, bromate, malonic acid and cerium(IV). The reaction studied in this work is a variation of the original BZ reaction, where malonic acid is substituted by acetone and oxalic acid. Chemical oscillators may have different oscillation patterns and might show an induction period or even a break between oscillations (sequential oscillations). Variations on acetone concentration[1] and temperature[2] may cause the appearance of sequential oscillations on this system. Herein we report the effects of changes on acetone and sulfuric acid concentrations, in batch. The concentrations of oxalic acid (0.1 M), bromate (0.02 M), and cerium(IV) (0.001 M) were fixed, while sulfuric acid and acetone concentrations were changed in the range from 1.25 M to 1.76 M and 0.20 M to 0.28 M, respectively. Sequential oscillations (Figure 1) were observed in the ranges of 1.65 M to 1.75 M sulfuric acid concentration ([acetone] = 0.20 M) and 0.22 M to 0.27 M acetone concentration ([$H_2SO_4$] = 1.50 M). Increasing further any of these concentrations make the break between the two groups of oscillations grows until it becomes an induction period. The results show also that changes on oscillations caused by shifts of sulfuric acid or acetone concentrations can be compensated by each other.

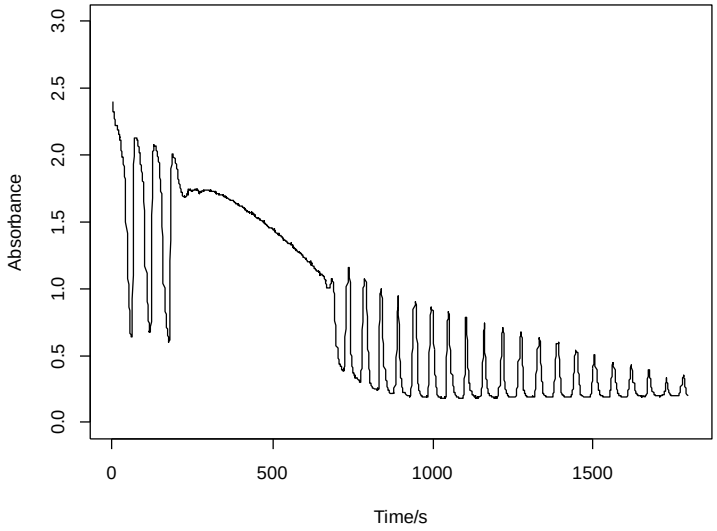


**Figure 1**: Sequential oscillations. Sulfuric acid 1.5 M, acetone 0.25 M, oxalic acid 0.1 M, sodium bromate 0.02 M, cerium(IV) 0.001 M.

1. Wittmann, M.; Stirling, P.; Bódiss, J. Temporary non-oscillatory states in the oxalic acid-acetone mixed substrate Belousov-Zhabotinskii reaction. *Chem. Phys. Lett.* **1987**,*141*, 241.
2. Monteiro, E. V.; Varela, H.; Faria, R. B. The effect of flow rate on the oscillatory activation energy of an oscillating reaction. *Chem. Phys. Lett.* **2017**, *684*, 219.

**Área: FIS** **Inscrição: 00160**

# The use of agro-industrial waste and *Moringa oleifera* leaves as antioxidants sources for soy oil biodiesel

**Marcia Gabriela Pianaro Valenga (PG),[1*] Nayara Lais Boschen (PG),[1] Paulo Rogério Pinto Rodrigues (PQ),[1] Guilherme Arielo Rodrigues Maia (PQ).[1]**

**vmarciagabriela@gmail.com**

*[1]Chemistry Department, Universidade Estadual do Centro-Oeste - UNICENTRO*

Key Words: Antioxidants, Barley waste, Biodiesel, Moringa leaves

## Highlights

Barley waste and *Moringa oleifera* leaves were used as natural antioxidants sources to soy oil metylic biodiesel. In the best condition it was obtained an induction time of 8,18±0,18 hours, at 110 °C.

## Abstract

Biodiesel were prepared through soy oil metylic transesterification, using alkaline catalysis. Antioxidants extraction from barley waste (BW) and moringa leaves (ML) was made according to the method proposed by Boschen[1], using acid environment. Concentrations were defined through a $3^2$ experimental design (Table 1). The response was obtained as induction time (IT), using the equipment Rancimat®. Software employed was STATISTICA®. Response surface (Figure 1) showed best results to BW and ML concentration of, respectively, 13 and 9 g $L^{-1}$, being the highest IT 7,80 hours.

**Table 1.** Variables of the experimental design

| Original independent variables | Coded variables and levels | | |
|---|---|---|---|
| | $x_1$ | $x_2$ | $x_3$ |
| | -1 | 0 | +1 |
| $X_1$= BW concentration (g $L^{-1}$) | 9 | 11 | 13 |
| $X_2$=ML concentration (g $L^{-1}$) | 3 | 6 | 9 |

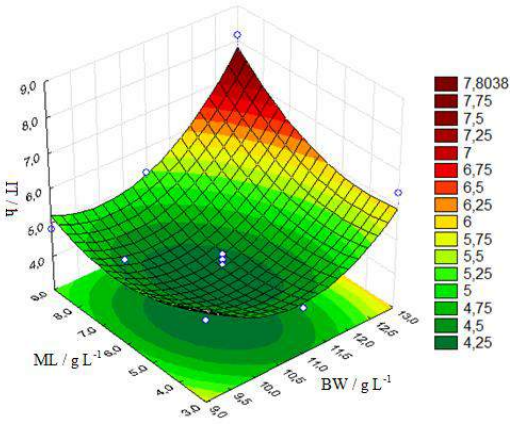


**Figure 1.** Response surface

Analysis of Variance showed all therms from the model were significant to 95% of trust. According to determination coefficient ($R^2$), the proposed model can explain 87,80% of the variation around the mean, being suitable since it is higher than 80%[2]. To F-test, $F_{calculated}$ was superior to $F_{tabulated}$ to all variables, showing the model had a significative regression.

Experimental measures were made using the best condition to define the practical IT possible to reach. The assays mean was 8,18±0,18 hours, which is in agreement with the minimum IT of 8,00 hours, established by ANP.[3] An control sample, without antioxidants addiction, was also produced and presented an IT of 4,04±0,08 hours. Therefore, for the best result there was more than a 100% increasement of the IT.

**References:**

[1] BOSCHEN, N. L. et al. BR1020160046394. 2016.
[2] MAIA, G. A. R.; et al. Acta Scientarum. 36, 4, 699-705, 2014.
[3] ANP. Disponível em: http://www.anp.gov.br. Acesso: 08 novembro 2016.

**Acknowledgements:**

**Área: FIS** **Inscrição: 00089**

# Study of the behavior of the methyl orange (MOR) dye in binary mixtures using amphiprotic solvents

**Ana C. Sant'Ana (IC),[1] Anayana Z. Dangui (IC),[1] Keller P. Nicolini (PQ),[1] Jaqueline Nicolini (PQ).[1*]**

**jaqueline.nicolini@ifpr.edu.br**

[1]*Colegiado de Química, Instituto Federal do Paraná – IFPR.*

Palavras-chave: *binary mixtures, molar fraction, methyl orange.*

## Highlights

Solvent plays an important role in the MOR solvation, by the alkyl groups present in the solvent molecules. The behavior is due to the effect of preferential solvation.

## Resumo/Abstract

The solvents influence on chemical and physical processes, reaction rates, mechanisms, selectivity, chemical equilibrium, position and intensity of spectral absorption bands, liquid chromatographic separations.[1] The behavior of MOR in binary mixtures of water (W) (Solvent 1, S1) and methanol (M), ethanol (E), *n*-propanol (NP), *iso*-propanol (IP) or *t*-butanol (NB) (cosolvent or solvent 2, S2) was studied in order to investigate the behavior of the MOR in amphiprotic solvents. The energy transition ($E_T$) values were plotted as a function of the molar fraction of the cosolvent ($X_2$) (Figure 1) and the experimental values for each binary mixture were fitted according equation described to Rosés et al.[2] The results (Table 1) show a good nonlinear fit (SD ≤ 0.191). The $E_T$(MOR) values are in agreement with the experimental values. The parameters which define the preferential solvation ($f_{2/1}$ and $f_{12/1}$) indicate a tendency for the indicator MOR to be solvated by the cosolvents (S2, R-OH) and by the mixture of solvent 1 (S1, water) with solvent 2 (S12), rather than S1. In mixed solvents the solutes can interact to a different degree with the components of the mixture and this difference in the interactions is reflected in the composition of the solvation microsphere. The results show new potentialities of the methyl orange indicator.

**Table 1.** Calculated Parameters for Methyl Orange (MOR) in Binary Mixtures at 25 °C[a].

| Binary mixture | $E_T(MOR)_1$ | $E_T(MOR)_2$ | $E_T(MOR)_{12}$ | $f_{2/1}$ | $f_{12/1}$ | SD ($x10^{-2}$) |
|---|---|---|---|---|---|---|
| W-M | 67,74 | 61,47 | 57,60 | 3,29 | 0.330 | 1,2 |
| W-E | 68,40 | 61,58 | 57,97 | 0,525 | 0.575 | 3,0 |
| W-NP | 58,33 | 61,65 | 55,29 | $7,3x10^{-2}$ | 0.185 | 9,6 |
| W-IP | 68,91 | 61,75 | 47,05 | 0,219 | 0.118 | 13.5 |
| W-TB | 69,22 | 61,57 | 48,00 | $6,1x10^{-2}$ | 0.095 | 19.1 |

[a] Obtained for the mixtures water (S1) with R-OH (S2).

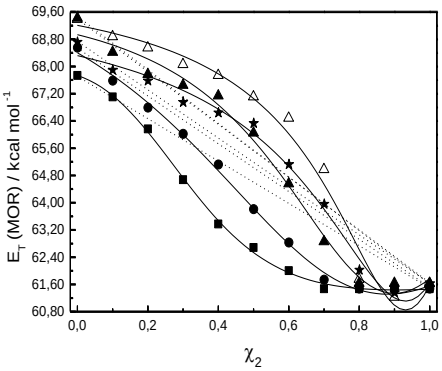


**Figure 1.** Influence of the cosolvent on the $E_T$(MOR) values, of water-ROH mixtures, the ROH component being (■) methanol. (●) ethanol (∗) *n*-propanol. (▲) *iso*-propanol. (Δ) *t*-butanol. (·····) Theoretical linear dependence for no preferential solvatation; (——) curve fitted with equation from Ref. 2.

[1] Reichardt, C.; Welton, T. Solvents and Solvent Effects in Organic Chemistry. *Wiley-VCH: Weinheim*, 2004.
[2] Rosés M., *et al*. *J. Chem. Soc., Perkin Trans. 2*, 1997, 1341.

**Área: FIS** **Inscrição: 01027**

# Effect of inhibitors and a bad solvent on a Brazilian crude oil: kinetics of asphaltene adsorption on gold surfaces of QCM electrode

**[1*]Lia B.S. Balestrin (PG), [1]Celso A. Bertran (PQ), [2]Mateus B. Cardoso (PQ), [1]Watson Loh (PQ).**

**lia.balestrin@iqm.unicamp.br**

*[1]Instituto de Química, UNICAMP; [2]Laboratório Nacional de Nanotecnologia,CNPEM*

Palavras Chave:asphaltene, QCM, kinetic, adsorption, crude oil.

## Highlights

Quartz crystal microbalance (QCM) associated to a microscopy technique can be used to determine the kinetics of asphatenes deposition. It is also possible to determine in crude oil systems the inhibitor capacity to avoid their deposition directly.

## Abstract

The kinetics of asphaltene adsorption was measured using a quartz crystal microbalance (QCM) with a gold surface. The measurements were done using heptane in the range of 0 to 115 % of the onset, determined by optical microscopy. The data suggested that, in low heptane concentrations (0-75% of the onset), the RLA (reaction-limited aggregation) model describes the deposition curves. While in high concentrations (95-115% of the onset), the DLA (diffusion-limited aggregation) and sedimentation models fit the data. (Figure 1) These data also suggest that adding different inhibitors to the formulation at 95% of the onset changes the mechanism to RLA model, where not every collision results in aggregation. However, only by combining this information with optical microscopy we could determine the inhibitor effects: hampering nucleation and asphaltene growth. Therefore, this work describes the adsorption kinetics of asphaltene perturbed by a flocculant and inhibitors, which is main topic for the design of asphaltene inhibitors or dispersants for crude oils. Besides, these data show that QCM is a good technique to be conducted directly in crude oil with no need analyze crude oil with no need for use of model systems or other sample treatments.

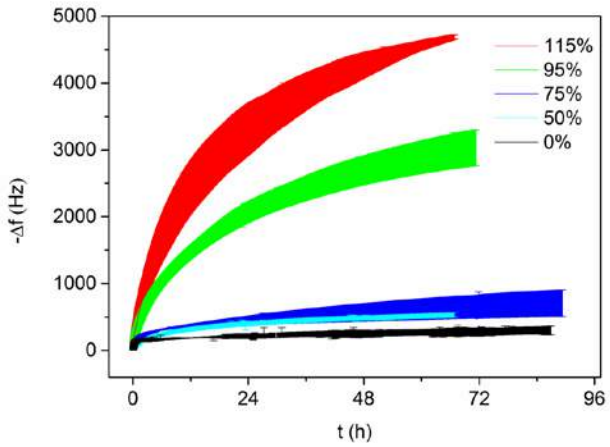


Figure 1: QCM results shown as change in frequency as a function of time of crude oil with different heptane contents.

**Área: FIS** **Inscrição: 01067**

# Estudo comparativo da eficiência de adsorção de diferentes classes de corantes texteis empregando residuo industrial

**Tainan Miguel (IC), Francielle Schmitz(PG); Ivonete O. Barcellos (PQ)*.**

*E-mail:* **tainan_miguel@hotmail.com**; *franci.schmitz@gmail.com;iob@furb.br.*
[1]*Departamento de Química. CCEN/FURB. Rua Antônio da Veiga, 140, CEP 89012-900 Blumenau, SC.*
Palavras Chave: *Adsorção, corante básico, corante direto, resíduo industrial, adsorvente alternativo.*

## Highlights

Comparative study on the adsorption efficiency of different classes textile dyes using industrial waste.
The textile industry is one of the largest water consumers in the world.
In this study, the potential use of an industrial waste as an adsorbent for the textile was investigated.

## Resumo/Abstract

A adsorção é uma técnica utilizada em processos de descontaminação de efluentes, na qual o contaminante presente na fase líquida é adsorvido por um material adsorvente[(1)].
Os métodos de adsorção, removem completamente a molécula de corante sem gerar fragmentos e, por essa razão, tornaram-se uma alternativa atraente para o tratamento de águas residuais[(2)]. O presente trabalho consiste em avaliar a eficiência da adsorção do corante básico Astrazon Azul FGGL 300% e corante direto Preto C.I 22 em resíduo da indústria de clarificação de óleo vegetal (RC) em diferentes granulometrias. A Figura 1 mostra o esquema da parte experimental.

**Figura 1:** Esquema experimental para a remoção do corante

A Figura 2(a,b) mostra os espectro de absorção das soluções do corante, antes e após o processo de adsorção no residuo (RC). Observa-se um grande decaimento da absorção do corante confirmada nas curvas dos espectros.

**Figura 2** (a) Corante básico (b) Corante direto no tempo zero (1), 1 hora de cinética (2) e tempo infinito (3)

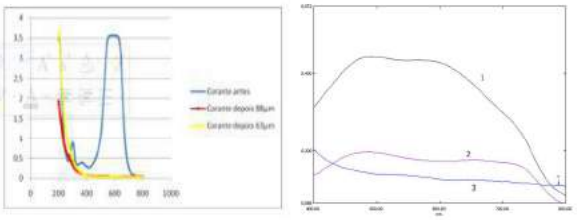

As Figuras 3 e 4 mostram a capacidade de remoção do corante com quantidades diferentes de adsorvente em diferentes temperaturas e nas granulometrias de 88 e 63 µm, respectivamente.

**Figura 3** Corante básico (a) 88 µm e (b) 63 µm

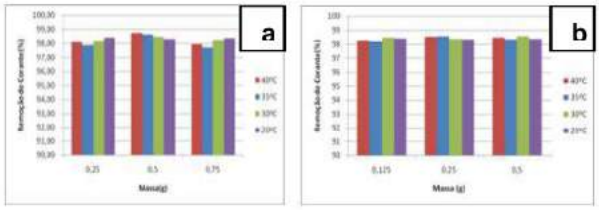


**Figura 4** Corante direto (a) 88 µm e (b) 63 µm

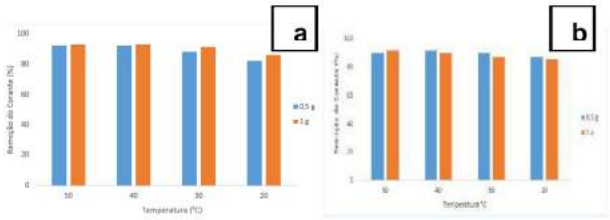


O RC apresentou excelentes propriedades de adsorção, onde a eficiência do adsorvente variou de 93% a 86% no caso do corante direto e em torno de 97% para o corante básico nas mesmas condições de temperatura e quantidade de adsorvente. A adsorção dos corantes em RC foi influenciado favoravelmente por um aumento da temperatura, entretanto não muito significativo pela granulometria.

## *Referências*

[1] *MENDES, C. R.;* ***Revista Matéria,****vol.20 nº4, p.1517-7076, 2015.*

[2]MITTERSTEINER, M; SCHMITZ, F; BARCELLOS, I. O. **Journal of Water Process Engineering**, v. 17, p. 181-187, 2017

**Área: FIS** **Inscrição: 00768**

# SOLUBILIDADE DE TIMINA (THY) EM ÁGUA DO MAR ARTIFICIAL PARA ESTUDOS DE QUÍMICA PREBIÓTICA

Daniely de Souza Carvalho (IC),[1] Adriana Clara da Silva (IC),[2] Cristine E. A. Carneiro (PQ).[3]
adriana.silva@ufob.edu.br; dannycarvalho97@gmail.com

[1, 2, 3] *Centro de Ciências Exatas e das Tecnologias, Universidade Federal do Oeste da Bahia – UFOB.*
*Palavras Chave: Química prebiótica, Água do mar, Timina, Origem da vida, Solubilidade, Temperatura.*

## Highlights

Solubility Of Timine In Artificial Sea Water For Prebiotic Chemistry Studies.
Prebiotic chemistry studies the reactions that may have contributed to the emergence of life on Earth. The behavior of thymine in various artificial sea water are the focus of this work.

## RESUMO/ABSTRACT

A química prébiótica estuda as reações que podem ter contribuído para o surgimento de vida na Terra. O objetivo deste trabalho foi avaliar a solubilidade da timina (Thy) em: (1) água ultrapura, (2) água do mar atual, (3) água do mar artificial de 3,2 bilhões de anos, (4) água do mar artificial de 4,0 bilhões de anos e (5) água do mar artificial de 4,0 bilhões de anos contendo P, Zn, Mn, Si e Fe. Para cada ambiente foram pesadas 8 mg de Thy e solubilizado em 1 mL da água, o sistema foi incubado a 40°C por 1 hora, depois mantido a 30, 35, 40, 45, 50, 55 e 60 C° por 24 horas e centrifugado durante 20 minutos. A solução final foi lida em 265 nm e a timina quantificada usando uma curva padrão preparada em cada tipo de água. Foram feitas medidas de pH antes e depois da adição de Thy. Na temperatura de 30 °C a Thy apresentou maior solubilidade em (1), em (2) ocorreu em 50 °C, em (3) e (5) em 60 °C e em (4) em 55 °C. A maior solubilidade (8,76 mg $mL^{-1}$) foi observada em (3) na temperatura de 60 °C, valor muito próximo do observado para a solubilidade da timina (8,70 mg $mL^{-1}$) em (4) a 55 °C. A menor solubilidade da base (0,57 mg $mL^{-1}$) foi observada em (5) a 35 °C.

**Área: FIS** **Inscrição: 00221**

# Análise Físico-Química e Determinação de Metais Tóxicos Presentes na Manipueira

**Ingrid K. L. Melo (IC),[1] Maria C. Tavares (PG),[1] Janesmar C. M. Cavalcanti (PQ),[2] José G. da S. Júnior (PQ),[3] Wander G. Botero (PQ),[1] Vinícius Del Colle (PQ).[1]***

**Ingrid-karen@live.com; delcolle@arapiraca.ufal.br**

*[1]Universidade Federal de Alagoas – Campus Arapiraca, UFAL; [2]Universidade Estadual de Alagoas – UNEAL – Campus Arapiraca; [3]Instituto Federal de Alagoas – Campus Marechal Deodoro*

Palavras Chave: *Manipueira, Metais, Caracterização físico-química, Meio ambiente*.

## Highlights

Physical-Chemical Analysis and Determination of Metals from Cassava Residual Water
The residual water, obtained from Cassava processing, is rich in organic compound and toxic metals and represents a dangerous risk for body water and soil near to house of flour. Then is relevant analyze chemically this material in order to advise the farm worker about the environmental risk of manipueira.

## Resumo/Abstract

A mandioca (*Manihot esculenta*) tem espaço importante na agroindústria brasileira. Seu processamento gera um efluente líquido denominado manipueira, cuja composição química abrange desde macro e micronutrientes, matéria orgânica e elementos tóxicos.[1] O descarte desse efluente é, muitas vezes, feito de forma inadequada e pode levar a contaminação de corposd'água ou ou do solo nas proximidades das 500 casas de Farinha existentes no estado de Alagoas.[2] Nesse sentindo, estudos de caracterização da manipueira são importantes, pois contribuem para o manuseio, descarte e aplicação adequados. Esse trabalho teve como objetivo comparar as características físico-químicas da manipueira filtrada em 0,45 µm e em filtro comum. A manipueira foi coletada em uma casa de farinha na cidade de Arapiraca – AL e armazenada a 4°C. Logo após, centrifugada para separação dos sólidos, passada em filtro qualitativo e membrana nitrocelulose de 0,45 µm. Os filtrados foram caracterizados quanto: pH, condutividade, carbono orgânico total (COT) por combustão e de metais por MP AES com digestão prévia com $HNO_3$ 65% (v/v) e $H_2O_2$ 35 % (v/v). Os resultados da caracterização estão apresentados na Tabela 1

**Tabela 1** – Resultados da caracterização da manipueira passada em filtro comum e em 0,45 µm.

| Efluente | COT (g $L^{-1}$) | pH | mS cm | Ba mg $L^{-1}$ | Cd mg $L^{-1}$ | Cr mg $L^{-1}$ | Ni mg $L^{-1}$ | Pb mg $L^{-1}$ | Zn mg $L^{-1}$ |
|---|---|---|---|---|---|---|---|---|---|
| Filtro comum | 24,6 | 3,48 | 24,4 | 0,60 | 0,08 | 0,51 | 0,14 | 0,86 | 18,3 |
| Filtro 0,45 µm | 23,9 | 3,55 | 20,1 | 0,47 | 0,05 | 0,22 | 0,17 | 0,48 | 2,12 |

Como observado na Tabela 1, a filtração em 0,45 µm leva a uma retenção de COT e, consequentemente, dos metais presentes na manipueira, seja por estarem associados ao mesmo ou por agregação até entupimento do poro. Os valores de COT refletem um potencial parcial da aplicação do material como biofertilizante. O pH para os efluentes estudados estão fora do padrão estabelecido pela Resolução n° 430 CONAMA (entre 5 e 9) para o descarte de efluente.[3] Já os valores referentes ao Ba, Cd, Ni e Pb e Zn do filtrado em 0,45 µm estão dentro dos limites máximos estabelecidos pelo CONAMA, enquanto Cr nos dois filtrado e Zn do efluente de filtro comum estão acima dos limites máximos, representando um problema ambiental como consequência do descarte inadequado. A filtração em 0,45 µm reduziu bruscamente os valores de Zn no efluente, apresentando-se como alternativa para a remoção de Zn da manipueira.

1 AVANCINI, S.R.P.; FACCIN, G.L.; TRAMONTE, R.; ROVARIS, A.A.; PODESTA, R.; SOUZA, N.M.A.; AMANTE, E. R. Cassava starch fermentation wastewater: Characterization and preliminary toxicological studies. Food and Chem. Tox., v. 45, pp. 2273–2278, 2007.
2 DUARTE, A. S.; ROLIM, M. M.; SILVA, E. F. DE F.; PEDROSA, E. M. R.; ALBUQUERQUE, F. S.; MAGALHÃES, A. G. Alterações dos atributos físicos e químicos de um Neossolo após aplicação de doses de manipueira. Rev.Bras. de Eng. Agr. e Amb., v. 17, n. 9, p. 938-946, 2013.
3 CONAMA, Conselho Nacional do Meio Ambiente, Resolução n° 430 de 2011.

**Área: FIS** **Inscrição: 00334**

# Surface modification of aseptic carton package for energy harvesting devices

**Kelly S. Moreira (IC),[1] Thiago A. L. Burgo (PQ).[2*]**

**kellymoreira.sc@gmail.com; thiago.burgo@ufsm.br**

[1]*Department of Chemistry, UFSM;* [2]*Department of Physics ,UFSM*

Keywords: *Triboelectric generators, Energy harvesting, Food packaging, Polymers, Surface modification*.

## Highlights

Triboelectric generators for energy harvesting systems were constructed using aseptic carton packages with a scalable low-cost surface modification process.

## Resumo/Abstract

Triboelectric generators are electrostatic generators based on tribocharging (or contact electrification). Most of the triboelectric generators are constructed using expensive materials like gold thin films [1] and costly processes such as photolithography. In this work, we used aseptic carton packages in a low-cost scalable process to construct a triboelectric generator with efficiency comparable to recent devices reported in the literature. In fact, aseptic carton packages, mostly based on either Tetra Pak or SIG Combibloc systems, are composed from laminates of liquid packaging board, foil, and polyethylene and naturally present all parts required by a triboelectric system. As shown in the Scheme 1, the triboeletrization is enhanced by the surface modification of polyethylene, such as chemical, physical and electric processes. In the first moment, the polyethylene surface was oxidized and used as face of the tribogenerator while another polyethylene sheet was kept intact, obtaining potentials as high as 200 Volts. We were capable to store generated by our device in 4 capacitors of 2.2 µF during 3.5 minutes, reached 2.5 Volts. Moreover, the voltages obtained here are in the same order of magnitude of nanoengineered devices that were recently described in the literature [2] and we believe that using aseptic carton packages and another surface modification, could be a reliable way to construct energy harvesting and scavenging devices that may to collect energy through daily activities, like walking or driving, and use it for devices that require low power density.

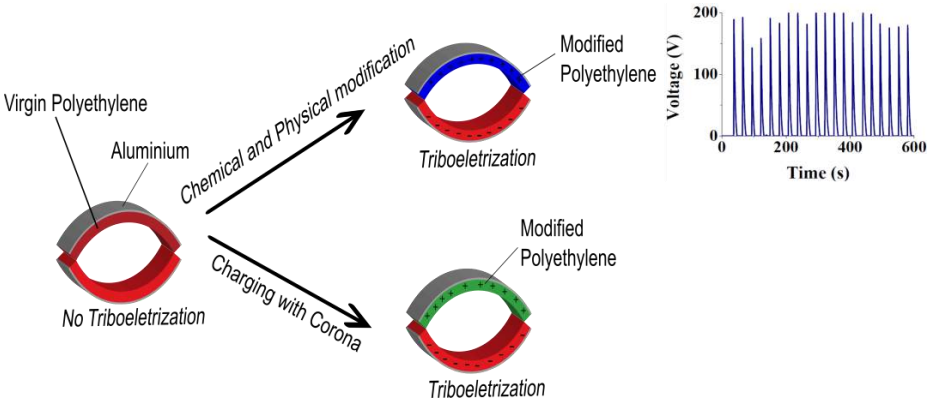


Scheme 1: Sandwich-type electrostatic generator using aseptic carton packages and low-cost processes.

Acknowledgments

References

[1] Meng, B.; Tang, W.; Zhang, X.; Han, M.; Liu, W.; Zhang, H. *Nano Energy* **2013**, *2* (6), 1101-1106.

[2] Yang, Y.; Zhu, G.; Zhang, H.; Chen, J.; Zhong, X.; Lin, Z.-H.; Su, Y.; Bai, P.; Wen, X.; Wang, Z. L. *ACS Nano* **2013**, *7* (10), 9461–9468.

**Área: FIS** **Inscrição: 00777**

# RAMAN SPECTROSCOPY APPLIED TO THE RESTORATION AND CONSERVATION OF CELLULOSE-SUPPORTED WORK OF ART

**Pâmella da Silva Campos (IC),[1] Aloisio Arnaldo N. de Castro (PQ),[2] Antonio Carlos Sant'Ana (PQ)[1]**

**pamellacampos@live.com; antonio.sant@ufjf.edu.br**

*[1]Laboratório de Nanoestruturas Plasmônicas, Depto. Química UFJF; [2]Laboratório de Conservação e Restauração de Papel, Museu de Arte Murilo Mendes, UFJF.*

Palavras Chave: *Vibrational spectroscopy, Carbonatation, Interdisciplinarity*.

## Highlights

Interdisciplinary perspective in the use of Raman spectroscopy in the fields of restoration and conservation. The understanding of carbonatation process in the restoration of cellulosic supports.

## Resumo/Abstract

This work presents, from an interdisciplinary perspective, when involving the areas of museum conservation and vibrational spectroscopy, a case study on the restoration of a set of three works of art by G. Rouault, J. Miró and P. Picasso from the collection of the Museu de Arte Murilo Mendes of the Universidade Federal de Juiz de Fora (UFJF).

The works of art were submitted to aqueous treatment, including cleaning by immersion in deionized water baths and in calcium hydroxide solution for deacidification. The deterioration levels related to cellulosic acidification over time and the chemical effects of the restoration process were evaluated by measuring the pH with a flat-membrane electrode and through Raman spectroscopy.

Fig 1: Mapping of the points analyzed by Raman spectroscopy in the artwork of J. Miró.

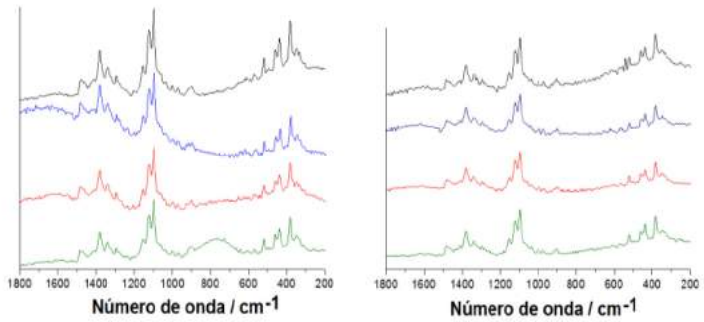


Fig 2: Raman spectra from the points 'a' and 'b', sets in left and right, respectively, in each step of the restoration process.

It can be observed that the heterogeneity in the restoration process was present in the studied regions of the artwork, since the action of the chemical components differs in the distinct areas which present different levels of degradation. In addition, the air carbonatation process presented slow kinetics, affecting expectations about impact of such restoration procedures on the conservation of the artworks.

These results seek to validate the importance of the use of Raman spectroscopy, in an interdisciplinary point of view, in the field of preservation and restoration of graphic documents, therefore, contributing to the strengthening of analytical studies of cultural objects made on cellulosic supports.

**Área: FIS** **Inscrição: 01273**

# Influência da relação molar metanol/óleo de macaúba na produção de biodiesel em reator de leito fixo

**Francisco C. A. Lima (PG),[1*] Fábio M. Silva (PQ),[1] Paulo A. Z. Suarez (PQ)[1], Matheus F. Cunha (IC)[1]**

**unb.tqb@gmail.com**

[1] *INCT-CATÁLISE, Laboratório de Materiais e Combustíveis, Instituto de Química, Universidade de Brasília (IQ-UnB, Campus Universitário Darcy Ribeiro*

Palavras Chave: *Biodiesel, Esterificação, Transesterificação, Metanólise, Catalisador heterogêneo, Reator de leito fixo*

## Highlights

Influence of the molar ratio methanol / macaúba oil on the production of biodiesel in a fixed bed reactor
A reactor (pilot plant) was developed to produce biodiesel using heterogeneous catalysts; Macauba oil was used as feedstock; The reaction in the fixed bed reactor was performed in different proportions of Methanolysis and its characterized products.

## Resumo/Abstract

O Brasil possui uma vasta diversidade ambiental e por sua vez, um amplo potencial energético na variedade de sementes e frutos oleaginosos que podem ser cultivados no seu solo. Este trabalho descreve o potencial do óleo extraído do fruto da palmeira *Acrocomia aculeata* (macaúba) para a produção de biodiesel por catálise heterogênea em planta piloto. Esta oleaginosa se mostra uma nova e promissora alternativa para a produção de biodiesel (combustível renovável). A produção em reator de leito fixo proporciona a otimização do processo em larga escala. Atualmente, a principal matéria-prima para produção de biodiesel é a soja, a qual possui constante competição com o mercado alimentício. Visando o aumento na produção de biodiesel no Brasil, este trabalho destaca a macaúba como uma boa alternativa à soja, uma vez que possui baixo impacto alimentício, pode ser cultivada em solos menos produtivos, seu fruto possui alto teor de óleo e é capaz de gerar um biodiesel de qualidade. Sabe-se que o biodiesel é menos poluente quando comparado com o diesel de origem fóssil, de modo que o incentivo a sua produção se encaixa nos parâmetros de desenvolvimento sustentável. Estas características fazem dessa palmeira uma excelente fonte para a produção de biodiesel. O cultivo dessa palmeira contribui para a geração de empego e complementação de renda de seus produtores, uma vez que todas as suas partes podem ter utilizações industriais como medicinal, cosmética, alimentícia, energética, artesanal e até mesmo na construção civil.

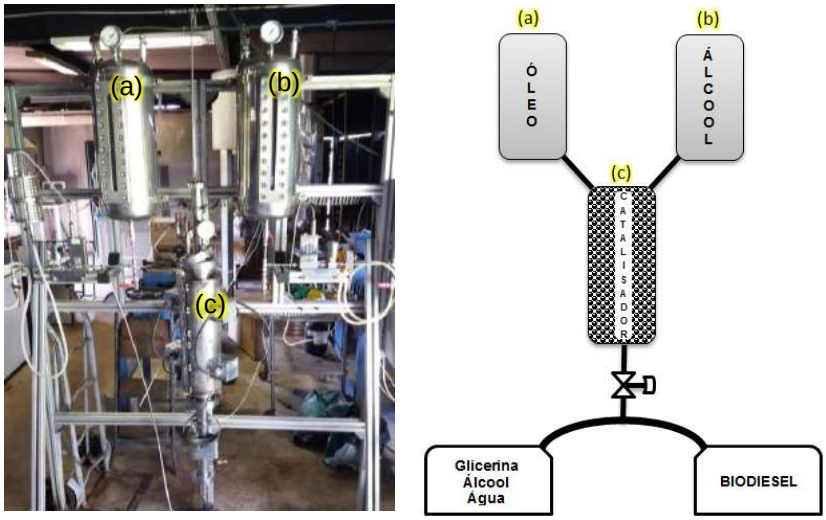


**Figura 1** Reator contínuo de leito fixo tubular e esquema da planta piloto projetada para produzir biodiesel usando catalisadores heterogêneos que operam em um fluxo contínuo: (a) estoque de matéria-prima graxa; (b) Estoque de álcool; e (c) reator tubular.

**Área: FIS** **Inscrição: 01292**

# New Approach For Calculation Of Enthalpy Of Formation From Computational Thermochemistry

**Vagner Roberto Batistela (PQ),[1*] Ana Paula de Sene (IC),[2] Abel Ornelas Dias (PG),[3] Douglas Vanzin (PG),[4] Leonardo Tsuyoshi Ueno (PQ)[5]**

***vagner.batistela@yahoo.com.br**

*[1]Department of Technology, UEM; [2]Department of Environment, UEM; [3]Department of Chemical Engineering, UEM; [4]Department of Chemistry, UEM; [5]Department of Chemistry, ITA.*

Keywords: *Thermochemistry, Molecular Modeling, Enthalpy of Formation, Trihalomethanes, G4, Ochterski.*

## Highlights

► New approach for calculation of enthalpy of formation from computational thermochemistry.
► The Ochterski method was modified in the contribution of atomic enthalpy at 0 K for that at 298.15 K.
► $\Delta H_f^0$ values calculated with this new approach were consistent with those of reference.

## Resumo/Abstract

The Ochterski method [(1)] is often used for calculation of standard enthalpies of formation ($\Delta H_f^0$) from thermochemical data obtained by molecular modeling. The method considers that a molecule is formed by the junction of isolated atoms and that the molecular $\Delta H_f^0$ at 298.15 K is obtained by a thermochemical cycle involving the molecule and its free atoms at 298.15 K and 0 K. In this work, it was considered that the term describing the enthalpy of atoms at 0 K should be substituted to 298.15 K for the cycle be closed. Structures of chlorinated and brominated trihalomethanes (TCM, BDCM, DBCM and TBM) were optimized in vacuum using *ab initio* G4 theory [(2)] and the values of $\Delta H_f^0$ at 298.15 K were determined by both classical and modified Ochterski method. Results are presented in Table 1.

**Table 1.** Standard enthalpies of formation ($\Delta H_f^0$) of chlorine and bromine trihalomethanes optimized with G4, 298.15 K. Values were calculated by classical Ochterski method and by the new approach, in kcal/mol.

| Molecule | $\Delta H_f^0$ classical | $\Delta H_f^0$ new approach (% error) | $\Delta H_f^0$ reference |
|---|---|---|---|
| TCM ($CHCl_3$) | + 2431.9 | -24.14 (1.8) | -24.59 ± 0.6 [(3)] |
| BDCM ($CHCl_2Br$) | + 2056.0 | -12.01 (1.3) | -12.17 ± 0.6 [(2)] |
| DBCM ($CHClBr_2$) | + 1680.0 | -0.06 (75.0) | -0.24 ± 0.74 [(2)] |
| TBM ($CHBr_3$) | + 1303.8 | +11.74 (11.3) | +13.24 ± 0.8 [(3)] |

One of the difficulties in calculating thermochemical parameters from molecular modeling is the quantum description of atoms with many electrons, as chlorine and bromine. In this work, the G4 method of optimization was used because it describes these atoms with accuracy. From Table 1, the values of $\Delta H_f^0$ calculated by the Ochterski method were all endothermic and overestimated by about 100 times compared to the references. However, with the proposed correction it was obtained values of $\Delta H_f^0$ quite close to those of reference. For the TBM, containing three bromine atoms, the margin of error was only 11.3%, acceptable considering the complexity of the electronic structure.

References

[1] J.W. Ochterski, Thermochemistry in Gaussian, 2000.
[2] P.J. Linstrom, W.G. Mallard (Eds.)., NIST Standard Reference Database, 69, 20899.
[3] J.Z. Dávalos, R. Notario, C.A. Cuevas, J.M. Oliva, A. Saiz-Lopez, Comput. Theor. Chem. 1099 (2017) 36–44.

**Área: FQ** **Inscrição: 01305**

# Computer Simulations of Chiromagnetic Nanoparticles

**Uallisson S. Santos (PG),[1] Jihyeon Yeom,[2] Nicholas A. Kotov (PQ),[2] André F. de Moura (PQ)[1,*]**

moura@ufscar.br

[1]*Department of Chemistry, UFSCar;* [2]*Department of Chemical Engineering, University of Michigan.*

Keywords: *Cobalt oxide spinel, Paramagnetic nanoparticles, Chirality imprinting, Magnetic circular dichroism, Ab initio molecular dynamics, Time-dependent Density Functional Theory.*

## Highlights

Chiral amino acids imprinted chirality on paramagnetic cobalt oxide spinel nanoparticles. The interplay between chirality and magnetism allowed light absorption modulation by magnetic field.

## Abstract

The light-matter interaction is one of our main tools for transmitting, processing and storing energy and information. We have recently demonstrated that imprinting chirality on paramagnetic cobalt oxide nanoparticles allows the absorption of light to be modulated by an external magnetic field over a wide range of wavelengths.[1] The chirality transfer mechanism involved doubly-coordinated cysteine molecules occupying and distorting octahedral positions around Co(III) atoms at the surface, as demonstrated by the B3LYP/6-31G geometry optimizations and ab initio molecular dynamics simulations. The DFT calculations also demonstrated that spin density is highly localized in the Co(II) atoms at the tetrahedral positions of the lattice. Calculated electronic circular dichroism was in excellent agreement with the experimentally measured spectra and provided a detailed description of the individual electronic transitions for both alpha and beta electrons. The behavior of paired and unpaired electrons was very distinct, with alpha electrons being preferably excited to LUMO, which was located on a Co(III) surface atom, whereas beta electrons close to the gap were excited to other orbitals besides LUMO (Figure 1). The possibility to pump electronic density into a surface site opens many possibilities in photocatalysis applications and magnetooptics.

References: (1) Yeom, J.; Santos, U. S.; Chekini, M.; Cha, M.; de Moura, A. F.; Kotov, N. A. *Science* **359**: 309-314 (2018).

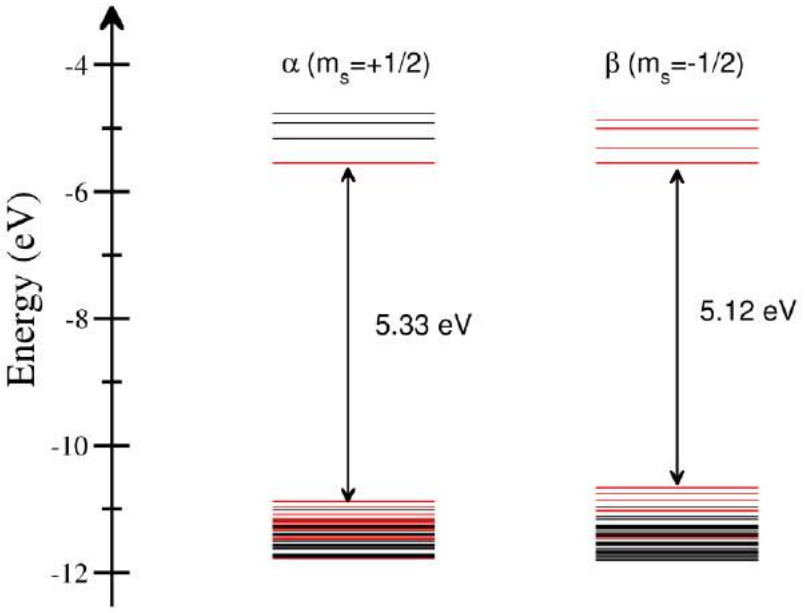


**Figure 1.** Orbitals from HOMO-30 to LUMO+3 for the $Co_3O_4$ NP. Red lines stand for orbitals with significant contributions to the ECD gap band.

**Área: FIS**
*(Inserir a sigla da seção científica para qual o resumo será submetido. Ex: ORG, BEA, CAT)*

**Inscrição: 01331**
*(Inserir o número de inscrição do autor que fez a submissão)*

# Microbial habitability of Europa sustained by radioactive sources

**Thiago Altair (PG),[1,2] Marcio G. B. de Avellar (PQ),[3] Fabio Rodrigues (PQ),[4] Douglas Galante (PQ),[1]**

**douglas.galante@lnls.br; thiago.ferreira@lnls.br**

*[1]Laboratório Nacional de Luz Síncrotron, CNPEM; [2]Programa de Pós-Graduação em Física Biomolecular, IFSC-USP; [3]Instituto de Astronomia, Geofísica e Ciências Atmosféricas, USP, [4]Instituto de Química, USP*

Palavras Chave: *radiólise, quimiossíntese, astrobiologia*

## Highlights

Water radiolysis can sustain a microbial ecosystem on the Jupiter`s moon Europa. It can can provide the chemical disequilibrium for the maintenance of life. Radiolysis can be a complementary energy source to hydrothermal activity.

## Resumo/Abstract

In this work, it is presented the feasibility of microorganisms like the *bacterium Candidatus Desulforudis audaxviator*, an extremophile found in a gold mine in South Africa surviving at depths up to 4 km, with temperatures between 45°C and 60°C, few nutrients available and some concentration of radioactive minerals such as uraninite, to survive in satellites or in planets like the Jovian moon Europa by extracting energy from the radioactive decay of uranium, thorium and potassium. Knowing the metabolic demands of *Candidatus Desulforudis audaxviator*, a simple ecosystem model is proposed with the basic ingredients to support this kind of microbial life. The Jovian moon Europa was chosen as a potential target to apply this model of ecosystem, due to the similarity of environments. Our study shows that, depending on the availability and state of the pyrite, the radiolytic habitability of Europa is possible, in a complementary way to the hydrothermal habitability. However, this case would be strongly dependent on the concentration of 40K of the oceans or on the seabed. The model also has a variety of modelling parameters that can be further constrained by future space missions to the Jovian system, thus allowing a better understanding of the capacity of the moon to sustain microbial life on its deep environments.

**Área: FIS** **Inscrição: 00783**

# Effect of macromolecule hydrophobicity on liquid-liquid equilibrium of aqueous two-phase system composed of $(NH_4)_2S_2O_3$

**Francielle O. Chagas (PG),[1] Beatriz M. Fontoura (PG),[1] Silvia J. R. Vargas (PG),[1] Luís H. M. da Silva (PQ),[1] Maria C. Hespanhol (PQ) [1,2]**

**francielle.chagas@ufv.br**

*[1]Grupo de Química Verde Coloidal e Macromolecular (QUIVECOM), [2]Grupo de Análises e Educação para a Sustentabilidade (GAES), Instituto Nacional de Ciências e Tecnologias Analíticas Avançadas (INCTAA), Departamento de Química, Centro de Ciências Exatas e Tecnológicas, Universidade Federal de Viçosa – MG.*

Key-word: Aqueous two-phase system, Phase diagram, Hydrophobicity, Intermolecular interaction.

## Highlights

Obtaining new phase diagrams. Effect of hydrophobicity in separation of phases. Decrease the water-macromolecule and electrolyte-macromolecule interactions contributed for the separation phases process.

## Abstract

Aqueous two-phase system (ATPS) is an efficient technique used in the extraction and purification of metals, biomolecules, enzymes, natural dyes, and microorganisms[1]. This system is recognized for being environmentally friendly because its components are nontoxic, biodegradable, and inexpensive[1]a. In addition, ATPS spends less time to phase splitting in contrast with conventional solvent extraction. In the present work, the phase diagrams for macromolecules (PEG1500, PPG400, pluronic10R5 or L35) + $(NH_4)_2S_2O_3$ + $H_2O$ were experimentally determined at 298.2 K. Fig.1 shows the phase diagrams for the L35, pluronic10R5 or PEG1500 + $(NH_4)_2S_2O_3$ + $H_2O$. The copolymers L35 and pluronic10R5 have segments of polypropylene oxide (PO) in your structure, while the PEG1500 shows only segments of ethylene oxide (EO). The copolymers are more hydrophobic than PEG1500, so the biphasic region is higher. However, the biphasic region of the ATPS with pluronic10R5 and L35 is similar. Fig. 2 shows the phase diagrams for the PPG400 and PEG1500 + $(NH_4)_2S_2O_3$ + $H_2O$ at 298.2 K. The phase separation process occurs at lower concentrations of polymer and electrolyte for ATPS formed by PPG than observed in the ATPS formed by PEG. This occurring because PPG is more hydrophobic than PEG, the PPG structure decreases the water-macromolecule and electrolyte-macromolecule interactions, favoring the phase separation process at lower ATPS component concentrations[2].

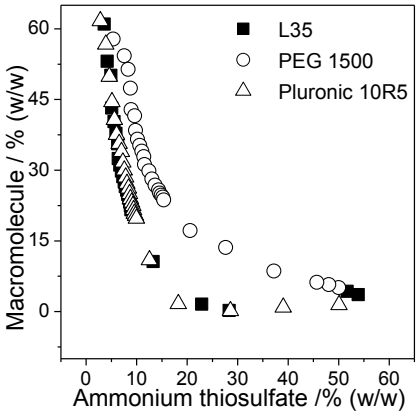


**Fig.1** The effect of hydrophobicity on the phase diagram of the L35, PEG 1500 and pluronic 10R5 + $(NH_4)_2S_2O_3$ + $H_2O$ ATPS

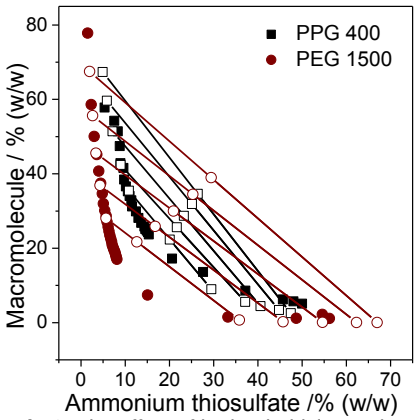


**Fig.2** The effect of hydrophobicity on the phase diagram of the PEG 1500 and PPG 400 + $(NH_4)_2S_2O_3$ + $H_2O$ ATPS

References

[1] P.R. Patrício, M.C.Mesquita, L.H.M.Silva, M.C.H.Silva. J. Hazardous Materials 193 (2011).

[2] P.R. Patrício, A. Mageste, L. R. de Lemos, R. M. Carvalho, L.H.M.Silva, M.C.H.Silva. Fluid Phase Equilibria 305 (2011).

Acknowledgements: FAPEMIG, CNPq, CAPES and INCTAA.

**Área: FIS** **Inscrição: 00933**

# Síntese e caracterização do monômero di-hidrogenofosfato de 10-metacriloxidecil (10-MDP)

**Paula Roberta Perondi Furtado (IC), Nataly Castro (PG), Rogério A. Gariani (PQ), Marcia M. Meier (PQ)*.**

**paularobertafurtado@gmail.com; marcia.meier@udesc.br**

*Programa de Pós-Graduação em Química, Universidade do Estado de Santa Catarina, UDESC.*

Palavras Chave: *Polímero, 10-MDP, monômero, adesivo, NMR*

## Highlights

Synthesis and characterization of di-hydrogen phosphate of 10-methacryloxidecil (10-MDP)
10-MDP has the capability to link chemically to dental hydroxyapatite, thus, is one component of dental adhesives. This work present a synthetic route to obtain 10-MDP with 83 % yield.

## Resumo/Abstract

Um dos compostos que vem sendo utilizado amplamente em adesivos dentais é o monômero di-hidrogenofosfato de 10-metacriloxidecil (10-MDP). O grupamento de ácido fosfórico do 10-MDP tem a capacidade de unir-se quimicamente à hidroxiapatita dental, atuando como um adesivo.[1]
O objetivo deste trabalho foi sintetizar 10-MDP e para isso primeiramente sintetizou-se seu precursor o 10-hidroxidecilmetacrilato (HDMA)[2]. Para a síntese do 10-MDP, adaptada de Ogliari e col. (2008)[3], utilizou-se acetona em pentóxido de fósforo e sob agitação constante adicionou-se 10-HDMA, obtendo-se rendimento de 83%. Como inibidor de polimerização utilizou-se 2,6-di-terc-butil-4-metilfenol. Espectro de FT-IR apresentou bandas características de νP-O do 10-MDP. No espectro de RMN$^{1}$H (Figura 1) há sinais característicos de $CH_2$ ligados a grupos eletronegativos em 3,6 a 4,1 ppm; hidrogênio ligado a carbono vinílico na região de 5,5 a 6,1 ppm; hidrogênios metilênicos na região de 1,0 e 1,7 ppm e hidrogênio de grupo metílico próximo a 2,0 ppm. O espectro de RMN$^{31}$P indicou o surgimento de dois sinais, sendo um muito mais intenso, indicando a presença de átomos de fósforo na estrutura. O procedimento utilizado para a síntese mostrou-se simples, eficaz e com um bom rendimento. A caracterização por RMN$^{1}$H e $^{31}$P e FT-IR confirmou a estrutura química do 10-MDP.

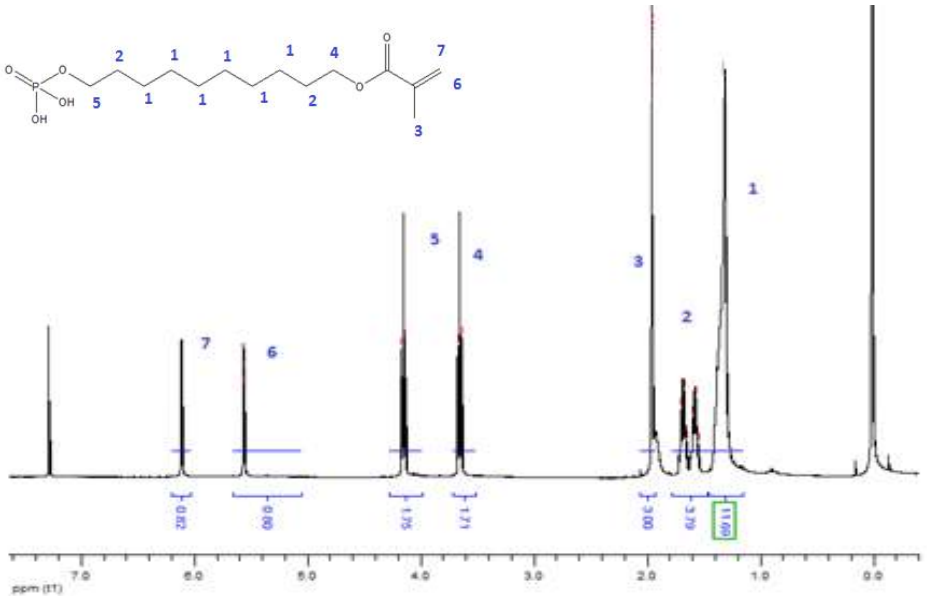


**Figura 1:** Espectro de RMN de $^{1}$H do monômero 10-MDP

1. LANDUYTA, K. et al. **Biomaterials**. 2007; 28: 3757–3785.
2. FURTADO, Paula Roberta P. *Síntese do monômero 10-hidroxidecil metacrilato (10-HDMA).* **Anais SBS-Sul**, 2017.
3. OGLIARI, F. et al. **Journal of Dentistry**. 2008; 36: 171-177.

**Área: _FIS_____ Inscrição: _01042_____**

# Encapsulação de monômero metacrílico: caracterização do complexo de inclusão e do polímero formado

**Rafael M. Savanhago (IC),[1] Marcia Margarete Meier(PQ)*[1]**

**rafael.savanhago@edu.udesc.com;**

[1]*Departamento de Química, Universidade do Estado de Santa Catarina, UDESC, Joinville/SC*

Palavras Chave: *Ciclodextrina, BisGMA, dental, inclusão, metacrilato, polímero*

## Highlights

Methacrylic monomer encapsulation: inclusion complex and polymer characterization
Dental composites properties is still a challenge topic. The presence of β-cyclodextrin(B-CD) increased 27% of flexural strength of methacrylic polymer due to inclusion complex formation.

## Resumo/Abstract

Apesar do crescente uso de compósitos dentais de matriz metacrílica, suas propriedades ainda são objeto de desenvolvimento visando mimetizar à estrutura dental natural nas propriedades físicas, químicas e estéticas. Este trabalho apresenta a caracterização do complexo de inclusão formado entre β-ciclodextrina(B-CD) e o monômero metacrílico 2,2-bis[4-(2-hidroxi-3-metacriloxipropoxi)fenil]-propano (Bis-GMA) e o efeito do complexo de inclusão na resistência à flexão (RF) de matrizes poliméricas.
Resultados de RMN$^1$H de Bis-GMA/B-CD 1:1(mol/mol) e 1:2(mol/mol) demonstram deslocamento químico dos sinais atribuídos aos anéis aromáticos do Bis-GMA, variando entre $\Delta\delta$=0,004 a 0,005 ppm (Figura 1). Espectros de FTIR indicam deslocamento do $\nu$C=O (1714,8,1719,0, 1723,0 cm$^{-1}$), e do $\nu$OH (3430,0, 3297,0 1:1, 3282,2), respectivamente para BisGMA, Bis-GMA/B-CD 1:1, Bis-GMA/B-CD 1:2. Os resultados espectroscópicos indicam a formação de forças intermoleculares entre Bis-GMA e B-CD.
Matrizes poliméricas foram preparadas por fotopolimerização (468nm) contendo 0% (controle) e 1,3 % m/m de B-CD. Após 30 dias de ensaio de absorção de água os grupos não apresentaram diferença estatística. Observou-se um aumento de 27% na RF no grupo contendo B-CD, indicando um provável aumento no ordenamento molecular do polímero formado.
Os resultados obtidos até o momento indicam que a presença de B-CD contribui no aumento da resistência à flexão de matrizes poliméricas, provavelmente pela formação do complexo de inclusão B-CD/Bis-GMA, no qual os anéis aromáticos podem estar alojados na cavidade de B-CD.

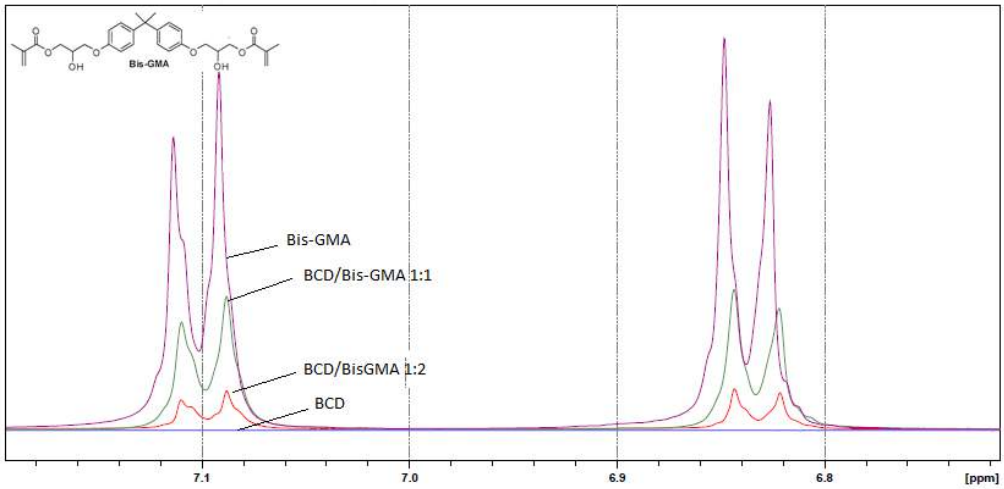


Figura 1: Espectro de RMN$^1$H de Bis-GMA, Bis-GMA/B-CD 1:1, Bis-GMA/B-CD 1:2 mol/mol e BCD, destacando os sinais atribuídos aos hidrohênios do anel aromático do monômero.

**Área: FOT** *(Inserir a sigla da seção científica para qual o resumo será submetido. Ex: ORG, BEA, CAT)*

**Inscrição: 00129** *(Inserir o número de inscrição do autor que fez a submissão)*

# The photodegradation behavior of two indium phthalocyanines and its influence on the photohaemolysis of human red blood cells

**André Romero da Silva (PQ),[1*] Luciene Cristina Duarte da Silva (IC),[2] Sulamita Loureiro Rocha (IC).[2]**

**aromero@ifes.edu.br**

*[1]Coordination of the Industrial Chemistry Course, IFES; [2]Coordination of Degree in Chemistry, IFES*

Palavras Chave: Photodegradation, Photohaemolysis, Phthalocyanine, Nanoparticles, PLGA-PEG.

## Highlights

The photobleaching of the free and encapsulated In(III)-1,4-tetrakis(benzyloxy)phenoxy-phthalocyanine (O-InTBPPc) and of In(III)-2,3-tetra(*terc*-butyl)phenoxy-phthalocyanine (M-InTTBPPc) was evaluated in organic and aqueous solvent. The free M-InTTBPPc was more photobleached in dimethylformamide (DMF) than It was the free O-InTBPPc, but the free M-InTBPPc suffered a lower photobleaching in phosphate buffer saline (PBS) solution than suffered the free O-InTBPPc. M-InTTBPPc encapsulated into PEGlated polylactide-co-glycolide (PLGA-PEG) nanoparticles was more photobleached in PBS solution than was the encapsulated O-InTBPPc. Consequently, the encapsulated O-InTBPPc was more efficient in causing photohaemolysis on the human red blood cells (HRBC).

## Resumo/Abstract

It is known phthalocyanines suffer photobleaching[1] and that much more the photosensitizer is photobleached, the greater is the intensity of photobiological damage[2]. O-InTBPPc or M-InTTBPPc was encapsulated into PLGA-PEG nanoparticles and the photobleaching of each free and encapsulated compound and its influence on the photohaemolysis were evaluated. Relative absorbance (AR) measurement was performed in DMF and PBS solution using a spectrophotometer. The free M-InTTBPPc was photobleached faster than It was the free O-InTBPPc in organic solvent when the laser power was increased from 1 to 22 mW since the AR was decreased from 0.54 to 0.10, while the value for the free O-InTBPPc was decreased from 0.89 to 0.24. The free O-InTBPPc was 1.9x more photobleached in PBS solution than was the free M-InTTBPPc, but the encapsulated O-InTBPPc was 2.7x lesser photobleached than was the encapsulated M-InTTBPPc. It was not observed a photodegradation dependence with the increase of the free O-InTBPPc concentration (2-15 µmol/L) as It was for the free M-InTTBPPc in organic solvent, probably due to a higher aggregate state of the M-InTTBPPc. Both free and encapsulated compounds were photobleached in the PBS solution with a little concentration dependence. The higher tendency of the encapsulated M-InTTBPPc to suffer photobleaching reduced its efficiency to cause photohaemolysis (lower than 9%) while the encapsulated O-InTBPPc caused a photohaemolysis around 70%. The free O-InTBPPc was also more efficiency than it was the free M-InTTBPPc to photohemolyze the HRBC. We thank CNPq, FAPES and IFES for financial support. *Reference:*
[1] Bonnett, R et al. *Tetrahedron* **2001**, *57*,9513. [2] Piffaretti, F. et al. *Dermatol.* **2013**, *227*, 214.

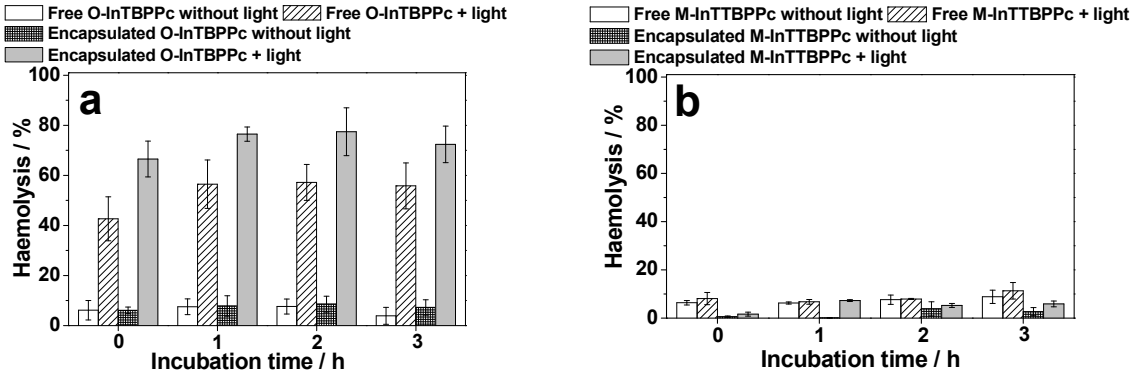


Figure 1 – Photohaemolysis caused by (a) O-InTBPPC and (b) M-InTTBPPc

**Área: FOT** **Inscrição:** 00196

# Synthesis and characterization of tetraporphyrins dispersed in peptide based low molecular weight gelators

**Sandra Valeria Vassilaides (PG),[1] Mauricio V. B. Pinheiro (PQ),[2] Klaus Krambrock (PQ),[2] Francesca Giutinni (PQ),[3] Wendel A. Alves (PQ).[1]***

s.valeria@ufabc.edu.br ; wendel.alves@ufabc.edu.br

*[1]Centro de Ciências Naturais e Humanas, Universidade Federal do ABC, 09210-580, Santo André, SP, Brazil; [2]Departamento de Física, ICEx, Universidade Federal de Minas Gerais, 31270-901, Belo Horizonte, MG, Brazil; [3]School of Pharmacy and Biomolecular Sciences, Liverpool John Moores University, Liverpool, UK.*

Palavras Chave: *Tetraporphyrin, singlet oxygen, hydrogel, photosensitizer, electron paramagnetic resonance*

## Highlights

The association of porphyrins with a short peptide-based hydrogel retained both the ability gel water typical of Fmoc-diphenylalanine (Fmoc-FF), and the optical behavior of photosensitizers.

## Resumo/Abstract

Nanostructured peptide hydrogels are interesting matrices for the incorporation of photosensitizers (PS), since they are biocompatible materials, pH sensitive, and with a higher surface area in the porous network.[1] In this work, *N*-(9-Fluorenylmethoxycarbonyl)-*L,L*-diphenylalanine (**1**) hydrogel (Fmoc-FF) was used as matrix to dispersed porphyrin monomers (**2**-**5**). The structural and chemical properties of the samples were investigated by different electron spectroscopy techniques, electron paramagnetic resonance (EPR) and scanning electron microscopy (SEM). The hydrogels were prepared with a mixture of water/DMSO (8:2, v/v) by using a concentration of 5 mg $mL^{-1}$ of Fmoc-FF with different concentrations of porphyrins (0.5-0.5 μg $L^{-1}$), previously dissolved in DMSO. Incorporation of PS in the hydrogel does not modify the absorption profile of the porphyrins, but the emission spectrum became quite different for **4** and **5** showing some effects of aggregation between neighboring molecules (data not shown). Fig. 1b shows the morphologies of the obtained samples. It can be seen that a network of entangled fibers with diameters ranging from 100-150 nm and lengths of up to a few micrometers, in coexistence with globular particles with a few tens of nanometer in diameter. The detection of $^1O_2$ has been performed in the presence of 2,2,6,6-tetramethylpiperidine (TEMP) by using spin-trapping EPR. The Fig. 1c shows efficiency comparison of $^1O_2$ generation where **4**>**2**>>**3**=**5** in the concentration equal to 50 μg $L^{-1}$ of porphyrin, which can be related to the donor/acceptor strength of porphyrin ring substituents, and homogeneity of PS dispersion in hydrogel matrix.

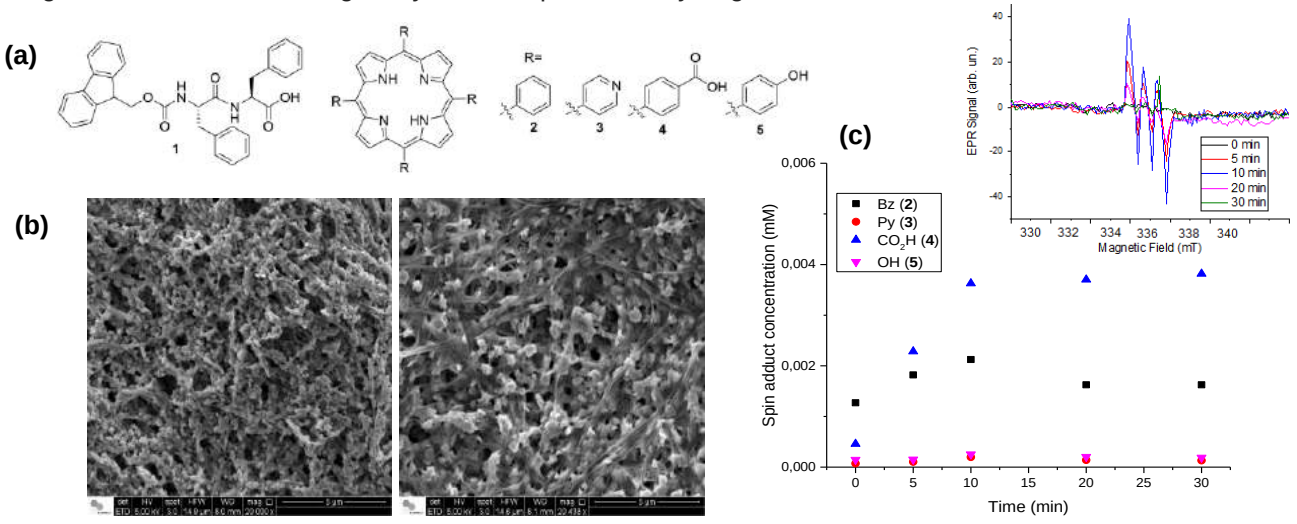


**Figure 1**: (a) Structures: **1** – Fmoc-FF; **2** – **5** tetraporphyrins; (b) SEM of hydrogel: (left) Fmoc-FF; (right) porphyrin **4**; (c) Spin adducts formation of TEMP-$^1O_2$ after illumination with white light. The concentration was determined from the double integration of the EPR signal for each sample. On top, the corresponding experimental EPR spectra are shown for the hydrogel containing embedded porphyrin **4** (50 μg $L^{-1}$).

**1.** Souza, S. F.; Kogikoski, S.; Silva, E. R.; Alves, W. A. *J. Braz. Chem. Soc.* **2017**, *28*, 1619-1629.

**Área: FOT**
*(Inserir a sigla da seção científica para qual o resumo será submetido. Ex: ORG, BEA, CAT)*

**Inscrição: 00215**
*(Inserir o número de inscrição do autor que fez a submissão)*

# Produção fotoquímica de $O_2$ e $H_2$ a partir da água usando um complexo triscarbonil de Mn(I) na ausência de oxidantes

**Rafael Cavalieri Marchi (PG),[1] Rose Maria Carlos (PQ).[1]***

**marchirc@ufscar.br; rosem@ufscar.br**

[1]*Departamento de Química, UFSCar, Laboratório de Fotoquímica Inorgânica e Bioinorgânica*

Palavras Chave: Fotossíntese artificial, evolução de hidrogênio e oxigênio moleculares, complexo de Mn(I), química sustentável, ressonância paramagnética de elétrons (RPE).

## Highlights

Photochemical Generation of $O_2$ and $H_2$ from Water using a Mn(I) triscarbonyl complex in the absence of oxidants. This work reports an artificial water splitting system based on Mn(I) complex to produce $H_2$(g) and $O_2$(g) in neutral aqueous solution in the absence of oxidants that resemble the natural photosynthesis.

## Resumo/Abstract

A busca por combustíveis que possam substituir as fontes fósseis se faz necessário. A inspiração por alternativas vem da fotossíntese natural pois as plantas verdes usam como substrato água e energia solar para a clivagem da molécula da água em $O_2$(g) e $H^+$, utilizando-se de um cluster de Mn como catalizador.[1]

$$2\ H_2O(l) \xrightarrow{Mn_4O_4\ (cat.)} O_2(g) + 4\ H^+(aq) \qquad \text{Eq. (1)}$$

Nosso grupo de pesquisa, trabalha com complexos *fac*-[Mn(phen)$(CO)_3$(imidazol)]$^+$ capaz de absorver luz e levar reações de transferências de elétrons.[2,3]

Este trabalho descreve um novo complexo de Mn(I)-Imidazol que é capaz de promover a clivagem da molécula de água em $O_2$(g) e o $H_2$(g) em condições brandas e sem a necessidade de oxidantes externos. O processo fotoquímico leva a formação e rompimento de ligações e alterações nos estados de oxidação do centro metálico demonstradas pelas técnicas de UV-vis, RMN- $^1$H e $^{13}$C, voltametria cíclica a diferentes pH, espectrometria de massas, ressonância paramagnética de elétrons (RPE) e por cálculos computacionais usando a teoria do funcional de densidade (DFT).

A liberação fotoquímica de $O_2$(g) e o $H_2$(g) pelo complexo foi demonstrada por espectrometria de massas, Figura 1. Os experimentos fotoquímicos acompanhados por RPE mostram os vários estados de oxidação alcançados pelo íon de Mn: um sinal crescente em $g$= 2,0 correspondentes aos centros de Mn(II) e uma componente crescente ($g_x$ ~ 9.85 e $g_y$ ~ 3.9) correspondente a Mn(IV), Figura 2.

O complexo é uma promissora ferramenta de pesquisa para se obter uma química sustentável uma vez que se usa apenas luz e condições brandas.

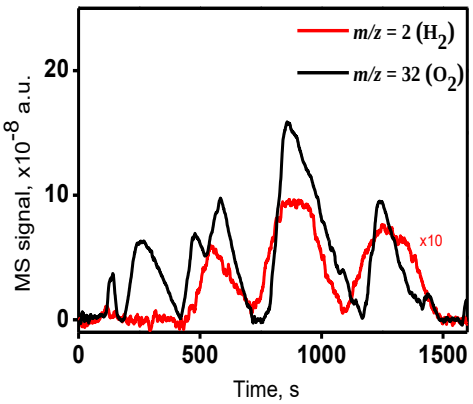


*Figura 1 Espectometria de massas*

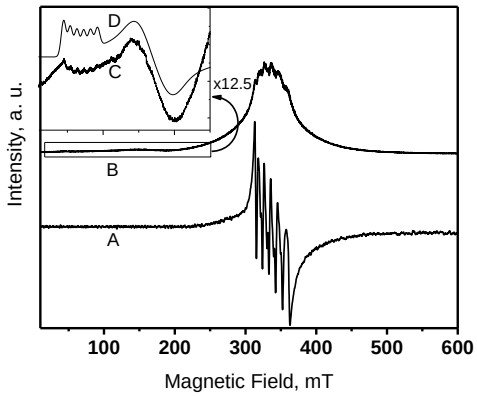


*Figura 2 Espectro de ERP mostrando os estados de oxidação do complexo de Mn(I)*

1. Tachibana, Y.; Vayssieres, L.; Durrant, J.R. *Nature Photonics* **2012,** 6, p. 511
2. Carlos, R. M.; Carlos, I. A.; Limaneto, B. S.; Neumann, M.G. *Inorg. Chim. Acta* **2000**, 299, 231
3. deAguiar, I; Inglez, S D.; Lima, F. C. A.; Daniel, J. F. S; McGarvey, B. R.; Tedesco, A. C.; Carlos, R. M. *Inorg. Chem.* **2008**, 47, 11519

**Área: FOT** **Inscrição: 00530**

# Photocatalytic treatment of wastewater from cassava processing by using NiO/Ni/$TiO_2$ composites

**Klebson Souza Santos[1](PG), Paula A. L. Lopes[1] (PG), Luciana A. Silva[1,2] (PQ)*.**

klebsonsouzaqa@gmail.com

*[1] Instituto de Química e [2] Instituto Nacional de Ciência e Tecnologia, INCT, de Energia e Ambiente, Universidade Federal da Bahia, Campus de Ondina, Salvador 40170-290, Bahia.*

Palavras Chave: wastewater, Cassava, Cyanide, Photocatalysis, Photodegradation.

## Highlights

The photocatalytic treatment of wastewater from cassava processing with the NiO/Ni/$TiO_2$ as a photocatalyst ($\lambda$ > 370 nm) decreases the cyanide content to 62% with the simultaneous ethene production.

## Resumo/Abstract

A água residual do beneficiamento da mandioca, denominada água de manipueira, apresenta uma grande carga de poluentes, com destaque para a linamarina, glicosídeo característico da planta de mandioca, hidrolisável a HCN. A atividade de diferentes compósitos de $TiO_2$ com níquel foi avaliada na fotodegradação desse efluente em atmosfera de argônio e $\lambda$ > 370 nm. Os produtos gasosos foram monitorados por cromatografia gasosa com TCD e FID com metanador e espectrometria de massa e a fase líquida analisada por volumetria de precipitação com $AgNO_3$ para determinação de $CN^-$. Os compósitos foram obtidos por impregnação de $TiO_2$ comercial (anatásio) com níquel por via úmida (Ni-$TiO_2$) e tratados termicamente em atmosfera de $H_2$ (Ni/$TiO_2$) e depois em ar (NiO/Ni/$TiO_2$). Os resultados da fotodegradação de $CN^-$ com o tratamento do efluente encontram-se na Tabela 1. Pode-se notar que a presença de Ni contribui para o aumenta da fotoatividade, assim como o tratamento térmico em $H_2/O_2$, com aumento da % de fotodegradação de 26,55% com o $TiO_2$ puro para 62,84% com NiO/Ni/$TiO_2$. A análise da fase gasosa indicou a formação de eteno durante o tratamento fotocatalítico da água de manipueira, ainda não quantificado mas confirmado pelo espectro de massa. A produção de eteno mantém relação com a fotodegração de cianeto, com aumento da área de pico em função do tempo de irradiação (Figura 2). Desta forma, o fotocatalisador mais ativo tanto na fotodegradação de cianeto quanto na produção de eteno é o NiO/Ni/$TiO_2$.

Tabela 1. % de fotodegradação de $CN^-$ para os diferentes fotocatalisadores.

| Fotocatalisador | Fotodegradação de de $CN^-$ (%) |
|---|---|
| $TiO_2$ comercial | 26,55 |
| Ni-$TiO_2$ | 38,78 |
| Ni/$TiO_2$ | 56,89 |
| NiO/Ni/$TiO_2$ | 62,84 |

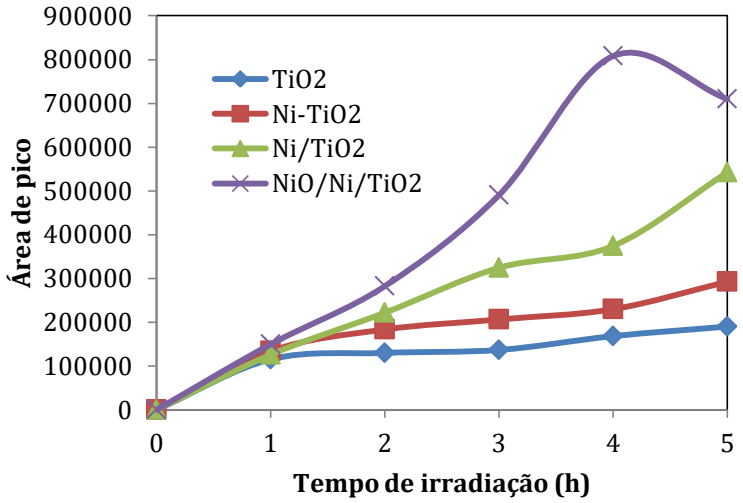


Figura 1. Área de pico do eteno em função do tempo de irradiação ($\lambda$ > 370 nm) de água de manipueira com diferentes fotocatalisadores.

**Área: FOT** **Inscrição: 00534**

# Amyloid Beta Monitoring Through a Ru(II) Complex: Luminescent Probe Candidate for Early Diagnosis of Alzheimer's Disease

**Mariana P. Cali (PG),[1] Rose M. Carlos (PQ).[1]***

**marianapcali@hotmail.com; rosem@ufscar.br**

*[1]Departamento de Química, UFSCar*

Keywords: *Ru(II) Complexes, Luminescent Probes, Alzheimer's Disease, Amyloid Beta Peptide*

## Highlights

Luminescent Ru(II) complex for early diagnosis of Alzheimer's Disease. Ruthenium complex interaction with the amyloid beta peptide. Analysis by FLIM, TEM and biophysical techniques.

## Resumo/Abstract

Alzheimer's disease is the most common cause of dementia in elderly people and it is responsible for the progressive decline of their cognitive and motor functions.[1] Once the disease has progressed, amyloid beta aggregates are found in the patient's brain and are known to disturb the normal brain function. With that in mind, a ruthenium metal complex was developed to, with its different sets of ligands, act as a probe to monitor in real time the aggregation process of amyloid beta through its luminescence.

The initial luminescence studies showed that our ruthenium complex does in fact bind to the amyloid beta protein from early stages of aggregation to fibril formation. The intrinsic fluorescence of the peptide is increased significantly in the presence of ruthenium complex. The aggregation process of many fragments of the $A\beta_{1-40}$ peptide– $A\beta_{1-28}$, $A\beta_{15-21}$, $A\beta_{11-22}$, $A\beta_{25-35}$ and $A\beta_{29-40}$ were tested with the complex. Our preliminary studies through emission lifetime have shown that there the complex is able to interact more significantly with the $A\beta_{11-22}$ and $A\beta_{1-28}$ and less significantly with $A\beta_{25-35}$ and $A\beta_{29-40}$.

It is possible to see that the aggregates increase in size with the incubation time and tend form plaques. Fibrils could be seen prominently in 120 minutes of incubation whereas in 240 minutes the fibrils tend to form fibril-plaques. When the complex was added in the 1:1 proportion is possible to see a significant difference in the size of aggregates in 240 minutes of incubation.

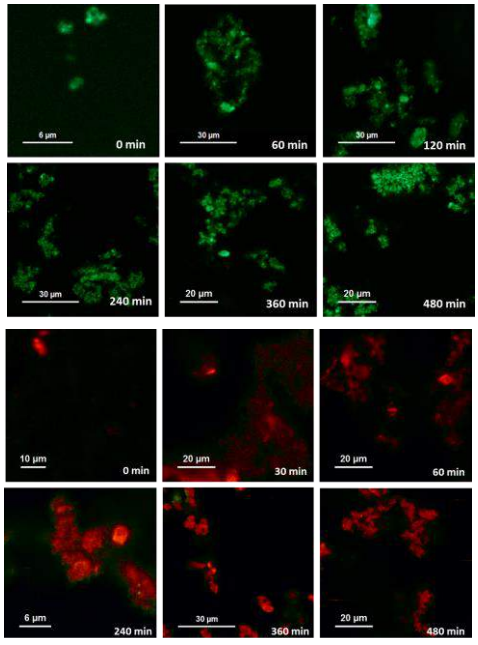


Figure 1: FLIM images of different aggregation stages of amyloid beta with and without complex.

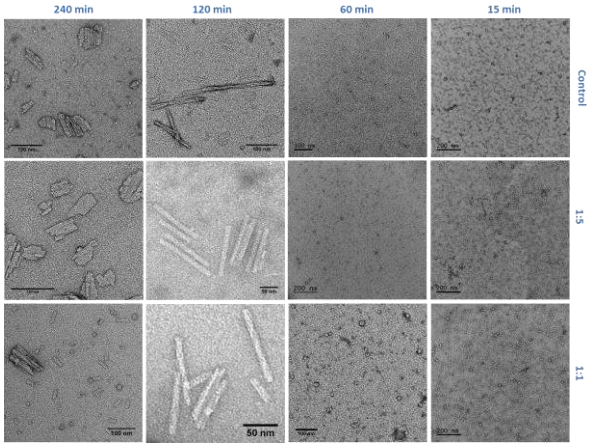


Figure 2: TEM images of amyloid beta with the complex in different proportions.

[1] S.Sadigh-Eteghad, B. Sabermarouf, A. Madji, M. Talebi, M. Farhoudi, J. Mahmoudi, Amyloid-beta: a crucial factor in Alzheimer's disease. *Medical Principles and Science*, n. 24, p. 1-10, 2015.

**Área: FOT** **Inscrição: 00545**

# A study of the photophysical and solvatochromic properties of naphtho[2,3-*b*]benzofuran-6,11-diones

**Rodolfo I. Teixeira (PG),[1*] Marlon D. Tonin (PG),[1] Nanci C. de Lucas (PQ)[1] and Simon J. Garden (PQ)[1]**

***rodolfoiteixeira@gmail.com**

[1]*Departamento de Química Orgânica, Instituto de Química, Universidade Federal do Rio de Janeiro (UFRJ).*

Keywords: fluorescence, 1,4-naphthoquinones, solvatochromism

## Highlights

Naphthobenzofurandiones with electron-donating groups displayed dramatic Stokes shifts of the fluorescence emission as a function of the solvent polarity.

## Resumo/Abstract

Naphthoquinones have been intensively investigated due to their biological activity.[1] The photochemistry of naphthoquinones has been thoroughly investigated in both organic solvents and aqueous solution.[2-3] Photoexcitation of 1,4-naphthoquinones leads to efficient intersystem crossing to the triplet state. Therefore, quinones generally do not exhibit fluorescence. In the present study, we have investigated the influence of solvent polarity on absorption and emission properties of naphtho[2,3-*b*]benzofuran-6,11-diones.

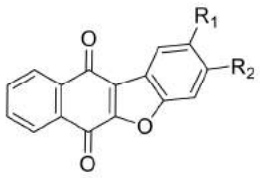


**1:** $R_1 = R_2 = H$
**2:** $R_1 = CH_3$; $R_2 = H$
**3:** $R_1 = Cl$; $R_2 = H$
**4:** $R_1 = OH$; $R_2 = H$
**5:** $R_1 = OCH_3$; $R_2 = H$
**6:** $R_1 = CO_2Me$; $R_2 = H$
**7:** $R_1 = H$; $R_2 = CH_3$
**8:** $R_1 = H$; $R_2 = OCH_3$

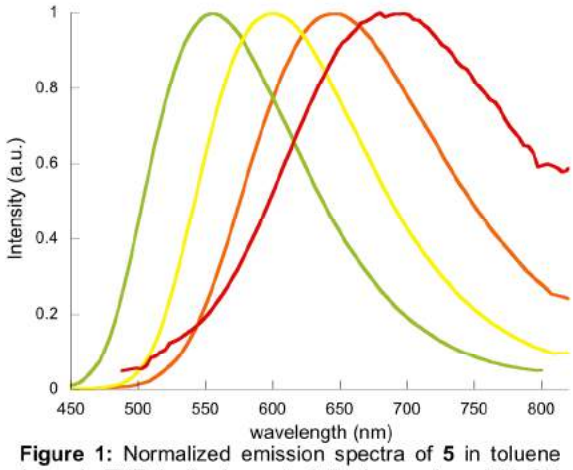


**Figure 1:** Normalized emission spectra of **5** in toluene (green), THF (yellow), acetonitrile (orange) and MeOH (red).

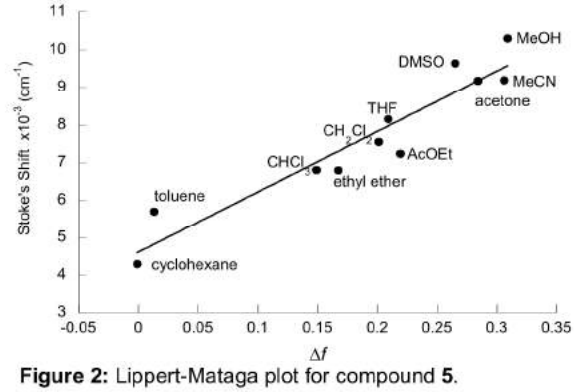


**Figure 2:** Lippert-Mataga plot for compound **5**.

The absorption spectra of compounds **1-8** reveal an intramolecular charger transfer (ICT) transition in the 390-420 nm region and a π,π* transition in the 330-360 nm region. Comparison of the absorption spectra for the compounds revealed a relative increase in intensity of the ICT transition with electron donating substituents in comparison to electron withdrawing substituents.

Compounds **4**, **5** and **8** exhibit fluorescence emission with a dramatic colour change as a function of the solvent polarity. For **5**, the emission in toluene is a greenish yellow whilst in MeOH the emission is red (Figure 1). Additionally, a diverse range of solvents was used to study the emission and the results are shown as a Lippert–Mataga plot (Figure 2, correlation R = 0.95). Therefore, simply monitoring the emission maxima should allow discrimination of polarity changes / differences between media. The fluorescence quantum yield and lifetime were also measured for **4**, **5** and **8** in toluene. The respective values are: **4** 0.01 (τ = 1.55 ns), **5** 0.04 (τ = 2.11 ns) and **8** 0.03 (τ = 8.18 ns).

In summary, an unusual property of a group of quinones that exhibit a large solvatochromic effect with respect to fluorescence emission as a function of the polarity of the environment has been described.

[1] da Silva, F. C.; Ferreira, V. F. *Current Organic Synthesis,* **2016**, 13, 334.
[2] Görner, H. Photochemistry and Photobiology. **2005**, 81, 376.
[3] de Lucas, N. C., *et. al. Photochemical & Photobiological Sciences*. **2012**, 11, 1201.

**Área: FOT** **Inscrição: 00598**

# Photocatalyzed [2+2]-cycloaddition of 3-(2-oxo-2-phenylethylidene)-2-oxindole by ruthenium complexes.

**Rodolfo I. Teixeira (PG),* Simon J. Garden (PQ) and Nanci C. de Lucas (PQ).**

***rodolfoiteixeira@gmail.com**

*Departamento de Química Orgânica, Instituto de Química, Universidade Federal do Rio de Janeiro (UFRJ).*

Keywords: photocatalysis, [2+2]-cycloaddition, visible light, energy transfer.

## Highlights

The intermolecular [2+2]-cycloaddition reaction of a 3-ylidene-2-oxindole was promoted, via energy transfer, by ruthenium (II) photocatalysts that were irradiated by a commercial 8 W household LED lamp.

## Abstract

Photocatalysis has become a prominent theme in organic chemistry as a unique and effective tool for electron or energy transfer processes under mild reaction conditions.[1] Ruthenium(II) complexes have demonstrated useful properties as photocatalysts.[2] Although $Ru(bpy)_3^{2+}$ has been extensively studied in photoredox systems, the ability of metal polypyridyl complexes to facilitate triplet sensitization via an energy transfer process has not been extensively investigated.[3] Therefore, in the present study we have investigated the ability of ruthenium complexes to photocatalyse a [2+2]-cycloaddition reaction.

The catalytic test was based upon the synthesis reported by Wu *et al.*[4] A mixture of **1** (0.10 mmol) and catalyst (4 mol%) were dissolved in 20 mL of MeOH and stirred whilst being irradiated by a commercial 8 W household LED lamp. The catalysts used were: rose bengal (as standard), $[Ru(bpy)_3](PF_6)_2$ (bpy = bipyridyl) and $[Ru(bpy)_2dppz](PF_6)_2$. The reaction scheme, catalyst structure and yields are shown in table 1. The energy transfer mechanism was investigated by Stern-Volmer quenching experiments of the transient absorption and of the emission from the ruthenium (II) triplet complexes. The Stern-Volmer plots for the ruthenium complexes showed quenching of the emission at 620 nm and of triplet absorption at 370 nm, both with a quenching constant of $6\text{-}7x10^9$ L $mol^{-1}$ $s^{-1}$.

In conclusion, ruthenium complexes catalysed the intermolecular [2+2]-cycloaddition of a 3-ylideneoxindole, via a triplet sensitization energy transfer process, with good product yield (75%) when irradiated by visible light from a commercial 8 W household LED lamp.

**Table 1:** Synthesis of a spirocyclobutano-oxindole from 3-(2-oxo-2-phenylethylidene)-2-oxindole

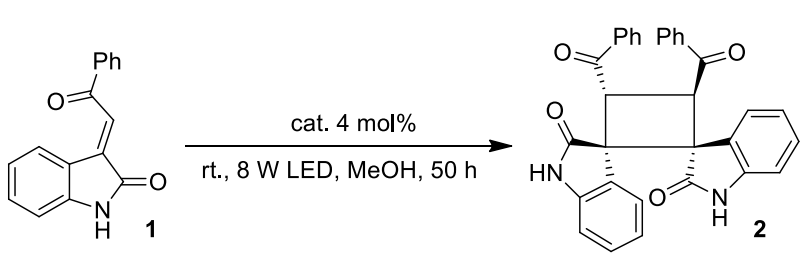


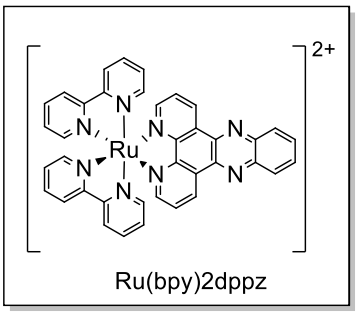


| **catalyst** | None | rose Bengal | $[Ru(bpy)_3](PF_6)_2$ | $[Ru(bpy)_2dppz](PF_6)_2$ |
|---|---|---|---|---|
| **Yield** | 4%[a] | 60%[b] | 74%[b] | 71%[b] |

[a]Yield was based on the difference between the absorption before and after irradiation. [b]isolated yield.

[1] Miranda, M. A.; Marin, M. L. *Curr. Opin. Green Sustain. Chem.* **2017**, 6, 139–149.
[2] Twilton, J.; Le, C. C.; Zhang, P.; Shaw, M. H.; Evans, R. W.; MacMillan, D. C.. *Nat. Rev. Chem.* **2017**, 1.
[3] Shaw, M. H.; Twilton, J.; MacMillan, D. W. C. *J. Org. Chem.* **2016**, 81 (16), 6898–6926.
[4] Wu, L. L.; Yang, G. H.; Guan, Z.; He, Y. H. *Tetrahedron*. **2017**, 73 (14), 1854–1860.

**Área: FOT** **Inscrição: 00617**

# Synthesis and photophysical studies of new fluorescent N-acylhydrazone and semicarbazone-7-NEt$_2$-coumarin dyes.

**Thiago M. Pereira (PG),[1] Fabio S. Miranda (PQ),[2] Arthur E. Kummerle (PQ).[1]***

**thm.pereira@hotmail.com; akummerle@hotmail.com**

*[1]Departamento de Química, UFRRJ; [2]Instituto de Química, UFF.*

Palavras Chave: *(Coumarin, fluorescence).*

## Highlights

The new coumarin derivatives were obtained by simple and easy protocol. The photophysical evaluation demonstrated spectral variations with the change of the 'R' group, mainly withdrawing groups.

## Resumo/Abstract

Coumarins are organic heterocycles present in plants and show several routes of obtaining and synthetic derivatization.[1] These have a range of applications which are extensively exploited, such as fluorescent chemical and biological probes.[2,3] The goal of this work is the synthesis of new coumarin derivatives from the condensation reaction between hydrazides (4b-h) to 3-acetyl-7-NEt$_2$-coumarin (1). The variation in R had the objective of modulating the electron density over the fluorophore, leading to different profiles of fluorescence. The 3-acetyl-7-NEt$_2$ (1) was obtained from 4-NEt$_2$-salicilaldehyde (2) and ethyl acetoacetate (3) in 24h by reflux, with 85% yielding. The synthesis of hydrazides (4b-h) was evaluated using aldehydes, which were oxidized to the corresponding esters in basic medium (KOH) using methanol and $I_2$, which were sequentially reacted with hydrazine hydrate. Hydrazones and semicarbazone (5a-h) were obtained reacting the excess (1.05eq) of hydrazides (4b-h) and semicarbazide with 3-acetyl-7-NEt$_2$-coumarin (1) at 75°C for 24h.

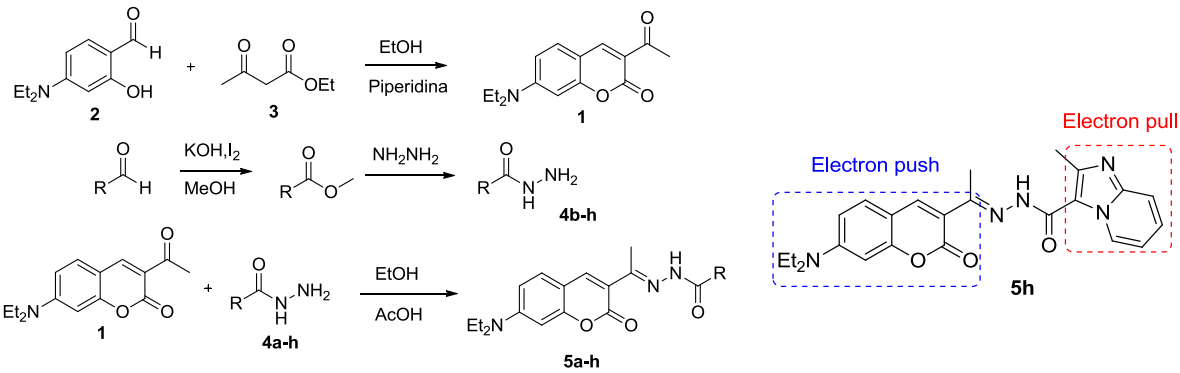


**5a**: R= NH2 (**77%**)
**5b**: R= Ph (**85%**)
**5c**: R=4-MeO-Ph (**83%**)
**5d**: R= 4-Cl-Ph (**91%**)
**5e**:R=benzo[1,3]dioxola (**80%**)
**5f**: R= 4-OH-Ph (**70%**)
**5g**:R=4-F-Ph (**70%**)
**5h**: R=[imidazopiridina] (**72%**)

The compounds described in here were obtained in a simple and easy way. All of compounds were structural analyzed by $^1$NMR and $^{13}$NMR. The photophysical analysis demonstrated variation in spectral properties (UV/Vis and fluorescence) with the change of the R group. Additionally, the photophysical characteristics make these compounds useful as fluorescence push-pull chemical and biological probes. Acknowledgments: FAPERJ-CNPQ-UFRRJ.

1 Ghouili A, et al.J Phys Chem Solids 2014;75:188-193.2 Danko M, et al. Dyes and Pigments 2011;90:129-138. 3 Winnik FM, et al. Colloids and Surfaces A: Physicochemical and Engineering Aspects 1996; 118: 1-39.

**Área: FOT** **Inscrição: 00634**

# Estudo por fotólise por pulso de laser da reatividade do triplete de dimetoxi-xantonas frente a doadores de energia, elétron e hidrogênio

**Romulo Correia Ferreira[1] (PG)*, Victor Gomes de Almeida[3] (IC) , Cosme Henrique Coêlho dos Santos de Oliveira[1] (PG), Antônio Eduardo da Hora Machado[2] (PQ), Dari Cesarin-Sobrinho[1] (PQ), José Carlos Netto-Ferreira[1] (PQ).**

*[1]Universidade Federal Rural do Rio de Janeiro. BR-465, Km 7, Seropédica, RJ, 23.890-000. ICE, Departamento de Química; [2]Universidade Federal de Uberlândia. Av. João Naves de Ávila, 2121 - Santa Mônica, Uberlândia - MG, 38408-100, Instituto de Química; [3]Universidade do Grande Rio Professor José de Souza Herdy. Rua Professor José de Souza Herdy, 1160 – Duque de Caxias, 25071-202.*

***romulorcf@yahoo.com.br**

Palavras Chave: *Fotólise por pulso de laser, xantona, triplete.*

## Highlights

Study by laser flash photolysis of the triplet reactivity of dimethoxy-xanthones to energy, electron and hydrogen donors. Studies by laser flash photolysis exhibited at xanthone irradiation in the presence of electron donor suppressors, results in the formation of its radical anion.[1,2] The irradiation of the xanthones led to the formation of their respective triplet excited states. From the suppression rate constants obtained, it was observed that in the presence of hydrogen donor suppressors, the cetyl radical derived from the respective xanthones was formed, and with an electron donor suppressor, the radical anion also formed from the xanthones.

## Resumo/Abstract

Estudos por fotólise por pulso de laser mostraram que a irradiação de xantona em presença de supressores doadores de elétron, resulta na formação do seu ânion radical,[1,2] enquanto que em presença de doadores de hidrogênio, tais como observa-se a formação do radical cetila correspondente.[2,3]

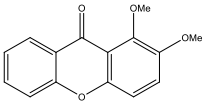


**1,2MX**

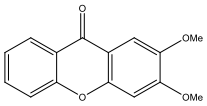


**2,3MX**

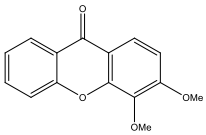


**3,4MX**

As xantonas estudadas apresentam espectro com máximo de absorção em 620 nm e tempo de vida em torno de 1,8 µs, em acetonitrila. Com 1-metil-naftaleno, supressor por transferência de energia, obteve-se para todas as xantonas uma constante de velocidade de supressão na ordem de $10^9$ $L.mol^{-1}.s^{-1}$ em acetonitrila, valor idêntico ao da constante de velocidade de difusão para esse solvente. Foram também obtidas as constantes de velocidade de supressão em presença de doadores de hidrogênio. Excetuando os álcoois, todos os outros supressores doadores de hidrogênio, operaram num processo controlado pela velocidade de difusão, formando radical cetila correspondente. Na presença de doador de elétron, observa-se a formação do ânion radical correspondente (Tabela 1).

| $K_q$ ($Lmol^{-1}s^{-1}$) | | | |
|---|---|---|---|
| **Supressores** | **1,2 MX** | **2,3 MX** | **3,4 MX** |
| **1-metil-naftaleno** | $1,14x10^9$ | $1,39x10^9$ | $8,95x10^9$ |
| **Fenol** | $1,84x10^9$ | $1,96x10^9$ | $2,10x10^9$ |
| **Trietilamina** | $1,25x10^9$ | $4,07x10^9$ | $1,50x10^9$ |

A irradiação das xantonas levou à formação de seus respectivos estados excitados triplete. A partir das constantes de velocidade de supressão obtidas observou-se que na presença de supressores doadores de hidrogênio ocorreu formação do radical cetila derivado das respectivas xantonas, e com supressor doadores de elétron houve formação do ânion radical também derivado das xantonas.

## Agradecimentos

UFRRJ, CNPq e CAPES.

1- Takaizumi, A. A. C.; Santos, F. R.; Silva, M. T.; Netto-Ferreira, J. C.;*Quim. Nova* 2009, *32*, 1799.
2- Whang, J.-T.; Pan, Y.; Zhang, L.-M.; Yu, S.-Q.; *Chin. J. Chem. Phys*.2007, *20*, 396.
3- Lathioor, E. C.; Leigh, W. J.; *Photochem. Photobiol.* 2006, *82*, 291.

**Área: FOT** **Inscrição: 711**

# Photodegradation of sodium diclofenac and toxicity monitoring

**Letícia S. Lima(IC),[1*] Marcelo M. Galdino(IC),[1] Danilo R. Souza (PQ).[1]**

**danilo.souza@ufob.edu.br; leticia.mano@hotmail.**

[1]*Centro de Ciências Exatas e das Tecnologias, UFOB*

Palavras Chave: *emerging contaminants; $TiO_2$, photodegradation, sodium diclofenac, toxicity assays.*

## Highlights

- Mitigation of emerging contaminants
- $TiO_2$ and application for photodegradation of diclofenac sodium
- Assays of reduction toxicicity using Artemias Salinas.
- Concentration reduction about 90 % and toxicity reduction about 80 %.

## Abstract

Emerging contaminants, also known as endocrine disrupters, are present in commercial products such as medicines, hygiene products, dyes foods and pesticides. Among them, diclofenac sodium, being biorecalcitrant and widely consumed by the population, guarantees its residual presence increasing in aquatic sources. A difficult degradation by traditional methods, the application of advanced oxidative treatments is becoming more feasible.

In the present work, diclofenac sodium samples were exposed to the process of photodegradation using $TiO_2$ and assays of toxicity reduction using Artemias Salinas. Initially diclofenac sodium samples were analyzed indicating that the estimated 50% DL was $4.41x10^{-4}$ $molL^{-1}$. This concentration as the initial reference, the photodegradation tests were carried out. With 60 minutes of photocatalytic exposure, the presence of diclofenac sodium was almost totally mitigated, and in 10 minutes it was estimated that 90% of degradation. Monitoring toxicity of the photogered residues indicated a reduction of about 80% in 30 minutes of photolysis.

**Área: FOT** *(Inserir a sigla da seção científica para qual o resumo será submetido. Ex: ORG, BEA, CAT)*

**Inscrição: 00752** *(Inserir o número de inscrição do autor que fez a submissão)*

# Estudo da interação entre azul de metileno e curcumina para uso em terapia combinada com antiangiogênica

**Rodrigo C. Silva (PG),[1] Cláudio R. Neri (TC),[2] Osvaldo A. Serra (PQ),[2] Yassuko Iamamoto,[2] Hilde H. Buzzá (PQ),[3] Iouri E. Borissevitch (PQ),[4] Pablo J. Gonçalves (PQ).[1]***

**rcosta2609@yahoo.com.br; pablo@ufg.br**

*[1]Instituto de Química, UFG; [2]Departamento de Química, FFCLRP-USP; [3]Instituto de Física de São Carlos, IFSC-USP; [4]Departamento de Física, FFCLRP-USP.*

Palavras Chave: *Azul de metileno, Curcumina, Complexação, Atividade antiangiogênica, Atividade fotodinâmica.*

## Highlights

Study of the interaction between methylene blue and curcumin for use in combination therapy.

Combined use of methylene blue and curcumin.
Methylene blue-curcumin complex with 1:4 stoichiometry.
Reduced aggregation trend and increased stability of curcumin.

## Resumo

A terapia fotodinâmica consiste no uso de um agente fotossensibilizador para geração fotoinduzida de oxigênio singlete visando o tratamento de diversas doenças, incluindo o câncer. A terapia antiangiogênica provoca a morte celular pela inibição do surgimento de novos vasos sanguíneos necessários à nutrição da massa tumoral. Assim, a combinação de fotossensibilizadores com agentes antiangiogênicos (AA) tem sido uma estratégia amplamente investigada visando o aumento da eficiência do tratamento. Neste trabalho, a combinação entre azul de metileno (AM), excelente fotossensibilizador, com a curcumina, um conhecido AA, foi avaliada por espectroscopia de infravermelho, UV-Vis e fluorescência. A estequiometria e constante de ligação foram determinadas pelos métodos Benesi-Hildebrandt e Klausen-Langmyhr e a estabilidade do complexo por CLAE-DAD. As atividades fotodinâmica e vascular foram determinadas pelo método do sensor químico e membrana corioalantóica em ovos de galinha, respectivamente. A combinação entre o AM com a curcumina formou um complexo cuja estequiometria foi de 1:4 com constante de ligação de $1{,}1.10^{18}$ $M^{-4}$, onde os grupos β-dicetona da curcumina interagiram com os grupos amino e enxofre do AM. O complexo diminuiu a tendência de agregação da curcumina e aumentou a estabilidade dessa espécie em solução aquosa. O complexo apresentou atividade fotodinâmica quando irradiado no vermelho (570 a 670 nm), não alterou o rendimento quântico de oxigênio singlete do AM (0,52) e apresentou grande redução da rede vascular da membrana corioalantóica pela ação sinérgica entre a atividade fotodinâmica do AM e antiangiogência da curcumina.

**Área: FOT** **Inscrição: 01008**

# Síntese e avaliação fotofísica preliminar de benzimidazóis bifenílicos

**Nathália S. de Araújo (PG),[1]* Táthyla C. da Rocha (IC),[2] Jose D. F. Villar (PQ),[1] Fabio da S. Miranda (PQ).[2]**

**nathaliasalesaraujo@gmail.com**

*[1]Departamento de Química, IME, Rio de Janeiro, RJ; [2]Instituto de Química, UFF, Niterói, RJ.*

Palavras Chave: *Benzimidazol, Luminescência, Bifenil.*

## Highlights

Synthesis and preliminary photophysical evaluation of biphenyl benzimidazoles. Investigation of electronic effect of different substituents on the luminescence of biphenyl benzimidazoles.

## Resumo/Abstract

O grupo de fotoquímica molecular da UFF vem trabalhando com a síntese e caracterização fotofísica de compostos heterocíclicos, destacando-se imidazóis e derivados.[1,2] Benzimidazóis e derivados tem sido investigados como protótipos para atividade anti-tumoral, anti-HIV e anti-microbiana, como cristais líquidos, intercaladores de DNA e sondas fluorescentes.[1,3] Neste trabalho está sendo reportada a síntese e o estudo fotofísico prévio de alguns benzimidazóis bifenílicos (ver esquema sintético na Figura 1).

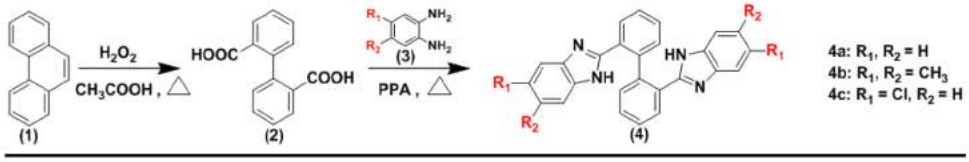


**Figura 1.** Rota sintética para obtenção dos compostos 4a, 4b e 4c

A figura 2 apresenta os espectros de emissão dos compostos preparados. O grupo metila causou um deslocamento batocrômico quando comprado com o derivado sem grupo substituinte. O benzimidazol substituído com cloro teve apenas um leve alargamento da largura de linha que afetou minimamente a sua cromaticidade.

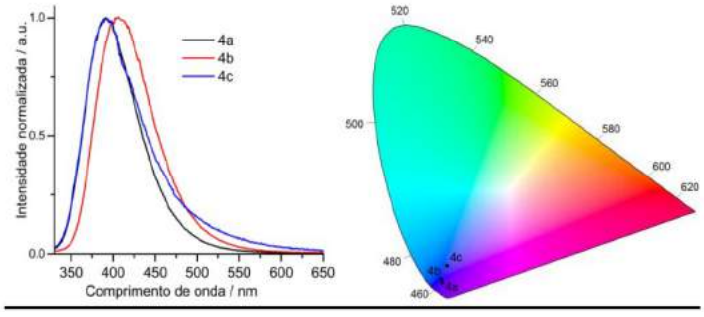


**Figura 2.** (Esquerda) Espectros de emissão em MeOH; (Direita) diagrama de cromaticidade.

Apesar de mais substituintes serem necessários para ter um melhor entendimento das tendências fotofísicas nessa classe de compostos, fica evidente a modulação da luminescência nas moléculas preparadas pelo efeito eletrônico causado pelo substituinte sob o anel benzimidazólico.

[1] Miranda, F. S. et al. *J. Mol. Struc.* **2009**, *938*, 1-9.
[2] Miranda, F. S. et al. *J. Mol. Struc.* **2014**, *1063*, 320-327.
[3] Stibrany, R. T. et al. *Inorg. Chem.* **2004**, *43*, 1472-1480.

**Área: FOT** **Inscrição: 01113**

# Preparation and characterization of fibroin hydrogels for potential application in photodynamic therapy

**Jose Eduardo U. Rojas[1] (PG), Francesca Giuntini[2] (PQ), Wendel A. Alves[1]* (PQ)**

joeullo@hotmail.com; wendel.alves@ufabc.edu

*[1]Centro de Ciências Naturais e Humanas, Universidade Federal do ABC, 09210-580, Santo André, Brazil; [2]School of Pharmacy and Biomolecular Sciences, Liverpool John Moores University, Byrom Street, Liverpool, L3 3AF, UK.*

Keywords: *Porphyrin, fibroin, hydrogels, photodynamic therapy, crosslinking, rheology, singlet oxygen.*

## Highlights

The objective is to show the ability of hybrid porphyrin-fibroin hydrogels to generate singlet oxygen after gelification. Silk fibroin hydrogels demonstrate a distinct efficacy as matrices for incorporation of new functional molecules to the application in photodynamic therapy and photothermal therapy.

## Resumo/Abstract

The research in to natural materials has notably increased in recent years due to the opportunity of combining biocompatibility with exceptional physical, mechanical, and chemical properties, which would be arduous to obtain following a synthetic route. Among these natural polymers, silk fibroin is attractive because of its optical transparency, outstanding mechanical robustness and compatibility with living systems, with the formation of non-inflammatory degradation products. In this study, we were capable to form translucid hydrogels from raw silk fibers at different concentrations and used them as matrix to incorporate a photosensitive molecule - sodium (4,4',4''-(20-(4-(3-carboxypropanamido) phenyl) porphyrin-5,10,15-triyl) tribenzenesulfonate - for future use in photodynamic therapy. The obtained hydrogels were characterized by different rheology techniques and spectrophotometry analysis to study the factors that are involved in the formation of the hydrogel, and to have information about silk fibroin (SF) properties after adding the porphyrin molecule to the matrix. The set of obtained results showed that the SF hydrogels have a shear thinning behavior, where the viscosity of the gel decrease whit the increase of the shear rate, and that it can be classified as thixotropic materials. This mean that the structure of the material needs time to recover after experience shear deformation. Also, we observed that the secondary structure of the fibroin is not affected by the addition of porphyrin in any concentration, it was confirmed by the negative Cotton signal around 220 nm in the circular dichroism spectra. The hybrid porphyrin-fibroin nanofibers were capable to generate singlet oxygen after gelification, and we proved that silk fibroin hydrogels are an excellent matrix to encapsulate other molecules to application in photodynamic therapy and photothermal therapy, leading to the formation of selfassembled peptide nanostructures with controllable phototherapeutic effects.

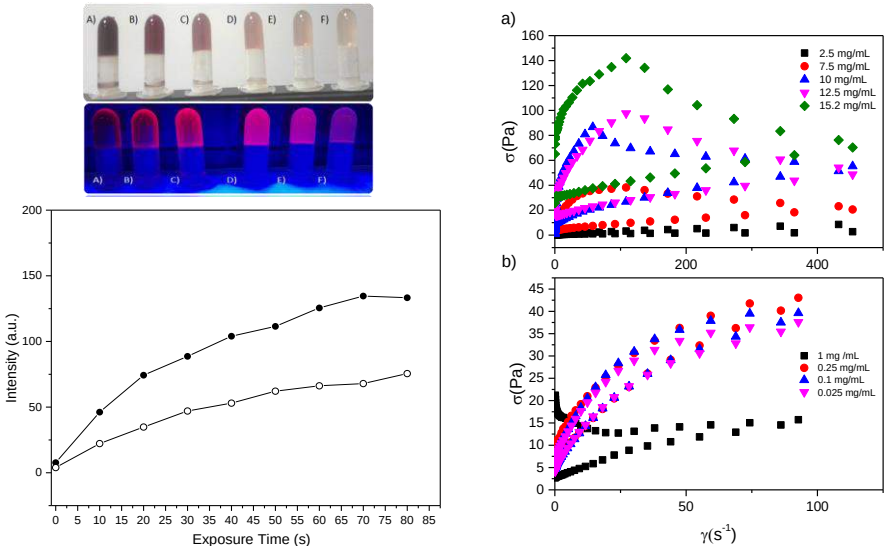


**Fig. 1-** (left) Fibroin/porphyrin hydrogels matrices and kinetic curve of generation of reactive oxygen species by using singlet oxygen sensor green (SOSG; Life Technologies, Carlsbad, CA) as the fluorescent probe for hibrid hydrogel (•) and porphyrin solution (o); (right) Flow rheograms of the hydrogels composed of (a) Fibroin and (b) Fibroin/porphyrin hydrogels. The flow rheograms shows the thixotropy behavior of the prepared hydrogels.

**Área: FOT** **Inscrição: 01168**

# Síntese e caracterização do complexo $[Ru(phen)_2(iso)]PF_6$

**Beatriz Pachel (IC)[1], Rafael C. Marchi (PG)[1], Danielle F. Silva (PQ)[1], João B. Fernandes (PQ)[1], Maria Fátima G. F. Silva (PQ)[1], Rose M. Carlos (PQ)[1].**

**biapachel@hotmail.com; rosem@ufscar.br**

*[1]Departamento de Química, UFSCar.*

Palavras Chave: Complexo Ru(II), antioxidante, produto natural, luminescência.

## Highlights

Synthesis and characterization of $[Ru(phen)_2(iso)]PF_6$ complex. Characterization of a complex containing a phenollic acid coordinated to the metal center and evaluation of its properties against reactive oxygen species (ROS).

## Resumo/Abstract

A presença de espécies reativas do oxigênio (ERO's) no meio biológico leva tanto a doenças degenerativas quanto a deterioração de alimentos. Compostos naturais como por exemplo os ácidos fenólicos apresentam propriedades antioxidantes. Estes possuem uma limitante para aplicação prática que a é baixa solubilidade em meio aquoso e a facilidade de oxidação.[1]

O complexo $[Ru(phen)_2(iso)]PF_6$ foi planejado para potencializar a atividade antioxidante dos ácidos fenólicos livres, uma vez que a quelação dessas moléculas à centros metálicos favorece a solubilidade e investigação biológica dessas interações.[2]

Para a caracterização, foram utilizadas técnicas espectroscópicas: espectroscopia eletrônica (UV-vis e luminescência), espectroscopia de infravermelho e ressonância magnética nuclear: O espectro de infravermelho obtido em KBr mostra o desparecimento do estiramento da carboxila do ácido isovanílico livre em 1700 $cm^{-1}$,com a coordenação no complexo, Figura 1. A Figura 2 mostra o deslocamento da absorção de MLCT (Ru—phen) no complexo precursor $[Ru(phen)_2(Cl)_2$, ($\lambda_{máx}$=555 nm) com a troca dos dois cloretos pelo grupo carboxi do isovanalato. O complexo Ru-iso apresenta emissão intensa com máximo em 600nm, similar ao $Ru(phen)3]^{2+}$ indicando que a emissão é proveniente dos estados excitados 3*MLCT. A semelhança entre o espectro de excitação e o espectro de absorção também sugerem que a emissão é provenietne do 3*MLCT. O deslocamento de Stokes grande (5520 $cm^{-1}$) indica que o complexo pode ser um bom sensor biológico uma vez que este não leva à reabsorção da emissão, Figura 3. Espera-se que este composto seja mais seletivo e consequentemente menos tóxico, podendo coletar informações fisiológicas importantes.

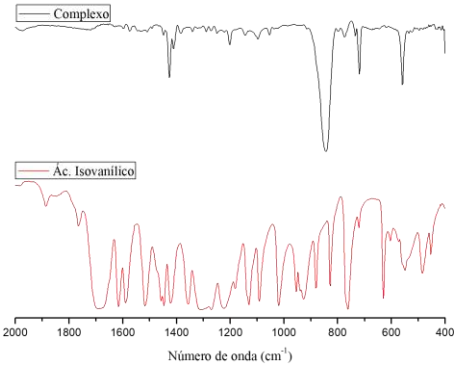


Figura 1 Espectro de IV $[Ru(phen)_2(iso)]^+$ e ácido isovanílico livre.

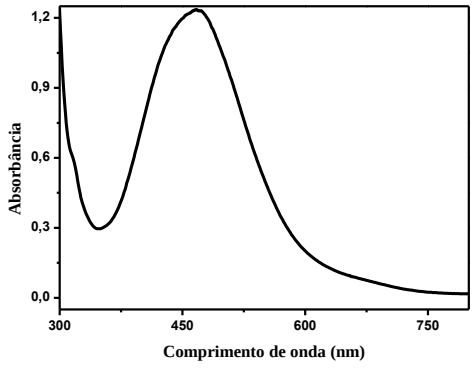


Figura 2 UV-vis $[Ru(phen)_2(iso)]^+$ em acetonitrila.

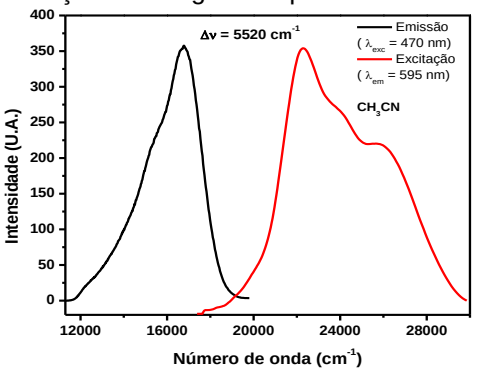


Figura 3 Luminescência $[Ru(phen)_2(iso)]^+$ em acetonitrila.

1. Nielsen, Inge Lise F. et al. *J. Nutr.*2006, 136, 404-408
2. Oliveira, R. M., de Souza Daniel, J. F., de Aguiar, I., Silva, M. F. D. G. F., Fernandes, J. B., & Carlos, R. M. *Journal of inorganic biochemistry* 2013, 129, 35-42.

**Área: FOT**
*(Inserir a sigla da seção científica para qual o resumo será submetido. Ex: ORG, BEA, CAT)*

**Inscrição: 01315**
*(Inserir o número de inscrição do autor que fez a submissão)*

# Nature-inspired fluorescent betalains

**Erick L. Bastos (PQ)***

**elbastos@iq.usp.br**

*Departamento de Química Fundamental, Instituto de Química, Universidade de São Paulo, São Paulo, SP, Brazil*

Keywords: Beetroots, betalains, fluorescence, natural products, nanomaterials, cell biology.

## Highlights

The structural modification of betalains allows the development of new functional dyes with tailored photophysical properties. Herein we describe the semisynthesis and photophysical characterization of several water-soluble artificial betalains.

## Resumo/Abstract

Sunlight provide plants with the energy necessary to produce oxygen from water and carbon dioxide. There are, however, several other phenomena involving the interaction of light and plant pigments. The yellow petals of most plants of the order Caryophyllales emit green fluorescence when irradiated with blue light [1]. Although the ecological and biological functions of fluorescence in plants is still matter of debate[2], this result contributed to promoting interest in water-soluble alkaloids named betalains[3].

Betalamic acid is the key biosynthetic precursor of the two classes of natural betalains: red betacyanins and yellow betaxanthins. The aldimine coupling between betalamic acid and cyclo-DOPA produce betacyanins, which have been used as antioxidants and show gene regulatory activity[4]. Betaxanthins are formed when cyclo-DOPA is replaced by other amino acids or amines. Betalains are imines or iminium salts and, therefore, are subject to hydrolysis and transimination[5]. Consequently, betalamic acid have been obtained from the hydrolysis of natural betalains (especially betanin, the main pigment of beetroots) and used to semisynthesize natural and artificial betalains.

Betalains have been used as natural additives for food, drugs and cosmetic products in the form of commercially available beet juice concentrate or beet powder. Additionally, natural and artificial betalains have been used in several technological applications, such as solar cells, nanoparticle fabrication, hydrogen-producing devices, fluorescent probes, and colorimetric sensors. The excitation of some of these compounds in the near-infrared results in yellow fluorescence with two-photon cross sections in water of 323 GM and 179 GM. Detailed NMR analysis allowed the study of electronic effects on the hydrolytic and photophysical properties of phenylbetalains. The fluorescence efficiency of the betalains is sensitive to the nature of the surrounding environment, increasing by as much as an order of magnitude in confined media. Increase in fluorescence efficiency was attributed to the destabilization of the charge transfer character of the excited state affecting the transition dipole moment of betalains.

Our research group have developed synthetic routes to a variety of functional semisynthetic derivatives and analogs of betalains[6–9]. In this work, I will present our results on the design and semisynthesis of betalains, neobetalains and quasibetalains and their application as smart fluorescent probes and as mediators in energy conversion systems.

[1] F. Gandía-Herrero, F. García-Carmona, J. Escribano, *Nature* 2005, **437**, 334.
[2] A. Iriel, M. G. Lagorio, *Naturwissenschaften* 2010, *97*, 915.
[3] M. I. Khan, P. Giridhar, *Phytochemistry* 2015, **117**, 267.
[4] T. Esatbeyoglu, A. E. Wagner, V. B. Schini-Kerth, G. Rimbach, *Mol. Nutr. Food Res.* 2015, **59**, 36.
[5] W. Schliemann, N. Kobayashi, D. Strack, *Plant Physiol.* 1999, *119*, 1217.
[6] F. H. Bartoloni, L. C. P. Gonçalves, A. C. B. Rodrigues, F. A. Dörr, E. Pinto, E. L. Bastos, *Monatsh. Chemie* 2013, **144**, 567.
[7] L. C. P. Gonçalves, S. M. Da Silva, P. C. DeRose, R. A. R. A. Ando, E. L. Bastos, *PLoS One* 2013, **8**, e73701.
[8] L. C. P. L. C. P. Gonçalves, B. M. B. M. Di Genova, F. A. F. A. Dörr, E. Pinto, E. L. Bastos, *J. Food Eng.* 2013, **118**, 49.
[9] L. C. P. Gonçalves, R. R. Tonelli, P. Bagnaresi, R. A. Mortara, A. G. Ferreira, E. L. Bastos, *PLoS One* 2013, **8**, e53874.

**Área: FOT** **Inscrição: 01423**

# Development of topical formulation containing methylene blue for photodynamic therapy

**Lucas A.G. da Costa (IC)[1*], Hanna K. de M. Pereira (IC),[1] Adriana Fontes (PQ),[2] Juliana de S. A. Falcão (PQ)[3], Beate S. Santos (PQ)[1]**

***lucasamadeusc2@hotmail.com**

*[1]Departamento de Ciências Farmacêuticas, [2]Departamento de Biofísica e Radiobiologia, UFPE; [3]Unidade Acadêmica de Saúde, UFCG*

Keywords: *Photosensitizer, Methylene Blue, Topical Formulation, Gels*

## Highlights

We developed semisolid gel formulations containing methylene blue to apply them as topical formulations in photodynamic therapy in the treatment of cutaneous infections.

## Resumo/Abstract

Methylene blue (MB) has already showed promising results in photodynamic treatment of cutaneous infections, but no topical formulation has been standardized yet[1]. A gel system is a proper option due to several advantages, *e.g.,* a longer contact time with the skin and excelent transparency allowing a greater light irradiation efficiency. In this study we prepared carbomer 940® (CBP) or hydroxyethylcellulose (HEC) based gels containing 0.15% methylparaben, triethanolamine s.q. pH ~7.0, distilled water or 10% hydroalcoholic solution or 10% urea solution s.q.t. and MB (1%) and tested their reactive oxygen species (ROS) production. Formulations presented a blue color (Fig. 1), pH ~7.0 and maximum spreadability close to 5,000 $mm^2$ for CBP and 6,500 $mm^2$ for HEC gels. Figure 1 presents the results of ROS production observed for all formulations.

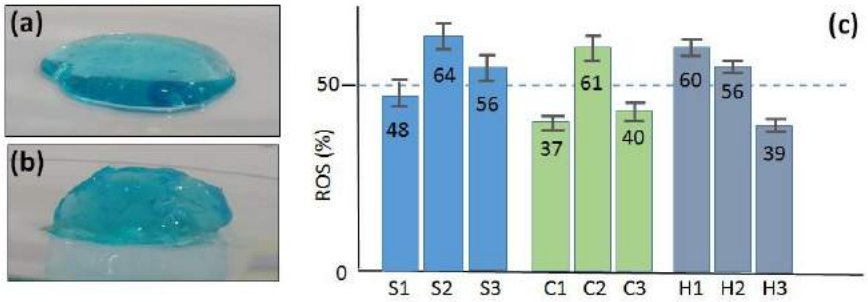


*Figure 1. Visual aspect of gels (a) HEC(H); (b) CBP(C). (c) ROS production of all systems compared to the aqueous solution of MB(S). 1 – water, 2 – ethanol, 3 – urea.*

The best formulations, in terms of ROS generation, were CBP with ethanol 10% (61% ROS) and HEC (60% ROS), presenting a 23% increase in relation to the aqueous solution of MB (48% ROS). These matrices provided a favorable physicochemical environment for the amplification of the photodynamic effect showing a great potential to be applied as topical formulations against cutaneous infections.

We thank CNPq, PROPESQ-UFPE and INCT-INFo for the support.

[1]TARDIVO, João Paulo et al. 2005. **Photodiagnosis and Photodynamic Therapy**, [s.l.] 2(3) 175-191.

**Área: INO** **Inscrição: 00016**

# Degradação do antibiótico levofloxacino catalisada por porfirinas de manganês

**Ana Luísa A. Lage* (PG), Mirra. A. N. da Silva (TC), Dayse C. S. Martins** (PQ)**

***analuisalage@gmail.com ****daysequimica@ufmg.br**

*Departamento de Química, Universidade Federal de Minas Gerais, Belo Horizonte – MG, Brasil.*

Palavras Chave: *Sistemas Biomiméticos, Catálise, Resistência Bacteriana, Metaloporfirinas, Fármacos*

## Highlights

**Degradation of the antibiotic levofloxacin catalyzed by manganese porphyrins**.
Pioneer work of degradation of a fluoroquinolone by porphyrins; Porphyrin degrade up to 81% of levofloxacin; Best degradation of levofloxacin was obtained by a second-generation porphyrin and $H_2O_2$.

## Resumo/Abstract

A degradação do antibiótico levofloxacino (LEV, Figura 1a) por catalisadores metaloporfirínicos (Figura 1b), na presença de $H_2O_2$, foi avaliada.

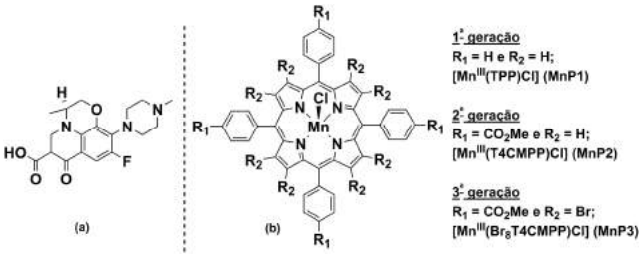


**Figura 1**. (a) Levofloxacino e (b) Porfirinas de manganês estudadas.

**Tabela 1**. Degradação (%) do antibiótico LEV por porfirinas de manganês, na presença de $H_2O_2$*

| Sistema | Branco** | MnP1 | MnP2 | MnP3 |
|---|---|---|---|---|
| **Tampão/ACN (85:15)** | 9 | 0 | 0 | 3 |
| **ACN** | 20 | 33 | 81 | 51 |

* Análise por HPLC/UV (290 nm); ** Sistema sem catalisador

Os sistemas envolvendo apenas acetonitrila como solvente levaram à maior degradação do LEV, quando comparados aos sistemas com Tampão/ACN. Além da decomposição rápida do oxidante em meio aquoso, a água é conhecida por ser um capturador de radical hidroxila, o que pode estar interferindo no processo de degradação do antibiótico. Dessa forma, acredita-se que o mecanismo dessas reações passa por processos radicalares. Ao se comparar os catalisadores, observa-se que a metaloporfirina **MnP2** levou à melhor degradação do LEV, com um aumento de 305% em relação ao sistema branco. Comparando-se as metaloporfirinas **MnP2** e **MnP3**, observa-se um decréscimo na degradação do antibiótico, o que pode estar ocorrendo devido à presença de grupos volumosos nas posições β-pirrólicas da porfirina, que distorcem seu macrociclo, dificultado a aproximação do substrato. O presente trabalho evidencia uma maneira alternativa de degradar o levofloxacino. Esses sistemas poderão contribuir para a identificação e quantificação dos prováveis metabólitos desse antibiótico em sistemas biológicos. É importante destacar que (a) não é necessário investir na síntese de um catalisador de 3ª geração (como a **MnP3**), que requer mais esforços de preparação, e (b) a porfirina **MnP2** é um catalisador promissor para a degradação da levofloxacino e para a degradação de outras classes de antibióticos e outros fármacos que ainda não foram estudados.

Agradecimentos: FAPEMIG, CNPq, CAPES

**Área: INO** **Inscrição: 00062**

# *trans*-[Ru(NH$_3$)$_4$(pyS)X] complexes: *syntheses, characterization and self-assembled monolayer* on gold

**Ingrid Aragão L. Azevedo (IC),[1] Caio Bezerra de Castro (PG)[1,2], Izaura C. N. Diógenes (PQ)[1], Tércio de F. Paulo (PQ)[1]***

**ingridy_3636@hotmail.com; tercio@dqoi.ufc.br**

*[1]Departamento de Química Orgânica e Inorgânica, UFC; [2]Departamento de Química, UFSCAR*

Palavras Chave: Self-assembled monolayers, Coordination compounds, Au-S interaction.

## Highlights

Syntheses and characterization of ruthenium tetraamine complexes; Formation of self-assembled monolayers on gold; The effect of the ligand *trans* on the Au-SR bond strength.

## Abstract

In Inorganic Chemistry, the term Coordination Compounds includes species formed by a transition metal atom or ion and one or more ligands (atoms, ions or molecules) that formally donate electron density to the metal species. Nowadays coordination compounds are used in diverse areas such as materials (catalysis), photochemistry, bioinorganic (Metallodrugs), inorganic physics (molecular wires) and electrochemistry (modified electrodes and biosensors). In this work, a series of complexes of the type *trans*-[Ru(NH$_3$)$_4$(pyS)X](PF$_6$)$_2$ , where pyS = mercaptopyridine and X = bpa (1,2-bis(4-pyridyl)ethane), bpe (1,2-bis(4-pyridyl)ethylene, py (pyridine), or 4,4´-bpy (4,4´-dipyridyl) (see Figure 1), were synthetized and characterized using conventional vibrational and electronic spectroscopic and electrochemical techniques. Furthermore, density functional theory (DFT) calculations were performed to help with the interpretation of experimental results. These complexes contain the ligand pyS, which allow the spontaneous adsorption (self-assembled) of such compounds on gold surfaces in consequence of the strong Au-S interaction.[1-2] Surface plasmon resonance (SPR) was used to monitoring the formation of self-assembled monolayers (SAM) of the complexes on gold and to calculate the amount of adsorbed species. As a perspective, it is intended to evaluate the effect of the ligand X on the strength of the Au-SR bonding.

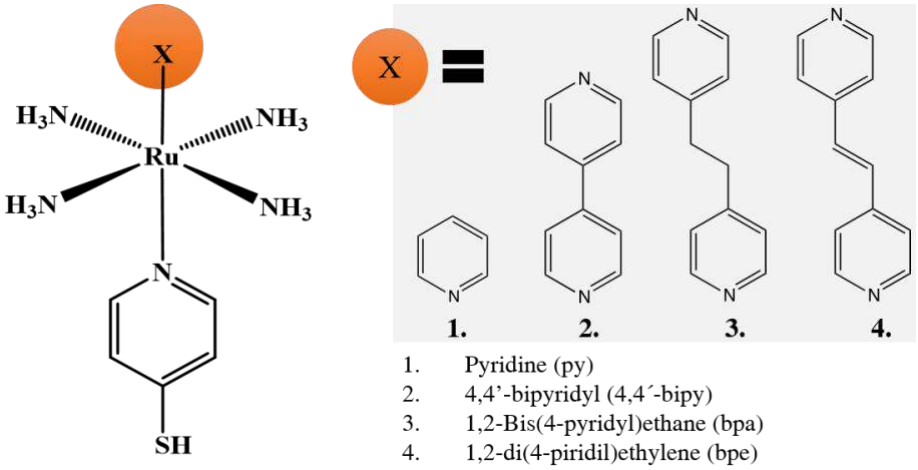


Figure 1. Structures of the series of the type *trans*-[Ru(NH$_3$)$_4$(pyS)X](PF$_6$)$_2$ complexes.

1. Hakkinen, H., The gold-sulfur interface at the nanoscale. *Nat Chem* **2012,** *4* (6), 443-455.
2. Kokkin, D. L.; Zhang, R.; Steimle, T. C.; Wyse, I. A.; Pearlman, B. W.; Varberg, T. D., Au–S Bonding Revealed from the Characterization of Diatomic Gold Sulfide, AuS. *The Journal of Physical Chemistry A* **2015,** *119* (48), 11659-11667.

**Area: INO** **Subscription: 00121**

# Stability study of the complex ion $[Cu(opba\text{-}dCl)]^{2-}$ in function of pH.

**Débora de O. Souza[1](IC)*, Emerson F. Pedroso[1](PQ), Rangel C. Q. Dutra[2](PQ)**

**debora.o.souza@live.com; pedroso@cefetmg.br**

[1]*Departamento de Química, Centro Federal de Educação Tecnológica de Minas Gerais, Av. Amazonas, 5855, BH, MG;*
[2] Fundação *Ezequiel Dias, Rua Conde Pereira Carneiro, 80, BH, MG;*

Keywords: Coordination compound ,*Stability study, pH variation.*

## Highlights

Automatic titrator for pH control; and UV-vis spectroscopy; Inorganic chemistry; Stability of the complex; Great range of work.

## Abstract

The coordination compounds present a wide range of applications, among them we can highlight biological activity, catalysts, magnetic devices and sensors. Depending on the application the compound should have a stability in function of pH variation. For this purpose, the aim of this work is to evaluate the stability of $Na_2[Cu(opba\text{-}dCl)]$ as a function of pH by UV-vis absorption spectroscopy.

An automatic titrator for pH control and an UV-vis spectrometer were used. The Uv-vis spectra were measured in the range of 400 to 1100 nm in a quartz cuvette at room temperature.

It is possible to observe that when the pH is below 4.38, an abrupt increase occurs at the bottom line of the spectrum, caused by the presence of precipitated particles (Figure 1). Also in this same pH the solution shows a greenish coloration, which indicates the decomposition of the complex ion and the consequent formation of an insoluble coordination polymer.

By analyzing the graph it was possible to define that the optimum pH range of work for this substance is 4.69 to 10.99. It suggests that in this range the complex does not decompose.

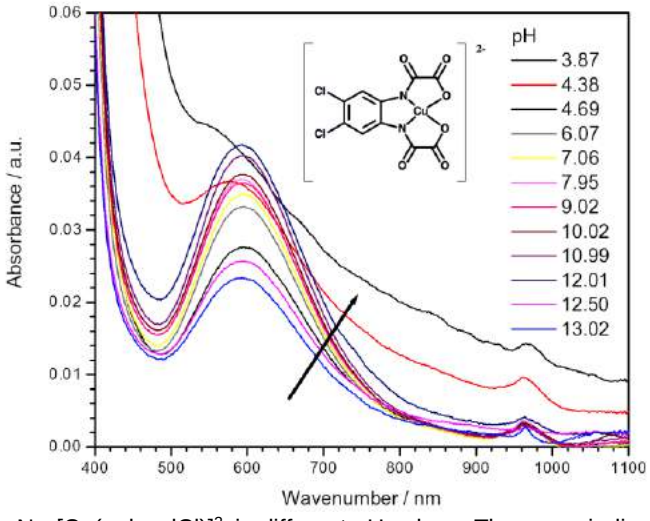


**Figure 1:** Complex spectrum $Na_2[Cu(opba\text{-}dCl)]^{2-}$ in different pH values. The arrow indicates the pH increase values.

Acknowledgement: CNPq, FAPEMIG, CEFET-MG.

References

[1] Fettouhi, M., Ouhahab, M., Cador, O., Boukhari, A., Mathonière, C., Kahn, O., New Metal Oxamates as Precursors of Low-Dimensional Heterobimetallics. **Inorganic Chemistry** (35),1996, p. 4937.

**Área: INO** **Inscrição: 00220**

# Indirect Detection of HO• Radical Produced by a Copper Complex under Electrolysis Conditions: Ascorbic Acid as Redox Probe

**Vitória S. Dibo (IC),[1] Dieric S. Abreu (PG),[1] Adolfo I. B. Ramos (PG),[1] Otaciro R. Nascimento (PQ),[2] Izaura C. N. Diógenes (PQ).[1*]**

**vitoriadibo@alu.ufc.br; izaura@dqoi.ufc.br**

*[1]Departamento de Química Orgânica e Inorgânica, UFC; [2]Instituto de Física de São Carlos, USP*

Palavras Chave: *Reactive Oxygen Species, Copper Complex, Electrocatalysis, Radical Generation*

## Highlights

Gold polycrystalline surfaces were spontaneously modified with a copper complex.
Oxidation reaction of ascorbic acid was used as redox probe for the detection of HO• produced by the adsorbed complex.

## Resumo/Abstract

Despite the nonexistence of free metal ions in healthy biological systems, under cellular acidosis or ischemic conditions, such ions are released and catalyze the production of HO• through Fenton or Haber-Weiss reactions. Copper compounds have been proposed as exogeneous sources of reactive oxygen species (ROS). In this work, we have used ascorbic acid (AA) as redox probe to indirectly prove the generation of ROS by $[Cu(4\text{-mbpy-Bz-SMe})_2]^{2+}$ adsorbed on gold (4-mbpy-Bz-SMe = (E)-1-(4'-methyl-[2,2'-bipyridine]-4-yl)-N-(4(methylthio)phenyl)methanimine). Using the modified gold surface as working electrode in solution containing AA, the voltammogram shows a one-electron wave centered at 0.23V whose current is dependent on the concentration of AA. Accounting that the $Cu^{II/I}$ redox wave is observed at 0.32 V, we suggest a ROS produced by the complex during the negative potential scan (0.5 to –0.1V) oxidizes AA to ascorbyl radical ($AA^{+\bullet}$) in a chemical step previous to the electrochemical one ($AA^{+\bullet} \rightarrow DAA + 1e^- + H^+$). The EPR spectrum of the electrolyzed solution (–0.2V) was acquired in the presence of DMPO and shows hyperfine splittings at $A^N$ = 15.0 and 15.2 G, consistent with the adduct OH-DMPO. We hypothesize that a dimeric copper compound formed on surface, Au/[$Cu^{I}$-O-O-$Cu^{I}$], is oxidized back to Au/[2$Cu^{II}$] during the reverse scan. In acidic and aerated medium, this oxidative step produces $H_2O_2$ which, in turn, reacts with the reduced adsorbed complex generating HO• and recovering the starting Cu(II) complex in a catalytic mechanism involving a Fenton like reaction.

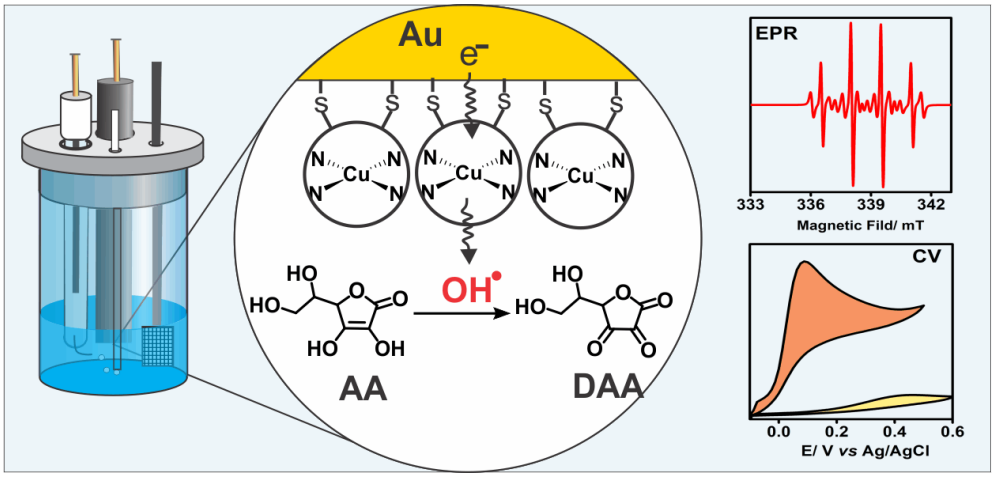


Figure 1 – Cartoon representation of the ascorbic acid oxidation by the copper complex adsorbed on gold.

**Área: INO** **Inscrição: 00276**

# Síntese e comportamento catalítico de porfirinas de Mn(III) na formação de carbonatos cíclicos utilizando $CO_2$ e epóxidos

**Jorge L. S. Milani (PQ),[2]* Alexandre M. Meireles (PG),[1] Werberson A. Bezerra (IC),[2] Dayse C. S. Martins (PQ),[1] Rafael P. Chagas (PQ),[2] Daniele Cangussu (PQ)[2]**

**alemoreira13@gmail.com; milani_jorge@yahoo.com.br**

*[1]Departamento de Química, ICEx, UFMG; [2]LABSINCO, Instituto de Química, UFG*

Palavras Chave: *Porfirinas, Carbonatos cíclicos, Dióxido de carbono, Catálise homogênea, Química verde.*

## Highlights

**Synthesis and catalytic behavior of Mn(III) porphyrins in the coupling of $CO_2$ and epoxides to cyclic carbonates.**

High active and selective new $Mn^{III}$ porphyrins were used in the chemical fixation of $CO_2$ into cyclic carbonates; Reaction behavior dependent of X axial ligand nature: chlorine provides the most active system.

## Resumo/Abstract

A reação de fixação de $CO_2$ em epóxidos, obedecendo aos princípios da química verde, tem sido uma forma promissora de obtenção de carbonatos cíclicos. Assim, as metaloporfirinas destacam-se como uma classe de catalisadores extremamente eficientes para a obtenção destes produtos, com altos rendimentos. Neste trabalho, descreve-se a obtenção de porfirinas de manganês ($Mn^{III}P$) inéditas e a avaliação da sua eficiência catalítica neste tipo de reação.

As $Mn^{III}P$ (Figura 1) foram obtidas por metodologia descrita na literatura e caracterizadas por espectroscopia UV-Vis, IV-FT, análise térmica, RMN $^1H$ (ligante porfirínico), CHN e espectrometria de massas. Os resultados (Tabela 1) são extremamente satisfatórios. O sistema desenvolvido é altamente ativo e com seletividade de 100% para o carbonato cíclico obtido a partir do óxido de estireno (SO).

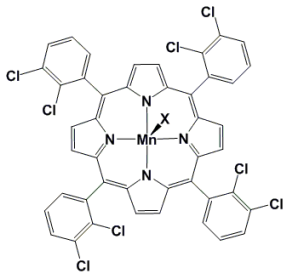

X = **$NO_3^-$**; [$Mn^{III}$T(2,3DCPP)$NO_3$] **(1)**
X = **$OAc^-$**; [$Mn^{III}$T(2,3DCPP)OAc] **(2)**
X = **$IO_3^-$**; [$Mn^{III}$T(2,3DCPP)$IO_3$] **(3)**
X = **$Br^-$**; [$Mn^{III}$T(2,3DCPP)Br] **(4)**
X = **$Cl^-$**; [$Mn^{III}$T(2,3DCPP)Cl] **(5)**
X = **$OH^-$**; [$Mn^{III}$T(2,3DCPP)OH] **(6)**

**Figura 1. C**atalisadores metaloporfirinicos estudados.

**Tabela 1.** Reações de fixação de $CO_2$ em SO, utilizando **1-6**.[a]

| Entrada | $Mn^{III}P$ | Tempo (h) | Conversão (%)[b] | TON[c] | TOF[d] |
|---|---|---|---|---|---|
| 1 | **1** | 1 | 60 | 29.940 | 29.940 |
| 2 | **1** | 5 | 97 | 48.544 | 9.709 |
| 3 | **2** | 1 | 70 | 35.211 | 35.211 |
| 4 | **2** | 5 | 100 | 50.000 | 10.000 |
| 5 | **3** | 1 | 55 | 27.624 | 27.624 |
| 6 | **3** | 5 | 93 | 46.729 | 9.346 |
| 7 | **4** | 1 | 68 | 33.784 | 33.784 |
| 8 | **4** | 5 | 98 | 49.020 | 9.804 |
| 9 | **5** | 1 | 80 | 40.000 | 40.000 |
| 10 | **5** | 5 | 100 | 50.000 | 10.000 |
| 11 | **6** | 1 | 58 | 28.902 | 28.902 |
| 12 | **6** | 5 | 96 | 48.077 | 9.615 |

[a]0,00125 mmol catalisador (0,002 mol%), 0,625 mmol TBAB (brometo de tetrabutilamônio, 1,0 mol%), SO (62,50 mmol), $P_{[CO2]}$ = 30 bar, T = 100 °C. [b] Conversões determinadas por RMN $^1H$. [c] TON = *Turnover number* ($n_{carbonato}/n_{catalisador}$). [d]TOF = *Turnover frequency* (TON $h^{-1}$).

Há uma forte dependência da ocorrência da reação com o ligante axial (X). Esse ligante, em posição *trans* ao oxigênio do epóxido, influencia diretamente a natureza da interação Mn-O(epóxido). Os catalisadores **2** e **5** apresentaram conversões de 100% em 5 horas de reação, sendo o complexo **5** (X=Cl), aquele que apresentou uma taxa de conversão inicial mais elevada (entradas 3 e 9), indicando que a troca de um ligante $OAc^-$ por $Cl^-$ aumenta a velocidade da reação. Dessa forma, os sistemas estudados são muito promissores, tendo TON e TOF comparáveis aos melhores sistemas descritos na literatura, como observado nas reações utilizando o complexo **5**. Uma otimização será feita no intuito de elevar as atividades em períodos mais curtos e em condições reacionais mais brandas.

Agradecimentos: FAPEMIG, FAPEG, CAPES, CNPq.

**Área: INO** **Inscrição: 00316**

# Energy transfer in trivalent europium diphenylphosphinate matrix associated with a β-diketone ligand

**Ana B. Lazzarini (IC)[1*], Paloma R. de Castro (IC), Luís F. B. Bim (PG)[1], Marco A. Cebim (PQ)[1]**

**bia.lazzarini@hotmail.com**

*[1]São Paulo State University (Unesp), Institute of Chemistry, Araraquara, São Paulo, Brazil, Department of General and Inorganic Chemistry, Luminescent Materials Laboratory.*

Keywords: *rare earth, energy, organic ligands, β-diketonate, photoluminescence spectroscopy.*

## Highlights

Improvement of energy transfer between diphenylphosphinate-$Eu^{3+}$ by the association with a β-diketonate ligand.

## Abstract

In recent years, the interest in coordination compounds has increased in which the aim is to maximize the so-called "antenna effect". In trivalent rare earth ($RE^{3+}$) complexes with organic ligands, the use of β-diketonates is highly targeted[1] since the $RE^{3+}$ small absorption coefficient is then compensated by both the great absorption capacity of the ligand and the efficiency of the energy transfer from this type of ligand to the cation $RE^{3+}$. In this work, we have attempted to demonstrate that the association of a β-diketonate ligand with europium diphenylphosphinate – $[Eu(dpp)_3]_n$ – can have a positive impact on the $RE^{3+}$ emission intensity, enhancing cross relaxation and allowing a more effective sensitization of trivalent rare earth ion. The preparation consisted of subjecting $[Eu(dpp)_3]_n$ – synthesized through the methodology proposed by Bim *et al.*[2] –, resuspended in ethanol, and an ethanolic solution of butylmethoxydibenzoylmethane – H*bmdm* – to reflux under constant stirring for 48 hours. From $Eu^{3+}$ $^5D_0 \rightarrow {}^7F_2$ transition in photoluminescence spectroscopy spectra[3] (Fig. 1.), it can be concluded there is only one crystallographic site type by which the trivalent rare earth ions are inserted. Moreover, considering the ratio between the integrated intensities of $^5D_0 \rightarrow {}^7F_1$ and $^5D_0 \rightarrow {}^7F_2$, it is possible to claim that those trivalent europium ions are distributed in high symmetrical sites. Therefore, further sequential experiments aim to study, analyze, and confirm the effectiveness of energy transfer in the association of $[Eu(dpp)_3]_n$ with H*bmdm*.

**Fig. 1. (a)** $[Eu(dpp)_3]_n$ excitation spectrum @ 77K with emphasis on the region between 300 and 500 nm (provided by *Bim et al.*), **(b)** $[Eu(dpp)_3]_n$ associated with H*bmdm* excitation spectrum @ room temp. with emphasis on the region between 350 and 500 nm and **(c)** $[Eu(dpp)_3]_n$ associated with H*bmdm* emission spectrum @ room temp. with selective excitations.

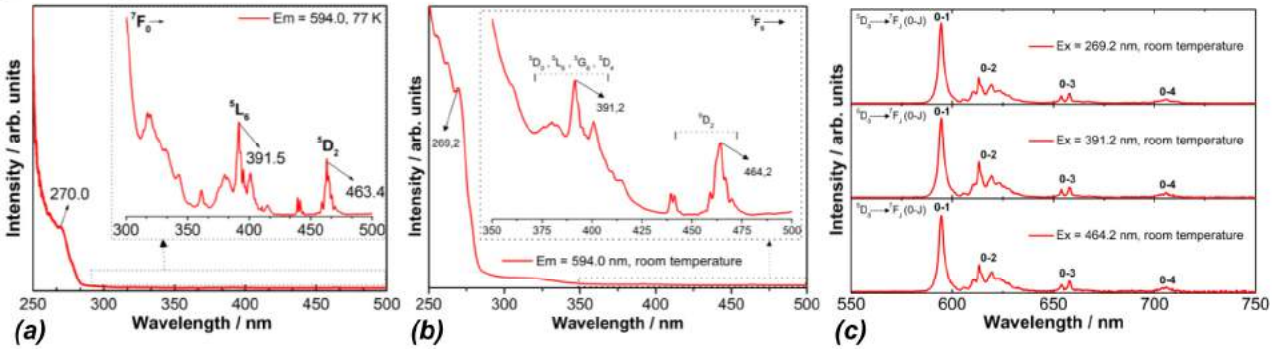


[1]RAJ, D. B. A., BIJU, S., REDDY, M. L. P.; **Dalton Trans.** (2009) 7519-7528.

[2]BIM, L. F. B., CEBIM, M. A.; STUCCHI, E. B. **A new overview on rare earth diphenylphosphinates**. In: Proceedings of the 18th International Conference on Luminescence. Internet: Aptor Software; 1 (2017) 1-484. ISBN: 978-85-63273-36-9

[3]BINNEMANS, K.; **Coordination Chemistry Reviews** 295 (2015) 1-45.

**Área: INO** **Inscrição: 00333**

# Helical Coordination Polymer from Manganese(II) 16-Metallacrown-6 Recognition of Zwitterionic L-Glutamate

**Thomaz A. Wioppiold (PG),[1] Ulrich Abram (PQ),[2] Ernesto S. Lang (PQ)[1]***

**tarrudaw@gmail.com; eslang@quimica.ufsm.br**

*[1]Laboratório de Materiais Inorgânicas, Departamento de Química, UFSM, Santa Maria/RS; [2]Freie Universität Berlin, Berlin, Germany.*

Palavras Chave: *Metallacrown, Molecular Recognition, Zwitterionic Receptor, Aroylbisthiourea, Coordination Polymer*

## Highlights

The incorporation of L-glutamate by a binuclear manganese(II) metallacrown leads to a complementary [2+2] structure. This phenomenon was investigated under x-ray diffraction and shows the formation of a helical coordination polymer influenced by the presence of $Mn^{2+}$ ions in solution.

## Abstract

The reactions between 2,5-furandicarbonylbis(*N*,*N*-diethylthiourea) ($H_2L^1$) and $Mn(OAc)_2$ in methanol gives a suspension of the neutral manganese(II) 16-Metallacrown-6 (16-$MC_{Mn}$-6) (**I**). The following treatment with an excess of L-glutamic acid results in a clear solution. Crystals were obtained by the slow evaporation of the solution in reasonable yield (> 60%) and the analysis by single crystal x-ray diffractions reveals the complementary behavior between the 16-$MC_{Mn}$-6 and the deprotonated amino acid $(Glu)^-$ in a complex with formula $\{Mn[16\text{-}MC_{Mn}\text{-}6]_2(Glu)_2\}_n$ (**II**). The manganese metallacrown act as a zwitterionic receptor[1] where one carboxylate oxygen and its vicinal ammonium group interact with one manganese(II) atom through coordinate bond and the oxygen-rich metallomacrocycle via hydrogen bonding, respectively. Two side-chain carboxylate chelates from two units coordinate to the second manganese(II) atom of the opposite unit to form a $\{[16\text{-}MC_{Mn}\text{-}6]_2(Glu)_2\}^{2-}$ structure. The charge is counterbalanced by the presence of free $Mn^{2+}$ ions coming from the original solution that also act as a linker between the [2+2] units resulting in a 1-D coordination polymer. The helical structural motif[2] (Scheme 1b) is the result of four metallacrowns screwing into the same axis (Scheme 1c). The IR spectrum of the compound **II** exhibits $\nu_{N\text{-}H}$ bands corresponding to the glutamate moiety in the region of 3200-3400 $cm^{-1}$. The full characterization of this compound is in progress, as well the assays to determine the association constant ($K_a$) and other thermodynamic parameters of the system.

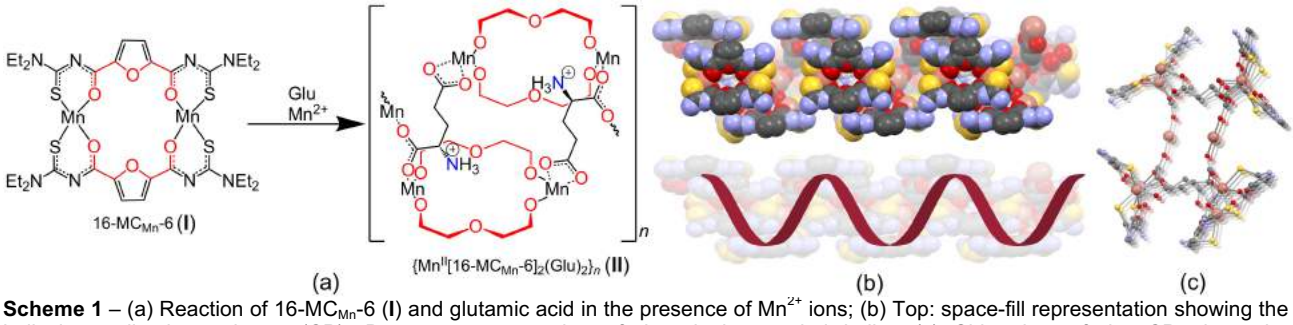


**Scheme 1** – (a) Reaction of 16-$MC_{Mn}$-6 (**I**) and glutamic acid in the presence of $Mn^{2+}$ ions; (b) Top: space-fill representation showing the helical coordination polymer (CP); Bottom: representation of the single-stranded helice (c) Side view of the CP along the crystallographic *a* axis. Color legend: carbon (dark grey), oxygen (red), nitrogen (light blue), sulfur (yellow), manganese (tea rose).

*Acknowledges*

CAPES CNPq Conselho Nacional de Desenvolvimento Científico e Tecnológico FAPERGS Fundação de Amparo à Pesquisa do Estado do Rio Grande do Sul

(1) Luis, S. V; Alfonso, I.; Galindo, F. In *Supramolecular Chemistry*; John Wiley & Sons, Ltd, 2012.
(2) Leong, W. L.; Vittal, J. J. *Chem. Rev.* **2011**, *111* (2), 688–764.

**Área: INO** **Inscrição:00370**

# Luminescent lanthanide MOFs based on ligand 4,4',4''-((benzene-1,3,5-triyltris(methylene))tris(oxy))tribenzoate ligand: syntheses, structures and photophysical properties

**Lanousse Petiote (PG),[*] Italo O. Mazali (PQ)[*] Fernando A. Sigoli[*] .**

**fsigoli@iqm.unicamp.br; lanoussepetiote@gmail.com**

[*]*Laboratory of Functional Materials- Institute of Chemistry – UNICAMP, Campinas, Brazil*

Key-words:*(Lanthanide organic frame-works, Crystal disorder, photoluminescence).*

## Highlights

Influence of crystalline structure disorder on photophysical properties of $Eu^{3+}$ containing MOF. Energy transfer process mechanism in co-doped Tb/Eu MOF.

## Resumo/Abstract

Lanthanide-containing metal–organic frameworks (LnMOFs) have been emerging as promising luminescent materials in the past few decades, such as light emitting materials and physical/chemical sensors. These hybrid materials combine the unique photophysical properties of lanthanide trivalent ions and the advantages of MOFs. Taking the advantage of the spatial regularity of the building blocks, different lanthanide ions can be inserted into a MOF aiming the white light generation or thermal optical ratiometric probes. This work reports on the photoluminescence studies, with emphasis on the relation between the crystal disorder, $Eu^{3+}$ luminescence and energy transfer processes mechanisms in the co-doped Tb/Eu of 4 isostructural LnMOFs namely LnL where L is the tricarboxylic ligand 4,4',4''-((benzene-1,3,5-triyltris(methylene))tris(oxy))tribenzoic (Figure **A**) and Ln is $Eu^{3+}$, $Gd^{3+}$, $Tb^{3+}$ or a mixture of them. The MOFs were synthesized under solvothermal conditions and characterized by single-crystal X-ray diffraction, powder X-ray diffraction, infrared spectroscopy, and photoluminescence spectroscopy. Single crystal. *P-DRX* and *FT-IR* data show that all compounds are monoclinic (space group p-1) and show a one-dimensional connected network (Figure **C**). The MOF GdL shows a broad band emission at 77K attributed to intra-ligand $\pi^* \rightarrow \pi$ transitions which disappear at room temperature (300 K). Upon ligand excitation, EuL and TbL show, in a microsecond time-scale, the typical luminescence of $Eu^{3+}$ (0.51 ms) and $Tb^{3+}$(0.88 ms) due to $^5D_0 \rightarrow {}^7F_{j=0,1,2,3,4}$ and $^5D_4 \rightarrow {}^7F_{j=6,5,4,3}$ respectively via the ligand “antenna effect” in the solid state at 77 and 300 K. Interestingly, photoluminescence spectrum of EuL (Figure **D**) shows the $^5D_0 \rightarrow {}^7F_1$ and $^5D_0 \rightarrow {}^7F_2$ transitions splitted, at least, in four and seven stark-components, respectively. Such spectroscopic features can be, possibly, attributed to the disorder in the DMF coordinated -molecules (Figure **B**).

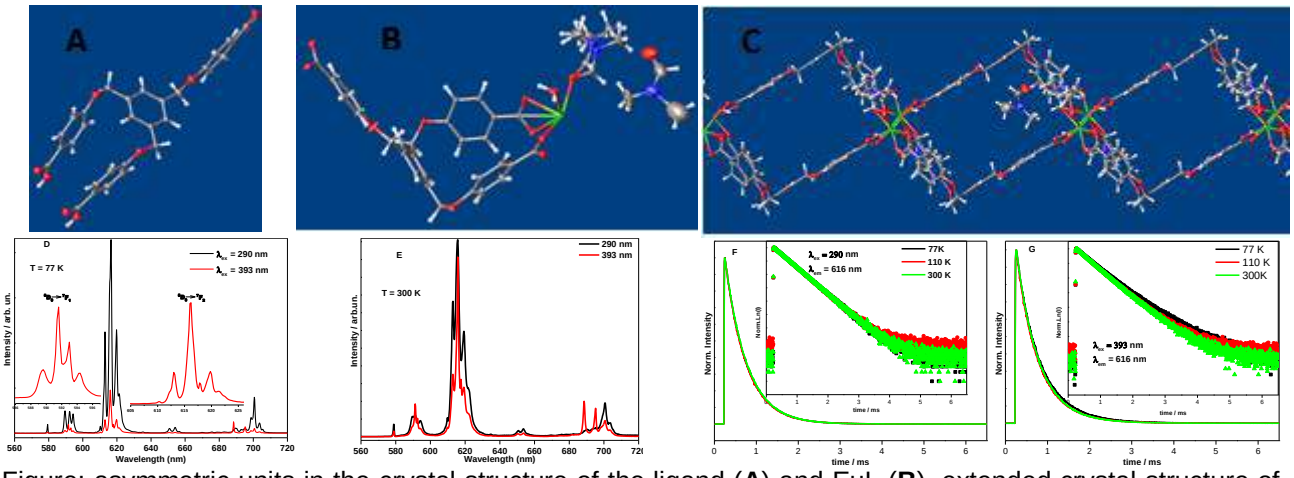


Figure: asymmetric units in the crystal structure of the ligand (**A**) and EuL (**B**), extended crystal structure of EuL (**C**), photoluminescence spectra vs $\lambda_{ex}$ (t) (**D** e **E**) and $^5D_0$ decay perfil vs t($\lambda_{ex}$) EuL (**F** e **G**).

**Área: INO** **Inscrição: 00391**

# Synthesis, characterization and antitumor activity of a 2,5-diketopiperazine copper coordination compound

**Fausthon Fred da Silva (PQ)[1]*, José F. da Silva Neto (PQ)[2], George C. Jimenez (PQ)[2], Daniela M. B. de Souza (PQ)[2], Eduardo H. L. Falcão (PQ)[3] e Severino Alves Júnior (PQ)[3]. *fausthon@quimica.ufpb.br**

*[1]Departamento de Química, UFPB; [2]Departamento de Morfologia e Fisiologia Animal, UFRPE; [3]Departamento de Química Fundamental, UFPE.*

Key words: *diketopiperazine, complex, antitumor*.

## Highlights

Diketopiperazines are precursors for biologically active molecules. The 2,5-piperazinedione-1,4-diacetic acid and its copper complex were obtained. The complex showed tumor inhibition of 63%.

## Abstract

Many cations have biological activities recognized within the human body; however, the choice of the ligand is a determining factor in the pharmacological properties of a complex. 2,5-diketopiperazines are cyclic peptides found as byproducts of protein degradation, used as models for protein studies and applied as precursors to antitumor agents. In this work, we synthesize 2,5-piperazinedione-1,4-diacetic acid ($H_2$PDA) and its copper complex. Ligand and complex were characterized by CHNS, TGA, FTIR, SEM, XRD and NMR. For the complex, spontaneous and antitumor activity assays were performed *in vivo*.

The $H_2$PDA was obtained using iminodiacetic acid via hydrothermal synthesis (Figure 1). The NMR and FTIR (Figure 2) analyzes are in agreement with the literature. The complex crystals were obtained crystals using open crystallization in water. CHNS and TGA analysis confirm the formula $[Cu(PDA)(H_2O)_{2,5}]$. The FTIR shows the carbonyl and C-O signals, displaced in relation to the ligand, indicating coordination. The stretch band O-H confirms the water in the structure. Eight Wistar rats received 66.66 mg/kg of the complex and presented a set of behavioural responses in characteristic periods of occurrence. Responses in the Central Nervous System (excitatory and depressants) and in the Autonomic Nervous System were observed. The tumor inhibition activity of the complex against the Ehrlich tumor was verified. A medium tumor volume of 7 $mm^3$, against 19 $mm^3$ for tumours of the control group (63% inhibition), were observed, however we noticed a slight increase in the rate of tumor growth.

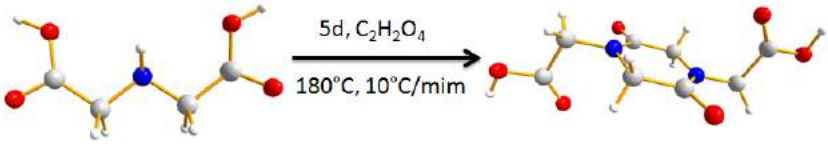


Figure 1: Synthesis of the $H_2$PDA (C=gray, H= white; O= red and N = blue).

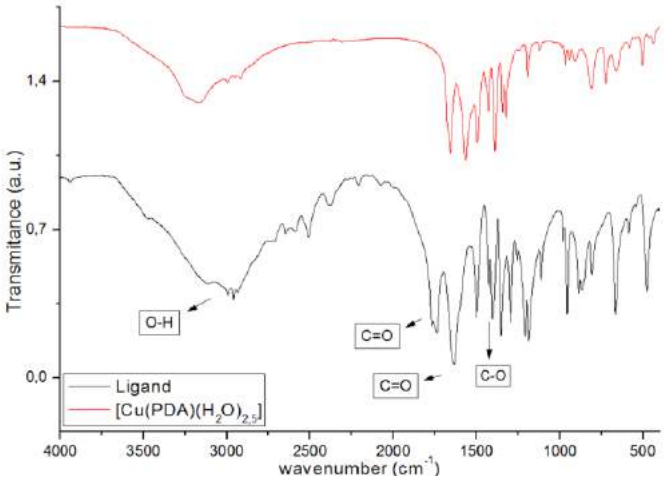


Figure 2: Infrared spectra of the ligand and the copper complex.

**Área:** INO **Inscrição:** 00406

# Particularities of trivalent europium luminescence in a pure phenylphosphinate matrix

**Gabriela L. E. Teotônio (IC)[1*], Luís F. B. Bim (PG)[1], Marco A. Cebim (PQ)[1]**

**gabrielaluciaeller@gmail.com**

[1]*São Paulo State University (Unesp), Institute of Chemistry, Araraquara, São Paulo, Brazil, Department of General and Inorganic Chemistry, Luminescent Materials Laboratory.*

Keywords: *rare earth metal, luminescence, symmetry, photoluminescence spectroscopy.*

## Highlights

Differences in the emission spectra of organophosphorylated complexes by changing the number of phenyl groups bound to the ligands.

## Abstract

Coordination compounds between trivalent rare earth cations ($RE^{3+}$) and organic ligands with high molar absorptivity, such as β-diketones and carboxylates, can generate molecular light conversion devices[1]. Curiously, there are few reports in the literature using phosphinates for this purpose. In order to overcome this gap, Stucchi's research group have been devoted for years to the study of optical and structural properties of polyphenolic complexes with $RE^{3+}$, in particular, of rare earth diphenylphosphinates – $[RE(dpp)_3]_n$ which proved to be good candidates for such application[2-5]. Similarly, the present work wishes to verify the capability of applying phenylphosphinate ligand to maximize cross relaxations between ligand-metal, resulting in high efficiency compounds for luminescence. Preparation of europium phenylphosphinate – $[Eu(mpp)_3]_n$, based on proposal of Bim and coworkers[6], was performed by direct reaction between a europium chloride and phenylphosfinic acid (H*mpp*) in a microprocessed thermostatic bath. Contrary to that reported by Abreu and coworkers[5] for $[RE(dpp)_3]_n$, photoluminescence spectroscopy of $[Eu(mpp)_3]_n$ at 298 K showed no changes in intensity of $Eu^{3+}$ hypersensitive transition $^5D_0 \rightarrow {}^7F_2$ suggesting that $Eu^{3+}$ ions are inserted in one crystallographic site (Figure 1). In addition, it is possible to infer through the ratio between $^5D_0 \rightarrow {}^7F_1$ and $^5D_0 \rightarrow {}^7F_2$ that it comes from a low symmetry site. Therefore, a slight variation in the ligand gives the coordination compound different symmetry properties. Future analysis will be carried out in order to determine the overall structure and optical properties of $[RE(mpp)_3]_n$.

***Fig. 1. (a) $[Eu(mpp)_3]_n$ excitation spectrum @ room temp. with emphasis on the region between 300 and 500 nm and (b) $[Eu(mpp)_3]_n$ emission spectrum @ room temp. with selective excitations.***

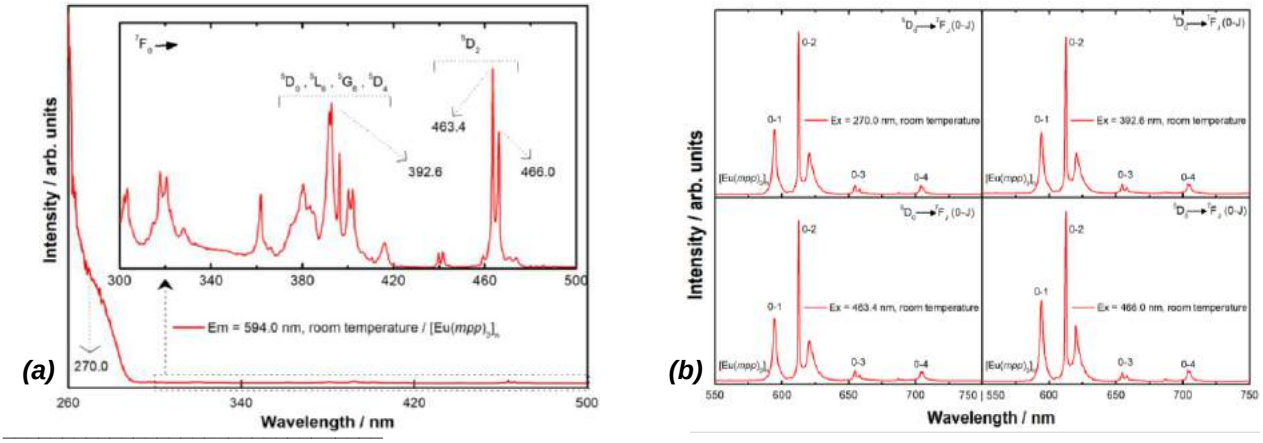


[1]ARMELAO, L. *et al.* **Coordination Chemistry Reviews** 254 (2010) 487–505.
[2]STUCCHI, E. B. *et al.* **Journal of Alloys and Compounds** 275–277 (1998) 89–92.
[3]SCARPARI, S. L.; STUCCHI, E. B. **Journal of Alloys and Compounds** 323–324 (2001) 740–742.
[4]FRANCISCO, C. S.; STUCCHI, E. B.; ABREU, E. M. **Journal of Alloys and Compounds** 418 (2006) 234–237.
[5]ABREU, E. M. *et al.* **Optical Materials** 35 (2013) 332–337.
[6]BIM, L. F. B., CEBIM, M. A.; STUCCHI, E. B. **A new overview on rare earth diphenylphosphinates**. In: Proceedings of the 18th International Conference on Luminescence. Internet: Aptor Software; 1 (2017) 1-484. ISBN: 978-85-63273-36-9

**Área: INO** **Inscrição:00455**

# Derivado de 1,3,4-oxadiazol como ligante em compostos β-dicetonados de Gadolínio.

**Maria Izabel Xavier Scapolan (IC),[1]Renata Danielle Adati (PQ),[1]*Eduard Westphal (PQ)[1]**

**izabelscapolan@gmail.com, renataadati@utfpr.edu.br**

*[1]Departamento Acadêmico de Química e Biologia, UTFPR.*

Palavras Chave: *Lantanídeos, 1,3,4-oxadiazol, β-dicetona, Composto de coordenação.*

## Highlights

1,3,4-oxadiazole derivative as ligand in β-diketonate gadolinium compounds. Due to its chelating capability and high UV-visabsorbance coefficient, a 1,3,4-oxadiazole + pyridine bidentate ligand was employed to synthesize a new lanthanide coordination compound.

## Resumo/Abstract

Complexos β-dicetonados de lantanídeos são amplamente investigados pois apresentam espectros de emissão com linhas finas e definidas. Transições eletrônicas de alguns lantanídeos podem apresentar intensa luminescência quando coordenado a ligantes que atuam como antenas, mecanismo conhecido como efeito antena [1]. Neste trabalho, tem-se por objetivo a síntese e caracterização de um novo composto de coordenação β-dicetonado contendo ligante derivado do heterociclo 1,3,4-oxadiazol. Para a síntese do composto, foi utilizada proporção estequiométrica de 1:3:1 de $GdCl_3$:tta:o-OXD (tta=2-tenoiltrifluoroacetona; o-OXD=2-(4-metoxi)fenil-5-(2-piridil)-1,3,4-oxadiazol); a solução aquosa contendo o metal foi adicionada lentamente à solução etanólica dos ligantes, previamente desprotonados por $NaOH_{(aq)}$(1 $mol.L^{-1}$). A mistura foi mantida sob agitação a ~65°C por 3h em atmosfera inerte. Ao final da reação e evaporação do solvente observou-se formação de uma cera alaranjada, a qual foi lavada com etanol e uma mistura de clorofórmio e éter de petróleo (1:2). O indício de sucesso da síntese do composto de coordenação pode ser confirmada por resultados dos espectros de infravermelho apresentados na Figura 1. O desaparecimento da banda em 1656,0 $cm^{-1}$ referente ao estiramento $\nu_{as}$(C=O) da β-dicetona indica a formação de quelato. A banda em 1537,9 $cm^{-1}$, atribuída à estiramentos $\nu_{as,s}$(C=N),também deslocada no espectro do complexo, é característica da coordenação por este grupo funcional. Na Figura 2 os deslocamentos dos máximos de absorção (UV-Vis) evidenciam mudanças no ambiente químico e sugerem a coordenação dos ligantes o-OXD e tta. Análises para a determinação estrutural do composto de coordenação estão em andamento.

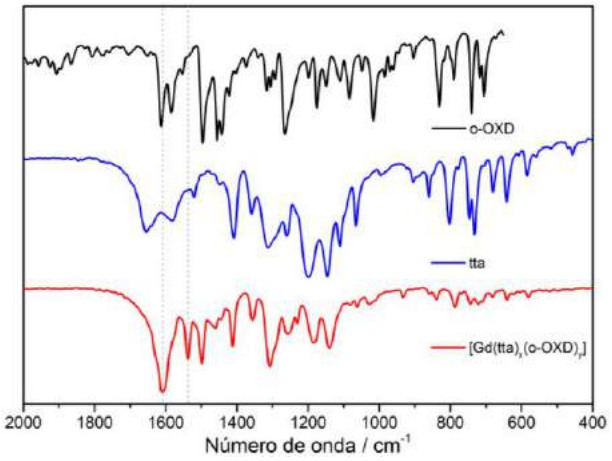


Figura 1: Espectros vibracionais na região do infravermelho dos ligantes o-OXD, tta e composto de coordenação.

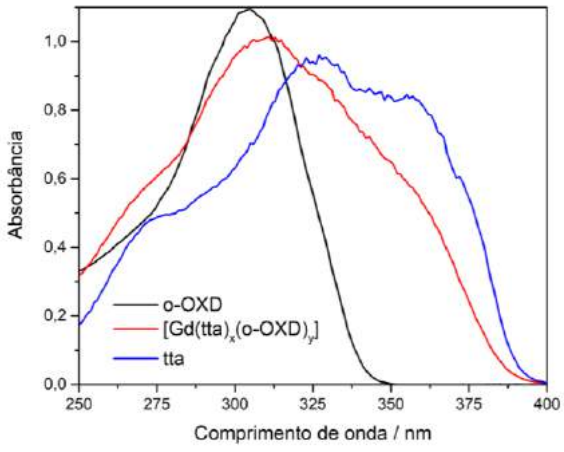


Figura 2: Espectros de absorção na região do UV-Vis dos ligantes o-OXD, tta e composto de coordenação.

[1] BINNEMANS, K. Rare-Earths beta-diketonates. In: _____ . GSCHMEIDNER, K. Jr.; BÜNZLI, J-C. G.; PECHARSKY, V. K. Handbook on the physics and chemistry of Rare Earths. Amsterdan: Elsevier, 2005. v. 35, cap. 225, p. 111-272.

**Área: INO** **Inscrição: 00464**

# Chemosensor based on HABA for detection of $F^-$, $CH_3COO^-$ and $PO_4^{3-}$ anions

**Caio H. dos Santos(IC)[1], Izilda A. Bagatin (PQ).[1]***

**ibagatin@gmail.com**

*[1]Departamento de Química, Laboratório de Química de Calixarenos, Espectroscopia Molecular e Catálise, ICAQF-UNIFESP, rua Arthur Riedel, 275, Diadema, Brasil, CEP 09972-270.*

Palavras Chave:*(sensor, phosphate, acetate, fluoride, 2-(4-hydroxiazobenzene)benzoic acid, selectivity).*

## Highlights

The limits of detection (LOD) of HABA for $F^-$, $CH_3COO^-$ and $PO_4^{3-}$anions were 2.5 x $10^{-7}$, 4.7 x $10^{-8}$, and 5.8 x $10^{-7}$ mol $dm^{-3}$.
HABA has better selectivity for detecting of $PO_4^{3-}$ even in the presence of interfering ions.

## Resumo/Abstract

Chelating systems selective and sensitive to ions are the goal of this work. Developing receptors capable of interacting with anions is a huge challenge, especially those using hydrogen bonds to interact with the analytes. The 2-(4-hydroxiazobenzene)benzoic acid (HABA) has two hydrogens groups available for interaction; one is the azo group and the other is the carboxylic acid group, enabling interaction with cations and anions. Several titrations of chromophore 2-(4-hydroxiazobenzene)benzoic acid were performed with cations ($Mg^{2+}$, $Hg^{2+}$, $Pb^{2+}$) and anions ($Cl^-$, $F^-$, $H_2PO_4^{2-}$, $CH_3COO^-$, $Cr_2O_7^{2-}$). However, only the interactions with fluoride, acetate, and phosphate were significant, showing the sensitivity of the ligand HABA by these anions, characterized by the displacement of the absorbance bands at 372 nm to 491 nm. The binding constants found to acetate, fluoride, and phosphate were 1.91 x $10^4$, 1.30 x $10^4$, and 1.28 x $10^4$ $mol^{-1}$ $dm^3$ respectively. $^1$H-NMR titrations confirmed binding constants similar to those of UV-vis, besides showing evidence of the analyte binding by the hydrogen of the carboxylic acid. The interaction has a 1:1 stoichiometry confirmed by the "Job´s plot."

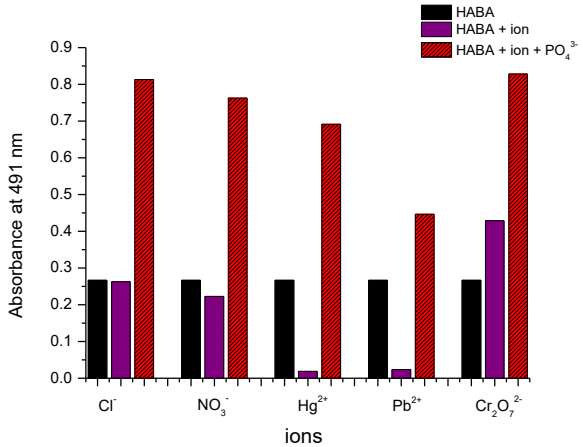


Figure 1 - Absorbance intensity of HABA (1 x $10^{-5}$ mol $dm^{-3}$) in the presence of interferent ions (10 equivalents).

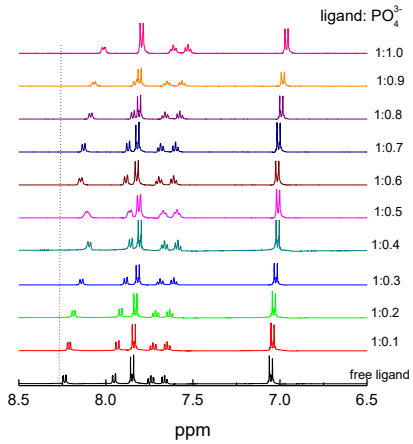


Figure 2 - Titration on $^1$H NMR of HABA with $PO_4^{3-}$ anion at 1 x $10^{-2}$ mol $dm^{-3}$.

**Área: INO** **Inscrição: 00573**

# Ruthenium(II) terpyridine complexes containing heteroaryl-2-imidazole ligands featuring catalytic activity for water oxidation

**Luis E.S.C. Huamaní (PG),[1]* Renan B. Guerra (PG),[1] Naheed Bibi (PG),[1] André L.B. Formiga (PQ).[1]**

**lsantacruzh@gmail.com**

*[1]Departament of Inorganic Chemistry, Institute of Chemistry – UNICAMP, P.O. Box 6154, 13083-970 Campinas, SP, Brazil*

Keywords: *Water splitting, Solar energy, Overpotential, Water oxidation catalysts, Ruthenium polypyridyl complexes, Ruthenium terpyridine aquo complexes.*

## Highlights

Herein, we changed the heteroaryl moiety of the ruthenium(II) terpyridine aquo complexes and studied the water oxidation-catalytic performance influenced by the heteroaryl-2-imidazole ligands.

## Abstract

Water splitting into $O_2$ and $H_2$ by using solar energy is a clean alternative to fossil fuels to supply the world energetic demands. Water oxidation ($2H_2O \rightarrow O_2 + 4H^+ + 4e^-$) is the most challenging step because it requires the use of overpotentials to obtain a good performance and is kinetically unfavorable as it implies proton-electron transfer steps, so water oxidation catalysts (WOC) have been developed to deal with these challenges. Among several WOC, ruthenium polypyridyl complexes have been widely studied as they meet the requirements needed for high-efficient water oxidation.[1] In this work, two new ruthenium(II) terpyridine aquo complexes $[Ru(OH_2)(Himpy)(tpy)]^{2+}$ **(1)**, and $[Ru(OH_2)(Himpa)(tpy)]^{2+}$ **(2)** have been synthesized and well characterized by UV-vis, $^1$H-NMR, and ESI-MS. Electrochemical measurements were performed to know the influence of σ-donor/π-acceptor properties of heteroaryl-2-imidazole ligands on water oxidation-catalytic performance.

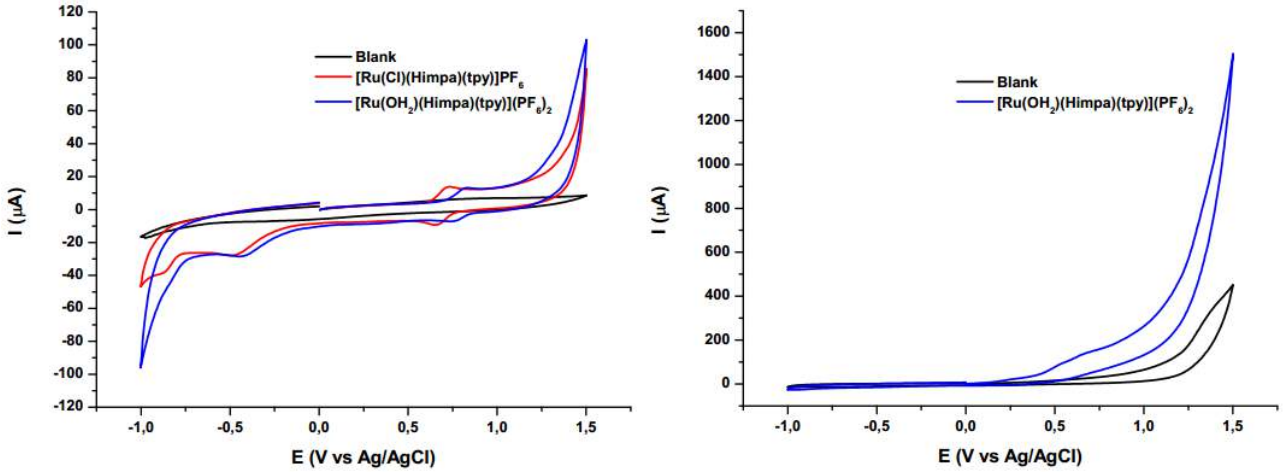


**Figure 1:** CV of complexes $[Ru(OH_2)(Himpa)(tpy)]^{2+}$ and $[RuCl(Himpa)(tpy)]^+$ in pH 1 $H_2SO_{4\,(aq)}$:acetone 4:1 (left) and pH 13 after adding NaOH (right). Working electrode - glassy carbon, scan rate – 0.1 V $s^{-1}$.

1. Duan, L.; Bozoglian, F.; Mandal, S.; Stewart, B.; Privalov, T.; Llobet, A.; Sun, L.; *Nature Chem.* **2012**, *4*, 418.

We would like to thank financial support from Fundação de Amparo à Pesquisa do Estado de São Paulo (FAPESP), Coordenação de Aperfeiçoamento de Pessoal de Nível Superior (CAPES) and Conselho Nacional de Desenvolvimento Científico e Tecnológico (CNPq).

**Área: INO** **Inscrição: 00576**

# Chemical fixation of carbon dioxide to cyclic carbonates catalyzed by zinc(II) complexes bearing 1,2-disubstituted-benzimidazole ligands

**Rafael Pavão das Chagas (PQ),* Jorge Luiz Sônego Milani (PQ), Danielle Cangussu (PQ), Gabriel Amorim Vilela (IC), Werberson de Almeida Bezerra (IC).**

**rafael.pchagas@gmail.com**

*LABSINCO – Laboratório de Síntese e Catálise Organometálica, Instituto de Química, Universidade Federal de Goiás.*

Keywords: *Carbon dioxide; Cyclic carbonate; Zinc complexes; Benzimidazole; Cycloaddition; Homogeneous catalysis.*

## Highlights

- Simple synthetic routes to the ligands and complexes.
- Efficient solvent-free catalytic system for the cycloaddition of diverse epoxides with $CO_2$.
- Low catalyst and cocatalyst loads.

## Resumo/Abstract

The cycloaddition reaction of carbon dioxide and epoxides to produce cyclic carbonates is an attractive transformation, since it uses $CO_2$ – an inexhaustible, cheap, nontoxic and non-flammable green source of carbon. Moreover, the high levels of $CO_2$ in the atmosphere due to anthropogenic emissions impel the chemistry community to seek ways to utilize $CO_2$ as a feedstock.

We report here a simple and inexpensive procedure to synthesize 1,2-disubstituted benzimidazole ligands and their utilization to readily produce and isolate four zinc(II) complexes of formula $[ZnCl_2(L)_2]$ (Figure 1) characterized by $^1H$ and $^{13}C$ NMR, elemental analysis, IR, ESI-HRMS and two of them had their structures determined by single-crystal X-ray diffraction.

The complexes were evaluated as catalysts for the coupling reaction between $CO_2$ and propylene oxide (PO) or styrene oxide (SO), under solvent-free conditions, showing high selectivity to cyclic carbonates (> 99%) and good catalytic activity. Selected results are showed in Table 1.

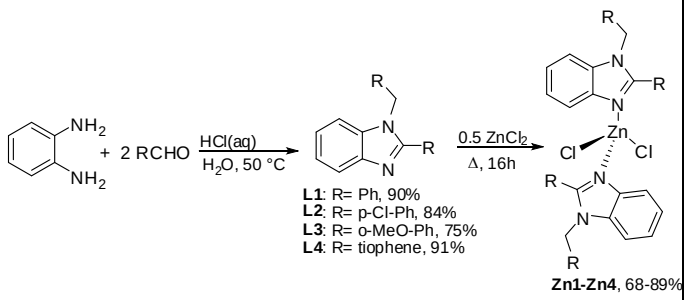


**Figure 1.** Synthesis of ligands and complexes **Zn1-Zn4**.

**Table 1.** $CO_2$ cycloaddition reaction using **Zn1-Zn4**.[a]

| Ent. | Cat. | T (°C) | t (h) | Conv. (%)[b] | TON[c] | TOF[d] |
|---|---|---|---|---|---|---|
| 1 | **Zn1** | 100 | 6 | 65 | 1623 | 270,56 |
| 2 | **Zn2** | 100 | 6 | 44 | 1106 | 184,37 |
| 3 | **Zn3** | 100 | 6 | 45 | 1136 | 189,39 |
| 4 | **Zn4** | 100 | 6 | 60 | 1488 | 248,02 |
| 5 | **Zn4** | 100 | **24** | 94 | 2358 | 98,27 |
| 6 | **Zn4** | 100 | **48** | 60 | 2994 | 62,38 |
| 7 | **Zn4** | **60** | 6 | 13 | 330 | 55,04 |
| 8 | **Zn4** | **80** | 6 | 37 | 936 | 156,05 |
| 9 | **Zn4** | **120** | 6 | 85 | 2119 | 353,11 |
| 10 | **Zn4** | **150** | 6 | 93 | 2315 | 385,80 |
| 11[e] | **Zn1** | 100 | 16 | 71 | 1773 | 110,82 |
| 12[e] | **Zn2** | 100 | 16 | 96 | 2404 | 150,24 |
| 13[e] | **Zn3** | 100 | 16 | 94 | 2358 | 147,41 |
| 14[e] | **Zn4** | 100 | 16 | 80 | 2000 | 125,00 |

[a] Reaction parameters: cat:cocat:PO = 1:1:2500, cat. (0.04 mol%), cocat. = TBAB (0.04 mol%); [b] Conversions determined on basis of $^1H$ NMR analysis; [c] mol of carbonate produced·mol(**1**)$^{-1}$; [d] TON·h$^{-1}$; [e] Reactions with SO.

A series of parameters were evaluated in the catalytic system, such as temperature, time, $CO_2$ pressure and type and amount of catalyst and cocatalyst. Complex **Zn4** was tested in the cycloaddition of $CO_2$ with seven different epoxides, under the standard conditions. Except for cyclohexene oxide, all epoxides were converted to their corresponding cyclic carbonates with good catalytic activity. Conversions were up to 100%, as for the epoxide glycidol.

Besides the simplicity of the synthetic methods to the ligand and to the complex, the benefit of our system, compared to other binary systems, is that we used lower catalyst and cocatalyst loads (up to fiftyfold less amount). Considering that the cost of the cocatalyst may have a deep impact in the whole process, we believe the utilization of smaller amounts of the base is a great advantage of our work.

**Acknowledgments:** FAPEG, CAPES, PPGQ/IQ/UFG.

**Reference:** J. L. S. Milani, I. S. Oliveira, P. A. Dos Santos, A. K. S. M. Valdo, F. T. Martins, D. Cangussu, R. P. das Chagas, *Chin. J. Catal.*, **2018** (*in press*), DOI: 10.1016/S1872-2067(17)62992-9.

**Área: INO** **Inscrição: 00592**

# Propriedades fotoluminescentes do $CeO_2$ dopado com Cobalto

**Mariana S. Tavares (IC), Glaucio B. Ferreira (PQ), José M. Siqueira Júnior (PQ)***

**marianat@id.uff.br; jmsiqueirajunior@id.uff.br**

*Departamento de Química Inorgânica, Instituto de Química, Universidade Federal Fluminense*

Palavras Chave: *Ceria, Photoluminescence, Chromaticity*

## Highlights

Photoluminescent properties of Cobalt doped $CeO_2$. This paper describes the photoluminescence and chromaticity study of $CeO_2$ doped with Cobalt using starch and precipitation with ammonia, which showed a correlation between emission wavelength and oxygen vacancy.

## Resumo/Abstract

Óxido de Cério (IV) ou céria nanoparticulada tem a estrutura da fluorita, em que os Oxigênios são situados ao longo de um mesmo plano, o que lhe confere uma alta mobilidade de Oxigênio na sua rede cristalina. A capacidade da céria de desenvolver prontamente vacâncias de Oxigênio é a chave para a sua eficácia como uma matriz dopante[1]. O Óxido de Cério (IV) tem desempenhado um importante papel na catálise[2]. Estudos anteriores estruturais[3] e espectroscópicos[4] mostraram a versatilidade do $CeO_2$ dopado com Cobalto.

O objetivo do trabalho foi realizar o estudo de fotoluminescência e cromaticidade (figuras 1 e 2, respectivamente) da fase do $CeO_2$ dopado com diferentes teores de Cobalto ($Ce_{1-x}Co_xO_{2-\delta}$, com x variando de 0,00-0,10) o qual foi sintetizado pelo método de precipitação em amônia.

Na figura 1, observam-se pequenos deslocamentos e alterações de intensidade do espectro de emissão no visível com relação ao Óxido de Cério não dopado. No diagrama de cromaticidade (figura 2), constatam-se variações de emissões. Ambos os resultados podem estar relacionados devido à transição eletrônica dos níveis de energia com defeitos da banda Ce 4f para banda O 2p, o que estão associados às deformações na superfície relativas ao aumento de vacâncias de Oxigênio[5].

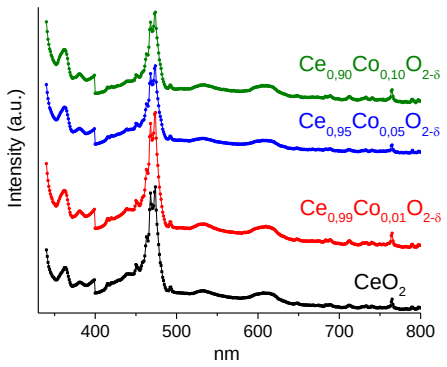


**Figura 1.** Espectro de fotoluminescência das amostras de Óxido de Cério dopado com Cobalto.

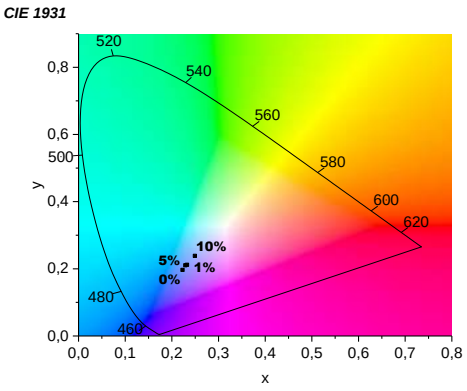


**Figura 2.** Diagrama de cromaticidade das amostras de Oxido de Cério dopado com Cobalto.

Os resultados obtidos indicam que a incorporação parcial dos metais de transição no retículo do $CeO_2$ está ligado ao aumento de vacâncias de oxigênio, o que está relacionado aos defeitos estruturais que são compensados, gerando uma transformação de Ce (IV) para Ce (III).

[1] TROVARELLI, A. Catalytic Properties of Ceria and $CeO_2$-Containing Materials. *Catalysis Reviews*, v. 38, p. 439–520, 1996.
[2] CHATTOPADHYAY, J.; SON, J.E.; PAK, D. Preparation and characterizations of Ni-alumina, Ni-ceria and Ni-alumina/ceria catalysts and their performance in biomass pyrolysis. *Korean Journal of Chemical Engineering*, v. 28, p. 1677–1683, 2011.
[3] TAVARES, M., VAZ, M., Ferreira, G., SIQUEIRA JR, J. Análise Microestrutural do $CeO_2$ Dopado com Cobalto. *23ª Reunião da Associação Brasileira de Cristalografia*, Vitória-ES, 2017.
[4] TAVARES, M., VAZ, M., Ferreira, G., SIQUEIRA JR, J. Estudo Estudo Estrutural da $CeO_2$ Dopada com Cobalto. *39ª Reunião Anual da Sociedade Brasileira de Química*, Goiânia-GO, 2016.
[5] WANG, G.; MU, Q.; CHEN, T.; WUANG, Y. TROVARELLI, A. Synthesis, characterization and photoluminescence of CeO2 nanoparticles by a facile method at room temperature. *Journal of Alloys and Compounds,* v. 493, p. 202-207, 2010.

**Área: INO** **Inscrição:00611**

# Amphiphilic complexes of terbium(III) and gadolinium(III) nanostructured micelles: synthesis, cytotoxic and apoptotic activities in tumor cells and MRI applications

**Simone R. Silva(PQ)[1], Arshad Islam(PG)[2], Érica C. Duarte(IC)[3], Dalton Dittz(PQ), Luiz A. Colnago(PQ)[5], Fernando F. Paiva(PQ)[6], Miriam T. P. Lopes(PQ)[4], Frédéric Frézard(PQ)[2], Cynthia Demicheli(PQ)[3]**

**simone.rodrigues@ufrr.br; arshad.cgl@gmail.com**

*[1]Departamento de química da Universidade Federal de Roraima, [2]Departamento de Fisiologia e Biofísica, Instituto de Ciências Biológicas da Universidade Federal de Minas Gerais, [3]Departamento de Química, Instituto de Ciências Exatas da Universidade Federal de Minas Gerais, [4]Departmento de Farmacologia, Instituto de Ciências Biológicas da Universidade Federal de Minas Gerais, [5]Embrapa Instrumentação, Empresa Brasileira de Pesquisa Agropecuária de São Carlos, SP, [6]Instituto de Física de São Carlos, Universidade de São Paulo.*

Palavras Chave: *Complexes, Micelles, Antitumor, N-alkyl-N-methylglucamine, MRI Applications, Theranostics*

## Highlights

Gd(III) nanostructured micelles and amphiphilic complexes of Tb(III) were obtained and evaluated for their cytotoxicity against metastatic melanoma B16F10 cell line and murine fibroblasts L292. The complexes were of $[Ln(L)_2]$ type, where Ln= Tb(III) or Gd(III), and L represents a ligand of the N-alkyl-N-methylglucamine surfactants including N-octanoyl-N-methylglucamine (L8), N-decanoyl-N-methylglucamine (L10) and N-dodecanoyl-N-methylglucamine (L12). The morphological characteristics of $Tb(L12)_2$ were determined by transmission electron microscopy. In aqueous solution, Gd(III) complexes self-aggregate, forming nanostructured micelles. Tb(III) complexes were found to have antitumor potential, with $Tb(L8)_2$ being the most efficient and less cytotoxic towards murine fibroblasts when compared to Gd(III) nanostructured micelles and Cisplatin. Analysis of the pro-apoptotic potential of $Tb(L8)_2$ complex and the ligand (L8) in supernatants of B16F10 cultures, by quantifying the cellular DNA using flow cytometry with propidium iodide, exhibited several fold increase in sub-diploid DNA compared to the control. The relaxivity of the $Gd(L8)_2$ and $Gd(L10)_2$ complexes did not show any significant change when measured at concentrations below and above the critical micelle concentration. T1-weighted images of Gd(III) nanostructured micelles showed a greater MRI contrast potential than the commercial contrast agent Gd-DTPA.

## Resumo/Abstract

Cationic amphiphilic complexes of Tb(III) and nanostructured micelles of Gd(III) with ligands of the N-alkyl-N-methylglucamine surfactant series were synthesized with a stoichiometric ratio 1:2 metal:ligands.

These complexes were found to form nanostructured micelles in aqueous solution and the morphological aspect of $Tb(L12)_2$ was accessed by transmission electron microscopy, showing the formation of nanoclusters in aqueous solution.

The Gd(III) micelles demonstrated improvement in the contrast of T1-weighted images, when compared to the commercial contrast agent Gd-DTPA (Magnevist®). The $Gd(L8)_2$ and $Gd(L10)_2$ micelles were found to have similar relaxivity values below and above the CMC, suggesting that their potential as CAs is independent of the concentration used. Considering the growth inhibition of cancerous cells, $Tb(L8)_2$ and $Gd(L12)_2$, among other complexes were the most active against metastatic melanoma cell line B16F10. Flow cytometry analysis showed that $Tb(L8)_2$ complex (the most selective among others) induced apoptosis at a concentration of 100 µM after 48 h and 1 µM after 72 h of treatment. This work establishes that this type of complexes have potential as anticancer agents and deserves to be investigated further. On the other hand, Gd(III) nanostructured micelles were shown to have potential as theranostic agents.

As a future perspective, the Gd(III) nanostructured micelles could be functionalized with a cancer specific ligand and utilized as a promising approach to selective drug delivery. Another possible application is to create an MRI dual modality agent, exploring the association of Gd(III) nanostructured micelles with fluorescent probes. This could improve the diagnostic efficacy by using magnetic resonance and a complementary technique such as positron emission tomography (PET) scan.

**Área: INO** **Inscrição: 00618**

# Titanium Films by Sol-Gel Process Doped $Yb^{3+}$ and $Er^{3+}$: thermal treatment effect

**Danielle C. Baldini (PG),* Emerson Henrique de Faria (PQ), Katia Jorge Ciuffi (PQ), Lucas Alonso Rocha (PQ), Eduardo José Nassar (PQ)***

**daniellecbaldini@hotmail.com; eduardo.nassar@unifran.edu.br**

*Universidade de Franca, Av. Dr. Armando Salles Oliveira, 201, Pq. Universitário, Franca/SP, CEP 14404-600, Brazil.*

Palavras Chave: *solar cell; spin-coating; luminescence;upconversion*

## Highlights

Titanium films deposited by spin-coating technique and sol-gel process presented transparency above 80%. The study showed the influence of the thermal treatment on the emission of the $Er^{3+}$ ion.

## Resumo/Abstract

The search for clean and renewable energy sources has been constantly studied to reduce environmental damage caused by energy generation. Solar radiation is a reality to generation of the electric energy, but part this energy is not used to produce electricity. This work aims to study the preparation of thin films based on titanium doped with $Yb^{3+}$ and $Er^{3+}$, the spin-coating technique was used setting the parameters; rotation at 3000rpm, volume alkoxide doped with lanthanide ions 50µL, acceleration and deceleration ramps 10 seconds, and the maximum rotation for 30 seconds. The study relates two thermal treatments in order to promote the upconversion mechanism, so in the one the films were submitted at 500ºC for 4h between the depositions and in the another, first all the depositions were carried out and to finalize the heat treatment in the conditions. The films without thermal treatment presented about 72% transparency from 350nm, after thermal treatment 83%. The X-rays diffraction showed begin crystallization of the $TiO_2$ (JCPDS#23-1446). The emission spectra of the films excited at 980nm showed the emission characteristic of the $Er^{3+}$ ion in the regions green (542nm) and red (660nm), corresponding to the transitions $^4S_{3/2} \rightarrow {}^4I_{15/2}$ and $^4F_{9/2} \rightarrow {}^4I_{15/2}$, respectively. The emission intensity is a function of the laser power, as shown in Figure 1a. However, the thermal treatment between depositions promoted decrease of the emission intensity, figure 1b.

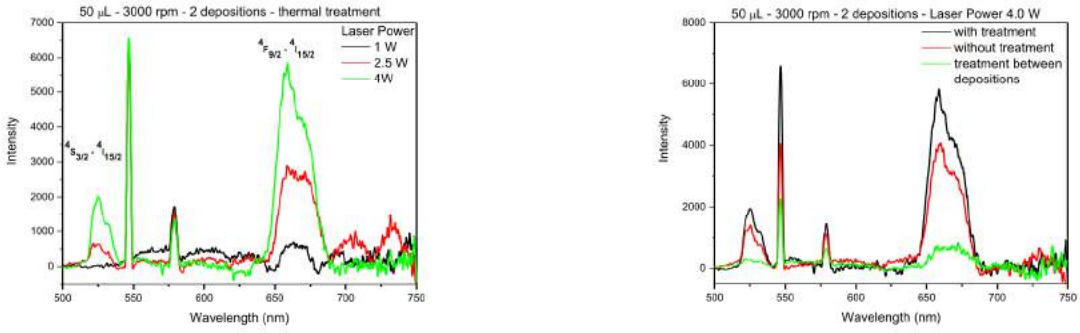


a b

**Figure 1:** Film emission spectrum Ti:$Yb^{3+}$,$Er^{3+}$. a) Laser power variation; b) different thermal treatments.

**Área: INO** **Inscrição: 00625**

# Oxidação de cicloexano por PhIO ou $PhI(OAc)_2$ em solventes da Química Verde catalisada por uma Mn-porfirina

**Rodrigo Oliveira Malheiros*** **(IC), Adriano S. Guimarães (PG), Alexandre Moreira Meireles (PG), Ana Luísa Almeida Lage (PG), Gilson de Freitas Silva (PQ)**

**roolimal@ufmg.com; gilson.freitas@gmail.com**

*Departamento de Química, Instituto de Ciências Exatas, Universidade Federal de Minas Gerais.*

Palavras Chave: *Porfirina de Manganês, Catalisador biomimético, Química verde, Oxidação de cicloexano*

## Highlights

Cyclohexane oxidation by PhIO or $PhI(OAc)_2$ in Green Chemistry solvents catalysed by an Mn-porphyrin. Dimethyl carbonate and ethyl acetate are good solvents for the cyclohexane oxidation catalyzed by Mn-porphyrins.

## Resumo/Abstract

Metaloporfirinas são conhecidas por seu uso como catalisadores em reações de oxidação de substratos orgânicos na presença de diferentes oxidantes. Esses catalisadores são importantes para a área de química verde devido à sua baixa toxicidade e à aplicação na oxidação de diferentes substratos orgânicos sob condições brandas, com possibilidade de uso de solventes verdes, incluindo água. Neste trabalho, realizou-se um estudo da oxidação de cicloexano catalisada pela metaloporfirina [$Mn^{III}$(T2PyP)Cl] (**MnP**) (Figura 1), obtida a partir da metodologia descrita na literatura. As reações foram realizadas nos solventes verdes carbonato de dimetila (DMC) e acetato de etila (EtOAc), utilizando-se iodosilbenzeno (PhIO) e iodobenzeno diacetato ($PhI(OAc)_2$) como oxidantes.

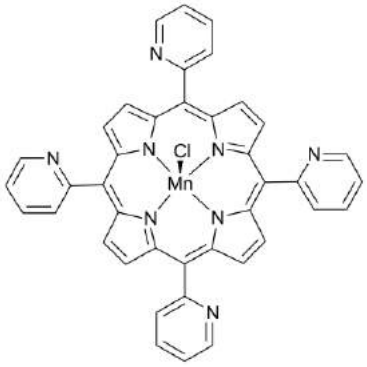


**Figura 1:** Estrutura da metaloporfirina [$Mn^{III}$(T2PyP)Cl].

**Tabela 1:** Rendimento dos produtos de oxidação do cicloexano por $PhI(OAc)_2$ ou PhIO, catalisada por [$Mn^{III}$(T2PyP)Cl], em DMC ou EtOAc e meio aeróbio.

| Oxidante | Solvente | ONA (%) | OL (%) | Sel. (%) | DES (%) |
|---|---|---|---|---|---|
| **PhIO** | DMC | 9 | 18 | 67 | 80 |
| | EtOAc | 11 | 15 | 58 | 91 |
| **$PhI(OAc)_2$** | DMC | 10 | 17 | 63 | 89 |
| | EtOAc | 11 | 21 | 66 | 100 |

Condições de reação: 25 °C, relação de quantidade de matéria MnP:oxidante:ciclo-hexano = 1:10:4650. ONA = rendimento de cicloexanona; OL = rendimento de cicloexanol; DES = destruição da MnP. SEL. [= 100 × rendimento cicloexanol / (rendimento cicloexanol + rendimento cicloexanona)].

As reações realizadas em DMC ou EtOAc como solventes levaram a rendimentos semelhantes para os produtos ONA e OL, independente do oxidante utilizado. Dessa forma, sugere-se que a mesma espécie ativa de alta valência ($Mn^{V}$=O) esteja sendo formada para ambos os oxidantes.

O maior grau de destruição do catalisador foi verificado nos sistemas usando $PhI(OAc)_2$, isso deve ocorrer porque esse oxidante é mais solúvel e gera diferentes espécies no meio de reação, as quais favorecem a oxidação do macrociclo. Por outro lado, o $PhI(OAc)_2$ é estável e disponível comercialmente, o que o torna mais atrativo considerando-se os princípios da Química Verde.

Finalmente, pode-se afirmar que a oxidação de cicloexano em solventes verdes é viável, permitindo a substituição dos solventes organoclorados geralmente usados nesses processos.

Agradecimentos: FAPEMIG, CAPES, CNPq.

**Área: INO Inscrição: 00729**

# Synthesis, chemical characterization and DNA interaction study of a new valproate zinc (II) ternary complex

**Paulo R. dos Santos (PG)[1]; Franco Smiderle(IC)[1]; Davi F. Back (PQ)[2]; Claus Tröger Pich (PQ)[3]; Sidnei Moura (PQ)[1].**

**prsantos.quimica@gmail.com**

*[1]Instituto de Biotecnologia, UCS; [2]Departamento de Química, UFSM, [3]Departamento de Biotecnologia, UFSC;.*

*Key words: Zinc (II);anticonvulsant prototype; DNA interaction.*

## Highlights

New ternary complex with valproate, zinc and nicotinamide as an anticonvulsant prototype. Interaction analyzes of the ternary complex of zinc with DNA *in vitro* show the low genotoxic activity.

## Abstract

Valproic acid (Valp) is an antiepileptic drug (AED) that has the broad spectrum across all types of seizures and epileptic syndromes. Some metal ions like zinc has been frequently incorporated into pharmaceuticals for therapeutic or diagnostic purposes and research. Zinc(II) complexes are stabilized with N-donor ligands. In this context, nicotinamide (Nic) is an important biological N-donor ligand present in metabolic process of mammalian organisms. Furthermore, that molecule has been shown to exert a number of anti-inflammatory and redox properties. In this way, was synthetized a new ternary complex with zinc and nicotinamide (complex **2**) as a new anticonvulsant prototype.

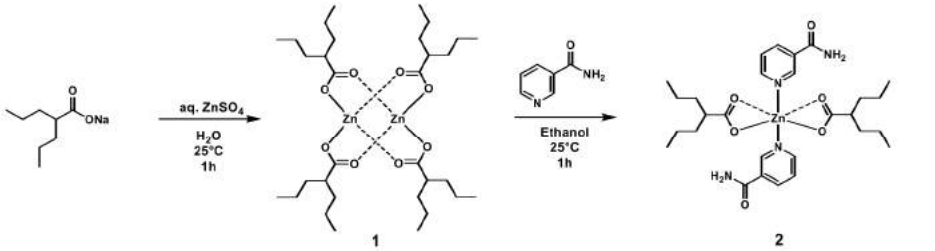


Figure 1. Synthesis of ternary complex with valproate, nicotinamide and Zinc(II).

$^{1}$HNMR and $^{13}$CNMR spectra have shown the stoichiometric ratio of the chemical reaction is 2 : 2 : 1 (Valp : Nic : Zn(II)). Therefore, crystallographic data have confirm this structure is a ternary structure in the solid state. The acute cytotoxicity test (24 h) of complex **2** against Artemia saline presented low toxicity compared to the starting material (sodium valproate). In other hand, Plasmidial DNA interaction assay (single and double DNA breaks analysis by electrophoresis) and CT-DNA interaction assay (double helix interaction type by circular dichroism spectrophotometry) have shown complex **2** has low genotoxic activity, when compared to the nicotinamide control trial, indicating that this ternary complex has potential application in the development of a new drug. Acknowledgment to FAPERGS - PRONUPEQ, Grant/Award Number: 16/2551-0000523-0.

**Área: INO** **Inscrição: 759**

# Synthesis, characterization and LB films construction of a ruthenium complex with a new methyl 9-hydroxyphenalene-5-carboxylate ligand

**Herbert Winnischofer (PQ),[1] Isis Mani Wahl Godoy (PG),[1] Eduard Westphal (PQ)[2].**

**hwin.ufpr@gmail.com; isismani@gmail.com.**

*[1]Departamento de Química, UFPR; [2]Departamento Acadêmico de Química e Biologia, UTFPR.*

Palavras Chave: Ruthenium complex, *Methyl 9-hydroxyphenalene-5-carboxylate, Langmir-Blodgett films, Thin film, Stearic acid.*

## Highlights

A ruthenium complex was synthetized with a new ligand named methyl 9-hydroxy-1-oxo-*1H*-phenalene-5-carboxylate. Langmuir-Blodgett films were constructed using a mix of the complex with stearic acid.

## Abstract

Ruthenium complexes with pyridine ligands have been extensively studied for decades because of their photochemistry and electronic properties. To modulate these properties, several ligands have been combined with the $[Ru(bpy)_2]^{2+}$ fragment to form new coordination compounds. One class that captured attention of our group is the polycyclic aromatic ligands like the phenalenyl unit. These multicyclical systems have interesting electronic properties that can be exploited in catalysis [1], spin memory devices [2], molecular electronics and in thin films.

In the present study a ruthenium 2,2'-bipyridine complex was synthetized with a new ligand named methyl 9-hydroxy-1-oxo-*1H*-phenalene-5-carboxylate (L). The complex $[Ru(bpy)_2L][PF_6]$ was characterized by $^1H$ NMR, $^{13}C$ NMR, UV-vis and FTIR spectroscopies. The cyclic voltammetry (CV) of the complex revealed three electrochemical processes.

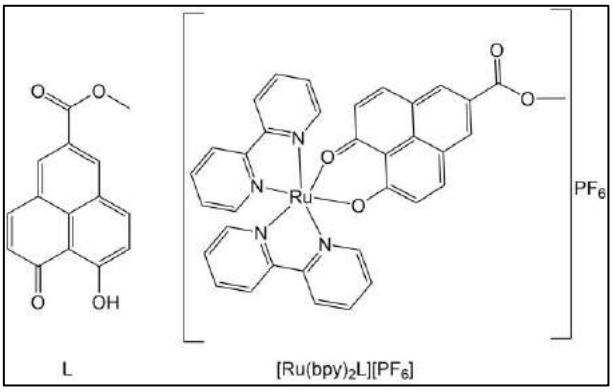


**Figure 1 –** Structure of the ligand L and $[Ru(bpy)_2L][PF_6]$ complex

Langmuir-Blodgett films were obtained from a mix of the complex $[Ru(bpy)_2L][PF_6]$ with stearic acid. The P×A curves revealed stable monolayer with collapse pressure above 50 $mN{\cdot}m^{-1}$. The UV-vis spectrum of the film show 3-nm bathochromic shift of the π–π* band compared to solution. The CV of the film revealed a reversible process with $E_{1/2}$=0.76 V attributed to the $Ru^{II/III}$ pair. In the next step, a new ligand containing long aliphatic chains is going to be prepared.

**References**

1. Pariyar, A. *et al. J. Am. Chem. Soc.* **137,** 5955–5960 (2015).
2. Raman, K. V. *et al. N ATU R E* | **493,** 509 (2013).

**Área: INO** **Inscrição: 00814**

# Chemical behavior of chloridotetrakis(ibuprofenato)diruthenium(II,III) metallodrug in acidic solution

**Marcio Hayashi (IC), Hanif-Ur-Rehman (PG), Denise de Oliveira Silva (PQ)***

**marcio.hayashi@usp.br; deosilva@iq.usp.br**

*Departamento de Química Fundamental, Instituto de Química, Universidade de São Paulo, São Paulo, SP, Brazil*

Keywords: *Diruthenium(II,III), Ibuprofen, Metallodrug, Nanoparticles.*

## Highlights

Diruthenium(II,III)-Ibuprofen metallodrug shows tendency to form nanoparticles in solution.
The chemical behavior may depend on the presence and nature of acids in the medium composition.

## Abstract

Reports from our group have shown that the diruthenium(II,III)-Ibuprofen metallodrug exhibits brain anticancer activity in glioma cell lines both *in vitro* (animal and human cells) and *in vivo* [1,2]. The lead RuIbpCl complex of formula $[Ru_2(Ibp)_4Cl]$, where Ibp = carboxylate anion derived from the non-steroidal anti-inflammatory drug ibuprofen, exhibits paddlewheel structure with four equatorially bridged Ibp anions while the chloride is axially coordinated to the mixed valence $Ru_2$(II,III) dimetal core. This complex shows polymeric structure in the solid state due to the formation of extended chains connected by Ru-Cl axial bridges. We also have found that the complex has tendency to form nanoparticles (NPs) which may depend on the composition of the solution medium, and additionally it might be affected by the presence of acids [3]. To investigate the role of the acid, in the present work we have studied the behavior of the metallodrug in medium containing three different acids: sulfuric, hydrochloric and acetic acid. In aqueous solution containing small amount of ethanol, the complex (at concentration below 200 μM) shows light pink color, which changes to yellow in the presence of acid. This color change is corroborated by the decrease of intensity of the visible absorption band at about 500-600 nm when the acid is added. Suspensions of acid:complex at the range 0 to 2.0 molar ratio, where the pH was maintained at 3.5-6.6, were monitored by measuring particle size (by DLS, dynamic light scattering) and zeta potential. The results showed that the acid has an effect on the formation of particles mainly contributing to decrease the particle size below 100 nm. Distribution of particles were related to acceptable PDI (polydispersity index), mostly at 0.1-0.4 values. However, although the systems were apparently homogeneous, the possibility of having mixture of nano-sized particles and molecular RuIbpCl in acidic medium cannot be ruled out. The nature of the acid seems to not have significant effect on the behavior of the complex since similar tendency was found for the three investigated acids, *i.e*., the sulfuric acid containing no potential coordinating species, the hydrochloric acid which contains the common chloride axially coordinated anion, and the acetic acid that contains potential equatorial coordinating acetate anions. Potential zeta measurements, however, suggests that the particle stabilization may depend on the nature of the acid, with the sulfuric acid contributing to decrease zeta potential to the lower limit value (~30 mV) in contrast to the other two acids which maintained the values above 30 mV. The results suggest the metallodrug chemical behavior may be modulated in acidic medium (FAPESP, CNPq).

[1] D. de Oliveira Silva, Ruthenium Compounds Targeting Cancer Therapy, in: Atta-ur-Rahman, M.I. Choudhary (Eds.), Frontiers in Anti-cancer Drug Discovery, vol. 4, Bentham Science Publishers, Sharjah, U.A.E., pp. 88–156, 2014. [2] Hanif-Ur-Rehman, Tatiana E. Freitas, Renata N. Gomes, Alison Colquhoun, Denise de Oliveira Silva. J. Inorg. Biochem. 165, 181–191, 2016. [3] Hanif-Ur-Rehman. Synthesis and Characterization of Axially Modified Diruthenium-Ibuprofenate Complexes and Studies of Interaction with Chitosan and Glycol Chitosan, PhD Thesis, Instituto de Química, USP, 2016.

**Área: INO** **Inscrição: 00823**

# Synthesis of magnetic composites by combustion method: Materials for photodegradation of methylene blue

**Matheus G. Ferreira (IC)[1*], Francisco M. S. Garrido (PQ)[1], Marta E. Medeiros (PQ)[1]**

**matheus.gomes@ufrj.br; chico@iq.ufrj.br; martam@iq.ufrj.br**

*[1] Departamento de Química Inorgânica, Instituto de Química - UFRJ*

Keywords: *magnetic oxides; combustion method; magnetic separation; dye photodegradation.*

## Highlights

Magnetic composites were prepared with ZnO, $ZnFe_2O_4$ and Vulcan-X by combustion synthesis. These composites have activity for methylene blue photo degradation and can be removed by a magnetic field.

## Resumo/Abstract

Fotocatálise tem como princípio utilização de luz para ativar um semicondutor, resultando na promoção de um elétron para a banda de condução e gerando uma lacuna na banda de valência. Tal lacuna apresenta energia suficiente para oxidar a água, gerando espécies radicalares •OH. O elétron excitado (banda de condução) pode ser transferido para a água reduzindo-a, gerando também a espécie •OH. Esta espécie radicalar apresenta alta reatividade, apresentando alta eficácia na degradação de corantes como o azul de metileno em meio aquoso. Neste trabalho, compósitos de ZnO, semicondutor ativo em processos fotocatalíticos, com o material magnético $ZnFe_2O_4$ e carbon black (Vulcan-X), foram preparados pelo método de combustão. Foram utilizadas as seguintes proporções (m/m/m) de ($ZnO/ZnFe_2O_3$/Vulcan-X): A = (1/0/0); B = (1/1/0); C = (2/2/1) e D = (3/3/4). A formação da fase wurtzita do ZnO nos quatro materiais e da fase cúbica da ferrita de zinco nos materiais B, C e D, foi confirmada por DRX (difratômetro Rigaku, radiação CuKα). Nos testes fotocatalíticos foi utilizada como fonte luminosa uma lâmpada LED, potência de 12 W, e solução de azul de metileno (MB) com 72 mg/L. Durante o teste, coletou-se alíquotas a cada 20 minutos, analisadas por espectroscopia UV-Vis, verificando-se uma progressiva diminuição na concentração do corante. Sendo que, depois de 140 minutos foi observada uma diminuição de 89% na concentração de MB, no teste com o material B (Figura 1), e 99% para o material A após 120 minutos.

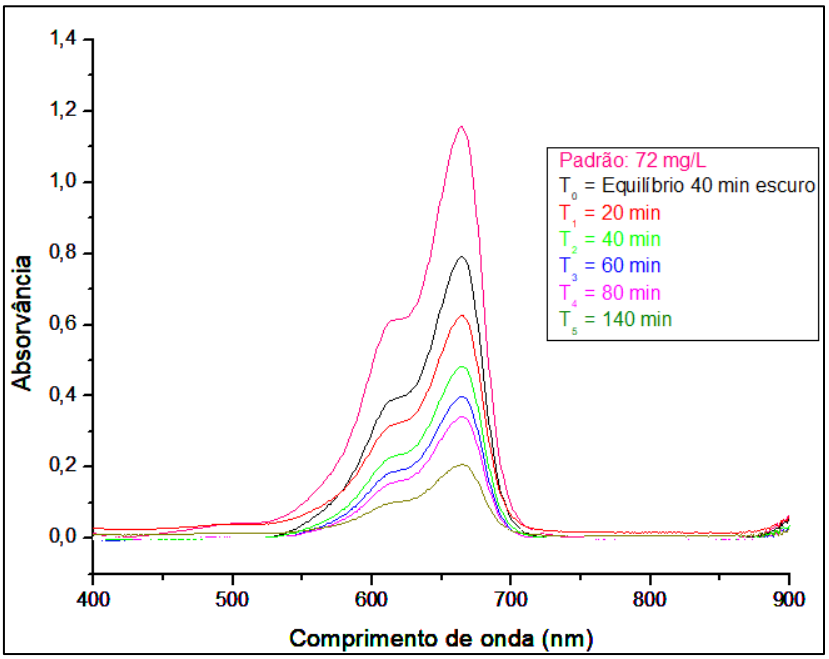

**Área: _INO_** **Inscrição: __00827__**

# Otimização da Síntese de um Complexo de Cobalto(III) Através de Síntese em Fluxo

**Caio M. Pacheco[1] (IC), Marcos V.P. Mello[2] (PG), Mauricio Lanznaster[2*] (PQ)**

**caiomp@id.uff.br; ml@id.uff.br***

*[1]Universidade Federal Fluminense, Instituto de Química; [2]Universidade Federal Fluminense, Instituto de Química, Programa de Pós-Graduação em Química da UFF*

Palavras Chave: *cobalto, PDAH, câncer, metalofármacos, síntese em fluxo.*

## Highlights

Synthesis Optimization of a Cobalt(III) Complex Through Flow Chemistry. A flow reactor system has been used for the preparation of precursors for the synthesis of Hypoxia Activated Prodrugs in large scale with high yields. The flow system provides greater reproducibility due to control of the reactional variables.

## Resumo/Abstract

Uma das barreiras ao tratamento de tumores sólidos é a presença de regiões pouco vascularizadas, denominadas regiões em hipóxia. Devido a essa condição, o tumor também apresenta uma maior capacidade redutora comparada a células normais[1], tornando-as um alvo potencial para o desenvolvimento de Pró-drogas Ativadas por Hipóxia (PDAHs).

Com o intuito de sintetizar PDAHs com alto rendimento, em larga escala e de forma reprodutível, foi utilizado o sistema de reação em fluxo Asia da Syrris[2], proporcionando um controle fino de diversas variáveis do processo reacional.

O presente trabalho descreve a síntese em fluxo do complexo precursor a PDHAs $[Co^{III}(py_2en)(NO_2)_2]ClO_4$ **(1)**. Através de mudanças nas variáveis do processo reacional, foi obtido um melhor rendimento comparado ao método de preparação pelo método clássico (“batelada”), que tem apresentado problemas de reprodutibilidade e rendimento (Figura 1). Após diversas reações, o solvente mais adequado para a reação foi água, com o fluxo de 1mL/min, e a concentração de até 0,3 mol/L do ligante tetradentado N,N’-bis(piridina)etilenodiamino e o hexanitrocobaltato de sódio. As caracterizações foram feitas através de espectroscopia na região do infravermelho e espectrometria de massas (ESI-MS).

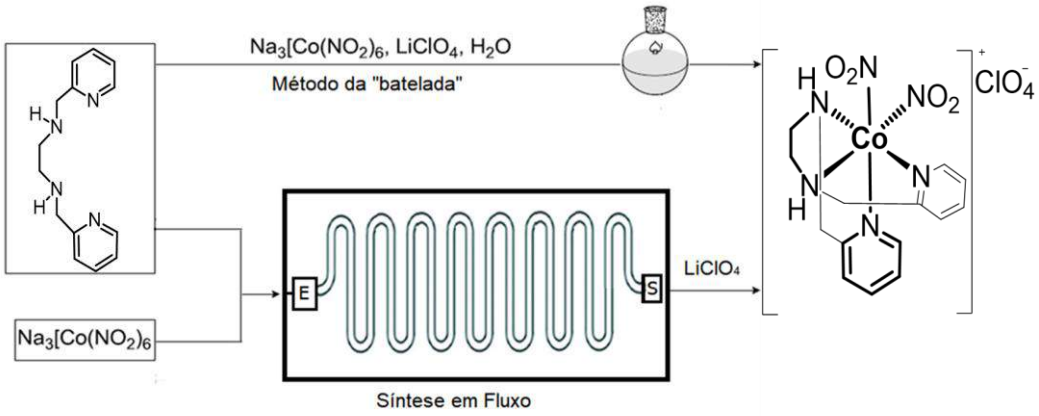


Figura 1: Esquema da síntese do complexo 1.

O complexo **1** foi obtido e caracterizado de forma reprodutível com rendimento de até 53%, superior ao método de “batelada”, podendo ser realizada em altas quantidades (>4g), evidenciando a grande praticidade e aplicabilidade do sistema de síntese em fluxo.

**Referências:**

[1]. Lin, A. J. *et. al. J. Med. Chem.* **1972**, 15 (12) 1247.
[2]. Degennaro, L. *et. al. J. Flow Chem.* **2016**, 6(3), 136.

**Área: INO** **Inscrição: 00844**

# Coumarin-*N*-acylhydrazone ligands and their Ru(II) complexes: Structure, characterization and antimicrobial activity

**Patrícia S. V. B. Almeida (PG),[1*] Thiago M. Pereira (PG),[1] Guilherme P. Guedes (PQ),[2] Arthur E. Kummerle (TC),[1] Leandro L. de Oliveira (PQ),[3] Amanda P. Neves (PQ).[1]**

**svb.almeida@gmail.com**

*[1]Departamento de Química, UFRRJ; [2]Departamento de Química Inorgânica, UFF; [3]Departamento de Biologia Geral, UFV.*

Keywords: *Ruthenium Complexes, Coumarin, Hydrazone, Antimicrobial activity.*

## Highlights

This work describes the synthesis, characterization and evaluation of the antimicrobial activity of new hybrid coumarin ligands and their $Ru^{II}$ complexes.

## Abstract

Metal-based drugs play an important part in the history of medicinal chemistry. Ruthenium complexes as well as coumarins and hydrazone derivatives have been studied and demonstrated significant biological activities[1,2], including antimicrobial, which has motivated this work. The synthetic methodology of the ligands and complexes is show in the scheme below.

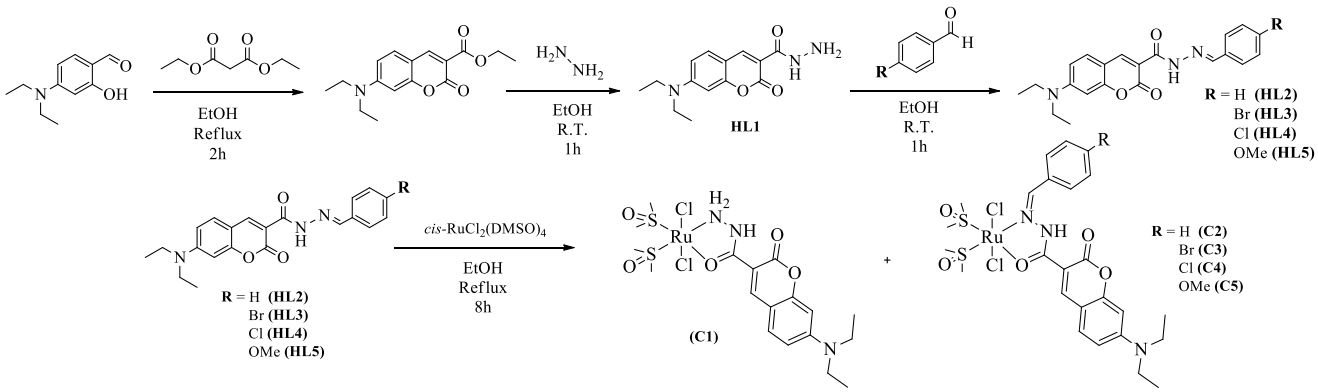


The compounds were characterized by IR, UV-Vis, $^1$H NMR and cyclic voltammetry and the data obtained are in accordance with similar compounds described in the literature[1,2,3]. The compounds HL2, HL4, C2 and C3 presented suitable crystals for X-ray diffraction analyses. The $Ru^{II}$ ion is in a distorted octahedral environment, equatorially coordinated by an ON chelate of the hydrazone ligand and two sulfur atoms of the DMSO ligands at *cis* positions. A pair of chlorine atoms at the axial positions completes the coordination sphere. The molecular structures are show in figure 1.

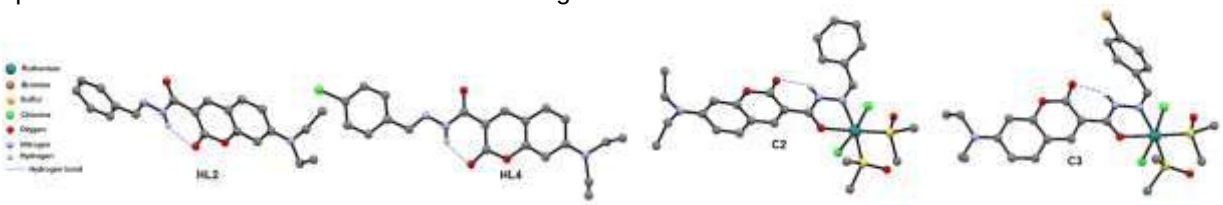


Figure 1: Molecular structures of HL2, HL4, C2 and C3.

The compounds were studied against 11 certified strains. The ligands and the metal precursor were not active against the bacteria tested at 200 mM. On the other hand, the complexes exhibited inhibition against gram-positive species with a MIC around 100 µM for C3 and C4.

[1] New J. Chem., 2016, 40, 8846; [2] Dalton Trans. 2016, 45, 3163; [3] Bioorg Med Chem Lett, 2017, 27, 223.

**Área: INO** **Inscrição: 00853**

# Synthesis, Crystal Structure and Magnetic Properties of a luminescent Europium(III) complex containing oxamate as a ligand.

**Thalyssa K.F.P. Viana (IC)[1*], Raphael C.A. Vaz (PG)[1], Isabela O. Esteves (IC)[1], Willian X.C. Oliveira (PQ)[1], Emerson F. Pedroso (PQ)[2], Cynthia L.M. Pereira (PQ)[1].**

**thalyssakfpv@hotmail.com; cynthialopes@ufmg.br**

*[1]Departamento de Química, Universidade Federal de Minas Gerais, Av. Antônio Carlos, 6627, Pampulha, BH, MG; [2]Centro Federal de Educação Tecnológica de Minas Gerais, Av. Amazonas, 5253, Nova Suíça, BH, MG.*

Keywords: *Coordination Compound, Crystal Structure, Molecular Magnetism, Magnetic Properties.*

## Highlights

The synthesis, crystal structure and magnetic properties of $Eu^{3+}$ oxamate complex are described in this work.

## Abstract

Recently, the obtention of coordination compounds containing lanthanides ions has attracted the interest of researchers worldwide due to their optical and magnetic properties.[1] The possibility of the association between magnetism and optical properties and the preparation of single ions present potential for future technological innovation.

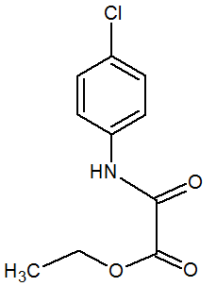


*Figure 1. Representation of the ligand used.*

The present work describes the synthesis and chemical characterization of an oxamate ligand showed in Figure 1, as well as its coordination to europium(III) ion. The synthesis of this ligand was done as reported previously.[2] To the obtention of the new Eu(III) complex, the synthesis was performed by means of direct addition of an aqueous solution of the metal ion to a solution containing the ligand.

Crystal structure of the metal complex was determined and it consists of four ligands coordinated to one $Eu^{3+}$ ion. Magnetic properties were measured and they are in agreement with the presence of one europium(III) ion. Initial tests in the UV chamber ($\lambda$= 254 and 366 nm) suggest that this complex is luminescent. Determination of quantum yield is the next step of this work.

**Acknowledgments:** CAPES, CNPq, FAPEMIG

**References**

1 CLEGG, W., ALEXANDRER J,COLE, JACQUELINE MEVANS, JOHN S OMAIN PETER,PARSONS, SIMON; WATKIN, D. J. **Crystal Structure Analysis Principles and Practice**. Second Edition. Oxford University Press, 2009.

2 FORTEA-PÉREZ, F. R. et al. Structural insight into the reaction mechanism of Pd-catalyzed nitrile hydration: Trapping the $[Pd(H_2O)_4]^{2+}$ cation through a supramolecular complex. **Inorganica Chimica Acta,** v. 443, 2016, p. 267-273.

**Área: INO** **Inscrição: 00887**

# Síntese, estrutura cristalina e caracterização vibracional de um ligante pirazólico funcionalizado e um novo complexo de $Co^{II}$

**Isac M. Dias*[1] (PG), Iuri C. Soares[1] (PG), Henrique C. S. Junior[2] (PG), Glaucio B. Ferreira[2] (PQ), Guilherme P. Guedes[1,2] (PQ) *marinhoisac@gmail.com**

[1] *Universidade Federal Rural do Rio de Janeiro, Departamento de Química, BR 465, km 7, Seropédica, RJ.*
[2] *Universidade Federal Fluminense, Instituto de Química, Alameda Barros Terra, s/n, Niterói, RJ*

Palavras Chave: *Ligante pirazólico, Susceptibilidade eletrofílica, Estrutura cristalina, Cobalto(II)*

## Highlights

Synthesis, crystal structures and vibrational characterization of a pyrazole ligand and a new $Co^{II}$ complex. Vibrational characterization. Strong intramolecular hydrogen bonding induces the monodentate coordination mode of the ligand.

## Resumo

Pirazóis funcionalizados são amplamente utilizados em síntese de complexos devido a sua versatilidade de modos de coordenação e suas comprovadas atividades farmacológicas[1]. Neste trabalho, descreve-se a síntese, a caracterização espectroscópica e estruturas cristalinas de um ligante pirazólico e seu respectivo complexo de $Co^{II}$. A síntese do pré-ligante está mostrada no esquema (A). A caracterização espectroscópica na região do infravermelho de cada etapa reacional foi feita realizado através de um estudo comparativo entre os espectros experimentais e os simulados por cálculos DFT/PBE D3 com função de base Def2-TZVP. As principais absorções e atribuições estão mostradas em (B). O pré-ligante foi caracterizado por RMN-$^1$H e difração de raios X por monocristal (DRX).

**(A)**

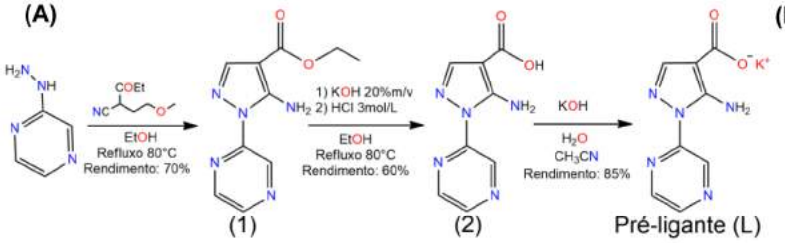


**(B)**

| | Experimental (Teórico) ($cm^{-1}$) | |
|---|---|---|
| | **υN-H** | **υC=O** |
| **1** | 3460(3696)<br>3340(3544) | 1678(1758) |
| **2** | 3443(3544)<br>3327(3406) | 1650(1689) |
| **L** | 3447(3559)<br>3320(3355) | 1617(1641)<br>1419(1411) |

Esquema de síntese em (A) e tabela com as principais vibrações para as etapas reacionais da síntese do pré-ligante (B)

A síntese do complexo foi realizada através da reação entre $CoCl_2$ e L, na proporção 1:2. A DRX por monocristal (C) mostrou que o complexo cristalizou em um sistema monoclínico com grupo de espaço $P2_1/c$ e parâmetros de célula a=12,7353(3)Å, b=7,1615(3)Å, c =12,3527(7)Å, β= 112,456(2)Å e V=1041,19(4)Å$^3$. O $Co^{II}$ está em um ambiente octaédrico distorcido, coordenado a dois L e a quatro moléculas de água. O cálculo da susceptibilidade eletrofílica (D) do pré-ligante desprotonado sugeriu que a coordenação pelo átomo de oxigênio $O^1$ é preferencial. Entretanto, tanto a estrutura cristalina quanto a análise por QTAIM[2] para o complexo mostraram que a coordenação pelo $O^2$ torna-se preferencial devido ao estabelecimento de uma forte ligação hidrogênio envolvendo este átomo e o ligante aqua adjacente, que estabiliza a estrutura.

**(C)**

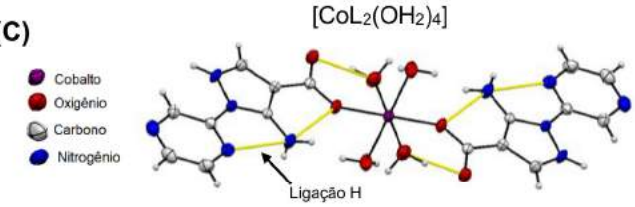


**(D)**

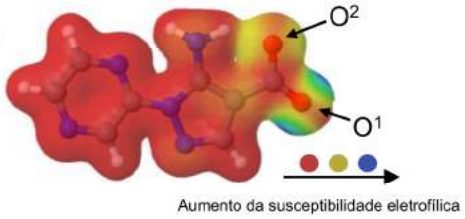


Estrutura cristalina do complexo em (C) e mapa da susceptibilidade eletrofílica do pré-ligante L em (D)

[1] *New J.Chem.* **2017**, 41,16
[2] *Phys. Rev. Lett.***1996**, 77,3865

**Área: INO** **Inscrição: 00942**

# Rigid Bipodal Ligand as Molecular Building Block to Construct New Metal-organic Frameworks

**Catiúcia R. M. O. Matos (PG) [1] and Célia M.Ronconi (PQ).[1,*]**

**catiuciarmom@gmail.com; cmronconi@id.uff.br**

[1] *Universidade Federal Fluminense, Instituto de Química, Programa de Pós-Graduação em Química da UFF, outeiro de São João Batista s/n, Campus do Valonguinho, Centro, 24020-141, Niterói, RJ, Brazil.*

*Keywords*: *Bipodal Dicarboxylic Ligand, Conjugate Rigid Spacer, photophysical properties*

## Highlights

In this work we describe the syntheses of a rigid bipodal ligand (**H2L1**) to be used as a molecular building block to construct new MOFs materials for sorption and photoluminescence studies.

## Resumo/Abstract

In a previous work of our group, four Coordination Networks (CNs) of Co (II), Cd (II), Er (III) and Gd (III) were obtained using the rigid ligand of 4,4'-ethynylenbenzoate. [1,2] The carboxylate ligand adopted different coordination modes which together with the preferred geometries of the metal ions formed the 1D, 2D and 3D CNs containing varied interpenetrations and rare topologies. As part of our ongoing research on rigid CNs, we prepared the rigid ligand **H2L1** with two triple bonds in the spacer to be included in our library of ligands.[3–5] Five steps of reactions have been performed to obtain **H2L1** ligand: the first one is an esterification to afford **1**, the second is a Sonogashira coupling to obtain **2**; the third step is a hydrodesililation to afford **3**; the fourth step is an Eglinton homo-coupling to afford **4**; finally the hydrolysis of **4** gives rise two coordination sites, see scheme below. The **H2L1** and **1**, **2**, **3** and **4** have been characterized by NMR $^{1}$H, IV, TGA and DSC. Also, **4** and **H2L1** had their photophysical properties evaluated in the solid state. **H2L1** showed strong emission at 492, 462 and 433 nm when excited at 367, 340, 316 nm due to the π conjugation.

Scheme 1: Synthetic route to obtain **H2L1** and the intermediates **1**-**4**.

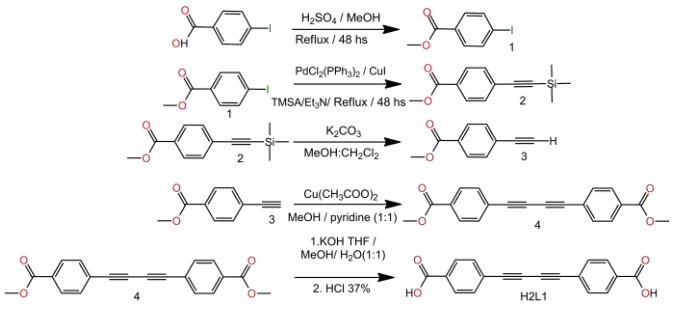


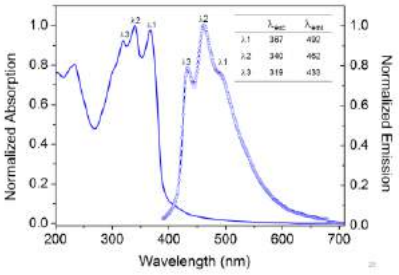


Figure 1: Normalized absorption (full line) and normalized emission (dashed line) of **H2L1** in the solid state.

The **H2L1** is being used as a building block in many synthetic trials for new MOFs (Metal-organic Framework) and CNs materials of *d* and *f* block elements for $CO_2$ capture and photoluminescent studies.

Acknowledgment: CAPES, PROPPI, LQSN, PPGQ-UFF, LAREMN, LAME, LAMATE, LDRX.

---

(1) Martins, V.; Resende, J. A. L. C.; Ronconi, C. M. *CrystEngComm* **2017**, *19*, 3103.
(2) Martins, V.; M. Ronconi, C. *Rev. Virtual Química* **2017**, *9*, 1318.
(3) Matos, C. R. M. O.; Monteiro, F. G. A.; Miranda, F. Da. S.; Pinheiro, C. B.; Bond, A. D.; Ronconi, C. M. *Cryst. Growth Des.* **2017**, *17*, 5965.
(4) Matos, C. R. M. O.; Miranda, F. Da. S.; Carneiro, J. W. de M.; Pinheiro, C. B.; Ronconi, C. M. *Phys. Chem. Chem. Phys.* **2013**, *15*, 13013.
(5) Matos, C. R. M. O.; Vitorino, L. S.; De Oliveira, P. H. R.; De Souza, M. C. B. V; Cunha, A. C.; Boechat, F. D. C. S.; Resende, J. A. L. C.; Carneiro, J. W. D. M.; Ronconi, C. M. *J. Mol. Struct.* **2016**, *1120*, 333.

**Área: INO** **Inscrição: 1025**

# Iron(III) complexes with tridentate Schiff bases derived from diaminomaleonitrile: Synthesis and characterization

**Thiago H. Döring (IC)*[1], Edward R. Dockal (PQ)[2], José W. da Cruz Júnior (PQ)[1].**

**jose.w.cruz@ufsc.br; thiago.doring@ufsc.br**

*[1]Departamento de Ciências Exatas e Educação, Universidade Federal de Santa Catarina (UFSC) Blumenau/SC.*
*[2]Departamento de Química, Universidade Federal de São Carlos São Carlos/SP.*

Keywords: Schiff bases, Iron(III) complexes, diaminomaleonitrile.

## Highlights

In this work, iron(III) complexes with tridentate Schiff bases synthesized from diaminomaleonitrile were synthesized and characterized by melting point, qualitative solubility, conductivity measurements and electronic spectroscopy.

## Resumo/Abstract

Schiff bases are compounds having an imine group, $R^1R^2C=NR$, which are formed by the condensation of a primary amine with a compound bearing a carbonyl group[1]. The understanding that the ligands coordinated with metals in natural systems are asymmetrical has aroused interest in the synthesis and characterization of asymmetric Schiff bases derived from amines suitable to form complexes with transition metals[2]. In this work, iron(III) complexes with tridentate Schiff bases derived diaminomaleonitrile (Figure 1) were synthesized by adaptation of published method[3]. The complex (1) was soluble in THF, methanol, ethanol and acetonitrile, being partially soluble in water and insoluble in hexane. Complex (2) was soluble in methanol and ethanol, partially soluble in water, THF and acetonitrile, and insoluble in hexane. The general characterization data are found in Table 1. Both complexes degraded instead of melting. The conductivity measurements, carried out in methanol, indicate the complexes as 1:1 electrolytes, possibly due to the exchange of a $Cl^-$ ligand by a solvent molecule. The electronic spectra, performed with methanolic solutions, presented three bands of high molar absorptivity, between 270 nm and 400 nm, attributed to the transitions $\pi \rightarrow \pi*$ e $n \rightarrow \pi^*$. Also, bands of low molar absorptivity, referring to the d-d transitions observed in 750 nm for complex (1) and 760 nm for complex (2). Vibrational Spectra and Elemental Analyses will be performed to corroborate the structures proposed and will be presented at 41st RASBQ.

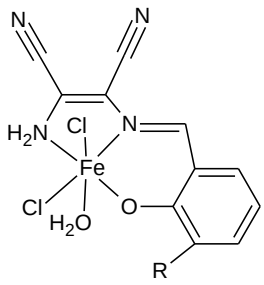


**Figure 1.** Proposed structures for the compounds obtained: (1) R=OH; (2) $R=OCH_3$.

**Table 1.** General characterization data of the complexes obtained.

| Complex | MW ($g \cdot mol^{-1}$) | Yield (%) | M.P. (ºC) | Conductivity ($\mu S\ cm^{-1}$) |
|---|---|---|---|---|
| (1) | 371,96 | 75,2 | 191 | 98,13 |
| (2) | 385,98 | 40,1 | 259 | 100,20 |

[1]Cozzi, P. G. *Chem. Soc. Rev.*, **33**, 410, 2004.
[2]Kureshy, R.I., *et al., J. Mol. Catal. A: Chem.*, **160**, 217, 2000.
[3] Costes,J-P; *et al, Inorg.Chim.Acta.* **274**, 73, 1998.

**Acknowledgements: CNPq.**

**Área: INO** **Inscrição: 1053**

# Oxamate-based Cobalt(II) Complex and dpss: Assembling of the {[Co(H$_2$O)$_6$][Co$_2$(H$_2$mpba)$_3$]}·2,2-dpss·2H$_2$O complex in the solid.

**Nathália R. de Campos (PG),[1*] Walace D. do Pim (PQ),[2] Antônio C. Doriguetto (PQ),[1] Ana Karoline S. M. Valdo[3] (PG), Felipe T. Martins (PQ),[3] Humberto O. Stumpf (PQ)[4], Maria Vanda Marinho (PQ).[1]**

**nathaliarodriguescampos@yahoo.com.br; maria.marinho@unifal-mg.edu.br.**

*[1]Instituto de Química, Universidade Federal de Alfenas, Campus Santa Clara, Alfenas, MG, 37130-001, Brazil;[2]Departamento de Química, Centro Federal de Educação Tecnológica de Minas Gerais, Belo Horizonte, MG, 30421-169, Brazil;[3]Instituto de Física, Universidade Federal de Goiás, Campus Samambaia, Goiânia, Go, 74690-900, Brazil; [4]Departamento de Química, Universidade Federal de Minas Gerais, Campus Pampulha, Belo Horizonte, MG, 31270-901, Brazil.*

*Keywords: coordination complex, oxamate ligands, cobalt(II), X-ray diffraction.*

## Highlights

- Formation of a triple-stranded dinuclear cobalt(II) complex stabilized by a cationic complex;
- Combination between the partially deprotonated 1,3-phenylenebis(oxamate) ($H_2mpba^{2-}$) and di(2-pyridyl)disulfide (dpss) ligands in the self-assembled process;
- Formation of a new polymeric network.

## Abstract

Oxamate-based coordination compounds are described with an extensive variety of structural arrangements and can be used as precursors in the synthesis of heterometallic systems, which have several potential applications in molecular magnetism and spintronics, for instance[1]. In this sense, cobalt(II) presents spin-orbit coupling, which could be responsible for fascinating magnetic behavior. Among the N/O-donor ligands, the oxamate-type stand out in the synthesis of metallic complexes, because they present different coordination modes, and two of them is depicted in Figure 1. In this work is presented a complex salt of formula {[Co(H$_2$O)$_6$][Co$_2$(H$_2$mpba)$_3$]}·2,2dpss·2H$_2$O (**1**). The anion is a dinuclear mesocate in which three partially deprotonated $H_2mpba^{2-}$ ligands chelate the cobalt(II) ions in a bisbidentade mode thorough the carbonyl groups (Figure 1). The cation is the hexaaquacobalt(II) complex, $[Co(H_2O)_6]^{2+}$ and the crystal structure is stabilized by the non-coordinated dpss ligand and water molecules. The three cobalt(II) ions in the structure exhibit an octahedral geometry connected to six oxygen atoms from oxamate (C=O) or from water molecules ($O_w$). Besides the single crystal X-ray diffraction (SXRD), **1** was characterized in a polycrystalline sample by FTIR, TG/DTA and PXRD and all the analysis are in agreement with the structure determined by the SXRD. Thermal analyses show a first mass loss near 100 ºC, corroborating the presence water molecules as crystallization solvents and the following losses were assigned to thermal decomposition of the ligands until de formation of cobalt(II) oxide (CoO).

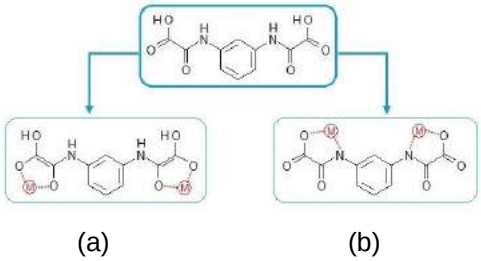


**Figure 1.** Representation of the $H_4mpba$ ligand and two examples of their coordination modes. In **1** was observed the (a) coordination mode.

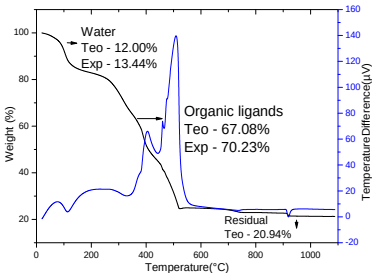


**Figure 2.** TG/DTA curves of **1**.

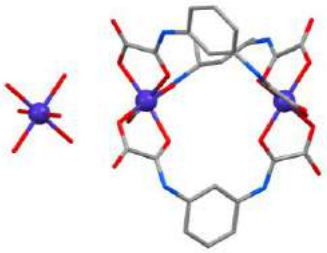

**Figure 3.** Crystalline structure of **1**. Dpss and water molecules were omitted for clarity.

[1] Pardo, E.; Ruiz-Garcia, R.; Cano,J.; et al. *Dalton transactions*, **2008**, 21, 2780.
[2] Kadam, R. M.; et al., *Chemical Physics Letters*, **2002**, 357, 457.

***Acknowledgments***
*Unifal, Fapemig, CNPq, Capes, FINEP (ref.134/08), RMQ-MG.*

**Área: INO** **Inscrição:01108**

# Síntese e caracterização do novo complexo metálico estrôncio com ligante 1-10-fenantrolina

**Gabriela Cristina M. Calisto (IC)**[1],**Simone Rodrigues Silva (PQ)**[1*]

**gabikalisto@gmail.com; simone.rodrigues@ufrr.br**

[1]*Departamento de Química – UFRR- Roraima/RR. CEP: 69310-000*

Palavras Chave: Bactericida, *Estrôncio, Síntese, Caracterização*

## Highlights

As bactérias parasitas provocam doenças aos seres vivos por meio da absorção de nutrientes de matérias orgânicas vivas. Para o combate de doenças bacterianas são utilizados antibióticos e vacinas. Entretanto, as bactérias estão cada vez mais resistentes aos fármacos devido ao uso irregular destes. Logo, o objetivo deste trabalho é obtenção do estanho e cobre com o ligante 1,10- fenantrolina.

## Resumo/Abstract

O complexo de estrôncio foi sintetizado a partir da solução aquosa contendo 3 mol de ligante (1,10-fenantrolina) para 1 mol do metal ($Sr(NO_3)_2$), formando uma solução incolor. O precipitado foi obtido pela evaporação lenta da solução. A purificação do precipitado ocorreu por meio da utilização do solvente clorofórmio, obtendo-se um complexo de coloração levemente rosa. O complexo obtido foi caracterizado através das técnicas de ponto de fusão, condutimetria e espectroscopia UV-Vis.

Através do ponto de fusão obtido para o complexo, mostrado na Tabela 1, foi possível observar diferenças significativas entre o valor do ponto de fusão do ligante, tal diferença pode está relacionado com a coordenação metal-ligante.

A condutividade foi realizado para o complexo e para o ligante em solução etanólica na concentração 1 $x10^{-3}$ M afim de obter o número de contra-íons presentes na estrutura do complexo. Como mostrado na Tabela 1, a condutividade do complexo de estrôncio foi de 175 µS, que quando comparado com os valores de referencias para eletrólitos citados por Geary (1971), observa-se que este valor está próximo da faixa de referência para eletrólitos 1:2 em etanol, o que indica que o complexo obtido apresenta dois contra-íons em sua estrutura.

**Tabela 1.** Temperatura de fusão e condutimetria do Complexo de Sr

| Amostras | Ponto de Fusão | Condutimetria |
|---|---|---|
| Fenantrolina | 117 °C | 3 µS |
| Complexo de Sr | 212 °C | 175 µS |

Foi realizada a obtenção de espectros eletrônicos na região do ultravioleta visível para o ligante e seu complexo utilizando-se como solvente etanol em temperatura ambiente, com a finalidade de se obter confirmação quanto à coordenação metal-ligante. Através dos dados espectroscópicos obtidos é possível observar surgimento de nova banda na região UV do complexo, diferentemente do ligante analisado.

**Figura 1**. Espectroscopia UV-vis do ligante 1,10 fenantrolina (vermelho) e do complexo de Sr (azul)

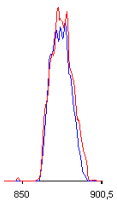


Logo, a síntese do composto levou a formação de um complexo na proporção 1:2 (metal/ligante). Os dados adquiridos pelas técnicas físico-químicas estão de acordo com a proposta e apontam que o ligante interage com o metal nitrato de estrôncio. Outras análises serão realizadas para a confirmação da estrutura do complexo. Além da atividade terapêutica do complexo.

**Área: INO** **Inscrição: 1118**

# Investigation of photodynamic efficiency of new porphyrin derivative

**Anderson Gomes (PG), Jacqueline A. Marques (PQ), Christiane P. F. Borges (PQ)**

**cpfborges@uol.com.br; derso321@hotmail.com**

*Programa de Pós-Graduação em Química Aplicada, Departamento de Química, Universidade Estadual de Ponta Grossa, Ponta Grossa, PR.*

Palavras Chave: *Porphyrin derivative, Photosensitizer, Photodynamic efficiency, Photo-oxidation, PDT*

## Highlights

Protonation reduces the photo-oxidation rate constant of BSA and the quantum yield of the singlet oxygen ($\Phi_\Delta{}^1O_2$) of new carboxy porphyrin. The photodynamic efficiency increases when violet LED is used.

## Resumo/Abstract

Photodynamic Therapy (PDT) involves the irradiation of a photosensitizer (PS) compound with light in appropriate wavelength to produce reactive oxygen species (ROS). Porphyrin derivatives are compounds of interest in PDT due to their photophysical properties. The evaluation of the PS efficiency to generate ROS is important to PDT. This work investigated the photodynamic efficiency of new carboxy porphyrin (TCPP) using two techniques that employ either bovine serum albumin (BSA) or uric acid (UA) as chemical dosimeters. The porphyrin synthesis was performed by the method adapted from Kostas *et al*[1]. The solutions were prepared in PBS (pH 7.2) and $NaHCO_3$/NaOH buffer (pH 10.5) and were illuminated with red and violet LED. The photo-oxidation rate constant of BSA ($k_f$) was investigated by the fluorescence intensity decay in the presence of PS and irradiation. The singlet oxygen quantum yield ($\Phi_\Delta{}^1O_2$) of porphyrin was investigated by monitoring the degradation of UA, the solutions were irradiated with LEDs and the photo-oxidation was followed by absorption decay in 292 nm[2]. The results show that the BSA oxidation is most efficient in pH 10.5, and that the $\Phi_\Delta{}^1O_2$ is higher in pH 10.5 than pH 7.2 (Table 1). The effect of different light sources could be observed, the irradiation with violet LED was more efficient than the red LED. The result show that TCPP has potential for use in PDT.

Table 1 - $k_f$ and $\Phi_\Delta{}^1O_2$ values for porphyrin in buffer 7.2 and 10.5 irradiated with violet and red LEDs. Values are represented by the mean of three measures ± standard deviation.

| pH | $k_f$ ($10^{-4}$ $s^{-1}$) violet | $k_f$ ($10^{-4}$ $s^{-1}$) red | $\Phi_\Delta{}^1O_2$ violet | $\Phi_\Delta{}^1O_2$ red |
|---|---|---|---|---|
| 7.2 | 5.84 ± 0.02 | 0.85 ± 0.04 | 0.57 | 0.08 |
| 10.5 | 7.63 ± 0.03 | 1.40 ± 0.02 | 2.40 | 0.09 |

References

[1]KOSTAS, I. D. *et al.* Tetrahedron Letters, **2007**, 48, 6688.
[2]GEROLA, A. P. *et al.* J. Photochem. Photobiol. A. **2012**, 232, 14.

Acknowledgments: Capes, C-LABMU/UEPG, Fundação Araucária, Fundo Paraná/SETI.

**Área: INO** **Inscrição: 01139**

# Síntese e avaliação da eficiência da 5,10,15,20-tetraquis(4-metiltiofenil)porfirina para Terapia Fotodinâmica

**Matheus H. I. Souto* (IC), Franciele S. Dias (IC), Dayse C. S. Martins** (PQ).**

***matheushignacio@hotmail.com; **daysequimica@ufmg.br**

*Departamento de Química, Instituto de Ciências Exatas, Universidade Federal de Minas Gerais*

Palavras Chave: *Porfirina, síntese, fotossensibilizador, câncer, TFD, luz.*

## Highlights

**Synthesis and evaluation of the efficiency of 5,10,15,20-tetrakis(4-methylthiophenyl)porphyrin for Photodynamic Therapy.** Uma porfirina tiolada foi obtida por adaptação de método relatado na literatura. Esta porfirina foi avaliada por meio do teste de Fischer e do ensaio de fotobranqueamento.

## Resumo/Abstract

As porfirinas têm sido estudadas como agentes fotossensibilizadores pois, quando submetidas a um comprimento de onda adequado, elas formam Espécies Reativas de Oxigênio (EROs) que atuam na apoptose de células tumorais. Devido à menor toxicidade em relação aos tratamentos convencionais a terapia fotodinâmica tem sido alvo de diversos estudos e novos agentes têm sido estudados. Neste trabalho, descreve-se a síntese da 5,10,15,20-tetraquis(4-metiltiofenil)porfirina (Figura 1) e a avaliação de sua eficiência como fotossensibilizador. Optou-se por uma porfirina com grupos substituintes contendo átomos de enxofre, devido a sua elevada afinidade com nanopartículas de ouro, que possuem certa atividade antitumoral e que poderão ter efeito amplificado se atuarem conjuntamente.

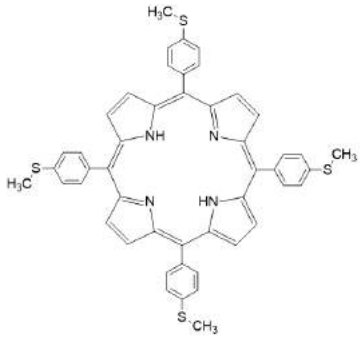


**Figura 1.** Estrutura da 5,10,15,20-tetraquis(4-metiltiofenil)porfirina ($H_2$T4MeSTPP).

**Tabela 1.** Atividade fotodinâmica (AF) comparada a composto comercial.

| Sistema de LED | Porfirina | |
|---|---|---|
| | Verteporfirina[1] | $H_2$T4MeSTPP |
| Branco | 208,00 | 3,5773 |
| Rosa | 7,31 | 0,8885 |
| Azul | 14,00 | 0,4899 |
| Verde | 58,00 | 0,5031 |
| Amarelo | 11,60 | 0,8112 |
| Vermelho | 4,69 | 0,2156 |

**Tabela 2.** Ensaio de fotobranqueamento (%) da $H_2$T4MeSTPP.

| Sistema de LED | | | | | |
|---|---|---|---|---|---|
| Branco | Rosa | Azul | Verde | Amarelo | Vermelho |
| 11,18 | 6,25 | 5,31 | 13,06 | 8,46 | 3,48 |

A $H_2$T4MeSTPP foi obtida segundo o método de Johnstone et colaboradores[2] e foi caracterizada por RMN $^1$H, espectrometria de massas e espectroscopia ultravioleta-visível. O teste de Fischer e o ensaio de fotobranqueamento foram realizados conforme procedimentos descritos na literatura e os resultados estão apresentados nas Tabelas 1 e 2. Apesar da porfirina ter apresentado baixo teor de fotobranqueamento (<12%), ela não apresentou AF importante, provavelmente devido a sua baixa solubilidade no sistema tampão pH = 7,4. Neste sentido, alterações estruturais na porfirina $H_2$T4MeSTPP têm sido estudadas a fim de aumentar sua solubilidade em sistemas aquosos, facilitando sua futura interação com nanopartículas de ouro.

**Agradecimentos**: UFMG, CNPq, CAPES, Fapemig.

[1]Monteiro, C. S. Dissertação de Mestrado, Depto de Química, UFMG, 2016. [2]Johnstone et all. Heterocycles, 1996(43) 7, 1423.

**Área: INO**
*(Inserir a sigla da seção científica para qual o resumo será submetido. Ex: ORG, BEA, CAT)*

**Inscrição: 01146**
*(Inserir o número de inscrição do autor que fez a submissão)*

# Properties and photocatalytic activity of $BiVO_4$ nanoflowers decorated with AuNP synthesized under conventional and microwave heating

**Fernando T. H. Hirata (IC),[1] Juliana S Souza (PQ) e [2] Paola Corio (PQ).[1]**

**fernando.hirata@usp.br; paola.corio@iq.usp.br**

*[1]Instituto de Química, USP; [2]Centro de Ciências Naturais e Humanas, UFABC*

Palavras Chave: *Fotocatálise, efeito plasmônico, nanomateriais, síntese assistida por micro-ondas*

## Highlights

- AuNP and $BiVO_4$ nanoflowers heterojunction with photocatalytic activity
- Microwave *vs* conventional heating on the synthesis of inorganic nanoparticles
- Plasmon enhanced photocatalytic effect

## Resumo/Abstract

Bismuth vanadate nanostructures are very promising materials for photocatalytic applications under visible light, due to its low band-gap energy (~2.4 eV). The photocatalytic activity can be intensified by the formation of heterojunctions with plasmon nanoparticles, which increase the local electron field near the semiconductor that give rise to an enhanced excitation process. Several time and energy consuming methods have been employed to obtain this kind of heterojunction. In this work we show the development of a synthetic protocol to obtain AuNP-decorated $BiVO_4$ nanoflowers, based on the polyol method, using either microwave and conventional (oil bath) heating. Both methods used polyvinylpyrrolidone (PVP) as caping agent, ethylene glycol as solvent, $HAuCl_4.4H_2O$ as Au source, a mixture of bismuth nitrate and ammonium metavanadate as $BiVO_4$ precursor (1:5 Au:Bi molar ratio), additionally the reactions were submitted to a reflux at 140°C. The synthesis performed under conventional heating took 4h whereas it took 10 minutes for the one performed under microwave heating. The material obtained under the two methods was the same, Figure 1a.
Methylene blue photodegradation experiments under visible light were conducted in a photocatalytic reactor. After 6h of irradiation pure AuNP were capable of degrade ~55% of the dye, pure $BiVO_4$ nanoflowers 77% and the heterojunction ~95%, Figure 1b. These results show the plasmon enhanced photocatalytic activity, for the catalysts obtained through the two methods, and how microwave assisted synthesis is promising as a green method to obtain inorganic architectures.

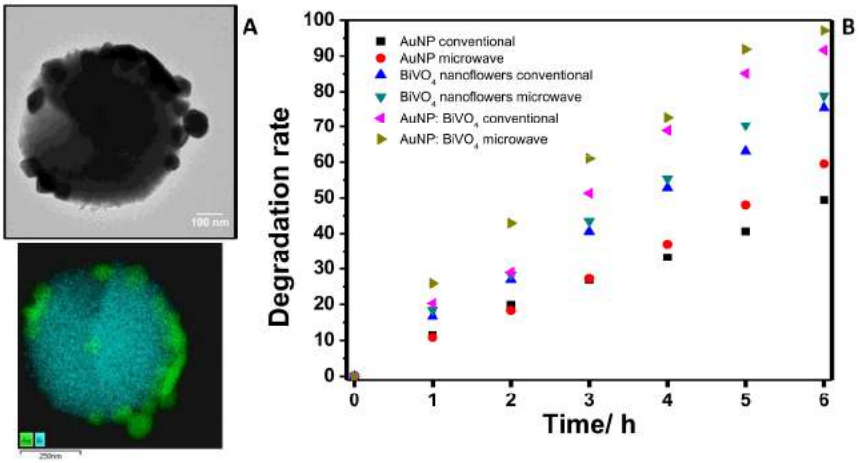


**Figure 1. (A)** Transmission electron microscopy and energy dispersive X-Ray mapping analysis images of AuNP-decorated $BiVO_4$ nanoflower. **(B)** Dye degradation rates as function of time.

[1]*Nano-Micro Letters*, 2011, **3**, 171-177.
[2]*Applied Catalysis B: Environmental*, 2016. **194**, 141-149.

**Acknowledgements:** FAPESP Grants # 2017/12688-8 and 12/13119-3.

**Área: INO** **Inscrição: 01245**

# Citotoxicidade de complexos de Ru(II) com diferentes tipos de isomeria

**Vanessa N. S. Campos (PG),[1] Ceslinolia M. Leite (PG),[2] Katia M. Oliveira (PG),[2] Thales E. M. Silva(IC)[3], João Honorato (PG),[2] Rodrigo S. Corrêa (PG),[4] Diego Martinez Otero, [5] Alzir A. Batista (PQ),[2] vanessa_niely@hotmail.com; vanessa_niely@hotmail.com**

*[1]Departamento de Química, UFMA; [2]Departamento de Química, UFSCar; [3] Universidade Federal de Alfenas (Poços de Caldas), [4] Universidade Federal de Ouro Preto, [5] Universidad Nacional Autónoma de México*

Palavras Chave: *Rutênio (II), Isomeria, Câncer, Bifosfinas.*

## Highlights

Cytotoxicity of Ru (II) complexes with different types of isomerism

Synthesis and evaluation of anticancer properties of ruthenium (II) complexes containing isomerism

Two complexes were characterized by various techniques and their cytotoxicity were evaluated.

## Resumo

Neste trabalho reportamos a síntese de dois novos complexos de rutênio (II): (**1**) [Ru(lap)(dppe)(bipy)]$PF_6$ e (**2**) [Ru(L-cis)(dppb)(bipy)]$PF_6$ (dppe = 1,2-bis(difenilfosfina)etano; dppb = 1,4-bis(difenilfosfina)butano; bipy=2,2'-bipiridina; lap = lapachol; L-cis = cisteína), os quais foram caracterizados por difração de raios X, RMN $^{31}P\{^1H\}$, $^1H$, $^{13}C$; espectroscopia de absorção na região do IV, UV/Vis; voltametria cíclica e de pulso diferencial; análise elementar e condutividade molar, bem como, avaliados quanto às suas atividades citotóxicas frente às linhagens de câncer de mama (MDA-MB-231) e não tumoral de mama (MCF-10A). O complexo **1** apresenta a formação de isômeros, onde um composto apresenta o oxigênio da carbonila do ligante lapachol *trans* ao átomo de fósforo do ligante dppe, e em outro, é o oxigênio da hidroxila que está *trans* ao mesmo átomo de fósforo. O composto **2** apresenta diastereoisômeros, mostrado pela duplicação dos sinais nos espectros de RMN. [1] Os resultados de citotoxicidade foram semelhantes para o composto **1** com $IC_{50}$ do isômero **A** (0,15 ± 0,01µM) e mistura de isômeros (0,13 ± 0,03µM), frente à linhagem tumoral MDA-MB-231. E o resultado de citotoxicidade da mistura diastereoisomérica do composto **2** frente a mesma linhagem tumoral (31,50 ± 5,20 µM). Este resultado é próximo ao obtido com o complexo com glicina, que apresenta apenas um isômero. Estudos estão sendo realizados com o [Ru(fosfo)(dppb)(bipy)]$PF_6$ (fosfo = fosfoetanolamina), cujos espectros de RMN mostram a presença de dois isômeros e será verificado se ambos têm a mesma citotoxicidade, contra a MDA-MB-231.

Referência:

1. Dos Santos ER, Mondelli MA, Pozzi LV, Correa RS, Salistre-de-Araujo HS, Pavan FR, et al. New ruthenium (II)/phosphines/diimines complexes: Promising antitumor (human breast cancer) and Mycobacterium tuberculosis fighting agents. Polyhedron. **2013**;51:292-7.

**Área: INO_____** *(Inserir a sigla da seção científica para qual o resumo será submetido. Ex: ORG, BEA, CAT)*

**Inscrição: 01302** *(Inserir o número de inscrição do autor que fez a submissão)*

# Identification of molecular species in solution by theoretical calculations: how far can we trust the models?

**João Madureira (PQ),[1*] Pedro Lucchetti (IC),[1] Gabriel M. Moreira (IC)**

**jmadureira@id.uff.br**

[1]*Departamento de Química Inorgânica – Instituto de Química, UFF*

Palavras Chave: *Iron(II) acetylacetonates, Molecular structure, Solution, Theoretical calculations, Cocoon.*

## Highlights

►Calculations show relevant $[Fe(acac)_2(H_2O)_n]$ structures in solution.
►Water properties can be reproduced with 80 – 100 molecules
►COCOON methodology does not rely on heavy basis sets or full size PBC.

## Resumo/Abstract

$[M^{II}(R,R'\text{-acac})_2]$ (M=Mn,Fe,Co,Ni,Cu,Zn) complexes are classic coordination compounds[1] applied as building blocks, catalysts or catalysts precursors for organometallic synthesis and materials preparation. Due to its low aqueous solubility, molecular structure determination relies on solid state data, particularly X-ray diffraction and infrared. Under anhydrous condition they precipitate as distorted octahedral oligomers[2] while they present themselves in the monomeric form in diluted solutions. The assumed preference for distorted octahedral geometry is assured by solvent molecules. If the synthesis uses hydrated materials two waters are assumed to be present. The known crystal structures are almost always the *trans* isomers, as seen in *trans*-$[Fe^{II}(acac)_2(H_2O)_2]$.[3]

Water is green chemistry favorite solvent and much effort has been applied to develop active catalysts in water. The determination of the molecular identities present in solution is fundamental to understand the mechanisms of action of the catalyst and to identify the relevant forms.

Solution conditions were simulated for $[Fe^{II}(acac)_2]$, $[Fe^{II}(acac)_2(H_2O)]$ and $[Fe^{II}(acac)_2(H_2O)_2]$ isomers, with DFT (gas phase and implicit solvent SMD model), Molecular Dynamics under PBC (with iron parameterized Force Field) and our newly developed explicit DFT method (Cocoon). They show several possible structures for five- and six-coordinate compounds. BSSE corrected Gibbs energies with different basis sets do not support *trans* isomer as the energy minimum, same as the kinetic calculations from the trigonal bipyramidal intermediate.

1-F.A.Cotton, Progr. Inorg. Chem., 1966, 7, 366.
2-S.Shibata, S.Onuma, A.Iwase, H.Inoue, Inorg. Chim. Acta, 1977, 25, 33
3-J.Laugier, J.P.Mathieu, Acta Cryst., 1975, B31, 631.

**Área: ____INO____ Inscrição:___00039____**

# Synthesis, characterization, cytotoxic and anti-*M. tuberculosis* activity of novel platinum(II) complexes.

**Maurício F. de Lima (IC)[1], Letícia P. de Oliveira (PG)[1]*, Zumira A. Carneiro (PQ)[2], Camila M. Ribeiro (PQ)[3], Drielly A. Paixão (PQ)[1], Marcos Pivatto (PQ)[1], Marcus V. N. de Souza (PQ)[4], Letícia R. de Souza Teixeira (PQ)[5], Sérgio de Albuquerque (PQ)[2], Fernando R. Pavan (PQ)[3], Wendell Guerra (PQ)[1]***

**mauriciolima@ufu.br; leticiapires@ufu.br**

*[1] Instituto de Química, Universidade Federal de Uberlândia, Campus Santa Mônica, Uberlândia, MG, Brazil;*
*[2] Departamento de Análises Clínicas, Toxicológicas e Bromatológicas, Faculdade de Ciências Farmacêuticas de Ribeirão Preto, Universidade de São Paulo, Ribeirão Preto, SP, Brazil;*
*[3] Faculdade de Ciências Farmacêuticas, Universidade Estadual Paulista, Laboratório de Pesquisa em Tuberculose, Campus Araraquara, Araraquara, SP, Brazil;*
*[4] Fundação Oswaldo Cruz, Instituto de Tecnologia em Fármacos–FarManguinhos, Manguinhos, Rio de Janeiro, RJ, Brazil;*
*[5] Departamento de Química, Universidade Federal de Minas Gerais, Belo Horizonte, MG, Brazil.*

Palavras Chave: *Platinum(II) Complexes, Fluoroquinolones, Cytotoxic Activity, Tuberculosis.*

## Highlights

Three new platinum complexes with fluoroquinolones have been synthesized and characterized. The complexes were more active than cisplatin, as well as some drugs used in the treatment of tuberculosis.

## Resumo/Abstract

This work describes the synthesis, characterization and in vitro evaluation against tumor cell lines and *Mycobacterium tuberculosis* of three new platinum(II) complexes. These complexes were synthesized as the scheme showed in Figure 1. The characterization was realized by elemental and spectroscopic (FT-IR) analysis, high-resolution mass spectrometry (HRESIMS) and nuclear magnetic resonance (NMR).

Figure 1 – General scheme of the complexes' synthesis and its proposed structure. L corresponds to ofloxacin (complex **1**), ciprofloxacin (**2**) and sparfloxacin (**3**).

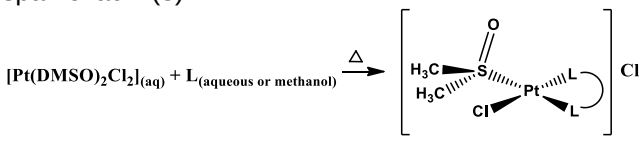


Table 1 – Elemental analysis and NMR signals of the complexes. ( ) Theoretical values.

| Complex | %C | %H | %N | $^{195}$Pt NMR (ppm) |
|---|---|---|---|---|
| **1** | 31,58 (31,63) | 3,88 (4,25) | 5,45 (5,53) | -2950 |
| **2** | 33,63 (33,78) | 3,50 (3,58) | 6,07 (6,22) | -3135 |
| **3** | 34,84 (34,25) | 4,04 (3,83) | 7,72 (7,61) | -2880 |

The elemental analysis, as described in Table 1, are in agreement with the proposed formulations. Also, the $^{195}$Pt NMR signals indicates the coordination sphere $PtN_2SCl$[1]. The FT-IR data also suggests that fluoroquinolones are coordinated in a bidentate manner by nitrogen atoms of the piperazine ring. Mass spectra, realized in acetonitrile, shows the presence of molecular ion $[M - Cl]^+$ for complexes **1** and **3**, and the molecular ion $[M - Cl + CH_3CN]^+$ for complex **2**, corroborating with the proposed structures. The complexes were stable in aqueous solution (1,5% DMSO, phosphate buffer), as verified by UV-Vis spectroscopy data.
The biological essays against *M. tuberculosis* (ATCC 27294) showed that all complexes were very active, with minimum inhibitory concentration (MIC) values compared to the first and second line drugs used in the treatment of tuberculosis. Complex **3** exhibited great potential against drug-resistant clinical isolates. The cytotoxic activity was evaluated against two breast cancer cell line (MCF-7 and MDA-MB-231). In this case, complex **3** was more active and more selective than cisplatin.

[1] Martins, E. T.; Baruah, H.; Kramarczyk, J. *et al. J. Med. Chem.* **2001**, 44.

**Área: INO** **Inscrição: 00057**

# Synthesis and characterization of gadolinium coordination compounds containing different classes of ligands.

**Daniel Hachiya de Oliveira (IC),[1] Eduard Westphal (PQ), [1] Renata Danielle Adati (PQ), [1]**

**danieloliveira@alunos.utfpr.edu.br**

*[1]Departamento Acadêmico de Química e Biologia, UTFPR – Campus Curitiba*

Keywords: Lanthanide, photoluminescence, Coordination Compound

## Highlights

Different classes of ligand were used to obtain Gd complexes. An inedited ligand, a benzoic acid derivative (dpdb), exhibit high UV absorption and coordinates efficiently to the Gd as chelating agent.

## Resumo/Abstract

The lanthanides ions has singular spectroscopic properties, such as strong emission lines and high color purity, allowing to synthesize luminescent coordination compounds and apply them in light emitting devices and luminescent markers. Although gadolinium is not a luminescent center, it can be used for complexes' structural study and ligands' triplet level determination. Here benzophenone-3 (bzf) and 2,2'-bipyridine (bipy) were used as ligands to obtain $[Gd(bzf)_3(bipy)]$ complex; bzf and $Gd(NO_3)_3$ were dissolved in ethanol and the pH were adjusted to 6-7 with triethanolamine, then bipy was dissolved in ethanol and added to the first solution, the result mixture was stirred at 50 °C for 6 h. A second complex, denoted $[Gd(dpdb)_3(H_2O)_2]$ was synthesized using 4-[(E)-(4-decyloxyphenyl)diazenyl]benzoic acid (dpdb), which was solubilized in DMSO and deprotonated with KOH, then $Gd(NO_3)_3$ solution was dropwised into dpdb one, then the solution was stirred at 50 °C for ~2 h. The infrared spectra show a carbonyl group displacement of bands associated with the bzf and dpdb ligands, and C-N bond in the bipy ligand. The plateau observed at 50-300 °C confirms that there no exist water molecules in the coordination sphere of gadolinium ion at $[Gd(bzf)_x(bipy)_y]$ complex (Figure 1c). On the other hand the $[Gd(dpdb)_x(H_2O)_y]$ display a 6,2% weight loss up to 96°C, indicating the presence of water molecules, as it was expected. Elementary analysis suggests different stoichiometries according to nitrogen percentage, higher than expected for both. The possibility of ionic complexes is being investigated.

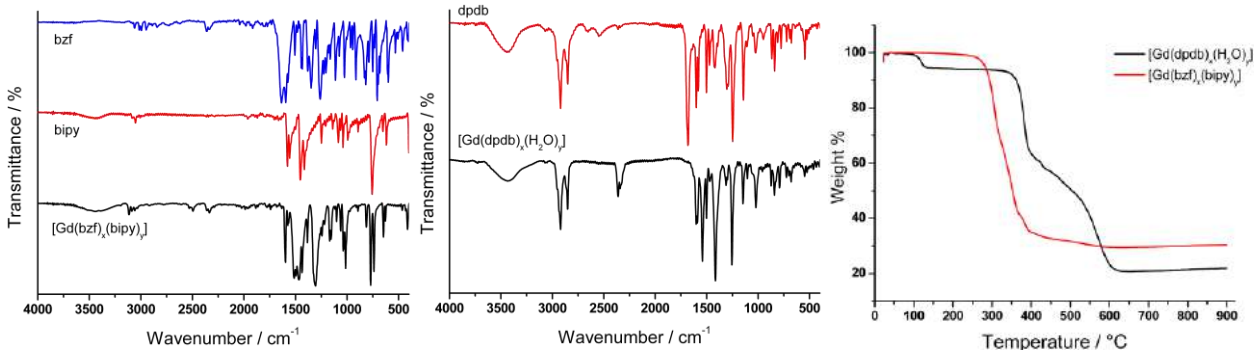


(a) (b) (c)

Figure 1: (a) Infrared spectra of bzf and bipy ligands and $[Gd(bzf)_3(bipy)]$; (b) infrared spectra of dpdb ligand and $[Gd(dpdb)_3(H_2O)_2]$; (c) TG curves of $[Gd(dpdb)_3(H_2O)_2]$ and $[Gd(bzf)_3(bipy)]$.

**Área: INO** **Inscrição: 0092**

# Reactions of organic and inorganic tellurium derivatives with 2,6-dipicolinoyl-bis(*N,N*-diethylthiourea)

**Sailer S. dos Santos (PQ),[1]* Hung H. Nguyen (PQ),[2] Ernesto S. Lang (PQ),[1] U. Abram (PQ),[3]*.**

**sailer.santos@ufsm.br; ulrich.abram@fu-berlin.de**

*[1]Department of Chemistry, Federal University of Santa Maria - UFSM, Brazil; [2]Department of Chemistry, Hanoi University, Vietnam; [3]Institut of Chemistry and Biochemistry, Freie Universität Berlin, Germany.*

Keywords: *Heterodentate chelator, Mixed $Te^{II}/Te^{IV}$ derivatives.*

## Highlights

Reactions of 2,6-dipicolinoylbis(*N,N*-diethylthiourea) with organic and inorganic tellurium compounds provided unexpected structures. A redox pathway took place to produce a rare $Te^{II}/Te^{IV}$ mixed derivative.

## Abstract

The *N,N*-dialkyl-*N*'-aroylthioureas ligands are versatile chelators which allow a variety of modifications in the periphery of their coordination sites. This feature may be useful to provide a rational design to a particular ligand. Figure 1 shows typical coordination modes for common *N,N*-dialkyl-*N*'-aroylthioureas, usually with κ*O,S*-chelation. The 2,6-dipicolinoyl-bis(*N,N*-dialkylthioureas) (Figure 2) have an extra nitrogen atom from the pyridinic moiety. Recently, these compounds were employed in the preparation of heterometallic coordination compounds, mixing first-row transition metals (M) with lanthanides (Ln) and main group metals.[1]

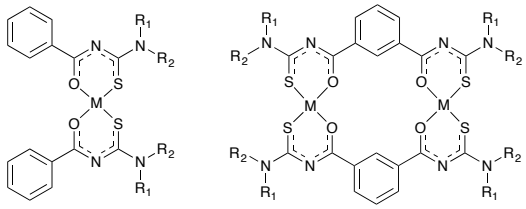

Figure 1. Common coordination modes of *N,N*-dialkyl-*N*'-aroylthioureas

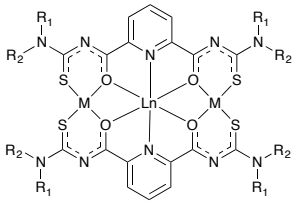

Figure 2. Structure of complexes derived from 2,6-dipicolinoyl-bis(*N,N*-dialkylthioureas)

In this work, we report the use of 2,6-dipicolinoyl-bis(*N,N*-diethylthiourea) (**L**) as a ligand to tellurium compounds. We worked with both inorganic and organic tellurium derivatives, since thiourea-based compounds behave as suitable ligands for the most common $Te^{II}$ and $Te^{IV}$ oxidation states. The reaction of **L** with the inorganic compound tellurium(IV) bromide ($TeBr_4$) provided compound **1**. Surprisingly, **1** was a $Te^{II}$ derivative owing the oxidation of some amount of the ligand, producing the reduction of Te. In this case, **L** acted as a κ*S,S'*-chelator, since the soft $Te^{II}$ is large enough to be "embraced" by both thiourea arms of the ligand (Figure 3). When starting from the organic derivative phenyltellurium(IV) bromide ($PhTeBr_3$), a $Te^{II}/Te^{IV}$ mixed-valence complex was produced (**2**). A partial reduction of the tellurium-based starting material was found in **2**. In this case, the $Te^{II}$ moiety behaved as a telluronium cation with κ*S,S'*-chelation from **L**, while the remaining $Te^{IV}$ atom appeared as a tellurolate anion (Figure 4).

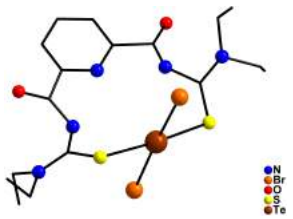

Figure 3. Molecular structure of complex **1**.

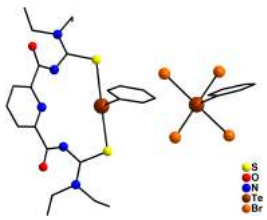

Figure 4. Molecular structure of complex **2**.

[1] H. H. Nguyen, J. J. Jegathesh, A. Takiden, D. Hauenstein, C. T. Pham, C. D. Le and U. Abram, *Dalton Trans.*, **2016**, 45, 10771.

**Área: INO** **Inscrição:00159**

# *Aromatic Beta-diamide and beta-monoketo-monoamide as promising ligands for Eu(III) and Tb(III) complexes with high luminescence*

**Larissa Alves-Corrêa (PG),[1]* Claudio L. Donnici (PQ),[1] Maria Helena Araujo (PQ),[1] Alex S. Borges (PQ),[2] Sérgio L. Scarpari (PQ),[3] Sidney J. L. Ribeiro(PQ)[3]**

**lalvescorrea@yahoo.com; cdonnici@terra.com**

*[1]LABSTOP – LABoratory of Synthesis&Tailoring of Optoelectrochemical molecular devices, Departamento de Química, UFMG; [2] Coordenadoria de Química-IFES, [3]Instituto de Química de Araraquara/UNESP – Araraquara - SP*

Key-words: *Europium, Terbium, Gadolinium, Complexes with amides, Luminescence*

## Highlights

Design and synthesis of novel functionalized dicarbonyl-amide derivatives as ligands for development of more stable and highly fluorescent Eu(III) and Tb(III) complexes.

## Abstract

Europium and terbium complexes with *beta*-diketones coordination are well-known for their luminescent properties, however there is almost none description of these complexes with amides. The present work describes the synthesis, characterization and luminescent studies with six complexes formed between the ligands **1A** and **1B** with europium, terbium and gadolinium. Ligands and complexes have been synthesized with reasonable yields and characterized by usual techniques. Eu(III) and Tb(III) complexes were luminescent, red and green, respectively. From the obtained spectroscopic data for Gd(III) complex the triplet energy of the ligand **1A** in 23980 $cm^{-1}$ could be achieved. **Eu1B** complex that had greater structural rigidity, showed higher thermal stability and quantum yield (**Eu1B**: 28.31%, **Eu1A** 8.03%) and these data corroborated the great importance from the structural rigidity for the highest luminescence. Complexes rate of decay measured values (**Eu1A**-0.685 ms;**Eu1B**-0.684 ms;**Tb1A**-0.487 ms;**Tb1B**-0.656 ms;**Gd1A**-1.501 ms,**Gd1B**-1.670 ms). These diamides are really promising ligands for the development of luminescent complexes with high efficiency and stability.

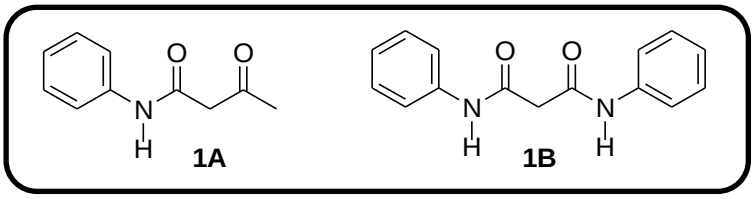


**ACKNOWLEDGMENTS:CNPq, FAPEMIG(CEX-PPM0281-17)**

1. Binnemans, K. *Handbook on the physics and chemistry of rare earths* **2005**, *35* (225), 107.
2. Eliseeva, S.,*el al.New J. Chemistry* **2011,** (6), 1165.
3. Chitnis, D. *et al.Optik - Int. J. Light Electron Optics* **2017**,*130*, 237.

**Área: INO** **Inscrição:00199**

# Synthesis and Characterization of Thiosemicarbazones and their Coordination Compounds

**Vinícius A. Costa (IC),[1*]Fabio D. Mota (IC),[1] Mauro A. Lima (PG),[1]; Fillipe Vieira Rocha (PQ),[1].**

**viniciuscosta1995@gmail.com;**

[1]*Departamento de Química, UFSCar;*

Keywords:*Thiosemicarbazones, Coordination Compounds.*

## Highlights

- Synthesis of new thiosemicarbazones and their complexes of Ni(II) and Pd(II);
- Insertion of a chloride at the 3-position of the ketone;
- Structural elucidation by NMR $^{1}H$, $^{13}C$, COSY and HSQC.

## Abstract

Thiosemicarbazones (TSC) appear as promising ligands in the synthesis of metal compounds with a possible activity against tumor cells [1]. Studies showed that thiosemicarbazones and their square planar complexes are important to interact with active site of the enzyme topoisomerase [2,3]. Therefore, in this work we synthesize some TSC ligands and their bis-chelated complexes of Ni(II) and Pd(II) once $d^8$ metals are great choice to achieve this geometry.

Synthesis of the thiosemicarbazone of interest consists in a condensation reaction between a ketone/aldehyde and a thiosemicarbazide in ethanolic medium catalyzed by acid. Synthesis of the Pd(II)/Ni(II) complexes is carried out by adding the ligand in proportions 2:1 (ligand:metal). Solutions were stirred at room temperature in acetonitrile over 24h. Figure 1 below represents the synthesis scheme of the compounds.

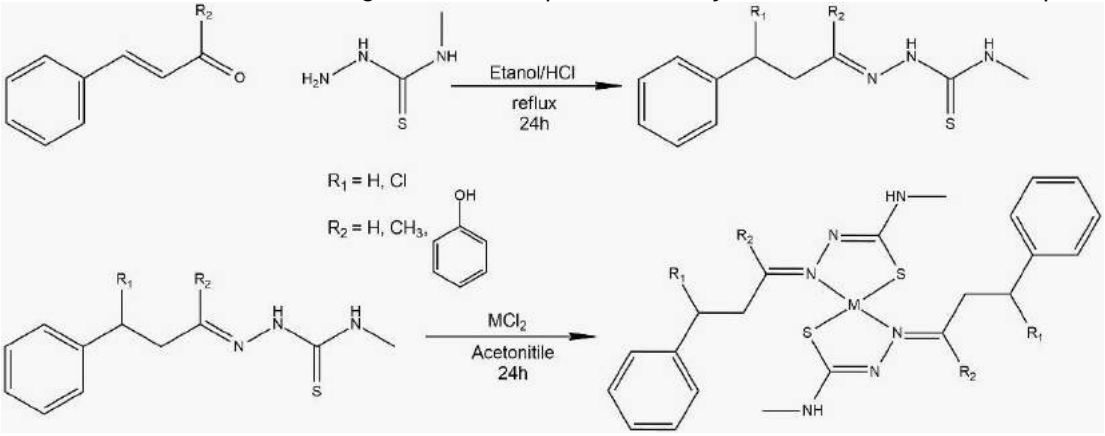


**Figure1. Schematic synthesis of the compounds**

All compounds obtained will be characterized by the following techniques: UV-Vis spectroscopy, infrared absorption spectroscopy, NMR and elemental analysis. Among the results, it was possible to observe the presence of the characteristic bands for thiosemicarbazone in the IR spectrum$\nu$C=S (763cm$^{-1}$);$\nu$C-N (1261cm$^{-1}$); $\nu$C=N (1535cm$^{-1}$);$\nu$N-H (3319cm$^{-1}$). No peaks were found in NMR spectra attributed to the olefin protons of the ketone. NMR techniques HSQC and COSY were crucial to confirm the break of double bond.

**Acknowledgments:**
FAPESP 2016/04201-9, CNPq, CAPES

**References:**

[1] H. Huang *et. al.*, J. Med. Chem. 53 (2010) 3048–3064.
[2] B. M.Zeglis*et. al.,*J. Med. Chem., 54(7)(2014)2391–2398.
[3]F. V. Rocha *et. al.*, J. Inorg. Biochem. 159 (2016) 165–168.

**Área: INO** **Inscrição: 00228**

# Novel Binuclear Chromium(III) Complexes with Potential Application as Building Blocks in Single Molecule Magnets Synthesis

**Bruno José Stoeberl (IC),[1] Francielli S. Santana (PG),[1] Siddhartha O. Giese (PQ),[2] David L. Hughes (PQ),[3] Jaísa F. Soares (PQ),[2] Dayane Mey Reis (PQ),[1*]**

**brunostoeberl@alunos.utfpr.edu.br; dayane@utfpr.edu.br.**

[1]Departamento Acadêmico de Química e Biologia, UTFPR; [2]Departamento de Química, UFPR; [3]School of Chemical Sciences & Pharmacy, UEA.

Palavras Chave: *Single-Molecule Magnets, Rational Synthesis, Chromium(III), Building Blocks.*

## Highlights

It is reported the obtainment of two novel binuclear building blocks based on chromium(III) exhibiting a large potential application for single-molecule synthesis by a rational single-product route.

## Abstract

Single-Molecule Magnets (SMMs) exhibit a large range of novel properties that arouse the interest of the technological and scientific communities. However, there is a lack of rational synthetic routes, since the majority of descriptions mostly involve one-pot and uncontrolled self-assembly routes, preventing the rationalization of the synthetic process, thus raising many difficulties in the study and improvement of the desired properties. The objective of this work is to develop a rational synthetic route for SMMs based on building blocks using $RC(CH_2OH)_3$ type pre-ligands in reaction with chromium(III) ions and to characterize the obtained products by spectroscopic and structural techniques. The building block approach is known by its large possibility of chemical tailoring, and while combined with the redox stability of chromium(III) ion, demonstrates an ability to direct the route into a high yield single-product route. We report the synthesis and characterization of three novel binuclear complexes of general formula $[Cr_2Cl_4\{RC(CH_2O)(CH_2OH)_2\}_2]$, where R = Me (complex 1, Fig.1), Et (complex 2, Fig.2) or $NH_2$ (whose structure is under refinement) obtained in mild synthetic conditions. For all products, FTIR spectroscopy suggests the obtainment of novel products whose structures were confirmed by single-crystal X-ray diffraction while the electronic and EPR spectra are compatible with the expected for the structures. Also, they are already being employed in a, still ongoing, synthesis of SMMs directed by the chemical stability of the chromium(III) ion to yield strictly one product.

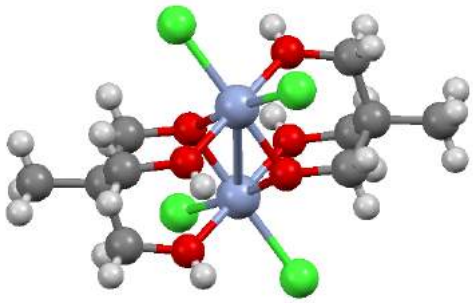

Fig.1: Schematic representation of complex 1.

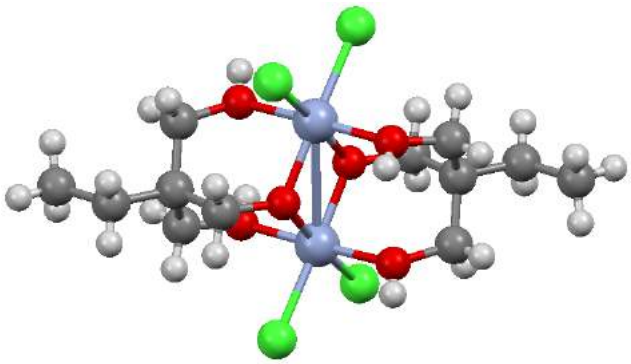

Fig.2: Schematic representation of complex 2.

**Área: INO** **Inscrição: 00283**

# Surface immobilization of carboxymethylated cashew gum (*Anacardium Occidentale L.*) on FeCo magnetic nanoparticles

**Maria Karolina da S. Oliveira* (PG), Leandro A. Costa (IC), Maria A. S. da Silva (PQ), Ana Rosa Richter (PG), Regina C. M. de Paula (PQ), Izaura C. N. Diógenes (PQ).**

**karolinacastelo@hotmail.com; izaura@dqoi.ufc.br**

*Departamento de Química Orgânica e Inorgânica, UFC*
Keywords: *FeCo alloy, Magnetic Nanoparticles, Cashew Gum, Colloidal Stability*

## Highlights

FeCo nanoparticles (NPs) produced by thermodecomposition were coated with carboxymethylated cashew gum producing FeCo@CMCG. Zeta potential of -36 mV was determined at pH 6.7 for FeCo@CMCG.

## Resumo/Abstract

Despite the exceptional magnetic properties exhibited by FeCo alloy nanoparticles (NPs), they cannot be directly used in biological applications due to oxidation processes and toxicity. As an environmental friendly approach, natural polysaccharide-coatings have been used to provide biocompatibility and chemical and colloidal stability in aqueous medium to magnetic NPs. The carboxymethylation of cashew gum (CG), which is a water-soluble polymer exudate from the cashew tree (*Anacardium occidentale L.*), ensures anchor groups for polymer attachment to NP. This work shows the results obtained on the characterization of FeCo NPs modified with carboxymethylated CG (CMCG) and the colloidal stability as function of pH. Hydrophobic $Fe_{59.86}Co_{40.14}$ NPs were synthesized from the reductive decomposition of $[Fe(acac)_3]$ and $[Co(acac)_2]$, acac = acetylacetonate under $H_2$ gas. The nanocrystals were transferred to aqueous phase and mixed with CMCG solution thus producing FeCo@CMCG materials. XRD patterns, Figure 1-A, show diffraction peaks assigned to the body-centered cubic structure of the FeCo alloy. FT-IR spectrum of FeCo@CMCG indicates the polymer grafting due to the vibrations at 1600 $cm^{-1}$ ($v_{as}COO^-$) and 1450 $cm^{-1}$ ($v_sCOO^-$) of the carboxymethyl moiety. DLS measurements, Figure 1-B, shows an increase in average hydrodynamic diameter for FeCo@CMCG, consistent with the polymer coating. Zeta potential measurements, Figure 1-C, indicate colloidal stability over the pH range due to the charged carboxylate groups that provide electrostatic repulsions (isoelectric point at pH 2.8). Zeta potential of -36 mV at pH 6.7 makes FeCo@CMCG attractive for biological applications.

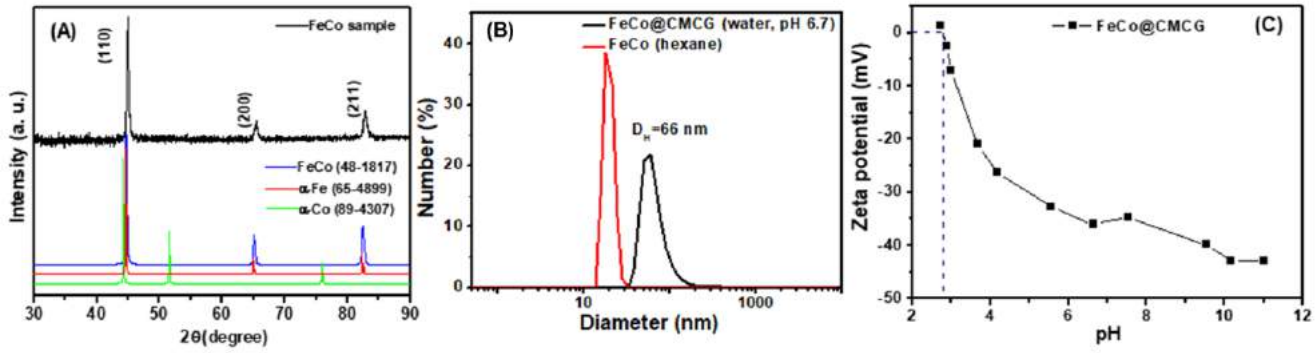


**Figure 1:** (A) XRD pattern of FeCo sample (black) with JCPDS cards, (B) DLS size distributions and (C) Zeta potential *versus* pH in water.

**Área: INO** **Inscrição: 00315**

# Lowering water oxidation overpotential of a mononuclear ruthenium(II) complex bearing ionizable imidazole moieties.

**Renan B. Guerra (PG),[1*] Luis E.S.C Huamaní (PG),[1] Naheed Bibi (PG),[1] André L.B. Formiga (PQ).[1]**

**renan.guerra@iqm.unicamp.br**

[1]*Departament of Inorganic Chemistry, Institute of Chemistry – UNICAMP, P.O. Box 6154, 13083-970, Campinas/SP, Brazil.*

Keywords: Water Oxidation Catalysis, Water Splitting, Homogeneous Catalysis, Ruthenium(II) Complexes, Electrocatalysis.

## Highlights

- A new mononuclear ruthenium(II) complex analogous to $[Ru(tpy)(bpy)OH_2]^{2+}$ was synthetized.
- $[Ru(H_2dimpy)(bpy)OH_2]^{2+}$ containing 2 imidazole moieties was characterized.
- Cyclic voltammetry showed a lower $Ru^{III}/Ru^{II}$ redox potential when compared to $[Ru(tpy)(bpy)OH_2]^{2+}$.
- In pH > 9, imidazole moieties are deprotonated, leading to even lower overpotentials.

## Abstract

The search for alternative and carbon-free source of energy is now of paramount importance for a sustainable development. The use of solar energy appears as one of the most promising alternatives through photoelectrochemical cells, and ruthenium-based water oxygen catalysts (WOC) are among the most used catalysts to achieve this goal. In this work we present the synthesis and characterization by UV-vis, $^1$H-NMR, ESI-MS, single crystal XRD, and cyclic voltammetry of a new mononuclear ruthenium complex, $[Ru(H_2dimpy)(bpy)OH_2](PF_6)_2$, bearing dissociable protons. Upon deprotonation at pH > 9, the $Ru^{III}/Ru^{II}$ redox couples are largely shifted to lower potentials. Cyclic voltammetry at pH = 13 showed that the complex displays catalytic current towards water oxidation at low overpotential (1.0 V), being a potential molecule to be used as a catalyst for water oxidation. Figure 1 shows CV's measurements in both acid and basic media. Even in acid conditions, when the imidazole moieties are protonated, the complex shows a lower $Ru^{III}/Ru^{II}$ redox couple (0.61 V) when compared to analogous $[Ru(tpy)(bpy)OH_2](PF_6)_2$ in pH = 1 (0.81 V)[1].

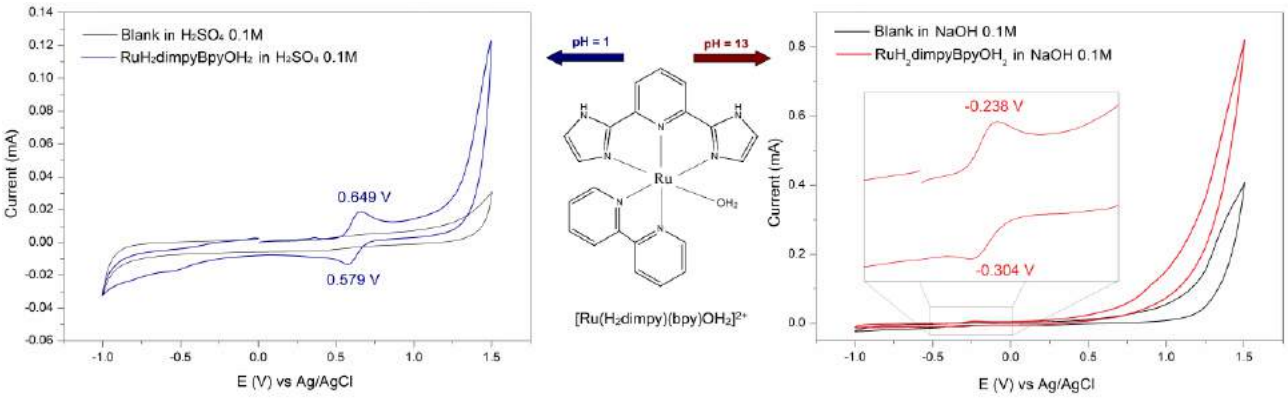


**Figure 1** – Cyclic voltammograms of $[Ru(H_2dimpy)(bpy)OH_2](PF_6)_2$ (2mM) in water:acetone (4:1), in acid and basic media. WE: Glassy carbon, CE: platinum wire, RE: Ag/AgCl, scan rate: 100 mV·s$^{-1}$.

[1]Okamura, M.; Yoshida, M.; Kuga, R.; Sakai, K.; Kondo, M.; Masaoka, S. Dalton Trans., 2012, **41**, 13081.

We would like to thank financial support from Fundação de Amparo à Pesquisa do Estado de São Paulo (FAPESP, 2013/22127-2), Coordenação de Aperfeiçoamento de Pessoal de Nível Superior (CAPES) and Conselho Nacional de Desenvolvimento Científico e Tecnológico (CNPq, 142440/2015-9).

**Área: INO** **Inscrição: 0323**

# Application of gold mining sludge in the preparation of materials for photo degradation of methylene blue

**Matheus G. Ferreira (IC)[1], José M. A. Grigorovski Júnior (IC)[1], Francisco M. S. Garrido (PQ)[1], Marta E. Medeiros (PQ)[1], Fernanda A. N. G. da Silva (PQ)[1], Vanessa P. R. Silva (PG)[1], Zuleica C. Castilho (PQ)[2].**

**chico@iq.ufrj.br; martam@iq.ufrj.br; matheus.gomes@ufrj.br;**

[1]*Departamento de Química Inorgânica, Instituto de Química – UFRJ*
[2]*CETEM – Rio de Janeiro*

*Palavras Chave: Vulcan-X; carbon black; dye photo degradation; gold mine sludge, pyrite.*

## Highlights

Composites of gold mine sludge with Vulcan-X and $CeO_2$ were prepared. These composites have activity for methylene blue degradation by photo Fento process.

## Resumo/Abstract

Drenagem ácida é um dos principais problemas da mineração de ouro, os minerais de sulfetos extraídos do interior da terra, descartados na superfície, reagem com água e oxigênio produzindo ácidos. O uso inovador destes rejeitos permitiria agregar valor ao processo de reciclagem viabilizando uma mineração limpa. O descarte de corantes na indústria têxtil também é considerado um problema ambiental atual. Neste trabalho o rejeito sólido de uma mina de ouro foi caracterizado e utilizado na preparação de materiais compósitos para a degradação do corante azul de metileno (MB) pelo processo foto Fenton, onde a pirita presente no rejeito atua como catalisador Fenton. Para a preparação do compósito, foi feita a mistura, em meio aquoso, entre Vulcan-X (50%) e o rejeito de mina (40%). Sendo levado em consideração o fato do Vulcan-X apresentar potencial zeta positivo enquanto que para o rejeito foi determinado, experimentalmente, um potencial zeta negativo. Através da impregnação com solução de nitrato de cério (IV) e amônio e calcinação a 300 $^0$C, foi adicionada, ao compósito, a fase $CeO_2$ (10%). As principais fases cristalinas identificadas por XRD, no material final, foram: $CeO_2$ (cúbica); $FeS_2$ (pirita) e Quartzo. O teste fotocatalítico (Figura-1), na presença de 48 mmol/L de $H_2O_2$, foi acompanhado por UV-Vis observando-se total eliminação do azul de metileno (concentração inicial de 150 mg/L), após 300 minutos de iluminação com lâmpada de LED (12 W), sendo que o material apresentou resultado similar por três reutilizações.

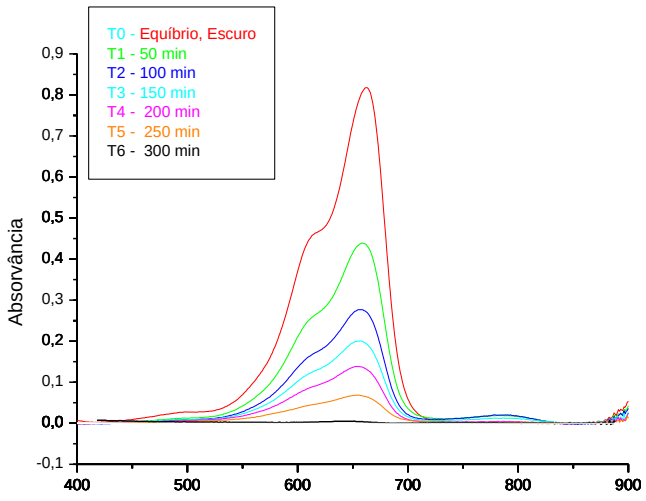


Figrua-1: Teste de foto degração de MB

**Área: INO** **Inscrição: 00364**

# INVESTIGATION OF THE ADDUCT BETWEEN CHLORITE AND CHLORINE DIOXIDE BY ELECTRONIC SPECTROSCOPY

**Gláucia W. Martins (PG), Roberto B. Faria* (PQ)**
**glauciawanzeller@yahoo.com.br; faria@iq.ufrj.br**
*Instituto de Química, UFRJ*

Palavras Chave: *Chlorite, Chlorine dioxide, Aduct, Electronic spectroscopy*

## Highlights

The dissolution of chlorine dioxide in aqueous solution of chlorite produces a brown solution with unclear nature. The UV-vis spectrum of this species is revealed for the first time.

## Resumo/Abstract

Sodium chlorite and chlorine dioxide have many applications in industry. They are often used as bleach and disinfectants instead of chlorine and sodium hypochlorite in the treatment of water and sewage. They are also employed in the bleaching of textiles and paper pulp because they do not produce undesirable chlorinated by-products.

However, dissolution of chlorine dioxide in chlorite solution, or the addition of HCl solution over solid or aqueous solution of sodium chlorite, produces a brown solution which composition is not well stablished yet. In this work we present the result of a spectroscopic study of these brown solutions.

The electronic spectra (UV-vis) we obtained show that the subtraction of the chlorine dioxide and chlorite spectra from the brown solution spectrum revels, for the first time, a low intensity band, with a maximum between 370 and 380 nm. This band can explain the increase of the absorption in the visible region which produces the observed brown color. This is the first time that a new band is shown in the solutions containing chlorite and chlorine dioxide, which explain the very well-known brown color of these solutions.[1,2] It is proposed that this color is due to the formation of an weak interaction aduct between the reagents.[1,2] We obtained also Raman spectra of these solutions but they did not show any new band, differently from that present in chlorite and chlorine dioxide solutions. As a conclusion, the nature of this aduct remains uncertain, but the electronic spectra we present here can be a starting point to reveal its structure.

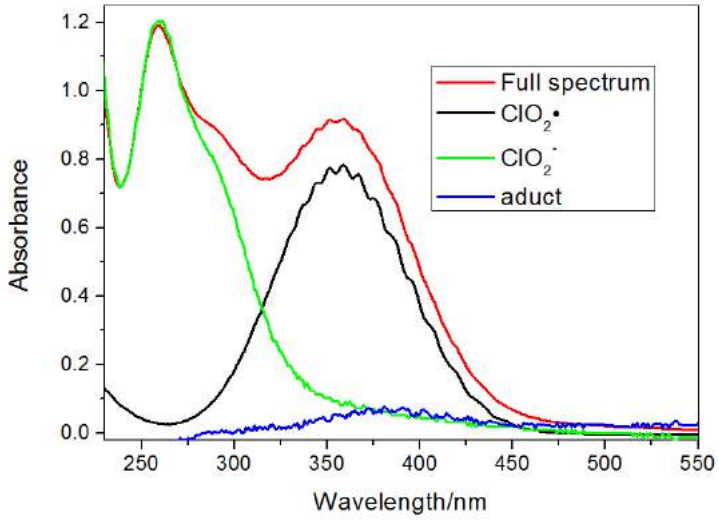


**Figure 1.** Electronic spectra of the brown solution (red) produced by the mixture of chlorine dioxide (black) and chlorite (green). The subtraction the last two from the first one reveals the spectrum of the aduct responsible for the formation of the brown color.

References:
1. Gordon, G.; Emmeneger, F.; *Inorg. Nucl. Chem. Lett.* **1966**, *2*, 395-398.
2. Körtvélyesi, Z.; Analytical methods for the measurement of chlorine dioxide and related oxychlorine species in aqueous solution, PhD Thesis, Miami University, 2004.

**Área: INO** **Inscrição: 00371**

# DINUCLEAR PLATINUM(II) COMPLEX WITH OXADIAZOL ADAMANTANE

**Jéssika Thayanne da Silva (IC)[1], Ana Luiza de A. Querino (IC)[1], Renata Diniz (PQ)[1], Heveline Silva (PQ)[1]***

**jessikathayanne@outlook.com; hevelinesilva@ufmg.br**

*[1]Departamento de Química, ICEX, Universidade Federal de Minas Gerais, Av. Antônio Carlos 6627, Pampulha, 31270-901, Belo Horizonte, Minas Gerais.*

Palavras Chave: *Platinum, dinuclear, oxadiazol.*

## Highlights

A dinuclear platinum complex was obtained with four bidentate bridging ligands.
X-ray crystallography confirms data from elemental analysis, infrared spectroscopy, $^{1}H$, $^{13}C$ and $^{195}Pt$ NMR.

## Abstract

The discovery of cisplatin, in the late's 1960's, enhanced the metallic compounds studies for cancer treatment. Despite its success in the clinic and its broad utilization in the treatment of several types of cancer, it may cause cell resistance and severe side effects. These factors motivated studies of a great number of platinum derivative compounds, such as bi- or tri-homonuclear complexes, that show different cellular uptake mechanisms and lower cell resistance[1]. With the aim to obtain a more effective and less toxic compound, a new dinuclear platinum complex was synthesized with heterocyclic 1,3,4-oxadiazolines ligands (ligand A) that could confer lipophilicity and potential anticancer activity.

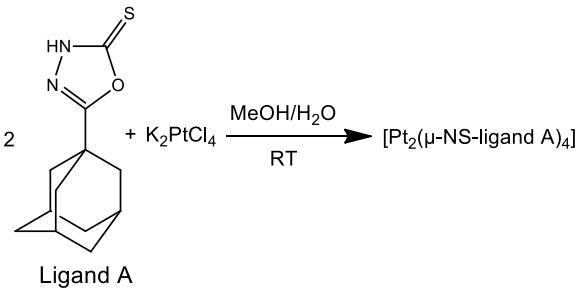

The complex was synthesized as shown above in 71% yield and was characterized by elemental analysis, X-ray crystallography, infrared and $^{1}H$, $^{13}C$ and $^{195}Pt$ NMR. Data suggests that a Pt dinuclear complex was obtained with four bridging ligands, each coordinated by the N and S atoms, as confirmed by single crystal X-ray analysis. $^{195}Pt$ NMR spectra showed a single signal at -3032,92 ppm, due to high symmetry[2]. The absence of υNH band in infrared spectra indicates that ligand A assumes its tautomeric form in complex 1.

| | Complex 1 | |
|---|---|---|
| | **Anal. Calc.** | **Found** |
| %C | 43,30 | 44,99 |
| %H | 4,54 | 4,82 |
| %N | 8,42 | 8,73 |

Activity against tumor cells are ongoing.

FAPEMIG, CNPQ

[1]Neves A.P., Vargas, M. D. *Rev. Virtual Quim.*, 2011, *3*, 196-209.
[2]Paschoal, D., Guerra, C. F., Oliveira, M. A. L., Ramalho, T. C., Dos Santos, H. F., *Journal of Computational Chemistry*, 2016, 2360-2373.

**Área: INO** **Inscrição: 00400**

# Estudo da coordenação dos ligantes 4-cloro e 4-nitro-benzaldeído-tiosemicarbazona derivados do R-(+)-limoneno com cobre(II)

**Bruno Ribeiro Santos (GR)[1]*; Ariane C. F. Beltrame (IC)[2]; Alisson F. Stocco (IC)[3]; Alessandra Stevanato (PQ)[2]; Fábio Vandresen (PQ)[2]**

**brunosantos.brs@hotmail.com; brunosantos.brs@hotmail.com**

[1]*Departamento de Engenharia Química, UTFPR – Câmpus Londrina.*
[2]*Departamento de Química, UTFPR – Câmpus Londrina.*
[3]*Departamento de Engenharia de Materiais, UTFPR – Câmpus Londrina.*

Palavras Chave: *Complexos de Cobre(II), Limoneno, Tiossemicarbazonas.*

## Highlights

Coordination study of 4-chloro and 4-nitro-benzaldehyde-thiosemicarbazone ligands derived from R-(+)-limonene with copper(II). Thiosemicarbazones and their copper complexes are substances of pharmacological interest. It is proposed to synthesize R-(+)- limonene complexes of 4-chloro and 4-nitro-benzaldeide-thiosemicarbazones.

## Resumo

O cobre é um composto metálico largamente presente no corpo humano em diversas funções reguladoras do organismo, garantindo baixa citotoxicidade. Sua capacidade oxidativa despertou interesse para seu uso terapêutico[1]. Os ligantes tiossemicarbazonas apresentam propriedades antifúngicas, antibacterianas e antitumorais. Estes foram obtidos por catálise ácida em refluxo durante cinco horas entre tiossemicarbazida e um aldeído (4-Cl-benzaldeído) ou (4-$NO_2$-benzaldeído). Foram caracterizados por infravermelho e RMN de $^{1}H$ e $^{13}C$ {$^{1}H$}. A unidade terpênica foi evidenciada pelos sinais δH/δC 5,36 ($^{1}H$, s) / 120,6; 1,48 ($^{3}H$, s / 24,5; 1,50 ($^{3}H$, s) / 24,2 e δH 1,64 ($^{3}H$, s) / 23,5. A tiossemicarbazona foi caracterizada pelos sinais δH 9,00-11,00 e 7,30-7,60 (NH), δH/δC 7,00-8,50 (CH=N) / 141,0 (C=N) e δC 174,4 (C=S). Os complexos foram sintetizados na razão molar 1:2 entre cloreto de cobre(II) e ligantes 4-cloro-benzaldeído-tiosemicarbazona (4-Cl-TSC-R-Lim, **L1**) ou 4-nitro-benzaldeído-tiosemicarbazona (4-$NO_2$-TSC-R-Lim, **L2**), sob agitação magnética à 70 °C durante duas horas. Os complexos foram analisados por IV e PF. No complexo [Cu(4-Cl-TSC-R-Lim)$_2$] (**C1**), observou-se deslocamento (C=S) de 822 a 833 $cm^{-1}$ e uma variação de 24 $cm^{-1}$ para a banda de (C=N). Para o complexo [Cu(4-$NO_2$-TSC-R-Lim)$_2$] (**C2**), observou-se a banda (C=S) em 846 $cm^{-1}$ e deslocamento (C=N) de 1564 $cm^{-1}$ para 1527 $cm^{-1}$. A Figura 1 ilustra os espectros obtidos para os complexos (**C1**) e (**C2**) e seus respectivos ligantes (**L1**) e (**L2**). Ref. [1] DENOYER, Delphine et al.. Metallomics, [s.l.], v. 7, n. 11, p.1459-1476, 2015. Royal Society of Chemistry (RSC).

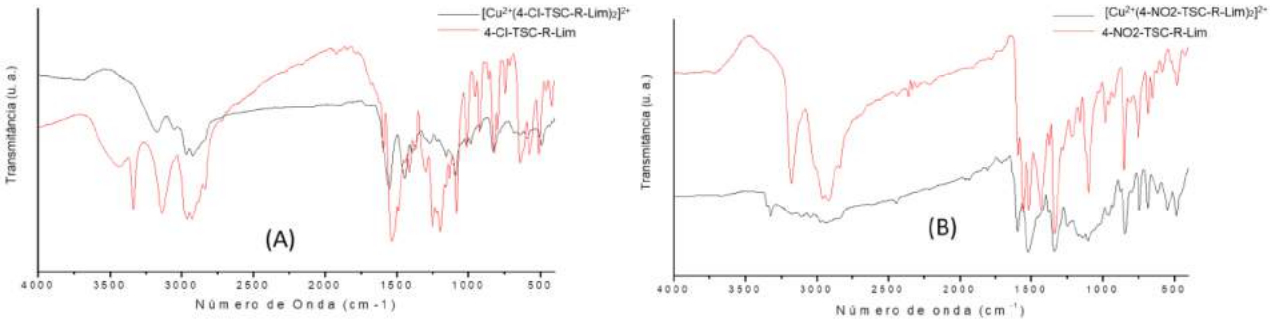


**Figura 1.** Espectros de absorção no IV: (**A**) do ligante 4-Cl-TSC-R-Lim (L1) e complexo [Cu(4-Cl-TSC-R-Lim)$_2$] (C1); (**B**) do ligante 4-$NO_2$-TSC-R-Lim (L2) e complexo [Cu(4-$NO_2$-TSC-R-Lim)$_2$] (C2).

**Área: *INO***
*(Inserir a sigla da seção científica para qual o resumo será submetido. Ex: ORG, BEA, CAT)*

**Inscrição: *00404***
*(Inserir o número de inscrição do autor que fez a submissão)*

# Estudo teórico da inclusão de complexos de platina (II) não covalentes em β-ciclodextrinas.

**João Marcos B. Candido (IC),[1*] Nathália M. Paixão (PG),[1] Luiz Antônio S. Costa (PQ)[1].**

**luiz.costa@ufjf.edu.br; joaomarcosbca@gmail.com**

*[1]Departamento de Química, NEQC – Núcleo de Estudos em Química Computacional, ICE, UFJF - Universidade Federal de Juiz de Fora, Juiz de Fora, MG 36036-330*

Palavras Chave: Complexos de Inclusão, ONIOM, Interações não Covalentes, Ciclodextrinas, DFT.

## Highlights

**Theoretical study of the inclusion of non-covalent platinum (II) complexes in β-cyclodextrins.**
This work aims to study non-covalent platinum (II) complexes included in β-cyclodextrin units using the ONIOM methodology with different conformations.

## Resumo/Abstract

Os compostos polinucleares de Platina (II) não covalentes têm se mostrado muito promissores contra células cancerosas devido a interações mais rápidas e efetivas em comparação com os compostos covalentes, como por exemplo, o complexo BBR3464[1]. Este trabalho tem como objetivo o estudo de propriedades estruturais e termodinâmicas da inclusão de complexos de platina (II) não covalentes em unidades de β-ciclodextrinas. Foram realizados cálculos de otimização e frequências harmônicas utilizando a metodologia ONIOM, definindo para a camada alta o funcional BHandH, com o conjunto de funções de base 6-31+G(d,p) para os átomos não metálicos e o ECP SDD para os átomos de platina e, para a camada baixa, o campo de força UFF. Além disso, as estruturas foram obtidas utilizando o modelo contínuo de solvente PCM, no qual a água foi utilizada como solvente. Foram inicialmente estudados dois modos de inclusão com estequiometrias diferentes. A Figura 1 demonstra os modos de inclusão analisados, em (a) está representado o complexo de inclusão com apenas uma unidade de β-ciclodextrina, em (b), (c) e (d) está representado o segundo modo de inclusão com duas unidades de β-ciclodextrinas, sendo possível apenas três configurações diferentes, devido à simetria do complexo. Até o momento a estrutura mais estável é a representada na Figura 1.c, conformação HT, devido ao menor valor da energia livre de Gibbs encontrada para a energia de interação do complexo formado, entre as unidades de β-ciclodextrinas e do complexo de platina(II).

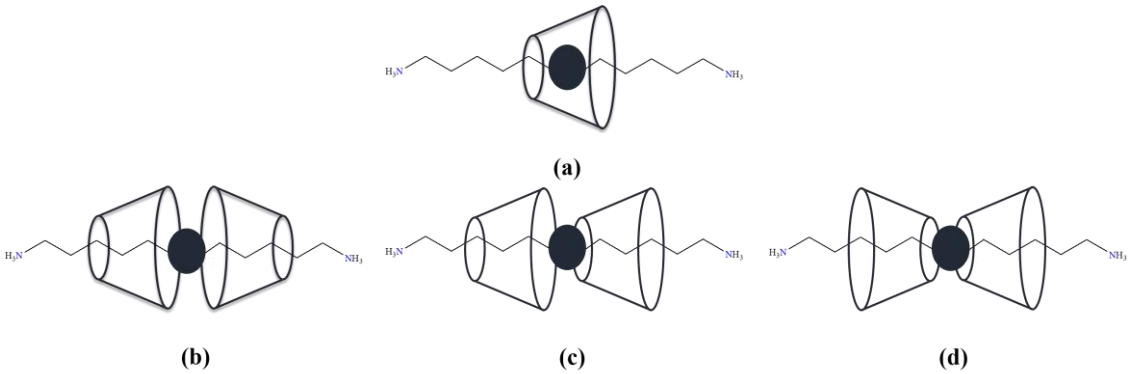


**Figura 1.** Modos de inclusão do complexo mononuclear de platina (II) com (a) uma unidade de β-ciclodextrina e com duas unidades em três configurações diferentes (b) HH, (c) HT e (d) TT.

1. A.L. Harris, *et. al.*, Inorganic Chemistry Communication, **44,** 9598-9600 (2005).

**Área: INO**
*(Inserir a sigla da seção científica para qual o resumo será submetido. Ex: ORG, BEA, CAT)*

**Inscrição: 434**
*(Inserir o número de inscrição do autor que fez a submissão)*

# DNA/BSA binding properties of metallo-tetrakis(1-naphtyl)porphyrins: the metal central ion effect

**Carolina Hahn da Silveira (PG),[1] Emanuelly Garoforo (IC)[1] and Bernardo A. Iglesias (PQ),[1*]**

**bernardopgq@gmail.com; carolinahahndasilveira@gmail.com**

[1]*Bioinorganic and Porphyrinoid Materials Laboratory, Department of Chemistry, Universidade Federal de Santa Maria, UFSM, ZIP CODE 97110-900, Camobi, Santa Maria – RS, Brazil.*

Palavras Chave: *Porphyrins, Metalloporphyrins, DNA, BSA.*

## Highlights

In this work, we demonstrate the ability of biomolecules (DNA and BSA) interact to metalloporphyrins in DMSO/Tris-HCl buffer media. We also present the thermodinamic parameters of these covalently interaction, depending on the metal ion nature.

## Resumo/Abstract

Porphyrins are an interesting class of heteroaromatic 18 π-electron aromatic macrocycles that have found wide applications in many fields, including biologic systems, medicine, catalysis and materials.[1] Such applications explore their optical, photochemical, photo-electrochemical, catalytic, binding and electrochemical properties.[2]
In this work, a new series of metallo-tetra-(naphytyl)porphyrins (2H, Zn, Cu, Ni, Co and Mn) are described. The structural and electronic properties were characterized by mass spectrometry, electronic absorption and emission spectroscopy, infrared spectroscopy and cyclic voltammetry. Also, the interaction of the porphyrin complexes and biomolecules (DNA and BSA) were evaluated as a function of the metal central ion coordinated of the porphyrin ring, showing significant influence on the electronic and biomolecule-binding properties.

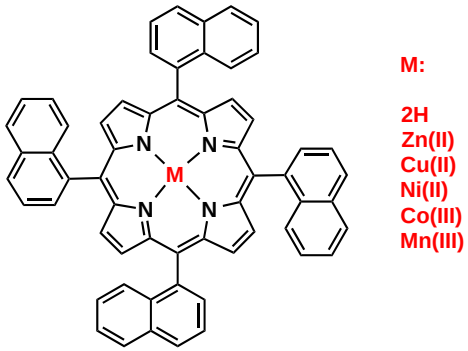


**Figure 1.** General representative structure of metalloporphyrins used in this study.

References

[1] Kadish, K.M.; Smith, K.M.; Guilard, R.; *The Porphyrin Handbook*; Academic Press, San Diego, **2010**, *vol.1-22*.
[2] Ralph, S.F.; *Current Topics in Medicinal Chemistry*, **2011**, *11*, 572-590.

**Área: INO** **Inscrição: 00593**

# Identificação de ácido acetilsalicílico em formulações farmacêuticas sólidas por espectroscopia de infravermelho

**Rayane D. Alhadas (IC),[1]* Bruna L. M. Vieira (IC),[1] Tatiana Alves Toledo (TM),[1] Denise B. A. Barbosa (FM)[1].**

***rayanealhadas@hotmail.com; tatiana.alves@ifsudestemg.edu.br**

[1]*Laboratório de Pesquisa e Experimento em Nanociência, Instituto Federal de Ciência e Tecnologia do Sudeste de Minas Gerais – Campus Juiz de Fora*

Palavras Chave: Ácido acetilsalicílico, fármaco, infravermelho, identificação.

## Highlights

Identification of acetylsalicylic acid in solid pharmaceutical formulations by infrared spectroscopy - The objective of this study was to identify AAS in commercial formulations by visual method and by infrared spectroscopy. The major bands have been observed and the differences are due to the excipients.

## Resumo/Abstract

O ácido acetilsalicílico (AAS) é o analgésico de maior popularidade e aceite social, com ação comprovada como analgésico e antitérmico, além de ser usado em distúrbios cardiovasculares [2,4]. A técnica de espectroscopia de infravermelho é uma metodologia simples e rápida que evidencia grupos funcionais e é útil para a identificação de medicamentos[3].
Objetivou-se identificar o AAS em formulações comerciais em comparação ao padrão analítico, utilizando a técnica de infravermelho.

Foram adquiridas duas apresentações distintas de AAS, comprimidos de 100mg e 500mg. O padrão é o reagente da Merck®. Seguindo a recomendação da Farmacopeia Brasileira (2010), foi realizada a identificação do princípio ativo, por método visual e por espectroscopia de infravermelho, utilizando pastilhas de KBr, entre 4000 e 400 $cm^{-1}$, com média de 128 varreduras com resolução de 2 $cm^{-1}$, no espectrômetro FT- IR Spectrum Frontier. Origin Pro 8 foi o software empregado na análise dos dados.

A identificação visual do princípio ativo apresentou uma escala de coloração, devido às concentrações diferentes entre as amostras (figura 1).

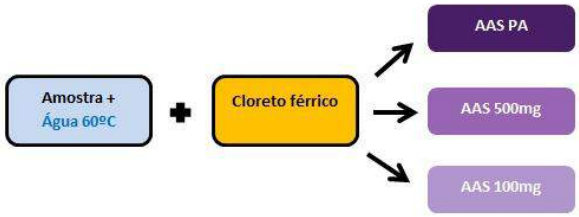


Os espectros de infravermelho (figura 2) dos medicamentos apresentaram perfis semelhantes ao padrão, apresentando as bandas características (figura 3) descritas na literatura [2,3]. As pequenas diferenças são atribuídas aos excipientes adicionados nas formulações [3].

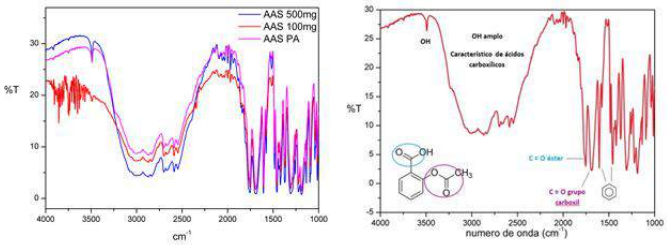


Como esperado, os espectros apresentaram similaridades, tanto com o padrão quanto com o relatado em literatura. As principais bandas características foram observadas e os pequenos deslocamentos e diferenças de intensidades são decorrentes dos efeitos produzidos pelos substituintes vizinhos oriundo dos excipientes.

Referências:.
[1]BRASIL. *Farmacopeia Brasileira*, 5ª ed. Agência Nacional de Vigilância Sanitária. Brasília: Anvisa, 2010. [2]BUNACIU, A. A., ABOUL-ENEIN, H.Y., FLESCHIN, S. *Canadian Journal of Analytical Sciences and Spectroscopy*, vol 51, n 5, 2006. [3]MORAIS, F.E., 2011. *Dissertação* (Mestrado em Química) - Universidade Federal do Rio Grande do Norte, Natal, RN. [4]XAVIER, M.P., SOUSA, S. F., *Revista Amazônia*, vol 1 (3), 2013.

**Área: INO** **Inscrição: 00601**

# The effect of the temperature on Brilliant Green dye bleaching catalyzed by zinc hydroxide nitrate

**Murilo G. Da Rocha (IC)[1,2], Geani M. Ucoski (PQ)[1], Shirley Nakagaki (PQ)[1], Guilherme S. Machado (PQ)[2]***

**murilo_goncalvesrocha@yahoo.com.br; *guimachado@ufpr.br**

*[1]Laboratório de Bioinorgânica e Catálise, Universidade Federal do Paraná, Departamento de Química, CP 19081, CEP 81531-990, Curitiba, Paraná, Brasil; [2]Laboratório de Bioinorgânica Marinha e Química Verde, Centro de Estudos do Mar, Universidade Federal do Paraná, Núcleo Mirassol, Balneário Mirassol, Caixa-Postal: 61 CEP: 83255-000, Pontal do Paraná, Paraná, Brasil.*

Key words: *layered hydroxide salts, bleaching catalysis, organic dye.*

## Highlights

Synthesis of zinc hydroxide nitrate and use as a catalyst on the Brilliant Green dye bleaching reaction. The effect of the temperature for the catalytic system was analyzed.

## Resumo/Abstract

Zinc hydroxide nitrate (ZHN), a compound belonging to the class of the layered hydroxide salts, was synthesized by the co-precipitation method [1] and characterized by powder x-ray diffraction and infrared spectroscopy. The ZHN solid was investigated as a catalyst in the oxidative bleaching of the Brilliant Green (BG) organic dye by hydrogen peroxide 11,24 mol $L^{-1}$. BG is a potential carcinogen that is frequently discarded or lost in the textile industry's wastewaters [2]. The dye bleaching reactions using ZHN in heterogeneous catalysis presented an expressive increase in the reaction rate constant (k) in comparison to the control reactions (without the catalyst). The progress of the catalytic reaction was monitored using UV-Vis analysis following the decrease of the main band of the BG dye at 625 nm. The best catalytic result was observed when using the molar ratio of 5000:100:1 (oxidant:dye:catalyst), at 45 $^{o}$C, in the absence of light. Under these catalytic conditions, it was observed rate constant of about 438 times bigger than that observed in the control reaction. The results emphasize the effect of the temperature on the catalytic result since only a little increase on the reaction temperature resulted in a great change on the rate constant (Table 1), indicating that the ZHN is a promising solid catalyst for BG dye bleaching. The possibility of the ZHN's reuse was also investigated and the proposition of a catalytic cycle is currently under investigation.

Table 1: Catalytic results obtained for the BG dye oxidative degradation by hydrogen peroxide under different reaction conditions[a].

| Temperature (º C) | Velocity constant k ($s^{-1}$) | Control reaction[b] velocity constant ($s^{-1}$) | Times of increase in the rate constant |
|---|---|---|---|
| **25** | $2.24 \times 10^{-4}$ | $1.9 \times 10^{-6}$ | 117.70 |
| **35** | $4.67 \times 10^{-4}$ | $2.0 \times 10^{-6}$ | 233.68 |
| **45** | $8.74 \times 10^{-4}$ | $2.0 \times 10^{-6}$ | 437.42 |

[a]oxidant:dye:catalyst molar ratio: 5000:100:1, using 19 mg of catalyst solid, solvent: water, different temperatures, reaction time: 1 h and under absence of light. [b]control reaction using only dye BG and the oxidant, without catalyst.

*References*

[1] Machado, G. S.; Arízaga, G. G. C.; Wypych, F.; Nakagaki, S. *J. Catal.* 2010, *274*, 130.
[2] Gessner, T.; Mayer, U. *Triarylmethane and Diarylmethane Dyes*, Ullmann's Encyclopedia of Industrial Chemistry, Wiley-VCH, Weinheim, 2002.

**Área: INO** **Inscrição: 00704**

# Study of crylene acid ligand coordinated to lanthanide compound

**Lucas do Prado Cardoso (IC),[1*] Michele do Rocio Gonçalves Dias (PG),[1] Cristiane Pilissão (PQ),[1] Renata Danielle Adati (PQ).[1]**

**lucascardoso@alunos.utfpr.edu.br**

[1]*Departamento Acadêmico de Química e Biologia, UTFPR*

Keywords: *Luminescence, Coordination compound, Octocrylene, Lanthanide.*

## Highlights

A lanthanide complex with crylene acid (CLN) was obtained, the FT-IR analysis confirmed metal coordination, chemical stoichiometry was suggested by $Gd^{3+}$ and $Eu^{3+}$ titration.

## Abstract

Carboxylic acids are commonly used in coordination chemistry with lanthanides ions, owing to the stronger binding to metal centre. In this work we report the coordination of crylene acid (CLN; 2-cyano-3,3-diphenyl-2-propenoic acid). According to our previous studies, CLN (Figure 1) is a chromophore obtained from the alkaline hydrolysis of octocrylene (OCR; 2-ethylhexyl 2-cyano-3,3-diphenyl-2-propenoate), as known there is no studies reporting lanthanide coordination compounds of CLN ligand. We report here the synthesis and characterization of lanthanide (gadolinium and europium) complex, LnCLN, due to: Possibility of determining ligand triplet state by GdCLN fluorescence analysis; Low cost of Gd compared with other $Ln^{3+}$; Similarity between $Gd^{3+}$ and $Eu^{3+}$ atomic radii; On other hand $Eu^{3+}$ complexes exhibit narrow bands and can be used as structural probe. To obtain LnCLN, 4.0 mmol CLN was solubilized in ethanol, 1.0 mmol $LnCl_3$ (pH 4.5) was slowly added to the solution. The system was kept in stirring and heating for ~1 h at 50 °C. After some days a solid (Figure 2) were obtained, filtered out, washed with ethanol and dried in a vacuum. FT-IR spectra of LnCLN compared with CLN ligand (Figure 3), show a $\nu_s$(C=O) band displacement of ~76 $cm^{-1}$ suggesting strong interaction between oxygen atoms from carbonyl groups and $Ln^{3+}$. The chemical stoichiometry of the complex, suggested by $Ln^{3+}$ titration using a standard EDTA solution, confirmed the 1:3 (metal:ligand) molar ratio. To verify charge transfer, CLN triplet state will be determined by GdCLN fluorescence analysis.

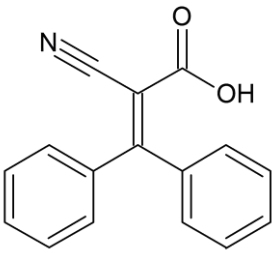


Figure 1. Molecular structure of CLN.

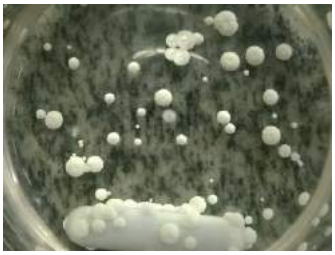

Figure 2. GdCLN coordination compound.

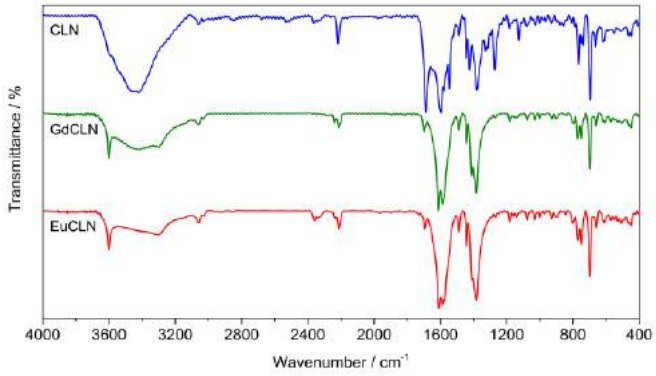


Figure 3. FT-IR spectra of the CLN, GdCLN and EuCLN.

Table 1. Infrared frequencies (wavenumber in $cm^{-1}$) for the CLN, GdCLN and EuCLN.

| | Wavenumber / $cm^{-1}$ | | | | | |
|---|---|---|---|---|---|---|
| Compound | **ν**C=O | **ν**C–O | **ν**C=C | **ν**C≡N | **ν**O–H | **δ**O–H |
| CLN | 1687 | 1273 | 1597 | 2220 | 3435 | 931 |
| GdCLN | 1612 | 1412 | 1587 | 2214 | 3425 | — |
| EuCLN | 1610 | 1410 | 1588 | 2214 | 3405 | — |

**Área: INO** **Inscrição:00756**

# Co(II) benzimidazoles complexes: Synthesis, characterization and catalytic studies to chemical fixation of $CO_2$ in cyclic carbonates

**Jorge Luiz Sônego Milani (PQ), Danielle Cangussu (PQ), Rafael Pavão das Chagas (PQ), Gabriel Amorim Vilela (IC), Ana Karoline S. M. Valdo (PG), Felipe Terra (PQ)**

**milani_jorge@yahoo.com.br**

*LABSINCO – Laboratório de Síntese e Compostos Organometálicos - Instituto de Química – Universidade Federal de Goiás – UFG*

Keywords: *Cobalt catalysts; Full characterization of Co(II) complexes; Cyclic carbonates.*

## Highlights

Co(II)-benzimidazoles complexes good activities and selectivity in the chemical fixation of $CO_2$ to cyclic carbonates

Complete characterization of Co complexes

## Resumo/Abstract

One of the most challenging environment problem is the control emissions of greenhouse gases; carbon dioxide levels in atmosphere are the highest since records began; the concentration of $CO_2$ in atmosphere has risen up from 280 ppm to 400 ppm during the last century and, the average global temperature has increased between 0.6 °C and 1 °C in the same period. New routes to transform $CO_2$ into desirable and economically competitive products are the main goal for chemists.[1]

In this sense, we developed five cobalt(II) benzimidazole complexes (Figure 1) which were characterized by $^1H$ and $^{13}C$ NMR, elemental analysis, IR, electronic spectra (diffuse reflectance and methylene chloride solution), ESI-HRMS, Raman and crystalline structure. The complexes had their catalytic performance studied in the $CO_2$ fixation reaction with an epoxide forming cyclic carbonates. The catalytic performance is showed in Table 1.

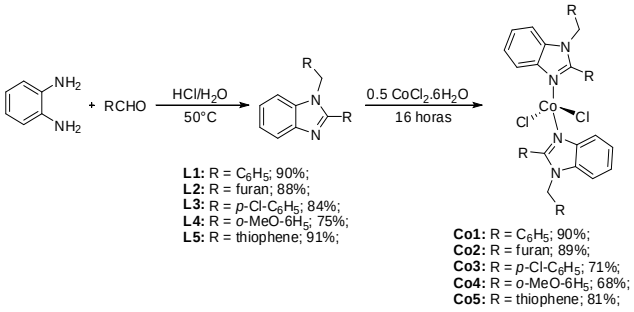


**Figure 1.** Synthesis of **Co1-Co5**.

In summary, we have synthesized five tetracoordinate cobalt complexes, calculated their field parameters, studied magnetic and structural behavior and a complete catalytic study was performed. All complexes were able to catalyze the cycloaddition reaction. Different types of bases were tested and TBAB was the best. An equilibrium between nucleophilic/leaving group ability of anion is responsible to the better conversion using TBAB. Temperature has a high impact in catalytic activities arising TON e TOF when increasing this variable.

**Table 1.** $CO_2$ cycloaddition reaction using **Co1-Co5**.[a]

| Ent. | Cat. | T (°C) | t (h) | Conv. (%)[b] | TON[c] | TOF[d] |
|---|---|---|---|---|---|---|
| 1 | Co1 | 100 | 16 | 85 | 1186 | 74 |
| 2 | Co2 | 100 | 16 | 71 | 993 | 62 |
| 3 | Co3 | 100 | 16 | 74 | 1029 | 64 |
| 4 | Co4 | 100 | 16 | 93 | 1308 | 82 |
| 5 | Co5 | 100 | 16 | 81 | 1138 | 71 |
| 6 | Co4 | 60 | 6 | 5 | 69 | 12 |
| 7 | Co4 | 120 | 6 | 100 | 1400 | 233 |
| 8[e] | Co4 | 100 | 48 | 94 | 2642 | 55 |
| 9[f] | Co4 | 100 | 6 | 53 | 749 | 125 |
| 10[g] | Co4 | 100 | 6 | 54 | 757 | 126 |
| 11[h] | Co4 | 100 | 6 | 66 | 927 | 155 |
| 12[i] | Co4 | 100 | 6 | 45 | 636 | 106 |
| 13[j] | Co4 | 120 | 6 | 81 | 2436 | 407 |

[a] Reaction conditions: catalyst (0.01 mmol, 0.07 mol%), cocatalyst (TBAB, 0.01 mmol, 0.07 mol%); $P_{[CO2]}$ = 30 bar,[b] Conversions determined on basis of $^1H$ NMR analysis. [c] Turnover number (mol of carbonate produced/mol catalyst).[c] Turnover frequency ($TON.h^{-1}$). [e] 2800 eq. of SO. [f] PPNCl. [g] TBAC. [h] TBAI. [i] DMAP. [j] 3000 eq of SO.

Reactions with different epoxides was performed in optimal conditions and the systems were active with all epoxides tested.

**Acknowledgements:**

FAPEG and CAPES.

**References**

1. Milani, J. L S.; Oliveira, I. S.; Dos Santos, P. A.; Valdo, A. K. S. M.; Martins, F. T.; Cangussu, D.; Das Chagas, R. P. *Chin. J. Cat., in press,* DOI: 10.1016/S1872-2067(17)62992-9.

**Área: INO**
*(Inserir a sigla da seção científica para qual o resumo será submetido. Ex: ORG, BEA, CAT)*

**Inscrição: 00792**
*(Inserir o número de inscrição do autor que fez a submissão)*

# Organically modified Urea-sepiolite to application in caffeine removal

**Evane da Silva* (PG),[1] Michelle Saltarelli (PQ),[1] Emerson H. de Faria (PQ),[1] Eduardo J. Nassar (PQ),[1] Katia J. Ciuffi (PQ),[1]**

**mi_saltarelli@yahoo.com.br; evanemuzambinho@yahoo.com.br**

***[1]Laboratório de Pesquisa Sol-Gel - Universidade de Franca, Av. Dr. Armando Salles Oliveira, 201 Pq. Universitário, CEP 14.404-600, Franca, SP.***

Keywords: *sepiolite, organoclays, adsorption, caffeine*

## Highlights

- ✓ Sepiolite were modified using urea functionalized alkoxide;
- ✓ No basal changes occurs after organomodification;
- ✓ The textural analyses confirmed functionalization SEP (149 $m^2.g^{-1}$) to SEP-TEMSPU (17 $m^2.g^{-1}$);
- ✓ Thermal analyses (TG/DTG/DSC) showns the characteristic decomposition of TEMSPU.

## Resumo/Abstract

This study aimed to assess the capacity of sepiolite (SEP) modified with Trietoxymethylsilanopropyl Urea (SEP-TEMSPU) to adsorb and remove caffeine from aqueous solutions. Powder X-ray diffraction (PXRD) revealed no increased basal spacing in the modified sepiolite proving that the clay present non-expansive characteristics. Thermal analyses (TG/DTG/DSC) for modified clay present a mass loss at 347.55 °C (7.86%), characteristic of the decomposition of organic matter resulting from TEMSPU, previously not observed for SEP. The infrared spectroscopy shows functionalization due to deformation vibrations of N-H bonds (1556 to 1263 $cm^{-1}$) and NH (3341 $cm^{-1}$) bonds in the urea. The C-H stretching at the propyl groups (2925-2921 $cm^{-1}$) is also a good indication for the modification, since the sepiolite does not have any peaks around this region. The textural analyses confirmed functionalization of the natural sepiolite too, there was a decrease in the specific surface area from SEP (149 $m^2.g^{-1}$) to SEP-TEMSPU (17 $m^2.g^{-1}$) due to the presence of the organic groups of the alkoxy. The maximum adsorption capacity at equilibrium (Figure 1) indicate that the sepiolite and urea-sepiolite constitutes an efficients and suitables caffeine adsorbents.

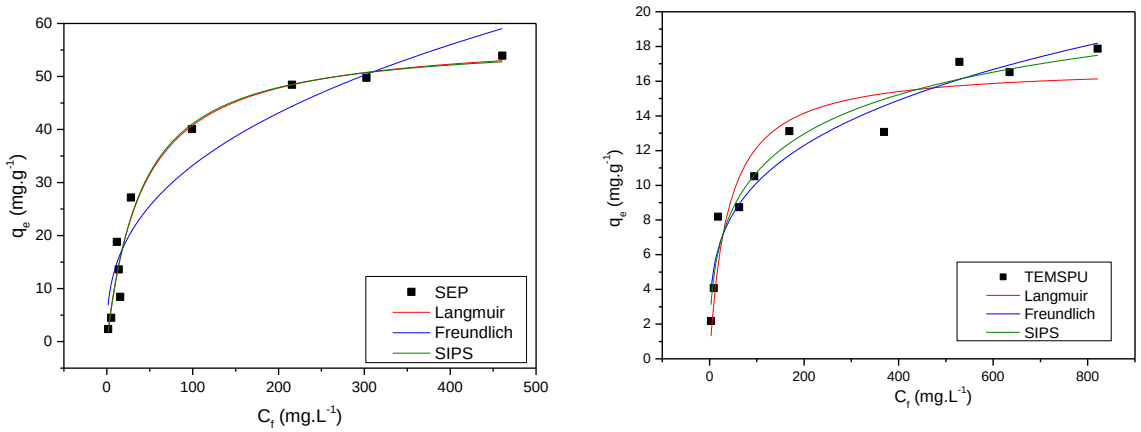


**Figure 1:** Equilibrium (symbol) and models (lines) Langmuir 1, Freundlich and Sips isotherms for the equilibrium data for caffeine adsorption on purified and modified sepiolita.

**Acknowledgments:** Brazilian Research funding agency FAPESP (2016/01501-1 and 2016/50322-2). E.H.d.F. and K.J.C. acknowledge CNPq grants (311767/2015-0 and 305398/2015-6, respectively). CAPES PNPD-1660297.

**Área: INO** **Inscrição: 00865**

# Lanthanide complex as potential nitric oxide luminescent probe

**Filipe Miranda Cabral (PG),[1] Gilmar Araújo Brito Júnior (PQ),[1] Italo Odone Mazali (PQ),[1] Fernando Aparecido Sigoli (PQ)[1]**

**filipemcabral@gmail.com; fsigoli@iqm.unicamp.br**

*[1]Laboratory of Functional Materials- Institute of Chemistry – UNICAMP, Campinas, Brazil*

Keywords: *Lanthanide, Complexes, Luminescence, Nitric Oxide.*

## Highlights

Development of a new organic ligand to act as nitric oxide luminescent probe. Nitric oxide detection using lanthanide complexes. Luminescence spectroscopy to detect nitric oxide in solution.

## Abstract

Nitric oxide plays an important role in the biological environment in the cardiovascular system, neurologic and immunologic system [1,2]. To track the nitric oxide in the biological environment fluorescent biomarkers such as 4,5-Diaminofluorescein diacetate (DAF-2 DA) [3], a diamine molecule, that shows fluorescence in presence of NO are used. Based on this molecule and in the work done by Yuan [4], we have developed the ligand 4-(3,4-diaminophenoxy)pyridine-2,6-dicarboxylic acid, from the chelidamic acid and 5-flouro-2-nitroaniline. The ligand was synthetized in 5 steps, purified and characterized, ($^{1}$H-NMR, $^{13}$C-NMR; MS, FITR). The lanthanide complex was synthesized using the follow methodology: the 4-(3,4-diaminophenoxy)pyridine-2,6-dicarboxylic acid was dissolved in water followed the addition of 3 equivalent of $K_2CO_3$, the mixture was stirred by 30 minutes, then the lanthanide chloride was added in a stoichiometry 3:1 ligand-metal, the mixture was stirred by 4 hours. The solid formed was separated by centrifugation, the supernatant was removed and the solid was dried in a vacuum oven overnight. The complex was analyzed by photoluminescence spectroscopy in presence and absence of NO. To ensure NO in solution we have used the molecule S-Nitrosoglutathione (GSNO) on tris-HCl buffer. The test with the europium(III) complex as NO probe was realized in a solution 5 x $10^{-5}$ mol $L^{-1}$ in tris-HCl buffer. The NO generator solution (GSNO) was prepared in a concentration 3 times higher to ensure 3:1 NO:complex molar ratio. The solution of GSNO was added to the complex solution and stirred for 30 minutes. The photoluminescence spectra (Figure 1) indicate the emission intensity increases 2.3 times in presence of NO. The europium complex synthetized shows a high potential to act as NO optical probe and considering that lanthanide emission can be obtained by time resolved fluorescence spectroscopy, probably a high level of detection may be achieve eliminating the fluorescence signal from biological environments.

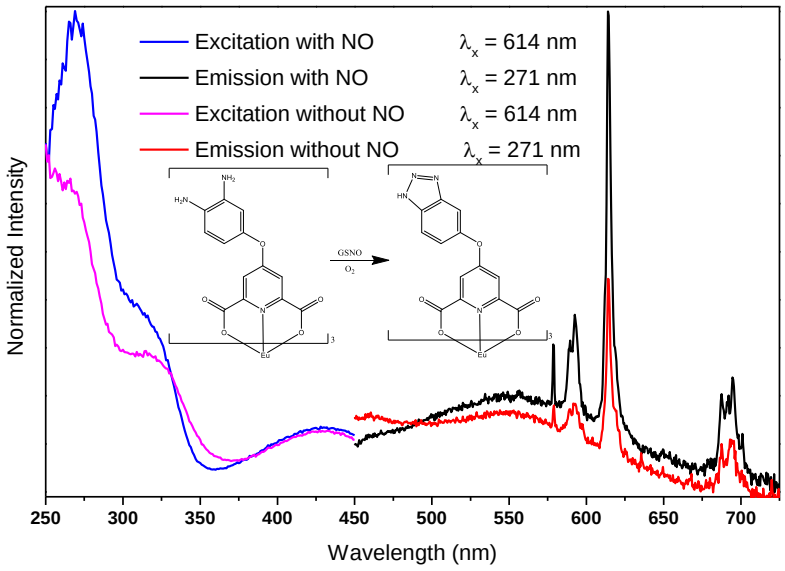


Figure 1: excitation and emission spectra of the europium complex in presence (black and blue lines) and absence of NO (pink and red lines), in the center of the figure is represented the reaction between the complex and GSNO.

1. Snyder S, Bredt DS. Biological roles of nitric oxide. Sci Am. 1992;266(5):28–35.
2. Nathan C, Xie Q wen. Nitric oxide synthases: Roles, tolls, and controls. Cell. 1994;78(6):915–8.
3. Nakatsubo N, Kojima H, Kikuchi K, Nagoshi H, Hirata Y, Maeda D, et al. Direct evidence of nitric oxide production from bovine aortic endothelial cells using new fluorescence indicators: Diaminofluoresceins. FEBS Lett. 1998;427(2):263–6.
4. Chen Y, Guo W, Ye Z, Wang G, Yuan J. A europium(III) chelate as an efficient time-gated luminescent probe for nitric oxide. Chem Commun (Camb). 2011;47(22):6266–8.

**Área: INO** **Inscrição: 00931**

# Iron (II) oxalate as precursor of magnetic composites for dye adsorption

**José M. A. Grigorovski Júnior (IC)[1*], Francisco M. S. Garrido (PQ)[1], Marta E. Medeiros (PQ)[1]**

**jmauricioagjr@gmail.com; chico@iq.ufrj.br**; **martam@iq.ufrj.br**

[1] *Departamento de Química Inorgânica, Instituto de Química - UFRJ*

Keywords: *Magnetic oxides; carbon black; Vulcan-X; magnetic separation; dye elimination.*

## Highlights

Magnetic iron (III) oxide composites were prepared with Vulcan-X using iron (II) oxalate as a precursor. These composites have high dye adsorption capacity and can be removed by a magnetic field.

## Resumo/Abstract

One of the main problems of textile industry is related to the environmental impact caused by the disposal of waste containing residual synthetic dyes. Removal of dyes from waste water can be achieved by a number of methods. The adsorption method using materials with high rate and capacity is preferred compared to others in terms of high efficiency, easy handling and cost-effectiveness. However, easy separation of the adsorbed dyes from the environment is an important issue which requires a suitable adsorbent such as a magnetic composite. Therefore, magnetic gama-$Fe_2O_3$ a cost-effective, air-stable and non-toxic material is a good choice to prepare magnetic composites to permit easy separation. Thermal decomposition of oxalates is an interesting route to prepare these materials. When heated at 300ºC, iron (II) oxalate generates iron (III) oxide with gamma structure, which shows the desired magnetic property. This paper has as objective the preparation of iron (III) oxide magnetic composites with 'carbon black' (Vulcan-X) by heating iron (II) oxalate. The application of this composite in methylene blue (MB) adsorption in aqueous solution was also evaluated. Composites Vulcan-X/gamma-$Fe_2O_3$ with nominal ration (w:w) of (4:1), (3:1), (2:1), (1:1) and (1:2) were prepared. The formation of gamma-$Fe_2O_3$ was confirmed by XRD. The adsorption capacity of Vulcan-X to MB was determined as 275 mg/g, whereas, the (1:2) composite shows the adsorption capacity of 121 mg/g. Figure 1 shows the results of adsorption of MB (60 $mgL^{-1}$) in (1:2) composite.

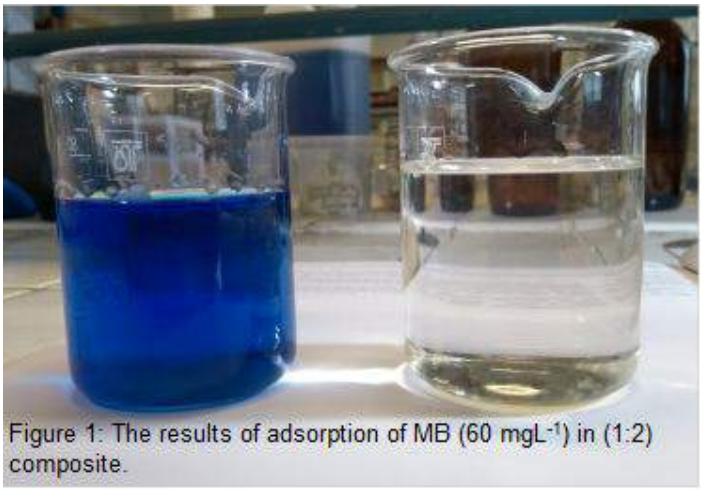

Figure 1: The results of adsorption of MB (60 $mgL^{-1}$) in (1:2) composite.

**Área: INO** **Inscrição: 00971**

# Synthesis of a new copper (II) complex with Benzoylpyridylthiourea: Characterization by X-ray diffraction

**Jhonathan Renner N. dos Santos (IC)[1], Michelle Pereira Quintino (PQ)[1,2], José Ricardo Sabino (PQ)[3]**
**jhonathanquimica@gmail.com**

*[1]PUC Goiás - Escola de Ciências Exatas e da Computação ; [2]Universidade Estadual de Goiás – Campus Itumbiara; [3] Universidade Federal de Goiás - Instituto de Física, Goiânia, GO*

Palavras Chave: *Thiourea, Copper complex, X-ray diffraction*

## Highlights

A new copper complex was synthesized with benzoylpyridylthiourea. It has been observed two different types of coordination of the copper ion with the thiourea sulfur atoms and a chloride.

## Resumo/Abstract

Thioureas derivatives are versatile organic compounds, which have biological activity acting as antioxidants, bactericide, fungicide and herbicide. Since thioureas have different atoms with electron donating properties (Nitrogen, Oxygen and Sulfur), this class of compounds can do different types of coordination with different metal cations.[1] Interest in copper complexes comes from their potential use as antimicrobial, antiviral, anti-inflammatory and antitumor agents[2] In this work, a new copper complex was obtained by reaction of a copper solution ($CuCl_2.2H_2O$ 1mmol) with a benzoylpyridylthiourea (2mmol) in ethyl acetate. Monocrystals for X-ray diffraction were obtained by evaporation. The structure of the ligand and the Ortep view of ligant (1) and the complex (2) are shown in figure 1.

**Figure 1.** Ortep view of the asymmetric unit of compounds **1** and **2**. Atoms in equivalent positions are highlighted. Some H atoms omitted.

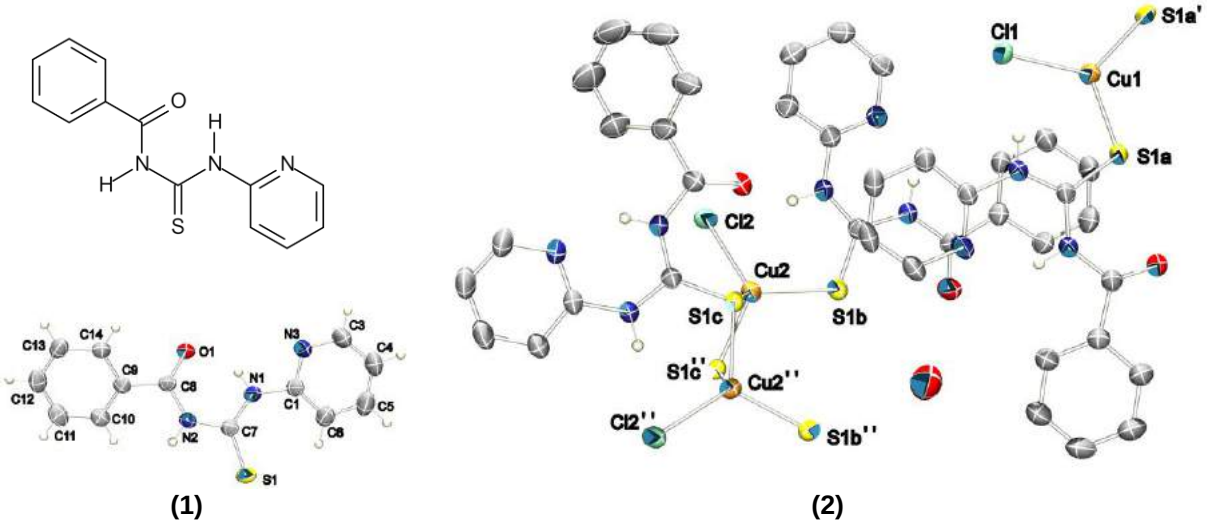


**(1)** **(2)**

In compound **2**, there are two kinds of coordination of the ion. Ion Cu1 resides on a 2-fold axis and is coordinated by two sulfur atoms and one chloride, while ion Cu2 is in a general position and coordinated by four atoms, three sulfur atoms from three different ligands and one chloride atom, showing a distorted tetrahedral environment.

References

[1] Abdwlah, B.H., Salh, Y.M. *Oriental Journal of Chemistry*, Vol. 26 (3), p. 763-773, **2010**.
[2] Santini, C., Pellei, M. et al. *Chemical Reviews*, 114 (1), p. 815-862, **2014**.

**Área: INO** **Inscrição: 01043**

# Síntese e caracterização química dos complexos de Sb(III) e Bi(III) com ligante bidentado para atuação como agentes leishmanicidas

**Dariane da Silva Lopes (IC),[1] Simone Rodrigues Silva (PQ)[1]**

**darianelopes3@gmail.com; simone.rodrigues@ufrr.br**

[1]*Departamento de Química, UFRR;*

Palavras Chave:*(Leishmaniose, Flebotomíneos, Parasitas, Complexos, Antimônio, Bismuto).*

## Highlights

A leishmaniose é uma doença provocada por parasitas, encontrados principalmente nos Países Tropicais e Bacias Mediterrâneas, causada por infecção de diferentes espécies de protozoários parasita do gênero Leishmania. O Estado de Roraima apresenta como foco principal a Leishmaniose Visceral, localizando-se principalmente nos municípios de Normandia, Pacaraima, Amajari e Uiramutã, onde quase toda população acometida é indígena, predominantemente da etnia Macuxi. Desta forma, o objetivo deste trabalho é realizar a obtenção e caracterização dos complexos de Sb(III) e Bi(III) com o ligante bidentado 1,10-fenantrolina para atuação como agentes leishmanicidas.

## Resumo/Abstract

Analisando a Tabela 1 verifica-se um aumento na temperatura de fusão e/ou decomposição dos complexos quando comparados ao ligante livre, sugerindo a coordenação do mesmo ao centro metálicos de Bi(III) e Sb(III). Outra evidencia da formação de um composto de coordenação foi a decomposição do complexo de Bi(III) em 210 °C.

A medida de condutividade dos complexos foi realizada com objetivo de observar a presença de eletrólitos nos complexos sintetizados em solução. Os testes foram realizados a partir de soluções preparadas dos complexos em DMSO numa concentração de 1,0 x $10^{-3}$ mol.$L^{-1}$ a 25 °C. Os resultados das medidas de condutância eletrolítica molar para o complexo Bi(III) e Sb(III) são apresentados na Tabela 1. Através dos dados condutimétricos obtidos é possível afirmar que o complexo de Sb(III) não há eletrólitos presentes, enquanto que o complexo de Bi(III) apresenta dois eletrólitos em sua estrutura.

**Tabela 1.** Intervalo de fusão e/ou temperatura de decomposição e os valores de de condutância eletrolítica em solução de DMSO para o ligante 1,10-fenantrolina e os complexos de Sb(III) e Bi(III).

| Composto | Temperatura de fusão e/ou ponto de decomposição (°C) | Condutimetria ($ohm^{-1}$ $cm^2$ $mol^{-1}$) |
|---|---|---|
| Phen | 117 | 3 |
| $[Sb(Phen)Cl_3]$ | 298 | 22,54 |
| $[Bi(Phen)_2NO_3](NO_3)_2$ | 210* | 85,52 |

**Figura 1.** Espectros UV-vis do ligante 1,10-fenantrolina e dos complexos de Sb(III) e Bi(III) na região de 600 – 800 nm em DMSO.

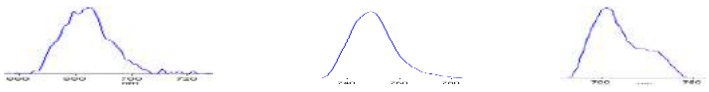

**Ligante** **Bi(III)** **Sb(III)**

Através da análise entre os espectros de absorção do ligante e dos complexos é possível observar diferenças significativas, em que as bandas de absorção no espectro dos complexos deslocaram-se para um comprimento de onda maior em comparação com o ligando livre. O espectro eletrônico mostra claramente a influência do centro metálico. Observa-se ainda um surgimento de uma nova banda para o complexo de Sb(III).

A partir dos resultados obtidos concluímos que houve a formação de complexos de Bi(III) e Sb(III), devido as alterações apresentadas nos estudos via ponto de fusão, análises condutimétricas e espectroscópicas. Novas análises estão sendo realizadas afim de se obter novas informações estruturais e terapêutica desses complexos.

**Área: INO Inscrição: 01056**

# Spectroscopy and electrochemical studies of phenanthroline derivatives $Cu^{2+}$, $Pd^{2+}$ and $Ru^{3+}$ complexes.

**Renan Santini Barbosa (IC)[1], Izilda A. Bagatin[1*](PQ).**

**renan.santini@hotmail.com; ibagatin@unifesp.br**

*[1]Departamento de Química, ICAQF; Laboratório de Química de Calixarenos, Espectroscopia Molecular e Catálise, UNIFESP, Diadema, SP, Brasil, CEP 09972-230*

Palavras Chave:*(1,10-phenanthroline-5,6-dione, coordination complexes, cyclic voltammetry).*

## Highlights

Potential luminescent and redox compounds.
Synthesis of coordination compounds containing 1,10-phenanthroline-5,6-dione and transition metals.
Spectroscopic and electrochemical studies of transition metals complexes.

## Resumo/Abstract

Coordination compounds[1] with luminescent or exciting electrochemical properties[2] could be formed with phenanthroline derivatives depending on the coordinated transition metal. In this work, we present the spectroscopic data of $Cu^{2+}$, $Pd^{2+}$ and $Ru^{3+}$ complexes with phenanthroline derivatives. Thus, the following complexes $[Cu(1,10\text{-phen-}5,6\text{-dione})(H_2O)_2]^{2+}$ **(1)**, $[Pd(1,10\text{-phen-}5,6\text{-dione})_2]^{2+}$ **(2)** and $[Ru(NO)Cl(1,10\text{-phen-}5,6\text{-dione})_2]^{2+}$ **(3)** were synthesized**.** The ligand showed $^1$H NMR (300 MHz, $CDCl_3$) signs at 9.14 ppm (a), 8.52 ppm (c) and 7.60 ppm (b), and IR frequency at 1684 $cm^{-1}$ ($\nu$C=O), 1662 $cm^{-1}$ ($\nu$C=N), and 1569 $cm^{-1}$ ($\nu$C=C). The coordination of each metal depicted different IR and $^1$H NMR spectra, as observed for the complex **(2),** IR frequency at 1690 $cm^{-1}$ ($\nu$C=O), 1653 $cm^{-1}$ ($\nu$C=N), and 1578 $cm^{-1}$ ($\nu$C=C) and $^1$H NMR signals (ppm, 300 MHz, DMSO-$_{d6}$) at 9.25 ppm, 8.80 ppm, 8.05 ppm. In turn the complex **(1)** depicted IR frequency at 1700 $cm^{-1}$ ($\nu$C=O), 1652 $cm^{-1}$ ($\nu$C=N), and 1575 $cm^{-1}$ ($\nu$C=C). Finally, the complex **(3)** depicted IR frequency at 1887 $cm^{-1}$ assigned to $\nu$N≡O, since IR frequency of $Ru(NO)Cl_3{\cdot}5H_2O$ occur at 1900 $cm^{-1}$. The cyclic voltammetry of the ligand and the complex **(2)** in DMF showed $E_{1/2}$ = -0,337V *vs* EPH and $E_{1/2}$ =-0,017V *vs* EPH, respectively, characteristic of the reversible pair of 1,10-phenanthroline-5,6-dione ligand.

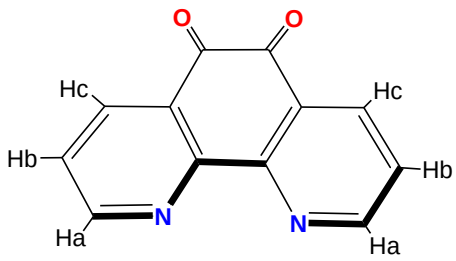


**Figure 1:** 1,10-phenanthroline-5,6-dione ligand.

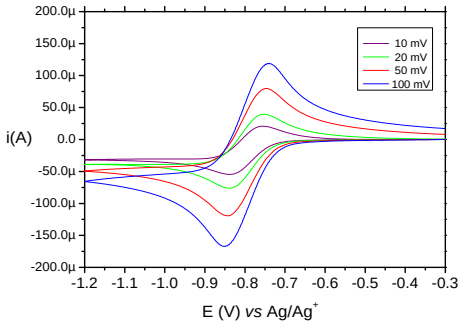


**Figure 2**: Cyclic voltammetry of 1,10-phenanthroline-5,6-dione ligand

[1] F. Calderazzo, G. Pampaloni, V. Passarelli, *Inorg. Chim. Acta* 330, **2002**, 136–142.
[2]T. Lazarides, A. Barbieri, C. Sabatini, F. Barigelletti, H. Adams, M. D. Ward, *Inorg. Chim. Acta* 360, **2007**, 814–824.

**Área: INO** **Inscrição: 1121**

# Complexos Binucleares de Fe(III)/Cu(II) e Co(III)/Cu(II) Contendo Bases de Schiff tetradentadas: Síntese e Caracterização.

**Igor Vinicius de França (IC)*[1], Edward R. Dockal (PQ)[2], José W. da Cruz Júnior (PQ)[1].**

**igorviniciusdefranca@gmail.com; jose.w.cruz@ufsc.br**

*[1]Departamento de Ciências Exatas e Educação, Universidade Federal de Santa Catarina (UFSC) Blumenau/SC.*
*[2]Departamento de Química, Universidade Federal de São Carlos São Carlos/SP.*

Palavras Chave: *Bases de Schiff Tetradentadas; Complexos Binucleares.*

## Highlights

Binuclear Complexes of Fe(III)/Cu(II) and Co(III)/Cu(II) Containing Tetradentate Schiff Bases: Synthesis and Characterization: Schiff Base complexes of Fe(III) and Co(III) were used to form binuclear Fe(III)/Cu(II) and Co(III)/Cu(II).

## Resumo/Abstract

Uma vez que o sítio ativo de muitas metaloenzimas apresenta uma ou mais pontes, tais como hidroxo unindo dois centros metálicos[1], complexos de Cu(II) com bases de Schiff têm sido empregados na tentativa de mimetizar enzimas de cobre responsáveis pela oxidação de compostos fenólicos[2]. Com isso, no presente trabalho, dois complexos binucleares de Fe(III)/Cu(II) e Co(III)/Cu(II) (FIGURA 1) foram sintetizados utilizando como ligantes complexos mononucleares de Fe(III) e de Co(III), contendo base de Schiff tetradentada derivada da 1,2-diaminotolueno e do 2,3-diidroxibenzaldeído, mediante procedimentos descritos na literatura[3,4]. A caracterização foi realizada por medidas de ponto de fusão, testes qualitativos de solubilidade, medidas de condutância e espectroscopia eletrônica. Os dados gerais dos complexos se encontram na Tabela 1. Observou-se, nos testes de solubilidade, que ambos são solúveis em dimetilformamida, e insolúveis em água e hexano. Também se observou que o complexo (A) solubilizou-se em clorofórmio. Observou-se que os dois complexos degradaram ao invés de fundir. As medidas de condutividade foram realizadas com soluções com concentração de $1x10^{-3}$ $mol{\cdot}L^{-1}$ em DMF, nas quais observou-se o complexo (A) é um eletrólito 1:1, enquanto o complexo (B) é não-eletrólito. Os espectros eletrônicos de ambos apresentaram bandas de alta absortividade, atribuídas às transições $\pi \rightarrow \pi*$ e $n \rightarrow \pi*$ na região entre 320 nm – 450 nm. Foi observada a banda d-d para os íons Cu(II) em 960 nm para (A) e em 800 nm para (B). Espectros vibracionais e análises elementares destes compostos estão sendo obtidos com o intuito de auxiliar na elucidação de suas estruturas e serão apresentados no evento.

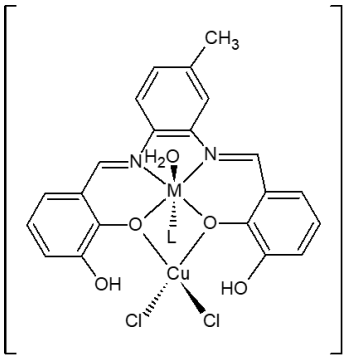


**Figura 1:** Estruturas propostas para os compostos binucleares obtidos: (A) M=Fe e L=$Cl^-$ e (B) M=Co e L=$OH^-$.

**Tabela1.** Dados gerais de caracterização dos complexos obtidos.

| Complexo | M. M. ($g{\cdot}mol^{-1}$) | Rend. (%) | P.F. (ºC) | Cond. ($\mu S\ cm^{-1}$) |
|---|---|---|---|---|
| (A) | 604,41 | 41,94 | >213 | 42,1 |
| (B) | 625,82 | 3,22 | >318 | 0,8 |

**Agradecimentos:** CNPq.

[1] Strater, N.; *et al., Angew. Chem. Int. Ed. Engl*., **1996**, *35*, 2024.;
[2] Larrow, J. F.; *et al. J. Org. Chem*. **1994,** 5, 1939.;
[3] Cavalheiro, E. T. G.; *et al*. *Thermochim. Acta*, **2001,** *370,* 129.;
[4] Gruber, S. J.; *et al*. *J. Inorg. Nucl. Chem*., **1968,** *30*, 1805.

**Área: INO** **Inscrição: 01218**

# Síntese, caracterização vibracional e estruturas cristalinas de dois novos polímeros de coordenação contendo um ligante pirazólico

**Iuri C. Soares (PG)[1], Helen A. Brito (IC)[1], Isac M. Dias (PG)[1], Henrique C. S. Junior (PG)[2], Glaucio B. Ferreira[2] (PQ), Guilherme P. Guedes (PQ)[1,2]**

**icsoares09@gmail.com**

*[1] Universidade Federal Rural do Rio de Janeiro, Departamento de Química, BR 465, Km 7 – Seropédica/RJ, Brasil.*
*[2] Universidade Federal Fluminense, Instituto de Química, Outeiro de São João Batista, s/n – Niterói/RJ, Brasil.*

*Palavras Chave: Pirazol, Polímeros de Coordenação, Density Functional Theory (DFT)*

## Highlights

Synthesis, vibrational characterization and crystalline structures of two new coordination polymers containing a pyrazole ligand. Coordination preferences of pyrazol-based ligands. Pyrazol-based ligand as a spacer.

## Abstract

Pirazóis têm sido amplamente utilizados na química de coordenação como bloco construtor de polímeros de coordenação, devido a sua versatilidade e possibilidades de funcionalização[1]. Neste trabalho será apresentada a síntese, caracterização espectroscópica, estrutura cristalinas de um pirazol funcionalizado e de seus respectivos complexos de cobre(II) e cobalto(II). A síntese do pirazol (**L1**) está demostrada na figura abaixo[2].

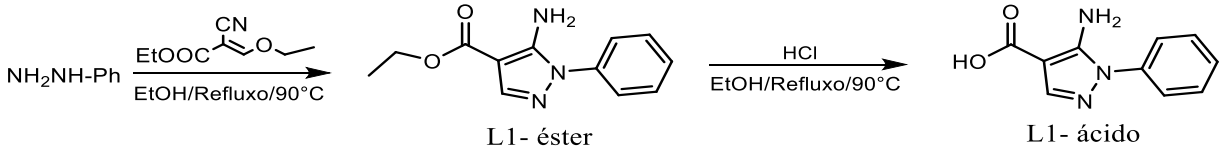


L1- éster L1- ácido

Os resultados experimentais das caracterizações por espectroscopia de absorção na região do infravermelho, e espectroscopia Raman para o precursor éster e o produto final estão em acordo com os calculados, obtidos por Density Functional Theory (**DFT**). Utilizando-se o sal potássico de L1, dois novos polímeros de coordenação foram obtidos ao reagir $Cu(ClO_4)_2$ ou $Co(ClO_4)_2$, juntamente com 1,10-fenantrolina e o **L1**$^-$ como espaçador em uma solução etanol: água**.** A estrutura do complexo de cobre trata-se de um polímero de coordenação 1D de fórmula $^1{}_\infty[Cu_2(L1)_2(phen)_2](ClO_4)_2(H_2O)_3$ (figuras **a** e **b**). Utilizando cálculos DFT, foi possível estimar um acoplamento antiferromagnético com J = -117 $cm^{-1}$ entre os íons de cobre(II). A caracterização do complexo de cobalto(II) encontra-se em andamento. Visando melhor compreensão dos possíveis modos de coordenação do pirazol, foi feita uma análise teórica da susceptibilidade eletrofílica dos orbitais de fronteira. Os resultados sugerem que a forma aniônica ($L1^-$) coordena-se primeiramente pelo carboxilato que causa a ativação do nitrogênio pirazólico como sítio de coordenação secundário **(c)**.

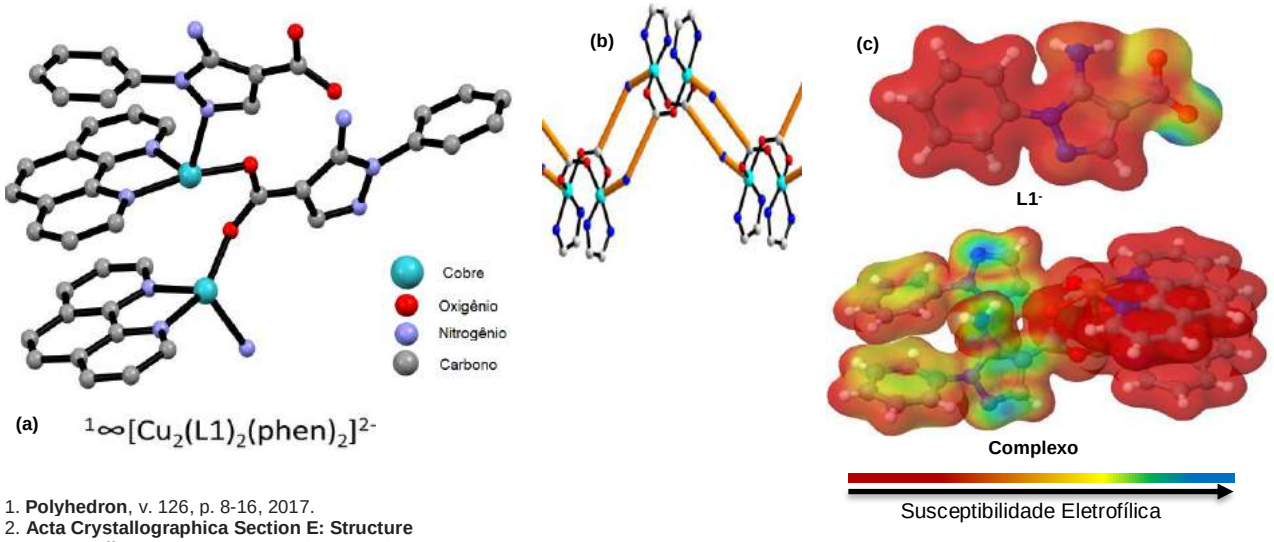


1. **Polyhedron**, v. 126, p. 8-16, 2017.
2. **Acta Crystallographica Section E: Structure Reports Online**, v. 64, n. 7, p. o1312-o1313, 2008.

**Área: INO** **Inscrição: 01295**

# Layered double hydroxides and acetylsalicylic acid: reactivity and desorption studies

**Isabelle N. de Oliveira (PG), Kárita K. S. Silva (IC), Cleiber C. Morais (PG), Renato Rosseto (PQ)***

**isabellenunesoliveira@gmail.com; renato.rosseto@ueg.br**

*Campus Anápolis de Ciências Exatas e Tecnológicas, BR 153 Km 98, Universidade Estadual de Goiás.*

Keywords: Nonsteroidal anti-inflammatory, Anionic clays, Drug sustained delivery.

## Highlights

Synthesis and application of layered double hydroxides for drug delivery. Use of inorganic nanocarriers for controlled release of nonsteroidal anti-inflammatory drugs.

## Abstract

The aim of this work was focused on the synthesis of Mg/Fe (2:1) and Ca/Fe (2:1) layered double hydroxides (LDHs) to incorporate acetylsalicylic acid (ASA) looking for drug controlled release. The LDHs and products obtained from LDHs and ASA reactions were characterized by X-ray diffraction, thermogravimetry, and scanned electron microscopy. The desorption kinetics of ASA from inorganic solids were performed at 25$^{o}$C and 40$^{o}$C in buffered solutions (artificial saliva, pH 6.8; simulated body fluid, 7.4), monitored by UV-vis spectroscopy. The results showed that the adsorption of ASA on LDHs was dependent on various factors, especially on pH and temperature reaction, and also observed the formation of iron/ASA complex and ASA decomposition. The desorption analysis of ASA from LDHs suggested an increase of drug solubility, and showed sustained release profile with 60 % and 70 % (at 25$^{o}$C and 40$^{o}$C, respectively) of the loaded drug being released up to 1h, and then an equilibrium stage reached after 4h, independently of solution pH or LDH. The presented results are promising to use these LDHs as carries to improve water solubility and chemical/ thermal stability of weakly water-soluble drugs. Details of the synthesis, characterization, thermal stability studies, and desorption kinetics of the compounds will be presented.

The authors acknowledge to the Programa de Bolsa de Incentivo à Pesquisa e Produção Científica (PROBIP/UEG), Universidade Estadual de Goiás/Pró-Projetos/Programas, PrP/UEG (Pró-Eventos/UEG), CAPES and FAPEG for sponsorships.

**Área: INO** **Inscrição:01332**
*(Inserir a sigla da seção científica para qual o resumo será submetido. Ex: ORG, BEA, CAT)* *(Inserir o número de inscrição do autor que fez a submissão)*

# Synthesis, spectroscopy of copper(II) catechol complexes

**Camilla P. Corrêa (IC), Bruna M. Chinelate (IC), Gabriel S. Martins (IC),Tatiana Alves Toledo (PQ), Denise B.A. Barbosa (PQ).**

**camillacorrea4@gmail.com; denise.barbosa@ifsudestemg.edu.br**

[1]*Departamento de Educação e Ciências-LPEN, Instituto Federal de Educação do Sudeste de Minas Gerais-campus Juiz de Fora*

Palavras Chave:*catechol, spectrocopy, coordination compounds.*

## Highlights

Synthesis, spectroscopy of copper(II) catechol complexes. Cu (II) complexes with the ligands 4-tert-Butylcatechol(1) and 4-ferrocenyl aniline (2) have been synthesized and characterized by FT-IR and EPR measurements.

## Resumo/Abstract

Catechol enzymes are important in many natural systems, being present in plants, insects and crustaceans. The catechol oxidases, for example, act in the catecholase activity, that is, they have the capacity to catalyze oxidation reactions involving the transfer of two electrons from a wide variety of o-diphenols to the respective o-quinones, causing the reduction of oxygen to water[1].In addition, these enzymes interact with organic compounds acting as a powerful building block for polymer networks with excellent mechanical properties. Many researches are developed using synthetic tactics so that new paramagnetic ligands with redox activity are obtained. Based on these, it is possible to obtain molecular materials where a paramagnetic metal ion is coordinated to an organic radical.Therefore, in this project, it is proposed the use of 4-tert-Butylcatechol(1), 4-ferrocenyl aniline(2), and copper(II) ions to investigate the kinetic mechanism of the structural organization of these polymeric compounds. the compound $[Cu(1)_2(2)_2]$ was obtained by solubilization 0.36 mmol (1) and 0.36 mmol (2) in ethanol. After was add 0.12 mmol $CuCl_2$. The mixture is refluxed at 50ºC for 3 hours. The formed black precipitate is filtered, washed with ethanol and dried. The product is recrystallized from ether. Yield: 83 mg (67.8%).IR(KBr, $cm^{-1}$) : 3553 (ν NH), 2959 (ν $CH_3$), 1591 (ν C-N), 1460 (ν C-O), 1263 (ν Ar-N), 1004-1106 (ν Fc).(Figure 1a) The Mössbauer spectroscopy study shows a characteristic doublet of Fe (II) with an isomeric displacement of 2.32 mm/s, and a quadrupolar unfolding of 0.32 mm/s (Figure 1b). The results obtained are in agreement with the proposed structure.The electrochemical characterization and structural of the compound is underway.
1

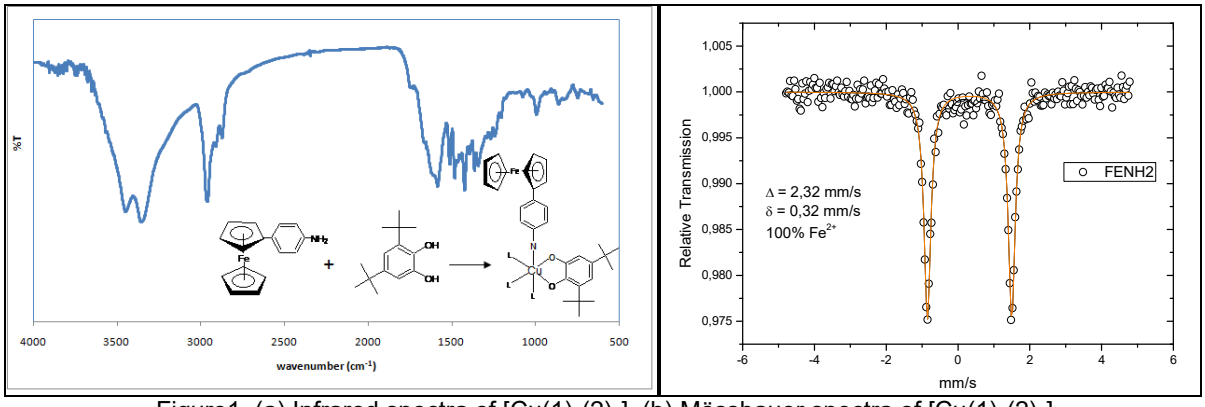


Figure1. (a) Infrared spectra of $[Cu(1)_2(2)_2]$. (b) Mössbauer spectra of $[Cu(1)_2(2)_2]$.

1.KLABUNDE, T.; EICKEN, C.; SACCHETTINI, J. C.; KREBS, B. Crystal structure of a plant catechol oxidase containing a dicopper center, Nature Structural Biology, v. 5, p. 1084-1090, 1998.
2.Wu, J.J.; Zhang, L.; Wang, Y.X.; Long, Y.H.; Gao, H.; Zhang, X.L.;Langmuir, 2011, 27,13684.

**Área: INO** **Inscrição: 01334**

# Spectroscopic studies of Copper I and II complexes by DFT calculations.

**Herisson F.S. de Oliveira (PG),[1] Rafael G. Silveira (PQ),[1,2] Fillipe V. Rocha(PQ),[1]**

**herissonoliveira2010@hotmail.com**

*[1]Departamento de Química, UFSCar; [2]Departamento de Química, Instituto Federal Goiano*

*Palavras Chave: Computacional Chemistry, Inorganic Spectroscopy, Copper Complexes, DFT Calculations.*

## Highlights

- Computational predictions of spectroscopic properties in Copper (I) and (II) complexes.
- Analysis of the influence of the metallic oxidation number on the structure and spectroscopic properties.

## Resumo/Abstract

Mechanistic studies have helped on elucidating the mode of action of metal complexes in cancer treatment.[1] Study the cell uptake and intracellular distribution of luminescent bioactive complexes[2], in order to identify the main targets is one of the most applied methods. Therefore, in this work we performed DFT calculations to predict some important thermodynamical and spectroscopical information of three different ligands and their copper (I)/(II) complexes. Compounds structures were planned to achieve adequate spectroscopical characteristics, possible luminescent properties and interact to DNA by intercalation due the presence of a planar aromatic organic system (Figure 1 A).

Optimization data showed that Cu(II) complexes have lower distortion of square planar geometry than Cu(I) analogues. Results demonstrated that the oxidation number determine the kind of transitions, we observed a MLCT band to the Cu(I) compounds and a band LMCT to Cu (II) complexes. Cu(II) complexes have better absorption in lower energies region (around 570 nm) (Figure 1B) compared to the Cu(I) compounds (around 420 nm). Then, Cu(II) compounds are more suitable to reach our objective, since this region is not affected by biomolecules absorptions and planar structure can help non-covalent interactions in the biological field.

The most promising compound was the $[Cu(DPOQ)_2]^{2+}$ (DPOQ = dipyrido[1,2,5]oxadiazolo[3,4b]quinoxaline) due the more rigid structure, smaller distortion angles and higher absorption wavelengths. Experimental studies will be performed to investigate the luminescent and biological properties of this complex.

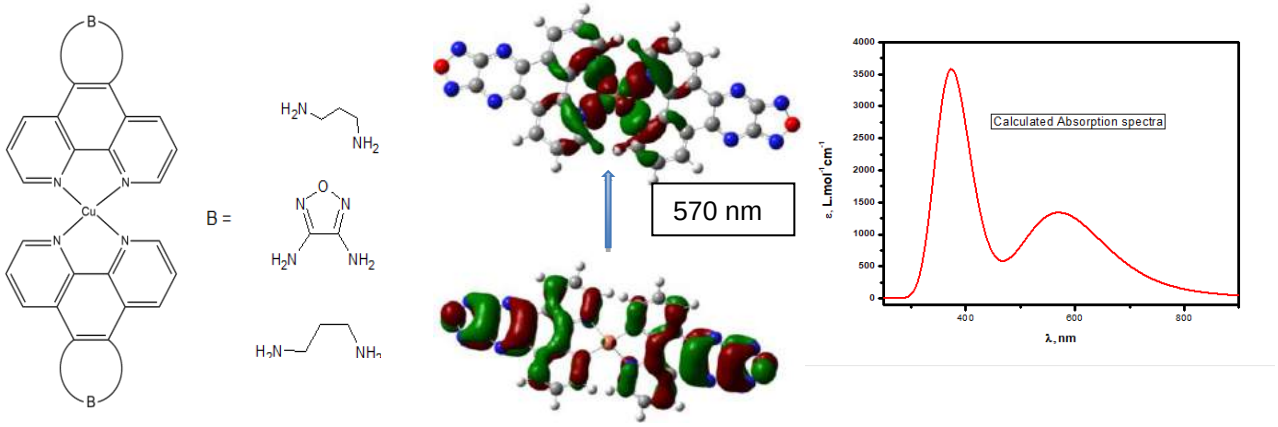


Figure 1. A. Proposed chemical structures for the compounds. B. Absorption spectra and correspondent electronic transition.

**Acknowledgments:**
FAPESP 2016/04201-9, CNPq, CAPES

**References:**

1- S. Dasari, P. B. Tchounwou; Eur. J. Pharmacol. 2014, 364.
2- C. A. Puckett, R.J. Ernst, J. K. Barton; Dalton Trans. 2010, 39 (5), 1159.

**Área: INO** **Inscrição: 01349**

# Synthesis and Characterization of $Cu_2O$ Thin Films for Photoelectrochemical (PEC) Applications

**João F. C. Coli (IC),[1] Cristiane B. Gonçalves (PG),[1]* Maximiliano Zapata (PQ),[1,2] Antônio C. Doriguetto (PQ)[1]**

joaofelipecoli@gmail.com; cristianebgquimica@gmail.com*

*[1]Instituto de Química, Universidade Federal de Alfenas, Alfenas, MG, 37130-001; [2]Departamento de Física, Universidade Federal de Minas Gerais, Belo Horizonte, MG, 31270-901, Brazil.*

Keywords: *Cuprous oxide, Thin films, Photocathodes, Photoelectrochemical*

## Highlights

- $Cu_2O$ photocathode for photoelectrochemical (PEC) water splitting process;
- Semiconductor material for sunlight energy absorption in visible region;
- New materials easy to prepare, low cost, and low toxicity to produce clean energy with minimal environmental impact.

## Resumo/Abstract

A huge number of semiconductor materials have been studied in photoelectrochemical (PEC) systems aimed to produce clean energy from water splitting under solar irradiation. Among them, $Cu_2O$, a promising photocatalyst due to its optimum band gap (1.9 - 2.2 ev) with high coefficient of absorption in the visible region, good electrical conductivity, and simple preparation[1-3].

The nanostructured $Cu_2O$ can be prepared by different methods, such as electrodeposition, which additionally allows the control of the morphology and orientation, changing the deposition parameters, such as electrolyte pH, temperature, time of deposition, among others[1-3].

In the present work, nanostructured $Cu_2O$ thin films were electrodeposited on FTO glasses substrates according to the method reported by Qi et al (2016)[1]. The depositions were performed during 1500 seconds, with a constant current density of -1mA.cm$^{-2}$, varying the temperature between 45 and 65 °C.

The thin film crystallinity was evaluated on a Rigaku Ultima IV (type II) X-ray diffractometer with θ-2θ geometry under the follow conditions: CuKα, radiation λ=1.5418 Å); scan rate of 1º 2θ min$^{-1}$ with a width step of 0.05º 2θ. The Bragg reflections in the experimental PXRD patterns match those ones in the PDF (#65-3288) data-base. The experimental PXRD patterns of the $Cu_2O$ thin films obtained here exhibit typical Bragg peaks corresponding to the (100), (111), (200), (211), and (220) planes of the $Cu_2O$ phase (Figure 1). The morphological and microstructural characterization of the $Cu_2O$ thin films are underway.

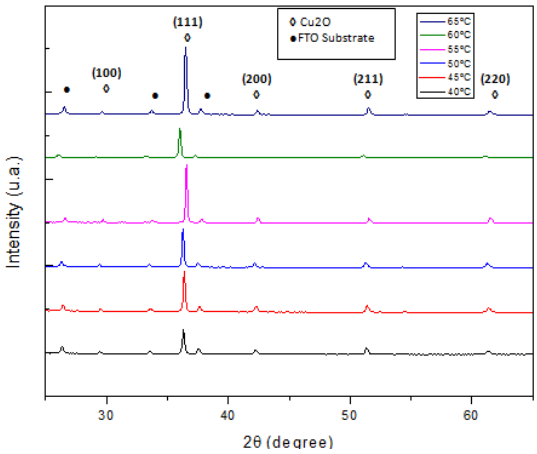


Figure 1: Experimental PXRD patterns of the $Cu_2O$ thin film deposited in FTO glass compared to the $Cu_2O$ phase (PDF (#65-3288))

[1]Qi, H.; Wolfe, J.; Fichou, D.; Chen, Z. *Nature,* **2016**.
[2]Azevedo, J.; Tilley, D.; Schreier, M. *et al*. *Nano Energy,* **2016,** 24,10-15.
[3]Paracchino, A.; Mathews, N.; Hisatomi, T. *et al*. *Energy & Environmental Science,* **2012**, 5, 8673-8681.

*Acknowledgments: PROBIC (UNIFAL-MG), FAPEMIG, CNPq, CAPES, FINEP, RMQ-MG.*

**Área: MAT** **Inscrição: 01383**

# Incorporation of papain in ordered mesoporous silica

**Danilo W. Losito* (IC),[1] Fúlvio G. Corazza (PG),[2] Patrícia S. Lopes (PQ),[2] Tereza S. Martins (PQ),[1]**

**dlosito77@gmail.com***

*[1]Departamento de Química, Instituto de Ciências Ambientais, Químicas e Farmacêuticas, UNIFESP; [2]Departamento de Farmácia, Instituto de Ciências Ambientais, Químicas e Farmacêuticas, UNIFESP.*

Palavras Chave: *SBA-15, Papain, Mesoporous silica, Cytotoxicity, Antimicrobial activity.*

## Highlights

Papain there is many applications, such as in foods, cosmetics, pharmaceutical products and as biocatalysts. However, due to its pool stability its commercial use is restricted.
In order to improve the performance of papain, it was incorporated into mesopores of SBA-15 due to excellent properties of this ordered mesoporous silica such as high surface area.
The papain confinement in the mesoporous of SBA-15 generates synergistic effects that enhance the stability of this enzyme.
The papain immobilized in SBA-15 showed interesting results as antimicrobial activity and low cytotoxicity.

## Resumo/Abstract

SBA-15 with highly ordered large mesopores, 2D hexagonal mesoporous structure and high surface area is very interesting for the incorporation of enzymes, such as papain that has poor stability. The goal of this work was to study the effect of incorporating papain into SBA-15 in relation the enzymatic and antimicrobial activity and cytotoxicity of papain. The papain (PPN) was incorporated into SBA-15 by incipient wetness impregnation (IWI) using post-synthesis methodology and water (W) and phosphate buffer solution (PBS) as solvent. The SBA-15:PPN mass ratio was equal to 2 (50 wt.%), 10 (10 wt.%) and 20 (5 wt.%). The SBA-15PPN samples were analyzed using different characterization techniques: small angle X-ray scattering (SAXS), $N_2$ adsorption-desorption isotherms (NAI), Fourier transformed infrared (FTIR) and scanning electron microscopy (SEM). The samples also were evaluated for its antimicrobial activity and cytotoxicity. SAXS (Fig 1) results showed reflections of a two-dimensional hexagonal mesoporous structure for all samples (SBA-15PPN), similar to SBA-15, indicating that the incorporation procedure does not change the pore structure of the SBA-15. SEM images also revealed that the SBA-15 particles in the samples (SBA-15PPN) are similar to pure SBA-15, retaining the well-defined wheat-like macrostructure clusters of pure SBA-15 (Fig. 2). Analyzing the NAI (Fig. 3) results we observed that the samples have smaller superficial area and pore volume when compared with pure SBA-15, so we concluded that papain is inside the mesopores. FTIR results showed significant shifts for the SBA-15PPN samples, indicating slightly interaction between the papain and silica.

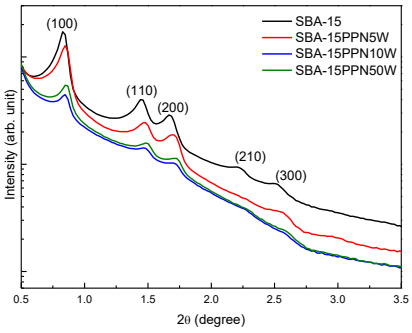


*Fig. 1. SAXS curves of SBA-15PPN*

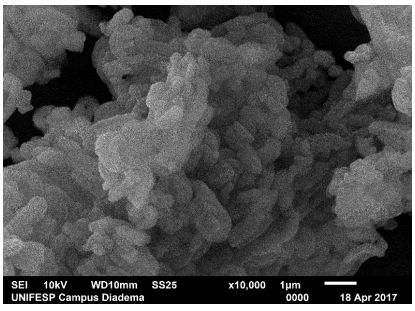


*Fig. 2. SEM image of SBA-15PPN50W*

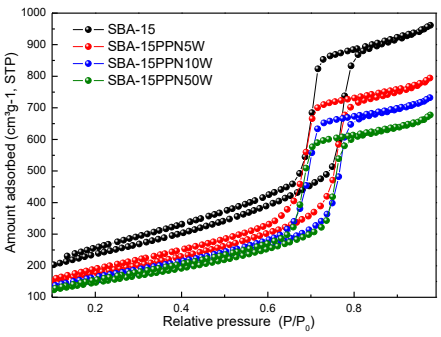


*Fig. 3. NAI of SBA-15PPN*

Cytotoxicity results (IC50 and IC10) for SBA-15 and SBA-15PPN samples showed that these materials are non-toxic. Antimicrobial activity results showed that SBA-15 decreased proliferation of Staphylococcus aureus, Candida albicans, Pseudomona aeruginoa and Escherichia coli by approximately 80%. However, the antimicrobial activity for SBA-15PPN samples drastically decreases, exhibiting a slight activity against Candida albicans.

*Acknowledgments*: The authors thank to NIPE-Unifesp and Laboratório de Cristalografia (IF-USP).

**Área: INO** **Inscrição: 01393**

# SÍNTESE, CARACTERIZAÇÃO E ATIVIDADE ELETROCATALÍTICA FRENTE RRO DE UM NOVO COMPLEXO DE NÍQUEL (II)

**Matheus M. Diniz (IC),[1] Fagner da S. Moura (PG),[1] Thaís D. Petizero (PG),[1] Annelise Casellato (PQ),[1] Marta E. Medeiros (PQ),[1] Francisco M. S. Garrido (PQ).[1]**

**casellato@iq.ufrj.br**

[1]*Departamento de Química Inorgânica (Instituto de Química, UFRJ);*

Palavras Chave: *complexo de níquel (II); voltametria cíclica; pilha a combustível; base de Schiff*

## Synthesis , characterization and eletrocatalitic activity front RRO of a new complex of nickel (II)

A nickel (II) complex was synthesized. This complex was characterized by spectroscopical and electrochemical techniques. This complex was developed to be tested as an electrocatalyst in fuel cells.

## Resumo/Abstract

A sociedade contemporânea tem-se voltado para discussões acerca de problemas econômicos e ambientais devido ao aumento da dependência dos combustíveis fósseis como principal fonte de energia. Neste contexto, as pilhas a combustível aparecem como uma alternativa promissora de geração de energia elétrica limpa e de alta eficiência. A platina é o principal eletrocatalisador desses dispositivos e devido a sua baixa disponibilidade e alto custo novos compostos de coordenação têm sido investigados como possíveis eletrocatalisadorse. Assim, o objetivo deste trabalho consiste na síntese, caracterização e investigação eletrocatalítica frente as reações de redução de oxigênio (RRO) em meio básico de um composto de coordenação contendo como íon metálico o níquel (II) coordenado a ligantes do tipo N,O-doador.

O complexo foi sintetizado em solução metanólica do respectivo ligante base de Schiff e em seguida adicionou-se à mistura solução metanólica de acetato de níquel (II) tetrahidratado sob agitação magnética por 2 horas.

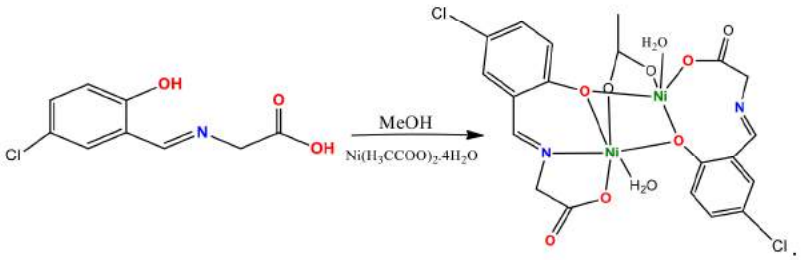


**Figura 1:** Esquema de síntese do complexo e provável estrutura.

Ao analisar o espectro no infravermelho do ligante com o do complexo é possível observar o deslocamento de bandas características para menores valores de energia, sugerindo a complexação.

A análise por espectroscopia eletrônica revelou valores de $\lambda_{máx}$ e absortividade molar de acordo com os encontrados na literatura para compostos de coordenação de níquel (II) semelhantes.

A voltametria cíclica do ligante e do complexo foram realizadas, quando comparadas é possível verificar um pico de potencial anódico no voltamograma do complexo ausente no ligante que ocorre em +0,91V, sugerindo que este processo oxidativo é exclusivo do complexo.

Os testes eletrocatalíticos foram realizados com soluções de NaOH 0,1 mol $L^{-1}$ em atmosfera inerte e em soluções saturadas com oxigênio

Na solução saturada com oxigênio foi possível verificar que tanto os picos de oxidação quanto os picos de redução relacionados ao complexo são intensificados. Além disso, em presença de oxigênio, é possível verificar o aparecimento de um novo pico de redução relacionado a redução do oxigênio molecular.

A partir desta caracterização do complexo, novos estudos vem sendo realizados para a fim de otimizá-lo como um eletrocatalisador em células a combustível.

**Área: INO** **Inscrição: 01401**

# Reactivity Studies on a Cobalt(III) Complex Towards the Development of Catechol-Based Bioreductive Prodrugs

**Aline F. M. da Silva (PG)[1*], Javier A. G. Gómez (PQ)[1] and Mauricio Lanznaster (PQ)[1]**

**alines@id.uff.br**

[1]*Instituto de Química, Universidade Federal Fluminense, CEP: 24020-141, Centro, Niterói, RJ.*

Keywords: *Cobalt Complexes, Catechol, Cancer, Bioreductive Prodrugs, Reactivity Assays*

## Highlights

The hypoxic region of a tumour can be a target for new therapies against cancer. A cobalt(III) complex was investigated as model for catechol-based bioreductive prodrugs.

## Abstract

The current treatments for cancer – chemo and radiotherapy – find resistance in solid tumours because of a hypoxic condition (low concentration of oxygen) that limit their efficiency. However, the hypoxic environment can be exploited for the development of bioreductive prodrugs. In this approach, a compound could circulate intact through the body, being selectively activated in the reductive environment of a tumour, with subsequent release of a cytotoxic ligand. Compounds like catechols, with antitumor potential, and cobalt complexes, whose metallic center has an inert (+3) and a labile (+2) oxidation state, are being investigated for the development of such systems. In this way, we present the synthesis (Scheme 1), characterization and preliminary reactivity assays of a cobalt(III) complex with tris(pyridin-2-ylmethyl)amine (TPA) and tetracholocatechol (TCC) ligands, [Co(TPA)(TCC)]$ClO_4$ (**1**), as model for catechol-based bioreductive prodrugs.

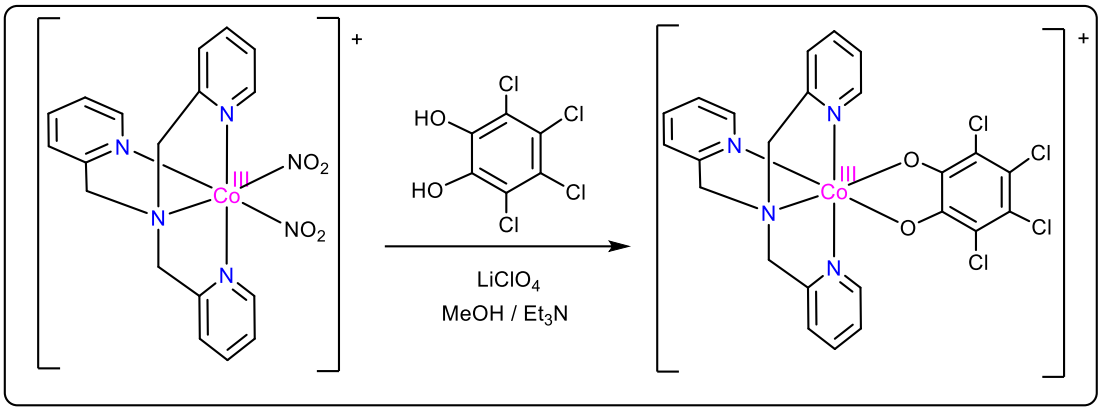


**Scheme 1.** Synthesis of **1.**

The complex was fully characterized by single crystal X-ray diffraction, IR, UV-Vis, ESI-MS and CHN elemental analysis. Cyclic voltammetry analysis revealed a pair of waves at -0.99V and -0.58V *vs* $Fc/Fc^+$, assigned to irreversible metal centered ($Co^{3+}/Co^{2+}$) reduction and oxidation processes, respectively. Reactivity assays, monitorated by UV-Visible spectroscopy in phosphate buffer at pH 6.2, 7.0 and 7.4, with ascorbic acid (reducing agent), under argon and oxygenated atmospheres, at 25 °C, showed no significant changes in the spectra during 24 hours, which indicates that both reduction and ligand dissociation did not take place. Additional studies are in progress to evaluate the reduction of **1** by other reducing agents.

**Área: INO** **Inscrição: 1422**

# Exploring DNA binding and cleavage, Topo I inhibition, and cytotoxic activity of two new Cu(II) compounds containing 4-aminoantipyrine.

**Ívina P. de Souza[1, 2](PG), Bárbara de P. Machado[1](IC), Alexandre B. de Carvalho[1](PG), Ildefonso Binatti[1](PQ), Andrew Kellett[3](PQ), Elene C. Pereira-Maia[2](PQ), Priscila P. Silva-Caldeira[1] (PQ) priscila@cefetmg.br**

*[1]Department of Chemistry, CEFET-MG; [2]Department of Chemistry, UFMG, Belo Horizonte, Brazil, [3]School of Chemical Science, Dublin City University, Dublin 9, Ireland.*

Keywords: *Cu(II) complexes*, *4-aminoantipyrine, cytotoxic activity, Topoisomerase I, DNA binding and cleavage*

## Highlights

- Synthesis of two new water-soluble casiopeína-like complexes;
- One of them showed promising cytotoxic activity, being able to inhibit the Topo I and cleavage the DNA at low concentrations.

## Abstract

In general, Casiopeínas®, a class of Cu(II) complexes with antitumoral activity, interact with DNA and induces cleavage by an oxidative mechanism. Two of these complexes are currently in clinical trials. However, Casiopeínas® exhibit very low solubility in aqueous media, which creates a pharmaceutical barrier. This work consist on the synthesis and characterization of two new water-soluble casiopeína-like complexes with the basic formula $[Cu(O{-}N)(N{-}N)(ClO_4)_2]$, in which O−N = 4-aminoantipyrine and N−N = 1,10-phenanthroline (**1**) or 2,2'-bipyridine (**2**). The complexes were characterized by elemental analyses, conductivity measurements, ESI-MS, EPR, FTIR and UV-vis spectroscopies. These complexes exhibit a distorted tetragonal geometry around copper, which is coordinated to two bidentate ligands in equatorial sites and two perchlorate ions weakly bonded in the axial positions (Fig. 1-a). In solution the complexes present as 2:1 electrolytes. The binding behaviors of the complexes to CT-DNA have been investigated by absorption spectra and viscosity measurements. These compounds were found to bind to DNA by non-classical intercalation mode, inhibit topoisomerase I activity (Fig. 1-b) and induce DNA cleavage by an oxidative mechanism involving the generation of ROS (Fig 1-c). The complex **1** presented a high nucleolytic activity generating single- and double-strand breaks at low concentration. Furthermore, both complexes inhibit the growth of K562 cells in a concentration-dependent manner with the $IC_{50}$ values (1.8 and 26 μM for **1** and **2**, respectively) lower than free ligands.

**Acknowledge**: FAPEMIG and CNPq.

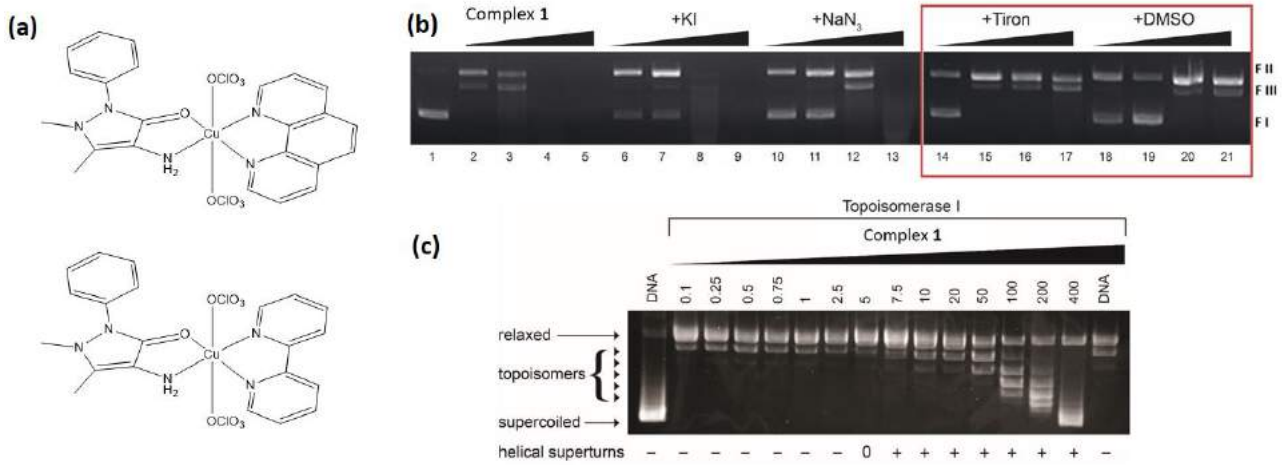


**Fig. 1 (a)** Proposed structures for complexes **1** (top) and **2** (botton). **(b)** Effect of ROS scavengers on the damages of superhelicoidal pUC19 incubated for 30 min, at 37 °C, pH = 7.2, with 1.0 mM Na-L-ascorbate, in absence and presence of increase concentration of **1** (2.5; 5.0; 7.5; 10,0 μM). **(c)** Topoisomerase I-induced DNA relaxation in the presence of **1**. Negative supercoiled pUC19 was incubed with **1** at the concentrations indicated on the top of the lanes prior to be treated with Topo I.

# Synthesis and characterization of Copper Metal-Organic Frameworks for adsorption of Phenol

**Anderson N. Carvalho (IC),[1] Geise Ribeiro (PQ).[1*]**

**andersonvga94@gmail.com; geise@unifei.edu.br**

[1] *Instituto de Física e Química, UNIFEI*

Palavras Chave: MOFs, Phenol, Adsorption

## Highlights

Synthesis and characterization of Copper Metal-Organic Frameworks for adsorption of Phenol. Solvothermal Synthesis of MOFs contend carboxylates and 4,4'Bipyridine. IR spectra showed satisfactory results for MOFs containg mixed linkers. IR spectra indicates possible adsorption of Phenol.

## Resumo/Abstract

The sucess of the Metal-Organic Frameworks (MOFs) has stimulated studies to verify the removal by adsorption of different environmental contaminants. Phenol is a highly toxic aromatic hydrocarbon deemed as a contaminant in both soil and water.

The objective of this work is to make a contribution to the development of new MOFs and use them as adsorbent for the contaminant phenol. Synthesis, characterization and evaluation of the adsorption of phenol in compounds of Copper containing carboxylates derived from Trimesic acid (BTC) and *p*-Fenilenediacetic acid (*p*-Fen) and 4,4' Bipyridine (Bpy) are described.

The IR spectra of the two compounds obtainded didn't showed strong bands arond 1700cm$^{-1}$ wich are characteristic of the C=O stretching of the COOH group, but bands are observed assigned to asymmetric and symetric stretching of the COO- group, indicating the coordination of the carboxylate to the metallic center. The spectra also showed a band at 1600 cm$^{-1}$ that has been defined on the literature as N=C stretching of compouds of Copper with Bpy.

The FT-IR spectra of Cu(BTCBpy) after interaction with Phenol showed a band around 3500cm$^{-1}$ and a large one proceeding it that are characteristic of the O-H stretching absorption of phenol.

IR spectra showed satisfactory results for MOFs containg mixed linkers and indicates possible adsorption of Phenol. Further Uv-vis sperctroscopy and HPLC studies wil be performed to truly confirm the adsorption.

**Área: INO** **Inscrição: 00081**

# Porfirinas de manganês imobilizadas em partículas magnéticas: catalisadores heterogeneizados para degradação do ciprofloxacino

**Aline C. Marciano* (IC), Ana L. A. Lage (PG), Sara S. Vieira (PQ), Maria H. Araújo (PQ), Dayse C. S. Martins** (PQ)**

**aline.capelao@gmail.com*; daysequimica@ufmg.br****

*Departamento de Química, Instituto de Ciências Exatas, Universidade Federal de Minas Gerais*

Palavras Chave: *Catálise heterogênea, Sistemas biomiméticos, Química verde, Antibióticos, Contaminantes ambientais*

## Highlights

**Immobilization of manganese porphyrins into magnetic particles: heterogenized catalysts for the degradation of ciprofloxacin**. Heterogenized catalyst degraded up to 92% of ciprofloxacin whereas in the homogeneous system, it was up to 81%. Best degradation of ciprofloxacin was obtained by heterogenized manganese porphyrin and *t*-BuOOH.

## Resumo/Abstract

A degradação do antibiótico ciprofloxacino (CIP, Figura 1a) foi avaliada na presença de $H_2O_2$ e *t*-BuOOH, utilizando-se uma porfirina de manganês [$Mn^{III}$(TPP)Cl] (**MnP**) como catalisador, em sistema homogêneo ou na sua forma imobilizada em suporte inorgânico (Figura 1b).

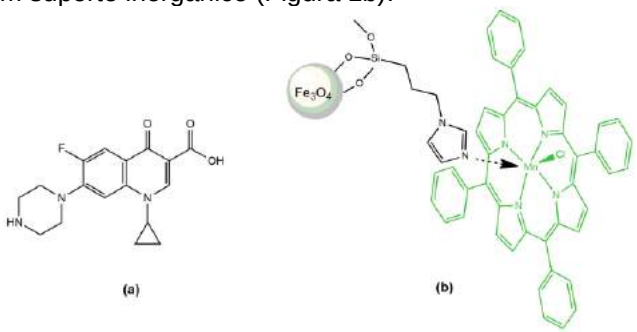


**Figura 1.** (a) Ciprofloxacino e (b) MnP imobilizada em suporte de óxido de ferro ($Fe_3O_4$) magnético recoberto por sílica modificada com grupo imidazol.

**Tabela 1**. Degradação (%) do CIP pela **MnP**, na presença de $H_2O_2$ e *t*-BuOOH.*

| Sistema | Homogêneo | | Heterogêneo | |
|---|---|---|---|---|
| | Branco** | MnP | Branco*** | MnP imobilizada |
| ***t*-BuOOH** | 57 | 81 | 88 | 92 |
| **$H_2O_2$** | 34 | 50 | 67 | 71 |

*Análise por UV-Vis (280 nm); ** Sistema na ausência de catalisador; *** Sistema na presença do suporte.

O material heterogeneizado preparado foi caracterizado por TG, DRX e BET. Análises de MEV ainda serão realizadas a fim de avaliar se o recobrimento total da partícula magnética foi obtido com sucesso. De maneira geral, os sistemas catalíticos contendo MnP levaram a um maior grau de degradação do CIP, indicando que os catalisadores porfirínicos são promissores nestes processos. Os sistemas heterogêneos levaram à maior degradação do CIP. A vantagem desses sistemas está na recuperação (com utilização de um imã) e reutilização do catalisador, etapa que está em desenvolvimento. A **MnP** imobilizada levou a uma maior degradação do CIP, com aumento de 4% e 7% em relação ao branco para *t*-BuOOH e $H_2O_2$, respectivamente. O alto valor de degradação do CIP no sistema em presença exclusiva de suporte pode estar relacionado a: (a) a atividade catalítica desse por meio de partículas de magnetita expostas, e (b) adsorção do substrato nos poros do material. Assim, destacam-se a necessidade de estudos mais aprofundados quanto ao recobrimento do catalisador heterogeneizado e o investimento na utilização de outros catalisadores porfirínicos, que possam aumentar a degradação do antibiótico nos sistemas heterogêneos.

Agradecimentos: FAPEMIG, CNPq, CAPES.

**Área: INO**
*(Inserir a sigla da seção científica para qual o resumo será submetido. Ex: ORG, BEA, CAT)*

**Inscrição: 00103**
*(Inserir o número de inscrição do autor que fez a submissão)*

# Determination of Point of Zero Charge of Super Fine Fibrous Peat

**Bruna P. Szpoganicz (PG),[1] Lino Meurer (IC),[1] Luiz Fernando D. Probst (PQ),[1] Bruno Szpoganicz (PQ)[1].**

**belabruna@yahool.com; bruno.s@ufsc.br.**

*[1]Departamento de Química, UFSC; Universidade Federal de Santa Catarina, CEP: 88040-900, Florianópolis – SC.*
Palavras Chave: Super Fine Fibrous Peat, Point of Zero Charge.

## Highlights

The SSF with PZC = 2.71 would be suited to adsorb positive ions in the treatment of effluents contaminated with cations.

## Resumo/Abstract

Peat is a natural material containing lignin, cellulose, and humic acid as its major constituents. These constituents are potentially very useful from an adsorption standpoint because they contain polar functional groups such as alcohols, aldehydes, carboxylic acids, ketones, and phenolic hydroxides, which can all be involved in heavy-metal adsorption. Peat is known to have excellent ion-exchange properties similar to natural zeolites, and it is a kind of soil, rich in organic materials, which has a porous structure (BALASUBRAMANIAN, et al., 2009; ZEHRA, et al, 2015).
Points of zero charge (PZCs) are pH values at which the surface charge components become equal to 0 under given conditions of temperature, applied pressure, and aqueous solution composition (SPOSITO, 2008). This does not mean that the surface has no charge at pH PZC, but rather that there are equal amounts of positive and negative charges. PZC values could help optimize the selection of a substrate for the treatment of a CND (BAKATULA, et al., 2018). Organic materials with low PZC such as peat, algae, wood ash and coconut shells would be better suited to treat effluents contaminated with cations, while other materials with high PZC values such as banana peel, orange peel and melon bark would be more appropriate to capture anions (FREITAS, et al., 2015; MAURYA, et al., 2014; MUKHERJEE, et al., 2011).
The point of zero charge was determined using 5 Erlenmeyer flasks with 1g of Super Fine Fibrous Peat (SFF) and adding aliquots of 10.0; 7.5; 5.0; 2.5 and 1.25 mL of 0.10 mol/L HCl. Another 5 flasks containing 1g of SFF Peat with equal volumes of 0.10 mol/L NaOH. Then 5 mL of 0.10 mol/L KCl and distilled water was added to make up the 100 mL volume, including a sample with only 0.10 mL KCl and water. These samples were shaken for a period of one hour, and the pH of each was measured (pH1). Then, 5 mL of 1M KCl was added to each sample and stirred again for a period of one hour and the pH of all was again measured (pH2). The pH of the samples was measured at a pH meter Titrino Plus 350 (Metrohm), equipped with a Ag/AgCl combined electrode from Metrohm. The plot of $\Delta(pH_1\text{-}pH_2)$ versus pH1 shows the value of PZC (Figure 1).

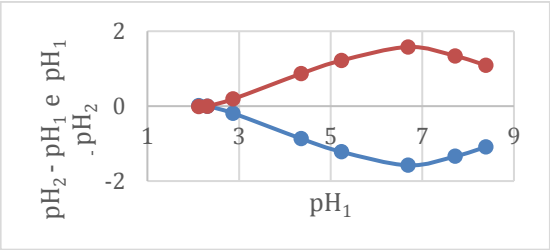


The SSF with PZC = 2.71 would be suited to adsorb positive ions in the treatment of effluents contaminated with cations.

[1] BAKATULA, E.N.; RICHARD, D.; NECULITA, C. M.; ZAGURY, G. J.; Determination of point of Zero charge of natural organic materials, **Enviromental Science and Pollution Research,** v. 12, 2018, 1-11.
[2] BALASUBRAMAIN, R.; PERUMAL, S. V.; VIJAYARAGHAVAN, K.; Equilibrium isotherm studies for the multicomponent adsorption of lead, zinc and cadmium onto Indonesian Peat. **Ind. Eng. Chem. Res.**.,v.48, 2009, p. 2093- 2099.
[3] FREITAS, F. B. A..; CÂMERA, M. Y. F.; MARTINS, D. F. F.; Determinação do PCZ de adsorventes naturais utilizados na remoção de contaminantes em solução Aquosa**, Blucler Chemistry Proceedings,** v. 3, 2015, p.1-8.
[4] MAURYA, et al.; Biosorption of Methylene blue by de oiled algal biomass: equilibrium, kinetics and artificial neural network modelling. **PLoS One**, v 9, 2014, p.12.
[5] MUKHERJEE, A.; ZIMMERMAN, A. R.; HARRY, W.; Surface chemistry variations among a series of Laboratory-produced biochards, **Geoderma**, v.163, 2011, p.247-255.
[6] SPOSITO, G.; ; **The Chemistry of Soils**, v.2. Oxford University Press, New York, 2008, p.12.
[7] ZEHRA, T.; LIM, L. B. L.; PRIYANTHA, N.; Removal behavior of Peat collected from Brunei Darussalam for Pb(II) ions from aqueous solution: equilibrium isotherm, thermodynamics, kinetics and regeneration studies. **Environ. Earth Science,** v.74, 2015, p. 2541-2551.

**Área: ___INO___ Inscrição:___00126___**

# Palladium complexes with oxadiazol and thiazolidine-adamantane ligands: the influence of heterocycle in Pd-S bond

**Josiane T. Silva (IC)[1], Gustavo M. Alvarenga (IC),[1] Heveline Silva (PQ)[1*].**

**josiane.teixeira@hotmail.com; hevelinequi@gmail.com**

*[1]Departamento de Química, ICEx, Universidade Federal de Minas Gerais, Belo Horizonte – MG, Brasil.*

Palavras Chave: *Palladium, Adamantane, Heterocycle.*

## Highlights

Palladium Metal complexes have shown great potential as antitumor agents.
Pd-S: covalent bond and coordinate bond.
Oxadiazol and thiazolidine are biologically important heterocycles.

## Resumo/Abstract

No processo de síntese dos complexos, o metal foi adicionado ao ligante (1:2), promovendo uma reação de substituição com deslocamento de ligantes cloro. (Figura 1)

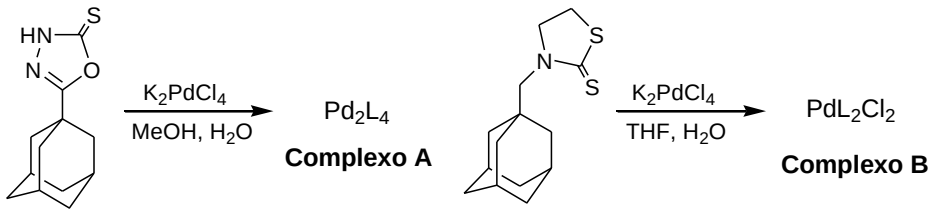


**Figura 1.** Síntese dos complexos

A caracterização dos complexos foi realizada por análise elementar (Tabela 1), espectroscopia na região do infravermelho e RMN de $^{1}H$ e $^{13}C$.
A síntese ocorreu de forma semelhante para os dois ligantes, mas as análises indicaram a complexação de forma bidentada em ponte para o derivado do Oxadiazol (Complexo A) e monodentada para o ligante derivado de Tiazolidina (Complexo B).

| | **Complexo A** | | **Complexo B** | |
|---|---|---|---|---|
| | Teórico | Experimental | Teórico | Experimental |
| **% C** | 49,91 | 51,45 | 47,22 | 48,82 |
| **% H** | 5,24 | 4,25 | 5,94 | 5,93 |
| **% N** | 9,71 | 9,96 | 3,93 | 5,07 |

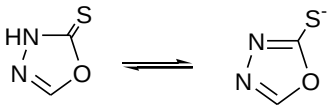


**Figura 2**. Tautomerismo tiona-tiol

No espectro de RMN de $^{1}H$ do Complexo A constatou-se a ausência do simpleto largo em δ 11,2 referente ao H de NH do ligante que muda sua forma tautomérica (Figura 2) ao ligar-se de forma covalente ao metal pelo S e coordenada pelo N. No RMN de $^{13}C$ observou-se o deslocamento químico do sinal em δ 170,5 para δ 172,70, referente ao carbono C-S. No espectro de IV as bandas em 3200 $cm^{-1}$ (N-H) e 1310 $cm^{-1}$ (C=S) do ligante estão ausentes no Complexo A. O CHN indica a ausência dos cloros. Para o complexo B, não foram observadas mudanças no espectro de infravermelho, visto que a ligação é coordenada pelo par de elétrons do S. O complexo resultante é neutralizado pelos ligantes cloro (a condutimetria foi compatível para complexos neutros nos dois casos). Os compostos têm diferentes labilidades em solução de DMSO, reforçando a diferença de coordenação dos ligantes.
Testes de citotoxicidade estão em andamento.

Garcia, A. et al. J Biol Inorg Chem **2016**, 273.

FAPEMIG, CNPQ

**Área: INO** **Inscrição:00178**

# Diphenylphosphine/Ru(II) complexes with antitumor activity: interactions with DNA and with HSA

**Adriana P.M. Guedes (PG),[1] Gregory F. Grawe (PG),[1] Celisnolia M. Leite (PG),[1] Elisângela de P. Silveira-Lacerda[2], Thales Eduardo M. Silva (IC)[3], Alzir A. Batista (PQ).[1]***

**adriana_quimica@hotmail.com; daab@ufscar.br**

*[1]Departamento de Química, UFSCar; [2]Departamento de Ciências Biológicas, UFG, [3]Universidade Federal de Alfenas, Campus Poços de Caldas*

Palavras Chave: *Diphosphine/Ru complexes, Antitumor activities, DNA and HSA interaction, Celular death.*

## Highlights

Ruthenium/diphenylphosphine complexes present good antitumor activities against human breast tumor cells (MDA-MB-2310) and lung tumor cells (A549), inducing cell death by apoptosis.

## Abstract

Ruthenium/phosphine complexes are good examples of potential antitumor metallodrugs[1]. Thus, given the promising results reported in the literature involving ruthenium/phosphine complexes as potential antitumor drugs, herein we synthesize, characterize and investigate new complex and their effect cultured MDA-MB-231 and A549 tumor cells. Here, we also study the binding of the complexes to DNA and HAS biomolecules. The complexes, with general formula $[Ru(tzdt)(bipy)(P\text{-}P)]PF_6$ and $[Ru(MIm)(bipy)(P\text{-}P)]PF_6$, where P-P= 1,1′-bis(diphenylphosphino)ferrocene and (oxydi-2,1-phenylene)bis(diphenylphosphine); bipy= 2,2'-bipyridine; tzdt= 2-mercapto-2-thiazoline) and MIm= 2-mercapto-1-methyl-imidazole. The MTT [3-(4,5-dimethylthiazol-2-yl)-2,5-diphenyl tetrazolium bromide] assay was used for the determination of the activity of the complexes. The IC50 for the complexes $[Ru(tzdt)(bipy)(POP)]PF_6$ and $[Ru(MIm)(bipy)(dppf)]PF_6$ are about 0.10 µM for the lung tumor cells A549 and about 0.29 µM for the breast tumor cells, respectively. The mechanism death for the cells, induced by the complexes are mainly by apoptosis. The complexes present weak electrostatic interaction with the DNA and their interaction with the HSA biomolecule occurs preferentially by the FA7 (site I). The complexes present promising results with $IC_{50}$ values comparable with the reference drug cisplatin and high selectivity indexes were found. The $IC_{50}$ of the complexes and their interaction with the biomolecules will be related with their structures.

## Acknowledgments

CNPq, CAPES e FAPESP

_____

1 Takarada, J. E.; Guedes, P. M. G.; Correa, S. C.; Silveira-Lacerda, E. de P.; Iacovelli, F.; Deflon, V. M.; Batista, A. A.; Desidere, A. *Arch. Biochem. Biophys.**2017**, 636, 28-41.*

**Área: INO** **Inscrição:00185**

# Pd (II) complexes as potential inhibitors of Topoisomerase II

**Mauro A. Lima (PG),[1]* Victor Deflon (PQ),[2] Fillipe V. Rocha (PQ)[1]**

**lima.mauroal@gmail.com**

[1]*Departamento de Química, UFSCar;* [2]*Instituto de Química de São Carlos, Universidade de São Paulo*

PalavrasChave: *Palladium, Thiosemicarbazone, Phosphines, Topoisomerase, Cancer, Cytotoxicity.*

## Highlights

- Synthesis and characterization of new Pd(II) complexes;
- Compound **1** 3 fold more cytotoxic than cisplatin;
- Palladium (II) complexes as inhibitors of topoisomerase II enzyme.

## Resumo/Abstract

Thiosemicarbazones are compounds that have been studied for their antitumor activity[1]. One of your targets is the enzyme topoisomerase II alpha[2]. Some cancer cells presents an over expression of this enzyme, therefore the design of new compounds that can inhibit the enzymatic cycle is an interesting pathway to combat these kind of cancer cells[3]. Presence of a metal ion, in general, increases the activity against the enzyme, furthermore, square-planar geometry showed an important characteristic to improve the interaction between substrate and enzyme. Motivated by these facts we synthesized and characterized by IR, NMR, UV-Vis, elemental analysis and X-ray diffraction new palladium(II) complexes bearing thiosemicarbazone and different phosphines as co-ligands of the type [PdCl(PPhR)(TSC)]. The ligand TSC and their complexes (1 and 2) were tested against two tumor cells line (MDA-MB-132 and A549). After, inhibition activity against topoisomeras II was analyzed by relaxation electrophoresis assay.

Spectroscopy techniques demonstrated the anionic N,S-chelate coordination of ligand TSC and the presence of phosphine in the coordination sphere of the metallic ion. We observed a displacement of 50 $cm^{-1}$ attributed to the vC=S vibration to less energetic region in the IR spectra. $^{31}P$ NMR showed only one peak in 27 ppm assigned to the phosphorus atom in a *trans* position to the nitrogen. These data were confirmed by the obtained structure (figure 1A). Cytotoxicity results showed that compounds **1** and **2** inhibit the cellular grow in the same range of cisplatin. However they not have any interaction with DNA, possibly the mechanism of action against tumor cells is different. These compounds can interrupt the enzymatic cycle of topoisomerase II in concentrations close to $IC_{50}$ (figure 1B) indicating a possible relationship.

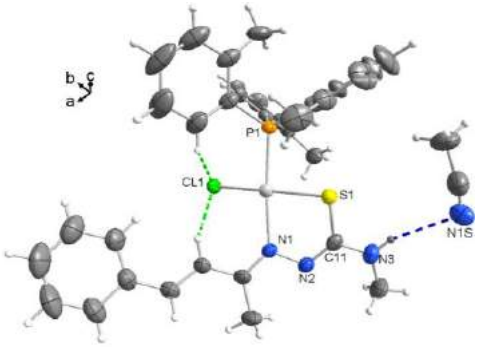


Figure 1A. Structure of compound **2**

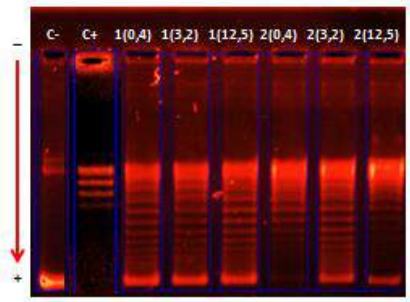


| IC-50 (μM) | |
|---|---|
| Nome | MDA-MB-231 |
| 1 | 0,89±0,2 |
| 2 | 3,43±0,8 |
| cisplatin | 2,50±0,2 |

Figure 1B. DNA relaxation assay by topoisomerase II.

**Acknowledgments:**
FAPESP 2016/04201-9, CNPq, CAPES

**References:**

1. Wilson, James T., *et al.* Chemical research in toxicology 29.4 (2016): 649-658.
2. Rocha, Fillipe V., *et al.* Journal of inorganic biochemistry 159 (2016): 165-168.
3. Sandhaus, Shayna, *et al.* Inorganic chemistry communications 64 (2016): 45-49.

**Área: INO** **Inscrição: 00222**

# Experimental and theoretical characterization of Sn(IV), Sb(III) and Bi(III) Xanthate

**Victor H. M. da Silva (IC),[1] Glaucio B. Ferreira (PQ) [2]**

**victormalamace@gmail.com; glauciobf@gmail.com**

*[1]Escola de Engenharia, Universidade Federal Fluminense, Rua Passos da Pátria 156, 24210-253, Niterói, RJ, Brazil, [2]Departamento de Química Inorgânica, Universidade Federal Fluminense, Outeiro de São João Batista s/n, 24020-141 Niterói, RJ, Brazil*

Palavras Chave: *Xanthate, Heavy Metals, Spectroscopy, Complex.*

## Highlights

Xanthate is an import group of ligands by its applications. The study reports the xanthate complexes with Sb, Sn and Bi. Experimental and theoretical characterizations have a good alignment for IR, Raman and UV spectra.

## Resumo/Abstract

The O-alkyldithiocarbonates, so-called xanthates (Xn) are a group of ligands that in metallic complexes derivatives can have extensively applications in pharmaceutical, fungicides, pesticides, thin films for phovoltaic devices and even in therapy for HIV infection. Xanthates have the propriety of decompose in broader temperature ranges and also it is easy synthesized, in large scale[1]. In the other hand, in literature there is a lack of structural and spectroscopic characterization study for some aryl xanthates, and a much smaller number of studies containing theoretical analyzes of this ligands and its complexes.

This study presents the experimental and theoretical characterization of several new alkyxanthates complex with Sn, Sb and Bi. The complexes was formed following the synthesis route described by literature[2,3] and by the equation (M = Sn, Sb, Bi; y= 4 for Sn and y=3 for Sb and Bi; R = etyl, i-propyl and n-butyl):

$$M^{+y} + y\ RXn^{-} \rightarrow \left[M(RXn)_y\right]$$

$$Sn^{+4} + 2Cl^{-} + 2RXn^{-} \rightarrow [Sn(RXn)_2Cl_2]$$

The characterization was performed in solid phase using IV, UV and Raman equipment from LAME-UFF. Theoretical study were submitted with the DFT method CAM-B3LYP/6-311+G(d,p) for light elements (C, O, S and H) and the ECP-LANL2DZ basis set to metals, using Gaussian 09 program.

This preliminary study of the xanthate complexes presents the experimental and theoretical IR spectra and the vibrational assigned of both spectra, as well as its geometries, described in literature as an octahedral complex, with two xanthate as a bidentate and two monodentate ligand (Cl or xanthate. The IR/Raman experimental characterization for structure found[3], confirmed the presence of xanthates through the bands shown in the table below. IR vibrational spectra simulated by the theoretical calculation permitted a refined assignment, mainly in low wavenumbers and resulted in a good approximation with the experimental spectra.

| Complex | Vibrational modes analysis ($cm^{-1}$) | | | | | | |
|---|---|---|---|---|---|---|---|
| | ν(C-H) | σ(HCH) | ν(C-O) | ν(C=S) | ν(C-S) | ν(Sn-S) | ν(Sn-Cl) |
| $[Sn(i\text{-}propyl)Xn)_2Cl_2]$ | 2977 | 1372 | 1241 | 1008 | 897 | 296 | 280 |
| $[Sn(i\text{-}propyl)Xn)_4]$ | 2977 | 1371 | 1242 | 1005 | 897 | 296 | # |

We intend to report the characterization of this entire row of xanthate complexes, for a good comprehension of its structure and synthesis. The comparison with the theoretical data will enhance this understanding of the molecules.

Acknolegment: CNPq, FAPERJ, PIBIC, PROPPi UFF, LAME-UFF and LMQC-UFF.

Reference: [1] B. Gupta, N. Kalgotra, S. Andotra, S. K. Pandey, Monatsh Chem 143 (2012) 1087-1095. [2] S. Ramachandra Rao, Xanthates and Related Compounds, Dekker,1971.[3] C. L. Raston, P. R. Tennant, A. H. White, G. Winter, Aust. J. Chem. 31 (1978) 1493-1500.

**Área: INO** **Inscrição: 00235**

# Spin crossover tuning through ligand design: Magnetic measurements, Mössbauer and crystal structures of two isomeric Fe(II) complexes with 2-aryl-imidazole ligands

Naheed Bibi (PG),[1] Luis E.S.C. Huamaní (PG),[1] Renan B. Guerra (PG),[1] Aline Alves Oliveira (PG),[3] Fanny Berón (PQ),[2] Andrea Paesano Júnior (PQ),[3] André L. B. Formiga (PQ).[1]

**formiga@iqm.unicamp.br**

[1]*Institute of Chemistry – UNICAMP;* [2]*Institute of Physics Gleb Wataghin – UNICAMP;* [3]*Department of Physics – UEM*

Palavras Chave: *Fe(II) complexes, Ligand design, Mössbauer Spectroscopy, Magnetic measurements*

## Highlights

The spin crossover behavior of two complexes of Fe(II) with 2-aryl-imidazole ligands were investigated using Mössbauer Spectroscopy and magnetic susceptibility measurements.

## Abstract

Designing coordination complexes that are stable and exhibit spin crossover (SCO) phenomenon are highly in vogue because of their applications in memory storage and switching devices. Imidazole has a bifunctional character i.e., the presence of pyrrolic and pyridinic N-atom, in addition to its -NH functional group which makes it a perfect candidate for manipulation of the ligand field strength, to trigger interesting electrochemical and magnetic properties in the corresponding metal complexes.

In the present work, Mössbauer Spectroscopy and magnetic susceptibility measurements were used to study the spin crossover phenomena in two complexes $[Fe(M)_3](ClO_4)_2$ **(1)** and $[Fe(Z)_3](ClO_4)_2$ **(2)**. Single crystals of both the complexes showed distorted octahedral form of the meridional isomers with a space group P 21 / c at 150 K. Mössbauer Spectroscopy (Figure 1) for complex (1) proves the existence of both HS and low spin configurations at ambient temperature whereas only LS state at a lower temperature (22K). However, complex (2) was found to exist in low spin only at a wide range from ambient temperature to 22K. Magnetic susceptibility experiments also endorsed the aforementioned results. Complex **(1)** was found to be a spin crossover compound with a spin transition at 225 K, whereas complex **(2)** had a stable magnetic behavior between 0–300 K. Therefore, ligand design can be considered as a potential tool to manipulate and fine tune the magnetic properties of these complexes.

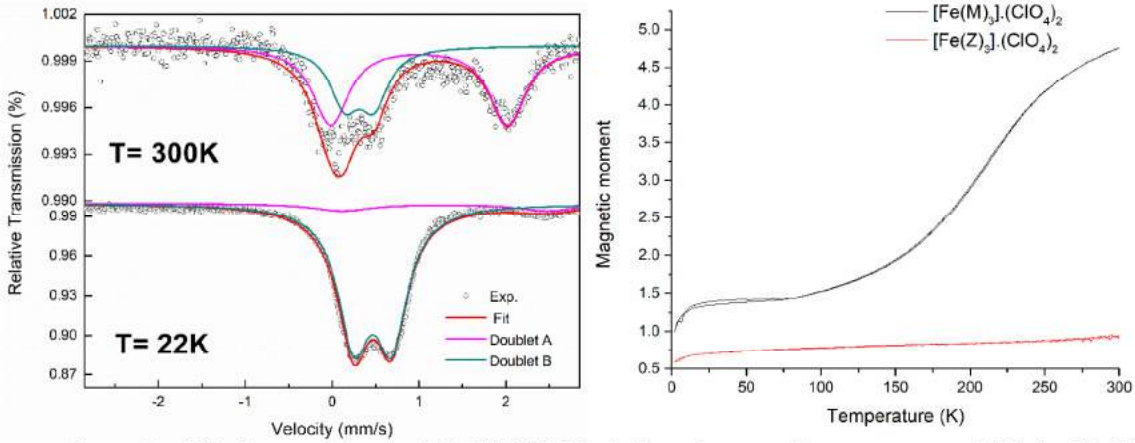


Figure 1 - Mössbauer spectra of $[Fe(M)_3](ClO_4)_2$ (left) and magnetic moments *vs.* T(K) for $[Fe(M)_3](ClO_4)_2$ and $[Fe(Z)_3](ClO_4)_2$ (right).

**References**

[1] Gütlich, P.; Gaspar A. B.; Garcia, Y. Spin state switching in iron coordination compounds. *Beilstein .J Org. Chem.* **2013**, *9* , 342–391.

We would like to acknowledge CAPES, FAPESP and CNPq for financial assistance.

**Área: INO** **Inscrição: 00243**

# Synthesis and structural characterization of multinuclear palladium(II) arylchalcogenolates compounds

**Natália V. Fagundes (IC),[1] Camila N. Cechin (PG),[1*] Bárbara Tirloni (PQ),[1] Ernesto S. Lang (PQ).[1]**

**natalia-fagundes@outlook.com; camilacechin@hotmail.com**

[1]*Departament of Chemistry, UFSM;*

Key-words: *palladium, chalcogenolate, oxidative addition*

## Highlights

This work reports the synthesis and characterization of multinuclear palladium(II) arylchalcogenolates compounds through oxidative addition reactions.

## Abstract

The study of organopalladium compounds have been incresing in the last few years due to the diversity applications, as in catalisys,[1] synthesis[2] and material science[3]. The palladium arylchalcogenolate coordination chemistry has attracted great interest in a variety of applications, mainly in organometallic chemistry, as catalists in C-C coupling reations.[4]

Considering the great importance in this class of compounds, the purpose of this work is to present the synthesis and structural characterization of three new multinuclear palladium(II) arylchalcogenolates.

The synthesis of these compounds were performed through oxidative addition reactions of $[Pd(bipy)py_2][(PF_6)_2]$ to $(ArTe)_2$ ligands, diaryl ditelurides, where Ar = Ph, Mes, *p*-$^t$Bu-$C_6H_4$. **Figure 1** shows the molecular structure of compounds **1**-**3**, elucidated by single-crystal X-ray diffraction.

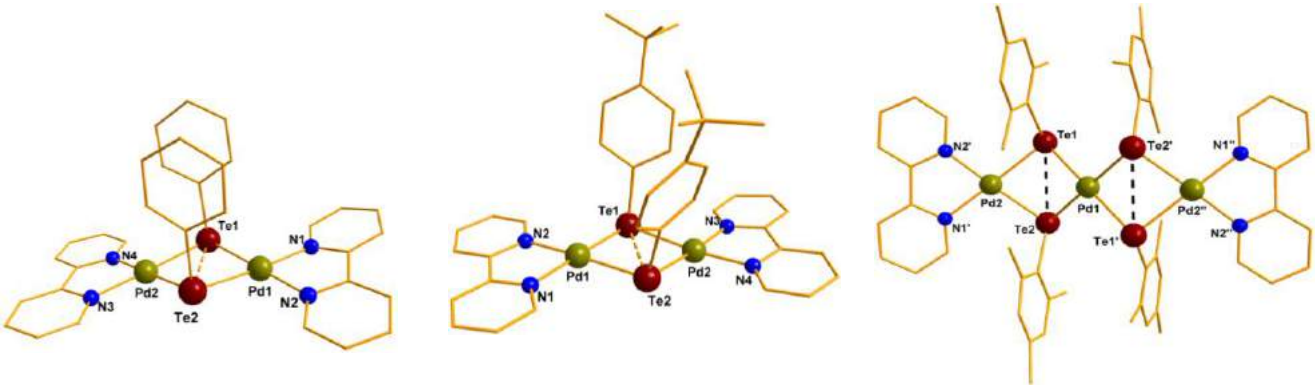


**Figure 1.** Molecular structure of compounds **1**, **2** and **3**, respectively.

The use of different $(ArTe)_2$ led to **1**-**2** (dinuclear) and **3** (trinuclear) due to the basicity variation among arylchalcogenolate ligands generated *in situ.* The enhanced basicity of $(MesTe)^-$ is verified by central palladium in **3**. Since $[Pd(bipy)py_2][(PF_6)_2]$ was used as palladium source, it was realized that $(MesTe)^-$ ligands substitute one bidentate bipy and two pyridyl ligands coordinated to palladium, leading a trinuclear compound. This fact did not happen to $(PhTe)^-$ and (*p*-$^t$Bu-$C_6H_4Te)^-$ in **1** and **2**.

For compounds **1**-**3** complementary analyzes were carried out, which corroborate with the structure elucidated by single crystal X-ray diffraction.

---

1. Dupont, J.; Consorti, C. S.; Spencer, J. *Chem. Rev.* **2005**, *105*, 2527.
2. Jain, V. K.; Chauhan, R. S. *Coord. Chem. Rev.* **2016**, *306*, 270.
3. Ghedini, M.; Aiello, I.; Crispini, A.; Golemme, A.; La Deda, M.; Pucci, D. *Coord. Chem. Rev.* **2006**, *250*, 1373.
4. Kumbhare, L. B.; Dutta, P. K. *J. Organomet. Chem.* **2016**, *805*, 59.

**Área: INO** **Inscrição: 00248**

# Degradação do antibiótico norfloxacino por $H_2O_2$ e $KHSO_5$, catalisada por porfirinas de manganês halogenadas

**Alexandre M. Meireles (PG), Ynara M. Idemori (PQ), Dayse C. S. Martins (PQ)**

**daysecsm@yahoo.com.br; alemoreira13@gmail.com**

*Departamento de Química, ICEx, Universidade Federal de Minas Gerais, UFMG.*

Palavras Chave: *Porfirinas de manganês, Catalisador, Fármaco, Química verde, Halogênio.*

## Highlights

**Norfloxacin degradation by $H_2O_2$ and $KHSO_5$ catalyzed by halogenated manganese porphyrins**
A green chemistry strategy for degradation of norfloxacin; Steric hindrance caused by the halogen atoms avoid the interaction between the active species and norfloxacin; Better degradation (22%) was obtained with $KHSO_5$ and [MnT2,3DCPPCl] as catalyst.

## Resumo/Abstract

Antibióticos são agentes que inibem o crescimento de microorganismos e sua ampla utilização, de forma indiscrimada, tem levado a sérios problemas ambientais, como a resistência bacteriana. Neste contexto, o emprego de catalisadores para favorecer a degradação destes compostos, associado aos princípios da química verde, tem ganhado atenção na comunidade científica. Assim, descreve-se a utilização de catalisadores porfirínicos de manganês (MnP) contendo átomos de halogênio na periferia do macrociclo (Figura 1) em reações de degradação do norfloxacino (NOR) por $H_2O_2$ ou $KHSO_5$ (Tabela 1).

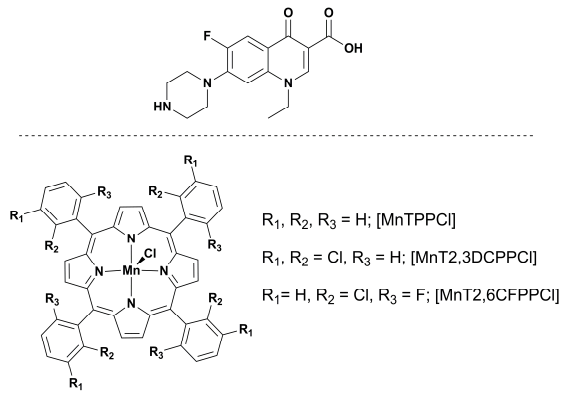


**Figura 1.** Estrutura do norfloxacino (a) e dos catalisadores metaloporfirínicos (b), utilizados neste trabalho.

**Tabela 1.** Reações de oxidação do norfloxacino por $H_2O_2$ e $KHSO_5$, na presença de MnP.

| Oxidante | Catalisador | [A]Degradação do NOR(%) | [B]Destruição da MnP(%) |
|---|---|---|---|
| $H_2O_2$ | - | 12 | - |
| | [MnTPPCl] | 18 | 85 |
| | [MnT2,3DCPPCl] | 20 | 72 |
| | [MnT2,6CFPPCl] | 16 | 66 |
| $KHSO_5$ | - | 6 | - |
| | [MnTPPCl] | 20 | 90 |
| | [MnT2,3DCPPCl] | 22 | 75 |
| | [MnT2,6CFPPCl] | 16 | 85 |

Condições de reação: relação em quantidade de matéria catalisador:norfloxacino:oxidante = 1:10:100. Agitação magnética, 25 ºC, sistema aeróbico, presença de luz. [A]A degradação do norfloxacino é calculada pela relação: [($Abs_{273}$ inicial - $Abs_{273}$ final)x100]/$Abs_{273}$ inicial]. [B]O grau de destruição dos catalisadores foi calculado a partir dos espectros de absorção na região do UV-Vis obtidos após o término da reação.

A presença dos catalisadores porfirínicos levou ao aumento da degradação do norfloxacino quando comparado às reações branco (ausência de MnP), para os dois oxidantes utilizados, porém o grau de degradação ainda é baixo. Nas reações com os catalisadores [MnT2,3DCPPCl] e [MnT2,6CFPPCl], os átomos de cloro e/ou flúor nas posições *–orto* podem promover um maior impedimento estéreo no catalisador, dificultando a aproximação do fármaco ao sítio ativo, se comparado ao catalisador [MnTPPCl]. Além disso, a clivagem homolítica da ligação O-O, nas reações com $H_2O_2$ pode ser desfavorecida em água, impedindo a formação dos radicais $HO^{\bullet}$, responsáveis por degradar o fármaco. Já nas reações com $KHSO_5$, o oxidante pode ser decomposto na presença de íons Mn(II) e/ou Mn(III), vindos da destruição dos catalisadores porfirínicos (Tabela 1), levando a uma diminuição nos valores de degradação para estes sistemas. Uma otimização do sistema será realizada no intuito de aumentar a eficiência da reação e permitir a identificação dos produtos de degradação do norfloxacino.

Agradecimentos: FAPEMIG, CNPq, CAPES.

**Área: INO** **Inscrição: 00277**

# Synthesis and Characterization of basic catalysts designed by Calixarenes or Silicas to take advantage of Glycerol.

**Daniela Machado(PG),[12] Eliezer L. Gomes (PQ),[1] Izilda A. Bagatin (PQ).[2]**

**machado.daniela23@gmail.com; ibagatin@unifesp.br**

*[1] Departamento de Engenharia Química, Laboratório de Catálise Heterogênea e Química Verde. Universidade Federal de São Paulo – Campus Diadema. Rua Prof. Artur Riedel, 275. Diadema - São Paulo – SP – Brasil. CEP 09972-270;*
*[2]Departamento de Química, Laboratório de Química de Calixarenos, Espectroscopia Molecular e Catálise. Universidade Federal de São Paulo – Campus Diadema. Rua Prof. Artur Riedel, 275. Diadema - São Paulo – SP – Brasil. CEP 09972-270.*

Palavras Chave: Basic Catalysis, Glycerol, Calixarenes, Hybrid Silicas.

## Highlights

Synthesis and characterization of basic catalysts;
Basic catalysis using hybrid silicas and calix[n]arenes activated;
Use of a potential residue: glycerol;

## Resumo/Abstract

The growing concern about environmental issues and the allocation of environmental liabilities pose a significant challenge. A process of great importance in the Brazilian economy is the production of biofuels, produced from a reaction of transesterification of glycerides with an alcohol in the presence of a catalyst. In this reaction besides biofuel, there is a generation of a co-product, the glycerol, used in several sectors as a humectant, but this one may not be absorbed by the market. Routes to valorize glycerol have been increased by their conversion into glyceryl carbonate with the use of a basic catalyst, making the production chain of biofuels more sustainable and economically practicable. In this context, hybrids silica and calixarene-derived arise, whose preliminary tests with calix[4]arene depicted a frequency at 1784cm$^{-1}$, on an IR spectrum, assigned to glyceryl carbonate, demonstrating their effectiveness when applied to the glycerol transcarbonation reaction. Calix[4]arene is a material belonging to the P121/n1 group being a widely crystalline material according to Figure 1, while the hybrid silicas are amorphous materials having pore structure organization. These materials are quite workable due to their thermal stability in the range of 78° C which is the temperature of the reaction medium.

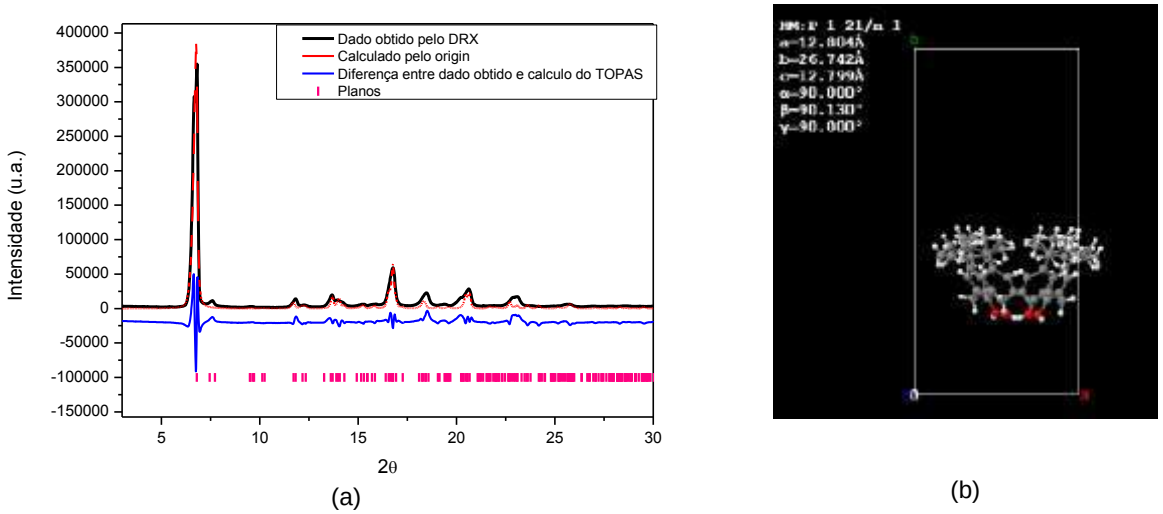


(a) (b)

**Figure 1** – (a) DRX of calix[4]arene (software TOPAS) (b) Structure of calix[4]arene.

**Área: INO** **Inscrição: 00330**

# Synthesis and analysis of a novel dinuclear bis(oxamate) type complex using $[Co_2(H_2mpba)_3]^{2-}$ mesocate as building block

**Cintia Almeida Simosono (IC),[1]* Nathália R. De Campos (PG),[1] Walace Doti do Pim (PQ),[2] Antônio C. Doriguetto (PQ),[1] Ana Karoline S. M. Valdo (PG),[3] Felipe T. Martins (PQ),[3] Humberto O. Stumpf (PQ),[4] and Maria Vanda Marinho (PQ).[1*]**

***cintiasimosono@hotmail.com; maria.marinho@unifal-mg.edu.br.**

*[1]Instituto de Química, Universidade Federal de Alfenas, Campus Santa Clara, Alfenas, MG, 37130-000, Brazil; [2]Departamento de Química, Centro Federal de Educação Tecnológica de Minas Gerais, Belo Horizonte, MG, 31270-901, Brazil;[3]Instituto de Física, Universidade Federal de Goiás, Campus Samambaia, Goiânia, Go, 74690-900, Brazil;[4]Departamento de Química, Universidade Federal de Minas Gerais, Campus Pampulha, Belo Horizonte, MG, 31270-901, Brazil.*

Keywords: *coordination chemistry, crystal engineering, supramolecular chemistry.*

## Highlights

- The complexing ability of cobalt(II) in solution by the 1,3-phenylenebis(oxamate) ligand
- Use of building blocks in the synthesis of new complexes
- Structural characterization of the complex –formation of metallamacrocycles

## Abstract

Use of Supramolecular Chemistry and Crystal Engineering concepts for solid-state structure formation is constantly increasing.[1] The development of new synthetic strategies trying to control the molecular ordering of organic or metal−organic building blocks to obtain desirable materials with interesting properties has been employed to the self-assembly of new compounds.[1-2] Therefore, in the present work a new compound of formula $[Co_2(H_2mpba)_3][Co(H_2O)_5(CH_3OH)]\cdot 2DMSO\cdot 2H_2O$ **(1)** was prepared by reacting $Co^{2+}$ ions and the $H_2mpba^{2-}$ dianion through the *in situ* methodology in methanol/dmso mixture. It is well known that the crystallization process is very important in order to get a better understanding of the crystal assembly and therefore, we investigate the solvent and cobalt(II) ion roles in the desired-crystal growing. The analysis by CHN, IR, TG/DTA indicated the formation of **1**. Analysis of the IR spectrum reveals νN-H at 3232 $cm^{-1}$, which confirms the partial deprotonation of the $H_4mpba$ preligand, as well as bands of the carboxylate portion and solvent molecules. TG/DTA curves are in according with the studies by single crystal X-ray diffraction, which show two independent crystallography cobalt(II) centers coordinated to three $(H_2mpba)^{2-}$ ligands (see Figure 1) and a third cobalt(II) ion coordinated to five water molecules and one methanol molecule forming the $[Co(H_2O)_5(CH_3OH)]^{2+}$ complex. Thus, for the first time, an anionic dinuclear unit $[Co_2(mpba)_3]^{2-}$ is stabilized by another cationic coordination complex, as shown in the crystal structure exhibited in Figure 2.

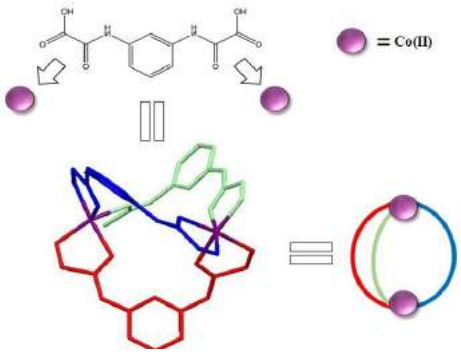


**Figure 1.** Combination of the $H_2mpba^{2-}$ with the cobalt(II) ion to form the $[Co_2(H_2mpba)_3]^{2-}$ dinuclear complex.

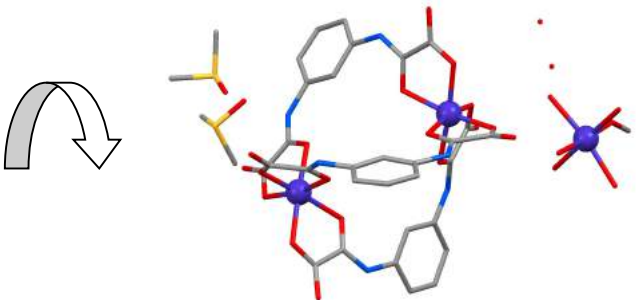

**Figure 2.** Molecular structure of **1** consisting of a mesocate of formula $[Co_2(H_2mpba)_3]^{2-}$ and $[Co(H_2O)_5(CH_3OH)]^{2+}$ as a stabilizing counterion. Hydrogen atoms were omitted for clarity.

[1]Ribeiro, E.O.; *et al, CrystEngComm,* **2017***, 19,* 5460; [2]Dhers, S.; *et al*, *Coord. Chem. Rev*. **2015**, *296*, 24.

***Acknowledgments***
*PIBIC/CNPq (Unifal-MG), Fapemig, CNPq, Capes, FINEP (ref.134/08), RMQ-MG.*

**Área: INO**
*(Inserir a sigla da seção científica para qual o resumo será submetido. Ex: ORG, BEA, CAT)*

**Inscrição: 00366**
*(Inserir o número de inscrição do autor que fez a submissão)*

# Complexos Fluorescentes de Lantânio-Espiropirano com Aplicações em Materiais Poliméricos.

**Izadora F. Reis (PG)[1] e Frederico B. de Sousa (PQ)[1*]**

**izadorafonseca@hotmail.com e fredbsousa@gmail.com**

*[1]Instituto de Física e Química, Universidade Federal de Itajubá – MG, Brasil.*
Palavras Chave: *Espiropirano, Lantânio, complexo, fotocromismo, reversibilidade, fluorescência.*

## Highlights

Lanthanum-Spiropyran Fluorescent complex for Polymeric Materials Applications. Spiropyrans are photochromic molecules.[1] Spiropyrans have been used in fields from chemistry to materials sciences. Concerning metal complexes spiropyrans have been used and colorimetric sensors.[2]

## Resumo/Abstract

A propriedade fotocrômica dos espiropiranos pode ser comprovada por espectroscopia eletrônica, em que se observa espectros de absorção separados (Figura 1a). Ao utilizá-lo como ligante na reação com Lantânio ($La^{3+}$) como centro metálico, ocorreu um deslocamento significativo na banda de absorção, bem como uma mudança de cor (Figura 1b), indicando a formação do complexo que foi isolado em etér. O produto (LaMC) apresentou fotocromismo e fluorescência, como propriedades de grande interesse, em que esta última foi evidenciada pelo espectro de emissão (Figura 1c). Também foi realizado um estudo cinético (Figura 1d) do complexo, afim de verificar a estabilidade do mesmo em solução de THF anidro. Observou-se um decaimento exponencial na coloração, indicando uma possível dissociação do complexo. Além deste, realizou-se um experimento de reversibilidade (Figura 1e) em solução de THF anidro, ou seja, medidas de absorção com emissão de radiação UV e luz branca de forma alternada, como resultado observou-se um pequeno decaimento na eficiência com 15 ciclos. Devido à instabilidade do complexo em solução, o mesmo foi imobilizado em matriz polimérica a base de policaprolactona, visando a produção de filmes (Figura 1f) e fibras com potencial aplicação na produção de materiais com propriedades únicas, como o fotocromismo e a fluorescência.

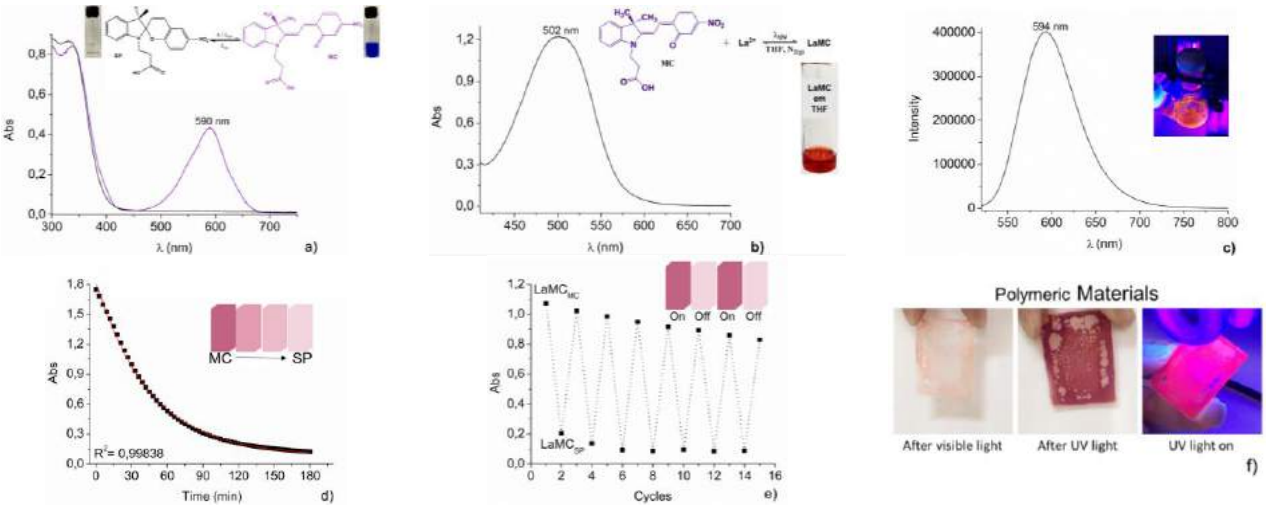


Figure 1: a) UV-visible spectra of SP and MC isomers, b) UV-visible spectrum of LaMC complex, c) emission spectrum of LaMC complex, d) kinetic behavior of LaMC complex in solution, e) cycles of UV and visible lights irradiation on LaMC complex and f) association of LaMC complex into polycaprolactone matrix.

Acknowledgements: This work was supported by CNPq, FAPEMIG, CAPES and LNBio.
[1] De Sousa, F. B., et al., J. Mater. Chem., 2010, 20, 9910-9917.
[2] Shiraishi, Y., et al., Chem. Commun., 2012, 48, 5485-5487.

**Área: INO**_____ **Inscrição: 00390**_____

*(Inserir a sigla da seção científica para qual o resumo será submetido. Ex: ORG, BEA, CAT)*

*(Inserir o número de inscrição do autor que fez a submissão)*

# Studies of chromium (VI) adsorption in *Eucalyptus grandis* bark.

**Anamaria D. P. Alexiou (PQ), Amanda dos S. Godim (IC), Paulete Romoff (PQ).**

**anamaria.alexiou@mackenzie.com; amandagondim_11@hotmail.com**

*Escola de Engenharia, UPM*

Palavras Chave:*(Chromium (IV), Eucaliptus grandi, Adsorption).*

## Highlights

- $K_2Cr_2O_7$(aq) solution was used as synthetic effluent.
- *Eucalyptus* bark is a lamellar material with microporous.
- 42% of chromium(VI) was removed of solution after 180min of contact with barks.

## Resumo/Abstract

*Eucalyptus* spp. are the most important fiber sources for pulp and paper industries; however, substantial amounts of biomass residues are generated, among which bark is the most abundant and is currently simply burned to produce energy. Chromium (VI) is a toxic metal and there is a great concern of researchers in removing this metal from aquatic environments. In this work, we report the use of *Eucalyptus* barks to remove chromium (VI) of synthetic effluent.

The barks were dried soon after collection and pulverized in a mill, and then stored. This material was treated according to Sarin and Pant work [1]. The adsorption test was performed by adding 75mL of synthetic effluent ( $6.83.10^{-4}$M $K_2Cr_2O_7$) to 375mg of treated *Eucalyptus* bark and the mixture was heated to 32$^{o}$C for 180 min. Every 30 minutes, 6mL of this solution was filtered and the UV-Vis spectrum of the filtrate was obtained.

The MEV image of *Eucalyptus* bark in figure 1a shows that it is lamellar and porous material. The blue points in the figure 1b show that chromium (VI) was adsorbed on the bark surface.

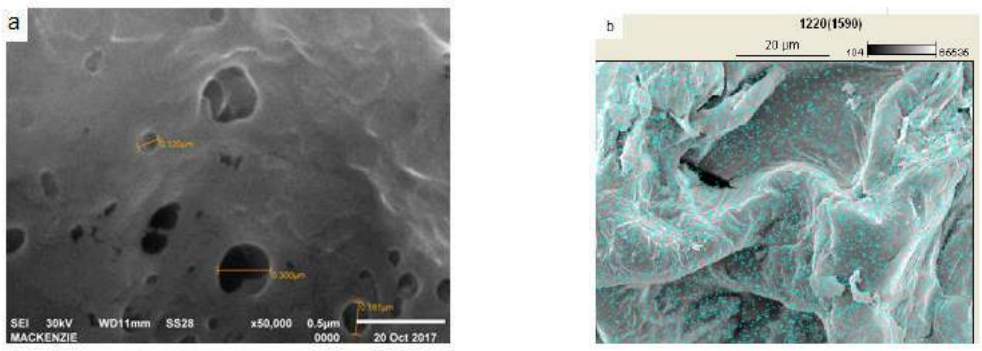


Figure 1. MEV image of eucalyptus bark before (a) and after contact with synthetic effluent (b).

UV Vis analysis of the filtrate determined the concentration of chromium remaining in solution, and the calculated percentage of removal was 42%.

Fundo Mackenzie de Pesquisa.

[1].SARIN, V; PANT, K. K.. *Bioresour. Technol.*, **2006**, 97, 15.

**Área: INO** **Inscrição:00438**

# Synthesis and characterization of new Zn(II) complexes designed as prototypes for chemotherapeutic treatment of bacterial infections

**Henrique J. de Arruda (PG),[1*] Felipe Vitório (PG),[1] Amanda P. Neves (PQ),[1] Arthur E. Kümmerle (PQ).[1]**

**henriqueufrrj@outlook.com**

[1]*Department of Chemistry, UFRRJ;*

Keywords: *(Coumarin derivatives, Zn(II) complexes, Imidazopyridine, biological activity).*

## Highlights

The main focus of this work was to explore the synthesis of new coumarin- imidazopyridine derivatives and their Zn(II) complexes. The compounds have been characterized by NMR and infrared spectra.

## Abstract

Nowadays is a worldwide necessity the demand for new bactericidal compounds, capable of effectively combating and even being active against multiresistant bacteria[1]. In this sense, the use of inorganic compounds has been described by several research groups, where the incorporation of a metal ion can result in improved biological activities, low resistance and tolerable side effects, when compared to the free organic ligands[2]. This work describes the synthesis and characterization of two coumarin derivatives (IM1 and IM2) and their respective $Zn^{II}$ complexes (IM1-Zn and IM2-Zn). The ligands and the metal complexes have been prepared according to the Scheme 1.

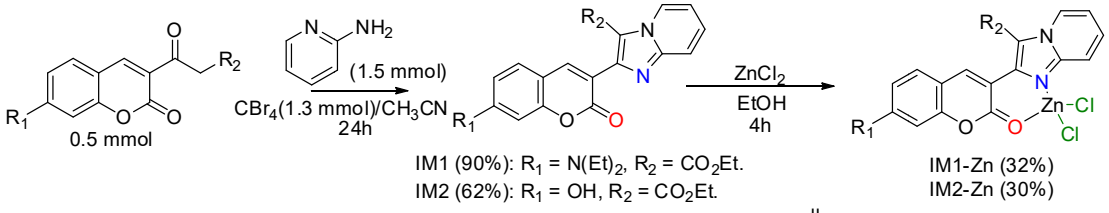


**Scheme 1:** Synthesis of the ligands IM1-IM2 and the $Zn^{II}$ complexes.

All compounds have been characterized by $^1$H NMR and Infrared spectroscopy. The $^1$H NMR spectra of IM1 and IM1-Zn are shown in Fig 1.

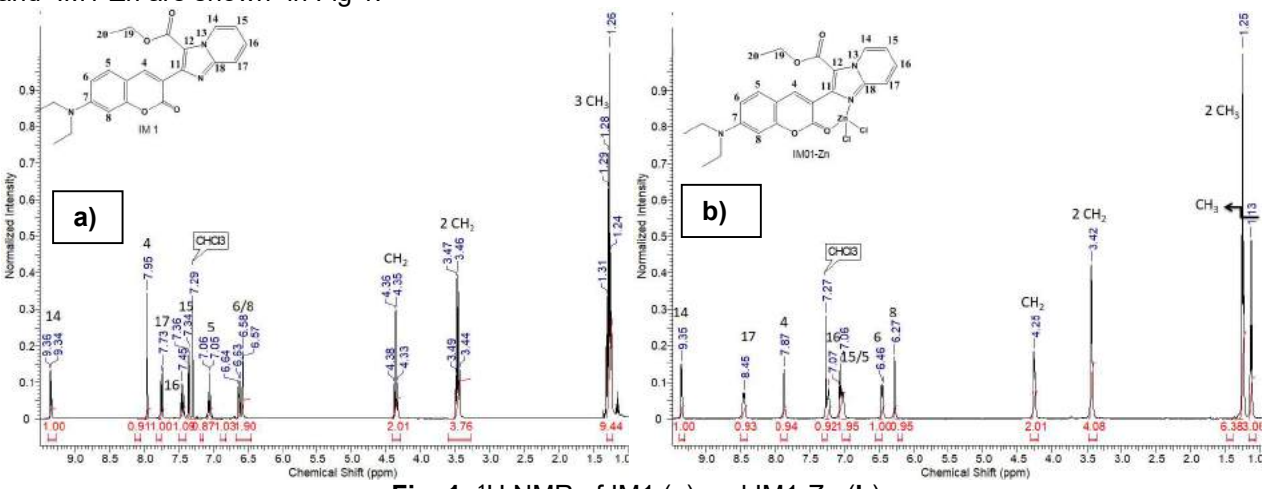


**Fig. 1:** $^1$H NMR of IM1 (**a**) and IM1-Zn (**b**).

The spectrum of the IM1-Zn showed that the signals of the hydrogens nearby the coordination points were shifted to lower field suggesting coordination through the iminic nitrogen and the carbonyl oxygen. The characterization of the compounds by other techniques such as X-ray diffraction and elemental analysis are underway.

[1] PANDEY, A and NEGI, P. S. Natural Product Research, 2017, 2, 1-4.

[2] SHI, Y.; SHOU, C-H. Bioorganic Medicinal Chemistry Letters. 2011, 21, 95.

**Área: _INO_____** **Inscrição:__ 00488_____**
*(Inserir o número de inscrição do autor que fez a submissão)*

# Investigation on formation of highly luminescent β-Diketone-Ln(III)-edta water-soluble complexes

**Ercules E.S. Teotonio (PQ),[1] Haryane M. Silva (PG),[1*] Wagner M. Faustino(PQ),[1] Hermi F. Brito,[2] Oscar L. Malta (PQ),[1,3] Maria Cláudia F. C. Felinto (PQ),[4]**

**teotonioees@quimica.ufpb.br; haryane_morais@hotmail.com**

*[1]Departamento de Química, UFPB; [2]Departamento de Química Fundamental – IQ-USP; [3]Departamento de Química Fundamental – UFPE;[4]Instituto de Pesquisas Energéticas e Nucleares-IPEN-SP*

Palavras Chave: *Lanthanide complexes, water-soluble, edta, β-diketone, photoluminescence*

## Highlights

Photophysical properties of three β-diketone-Lanthanide-edta water-soluble complexes were investigated. A very strong red and green luminescence have been observed in aqueous solutions. $Eu^{3+}$ and $Tb^{3+}$ systems are promising as red and green optical markers for bioassay or bioimaging.

## Resumo/Abstract

In the last decades, a special attention has been devoted to the development of water-soluble trivalent lanthanide ($Ln^{3+}$) complexes exhibiting strong emission intensities. In particular, Ln-edta complexes (edta: ethylenediamintetraacetate) present high stability in both solid and aqueous solutions. The water molecules coordinated to the lanthanide ion in these complexes may be substituted by other kind of ligands, which act as efficient luminescence sensitizer via *antenna effect*. This indirect excitation process can overcome the very low molar absorption of the 4f-4f electronic transitions. In this work, we have investigated systematically the photoluminescent properties and formation of β-diketone-Eu-edta (where β-diketone: tta=thenoyltrifluoroacetonate or btfa=benzoyltrifluoroacetonate) and acac-Tb-edta (acac=acethylacetonate) complexes, in aqueous solution. In order to investigate the formation of Ln-edta-β-diketonate complexes, luminescence spectral data were recorded for aqueous solutions containing different Ln-edta and β-diketone molar ratios (Fig. 1). A very strong red luminescence has been observed by addition of tta or btfa ligand to the Eu-edta complex solution. As the β-diketonate:Eu-edta molar ratio increases, the intensity parameter ($\Omega_2$ ) values undergo asymptotic behavior, reaching its maxima values when the β-diketonate quantities are approximately equivalent to the initial quantity of precursor complex in solution. The formation of acac-Tb-EDTA complex in aqueous solution was investigated taking into account the full width at half maximum ($\Delta\lambda$) band assigned to the $^5D_4 \rightarrow {}^7F_5$ transition at 547 nm. The $\Delta\lambda$ versus acac:Tb-edta molar ratio curve (Fig. 1) shows a saturation profile when the molar ratio is close to 1. These luminescent results give evidences of water molecules were substituted by one β-diketonate molecule in the first coordination sphere of the $Eu^{3+}$ and $Tb^{3+}$ ions, and that these $Ln^{3+}$ systems are promising to act as red and green optical markers for bioassay or bioimaging.

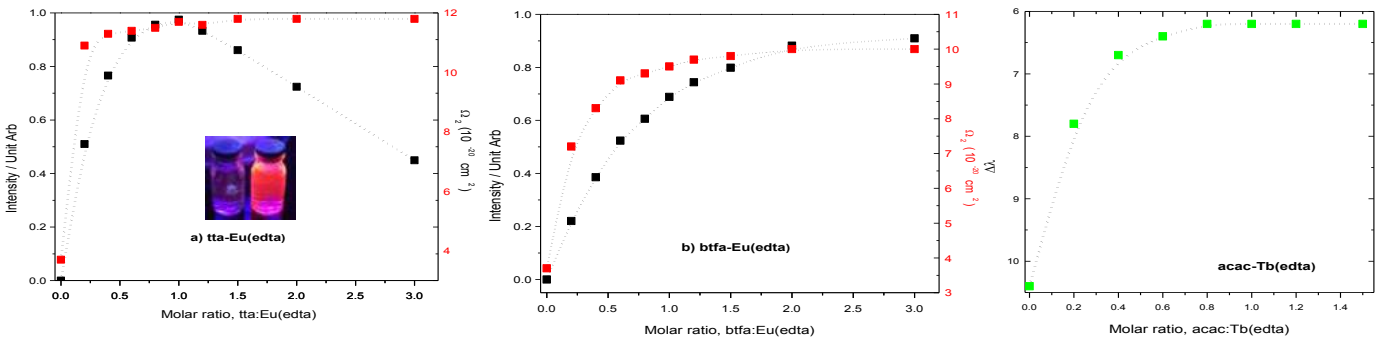


Fig. 1: Luminescence data for tta-Eu-edta (A), btf-Eu-edta (B) and acac-Tb-edta complexes in aqueous solution.

- **Área: INO** **Inscrição: 00508**

# Perylene-derived calix[4]arenes with potential application in luminescent systems

**Giulia Murbach de Oliveira (IC),[1] Izilda A. Bagatin (PQ),[1]**

**giuliamurbachdeoliveira@outlook.com; ibagatin@gmail.com**

[1]*Departamento de Química, Laboratório de Química de Calixarenos, Espectroscopia Molecular e Catálise, ICAQF - UNIFESP, Diadema, Brasil, CEP 09972-270.*

Palavras Chave: *Calixarene, Perylene, Luminescence*

## Highlights

Calix[4]arenes functionalized in both its upper and lower rims for luminescent applications.
Synthetic route to attach the insoluble perylene-dye to the calixarene.

## Resumo/Abstract

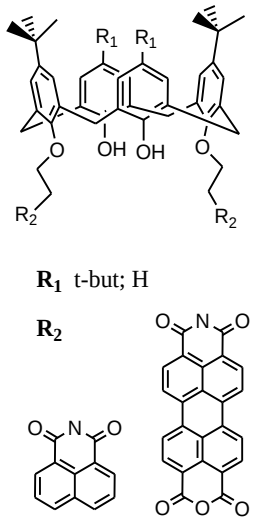


Figure 1

In this work, perylene-derived molecules, chromophores which possess high quantum yields, were attached to calix[4]arene matrix as a means of creating macromolecules (figure 1) which can be utilized in the development of OLEDs, or as biological markers. The relevance of this work lies in the combination of both perylene chromophores and calixarenes merging their unique properties. Perylene-derived molecules, as an example of the perylene-3,4,9,10-tetracarboxylic dianhydride used in this work, have high lightfastness and are very stable electron-receptors[1], but are very insoluble. Calixarenes, on the other hand, are macrocycles which allow functionalization and intermolecular interactions in both its upper and lower rims and have been used in many applications in the host-guest and supramolecular chemistry[2].

In this context, functionalizing calixarenes with such chromophores makes the chromophores soluble in several solvents, and therefore, useful for the applications above-mentioned. The compounds synthesized were the ligand perylene-3,4,9,10-tetracarboxylic acid monoanhydride monopotassium carboxylate **(1)**; 5,11,17,23-tetra(tert-butyl)-25,27-dicyanomethoxy-26,28-dihydroxy-calix[4]arene **(2)**; 5,11,17,23-tetra(tert-butyl)-25,27-diaminoethoxy-26,28-dihydroxy-calix[4]arene **(3)**; 5,11,17,23-tetra(tert-butyl)-25,27-bis(1,8-naphthalic anhydride)-26,28-dihydroxy-calix[4]arene **(4)**; 5,17-bis(tert-butyl)-25,27-dicyanomethoxy-26,28-dihydroxy-calix[4]arene **(5)**; 5,17-bis(tert-butyl)-25,27-diaminoethoxy-26,28-dihydroxy-calix[4]arene **(6)**, among others. The analysis of the reactions was carried out with $^1$H NMR and infrared spectroscopy. The analysis of the infrared spectrum proved the preparation of the ligand **(1)** by the shift from the anhydride band at 1773 cm$^{-1}$ to the carboxylic acid band at 1713 cm$^{-1}$. The inspection of the $^1$H NMR spectra allowed the examination of the functionalized calixarenes, as well as its conformations. $^1$H NMR data indicates the presence of **(2)** from the calix[4]arene matrix because of the occurrence of the two t-butyl singlets at 0.89 and 1.33 ppm (18H each), the ether at 4.32 ppm (4H) and the two m-ArH singlets at 7.13 (4H) and 6.74 ppm (4H). The reduction of **(2)** forming **(3)** is noticed by the approximation of the two t-butyl singlets at 1.23 and 1.12 ppm, by the presence of the $NH_2$ hydrogens at 5.13 ppm (s, 4H) and because of the hydrogens of the ether depicted at 3.38 ppm (t, N-$CH_2$, 4H) and 4.12 ppm (t, O-$CH_2$, 4H). The ligand **(4)**, in turn, showed the absence of the $NH_2$ hydrogens and the presence of the 1,8-naphthalic anhydride hydrogens at 7.77 ppm (dd, 4H), 8.69 ppm (dd, 4H), and 8.18 (dd, 4H). The loss of two t-butyl groups in **(2)**, producing **(5)** was validated by the presence of only one t-butyl singlet at 0.92 ppm (18H) and also by the presence of three m-ArH shifts at 7,14 ppm (d, 4H), 6,79 ppm (t, 2H) and 6,75 (s, 4H). The reduction of **(5)** to make (**6**) was ascertained by the shift of the t-butyl singlet from 0.92 ppm to 1.12 ppm (s, 18H) and by the presence of the ether at 3.38 ppm (N-$CH_2$, 4H) and 4.12 ppm (O-$CH_2$, 4H)

1 Langhals, H. Cyclic carboxylic imide structures as structural elements of high stability – novel developments in perylene dye chemistry. *Heterocycles*, 4, 477-500, **1995**

2 Gutsche, C. D. Calixarenes: An introduction**,** *Royal Society of Chemistry Publishing*, Cambridge, **2008**

**Área: INO** **Inscrição: 00520**

# Complexos de Fe(II), Mn(II) e Zn(II) derivados de um ligante do tipo oxamato funcionalizado: Síntese e Caracterização

**Jhonny Willians de O. Maciel (PG),[1*] Lucas H.G. Kalinke (PG),[1] Ana Karoline S.M. Valdo (PG),[1] Felipe Terra Martins (PQ),[1] Danielle Cangussu de Castro Gomes (PQ).[1]**

**jhonnywmaciel@gmail.com**

[1]*Instituto de Química, UFG*

Palavras Chave: *Oxamato, Fe(II), Mn(II) e Zn(II).*

## Highlights

**Fe(II), Mn(II) and Zn(II) complexes derived from a functionalized oxamate-type ligand : Synthesis and Characterization.**

In this work, we present the preparation and structural results concerning the formation of complexes between the Iron(II), manganese(II) and zinc(II) ions with the N-(4-carboxyphenyl)oxamic acid ($EtH_2pcpa$).

## Resumo/Abstract

A preparação e compostos de coordenação com ligantes do tipo oxamato tem sido bastante explorada nas últimas décadas com inúmeros exemplos de onde a estratégia de síntese leva a diferentes topologias estruturais e propriedades físicas.[1] Neste trabalho, apresentamos os resultados estruturais relativos a formação de complexos entre os íons de Ferro(II), Manganês(II) e Zinco(II) com o ligante ácido N-(4-carboxifenil) oxâmico etil éster ($EtH_2pcpa$).

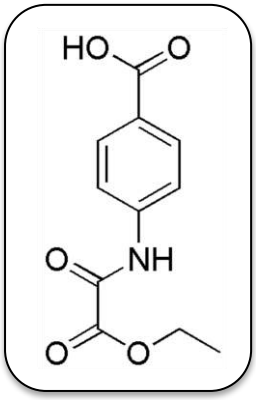


**Figura 1.** Esquema do ligante $EtH_2pcpa$.

Para a síntese dos complexos foi utilizada a técnica de difusão lenta em tubo na forma de H, e após três semanas, observou-se o aparecimento de cristais ao longo dos tubos. As estruturas dos três novos complexos metálicos de fórmula $[Fe(H_2pcpa)_2(H_2O)_2]$ **(1)**, $[Mn(Hpcpa)(H_2O)_3]_n \cdot 1/2H_2O$ **(2)** e $[Zn(Hpcpa)(H_2O)_3]_n \cdot 1/2H_2O$ **(3)** foram determinadas por difração de raios-X de monocristal. O complexo **1** formou cristais laranja amarronzado, a estrutura de **1** consiste em um monômero de Fe(II). Cada íon de Fe(II) é hexacoordenado com esfera de coordenação composta de duas moléculas de água posicionadas em *trans* e quatro oxigênios-oxamato de dois ligante $H_2pcpa^{-1}$. Os produtos **2** e **3** formaram cristais transparentes incolores, cadeias em ziguezague neutras de íons Mn(II) e Zn(II), respectivamente, unidos por ligantes $Hpcpa^{-2}$, cada íon é hexacoordenado com as três moléculas de água posicionadas em *Mer*, dois oxigênios-oxamato de um ligante $Hpcpa^{-2}$ e um oxigênio-carboxilato de um outro grupo do $Hpcpa^{-2}$, que constrói um octaedro. A separação intracadeia Mn···Mn no complexo **2** é de 11,456 Å e Zn···Zn no complexo **3** é de 11,325 Å.

Agradecimentos: CNPQ, CAPES, FAPEG e UFG.

Referências:

[1] T. L. Oliveira *et al.*, “Cobalt ( II ) and copper ( II ) assembling through a functionalized oxamate-type ligand,” *Polyhedron*, vol. 81, pp. 105–114, 2014.

**Área: INO** **Inscrição: 00562**

# SYNTHESIS, CHARACTERIZATION AND BIOLOGICAL ACTIVITY OF COMPLEX NITROSYLS

**[1,3]Iury A. Paz (PG)*, [2]Carlos Daniel S. Silva (PQ),[1]Luiz G.F. Lopes (PQ),[1] Eduardo H. Sousa (PQ), [3]Nilberto R.F.Nascimento (PQ)**

**iury.paz@hotmail.com**

*[1]Laboratório de Bioinorgânica, Departamento de Química Orgânica e Inorgânica, UFC-Campus do Pici; [2]Departamento de Química, IFBA-Salvador; [3]Laboratório de Fisiofarmacologia cardiovascular e renal, ISCB, UECE-Campus Itaperi*

Palavras Chave: *Cardiovascular Diseases, Hipertension, Nitric Oxide, Metal complexes, Complex Nitrosyls.*

## Highlights

NO-releasing complexes, obtaining vasodilator activity through the GCs-cGMP pathway, being possible antihypertensive drugs.

## Resumo/Abstract

Cardiovascular diseases are one of the leading causes of death worldwide, often caused by endothelial dysfunction. In medical emergencies, sodium nitroprusside (SNP), $Na_2[Fe(CN)_5NO]$, is widely used. However, this drug causes undesirable effects, such as strong hypotension and release of cyanide in the body. In view of this, novel compounds which may act as NO-releasers in vivo are desirable. In this work, coordination compounds containing 5-azaindole and nitrosyl group were synthesized and characterized by spectroscopic and electrochemical techniques and vasodilation experiments were performed on aortic rings of wistar rats. The complexes cis-$Ru(NO)(phen)_2(5\text{-aza})](PF_6)_3$ (FOR095) and cis-$[Ru(NO)(bpy)_2(5\text{-aza})](PF_6)$ presented NO stretching frequency around 1943 $cm^{-1}$, characteristic of the nitrosyl ($NO^+$) group. In the UV-VIS region, internal ligand electron transfer bands and MLCT bands were observed for this type of compounds. By the nuclear magnetic resonance technique, the compound FOR095, it was obesrved signals related to the presence of 22 H atmos, confirming part of the proposed structure. In the cyclic voltammogram, potential waves were observed for the redox process centered on the nitrosyl group - $\{RUNO\}^{6/7}$. The chemical reduction by azide corroborates this assignment. The FOR095 complex had vasodilator action on wistar rat rings, with similar efficacy to the SNP, and obtaining a total block in the presence of ODQ, indicating a mechanism dependent on nitric oxide.

**Área: INO** **Inscrição: 00581**

# Bright Orange-Red Emission in a New Heteroleptic $Cu^{I}$ complex Based on Phosphine/Pyrazoline Ligands

**Lis R. V. Favarin[1] (PG), Guilherme B. Laranjeira[1] (PG), C. F. A. Teixeira[1] (PG), Leandro M. Lima[1] (IC), L. M. C. Pinto[1] (PQ), L. Bezerra[1] (PG), Amilcar. M. júnior[1] (PQ), A. P. Duarte[1] (PQ), Lucas Pizzuti[2] (PQ), Davi F. Back[3] (PQ), Gilberto Maia[1] (PQ) Gleison A. Casagrande[1*] (PQ)**

**gleisoncasag@gmail.com**

*[1]Instituto de Química - UFMS-MS; [2]FACET-UFGD-MS; [3] Departamento de Química – UFSM-RS*

Palavras Chave:*(Copper (I) Complexes, Pyrazolines, Luminescent Copper Compounds).*

## Highlights

A new mononuclear heteroleptic $Cu^{I}$ complex based on mixed phosphine/thiocarbamoyl-pyrazoline ligands was synthesized and structurally characterized. The complex exhibited distorted tetrahedral coordination geometry around metallic atom and interesting photophysical properties as strong absorption in the UV-Vis range and bright orange-red emission observed in the solid state upon excitation of the prepared compound at $\lambda_{ex}$ =290 nm. As shown by TD-DFT studies, the absorption and emission behavior of this new compound proved primarily to be related to HOMO and HOMO-1 to LUMO orbitals involving ((M+X)LCT $Cu(d^{10})\rightarrow\pi^{*}(S=C–N_{pyrazoline\ ring})$) electronic transitions. The complete characterization of this new Copper(I) complex also included X-Ray studies, elemental analysis, IR spectroscopy, cyclic voltammetry and absorption/emission studies.

## Abstract

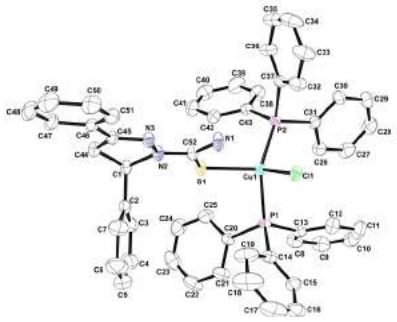

Crystal structure (X-ray) of new $Cu^{I}$ complex synthesized from $(PPh_3)_2CuCl$ and 1-thiocarbamoyl-3,5-diphenyl-4,5-dihydro-1*H*-pyrazole

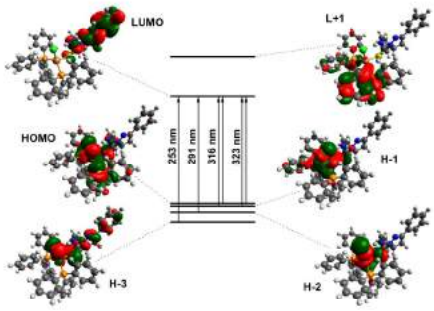


TD-DFT studies with emphasis on the HOMO and HOMO-1 to LUMO involving ((M+X)LCT $Cu(d^{10})\rightarrow\pi^{*}(S=C–N_{pyrazoline\ ring})$) electronic transitions.

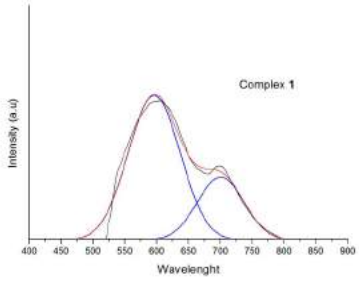


Emission spectrum of title complex measured in solid state at 298 K ($\lambda_{ex}$ = 290 nm) and its deconvolution into two Gaussian components.

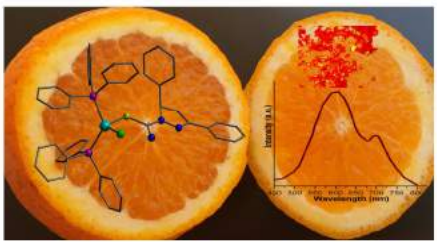

Bright orange-red emission at 604 and 715 nm under ($\lambda_{ex}$ = 290 nm).

**Área: INO** **Inscrição: 00613**

# Investigação de um Complexo Cobalto(III)-4-cloroacetoacetato de etila como Possível Plataforma Biorredutível para Liberação de Fármacos

**Marcos Vinícius P. de Mello (PG), Javier Alexander G. Gomez (PQ), Mauricio Lanznaster (PQ)***

**mvpmello@id.uff.br; ml@id.uff.br***

[1]*Bio&Nano, Instituto de Química, Universidade Federal Fluminense, Campus Valonguinho, Niterói, RJ.*

Palavras Chave: Cobalto(III), Metalofármaco, Entrega controlada de fármacos, Hipóxia, PDAH, Câncer.

## Highlights

Investigation of Cobalt(III)-ethyl-4-chloroacetoacetate Complex as a Bioreductive Platform for Drug Delivery

A novel cobalt(III) complex was obtained. A *quasi*-reversible process was observed for the couple $Co^{3+}/Co^{2+}$. Simulations of the hypoxic tumor environment were performed by UV-Visible spectroscopy.

## Resumo/Abstract

Regiões hipóxicas limitam tratamentos anticâncer como a quimio- e radioterapia em certos tipos de tumores sólidos.[1] No entanto, mesmo sendo um obstáculo, elas podem ser utilizadas para o desenvolvimento de *PDAHs,* que são capazes de atingir o ambiente hipóxico tumoral, liberando um fármaco seletivamente.[2,3] Complexos de cobalto tem sido estudados como potenciais *PDAHs,* devido a seus dois estados de oxidação acessíveis. A coordenação do fármaco ao $Co^{3+}$, inerte, inibe sua toxicidade e permite seu carreamento pelo corpo, e a liberação do fármaco ocorre seletivamente no ambiente hipóxico, onde o metal é reduzido a sua forma +2, lábil.[2,3] Este trabalho descreve o estudo de um novo complexo de cobalto(III) como possível plataforma biorredutível para liberação de fármacos. O complexo **1** foi obtido pela reação entre o ligante 4-cloroacetoacetato de etila e um complexo precursor $[CoCl_2(py_2en)]ClO_4$. A estrutura obtida por difração de raios X mostra o ligante $py_2en$ em conformação cis-β [2] (Fig. 1 **A**). Um processo *quasi* reversível para o par $Co^{3+}/Co^{2+}$ foi observado, com $E_{1/2}$ igual a -0,09 V vs. EPH **(B).** O monitoramento de solução por UV-Vis evidencia alta estabilidade de **1** em diferentes meios **(C)**. A simulação da redução do complexo e dissociação do ligante acetoacetato no ambiente tumoral em condições de hipóxia foi realizado através do monitoramento por UV-Vis da redução química de **1** em diferentes concentrações de $O_2$.

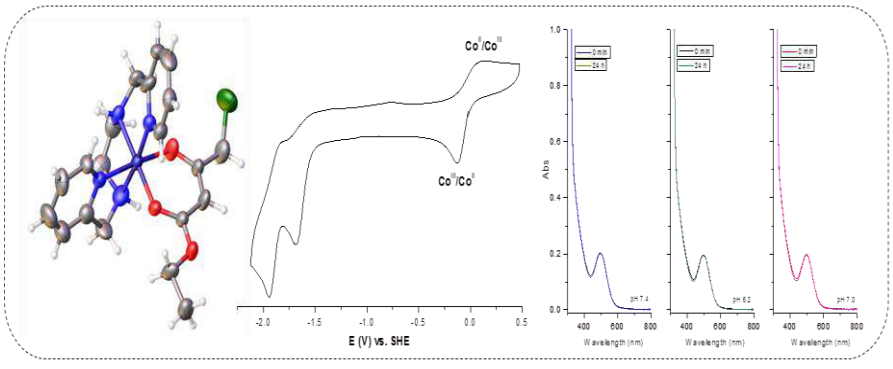


Fig. 1. (A) Representação OLEX[4] de 1 (contra-íon omitido para melhor visualização); (B) Voltamograma cíclico de **1** em MeCN com $TBAClO_4$ 0.1 $mol{\cdot}L^{-1}$. Trabalho: carbono; Ref.: Ag/AgCl (MeCN-$TBAClO_4$ 0.1 $mol{\cdot}L^{-1}$; Aux.: Pt; Ref. int.: $Fc/Fc^{+}$; (C) Espectros UV-Vis de **1** em tampão fosfato/dmso (9:1) 1 x $10^{-3}$ $mol{\cdot}L^{-1}$ monitorados por 24 h em pH 6.2, 7.0 e 7.4.

(1) Lippard, S. J.; Graf, N. *Adv. Drug Deliv. Rev.* **2012**, 64, 993; (2) Lanznaster, M.; *et al. J. Inorg. Biochem*. **2014**, 132, 37 ; (3) Renfrew, A. Bryce, N. S.; Hambley, T. *Chem. Eur. J.* **2015**, 21, 15224; (4) Dolomanov, O.V.; et al. J. Appl. Crystallogr. **2009**, 42, 339; (5) Gagne, Robert. *et al. Inorg. Chem.* **1980**, 19, 2854.

**Área: INO** **Inscrição: 00640**

# Sínteses de decavanadatos contendo complexos de cobalto(II), cobre(II) e níquel(II)

**Luiza B. P. Leme (IC),[1] Juliana M. Missina (PG),[1] Kahoana Postal (PG),[1] Maurício P. Franco (PG),[1] Francielli S. Santana (TC),[1] David L. Hughes (PQ),[2] Jaísa F. Soares (PQ)[1], Giovana G. Nunes (PQ)[1*]**

**luizabudel.leme@gmail.com; nunesgg@ufpr.br**

*[1]Departamento de Química, UFPR, Curitiba, PR, Brasil; [2]School of Chemistry, University of East Anglia, Norwich, NR47TJ, UK*

Palavras Chave: *Decavanadato, Cobalto(II), Cobre(II), Níquel(II), Tris(hidroximetil)aminometano.*

## Highlights

Synthesis of decavanadates with cobalt(II), copper(II) and nickel(II) complexes. Spectroscopic and diffractometric characterization. Biological applications involving angiogenesis in tumors. Decavanadate associated with cobalt, copper and nickel aquacomplexes.

## Resumo/Abstract

Recentemente o ânion decavanadato $[H_xV_{10}O_{28}]^{6-x}$ ($V_{10}$) demonstrou ação antidiabética e anticâncer.[1] Visando a avaliar o efeito do $V_{10}$ combinado com outros metais no processo de angiogênese, estamos interessados no desenvolvimento de rotas sintéticas que permitam a obtenção de compostos heterometálicos puros e em bons rendimentos. Para tal, a reação entre $NH_4VO_3$, $(CH_3)_4NCl$ e $MCl_{2(aq)}$ (5:1:1) (M= $Co^{II}$, $Cu^{II}$ e $Ni^{II}$) em solução aquosa (pH 4,5) produziu cristais laranja, com rendimentos de 60%, 44% e 53%, respectivamente. Os espectros Raman apresentaram bandas em 963 $cm^{-1}$ ($\nu$(V=O)), 800 a 200 $cm^{-1}$ ($\delta$ e $\nu_s$(V–O–V)), características do $V_{10}$. Os espectros de IV mostraram bandas em 960 $cm^{-1}$ ($\nu$(V=O)), 804 a 522 $cm^{-1}$ ($\nu_s$ e $\nu_{ass}$(V–O–V)) e 1616 e 1618 $cm^{-1}$ do cátion amônio. A análise de DRX-monocristal revelou a obtenção dos produtos $\{(NH_4)_2[Co(H_2O)_6]_2[V_{10}O_{28}]\}\cdot 4H_2O$ ($CoV_{10}$), $\{(NH_4)_2[Cu(H_2O)_6]_2[V_{10}O_{28}]\}\cdot 2H_2O$ ($CuV_{10}$) e $\{(NH_4)_2[Ni(H_2O)_6]_2[V_{10}O_{28}]\}\cdot 4H_2O$ ($NiV_{10}$), sendo $CuV_{10}$ inédito. O espectro de RPE de $CuV_{10}$ apresentou um sinal em g = 2,1, característico de espécies contendo cobre(II). Os teores de metal foram compatíveis com os valores teóricos para as estruturas. Quando a síntese foi realizada em tampão tris(hidroximetil)aminometano empregando $V_2O_5$ e $CuCl_2$ (2,5:1), obtiveram-se cristais laranja que foram caracterizados por DRX-monocristal como $[Cu(H_2O)_5NH_3C(CH_2OH)_3]_2[V_{10}O_{28}]\cdot 6H_2O$. O efeito dos polioxovanadatos $CoV_{10}$, $CuV_{10}$ e $NiV_{10}$ na formação de vasos sanguíneos está sendo avaliado em modelos de membrana corioalantóica.

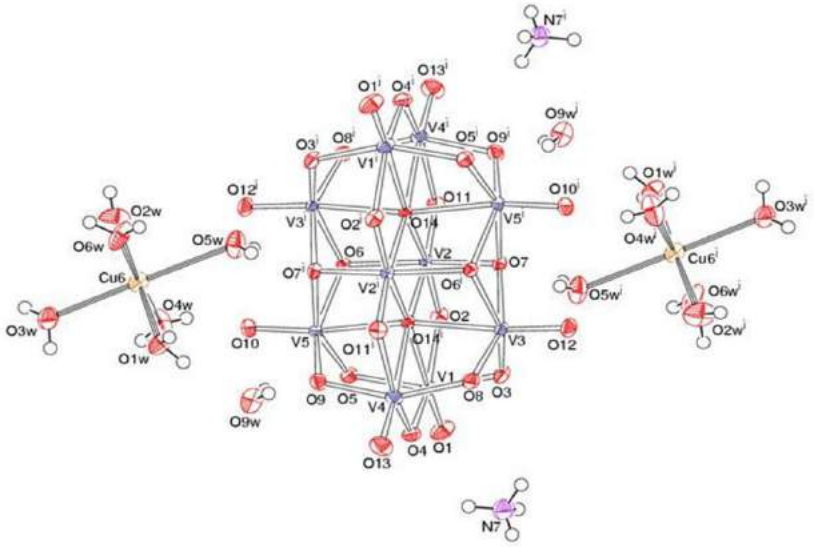


Figura 1. Diagrama ORTEP de $\{(NH_4)_2[Cu(H_2O)_6]_2[V_{10}O_{28}]\}\cdot 2H_2O$ ($CuV_{10}$).

[1]. REHDER, D. *Future Med. Chem*., v. 4, n. 14, p. 1823-37, **2012**.

**Área: INO** **Inscrição: 00755**

# Synthesis and characterization of $Fe_3O_4$@$SiO_2$ core-shell magnetic nanoparticles.

**Vanessa Cezar Ribas (IC), Vladimir Lavayen (PQ), Jacqueline Arguello da Silva* (PQ).**

**vanessa.ribas@ufrgs.br; jackiearguello@iq.ufrgs.br**

*Departamento de Química, UFRGS.*

Keywords: Core-shell structures, Magnetite, Stöber silica.

## Highlights

Spherical core-shell Fe3O4@SiO2 structures. Magnetic susceptibility, spectroscopy and microscopy analysis.

## Resumo/Abstract

Magnetic nanoparticles, such as magnetite ($Fe_3O_4$ NPs), have gained considerable attention due to their high potential application in medicine, chemistry, material engineering and biomedicine. However, these materials are susceptible to slow oxidation by atmospheric oxygen, as well as being relatively unstable and poorly dispersed in aqueous media. Core-shell structures represent attractive alternatives to overcome such disadvantages by combining core magnetic properties with shell stability and dispersibility, usually composed of polymers, metal nanoparticles or silica. This work reports the synthesis of $Fe_3O_4$ NPs by precipitation of ferrous hydroxide followed by partial oxidation to magnetite. Subsequent, core-shell sphere structures ($Fe_3O_4$@$SiO_2$) were obtained through the Stöber method. Both materials, $Fe_3O_4$ NPs and $Fe_3O_4$@$SiO_2$, were characterized by scanning electron microscopy (SEM), X-ray powder diffraction (XRD) and Infrared spectroscopy. The SEM images reveal the formation of $Fe_3O_4$ nanoparticles with octahedral morphology (Fig. 1A), while the silica-coated nanoparticles adopted spherical shape (Fig. 1B). The diffraction peaks correspond to $Fe_3O_4$ planes (220), (311), (222), (400), (422), (511), (440), (620), (533), (622) and (444) (Fig. 1C). Besides the magnetite diffraction pattern, the $Fe_3O_4$@$SiO_2$ exhibits a wide band corresponding to amorphous silica in the range of 20-27°. The FT-IR spectra exhibit the Si-O-Si asymmetric stretching vibration at 1020-1100 $cm^{-1}$. Finally, the magnetic susceptibilities were measured; the saturation magnetization values of $Fe_3O_4$@$SiO_2$ (12,5 emu/g) are much lower than that of $Fe_3O_4$ NPs (81,0 emu/g), probably because of the thick shells coated on magnetic nanoparticles.

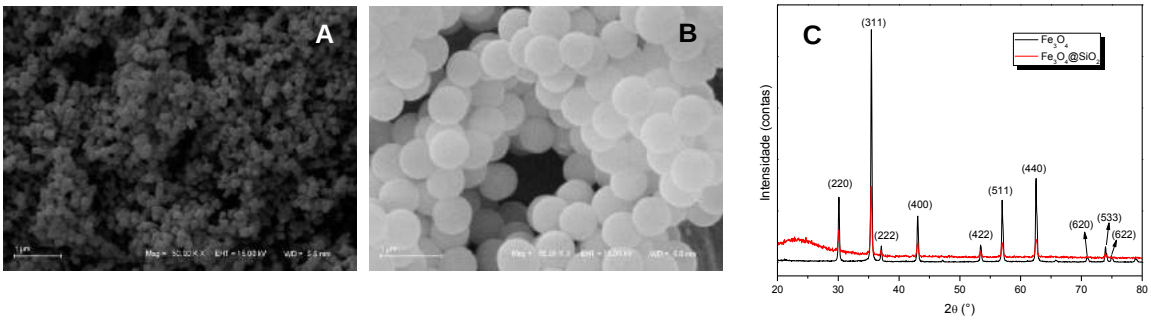


**Fig. 1.** SEM images of $Fe_3O_4$ (A) and $Fe_3O_4$@$SiO_2$ (B). $Fe_3O_4$ (black line) and $Fe_3O_4$@$SiO_2$ (red line) diffractograms(C).

**Acknowledgments:** INCTBio, CNPq and PROPESQ-UFRGS.

**Área: INO**
*(Inserir a sigla da seção científica para qual o resumo será submetido. Ex: ORG, BEA, CAT)*

**Inscrição: 00781**
*(Inserir o número de inscrição do autor que fez a submissão)*

# Visible-light photocatalytic response of titanate nanotubes (TiNT) – polyheptazine (HPZ) hybrid

**Vinícius A. Almeida (IC),[1] Juliana S Souza (PQ).[1]***

**juliana.souza@ufabc.edu.br**

[1]*Centro de Ciências Naturais e Humanas, UFABC*

Palavras Chave*(Titanate nanotubes, polyheptazine, photocatalysis, nanomaterials.*

## Highlights

- Photocatalyst based on TiNT-HPZ hybrid material.
- Development of a novel strategy to obtain nitrogen-doped TiNT.
- Charge transfer process between polyheptazine and TiNT under visible-light.

## Resumo/Abstract

TiNT have been extensively studied due to its properties that allows it to be applied in photodegradation of organic dyes. However, due to its high band gap energy it can only absorb UV light. TiNTs can be sensitized to visible light by doping them with nitrogen, which can be made through several strategies.[1] Here we report the development of a new method of doping TiNT with nitrogen, which consists of the polymerization of polyheptazine directly onto the nanotubes surface (Figure 1a), using as monomer source the product of urea pyrolysis.[2] The properties of the obtained hybrid were experimentally determined by a careful analysis of its spectroscopy properties, surface area analysis, zeta potential data, crystalline structure determination and electron microscopic imaging. All results were compared to those obtained for the P25-polyheptazine hybrid, since P25 is a reference material in photocatalysis field.

Rhodamine B was used as dye to evaluate the photocatalytic activity of the hybrid materials under visible light; Figure 1b show the degradation rates obtained as function of time. The presence of the polymer increases the efficiency of both hybrid materials, due the photoinduced charge transfer from LUMO and direct charge transfer from HOMO of polyheptazine to the conduction band of the TiNT, Figure 1c. Besides that, the TiNT-HPZ hybrid show higher performance, which we believe be ascribed to the presence of polymer between the layers of the multi-lamelar structure of TiNT, whereas P25 have polymer only over its surface.

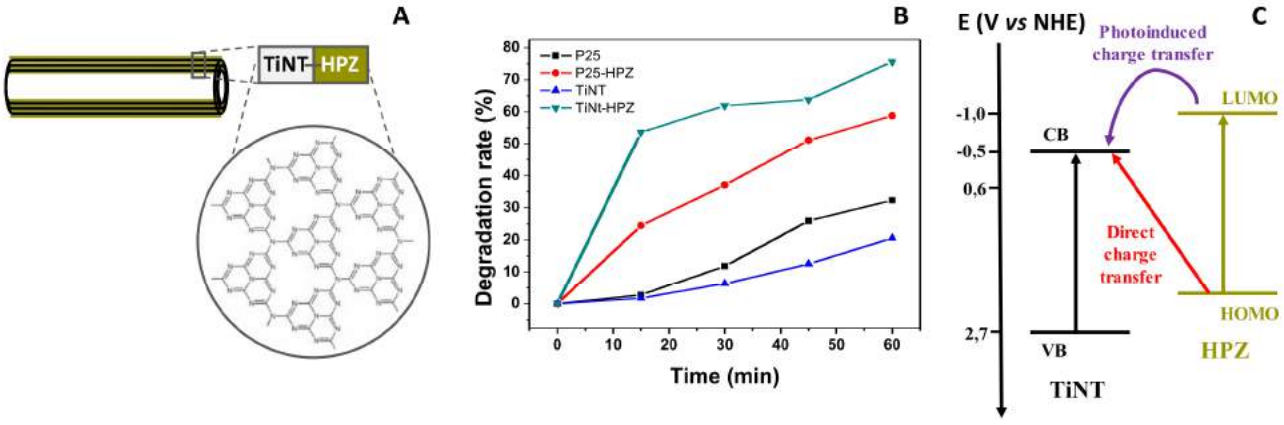


**Figure 1. (A)** Schematic representation of the TiNT modified at the surface by polyheptazine. **(B)** Degradation rates of rhodamine B as function of time using P25, P25-HPZ, TiNT and TiNT-HPZ as photocatalysts under simulated sunlight irradiation. **(C)** Schematic representation of the charge transfer processes that occurs when the TiNT-HPZ is irradiated by simulated sunlight.

[1]*J Mol. Catal. A*, 2014, **394**, 48–56
[2]*Phys. Chem. Chem. Phys.*,2011,**13**,21511–21519

**Acknowledgement:** FAPESP Grant #2017/11395-7.

**Área: INO** **Inscrição: 00816**

# Glifosato como ligante frente ao chumbo divalente.

**Emanoel Hottes (PG),[1] Sumaia Hottes (IC),[2*] Marcelo H. Herbst (PQ),[1]**

**emanoelhottes@yahoo.com.br; sumaiahottes@hotmail.com**

*[1]Departamento de Química, UFRRJ; [2]Departamento de Engenharia Química UFRRJ.*

Palavras Chave: *Glifosato, complexos de chumbo (II), síntese e caracterização.*

## Highlights

The complexation of glyphosate towards divalent lead was investigated. The results obtained indicated that the reaction path did not directly affect the obtained product.

## Resumo/Abstract

O glifosato é o herbicida mais utilizado em todo mundo. No contexto da química inorgânica, sua relevância reside na sua capacidade de se coordenar fortemente a diferentes íons metálicos, fenômeno relacionado ao seu comportamento bioquímico e ambiental. Desta forma este trabalho teve como objetivo estudar a complexação do glifosato frente ao chumbo (II), tendo em vista a escassez de estudos disponíveis na literatura para este sistema [1]. A complexação foi estudada em fase heterogênea, em suspensão aquosa a 80°C ou 60°C e pH ácido. Duas rotas distintas foram investigadas, uma a partir do PbO, e outra, tendo como precursores o carbonato e o hidróxido de Pb(II). As sínteses foram feitas variando-se também as proporções metal - ligante, sendo estas respectivamente 1:1, 2:1 e 1:2. Foram obtidos produtos insolúveis e policristalinos, que foram caracterizados por CP-MAS RMN de $^{31}P$, infravermelho e difração de raios-X de pó. Os espectros vibracionais dos produtos mostram para todos os casos alteração nas absorções dos grupos carboxilato e fosfonato, sugerindo coordenação pelos oxigênios dos referidos grupos, enquanto os espectros de RMN de $^{31}P$ mostraram que o grupo fosfonato possuía apenas um modo de coordenação, uma vez observado um único sinal para fósforo nos espectros. Por meio de análise comparativa da difração de raios-X de pó observou-se que todos os compostos obtidos possuíam formas de empacotamento similares aos dos fosfonatos de Pb(II).

1- Kobyoecka, J. *et al*., Monatsh. Chem., v. 131, 1 – 11, 2000.

**Área: INO**
*(Inserir a sigla da seção científica para qual o resumo será submetido. Ex: ORG, BEA, CAT)*

**Inscrição: 00924**
*(Inserir o número de inscrição do autor que fez a submissão)*

# Effects of New Ruthenium Amphiphile Compounds on Peptides Aggregation

**Bruna M. Soares (PG),[1] Herbert Winnischofer (PQ),[2] Jaqueline Pazinato (PG),[2] Eduard Westphal (PQ),[3] Francesca Cavalieri (PQ),[4] Wendel A. Alves (PQ).[1]***

**wendel.alves@ufabc.edu.br**

*[1]Centro de Ciências Naturais e Humanas, Universidade Federal do ABC, 09210-580, Santo André, Brazil; [2]Departamento de Química, Universidade Federal do Paraná, Curitiba 81531-990, Brazil; [3]Departmento de Química e Biologia, Universidade Tecnológica Federal do Paraná, Curitiba, Paraná, 81280-340, Brazil; [4]Department of Chemical and Biomolecular Engineering, University of Melbourne, Melbourne 3010, Australia.*

Keywords: *Supramolecular chemistry, Peptides, Ruthenium complex, Amyloid-β, Alzheimer's disease.*

## Highlights

Ability of a new ruthenium complex to induce inhibition and disruption of aggregates from peptides applied as amyloid-β models. Effects were observed even at low concentrations of the ruthenium complex.

## Abstract

Alzheimer's disease (AD) is a neurodegenerative disease with no certain cure, the most typical form of dementia. An ubiquitous observation in AD patients is the formation of plaques in their gray matter.[1a] The dominant components of these plaques are peptides known as amyloid beta (Aβ).[1b,1c] In our studies, we applied a new ruthenium complex ($[\eta^6$-$(C_6H_6)RuClL]PF_6$, L = 2-(4-dodecyloxyphenyl)-5-(2-pyridyl)-1,3,4-oxadiazole; RuL, Figure IA) as an Aβ aggregation inhibitor and disruptor using two peptides as amyloid-β models, which is a simpler strategy to evaluate the aggregation process. The first peptide (Figure IB) is an alternating arginine/phenylalanine octapeptide that forms amyloid-type β-sheet rich fibrils and other amyloid-like analogs.[2] The second one contains L-proline as the amine termination (Figure IC). In our thioflavin T (ThT) assays, peptides alone showed complete aggregation, whereas peptides coincubated with RuL exhibited significantly reduced aggregation (Figure II). Besides that, we have also developed studies regarding the disruption of mature peptide aggregates (Figure III). For this purpose, a RuL solution was added in an aged peptide+ThT solution. It was verified that after a period of ~10 minutes the addition of RuL led to aggregates disarrangement. We expect to provide a full description of the inhibition and disruption processes of the peptide aggregates in solution. The main goal is unveil the *in-situ* structure of self-assemblies and verify how the ruthenium complex acts on the structures. Our findings are expected to contribute for understanding the amyloid cascade and provide subsidies for therapeutic applications of ruthenium complexes in AD.

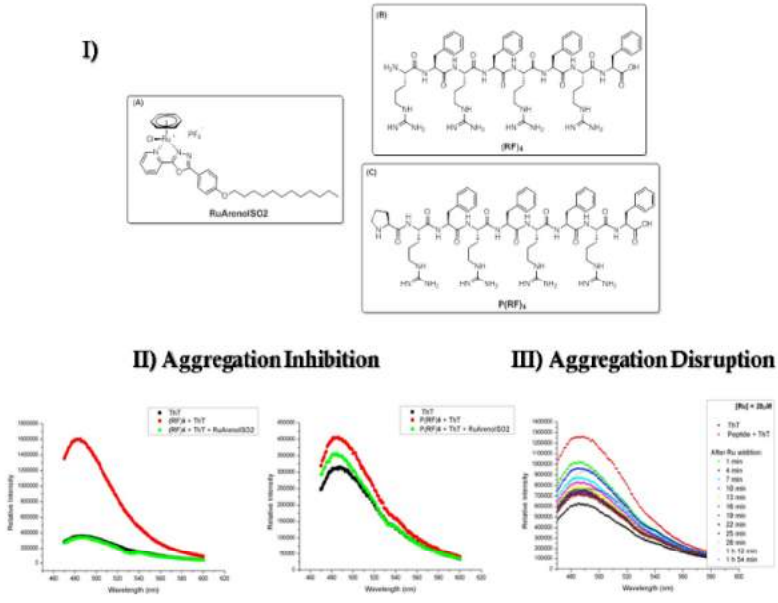


**Figure 1.** I) Chemical structures of the compounds applied in this study, II) Fluorescence spectrum of the peptides, ThT and RuL complex in the same formulation, 1 hour after sample preparation; III) Fluorescence spectrum of the peptide $(RF)_4$ and ThT before and after the addition of the RuL complex.

**References:**

**1**. (a) J. Hardy, D. Selkoe, *Science* **2002**, *297*, 353-356; (b) M. Goedert, M.G. Spillantini, *Science* **2006**, *314*, 777-781; (c) I.W. Hamley, *Angew. Chem. Int. Ed.* **2007**, *46*, 8128-8147.

**2**. C.C. Decandio, E.R. Silva, I.W. Hamley, V. Castelletto, M.S. Liberato, V.X. Oliveira Jr., C.L.P. Oliveira, W.A. Alves, *Langmuir* **2015**, *31*, 4513-4523.

**Área: INO** **Inscrição: 01029**

# Electrocatalytic activity of water oxidation by coordination polymer Co-pentacyanidoferrate(II)

**Bruno M. Pires (PG)[1], Stefan Strohauer(PG)[1,2], André L. B. Formiga (PQ)[1], Juliano A. Bonacin (PQ)[1*]**

***jbonacin@g.unicamp.br**

*[1]Institute of Chemistry, University of Campinas, Campinas, SP; [2]Institute of Physics, Goethe-Universität, Frankfurt am Main, Frankfurt-German*

Palavras Chave: *water splitting, water oxidation, oxygen evolution reaction, Prussian blue, electrocatalysis*

## Highlights

Electrocatalytic properties of Co-pentacyanidoferrate(II) on water oxidation
High stability and performance for water oxidation even at pH=7
Over potential of 0.46 mV and Tafel slope of 146 mVdec$^{-1}$

## Resumo/Abstract

Strategies to develop new sources of green and sustainable energy to attend the global demand is a challenge for the scientific community. A promising alternative is the production of hydrogen from the process of water splitting. Water is an abundant molecule on Earth and can be decomposed into $H_2$ and $O_2$. Although the process seems simple, the water oxidation is thermodynamically and kinetically unfavorable and therefore requires a catalyst to overcome the energetic barrier. The challenges in the development of catalysts for water oxidation are: design of materials that operate under conditions of low overpotential; stability under conditions of strong oxidation; composition based on abundant elements in nature; high stability and robustness. Thus, the goal of this work was to evaluate the electrocatalytic properties for water oxidation by the coordination polymer produced by the reaction between cobalt(II) and $[Fe(CN)_5(isn)]^{4-}$, (isn =isonicotinate). The films were deposited on FTO-electrodes. First the cobalt was reduced on the electrode and after this, the complex was deposited electrochemically (+0.3 V-vs-SCE for 6 hours). Figure-A presents the cyclic voltammograms of the Co-$[Fe(CN)_5(isn)]^{4-}$ (Prussian blue analogous) in different pH. Efficiency of the catalysis supported in the FTO substrates was evaluated by obtaining the Tafel plots of water oxidation and the determination of the over potential that were 146 mVdec$^{-1}$ and 0.46 mV, respectively (Figure-B). The observed performance values are compatible with the best results described in the literature for this class of catalyst.

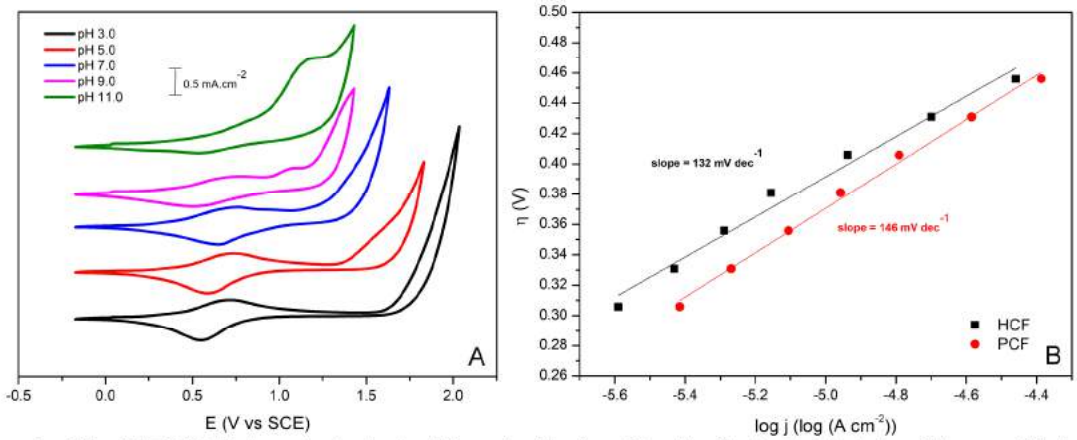


Figure **A.** CV of FTO/CoFeisn electrode in different pHs (v= 50 mV.s$^{-1}$). **B.** Tafel plots of the modified FTO substrates (HCF – hexacyanidoferrate and PCF – pentacyanidoferrate).

**Área: INO** **Inscrição: 00966**

# Iron (III) dinuclear metallacycle cavity as an effective ammonia storage system

**Ingrid F. Silva (PG),[1] Ivo F. Teixeira (PG),[2] Wdeson P. Barros (PQ),[3] Carlos B. Pinheiro (PQ),[4] Ana Paula C. Teixeira (PQ),[1] Humberto O. Stumpf (PQ).[1]***

**ingridfernandesilva@hotmail.com; stumpf@ufmg.br**

*[1]Departamento de Química, ICEx, UFMG; [2]Departamento de Química Fundamental, Instituto de São Paulo, Universidade de São Paulo; [3]Instituto de Química, Universidade Estadual de Campinas; [4]Departamento de Física, ICEx, UFMG.*

Keywords: Adsorption, Supramolecular Chemistry, Oxamate, Ammonia.

## Highlights

- Hydrogen transport and storage in ammonia form is an efficient and cheap process.
- The metallacycle was tested for adsorption of a number of compounds and it presented an impressive selectivity for nitrogen compounds having an outstanding capacity to ammonia adsorption.

## Resumo/Abstract

Ammonia has a large volume energy density, consequently it has a high potential to be used as fuel and energy reservoir in the future.[1] In this work, the action of a dinuclear metallacycle of $Fe^{III}$ (Fe(opba)), which the crystalline structure is shown in Figure 1, with an outstanding capacity to adsorb ammonia (11.3 mmol $g^{-1}$) was investigated, showing a strong preference by nitrogenous compounds, especially short chain amines (Figure 2). Adsorption results, suggest that the Fe(opba) cavity has an essential role in the adsorption mechanism, being the responsible by the size selectivity during the adsorption process. In order to better understand the ammonia adsorption mechanism, the Fe(opba) was fully characterized before and after the adsorption process. The results of thermogravimetric-mass spectrometry and ammonia isotherm experiments reveal that 8 ammonia molecules are physisorbed by the complex cavity (free ammonia) and 4 molecules are chemisorbed (coordinated ammonia) per dinuclear metallacycle unit. Others characterizations also confirmed the adsorption mechanism proposed confirming a structural modification to the compound before and after the adsorption. In addition, reuse tests have shown that despite some loss of efficiency the compound is capable of desorbing most of the ammonia and can be used in consecutive cycles, being a potential ammonia storage or adsorbent for the removal of ammonia in effluents.

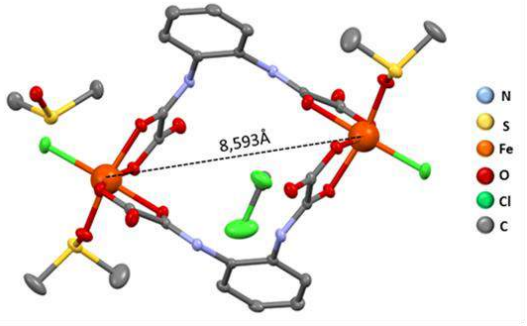


**Figure 1.** Crystalline structure of the complex $[Fe_2(opba)_2Cl_2(dmso)_2]\cdot CH_2Cl_2\cdot dmso]$. The hydrogen atoms were omitted for better viewing.

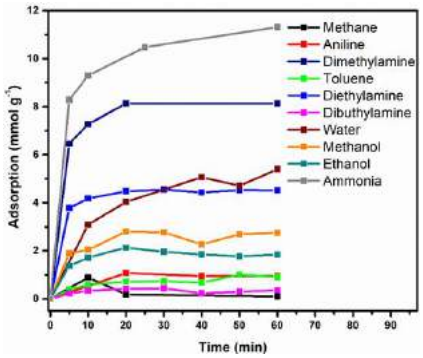


**Figure 2.** Adsorption curves, as a function of time, for a series of compounds (amines, alcohols and hydrocarbons) per gram of complex, for one hour at 25 °C under atmospheric pressure.

1. Rees, N. V. & Compton, R. G. Carbon-free energy: A review of ammonia and hydrazine based electrochemical fuel cells. *Energy Environ. Sci*. **4**, 1255–1260 (2011).

*Acknowledgments: FAPEMIG, CNPq and CAPES are acknowledged for financial support.

**Área:___INO_____** *(Inserir a sigla da seção científica para qual o resumo será submetido. Ex: ORG, BEA, CAT)*

**Inscrição: _01049_** *(Inserir o número de inscrição do autor que fez a submissão)*

# Oxidation catalysts based on ironporphyrin supported on diatomaceous earth.

**Marcus. V. do Prado[1] (PG),[1] Eduardo J. Nassar[1] (PQ), Emerson H. de Faria[1] (PQ), Katia J. Ciuffi[1] (PQ), B. González[2] (PQ), M.A. Vicente[2] (PQ), R. Trujillano[2] (PQ), Vicente Rives[2] (PQ).**

*marcusvprado7@gmail.com and/or katia.ciuffi@unifran.edu.br*

[1] Universidade de Franca (UNIFRAN), Grupo de Pesquisa em Materiais Lamelares Híbridos (GPMatLam). Av. Dr. Armando Salles Oliveira, 201 Franca-SP, CEP 14404-600.
[2]GIR-QUESCAT, Departamento de Química Inorgánica, Universidad de Salamanca, 37008 Salamanca, Spain.

Keywords: *ironporphyrin, emerging organic pollutant, heterogeneous catalysis, oxidation*

## Highlights

- ✓ Ironporphyrin was immobilized via covalent bonds onto diatomaceous earth.
- ✓ Diatomaceous earth increased the chemical and thermal stability of ironporphyrin.
- ✓ Parameters time, concentration of catalysts and drug, using of UV-light, were tested.

## Resumo/Abstract

The search for new and inventive catalysts that can mimetize certain reactions carried out by animal enzymes, such as by Cytochrome P450 and their synthetic models (for instance, synthetic porphyrins), is in the highlight for the last decades and equally important is the search for new matrices that can support these synthetic models. Not only the synthetic path to obtain the catalyst is important, but the conditions governing their optimal reaction pathways, such as pH or substrate concentration.

Synthetic metalloporphyrins have been successfully used as biomimetic catalysts in many oxidation reactions. However, their high cost and the difficulties inherent to homogeneous catalysis have prevented their large-scale application. Catalyst heterogeneization aims to overcome these drawbacks in addition to mimicking enzyme site isolation, improving reaction selectivity. New matrices are essential to reach this target.

Hybrid materials consisting of Diatomaceous Earth (DE) amino-functionalized with aminopropyltriethoxysilane (DE-APTES), followed by grafting with [meso-tetrakis(pentafluorophenyl) porphinato]iron(III), (DE-APTES-FeTFPP), have been here studied. The UV–Vis spectrum exhibited a Soret band at 416 nm, characteristic of ironporphyrin located in a confined space (the amount of FeFFPP per gram of DE was 20.0 mg/g). Leaching studies of FeTFPP from DE and DE-APTES confirmed that ironporphyrin was entrapped and not just adsorbed on the silica surface. IR spectroscopy confirmed that FeTFPP was grafted onto DE-APTES via the amine groups (amine band at 1570 $cm^{-1}$). DE displayed typical quartz and cristobalite crystalline phases and amorphous porous silica, the intensity of its characteristic reflection at $2\Theta = 22^{o}$ decreasing in the presence of FeTFPP; the ironporphyrin influenced the organization of the material, as confirmed by SEM analysis.

Tests using DE-APTES-FeTFPP as catalysts in the epoxidation of cyclooctene, showed complete selectivity to the epoxide. The degradation of caffeine, confirmed the ability of DE as a promising natural support for ironporphyrin catalysts. Caffeine degradation was influenced by pH, substrate and catalyst concentration.

**Acknowledgments:**

This work was carried out in the frame of a Spain−Brazil Interuniversity Cooperation Grant, funded by MEC (PHBP14/ 00003) and CAPES (317/15), and a Universidad de Salamanca−FAPESP (2016/50322-2) Cooperation Grant. The Brazilian group acknowledges support from Brazilian Research funding agency FAPESP (2016/01501-1 and 2013/19523-3). E.H.d.F. and K.J.C. acknowledge CNPq grants (311767/2015-0 and 305398/2015-6, respectively).

**Área: INO** **Inscrição: 01279**

# Compostos de $\eta^6$-arenorutênio(II) com ligantes fenilazo e feniloxadiazo: estabilidade, cinética de substituição de ligantes e atividade citotóxica em modelo de glioma humano.

**Jaqueline Pazinato (PG),[1*] Elizangela Cavazzini Cesca (PG),[1] Herbert Winnischofer[1] (PQ), Eduard Westphal[2] (PQ), Hugo Gallardo[3] (PQ) e Sheila M. B. Winnischofer[4] (PQ)**

**jaquelinepazinato@gmail.com**

*[1]Departamento de Química, UFPR; [2]Departamento de Química, UTFPR; [3]Departamento de Química, UFSC; [4]Departamento de Bioquímica, UFPR.*

Palavras Chave: $\eta^6$-arenorutênio(II), Estabilidade, Cinética e Solvólise.

## Highlights

$\eta^6$-Areneruthenium(II) compounds with phenylazo and phenyloxadiazo based ligands were characterized by their chemical stability in solution, the kinetics of ligand substitution and the cytotoxic activity in human glioma models.
Substitution reactions occurs in solution of the $\eta^6$-areneruthenium(II) complexes with loss of the arene ligand.
The arene loss reaction does not influence the cytotoxicity of the compounds.

## Resumo/Abstract

Os complexos de $\eta^6$-arenorutênio(II) podem sofrer hidrólise na ligação Ru-Cl, formando espécies de aquorutênio, que são mais reativos a substituição.[1] O complexo resultante pode ligar-se às nucleobases do DNA, como a guanina N7, enquanto que os ligantes aromáticos podem se intercalar no DNA. Essa interação pode provocar alterações no ciclo e levar a morte celular. No entanto, apesar dessa relativa labilidade do ligante cloreto devido ao efeito *trans*-labilizante promovido pelo ligante benzeno, Dougan *et al.*[1] demonstraram que tanto o ligante cloreto quanto o benzeno são susceptíveis a substituição. Neste trabalho realizamos ensaios para verificar a estabilidade, a substituição de ligantes e a cinética de reação de substituição nos complexos de $\eta^6$-arenorutênio(II) em solução aquosa e em DMSO. O espectro UV-vis obtido em solução aquosa e em DMSO mostrou uma diminuição na intensidade e deslocamento para UV após um período de 72 horas e temperatura ambiente, indicando que a espécie inicial está sendo consumida e outra espécie está sendo formada. Esse processo também foi acompanhado por espectroscopia RMN de $^1$H em $(CD_3)_2SO$. Após 6 horas foi observado o surgimento de um sinal de deslocamento químico δ=7.4 ppm, que aumentou gradativamente de intensidade durante 72 horas de monitoramento. Esse sinal foi atribuído ao hidrogênio do benzeno livre, formado pela perda do ligante areno. Após 72 horas, a intensidade desse sinal equivale a aproximadamente 30% do complexo no início do experimento. Outros sinais que surgiram em δ= 4 ppm são coerentes com o hidrogênio da molécula de DMSO coordenada ao centro metálico. As curvas cinéticas obtidas por espectroscopia UV-vis foram ajustadas para uma cinética de primeira ordem, e os valores de $k_{obs}$ obtidos para os complexos **2a** ([($\eta^6$-$C_6H_6$)Ru(2-(4'-dodeciloxifenilazo)piridina)Cl]), **2b** ([($\eta^6$-$C_6H_6$)Ru(2-(4'-metoxifenilazo)piridina)Cl]), **4a** ([($\eta^6$-$C_6H_6$)Ru(2-{(4-dodeciloxifenil)-1,3,4-oxidiazol-2-il}piridina)Cl]) e **4b** ([($\eta^6$-$C_6H_6$)Ru(2-{(4-metoxifenil)-1,3,4-oxidiazol-2-il}piridina)Cl]) variaram entre 1,67-6,94x$10^{-4}$ $s^{-1}$. Esse valores correspondem a uma reação de substituição lenta se comparada com outros relatos na literatura de compostos similares. Os compostos **2a**, **2b** e **4a** foram altamente citotóxicos para células de glioma U251, U87MG e T98G; **2a**: $IG_{50}$ (μmol·$L^{-1}$) = 5,9 (U251); 4,9 (U87MG); 5,5 (T98G ); **2b:** $IG_{50}$ (μmol·$L^{-1}$) = 8,0 (U251); 4,9 (U87MG); 24,7 (T98G ); **4a** $IG_{50}$ (μmol·$L^{-1}$) = 6,1 (U251); 5,66 (U87MG); 12,4 (T98G ). No entanto, o composto **4b**, apesar de sofrer solvólise na mesma taxa que os demais compostos, esse apresentou baixa citotoxicidade para as linhagens estudadas. Deste modo, a reação de substituição ocorrida nos compostos e o benzeno livre parece não ter correlação com o efeito citotóxico sobre as linhagens de glioma. Os compostos **2a** e **2b** apresentam comportamento redox dentro da faixa compatível com biomoléculas eletroativas e isso poderia estar associado a um desbalanço redox dentro da célula que levaria a morte. São necessários mais estudos para entender os mecanismos de ação desses compostos nas células tumorais.

[1]Dougan, S.J. et al. Inorganic Chemistry, 45, 26, 2006.

**Área: INO** **Inscrição: 01326**

# Complexos de Cu (I) que incorporam trifenilfosfina e aciltioureias: avaliação de suas propriedades citotóxicas

**[1]Ceslinolia M. Leite (PG), [2]Eduardo E. Castellano (PQ), [1]Alzir A. Batista (PQ)**

**celisnolia@hotmail.com**

*[1]Departamento de Química, UFSCar; [2]Instituto de Física, IFSC/ USP-SC*

Palavras Chave: *Cobre (I),Trifenilfosfina, Aciltioureias, Câncer.*

## Highlights

Complexes of Cu (I) incorporating triphenylphosphine and acylthioureas: evaluation of their cytotoxic properties

Copper complexes (I) as possible anticancer drugs;

Acyl thioureas exhibit cytotoxic activity in tumor cells;

Synthesis and characterization of 4 new complexes of Cu (I)

## Resumo/Abstract

Os complexos baseados em cobre têm sido investigados na suposição de que os metais endógenos podem ser menos tóxicos para as células normais em relação às células cancerosas, uma vez que, as células tumorais possuem uma resposta diferencial ao metabolismo do cobre (SANTINI et al., 2014). Somado a isto, as aciltioureias têm chamado a atenção da química de coordenação pela variedade estrutural devido às substituições dos H, podendo se coordenar de diversas maneiras, o que proporciona diversas possibilidades de estrutura para os compostos de coordenação (SHEEBA et al., 2014). Neste trabalho reportamos a síntese de quatro novos complexos de cobre (I): (**1**) $[Cu(DMB)(PPh_3)_2]$ (**2**) $[Cu(DMB)(PPh_3)_2]NO_3$ **(3)** $[Cu(DMT)(PPh_3)_2]$ e **(4)** $[Cu(DMT)(PPh_3)_2]NO_3$ (DMB: N,N-dimetil-N'-benzoiltioureia; DMT: N,N-dimetil-N'-2-tiofenocarboniltioureia). Na caracterização por RMN $^{31}P\{^1H\}$ os complexos apresentaram um singleto. No IV, a banda do grupo carbonila das aciltioureias indica que os ligantes estão coordenados, sendo observado uma diminuição da frequência desta banda. Na condutividade molar os compostos **1** e **3** mostraram-se neutros, enquanto os compostos **2** e **4** eletrólitos 1:1. A difração de raios X confirmou as estruturas propostas. Na avaliação da citotoxicidade frente às linhagens de células de câncer de pulmão (A549) e mama (MDA-MB-231) os compostos apresentaram valores de $IC_{50}$, entre 3 e 7 μM. Na avaliação da interação dos compostos com BSA por espectroscopia de fluorescência, os valores de $K_b$ foram da ordem de $\mathbf{10^3}$ indicando interação moderada.

Referências:

SANTINI; et al. Advances in Copper Complexes as Anticancer Agents. *Chem. Rev*. **114**: 815, 2014

SHEEBA, et al. Chiral ($\eta^6$-p-cymene)ruthenium(II) complexes containing monodentate acylthiourea ligands for efficient asymmetric transfer hydrogenation of ketones. *Organometallics*, **33**: 540, 2014.

**Área: INO**
*(Inserir a sigla da seção científica para qual o resumo será submetido. Ex: ORG, BEA, CAT)*

**Inscrição: 00920**
*(Inserir o número de inscrição do autor que fez a submissão)*

# Outstanding Optical Properties from Partial Substitution of Pb by Sn in Cs-Pb-Sn-Br Nanocrystals

**Ana Beatriz Ferreira Vitoreti (PG),[1,2,3] Said Agouram (PQ),[4] Mauricio Solis de la Fuente (PQ),[5] Vicente Muñoz-Sanjosé (PQ),[4] Marco Antônio Schiavon (PQ),[2] Ivan Mora-Seró (PQ)[1*]**

***aninhavitoreti@yahoo.com.br; sero@uji.es***

*[1] Institute of Advanced Materials (INAM), Universitat Jaume I, 12006 Castelló, Spain; [2] Department of Natural Science, Federal University of São João del-Rei, 36301-160 São João del-Rei, Brazil; [3] CAPES Foundation, Ministry of Education of Brazil, Brasília, 70040-020, Brazil; [4] Department of Applied Physics and Electromagnetism, University of Valencia, 46100 Valencia, Spain; [5] Lawrence Berkeley National Laboratory, Energy Technologies Area 1 Cyclotron Rd., 94720, California, United States of America.*

Palavras Chave: *Perovskite nanocrystal, $CsPbBr_3$, $CsPb_{1-x}Sn_xBr_3$, mixed-metal cation, tin-substituted perovskite nanocrystal.*

## Highlights

Perovskite NCs are one of the most promising materials. There is a great effort in order to substitute the Pb by a less hazardous element, as Sn, without any reduction of the optimal properties.

## Resumo/Abstract

As perovskite-based optoelectronic performance is striking for such novel technology,[1] the Pb component toxicity in these perovskite optoelectronics devices it's a major concern for its large-scale applications. Despite the great effort carried out in order to substitute the Pb by a less hazardous element, lead-free perovskite still more unstable than lead-containing perovskites and presenting lower performance.[2,3] Inspired by recent research about lead-less perovskite with mixed-cation, in this work we demonstrate the colloidal preparation of Cs-Pb-Sn-Br NCs with Sn substitution rate up to x=0.19. We have made a systematic study varying different synthesis parameters as precursor ratio, temperature or reaction time. We show that the synthesis temperature and the amount of ligand played an important role in the kind of Cs-Pb-Sn-Br compounds synthesized, size of nanocrystals, on colloidal stability and in optical properties. We observe by the first time a positive effect in terms of enhancement of the optical properties when Sn substitutive partially Pb. Sn-replacing not only enhances the PLQY of 7.3% in $CsPbBr_3$ to 73.4% in $CsPb_{0.93}Sn_{0.07}Br_3$ but also the nanocrystals crystallinity. High performance is based on the stabilization of $Sn^{2+}$ in the NCs for several months as it has been determined by XPS measurements, opening an interesting research way in Pb-less perovskite with excellent optoelectronic properties.

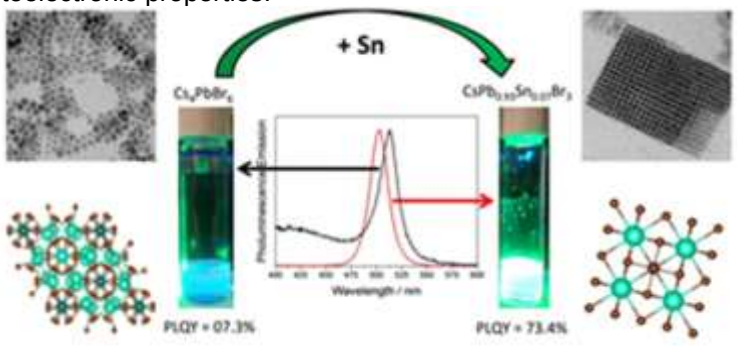


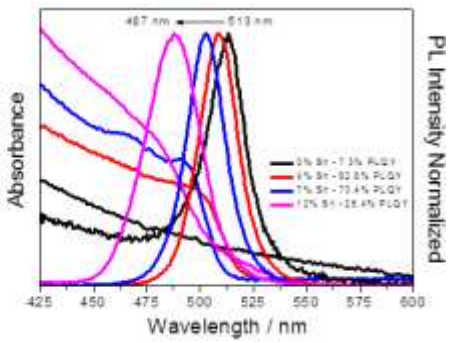


[1]Gonzalez-Carrero, S., et al.; Opt Express, 2016, 24, 285.
[2]Swarnkar, A., et al.; ACS Energy Letters, 2017, 2, 1089.
[3]Swarnkar, A., et al.; ACS Energy Letters, 2018, 286.
**ACKNOWLEDGMENTS:** FAPEMIG, CNPq, CAPES, RMQ, ERC.

**Área: INO** **Inscrição:_____**

# Aplicação de palygorskita organofilizada na remoção de glifosato em efluente aquoso.

**Carla Napoli Barbato (PQ),[1] Patricia Viana Rodrigues* (IC),[2,3] Luiz Carlos Bertolino (PQ),[3] Fernanda Arruda Nogueira Gomes Silva (PG),[2] Vitor Schwenck Brandão (PQ),[3].**

**Carla.barbato@ifrj.edu.br; p.vianaaa@yahoo.com.br**

*[1]Instituto Federal de Educação, ciência e Tecnologia do Rio de Janeiro - Unidade Duque de Caxias; [2]Instituto de Química, UFRJ, [3]Centro de Tecnologia Mineral*

Palavras Chave: *(Palygorskita, organofilização, adsorção, herbicida, glifosato)*

## Highlights

Application of organophilized palygorskite in the removal of glyphosate from aqueous effluent. Palygorskite is a clay mineral that after organophilization can be used to remove glyphosate from aqueous effluent by means of adsorption. Glyphosate is the active principle of some herbicides.

## Resumo/Abstract

A partir de 1960 com a Revolução verde houve o estímulo a aplicação de herbicidas visando o aumento da produção agrícola, o que contribui para a contaminação do solo, corpos d'água e problemas à saúde humana. O glifosato é um composto usado como principio ativo em herbicidas e é predominantemente aniônico em meio aquoso. A palygoskita é um argilomineral com fórmula de célula unitária $Mg_5Si_8O_{20}(OH)_2(OH_2)_4.4H_2O$, a qual pode ser utilizada para remover glifosato de efluente aquoso devido a sua alta área superficial específica e capacidade de troca catiônica. Estudos indicam que é necessário a organofilização da palygorskita a fim de mudar sua carga superficial negativa para positiva (XI et al., 2010). O estudo teve como objetivo principal a remoção de glifosato de meio aquoso por meio da adsorção utilizando palygoskita oriunda de Guadalupe (PI) previamente organofilizada com brometo de cetiltrimetil amônio (CTAB) na proporção 1:1 (p/p) e com granulometria abaixo de 20 µm. Nos ensaios de adsorção em batelada utilizou-se 20 mL de efluente e realizou-se um planejamento $2^{(4-1)}$, no qual as variáveis independentes foram massa, concentração de glifosato, tempo de agitação e pH. A concentração de glifosato foi obtida por meio da quantificação de fósforo pela espectrometria de Emissão Atômica por Plasma Acoplado Indutivamente. Os resultados dos ensaios de adsorção indicaram que adsorveu cerca de 86% de glifosato.

XI, Y.; MALLAVARAPU, M.; NAIDU, R. Adsorption of the herbicide 2,4-D on organo-palygorskite. Applied Clay Science, v.49, p.255-261, 2010.

**Área: MAT**
*(Inserir a sigla da seção científica para qual o resumo será submetido. Ex: ORG, BEA, CAT)*

**Inscrição:00936**
*(Inserir o número de inscrição do autor que fez a submissão)*

# Temperature Induced Optical Changes in Type II Metallopolymer based in Fluorene-Terpyridine Europium Complex.

**Denis A. Turchetti (PQ)[1,2], Alisson J. Santana (PG)[2], Luís G.T.A. Duarte (PG)[3], Raquel A. Domingues (PQ)[4], Tereza D.Z. Atvars (PQ)[3], Leni C. Akcelrud (PQ)[2].**

**denisturc@gmail.com;**

*[1]Instituto de Física de São Carlos, USP; [2]Departamento de Química, UFPR; [3]Instituto de Química, UNICAMP; [4]Instituto de Ciência e Tecnologia, USP.*

Keyword: *metallopolymer, Europium, Fluorene, Thermochromism, electron-phonon*

## Highlights

Photophysical Properties of metallopolymer containing fluorene, terpyridine and europium complex. Interpretation of the thermochromic effects in solid state.

## Resumo/Abstract

Thermochromic polymers are emerging as an important class of temperature sensors. The luminescent thermometry explores six parameters to analyze the luminescent emission of a given material: intensity, band shape, spectral position polarization, lifetime and bandwidth. In this contribution, the photophysical properties, with special emphasis on thermochromism of a π-conjugated polymer-$Eu^{3+}$ in the solid state, were studied. Absorption/emission spectra and lifetime measurements were carried out to explore the interaction of the europium complex with the polymer. For comparison purposes the same measurements were made with a model compound (representing the complexed sites in the metallopolymer) and with the corresponding conjugated polymer without complexation. The range of temperature studied was of 20 to 400 K. The most striking feature of this system is that the polymer emission, in the metallopolymer, becomes less sensitive to temperature variations. This effect was interpreted as a strong stiffening of the polymer chain that hindered electron-phonon interactions.

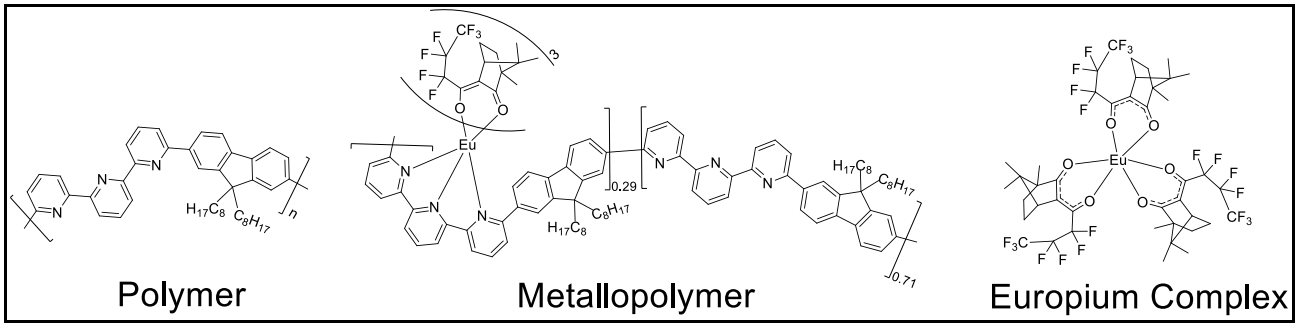

**Área: MAT** **Inscrição: 00922**

# Síntese de Filmes de Nanopartículas de Ouro e Polímero Luminescente em Substrato de Sílica para Aplicação em Sensores Óticos

**Carla Requena Klimpovuz* (IC)[1], Hellen V. C. Da Silva (IC)[2], Denis A. Turchetti (PG)[2], Leni Campos Akcelrud (PQ)[2], Marcela Mohallem Oliveira (PQ)[1].**

**carlaklimpovuz@yahoo.com.br**

*[1]Grupo de Química de Nanomateriais – GQNano, Departamento Acadêmico de Química e Biologia – DAQBi, Universidade Tecnológica Federal do Paraná – UTFPR; [2]Laboratório de Polímeros Paulo Scarpa – LaPPS, Departamento de Química – DQ, Universidade Federal do Paraná – UFPR.*

Palavras Chave: *Nanopartícula de ouro, Absorção plasmon, Polímero luminescente, Sensores óticos.*

## Highlights

Synthesis of Gold Nanoparticles and Luminescent Polymer Films on Silica Substrate for Optical Sensors Application.
Nanomaterials segment is based on matter manipulation and its use in technologies such as optical sensors. Gold nanocomposites are used in this area due to their optical properties and high stability.

## Resumo

Nanopartículas de ouro (AuNPs) são objeto de intensos estudos por apresentarem características diferenciadas daquelas encontradas no sólido estendido. AuNPs são detentoras de propriedades óticas altamente atrativas devido à variação da absorção *plasmon* com mudanças na forma, tamanho e meio que as cerca,[1] potencializando a sua aplicação em dispositivos óticos. A junção de AuNPs com polímeros luminescentes também é colocada em voga por conta da alteração das propriedades dos constituintes do nanocompósito, possibilitando o aumento na gama de aplicações.[2]
O esquema expõe simplificadamente o que foi realizado neste trabalho.

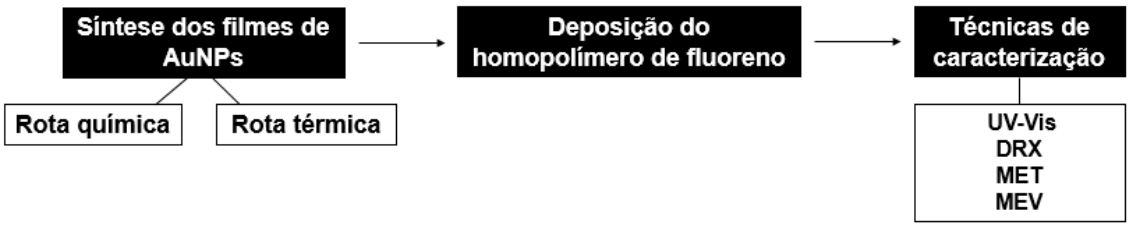


Os espectros UV-Vis do filme de Au NPs apresentaram bandas referentes à absorção *plasmon*, com diferenças nos espectros para cada uma das rotas. A DRX indicou picos referentes à $Au^0$ cfc. As imagens de MET e MEV indicaram o formato esférico e a diferença de tamanhos entre as AuNPs obtidas pelas diferentes rotas. Para o nanocompósito de AuNPs e polímero luminescente, observou-se interação entre os componentes através de variações nos espectros UV-Vis e nas imagens de microscopia.
Para as AuNPs, ambas as rotas se mostraram funcionais, sendo que a última apresentou resultados surpreendentes no que diz respeito ao controle de tamanho, homogeneidade, estabilidade e reprodutibilidade. A deposição do polímero sobre os filmes de AuNPs resultou em características diferenciadas provenientes da sinergia entre os componentes.

[1] Oldenburg, S. J.; et al., **Chem. Phys. Lett.**, v. 288, p. 243-247, 1998.
[2] Oliveira, H. P. M.; et al., **Química Nova**, v. 29, p. 227-286, 2006.

**Área: MAT** **Inscrição: 00084**

# Thermal processing optimization to obtain composites for controlled release of fertilizer

**Camila G. Chiaregato* (IC)[1], Roselena Faez (PQ)[1].**

**camilachiaregato@gmail.com**

[1]*Laboratório de Materiais Poliméricos e Biossorventes (LAB MPB), UFSCar, Araras.*

Palavras Chaves*: PHB, Sugarcane Bagasse, Controlled Release, Thermal Processing, Potassium Nitrate.*

## Highlights

Soil fertilization needs possible solutions. Composites of PHB and sugarcane bagasse have potential as a material for controlled release of fertilizers. Optimize this process is the first stage.

## Abstract

Development of slow/controlled release materials has expanded and demonstrated a potential to increase field productivity by delivering the nutrient in a spaced form and synchronized with the needs of the plant, as well decreasing nutrient losses[1]. Optimizing the processing is a demand. The aim of this work was to study the thermal processing (mixer chamber of Haake rheometer) of composites based on Poly(3-hydroxybutyrate) (PHB), sugarcane bagasse (BCA)[2] and potassium nitrate ($KNO_3$) as a controlled release material. The parameters fiber content (10, 20 and 30 wt.%) and $KNO_3$ sorbed by BCA (BCAS) and non-sorbed (BCA) were evaluated and the temperature and rotation (165° C and 50 rpm) and $KNO_3$ content (50 wt.%) were kept constant. For BCA10 (a), BCA20 and BCA30, the processing was finalized after the stable plateau torque, figure 1 (a). However, after processing, it was visible to the naked eye that the composites had heterogeneous points. To improve homogeneity, BCA10 (b) was processed in two steps, initially, the PHB was placed and, in 7 min, the mixture of BCA and $KNO_3$ was added, finishing in 15 min. As the nutrient content in the composition is high, it was not possible, for all the nutrient be aggregated by the polymer. For the composites BCAS10, BCAS20 and BCAS30, the nutrient was first sorbed by the fiber and then processed under the same conditions as BCA10 (b). Evaluating all conditions, the composite with sorbed nutrients has better homogeneity.

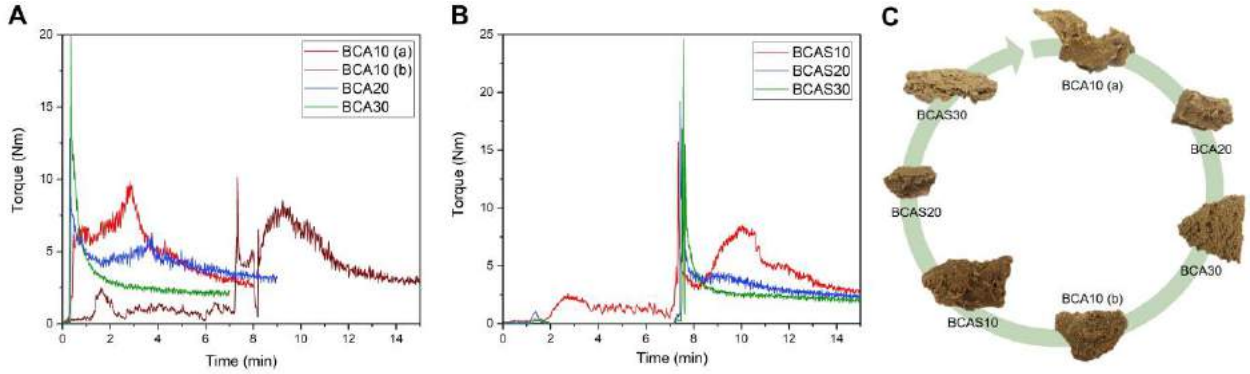


Figure 1: Torque curves a) composites with non-sorbed nutrients; b) composites with sorbed nutrients; c) images of composites obtained by thermal processing.

1 AZEEM, B. et al. Review on materials & methods to produce controlled release coated urea fertilizer. **Journal of Controlled Release**, v. 181, p. 11–21, 2014.
2 PICKERING, K. L.; EFENDY, M. G. A.; LE, T. M. A review of recent developments in natural fibre composites and their mechanical performance. **Composites Part A: Applied Science and Manufacturing**, v. 83, p. 98–112, 2016.

**Área: MAT** **Inscrição: 00832**

# Efeito da temperatura na molhabilidade de fibras de blendas de Ecovio®/PNIPAAm eletrofiadas

**Liege Aguiar Pascoalino (IC)[1], Edvani Curti Muniz (PQ)[2], Priscila Schroeder Curti (PQ)[1*].**

**liegeaguiar@gmail.com; priscilacurti@utfpr.edu.br**

*[1]Departamento Acadêmico de Química, UTFPR – Câmpus Londrina; [2]Programa de Pós-Graduação em Ciência e Engenharia de Materiais, UTFPR – Câmpus Londrina*

Palavras Chave: *Ecovio®, PNIPAAm, Eletrofiação, Blendas, Fibras.*

## Highlights

Temperature effect on the wettability behavior of the electrospun Ecovio®/PNIPAAm mats. Biocompatible and thermo-responsive PNIPAAm smart polymer. Hydrophylic-hydrophobic behavior of electrospun Ecovio®/PNIPAAm mats. The wettability behavior changed in function of the temperature.

## Resumo

A eletrofiação é uma técnica versátil e de baixo custo, capaz de produzir fibras poliméricas contínuas e uniformes com alta razão área/volume e diâmetros na faixa micro a nanométrica[1]. O Ecovio® é um polímero biodegradável produzido pela BASF, apresentando boa resistência mecânica e módulo de elasticidade[2]. O poli (N-isopropilacrilamida) (PNIPAAm) é um polímero termorresponsivo, que possui comportamento hidrofílico-hidrofóbico reversível em torno de 32ºC em meio aquoso, sendo muito aplicado na área de biomateriais[3]. Nesse trabalho, a molhabilidade de fibras de Ecovio®/PNIPAAm eletrofiadas foi avaliada, em função da temperatura, por meio de medidas de ângulo usando água mili-Q. Observou-se que não ocorreu molhabilidade das fibras de Ecovio® puro (comportamento hidrofóbico), pois na faixa de temperatura estudada (25-45°C) os valores de ângulo de contato ficaram acima de 130º (Fig.1).

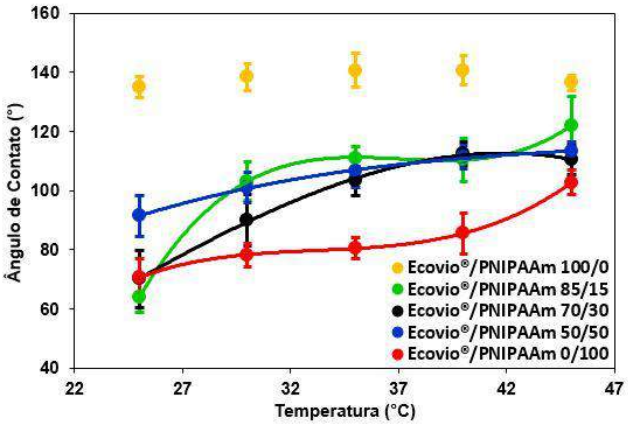


**Figura 1 -** Medidas de ângulo de contato formada entre a gota de água e a superfície das fibras de Ecovio®/PNIPAAm eletrofiadas, em função da temperatura.

A adição de PNIPAAm alterou significativamente os valores de ângulo de contato das fibras de Ecovio®/PNIPAAm eletrofiadas (Fig. 1). Abaixo de 30-32°C, ocorreu o molhamento dessas fibras, principalmente nas proporções mássicas de 15% e 30% de PNIPAAm, indicando o seu comportamento hidrofílico. Acima de 30-32°C, as fibras tornaram-se hidrofóbicas (valores de ângulos de contato acima de 90°), devido à mudança conformacional das cadeias poliméricas do PNIPAAm, acarretando em uma menor molhabilidade. Tais resultados indicam que as fibras de Ecovio®/PNIPAAm eletrofiadas apresentaram a transição hidrofílica-hidrofóbica característica do PNIPAAm, sendo mais evidente para as proporções mássicas de 15% e 30% de PNIPAAm. Assim, provavelmente essas fibras apresentam potencialidade de aplicação na área de adesão/descolamento celular.

[1] Corradini, E. et al. In: E. Longo; F.A.L.Porta (editors) Recent Advances in Complex Functional Materials From Design to Application. Springer, Cham, Switzerland, 83-128, 2017.
[2] Freitas, A.L.P.de L. et al. Polym Testing, 62, 189–195, 2017
[3] BRUN-GRAEPPI, A.K.A.S. et al. Progress in Polymer Science, 2010.

**Área: MAT** **Inscrição: 00854**

# Electrochemical vs Chemical: The most efficient synthesis method for a new ternary nanocomposite GO/$WO_3$NW/PAni

**Caroline B. Aquino (PG),[1,2] Danilo A. Nagaoka (PG),[1,2] Eduardo G. Cândido (IC),[2] Maria M. Machado (PQ),[1,2] Pedro H. C. Camargo (PQ),[3] Sergio H. Domingues (PQ).[1,2]***

**carolinebrambilla.aquino@gmail.com; shdomingues@makcenzie.br**

*[1] MackGraphe - Graphene and Nanomaterials Research Center, Mackenzie Presbyterian University, São Paulo, Brazil;*
*[2]Engineering School, Mackenzie Presbyterian University, São Paulo, Brazil;*
*[3]Department of Fundamental Chemistry - Institute of Chemistry, University of São Paulo, Brazil.*

Keywords:(*Graphene oxide, Tungsten oxide nanowire, Polyaniline, Chemical and electrochemical Polymerization, Supercapacitor).*

## Highlights

We performed the evaluation of different methodologies for the synthesis of a novel ternary nanocomposite based on graphene oxide, tungsten oxide nanowire and polyaniline.

## Abstract

In this work, we have investigated the efficiency of two different methodologies, chemical and electrochemical, to synthesize a novel ternary nanocomposite based on the combination of graphene oxide (**GO**), tungsten oxide nanowire (**$WO_3$NW**) and polyaniline (**PAni**). In fact, these materials present high superficial area, fast charge/discharge process and stability, which contribute to increase their capacitive properties, making them suitable to be applied as supercapacitors. For this purpose, the previously prepared **GO**[1] and **$WO_3$NW**[2] were employed in the chemical and electrochemical polymerization[3], respectively leading to the **C-GO/$WO_3$NW/PAni and E-GO/$WO_3$NW/PAni** samples, as shown in **Figure 1**.

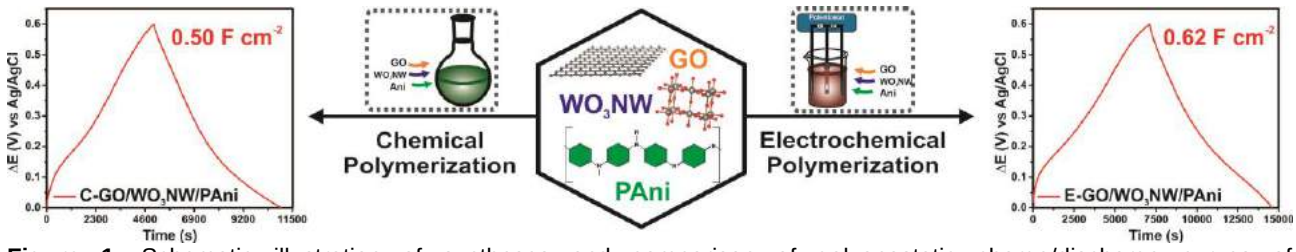


**Figure 1.** Schematic illustration of syntheses and comparison of galvanostatic charge/discharge curves of nanocomposites.

Raman spectroscopy and scanning electron microscopy confirmed the successful synthesis of both nanocomposites, showing the coexistence of the three components. The electrochemical evaluation attested a better electrochemical response for the nanocomposites when compared to the control samples. The capacitive values found, of 0.62 F $cm^{-2}$ for **E-GO/$WO_3$NW/PAni** and 0.50 F $cm^{-2}$ for **C-GO/$WO_3$NW/PAni** proved the materials to have a promising performance as supercapacitor. Besides, the nanocomposites exhibited high stability, with retention capacitance of about 60% after 1600 cycles. Overall, we described the synthesis of novel ternary nanocomposites through different versatile and environmental friendly routes that allow us to design and modulate the final material according to the capacitive behavior desired.

Acknowledgements: Mackenzie Presbiterian Universisty (UPM), FAPESP (SPEC 2012/50259-8 and 2015/10149-7), MackGraphe, Department of Fundamental Chemistry (USP), CNPq (403544/2016-5), Materials Chemistry Group (GQM – UFPR).
References: [1] Domingues, S. H. *et. al*. *Chemical Communications* **2011**, 47, 2592. [2] Gu, Z. *et. al*. *Journal of Solid State Chemistry* **2007**, 180, 98. [3] Ma, J. *et. al*. *Ionics* **2013**, 19, 1405.

**Área: MAT**
*(Inserir a sigla da seção científica para qual o resumo será submetido. Ex: ORG, BEA, CAT)*

**Inscrição: 00686**
*(Inserir o número de inscrição do autor que fez a submissão)*

# Synthesis and characterization of superparamagnetic iron oxide nanoparticles covered with methylene blue and hypericin molecules.

**Victor H. Toledo (IC),[1]* Martha S. Ribeiro (PQ),[2] Tania M. Yoshimura (PG),[2] Saulo P. Toledo (PG),[2] Paula S. Haddad (PQ),[1]**

**victorhlatoledo@gmail.com**

*[1]Departamento de Química, UNIFESP; [2] Centro de Lasers e Aplicações, IPEN-CNEN/SP*

Palavras Chave: *Nanoparticles, Superparamagnetism, Singlet Oxygen, Methylene blue, Hypericin, Silica.*

## Highlights

Synthesis of nanoparticles by co-precipitation. Functionalization with photoactive molecules. Structural and spectroscopic characterization. Measurement of $^1O_2$ generation. Biological assay in *E. coli*.

## Resumo/Abstract

The present study is focused on the synthesis and characterization of methylene blue and hypericin-containing silica-coated superparamagnetic nanoparticles with great potential for photodynamic therapy (PDT). The photoactive molecule (PM) when exposed to light reacts with molecular oxygen and generates singlet oxygen ($^1O_2$) which is cytotoxic. Superparamagnetic iron oxide nanoparticles (SPIONs) were prepared with a mixture of iron (II) and (III) chlorides in the presence of a base by co-precipitation and its surface was covered with tetraethylammonium. SPIONs were coated with a double layer of silica, tetraethylortosilicate (TEOS) and sodium silicate ($Na_2SiO_3$), generating the SPIONs-$Na_2SiO_3$-TEOS-PM compound, as shown below.

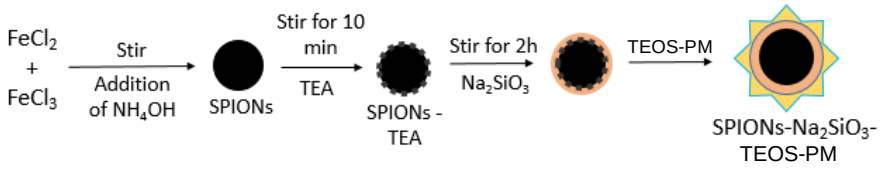


As-synthesized nanoparticles were characterized by Fourier transform infrared spectroscopy, X-ray diffraction, and SQUID magnetic measurements. X-ray powder diffraction technique confirmed the formation of the magnetite. By using the Scherrer equation for 311 reflection, it was observed that the average crystallite sizes were 18 nm. By infrared spectroscopy, it is possible to note characteristics bands of iron- oxygen, besides others bands associated to silicate groups. The nanocomposites presented magnetic behavior at room temperature due to the presence of magnetite ($Fe_3O_4$) core. Indirect measurements of $^1O_2$ release were performed using a red light (630-650nm, P=25mW) and reagent, 1,3-Diphenylisobenzophuran, with SPIONs-$Na_2SiO_3$-TEOS-PH, observing the absorption decay in UV-vis. $^1O_2$ is spontaneously released in aqueous solution at levels required for biomedical applications and tests with bacteria show promising nanoparticles applications.

**Área: MAT** **Inscrição: 00728**

# Cerium (IV) hydrogenphosphate as an intercalation matrix for Pd(II)

**João Paulo Pereira Duarte (IC),[1]*Luiz Diego Silva Rocha (PG),[1]Roseli Martins de Souza (PQ),[1]Marta Eloisa Medeiros (PQ),[1]Luiz Fernando Brum Malta (PQ).[1]**

**jpaulop.duarte@gmail.com**

[1]*Instituto de Química, UFRJ.*

Palavras Chave: *Ion exchange, layered matrix, hydrothermal treatment, intercalation*

## Highlights

Cerium hydrogenphosphate is an ion-exchange layered material
It forms self-supported films
Palladium was intercalated via ion-exchange process
The nanocomposite can be used in organometallic cataysis

## Resumo/Abstract

Cerium (IV) acid phosphate (CeP) belongs to the class of acid phosphates of tetravalent metals. In particular, this material assumes the form of fibrous self-supported sheets [1]. It presents the property of ion-exchange towards cations. In the present work it is intended to incorporate palladium in layered matrix of varying cristallinities as an effort to obtain nanocoposites for organometallic catalysis.
CeP was synthesized according to previous work [2]. 6 mol $L^{-1}$ $H_3PO_4$ aqueous solution was added dropwise to a 0.05 mol $L^{-1}$ $(NH_4)_2Ce(NO_3)_6$ aqueous solution at 90ºC and the mixture was kept at this temperature for 0h, 2h and 4h. The solids were characterized by XRD, FTIR and TGA.
The XRD patterns (Fig. 1) show the improvement in cristallinity as the treatment time is increased. For the 4hour-time treated material, the most cristalline, we proceeded to the ion-exchange process with Pd (Fig. 2a). It was observed a dramatic decrease of peak intensity but there was no change concerning the 2θ value of the interlayer space peak (2θ~8.0º). The FTIR spectra (Fig.2b) show that PO-H stretching mode at 2380 $cm^{-1}$ loses intensity after Pd impregnation signaling ion-exchange. TGA curves point to 3.8 and 2.8 $H_2O$ for CeP and CeP-Pd hydration evidencing partial dehydration after intercalation. ICP-OES, Raman and SEM characterizations are underway.

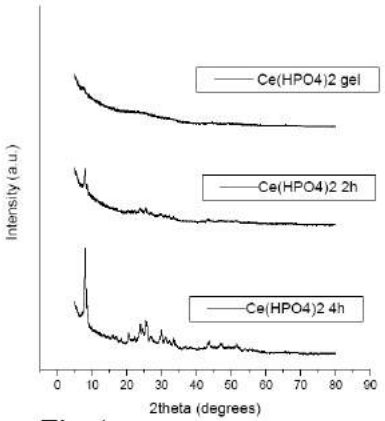


Fig.1

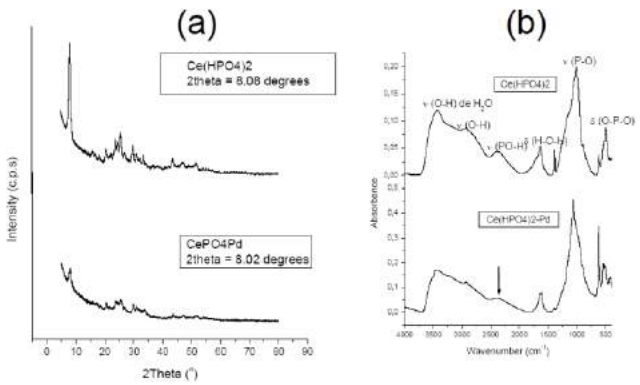


Fig. 2

1 C. Verıssimo and O.L. Alves: J. Mater. Chem. 13, 1378 (2003).
2 R. Romano and O. L. Alves J. Incl. Phen. Macro. Chem. (2005) 51: 211–217

**Área: MAT** **Inscrição: 00526**

# Preparation of graphene oxide (GO) membranes with potential application in water desalination

**Marianne Ferreira de Barros (IC)[2]*, Sofia de Carvalho Britto Sousa (IC)[2], Carolina Miranda Tecchio (TM)[1], Lucas dos Santos Fernandes (IC)[2], Isadora Vinseiro Martins (IC)[2], Cláudia Karina Barbosa de Vasconcelos (PQ)[2], Marcelo Machado Viana (PQ)[1]**

**marcelomachado@ufmg.br; marianne.barros@hotmail.com**
[1]Departamento de Química - ICEx, *Universidade Federal de Minas Gerais;* [2]Departamento de Engenharia Química - IPUC, Pontifícia Universidade Católica de Minas Gerais

*Keywords: Desalination, Graphene Oxide, Membranes, Nanotechnology.*

## Highlights

Synthesis of graphene oxide by using microwave radiation and chemical exfoliation. Preparation of GO porous membranes with controlled thickness and potential application in water desalination.

## Abstract

The desalination is one of the most promising approaches to mitigate the water shortage increasing the water supply beyond what is available in the world. Reverse osmosis and multistage flash distillation has been mainly used to seawater desalination, however these processes consume large amounts of thermal and electric energy [1]. Some studies have demonstrated that graphene-like membranes can be used for this purpose due to their chemical and mechanical stability and also high fluid permeability and ion rejection rate [1]. In this work, multilayer structures formed by porous GO have been prepared and investigated for their ability of ionic and molecular separation. The GO membranes with controlled thickness were prepared using chemical route involving acids and microwave radiation. These membranes were characterized by X-ray diffractometry (XRD), infrared spectroscopy (FTIR), thermogravimetry (TG-DTA) and scanning electron microscopy (SEM) (Figure 1). The GO membranes with 350 nm of thickness deposited on commercial polyvinylidene fluoride (PVDF) showed good thermal stability and an interplanar distance of 0.74 nm. According to literature, these results demonstrate the potential to application as ionic and molecular sieves. The deionized water flux across the GO membrane measured was 35.6 Kg $m^{-2}$ $h^{-1}$. New experiments of water permeability and salt rejection, evaluated by ionic conductivity in solution, are now in progress.

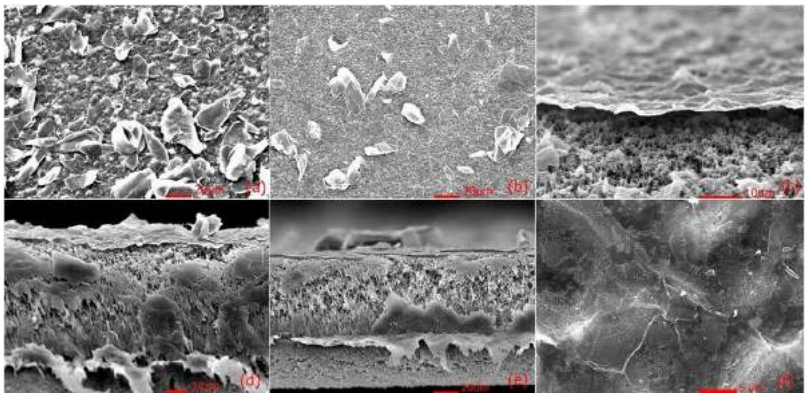

Figure 1. SEM images of GO membrane: (a, b) graphene oxide sheets, (c, d, e) cross-section and (f) carbon dots on the surface.

Acknowledgment: We thank FAPEMIG, CNPq, and Capes for financial support.

[1] Shahin H., Mady E., Graphene Membranes for Water Desalination, NP G Asia Materials, 9, e427, 2017.

**Área: MAT** **Inscrição: 00547**

# Three-dimensional graphene nanofilters for heavy metal ions removal from water: a combined experimental and theoretical study

**Bianca Lino (IC),[1] Victória Ximenes (IC),[1] Gabriel R. L. Reis (IC),[1] José R. Bordin (PQ)[1] and Carolina F. de Matos (PQ)[1*]**

**carolinamatos@unipampa.edu.br;**

[1]*Campus Caçapava do Sul, Universidade Federal do Pampa-UNIPAMPA*
Key words: *Three-dimensional Graphene, Nanofilters, Heavy Metals.*

## Highlights

Thermochemical preparation of Three-dimensional graphene nanofilters for heavy metal removal from water. Theoretical and experimental: nanofilters are selective to certain metal ions.

## Abstract

In this work we propose a simple, low cost and “green” route for preparation of Three-dimensional graphene based materials filters (3D-rGO) for heavy metal removal from water. 3D-rGO nanofilters where obtained from the reduction of graphene oxide (GO) under very specific conditions. A flow-directed assembly was used to assemble GO sheets into layered films. In this procedure, aqueous GO dispersions were filtered through a porous membrane. After these procedures the films were peeled off from the membranes. The freestanding GO layered films were put into a flask with the reducing agent solutions (ascorbic acid). Each flask was then sealed in a stainless steel autoclave and heated in different conditions. After this, the 3D-rGO nanofilters obtained were washed with deionized water and dried at 60°C. The nanofilters were characterized by SEM, XRD, Raman and FTIR spectroscopies. Simple reaction variations promoted significant morphological changes (including pore size distribution). Controlling the synthesis parameters was possible to modulate the adsorptive properties of the 3D-rGO nanofilters. In other words, was possible to make it more selective to certain types of metal ions. Atomistic Molecular Dynamics simulations were employed to analyze the blockage and adsorption properties of a membrane composed of three layered porous graphene The theoretical results indicates that the membrane is able to block and adsorb more than 90% of the monovalent and divalent cations and 100% of the trivalent cations regardless the simulated opening in the sheets, corroborating experimental data.

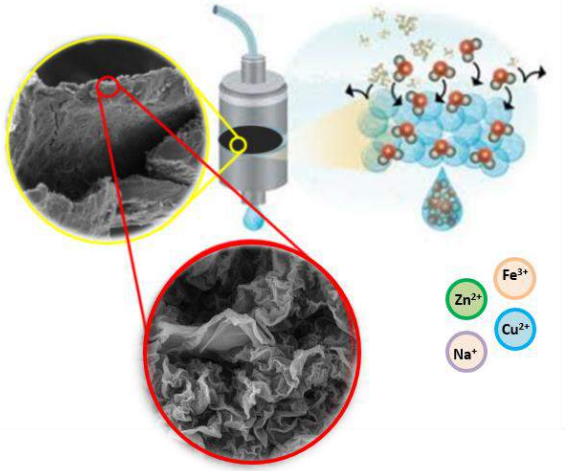

**Área: MAT**
*(Inserir a sigla da seção científica para qual o resumo será submetido. Ex: ORG, BEA, CAT)*

**Inscrição: 649**
*(Inserir o número de inscrição do autor que fez a submissão)*

# $Er^{3+}$ and $Yb^{3+}$ up conversion on oxide matrix obtained by non-hydrolytic sol-gel

**Camila J. Granito (IC), Filipy H. P. de Andrade (IC), Maria F. Ferreira (IC), Danielle C. Baldini (PG), Emerson H. de Faria (PQ), Katia J. Ciuffi (PQ), Lucas A. Rocha (PQ), Eduardo J. Nassar* (PQ).**

**eduardo.nassar@unifran.edu.br**

*Universidade de Franca*

Palavras Chave: *Up conversion, energy transfer, solar cells.*

## Highlights

The different matrix doped with different ion concentration of the $Er^{3+}$ and $Yb^{3+}$ can affect the lanthanide ion emission. The $Yb^{3+}$ increase the energy transfer of the $Yb^{3+}$ to $Er^{3+}$.

## Resumo/Abstract

In this work the yttrium-aluminum [1] and gadolinium-aluminum [2] oxide were prepared by non-hydrolytic sol-gel methodology. The matrices were synthesized with $Er^{3+}$ and $Er^{3+}/Yb^{3+}$, the molar ratio was 1%. The samples were treated at 800°C during 4 h. The samples were characterized by X-rays (XRD) diffraction and up conversion photoluminescence (PL). The XRD present peaks ascribed to the different oxides, yttrium, yttrium aluminum garnet, gadolinium and gadolinium aluminate peroviskite. The emission spectrum were use to laser system with excitation wavelength fixed at 980 nm and 2.0 W power. The samples containing only $Er^{3+}$ ion present bands in the green (542 nm) and red (660 nm) regions, correspondent to $^4S_{3/2} \rightarrow {}^4I_{15/2}$ and $^4F_{9/2} \rightarrow {}^4I_{15/2}$ transitions, respectively, the similar intensity was observed. The samples containing $Er^{3+}$ and $Yb^{3+}$ the emission spectrum present the bands in the same regions, however as band in the red region is more intense than green. The increase in the intensity of transition $^4F_{9/2} \rightarrow {}^4I_{15/2,}$ is an indicative that the excited state $^2F_{9/2}$ of the $Yb^{3+}$ ion transfer energy to the $^4F_{9/2}$ level. The incorporation of the $Yb^{3+}$ ion as sensitizer showed an increase on emission of the activator $Er^{3+}$ ion. The matrices present different behavior in the emission of the $Er^{3+}$ ion. The figure 1 presents the emission spectrum to the samples.

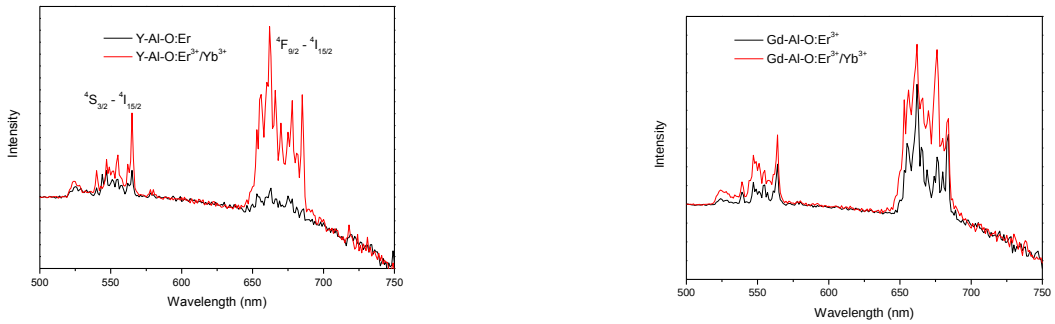


a b

**Figure 1:** Emission spectra to the samples without $Yb^{3+}$ and with $Yb^{3+}$ into Y-Al-O (a) and Gd-Al-O (b) matrices.

**CNPq, CAPES e FAPESP**

[1] E. J. Nassar, L. R. Ávila, P. F. S. Pereira, C. Mello, O. J. de Lima, K. J. Ciuffi, L. D. Carlos, J. Lumin. *111* (2005) 159-166.
[2] M. G. Matos, P. S. Calefi, K. J. Ciuffi, E. J. Nassar, Inor. Chim. Acta, 375 (2011) 63-69.

**‘’’Área: MAT** **Inscrição: 0415**
*(Inserir o número de inscrição do autor que fez a submissão)*

# Swelling behavior of gelatin/dextran hydrogel crosslinked by Diels-Alder click chemistry

**Rodolfo D. Piazza* (PG)[1], João Victor Brandt (PG)[1], Rodrigo F. C. Marques (PQ)[1], Miguel Jafelicci Jr (PQ)[1]**

**rodolfo.piazza@gmail.com; jafeli@iq.unesp.br**

[1]*Laboratory of Magnetic Materials and Colloids, Department of Physical–Chemistry, São Paulo State University- UNESP*

Key Words: Sensitive-hydrogels; Click chemistry; Diels-Alder.

## Highlights

Diels-Alder click chemistry. pH responsive hydrogels. Swelling behavior.

## Resumo/Abstract

Hydrogels are three-dimensional network of hydrophilic polymers which are widely used in biomedical applications, such as tissue engineering, regenerative medicine, cellular immobilization, and drug delivery systems. The hydrogels could be chemically crosslinked or molecularly tangled, through ionic, hydrophobic and/or H-bonding interactions. However, most of the synthetic routes to promote chemical crosslinking in hydrogels use initiators and the sub-products of the reaction may introduce toxicity into the platform (1,2). In the last decade, the click reaction emerges as an alternative of crosslinking due to high selectivity and reactivity. In the present work, gelatin and dextran were derivatized to further chemical crosslinking by Diels-Alder click reaction to study the swelling properties in different media. The derivatization reaction was confirmed by $^{1}$H-NMR spectroscopy, which the peak at 6.28 ppm correspond to the maleimide group grafted on gelatin and the protons of furoic acid could be observed at 6.64, 7.26 and 7.72 ppm in dextran sample. The swelling property of Diels-Alder hydrogel was evaluated in water, phosphate buffer solution (PBS pH 7.4) and gastric fluid simulated (GFS pH 2.0). In water the hydrogel swells 377%, while in PBS and GFS the swelling capacities were 458% and 641%, respectively. This behavior could be attributed to surface charges of the polymer chains according to pH of solution medium. The swelling mechanism was studied based on Peppas equation (3), which results in non-Fickinian mechanism, where the diffusion and relaxation of the polymer chain occur simultaneously.

1 Meng, X.; Edgar, K.J. “Click” reactions in polysaccharide modification. **Progress in Polymer Science**, p. ASAP, 2015.
2 Buwalda, S.J.; Boere, K.W.M.; et al. Hydrogels in a historical perspective: from simple networks to smart materials. **Journal of Controlled Release**, v. 190, p. 254–73, 2014.
3 Ritger, P.L.; Peppas, N.A. A Simple Equation for Description of Solute Release II. Fickian and anomalous release from swellable devices. **Journal of Controlled Release**, v. 5, p. 23–36, 1987.

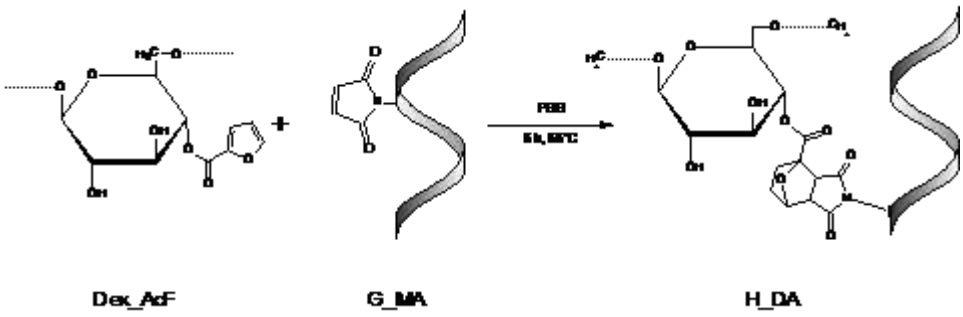


Figure. Schematic illustration to Diels-Alder crosslinking reaction.

**Área:a MAT** **Inscrição: 00439**

# Effect of functionalization of porous silica as nanoreactor for preparation of fluorescent Carbon Dots

**Albina Mikhraliieva (PG),[1] Henrique B. da Motta (IC),[1] Volodymyr Zaitsev (FM)[1]*.**

**mialnr@gmail.com; vnzaitsev@gmail.com**

[1]*Departamento de Química, PUC-RIO*

Palavras Chave: *Carbon Dots, Fluorescence, Silica gel, Citric acid.*

## Highlights

A simplified method for preparation Carbon Dots. Combination of classical pyrolysis of citric acid and a thermal-resistant reservoir promotes formation of fluorescent particles.

## Resumo/Abstract

Fluorescence (FL) detection has excellent sensitivity, short response time but requires compounds either to have native fluorescence or to be chemically modified to induce fluorescence. Carbon Dots (CDs) are new one kind of carbon materials that exhibit high fluorescence. These small particles (size smaller than 10 nm) have non-toxic carbon structure and can be modified with different functional groups. Crucial step of fabrication these fluorescent nanomaterials is synthesis approach. Composition, structure and final properties of CDs depend on the initial materials used as sources of carbon and the conditions of production (temperature, pressure, solvent) employed. As a result, CDs represent a mixture of particles with different sizes. Complex separation methods are used to obtain unimodal distribution of particle size. Controlling the morphology and size distribution of CDs during synthesis is a problem, therefore a new and simple method is required. We proposed to overcome those difficulties by using an external support capable of restricting the size and shape of the nanostructures generated. Porous silica material can be used as nanoreator of the CDs formation. During thermal decomposition of citric acid at high temperature in the absence of oxygen, particles that emit blue light are formed. It was found that silica gel modified with amine groups promotes retention of high fluorescent nanoparticles in dispersion after etching of support. Emission spectra did not change the band position (λem = 445 nm) after excitation at different wavelengths, which attest to narrow size distribution of prepared particle.

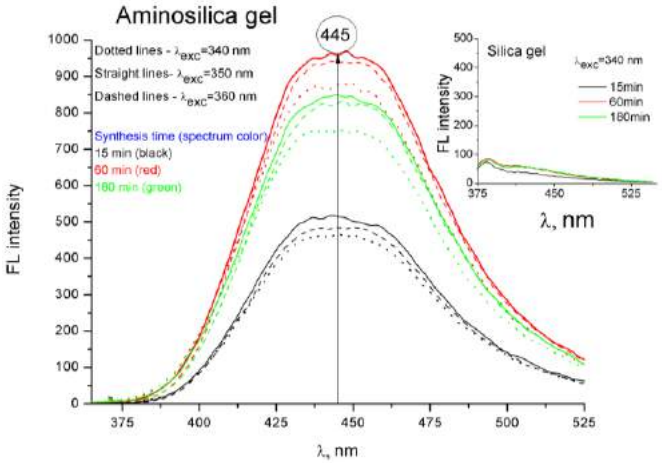


Figure 1. Emission spectra of aqueous CDs dispersions from silica gel e aminosilica supports

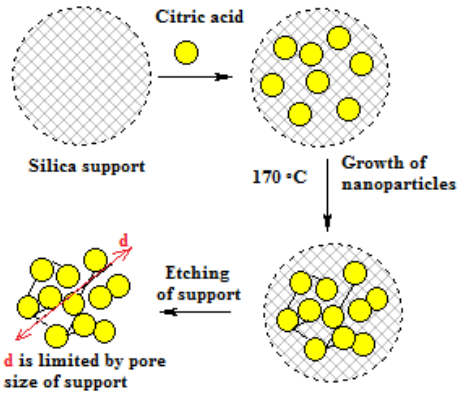


Figure 2. Schematic preparation of CDs

**Área: MAT** **Inscrição:** 00468

# UTILIZAÇÃO DA TÉCNICA DE REELS E DO MÉTODO DFT PARA A OBTENÇÃO DO GAP DOS COPOLÍMEROS PFO-DBT E PSiF-DBT

**Vanessa F. dos Santos (IC)[1], Sérgio de P. Machado (PQ)[1]*, Maria Luiza M. Rocco (PQ)[1]***

**vanessa.farelo@hotmail.com; sergiopm@iq.ufrj.br; luiza@iq.ufrj.br**

[1] *Instituto de Química, Universidade Federal do Rio de Janeiro, Rio de Janeiro 21941-909, Brasil*

Palavras Chave: *REELS, DFT, PFO-DBT, PSiF-DBT*

## Highlights

APPLICATION OF REELS AND DFT FOR OBTAINING THE GAP OF PFO-DBT AND PSiF-DBT COPOLYMERS

Experimental and theoretical gaps of PFO-DBT and PSiF-DBT were compared using REELS and DFT. The influence of unconjugated side chains and substitutions at strategic points were also studied.

## Resumo/Abstract

Apesar de representar pequena parcela da geração de energia elétrica mundial, a energia solar vem ganhando espaço e novos materiais para células solares orgânicas estão sendo construídos através da combinação de grupos químicos com diferentes afinidades eletrônicas – os chamados copolímeros.

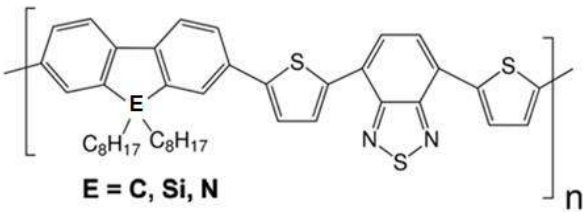


**Figura 1**. Estrutura do copolímero PSiF-DBT, onde E = Si e do PFO-DBT, onde E = C.

Dessa forma, este trabalho teve por objetivo estudar e comparar, através do método DFT (*Density Functional Theory*) e da técnica de REELS (*Reflection Electron Energy Loss Spectroscopy*), os valores para o *gap* ($E_{LUMO}$-$E_{HOMO}$) dos copolímeros PFO-DBT e PSiF-DBT (Figura 1), visando a aplicação em células solares. Além disso, foi verificada a influência, no *gap*, do crescimento das cadeias laterais não conjugadas e da cadeia polimérica.

As análises por REELS dos filmes de PFO-DBT e de PSiF-DBT foram conduzidas no equipamento ESCALAB 250Xi, as quais forneceram os valores para o *gap* eletrônico dos copolímeros. O procedimento teórico foi realizado pelo programa *gaussian09*, com o funcional B3LYP e a base LanL2DZ.

Os *gaps* eletrônicos obtidos para o PFO-DBT e o PSiF-DBT foram **1,81 eV** e **1,87 eV**, respectivamente. Já o método DFT mostrou que as cadeias laterais não conjugadas não influenciaram significativamente no valor do *gap* (Tabela 1), mas este apresentou um comportamento exponencial com o crescimento da cadeia polimérica (Figura 2) em ambos os casos. Diante disso, estes copolímeros representam excelentes opções para o emprego em células solares orgânicas, contribuindo para novos avanços neste tipo de tecnologia.

Este trabalho tem colaboração com o grupo da professora Lucimara S. Roman, da UFPR.

**Tabela 1**. Variação do *gap* (eV) com o crescimento das cadeias laterais do PFO-DBT e do PSiF-DBT.

| **Valores do *gap* (eV) em função do número de carbonos em cada cadeia lateral** | | | | | |
|---|---|---|---|---|---|
| | Zero | Um | Quatro | Seis | Oito |
| PFO-DBT | 2,14 | 2,13 | 2,13 | 2,12 | 2,13 |
| PSiF-DBT | 2,17 | 2,14 | 2,13 | 2,13 | 2,14 |

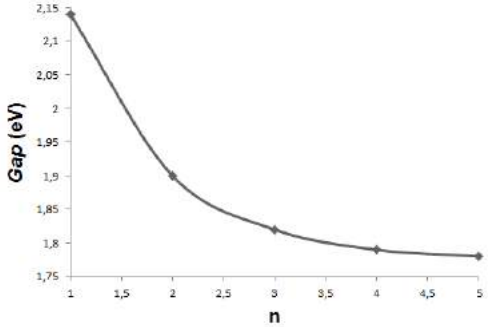


**Figura 2**. Variação do *gap* (eV) com o crescimento da cadeia polimérica do PSiF-DBT.

**Área: MAT** **Inscrição: 00878**

# Development of active SERS platform via self-assembly monolayers of AuNRs

**Jaciara Bär (PG),[1] Anerise de Barros (PQ),[1] Davi H.S. Camargo (PG),[2] Larissa H. Oliveira (PQ),[1] Luis O.Z. Falsetti (IC),[2] Fernando A. Sigoli (PQ),[1] Diego P. Santos (PQ),[1] Carlos C.B. Bufon (PQ),[2] Italo O. Mazali (PQ).[1]***

**jaciara.bar@iqm.unicamp.br; mazali@iqm.unicamp.br**

*[1] Functional Materials Laboratory - Institute of Chemistry, University of Campinas, Brazil. [2]Functional Devices and Systems - Brazilian Nanotechnology National Laboratory (LNNano - CNPEM) - Brazil.*

Keywords: *SERS, plasmonic, nanorods, gold, self-assembly.*

## Highlights

Self-assembled monolayers of aligned-AuNRs using cucurbit[7]uril to SERS application. Development of SERS sensor for detection of analyte at ultra-low concentrations.

## Abstract

Gold Nanorods (AuNRs) have attracted extensive attention and scientific interest due to their special optical properties. In particular, the study of the interaction between electromagnetic radiation and metallic nanostructures is rapidly growing, with analytical applications such as plasmonic devices for Surface-Enhanced Raman spectroscopy (SERS) [1,2]. In this work, we investigated the obtaining of self-assembled monolayers (SAM) of aligned-AuNRs, via supramolecular alignment using cucurbit[7]uril (CB[7]), onto silicon substrates. For this, the silicon substrates were fabricated with submicrometer channels by lithography and etching processes, and then functionalized with (3-mercaptopropyl)trimethoxysilane. Finally, the AuNRs_CB[7] were deposited by immersion in channels. Analysis by UV-vis absorption suggests the inter-rod interaction between AuNRs and CB[7] promoting the self-alignment of AuNRs, which is indicated by the red-shift of the longitudinal surface plasmon resonance band (LSPR) from 735 nm to 762 nm and confirmed by SEM-FEG images. The Raman spectra for the substrates modified with AuNRs_CB[7] were collected using rhodamine 6G as probe molecule and we also investigated the effect of wet and dry states in the Raman analysis. The results indicated that the wet condition shows greater intensity in the spectrum compared to the dry condition, an effect associated with the dielectric component of the analyzed environment. Theoretical data confirmed this effect and also showed that the wet condition is in the resonance region and covers the SERS spectrum. The system has shown to be very effective and promising for SERS sensor applications for molecules at ultra-low concentrations.

[1] Shiohara, A.; Wang, Y.; Liz-Marzán, L.M. J. Photochem. Photobiol., C, 21 (2014) 2–25.
[2] Cao, J.; Sun, T., Grattan, K.T.V. Sens. Actuators, B, 195 (2014) 332–351.

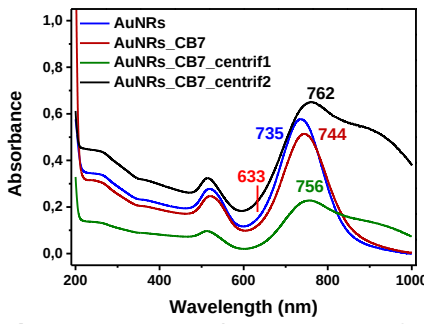


**Figure 1:** UV-vis spectra of suspension AuNRs_CB[7].

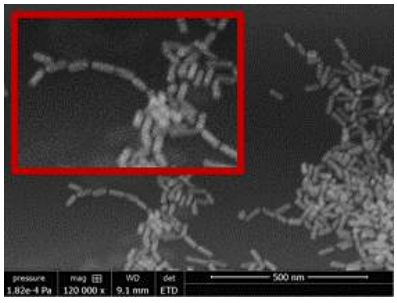

**Figure 2:** SEM image of AuNRs_CB[7] into channel of Si substrate.

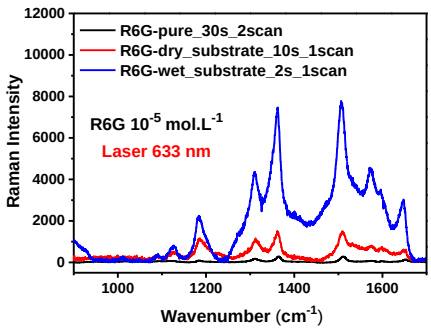


**Figure 3:** Raman spectra of R6G on the substrate with AuNRs_CB[7] under different conditions.

**Área: MAT** **Inscrição: 00349**

# Pseudocapacitors from crumpled graphene balls/mixed transition metal oxides composites

**Larissa H. Nonaka (IC)[1], Estéfani T. Barce (IC)[1], Victor H.R. Souza (PQ)[1*]**

**larissaharumi123@hotmail.com; victorsouza@ufgd.edu.br**

*[1] Laboratório de Materiais Cerâmicos Avançados (LMCA), Faculdade de Ciências Exatas e Tecnologia (FACET), Universidade Federal da Grande Dourados (UFGD).*

Keywords: *Crumpled graphene balls, Mixed transition metal oxides, Pseudocapacitors.*

## Highlights

- One step synthesis of crumpled graphene balls/mixed transition metal oxides.
- Aggregation-resistant composites with accessible surface area.
- 3D composites for energy storage materials.

## Abstract

Restacking of graphene is one of the issues which compromises the properties of this carbon nanostrucuture and decrease their solution processability. Changing the 2D structure of graphene into a 3D structure simply crumpling it like a paper ball is a clever solution to keep this material with high accessible surface area and resistant to aggregation.[1] The charging storage properties of raw crumpled graphene and composites with metal oxides is beginning to be explored since this metals precursors present excellent pseudocapacitive response.[2] Mixed transition metal oxides is an option to enhance the pseudocapacitive properties of this class of charge storage materials since they exhibit higher electron conductivity.[3] Herein, we show a new approach to obtain composites made of crumpled graphene balls and mixed transition metal oxides in one single step. Graphene oxide was obtained by a modified Hummer's method; and crumpled graphene balls and mixed transition metal oxides composites were synthesized nebulizing a graphene oxide/metal precursors (iron and manganese) dispersion into a tubular furnace.[1] The scanning electron microscope (SEM) micrograph in Figure 1 shows the crumpled graphene ball decorated by the metallic species. The cyclic voltammetry measurements presented a quasi-rectangular shape, which is typical for pseudocapacitive materials, but charge-discharge measurements presented low value of specific capacitance (around 30 F/g). Different graphene oxide/metal precursors ratios will be explored to enhance the capacitive properties of the composite.

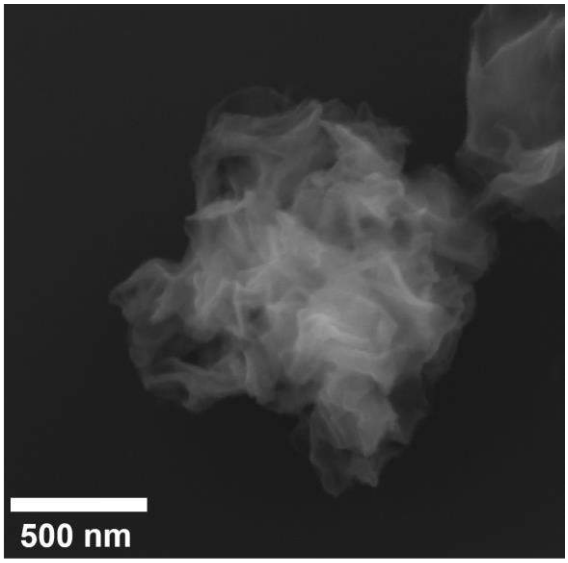


**Figure 1 –** SEM micrograph of crumpled graphene ball/mixed transition metal oxide.

[1] J. Luo, H.D. Jang, T. Sun, L. Xiao, Z. He, A.P. Katsoulidis, M.G. Kanatzidis, J.M. Gibson, J. Huang, ACS Nano, 5 (2011) 8943-8949.
[2] C. Lee, E.H. Jo, S.K. Kim, J.-H. Choi, H. Chang, H.D. Jang, Carbon, 115 (2017) 331-337.
[3] L. Lin, S. Tang, S. Zhao, X. Peng, N. Hu, Electrochimica Acta, 228 (2017) 175-182.

**Área: MAT** **Inscrição: 373**

# Obtenção de fibras a partir da blenda polimérica de PCL e PBAT para liberação de sulfadiazina de prata

**Janice C. Hardt (PG),[1] Douglas C. Dragunski (PQ),[1] Josiane Caetano (PQ),[1*] Andressa G. Rosenberger (PG),[1]**

**janice.hardt@hotmail.com; caetanojosi@gmail.com**

[1]*Universidade Estadual do Oeste do Paraná, UNIOESTE*

Palavras Chave: *eletrofiação, fibras, PCL, PBAT, queimaduras, pele.*

## Highlights

Fiber obtainment from PCL and PBAT polymer blends for the release of silver sulfadiazine.
Use of a polymeric blend to produce films by electrospinning incorporating silver sulfadiazine for controlled release in the treatment of burns.

## Resumo/Abstract

Neste trabalho utilizou-se para produção da blenda polimérica os polímeros, poli(ε-caprolactona) (PCL) e o poli(butileno-adipato-co-tereftalato) (PBAT), pelo processo de eletrofiação, para liberação controlada do fármaco sulfadiazina de prata. Inicialmente incorporou-se o fármaco a uma solução da blenda polimérica com condições previamente definidas, concentração da solução de 20%m/V, sendo 75%m/m PBAT e 25%m/m de PCL, concentração do fármaco de 10%m/m, distância ao coletor de 12cm, tensão de 15kV e vazão de 1,0mL/h, obtendo-se fibras com descontinuidades, *beads*, que foram verificadas em imagens obtidas por Microscopia Eletrônica de Varredura. Mesmo com a presença dos *beads* obteve-se um filme, com o qual foram realizados testes prévios para verificar se a liberação do fármaco do filme era efetiva em tampão fosfato pH 5,5 que simula as condições da pele. Após o filme ter sido deixado em tampão por aproximadamente 5h, verificou-se que não havia mais oscilações na concentração do fármaco que estava sendo liberada pelo filme. Com o filme contendo a sulfadiazina e com o filme em que o fármaco foi liberado, realizou-se análises térmicas. Na termogravimetria observou-se que para o filme contendo a sulfadiazina, a degradação se iniciou antes que no filme em que foi liberado, isto porque a primeira perda de massa em aproximadamente 305ºC refere-se ao fármaco, representando a efetiva liberação do fármaco do filme. Por meio da Calorimetria Diferencial Exploratória não foram observadas diferenças significativas, pois as variações nos calores e temperaturas de fusão para os dois termogramas foram pequenas.

**Área: MAT** **Inscrição: 00973**

# Porous ceramic based on phlogopite from the polymeric sponge method

**Alley M.S. Procópio (PG),[1] Mercês C. Silva (PQ),[1] Francisco M. Filho (PQ),[1*]**

**alleymichael1987@gmail.com; franciscomoura@unifei.edu.br**

*[1]Universidade Federal de Itajubá, Rua Irmã Ivone Drumond, 200, Distrito Industrial II, Itabira-MG*

Keywords: *Porous ceramic, Polymeric sponge, Phlogopite.*

## Highlights

Porous ceramic based on phlogopite, mineral of chemical formula $KMg_3(AlSi_3O_{10})F_2$.
Polymeric sponge method or the replica technique.
Characterization of the ceramic body by TG/DTG, Dilatometry and MEV.

## Resumo/Abstract

Porous ceramics are technologically great applicability materials, their characteristics and properties as mechanical resistance, low density and thermal conductivity, high surface areas make them attractive for use as filter media, catalytic support, thermal and acoustic insulation[1-3]. Its obtainment is by the conventional method of the PU polymeric sponge coated with ceramic suspension, posteriorly drought, calcined and sintered[4]. This method allows obtaining micrometric pores, with structure interconnected and identical to the substrate[4]. In this work, a porous ceramic based on phlogopite was obtained using the replica method. The methodology used in the production of the ceramic suspension (pH = 9) was: 25.0 g phlogopite, 1.0 mL NaSiO3 and 40.0 mL distilled water, a ball mill with a speed 600 rpm/24h. The sponge was measured and dipped to the ceramic suspension, the excess removed and dried at 25ºC. The samples were treated thermally at 400°C/1h, then calcined at 900°C and sintered at 1300°C/2h. The TG/DTG analysis, maximum mass loss occurred at 500ºC, by dilatometry, maximum sintering temperature occurred at 1200ºC and by MEV, the pores presented hexagonal and uniform geometries with 500µm. The obtained porous ceramic had good mechanical resistance and interconnected pores, regular and large.

References:
[1]Romano, R. C. O.; Pandolfelli, V. C. Cerâmica. 2006, 52, 213.
[2]Sifontes, A. B. et al. J. Mater. Sci. 2009, 44, 4507.
[3]Falk, G. S. et al. Cerâmica. 2014, 60, 102.
[4]Sharif, S. M. et al. Int. J. Sci. Technol. Res. 2013, 2, 283.

Acknowledgement: UNIFEI, CAPES, PPGMQ, Limav.

**Área: MAT**
*(Inserir a sigla da seção científica para qual o resumo será submetido. Ex: ORG, BEA, CAT)*

**Inscrição: 00514**
*(Inserir o número de inscrição do autor que fez a submissão)*

# Influence of different fuels in the combustion synthesis of copper vanadate and its application in photocatalysis

**Luan P. Camargo (IC),[1] Adriana C. Lucilha (PQ),[1] Luiz H. Dall'Antonia (PQ).[1*]**
**luanpcamargo@gmail.com; luizh@uel.br**

[1]*Departamento de Química, UEL*

Palavras Chave: *$Cu_2V_2O_7$, Citric Acid, Glycine, Urea, Discoloration, Methylene Blue.*

## Highlights

Citric acid, glycine and urea used as fuel in the combustion synthesis of copper vanadate.
Methylene Blue photocatalytic decolloration under visible light.

## Resumo/Abstract

Copper vanadate Nanoparticles were produced by combustion synthesis using different fuels: citric acid, glycine and urea. The nanoparticles were characterized by X-ray diffraction, which indicated that the phase of greatest abundance was the α-$Cu_2V_2O_7$, whereas the β-$Cu_2V_2O_7$ 7 phase was also obtained, however in a small amount. This mix of phase can be due the variation in the flame temperature during the synthesis process[1,2]. By thermogravimetry analysis it was possible to verify that the formation process for samples synthesized with citric acid and glycine occurred in two events, whereas for urea three events were observed. By the diffuse reflectance analysis, it was possible to verify that the synthesized materials have band gap energy values between 2.12 and 2.15 eV (Fig. 1), which includes absorption in the region of visible light. The surface area of the synthesized compounds were evaluated via adsorption BET isotherm, with values of 4.822; 3.539 and 4.207 $m^2/g$ for citric acid, glycine and urea, respectively. The results of the discoloration of a solution of methylene blue were simulated as a pseudo second order reaction and the highest value of reaction constant was found for the copper vanadate synthesized using citric acid as fuel. This result indicates that the higher value of the surface area may be the preeminent factor for a greater discoloration rate constant.

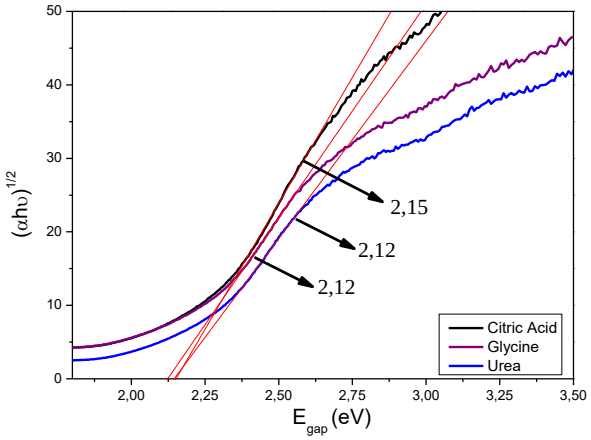


**Figure 1** - Diffuse reflectance specta for copper vanadate samples synthesized with citric acid, glycine and urea.

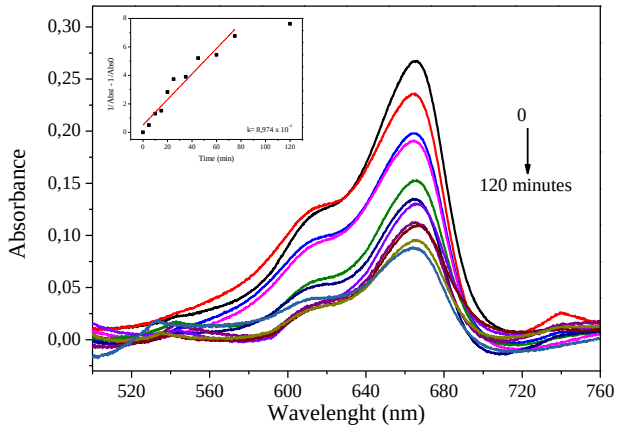


**Figure 2** - Absorption spectra for methylene blue discoloration under visible light irradiation, in the presence of the semiconductor obtained by the citric acid fuel.

[1]SIVAKUMAR, V. et al. *J. Mater. Sci. Mater. Electron*. **2014**, 25, 1485-1491
[2]PALACIO, Luz Amparo et al. *Catalysis Today*. **2008**, 133-135, 502-508.

**Área: MAT** **Inscrição: 00321**

# Synthesis of Nickel Molybdates – a comparative study of co-precipitation and sol-gel method

**Maíra V. Da Silva (PG),[1*] Kisla P. F. Siqueira (PQ)[1]**

**mairaufop@hotmail.com**

[1]*Laboratório de materiais cerâmicos, ICEB II nº 65, Departamento de Química, UFOP – Campos Morro do cruzeiro, MG*

Palavras Chave: Nickel molybdate, Sol-gel method, Edible gelatin, X-ray diffraction.

## Highlights

Synthesis of Nickel Molybdate using the sol-gel protein method has been proposed for the first time and edible gelatin was used;
Co-precipitation method was used for comparison purpose.

## Resumo/Abstract

Inorganic compounds of the class of metallic molybdates are of great scientific importance due to their diverse properties.Nickel molybdate is a luminescent material with large applications such as electronic and dielectric devices. It has already been produced by several synthetic routes, however the synthesis using the sol-gel protein method has been proposed by the first time by our group, in order to investigate the feasibility of the method and its implications on the final properties of the products. It is known that the synthesis methodology directly affects the properties of the product. Thus, in this work it was used co-precipitation and sol-gel methods using edible gelatin in the last. The parameters time, pH, temperature and reaction rate were adjusted for each synthesis. Furthermore, a thermal study was performed in order to obtain polymorphic forms of the material with have specific colors. It were observed a change in coloration from green to yellow when occurred the transition from β to α phases. Firstly, the products were characterized by the X-ray diffraction. The results were indexed by ICDD cards. Thermogravimetric analyzes, Raman spectroscopy and UV-vis absorption were performed in order to contribute to the interpretation of phase transitions and properties of the products obtained by the two methods.

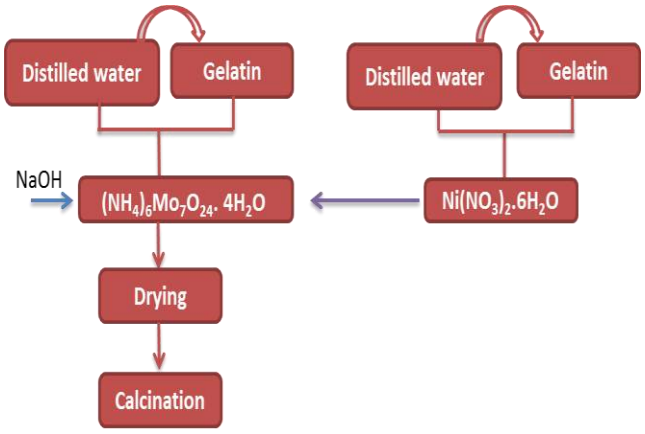


Figure: Sol-gel method synthesis.

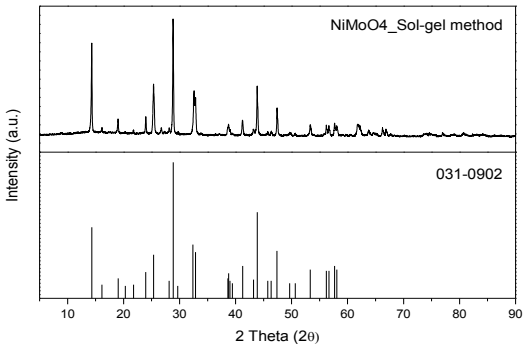


Figure: XRD pattern.

References:

[1] Ghazal Kianpour, et.al; J. Mater Sci: Mater Electron, (2016);
[2] José A. Rodriguez, et.al; J. Phys. Chem. B 1998, 102, 1347-1355.

Acknowledgment: FAPEMIG, CNPq, UFOP.

**Área: MAT** **Inscrição: 00200**

# Structure determination of NVP-AS co-crystal at different temperatures

**Rogeria Nunes Costa (PG),[1*] Sana Siedler (PG),[2] Simone G. Cardoso (PQ),[2] Yamila G. Linck (PQ),[3] Lucía Reviglio (PG),[3] Gustavo A. Monti (PQ),[3] Alexandre M. G. Carvalho (PQ),[4] Jackson A. L. C. Resende (PQ),[5] Helvécio V. A. Rocha (PQ),[6] Silvia Lucia Cuffini (PQ).[1]**

**rogeria.ncosta@gmail.com**

*[1]Institute of Science and Technology, UNIFESP – Brazil; [2]Center of Healthy Sciences, UFSC – Brazil; [3]Faculty of Mathematics, Astronomy, Physics and Computing, UNC – Argentina; [4]Brazilian Synchrotron Light Laboratory, CNPEM – Brazil; [5]Institute of Exact and Earth Sciences, UFMT – Brazil; [6]LaSiFA, FIOCRUZ – Brazil.*

Palavras Chave: *Nevirapine, Salicylic acid, Co-crystals, X-Ray diffraction, Structure determination.*

## Highlights

Co-crystallization as strategy to improve drug properties. Preparation and solid-state characterization of nevirapine co-crystals. Structural organization of a co-crystal in different temperatures.

## Resumo/Abstract

Co-crystallization is a strategy frequently used in pharmaceutical area to improve drug properties.[1,2] Nevirapine (NVP) is an antiretroviral drug that presents low solubility, which implies in low bioavailability and difficulties in formulation process. Based on this, different strategies are applied to obtain co-crystals of NVP. A pharmaceutical co-crystal is a crystalline structure formed between an active pharmaceutical ingredient (API) and another molecule pharmaceutically acceptable. The crystalline structure of NVP-salicylic acid (NVP-SA) had already been reported in the literature at low temperature.[3] This co-crystal was obtained by our group and differences were observed in the crystalline phases at room and low temperature (figures 1 and 2). X-Ray diffraction (XRD) experiments using synchrotron radiation source (XRD1 - LNLS)[4] (figure 3), thermal analysis and solid-state Nuclear Magnetic Resonance (ss-NMR) were used to characterize these materials. A study was conducted in order to determine the structures and identify the behavior of this co-crystal from room temperature to 100K. At room temperature, SA molecule is located on an inversion center, which allows describe two positions of this molecule in occupational disorder. However, when cooling is carried out, the molecule is stabilized in one position, inducing the loss of the symmetry center located in the SA molecule. This allows to describe the phase transition in the co-crystal.

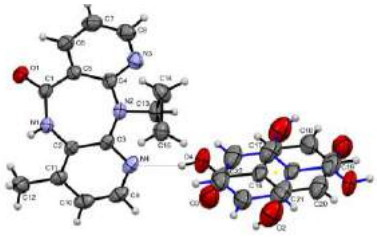

Figure 1. Representation of co-crystal asymmetric unit at room temperature (thermal ellipsoids at 50% probability level)

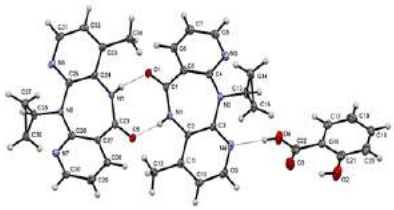

Figure 2. Representation of the co-crystal asymmetric unit at 100K (thermal ellipsoids at 50% probability level)

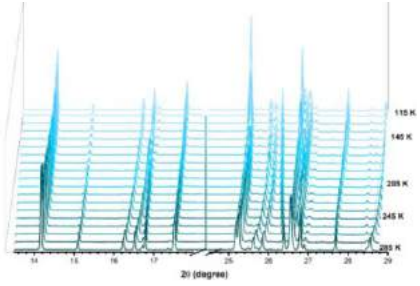

**Figure 3.** XRD pattern depending on temperature.

1. Shan, N. *et al. Expert Opin. Drug Metab. Toxicol.* **10,** (2014).
2. Domingos, S. *et al. J. Pharm. Pharmacol.* **67,** 830–846 (2015).
3. Caira, M. R. *et al. CrystEngComm* **14,** 2541–2551 (2012).
4. Carvalho, A. M. G. *et al. J. Synchrotron Radiat.* **23,** 1501–1506 (2016).

**Área: MAT** **Inscrição:00245**

# Coating of organosilicon thin films protecting polypropylene against photodegradation

**Amanda S.M. Freitas (PG),[1] Felipe O. Fernandes (IC),[2] Elidiane C. Rangel (PQ),[2] Nilson C. Cruz (PQ),[2] Adriana O. Delgado-Silva (PQ),[1] Walter R. Waldman (PQ).[1]***

**walter.waldman@gmail.com**

*[1]Departament of Physics, Chemistry and Mathematics, UFSCar; [2]Technological Plasmas Laboratory, UNESP*

Keywords: *photodegradation, polypropylene, plasma, organosilicon, coating.*

## Highlights

Organosilicons thin films protected polypropylene films against photodegradation, showing a decisive role in the evolution of the surface cracking and up to 55% fewer carbonyls than the control samples.

## Abstract

Photodegradation of polymers limits the options for its use outdoor and reduces its useful life. Deposition of thin films of organosilicon by plasma on polymers can increase their resistance to photodegradation without interfering in aspects such as color and brightness due to the transparency and nanometric dimension of these films. Polypropylene (PP) films were pre-treated with oxygen plasma (5 minutes - $7{,}5.10^{-2}$ Torr - 50W), and treated with a plasma of 1:1 oxygen and hexamethyldisiloxane (15, 30, 45, 60 minutes - $2{,}3.10^{-2}$ Torr - 80 W) (Seufitellis, 2015). Homogeneous and continuous films were obtained, with a thickness between 50 and 550 nm and roughness between 26 and 52 nm. Scanning Electron Microscopy was used to follow the surface cracking as a function of photodegradation time (Figure 1). After 196 hours of UV-C photodegradation we had mainly two findings: 1) PP samples without coating showed less, but deeper and broader crackings than the PP coated with organosilicon thin films, and 2) In all coated samples the crackings followed the same pattern of deposition. Despite the visual modification of the coating after 196 hours of UV-C photodegradation, there was no observable detachment of the coatings from the PP substrate. These findings showed a role of the organosilicon thin film in the evolution of cracking as a function of photodegradation time. Additionally, we have observed, using FTIR, lower carbonyl and vinyl formation for the coated samples than the found for the PP without coating.

| After 196 hours of UV-C | | | |
|---|---|---|---|
| PP (control) | | PP coated with organosilicon thin film | |
| 2,000x | 20,000x | 2,000x | 20,000x |
| 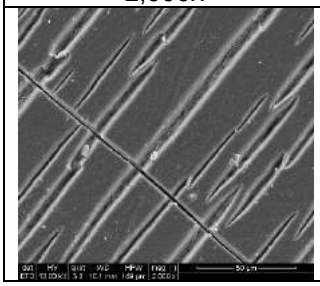 | 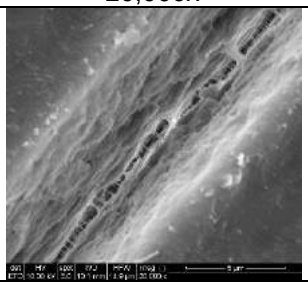 | 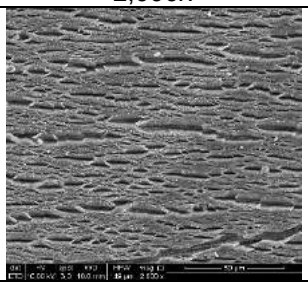 | 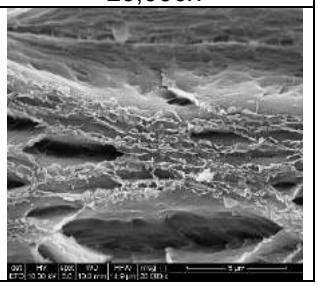 |

Figure 1: Micrographs of PP without and with organosilicon thin films after 196 hours of UV-C photodegradation. Coated samples showed in this figure were obtained after 60 minutes of plasma deposition.

## References

Monique Seufitellis Curcio. Fotocatalisadores de $TiO_2$ sol gel suportados em polipropileno com filme de organossilicone depositado por plasma: fotoestabilidade e remediação de formaldeído em fase gasosa. 2015. Tese de Doutorado em Ciências Naturais - UENF. Orientador: Maria Cristina Canela.

**Área: MAT**
*(Inserir a sigla da seção científica para qual o resumo será submetido. Ex: ORG, BEA, CAT)*

**Inscrição:__00050___**
*(Inserir o número de inscrição do autor que fez a submissão)*

# Incorporation of carbon SWNT in polymer blends based on Nylon 66 and Silk Fibroin for application in engineering materials.

**Luciano Moura de Souza (PG),[1]Fernando ReinoldoScremin (PQ),[1]Paulo Rodrigo Stivall Bittencourt (PQ)[1]**

**lucianomourasouza@gmail.com; paulob@utfpr.edu.br**

*[1]Departamento Acadêmico de Química, Universidade Tecnológica Federal do Paraná - Medianeira*

Palavras Chave: Young modulus, Texturometer, Bombix mori, Carbon Nanotube.

## Highlights

Polymer blends Nylon 66/silk (Bombix mori) fibroin is possible due to their solubility in formic acid. The incorporation of SWNT occurred due to their suspension in solution, resulting improvements in the mechanical properties.

## Resumo/Abstract

Silk Fibroin (SF) and nylon (Ny) could be good candidates to modify each other, because SF's similar chemical structure with Ny, may lead to a possible miscibility between the components, and there is a chance that the molecular chain of SF and nylon might mutually aggregate to form a new ordered structure, which may then change the crystallization behavior or even improve the properties of SF. In this case the use of SWNT can improve the product properties.(Liu *et al.*, 2004)

This work presents a methodology for the incorporation of SWNT aiming at the improvement of the mechanical properties. SF and Ny were dissolved in formic acid solution and a SWNT suspension was added in defined compositions resulting in a solution with high stability.

The polymer films were obtained by casting method and analyzed by texturometer. The results obtained for Ny66:SF blends with SWNT can be observed in table 1:

Table 1: Tensile properties of Ny66:SF blends with SWCNT with different contents

| Tensile Properties | | | | | | | | | |
|---|---|---|---|---|---|---|---|---|---|
| Composition | 40:60 (%) | | | 50:50 (%) | | | 60:40 (%) | | |
| SWNT / Ny66:SF | *a | *b | *c | *a | *b | *c | *a | *b | *c |
| 0,00% | 4,00 | 3,40 | 1,24 | 3,61 | 3,06 | 1,11 | 6,32 | 3,57 | 2,50 |
| 0,25% | 3,28 | 3,10 | 0,76 | 3,59 | 4,57 | 0,77 | 6,30 | 2,11 | 1,92 |
| 0,50% | 2,64 | 3,64 | 0,64 | 3,09 | 4,18 | 0,70 | 8,59 | 3,92 | 2,31 |
| 1,00% | 4,78 | 3,00 | 1,17 | 3,47 | 2,74 | 1,12 | 4,45 | 2,11 | 2,00 |

*a - Tensile Strengh / MPa *b - Elastic Modulus / MPa *c- Elongation at Break / %

It is observed that the higher Ny content in the blends improves the mechanical properties as observed in the results of the tests without the SWNT. The presence of SWNT tends to improve the properties of the material when the Ny content is high and does not affect significantly in the other compositions this fact can be related due the greater interaction between SWNT and Nylon 66.

Liu, Y., Shao, Z., Zhou, P. & Chen, X. (2004). Thermal and crystalline behaviour of silk fiborin/nylon 66 blend films. *Polymer*, **45**, 7705–7710.

**Área: MAT** **Inscrição: 00097**

# Spray-dried materials components ratio evaluation by TGA

**Débora França (PG),[1,2*] Roselena Faez (PQ).[1]**

**deboraf@usp.br**

*[1]Departamento de Ciências da Natureza, Matemática e Educação (DCNME), UFSCar; [2]Programa de pós-graduação em Engenharia e Ciência de Materiais, USP*

Palavras Chave: Characterization, Spray Dryer, CRF, Chitosan, Fertilizer.

## Highlights

Spray drying process to obtain controlled release fertilizer. Alternative use of TGA to determine the real component ratio in the sample.

## Resumo/Abstract

Controlled release fertilizers based on chitosan (Ch), TPP, $KNO_3$, and MMt have been prepared by Spray Dryer with different atomizer nozzles (2FN and 3FN)[1]. However, one of the disadvantages of spray drying technique is the loss of material adhered on glass wall of drying chamber affecting the initial ratio formulation. TGA was suggested to determine the real content of Ch, nutrient and clay. TG curves of pure components were separately analyzed and interpreted to obtain the values of the $KNO_3$ in each sample. After, they were compared to the results from spectroscopic techniques. DSC, FTIR and DRX were performed to evaluate the interactions among all components. These analyses supported the formation of (i) $NaNO_3$ from the exchange cations into the MMt layers (DRX:2θ = 29.46º and 41.01º); (ii) chitosan salts from interactions between amine groups and free nitrates from $KNO_3$ (DRX:2θ = 27°, DSC exothermic peak around 300°C). $KNO_3$ content in the samples obtained by 2FN was close to those of theoretical, but it was larger for 3FN materials. Also, the TGA confirm that the samples sprayed by 3FN have higher Ch and lower $KNO_3$ content than those prepared by 2FN, due to the extra layer of Ch (shell). All results were corroborated by the values obtained from Flame Photometry measurements (not shown). TGA was very useful to determine the real content of the spray-dried materials since the ratio composition was altered during the process.

Figure 1. TGA curves used to determine the amount of KNO3 in each CFR material

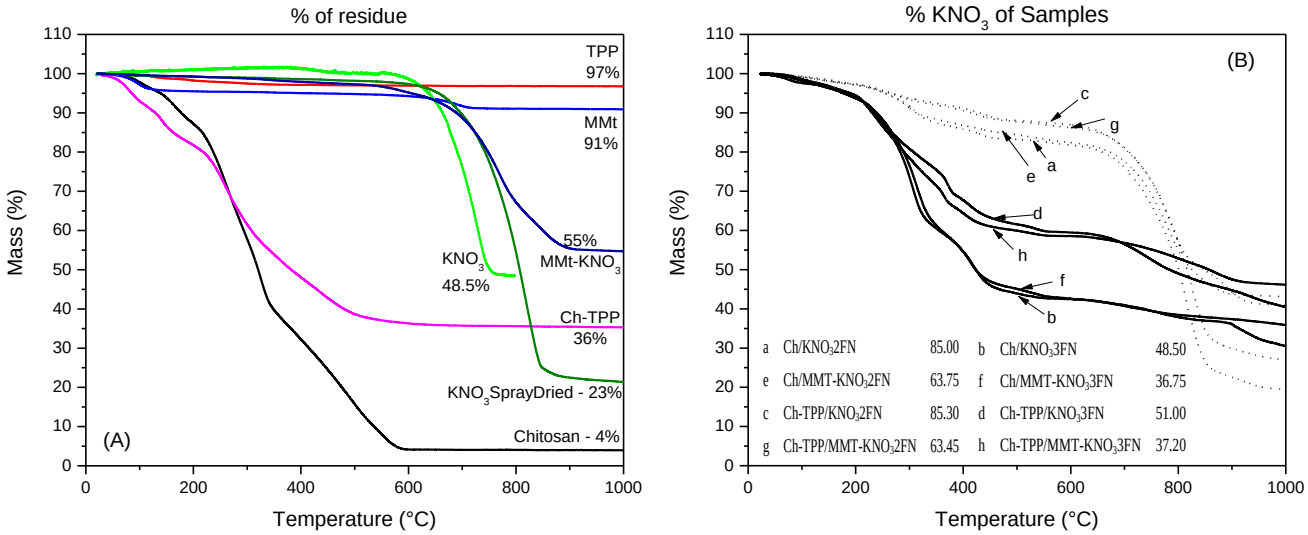


**Reference**

[1]França, D. (2017). *Estruturas biopoliméricas fertiliberadoras obtidas pela técnica de secagem por atomização (spray drying)*. Master's Dissertation, Faculdade de Zootecnia e Engenharia de Alimentos, University of São Paulo, Pirassununga. Retrieved 2018-01-16, from http://www.teses.usp.br/teses/disponiveis/74/74133/tde-22112017-102140/

**Área_____MAT_____ Inscrição:____0060_____**

# Synthesis of Donor-Acceptor (D-A) Hybrids Based on Functionalized Thiophene-imides for High Fluorescent Material Development

**Marina de Ávila Costa (PG),[1]* Claudio LuisDonnici (PQ) [1]**

**marinaac@ufmg.br**

[1] ***LABSTOP*** *– LABoratory of Synthesis&Tailoring of Optoelectrochemical molecular devices - Departamento de Química - ICEX, Universidade Federal de Minas Gerais – BH – MG*

Key Words: *Fluorescence, Charge-Transfer, Donor-acceptor systems ,thiophene-imide*

## Highlights

Design and development of highly fluorescent novel hybrid materials through the junction of Donor-Acceptor units obtained via an easy functionalization in thiophene-imide moiety

## Resumo/Abstract

Nowadays, high efficient and low cost organic fluorescent semiconductor materials are extremely important for the development of new technological photoelectronic devices. These materials have been obtained from hybrid systems containing two sub-units: one with higher electronic density (electron donor (**D**)), and another one with lower electronic density (electron acceptor (**A**)).[1-3] These **D**onor-**A**cceptor (**D-A**) or ambipolar systems with high conjugation increases the quantum efficiency. This work presents the synthesis and the study of photophysical properties of novel **D-A** hybrids: N-aryl-thiophenoimides **1** and **2** (Figure 1) formed by thiophene-dicarboxy (**A**) and two fluorescent amino units (**D**). Derivatives **1** and **2** were obtained (80% yield) by imide condensation reactions between the 3,4-dicarboxythiophene anhydride and the corresponding amines. The conjugation and the occurrence of locally excited state (LE) and/or inter-chain charge-transfer state (CT) were investigated by UV-Visible, photoluminescence spectroscopy (PL), and solvatochromic experiments applied to the final hybrid and the initial sub-units. **1** and **2** show strong light emissions at 540 and 570 nm and, in fact, these hybrids exhibited usual redshift values in UV absorption (≅ 21-30 nm) in comparison to the corresponding precursors. However, much higher redshitf values were obtained in PL emission (≅ 180-210 nm), since generally the measured values are lower than 100 nm[3]. These novel thiopheneimide hybrids seem to be promising materials as novel luminescent materials.

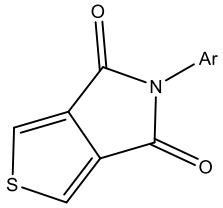


**1** - Ar = 2-aminofluorene
**2** - Ar = 2-aminodibenzofuran

**Figure 1** – Chemical structures of N-aryl-thiopheneimides **1** and **2** investigated in this work

**ACKNOWLEDGMENTS:CNPQ,FAPEMIG(CEX-PPM 0281-17)**

1- Li, W.,*et al. Top Curr Chem*,**2016**,*374*,1
2- Cheng XB, *et al*.*Tetrahedron*,**2012**,*68,*5375.
3- Li, W. J.; et, al.*Adv. Funct. Mater*.**2014**,*24*,1609.

**Área: _MAT_** **Inscrição: _00018_____**

# Study of the adsorption of tannic acid by clay modified with polyethylenimine

**[1]Ruan R. Henriques (PG), [2]Gustavo G. Celestino (IC),[2] Ana L. Shiguihara (PQ), [3] Vera R. L. Constantino (PQ), [1] Bluma G. Soares(PQ), [2] Jorge Amin Jr. (PQ)**
**ruanhenriara@gmail.com; jorgejunior@macae.ufrj.br**

*[1]Instituto de Macromoléculas, UFRJ; [2] Universidade Federal do Rio de Janeiro-Campus Macaé, [3]Instituto de Química-USP, São Paulo.*

Palavras Chave: *Ácido tânico, Argila, Polietilenimina.*

## Highlights

Study of the adsorption of tannic acid by clay modified with polyethyleneimine. Montmorrilonite was modified with different amounts of polyethylenimine. The adsorption process of tannic acid on montmorrilonite modified with polyetheylenimine was investigated.

## Resumo/Abstract

A produção de substratos alternativos para o processo de adsorção é de grande interesse tecnológico, pois podem ser empregados nos processos de tratamento de efluentes industriais. Dentre as possibilidades de adsorventes têm-se os argilominerais, entretanto, estes adsorventes apresentam limitações para adsorção de espécies neutras ou carregadas negativamente. Portanto, o objetivo desse trabalho foi modificar a argila montmorilonita (MMT) com diferentes quantidades de polietilenoimina (PEI), 0,1 e 0,4% (m/m), e estudar o processo de adsorção do ácido tânico (AT) sobre estes novos materiais. A argila MMT e a argila modificada com o PEI foram caracterizadas por espectroscopia no infravermelho (FTIR), difratometria de raios X e análise termogravimétrica (TGA). A quantidade de AT adsorvido foi determinada por espectrofotometria UV-Vis. O espectro FTIR das argilas preparadas com 0,1 e 0,4% (m/m), nomeadas como MMTPEI1 e MMTPEI4, apresentaram bandas em 2931, 2839 e 1312 $cm^{-1}$ que são atribuídas aos grupos $CH_3$, $CH_2$ e CN do PEI, indicando a sua incorporação na MMT. Os difratogramas de MMTPEI1 e MMTPEI4 mostraram que o PEI está revestindo a MMT. As curvas TGA mostraram que houve uma incorporação de 9,7 e 18,5 % de PEI nas argilas MMTPEI1 e MMTPEI4, respectivamente. A Figura 1 mostra que a maior quantidade de AT adsorvido ocorreu para a argila MMTPEI4, alcançando um patamar máximo de adsorção em 562 $mg.g^{-1}$ a 25°C. Os resultados experimentais mostram que a MMT modificada com o PEI tem um grande potencial na adsorção de ácido tânico.

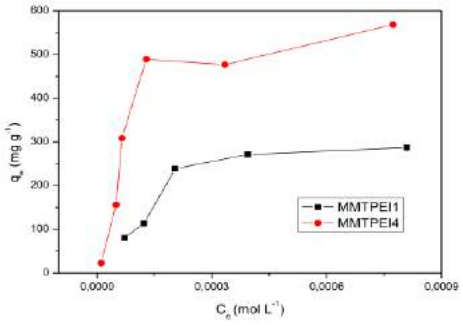


Figura 1: Isotermas de adsorção do ácido tânico sobre MMTPEI1 e MMTPEI4 a 25°C em pH 4.

**Área: MAT** **Inscrição: 00247**

# Kinetics of adsorption of methylene blue dye in mesoporous silica encapsulated magnetite nanoparticles

**Ricardo M. A. Silva (IC),[1] Lucas S. Rodrigues (IC),[1] João A. D. Silva (PQ).[1]***

rmontserrat98@gmail.com; jdsilva@iff.edu.br

[1]*IFFluminense, campus Cabo Frio*

Key words: *mesoporous sílica, magnetite, sorption*

## Highlights

Kinetics of adsorption of methylene blue dye in mesoporous silica encapsulated magnetite nanoparticles. High initial adsorption rate. High kinetics rate constant.

## Resumo/Abstract

O descarte inadequado de insumos químicos pode provocar danos ambientais além de ser economicamente contraproducente. O presente trabalho visa o desenvolvimento de sílica mesoporosa nucleada com magnetita para recuperação de insumos químicos de interesse em leitos aquáticos e posterior dessorção do insumo para reaproveitamento industrial. Para tal, primeiramente produziu-se magnetita por reação de co-condensação entre os íons de $Fe^{2+}$ e $Fe^{3+}$. Em seguida, revestiu-se as nanopartículas de magnetita com sílica mesoporosa (surfactante CTAB). A sílica produzida foi empregada como adsorvente da molécula modelo azul de metileno (AM) em soluções aquosas.

A quantidade de AM remanescente em solução foi quantificada através de espectrofotometria na região do UV-Vis (Figura 1).

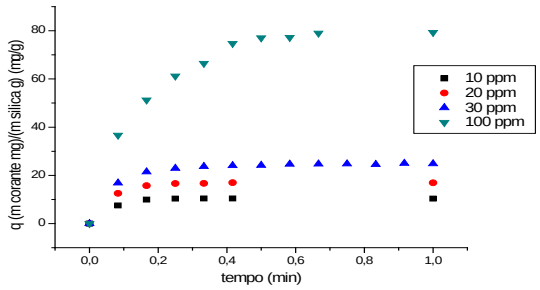


Figura 1: Dados experimentais da cinética de adsorção do AM na sílica produzida.

Os dados obtidos foram modelados obtendo como melhor resultado o mecanismo de adsorção de pseudossegunda ordem (equação abaixo) como apresentado na Figura 2.

$$\frac{t}{q} = \frac{1}{k_2 q_e^2} + \frac{t}{q_e}$$

$$h = k q_e^2$$

- h = velocidade inicial de adsorção)

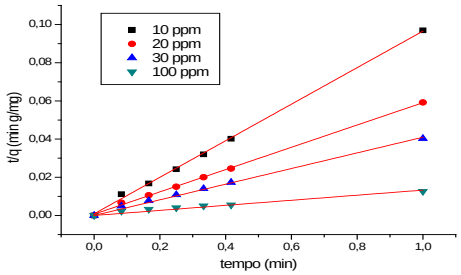


Figura 2: Modelagem de pseudossegunda ordem dos dados de adsorção.

A partir da modelagem das curvas pôde-se determinar os seguintes parâmetros cinéticos:

Tabela 1: Parâmetros cinéticos obtidos a partir da modelagem

| Conc. (ppm) | $R^2$ | $K_2$ (g/ mg min) | $q_{e\ calc.}$ (mg/g) | h **(mg/g min)** |
|---|---|---|---|---|
| **10** | 0,9985 | 10,792 | 10,45 | 1178 |
| **20** | 0,9989 | 5,061 | 17,13 | 1485 |
| **30** | 0,9990 | 1,627 | 25,47 | 1055 |
| **100** | 0,9838 | 0,157 | 85,80 | 1152 |

A sílica produzida apresentou um elevado valor da velocidade inicial de adsorção (1217,5 mg/g min) quando comparada a outros trabalhos semelhantes[1] assim como elevada constante de velocidade ($k_2$) e pequeno tempo para atingir o equilíbrio[2]. Acredita-se que ocorra um efeito sinérgico entre a sílica e magnetita no processo de adsorção. Dessa forma, O sistema apresenta grande aplicabilidade industrial devido à alta velocidade inicial e capacidade de adsorção. Além disso, a dessorção do corante foi testada na presença de etanol apresentando bons resultados.

Agradecimentos: CNPq, IFF-Campus Cabo Frio.

[1] Gurses, A.; Doğar, Ç.; Yalçın, M.; Açıkyıldız, M.; Bayrak R.; Karaca, S.; *J. Hazard. Mater.* **2006**, *131*, 217-228.

[2] Fisli, A.; Syusuf S.; Ridwan; Krisnandi, Y. K.; Gunlazuardi J.; *Adv. Mater. Res. (Durnten-Zurich, Switz.)*, **2014**, *896,* 525-531.

**Área:** MAT **Inscrição: 00226**

# Nanogold on porous glass as a passive sampler for monitoring of gaseous elemental mercury in artisanal gold mining

**Elias B. Santos (PQ),[1] Paleah Moher (PQ),[2] Stacy Ferlin (IC)[3], Anne Helene Fostier (PQ),[3] Italo O. Mazali (PQ),[3] Kevin Telmer (PQ),[2] Alexandre G. Brolo (PQ),[2]**

**santos.barros@unifesp.br**

*[1]Instituto de Ciência e Tecnologia, UNIFESP; [2]University of Victoria, UVic, Canadá; [3]Instituto de Química, UNICAMP.*

Palavras Chave: *Ouro nanométrico, Vidro poroso, Amostrador passivo, Mercúrio gasoso, ASGM.*

## Highlights

A portable passive sampler for monitoring of gaseous elemental mercury (GEM) exposure in artisanal and Small-scale gold mining (ASGM) is introduced. The sampler was prepared via direct reduction of gold into porous Vycor glass (PVG) discs (PVG/Au). The material was characterized by transmission electron microscopy and UV-vis spectroscopy, which allowed confirming the formation of nanogold. Laboratory experiments showed the viability of using PVG/Au as passive sampler for monitoring of $Hg^0$. PVG/Au samplers were deployed in an ASGM area ant it was able to indicate personal mercury exposure. This complete work was recently published in the journal Scientific Reports – Nature.

## Resumo/Abstract

Mercury contamination is a major workplace hazard in artisanal gold mines in developing Countries, particularly in Africa, Asia and South America. There are no portable and cheap methods able to alert workers of mercury exposure *on site* in remote locations. In this work, a miniaturized mercury sampler prepared by the direct reduction of gold into the porous nanostructures of Vycor® glass is introduced. Mercury retention on the PVG/Au sampler induces significant color changes, due to the formation of Au-Hg amalgam that affects the surface plasmon resonance characteristics of the material. The color change can potentially be quantified by the analysis of pictures obtained with a cell phone camera. Laboratory experiments showed the viability of using PVG/Au as passive sampler for monitoring of $Hg^0$. PVG/Au samplers were then deployed in an artisanal and small-scale gold mining area in Burkina Faso, Africa, and it was able to indicate personal mercury exposure. The amount of mercury quantified in the samplers for all miners was higher than the current personal exposure limit set by the US Occupational Safety & Health Administration (OSHA). The colorimetric analysis (RGB histograms of the images) of the sampler before and after exposure to $Hg^0$ indicates the presence of GEM in the environment (Figure 1). Figure 2 shows the PVG/Au samplers before and after the field test. The color change is related to the amounts of mercury in the sampler, indicating high exposure of the miners to GEM.

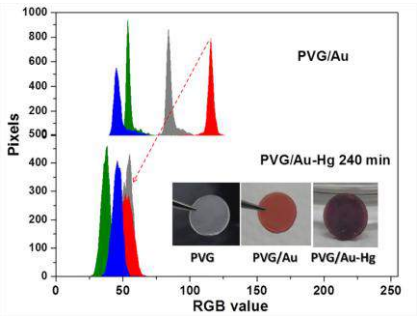


**Figure 1.** From left to right: PVG disc (colorless), PVG/Au disc (red), and PVG/Au after exposure to $Hg^0$ vapor.

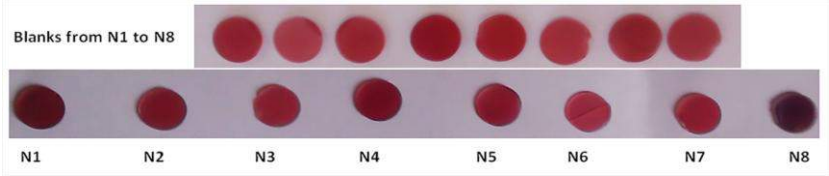


**Figure 2.** PVG/Au samplers before and after their application in the ASGM during the burning of Au-Hg amalgam.

**Área: MAT** **Inscrição:00666**

# *Novel Conducting, Biocompatible and Biodegradable Copolymer PEDOT-co-PLLA for Biomedical Applications*

**Aruã C. da Silva (PG)[1], Ana T. S. Semeano(PG)[1], Alexander H. Ulrich (PQ)[1], Michael J. Higgins (PQ)[2] Susana I. Cordoba de Torresi (PQ)[1]**
**aruacs@iq.usp.br; storresi@iq.usp.br**

*[1] Universidade de São Paulo, Instituto de Química, Av. Prof. Lineu Prestes, 748 –São Paulo – SP – Brazil*
*[2]University of Wollongong, Intelligent Polymer Research Institute, Innovation Campus, Squires Way, NSW 2522, Australia*

Palavras Chave:*Conducting, Biodegradable, Biomaterial, Tissue Engineering, Regenerative Medicine.*

## Highlights

- ✓ Novel Conducting and Biodegradable copolymer based on PEDOT-*co*-PDLLA;
- ✓ Atomic Force Microscopy applied to understand interaction between Fibronectin and Biomaterial surface, as KPFM, C-AFM and Force Spectrocopy Mapping;
- ✓ Biocompatible with Embryonic Stem Cells with excellent growth and differentiation for Neural Cells;

## Abstract

Electroactive biomaterials are a new generation of “smart” biomaterials based on conducting polymers. Poor molecular interaction with cells is the main challenge to face for the use of conducting polymers as biomaterials, even though that their biocompatibility can be highly improved by doping with specific anions but, despite this, electroactive polymers still present low or none biodegradability.

The challenges for developing biomaterials for active scaffolds by electrical stimulation are: (1) the difficulty of working with conducting polymers which can only be obtained over electrodes by electrochemical synthesis; (2) to achieve surface chemistry which enables surface charge keeping biocompatibility for living cells culture and (3) poor compatibility between conducting and biodegradable polymers. Here we developed the synthesis of a novel electroactive, biodegradable and biocompatible copolymer (PEDOT-*co*-PDLLA) in different proportions of PEDOT:PDLLA (1:5; 1:25 and 1:50) which joins the properties of both homopolymers in a single biomaterial. Furthermore, we characterized/studied its surface properties as work function, charge/current distribution and surface chemistry by using Conductive Atomic Force Microscopy and Force Spectroscopy with an AFM-tip functionalized with Fibronectin as model protein. Additionally, the biocompatibility of PEDOT-*co*-PDLLA was investigated with Embryonic Stem Cells, showing an excellent growth and differentiation for Neural Cells with better results for PEDOT-*co*-PDLLA 1:50 in good agreement with AFM studies.

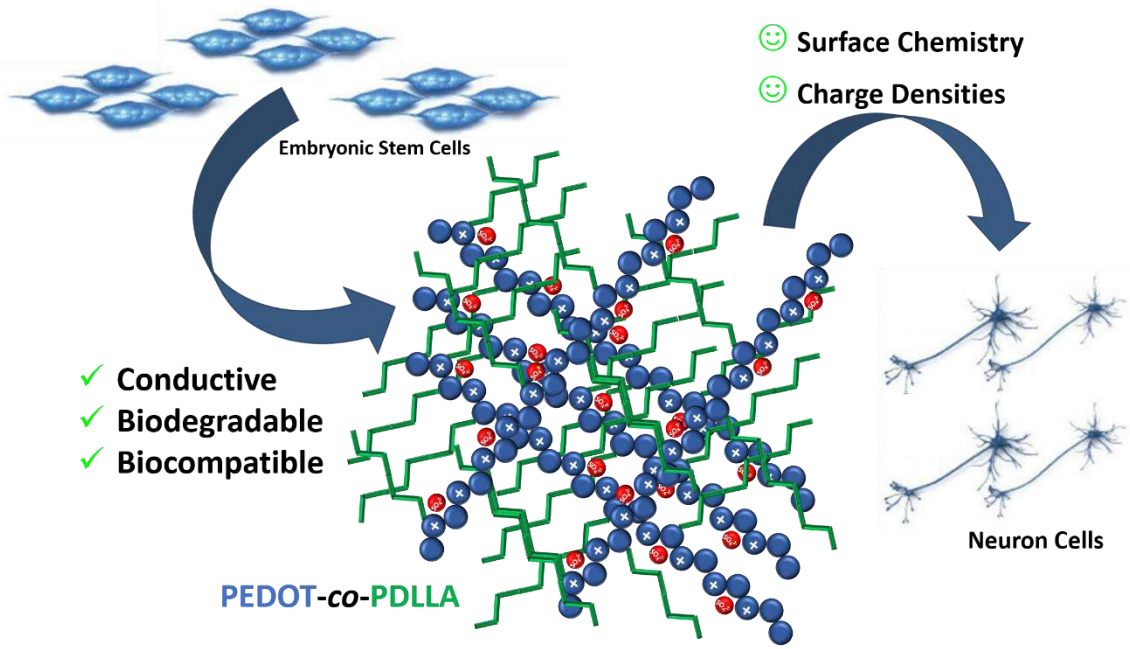

**Área: MAT** **Inscrição: 00448**

# Polythiophene/Au and polythiophene/Au/CNTs nanocomposite thin films to organic solar cell application

**Camila S. Inagaki (PG)[1], Marcela M. Oliveira (PQ)[2], Lucas F. Lima (PG)[3], Matheus F. F. Neves (PG)[3], Lucimara S. Roman (PQ)[3], Aldo J. G. Zarbin (PQ)[1*]**

**camila.suemi@gmail.com; aldozarbin@ufpr.br**

*[1]Department of Chemistry, Federal University of Paraná (UFPR), Centro Politécnico, CP 19081, CEP 81531-990, Curitiba, PR, Brazil; [2]Department of Chemistry and Biology, Federal Technological University of Paraná (UTFPR), Curitiba, PR, Brazil; [3]Department of Physics, Federal University of Paraná (UFPR), Centro Politécnico, CP19044, CEP 81531-990, Curitiba, PR, Brazil.*

Keywords: *Polythiophene, gold nanoparticles, carbon nanotube, thin film, photovoltaic devices*

## Highlights

Gold nanoparticles homogeneously dispersed in the polythiophene thin film were obtained, with size of ≈3 nm. Photovoltaic devices based on annealed films showed an efficiency of 0,8%.

## Resumo/Abstract

This work shows a facile one-pot synthesis and processing as thin film of a nanocomposite of polythiophene (PT)/gold nanoparticles (AuNPs) and PT/AuNPs/carbon nanotubes (CNTs), using the liquid-liquid interfacial polymerization method.[1,2] This method consists in a redox reaction between the thiophene (reducing agent) solubilized in n-hexane and a $HAuCl_4$ (oxidant) aqueous solution, in which both the PT and AuNPs are formed simultaneously, yielding a self-assembled thin film at the liquid-liquid interface.[3] In the nanocomposite with CNTs, a dispersion of CNT in n-hexane is added in the system. Several films were obtained varying both the reaction time and the amount of thiophene, which were easily deposited over substrates and extended characterized through different techniques. Short reaction times yields PT films highly decorated with AuNPs, in which most of NPs present size of ≈3 nm. However, long reaction times and high amounts of thiophene produce thicker and less transparent films with agglomerated AuNPs. Electrochemical studies showed that PT present electrochromic properties, in which a red and blue colors could be observed referent to the reduced and oxidized state respectively.[1] The *J vs. V* curves of the photovoltaic devices, using PT/AuNPs and PT/AuNPs/CNT films, showed that the films containing smaller size of AuNPs and less quantity of CNT exhibit a more rectifier behavior. An annealing of 200 °C/30 min was performed for the best device containing PT/AuNPs and the efficiency were increased by almost two times. The photovoltaic parameters are shown in Table 1.

Table 1 – Photovoltaic parameters of the devices fabricated using PT/AuNPs and PT/AuNPs/CNT films as electron donor materials. These films were synthesized with 4.5 hour of reaction and 100 µL of thiophene.

| Film | *Annealing* | $J_{sc}$ (mA cm$^{-2}$) | $V_{oc}$ (V) | *FF* (%) | Ƞ (%) |
|---|---|---|---|---|---|
| PT/AuNPs | No | -0,535 | 0,17 | 30,00 | 0,0500 |
| PT/AuNPs | Yes*[1] | -1,088 | 0,23 | 32,90 | 0,0820 |
| PT/AuNPs/NTC*[2] | No | -0,053 | 0,39 | 20,41 | 0,0042 |

*1- Annealing of 200 °C for 30 minutes.
*2- Film with 0,0025 mg of CNT.

[1]Salvatierra, R. V. et al, Chem. Comm. 52 (8), 1629-1632, 2016; [2]Salvatierra, R. V. et al, Chem. Mater. 22, 5222-5234, 2010; [3]Oliveira, M. M. et al, J. Phys. Chem. C 112, 18783-18786, 2008.

**Área: MAT** **Inscrição:00125**

# A new route for preparing multi-oxide nanocomposites of nanoparticles-decorated nanotubes

**Carlos S.B. Dias (PQ),[1] Flavio Garcia (PQ),[2] Italo O. Mazali (PQ),[3] Mateus B. Cardoso (PQ),[1,4] Juliana Martins de Souza e Silva (PQ).[5]***

**mazali@iqm.unicamp.br; juliana.martins@physik.uni-halle.de**

*[1] Brazilian Synchrotron Light Laboratory (LNLS – CNPEM), Brazil; [2] Brazilian Center for Research in Physics (CBPF), Brazil; [3] Institute of Chemistry, University of Campinas, Brazil; [4] Brazilian Nanotechnology National Laboratory (LNNano - CNPEM) - Brazil; [5] Institute of Physics, Martin-Luther-Universität Halle-Wittenberg, Germany.*

Key words: *Nanoparticle; Nanocomposite; Hematite; Semiconductor Oxide; Nanotube*

## Highlights

We present a versatile synthetic method to prepare nanohybrids composed of nickel oxide (NiO) nanoparticles decorating hematite (alpha-$Fe_2O_3$) nanotubes with potential catalytic and biological applications.

## Resumo/Abstract

The development of synthetic methods to prepare novel metal oxide nanocomposites is a field of materials chemistry with many technological implications. First, new properties can emerge due to the synergistic interactions between distinct metal-oxide phases combined in one single nanocomposite. Second, particular morphologies can be obtained by adjusting the nanocomposites' architecture to fulfill the needs of specific technological applications. Here, to address the need for new synthetic methods, we present a direct route for preparing multi-oxide inorganic nanocomposites with the specific architecture of nanoparticles decorating nanotubes. We impregnated hematite nanotubes with a metallo-organic precursor of nickel and, subsequently, we thermally decomposed it, in sequential impregnation-decomposition cycles (IDC). Materials were characterized (XRD, SEM, TEM, EELS) and the nanocomposite obtained is composed of NiO nanospheres grown on the walls of hematite nanotubes (Figure 1). Hematite nanotubes were morphologically and chemically stable during the synthetic process, thus having a potential use for different applications that require $Fe_2O_3$ stability. Virtually any individual metallo-organic precursor/combinations of precursors can be used in the synthetic route presented here. Therefore, it could be explored to obtain tailored nanocomposites consisting of controlled-size nanoparticles with different oxides combinations decorating the walls of nanotubes, with potential use in catalysis and biomedicine.

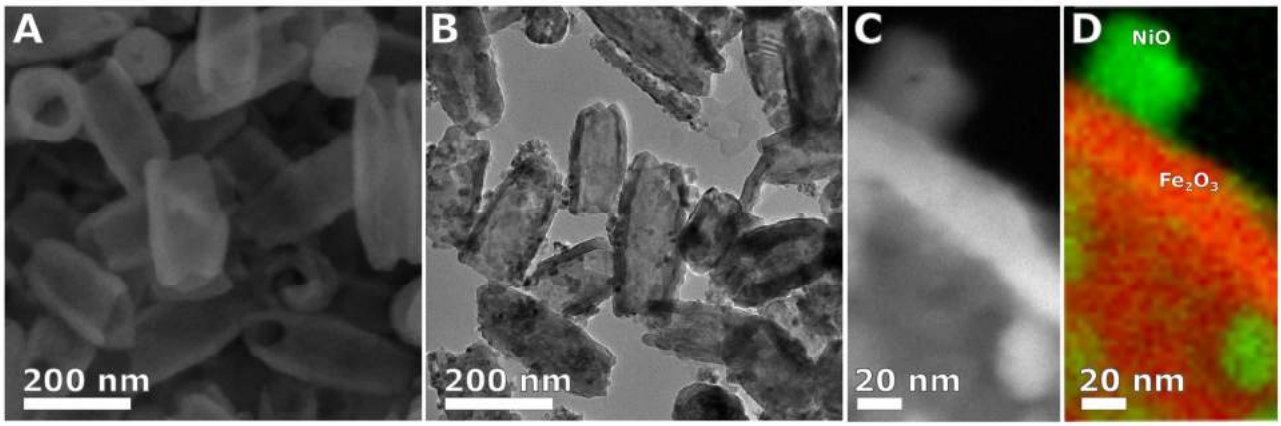


**Figure 1.** Morphology of the hematite nanotubes before and after the impregnation-decomposition cycles with nickel(II) 2-ethylhexanoate. A) Dark-field TEM image of the synthesized hematite nanotube before the IDC procedure, (B) and (C) are, respectively, bright- and dark-field TEM images of the NiO-hematite nanocomposites obtained after submitting the hematite nanotubes to the IDC procedure. (D) Chemical mapping (iron L-edge and nickel L-edge) based on the EELS measurements of the region shown in (C). Spherical NiO nanoparticles are mostly located in the inner walls of the hematite nanotubes.

**Área: MAT** **Inscrição: 01351**

# Extracellular Matrix Digestion Products for Tissue Engineering

**Gabriela M.M. Lobato (PG)[1*], Flávia V. Winck (PQ)[1], Luiz H. Catalani (PQ)[1].**

**gmmlobato@gmail.com; catalani@usp.br**

[1]*Institute of Chemistry, USP*

Key words: *Tissue Engineering, Hydrogel, Extracellular Matrix.*

## Highlights

Implants used in tissue regeneration (TE) still fail to mimic properties of extracellular matrix (ECM). Decellularized ECM has been used as scaffold for TE. Hydrogels from digested dECM is an alternative for processable ECM scaffolds.

## Resumo/Abstract

Facing the medical needs regardless tissue engineering, we´re trying to develop an injectable hydrogel from digested ECMs. The digestion protocol was modified from [1] using trypsin, pepsin and collagenase. Glycosaminoglycan (GAGs) and peptides quantification were performed after continuous and stepwise digestion, showing that regardless the substrate and enzyme, the stepwise process yields a higher amount of GAGs and peptides, so a less degraded product.

ECMs were also analyzed by proteomics, as in [2], to identify its composition. For tendon ECM: cadherin EGF LAG seven-pass G-type receptor 1, leucine rich-repeat containing 9, dynein axonemal heavy-chain and collagen alpha-1 (IV); pericardium ECM: folliculin interactin protein 2, TGF-beta receptor type-1, fibrillin-1, periostin, collagen alpha-1 (XII) chain, zinc-finger C2H2-type, histone H4, prolargin, collagen alpha-2 (1) chain, collagen type VI alpha-1 chain, lumican, annexin A5, anion exchange protein, olfactomedin like, collagen type VI alpha-3 chain, collagen type VI alpha-2 chain and protein kinase C-delta type; bone ECM: complement C3, collagen alpha-2(1) chain; ring finger protein 187 and ciliary rootlet coiled-coil. After proteomic, we verified that pericardium ECM has a highly diverse pool of proteins, differently from the other ECM types. Therefore, it is expected that after *in vitro* assays with stem cells, samples treated with pericardium ECM digested in stages might show better results for tissue regeneration.

[1] Williams C., *et al. Adv Healthc Mater*. 2015; 4(10):1545-1554.
[2] Flores I. L., *et al. Clinical Science*. 2016; 130: 785-799.

**Área:** MAT **Inscrição:** 01368

# Fast and efficient graphene oxide (GO) reduction by using a lab-made UV photoreactor

**Eduarda I. de Castro (IC)*, Nei C. O. Sousa (PG), Jairo J. Pedrotti (PQ)**

**eduardaiorio@hotmail.com**

*MackGraphe - Graphene and Nanomaterials Research Center – Mackenzie Presbyterian University – Rua da Consolação, 896 – São Paulo, SP – CEP 01302-907.*

Keywords: Graphene oxide, UV radiation, lab-made photoreactor, photochemical reduction.

## Highlights

- A photoreactor was fabricated and applied for graphene oxide reduction.
- Higher efficiency of rGO production was assured with irradiation time ≥ 30 min of 1 mg $L^{-1}$ GO dispersion.

## Abstract

The graphene oxide (GO) consists of an oxidized graphene layer decorated with hydroxyl, epoxide, carbonyl and carboxylic groups. The oxygen groups in the GO structure confer to it an insulator property [1]. To enhance its conductivity, the oxygen groups must be removed by a process of reduction, recovering the $sp^2$ domains. The most common chemical method used for GO reduction utilizes sodium borohydride or hydrazine, which are well known by their high reactivity and toxicity. In order to overcome these drawback associate to use of strong reducing agents, the photochemical reduction methods are very attractive, because they are low time consuming, produce low amounts of chemical residues and does not insert functional groups into the graphene structures [2]. In this work, an UV photoreactor was fabricated and its performance was evaluated for graphene oxide reducing. The photoreactor utilizes a 250 W high-pressure mercury lamp as source of UV radiation and four quartz tubes of 10 mL with 10-mm thickness to put the samples. Aliquots of 4 mL of 1mg $L^{-1}$ GO dispersions in DI water were UV irradiated for 15, 30, 45 and 60 minutes. The irradiation of the GO dispersion leaded to darkening of the color solution (Fig. 1B) and to significant changes in its absorption spectrum (Fig.1C). The position of the band with higher intensity depends on the degree of oxidation of the GO. The results show that the irradiation time of the GO dispersion leads to a shift of the maximum band from 229 nm to 261 nm until 30 min exposure solution, due to conversion of the oxidized material to its reduced form resulting of the increase in the extent of the aromatic clusters of $sp^2$-hybridized carbon.

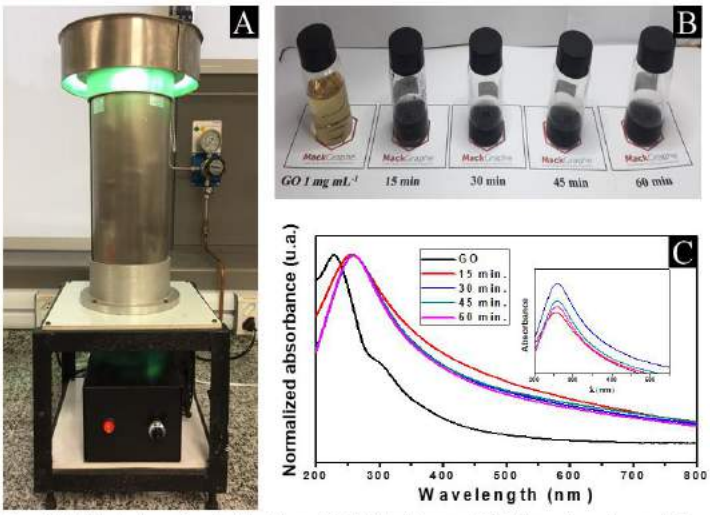


Fig. 1 (A) UV photoreactor digital picture. (B) Digital pictures of GO dispersions (1 mg $mL^{-1}$) before and after UV irradiating for 15,30, 45 and 60 min. (C) UV-Vis absorption spectra of GO dispersions before and after UV irradiating.

Acknowledgment: MACKPESQUISA and FAPESP (#2012/50259-8)

1. Dreyer, D. R., Park, S., Bielawski, C. W., & Ruoff, R. S. The chemistry of graphene oxide. *Chemical Society Reviews*, *39* (1), 228-240, 2010.
2. Koinuma, M.; Ogata, C.; Kamei, Y.; Hatakeyama, K.; Tateishi, H.; Watanabe, Y.; Taniguchi, T.; Gezuhara, K.; Hayami, S.; Funatsu, A.; Sakata, M.; Kuwahara, Y.; Kurihara, S.; Matsumoto, Y. Photochemical Engineering of Graphene Oxide Nanosheets. *The Journal of Physical Chemistry,* 116, 19822-19827, 2012.

**Área: MAT** **Inscrição: 01287**

# Estudo de reações biocatalíticas envolvendo microrganismos funcionalizados com óxidos metálicos.

**Cristian L. da C. Almeida (PG)[1*], Verônica Maciel Bispo (PG)[1], Débora de A. Santana (PQ)[2], Regina Geris (PQ)[1] e Marcos Malta (PQ)[1]**

**cristian.lins@gmail.com; cristian.lins@gmail.com**

[1]*Instituto de Química, Universidade Federal da Bahia, Campus Ondina, Salvador (BA), Brasil*
[2]*Departamento de Ciências Exatas e da Terra, Universidade do Estado da Bahia, Campus I, Salvador (BA), Brasil*

Palavras Chave: *Biotransformação, Bio-híbrido, Fungos Filamentosos*

## Highlights

1) Fungi cells of species *A. niger* were functionalized with $TiO_2$ e $WO_3$ particles, forming bio-hybrids *A. niger/$TiO_2$ and A. niger/$WO_3$.*
2) The bio-hybridss were applied in reations of the glycerol's biotransformation producing appreciated quantities of tartaric and lactic acid.

## Resumo/Abstract

Neste trabalho utilizamos células fúngicas viáveis, funcionalizadas com óxidos inorgânicos em sua parede celular, com a finalidade de promover reações de biotransformação em amostras contendo glicerol como substrato. Os bio-híbridos formados por *A. niger*/$TiO_2$, *A. niger*/$WO_3$, *P. Macrosporus*/$TiO_2$ e *P.Macrosporus*/$WO_3$ foram obtidos após 4 dias, cultivando as espécies fúngicas em soluções contendo uma fonte de carbono e partículas submicrométricas de $TiO_2$ ou $WO_3$. Em seguida, uma alíquota de 15 mL de glicerol foi adicionado e levada para um processo de fermentação durante 10 dias. O caldo fermentado resultante passou por um processo de extração utilizando uma mistura de solventes orgânicos. Em seguida, o extrato obtido foi analisado por HPLC (Figura 1). Resultados preliminares mostraram que células funcionalizadas com óxidos metálicos consumiram o glicerol, gerando produtos de maior valor agregado como os ácidos tartárico e lático.

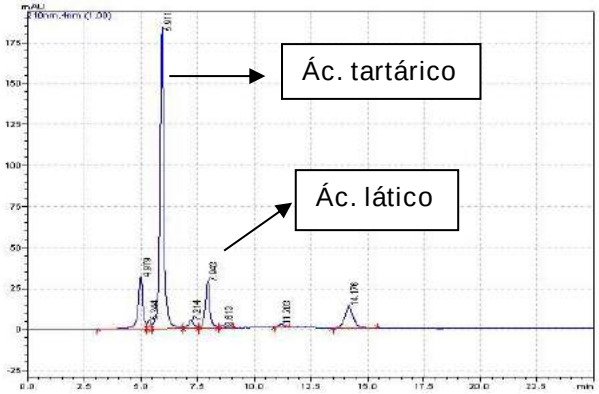


Figura 1: Cromatograma do extrato originado do caldo de reação do híbrido *A. niger*/$WO_3$

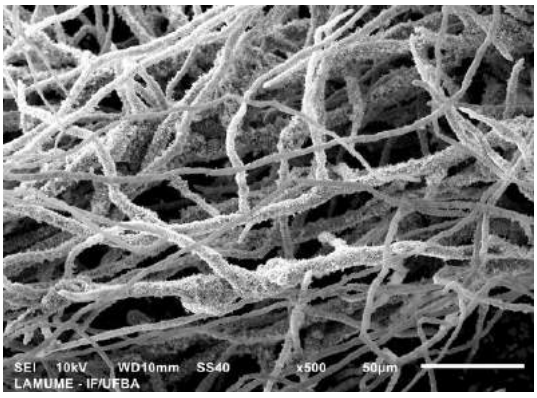


Figura 2: SEM do bio-híbrido *A. niger*/$WO_3$

1. West, T.P. Fungal biotransformation of crude glycerol into malic acid. **Zeitschrift fur Naturforschung - Section C Journal of Biosciences**, v. 70, n. 5–6, p. 165–167,
2. FAKHRULLIN, R. F. Et al. Cyborg cells: functionalisation of living cells with polymers and nanomaterials. **Chem. Soc. Rev**., 2012.
3. FONTES, A. M., GERIS, R., SANTOS, A. V., PEREIRA, M. G., RAMALHO, J. G. S., SILVA, A. F., MALTA, M. Bio-inspired gold microtubes based on the morphology of filamentous fungi. **Biomaterials Science**, 7, 2014.
4. MACIEL, V. M. B.; **Funcionalização de células fúngicas com óxidos de metais de transição para o desenvolvimento de estruturas híbridas biomiméticas.** 121 f. Dissertação (Mestrado) - Instituto de Química, Universidade Federal da Bahia, 2016

**Área: MAT** **Inscrição: 01316**

# Photoluminescence and scintillation of $GdOCl:Eu^{3+}$ obtained from homogeneous precipitation method.

**Maike O. Krauser (PG)[1,2], Marian R. Davolos[1], Marco A. Cebim[1]***

**maike_krauser@uft.edu.br; *mcebim@iq.unesp.br**

*[1]Unesp, Instituto de Química, Araraquara, SP, Brasil; [2]UFT, Química Ambiental, Gurupi, TO, Brasil*

Palavras-chave: *Rare earth, Europium (III), Luminescence, Scintillation.*

## Highlights

$GdOCl:Eu^{3+}$ was obtained by homogeneous precipitation method.
Scintillation under X-ray excitation was evaluated.

## Resumo/Abstract

Gadolinium oxychlride (GdOCl) doped with $Eu^{3+}$ exhibit strong red-luminescence when excited with ionizing radiation, which are useful in lamp and display application. In this work it is shown luminescence and scintillation properties of $GdOCl:Eu^{3+}$ 1% at., obtained from the solid state reaction among $Gd(OH)CO_3.nH_2O$ 1%, homogeneous precipitation, with ammonium chloride salt ($NH_4Cl$) in dynamic atmosphere of 900°C nitrogen gas. The obtained material presents the crystalline phase regarding the GdOCl PDF 12 798 of tetragonal structure and spatial group P4/nmm, without the presence of spurious crystalline phases. The data obtained through the vibration spectroscopy in the infrared region support the X-ray diffraction data, making it possible to observe only stretches regarding the presence of water ($H_2O$) and carbonates ($CO_2$ e $CO_3^{2-}$). Different from the precursor gadolinium hydroxide carbonate ($GdOHCO_3.nH_2O$), the material presented spheroidal micrometric conglomerates observed through scanning electron microscopy, figure 1. The emission spectrum, figure 2, obtained from the luminescence spectroscopy with excitement in the UV region and X-ray presents the intraconfigurational transitions of the ions $Eu^{3+}$ $^5D_0 \rightarrow {}^7F_J$ J = 0, 1, 2, 3 e 4, standing out with high intensity, the hypersensitive transition $^5D_0 \rightarrow {}^7F_2$ in 622 nm, independent from the utilized excitement, being it in the $Gd^{3+} \rightarrow Eu^{3+}$ in 273 nm, in the transition $^7F_0 \rightarrow {}^5L_6$ or X-ray. The $GdOCl:Eu^{3+}$ when submitted to long periods under X-rays excitement it stands out the low reduction in the emission intensity, during 240 minutes excitement the reduction is lower than 4%.

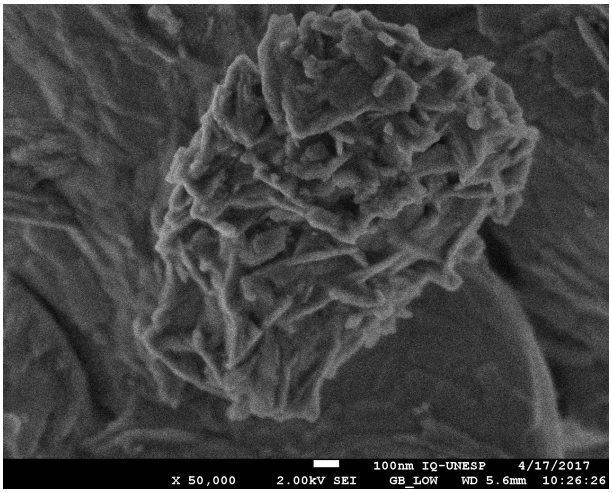


Figure 1. Field emission gun scanning eléctron microscopy (FEG-MEV) of $GdOCl:Eu^{3+}$ 1%.

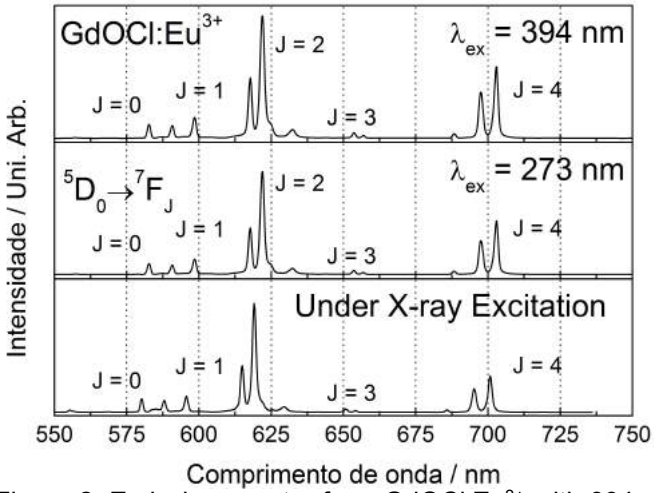


Figure 2. Emission spectra from $GdOCl:Eu^{3+}$ with 394 nm; 273 nm and X-ray excitation.

- LEE, S.-S. et al. Morphology-dependent photoluminescence property of red-emitting LnOCl:Eu (Ln=La and Gd). Journal of Solid State Chemistry, v. 180, n. 12, p. 3529-3534, 2007.
- M.A.Cebim, H.H.S.Oliveira, N.Barelli, M.R.Davolos, Sistema para realização de medidas de luminescência com excitação por raios X, Quim. Nova, 34 (2011) 1057-1062

**Área: MAT** **Inscrição:01051**

# Preparação de catalisadores de óxido de ferro a partir do minério de ferro

**Jefferson R. L. Santos (IC)[1], Alan Paulo da Silva Mendes (IC)[1], André R. Martins (PQ)[2], Simone Pereira de Lima (PQ)[1], Maria do Carmo Rangel (PQ)[3]**

**simone.lima@ifba.edu.br**

*[1]Instituto Federal da Bahia, Campus Salvador, 40301-015, Salvador, Ba, Brasil; [2]Instituto Federal da Bahia, Campus Porto Seguro, Ba, Brasil; [3]Universidade Federal da Bahia, Ondina, Salvador, Ba.*

*Palavras Chave: Catalisadores, Ferro, Óxido de nióbio, POAs.*

## Highlights.

Catalysts prepared from iron ore were prepared and characterized. It was found that magnetite was produced regardless the presence of niobia the solids being suitable for Fenton reaction.

## Resumo/Abstract

Diversos resíduos têm sido dispostos no meio ambiente de forma inadequada, impactando negativamente na vida aquática e na qualidade de vida do ser humano. Entre diversas alternativas, os processos oxidativos avançados têm sido reconhecidos como um meio promissor para o tratamento de efluentes contaminados. Nesse trabalho, foram sintetizados catalisadores que serão utilizados na remoção do fenol presente em correntes aquosas, através de processos oxidativos avançados (POAs), tal como o processo Fenton, que combina peróxido de hidrogênio com íons $Fe^{2+}$, providos pelo catalisador. Foram obtidos sólidos baseados em óxido de ferro (obtido a partir do minério), suportado em óxido de nióbio. As amostras foram preparadas por precipitação e calcinadas a 400 ºC. Para efeito de comparação foram preparadas amostras a partir do nitrato de ferro p.a. Os sólidos foram caracterizados por difração de raios X, medida de área superficial especifica e microscopia eletrônica de varredura. Os difratogramas indicaram a presença de magnetita em todas as amostras, que é a fase de óxido de ferro ativa na reação de Fenton. A área superficial especifica da nióbia foi 104 $m^2.g^{-1}$, nota-se que a adição de ferro diminui o valor da área superficial. A área da amostra obtida com o minério foi 6 $m^2.g^{-1}$, enquanto aquela obtida a partir do nitrato de ferro foi 60 $m^2.g^{-1}$. Essa diferença nos valores de área pode ser atribuída a presença das impurezas contidas no minério. Os resultados mostraram que o minério de ferro pode ser usado para a obtenção de sólidos baseados em magnetita suportada, ou não, em óxido de nióbio.

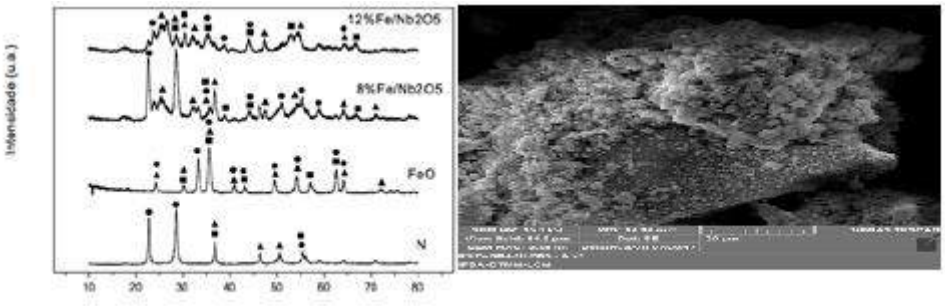


**Figura 1.** Difratogramas de raios X das amostras de óxido de ferro, 8% $Fe/Nb_2O_5$, 12% $Fe/Nb_2O_5$ e FeO, preparadas a partir do reagente do minério, e N (óxido de nióbio). ▪ Magnetita, • Hematita, ▲ Fe(NbO4). **Figura 2**. Microscopia eletrônica de varredura da amostra 8% $Fe_3O_4/Nb_2O_5$

### Agradecimentos

Os autores agradecem à FAPESB/IFBA e PRPGI/IFBa pelo apoio financeiro e à CBMM pela doação do precursor do óxido de nióbio.

### Referências

Levec, J., Pintar, A.; Catalytic oxidation of aqueous solutions of organics. An effective method for removal of toxic pollutants from waste Waters, Catal. Today 24, 51-58 (1995).

Paczésniak, T.; Sobkowiak, A.; The influence of solvent on the reaction between iron(II), (III) and hydrogen peroxide, J. Mol. Catal. A: Chem. 194, 1-11(2003).

**Área: MAT** **Inscrição:1079**

# Synthesis and characterization of chitosan-based nanocarriers for siRNA release

**Grazieli O. Martins (PG),[1*] André M. M. Junior (PG),[1] Aline M. F. Lima (PQ),[1] Maicon S. Petrônio (PQ),[1] Vera A. O. Tiera (PQ),[1] Marcio J. Tiera (PQ)[1]**

**mjt@ibilce.unesp.br; grazi.martins2@gmail.com**

[1]*Departamento de Química e Ciências Ambientais, UNESP-IBILCE*

Keywords: *Chitosan, Diethylaminoethyl (DEAE), Gene therapy, Nanoparticles, Polycations, siRNA*

## Highlights

Derivatives of chitosan were synthesized and characterized.
Derivatives complexed siRNA-CCR2 into low polydispersity spherical nanoparticles of 150 nm in size.

## Abstract

Small interfering RNA (siRNA) has been widely investigated due to its potential to treat diseases by the silencing of targeted genes[1]. However, the intracellular delivery of siRNAs molecules remains as an ongoing challenge due to their negative charges and susceptibility to degradation by endogenous enzymes. The development of nanosized carriers is a need to overcome the extra and intracellular barriers. Thus, chitosan derivatives containing tertiary amino groups and varied degrees of acetylation were synthesized and characterized by gel permeation chromatography (GPC) and $^1$H-NMR techniques. The complex coacervation process at varied charge ratios was employed to prepare nanoparticles with siRNA-CCR2 and the interaction was studied by gel retardation assay, dynamic light scattering and FEG-SEM. The derivatives efficiently complexed the siRNA at low charge ratios and formed spherical particles of 150 nm in size with zeta potentials varying from +10 to +13 mV. Cell viability studies showed that the modifications resulted in derivatives of low cytotoxicity and that imparting a moderated amphiphatic character to chitosan is a promising way to condense siRNA into nanoparticles.

**Figure 1.** Structure of diethylaminoethyl chitosans derivatives and siRNA-CCR2 nanoparticles obtained by the coacervation process.

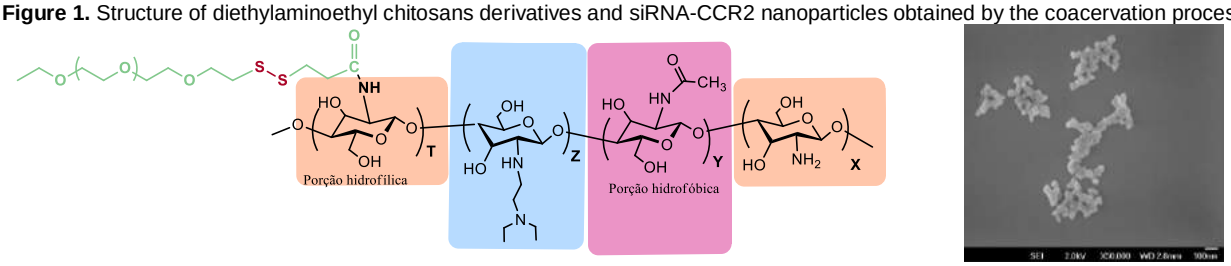


**Table I. Physicochemical properties of synthesized amphiphatic DEAE-CH derivatives**

| Polymer | Monomer* (%) X | Y | Z | $\bar{M}_w$ (KDa) | $\bar{M}_n$ (KDa) | Pdi $\left(\frac{\bar{M}_w}{\bar{M}_n}\right)$ |
|---|---|---|---|---|---|---|
| $CH_{20}$-$DEAE_{15}$ | 67.8 | 19.4 | 12.8 | 183.6 | 66.6 | 2.76 |
| $CH_{20}$-$DEAE_{25}$ | 55.3 | 20.2 | 24.5 | 181.9 | 67.8 | 2.68 |
| $CH_{30}$-$DEAE_{15}$ | 59.7 | 29.5 | 10.8 | 179.3 | 67.4 | 2.66 |
| $CH_{30}$-$DEAE_{25}$ | 48.0 | 27.7 | 24.3 | 184.9 | 70.0 | 2.64 |

* Data (%) obtained by $^1$H NMR at 80 °C. X= degree of deacetylation, Y = degree of acetylation and Z= degree of substitution by DEAE groups.

## References

1. SHI, Q.; PICOLA, I. P. D.; RONDON-CAVANZO, E. P.; TIERA, M. J. et al., In vivo Therapeutic Efficacy of TNF-α silencing by FA-PEG-DEAE-Chitosan-siRNA Nanoparticles in CAIA Mice, 2018, in press.

**ACKNOWLEDGEMENTS:** FAPESP 2017/10331-5 and Embrapa Instrumentação, São Carlos, Brazil

**Área: MAT** **Inscrição: 00528**

# Study of dye-modified Ag/$TiO_2$ nanocomposites for application in photocatalysis

**Gabriella Correia de Almeida (IC)[*1], Nelcy Della Santina Mohallem (PQ)[1], Marcelo Machado Viana (PQ)[1]**

**gabriellacorreiadealmeida@gmail.com**

[1]*Departamento de Química, Instituto de Ciências Exatas, Universidade Federal de Minas Gerais*

*Keywords: Titanium dioxide, Natural dye, Photocatalysis, Silver.*

## Highlights

Tailoring the crystalline phases of $TiO_2$ nanoparticles by using microwave radiation and pH control. Modification of $TiO_2$ nanoparticles for application in photodegradation of methylene blue dye.

## Abstract

Among the current environmental problems, we can highlight the considerable increase in the levels of wastewater discharges polluted. A great effort has been made to develop technologies, mainly involving the photocatalysis process to treat contaminated water. This process is based on the electronic excitation of semiconducting oxides, such as titanium dioxide ($TiO_2$). The photoactivity of $TiO_2$ depends on its crystalline phase and its textural, structural and morphological properties play an important role in the photodegradation efficiency of dyes. A strategy to improve the photoactivity of the $TiO_2$ is the combination with silver nanoparticles and dye molecules enabling the increase in the recombination time of the electron/hole pairs and the range of light absorption. In this work, the synthesis of $TiO_2$ nanoparticles was carried out from titanium tetrachloride and microwave radiation. Surface modification of the oxide was performed using natural dye from jabuticaba and silver nanoparticles. To prove the surface modification with dyes, UV-vis and fluorescence spectroscopy were used. The X-ray diffraction showed the presence of the anatase phase in syntheses performed in basic conditions and in acidic conditions, rutile phase was observed. XRD also provided crystallite size, and these were confirmed by transmission electron microscopy (TEM) (Figure 1). Through gas adsorption, the oxides showed specific surface areas varying from 40 $m^2g^{-1}$ to 200 $m^2g^{-1}$. The photocatalytic test using structurally modified $TiO_2$ showed a greater potential for methylene blue degradation.

Acknowledgment: We thank FAPEMIG, CNPq, and Capes for financial support.

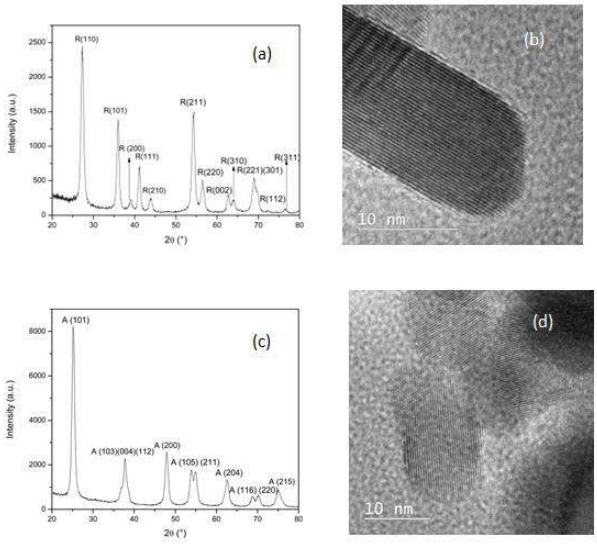


Figure 1. (a) XRD and (b) TEM to rutile phase; (c) XRD and (d) TEM to anatase phase.

**Área: MAT** **Inscrição: 00749**

# Anti-scaling performance of a textured copper-based Slippery Liquid-Infused Porous Surface (SLIPS)

**Gabrieli do Amaral Diniz (IC), Eduarda Sofiatti (IC), Maria F.B. Sousa (PQ), Celso A. Bertran (PQ)**

**bertran@iqm.unicamp.br; mfabr@iqm.unicamp.br**

*Instituto de Química, UNICAMP*

Palavras Chave:*SLIPS, Anti-scaling, Calcium carbonate, Textured copper.*

## Highlights

Copper-based lubricated slippery surface presents an effective inorganic anti-scaling property.
Copper-based lubricated surfaces are stable under inorganic scaling test conditions.
Perfluorinated oil Krytox is a good lubricant to produce inorganic anti-scaling SLIPS.

## Resumo/Abstract

Surfaces termed “SLIPS” (Slippery Liquid-Infused Porous Surface) present quite singular properties, for instance, self-healing and self-cleaning, which make them very promising for a broad range of applications in so diverse fields such as medical, avionic, oil and gas industries, among others. SLIPS are designed surfaces with controlled wettability based on the embedding of a lubricant non-polar fluid into textured or porous materials having the ability to repel aqueous and/or oily liquids. Considering that scaling is a crucial problem in many industrial facilities, in this work the anti-scaling ability of textured copper-based SLIPS was evaluated. Texturing of copper plate (2.0 x 3.0 x 0.2 cm) was achieved by oxidation with 2.0 M NaOH solution during 24 hours followed by intensive washing with deionized water. The textured material was modified by thiolation (perfluorodecanothiol 5 x $10^{-3}$ mol $L^{-1}$ in ethanol, during 24 h), then impregnated with the perfluorinated oil Krytox to produce the SLIPS. The water contact angle with the thiolated-copper and the SLIPS surfaces were $150^{o}$ and $116^{o}$, respectively. Both surfaces were submitted to scaling tests by immersion into calcium carbonate supersaturated brine and were assessed by scanning electronic microscopy (SEM) and/or atomic force microscopy (AFM). AFM images of the $CaCO_3$ deposited onto these materials (Figure1b;1d) showed that the number of nucleation sites onto the SLIPS surface decreased when compared with the thiolated surface: only one crystal can be seen in image d; other bright spots are part of the textured-surface.

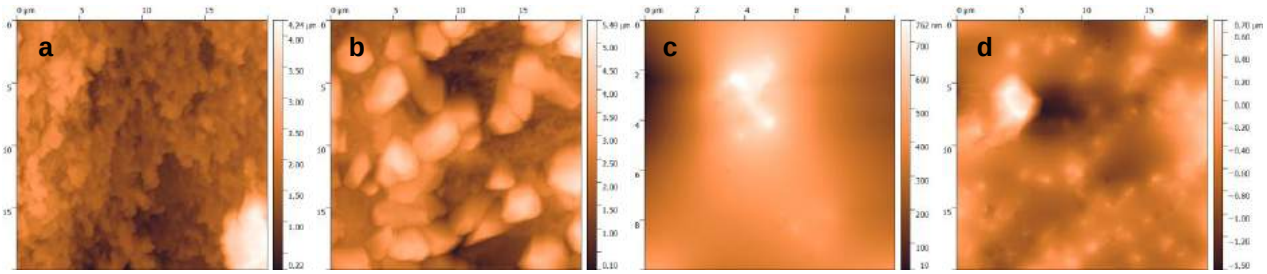


Figure 1 – AFM images of Textured Thiolized-Copper and Copper-SLIPS, before (1a,1b) and after scaling experiments (1b,1d), respectively.

**Área: MAT** **Inscrição: 00941**

# Síntese e caracterização de um novo candidato a sistema veiculador de fármaco empregando-se nanopartículas magnéticas e pilar[n]arenos

**Tamires S. Fernandes (PG),[1] Evelyn C. S. Santos (PG),[1] Vinicius G. C. Madriaga (IC),[1] Carolina V. Barroco (IC),[1] Vanessa Nascimento (PQ),[1] Célia M. Ronconi (PQ).[1*]**

**tamires_soares@msn.com; cmronconi@id.uff.br***

*[1]Universidade Federal Fluminense, Instituto de Química, Outeiro São João Batista, s/n, Campus do Valonguinho, Centro, 24020-141, Niterói, RJ, Brasil.*

Palavras Chave:*(Sistemas Veiculadores de Fármacos, Nanopartículas Magnéticas, Pilar[n]arenos).*

## Highlights

Synthesis and characterization of a new drug delivery system candidate based on magnetic nanoparticles and pillar[n]arenes. We present the results of a drug delivery candidate material based on iron magnetic nanoparticles and carboxylatopillar[5]arene for future application in tuberculosis treatment with the isoniazid drug.

## Resumo/Abstract

Sistemas Veiculadores de Fármacos (SVF) são dispositivos moleculares capazes de entregar um determinado fármaco diretamente a um alvo desejado. Esse tipo de sistema representa um avanço no tratamento das mais diversas doenças, uma vez que é capaz de diminuir os efeitos adversos, os tempos de tratamento e as dosagens de medicamentos necessárias.[1] Neste trabalho, está apresentada a síntese e caracterizações de um novo candidato a SVF (FeNP-CP[5]A) baseado na interação de nanopartículas magnéticas de óxido de ferro (FeNP) com compostos macrocíclos do tipo pilar[5]arenos funcionalizados com grupos carboxilato (CP[5]A). Esse sistema será, posteriormente, empregado como veiculador do fármaco isoniazida (INH) utilizado no tratamento da tuberculose. Para a obtenção do material (esquema abaixo), primeiramente foram sintetizadas as nanopartículas magnéticas pelo método de coprecipitação[1] e o CP[5]A através de 5 etapas reacionais[2]. Posteriormente, o FeNP-CP[5]A foi obtido através da agitação mecânica dos mesmos em meio aquoso por 48 h. O FeNP-CP[5]A e seus precursores vêm sendo caracterizados por diversas técnicas. Pelo espectro de IV (figura 1) é possível confirmar a formação do FeNP-CP[5]A através das bandas em 1539 (νC=O (1)), 1400 (νC=C$_{arom}$ (2)), 1198 (νC-O (3)) e 1062 (δC-H$_{arom}$ (4)) cm$^{-1}$ referentes à presença do CP[5]A. Como perspectivas deste trabalho temos a complementação das caracterizações do material pelas técnicas de TEM, DLS, ZP, medidas magnéticas, entre outras e o início dos testes com o fármaco.

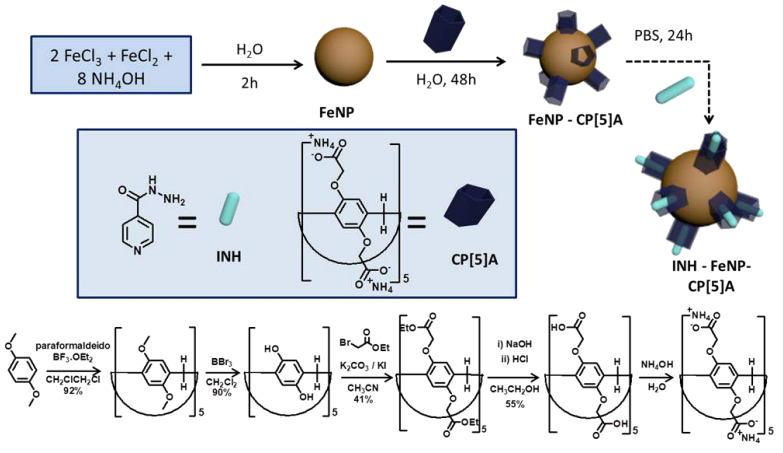


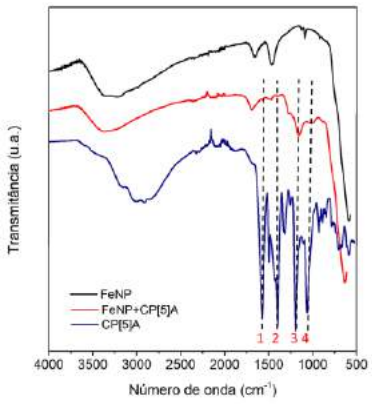


**Figura 1**: Espectro de IV do FeNP-CP[5]A e seus precursores.

**Agradecimentos:** CAPES, CNPQ, FAPERJ, PPGQ-UFF, LQSN, LAMATE, LAME, LaReMN.

(1) Santos, E. C. S.; Watanabe, A.; Vargas, M. D.; Tanaka, M. N,; Garcia, F.; Ronconi, C. M. *New J.Chem.* **2018**, 42, 671.
(2) Xia, D.; Yu, G.; Li, J.; Huang, F. *Chem. Commun.*, **2014**, 50, 3606.

**Área: MAT** **Inscrição: 00999**

# Quantification and separation of rare earth elements from fluorescent lamp phosphors and synthesis of luminescent nanoparticles

**Gabriel A. Freitas (IC), Alex R.H.L. Cruz (PG), Helmut I. Padilla-Chavarría (PG), Adriana Gioda (PQ), Tatiana D. Saint'Pierre (PQ), Jiang Kai* (PQ).**

***jkai@puc-rio.br***
*Departamento de Química, Pontifícia Universidade Católica do Rio de Janeiro.*
Palavras Chave: *Rare earth elements, fluorescent lamp phosphor, quantification, separation, reutilization.*

## Highlights

Reutilization of rare earth elements collected from fluorescent lamps for the preparation of highly luminescent nanoparticles.

## Resumo/Abstract

Fluorescent lamps (FL) are largely used due to their higher efficiency and longer life span as compared to incandescent bulbs. Phosphors found in such lamps contain Rare Earth Elements (REE), which are chemically very similar and have a wide range of applications. Their reutilization is thus vital, not only for the industrial sector, but also for environmental reasons since this process relies on the recycling of electronic waste (more specifically FLs).
This project aims at the quantification, separation and reutilization of REE obtained from FLs (specially Y, Eu and Tb) by methods of filtrations, dilutions in acidic environments and co-precipitation with an organic compound, trimesic acid (TMA).

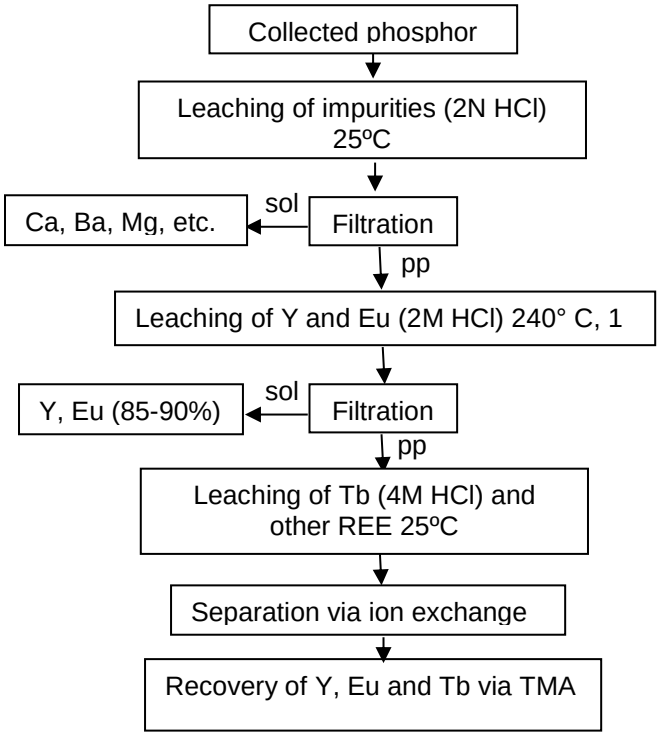


**Picture 1.** Diagram showing the steps of separation.

| Element | 1ª step | 2ª step | 3ª step |
|---|---|---|---|
| Y | 6,64±0,82 | 29,78±1,32 | 0,17±0,07 |
| Eu | 0,52±0,04 | 1,58±0,06 | 0,013±0,005 |
| Tb | 0,058±0,006 | 0,052±0,044 | 0,016±0,005 |
| Ba | 9,583±0,166 | 0,345±0,020 | 0,024±0,010 |
| Ca | 7183±356 | 1277±339 | 5,85±2,225 |

**Table 1.** Leaching rates in three stages ug.g$^{-1}$.

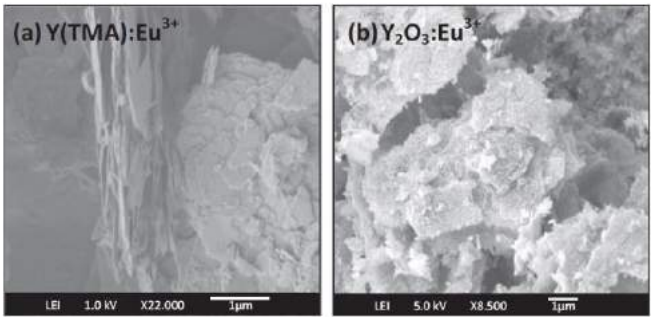


**Picture 2.** MEV de RE(TMA) and $RE_2O_3$:$Eu^{3+}$.[2]

**Agradecimentos:** CNPq, CAPES, FAPERJ, PUC-Rio.

**Área: MAT** **Inscrição: 01013**

# Study of the interactions between carboxymethylcellulose and ethylenediamine for synthesis of nanoparticles

**Braulio de Vilhena Amorim Tostes (IC),[1] Dirliane Santos Duarte (IC)[1], Indira Carolina Brito Pires (IC)[1] Douglas de Britto (PQ).[2]***

**bvatostes@hotmail.com; douglas.britto@embrapa.br**

*[1]Instituto Federal de Educação, Ciência e Tecnologia do Sertão Pernambucano; [2]Embrapa Semiárido*

Keywords: Polyelectrolyte, Ionic Gelling, Desalination, Colloids.

## Highlights

Carboxymethylcellulose and ethylenediamine forms suspension in presence of ethanol. The acid media increases the precipitation rate. The characterization attested the ionic interaction.

## Resumo/Abstract

In Brazil, there are areas where drinking water is scarce, mainly in the semi-arid region, where the mean annual precipitation is low (<500 mm/year). One alternative for obtaining drinking water is through the groundwater, however, contaminations or high salt content prevent its use for human consumption and farming activities. An alternative for the removal of these solutes is through nanoparticles and ionic interaction. Thus, this work reports the preparation of a new nanoparticle system, from carboxymethylcellulose (CMC) and ethylenediamine (EDA), aiming the interaction and removing of soluble ions. The synthesis was performed from 50.0 $cm^3$ of CMC (5.0 mg $cm^{-3}$) with 3.5 $cm^3$ of EDA in acid and neutral media. The ionic interaction was accompanied by turbidity variation (UV-Visible spectroscopy), during ethanol addition. The precipitated was characterized by FTIR spectroscopy. Effective interaction between CMC and EDA was observed. In neutral medium, the CMC-EDA interaction occurred upon addition of 0.5 $cm^3$ of ethanol with high turbidity and precipitated at 1.0 $cm^3$ of ethanol. For pure CMC (control), the turbidity did not vary, forming only a clear gel that become denser at 6.0 $cm^3$ of ethanol (Figure 1a). In acid media, the precipitation was faster, forming a high turbidity suspension (Figure 1b). The characterization by FTIR showed that interaction between CMC and EDA occurred, mainly in the acid medium, where it was possible to identify in the precipitate, NH bands due stretching (3200 $cm^{-1}$) and angular deformation (1601 $cm^{-1}$), characteristics of EDA.

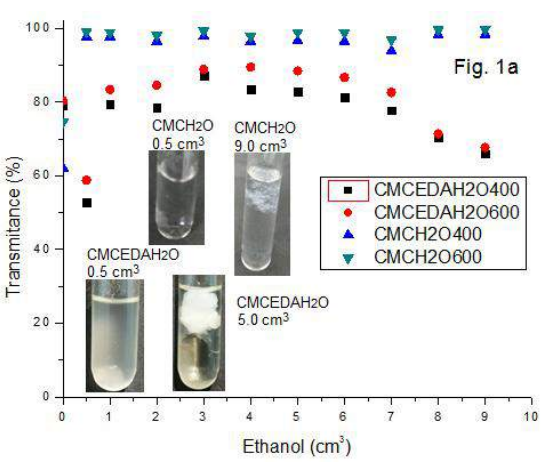


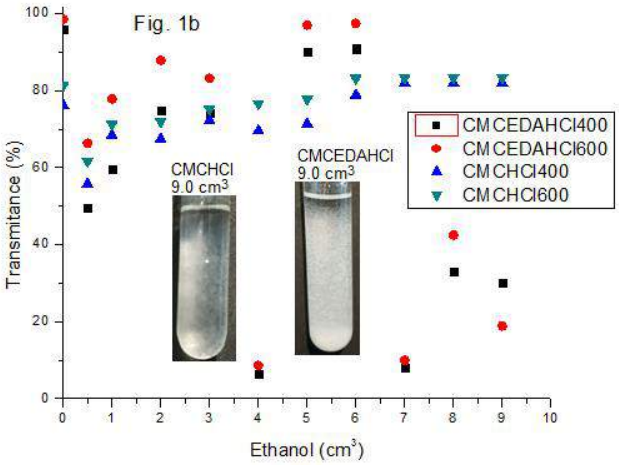

**Área: MAT** **Inscrição: 00426**

# Thermal stability of the Green Coffee Cake as a response to the study of the water vapor blast process for the production of high value materials.

**Elisa B. de Brito (PG)[1], Lucas T.G.Pimenta (IC)[1], Suellem C. Barbosa (PQ)[1], Maria de Fátima V. Marques (PQ)[1].**

**elisabrito@ima.ufrj.br**

*1Catalysis laboratory for polymerization, IMA-UFRJ, 21941-598, Rio de Janeiro, RJ*

Keywords:Cellulose, Biopolymer, Steam explosion, Residue, Green coffee.

## Highlights

Thermal stability of agricultural residue fiber. Evaluation of vapor explosion parameters.

## Abstract

Natural fibers are structures widely used in polymeric composites as a reinforcing agent. This work aims at evaluating the properties of green coffee cake (TCV), a residue of the coffee industry, after the explosion of water vapor, a technique that subjected the lignocellulosic material to high temperature and pressure, followed by rapid depressurising, as a form of break part of its structure and expose cellulose, a biopolymer that presents excellent thermal and mechanical properties[1,2].

The TCV used in this study (Cooxupé LTDA, MG) was moistened for 24 hours and transferred to 1L autoclave of BuchiGlassuster, where it was heated at 180 ° C to 2 bar under nitrogen. The reactor depressurising was performed in 10 min cycles and the process was repeated for another 4 cycles. The samples were characterized by thermogravimetry (TGA) to evaluate the thermal stability of the fiber after the explosion cycles (Figure 1, Table 1).

**Figure 1**: Thermogravimetric analysis (TGA / DTG) for the steam explosion cycles and **Table 1:** Data on the TG and DTG curves of the vapor blast cycles.

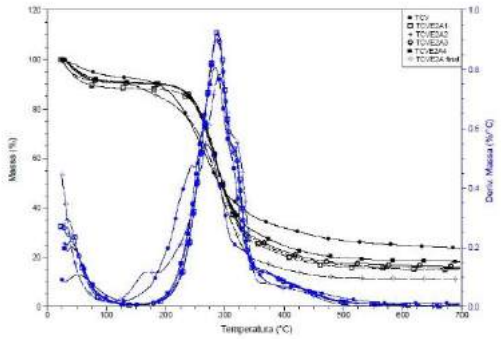

| Sample | Moisture (%) | T*onset* (ºC) | Tmáx (ºC) | Residue (%) |
|---|---|---|---|---|
| **TCV** | 7,03 | 221 | 270 | 23,8 |
| **TCVE2A1** | 11,50 | 252 | 287 | 15,0 |
| **TCVE2A2** | 9,13 | 251 | 287 | 15,5 |
| **TCVE2A3** | 9,57 | 252 | 287 | 16,3 |
| **TCVE2A4** | 8,96 | 245 | 284 | 18,3 |
| **TCVE2Afinal** | 9,47 | 242 | 290 | 11,1 |

The initial mass loss, between 25-125 ºC, and the following losses were identified, between 180-200ºC, concerning the degradation of hemicellulose, between 220-260ºC, cellulose degradation and between 280-500ºC to lignin degradation. Samples after blasting have a higher degradation temperature than the standard sample, showing greater thermal stability of the fibers after treatment, indicating that the process removed some of these amorphous components, as confirmed in the infrared spectra (FTIR), which present bands with lower intensity in the vibrations related to hemicellulose and lignin.

The thermal stability of the TCV fibers after 3 cycles of steam explosion increased compared to the original fiber, indicating the removal of amorphous components from the fiber, increasing the cellulose content, more hydrophilic.original.

[1]BORDES, P.; POLLET, E.; AVÉROUS, L.; Biodegradable polyester/nanoclay systems.Progress in Polymer Science. 2009,*34*, 125.

[2] KLEMM, D.; KRAMER, F.; MORITIZ, S; LINDSTROM, T.; ANKERFORS, M.; GRAY, D.; DORRIS, A. Nanocelluloses: A New Family of Nature-Based Materials. Angewandte Chemie International Edition, v. 50, n. 24, p. 5438-5466, jun. 2011.

**Área: MAT** **Inscrição: 00708**

# Efficient amine functionalization of carbon nanotubes with triethylenetetramine through microwave assisted reaction for applications in nanofluids.

**Tiago G. de O. Silveira (IC),[1] Victor Emanuel M. M. Monteiro (IC),[1] Ana Paula Silva (IC),[3] Jesús A. Nuncira Valencia (PG),[2] Vinicius Caliman (PQ),[1] Glaura Goulart Silva (PQ).[1]***

**tiago.silveirago@gmail.com; glaura.goulart@gmail.com**

*[1]Departamento de Química, UFMG; [2]Departamento de Engenharia Química UFMG; [3]Centro Universitário UNA.*

Palavras Chave: *Carbon Nanotubes, Triethylenetetramine, Surface Chemical Functionalization, Physicochemical Properties.*

## Highlights

The chemical surface modification of carbon nanotubes with triethylenetetramine through microwave-assisted reaction was performed as a high yield and low environmental impact alternative, allowing to save energy and reaction times. The structure and properties of the modified nanomaterial were characterized to propose them for applications in polymer-water based nanofluids.

## Resumo/Abstract

Carbon nanotubes (CNT) exhibit outstanding physicochemical properties, which allow them to be used in several polymer applications, as reported previously by our group[1-3]. However, they tend to form stable aggregates, which lead to unwanted changes in their properties[4]. In order to counteract this, surface chemical functionalization of CNT with amino groups is as an alternative to improve dispersion behavior of CNT in polymer-water based fluids. Nevertheless, chemical routes for surface amino-modifications are still being optimized with respect to yield and environmental impact[5].

In this work, a low-cost and green chemistry route to functionalize oxidized-CNT (ONTC) with triethylenetetramine (TETA) was applied to control reaction parameters such reagents and time. The modified nanomaterial was fully characterized by all relevant techniques such as CHNO, FTIR, Raman, SEM, TEM, and others. Thermogravimetric curves showed 12% mass loss in the 120 - 400 °C range for ONTC-TETA, which is assigned to the thermal decomposition of the amino and carboxyl groups. Zeta potential measurements of aqueous dispersions displayed a surface charge of 21 ± 1 mV at 25 °C. Rheology measurements demonstrated the superior viscosity (increase of 180% at a shear rate of 1 $s^{-1}$ ) in partially hydrolyzed polyacrylamide (HPAM) aqueous solutions when adding amounts of 1% of ONTC-TETA. These results indicate a great progress for the implementation of ONTC-TETA-HPAM nanofluids in energy applications such as enhanced oil recovery.

The authors acknowledge Petrobras, Fapemig, and CNPq for the financial support. Also, the Technology Center for Nanomaterials (CTNano) of the UFMG is acknowledged for help in structural characterizations. Microscopic Center of UFMG is acknowledged for SEM and TEM images.

References:

[1]Soares, M. C. F.; *et al*. J. Polym. Res. 2013.
[2]Lopes, M. C.; *et al*. J. Appl. Polym. Sci. 2014.
[3]da Silva, W. M.; *et al*. J. Appl. Polym. Sci. 2015.
[4]Samanta, S. K.; *et al*. Acc. Chem. Res. 2014.
[5]Punetha, V. D.; *et al*. Prog. Polym. Sci. 2017.

**Área:** MAT **Inscrição:** 01377
*(Inserir o número de inscrição do autor que fez a submissão)*

# Activated material obtained from shale by-products for sulfur removal of fuel oil

**Antonio S. Mangrich* (PQ), Andréa B. A. Drabecki (PG), Juliana Schultz (PQ)**

**mangrich@ufpr.br; andrea_appolinario@yahoo.com.br**

*Departamento de Química, UFPR*
*Palavras Chave: Shale, Adsorption, Desulfurization, Shale fuel oil.*

## Highlights

Adsorption as alternative hydrodesulfurization
Adsorbent material from shale by-products
Reducing sulfur content of shale fuel oil
Magnetization of materials prepared at 600 °C (magnetite or spinel ferrite formation)

## Resumo/Abstract

The concern about environmental contamination by sulfur-containing gases has increasing restrictive legislation of fuels. There are studies of alternative processes to hydrodesulfurization, such as oxidative, extractive, and by adsorption. Adsorbents like activated coals, zeolites and others materials are used. The shale industrialization needs to reduce sulfur content in shale fuel oil, at below 1.00 % wt. In this work, materials are produced with two shale-processing by-products: spent shale (the rock after the processing) and shale fines (rock in granulometry inferior to that used in the process) for partial removal of sulfur compounds from shale oil. These materials are produced according to Table 1, in two granulometries each one (bigger at 2 mm to 3,36 mm and smaller at 0,177 a 0,250 mm).

Table 1. Produced materials

| Material | By-products | Final Temperature | Copper source |
|---|---|---|---|
| FXm350S | shale fines | 350 °C | $CuSO_4$ |
| XRm350S | spent shale | 350 °C | $CuSO_4$ |
| XRm600S | spent shale | 600 °C | $CuSO_4$ |
| FXm600S | shale fines | 600 °C | $CuSO_4$ |
| XRm600Cl | spent shale | 600 °C | $CuCl_2$ |
| FXm600Cl | shale fines | 600 °C | $CuCl_2$ |
| FXm350Cl | shale fines | 350 °C | $CuCl_2$ |
| XRm350Cl | spent shale | 350 °C | $CuCl_2$ |

Tests of adsorption with these materials and determination of the sulfur content in the shale fuel oil were carried out. The total copper content on the prepared materials was confirmed by ICPOES analysis at concentrations of 1.80 to 8.13 % wt, and the results of the EPR analysis proved the presence of Cu(II) and the magnetization of the materials prepared at 600 °C (e.g. Figure 1), probably due to the magnetite or spinel ferrite formation. The capacity of the adsorbent materials prepared was 0.05 to 0.16 mg S / g of the adsorbent and as can be seen in the Figure 2 it was not possible to establish correlation with copper content.

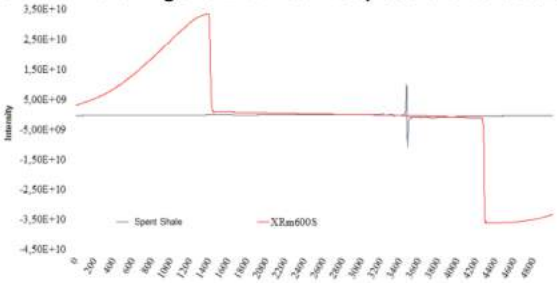


Figure 1. EPR sprectra

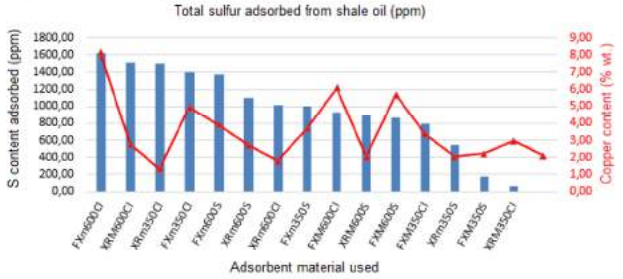


Figure 2. S adorbed and Cu content

**Área: MAT** **Inscrição: 01359**

# Core-shell nanofibers as drug carriers for transdermal delivery of drugs with antimalarial activity

**Laura Rebouças (PG),[1*] Ana Paula S. Immich (PQ)[2] e Luiz Henrique Catalani (PQ).[1]**

**lauraoreboucas@gmail.com; catalani@usp.br**

*[1]Instituto de Química, USP; [2]Departamento de Engenharias, Campus Blumenau, UFSC*

Key Words: *Malaria, Coaxial fibers, Transdermal device, Controlled drug delivery, Electrospinning, nanofibers.*

## Highlights

Malaria treatment is long and grueling, hampering patient adherence. A transdermal device would facilitate the treatment and improve effectiveness. Core-shell electrospun fibers are proposed as device to control the drug release.

## Abstract

The treatment of malaria requires a great dedication from the patient, where the medicine needs to be used for several days, compromising patient adherence to the treatment - especially children - with a high recurrence rate[1]. Thus, this project has as goal the development of a transdermal device to administrate antimalarial drugs, including Artemether-Lumefantrine[2] and Piperaquine-Dihydroartemisinin combinations, as well as a melatonin derivative[3].

Core-shell electrospun nanofibers are being tested, the pair of polymer models can be PET/PCL or PET/Nylon-6,6, with the drug in the core of fibers, while the release assay is carried out in PBS/isopropanol.

To confirm the core-shell architecture, the fibers were analyzed by TEM. Gold nanoparticles were included to enhance contrast. AuNP were synthesized *in situ* for a better dispersion (Figure 1), reducing $HAuCl_4$ with $NaBH_4$ inside PET solution.

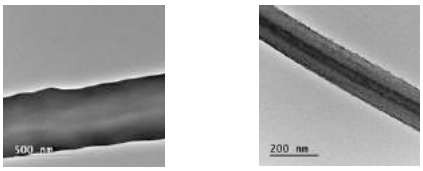


(a) (b)

Figure 1: TEM images of core-shell nanofibers: (a) plain fibers PET/PET; (b) PET+AuNP/Nylon.

Ibuprofen was initially chosen as a model drug, since its Log P (3.97) is very similar to Artemether (3.53). Maximum loading capacity of ibuprofen in monoaxial PET fibers was determined as 90 mg/g of polymer. However, the releasing kinetics showed to be too slow, compromising the application. Other polymers, like nylon-6,6 and PCL are under scrutiny.

[1] Lalloo, D.G. et al., 2016. *J Infect (2016)*. 1-15
[2] Balducci, A.G. et al., 2015. *J Drug Deliv Sci Tec*, 32, 1–7.
[3] Schuck, D.C. et al., 2014. *Eur J Med Chem*, 78, 375–382.

**Área: MAT** **Inscrição: 1182**

# Copolymers used as additives for fuels

**Aline S. Muniz (PQ)*, Fernando A. Ferraz (PQ), Angelo R.S. Oliveira (PQ), Maria Aparecida F. César-Oliveira (PQ)**

**alinemuniz@ufpr.br; mafco@quimica.ufpr.br**

*LEQUIPE - Laboratory of Polymer Chemistry and Organic Synthesis, Department of Chemistry, UFPR - Federal University of Parana, Curitiba, Parana, Brazil.*

Palavras Chave: *biodiesel, antifreeze, methacrylate copolymers, acrylate copolymers, pour point, polymeric additives.*

## Highlights

The copolymers with low molar mass, synthesized, can hinder the crystalline networks formation that occur on fuels in cold weather conditions allowing the incorporation of more biodiesel in diesel oil.

## Abstract

New sources of clean and sustainable energy generation have been investigated in recent years, as there is a growing concern to reduce environmental pollution as well as to reduce greenhouse gas emissions that contribute to global warming. The copolymers with low molar mass (<Mw> 4000 g/mol) were herein synthesized through free radical polymerization of various acrylic compounds. The performance of them as additive showed that they can hinder the crystalline network formation, that occur on fuels in colder regions. For example, the use of M14A14 decrease the pour point (PP) of neat biodiesel (B100) to -9°C and blend B5 to -22 °C and the additive M14A16 decrease the PP of blend B20 to -35°C, corresponding to an excellent result, that allow the incorporation of a larger amount of biodiesel in diesel oil, composing blends of higher levels than the current values, independent of the country region and the season of the year. The feasibility of increasing the insertion of biodiesel in the Brazilian energy matrix, either by encouraging the use of B100 or by increasing the biodiesel content in blends with diesel oil, results in the use of increasing amounts of biodiesel, which favors aggregation of value to the national raw materials, develops the national industry, expands the generation of employment and income in its production chain besides being a renewable energy source that favors the reduction of emissions of greenhouse gases.

Pictorial representation of the biodiesel cooling behavior.

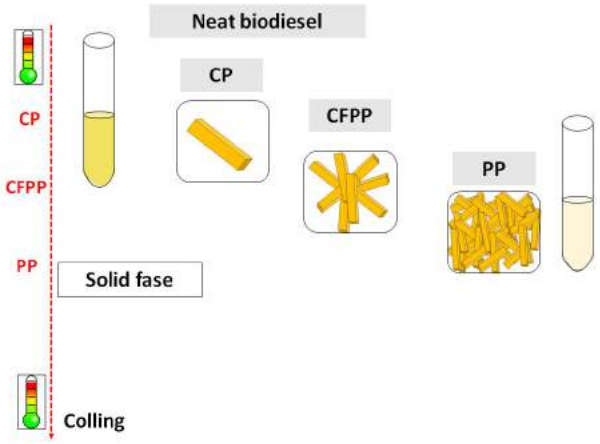


Soybean biodiesel cooled with additive (A) and without additive (B).

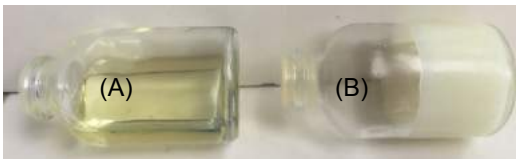


Effect of the polymeric additives as pour point depressant on B100.

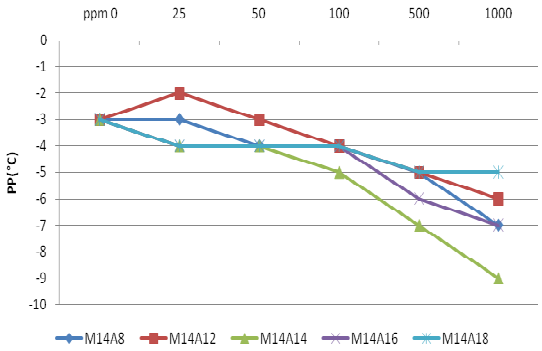


Effect of the polymeric additives as pour point depressant on B20 (20% B100 + 80% diesel oil).

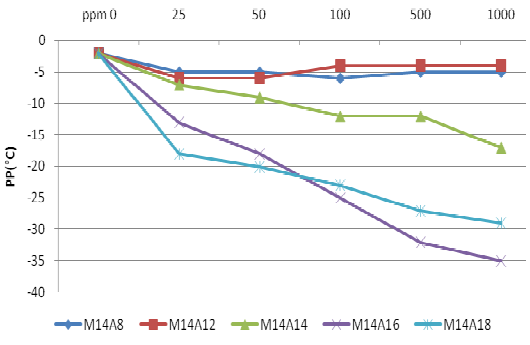

**Área: MAT** **Inscrição: 01247**

# Hierarchical structured materials formed by combination of zeolite crystals and bacterial cellulose fibers

**Raquel de A. Bessa (PG),[1] Anderson Luiz P. Castro (IC),[1] André Luís S. Pereira (PG),[1] Morsyleide de F. Rosa (PQ),[2] Adonay R. Loiola (PQ).[1*]**

**adonay@ufc.br**

*[1]Departamento de Química Orgânica e Inorgânica, UFC; [2]Embrapa Agroindústria Tropical*

Keywords: Zeolite, Bacterial Cellulose, Hierarchically Structured, Composites.

## Highlights

Zeolite/bacterial cellulose composites in cartridge form with hierarchical architecture have been obtained. Their structure suggest high potential for adsorption as the access into the pores is optimized.

## Abstract

Hierarchical materials integrate different kinds of porosity enhancing mass transport and diffusion within the crystals, ideally while maintaining the intrinsic zeolitic properties and can be achieved using post-synthesis methods such as zeolitization of preformed solids.[1] Many adsorbents and catalysts may use this approach and, among them, the zeolites are highlighted once mass transference issues due to densification, which limits the access of molecules to the active sites in the inner channels and consequently makes its applications difficult, can be worked. Zeolites have well-defined microporous system formed by tetrahedral silicon and aluminum atoms linked by oxygen atoms.[2] Bacterial cellulose is a biomaterial with several interesting characteristics such as high water holding capacity, crystallinity and purity that have recently attracted attention, especially for composite development. It possesses a three-dimension structure and large surface area that stabilizes adsorbed particles, enabling stable composites.[3] Macro and mesopores present at the bacterial cellulose structure have been regarded as a feasible alternative to mass transference problems caused by the zeolites compaction that prevents the specific molecules access to the micropores. Thus, herein we propose the synthesis of composites by means of impregnation of zeolite crystals on bacterial cellulose forming cartridges with high surface area.

Zeolite A was synthesized by hydrothermal method and then added to a suspension of functionalized cellulose prepared via bacterial route and them mixed by ultrasonification. The solids cartridges were prepared by lyophilization.

*Figure 1: Schematic representation of zeolite/celulose cartridges*

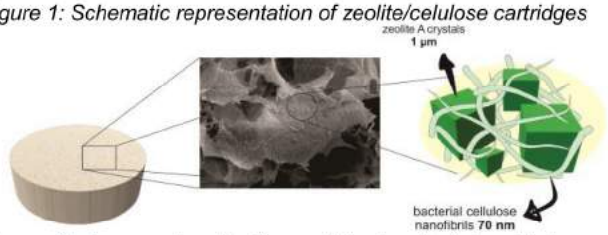


Figure 1 shows sheets formed by bacterial cellulose nanofibrils entwining the zeolite crystals, evidencing no aglomerations. X-ray diffraction patterns of zeolite A, cellulose and composites are presented in Figure 2, showing that zeolite crystals are preserved in the concentrations tested.

*Figure 2. X-ray diffratograms of the cartridges varying the weight proportion of cellulose (C) and zeolite (A): a) C0,5%; b) C0,5%A0,5%; c)C0,5%A1,0%; d) and h) A100%; e)C1,0%; f) C1,0%A0,5%; g)C1,0%A1,0%.*

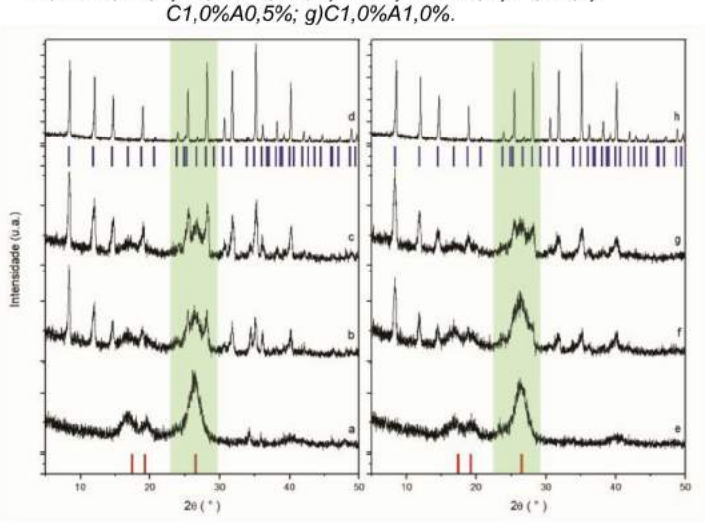


## References

1 SERRANO, D. P. et. al. **Chemical Society Reviews,** v. 42, n. 9, p. 4004-4035, 2013.
2 LOIOLA, A. R. et al. **Journal of Materials Chemistry,** v. 18, n. 41, p. 4985-4993, 2008.
3 SOHEILMOGHADDAM, M. et al. **Carbohydrate Polymers,** v. 106, p. 326-334, 2014.

**Área: MAT** **Inscrição:01356**

# Irreversible low-temperature dehydration of $H^+$-exchanged titanate nanostructures.

**Flávio M. Vichi (PQ),[1] Marina Moraes Leite (PG),[1*]**

**fmvichi@iq.usp.br; marina.leite@usp.br**

[1]*Departamento de Química Fundamental, Instituto de Química - USP;*

Palavras Chave: *Titanate Nanostructures, Acid Treatment, Dehydration*

## Highlights

$H^+$-exchanged titanate nanostructures (TNS) dehydrate at 150 °C. The dehydration leads to an irreversible crystal transformation to a different titanate, but not $TiO_2$.

## Resumo/Abstract

TNS find potential applications in energy conversion and water remediation, especially as absorbents of heavy metals.[1] TNS are obtained by the alkaline hydrothermal treatment of $TiO_2$. Despite the controversy regarding their crystal structure, it is known that they are layered $Na^+$-titanates that can be converted into $H^+$-titanates with acid treatment. We show that $H^+$-titanates undergo a crystal transformation at temperatures as low as 150 °C, due to irreversible dehydration.

TNS were obtained by treating $TiO_2$ with 30 wt% NaOH solution at 140 °C for 24h. $H^+$-exchange was achieved by soaking the powders in HCl solution at pH 1,5. The powders were dried at 60 °C for 24h, and heated at 150 °C for 2h. Samples were characterized by FTIR, Raman and UV-Vis (DRS) spectroscopies; XRD; TG-MS; ICP-OES; TEM; and BET.

$H^+$-exchanged sample has a BET surface area of 368 $m^2.g^{-1}$. Nanotubes and nanosheets were observed by TEM. Samples treated at 150 °C absorbed light throughout the visible range. DTG on Fig. 1 (a) shows that the $H^+$-titanate exhibits a broad weight loss centered at 106 °C corresponding to loss of $H_2O$. This dehydration leads to a shift toward higher angles in the XRD peak around 10° caused by the interlayer space contraction from *ca.* 10.4 Å to 8.6 Å (Fig. 1 (b)). Raman spectra on Fig 1 (c) reveal a shoulder next to the typical TNS band at 270 $cm^{-1}$ after dehydration. Anatase was not detected by XRD or Raman, indicating a different type of phase transformation at low temperature. Considering the proposed models for the crystal structure of TNS and the decrease of interlayer distance with the heat treatment, we believe that the dehydration of TNS at 150 °C may follow the equation:

$3\ H_2Ti_2O_5 \cdot H_2O \rightarrow H_2Ti_3O_7 + 4H_2O$

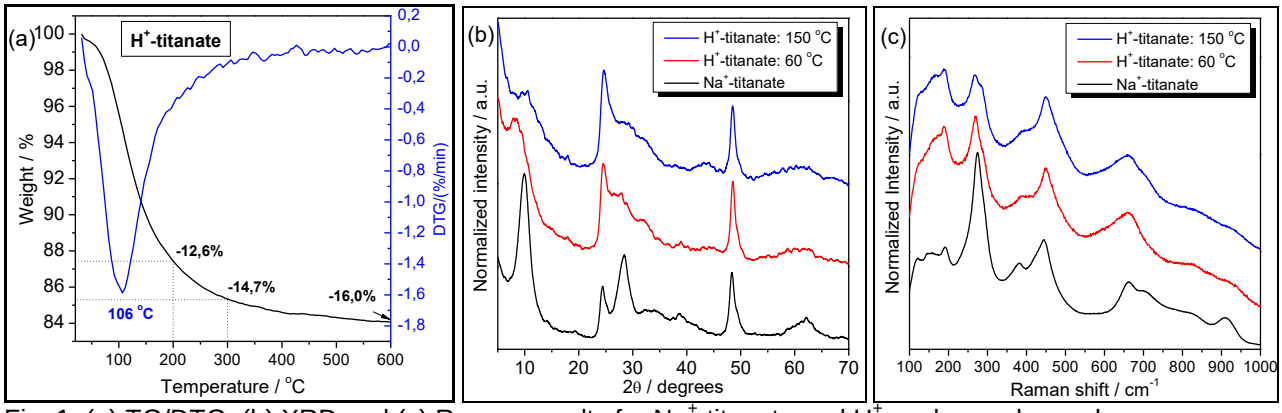


Fig. 1. (a) TG/DTG; (b) XRD and (c) Raman results for $Na^+$-titanate and $H^+$-exchanged samples.

References:

[1]Ge M, Cao C, Huang J, Li S, Chen Z, ZHANG KQ, et al. A Review of One-dimensional $TiO_2$ Nanostructured Materials for Environmental and Energy Applications. J Mater Chem A. 2016;4:6772–6801.

**Área: MAT** **Inscrição: 01303**

# Graphene Oxide functionalized with (3-Aminopropyl) triethoxysilane and its applications in composites.

**Tiago Serodre (PG)[1], Valdirene Gonzaga Resende (PQ)[2], Adelina Pinheiro Santos (PQ)[1], Clascídia Aparecida Furtado (PQ)[1]**

**tms@cdtn.br; tserodre@hotmail.com**

*[1]Laboratório de Química de Nanoestruturas de Carbono, CDTN. Brazil*
*[-2]Vale S.A. Brazil*

Keywords:*(Graphene oxide, Nanomaterial, Nanocomposites).*

## Highlights

- Graphene Oxide was functionalized with (3-Aminopropyl) triethoxysilane.
- The effects of the functionalized GO was assessed in silicate composites
- The mechanical strength of the composites was tested

## Abstract

Graphene oxide (GO) is a promising nanomaterial, coupling the superlative mechanical and electrical properties of graphene with ease in production from graphite and high dispersability in aqueous media[1]. Similarly, water-soluble sodium silicates (SS) are very versatile substances which find application in many fields of industry and engineering, such as adhesives, binders in foundries, and soil stabilizers and hardening agents in civil engineering, among others [2] The addition of small quantities of nanomaterials into sodium silicate matrices brings the possibility of increasing greatly the mechanical properties of the resulting composites.[3],[4]
Is this study, we have evaluated the functionalization of GO with (3-Aminopropyl) triethoxysilane (APTES) as means of rendering the nanomaterial better dispersible in the liquid SS, as well as creating functional groups on its surface which can crosslink with the SS matrix once it is polymerized, improving the mechanical properties thereof. The functionalization of the GO was evaluated through FTIR, potentiometric titration and thermogravimetric techniques. The dispersions were studied through UV-vis spectroscopy, and, finally, the mechanical properties of the composites were assessed in compressive mechanical tests.

[1] D. Marcano et al. “Improved Synthesis of Graphene Oxide” ACS Nano, 4 (8), 2010.

[2] G. Lagaly, W. Tufar, A. Minihan, and A. Lovell, “Silicates,” in Ullmann’s Encyclopedia of Industrial Chemistry, 2000.

[3] J. Wang, Z. Fan, and H. Wang, “An improved sodium silicate binder modified by ultra-fine powder materials,” China Foundry, vol. 4, no. 1, 2007.

[4] US 2013/0243973 A1 (2013) Vale S. A., invs.: F. C. Dutra, H. P. Pimenta, V.G. de Resende, A.A.M. Borges.

**Área: MAT** **Inscrição: 01335**

# Colloidal stability of silica nanoparticles during bioconjugation reactions with a silylated amyloidogenic peptide

**Carla C. Decandio (PG),[1] Michelle S. Liberato (PQ),[2] Mateus B. Cardoso (PQ),[2] Wendel A. Alves* (PQ).[1]***

carla.decandio@ufabc.edu.br; wendel.alves@ufabc.edu.br

*[1]Centro de Ciências Naturais e Humanas, Universidade Federal do ABC, Santo André, Brazil; [2]Brazilian Nanotechnology National Laboratory (LNNano), CNPEM, Campinas, SP, Brazil*

Keywords: *hybrid peptides, silica nanoparticles, active dressings, surface modification, cross-β structure.*

## Highlights

A simple method for silica nanoparticle dressing functionalization with peptides is presented. The grafting proceeds in a single step, by incubation with a hybrid silylated amyloidogenic peptide.

## Resumo/Abstract

Silica nanoparticles functionalized with bioactive biomolecules have been studied extensively in last year, because of their potential application as selective response of biosensors, drug delivery systems and “smart” material. Molecular self-assembly of oligopeptides into well-ordered nanostructures provide us models to exploring development of new materials, and the involvement of peptide aggregates in several degenerative diseases.[1] Recently, we have shown a systematic fibrillation behavior of an alternating $[RF]_{n=1-5}$ peptide (R = L-arginine, F = L-phenylalanine), which exhibit physicochemical properties of a beta-amyloid protein.[2] In order to create new properties and to stimulate particular desired functionalities, we proposed the synthesis of a silylated octapeptide $[(CH_3CH_2O)_3Si\text{-}G(RF)_4]$ (where G = L-glycine), by using solid-phase peptide synthesis, and its conjugation with 3-(triethoxysilyl)propyl isocyanate. At the same time, $SiO_2$NPs were prepared by using Stöber-based solvent varying method, which allows obtaining nanoparticles with a narrow size distribution and diameter of ~90 nm (as shown in the SEM micrograph below), followed by surface functionalization for colloidal stabilization, by incorporating different amounts of $[(CH_3CH_2O)_3Si\text{-}G(RF)_4]$ and sulfobetaine siloxane (SBS) in aqueous solution. In the proportion of (1:9, m/m), the functionalization was successfully achieved, obtainingæaazetaapotentialavalueaofa−51 mV and a hydrodynamic diameter of 110 nm for $SiO_2$-NPs, and −44 mV and a hydrodynamic diameter of 119 nm for peptide-dressed silica nanoparticles in aqueous solution. In addition, XPS analysis (Figure 1B) showed a peak with a binding energy of 400 eV, which was assigned to the N(1s) in the silylated peptide. Future studies for cellular targeting are underway.

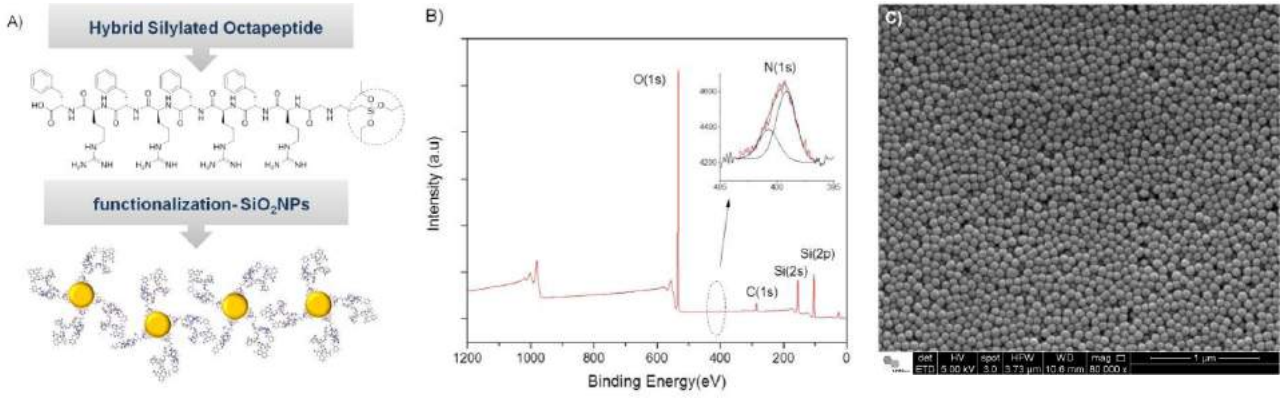


Fig.1. (A) Functionalization of $SiO_2$NPs with $[(CH_3CH_2O)_3Si\text{-}G(RF)_4]$, (B) XPS of $SiO_2$NPs@$[(CH_3CH_2O)_3Si\text{-}G(RF)_4]$, (C) Top-view SEM images of $SiO_2$NPs.

**References: 1.** Decandio, C.C.; Silva, E.R.; Hamley, I.W.; Castelletto, V.; Liberato, M.S.; Oliveira Jr., V.X., Oliveira, C.L.P.; Alves, W.A. Self-Assembly of a Designed Alternating Arginine/Phenylalanine Oligopeptide. *Langmuir* **2015**, *31*, 4513-4523; **2.** Silva, E.R.; Listik, E.; Han, S.W.; Alves, W.A.; Soares, B.M.; Reza, M.; Ruokolainen, J.; Hamley, I.W. Sequence length dependence in arginine/phenylalanine oligopeptides: implications for self-assembly and cytotoxicity. *Biophys. Chem.* **2018**, *233*, 1-12.

**Área: MAT** **Inscrição: 00748**

# Polyethylene Glycol Conjugation to Amyloidogenic Peptide via Click Reaction

**Wallace S. G. Pereira[1] (PG), Ana C. Domakoski[1] (PQ), Sandra V. Vassiliades[1] (PG), Francesca Cavalieri[2] (PQ), Wendel A. Alves[1]* (PQ).**

**wallace.sena@ufabc.edu.br; wendel.alves@ufabc.edu.br**

*[1]Centro de Ciências Naturais e Humanas, Universidade Federal do ABC, 09210-580, Santo André, Brazil; [2]Department of Chemical and Biomolecular Engineering, University of Melbourne, Melbourne 3010, Australia.*

Keywords: *Peptide copolymers, polyethylene glycol (PEG), Cross-β structure, click reaction, solid phase synthesis.*

## Highlights

We have used the click reaction in order to obtain a peptide-PEG conjugate containing an alternating $[RF]_5$ decapeptide (R = arginine, F = phenylalanine) conjugated to PEG of molar mass 1500.

## Resumo/Abstract

Recently, we have investigated the aggregation and cytotoxicity of short amyloid-like peptides with general form $[RF]_n$ (n = 1-5).[1] The sequences selected have been shown to be critical in fibrillization. We will also investigate the self-assembly of copolymers of the peptide with poly(ethylene glycol), PEG. PEG is a water soluble polymer that has been approved for pharmaceutical applications. The PEG will be attached to peptide fragments designed to bind to the full disease-causing peptide. We expect it will provide steric stability to peptide fibrils, forming a coating layer that prevents aggregation into larger aggregates as observed as a symptom of amyloid disease. The present work aims at the synthesis of the **2** copolymer using the click reaction as a key step. Click reaction is an interesting synthetic strategy to formation of a stereospecific triazole ring. To obtain the intermediates, **3** was dried in a vacuum oven and then monotosilated in the presence of triethylamine (TEA) in 81% yield (Scheme 1). The Tosyl-hydroxyl-PEG (PEGOTs) were used in the reaction with $NaN_3$ leading to formation of **4** (46%). In parallel, the amino group in side chain of lysine was deprotected and used in conjugation reaction with the activated propyolic acid, leading to **6** (33%). The reaction between **4** and **6** was performed in the presence of *t*-butanol, $CuSO_4$ and ascorbic acid, obtaining copolymer **2** (37%). Currently, steps **c, d** and **e** are being optimized concomitantly with the coupling between **2** and **1**, for the formation of **7**.

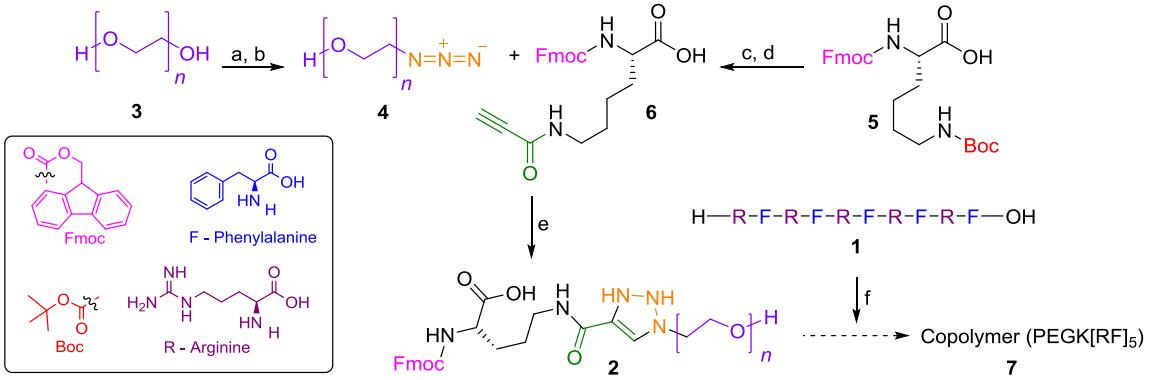


**Scheme: 1 – $[RF]_5$; 2 – Fmoc-Lys-PEG (PEGK); 3 – Polyethylene glycol (PEG 1500)**; **4 – $PEGN_3$; 5 – Fmoc-Lys(Boc)-OH (K); 6 – Fmoc-Lys-alkyne**. **a) 3,** 1,5 eq. 4-Toluenesulfonyl chloride (TsCl), 1,5 eq TEA, $CH_2Cl_2$, rt, 18h (81%); **b)** Tosyl-hydroxyl-PEG, 5 eq. $NaN_3$, $CH_3CN$, overnight, 90°C (46%); **c) 5**, TFA, $CH_2Cl_2$, 18h, rt (**I** - 98%). **d)** *i* **-** propiolic acid, 1,5 eq. NHS, EDC 1,5 eq, 18h, rt (**II** - 71%); *ii* **-** 1,0 eq. **I**, 1,0 eq. **II**, 0,1 eq. DMAP, $CH_2Cl_2$, overnight, rt (33%), **e)** 1,0 eq. **4**, 1,0 eq. **6,** 3 eq. sodium ascorbate, 3 eq. $CuSO_4 \bullet 5H_2O$, *tert*-butanol, 18h, rt (37%). **f)** Solid phase peptide synthesis.

**Reference: 1.** (a) Decandio, C.C.; Silva, E.R.; Hamley, I.W.; Castelletto, V.; Liberato, M.S.; Oliveira Jr., V.X., Oliveira, C.L.P.; Alves, W.A. Self-Assembly of a Designed Alternating Arginine/Phenylalanine Oligopeptide. *Langmuir* **2015**, *31*, 4513-4523; (b) Silva, E.R.; Listik, E.; Han, S.W.; Alves, W.A.; Soares, B.M.; Reza, M.; Ruokolainen, J.; Hamley, I.W. Sequence length dependence in arginine/phenylalanine oligopeptides: implications for self-assembly and cytotoxicity. *Biophys. Chem.* **2018**, *233*, 1-12.

**Área: MAT** **Inscrição:01069**

# Influence of reagents concentrations during synthesis for silver nanoparticles stability.

**Amanda Novais de Abreu (IC),[1*] Gabriella Silva (IC),[1] Deangelis Damasceno (PQ),[1] Monise C. R. Casanova Coltro (PQ),[1] Categorias: Pesquisador (PQ), Prof. de ensino fundamental/médio (FM), Pós-graduando (PG), Estudante de graduação (IC), Técnico de Nível Superior (TC) e Técnico de Nível Médio (TM).**

**monisec@gmail.com; mandsnovais16@gmail.com**

[1]Instituto Federal de Educação, Ciência e Tecnologia de Goiás, Campus Senador Canedo. Rua Firmino Rodrigues do Nascimento, Quadra 1F, lotes 21 e 22, Jardim Todos os Santos, Senador Canedo. Goiás.

Palavras Chave: synthesis, nanoparticles, silver, stability

## Highlights

Smaller diameter nanoparticles are obtained when PVA is used
Silver nanoparticles with higher concentration sodium tetrahydridoborate are smaller

## 2Resumo/Abstract

Mettalic nanoparticles have outstanding optical, electronic and mecanical properties. Some of these properties comes from the interaction between eletromagnetic field in specific frequencies that can induct a ressonance oscilation of free surface electrons on nanoparticles which is called surface plasmonic ressonance (SPR).

The obtainment of silver nanoparticles is based on a oxidation- redution reaction of a silver salt and a reduction agent, Sodium tetrahydridoborate – a powerful reduction agent which favors the reaction velocity making it higher and providing smaller particles when compared to weaker reduction agents. As a stabilizing agent for silver nanoparticles, polyvinil alcohol (PVA) was used.

Although synthesis of silver nanoparticles is not new, stability is a crucial factor for a good aplicability of silver nanoparticles. On this purpose, a range of variables can influence silver nanoparticles stability such as concentration of silver nanoparticles and reduction agent, reaction temperature, the lasting of the reduction process, storage.

In this work, the variation of silver salt, sodium tetrahydridoborate and PVA concentractions during nanoparticles synthesis were evalluated in order to understand their influence on silver nanoparticles stability. This was obtained through nanoparticles diameter analysis through transmission eléctron microscopy (TEM) and Ultraviolet and visible spectroscopy.

Results show that smaller diameter nanoparticles are obtained when PVA is used as a stabilizing agent when compared to nanoparticles obtained with just silver nitrate and sodium tetrahydridoborate. Silver nanoparticles synthesized with higher concentration sodium tetrahydridoborate are smaller when compared to the ones obtained with a smaller sodium tetrahydridoborate concentration.

**Área: MAT** **Inscrição: 01083**

# Hydrophobic and Electrostatic Effects of Chitosan Derivatives on the Antifungal Activity against *Aspergillus flavus*

**Hemelen Caroline Amoroso (IC),[1*] Márcio J. Tiera (PQ),[1] Aline M. F. Lima,[1] Odílio B. G. Assis (PQ),[2] Vera A. O. Tiera (PQ).[1]**

**verapoli@ibilce.unesp.br**

[1] *Departamento de Química e Ciências Ambientais, – UNESP, São José do Rio Preto, São Paulo, Brazil.*
[2] *Embrapa Instrumentação, Rua XV de Novembro, 1452, C.P. 741, 13560-970 São Carlos, Brazil.*

Keywords: Chitosan, ketoglutaric derivatives; Aspergillus flavus; antimicrobial.

## Highlights

Amphiphilic derivatives of chitosan were synthesized and characterized.
Anionic and hydrophobic groups strengthened the hydrophobic interactions and increased of inhibition of the fungal growth.

## Resumo/Abstract

In this work, chitosan derivatives containing anionic and hydrophobic groups were obtained by means of grafting with α-ketoglutaric acid (Ket) and dodecyl groups. The derivatives were characterized by 1H-NMR and FTIR techniques and their associative behavior in aqueous solution was studied by fluorescence spectroscopy. The insertion of both groups strengths hydrophobic interactions and DLS measurements showed that self-association leads to the formation of micrometric aggregates whose superficial charge depends on pH. Mycelial growth inhibition assays against *A. flavus* fungus were performed in the presence of increasing concentrations of the different polymers[1]. All the derivatives showed higher inhibitory effects than deacetylated chitosan (CH). The insertion of anionic groups reinforced the hydrophobic interactions and the ketoglutaric derivatives (DS = 15 and 25%) inhibited the growth of the fungus in 80% in the concentration of 2.0 g / L. The insertion of dodecyl groups and ketoglutaric acid provided zwitterionic derivatives that exhibited higher antifungal activities, which was attributed to hydrophobic interactions between the amphiphilics and the hydrophobic constituents of the cell wall.

Figure 1. $^{1}$H-NMR spectrum of the amphiphilic QCETO15D7 and general scheme of the comparative study of the ketoglutaric derivatives of chitosan.

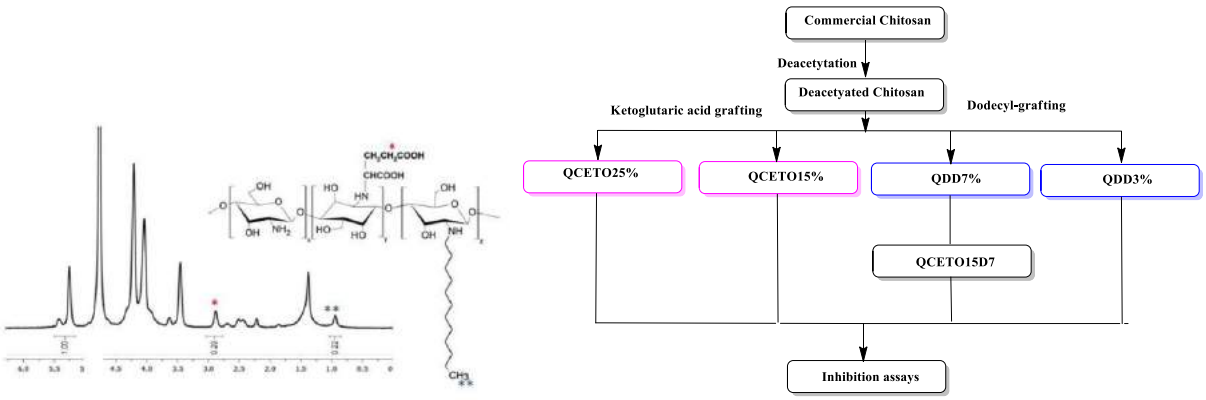


## ACKNOWLEDGEMENTS

FAPESP 2016/15736-0. EMBRAPA Instrumentação – São Carlos.

## REFERENCES

[1]FELIX VIEGAS DESOUZA, R. H.; TAKAKI, M.; PEDRO,R. d. O.; GABRIEL, J. d. S.; TIERA, M. J.; DEOLIVEIRA TIERA,V.A. Hydrophobic Effect of Amphiphilic Derivatives of Chitosan on the Antifungal Activity against Aspergillus flavus and Aspergillus parasiticus.Molecules 2013, 18,4437-4450.

**Área: MAT** **Inscrição:01100**

# PREPARAÇÃO E CARACTERIZAÇÃO DE FILMES DE ZEÍNA CONTENDO PONTOS QUÂNTICOS DE ZnO

**Francielle Schmitz (PG),[1] Ana Luiza Einloft Petter da Silva(IC),[1] Izabel C. Riegel Vidotti (PQ),[2] Lizandra M. Zimmermann (PQ).[1*]**

**E-mail: franci.schmitz@gmail.com; lmz@furb.br**

*[1]Departamento de Química. CCEN/FURB. Rua Antônio da Veiga, 140, CEP 89012-900 Blumenau, SC;*
*[2]Departamento de Química, UFPR; Av. Cel. Francisco H. dos Santos, 100, 81531-980 Curitiba – PR.*
Palavras Chave: *Pontos quânticos, óxido de zinco, zeína*, filmes de biopolímeros, nanocompósitos.

## Highlights

**Preparation and characterization of zein films with ZnO quantum dots (QDs)**. Nanocomposites films of zein biopolymer and ZnO QDs were prepared with good textural properties. They can be used for many applications, such as coating for food packaging, sensing and UV-blockers.

## Resumo/Abstract

Os Pontos Quânticos (Quantum Dots, QDs) são nanopartículas de materiais semicondutores de dimensões que variam de 2 a 10 nm, com propriedades distintas, como de elevada absorção e baixa tendência de fotodegradação. Em especial, os QDs de ZnO têm recebido especial atenção por serem ambientalmente amigáveis. Desta forma, o presente estudo objetiva o desenvolvimento de metodologias e técnicas para a síntese de nanopartículas de ZnO para a preparação de filmes com o biopolímero zeína. A Figura 1 esquematiza a preparação do nanocompósito.

A Figura 2 mostra o crescimento dos QDs durante 120 min, através das análises de UV-vis e fluorescência. No espectro de absorção da zeína é possível constatar que há sobreposição na região de absorção com os QDs. Disso advém a possibilidade de obtenção de um nanocompósito com excelentes propriedades bloqueadoras de UV. Os filmes obtidos também são fluorescentes, devido principalmente à emissão azul da zeína (Figura 1). A combinação de QDs de ZnO com o biopolímero zeína é promissora, produzindo filmes com bom aspecto textural para serem utilizados em diversas aplicações que demandem da atividade bloqueadora de UV, antimicrobiana, tais como em embalagens de alimentos e de sensoriamento para diversos analitos, considerando-se a resposta óptica de fluorescência tanto do ZnO como da zeína.

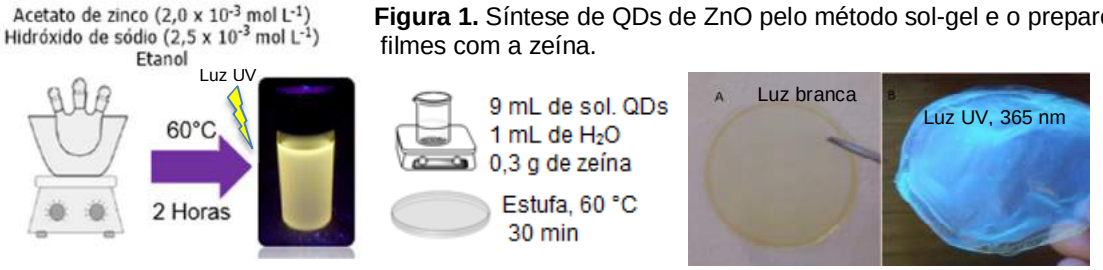


**Figura 1.** Síntese de QDs de ZnO pelo método sol-gel e o preparo dos filmes com a zeína.

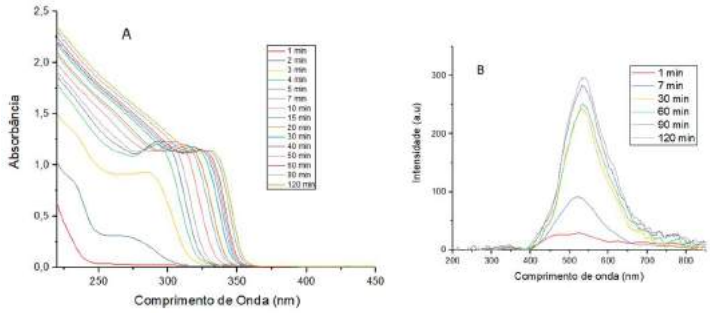


**Figura 2.** Espectros da dispersão coloidal de QDs de ZnO (A) de UV-vis (B) de emissão de fluorescência, com excitação em 330 nm.

Agradecimentos:
Furb, UFPR, Fapesc e Capes.

Referências

1. Zimmermann, L. M.; Baldissera, P. V.; Bechtold, I. H. *Mat. Res. Exp*,**2016,** 3, 7, 075018.

**Área: MAT** **Inscrição: 00926**

# Chitosan/waste coffee grounds composite: An efficient and eco-friendly adsorbent for removal of pharmaceuticals contaminants from water

**Emanuele F. Lessa (PG)*, Matheus L. Nunes (IC), André R. Fajardo (PQ)**

**drefajardo@hotmail.com; emanuelef.lessa@hotmail.com**

*Laboratório de Tecnologia e Desenvolvimento de Compósitos e Materiais Poliméricos (LaCoPol), Centro de Ciências Químicas, Farmacêuticas e de Alimentos, Universidade Federal de Pelotas (UFPel), Campus Capão do Leão s/n, 96010 900, Pelotas-RS, Brazil.*

Keywords: chitosan; coffee grounds; chitosan composites; adsorption; pharmaceutical contaminants; emerging contaminants.

## Highlights

>Chitosan/waste coffee grounds (WCG) composites were prepared;
>WCG-containing composites enhances the adsorption of pharmaceuticals from water;
>The composite is reusable in consecutive adsorption processes.

## Resumo/Abstract

Waste coffee-grounds (WCG), a poorly explored source of biocompounds, were combined with chitosan (Cs) and poly(vinyl alcohol) (PVA) in order to obtain composites. Overall, WCG showed a good interaction with the polymeric matrix and good dispersibility up to 10 wt-% (**Fig. 1**).

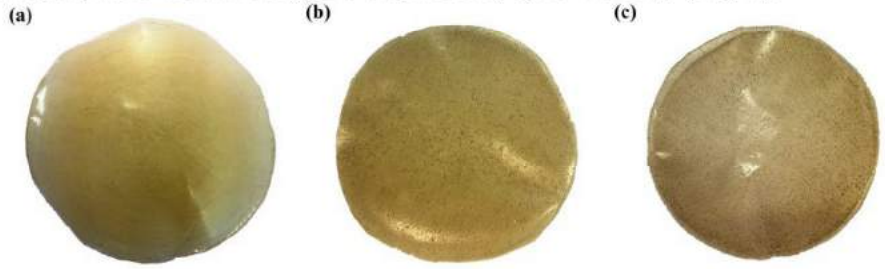


**Fig. 1**. Photographic images of composites prepared with (a) 0 wt-%, (b) 5 wt-% and (c) 10 wt-% of WCG.

At 5 wt-% WCG, the composite exhibited a noticeable enhancement (from 10 to 44%) of the adsorption of pharmaceuticals (metamizol (MET), acetylsalicylic acid (ASA), acetaminophen (ACE), and caffeine (CAF)) as compared to the pristine sample. The highest removal efficiency was registered at pH 6 and the removal followed the order ASA > CAF > ACE > MET. For all pharmaceuticals, the adsorption kinetics was found to follow the pseudo-second order model, while the adsorption mechanism was explained by the Freundlich isotherm. Reuse experiments indicated that the WCG-containing composite has an attractive cost-effectiveness since it presented a remarkable reusability in at least five consecutive adsorption/desorption cycles (**Fig. 2**).

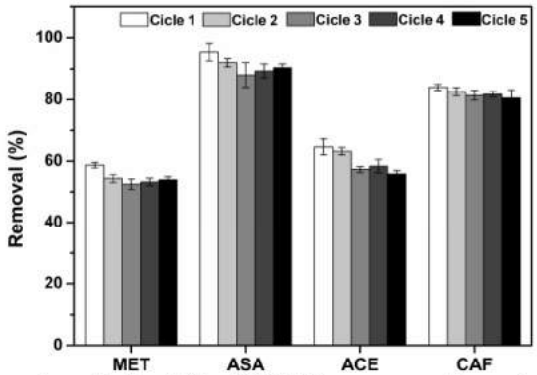


**Fig. 2.** Reusability of composite with 5 wt-% of WCG in consecutive adsorption/desorption cycles.

**Área: MAT** **Inscrição: 00875**

# Synthesis and Characterization of a Conjugated Metallopolymer Complexed with Terbium Ions.

**Emerson C. G. Campos (PG),[1*] Cristiano Zanlorenzi (PQ),[2] Denis A. Turchetti (PQ),[2] Leni C. Akcelrud (PQ)[2]**

**emerson.cg.quimica@gmail.com**

*[1]Programa de Pós-Graduação em Engenharia e Ciência dos Materiais (PIPE), UFPR; [2]Departamento de Química, UFPR.*

Keywords: *Metallopolymer, Terbium complexes, Conjugated polymer, Photophysical properties.*

## Highlights

Synthesis and characterization of a metallopolymer containing complexed Tb ions.
Photophysical properties of the conjugated polymer and of its non-conjugated counter part and of a model compound.

## Resumo/Abstract

Metallopolymers are hybrid structures in which metallic centers are linked to some of the repeating units, in order to obtain advantages from both parts: the properties from the metallic centers (optical, magnetic, electronic) and from the organic structure. Apart from the well-known mechanical features such as flexibility, easy processing and low cost of production other characteristics (electric conductivity, electrochromism, luminescence, high rate of carrier mobility), are added to the final material. In this line of pursuit, the synthesis of a metallopolymer was performed in two steps: first, the synthesis of the conjugated polymer poly[(9,9'-diexylfluorene-2,7-il)-alt-6,6"-(2,2':6',2"-terpyridine)] (LaPPS75) composed of fluorene (flu) and terpyridine (tpy) units, synthezised by Suzuki coupling, and in the second, the synthesis of the metallopolymer by *in-situ* reaction by adding to the polymer (LaPPS75), organic ligand acetylacetonate (acac) and terbium salt respecting the proportions 1:3:1, originating the LaPPS75Tb, (LaPPS75 complexed with Tb ions in the tpy sites). The structural and photophysical characterizations were performed $^{1}H$ and $^{13}C$ NMR, FTIR, UV-Vis and emission measurements in solution. The metallopolymer (LaPPS75Tb) showed photophysical behavior dependent on the chemical environment, in particular it was observed that the emission of the metal occurs only in DMSO solution. Curiously, all other solvents act as quenching agents in the emission of the metal, as shown in the Figure. With such characteristics this structure becomes potentially applicable in OLED's devices, chemical sensor, photoconductors, electrocatalysts, etc.

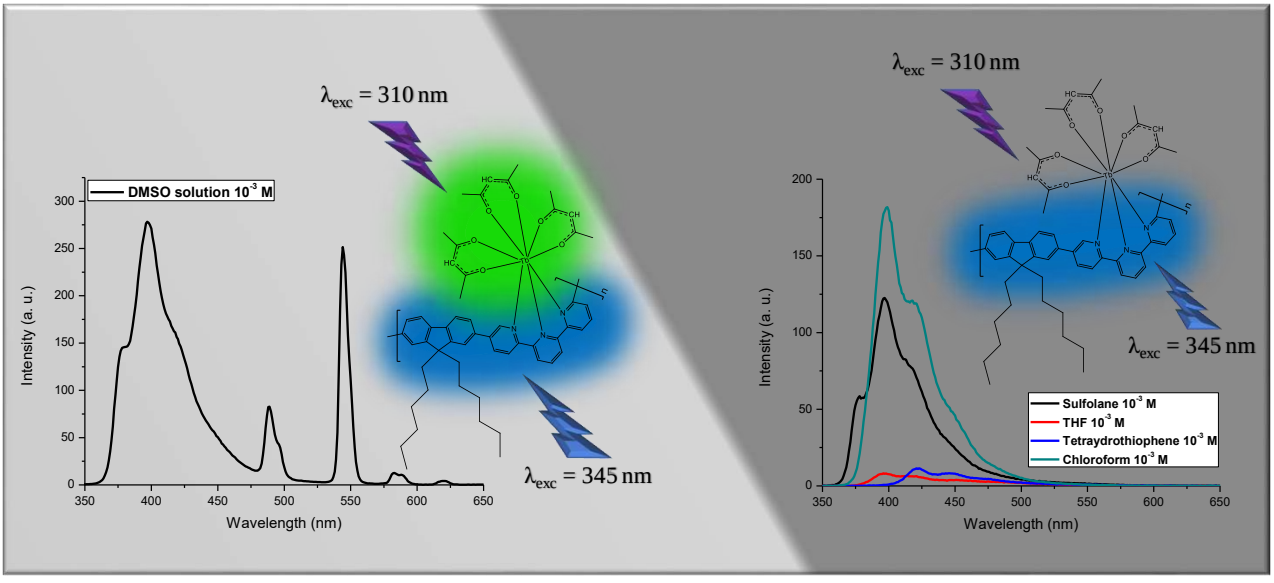

**Área: MAT** **Inscrição: 01001**

# Optimization of the Ni/Al layered double hidroxide synthesis by factorial design

**Luiz Diego Silva Rocha (PG),[1] Lucas Alex do Nascimento (IC),[1] Breno Guanabara Correa (IC),[2] Raquel Veríssimo dos Santos (PG),[2] Jaqueline Dias Senra (PQ),[2] Luiz Fernando Brum Malta (PQ).[1]***

**ldrocha@ufrj.br; lfbmalta@iq.ufrj.br**

*[1]Instituto de Química, UFRJ; [2]Instituto de Química, UERJ*

Palavras Chave: *LDH, Synthesis optimization, Crystal size, Catalyst*

## Highlights

Ni/Al LDH synthesis was optimized
Evaluated parameters were precipitation pH, Ni:Al ratio and precipitate washing and isolation
The responses were crystal size, $CO_3^{2-}$ content and the thermal stability

## Resumo/Abstract

LDH materials are based on a metallic M2+/M3+ hidroxide network. These are layered materials in which the interlayer space is occupied by anions to compensate the interlayer positive charge hence being anion exchangers. This property allows inserting anionic homogenous catalysts between layers giving rise to heterogenous catalysts.[1] To accomplish the liquid phase catalysis the layered structure must exhibit thermal stability as high as possible, low carbonate content (for the ease of ion exchange), cristallinity and high surface area.

Ni/Al LDHs were synthesized applying the varying pH approach. For optimization it was employed a $2^4$ factorial desing: the varied parameters were those of Table 1. Samples were characterized by XRD, FTIR and TGA.

From XRD patterns it was calculated the mean crystal size using the Scherrer formula.[2] These data permited to evidence which conditions set afforded the most crystalline sample (D = 7.1 nm): precipitation pH = 11, no washing, Ni:Al 3:1 and isolation by filtration. However this XRD pattern presented 2nd phase peaks. Similar condition sets were inspected and that applying pH = 8 and washing presented same crystallinity level (D = 5.2 nm). In addition FTIR evidenced this sample has the lowest carbonate content (bands at 1400 and 1360 $cm^{-1}$)[3] and TGA showed it is one of the most thermal stable. ICP-OES, BET and SEM characterizations are underway.

Table 1

| Level/Parameter | pH | Washing | Molar ratio (Ni:Al) | Isolation |
|---|---|---|---|---|
| **+** | 11 | Yes | 3:1 | Filtration |
| **-** | 8 | No | 2:1 | Centrifugation |

1. Silva AC et al J Nanometer. 2013, 2013, 1.
2. Weller MT Inorganic Materials Chemistry, Oxford University Press, 1994.
3. Toledo TV et al Quim. Nova. 2011, 34:4, 561.

**Área: MAT** **Inscrição: 01018**

# Avaliação dos engaços de uva *BRS Violeta* e *Vitis Labrusca Isabel* como potenciais precursores de carvão ativado para fins de adsorção

**Indira C. B. Pires (IC),[1] Braulio de Vilhena A. Tostes (IC),[1] Débora S. C. dos Anjos (PQ),[2] Kamilla B. S. Costa (PQ).[2*]**

**indirabrito98@gmail.com; kamilla.barreto@ifsertao-pe.edu.br**

*[1]Licencianda em Química, Campus Petrolina, IF Sertão-PE, Petrolina-PE; [2]Docente, Coordenação de Licenciatura em Química, Campus Petrolina, IF Sertão-PE, Petrolina-PE.*

*Palavras chave: Materiais lenhosos, Engaço uva, Carvão ativado, Adsorção.*

## Highlights

**Evaluation of BRS Violeta and Vitis Labrusca Isabel grapes stalks as potential raw of activated carbon by adsorption process.** Agroindustrial waste to produce activated carbon benefits the environment. Grapes stalks are cheap and abundant in São Francisco Valley. They showed potential to obtain activated carbon to adsorption.

## Resumo/Abstract

Devido à produção anual superior a 20 milhões de Kg de uva, na região do Vale do São Francisco, o presente trabalho investiga a potencialidade dos engaços *BRS Violeta* (E-In Vio) e *Vitis Labrusca Isabel* (E-In Isa) como precursores de carvão ativado (CA) para fins de adsorção. Os engaços *in natura* (E-In) foram secos, triturados e peneirados. As amostras foram calcinadas sob atmosfera inerte ($700^0$C,60min). Realizou-se a caracterização por IV, MEV, TG, área superficial e teores de cinza. Por IV, observa-se bandas em 1737cm$^{-1}$ (C=O, lignina e hemicelulose), em 2919cm$^{-1}$ (-$CH_2$, lignina, hemicelulose e celulose) e em 1428cm$^{-1}$ (-CH, alifática de ligninas) (Fig.1). Por MEV, observa-se morfologia de estrutura fibrosa e maciça (E-In) e a presença de poros nos carvões (Fig.2). Já por TG, evidenciou-se perdas de hemicelulose (143-210°C, E-In Vio e 136-215°C, E-In Isa) e celulose (210-354°C, E-In Vio e 215-364°C, E-In Isa) (Fig.3). Pelo método BET, constatou-se aumento na área superficial de 0,4572 (E-In Isa) para 1,8248 m$^2$.g$^{-1}$ (C Isa), ressaltando assim a importância do processo de carbonização para aprimoramento do material. Quanto aos teores de cinza, obteve-se 9,97% (E-In Vio) e 7,20% (E-In Isa). Estudos demonstram que bons precursores de CA possuem baixos teores de cinza[1]. Os engaços de uva apresentaram-se como potenciais precursores para a obtenção de CA para fins de adsorção de metais e/ou corantes.

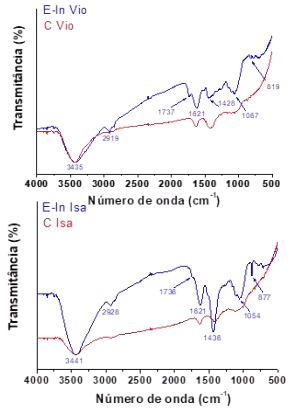


**Fig. 1.** IV: a) E-In Vio e C Vio b) E-In Isa e C Isa.

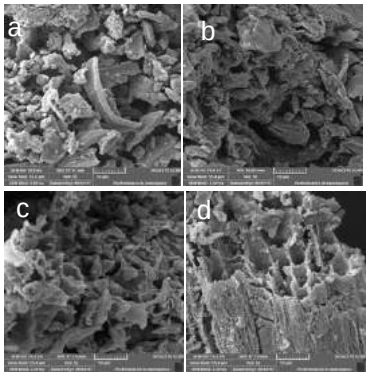


**Fig. 2.** Mev: a) E-In Vio b) E-In Isa c) C Vio d) C Isa.

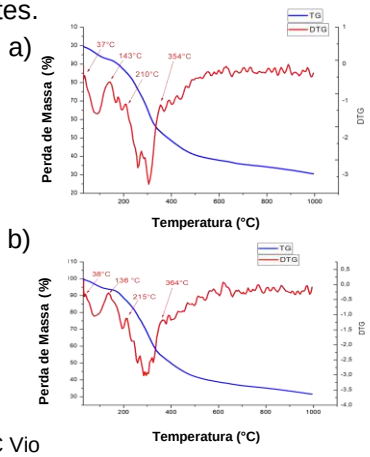


**Fig. 3**. TG/DTG: a) E-In Vio b) E-In Isa.

**Tabela 1.** Área Superficial, volume e tamanho dos poros.

| Amostras | Área Superficial BET (m².g$^{-1}$) | Volume Dos Poros (cm³.g$^{-1}$) | Tamanho dos Poros (Å) |
|---|---|---|---|
| E-In Isa | 0,4572 | 0,000165 | 659,817 |
| C Isa | 1,8248 | 0,002393 | 942,835 |

**Referências:** [1]PRADO, R.G. Programa de pós-graduação em agroquímica, UFLA, 2010.

**Agradecimentos:** PIBIC IF Sertão-PE, CETENE, UNIVASF.

**Área: MAT** **Inscrição:00885**

# A photodispositive based on reduced graphene oxide modified with polyethylenimine to deliver amphotericin B

**Letícia S. Vitorino (IC)*, Isabela A. Albuquerque Bessa (IC), Thiago Custódio (PG), Evelyn C. S. Santos (PG), Célia M. Ronconi (PQ).**

leticia_vitorino@id.uff.br; cmronconi@id.uff.br

*Universidade Federal Fluminense, Instituto de Química, Programa de Pós-Graduação em Química da UFF, Outeiro de São João Batista s/n, Campus do Valonguinho, Centro, 24020-141, Niterói, RJ, Brazil.*

Keywords: *leishmaniasis, reduced graphene oxide, amphotericin B, polyethylenimine, drug delivery system, near-infrared light absorbance*

## Highlights

Nanodispositives based on functionalized rGO increases water solubility of AmB and can be employed in the treatment of cutaneous leishmaniasis by drug release under NIR light absorbance.

## Resumo/Abstract

Amphotericin B (AmB) is an antifungal used to treat leishmaniasis symptoms but presents low water solubility and severe side effects, such as nephrotoxicity.[1] Aiming to enhance drug solubility and reduce drug´s toxicity, new drug delivery systems (DDSs) based on functionalized reduced graphene oxide (rGO) have been developed. These DDSs have good biocompatibility, high drug loading efficiency and excellent near-infrared (NIR) light absorbance, which can be used to stimulate drug release.[2] Thus, herein, we report the synthesis, characterization and drug loading of a new photodispositive based on rGO modified with polyethylenimine (PEI). To prepare rGO-PEI, graphene oxide was obtained by a modified Hummers method[3] followed by exfoliation, coated with PEI and reduced with hydrazine hydrate. The device was evaluated by ATR-IR, which showed the absence of C-O-C and C=O bands indicating the reduction step was successful carried out. The bands of C-H and C-N indicated the presence of PEI. TEM analysis (Fig. 1a) showed a two dimensional structure formed by thin and wrinkled sheets. Zeta potential measurements revealed a positive charge surface up to pH = 9 due to the protonated amino groups of PEI. The device was loaded with AmB to yield rGO-PEI-AmB with loading efficiency of 96%. AmB release from rGO-PEI-AmB in a dispersion of 2.36 mg/mL was investigated at pH = 4.5, under NIR irradiation (λ=800 nm) and monitored by UV-Vis spectroscopy. AmB was released under NIR irradiation. This material will be further tested for cutaneous leishmaniasis.

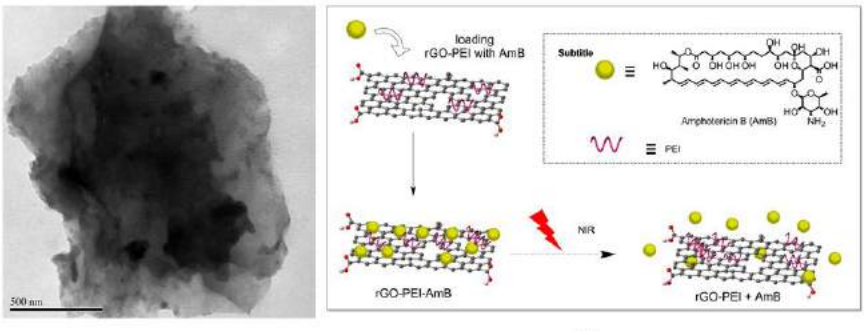


**Figure 1: (a)** TEM image of rGO-PEI and **(b)** Scheme of loading rGO-PEI with AmB and release with NIR light.

**Acknowledgements:** UFF, CNPq, CAPES, LAMATE, LAME, Plataforma de Microscopia do IB-UFF.

[1] Chávez-Fumagalli, M. A. *et al.*, *Rev Soc Bras Med Trop.*, **2015**, *48*, 235-242.
[2] Robinson, J. T. *et al. J. Am. Chem. Soc.*, **2011**, *133*, 6825–6831.
[3] Santos, T. C., Ronconi, C. M. *J. $CO_2$ Util.*, **2017**, *20*, 292-300.

**Área: MAT_____** *(Inserir a sigla da seção científica para qual o resumo será submetido. Ex: ORG, BEA, CAT)*

**Inscrição: 00740____** *(Inserir o número de inscrição do autor que fez a submissão)*

# Desenvolvimento de nanocompósito argila aniônica/carvão hidrotérmico para uso como adsorvente multifuncional

**Roberta Laiz B.S. Albano (PG)[1]*, Odair P. Ferreira (PQ)[1]**

**opferreira@gmail.com; robertalaizalbano@gmail.com**

[1] *Laboratório de Materiais Funcionais Avançados (LaMFA), Departamento de Física, Universidade Federal do Ceará*

Palavras Chave*: Hidróxido duplo lamelar, Celulose, Carbonização hidrotérmica, Nanocompósito, Adsorção.*

## Highlights

## Development of anionic clay/hydrochar nanocomposite for application as multifunctional adsorbent

Cellulose and anionic clay as raw materials; Hydrothermal carbonization to prepare anionic clay/hydrochar nanocomposites; Multifunctional materials for adsorption of anionic and cationic dyes.

## Resumo/Abstract

O presente trabalho buscou desenvolver materiais multifuncionais (nanocompósitos) envolvendo argila aniônica (hidróxidos duplos lamelares) e carvão hidrotérmico produzidos via carbonização hidrotérmica (HTC) da celulose na presença da argila, visando seu emprego na adsorção simultânea de espécies químicas catiônicas e aniônicas. As argilas aniônicas são materiais adsorventes e/ou trocadores aniônicos e os carvões hidrotérmico, devido suas características de superfície (grupos oxigenados), são materiais adsorventes catiônicos. A HTC apresenta-se como uma metodologia promissora para agregar valor aos resíduos de biomassa/biomoléculas, sendo a biomassa uma fonte de matéria-prima renovável e abundante para a produção de materiais carbonáceos de forma sustentável. Os nanocompósito formam produzidos via HTC da celulose na presença da argila aniônica, constituída de $Mg^{2+}$, $Al^{3+}$ e $SO_4^{2-}$ na razão $Mg^{2+}/Al^{3+}$ igual a 2, e utilizando tempos 4 e 24 h e temperaturas 230 e 250 ºC para as reações hidrotérmicas. Estes materiais foram caracterizados quanto suas propriedades composicionais, térmicas, estruturais, texturais e morfológicas. Ensaios prévios de adsorção com corantes catiônico (Azul de Metileno) e aniônico (Azul Reativo 19) foram realizados com os sistemas preparados. Estes resultados indicaram que o nanocompósito preparado a 230 ºC e 4 h reação apresentou os resultados mais promissores quanto à interação com os corantes catiônico e aniônico (Figura 1). Portanto, o nanocompósito produzido possui multifuncionalidade, sendo caracterizado pela sua capacidade de adsorção de espécies químicas carregadas positivamente e negativamente, podendo ser aplicados como novo adsorvente em remediação ambiental.

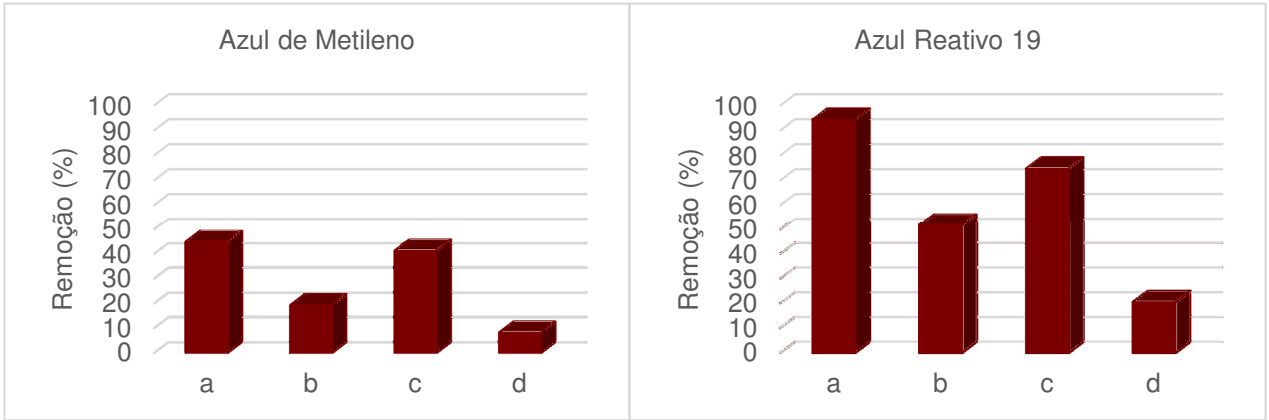


**Figura 1:** Eficiência de remoção dos corantes Azul de Metileno e Azul Reativo 19 para os compósitos **(a)** Mg-Al/C (230 ºC, 4 h); **(b)** Mg-Al/C (230 ºC, 24 h); **(c)** Mg-Al/C (250 ºC, 4 h); **(d)** Mg-Al/C (250 ºC, 24 h). *Concentração dos corantes: Azul de Metileno 50 mg/L; Azul Reativo 19 100 mg/L. Dosagem: 1 g/L. Condições dos ensaios: agitação constante por 4 h à temperatura de 25 ºC.*

**Área: MAT** **Inscrição: 01137**

# Oleylamine-mediated synthesis of unusual 4H (*hcp*)/*fcc* phase in gold nanorods

**Daniel A. de Moraes (PG)[1], João B. Souza Jr. (PG)[1], Vishnu Mogili (PQ)[2], Fabio F. Ferreira (PQ)[3], Laudemir C. Varanda (PQ)[1,*]**

**lvaranda@iqsc.usp.br**

*[1]Colloidal Materials Group, Chemistry Institute of São Carlos – USP, São Carlos, Brazil; [2]Electron Microscopy Laboratory - LNNano, Campinas, Brazil; [3]Center for Natural and Human Science, UFABC, São Paulo, Brazil*

Palavras Chave: *gold nanorods, oleylamine-mediated route, 4H hcp phase, stacking fault, HRTEM.*

## Highlights

The oleylamine-mediated method was used to synthesize Au nanorods in an unusual hexagonal-close package (4H *hcp*) phase. The *hcp* phase in a mixture of the *fcc* phase were assigned to the Au atoms stacking fault and confirmed by X-ray diffraction and high-resolution transmission electron microscopy.

## Resumo/Abstract

Crystal structures control is one of the key challenges in the functional inorganic nanostructures. Noble metals (Au, Ag, Pt, and Pd) typically crystallize in the face-centered cubic (*fcc*) phase at ordinary conditions. Recently, Zhang *et al.,* obtained gold nanosheets using 1-amino-9-octadecene[1] and nanoribbons in mixture of oleylamine and 1,2-dichloropropane[2] in a hexagonal close-package (*hcp*) phase. In this work, we synthesized Au nanorods with average diameter of 10 nm and length ranging from 30 to 550 nm in the unusual 4H *hcp* structure using oleylamine as both, reducing agent and solvent. The synthesis was carried out at 65° C for 24h under $N_2$ flow in a reflux system and using the $HAuCl_4.3H_2O$ as precursor. X-ray diffraction patterns showed a mixture of 4H *hcp* and *fcc* phases, which were confirmed by Rietveld refinement using the stacking fault model resulting in the 20% of the 4H *hcp* phase. Figure 1 presents high-resolution transmission electron microscopy (HRTEM) images shown 4H *hcp* nanorods with the *fcc* phase located preferably at the end of the nanorods. The HRTEM image in the Figure 1c shows the atomic spacing of 2.4 Å and 2.5 Å assigned to the (004) and $(1\bar{1}0)$ planes of the 4H phase, respectively. UV-Vis-NIR results show a low intensity band at 520 nm and a broadned band from 800 nm to the NIR assigned to transversal and longitudinal localized surface plasmon resonance (LSPR), respectively covering the therapeutic window. In conclusion, the unusual 4H *hcp*-Au nanorods were synthesized using a simple oleylamine-mediated route with potential application as sensor, catalyst and biomarker. **Acknowledgement:** FAPESP and CNPq for financial support.

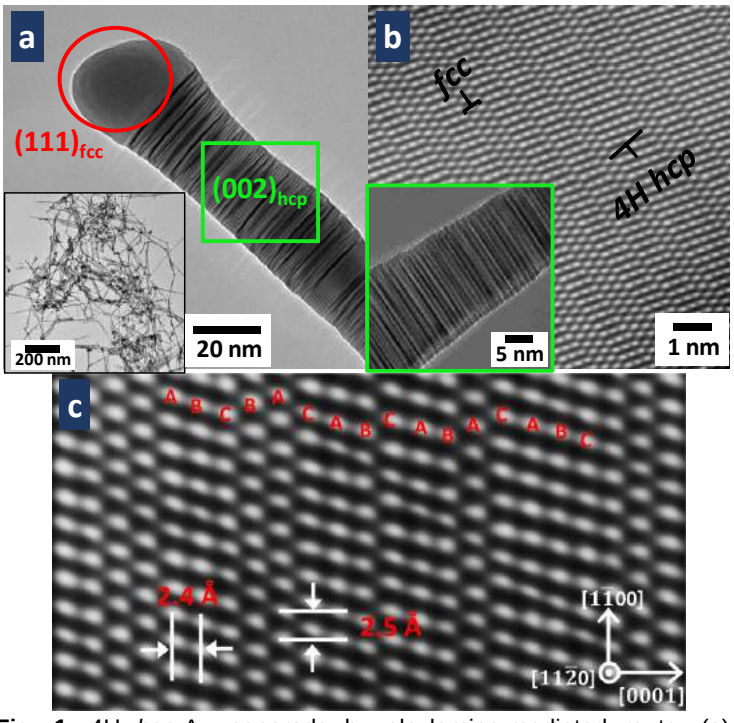


**Fig. 1.** 4H *hcp*-Au nanorods by oleylamine-mediated route: (a) HRTEM of individual nanorod shown *fcc* and *hcp* domains and low magnification TEM image (inset), (b) HRTEM of *hcp* region (inset) and stacking fault structure, and (c) HRTEM of the 4H *hcp*-Au phase.

[1] X. Huang, et. al, *Nature Communications*. 2:292, **2011**.
[2] Z. X. Fan, et. al, *Nature Communications*. 6:7684, **2015**.

**Área: MAT**
*(Inserir a sigla da seção científica para qual o resumo será submetido. Ex: ORG, BEA, CAT)*

**Inscrição: 00843**
*(Inserir o número de inscrição do autor que fez a submissão)*

# 45S5 Bioglass Scaffold to repair bone tissue damages

**Mariana de Oliveira Silva (PG),[1*] Celso Aparecido Bertran (PQ).[1]**

**mariana.oliveira@iqm.unicam.br; bertran@iqm.unicamp.br**

[1]*Instituto de Química, Unicamp*

Scaffold, Bioglass, Tissue damage

## Highlights

Development of a scaffold made with 45S5 Bioglass particles, binding them with 45S5 sol-gel. Production of pores using surfactant and hydrogen peroxide and flash sintering to avoid crystallization.

## Resumo/Abstract

The 45S5 Bioglass® is one the most promising materials to be used in bone tissue damages, especially due to its biocompatibility, bioactivity and osteoinduction. However, the production of BG 45S5 scaffolds with a good compromise between porosity and mechanical properties results in the crystallization of the glass because of its small sintering window, lowering the properties that make it such an interesting material. In this work, 45S5 scaffolds were produced using particles of this glass made by melt and quenching together with the "Fritas" method, binding them using a 45S5 Bioglass® film produced by sol-gel, and surfactant and hydrogen peroxide to produce pores. The characterization of the final material was made with microscopy and XRD. A non-crystalline white scaffold (Figure 1) with pores between 50 and 100 μm was obtained. The sol-gel did not cover the particles homogeneously as it was indicated by the SEM image (Figure 2) where some rough regions are observed.

Figure 1. Scaffold picture

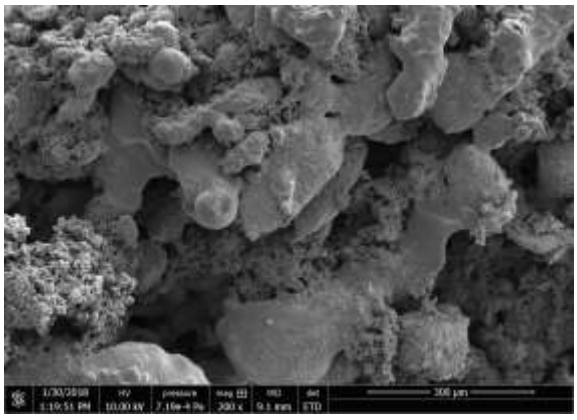

Figure 2. SEM image of the 45S5 Bioglass® Scaffold

**Área: MAT**
*(Inserir a sigla da seção científica para qual o resumo será submetido. Ex: ORG, BEA, CAT)*

**Inscrição: 01374**
*(Inserir o número de inscrição do autor que fez a submissão)*

# Silica MCM-48 nanoparticles functionalized with diphenylsilane as BTEX adsorbent.

**Daniel Santos Garcia Osório (PG)[1], Helton Pereira Nogueira (PG)[1], Koiti Araki (PQ)[1]**

**koiaraki@iq.usp.br; danielg1@usp.br; helton.nogueira@usp.br**

[1]*Departamento de Química Fundamental, Instituto de Química, Universidade de São Paulo (IQ-USP)*[1]

Palavras Chave: *MCM48, "BTEX", Cromatografia, Adsorção.*

## Highlights

- Synthesis of diphenylsilane-functionalized MCM-48 silica for efficient removal of BTEX
- Functionalized MCM-48 silica with high surface area as BTEX adsorbent
- Regular shape of pores allowing easy access to active sites without obstruction of channels.

## Resumo/Abstract

O BTEX (mistura de benzeno, tolueno, etil-benzeno e xileno) destaca-se pelo seu potencial de contaminação e toxicidade à saúde humana e ambiental, podendo provocar os mais diversos efeitos incluindo danos ao fígado, rins, coração, pulmões e sistema nervoso. Frente a esse problema, os adsorventes baseados em sílica são uma alternativa para remover eficientemente os BTEXs dos corpos d'água. A preparação das nanopartículas de sílica mesoporosa MCM-48 foi baseada no método de Stöber modificado (Kim, Chung, and Lin 2010). Proporções estequiométricas do material preparado foram funcionalizadas com dimetoxidifenilsilano. As análises por FTIR (Fig. a) revelou que a sílica funcionalizada com grupos fenil apresenta bandas em 3079 e 3059 $cm^{-1}$ correspondentes as vibrações de estiramento C-H do anel benzênico, além das bandas em 2925, 2851, 2985 e 2954 $cm^{-1}$ atribuídas ao estiramento e flexão da ligação C-H do grupo metoxi. As bandas em 1432 e 1385 $cm^{-1}$ foram atribuídas a vibração C=C do anel aromático, e as bandas em 700 e 740 $cm^{-1}$ a deformação angular fora do plano do benzeno. No DRX (Figura b) aparecem picos intensos atribuídos aos planos cristalinos (211) e (220), além de picos menos intensos correspondentes aos planos (321), (400), (420), (332), (422) e (431). Esses picos são característicos da meso-estrutura do MCM-48 que tem poros com simetria Ia3d, e área superficial de 1011 $m^2.g^{-1}$ determinada pelo método BET As imagens de MET revelaram os tamanhos e morfologias das amostras de sílica MCM 48 pura e funcionalizada. O tamanho da partícula do material preparado está na faixa de 95 ± 15 nm que permanece mais ou menos constante mesmo depois dos processos de funcionalização (Figura c).

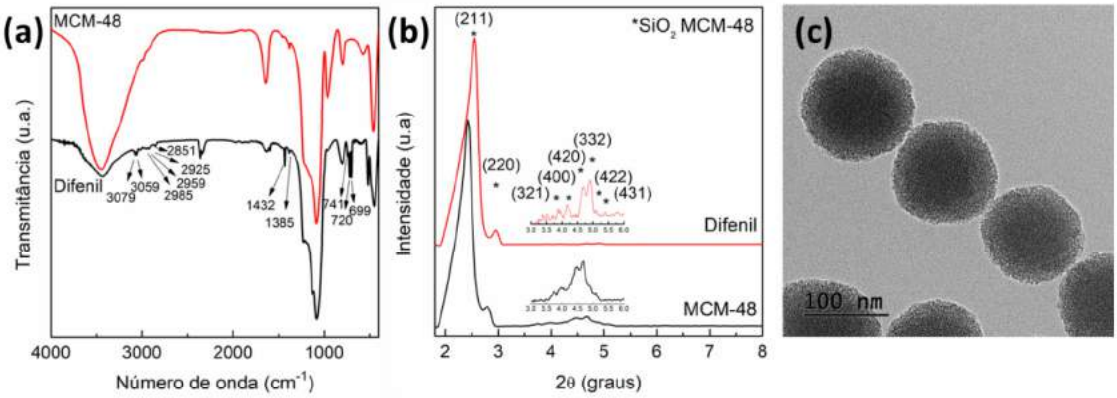

**Área: MAT**
*(Inserir a sigla da seção científica para qual o resumo será submetido. Ex: ORG, BEA, CAT)*

**Inscrição: 00689**
*(Inserir o número de inscrição do autor que fez a submissão)*

# Relation between porosity, particle size and adsorption efficiency of methyl methacrylate-based crosslinked polymer resins

**Maximiliano F. Martins (IC),[1]*Carla M. F. Silva (PQ),[2] Elizabete F. Lucas (PQ),[3]Queli A. R. Almeida (PQ),[1]Thiago M. Aversa (PQ).[1]**

**thiago.aversa@ifrj.edu.br; maxfmartins@gmail.com**

*[1] Federal Institute of Education, Science and Technology of Rio de Janeiro, IFRJ; [2] Macromolecules Institute, Federal University of Rio de Janeiro, IMA/UFRJ; [3] Metallurgy and Materials Engineering, Federal University of Rio de Janeiro, PEMM/UFRJ*

Keywords:*suspension polymerization, crosslinked polymer, porosity, particle size, adsorption*

## Highlights

Suspension polymerization is an important process to obtain spherical polymers (beads).
Porosity could be affected by polymerization mechanical stirring.
Adsorption is directly affected by bead particle size.

## Abstract

Suspension polymerization is a heterogeneous polymerization process in which a phase containing monomer(s) and initiator is dispersed in a continuous phase. The polymer particles obtained from this technique commonly have spherical morphology. Several factors can affect the characteristics of the obtained material. However, the stirring speed is the one that most significantly interfere the particle size: the higher the speed, the smaller the particle size [1]. For polyvinyl chloride (PVC), it is known that the stirring speed affects the porosity of the particles, but this is not reported for other types of polymers [2]. Thus, the aim of this work was to evaluate the relation between the polymer beads particle size and its porosity, also evaluating the adsorption capacity. For this, three porous polymeric resins based on trimethylolpropane trimethacrylate (TMPTMA) and methyl methacrylate (MMA) were obtained using only varying the mechanical stirring speed: 460 RPM, 310 RPM and 250 RPM. Preliminary adsorption tests revealed that the higher the agitation speed, the lower the adsorption efficiency, and in the next step quantitative analysis of porosity will be carried out.

[1] GOKMEN, M. T.; DU PREZ, F. E. Porous polymer particles – A comprehensive guide to synthesis, characterization, functionalization and applications. **Prog.Poym.Sci.** v. 37, p. 365-405, 2012.

[2] ALEXOPOULOS, A. H.; KIPARISSIDES, C. One the prediction of internal particle morphology in suspension polymerization of vinyl chloride. Part I: The effect of primary particle size distribution. **Chem. Eng. Sci.** v. 62, p. 3970-3983, 2007.

**Área: MAT** **Inscrição: 00605**

# Atividade Antimicrobiana e Caracterização de Filmes de Amido de Mandioca/Quitosana Reforçados com Fibras de Cana-de-Açúcar

**[1]Paula C. Ireno Franco (PG), [1*]Mary Leiva Faria (PQ), [2]Ana P. Bilck (PQ), [1]Elaine A. S. Menegon(PQ)**

**paulaconsolif@hotmail.com; ml.faria@uol.com.br**

*[1]Fundação Educacional do Município de Assis -FEMA/IMESA, [2]Departamento de Química-UEL*

Palavras Chave: *Biofilme, Amido, Fibra, Quitosana.*

## Highlights

Antimicrobial Activity and Characterization of Cassava Starch/Quitosan Films Reinforced with Sugarcane Fiber - Polymeric blends of starch/chitosan/sugarcane fiber were produced, characterized and antimicrobial activity evaluated.

## Resumo/Abstract

Filmes produzidos de amido de mandioca, plastificados com glicerol e com a adição de 15% fibras de cana de açúcar (F15) levaram à formação de compósitos poliméricos com boas propriedades de barreira. Porém, ensaios em massa de pastel indicaram que os filmes ainda se apresentavam bastante higroscópicos para serem empregados como embalagem ativa. Assim, com a finalidade de se obter filmes com melhores propriedades físicas e funcionais, o objetivo deste trabalho foi verificar a influência da quitosana nas propriedades mecânicas e de barreira da blenda polimérica amido/quitosana/fibra cana-de-açúcar, bem como na atividade antimicrobiana destes filmes contra *E. coli*. Os filmes foram produzidos com amido de mandioca (3 g/100g solução filmogênica), glicerol (30g/100g amido), fibra (15 g/100g amido) e quitosana (0.25g, 0.5g e 1g/100g solução filmogênica). Todos os filmes foram produzidos pela técnica de *casting.* A adição de quitosana aumentou a permeabilidade ao vapor de água quando comparado ao filme controle (FC-F15). As propriedades mecânicas destas formulações constam da tabela 1.

**Tabela 1. Propriedades Mecânicas dos Filmes**.

| Formulação | Resistência Máxima a Tração (MPa) | Alongamento na ruptura (%) | Módulo de Young (MPa) |
|---|---|---|---|
| FC-F15 | 0,59 (±0,1) | 15,36(±3,5) | 3,23(± 0,5) |
| F-0,25 | 6,091(±1.3) | 37,38(±6.1) | 242,89(±27.5) |
| F-0,50 | 6,946(±1.2) | 43,91(±9.2) | 261,56(±30.7) |
| F-1,00 | 8,049 (±0.7) | 22,99(±4.4) | 299,49(±20.1) |

Conclui-se que a adição de quitosana à blenda amido/fibra cana-de-açúcar, melhorou as propriedades mecânicas dos filmes, entretanto, não melhorou as propriedades de barreira, tornando inviável a aplicação dos filmes em massas de pastel. O teste do halo confirmou a atividade antimicrobiana da quitosana, visto que a *Escherichia coli* mostrou-se sensível frente à todas as concentrações da quitosana empregada nos filmes.

VASCONEZ, M. B.; FLORES, S. K.; CAMPOS, C. A.; ALVARADO, J.; GERSCHENSON, L. N., *Food Research International*, **2009**, 42**,** 762.

**Área: MAT**_____ **Inscrição:_00730**_____
*(Inserir a sigla da seção científica para qual o resumo será submetido. Ex: ORG, BEA, CAT)* *(Inserir o número de inscrição do autor que fez a submissão)*

# Controlled delivery fertilizer: from agro-residues to agribusiness

**Roselena Faez (PQ),[1] You-Lo Hsieh (PQ)[2]**

**faez@ufscar.br**

*[1]Laboratório de Materiais Poliméricos e Biossorventes, DCNME, UFSCar-Araras; [2]University of California- Davis.*

Palavras Chave: Potassium nitrate, cellulose, sugarcane bagasse, ferti-release.

## Highlights

Controlled delivery fertilizer based on cellulose-based fiber and chitosan. Three-layer films assembly. Cellulose fiber and TEMPO-CNF improve ionic interaction with potassium nitrate.

## Resumo/Abstract

Controlled delivery system is a remarkable research area since with strategic materials the chemical substances such as agrochemical can target the soil and plant with improve efficacy. Cellulose is the most abundant natural biopolymer and agricultural residues such as sugarcane bagasse (SCB) and rice straw are interesting sources for obtaining low cost materials. Approximately 280-300 kg of bagasse (50% moisture) are generated per ton of sugarcane. In these work we prepared a three-layer assembly material based on chitosan and crude SCB or cellulose-rich material extracted from SCB by alkali and acidified chlorite-alkali sequential treatments and TEMPO. The release is modulated according to the fiber used. As more pure the cellulose-based fibers higher the homogeneity and slower the fertilizer release. Additionally, the small amount of TEMPO-CNF in the films (0.1 wt.%) decreases the release. As an example, Fig. 1 shows the comparative potassium release profile from three-layer films containing CNF in the core. A high delay in release is observed for films with CNF. Two lag times were verified, up to 1h (releasing 25%) and up to 48h (releasing only 35% of the total potassium). This behavior is explained by the increase of negative and positive charges in the system that contributes to improve the ionic interaction with $KNO_3$ salt. The presence of CNF increases the negative charge that can interact with potassium cation and nitrate anion with positively charged chitosan. The K-containing core-coating assembling demonstrates to be a promising material to be used as slow or controlled delivery fertilizer.

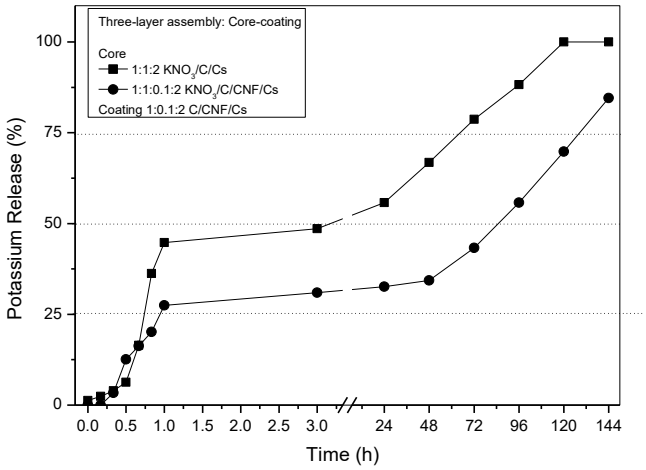


Figure 1. Potassium release from 1:1:2 $KNO_3$/C/Cs coated with 1:0.1:2 C/CNF/Cs

**Área: MAT** **Inscrição: 01091**

# Glycerol oleate reaction with citric acid to produce solid and liquid products for different applications

**Fernanda G. Mendonça (PG),[1]* Izadora R. S. Menezes (IC),[1] Philipe X. Fonseca (IC),[1] Mariana de S. Gomes (PG),[1] Mariana R. D. Santos (IC),[1] Adriana B. Salviano (PG),[1] Paulo S. Martins (PQ),[2] Rochel M. Lago (PQ)[1]**

**nandagm@ufmg.br**

*[1] Departamento de Química, ICEx, Universidade Federal de Minas Gerais, Belo Horizonte - MG, Brazil; [2] Fiat Chrysler Automobiles Latam, Betim - MG, Brazil*

Palavras Chave: *Glycerol, Oleate, Citric acid, Hydrophilic polymers, Amphiphilic molecules*

## Highlights

- Glycerol oleate was combined with citric acids to produce unique solid and liquid products
- Solids are based on hydrophilic polymers with water absorption capacity
- Liquids are amphiphilic molecules with potential to act as pH-responsive switches

## Abstract

This work studies the combination of glycerol oleate with citric acid, leading to the formation of unique liquid and solid products. Oleic acid was combined with glycerol in a first step (160 ºC, 5h). Citric acid was added to the medium on a second step (140 ºC, 2h). Three molar proportions of the reactants were studied.

CHN, TG, potentiometric titration and FTIR analyses indicate that solid products are formed essentially by a crosslinked polymer based mainly on glycerol and citric acid. Solids are highly hydrophilic absorbing ca. 300% water, and also showed interaction with cationic dye methylene blue.

Liquid products are formed by amphiphilic molecules based on the combination of glycerol oleate with citric acid in different proportions. Potentiometric titrations indicated that these molecules presented pH-controlled hydrophilicity, acting as molecular switches. Figure 1 shows a possible scheme of products obtained during performed reactions.

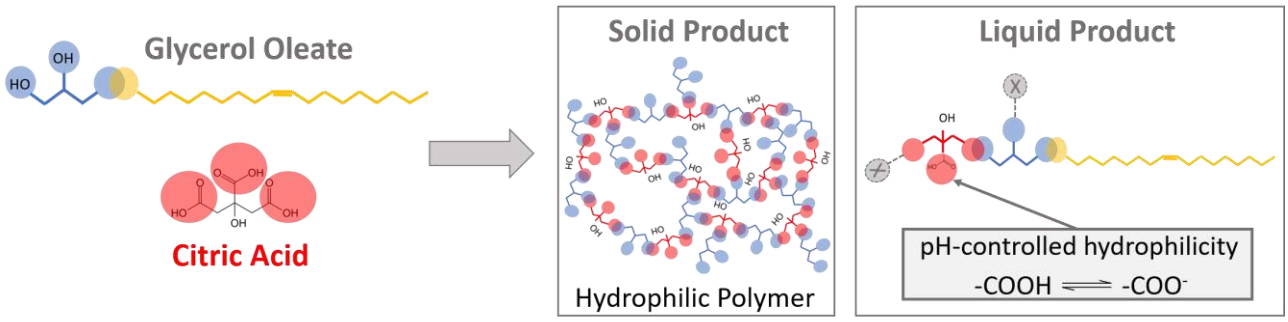


**Figure 1.** Scheme of reaction through glycerol oleate and citric acid to obtain a solid and a liquid product.

More detailed studies are currently going on to develop applications for these materials.

**Acknowledgments:** CNPq, FAPEMIG, INCT-MIDAS and FCA Automobiles.

**Área: MAT** **Inscrição:00590**

# PEPTIDE-GRAPHENE COMPOSITE MATERIAL IN THE DEVELOPMENT OF ENERGY STORAGE DEVICES

**Thiago C. Cipriano (PQ), Roberto M. Torresi (PQ).**

**thiagoc@iq.usp.br; rtorresi@iq.usp.br**

*Instituto de Química, USP;*

Key words; Diphenylalanine, graphene oxide, super capacitor,

## Highlights

Nanocomposites of diphenylalanine (FF) and carbon-based materials provide an opportunity to overcome drawbacks associated with using FF micro- and nanostructures in nanobiotechnology applications. In this study, FF/reduced graphene oxide (rGO) composites were found to self-assemble into layered micro- and nanostructures, which exhibited interesting electronic properties to use in energy storage application.

## Abstract

Peptide-based nanostructures of FF derived from natural amino acids are superior building blocks for biocompatible devices. Graphene is considered an ideal two-dimensional reinforcing component for hybrids or composite materials, possessing an extremely large surface area, superior carrier transport, mechanical flexibility and thermal/chemical stability, among a host of notable characteristics[1,2,3]. In this work, layered FF-rGO nanocomposite materials were investigated. Using Raman spectroscopy, it is possible to prove that graphene is present in the peptide structures. Analyzing the composite spectrum, it is not possible to identify the CH band in 1200 $cm^{-1}$ typical of the FF, indicating the interaction of the aromatic rings with the rGO. Possibly this band is overlapping by the typical D band of graphene compounds, indicative of structural disorder. The typical band of FF compounds in 1580 $cm^{-1}$, related to the presence of the aromatic rings, seems to compose and shift the typical G-band of carbon compounds. In S.E.M images a decrease in the size of the microstructures was observed as a larger amount of graphene was added, a result corroborated by the increase of the D band observed in the Raman spectra. In the T.E.M images it is possible to clearly observe the graphene sheets adhered in the peptide matrix. Cyclic voltammetry data indicate that the material exhibits capacitive properties that vary as a function of the amount of graphene added in the matrix, more studies being carried out to quantify the influence of graphene amount on the peptide. The results obtained indicate that the composite material FF-rOG is very promising from the point of view of charge accumulation and that it will be possible to obtain control of this flow by adequately quantifying the amount of graphene dispersed in the peptide.

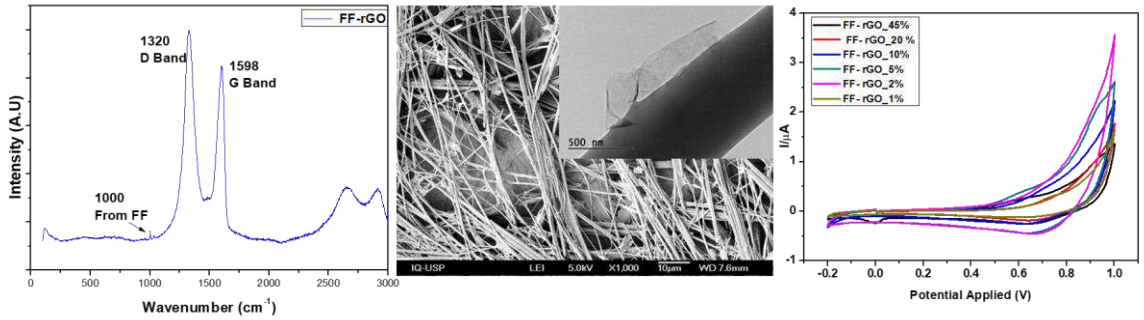


*Figure 1. left - Raman Spectro of composite material indicate the main band from FF and rGO, S.E.M image from FF-rGO in the insertion T.E.M showing the graphene layer in the peptide matrix. Right - image show the several voltammograms of different mass proportion of composite.*

[1] Ryan,K. at all. *Adv. Mater*.**2017**, 18, 172-179 . [2] Han, H. T. at all. *Adv. Mater*. **2010**, 22, 2060–2064

[3] Cipriano,T at all. *ACS Appl. Mater. Interfaces*. **2014**, 6, 21408−21415. Acknowledge to FAPESP grant nos. 2015/26308-7 and 2017/11784-3.

**Área: MAT** **Inscrição: 00655**

# Preparation and use of Porous $TiO_2$ in Adsorption and Photocatalytic Degradation of Organic Dyes in Water

**Kariny C. Vieira (IC),[1]Humberto O. Stumpf (PQ),[2]Walace D. do Pim (PQ)[1*]**

Kariny.quimica@hotmail.com; walacedopim@cefetmg.br

*[1]Departamento de Química, Centro Federal de Educação Tecnológica de Minas Gerais; [2]Departamento de Química, Instituto de Ciências Exatas, Universidade Federal de Minas Gerais.*

*Key words: porous $TiO_2$,solvothermal syntheses, adsorption, photocatalysis, dyes removal.*

## Highlights

- Solvothermal syntheses were employed to prepare porous $TiO_2$.
- Decanoic acid was used as template during the sol-gel process.
- Materials applied as adsorbent and as photocatalyst to dyes removal.

## Abstract

Photocatalysis has been widely used in environmental remediation, such as in the degradation of dyes and emerging contaminants in wastewaters.[1] Among several materials used in the literature, $TiO_2$ seems to be very promising for this purpose.[2] In this work it was used a route to obtain porous $TiO_2$ employing sol-gel method using decanoic acid as template under various synthetic conditions, in order to increase the surface area of the materials. This work describes the syntheses and characterization of four of these materials, as well as a preliminary application of them as adsorbents and as photocatalysts in the reactions of degradation of methylene blue and indigo carmine dyes in aqueous solution. The synthesis of materials in the presence of decanoic acid and the precursor titanium(IV) tetraisopropoxide (TTIP) were performed by varying NaOH concentration and ratio of solvents ($H_2O$ / ethanol). The materials were characterized by TGA, PXRD, SEM, FTIR and Raman spectroscopies and showed that the materials were successfully obtained. Analysis of contact angles formed by a drop of water in the pastille of each material made it possible to confirm the hydrophobization of the materials by decanoic acid. The discoloration of the dyes solutions was monitored by using a UV-Vis spectrophotometer. After the adsorption tests, the materials were used as photocatalysts in the degradation of the dyes in a chamber in the presence of UV radiation. All materials presented satisfactory results, and two of them removed practically 100% of the dyes.

### REFERENCES

1- Nogueira, R. F. P; Jardim, W.F. A fotocatálise heterogênea e sua aplicação ambiental. **Química Nova**, v.21, n.1, p. 69-72, 1998.
2- Cervantes, T. N. M.; Zaia, D. A. M.; Santana, H. de. Estudo da fotocatálise heterogênea sobre Ti/$TiO_2$ na descoloração de corantes sintéticos. **Química Nova**, v. 32, n.9, p. 2423- 2428.

### ACKNOWLEDGEMENTS

FAPEMIG, CAPES and CNPq.

**Área: MAT**
*(Inserir a sigla da seção científica para qual o resumo será submetido. Ex: ORG, BEA, CAT)*

**Inscrição: 00417**
*(Inserir o número de inscrição do autor que fez a submissão)*

# Photoluminescence and scintillation of $Gd_2O_2S$:Y,Lu,Eu spherical particles

**Giovanni F. Requena (IC),[1] Vagner A. Moralles (PG),[1] Maike O. Krauser (PG),[1,2] Marco A. Cebim (PQ),[1] Marian R. Davolos (PQ),[1*]**

**davolos@ig.unesp.br**

[1]*Unesp, Instituto de Química, Araraquara, SP, Brasil; UFT, Química Ambiental, Gurupi, TO, Brasil*

Palavras Chave: *Rare earth oxysulfides. Europium(III). Luminescence. XEOL.*

## Highlights

Spherical and crystalline particles were obtained by the homogeneous precipitation.
The co-doped samples preserve the material structural and optical properties.

## Resumo/Abstract

The terbium doped gadolinium oxysulfide is a high performance scintillator and, due to its properties, is applied in dosimetry, high energy physics and medical imaging. Being a wide applied scintillator, the optimization of its properties becomes a key goal. To reach this goal a percentage of gadolinium was replaced by lutetium, creating a system that presents a greater absorption range of ionizing radiation, and by yttrium, decreasing the variations of ionic radii caused by the substitutions. To analyze the effects of substitution on the material, $Eu^{3+}$, a spectroscopic probe, was used as the luminescence activator, replacing $Tb^{3+}$. Spherical particles were obtained by homogeneous precipitation with urea and, subsequently, sulfurization under inert atmosphere. From the structural results the obtained samples do not contain significant amounts of molecular species impurities, are crystalline, and do not present spurious phases. The optical results show that the emission spectra profile of each sample do not change with the presence of the co-dopants, being an indicative that the activator occupies the same symmetry sites independently of the percentage of co-doping and of chemical environment. However, through the refinement of photoluminescence spectroscopy results, it is observed that even the activator being in the same symmetry sites, the symmetry of $Eu^{3+}$ changes with the increase of co-dopants percentages. Therefore, it is emphasized that the proposed modification preserves the structural and optical properties of the materials and that the obtained compounds have the potential to be applicable as scintillators.

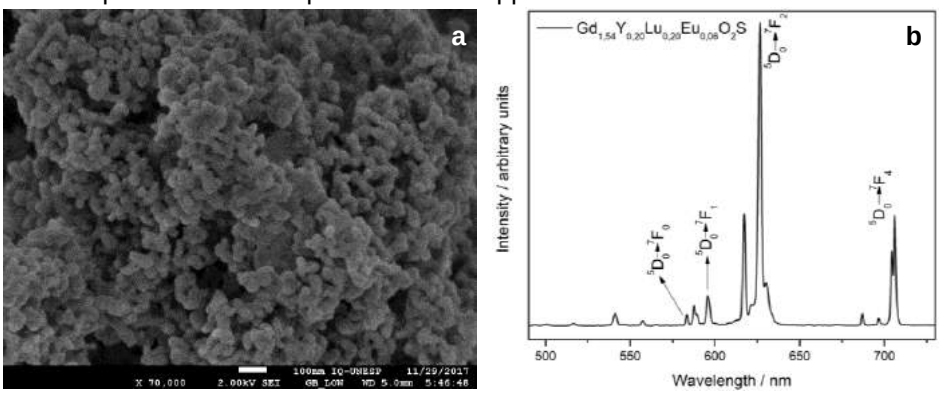


**Figure 1 - Characterization of $Gd_{1,54}Y_{0,20}Lu_{0,20}Eu_{0,06}O_2S$:**
**(a) Field emission gun scanning electron microscopy (FEG-MEV); (b) X-ray excitation optical luminescence spectrum (XEOL).**

- A.M.Pires, M.R.Davolos, E.B.Stucchi, $Eu^{3+}$ as a spectroscopic probe in phosphor based on spherical fine particle gadolinium compounds, Inter. J. Inorg. Mat. 3 (2001) 785-790
- M.A.Cebim, H.H.S.Oliveira, N.Barelli, M.R.Davolos, Sistema para realização de medidas de luminescência com excitação por raios X, Quim. Nova, 34 (2011) 1057-1062

**Área: MAT** **Inscrição: 00443**

# *STUDY OF LCC AND QUITOSANA GEL TOXICITY* : PARAMETRISATION IN ARTHROPOD TEST.

**Francisco Cardoso Figueiredo (FM),[1] Thamires Pereira dos Santos (PG)[1], Raimundo Oliveira Lima Júnior (PQ)[2], Natália da Silva Ferreira (IC)[1], José Ribeiro dos Santos Júnior (PQ)[1].**

fcfigueiredo19@hotmail.com

[1]Federal University of Piaui, [2]Federal Institute of Piauí
Key words: Carrapaticida, LCC, Chitosan, Arthropod.

## Highlights

Product applied to *Tribolium sp* to verify the concentrations to favor the mortality. The result show that LD50 was reached within one hour.

## Resumo/Abstract

In this work a gel was developed from the mixture of different concentrations of cashew liquid - LCC and chitosan, from 1 to 100 mg of LCC dispersed in chitosan. The mixtures were tested for their degree of toxicity. The gel should be applied in tick combat. Because it is a natural product and therefore causes the least harmful effects on the environment compared to known drugs that are artificially synthesized and have effects on several living species, since ticks are known for resistance. The toxicity of this compound was initially tested on arthropods using the standard Tribolium castaneum. The known populations of arthropods (70 animals) were contacted with the gel at concentrations of 1, 5, 10, 50, 100 mg / L. The mortality of the specimens was observed over time for the definition of DL 50. A Figure 1 shows the population decay according to the concentration and the contact time. Among the population reduction curves analyzed it was found that the highest concentration eliminated all individuals in less than one hour, which reveals the potential of the product for more specific tests in the different species of ticks and other arthropods.

**Figure 1: Analysis of the population of Tribolium castaneum as a function of time for defined concentrations of LCC and chitosan**

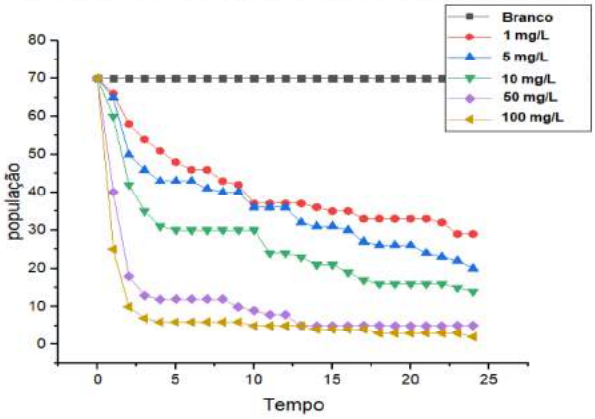

**Área: MAT** **Inscrição: 00726**

# Two Routes Comparison for Silver and Gold Nanoparticles Deposition on Silica Substrate for Future Application in Optic Sensors

**Amanda Figueiredo Pereira (PG),[1] Marcela Mohallem Oliveira (PQ).[1*]**

**mandinha_fp@yahoo.com.br; marcelam@utfpr.edu.br**

[1]*Grupo de Química de Nanomateriais – GQNano, Departamento Acadêmico de Química e Biologia - DAQBi, Universidade Tecnológica Federal do Paraná - UTFPR*

Palavras Chave: *Nanopartículas de Ouro, Nanopartículas de Prata, Nanopartículas Metálicas Mistas, Sensores Ópticos, Absorção Plasmon.*

## Highlights

Compare which of two deposition routes of metal nanoparticle on a specific substrate is the one of most promising to develop innovative technologies in optical sensors.

## Resumo/Abstract

As nanopartículas são materiais que apresentam propriedades interessantes quando comparadas com as do mesmo material em tamanho estendido.[1] Dentre as propriedades interessantes estão as ópticas, advindas da ressonância plasmon de superfície localizado (RPSL). A aplicação desse fenômeno em sensores ópticos é extremamente promissora em função da possibilidade de intensificação do sinal recebido, aumentando assim a sensibilidade e a seletividade do sensor.[2]

Neste trabalho foram propostas duas rotas de deposição de nanopartículas de ouro, prata e ambos os metais em lamínulas de sílica. A primeira envolve um método químico de redução, sendo esta tradicionalmente utilizada em trabalhos do GQNano. A segunda envolve a deposição das nanopartículas pelo método térmico, onde o resultado foi um filme mais uniforme e estável. Ambos os filmes obtidos apresentam diferenças como cor e homogeneidade. As técnicas utilizadas para a elucidação e comparação dos materiais foram a espectroscopia UV-Vis, difração de raios X e microscopia eletrônica de transmissão, onde notamos a obtenção de filmes de nanopartículas metálicas, com características diferentes, como tamanho médio e distribuição sobre o substrato, de acordo com a rota escolhida.

**Agradecimentos:**
CNPq, CAPES, Fundação Araucária, INCT em Nanomateriais de carbono, GQM-UFPR, CME-UFPR, PPGQ-UTFPR.

**Referências:**
[1] KHAN, I.; SAEED, K.; KHAN, I. *Arabian Journal of Chemistry*, **2017**.
[2] GOUVÊA, Paula M. P. et al. *J.Appl. Phys.,* **2011**, 109, 10.

**Área: MAT** **Inscrição: 00232**

# Polyaniline against black phosphorus degradation: a long-term stability study

**Jéssica E S Fonsaca (PG),[1] Sergio H Domingues (PQ),[2] Elisa S Orth (PQ),[1] Aldo J G Zarbin (PQ),[1*]**

**je.fonsaca@gmail.com; aldozarbin@gmail.com[*]**

*[1]Department of Chemistry, Federal University of Paraná (UFPR) – Curitiba - PR; [2]Graphene and Nano-materials Research Center – Mackgraphe – Mackenzie Presbyterian University – Sao Paulo – SP.*

Keywords: *Black phosphorus, Polyaniline, Thin film, Stability.*

## Highlights

The interfacial method was employed to obtain homogeneous and self-standing thin films of black phosphorus (BP) protected by polyaniline, considerably slowing down BP degradation under air exposure.

## Abstract

The interest in exploring the properties of black phosphorus (BP)[1] has been growing as well as the concern in protecting it against its high instability in air. Thus, we have synthesized a BP-polymeric nanocomposite through the liquid/liquid interfacial method[2], aiming to overcome BP deterioration. Aniline was polymerized in a deaerated dispersion of BP and, after the solvent exchange to a biphasic system, a self-standing film of BP covered by polyaniline (PANI) was observed at the interface.[3] Raman spectroscopy confirmed the coexistence of both materials in the resulting film. Infrared spectra showed the presence of bands related to modes of phosphorus oxidation for bare BP, attesting its unstable nature, and the absence for BP/PANI, suggesting a protective role of PANI on BP. Thus, both bare and capped materials were exposed to the same ambient conditions and evaluated through different techniques (**Figure 1**).

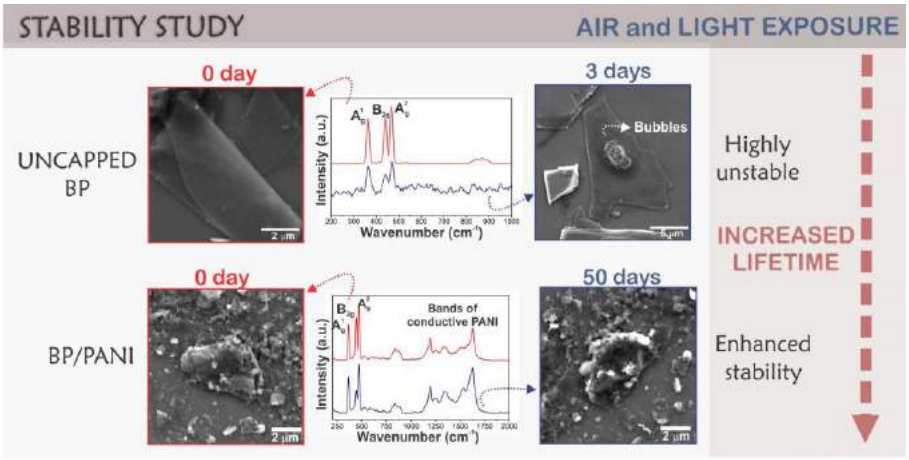


**Figure 1 -** Stability study of bare BP and BP/PANI nanocomposite.

Scanning electron microscopy images alarmed the beginning of degradation of the uncapped material with only 3 days of exposure, showing the characteristic bubbles on BP surface. The same was observed through Raman, indicated by the gradual decrease in the intensity of BP bands that completely disappear with its total degradation (at about 10 days). The PANI-covered material, however, has taken about 50 days for the same process to begin, reaching an increase of about 1500% in the stability, and it is still under monitoring. Overall, this work enlightens to new possibilities towards the development of thin films suitable to be designed and applied in different BP-based materials.

Acknowledgementes: CNPq, CAPES, Fundação Araucária, NENNAM, INCT-Nanocarbon, L'Oréal-UNESCO-ABC.
References: [1] Li, L. *et al*. *Nat Nano* **2014**, 9, 372. [2] Salvatierra, R. *et. al. Chem. Mat.* **2010**, 22, 5222. [3] Fonsaca, J. E. S. *et. al. Sci. Rep.* **2017**, 7, 10165.

**Área: MAT** **Inscrição: 0300**

# Adsorption of metformin hydrocloride by ecovio® solution in electrospinning and activated carbon

**Ana C. R. Meira (PG),[1] Aparecido N. Módenes (PQ),[1] Douglas C. Dragunski (PQ),[1] Paulo R. S. Bittencourt (PQ).[2]**

**ana.meira@unioeste.br; anmodenes@yahoo.com.br**

[1]Graduate Degree Program in Chemistry, UNIOESTE - Toledo; [2] Chemistry Department, UTFPR - Medianeira

Keywords: *Adsorption, Metformin Hydrocloride, Actived carbon, Ecovio®, Electrospinning.*

## Highlights

The enhancement in consumption of human and veterinary medicines has increased the contamination of wastewater and surface water, and activated carbon has been revealed to remove this contaminant.

## Resumo/Abstract

The presence of medicinal products in the environment causes several changes in aquatic and plant life when present in surface water, wastewater and soil[1]. Metformin (Met) is marketed as metformin hydrochloride, an active ingredient for the treatment of type 2 diabetes mellitus[2]. The main impact caused by the presence of Met in rivers and lakes is the feminization of fish and small animals[3].

In order to remove this contaminant tested as adsorbents: ecovio® solution in electrospinning, (Figure 1), and activated carbon from the biomass of the Musa cavendish banana, in a batch process and quantified by Uv-Vis spectroscopy. The results showed which the highest rate of adsorption occurred for the actived carbon with KOH tratament, $q_{exp.}$ of approximately 53.28 $mg.g^{-1}$, and modification of the ecovio® solution in electrospinning, using dichloro methane (DCM) as a solvent, increased its adsorption capacity by the increase of its porosity (Table 1).

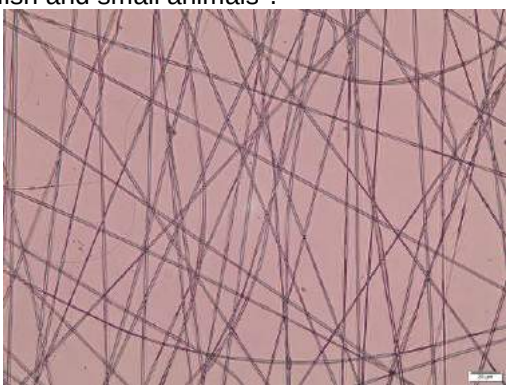

Fig 1. Images of optical microscopy the fibers of ecovio® by electrospinning. Experimental conditions: ecovio® 15% m/V; rate: 0,5 $mL.h^{-1}$; 14 kV; 12 cm.

Table 1 – Results obtained from batch adsorption experiments. Experimental conditions: $[Met]_{inicial}$ 500 $mg.L^{-1}$; T: 30 °C; volume of solution 50 mL.

| ADSORBENT | $q_{(exp.)}$ ($mg.g^{-1}$) | ADSORBENT | $q_{(exp.)}$ ($mg.g^{-1}$) |
|---|---|---|---|
| BIOMASSA (BM) 30 °C | 2,19 | BM/KOH | 53,28 |
| BIOMASSA 60 °C | 4,82 | BM/NaOH | 11,88 |
| BIOCHAR (BC) 400 °C | 33,15 | BC/ZnCl | 10,99 |
| BIOCHAR 650 °C | 37,99 | CARVÃO ATIV. COM. | 12,64 |
| BIOCHAR 900 °C | 35,88 | ECOVIO | 0,21 |
| $BM/H_3PO_4$ | 3,32 | ECOVIO/DCM | 2,93 |
| $BC/H_3PO_4$ | 9,22 | ECOVIO/NaCl | 1,41 |

In future works, the activated carbon produced will be added to ecovio® solution in electrospinning and will be evaluate its mechanism and adsorption capacity.

**References**

[1]DIETRICH, D.R. et al. **Toxicology Letters**. v. 131(1–2), p. 1-3, 2002.
[2]COSTA, A.F.; et al. **Cadernos de Saúde Pública**. v. 33, 2017.
[3]NIEMUTH, N. J. et al. **Chemosphere**. v. 135, p. 38-45, 2015.

The authors would like to thank Universidade Estadual do Oeste do Paraná and Universidade Tecnológica Federal do Paraná.

**Área: MAT** **Inscrição: 00320**

# Investigation of the structural and optical properties of cobalt molybdate – A possible temperature indicator

**Rosiane K.S.Costa*(PG),[1] Stéfani C. Teles (IC),[1] Kisla P.F.Siqueira (PQ)[1]**

**rosianekeilasc@yahoo.com.br**

[1]*Laboratório de Materiais Cerâmicos, ICEB II n°65, Departamento de Química, UFOP-Campus Morro do Cruzeiro, Ouro Preto - MG.*

Palavras Chave: *Thermochromism, Multifunctional material, Synthesis, Molybdates.*

## Highlights

Cobalt molybdates exhibit polymorphic forms with characteristic colors. The materials were synthesized by copreciptation and their structural and optical properties were studied in detail.

## Resumo/Abstract

Cobalt molybdates ($CoMoO_4$) have been considered important ceramic materials with wide scientific interest due to their interesting properties, such as, magnetic, catalytic, photoluminescent, piezochromic or thermochromic. Thermochromic properties of molybdates were investigated in this work; i.e., the phenomenon of the color changes of the material when subjected to different temperatures. Three polymorphic forms of the material (hydrated, beta and alpha phase) were synthesized by copreciptation reaction under suitable temperature and time conditions. The hydrated phase was obtained at 70ºC while the beta and alpha one, were obtained after thermal treatment in the range from 300 to 600 °C. All the materials were characterized by X-ray diffraction and Raman spectroscopy. The results showed that although the three polymorphic forms could be produced, only the beta phase exhibited the thermochromic property. Thus, the cobalt molybdates changed their color from purple to green when occured the phase transition from beta to alpha, at around 600 °C. The results support the idea that cobalt molybdates are promising for monitoring industrial processes that occur at about 600°C.Thus, the sudden change in color of materials from purple to green could facilitate visual monitoring of the process by the operator.

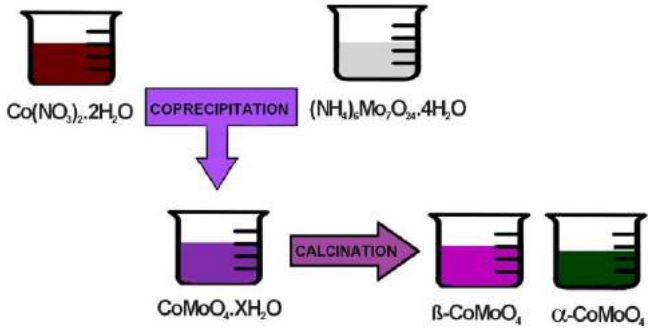


Figure 1:Scheme of the synthesis of the materials

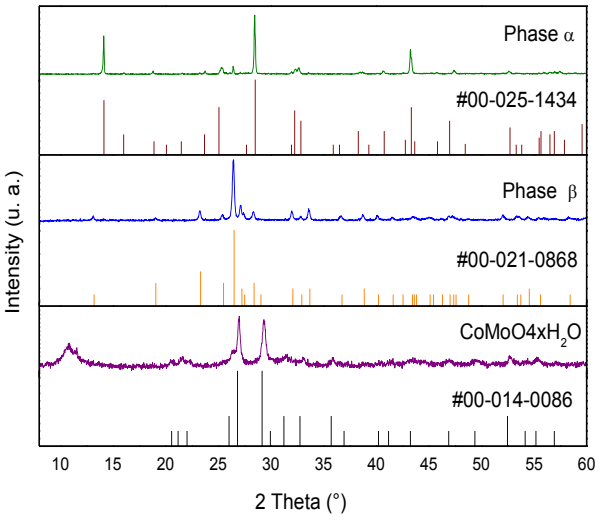


Figure 2:XRD patterns of polymorphic forms of molybdates

References:
[1] EDA, K;et al Journal of Solid State Chemistry, n°178, 2791–2797, 2005

[2] GUTIERREZ, V. B; et al. Dalton Transactions, n° 42, 13622–13627, 2013

Acknowledgment: FAPEMIG, CNPq, UFOP.

**Área: MAT** **Inscrição: 00352**

# Electrical conductive films of reduced graphene oxide and polyaniline prepared from a solid gel

**Vitor H.N. Martins (IC),[1] Victor H.R. Souza (PQ),[1*].**

**vitorhugotl@icloud.com; victorsouza@ufgd.edu.br**

*[1] Laboratório de Materiais Cerâmicos Avançados (LMCA), Faculdade de Ciências Exatas e Tecnologia (FACET), Universidade Federal da Grande Dourados (UFGD).*

Keywords: *graphene oxide, polyaniline, self-assembled films, doctor blade technique.*

## Highlights

- Self-assembled films made of reduced graphene oxide and polyaniline.
- Doctor blade technique to produce films with high electrical conductive properties.

## Abstract

The ability to process materials into thin films is required for new technologies which aim the production of thinner devices. Graphene oxide (GO) is one of these promising materials due to its higher processability in water and different techniques that can be explored to produce such films, as drop-casting, spin-coating, vacuum filtration, and so on.[1] Doctor blade technique is another affordable way to produce films in which a high viscosity mixture is casting over a substrate, covering all its surface. Inspired by adhesive and conducting thin films from graphene oxide and poly(3,4-ethylenedioxythiophene):poly(styrenesulfonate)[2], the present work presents the production of self-assembled films of reduced graphene oxide and polyaniline (PAni) prepared using the doctor blade technique to cast a solid gel made by graphene oxide and the conducting polymer. Graphene oxide was obtained using a modified Hummer's method. The solid gel (Figure 1 (a)) was produced using a 2% or 1 % GO dispersion mixed to the polyaniline. Self-assembled films were further obtained casting the solid gel over glass substrates, drying it at 70 °C, followed by reduction of graphene oxide exposing it to hydrazine vapor. Foldable films were produced (Figure 1 (b)), and the conductivity measured using a four-points probe of the 2%GO/2%PAni film was 19.1 ± 4.0 S $cm^{-1}$. An application on energy storage devices will be further explored.

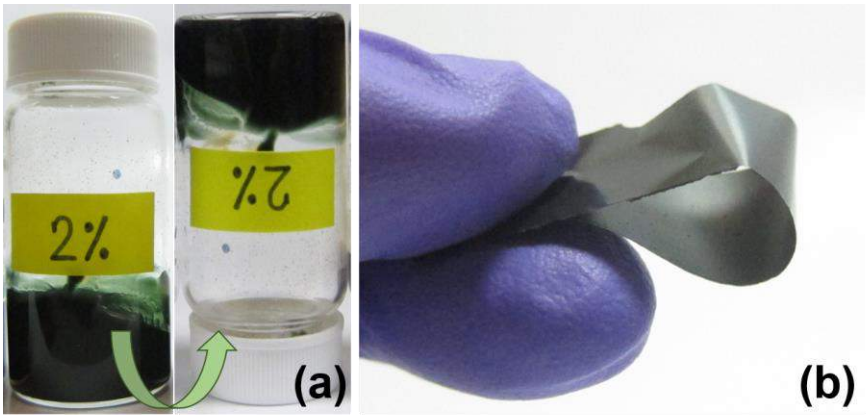


**Figure 1 –** (a) Solid gel made of graphene oxide and polyaniline; (b) Foldable self-assembled film of reduced graphene oxide and polyaniline.

[1] G. Eda, M. Chhowalla, Advanced Materials, 22 (2010) 2392-2415.
[2] V.C. Tung, J. Kim, L.J. Cote, J. Huang, Journal of the American Chemical Society, 133 (2011) 9262-9265.

**Área: MAT** **Inscrição: 00207**

# Biopolymeric Films of Diethylaminoethyl-Chitosan Derivatives: Potential Application as Antimicrobial Coatings

**Otávio da Mata Cunha (PG),[1*] Márcio J. Tiera (PQ),[1] Aline M. F. Lima,[1] Odílio B. G. Assis (PQ),[2] Vera A. O. Tiera (PQ).[1]**

**otavio.cunha_@hotmail.com**

*[1] Departamento de Química e Ciências Ambientais, – UNESP, São José do Rio Preto, São Paulo, Brazil.*
*[2] Embrapa Instrumentação, Rua XV de Novembro, 1452, C.P. 741, 13560-970 São Carlos, Brazil.*

Keywords: Chitosan, Diethylaminoethyl derivatives; Cytotoxicity; Mechanical Properties.

## Highlights

Amphiphilic derivatives of chitosan exhibited very low cytotoxicity effects on fibroblast cells.
Biopolymeric films were prepared and displayed improved mechanical properties and potential as antimicrobial coatings.

## Resumo/Abstract

The objective of this study was to evaluate the mechanical properties of films prepared by casting aiming their application as antimicrobial coatings. We present the synthesis, mechanical properties and cytotoxicity evaluation of biopolymeric films of chitosan. Derivates containing 40 mol % of diethylaminoethyl groups (DEAE) and 3% of dodecyl groups (DD) were prepared as described by GABRIEL et al., 2015[1]. The mechanical properties were obtained by elastic modulus, maximum tensile strength stress and percentage of elongation. Cytotoxicity was performed using 3T3 cells cultured in 96-well plates. The films exhibited significant differences in their mechanical properties, demonstrating that the chemical modification in the chitosan structure resulted in a decrease the elastic modulus and maximum tensile strength providing an increase in elongation at break without use of plasticizers. The results indicated that the chemical modification of chitosans of medium Mw is a promising strategy to obtain antimicrobial films of good malleability.

**Table 1.** Characterization data of high molecular weight chitosan and chitosan derivates.

| Polymers | DS (%)* DEAE | DS (%)* DD | Mw (kDa)** | Elastic Modulus (MPa) | Tensile Strength (MPa) | Elongation at break (%) |
|---|---|---|---|---|---|---|
| **CH** | - | - | 282 | 13,54 ± 0,5 | 44,93 ± 5,88 | 3,8 ± 0,68 |
| **CH-DEAE** | 40 | - | 266 | 6,93 ± 0,60 | 39,13 ± 0,94 | 6,55 ± 1,50 |
| **CH-DEAE-DD** | 40 | 3 | - | 7,06 ± 0,7 | 24,50 ± 3,88 | 17,83 ± 2,42 |

*Determined by $^1$H NMR. **Determined by GPC.

**Figure 1.** Cell viability of the polymers at various concentration in 3T3 cells.

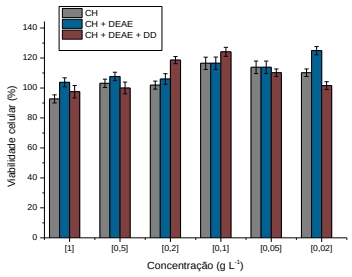


The cytotoxicity study, figure 1, showed that all the derivates exhibited low cytotoxicity and cell viabilities remained above 90%, demonstrating potential for application as a protective coating of seeds and fruits.

## ACKNOWLEDGEMENTS

FAPESP 2017/13762-7 e 2016/15736-0. EMBRAPA Instrumentação – São Carlos.

## REFERENCES

[1]GABRIEL, J. S.; TIERA, M. J.; TIERA, V. A. O. Synthesis, characterization, and antifungal activies of amphiphilic derivatives of diethylaminoethyl chitosan against Aspergillus flavus. **Journal of Agricultural and Food Chemistry**, v. 63, p. 5725-2531, 2015

**Área: MAT** **Inscrição: 01259**

# Tri-ureasil hybrid gel as biofilm forming for controlled release of cubebin.

**Natana A.M. Jesus (PG),* Marcio L.A. Silva (PQ), Wilson Cunha (PQ), Denise C. Tavares(PQ), Ricardo A. Furtado (PG), Eduardo F. Molina (PQ).**

**natana_martinz@hotmail.com; eduardo.molina@unifran.edu.br**

*Universidade de Franca, Av. Dr. Armando Salles Oliveira, 201, Franca-SP*

Palavras Chave:Hybrid, Tri-Ureasil, Controlled release.

## Highlights

In this work we report the effects of catalyst amount on tri-ureasil hybrid gel prepared by sol-gel route, aiming to control the film forming time. The release of cubebin through this gel was studied.

## Resumo/Abstract

Due to their numerous favorable characteristics, specifically the excellent film-forming properties, processability, biocompatibility, non-toxicity, hydrophilicity control and chemical resistance, films derived from ureasil gels, recently have attracted great attention and have been used for pharmaceutical purposes [1]. Considering a steadily increasing attention paid to organic–inorganic hybrid film forming gels due to a wide range of potential applications, this work has investigated a tri-ureasil hybrid gel as a biofilm forming and potential application as cubebin release system. (-)-Cubebin is an important dibenzylbutyrolactone lignin also kwon as 2,3-bis(3,4 methylenedioxybenzyl)-butyrolactol. Cubebin extracted from *Piper cubeba* seeds has been showed anti-inflammatory, analgesic, vasorelaxant, trypanocidal, antimycobacterial and antiprotozoal activities [2]. The hybrid films show versatile shaping, highly transparency and flexibility. the augment of HCl amount promotes an increase in the speed of reactions leading to a decrease of film formation time. When we used a catalyst/hybrid ratio equal to 2 (v/m) an average gel time of 5 min was observed. All films does not showed a statistically significant reduction in cell viability in relation to negative control group, demonstrating that hybrids were biocompatibles. The hydrophobic nature and the lower water retention of the polymer chains present in the hybrids, favor the dissolution and the slow release of cubebin in water. In sum, the tri-ureasil hybrid may provide several advantages as biofilm forming that offers new opportunities to development of drug delivery systems containing organic species that possess analgesic, anti-histaminic, anti-inflamatory, antitumor and antimicrobial activities.

[1] Junior JAO, Carvalho FC, Soares CP, Chorilli M, Chiavacci LA. Development of cutaneous bioadhesive ureasil-polyether hybrid films. Int J Polym Sci 2015;2015(3):1-7.Molina EF, Marçal L, Carvalho HWP, Nassar EJ, Ciuffi KJ. Polym Chem 2013;4:1575-1582.

[2]Carvalho MT, Rezende Kc, Evora PR, Bastos JK, Cunha WR, Andrade e Silva ML, Celotto AC. The lignan (-)-cubebin inhibits vascular contraction and induces relaxation via nitric oxide activation in isolated rat aorta. Phytother Res 2013;27:1784-1789.

**Área: MAT** **Inscrição:00860**

# Structure-property relations of chiral polyfluorene derivatives

**Cristiano Zanlorenzi (PQ),[1*] Bruno Nowacki (PQ),[1,2] Alexander Baev (PQ),[2] Paras N. Prasad (PQ),[2] Leni Akcelrud(PQ),[1]**

**cristizan@yahoo.com.br; akleniak@gmail.com**

*[1]Laboratório de Polímeros Paulo Scarpa (LaPPS), UFPR; [2] Institute for Lasers, Photonics, and Biophotonics. University at Buffalo.*

*Keywords: Chiral polymers, Polyfluorene derivatives, Chirality parameter, Helical polymers, Theoretical calculations.*

## Highlights

Synthesis of polymers for chiral photonics;
Correlation between structure and optical activity of polyfluorene derivatives;
Influence of extrinsic and intrinsic parameters in the chirality parameter.

## Resumo/Abstract

There has been growing interest in studying chiral polymers both theoretically and experimentally due to their potential application in the field of negative refractive index metamaterials. Large optical activity of these polymers, combined with their excellent flexibility and processability holds a great promise for a wide range of technological applications. In order to prepare such materials, its desirable that the polymer backbone presents a helical assembly behavior, generally incorporating asymmetric chiral centers to the monomer units. The resulting materials are characterized by a chirality parameter, *κ*, and can be measured by the circular dichroism (CD) technique. In this way, the synthesis along with a systematic study of a series of chiral polyfluorene derivatives was made, aiming to identify the main properties controlling the chiroptical activity of polymer films. For each polymer, five empirical/theoretical properties were chosen, due to their effect on the chirality parameter: glass transition temperature, dissymmetry factor, molar mass, helix tightness and the inverse of interconversion energy. A radar graph was built, exhibiting the influence of these five parameters and their interplay. The polygonal area in the radar graph and *κ* presented a direct relationship. Such graph can provide prescreening of polymer properties, based on both experimental measurements and theoretical considerations and help to choose the right combination of parameters, leading to a material with the best properties.

Figure 1. a) Synthesized structures, (b) radar graph and (c) resulting polygon area graph related to five properties.

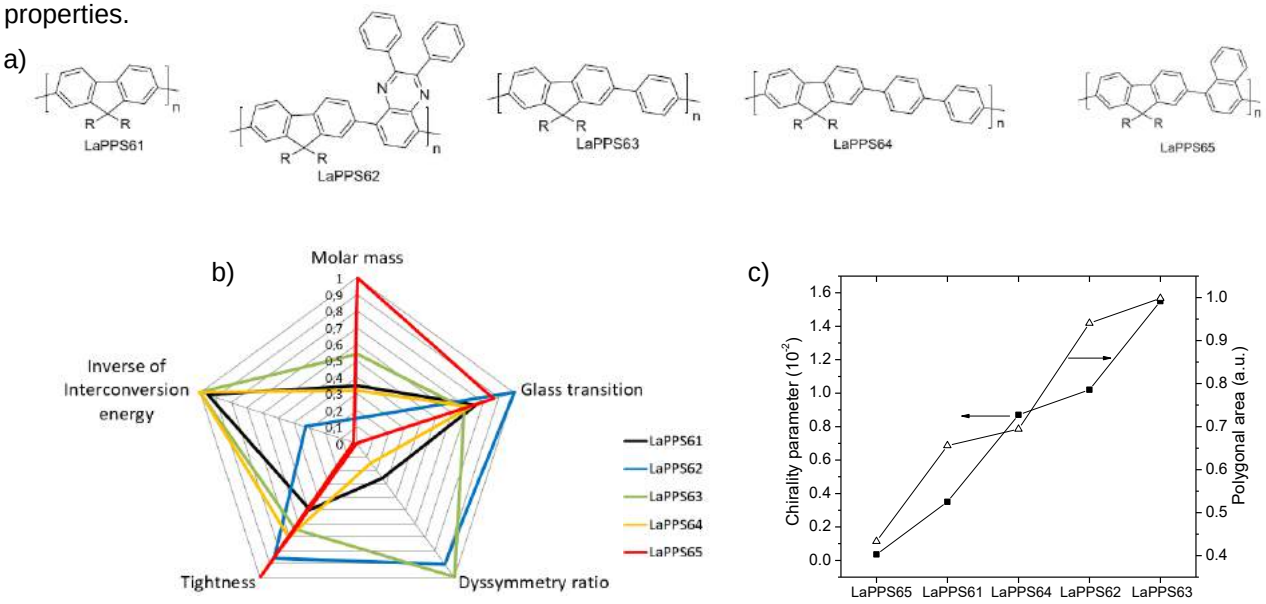

**Área: MAT**
*(Inserir a sigla da seção científica para qual o resumo será submetido. Ex: ORG, BEA, CAT)*

**Inscrição: 00255**
*(Inserir o número de inscrição do autor que fez a submissão)*

# Hydrophobic papers based on cellulose coated with recycled polystyrene

**Ariane de V. S. Cebrian (IC),[1*] Fernando E. Maturi (PG),[1] Hernane S. Barud (PQ),[2] Robson R. Silva (PQ),[3] Sidney J. L. Ribeiro (PQ),[1] Márcia B. Cardoso (PQ)[4].**

**avscebrian@hotmail.com**

*[1]Institute of Chemistry - São Paulo State University (UNESP); [2]University of Araraquara (UNIARA); [3]São Carlos Institute of Physics - University of São Paulo (USP); [4]Institute of Technological Research (IPT)*

Palavras Chave: *Cellulose, Polystyrene, Limonene, Hydrophobic papers, Airbrush.*

## Highlights

The project seeks the recycling of expanded polystyrene waste through its dissolution in green solvent for cellulose coating and the obtaining of hydrophobic surfaces using the airbrush technique.

## Abstract

Polystyrene (PS) is a synthetic polymer mainly produced in the expanded form (expanded polystyrene, EPS), commercially known as Styrofoam™, which is composed by only 2 wt% of PS. The mechanical and thermal recycling of EPS are not favored due to low density and release of toxic gases to the environment, respectively. The chemical recycling is an alternative approach for the EPS recycling because the dissolution in a solvent prevents the polymer degradation and there is no gas release into the environment. The use of d-limonene extracted from orange peel as a solvent is attractive since it comes from a renewable source and reduces about 95% of the original EPS volume. The resulting solution can be tailored to fabrication of hydrophobic surfaces, such as hydrophobic papers. In this way, different EPS solutions were acquired through the dissolution of EPS packages in d-limonene, followed by the application into cellulose surface using the airbrush technique, as show in figure 1. The concentrations of EPS solutions used were 10%, 15% and 20%. All samples were characterized by contact angle, differential scanning calorimetry (DSC), thermogravimetric analysis (TGA) and vibrational infrared spectroscopy (IR). Initial results show that the contact angle increases as the concentration of the EPS solution increases, indicating that there is an increase in the hydrophobicity of the cellulose surface.

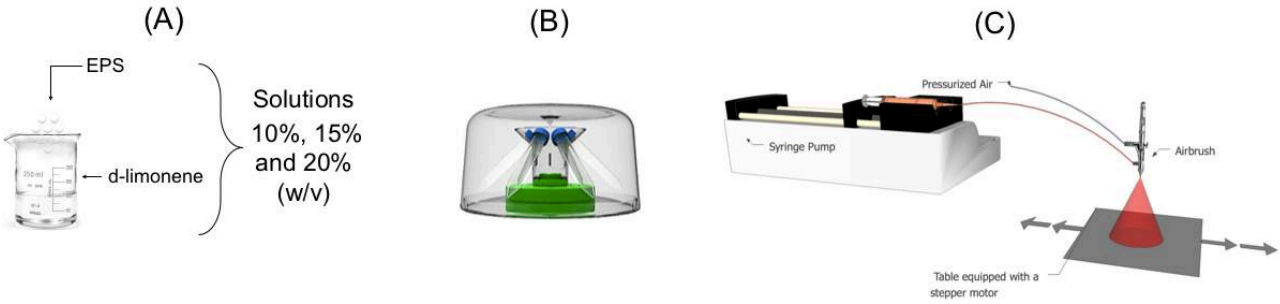


**Figure 1.** Scheme of the cellulose coating process. Dissolution of the expanded polystyrene packages (A), centrifugation of the solution for removal of impurities (B) and coating of the papers using the airbrush technique (C).

Acknowledgments: FIPT, CNPq and Fapesp.

**Área: MAT** **Inscrição: 00035**

# Accelerated aging study on rheological properties of synthetic bitumens

**Ricardo S. Souza (PG)[1,2], Leila Léa Y. Visconte (PQ)[1], Valéria G. Costa (PQ)[2]**

*Email: ricardo.souza@ima.ufrj.br*

*1 Instituto de Macromoléculas Profa. Eloisa Mano – IMA - UFRJ, Av. Horácio Macedo 2030, Centro de Tecnologia, Bl. J, Cidade Universitária, Ilha do Fundão, Rio de Janeiro, RJ, Brasil, CEP: 21941-598*

*2 Instituto Nacional de Tecnologia – INT, Av. Venezuela 82 sl. 106, Saúde, Rio de Janeiro, RJ, Brasil, CEP:20081-312*

Palavras Chave: *synthetic bitumen, polypropylene, viscosity, storage modulus, loss modulus*

## Highlights

Bitumen catalytic cracking petroleum is widely used in the construction industry as one of the components of the binder and mineral aggregates of pavement asphalt cement (PAC). However, this material presents great limitations of use in different temperatures. One of the alternatives studied is the formulation of binders of oil/polymer mixtures which, when compared to traditional and modified bitumen (traditional bitumen with addition of polymeric material to modify its final properties) present better performance [1] [2]. Exposure of the material to external agents (weathering) can cause changes in the characteristics of the material and thus modify its performance, sometimes shortening the life time in ideal conditions. The objective of this work was to investigate the behavior of formulated binders, whose materials were of post-consumed origin, simulating the effect of aging degradation on the rheological properties of the samples.

## Resumo/Abstract

For this work, the binder's formulations were made using recycled polypropylene and post-consumed paraffinic oil. The samples were made on IKA Eurostar 20 mechanical stirrer with mixing blade with four propellers. A heating bath was used at 170°C. The samples were mixed up at 500 rpm and the mixing time was 2 min. The proportions of the mixtures were 5, 10 and 20 % (m/v). The accelerated aging test was carried out in the QUV aging chamber of the company Q-lab, according to ASTM G-154 cycle 1. The rheological analyzes were performed on Rheometer oscillating disc Haake Mars II (Thermo Scientific), viscosity curves were performed in ascending-descendants ramp with shear rate from 0 to 200 $s^{-1}$ for 3 min. The analyzes were performed at 150°C. Frequency sweep curves were performed with controlled stress of 1 Pa with variation of oscillation frequency of 0.1 to 100 rad/s, the temperature used was 25 and 125 ºC.

Observing the values obtained in the flow curve analysis, it is possible to observe an increase in viscosity values at low shear rates in the samples with 15% and 20% polymer mass in the composition of the synthetic bitumen, the sample with 15% PP obtained an increase of 3.5 Pas, while the 20% sample obtained an increase of 1Pas, however these samples obtained a slight decrease in the viscosity values when the shear rate was increased; the aged samples showed a more pronounced pseudo-plastic characteristic.

Observing the results obtained for the frequency sweep test of the samples before aging and after aging, the aged samples analyzed at a temperature of 25°C showed a slight increase in the values of storage modulus (G'), except the sample with 20% of the polymer in the composition, and the loss modulus (G") also showed increase in its values in relation to the samples before aging. Those samples that were analyzed at 125°C did not present the same tendency to increase the values of G' and G" of the samples that were aged in relation to the unaged samples. The action of aging may have caused the samples to stiffen, causing them to increase in their modulus values, but at the same time this enrichment is no longer observed by the softening of the sample. Stiffness at low temperatures can decrease the resistance that would cause successive deformations, causing a decrease in its useful life

[1]Fuentes-Audén, C. et. al. Polymer Testing. **2007**, 26 (3), 323
[2]Fuentes-Audén, C. et. al. Polymer Engineering and Science. **2012**, 52, 242

**Área: MAT** **Inscrição: 628**

# Gold Electrodeposition on Porous Polymeric Templates for Raman Spectroscopy

**Rafael N. P. Colombo (PG)[1], Rodrigo V. Moreira (PG)[1], Dalva L. A. de Faria (PQ)[1], Susana I. C. de Torresi (PQ)[1]**

**rafanericol@hotmail.com**

[1]*Instituto de Química, USP*

Palavras Chave:*Electrodeposition, Gold, SERS, Nanoparticles, Template, Breath-figure*

## Highlights

A low-budget and rapid method was developed to synthesize gold substrates for Raman spectroscopy.
With inherent stability and portability of solid state, substrates do show promising results with Rhodamine.

## Abstract

Usual approaches for SERS active substrate confection rely mainly on top-down lithographic procedures, with several advantages as precision and reproducibility, yet at the price of costly equipments and time-consuming protocols. Among the bottom-up alternatives, spin-coated porous PMMA films were produced on top of a conducting substrate in a single-step fashion, therefore delimiting confined electroactive regions inside the pores of a few hundreds of nanometers in diameter. This methodology allows the electrodeposition of a range of materials with controllable geometry and filling, such as agglomerated gold nanoparticles and flat disks, presenting both good stability and reproducibility [1]. The SEM micrographs are shown in Figure 1.

**Fig 1.**SEM micrographs of electrodeposited Au with polymeric mask still present, different electrochemical conditions lead to formation of (left) flat particles and (centre and right) agglomerated nanoparticles.

Raman measurements, Figure 2, were acquired after addition of Rhodamine 6G $10^{-5}$ M on both structured surfaces and spectra were collected on randomly selected sample spots, with laser excitation on 633 nm and 785 nm wavelengths, exhibiting good reproducibility.

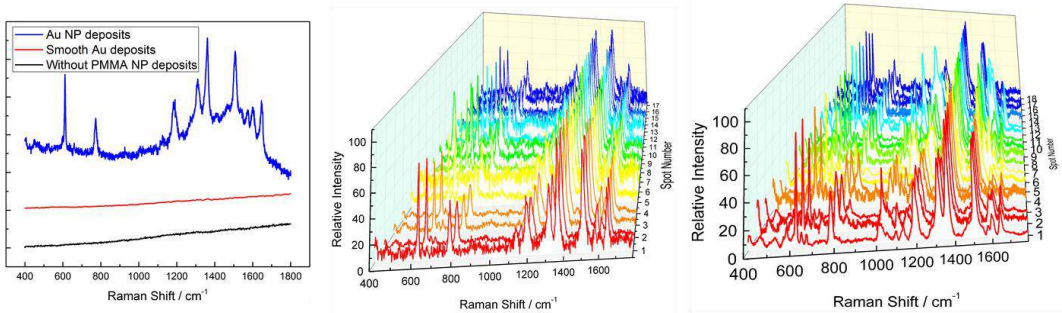


**Fig 2.** Raman spectra after Rhodamine addition on blank, flat gold and nanoparticles (left), spectra collected on multiple spots at excitation of 633 nm and 785 nm (centre and right, respectively).

[1] Colombo RNP, Petri DFS, Torresi SIC, Gonçales VR, Electrochim. Acta, 158, 2015, 187-195.

**Área:** MAT **Inscrição:** 00085

# Dye-sensitized solar cells based on $TiO_2$ nanoparticles

Sthéfany Zaida S. do Amparo[1]*(IC), Gabriella C.de Almeida[1] (IC), Ana Luisa Almeida Lage[1](PG), Dayse Carvalho da Silva Martins[1](PQ), Nelcy Della Santina Mohallem[1] (PQ), Marcelo Machado Viana[1] (PQ).

***sthefany_zaida@hotmail.com**

[1] *Departamento de Química, Instituto de Ciências Exatas, Universidade Federal de Minas Gerais*

Keywords: *Titanium dioxide, Solar cells, Dyes, Jabuticaba, Porphyrin.*

## Highlights

Preparation of $TiO_2$ nanoparticles surface-modified by porphyrin molecules. Evaluation of the efficiency of solar cells of titanium dioxide sensitized by natural or artificial dyes.

## Abstract

Photovoltaic devices are based on the photovoltaic effect, which is the appearance of an electric power in a semiconductor material when exposed to light [1]. Among these devices, the dye-sensitized solar cells (DSSC) stand out as a promising solution to the sustainable energy. The most widely used semiconductor in DSSC is titanium dioxide ($TiO_2$) due to its resistance to continuous electron transfer. In this work, $TiO_2$ was obtained by the precipitation method from titanium tetrachloride using microwave radiation. Anatase $TiO_2$ nanoparticles with crystallite sizes of 15 nm was obtained after temperature and pH control. The nanomaterial was characterized by transmission electron microscopy, fluorescence spectroscopy, X-ray diffraction and thermogravimetric analysis. $TiO_2$ nanoparticles showed good efficiency in the photodegradation of methylene blue dye, which proves their potential to be applied in DSSC. DSSC devices were made using indium doped tin oxide (ITO) slides with natural dye of jabuticaba or tetrakis(4-carboxyphenyl)porphyrin (Table 1).

**Table 1-** DSSC composition prepared in this work

| | Components | DSSC I | DSSC II |
|---|---|---|---|
| PHOTOELECTRODE | Semiconductor | $TiO_2$ | $TiO_2$ |
| | Catalyst | Graphene | Graphene |
| COUNTER ELECTRODE | Electrolyte | $I^{3-}$ / $I^-$ ions | $I^{3-}$ / $I^-$ ions |
| | Photon absorber | Natural dye extracted from jabuticaba | Artificial dye (porphyrin) |

The fluorescence technique confirmed the surface modification of $TiO_2$ nanoparticles with the porphyrin molecules (Figure 1). The solar cells were characterized from a current versus voltage curve using a UVA lamp of 350 nm at 15 W and the efficiency measurements are underway (Table 2).

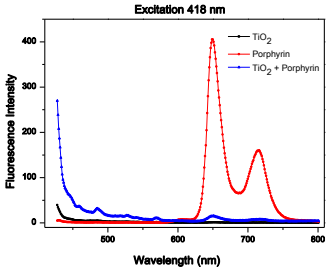


**Figure 1-** Fluorescence spectra for $TiO_2$, porphyrin and $TiO_2$ + porphyrin.

**Table 2-** Efficiency of the solar cells

| Device | Efficiency (%) |
|---|---|
| **DSSC I** | 1.24 |
| **DSSC II** | underway |

Acknowledgment: We thank FAPEMIG, CNPq, and Capes for financial support.

[1] Grätzel, Michael, J Photoch Photobio C, 4, 2003, 145

**Área: MAT** **Inscrição: 0009**

# Corrosive process study at a central of water treatment and distribution in Potiretama – CE rural area

**Josy Eliziane T. Ramos (PQ),[1] Sanderlir S. Dias (PQ),[1] Ronnielbe A. Moura (IC).[1]***

**Josy.ramos@ufersa.edu.br; ronnielbeavelino@gmail.com**

[1]*Departamento de Ciências Exatas e Naturais - DECEN, UFERSA;*

Palavras Chave: *Corrosão, Triângulo da corrosão, Proteção, Concreto.*

## Highlights

Corrosion forms, corrosive medium and operational conditions were identified for the Corrosion Triangle construction, to define the best protection technique that could minimize this process.

## Resumo/Abstract

The corrosive phenomenon is a process of metallic materials deterioration that occurs due to the medium and metal interaction. As this process is spontaneous, it entails enormous losses for all metallics segments. A theoretical review was developed and, later, *in situ* visits were carried out that allowed the objects registration in a corrosive process. From the studied parts evaluation, it was possible to observe the corrosion forms, the corrosive medium identification and operational conditions that were subjected and, then, the Corrosion Triangle was constructed, in order to propose techniques to soften the impacts caused by the corrosive phenomenon. The adductor presented numerous corrosion forms, with highest prevalence being uniform corrosion. This uniform corrosion caused complete destruction of several adductor elements, as well as partial destruction of others. Another corrosion found was in concrete, a corrosion that can be fatal to the entire structure. Figure 1 shows the uniform corrosion in a joint part (1a) and corrosion in wall of the reservoir concrete (1b). The reservoir presented cracks and holes caused by iron corrosion inside its structure, and these caused water leakage. For such situations, the best technique would be the joint replacement due to its advanced corrosive process and, in the reservoir case, the precast concrete rings replacement to avoid a total water supply stoppage in the rural area region.

Figure 1: uniform corrosion in a joint part (1a) and corrosion in wall of the reservoir concrete (1b).

1a

1b

**Área: MAT** **Inscrição: 00216**

# Nanoencapsulação do extrato do fruto de *Guazuma ulmifolia* Lam. utilizando poli (ácido lático-co-ácido glicólico)

**[1]Anna Flavia Dias Zafred* (IC), [2]Mara Núbia Guimarães dos Santos (PG), [1]Ana Paula Terezan (PQ), [2]Jaqueline Rodrigues da Silva (PQ), [2]Ricardo Bentes de Azevedo (PQ), [1]Lucília Kato (PQ), [1]Cecília Maria. Alves de Oliveira (PQ), [1]Denilson Rabelo (PQ), [1]Patrícia P. Confessori Sartoratto (PQ)**

**patricia@ufg.br; annaflavia.zafred@gmail.com**

*[1]Instituto de Química, UFG, Goiânia-GO, Brasil; [2] Instituto de Biologia, UnB, Brasília-DF, Brasil*

Palavras Chave: *nanoencapsulação, Guazuma ulmifolia, mutamba, PLGA*

## Highlights

Nanoencapsulation of extract of the fruits of *Guazuma ulmifolia* Lam. using poly (lactic acid-co-glycolic acid). The extract was encapsulated in PLGA by the emulsion-solvent technique. Polymer molecular weight affected the average nanoparticle diameter and polydispersion, while encapsulation efficiency remained constant.

## Resumo/Abstract

Os extratos da folhas e cascas da *Guazuma ulmifolia* Lam. (mutamba) apresentam efeitos hipoglicemiantes, leishmanicida e anticolinesterase associados à presença de polifenóis (1). Já os frutos, comestíveis, embora menos investigados, seus extratos de média polaridade apresentam alto potencial antioxidante, associado ao alto teor de compostos fenólicos. Sabe-se também que, em geral, a baixa solubilidade, estabilidade e biodisponibilidade dos fenólicos limitam suas aplicações e que, a nanoencapsulação destes em polímeros biodegradáveis e biocompatíveis aumenta a absorção, protege contra degradação e prolonga o tempo de circulação (2). Neste contexto, este trabalho apresenta o estudo inicial da nanoencapsulação, em PLGA, de compostos extraídos de frutos da mutamba. Um extrato de média polaridade (ExD) foi obtido por partição líquido-líquido (água/diclorometano) do extrato metanólico dos frutos da mutamba (coletados no resquício da Mata Subcaducifólia Estacional, Campus da UFG, Goiânia/GO). A encapsulação em PLGA (50:50) foi realizada pelo método de emulsão–evaporação de solvente, no qual a fase orgânica foi constituída de PLGA (38-54 kDa ou 5–15 kDa) e ExD, dissolvidos em diclorometano. A fase aquosa foi composta de água e PVA. Para comparação, foram realizados procedimentos na ausência de ExD. As amostras foram caracterizadas por espalhamento dinâmico de luz e microscopia eletrônica de transmissão. A eficiência de encapsulação foi determinada a partir de medidas por espectrofotometria na região do ultravioleta. Os resultados estão resumidos na Tabela 1. O uso de PLGA de maior massa molecular resultou em nanopartículas esféricas de menor diâmetro médio e menor índice de polidispersão. A eficiência de encapsulação foi semelhante para ambos os polímeros.

Tabela 1. Diâmetro hidrodinâmico (Dh), índice de polidispersão (IPD) e eficiência de encapsulação (EF) do extrato em nanopartículas (NP) de PLGA.

| Amostra * | ExD/PLGA (% m/m) | $D_h$ (nm) | IPD | EF (%) |
|---|---|---|---|---|
| NP-A10 | 10 | 214 | 0,14 | 26,6 |
| NP-B10 | 10 | 373 | 0,57 | 23,0 |
| NP-A5 | 5 | 164 | 0,09 | 43,1 |
| NP-B5 | 5 | 269 | 0,51 | 40,6 |
| NP-A | 0 | 231 | 0,13 | - |
| NP-B | 0 | 186 | 0,30 | - |

*A- PLGA de 38-54 kDa; B- PLGA de 5–15 kDa

(1) Lopes, G. C; Rocha, J. C. B, Almeida, G. C.; Mello, J. C. P. J. Braz. Chem. Soc., 20, 1103-1109, 2009.
(2) Wanga, S.; Sua, R.; Niea, S.; Suna, M.; Zhanga, J.; Wub, D.; Moustaid- Moussaa, N. J. Nutr. Biochem., 25, 363–376, 2014.

Agradecimentos ao CNPq e a Fapeg

**Área: MAT** **Inscrição: 00358**

# Synthesis of a luminescent hybrid of silica and Iridium complex for biomarker application

**Alessandra Mara G. Mutti (PG)[1], João Antonio O. Santos (PG)[1], Felipe S. M. Canisares (PG)[1], Ana Maria Pires (PQ)[1], Sergio A. M. Lima (PQ)[1*].**

***samlima@fct.unesp.br**

[1]*Departamento de Química e Bioquímica, FCT-UNESP, Presidente Prudente – SP.*

Key-works: *Silica, Iridium, Complex, Biomarker, Luminescence, Surface modification.*

## Highlights

Luminescent $Ir^{3+}$-complex; spherical non-toxic and biocompatible silica ($SiO_2$) particles; anchoring $Ir^{3+}$-complex on the surface of silica; red intense luminescent silica particles.

## Resumo/Abstract

Luminescent silica are interesting and versatile materials performing specific tasks by linking functional molecules on the surface, and can be applied as biomarkers[1], since it is biocompatible and non-cytotoxic[1,2]. Phosphorescent Iridium complexes exhibit high quantum yields[3], and color modulation through the modification of the ligands. By combining these characteristics of both, it is possible to produce a hybrid that emits in a region other than the auto-fluorescence of the biological medium, making them promising for application as biomarker. The purpose of this work is to investigate the coordination of an $Ir^{3+}$-complex with aminofunctuonalized $SiO_2$ through an amidic bond. The $SiO_2$-$NH_2$ was synthesized via sol-gel using TEOS and APTES. The $Ir^{3+}$-complex was prepared from a precursor dimer ($[Ir_2(ppz)_4Cl_2]$) with the biquinoline carboxylic diacid (bqda). Finally, the $Ir^{3+}$-complex carboxylate groups were activated with the crosslinker EDC, which were conjugated to the $NH_2$ groups present on the particles, yielding the luminescent hybrid. By SEM (Fig. 1a), the obtained $SiO_2$-$NH_2$ are spheroidal shaped (178±9 nm). The Si-O and N-H vibrational modes were observed by FTIR. Through $^{29}$Si-NMR were detected Si atoms as $Q^{4,3,2}$ groups. The $Ir^{3+}$-complex formation was first confirmed by FTIR, showing that the ligand was coordinated to Ir-complex through the quinoline group. Photoluminescence Spectroscopy showed a large and intense emission band in the red region with high color purity (Fig. 1b and c), which is also present after incorporation on the particles, confirming the luminescent hybrid formation.

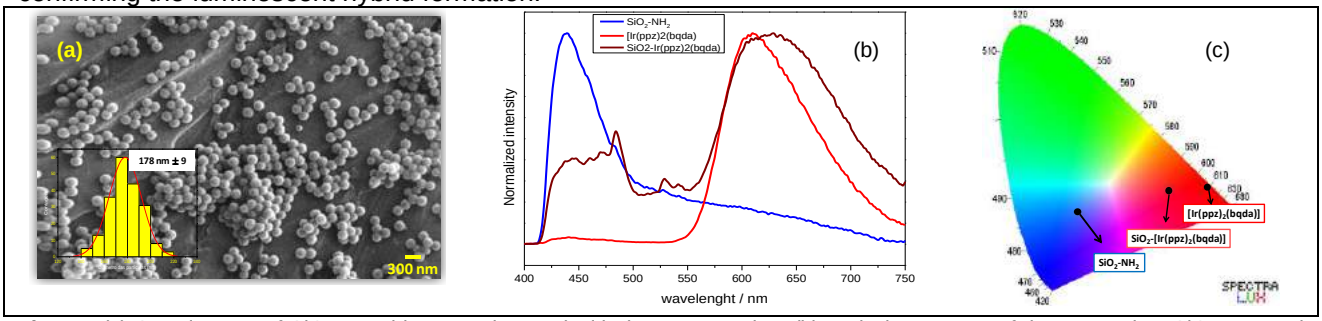


**Fig. 1 –** (a) SEM images of $SiO_2$-$NH_2$; histogram inserted with the average size; (b) Emission spectra of the Ir-complex, $SiO_2$-$NH_2$ and $SiO_2$-Ir complex; (c) Color diagram and color purity of $SiO_2$-$NH_2$ (37%), $[Ir(ppz)_2(bqda)]$ (98%) and $SiO_2$-$[Ir(ppz)_2(bqda)]$ (55%).

Acknowledgements: FAPESP, CAPES, LabMEV, NMR – IQ/UNESP. Refs.: [1]BAE, S. W. et al. *Chem. Comm.* 2012, 48, 2270–82. [2]AL-RAWI, M, et al. *Inorganic Compounds*, 2011, 85, 813–826.. [3] CAMARGO, A. S. S. et al. *J. Phys. Chem*, 2013, 117, 2966-2975.

**Área: MAT**
*(Inserir a sigla da seção científica para qual o resumo será submetido. Ex: ORG, BEA, CAT)*

**Inscrição: 01283**
*(Inserir o número de inscrição do autor que fez a submissão)*

# Simultaneous oxygen and temperature ratiometric optical probes based on an europium(III) complex and anthracene covalently bounded to pdms.

**Diogo A. Gálico (PG),[1] Ítalo O. Mazali (PQ),[1] Fernando A. Sigoli (PQ).[1*]**

**dagbau@hotmail.com; fsigoli@iqm.unicamp.br**

*[1]Laboratory of Functional Materials – Institute of Chemistry, University of Campinas - UNICAMP*

Palavras Chave:*Lanthanide, pdms, Temperature probe, Oxygen probe.*

## Highlights

Simultaneous temperature and oxygen optical probing. Probes chemically bounded to the pdms. Ratiometric probing based on anthracene and $Eu^{3+}$ emissions. Anthracene→$Eu^{3+}$ energy transfer.

## Resumo/Abstract

Simultaneous probing of oxygen and temperature is widely applied in several areas such as blood analysis, bioreactor fluids, chemical industry, aerodynamic research and in the monitoring of food quality control [1]. The use of luminescent probes have the advantages of contactless measurements and the possibility of large and/or micro scale imaging [2]. In this context, the application of lanthanides complexes or nanoparticles for optical probes it is interesting due to the long emission lifetimes, narrow emission bands and large pseudo-Stokes shifts [3]. In this work we chemically attached the $[Eu(bzac)_3(H_2O)_2]$ complex (red emitter) and the anthracene group (eant - blue emitter) in a pdms matrix resulting on a self-supportable membrane (structural scheme in Fig. 1-a) with high thermal sensitivity to temperature and oxygen level variation (Fig. 1-b). The ratio between the anthracene (380-565 nm range) and europium(III) (602-640 nm range) emissions was used in the luminescent probing. For the temperature probing, the system shows an operational range of 203-323 K and a maximum relative sensitivity of 2.69 % $K^{-1}$ at 233 K. The oxygen dependence of the emission was measured at 25, 30, 35 and 40 °C and a temperature correction surface (Fig. 1-b) was developed. The results also indicate the existence of an energy transfer from anthracene to europium(III) in this system even though these species are not bound chemically.

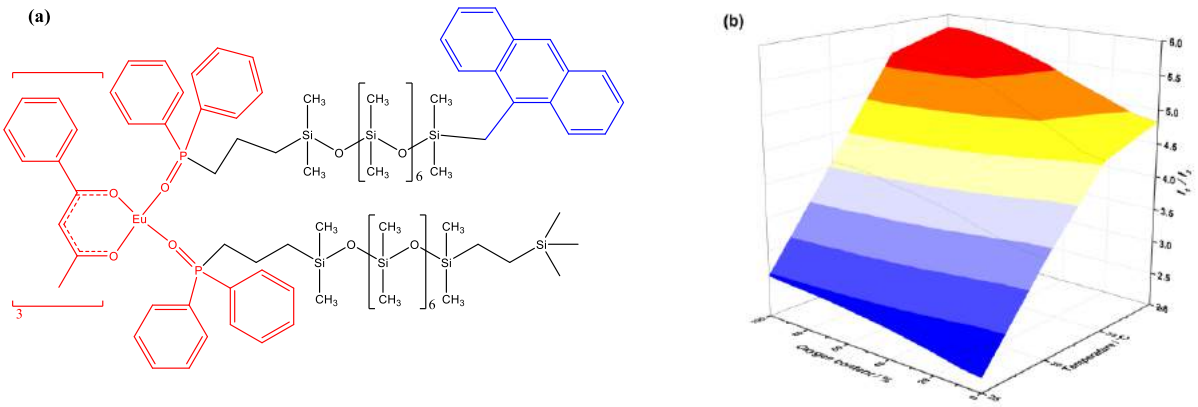


**Figure 1:** (a) Structural scheme of the pdms-eant(0.1%)-edppo(1%)-$[Eu(bzac)_3]$(0.25%) membrane and (b) simultaneous temperature (25-40 °C range) and oxygen ratiometric probing.

[1] M.I.J. Stich, L.H. Fischer, O.S. Wolfbeis, Chem. Soc. Rev. 39 (2010) 3102.
[2] X. Wang, O.S. Wolfbeis, R.J. Meier, Chem. Soc. Rev. 43 (2014) 3666.
[3] C.D.S. Brites, P.P. Lima, N.J.O. Silva, A. Millán, V.S. Amaral, F. Palacio, L.D. Carlos, Nanoscale. 4 (2012) 4799.

**Área: MAT** **Inscrição: 00868**

# Synthesis, Characterization and Photophysical Properties of a Fluorene-Benzothiadiazole / Fluorene-Terpyridine Block Copolymer

**Alisson J. Santana (PG),[1*] Denis A. Turchetti (PQ),[1,2] Leni C. Akcelrud (PQ),[1].**

**nossila.08@hotmail.com; nossila.08@hotmail.com**

*[1]Departamento de Química, UFPR; [2]Departamento de Física, USP*

Palavras Chave: *Block copolymers, Conjugated polymers, Photophysics.*

## Highlights

Alternating copolymers containing fluorene bonded to benzothiadiazole and terpyridine were synthesized. The polymer showed two emission bands.

## Resumo/Abstract

In the steadily growing field of electronic devices, several types of polymer systems and device architectures have emerged as attractive means to improve the performance and chemical stability of the devices. One approach is a block copolymer synthesis[1]. In this work we report the synthesis, characterization and photophysical properties of a copolymer built up by blocks, based on the fluorene-benzothiadiazole segment linked either to fluorene-terpyridine units, in an alternated fashion. The block copolymer, Poly(9,9'-n-dihexyl-2,7-fluorene)-alt-4,7-(2,3,5-benzothiadiazole)-co-(9,9'-dihexyl-2,7-fluorene)-alt-6,6'-(2,2':6,2''-terpyridine) (LaPPS76) was synthesized through the Suzuki route[1,2]. The polymer was characterized using elemental analysis, GPC, NMR, TGA, DSC, UV-Vis and fluorescence spectroscopy. The LaPPS76 (ratio between blocks is 70/30), presents two dominant electronic transitions: a $\pi$-$\pi^*$ transition at 340 nm and a transition with internal charge transfer (ICT) in 435 nm. Also the polymer shows two emission bands: at 380 nm and another in 535 nm. The analysis of this spectrum leads to the conclusion that the first band is relative to the fluorene-terpyridine block and the second to the fluorene-benzothiadiazole segment.

(1) Zanlorenzi, C.; Cassemiro, S. M.; Grova, I. R.; Akcelrud, L. Photophysical Behavior of Block Copolymers Containing EDOT, Thiophene, and Benzodiathiazole Units Linked to Fluorene. *J. Polym. Sci. Part B Polym. Phys.* **2016**, *54* (9), 908–915.

(2) Yan, C.; Sun, Z.; Guo, H.; Wu, C.; Chen, Y. Thiophene-Fused 1,10-Phenanthroline toward a Far-Red Emitting Conjugated Polymer and Its Polymer Dots: Synthesis, Properties and Subcellular Imaging. *Mater. Chem. Front.* **2017**, *1* (12), 2638–2642.

**Área: MAT** **Inscrição:01369**

# Study of the Association of Few-walled Carbon Nanotubes with the Semiconductor Complex $Bu_4N[Ni(dmit)_2]$.

**Matheus Kley Rodrigues (IC),[1] Luciano Roni Silva Lara (PQ),[1] Raquel Vieira Mambrini (PQ),[2] Walace Doti do Pim(PQ),[2] Humberto Osório Stumpf.[1]***

**larovkzki@gmail.com; stumpf@ufmg.br**

*[1]Departamento de Química, UFMG; [2] Departamento de Química, Centro Federal de Educação Tecnológica de Minas Gerais.*

Keywords: *few-walled carbon nanotubes, dmit, nickel, magnetism.*

## Highlights

- FWCNTs can exhibit adjustable electronic properties because of their high response to the surrounding chemical environment.
- It was obtained a new composite based on Few-walled Carbon Nanotubes (FWCNTs) and $[Bu_4N][Ni(dmit)_2]$ [dmit = 1,3-Dithiola-2-tiona-4,5-dithiolate];
- The interaction between the components was investigated by Raman Spectroscopy and TEM images show that the complex was well dispersed in the CNTs surface.
- Preliminary magnetic study showed a blocking temperature near 260 K.

## Resumo/Abstract

The development of new materials with potential application in spintronics is motivating and our group has concentrated efforts to obtain materials based on coordination compounds and carbon nanotubes for this purpose. The investigation of the interactions between these entities has also been of great interest.[1] This work aims to prepare and study composites based on FWCNTs and the complex $[Bu_4N][Ni(dmit)_2]$, which has shown promise due to its electronic properties. The complex was prepared accordingly to the literature and the CNTs are from a commercial source.[2] Initially, the FWCNTs were dispersed in chloroform by using a titanium tip ultrasound in an ice bath and a solution of the complex was added to the suspension and system was kept under stirring for 90 min. The material was separated by centrifugation (5000 rpm), washed, and dried under vacuum for 48 h. The composite was preliminarily characterized by FTIR, Raman spectroscopy, thermal analyses, TEM images with chemical mapping and magnetic measurements. TEM images show that the composite was successfully prepared with a great dispersion of the complex in the surface of CNTs. Magnetization measurements were performed in a SQUID magnetometer from 2 to 300 K and the maximum applied field was of 7 T. The ZFC/FC curves showed a blocking temperature ($T_B$) near 260 K. This hybrid material will be studied further to verify its semi-conductive properties and potential application in the field of electronic materials.

### REFERENCES

[1] (a) Silva, I. F.; do Pim, W. D.; Teixeira, I. F.; Barros, W. P,; Teixeira, A. P. C.; do Nascimento, G. M.; Pereira, C. L. M.; Stumpf, H.O. *J. Phys Chem. C* **2016**, *120*,1245; (b) do Nascimento, G. M.; Barros, W. P.; Kim, Y. A.; Muramatsu, H.; Hayashi, T.; Endo, M.; Pradie, N. A.; Fantini, C.; Pimenta, M. A.; Dresselhaus, M. S.; et al. *J. Raman Spectrosc*. **2012**, *43*,1951.

[2] (a) Steimecke, G.; Hoyer, E. *Zeitschrift Fur Chemie* **1979**, *19*, 268; (b) Nakamura, Y.; Kato, R.; Kishida, H., *J. Phys. Soc. Jpn*, **2015**, *84*, 44715.

### ACKNOWLEDGMENTS

CNPq, CAPES and FAPEMIG.

**Área: MAT** **Inscrição: 01267**

# A scalable new platform to produce all-carbon low-cost paper-based electrodes

**João P.F. Bertacchi (PG),[1] Fernando Galembeck (PQ).[1]**

**joao.bertacchi@iqm.unicamp.br; fernagal@iqm.unicamp.br**

[1]*Department of Physical Chemistry, Institute of Chemistry, UNICAMP*

Keywords: EDLC, *supercapacitor, graphite, activated carbon, cellulose, paper.*

## Highlights

A new scalable platform to make high-performance, non-metallic and flexible conductive materials formed by graphite coatings on cellulose. Supercapacitors with outstanding areal capacitance.

## Resumo/Abstract

This work is based on a scalable new platform to produce graphite-coated paper as a high-performance, flexible and low-cost conductive material.[1,2] Dispersions of activated carbon and/or graphite in an alkaline cellulose solution were prepared with different compositions and sprayed on filter paper. Coated paper sheets were assembled as symmetric capacitors and tested in galvanostatic charge-discharge cycling experiments using different current densities. The results in Figure 1 compare favorably to the state-of-the-art all-carbon paper-based supercapacitors in the literature (e.g., 80 $mF.cm^{-2}$ for graphene oxide in cellulose tissues).[3] They also surpass the performances of hybrid supercapacitors that include manganese oxide nanoparticles within the paper/graphene matrix, yielding 175 $mF.cm^{-2}$).[4] Thus, blending activated carbon with graphite exfoliated by soluble cellulose provides an excellent combination of electrical conductivity and interfacial activity required to make high-performance supercapacitors.

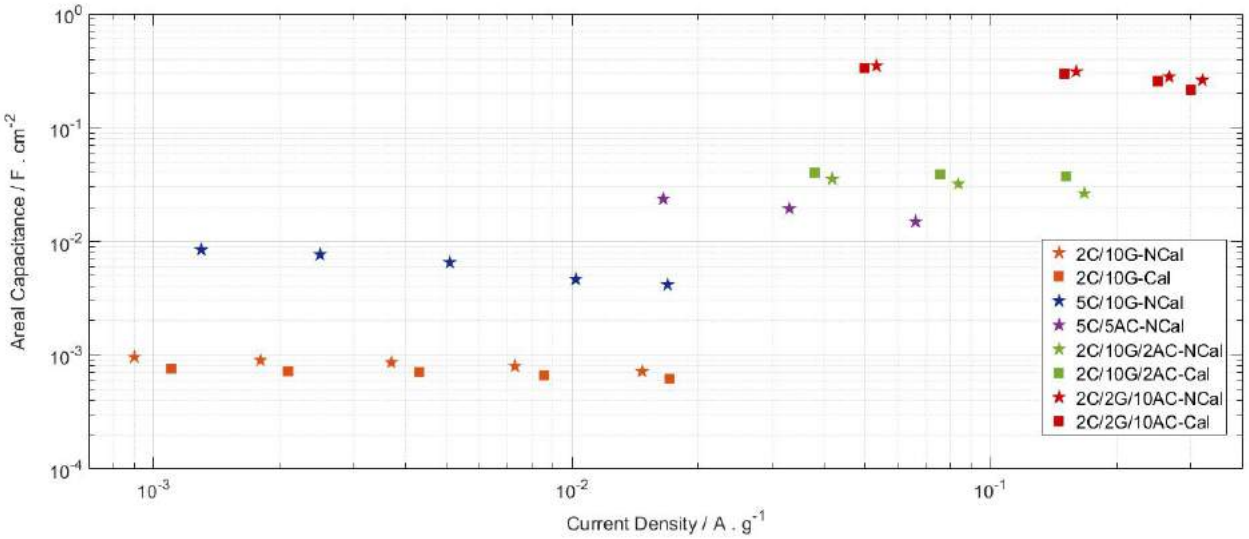


Figure 1: Areal capacitance of the assembled devices tested at different current densities (per gram of applied dispersion). ★: non-calendered electrodes. ■:calendered electrodes. C, G, AC refer to the percent weight of cellulose, graphite and activated carbon in the dispersions used to prepare the electrodes, e.g.: 2C/2G/10AC was prepared using a 2% graphite plus 10% activated carbon dispersion in 2% cellulose aqueous solution.

References:

[1] Ferreira, E.S., da Silva, *et al*. *Nanoscale*, 9, 2017, pp.10219-10226
[2] Galembeck, F., Ferreira, E.S. *Patent No:* WO2016119032A1, 2016.
[3] Sevilla, M., *et al*. *Energy Storage Materials*, *5*, 2016, pp.33-42.
[4] Feng, J.X., *et al*. *Journal of Materials Chemistry A*, *2*(9), 2014, pp.2985-2992.

**Área: MAT** **Inscrição: 01367**

# Development of materials based on calcium polyphosphate/alginate for bone cement applications

**Joalen P. Monte (IC),[1]* Graziela B. A. Silva (IC), [2] Juliana S. A. Falcão (PQ)[3], Beate S. Santos (PQ)[4]****

***joalenpm@gmail.com; **beate_santos@yahoo.com.br**

*[1]Fundamental Chemistry Department, UFPE, Pernambuco, Brazil; [2]UFRPE – UACSA, Pernambuco, Brazil; [3]UFCG, Pernambuco, Brazil. [4]Pharmaceutical Sciences Department, UFPE, Pernambuco, Brazil;*

Palavras Chave: *Bone Substitutes, Biomaterial, Calcium Polyphosphate.*

## Highlights

This work presents new calcium polyphosphate/alginate composites as potential biomaterials for bone cement/prosthesis applications.

## Resumo/Abstract

Calcium phosphate based materials are biocompatible and chemically similar to hydroxyapatite, the main component of bone tissues.[1,2] We prepared different composites based on sodium polyphosphate, sodium alginate and calcium chloride by dissolving both polymers in aqueous medium at 80ºC and adding $Ca^{2+}$ ions under vigorous stirring. The TGA of the dried composites showed 60-75% of alginate incorporation while Raman spectroscopy/microscopy revealed the characteristic vibrational frequencies of the polymer and the polyphosphate anion (Fig.1(a)). The morphology of the materials examined by SEM shows that the CPP particles are composed of crystalline flakes (Ca/P~1) (Fig.1(b)) while the final CPP/alginate composites show a unique pattern, suggesting the coating of the micrometer sized crystals by a film of calcium alginate (Fig1(c)).

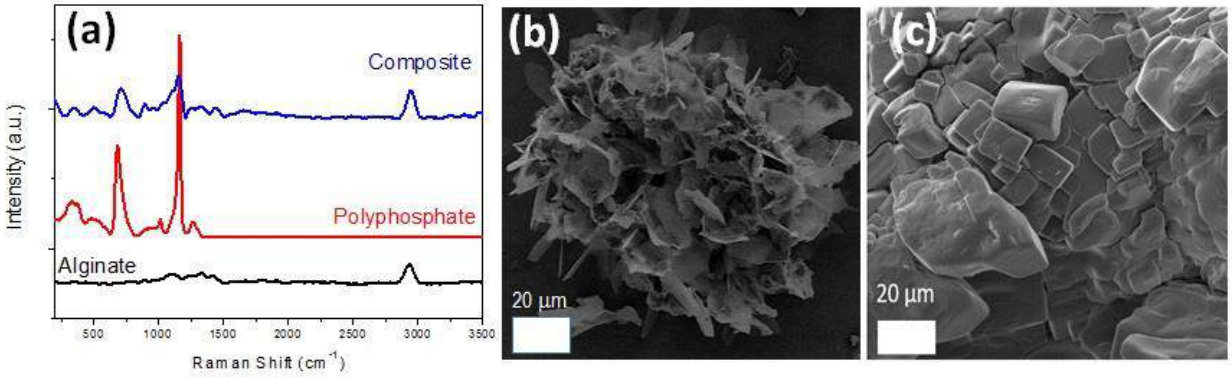


*Figure 1. Raman spectra of sodium alginate, sodium polyphosphate and of the calcium polyphosphate composite (a); SEM images of the CPP (b) and the alginate composites (c).*

The X-Ray diffraction pattern of CPP present a great crystallinity with no distinguishable phase, while the composites present a more amorphous pattern. The overall results show that these composites are promising bone substitute materials.

We thank CNPq and Propesq-UFPE for the encouragement.

1. Yang, L.; Zhong, C.;*Front. Mater. Sci.*, ***2013**, 7(4), 313-334.*
2.Low, K. L.; et al. Calcium phosphate-based composites as injectable bone substitute materials. *J. Biom. Mater. Research, **2010**, 94B, 273-286.*

**Área: MAT** **Inscrição: 01376**

# Preparation and characterization of ashes from cassava and sugarcane bagasse wastes

**André Vinícius Bueno de Oliveira (IC),[1] Tânia Mara Rizzato da Silva (TM),[1] Sílvia Luciana Fávaro (PQ),[2] Vagner Roberto Batistela(PQ).[1*]**

**andrebueno2002@hotmail.com; vagner.batistela@yahoo.com.br**

*[1] Department of Technology, UEM. [2] Department of Mechanical Engineering, UEM.*

Keywords: *residue, waste, ash, cassava, sugarcane, sustantability.*

## Highlights

- Preparation and characterization of ashes from cassava and sugarcane bagasse wastes.
- Characterization of wastes *in natura* and their ashes by $pH_{zpc}$, FTIR and SEM.
- Ashes can be applied as adsorbents for cationic species.

## Resumo/Abstract

An important form of destination of sugarcane (SUC) and cassava (CAS) agroindustrial wastes is their application as adsorbent materials. In this work, ashes of sugarcane bagasse and cassava residue were prepared by the following steps: washing, basic treatment with NaOH 0.10 mol.$L^{-1}$ for 24 h, drying at 105$^{o}$C for 24 h, carbonization and calcination at 600$^{o}$C for 6 h. The low yields of 6.8 % for SUC and 4.1 % for CAS indicated high content of organics in the wastes. Zero point of charge of the materials were 7.69 and 9.07 for SUC and CAS *in natura* and for their ashes were 10.27 and 10.63, resulted from the treatment with base in their preparation. As consequence, ashes present superficial negative charge which is very important for adsorption of cationic species. Due to the preparation of ashes, bands in 3334 and 1032 $cm^{-1}$ of alcohol groups disappeared and a new band at 880 $cm^{-1}$ appeared, what indicates that cellulose and starch from materials *in natura* were converted to aromatic hydrocarbons. SEM micrographs showed that SUC has fibrous structure and its ashes presented irregular shape clusters without fibrous aspect. CAS residue *in natura* presents porous structure and its ashes have clusters of smaller spacings.

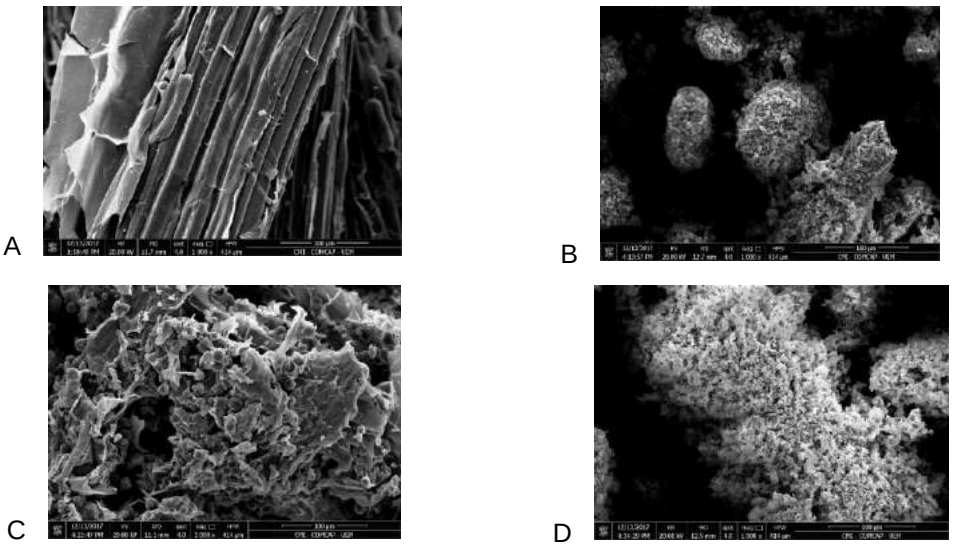


**Figure 1.** SEM micrographies of SUC *in natura* (1), SUC ashes (2), CAS *in natura* (3) and CAS ashes (4). Magnifications of 1000x.

**Área: MAT** **Inscrição:01345**

# Synthesis and characterization of AuPd and AuPt bimetallic nanoparticles for biointegration with microorganisms

**Sarah Mariana F. Santana*** **(PG), Verônica Maciel Bispo (PG), Regina Geris (PQ) and Marcos Malta (PQ).**

**sarahmariana.289@gmail.com**

*Institute of Chemistry, Federal University of Bahia, Campus Ondina, Salvador (BA), Brazil*
Keywords: Nanoparticles, AuPd, AuPt, Plasmonic band.

## Highlights

1) AuPd and AuPt nanoparticles were obtained through sequential reduction of $Pd^{2+}$ and $Pt^{2+}$ over Au-NPs.
2) Plasmonic band of Au-NPs decreased at higher concentrations of Pd and Pt atoms.
3) Microorganisms were cultivated in these solutions to assimilate nanoparticles on their cell wall.

## Abstract

Recently, the preparation of fungi/Au-NPs bio-hybrids have gained interest due to possible applications beyond the classical biotechnological use of such microorganisms. For instance, our group have demonstrated the production of mycelia-like gold microtubes using Au-NPs/fungus as biotemplates[1]. The addition of a second metal in the structure of Au-NPs has been widely used to improve the performance of these materials as catalysts[2]. In this work, we present some results regarding the controlled addition of Pd and Pt metals on the surface Au-NPs, and subsequent cultivation of filamentous fungi in these colloidal solutions. In these experiments, we have varied the concentration of both $Pd^{2+}$ and $Pt^{2+}$ (0.5, 2.0, 5.0, 20.0, 50.0 and 70% (w / w)) in Au-NPs solutions, proceeding a subsequent metal reduction using ascorbic acid. The UV-vis spectra of solutions containing AuPd and AuPt nanoparticles (Figure 1) are presented below.

Figure 1: Absorption spectra in the UV-vis region for solutions of AuPd and AuPt NPs with different concentrations of $Pd^{2+}$ and $Pt^{2+}$.

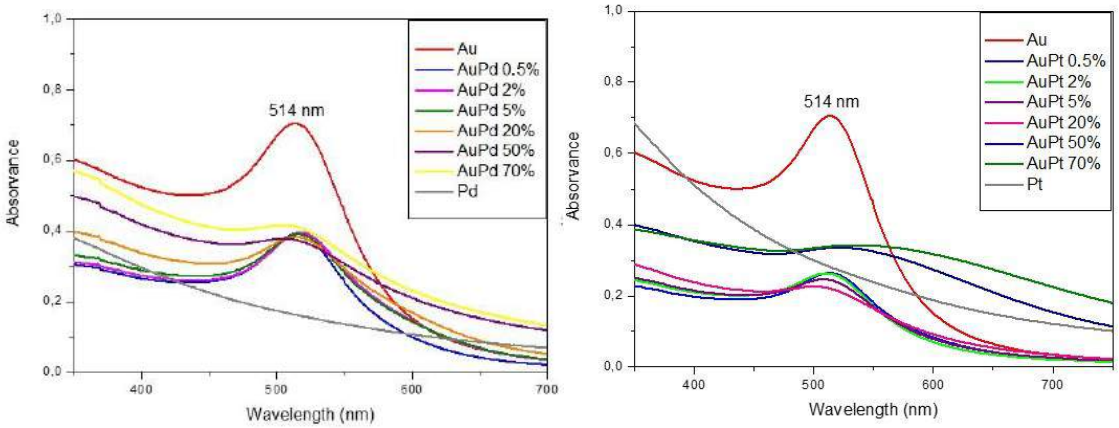


The maximum absorption of the plasmonic band for Au-NPs is located at ≈ 514 nm. It can be observed that plasmonic band decreases at higher concentrations of Pd and Pt atoms, indicating an efficient deposition of these metals on the surface of the Au-NPs. These results may be useful for selecting the best concentration of Pd and Pt to favor the deposition of bimetallic NPs in microorganisms to produce bio-hybrids materials.

[1]Fontes A. M, Geris R., dos Santos A. V., Pereira M. G., Ramalho J. G. S., da Silva A. F., Malta M., Biomater. Sci., 2, 2014, 956.
[2]Nutt M. O, Hughes J.B., Wong M. S., Environ. Sci. Technol., 39, 2005,1346.

Acknowledgement: CNPq and FAPESB.

**Área: MAT** **Inscrição: 00859**

# Conjugated polymer to gold nanoparticles passivation. Synthesis, characterization and photophysics interpretation.

**Hellen Vienna C. Silva (IC),[1] Carla R. Klimpovuz (IC),[2] Denis A. Turchetti (PQ),[1] Marcela M. Oliveira (PQ),[2] Leni C. Akcelrud (PQ),[1*].**

**hellen.vienna.hv@gmail.com; akleniak@gmail.com**

*[1]Departamento de Química, UFPR; [2]Departamento de Química, UTFPR.*

*Palavras Chave: Conjugated polymers, metallic nanoparticle, Electrostatic interaction.*

## Highlights

Synthesis, structural and photophysical characterization of fluorene copolymer;
Thiol groups as interaction sites for gold nanoparticles;
Photophysical properties of polymer passivated nanoparticles.

## Resumo/Abstract

The association of gold nanoparticles with polymer chains in optical sensors provides a means of enhancing the differences of refraction index which are probed by the device, increasing its reaching and selectivity (Scientific American, 2007, v. 296, n. 4, p. 56-63). Here the synthesis of a thiol containing polyfluorene derivative [poly(9,9´-diyl)bis(hexane-1-thiol-fluorene-alt-2,7-dihexyfluorene)] (LaPPS79) are described, along with the corresponding system in which the polymer acts as a passivating agent for gold nanoparticles, shown in scheme 1. The properties of the pristine polymer and those of the system polymer/gold nanoparticles when compared showed an increase in the intensity and a redshift of the plasmon band of the nanoparticles. The formation of an ordered system was also observed by transmission electron microscopy.

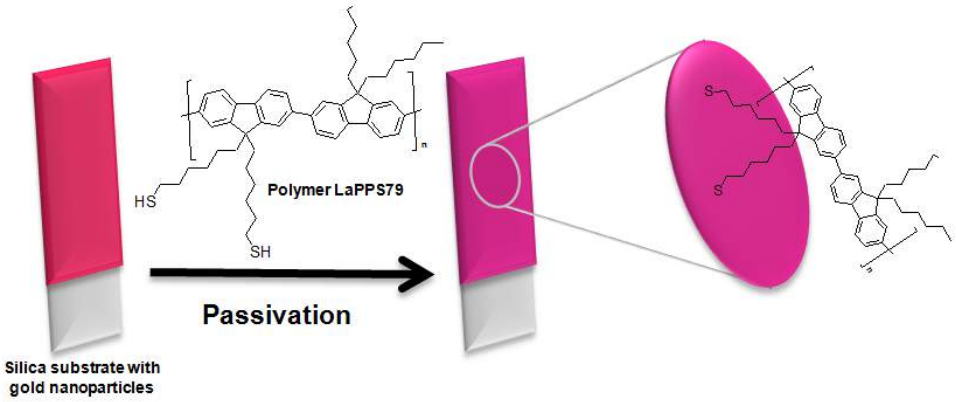


Scheme 1: Surface modification of gold nanoparticles with LaPPS79.

**Área: MAT** **Inscrição: 00813**

# Intensified Raman spectrum of 4-MBA on nonstoichiometric $CeO_2$

**Alice C. Reinaldo (IC),[1] Isaías de Castro Silva (PG),[1] Fernando A. Sigoli (PQ),[1] Italo O. Mazali (PQ).[1*]**

**isaias.silva@iqm.unicamp.br; mazali@iqm.unicamp.br**

[1]*Institute of Chemistry, University of Campinas, Brazil.*

Keywords: *Raman spectroscopy, Cerium(IV) oxide, Nanoparticles, SERS.*

## Highlights

We report the observation of the intensified Raman spectrum of 4-mercaptobenzoic acid (4-MBA) adsorbed in small quantities on reduced nanorods of cerium(IV) oxide ($CeO_2$-NR).

## Abstract

Typical nanoparticles applied for the intensification of the Raman spectrum of organic molecules are metallic ones[1]. However, the intensification of the Raman spectrum can also be observed when semiconductor nanoparticles are applied, where other mechanisms of intensification, beside surface plasmon resonance in metallic nanoparticles, are responsible for the intensification[1]. In this work $CeO_2$-NR were synthesized by hydrothermal synthesis, and characterized by X-ray diffraction and transmission electronic microscopy (TEM) (Figure 1). The $CeO_2$-NR was reduced by sodium borohydride ($NaBH_4$) through solid state reaction, in order to generate oxygen vacancies. The molecule 4-MBA was adsorbed on reduced $CeO_2$-NR from a $10^{-3}$ mol.$L^{-1}$ ethanol solution free of oxygen and after adsorption, the solid was washed several times in order to remove non-adsorbed molecules. It is possible to observe the bands attributed to 4-MBA (Figure 2), and the displacement for lower wavenumbers of $T_{2g}$ band of $CeO_2$, which is related to the generation of oxygen vacancies after reduction with $NaBH_4$[2]. Because of the small quantities of molecules adsorbed we can call this a phenomenon of intensification, and this may be related to electronic transitions that only occur in the presence of oxygen vacancies on $CeO_2$.

1 - Lombardi; Birke *J. Phys. Chem. C* 2014, **118**, 11120.
2 - Silva; Sigoli; Mazali *J. Phys. Chem. C* 2017, **121**, 12928.

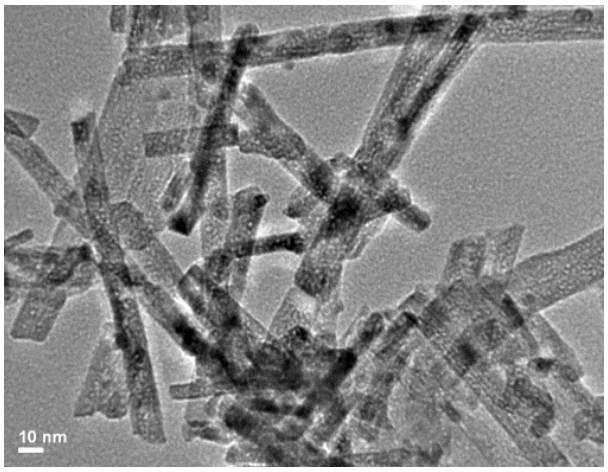


Figure 1. TEM images of $CeO_2$-NR.

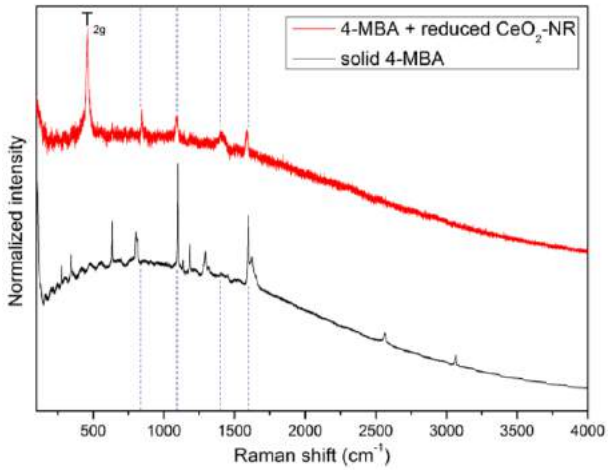


Figure 2. Raman spectra of pure 4-MBA (black) and 4-MBA adsorbed on $CeO_2$-NR (red).

**Área: MAT**
*(Inserir a sigla da seção científica para qual o resumo será submetido. Ex: ORG, BEA, CAT)*

**Inscrição: 01322**
*(Inserir o número de inscrição do autor que fez a submissão)*

# HIDROGÉIS NANOESTRUTURADOS CONTENDO NANOWHISKERS DE CELULOSE PARA LIBERAÇÃO TÓPICA DE FÁRMACO

**Bruno Carlos Melo (IC)[1], Francisco Helder Almeida Rodrigues (PQ)[1]**

brunocarlosmelo1994@gmail.com; almeida_quimica@yahoo.com.br
[1]*Coordenação de Química, UVA*
Palavras Chave: *Hidrogel; Intumescimento; Difusão; Microesferas; Lliberação tópica.*

## Highlights

Nanostructured hydrogels containing cellulose nanowhiskers for topical drug delivery systems.

The objective of the work dealt with in the optimization of hydrogels synthesis and obtaining nanostructured hydrogels with cellulose nanowhiskers, and evaluating its degree of swelling and diffusion coefficient.

## Resumo/Abstract

Hidrogéis são redes tridimensionais de polímeros hidrofílicos química ou fisicamente reticulados mantendo sua integridade estrutural quando intumescido[1]. O alginato de sódio (NaAg) é um biopolímero aniônico, composto de cadeias lineares de ácido α-L-glucurônico e β-D-manurônico, apresentando grupos hidrofílicos que quando inseridos em meio contendo íons bi ou trivalentes, forma hidrogéis capazes de encapsular uma série de substâncias[2]. No presente trabalho, hidrogéis foram sintetizados através da reticulação entre soluções de NaAg (1, 2 e 3% m/v) e $CaCl_2$ (1, 2,5 e 5% m/v); na ausência e presença de NWCs (1 e 2 % m/m), e avaliados quanto aos parâmetros de transporte líquido e intumescimento em água destilada, com vistas a uma possível utilização como veículos carreadores em sistema de liberação tópica de fármacos. Verificou-se que o grau de intumescimento aumenta com o acréscimo de alginato de sódio e diminui com o aumento da concentração de $CaCl_2$ (Figura 1a), por haver um incremento de grupos hidrofílicos na cadeia polimérica e devido ao caráter forte de dissociação do $CaCl_2$ levando a um maior número de interações entre cátions $Ca^{2+}$ e grupos hidrofílicos, diminuindo as dimensões dos interstícios estruturais, respectivamente. Por outro lado, observou-se um acréscimo no intumescimento com a inserção de 1 e 2% de NWCs em hidrogéis com 1% de alginato (Figura 1b).

**Figura 1.** Avaliação do grau de intumescimento (Q).

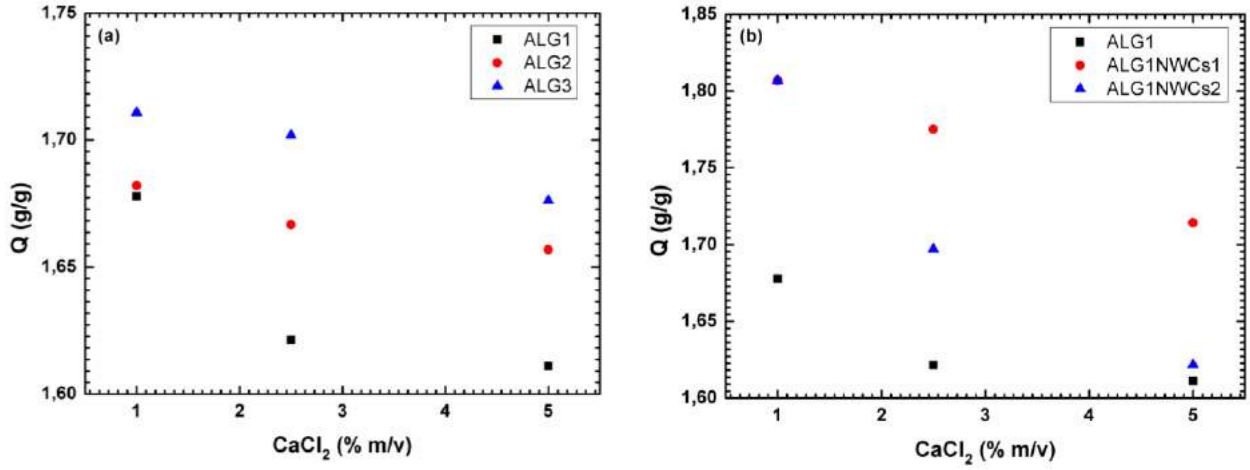


Agradecimentos: Ao CNPq, à FUNCAP (BP2-0107-00085.01.00/15) e à UVA.

[1]*Spangnol, C.; Rodrigues, F.H.A.; Pereira, A.G.B.; Farjado, A.R.; Rubira, A.F.; Muniz, E.C. Cellulose.* ***2012****, 19, 1225.*
[2]*Fernandes, R.S.; de Moura, M. R.; Aouada, F. A. Química Nova.* ***2017****, 40, 60.*

**Área: MAT** **Inscrição: 01071**

# Reuse of silica gel contaminated with organic compounds in the synthesis of silicate glasses

**Isabela Ferreira Gomes (IC),[1*] Camila Ferreira Da Silva (PG),[2] Leandro Ferreira Pedrosa (PQ),[1] Gisele Ribeiro (PQ),[2] Sebastião Ribeiro (PQ),[3] Michele Lemos de Souza (PQ),[1,2] Ladário Da Silva (PQ),[1,2] Elivelton Alves Ferreira (PQ).[1,2*]**

***isabela_ferreira@id.uff.br; eliveltonalves@id.uff.br**

[1]*Instituto de Ciências Exatas (ICEx), UFF, Volta Redonda-RJ CEP 272131-145, Brasil*

[2]*Programa de Pós-Graduação em Engenharia Metalúrgica (PPGEM), UFF, Volta Redonda-RJ CEP 27255-125, Brasil*

[3]*Escola de Engenharia de Lorena, Universidade de São Paulo, Lorena-SP CEP 12600-970 Caixa-postal: 116, Brasil*

Keywords: *glass, silica gel, Raman Spectroscopy and Ellipsometry*.

## Highlights

Silica gel is used as an adsorbent to isolate natural compounds, but it is an expensive process that generates contaminated solid waste. In this work, we propose the reuse of silica gel in the production of Soda-Lime glasses.

## Abstract

Silica gel is an amorphous silicon acid used in organic chemistry laboratory intensively to isolate organic compounds. It has a high cost and it generates solid waste contaminated with organic compounds. [1-3] In the present work was proposed to synthesize Soda Lime glass from the silica gel with the presence of the contaminants from a synthesis of boron-dipyrromethene compound (BODIPY). The possible applications of this class, such as in the manufacture of bottles, windows, blocks of glass for construction, food packaging, among others [4] highlights its environmental and technological relevance. Silica gel was used as a vitreous former without prior use and with contamination for the synthesis of the vitreous material. The methods utilized was melting at 1400 °C and cooling at room temperature. The Raman Spectroscopy and Ellipsometry results showed that the presence of the organic contaminant does not modify physically and chemically this material. In Figures A and B can be observed that the glass produced from the silica gel contaminated shown refractive index values (n) practically constant in the regions from the ultraviolet to the infrared of 1.45. On the other hand, there was a decreasing of the coefficient of extinction (k) from 0.2 to 0.1 with a wavelength (λ) increase from 300 nm to 400 nm. Nevertheless, k values were approximately equal to 0.1 for λ values greater than 400 nm. These results are consistent with those of the sample without previous contamination.

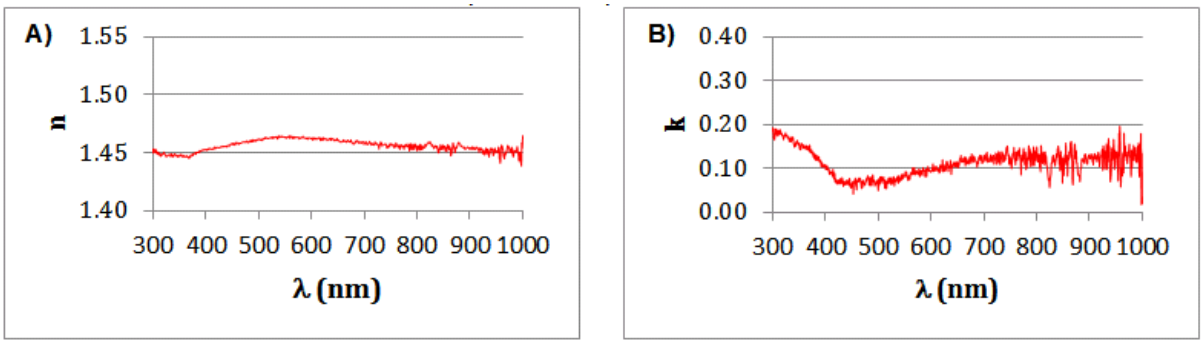


*Refractive index (Figure A) and Coefficient of extinction (Figure B) as a function of the wavelength of Soda-Lime glass synthesized from silica contaminated with substances derived from the synthesis of BODIPY.*

REFERERENCES

[1] Teixeira, S. C. G.; et al. *Quim. Nova*, **2003**, *26*, 931-933.
[2] Collins, C. H.; et al. Fundamentos de Cromatografia, Editora da UNICAMP, Campinas, SP, **2006**.
[3] Patrícia S. S. A.; et al. *Quim. Nova*, **2010**, 33 212-215.
[4] Alves, O. L. *Quim. Nova na Escola*, **2001**, edição especial, 9-20.

**Área: MAT_____** *(Inserir a sigla da seção científica para qual o resumo será submetido. Ex: ORG, BEA, CAT)*

**Inscrição: 01086** *(Inserir o número de inscrição do autor que fez a submissão)*

# Electronic structure, morphology and charge transport of GO-PEDOT:PSS blends for organic photovoltaics

**Soheila Holakoei (PG),[1] Lucas F. Lima (PG),[2] Bruno G.A.L. Borges (PQ),[1] Carolina F. de Matos (PQ),[3] Aldo J. G. Zarbin (PQ),[4] Lucimara S. Roman (PQ),[2] Cássia C. Turci (PQ),[1] Maria Luiza M. Rocco (PQ).[1]***

*luiza@iq.ufrj.br

[1]*Instituto de Química, Universidade Federal do Rio de Janeiro, 21941-909, Rio de Janeiro, RJ, Brazil*
[2]*Departamento de Física, Universidade Federal do Paraná, 81531-990, Curitiba, PR, Brazil*
[3]*Departamento de Química, Universidade Federal do Pampa, 96570-000, Caçapava do Sul, RS, Brazil*
[4]*Departamento de Química, Universidade Federal do Paraná, 81531-990, Curitiba, PR, Brazil*

Keywords: *Photovoltaics, NEXAFS, Morphology, Core-hole clock method*

## Highlights

Organic photovoltaics (OPVs) present important advantages such as flexibility, thinness, and simple manufacturing process [1]. In this study, the electronic structure and molecular orientation of thin films of GO-PEDOT:PSS with the composition of 1, 5, 10 and 100 w/w% of PEDOT:PSS were investigated by Near-Edge X-ray Absorption Fine Structure (NEXAFS) spectroscopy [2] using two different detection modes: total electron yield (TEY) and fluorescence yield (FY), at different X-ray incident angles. Ultrafast electron dynamics in the low-femtosecond regime was assessed by resonant Auger spectroscopy using the Core–Hole Clock (CHC) method [3] at the sulfur 1s absorption edge. All these experiments were performed for two series of cooled and not-cooled samples, aiming to monitor the change in electronic and structural properties caused by the thermal treatment.

## Abstract

Sulfur 1s TEY and FY NEXAFS spectra of GO-PEDOT:PSS 5% are shown in Figure 1. These spectra were measured at the soft X-ray spectroscopy (SXS) beamline of the Brazilian Synchrotron Light Laboratory (LNLS), Campinas, São Paulo.

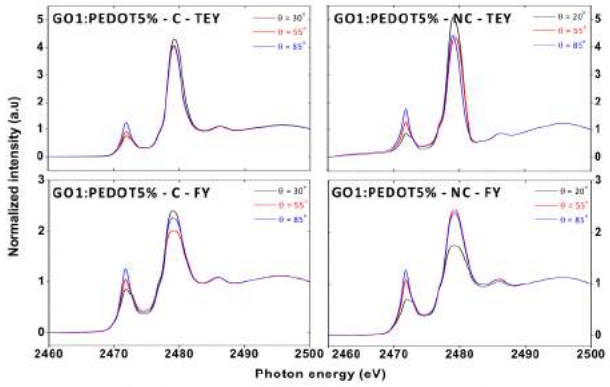


**Figure 1:** Sulfur 1s TEY and FY NEXAFS spectra of GO-PEDOT:PSS (5%) measured at three different incidence angles.

These spectra show two main absorption peaks. The first one which is composed of two features corresponds to the overlapping of the S1s → π* and S1s → σ* transitions in PEDOT at 2472 and 2473.2 eV, respectively. The higher intensity peak corresponds to sulfur 1s transitions in PSS. A strong angular dependence for PEDOT at both transitions, especially at the S1s → π*, in cooled and not-cooled samples, can be observed, which is more intense in the FY mode. At normal incidence, the intensity of the S1s → π* transition is higher, indicating that the PEDOT unit is preferably oriented perpendicular to the substrate surface. For PSS the corresponding peak (at 2479 eV) shows weak polarization dependence. The core-hole clock (CHC) method was employed to calculate the charge transfer time ($\tau_{CT}$) from the ratios of the spectators and normal Auger signals using the sulfur core-hole lifetime of 1.27 fs [4] as an internal reference clock. From the CHC method it was possible to show that the GO-PEDOT:PSS 5% blend has the lowest charge transfer time in comparison with other GO-PEDOT:PSS blends. As a conclusion, the reduction of $\tau_{CT}$ leads to higher electron mobility, which means that the electron delocalization dynamics of PEDOT:PSS (5%) film is enhanced by the presence of the graphene oxide. This result is in complete agreement with electrical tests performed for the GO-PEDOT:PSS blends.

This work was partially supported by LNLS, Brazil. Special thanks to CAPES and CNPq for financial support.

### References

1. B. Kippelen, Jean-L. Bredas, Organic photovoltaics, Energy Environ Sci, 2 (2009) 251-261.

2. J. Stöhr, NEXAFS spectroscopy, Springer, Berlin, 1992.

3. D. Menzel, Ultrafast charge transfer at surfaces accessed by core electron spectroscopies, Chemical Society Reviews, 37 (2008) 2212-2223.

4. J.L. Campbell, T. Papp, At. Data Nucl. Data Tables, 77 (2001) 1-56.

**Área: MAT** **Inscrição:** 01129

# Rare Earth Oxide-Based Nanoparticles with Application in Photodynamic Therapy for Cancer

**Bianca Almeida da Silva (PG),[1] Helmut Isaac Padilla-Chavarría (PG),[1] Volodymyr Zaitsev (PQ),[1] Edith Alejandra C. Mendivelso (PQ),[2] Luiz Anastacio Alves (PQ),[2] Yutao Xing (PQ),[3] Jiang Kai (PQ).[1]***

**bianca.aalmeida@hotmail.com; jkai@puc-rio.br**

*[1]Departamento de Química, PUC-Rio; [2]Laboratório de Comunicação Celular, Fiocruz; [3]Instituto de Física, UFF*

Keywords: *Nanoparticles, Rare Earth Oxides, Photodynamic Therapy, Cancer.*

## Highlights

Rare earth oxide-based nanoscintillators suitable to generate reactive oxygen species that elicit cell death in photodynamic therapy against tumors when coated with a photosensitizing material.

## Abstract

Photodynamic therapy is a non-invasive technique approved for the treatment of cancer. A photosensitizer (in this case, methylene blue) is activated by absorption of light of a specific wavelength to generate reactive oxygen species, which are toxic to cells[1]. Therefore, our aim is to synthesize and optimize doped rare earth oxide-based nanoparticles that, when excited by X-ray radiation, emit in the visible region, activating the photosensitizer.

Nanoparticles were synthesized by PVA-assisted sol-gel route[2], preparing a solution of 0,2 mol/L $GdCl_3 \cdot 6H_2O$ and mixing it with another solution of 0,2 mol/L $LnCl_3 \cdot 6H_2O$, adding PVA 10% (w/v), where Ln = Eu, Sm, Tb and Tm. After 30 min of stirring, solution was dried at 100 °C for 24 h, kept at 200 °C for 5 h, and calcined at 1000 °C for 5 h.

Structural and luminescence properties were determined. DLS showed that $Gd_2O_3$:$Eu^{3+}$ systems have hydrodynamic radius between 140-200 nm. SEM images confirmed that $Gd_2O_3$ NPs doped with $Sm^{3+}$ and $Eu^{3+}$ have different size and shape distributions. Total excitation showed that NPs have a bandgap of 5.25 eV. Figure 1 shows excitation and emission spectra of $Gd_2O_3$:$Ln^{3+}$.

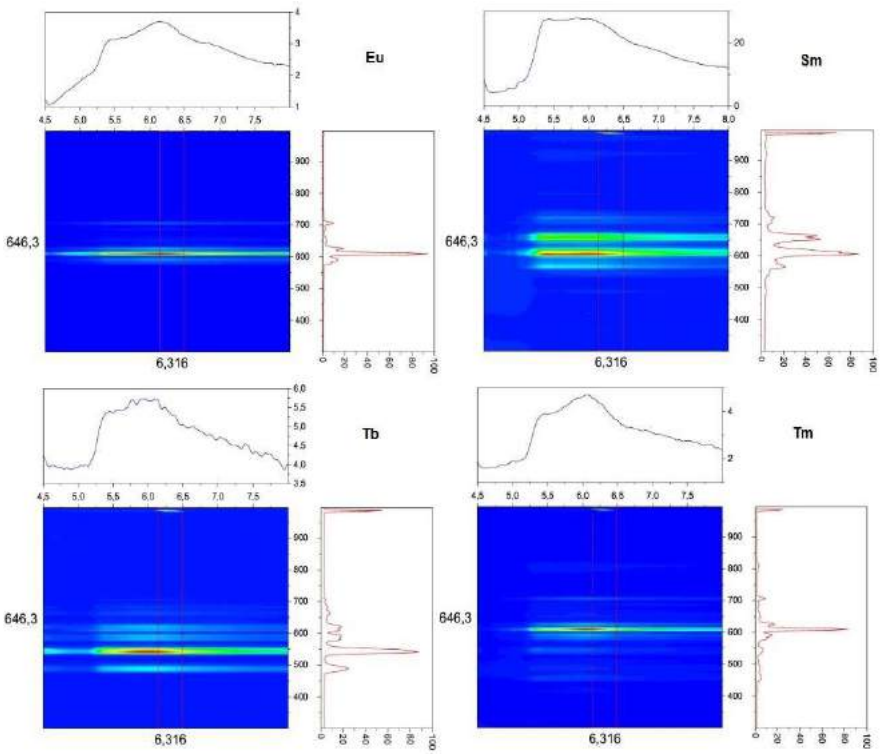


**Figure 1:** Emission and excitation of synthesized nanoparticles.

It was observed that $Eu^{3+}$ and $Sm^{3+}$ are the most suitable emitters for the use with photosensitizer. It is concluded that it is necessary to optimize size and shape distribution of these NPs.

[1]Kamkaew, A.; et al. *ACS Nano*, 10, 3918-3935, 2016.
[2]Sobral, G. A.; et al. *J. Phys. Chem. Solids*, 98, 81–90, 2016.

**Área: ___MAT_____** *(Inserir a sigla da seção científica para qual o resumo será submetido. Ex: ORG, BEA, CAT)*

**Inscrição:___ 00880__** *(Inserir o número de inscrição do autor que fez a submissão)*

# Photoelectrochemical degradation of methylene blue dye on Ti/$TiO_2$ nanotubes electrode.

**Johan R. González-Moya (PQ),[1]* Isabella M. Santos (IC),[2] Giovanna Machado (PQ),[1] giovannamachado@uol.com.br; jglez82@gmail.com**

[1]*Centro de Tecnologias Estrategicas do Nordeste, CETENE;*
[2]*Instituto Federal de Educação, Ciência e Tecnologia de Pernambuco, IFPE*

Palavras Chave: *photoelectrochemical dye degradation, water remediation, $TiO_2$ nanotubes, anodization.*

## Highlights

Water remediation by photoelectrochemical degradation of dyes using $TiO_2$ nanotubes supported on Ti electrodes.

## Resumo/Abstract

The textile industry is well developed in Pernambuco generating a lot of jobs in the region, but also generates a lot of wastewater deeply colored with dyes. With the aim of diminish the water contamination different methodologies are being investigated for the removal/degradation of dyes such as: microbiological, photocatalytic and electrochemical oxidation.[1–3] One interesting method is the photoelectrochemical oxidation combining electrochemical oxidation and photocatalysis. $TiO_2$ is a good material for photocatalysis and combining with electrodes could be used in photoelectrochemical process. In this work we evaluated the photoelectrochemical degradation of methylene blue (MB) as a model dye using $TiO_2$ nanotubes obtained by anodization in Ti foil as electrode. We used the two electrodes system with the Ti/TiO2 as anode and Ti metallic as cathode and using the potentiostatic method for oxidation with a bias of 3 V and simultaneous solar simulated irradiation during the 3 hours of 75 mL of 10 ppm MB. The degradation of MB was evaluated by decolorization measuring the absorbance in the 664 nm maxima with a UV-Vis spectrophotometer and the mineralization by the total organic carbon content (TOC). With the photoelectrochemical process we obtained the 84 % of decolorization (Figure 1) and 20 % of TOC abatements. The photoelectrochemical process was superior to the electrooxidation and photocatalysis itselfs in the same conditions because the formation of more oxidizing species capable to degrade the dye. The $TiO_2$ nanotubes obtained by anodization have a good potential for dye degradation by photoelectrochemical process.

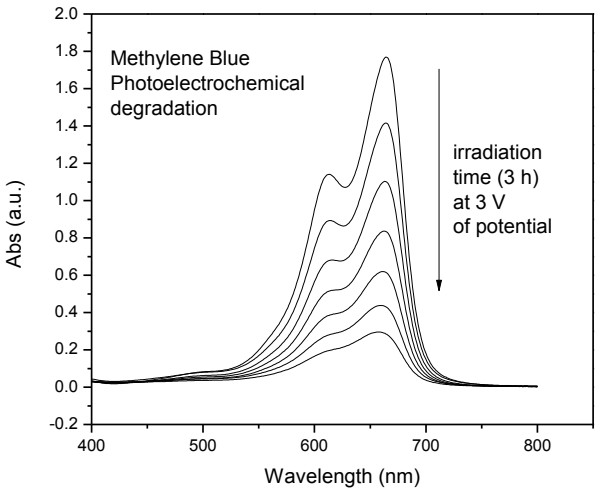


Figure 1. Photoelectrochemical degradation of MB.

### References

(1) Hussain, S. T.; Mazhar, M.; Siddiqa, A.; Javid, H.; Siddiq, M. Cu-S Coped TiO 2 NanoPhotocatalyst for the Degradation of Environmental and Industrial Pollutants. **2012**, 21–30.

(2) Wächter, N.; Pereira, G. F.; Rocha-Filho, R. C.; Bocchi, N.; Biaggio, S. R. Comparative Electrochemical Degradation of the Acid Yellow 49 Dye Using Boron-Doped Diamond, β-PbO 2 , and DSA ® Anodes in a Flow Reactor. *Int. J. Electrochem. Sci* **2015**, *10* (November 2014), 1361–1371.

(3) Esquivel, K.; García, M. G.; Rodríguez, F. J.; Ortiz-Frade, L. a.; Godínez, L. a. Study of the Photo-Electrochemical Activity of Cobalt- and Nickel-Doped TiO2photo-Anodes for the Treatment of a Dye-Contaminated Aqueous Solution. *J. Appl. Electrochem.* **2013**, *43* (4), 433–440.

**Área: MAT** **Inscrição:_01009_____**

# UV-Shielding and enhanced thermal stability of poly(vinyl alcohol)/graphene composites

**Regina D.E Carvalho (PG),[1*] Renata H. de Carvalho (IC),[1*] Virginia R. da Silva (PQ),[1] Max P. Ferreira (PQ),[1] Adelina P. Santos (PQ),[1] Clascídia A. Furtado (PQ).[1]**

**clascidia@yahoo.com; *duque_strada@yahoo.com.br; *natinha48@hotmail.com**

*[1]Laboratório de Química de Nanoestruturas de Carbono, Centro de Desenvolvimento da Tecnologia Nuclear, Belo Horizonte, Minas Gerais, Brazil.*

Keywords:*(Composite, Poly(vinyl alcohol), , Graphene, Radiation shielding, Kinect of degradation)*

## Highlights

- UV radiation attenuators based on flexible PVA/graphene composites were obtained.
- Kinetic studies showed the influence of few layer graphenes on the thermal degradation of PVA/graphene composites.

## Abstract

UV radiation has short wavelength and high energy. Even though UV radiation is widely used in industrial processes and applications such as in detectors and medical diagnosis, prolonged exposure to it may result in harmful health effects and degradation on skin, eyes, and immune system of humans. Protection is therefore needed, and alternative UV shielding materials with enhanced performance and versatility are still required [1]. Alternatively, polymer-based shield material are being produced, because they are lightweight, conformable, and may be designed to include non-toxic materials. Attenuation is obtained by combining the load and structural material [2]. Graphene is a two-dimensional (2D) material with monatomic thickness with excellent properties, such as high electron mobility, high thermal conductivity, high mechanical strength, in addition to high transparency and surface area, making it a promising material for use in nanocomposites [3]. In this paper, few-layer graphene based nanocomposites of poly (vinyl alcohol) were tested for shielding of UVC (100−280 nm), UVB (280−315 nm) and UVA (315−400 nm) radiation. The nanocomposites were characterized by TGA, Raman and IR spectroscopy. Kinetic studies showed an increase of the activation energy of decomposition with the addition of graphene to the polymer matrix. The incorporation of graphenic nanostructures resulted in flexible films with also enhanced UV shielding properties. The results are promising and the absorbance of UV at 300 nm can be up to 80% for the nanocomposites with around 70% of transparency in visible spectral range and concentration as low as 0.5 wt% of nanocarbon.

Acknowledgements: CNEN, FAPEMIG, CAPES, CNPq, SisNano, and the Brazilian Nanocarbon Institute.

[1] K. Sabira, P. Saheeda, S. Jayalekshmi, Mater. Lett. 200, (2017),125-127.

[2] L. Ran et al, Compos. Sci. Technol. 143, (2017), 27-74.

[3] K. S Novoselov, A K Geim, S. V Morozov et al, Science.306, (2004), 666 – 669.

**Área: MAT** **Inscrição:00855**

# From graphite to graphene: improving the Hummers method to produce high quality reduced graphene oxide (rGO)

**Danilo A. Nagaoka (PG),[1,2] Sergio H. Domingues (PQ).[1*,2]**

**danilo.nagaoka@gmail.com; shdomingues@mackenzie.com**

*[1]MackGraphe – Graphene and Nano-materials Research Center, São Paulo, Brazil, Mackenzie Presbyterian University, São Paulo, Brazil; [2]Engineering School, Mackenzie Presbyterian University, São Paulo, Brazil.*

Key words: *improved Hummers method, reduced graphene oxide, graphite exfoliation.*

## Highlights

High quality reduced graphene oxide (rGO) obtained through a simple modified Hummers method, leading to flexible thin films with low Rs values.

## Abstract

Chemical exfoliation of graphite is one of the promising candidates for large-scale production of graphene-like materials.[1] The modified Hummers method is a standard procedure for chemical exfoliation, it consists in three main steps (i) oxidation of graphite to obtain the graphite oxide followed by (ii) the dispersion of the graphite oxide in different solvents in order to produce homogeneous suspensions, and, finally (iii) the suspension reduction to obtain the reduced graphene oxide (rGO), which is a graphene derivative that presents vacancies and defects in its structure, inducing a decrease of several properties, *e.g.* electrical conductivity and thermal stability.[2] To overcome the defect generation we present a simple approach in Hummers method, to obtain high quality rGO, based on a strict control of temperature and chemical addition ratio during the oxidation process, as described in step (i). **Figure 1** summarizes our results and presents a comparison between the Raman results of a standard rGO and our procedure. The defect distance and the $I_D/I_G$ ratio were calculated resulting in values to our material higher than 20 nm and 0.27 respectively, which could be comparable to CVD graphene. Also, we prepared flexibles thin films of rGO deposited over PET, which presented Rs values below 300 Ω/□ with 75% of transmittance at 550 nm. Thus, we were able to produce rGO with characteristics similar to pristine graphene, through a simple route with high yield, promising to be employed in different graphene-based flexible devices.

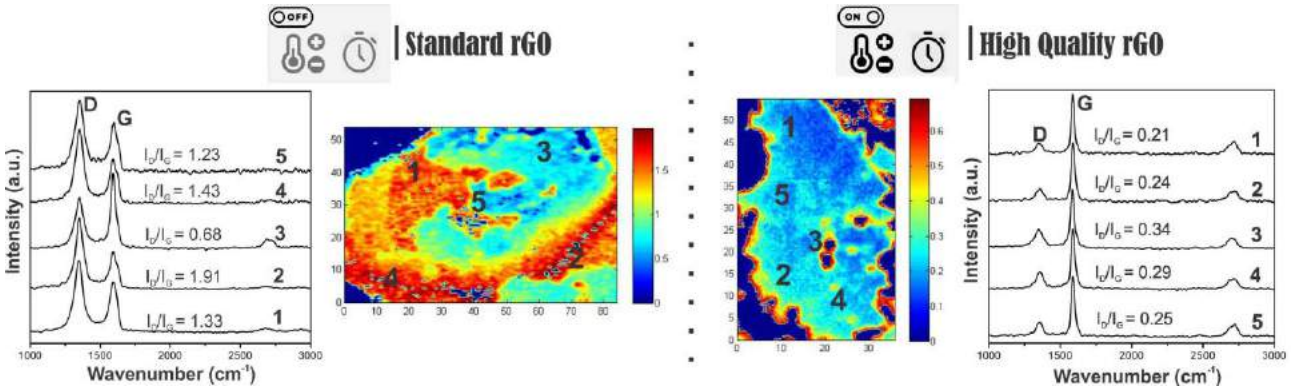


**Figure 1 –** Raman mappings along with the indicated spectra of standard and high quality rGO.

**Acknowledgments**

Authors acknowledge Presbyterian Mackenzie University (UPM), GQM-UFPR, CNPq (403544/2016-5) and FAPESP (SPEC 2012/50259-8).

**References**

[1] Soldano, A. Mahmood, E. Dujardin, Carbon **2010,** 48, 2127.
[2] Eigler, et al. Adv. Material, 2013, 25, 3583-3587.

**Área: MAT** **Inscrição: 00862**

# Unraveling the Differences in the Activity and Stability of Non-enzymatic Electrochemical Sensors by Controlling Surface Facets

**Anderson G.M. da Silva (PQ),[1] Fabián A.C. Pastrián (PG),[1] André H.B. Dourado (PG),[1] Ana P. de Lima Batista (PQ),[1] Antonio G.S. de Oliveira-Filho (PQ),[2] Pedro H.C. Camargo (PQ),[1] Susana I.C. de Torresi (PQ)[1]* andersondeob@gmail.com; storresi@iq.usp.br**

*[1]Departamento de Química Fundamental, Instituto de Química, Universidade de São Paulo, Av. Prof. Lineu Prestes, 748, 05508-000, São Paulo, SP, Brazil*

*[2]Departamento de Química, Faculdade de Filosofia, Ciências e Letras de Ribeirão Preto, Universidade de São Paulo, 14040-901, Ribeirão Preto, SP, Brazil*

Palavras Chave: $Cu_2O$, Surface Facets, Electrochemical Sensors, *Glucose.*

## Highlights

We unraveled the effect of {111} and {100} surface facets over the electrochemical sensing activities and stabilities. Systematic understanding by a combination of theoretical and experimental design.

## Resumo/Abstract

By a combination of theoretical and experimental design, we untraveled the effect of {111} and {100} surface facets over the non-enzymatic electrochemical sensing activities, selectivities. We employed $Cu_2O$ cubes, cuboctahedrons, and octahedrons as model substrates (Figure 1), and glucose as the analyte, in which their activities and stabilities displayed a shape-dependent behavior as shown in Figure 2. We started by theoretically investigating the potential energy curves for glucose adsorption at Cu2O {111} and {100} surface facets. We found that the glucose adsorption energy was significantly higher for {100} relative to the {111} facets. Then, we experimentally observed that their electrochemical sensing performances displayed a shape-dependent behavior. While the activities followed the order: cubes > cuboctahedrons > octahedrons, their stabilities showed an opposite trend. The higher activity enabled by {100} facets was explained by its stronger interaction with glucose. On the other hand, the higher stability enabled by {100} facets could be explained based on its weaker adsorption of $O_2$ relative to the {100} surface, that led to lower reactivities towards the $Cu_2O$ to CuO oxidation.

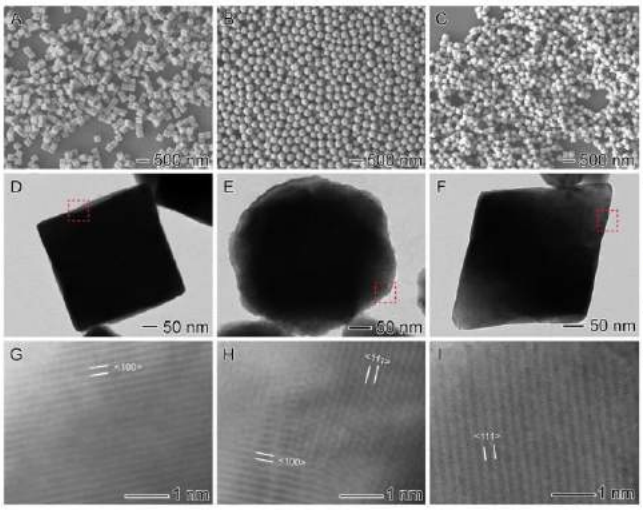


**Figure 1.** SEM (A-C) and HRTEM (D-I) images of $Cu_2O$ cubes (A, D, and G), cuboctahedrons (B, E, and H), and octahedrons (C, F, and I).

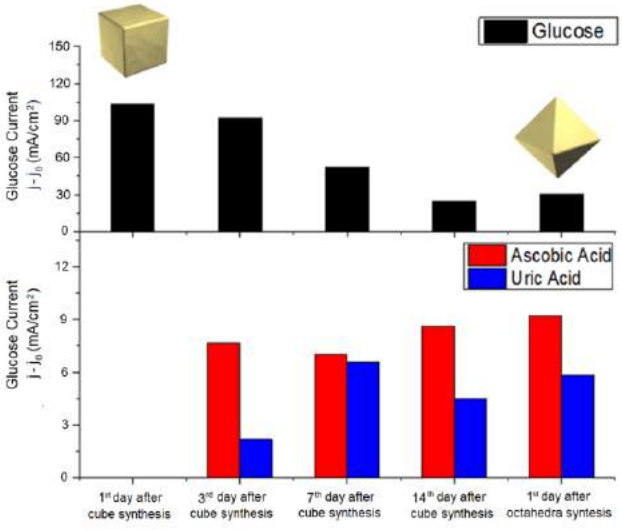


**Figure 2.** Activity and selectivity for the electrochemical detection of glucose employing freshly prepared $Cu_2O$ cubes and octahedrons relative to the same samples after they had been stored several days in aqueous solutions.

**Área: MAT** **Inscrição: 00398**

# Sínteses de cristais líquidos iônicos e estudo de suas propriedades mesomórficas

**Saúl Ovalle Perez[a] (PG), Eduard Westphal[b] (PQ) e Hugo Gallardo[a*] (PQ)**

**hugo.gallardo@ufsc.br;**

*[a]Department of Chemistry, Federal University of Santa Catarina, Florianópolis, Brazil; University of Santa Catarina, Florianópolis, Brazil. [b]Department of Chemistry and Biology, Federal University of Technology - Parana, Curitiba, Brazil.*

Palavras Chave: *Cristal líquido iônico, Tolano, N-metilimidazólio*

## Highlights

Synthesis of ionic liquid crystals and their mesomorphic properties. The mesomorphic properties were mesophases with 1- to 3-dimensional molecular organization when the number of terminal alkoxy chains and/or the spacer chain were increased

## Resumo/Abstract

Os cristais líquidos iônicos são uma classe importante de materiais orgânicos com propriedades intrínsecas de um liquido iônico (condutividade iônica) e cristal líquido (fluidez e auto-organização); essa combinação torna-os promissores para diversas aplicações tecnológicas como baterias,[1] sensores,[2] células solar,[3] etc. No presente trabalho foram sintetizados e caracterizados sete novos cristais líquidos iônicos contendo o mesmo núcleo mesógenico, um grupo tolano unido ao heterociclo 1,2,3-triazol, com diferente número de cadeias terminais e do tamanho da cadeia espaçadora; esta última, responsável de conectar o núcleo mesógenico com a parte iônica da molécula (íon *N*-metilimidazólio) como é apresentado na figura 1. As propriedades liquido cristalinas e térmicas foram estudadas por calorimetria diferencial de varredura, analises termogravimétrico, microscopia óptica de luz polarizada, difração de raios X e espalhamento de raios X em baixo ângulo. Todos os compostos foram estáveis termicamente. O composto **I-12** apresentou uma organização molecular bilamelar, esmética bilamelar A e C. Os compostos **II-4**, **2-8** e **II-12** exibiram mesofases colunares, obliqua e hexagonal, pelo incremento no número de cadeias terminal. O incremento na cadeia espaçadora favoreceu a formação de uma mesofase cubica bicontinua e micelar com empacotamento hexagonal compacta. Finalmente, os compostos **III-4**, **III-8** e **III-12** com três cadeias terminal só apresentaram fases colunares, sendo desfavorecida a colunar obliqua com o incremento na cadeia espaçadora.

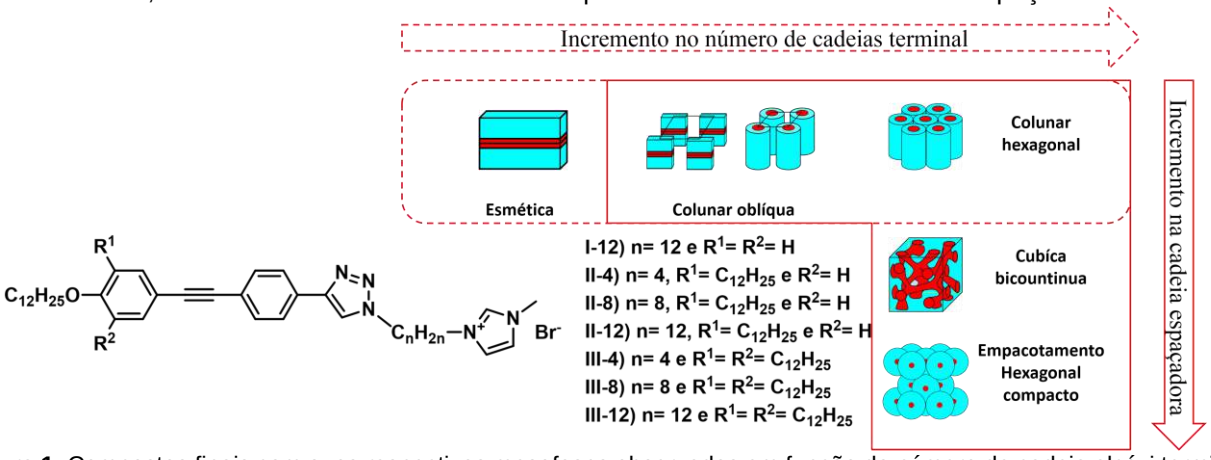


**Figura 1**. Compostos finais com suas respectivas mesofases observadas em função do número de cadeia alcóxi terminal e cadeia espaçadora. A cor celeste e vermelho representa a parte apolar e iônica da molécula, respectivamente.

**Agradecimento:** UFSC, CAPES, CNPq, INCT-Catálise e INCT/INEO pelo suporte financeiro. Aos laboratórios CEBIME, LDRX (CFM/UFSC) e LNLS (Proposta 20160735 e 20170154) pelos acesso e/ou analises.

1 DEVAKI, S. J.; SASI, R. Ionic Liquids/Ionic Liquid Crystals for Safe and Sustainable Energy Storage Systems. 2017.

2 ATTA, N. et al. Ionic Liquid Crystals Modifier for Selective Determination of Terazosin Antihypertensive Drug in Presence of Common Interference Compounds. ***Crystals*****,** v. 7, n. 1, p. 27, 2017.

3 CHEN, L.; XIE, C.; CHEN, Y. Self-Assembled Conjugated Polyelectrolyte–Ionic Liquid Crystal Complex as an Interlayer for Polymer Solar Cells: Achieving Performance Enhancement via Rapid Liquid Crystal-Induced Dipole Orientation. ***Macromolecules*****,** v. 47, n. 5, p. 1623-1632, 2014.

Area: MAT Subscription: 00286

# Use of expanded polystyrene in increasing hydrophobicity in ceramic electrical insulators in transmission lines

**Rafaela G. Ferreira[1](IC)*, Débora de O. Souza[1](IC),Claudinei R. Calado[1](PQ)**

[1]*Department of Chemistry of the Federal Center of Technological Education of Minas Gerais*
**rafahh97@gmail.com*
Keywords: *EPS*, Organic solvents, Ceramic surfaces.

## Highlights

Ceramic surfaces. Coating materials. Decrease in maintenance costs. Improvements regarding commercial coatings. Transformation of hydrophilic surfaces into hydrophobic.

## Abstract

The deposition of dirt on ceramic electrical insulators (CEI) can induce the appearance of a leakage current, causing drops in the electric transmission lines. This work aims at the deposition of hydrophobic polymer films capable of avoiding the formation of conductive surfaces on the CEI (Figure 1 (c)). This coating seeks to reduce maintenance costs of transmission lines, as well as the use of scrap polymer material, expanded polystyrene (EPS).

It was used 0.1 g of EPS solubilized in 10 mL of THF, acetone / cyclohexane (7:3), chloroform and toluene to obtain the hydrophobic resin. The solution was deposited using a drip technique (Pasteur pipette) on the CEI. The film was oven dried at 80 °C for 15 minutes. The contact angle was measured using a Kruss GMBH goniometer.This procedure was repeated using EPS resin doped with 2.2% magnesium stearate by mass.

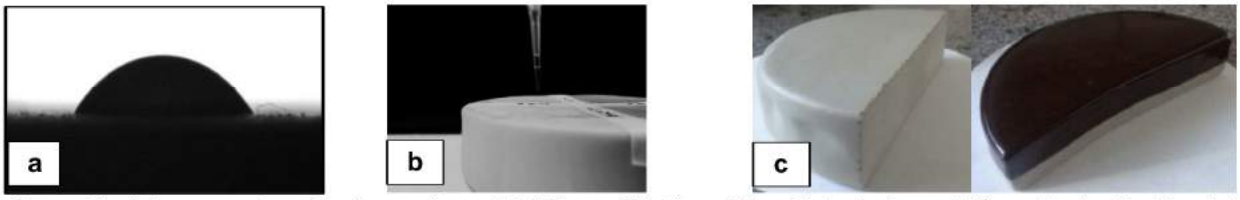


**Figure 1:** a) Image captured by the equipment; b) Exemplification of the drip technique; c) Ceramic electrical insulators.

It was observed that the contact angle for the coated samples was higher than that observed for the uncoated sample and coated by commercial products (Table 1). The best result observed was the Chloroform + Mg 2.2% sample, which presented an angle of 119.21°. These results indicate that doped EPS resins are efficient in obtaining hydrophobic surfaces. Future tests should show if they will be efficient in reducing CEI leakage current.

**Table 1**: Solvent x contact angle.

| Solvent | Angle |
|---|---|
| Uncoated | 55,10° |
| Commercial sample 1 | 70,08° |
| Commercial sample 2 | 69,60° |
| THF | 90,70° |
| THF + Mg 2,2% | 89,92° |
| THF + Zn 1,1% | 91,90° |
| Acetone/Cyclohexane (7:3) | 70,03° |
| Acetone/Cyclohexane (7:3) + Mg 2,2% | 75,07° |
| Toluene | 87,66° |
| Toluene + Mg 2,2% | 78,00° |
| Chloroform | 77,44° |
| Chloroform + Mg 2,2% | 119,21° |

**Acknowledgement:** CNPq, FAPEMIG, CEFET-MG.

**References:** [1] **FERREIRA**, Carla Regina. **Obtenção de superfície super-hidrofóbica a partir de nanocompósitos de PS e EPS com nanopartículas de ZnO modificadas**. CEFET-MG, 2016

**Área: ___MAT_____ Inscrição:__00745____**

# Thin films of ternary nanocomposites between carbon nanotubes, Prussian blue and polyaniline.

**Ariane Schmidt (PG),[1] Samantha Husmann (PQ)[1], Aldo J. G. Zarbin(PQ)[1]**

**arianeeschmidt@gmail.com; aldozarbin@ufpr.br**

[1]Departamento de Química, Universidade Federal do Paraná (UFPR) Centro Politécnico – Jd. das Américas – 81531-990 – Curitiba – PR - Brasil

Keywords: *carbon nanotubes, Prussian blue, polyaniline, nanocomposites.*

## Highlights

Ternary nanocomposites between carbon nanotubes, Prussian blue and polyaniline were synthesized by interfacial polymerization and electrochemically deposition and successfully characterized.

## Resumo/Abstract

The formation of nanocomposites is a way to improve the properties or give new properties to materials. In this perspective, nanocomposites between Prussian blue (PB) and carbon nanotubes (CNT) are very attractive due the synergistic properties resulting from the electrochemical and electrochromic properties of PB and the different properties of CNTs. Our researcher group developed a new route do synthesized these materials by a liquid-liquid interfacial polymerization and the PB can be formed using a heterogeneous reaction with ferric species inside the CNT cavities. Thereby, the objective of this work is prepared ternary nanocomposites between carbon nanotubes, Prussian blue and polyaniline. Polyaniline (PAni) is a conductor polymer which is interesting because of a low cost of monomer and that can be easily synthesized in its more conductive form, the so-called esmeraldine salt. Two synthetic approaches were used to synthesize the ternary composite:.one of them consisting in liquid-liquid interfacial polymerization with PB being formed in aqueous acidic media together with PAni, and the second one is an electrochemical synthesis of both PB and PAni over CNTs films. The formation of nanocomposite was confirmed by different characterization techniques, as XRD and UV-Vis spectroscopy. SEM images show the CNT decorated with both PAni and nanocubes of PB (Figure 1); Raman spectra shows that. PAni was majority in emeraldine salt structure, as well as the presence of CN band, characteristic of PB. The synthesis through interfacial polymerization enables a better processability of the material.

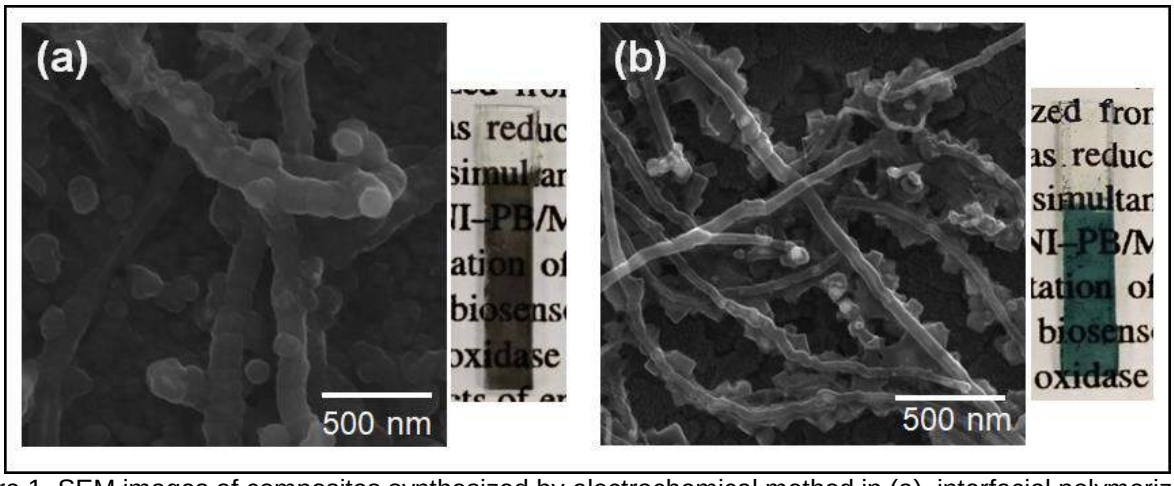


Figure 1. SEM images of composites synthesized by electrochemical method in (a), interfacial polymerization in (b) and the respective digital photograph of the films.

**Área: MAT** **Inscrição: 00511**

# Aqueous dispersions of carbon nanotubes without passivation or functionalization

**João P. V. Damasceno (PG)[1], Aldo J. G. Zarbin (PQ)*[1].**

**joaopaulovd@gmail.com; aldozarbin@ufpr.br**

*[1]Chemistry Department, Federal University of Paraná - UFPR, Curitiba.*

Key Words: Carbon Nanotubes Dispersions, Aqueous Dispersions, Conducting Thin Films.

## Highlights

Preparation of aqueous dispersions of carbon nanotubes without passivant agents or surface functionalization and processing of these dispersions in conductive and transparent thin films.

## Abstract

Carbon nanotubes (CNTs) form bundles due to their high surface energy, which difficult preparation of complex materials and devices. One way to overcome this problem is dispersing them in liquid media, separating individual entities from bundles and simplifying the storage, transportation and processing. Stable aqueous dispersions of nanotubes are very difficult to be obtained, and they are usually achieved using passivant agents or by inserting functional groups on the CNTs surface[1]. In this work we propose an innovative method based on literature[2] to prepare stable aqueous dispersions of single-walled and multi-walled carbon nanotubes that does not require passivant agents or surface functionalization. Solid carbon nanotubes were sonicated with commercial tetrahydrofuran, which contains a phenolic compound that generates electrical charges on materials. Organic dispersions of highly charged carbon nanotubes were added to deionized water, filtered, and purged with air to eliminate most of tetrahydrofuran, resulting in non-passivated and non-functionalized aqueous dispersions. These aqueous samples were also used to prepare thin films in liquid-liquid interfaces following a method proposed by our research group[3]. Aqueous dispersions presented zeta potentials between -20 and -30 mV and Raman spectroscopy performed *in situ* confirmed charge transference that is responsible for the surface electric potentials of nanotubes dispersions. Thin films were deposited over glass substrates up to three consecutive times because of the low concentration of aqueous samples, and presented sheet resistance of about 30 kΩ $\square^{-1}$ and transmittance next to 80 % at 550 nm.

[1] J. N. Coleman, *Adv. Funct. Mater.* **2009**, *19*, 3680–3695.
[2] G. Bepete, E. Anglaret, L. Ortolani, V. Morandi, K. Huang, A. Pénicaud, C. Drummond, *Nat. Chem.* **2017**, *9*, 347–352.
[3] V. H. R. Souza, S. Husmann, E. G. C. Neiva, F. S. Lisboa, L. C. Lopes, R. V. Salvatierra, A. J. G. Zarbin, *Electrochim. Acta* **2016**, *197*, 200–209.

**Área: MAT**

**Inscrição: 00848**
*(Inserir o número de inscrição do autor que fez a submissão)*

# Characterization of the Pani/$MoO_3$ hybrid for ethanol electrooxidation

**Fernando Ratuchne (PG)*,[1] Cristiane Antoniazzi (PG),[1] Marins Danczuck (PQ),[1] Eryza G. de Castro (PQ)[1]**

**fratuchne@hotmail.com; eryza.castro@gmail.com**

*[1]Departamento de Química, UNICENTRO;*

Palavras Chave: *Conducting Polymer, Metal Oxide, Hydrogen Production, Electrocatalysis*

## Highlights

Pani/$MoO_3$ presents bands in the UV-Vis and FTIR characteristics. Cyclic Voltametry suggests an interaction of $MoO_3$ with amine group of Pani. Pani/$MoO_3$ is promising for the electrooxidation of ethanol.

## Resumo/Abstract

Polyaniline (Pani) stands out for its low cost of production, easy synthesis and doping/dedoping, high conductivity and optical, electronic and electrochemical properties. Due to the difficulty in its processability and low thermal, mechanical and electrochemical resistance, it is tried to synthesize hybrid materials of Pani with metal oxides and polymeric materials. Materials composed of semiconductor oxides and Pani are studied for their magnetic, optical and catalytic properties, which arise from electron transfer reactions between the polymer and the oxide, providing wide applications in the fields of electronics and optics. The Pani was modified with $MoO_3$ and the optical, thermal and electrochemical properties of these materials were studied by UV–Vis, FTIR, TG and CV analysis. From UV-Vis and FTIR, the formation of composites was confirmed by presence the characteristic bands of emeraldine salt. The TG results showed that Pani/$MoO_3$ hybrids presented greater thermal stability than the Pani. Voltamograms show that hybrids have the 2 par of peaks characteristics of Pani and upper current density at high scan rates studied. The lower intensity of the peaks pair at ~0.83/0.78V indicates that $MoO_3$ particles stabilize the amine groups of Pani, its making the oxi-reduction reactions of these sites less favorable, which agrees with the decrease in the intensity of the $\nu(CN^{\cdot+})$ band at 1222 $cm^{-1}$ in FTIR spectra. Preliminary tests show that Pani/$MoO_3$-5% has promising behavior in ethanol electrooxidation as is showing in the Figure 1.

Figure 1. Current of the materials obtained in $H_2SO_4$ (0.5 mol $L^{-1}$) and in $H_2SO_4$ (0.5 mol $L^{-1}$) + 5% Ethanol, using cyclic voltammetry, velocity of 100 $mVs^{-1}$, three-electrode system with Ag/AgCl electrode (3M) as reference electrode and carbon paste as working electrode.

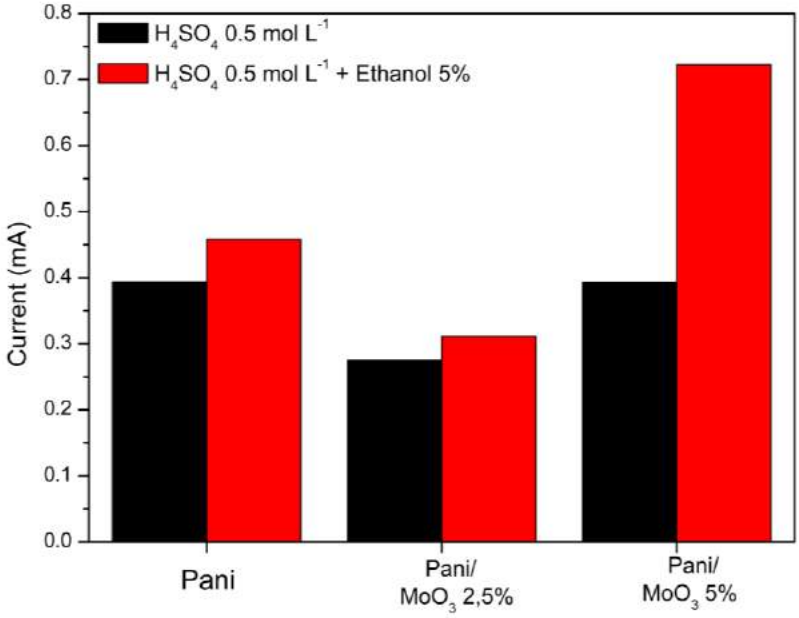

**Área: MAT** **Inscrição: 00685**

# Charcoal and activated carbon from yeast biomass residues

**Mikaela Santos (IC),[1] Viviane F. Melo (Bel.),[1] Helen Modesto (IC)[1], Jenny S. Komatsu (PQ),[2] Wagner A. Carvalho (PQ),[2] Geórgia Labuto (PQ),[1]**

**myykaela.s@gmail.com; geolabuto@gmail.com**

*[1]Departamento de Química, UNIFESP; [2] Centro de Ciências Naturais e Humanas, UFABC*

Palavras-Chave: *yeast biomass, yeast biomass from β-glucan extraction, mesoporous carbon*

## Highlights

Development of new use alternatives for yeast biomass residues.
Production of activated carbons with high surfaces areas.
Production of mesoporous activated carbons.

## Resumo/Abstract

Charcoals (C) and activated carbons (AC) are prepared from several materials, which must be cost-effective and easily activated. Using biomass residues from industry valorize these materials and boost up the bioeconomy (Labuto and Carrilho, 2016). The ethanol industry generates around 30g of yeast biomass/liter of alcohol produced. This residue has 43% of carbon and potentially can be converted in C and AC (Costa, 2004, Labuto et al., 2015). In the present work, we produced C and AC from yeast biomass residues (YB) from ethanol industry and yeast biomass residue from the β-glucan extraction (YR). For the C production, known masses of YB or YR were submitted to a heating program (ramp 10ºC/min, 60min at 500°C) under a $N_2$ atmosphere, in a tubular furnace equipped with a quartz reactor and quartz sample holder. After heating program, the reactor was opened (200°C) and the materials produced were removed from the reactor (100°C). The AC production employed a procedure established in the patent process BR 1020170030059 (INPI). The procedures recovered around 26% m/m (C) and between 22 and 43% m/m (AC). Surface areas of ACs ranged between 1030 and 1398 $m^2g^{-1}$, with 78 to 90% of micropores, been a high quality activated carbons with commercial potential.

**References:**

Costa, L.F. Revista Eletrônica Nutritime, 1 (2004), 01-06.
Labuto, G. et al. Revista Ambiente & Água, 10 (2015), 510-519.
Labuto, G.; Carrilho, E.N.V.M. In: M.N.V. Prasad, Bioremediation and Bioeconomy, 1ed.; 2016, v.1, p.569-586.

**Acknowledgment:**

CNPq, FAPESP (Process:2016/06271-4, 2017/13074-3).

**Área: MAT** *(Inserir a sigla da seção científica para qual o resumo será submetido. Ex: ORG, BEA, CAT)*

**Inscrição: 00693** *(Inserir o número de inscrição do autor que fez a submissão)*

# Effect of glass powder as reinforcing filler in the production of recycled polypropylene composites

**Ian S. Costa (IC)[1]*, Larissa A. Almeida (TM)[1], Julio Cesar J. Junior (PQ)[2], Ana Lucia N. da Silva (PQ)[2], Rachel O. Nasser (PQ)[3], Thiago M. Aversa (PQ)[1]**

**iansantosc@gmail.com**

*[1] Federal Institute of Education, Science and Technology of Rio de Janeiro, IFRJ; [2] Macromolecules Institute, Federal University of Rio de Janeiro, IMA/UFRJ; [3] Federal Institute of Education, Science and Technology of Rio Grande do Sul, IFRS*

Keywords: *Composite; Mechanical and Thermal Properties; Polypropylene; Glass powder; Recycling*

## Highlights

Glass powder could be a good reinforced filler on recycled polypropylene composites.
Composite becomes more rigid increasing the glass powder content.
Melt flow index reduces as the glass powder content increases.

## Abstract

Polypropylene (PP) is a polyolefin that exhibit good thermal and mechanical properties and low cost and its recycled form had already been employed in composites with sawdust and glass fiber, for example[1,2]. Therefore, this work aims to evaluate the thermal and mechanical properties of composites of post-consumer polypropylene and glass powder from automotive industry waste. For this, the materials (polypropylene and glass powder) were processed in a twin screw extruder. The number of experiments was based on a $2^k$ factorial design, with k = 2 factors: glass powder content and screw rotation speed. Glass powder was only analyzed for particle size. Composites were analyzed by melt flow index (MFI), scanning electron microscopy (SEM) and mechanical tests: tensile strength test and notched Izod impact. It was observed an increase of the elastic modulus and lower impact resistance, indicating an increase of hardness for the composites with higher glass powder content and lower screw rotation. Thus, it can be observed that the recycled polypropylene matrix added with glass powder undergoes significant changes in its properties, being able to confer to these materials the possibility of application, reflecting in a valorization of the recycled material.

[1] LI, T.Q.; NG, C.N.; LI, R.K.Y. Impact behavior of sawdust/recycled–PP composites. **J. Appl. Polym. Sci.**, v. 81, p.1420-1428, 2001.

[2] MÄDER, E.; RAUSCH, J.; SCHMIDT, N. Commingled yarns - processing aspects and tailored surfaces of polypropylene/glass composites. **Composites Part A**, v. 39, p. 612-623, 2008.

**Área: MAT** **Inscrição: 00515**

# Functionalization of fungal cells with transition metal oxides for the development of biomimetic hybrid structures

**Verônica Maciel Bispo (PG),[1*] Regina Geris (PQ)[1] and Marcos Malta (PQ)[1].**

**Veronica.bastos@ufba.br**

[1]*Instituto de Química, UFBA, Campus Ondina, Salvador (BA), Brazil*

Palavras Chave: *Biomaterials, Biotemplates, Self-assembly, Fungi, Inorganic oxides.*

## Highlights

1) Self-assembly of transition metal oxides with fungal cells, resulting in the synthesis biomimetic of microstructures.
2) The analysis of OM, SEM, EDS, XRD, TG and Raman spectroscopy techniques showed the formation of microtubular structures in which the oxide particles are deposited uniformly on the cell wall of the fungi.
3) The bio-hybrids calcined revealed the formation of a novel microtubule biomimetic structure $WO_3$ and $TiO_2$ with potential applications of these biosystems.

## 4) Resumo/Abstract

Novel bio-hybrid consisting of fungi/$TiO_2$ and fungi/$WO_3$ were synthesized by culturing the fungal species in solutions containing a carbon source and submicrometric particles of $TiO_2$ or $WO_3$. In this strategy, inorganic particles were assimilated over the fungal surface resulting in biomimetic tubular microstructures.
Bio-hybrids were characterized through optical microscopy (OM), scanning electron microscopy (SEM), microanalysis by energy dispersive X-ray spectroscopy (EDS), thermogravimetric analysis (TGA), X-ray diffraction (XRD) and Raman spectroscopy. These set of the analysis confirm the formation of microtubular structures with a thickness varying from 1.5 to 2.5 µm (Figure 1). XRD data (Figure 2) indicated that crystalline phase of the inorganic components remains unchanged after assimilation by microorganisms. Finally, results of SEM, EDS and Raman analyses of the calcined bio-hybrid fungi/$WO_3$, revealed the formation of an original $WO_3$ biomimetic structure with a thickness of the approximately 2.5 µm. To conclude, a mechanism has been proposed to elucidate the process of assimilation of the particles in the fungal cell wall and potential applications of these biosystems.

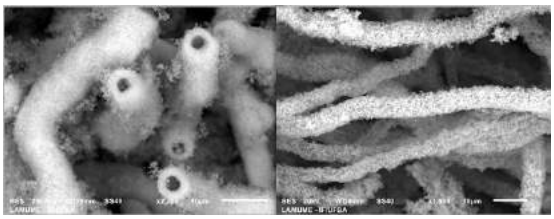

Figure 1 – SEM of Bio-hybrids

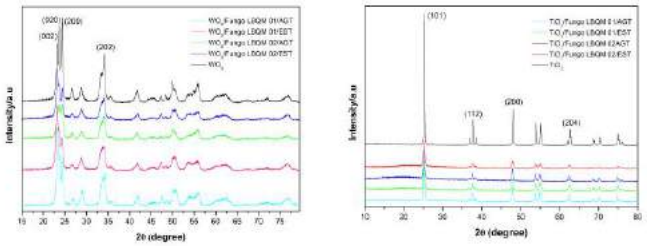


Figure 2 – XRD analysis of Bio-hybrids

## References

1. BRUSHAN, B. Biomimetics: lessons from nature – an overview. Phil. Trans. R. Soc. A, 367, 1445–1486, 2009.
2. FAKHRULLIN, R. F. Et al. Cyborg cells: functionalisation of living cells with polymers and nanomaterials. Chem. Soc. Rev., 2012.
3. FONTES, A. M., GERIS, R., SANTOS, A. V., PEREIRA, M. G., RAMALHO, J. G. S., SILVA, A. F., MALTA, M. Bio-inspired gold microtubes based on the morphology of filamentous fungi. Biomaterials Science, 7, 2014.
4. Bigall, N.C.; Reitzig M.; Naumann, W.; Simon, P.; van Pée, K.H.; Eychmüller. A. Fungal Templates for Noble-Metal Nanoparticles and Their Application in Catalysis. Angew. Chem. Int., 47, 7876–7879, 2008.

**Área: MAT**
*(Inserir a sigla da seção científica para qual o resumo será submetido. Ex: ORG, BEA, CAT)*

**Inscrição: 00536**
*(Inserir o número de inscrição do autor que fez a submissão)*

# Frontier micro/mesoporous silica obtained by the hydrolysis of TEOS in pressurized aqueous $CO_2$

**Manuel E.G. Winkler (PG)[1*], Marcos H. Kunita (PQ)[1‡], Edvani C. Muniz[1], Adley F. Rubira (PQ)[1].**

**manuelgw@gmail.com; afrubira@gmail.com**

[1]*Departamento de Química, UEM.*
[‡] *In memoriam*

Palavras Chave: *$CO_2$ utilization, aqueous $CO_2$ as a catalyst, self-neutralizing process, TEOS hydrolysis, micro/mesoporous silica.*

## Highlights

A self-neutralizing acid hydrolysis of TEOS was developed replacing common acids for aqueous $CO_2$, leading to frontier micro/mesoporous silica with properties tailored by the applied $CO_2$ pressure.

## Resumo/Abstract

Micro and mesoporous silica are materials with great applicability on the adsorption of gases and water-pollutant[1,2]. A well-established $SiO_2$ synthesis is the acid hydrolysis of TEOS in ethanol[3], which requires the neutralization of the reaction wastes to perform an appropriate discard. We contour this advantage replacing the commonly used acids, like HCl and $H_2SO_4$, for pressurized aqueous carbon dioxide in a batch reactor. The adopted pressure and temperature conditions allowed the achievement of the pH ~ 3, which after the pressure relief neutralizes spontaneously. Frontier micro/mesoporous silicas were prepared as follows. Briefly, 5 mL of TEOS was added to the reactor, which was sealed and heated to 70ºC. The system was pressurized with $CO_2$ and then 45 mL of water was injected resulting in the final pressures of 5, 40, 65 and 83 bar (samples $P_5$, $P_{40}$, $P_{65}$, $P_{83}$). After 6 hours under stirring, the silica gel was collected, washed with acetone and centrifuged at 10,000 rpm at 25ºC. Lastly, the solid was macerated into mortar and pistil of agate. Textural analysis of the final products revealed materials with their characteristics in the border of micro/mesoporous classification (Table 1). The micro and mesoporous character can be tailored by the adopted $CO_2$ pressure on the hydrolysis step, higher $CO_2$ pressure leads to smaller mean pore size as denoted by the TEM images of $P_5$ and $P_{83}$ (Figure 1A and B) and by the mean pore size of all samples (Table 1).

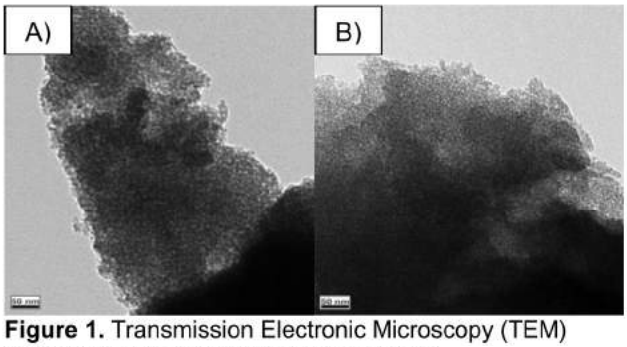


**Figure 1.** Transmission Electronic Microscopy (TEM) images of A) $P_5$ and B) $P_{83}$ $SiO_2$ particles.

**Table 1.** Textural properties of frontier micro/mesoporous silica obtained by the acid hydrolysis of TEOS performed in aqueous $CO_2$.

| Sample | Mean pore size (nm) | BET surface specific area ($m^2\ g^{-1}$) | Total pore volume ($cm^3\ g^{-1}$) | Micropore volume ($cm^3\ g^{-1}$) |
|---|---|---|---|---|
| $P_5$ | 4 | 724 | 0.406[a] | 0.114[a] |
| $P_{40}$ | 3 | 745 | 0.433[a] | 0.108[a] |
| $P_{65}$ | 3 | 908 | 0.495[a] | 0.106[a] |
| $P_{83}$ | 2 | 732 | 0.361[a] | 0.147[a] |

[a]Calculated by NLDFT.

References

[1] TSAI, C. H.; *et al. Journal of Hazardous Materials* 309, p. 236-248, **2016**.
[2]LI, H.; *et al. Microporous and Mesoporous Materials* 237, p. 222-227, **2017**.
[3]CATAURO, M.; PACIFICO, S. *Materials* 10(7), p. 840-853, **2017**.

**Área: MAT** **Inscrição: 00312**

# Mixed matrix membranes Synthesis with MIL-101(Cr) for gas separation

Gabriela H.G. dos Santos (PG),[1] Jussara L. Miranda (PQ),[1] Luiza C. de Moura (PQ),[1*] Helen C. Ferraz (PQ). [2]

**gabrielahgsantos@gmail.com; lcmoura@iq.ufrj.br**

[1]*Instituto de Química, UFRJ;* [2]*Programa de Engenharia Química, UFRJ*

Palavras Chave:*MIL-101(Cr), MOF, Mixed matrix membranes, gas separation*

## Highlights

This work consists in the synthesis and characterization of mixed matrix membranes with metal organic framework MIL-101(Cr) (MM101) for gas separation.

## Resumo/Abstract

Mixed matrix membranes can be composed of a metal organic framework (MOF) and a polymer matrix, taking advantage of the good properties of MOFs and the low cost and permeability of polymer membranes They are promising materials for gas separation due to their selectivity and reasonable cost. MMs have several applications and be designed for purification of natural gas or even in CO2-rich pre salt reservoirs.
In this work, MMMs were synthesized with MIL-101(Cr) (MM101) that presents high adsorption capacity.
The synthesis of MIL-101(Cr) was done employing hydrothermal method according to Ferey[1]. The characterization of MIL-101(Cr) was done by XRD, FTIR, BET and thermal analysis. MMMs were synthesized using different MIL-101/polymer ratios. MM101s were characterized by thermogravimetric analyses, BET, FTIR and Scanning Electron Microscopy (SEM).
The diffractogram of MIL-101(Cr) presented peaks at 8.5° and 9° similarly to the literature, showing good cristanility (Fig. 1). FTIR of MIL-101 (Cr) presented bands in the region of 3500 and 3100 $cm^{-1}$, indicating the presence of water and solvents in the pores. Symmetric and asymmetric bands of coordinated carboxylate groups were observed in the region of 1550 and 1400 $cm^{-1}$, corroborating the presence of bridge carboxylates in MIL-101 (Cr). MM101 presented a good MIL-101 dispersion and homogeneity according to SEM analyses (Fig. 2).
It can be concluded that MM101 has been satisfactorily obtained. MM101 is being tested towards $CO_2$ permeability and selectivity in relation to other gases such as $N_2$ and $CH_4$.

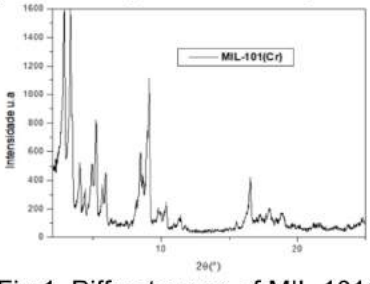


Fig.1. Diffractogram of MIL-101(Cr)

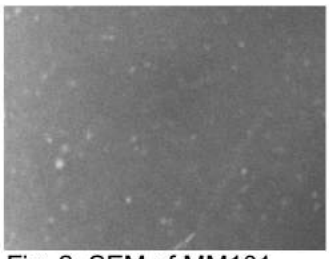

Fig. 2. SEM of MM101

[1]Férey G., et al; Science. 309 (5743),2040-2042, 2005.
[2]Cambridge Structural Database.
[3]Rodrigues M. Separation and Purification Tecnology. 192, 491-500, 2018.

**Área: MAT**
*(Inserir a sigla da seção científica para qual o resumo será submetido. Ex: ORG, BEA, CAT)*

**Inscrição: 00305**
*(Inserir o número de inscrição do autor que fez a submissão)*

# Removal of $Cu^{2+}$ ions from aqueous solutions using starch-g-poly(acrylic acid)/rice husk ash: adsorption kinetics

**B. C. Melo (IC)[1], Ana Jéssica R. da Rocha (IC)[1], Varneir A. Cardoso (IC)[1], Carlos E. de C. Magalhães (PQ)[2], Francisco Helder A. Rodrigues (PQ)[1]**
brunocarlosmelo1994@gmail.com; almeida_quimica@yahoo.com.br
*[1] Coordenação de Química, UVA; [2]Coordenação de Química, UECE*
Keywords: *Superabsorbent hydrogel; Hydrogel composite, Rice husk ash; $Cu^{2+}$ ions; Wastewater remediation.*

## Highlights

A set of superabsorbent hydrogels composites were prepared and used to adsorb $Cu^{2+}$ from the aqueous solution.
Adsorption kinetics followed the pseudo-second-order model, which is based on the chemisorption phenomenon.

## Resumo/Abstract

A series of superabsorbent hydrogels composites based on the biopolymer starch (St) grafted poly(acrylic acid) and rice hull ash (RHA) were synthesized by solution polymerization according to the procedure described Azevedo et al.[1], with the interest in the study of these systems as alternative adsorbents the of metal ions from aqueous solutions. The hydrogels were characterized by evaluated for adsorption kinetics for the $Cu^{2+}$ ions. In order to examine the controlling mechanism of adsorption processes such as mass transfer and chemical reaction, the pseudo first order and pseudo-second order equations were used to test the experimental data. Table 1 presents results obtained for the pseudo first-order and pseudo second-order model.

**Table 1.** Kinetics parameters of $Cu^{2+}$ ions adsorption on starch-g-poly(acrylic acid)/rice husk ash.

| RHA wt% | 0 | 1 | 5 | 10 | 20 | 30 |
|---|---|---|---|---|---|---|
| $q_e$,cal | 276 | 279 | 284 | 294 | 273 | 267 |
| $q_e$,exp | 208 | 201 | 175 | 171 | 200 | 177 |
| $k_1(10^{-2})$ | 5,26 | 5,11 | 4,98 | 4,94 | 4,80 | 3,89 |
| $R^2$ | 0,9679 | 0,9662 | 0,9113 | 0,9035 | 0,9753 | 0,9111 |
| $q_e$,cal | 293 | 295 | 298 | 309 | 289 | 278 |
| $k_2(10^{-4})$ | 4,04 | 4,18 | 4,72 | 4,85 | 3,94 | 3,87 |
| $R^2$ | 0,9976 | 0,9977 | 0,9974 | 0,9974 | 0,9979 | 0,9979 |

The correlation coefficients $R^2$ for the pseudo-second-order kinetic plots for all the hydrogels studied are above 0.997, suggest that the pseudo-second-order kinetic model can describe well the experimental data, and meaning that the adsorption process of $Cu^{2+}$ onto these adsorbents is probably controlled by the chimisorption phenomenon[2]. Moreover, the calculated equilibrium adsorption capacities qe,cal also agree with the experimental data in the case of pseudo-second order kinetics. In addition, it is obvious that when 10 wt% RHA is introduced into the hydrogel, the resulting adsorbent has faster initial adsorption rate and higher final adsorption capacity. That is, an appropriate addition of RHA into the polymeric networks can promote the adsorption of $Cu^{2+}$ onto the hydrogels.

Acknowledgments: To CNPq, FUNCAP (BP2-0107-00085.01.00 / 15), UECE and UVA.

[1]Azevedo, A.C.N. de; Vaz, M.G.; Gomes, R.F.; Pereira, A.G.B.; Fajardo, A.R.; Rodrigues, F.H.A. *Iranian Polymer Journal.* **2017**, *26*, 93.
[2]Souza, K.C.; Antunes, M.L.; Conceição, P.F.T. *Quimica Nova.* **2013**, *36*, 651.

**Área: MAT** **Inscrição: 00731**

# Evaluation of silicone rubber hydrophobicity after different periods of accelerated photo-ageing

**Ana Paula Munaro (PG),[1,2] Aline S. Salum(PQ),[2] Fábio S. Richart (PQ),[2] Francyele I. C. Silva (PQ),[2] José Molinari (TC),[3] Marilda Munaro (PQ),[2] Leni Akcelrud (PQ).[1]***

**anapaulamunaro@gmail.com; akleniak@gmail.com.**

*[1]Departamento de Química, UFPR; [2]Instituto de Tecnologia para o Desenvolvimento, Institutos Lactec; [3]Companhia Paranaense de Energia, Copel Distribuição.*

Palavras-Chave: *Silicone rubber, Photodegradation, Hydrophobicity, Surface roughness.*

## Highlights

Hidrophobicity has direct relation to the surface appearance.
Weathering results in an increase of the contact angle and also in the surface roughness.
UV radiation may accelerate the diffusion process of LMW.

## Abstract

In recent years, due to the advantages of silicone rubber (SR) insulators such as low cost, light weight, high mechanical strength, hydrophobic surface and good dielectric properties compared with porcelain and glass insulators, they have been widely used over the world for electrical power transmission and distribution systems. These materials are prone to decomposition under different environmental conditions, the main deleterious factors leading to the elastomer´s degradation include solar radiation, humidity, temperature cycles and pollution, acting simultaneously and in various degrees, depending on the environment, making the study and the forecast of life span of the silicone rubber based equipments rather complex. In an attempt to contribute to this important problem we underwent a systematic study of the photodegradation of SR in simulated environment. Samples were subjected to accelerated weathering in a Weather-Ometer chamber for 4500 hours. During this time, were evaluated the hydrophobicity, topography by Atomic Force Microscopy and the element composition on the surface by Energy Dispersive Spectrometer. The results indicate that hydrophobicity increases for all composites after the weathering, probably due to increase in surface roughness of composites, which could be attributed to the exposure of the fillers, such as silica and aluminum trihydrate. In addition, it has been observed micron-sized crackles formation on the surface which may be facilitate the diffusion of low molecular weight (LMW) compounds from the bulk sample to surface, which are one of the responsible factors for the hydrophobic surface of SR.

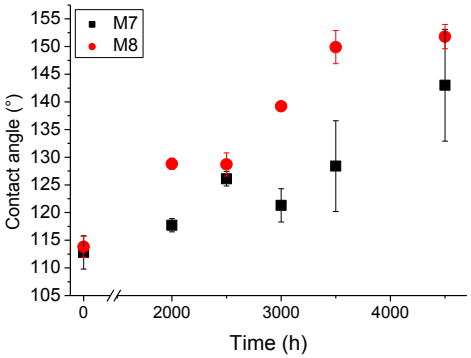


Figure 1. Hydrofobicity of M7 e M8 samples.

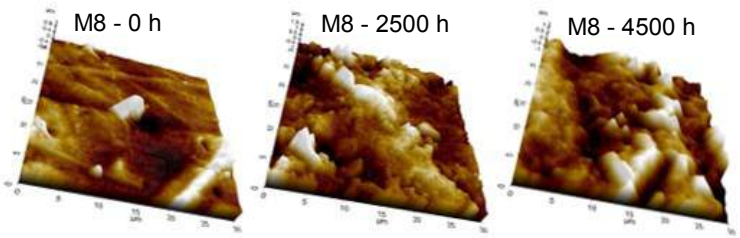


Figure 2. Topography changes of M8 sample by AFM.

**Área: MAT** **Inscrição: 00706**

# Comparison of Hybrid Conjugates Containing Amyloidogenic Peptides and Gold Nanoparticles

**Juliane N.B.D. Pelin (PG), Wendel A. Alves* (PQ).**

juliane.pelin@ufabc.edu.br; wendel.alves@ufabc.edu.br

*Centro de Ciências Naturais e Humanas, Universidade Federal do ABC, 09210-580, Santo André, Brasil.*

Keywords: *Peptide assemblies, Gold nanoparticles, Amyloids, Inhibitors, Crystal nucleation and Growth.*

## Highlights

Study of the nucleation process of the metal particles on peptide sequences that self-organize in a β-sheet-like structures based on *L*-phenylalanine (F), *L*-arginine (R) and *L*-cysteine (C) amino acids.

## Resumo/Abstract

Cooperative binding of nanoparticles can influence the aggregation properties of peptides or proteins, being beneficial or deleterious to the formation of amyloid structures. In this work, we have investigated the effect of gold nanoparticles (AuNPs) on the aggregation of two short amyloid-like peptides, CFF and $(RF)_4$ in aqueous medium.[1,2] For CFF, we have shown that the structure of the resulting scaffolds were dependent on the nanoparticle synthesis route, i.e., by using sodium borohydride ($NaBH_4$) as a reducing agent, or by using the peptide-catalyzed redox technique for the synthesis and stabilization of AuNPs under heating at 60°C. For both methods, it was verified that the systems self-organize as polydisperse globules, with the presence of flexible parts. Besides the hybrids can promote electron transfer from the metallic nanoparticles to the CFF surface, creating an n-type semiconductor and causing a peak shift of the phenylalanine absorption band.[2] In the case of $[RF]_4$ system, the $NaBH_4$ strategy for the nucleation of AuNPs has been used, indicating the presence of polydisperse globules. It has an absolute zeta potential equal to +22.5 mV, which forms an p-type semiconductor. Small-angle X-ray scattering (SAXS) and dynamic light scattering (DLS) showed nanosized particles for both systems, in agreement with transmission electron microscopy (TEM) images (Fig. 1). Also, depending on the $[HAuCl_4]$/[peptide] ratio were formed different polymorphs in solution. As next step, we will investigate the use of these hybrids on plasmonic catalysts based on the reduction of 4-nitrophenol.

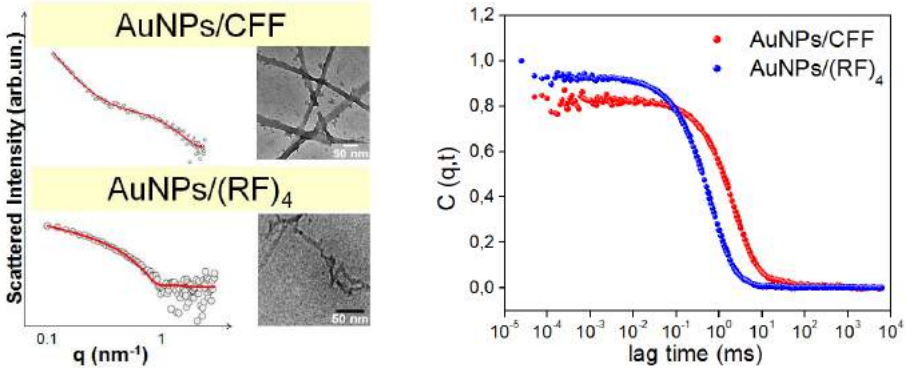


**Figure 1.** SAXS profiles, TEM images and correlation curves for the conjugates containing AuNPs and peptides CFF and $(RF)_4$ within their respective critical aggregation concentration.

[1] Pelin, J.N.B.D.; Gatto, E.; Venanzi, M.; Cavalieri, F.; Silva, E.R.; Oliveira, C.L.P.; Souza, J.S.; Martinho, H.; Alves, W.A. Hybrid Conjugates Formed between Gold Nanoparticles and an Amyloidogenic Diphenylalanine-Cysteine Peptide, *manuscript submitted*, **2018**.

[2] Silva, E.R.; Listik, E.; Han, S.W.; Alves, W.A.; Soares, B.M.; Reza, M.; Ruokolainen, J.; Hamley, I.W. Sequence length dependence in arginine/phenylalanine oligopeptides: implications for self-assembly and cytotoxicity. *Biophys. Chem,* **2018**, *233*, 1-12.

**Área: MAT** **Inscrição: 00202**

# Isolation of cellulose and cellulignin from sugarcane bagasse by green chemical treatments

**Lucas Luiz Messa (PG),[1,2]* Roselena Faez (PQ).[1]**

**messalucas@hotmail.com**

*[1]Laboratório de Materiais Poliméricos e Biossorventes (Lab MPB), UFSCar, Araras, São Paulo - Brasil; [2]Universidade de São Paulo - FZEA, Pirassununga, São Paulo - Brasil.*

Keywords*: Residue; mercerization; bleaching.*

## Highlights

Sugarcane bagasse and its byproducts fibers offer a great potential as reinforcement in biodegradable biocomposites. Cellulose and its derivatives fibers were successfully obtained by efficient and green chemical treatments.

## Resumo/Abstract

In recent years, there has been growing interest in developing environmentally friendly technologies that enable the use of green and sustainable processes and products due the necessity to preserve the environment[1]. In this context, natural fibers are being extensively studied for many applications, due to their unique characteristics, such as biodegradability, abundance and high specific properties[2]. In Brazil, sugarcane bagasse is a waste generated in large quantities by the agro-industry, and is composed of 40-50% cellulose, 25-35% hemicellulose and 18-24% lignin[3], which allows the use of this residue as source of cellulose for the development of biodegradable composites. In this work, cellulose was isolated from sugarcane bagasse by mercerization (4% NaOH, 70ºC, 5 minutes, twice), followed by bleaching (4% $H_2O_2$, 45ºC, 6 hours, pH 11.5). Chemical treatments of bagasse were effective in removing most hemicelluloses and lignin to yield 46.5% cellulose-rich solid. Micrographs showed a decrease in the degree of fiber aggregation, possibly caused by the partial removal of lignin and hemicellulose (Figure 1A). The FTIR spectra of treated fibers (Figure 1B) confirmed the removal of amorphous constituents, showing a decrease in the intensity of bands characteristic of hemicellulose and lignin, while XRD results showed that the treatments favored the increase of fiber crystallinity (Figure 1C). However, results indicated the efficiency of the milder chemical treatments, important aspects that point out the potentiality of this raw material as source of cellulose for the development of biocomposites.

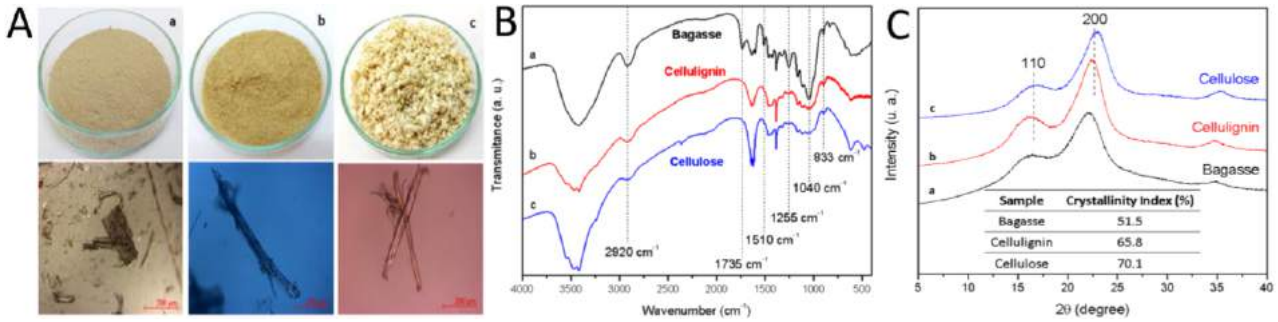


Figure 1. (A) optical images for (a) bagasse, (b) cellulignin and (c) cellulose; (B) FTIR spectra of bagasse during isolation process following: (a) water washing, (b) mercerization and (c) de-lignification; (C) XRD of cellulosic samples and Crystallinity index (CrI).

[1]Bharath, K. N.; Basavarajappa, S. *Sci Eng Compos Mater*, v. 23, n. 2, p. 123–133 (2016);
[2]Ramesh, M.; Palanikumar, K.; Reddy, K. H. *JRSE*, v. 79, p. 558–584 (2017);
[3]Mandal, A.; Chakrabarty, D. *Carbohydr Polym*, v. 86, n. 3, p. 1291–1299 (2011).

**Área: MAT**
*(Inserir a sigla da seção científica para qual o resumo será submetido. Ex: ORG, BEA, CAT)*

**Inscrição: 00977**
*(Inserir o número de inscrição do autor que fez a submissão)*

# Preparation of $BiVO_4$-decorated ZnO nanorods for oxygen evolution using photo-electrocatalysis

**Rafael M. de Almeida (PG), André Luiz Martins de Freitas (PG), Juliana dos Santos de Souza (PQ), Flavio Leandro de Souza (PQ), Wendel A. Alves* (PQ)**

r.mascarenhas@ufabc.edu.br; wendel.alves@ufabc.edu.br

*Centro de Ciências Naturais e Humanas, Universidade Federal do ABC, 09210-580, Santo André, SP, Brazil.*

Keywords: *multihierarchical electrode, photoelectrocatalysis, water splitting.*

## Highlights

We show that both the glass substrates - indium tin oxide (ITO) or fluorine doped tin oxide (FTO) - and the heat treatment process affect the self-assembled $BiVO_4$-decorated ZnO heteronanostructures, and its photoelectrocatalytic oxygen evolution reaction.

## Resumo/Abstract

The use of semiconductor heterojunction nanostructures to obtain hierarchical electrodes have been widely investigated, especially in the field of energy conversion and photoelectrocatalysis.[1] Zinc oxide nanorod (ZnONR) is a suitable catalyst for photoelectrochemical water splitting applications, however it only absorbs UV radiation.[1-2] On the other hand, bismuth vanadate ($BiVO_4$), exhibit high visible light absorptivity due to its small band gap energy (2.4 eV).[1] In this work, we have studied the role of the ITO and FTO bottom electrode on the self-assembled stability of $BiVO_4$-ZnO nanostructure architecture, and the effect of heat-treatment at 600 °C for 1 h. To grow the ZnONR films, a two-step method based on the literature with minor modifications was used.[2] $BiVO_4$ nanostructures were prepared through precursor mediated growth method and decorated on the surface of ZnONRs by using a colloidal $BiVO_4$ solution (previously ultrasonicated). The structural and chemical properties of the films were investigated by X-ray diffraction, X-ray photoelectron spectroscopy and scanning electron microscopy. Fig. 1 shows the morphologies of the obtained samples. It can be seen that ZnONRs with 100-200 nm in diameter were successfully synthesized on both substrates. The $BiVO_4$ nanofibers are well dispersed on the surface, and penetrates completely between the rods, as shown in Fig. 1B. According to the XRD analyses, $BiVO_4$ takes the monoclinic structure and ZnONR takes the wurtzite structure. However, for the calcined samples, we have observed a slight growth in the (002) plane by monitoring the Bragg peak intensity. As shown in Fig. 1, the current was directly generated from the designed photoanode as no current was detected when applying a linear sweep within a range from −0.5 to +1.0 V in the darkness. Compared with pristine ZnONRs, the ZnONRs coated with $BiVO_4$ film shows higher photocurrent density under light illumination, which can be related to the increase of light absorption capability of ZnO. However, the ZnONR films grown in FTO substrate showed better photocurrent density stability than ZnONR/ITO electrodes. The heat-treated $BiVO_4$-ZnONR electrodes exhibit a lower response compared with electrodes based on ZnONR films.

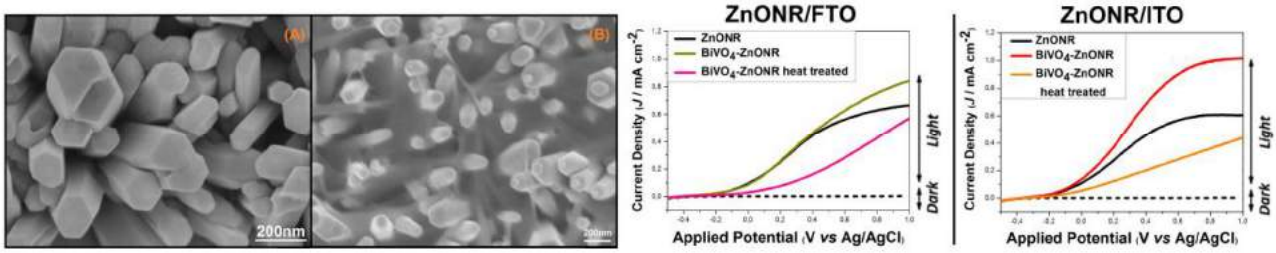


**Fig. 1-** (left) Top-view SEM images of pristine ZnONRs (A) and coated with $BiVO_4$ nanostructures (B); (right) Photocurrent (J) vs. voltage ($V_{RHE}$) curves without and with sunlight irradiation for both modified FTO and ITO electrodes, respectively, measured using a scan rate of 10 mV $s^{-1}$. Electrolyte: 0.5 mol $L^{-1}$ $Na_2SO_4$. The sunlight was simulated using an ozone-free xenon-lamp coupled with 1.5 Global filter and intensity adjusted at 100 mW.$cm^{-2}$.

[1]A. Kudo, Y. Miseki, *Chem. Soc. Rev.* **2009**, *38*, 253-278.
[2]J.S. Souza, W.M. Carvalho, F.L. Souza, C. Ponce-de-Leon, D.V. Bavykin, W.A. Alves, *J. Mater Chem. A* **2016**, *4*, 944-952.

**Área: MAT** **Inscrição: 01073**

# Importance of corrosion resistence of the cannula test in control quality of hypodermic needles

**Renata de F. D. Vale (TC),[1] Anna Maria B. S. Fust (TC),[1] Lilian de F. Venâncio (TC),[1] Kátia C. Leandro (PQ),[2] André L. Gemal (PQ),[3] Filipe S. Q. da Silva (PQ),[4] Michele Feitoza-Silva (PQ),[1] Carolina M. de Carvalho (PG).[1]***

**renata.dalavia@incqs.fiocruz.br; caroldemesquita@hotmail.com**

*[1]Departamento de Química, INCQS-FIOCRUZ; [2]Programa de Pós-graduação em Vigilância Sanitária, INCQS-FIOCRUZ; [3]Instituto de Química – UFRJ; [4]Vice-Diretoria de Ensino e Pesquisa, INCQS-FIOCRUZ;*

Palavras Chave*: Corrosion, Hypodermic needles, Health Surveillance*

## Highlights

Quality control of hypodermic needles.
Corrosion resistance with enlarged view.

## Resumo/Abstract

Hypodermic needles are products that poses medium risk to the user health, according to Anvisa's risk classification. This study aims to discuss the importance of the corrosion resistance test in hypodermic needle cannulas in product quality control. Samples of hypodermic needles used in 17 Brazilian States have been selected. The cannula were evaluated according to NBR ISO 9626/2003 and NBR 9259/1997. The results were analyzed using an adapted scale that classifies the extent of the corrosive damage based on the macroscopic findings. Additionally, the samples that presented corrosion in at least one of the evaluated units were considered unsatisfactory. 174 batches of needle samples from 9 different registry holders were analyzed. According to the methodology of NBR ISO 9626/2003, 100% of the samples were considered satisfactory. However, according to the methodology of NBR 9259/1997, 169 samples were rejected, that is, 97.1% of the samples. Irregularities may jeopardize the quality of the product and result in risks to consumer health. For being a product certified since 2011, it is necessary to reflect on the importance of the corrosion resistance test and the compulsory certification for health surveillance. Thus, the confirmation that certification does not guarantee health quality reiterates the importance of the public health laboratory and the continuous monitoring by health authorities in Brazil.

**Área: MAT** **Inscrição: 01102**

# Proposed regulatory change in view of the silicone quantification test in hypodermic syringes

**Michele Feitoza-Silva (PQ),[1] Renata de F. D. Vale (TC),[1] Anna Maria B. S. Fust (TC),[1] Lilian de F. Venancio (TC),[1] Kátia C. Leandro (PQ),[2] Cristovão de S. Alves (PG).[1]***

**michele.feitoza@incqs.fiocruz.br; cristovao.s.alves@hotmail.com**

*[1]Departamento de Química, INCQS-FIOCRUZ; [2]Programa de Pós-graduação em Vigilância Sanitária, INCQS-FIOCRUZ*

Palavras Chave: *Syringes, Lubricants, Regulacion, Product surveillance postmarketing, Silicone oil, Metrological certification*

## Highlights

Quantification of silicone in hypodermic syringes.
Amendment of the technical regulation.

## Resumo/Abstract

With the increasing advance in diagnostic and therapeutic technologies, more and more health products are available in the market, and consequently, actions directed to their control and monitoring are necessary. Single-use hypodermic syringes (SuHS) are medical devices widely used in a variety of health services and are commonly used in medication administration. They are usually made of high quality plastic and internally lubricated with medical grade polydimethylsiloxane (silicone oil). The current legislation establishes the limit of 0.25 mg/cm² of lubricant per syringe, and the aspect evaluation, by visual inspection, as a method of analysis. Thus, this study aims to evaluate the applicability of the aspect evaluation assay on the presumption of excess lubricant in SuHS commercialized in Brazil, by comparing results obtained in the aspect and extraction/quantification assays (standardized method). Nineteen batches of SuHS were analyzed, totaling 168 units. All samples failed in the aspect evaluation for presenting excess silicone inside. The extraction/quantification assay of the same samples showed that only 2 samples had a mean lubricant content above the standard, ie 87.5% of the failures in the lubricant aspect evaluation would not occur in the extraction/quantification assay. This result highlights the need for regulatory changes regarding the subjective form of lubrication analysis (visual inspection) in SuHS currently used, and suggests the extraction/quantification test as a more accurate and reliable alternative, minimizing the possibility of errors in analysis of metrological certification.

**Área:** MAT **Inscrição: 00424**

# Electrochemical application of all-chemically synthesized graphene/iron oxide composites

**Jonathan dos Santos (IC)*, Laís C. Lopes (PG), Aldo J. G. Zarbin (PQ)**

**jonathan.santos@ufpr.br; aldozarbin@ufpr.br**

*Department of Chemistry, Federal University of Paraná (UFPR), Curitiba, PR, Brazil..*

Key words: *Chemical synthesis of graphene, Thin film, electrochemistry, Liquid/liquid interface, iron oxide, Supercapacitor.*

## Highlights

The total chemical synthesis in one step of graphene from benzene at liquid-liquid interface described in this work presents remaining species of iron oxides after synthesis giving promising properties for use in electrochemical devices such as capacitors

## Abstract

Graphene is a one-atom thick structure composed of $sp^2$ hybridized carbons arranged in a two-dimensional hexagonal reticulum, presenting unique properties, such as exceptional charge transport and optical properties, which give great applicability in different areas. In this work, we report the applications of the total chemically-synthesized graphene from benzene, obtained as thin films at liquid-liquid interface. The samples were fully characterized and a set of samples were prepared varying i) post-synthesis treatment (without treatment, HCl and $NH_4OH$-treated), and ii) the number of layer of thin film deposited on the substrate for electrochemical tests: cyclic Voltammetry (CV) and charge and discharge (CD) to evaluate the applicability of graphene/iron oxide composites in electrochemical devices. In the cyclic voltammetry tests we studied two electrolytes, different potential window and scan speeds. The CV tests showed cathodic and anodic peaks relative to redox processes of iron species present in the film, and showed voltammogram area increasing with the deposition, indicating a rise in the capacitance of the material. The CD tests showed a characteristic capacitor profile for all samples, and from these tests it was possible to determine the capacitance values. Figure 1 shows the studied samples composed by 2 layers film. The sample without treatment after the synthesis presented the best results in higher current densities, with values of capacitance up to 30 F $g^{-1}$. Thus, the sample without post treatment has been shown to be the most promising samples to applications in capacitors.

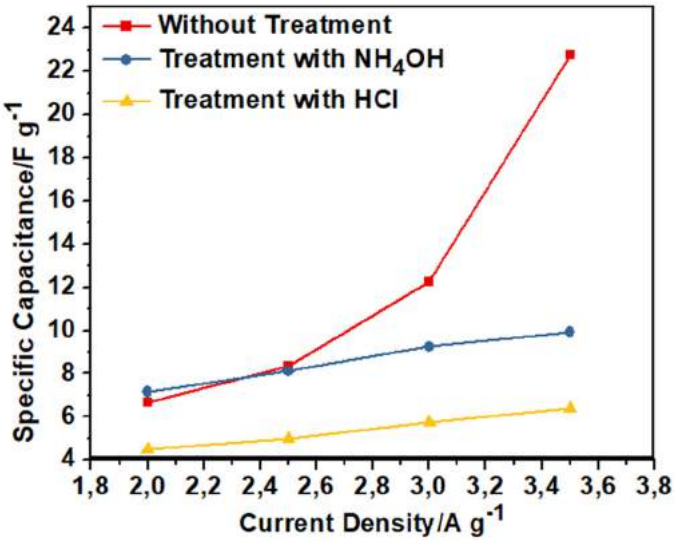

**Área: MAT** **Inscrição: 00661**

# Activity of immobilized porcine pancreatic lipase into mesoporous silica SBA-15 in transesterification reactions

**Igor Nuno dos Santos Rocha (IC)[1], João André Duarte Silva (PQ)*[1]**

**igornunotg@gmail.com; jdsilva@iff.edu.br**

[1]*Instituto Federal Fluminense de Ciência e tecnologia – Campus Cabo Frio, IFF;*

Palavras Chave: *biocatalisador, enzima, sílica, transesterificação.*

## Highlights

Activity of immobilized porcine pancreatic lipase into mesoporous silica SBA-15 in transesterification reactions. Porcine pancreatic lipase was immobilized on mesoporous silica. The catalytic activity of the system was tested in olive oil.

## Resumo/Abstract

Os silicatos mesoporosos têm sido utilizados para diversos fins industriais em especial nas áreas de catálise e adsorção. O presente trabalho visa efetuar a imobilização da Lipase de Pâncreas de Porco (LPP) na sílica SBA-15 e verificar o impacto desse processo na atividade catalítica da enzima.

Essa imobilização foi realizada a partir de 0,1 g de LPP com 1,0 g de sílica em 10 mL de solução tampão pH 7.

Tanto a enzima imobilizada quanto a livre foram submetidas a estudo cinético frente a reação de transesterificação do óleo de oliva/goma arábica tamponada em pH 7. Após 24 h o ácido livre foi determinado titrimeticamente com NaOH 0015 M (fenolftaleína)[1]. (Figura 1)

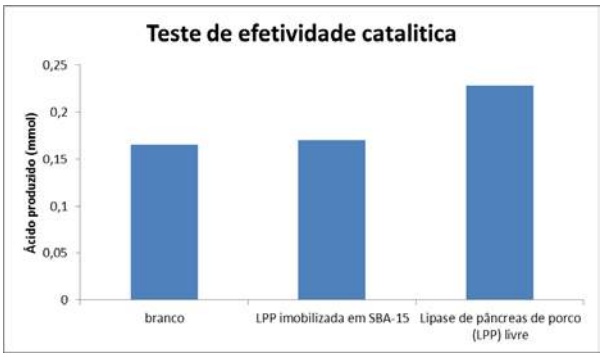


Figura 1: Resultado da catálise enzimática do óleo de oliva em termos de quantidade de ácido liberado.

A comparação entre as atividades da enzima livre e imobilizada é apresentada na Figura 2.

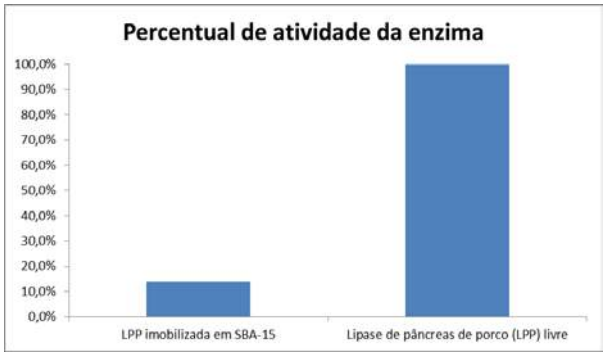


Figura 2: Comparação entre as atividades da lipase livre e da lipase suportada em sílica.

A partir dos resultados constata-se e a imobilização da enzima. Entretanto, a atividade da enzima imobilizada é menor do que a livre. Essa observação pode ser justificada pela dificuldade de difusão do substrato nos mesoporos da sílica em função da elevada viscosidade da emulsão formada pelo sistema óleo/goma arábica. Apesar a baixa eficiência, o sistema proposto pode ser reutilizado em outras reações de transesterificação.

Futuramente serão avaliadas atividades da LPP em sílica mesoporosa contendo compostos, tais como líquidos iônicos, de amplificam a atividade de lipases[2].

Agradecimentos: CNPq, IFF – Campus Cabo Frio.

1. Melo, A. F., Tese (Doutorado), UFRJ, 2012.
2. Kragl, U.; Eckstein, M.; Kaftzik, N.; *Curr. Opin. Biotechnol.* **2002**, *13*, 565.

**Área: MAT** **Inscrição: 00798**

# Thin films of nanocomposites between graphene and nickel hexacyanoferrate nanoparticles applied in energy storage

**Eduardo G. C. Neiva (PQ),[1]* Aldo J. G. Zarbin (PQ).[2]**

**eneiva@furb.br**

*[1]Department of Chemistry, University of Blumenau (FURB), Blumenau, SC, Brazil; [2]Department of Chemistry, Federal University of Paraná (UFPR), Curitiba, PR, Brazil;*

Key words: *Graphene, Nickel hexacyanoferrate, Thin films, Lithium, Sodium and Potassium aqueous batteries.*

## Highlights

Synthesis of nanocomposites between graphene and nickel nanoparticles through the polyol method;
Thin films deposition using the biphasic system;
Electrochemical preparation of nickel hexacyanoferrate.

## Abstract

The development of new energy storage devices with high energy and power densities is directly related with the synthesis of new materials with defined structural and morphological characteristics that supplies a high and fast electroactivity. An interesting approach to achieve these requirements is through the synthesis of nanocomposites of the electroactive material with graphene, which enables a good conductivity to the final material and favoring higher power densities. Nanoparticles of metallic hexacyanoferrates have been widely studied as electroactive materials for aqueous batteries due their interesting characteristics as open framework structure, good durability and fast kinetics. In this way, this work aims the synthesis and characterization of nanocomposites between reduced graphene oxide (rGO) and metallic nickel, their processing as thin films and use for the synthesis of nickel hexacyanoferrate nanoparticles and their application for aqueous batteries. The rGO/nickel nanocomposites with different mass proportions were synthesized by the polyol method at 200 °C for 2 hours starting from graphene oxide (GO) solution in ethylene glycol containing nickel acetate.[1] These materials were characterized by X ray diffraction (XRD), infrared spectroscopy (FT-IR), scanning electron microscopy (SEM), X-ray spectroscopy (EDS) and Raman spectroscopy. Next, the materials were processed as thin films using a liquid-liquid interface and deposited over ITO substrates. These thin films were employed in the electrochemical synthesis of nickel hexacyanoferrate through voltammetric cycling in $[Fe(CN)_6]^{3-}$ 1 mmol $L^{-1}$ and KCl 0.1 mol $L^{-1}$ aqueous solution with pH 6 and 3. These nanocomposites were characterized by XRD, Raman spectroscopy, SEM, EDS and UV-Vis spectroscopy. They were also evaluated by cyclic voltammetry and charge-discharge measurements in lithium, sodium and potassium aqueous solutions, as well as their stabilities through successive cycling. The impacts in the crystalline structure of the nickel hexacyanoferrates cause by the voltammetric cycling in different alkaline metal ion solutions were monitored by XRD. The synthesis conditions led to the reduction of the GO to rGO and the obtaining of nickel particles with face centered cubic structure. However, the nanocomposite with 10.5 % of nickel (rGONi-1) produced nanoparticles with sizes in the range from 10 to 40 nm, while the rGONi-2 (46.9 % of nickel) led to micrometric particles with sizes in the range from 0.5 to 5 µm. When used as precursor for the synthesis of nickel hexacyanoferrate, the rGONi-2 thin film cycled in $[Fe(CN)_6]^{3-}$ aqueous solution with pH 3 produced the higher amount of desired material, where few voltammetric cycles (10 – 30) were enough to produce the hexacyanoferrate. The rGONi-1 lead to nickel hexacyanoferrate nanoparticles with sizes ranging from 20 to 60 nm, while in the nickel sample synthesized without the GO lead to hexacyanoferrate particles deposited over the nickel micrometric particles and the ITO electrode. However, both rGONi-2 cycled at pH 6 and 3 produced a very high amount of nickel hexacyanoferrate, leading to the appearing of plates over the rGO layers. The higher voltammetric stabilities were verified using KCl and NaCl electrolyte solutions, but the use of $Na^+$ affected significantly the structure of the hexacyanoferrates. When evaluated by charge-discharge, the hexacyanoferrates produced using the rGONi-2 cycled in pH 3 led to the higher capacities, as high as 78.4 mA h $g^{-1}$, and energy and power densities (39.1 W h $kg^{-1}$ and 0.2 kW $kg^{-1}$, respectively) when analyzed in KCl medium.

[1] NEIVA, E. G. C. et al, One material, multiple functions: graphene/$Ni(OH)_2$ thin films applied in batteries, electrochromism and sensors. **Scientific Reports**, v. 6, p.33806, 2016.

**Área:** MAT *(Inserir a sigla da seção científica para qual o resumo será submetido. Ex: ORG, BEA, CAT)*

**Inscrição:** 01413 *(Inserir o número de inscrição do autor que fez a submissão)*

# $Ag_2WO_4$ polymorphs: selective synthesis and characterization

**Roman Alvarez-Roca (PQ)[1]*, Pablo S. Lemos (PG)[1], Elson Longo (PQ)[1]**

**cortes116@yahoo.es**

[1] *LIEC/CDMF-DQ, Universidade Federal de São Carlos*

Keywords: *silver nanoparticle, morphology, silver tungstate*

## Highlights

The availability of facile methods to prepare metastable phases available further properties and unusual applications.

## Abstract

Controlling the synthesis of metastable polymorphs of an inorganic material is a further step in the design of novel properties and unexplored applications. In contrast to their thermodynamically more stable counterparts, metastable phases have been elusive due to their propensity to convert to the stable phase. In this work, we report a simple procedure to effectively control for the synthesis of the crystalline polymorphs of $Ag_2WO_4$. The different polymorphs; the stable α- and metastable β- and γ-$Ag_2WO_4$; were prepared via controlled precipitation under ambient conditions over mixture of the precursor salts ($AgNO_3$ and $Na_2WO_4$) at adequately select values of concentration and salts stoichiometric ratio. These crystals were structurally characterized by X-ray diffraction (XRD). The shapes and sizes were observed by field emission scanning electron microscopy (FE-SEM). Their optical properties were analyzed by Photoluminescence emission (PL). Finally, the possible mechanism of nucleation and stabilization of the phases is discussed based on driven of the short-range structural and electronic changes of their diverse constitutive clusters [$WO_x$] and [$AgO_y$] (x = 4-6 and y=2, 4-7). This process and the concentration and stoichiometry dependence of the polymorphms is displayed in figure 1. The availability of a facile method to prepare different $Ag_2WO_4$ polymorphous is expected to catalyze further empirical studies on the elusive and little-studied metastable phase.

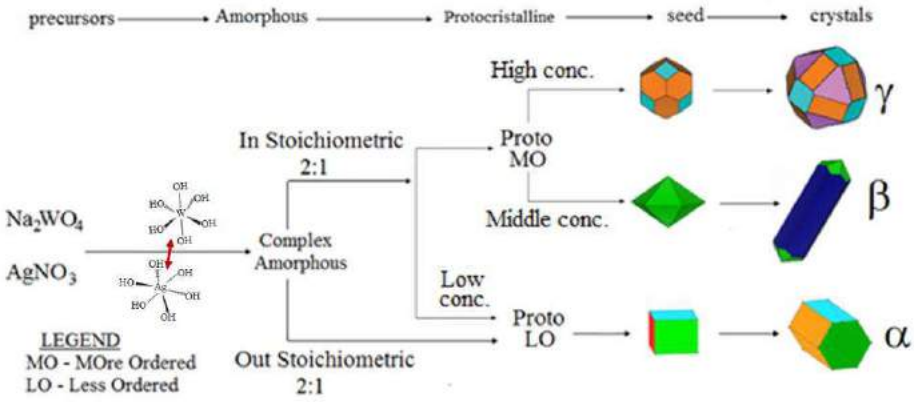


**FIGURE 1**. Schematic diagram of nucleation processes for different $Ag_2WO_4$ phases. The equilibrium of the phases is a function of the concentration and molar stoichiometry.

**Área: MED** **Inscrição: 01343**

# Serine protease from *Bothrops asper* snake venom and its inhibition by hesperetin

**Giovanna R. Grillo (IC) *, Roney V. dos Santos (PG), Ljubica Tasic (PQ).**

**gigrillo@gmail.com**

*Department of Organic Chemistry, UNICAMP*

Key words: *Snake venom, Serine protease, Hesperetin.*

## Highlights

Our focus is the characterization and activity of a serine protease, named BaSP1, derived from *Bothrops asper* snake venom and its inhibition in the presence of hesperetin.

## Abstract

Serine proteases cause hemostatic changes in victims of ophidian accidents. The catalytic mechanism of these enzymes involves a catalytic triad formed by His57 – Asp102 – Ser195 residues.

Our research started with isolation and purification of the target protein from the *Bothrops asper* snake venom. To isolate and purify BaSP1, we have used FPLC techniques. In the first step, exclusion chromatography and, thereafter, affinity chromatographic step were applied. To verify the BaSP1's purity, a reversed-phase chromatography was performed. The protein was biophysically and biochemically characterized. Circular dichroism (CD) was used to verify the BaSP1 2D structure and fluorescence for folding evaluation.

The other research target was BaSP1 potential inhibitor, hesperetin (Hst). This compound was obtained after hesperidin extraction from orange peels and its subsequent hydrolysis. Hst was characterized by TLC, UV-Vis, CD, FT-IR, NMR ($^{1}$H and $^{13}$C NMR) and MS.

Afterwards, the enzyme (BaSP1) and the inhibitor (Hst) interaction was evaluated and enzymatic assays were performed to verify the inhibitory capacity of Hst. Figure 1 and Table 1, show the reduction of $V_{MAX}$ and $K_M$ when Hst was added to an enzyme solution.

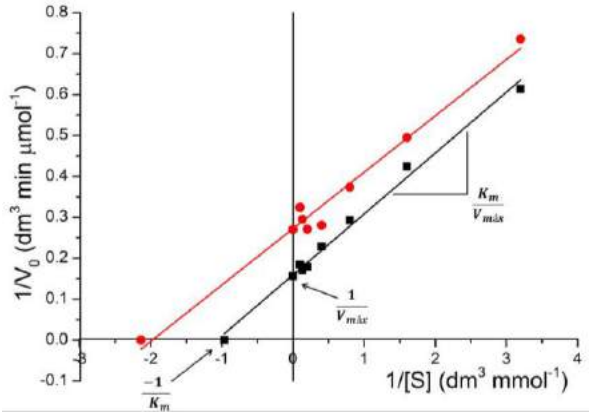


**Figure 1** - Lineweaver-Burk plots obtained in BaSP1 and hesperetin (Hst) experiment. The black (BaSP1) and red lines represent the target enzyme activity assays in the absence and presence of hesperetin, respectively.

**Table 1** - Values obtained from the Lineweaver-Burk plot (Figure 1) when monitored BaSP1 activities in the presence and absence of hesperetin:

| | $K_M$ (mmol dm$^{-3}$) | $V_{MAX}$ (µmol dm$^{-3}$ min$^{-1}$) | Slope |
|---|---|---|---|
| Protein BaSP1 | 1.0352 | 6.3981 | 0.1488 |
| BaSP1 and Hst | 0.4684 | 3.7071 | 0.1378 |

We have successfully obtained both target entities, BaSP1 and Hst. According to biochemical and biophysical test results, BaSP1 was folded and active. Hesperetin was shown to be a potential inhibitor of BaSP1, once there were observed alterations in BaSP1 features when Hst was added.

Special thanks to FAPESP (Process number: 2016/21682-0) and to CNPq for financial supports.

[1] R. Vander dos Santos *et al. Toxicon* 143 (**2018**) 36e43

**Área: MED** **Inscrição: 01362**

# Discovery of new *Plasmodium* cGMP-dependent protein kinase potential inhibitors with antiplasmodial and transmission blocking activities

**Gustavo C. Cassiano (PQ),[1] Kaira C.P. Tomaz (PG),[2] Marília N. N. Lima (PG),[2] Bruno J. Neves (PQ),[2] Tatyana A. Tavella (PG),[1] Melina Mottin (PQ),[2] Rodolpho C. Braga (PQ),[2] Juliana Calit (IC)[3], Pedro V.L. Cravo (PQ),[4] Daniel Y. Bargieri (PQ)[3], Carolina Horta Andrade (PQ),[1,2] Fabio T.M. Costa (PQ).[1*]**

**carolhandrade@gmail.com; fabiotmc72@gmail.com**

*[1]Laboratory of Tropical Diseases, UNICAMP, Brazil; [2]LabMol - Laboratory for Molecular Modeling and Drug Design, UFG, Brazil; [3]Department of Parasitology, Institute of Biomedical Sciences, USP, Brazil; [4]Institute of Tropical Medicine and Hygiene, UNL, Portugal.*

Keywords: Malaria, Virtual Screening, Pharmacophore, PKG, QSAR, Experimental evaluation.

## Highlights

Discovery of novel scaffolds against asexual blood stages of *P. falciparum* and sporogonic development of *P. berghei*. Virtual screening to identify novel antiplasmodial and transmission blocking compounds.

## Abstract

In the absence of an effective vaccine, rapid treatment is vital for effective malaria control. However, among the greatest challenges in battling malaria is the recurrent emergence and spread of parasite resistance to antimalarial drugs, highlighting the importance to develop new antimalarials with novel modes of action.[1] Using bioinformatics tools, we interrogate the *Plasmodium falciparum* and *P. vivax* proteomes to identify protein kinases that may represent potential drug targets for the parasite life cycle. PKG was selected because: 1) is essential for asexual blood stage; 2) is conserved between *Plasmodium* species; 3) has low identity with human ortholog.[2] After, we integrated a QSAR-based virtual screening with ligand-based pharmacophore models for the discovery of novel potential *Plasmodium* PKG inhibitors. The computational approach allowed us to select 19 compounds for further experimental evaluation. The *in vitro* assays against asexual blood stage of *P. falciparum* (3D7 strain) showed that two compounds, LDT-146 and LDT-147, presented activity at low nanomolar concentrations ($IC_{50}$ = 15 nM and 105 nM, respectively). In addition, these compounds exhibited low cytotoxicity in mammalian cells (COS-7), resulting in high selectivity towards malaria parasites. Furthermore, some compounds also showed good *in vitro* inhibition of *P. berghei* ookinete formation, demonstrating that hit-to-lead optimization based on these compounds may also lead to new antimalarials with transmission blocking activity. In future studies, we aim to perform enzymatic assays against plasmodial PKG aiming to study the mechanism of action of those compounds.

**Table 1.** *In vitro* evaluation of selected hits against asexual blood stage of *P. falciparum* 3D7 strains, cytotoxicity on mammalian cells (COS7) and selectivity index.

| ID | 3D7 | COS-7 | SI |
|---|---|---|---|
| | $IC_{50}$ (µM) | $CC_{50}$ (µM) | |
| LDT-146 | 0.015 ± 0.002 | 5.888 | 392.5 |
| LDT-147 | 0.105 ± 0.018 | 7.541 | 71.8 |

$IC_{50}$: half maximal inhibitory concentration on 3D7 strains; $CC_{50}$: half maximal cytotoxic concentration on COS-7 cells; SI: Selectivity index calculated by CC50/IC50; The data are expressed as mean ± SD of 3 independent assays.

[1]WHO. World malaria report **2015**, http://www.who.int/malaria/publications/world-malaria-report-2015/report/en/.
[2]Solyakov, L.; Halbert, J.; Alam, M.M.; et al. *Nat. Commun.* **2011**, 2, 565.

**Área: MED** **Inscrição: 01348**

# Synthesis, acute toxicity, antioxidant and antinociceptive activity of new sulfonamides derived from carvacrol

**Aldo S. de Oliveira (PQ),[1*] Inês M.C. Brighente (PQ),[2] Ricardo J. Nunes (PQ),[2] Rosendo A. Yunes (PQ),[2] Catharina Nucci-Martins (PG),[3,4] Adair R.S. Santos (PQ),[3].**

***aldo.sena@ufsc.br**

*[1]Department of Exact Sciences and Education, UFSC; [2]Departament of Chemistry, UFSC, [3]Department of Physiological Sciences, UFSC; [4]Department of Structural and Functional Biology, UNICAMP.*

Key words: Carvacrol, Sulfonamides, Nociception, Antioxidant activity.

## Highlights

We synthesize new sulfonamides derived from carvacrol. Acute toxicity and antioxidant tests were performed. The antinociceptive activity was made through model of pain induced by glutamate.

## Resumo/Abstract

Carvacrol possesses a variety of pharmacological properties.[1] Recently we have reported the preparation of sulfonamides derived from carvacrol, who showed excellent results in antibacterial activity against resistant *S. aureus strains*.[2] From the fifteen compounds synthesized we selected new five (S1-S5, **Scheme 1**), based on the preliminary antioxidant assays, for the verification of acute toxicity and antinociceptive activity.

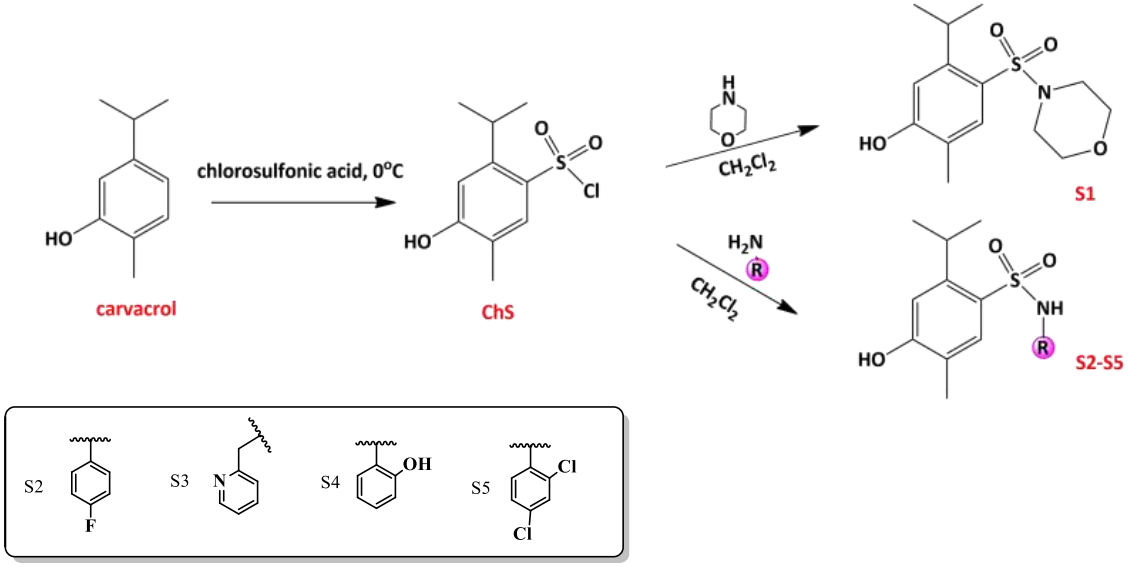


**Scheme 1**. Synthesis of the sulfonamides derived from carvacrol

The compounds showed low toxicity, $DL_{50}$ above 1000 mg/kg. All compounds were active in all tested antioxidant assays: iron chelating activity, reducing power and total antioxidant. The highlight was for the compounds S1 and S4, more active or of activity comparable to BHT and routine.
We used the model of nociception induced by intraplantar injection of glutamate on rats, analyzed the reduction of edema formed and verified the effect on the locomotor activity of the animals (open-field assay). The systemic treatment of rats with the carvacrol and S1-S5 significantly inhibits nociception induced by injection of 20 mmol/ i.pl. glutamate. The compound S1 (0.003 and 0.03 mg/kg, i.g) was only able to reduce paw edema. Thus, S1, S2, S3 and S5 at doses up to 0.03 mg/kg has an interesting potential analgesic to treat acute pain without causing sedation in the central nervous system.

1. de Santana Souza, M. T.; et al. *Biomedicine & Pharmacotherapy* 96: 313–319, 2017.
2. de Oliveira, A. et al. *Journal of Biosciences and Medicines*, 4, 105-114, 2016.

**Área: MED** **Inscrição: 01212**

# Structure-Activity Relationships for a Series of Benzimidazole Derivatives as Cruzain Inhibitors

**Leonardo L.G. Ferreira (PQ)[1], Ivani Pauli (PQ)[1], Mariana L. de Souza (PQ)[1], Glaucius Oliva (PQ)[1], Rafaela S. Ferreira (PQ)[2], Marco A. Dessoy (PQ)[3], Brian W. Slafer (PQ)[3], Luiz C. Dias (PQ)[3] and Adriano D. Andricopulo (PQ)[1]**

**leonardo@ifsc.usp.br; aandrico@ifsc.usp.br**

*[1]Laboratory of Medicinal and Computational Chemistry (LQMC), Physics Institute of Sao Carlos (IFSC) – University of Sao Paulo (USP); [2]Department of Biochemistry and Immunology – Federal University of Minas Gerais (UFMG); [3]Institute of Chemistry – University of Campinas (UNICAMP)*

Keywords: QSAR, *Trypanosoma cruzi*, Cruzain, Chagas Disease.

## Highlights

Cruzain is a validated target for drug discovery. Benzimidazole derivatives were synthesized and evaluated. Chemometric models were built to guide the design of optimized cruzain inhibitors.

## Abstract

Chagas disease affects 8 million people worldwide, mostly in Latin America, causing more than 10,000 deaths per year and putting at risk of infection more than 25 million people. Pharmacotherapy of Chagas disease is restricted to a few options whose inefficacy and associated adverse effects demonstrate the urgent demand for novel, safe and effective drugs[1]. In this study, 3D quantitative structure-activity relationship (QSAR) models were developed for a series of inhibitors of the major cysteine protease from *Trypanosoma cruzi* (cruzain, EC 3.4.22.51)[2] using the Comparative Molecular Similarity Index Analysis method (CoMSIA). The data set consists of 27 molecules synthesized and evaluated in our laboratory, having a benzimidazole core as the mutual substructure. Training and test sets were selected by applying a principal component analysis on the entire series. The molecular alignment was obtained by a structure-based approach, whereby the inhibitors were docked into the binding site of cruzain. The final CoMSIA model, weighted by the standard deviation*coefficient (Stdev*Coeff) region focusing technique, displayed suitable statistical consistency ($r^2$ = 0.98 and $q^2$ = 0.75) and predictive ability for test set compounds ($r^2_{pred}$ = 0.82). The 3D contour plots revealed relevant properties of the inhibitors closely related with their corresponding biological activity (**Figure 1**). These findings support the use of the CoMSIA model to guide the conception of novel cruzain inhibitors within the chemical space delimited by the studied benzimidazole series.

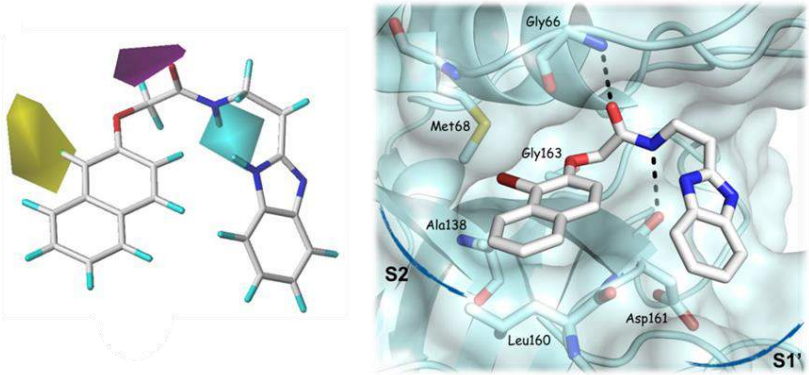


**Figure 1**. Hydrophobic and hydrogen bond donor/acceptor contour maps for a data set inhibitor along with its binding mode in the active site of cruzain. Inhibitor and amino acid residues are shown as sticks, and hydrogen bonds as dashed lines. Yellow, magenta and cyan plots indicate regions where hydrophobic, acceptor and donor groups, respectively, correlate with activity increment.

**References**

1. WORLD HEALTH ORGANIZATION. 2018. Disponível em: <http://www.who.int/chagas/en/>
2. Ferreira, L. G.; Andricopulo, A. D. *Pharmacol. Ther*. **2017**, 180, 49.

**Área: MED** **Inscrição: 01191**

# Identificação de novos candidatos a agentes antitumorais

**Carolina T. Martins (IC),[1] Ellen M.G.Silva (IC),[1] Luma G. Magalhaes (PG),[1] Eduardo B. Mass (PG),[2] Dennis Russowsky (PQ),[2] Adriano D. Andricopulo (PQ)[1]*.**

**carolina.teixeira.martins@usp.br; aandrico@ifsc.usp.br***

*[1] Laboratório de Química Medicinal e Computacional, Centro de Pesquisa e Inovação em Biodiversidade e Fármacos,Instituto de Física de São Carlos, Universidade de São Paulo, São Carlos-SP, Brasil; [2] Instituto de Química, Departamento de Química Orgânica -Universidade Federal do Rio Grande do Sul, Porto Alegre –RS*

Palavras Chave: *Câncer, Planejamento de Fármacos, Ensaios Celulares.*

## Highlights

**Identification of new antitumor candidates**

We present the study of the bioactivity of hybrids of dihydropirimidinone-chalcones, chalcones and dihydropirimidinones under cytotoxicity and migration assays employing a tumor and a normal cell line.

## Resumo/Abstract

O câncer é um conjunto de doenças ocasionadas pela proliferação descontrolada de células anormais do organismo.[1] Apesar de vasta, a terapia atualmente disponível apresenta limitações como alta toxicidade e baixa biodisponibilidade.[2] Nesse contexto, o desenvolvimento de terapias mais seguras e eficazes se faz necessária. Com o objetivo de identificarmos novos candidatos a agentes antitumorais, três séries de compostos (chalconas; dihidropirimidinonas e híbridos de dihidropirimidinonas-chalconas) foram avaliadas em ensaios celulares empregando a linhagem tumoral MDA-MB-231. A citotoxicidade dos compostos foi investigada em células tumorais e normais (HFF1) e a capacidade de inibição da migração celular por meio de ensaios qualitativos (*wound healing*) e quantitativos (câmara de Boyden). Os efeitos dos compostos sobre a organização do citoesqueleto e da cromatina foram investigados por meio de estudos de imunofluorescência. Inicialmente, uma triagem com 15 representantes das três classes químicas estudadas permitiu a identificação de 12 compostos ativos, a exemplo da chalcona **(1)** e do híbrido **(2)**, que se destacaram por sua significativa ação citotóxica (Figura 1). Parâmetros de $CC_{50}$ (concentração citotóxica em que 50% das células estão inviáveis) foram investigados para as linhagens tumoral e não tumoral.

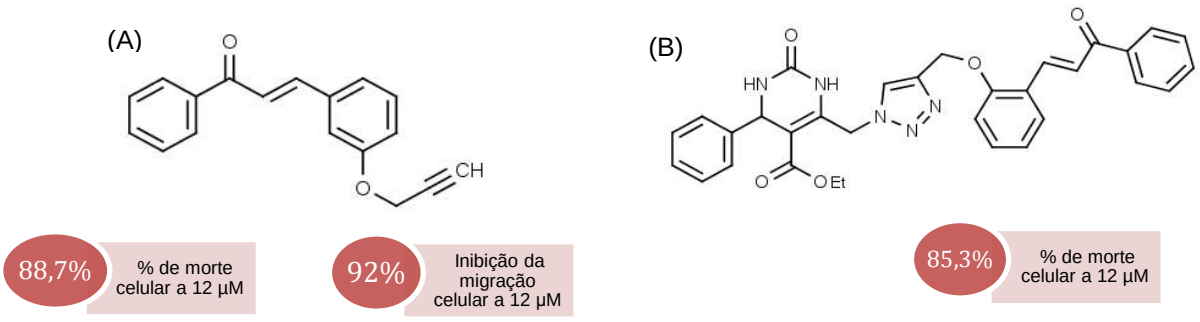


**Figura 1**: A) Composto **1**. B) Composto **2**.

A migração celular é fundamental para o processo de metástase. Desta forma, a capacidade dos compostos em inibir este processo foi avaliada. O ensaio *wound healing* permitiu a identificação de 2 compostos ativos, entre os quais, a chalcona **1** (Figura 1). Os resultados obtidos indicam que as séries estudadas apresentaram *hits* interessantes para o planejamento e síntese de novos ligantes promissores da proteína alvo.

[1] INSTITUTO NACIONAL DO CANCER (INCA). Disponível em: < http://www.inca.org.br> .
[2] AVENDANO, C.; MENENDEZ. J.C.; **Medicinal Chemistry of Anticancer Drugs**. 2008.

**Área: MED** **Inscrição: 01141**

# Screening of the MMV Pathogen Box on *Schistosoma mansoni* juvenile worms for antischistosomal drug discovery

**João M. R. Neto (PG)[1], Walter C. G. Valente (TC)[1], Mônica E. T. A. Chino (TC)[1], Elid F. C. L. Chaves (TC)[1], Mayara K. da S. Santos (IC)[1], Giuliana V. Schirato (PQ)[1], Antônia L. Santos (PQ)[1], Rafael F. Dantas (PQ)[1], Mario R. Senger (PQ)[1], Floriano P. S. Junior (PQ)[1]*.**

**joao.neto@ioc.fiocruz.br; floriano@ioc.fiocruz.br***

*[1]Laboratório de Bioquímica Experimental e Computacional de Fármacos (LaBECFar), Instituto Oswaldo Cruz – FIOCRUZ. Rio de Janeiro-RJ, Brazil.*

Palavras Chave: *Schistosomiasis, Phenotypic Screening, XTT assay, anti-helminthic drug development.*

## Highlights

Seven highly-active anti-juvenile *S. mansoni* molecules were identified. The most active one, a N,N-disubstituted carboxamide is a known anti-onchocercarial. This finding may lead to a broad spectrum anti-helminthic in the future.

## Resumo/Abstract

Schistosomiasis is a helminth infection caused by parasitic *Schistosoma sp*. worms. It is spread over the tropical regions of the world with more than 200 million people affected and an estimated 800 million at risk. The parasite juvenile stage is highly relevant for finding new schistosomicidal compounds because it is more resistant to praziquantel (PZQ), the single drug currently used in chemotherapy. In this study, we used the tetrazolium salt XTT biochemical viability assay on *S. mansoni* juvenile worms to screen the 400 compounds in the pathogen box (PB) from Medicines for Malaria Venture (MMV). Assay standardization demonstrated Z' of 0.40 using 48h of incubation (Figure 1A). At the screening concentration of 10 µM, 36 compounds were identified as hits with seven most-promising compounds presenting 7-23% residual viability and 29 compounds bringing residual viability to 23-43% (Figure 1B). Considering original activity annotation in the PB, 35% acts on tuberculosis, 19% kinetoplastids, 14% schistosomiasis and 13% on malaria. From the schistosomiasis disease set of 12 compounds, only 7 were considered hits in this anti-juvenile screening. From 20 reference compounds (known anti-infectives) tested, 4 were hits using XTT assay: PZQ, mefloquine, posaconazole and benznidazole. Until now, the last 2 drugs have never been described as anti-schistosomal compounds. Finally, the most active compound belongs to the anti-onchocercarial set and it's structure displays a N,N-disubstituted carboxamide carrying hydrophic 4-methoxyphenyl and 2-(6-methylpyridin-2-yl)ethyl moieties. Ongoing follow-up studies include dose-response curves, cytotoxicity and in *vivo* experimental chemotherapy.

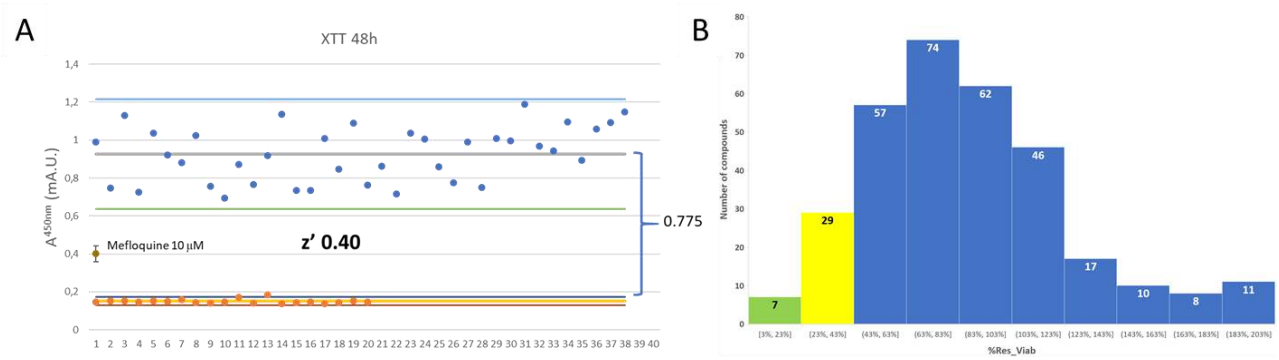


Figure 1: A) Viability measurements for control live (blue dots) and dead (orange dots) juveniles within 48h incubation time with XTT assay reagent, while mefloquine activity was used as internal control. B) Histogram for the percent residual viability of *S. mansoni* after 48h incubation with MMV library (highest activity - green; potential hits - yellow).

**Área: MED** **Inscrição: 01114**

# ADME-T and pharmacokinetic parameters of antitrypanosomal / antitumoral analogues of licarin A

**Thiago R. Morais (PG),[1*] João Paulo S. Fernandes (PQ),[1] Patricia Sartorelli (PQ)[1], André G. Tempone (PQ),[2] Natália Girola (PG),[3] Ana C. B. Fortuna (PQ),[4] Amílcar C. Falcão (PQ),[4] João Henrique G. Lago (PQ).[5]**
**E-mail: thiago_rahal@hotmail.com**

*[1]Instituto de Ciências Ambientais, Químicas e Farmacêuticas – UNIFESP, SP; [2] Centro de Parasitologia e Micologia - Instituto Adolfo Lutz, SP – São Paulo; [3]Departamento de Microbiologia, Imunologia e Parasitologia – UNIFESP, SP; [4]Centro de Neurociências e Biologia Celular – Universidade de Coimbra – Portugal; [5]Centro de Ciências Naturais e Humanas, UFABC, SP.*

Keywords: Pharmacokinetics, PAMPA assay, *blood brain barrier* (BBB), *ex vivo*, antitumoral, antitrypanosomal.

## Highlights

This work reports the preparation and evaluation of antitrypanosomal/antitumoral activity of several semisynthetic derivatives of licarin A. Additionally, bioactive compounds were analyzed by ADME-T and the pharmacokinetic parameters were determined by PAMPA (GIT/BBB). As results, were obtained compounds which could be used as new scaffolds to trypanosomiasis or cancer treatment.

## Abstract

This study aims to present combined techniques to attend pre-clinical screening using a bioactive semisynthetic derivatives of licarin A correlating SAR study and its pharmacokinetics involved as early stage of pre-clinical trials based on ADME-T profiling. Experimentally, were prepared different derivatives of licarin A (**L1**): methyl (**L2**), acetyl (**L3**), allyl (**L4**) and 2-allyl-3-hydroxyl (**L5**) (fig.1) which exhibited antitrypanosomal against trypomastigotes of *T. cruzi* and cytotoxicity against different tumor cells. Among the tested compound, **L5** was most promising derivative due to its antitrypanosomal ($IC_{50}$ = 5.0 ± 0.8 µM) and cytotoxic ($IC_{50}$ = 7.0 ± 0.7 µM - against HL-60 cells) potential compared to positive controls benznidazole ($IC_{50}$ = 16.4 ± 0.9 µM) and cisplatin ($IC_{50}$ = 10.0 ± 1.0 µM). Compounds **L1 – L5** were submitted to *in vitro* screening tests by parallel artificial membrane permeability assays (PAMPA) to evaluate their apparent permeability (Papp) through gastro-intestinal tract (GIT) and blood-brain barrier (BBB) models. Obtained results appointed to 67% of compounds with good to optimal intestinal permeability, especially monomeric units (pharmacophore-like) (Papp > $1.1\times10^{-6}$ cm/s), and 46% of these are also expected to exhibit good permeability through blood-brain barrier (Papp > $2.0\times10^{-6}$ cm/s). These findings are consistent to a rational design with a high transport rate by passive transcellular pathway. Although, another experiment were performed using chamber apparatus (Ussing), assembled with mouse intestine segments, an *ex vivo* method. Then bioactive compounds were Papp measured (n = 3) by quantitative UFLC, and was observed that monomers were well absorbed through the membranes than corresponding lignans. Moreover, a set of *in silico* tool SwissADME were run in comparison to previously *in vitro* experiments. Those results also suggested a low extent of plasma protein binding for most compounds (Papp<$1.0\times10^{-5}$cm/s), and these findings were also supported by *in silico* data. In both PAMPA models, compound **L5** represented the most promising derivative and should be considered in the subsequent studies of the development of new structurally related drug candidates. Further cell-based experiments will be executed about cell death pathway and correlated parasitic mechanisms of action to assess their interference on the efflux transporters *e.g.* permease glycoprotein (P-gp) and BCRP, helping understand more about drug resistance and molecular targeting on Drug Delivery systems.

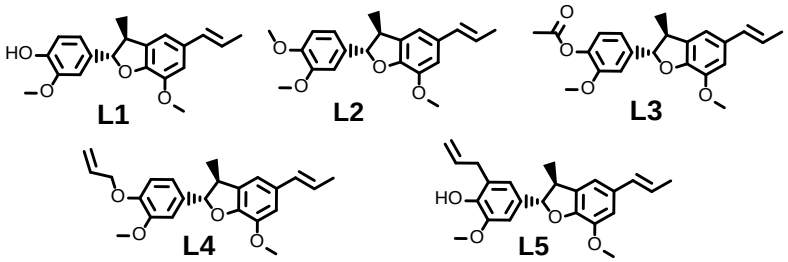


Figure1. Licarin A (**L1**) and semissynthetic derivatives.

**Acknowledgments**: FAPESP, CNPq and CAPES (PDSE n. 88881.134147/2016-01).

**Área: MED** **Inscrição: 01084**

# A new 3-nitro-1,2,4-triazole derivative is more potent and selective than benznidazole against *Trypanosoma cruzi*

**Frederico S. Castelo-Branco (PQ),[1] Rodolfo R. F. França (PG),[1,2] Cheyene A. C. Menozzi (PG),[1,2] Mayara dos Santos Baptista (IC),[1] Policarpo Ademar Sales Júnior (PQ),[3] Silvane Maria Fonseca Murta (PQ),[3] Álvaro José Romanha (PQ),[3] Angelo da Cunha Pinto (PQ) (*in memoriam*),[4] Nubia Boechat (PQ).[1]***

**frederico.branco@far.fiocruz.br; nubia.boechat@far.fiocruz.br**

*[1]Departamento de Síntese de Fármacos, Farmanguinhos/FIOCRUZ; [2]Instituto de Ciências Biomédicas, UFRJ; [3]Laboratório de Parasitologia Celular e Molecular - CPqRR/FIOCRUZ; [4]Instituto de Química, UFRJ.*

Keywords: Nitrotriazole, Azole, *Trypanosoma cruzi*, Chagas disease.

## Highlights

A novel 3-nitro-1,2,4-triazole derivative (**6**) showed potent activity against *Trypanosoma cruzi*, being more selective and almost 4-fold more potent than the reference antichagasic drug benznidazole.

## Abstract

The aim of this work was the development of substances containing 1,2,4-triazole, 3-nitro-1,2-4-triazole and 2-nitroimidazole nuclei to evaluate the contribution of these heterocycles to the activity against *Trypanosoma cruzi* (Tc), the causative of Chagas disease. Such compounds were based on the structure of substance **1** and fluconazole, substances with important anti-Tc activity,[1] as well as benznidazole, the reference antichagasic drug (Fig.1). The derivatives were obtained through a simple two or three-step route. The *in vitro* evaluation was carried out in an intracellular model containing both amastigote and trypomastigote forms of Tc. The results showed that the 3-nitro-1,2,4-triazole nucleus promotes higher potency than 2-nitroimidazole, in addition, both are superior to 1,2,4-triazole, emphasizing that the presence of the nitro group is important for anti-Tc activity. Another interesting result is that when the derivatives had their carbonyls reduced to hydroxyls, there was an increase in anti-Tc potency. The derivatives containing the biphenyl moiety are in biological evaluation at the present date. The most promising substance in the series was the 3-nitro-1,2-4-triazole derivative **6** with the hydroxyl derivative, whose $IC_{50}$ was 0.39 μM, being approximately 4-fold more potent than benznidazole. In addition, this derivative showed low cytotoxicity, with $CC_{50}$ of 1200 μM, which led to a high selectivity index of 3080, more than twice as high as benznidazole.

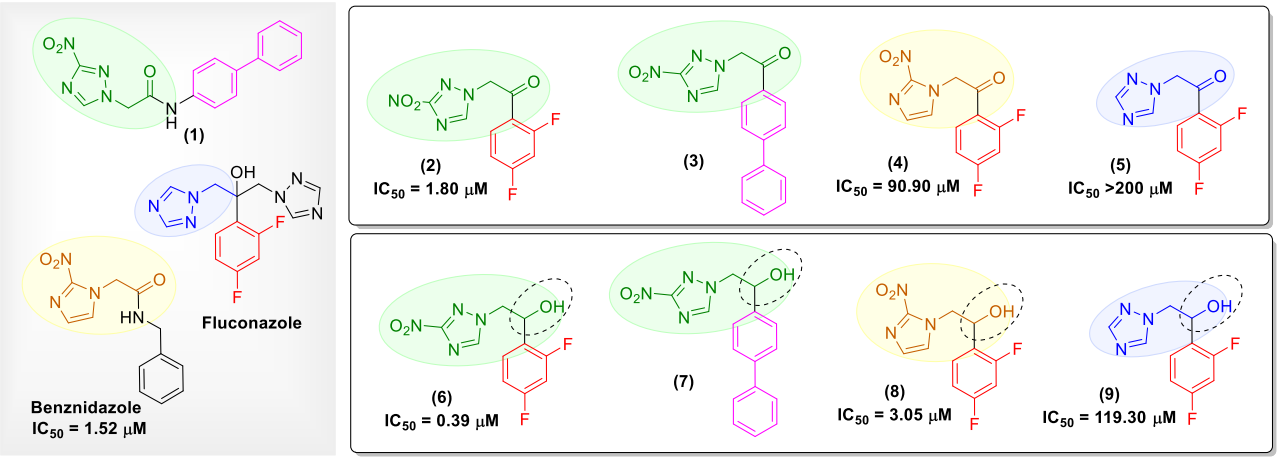


**Figure 1.** Design of the azolic compounds and their activity against Tc.

**Acknowledgments**: FAPERJ, CNPq.

[1] Papadopoulou, M.V. *et al. J. Med. Chem*. **2015**, 58, 1307.

**Área: MED** **Inscrição: 00997**

# Analysis of the biological activity of antidiabetic compounds using CoMFA models

**Simone Q. Pantaleão (PG),[1*] Angélica N. Lima (PQ),[1] Eric A. Philot (PQ),[2] Ana Lígia Scott (PQ),[2] Káthia M. Honório (PQ).[1,3]**

*simone.queiroz@ufabc.edu.br

*[1]Centro de Ciências Naturais e Humanas, UFABC; [2]Centro de Matemática, Computação e Cognição, UFABC; [3]Escola de Artes, Ciências e Humanidades, USP.*

Key words: (*Diabetes, DPP-4, Docking, CoMFA*).

## Highlights

Diabetes is a chronic disease involving failures in insulin production, compromising the glucose transport. Such process is signaled by incretins known as GLP-1 and GPI, which are degraded by the DPP-4 enzyme.

## Abstract

As a prerequisite for obtaining the bioactive conformations of the 54 molecules of interest, the docking technique was employed using GOLD[1] program. After obtaining the alignment, the PLS (Partial Least Squares) technique was used to perform the CoMFA analyzes and to generate the values of $r^2$ (regression coefficient) and $q^2$ (correlation coefficient with crossvalidation) using the Sybyl $X^2$ package. The internal validations were performed using the leave one out (LOO) method. The parameters tested for the distances between grid points were: 0.5; 1.0; 1.5 and 2.0Å; and the weight values (w) were: 0.3, 0.5, 0.7 and 0.9; checking without/with region focus. The parameter that was the most adequate for the construction of the model consisted of distance equals to 1.0 Å and the weight of 0.5 between the points of the grid. The next step was to separate the training and test sets to verify the predictive capacity of the model (42 molecules in the training and 12 structures in the test sets). The MATLAB[3] package was used for splitting the compound sets. The best model was the one obtained with w = 0.5 and d = 1.0Å ($q^2$ = 0.863 and $r^2$ = 0.991); the stereochemical and electrostatic fields were calculated with Lennard-Jones and Coulomb potentials. By analyzing the contour maps for the least (molecule 1) and the most active (molecule 40), the contribution regions of these ligands for the biological activity in the DPP-4 enzyme were identified, which will aid in the design of new bioactive ligands.

## References

[1]Jones, G.; Willett, P.; Glen, R. C.; Leach, A. R.; Taylor, R., Development and validation of a genetic algorithm for flexible docking. Journal of molecular biology 1997, 267 (3), 727-748.
[2]Sybyl-X Molecular Modeling Software Packages, Version 2.0. TRIPOS Associates, Inc; St. Louis, MO, USA: 2012.
[3]Gilat, A., MATLAB: An Introduction with Applications. Wiley, 2004.

## Acknowledgments

The authors would like to thank FAPESP, CAPES and UFABC for the financial support.

**Área:** MED **Inscrição: 00917**

# DESIGN, SYNTHESIS AND ANTI-*PLASMODIUM FALCIPARUM* ACTIVITY OF NOVEL BIS-TRIFLUOROMETHYLQUINOLINES DERIVATIVES

**Marília Oliva Gandi (IC),[1,2] Alcione Silva de Carvalho (PQ),[2] Jorge Souza Mendonça (PQ), [2] Antoniana Ursine Krettlie (PQ) [3] e Núbia Boechat[2]* (PQ).**

**alcione.carvalho@far.fiocruz.br; nubia.boechat@far.fiocruz.br***

*[1]Faculdade de Farmácia UNIG; [2]Departamento de Síntese de Fármacos, FIOCRUZ; [3] Laboratório de Malária, René Rachou, FIOCRUZ*

Palavras Chave: *Bis-trifluoromethylquinolines; Trifluoromethylquinolines; Adducts; Anti-Plasmodium falciparum; Antimalarilal.*

## highlights

Preliminar *in vitro* assay of novel bistrifluoromethylquinoline indicate that this system to be promising for the planning of a leader with anti-*plasmodium* agent due to have shown excelent activity.

## Resumo/Abstract

A OMS preconiza a quimioterapia combinada à base de derivados de artemisinina com as quinolinas (ACT) no combate contra o *P. falciparum,* como **ASAQ** ou **ASMQ** (Fig.1).[1,2] Entretanto, apesar do avanço da quimioterapia, já existem cepas resistentes aos medicamentos.[1,2] O planejamento, a síntese e a avaliação anti-*plasmodium* de novos 2,8-bis(trifluorometil)quinolínicos (**1-3**), objetivo alvo do presente trabalho, foi proposto com intuito de investigar a importância desses novos compostos para atividade anti-*plasmodium,* já que existem resultados promissores de sistema bisquinolínico com alta atividade antimalarial [3] (Fig 1).

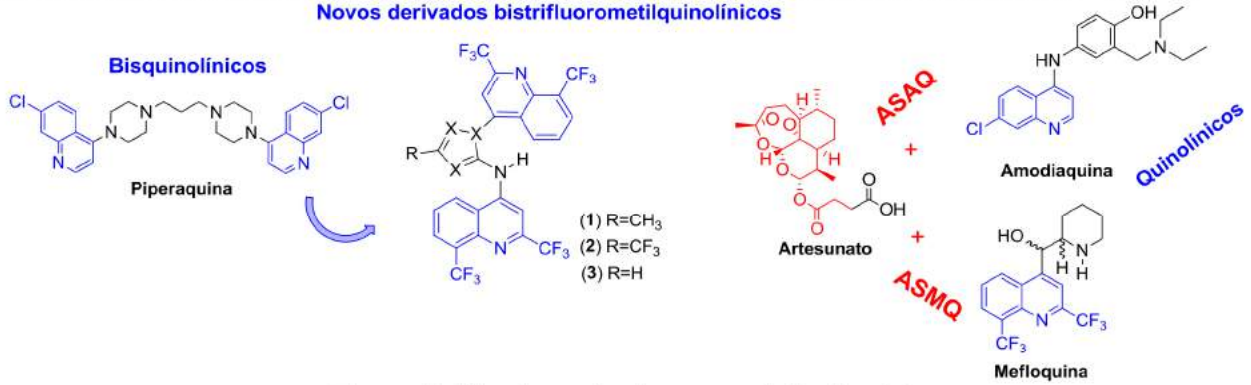


**Figura 1:** Planejamento dos novos derivados **1-3**.

Os compostos **1-3** foram sintetizados a partir da reação de condensação e ciclização da 2- trifluormetilanilina com 4,4,4-trifluoroacetoacetato de etila, seguida da reação de cloração com oxicloreto de fósforo fornecendo o intermediário-chave clorado. Este foi então convertido aos produtos finais **1-3** pela reação de substituição nucleofílica aromática do intermediário clorado com os respectivos aminos recém preparados. A avaliação *in vitro* da atividade contra o clone $W_2$ de *P. falciparum* dos novos derivados **1-3,** a atividade da citotoxicidade em células renais de macaco e o Índice de Seletividade (IS) estão em andamento. Analisando os resultados preliminares do composto **1** mostrou ser uma substância bastante promissora, devido ter apresentado a atividade anti-*Plasmodium falciparum* em escala nanomolar e com alto IS. Cabe ressaltar, que o protótipo mefloquina é em escala micromolar.

**Agradecimentos:** FAPERJ; CIEE; FARMANGUINHOS; FIOCRUZ.

**Referências:**

1-https://www.dndi.org/diseases-projects/malaria/
2-http://www.who.int/malaria/publications/world-malaria-report-2016/report/em/
3- Alistair J. Fielding *et al*, (2017) *Chem. Eur. J.*, *23*, 6811

**Área: __MED_____ Inscrição: _00851__**

# Construction and Validation of 3D Chemical Similarity Models of Triclosan

**Philipe de Oliveira Fernandes (IC),[1] Isabella D. Franco (IC),[2] Vinícius G. Maltarollo (IC),[2].**

**philipe.of@gmail.com**

*[1]Departamento de Química, Instituto de Ciências Exatas, Universidade Federal de Minas Gerais; [2]Departamento de Produtos Farmacêuticos, Faculdade de Farmácia, Universidade Federal de Minas Gerais*

Palavras Chave: *Molecular Modelling, 3D Similarity Chemical Model, Antimicrobial, Triclosan.*

## Highlights

3D chemical similarity models were created and validated based on triclosan analogs, and the results showed high values of AUC and accuracy. Hypothesis tests demonstrate the importance of each color feature present in these models.

## Resumo/Abstract

Antimicrobial resistance is a global healthcare problem, that is why the development of new drugs which act through different modes of action is crucial. Triclosan is a widely used broad spectrum antibacterial and is considered interesting because it works in the fatty acid biosynthesis II pathway, present only in bacteria. This research focused on building and validating 3D similarity models for applying in a drug design campaign for new active compounds.

The queries were built from the three most actives compounds present in Gerusz's work[1] using the lower energy conformers obtained with OMEGA. These queries were constructed exhaustively, reaching all combinations using vROCS, to evaluate how the features present in the models influence the ability of distinguish active compounds ($IC_{50}$ < 1 µM) from inactive compounds ($IC_{50}$ > 1 µM) and decoys (1:36 proportion for each active compound). The best models were submitted to a confusion matrix. All results were used in statistical analysis.

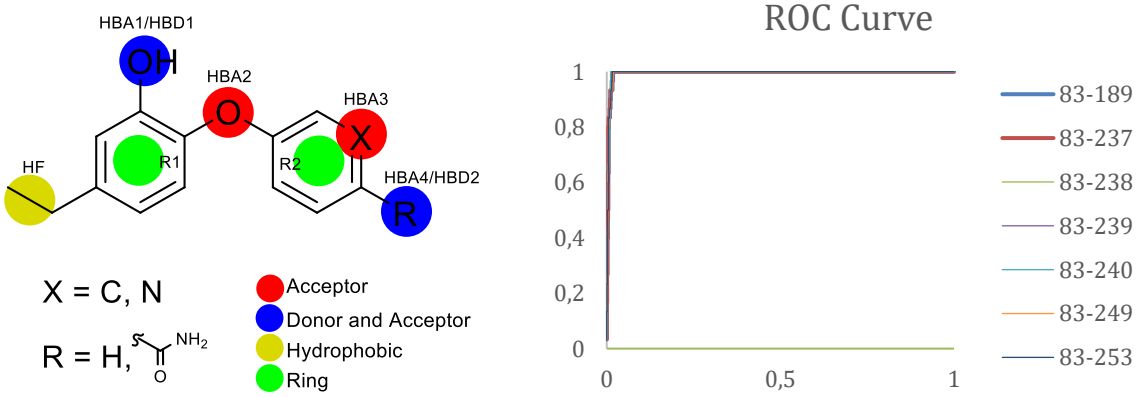


Figure: Features of models and ROC curve with the seven best queries

448 queries were created and validated, deleting features presents (hydrophobic groups, rings, hydrogen bond acceptor and donor). The queries analysis was based on the area under the ROC curve (AUC) values (0,996) and accuracy (>97%). The Mann-Whitney test indicates that HF, HBD1, HBA2, HBD2 e HBA 4 groups are important for increase AUC and enrichment values. The authors would like to thank OpenEye Scientific Software for the academic license, CNPq and FAPEMIG funding.

**Reference**

1) Gerusz et al, *Journal of Medicinal Chemistry* 2012, 55, 991

**Área:** *MED* **Inscrição:** 0836

# Planejamento, síntese e avaliação biológica de novos derivados carbohidrazonamidas candidatos a protótipos tripanocidas

**Mayara Salles Souza do Nascimento[1,2] (PG); Raíssa Lamin Teixeira[3] (IC); Juliana M. Chaves Barbosa [4] (IC); Kelly Salomão[4] (PQ); Solange C. Lisboa[4] (PQ); Samir A. Carvalho[1] (PQ); Edson F. da Silva[1,3] (PQ); Carlos Alberto Manssour Fraga[2]* (PQ)**

*[1]Fiocruz- Fundação Oswaldo Cruz, Instituto de Tecnologia em Fármacos – Farmanguinhos, Rio de JaneiroRJ; [2]Universidade Federal do Rio de Janeiro; Instituto de Ciências Biomédicas; Rio de Janeiro, RJ; [3]Unigranrio – Universidade do Grande Rio, Duque de Caxias, Rio de Janeiros, RJ; [4]Fiocruz- Fundação Oswaldo Cruz; Laboratório de Biologia Celular, Instituto Oswaldo Cruz, Rio de Janeiro, RJ.*

edson.ferreira@far.fiocruz.br; cmfraga@ccsdecania.ufrj.br

***Palavras Chave:*** *Carbohidrazonamidas, Atividade Tripanocida, Doença de Chagas*

## Highlights

Planning, synthesis and biological evaluation of new carbohydrazonamide derivatives candidates for trypanocidal prototypes

The five new compounds were avaluated against *T. cruzi*. Thus, we can identify two compounds (4) [$IC_{50}$= 9,5 µM] and (5) [$IC_{50}$= 12,9 µM], which showed significant activity when compared to benznidazole [$IC_{50}$= 10,3 µM].

## Resumo/Abstract

A doença de Chagas (DC) ou a tripanossomíase americana é uma doença parasitária importante causada pelo parasito hemoflagelado *Trypanosoma cruzi*[1]. De acordo com a OMS, há 5-6 milhões de pessoas contaminadas e cerca de 70 milhões de pessoas estão em áreas de risco. Esta doença mata mais de 7.000 pessoas por ano na América Latina1. Nifurtimox (Nf) e benznidazol (Bz) são os únicos dois fármacos utilizados no tratamento de DC[2]. Portanto, o planejamento estrutural foi feito com base na ferramenta de Hibridação Molecular de 5-nitroimidazole e N-acil-hidrazona para potencializar a atividade tripanocida. Assim, este trabalho visa o planejamento, síntese e avaliação bilógicas de novos derivados carboidrazonamidas funcionalizadas, candidatos a protótipos tripanocidas. Foram sintetizados 5 novos derivados de carbohidrazonamida em rendimentos razoáveis, utilizando reações clássicas de química orgânica. Os intermediários, assim como os 5 novos derivados, foram caracterizados por técnicas de análises. Os novos derivados foram avaliados contra *T. Cruzi*, na forma tripomastigotas, tabela 1. Assim, podemos identificar dois compostos (4) [$IC_{50}$ = 9,5 µM] e (5) [$IC_{50}$ = 12,9 µM], os quais mostraram atividades significativas quando comparados ao padrão benznidazol [IC50 = 10,3 µM].

**Tabela 1: Atividade tripanocida "*in vitro*" sobre a forma tripomastigota de *T. cruzi* (cepa Y), e citotoxicidade sobre células de macrófagos peritoneais de camundongos suíços, das novas carboidrazonamidas**.

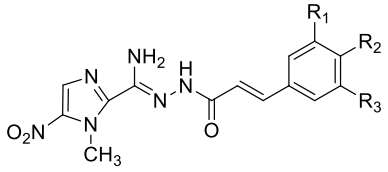


(1-5)

| | $R_1$ | $R_2$ | $R_3$ | *T.cruzi* [a] | Macrófagos | IS |
|---|---|---|---|---|---|---|
| **1** | H | F | H | 120,60 ± 14,69 | 98,33 ± 16,07 | 0,81 |
| **2** | H | Cl | H | 127,04 ± 14,69 | 21,30 ± 2,60 | 0,16 |
| **3** | H | Br | H | 119,70 ± 18,91 | 185,00 ± 21,79 | 1,54 |
| **4** | H | $NO_2$ | H | 9,50 ± 1,15 | 79,69 ± 25,24 | 8,38 |
| **5** | H | OH | H | 12,85 ± 1,94 | 423,33 ± 58,38 | 32,94 |
| **Bnz** | - | - | - | 10,26 ± 1,36 | >4000 | >389,86 |

ND = Não determinado, IS = índice de seletividade, [a] $IC_{50}$ µM.

[1] RASSI, A. Jr., *et al*. Infect. Dis. Clin. North Am. **2012,** v.26, p. 275-91,.

[2] WILKINSON, S.R., *et al.* Curr. Top. Med. Chem**. 2011,** v.11,p. 2072-2084, 2011

**Área: MED** **Inscrição: 00738**

# Interaction models of the protein Phosphoethanolamine Methyltransferase from *Haemonchus contortus* relating drugs and lignans through molecular docking

**Aline Féboli (PG),[1]* Alexandre Borges (PQ),[2] Rosangela da Silva de Laurentiz (PQ)[1]**

**alinefeboli23@gmail.com**

[1]*Departamento de Física e Química, UNESP - Universidade Estadual Paulista - Faculdade de Engenharia de Ilha Solteira*
[2] *Pós-Doutorando – Faculdade de Ciências farmacêuticas – Universidade de Campinas*

Palavras Chave: *Anti-helmínticos naturais, Hinoquinina, Albendazol, Docking consensual.*

## Highlights

Natural products as alternative to synthetics anthelmintic to control parasitosis gastrointestinal in sheep
Anthelmintic activity of lignans from Piper cubeba
Interaction models of the protein-albendazole and protein-lignans

## Abstract

Alternatives to the use of synthetic anthelmintics to control parasitosis in sheep, mainly caused by the nematode *Haemonchus contortus*, have been studied, among them, the use of natural products [1]. In vitro studies with the cubebin, dihydrocubebin and hinokinin, lignans isolated from *Piper cubeba*, against eggs and different larval stages of *H. contortus* demonstrated the action of these lignans, with hinokinin being the most effective ($IC_{50}$ <70 µg / mL) without differences with the albendazole control. Molecular docking studies of lignans and albendazole (as an interaction model) were performed using Phosphoethanolamine methyltransferases (PDB 4KRG), which acts on the synthesis of the cell membrane of the nematode. The consensual docking study used the Maestro 10.1 and GOLD 5.1 softwares. The results of the overlap of the poses (fig.1) obtained from albendazole and lignans showed that they occupy the same region of the active site of protein. Cubebin presented a different interaction model of albendazole, presenting in common the hydrophobic interaction with Leu124. The hinokinin presented an interaction model similar to albendazole with hydrophobic interaction Phe81, Leu124 and hydrogen bonding Asp105, as well as dihydrocubebin with hydrophobic interaction with Phe81, Leu124 and hydrogen bonding with Asn124. These results demonstrate that the *in vitro* action of these two lignans may be related to the deactivation of this enzyme according to the model of interaction of albendazole.

Figura 1: Overlap of consensual docking poses, albendazole (blue), cubebin (green), dihydrocubebin (magenta) and hinokinin (gray).

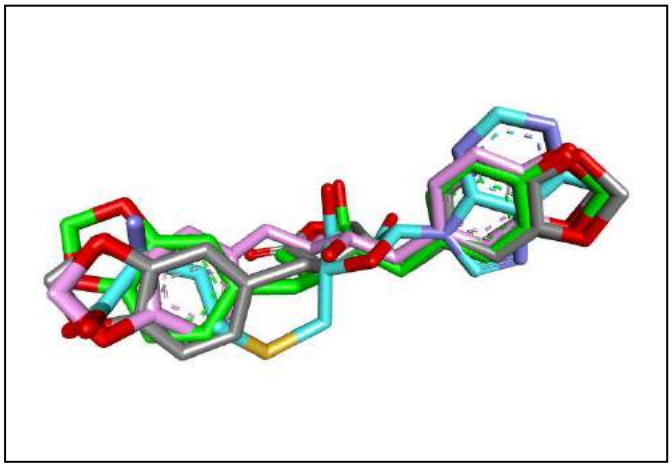

**References:** [1] W. H. Witola; K. Matthews; M. McHugh. International Journal for Parasitology. 6 (2016) 44-53.

**Área: MED** **Inscrição: 00674**

# PLASMONIC PHOTOTHERMAL CANCER THERAPY WITH REDUCED GRAPHENE OXIDE CORE/SHELL NANOCOMPOSITES

**Kostiantyn Turcheniuk (PG),[1] Tetiana Dumych (PG),[1] Rostyslav Bilyy (PG),[2] Mykhailo Nazarkovskyi (PG),[3] Volodymyr Zaitsev (PQ)[3]*.**

**vnzaitsev@puc-rio.br**

*[1]Institut d'Electronique, de Micro´electronique et de Nanotechnologie Universit´e Lille1; [2] Lviv National Medical University, Ukraine; [3] PUC-Rio, Brazil*

Palavras Chave: *Plasmonic cancer therapy, reduced graphene oxide, Au nanorods, functional nanocomposites*

## Highlights

Photothermal conversion and anticancer efficiency of core/shell metal nanoparticles (NPs) is improved by changing the particles geometry and composition. Au nanorods and bimetallic AuPd nanoparticles covered with reduced graphene oxide is greatly improved the solubility and anticancer efficiency.

## Resumo/Abstract

Gold nanoparticles (Au NPs) and reduced graphene oxide (rGO) mediated hyperthermia are the two most widely explored systems used for the photothermal ablation of cancer cells. We show that the photothermal conversion and efficiency of these nanomaterials can be improved not only by combining them into one material, but also by changing the particles geometry, forming Au nanorods or bimetallic AuPd nanoparticles. The Au and AuPd NPs were covered with rGO and covalently functionalized with poly(ethylene glycol) (PEG) chains. It is greatly improved the solubility and stability of the nanocomposites in biological media and ensured its biocompatibility towards cancer cells. We show that Au NRs@rGO-PEG are ideal multifunctional theranostic nanostructures that can exert efficient photothermal destruction of tumors in mice upon low doses of NIR light excitation and can act as fluorescent cellular markers due to the presence of a NIR dye integrated onto the rGO shell. The nanocomposite was successfully used for the in vitro photothermal ablation of HeLa cells. At 1 W $cm^{-2}$, the total killing of HeLa cells was achieved through irradiation nanocomposites incubated cells for 10 min at a particle concentration of 20 mg $mL^{-1}$.

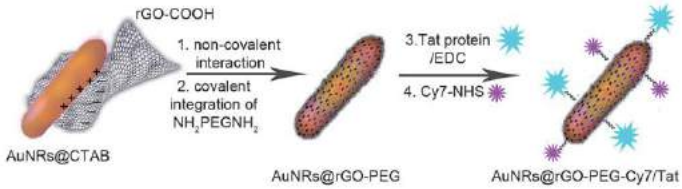


Illustration of the preparation of pegylated fluorescently labeled, Tat-protein modified Au NRs@rGO-PEG-Tat/Cy7

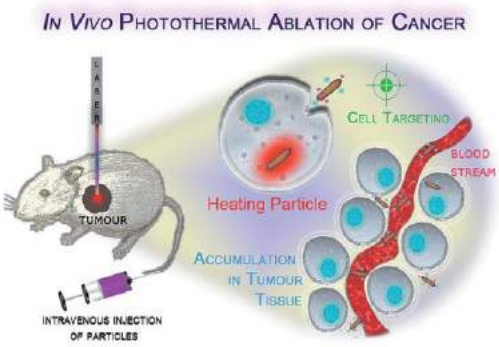

**Área: MED** *(Inserir a sigla da seção científica para qual o resumo será submetido. Ex: ORG, BEA, CAT)*

**Inscrição: 00635** *(Inserir o número de inscrição do autor que fez a submissão)*

# Blind docking and Semi-Empirical Studies of β-Tubulin Inhibitors

**Harold H. Fokoue (PQ),[1]Teiliane R. Carneiro (PQ),[1] Eliezer J. Barreiro (PQ),[1] Lídia M. Lima (PQ), [1]Carlos M. R. Sant'Anna (PQ) [1,2]**

**hfokoue@gmail.com; santanna@ufrrj.br**

*[1]Instituto Nacional de Ciência e Tecnologia de Fármacos e Medicamentos (INCT-INOFAR; http://www.inctinofar.ccs.ufrj.br/), Laboratório de Avaliação e Síntese de Substâncias Bioativas (LASSBio®, http://www.lassbio.icb.ufrj.br) Universidade Federal do Rio de Janeiro, CCS, Cidade Universitária, Rio de Janeiro-RJ, Brasil*
*[2]Departamento de Química, Universidade Federal Rural do Rio deJaneiro, Seropédica 23890-000, RJ, Brasil.*

Palavras Chave: *Tubulin, Cytotoxic activity, Cancer, CA4, Blind docking Study, sulfur-oxygen interactions*.

## Highlights

Blind docking studies are indicative that tubulin polymerization modulators Combretastatin-4, LASSBio-1586 and LASSBio-1920 bind almost exclusively to the colchicine-binding site of tubulin. Intermolecular sulfur-oxygen interactions enhanced LASSBio-1920 inhibition.

## Resumo/Abstract

Combretastatin-A4 (CA-4), a natural product, is known for its anti-tumor activity due to its antitubulin properties. CA-4 displays nanomolar cytotoxic activity and its mechanism of action involves reversible, high affinity binding to the colchicine site of tubulin.

The ability of compounds CA-4, LASSBio-1586 and LASSBio-1920 to modulate tubulin polymerization was verified by studying their effects on microtubule dynamics, employing the tubulin polymerization assay kit (BK006P). In a concentration of 10 µM CA-4, LASSBio-1586 and LASSBio-1920 induced 70%, 65% and 75% respectively the tubulin polymerization[1].

Blind docking studies with the Swiss Dock server predicted that all three ligands bind almost exclusively to the colchicine binding site of tubulin (PDB code 1SA0), with the most stable interaction poses, according to the Gibbs free energy for interaction ($\Delta G_{int}$) at that site (Figure 1A-C). The best values of $\Delta G_{int}$ of CA-4, LASSBio-1586 (7a), LASSBio-1920 (7h) were, respectively, -8.49 kcal/mol, -8.41 kcal/mol and -8.81 kcal/mol, in qualitative accordance with the observedtubulin polymerization data[1].

We performed semi-empirical studies using MOPAC2016, with PM7 method, to calculated the enzyme-ligand interaction enthalpies for CA-4 ($\Delta H_r°$=-41.93 kcal/mol), LASSBio-1586 ($\Delta H_r°$=-36.41 kcal/mol) and LASSBio-1920 ($\Delta H_r°$=-39.07 kcal/mol). The calculated logP with Percepta were, respectively, 2.93, 2.43 and 3.25.It seems that the liposolubility is important for the tubulin polymerization.We also observed that only LASSBio-1920 and *N*-deacetyl-*N*-(2-mercapto-acetyl)colchicine (DAMA-colchicine) trimethoxy-phenyl groups are orientedso as to establish intermolecular sulfur-oxygen interaction[2] with the sulfur atom of Cys241B (Figure 1A-C), a kind of interaction that is now being recognized as very important in biological systems.

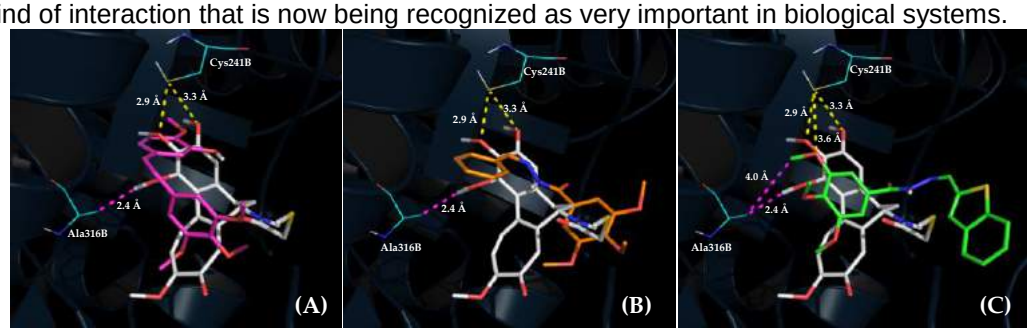


**Figure 1.** Superposition of the DAMA-colchicine (C atoms in white) structure co-crystalized with beta tubulin (cartoon representation, PDB code: 1sa0) and the more stable blind docking poses of CA-4 (carbon atoms in magenta) (**A**), LASSBio-1586 (orange, **7a**) (**B**) and LASSBio-1920 (green, **7h**) (**C**) in colchicine binding site.Sulfur is represented in yellow, oxygen in red, nitrogen in blue; interaction between sulfur and oxygen atoms as dashed yellowlines and hydrophobic interactions as dashed magenta lines[1].

**References:** [1]*Lett. Drug. Des. Discov.*, **14**, 1, 2017; [2]*J. Chem. Inf. Model.*, **55**, 2138, 2015.
**Acknowledgements:** FAPERJ, CAPES, INCT-INOFAR

**Área: MED** **Inscrição:569**

# Drug Design based on vouacapanic derivative with antileukemic activity

**Cleison Carvalho Lobato* (PG),[1,2,3] Rosivaldo dos Santos Borges (PQ),[2,3] Carlos Henrique Tomich de Paula da Silva (PQ),[3,4] Cleydson Breno Rodrigues dos Santos (PQ),[2,3,4]**

**breno@unifap.br; cleison@unifap.br**

*[1]Colegiado de Ciências Biológicas, Campus Binacional-Oiapoque, Universidade Federal do Amapá; [2]Laboratório de Modelagem e Química Computacional, Universidade Federal do Amapá; [3]Programa de Pós-Graduação em Química Medicinal e Modelagem Molecular, Universidade Federal do Pará; [4]Laboratório Computacional de Química Farmacêutica e Ensaios Biológicos, Universidade de São Paulo-Ribeirão Preto.*

**Keywords:** *Drug-design; Chronic myeloid leukemia; Virtual screening; Molecular docking.*

## Highlights

Virtual Screening is used on compounds selection through structural similarity. Molecular docking shows the way of ligand-receptor interactions. Also, pharmacokinetic and toxicological properties was predicted.

## Abstract

Leukemia is a neoplasm of hematopoietic tissue originating from the bone marrow and can be classified according to the cell line involved as myeloid and lymphoid. The studies have evidenced the essential role of the control of BCR-ABL tyrosine kinase activity for the treatment of chronic myelogenous leukemia (COWAN-JACOB et al., 2007). The main objective of this work is drug design that act as inhibitors of ABL tyrosine kinase activity, responsible for the proliferation of these tumor cells. Among the naturally occurring compounds with activity in K562 chronic myeloid leukemia tumor cells, the vouacapanic derivative 16-(N,N-Diethylamino)methylene-6α-hydroxivouacapan-7β,17β-lactone has such proven biological activity (EUZEBIO et al., 2010). Virtual screening was performed to obtain similar structures from the vouacapanic derivative with potential activity in the K562 cells. The structures obtained by virtual screening were submitted to studies of predictions of pharmacokinetic and toxicological properties, as well as, molecular docking study with the BCR-ABL tyrosine kinase receptor, extracted from the protein databank (PDB ID 1IEP) to predict the binding affinity between the protein-ligand complexes. A compound which showed the better binding affinity was ZINC38664626**,** has had good pharmacokinetic and toxicological parameters, showing to be a promising compound to be used as a drug.

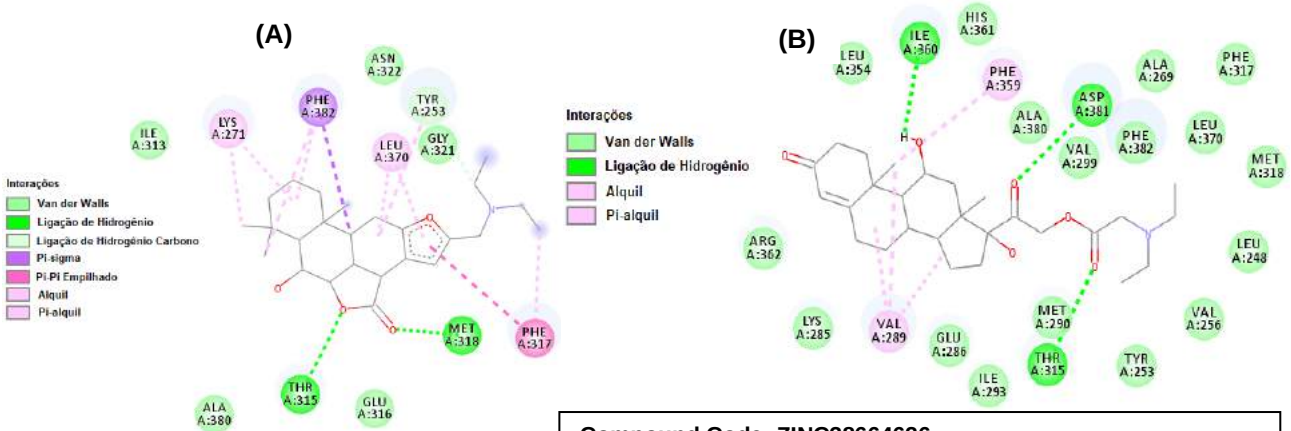


**Compound Code: ZINC38664626**
Binding Affinity: -13.7 kcal/mol
QikProp Properties: Percentage of Human Oral Absorption – 72%
Caco-2 permeability – 50.930
MDCK cell permeability – 21.909
$LogP_{o/w}$ – 2.377
#stars - 0

**Figure 1.** Representation of the modes interactions proposed through studies of docking simulations in two dimensions for 16-(N,N-Diethylamino)-methylene-6α-hydroxivouacapan-7β,17β-lactone (A) and ZINC-38664626 (B) and results obtained in the studies of pharmacokinetic predictions, for ZINC-38664626, obtained with the program QikProp

**Área: MED** **Inscrição: 00552**

# Sirtinol analogues design and molecular docking in the search for *Trypanosoma cruzi* Sirtuin 2 inhibitors

**Evelin Fornari Pereira, (PG)[1*]; Glaucio M. Ferreira, (PG)[1]; Wítor Ferraz, (IC)[1]; Gustavo H. G. Trossini, (PQ)[1]. evelin.fornari@usp.br**

[1]*Faculdade de Ciências Farmacêuticas da Universidade de São Paulo, São Paulo, Brasil.*

Palavras Chave: *Chagas' disease, Docking, Sirtuin 2, LBDD.*

## Highlights

Analogues of sirtinol designed and molecular docking study using LBDD (ligand based drug design) to inhibit the enzyme Sir2 *for Trypanossoma cruzi* as antichagasic candidates.

## Resumo/Abstract

Neglected diseases are caused by infectious and parasitic agents. These diseases are prevalent in tropical areas and poor and in developing countries have been presenting medical relevance. Among the negleted diseases, Chagas' disease is endemic in Latin America and has spread to other continents by migratory movements. Actually, there are only two drugs available to the treatment - Nifurtimox and Benznidazole, but they are effective only in the acute phase of disease and they present several side effects. The research of new antichagasic agents at the national and international levels and in the majority carried out academically, no therapeutic alternatives for the disease have been found yet, thus persisting the urgent need for the discovery and development of new antichagasic agents. The currently strategy in drug discovery involves the choice and selection a specific biochemistry target. In case, sirtuin 2 (silent information regulator 2) were shown to be essential for the in vitro growth of T. cruzi. As reported that trypanosomatids in general, overexpression of Sir2 is related to the survival of amastigotes forms. Sir2 inhibitors like sirtinol showed efficacy against *T. cruzi* growth. Thus, these evidences indicate that the Sir2 of trypanosomatids can be considered as biological targets in the search and development of new antichagasic drugs. In this study we used ligand based drug design (LBDD) to planning sirtinol analogues Sir2 candidates. To understand the correlation among 12 designed analogues and Sir2 protein were performed docking studies in the Sir2 model preview models constructed by our group. These analogues were built substituting 1-phenylethanamine for other primary amines. The docking studies show that the analogues are presenting a good complementarity with Sir2 active site. These results suggest that new designed molecules can be Sir2 inhibitors and antichagasic candidates.

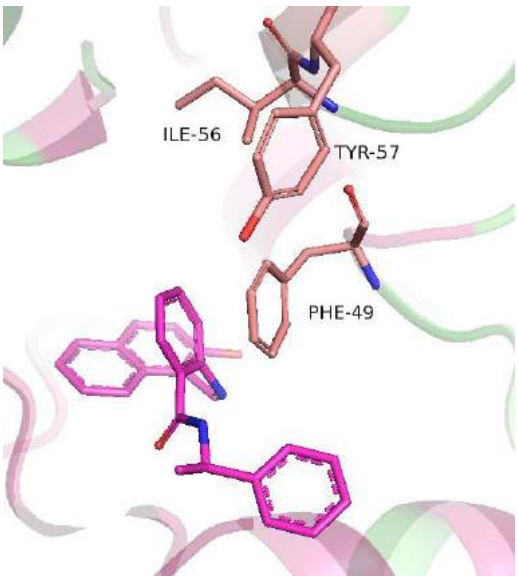


**Figure 1.** Best ranked sirtinol docking study

**Área: MED** **Inscrição: 00509**

# Estudos visando a síntese e avaliação farmacológica de compostos heterocíclicos candidatos a protótipos de fármacos inovadores para o tratamento da doença de Alzheimer

**Vanessa S. Gontijo* (PQ),[1] Mayara Chagas Rosa (IC),[1] Newton G. Castro (PQ),[2] Claudio Viegas Junior (PQ)[1].**

***vanessagontijo@yahoo.com.br**

*[1]Departamento de Química, UNIFAL-MG; [2]Laboratório de eletrofisiológia. Instituto de Ciências Biomédicas. Centro de Ciências da Saúde, UFRJ.*

Palavras Chave: 1,2,3-triazoles, Click Chemistry, *Alzheimer's disease, Acetylcholinesterase, MTDLs.*

## Highlights

Studies aiming at the synthesis and pharmacological evaluation of heterocyclic compounds candidates for innovative prototypes of drugs for the treatment of Alzheimer's disease. Anticholinesterase activity. Triazole compounds in medicinal chemistry.

## Resumo/Abstract

A doença de Alzheimer (DA) foi descrita pela primeira vez pelo médico alemão Alois Alzheimer, em 1906[1]. Esta patologia é caracterizada pela diminuição progressiva da memória recente e declínio severo de cognição, associados com degradação de neurônios colinérgicos em muitas áreas do Sistema Nervoso Central (SNC). Os compostos heteroaromáticos triazólicos possuem larga aplicação na química medicinal sendo atribuída a esta classe de heterociclos várias propriedades biológicas. A importância dos compostos triazólicos é incontestável, particularmente no que se refere ao fato de que alguns deles são fármacos mundialmente consumidos[2].

O objetivo geral deste trabalho é a síntese e a avaliação compostos com perfil de atividade multialvo, com propriedades inibitórias da AChE, antioxidante e neuroprotetora, representando inovação radical no desenho de candidatos a protótipos de fármacos para o tratamento da Doença de Alzheimer. A estratégia de síntese adotada para obtenção dos compostos *N*-benzil-triazolilacilidrazônico **3a-i** (Esquema 1) teve como etapa chave uma reação do tipo CuAAC (cicloadição alcino-azida catalisada por cobre)[3]. Foi obtida uma série de 9 diferentes derivados *N*-benzil-triazolilacilidrazônicos com diferentes funcionalizações de acordo com o precursor alcino terminal empregado.

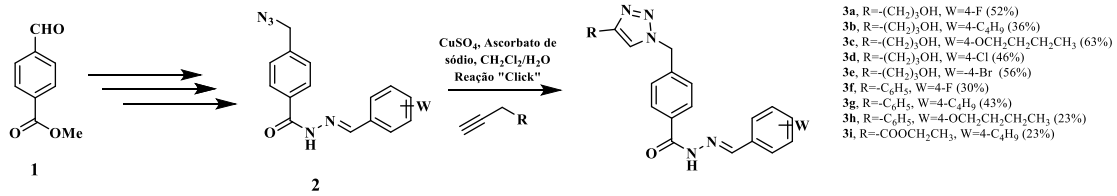


***Esquema 1.*** *Rota para a síntese da série de derivados N*-benzil-triazolilacilidrazônicos **3a-i**

A avaliação farmacológica *in vitro* da inibição da atividade de AChE revelou o composto **3f** como o mais ativo da série, mas com uma potência inibitória relativamente fraca ($IC_{50}$= 95,1 µM). No momento esta substância está sob avaliação da seletividade AChE x BuChE, mecanismo de ação, citotoxicidade e potencial antioxidante e quelante de biometais $Zn^{2+}$, $Fe^{2+}$ e $Cu^{2+}$, podendo representar um novo protótipo de candidato a fármaco multialvo para doenças neurodegenerativas, especialmente a DA.

[1]Moller, H.J.; Graeber, M.B. *Eur. Arch. Psychiatry Clin. Neurosci.* **1998**, *248*, 111-22. [2]Prusiner, P.; Sundaralingam, M. *Acta Crystallografic B*, **1976**, *32*, 419-426. [3]Gontijo, V.S *et al*. *Med. Chem. Res.* **2014**, 11, 89.

Agradecimentos: FAPEMIG, CAPES, CNPQ, UNIFAL, UFRJ.

**Área: MED** **Inscrição: 00425**

# Synthesis, cytotoxicity and *in vitro* evaluation of antileishmanial activity of benzoylguanidines

**Kaio M.S. Silva (PG),[1*] Marciéli Fabris (PG),[1] Tiago O. Brito (PG),[1] Fernando C. Macedo Jr. (PQ),[1] Bruna T.S. Bortoleti (PG),[2] Wander R. Pavanelli (PQ),[2] Ivete C. Costa (PQ),[2] Marcelle L.F. Bispo (PQ).[1]**

**marcieli.fabris@gmail.com; kmlancret@gmail.com**

*[1]Department of Chemistry, UEL; [2]Department of Pathological Sciences, UEL.*

Keywords: *Benzoylguanidines, Leishmania amazonensis, Antileishmanial activity*.

## Highlights

Synthesis of *N*-substituted benzoylguanidines from their corresponding benzoylthioureas. Evaluation of antileishmanial activity. Benzoylguanidines showed considerable antileishmanial activity.

## Resumo/Abstract

Leishmaniasis is a tropical and neglected disease, which is responsible for 20,000 to 30,000 deaths per year.[1] However, the current standard treatment shows adverse effects and high toxicity.[2] In this context, it is necessary the development of new antileishmanial agents more active and selective. Therefore, in the present work, we report the synthesis of *N*-substituted benzoylguanidines from their corresponding benzoylthioureas, in order to evaluate the antileishmanial activity of this class of substances and, after that, to perform a structure-activity relationship study, aiming to identify the key points for the biological activity of these compounds. Thus, benzoylguanidines (**1-7**) were prepared according to the synthetic route outlined in Scheme 1. The solids were obtained in good yields (59-91%) and were fully characterized by melting point and spectroscopic techniques. Afterwards, the benzoylguanidines were evaluated against promastigotes forms of *Leishmania amazonensis* and their cytotoxicities in host cells was tested by MTT assay. In this series, the compounds that have electron withdrawing groups attached to the benzene ring (**5-7**) show the higher antileishmanial activities (% cellular viability range to 19 and 52 in 25 µg/mL). Conversely, the cytotoxicity of these compounds also was more significant, being the derivatives **1-4** less cytotoxic than **5-7**, which could indicate that the electronic factor is an important parameter to modulate the activity and cytotoxicity of this class of compounds. These results provide evidence to support the proposition that benzoylguanidines have antileishmanial potential.

**Scheme 1.** Synthetic route to preparation of benzoylguanidines (**1-7**).

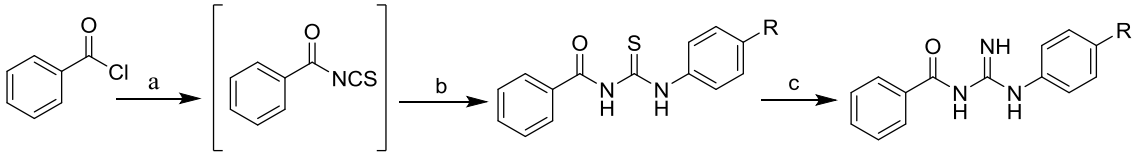


**1**: R=H; **2**: R= OH; **3**: R=OMe
**4**: R= *t*-Bu; **5**: R= Cl; **6**: R=Br
**7**: R= $NO_2$

**Reagents and conditions:** a) $NH_4SCN$, dry acetone, reflux, 15 min; b) Corresponding amines, acetone, 30 min-3h, 70-99%; c) $NH_4OH$, $Et_3N$, $NaBiO_3$, $BiI_3$, reflux, 3-4 h, 59-91%.

1- World Health Organization: Leishmaniasis: 2017 <http://www.who.int/mediacentre/factsheets/fs375/en/>
2- Alvar J, Vélez ID, Bern C et al. PLoS One. 2012; 7(5):35671.

**Área: MED** **Inscrição: 00327**

# Antibacterial activity of new 2-amino-1,4-naphtoquinones

**Carla Cristina da Silva (PG),[1] Rojane de Oliveira Paiva (PQ),[2] Gisela Lara da Costa (PQ),[2] Aurea Echevarria (PQ)[1*]**

**carla.ufruralrj@gmail.com; echevarr@ufrrj.br**

[1]*Departamento de Química, UFRRJ*
[2]*Laboratorio de Taxonomia, Bioquímica e Bioprospecção de Fungos, Instituto Oswaldo Cruz, FIOCRUZ*

Palavras Chave: *Naphtoquinones, Antibacterial Activity, 2-Aminonaphtoquinones, Microwave Irradiation*

## Highlights

Synthesis of 2-amino-1,4-naphtoquinones were performed by microwave and ultrasound irradiation.
The antibacterial activity was assessed by MICs values using the *p*-iodonitrotetrazolium chloride assay.

## Resumo/Abstract

1,4-Naphtoquinone pharmacophore in known to pronounced biological effects in 1,4-naftoquinone-derivatives such as antitumor, antimycobacterial, antiparasitic. Moreover, the incorporation of N-atom on C-2 and C-3 of 1,4-naphtoquinone structure has led to compounds with diversified biological activities including the antibacterial. Thus, considering the importance of this class and the known the bacterial resistance, we synthesized seven 2-amino-1,4-naphtoquinones, and evaluated the biological effect against gram-positive and gram-negative strain of bacteria.

The preparation of 2-aminonaphtoquinones was carried out by alternative methodologies without using the usual mono or dichloride-derivative. The use of ultrasound (method A/B) or microwave (method C) irradiation made possible to obtain the compounds, in reasonable yields, directly of 1,4-naphtoquinone and amine. The yields and process are show in Scheme-1 and Table-1.

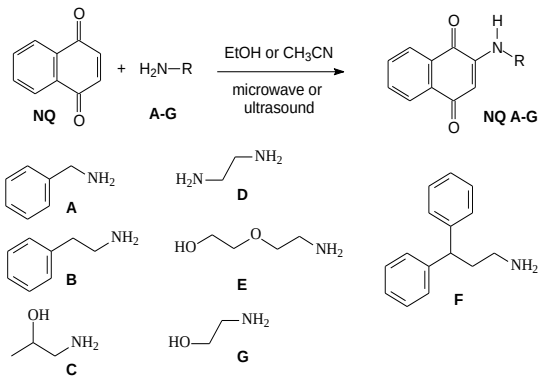


Scheme 1

**Table 1.** Methods and yields to obtain the 2-amino-1,4-naphto-quinones

| Compound | Method | | |
|---|---|---|---|
| | A[a] | B[b] | C[c] |
| **NQA** | 47 | 75 | 71 |
| **NQB** | 32 | 52 | 53 |
| **NQC** | 37 | 15 | 71 |
| **NQD** | 27 | 47 | 71 |
| **NQE** | 65 | 52 | 29 |
| **NQF** | 58 | 44 | 67 |
| **NQG** | 20 | 42 | 39 |

[a]ultrasound/ethanol; [b]ultrasound/ MeCN; [c]microwave/MeCN

After, antibacterial activities of compounds were evaluated against 9 bacteria strains, (*Bacillus subtilis*, *Enterococcus faecalis*, *Staphylococcus aureus, Bacillus cereus*, *Escherichia coli*, *Klebsiella pneumoniae*, *Pseudomonas aeruginosa*, *Acinetobacter baumannii and Klebsiella pneumoniae* β-lactamase resistant). The assays were carried out according to the broth microdilution technique using 96-well microplates, and the effect revealed by *p*-iodonitrotetrazolium assay. The minimum inhibitory concentration (MIC) was evaluated for each compound and clorafenicol used as positive control.

The results showed the NQA, NQC and NQG the most active compounds for all bacteria. Highlighting, the activity against the *K. pneumoniae* resistant, when **NQG** showed the best effect with MIC=31.2μg/mL and the clorafenicol MIC=125μg/mL.

In conclusion, the alternative method to preparation of amino-naphtoquinones was efficient, and their antibacterial effects very promising.

**Área: _MED_____** *(Inserir a sigla da seção científica para qual o resumo será submetido. Ex: ORG, BEA, CAT)*

**Inscrição:__00236_____** *(Inserir o número de inscrição do autor que fez a submissão)*

# Theoretical Investigation of thiosemicarbazones and dialkylphosphorylhydrazones as Proposed Serine Proteases Inhibitors

**Bruno H. M. Mendes (IC),[1*] Carlos M. R. Sant'Anna (PQ),[1]**

**santanna@ufrrj.br; brunohmmufrrj@gmail.com**

[1]*Departamento de Química, UFRRJ.*

Palavras Chave: *Snake venom, Serine Protease, Thiosemicarbazones, Dialkylphosphorilhydrazones, Molecular Docking*

## Highlights

A comparative model of a *Bothrops jararaca* serine protease was constructed and used to obtain and compare its complexes with thiosemicarbazones and dialkylphosphorylhydrazones by molecular docking.

## Resumo/Abstract

Serine proteases (SP), metalloproteases (MP) and phospholipases A2 are the main toxins present in snake venom. They are found in poisons of various snake families, including Viperidae, the main responsible for snakebites in Brazil. Previous results from our group[1] led to the patenting of thiosemicarbazones (TSC) with inhibitory action on MP and anti-hemorrhagic action. The objective of this work is to use theoretical methods to study the modes of protein-ligand interaction for the design of SP inhibitors. We included in this study, besides TSC, dialkylphosphorylhydrazones (DAP) synthesized by our group[2], since compounds of the class of phosphonates presented excellent SP inhibition.[3]

TSC and DAP structures (figs. 1 and 2) were constructed with Spartan'14 (Wavefunction, Inc.), and the energy was minimized using the PM6 method. A comparative model of *Bothrops jararaca* SP was constructed with Swiss-Model using as a template the structure with PDB code 2AIP (resolution of 1.65 Å, 75% identity, estimated quality (QMEAN) of 0.79 for the model). A duplicate docking study of the compounds in the model with the ChemPLP function (GOLD 5.5, CCDC) was carried out. The averages of the scores are listed (table 1). The data indicate that, in general, the DAP are the best ligands for *B. jararaca* SP, with the **4f** ligand being the best.

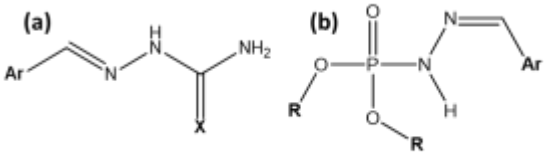


**Figura 1**: Estrutura principal das TSC (a) e das DAF (b)

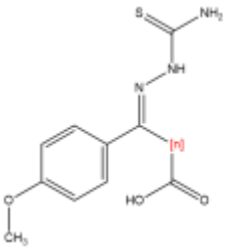


**Figura 2**: Modificação estrutural proposta para a molécula 23 da série das TSC. O espaçador "n" pode variar entre 2 e 3 grupos CH2, gerando as moléculas modificadas 23b e 23c, respectivamente.

**Tabela1**: Padrão de substituição das TSC e das DAF e médias de pontuação geradas pelo programa GOLD.

| TSC | X | Ar | Médias | DAF | R | Ar | Médias |
|---|---|---|---|---|---|---|---|
| **22** | S | Fenil | 36,97 | **4a** | Et | 4-piridil | 48,78 |
| **23** | S | 4-OMe- Fenil | 35,34 | **4b** | Bu | 4-piridil | 58,34 |
| **23b*** | S | 4-OMe- Fenil | 50,25 | **4c** | *iso*-Pr | 4-piridil | 49,07 |
| **23c*** | S | 4-OMe- Fenil | 49,45 | **4d** | *iso*-Bu | 4-piridil | 44,42 |
| **24** | S | 4-Cl-Fenil | 34,58 | **4e** | Et | 3-piridil | 49,58 |
| **25** | S | 3-OH,4-OMe- Fenil | 35,10 | **4f** | Bu | 3-piridil | **64,67** |
| **26** | S | 2-Furanil | 37,50 | **4g** | *iso*-Pr | 3-piridil | 50,61 |
| **27** | S | 4-Br- Fenil | 32,82 | **4h** | *iso*-Bu | 3-piridil | 46,65 |
| **53** | O | 2,4-OH-Fenil | 47,54 | **4i** | Et | 2-piridil | 47,41 |
| **54** | O | 3-OH -Fenil | 40,81 | **4j** | Bu | 2-piridil | 61,57 |
| **55** | O | 4-OH-Fenil | 46,95 | **4k** | *iso*-Pr | 2-piridil | 49,31 |
| **56** | O | 3-OH,4-OMe-Fenil | 35,61 | **4l** | *iso*-Bu | 2-piridil | 44,80 |
| **57** | O | 4-COOH-Fenil | 35,17 | **4m** | *sec*-Bu | 5-Br-3-piridil | 49,30 |
| **58** | O | 4-OMe-Fenil | 37,46 | **4n** | *sec*-Bu | 2-Br-3-piridil | 46,32 |
| **59** | O | 4-Cl-Fenil | 37,17 | **4o** | *sec*-Bu | 3,5-Cl-4-piridil | 46,59 |

[1]Ferreira et al., *ACS Med Chem. Lett.* 2017, **8**, 1136.
[2]Da Matta et al. *Eur. J. Med. Chem.* 2015, **101**, 1.
[3]Sieczyk and Oleksyszyn, *Curr. Med. Chem.* 2009, **16**, 1673.

**Área: MED** *(Inserir a sigla da seção científica para qual o resumo será submetido. Ex: ORG, BEA, CAT)*

**Inscrição: 00139** *(Inserir o número de inscrição do autor que fez a submissão)*

# Synthesis and cytotoxicity activity of new analogs of *Santacruzamate A*

**Silmara N. Andrade (PG),[1] Diego E. L. Seckler (IC),[2] Tulio R. Freitas (PG),[1] Renata R. Nunes (PG),[1] Fernanda C. G. Evangelista (PG),[3] Jorge L. Humberto (PQ),[2] Adriano P. Sabino (PQ),[3] Alex G. Taranto (PQ),[1] Fernando de Pilla Varotti (PQ),[1] Flaviane F. Hilário (PQ).[2*]**

**silmaranunesandrade@hotmail.com; flavianehilario@iceb.ufop.br**

*[1]Núcleo de Química Biológica da UFSJ – NQBio; [2]Departamento de Química da UFOP; [2]Departamento de Análises Clínicas e Toxicológicas da UFMG.*

*Keywords: Cancer, Mode of action, HDAC*

## Highlights

HDAC is considered as an anticancer drug target. HDAC inhibitors (iHDAC) regulate events such as cell survival, differentiation and apoptosis in tumor cells. iHDAC are a potential anti-cancer agents.

## Resumo/Abstract

Cancer development is not restricted to the genetic alterations, but may also involve epigenetic changes. In this context, Histone Deacetylase (HDAC) plays a vital role in the epigenetic regulation of gene expression. Then, a novel series of synthetic analogs of *Santacruzamate A* with zinc-linked group (ester and carbamate) were designed and synthesized as potential HDAC inhibitors. The synthetic route for these compounds is outlined in Scheme 1 and involved coupling reaction between carboxylic acid and amines, Williamson ether synthesis using phenolates and methanesulfonate, and copper(II) catalyzed click reaction. Compounds IDH1 to IDH7 presented best results of biding energy (kcal/mol) against HDAC4 compared to crystallographic ligand. The compound most potent and selective of the serie, IDH-1 exhibited remarkably enhanced anticancer potency against three kinds of cancer cell lines, in which MTT assay was performed against MCF-7 (breast cancer), MDA-MB-231 (breast cancer), TOV-21G (adenocarcinoma), and non-tumor cell line WI-4-26VA (lung fibroblast) with $IC_{50}$ values for tumor cells ranging from 24.3-44.93μM, compared with Etoposide (12-18.57μM) and Doxorubicin (2.1-4.37μM). Further investigation showed that IDH-1 could promote DNA damage and an increase on the levels of caspase 3 and 9, p21, TP53 and BAK, suggesting cell death of tumor cells MDA-MB-231 and TOV-21G by apoptosis through the intrinsic pathway. This study demonstrated that synthetic analogs of *Santacruzamate A* with zinc-linked group are effectives for improving both HDAC inhibitory activity and antitumor activity. The most potent compound, IDH-1, could be promising candidate for cancer therapy.

**Scheme 1**: Synthesis of new histone deacetylase (HDAC) inhibitors

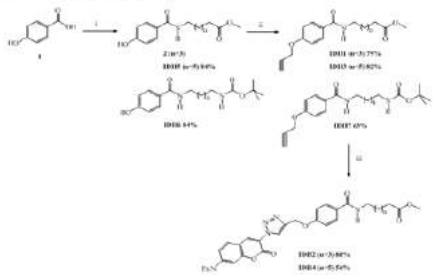

**Table 1**: Docking of the IDH compounds against different HDAC subtypes..

| Compound | HDAC2 | HDAC3 | HDAC4 | HDAC7 |
|---|---|---|---|---|
| IDH1 | -7.2 | -4.1 | -6.5 | -7.2 |
| IDH2 | -7.6 | -4.6 | -7.4 | -8.2 |
| IDH3 | -7.9 | -4.9 | -7.2 | -7.4 |
| IDH4 | -8.3 | -5.0 | -7.6 | -8.2 |
| IDH5 | -7.5 | -5.6 | -8.5 | -7.9 |
| IDH6 | -7.1 | -5.7 | -1.2 | -8.7 |
| IDH7 | -7.3 | -4.5 | -4.8 | -7.5 |
| Ligand Crystal. | -9.9 | -6.3 | -3.8 | -10.4 |
| RMSD | 0.3702 | 1.0160 | 1.7727 | 1.7993 |

**Table 2.** $IC_{50}$ values obtained in *in vitro* assays MCF-7, MDA-MB-231, TOV-21G and WI-4-26VA cell lines.

| COMPOUNDS | IC50 (μM)[a] | | | | Selective Index (SI)[b] | | |
|---|---|---|---|---|---|---|---|
| | MDA-MB-231 | MCF-7 | TOV-21G | WI-26VA4 | MDA-MB-231 | MCF-7 | TOV-21G |
| IDH-1 | 26.8±8.2 | 44.93±4.61 | 24.3±6.3 | 128.81 ±17.6 | 4.81 | 2.87 | 5.3 |
| IDH-2 | 22.02±3.77 | 29.93±3.79 | 21.01±1.19 | 27.35 ±6.23 | 1.24 | 0.93 | 1.3 |
| IDH-3 | 51.94±6.56 | 42.82±5.43 | 26.36±6.94 | 76.36±23.64 | 1.47 | 1.78 | 2.9 |
| IDH-4 | 19.48±1.83 | 22.91±8.4 | 23.02±7.98 | 15.67±2.61 | 0.80 | 0.68 | 0.68 |
| IDH-5 | 100<IC <1000 | 99.2±34.1 | 100<IC <1000 | 73.28±22.16 | ND | 0.74 | ND |
| IDH-6 | 34.93±8.9 | 38.99±13.67 | 50.51±14.86 | 35.71±20.81 | 1.02 | 0.92 | 0.71 |
| IDH-7 | 71.34±21.36 | 75.04±4.4 | 45.74±16.02 | 48.47± 18.7 | 0.68 | 0.65 | 1.06 |
| Etoposide | 12.0±1.07 | 16.84±5.44 | 18.57±3.91 | 8.65±0.23 | 0.72 | 0.51 | 0.47 |
| Doxorubicin | 2.3±0.55 | 2.1±0.7 | 4.37±1.06 | 1.9±0.9 | 0.83 | 0.9 | |

[a] IC50 values are indicated as mean ± SD of three independent experiments.
[b] Selective Index (SI) for these compounds was deduced as the ratio of IC50 of the compound in normal cells over IC50 of compound in cancer cells.

**Figure 1.** Relative quantification of *TP53*, *p21* and *BAK* gene in MDA-MB-231 (a) and TOV-21G (b) line at different concentrations of compound **IDH-1** (*p<0.05).

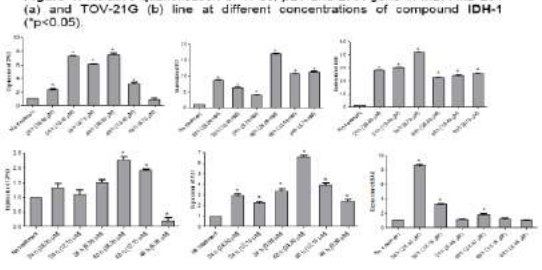

**Área: MED** **Inscrição: 00106**

# Risk Assessment for synthetic cannabinoids: an application in criminal science

**Jade Simões de Castro (FM),[1,2] Caio Henrique Pinke Rodrigues (PG),[1] Eduardo Borges de Melo (PQ),[3] Aline Thaís Bruni (PQ),[1,2*]**

**j.castro@usp.br ; aline.bruni@usp.br**

*[1]Departamento de Química, FFCLRP – USP – RP*
*[2]Instituto Nacional de Ciência e Tecnologia Forense (INCT Forense), Ribeirão Preto/SP*
*[3]Laboratório de Química Medicinal e Ambiental Teórica (LQMAT), UNIOESTE, campus Cascavel, PR.*

Keywords: *Synthetic Cannabinoids; In Silico Toxicity; New Psychoactive Substances, Risk Assessment, Criminal Science*

## Highlights

Synthetic cannabinoids (CB) have increased in use.
We studied a series of CB regarding to toxicity.
Partial Least Squares models were obtained.
Both experimental and *in silico* values were able to give information about risk assessment.

## Abstract

Synthetic cannabinoids are commonly sprayed on herbal products to reproduce the cannabis recreational effects and are known as ‘‘spice’’. According to UNODC (United Nations Office on Drugs and Crime) the toxic effects of these drugs are still unknown. Many harm effects and fatalities have been associated to synthetic cannabis. Physicochemical and pharmacological properties are not easily found. Knowledge about these substances are important to criminal science: they can provide information to drive efforts for both law enforcement as for harm reduction policies. In this sense, *in silico* methods are an alternative to understand the behavior of these new substances, once experimental measures are commonly time-consuming and may involve high costs. The main goal of this work was to evaluate a series of heterocyclic compounds, 1,3disubstituted indole and 2-azaindole derivatives identified in forensic samples. Molecular structures were studied by means of ORCA 4.0.1 package. Toxicological variables were calculated by ACD/I-Lab 2.0: LogP and LD50 for many human (blood, duodenum etc.) and animal (rat and mouse). We also used experimental values of human $CB_1$ and $CB_2$ receptors based on affinities obtained in radioligand binding studies (Forensic Toxicol. (2016) 34:329–343). Toxicological values were used as dependent variables and Partial Least Squares regression was performed on Pirouette® Package. Ten regression models were obtained against the structural properties. Both *in silico* as experimental values were able to give information about the toxicological behavior of CBs and give insights about risk assessment.

**Área: MED** **Inscrição:00068**

# Drug Discovery applied to Agrobusiness: prediction of *Riphicephalus microplus* Acetylcholinesterases isoforms, an important target in the development of carrapaticides

**Isabela de Oliveira Estela (IC)[1], Humberto Fonseca de Freitas (PQ) [1], Samuel Silva da Rocha Pita (PQ)[1*]**

**Isabelaestrela012@gmail.com; samuelrpita@gmail.com**

[1]*Laboratório de Bioinformática e Modelagem Molecular, Faculdade de Farmácia, UFBA, 40170-115, Salvador-Bahia*
Keywords: Acetylcholinesterase, *Rhipicephalus microplus, Cattle Tick, Comparative Modeling*

## Highlights

The Cattle Tick generate loses of billions of dollars in livestock. Computational methods can be helpful in search for more effective control strategies based on the structure of Acetylcholinesterase.

## Abstract

*Rhipicephalus microplus* is the cause of severe anemia in cattle and it is also responsible for the transmission of pathogens that increased the mortality of the herds. The knowledge of Acetylcholinesterases 1, 2 and 3 from *R. microplus* (RmAChE 1, 2, and 3) 3D structures could be helpful in the search for new anticholinesterases compounds. The three isoforms present significant sequential differences which may reflect in biological function distinction, for instance, in catalytic efficiency. In order to understand these differences from the structural point of view, comparative models of the three isoforms were built using Modeller v.9.18. The best models of each isoform presented energetical, stereochemical and folding quality compatible to X-ray structures used as templates. At first, the volume of the inhibitors interaction sites and the electrostatic profile were investigated by using the servers PDBsum and APBS-pdb2pqr, respectively. This preliminary analyzes showed that RmAChE2 presents an additional volume of 13% at the catalytic site (Ser219, Glu319 and His439) (Fig 1B - middle) when compared to the other two isoforms. The major volume of RmACHE2 allows the accommodation of bulky binders/substrates and could be related to the metabolic detoxification in the tick performed by this isoform. The three isoforms presented distinct electrostatic profiles: RmAChE1 predominates negative charges (Fig 1C - Upper); RmAChE2 concentrate positives charges (Fig 1C - middle); and RmAChE 3 shows a more homogeneous charge distribution (Fig 1C - Lower). The differences in electrostatics potential can play a significant role on interaction of ligands with different charges in the activity site of each isoforms. As prospects, site probing analyzes will be performed to characterizes in detail the site of interaction of each isoform and compare to mammalian (*Hs*AchE e *Hs*BuChE) isoform in order to screening selective ligands to *Rm*AChEs.

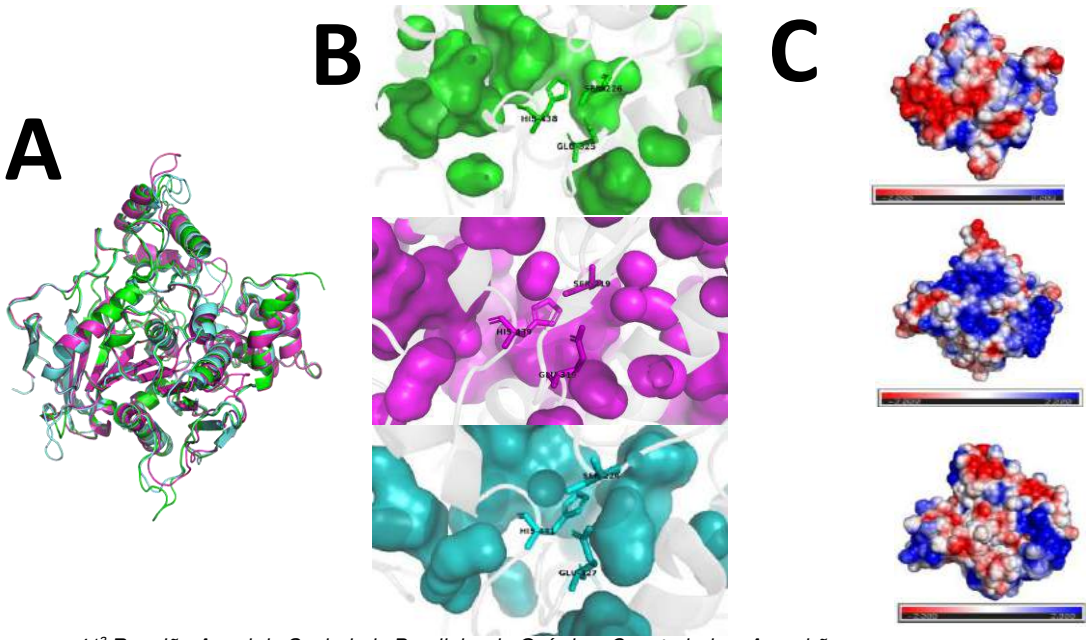


**Figure 1:**
**A) Aligned cartoon structures of RmAChE1 (green), RmAChE2 (magenta) and RmAChE3 (cyan); B) Catalytic site cavity shown on surface for the 3 isoforms with catalytic triad in stick: RmAChE1 in green, RmAchE2 in magenta and RmAChE3 in cyan;**
**C) Electrostatic potential map of the three isoforms. Regions with predominance of negative (colored red) and positive (Blue colored) charges.**

**Área: MED** **Inscrição: 01024**

# Synthesis and Biological Evaluation of the Coumarins Derivatives as Potential Inhibitors of the Production of the *Pseudomonas aeruginosa* Virulence Factor Pyocyanin

**Carine Assunção de Oliveira Maciel (IC),[1] Thamires Quadros Froes (PG),[2] Luana da S. M. Forezi (PQ),[3] Mariana F. C. Cardoso (PQ),[3] Dora C. S. Costa (PG),[3] Vitor F. Ferreira (PQ),[4] Fernando de C. da Silva (PQ),[3*] Marcelo S. Castilho (PQ),[1,2,*]**

cabiles44@hotmail.com; castilho@ufba.br*

*[1] Faculdade de Farmácia da Universidade Federal da Bahia, Bahia, Salvador, BA, Brazil.; [2]Programa de pós-graduação em Biotecnologia da Universidade Estadual de Feira de Santana, Feira de Santana, BA, Brazil; [3]Universidade Federal Fluminense, Instituto de Química, Departamento de Química Orgânica, Niterói, RJ, 24020-150, Brazil; [4]Universidade Federal Fluminense, Departamento de Tecnologia Farmacêutica, Faculdade de Farmácia, Niterói, RJ, 24241-002, Brazil*

Keywords: *Bacterial Resistance, Pyocyanin biosynthesis inhibition, Coumarin, SAR.*

## Highlights

Bacterial resistance is a worldwide problem whose solution depends on virulence modulation. Herein we report that coumarin derivatives are micromolar inhibitors of pyocyanin production, one of the main *P. aeruginosa* virulence factors.

## Resumo/Abstract

Coumarin derivatives **2a-m** and **3a-j** were obtained, in good to moderate yields, by Knoevenagel condensation of 4-hydroxycoumarin (**1**) with aldehydes in the presence of different thiol (Figure 1A). Single concentration assays suggest that several coumarin derivatives inhibit pyocyanin biosynthesis but those with a secondary carbon at C-3 position have better antibacterial activity than those with one additional substituent (Figure 1B).

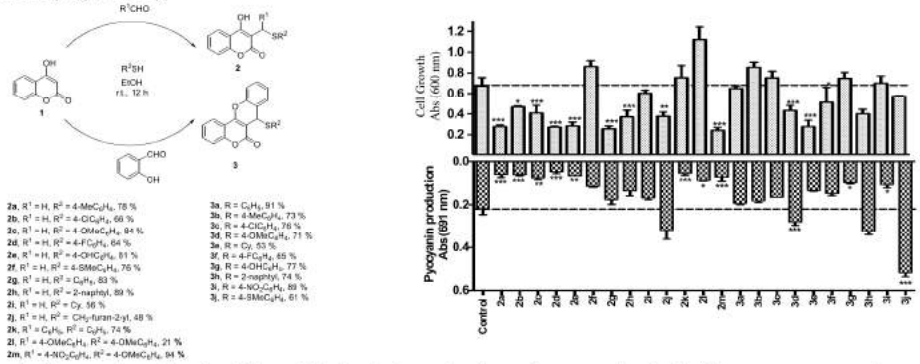


**Figure 1.** General synthesis (A) and biological evaluation of coumarin derivatives as pyocyanin production inhibitors (B)

Compounds that kill the bacteria are prone to select resistant strains, then only di-substituted coumarin derivatives were further investigated. Concentration-response curves suggest that shows that $OCH_3$ substituted rings have a detrimental effect on potency **2k** ($EC_{50}$ 6.66 ± 1.65 μM *vs* **2l** ($EC_{50}$ 41.79 ± 13.44 μM). A similar trend is observed for $NO_2$ on *para* position ($EC_{50}$ 72.62 ± 21.69 μM). This might be due to electronic or steric effects, but the fact that OH substitution partially restores the biological activity (**3g** $EC_{50}$ 49.89 ± 13.78 μM) led us to conclude that electronic effects are pivotal to the compounds´ potency.

Financial support: FAPESB, FAPERJ, CNPq, CAPES

**Área: MED**
*(Inserir a sigla da seção científica para qual o resumo será submetido. Ex: ORG, BEA, CAT)*

**Inscrição: 01329**
*(Inserir o número de inscrição do autor que fez a submissão)*

# Design of new analogs and investigation of *Sm*TGR inhibition by fragments identified by X-ray crystallography

**Lauro R. de Souza Neto[1] (PG), Nicholas Furnham[2] (PQ), Ray Owens[3] (PQ), Anil Verma[3] (TC), José B. Neto[4] (PQ), Frank von Delft[4] (PQ), Luciano P. Gomes[1] (TC), Bruna M. Mesquita (PG)[5], Sabrina B. Ferreira[5] (PQ), Rafael F. Dantas[1] (PQ), Floriano P. Silva-Jr[1] (PQ)*.**

**lribeirods@gmail.com; floriano@ioc.fiocruz.br**

*[1]Laboratory of Experimental and Computational Biochemistry of Drugs, Oswaldo Cruz Institute, FIOCRUZ, Rio de Janeiro, Brazil; [2]Department of Infection and Immunity, London School of Hygiene and Tropical Medicine, UK; [3]Oxford Protein Production Facility, Oxford University, UK; [4]Diamond Light Source, Rutherford Appleton Laboratory, United Kingdom; [5]Laboratory of Organic Synthesis and Biological Prospecting, Institute of Chemistry, Federal University of Rio de Janeiro.*

Keywords: Schistosomiasis, *Sm*TGR inhibitors, Fragment-based Lead Discovery, X-ray crystallography, Rational Drug Design.

## Highlights

*Sm*TGR ligands were identified in a fragment-based lead discovery campaign. All hits were evaluated for enzyme inhibition but no significant activity was observed. Novel designed analogs are being synthesized for improved activity.

## Abstract

Schistosomiasis is a disease caused by parasites of the genus *Schistosoma*. Praziquantel is the only available drug, which makes the development of new therapeutic options more urgent. Thioredoxin Glutathione Reductase of *S. mansoni* (*Sm*TGR) is a flavoenzyme that plays a pivotal role in the redox homeostasis of the parasite, besides being a validated therapeutic target.

In the early phases of this work, molecular fragments were identified as *Sm*TGR ligands in a fragment-based lead discovery campaign using X-ray crystallography. Among the 474 fragments screened, we were able to identify 16 ligands modeled at 10 different sites in the *Sm*TGR monomer (Fig. 1). This work aimed to investigate the fragments' inhibitory activity and synthesize new designed analogues.

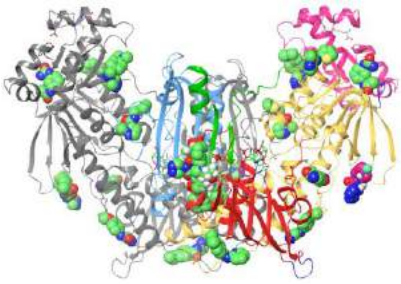

**Fig. 1 –** *Sm*TGR dimer and ligands represented as green spheres.

So far, we have assayed hits from crystallography screening for enzyme inhibition (Fig. 2). The results showed that the small differences observed in the activity levels are not statistically significant. This could be explained by the high Kd associated with small molecular fragments (MW <300 Da), which can reach the high mM range.

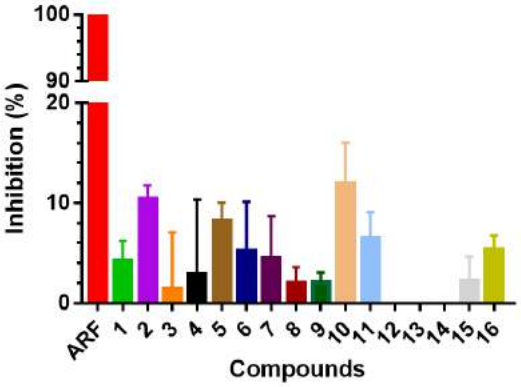


**Fig. 2 -** SmTGR assay. The assayuses NADPH and DTNB as substrates. The fragments were screened at 2 mM, including Auranofin (ARF) which was used as positive control.

Based on the binding modes, new fragments analogues were designed and are currently in the synthesis step. In addition, a search in the ZINC database allowed the identification of 3022 molecules containing our fragments as substructures. Among these, 153 were predicted by docking as possible ligands (*vHits*). New assays using both rationally designed analogs and *vHits* will be performed to evaluate the inhibition potential of these molecules.

**Área: MED** **Inscrição: 01198**

# Development of a protocol for the virtual screening of a series of small-molecules ligands of the tubulin colchicine binding site

**David L. Palomino-Salcedo (PG),[1] Luma G. Magalhães (PG),[1] Glaucius Oliva (PQ),[1] Adriano D. Andricopulo (PQ).[1*]**

**palomino@ifsc.usp.br; aandrico@ifsc.usp.br**

[1]*Instituto de Física de São Carlos, USP*

Palavras Chave: *Molecular Dynamics, Molecular Docking, FEP, Tubulin, Microtubule.*

## Highlights

We have developed a protocol to perform a virtual screening to identify new small-molecule ligands as tubulin-binding agents with anticancer properties (colchicine binding site).

## Resumo/Abstract

Microtubules are cytoskeletal polymers composed of αβ-tubulin heterodimers, an extensive network of filaments that span the cell interior. [1] Interrupting the correct formation of microtubules lead to cell apoptosis, which is widely recognized as an attractive approach for the design of potent anticancer agents. The chemotherapeutic class of tubulin-binding agents (TBA), such as like taxanes, vinca alkaloids and epothilones, are well-known binders of β-tubulin able to suppress the dynamics of spindle microtubules, disturbing the chromosomal segregation and inducing cell death. In humans, microtubules are composed of eight α-tubulin isotypes and seven β-tubulin isotypes in mixed combinations. These isotypes have high degree of structural homology, but a vastly divergent sequence at their carboxy-terminal tail. Tubulin isotypes play an important role in microtubule dynamics. [2] Some isotypes present different binding affinities for a variety of anticancer agents. However, the reasons underlying the magnitude of the binding affinities are not well understood at the molecular level. Therefore, we have developed a protocol to perform a virtual screening to investigate the binding-affinity of a series of small-molecule ligands (acridone derivatives) to the tubulin colchicine site. First, we performed a molecular dynamics simulation to evaluate an *average* structure, using cluster analysis. Second, using the resulting structure, we executed a molecular docking strategy with a library of ligands with known $IC_{50}$ values. Finally, we calculated the affinity energy using the Free Energy Perturbation method. Our results clearly show that this protocol succeeds in predicting new candidate molecules with high binding affinity to the tubulin colchicine binding site.

References

[1] Parker, Amelia L., et al. "An emerging role for tubulin isotypes in odulating cancer biology and hemotherapy resistance." International journal of molecular sciences 18.7 (2017): 1434.

[2] Kumbhar, Bajarang Vasant, et al. "Exploring the origin of differential binding affinities of human tubulin isotypes αβII, αβIII and αβIV for DAMA-colchicine using homology modelling, molecular docking and molecular dynamics simulations." PloS one 11.5 (2016): e0156048.

**Área: MED** **Inscrição: 01157**

# Study of the molecular interactions between DPP-IV and some inhibitors used for the treatment of type II diabetes mellitus

**Michelle C. M. R. Martins (PG),[1*] Simone Q. Pantaleão (PG),[1] Káthia M. Honório (PQ).[1,2]**

***melo.reis@ufabc.edu.br**

*[1]Centro de Ciências Naturais e Humanas, UFABC; [2]Escola de Artes, Ciências e Humanidades, USP.*

Key words: (*Diabetes, DPP-IV Inhibitors, Docking, GOLD, BINANA*).

## Highlights

Study of the molecular interactions between DPP-IV and some inhibitors for the treatment of type II diabetes mellitus. Understanding the inhibitory profile of compounds derived from omarigliptin, whose results revealed the biological importance of atoms such as nitrogen and fluoride in the structure of the studied molecules.

## Abstract

Type II diabetes mellitus is a metabolic disorder that involves a failure in the secretion and / or action of insulin in the body.[1] One of the strategies involved in its treatment is the inhibition of DPP-IV, being interesting the analysis of the interactions between this enzyme and bioactive compounds of interest, using the technique known as molecular docking. In this work, 7 derivatives of omarigliptin[2,3] were docked at the binding site of DPP-IV using GOLD[4] program and the possible interactions were analyzed, considering the following parameters: (i) flexibilization of residues with basic character (e.g. Arg125); (ii) residues with acid character (Glu206); (iii) residues with polar character (Ser630, Tyr547 and Tyr666); (iv) two molecules of structural water; (v) and Goldscore as scoring function. Additionally, we evaluated the selected compounds with the BINANA[5] tool (BINding ANAlyzer) to identify the main characteristics of the ligand-DPP-IV interactions observed. From the obtained results, it was observed that the interactions between the previously mentioned residues and nitrogen and fluoride atoms of the inhibitors are of the hydrogen bonding type, saline bridge and hydrophobic contacts at the active site of DPP-IV. In the case of the most active compounds there was also interaction with water molecules of the DPP-IV enzyme. Therefore, the results obtained here can help the design of new candidates to inhibit DPP-IV.

## References

[1]Baynes, J.; Dominiczan, M.H.; Medical Biochemistry, Cap.20, Rio de Janeiro, Elsevier, 2007.
[2]Chem, P. et al. Bioorg. Med. Chem. Lett. 2015, 25, 5767–5771.
[3]Cox, J. M. et al. Bioorg. Med. Chem. Lett. 2016, 26, 2622-2626.
[4]Jones, G. et al. J. Mol. Biol. 1997, 267, 727-748.
[5]Durrant, J. D. & McCammon, J. A. J. Mol. Graph. Model. 2011, 29, 888-893.

## Acknowledgments

The authors would like to thank FAPESP, CAPES and UFABC for the financial support.

**Área: MED** **Inscrição: 01116**

# Chemoinformatics Strategies for a Series of Antichagasic Compounds

**Alex R. Medeiros (IC), Leonardo L. G. Ferreira (PQ), Rodolpho C. Braga (PQ), Adriano D. Andricopulo (PQ)**

**alex.medeiros@usp.br; aandrico@ifsc.usp.br**

*Laboratory of Medicinal and Computational Chemistry (LQMC), Physics Institute of Sao Carlos (IFSC) – University of Sao Paulo (USP)*

Keywords: Molecular Modeling, *Trypanosoma cruzi*, Cruzain.

## Highlights

Chagas disease is endemic in Latin America. Cruzain is a validated molecular target for drug discovery. Chemoinformatics is a valuable tool in designing novel cruzain inhibitors.

## Abstract

Chagas disease is a neglected tropical disease (NTD) that affects 8 million people worldwide, especially in Latin America where it is endemic[1]. Currently, the available chemotherapy features high toxicity along with poor efficacy, mainly in the chronic phase of the disease. In this context, there is an urgent need for novel, safe and effective compounds for Chagas disease therapy. To that end, the cysteine protease cruzain (EC 3.4.22.51) from the etiological agent of the disease, the protozoan*Trypanosoma cruzi*, has been broadly explored in current drug discovery programs[2].The present study aims to identify novel compounds suitable for molecular optimization by using chemoinformatics tools, such as virtual screening, along with a set of in house-validated and highly active cruzain inhibitors. By integrating scaffold decomposition methods and structure-based 3D pharmacophore modeling, a virtual screening cascade was devised to identify novel cruzain inhibitors. Initially the dataset was structurally decomposed to correlate two-dimensional molecular fragments and biological activity. Next, the dataset molecules in complex with cruzain were used to identify 3D features responsible for enzyme-inhibitor recognition (**Figure 1**), which were subsequently used as a classification criteria for active/inactive compounds. Finally, the outlined models were applied to screen an external dataset with the view to address the accuracy and validate the overall chemoinformatics approach.

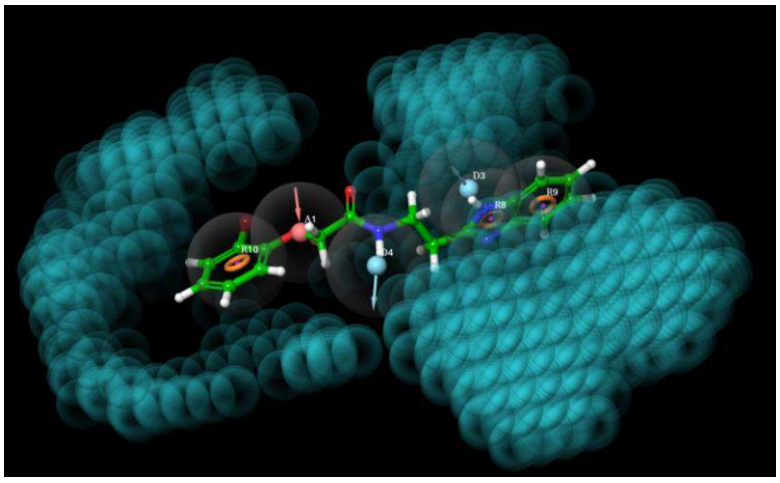


**Figure 1**. Inhibitor in the binding cavity of cruzain and the identified features used to generate the phamacophore.

**References**

1. Pérez-Molina, J. A.; Molina, I. *Lancet* **2018**, *391*, 82.
2. Ferreira, L. G.; Andricopulo, A. D. *Pharmacol. Ther*. **2017**, 180, 49.

**Área: MED** **Inscrição:** 01089

# New pyrazolopyrimidines as Inhibitor of *L. amazonensis* Arginase

**Luiz C. S. Pinheiro (PQ)[1], Lívia M. Feitosa (PG)[1], Flávia F. Silveira (PG)[1], Maria de Lourdes G. Ferreira (PQ)[1], Danielle L. Souza (IC)[1], Julio A. A. S. S. Come (PG)[2], Lucas V. B. Hoelz (PQ)[1], Edson R. Silva (PQ)[2], Nubia Boechat (PQ)[1]***

**luiz.pinheiro@far.fiocruz.br; nubia.boechat@far.fiocruz.br**

[1]*Departamento de Síntese de Fármacos, Farmanguinhos - FIOCRUZ, Fundação Oswaldo Cruz. RJ, Brazil.*
[2]*Departamento de Medicina Veterinária, Faculdade de Zootecnia e Engenharia e Alimentos, Pirassununga, SP, Brazil.*

Keywords: *Leishmaniasis, arginase, pyrazolopyrimidine*

## Highlights

The 1-phenyl-1*H*-pyrazolo[3,4-*d*]pyrimidine derivative exhibited *L. amazonensis* arginase inhibition.
The new compound **4a** (R = H) was more potent than the prototype.

## Abstract

Our group has synthesized a series of triazolo[1,5-*a*]pyrimidine derivatives as a quinoline bioisostere with the aim to study the antiparasitic activity of these compounds (1).
During our search for new compounds that can be used to treat of leishmaniasis, we have demonstrated the importance of prototype I, a triazolo[1,5-*a*]pyrimidine linked to the thiosemicarbazide group that inhibited the arginase enzyme of *L. amazonensis* with $IC_{50}$ of 16.5 µM (2).
In an effort to enhance the activity of triazolopyrimidine prototype **I**, this work has as objective the design and synthesis of new series of compounds by the exchanging between the triazolo[1,5-*a*]pyrimidine ring (green) by a 1*H*-pyrazolo[3,4-*d*]pyrimidine ring (red) which are bonded to the thiosemicarbazide group (blue) (Figure 1).

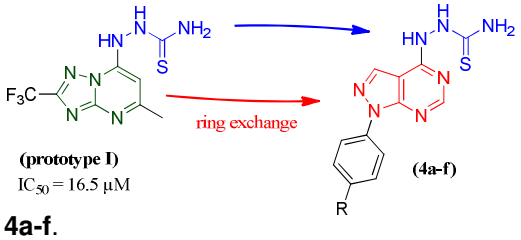


**Figure 1:** Planning of compounds **4a-f**.
Reaction of aminopyrazoles **(1a-f)** with formic acid at 100 °C, produced the derivatives 1-phenyl-1*H*-pyrazolo[3,4-*d*]pyrimidin-4(7*H*)-ones **(2a-f)** with 73-89% yield. Which was treated with $POCl_3$ under reflux to obtain the derivatives 4-chloro-1-phenyl-1*H*-pyrazolo[3,4-*d*]pyrimidines **(3a-f)** in 78-97% yield. The reaction between the derivatives **3a-f** and thiosemicarbazide was performed in DMF at 25 °C, to obtain the new derivatives 2-(1-phenyl-1*H*-pyrazolo[3,4-*d*]pyrimidin-4-yl)hydrazinecarbothioamides **(4a-f)** with 23-50% yield (Figure 2).

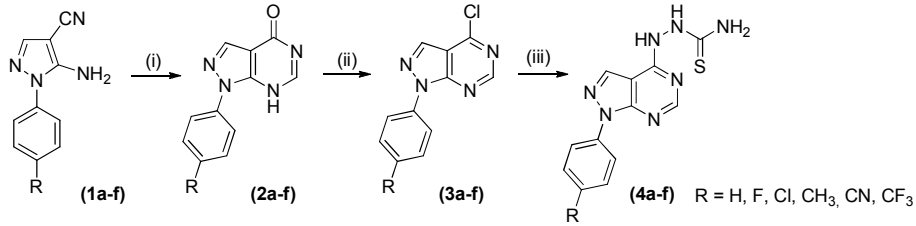


*Reagents and conditions*: (i) $HCO_2H$, 100 °C, 12h; (ii) $POCl_3$, reflux, 24h; (iii) thiosemicarbazide, DMF, 25 ºC, 12h.
**Figure 2:** Synthesis of compounds **4a-f**.
Among the 1-phenyl-1*H*-pyrazolo[3,4-*d*]pyrimidines synthesized, the compound **4a** (R = H) was the most active exhibited arginase inhibition whith $IC_{50}$ values of 12 µM, more potent than the prototype **I**. It is possible to state that the 1*H*-pyrazolo[3,4-*d*]pyrimidine system is promising as a prototype for the design of new agents against *Leishmania sp.*.

**ACKNOWLEDGEMENTS**: CNPq, CAPES, FAPERJ and PDTIS/FIOCRUZ

**REFERENCES**

(1) Boechat, N. et al. *Molecules*, **2012**, 17, 8285-8302.
(2) Silva, E.R. et al. *Chem Biol Drug Des*, **2015**, 86, 969-978.

**Área: MED** **Inscrição: 01035**
*(Inserir o número de inscrição do autor que fez a submissão)*

# Multivariate QSAR study of Modafinil derivatives with molecular descriptors derivated from SMILES notations and free softwares.

**Eduardo Borges de Melo (PQ),[1,2] Aline Thais Bruni (PQ)[2,3].**

**eduardo.b.de.melo@gmail.br**

[1]*Laboratório de Química Medicinal e Ambiental Teórica (LQMAT), UNIOESTE, campus Cascavel, PR.*
[2]*Departamento de Química, FFCLRP – USP – RP*
[3]*Instituto Nacional de Ciência e Tecnologia Forense (INCT Forense), Ribeirão Preto/SP*

Keywords: drug dependence, QSAR, DAT, SMILES, open softwares.

## Highlights

- There are no approved medications for the treatment of stimulants abuse drugs.
- A QSAR study with DAT inhibitors was carried out.
- The model was according with available data on the mechanism of action.

## Resumo/Abstract

Despite many years of research, there are no approved medications for the treatment of reliance on stimulants such as cocaine, and treatment is focused on psychotherapy and abstinence, but about 50% of the individuals end up having relapses, mainly due to the symptoms of abstinence. The dopamine transport receptors (DAT) is a biological target for development of agents for treatment of psychostimulant dependence. This study aimed to obtain a QSAR model based on a set of 49 sulfanyl ethyl piperazines (all Modafinil derivatives) assayed as DAT inhibitors. We used only 2D molecular descriptors with the SMILES notation obtained in free platform ChemDes (http://www.scbdd.com/chemdes). The Variable selection (with Ordered Predictors Selection approach) and the model building were carried out in the QSAR Modeling (http://lqta.iqm.unicamp.br). The validation was performed in the same software and in the Xternal Validation 1.2 (https://sites.google.com/site/dtclabxvplus). A PLS model with good internal and external statistical features was obtained with four molecular descriptors: two BCUT weighted by polarizability and volume, one minimum E-state value, and one MOE-type descriptor based on partial charges and surface area. The presence of electronic characteristics agrees with reported information that the mode of binding of both Modafinil and cocaine to the DAT receptor is dependent on hydrogen bonds. Results show that the obtained model, although simple, have potential and may be suitable to propose new derivatives and for use in virtual screening studies.

**Área: MED** **Inscrição:00918**

# Thiosemicarbazones indole-based derivatives: Anticancer activity and Docking Studies towards topoisomerase inhibition

**Túlio R. Couto (PQ)[1*], Leiliane A. Silva (IC)[1], Lucas M. S. Rodrigues (IC)[1], Eduardo C. Aguiar (PQ)[1], Jamerson F. Oliveira(PQ)[2], Thalita S. Lima(PG)[2], Sybelle C. B. L. Pedrosa(PQ)[2], Maria C. A. Lima(PQ)[2].**

**tulio.couto@ufrpe.br**

[1]*Unidade Acadêmica de Serra Talhada (UAST) – UFRPE;*
[2]*Departamento de Antibióticos, Universidade Federal de Pernambuco – UFPE*

Palavras Chave: *Docking, Interação com DNA, Química Medicinal, Topoisomerase.*

## Highlights

Five thiosemicarbazones indole-based derivatives were submitted to in vitro antitumoral tests, and the results were compared to docking studies towards the topoisomerase enzyme.

## Resumo

No desenvolvimento de novas entidades terapêuticas para o tratamento do câncer, uma das estratégias utilizadas é a inibição da enzima topoisomerase, por ter papel importante na replicação do DNA.[1] Neste sentido, uma série de derivados indólicos tiossemicarbazona (Figura 1) foram sintetizados e posteriormente submetidos a testes de atividade antitumoral in vitro.[2] Para determinação do mecanismo de ação antitumoral, o agente de atividade mais pronunciada foi submetido ao teste de interação com a topoisomerase 2 alfa, que indicou que o composto foi capaz de inibir a enzima. Posteriormente, a análise de docking para a topoisomerase foi realizada para toda a série de compostos. Os dados de docking e atividade in vitro obtidos para estes compostos estão descritos na Tabela 1.

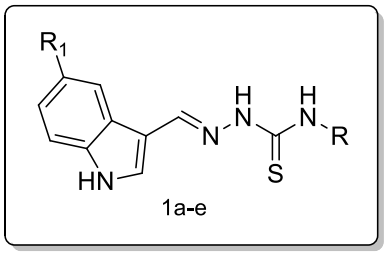


Figura 1.

Tabela 1. Atividade antiproliferativa in vitro (GI50 em µM) e Docking (kcal/mol) de derivados indólicos tiossemicarbazona

| **Linhagens** | **1a** R = 1-naftil $R_1$ = Br | **1b** R = 1-naftil $R_1$ = H | **1c** R = p-toluil $R_1$ = H | **1d** R = 2-fenetil $R_1$ = Br | **1e** R = 2-fenetil $R_1$ = H | **Dox** |
|---|---|---|---|---|---|---|
| U251 | 7.32 | 0.92 | 8.11 | 7.49 | 77.90 | 0.14 |
| MCF 7 | 0.95 | 0.25 | 2.52 | 6.81 | 15.54 | 0.07 |
| NCI-ADR/RES | 6.18 | 6.48 | 1.46 | 7.14 | 38.74 | 0.77 |
| 786-0 | 6.56 | 0.25 | 3.99 | 7.58 | 76.29 | 0.11 |
| NCI-H460 | 6.99 | 0.38 | 11.72 | 8.48 | >100 | 0.09 |
| OVCAR-3 | 1.60 | 0.21 | 3.88 | 8.22 | >100 | 0.22 |
| HT-29 | 6.56 | 0.01 | 1.45 | 7.87 | >100 | 0.23 |
| K562 | 5.29 | 0.01 | 0.16 | 2.12 | 0.17 | 0.93 |
| **Docking** | **-10.7** | **-10.36** | **-9.03** | **-10.01** | **-9.34** | **–** |

A análise das energias de interação entre o ligante e receptor mostraram correlação com os dados in vitro obtidos para esta série de compostos. As estruturas 1a e 1b, que obtiveram os melhores resultados de interação com o sítio ativo da topoisomerase, apresentaram excelentes resultados na análise in vitro. Estes dados, junto aos testes de inibição da topoisomerase realizados para a estrutura **1b** sugerem que a topoisomerase pode ser um alvo de ação antitumoral desta série de compostos.

1. Pommier, Y., Leo, E., Zhang, H. & Marchand, C. DNA topoisomerases and their poisoning by anticancer and antibacterial drugs. *Chem. Biol.* **17,** 421–433 (2010).
2. Oliveira, J. F. *et al.* Thiosemicarbazones and 4-thiazolidinones indole-based derivatives: Synthesis, evaluation of antiproliferative activity, cell death mechanisms and topoisomerase inhibition assay. *Eur. J. Med. Chem.* **136,** 305–314 (2017).

**Área: MED** **Inscrição: 00881**

# Molecular modeling studies upon the hybrid prophylactic agent between 7-methoxytacrine (7-MEOTA) and 4-pyridinealdoxime (4-PA) with different spacer lengths

**Jorge Alberto Valle da Silva (PG),[1] Eugenie Nepovimova (PQ),[2] Teodorico Castro Ramalho (PQ),[3] Kamil Kuca (PQ),[1] Tanos Celmar Costa Franca (PQ),[1,4,*]**

tanosfranca@gmail.com

[1]*Laboratory of Molecular Modeling Applied to the Chemical and Biological Defense (LMCBD), Military Institute of Engineering, Rio de Janeiro/RJ, Brazil;* [2]*Biomedical Research Centre, University Hospital Hradec Kralove, Hradec Kralove, Czech Republic;* [3]*Laboratory of Molecular Modeling, Chemistry Department, Federal University of Lavras, Lavras, MG, Brazil;* [4]*Center for Basic and Applied Research, Faculty of Informatics and Management, University of Hradec Kralove, Hradec Kralove, Czech Republic.*

*Keywords: Acetylcholinesterase, Molecular modeling, Aldoxime, Spacer, 7-MEOTA-4-PA.*

## Highlights

- Hybrids between 7-methoxytacrine (7-MEOTA) and 4-pyridinealdoxime (4PA) can work as good prophylactic agents for intoxication by organophosphates;
- The hybrid with a 5-carbon length-spacer connecting 7-MEOTA and 4PA is promising for reactivation of acetylcholinesterase (AChE) inhibited by the neurotoxic agent VX;
- Molecular modeling studies of hybrids with spacers from 1 - 10 carbons long, pointed to the 4 and 5-carbon length spacers as the best for optimizing interactions inside human AChE inhibited by VX.

## Resumo/Abstract

The novel prophylactic agent 7-methoxytacrine-4-pyridinealdoxime hybrid (called here hybrid 5C) is a hybrid between 7-methoxytacrine (7-MEOTA) and 4-pyridinealdoxime (4-PA) with a 5-carbon length-spacer connecting both molecules. This compound was former designed as a prophylactic agent for intoxication by organophosphates (OP), able to form a complex with acetylcholinesterase (AChE) and reactivate this enzyme in case of OP inhibition. In order to check if the 5 carbons spacer is the ideal to maximize the interactions of this compound inside human AChE (*Hss*AChE), we performed in this work docking, molecular dynamics and mmpbsa studies on a series of analogues of the hybrid between 7-MEOTA and 4-PA, varing the spacer-length from 1 to 10 carbons long. Our results helped to elucidate the interactions of these compounds with the different binding sites inside *Hss*AChE and pointed to the 4 and 5 carbons long as the best spacers for optimizing these interactions.

# 3'-Hydroxychalcones against multidrug-resistant *Mycobacterium tuberculosis*: Design using Topliss' method, synthesis and bioassay

**Leticia R. Assis (PG),[1] Ligia O. Rodrigues (PG),[1] Débora L. Campos (PG),[2] Camila M. Ribeiro (PG),[2] Isabel C. Silva (PQ),[2] Fernando R. Pavan (PQ),[2] Luis O. Regasini (PQ).[1]***

**leticia-rda@hotmail.com; regasini@ibilce.unesp.br**

*[1]Laboratório de Química Verde e Medicinal (LQVM), Departamento de Química e Ciências Ambientais, Instituto de Biociências, Letras e Ciências Exatas (IBILCE), UNESP, São José do Rio Preto, SP, Brasil; [2]Departamento de Ciências Biológicas, Faculdade de Ciências Farmacêuticas, UNESP, Araraquara, SP, Brasil.*

Palavras Chave: Chalcone, Tuberculosis, *Mycobacterium*, Topliss, SAR, Multidrug-resistance

## Highlights

4-nitro-3'-hydroxychalcone (**12**) and 4-piridinyl-3'-hydroxy-chalcone (**19**) demonstrated potent activity against MDR clinical isolates of *M.tuberculosis*, exhibiting MIC values ranging from 27.3 to 39.9µM.

## Abstract

Chalcones are privileged scaffold in Medicinal Chemistry, due to their broad spectrum of bioactivities, easy and versatile synthesis.[1] Among these, metochalcone and sofalcone have been marketed as choleretic and antiulcer drugs.[2] As part of our continuing investigation for novel antitubercular agents, we synthesized 45 hydroxychalcones by Claisen-Schmidt reaction[3], resulting in yields of 45-98%.

**Scheme.** General reaction for synthesis of 3'-hydroxychalcones

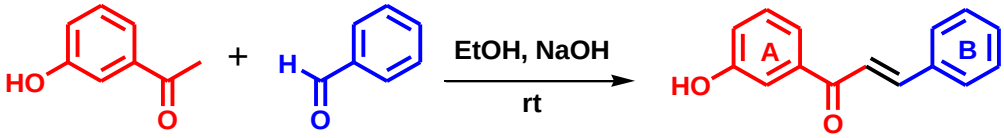


Chalcones presented hydroxyl on rings A and B at positions *ortho*, *meta* and *para*. The major substituents on ring B were electron-withdrawing atoms/group (halogens, $CF_3$, $OCF_3$ and $NO_2$), indicated by Topliss' decision tree. Bioisosteric hypothesis was investigated by replacement of phenyl ring B by furanyl, thienyl, pyridinyl and naphthyl rings. Twelve hydroxychalcones substituted by electron-withdrawing and hydrophobic groups exhibited activity against H37Rv (sensitive and ATCC strain)[4], demonstrating MIC values ranging from 4.6 to 14.7µM. These chalcone were selected to evaluation against human pneumocytes[4]. Three chalcones exhibited low toxicity $IC_{50}$ > 100µM and were assayed against resistant clinical isolates. For clinical strains A (resistant to isoniazid), B (resistant to isoniazid and rifampicin) and C (resistant to isoniazid, rifampicin and moxifloxacin), **12** displayed MIC values of 39.9, 33.9 and 27.7µM, respectively. For clinical strains D (resistant to isoniazid, rifampicin and amikacin), **19** presented MIC value of 27.3µM.

**Figure.** Structure of 3'-hydroxychalcones with activity against MDR *Mycobacterium tuberculosis*

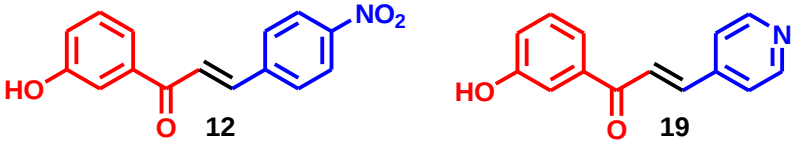


Additionally, bioactive 3'-hydroxychalcones were subjected to *in silico* analysis to predict their drugability. All compounds did not violate their Lipinski's and Veber's boundaries, and potent antitubercular hydroxychalcones exhibited absorption percentage ranging from 80.3 to 96.1. These values corroborated their ability to penetrate into highly hydrophobic mycolic acid layer of *M. tuberculosis* and blood-brain membrane, which is relevant barrier to drugs to act against tuberculous meningitis.[5]

[1]Zhuang et al. **Chem. Rev.** 117, 772, 2017. [2]Sahu et al. **Curr. Med. Chem.** 19, 209, 2012. [3]Mahapatra et al. **Eur. J. Med. Chem**. 101, 496, 2015. [4]Fernandes et al., **J. Med. Chem.** 60, 8647, 2017. [5]Polaquini et al. **Molecules** 22, 1685, 2017.

**Área: MED** **Inscrição: 00819**

# Sulfation of the ß-1,3;1,6-D-glucan botryosphaeran and evaluation of its derivatives against herpes and dengue viruses

**Bruce A. L. Sacchelli (PG),[1] Thainá M. Bernardes (IC),[1] Aneli M. Barbosa-Dekker (PQ),[1] Lígia C. F. Galhardi (PQ),[2] Rosa E. C. Linhares (PQ),[2] Alexandre Orsato (PQ).[1*]**

**orsato@uel.br[*]**

[1]*Departamento de Química, CCE/UEL;* [2]*Laboratório de Virologia, CCB/UEL.*

Palavras Chave: *Botryosphaeran; β-glucan; sulfation; antiviral activity; dengue fever; herpes.*

## Highlights

Sulfated polysaccharides are known to have antiviral activity. Botryosphaeran, a beta-glucan, was synthetically sulfated and its derivatives presented activity against herpes and dengue viruses.

## Abstract

Viral diseases, such as dengue and herpes, are a threat to public health. A specific treatment for dengue fever is still not available. Herpes is treated mainly with acyclovir, but resistant strains to this drug are increasing. Sulfated polysaccharides are known to present antiviral activity against enveloped viruses that cause these diseases. Botryosphaeran is an exopolysaccharide (EPS) of the fungus *Botryosphaeria rhodina*.[1] This work proposed the sulfation of this biopolymer (Fig. 1) in order to enhance its antiviral activity.

*Figure 1. Sulfation of Botryosphaeran with chlorosulfonic acid*

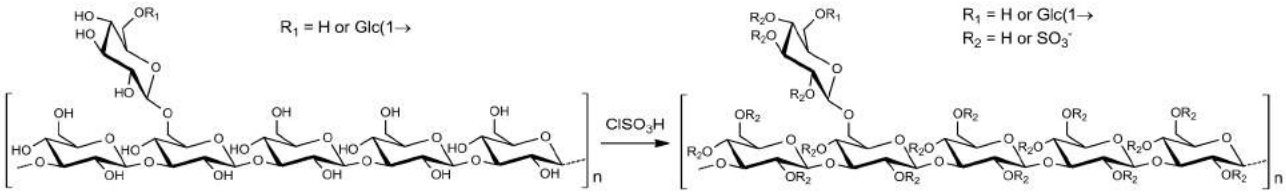


The sulfation was performed with chlorosulfonic acid, as described by Mendes et al (2009).[2] The presence of sulfate groups in the products was demonstrated by infrared spectroscopy. Different degrees of substitution (DS) were found when the EPS was submitted to one (DS=0.4) or three cycles of sulfation (DS=0.5). The highest DS (1.1) was obtained for this EPS that underwent a process of aqueous solubilization and filtration prior to sulfation. Table 1 shows the $IC_{50}$ of botryosphaeran and its derivatives against Herpes Simplex Virus (HSV).

*Table 1. $IC_{50}$ of botryosphaeran and its derivatives against HSV.*

| Sample | Degree of substitution | $IC_{50}$ (HSV) |
|---|---|---|
| Botryosphaeran | - | 41.7 μg $mL^{-1}$ |
| S1 | 0.4 | 3.0 μg $mL^{-1}$ |
| S3 | 1.1 | 2.4 μg $mL^{-1}$ |

The increasing activity can be related to the higher DS value, considering that the same tendency was observed when the same samples were tested against Dengue virus (DENV-3). The highest sulfated botryosphaeran (S3) displayed 90% and 73% inhibition against DENV-3 at 100 and 50 μg $mL^{-1}$, respectively.

**1.** BARBOSA A. M. et al. ***Carbohydr. Res.*** 338, 1691–8, 2003. **2.** MENDES, S. F. et al. ***Int. J. of Biol. Macromol.***, 45, 305–309, 2009.

**Área: MED**
*(Inserir a sigla da seção científica para qual o resumo será submetido. Ex: ORG, BEA, CAT)*

**Inscrição: 00722**
*(Inserir o número de inscrição do autor que fez a submissão)*

# Synthesis, antileishmanial activity and protease inhibition of benzoxazoles derivatives.

**Laís R. S. Folquitto (PG),[1*] Priscila F. Nogueira (IC),[1] Patrícia F. Espuri (PG),[2] Vanessa S. Gontijo (PQ),[1] Thiago B. De Souza (PQ),[3] Marcos J. Marques (PQ),[2] Diogo T. Carvalho (PQ),[4] Wagner A. S. Júdice (PQ),[5] Danielle F. Dias (PQ).[1]**

**lais.folquitto@gmail.com; lais.folquitto@gmail.com**

*[1]Institute of Chemistry, UNIFAL-MG; [2]Institute of Biomedical Sciences, UNIFAL-MG; [3]Industrial Pharmacy Department, UFSM; [4]College of Pharmaceutical Sciences, UNIFAL-MG; [5]Interdisciplinary Center of Biochemical Research, UMC.*

Keywords: *Benzophenone, Acetophenone, Leishmania amazonensis, Antiproteolytic activity, rCPB2.8, rCPB3.0.*

## Highlights

- Ten benzoxazole derivatives were obtained;
- They showed good results as inhibitors of proteases and against *Leishmania amazonensis*;
- Derivatives **4d** and **2b** showed significant results.

## Resumo/Abstract

The pathology Leishmaniasis is caused by protozoa of the genus *Leishmania*, infecting individuals in several parts of the world, including many cases in Brazilian territory, according to World Health Organization[1]. Due to the scarcity of drugs used for the treatment of this disease and also registered resistance cases, the need for development of new compounds with antileishmanial activity arouse interest in researchers and so the search for different targets of drugs design, like proteases, which are very important to virulence and survival of parasites[2]. In light of that, this work describes the synthesis of ten benzoxazoles derivatives, which were obtained in three-step route from 4-hydroxybenzophenone and 4-hydroxyacetophenone, along with their proteases inhibition and antileishmanial activities. Benzoxazoles derivatives and synthetic intermediates and precursors were evaluated according to their proteases inhibition against cysteine (papain and rCPB2.8 and rCPB3.0, specifics of genus *Leishmania*) and serine (trypsin) proteases. All compounds present meaningful values of $IC_{50}$ (0.0075–0.7612 μM), better than standards E64 (1.7821 μM) and TLCK (7.2318 μM). Afterwards, they were *in vitro* assayed against promastigote forms of *Leishmania amazonensis*, wherein the most actives compounds were evaluated against amastigote forms and their cytotoxicity activity. The benzoxazole derivative from benzophenone **4d** and synthetic intermediate **2b** were the most actives compounds with values of $IC_{50}$ 90.3 and 130.9 μM, respectively, besides significant values of selectivity indexes, comparing to standards drugs pentamidine and amphotericin B. Therefore, these compounds may be more explored to improve their potential antileishmanial.

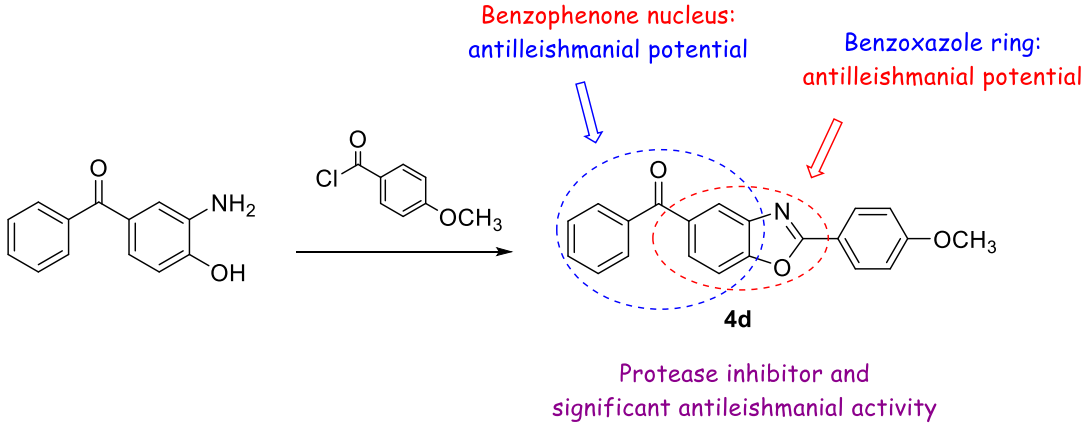


References: [1]WHO (2015) <http://www.who.int/mediacentre/factsheets/fs375/en/>.
[2]Das P. et al. (2013) Indian J. Biochem. Biophys. 50:363–376.

Acknowledgements:
FAPEMIG CAPES CNPq

**Área: MED** **Inscrição: 00659**

# Synthesis of thiosemicarbazide derivatives with antimicrobial activity

**Maria Luísa Leandro de Lima (IC)[1], Rafael Matos Ximenes (PQ)[1], Kêsia Xisto da Fonseca Ribeiro de Sena (PQ)[1], Julianna Ferreira Cavalcanti de Albuquerque (PQ)[1]*.**

**julianna@ufpe.br**

[1]*Departamento de Antibióticos, UFPE, Recife, Brasil*

Keywords: *Thiosemicarbazide, Thiosemicarbazone, antimicrobial activity*.

## Highlights

Three new thiosemicarbazide derivatives were synthesized with yield above 70%. Compounds were tested for their antimicrobial activity. All compounds were active mainly against *Candida albicans*.

## Resumo/Abstract

Thiosemicarbazone derivatives have been studied due to their biological activities, as antibacterial, antiviral, antitumor, and antiprotozoal[1,2]. Compounds were synthesized with equimolecular amounts of reagents and accompanied by TLC (Fig.1). Three new compounds were synthetized: compound Ju-840 (MP 205-206 ºC, Yield 73%), compound Ju-852 (MP 213-214ºC, Yield 90 %), and compound Ju-882 (MP 189-190 ºC, Yield 99,8 %). Given the high bacterial/fungal resistance to known antibiotics in hospital environment, the need has arisen to find new and more effective drugs. Towards this objective, compounds were assessed for their antimicrobial activity against clinical relevant microorganisms (Table 1). Thiosemicarbazide derivatives were active against Gram-positive bacteria and yeast, except for compound Ju-852, which was active only for yeast.

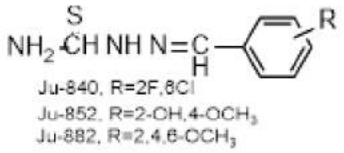


**Figure 1.** Thiosemicarbazide derivatives.

**Table 1.** Antimicrobial activity evaluated through disk diffusion method. Results are expressed in mm of inhibition zones (mean ± SD).

| Micro-organisms | | Thiosemicarbazide derivatives | | | Ref. drug |
|---|---|---|---|---|---|
| | | Ju-852 | Ju-840 | Ju-882 | Kanamycin |
| Gram-positive bacteria | 1 | 0 | 15±0.57 | 15±0.82 | 23 |
| | 6 | 0 | 12±0.63 | 12±0.72 | 28 |
| | 138 | 0 | 0 | 0 | 0 |
| | 16 | 0 | 20±0.74 | 15±0.80 | 14 |
| Gram-negative bacteria | 39 | 0 | 0 | 0 | 20 |
| | 224 | 0 | 0 | 0 | 15 |
| | 398 | 0 | 0 | 0 | 15 |
| Mycobacterium | 71 | 0 | 0 | 0 | 40 |
| Yeast | 1007 | 13±0.91 | 25±0.71 | 27±0.83 | nt |

**Note:** 1 *Staphylococcus aureus*, 6 *Micrococcus luteus*,138 *Enterococcus faecalis,* 16 *Bacillus subtilis*, 39 *Pseudomonas aeruginosa*, 224 *Escherichia coli*, 398 *Serratia marcescens*, 71*Mycobacterium smegmatis*, 1007 *Candida albicans*, nt = not tested.

**References**

[1]Bharti, N.; Husain, K.; Garza, M. T. G. et al. Bioorg. Med. Chem. Lett, 12 (23), 3475-3478, 2012.
[2]Tenório, R. P.; Góes, A.J.S.; Lima, J.G. et al. Quim. Nova, 28 (6), 1030-1037, 2005.

**Área: MED** **Inscrição: 00571**

# Pharmacokinetic and Docking studies of Thiazolidinedione derivatives inhibitors of Trypanothione Reductase of *Trypanosoma cruzi* (TcTR)

**Clarissa M. S. Peralva (IC),[1] Kamel Metwally (PQ), [2] Samuel S. da R. Pita (PQ)[1*]**

**cperalva411@hotmail.com; samuelrpita@gmail.com**

*[1]Laboratório de Bioinformática e Modelagem Molecular (LaBiMM), Faculdade de Farmácia, Universidade Federal da Bahia, Ondina, CEP: 40170-115, - Salvador- BA- Brasil;* [2] Department of Medicinal Chemistry, Zagazig University, Zagazig, Egypt.

Keywords: *Trypanosoma cruzi*, *Trypanothione Reductase, Pharmacokinetic Properties, Docking, Drug Discovery.*

## Highlights

Chagas disease affects to 6-7 million people worldwide. The TcTR is a validated target for anti-trypanosoma drugs. Computational methods have been helping the research of new TcTR inhibitors that could lead in new drugs.

## Abstract

Since its discovery in 1908 until nowadays there is any effective treatment for Chagas' disease, mainly at its chronic phase. *Trypanosoma cruzi* Trypanothione Reductase (TcTR) is a validated molecular target and the search for new compounds capable of promoting its rupture or blockage of its catalytic activity could result in promising anti-trypanosoma/Chagas' compounds. Thus, we selected a series of Thiazolidinedione derivatives aiming that they will inhibit TcTR. Firstly, we analyzed their pharmacokinetics and toxicology properties from pkCSM server (http://biosig.unimelb.edu.au/pkcsm/prediction) and we noted that: ***i)*** All compounds had an ideal values for intestinal absorption (IA ≥ 75%); ***ii)*** poor CNS penetration (Log PS ≤ -3); ***iii)*** they do not inhibit hERG and ***iv)*** all compounds were not substrates (and inhibitors) of the P-glycoprotein, except *KAM-2*, *KAM-3*, *KAM-4*, *KAM-5*, *KAM-6*, *KAM-7* e *KAM-15*. Afterwards, we employed Autodock 4.2.6 to analyze the interactions among Thiazolidinediones and TcTR. The best binding energy for the TcTR complexes were obtained with **KAM-4** (-10.69 kcal/mol) and **KAM-2** (-9.97 kcal/mol) and the worst, **KAM-13** (-8.55 kcal/mol). We evaluated the TcTR active site interactions with Thiazolidinedione and our results showed that better inhibitors (**KAM-4** and **KAM-2**, **Figure 1-A**) interacted with the main active site residues (*Cys-58*, *His-461*, *Thr-463*, *Glu-466* and *Glu-467*), whereas **KAM-13** (worst energy) interacted a little far away from active site (**Figure 1-B**). Then we concluded that the interaction of Thiazolidinedione derivatives at TcTR could help in the discovery of new anti-trypanosoma drugs.

**Figure 1.** Main interactions of best docking poses of Thiazolidinedione derivates (**KAM-2**, **KAM-4** and **KAM-13**) at Trypanothione Reductase of *Trypanosoma cruzi* (TcTR). TcTR structure is represented in gray cartoon, their catalytic residues (cyan) and ligand in sticks. **A) KAM-2** (magenta) and **KAM-4** (orange). **B) KAM-13** (green).

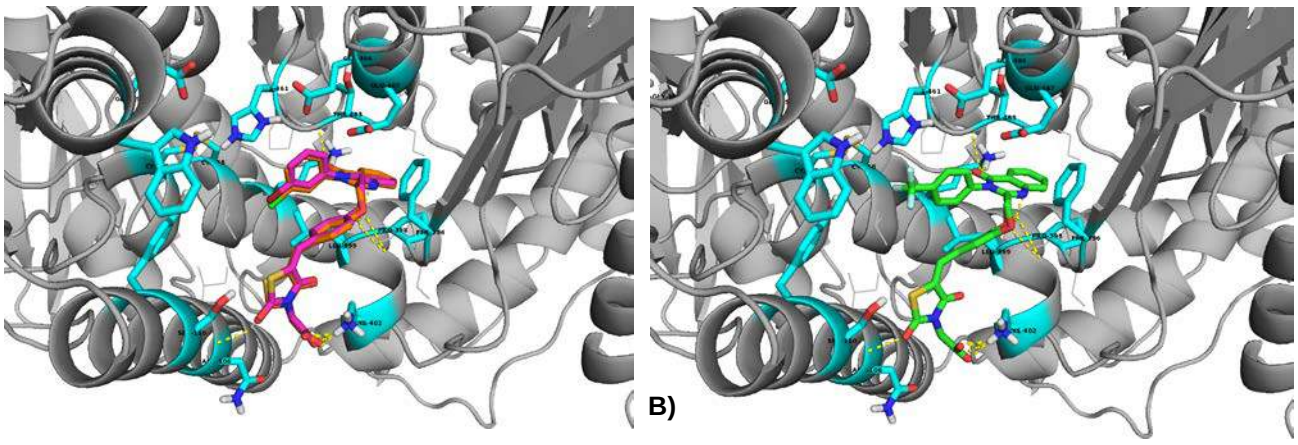

**A)** **B)**

**Área: MED** **Inscrição: 554**

# Discovery of Marinoquinolines as Potent and Fast-Acting *Plasmodium falciparum* Inhibitors with In Vivo Activity

**Anna Caroline C. Aguiar (PQ),[1] Michele Panciera (PQ),[2] Eric F. S. dos Santos (PG),[2] Maneesh K. Singh (PG),[3,4] Mariana L. Garcia (PG),[1] Guilherme E. de Souza (PG),[1] Myna Nakabashi (PQ),[4] Célia R. S. Garcia (PQ),[3] Glaucius Oliva (PQ),[1] Carlos Roque D. Correia (PQ),[2] Rafael V. C. Guido (PQ),[1]***

***rvcguido@ifsc.usp.br**

*[1]Sao Carlos Institute of Physics, University of Sao Paulo, Av. Joao Dagnone, 1100 Jardim Santa Angelina, São Carlos, SP, 13563-120, Brazil; [2]Institute of Chemistry, State University of Campinas, Josue de Castro St., Campinas, SP, 13083-970, Brazil; [3]Department of Parasitology, University of Sao Paulo, São Paulo, SP, 05508-000, Brazil; [4]Department of Physiology, University of Sao Paulo, Rua do Matão 101, travessa 14, São Paulo, SP, 05508-090, Brazil*

Palavras Chave: malaria, inhibitor, Plasmodium falciparum, marinoquinoline.

## Highlights

We used a combination of synthesis and SAR/QSAR studies to discover marinoquinoline derivatives as inhibitors of *P. falciparum* with noticeable in vivo activity. The compounds are new lead candidates for antimalarial development.

## Resumo/Abstract

Malaria is one of the most prevalent parasitic infection in the world. The disease affects 262 million people each year, and in 2015 it was estimated to have caused 429,000 deaths. We report a comprehensive study to discover marinoquinoline derivatives as a new class of compound with antiplasmodial activity. We synthesized and evaluated the inhibitory activity against *P. falciparum* 3D7 strain and conducted a structure−activity relationship study, focusing on the improvement of potency and maintaining low cytotoxicity. Next, we devised 2D and 3D QSAR models, which we prospectively validated, to discover new marinoquinoline derivatives with enhanced potency. The most potent compound **50** ($IC_{50}^{3d7}$ = 39 nM; $IC_{50}^{K1}$ = 41 nM) is a fast-acting inhibitor with noticeable activity in the early stage of intraerythrocytic cycle and liver stages of development. Moreover, the compound showed considerable selectivity index (SI > 6410) and additive effect in combination with artesunate. Mechanism of action investigation indicated concentration-dependent interference in heme species sequestration (Figure 1). Compound **50** showed an excellent tolerability in non-infected mice (all mice survived up to 30 days) and interesting oral efficacy at 50 mg/Kg in the *P. berghei* malaria mouse model (62 % of parasitemia reduction on day 5 and 56 % on day 9 post-infection) thus being considered as a lead compound for the discovery of new antimalarial agents.

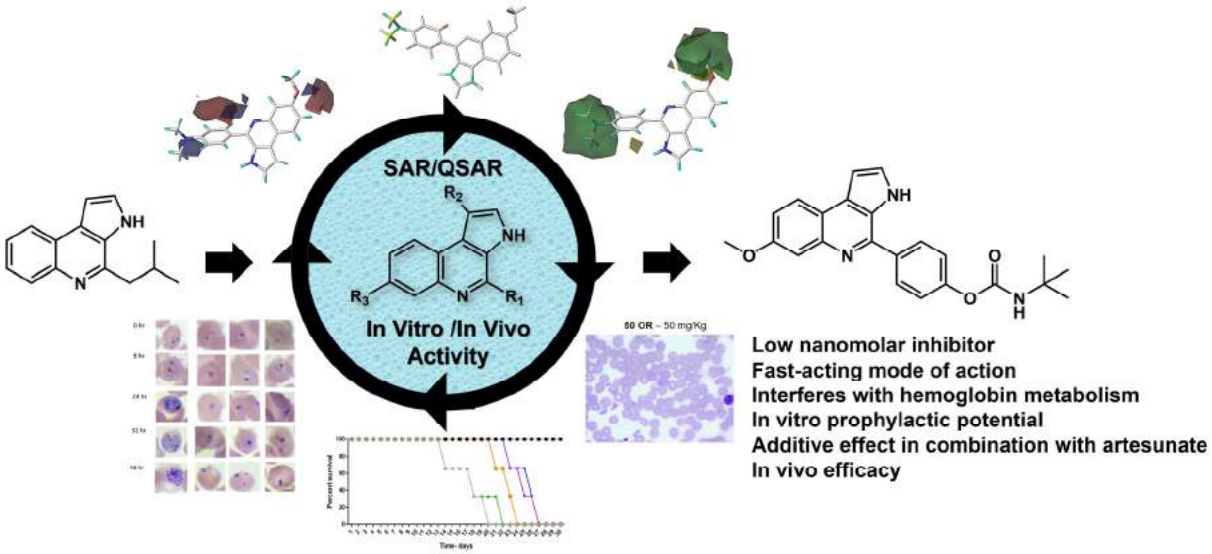


**Figure 1**. Integrated strategies to discover marinoquinoline derivatives as new lead candidates.

**Área: MED** **Inscrição:00522**

# Molecular Modeling of Thiosemicarbazones, CandidateDual Inhibitors of Snake Venoms Metalloproteases andPospholipases A2

**Nathally Lima do Nascimento (IC),[1]Catarina De Nigris Del Cistia (PG),[2]Arthur E. Kürmmerle (PQ)[1], Carlos Mauricio R. Sant'Anna (PQ)[1]***

**nathylnasc@gmail.com; santanna@ufrrj.br**

*[1]Departamento de Química, UFRRJ; [2]Departamento de Matemática, UFRRJ.*

Palavras Chave:*snakebites,thiosemicarbazones, molecular docking, semiempiricalmethod.*

## Highlights

Molecular docking and semiempirical calculations were used to verify the potential snake venom $PLA_2$inhibitory activity of thiosemicarbazones, previously identified by us as metalloproteases inhibitors.

## Resumo/Abstract

This project aims to obtain compounds to treat victims of snakebites, which are responsible for many deaths and amputations worldwide. The toxic effect of venoms occurs primarily by the action of metalloproteases and phospholipases $A_2$ ($PLA_2$). Our group employed rational design to propose thiosemicarbazones (INPI: BR 2016 003490 6) which were synthesized and showed inhibitory activity against a venom metalloprotease and also *in vivo* anti-hemorrhagic action[1]. Here we present the results of atheoretical investigation of the most active thiosemicarbazones (figure 1), to verify their potential activity as $PLA_2$ inhibitors.

Two $PLA_2$ X-ray structures from *Bothrops jararacussu* available in the Protein Data Bank, 1ZL7 and 1ZLB, the first containing a $Ca^{2+}$ ion, were used for a triplicate docking study with the GOLD program (CCDC), using Goldscore as the scoring function. The highest fitness scores were obtained with the $Ca^{2+}$ containing structure. The best poses of the 3 thiosemicarbazones into 1ZL7 were then used as input files for calculations with the semiempirical PM6 method of the MOPAC2016 program (Stewart Computational Chemistry) to obtain data to calculate the enthalpy of interaction ($\Delta H_{int}$). The three structures produced favorable $\Delta H_{int}$, with 23b presenting the best result (figure 2). As the 3 thiosemicarbazones are also metalloprotease inhibitors, these theoretical results are indicative that all compounds are dual inhibitors candidates, which could improve their therapeutic efficacy for snakebites treatment.

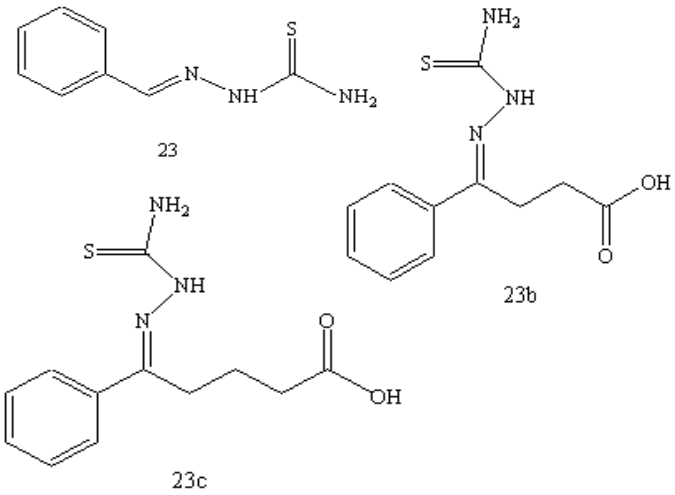


Figure 1: Structure of the compounds 23,23b e 23c.

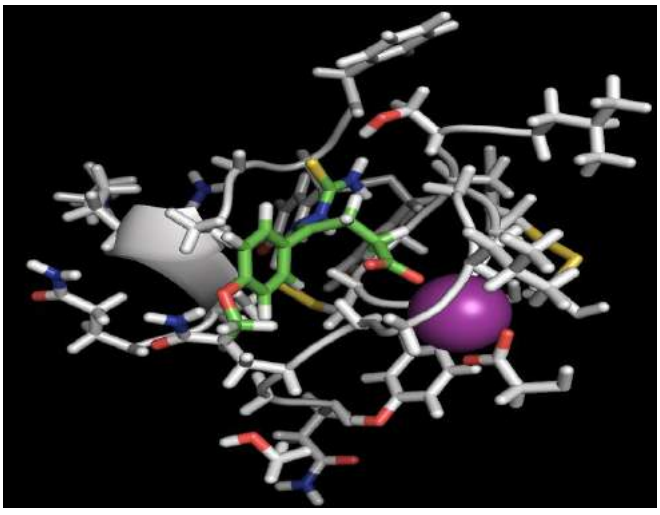

Figure 2: Interaction between the compound 23b (green) and 1ZL7 active site (gray).

[1]FERREIRA, F. B. et al.,*ACS Med Chem. Lett.***2017**, 8, 1136-1141

**Aknowledgments:** CNPq, CAPES, Faperj.

**Área: MED** **Inscrição: 00431**

# CHALCONES SYNTHESIS BY CLAISEN-SCHMIDT CONDENSATION AND EVALUATION OF LARVICIDAL ACTIVITY IN *Aedes aegypti*

**Gabriella Barroso Souza (PG),[1*] Péricles B. Alves (PQ),[1] André L. B. S. Barreiros (PQ),[1] Marizeth L. Barreiros (PQ),[1] Sócrates C. de Holanda Cavalcanti (PQ),[2] Thaysnara B. Brito (PG),[2] Emmanoel Vilaça Costa (PQ).[3]**

**gabriella_souza25@hotmail.com**

*[1]Departamento de Química-UFS, [2]Departamento de Farmácia UFS; [3]Departamento de Química- UFAM.*

Keywords: *Synthesis, Chalcones, Aedes aegypti, Larvicidal activity.*

## Highlights

Use of chemical agents with biological potential is efficient in the prevention and treatment of diseases. This study synthesized and characterized four chalcones for larvicidal activity evaluation.

## Resumo/Abstract

Among the neglected tropical diseases (NTDs) that have been spread, Dengue, Chikungunya and Zika, are considered a great threat causing millions of death worldwide. The main factors contributing to the occurrence of such diseases are urbanization, climate change, lack of urban planning, intense people movement, lack of basic sanitation, and the indiscriminate use of insecticides. The chalcones were subjected evaluation of larvicidal activity against *Aedes aegypti* in order to contribute to the diversity of synthetic organic molecules in the study of structure versus activity of bioactive substances aiding in *Aedes Aegypti* vector control. The methodology used to obtain chalcones was Claisen-Schimidt aldolic condensation, which consists of the coupling between acetophenone and its derivatives with different aromatic aldehydes. Obtained chalcones were characterized using FTIR, HRMS, $^{1}$H-NMR, and $^{13}$C-NMR. (E) -1,3-diphenyl-prop-2-en-1-one (C-1), (*E*)-1-phenyl-3-*α*-naphtylprop-2-en-1-one (C-2), (*E*)-1-(4'-methoxyphenyl)-3-*α*-naphtyilprop-2-en-1-one (C-3) and (*E*)-1-(4'-methoxyphenyl)-3-(4-methoxyphenyl)-prop-2-en-1-one (C-4) were synthesized. The reaction is carried out on magnetic stirring for 3h in basic medium, using ethanol as the solvent at room temperature. After this time, the reaction mixture is stored in a refrigerator for 24 hours and in the next day is vacuum filtered. The reaction yield varied from 81% to 95%. The results of *Aedes aegypti* larvicidal test were: Chalcones C-1 and C-2 exhibited the best results with $CL_{50}$ 6.08 ppm and 39.88 ppm and C-3 and C-4 presented moderate activity $CL_{50}$ 634.86 ppm and 104.52 ppm.

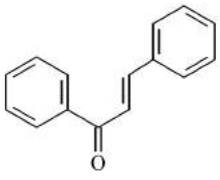


**C-1**

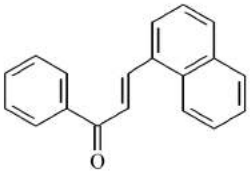


**C-2**

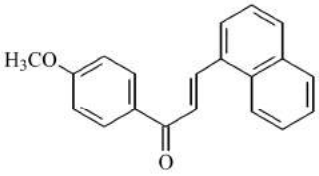


**C-3**

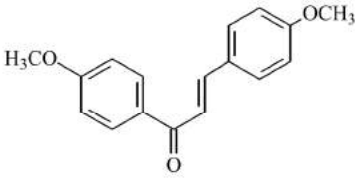


**C-4**

**Área: MED** **Inscrição: 357**

# Evaluation of the interaction of β-carbolines derivatives with DNA by molecular fluorescence and correlation with antiproliferative activity

**Marina de M. Silva (PG)[1], Karlly T. de O. Pereira (PG)[1], Valeria A. Barbosa (PQ)[2], Maria H. Sarragiotto (PQ)[2], Josué Carinhanha C. Santos (PQ)[1] e Isis M. Figueiredo (PQ)[1]**

**Marina-nina14@hotmail.com; karlly_thay@hotmail.com**

[1]*Instituto de Química e Biotecnologia, Universidade Federal de Alagoas.*
[2]*Departamento de Química, Universidade Estadual de Maringá.*

*Key words: DNA interaction; β-carbolines; action mechanism; antiproliferative activity*

## Highlights

β-carbolines interact by intercalation with DNA indicating the possible mechanism of action. Correlation between $K_b$ and $GI_{50}$ values for colon and kidney cancer cell lines was stablished.

## Abstract

The biological activities of many anticancer drugs may be often explained in terms of their interactions with nucleic acids[1,2]. Therefore, this study have tried to establish the relationship between the binding constants ($K_b$) values with DNA and *in vitro* activity parameters to evaluate the action mechanism responsible for the antiproliferative activity. Thus, the interaction of the β-carbolines **9e**, **9c**, **10b** and **17a** (**Fig. 1a**) which showed a pronounced antiproliferative activity[3], were evaluated with ctDNA (*Calf thymus*) through molecular fluorescence. The strength of the interaction, expressed as $K_b$ ranged from 2.45 to 118.7×10$^4$ M$^{-1}$. The binding mode was studied through the quenching effect of KI and by competition assays with ethidium bromide (BE). In the KI study, it can be seen that the $K_{SV}$ (Stern-Volmer quenching constant) values were reduced in the presence of DNA suggesting intercalation mode interaction, which was confirmed by the BE assay. Finally, the correlation analysis showed that for colon cell line (HT-29) there was a linear inverse trend, while for kidney cell line (786-0), there was an inverse exponential relation (**Fig 1b**). Due the analyzed variables ($K_b$ *vs* $IG_{50}$) were inversely proportional, the main action mechanism of these compounds may be related to DNA target. These data are in agreement with works found in the literature[1,2]. For the other strains assessed it was not possible to establish a good correlation (r < 0.3) indicating that compounds tested show a certain selectivity for colon and kidney cancer cell lines.

**Fig.1.** a) β-carbolines structures; b) The correlation between $K_b$ values and antiproliferative activity ($GI_{50}$) for colon and kidney cell lines.

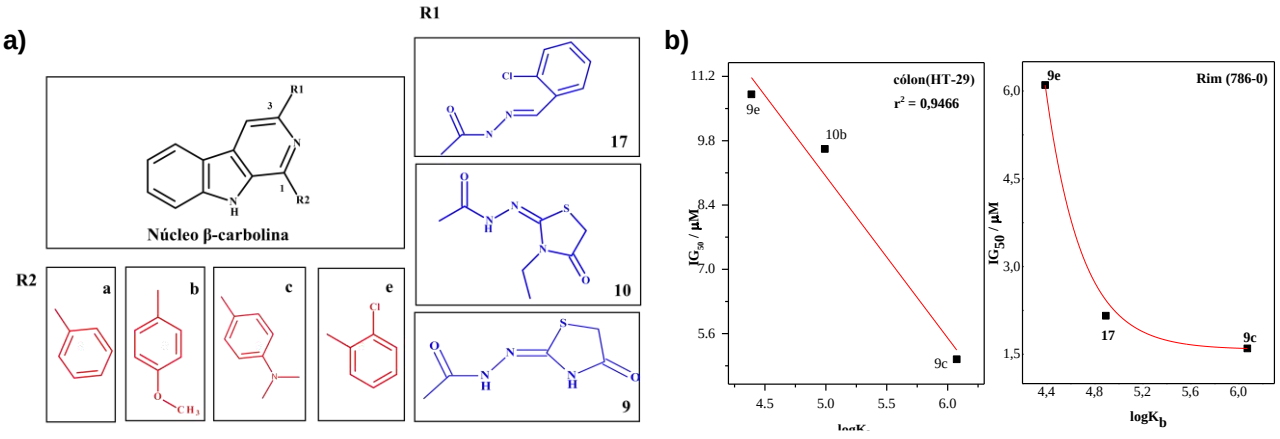


[1] SILVA, M. M. et al. ***J. Braz. Chem. Soc.*** 27, 9, 1558-1568, 2016.
[2] SAVARIZ, F. C. et al. ***Bioorg. Med. Chem.*** 22, 6867-6875, 2014.
[3] BARBOSA, V. A., et al. ***Europ. J. Med. Chem.*** 124, 1093-1104, 2016.

**Área: MED** **Inscrição: 287**

# $H_2S$-Donating monastrol: A new calcium channel modulator

**Taniris Cafiero Braga (PG),[1] Kathleen Viveiros Soares (IC),[1] Itamar Couto Guedes de Jesus (PG),[2] Silvia Guatimosim (PQ),[2] Ângelo de Fátima (PQ),[1]**

**E-mails: niratis@gmail.com (TCB) and angelodefatima@gmail.com (AF)**

*[1] Department of Chemistry, UFMG, Brazil; [2] Department of Biochemistry and Immunology, UFMG, Brazil.*

Keywords: *Monastrol, hydrogen sulfide, cardiomyocyte, calcium, calcium channel.*

## Highlights

► A novel hybrid Monastrol-$H_2S$ was prepared in 5 steps with 8% overall yield. ►Monastrol-$H_2S$ showed similar results as nifedipine at calcium transient dynamics in cardiomyocytes.

## Resumo/Abstract

The $H_2S$ and Biginelli's adducts can be considered as potentials calcium channel modulators.[1,2] In ventricular myocytes, the intracellular $Ca^{2+}$ transient is responsible for triggering cardiomyocyte contraction.[3] Therefore a hybrid monastrol-$H_2S$ (**9**) was synthetized and evaluated by calcium transient activity (Fig.1). The synthesis of **9**, started by Biginelli's cyclic condensation followed by hydrolyses furnishing **4** (46% yield, 2 steps). The linker **7** was prepared by protecting 2-bromoethan-1-amine with *di-tert-butyl*-dicarbonate with 73% yield. Then, $H_2S$ releasing core **6** was prepared by condensation between *trans*-anethole and sulfur followed by a methoxy deprotection with 18% yield. The nucleophilic bimolecular substitution of **6** with **7** was followed by an amine deprotection furnishing **8** with 68% yield. Finally, **4** and **8** was coupling providing **9** with 64% yield. The cardiomyocytes was treated using compounds monastrol, **6** and **9** in concentration between 100nM-10μM. The fluctuation in $Ca^{2+}$ release was recorded in electrically stimulated Fluo4/AM-loaded cardiomyocytes. Monastrol and **9** did not show significance change in the calcium transient. Besides **6**, in 100 μM, showed cytotoxic to cardiomyocytes. Fortunately, **9** showed a diminishing of calcium transient comparable with the control nifedipine. In summary, monastrol-$H_2S$ was obtained in 5 step with 8% overall yield. The magnitude of the effect evoked by **9** is similar to nifedipine. Therefore, **9** is considered a potential calcium modulator.

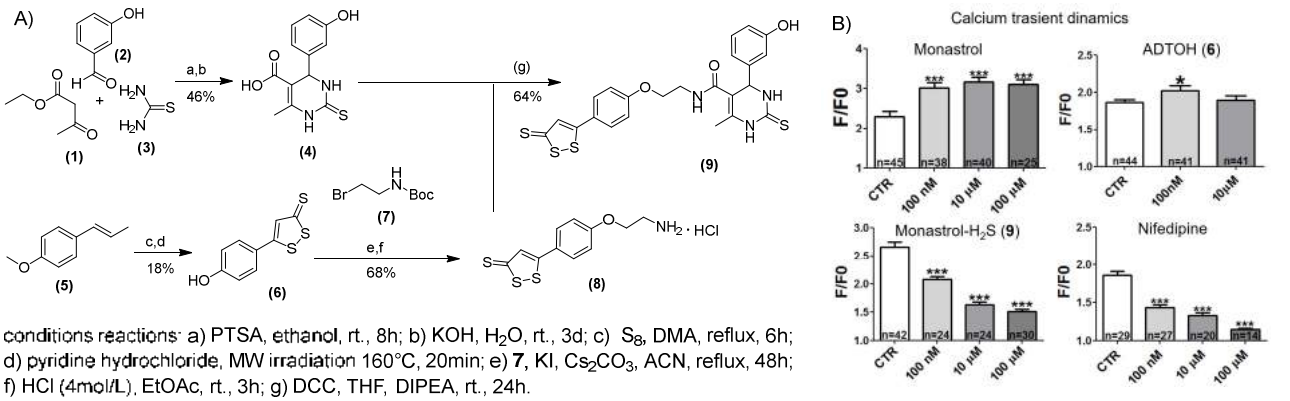


conditions reactions: a) PTSA, ethanol, rt., 8h; b) KOH, $H_2O$, rt., 3d; c) $S_8$, DMA, reflux, 6h; d) pyridine hydrochloride, MW irradiation 160°C, 20min; e) **7**, KI, $Cs_2CO_3$, ACN, reflux, 48h; f) HCl (4mol/L), EtOAc, rt., 3h; g) DCC, THF, DIPEA, rt., 24h.

**Figure 1:** A) Synthetic strategy to obtain monastrol-$H_2S$ (**9**). B) Calcium transient dynamics in cardiomyocytes treated by monastrol, ADTOH (**6**), monatrol-$H_2S$ (**9**) and nifedipine in concentrations 100nM-10μM.

Acknowledgment: FAPEMG, CNPq and CAPES.

[1] Nature. **2002**, 415(6868):198-205.
[2] J. Adv. Res. **2015**, 6(3): 363-373.
[3] Bull. Exp. Biol. Med. **2011**, 2(151): 163-166.

**Área: MED** **Inscrição: 00204**

# Molecular modeling studies of the nicotinic acetylcholine receptor (nAChR) α7: Validation and analysis of bioactive compounds

**Natália Fernanda Frediani Pirolla (PG)[1*], Victor S. Batista (PG)[1], Nailton M. Nascimento-Júnior (PQ)[1].**

**naty_frediani@hotmail;** nailtonjr@iq.unesp.br

[1]*Universidade Estadual Paulista "Júlio de Mesquita Filho", Laboratório de Química Medicinal, Síntese Orgânica e Modelagem Molecular (LaQMedSOMM), Instituto de Química, Departamento de Química Orgânica, Rua Professor Francisco Degni, 55, Jardim Quitandinha, CEP 14800-060, Araraquara-SP, Brasil.*

Palavras Chave: *nAChRs α7, Alzheimer´s disease, Molecular docking, Lobeline, Agonist activity.*

## Highlights

The nAChRs α7 are related with neuroprotective effects, attenuating β-amyloid protein-induced neurotoxicity. The agonist modulation of this receptor is a promising approach for the treatment of Alzheimer's disease[1]. Based on the crystallographic structure of the nAChRs α7, co-crystallized with lobeline (PDB ID: 5AFN)[2], redocking validation as well as *in silico* analysis of agonists with *in vitro* activity from literature were performed. The ligands were built with protonation states at physiological pH, using Discovery Studio Visualizer program and optimized through semi-empirical PM7 method using MOPAC2016. The redocking validation of nAChRs α7 model was based on the analysis of different scoring functions[3] (ChemPLP, ChemScore, GOLDScore, ASP) to evaluate ligands spatial orientation (RMSD) and relevant ligand-receptor interactions. Discovery Studio was used to analyse the predicted interactions, which were performed on GOLD and visualized through PyMol program. The ASP scoring function presented lower RMSD value, predicting key interactions between lobeline binding site residues and the selected molecules. Lobeline residues (Q55, Q114, Y191, W145, C186, S144, Y184, L36, I165, Y91, K141, W53 and N92) were frequently observed in the most active compounds of literature. So, they can be used to help the virtual screening of novel substances against the nAChRs α7.

## Abstract

The crystallographic structure of the nAChRs α7, co-crystallized with lobeline[2] **(1) (Figure 1)** (PDB ID: 5AFN) was used in the molecular modeling validation step and analysis of bioactive compounds from literature. For this purpose, the compounds were selected based on structural similarities with **1**, including the presence of aromatic subunits and subunits with basic or positively charged nitrogen atoms, as can be observed in **1** and quinucline analog **(2)**. Between all the scoring functions evaluated on redocking validation, ASP has shown the best results, presenting lower RMSD value = 0.5252 and the atoms position of co-crystallized ligand was exactly overlapped on redocking ligand, as observed in **3 (Figure 1)**. In addition, the *in silico* model predicted well the key interactions between residues and the molecules selected from the scientific literature. The most active compounds frequently presented interactions shown in **Table 1**. So, this methodology can be used in virtual screening of novel compounds, in combination of docking results from bioactive compounds from literature.

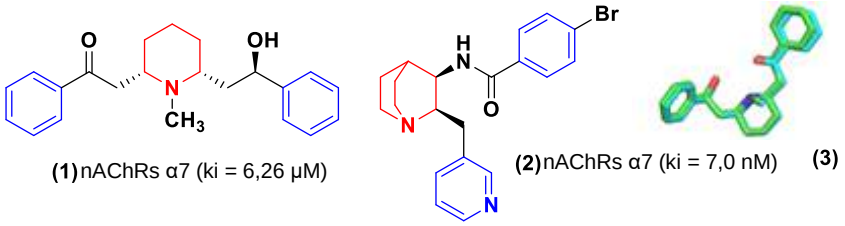


**(1)** nAChRs α7 (ki = 6,26 μM) **(2)** nAChRs α7 (ki = 7,0 nM) **(3)**

**Figure 1:** Lobeline **(1)**, quinuclidine analog **(2)** chemical structures and overlap of the atoms position of co-crystallized ligand and redocking ligand, predicted by scoring function ASP **(3)**.

**Table 1:** Residues from crystal structure that interact with lobeline.

| | |
|---|---|
| Q55 | L36 |
| Q114 | I165 |
| Y191 | Y91 |
| W145 | K141 |
| C186 | W53 |
| S144 | N92 |
| Y184 | - |

Acknowledgements:
CAPES (scholarship), CNPQ, PROPe: Process 840, INCT-INOFAR: Process 573.564/2008.

[1]Cheng, Q; Yakel, J. Biochemical Pharmacology, 2015, 97, 439-444./ [2]Spurny, R. et al. Science. 2015, 112, 2543-2552./ [3]Cleves, A. E; Jain, A. N. Journal of Computer-Aided Molecular Design, 2015, 29, 485-509.

**Área: MED** **Inscrição: 0110**

# *In vitro* Screening of chalcones against urease activity

**Richele P. Severino (PQ)[1], Tainara da F. Rosa (IC),[1] Léia C. Mendes (IC),[1] Rosa S. Lima (PG),[2] Mirian R. C. de Castro (PG),[2] Aline Bernardes (PG),[2] Caridad N. Perez (PQ),[2] Lorena R. F. de Sousa (PQ),[1*].**

**richeleps@yahoo.com.br; lorennarf@yahoo.com.br***

*[1]Unidade Acadêmica Especial de Química, UFG, Regional Catalão, Catalão-GO; [2]Instituto de Química, UFG, Goiânia-GO.*

Key words: *Urease, Chalconas, Helicobacter pylori, Gastrite*.

## Highlights

On the view of antimicrobial activity of chalcones and the relationship of urease activity as virulence factor of ureolytic bacteria, we have investigated diverse chalcones against urease enzyme.

## Resumo/Abstract

Chalcones are natural compounds precursors of flavonoids on metabolic pathway in plants. These molecules have been showed a range of biological activities, such as antitumor, anti-inflammatory, antimicrobial, among others.[1]

*Helicobacter pylori* is a bacteria commonly found in digestive tract, and infections by *H. pylori* can lead to gastric ulcers in the stomach. Urease activity is the main virulence factor of *H. pylori*, responsible for pH changes on environment conditions for their development.[2,3] Among chalcones with antibacterial activity, sofalcone is in clinical trials for treatment of *H. pylori* infection.[4]

In this view synthetic chalcones with structural diversity were screened against urease using Berthelot reaction[5,6] (Figure 1). $IC_{50}$ was determined for the compounds with higher enzyme inhibition (Table 1), and chalcones that exhibited effective antiurease activity (Figure 2) will be further investigated on *H. pylori*.

**Figure 1. Inhibition of compounds tested**

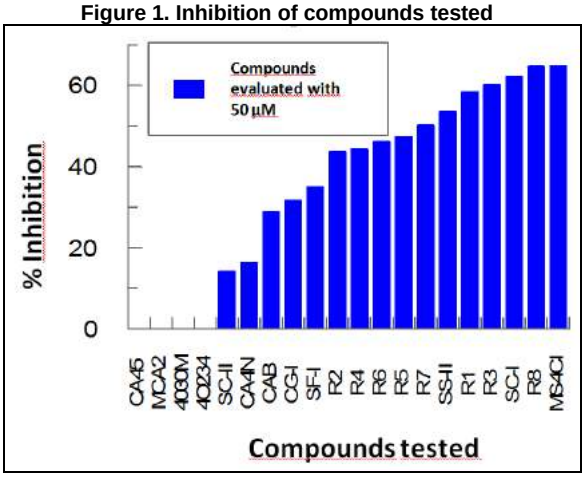


**Figure 2. Chalcones with significant inhibitory activities**

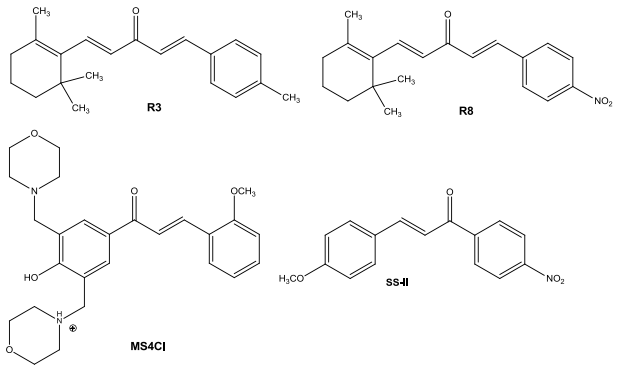


**Table1: $IC_{50}$ values of compounds against urease**

| Compounds | $IC_{50}$ (µM) |
|---|---|
| R3 | 33,68 ± 2,09 |
| R8 | 25,08 ± 2,43 |
| SS-II | 42,06 ± 3,47 |
| MS4Cl | 29,43 ± 2,41 |

[1]Prashar H. et al. *Inter J Pharm Sci Res.* **2012**; 3: 13-1927.
[2]Algood HMS, Cover TL. *Clin Microbiol Rev* **2006**; 19: 597-613.
[3]Stingl K, et al. *Trend Microbiol* **2002**; 10: 70-74.
[4]Masayuki, MDS, et al. *J of Clinical Gastroenterol* **1998**; 27: S183-186.
[5]Ali SL, et al. *International J of Pharma Research and Health Sciences* 2015; 3: 891-894.
[6]De Sousa LRF, et al. *J. Nat. Prod.* **2014**, *77*, 392.

Área: MED

**Inscrição: 00076**

# Biochemical characterization of new *Schistosoma mansoni* aspartic proteases inhibitors identified by virtual screening

**Bárbara F. Gomes[1] (IC), Mario R. Senger[1] (PQ), Bruno J. Neves[2] (PQ), Raymond Owens[3] (PQ), Nicholas Furnham[4] (PQ), Carolina H. Andrade[5] (PQ), Floriano P. Silva-Júnior[1] (PQ)*.**

**floriano@ioc.fiocruz.br**

*[1]Laboratory of Experimental and Computational Biochemistry of Drugs, Oswaldo Cruz Institute, FIOCRUZ; [2]Laboratório de Quimioinformática, Centro Universitário de Anápolis - UniEVANGÉLICA; [3]Oxford Protein Production Facility, UK; [4]London School of Hygiene and Tropical Medicine, UK; [5]Laboratory for Molecular Modeling and Drug Design, Faculty of Pharmacy, Federal University of Goias.*

Key words: *Schistosomiasis, Cathepsin D, Drug Discovery, Neglected Tropical Diseases, Computer Aided Drug Design.*

## Highlights

Aspartic proteases are validated targets for the development of new antischistosomal drugs. In this work, we want to identify inhibitors of these enzymes, using computational and experimental methods.

## Abstract

Schistosomiasis is an important parasitic disease caused by trematodes of the gender *Schistosoma*. Praziquantel (PZQ) is the drug of choice for the treatment of schistosomiasis. There is, however, a concern with the appearance of isolates resistant to PZQ.

Cathepsin D-like aspartic proteases are involved in the host's haemoglobin digestion, being essential in the life cycle of these parasites. One such enzyme, SmCD1, has been investigated for drug development.

Virtual screening has been widely used in the early stages of drug discovery, because it allows the identification of possible hits, even before they are tested *in vitro* or *in vivo*. Several compounds with schistosomicidal activity have been identified in this way, including protease inhibitors[1,2].

Initially, a virtual screening of 20,000 compounds belonging to two commercial libraries, Microformat and DIVERSet-EXP, was performed on SmCD1 enzyme (Figure 1). The 50 most promising candidates as inhibitors were selected, and subsequently screened on: 1) worms' aqueous extract (WAE); 2) pig pepsin enzyme; and 3) recombinant SmCD1 enzyme, already cloned and expressed by the group in HEK293 cells.

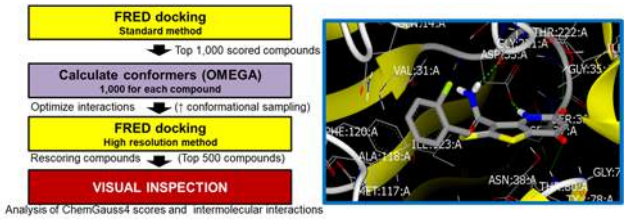


Figure 1: Virtual screening workflow.

The enzymatic assays were performed as follows: pH 3.5; 5 µM of Abz-AIAF/FSRQ-EDDnp-based fluorescence octapeptide (FRET) substrate[3] ($\lambda_{em}$: 420 nm, $\lambda_{ex}$: 310 nm), 20 µg extract or 0.5 µg pepsin/SmCD1.

Results for the most interesting compounds are shown below.

Table 1: Screening results at 10 µM for selected compounds.

| | % inhibition | | |
|---|---|---|---|
| **Inhibitor** | Pepsin | WAE | SmCD |
| **1** | 25.5 | 15.9 | 4.5 |
| **2** | 41.0 | n.d. | 12.8 |
| **5** | 46.3 | 18.1 | 15.5 |
| **10** | 8.6 | 13.8 | 31.0 |
| **17** | 33.5 | 12.6 | 2.0 |
| **19** | 34.5 | 15.0 | n.d. |
| **22** | 26.0 | 21.4 | 5.0 |
| **32** | 38.0 | n.d. | 12.2 |
| **50** | n.d. | 26.6 | 3.4 |

n.d. = not detected.

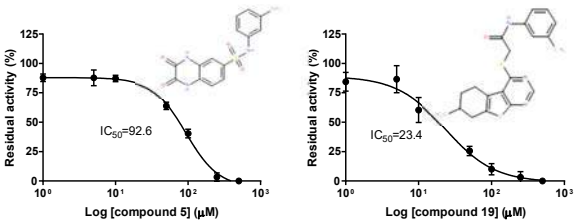


Figure 2: Concentration-response plots for $IC_{50}$ determination on pepsin enzyme.

Overall, most compounds showed highest activity against the digestive enzyme, pepsin, with some compounds presenting $IC_{50}$ values in the mid µM range. Conversely, compounds **10** and **50** preferably inhibited SmCD1 and WAE, respectively.

[1]Neves, B.J.; et al. *J. Med. Chem*., 59: 7075–7088, **2016** .
[2] Melo-Filho, et al. *J Chem Inf Model*. 56: 1357–1372, **2016**.
[3] Pimenta et al., *Biochim Biophys Acta.* 1544:113-22, **2001.**

**Área: MED** **Inscrição: 01205**

# *In vitro* inhibition of *Helicobacter pylori*, interaction studies and molecular docking of lichen natural products with jack bean urease

**Camila da S. Nunes (PG),[1]*, Thamilla Maria S. Maciel (PG)[1], Tiago C. A. Lage (PG)[2], Yane C. C. Mota (PG)[3], Carla Masia (PG)[4], Ângelo de Fátima (PQ)[5], Sergio A. Fernandes(PQ)[2], Luzia Modolo (PQ)[3], Francesca Sisto (PQ)[4], Josué C. C. Santos (PQ)[1], Isis M. Figueiredo (PQ)[1] nunescamila0@gmail.com**

[1] Instituto de Química e Biotecnologia, Universidade Federal de Alagoas, Maceió, AL, Brazil; [2] Departamento de Química, Universidade Federal de Viçosa, Viçosa, MG, Brazil; [3] Departamento de Botânica, Universidade Federal de Minas Gerais, Belo Horizonte, MG, Brazil. [4] Department of Biomedical, Surgery and Dental Sciences, Università degli Studi di Milano, Milano, Italy. [5] Departamento de Química, Universidade Federal de Minas Gerais, Belo Horizonte, MG, Brazil;

Palavras Chave: *urease, H. pylori, usnic acid, fumarprotocetraric acid, protein interaction, docking molecular.*

## Highlights

Lichen secondary metabolites inhibited the ureolytic activity of jack bean urease based on different mechanisms of action confirmed by theoretical studies, fluorescence and enzymatic assays.

## Resumo/Abstract

Compounds able to inhibit the activity of *H. pylori* urease have been used for treatment of diseases associated with infections caused by this bacterium. Then, the development of urease inhibitors has been an interesting approach for the treatment of *H. pylori*-associated diseases[1]. This work focused on the *in vitro* evaluation of the inhibitor potential of lichen secondary metabolites like usnic acid isomers [(S)-(-)-UA and (R)-(+)-UA] and fumarprotocetraric acid (FUM) through of kinetics and spectroscopic studies with *jack bean* at pH 7.4. All lichen compounds tested interact with urease by statistic quenching mechanism and change the native protein structure. The complexes were mainly stabilized by electrostatic forces and according $K_b$ values to the following order of affinity: (R)-(+)-UA > (S)-(-)-UA > FUM. The (S)-(-)-UA, acts as mixed inhibitor while (R)-(+)-UA and FUM are competitive ones. Moreover, minimum inhibitory concentrations for the lichen metabolites tested were lower (from 2- to 7.8-fold) than those of omeprazole against five *H. pylori* strains tested. Finally, we explored the binding mode of the isomers in the active site of jack bean and *H. pylori* ureases (Fig. 1), using docking molecular. The (R)-(+)-UA isomer showed stronger interaction in the active site with both ureases evaluated. The docking results indicate that the (R)-(+)-UA showed better binding affinity than (S)-(-)-UA corroborating with experimental results. Overall, the lichen metabolites tested are lead compounds for the design of more efficient urease inhibitors for the treatment of *H. pylori* infections.

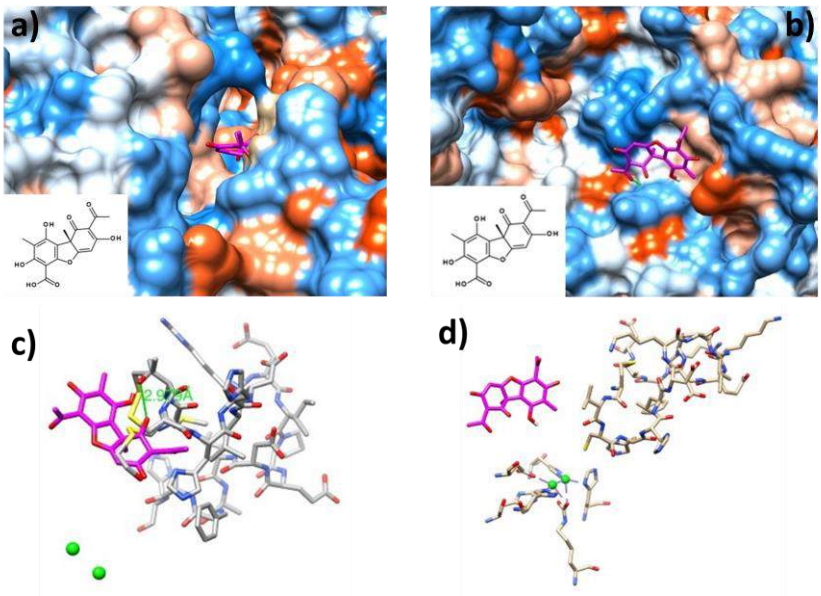


**Fig. 1**. a) Hydrophobic surface of the jack bean urease (PDB: 3LA4) with the ligand in the active site cavity. b) Hydrophobic surface of the H. pylori urease (PDB: 1E9Z) with the ligand in the active site cavity. c) Binder interactions with the amino acids of the active site in the jack bean urease (-6.9 kcal mol $^{-1}$). d) Binder interacting by hydrogen bonds and hydrophobic interactions with the amino acids of the active site in the H. pylori urease (-6.3 kcal mol $^{-1}$).

[1] X. Y. Jiang, L. Q. Sheng, C. F. Song, N. N. Du, H. J. Xu, Z. D. Liu and S. S. Chen, *New J. Chem.*, 2016, **40**, 3520.

**Área: MED** **Inscrição: 01167**

# Caracterização de novos agentes perturbadores de microtúbulos com propriedades anticâncer

**Ellen Maria Giliotti Silva (IC),[1] Carolina Teixeira Martins (IC),[1] Luma Godoy Magalhães (PG),[1] Eduardo Bustos Mass,[2] Dennis Russowsky (IC),[2] Adriano Defini Andricopulo (PQ).[1*]**

**ellen.giliotti.silva@usp.br; aandrico@ifsc.usp.br***

*[1]Laboratório de Química Medicinal e Computacional – LQMC, Centro de Pesquisa e Inovação em Biodiversidade e Fármacos – CIBFar, IFSC – USP; [2]Instituto de Química - Universidade Federal do Rio Grande do Sul – UFRGS*

Palavras Chave: *Tubulina, Câncer, Planejamento de Fármacos, Ensaios Bioquímicos.*

## Highlights

**Characterization of new modulators of microtubules with anticancer properties.**

We studied the effects of a series of chalcones, dihydropyrimidinones and hybrids of dihydropyrimidinone-chalcones on the tubulin polymerization and the progression of cell cycle.

## Resumo/Abstract

Os microtúbulos são polímeros formados pela dinâmica funcional de polimerização e despolimerização da proteína tubulina, e desempenham papel essencial na migração e divisão celular.[1] Estes processos são fundamentais na progressão do câncer. Desta forma, compostos que interferem na dinâmica de polimerização da tubulina são de grande interesse.[2] O objetivo deste trabalho é identificar novos compostos com atividade moduladora da tubulina, a partir de três séries químicas: Híbridos de dihidropirimidinona-chalconas; chalconas e dihidropirimidinonas. A triagem de 15 representantes destas classes químicas em ensaios de polimerização da proteína tubulina *in vitro* permitiu a identificação de 6 compostos capazes de inibir a polimerização da mesma, de forma similar ao observado para o composto padrão colchicina. Os compostos mais potentes foram identificados e o resultado dos ensaios de polimerização da tubulina nos levou a investigar o efeito dos mesmos sobre a progressão do ciclo celular (Figura 1A), uma vez que moduladores de microtúbulos o interrompem na fase $G_2$/M por meio da inibição da formação das fibras do fuso mitótico. Por exemplo, o resultado obtido para o composto **1** (Figura 1B) mostra que, de forma semelhante ao que foi observado para a colchicina, há um acúmulo de células na fase $G_2$/M, sugerindo que a modulação da tubulina também ocorre intracelularmente. Estudos de modelagem molecular foram conduzidos para caracterizar o modo de ligação dos compostos na proteína tubulina, fornecendo informações sobre os requisitos estruturais mais importantes envolvidos.

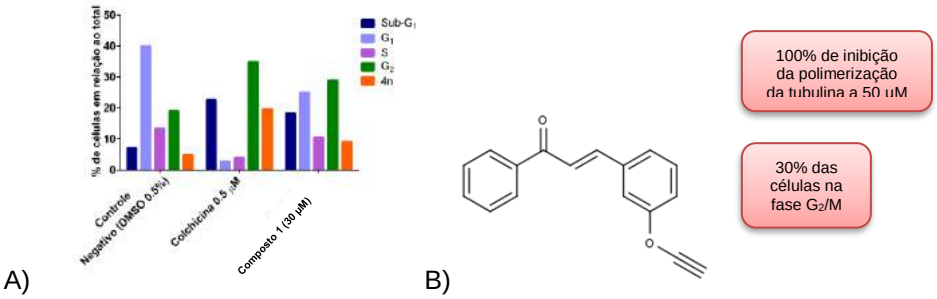


A) B)

Figura 1. A) Progressão do ciclo celular analisada pela técnica de citometria de fluxo. B) Composto representativo da série de moduladores bioativos (Composto **1**).

[1] Dumontet, C. et al. Nat Rev Drug Discovery. 2010, 9, 790–803.
[2] PROTA, A. E. et al. Molecular mechanism of action of microtubule-stabilizing anticancer agents. Science, v. 339, n. 6119, p. 587–590, 2013.

**Área: MED** **Inscrição: 01140**

# Construction and validation of QSAR models for thiazole derivatives with antifungal activity

**Iasmin N. S. Teixeira (PG),[1*] Vinicius G. Maltarollo (PQ),[1] Renata B. Oliveira (PQ)[1]**

**renatabo.ufmg@gmail.com; iasminnst@ufmg.br**

[1]*Departamento de Produtos Farmacêuticos, Faculdade de Farmácia, Universidade Federal de Minas Gerais*

Keywords: *HQSAR, CoMFA, CoMSIA*

## Highlights

Construction and validation of 2D and 3D QSAR models for antifungal prediction. All constructed models were validated according internal and external validation metrics using OECD guidelines.

## Abstract

*Cryptococcosis* is an infectious disease with worldwide distribution and clinical relevance, mainly caused by *C. neoformans* and *C. gattii*. Cryptococcal meningitis is one of the most important HIV-related opportunistic infections and it is associated with significant mortality (~600,000 deaths/year).[1] Aiming to develop new substances with antifungal activity against *C. neoformans,* 2D and 3D-QSAR studies were carried using a series of 29 thiazole derivatives with determined minimum inhibitory concentration (MIC). The 2D structures were constructed and a conformational analysis generated the lowest energy conformations and, after, they were aligned according common scaffold. Antifungal space (pMIC for *C. neoformans* inhibition), drug-like space (molecular weight, ClogP, number of hydrogen bond donors and acceptors, fraction of $sp^3$ carbons, and number of rotatable bonds), and structural space (MACC fingerprints) were considered for individual hierarchical cluster analysis (HCA) which guided training and test sets (4:1) separation. Then, 2D (HQSAR) and 3D (CoMFA and CoMSIA) QSAR models were constructed (Sybyl X 2.1) by using different parameter combinations and internally validated. After generation and comparison of their robustness, the five most robust models were selected and submitted to external validations, according to OECD guidelines. As a result, all selected models presented higher $Q_{2(F1)}$, $Q_{2(F2)}$, $Q_{2(F3)}$ and CCC values (>0.6) than other models, showing their acceptable predictive power. Therefore, the three employed techniques as well as constructed models could be employed to predict the biological activities of new proposed substances in the design of new antifungal agents.

| | HQSAR | CoMFA | CoMSIA |
|---|---|---|---|
| **Model** | A/C/DA | S/E | D/E |
| **Parameters** | 8 to 11 atoms / HL = 61 | w = 0.5 / d = 1 | w = 1.1 / d = 1.5 |
| **$Q^2$** | 0.854 | 0.741 | 0.876 |
| **$R^2$** | 0.966 | 0.979 | 0.939 |
| **$Q^2_{(F1)}$** | 0.957 | 0.871 | 0.880 |
| **$Q^2_{(F2)}$** | 0.954 | 0.863 | 0.872 |
| **$Q^2_{(F3)}$** | 0.959 | 0.879 | 0.887 |
| **CCC** | 0.977 | 0.926 | 0.937 |

*Table 1. Internal and external validation metrics for the most robust models generated with each QSAR technique. HQSAR parameters: A=atoms; C=connections and; DA=H-bond donor and acceptor; HL: hologram length; CoMFA and CoMSIA parameters: S=steric; E=electrostatic; D=H-bond donor; w=weight factor; d=distance factor; $Q^2$: internal validations coefficient; $R^2$:calibration coefficient; $Q^2_{(F1)}$: predictive $R^2$; $Q^2_{(F2)}$: Schüürmann $q^2$; $Q^2_{(F3)}$: Consonni et al. $q^2$; CCC: concordance correlation coefficient.*

**Acknowledgements**
FAPEMIG, CNPq, UFMG

**References**

1. B.J. Park et al. AIDS. 23 (2009) 525–530.

**Área: MED** **Inscrição: 01105**

# Biotransformation of taxifolin by *Beauveria bassiana* ATCC 7159

**Larissa F. M. Werworn (IC),[1] Sérgio L. F. do Nascimento (IC),[1] Adilson P. Sinhorin (PQ),[2] Valéria de Oliveira (PQ),[3] Francine Pazini (PQ).[1*]**

**lara.tof@hotmail.com; francinepazini@gmail.com**

*[1]Instituto de Ciências da Saúde, UFMT; [2] Instituto de Ciências Naturais, Humanas e Sociais UFMT; [3] Faculdade de Farmácia, UFG.*

Keywords: *Biotransformation, Taxifolin, Filamentous fungi.*

## Highlights

Filamentous fungi have an enzymatic system able to catalyze a huge variety of reactions.

Biotransformation by filamentous fungi is an alternative to prepare a biodiversity of new compounds.

Taxifolin is a flavanone that has stereochemistry and antioxidant, anti-inflammatory and antitumor actions known.

*Beauveria bassiana* was able to biotransform taxifolin into four metabolites.

## Abstract

Filamentous fungi are rich source of enzymes, able to catalyze a huge variety of reactions selectively, modifying the structure of compounds, aiming to obtain more satisfactory biological activities and/or to reduce the undesired effects[1]. In this sense, the biotransformation of taxifolin (figure 1), a dihydroflavonol that has antioxidant, anti-inflammatory, and antitumor actions, by filamentous fungi is a viable alternative to obtain new molecules[2,3]. For this purpose, a screening assay with ten filamentous fungi strains was performed. Then, taxifolin was incubated in liquid medium containing *Beauveria bassiana* for 96 hours in a semi-preparative assay, where 4 different derivatives (3 more polar and 1 less polar – figure 2) were produced, detected by HPLC and separated by TLC. The HPLC analysis were performed in gradient elution. The mobile phase consisted of acetonitrile and water, and the stationary phase consisted of a C18 colum. After, IR spectroscopy, MS and NMR experiments will be performed to elucidate the structure of the formed derivatives. This study demonstrated that *Beauveria bassiana* ATCC 7159 was able to biotransform taxifolin, being a promising alternative to prepare a biodiversity of compounds with possible biological activities.

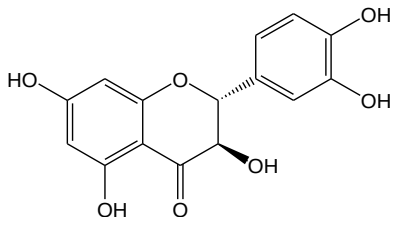


Figure 1: Chemical structure of taxifolin.

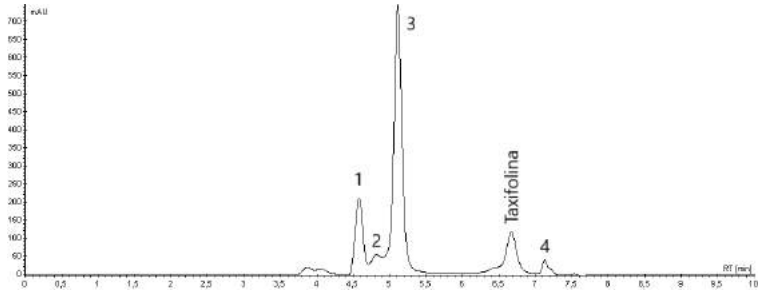


Figure 2: HPLC chromatogram of derivatives of taxifolin.

1.AZERAD, R.. **Bull. Soc. Chim.**, v.132, p.71-51. 1995
2.SATUÉ, M. *et al*.. **Biochemical Pharmacology**, v. 86, p. 1476-1486, 2013.
3.XIE, X. *et al*.. **Molecular Vision**, v. 23, p. 520-528, 2017.

**Acknowledgments**: To FAPEMAT for the financial support.

**Área: MED** **Inscrição: 01068**

# Antitumor Activity of Mesoionic Salts in Osteosarcoma

**Danilo Sousa-Pereira (PG),[1] Luma Duarte Barbosa (PG),[2]* Cristiane Frauches-Santos (PG),[1] Vinicius Cruz (IC),[2] Ana Carolina Leal (PQ),[2] Amanda dos Santos Cavalcanti (PQ),[2] Aurea Echevarria (PQ),[1]**

**sousadanilo90@gmail.com; luma_duarte@hotmail.com**

*[1]Departamento de Química-ICE, UFRRJ, Seropédica-RJ; [2]Instituto Nacional de Traumatologia e Ortopedia Jamil Haddad-INTO, Rio de Janeiro-RJ.*

Key Words: *Osteosarcoma, Mesoionic, Chemotherapy, Heterocyclic Compounds, Preclinical Research, Cancer.*

## Highlights

Mesoionic salts showed to be cytotoxic against osteosarcoma by inducing cell death by apoptosis after treatment. These compounds may be potential candidates for the treatment of this bone malignancy.

## Abstract

Among the bone tumors the Osteosarcoma (OS) is the most common in childhood and adolescence. For treatment there are few options of chemotherapeutic agents and the available ones cause side effects. The identification of new compounds with promising application in osteosarcoma is relevant to the treatment of this disease. The mesoionic salts belong to a class of heterocyclic compounds with antitumor activity that has been verified in different tumors such as melanoma and hepatocarcinoma. The present study aimed to evaluate the antitumor effect in vitro of mesoionic salts of 1,3,4-thiadiazolium-2-arylamine in osteosarcoma cells. The compounds were synthesized as shown in Scheme. By the MTT reduction assay, it was found that the **MIC-F** and **MIC-NO$_2$** salts reduced the relative viability of the MG-63 osteosarcoma cells, while the **MI-3,4F** and **MI-4F** salts were not able to reduce the cell viability after treatment for 24 and 48 hours (Table). By counting cells with trypan blue, it was found that treatment with the **MIC-NO$_2$** and **MIC-F** salts, for 24 and 48 hours, reduced the viability of MG-63 cells and were therefore cytotoxic (Figure). The analysis of annexin-V and propidium iodide by flow cytometry revealed that treatment with **MIC-NO$_2$** and **MIC-F** induced cell death by apoptosis. Thus, among the four mesoionic salts evaluated in this study, only **MIC-NO$_2$** and **MIC-F** had cytotoxic effects on MG-63 osteosarcoma cells and, therefore, may be potential candidates for the development of drugs targeted to the treatment of this disease.

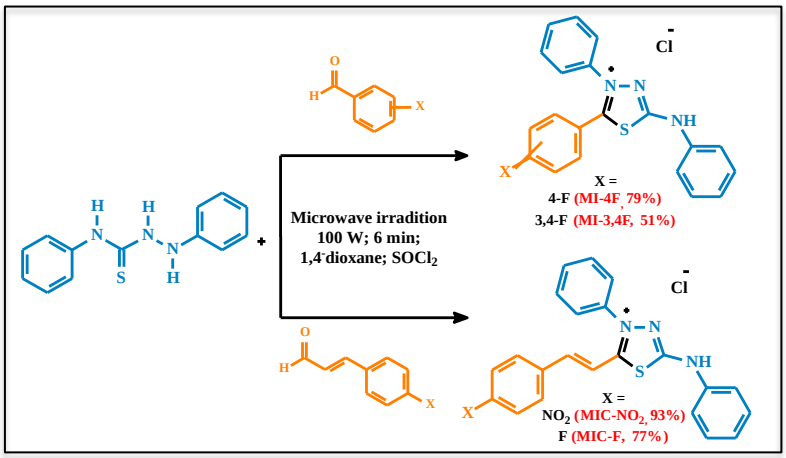


**Scheme.** The synthetic route for the preparation of mesoionic compounds.

**Table.**
Concentration Inhibitory ($IC_{50}$) of mesoionic salts on the lineage Cell of Osteosarcoma MG-63.

| Mesoionic/$IC_{50}$ (μM) | 24 h | 48 h |
|---|---|---|
| **MIC-F** | 4.36 ± 0.08 | 1.93 ± 0.20 |
| **MIC-NO$_2$** | 4.78 ± 0.02 | 2.02 ± 0.05 |
| **MI-4F** | 61.19 ± 0.27 | 36.49 ± 0.17 |
| **MI 3,4-F** | 1674 ± 1.77 | 45.59 ± 0.13 |

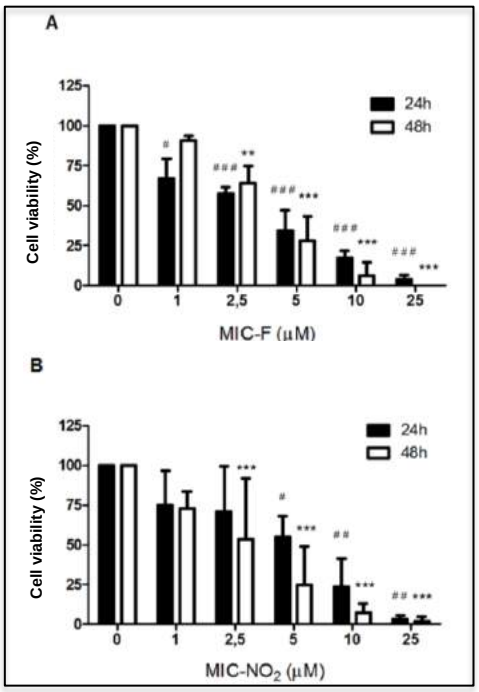


**Figure.** Cytotoxicity of the MIC-F (A) and MIC-NO$_2$ (B) salts (1, 2.5, 5, 10 and 25 μm) on the Osteosarcoma cells.

**Área: MEDA** **Inscrição: 00955**

# Synthesis and antileishmanial activity of novel β-carboline-1,3,5-triazine hybrids

**Paula Baréa (PG),[1*a] Valéria A. Barbosa (PQ),[1a] Mariana S. Leoncio (IC),[1a] Jéssica C. de Paula (PG),[2a] Willian F. da Costa (PQ),[1a] Celso V. Nakamura (PQ),[2a] Maria H. Sarragiotto (PQ).[1a]**

**vabarbosa2@uem.br; apbarea3@gmail.com**

*[1]Departamento de Química, UEM; [2]Departamento de Análises Clínicas, UEM*

Palavras Chave: *β-carboline, 1,3,5,-triazine, antileishmanial activity, Leishmania amazonensis.*

## Highlights

Novel hybrids β-carboline-1,3,5-triazine were synthesized and evaluated for their antileishmanial activity; Hybrid **4a** displayed potent antileishmanial activity and high selectivity index against *Leishmania amazonensis* promastigotes.

## Resumo/Abstract

Leishmaniasis is caused by protozoan parasites of the genus *Leishmania,* and according to World Health Organization (WHO) it is endemic in 97 countries and territories.[1] The ineffectiveness of current treatments for leishmaniasis,[2] as well as the antileishmanial potential of both *β*-carboline and 1,3,5-triazine nucleus motivated us to synthetize *β*-carboline-1,3,5-triazine hybrids in order to obtain new compounds with potent antileishmanial activity and low toxicity. The novel *β*-carboline-1,3,5-triazine hybrids were obtained from methyl *β*-carboline-3-carboxylates (**1a-c**) intermediates, which were prepared according the methodology described by our research group.[3] Reaction of **1a-c** with ethylenediamine afforded the corresponding *β*-carboline-3-carboxamides **2a-c** (**Scheme 1**). Treatment of **2a-c** with a suspension of cyanuric chloride in a mixture of water/acetonitrile 1:1, at 0 °C, followed by addition of sodium hydroxide solution, gave the compounds **3a-c** in good yields (55-87%). For the synthesis of *β*-carboline-1,3,5-triazine hybrids **4a-c** (**Scheme 1**), the intermediates **2a-c** were subjected to reaction with cyanuric chloride as previously described, followed by addition to the reaction mixture, without previous treatment, of 10 equivalents of isopropylamine and heating at 70 °C for 48 hours to provide the desired products in good yields (48-75%).

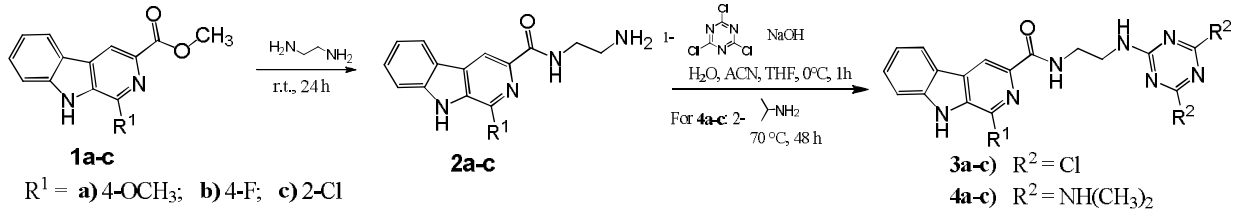


**1a-c**

$R^1$ = **a)** 4-$OCH_3$; **b)** 4-F; **c)** 2-Cl

**2a-c**

**3a-c)** $R^2 = Cl$

**4a-c)** $R^2 = NH(CH_3)_2$

**Scheme 1:** Synthetic route for preparation of β-carboline-1,3,5-triazine hybrids **3a-c** and **4a-c**.

The hybrids synthesized were evaluated *in vitro* against promastigote forms of *Leishmania amazonensis* (**Table 1**). Analysis of $IC_{50}$ data showed that the replacement of chlorine atoms of **3a** by isopropylamino group in **4a** increased the antileishmanial activity by about 10 times. On the other hand, the insertion of the isopropylamino group led to a loss of the activity for compound **4c,** compared to **3c**. Both hybrids **3b** and **4b** were inactive. These results show that **4a** is a promising antileishmanial agent.

**Table 1:** Antileishmanial activity data for compounds **3a-c** and **4a-c** against *L. amazonensis*.

| Comp. | Promastigotes $IC_{50}$ (μM) | J774A1 $CC_{50}$ (μM) | IS PRO | Comp. | Promastigotes $IC_{50}$ (μM) | J774A1 $CC_{50}$ (μM) | IS PRO |
|---|---|---|---|---|---|---|---|
| **3a** | 67.5 ± 0.1 | 201.3 ± 3.9 | 3.0 | **4a** | **6.2 ± 1.4** | 145.7 ± 10.1 | **23.5** |
| **3b** | >100 | n.t | n.d | **4b** | >100 | n.t | n.d |
| **3c** | **7.6 ± 2.02** | 28.5 ± 3.6 | 3.8 | **4c** | >100 | n.t | n.d |

[1]World Health Organization. Avaible in: http://www.who.int/gho/neglected_diseases/ leishmaniasis/en/. Accesed 29 aug. 2017; [2] P. Mitropoulos, P. Konidas, M. Durkin-Konidas, *J. Am. Acad. Dermatol.* **2010**, 309-322; [3] L.T.D. Tonin, M.R. Panice, C.V. Nakamura, K.J.P. Rocha, A.O. Dos Santos, T. Ueda-Nakamura, W. Ferreira Da Costa, M.H. Sarragiotto, Biomed. Pharmacother., 64 (2010), pp. 386-389.

**Área: MED** **Inscrição: 00890**

# Development of new potential *Mycobacterium tuberculosis* enoyl-ACP reductase inhibitors.

**Fernanda Lima de Azevedo Maia (IC),[1*]Raoni Schroeder B. Gonçalves (PQ),[1]Joyce Cristina Castro (IC),[1]Laudicéa do Nascimento Oliveira (PG),[1]Lucas Souza Mathias (IC),[1]Magaly Girão Albuquerque (PQ),[1]Camilo Henrique da Silva Lima (PQ),[2]**

**fernandaazevedomaia@ufrj.br; raoni.schroeder@iq.ufrj.br**

*[1]Instituto de Química, Departamento de Química Orgânica, UFRJ, Universidade Federal do Rio de Janeiro.[2]UFF, Universidade Federal Fluminense.*

Palavras Chave:*Chalcona, Tuberculose, Síntese Orgânica*

## Highlights

Development of new *Mycobacterium tuberculosis* enoyl-ACP reductase (InhA) inhibitors.

## Resumo/Abstract

A Tuberculose (TB) é uma doença crônica e infectocontagiosa cujo agente etiológico é o *Mycobacterium tuberculosis*. Em 2016, cerca de 10,4 milhões de pessoas apresentaram a doença, sendo a TB uma das 10 principais causas de morte no mundo.[1] O tratamento de primeira escolha é extenso (6 meses) e possui efeitos colaterais adversos, contribuindo para a interrupção da medicação. Tal ação promove a evolução da TB multirresistente (MDR-TB) e TB extremamente resistente (XDR-TB). Nesses casos, fármacos de segunda escolha são administrados, elevando o tempo de tratamento e apresentando menor eficácia.

Nesse contexto, o presente trabalho tem como objetivo o desenvolvimento de novos fármacos para o combate à TB. O alvo farmacológico escolhido foi a enzima enoil-ACP redutase (InhA), que participa da biossíntese de ácidos micólicos, componentes essenciais da parede celular bacteriana. A isoniazida (INH), principal fármaco utilizado no combate da TB é capaz de inibir essa enzima. No entanto, a INH é um pró-fármaco que depende da ação da enzima catalase-peroxidase micobacteriana (KatG), que leva à formação do complexo INH-NAD, o qual é ativo frente à bactéria. Tendo em vista que a maioria das cepas resistentes à INH possuem mutações na KatG, o desenvolvimento de inibidores da InhA que não dependam da pré-ativação da KatG é uma promissora estratégia.

Através de estudos de Modelagem Molecular foi construído um mapa farmacofórico para a identificação de novos potenciais inibidores da InhA.[2,3] Em seguida, esse mapa foi utilizado em um screening virtual através do banco de dados ZINC (http://zinc.docking.org/), onde o composto 1 [ID do ZINC: 4026219; (E)-1-(8-hidroxi-4-metoxi-1-naftil)-3-fenil-prop-2-en-1-ona] foi identificado como um novo hit. A partir desse composto foi proposta uma série de derivados contendo diferentes substituintes na fenila, conforme descrito no **esquema 1**. Os derivados propostos foram obtidos em três etapas tendo como material de partida o 1,5-di-hidroxinaftaleno.

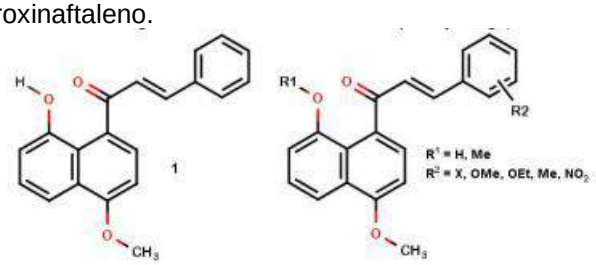


**Esquema 1.** Um novo composto (1) foi identificado e propôs-se uma série de derivados.

[1] WHO (**2016**) [http://www.who.int/mediacentre/factsheets/fs104/en/]. [2] Lima, C.H.S (**2015**) Doctoral Thesis, IQ-UFRJ. [3] Lima, C.H.S. et al. (**2015**) Int J Mol Sci, 16:23695

**Área: MED**_____ **Inscrição:00839**_____
*(Inserir a sigla da seção científica para qual o resumo será submetido. Ex: ORG, BEA, CAT)* *(Inserir o número de inscrição do autor que fez a submissão)*

# Planejamento, síntese e avaliação biológica de novos derivados 4-nitroimidazólicos candidatos a agentes tripanocidas

**Giulianna P. Alcântara (PG),[1,2] Juliana M. Chaves Barbosa (IC),[3] Kelly Salomão (PQ),[3] Solange L. de Castro (PQ),[3] Samir A. Carvalho (PQ),[1] Edson F. da Silva (PQ),[1,4] Carlos A. M. Fraga (PQ)[5*].**

**samir.carvalho@far.fiocruz.br; cmfraga@ccsdecania.ufrj.br***

*[1]Fiocruz- Fundação Oswaldo Cruz, Instituto de Tecnologia em Fármacos – Farmanguinhos Rua Sizenando Nabuco, 100, Manguinhos, 21041-250 Rio de Janeiro, RJ; [2]Universidade Federal do Rio de janeiro; Instituto de Química; Av. Athos da Silveira Ramos, 149, bl. A; CEP:21941-909- Cidade Universitária- Rio de janeiro, RJ; [3]Fiocruz- Fundação Oswaldo Cruz; Laboratório de Biologia Celular, Instituto Oswaldo Cruz; [5]Universidade Federal do Rio de Janeiro; Instituto de Ciências Biomédicas; PO Box 68023, 21941-902 Rio de Janeiro, RJ, Brazil; [4]Unigranrio – Universidade do Grande Rio; Rua Prof. José de Souza Herdy, 1160 – 25 de Agosto – Duque de Caxias; CEP 25071-202 – Rio de Janeiro – RJ; [5] Programa de Pesquisa em Desenvolvimento de Fármacos, Instituto de Ciências Biomédicas, Universidade Federal do Rio de Janeiro, PO Box 68023, 21941-902, Rio de Janeiro, RJ, Brazil.*

Palavras Chave: *Trypanosoma, Nitroimidazol, Citotoxicidade.*

## Highlights

Planejamento, síntese e avaliação biológica de novos derivados 4-nitroimidazólicos candidatos a agentes tripanocidas. Foram sintetizados 5 novos derivados 4-nitroimidazólicos e sua atividade tripanocida e de citotoxicidade foi avaliada em teste *in vitro*. Os novos derivados apresentaram atividade tripanocida moderada e baixa citotoxicidade.

## Resumo/Abstract

A doença de Chagas (DC) é uma zoonose causada pelo *Trypanosoma cruzi*. Esta parasitose endêmica representa um grave problema de saúde pública nos países tropicais. Atualmente a terapia utilizada no Brasil tem eficácia limitada, sendo apenas eficiente na fase aguda da doença. Carvalho *et al*. sintetizaram novas *N*-acilidrazonas, que em testes *in vitro*, foram duas vezes mais ativas do que o medicamento de referência Benznidazol[2]. O objetivo deste trabalho é o planejamento, síntese e avaliação biológica de uma nova família de análogos de benznidazol, estruturalmente planejados, explorando a hibridação molecular do benznidazol com *N*-acilidrazonas, a fim de potenciar o perfil tripanocida. Os novos análogos foram sintetizados em bons rendimentos, identificados por técnicas de análise e sua atividade tripanocida e de citotoxicidade foi avaliada em teste *in vitro* (Tabela 1).

Tabela 1 - Atividade tripanocida *in vitro* e citotoxicidade dos derivados 4-nitroimidazólicos.

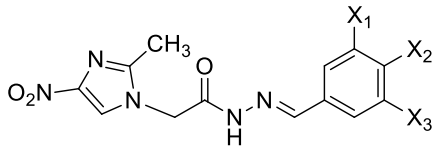


| $X_1$ | $X_2$ | $X_3$ | $IC_{50}$ [a] Tripomastigota | $IC_{50}$ [a] Citotoxicidade |
|---|---|---|---|---|
| H | H | H | 409 ± 39 | >1000 |
| H | F | H | 610 ± 41 | >1000 |
| H | Cl | H | 207 ± 80 | 867 ± 57 |
| H | Br | H | 320 ± 40 | 678 ± 63 |
| H | $OCH_3$ | H | >500 | >1000 |

[a] $IC_{50}$ expresso em µM.

Os derivados mostraram atividade moderada na forma tripomastigota e não foram citotóxicos na concentração testada demostrando.

[1] Dias, L.C. *et al*. Química Nova.**2009**, 32, 2444-2457.
[2] Carvalho, S.A. *et al*. Bioorganic & Medicinal Chemistry Letters. **2004**,14,5967-5970.

**Área: MED**
*(Inserir a sigla da seção científica para qual o resumo será submetido. Ex: ORG, BEA, CAT)*

**Inscrição: 00831**
*(Inserir o número de inscrição do autor que fez a submissão)*

# Docking studies of alkaloids from *Prosopis juliflora* against Acetylcholinesterase 1 of *Riphicephalus microplus* (RmAChE1)

**Samuel S. da R. Pita (PQ)[1*], Alexsandro Branco (PQ)[2], Hélimar G. de Lima (PG)[3], Maria J. M. Batatinha (PQ)[2], Humberto F. de Freitas (PQ)[1*]**

**samelrpita@gmail.com; humbarato@gmail.com**

*[1] Laboratory of Bioinformatics and Molecular Modeling (LaBiMM), Faculty of Pharmacy, Federal University of Bahia, 40170-115, Salvador-Bahia, Brazil; [2] Health Department, State University of Feira de Santana, Feira de Santana- Bahia, Brazil; [3] Laboratory of Veterinary Toxicology (LaTox), Hospital of Veterinary Medicine, Federal University of Bahia, 40170-115, Salvador-Bahia, Brazil*

Keywords: *Rhipicephalus microplus,*Acetylcholinesterase*, alkaloids, docking*

## Highlights

Cattle tick is a problem in agro-industry. Current acaricides (inhibitors of Acetylcholinesterase) has been developing resistance. New acaricides could be developed from Brazilian diversity and the RmAChE 1 is the main target.

## Resumo/Abstract

The bovine tick (*Rhipicephalus microplus*) is the vector of several cattle diseases. Traditional acaricides (organophosphates / carbamates) inhibit Acetylcholinesterase 1 of *R. microplus* (RmAChE1), however, they are faced with the onset of resistance. Preliminary studies, using a methanolic fraction of *Prosopis juliflora*, reported inhibition of RmAChE1. A characterization of this fraction (HPLC-DAD / HPLC-MS) revealed the presence of 3 major alkaloids (**Figure 1**), suggesting that these molecules could be responsible for its inhibitory effects. Aiming to investigate the interaction between these alkaloids and RmAChE1, docking studies with GOLD 5.5 program were performed. The results suggest that the alkaloids preferentially occupy the catalytic sites, the anionic subsite and the peripheral anionic site (PAS), especially the group 2- (hydroxymethyl) -3-piperidinol (Prosopine, **Fig. 1A**) and 2-methyl- 3-piperidinol (Juliprosinene and Juliprosopine, **Fig. 1B** and **1C**). These groups interact through hydrogen bond with residues of Serine 222, Histidine 460 (catalytic site) and Tyrosine 144 (PAS) and cation-π interactions with the Tryptophan 103 residue (**Fig. 1B**). Cation-π interactions were also observed between Tyrosine residue 144 of RmAChE1 and 2,3-Dihydro-1H-indolizine subunit (**Fig. 1B**) or hexahydroindolizine (**Fig. 1C**). Then, we concluded that *P. juliflora* alkaloids occupy the sites of interactions common to classical acetylcholinesterase inhibitors (*e. g.*, huprine / donepezil), thus justifying their inhibition in RmAChE1. Additionally, the structural singularity of these alkaloids and their interaction profiles are exploited to synthesize new alkaloids or other, structurally simpler, allowing the development of new acaricides based on Brazilian biodiversity.

**Figure 1.** Mode of interaction of the alkaloids obtained by molecular docking against Acetylcholinesterase 1 of *R. microplus* (RmAChE1): **A)** Prosopine, **B)** Juliprosinene and **C)** Juliprosopine

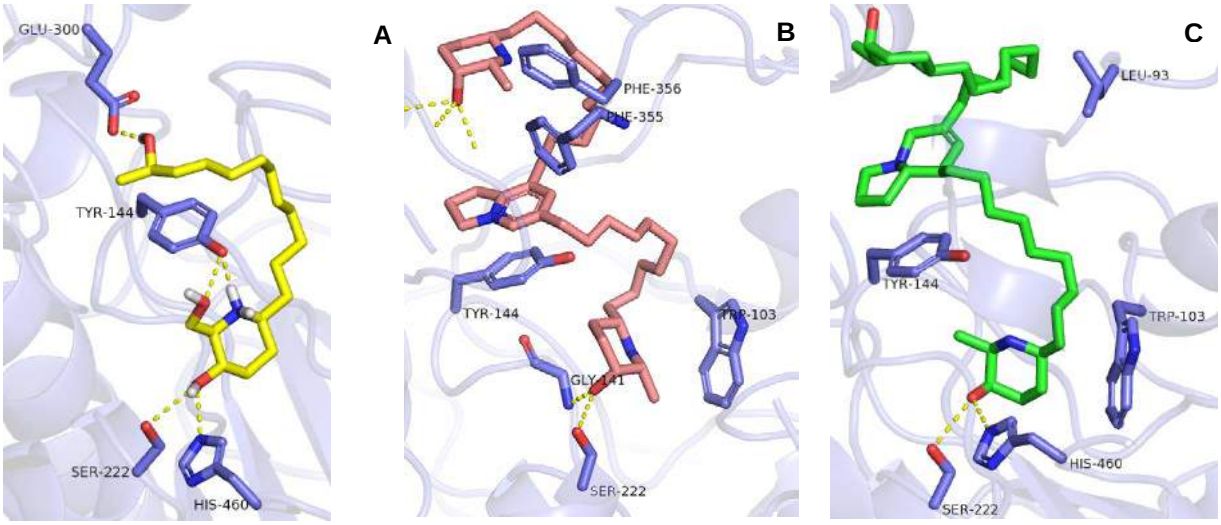

**Área: MED**
*(Inserir a sigla da seção científica para qual o resumo será submetido. Ex: ORG, BEA, CAT)*

**Inscrição:00733**
*(Inserir o número de inscrição do autor que fez a submissão)*

# Molecular modeling and prediction toxicity studies of organozinc metallodrugs candidate to anticancer agents

**Paulo R. Santos (PG),[1] Mariana S. Fernandes (IC),[2] Alisson F. Oliveira (PG),[2] Fávero R. Paula (PQ),[2] Eduardo B. Melo (PQ)[3], Pablo Machado (PQ),[4] Sidnei M. Silva (PQ).[2]***

**faveropaula@unipampa.edu.br; smsilva11@ucs.br**

*[1]Programa de Pós-Graduação em Biotecnologia, UCS; [2]Programa de Pós-Graduação em Ciências Farmacêuticas, UNIPAMPA; [3]Programa de Pós-Graduação em Ciências Farmacêuticas, UNIOESTE, [4]Instituto Nacional de Ciência e Tecnologia em Tuberculose, PUCRS.*

Palavras Chave: *Organozinc, physicochemical properties, molecular modeling*.

## Highlights

Molecular modeling models, physicochemical properties, and prediction toxicity studies of organozinc metallodrugs compounds are important to study some candidate to new anticancer agents.

## Resumo/Abstract

Cancer is a set of diseases that affect tissues of the human body and may cause the death of carrier patients. Four metallodrugs zinc complex of the valproate (PRS 01 and 02), diclofenac (PRS 3) and ibuprofen (PRS 4), candidates to new antitumor drugs, synthesized by Prof. Sidnei Moura e Silva, UCS, were submitted to molecular modeling, the determination of physicochemical properties (described in rule of five) and toxicity prediction studies aiming to support the drug development. Spartan 08 software and DFT/B3LYP-6.31G* methods were used in the molecules structural geometry optimization. Molinspiration Chemoinformatics and Marvin Sketch 6.2.1 were used to calculate the physicochemical properties such as logP, TPSA, molecular weight and volume, number of acceptor and donor hydrogen bond, and ClogD. AdmetSAR and Protox were the software used in toxicity prediction. All PRS chemical structures were modeled and these compounds showed values of TPSA, number of acceptor and donor hydrogen bond properties similar with other anticancer drugs. All PRS compounds showed molecular weight values which are considered a deviation of rule of five. ClogD values of PRS (Table I) turn the PRS 2 and 3 better to oral administration than 1 and 4 because the range of 1 to 3 is better to intestinal absorption. No carcinogenic and genotoxic effects for all PRS metallodrugs were predicted by software.

Table I - Physicochemical values of molecular weight and ClogD for all PRS compounds.

| PRS Compounds | Molecular weight | ClogD |
|---|---|---|
| **1** | 510.01 | 2.21 |
| **2** | 598.07 | 0.35 |
| **3** | 799.22 | 8.52 |
| **4** | 722.21 | 2,79 |

**Acknowledgments:** FAPERGS - PRONUPEQ process number: 16/2551-0000523-0.

**Área: MED** **Inscrição: 00668**

# Construction and Validation of HQSAR models for cell permeability, human intestinal absorption and oral bioavailability

**Ingrid A. Almeida (IC),[1] Vinicius G. Maltarollo (PQ),[1]***

**maltarollo@ufmg.br**

[1]*Departamento de Produtos Farmacêuticos, Faculdade de Farmácia, Universidade Federal de Minas Gerais*

Keywords: *HQSAR, Permeability, Oral bioavailability, Absorption*

## Highlights

Three datasets were used to generate QSAR models with internal validations. Two robust models were obtained according $Q^2$ value. External validations will be implemented as next steps.

## Abstract

Early stages of drug development benefits from pharmacokinetic studies, making research more efficient and less expensive.[1] Accordingly, HQSAR models were generated (Sybyl X 2.1) using three known datasets with experimentally determined properties for Caco-2 cellular permeability (P, 1272 compounds),[2] human intestinal absorption (HIA, 506 compounds)[3] and oral bioavailability (F, 261 compounds).[4] Datasets were curated and had their molecular structures determined, followed by descriptors calculation, such as logP, molecular weight, H-bond donor and acceptors, PSA, number of rotatable bonds, fingerprints and others. Molecules with drug-like properties (that fit at least 3 of Lipinski's rules) were then separated into two sets for model generation: training and test (4:1) through HCA method. For each subset, 1140 models were exhaustively constructed, by using different parameter combinations and were considered internally robust when calculated $Q^2 > 0.6$ (according to OECD). Selected models, from all datasets and curation (complete and drug-like datasets), will undergo subsequent external validation, however Table 1 results shows that both P and HIA models were acceptable ($Q^2 > 0.6$) and preliminary results indicate that HIA model has acceptable predictive power ($Q^2F1$, $Q^2F2$, $Q^2F3$ and CCC coefficients are all above 0.6). Onward, physicochemical interpretation of all six models will be carried and generated models will be employed in a consensus model for general permeability.

| | P | HIA | F |
|---|---|---|---|
| $F_{dist}$ | A/H | A/C/Ch/DA | A/B |
| $F_{size}$ | 4 a 7 | 1 a 4 | 6 a 8 |
| ***HL*** | 401 | 307 | 199 |
| ***PCs*** | 28 | 21 | 7 |
| $Q^2$ | 0.628 | 0.690 | 0.567 |
| $R^2$ | N/A | 0.913 | 0.812 |

*Table 1: Summary of the statistical validations of most robust models from drug-like subsets. $F_{dist}$: fragment distinction; $F_{size}$: fragmentsize in atoms; HL: Hologram length in bins; PCs: number of principal components; A: Atoms; B:Bonds; C: Connections; Ch: Chirality; H:Hydrogen atoms; DA: Donors and acceptors of hydrogen bonding. *$R^2$ value for P model was not collected due internal software error.*

### Acknowledgements

FAPEMIG, CNPq and UFMG.

### References

1. Moore A. EMBO Reports. 2003; 4:114-117.
2. Wang N, et al. J. Chem. Inf. Model. 2016; 56:763−773.
3. Moda TL, Andricopulo AA. Bioorg. Med. Chem. Lett. 2012; 22:2889–2893.
4. Moda TL, et al. Bioorg. Med. Chem. 2007;15:7738–7745.

**Área:** MED **Inscrição:** 00620

# Antiglycation activity of new derivatives of lipoic acid

**Natália Machado Pereira de Oliveira Torres (PG),[1] Ana Carolina Silva Batista, (IC),[1] Philipe de Oliveira Fernandes (IC),[1] Rafael Araujo Silva (IC),[1] Jadriane de Almeida Xavier (PG),[2] Marília Oliveira Fonseca Goulart (PQ),[2] Rosemeire Brondi Alves (PQ),[1] Rossimiriam Pereira de Freitas (PQ)[1]*.**

**mpotnatalia@gmail.com; rossipfreitas@gmail.com**

*[1]Departamento de Química, UFMG; [2]Instituto de Química e Biotecnologia, UFAL*

Keywords: *Antiglycation, Glycation, Lipoic acid*

## Highlights

Synthesis of novel lipoic acid derivatives; antiglycation activity of new lipoic acid derivatives based on bovine serum albumin fructose/methylglyoxal model systems.

## Abstract

Glycation is a non-enzymatic reaction between reducing sugars and amino group of biomolecules, forming advanced glycation end-products (AGEs). These products are also formed by other metabolic routes and are associated with various physiological dysfunctions such as atherosclerosis, osteoporosis, asthma, arthritis, sarcopenia, Alzheimer's disease, cancer and various diabetic complications. Due to these biological actions, the search for molecules that inhibit the formation of AGEs is extremely important. Studies have shown that several extracts of plants, fruits and vegetables have antiglycation activity. The present work aims at the synthesis and preliminary evaluation of antiglycation activity of new lipoic acid derivatives obtained by classic coupling using natural (lupeol and eugenol) or synthetic compounds (coumarin and diamine). The new esters **2a, 2b** and **2c** and amides **2d** and **2e** (Scheme 1) were obtained with yields ranging from 51 to 90%.

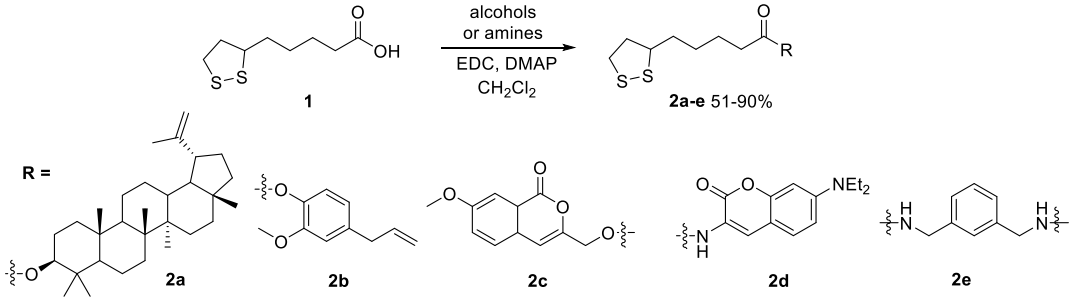


**Scheme 1.** Synthesis of new esters and amides of lipoic acid.

The antiglycation activity of the new derivatives was evaluated through two methods: bovine serum albumin-fructose/glucose model -BSA+(F+G)- and bovine serum albumin-methylglyoxal model -BSA+MG. Both assays measure the inhibition of AGEs formation by monitoring a reaction between a reducing sugar and a protein in the presence of an inhibitor. In the first assay, compound **2e** was the most active, inhibiting the formation of AGEs by 76% at higher concentration. In the BSA+MG assay, compounds **2a** and **2b** were the most active, inhibiting the formation of AGEs by 34% (Figure 1). Aminoguanidine (AMG) was used as positive control.

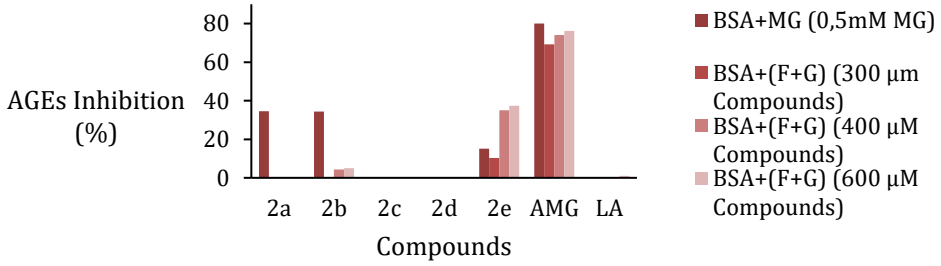


**Figure 1.** Inhibition of AGEs formation by new derivatives of lipoic acid.

**Acknowledgment**: FAPEMIG, CAPES and CNPq.

**References:**

Barbosa, J. H. P.; Souza, I. T.; Santana, A. E. G.; Goulart, M. O. F. *Química Nova,* **2016**, 39, 608.

**Área: MED** **Inscrição: 00555**

# In vitro leishmanicidal activity of dihydroquinoline lactones

**Rosangela S. Laurentiz (PQ)[1*], Ana P. R. Pissurno (PG)[1], Lizandra Guidi Magalhães (PQ)[2].**

**rosangela@dfq.feis.unesp.br**

*[1]Departamento de Física e Química, UNESP - Universidade Estadual Paulista - Faculdade de Engenharia de Ilha Solteira,*
*[2] Núcleo de Ciências Exatas e Tecnológicas da Universidade de Franca*

Palavras Chave: *Reação multicomponentes*, *Leishmania amazonensis, Índice de seletividade*

## Highlights

Synthesis of dihydroquinoline lactones derivatives
Activity against *Leishmania amazonensis*

## Resumo/Abstract

A series of dihydroquinoline lactones derivatives **4ae-be** were synthesized from a MW assisted-multicomponent reaction between tetronic acid (1), anilines **2a-b** and aromatic aldehydes **3a-e**, in $H_2O$ for 15 min (Scheme 1). These compounds were initially subjected to screening for *in vitro* leishmanicidal activity against the promastigote form of *Leishmania amazonensis* in concentration of 50 µg/mL. Screening results indicate that all of the synthesized compounds were actives. However, only compounds with parasite lysis higher than 80% were evaluated at lower concentrations for $IC_{50}$ determination. The cytotoxic concentration ($CC_{50}$) of the more actives compounds ($IC_{50}$ < 4.0 µg/mL) was also determinate on macrophage peritoneal. Compounds **4ac** e **4be** were more potent than other derivative with $IC_{50}$ value of 2.61 µg/mL and 3.57 µg/mL, respectively, and selectivity indexes (SI) 29.7 and 20.4 fold higher than those of the reference drug amphotericin (Table 1). The presence of the nitro group allied to the methylenedioxy group in benzylic ring in **4be** increased the selectivity index, as evidenced by the much lower selectivity index of the parent compound **4bd**. Regarding **4aa** and **4ac**, the presence of the $CF_3$ group, smaller and more lipophilic, favored the increase of the selectivity index to **4ac**. The experimental data suggest that these compounds may be further investigated as possible targets for development of new drug for treatment of cutaneous leishmaniosis.

**Scheme 1**. Synthesis of dihydroquinoline lactones derivatives **4ae**-**4be**

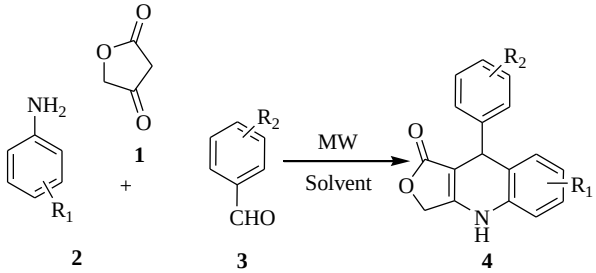


$R_1$: 3,4,5-$(OCH_3)_2$ (**2a**)
3,4-($OCH_2O$) (**2b**)

$R_2$: 4-Bn, 3-$OCH_3$ (**3a**)
4-$CH_3S$ (**3b**)
4-$CF_3$ (**3c**)
6-$NO_2$-3,4-$(OCH_3)_2$ (**3d**)
6-$NO_2$-3,4-($OCH_2O$)(**3e**)

| | Yield (%) |
|---|---|
| **4aa** | 85 |
| **4ab** | 81 |
| **4ac** | 79 |
| **4ad** | 76 |
| **4ae** | 70 |
| **4ba** | 84 |
| **4bb** | 81 |
| **4bc** | 88 |
| **4bd** | 69 |
| **4be** | 71 |

**Table 1**. Leishmanicidal activity of the dihydroquinoline derivatives **4aa**-**4ba**

| | Lysis (%) | $IC_{50}$ | $CC_{50}$ | SI |
|---|---|---|---|---|
| **4aa** | 94.9±3.2 | 2.58 | 2.92 | 1.13 |
| **4ab** | 92.3±2.7 | 12.92 | --- | ----- |
| **4ac** | 89.9±4.3 | 2.61 | 58.38 | 22.31 |
| **4ad** | 50.3±3.2 | ---- | ---- | ---- |
| **4ae** | 100 ± 0 | 14.73 | --- | --- |
| **4ba** | 79.67±2.4 | --- | | |
| **4bb** | 16.7±13.9 | ---- | | |
| **4bc** | 35.97±2.5 | ---- | | |
| **4bd** | 100 ± 0 | 1.07 | 5.74 | 5.03 |
| **4be** | 95.9±3.1 | 3.57 | 53.73 | 15.05 |
| | Amphotericin | 0.60 | 0.45 | 0.75 |

**Área: MED** **Inscrição: 00551**

# Simplificação Molecular como Estratégia para Descoberta e Otimização de Candidatos a Fármacos Antituberculose

**Ana Flávia Borsoi (IC),[1] Kenia Pissinate (PQ),[1] Cristiano Valim Bizarro (PQ),[1] Luiz Augusto Basso (PQ),[1] Pablo Machado (PQ).[1]* ana.borsoi@acad.pucrs.br; pablo.machado@pucrs.br**

[1]*Instituto Nacional de Ciência e Tecnologia em Tuberculose (INCT-TB), Centro de Pesquisa em Biologia Molecular e Funcional (CPBMF), Pontifícia Universidade Católica do Rio Grande do Sul, Porto Alegre, RS, Brasil.*

Palavras Chave: *Mycobacterium tuberculosis*, Planejamento, Estabilidade metabólica.

## Highlights

Molecular Simplification as a Strategy for Discovery and Optimization of Antituberculosis Drug Candidates

Compound with minimum inhibitory concentration (MIC) value in the submicromolar range;
The simplicity of the route, easily accessible reactants, and high purity make the synthetic protocols attractive.

## Abstract

Human tuberculosis (TB) is an infectious disease caused mainly by *Mycobacterium tuberculosis* (Mtb), and has been responsible for the deaths of thousands of people annually.[1] Recently, the antimycobacterial activity of 2-(quinolin-4-yloxy)acetamides (**Figure 1**) and their derivatives has been reported by our research group.[2] The compounds have been active against resistant and non-resistant Mtb strains and have exhibited selective inhibition of bacillus growth. Despite the excellent *in vitro* activity, this class of compounds showed only moderate *in vivo* activity. This result can be attributed to the metabolic instability of the acetamide group. Therefore, the present work has the objective of synthesizing and characterizing compounds that do not present the acetamide group in a strategy of molecular simplification.

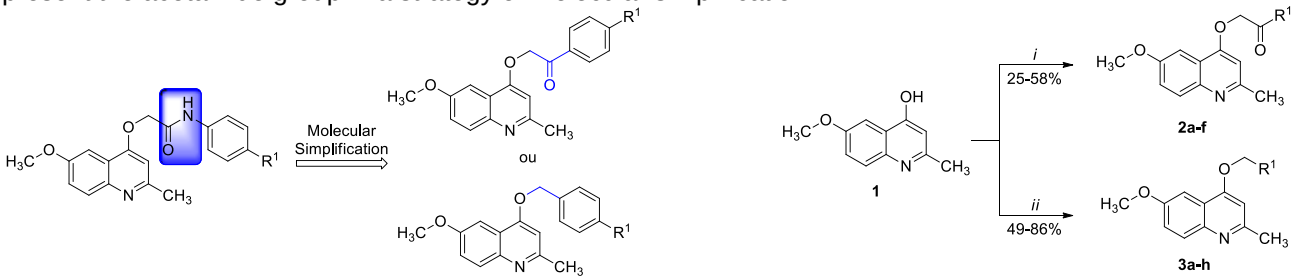


**Figure 1**. Molecular simplification 2-(quinolin-4-yloxy)acetamides. **Scheme 1**. Conditions: *i* and *ii*: alkyl halide DMF, $K_2CO_3$, 25 °C, 18 h.

The 2-(quinolin-4-yloxy)acetamides **2** and **3** were obtained from reaction of 6-methoxy-2-methylquinolin-4-ol (**1**) and alkyl halides using potassium carbonate ($K_2CO_3$) as base. The reactants were stirred for 18 h at 25 °C leading to products with 25–86% yields (**Scheme 1**). The synthesized compounds **2** and **3** were tested in whole-cell assay against Mtb H37Rv, using the first-line drug isoniazid as reference. The most active compound **3f** ($R^1$ = $(Cl)_2$-3,4-$C_6H_3$) inhibited the Mtb growth with an MIC of 0.3 µM while isoniazid had MIC of 1.46 µM. These initial findings encourage us to follow up with these molecules for the next stages of development.

References
[1]Global tuberculosis report 2016, World Health Organization.
[2]Giacobbo, B.C., et al., New insights into the SAR and drug combination synergy of 2-(quinolin-4-yloxy)acetamides against *Mycobacterium tuberculosis*. *Eur. J. Med. Chem.*, **2017**, 126, 491.

**Área: MED** **Inscrição:00483**

# Síntese e avaliação farmacológica de acilhidrazonas como protótipos de fármacos multialvos para o tratamento da doença de Alzheimer

**Daniela Corrêa Santos[1] (IC); Thayssa L. C. Nogueira[1] (IC); João V. F. Quimas[1] (IC); Ruan R. Henriques[2] (PG); Marcos Antonio de A. Lopes Junior[1] (PG), Leandro L. de Carvalho (PQ)[1]; Nelilma C. Romeiro[1] (PQ); Leandro L. Silva[1] (PQ); Andréa L. Ferreira de Souza[1]* (PQ)**

**daniela.csantos97@gmail.com; andrealuzia@gmail.com***

*[1]UFRJ – Campus Macaé, [2]UFRJ – Centro de Tecnologia.*

*Palavras Chave: acilhidrazonas, doença de Alzheimer, AChE, MPO, antioxidante, quelante.*

## Highlights

Synthesis and pharmacological evaluation of acylhydrazones as multi-target drugs prototypes for the treatment of Alzheimer's disease.

- The compounds show MPO inhibitory and antioxidant activities.
- The activities antioxidant and MPO-peroxidase inhibition correlate positively, r = 0.8.
- Compound **1k** also inhibited AChE and selectively chelated $Zn^{+2}$ e $Fe^{+2}$.

## Resumo/Abstract

**Introdução:** A doença de Alzheimer (DA) está relacionada ao peptídeo β-amilóide aumentado, proteína-*tau* hiperfosforilada, perda de neurônios e baixos níveis de acetilcolina, sendo estes tratados com inibidores da acetilcolinesterase (AChE). Evidências apontam ainda para o papel do estresse oxidativo, do qual participam a desregulação dos íons de metais de transição redox e a mieloperoxidase (MPO), encontrada em torno de placas β-amilóide.[1] Essa natureza multi-fatorial da DA exige derivados com ação multialvo para seu efetivo tratamento, sendo os derivados acilidrazônicos bons candidatos, tanto por sua capacidade sintética, quanto por diversas atividades biológicas relevantes.[2]

**Objetivos:** Sintetizar Bases de Schiff (acilhidrazonas **1a-o**) pela condensação da isoniazida com respectivos aldeídos sob irradiação de micro-ondas (Esquema 1) e avaliar suas atividades frente alvos atraentes para o desenvolvimento de fármacos anti-DA (Tabela 1).

**Resultados:** Dos 15 derivados sintetizados e avaliados, diversos foram capazes de inibir tanto a atividade clorinante, quanto a peroxidase da MPO, sendo que esta última parece estar relacionada à atividade antioxidante dos derivados (r = 0,8). O derivado **1k** possui ainda atividade inibitória sobre a AChE, além de complexar de modo seletivo os íons metálicos $Zn^{+2}$ e $Fe^{+2}$, caracterizando assim seu perfil multialvo.

**Conclusão:** O derivado **1k** pode ser considerado um bom candidato a protótipo de fármaco multialvo para o tratamento da DA, visto que atua como inibidor das enzimas MPO e AChE, possui perfil antioxidante e é capaz de quelar biometais.

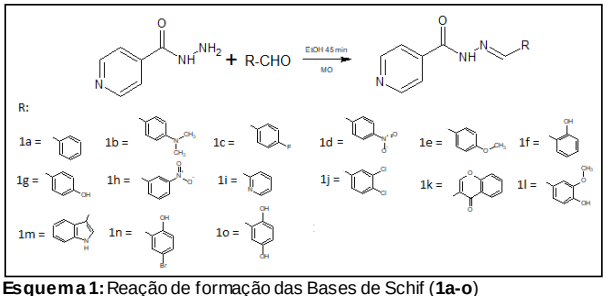


**Esquema 1:** Reação de formação das Bases de Schif (**1a-o**)

**Tabela 1: Avaliação farmacológica dos derivados 1a-o.**

| Substância (100 µM) | AA[a] (%) | AChE[b] (% Inibição) | MPO (% Inibição) | |
|---|---|---|---|---|
| | | | Peroxidase[c] | Clorinante[d] |
| Veículo | 0,15 | 6,9 | -5,0 | 1,8 |
| 1a | 3,3 | 16,5 | -7,2 | 74,9* |
| 1b | 6,3 | 6,9 | -10,4 | 97,0* |
| 1c | 8,1 | 16,3 | 4,2 | 79,0* |
| 1d | 2,5 | 12,7 | -0,8 | -47,5* |
| 1e | 2,4 | 8,0 | -2,1 | 59,3* |
| 1f | 5,3 | 3,0 | 36,2* | 92,2* |
| 1g | 28,7 | 10,0 | -37,9* | -31,2 |
| 1h | 3,9 | 14,0 | 3,0 | -9,3 |
| 1i | -0,6 | 24,5 | 25,9* | 60,0* |
| 1j | 2,0 | 36,2 | 5,6 | -13,8 |
| **1k** | 82,2* | 54,2* | 96,8* | 80,0* |
| 1l | 76,7* | 23,1 | 62,5* | 18,1 |
| 1m | 28,8 | 5,5 | 57,2* | 101,6* |
| 1n | 3,9 | 6,8 | 13,1 | 98,1* |
| 1o | 92,4* | 0,3 | 93,1* | 38,0 |
| Isoniazida | 91,3* | 5,8 | 96,1* | 88,6* |
| Quercetina | 96,3* | - | - | - |
| Rivastigmina | 0,2 | 59,6* | - | - |

[a]Atividade antioxidante (AA) determinada pelo método do DPPH.[6]
[b]Inibição da AChE (Eletrocphorus eletricus) através do métod de Ellman.[3]
[c]Inibição da atividade peroxidase da MPO (rato) pela oxidação do TMB.[4]
[d]Inibição da MPO (rato) foi medida pelo método da taurina.[5]

**Referências.** [1]*Curr.Med.Chem.*18(32):4949-75.2011.
[2]*Eur.J.Of.Med.Chem.45:3019-3026.2010.*
[3]*Biochem.Pharmacol.7:88-95.1961.*
[4]*Methods.Enzymol*.233:502-12.1994.
[5]*J.Immunol.Methods.*126(1):125-33.1990.
[6]*LWT.Food.Sci.Technol*.28:25–30.1995.
[7]*Eur.J.Med.Chem.*63:299-312.2013.

**Área: MED** **Inscrição:00389**

# Estudos computacionais utilizados na procura de potenciais inibidores da enzima arilalkilamina N-acetiltransferase do mosquito Aedes Aegypti

**Derli Ranieri Costa Dantzger (IC),[1] Luciana Scotti (PQ),[2] Marcus Tullius Scotti (PQ),[2] Hamilton Mitsugu Ishiki (PQ)[1]**

**hamilton@unoeste.br**

[1]*Universidade do Oeste Paulista;* [2] *Universidade Federal da Paraíba.*

Palavras Chave: *PRODUTOS NATURAIS, DOCKING, MODELAGEM MOLECULAR*

## Highlights

Use of computational studies to search potential inhibitors of arylalkylamine N-acetyltransferase enzyme from Aedes Aegypti.
27 compounds derived from natural products were docked with the arylalkylamine N-acetyltransferase enzyme.
All the studied molecules showed a good interaction with the studied enzyme.

## Resumo/Abstract

The transmission of endemic diseases is mainly allocated to mosquitoes such as Aedes aegypti, responsible for various sickness such as yellow fever, dengue and chikungunya fever. The need to find new environmentally friendly compounds having insecticidal properties leaded to the study of 27 potential inhibitors derived from natural products found in the Núcleo de Bioensaios Biossíntese e Ecofisiologia de Produtos Naturais (NuBBE) databank. These compounds were docked with the arylalkylamine N-acetyltransferase enzyme from Aedes aegypti, extracted from PDB (PDB ID=4FD5). The molecular geometries of all compounds were optimized using ab initio calculations.
Two distinct software, namely iGEMDOCK and AUTODOCK, were used to perform the docking calculations. In the iGEMDOCK program, the docking results presented a range of energies from -5.6 to -22.6 kcal/mol and in the AUTODOCK program, the results presented a range of energies from -7.51 to -10.11 kcal/mol.
The results derived from both software showed that 13 molecules presented similar interaction energies and were docked in the same site. Others molecules were docked near the active site. Only the compound (2R)-7,4'-diethoxy-5-hydroxy-3'-methoxy-6,8-dimethylflavanone appeared in the ranking of the five best results obtained for both software.

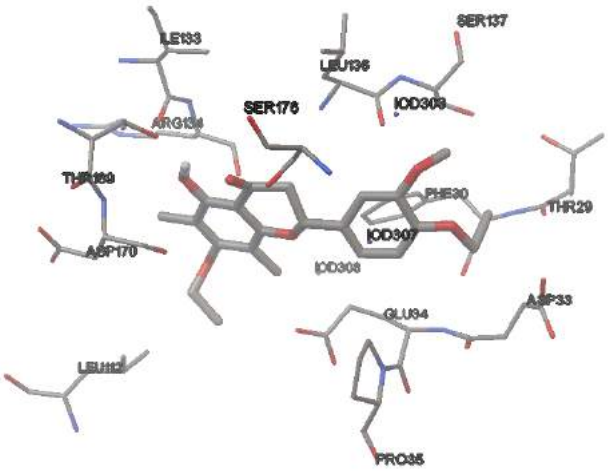


Figure 1. Interaction between compound (2R)-7,4'-diethoxy-5-hydroxy-3'-methoxy-6,8-dimethylflavanone and the active site of arylalkylamine N- acetyltransferase enzyme.

Additionally, it was observed that all the studied molecules showed a good interaction with the studied enzyme.

**Área: MED** **Inscrição: 00304**

# Molecular modeling studies of the nicotinic acetylcholine receptor (nAChRs) α4β2: Validation and analysis of bioactive compounds

**Victor S. Batista (PG),[1*] Nailton M. Nascimento-Júnior (PQ).[1]**

**sbatista.victor@gmail.com; nailtonjr@iq.unesp.br**

*[1]Universidade Estadual Paulista "Júlio de Mesquita Filho", Laboratório de Química Medicinal, Síntese Orgânica e Modelagem Molecular (LaQMedSOMM), Instituto de Química, Departamento de Química Orgânica, Rua Professor Francisco Degni, 55, Jardim Quitandinha, CEP 14800-060, Araraquara-SP, Brasil.*

Palavras Chave: *nAChRs α4ß2, Nicotine addiction, Molecular docking, Redocking, Binding affinity*

## Highlights

The nAChRs are pentameric ligand-gated ionic channels that respond to the endogenous neurotransmitter acetylcholine, with the α4β2 subtype being highly expressed in human brain. Nicotine addiction involves the modulation of this receptor. Tabagism is one of the world's leading preventable causes of death, killing around 5 million people each year. Only 10% of smokers effectively quit smoking without medication and the only FDA approved drug acting on the nAChRs α4β2 is varenicline, an expensive treatment. Our approach to the matter is based on the use of this receptor's crystal structure, co-crystalized with nicotine, to perform *in silico* validation of a computational docking methodology based on redocking and on the evaluation of the presence of relevant ligand-receptor interactions for a series of 28 nicotinic ligands with *in vitro* activities (Ki) gathered from the scientific literature. Discovery Studio Visualizer (DSV)[1] was used to built the ligands and analyse interactions predicted through docking, which was performed on GOLD Suite software. Ligand's geometry optimization was performed through PM7 semi-empirical method using MOPAC.[2] The ASP scoring function performed well in predicting key interactions between binding site residues and the selected molecules. The validated model can be applied on virtual screening of novel ligands.

## Abstract

The crystal structure of the nAChRs α4β2 was obtained from PDB (PDB ID: 5KXI). [3] The interactions between nicotine and the binding site residues were: W156 interacting with the pirrolidine basic nitrogen (pi-cation and backbone hydrogen bonding) and hydrophobic interactions with Y204, L121, T157, C199, C200, W57 and Y197. Docking parameters: explicit hydrogens, anhydrous binding site, rigid docking, ligand's ionization state predicted by MarvinSuite for pH 7.4 and 50 docking poses**.** The choice of the scoring function was based on the lowest RMSD between heavy atoms of co-crystalized ligand and docked nicotine. ASP function yielded the best result, as shown in **Table 1**. Binding interactions for docked nicotine are represented in **Figure 1**. For the nicotinic ligands, the scoring function predicted interactions with the following key residues: W156 (100%), Y204 (86.7%), L121 (93.3%), T157 (30%), C199 (30%), C200 (96.7%), W57 (66.7%) and Y197 (30%). 10 out of 28 nicotinic ligands were predicted to be spatially oriented closely to what is observed for co-crystalized nicotine, as shown in **Figure 2**.

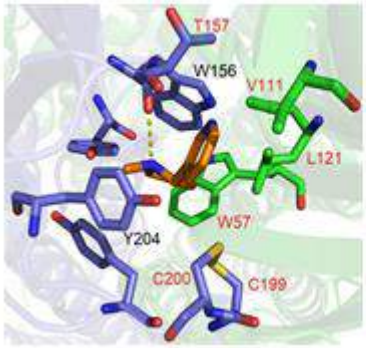


Figure 1: Binding interactions predicted by ASP scoring function. Red labels indicate hydrophobic contacts and black labes pi-cation interactions. Yellow dashed lines stands for hydrogen bonds. Hydrogens omitted for clarity.

| Scoring Function | RMSD | Score |
|---|---|---|
| ASP | 0.5275 | 36.1745 |
| GoldScore | 2.2876 | 63.8235 |
| ChemScore | 4.6723 | 28.0499 |
| CHEMPLP | 1.9598 | 49.26670 |

Table 1: RMSD and score for each of the GOLD software scoring functions.

Figure 2: Superposition of nicotinic ligands which mimics co-crystalized nicotine orientation.

Acknowledgements:
CAPES (scolarship), CNPQ, PROPe: Process 840, INCT-INOFAR: Process 573.564/2008

[1] BIOVIA, Discovery Studio Visualizer, v.17.0.2.1076, San Diego: Dassault Systèmes, 2017./ [2] MOPAC2016, James J. P. Stewart, Stewart Computational Chemistry, Colorado Springs, CO, USA/ [3]Morales-Perez *et al.*, Nature, 2016, 538, 411-415.

**Área:** MED **Inscrição:** 00225

# Síntese e avaliação farmacológica de derivados de dihidropirimidinonas inibidores duais MPO/AChE para o tratamento da Doença de Alzheimer.

**Thalita Corrêa C. de Oliveira*[1,4] (PG), João V.F. Quimas[2,4] (IC), Thayssa L. C. Nogueira[2,4] (IC), Júnia Maria Dutra Bastos[1,4](IC)Nelilma C.Romeiro[3,4], Leandro L. Silva[2,4](PQ) e Andréa L. F. Souza[*1,4] (PQ)**

***thalitaoliveiraufrj@gmail.com; andrealuzia@gmail.com****

*[1]LACASO-Laboratório de Catálise Aplicada e Síntese Orgânica; [2]Laboratório LIP-Laboratório Integrado de Pesquisa; [3]LICC- Laboratório integrado de Computação Científica.*

*[4]UFRJ – Campus Macaé, Av. Aluizio da Silva Gomes, 50, Granja dos Cavaleiros, Macaé - RJ - Brasil.*

Palavras Chave: *DHPM,Mieloperoxidase, Acetilcolinesterase, Multialvo, Estresse oxidativo, Reação de Biginelli.*

## Highlights

Synthesis and pharmacological evaluation of dihydropyrimidinone derivatives as MPO/AChE dual inhibitor for the treatment of Alzheimer's Disease.

- Synthesized dihydropyrimidinones inhibited both enzymes.
- The compounds **1d** and **1f** were more effective for AChE, while **1j** completely inhibited MPO.
- Different structural alterations point was determinant to different activities.

## Resumo/Abstract

**Introdução:**O tratamento da doença de Alzheimer (DA),é problemático devido a sua complexa fisiopatologia,envolvendo muitas vias, cujos principais alvos são perda neuronal, enrolamentos neurofibrilares,placa β-amilóide e níveis reduzidos de acetilcolina, tratado com inibidores da acetilcolinesterases (AChE).Atualmente,propõe-se reduzir o estresse oxidativo , destacando o papel pró-oxidante da mieloperoxidase (MPO), enzima presente apenas na microglia reativa circundante à placa β-amilóide, participando assim da patogênese da DA.[1]Na busca por moléculas multipotentes os derivados de diidropirimidinonas (DHPM) mostram-se promissores, pois podem atuar sobre a MPO[2] e a AChE[3].

**Objetivos:**Através da reação de Biginelli,uma clássica reação multicomponente que envolve a mistura de uma dicetona, uréia(ou tioureia) e um aldeído (Figura 1),sintetizar DHPMs que possam atual de forma dual MPO/AChE.

**Resultados:**Para a inibição da AChE tanto a presença do O (**1j-m**) no anel, quanto a metila (**1g-i**), parecem ser desfavoráveis, enquanto enxofre e etoxila são favoráveis (**1a-f**). Assubstituições no anel benzênico não foram determinantes para a ação antiocolinesterásica, no entanto, para a inibição da MPO foi a alteração mais relevante, sendo perdida na presença do grupo nitro(**1k-l**) e aumentada pelo Flúor (**1m**) ou do dimetilamino (**1j**)

**Conclusões/perspectivas:**A inibição das duas enzimas foi influenciada por alterações em pontos distintos da molécula, de modo que troca do O pelo S no derivado **1j**deverá produzir bom candidato a protótipo inibidor dual MPO/AChE potencialmente útil no tratamento da DA.

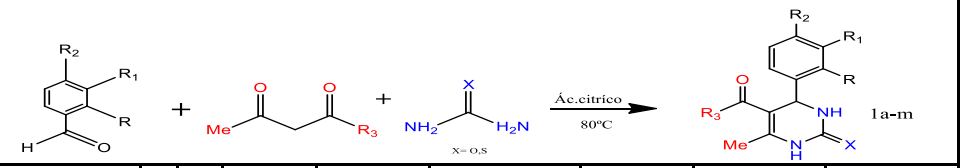


| Derivado (100 µM) | X | R | $R_1$ | $R_2$ | $R_3$ | Ponto de fusão (ºC) | %inibição da MPO[a] | %inibição da AchE[b] |
|---|---|---|---|---|---|---|---|---|
| 1a | S | H | H | $OCH_3$ | $OCH_2CH_3$ | 145-146 | 64,1*** | 41,4*** |
| 1b | S | H | $OCH_3$ | OH | $OCH_2CH_3$ | 215-217 | 43,5*** | 46,3*** |
| 1c | S | H | H | F | $OCH_2CH_3$ | 210-212 | 55,6*** | 52,2*** |
| 1d | S | H | H | H | $OCH_2CH_3$ | 205-206 | 58,3*** | 57,9*** |
| 1e | S | H | H | OH | $OCH_2CH_3$ | 202-204 | 71,5*** | 45,0*** |
| 1f | S | H | H | $CH_3$ | $OCH_2CH_3$ | 179-181 | 37,0*** | 57,2*** |
| 1g | S | H | H | H | $CH_3$ | 218-220 | 59,3*** | 30,6** |
| 1h | S | H | H | OH | $CH_3$ | 259-260 | 66,0*** | 20,3 |
| 1i | S | H | H | $OCH_3$ | $CH_3$ | 178-180 | 61,2*** | 28,3* |
| 1j | O | H | H | $N(CH_3)_2$ | $OCH_2CH_3$ | 256-258 | 99,5*** | 14,3 |
| 1k | O | H | $NO_2$ | H | $OCH_2CH_3$ | 190-192 | 24,5 | 37,6*** |
| 1l | O | H | H | $NO_2$ | $OCH_2CH_3$ | 169-170 | -28,2 | 26,0* |
| 1m | O | H | F | H | $OCH_2CH_3$ | 230-232 | 85,9*** | 32,4** |
| Veículo | | | | | | | -1,2 | 7,9 |
| Rivastigmina | | | | | | | ND | 58,4*** |
| Isoniazida | | | | | | | 88,64*** | ND |

[a]inibição da AChE (Eletrocphorus eletricus ) foi medida através do método de Ellam [4]. [b]inibição da MPO (rato) foi medida pelo método da taurina [5],*p<0,05**p<0,01***p<0,001, Anova de uma via(''Dunnett's Multiple Comparison Test') ,quando comparado ao grupo DMSO (veículo );ND= não determinado.

**Referências:**

[1]DOI:10.274/092986711797535245

[2]US2016/0326121A1

[3]DOI:10.1002/jbt.21897

[4]DOI:10.1016/00062952(61)901459

[5]DOI:10.1016/S00766879(94)3305-5

**Área: MED**
*(Inserir a sigla da seção científica para qual o resumo será submetido. Ex: ORG, BEA, CAT)*

**Inscrição: 1581**
*(Inserir o número de inscrição do autor que fez a submissão)*

# Novel Azido and Glucuronamide-based Nucleosides of Potential Therapeutic Interest

**Nuno M. Xavier (PQ),[1*] Rita G. Pereira (PQ),[1] Radek Jorda (PQ),[2] Eva Řezníčková (PQ),[2] Vladimír Kryštof (PQ),[2] Anne Loesche (PG),[3] René Csuk (PQ),[3] Nathalya Mesquita (PQ),[4] Glaucius Oliva (PQ)[4]**

**nmxavier@fc.ul.pt**

[1]Centro de Química e Bioquímica, Faculdade de Ciências, Universidade de Lisboa, Portugal
[2]Laboratory of Growth Regulators, Palacký University & AS CR, Czech Republic
[3]Bereich Organische Chemie, Martin-Luther-Universität Halle-Wittenberg, Germany
[4]Instituto de Física de São Carlos, Universidade de São Paulo, Brazil

Palavras Chave: *Nucleosides, Carbohydrate/nucleoside chemistry, Bioactive molecules, Lead molecules*

## Highlights

. Structurally novel furanosyl and pyranosyl nucleosides based on 5/6-azido glucosyl and on D-glucuronamide templates were synthesized.
. Some nucleosides displayed potent antiproliferative effects in cancer cells or exhibited effective inhibition of acetylcholinesterase, along with low neurotoxicity.
. Their $GI_{50}$ or $K_i$ values were in the low micromolar concentration range, similar or close to those of standard drugs, qualifying them as promising lead compounds for cancer or for Alzheimer's disease.
. Some compounds revealed their capability to inhibit an essential non-structural enzyme for Zika-virus replication.

## Resumo/Abstract

The development of novel nucleosides, nucleotides and analogs/mimetics has attracted much attention in organic and in medicinal chemistry, due to the variety of biological properties that these groups of compounds are prone to exhibit. Various examples of nucleoside and nucleotide analogs became clinically-used anticancer or antiviral agents, acting through interference with nucleotide-dependent events [1], while some reports also demonstrated the ability of these types of molecules to display antimicrobial effects [2] or to inhibit cholinesterases [3].
The search for new bioactive nucleos(t)ide analogs that may show innovative mechanisms of action and open new therapeutic opportunities remains of interest.

In this context, in this communication we present the synthesis and biological evaluation of novel nucleosides constructed on 5- or 6-azido glucosil moieties and on D-glucuronamide-based systems, which are rather unexploited glycosyl units in nucleoside chemistry. As N-heteroaromatic motifs, purine, uracil and triazole derivatives were included in the structures. The synthetic strategies employed furanose and pyranose precursors and involved *N*-glycosylation, sugar azidation or "click" 1,3-dipolar cycloaddition as key steps.

Some molecules were shown to display potent antiproliferative activities in cancer cells and to act *via* pathways that may be valuable to circumvent chemotherapy resistance. Enzymatic assays on relevant therapeutic targets revealed low micromolar inhibitors of acetylcholinesterase, while showing low neurotoxicity, qualifying them as promising lead molecules for Alzheimer's disease. Moreover, some nucleosides showed their ability to inhibit an essential non-structural enzyme for Zika-virus replication, motivating further research concerning their potential use as anti-flavivirus agents.

*Acknowledgements:* Fundação para a Ciência e Tecnologia (FCT) is acknowledged for funding (IF/01488/2013/CP1159/CT0006).

References:
[1] J. Shelton, X. Lu, J. A. Hollenbaugh, J. H. Cho, F. Amblard, R. F. Schinazi, *Chem. Rev.* **2016**, *116*, 14379.
[2] M. Serpi, V. Ferrari, F. Pertusati, *J. Med. Chem.* **2016**, *59*, 10343.
[3] a) N. M. Xavier, S. Schwarz, P. D. Vaz, R. Csuk, A. P. Rauter, *Eur. J. Org. Chem.* **2014**, *2014*, 2770; b) D. Batista, S. Schwarz, A. Loesche, R. Csuk, P. J. Costa, M. C. Oliveira, N. M. Xavier, *Pure Appl. Chem.* **2016**, *88*, 363.

**Área: MED** **Inscrição: 00116**

# Molecular modeling studies of the *Penicillium Camembertti* Lipase (PCL) enzyme: Docking and validation of bioactive compounds

**Thaíz R. Ribeiro (PG),[1*] Victor S. Batista (PG),[1] Nailton M. Nascimento-Jr. (PQ).[1]**

**nailtonjr@gmail.com; gisele1640@hotmail.com**

[1]*Universidade Estadual Paulista "Júlio de Mesquita Filho", Laboratório de Química Medicinal, Síntese Orgânica e Modelagem Molecular (LaQMedSOMM), Instituto de Química, Departamento de Química Orgânica, Rua Professor Francisco Degni, 55, Jardim Quitandinha, CEP 14800-060, Araraquara-SP, Brasil.*

Palavras-Chave: *Molecular docking, DAGL-α, PCL enzyme, Obesity, Inhibitory activity*

## Highlights

*Penicillium camembertii* lipase (PCL) is a mono, di-acylglycerol lipase, showing a canonical α/β hydrolase fold and the catalytic triad Ser-Asp-His[1]. In addition, its high structural similarity and the preservation of the catalytic residues arrangement allow its use as surrogate for the DAGL-α enzyme structure in computational studies, considering there are no crystal structures available for this enzyme. Based on the crystallographic structure of the PCL enzyme, *in silico* analysis of inhibitors with in vitro activity ($IC_{50}$) gathered from the scientific literature was performed. The ligands were built respecting protonation states for intracellular pH, using Discovery Studio Visualizer (DSV) software and optimized through semi-empirical PM7 method using MOPAC2016. The docking of these ligands on PCL enzyme was performed using different scoring functions (ChemPLP, ChemScore, GOLDScore and ASP) to evaluate ligands spatial orientation as well as relevant ligand-biomacromolecule interactions. The ChemPLP scoring function performed well in general[2]. DSV was used to analyze interactions predicted by GOLD Suite software for the best scored of 50 docking poses for each ligand. After validation, the model can be applied in the virtual screening of novel compounds designed as DAGL-α inhibitors.

## Abstract

The endocannabinoid system is a proven signaling pathway for appetite control, indirectly influencing the energy balance and therefore straight involved with obesity. An alternative for the modulation of this system would be sn-1-diacylglicerol lipase α inhibition, generating a signaling cannabinergic decrease and consequent orexia inhibition. Aiming to understand how substances with inhibitory activity towards the enzyme interact, the crystal structure of the PCL enzyme was obtained from PDB (PDB ID: 5CH8). To analyze similarities between crystallographic structure of PCL and DAGL-α, the primary sequence of DAGL-α was obtained through the NCBI proteomic server and after identifying the best correlation between the amino acid residues using the Swiss Model server, it was found that a high structural similarity and the preservation of the catalytic residues could be observed. In parallel, substances with high inhibitory activity against DAGL-α were gathered, as it can be observed for the sulfonamides **1** and **2**[3] **(Figure 1)**. The rigid molecular docking was carried out between the constructed substances and the *in silico* model, where the interactions between the amino acid residues and the previously designed molecules were observed through careful analysis. From these interactions, were frequently observed the residues R87, V86, K270, D267 also S145 **(3)**, which can be used as markers for future virtual screening of novel compounds.

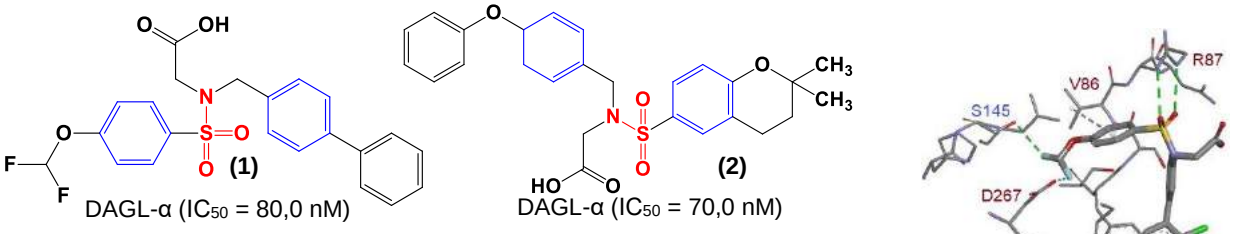


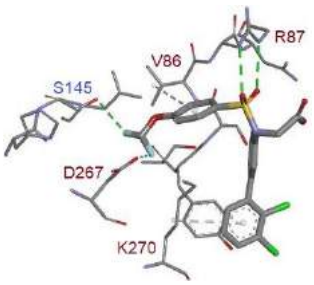


(3)

**Figure 1:** High potent sulfonamides with inhibitory activit against DAGL-α **(1 and 2)**. One of the predicted docking poses, showing interactions between residues of PCL enzyme and the inhibitor **(3)**.

Acknowledgements:
CNPQ (scholarship), PROPe: Process 840, INCT-INOFAR: Process 573.564/2008.

[1]Tang, Qingyun et al., Chemistry Select, 2016, 1, 836-839./ [2]Li, Yan et al., Journal of chemical information and modeling, 2014, 54, 1717-1736./ [3]Janssen, Freek J. et al., Journal of medicinal chemistry, 2014, 57, 6610-6622.

**Área: MED** **Inscrição: 00101**

# Structure-activity methods applied to NPS amphetamines e cathinones in order to predict risk assessment

**Eduardo Borges de Melo (PQ),[1,2] Caio Henrique Pinke Rodrigues (PG),[2] João Paulo Ataíde Martins[3] (PQ), Aline Thais Bruni (PQ)[2,4].**

**aline.bruni@usp.br**

[1]*Laboratório de Química Medicinal e Ambiental Teórica (LQMAT), UNIOESTE, campus Cascavel, PR.*
[2]*Departamento de Química, FFCLRP – USP – RP*
[3]*Departamento de Química, Universidade Federal de Minas Gerais (UFMG).*
[4]*Instituto Nacional de Ciência e Tecnologia Forense (INCT Forense), Ribeirão Preto/SP*

Keywords: Forensic chemistry; QSAR; NET; Amphetamines; Cathinones.

## Highlights

New synthetic recreational drugs circumvent legal prohibitions.
*In silico* models can be used to determine the toxicological risk.
The QSAR model is able to predict the risk of some derivatives.

## Resumo/Abstract

New psychoactive substances (NPS) have been created to circumvent legal prohibition of abuse drugs. This phenomenon brings difficulties in detecting the risk of using these new substances since their health effects are unknown. Nevertheless, *in silico* methods present great potential to study NPS. They are able in make predictions for toxicity in a less time-consuming way, giving a positive feedback since these new drugs are in constant expansion. This study aimed to build a QSAR model able to verify the potential risk of new synthetic recreational drugs derived from amphetamines and cathinones. For this purpose, a data set consisting of 23 derivatives with *in vitro* affinity against the norepinephrine transporter (NET) receptor was selected. We used geometric molecular descriptors (AM1 level) obtained in free platform ChemDes, and the Ordered Predictors Selection (OPS) for variable selection. A PLS model was obtained with good internal ($R^2$=0.914; *SEC*=0.167; $Q^2_{LOO}$=0.835; *SEV*=0.231) and external (average of 7 different test sets: $R^2_{pred}$=0.754; *SEP*=0.246) statistical features. This model was able to accurately predict the risk range of three previously selected derivatives: methedrone (low), ethcathinone (medium), and methamphetamine (high). These data were used to create a simple free program in JAVA to help those interested in using it to determine the risk of new synthetic drugs of abuse of this class, which can be requested from the authors. These results show the potential of using *in silico* methods as an important support tool for the forensic sciences.

**Área: ORG** **Inscrição: 0020**

# β-hydroxy(amino)amides: enzymatic catalysis via nitrile hydratases and ketoreductases

**Éverton A. Tordato (PG), Lucas Henrique C. Machado (IC), Cintia D.F. Milagre (PQ)***

cintiamilagre@iq.unesp.br

*Instituto de Química, UNESP – Araraquara*

Palavras Chave: *Enzymes, beta-Hydroxyamides, Nitrile hydratase, Ketoreductases, Biocatalysis*

## Highlights

β-Hydroxy(amino)(keto)amides were obtained;
Nitrile hydratases and ketoreductases were screened for enzymatic activity and substrate scope;
Enantiomeric excess of 99% were achieved.

## Resumo/Abstract

The long-awaited global goal of sustainable development can be facilitated, in the context of chemical processes, by the use of biocatalysts in the organic synthesis.[1] Optically active β-hydroxy(amino)amides are important building blocks for the synthesis of active pharmaceutical ingredients, such as, fluoxetine, nisoxetine, tomoxetine and levamisole.[2] Herein, β-hydroxy(amino)amides were obtained through enzymatic catalysis. Two classes of enzymes were evaluated: (1) nitrile hydratase (NHase) which converts a nitrile into the correspondent amide (Scheme 1) and (2) ketoreductases (KRED) for the conversion of ketone into secondary alcohols (Scheme 2).

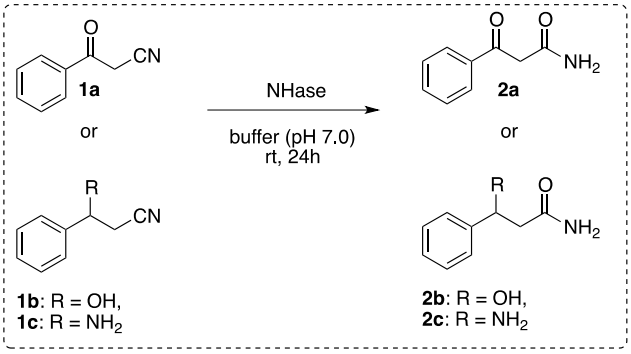


**Scheme 1:** Enzymatic nitrile hydration

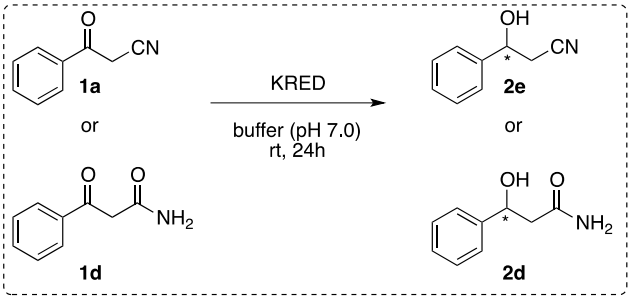


**Scheme 2:** Enzymatic ketone reduction

Thirteen commercial nitrile hydratases were screened with three substrates: 3-oxo-3-phenylpropanonitrile (**1a**), 3-hydroxy-3-phenylpropanonitrile (**1b**) and 3-amino-3-phenylpropanonitrile (**1c**) affording conversions in the range of 86-100% for cobalt-dependent enzymes. No stereoselectivity were observed for any evaluated enzyme. On the other hand, three microorganisms containing ketoreductases were screened with 3-oxo-3-phenylpropanonitrile (**1a**) and 3-oxo-3-phenylpropanoamide (**1d**) giving conversions and stereoselectivity of 3.2-100% and 94-100%, respectively. Data obtained in this work are being used for enzymatic cascade reactions development. One of the most prominent advantages related to the implementation of these multi-step one-pot biotransformations is their step economy. Carrying out several reactions in direct succession without purification of intermediates helps to maximize the overall yield and minimize the use of reagents, catalysts and solvents yielding a more sustainable process.

[1]Sheldon, R. A.; Pereira, P.C.; *Chem. Soc. Rev*. **2017**, 46, 2678.
[2] Garcia-Junceda, E.; Lavandera, I.; Rother, D.; Schrittwieser, J. H.; *J. Mol. Catal. B: Enzym.* **2015,** *114,* 1.

**Área: ORG** **Inscrição: 00040**

# Relevance of kinetic data of cellulose acylation to the synthesis of cellulose mixed esters

**Thaís de A. Bioni (PG),[1*] Omar A. El Seoud (PQ),[1]**

**tha.bioni@usp.br**

[1]*IInstitute of Chemistry, University of São Paulo*

Keywords: Ionic liquid, Cellulose, *Kinetics, Mixed Esters*

## Highlights

The properties of the commercially important cellulose mixed esters, e.g., acetate (Ac)/propionate (Pr) depend on the relative degree of substitution by each acyl group, e.g., $DS_{Ac}/DS_{Pr}$. It is difficult to control this ratio in the industrial (heterogeneous) process; homogenous acylation permits a better control. We show that the ratio between the third-order rate constants ($k_{Ac}/k_{Pr}$) is similar to that between $DS_{Ac}/DS_{Pr}$, i.e, kinetic data permit prediction, hence control of mixed ester composition.

## Abstract

Using solution conductivity, we studied the acylation of microcrystalline cellulose (MCC) by acetic- and propionic anhydride (1 $Ac_2O$: 1 $Pr_2O$), and by *N*-acetyl, and *N*-benzoylimidazole (1 AcOIm: 4 BzOIm). The reaction was carried out under homogeneous conditions in a mixture of the ionic liquid (IL) 1-allyl-3-methylimidazolium chloride and the molecular solvents dimethyl sulfoxide (DMSO) and *N,N*-dimethylacetamide (DMAc). The reaction third-order rate constants (first order in MCC, the anhydride, and the IL) were calculated; their ratios were similar to the corresponding degrees of substitution. That is, kinetic data permit prediction of product composition. Table 1 shows results obtained for acylation with $Ac_2O/Pr_2O$ and AcOIm/BzOIm in IL/DMSO. Fig. 1 Ilustrates the $^1$H NMR spectrum of the ester obtained in IL/DMSO.

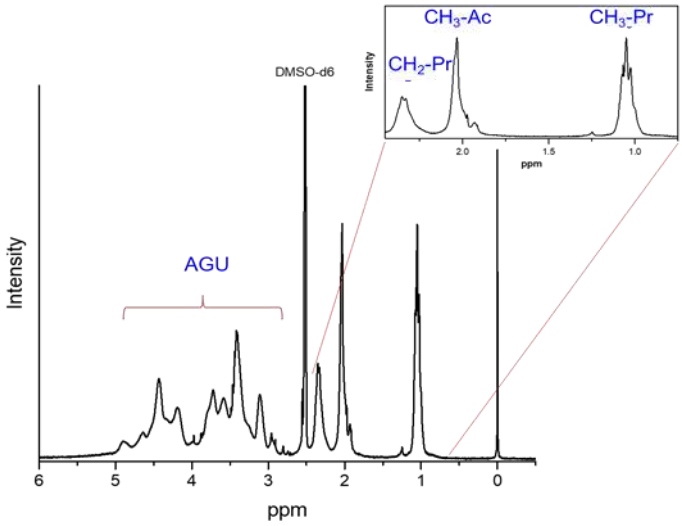


**Fig 1.** Cellulose acetate propionate synthesized in IL/DMSO, **$DS_{Ac}/DS_{Pr}$=1.24**.

**Table 1.** Third order constants for acylation of MCC in IL/DMSO at 40 °C.

| $k_{3Ac2O}$ | $k_{3Pr2O}$ | $k_{3Ac2O}+k_{3Pr2O}$ | $k_{3Ac2O}/k_{3Pr2O}$ | $DS_{Ac}/DS_{Pr}$ |
|---|---|---|---|---|
| 2,344E-3 | 1,910E-3 | 2,224E-3 | 1,23 | 1,24 |
| $k_{3AcOIm}$ | $k_{3BzOIm}$ | $k_{3AcOIm}+k_{3BzOIm}$ | $k_{3AcOIm}/k_{3BzOIm}$ | $DS_{Ac}/DS_{Bz}$ |
| 13,45E-3 | 12,71E-3 | 13,21E-3 | 1,06 | 0,71 |

It was possible to observe relationship between the ratio of DS and $k_3$ to the formation of cellulose acetate propionate, showing that the synthesis has kinetic control. In the case of the cellulose acetate/benzoate mixed ester, the ratios of DS and $k_3$ were slightly different, probably because of steric requirement of the rigid benzene ring.

We thank FAPESP (2014/22136-4) for financial support and CAPES for fellowship to T. Bioni.

**Área: ORG** **Inscrição: 00044**

# QUANTIFICAÇÃO DE ÉSTERES METÍLICOS POR ANÁLISE TERMOGRAVIMÉTRICA APLICANDO PARÂMETROS CINÉTICOS

**Michelle Budke Costa (PQ),[1] Nathieli Thomas (PG),[1*] Fernanda Gato (PG),[1] Daniel Marcos Dal Pozzo (PG),[1] Fernando Reinoldo Scremin (PQ)[1].**

**michellebudke@gmail.com; nathieli93@hotmail.com**

*[1]Departamento de Química, UTFPR.*

Palavras Chave: Análise Termogravimétrica, ésteres metílicos, parâmetros cinéticos.

## Highlights

Quantification of methyl esters by thermogravimetric analysis applying kinetic parameters. Mathematical Modeling Applied Transesterification Reaction. Thermogravimetric Curves of Methyl Esters. Transesterification reaction of crude Macauba almond oil. Mathematical determination of kinetic parameters in organic reactions. Pseudo-homogeneous model of second order. Pseudo-homogeneous model of first order.

## Resumo/Abstract

A aplicação de modelos matemáticos que visem a quantificação do teor de ésteres são úteis para prever o comportamento cinético de reações de transesterificação. Neste trabalho, foram aplicados dois modelos para estimar os parâmetros cinéticos frente aos dados experimentais obtidos a partir de análises termogravimétricas (TGA). A Análise Termogravimétrica é uma técnica utilizada como método inovador na quantificação de ésteres alquílicos, pois analisa a estabilidade térmica do material, em função da perca de massa pelo aumento da temperatura. Foram realizadas transesterificações com óleo de amêndoa de macaúba, utilizando metanol e ácido p-toluenosulfônico (p-TS) como catalisador. O perfil temogravimétrico do produto da reação de transesterificação apresentou dois processos bem definidos, o primeiro em torno de 210 ºC (eliminação do éster) e o segundo, em torno de 365 ºC (eliminação do triglicerídeo residual). A deconvolução de ambas as curvas gerou um fator de dispersão excelente ($R^2$=0,9992) e obteve-se o perfil do teor dos ésteres metílicos em função do tempo (Figura 1).

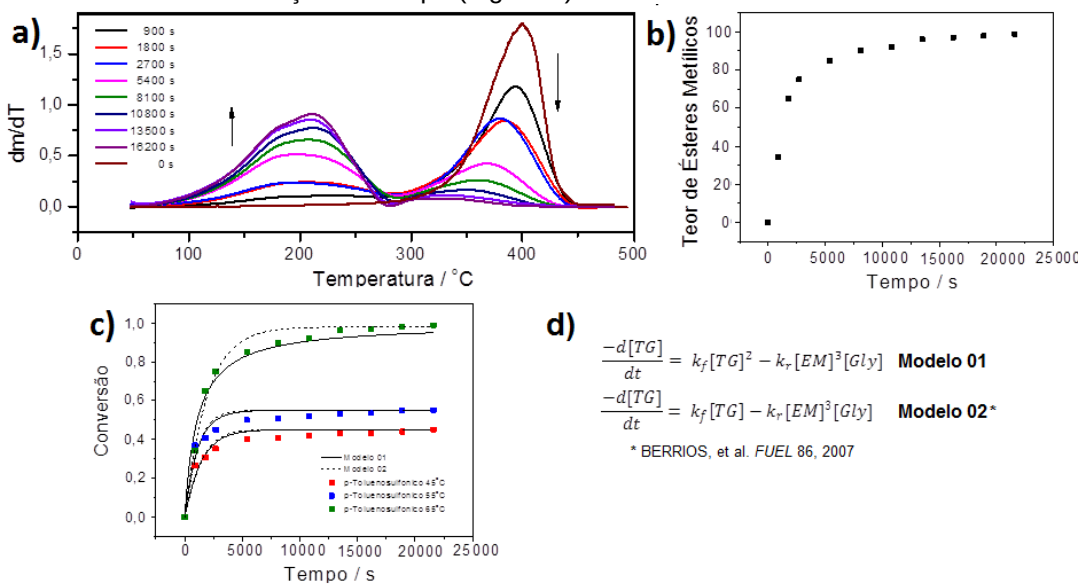


**Figura 1**. a) Perfil termogravimétrico diferencial, b) perfil do teor de ésteres metílicos em função do tempo, c) ajuste dos modelos cinéticos proposto para a reação de transesterificação metanólica do oleo da amendoa de macauba catalisada por ácido p-TS e d) modelos utilizados.

Com o perfil do teor de ésteres em função do tempo, determinou-ser os parâmetros cinéticos da reação com $R^2$ médio de 0,958 para o modelo 01 (pseudo-homogêneo de segunda ordem) e 0,970 para o modelo 02 (pseudo-homogêneo de primeira ordem). Ambos os modelos demonstraram excelente correlação, descrevendo adequadamente a reação.

**Área:** *ORG*

**Inscrição:** 00078
*(Inserir o número de inscrição do autor que fez a submissão)*

# Synthesis of Carboxyl-functionalized ionic liquids from cyclic anhydrides.

**Tânia M. Cassol (PQ),[1*] Guilherme H. Berton (IC),[1] Talita J. Ramos(PG),[2] Severino A. Junior(PQ),[2*]**

tcassol@utfpr.edu.br.; salvesjr@ufpe.br.

*[1]Departamento de Química e biologia UTFPR- Francisco Beltrão; [2]Departamento de Química Fundamental UFPE- PE*

Palavras Chave:*( Room temperature ionic liquids (RTILs), Carboxylic acids, cyclic anhydrides, Ionogels, Lanthanides ions).*

## Highlights

We describe here for the first time Room temperature ionic liquids (RTILs), imidazole-based cations with appended carboxylic acids as terminals, which are directly derived from the cyclic anhydrides.
All structures are easy preparation (up-scaling into kg scale possible); melting point < 100 °C aligned with thermal stability up to 100 °C; 3) chemical stability in water and common organic solvents;

## Resumo/Abstract

Room temperature ionic liquids (RTILs) are ILs with melting points below room temperature. Typically, a RTIL consists of nitrogen or phosphorous-containing organic cations and large organic or inorganic anions.[1] The wide range of possible cation and anion combinations allows for a large variety of tunable interactions and applications[1,2] what makes the Ionic Liquids one class of compounds that grows rapidly and with them all the research areas among them the complexation with lanthanides salts shows that unique luminescent proprieties.[3]

In this work, we show a new methodology for obtaining novel Carboxil functionalized ionic liquids with high yield and purity based on procedure proposed by Riidsger et. all.[4] Figure 1.

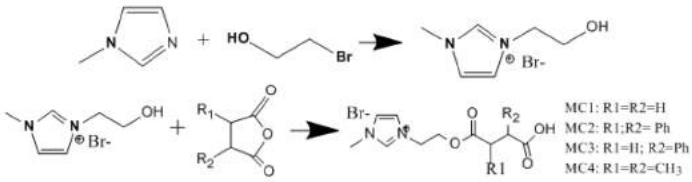


Fig. 1.
General synthetic procedure employed to prepare the new monocationic carboxylate-ionic liquids

The products were characterized by several spectroscopic techniques. We also performed the measurements of melting point, thermogravimetric and elemental analysis that prove the proposed structures for ionic liquids, which are unprecedented in the literature. Figure 2

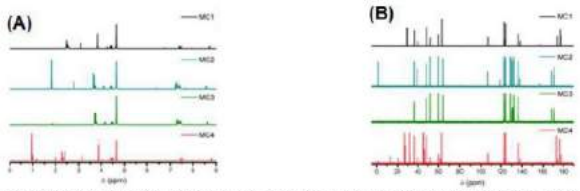


Figure 2. Spectrum to elaborated ionic liquids. (A) NMR spectrum 1H; (B) NMR 13C spectrum;

The Room temperature ionic liquids are been studied for the coordination of lanthanide ions (Eu or Gd). Ionogels to combine the properties of the ionic liquids and luminescence of lanthanides salts.

Acknowledgements
This work was supported by CNPq, CAPES, LAC-UFPE and FACEPE.

References
[1] Adv. Synth. Catal. 2006, 348, 243-248.
[2] Chem. Lett. 2004, 33, 1590-1591.
[3] Eur. J. Inorg. Chem. 2010, 2569–2581.
[4] Topics in Catalysis, 2006, 40, 91-102.

**Área: ORG . Inscrição: 00109 .**

# Mechanochemical the synthesis of enaminones

**Edson Evangelista (PG),[1] Silvio Cunha (PQ)[1,2]**

**Edson.te@hotmail.com; silviodc@ufba.br**

[1]*Instituto de Química, Universidade Federal da Bahia, Campus de Ondina, 40170-290, Salvador – BA.*
[2]*INCT-Instituto Nacional de Ciência e Tecnologia em Energia e Ambiente, Campus de Ondina, Salvador – BA*

Key words:*(enaminones, green chemistry, mechanochemistry).*

## Highlights

Enaminones were obtained in good yields under of mechanochemical condition without the use of solvents or catalysts.

## Resumo/Abstract

Enaminones are important intermediates in the construction of *N*-heterocycles (Figure 1), so their synthesis has become the target of numerous studies over the years in order to develop more efficient methodologies to obtain them.[1,2] The study of the reactivity of enaminones is favored by important aspects of this type of compound, such as the ease with which they are synthesized, isolated and stored, generally under atmospheric conditions and at room temperature. This is due to the carbonyl group that is conjugated to the enamine moiety, which confers a strong stability to this system.[3] Over the years, several methodologies for the synthesis of enaminones have been developed and perfected from the original procedures. In addition to reducing reaction time, increasing yield and process efficiency, most methods are focused on Green Chemistry parameters.[1]

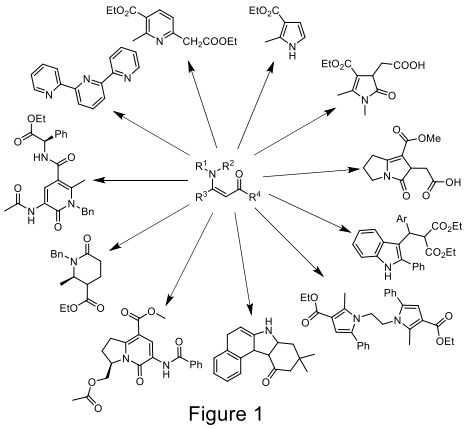

Figure 1

With the resurgence of mechanochemistry, a new frontier was established allowing the development of current methodologies, aiming for greater energy efficiency and an increase in the scale. In this work, different primary amines, secondary amines and diamines were used as the starting material for 1,3-dicarbonyl compounds to obtain *β*-enamino esters and ketones.

The procedures were performed using the planetary ball mill, and the synthesis occurred without the presence of solvent or catalyst, and with simple and cleaner purification procedures, affording enaminones in reasonable to good yields around (Figure 2). In one example, we could prepare from 0.6 to 60.0 g of enaminone from ethanolamine and methyl acetoacetate, illustrating the scale up viability of the mechanochemical approach.

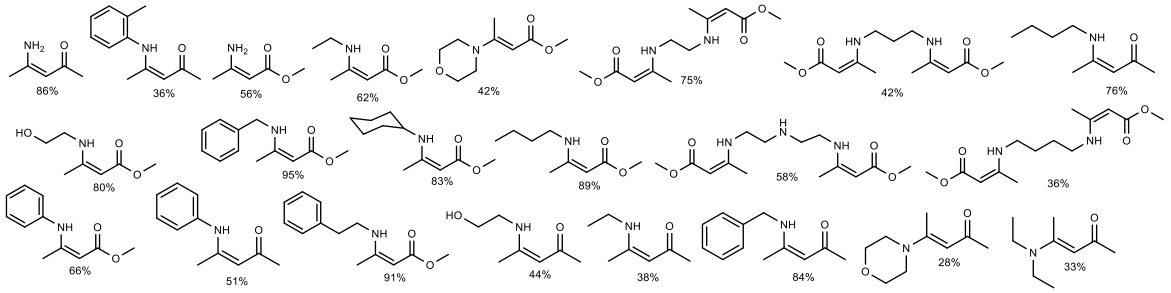

Figure 2

*1 - Ferraz, H. M. C; Gonçalo, E. R. S.; Quim. Nova; 2007, 30, 957. 2 - Govindh et.al., Org. Commun. 2012, 5:3, 105-119; 3 - Negri, G.; Kascheres, C. and Kascheres, A. J.; J. Heterocyclic Chem., 41, 461(2004). 4 - Stolle, A.; Ranu, B.; Ball Milling Towards Green Synthesis: Applications, Projects, Challenges. (RSC) Publishing, 2015, cap. 10, p. 241-276.*

**Area: ORG** **Submission Number: 00152**

# Pentacyclic triterpenes and the cytotoxic potential of *Vochysia divergens* Pohl stem extract

**Letícia P. Pimenta (PG),[1*] Rita C. N. Pedroso (PG),[1] William P. Souza (PG),[2] Alexander B. Valerino-Diaz (PG),[3] Lourdes C. dos Santos (PQ),[3] Marcos A. Soares (PQ),[2] Denise C. Tavares (PQ),[1] Márcio L. A. Silva (PQ),[1] Wilson R. Cunha (PQ),[1] Patrícia M. Pauletti (PQ),[1] Ana H. Januário (PQ),[1] leticia_pimenta94@hotmail.com**

*[1]Natural Products Research Group, University of Franca, Franca, SP, 14404-600, Brazil; [2]Department of Botany and Ecology, University Federal de Mato Grosso, Cuiabá, MT, 78060-900, Brazil; [3]UNESP-São Paulo State University, Chemistry Institute-Araraquara, SP, 14800-901, Brazil*

Keywords: *Cytotoxicity, HPLC-RI, Pentacyclic triterpenes, Vochysia divergens, Vochysiaceae.*

## Highlights

Five triterpenes belonging to the classes lupan, oleanane, and ursane were isolated from the ethanolic extract of *Vochysia divergens* stem (VC) by HPLC-RI and identified by NMR; the VC cytotoxic potential was evaluated.

## Abstract

*Vochysia divergens* Pohl is a native species of the Pantanal biome. It is popularly known as Cambará. Literature data have revealed the presence of the triterpenes oleanane, ursane, and lupan in the stem of this species[1]. Our research group has shown that, at 100 µg/mL, the ethanolic extract of this species reduces the motor activity of adult *Schistosoma mansoni* worms by 100% within 24 h. This study aimed to isolate the aforementioned triterpenes by HPLC-RI and to evaluate the cytotoxicity of the ethanolic extract of *V. divergens* stem (VC). The triterpenes divergioic acid (**1**) and sericic acid (**2**) and a mixture containing 24-hydroxytormentic acid (**3**), 4-*epi*-sericoside (**4**), and 4-*epi*-niga-ichigoside F1 (**5**) were obtained from a VC fraction after it was submitted to sephadex column and HPLC-RI. NMR experiments (1D and 2D) helped to elucidate the structures of the compounds. VC cytotoxicity to a normal line of human lung fibroblast cells, GM0792A, was evaluated by the *in vitro* toxicology colorimetric assay – Kit XTT; VC was tested at concentrations ranging from 9.8 to 1.250 µg/mL. The assay revealed that VC was not cytotoxic against the tested cell line: $IC_{50}$ was equal to or higher than 1.250 µg/mL. Compounds **1**, **2**, and **4** presented anti-inflammatory activity[2]. Compound **3** exerted marked antinociceptive action in mice[3]. Compound **4** displayed anti-*H. pylori* activity against three metronidazole-resistant strains[4]. Studies to evaluate the potential of these compounds against *S. mansoni* are underway.

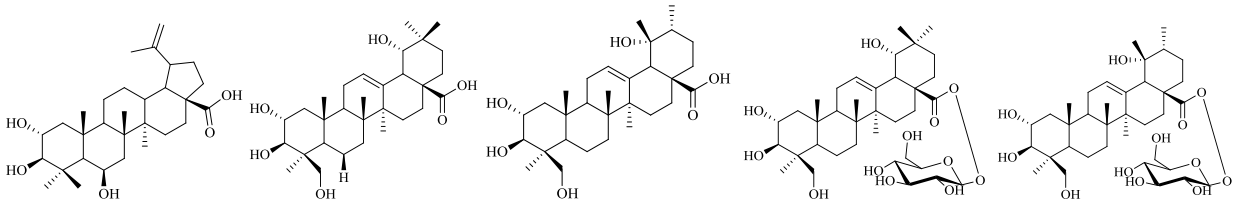

**1** **2** **3** **4** **5**

[1] Carnevale Neto, F.; Pilon, A. C.; Silva, D. H. S.; Bolzani, V. S.; Castro-Gamboa, I. *Phytochem Rev.*, 10, 413-429, 2011.
[2] Huang, J.; Wang, Y.; Li, C.; Wang, X.; He, X. *Industrial Crops and Products* 91, 302–309, 2016.
[3] Beirith, A.; Santos, A. R.; Calixto, J. B.; Hess, S. C.; Messana, I.; Ferrari, F.; Yunes, R. A. *Planta Med.*, 65, 50-55, 1999.
[4] De Leo, M.; De Tommasi, N.; Sanogo, R.; D'Angelo, V.; Germanò, M. P.; Bisignano, G.; Braca, A. Phytochemistry 67, 2623–2629, 2006.

**Área: ORG** **Inscrição: 00192**

# Use of Trichloroisocyanuric Acid for the Conversion of Amides to Amines via Hofmann Degradation

**Gustavo A. Bastos (IC) and Marcio C. S. de Mattos* (PQ)**

**gustavobasttos@gmail.com; mmattos@iq.ufrj.br**

*Departamento de Química Orgânica, Instituto de Química, UFRJ*

Palavras Chave: *Hofmann degradation, Electrophilic halogenation, N-Halocompound, Amine, Amide, Green chemistry*

## Highlights

- One pot preparation of amines from amides
- Safe reagents and simple reaction conditions
- Green methodology

## Resumo/Abstract

The Hofmann degradation is the conversion of a primary amide to a primary amine with one fewer carbon atom. This methodology, known since 1881, involves the reaction of the amide with an halogen in the presence of aqueous bases, being the formation of a *N*-haloamide intermediate one key step to its success.[1] In recent years, we have been exploring the chemistry of trichloroisocyanuric acid (TCCA) as a green reagent for electrophilic chlorination of diverse substrates.[2] Herein we show our results of its use for the *N*-chlorination of amides followed by Hofmann degradation to amines.

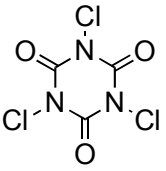

(TCCA)

Optimization of the reaction conditions using benzamide as a model substrate for the Hofmann degradation showed the best yield of aniline (54%) was obtained using aqueous acetonitrile as solvent and NaOH as base, in a molar ratio of 1 / 0.34 / 5.5 (amide / TCCA / NaOH). Using these conditions, diverse amines were obtained from the corresponding amides in 14 – 78% isolated yield in a one pot process. As can be seen in Scheme 1, the methodology proved to be efficient for the preparation of anilines and cyclohexylamine from the corresponding benzamides and cyclohexanecarboxamide, respectively. However, using a linear primary amide (e.g. decanamide) as substrate, a mixture of nonylamine and the nitrile was obtained.

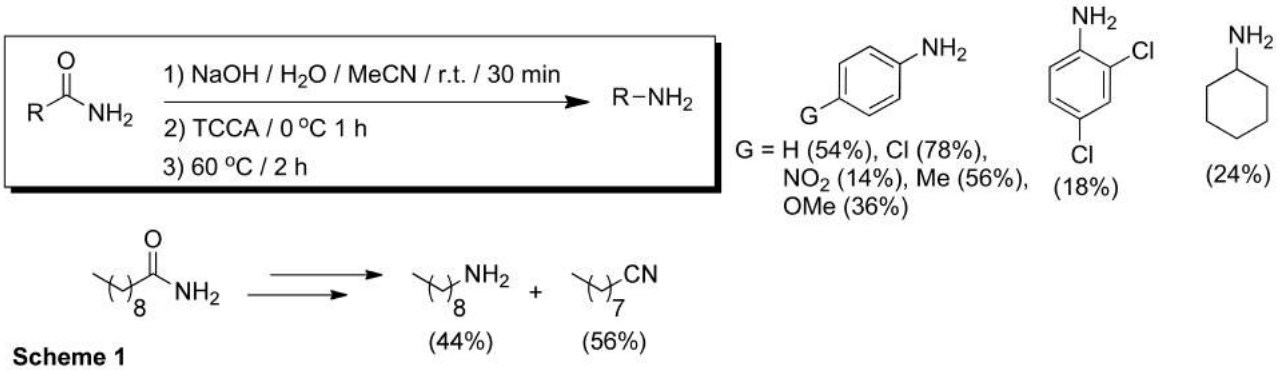


**Scheme 1**

In summary, we propose a new green methodology for the Hofmann degradation of amides using trichloroisocyanuric acid. To show the utility of our methodology, aniline was obtained in 54% from the reaction of benzamide and TCCA, while traditional conditions using toxic and corrosive $Cl_2$ gave aniline in only 30% yield.[3]

1. Kürti, L.; Czakó, B. *Strategic Applications of Named Reactions in Organic Synthesis*. Elsevier, 2005.
2. de Mattos, M. C. S.; Mendonça, G. F. *Cur. Org. Synth.* **2013**, *10*, 820.
3. Liguori, L.; Bjorsvik, H. R. *Org. Process Res. Dev*. **2011**, *15*, 997.

(financial support: CNPq)

**Área: ORG** **Inscrição: 00242**

# New chiral oxazolidine-dihydropyridines

**Rebeca Garcia Moura (PG), Daniel Y. R. Palma (IC), Claudio Di Vitta (PQ), Liliana Marzorati (PQ)***

**rebeca.garcia.moura@usp.br; lmarzora@iq.usp.br**

***Instituto de Química, Universidade de São Paulo***

Key words: *Pyridinium salts, Oxazolidines, Diels-Alder adducts, Isoquinuclidines.*

## Highlights

Pyridinium betaines of chiral pyridinium salts, bearing a β-hydroxy substituent linked to the heterocyclic nitrogen atom, underwent “in situ” cyclization, leading to oxazolidine-dihydropyridines. The latter compounds were submitted to Diels-Alder cycloaddition with *N*-methylmaleimide, affording new chiral isoquinuclidines.

## Abstract

2,4,6-Triphenyl-*N*-methyl-pyridinium ylides can be prepared by deprotonation of the methyl *N*-substitutent. Usually, aqueous alkali performs well and “one pot” aldol addition of such ylides to aromatic aldehydes leads to *N*-β-hydroxy pyridinium salts. Such intermediate products cyclize “in situ” to oxazolidine-dihydropyridines[1].

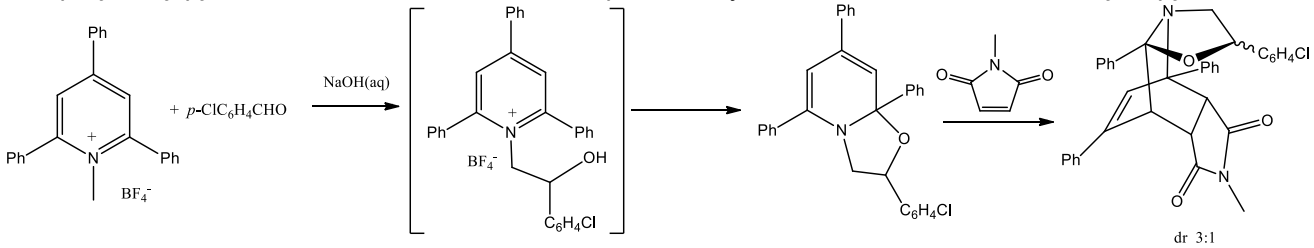


Encouraged by such preliminary results, we envisaged a preparative route to chiral isoquinuclidines. To this end, four chiral 2,4,6-triphenylpyridinium tetrafluoroborates were prepared from 2,4,6-triphenylpyrilium tetrafluoroborate and enantiomerically pure β-aminoalchools[2].

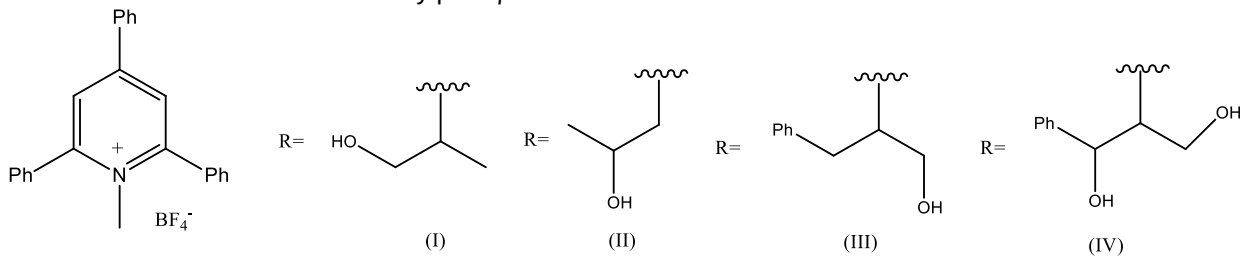


As expected, treatment of pyridinium salts (**I - IV**) with aqueous sodium hydroxide (20%m/v) afforded the corresponding oxazolidines-dihydropyridines in moderate yields, as mixtures of diastereoisomers:

| 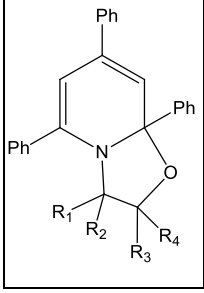 | | **Yield (%)** | **Diastereomeric ratio** |
|---|---|---|---|
| | $R_1 = CH_3, R_2 = R_3 = R_4 = H$ | 45 | 1:1 |
| | $R_1 = R_2 = R_3 = H, R_4 = CH_3$ | 43 | 1:1 |
| | $R_1 = PhCH_2, R_2 = R_3 = R_4 = H$ | 55 | 1.4:1 |
| | $R_1 = Ph, R_2 = R_3 = H, R_4 = CH_2OH$ or $R_1 = PhCHOH, R_2 = R_3 = R_4 = H$ | 68 | 10:1 |

The Diels-Alder reaction employing *N*-methylmaleimide as dienophile afforded the corresponding adducts as mixtures of diastereoisomers that could be isolated by column chromatography on silica gel.

References: 1. J.M.Nakagawa, *Master Dissertation*, **2015** .
2. A.R. Katritzky; R.T. Langthorne; R.C. Patel; G. Lhommet, *Tetrahedron Lett.* **1981**,*37*, 2383.

**Área: ORG .** *(Inserir a sigla da seção científica para qual o resumo será submetido. Ex: ORG, BEA, CAT)*

**Inscrição: 00251 .** *(Inserir o número de inscrição do autor que fez a submissão)*

# Substituent effect evaluation on spectroscopic properties of Schiff bases derived from diaminomaleonitrile and salicylaldehydes

**Lucas S. Mello (PG),[1] José W. Cruz Junior (PQ),[2] Edward R. Dockal (PQ).[1]**

**lucasdosantosmello@gmail.com; erdockal@gmail.com**

*[1]Laboratório de Sínteses Inorgânicas, Catálises e Cinética, Departamento de Química, UFSCar – São Carlos/SP; [2]Laboratório de Química Inorgânica, Departamento de Ciências Exatas e Educação, UFSC – Blumenau/SC.*

Palavras Chave: *Schiff base, Salen-type, Diaminomaleonitrile*

## Highlights

- Synthesis of Schiff bases derived from diaminomaleonitrile and salicylaldehydes;
- Characterization by physical methods;
- Substituent effect evaluation;

## Resumo/Abstract

Schiff bases are organic compounds that are usually prepared by the reaction between a primary amine and an active carbonyl compound, first described by Hugo Schiff in 1864.[1] Diaminomaleonitrile is a hydrogen cyanide tetramer which is an electron rich diamine with low basicity and low nucleophilicity, due to the electron withdraw effect caused by its conjugated cyano groups.[2] So it reacts with carbonyl compounds to give monocondensated Schiff bases even in excess of carbonylic compound.[3]

In the work, seven monoiminated Schiff bases were obtained from the reaction between diaminomaleonitrile and salicylaldehyde or substituted salicylaldehyde. The products were characterized by physical methods and the substituent effect was evaluated by infrared and UV-Vis spectrometry and $^1$H NMR.

The medium yield of the reactions was 90 % and the compounds were soluble in polar organic solvents such as DMSO, *N,N*-DMF and THF and were insoluble in water and hexane. Vibrational spectra shows characteristic $\nu$N-H$_2$ (3484-3192 cm$^{-1}$), $\nu$C≡N (2246-2205 cm$^{-1}$), $\nu$C=N (1645-1624 cm$^{-1}$) and $\nu$C-O (1304-1230 cm$^{-1}$) bands. Characteristic $^1$H NMR peaks were observed as follows: 8,95-10,66 ppm (s, OH); 8,45-8,61 (s, -N=CH-) and 7,56-7,90 (-NH$_2$). When substituted in the position 3, the imine hydrogen is observed at higher chemical shifts. 4-substitued Schiff bases have the higher chemical shift for phenolic hydrogen. The methoxy-substituted compounds have higher chemical shift for amine hydrogen. The Electronic spectra morphologies were defined by the substituent position rather than its chemical nature, however, methoxy-substituted compounds shower a hyperchromic effect.

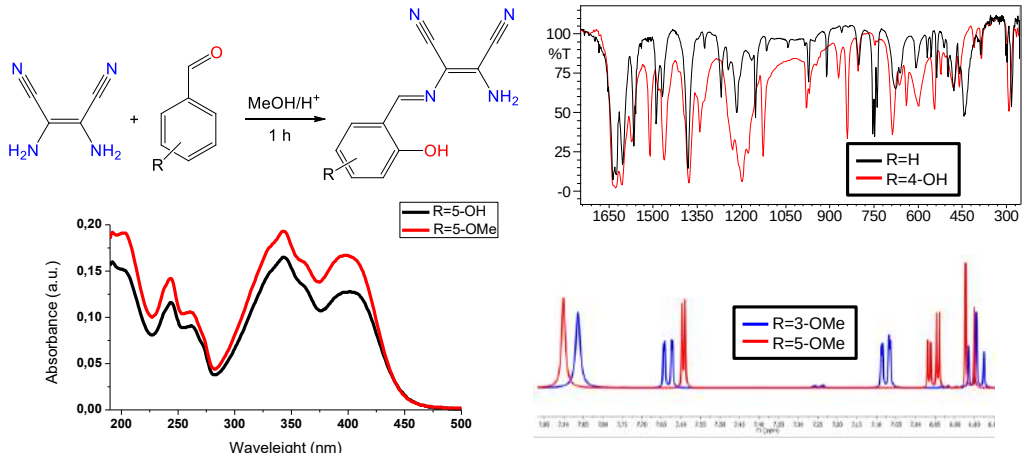


Figure 1. Synthetic methodology and spectra comparison (R=H, OH or OMe).

[1] Cozzi, P. G. *Chem. Soc. Rev.* **2004**, *33* (7), 410.
[2] MacLachlan, M. J. *et al*. *Inorg. Chem.* **1996**, *35* (19), 5492.
[3] Iwamoto, T.; Suzuki, H. *Chem. Lett.* **1976**, *5* (4), 343.

**Área: ORG** **Inscrição: 00263**

# Synthesis and characterization of non-symmetric dimeric ionic liquid crystals derived from 1,3,4-oxadiazole heterocycle.

**Monike da Silva Kutz (IC),[1] Fernando Molin (PQ).[1]**

**monikekutz@gmail.com; fmolin@gmail.com**

[1]*Departamento Acadêmico de Química e Biologia, Universidade Tecnológica Federal do Paraná.*

Palavras Chave: *Liquid Crystals, Luminescent Materials, 1,3,4- oxadiazole.*

## Highlights

After 130 years of the discovery of liquid crystals, several technological applications are being studied and developed, providing technological advances to scientific environment and to society.

## Resumo/Abstract

With the increase in manufacturing and consumption of electronic devices, such as organic light emitting diodes (OLED), organic field effect transistors (OFETs) and organic photovoltaic devices (OPVs), there was an increasing interest in the production of materials that are renewable[1], flexible, cheaper, easier to synthesize, and with reduced energy consumption, when compared to conventional devices.[2] Thereby the field of organic electronics has been developing, no longer being an area of pure academic interest, but enabling real day-to-day applications[1]. Within the organic electronics, the liquid crystals (LCs) have been gaining notoriety due to their intermediary properties to the crystalline solid and the isotropic liquid, possessing long-range orientational order, characteristic of crystals, and flowing like liquids[3]. LCs containing in their structure one, or more, heterocycles are being exploited as a result of their versatility,[4] thus, dimeric LCs derived from 1,3,4-oxadiazole heterocycle have been studied because of the high quantum yield of luminescence and stability thermal[5]. In order to study the p roperties of dimeric ionic LCs, the objective of this work was to synthesize and characterize two new molecules derived from 1,3,4-oxadiazole heterocycle, wherein each mesogenic group, oxaphenol (II) and oxapiridine (IV), were synthesized from the tetrazole (I), reacting it with the respective acyl chlorides in the presence of dry pyridine. The structural alteration was the variation of the size of the alkyl chain spacer of the mesogenic groups, in order to conclude that the presence of mesophases is affected by steric effects.

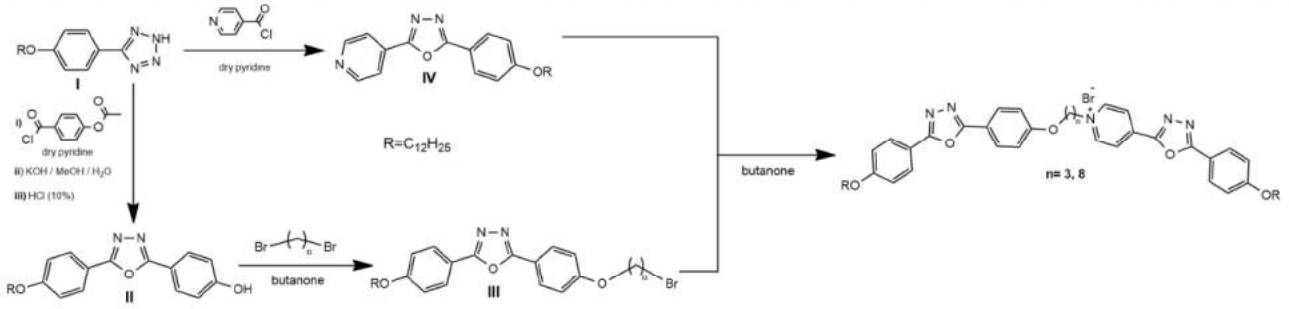


*Figure 1: Synthetic route of dimeric ionic liquid crystals derived from 1,3,4-oxadiazole heterocycle.*

**Referências.**

(1) Bushby, R. J.; Kelly, S. M.; O'Neill, M. *Liquid Crystalline Semiconductors - Materials, Properties and Applications*; Springer Series, **2013**; Vol. 169.

(2) Ruiz, C.; Hennrich, G. Organic Semiconductors toward Electronic Devices: High Mobility and Easy Processability. *J. Phys. Chem. Lett.* **2012**, *3*, 1428–1436.

(3) Khoo, I.-C. *Liquid Crystals Beyond Displays*; Wiley, **2007**, 368p.

(4) Selvarasu, C.; Kannan, P. Bent Shaped 1,3,4-Oxadiazole/Thiadiazole heterocyclic rings containing liquid crystals. *J. Chem. Sci.* **2015**, *127* (10), 1831–1838.

(5) Taylor, P.; Srivastava, R. M.; Filho, R. A. W. N.; Schneider, R.; Vieira, A. A.; Gallardo, H. Synthesis , optical properties and thermal behaviour of 1 , 3 , 4 - oxadiazole - based twin dimers. *Liq. Cryst.* **2008**, *35* (April 2013), 737–742.

**Área: ORG** **Inscrição: 00306**

# Chemical composition of essential oil from inflorescences from male and female specimens of *Baccharis punctulata* DC.

**Murilo S. de Oliveira (IC),[1] Jociani Ascari (PQ),[1] Domingos S. Nunes (PQ),[2] Dilamara Riva Scharf (PQ)[3], Edésio Luiz Simionatto (PQ)[3], Gustavo Heiden (PQ)[4]**

murilo_tinelli@hotmail.com

[1]*Coordenação de Ciências Biológicas - Universidade Tecnológica Federal do Paraná, Campus Santa Helena, UTFPR, PR Brasil.*
[2]*Departamento de Química – Universidade Estadual de Ponta Grossa, UEPG, PR, Brasil.*
[3] *Departamento de Química – Universidade Regional de Blumenau, FURB, SC, Brasil.*
[4] *Embrapa Clima Temperado, RS, Brasil.*

*Keywords: Baccahris punctulata, inflorescences, male and female specimens, essential oil, GC-MS-FID.*

## Highlights

In this work, the essential oils from the male and female inflorescences of B. *punctulata* DC were analyzed for the first time. GC-MS-FID analyzes showed high proportions of spathulenol and elemol in female and male inflorescences, respectively.

## Resumo/Abstract

The genus *Baccharis* (Asteraceae) has approximately 400 species distributed in great part in Argentina, Mexico and Brazil. The species consisting of dioecious or rarely monoic plants. Species of this genus are widely used in South America in traditional medicine for the control and treatment of diseases, in addition to their economic and environmental importance. The species *Baccharis punctulata*, popularly known as "Chilka saru saru" is used in medicine by rural communities in Bustillo Province in Bolivia for the treatment of asthma, dislocations and bruises. It is observed that only in a few studies on essential oils, it has been taken into account that the species of this genus are dioecious, and there may be differences between the secondary metabolism of male and female specimens of the same species. The objective of this work was to analyze the chemical composition of the essential oils of the inflorescences of male specimens (BPIM) and female (BPIF) collected in the western region of Paraná. The essential oils were obtained by hydrodistillation during 3h, yielding 0.34% (w/w) for BPIM and 0.15% (w/w) for BPIF. The chemical analyzes performed by GC-MS-FID demonstrated the occurrence of sesquiterpenes in a greater proportion in BPIM, being: elemol (26.29%), β-caryophyllene (8.59%) and bicyclogermacrene (6.43%) and in BPIF, spathulenol (22.52%), β-caryophyllene (12.20%), and the monoterpene β-ocimene (11.12%). The results suggest that the composition of the essential oils from this plant species varies with the individual development of the female and male specimens.

**Área: ORG** **Inscrição: 00322**

# Synthesis and Theoretical Studies of the Rotational Barrier of 2,4,6-Trifenetil-1,3,5-triazine

**Catarina De Nigris Del Cistia (PQ),[1,2] Igor Resendes Barbosa (IC),[2] Aurea Echevarria (PQ),[2] Carlos Mauricio R. Sant'Anna (PQ).[1,2]***

**catarina@ufrrj.br; santanna@ufrrj.br**

*[1]ICE, Departamento de Matemática, UFRRJ; [2]Instituto de Química, UFRRJ. Seropédica, Rio de Janeiro, Brasil.*

Palavras Chave: *1,3,5-triazines, atropisomers, rotational barrier, DFT, NMR.*

## Highlights

NMR data indicated the presence of atropisomers for the compound. DFT calculations were used to determine the rotational barrier to identify which bond rotation is responsible for the atropisomerism.

## Resumo/Abstract

The 1,3,5-triazine derivatives are of synthetic interest because of their wide range of applications. Literature reports antimicrobial, anti-HIV, anti-cancer, anti-malarial, leishmanicidal and others activities, reinforcing their medicinal importance. The 2,4,6-triphenethyl-1,3,5-triazine (**figure 1**) was prepared from the cyanuric chloride and excess sodium carbonate in THF. The $^{13}C$ NMR spectrum showed double signals for each aliphatic C (δ42.4 and 42.1 for $CH_2$-N, δ36.3 and 35.9 for $CH_2$-Ar) which coalesced under heating, indicating the existence of atropisomers.

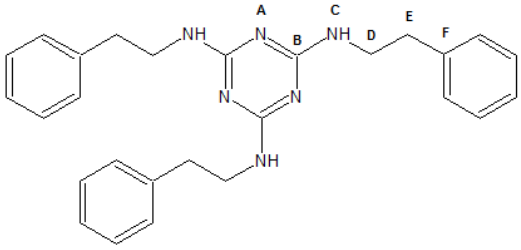


**Figure 1:** 2,4,6-triphenethyl-1,3,5-triazine.

For the theoretical determination of the rotational barriers, 3 dihedral angles were evaluated: d1(A,B,C,D), d2(B,C,D,E) and d3(C,D,E,F) (**figure 1**). The compound was constructed, energy-minimized and each dihedral angle was systematically varied between -180$^0$ and 180$^0$ with a 30$^0$ increment for determination of the respective energies with the Density Functional Theory (DFT) method (B3LYP functional, 6-31G* basis set), by means of the Spartan'14 program (Wavefunction, Inc.). Each dihedral angle showed different energy patterns and energy barriers (**figure 2**).

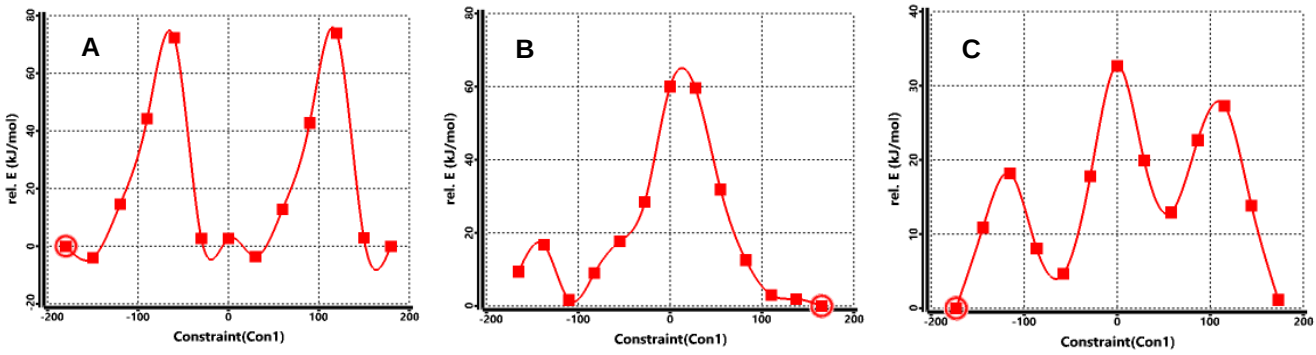


**Figure 2:** Relative energy for the dihedral angles torsion [constraint (Con1)] for dihedrals d1 (**A**), d2 (**B**) and d3 (**C**), respectively.

As we can see, the first dihedral presented a torsional barrier of ~80 kJ/mol (~20 kcal/mol), which is the lower limit for the existence of Class 2 atropisomers, related to a $t_{1/2}$ in the order of minutes.[1] The remaining dihedral angles have barriers that are too low to explain the observation of atropisomers by the MNR methodology. Studies are in progress to include also in the calculation of the torsional barrier the influence of the solvent utilized in the NMR analysis.

[1] LaPlante *et al.*, *ChemMedChem*, **2011**, 6, 505-517.

**Área: ORG** **Inscrição: 00354**

# A study of extraction of natural products from renewable sources: naringin from grapefruit peels and hesperidin from orange peels.

**Maria V. M. Cortez (IC),[2] Anna V. J. Nunes (IC),[2] Elivana L. França (PG),[1,2] Maria C. K. Sakukuma (PG),[1,2] Jorge M. David (PQ),[1,2] Mauricio M. Victor (PQ).[1,2*] mmvictor@ufba.br**

*[1]Instituto de Química, UFBA, Campus de Ondina, Salvador/BA, 40170-115; [2] Instituto Nacional de Ciência e Tecnologia em Energia e Ambiente – INCT E&A, Salvador/BA, 40170-070.*

Key words: *grapefruit albedo, orange albedo, naringin, hesperidin, natural products.*

## Highlights

The albedo of grapefruit and orange were used as source of known flavones naringin **1** and hesperidin **2** (Figure 1), respectively, by the modification of known process, which involves extraction with methanol and crystallization in water with the addition of dichloromethane. The direct method developed decreased times and led to higher yields of natural products (4.1% w/w of naringin and 2.5% w/w of hesperidin).

## Resumo/Abstract

The original method to obtain naringin from grapefruit albedo involves extraction with methanol and crystallization in water with addition of dichloromethane after 3-day air-drying stage, requiring about 10 days for all process, furnishing naringin in 2.4% w/w yield.[1] Due its biological properties, we decided to investigate modification of methodology according descriptions listed below:

- Method A:[1] air-dried albedo (3d), room temperature methanol extraction (3d) and crystallization (3-4d);
- Method B: air-dried albedo (3d), hot methanol extraction (3,5h) and crystallization (3-4d);
- Method C: fresh albedo, hot methanol extraction (3,5h) and crystallization (3-4d).

After peeling the fruits using a knife to separate the exterior flavedo, the albedo was cut into small pieces. To dry experiments, the grapefruit albedo was air-dried for 3 days, followed by oven drying overnight. The orange albedo was only air-dried for 3 days or until constant weight. The loss of mass obtained from fresh to dry albedo was of 24.4% for grapefuits and 33.1% for oranges, and these results were used as basis to calculate the dry-based yields (%) of the process performed with fresh albedo. Table below shows the comparatives between extractions from both fruits:

| Entry | Method A | | Method B | | Method C | |
|---|---|---|---|---|---|---|
| | Grapefruit | Orange | Grapefruit | Orange | Grapefruit | Orange |
| 1 | 2.5% | 1.1% | 2.8% | 2.6% | 4.2% | 2.9% |
| 2 | 2.1% | 1.0% | 2.4% | 2.4% | 3.9% | 3.5% |
| 3 | 2.1% | 0.9% | 2.7% | 2.6% | 4.3% | 2.0% |
| **Average** | **2.2%** | **1.0%** | **2.6%** | **2.5%** | **4.1%** | **2.8%** |

The success of modification of extraction methodology on grapefruit is due to significant reduction of total time required, from 10 to 3-4 days, depending on the recrystallization time, and to improvement on yields, furnishing about 70% more than the method used as basis for this work.[2]

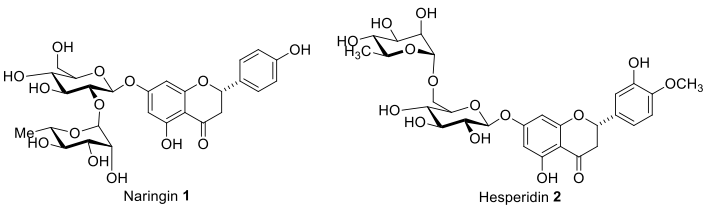


Figure 1

Success of this methodology prompted us to perform extraction of hesperidin from orange albedo, due its similarity to the naringin molecular structure. In dry-based albedo experiments (methods A and B), hesperidin yields increased significantly, different from naringin extractions. However, moving from room temperature to hot extraction with methanol (method C) is not possible to confirm the same yield improvement in hesperidin extraction due to variability of results obtained in the process performed with orange fresh albedo (entries 1-3, method C).

[1] Sudto, K.; Pornpakakul, S.; Wanichwecharungruang, S. *Int. J. Food Sci. Tech*. **2009**, *44*, 1737–1742.
[2] Victor, M. M.; David, J. M.; Sakukuma, M. C. K.; França, E. L.; Nunes, A. V. J. *Green Process. Synth*.: doi.org/10.1515/gps-2017-0112.

**Área: ORG** *(Inserir a sigla da seção científica para qual o resumo será submetido. Ex: ORG, BEA, CAT)*

**Inscrição: 401** *(Inserir o número de inscrição do autor que fez a submissão)*

# Solvent effect on the conformational preference of some 1,3-disubstituted acyclic compounds by $^1$H NMR

**Lucas J. Karas (PG),[1]* Patrick R. Batista (PG),[1] Renan V. Viesser (PG),[2] Cláudio F. Tormena (PQ),[2] Roberto Rittner Neto (PQ),[2] Paulo R. de Oliveira (PQ)[1]**

**poliveira@utfpr.edu.br; lucaskaras@gmail.com**

*[1]Departamento Acadêmico de Química e Biologia, Universidade Tecnológica Federal do Paraná, Campus Curitiba, Sede Ecoville, Rua Deputado Heitor de Alencar Furtado 5000, Bloco C, CEP 81280-340, Curitiba-PR, Brasil; [2]Laboratório de Físico Química Orgânica, Instituto de Química, Universidade de Campinas, Caixa Postal 6154, 13083-970, Campinas, SP, Brasil*

Keyword: *Conformational analysis, hydrogen bond, acyclic compounds, NMR, Solvent effect.*

## Highlights

Solvent influences the conformational equilibrium of these compounds
The O-H···O intramolecular hydrogen bond influenced in the conformational equilibrium of these compound

## Resumo/Abstract

The term conformational analysis refers to two aspects of studies, determination of the molecular geometry and energy of the confomers, followed by determination of which steric and electronic interactions are responsible for the stabilization of each conformer.[1] This work had as objective to investigate how the solvent and the intramolecular hydrogen bonding (IHB) affect the conformational preference of some 1,3-disubstituted acyclic compounds (Figure 1),[2] and what is the effect of the different alkyl substituents on these compounds by $^1$H NMR.

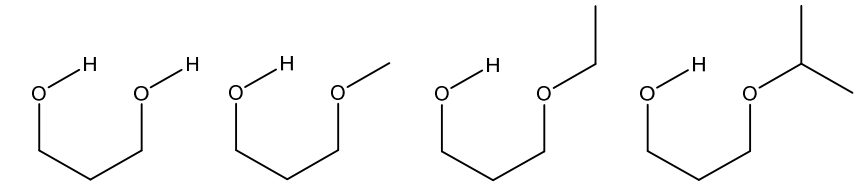


Figure 1. Structure of the 1,3-disubstituted acyclic compounds studied.

$^1$H NMR spectra were obtained on a Bruker Avance III spectrometer, operating at 600.17 at concentrations of 0.05 mol $L^{-1}$ using TMS as reference. The effect of the solvent on the conformational equilibrium of the compounds **1**-**4** were analyzed using the values of vicinal coupling constants ($^3J_{HH}$) obtained in different solvents along with the theoretical $^3J_{HH}$ values obtained for the stable conformers of each compound using the BHandH/EPR-III. Experimental $^3J_{H1H2}$ results increase with increasing polarity of the solvent for all compounds. In $CCl_4$ the values are close to 5.60 Hz, whereas in DMSO-$d_6$ and Pyridine-$d_5$, the values are higher, around 6.40 Hz. These results indicate that the conformational equilibria of 1,3-dissubstituted acyclic compounds change to hydrogen-bonding conformations in non-polar solvents and for non-hydrogen-bonding conformations in polar solvents.

1. Ribeiro, D. S.; Rittner, R. *J. Org. Chem.*, 68, 17, 6780, 2003.
2. Karas, L.J.; Batista, P.R.; Viesser, R.V.; Tormena, C.F.; Rittner, R.; Oliveira, P.R. *Phys. Chem. Chem. Phys.* 19, 16904, 2017.

**Área: ORG** **Inscrição: 00428**

# Three-component Synthesis of Arylidene-succinimides via *in situ* Wittig Reaction

**Fernando A. Barretto (PG),[1,2] Silvio Cunha* (PQ),[1,2].**

**fernando.barrettto@hotmail.com; silviodc@ufba.br**

[1] *Instituto de Química, UFBA, Campus Ondina, 40170290, Salvador - BA.*
[2] *INCT-Instituto Nacional de Ciência e Tecnologia em Energia e Ambiente, Campus de Ondina,* Salvador - BA

Palavras Chave: *(Multicomponent reaction, Wittig reaction, Maleimides).*

## Highlights

Diverse *N*-aryl substituted arylidene-succinimides were obtained by multicomponent reaction of *N*-substituted maleimides with salicylaldehydes and triphenylphosphine.

## Resumo/Abstract

The three-component reactions are characterized as convergent synthesis, because the three reagents lead to a product which contains most of all atoms of the reagents[1]. Arylidene-succinimides are system which present the C=C-C=O electrophilic moiety, susceptible to the Michael addition. Wittig reaction is the most of important reaction that promote olefination.[2] Therefore, to access a set of arylidene-succinimides[3,4] we describe herein a three-component reaction of *N*-substituted maleimides **(a)**, salicylaldehyde **(b)** and triphenylphosphine **(c)** in methanol at room temperate to obtain E-arylidene-succinimides isomer as major isomer, Scheme 1. Fortunately, the purification process was simple because the products precipitated. A representative set of derivatives could be obtained in reasonable yield and reaction time. The proposed mechanism should involve a *in situ* preparation of stabilized phosphorous ylide from *N*-substituted maleimides and triphenylphosphine followed by Wittig reaction with salicylaldehyde to form the arylidene-succinimides.

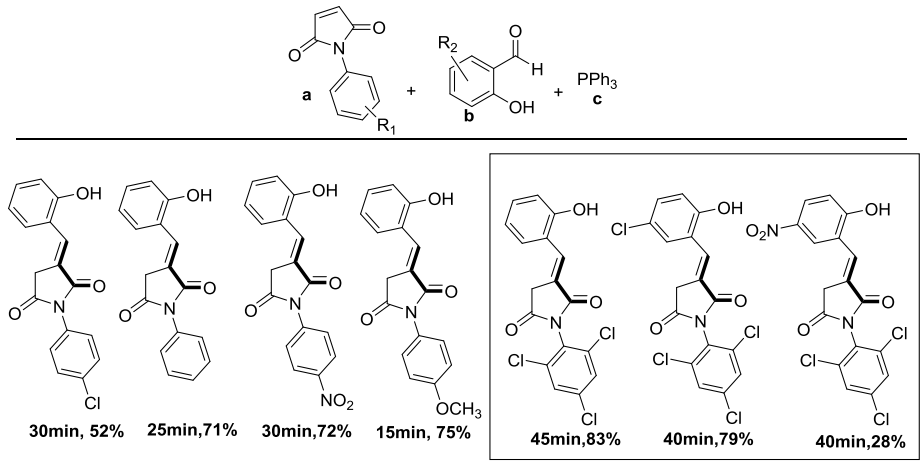


Scheme 1: Synthesis of (E)- Arylidene-succinimides

Therefore, we developed a three-component synthesis of new series of arylidene-succinimides via *in situ* Wittig reaction with easy purification and high diastereoselective.

**Acknowledgment:**
CNPq, CAPES and FAPESB

[1] *BATALHA, P. N. Rev. Virtual Quim., 4, 13-45,* ***2012****.*
[2] *TSOLOMITI, G. et al. Heterocycle Comunication, 12, 3-4,* ***2006****.*
[3] *YIAN, LIN, et al. Chin. J. Chem. 29, 1906-1910,* ***2011****.*
[4] *BAYAT, M. HOSSEINI, S. R. ASMARI, E. Phosphorus, Sulfur, and Silicon, 192, 98-102,* ***2016****.*

**Área: ORG** **Inscrição:** 00480

# A new multicomponent synthesis of pyrimido[4,5-b]quinolinetetraones

**Lourenço Luis Botelho de Santana (PQ)[3], Glauber Antonio Albuquerque Dourado (PG)[1,2*], Silvio Cunha (PQ)[1,2].**

**llsantana@uneb.br; glauberantonio.albuquerque@gmail.com**

[1]*Instituto de Química, Universidade Federal da Bahia, Campus de Ondina, 40170-290, Salvador – BA.*
[2]*INCT-Instituto Nacional de Ciência e Tecnologia em Energia e Ambiente, Campus de Ondina, Salvador – BA*
[3]*Departamento de Ciências da Vida, Universidade do Estado da Bahia Fac. Farmácia, 41195-000, Salvador – BA*

Key words: *Multi-component reactions, Heterocyclics, 2-amino-1,4-naphthoquinone, cycloaddition.*

## Highlights

Development of two new MCRs synthesis of pyrimido [4,5-b]quinolinetetraones and pyrimido [4,5-b] using aldehydes, 2-amino-1,4-naphthoquinone and barbituric acids.

## Abstract

The synthesis of pirimido [4,5-b]quinolinestetraones is a topic of interest due to their biological properties.[1,2] A new synthetic route was developed in a tricomponent form using a mixture of 2-amino-1,4-naphthoquinone (1), aromatic aldehydes (3a-f) and barbituric acid (2), producing 4a-e. Several conditions were tested, and the best result was obtained using reflux in acetonitrile and aminosulfonic acid as catalysis. This new methodology creates another option for the synthesis of this product. Replacing the reaction solvent by ethanol and removing the catalyst to adapt the process to the principles of green chemistry, a new reaction pattern was observed. The pyrimido [4,5-b]quinolinone-tetraones 5a-f were obtained with the formation of an exocyclic double bond, different from the pyrimido [4,5-b]quinolines-tetraones, where this double bond is endocyclic.

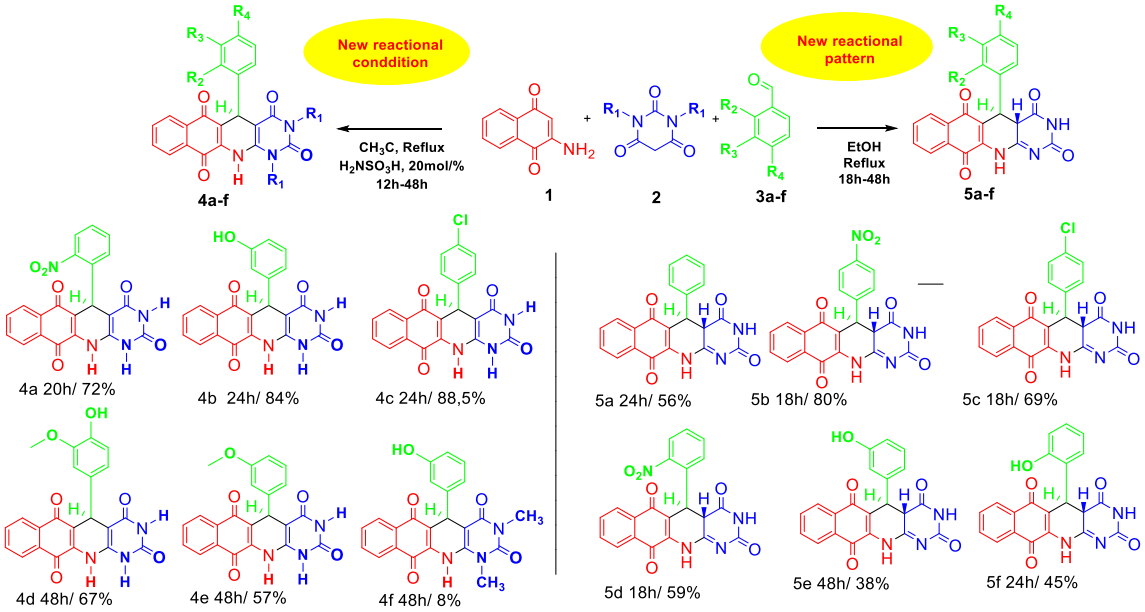


Therefore, change the reaction condition, we developed a new method for the preparation of pyrimido[4,5-b]quinolinetetraones, and a catalyst-free method to a new series of pyrimido[4,5-b]quinolinonetetraones

Acknowledgement:
CNPQ, INCT, UFBA

[1]Azizian, J., Delbari, A. S., Yadollahzadeh, K. *Synth. Commun*. 2014, (44), 3277.
[2]Bharti, R., Kumari, P., Parvin, T., Choudhury, L. H. *RSC Adv*. 2017, (7), 3928.

**Área: ORG** **Inscrição: 00484**

# Síntese de 2,5-dicloro-3,6-*bis*[(quinolon-6-il)amino]-1,4-benzoquinonas com potencial atividade antipriônica.

**Amanda R. P. Costa (IC)[1], Rodrigo C. da Silva (PG), Pedro N. Batalha (PQ)*, (PQ), Fernanda da C. S. Boechat (PQ), Maria Cecília B. V. de Souza (PQ)**

**amandarpc@id.uff.br; pedronettobatalha@gmail.com**

[1]*Departamento de Química Orgânica, UFF*

Palavras Chave: *benzoquinona, quinolona, Doenças do Príon, atividade antipriônica*

## Highlights

Synthesis of 2,5-dichloro-3,6-*bis*[(quinolon-6-yl)amino]-1,4-benzoquinones with potential antiprionic activity. New agents for the treatment of príon diseases. Quinone based bioactive substances. Quinone-quinolone conjugates as bioactive candidates. Non classical activities for quinolone derivatives.

## Resumo/Abstract

As doenças de Príon, decorrentes de encefalopatias espongiformes transmissíveis (EETs) foram descobertas por Stanley B. Prusiner, que definiu os príons como partículas proteináceas ($PrP^C$) transmissíveis e infecciosas que carecem de ácido nucléico e cuja conformação rica em α-hélices pode sofrer alterações e ser convertida em sua isoforma infectante $PrP^{Sc}$ propensa à agregação e acúmulo. As doenças de Príon são condições neurodegenerativas incuráveis que afetam mamíferos.

Hoang e Salvatore e colaboradores, descreveram a atividade anti-Príon de compostos bivalentes contendo arcabouço 2,5-diaminobenzoquinônicos. Considerando também a versatilidade biológica associada à derivados de quinolonas, este trabalho envolve a síntese de uma série de conjugados de benzoquinona e quinolona potencialmente capazes de diminuir o acúmulo da isoforma $PrP^{Sc}$.

Inicialmente 4-nitroanilina (**1**) foi convertida na 6-nitroquinolona (**2**), a partir da sua condensação com etoximetilenomalonato de dietila (EMME), seguida de ciclização térmica com difeniléter. O intermediário **2** foi então *N*-alquilado utilizando diferentes haletos de alquila (R-X) em meio alcalino de DMF, seguida da redução química do grupo nitro por hidrogenação catalítica ou tratamento com ferro em pó em solução aquosa de cloreto amoniacal. Os aminoésteres quinolônicos (**3a-d**) foram ainda convertidos nos respectivos aminoácidos **3e-h** via uma etapa de hidrólise alcalina.

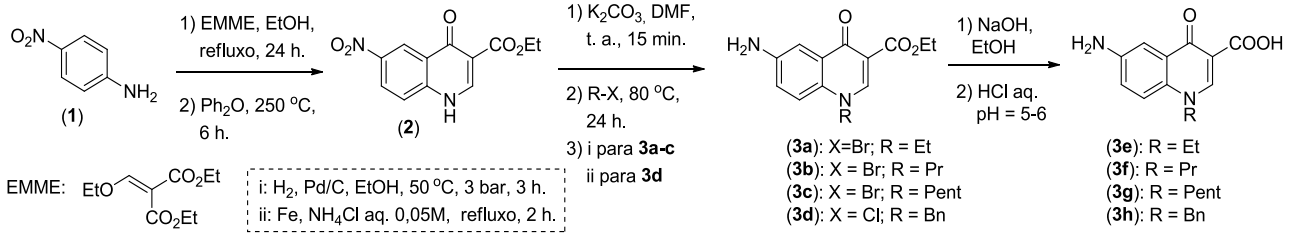


Os intermediários **3a-h** foram então reagidos com cloranil **(4)** em etanol, obtendo-se os conjugados **5a-e** com bons rendimentos. Estas substâncias foram devidamente caracterizadas por métodos espectroscópicos e terão sua atividade antipriônica avaliada.

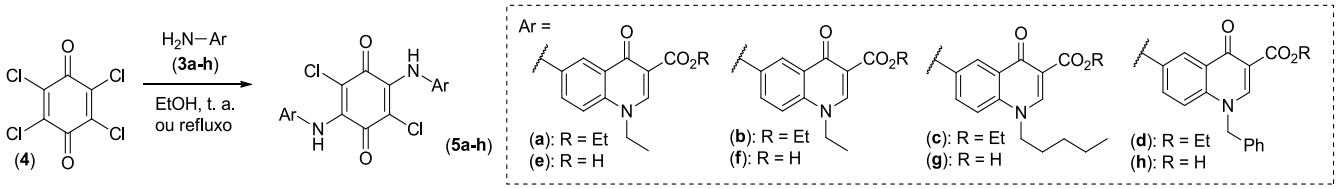


Agradecimentos: CAPES, CNPq, FAPERJ, PPGQ-UFF, PROAP-UFF.

**Área:** ORG **Inscrição:** 516

# Síntese e aplicação de organocatalisadores bifuncionais em reações de Michael estereosseletivas envolvendo nitrociano-compostos.

**Priscila M. A. Soares (PG), Elisângela Vinhato (PQ), Alessandro Rodrigues (PQ)***

**primarruda@yahoo.com.br; alessandro.rodrigues@unifesp.br**

*Departamento de Química, Universidade Federal de São Paulo, Diadema, SP, Brasil*

Palavras Chave: *Organocatálise, Cinchona, Reações de Michael, Síntese Orgânica*.

## Highlights

**Synthesis and application of bifunctional organocatalysts in stereoselective Michael reactions involving nitrocyano-compounds**.

Synthesis and evaluation of chiral organocatalysts in enantioselective Michael reactions.
Organocatalysts based on *Cinchona* alkaloids have been synthesized and evaluated for enantioselective nitrocyano-compounds synthesis.

## Resumo

O objetivo desse trabalho foi sintetizar organocatalisadores quirais bifuncionais derivados de alcaloides da *Cinchona*, sendo 2 novos (**I** e **II**) e outros 4 já descritos na literatura (**III**,[1] **IV**,[2] **V**[3] **e VI**[4]). Tais organocatalisadores foram testados frente a reações do tipo Michael entre etil 2-ciano-3-fenilpropanoato **1** e o *trans*-nitroestireno **2** formando o aduto de Michael **3** inédito.

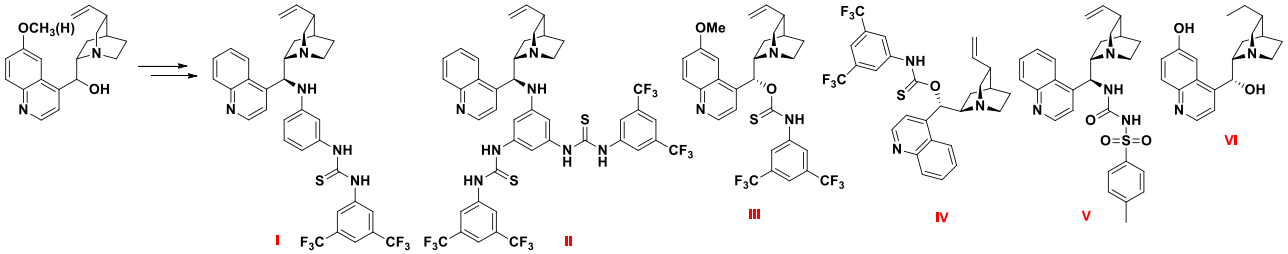


Estes catalisadores foram aplicados na reação de Michael e as condições experimentais como temperatura, solvente, quantidade de catalisador e tempo reacional foram variados. A Tabela apresenta resultados selecionados dos testes reacionais realizados. O melhor resultado foi obtido empregando-se o organocatalisador **VI** na formação do aduto de Michael **3** com excesso enantiomérico de 84%, 100% de conversão, a -80 ºC em meio de éter dietílico.

**Tabela.** Resultados obtidos com os organocatalisadores (**I-VI**) na reação de Michael[a]

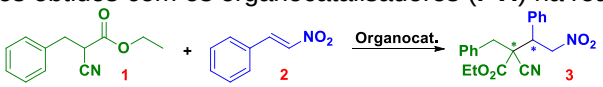


| Entrada | Organocat. | Quant. de organocat. | Solvente | T(°C) | Tempo | rd[b] | ee (%)[b] *maj (min)* | Conv.(%)[c] |
|---|---|---|---|---|---|---|---|---|
| 1 | I | 20 mol% | Tolueno | -80 | 168 h | -[d] | 25 (6) | 100 |
| 2 | II | 20 mol% | Tolueno | -80 | 168 h | 1:1,3 | 39 (15) | 100 |
| 3 | III | 20 mol% | Tolueno | -20 | 168 h | -[d] | 14 (13) | 100 |
| 4 | IV | 20 mol% | Tolueno | -80 | 168 h | 1:1,2 | 10 (0,1) | 100 |
| 5 | V | 20 mol% | Tolueno | -80 | 168 h | 1:0,9 | 21 (6) | 100 |
| 6 | V | 20 mol% | Tolueno | -20 | 168 h | 1:0,9 | 27 (6) | 100 |
| 7 | VI | 10 mol% | Tolueno | -80 | 48 h | 1:0,3 | 80 (3) | 100 |
| 8 | VI | 20 mol% | THF | -80 | 24 h | 1:0,3 | 74 (3) | 100 |
| 9 | VI | 20 mol% | THF | -20 | 24 h | 1:0,4 | 57 (2) | 100 |
| 10 | VI | 10 mol% | $O(Et)_2$ | -80 | 48 h | 1:0,2 | 84 (1) | 100 |

[a] As reações foram feitas utilizando-se **1** (0,15 mmol), **2** (0,10 mmol) em 0,2 mL de solvente; [b] Determinada por RMN $^1$H; [c] Determinado por CLAE, coluna: CHIRALCEL® AD-H, condições: hexano/isopropanol 93:7, 0,3 mL/min, 204 nm; [d] não foi possível determinar.

O organocatalisador **VI** se mostrou o mais eficiente na formação do aduto de Michael **3** nas condições reacionais investigadas até o momento. Demais experimentos estão sendo realizados objetivando maior estereosseletividade para posterior aplicação em outros derivados do *trans*-nitroestireno.

(1) Tripathi, C. B.; Mukherjee, S. *Angew. Chemie Int. Ed.* **2013**, *52*, 8450.
(2) Zhou, L.; *et al. J. Am. Chem. Soc.* **2010**, *132*, 15474.
(3) Zhang, W.; *et al. J. Am. Chem. Soc.* **2010**, *132*, 3664.
(4) Wąsińska-Kalwa, M.; *et al. Tetrahedron* **2018**, *74*, 3085.

Fomento Proc. 2016/21676-0

**Área: ORG** **Inscrição:557**

# Palladium-Catalyzed Carbonylative α-Arylation of Azlactones

**Danielle L. J. Pinheiro (PG),[1,2*] Dennis U. Nielsen (PQ),[2] Giovanni W. Amarante (PQ),[1] Troels Skrydstrup (PQ)[2]**

***dane_jf@hotmail.com**

*[1] Departamento de Química, Universidade Federal de Juiz de Fora, Juiz de Fora- MG, Brasil; [2] Inano, Aarhus University, Aarhus- Denmark.*

Palavras Chave: *Carbonylation, Palladium, Azlactones, α-Arylation, Isotope labeling.*

## Highlights

For the first time a chemoselective Palladium-catalyzed carbonylation of α–carbon of azlactones is demonstrated. The methodology was developed using an ex situ generation of CO in the *two chamber system*. A wide range substrate scope of aryl iodides and azlactones was obtained with good yields. Control experiments revealed the mechanism proceeds via direct carbonylation of α carbon of azlactones. The method also provided access to $^{13}$C-labeled compounds in larger scale, which were further used in the synthesis of very important heterocycles.

## Resumo/Abstract

The method applies the Pd-catalyzed decarbonylation process, releasing stoichiometric amount of CO in one chamber, which is consuming in the second chamber. In this work, the direct carbonylation of the α–carbon of azlactones using the two-chamber system is described. At first, it was evaluated different conditions in chamber 1 and 2. (Scheme 1). Having established the best reaction condition, various aryl iodides and azlactones were well tolerated. A substrate scope containing 22 new compounds were synthesized with good yields, up to 88%.

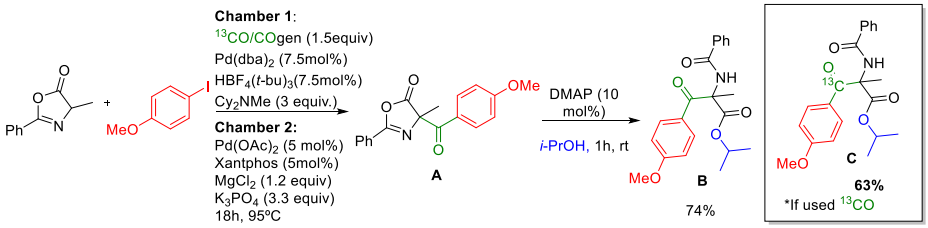


**Scheme 1**: Palladium-Catalyzed Carbonylative α-Arylation of Azlactones.

Control experiments revealed the direct carbonylation of α carbon of azlactones, being an ester intermediate via Steglich rearrangement unlikely. The reaction with $^{13}$COgen furnished the product **C** with of 63% yield. Next, **C** was used to provide an anti-inflammatory analogue, pyrazolone **D,** a new non-natural amino acid **E**, and the oxazol **F** in good yields (Scheme 2).

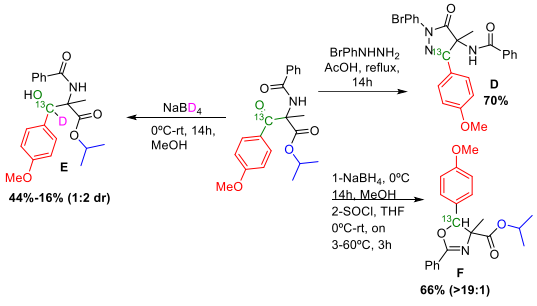


**Scheme 2:** Synthesis of labeled compounds.

In summary, a protocol for the direct Pd-catalyzed carbonylative α-arylation of azlactones has been described. Besides the good yields for the final products, different transformations with $^{13}$C-labeled were also demonstrated.

# Abordagens complementares nas sínteses totais de (+)- e (-)-bernumidina

**Bianca K. Corrêa (PG), Tamiris R. C. Silva (PG), Cristiano Raminelli (PQ)***

**tamiris.cipriano@gmail.com; raminelli@unifesp.br**

*Instituto de Ciências Ambientais, Químicas e Farmacêuticas, Universidade Federal de São Paulo, Diadema, SP, Brasil*

Palavras Chave: *Resolução cinética dinâmica quimioenzimática, Hidrogenação enantiosseletiva, Bernumidina.*

## Highlights

Complementary approaches in the total syntheses of (+)- and (-)-bernumidine. Chemoenzymatic dynamic kinetic resolution and enantioselective hydrogenation in the total syntheses of benzylisoquinoline alkaloids, which are potential ligands of μ opioid receptor.

## Resumo/Abstract

Empregamos resolução cinética dinâmica quimioenzimática[1] e hidrogenação enantiosseletiva[2] nas etapas chaves das sínteses totais dos alcaloides benzilisoquinolínicos (+)-bernumidina (**1a**) e (-)-bernumidina (**1b**), que são potenciais ligantes de receptores μ opioides.[3]

As abordagens para obter (+)-**1a** e (-)-**1b** estão delineadas na análise retrossintética apresentada no **Esquema 1**.

**Esquema 1.** Análise retrossintética para (+)-bernumidina (**1a**) e (-)-bernumidina (**1b**).

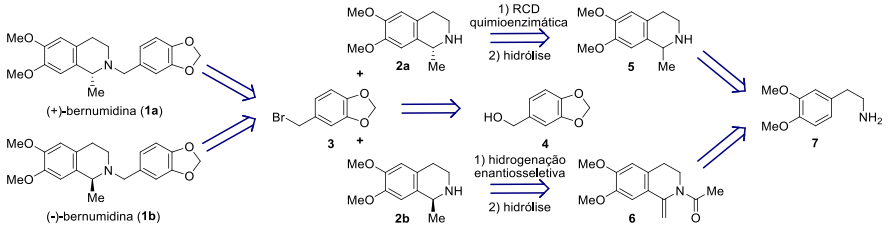


Iniciamos as sínteses da (+)-**1a** e da (-)-**1b** convertendo 3,4-dimetoxifenetilamina (**7**) nos intermediários **5** e **6** através de transformações de grupos funcionais. Posteriormente, o intermediário **5** foi submetido à reação de resolução cinética dinâmica quimioenzimática, resultando no composto **11** em 68% de rendimento e excesso enantiomérico de 99%. O intermediário **6** foi submetido à reação de hidrogenação enantiosseletiva, resultando no composto **12** em rendimento de 94% e 90% de excesso enantiomérico. Os compostos **11** e **12** foram submetidos a reações de hidrólise básica e alquilações promovendo a formação da (+)-**1a** e da (-)-**1b** (**Esquema 2**).

**Esquema 2.** Rotas sintéticas para (+)-bernumidina (**1a**) e (-)-bernumidina (**1b**).

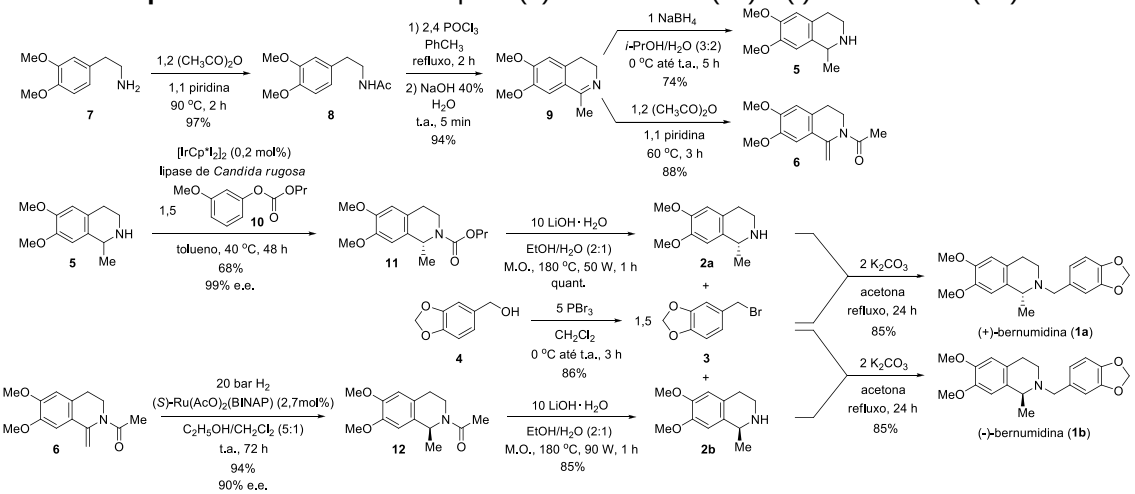


(+)-Bernumidina (**1a**) e (-)-bernumidina (**1b**) foram obtidas por abordagens complementares, em 6 etapas reacionais, com rendimentos globais de 39% e 55%, respectivamente.

1. Blacker, A. J.; Stirling, M. J.; Page, M. I. *Org. Process Res. Dev.* **2007**, *11*, 642.
2. Kitamura, M.; Hsiao, Y.; Ohta, M.; Tsukamoto, M.; Ohta, T.; Takaya, H.; Noyori, R. *J. Org. Chem.* **1994**, *59*, 297.
3. Kaserer, T.; Lantero, A.; Schmidhammer, H.; Spetea, M.; Schuster, D. *Sci. Rep.* **2016**, *6*, 21548.

**Área: ORG** **Inscrição: 00596**
*)*

# Synthesis of New Schiff Bases (N-Aryl)Phosphoramidic. Possible Microbiocidal

**Letícia Oliveira Dinalo (IC),[1] Paulo H. F. Lousa (PG),[1] William P. Macedo (PQ),[1]***

**william.macedo@ueg.br; wpmac2002@yahoo.com.br**

[1]*Centro de Ciência Exatas e Tecnológicas, UEG- Campus Henrique Santillo; Anápolis-GO*

Palavras Chave:*(Bases de Schiff, (N-aryl)phosphoramidic, Microbiocidal, Biological Activities)*

## Highlights

This work is devoted to obtaining a series of new derivatives of Schiff bases (N-aryl)phosphoramidic, by condensation reactions between amino (N aryl)phosphoramidates and aromatic aldehydes. Once obtained, the Schiff bases will be evaluated as microbiocidal agents.

## Abstract

Schiff bases are products of the reaction of primary amines with aldehydes or ketones and represented by the azomethine group (-CR = N-). Bases are considered pharmacophores of multiple actions[1]. Krátký, reported the strong inhibition of strains *of Staphylococcus aureus* by the action of the Schiff base (**1**)[1]. Another class of compounds of relevance is the class of phosphoramidates that stand out in medicinal chemistry. The Phosphoramidates are found in prodrugs by potentiating the original drug. For example, Kolodziej et al., Obtained a series of prodrugs (AZT-arylphosphoramidates), and all derivatives showed superior viral inhibition to standard AZT, with emphasis on (**2**) and (**3**) [2].

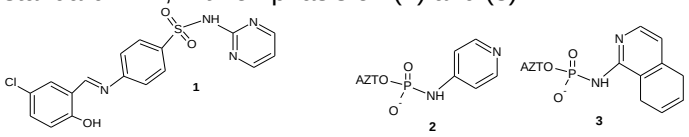


In this way, this work proposed two reactional steps to obtain a series of Schiff Bases (N-aryl) phosphoramidic. The first is to obtain intermediate (**6**)[3]. The second is the reaction of **6** with selected aldehydes[4]. (Scheme-1).

Scheme-1: Pathway to the Synthesis of Phosphoramidic Schiff Bases (8a- i).

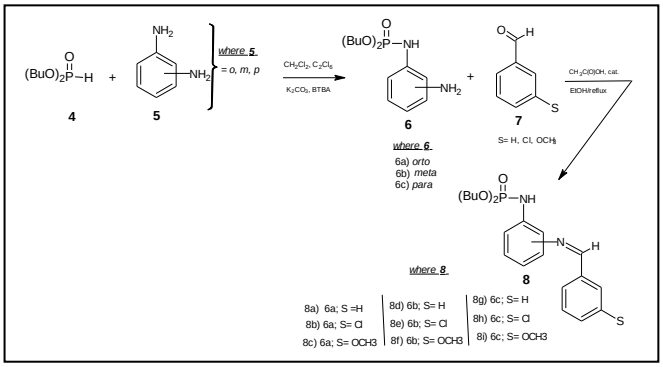


However, *6* has already been obtained and characterized. The reaction aiming at synthesis **8** is already in progress, but adjustment is being implemented to obtain **8a**. After obtaining 8, the biological tests will start with research groups of interest.

1- Krátký, M.; Dzurková, M.; Janoušek, J.; Koneˇcná, K.; Trejtnar, F.; Stolaˇríková, J.; Vinšová, J. *Molecules*. **2017**, 22, 1573.
2- Kolodziej, K.; Romanowska, J.; Stawinski, J.; Boryski, J.; Dabrowska, A.; Lipniacki, A.; Piasek, A.;Kraszewski, A.; Sobkowski, M. Synthesis,. *Eur. J. Med. Chem*. **2015**, 100, 77-88.
3- Souza, M. C.; Macedo, W. P.; Torres, T. S.; Pedrosa, L. F.; Alt, H. G. *Phosphorus, Sulfur, and Silicon and the Related Elements.* **2006**. v. 181, n. 8, p. 1885-1893,
4- Singh, T. S.; Paul, P. C.; Pramanik, H. A. R.. *Spectrochimica Acta Part A:.* **2014** v. 121, p. 520-526,

Agradecimentos**:: FAPEG**

**Área: ORG** **Inscrição: 00631**

# Synthesis and Biological Screening of tetrazolyl-4-oxoquinolines as Antitumor Agents

**Thiago M. do Vale (IC),[1] Pedro Henrique Ramos de Oliveira[1], Patricia Dias Fernandes (PQ)[2], Nathalia M. C. Tolentino (PG),[1] Maria Cecília B. V. de Souza (PQ),[1] Fernanda da C. S. Boechat (PQ)[1*]**

**thiagomota_tm@hotmail.com; fernandacostasantos@id.uff.br**

[1] *Instituto de Química, Universidade Federal Fluminense. Outeiro de São João Batista, s/n, Centro, Niterói, RJ, Brasil. CEP: 24020-141*
[2] *Universidade Federal do Rio de Janeiro, Instituto de Ciências Biomédicas, Laboratório de Farmacologia da Dor e da Inflamação. 21901-902, Brasil.*

Key-words: *Tetrazoles, quinolones, cancer.*

## Highlights

The aim of this work was the synthesis of new tetrazolyl-4-oxoquinoline derivatives and the evaluation of their antitumor activity aiming the search of new candidates for cancer treatment.

## Resumo/Abstract

Quinolones and their derivatives are widely used in the clinic for their antibacterial activity.[1] The main mechanism of action for this activity is the inhibition of topoisomerase IV enzymes, essential for bacterial DNA replication.[2] Given its homology with human topoisomerase II, anticancer activity of oxoquinolines via inhibition of this enzyme has been widely discussed in the literature.[1]

Tetrazoles are considered strategic from the point of view of medicinal chemistry by increasing metabolic stability and even potentiating pharmacological activity. In particular, tetrazole derivatives have important antitumor activity.[3] In this work, tetrazolyl-oxoquinolines were designed from the conjugation between quinolones and the tetrazole unit, with the objective of investigating how the insertion of the tetrazole unit directly attached to the C-6 carbon of the quinolone nucleus may contribute to the expression of the antitumor activity of these substances.

New derivatives were obtained in good yields (73-89%) and were characterized by physical methods of analysis. The previous evaluation of the antitumor activity of these substances indicates antitumor activity for the cell lines that have been tested, without expression of hemolytic activity.

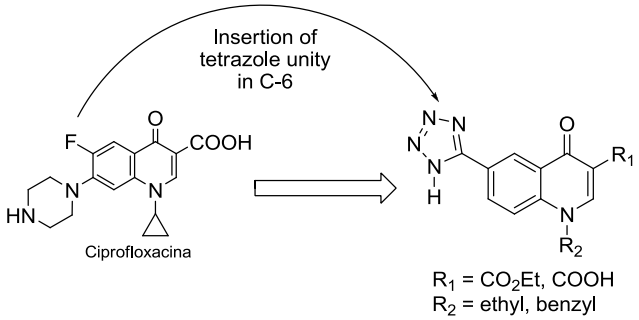


**Scheme 1**: Design of new tetrazole derivative as antitumor agents.

**Table 1:** Antitumoral activity for oxoquinolines **4a-b, 5a-b** and **6a-b**.

| Compound | IC50μM | | |
|---|---|---|---|
| | MCF-7 | MDAMB-231 | A549 |
| **Doxorrubicin** | 0,8 | 1,1 | 1,3 |
| **4a** | 18,7 | > 30 | 28,9 |
| **4b** | 21,9 | > 30 | 14,6 |
| **5a** | 15,6 | > 30 | 19,4 |
| **5b** | 24,3 | > 30 | 18,8 |
| **6a*** | NT | NT | NT |
| **6b** | 11,3 | > 30 | 27,6 |

*NT=not tested

Acknowledgments: CAPES, CNPq, FAPERJ

[1]Forezi, L.S.M., *et. al., Molecules* **2014**, *19*, 6651-6670.
[2]Ostrovskii, V.A.; Trifonov, R.E.; Popova, E.A. *Russ. Chem. Bull.* **2012**, *4*, 768-780.
[3] Demko, Z.P., Sharpless, K.B *J. Org. Chem* **2001**, *66*, 7945–7950.

**Área: ORG**
*(Inserir a sigla da seção científica para qual o resumo será submetido. Ex: ORG, BEA, CAT)*

**Inscrição: 00658**
*(Inserir o número de inscrição do autor que fez a submissão)*

# Enantioselective Heck–Matsuda Reaction on Dihydrofurans: Synthesis of Isobenzofuranones and Isochromanones

**Emilio C. de Lucca Jr. (PQ),[1] Shivashankar Kattela (PQ)[1], and Carlos Roque Duarte Correia (PQ)[1]**

**emilio.luccajr@iqm.unicamp.br; roque@iqm.unicamp.br**

[1]*Instituto de Química, Universidade Estadual de Campinas, C.P. 6154, CEP 13084-971, Campinas-SP, Brasil*

Palavras Chave: *Enantioselective Catalysis, Heck Reaction, Palladium, Organometallics, Aryldiazonium Salts.*

## Highlights

Isobenzofuranones and isochromanones constitute ubiquitous scaffolds in many natural and unnatural products possessing important pharmacological activity. Therefore, efficient and practical methods to obtain these cores are still a challenge to the synthetic chemists. Herein we disclose a new Pd-catalyzed route to isobenzofuranones and isochromanones in an enantioselective manner by a Heck–Matsuda reaction.

## Resumo/Abstract

Using the functionalized aryldiazonium salt **1** and the electron-rich olefin **2** in a Heck–Matsuda reaction, we envisioned that after the arylation and palladium hydride migration along the carbon chain, a lactol **3a** would be formed and that this intermediate could react with $NaBH_4$ to deliver isobenzofuranone **4a** (Scheme 1). After an optimization process, varying solvent, ligand, catalyst loading, temperature, and base, we found that compound **4a** could be isolated in 55% yield and 97% *ee*.

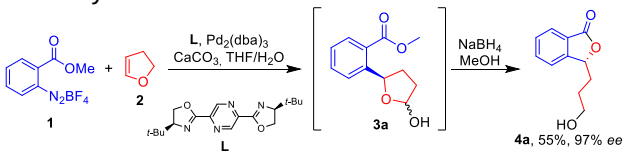


**Scheme 1**

We then explored the scope for this new Heck–Matsuda reaction, varying the arenediazonium salts (Figure 1).

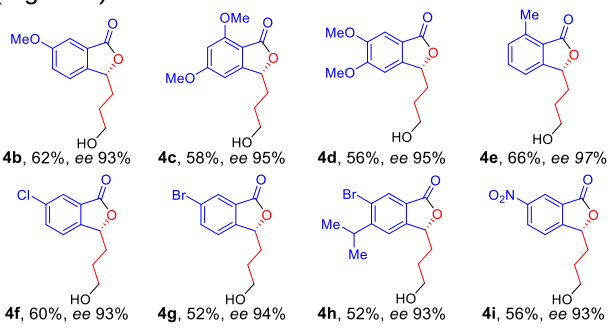


**Figure 1**

With these results in hand, we moved to the synthesis of isochromanones using 2,5-dihydrofuran. After an optimization process and scope evaluation, compounds **5a–g** were obtained in moderated yields and high *ee* (Figure 2).

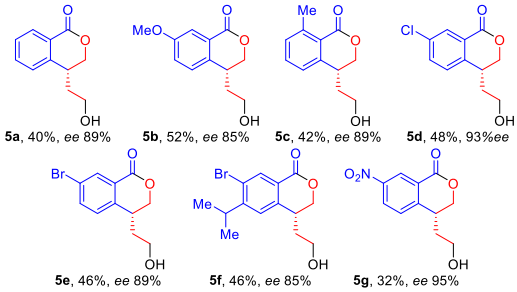


**Figure 2**

Finally, the value of the lactol **3a** was evaluated in the synthesis of the natural product butylphtalide (**6**) and medicinally core structures **7** and **8** (Scheme 2).

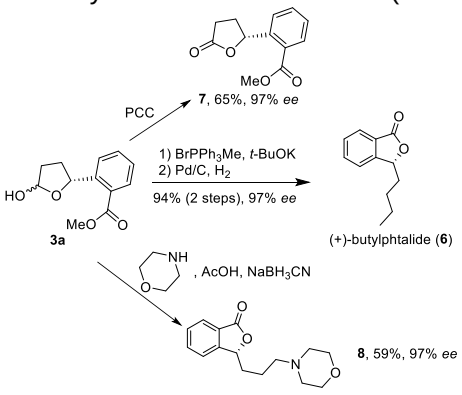


**Scheme 2**

We have developed a new enantioselective synthesis of isobenzofuranones and isochromanones through a Heck–Matsuda reaction.

We thank FAPESP, CNPq, and CAPES for financial support.

**Área: ORG** **Inscrição:00695**

# Syntheses of Sulfides via Wittig Reaction using Thiosulfonates

**Igor M. R. de Moura (IC),* Arisson T. da Silva (PG), Paulo H. Menezes (PQ)**

***igor_mota_moura@hotmail.com**

*Universidade Federal de Pernambuco, Depto de Química Fundamental, Recife-PE, Brazil*
Key Words: *sulfides; thiosulfonates; phosphonium salts*

## Highlights

The use of thiosulfonates and phosphonium salts for the synthesis of sulfides is described.
Non-symmetrical sulfides can be prepared without the use of thiols in good yields.

## Abstract

The sulfur compounds are widely used in organic synthesis and the importance of sulfides, sulfoxides and sulfones not only to increase the structural complexity of organic molecules but also in asymmetric reactions is unquestionable.[1] The most common pathway to synthesize sulfides is based on the use of thiols and halides,[2] however this strategy has some limitations, especially with regard to the use of thiols, compounds with an unpleasant odor.

Thus, despite the plethora of methods for the synthesis of sulfides, the development of a simple and reliable method for the synthesis of this class of compounds would be of the great interest. In this context, thiosulfonates have been widely used in many reactions due to their greater stability and ease of handling.[3]

This work describes the use of thiosulfonates and commercially available phosphonium salts for the synthesis of sulfides. In the course of developing milder reaction conditions, thiosulfonate **1** and phosphonium salt **2,** were used as model compounds and treated at room temperature with different bases and solvents. The progress of the reaction was monitored by TLC and the results are depicted in Table 1.

**Table 1.** Synthesis of sulfide **3** based on the reaction of thiosulfonate and a phosphonium salt[a]

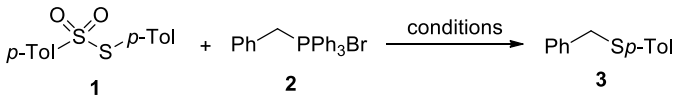


**1** **2** **3**

| Entry | conditions | | Time (h) | 3 (%)[b] |
|---|---|---|---|---|
| | Base (equiv.) | Solvent | | |
| 1 | $K_2CO_3$ (2) | $CH_2Cl_2$ | 72 | 44 |
| 2 | *t*-BuOK (2) | $CH_2Cl_2$ | 1 | 43 |
| 3 | KOH (2) | DMF | 24 | - |
| 4 | imidazole (2) | $CH_2Cl_2$ | 24 | - |
| 5 | $Et_3N$ (2) | $CH_2Cl_2$ | 72 | 45 |
| 6 | $Et_3N$ (10) | $CH_2Cl_2$ | 24 | 80 |

[a] *Reaction conditions:* Reactions were performed with **1** (0.4 mmol) and **2** (0.5 mmol) using the indicated amount of base in the appropriate solvent (5 mL) at 25°C. [b]Isolated yield.

From Table 1 it can be seen that the most efficient method for the synthesis of sulfide **3** was when triethylamine was used as a base in dichloromethane (Table 1, entry 6).

In summary, we have shown an efficient method for the synthesis of non-symmetrical sulfides from thiosulfonates and phosphonium salts. The method is simple, fast and general allowing further applications in the synthesis of more complex compounds.

We are grateful for financial support from CNPq and FACEPE.

1. Back, T. G.; Clary K. N.; Gao, D.; *Chem. Rev*., **2010**, *110*, 4498–4553
2. Kwong, F. Y.; Buchwald, S. L. *Org. Lett.* **2002,** *4*, 3517-3520.
3. Tranquilino, A.; Andrade, S. R. C. P.; da Silva, A. P. M.; Menezes, P. H.; Oliveira, R. A.*Tetrahedron Lett.* **2017,** *58*, 1265-1268.

**Área: ORG** **Inscrição:00715**
*(Inserir o número de inscrição do autor que fez a submissão)*

# Síntese de Cristais Líquidos Liotrópicos e sua Aplicação como Meio de Alinhamento para Obtenção de Parâmetros Anisotrópicos em RMN.

**Danilo G. B. da Silva (PG),[1] Fernando Hallwass (PQ),[1*] Armando Navarro-Vázquez (PQ)[1*]**

**hallwass@ufpe.br; armando.navarro@ufpe.br**

*[1]Departamento de Química Fundamental, UFPE;*

Palavras Chave: *Fases cromônicas, Cristais líquidos, Bisperilenimidas, Elucidação estrutural, RMN, RDC.*

## Highlights

Synthesis of Lyotropic Liquid Crystals and their Application as Alignment Media for Obtaining Anisotropic NMR Parameters. Liquid crystals (bisperylenimides) were synthesized and their application as alignment media to obtain anisotropic NMR parameters was studied. Coexistence of iso- and anisotropic phase was observed.

## Resumo/Abstract

Neste trabalho foram sintetizados cristais líquidos de derivados da bisperilenimidas e investigada a aplicação destes como meio de alinhamento para obtenção de parâmetros anisotrópicos de RMN. Foram testadas três metodologias de síntese e diferentes aminoácidos (glicina, L-valina, L-leucina e L-iso-leucina). O melhor resultado foi obtido utilizando-se a L-valina, formando a di (L-valina) perileno-3,4,9,10-bis (dicarboximida) dipotássica (**1**) (Figura 1). Os valores de deslocamento químicos foram comparados com os dados da literatura [1], confirmando a presença do composto **1** e foram atribuídos os sinais dos espectros de RMN $^{1}H$ e $^{13}C$, com auxílio dos experimentos gCOSY $^{1}H$-$^{1}H$, *g*HSQC $^{1}H$-$^{13}C$ e *g*HMBC $^{1}H$-$^{13}C$. Foi realizado o estudo para observar a formação de fases liotrópicas anisotrópicas em diferentes concentrações (0,3 e 0,5 M) e diferentes temperaturas (23, 27 e 60ºC) através dos espectros de RMN de $^{2}H$. A solução com 0,5 M e temperatura de 23ºC apresentou, no espectro de RMN de $^{2}H$, um desdobramento do sinal, indicando a existência da fase anisotrópica (Figura 1). Para aumentar o grau de orientação do cristal líquido, adicionou-se NaCl (10 e 20 mg) na solução. Por fim, foi utilizada a sacarose como molécula teste para as medidas do acoplamento dipolar residual (RDC). A coexistência das fases isotrópica e anistotrópica em uma relação de aproximadamente 1:1 permitiu a medida simultânea dos acoplamentos próton-carbono em ambas as fases na mesma amostra e, portanto, a extração direta dos RDCs.[2]

Figura 1. Estrutura do composto **1** e seu espectro de RMN $^{2}H$ em $D_2O$ 0,5 M a 23ºC.

Referências:

1. Suk-Wah, T-C., Liming, H., Aryal, G., Wonewoo, S., Delfin, M., Isaac, K. I., Proc. SPIE 6911, Emerging Liquid Crystal Technologies III, 691107, **2008**;
2. Reller, M., Wesp, S., Koos, M.R. M., Reggelin, M. K. Luy, B. *Chem. Eur. J.*, 23 13351-13359, **2017**.

Agradecimentos: FACEPE (APQ-0507-1.06/15) e CAPES.

**Área: ORG** **Inscrição: 00747**

# Synthesis and photophysical investigation of new quinoline derivatives

**Bruna Pastrello (PG)[1], Giovanny Carvalho dos Santos (PG)[1], Luiz Carlos da Silva Filho(PQ)[1], Valdecir Farias Ximenes(PQ)[1]**

**bpastrello@fc.unesp.br; bpastrello@fc.unesp.br**

[1]*Departamento de Química, Faculdade de Ciências, UNESP, Bauru.*

Keywords: Quinoline Derivatives, Photophysical Properties, Alkylation, Biphenylation

## Highlights

Due to their multiple applications, the development of new methods for synthesis of quinoline derivatives is of paramount importance. Here, quinoline derivatives with extended electron delocalization was synthesized. The effect of the substituent groups on their maximum of absorption was determined.

## Abstract

The development of new synthetic methods for quinoline derivatives is of paramount importance. These family of compounds have a variety of applications, including organic electronics and optoelectronics devices with highly efficient electron transport capacity, thermal stability, efficient photoluminescence and good film form properties[1]. Here, we describe a facile synthetic procedure and the optical characterization of quinolines with different substituents in six position the of heterocyclic backbone. Firstly, through one-pot technique, it was synthesized the nitroquinoline (N), which was reduced to obtain the aminoquinoline (NR). Then, two reactions were performed with the aminoquinoline: 1) Alkylation (NRA)[2] and 2) biphenyltation (NRB)[3]. The scheme for the general synthesis can be seen in Figure 1.

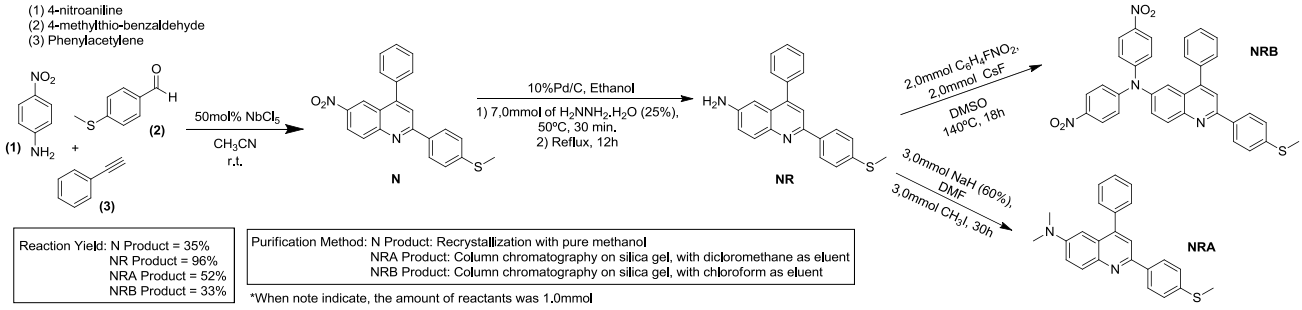


**Figure 1.** Scheme for synthesis of quinoline derivatives

Figure 2 shows the UV-Vis absorption spectra of the quinoline derivatives. A red-shift in the maximum absorbance in different substituents was obtained as follow: 358nm (-$NO_2$), 372nm (-$NH_2$), 388nm (-$N(CH_3)_2$) and 395nm (-$N(Ar\text{-}NO_2)_2$).

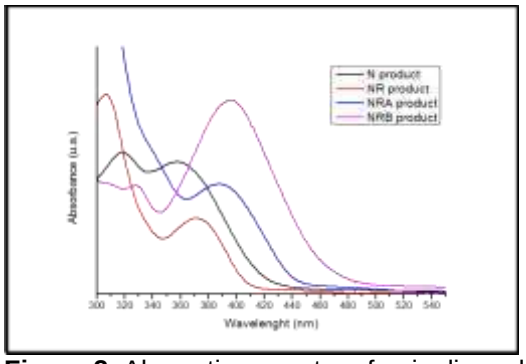


**Figure 2.** Absorption spectra of quinolines derivatives

In summary, this facile synthetic procedure was able to generate quinolines with extended electron delocalization, a desire characteristic for application in optoeletronics devices.

[1]SANTOS, G. C. *et al*. J. Fluoresc. 2017, Jan; 27 (1): 271-280. DOI 10.1007/s10895-016-1954-5
[2]KOMATSU, H. *et al*. Chemistry. 2013, Feb; 19(6): 1971-1977. DOI: 10.1002/chem.201202809
[3]NEDELTCHEV, A. K. *et al*. Tetrahedron. 2010, Oct; 66 (48): 9319-9326. DOI: 10.1016/j.tet.2010.09.108

**Área: ORG** **Inscrição: 808**

# Síntese de oxazolidinonas *via* reação de cloroaminociclização promovidas por sais de Pd(II)

**Bruna L. Papa (PG), Elisângela Vinhato (PQ), Alessandro Rodrigues (PQ)***

**b.papa@unifesp.br; alessandro.rodrigues@unifesp.br**

*Departamento de Química, Universidade Federal de São Paulo, Diadema, SP, Brasil*

Palavras Chave: *cloroaminociclização, oxazolidinonas, paládio*

## Highlights

Oxazolidinones synthesis via chloroaminocyclization reaction promoted by Pd(II) salts.

A new methodology aiming the synthesis of structurally more complex oxazolidinones catalyzed by Pd(II)-Cu(II) system have been developed. Nine novel oxazolidinones were synthesized up to 92% yield.

## Resumo

Em 2004 Lu[1] reportou a haloaminação de alcenos terminais catalisada por $PdCl_2$ com alta régio- e diastereosseletividade na formação de oxazolidinonas. Em 2009, Christie e colaboradores[2] demonstraram que a presença de cobre(II) é essencial para a formação da oxazolidinona *via* haloaminação com alta diastereosseletividade >25:1 (*trans*/*cis*), sem cobre(II) a amida alílica é formada por rearranjo sigmatrópico-[3,3] formal (Esquema 1).

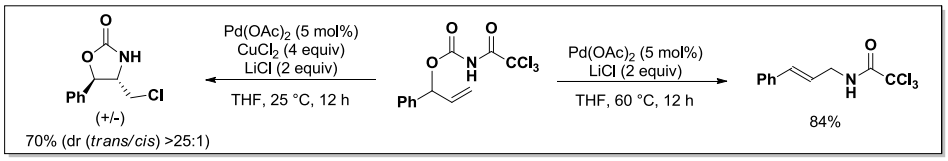


**Esquema 1**

As metodologias de Lu e Christie são limitadas à alcenos terminais ou ligados à grupos alquílicos simples. Tal limitação nos instigou a desenvolver uma nova metodologia para a síntese de oxazolidinonas mais complexas estruturalmente. Para a etapa de otimização foi utilizado o carbamato **4a** (derivado do álcool cinâmico) como modelo. Diversos fatores foram avaliados: 10 sais de Pd(II), quantidade de $CuCl_2$, quantidade de LiCl, tempo reacional, temperatura, solvente, quantidade de catalisador e concentração. A condição reacional optimizada (Esquema 2) levou a formação de **5a** em 65% de rendimento, tendo seu escopo verificado frente a outros 8 carbamatos análogos (**4b-i**). A síntese de **5a-i** foi realizada em triplicata e os rendimentos apresentados da média obtida.

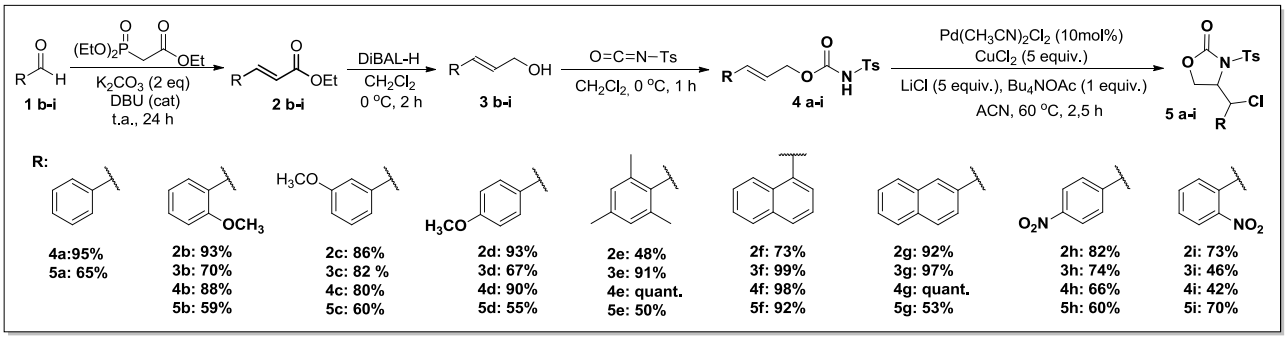


**Esquema 2**

Uma metodologia para a síntese de nove oxazolidinonas inéditas foi desenvolvida em rendimentos optimizados de até 92%. Além disso, um ciclo-catalítico para a reação de cloroaminociclização foi proposto e está sendo estudado por espectrometria de massas e cálculos computacionais (M06-2X/6-31G(d), LanL2DZ).

1. Lei, A., Lu, X. & Liu, G. *Tetrahedron Lett*. **2004**, *45*, 1785.
2. Warrington, A. D., Lunniss, C. J. & Christie, S. D. R. *Synthesis* **2009**, 148.

Bolsa Proc. 2016/17328-7
Fomento Proc. 2016/21676-0

**Área: ORG** **Inscrição: 00863**

# Synthesis of isocoumarins and 3,4-dihydroisocoumarins for antiproliferative activity

**Lucas da S. Santos (PG)*, Rafael T. Chapadeiro (IC), Rossimiriam P. de Freitas (PQ), Rosemeire B. Alves (PQ)**

**rosebrondi@yahoo.com.br; lucas.ssmg@gmail.com**

*Departamento de Química, ICEx, UFMG;*

Key words: *Isocoumarins, 3,4-Dihydroisocoumarins, Antiproliferative Activity.*

## Highlights

synthesis of novel isocoumarins and 3,4-dihydroisocoumarins;
synthesis of compounds with a possible antiproliferative activity.

## Abstract

Isocoumarins (1) and 3,4-dihydroisocoumarines (2) are lactones of natural origins that arouse the interest of synthetic and medicinal chemists as they present several biological applications such as antitumor, antimalarial, antifungal, anti-inflammatory, antimicrobial, among others activities. In addition, these compounds are important intermediates for the synthesis of other natural products.[1,2]

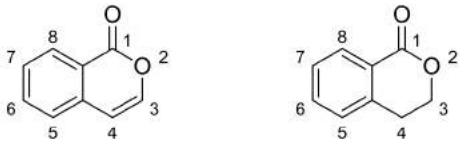

Isocoumarin (1) 3,4-dihydroisocoumarin (2)

Figure 1. Chemical structure of the basic skeletons of isocoumarins (1) and dihydroisocoumarins (2).

Due to the important biological activities presented by these lactones this work involved the obtention of novel isocoumarins and 3,4-dihydroisocoumarins derived from 2-bromo-5-methoxybenzoic acid in order to assess their antiproliferative activity. The synthetic route used in this work is presented in Figure 2. The route proved to be efficient for obtaining these lactonic derivatives.

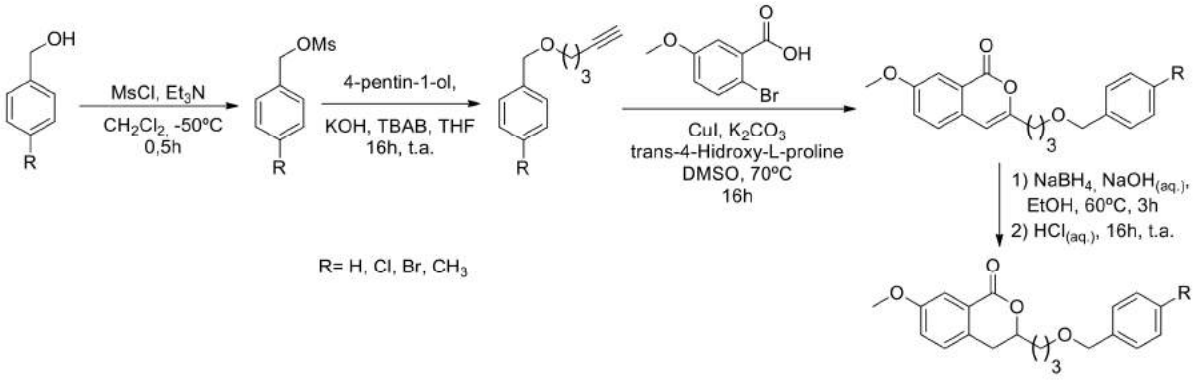


Figure 2. Synthetic route for the preparation of the isocoumarin compounds and their 3,4-dihydroisocoumarin analogues.

1. PAL, S.; CHATARE, V.; PAL, M. Isocoumarin and Its Derivatives: An Overview on their Synthesis and Applications. **Current Organic Chemistry,** v. 15, n. 5, p. 782-800, 2011.
2. SIMIC, M. et al. Functionalised isocoumarins as antifungal compounds: Synthesis and biological studies. **Bioorganic & Medicinal Chemistry Letters,** v. 26, n. 1, p. 235-239, 2016.

**Agreements:** CAPES, FAPEMIG, CNPq, UFMG

**Área: ORG** **Inscrição: 00908**

# Direct sequential C-H iodination/organoyl-thiolation of quinonoid deactivated systems: A new frontier for potent trypanocidal quinones

**Guilherme A. M. Jardim (PG),[1] Willian X. C. Oliveira (PQ),[1] Rossimiriam P. de Freitas (PQ),[1] Rubem F. S. Menna-Barreto (PQ),[2] Thaissa L. Silva (PQ),[3] Marilia O. F. Goulart (PQ).[3] Eufrânio N. da Silva Júnior[1]* (PQ)**

**eufranio@ufmg.br**

*[1]Department of Chemistry, UFMG; [2]FIOCRUZ, Rio de Janeiro; [3]Federal University of Alagoas*

Keywords:*(C-H activation, naphthoquinone, trifluoromethylthiolation, organoyl-thiolation, Chagas disease).*

## Highlights

We report a sequential C-H iodination/organoyl-thiolation of naphthoquinones and their potent trypanocidal activity. Under a combination of AgSR with a copper source, sulfur-substituted benzenoid quinones were prepared in high yields (generally > 90%). This provides an efficient and general method for preparing A-ring modified naphthoquinoidal systems, recognized as a challenge in quinone chemistry.

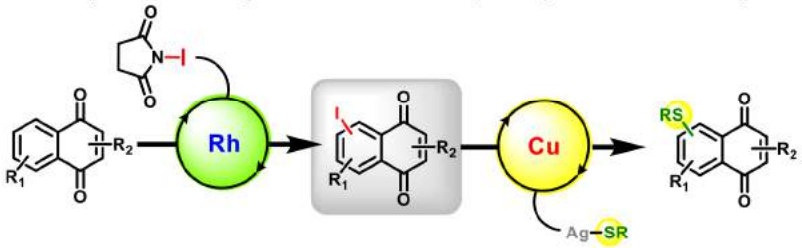


## Resumo/Abstract

1,4-Naphthoquinones (1,4-NQs) are considered privileged structures implicated in important biological processes.[1] Due of their biological importance, scientific endeavor has been devoted aiming at new synthetic methods for preparing 1,4-NQs with potential applicability against illness such as Chagas disease.[2] Recently, our research group have demonstrated the effectiveness of $[RhCp^*Cl_2]_2$ for the first catalytic directed *ortho*-functionalizations of simple (non-bias) 1,4-NQs by using different electrophilic iodine or bromine sources.[3] This methodology opened way for new modification on the benzenoid ring of 1,4-NQs as for example, copper catalyzed organoyl-thiolation reactions:

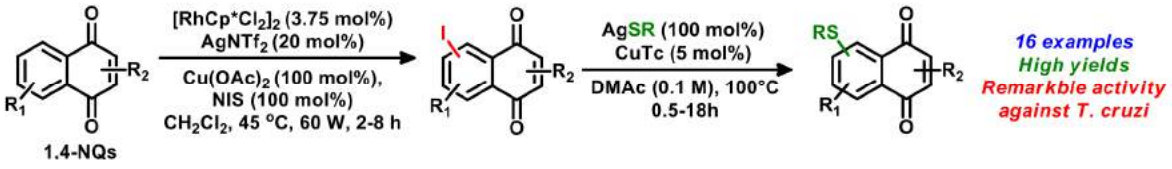


Herein our strategy was based on the general and powerful method to install iodine at C-5 with high yield and regioselectivity and subsequently to combine AgSR salts with a copper source, achieving the thiolated adducts in only two steps via a direct sequential C-H iodination/organoyl-thiolation protocol. Sixteen new compounds were synthesised and tested against *T. cruzi*, showing remarkable activity (examples showed values almost 40 times more active than benznidazole, the standard drug). Eleven structures were solved by X-ray crystallography and electrochemical studies were also performed. Exploratory reactions were conducted and the mechanism of the reaction was also proposed.

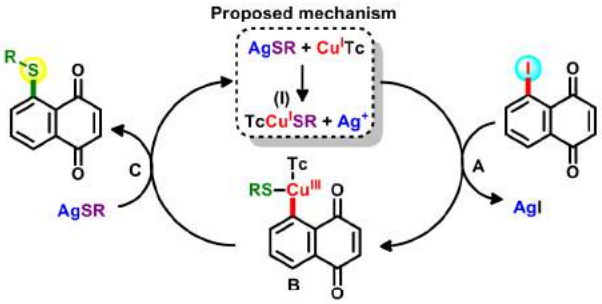


1. Monks et. al., *Toxicol. Appl. Pharmacol.*, 1992, **112**, 2. 2. Da Silva Júnior et. al. *J. Braz. Chem. Soc.*, 2014, **25**, 1780. 3. Jardim et. al. *Chem. Sci.*, 2016, **7**, 3780.

**Área: ORG** **Inscrição 00963**

# Enantioselective Heck−Matsuda Arylation of the Non-activated Cyclopentene

**Tomaz H. D. Chorro (IC),[1] Ellen C. Polo (PQ),[1] Carlos R. D. Correia (PQ).[1]**

**tomazchorro@gmail.com; roque@iqm.unicamp.br**

[1]*Institute of Chemistry, University of Campinas - UNICAMP, Campinas, São Paulo, Brasil.*

Keywords: *Palladium, Enantioselective Catalysis, Heck−Matsuda Reaction, cyclopentene, directing group.*

## Highlights

A series of natural and non-natural biologically active compounds have a cyclopentane ring in their structure. Recent work of our research group demonstrated the critical importance of directing groups in olefins such as cyclopentene to provide Heck−Matsuda products in excellent diastereo- and enantioselective manner. Herein we present enantioselective Heck−Matsuda studies involving a non-activated cyclopentene which further highlights the critical role of directing groups.

## Abstract

The Heck reaction, an important palladium catalyzed cross-coupling process, has emerged as a useful tool to construct C-C bonds. The Heck−Matsuda reaction is a very practical and efficient version of this reaction using arenediazonium salts as arylating agent under open-flask and mild conditions to provide enantioriched building blocks as attractive intermediates in organic synthesis.

Recent work from our group demonstrated the enantioselective arylation of 3-cyclopentene-1-ol (**2**) to afford 4-aryl-cyclopentenols (**3**) in high yields and *ee*'s (Scheme 1). DFT calculations have shown that the free hydroxyl group of the 3-cyclopentenol acts as a directing group in the migratory insertion step leading to the preferentially formation of Heck−Matsuda products (**3**) in a *cis*-configuration.

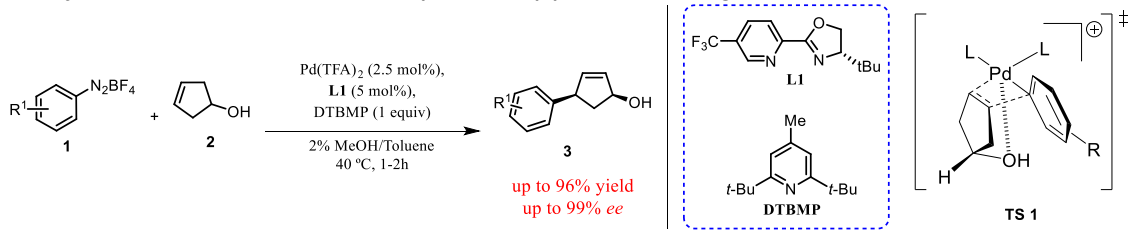


**Scheme 1.** Enantioselective Heck reaction of 3-cyclopenten-1-ol (**2**).

In this context, we decided to further evaluate the importance of the hydroxyl group by studying the Heck-Matsuda arylation of the cheap and commercially available cyclopentene (**5**), a cyclic and symmetric olefin, lacking a directing group. Initially a number of *N,N* ligands were screened to evaluate the influence of the catalyst in the reaction (Scheme 2). Next, we turned our attention to optimize bases, solvents, and reaction temperature.

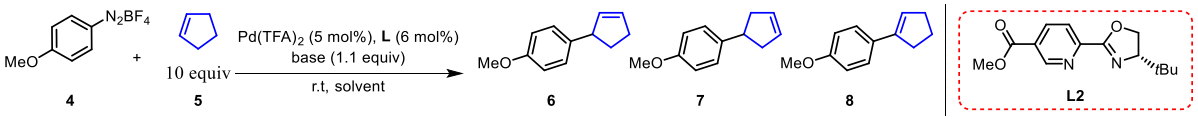


| Entry | Base | Ligand | Solvent | Yield (%) | Selectivity (**6:7:8**) | *e.r.* |
|---|---|---|---|---|---|---|
| 1 | NaOAc | L1 | MeOH | 31 | 29:2:0 | 45:55 |
| 2 | DTBMP | L1 | MeOH | 99 | 78:6:15 | 46:54 |
| 3 | NaOAc | L1 | 2-Methyl THF | 50 | 44:6:0 | 20:80 |
| 4 | NaOAc | L2 | 2-Methyl THF | 58 | **57:1:0** | **16:84** |

**Scheme 2.** Enantioselective Heck reaction of cyclopentene (**5**).

After extensive optimization, we obtained allylic product (**6**) in good yield and enantiomeric excess. The reaction proved to be highly dependent on the reaction conditions, thereby providing additional evidence to the importance of the hydroxyl directing group. We thank FAPESP, CNPq, and CAPES for financial support.

**Área: ORG** **Inscrição: 00975**

# Strong conformational preference of *cis*-2-fluoro- and *cis*-2-chlorocyclohexylamine measured by DNMR

**Ernani A. Basso (PQ),[1]* Camila B. Francisco (PG),[1] Cleverton S. Fernandes (PG),[1] Ulisses Z. Melo (PG),[1] Vanessa T. Paschoalino (IC).[1]**

**eabasso@uem.br**

[1]*Chemistry Department, UEM.*

Palavras Chave: *DNMR, Cyclohexylamine 2-substituted, Conformations, Equilibrium.*

## Highlights

Use of low temperature NMR to identify the individual conformers
Strong conformational preference insensitive to halogen size
Substituent effects in conformations of *cis*-2-halocyclohexylamines

## Abstract

Considering a lack of studies about the conformational analysis of 2-substituted cyclohexylamines, the conformational preference of *cis*-2-halocyclohexylamines (F and Cl) were investigated in this work, using DNMR.
NMR spectra were acquired on a spectrometer Bruker Avance III HD, operating at 500.13 and 125.77 MHz for $^{1}H$ and $^{13}C$ nuclei, respectively, in solutions with concentration of 0.01 mol $L^{-1}$ in $CD_2Cl_2$ and $CD_3OD$, using TMS as internal reference. The temperature was varied from 25 to -80ºC.
By low temperature NMR, the chemical shifts (δ), coupling constants (*J*) and half-height line widths (W), shown in Table 1, allow the identification of each conformer individually. The percentage of each conformer in equilibrium were determined by integration of $^{1}H$ and $^{13}C$ spectra at -80ºC.

**Table 1.** Chemical shifts (δ, ppm), coupling constants ($^{3}J_{H-H}$, Hz), half-height line width (W, Hz) and percentage of **ea** conformer for *cis*-2-halocyclohexylamines in $CD_2Cl_2$ and $CD_3OD$ at -80ºC

| | | | $CD_2Cl_2$ | | | | $CD_3OD$ | | | |
|---|---|---|---|---|---|---|---|---|---|---|
| X | H | δ | $^{3}J_{H-H}$ | W | % **ea**[a] | δ | $^{3}J_{H-H}$ | W | % **ea**[a] |
| **F** | H1a | 2,62 | 11,86[b] | 22,76 | 90 | 2,58 | 12,01[b] | 20,59 | 95 |
| | H1e | 3,37 | [c] | 16,89 | | 3,21 | [c] | 12,52 | |
| | H2a | 4,55 | [c] | 23,18 | | 4,48 | [c] | 23,11 | |
| | H2e | 4,72 | [c] | 10,16 | | 4,65 | 2,56[b] | 8,10 | |
| **Cl** | H1a | 2,81 | 11,48 | 20,61 | 90 | 2,78 | 11,51 | 20,73 | 94 |
| | H1e | 3,25 | 3,33 | 10,54 | | 3,10 | 3,31 | 11,32 | |
| | H2a | 4,17 | 10,69 | 22,46 | | 4,19 | 12,16 | 22,47 | |
| | H2e | 4,46 | [c] | 10,15 | | 4,41 | [c] | 8,10 | |

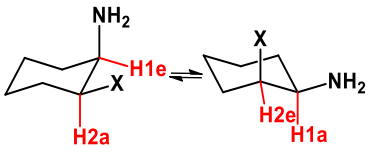

**ae** **ea**

[a]Average of $^{1}H$ and $^{13}C$ signals integration
[b]Measure of $^{3}J_{H-H}$ coupling disregarding the $^{2}J_{H-F}$ coupling
[c]The coupling constants were not measured due the loss of signal resolution at -80ºC.

The equilibrium is strongly shifted towards the **ea** conformer, with 90% in population for **F** and **Cl** in $CD_2Cl_2$, while the populations in $CD_3OD$ were of 95 and 94% for **F** and **Cl**, respectively. It shows that the equilibrium is little sensitive to solvent and insensitive to halogen atomic radii.
Although the axial preference for F and Cl in similar systems has already been reported,[1,2] it was not so pronounced as observed in this work. The strong preference for **ea** conformer is quite surprising, and may be an indication that hyperconjugative interactions govern the conformational preference of these systems. Carbon-halogen bond has been pointed as very significant in hyperconjugation,[3] which was confirmed by NBO calculations using software Gaussian 09.[4]

[1]Basso, E. A., et al. *J. Org. Chem.* **76,** 145–153 (2011).
[2]de Oliveira, P. R.; Rittner, R. *Magn. Reson. Chem.* **46,** 250–255 (2008).
[3]Alabugin, I. V.; Zeidan, T. A. *J. Am. Chem. Soc.* **124,** 3175–3185 (2002).
[4]Glendening, E. D. et al. NBO 5.0. Theoretical Chemistry Institute, University of Wiscosion: Madison, 2001.

**Área: ORG** **Inscrição 01004**

# Resolução Cinética de Derivados de 1-Feniletanol mediadas por Lipase B de *Candida Antarctica* imobilizada em batelada e fluxo contínuo

**Luísa S. de Melo (IC) [1], João C. C. da S. Junior (IC),[1] Pedro Pereira Felner (IC), [1] Larissa C. de Souza (IC),[1] Anderson R. Aguillón (PG),[1] Raquel A. C. Leão (PQ),[1,2] Leandro S. M. Miranda (PQ),[1] Rodrigo O. M. A. de Souza (PQ),[1*]**

**luisasaisse@gmail.com; *souzarod21@gmail.com**

*[1]Grupo de Biocatálise e Síntese Orgânica, Instituto de Química, Universidade Federal do Rio de Janeiro, Rio de Janeiro, RJ 21941-909; [2]Faculdade de Farmácia, Universidade Federal do Rio de Janeiro, RJ, Brazil, 21941-170.*

Palavras Chave: *Resolução cinética, Enantiosseletividade, Novozyme 435, Acetofenonas substituídas.*

## Highlights

Resolução Cinética de Derivados de 1-Feniletanol mediadas por Lipase B de Candida Antarctica imobilizada em batelada e fluxo contínuo: The enantioselectivity in the kinetic resolution of 1-phenylethanol derivatives, with the use of commercial lipase B from Candida antarctica (N435) as a catalyst, from substituted acetophenones.

## Resumo/Abstract

Atualmente, o setor farmacêutico tem investido muitos recursos na obtenção de fármacos enantiomericamente puros, os quais possuem como vantagens a redução na variabilidade de resposta dos pacientes, diminuição dos efeitos colaterais, entre outros. Dentre as metodologias para a separação enantiosseletiva está a resolução cinética, que utiliza as diferentes velocidades reacionais dos enantiômeros para reagir preferencialmente com o catalisador.[1] Estes catalisadores podem ser tanto químicos quanto biológicos, e dentre os biológicos, destacam-se as lipases que podem apresentar elevadas enantio-/regiosseletividade em condições reacionais brandas. Nesse contexto, este trabalho visa determinar a enantiosseletividade na resolução cinética de derivados de 1-feniletanol (**2a-j**) empregando a lipase comercial de *Candida antarctica* (CAL B) Novozyme 435 (**N435**) como catalisador, tendo como precursor as acetofenonas substituídas (**Figura**).[2] Até o momento, os resultados obtidos por cromatografia (CG-FID), das resoluções cinéticas de **2a-c**, tem apresentado excelentes resultados, bem como boa resolução dos sinais no método empregado, com conversões de 48, 37 e 19%, respectivamente e ee de 99%. Logo, os resultados preliminares, dos três padrões avaliados (**1a-c**), apresentam boas perspectivas para a resolução dos enantiômeros de interesse, levando a investir no aumento desse escopo (**1d-j**).

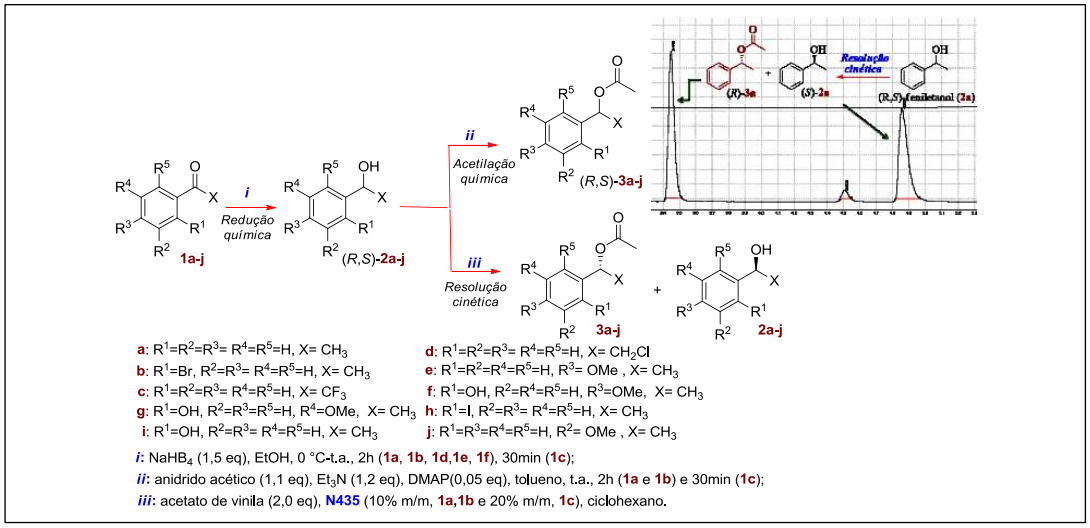


**Figura**: Rota sintética de obtenção dos enantiômeros puros.

(1) de Souza, R. O. M. A.; et al. *J. Org. Chem*. **2009**, 74, 6157-6162.
(2) Schulte, B. et al. *Tetrahedron* **2008**, *64,* 11852-11859.

**Área: ORG** **Inscrição: 01090**

# Estudos visando às sínteses totais de (*R*)- e (*S*)-nuciferina

**Givago P. Perecim (PG), Erika A. I. Rivero (IC), Diogo Oliveira-Silva (PQ), Cristiano Raminelli (PQ)***

**givagoperecim@gmail.com; raminelli@unifesp.br**

*Instituto de Ciências Ambientais, Químicas e Farmacêuticas, Universidade Federal de São Paulo, Diadema, SP, Brasil*

Palavras Chave: *Sínteses totais, Benzino, Nuciferina.*

## Highlights

Study toward the total syntheses of (*R*)- and (*S*)-nuciferine. Total syntheses of aporphine alkaloids are being carried out employing chiral auxiliary and benzyne chemistry.

## Resumo/Abstract

A química de benzino tem encontrado aplicações em química orgânica, incluindo sínteses de produtos naturais e preparações de materiais funcionais.[1] Neste contexto, pretendemos realizar as sínteses totais de (*R*)- e (*S*)-nuciferina (**1**),[2] utilizando abordagem que emprega auxiliar quiral e química de benzino.

Nossa abordagem para obter (*R*)- e (*S*)-nuciferina (**1**) está delineada na análise retrossintética apresentada no **Esquema 1**.

**Esquema 1.** Análise retrossintética para (*R*)- e (*S*)-nuciferina (**1**).

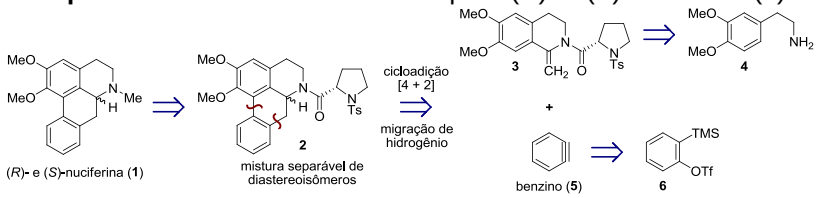


Iniciamos a síntese de (*R*)- e (*S*)-nuciferina (**1**) convertendo 3,4-dimetoxifenetilamina (**4**) no dieno quiral **3** através de transformações de grupos funcionais. Posteriormente, realizamos a reação entre o composto **3** e o precursor de benzino **6** resultando em uma mistura contendo os diastereoisômeros **2a** e **2b** na proporção de 2:1, de acordo com análise por CL-EM. Realizamos a separação dos diastereoisômeros **2a** e **2b** via CLAE preparativa, os quais foram obtidos em rendimentos que estão em fase de otimização. Em seguida, submetemos o diastereoisômero majoritário **2a** a reações de hidrólise básica e de *N*-metilação promovendo a formação de (*S*)-nuciferina (**1a**) (**Esquema 2**).

**Esquema 2.** Rota sintética para (*R*)- e (*S*)-nuciferina (**1**).

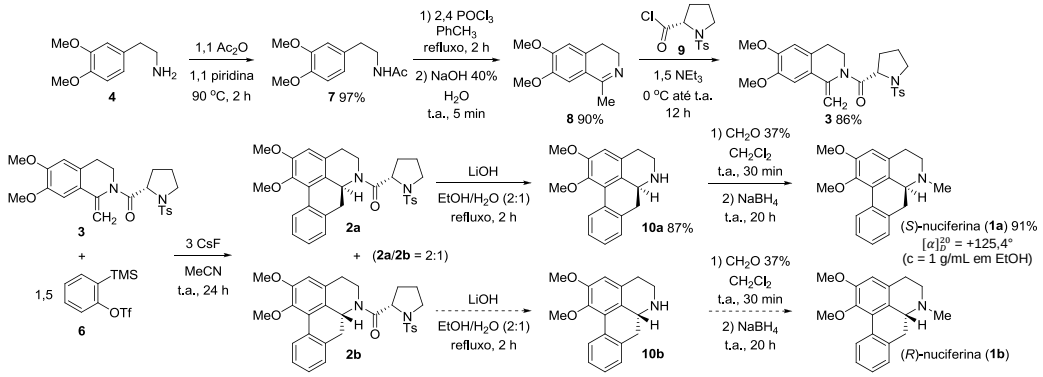


(*S*)-nuciferina (**1a**) foi sintetizada em 6 etapas reacionais. O rendimento global ainda não foi obtido devido ao fato do rendimento da etapa chave estar sendo otimizado.

1. Perecim, G. P.; Rodrigues, A.; Raminelli, C. *Tetrahedron Lett.* **2015**, *56*, 6848.
2. Munusamy, V; Yap, B. K; Buckle, M. J. C.; Doughty, S. W.; Chung, L. Y. *Chem. Biol. Drug. Des.* **2013**, *81*, 250.

**Área: ORG** **Inscrição: 01187**

# Síntese de Selenoésteres mediante rearranjo sigmatrópico entre selenoacetilenos e difenilsulfóxido catalisada por ácido tríflico

**Lucas L. Baldassari (PG),[1] Anderson Mantovani (PQ),[1] Nuno Maulide (PQ)[2] e Diogo S. Lüdtke (PQ).[1]***

**lucas-loss@hotmail.com; dsludtke@iq.ufrgs.br**

*[1]Departamento de Química Orgânica, Programa de Pós-Graduação em Química, UFRGS; [2]Institute of Chemistry, University of Vienna.*

Palavras Chave: *Selenoacetilenos, Selenoester, Catálise Ácida, Rearranjo [3,3] Sigmatrópico.*

## Highlights

Title: “Synthesis of α-aryl selenoesters trought sigmatropic rearrangement between selenoacetylenes and diphenylsulfoxide catalyzed by triflic acid.” In this work, the development of a new methodology for the synthesis of selenoesters will be described. The reaction involves the use of selenacetylenes and diphenylsulfoxide, catalyzed by triflic acid. The reaction mechanism goes through the activation of the alkyne and subsequent [3,3] sigmatropic rearrangement for the formation of the product.

## Resumo/Abstract

A síntese de selenoésteres vem atraindo a atenção da comunidade científica nos últimos anos. Tais compostos são reconhecidamente importantes por apresentar pronunciada atividade biológica.[1] Além disso, selenoésteres são importantes blocos construtores em síntese orgânica, uma vez que são excelentes fontes de radicais acila[2], o que os torna interessantes intermediários sintéticos para a formação de moléculas mais complexas. Nosso grupo de pesquisa tem voltado sua atenção para a ativação de triplas ligações pelo ácido tríflico[3], e nesse contexto, este trabalho abordará o desenvolvimento de uma nova metodologia para a síntese de selenoésteres, mediante a reação entre selenoacetilenos e difenilsulfóxido, através de um rearranjo [3,3] sigmantrópico catalisado por TfOH (Figura 1).

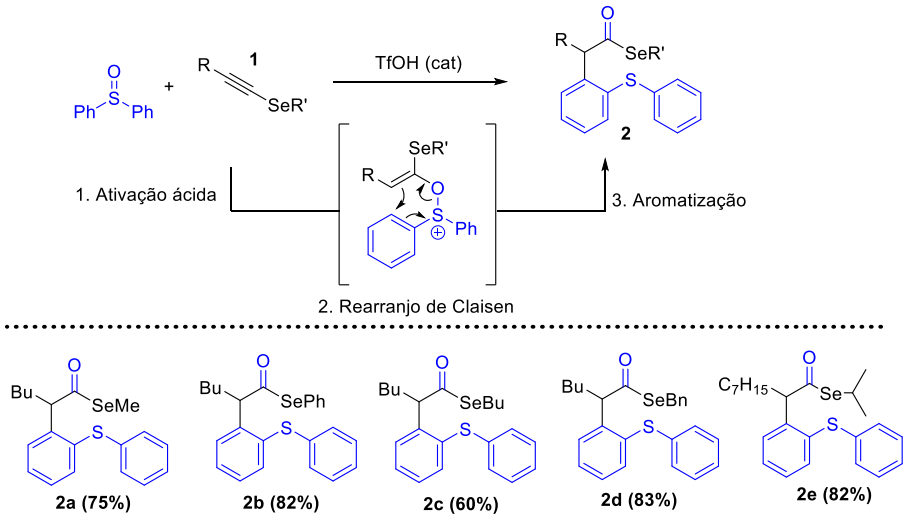


**Figura 1**. Estratégia e síntese de Selenoésteres.

Após serem avaliados os parâmetros reacionais, tais como temperatura, tempo, quantidade de ácido tríflico e de nucleófilo, foi utilizada a condição otimizada para a obtenção de diversos selenoésteres em bons rendimentos (60-83%). A reação tolerou a presença de substituintes alquílicos, benzílicos e arílicos ligados ao átomo de selênio.

Neste trabalho foi realizada a síntese de diversos selenésteres através de um rearranjo de Claisen entre selenoacetilenos e difenilsulfóxido em bons rendimentos. Estudos sobre a ativação dos selenoésteres com ácido tríflico, bem como o aumento do escopo reacional estão sendo realizados atualmente.

Referências
1- *Eur. J. Med. Chem.* **2014**, *73*, 153.
2- *Tetrahedron Lett.* **1983**, *24*, 4355.
3- *Angew. Chem. Int. Ed.* **2017**, *56*, 15723.

**Área: ORG** **Inscrição: 01228**

# Heterociclo Quinoxalina Aplicado à Preparação de Cristais Líquidos: Síntese, Mesomorfismo e Propriedades Físicas

**Leonardo de O. Aguiar (PG), Suélem P. de Souza (IC), André A. Vieira (PQ)***

**leonardoaguiar.1995@hotmail.com; vieira.andre@ufba.br***

*Instituto de Química, UFBA, 40170-115. Salvador, Bahia, Brasil.*

**Palavras Chave:** ***Cristais Líquidos, Fotoluminescência, Quinoxalina.***

## Highlights

**Quinoxaline Heterocycle Applied to the Preparation of Liquid Crystals: Synthesis, Mesomorphism and Physical Properties.** This work describes the synthesis and study of properties of 5,8-π-extended quinoxaline derivatives. All the obtained compounds exhibited liquid crystalline phases and strong green photoluminescence.

## Abstract

Cristais Líquidos Luminescentes (CLLs) constituem uma classe de materiais com promissora capacidade de aplicações na vida moderna[1]. Em especial, CLLs calamíticos, com formato de bastão, contribuem para o desenvolvimento de materiais inovadores, como os displays de cristais líquidos (LCDs), por exemplo. Uma das estratégias mais utilizadas para obtenção de CLLs calamíticos é incorporar um heterociclo a estruturas anisotrópicas[2]. Neste trabalho, são descritos a síntese, caracterização e o estudo de propriedades térmicas e fotofísicas de CLLs calamíticos contendo o heterociclo quinoxalina. Os derivados da quinoxalina são conhecidos por apresentarem bom desempenho na construção de polímeros, OLEDs e exibirem pronunciada atividade biológica[3]. Para contribuir com a investigação dos derivados da quinoxalina, é proposta a funcionalização deste heterociclo nas posições 5 e 8[4], variando os grupos periféricos acoplados. A rota sintética para preparar os compostos finais **5a-d** (**Esquema 1**) inicia com o composto 4,7-dibromo-2,1,3-benzotiadiazol, envolve reação de extrusão redutiva de enxofre, seguida pela ciclização utilizando glioxal e a reação final de acoplamento cruzado de Sonogashira, para obter os desejados derivados 5,8-π-estendidos da quinoxalina com bons rendimentos (73-84%). Todos os compostos foram caracterizados por espectroscopia na região do infravermelho e RMN. As propriedades térmicas foram avaliadas por DSC, TGA e MOLP. Os compostos finais exibiram fases líquido-cristalinas típicas de CL calamíticos. As propriedades fotofísicas foram estudadas por espectros de absorção e emissão em solução em clorofórmio. Estes compostos apresentaram intensa luminescência verde, com máximos de absorção entre 409-419 nm e emissão entre 511-521 nm.

**Esquema 1:** Rota sintética para os compostos-alvo (5a-d)

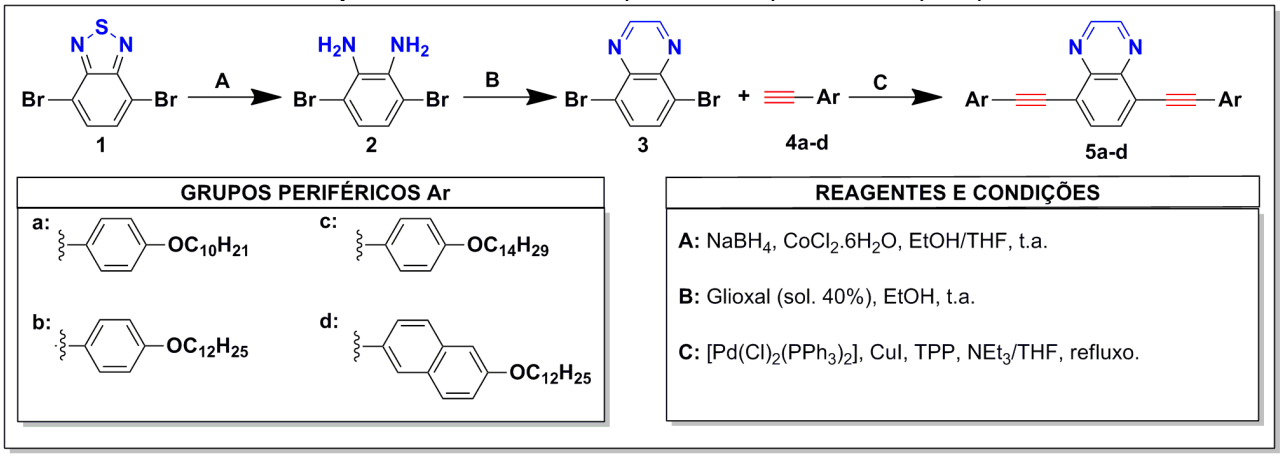


**Referências:** [1]Aguiar, L.O. et al. *Liquid Crystals*, **2018**, 45, 49-58; [2]Grosh, T., Lehmann, M. *J. Mater. Chem. C*, **2017**, 5, 12308-12337; [3]Yuan, J. et al. *J. Mater. Chem. C*, **2017**, 5, 1858; [4]Mancilha, F.S. et al, *Eur. J. Org. Chem*. **2006**, 4924–4933.

**Área: ORG** **Inscrição:__01299_____**

# Síntese de *N*-ftalimidas derivados do Eugenol e avaliação da sensibilidade de cepas de *Candida Albicans* frente à estes compostos.

**Karoline da Silva Santana (IC),[1] Caroline Menditi Silva (TM),[1] Luisa Luz Marçal (PQ)[1*]**

**santanakaroline18@gmail.com; luisa.marcal@ifrj.edu.br***

[1]*Instituto Federal de Educação Ciência e Tecnologia do Rio de Janeiro, IFRJ – Campus Nilópolis.*

Palavras Chave: *(Imidas cíclicas, N-ftalimidas, Eugenol, Antifúngicos, Candidiase).*

## Resumo

Imidas cíclicas têm sido extensamente estudadas devido seu potencial contra uma vasta série de doenças ou efeitos nocivos que afetam comumente os seres humanos, dentre elas: câncer, inflamações, dor, doenças causadas por fungos e bactérias, dentre outras. O mesmo pode ser observado do eugenol (4-alil-2-metoxifenol), um importante representante da classe dos compostos naturais encontrado no óleo de cravo, mais frequentemente extraído da planta *Syzigium aromaticum,* conhecida popularmente como Craveiro da Índia. Este composto atrai a atenção de muitos pesquisadores, por sua ampla gama de fatores biológicos, tendo destaque para a atividade antifúngica, e por sua versatilidade química.Tendo em vista o amplo potencial terapêutico da classe de imidas cíclicas, em especial as *N*-ftalimidas, que apresentam destaque nas atividades antifúngicas, e com base no potencial antifúngico relatado para o eugenol, pretende-se neste trabalho um estudo da sensibilidade de cepas de *Candica Albicans bucal,* frente a *N*-ftalimidas derivadas de eugenol, obtidas via condensação desses dois arcabouços (esquema 1), visando aumentar o potencial bioativo das estruturas finais planejadas.

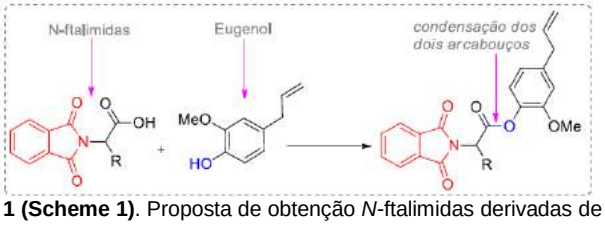


**Esquema 1 (Scheme 1)**. Proposta de obtenção *N*-ftalimidas derivadas de eugenol.

A abordagem sintética para tal proposta se baseia na síntese inicial de N-ftalimidas derivadas de aminoácidos (a partir do método clássico de condensação de aminas primárias com anidrido ftálico) e posterior condensação destas com eugenol (em uma reação de esterificação do eugenol, em meio TCCA/PPh3, seguindo a proposta de Rodrigues, *et al*, 2005.[€]

## Abstract

**Synthesis of N-phthalimides derived from Eugenol and evaluation of the sensitivity of Candida albicans strains against these compounds.**

Cyclic imides have been extensively studied because of their potential against a wide range of diseases or harmful effects that commonly affect humans, among them: cancer, inflammation, pain, diseases caused by fungi and bacteria, among others. The same can be observed for eugenol (4-allyl-2-methoxyphenol), an important representative of the class of natural compounds found in clove oil, most often extracted from the plant Syzigium aromaticum, popularly known as Craveiro of India. This compound attracts the attention of many researchers, due to its wide range of biological factors, highlighting the antifungal activity, and its chemical versatility. Considering the broad therapeutic potential of the class of cyclic imides, especially N-phthalimides, which are prominent in antifungal activities, and based on the antifungal potential reported for eugenol, this study intends to study the sensitivity of strains of Oral Candica Albicans, against eugenol-derived N-phthalimides, obtained by condensation of these two frameworks (scheme 1), aiming to increase the bioactive potential of the planned final structures. The synthetic approach to such a proposal is based on the initial synthesis of N-phthalimides derived from amino acids (from the classical method of condensation of primary amines with phthalic anhydride) and subsequent condensation of these with eugenol (in an esterification reaction of eugenol, TCCA / PPh3, following the proposal of Rodrigues, *et al*, 2005.[€]

[€]*Tetrahedron Letters* **46,** 5945–5947 (2005).

**Área: ORG** **Inscrição: 01341**

# Zinc-promoted, L-proline catalyzed allylation of aromatic aldehydes with allyl bromide in aqueous medium

**[1*] Renato A. Silva (PQ), [1] Fabrícia A. M. Souza (IC), [1] Túlio R. Couto (PQ).**

**renato.augusto@ufrpe.br**

[1]*Unidade Acadêmica de Serra Talhada (UAST), UFRPE*

Palavras Chave: *Alilação, Catálise orgânica, Álcoois homoalílicos.*

## Highlights

The allylation of aromatic aldehydes has been achieved in aqueous acidic medium using non-activated zinc dust catalyzed by L-proline.

## Resumo/Abstract

Álcoois homoalílicos são precursores bastante utilizados em reações de Prins, de epoxidação e de oxidação do grupamento vinílico terminal e como blocos na síntese de produtos naturais ou não-naturais. [1] A literatura descreve diversas metodologias para formação de ligações C-C para obtenção de álcoois homoalílicos por meio de reações mediadas por Al, Sn e In. Porém, em sua maioria, estas reações envolvem o uso de catalisadores caros e complexos, além de condições reacionais anidras e inertes. [2] No presente trabalho a reação do tipo Barbier em meio aquoso na presença de L-prolina foi estudada (figura 1).

**Figura 1.** Alilação de aldeídos aromáticos catalisada por L-prolina e promovida por zinco em meio aquoso.

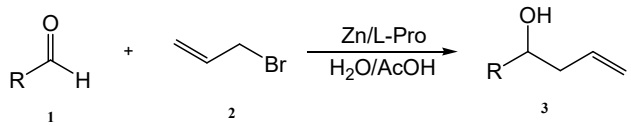


1 2 3

Estudos preliminares da reação entre 4-F-benzaldeído **1**, brometo de alila **2** e zinco em pó não-ativado foram realizados na ausência e na presença de L-prolina em meio aquoso ácido (tabela 1, entrada 1-3). O aumento da L-prolina provocou um aumento na conversão do 4-F-benzaldeído a 1-(4-fluorofenil)but-3-en-1-ol e diminuição do tempo reacional. Resultados similares foram observados na conversão de 4-OMe-benzaldeído a 1-(4-metoxi)but-3-en-1-ol (tabela 1, entrada 4-6)**.** Mais 5 aldeídos aromáticos foram testados com L-prolina (80% em mol) e em consequência bom rendimentos foram obtidos na formação dos álcoois homoalílicos (tabela 1, entrada 7-11)**.** Portanto, aldeídos aromáticos são alilados com brometo de alila na presença de L-prolina e zinco em meio aquoso ácido para gerar álcoois homoalílicos.em bons rendimentos.

**Tabela 1.** Estudo da influência da L-prolina na conversão de aldeídos aromáticos a álcoois homoalílicos.

| Entrada | ALDEÍDO | L-Prolina (% em mol) | TEMPO | CONVERSÃO |
|---|---|---|---|---|
| 1 | 4-F-benzaldeído | 0 | 4 h | 20 |
| 2 | 4-F-benzaldeído | 20 | 30 min | 87 |
| 3 | 4-F-benzaldeído | 80 | 15 min | 98 |
| 4 | 4-OMe-benzaldeído | 0 | 4 h | 5 |
| 5 | 4-OMe-benzaldeído | 20 | 8 h | 85 |
| 6 | 4-OMe-benzaldeído | 80 | 1 h | 92 |
| 7 | 2-F-benzaldeído | 80 | 1 h | 98 |
| 8 | 2-OMe-benzaldeído | 80 | 1 h | 98 |
| 9 | Benzaldeído | 80 | 1 h | 90 |
| 10 | 2-Naftaldeído | 80 | 1 h | 93 |
| 11 | 2-OH-benzaleído | 80 | 1 h | 95 |

**Agradecimentos**: A UAST-UFRPE pelo espaço disponibilizado e a FACEPE pela bolsa de iniciação científica de Fabricia A. M. Souza.

[1] (a) Pastor, I. M.; Yus, M. *Current Org. Chem.* **2012**, *16*, 1277. (b) Riera, A.; María, M. *Molecules* **2010**, *15*, 1041.
[2] Denmark, E. S.; Fu, *J. Chem. Rev.* **2003**, *103* (8), 2763.

**Área: ____ORG_____** *(Inserir a sigla da seção científica para qual o resumo será submetido. Ex: ORG, BEA, CAT)*

**Inscrição:___1412____** *(Inserir o número de inscrição do autor que fez a submissão)*

# Arylation of $\beta$-Ketosulfoxonium Ylides With Arynes: A Direct Synthesis of Pro-chiral Ylides and Mono-Arylated Ketones

**Alexánder G. Talero (PG),[1] Bruna S. Martins (PQ),[1] Antonio C. B. Burtoloso (PQ).[1]***

**alexandergaray@usp.br; antonio@iqsc.usp.br**

[1]*Instituto de Química de São Carlos, Universidade de São Paulo, IQSC-USP, CEP 13560-970.*

Palavras Chave: *Sulfoxonium ylides, Arynes, Pro-chiral, Arylation, Aryl ketones.*

## Highlights

A selective mono-Arylation of $\beta$-ketosulfoxonium ylides using aryne chemistry permits the flexible synthesis of pro-chiral sulfur ylides. These these pro-chiral sulfur ylides were also successfully converted into $\alpha$-aryl ketones through ylide cleavage in good yields.

## Resumo/Abstract

Sulfoxonium ylides, particularly pro-chiral ylides, are important targets with great potential in organic synthesis. New emerging methodologies using sulfoxonium ylides involved in the C-C bond formation put a limit on generation of new stereocenters due to limited availability of pro-chiral ylides. There is no direct and general protocol available in literature to access these synthetically important ylides. To the best of our knowledge, these versatile ylides can only be synthesized via multi step protocol passing through diazo counterpart as intermediate. Thus, we focused on to develop a methodology for smooth delivery of the above-mentioned ylide in a single step. Herein, we describe the synthesis of pro-chiral ylides by an arylation of $\beta$-ketosulfoxonium ylides, employing aryne chemistry, carried out under mild conditions in appreciable yields (45-84%). Moreover, these ylides upon reductive cleavage furnished aryl ketones in good yields (63-94%) offering a new and convenient approach for selective monoarylation of ketones. Studies are also underway to explore the possiblity of using these pro-chiral ylides in the total synthesis of a bioactive natural product.

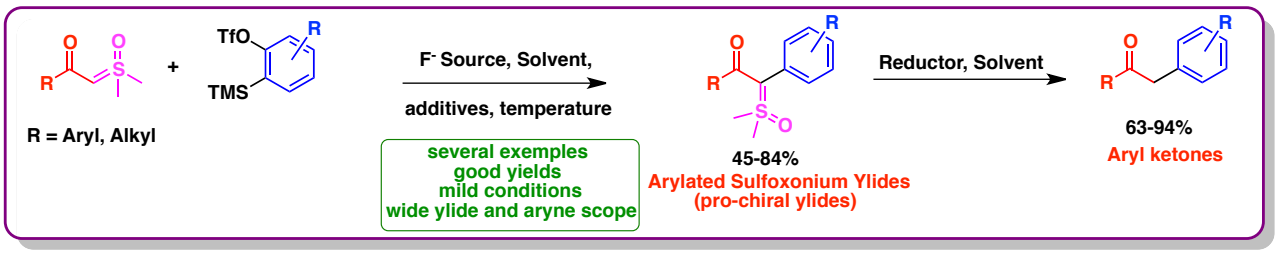

**Área: ORG** **Inscrição: 0021**

# Continuous Flow Enzymatic Kinect Resolution of Benzylic Alcohols: Development of a Low-Cost Homemade Bioreactor

**Gabriel O. Januário (IC), Humberto M. S. Milagre (PQ)***

**humbertomilagre@iq.unesp.br**

*Institute of Chemistry, UNESP - Araraquara, SP*

Keywords: *enzymatic kinetic resolution, bioreactors, continuous flow, solvents, lipase, calcium alginate.*

## Highlights

Development of a low-cost homemade bioreactor.
Enzymatic Kinect resolution of benzylic alcohols.
Continuous flow enzymatic reaction.

## Resumo/Abstract

The continuous-flow process represents an attractive trend applied in organic synthesis and when combined with enzymatic kinetic resolution is an effective methodology to achieve enantiomeric pure compounds.[1] In this work, we developed a homemade continuous-flow bioreactor packed with lipase immobilized in calcium alginate beads to perform the enzymatic kinetic resolution of racemic benzylic alcohols. The bioreactor was build using low-cost materials such as falcon centrifuge tubes, peristaltic pump tubing and connections. A column type bioreactor (8.8 cm × 1.6 cm) with 12,5 mL of total volume and 4,4 mL of working volume, equipped with an external system of thermostatic water operated in an up-flow mode (PFTR). Reaction conditions parameters such as: i) organic reactions (hydrolysis or esterification), ii) enzymes, iii) solvents (aqueous, buffer and organic solvents), iv) temperature and v) substrate were evaluated. The best result corresponds to the hydrolysis of (rac)-1-phenylethyl acetate catalyzed by the lipase from *Burkholderia cepacia* (immobilized in 1,0 mm alginate beads) in water at 40 °C, which reached the best conversion (42%), enantiomeric excess (> 99%) and volumetric productivity of 0.17 mmol $L^{-1}$ $min^{-1}$, during a three-days period of operation.

[1] Angajala, G.; Pavana, P.; Subashini, R. *Biocatalysis and Agricultural Biotechnology* **2016**, *7*, 257–270.

**Área:ORG** **Inscrição: 00063**

# Estudo da oxidação catalisada por Lacase de amidas derivadas da tiramina

**Viviane M. de Aguiar (PG),[1*] Leandro S. de Mariz e MIranda (PQ),[1] Raoni S. B. Gonçalves (PQ),[1] Rodrigo E. da Silva (IC),[1]**

**viviane.mrag@gmail.com; viviane.mrag@gmail.com**

[1] *Instituto de Química, Departamento de Química Orgânica, UFRJ, Universidade Federal do Rio de Janeiro.*

Palavras Chave: *Lacase, Tiramina, Biocatálise, Síntese Orgânica*

## Highlights

Laccase oxidative study of amides derived of tyramine.
Unpublished synthesis of tyramine derivatives.Biocatalytic reaction mediated by oxidoreductasesLaccase*Trametesversicolor*.

## Resumo/Abstract

Lacase (EC 1.10.3.2) é uma enzima capaz de catalisar a oxidação de uma grande variedade de compostos com a concomitante redução do oxigênio à água.[1] A tiramina, uma amina primária fenólica oriunda da descarboxilação da tirosina possui alguns importantes derivados com atividade biológica, apresentando-se como um intermediário na biossíntese de alcalóides da família *Amaryllidaceae*, por exemplo, a Galantamina.[2] Neste trabalho, será apresentado o estudo da utilização de Laccase (T*rametes versicolor)* na oxidação de dois derivados inéditos **(3- a,b)** da tiramina. Esses, foram obtidos com rendimento global acima de 40% a partir do aldeído correspondente e utilizados como substratos a fim de investigar a influência do pH, solvente, agitação e a presença do mediador (ABTS) no perfil de produtos da reação como exemplificado na **figura** abaixo. Análises preliminares sugerem que tenha ocorrido a dimerização dos derivados **3a** e **3b.**

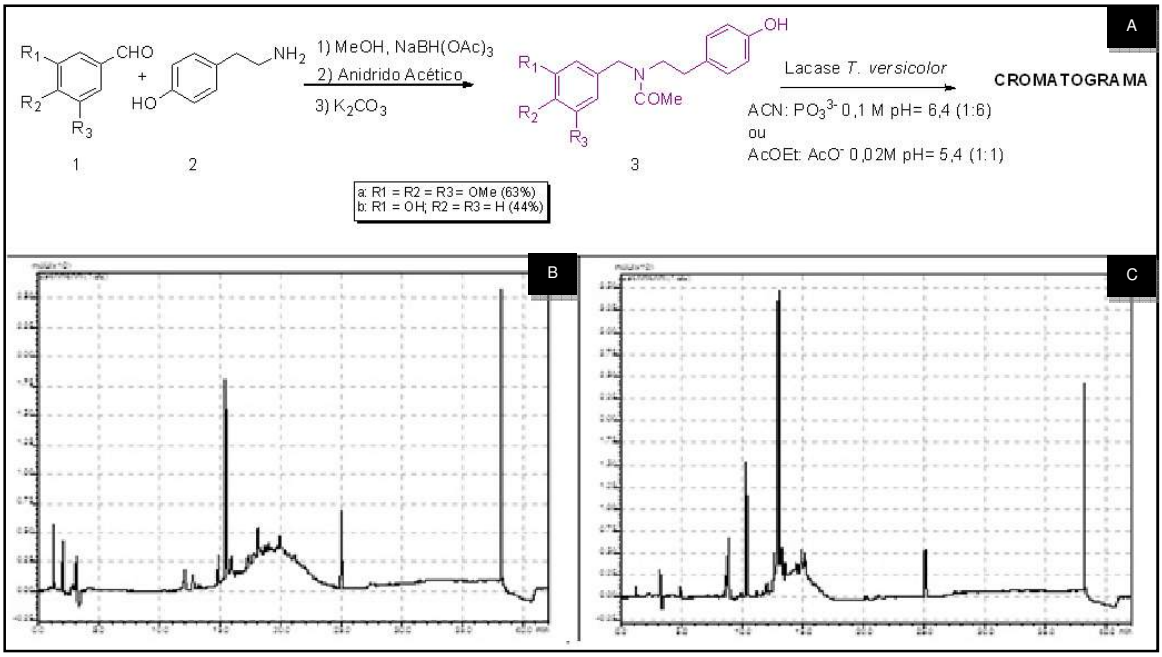


**Figura:(A)**Esquema reacional geral;**(B)**Cromatograma do produto reacional de **3a** de maior conversão com a Lacase(condição: agitação magnética: T= ambiente, ACN:Tampão $PO_4^{3-}$ 0,1M pH= 6,4 (1:6), $O_2$ atm – ABTS);**(C)**Cromatograma do produto reacional de **3b** de maior conversão com a Lacase (condição: agitação magnética: T= ambiente, ACN:Tampão $PO_4^{3-}$ 0,1M pH= 6,4 (1:6), $O_2$ atm – ABTS).

[1] COUTO, S. R., *et. al.*, Bio. Adv., 2006, **24**: p. 500-513
[2] Kuglstatter, A., et al., Bio. &Med. Chem. Lett., 2008. **18**(4): p. 1304-1307.

**Área: ORG**
*(Inserir a sigla da seção científica para qual o resumo será submetido. Ex: ORG, BEA, CAT)*

**Inscrição:00095**
*(Inserir o número de inscrição do autor que fez a submissão)*

# Estudo Sintético da δ-decalactona e Derivados

**Maísa Borges Costa (PQ), [1] Eduardo Lopes de Paula (PG), *[1] Anderson Silva Feliciano (IC)[1]**

**maisa.costa@ueg.br**

*[1]-Laboratório de Síntese, Isolamento e Modificações de Compostos Orgânicos (LabSIMCO) – Campus de Ciências Exatas e Tecnológicas Henrique Santillo – Universidade Estadual de Goiás (UEG-CCET); Caixa Postal 459, Cep. 75132-400 – Anápolis-Go –Brasil*

Palavras Chave: *Aeollanthus suaveolens, δ-decalactona*, *Atividades farmacológicas*

## Highlights

Synthetic Study of δ-decalactone and Derivatives

This work aimed at the synthetic study of lactone δ- (1) and its derivatives for further evaluation of its biological potential

Intramolecular cyclization reaction

## Resumo/Abstract

A espécie *Aeollanthus suaveolens* Mart. Ex Spreng, uma espécie aromática de origem africana, conhecida no Brasil, mais comumente na Amazônia, apresenta dentre as diversas atividades farmacológicas, os efeitos sedativos, ansiolítico, analgésico e também anticonvulsivante (ELISABETSKY, 2007; OLIVEIRA et al., 2004).

Seu óleo essencial é constituído, principalmente por lactonas (TUCKER; MACIARELLO; ALKIRE, 1995). Pesquisas sobre o potencial aromático das lactonas são amplos, porém poucos são os estudos relacionados a outras atividades farmacológicas (BORATYNSKI et al., 2016).

Diante do exposto, este trabalho objetivou o estudo sintético da δ-decalactona (**1**) e derivados, para posterior avaliação do seu potencial biológico. A metodologia sintética (Esquema 1) baseou-se em reações de condensação aldólica, ciclização de Michael e redução para a obtenção do 3,4-diidro-6-((*E*)-pent-1-enil)-piran-2-ona **(4)**, uma lactona inicialmente insaturada. Posteriormente, serão realizados ensaios biológicos com os compostos obtidos.

**Esquema 1 -** Metodologia para a síntese da δ-decalactona e seus derivados sintéticos.

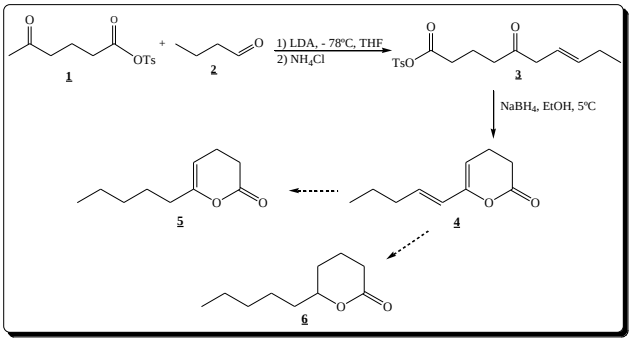


Análises de RMN $^{1}H$ e $^{13}C$ bidimensional estão em andamento para a total elucidação estrutural do composto **4**.

**Agradecimentos**

Os autores agradecem a CCET/UEG e aos órgãos de fomento à pesquisa como a CAPES e ao ProBIP/2016.

**Referências Bibliográficas**

BORATYNSKI, F.; DANCEWICZ, K.; PAPROCHA, M.; GABRY, B. Chemo-Enzymatic Synthesis of Optically Active γ- and δ-Decalactones and Their Effect on Aphid Probing, Feeding and Settling Behavior. Plos One, v. 07, p.1-18, 2016.

ELISABESTSKY, E. Phytotherapy and new paradigma of drugs mode of action. Science Et techina, v.12, p.459-464, 2007

OLIVEIRA, A. S. C.; COSTA, L. M. L.; ZOGHBI, M. G. B.; CONCEIÇÂO, C. C. C.; MOTA, M. G. C. Rendimentos dos principais componentes químicos do óleo essencial de *Aeollanthus suaveolens* (Mart ex K. Spreng) em diferentes partes vegetativas. In: XVIII Simpósio de Plantas Medicinais do Brasil, p.513, 16 a 19 de novembro, Manaus - AM, 2004.

TUCKER, A. O.; MACIARELLO, M. J.; ALKIRE, B. H. Essential Oil of *Aeollanthus suaveolens* Mart, ex Spreng. (Lamiaceae). Journal of Essential Oil Research, v. 13, p.198-199, 2001.

**Área: ORG** **Inscrição: 00140**

# Solvent-free synthesis of $\alpha$-acylated $\beta$-thioenaminones

**Jamille Silveira Matos (PG),[1] Silvio Cunha (PQ).[1*]**

**jamille_smatos@yahoo.com.br; silviodc@ufba.br.**

[1]*Instituto de Química, UFBA; INCT-Instituto Nacional de Ciência e Tecnologia em Energia e Ambiente, Campus de Ondina, Salvador – BA, Brasil.*

Palavras Chave: *Solvent-free, $\alpha$-Acylated $\beta$-thioenaminones, Alternative green route*.

## Highlights

A series of $\alpha$-acylated $\beta$-thioenaminones was prepared from enaminones and phenyl isothiocyanate under solvent-free condition at room temperature, with or without ultrasound irradiation.

## Resumo/Abstract

$\alpha$-Acylated $\beta$-thioenaminones compounds are intermediates that may be conveniently prepared from enaminones using montmorillonite as solid support at 40ºC.[1] Herein, these compounds were prepared from an alternative green route. Reactions of enaminones **1a-e** with phenyl isothiocyanate **2** under solvent-free condition at room temperature afforded a mixture of regioisomeric $\alpha$-acylated $\beta$-thioenaminones **3a-e**. This was confirmed by $^1$H NMR with the presence of the signals corresponding for both *Z* and *E* isomers in the 3:1 proportion. Under the same condition only one stereoisomer was obtained for the compounds **3f,g**. As can be seen in **Scheme 1**, compounds **3a,b,e,f,g** were obtained from enaminones with group R1 = H, n-butyl and $CH_2CH_2OH$ in good yields and compounds **3c,d** were obtained from enaminones with group R1 = Ph in poor yields.

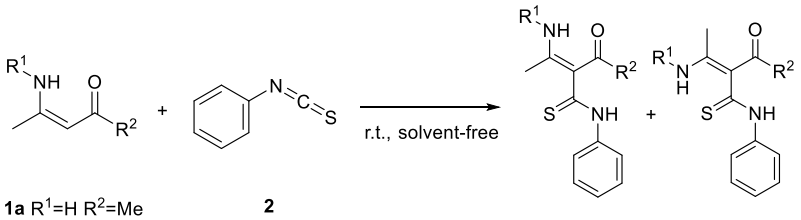


**1a** $R^1$=H $R^2$=Me
**1b** $R^1$=H $R^2$=OEt
**1c** $R^1$=Ph $R^2$=Me
**1d** $R^1$=Ph $R^2$=OEt
**1e** $R^1$=n-butyl $R^2$=OMe
**1f** $R^1$=H $R^2$=OMe
**1g** $R^1$=$CH_2CH_2OH$ $R^2$=Me

**2**

**3a** 73%
**3b** 66%
**3c** 25%
**3d** 25%
**3e** 78%
**3f** 56%
**3g** 67%

**Scheme 1**. Synthesis of $\alpha$-acylated $\beta$-thioenaminones.

To the reaction of enaminone **1h** with phenyl isothiocyanate **2** under solvent-free condition and ultrasound irradiation at room temperature **(Scheme 2)**, was obtained also as a mixture of isomers in the 3:1 proportion: ethyl (Z)-3-amino-2-(phenylcarbamothioyl)but-2-enoate and ethyl (E)-3-amino-2-(phenylcarbamothioyl)but-2-enoate (**3h**), in moderate yield.

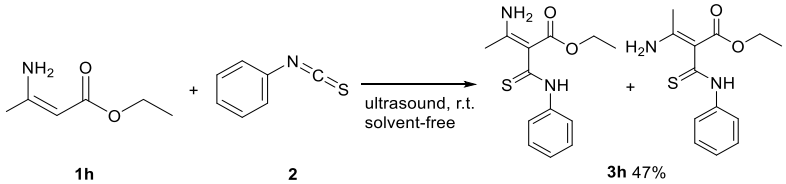


**1h** **2** **3h** 47%

**Scheme 2**. Synthesis of $\alpha$-acylated $\beta$-thioenaminones.

The solvent-free condition was efficient to the synthesis of stereoisomeric $\alpha$-acylated $\beta$-thioenaminones and is an alternative green route. The synthetic application of such compounds to the synthesis of complex heterocycles is under investigation.

[1] Braibante, M. E. F.; Braibante, H. S.; Missio, L. J.; Andricopulo, A. Synthesis. **1994**, 09, 898.

**Área: ORG** **Inscrição: 00148**

# Síntese e caracterização de novos derivados piperazínicos, análogos ao SQ109: Potenciais agentes antituberculose

**Mauricio F. Saraiva (PQ), Dijovani B. dos Reis (PG)**

**saraivaunifei@gmail.com; dijovani.reis@gmail.com**

*Instituto de Física e Química, Universidade Federal de Itajubá UNIFEI.*

Palavras Chave:*Tuberculose, SQ109, terpenóides.*

## Highlights

SQ109 is an antitubercular drug actually under phase II of clinical trials[1]. This work describe synthesis and characterization of new piperazinyl derivatives, analogues of SQ109: Potential anti-tuberculosis agents.

## Resumo/Abstract

We have previously described the synthesis and anti-tuberculosis activity of a series of diaminated terpenoids[2]. In order to increase the lipophilicity and to try improve the anti-tuberculosis activity we have now introduced the adamanta-1-carboxamide on the primary amine of these terpenoids. The obtained compounds are analogues of SQ109[3] a promising molecule in the fight against tuberculosis.
The synthetic pathway for the preparation of the compounds **6a-c** was made on four steps, starting from 1-adamantane carboxylic acid **1**, by transformation on acyl chloride derivative, this last one was reacted with piperazine to furnished the amide **3** in 66% of yield. After, the allylic bromide **5** prepared from respectively alcohol, reacted with the free amine of **3** to furnish the SQ109 analogues **6a-c** in good yields 70-90%.

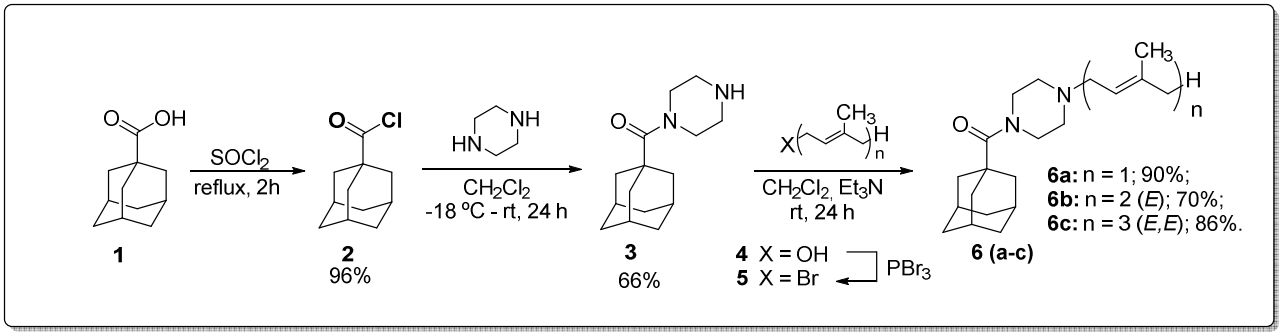


The obtainded compounds were characterized by IR, $^{1}H$ NMR, $^{13}C$ NMR and will be send to anti-tuberculosis activity evaluation.

### References

[1] WHO, *Global Tuberculosis Report*, **2016**.
[2] Reis, D. B.; Saraiva, M. F.; *et al Biomedicine and Pharmacotherapy*. ***2016***, 84, *1739-1747.*
[3] Onajole, O. K. *et al. European journal of medicinal chemistry*. **2012**, *54*, 1-9.

### Acknowledgement:

We acknowledgement, CAPES for the fellowship, RQMG by financial support and UFJF by NMR spectra.

**Área: ORG** **Inscrição:00161**

# Synthesis of new inhibitors of cathepsin K with potential use in osteoporosis therapy

**Talita B. Gontijo (PG),[1]Eufrânio N. da Silva Júnior (PQ)[1], Rossimiriam P. Freitas (PQ)[1].**

**talitabarbaragontijo@gmail.com; rossipfreitas@gmail.com.**

*[1]Departamento de Química, ICEX- UFMG.*

Palavras Chave: *Osteoporosis; Cathepsin K inhibitors; Dipeptides.*

## Highlights

Cathepsin K inhibitors: a promising approach in the treatment of osteoporosis; synthesis of new dipeptides and azadipeptides.

## Resumo/Abstract

Osteoporosis is a metabolic bone disease characterized by decreased bone mass and increased susceptibility to fractures. Currently, research in anti-osteoporosis therapies have been considered important in several areas, being the development of selective cathepsin K inhibitors pursued by many companies. Cathepsin K is a lysosomal cysteine protease found in the osteoclasts, being responsible for the degradation of organic components in the bone matrix.[1]Some inhibitors of cathepsin K have undergone clinical trials, such as odanacatib–discontinued in phase III-, and ONO 5333 - in phase II (Figure 1).[2]

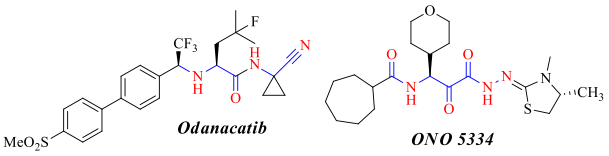


**Figure 1:** Inhibitors of cathepsin K

Recent studies have pointed out others azadipeptides and dipeptides derivatives active and selective to cathepsin K; therefore, structural modifications in these molecular skeletons are a promising strategy in the search for anti-osteoporosis therapies. In this work, different synthetic routes were developed to yield the new azadipeptide **5** and the new dipeptide derivative **9** (Scheme 2), which are being evaluated as cathepsin K and osteoclastogenesis inhibitors.

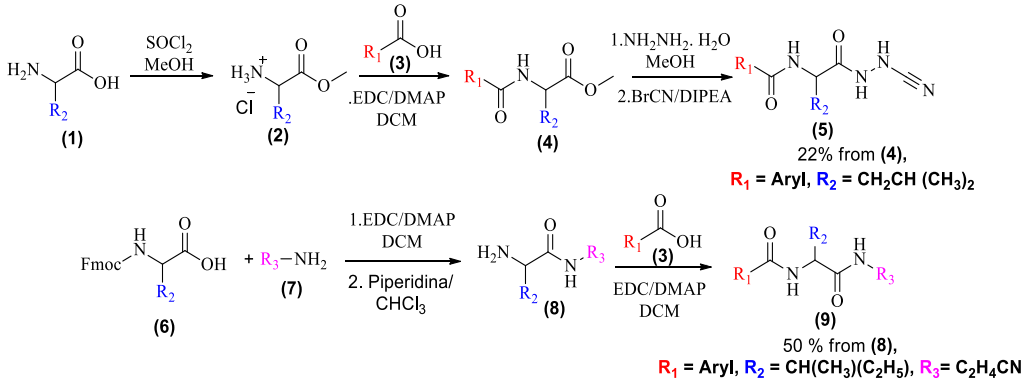


**Scheme 2:** Synthesis of new azadipeptides and dipeptides.

1. Leung, P. et al. *Bone.* **2011**, 49, 623-635.
2. Mukherjee, K. et al. *Biochemical Pharmacology*. **2016**, 117 10–19

**Aknowledgment:** CNPq, CAPES, FAPEMIG, UFMG.

**Área: ORG** **Inscrição: 00206**

# Synthesis of new compounds based on Lawsone via a multi-component reaction

**Mariana F. do C. Cardoso (PQ)[1], Luana M. Forezi (PQ)[1], Carolina C. Gil (IC)[1], Tayná S. dos Santos (IC)[2], Geraldo R. de Paula (PQ)[2], Lenise A. Teixeira (PQ)[2], Fernando de C. da Silva (PQ)[1], Vitor F. Ferreira (PQ)[2].**

**marianafcc83@hotmail.com**

[1]*Universidade Federal Fluminense, Campus do Valonguinho, Niterói-RJ, Brazil*
[2]*Universidade Federal Fluminense, Faculdade de Farmácia, Niterói-RJ, Brazil*

Palavras Chave: *Lawsone, naphthoquinones, Bacterial infections, Gram-positive bacteria*

## Highlights

The synthesis of several new compounds based on the 1,3-dicarbonyl scaffolds lawsone was developed using tandem four-component reactions involving the reagents benzylamine, methyl chloroformate and an appropriate aldehyde. These reactions generated a serie of naphthoquinones **5a-i** that are structurally related to lawsone.

## Abstract

Tandem multi-component reactions (MCR) are convergent syntheses that begin with three or more reactants and, preferably, end with only one formed product that contains all of the starting atoms.[1] Naphthoquinones play vital roles in several biological processes and are considered to be of great importance in medicinal chemistry. Naphthoquinones are often associated with various biological activities, including anticancer, antibacterial, antimalarial, trypanocidal, tuberculostatic and fungicidal activities.[2]

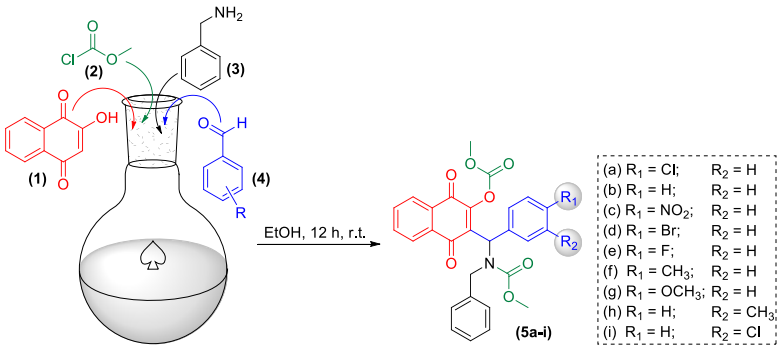


Scheme 01. Synthesis of compounds **5a-i**

Lawsone (1) is a 1,3-dicarbonyl compound that have been extensively used by synthetic organic chemists because of their peculiar chemical structures and their relationships with biologically important natural products. Indeed, this natural product has a large variety of biological activity that has been studied in recent decades and stimulated the synthesis of a large number of synthetic analogues.

With this aim in mind and as a further extension of our studies of the chemistry of naphthoquinones, we have prepared a new serie of compounds **5a-i**, which are structurally related to lawsone (1), via a four-component reaction using lawsone (1) as a starting material.

The resistance phenomenon has allowed bacterial infections to continue emerging more than 50 years after antimicrobials were introduced in clinical practice. This problem shows great interest in the development of new molecules that act as antimicrobials. Gram-positive bacteria can cause infections in patients in the hospital setting and also in the community. In this work we evaluated 32 Gram positive isolates, belonging to genus *Staphylococcus*, *Enterococcus* and *Streptococcus*, resistant and sensitive to the main antimicrobials used for therapy. Bacteria were analyzed by diluting different concentrations of the compound on Muller Hinton agar with subsequent addition of the isolates using the Steers replicator`s. The compound - HM-02 was the most effective because most of the isolates showed minimal inhibitory concentration (MIC) ≤ 256 µg / mL. All methicillin-resistant *Staphylococcus aureus* (MRSA) showed MIC ≤ 128 µg/mL. It demonstrates this compound is a potential promise as anti-*S. aureus*.

1. Parsons, P. J.; Penkett, C. S.; Shell, A. J.; *Chem. Rev.* **1996**, *96*, 195.
2. da Silva, F. C.; Ferreira, V. F.; *Curr. Org. Synth.* **2016**, *13*, 334.

**Área: ORG** **Inscrição 00218**

# Continuous flow biocatalyzed process enhanced production of (*R*)-1,2-propanediol mediated by Immobilized Candida Antarctica Lipase B

**Anderson R. Aguillón (PG)[1], David N. Câmara (IC),[1] Stefania P. de Souza (PQ),[1] Raquel A. C. Leão (PQ),[1,2] Leandro S. M. Miranda (PQ),[1] Rodrigo O. M. A. de Souza (PQ),[1]**

**anthersonr@gmail.com; souzarod21@gmail.com**

*[1]Grupo de Biocatálise e Síntese Orgânica, Instituto de Química, Universidade Federal do Rio de Janeiro, Rio de Janeiro, RJ 21941-909; [2]Faculdade de Farmácia, Universidade Federal do Rio de Janeiro, RJ, Brazil, 21941-170.*

Palavras Chave: *Continuous-flow, lipase, kinetic resolution, (R)-1,2-propanediol*

## Highlights

Enantiopure (R)-ether with excellent conversions and high productivities, optimized kinetic resolution on flow conditions, the reduction of reaction time from hours to a few minutes.

## Resumo/Abstract

Enantiomerically pure (*R*)-1,2-propanediol has important applications as a building block in the manufacture of pharmaceutical products such as antiviral agents and pheromones.[1] Several strategies have been successfully applied to the resolution of (*R*,*S*)-1,2-propanediol (**1**) and its derivatives. Taking advantage of the ability of some lipase to resolve racemic mixtures with a high level of stereoselectivity, some authors have applied it on the resolution of (*R*,*S*)-**1** using bulky ether protecting groups on the primary alcohol in order to enhance selectivity on kinetic and dynamic resolution.[2] However, the methodologies developed so far suffers from long reaction times leading to the desired product (up to 24 hours).

In our continuous effort on developing biocatalyzed continuous-flow process as key green emerging research area for sustainable manufacturing,[3] we reported our results on the kinetic resolution of (*R*,*S*)-1-(trityloxy)propan-2-ol, (*R*,*S*)-**2**, using a packed-bed containing lipase B from *Candida antarctica* immobilized on acrylic resin (Novozyme435) on continuous-flow.

The continuous flow reactors allowed to reduce the reaction time, going from 6 h in batch to 7 min in flow, keeping the values of conversion and selectivity during the reaction procedure (49% and >99% conversions and enantiomeric excess, respectively) and increasing the productivity of the process in all stages. In addition, the continuous flow reactor increased the productivity of kinetic resolution of (*R*,*S*)-**2** to 300% in comparison with batch reactor, after its optimization, and allowed continuous operation for 8 h in the kinetic resolution reaction.

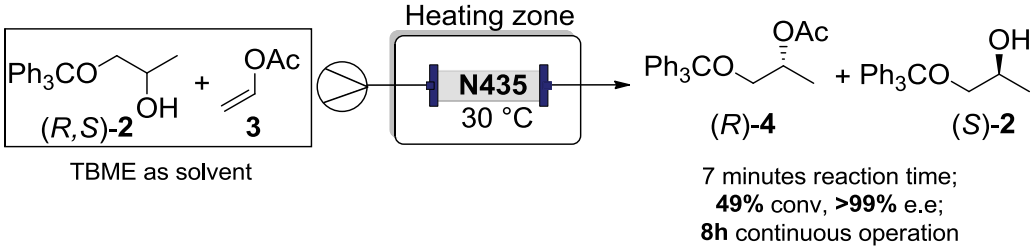


(1) Douglas, C. C.; Cooney, C. L. *Nat. Biotechnol.* **1986**, *4*, 651.
(2) Kim, M. J.; Choi, Y. K.; Choi, M. Y.; Kim, M. J.; Park, J. *J. Org. Chem.* **2001**, *66* (13), 4736.
(3) Leão, R. A. C.; de Souza, S. P.; Nogueira, D. O.; Silva, G. M. A.; Silva, M. V. M.; Gutarra, M. L. E.; Miranda, L. S. M.; Castro, A. M.; Junior, I. I.; de Souza, R. O. M. A. *Catal. Sci. Technol.* **2016**, *6* (13), 4743.

**Área: ORG** **Inscrição: 00244**

# Synthesis and condensation of amides derivatives from nonsteroidal anti-inflammatory drugs (NSAIDs) in "environmentally friendly" conditions.

**Daniel de Carvalho Santos (PG), Felipe Peixoto Ponquio (IC), Adriana Karla C. A. Reis[1*] (PQ)**

**carvalho.daniiel@gmail.com**; **adrianakarla.amorim@gmail.com**

[1]*Departamento de Química, Universidade Federal de São Paulo, Diadema, SP, Brasil*

Palavras Chave: *nonsteroidal anti-inflammatory drugs, amides, coupling reactions, environmentally friendly methodologies, microwave irradiation.*

## Highlights

In this study we synthesized amides derived from nonsteroidal anti-inflamatory-drugs (NSAIDs), with the proposal to synthesize novel amides that can be used as prodrugs, since similar compounds derived from other anti-inflammatory drugs (both amides and substituted products) have anti-inflammatory activities and there are indications that they may be used as anticancer compounds.[1-2] This motivated us to prepare and study this class of compounds.

## Abstract

This project aims to the synthesis of six amides derived from three important nonsteroidal anti-inflammatory drugs (NSAIDs): naproxen, ibuprofen and ketoprofen. Those compounds can be used as chiral derivatization reagents (CDRs) in the synthesis of sulfanyl derivatives, which can have an antitumoral biological potential, corroborating to the development of drugs in the field of chemoprevention. The interest amides were prepared by reacting the NSAIDs with heterocyclic aromatic amines (imidazole or 3-amino-1,2,4-triazole) by classical methods and also by microwave irradiation from coupling reactions via acid chlorides and coupling reagents such as DIC and CDI, in different solvents: acetonitrile, dichlorometane and dimethyl carbonate. The results obtained for the reactions with acid chloride were shown to be the most efficient and those via CDI enabled a new route of synthesis to be explored. For the reactions performed with DIC as the coupling reagent a lower yield due to the formation of by-products was observed. However, such reactions have responded satisfactorily to the environmentally friendly methodologies, thus becoming a very relevant alternative for the preparation of the interest compounds.

**Scheme 1.** (a) NSAIDs structures utilized in the development of this work (b) Main amides of interest

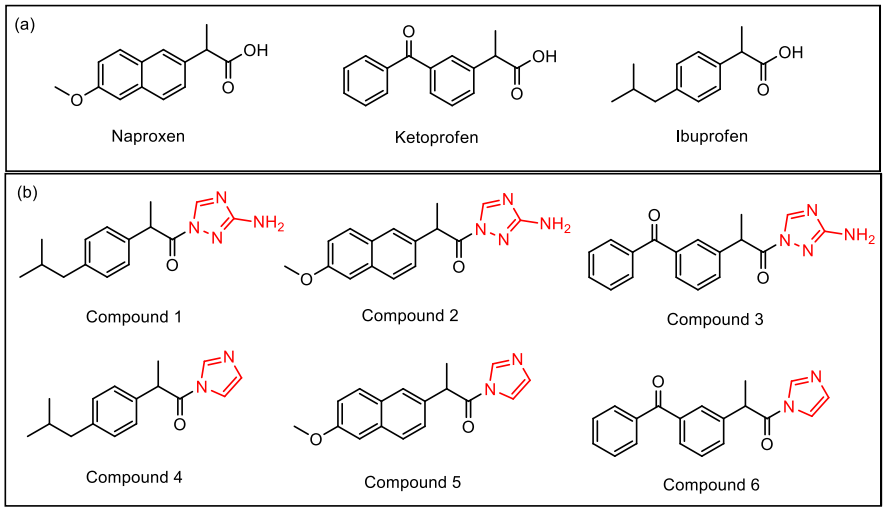


## References

[1] Allegretti, M.; Bertini, R.; Cinzia, B.i; Sabbatini, V.; Caselli, G.; Cesta, M. C.; Gandolfi, C.; Colotta, F.; *PCT Int. Appl*. **2001**, WO 2001058852 A2 20010816

[2] Wang, Pei-Yun; Chen, Ying-Ju; Wu, An-Chi; Lin, Yi-Sheng; Kao, Min-Fang; Chen, Jin- Ru; Ciou, Jyun-Fen; Tsai, Shau-Wei; *Advanced Synthesis Catalysis,* **2009**, 351,2333- 2341.

**Área: ORG** **Inscrição: 00275**

# Catalyst-free synthesis of pyridazinones from 3-hydroxy-indole-2-ones

**Geiziane A. Santos (PG),[1] Silvio Cunha (PQ)1,[2*]**

**geisy-alves1@hotmail.com; silviodc@ufba.br**

[1]*Instituto de Química, Universidade Federal da Bahia, Campus de Ondina, 40170-290, Salvador – BA.*
[2]*INCT-Instituto Nacional de Ciência e Tecnologia em Energia e Ambiente, Campus de Ondina, Salvador – BA*

Key words: *(Pyridazinones, Isatin, Hydroxy-indole-2-ones).*

## Highlights

Reaction of 3-hydroxy-indole-2-ones with hydrazine afforded pyridazinones in good yields.

## Resumo/Abstract

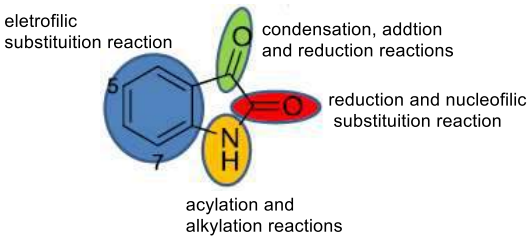


Figure 1

Isatin is an attractive and versatile molecule because allow different kind of reactions (Figure 1). 3-Hydroxy 2-oxindoles are isatin derivatives, which possess a carbonyl group at the 2 position of the 5-membered ring and a quaternary carbon center at the 3-position and are important synthetic targets.[3] Pyridazinone is a core found in diverse compounds with many biological activities.[4] Recent methodologies have been developed in the synthesis of pyridazinones[5]. In this work, we reported a new synthetic approach to pyridazinones **5a-e** from 3-hydroxy-indole-2-ones, **4a-e**. Compounds, **4a-e** were obtained from isatin **1a-c**, and symmetric ketones **2** or **3** with diethylamine as catalyst at room temperature. Reaction of **4a-e** with hydrazine as nucleofile and ethanol afforded the final products **5a-e** in a simple step with easy purification and excellent yields, wherein two new bonds N-C were formed, Scheme 1.

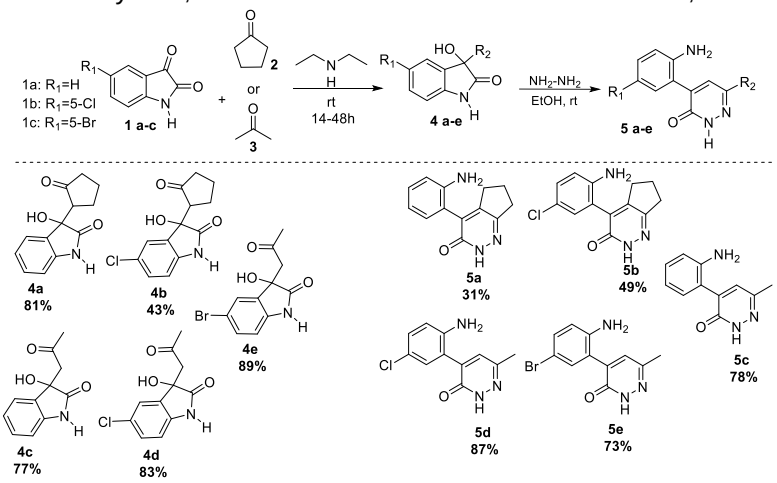


Therefore, we developed a catalyst-free synthesis of new series of 3-hydroxy-indole-2-ones and polyfunctionalized pyridazinones from isatin derivatives.

Acknowledgement:
FAPESB, INCT, UFBA

[1]Ferreira, V. F., Martinez, S. T. *Rev. Virtual Quim*., 2017, *9,* (3), 1154-1183; [2]Yan, T., Wang, X., Sun, H., Liu, J., Xie, Y. *Molecules.* 2013, *18*, 14505-14518; [3]Peddibhotla, S. *Curr. Bioact. Compd.* 2009, *5*, 20–38; [4]Verheelst, T.; Liu, Z.; Maes, J.; Maes, B. U. W. *J. Org. Chem*. 2011, 76, 9648.

**Área: ORG** **Inscrição: 00309**

# Dynamic kinetic resolution of amines with nickel catalysts supported on mixed oxides of lanthanum and alkaline earth metals

**Lucas A. Silva (IC),[1] Sânia M. Lima (PQ),[2] Fernanda A. Siqueira* (PQ),[1] Thayná N.C. Fernandes (IC),[1]. lucas.ads.eq@gmail.com; famsiq@gmail.com***

*[1]Departamento de Química, UNIFESP; [2]Departamento de Engenharia Química UNIFESP*

Keywords: *Chiral amines, Nickel, Synthesis, Catalysis.*

## Highlights

Chiral molecules are important for the synthesis of biological active compounds. Dynamic kinetic resolution is a promising methodology to produce pure enantiomers. Novel nickel catalysts have been used in this methodology. The desired acetamide was obtained in excellent enantioselectivity.

## Abstract

Enantiomerically pure amines are widely used in the pharmaceutical industry as building blocks for the synthesis of compounds with biological activities[1]. This project aims the synthesis of a chiral acetamide by the technique of dynamic kinetic resolution with different nickel catalysts supported in mixed oxides of lanthanum and alkaline earth metals. In this methodology the resolution and *in situ* racemization of the undesired enantiomer occurs due to the presence of a metal catalyst and a biocatalyst. In this sense, this synthesis pathway allows the achievement of a theoretical yield and enantiomeric excess of 100%[2]. The results obtained showed the efficiency of the nickel catalysts leading to excellent enantiomeric excesses. A summary are shown in table 1. The advantage in using nickel consists in the low cost associated with its commercialization in comparison to the catalysts of palladium and ruthenium, making the application of this system in a large scale economically viable.

**Table 1** - DKR results of 1-phenylethylamine with nickel catalysts in different temperatures

| Entry | Catalyst | Temperature | Conversion (%) | E.E (%) | Yield* (%) |
|---|---|---|---|---|---|
| 1 | LaO.9MgO, $NiO_3$ | 75 | 64 | 96 | 87 |
| 2 | LaO.9BaO, $NiO_3$ | 75 | 70 | 95 | 60 |
| 3 | LaO.9CaO, $NiO_3$ | 75 | 75 | 98 | 33 |
| 4 | LaO.9SrO, $NiO_3$ | 75 | 75 | 98 | 85 |
| 5 | LaO.9MgO, $NiO_3$ | 90 | 65 | 91 | 78 |
| 6 | LaO.9BaO, $NiO_3$ | 90 | 70 | 91 | 45 |
| 7 | LaO.9CaO, $NiO_3$ | 90 | 74 | 90 | 47 |
| 8 | LaO.9SrO, $NiO_3$ | 90 | 76 | 96 | 51 |
| 9 | LaO.9MgO, $NiO_3$ | 100 | 65 | 92 | 58 |
| 10 | LaO.9BaO, $NiO_3$ | 100 | 70 | 87 | 71 |
| 11 | LaO.9CaO, $NiO_3$ | 100 | 65 | 92 | 66 |
| 12 | LaO.9SrO, $NiO_3$ | 100 | 70 | 79 | 67 |

* Yield refers to the purified product and the percentage is relative to the converted amount.

**References**

[1] - PARVULESCU, A. N.; JACOBS, P. A.; DE VOS, D. E.. *Adv.Synth. Catal.* **2008**, *350*, 113–121,.
[2] - PÀMIES, O.; BÄCKVALL, J. E. *Chem. Rev.* **2003**,*103*, 3247–3261.

**Área: ORG** **Inscrição: 00341**

# Synthesis of Novel *N*-heterocycles from Biomass-derived Building Block Dimethyl Itaconate

**Guilherme J. S. R. dos Santos (IC),[1] Fernanda P. Ludwig (PG)[1] Alcione Viero de Bastos (PG),[1] Valéria D. O. Bareño (PG)[1], Sidnei Moura e Silva (PQ),[2] Alex F. C. Flores (PQ),[1] Darlene C. Flores (PQ)[1]**

**gui.srodrigues@hotmail.com;**

*[1]Núcleo de Estudo Estrutural e Sìntese de Heterocíclos, Escola de Química e Alimentos – Universidade Federal do Rio Grande, Campus Carreiros – Avenida Itália, km 08, CEP 92201-900, Rio Grande, RS, Brasil*
*[2]Laboratório de Produtos Naturais e Sintéticos, Instituto de Biotecnologia – Universidade de Caxias do Sul – Rua Francisco Getúlio Vargas, 1130, CEP 95070-560, Caxias do Sul, RS, Brasil*

Palavras Chave: *itaconic acid, pyrrolidinone, pyrazoles*

- Use of green building block dimethyl itaconate;
- Easy diversification of products from 1-$NH_2$-pyrrolidinyl hydrazides precursors;
- The route proposed allows to obtain novel polyfunctional azoles.

## Resumo

### Introdução

When it comes to energy production, a number of renewable technologies are available that can eventually make it possible to replace fossil fuels including wind, solar, biomass, etc. However, when the issue is the chemical industry, biomass is the real alternative to petroleum-based resources.[1] A promising platform chemical, which can be derived from renewable feedstock and have been pursued by researchers, is *itaconic acid* and/or its derivative compounds such as ester. These functionalized dicarboxylic acid or derivative esters can be utilized in polymers fabrication or heterocycles synthesis. [2] The development of heterocycles synthesis that involve compounds attainable from biomass will likely have positive implications in the future production of the aforementioned value-added products.
According to what was shown above, we present in this work a synthetic route for novel 1-amino-pyrrolidinonyl-pyrazoles from bio-based building block dimethyl itaconate as alternative for petrochemical-based.

### Resultados e discussão

The synthesis of the 4-carboxyethyl-6-pyridazinone **2** and 1-amino-5-pyrrolidinone-3-carbohydrazide **3** are outlined in the Scheme **1.** The condensation of hydrazine monohydrate with dimethyl itaconate in alcohol outcome in the compound **2** or **3**. The formation of the heterocycles **2** or **3** is controlled by the amount of hydrazine and reactional time used. The condensation [3 + 2] of hydrazide **3** with 1,3-dielectrophiles **4** e **5a-g** was investigated, **Scheme 2**. The hydrazide **3** were reacted com methyl acrylate **4** in methanol reflux forwarding polyfunctional pyrazoles **6** in excellent yields. The same hydrazide **3** were reacted with the enones **5a-g** leading to *N*-acyl-pyazoles derivatives **7a-g**. All the novel biheterocycles synthetised were characterized based on $^1$H and $^{13}$C NMR spectroscopy and MS-MS.

Esquema 1

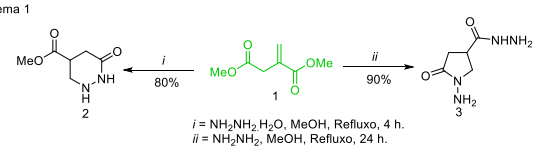


Esquema 2

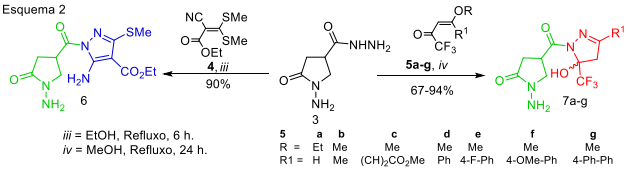


### Conclusão

In conclusion, we have developed a convenient and new approach for the synthesis of interesting *N*-acyl-pyazoles derivatives from dimethyl itaconate. This methodology can be used to afford improved molecular diversity simply changing in the hydrazide portion or electrophiles. The results of our studies have already been published,[3] Further, investigation on this type of reactions currently in progress in our laboratories.

### Referências

**1**. S. K. Ritter, *Chem. Eng. News*, **2004**, *82*, 31–34; (b) Werby, T. *&* Petersen, G. *Top Value Added Chemicals from Biomass*, ed., US Department of Energy, **2004.**
**2**. A. M. Medway and J. Sperry, *Green Chemistry*, **2014**, 16, 2084-2101. DOI 10.1039/c4gc00014e
**3.** Pereira, B. A.; Bastos, A. V.; Teixeira, W. K. O.; Silva, S. M.; Flores, A. F. C.; Flores, D. C. *Molecular Diversity*, **2017**, *21*, 1021-1026. DOI 10.1007/s11030-017-9771-6

**Área: ORG** **Inscrição: 00355**

# Resolução cinética dinâmica da (±)-1-feniletilamina catalisada por níquel suportado em óxidos mistos de metais lantanídeos

**Thayná N. de C. Fernandes (IC),[1] Lucas A. Silva (IC),[1] Sânia M. de Lima (PQ),[2] Fernanda A. Siqueira* (PQ),[1]**

**tthayyna@gmail.com; famsiq@gmail.com***

[1]*Departamento de Química, UNIFESP – Diadema*; [2] *Departamento de Engenharia Química, UNIFESP – Diadema*.

Palavras Chave: *Resolução cinética dinâmica, racemização, níquel, catálise, aminas quirais.*

## Highlights

Dynamic kinetic resolution of (±)-1-phenylethylamine with nickel catalysts on mixed oxides of lanthanides. The DKR is a simple and effective route to prepare chiral compounds. In this project it was proposed the use of nickel catalysts for the racemization step of the DKR. Excellent results were obtained.

## Resumo

As aminas enantiomericamente puras possuem diversas aplicações nas indústrias farmacêutica e agroquímica[1]. A síntese enantiosseletiva é extremamente relevante para obtenção destas aminas, uma vez que enantiômeros podem apresentar atividades biológicas distintas. Neste projeto foi proposto o estudo da resolução cinética dinâmica (DKR – do inglês Dynamic Kinetic Resolution) para a síntese de aminas assimétricas. Essa metodologia consiste em duas etapas. A primeira se caracteriza pela resolução cinética enzimática utilizando uma enzima estereosseletiva (Lipase *Candida antarctica* B) e acetato de etila como agente acilante. A segunda etapa é a racemização catalisada por um metal, a qual ocorre via processo redox, etapa que tem por objetivo racemizar o enantiômero indesejado. A maioria dos trabalhos descritos na literatura mostra o uso de catalisadores caros, como paládio ou rutênio[2], o diferencial deste é o uso do níquel como catalisador, que é um metal mais barato e pouco encontrado em trabalhos científicos. Para a avaliação da atividade dos catalisadores de níquel foram feitas reações em diferentes condições, envolvendo variação de suportes e temperaturas. Os resultados obtidos encontram-se relatados na tabela 1.

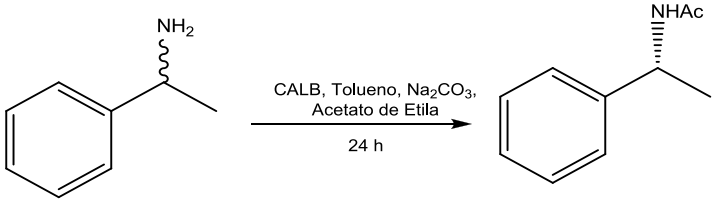


Tabela 1 – Resultados das DKR da (±)-1-feniletilamina com níquel como catalisador e diferentes temperaturas

| Entrada | Catalisador | Temperatura (°C) | Conversão (%) | ee (%) |
|---|---|---|---|---|
| **1** | LaO.9CeO, $NiO_3$ | 75 | 78 | 94 |
| **2** | LaO.9PrO, $NiO_3$ | 75 | 73 | 96 |
| **3** | LaO.9SmO, $NiO_3$ | 75 | 71 | 98 |
| **4** | LaO.9CeO, $NiO_3$ | 90 | 65 | 91 |
| **5** | LaO.9PrO, $NiO_3$ | 90 | 63 | 89 |
| **6** | LaO.9SmO, $NiO_3$ | 90 | 65 | 80 |
| **7** | LaO.9CeO, $NiO_3$ | 100 | 39 | 77 |
| **8** | LaO.9PrO, $NiO_3$ | 100 | 59 | 88 |
| **9** | LaO.9SmO, $NiO_3$ | 100 | 62 | 85 |

*Rendimento calculado a partir da quantidade de (±)-1-feniletilamina convertida.

Referências:
[1] PARVULESCU, A. N.; JACOBS, P. A.; DE VOS, D. E. *Adv.Synth. Catal.* **2008**, *350*, 113–121,
[2] VERHO, Oscar; BACKVALL, J. *J. Am. Chem. Soc.* **2015**, *137*, 3996-4009.

**Área: ORG** **Inscrição: 00411**
*(Inserir o número de inscrição do autor que fez a submissão)*

# Synthesis and leishmanicidal activity of eugenol triazolic derivatives

**Róbson Ricardo Teixeira (PQ),[1*] Poliana Aparecida Rodrigues Gazolla (PG),[1] Wallace Pacienza Lima (PQ),[2] Maria Paula Gonçalves Borsodi (IC),[2] Bartira Rossi Bergmann (PQ),[2] Adalberto Manoel da Silva (PQ).[3*]**

**robsonr.teixeira@ufv.br;**

[1]Departamento de Química, UFV; [2]Instituto de Biofísica Carlos Chagas Filho, Laboratório de Imunofarmacologia, UFRJ; [3]Instituto Federal de Educação, Ciência e Tecnologia Catarinense, Campus Araquari

Palavras Chave: eugenol, leishmanicidal activity, triazole, click chemistry

## Highlights

It is described the synthesis of a series of twenty-six eugenol derivatives bearing triazolic functionalities and the evaluation of their leishmanicidal activity.

## Resumo/Abstract

Eugenol (4-allyl-2-methoxy phenol) is a natural product found in several aromatic plants. It presents important biological activities including leishmanicidal [1,2]. It is herein described the synthesis and the evaluation of the leishmanicidal activity of eugenol derivatives bearing 1,2,3-triazole functionalities. Eugenol was extracted *via* hydrodistillation from dried flower buds of *Eugenia caryophyllata* (=*Syzygium aromaticum*). Alkylation reactions of eugenol afforded terminal alkynes in good yields. The key reaction involved in the preparation of eugenol derivatives with triazolic moieties corresponded to the Copper(I)-catalyzed Azide-Alkyne Cycloaddition (CuAAC), also known as click reaction, between alkynylated eugenol derivatives and different benzyl azides. Reactions were conducted in EtOH/$H_2O$ (1:1 v/v) at room temperature and afforded compounds with synthetically useful yields (77%–91%, **Scheme 1**).

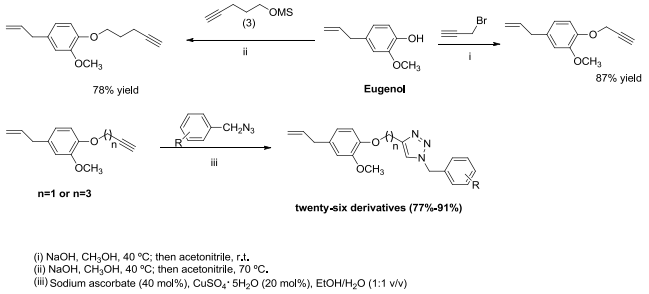


**Scheme 1** – Reactions involved in the preparation of eugenol triazolic derivatives.

In most cases, click reactions last less than 1 minute. The evaluation of the twenty-six synthesized compounds on promastigotes of *Leishmania amazonensis* (WHOM/BR/75/Josefa) showed that eugenol derivatives present leishmanicidal activities with varying degrees of effectiveness. The most active compound 4-(3-(4-allyl-2-methoxyphenoxy)propyl)-1-(4-methylbenzyl)-*1H*-1,2,3-triazole (**7k**) ($IC_{50}$ = 7.4±0.8 µmol $L^{-1}$) also targeted *Leishmania* parasites inside peritoneal macrophages ($IC_{50}$ = 1.6 µmol $L^{-1}$) without interfering with cell viability. The cytotoxicity of **7k** against macrophage cells presented $IC_{50}$ of 211.9 µmol $L^{-1}$ and the selective index was equal to 132.5. Under similar conditions, compound **7k** was more effective than glucantime and pentamidine, two drugs currently in the clinic. It is believed that eugenol triazolic derivatives may represent a scaffold to be explored toward the development of new agents to treat leishmaniasis.

**References**: [1] J. Alvar, I. D. Vélez, C. Bern, M. Herrero, P. Desjeux, J. Cano, J. Jannin, M. den Boer, Leishmaniasis worldwide and global estimates. *PLoS One* 7 (2012) e35671; [2] G. P. Kamatou, I. Vermaak, A. M. Vijoen. Eugenol – from the remote Maluku Islands to the international market place: a review of a remarkable and versatile molecule, *Molecules* 17 (2012) 6953-6981.

**Acknowledgements:** The authors are grateful to FAPEMIG (CEX-APQ-02957-17), CNPq and CAPES for financial support.

**Área: ORG** **Inscrição:** 00452

# Mechanochemical chlorination of acetamides *via* chemometric optimization

**Daniel Moreira Araújo (PG),[1*] Silvio Cunha (PQ).[2]**

**danielm.araujo@yahoo.com.br; silviodc@ufba.br**

[1]*Instituto de Química, Universidade Federal da Bahia, Campus de Ondina, 40170-290, Salvador – BA.*
[2]*INCT-Instituto Nacional de Ciência e Tecnologia em Energia e Ambiente, Campus de Ondina, Salvador – BA*
Palavras Chave: *Chemometric, TCCA, Chlorination, Mechanochemistry, Green chemistry.*

## Highlights

Using mechanochemistry, the reactional parameters of the chlorination of aromatic acetamides using TCCA (trichloroisocyanuric acid) were optimized applying Doehlert Matrix.

## Resumo/Abstract

Statistics helps researchers and practitioners in chemistry and other fields understand the results of their experiments. In this context, Chemometrics is a consolidated area in the activities of chemists. Despite the importance and variety of its applications, the use of chemometric optimization in synthetic organic chemistry are still rare.[1] Besides, the use of mechanochemistry is a new frontier of synthetic methodology.[2] For inserting parameters of green chemistry as reactions in the absence of solvents, this leads to explore synthesis of compounds with wide significance as building blocks. Aromatic halogenated compounds have key applications as precursors for a variety of cross-coupling, including Suzuki, Heck and Ulmann couplings.[3] Thus, we investigated the chlorination of aromatic acetamides using TCCA (trichloroisocyanuric acid) in a planetary mechanochemical equipment with agate reactor, applying the Doehlert Matrix, which is a planning widely used in methodological optimization. The factors studied were: Frequency (RPM) and Time (min.), since the previously applied two level Full factorial design showed that the number of balls is not significant. The response surface applied by the Doehlert Matrix Figure 1 showed that the critical factors were 446 RPM and 77 min. This condition was applied to other acetamides Scheme 1.[4-6] The method will be applied to others acetamides.

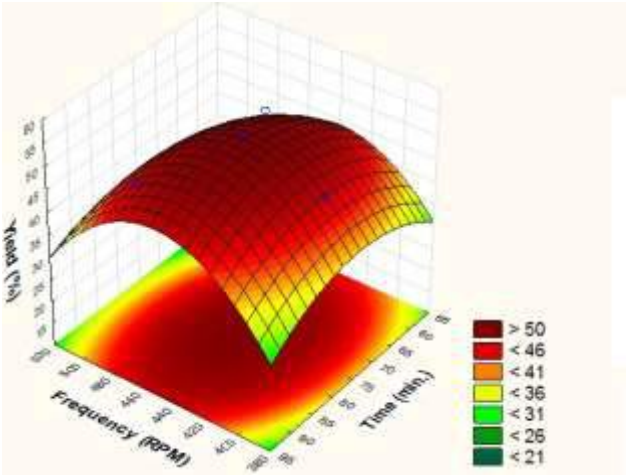


**Figure 1**: Doehlert matrix response surface

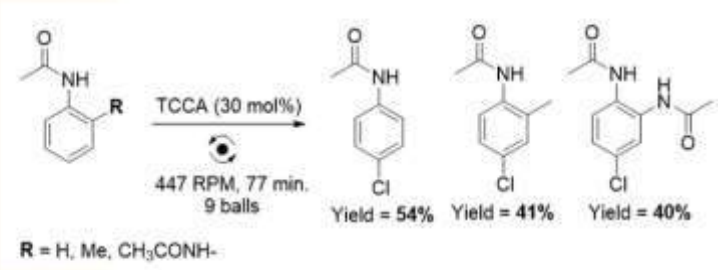


**Scheme 1**: Aromatic halogen Acetamides synthesized.

[1] Ferreira, L. C. S., Introdução às técnicas de Planejamento de Experimentos, Ed. Vento Leste, pg. 15, 2015.
[2] Hernández, J. G.; Bolm, C.;J. Org. Chem.2017, 82, 2733.
[3] Huang, B.; Zhao, Y.;Yang, C.; Gao, Y.; Xia, W.; Org. Lett. 2017, 19, 3779-3802.
[4] Vasconcellos, M. L. A. A.; Lima Junior, C. G.; Quim. Nova, 2009, 32, 244.
[5] Vecchiotti, V. L.; Gass. chim. ital. 1929, V59, P525-43.
[6] Molchanov, L. V.; Khimiya Prirodnykh Soedinenii 1983, (2), P207-9.

**Área: ORG** **Inscrição: 00479**

# Synthesis of indol sulfoxides and sulfones as broad spectrum antibacterials against the ESKAPE pathogens

**Edilma E. Silva (PG) and Gustavo P. Silveira (PQ)***

*Departamento de Química Orgânica, Instituto de Química, UFRGS.*
Palavras Chave: *ESKAPE pathogens, Sulfoxide, Sulfone, Indole, Antibacterial, Toxicity.*

## Highlights

A library of indol sulfoxides and sulfones was synthesized.Compounds presented modarate activities against the ESKAPE pathogens. Best lead showed broad spectrum activiy, low toxicity and citotoxicity.

## Resumo/Abstract

Recently, we presented the screening of a set of 17 indole-sulfides against the ESKAPE panel of bacteria. These compounds demonstrated high to moderate activity (MICs 2-8 μg/mL) against Gram-positive bacteria.[1] A second generation library of 15 sulfoxi- and sulfone-indoles was synthesized from the respective sulfide using 1 or 2 equivalents of *m*-CPBA (Scheme), respectively, and screened against the same panel of microrganism to improve pharmokinetics and toxic parameters.

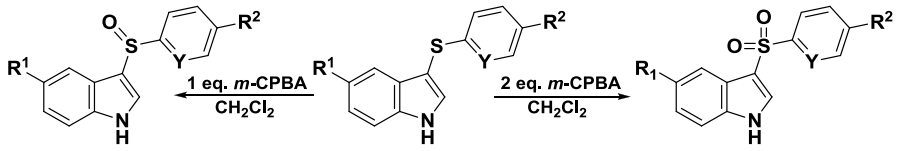


**Scheme**: synthesis of sulfoxi- and sulfone-Indoles by oxidation with *m*-CPBA.

None of the compounds showed cytotoxicity or mutagenicity at concentrations of 32 μg/mL. The best coumpund of the library, **EE29**, demonstrated broad spectrum activies (MICs 4-32 μg/mL, Table) and very low capacity of blood cells hemolysis (Table) at 10 μg/mL. This sulfone was classified as nonirritant using the Hen´s Egg Test on the Chorioallantoic Membrane (HET-CAM).[2] **EE29** showed genotoxicity at 32 μg/mL statistically similar to the negative control used in the test.

**Table**: MICs against the ESKAPE pathogens and hemolysis of **EE29**.

| | cLog P | *E. coli* | *S. aureus* | *E. faecalis* | *E. faecium* | *K. pneumoniae* | *P. aeruginosa* | *A. baumannii* | *Enterobacter* | Hemolysis 10μg/mL(%) 1μg/mL(%) |
|---|---|---|---|---|---|---|---|---|---|---|
| 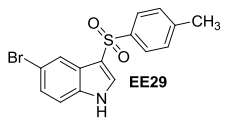 EE29 | | | | | | | | | | **0,78** |
| | **4.43** | **32** | **4** | **32** | **16** | **16** | **16** | **32** | **8** | **1,57** |

MICs expressed in μg/mL

In conclusion, a library of sulfoxi- and sulfone-indoles was prepared as a second generation of new antibacterials based on the respective sulfides. Coumpound **EE29** was able to keep the activiy observed against Gram-positive bacteria but also demonstrated potency against Gram-negative ones. Besides its broad spectrum, **EE29** presented much better toxicity profile and lipophilicity (cLog P 4.43) which will allow us to use this substance in topic formulations to treat infections caused by the ESKAPE pathogens.

1. Silva, E.E.; Silveira, G.P. et. al. *RASBQ* **2016**, MED 052.
2. Batista, B.G.; Silveira, G.P. et. al. *Chemistry Select* **2017**, 2, 11926.

**Área: ORG** **Inscrição: 00490**

# Emprego de partículas magnéticas modificadas com calix[4]arenos como catalisadores heterogêneos para síntese de xantenonas

**Gabrielle Castro Souza (IC)[1,]*, Carlos Henrique Callegario Zacchi (PG)[1], Ângelo de Fátima (PQ)[1], Maria Helena de Araújo (PQ)[1].**

*E-mails: Gabicssouza1@hotmail.com (GCS) and adefatima@qui.ufmg.br (AF)

[1]*Departamento de Química, UFMG, Brasil.*

Palavras Chave: *Partículas magnéticas; calixarenos; catálise heterogênea; xantenonas.*

## Highlights

►Use of magnetic particles modified with calix [4] arenes as heterogeneous catalysts for xanthenone synthesis ►Otimization of xanthenone synthesis catalyzed by calix modified magnetic particles [4] arenes. ► Magnetic particles had a pronounced catalytic effect on the synthesis of xanthenone (50-86% yield).

## Resumo/Abstract

As xantenonas (Esquema 1) são compostos heterocíclicos com propriedades biológicas e medicinais notáveis, tais como antivirais, antiinflamatórios, atividades antiproliferativas e antibacterianas.[1] Para a síntese de xantenonas utilizam-se abordagens de reações multicomponentes (RMC), empregando um composto fenólico, aldeídos e compostos 1,3-dicarbonilícos sob efeito de um catalisador ácido.[1] As partículas magnéticas tem recebido destaque pelo fato de oferecerem "vantagens limpas" para a catálise de uma reação de síntese orgânica. Dentre as vantagens em se utilizar esse tipo de catalisador, pode-se destacar: superfície passível de modificações, facilidade de remoção do meio de reação, e posterior recuperação.[2] O ácido *p*-sulfônico calix[4]areno já foi empregado como catalisador na síntese de xantenonas em meio homogêneo. Tendo em vista as vantagens da catálise heterogênea e as partículas magnéticas, utilizou-se partículas magnéticas modificadas com calix[4]areno (CX4-NP) para a síntese de xantenonas.

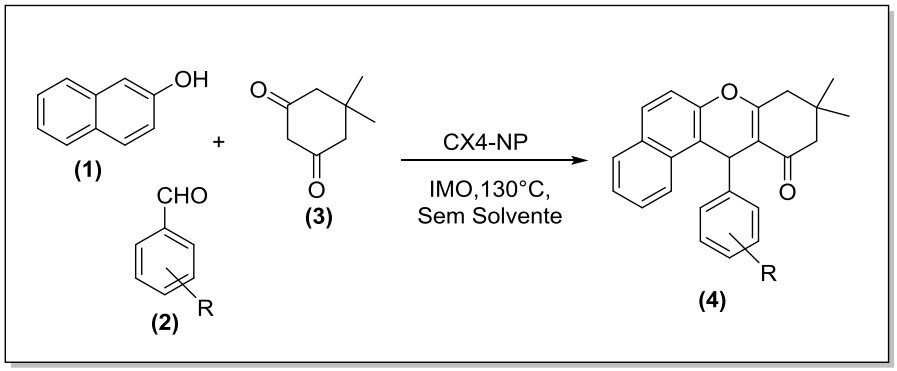


**Esquema 1.** Síntese das Xantenonas (**4**)

As condições de reação foram otimizadas (temperatura, solvente, catalisador) e apresentadas no Esquema 1. Os rendimentos ficaram entre 50-86%. O produto foi caracterizado por espectroscopia de RMN de $^{1}H$ e $^{13}C$ e DEPT-135. As próximas etapas do trabalho consistirão em utilizar diferentes aldeídos aromáticos e avaliar a atividade do catalisador quanto o reuso. Agradecimentos: FAPEMIG, CAPES e CNPq.

**Referências.**

[1] da Silva, D.L. *et al., Org. Biomol. Chem.* **2015**, *13*, 3280.
[2] Mojtahedi, M. M. *et al., Tetrahedron Lett.* **2009**, *50*, 2322.

**Área: ORG** **Inscrição:00523**

# Synthesis of quinolinyl lactones

**Ana Paula da Rocha Pissurno (PG),[1] Rosangela da Silva de Laurentiz (PQ),[1]**

**anapauladarochapissurno@gmail.com**

*[1]Departamento de Física e Química, UNESP - Universidade Estadual Paulista - Faculdade de Engenharia de Ilha Solteira.*

Palavras Chave: Organic Synthesis, Quinolinyl Lactones, Microwaves, Domino Reaction.

## Highlights

Synthesis of quinolinyl lactones via a domino reaction.
A fast and efficient synthetic route with the use of microwaves.

## Resumo/Abstract

The combination of pharmacophoric moieties of different bioactive substances can produce a new hybrid molecule with improved biological efficacy and affinity, a modified selectivity profile, and different and/or dual modes of action, and may reduce undesired side effects[1]. The combination of lactone and quinoline rings provides quinolinyl lactones, which are azo-analogues of arylnaphtalene lignan lactones. Despite the biological and synthetic importance of these compounds, there are few publications reporting efficient syntheses for obtained these azo-derivatives [2,3]. Therefore, the objective of this work was to synthesize, more efficiently, quinolinyl lactones through a domino reaction initiated by the MW-assisted reaction between tetronic acid (**1**) and 3,4-dimethoxy aniline (**2**) in acetonitrile. After the formation of the intermediate 4-azo-butenolide (**3**)[4], trifluoracetic acid and the aromatic aldehyde (**4**) were added at reactive vessel (Scheme 1). Derivatives **6a-e** were obtained in yield ranging from 80 to 90% (Scheme 1) in a total reaction time of 1 hour.

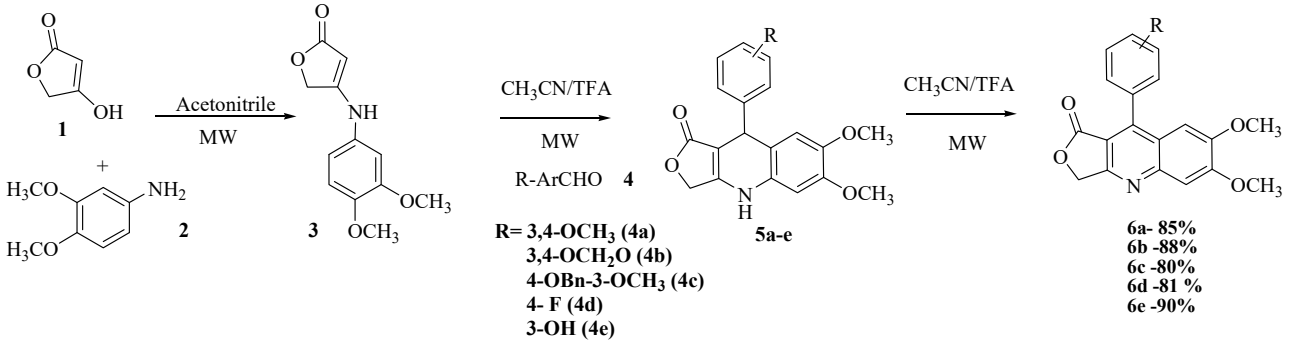


When only TFA was used, the reaction occurred slowly with yields lower than 40% and formation of several by-products. Other acids were also evaluated, but the results were not satisfactory. The use of the CH3CN/TFA mixture (2: 1) decreased the reaction time and favored the oxidation process of the intermediate 5. The advantage of this synthetic route over that described in the literature[3] is that it is not necessary use a strong oxidizing agent; moreover this route provide the desired product more quickly and efficiently.

[1] Viegas-Junior C. et.al. *Current Medicinal Chemistry*, **2007**, 14, 1829.
[2] Ogiku, T. et.al. *Tetrahedron Letters*, **1990**, 38, 5487.
[3] Hitotsuyanagi, Y. et.al. *Tetrahedron Letters,***1997**, 48, 8295.
[4]Pissurno, A. P. R; Laurentiz, R.S. *Synthetic Communications*, **2017**, 47, 1874.

FAPESP CAPES

**Área: ORG** **Inscrição: 00566**

# Use of humic substances as a biostimulant in *Solanum lycopersicum*

**Brenda H. S. L. Orlando (IC)[1] Dhaniella C. de B. Oliveira (IC)[2], Gleidson M. Pereira (PQ)[3]**

**brendasantosheloisa@gmail.com ; dhaniella.admm@gmail.com**

*[1]Undergraduate in Licentiate in Natural Sciences-Chemistry (UEPA); [2]Undergraduate in Licentiate in Natural Sciences-Chemistry (UEPA) [3]Environmental Engineering Department (UEPA)*

Palavras Chave: Biostimulant, Humic Substance, *Solanum lycopersicum,* Tomato

## Highlights

Humic substances contribute most of the cationic exchange of soils. The objective of this study was to verify the performance of humic substances as a biostimulant in *Solanum lycopersicum* seedlings.

## Abstract

Humic substances come from the chemical and biological degradation of organic residues and are naturally found in the soil. They play a key role in the production of plants because they can store lipids, carbohydrates, water and stimulant proteins to plant growth, nutrientes that are slowly released for plant nutrition, (Cunha, 2007). These substances can still absorb heat and alter soil temperature, encouraging germination, biological activity and consequently plant growth. Figure 1 represents the methodology used.

Figure 1.: Methodology

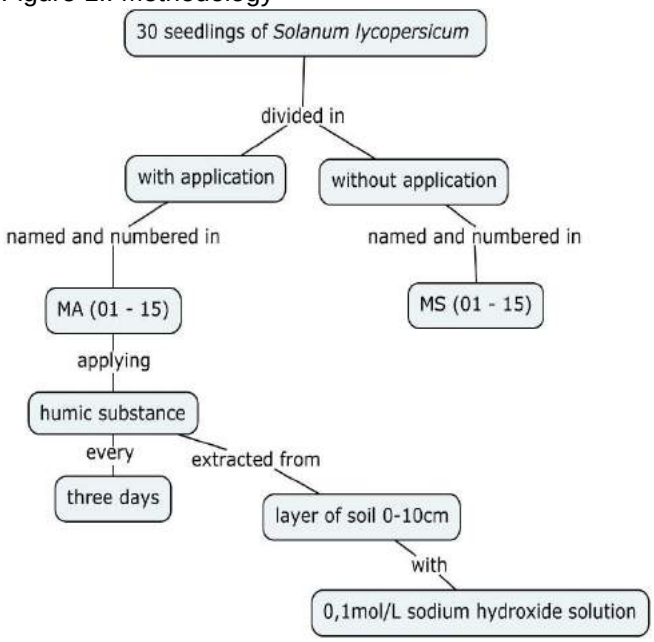


On the third day of seed development, the difference between MA and MS was already visible. According to Botero (2010) the humic substances are able to increase the speed of the germination rates of the plant, anticipating the vegetal growth of these. This early growth occurred in the work by the application of the substance, can be observed in figure 2 and 3, which compare the development of the MA and MS seedlings in the 3rd (Figure 2) and in the 14th day (Figure 3) in nursery.

Figure 2. MS germination (left) MA (right)

Figura 3: Leaves in MS (left) and MA (right)

Through the obtained results, it is verified that the humic substances have a great biostimulating potential, favoring the speed of growth of the *S. lycopersicum* (tomato) seedlings.

REFERENCES

BOTERO, W. G. (2010) Substâncias húmicas: interações com nutrientes e contaminantes. Tese (Doutorado em Química) Instituto de Química, Universidade Estadual Paulista. Araraquara-SP

CUNHA, T. J.; MADARI, B. E.; BENITES, V. M.; CANELLAS, L. P.; NOVOTNY, E.H.; MOUTTA, R. de O. TROMPWSKY, P. M; SANTOS, G. A. (2007). Fracionamento químico da matéria orgânica e características de ácidos húmicos de solos com horizonte a antrópico da Amazônia (Terra Preta). Revista ACTA Amazônica, vol. 37 (1), 2007: p.91-98

**Área: ORG** **Inscrição: 00582**

# Efficient Synthesis of *N*-phenethylarylthioamides by Kindler Reaction

**Paula Romanhi[1] (IC), Thiago da S. Pontes[1] (IC), Gustavo S. Proença[1] (IC), Cindy J. de Oliveira[1] (IC), Pedro R. Viegas[1] (IC), Beatriz G. de Castro[1] (IC), Luana A. Machado[2] (PG), Marcos C. de Souza[2] (PQ), Leandro F. Pedrosa[1]* (PQ).**

**paularomanhi@id.uff.br; leandropedrosa@id.uff.br**

[1] *Institute of Exact Sciences, Department of Chemistry, UFF, CEP 27213-145, Volta Redonda, RJ, Brazil.*

[2] *Institute of Chemistry, Department of Organic Chemistry, UFF, CEP 24020-141, Niterói, RJ, Brazil.*

Keywords: Kindler reaction, Thioamides, Multicomponent reaction.

## Highlights

A small library of arylthioamides was easily synthesized with good to excellent yields. The synthetic strategy involves greener approach for the Kindler Reaction under microwave irradiation.

## Resumo/Abstract

In recent years, the thioamides are often appeared in the literature as intermediates in medicinal chemistry and biological, but also in organic synthesis for the preparation of heterocycles containing sulphur.[1] Thioamides are traditionally prepared by thionation of the corresponding amides with phosphorus pentasulfide or Lawesson's reagent as thionating agent. Because sulfur is nontoxic, stable under ambient conditions, easy to handle, and readily available, its use in the preparation of thioamides is highly desirable as exemplified by the Kindler reaction, starting from aldehydes, elemental sulfur and amines.[2] This reaction has found in the past a bad reputation because of long reaction time, difficult conditions of reaction and formation of hydrogen sulfide toxic to humans and the environment. In the quest to find methods of catalytic synthesis responding to the new requirements of green chemistry, optimization conditions have made the Kindler reaction more attractive.[3] Therefore, the establishment of an effective, practical and green strategy for the formation of thioamides remains highly desirable. For this purpose, we have used an easy synthetic green approach to prepare *N*-phenethylarylthioamides (**3a-p**) by Kindler reaction (**Scheme 1**).

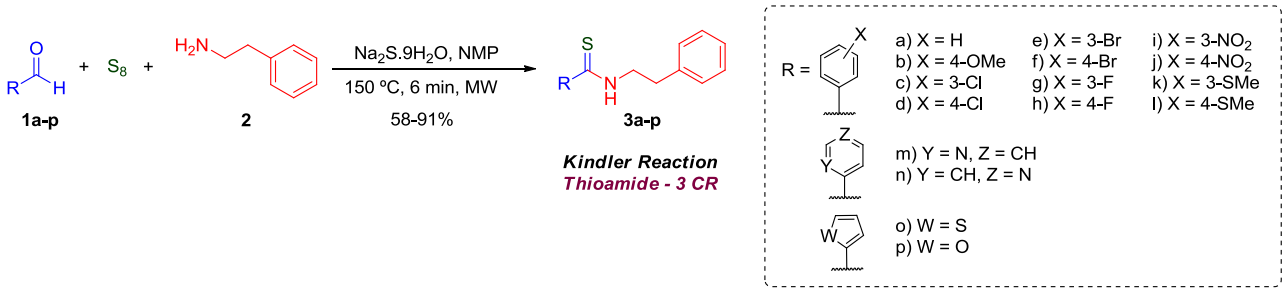


**Scheme 1.** Microwave-promoted three-component Kindler Reactions.

In this work we used the Kindler reaction under microwave irradiation using aryl aldehydes (**1a-p**), 2-phenylethylamine (**2**), sulfur, $Na_2S.9H_2O$ as catalyst and *N*-methylpyrrolidone (NMP) as solvent at 150°C for 6 minutes.[3] On average, aryl aldehydes substituted with electron-rich, neutral and deficient groups generated *N*-phenethylarylthioamides (**3a-p**) in 58-91% yields after recrystallization from boiling ethanol. Structures were confirmed by IR and NMR analysis. In summary, sixteen *N*-phenethylarylthioamides have been prepared with good to excellent yields. The protocol features broad substrate scope, nice yields, operability and commercially available and inexpensive raw materials, showing its practical synthetic value in organic synthesis.

REFERENCES

[1] Nguyen, T. B.; et al. *Org. Lett.*, **2012**, *14*, 4274-4277.

[2] X., Li; et al. *Asian J. Org. Chem.*, **2016**, *5*, 1353-1358.

[3] Priebbenow, D. L.; et al., *Chem. Soc. Rev.*, **2013**, *42*, 7870.

[4] Zbruyev, O. I.; et al. *J. Comb. Chem.* **2003**, 5, 145-148.

**Área: ORG** **Inscrição: 00604**

# Synthesis and luminescent properties of new naphthoquinoline lactones derivatives

**Fernanda A. Santos (PG),[1] Rosangela S. de Laurentiz (PQ).[1]**

**feh.amorim23@gmail.com**

*[1]Departamento de Física e Química, UNESP - Universidade Estadual Paulista - Faculdade de Engenharia de Ilha Solteira*

Palavras Chave: Naphthoquinoline, Multicomponent reaction, Microwave, Luminescence.

## Highlights

Naphthoquinoline lactones derivatives were obtained via microwave assisted MCR in excellent yields.
Naphthoquinoline lactones derivatives synthesized presented interesting luminescent properties.

## Resumo/Abstract

A series of naphthoquinoline lactones, with different R groups, were synthesized under microwave irradiation in two steps and total reaction time of 50 minutes. First step consisted in a multicomponent reaction (MCR) between tetronic acid (**1**), aromatic aldehyde (2) and amino anthracene (**3**). The use of ethanol and MW favors the subsequent oxidation step with DDQ, to provide derivatives **4,** without need for isolation of the dihydroquinolinic intermediate (Scheme 1).

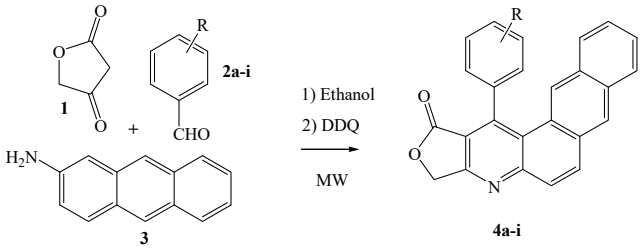


**Scheme 1.** Synthetic route to obtain derivatives **4a-i**

**Table 1.** Yield and Absorption and emission λ max (nm) for derivatives **4a-i**.

| Compound (R) | Yield | Abs | Emis |
|---|---|---|---|
| **4a: 3-$OCH_3$-4-OBn** | 91% | 325, 411 | 509 |
| **4b: 4-F** | 93% | 324, 347 | 497 |
| **4c: $SCH_3$** | 95% | 326, 408 | 506 |
| **4d: 3,4-$(OH)_2$** | 91% | 325, 350 | 598 |
| **4e: 3,4,5- $(OCH_3)_3$** | 94% | 325, 313 | 454 |
| **4f: 3-$OCH_3$-4-OH** | 91% | 324, 347 | 477 |
| **4g: 3-OH** | 90% | 325, 313 | 451 |
| **4h: 3-OCH3** | 96% | 325, 313 | 516 |
| **4i: 3,5-$(OCH_3)_2$-4-OH** | 94% | 324, 347 | 452 |

UV/Vis and fluorescence studies showed interesting luminescent properties of derivatives **4**. UV/Vis analysis showed that derivatives **4a-i** absorbed in the region of blue 300 - 400 nm (Table 1). No significant difference was observed in the absorption concerning the substituent of the benzyl ring. Regarding to the fluorescence data it is evident that the nature of the substituent significantly affects the intensity and wavelength of the emission band. The higher λ max emission (598 nm) was observed for compound **4d,** which has two hydroxyl groups as substituent. Irradiation of **4d** can result in ESIPT from the 4-OH to the nitrogen atom on the attached quinolinic ring to give the quinone, which can make an intramolecular hydrogen bond with 3-OH.[1] The formation of dimers of **4d** is also a hypothesis being studied.[2] The luminescent properties of **4d** are being investigated for possible application in OLEDs.

[1] Lukeman M, Burns MD, Wan P. Can. J. Chem., 89: 433-440, 2011.
[2] Naik LR, Math NN. Indian J. Pure Appl. Phys., 43, 743-749, 2005.

**Área: ORG** **Inscrição:00648**

# ESTUDO DE DERIVADOS PIRAZÓLICOS COMO INIBIDORES DE CORROSÃO

**Cinthia E. B. Maia (PG)*, [1] Gilberto A. Romeiro (PQ),[1] Marcia C. C. Velloso (PQ),[1] Guilherme C. Silva (IC),[1] e Mylenna V. Ferro (IC),[1]**

cbarrosmaia@gmail.com*; mvferro@id.uff.br

*[1]Universidade Federal Fluminense; Instituto de Química; Programa de Pós Graduação em Química; Outeiro de São João Batista, S/N; Valonguinho; Centro; Niterói; Rio de Janeiro; CEP:*

Palavras chave*: Corrosão, Inibidores, Derivados de pirazol.*

## Highlights

Pyrazole derivates that presented good anticorrosive activity have active centers linked to the S, O, N elements and to de phenyl group.

Inductive effects change anticorrosive activity.

## Resumo/Abstract

Corrosion processes are responsible for numerous losses, especially in the industrial sector. Inhibition of corrosive reactions can be controlled by various types of organic and inorganic compounds. Pyrazole, due to its molecular characteristics, has great potential for application in several, including as anticorrosive. In the present study, the corrosion capacity of 31 molecules derived from pyrazole was evaluated using experimental techniques and theoretical calculations. Of these, 17 were synthesized and evaluated as corrosion inhibitors using mass loss, linear polarization and scanning electron microscopy (SEM) assays. The metal used in the tests was ASTM A36 carbon steel in 1 mol.$L^{-1}$ solution of HCl (test solution). The experimental results showed that all pyrazole derivatives inhibit the corrosive process at 40 °C. However, the efficiency of the molecules decreases with increasing temperature to 50 ° C. In addition, it has been observed that the inhibition efficiency increases with increasing inhibitor concentration. Among the molecules studied, 1-(2-benzotiazoil)-3-methyl-pirazol-5-one (1), HOMO (2) and LUMO (3) representations, showed the highest inhibition efficiency of 94.95% to 400 mg.$L^{-1}$ in all used methods.

(1)

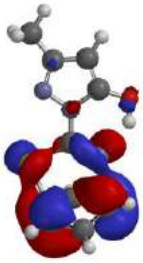

(2)

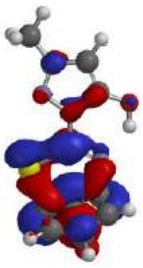

(3)

The Langmuir and Freudlich models were applied and it was observed that most of the inhibitors obey the Langmuir isotherm. SEM studies confirmed the formation of adsorbed films on the metal surface. Functional density theory (DFT) was used to understand the structure-efficiency relationship of inhibitors. It has been observed that withdrawal groups present in the molecules contribute more effectively than donor groups. A good relationship between theoretical and experimental results was obtained. Therefore, the gravimetric, electrochemical and theoretical results agree, showing that the inhibitors studied have a great anti-corrosion potential.

**Área: ORG** **Inscrição:00707**

# Synthesis of new *bis*-1,2,3-triazoles derivatives containing carboxylic acid groups: potential inhibitors of osteoclastogenesis

**Wallace J. Reis* (PG), Rosemeire B. Alves (PQ), Rossimiriam P. Freitas (PQ).**

**wallace.qui08@yahoo.com.br; rossipfreitas@gmail.com**

*Department of Chemistry, ICEx-UFMG, Av. Antônio Carlos, 6627, CEP 31270-901, Belo Horizonte, Minas Gerais.*

Palavras Chave:*Osteoporosis, 1,2,3-Triazoles, Carboxilic Acids, Osteoclastogenesis*

## Highlights

Synthesis of new *bis*-1,2,3-triazole-4-carboxylic acids; triazoles and long-chain acids as non-classical bioisosteres of phosphonates.

## Resumo/Abstract

Osteoporosis is a skeletal disease characterized by low bone mineral density, resulting in bones that are highly susceptible to fracture.[1] Osteoclasts are responsible of remodeling and bone resorption process, on this, therapies that inhibit the osteoclasts formation (osteoclastogenesis) are currently the focus of osteoporosis prevention. Studies has shown that 1,2,3-triazoles containing long-chain fatty acids inhibit the development *in vitro* of osteoclasts (Figure 1).[2]

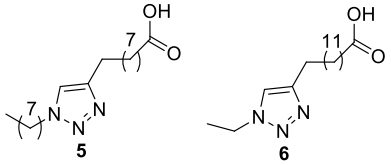


**Figure 1**: Long-chain triazolyl acids as inhibitors of osteoclastogenesis.

Recent investigation has indicated triazoles as non-classical bioisosteres of phosphonates,[3,4] and bisphosphonates dominate the antiresorptive therapy for osteoporosis. So, in this work we investigated the synthesis of new *bis*-1,2,3-triazole-derivatives containing carboxylic acids with potential application in the osteoclastogenesis process. Although all attempts for the click step involving compound **2a** were unsuccessful (under investigation), the compound **4a** was easily obtained with good global yield (Scheme 1).

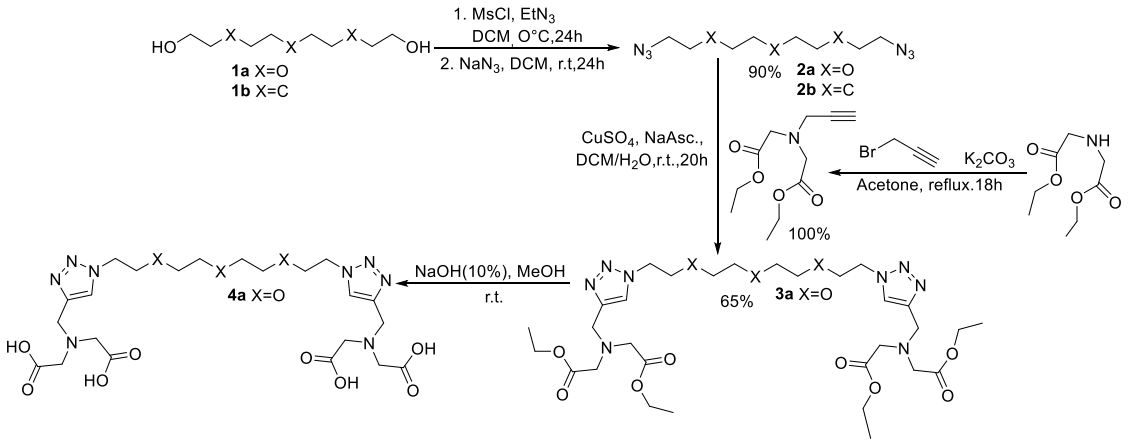


**Scheme 1**: Synthetic route for a new *bis*-1,2,3-triazole containing carboxylic acid groups.

Acknowledments: UFMG, Capes, CNPq and Fapemig

1 Silva, A. C. V.; da Rosa, M. I.; Fernandes, B.; Lumertz, S.; Diniz, R. M.; Damiani, M. E. F. R.; *Rev. Bras. Reumatol*. **2015**, 3, 223-228.
2 Marshall, J. A.; Lin, J.; Grey, A.; Reid, I. R.; Cornish, J.; Denny, W. A.; *Bioorg. Med. Chem*. **2013**, 21, 4112-4119.
3 Stroppa, P. H. F.; Antinarelli, l. M. R.; Carmo, A. M. L.; Gameiro, J.; Coimbra, E. S.; da Silva, A. D.; *Bioorg. Med. Chem*. **2017**, 25, 3034–3045.
4 Gontijo, V. S.; Espuri, P. F.; Alves, R. B.; de Camargos, L. F.; dos Santos, F. V.; Judice, W. A.; Marques, M. J.; Freitas, R. P.; *Eur. J. Med. Chem*. **2015**, 101, 24-33.

**Área: _ORG_____ Inscrição:__00724___**

# Oxone-Mediated Direct α-Hydroxylation of β-Dicarbonyl Compounds

**Marcelo V. Marques (TC),[1,2*] Marcos M. Peterle (PG),[1] Marcus M. Sá (PQ)[1]**

[1]*MESOLab, Departamento de Química, UFSC, Florianópolis/SC*
[2]*Lab. de Ciências, Departamento de Desenvolvimento Educacional, IFC, Fraiburgo/SC* marcelo.marques@ifc.edu.br

Keywords: *α-Hydroxylation, α-Hydroxy malonates, α-Hydroxy-γ-lactone, Oxone, Green chemistry*

## Highlights

A simple method to perform the α-hydroxylation of functionalized 1,3-dicarbonyl compounds was developed using Oxone in aqueous medium, which was successfully applied in the racemic synthesis of harzialactone.

## Abstract

During the studies dealing with the base-mediated epoxidation of γ,δ-unsaturated malonates **1** with Oxone, *en route* to functionalized cyclopropanecarboxamides[1] and γ-lactones,[2] we found that epoxide **2a** could be efficiently prepared from **1a** in an EtOAc-$H_2O$ biphasic system, while the α-hydroxylated epoxide **3a** was obtained under homogeneous conditions (Scheme 1). Due to the synthetic potential of this transformation,[3] we proceeded with further studies to establish the scope and limitation of the Oxone-mediated α-hydroxylation of malonates and γ-lactones. In this work, we report a green route to α-hydroxy-β-dicarbonyl compounds in aqueous medium under mild alkaline conditions (phosphate buffer, pH 8) at r.t.

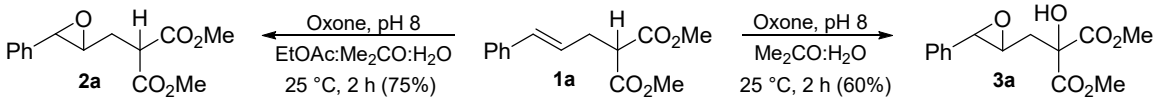


**Scheme 1.**

The α-hydroxylation of 1,3-dicarbonyl compounds **1-2** were performed by combining Oxone and basic medium, with yields ranging from 33 to 90% (Scheme 2). Malonates containing unsaturation (**1a** and **1b**, R = allyl) suffered overoxidation in the presence of Oxone (2.5 equiv) to give the hydroxylated epoxides **3a** and **3b** in good yields. The direct α-hydroxylation of epoxy malonates **2a** and **2b** was also performed to furnish **3a** and **3b** cleanly and in yields comparable to the one-pot method from **1**. Unsubstituted malonates **1c,d** were also hydroxylated, but the isolated yields were lower possibly due to losses during aqueous work-up.

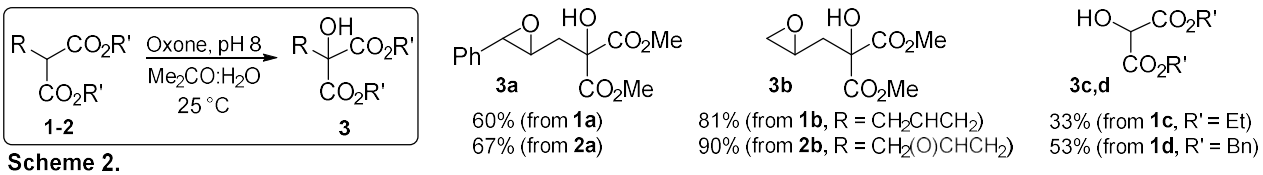


**Scheme 2.**

The α-hydroxylation was successfully employed in the racemic synthesis of harzialactone A (**6a**), a natural product from marine sponge.[4] Thus, α-hydroxylation of lactones **4a,b** followed by microwave-assisted Krapcho descarboxylation of **5a,b** led to the expected γ-lactones **6a,b** as mixtures of *syn:anti* diastereomers (Scheme 3).

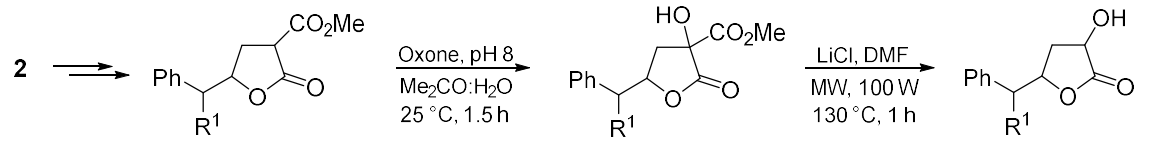


**Scheme 3.**

**4a** $R^1$ = H
**4b** $R^1$ = OH

**5a** $R^1$ = H (76%, dr = 3:1)
**5b** $R^1$ = OH (47%, dr = 2:1)

**6a** $R^1$ = H (49%, dr = 3:1)
**6b** $R^1$ = OH (24%, dr = 2:1)

References

[1] Marques, M. V.; Sá, M. M. *J. Org. Chem.* **2014**, *79*, 4650.
[2] Oliveira, C. C.; Marques, M. V.; Godoi, M. N.; Regiani, T.; Santos, V. G.; Santos, E. A. F.; Eberlin, M. N.; Sá, M. M.; Correia, C. R. D. *Org. Lett.* **2014**, *16*, 5180.
[3] Christoffers, J.; Baro, A.; Werner, T. *Adv. Synth. Catal.* **2004**, *346*, 143.
[4] Pawar, V. U.; Ghosh, S.; Chopade, B. A.; Shinde, V. S. *Bioorg. Med. Chem. Lett.* **2010**, *20*, 7243.

**Área: ORG** *(Inserir a sigla da seção científica para qual o resumo será submetido. Ex: ORG, BEA, CAT)*

**Inscrição: 00761** *(Inserir o número de inscrição do autor que fez a submissão)*

# Dienone-amide produced by the bioluminescent mushroom *Neonothopanus gardneri*

**Maria D. D. A. Oliveira[1*](PG); Teresinha J. A. S. Andrade[2,*](PQ); Dulce Helena S. Silva[3] (PQ); Cassius V. Stevani[5] (PQ); Joaquim S.C. Junior[4] (PQ); Antonia M.G.L. Citó (PQ)[1]**

*[1]maralves013@gmail.com; [2]aguiarte10@gmail.com* ; dhsilva@iq.unesp.br*

[1] *Federal University of Piauí, Department of Chemistry, Campus Ministro Petrônio Portela, Teresina, PI, Brazil.*

[2] *Federal Institute of Maranhão, Department of Chemistry, Campus Presidente Dutra, MA, Brazil.*

[3] *Institute of Chemistry - Sao Paulo State University, Araraquara, SP, Brazil*

[4] *Institute of Chemistry, University of Sao Paulo, Sao Paulo, SP, Brazil*

[5] *Federal Institute of Piauí, Department of Chemistry, Campus Central, Praça da Liberdade, Teresina, PI, Brazil.*

Keywords: *Neonothopanus gardneri*, bioluminescent mushroom. Secondary metabolites. Dienone-amide.

## Highlights

Isolation and structural elucidation of a novel long chain dienone-amide from the luminescent mushroom *Neonothopanus gardneri,* widespread in Cocais Forest, a transitional biome between the Amazon Forest and Caatinga.

## Abstract

The acetonitrile fraction (MeCN-Ng, 2.52 g) obtained from *Neonothopanus gardneri* mushrooms was fractionated by reverse phase C18 flash chromatography eluted with $H_2O$:$CH_3OH$ gradient, and yielded eight subfractions (Ng1-Ng8). Subfraction Ng3 (165 mg) was chromatographed by RP-HPLC-UV and afforded a long chain dihydroxy-dienone amide (**1**, 4.1 mg), obtained as a dark yellow solid. Its UV-Vis spectrum showed $\lambda_{max}$ 273 nm, whereas IR data evidenced bands for hydroxy groups (3449 $cm^{-1}$), carbonyl group (1731 $cm^{-1}$) and $sp^3$ C-H bonds (2922-2853 $cm^{-1}$). The $^1$H NMR spectrum and HSQC experiment showed signals for a terminal methyl at δH 0.93 (δC 12.9), two hydroxymethine hydrogens at δH 3.52 (δC 73.9) and δH 4.10 (δC 74.6), in addition to three broad double doublets at δH 7.30 (δC 142.8), δH 6.33 (δC 143.8) and δH 6.51 (δC 129.1), and one broad doublet at δH 6.23 (δC 129.0) for olefinic hydrogens. Additional signals between δH 2.62 and δH 1.35 appeared as double triplets, triplets or multiplets and were assigned to methylene hydrogens of compound **1**. The $^{13}$C NMR and DEPT135 spectra associated with HMBC and HSQC experiments evidenced signals for two carbonyls at δC 202.4 (C 13) and 176.3 (C1), six methynes, nine methylene and one methyl carbon, consistent with the proposed structure for compound **1**. This is the first report in the literature on the chemical investigation of fruiting bodies of *N. gardneri*, which resulted in the isolation and identification of the new 6,7-dihydroxy-13-oxo-octadeca-9,11-dienamide.

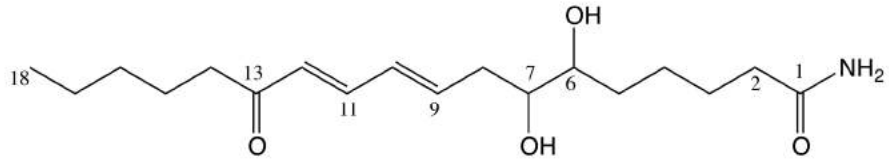


**1**

[1] CAPELARI, M.; DESJARDIN, D.E.; PERRY, B.A.; ASAI, T.; STEVANI, C.V. *Neonothopanus gardneri:* a new combination for a bioluminescent agaric from Brazil. Mycologia, v. 103, p. 1433–1440, 2011.

[2] KIRK, P.M., CANNON, P.F., MINTER, D.W. & STALPERS, J.A. *Ainsworth & Bisby's Dictionary of the Fungi*. Ed.10, CABI Europe – UK, 2008,771.

**Área: ____ORG____ Inscrição:____00846____**

# Synthesis of polycatenar photoisomerizable liquid crystals based on an expanded acylhydrazone core

**Wilson A. De Oliveira (IC)[1], Eduard Westphal (PQ)[1*]**

**Wilson.2.0.wi@gmail.com; eduardw@utfpr.edu.br**

[1]*Departamento Acadêmico de Química e Biologia, UTFPR*

Palavras Chave: *Acylhydrazones, Liquid crystals, Photoisomerization, Polycatenar, Organic Synthesis*

## Highlights

Five new molecules based on an expanded acylhydrazone core were synthesized and show *E-Z* photoisomerization. The liquid crystalline behavior is strongly dependent on the molecular structure.

## Abstract

Liquid Crystals (LC) are known as the fourth state of matter, showing simultaneously properties from the solid (organization and anisotropy) and the liquid state (fluidity), besides unique characteristic not found in both.[1] This makes these materials attractive to a wide variety of applications, like in displays, smart windows, thermometers, photovoltaic cells, semiconductors, among many others.[1,2] Acylhydrazone is a functional group that shows reversible *E-Z* photoisomerization under the incidence of UV light[3] and has not been much explored in the synthesis of LC. Therefore, the properties of these new liquid cristalline materials may be reversible modulated from a macroscopic level. In order to continue our investigations on how changes in molecular structure affects the properties of these materials, five new compounds derived from an expanded acylhydrazone core were synthesized (Figure 1). The molecules differ on the number and position of long alkoxy chains. All compounds were synthesize in good yield and had their structure and purity confirmed by NMR. TGA measurements show that they are stable up to 250 °C, while POM (Figure 2), DSC, XRD and SAXS (using Synchrotron radiation) confirm their liquid crystalline behavior. Compound **1-HDZES-1** shows a SmC mesophase between 198 °C and 212 °C while **3-HDZES-3** shows a $Col_h$ mesophase, ranging from below the room temperature until 118 °C. This strong difference in the molecular arrangement with the change on the number of alkoxy chains indicates an interesting polycatenar behavior. Preliminary studies confirm photoisomerization in chloroform solution.

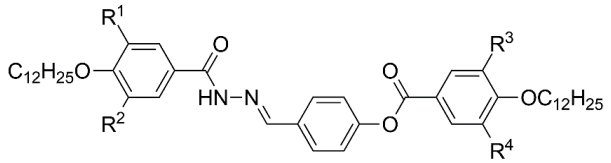


| | $R^1$ | $R^2$ | $R^3$ | $R^4$ |
|---|---|---|---|---|
| **1-HDZES-1** | H | H | H | H |
| **1-HDZES-3** | H | H | $OC_{12}H_{25}$ | $OC_{12}H_{25}$ |
| **3-HDZES-1** | $OC_{12}H_{25}$ | $OC_{12}H_{25}$ | H | H |
| **3-HDZES-3** | $OC_{12}H_{25}$ | $OC_{12}H_{25}$ | $OC_{12}H_{25}$ | $OC_{12}H_{25}$ |
| **2-HDZES-2** | H | $OC_{12}H_{25}$ | $OC_{12}H_{25}$ | H |

**Figure 1.** Structure of synthesized molecules.

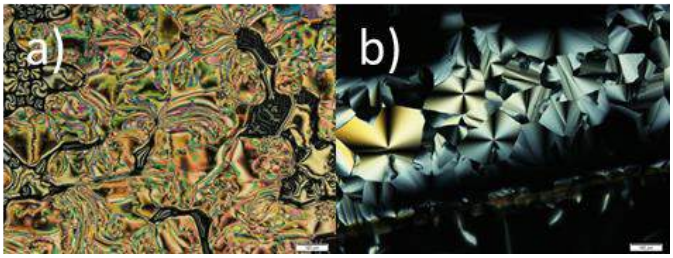


**Figure 2.** Textures observed by POM for the (a) SmC mesophase of **1-HDZES-1** at 207 °C and (b) $Col_h$ mesophase of **3-HDZES-3** at 115 °C.

[1] R.J. Bushby, S.M. Kelly and M. O'Neill, Liquid Crystalline Semiconductors, Springer, The Netherlands, 2013.
[2] Goodby, J.W.; Collings, P.J.; Kato, T.; Tschierske, C.; Gleeson, H. F.; Raynes, P., eds. Handbook of Liquid Crystals. 2nd ed. 2014.
[3] Su, X.; Aprahamian, I. Chemical Society Reviews, 43(6), 1963-1981, 2014.

**Área:** *ORG* **Inscrição:** 00888

# Laccase-catalyzed synthesis of dimers from 2,6-DMP: Optimization of TMBP synthesis and evaluation of its antioxidant action in biodiesel

**Jéseka G. Schirmann (PG),[1*] Robert F. H. Dekker (PQ),[2] Dionísio Borsato (PQ),[1] Aneli M. Barbosa-Dekker (PQ).[1]**

**jeseka_6@hotmail.com**

[1]*Departamento de Química, UEL;* [2]*UTFPR-Londrina*

Palavras Chave: *Botryosphaeria rhodina MAMB-05, laccase, biocatalysis, antioxidant action*

## Highlights

Selective synthesis of 2,6-DMP dimers by *B. rhodina* laccase
The laccase catalyzed TMBP synthesis was optimized by design matrix
TMBP as an antioxidant for biodiesel and its efficacy in relation to BHT

## Abstract

Laccases are multicopper oxidative enzymes catalyzing the reduction of molecular oxygen to water with the simultaneous abstraction of an electron from a donor substrate in the reduced form, which in turn, is oxidized.[1] Laccases catalyze the synthesis of different phenolic compounds. The ascomyceteous fungus, *Botryosphaeria rhodina* MAMB-05 is ligninolytic, and a good producer of laccases.[2] The objective of this work was to evaluate the potential of laccase as a biocatalyst for organic synthesis. This enzyme was used to selectively synthesize three dimeric products (Fig. 1) from 2,6-dimethoxyphenol (2,6-DMP). The variables that most influenced the enzymatic synthesis of the dimer, TMBP (**II**) by laccase were chosen, and a factorial-design was developed to optimize the synthesis of this dimer (Fig. 2). TMBP produced was evaluated as an antioxidant agent for biodiesel, and was compared to the commercial biodiesel antioxidant BHT. The evaluation of TMBP as an antioxidant for biodiesel was tested by the accelerated method (EN14112), by measuring the oxidative stability of biodiesel samples. The induction period (IP) value of a biodiesel sample containing TMBP was of 6.67 h, while the control sample showed an IP of 3.67 h. The induction period of the sample containing TMBP was superior to the minimum of 6.0 h established by legislation (EN 14214), attesting the efficacy of antioxidant action of TMBP. The antioxidant action of BHT resulted in an IP value of 6.28 h. TMBP could be a new alternative for this industrial application.

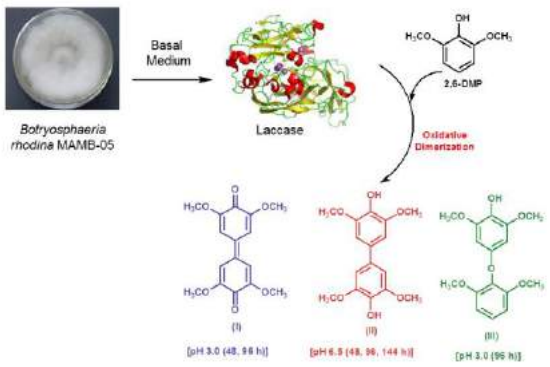


**Figure 1.** *Botryosphaeria rhodina* MAMB-05 laccase-catalysed selective synthesis of dimeric products from2,6-DMP according to pH and reaction time.

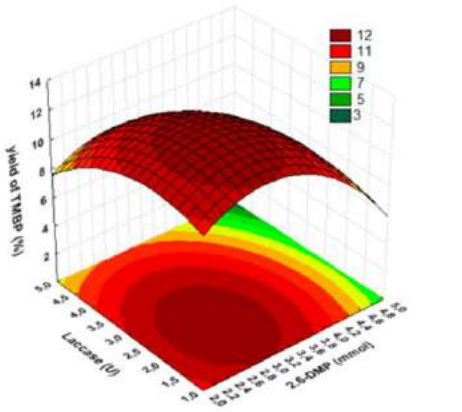


**Figure 2.** Three-dimensional surface response for the synthesis of TMBP by laccase. Time was fixed at 120 h, and the reaction was carried out at pH 6.5.

[1] Cannatelli, M.D., Ragauskas, A.J., The Chemical Record, 17, 2017, 122-140.
[2] Dekker, R.F.H., Barbosa, A.M., Enzyme and Microbial Technology, 28, 2001, 81-88.

**Área: ORG** **Inscrição: 00939**

# Síntese e Estudo de Cristais Líquidos Assimétricos Derivados do Heterocíclico 2,1,3-benzotiadiazol

**Eunice C. de Jesus (IC), Thaiane O. B. Silva (IC), Elias R. Silva (PG), André A. Vieira(PQ)***

nicecerqueira10@gmail.com ; vieira.andre@ufba.br*

*Instituto de Química, Universidade Federal da Bahia-UFBA, 40170-110, Salvador, BA, Brasil*

Palavras Chave: *Cristais líquidos, Assimetria, Luminescência, 2,1,3-Benzotiadiazol.*

## Highlights

Synthesis and Study of Asymmetric Liquid Crystals Derived from the 2,1,3-benzothiadiazole: A new series of asymmetric molecules able of presenting mesomorphism was synthesized and characterized. The final compounds had their thermal and photophysical properties investigated.

## Resumo/Abstract

Uma ampla variedade de cristais líquidos (CL) funcionalizados tem sido sintetizados e investigados afim de explorar suas aplicações em dispositivos opto-eletrônicos.[1] O mercado desses materiais tem crescido rapidamente devido as aplicações em células fotovoltaicas orgânicas (OPVs), diodos emissores de luz orgânicos (OLEDs), transistores orgânicos de efeito de campo, nanopartículas fluorescentes e sensores.[2]
O heterociclo 2,1,3-benzotiadiazol (BTD) é um núcleo muito utilizado na construção de CL, pois confere estabilidade térmica e química as moléculas, além de conferir elevada luminescência em sistemas pi-conjugados. Contudo, observa-se que a maior parte dos CL derivados do BTD reportados na literatura são simétricos.[3] Sendo assim, neste trabalho apresentamos a síntese, caracterização e estudo de uma série inédita de CL assimétricos luminescentes derivados do heterociclo BTD. O projeto almeja analisar o efeito de grupos doadores e retiradores de elétrons nas propriedades fotofísicas, além de analisar o impacto da assimetria nas propriedades térmicas. A rota sintética utilizada na preparação dos compostos-alvo (**7a-d**) é apresentada na **Esquema 1.**

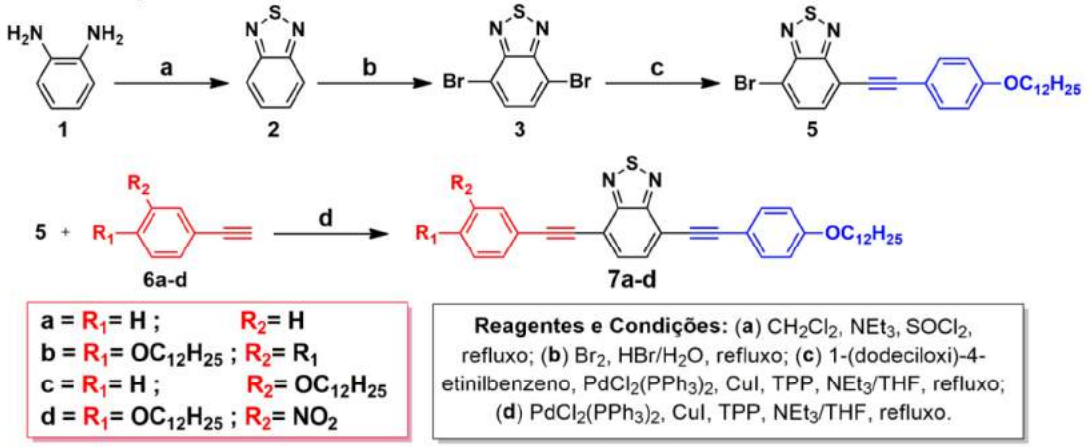


**Esquema 1.** Rota sintética utilizada para obtenção das moléculas-alvo **7a-d.**

Todas as moléculas finais (**7a-d**) e intermediários foram caracterizados por espectrometria de IV e RMN de $^{1}H$ e $^{13}C$. Os estudos para determinação das propriedades térmicas de **7a-d** foram realizados por microscopia óptica de luz polarizada (MOLP) e calorimetria de varredura diferenciada (DSC). As propriedades fotofísicas foram investigadas a partir da determinação de valores de absorbância, fluorescência, rendimento quântico e solvatocromismo para os compostos finais. Como resultado desses estudos observamos a presença da fase cristal líquido nesses materiais e a forte luminescência característica do BTD.

**Referências:** [1] Wöhrle, T., *Chem. Rev.* **2016**, v.*116*, p.1139–1241. [2] Frizon, T. E. A., *Dye. Pigment.* **2016**, v.*135*, p.26–35. [3] Aguiar, L. de O., *Liq. Cryst.* **2018**, v.*45*, p.49–58.

**Área: ORG**
*(Inserir a sigla da seção científica para qual o resumo será submetido. Ex: ORG, BEA, CAT)*

**Inscrição: 00965**
*(Inserir o número de inscrição do autor que fez a submissão)*

# Cleaving Paraoxon with Hydroxylamine: Ammonium Oxide Isomer Favors a Frontside Attack Mechanism

**Marcelo F. Lima (PQ)[1]*, Priscilla Amanda Urbano da Cruz (IC)[2], Maria Eduarda Camilo Fernandes (PG)[1], Carlos Polaquini (IC)[1], Elizabeth L. M. Miguel (PG)[3], Josefredo R. Pliego Jr. (PQ)[3], Leandro Scorsin (PG)[4], Bruno Surdi de Oliveira (IC)[4], Faruk Nome (PQ)[4]**

**mflima@sjrp.unesp.br**

*[1]Laboratório de Química Bio-orgânica Ambiental, Departamento de Química e Ciências Ambientais; IBILCE, UNESP, São José do Rio Preto-SP, Brasil. [2]Câmpus Universitário do Araguaia, UFMT – Universidade Federal de Mato Grosso, Instituto de Ciências Exatas e da Terra, Laboratório de Química Bio-orgânica do Araguaia, Barra do Garças-MT, Brasil. [3]Departamento de Ciências Naturais, Universidade Federal de São João del-Rei, São João del-Rei-MG, Brasil. [4]Departamento de Química, Laboratório de Catálise e Fenômenos Interfaciais, Universidade Federal de Santa Catarina, Florianópolis-SC, Brasil.*

Keywords: Paraoxon, Hydroxylamine, Dephosphorylation, Mechanism, Frontside attack.

## Highlights

In the study of the mechanisms for the dephosphorylation of paraoxon by hydroxylamine we have found out that there is a frontside attack alternative route still unexplored in the literature.

## Resumo/Abstract

A detailed molecular understanding of the mechanisms of the dephosphorilation of phosphate triesters due to nucleophilic attack can be very useful for the design of nucleophiles that are more efficient.[1] In this work, we report a combined experimental and theoretical study[2] of the reaction of hydroxylamine with paraoxon. The profile of the reaction rate according to pH was determined, and it was found that protonated hydroxylamine was unreactive, while the neutral form reacted via the zwitterion tautomer, with an overall free energy barrier of 23.0 kcal $mol^{-1}$. The anionic form was the most reactive, with a free energy barrier of 18.1 kcal $mol^{-1}$. Computational calculations revealed two mechanisms for the nucleophilic attack of the zwitterion form: the usual backside attack and a new frontside attack mechanism. The former proceeded according to a two-step associative mechanism, while the latter was a concerted single-step mechanism involving attack of the hydroxylamine oxygen on the phosphorus center (Figure 1) and interaction of the $NH_3^+$ group with the oxygen of the P=O group.

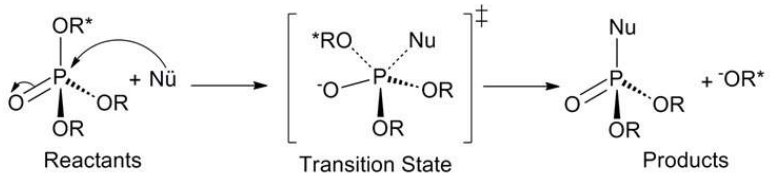


Figure 1. Proposed reaction mechanism for the dephosphorylation of paraoxon by hydroxylamine under neutral pH conditions.

The calculations indicated that the free energy barrier for the frontside attack was more favorable than the backside attack by 3 kcal $mol^{-1}$, supporting the notion that the observed reaction occurs by frontside attack. The reaction with the anionic hydroxylamine form occurred according to a single-step concerted ANDN mechanism.

References:

1- Kirby, A. J.; Nome, F. Accounts of Chemical Research. 2015, 48, 1806.
2- de Lima, G. F.; Pliego Jr, J. R.; Duarte, H. A. Chemical Physics Letters. 2011, 518, 61.

**Área: ORG** **Inscrição: 00982**

# Study of sulfamide and its *N,N'*-diindolyl derivative as anion carriers

**Matheus P. Freitas (PQ),[1] João G. P. Mendonça (PG),[1,2] Rodrigo A. Cormanich (PQ),[3] Sergio A. Fernandes (PQ)[2]**

**matheus@dqi.ufla.br; joaoquimica@live.com; cormanich@iqm.unicamp.br; santonio@ufv.br**

*[1]Departamento de Química, UFLA; [2]Departamento de Química, UFV; [3]Instituto de Química, UNICAMP*

Palavras Chave: sulfamida, carreadores de ânions, RMN, cálculos teóricos.

## Highlights

$^1$H NMR data showed that sulfamide binds to anions. *N,N'*-diindolylsulfamide was calculated to capture anions through hydrogen bonds. The binding strength increases according to $Cl^-<H_2PO_4^-<AcO^-<F^-$.

## Abstract

Anion carriers play an important role in phase transfer processes and membrane cell permeation. Sulfamide and *N,N'*-diindolylsulfamide (**DIS**), Figure 1, can bind anions ($X^-$) through hydrogen bonds and then be employed in anion transportation. Since the p*K*a of methanesulfonamide in DMSO (17.5) is lower than that for acetamide and urea (25.5 and 26.9, respectively),[1] the high acidity of the sulfamide hydrogens can improve the ligand-anion interactions if compared to the known *N,N'*-diindolylurea (**DIU**) and *N,N'*-diindolylthiourea (**DIT**).[2]

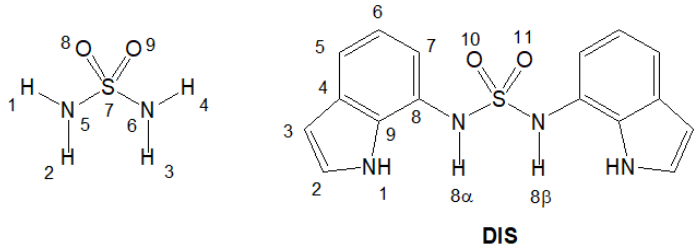


**Figure 1.** Chemical structures of sulfamide and its *N,N'*-diindolyl derivative (**DIS**).

Sulfamide was mixed with an anion source (as tetrabutylammonium salt) in 1:1 proportion and then analyzed by $^1$H NMR spectroscopy in DMSO-$d_6$ solution (*ca.* 20 mg $mL^{-1}$). **DIS** was theoretically evaluated: possible geometries for the **DIS**-$X^-$ complexes were optimized at the ωB97X-D/6-311++g(d,p) level, the same method applied for the natural bond orbital (NBO) calculations, and the quantum theory of atoms in molecules (QTAIM) calculations were carried out using the wavefunctions obtained from the optimizations.

For sulfamide, there is a broadening in the $^1$H NMR signal ($Cl^-<H_2PO_4^-<AcO^-<F^-$) as it complexes to the anion; actually, the proton signal for the sulfamide-$F^-$ complex disappeared, probably due to deprotonation by the anion. On the other hand, **DIS** is expected to bind anions without deprotonation of H(N) due to an influence of the indolyl groups, such as in the analogous **DIU** and **DIT** compounds, which have already been tested elsewhere as anion carriers.[2] Indeed, theoretical calculations showed that **DIS** interacts with anions through hydrogen bonds. Both the NBO (by means of the $n_{X^-} \rightarrow \sigma^*_{N\text{-}H}$ interaction energy) and QTAIM (by means of the charge on H(N) hydrogens engaged in hydrogen bonds) analyses indicate that the **DIS**:$X^-$ interaction strengthens according to the tendency observed above for the sulfamide-anion complexes ($Cl^-<H_2PO_4^-<AcO^-<F^-$).

Overall, **DIS** appears to be a prospective anion carrier with promising applications in phase transfer processes and membrane cell permeation.

**References**

1. D. H. Ripin and D. A. Evans, Evans pKa Table, available at the http://evans.rc.fas.harvard.edu/pdf/evans_pKa_table.pdf
2. D. Makuc, J. R. Hiscock, M. E. Light, P. A. Gale, J. Plavec, *Beilstein J. Org. Chem.* **2011**, *7*, 1205.

* Authors are grateful to FAPEMIG, FAPESP, CAPES and CNPq for the financial support of this research, for a scholarship and fellowships.

**Área: ORG** **Inscrição: 01021**

# Synthesis of aryl-amides derived from L-cysteine – potential double inhibitors of HIV1-PR and renin

**Aline S. Serralbo (IC)[1], Luiz S. Longo Jr. (PQ)[2], Adriana K. C. A. Reis (PQ)[1*]**

**aline_sserralbo@hotmail.com; adrianakarla.amorim@gmail.com**

[1]*Departamento de Química, Universidade Federal de São Paulo*
[2]*Departamento de Ciências Farmacêuticas, Universidade Federal de São Paulo*

Keywords: *Organic Synthesis, Arylamides, Coupling Reagents, NMR, Protease Inhibitors.*

## Highlights

In this work, functional and structural studies of HIV-1 and renin proteases were combined, allowing the design of new compounds that are potential inhibitors of both proteases, in order to eliminate side effects such as hypertension and facilitate the treatment of AIDS. The aim of this study was to synthesize two series of arylamides with structural similarity to Nelfinavir (a drug mainly used in antiretroviral therapy), using alternative methodologies to those described in the literature.

## Abstract

Polytherapies that rely on the combined use of reverse transcriptase inhibitors and HIV protease inhibitors are the most effective currently known AIDS chemotherapies. However, patients receiving Antiretroviral Therapies (ART) are prone to develop hypertension, among other undesirable side effects caused by the use of these medications. HIV-1 protease and renin are aspartic proteases, a small group of proteins that share common resources, which play major roles in the evolution of AIDS and hypertension, respectively. Structural and functional features common to HIV-1 protease and renin have led us to design dual-potential inhibitors, synthesizing new arylamides with structural similarity to the commercial antiretroviral agent Nelfinavir, aiming to provide these compounds with the capacity to inhibit these proteases. Two series of arylamides were prepared *via* coupling reactions of benzoic acids (series **I**) and anilines (series **II**) with *S*-trityl-*L*-cysteine derivatives (Scheme 1).[1,2] These methodologies proved to be efficient with relatively clean reactions; however some of the procedures need to be optimized. The molecular structures of the compounds were characterized by $^{1}H$, $^{13}C$ NMR spectroscopic data and two-dimensional techniques.

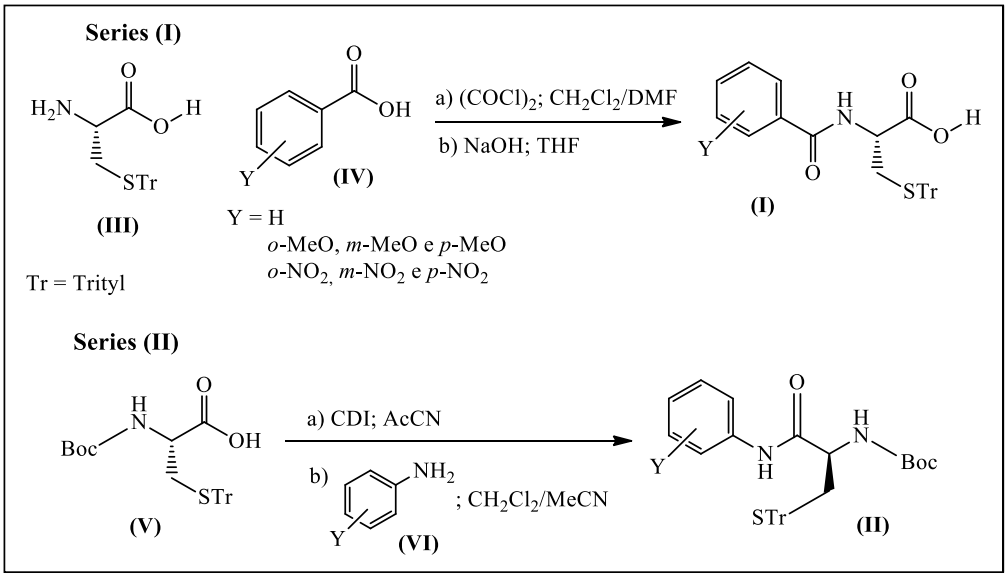


**Scheme 1.** Simplified routes of synthesis of series (**I**) and (**II**) of arylamides.

**References: 1.** PEARSON, A. J.; ROUSH, W. R. ***Handbook of Reagents for Organic Synthesis: Activating Agents and Protecting Groups***, p. 333, 335-338, 370–373, 1999; **2.** PATEL, K. RINKU et al. ***Asian J. Pharm. Res.*** 2013; v. 3, 3, p. 125-131.

**Área: ORG** **Inscrição: 01122**

# Selective functionalization of N-heterocyclic substrates using the TMPLi/$ZnCl_2$ system

**Rodolfo Hideki Vicente Nishimura (PG), Valter Eduardo Murie (PG), Giuliano Cesar Clososki (PQ)*.**

**gclososki@fcfrp.usp.br.com**

[1]*Núcleo de Pesquisas em Produtos Naturais e Sintéticos, Universidade de São Paulo, Ribeirão Preto – SP, Brasil*

Palavras Chave: *N-heterocycles, Selective functionalization, Metalation, Organozinc compounds, Verubulin*

## Highlights

Selective metalation of sensitive N-heterocycles studied, Reactivity with different electrophiles evaluated, Methodology to the synthesis of analogs of antitumoral verubulin developed.

## Resumo/Abstract

According to recent analyses of the US Food and drug administration, 59% of the approved drugs contain a nitrogen heterocycle.[1] Lithium amides play an important role in the directed functionalization N-heterocycles, however, the high reactivity of organolithium reagents is a drawback when dealing with substrates bearing sensitive functional groups. In addition, a number of N-heterocyclic rings are prone to nucleophilic attack of reactive organometallic species leading to undesirable products. The complexation of organic substrates with $ZnCl_2$ prior to the addition of the base has already proved to be an interesting strategy to overcome this problem since the corresponding organozinc derivatives are much more stable.[2] Given our interest in the functionalization of aromatic and heterocyclic compounds with organometallic reagents,[3] herein we wish to report the selective metalation of a number of important N-heterocyclic compounds using the base TMPLi (TMP = 2,2,6,6-tetramethylpiperamidyl) in the presence of $ZnCl_2$.2LiCl. Interestingly, after reaction of the organozinc intermediates with different electrophiles, the functionalized derivatives, some of them new compounds, were obtained in reasonable to good yields. Finally, application of the strategy to synthesize an analogue of antitumoral Verubulin illustrates that this approach has a great potential for application in Medicinal Chemistry (Scheme 1).

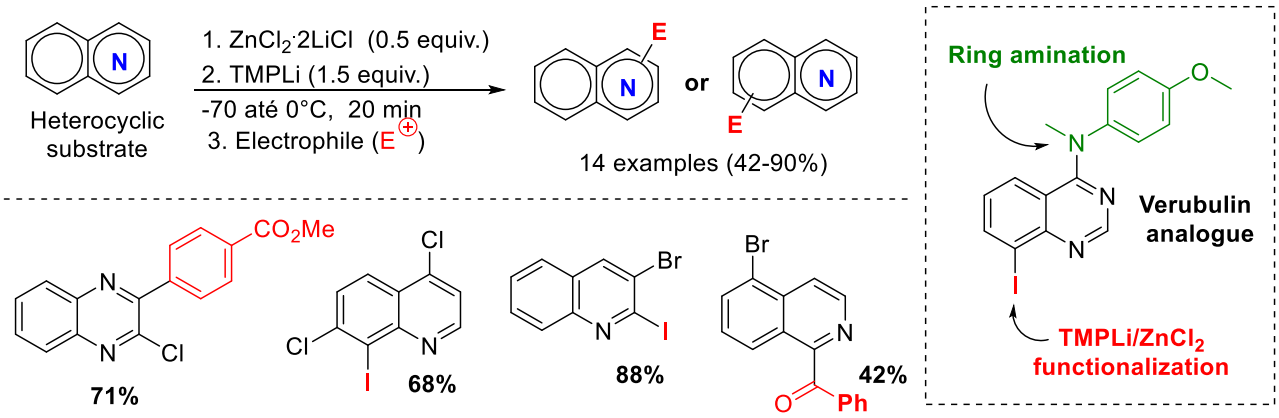


**Scheme 1**

**References:**

1. Vitaku, E.; Smith, D. T.; Njardarson, J. T. *J. Med. Chem*. **2014**, 57, 737, 10257.
2. dos Santos, F.; Batista, J.; Vessecchi, R.; Clososki, G. C., *Synlett* **2015**, 26, 2795.
3. a) Bozzini, L. A.; Batista, J. H. C.; de Mello, M. B. M.; Vessecchi, R.; Clososki, G. C. *Tetrahedron Lett.* **2017**, 58, 4186. b) Murie, V. E.; Nishimura, R. H. V.; Rolim, L. A.; Vessecchi, R.; Lopes, N. P.; Clososki, G. C., *J. Org. Chem.* **2018**, *83*, 871.

**Área: ORG** **Inscrição: 01196**

# Pirrol-2,3-diona: Intermediário-chave para Acessar 4-(2-amino-2-oxoacetil)-5-aril-*N*-arilpirazóis Regiosseletivamente

**Michael J. V. da Silva (PG), Géssica M. Ribeiro (PG), Fernanda A. Rosa (PQ)***

**dasilvamjv@gmail.com; farosa@uem.br**

*Departamento de Química, Universidade Estadual de Maringá (UEM), 87030-900, Maringá PR, Brasil*

Palavras Chave: *N-arilpirazol polifuncionalizado, β-enaminodicetona, Síntese Regiosseletiva.*

## Highlights

**Pyrrol-2,3-dione: Key-intermediate to Access 4-(2-amino-2-oxoacetyl)-5-aryl-*N*-arylpyrazoles Regioselectively**

- Regiochemical control of the cyclocondensation reaction of *β*-enamino diketones with arylhydrazines by in situ generated pyrrol-2,3-dione intermediate.
- Highly regioselective synthetic method for the preparation of 4-(2-amino-2-oxoacetyl)-5-aryl-*N*-arylpyrazoles in a one-pot procedure.

## Resumo/Abstract

O núcleo pirazólico constitui uma importante classe heterocíclica presente em uma série de fármacos com diversas atividades terapêuticas.[1] Assim, o desenvolvimento de metodologias sintéticas para acessar esse núcleo é de grande interesse. Neste contexto, nosso grupo de pesquisa (SINTHET) tem desenvolvido metodologias altamente regiosseletivas para síntese de *N*-arilpirazóis polifuncionalizados via ciclocondensação de β-enaminodicetonas com arilidrazinas.[2,3] Em continuação aos nossos trabalhos, propomos a síntese de 4-(2-amino-2-oxoacetil)-5-aril-*N*-arilpirazóis **4a**-**x** a partir da reação das β-enaminodicetonas **1a-l**[3] com arilidrazinas, gerando o intermediário pirrol-2,3-diona **3a**-**l** in situ (**Esquema 1**).

Inicialmente, observamos que o tratamento da *β*-enaminodicetona **1a** com DBU, em $CH_2Cl_2$ a temperatura ambiente, levou a formação do intermediário diidroxipirrol-1-ona **2a**, o qual se apresentou instável, dificultando seu isolamento. Assim, o intermediário **2a** foi gerado *in situ* e imediatamente desidratado utilizando TsOH, levando à formação da pirrol-2,3-diona **3a**. Em seguida, fenilidrazina foi adicionada ao meio reacional, levando à formação do pirazol desejado **4a** (72%) de forma altamente regiosseletiva (**Esquema 1**). Por fim, examinamos o escopo dessa reação variando as propriedades eletrônicas e estéricas dos substratos, onde foi possível obter uma série de 24 novos *N*-arilpirazóis de forma altamente regiosseletiva e com bons rendimentos (63-80%).

Dessa forma, a metodologia desenvolvida é de grande relevância sintética, visto que os produtos 4-(2-amino-2-oxoacetil)-5-aril-*N*-arilpirazóis **4a**-**x** foram obtidos de forma altamente regiosseletiva, em contraste com a metodologia anteriormente relatada por nosso grupo de pesquisa, na qual pirazóis análogos (**B**) (**Esquema 1**) foram obtidos com regiosseletividade moderada.[2]

**Esquema 1.**

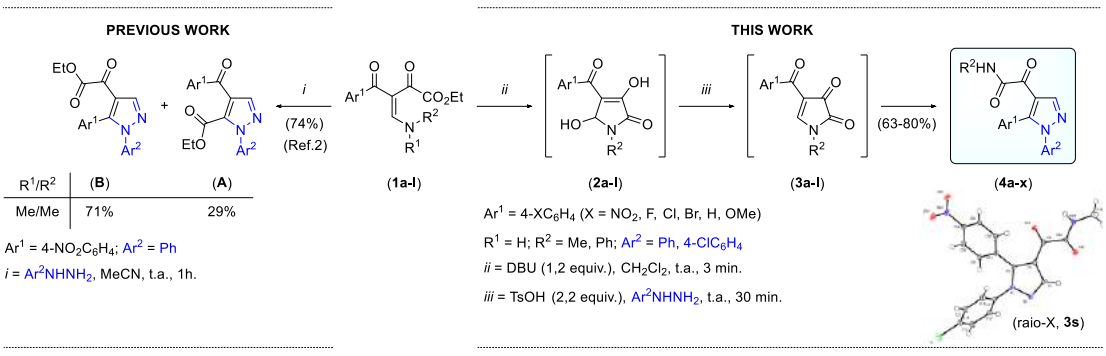


[1] KHAN, M. F. et al. *Eur. J. Med. Chem.* **2016**, *120*, 170. [2] SOUZA, T. F. et al. *Asian J. Org. Chem.* **2017**, *6*, 627. [3] da SILVA, M J. V. et al. *J. Org. Chem.* **2017**, *82*, 12590.

**Área: ORG** **Inscrição: 01278**

# Synthesis, X-Ray Structure of new complex with Paddle-Wheel SBUs

**Mateus C. Silva (IC)[*], Gabriel Salzer (IC)[1], Everton P. Barbosa (PQ)[2], Tatiana Alves Toledo (PQ)[1], Denise B.A. Barbosa (PQ)[1]**

**mateuscoimbra056@gmail.com; denise.barbosa@ifsudestemg.edu.br**

*[1]Departamento de Educação e Ciências-LPEN, Instituto Federal de Educação do Sudeste de Minas Gerais-campus Juiz de Fora; [2]Instituto Federal de Educação de São Paulo – campus Capivari.*

Palavras Chave: *cobre, polímero de coordenação, SBUs*

## Highlights

Synthesis, X-Ray Structure of new complex with Paddle-Wheel SBUs. In this work we show a new compound $[Cu(C_2H_3ClO_2)_2MnO_3(C_2H_3ClO_2)CuCl(C_2H_3ClO_2)]H_2O$. Secondary building units (SBUs) were employed for study the differents ligand coordination modes and metal coordination environments using linkers (urea and monocloacetic acid).

## Resumo/Abstract

The construction of extended solids from molecular building blocks is interesting due to the advantages it for the design of materials. The use of discrete molecular units in the assembly of extended networks is an synthetic approach permits reactions to take place at or near room temperature, where the structural integrity of the building units can be maintained throughout the reactions. We have focused on the study of crystalline materials to an understanding of the design, synthesis, and properties of materials. In particular, we have be interested in the magnetic materials due to their potential applications in technologies devices. Here, we present the development of MOFs using (SBUs) for understanding and predicting topologies of structures. The SBUs was first synthesized.(Figure1a).The complex was obtained by the addition of KMnO4 (7.02 mmol). The resulting solution was stirred for 3 h and left undisturbed at ambient temperature. The crystals was characterizated. This complex crystallizes in the triclinic space group P-1; The asymmetric unit contains 3 different units. One contains 2 copper atoms and 4 coordinated monochloroacetic acids. The axial chlorine atoms are coordinated to a manganese atom which is coordinated to 3 oxygen and a monochloroacetic acid. The other unit consists of 2 copper atoms coordinated to 4 monochloroacetic acids. The other unit is constituted by a copper atom coordinated to 2 monochloroacetic acids. The three units are interconnected by hydrogen bonds. (Figure b).The topology and others characterizations are in progress.

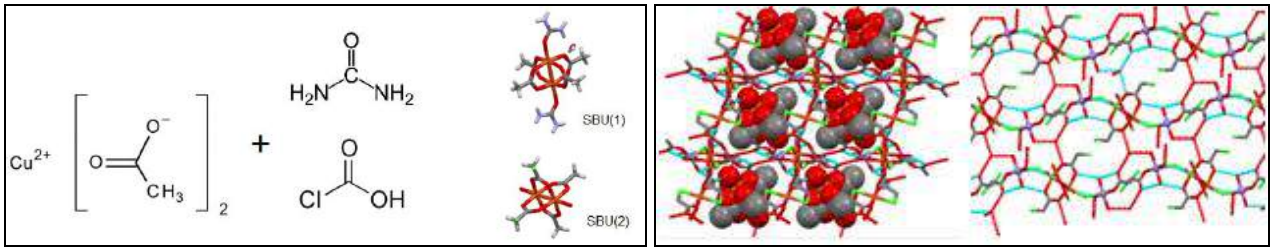


Figure1. (a) Synthesis of paddle wheel frameworks. (b) Packing with hydrogen bonds.

CHANDRASEKHAR, V. *Inorganic and Organometallic Polymers*. New York: Springer, 2005.
YING, H.,ZHANG, Y.,CHENG, J., *Dynamic urea bond for the design of reversible and self-healing polymers*. Nature Communications,2014.

**Área: QO** **Inscrição: 01323**

# Relationship between Hammett's parameters and in silico density functional with tandem mass ESI-CID fragmentation: Dihydropyridines as prototype

**Paulo R. dos Santos (PG)[1]; Claudio M. P. Pereira (PQ)[2]; Favero R. de Paula (PQ)[3]; Sidnei Moura (PQ)[1].**

**prsantos.quimica@gmail.com**

*[1]Instituto de Biotecnologia, UCS; [2]Departamento de Química, UFPEL; [3]Departamento de Farmácia, UNIPAMPA.*

*Key words: density functional theory; dihydropyrimidinones; Hammett theory; MS-MS fragmentation.*

## Highlights

This study have demonstrated the correlation between Hammett's parameters with DHPMs m- and p-substituents fragmentation by mass spectrometry( CID collision).

## Abstract

Over the years, with the instrumental analysis evolution, the relationships between the carried- out results with the data of theoretical analysis in silico and the Hammett's parameters have been reported. They have been very useful for chemical characterization of small organic molecules. Thus, this work aims at showing the feasibility and limitations for Hammett's and density functional theory applications in electrospray ionization–collision-induced dissociation (ESI-CID) fragmentation provision. For this, 13 dihydropyrimidinones para, meta, and orto monosubstituted were studied using ESI and CID in positive mode. As a result, it was observed that the main fragmentation includes the isocyanate and ethanol loses at low energy. Nevertheless, at higher energies, radical ions formed by McLafferty rearrangement were observed. The Hammett plots were correlated fragmentation profiles, showing good linearity for the $[M + H]^+$, which does not occur to radical ions and carbocation's. These tendencies had demonstrated that the stability of protonate and activation energy of secondary ions changes with the pKa. The density functional theory studies indicated that, both nitrogen atoms in the dihydropyrimidinone's prototypes are capable of being protonated. However, the activation energy of fragmentation products is not changed. Therefore, this work has shown information, which can be useful to understand tandem mass spectrometry in ESI-CID conditions for small organic molecules series. This is the first step for normalization of fragmentation pathway.

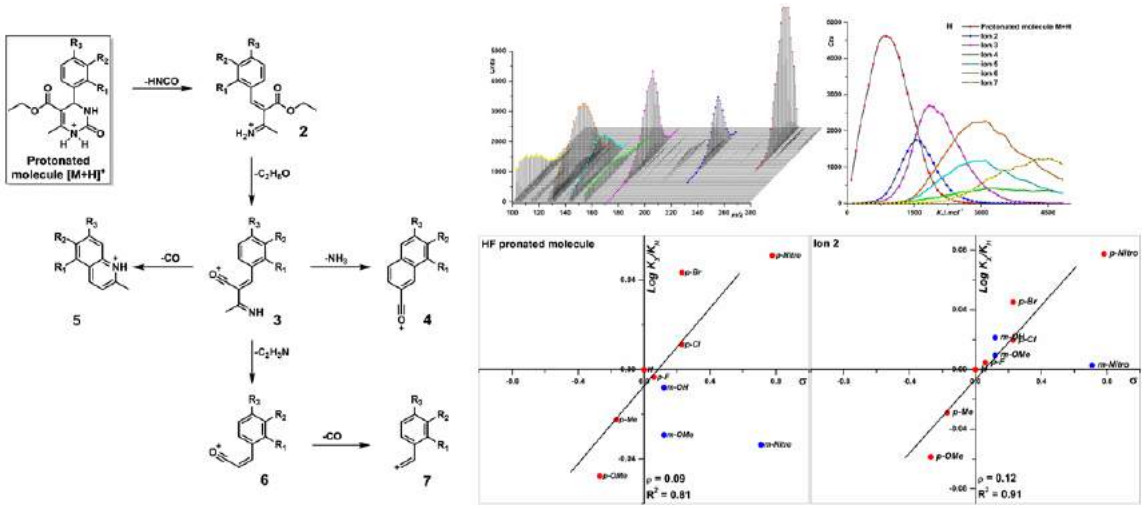


Figure. Scheme for ionization pathways, fragmentation and Hammett plots.

Acknowledgment to FAPERGS - PRONUPEQ process, Grant/Award Number: 16/2551-0000523-0, CNPq INCT Forense, Grant/Award Number: 465450/2014s-8.

**Área: ORG**
*(Inserir a sigla da seção científica para qual o resumo será submetido. Ex: ORG, BEA, CAT)*

**Inscrição: 01373**
*(Inserir o número de inscrição do autor que fez a submissão)*

# Synthesis of 5-aminotetrazoles from thioureas using trichloroisocyanuric (TCCA)

**Andressa C. D. Silva (IC),[1] Tiago L. Silva (PQ).[1]***

**adutra@ufrj.br; tiagolds@iq.ufrj.br**

[1] *Laboratory of Catalysis and Synthesis - LACOS – Institute of Chemistry – Federal University of Rio de Janeiro (UFRJ).*

Palavras Chave: Aminotetrazoles, thioureas, TCCA

## Highlights

5-aminotetrazoles is usually afforded using toxic and expensive reagents[2]. This work provides a new methodology to obtain 5-aminotrtazoles using Trichloroisocyanuric acid as a green catalyst.

## Abstract

Aminotetrazoles belong to a class of molecules that have biological activity as an epigenetic modulator. In addition, it plays a very important role in agronomy, being heterocyclic compound important for microbial activity in soil enrichment. The 5-aminotetrazoles are synthesized from methodologies that require the use of toxic and costly desulfurization agent.

Trichloroisocyanuric acid (TCCA) is an organic N-chlorine amine applied commercially in the treatment of swimming pools and also in the disinfection of drinking water. The advantages of TCCA are low cost and low toxicity. Also, according to the literature, it has already been used as a desulfurization agent[3]. From 1 mmol of thiourea **1** was added 1 mmol of triethylamine, $Et_3N$, and 0.4 mmol of trichloroisocyanuric acid **2** in DMF at room temperature and after 24 hours we obtained the corresponding aminotetrazole **3** in (**Scheme 1**).

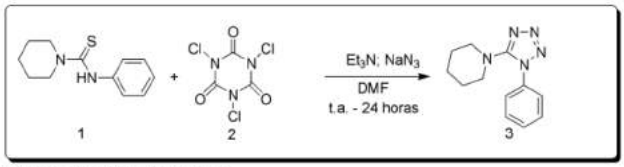


**Scheme 1** – reaction of synthesis of-aminotetrazole

Up to now, we have tested diferente solvent in order to achieve better yields of **3 ( Table 1)**. Despite this low yiels, we are optimizing reactional conditions and changing others parameters in reaction such as temperature, heat source (microwave) and bronsted base.

| SOLVENTE / TEMPERATURA -BANHO | RENDIMENTO |
|---|---|
| (DMF) /100ºC | 10% |
| (MeOH) / refluxo | 25% |
| (THF)/ refluxo | 10% |
| ($CH_2Cl_2$)/ 60ºC | 5% |
| ($H_2O$)/ refluxo | 5% |
| ($CH_3CN$) / refluxo | 20% |

**Table 1** –Solvents tested to obatain 5 aminotetrazole **3**

**Reference**:

1- V. Kumar, G. Rosse, *Medicinal Chemistry Letters,* **2016**,7, 132.
2- Chaudari, P.S.; Pathare, S.P. *et al. Journal of Organic Chemistry* **2012**, 8, 3716.
3 - Basu, N. Maijs, S.K. et al. *Carbohydate Research* ***2013***, 10, 10

**Área: ___ORG_____ Inscrição:___ 01439____**

# A multidimensional liquid chromatography method for monitoring on flow the activity of PNP-Mt immobilized enzyme

**Ananda C. de Castro (IC) [1], Leonardo K. B. Martinelli (PQ) [2], Diógenes S. Santos (PQ) [2], Luiz Augusto Basso (PQ)[2], Marcela C. de Moraes (PQ) [1]***

**ananda_villa@hotmail.com; mcmoraes@id.uff.br**

*[1]Instituto de Química, Universidade Federal Fluminense, UFF; [2]Pontifícia Universidade Católica do Rio Grande do Sul, PUC-RS*

Keywords: Multidimensional Liquid Chromatography, Biochromatography, Purine Nucleoside Phosphorylase, Tuberculosis.

## Highlights

A LC×LC method was developed and validated for monitoring on flow the PNP-Mt activity
PNP-Mt was covalently immobilized onto the internal surface of fused silica capillaries
Kinetic studies were conducted with the immobilized PNP-Mt

## Resumo/Abstract

Purine Nucleoside Phosphorylase (PNP) is a key enzyme in the purine salvage pathway and catalyzes the cleavage of deoxyribonucleosides to the corresponding purine base and sugar-1-phosphate in presence of inorganic phosphate (Pi). PNP from Mycobacterium tuberculosis (MtPNP) has been considered an attractive target for drug development against tuberculosis [1]. Therefore, the development of analytical tools for the fast identification of specific inhibitors for this enzyme has become an interesting task. A promising approach is the use of immobilized enzymes reactors (IMERs) for on-flow screening studies. MtPNP-IMER was prepared by the covalent immobilization onto a fused silica capillary, based on previously published conditions for human PNP [2]. For the on-flow multidimensional chromatography activity assay, the MtPNP-IMER was inserted in the first dimension (HEPES 100 mM pH 7.4, 0.05 mL/min) and an octyl column (Phenomenex Chrospher RP-8, 150 x 4.6 mm, 5 uM, 100 Å) in the second dimension. Inosine and the formed hypoxanthine, respectively substrate and product of the enzymatic reaction, were separated in the analytical column by the use of a mobile phase containing 1% TEA pH 6.0:MeOH (95:5), at a flow rate 0.8 mL/min, and λ = 280nm.
The estimated amount of MtPNP immobilized onto each capillary was 130.5 ± 32.3 µg of total protein, indicating that the immobilization procedure was efficient. The MtPNP activity was monitored by the direct quantification of formed hypoxanthine. Kinetic studies showed that the $K_M$ value for the substrate inosine using the immobilized enzyme (41µM) is similar to that one measured for the enzyme in solution (40±3µM).
These results revealed that the immobilized MtPNP retained its catalytic activity and represents a useful way of reutilizing the same amount of enzyme in diverse assays, including in the screening of new MtPNP inhibitors.

[1] R.G. Ducati et al./Archives of Biochemistry and Biophysics 486 (2009) 155–164
[2]Moraes, M. C.; et all. Capillary bioreactors based on human purine nucleoside phosphorylase: A new approach for ligands identification and characterization. Journal of Chromatography (Print) JCR, v. 1232, p. 110-115, 2012.

**Área: ORG** **Inscrição: 00066**

# Bidirectional synthesis of symmetric bis-benzoxazines by Mannich reaction of eugenol and diamines

**Rosiene R. Mattos (PG),[1,2] Silvio Cunha (PQ),[1,2]**

**rosiene.mattos@ufba.br; silviodc@ufba.br**

[1]*Instituto de Química, Universidade Federal da Bahia, Campus de Ondina, 40170-290, Salvador – BA.*
[2]*INCT-Instituto Nacional de Ciência e Tecnologia em Energia e Ambiente, Campus de Ondina, Salvador–BA.*

Palavras Chave:*(Eugenol, Benzoxazine, Diamine).*

## Highlights

Polyfunctionalized bis-benzoxazines were prepared by the Mannich reaction of eugenol, aliphatic diamines and formaldehyde.

## Resumo/Abstract

Benzoxazines are a new class of thermoset material such as phenolic and epoxy resins[1]. The modification benzoxazine monomers give different properties to the material. The synthesis of benzoxazines occurs by the Mannich reaction employing a phenol, an amine and formaldehyde (Scheme **1**). Benzoxazines also have biological properties, such as antireserpinic, anti-inflammatory and analgesic[1]. Eugenol has antithymosinase, antibacterial, antifungal, antiacne activities[2].
In this work, reactions of eugenol (**1**), formol (**2**) and diamines such as diamines and urea (**5**) at room temperature in methanol as solvent afforded the corresponding bis-benzoxazines**,** Scheme 1.

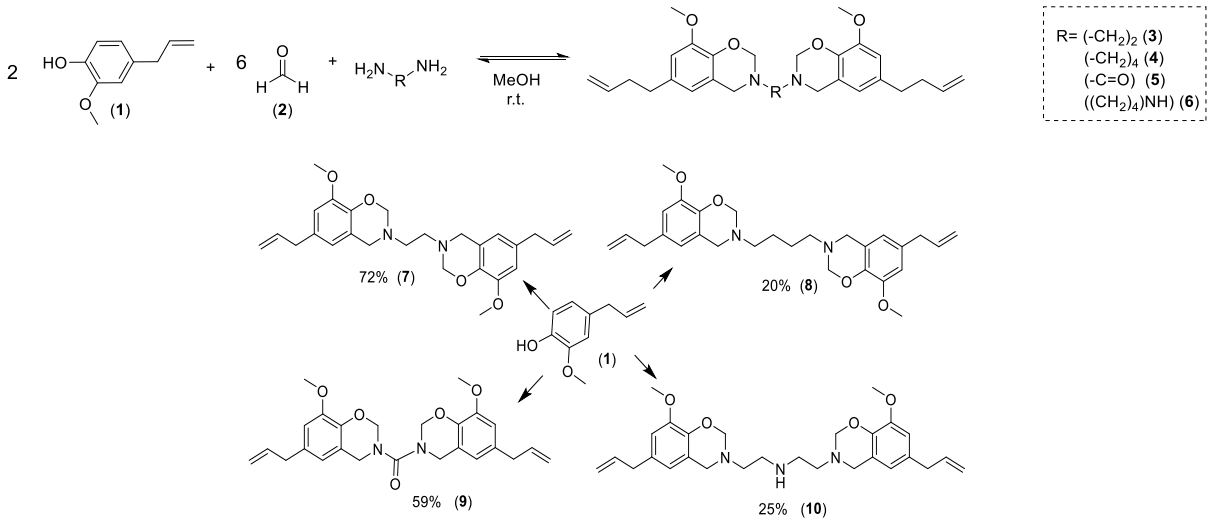


Scheme **1**: Synthesis of bis-benzoxazines symmetric.

The bis-benzoxazines are new compound, which were synthesized in moderate to good yields (20- 72%), in a bidirectional approach.

[1] Dumas, L., Bonnaud, L., Olivier, M., Poorteman, M., Dubois. P., *J. Mater. Chem. A*, **2015**,3, 6012-6018.
[2] Rudyanto, M., Ekowati, J., Widiandani, T., Honda, T., *Int J Pharm Pharm Sci*, **2014**,6, 2, 465-467.

**Área: ORG** **Inscrição: 00108**

# Multicomponent synthesis of 5-aminotetrazoles and bistetrazoles promoted by bismuth nitrate pentahydrate

**Iva S. de Jesus (PG),[1] Silvio Cunha (PQ)[1].**

**ivasouza.quimica@gmail.com; silviodc@ufba.br**

[1]*Instituto de Química, Universidade Federal da Bahia, Campus de Ondina, 40170-290, Salvador – BA. INCT-Instituto Nacional de Ciência e Tecnologia em Energia e Ambiente, Campus de Ondina, Salvador – BA*

Palavras Chave: *Bismuth, 5-aminotetrazoles, Multicomponent synthesis.*

## Highlights

Multicomponent reaction of $NaN_3$, phenyl isothiocyanate and amines mediated by $Bi(NO_3)_3{\cdot}5H_2O$ under microwave heating allowed the synthesis of 5-aminotetrazoles and bis-5-aminotetrazoles.

## Abstract

Tetrazol is a five-membered heterocyclic characterized by the presence of four *N*-atoms and one C-atom.[1,2] This heterocycle has diverse applications, for example as bioactive compounds.[2] In particular, 5-aminotetrazoles show anti-allergic, antiviral, and anti-inflammatory activities.[3,4] Therefore, new synthetic approaches have been reported in the literature. In this study we describe the multicomponent reaction of amine with phenyl isothiocyanate and $NaN_3$ in the presence of $Bi(NO_3)_3{\cdot}5H_2O$ in $CH_3CN$ as solvent, performed in a microwave reactor. Very short reaction time were observed to both aliphatic and aromatic amines, Scheme 1. The Bi(III) should behaves as thiophilic soft Lewis acid that coordinated to the *in situ* formed thiourea. The regioselectivity appears to be governed by the difference in basicity among the two thiourea's nitrogen. The most basic nitrogen promotes the elimination of the sulfur complexed to bismuth. Thus, this nitrogen belongs endocyclic in the formed tetrazole. When the difference of basicity decreases, mixture of regioisomers was observed.

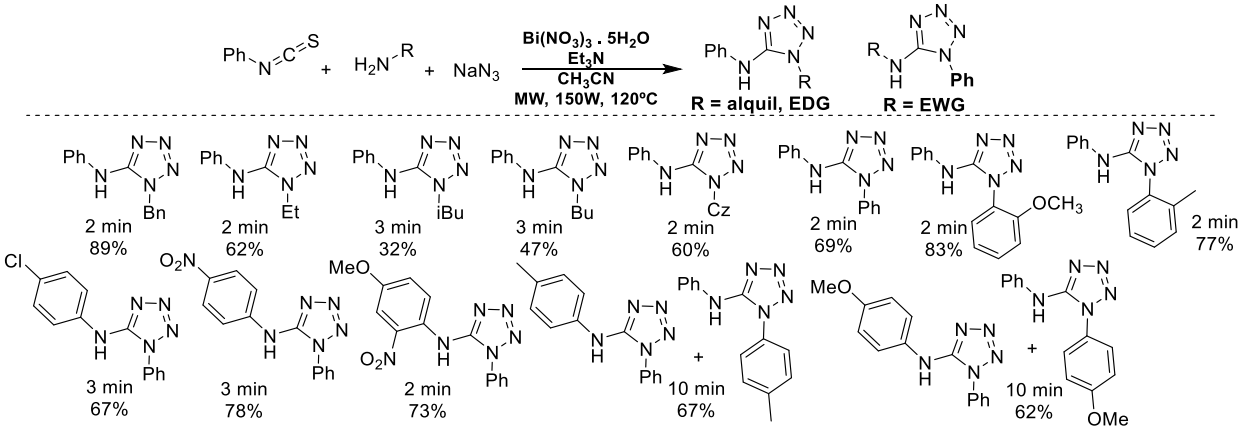


**Scheme 1.** Synthesis of 5-aminotetrazoles.

The synthesis of bis-5-aminotetrazoles was also achieved under the same reaction conditions, using aliphatic diamines, Scheme 2.

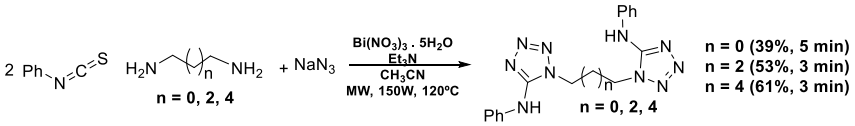


**Scheme 2.** Synthesis of bis-5-aminotetrazoles.

The three-component reaction of $NaN_3$, phenyl isothiocianate and amines/diamines promoted by Bi(III) under microwave radiation is an effective and green method to the synthesis of 5-aminotetrazole and bis-5-aminotetrazoles.

**ACKNOWLEDGEMENTS**

The authors thank CNPq, CAPES and FAPESB.

[1] Katritzky, A. R.; Rogovoy, B. V.; and Kovalenko, K. V.; *J. Org. Chem.* **2003**, *68,* 4941.
[2] Telvekar, V. N.; Jadhav, N. C.; Jagadhane, P. B.; Patel, K. N.; *Tetrahedron Lett*. **2013**, 54, 101.
[3] Galindo C. L. E.; Jácome A. I.; Martínez, K. M. C.; *Molecules,* **2015**, *20,* 1519.
[4] Patel, B. K.; Yella, R.; Khatun, N.; Rout, S. K. *Org. Biomol. Chem*. **2011**, 9, 3235.

**Área: ORG** **Inscrição: 00187**

# Aplicação de Carbodiimidas na Síntese de Anestésicos Locais

**Marco A. M. Bezerra (PG), João V. P. Pimentel (IC), Leandro S. M. Miranda (PQ), Rodrigo O. M. A. de Souza (PQ)**

**macenamarco@gmail.com; souzarod21@gmail.com**

*Grupo de Biocatálise e Síntese Orgânica, Instituto de Química, Universidade Federal do Rio de Janeiro, Rio de Janeiro, RJ 21941-909.*
Palavras Chave: *Carbodiimidas, Anestésicos, Bupivacaína, EDC*

## Highlights

**Carbodiimides application on Local Anesthetic Synthesis:** This work presents a milder alternative than acid chloride for local anesthetic synthesis.

## Resumo/Abstract

A classe das amino-amidas é a mais utilizada entre os anestésicos locais[1]. Dentre as estratégias utilizadas para o acoplamento de amida, a via cloreto de ácido é a mais utilizada para essa classe de fármacos. Entretanto, os reagentes empregados nessa etapa são corrosivos e também elevam os custos do processo com tratamento de efluentes. O presente trabalho tem como objetivo apresentar alternativas mais brandas para a síntese da mepivacaína (**1**), ropivacaína (**2**) e bupivacaína (**3**), utilizando carbodiimidas nas reações de amidação, pois estas não são corrosivas e oferecem maior simplicidade no isolamento[2]. As carbodiimidas são muito utilizadas na síntese de fármacos, sendo o cloridrato de *N*-(3-Dimetilaminopropil)-*N*′-etilcarbodiimida (EDC) a mais popular[3]. Em estudos preliminares reagiu-se o ácido pipecólico (**4**) com 2,6-dimetilanilina (**5**) utilizando EDC, para a obtenção do intermediário *N*-(2,6-dimetilfenil)piperidina-2-carboxamida (**6**). Após 12 horas de reação o produto foi detectado por cromatografia em camada delgada, entretanto, o baixo rendimento obtido não possibilitou o isolamento. Logo, pretende-se partir do ácido picolínico (**7**), utilizando o mesmo procedimento, mas visando à obtenção do intermediário piridínico (**8**). Pretende-se avaliar a influência da temperatura sobre essas amidações e o seu comportamento frente a diferentes carbodiimidas.

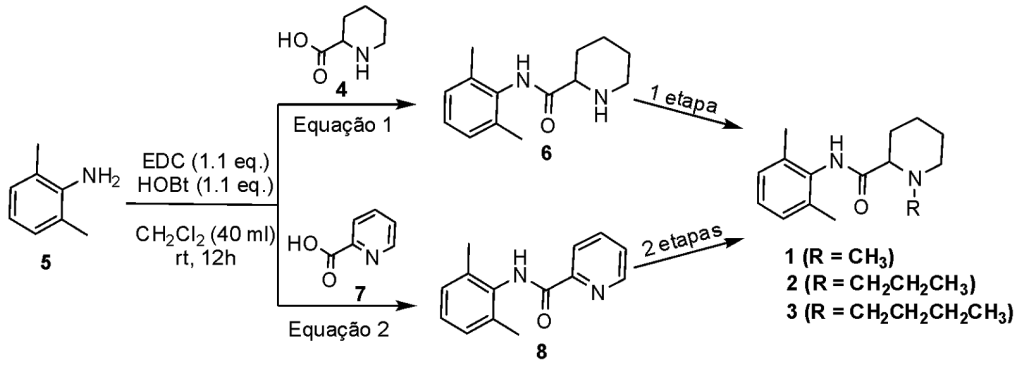


(1) Becker, D. E.; Reed, K. L. *Anesth. Prog*. **2006**, 53 (3), 98-109.
(2) El-Faham, A.; Albericio, F. *Chem. Rev.*, **2011**, 111 (11), 6557–6602.
(3) Dunetz, J. R.; Magano, J.; Weisenburger, G. A. *Org. Proc. Res. Dev*. **2016**, 20 (2), 140-177.

**Área: Org** **Inscrição:00269**

# Assignment of the relative and absolute stereochemistry of two novel epoxides using NMR and DFT-GIAO calculations

**Antônio J. Demuner (PQ),[1] Elson S. Alvarenga (PQ),[1] Vinícius M. Viana (IC),[1] Fernanda C. Moraes (PG).[1]***

**elson@ufv.br;**

[1]*Departamento de Química, UFV;*

Palavras Chave: *D-mannitol, Enantioselective synthesis, DFT, Diels-Alder, Epoxide.*

## Highlights

Two novel epoxides were synthesized and their structures were fully determined with the aid of high field nuclear magnetic resonance, infrared, mass spectrometry, and DFT theoretical calculations.

## Resumo/Abstract

Considering the potential biological application of isobenzofuranones[1], especially as agrochemical defensives, two novel epoxides were synthesized. The structures of these compounds were fully determined with the aid of high field nuclear magnetic resonance, infrared, mass spectrometry, and DFT theoretical calculations. Besides analyses of the 2D NMR spectra, the assignments of the nuclei at the epoxide ring were also inferred from information obtained by theoretical calculations. The calculated $^{1}$H and $^{13}$C NMR chemical shifts for eight candidate structures (Figure 1: en1-en4 and ex1-ex4) were compared with the experimental chemical shifts of **1** and **2** (Figure 2) by measuring the mean absolute errors (MAE) and by the DP4 statistical analysis[2].

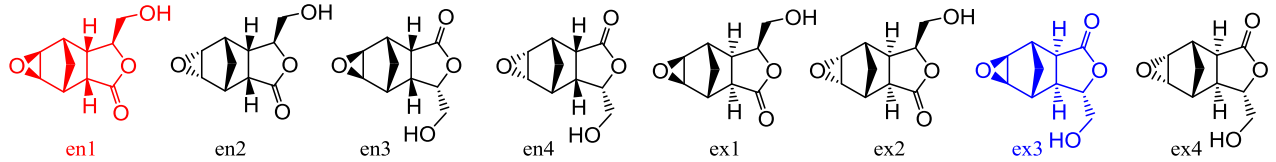


Figure 1: Candidate structures for epoxide **1** (en1-en4) and **2** (ex1-ex4).

The multiplicities of the hydrogens located at the bridge of the bicycle are distinct for epoxides **1** and **2** due to W coupling, and this feature was employed to confirm the assignment of these nuclei.

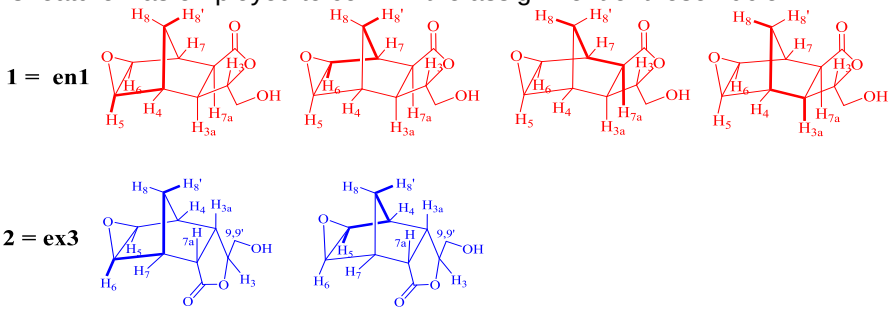


Figure 2: Representation of the W coupling highlighted in bold for the epoxide **1** and **2**.

The structures and relative configurations of **1** and **2** were determined by NMR spectroscopy assisted with theoretical calculations and due to the enantioselective synthesis starting from a chiral polyol (D-mannitol), the absolute configurations of the epoxides were also defined.

**Acknowledgements:** CAPES, CNPq, FAPEMIG, RMQuímica, UFV.

**References**:

1- Tetrahedron. 67 (2011) 3003–3009. doi:10.1016/j.tet.2011.02.029.
2- J. Org. Chem. 73 (2008) 4053–62. doi:10.1021/jo8003138.

**Área: ORG** **Inscrição: 00314**

# Rare Earth Triflate-Catalyzed Gröebke-Blackburn-Bienaymé Reaction under Microwave Heating to Access Imidazo[2,1-b]thiazoles

**Nicolas S. Anjos (IC)[1], Everton S. C. Fiorentino (IC)[1], Luiz S. Longo Jr*. (PQ)[1]**

**nicolasdosanjos@hotmail.com;** luiz.longo@unifesp.br*

[1]*Departamento de Ciências Farmacêuticas, Instituto de Ciências Ambientais, Químicas e Farmacêuticas Universidade Federal de São Paulo – campus Diadema*

*Keywords:* imidazo[2,1-b]thiazoles; multicomponent reaction; metal triflates; Groebke-Blackburn-Bienaymé reaction.

## Highlights

Imidazo-[2,1-b]thiazoles can be obtained in moderate to good yields by the Gröebke-Blackburn-Bienaymé reaction using rare earth triflates (Gd, La, Sc, Yb) as Lewis acid catalyst under heating by microwave irradiation.

## Abstract

The Gröebke-Blackburn-Bienaymé reaction (GBB)[1] is a multicomponent reaction involving aldehydes, isocyanides and amidines to obtain nitrogen-based heterocycles such as imidazo[1,2-a]pyridines and imidazo[2,1-b]thiazoles. In this study, we screened several metal triflates [$M(OTf)_3$, M = Gd, La, Sc, Yb] as Lewis acid catalyst for the GBB reaction to access imidazo[2,1-b]thiazoles. Initially we studied a model reaction with 2-aminothiazole, benzaldehyde and *terc*-butylisocyanide to prepare **1**, which was obtained in moderate yields regardless the catalyst used (48-53%; Table 1, entries 1-4). When the reaction time was increased from 90 to 180 min, we have observed a significant increase in the yield of **1** (68%, entry 5). Since the best condition was established to obtain **1**, we applied the same condition to synthetize new imidazo[2,1-b]thiazoles **2-5** by the variation of the aldehyde component (aliphatic and aromatic; entries 6-9). Our group earlier reported the same protocol for GBB reaction to access imidazo[1,2-a]pyridines.[2] In general, the yields obtained for imidazo[1,2-a]pyridines were higher (typically higher than 80%), compared to the yields obtained for imidazo[2,1-b]thiazoles.

**Table 1.** GBB reaction to prepare imidazo[2,1-b]thiazoles **1-5** using metal triflates as catalyst.[a]

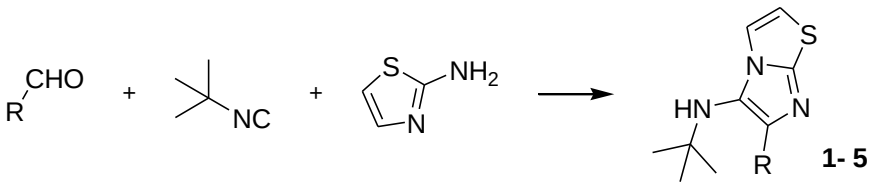


| Entry | R | Catalyst | Time | Yield |
|---|---|---|---|---|
| 1 | $C_6H_5$ (**1**) | $La(OTf)_3$ | 90 min | 48% |
| 2 | $C_6H_5$ (**1**) | $Sc(OTf)_3$ | 90 min | 51% |
| 3 | $C_6H_5$ (**1**) | $GdOTf)_3$ | 90 min | 49% |
| 4 | $C_6H_5$ (**1**) | $Yb(OTf)_3$ | 90 min | 53% |
| 5 | $C_6H_5$ (**1**) | $Gd(OTf)_3$ | 180 min | 68% |
| 6 | 4-$NO_2$-$C_6H_4$ (**2**) | $Gd(OTf)_3$ | 180 min | 54% |
| 7 | 4-$OCH_3$-$C_6H_4$ (**3**) | $Gd(OTf)_3$ | 180 min | 62% |
| 8 | *n*-$C_3H_7$ (**4**) | $Gd(OTf)_3$ | 180 min | 88% |
| 9 | *i*-$C_3H_7$ (**5**) | $Gd(OTf)_3$ | 180 min | 91% |

(a) ***Reagents and conditions:*** 2-aminothiazole (0,5 mmol), benzaldehyde (0,5 mmol), *terc*-butylisocynide (0.5 mmol), MeOH (1,0 ml), 5 mol% of $M(OTf)_3$,150ºC, closed vial (MICROWAVE 300 – Anton Paar®).

References:

1. (a) Groebke, K.; Weber, L.; Mehlin, F. *Synlett* **1998**, 661; (b) Blackburn, C.; Guan, B.; Fleming, P.; Shiosaki, K.; Tsai, S. *Tetrahedron Lett.* **1998**, *39*, 3635; (c) Bienaymé, H.; Bouzid, K.; *Angew. Chem. Int. Ed.* **1998**, *37*, 2234.
2. Gibeli, M. M.; Silva, G. A.; Santos, G. F. D.; Fernandes, P. C. S.; Longo Jr., L. S. *"A Comparative Study of Groebke-Blackburn-Bienaymé Reactions Catalyzed by $M(OTf)_3$ under Microwave Heating."* In: 39a Reunião Anual da Sociedade Brasileira de Química, 2016, Goiânia. (QO-034).

**Área: Org** **Inscrição: 00345**

# Systematic studies toward iodocyclization of (Z)-thiobutenynes using water as solvent: Ecofriendly synthesis of 3-Iodothiophenes

**Diego B. Carvalho (PG),[1] Camila B. Andrade (PG),[1] Ozildéia Soares (PG),[1] Cristiane Y. K. Shiguemoto,[a] Adriano C. M. Baroni (PQ)[1*]**

**adriano.baroni@ufms.br**

[1] *Faculdade de Ciências Farmacêuticas, Alimentos e Nutrição, Universidade Federal do Mato Grosso do Sul, 79070-900, Campo Grande-MS*

Palavras Chave: (Z)-thiobutenynes, Iodocyclization, $H_2O$, 3-Iodothiophenes

## Highlights

In this work, were synthesized 3-iodothiophenes through iodocyclization (of Z)-thiobutenynes using water as solvent.

## Introduction

The use of water as a solvent in synthetic organic chemistry has been subject of intense research in recent decades. Despite the low solubility of organic reagents in this medium, the use of co-solvents, surfactants and increase of temperature can guarantee the success of the reactions.[1]

In this work we performed a systematic study of synthesis of 3-iodothiophenes **2a-d** with different patterns, using $H_2O$ as the solvent, in order to find the best reaction condition, and thus to replace the toxic solvents $CH_2Cl_2$ and 1,2-dichloroethane commonly employed in iodocyclization reactions.[2]

## RESULTS AND DISCUSSION

In the first attempted, iodocyclization of (Z)-thiobutenynes **1a** was performed using $I_2$ as electrophilic source, in $H_2O$ as solvent, and 3-iodothiophene **2a** was obtained in 80% yield. However, when it was used (Z)-thiobutenyne **1b** containing alkyl group ($C_4H_9$), the product **2b** was obtained in moderate yields (36%). Use of CTAB as surfactant not improved yields of **2b**.

These results, prompted us to investigate other reaction conditions. Therefore, we hypothesized that use of $I_2$/KI system, could improve yields of **2b** due better solubility of $I_3^-$ anion in water. Thus, 3-iodothiophene **2b** was obtained in 73% yield. However, iodocyclization of (Z)-thiobutenyne **1d** using $I_2$/KI system provided **2d** in moderate 33% yield after 1 h at 100 °C. The $I_2$/KI system is a good alternative for synthesis of trisubstituted 3-iodothiophene **2a-c**, but new studies were carried out for obtain disubstituted 3-iodothiophene **2d**.

Due oxidants properties of Oxone®, we used this reagent to transform KI in eletrofilic species of iodine ($I^+$ or HOI) and iodocyclization reaction with **1d** provided 3-iodothiophene **2d** in 79% at 100 °C.

In Table 1 are showed a comparative study of iodocyclization of **1a-d** with $I_2$, $I_2$/KI and KI/Oxone® system.

**Table 1.** Synthesis of 3-iodothiophenes **2a-d**

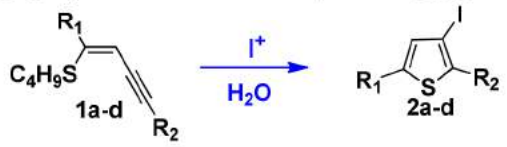


| iodothiophene | Reaction conditions[a,b] | Yield (%)[c] |
|---|---|---|
| 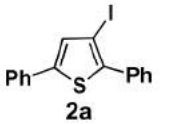 2a | $I_2$ ($CH_2Cl_2$)[2] | 80 |
| | $I_2$ (1.2 equiv)[a] | 80 |
| | $I_2$ (1.2 equiv) / KI (3.6 equiv)[a] | 83 |
| | KI (2.4 equiv) / Oxone® (0.8 equiv)[a] | 87 |
| 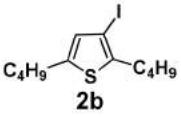 2b | $I_2$ (1.2 equiv) | 36 |
| | $I_2$ (1.2 equiv) / KI (3.6 equiv)[a] | 73 |
| | KI (2.4 equiv) / Oxone® (0.8 equiv)[a] | 81 |
| 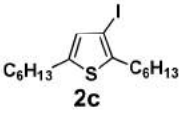 2c | $I_2$ (1.2 equiv)[a] | 31 |
| | $I_2$ (1.2 equiv) / KI (3.6 equiv)[a] | 61 |
| | KI (2.4 equiv) / Oxone® (0.8 equiv)[a] | 74 |
| 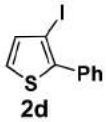 2d | $I_2$ (1.2 equiv)[b] | 28 |
| | $I_2$ (1.2 equiv) / KI (3.6 equiv)[b] | 33 |
| | KI (2.4 equiv) / Oxone® (0.8 equiv)[b] | 79 |

[a] room temperature. [b] 100 °C. [c] yield of isolated products.

## CONCLUSION

The best reaction condition of iodocyclization in $H_2O$ occurred in KI / Oxone® system, with yields ranging from 74 to 87%. The iodocyclization using $H_2O$ as solvent showed to be more efficient than in $CH_2Cl_2$.

## ACKNOWLEDGMENTS

FUNDECT-MS, CNPq, CAPES

[1] Fokin, V. V. et al *Chem. Reviews* **2009**, 109, 725.
[2] Baroni, A. C. M et al *Tetrahedron Lett*, 2014,

**Área: ORG** **Inscrição:00416**

# Síntese de Cristais Líquidos Iônicos derivados do núcleo Tristriazolotriazina

**Bruna do Nascimento Dutra (IC),[1*] Fernando Molin (PQ).[1]**

**brunadutra@alunos.utfpr.edu.br; fmolin@utfpr.edu.br.**

[1]*Departamento de Química e Biologia, UTFPR.*

Palavras Chave: *Cristais líquidos, Cristais líquidos iônicos, Tristriazolotriazina, Discóticos*.

## Highlights

Synthesis of Ionic Liquid Crystals derivated from the Tristriazolotriazine core. Synthesis of potencial discotics ionic liquid crystals derivated from tristriazolotriazines already described on literature. The only structure modification on these molecules is the alkylation of the nitrogen on the triazole ring.

## Resumo/Abstract

Nos últimos tempos, os materiais orgânicos vêm sendo cada vez mais explorados, tanto na pesquisa quanto na indústria, em razão de sua alta aplicabilidade em dispositivos eletrônicos e optoeletrônicos. Por conta disso, há uma grande procura por materiais orgânicos como uma próspera alternativa, devido ao seu fácil processamento, suas características facilitarem a produção de dispositivos semicondutores flexíveis, de baixo peso molecular e, principalmente, ao seu baixo custo de produção, principalmente os cristais líquidos (CLs). O centro rígido tris-[1,2,4]-triazolo-[1,3,5]-triazina (TTT) é um heterociclo simétrico em forma de disco muito utilizado como precursor para cristais líquidos discóticos (CLDs), sintetizado por meio da conversão de nitrilas em tetrazóis através da clássica reação com $NH_4Cl$ e $NaN_3$ em DMF[1-3]. Também é possível obter-se cristais líquidos iônicos com características particulares de condutividade, provenientes da capacidade condutiva dos líquidos iônicos em conjunto da fluidez e anisotropia dos CLs. No presente trabalho foram sintetizadas três novas moléculas por meio de modificação estrutural do 4-dodeciloxifenil TTT. Este composto não apresenta comportamento líquido cristalino e já é descrito na literatura[3]. Os produtos finais foram obtidos através da alquilação dos nitrogênios do grupo triazol, variando-se o número de cadeias alquílicas flexíveis do brometo benzílico utilizado. As propriedades térmicas e fotofísicas dos produtos estão sendo estudadas.

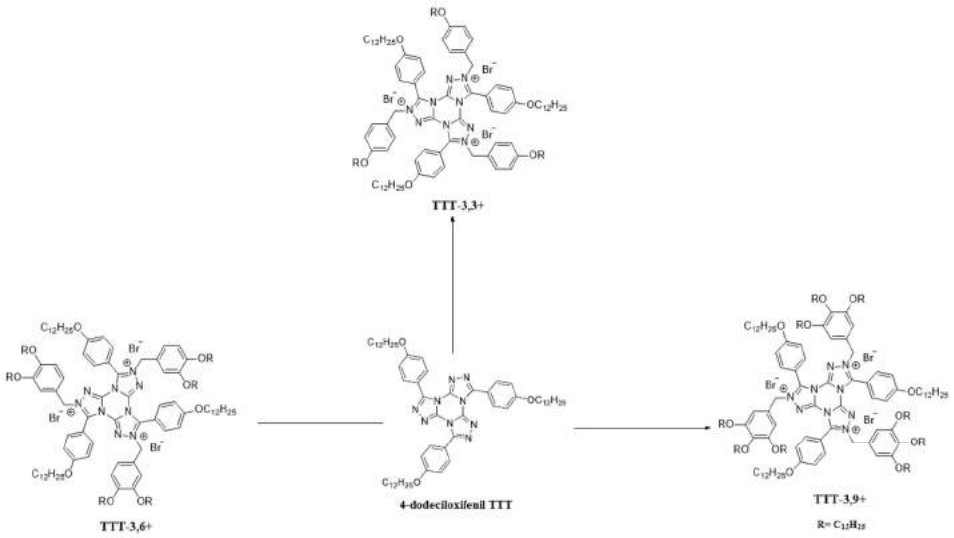


Figura 1 Esquema para obtenção das três moléculas finais desejadas a partir de uma molécula já descrita na literatura.

[1] Liquid Crystal, 2011, 6, (38) 679 - 688
[2] Langmuir, 2012, 28, (31), 11590 – 11598.
[3] Chem. Commum., 2008, 5134 – 5136.

**Área: ORG** **Inscrição: 00427**

# An 8-Step Approach for the Total Synthesis of (−)-Pleocarpanone

**Luiz F. T. Novaes (PG),[1] Julio C. Pastre (PQ),[1]**

**juliopastre@iqm.unicamp.br**

[1]*Intitute of Chemistry, University of Campinas (UNICAMP), Campinas, SP, Brazil*

Keywords: *Total synthesis, Terpene, Guaiane, Catalysis, Pleocarpanone.*

## Highlights

(−)-Pleocarpanone has been assembled in only 8 steps from a cheap monoterpene.
This work employed 4 catalytic reactions: Stille cross-coupling, 1,4-addition, ring-closing metathesis and alkene hydration.

## Abstract

Pleocarpanone is a natural norsesquiterpene with a guaiane carbon skeleton. This class of natural products present diverse biological activities and have attracted the interest of many synthetic chemists. The isolation of this natural product from the plant *Pleocarphus revolutus* was first reported in 1977 by Sammes and co-workers.[1] The stereochemistry was confirmed after its first total synthesis in 2007 by Snapper and co-workers,[2] however, their synthesis required 18 steps from an expensive starting material (**Scheme 1A**).

Our group has been interested in the pursuit of concise and efficient approaches toward the synthesis of natural products, as privileged scaffolds, which could be applied in our medicinal chemistry program. Since pleocarpanone has no biological activity reported so far, and only one synthesis has been reported, we designed an 8-step approach from the cheap monoterpene (−)-perillyl alcohol, in order to obtain reasonable quantities of pleocarpanone, enabling its biological evaluation (**Scheme 1B**).

Our synthesis started with the conversion of alcohol **1** into phosphonate **2**, taking advantage of its allylic position (**Scheme 1C**). Next, the more electron-rich alkene was selectively cleaved during an ozonolysis, following an intramolecular Horner-Wadsworth-Emmons olefination. After that, an allyl group was installed in two steps: α-iodination of enone **3**, and a Stille cross-coupling with allyltributylstannane. The remaining carbons were attached *via* copper-catalyzed 1,4-addition, which provided a mixture of four possible isomers. The second ring was forged by a ring-closing metathesis reaction of the isomeric mixture, and the synthesis was finished after a Mukaiyama hydration. Despite this initial success reported herein, this synthesis is currently under optimization, especially concerning the selectivity in the conjugate addition.

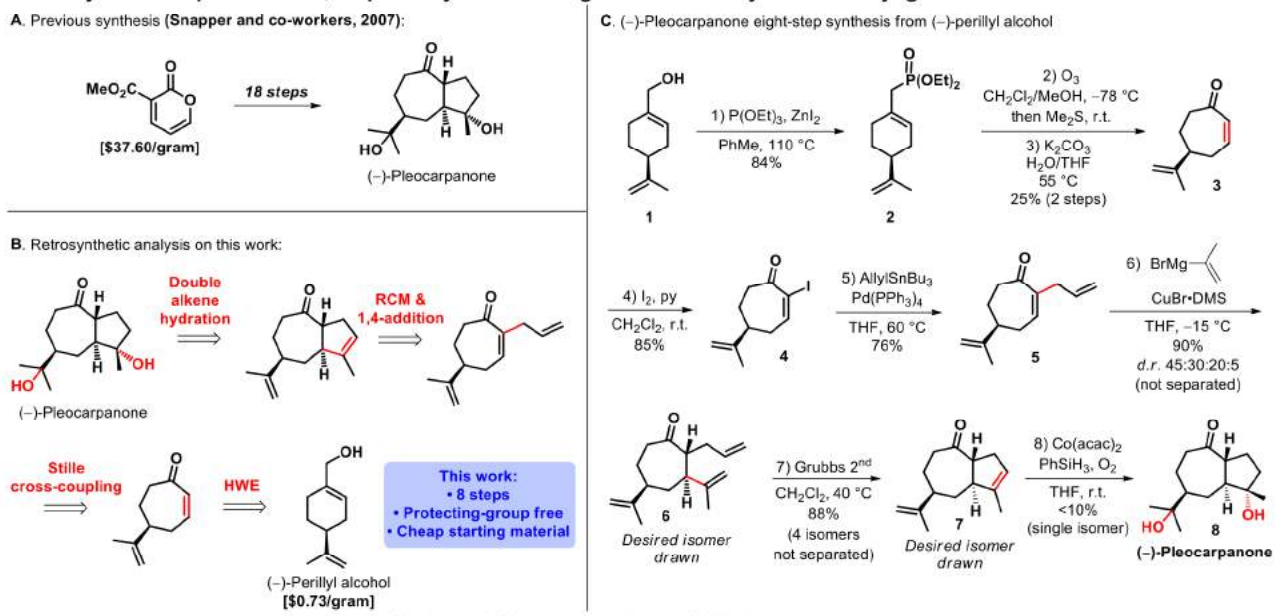


**Scheme 1**.Concise Synthesis of (−)-Pleocarpanone.

References:
[1] Silva, M.; Wiesenfeld, A.; Sammes, P. G.; Tyler, T. W. *Phytochemistry* **1977**, *16*, 379-385.
[2] Williams, M. J.; Deak, H. L.; Snapper, M. L. *J. Am. Chem. Soc.* **2007**, *129*, 486-487.

**Área: ORG** **Inscrição: 00467**

# Preparation of magnetic particles modified with calixarenes and evaluation as catalyst in Biginelli reaction

**Carlos Henrique Callegario Zacchi (PG) [1,*] Sara Silveira Vieira (PQ)[1], José Domingos Ardisson (PQ)[2], Ângelo de Fátima (PQ)[1], Maria Helena Araujo (PQ)[1].**

*E-mails: carloshzacchi@yahoo.com.br (CHCZ) and adefatima@qui.ufmg.br (AF)

*[1] Departamento de Química, UFMG, Brasil; [2]Laboratório de Física Aplicada, CDTN, Brasil.*

Keywords: *Magnetic particles; calixarenes; heterogeneous catalysis; Biginelli's reaction.*

## Highlights

►The obtained particles showed pronounced catalytic effect on the synthesis of Biginelli adducts (55-88% yields). ► Significant efficacy of the particles was observed even after five reuse cycles.

## Resumo/Abstract

Dihydropyrimidinones (DHPMs) are obtained from the Biginelli reaction, requiring acid catalysts to increase the yield. The *p*-sulfonic acid calix[4]arene has already been used, in homogeneous medium, in this reaction [1]. However, solid catalysts have many advantages over homogeneous catalysts. Thus, systems that can use this acid supported on a solid can be an important alternative for the synthesis of DHPMs [2]. The use of magnetic particles as supports of catalyst unites the efficiency of a heterogeneous catalyst to its magnetic capacity [3]. In this context, the synthesis of the DHPMs was carried out using the magnetic particles modified with calixarenes, according to Scheme 1.

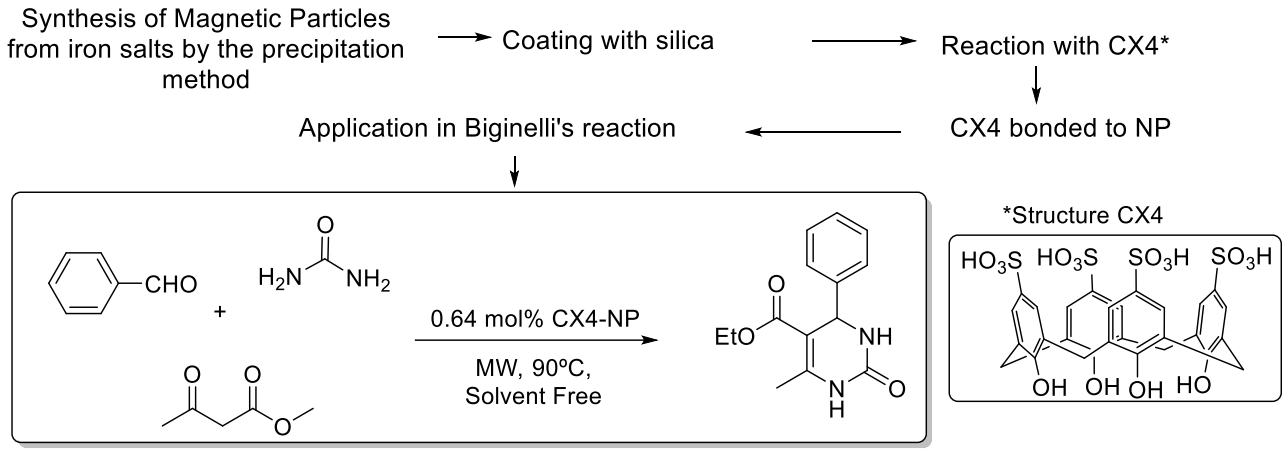


Scheme 1. Procedure of synthesis of the catalyst and application in the Biginelli reaction.

The reaction conditions were optimized (temperature, solvent, catalyst) and shown in Scheme 1. Then, different aromatic aldehydes were tested, and yields ranged from 55-88%. The catalyst maintained its constant activity after five cycles of reuse (80-88% yield). The next steps will be to apply the catalyst to other multicomponent reactions and glycerol valuation reactions. **Acknowledgments:** FAPEMIG, CAPES and CNPq.

**References.**

[1] da Silva, D.L. *et al.*, *Tetrahedron Lett.* **2011**, *52*, 6328.
[2] Liu, Y. *et al.*, *Appl. Surf. Sci.* **2018**, *427*, 575.
[3] Bodaghifard, M.A. *et al.*, *J. Iran Chem. Soc.* **2017**, *14*, 365.

**Área: ORG** **Inscrição: 00481**

# Síntese de aciclonucleosídoes fosfonatos quinolônicos, ANPs, possíveis compostos anti-CHIKV

**Letícia V. Faro (PQ),[1] Fernanda C. S. Boechat (PQ),[1] Marcos C. de Souza (PQ),[1] Izabel C. N. P. Paixão (PQ),[2] Maria Cecília B. V. de Souza (PQ).[1]***

**leticiafaro@gmail.com; gqocica@vm.uff.br**

*[1]Instituto de Química, Departamento de Química Orgânica, UFF; [2]Instituto de Biologia, Departamento de Biologia Celular e Molecular, UFF*

Palavras Chave: *Aciclonucleosídeo, Quinolona, Fosfonato, Chikungunya.*

## Highlights

Synthesis and biological evaluation of new 4-oxoquinoline acyclonucleoside phosphonates (ANPs) potential anti-CHIKV substances.
The increasing number of cases of CHIKV infections makes this disease a serious health problem in Brazil. It is urgent to find a treatment capable of reducing the effects of the CHIKV infections.

## Resumo/Abstract

O vírus CHIKV, causador da febre chicungunya, tem como vetores as espécies *Aedes aegypti* e *Aedes albopictus e,* atualmente, não há vacinas ou abordagens terapêuticas específicas para prevenir ou tratar infecção por CHIKV. Esta é considerada um grave problema de saúde no Brasil e é urgente encontrar um tratamento capaz de diminuir os efeitos da doença. Face ao amplo escopo de atividades biológicas dos compostos quinolônicos, e a resultados relacionados a síntese e estudos de atividade biológica de novos derivados quinolônicos, em especial antiviral, obtidos em trabalhos de nosso grupo de pesquisas, assim como a estudos citados na literatura envolvendo medicamentos como a ribavirina e a cloroquina, capazes de inibir o vírus CHIKV *in vitro*, está sendo realizada neste trabalho a síntese e a investigação do perfil anti-CHIKV de aciclonucleosídeos quinolônicos do tipo fosfonatos. Neste sentido, foram preparadas 1-[(diisopropoxifosforil)metil]-4-oxo-1,4-diidroquinolina-3-carboidrazidas (**4**), a partir da reação substituição nucleofílica à carbonila do grupamento éster dos derivados **3**, tendo-se hidrazina como nucleófilo. As substâncias **3** foram resultantes de reação de *N*-alquilação das quinolonas (**1**) com diisopropil(tosilmetoxi)fosfonato (**2**). Estes ANPs quinolônicos **4** estão em avaliação quanto sua atividade anti-CHIKV.

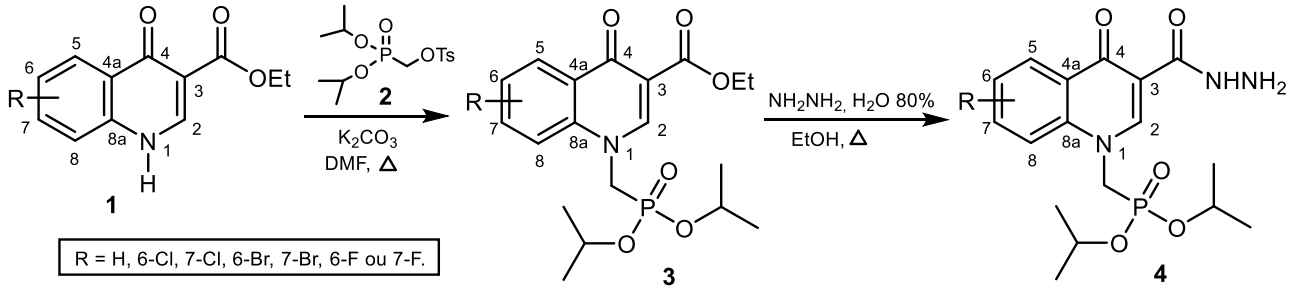


**Esquema 1.** Esquema reacional para obtenção dos derivados aciclonucleosídos quinolônicos fosfonatos **4**.

# Síntese de Sílicas Ativas: avaliação da matriz e de adsorção de Boro.

**Jean E. F.C.Rodrigues[1] (TM), Davi S. Assis[1] (TM), Juliana M.Souza[2] (PG), Ricardo J. Cassella[2] (PQ), Marcos T. Couto[1] (PQ)***

marcos.couto@ifrj.edu.br

[1] *Coordenação de Química,Campus Rio de Janeiro, IFRJ;* [2] *Departamento de Química Analítica, IQ, UFF*

Palavras Chave: Coluna de Pré-concentração; sílicas funcionalizadas; Boro

## Highlights

Synthesis of Active Silicas: matrix evaluation and Boron adsorption. This work functionalized a silica with amino sugar in the adsorption of boron. The adsorption capacity and TGA analysis were measured.

## Resumo/Abstract

A sílica é um material que pode ser usado como fase estacionária em diversas metodologias de fase heterogênea. Este trabalho incorporou à superfície de sílica 240-400 mesh a substância N-metilglucamina como estratégia na adsorção de boro, em sua forma de ácido bórico. A matriz de sílica funcionalizada foi sintetizada: após a ativação da sílica em meio fortemente ácido, a sílica foi funcionalizada com 3-cloro-propil-trietoxisilano.[1] A incorporação da N-metilglucamina ocorreu em metodologia de Tamborini et al.[2] A matriz sílica/glucamina foi testada frente a uma amostra de ácido bórico diluída e os resultados serão discutidos. O Boro foi determinado de forma indireta. A fase aquosa foi recolhida após contato com a sílica funcionalizada para determinação do analito por espectrofotometria de absorção molecular na região do ultravioleta-visível. Utilizou-se Azometina – H para a determinação do Boro não adsorvido à sílica. As análises da adsorção de boro foram realizadas e a solução resultante foi avaliada, apresentando uma adsorção superior a 95% da amostra inicial, sempre em triplicata. A metodologia comparou o branco da sílica ativa, não-funcionalizada, para a identificação da adsorção da amostra na sílica pura de boro livre. A matriz foi avaliada em análise de termogravimetria, Calorímetro Diferencial de Varredura, Espectroscopia de Infravermelho, RMN de sólido e difração de raio X para avaliação de sua estrutura e estabilidade, e serão discutidos.

**Referências**

**1** Yang,X.Y.; Chem. Soc. Rev.,2017,46,48

**2** Tamborini, S.;.;Inorg. Chim. Acta;2014; 410, p.28

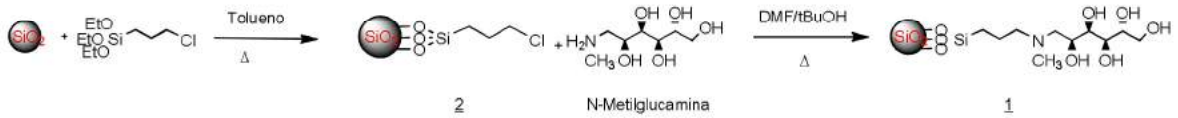


2 N-Metilglucamina 1

**Área: ORG** **Inscrição: 00525**

# Síntese de quinolonas conjugadas a triazóis e investigação de sua atividade leishmanicida

**Vanessa G. Oliveira (PG),[1]* Pedro F. Regufe (IC),[1] Miriam F. O. Lima (IC),[1] Viviane dos Santos Faiões (PQ),[2] Juliana da Silva Pacheco (PG),[2] Fernanda C. S. Boechat (PQ),[1] Caio Torres-Santos (PQ)[2], Fernando C. da Silva (PQ),[1] Maria C. B. V. de Souza (PQ)[1]**

**vanessagama@id.uff.br**

[1]*Universidade Federal Fluminense, Departamento de Química Orgânica - Instituto de Química – CEG – Outeiro de São João Batista-s/n° - Valonguinho - 24020-150 - Niterói – RJ*

[2] *Fundação Osvaldo Cruz, Laboratório de Bioquímica de Tripanosomatídeos, Instituto Oswaldo Cruz, Rio de Janeiro, RJ, Brazil.*

Palavras Chave: *Quinolona, triazol, leishmania, antiparasitária.*

## Highlights

Synthesis of quinolones conjugated to triazoles and investigation of their leishmanicidal activity

Non-classical activity of quinolones
Conjugation between the quinolone and triazole nuclei
Promising leishmanicidal actitivity

## Resumo/Abstract

**Introdução:** Muitos derivados 4-quinolônicos possuem perfil antibacteriano sendo que diversos deles são inclusive largamente empregados na clínica para tratamento de infecções bacterianas. Contudo, são muitos os relatos na literatura sobre quinolonas com atividades biológicas não clássicas, tais como antitumoral, antiviral e antiparasitária. [1] Outro núcleo heterocíclico presente em estruturas de substâncias para as quais são descritas atividades biológicas diversas, como por exemplo anti-leishmania, é o 1,2,3-triazólico. [2] Neste trabalho, preparou-se quinolonas conjugadas a triazóis e se fez estudos visando a avaliação do potencial leishmanicida destes compostos.
**Resultados:** Para a obtenção dos conjugados desejados, foram sintetizadas inicialmente as quinolonas **1.** [3] Estas foram em seguida *N*-alquiladas com brometo de propargila, obtendo-se os derivados do tipo **2**. Sua reação com diferentes aril ou alquilazidas, através de cicloadição 1,3-dipolar, levou às triazoloquinolonas **3** desejadas. Estas substâncias foram avaliadas quanto a sua atividade anti-promastigota de *L.amazonenses*.

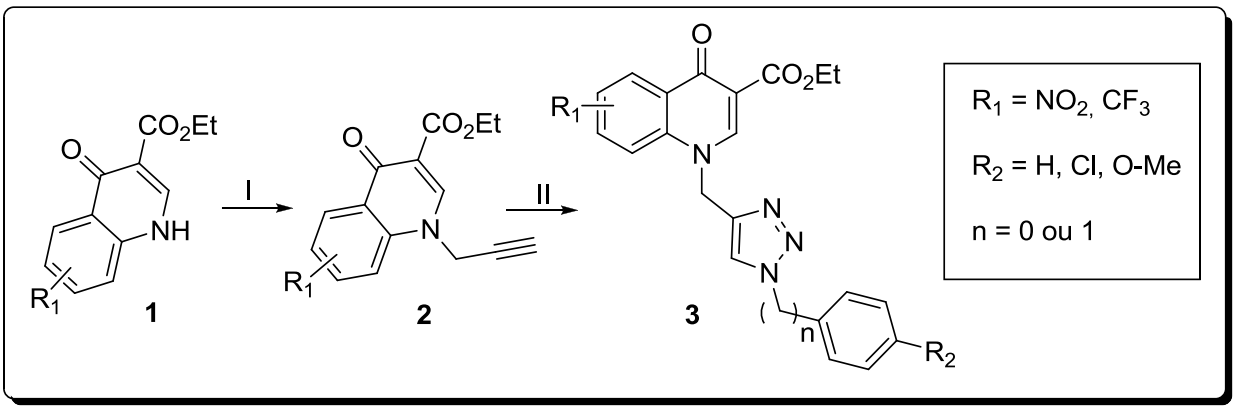


**Esquema 1**: Rota sintética para obtenção da quinolonas triazólicas do tipo **3**. I) $K_2CO_3$, DMF, brometo de propargila, aquecimento, 48 h. II) $N_3(CH_2)_nPhR_2$, $CuSO_4$, ascorbato de sódio, DMF, 24 h.

**Área: ORG** **Inscrição: 00568**

# Synthesis of 4-quinolone-porphyrin conjugates as potential photosensitizers

**Fernanda S. Sagrillo (PG),[1*] Ana T. P. Gomes (PQ),[2] Alan G. de Souza (IC),[1] Amanda R. P. Costa IC),[1] Fernanda da C. S. Boechat (PQ),[1] Maria Cecília B. V. de Souza (PQ),[1] Maria Graça P. M. S. Neves (PQ),[2] José A. S. Cavaleiro (PQ).[2]**

**fernandasagrillo@id.uff.br**

*[1] Universidade Federal Fluminense, Instituto de Química - Outeiro de São João Batista, s/nº. Campus do Valonguinho - Centro - Niterói - RJ, CEP: 24020-150, Brazil; [2] University of Aveiro, Departament of Chemistry and QOPNA, 3810-193, Aveiro, Portugal.*

Key-words: *Quinolones, Porphyrins, Photodynamic inactivation*

## Highlights

The aim of this work was the synthesis of new 4-quinoloneporphyrin conjugates and their future evaluation as photosensitizers (PS) aiming their application on photodynamic inactivation of microorganisms (PDI)

## Abstract

Photodynamic inactivation (PDI) is an approach that has gained prominence as a new form to inactivate microorganisms. In this therapy the vital constituents of the microorganisms are destroyed through a non-specific attack by reactive oxygen species (ROS) produced by dyes known as photosensitizers after their light activation in the presence of oxygen. On a strategy to obtain new PS, in this work it was prepared a series of 4-quinoloneporphyrin conjugates **5** (Scheme 1) to evaluate their potential as photosensitizer on bacterial inactivation. The key step for obtaining the new conjugates involved the Heck reaction between 2-bromo-5,10,15,20-tetraphenylporphyrinatozinc(II) (**1**) and the 1-allyl-4-quinolone substrates **2a-e**. Table 1 shows the results obtained from **1** and (**2b**) under different experimental conditions.

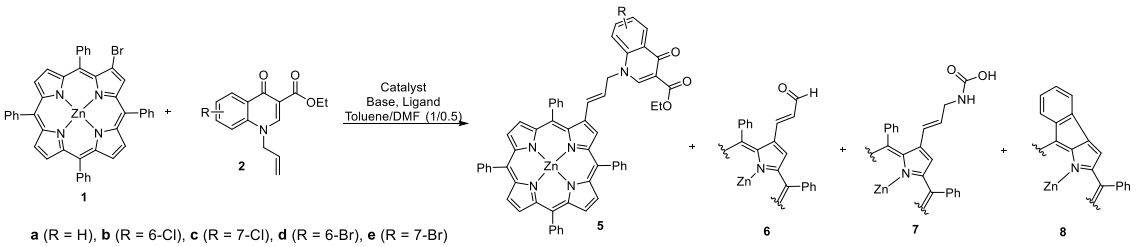


**Scheme 1.** Heck reaction between porphyrin **1** and 1-allyl-4-quinolone derivatives **2**.

**Table 1.** Catalyst, base, ligand, reaction time, and yields of the Heck reactions between **1** and **2b** (Toluene/DMF, 1:0.5).

| Entry | Catalyst | Base | Ligand | Time (h) | % 5 | % 6 | % 7 | % 8 | % 1 recov. |
|---|---|---|---|---|---|---|---|---|---|
| **1** | $Pd(OAc)_2$ | $K_2CO_3$ | TBAB | 3 | 13 | 15 | 5 | 6 | 5 |
| **2** | $Pd(OAc)_2$ | $Cs_2CO_3$ | TBAB | 29 | trace | 19 | trace | 10 | 32 |
| **3** | $Pd(OAc)_2$ | KOAc | TBAB | 2 | 33 | 1 | 19 | 10 | 6 |
| **4** | $Pd(OAc)_2$ | KOAc | $PPh_3$ | 2 | 42 | 3 | 9 | 10 | 5 |
| **5** | Tetrakis | KOAc | TBAB | 3 | 20 | 18 | 13 | 12 | 14 |

The best results were obtained under the conditions of entry 4 (Table 1) which were efficient extended to the other quinolones **2**. The structures of the new conjugates **5** and of the secondary products **6**-**8** also formed in these reactions were fully confirmed by spectroscopic techniques. All the conjugates **5** after hydrolysis and demetallation were able to generate singlet oxygen confirming their potential as PS.

Acknowledgments: CAPES, PDSE-CAPES, CNPq, FAPERJ, UFF-PROAES, University of Aveiro, Departament of Chemistry and QOPNA.

**Área: ORG** **Inscrição:00595**

# Chemical characterization of pyriproxifene by chromatography (HPLC-PDA and CG-MS)

**Patrícia S. Alves[1] (PG), Josiane M. S. Costa[3,*](IC), Maria D. A. Oliveira[2] (PG), Teresinha J. A. S. Andrade[4] (PQ), Joaquim S. Costa Júnior[3] (PQ)**

**patricia_silva_alves@hotmail.com; josianemarciel@outlook.com[*]**

[1] *State University of Piauí, Department of Chemistry, Campus Torquato Neto, Teresina, Piauí, Brazil.*

[2] *Federal University of Piauí, Department of Chemistry, Campus Senador Petrônio Portela, Teresina, Piauí, Brazil.*

[3] *Federal Institute of Piauí, Department of Chemistry, Campus Central, Praça da Liberdade, Teresina, Piauí, Brazil;*

[4]*Federal Institute of Maranhão, Department of Chemistry, Campus São Raimundo das Mangabeiras, Maranhão, Brazil.*

Keywords: *pyriproxifene, Aedes aegypti, microcephaly, water, HPLC-PDA.*

## Highlights

Chemical characterization of pyriproxifene by chromatography (HPLC-PDA and CG-MS). Combat the proliferation of larvae *Aedes aegypti*. Pyriproxyfen has been used in control of drinking water assessment in Brazil for human consumption. Correlated with emerging cases of microcephaly in the Americas.

## Resumo/Abstract

The pyriproxyfen has been used in control of drinking water assessment in Brazil for human consumption[1], in order to combat the proliferation of larvae *Aedes aegypti*. However, biological and chemical studies of this larvicide are still recent, so this work is intended to make a screening of insecticide through chromatographic techniques. In HPLC-PDA, 1 mg of the insecticide was used, solubilized Rock in mixture acetonitrile-methanol (80:20), and subjected to the process of clean up in Cartridge Chromabond ® C18ec (previously activated with MeOH), filtered with 0.45 µm membrane, injected into a Shimadzu analytical liquid chromatograph, model LC20A, controller CBM-20, with UV detector, and isocratic method of 0-60 minutes and flow 1.0 ml/min, C18 column (250 x 4.6 mm, particle size 5 µm), Macherey-Nagel brand. In the analysis CG-MS, was injected 10 µL of analyte splitless mode injection, use one capillary column RTX-5MS, model TQ8030 (length 30m, 0, 25mm ID., DF 0.25 µm), coupled to a mass spectrometer. The oven temperature was programmed in: 80 °C (2 min), 20 °C/min at 180 °C and 5 °C/min to 280 °C (3 min), whose gas carrier helium to 1 µL/ min with linear speed 44.5 cm/s and initial pressure 100 kPa. In the analysis of the insecticide by HPLC-PDA in λ of 272 nm (Figure 01), it can be seen the presence of two intense peaks with Retention times (TR) of 3,39min e 4,04min, respectively, corresponding to the wavelengths characteristic of the pyriproxyfen (λ 272 nm) and pyridalyl (λ 208 nm), according to a literature[2]. The analysis of insecticide by HPLC-PDA and GC-MS allowed the identification the pyriproxyfen and pyridalyl.

[1]WHO [World Health Organization]. Dengue. Guidelines for diagno-sis, treatment, prevention and control–New edition. Geneva,Switzerland, 2009.

[2]FAROUK, M.; HUSSEIN, L. A.; EL AZAB, N. F. New HPLC and fluorometric methods for the determination of pyriproxyfen and pyridalyl insecticide residues in tomatoes. Journal of AOAC International, v. 97, p. 188-196, 2014.

**Área: ORG** **Inscrição:0607**

# Optimization of the solvent mixture for extraction of phenolic compounds with antioxidant activity from *Byrsonima basiloba Juss*.

**Thais Cândido Roberto (IC)[1], Bruna Scaramboni (PG)[2], Catarina dos Santos (PQ)[1]. csantos@assis.unesp.br**

*[1]Departamento de Ciencias Biológicas, UNESP-Assis; [1]Departamento de Biotecnologia, UNESP-Assis*

Palavras Chave: i-optimal design, *phenolic compounds, flavonoids, $EC_{50}$, ABTS.*

## Highlights

The antioxidant activities from *Byrsonima* sp. leaves are usually assigned to their phenolics. From a selection of mixture of 15 extraction solvents ($H_2O$, EtOH and MeOH), obtained *via* an experimental i-optimal design of mixture, we found one proportion of solvent, which lead an extract with a best antioxidant activity and greater phenol and flavonoid contents.

## Abstract

The antioxidant activities from *Byrsonima* sp. leaves are usually attributed to their phenolic acids, flavonoids and tannins[1]. By a selection of mixture of 15 extraction solvents ($H_2O$, EtOH and MeOH), *via* an experimental i-optimal design of mixture (Design Expert 10.1, Stat-Ease Corporation), we found a proportion of solvents with maximum phenolics compounds extraction with the most efficient antioxidant activity. For each extract was used 5 g of dried and crushed leaves of *B. basiloba*/50 ml of the mixture of solvents (collected in Assis-SP). The solution was kept under dynamic maceration for 2h and filtered. The residue was reextracted twice more. The extracts were analyzed to concentration of total phenolics and flavonoids[2]and antioxidant activities[3,4]. Statistical analyzes were made with levels of 95% significance. The best solvent mixtures obtained for phenol and for flavonoid content were EtOH:MeOH 55:45 v/v (157.92± 5.35 mg galic acid/g extract) and 79:21 EtOH:MeOH v/v (12.57±6.89 mg quercetin/g extract), respectively. But, the best antioxidant activity was observed for solvent ratio of 33:34:33 EtOH:MeOH:$H_2O$ v/v/v ($EC_{50}$, 8.86 ± 2.53 mg extract/ml and 3.64±7.24 µM Trolox/mg dry extract). In this mixture of solvent, phenolic and flavonoid content were 130,97±1,99 mg galic acid/g extract and 8,17±4,49 mg quercetin/g extract, respectively. All the parameters tested, the linear model had a significant result (phenol p=0,0443, F=4,33) (flavonoids, p=0,0443, F=4,33) ($EC_{50}$: p<0.0196, F=5.56; ABTS p<0.0433, F=4,37). (Equation 1-4) (Figure 1 A-D).

$$\textbf{Phenol} = 122{,}09 * \text{etanol} + 150{,}51 * \text{methanol} + 114{,}98 * \text{water} \quad (1)$$

$$\textbf{Flavonoids} = 12{,}08 * \text{ethanol} + 9{,}66 * \text{methanol} + 2{,}92 * \text{water} \quad (2)$$

$$\textbf{EC}_{\textbf{50}} = 11{,}26^{*}\ \text{ethanol} + 9{,}76^{*}\text{methanol} + 20{,}75^{*}\text{water} \quad (3)$$

$$\textbf{ABTS} = 3{,}18^{*}\ \text{ethanol} + 3{,}59^{*}\ \text{methanol} + 2{,}46^{*}\ \text{water} \quad (4)$$

These results, compatible with the literature, were corroborated by the mathematical model proposed for this project.

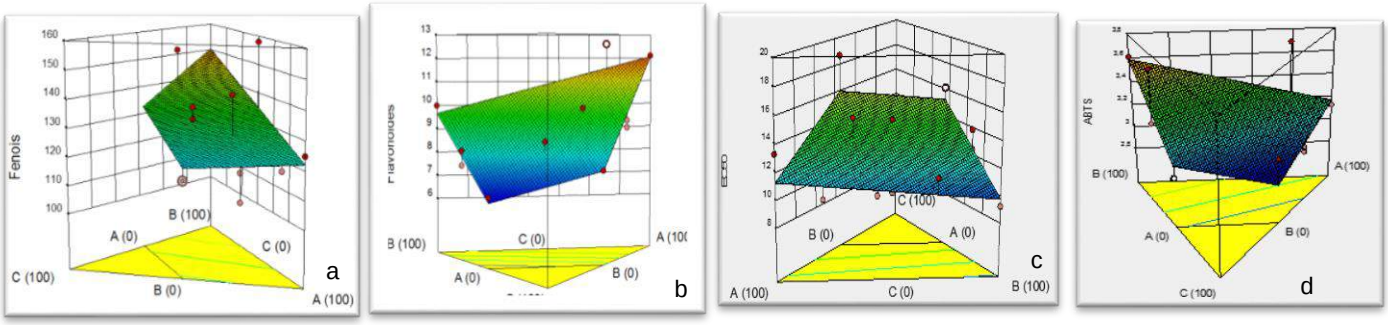


Figure 1. Influence of solvents (A:EtOH, B:MeOH, C:$H_2O$) in the extraction of a) phenol and b) flavonoids c) $EC_{50}$ d) ABTS.

[1]LONNI, A. A. S. G.; et al. *Analytica Chimica Acta*. **2012**, 57, 60.[2]KALIA, K., et al. **J. Agr. Food Chem**. 2008, 56, 10129. [3]ENUJIUGHA, V.N. et al. **Food and Nutrition Sciences**. **2012,** 3, 7. [4]RUFINO, M.S. M., et al. **Embrapa Agroindústria Tropical,** Comunicado técnico 128, junho de 2007.

**Área: ORG** **Inscrição: 00652**

# Synthesis of 2-aminothiazoles using α-bromoketones and thiourea in PEG-400

**Gabriela F. Matos (PG)[1], Achiles S. Ferreira (PG)[1], Rafael P. das Chagas (PQ)[1*], Olga S. do R. Barros (PQ)[1*].**

**gfmatoss@gmailcom; olgabarrros@gmail.com**

*[1]Instituto de Química, UFG.*

Palavras Chave: *2-Aminothiazoles, PEG-400, Synthesis, Thiourea.*

## Highlights

- Simple and efficient method for the synthesis of 2-aminothiazoles
- Alternative solvent PEG-400

## Resumo/Abstract

Aminothiazoles are a very important class of heterocycles. They have important biological properties and several applications in medicinal chemistry, such as: anti-allergic,[1] anti-coagulant,[2] antibacterial,[3] anti-inflammatory,[4] antidepressant,[5,6] and antifungal agents.[6] Most of the reported methodologies for their synthesis use hazardous solvents and require severe conditions or complicated procedures. In this work, we have developed an alternative methodology to synthesize 2-aminothiazoles through the reaction between α-bromoketones and thiourea using PEG-400 as a solvent, under mild conditions.

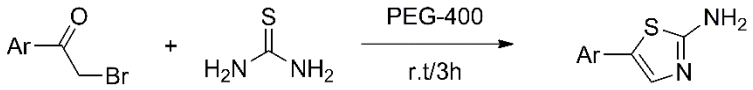


Ar: Ph, p-Br, p-$NO_2$, p-OM and Thiophene

| Ar[a] | Yield (%)[b] |
|---|---|
| Ph | 92 |
| p-OMe | 96 |
| p-Br | 43 |
| p-$NO_2$ | 72 |
| Thiophene | 72 |
| Cyclopentadiene | 50 |
| Ph[c] | 60 |
| Ph[d] | 90 |

[a]All products were identified by $^1$H and $^{13}$C NMR. [b]Isolated yields. [c] Thiourea was replaced by 1,3-diisopropyl-2-thiourea; product: 2-imino-1,3-thiazoline derivative. [d] Thiourea was replaced by selenourea; product: 2-aminoselenazol derivative.

In summary, an efficient methodology for the synthesis of a series of substituted 2-aminothiazoles is described. The main advantage of this method is the utilization of the non-hazardous alternative solvent PEG-400, under mild reaction conditions and a short reaction time. The scope of the reaction is still being extended and we should be able to soon report reactions using substituted thiourea and its derivatives urea and selenourea, as well as other α-bromoketones.

**Acknowledgements: UFG, CNPq, CAPES and FAPEG**

**References:**

1. Ohkubo, M., Kuno, A., Nakanishi, I. & Takasugi, H. *Chem. Pharm. Bull.* **43,** 1497–1504 (1995).
2. Jimonet, P. *et al.* Riluzole Series. *J. Med. Chem.* **42,** 2828–2843 (1999).
3. Rudolph, J., Theis, H., Hanke, R., Endermann, R. & Johannsen, L. *J. Med. Chem.* **44,** 619–626 (2001).
4. Jayashree, B. S., Anuradha, D. & Venugopala, K. N. *Asian J. Chem.* **17,** 2093–2097 (2005).
5. Asha, H. *et al.* RSC Advances agents. *R. Soc. Chem.* **5,** 96809–96828 (2015).
6. Das, D., Sikdar, P. & Bairagi, M. *Eur. J. Med. Chem.* **109,** 89–98 (2016).

**Área: ORG** **Inscrição: 678**

# Regiospecific Synthesis and Antitumor Evaluation of Thioethers Derived from Juglone

**Carinne B. S. M. R. Gomes[1] (PG); Caroline S. Moreira[1] (PG); Luana S. M. Forezi[1] (PQ); Pâmella S. Cordeiro[1] (IC); Vanessa do Nascimento[1] (PQ); Raquel C. Montenegro[2] (PQ); Vitor F. Ferreira[3] (PQ); David R. da Rocha[1*] (PQ)**

***davidrocha@id.uff.br**

*[1]Universidade Federal Fluminense, Departamento de Química Orgânica, Niterói, RJ; [2]Universidade Federal do Ceará, Departamento de Fisiologia e Farmacologia, Fortaleza, CE; [3]Universidade Federal Fluminense, Faculdade de Farmácia, Niterói, RJ*

Palavras Chave: *Naphtoquinones, Regiospecific synthesis, Leukemia*

## Highlights

Regiospecific synthesis of Juglone derivatives
Antitumor Evaluation of Thioethers Derived from Juglone
Compouds with high activity, selective against leukemic cells and safe for normal cells

## Resumo/Abstract

13 thioethers were synthesized, of which 12 are unpublished. The methodology employed was much higher than previously reported in the literature, since it allowed the production of purifiable thioethers using simpler techniques and in higher yields. Compounds were evaluated for their anticancer properties, showing excellent results and selectivity against HL60 leukemia, K562 lucena (resistant chronic myelogenous leukemia (MDR) and K562 (chronic myeloid leukemia) cells). Highlighting the lines K562 and K562Lu.

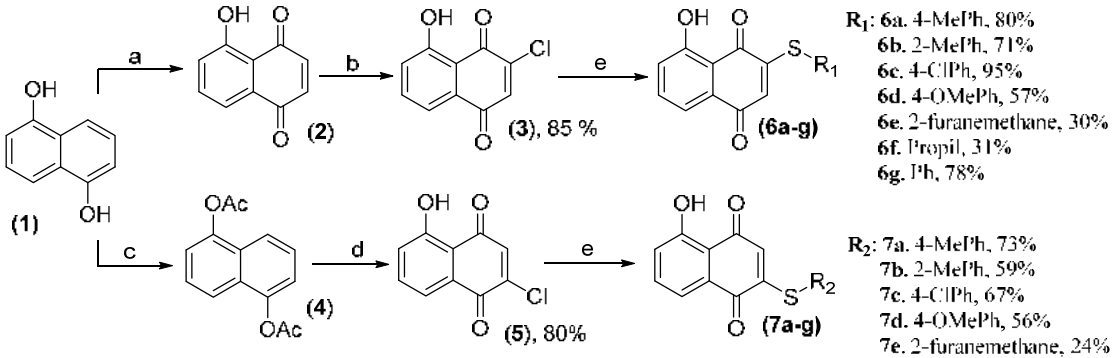


**Scheme 1.** Regiospecific synthesis of thioethers **6a-g** and **7a-g**

**Área: ORG** **Inscrição: 00713**

# Theoretical insights on the racemization of azlactone rings

**Pedro P. de Castro (PG),[1] Gabriel M. F. Batista (IC),[1] Hélio F. dos Santos (PQ),[1] Giovanni W. Amarante (PQ).[1]***

**pedro_possa@hotmail.com; giovanni.amarante@ufjf.edu.br**

[1]*Chemistry Department, Federal University of Juiz de Fora.*

Keywords: *Azlactone, Heterocycle, Racemization, Density Functional Theory (DFT).*

## Highlights

We hereby present a theoretical study on the racemization of azlactones. Two hypotheses were investigated, with the base mediated racemization being the most viable and consistent with experimental data.

## Resumo/Abstract

Azlactones are versatile heterocycles employed in a diversity of transformations; the main drawback of the use of these cycles consists in the complete epimerization of the α-carbonyl stereocenter during its preparation (Scheme 1).

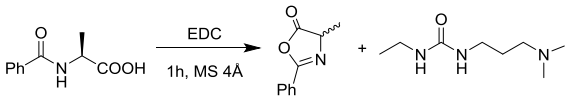


**Scheme 1.** Azlactone preparation, evidencing the complete racemization of the stereocenter.

Although this process is well known, the reaction step in which it occurs and how this racemization takes place is still unclear. Therefore, we hereby present a theoretical study using density functional theory (DFT) and employing the B3LYP/6-31G(d) level of theory to explain how the racemization of azlactones occurs. Two hypotheses were investigated: the keto-enol tautomerism (Figure 1A) and the base mediated racemization (using triethylamine as base), through an enolate intermediate (Figure 1B).

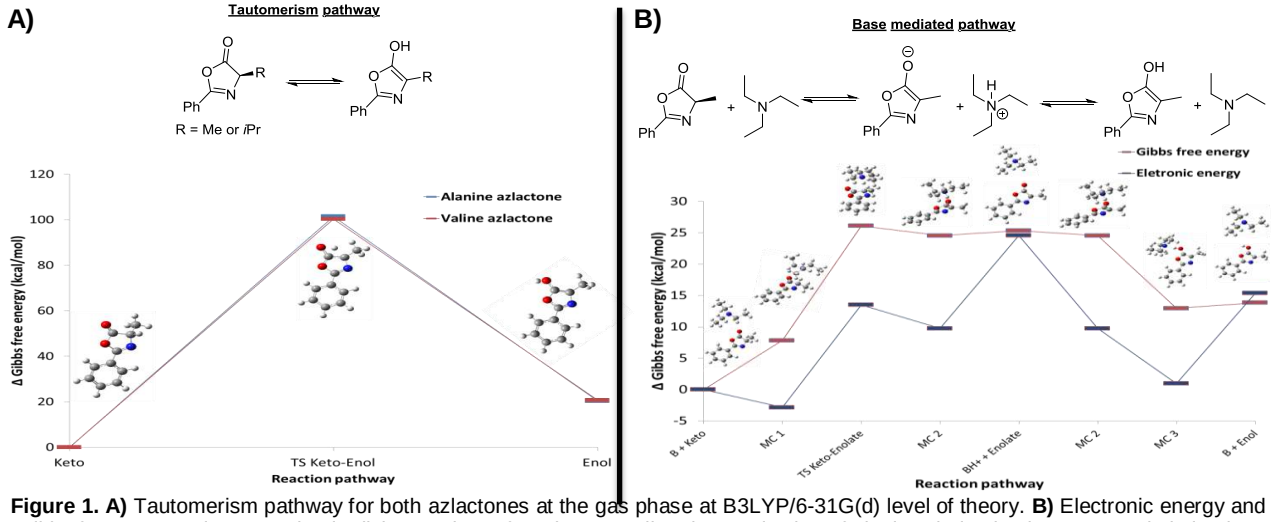


**Figure 1. A)** Tautomerism pathway for both azlactones at the gas phase at B3LYP/6-31G(d) level of theory. **B)** Electronic energy and Gibbs free energy along reaction in dicloromethane for a base-mediated racemization of alanine-derived azlactone. B: triethylamine; $BH^+$: protonated triethylamine; MC1: molecular complex keto + base; MC2: molecular complex enolate + $BH^+$; MC3: molecular complex enol + base

The results showed that the tautomerism pathway is unlikely to occur and that the base mediated pathway is consistent with experimental data and can spontaneously occur at room temperature. The same pathway was evaluated for a 2-alcoxy azlactone, showing a slower epimerization ratio, consistent with literature data. Based on this proposal, the percentage of keto and enol species were determined for a wide scope of azlactones by the difference in Gibbs free energy between these species, resulting in an experimental $\%_{Keto}$ higher then 99.99% in all cases, in accordance with experimental observations. Finally, we hereby suggest a new role for the catalysts involved in DKR reactions, in which in addition to influencing in a stereosective manner the ring-opening reactions, these catalysts are also necessary to mediate the racemization process.

Acknowledgements: CAPES, FAPEMIG, CNPq and Rede Mineira de Química for financial support.

**Área: ORG** **Inscrição: 00735**

# Desenvolvimento de Novos Biocatalisadores Imobilizados Contendo Lipases para a Produção do Carbonato de Glicerila em batelada e fluxo contínuo

**Marcelo A. Nascimento (PG),[1]Larissa E. Gotardo (IC),[1] Leonardo Raul (IC),[1]Raquel A. C. Leão(PQ),[1,2] Ivaldo Itabaiana Jr.(PQ),[1,3]Rodrigo O. M. A de Souza (PQ).[1]***

**marceloavelar@id.uff.br, souzarod21@gmail.com**

*1- Grupo de Biocatálise e Síntese Orgânica, Instituto de Química, Universidade Federal do Rio de Janeiro, Rio de Janeiro, RJ 21941-90;. 2-Faculdade de Farmácia, Universidade Federal do Rio de Janeiro, RJ, Brazil, 21941-170; 3-Departamento de Engenharia Bioquímica, Escola de Química, Universidade Federal do Rio de Janeiro, Rio de Janeiro,RJ 21941-910.*

Palavras Chave: *Imobilização, Lipases, Carbonato de glicerila.*

## Highlights

Development of New Immobilized Biocatalysts Containing Lipases for Batch and Continuous Flow Glyceryl Carbonate Production. New approaches for the production of glycerol carbonate and biodiesel.New biocatalysts with immobilized from porcine pancreas and *Candida antarctica* B. Synergic biocatalysts.

## Resumo/Abstract

O Carbonato de glicerina (CG) é um coproduto da produção do biodiesel com elevado potencial de aplicação pela indústria química, podendo ser produzido por via química ou através da transesterificação de óleos vegetais na presença de biocatalisadores como as lipases (triglicerolacil-hidrolases, E.C. 3.1.1.3).[1] Porém, alguns processos permanecem limitados devido ao alto custo desses biocatalisadores; sendo assim, a técnica de imobilização se mostra como uma alternativa importante para a sua utilização na síntese orgânica.[1]Este trabalho propõe a imobilização das lipases Pancreática suína(PPL) e *Candida antarctica* B (CalB) em quatro suportes resinosos distintos, sendo dois com grupos epóxidos (Purolite®) e outros dois com grupos octadecil (Purolite®) através dos métodos de adsorção e ligação covalente uni- e multipontual para aplicação na síntese do CG.[2]Um *screening* realizado investigou a influência do pH, temperatura e força iônica do meio reacional, além da atividade enzimática dos biocatalisadores. Como resultado, os suportes contendo lipase Pancreática suína apresentou melhores resultados para a atividade de hidrólise e a lipase *Candida antarctica* B para a atividade de esterificação, ambas imobilizadas em suporte epóxido Purolite®. Uma vez sendo a reação principal uma transesterificação do óleo vegetal, foi realizado um híbrido[3] na proporção (1:1) desses biocatalisadores e aplicado na síntese do carbonato de glicerila, obtendo uma conversão de 96% e seletividade >99% **(Figura)**, resultado proeminente comparado ao obtido na referência N435 de 87%.[4] Outros óleos estão sendo investigados, tais como: Palma, Macaúba e Linhaça.

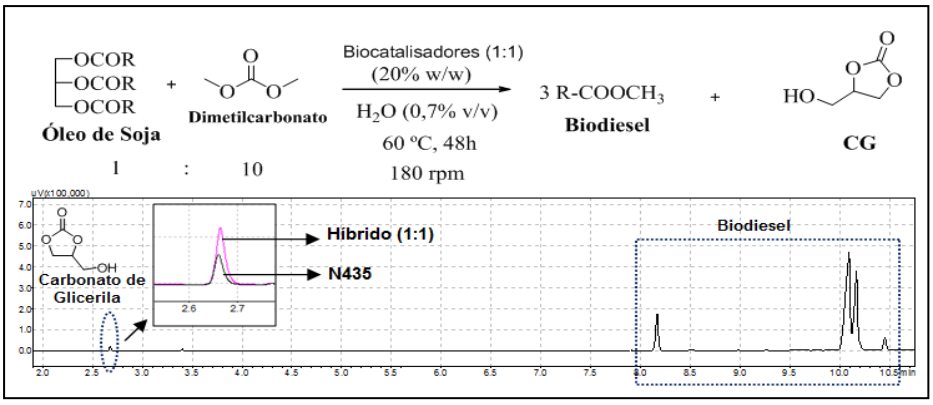


**Figura**: Cromatograma do híbrido do biocatalisador imobilizado em suporte Purolite® (ECR8205F e ECR8214F) lipases *Candida antarctica* B e Pancreática suína, respectivamente. Imagem ampliada: Comparação com a comercial N435. Análise realizada em CG-DIC (Shimadzu CG2010 – DB-5HT coluna capilar).

**Referências:** [1] Souza, S. P. et al. *J Chem Technol Biotechnol* **2018**, *93*,105–111.[2]Mateo, C. et al. *Enzyme Microb Technol***2007***, 40*, 1451–*1463.*[3]Norjannah, B. et al. *RSC Adv* **2016***, 6, 60034–60055.*[4]Go, A. R. et al.*Enzyme Microb Technol* **2013**, *53***,** 154–158.

**Área:** ORG **Inscrição:** 767

# Reações de Bromoaminociclização Enantiosseletivas

**Jullyane E. Matsushima (IC), Alessandro Rodrigues (PQ)***

**jumatsushima@outlook.com; alessandro.rodrigues@unifesp.br**

*Departamento de Química, Universidade Federal de São Paulo – UNIFESP*

Palavras Chave: *bromoaminociclização, enantiosseletividade, organocatálise, carbamatos alílicos*

## Highlights

Enantioselective Bromoaminocyclization reactions.

Development of a new methodology of enantioselective bromoaminocyclization of allyl-tosylcarbamates by organocatalysts.
Regio- and stereoselective control in bromoaminocyclization reactions of allylic carbamates.

## Resumo

Pan e colaboradores,[1] descreveram uma abordagem eficiente para reações de bromoaminociclização enantiosseletivas de carbamatos alílicos promovidas por catalisadores de escândio complexados a fosfinóxidos quirais. No presente trabalho, resolvemos desenvolver uma nova metodologia empregando organocatálise na reação de Pan. Considerando-se o elevado custo do $Sc(OTf)_3$, a organocatálise surge como abordagem alternativa. A reação de bromoaminociclização encontra-se em fase de otimização utilizando-se o carbamato cinâmico como modelo, na qual foram aplicados 17 organocatalisadores diferentes em condição reacional padrão (Esquema 1) em escala de 0,2 mmol. Para esta etapa, foram mantidas a temperatura, o tempo reacional, e o solvente, resultando no organocatalisador **XV** como o mais eficiente até o momento, conversão de 74% e 27% ee. A maioria dos organocatalisadores aplicados apresentou atividade, apesar das conversões modestas. Cabe ressaltar que sem a presença de organocatalisador não foi observada a formação de produto, sendo o carbamato **2** recuperado. Os resultados indicam que a reação ocorre de maneira régio- e diastereosseletiva com a formação exclusiva do ciclo de 6 membros com os substituintes -Br e -Ph em relação *trans*.

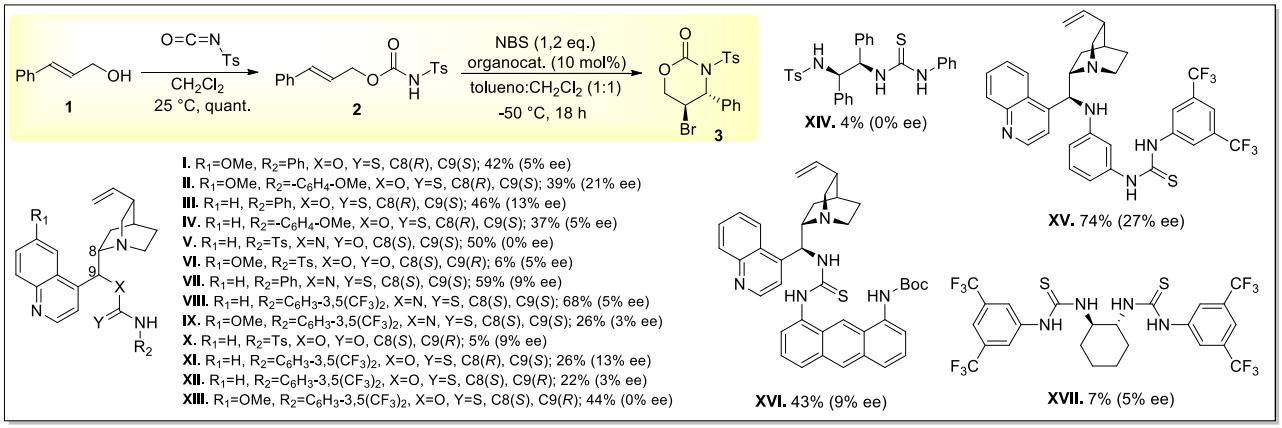


**Esquema 1.**

Na próxima etapa do trabalho, a otimização será concluída visando resultados mais eficientes. Após a finalização da otimização das condições reacionais, será investigada a limitação da metodologia frente a carbamatos estruturalmente mais complexos. No momento, estudos mecanísticos por espectrometria de massas e cálculos teóricos estão se iniciando objetivando o entendimento do processo e a ampliação da metodologia.

1. Pan, H.; *et al. Org. Lett.* **2016**, *18*, 896.

Fomento Proc. 2016/21676-0

**Área: ORG** **Inscrição: 00861**

# Synthesis of analytical standards of 25I-NBOMe and 25I-NBOH for forensic purposes

**Marcelo Pereira Queiroz (IC)[1,*], Wellington Alves de Barros (PG)[1], Leonardo da Silva Neto (PQ)[1], Clésia Cristina Nascentes (PQ)[1], Ângelo de Fátima (PQ)[1].**

*E-mail: marcelopq123@gmail.com (MPQ) and adefatima@qui.ufmg.br (AF)

[1]*Department of Chemistry, UFMG, Brazil.*

Keywords: *Phenylethylamine, 25I-NBOH, 25I-NBOMe, Serotonin receptors, Organic synthesis, Analytical standard.*

## Highlights

► 25I-NBOH e 25I-NBOMe were synthesized with high purity levels and at low cost. ►These analytical standards will be used in further studies.

## Abstract

*N*-Substituted phenylethylamines such as 25I-NBOH (**1**) and 25I-NBOMe (**2**) have been commercialized as recreational drugs, usually replacing lysergic acid diethylamide (LSD).[2] However, compared with LSD, few information is known about the pharmacological effects of this class of substances. Therefore, an efficient and accessible preparation of analytic standard is required to enable the studies with the class. Initially, **4** was obtained, as yellow solid (79%), through Henry's reaction between **3** and nitromethane, followed by dehydration of the Henry's adduct.[3] Substance **4** was reduced with $LiAlH_4$, resulting in **5** with 74% yield. Amine **6** was obtained through a eletrophilic aromatic substitution of **5** with iodine in the presence of $Ag_2SO_4$ at room temperature with 68% yield.[4] The reductive amination of **6** with 2-methoxybenaldehyde, using $NaBH_4$ as reducing agent, furnishes 25I-NBOMe (**2**) (61%). Similarly, 25I-NBOH (**1**) was obtained reacting **6** with salicylaldehyde (40%).[1]

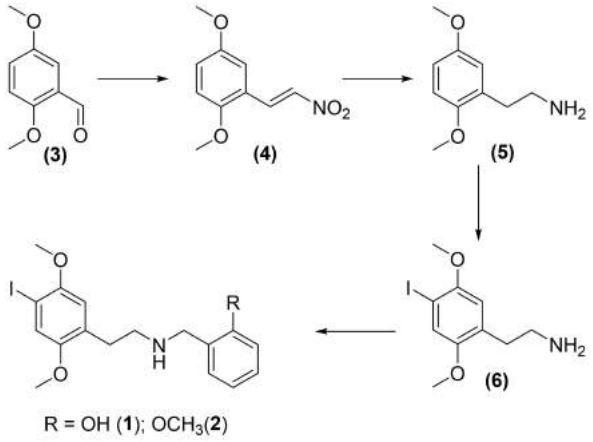


**Scheme 1.** Synthesis of 25I-NBOMe and 25I-NBOH from 2,5-dimethoxybenzaldehyde (**3**).

Both analytical standards were characterized by GC-MS, $^1$H NMR and $^{13}$C NMR, showing high purity levels and obtained at low cost. These results could provide more accessible advances in the forensic and pharmacological areas for these substances. **ACKNOWLEDGMENT:** FAPEMIG, CAPES e CNPq.

[1]Hansen, M. *et al ACS Chem. Neurosci.* **2014**, *5*, 243.

[2]Ninnemann, A. & Stuart, G. L. J. *Studies on Alcohol and Drugs*. **2015**, 74, 977.

[3]Anderson, W. K. *et al J. Org. Chem.* **1987**, 3, 2945.

[4]Karlsen, M. *et al J. Label. Compd. Radiopharm.* **2014**, *57*, 378.

**Área: ORG** **Inscrição: 00903**

# Synthesis and Antifungal Evaluation of α amino acids

**Alan F. de Araújo (FM)*,[1] Adriana P. Ferreira (IC),[2] Priscila S. V. Lima (PG),[3] Helivaldo D. S. Souza (PG),[3] Daniele de F. Silva (PG),[4] Edeltrudes O. Lima (PQ),[4] Petrônio F. A. Filho (PQ),[3] Rafael F. de Oliveira (PG),[3] Min-Fu N. Huang (PG),[3] Alex de Meireles Neris (PG).[3]**

**alanferreiraq@hotmail.com***

*[1]Instituto Federal da Paraíba, IFPB; [2]Departamento de Química, IFPB; [3]Departamento de Química, UFPB; [4]Departamento de Ciências Farmacêuticas, UFPB.*

Keywords: *Synthesis, Amino acids, Antifungal activities.*

## Highlights

The α-amino acids were synthesized in 2 steps and inhibited the growth of Candida strains with MIC of 256 µg.mL-1.

## Resumo/Abstract

Amino acids are compounds which contain two functional groups: an amino group and a carboxylic acid group bonded to α carbon. In addition, the α carbon is bonded to R groups that differentiate each other[1]. These compounds have been precursor in several searches from non-linear optics and the synthesis of a series of derivatives in order to develop more efficient medicines to combat various diseases like depression and Parkinson's disease. The α amino acids derivatives may demonstrate an increase in biological activity when It is used as adjuvants[2]. This work presents the synthesis and characterization of α amino acids in two steps: (i) reactions of aromatic *p*-substituted aldehydes (**1a-d**) in order to obtain α amino nitriles (**2a-d**) and (ii) its hydrolysis with a 6M solution of HCl to obtain the a amino acids (**3a-d**), like the reaction scheme below.

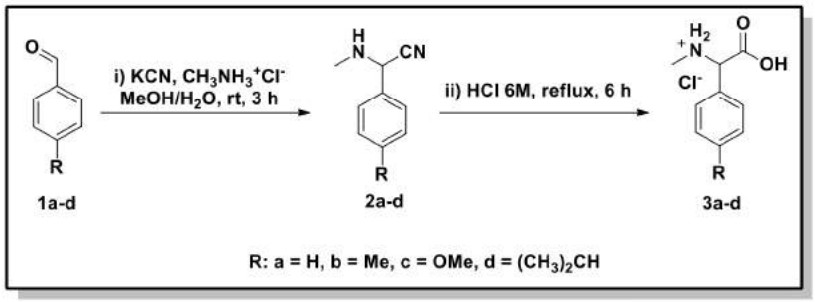


Reaction scheme of the α amino acids

The compounds (**3a-d**) were purified by recrystallization in EtOH/water 1:1 with 61-70% yield and characterized by spectroscopic methods (IR, MNR $^1H$ e $^{13}C$). Antifungal activities of the *Candida albicans* ATCC 76485 and *Candida tropicalis* LM 98 were investigated. All of compounds inhibited the growth of *Candida* strains with MIC of 256 µg.mL$^{-1}$. The synthetic routes of the synthesis of the α amino acids were carried out in a simple and effective way with good yields. The results of the investigation can be considered from great to moderate considering the established parameters[3].

1. Hughes, A. B. *Amino Acids, Peptides and Proteins in Organic Chemist.* **2009**, ISBN: 978-3-527-32096-7.
2. Kobayashi, K. S., et. Al. *National Institutes of Health*. **2011**. 7(3): 180–197.
3. Sartoratto, A.; et al. *Braz. Jour. of Microbiol*. **2004**, v. 35, p. 275-280

**Área: ORG** **Inscrição: 00948**

# Expanding the Redox-Relay Strategy: Accessing Carbonylated Compounds from Alkenyl Silyl and Methyl Ethers by Heck Arylations

**Henrique Esteves (PG),[1]* Vitor H. Menezes da Silva (PQ),[1] Carlos Roque D. Correia (PQ).[1]**

**estevesh@outlook.com**

[1]*Institute of Chemistry, UNICAMP – Campinas, SP, Brazil*

Keywords: *Heck-Matsuda arylation, Distal functionalisation, Redox-relay mechanism.*

## Highlights

Methanol and fluoride promote nucleophilic-assisted redox-relay process in Heck-Matsuda arylations of silyl and alkenyl ethers. The redox-relay is supported by isotopic labelling and DFT calculations.

## Abstract

The redox-relay strategy occurring in the Heck reactions[1] consists in the migration of a palladium hydride intermediate through successive migratory insertions along the carbon chain, followed by a terminal redox process, usually converting an alcohol into the corresponding aldehyde or ketone (Scheme 1, $R^1$ = H). This redox scenario allows access to distal functionalised aryl ketones. Recently, we reported a novel variant of this reaction[2] converting methyl and silyl-protected alkenols into the corresponding aryl ketones under Heck-Matsuda arylation conditions in excellent yields. Careful analysis of the reaction allowed us to isolate TBDPSOMe and TBDPSF derivatives as by-products. Kinetic data by *in situ* $^1$H NMR indicated that methanolysis and fluoride mediated deprotection occurs concomitantly, while fluoride ions from $BF_4^-$ convert TBSPSOMe into the TBDPSF derivative (Scheme 2). These finds suggest that the alkenyl silyl ethers, and presumably methyl ethers, undergo either a nucleophilic-assisted redox-relay process (Scheme 1, *path a*), or an anchimeric-assisted palladium reductive elimination (Scheme 1, *path b*), followed by methanolysis and/or fluorination of the silyl/methyl group bound to a putative oxonium intermediate. Both pathways would lead to the formation of the carbonylated product and regeneration of Pd(0). DFT calculations for alkenyl methyl ether redox-relay step favour the transition state through *path a* (Scheme 1) instead of the oxonium hypothesis.

**Scheme 1**

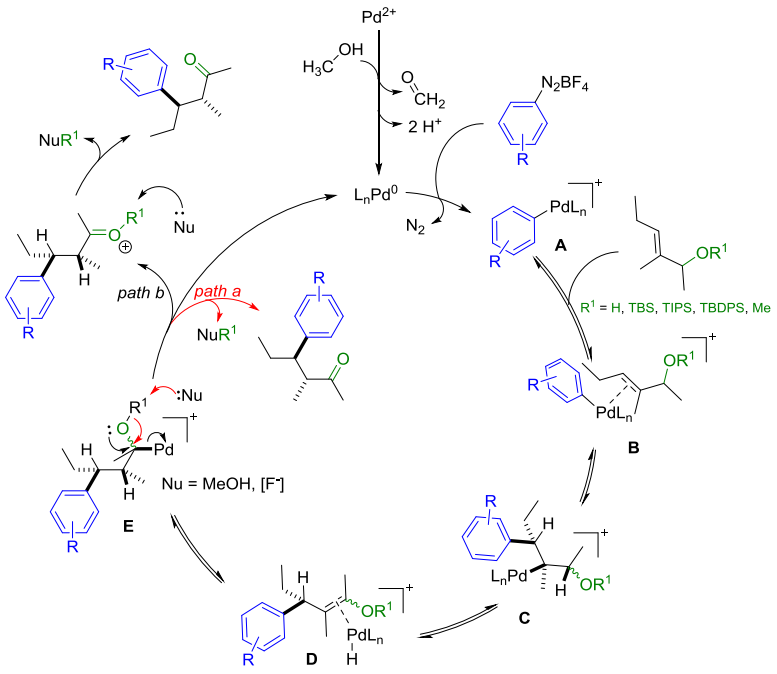


**Scheme 2**

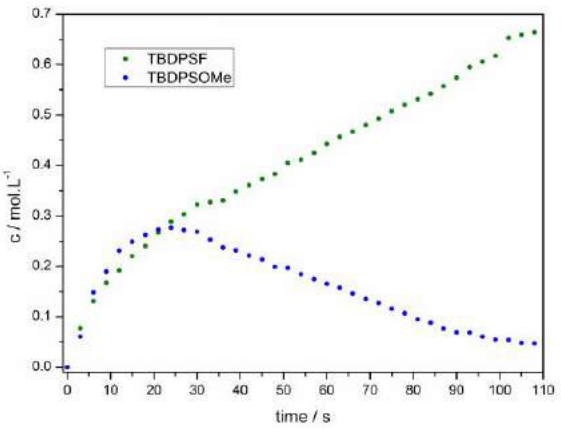


[1] Werner, E. W.; Mei, T.-S.; Burckle, A. J.; Sigman, M. S. *Science*. **2012**, *338*, 1455.
[2] Frota, C.; Polo, E. C.; Esteves, H.; Correia, C. R. D. *J. Org. Chem*. **2018**, doi: 10.1021/acs.joc.7b03098.

**Área: ORG**
*(Inserir a sigla da seção científica para qual o resumo será submetido. Ex: ORG, BEA, CAT)*

**Inscrição: 00974**
*(Inserir o número de inscrição do autor que fez a submissão)*

# Silver-Catalyzed Direct Selenylation of Indoles

**Elise A. M Rios[1*] (PG), Daniel da S. Rampon[1](PQ)**

**elise.maluf@gmail.com; danielrampon@ufpr.br**

*Laboratory of Polymers and Molecular Catalysts (LAPOCA), Department Of Chemistry, Federal University of Paraná-UFPR, Curitiba, PR, Brazil*

Keywords: *Direct Selenylation, Indoles, Silver, Organoselenium*

## Highlights

The direct functionalization of the indole nucleus is an important synthetic task since they are widely used in pharmaceutical, biological and material applications. On the other hand, organoselenium compounds are recognized for their biological activities and synthetic applicability, making them attractive targets. Therefore, the advantages of silver catalysis were evaluated for direct selenylation of indoles.

## Abstract

The functionalization of indole core has received considerable attention since this heterocycle is an important structural unit in many bioactive compounds and organic materials with technological interest.[1] Among them, 3-chalcogenylindoles are an emergent class of synthetic structures due their potential therapeutic values in the treatment of different diseases such cancer, cardiovascular, and bacterial diseases.[2] The methodologies reported for the preparation of 3-selenylindoles commonly involve the direct chalcogenylation of indole nucleus with various electrophilic organochalcogen reagents, then catalytic versions of these reactions employing safe diorganoyl dichalcogenides attracted interest. In the other hand, Ag-catalyzed reactions appeared as important synthetic tool for a variety of organic transformation.[3] This fact prompted us to explore a Ag-catalyzed regioselective C3 direct selenylation of indole. The suitable reaction conditions were developed with *1H*-indole and diphenyl diselenide with Ag(I) salts and dimethyl sulfoxide as solvent. First, we use 10 mol% of $AgNO_3$ due low cost and availability, at a temperature of 100°C for 24 hours (GC yield = 35%, anthracene as internal standard). Then, another silver salts were investigated in the same conditions, affording the follow GC yields: $Ag_2CO_3$ (21%), $Ag_2O$ (82%) (Scheme 1) and $Ag_2SO_4$ (77%). The effects temperature, solvent, catalyst source and catalyst amount are under evaluation.

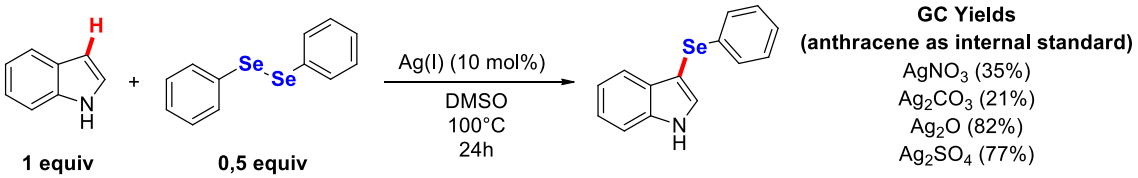


**Scheme 1**: Direct Selenylation of Indoles using Ag(I) salts as catalyst.

## Conclusions

The regioselective direct selenylation on C3 position of 1*H*-indoles was developed with use of silver salts as catalysts and the effect of each condition such as temperature, solvent effect and reaction is still been evaluated.

## References

[1] Lee C. W.; Adv. Mater. 2013, 25,5450 (b) Wang, Z.; et al.; Angew. Chem. Int. Ed. 2011, 50, 5365. [2] De Martino, G.; et al.; Med Chem. 2004, 47, 6120 (b) Funk, C. D.; Nat. Ver. Drug Discovery, 2005, 4, 664. [3] Longmire J.M. et al.; Am. Chem. Soc., 2002,124, 13400 (b) Liu, J.; et al.; Angew. Chem. Int. Ed., 2013, 52, 6953 (c) Shi, G.; et al.; Org. Lett.2015, 17, 38.

**Área: ORG**
*(Inserir a sigla da seção científica para qual o resumo será submetido. Ex: ORG, BEA, CAT)*

**Inscrição: 00992**
*(Inserir o número de inscrição do autor que fez a submissão)*

# *Push-pull* systems: A very useful building blocks for the preparation of biological active heterocycles.

**José Bitencourt (PG),[1] Carolina Passarelli (PQ),[1] José Costa (PG)[1], Manuel Almeida (PQ),[1] Nathally Pedroso (IC)[1], Ednilza de Lima (IC)[1], Jaqueline da Silva (IC)[1], José Quincoces (PQ)[1]**

**jose.bitencourt@aedu.com**

[1] *Department of Biotechnology, Anhanguera University of São Paulo, UNIAN*

Keywords: *push-pull* compounds; synthesis of heterocycles; organic synthesis

## Highlights

*Push-pull* compounds: properties and use in the synthetic route. Olefins substituted by electron donors and with electron accepting substituents; polarization of π bond; obtaining heterocycles.

## Resumo/Abstract

**INTRODUCTION:** *Push–pull* olefins are compounds containing electrondonating groups (RS) and electron-withdrawing groups (CN) at the opposite ends of a double bond, have attracted considerable attention due to their unusual physicochemical properties, such as high stability, easy E/Z-isomerization, and significant charge transfer, that make them suitable for nucleophilic attack. Such compounds are very useful building blocks and widely used in organic synthesis. (Scheme 1).

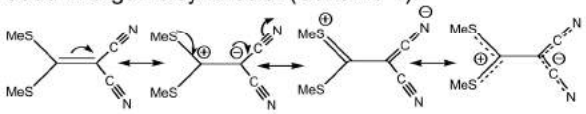

**Scheme 1 - Resonant structures of a *push-pull* alkene**

**DISCUSSION:** Heterocycles form two thirds of all organic compounds in Nature. There are many heterocycles that are part of our body and many drugs have some type of heterocycles.

Our research group has developed nearly 100 patents in recent years, in the field of Synthesis of Heterocycles, starting from *push-pull* systems. In reaction scheme 2, it is possible to observe that the primary nucleophilic attack of hydrazine hydrate occurs at the carbon atom of the double bond that is bound to electron donor groups, as can be seen in the resonant structures of scheme 1. The *push-pull* route has already been used to obtain drugs of recognized biological importance, such as 4-hydroxy-pyrazolo [3,4-d]pyrimidine, or allopurinol[1]. Important antiarthritic drug, which has antitumor and antileukemic activity.

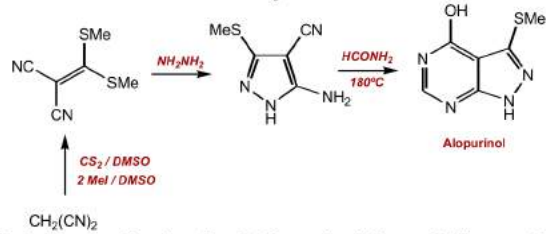


**Scheme 2 – Synthesis of allopurinol through the *push-pull route***

The following is a reaction scheme 3 in which some of the heterocycles obtained by us can be appreciated in a few steps of synthesis[2-3].

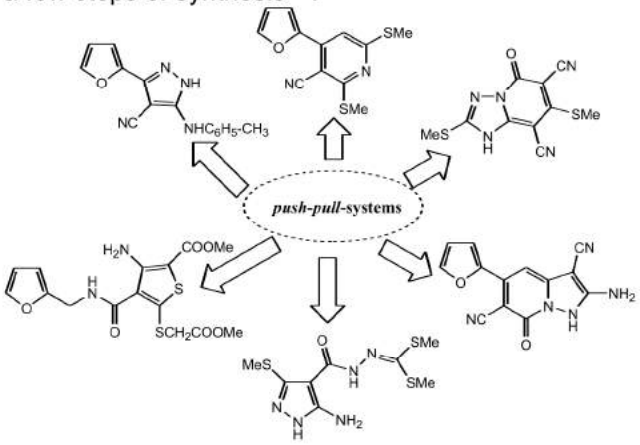


**Scheme 3: Some of the heterocycles obtained by our group starting from *push-pull* systems.**

In reviewing the Heterocycles books on the market, we find that there is no book on this subject and none of them contains the experimental procedures for synthesizing the starting materials of the various types of heterocycles, monocyclics and condensates. For this reason, our group decided to publish a book about the Synthesis of Heterocycles starting from *push-pull* systems this year. This book will also explain the reaction mechanisms and its theoretical basis for the synthesis of the most diverse types of heterocycles and the reaction conditions for the realization of experiments in this field.

**CONCLUSION**: Due to the higher reactivity of the compounds that present *push-pull* characteristics, the use of this pathway stands out, because the derivative is obtained with fewer reaction steps and higher yields.

**REFERENCES:** [1]Bioorganic Med. Chem. 21(2013) 5657-68; [2]German-Patents DD 294942, 1991; DD 288382 1991, C.A. vol. 115, 71595b 1991 ; DD 288383 1991, C.A. vol. 115, 49735 a, 1991 ; [3]Journal für Praktische Chemie. Chemiker-Zeitung, v. 342, n.4, p. 389-395, 2000; Heterocyclisations in the Sugar Chemistry by utilizing *push-pull* activated C-C double Bonds. Target in Heterocyclic Systems 2001, V.5, p. 299-326.

**Área: ORG** **Inscrição: 01023**

# Sand-Starch mixtures as stationary phases: Low-cost Columm Chromatography for dyes purification in Organic Chemistry class

**Bruna Costa Cerqueira (IC),* Rodrigo De Paula (PQ)**

**brunacerqueiraquimica@gmail.com**

*Centro de Formação de Professores/CFP, Universidade Federal of Recôncavo Bahia - UFRB, Campus Amargosa, 45.300-000, Amargosa/BA*

Keywords: low-cost materials, column chromatography, organic chemistry, stationary phase, experiment, purification

## Highlights

Considering the chromatography as the main method for organic chemistry purification, this work deals with the use of low-cost materials as stationary phase in an handcraft column chromatography.

## Resumo/Abstract

Amongst the many contents to be discussed, the Introductory Organic Chemistry classes in Brazilian Universities also brings the purification methods in their curricular subjects to deal with. It is well established that chromatographic methods are the best choice for many organic chemists around the world[1]. Besides, it is very common to teach paper chromatography as the single example relatively to this technique, becoming the knowledge neither enough nor attractive to student. By one side, such fault is understood due to the expensive costs related to usual stationary phases (*e.g.* $SiO_2$). Based on chomatography´s principle (chroma: color and graphy: written), an interesting experiment can be carried out with colored compounds which represents some important feature in social daily. Food dyes are good choices to be used since a lot of commercial food employs concerning amounts of such compounds and its human consumption must be avoided according Health Agencies[2].

The purpose of this work was developing an alternative chromatographyc system based in commercial and common materials to be used to elucidate a experimental chromatographyc routine. Then, mixtures of sand (from river and sea) and starch were evaluated to achieve best separation of food dyes using ethyl alcohol, water and their mixtures. Figure 1 shows the column during dyestuff elution and each different color which can be seen.

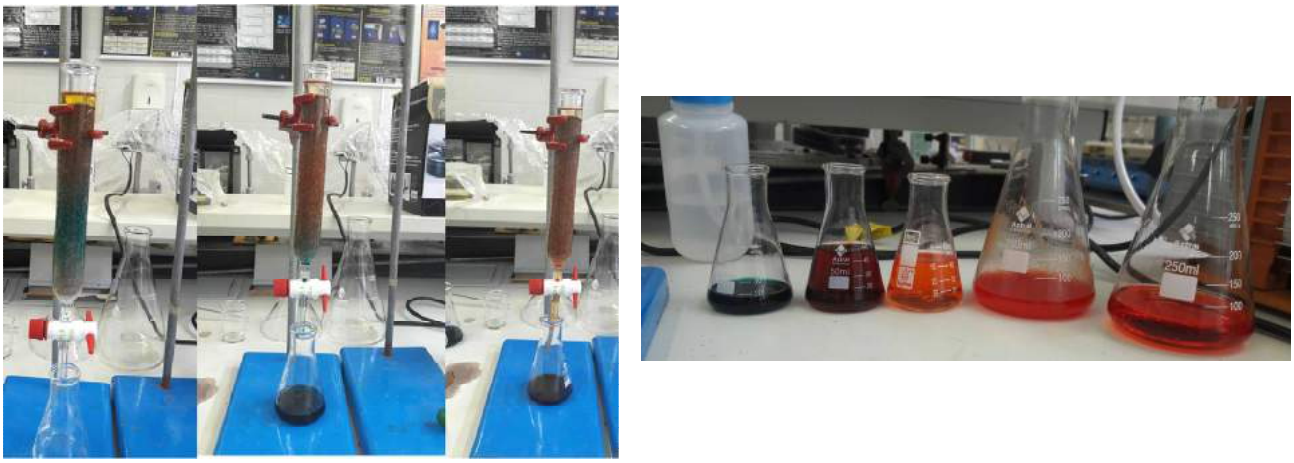

Figure 1. Left: Column chromatography of dyestuff through 100% sand river; Right: Food dyes collected

In addition to chromatography theory as well, discussions about molecular interactions, polarity and all steps in puification processes can enrich the class. Our first results showed good separation when food dyes containing amaranto, tartrazine and brilliant blue where submitted to this chromatographic column.

**References:** [1]Mohrig, J.R., Hammond, C.N., Schatz, P.F; In: Techniques in Organic Chemistry, 3rd. Edition, WH Freeman Company, USA, **2010**; [2]Prado, M.A., Godoy, H.T., *Alim. Nutr*, **2003**, *14(2)*, 237-250.

**Área: ORG** **Inscrição: 01159**

# Unequivocal Structural Assignments of Three Cardanol - Derived: An Experimental and Theoretical Approach

**Layla R. Barbosa (PG),[1] Valdemar L. Junior (PQ)*,[1] Adilson Beatriz (PQ),[2] Álvaro C. Neto (PQ).[1]**

**laylarosario@gmail.com; vljuniorqui@gmail.com**

*[1]Departamento de Química, UFES; [2]Instituto de Química, UFMS.*

Palavras Chave: *NMR calculations, GIAO model, Assigments, Cardanol, CNSL.*

## Highlights

Chemical shift calculations using DFT/B3LYP method. Complete NMR assignment for three cardanol-derived.

## Resumo/Abstract

Since a few decades, NMR chemical shift calculations have been used to interpret experimental spectroscopic data and to assign the structures of complex molecules.[1] The combination of NMR and computational chemistry techniques has emerged as a powerful tool to determine the connectivity, conformation and stereochemistry of challenging systems.[2] Theoretical methods (especially DFT) permit shielding tensors and spin-spin coupling constants to be calculated with highly reliable results.[3,4]
We present here a complete NMR assignment for three cardanol-derived (**1**, **2** and **3**). These studies were performed using 1D and 2D NMR techniques and compared with the theoretical predictions of the chemical shifts using DFT calculations.

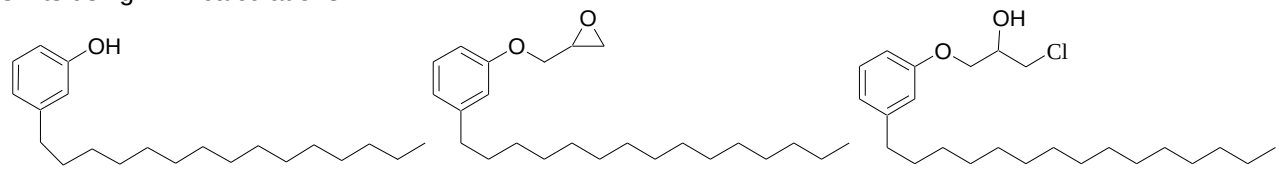


Figure1. Cardanol-derived studied in the present work.

Cardanol is a material obtained from cashew nut shell liquid (CNSL), which is a byproduct of cashew nut processing and represents a powerful phenolic pollutant.[5,6] It can be considered as a building block for chemical synthesis and adds value to the CNSL.[7]
GIAO model at DFT/B3LYP theory level using cc-pVTZ basis (with and without solvent) set was employed for calculations of $^{1}H$ and $^{13}C$ NMR chemical shifts (δ), using Gaussian03 program.[8]
From correlation between the theoretical and experimental data, it was concluded that the model used was effective for calculating δ for the studied compounds.
From compound **1** it was found that the mean deviation (MD), standard deviation (SD) and linear correlation factor (R) for all the calculations were generally better when using solvent.
Another conclusion was that the model used was effective for calculating δ for the studied compounds.

Table 1. Statistical analysis results for $^{13}C$ and $^{1}H$ chemical shift.

| | $^{13}C$ Chemical shift | | | $^{1}H$ Chemical shift | |
|---|---|---|---|---|---|
| | Without Solvent | With Solvent | | Without Solvent | With Solvent |
| SD | 3.3 | 3.1 | SD | 0.20 | 0.15 |
| MD | 5.4 | 5.9 | MD | 0.21 | 0.21 |
| R | 0.99614 | 0.99613 | R | 0.9964 | 0.99597 |

**References:**

1. Mohamed.s. H., et al. Journal of Molecular Structure, 1141, 436-440, 2017.
2. Aímola, T. J., et al. Org. Biomol. Chem., 13, 2140–2145, 2015.
3. Queiroz, L. H. K., et al, Magn. Reson. Chem., 49, 140–144, 2011;
4. Barbosa, L. R., et al, Magn. Reson. Chem., 52, 318-328, 2014.
5. Biswas, A., et al. J. Braz. Chem. Soc., Vol. 27, No. 6, 1078-1082, 2016.
6. Calo, E., et al. Green Chem, 9: 754, 2007.
7. Braga, F.C. et al. Dyes and Pigments, 141, 235-244, 2017.
8. M. J. Frisch et al, Gaussian 03, Revision C.02, Gaussian, Inc., Wallingford CT, 2004.

**Área: ORG** **Inscrição: 01214**

# Synthesis of new nitroxides modified with disulfide functionality to be used as spin label

**Ana Carolina Silva Batista (IC),[1] Fabíola Suelen dos Santos (PG),[1] Rossimiriam Pereira de Freitas (PQ).[1]**

**anacsbat@gmail.com, rossimiriam@qui.ufmg.br**

*[1]Departamento de Química, Instituto de Ciências Exatas, UFMG, Av. Antônio Carlos, 6627 31270-901 Belo Horizonte, MG*

Key words: *Label, Spin, EPR, Disulfide, Lipoic acid*

## Highlights

Synthesis of spin labels from lipoic and 11-mercaptoundecanoic acid; EPR studies of spin-labeled Au nanoparticles.

## Resumo/Abstract

Spin labels are molecules that contain a stable diamagnetic fragment, [1] such as the nitroxide group present in the 2,2,6,6-tetramethylpiperidine-1-oxyl compound (TEMPO) and derivatives. The synthesis of these labels is a strategy used to allow molecules that do not have a mismatched electron to be analyzed by Electronic Paramagnetic Resonance (EPR)[1], which is a technique that detects electron-nucleus and electron-electron interactions, obtaining information about the environment next to the unpaired electron. The objective of this work is the synthesis of spin labels containing disulfide groups that can be coupled to the surface of gold nanoparticles for molecular dynamics studies. Lipoic acid **1** and 11-mercaptoundecanoic acid **5** (MUA) were chosen to be coupled to TEMPO derivatives (TEMPOL **3** and 4-amino-TEMPO **2**) since they have sulfur atoms that have a great affinity for gold. The synthesis of the labels was performed according to the route shown in Scheme 1.

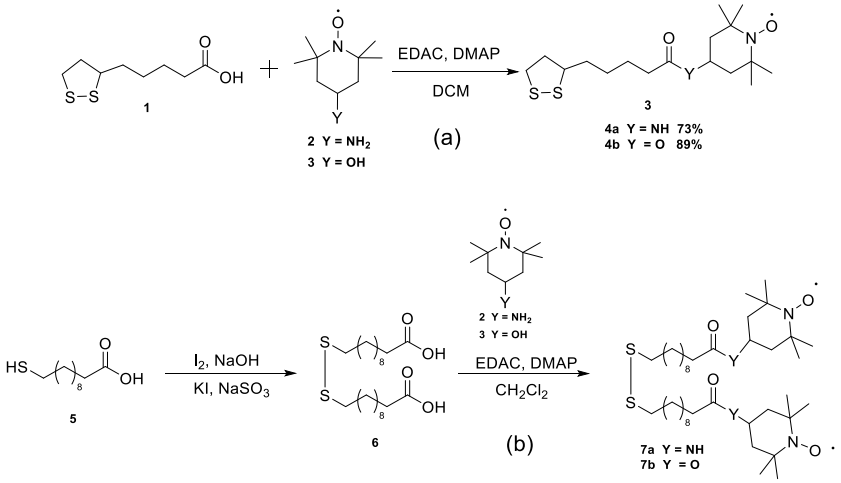


Scheme 1: Synthesis of spin labels using (a) lipoic acid and (b) MUA.

Using this methodology, it was possible to obtain and characterize diamagnetic lipoic and MUA acids derivatives with good yields, which are being used as probes for EPR studies of spin-labeled Au nanoparticles.

**References**:

**1** Fielding, A. J.; Concilio, M. G.; Heaven, G.; Hollas, M. A.; New developments in spin labels for pulsed dipolar EPR. Molecules, 2014, 19, 16999-17025.

**Aknowlegments**: FAPEMIG, Capes, CNPq, UFMG.

**Área: ORG** **Inscrição:** 01282

# A Practical Synthesis of densely substituted 2H-furo[3,2-*b*]benzopyran-2-ones

**Wilson Elias Rozo Nuñez (PG),[1*] Silvio Cunha (PQ).[2]**

**wilson.rozo@uptc.edu.co; silviodc@ufba.br**

[1]*Instituto de Química, Universidade Federal da Bahia, Campus de Ondina, 40170-290, Salvador – BA.*
[2]*INCT-Instituto Nacional de Ciência e Tecnologia em Energia e Ambiente, Campus de Ondina, Salvador – BA*
Palavras Chave: *2H-Furo[3,2-b]benzopyran-2-one, pulverolide, aurantricholide.*

## Highlights

A simple and efficient synthesis of new derivatives of the 2H-Furo[3,2-*b*]benzopyran-2-one, has been described.

## Resumo/Abstract

2H-Furo[3,2-*b*]benzopyran-2-one is a rare heterocycle that belongs to a class of natural pigments known as pulverolide and aurantricholide (A and B).[1] Their occurrence was described when they were isolated from the fungi *Pulveroboletus ravenelii* and *Tricholoma aurantium*. There are few methods described for the construction of this heterocyclic nucleus, which are characterized as impractical routes with low yields.[2] Subsequently, Oliveira proposed a one-step route for the construction of the 2H-furo[3,2-b] furobenzopyran-2-one nucleu.[3] To know the scope of this new route, we investigated the synthesis of new derivatives.
The methodology developed takes advantage of the ambidentate characteristics of 3,4-dibromofuran-2(*5H*)-one(furanone). The synthesis involves the reaction of furanone and salicylaldehydes in the presence of $Et_3N$ as a base and methanol as a solvent, at room temperature (Scheme 1).

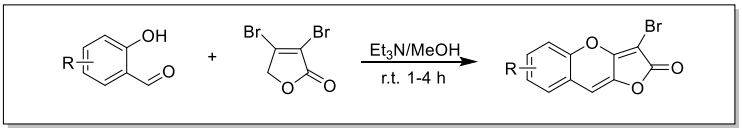


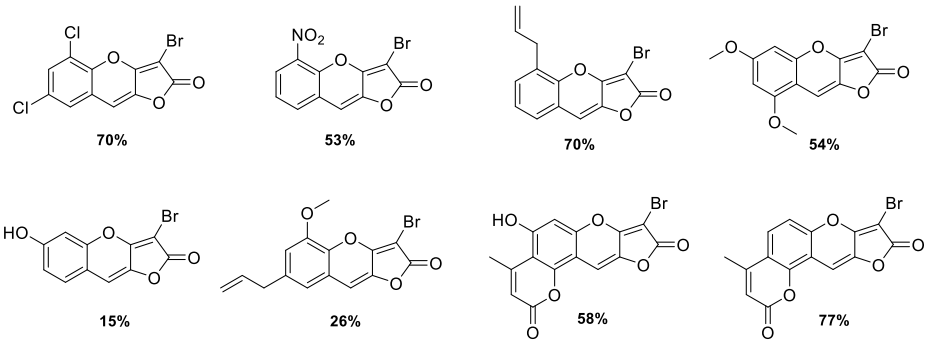


**Scheme 1**: New derivatives synthesized

A simple and efficient synthesis method of new derivatives of the 2H-Furo[3,2-*b*]benzopyran-2-one nucleu, has been described. A faster reaction, high purity of products and moderate yields (15-77%) compared to the described methods are the advantages of present protocol.

**Acknowledgement**
The authors thank INCT, CNPq and FAPESB.

**References**

1. Zhang, L.; Wang, F.; Dong, Z. J.; Steglich, W.; Liu, J. K. Heterocycles 2006, 68, 1455.
2. Yang, W; Liu, J.; Zhang, H. Tetrahedron Letters, 2010, 51, 4874.
3. Oliveira, Caio C. Estudo da reatividade da 3,4-dibromofuran-2(5H)-ona e aplicação na sintese de heterociclos funcionalizados. 2010, UFBA. Tesis de Mestrado.

**Área: ORG** **Inscrição: 01339**

# Síntese de um novo ligante quiral do tipo sanduíche cobaltoceno-imidazolina

**Elisângela Vinhato (PQ)*, Isabella Andrade Souza (IC)**

**evinhato@unifesp.br;**

*Departamento de Química, UNIFESP – Universidade Federal de São Paulo, Diadema, São Paulo, Brasil.*

Palavras Chave: *Cobaltoceno, Imidazolina, Síntese Enantiosseletiva, Ligante Quiral.*

## Highlights

Synthesis of a new type of chiral cobaltocene-imidazoline ligands
A new type of ligand containing cobaltocene and imidazoline was synthesized.
Development of chiral imidazoline ligands for Cu(II)-catalyzed enantioselective pyrrolidine derivatives synthesis.

## Resumo

A aplicação de metais de transição complexados a ligantes quirais é uma das ferramentas mais poderosas e utilizadas para controlar a estereoquímica na formação de novas ligações C-C/C-heteroátomo. Neste contexto, o desenvolvimento de ligantes quirais contendo um ou mais anéis imidazolínicos quirais têm surgido recentemente na literatura[1] para complementar e ampliar o escopo da catálise enantiosseletiva.

Neste trabalho, um novo ligante do tipo cobaltoceno-imidazolínico **I** foi projetado para aplicação na síntese enantiosseletiva de anéis pirrolidínicos. O Esquema 1 apresenta a rota sintética para a síntese do ligante **I**.

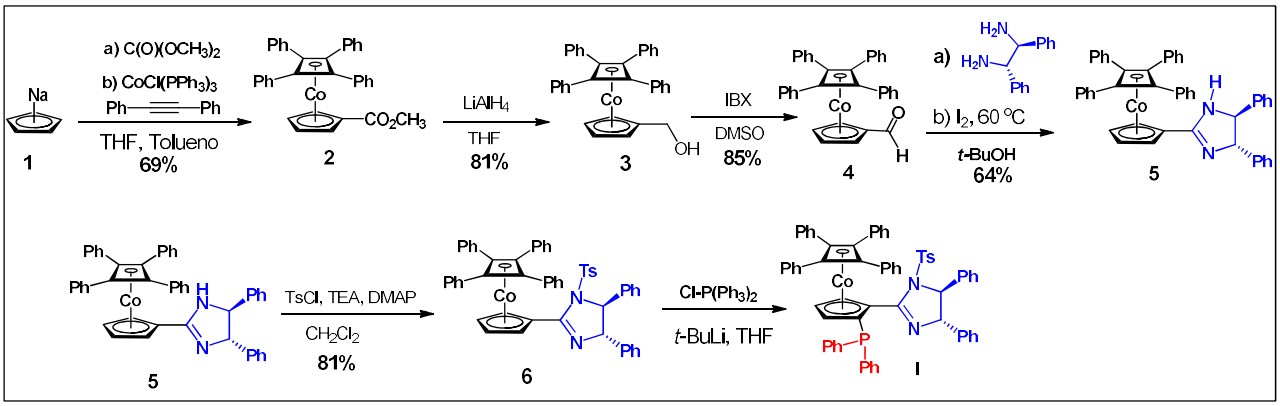


O intermediário **2** foi sintetizado[2] em quatro etapas reacionais. Sendo que as duas primeiras consistiram na síntese do $CoCl(PPh_3)_3$ que foi obtido com rendimento de médio de 57%. Em seguida, preparou-se o NaCp seguido de reação com carbonato de dimetila em THF sob refluxo de 4 horas. Na sequência adicionou-se o $CoCl(PPh_3)_3$ e difenil acetileno em tolueno obtendo o produto **2** em 69% de rendimento. A redução de **2**, foi feita utilizando $LiAlH_4$ em THF isolando o **3** em 81% de rendimento. A oxidação parcial de **3** foi realizada de forma inédita, desenvolvida com IBX em DMSO para isolar **4** com 85% de rendimento. A síntese de **5** (inédito) foi realizada com DPHEN em presença de $I_2$ em $^t$BuOH em 64% de rendimento, o qual foi tosilado resultando em **6** com 81% de rendimento. A última etapa será realizada com $ClPPh_2$ com $^t$BuLi como base. E após finalizado o ligante será caracterizado e usado na síntese de pirrolidinonas quirais em presença de sais de Cu(II).

1- Arai, T.; Tokumitsu, C.; Miyazaki, T.; Kuwano, S.; Awata, A. *Org. Biomol. Chem.* **2016**, *14*, 1831.
2- Anderson, C. E.; Overman, L. E.; Richards, C. J.; Watson, M. P.; White, N. *Org. Synth.* **2007**, *84*, 139.

FAPESP Fomento Proc. 2016/21676-0

**Área: ORG** **Inscrição: 01396**

# Novel 4-arylaminoquinoline-3-carbonitriles as Inhibitors of HIV-1 Reverse Transcriptase

**Alice M. R. Bernardino (PQ)[1], Beatriz C. L. Melo (PG)[1], Gustavo Polillo (PG)[1], Helena S. Pereira (PQ)[2], Izabel C. P. Paixão (PQ)[2], Michele S. Ribeiro (PG)[2] and Julio C. Borges (FM)[3].**

**julio.borges@ifrj.edu.br**

[1]Universidade Federal Fluminense – Dpto. de Química Orgânica – Instituto de Química – Outeiro São João Batista, s/n-Valonguinho, 24020-150, Niterói/R; [2]Universidade Federal Fluminense, Instituto de Biologia, Programa de Pós-Graduação em Ciências e Biotecnologia, Departamento de Biologia Celular e Molecular, Campus do Valonguinho, CEP 24210-150, Niterói, RJ, Brazil; [3] Instituto Ferderal de Educação Ciência e Tecnologia do Rio de Janeiro – Campus Nilópolis - Rua Lucio Tavares, 1045 – CEP 26530-060, Nilópolis/RJ.

Palavras Chave: quinoline, synthesis, HIV-1, reverse transcriptase.

## Highlights

Fourteen quinoline derivatives were prepared.
They were evaluated on the activity reverse transcriptase (RT) of HIV-1.
Most of the synthesized compounds showed significant *in vitro* inhibition of RT.

## Resumo/Abstract

The human immunodeficiency virus type 1 (HIV-1) was discovered in 1983 and is part of a subfamily of retroviruses called Lentivirus. HIV is the causative agent of acquired immunodeficiency syndrome (AIDS).[1] It destroys immune system leaving the victim vulnerable to opportunistic infections.[3] Reverse transcriptase is considered a key enzyme in the replication cycle of retroviruses and has been widely used as a tool to search compounds having antiviral potential.[2]
With regard to the search for new prototypes, with antiviral action, the presence of the quinolynic nucleus is very interesting, since it is present in several molecules that showed this activity.[3] Thus, we report the synthesis of 14 derivatives of the 4- arylaminoquinoline-3-carbonitrile to avaliate its potential as an antiviral agent.

The 4-arylaminoquinoline-3-carbonitrile derivatives **(3a-n)** were readily prepared from 4-chloroquinolines[4], that can be readily made by methodology similar to the Gould-Jacobs.[5]

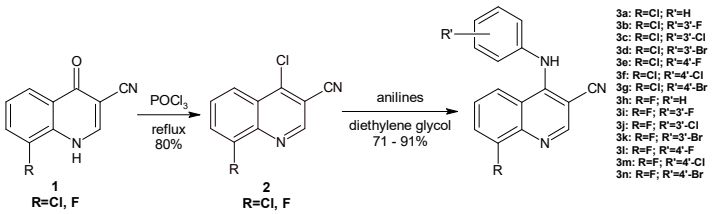


The 4-arylaminoquinoline-3-carbonitrile derivatives were evaluated on their ability to inhibit HIV-1 reverse transcriptase enzyme. The results highlighted that derivative **3h** ($IC_{50}$ < 8 μM) turned out to be more active. Our results show that derivatives **3a-n** displayed low cytotoxicity ($CC_{50}$ ≥ 100 μM).

1. Gallo RC, Montagnier L. *N Engl J Med*. **2003**, *349*, 2283.
2. Li G *et al.Retrovirology*. **2015**, *12*, 18.
3. [8]Hameed A *et al*. *Bioorg Chem.* **2016**, *65*, 175.
4. Borges, JC *et al. J Braz Chem Soc*. **2014**, *25*, 980.
5. Bernardino AMR et al. *Bioorg Med Chem*. **2006**, *14*, 5765.

**Área: ORG** **Inscrição: 00141**

# Síntese de Dihidropirimidinonas e avaliação de interação com o ssDNA

**Laís A. Schmoeller (IC),[1*] Felipe Wodtke (PG),[1] Fernando R. Xavier (PQ),[1] Rogério A. Gariani (PQ),[1].**
***lais_albert@hotmail.com**

[1] *Laboratório de Síntese e Catálise (SinCa)- Departamento de Química, Centro de Ciências Tecnológicas, Universidade do Estado de Santa Catarina – UDESC*

Palavras Chave: *Biginelli, Dihidropirimidinonas, ssDNA, Intercalação.*

## Highlights

Synthesis of Dihydropyrimidinones and evaluation of interaction with ssDNA. Synthesis of dihydropyrimidinones by traditional methods. Study of intercalation of salmon DNA with dihydropyrimidinones by molecular absorption spectroscopy (UVvis).

## Resumo/Abstract

A síntese de Biginelli foi descoberta em 1891 pelo italiano Pietro Biginelli, e desde então foram descobertas diversas aplicações na área farmacológica. A molécula de Biginelli (dihidropirimidinona) apresenta similaridade com as estruturas das bases nitrogenadas timina e citosina, apresentando então uma real possibilidade de interação do tipo *''π-stacking''* com as bases nitrogenadas do DNA. Assim o objetivo desse trabalho é de sintetizar adutos de Biginelli, bem como, caracteriza-los via RMN e CG/EM. Por fim, analisar o tipo de interação que ocorrerá entre os compostos sintetizados com DNA via espectroscopia de absorção molecular (UV-Vis).

Esquema 1: Rota sintética para obtenção das dihidropirimidonas e seus respectivos valores de $K_b$.

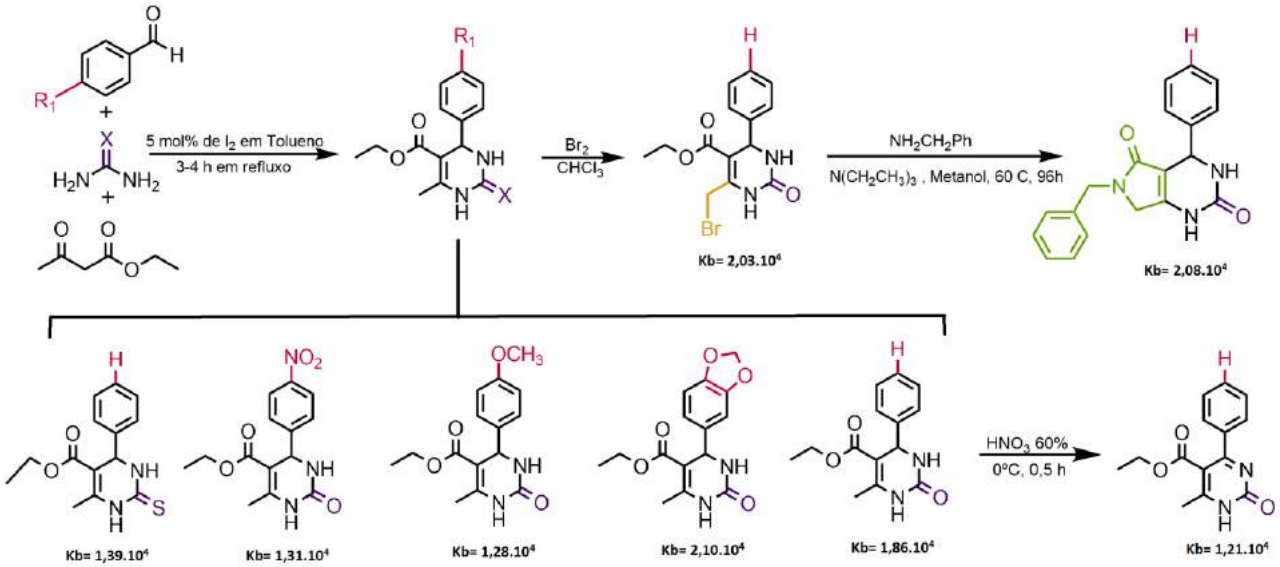


As sínteses dos adutos de biginelli (dihidropirimidinonas) ocorreram em rendimentos razoáveis e os compostos foram devidamente caracterizados. Através dos resultados obtidos pela titulação espectrofotométrica dos adutos de Biginelli com ssDNA, pode-se observar que, de fato, ocorre uma interação entre os compostos sintetizados e este ácido nucleico através do fenômeno de intercalação. Tal fato é suportado pelos fenômenos de hipocromismo e batocromismo observado durante os experimentos, para todos os compostos testados. Através dos cálculos pertinentes, foi possível a obtenção de valores de constante de ligação intrínseca ($K_b$) na ordem de $10^4$, o que indica uma magnitude satisfatória de interação entre os compostos sintetizados e o ssDNA.

**Referências:** Suresh and Jagir S. Shandu. *Reviews and Accounts* ,***2010***,*pg.* 66-133/ R.S. Bhosale *et al*. *Tetrahedron Lett*. 45,**2004**, pg.9111-9113/ T.George *et al. Synthesis* ,**1975** ,pg.405-407/ A. Puchala *et al. J. Heterocyclic Chem*., 38, **2001**, pg. 1345-1352.

**Área: ORG**
*(Inserir a sigla da seção científica para qual o resumo será submetido. Ex: ORG, BEA, CAT)*

**Inscrição: 41578**
*(Inserir o número de inscrição do autor que fez a submissão)*

# Synthesis of carbohydrate-linked pentadienone derivative with antitumor properties

**Carolina Passarelli (PQ),[1,2,3] Dirk Michalik (PQ),[2] José Costa (PG)[3], Manuel Almeida (PQ),[3] Durvanei Maria (PQ)[4], Anderson Ribeiro (PQ),[1] Christian Vogel (PQ) [2], José Quincoces (PQ)[3]**

**carol_passarelli@hotmail.com**

*[1]Center of Natural and Human Sciences, UFABC; [2]Chemistry Department, Rostock University; [3]Anhanguera University, UNIAN; [4] Laboratory of Biochemistry and Biophysics, Butantã Institut*

Keywords: *carbohydrate synthesis, biological activity, cancer, MTT assay, pentadienone derivative*

## Highlights

Association of curcumin derivative with carbohydrate;
Potentiation of the pharmacological action;
Improve specific interactions with lectin on the surface of cells.

## Abstract

**INTRODUCTION:** Alternatives are constantly investigated in the field of oncology. In this regard, natural compounds, like curcumin, are promising because of their excellent biological activities and low toxicity[1]. The work aims to improve the activity and selectivity of a curcumin derivative, binding to carbohydrate. The effect of carbohydrate-bound compounds is due to the specific interactions between carbohydrates and lectins in the cancer cell wall. The receptors for carbohydrate binding have been described on the tumor cells[2].
**RESULTS AND DISCUSSION:** From L-Ramnose the total acetylation of the free OH groups was carried out. In the next step, the acetylated anomeric carbon was replaced with bromine by treatment with hydrogen bromide. Using the Helferich glycosylation, it was possible to obtain the following allylic derivative. Cleavage of the acetyl groups was performed under Zemplen deacetylation conditions, followed by the benzylation reaction, to protect the free OH groups. Deprotection of the allyl group in the presence of $PdCl_2$ was performed successfully. From this point the respective trichloroacetoimidate derivate ***8*** was synthesized, with TMSOTf as Lewis acid.

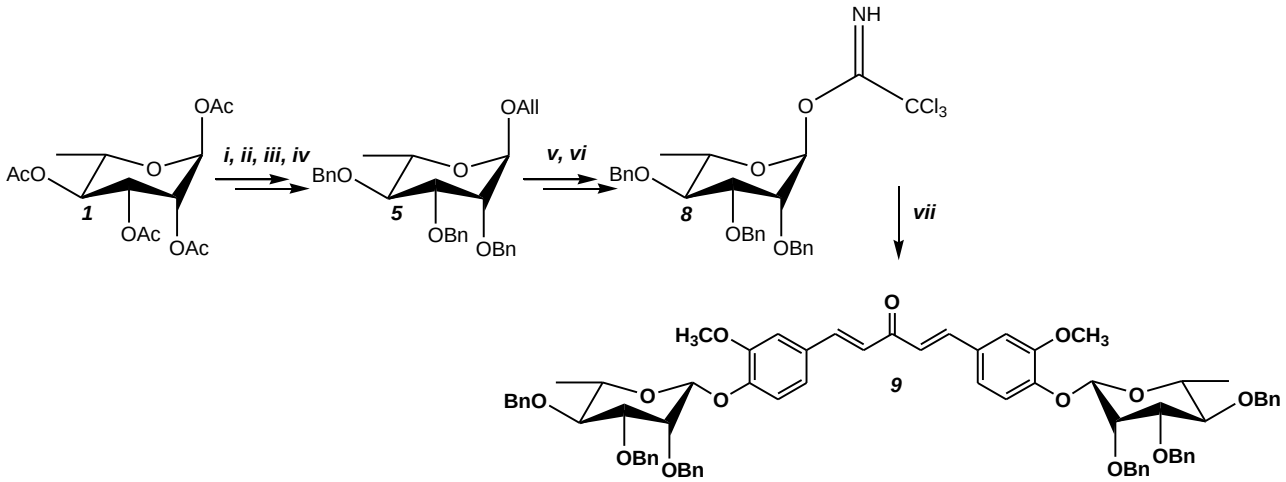


*Scheme 1 – (i) HBr 40% in AcOH, 1,5 Hrs., RT.; (ii) AllOH, $Hg(CN_2)$, MS 4A,16 Hrs., RT.; (iii) $MeO^-Na^+$, 1 Hr., RT; (iv) NaH, BnBr, 24 Hrs., RT.; (v) MeOH:$CH_2Cl_2$ (1,6:1), $PdCl_2$, 16 Hrs.; (vi) $CH_2Cl_2$, MS 4A, $Cl_3CCN$, 16 Hrs; (vii) O-glycosylation reaction between 2 mols of compound 8 and one mole of 1,5-bis(4-hydroxy-3-methoxyphenyl)penta-1,4-dien-3-one in TMSOTf and $CH_2Cl_2$,* 16 Hrs.

The association of the sugar ***8*** to the chalcone *1,5-bis(4-hydroxy-3-methoxyphenyl)penta-1,4-dien-3-one* gave the new analogue, ***9***. The MTT biological assay was performed and showed $IC_{50}$ of 2.66 µM, 14.94 µM, and 1.023 µM, 6.492 µM, for the 4T1, MCF7, SCC9 and SCC25 lineages respectively.
**CONCLUSIONS:** Considering the $IC_{50}$ value in µM of traditional drugs for the treatment of cancer, like doxorubicin and paclitaxel, the derivative ***9*** showed promise. It presented a lower value of $IC_{50}$ and it is non-toxic to the normal cell lines like HUVEC and MACRF.
**REFERENCES:** [1] Res. Treat., 2014, 46, 2-18. [2]*Science* 1989,*246*,227-246.
***ACKNOWLEDGMENTS:*** *DAAD and CAPES for financial support*

**Área: ORG**
*(Inserir a sigla da seção científica para qual o resumo será submetido. Ex: ORG, BEA, CAT)*

**Inscrição: 00809**
*(Inserir o número de inscrição do autor que fez a submissão)*

# PRODUCTION OF BIODIESEL WITH HOMOGENEOUS CATALYSTS BY MICROWAVE IN ETHANOL

**Pamela R. A. da Costa (IC)[1]; Sonara G. S. Cassa (IC)[1]; Thiago M. Aversa (PQ)[1]; Queli A. R. de Almeida (PQ)[1*]**

**pamelacatiara@yahoo.com.br; queli.passos@ifrj.edu.br**

[1] Federal Institute of Science and Technology of Rio de Janeiro , IFRJ - Duque de Caxias

Keywords: Biodiesel, Ethanol, Microwave, Residual Oil

## Highlights

Using of microwave as a search for energy efficiency;
New technology for biodiesel production;
Improvement of synthetic methodologies.

## Resumo/Abstract

Biodiesel is a "clean" fuel and an excellent alternative energy, bringing a series of environmental, economic and social advantages. The production of biodiesel may occur in the presence of short chain alcohols and basic or acid catalysts through shaking and heating[1]. According to literature, the microwave irradiation (MW) promote superior benefits over the conventional heating method to biodiesel preparation from coconut, palm and soybean oils, with using of methanol, one toxic solvent and different basic catalysts[2]. This work presents the biodiesel production using the microwave and homogeneous catalysts (KOH and $H_2SO_4$) in ethanol. The ethanol is a viable alternative to methanol because it is non-toxic and comes from a renewable source[3]. The results and conditions used in the reactions are described in Table 1. The route proposed in this work are a great alternative to conventional heating processes, favoring high conversions, lower reaction time and energy expenditure.

| Residual Oils | Ethanol 1,5% KOH, **3h** | Ethanol 1,5% KOH, **MW 20min** | Ethanol 1,0% $H_2SO_4$, **MW 20min** |
|---|---|---|---|
| Soyaben (A.I. 0,54) | 80% (A.I 0,40) | 71% (A.I 0,40) | 80% (A.I 0,40) |
| Corn (A.I. 0,54) | 75% (A.I 0,35) | 50% (A.I 0,34) | 85% (A.I 0,34) |
| Sunflower (A.I 0,30) | 40% (A.I 0,65) | 58% (A.I 0,70) | 90% (A.I 0,65) |
| Canola (A.I 0,55) | 76% (A.I 0,40) | 85% (A.I 0,40) | 95% (A.I 0,35) |

A.I – Acidity Index (mg KOH/g)

**Table 1:** Results obtained for the formation of biodiesel in microwaves

All the raw materials and biodiesel were characterized by the acidity index and the biodiesel were also by GC-MS indicating a conversion of over 96.5% of the residual oil in biodiesel, within the established limits.

**References:**

1- Sarin, A. Biodiesel: Production and Properties, The Royal Society of Chemistry, 2012.
2- Nomanbhay, S.; Ong, M. Y. A Review of Microwave-Assisted Reactions for Biodiesel Production, Bioengineering, 4, 57, 2017.
3- Lima, J. R. O. *et al.* Biodiesel de babaçu (orbignya sp.) obtido por via etanólica, Quimica Nova, 30, 600, 2007.

**Acknowledgements:** CNPq, IFRJ

**Área: ORG** **Inscrição:**_____
*(Inserir o número de inscrição do autor que fez a submissão)*

# Synthesis, characterization and cytotoxic activity of chalcones

**Telma Leda Gomes de Lemos (PQ),[1] Irvila Ricarte de Oliveira (PQ), [1] Maria Teresa Salles Trevisan (PQ), [1] Danilo Damasceno Rocha (PQ),[2] Manoel Odorico de Moraes Filho (PQ),[2] Iolanda Frota de Farias (PQ).[1]***

**tlemos@dqoi.ufc.br; iolandafrota1@gmail.com**

*[1]Departamento de Química Orgânica e Inorgânica, UFC; [2]Departamento de Fisiologia e Farmacologia, UFC*

Palavras Chave: *Chalconas sintéticas, cytotoxic activity , Spectroscopic date*.

## Highlights

The chalcones were synthesized by aldol condensation reaction using base catalysis. The substances were characterized by IR, GC-MS, $^{1}H$ and $^{13}C$ NMR. Cytotoxic tests showed good results.

## Resumo/Abstract

Synthesis of organic substances is an important part of the process of discovery and development of new drugs. The use of active molecules from natural products as a model, or prototype molecules for the synthesis of more biologically active analogous structures, has contributed significantly to obtain new therapeutic agents. Chalcones are among the substances synthesized for the purpose of being applied as bioactive molecules. Compounds **1**-**18** (**Fig. 1**) were synthesized by the Claisen-Schmidt condensation of aromatic ketones with aromatic aldehydes, affording exclusively the *E*-isomer in good yields.

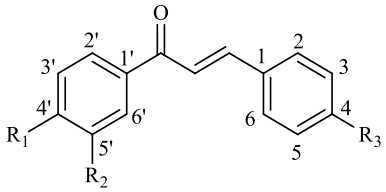

**1**. $R_1 = R_2 = R_3 = H$
**2**. $R_1 = R_2 = H$, $R_3 = OCH_3$
**3**. $R_1 = H$, $R_2 = R_3 = OCH_3$
**4**. $R_1 = R_2 = F$, $R_3 = H$
**5**. $R_1 = R_2 = Cl$, $R_3 = H$
**6**. $R_1 = R_2 = Br$, $R_3 = H$
**7**. $R_1 = R_2 = F$, $R_3 = OCH_3$
**8**. $R_1 = R_2 = Cl$, $R_3 = OCH_3$
**9**. $R_1 = R_2 = Br$, $R_3 = OCH_3$

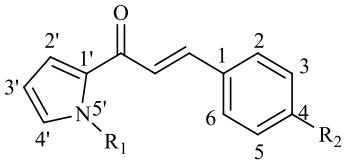

**10**. $R_1 = R_2 = H$
**16**. $R_1 = CH_3$, $R_2 = OCH_3$

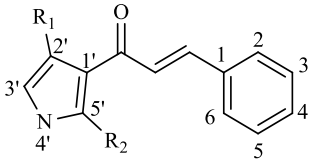

**11**. $R_1 = R_2 = CH_3$

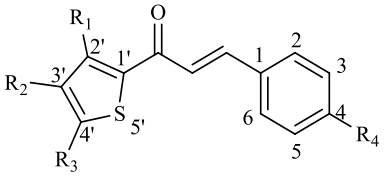

**12**. $R_1 = R_2 = R_3 = R_4 = H$
**13**. $R_1 = R_2 = H$, $R_3 = Br$, $R_4 = H$
**14**. $R_1 = H$, $R_2 = CH_3$, $R_3 = R_4 = H$
**15**. $R_1 = CH_3$, $R_2 = R_3 = R_4 = H$
**17**. $R_1 = CH_3$, $R_2 = R_3 = H$, $R_4 = OCH_3$
**18**. $R_1 = R_3 = H$, $R_2 = CH_3$, $R_4 = OCH_3$

**Fig. 1.** Structure of synthesized chalcones

All compounds were evaluated for their cytotoxic activity against SF-295 (human glioblastoma), PC-3 (prostate) and HCT-116 (colon) human cancer cell lines. They were first test at an initial concentration of 25 µg/ml. The cytotoxic activity tests showed good results, with high percentage of inhibition of tumor cell growth for some of them. The presence of a methoxyl group in ring B, decreased the activity. The synthesis procedure and purification methodologies used proved to be efficient, since chalcones were obtained with good yields. .

**Área: Org.** **Inscrição:00361**

# Biocatalytic Promiscuity: Use of lipases as catalyst on Henry reaction.

**Maria Clara S. Durigon (IC)[1*], Michele do Rocio Gonçalves Dias[1] (PG), Nádia Krieger[2] (PQ), Gustavo Henrique Couto[1] (PQ), Cristiane Pilissão[1] (PQ)**

**mariadurigon@alunos.utfpr.edu.br.**

[1] Departamento de Química e Biologia (DAQBi), UTFPR; [2] Departamento de Química - UFPR.

Palavras Chave: *Enzymatic Catalysis, Promiscuity, Nitroaldol, immobilization, Lipase.*

## Highlights

This study used lipases as catalyst in the Henry reaction with p-nitroaldehyde and nitromethane which provides a simple efficient method for the synthesis of β-nitroalcohols. The present method has many advantages including the mild and green reaction conditions, simplicity and good yield.

## Resumo/Abstract

Biocatalytic promiscuity, a new frontier extending the use of enzymes in organic synthesis, has attracted much attention and expanded rapidly in recent years.[1-2] This present study was aimed to evaluate the catalytic activity of different lipases free or immobilized in carbon nanotube – MWCNTs Pristine in the Henry reaction. The commercial lipases from *Lipozyme 435* and *Pancreatic pig* (PPL) and the native lipases LIPC12 (metagenomic lipase) and Papain lipase, as well as L-Proline were used as catalyst using p-nitrobenzaldehyde (1 mmol) and nitromethane (2 mmol), in DMSO (5 mL) and water (0.5 mL) for 48h, as shown on scheme 1. The conversions were calculated by 1H NMR.

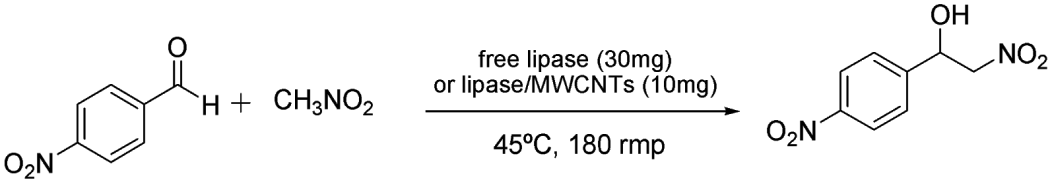


**Scheme 1**: Henry reaction catalyzed by lipase in DMSO and water.

To evaluate the promiscuity of the lipases in the Henry reaction, initially evaluated different lipases free or immobilized in MWCNTs, the results is shown in **figure 1.**

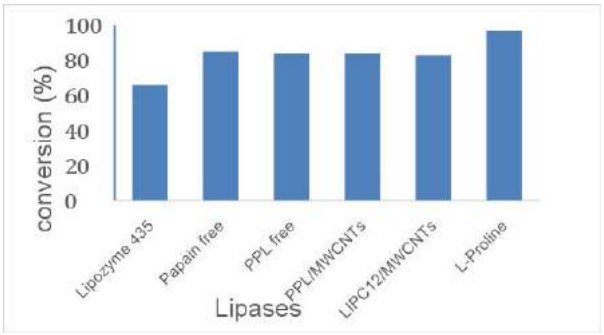


Figure 1 – Effect of the use of lipases in the nitroaldol reaction. Quantification by $^1$H NMR.

The system presented excellent results using the lipases free and immobilized, being that the conversions were of 66-85%. When used the L-Proline the conversion was of 97%. These results showed that lipases have great potential to be exploited in different types of reaction within the organic synthesis.

Acknowlegments: CNPq, CAPES, DAQBi-UTFPR, PPGQ-UTFPR, UFPR.

References

1. Tang, R. C. *et al*. *J. Mol. Catal. B. Enzym*. **2010**, *63*, 62-67.

2. Le, Z *et al*., Green Chemistry Letters and Reviews **2013**, *6*, 277-281.

**Área: QPN** **Inscrição: 00008**

# COMPOSIÇÃO QUÍMICA E ATIVIDADE BIOLÓGICA DO ÓLEO ESSENCIAL DA SEMENTE DE *Schinus molle*

**Vânia M. M. Valente (PQ),[1] Nathany K. Morais (IC),[2]* Patrícia M. Valente (PG),[3]**

**vvalente@ufv.br; nathanyk.morais@gmail.com**

*[1]Instituto de ciências Exatas e Tecnológicas, UFVCRP; [2]Instituto de Ciências Biológicas e da Saúde, UFVCRP; [3]Centro de ciências Agrárias UFES*

Palavras Chave: Antifúngico, inseticida, antibiótico.

## Highlights

CHEMICAL COMPOSITION AND BIOLOGICAL ACTIVITY OF SEED ESSENTIAL OIL OF *Schinus molle*
The green seed: camphene, p-cymene, α-Humulene and Germacrene D; and mature seed: α-tujene, camphene and sabinene .
Insecticidal activity with a 100% mortality rate against *S. zeamais* and *M. rosae*.

## Resumo/Abstract

A *Schinus molle* é utilizada em paisagismo, apresenta óleo essencial com importantes atividades antimicrobianas, podendo ser uma alternativa para o tratamento de micro-organismos resistentes. O objetivo deste estudo foi verificar a composição química do óleo essencial da sua semente, seu efeito antifúngico sobre *Aspergillus niger* e *Peniciulium expansum*, sua atividade antibacteriana sobre *Escherichia coli, Serratia marcescens, Staphylococcus aureus* e *Bacillus cereus* e atividade inseticida sobre *Sitophilus zeamais* e *Macrosiphum rosae*. O óleo das sementes frescas foi extraído em Clevenger e a composição química determinada por cromotografia gasosa acoplada à espectrometria de massas, sendo os seguintes compostos majoritários na semente verde: canfeno (14,4%), p-cimeno (15,1%), copaeno (9,9%), α-Humulene (29,8%) e Germacreno D (12,6%) e na semente madura: α-tujeno (15,2%), canfeno (45,2%) e sabineno (17,5%). Os halos de inibição dos óleos observados sobre as bactérias comparados aos halos obtidos pelo branco (água, 5 mm) e o antibiótico ácido nalidíxico (0,9 - 3,1 mm) foram pequenos, o maior valor foi observado sobre *E. coli* (9 mm). A atividade antifúngica observada teve 15,4% de inibição no crescimento micelial de *A. niger* com o óleo da semente verde e 26% de inibição pelo óleo da semente madura. Em *P. expansum* foram observadas inibições de 29,1% e 36,8% pelos óleos das sementes verdes e maduras, respectivamente. A atividade inseticida sobre *S. zeamais,* empregando 50 µL de óleo, e *M. rosae*, empregando 25 µL de óleo, teve índice de mortalidade de 100%.

**Área: QPN** **Inscrição: 00023**

# Antifungal activity of the essential oil of *Campomanesia macrobracteolata* and *Protium* sp. against *Thielaviopsis paradoxa*

**Kézia Roncati dos Santos (PG),[1†] Jéssyca Paes Dutra (PG),[2] Jaquelini Luber (PG),[3] Rodrigo Rezende Kitagawa (PQ),[2] Warley de Souza Borges (PQ),[1*]**

**[*]warley.borges@ufes.br; [†]kezia_coq@hotmail.com**

*[1]Departamento de Química, UFES; [2]Departamento de Ciências Farmacêuticas, UFES, [3]Departamento de Biologia, UFES*

Palavras Chave: *Óleo essencial, fungo, atividade fungicida, Thielaviopsis paradoxa*

## Highlights

Antifungal activity of the essential oil of *Campomanesia macrobracteolata* and *Protium* sp. against *Thielaviopsis paradoxa.*
Fungi cause great damage to agriculture.
*Thielaviopsis paradoxa* causes great damage to the pineapple culture.
Essential oils with great antifungal potential.
Extraction of essential oil and antifungal test by the microdilution method against *Thielaviopsis paradoxa*.

## Resumo/Abstract

Natural products, especially the essential oils of plants, play an important role in the discovery of new antifungal agents. With the increase of microbial diseases and many reports on microorganisms' resistance to antifungal drugs, the importance of studies of natural products with antifungal properties increases. Thus, the development of protective products with natural origin as an alternative to synthetic fungicides is currently in the spotlight. Due to this fact, the aim of this study was to find new antifungal agents among essential oils from two species: *Campomanesia macrobracteolata* (leaves and fruits) and *Protium* sp. (leaves and stems with flowers). The essential oil from the different parts of the plants was obtained by hydrodistillation in a Clevenger-type apparatus, and the composition of the essential oils determined by the GC-MS analysis. The antifungal activity of essential oils was evaluated against *Thielaviopsis paradoxa* and was determined by a microdilution assay. The essential oil of the fruits from *Campomanesia macrobracteolata* presented concentrations of 200 and 400 μg $mL^{-1}$ capable of inhibiting 50 and 100%, respectively. At the concentration of 800 μg $mL^{-1}$, essential oil of the leaves from *Campomanesia macrobracteolata* inhibited 100%. The essential oil from the leaves and stems of *Protium* sp. on the concentrations of 200 and 400 μg $mL^{-1}$, inhibited the fungus *Thielaviopsis paradoxa* in 25 and 100%, respectively. Results revealed that the two species are able to produce substances that inhibit the growth of this fungus.

**Área: QPN** **Inscrição: 00026**

# Variabilidade composicional em óleo essencial de flores de *Caesalpinia pulcherrima* (L.) SW

**Francisco E.A. Catunda Júnior (PQ),[1,2]* Águida M.A. Azevedo (PG),[2] Eriberto P. Sá Júnior (PG),[2] Mário G. de Carvalho (PQ),[3] Thiago F. Araújo (PQ).[1,2]**

***cearajr@gmail.com**

*[1]Centro de Ciências Exatas, Naturais e Tecnológicas, UEMASUL; [2]Mestrado em Biotecnologia, UNINTA; [3]Departamento de Química, UFRRJ*

Palavras Chave: *Caesalpinia pulcherrima, Flores, Óleo essencial, α-Pineno, E-Cariofileno, Germagreno D.*

## Highlights

Compositional variability in flowers essential oil of *Caesalpinia pulcherrima* (L.) SW

Essential oil variation in flowers was evaluated for the first time

Chemical composition in flowers essential oil was grouped in chemotypes

Main essential oil components in flowers were sesquiterpenes

## Resumo/Abstract

A *Caesalpinia pulcherrima* (*Fabaceae*), também conhecida como flamboyazinho é uma planta ornamental, da família das leguminosas, originária da Índia e América Central. Na índia, estudos farmacológicos revelaram que a espécie apresenta várias propriedades medicinais, das quais o uso no tratamento contra úlcera, tumores, dermatites, disenteria, diversas infecções, além da ação abortiva. (SUDHAKAR *et al*., 2006; EUFRÁSIO *et al*., 2009; SHARMA; RAJANI 2011). Flores de *C. pulcherrima* foram coletadas em três cidades da região noroeste do Ceará. Uma variabilidade significante no rendimento dos óleos essenciais, após extração por hidrodestilação, foi observada entre as espécimes de cores investigadas (variando de 0,006 a 0,053 %) e na composição química. As análises dos óleos essenciais foram feitas por CG-DIC e CG-EM, e um total de quarenta e oito constituintes foram identificados. α-Pineno (0,67 – 25,65 %), α–copaeno (3,49 – 25,52 %), E-cariofileno (1,64 – 20,56 %), germacreno D (4,69 – 33,42 %) e óxido de cariofileno (1,61 – 49-13 %), foram identificados como constituintes majoritários dos óleos essenciais, dependendo da espécime de cor analisada. A espécime de cor laranja apresentou alto teor de hidrocarbonetos monoterpênicos, enquanto de demais cores, amarela, vermelha e rosa, tiveram como majoritários hidrocarbonetos sesquiterpênicos. Vale ressaltar que a variação da composição química do óleo essencial das flores de *C. pulcherrima* está sendo relatada pela primeira vez.

SHARMA, V.; RAJANI, G.P. *Indian Journal of Pharmacology*. 2011. 43, 168-171
SUDHAKAR et al. Fitoterapia. 2006, 77, 5, 378-380
EUFRÁSIO et al. CCAB/UVA, 2009. Sobral – CE.

**Área: QPN** **Inscrição: 00157**

# Chemical composition and antimicrobial activity of essential oil obtained from two species of the Lauraceae family

**Eduardo J. Coutinho (IC),[2] Érica R. Costa (PG),[1] Gabriela M. Louro (PG),[1] Cleber L. Nicolau (PG),[1] Jaqueline C. M. da Silva (PG),[1] Crescencio C. S. Filho (IC),[2] Shaline. S. L. Fernandes (PG), [2] Marcia R. P. Cabral (PG),[3] Euclésio Simionatto (PQ).[1] eduardo.jcoutinho@gmail.com; erica_rodrigues23@hotmail.com**

*[1] Programa de Pós-Graduação em Recursos Naturais da Universidade do Estado de Mato Grosso do Sul, PGRN/UEMS; [2] Curso de Química Licenciatura da Universidade Estadual de Mato Grosso do Sul, PIBIC/UEMS; [3] Universidade Estadual de Maringá, UEM.*

Palavras Chave: *Extração, Óleo essencial, Ocotea catharinensis, Cinnamomum verum, Antimicrobianos.*

## Highlights

The extraction of the essential oil from the leaves of the species *O.catharinensis* and *C. verum* was carried out by hydrodistillation, after the chemical characterization the oils were tested against three bacteria.

## Resumo/Abstract

**Introdução:** As espécies da família Lauraceae apresentam-se distribuídas em regiões tropicais e subtropicais, com aproximadamente 3000 espécies. Espécies desta família são ricas em metabólitos secundários que compõe óleos.[1] O objetivo deste estudo é a caracterização química e atividade antimicrobiana dos óleos essenciais extraídos de duas espécies *Ocotea catharinensis* e *Cinnamomum verum*. **Resultados e Discussão:** A coleta das espécies foi realizada em Naviraí-MS, o rendimento do óleo essencial foi de 0,44% para *O. catharinensis* e 0,12% para *C. verum.* Após a extração por hidrodestilação os óleos foram submetidos à cromatografia (CG-EM) (Figura 1 e 2) e identificação dos constituintes principais.

**Figura 1.** Perfil químico do óleo da *O. catharinensis*

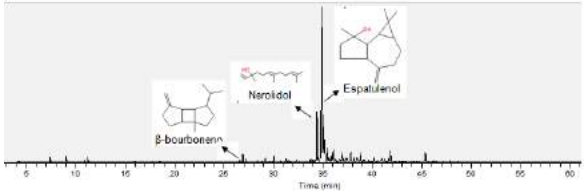


**Figura 2.** Perfil químico do óleo da *C. verum*

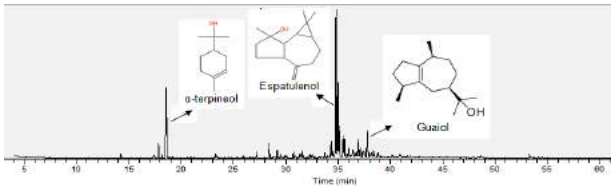


Realizaram-se também os testes de atividade antimicrobiana, sendo que para o teste de disco difusão e de concentração inibitória mínima (CIM) foram testadas bactérias gram-positivas e gram-negativas, todas as bactérias testadas foram sensíveis aos óleos (Tabela 1).

**Tabela 1.** Teste de disco difusão dos óleos essenciais e controle.

| Óleos essenciais | *B. cereus* (halo**) | *E. coli (halo)* | *S. aureus (halo)* | Interpretação* |
|---|---|---|---|---|
| ***O. catharinensis*** | 20,56 | 20,34 | 18,65 | S |
| ***C. verum*** | 20,97 | 18,50 | 20,76 | S |
| ***Antibiótico*** | 34,31 | 32,05 | 27,27 | S |

Legenda: R=resistente (halo ≤ 12 mm); I= intermediário (halo 13-17 mm) S= sensível (≥ 18 mm).

O teste de concentração inibitória mínima (CIM) mostrou a concentração necessária para cada óleo essencial testado inibir o crescimento das bactérias conforme mostra a tabela 2.

**Tabela 2. C**oncentração (CIM) de óleo essencial necessária para inibir o crescimento das bactérias

| | *B. cereus* (µg/mL) | *E. coli* (µg/mL) | *S. aureus* (µg/mL) |
|---|---|---|---|
| ***O. catharinensis*** | 2250 | 18000 | 9000 |
| ***C. verum*** | 9000 | 2250 | 2250 |

CIM* Forte= até 500 µg/mL, Moderada= 600 a 1600 µg/mL, Fraca= > 1600 [2]

**Conclusão:** Os óleos essenciais apresentaram composição química similar, e ambos foram ativos frente às bactérias testadas apresentando atividade antimicrobiana quando testados na forma bruta, o próximo passo são os testes de sinergismo.

**Referências:** [1] Grecco, S.S., Lorenzi, H., Tempone, A.G., Lago, J.H.G. (2016). Update: biological and chemical aspects of Nectandra genus (Lauraceae). Tetrahedron: Asymmetry. 27: 793-810.

[2] SARTO, Marcella P. Mansano; JUNIOR, Gerson Zanusso. Atividade antimicrobiana de óleos essenciais. **Revista Uningá Review**, v.20, n./1, p.98-102, 2014. **Agradecimentos:** UEMS/PIBIC, PGRN, FUNDECT.

**Área:___QPN_____ Inscrição:__00420__**

# Chemical composition of leaves and fruits essential oils from *Schinus terebinthifolius* genders cultivated at Ceará-Brazil

**Francisco Matheus F. Dias (IC),[1] Francisco Robson P. Azevedo (IC),[1] Priscila T. da Silva (IC),[1] Hélcio da Silva Santos (PQ),[1] Tigressa Helena S. Rodrigues (PQ),[1]* Paulo Nogueira Bandeira (PQ),[1]** Categorias: Pesquisador (PQ) e Estudante de graduação (IC).

**matheusd47@gmail.com; thelenasr@yahoo.com.br**

[1]*Curso de Química, Universidade Estadual Vale do Acaraú (UVA)*

*Palavras Chave: S. terebinthifolius genders, Volatile composition, Terpenes, Gas chromatography.*

## Highlights

- *S. terebinthifolius* essential oils from leaves and fruits shown different chemical compositions.
- Volatiles from *S. terebinthifolius* could be used to differentiate the male and female genders.

## Resumo/Abstract

*S. terebinthifolius* is a diootic plant largely found in the Brazilian coast, and all parts of the species are medicinal, being popularly known as antipyretic, analgesic and depurative. The main objective of this work was to determinate the volatile compounds of leaves and fuits from *S. terebinthifolius* male and female trees located at Ceara state in Brazil collected during dry season. The essential oils were obtained from leaves (both genders) and fruits (female only, green and red separately) by hydrodistilation. Chemical composition was determinated by gas chromatography with spectrometry (GC-MS and GC-FID) using data base from equipment and Kovats index calculation. Results exhibited different composition in essential oil leaves in both genders. In male leaves, D-Limonene (96%) was the major compound identified with other monoterpenes, α-Pinene (1%), Myrcene (1%), while β-Caryophyllene (0.5%) was the only sesquiterpene. In female essential oil leaves, δ-3-Carene (27%), β-Caryophyllene (30%), Spathulenol (5%) and Caryophyllene oxide (5%) were the mainly compounds, and sesquiterpens represented 48% of total oil composition. *S. terebinthifolius* fruits (green and red) shown distinct results, although the monoterpenes were 87 – 90% of both essential oils. D-Limonene (39%), Terpinen-4-ol (31%) and Sabinene (8%) were presented in green fruits; while Terpinen-4-ol (64%), Cis-p-menth-2-en-1-ol (4%) and Cis-piperitol (4%) were the main constituents determinated in red fruits, at mature conditions. Accordingly to this study, the *S. terebinthifolius* essential oil information shows the possibility to differentiate both genders and its chemical potential for futher biological applications.

**Área: QPN** **Inscrição:_00476__ __**

# Chemical composition and antimicrobial activity of essential oil *Psidium Myrtoides* O. Berg

**Renieidy F.C. Dias (PG)*,[1] Francisco J. T. Aquino (PQ),[1] Sérgio A L Morais,[1] Evandro A Nascimento,[1] Alberto de Oliveira,[1] Luis C. S. Cunha, (PQ),[2] Maria A. L. V. Ambrósio (PQ),[3] Carlos H. G. Martins(PQ)[3], João M. Souza (IC)[4]. Email: flavia.dias@ufu.br**

*[1]Núcleo de Pesquisa em Produtos Naturais, Universidade Federal de Uberlândia, CEP 38400-902, Uberlândia-MG; [2]Núcleo de Estudos em Alimentos e Produtos Naturais – Instituto Federal de São Paulo, CEP 18707-150, Avaré-SP. [3]Laboratório de Pesquisa em Microbiologia Aplicada, Universidade de Franca, CEP 14404-600, Franca-SP,. [4]Núcleo de Bioprospecção em Produtos Naturais – Instituto Federal do Triângulo Mineiro, CEP 38064-790, Uberaba-MG*

Keywords: Essential oil; Psidium *Myrtoides O. Berg; Sesquiterpenoid; CG-MS; Antimicrobial Activity.*

## Highlights

In this study, chemical composition and antimicrobial activity of the essential *Psidium Myrtoides* O.Berg were reported firstly. The essential oils were extracted by hydrodistillation and the components were identified by gas chromatography coupled to mass spectrometry (GC-MS). A total of 26 chemical components were identified, accounting for only sesquiterpene in the essential oil.

## Resumo/Abstract

*Psidium Myrtoides* O.Berg is known as Araçá-Roxo in Brazil. The plant belongs to the family Myrtaceae, which comprises about 145 genus and 5,970 species in the world (The Plant List). Most species of the genus *Psidium* produce essential oils (Chalannavar et al., 2014). The essential oil (EO) the fresh leaves from the aerial parts of *Psidium Myrtoides* O.Berg was obtained by hydrodistillation and analysed by GC–MS. The highest percentage of compounds were sesquiterpenes hydrocarbons (61,25%), followed by oxygenated sesquiterpenes (38,75%). Twenty-six compounds were identified which represent of the total composition of the EO. The major components of the EO were α-Copaene (7,55%), trans-caryophyllene (22,91%), α-humulene (7,1%), α-cadinene (4,52%), oxide caryophyllene (7,58%), and α -bisabolone (10,41%). The EO of the fresh leaves and dry leaves *Psidium Myrtoides* O.Berg was tested against seven bacterial and three yeasts by the broth microdilution method. The oils of the fresh and dry leaves exhibited moderate activity against *Streptococcus sanguinis and Streptococcus mutans* with inhibitory concentrations (MICs) of 200 and 400 µg/mL,respectively. The EO fresh and dry leaves showed an relevant potential to inhibit the growth of *Candida Glabrata* with MIC values 187,5 µg/mL and 46,5 µg/mL, respectively. Both oils also showed activity against *Candida albicans* and *Candida tropicalis* with MIC values ranging from 1500 to 3000 µg/mL.

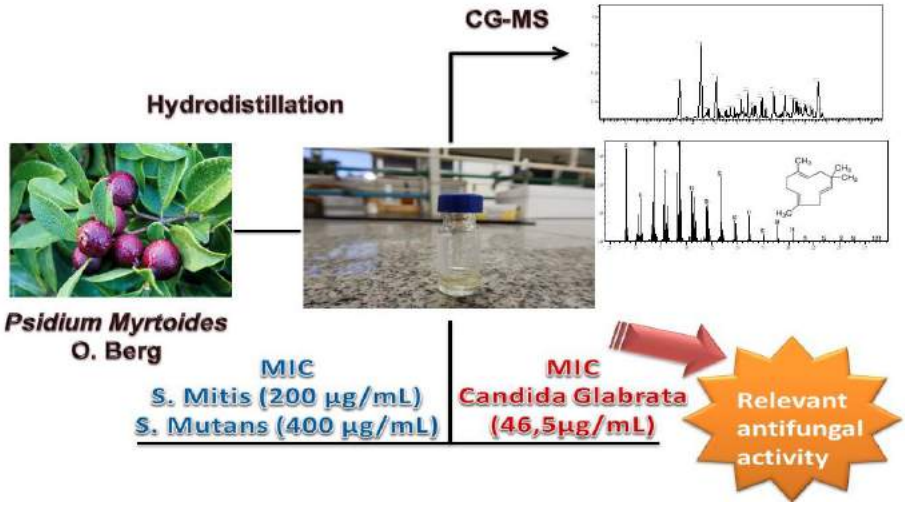


Acknowledgments:CAPES, UFU, UNIFRAN, FAPEMIG.

References: Chalannavar, R.K., Baijnath, H., Odhav, B. (2014). *The Chemical Composition of Leaf Essential Oils of Psidium guajava L. (White and Pink fruit forms) from South Africa.* TEOP 17 (6), 1293–1302.

**Área: QPN** **Inscrição: 00506**

# Avaliação da ação fotoprotetora do extrato aquoso de *Campomanesia adamantium*

**Larissa Gaiola(IC),[1*] Taline Baganha Stefanello Catalan (PG),[1] Claudia Andrea Lima Cardoso (PQ).[1]**

**larigaiola@gmail.com**

[1]Centro de Estudos em Recursos Naturais, Laboratório de Análise Instrumental, UEMS.

Palavras Chave: Protetor solar, FPS, guavira

## Highlights

Evaluation of the photoprotective action of the aqueous extract of *Campomanesia adamantium*.
The substances of natural origin can have the potential to a solar protection.
The *C.adamantium* showed ascending FPS according to the concentration of the extract.
The aqueous extract of *C.adamantium*a presented antioxidant action.

## Resumo/Abstract

Extratos podem atuar como fotoprotetores dependendo do valor do fator de protecão solar (FPS). O objetivo deste estudo foi avaliar a ação fotoprotetora[1], atividade antioxidante[2]e teor de compostos fenólicos[3] do extrato aquoso de *Campomanesia adamantium.* As folhas secas foram utilizadas na proporção de 20 g/L de planta-água para obtenção do extrato. O extrato liofilizado foi diluído em etanol 95% nas concentracões de 2%,3%, 4% e 8%. A concentração que apresentoua melhor resposta foi incorporada à base semissólida (Figura 1). No extrato incorporado a base semissólida foram realizadas as análises de estabilidade, durante 3 meses, não apresentando formação de fase, mantendo o odor adocicado, pH6 - 6,5 e o FPS variou 9,5 %.

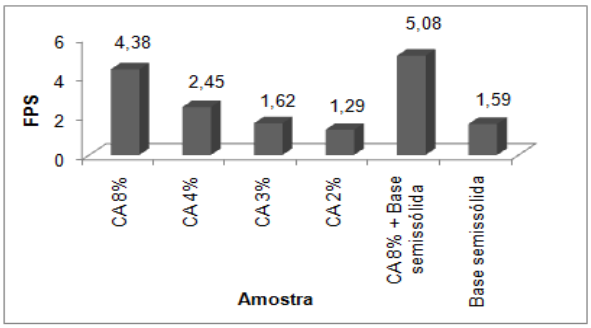


Figura 1 – Resultados obtidos de FPS para o extrato aquoso de *C.adamantium*

Segundo a lesgistação brasileira, cosmeticos com função fotoprotetora devem apresentar FPS de no mínimo 6. Contudo, segundo a mesma legislação o produto multifunctional, no caso o extrato aquoso de *C.adamantuim*, pode apresentar FPS 2. A atividade antioxidante foi de 30,18µg/mL empregando o radical livre DPPH e o teor de compostos fenólicos foi de 728,70mg/g, considerando-se um extrato com potencial antioxidante.

1-MANSUR, J.S.; BREDER, M. N. R.; MANSUR, M. C. D'.; AZULAY, R. David.**Anais Brasileiros de Dermatologia,** v.61, n. 3 p.121-124, 1986.
2-KUMARAN, A.; KARUNAKARAN, R. J. **FoodChemistry**. v. 97, p. 109-114, 2006.
3-DJERIDANE, A.; YOUSFI, M.; NADJEMI, B.; BOUTASSOUNA, D.; STOCKER, P.; VIDAL, N. **Food Chemistry**, v.97, p.654-660, 2006.

**Área: QPN** **Inscrição:___00614___**
*(Inserir o número de inscrição do autor que fez a submissão)*

# Antimicrobial activity of the essential oil of leaves of *Banisteriopsis malifolia* (Ness & Martius) B. Gates

**Roberto Chang (PQ)[1], Vanessa E. X. Martins (PG)[1*], Helena M. T. Silingardi (PQ)[2], Evandro A. Nascimento (PQ)[1], Luís C. S. Cunha (PQ)[3], Carlos H. G. Martins (PQ)[4], Maria A. L. V. Ambrósio (PQ)[4], Lorraine A. Garcia (IC)[4], Sérgio A. L. Morais (PQ)[1], Francisco J. T. de Aquino (PQ)[1].**

**chang@ufu.br; vanellenxm@hotmail.com**

*[1]Nucleus of Research in Natural Products, Federal University of Uberlândia, CEP 38400-902, Uberlândia/MG; [2]Institute of Biomedical Sciences, Federal University of Uberlândia, CEP 38400-002, Uberlândia/MG; [3]Nucleus of Bioprospecting in Natural Products, Federal Institute of Triângulo Mineiro, CEP 38064-790, Uberaba/MG; [4]Laboratory of Research in Applied Microbiology, University of Franca, CEP 14404-600, Franca/SP.*

Keywords: Essential oil, *Banisteriopsis malifolia*, biological activity, GC/MS.

## Highlights

The species *Banisteriopsis malifolia* (Ness & Martius) B. Gates (Malpighiaceae), a.k.a "flor-do-dia", is a native plant from Cerrado[4]. However, to date, only phenological and morphological studies of the plant have been carried out[5], which has aroused interest on studies related to the chemical Composition and the evaluation of the biological activity of this species. The essential oil of *B. malifolia* was characterized by GC/MS, and submitted to biological activity assays against oral microorganism by broth microdilution method.

## Resumo/Abstract

The oral cavity is an environment conducive to the growth of several microorganisms such as bacteria, responsible for periodontal diseases and dental caries.[1] In addition, studies have associated oral bacteria with various systemic diseases such as cardiovascular and intestinal diseases, rheumatoid arthritis, adverse effects on pregnancy, diabetes, among others.[2] The microbial resistance has been a major problem in the treatment of these diseases, which motivates the search for new antibacterial agents.[3] In this sense, this work aims to study the species *Banisteriopsis malifolia* (Ness & Martius) B. Gates (Malpighiaceae), popularly known as flower-of-the-day, a native, tropical and common plant from the Cerrado.[4] However, only phenological and morphological studies of this plant have been carried out [5], which aroused the interest in studies related to the chemical composition and the evaluation of the biological activity of this species. The essential oil of leaves of *B. malifolia* was obtained by hydrodistillation and the main compounds identified by GC/MS were (Z)-hex-3-enol (17.99%, RT 3.875 min); phytol (79%, RT 49.064 min) and a long chain alkane (18.43%, RT 73.380 min), being these compounds commonly found in oils of plants of this genus.[6] The antibacterial activity was evaluated against microorganisms of the oral cavity by broth microdilution method for the determination of Minimum Inhibitory Concentration (MIC). The oil concentrations tested were between 400 and 0.195 $\mu gmL^{-1}$ and tested against aerobic bacteria: *Streptococcus mutans* (MIC>400 $\mu gmL^{-1}$), *Streptococcus mitis* (MIC=400 $\mu gmL^{-1}$), *Streptococcus sanguinis* (MIC>400 $\mu gmL^{-1}$) and anaerobic bacteria: *Porphyromonas gingivalis* (MIC>400 $\mu gmL^{-1}$), *Fusobacterium nucleatum* (MIC>400 $\mu gmL^{-1}$) and *Actinomyces naeslundii* (MIC=400 $\mu gmL^{-1}$). The antimicrobial activity is considered good for MICs below 100 $\mu gmL^{-1}$ and moderate between 100 and 500 $\mu gmL^{-1}$.[7] The biological activity assays against oral microorganisms showed moderate activity against aerobic bacteria *Streptococcus mitis* and anaerobic bacteria *Actinomyces naeslundii*, showing interesting results regarding this species. Biological assessments with leaf extracts of *B. malifolia* are in progress.

Acknowledgments: UFU, UNIFRAN, FAPEMIG.
References: [1]Wade, G. W. *Pharmacol Res.* **2013**, 69(1), 137-43. [2]Chimenos-Küstner, E. *et al*. *Med Clin.* **2017**, (in press). [3]Anantaworasakul, P. *et al. Pharm Biol.* **2017**, 55(1), 1256–1262. [4]Gates, B. 1982. New York: The New York Botanical Garden. [5]Ferreira, C. A. 2013. Dissertação de mestrado em Ecologia e RN, UFU-MG. [6]Nunes, B.C. *et al.* 29ª Encontro Reg. Da Sociedade Brasileira de Química, Belo Horizonte, nov. 2015. [7]Holetz, F. B. *et al. Memorias do Instituto Oswaldo Cruz.* **2002**, 97(7), 1027-1031.

**Área: QPN** **Inscrição:00697**

*(Inserir o número de inscrição do autor que fez a submissão)*

# Chemical composition of essential oils of seven *Piper* species (Piperaceae) from Marambaia Island, Mangaratiba, RJ (Brazil)

**Ygor Jessé Ramos (PG)[1,2], Davyson de Lima Moreira (PQ)[1,2,3].**

**ygorjesse@gmail.com; davysonmoreira@hotmail.com**

*[1]Pós-graduação em Biologia Vegetal – Universidade do Estado do Rio de Janeiro (UERJ), Rio de Janeiro, RJ; [2]Departamento de Produtos Naturais - Farmanguinhos – Fundação Oswaldo Cruz, Rio de Janeiro – RJ; [3] Laboratório de Toxicologia Ambiental – DCB – ENSP - Fundação Oswaldo Cruz, Rio de Janeiro – RJ.*

*Keywords: Monoterpenes, Sesquiterpenes, Arylpropanoids, C6-C4-derivatives.*

## Highlights

Chemical diversity of seven *Piper* species; *Piper* species rich in terpenes and arylpropanoids. *Piper* species as source of volatile natural compounds.

## Resumo/Abstract

The Piperaceae family is distributed predominantly in the Neotropical region, and has its largest number of species belonging to the genus *Piper* L., which is represented by individuals with chemical varieties in essential oils (EO) and with recognized biological activities[1]. Marambaia Island is located in the municipality of Mangaratiba, in the bay of Sepetiba, South of the Rio de Janeiro State (23°04'S and 43°53'W). This area is surrounded mainly by Submontane Dense Ombrophylous Forest, in which already has an account of plant diversity and the presence of the genus *Piper* which may represent economic importance for local communities[2]. The aim of this study was to perform a chemical study of the EO composition from fresh leaves (150g), extracted by hydrodistillation in a Clevenger-type apparatus (3 hours) of seven *Piper* species from Marambaia Island: *Piper anisum* (Spreng.) Angely. (**Pas**); *Piper arboreum* Aubl var. *arboreum* (**Pab**); *Piper caldense* C. DC. (**Pcd**); *Piper diospyrifolium* Kunt. (**Pdp**); *Piper lepturum* Kunt. (**Plt**); *Piper lepturum* var. *angustifolium* (C.DC.) Yunck. (**Pla**); and *Piper mollicomum* Kunth. (**Pmc**). The EO compounds were identified and quantified by Gas Chromatography coupled to Mass Spectrometry (GC-MS) and GC coupled to the Flame Ionization Detector (GC-FID), respectively, in triplicate. GC-MS and GC-FID analyzes were performed using a HP-5ms column (30 m x 0.32 mm i.d. x 0.25 µm, particle size), temperature programing from 60 $^{o}$C to 240 $^{o}$C (3 $^{o}$C/ min) and flow rate at 1mL/min. The retention indices were calculated from a hydrocarbon homologous series (C8-C26, Sigma-Aldrich) to confirm the identification of the compounds. The results are listed in Table 1, which shows the major identified compounds of each species.

**Table 1.** Major constituents identified in the essential oils of *Piper* species from Marambaia Island.

| Species | Major Components % (Average ± Standard Deviation) | Yields % |
|---|---|---|
| **Pas** | 1-butyl-3,4-methylenedioxybenzene (77.16 ± 0.15) | 0.32 |
| **Pab** | (*Z*)-Caryophyllene (30.97 ± 0.27); Germacrene D (16.24 ± 0.20); (*Z*)-*beta*-Ocimene (16.06 ± 0.22) | 0.85 |
| **Pcd** | Eucalyptol (13.22 ± 0.08); Dillapiol (12.98 ± 0.09); Camphor (12.95 ± 0.18); Apiole (12.45 ± 0.12) | 0.21 |
| **Pdp** | (*E*)-Nerolidol (11.67 ± 0.11); Germacrene D (9.03 ± 0.21); *beta*-Elemene (7.84±0.17); | 1.23 |
| **Plt** | (*E,E*)-alpha-Farnesene (30.71 ± 0.19); (*E*)-Isosafrole (23.64 ± 0.11); (*Z*)-Caryophyllene (20.95 ± 0.08) | 0.56 |
| **Pla** | (*Z*)-gamma-Bisabolene (52.39 ± 0.87); Myrcene (12.73 ± 0.54); (*E*)-gamma-Bisabolene (11.72 ± 0,61) | 0.34 |
| **Pmc** | Eucalyptol (59.52 ± 0.36); alpha-Pinene (20.78 ± 0.09); beta-Pinene (14.30 ± 0.10) | 0.90 |

The results showed interesting chemiodiversity at the intra- and inter-species level with presence of monoterpenes, sesquisterpenes, arylpropanoids and C6-C4 derivatives.

[1] Santos, P.R. et al. Phytochemistry, 58(4), 547-551, 2001.
[2] Carvalho, D.C.; Conde, M.M.S. *Série Técnica Floresta e Ambiente*. 4(4): 001-026, 2014.

**Área: QPN** **Inscrição: 00805**

# Extraction of the essential oil from the leaves of Piper hispidinervum using supercritical $CO_2$.

**Edesio Luiz Simionatto (PQ),[1*] Dilamara Riva Scharf (PQ),[1] Gabriel Henrique Wientage (IC),[1] Bruna Heloisa Klinkowski (IC),[1] Julia Salamoni (IC),[1] Lúcio Cardozo Filho (PQ).[2]**

**edesio@furb.br**

*[1]Departamento de Química, FURB – Fundação Universidade Regional de Blumenau; [2]Departamento de Engenharia Química UEM – Universidade Estadual de Maringá.*

Palavras Chave: *Piper hispidivervum, Extração supercrítica, Safrol, Pentadecano, Óleo essencial*.

## Highlights

The essential oil obtained shows the presence of safrole and pentadecane.
The safrole content is lower than in the oil obtained by hydrodistillation.

## Resumo/Abstract

Este estudo avaliou a extração do óleo essencial das folhas da *Piper hispidinervum*, popularmente conhecida como pimenta longa, utilizando extração supercrítica com $CO_2$. O experimento foi realizado a uma temperatura de 40 $^{o}$C e pressão de 200 bar. As folhas e ramos jovens foram secos a sombra durante 10 dias antes da extração. O rendimento de óleo essencial obtido na condição supercrítica foi semelhante ao óleo essencial obtido por hidrodestilação, na faixa de 3,0 %. A análise cromatográfica por GC-FID destes dois óleos, comparada com padrões, apresenta dois perfis cromatográficos diferentes: o óleo essencial obtido por extração supercrítica que apresenta safrol (50%) e pentadecano (15%) como constituintes majoritários (Figura b), enquanto o óleo obtido por hidrodestilação apresenta safrol (88%) e terpinoleno (6%) (Figura a). O pentadecano foi isolado através do fracionamento do óleo utilizando coluna cromatográfica e confirmado com padrão analítico. O pentadecano foi também encontrado no produto da extração supercrítica das folhas da *Piper pescatorum* (PIMENTEL). O cultivo da espécie Piper hispidinervum no Vale do Itajaí-SC é estudado na perspectiva que esta planta possa ser uma fonte alternativa de safrol, em substituição a canela sassafrás (RIVA). Neste sentido, os resultados obtidos apontam que a hidrodestilaçção produz um óleo essencial com teor de safrol superior ao óleo obtido por extração supercrítica.

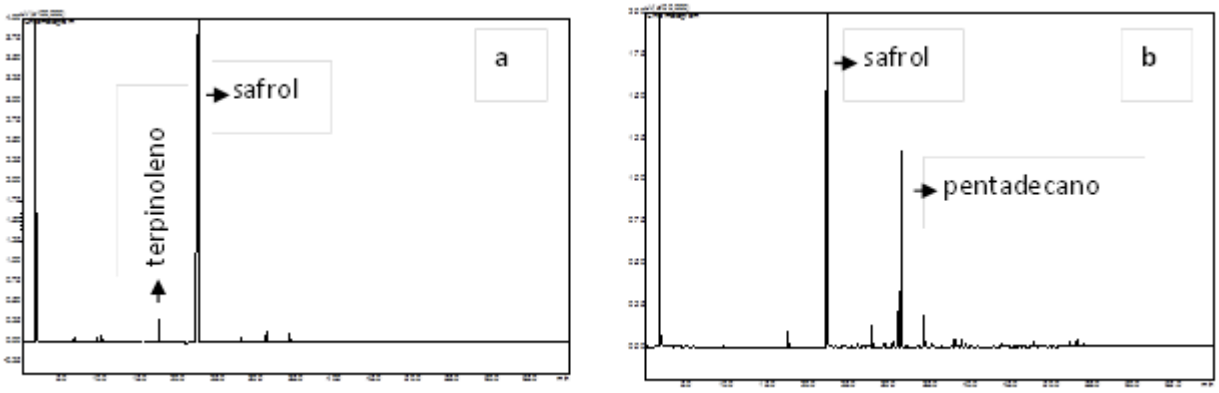


RIVA, D. et al. Acta Amazonica. v. 41, p. 297-302, 2011.
PIMENTEL, F.A. et al. Industrial Crops and Products. v. 43, p. 490-495, 2013. .

**Área: QPN** **Inscrição: 00817**

# The influence of abiotic factors on the production of essential oils of *Eugenia uniflora*

**Miriam Sannomiya (PQ),[1*] Renata de Oliveira Santos (IC),[1] Fabiana C. Pioker (PQ),[1] Rosely A. Liguori Imbernon (PQ).[1]**

**miriamsan@usp.br**

[1]*Escola de Artes, Ciências e Humanidades, USP- Campus Leste*
Palavras Chave:*(Eugenia uniflora, essential oil, seasonality)*

## Highlights

The chemical analyzes of the different leaf extracts of 4 individuals of *Eugenia uniflora* showed a difference in the chemical profile due to its location as well as the seasonality. Two specimens occurring in an area with an intense flow of urban transport means. Two other specimens occurring in a preserved area of an inner city. A large variety of secondary metabolites was observed on the spring, it be associated with high $O_3$ during this season. The defense system of the organism against herbivores. The copper content in the collected water can be contributed to the variation of metabolites.

## Resumo/Abstract

*Eugenia uniflora* L., popularly known as "cherry"; refers to a highly adapted to urban environments species and highly contaminated by airborne pollutants[1]. The studies show that individuals occurring in urban and rural centers respond differently to the effects of pollution in relation to their anatomical features, showing that this is a bioindicator species of the air quality. In this sense, a comparative study of the essential oil present in the leaves of *E. uniflora* specimens occurring in the metropolitan region of São Paulo and in a preserved area of Mogi Cruzes-SP as well as the study of chemical composition in different seasons, associated with the heavy metal content in water, can allow a better understanding of the contribution of each of these variables in the production of secondary metabolites.

The chemical analyzes by TLC anda GC/MS of the different leaf extracts of 4 individuals of *Eugenia uniflora* showed a difference in the chemical profile due to its location as well as the seasonality. Regarding the essential oils, it was possible to observe that the samples collected in the Mogi das Cruzes (São Paulo-Brazil) Park show a greater diversity of secondary metabolites than the samples that occur in the vicinity of the School of Arts, Sciences and Humanities (USP-Campus Leste), the which is located in the Tietê Ecological Park, in the vicinal of the Ayrton Senna highway. A great quantity and diversity of secondary metabolites were produce during spring. This production could may be associated with high $O_3$ during this season, either those compounds could be used as a defense system of the organism against herbivores or the production could be furnished to the flowers for the period of pollination of the plant[2]. A factor for the increment of secondary metabolites in the essential oils in the leaves of all the collections carried out in the Municipal Tropical Park Francisco Affonso de Mello, is possibly also associated with the copper content in the collected water, which presented a value of 45 times greater than the allowed by CONAMA[3]. It is known that bivalent metal ions can act as cofactors in the production of some secondary metabolites.

[1]ALVES, E.S.; TRESMONDI, F.; LONGUI, E.L.; Análise estrutural de folhas de *Eugenia uniflora* L. (Myrtaceae) coletadas em ambientes rural e urbano, SP, Brasil. *Acta bot bras*, **v. 2**, 241-248, 2008.

[2]TAIZ, L. & ZEIGER, E. Fisiologia Vegetal. 3ª ed. Artmed: Porto Alegre, 719 p, 2004.

[3]PICAUD, S.; OLOFSSON, L.; BRODELIUS, M.; BRODELIUS, P. E. Expression, purification, and characterization of recombinant amorpha-4,11-diene synthase from *Artemisia annua* L. Archives of Biochemistry and Biophysics, v.436, n. 2, p. 215-226, 2005.

**Área: QPN** **Inscrição:01063**

# Chemical study of flowers from two species of *Croton* visited by bees: velame (*Croton heliotropiifolius* Kunth) and marmeleiro (*Croton sonderianus* Muell. Arg.)

**Sonia P. Cabrera (PG),[1,2]* Telma M. G da Silva (PG),[2] Celso A. Camara (PQ), [2] Tania M S. Silva (PQ),[2]**

**soniapereira196@gmail.com**

*[1]Programa de Pós-Graduação em Química, DQF- UFPE; [2]Laboratório de Bioprospecção fitoquímica-DQ-UFRPE*

Palavras Chave: *Flores, Croton, estudo químico, Flavonoides*

## Highlights

- Chemical composition of flowers from *Croton heliotropiifolius* and *Croton sonderianus*
- The species are visited by bees
- Presence of the same glycosylated flavonoids in two species

## Resumo/Abstract

A região semi-árida do Nordeste Brasileiro é rica em espécies vegetais do gênero *Croton* e abelhas nativas. Os insetos e as flores coevoluíram com benefícios para os dois lados. No caso das abelhas, visitantes florais especializados, essa troca é obrigatória, pois as abelhas obtêm todo o seu alimento nas flores, as quais se beneficiam desta interação produzindo frutos com maior diversidade genética. As flores de *Croton heliotropiifolius* e *Croton sonderianus* (visitadas pelas abelhas) foram estudadas quimicamente utilizando técnicas cromatográficas e espectroscópicas. Foi possível analisar por UPLC-PDA-qTOF-MS/MS o perfil cromatográfico, isolar e identificar os principais constituintes químicos por RMN de $^{1}H$ e $^{13}C$. Nas duas espécies foi verificado a predominância de flavonoides, sendo que os glicosilados (rutina, quercitrina, isoquercitrina, tilirosídeo e 3'-metoxi-tlirosídeo) e seus isômeros foram observados nas duas espécies. Os flavonoides do tipo agliconas (3,7-dimetoxi-quercetina e 3,7,3'-trimetoxi-quercetina) só foram identificados nas flores de marmeleiro. É possível concluir que existe semelhança na composição química (flavonoides glicosilados) nas flores das duas espécies analisadas e que são visitadas por abelhas, principalmente as nativas.

Agradecimentos: CNPq e FACEPE.

**Área: QPN** **Inscrição: 01104**

# Chemical composition of the volatile oil from two *Xylopia* species from the State of Pará, Brazil

**Márcia M. Cascaes (PG),[1*] Eloisa H. A. Andrade (PQ),[1,2] Erick M. Sousa (IC),[2] Lidiane D. Nascimento (PG),[1] Giselle M. S. P. Guilhon (PQ),[3] Tainá O. Anjos (IC),[1] Soluan F. M. Pereira (IC),[1] Jorge Oliveira (PQ)[1].**

**cascaesmm@gmail.com**

*[1]Museu Paraense Emílio Goeldi; [2] Faculdade de Engenharia Química, UFPA; [3]Programa de Pós-graduação em Química, UFPA.*

*Palavras Chave:* Annonaceae, *Xylopia*, Essential oils, Chemical composition.

## Highlights

The yield and the chemical composition of the volatiles from *Xylopia emarginata* Mart. *and Xylopia frutescens* Aubl. (Annonaceae) were diferent.

## Abstract

### INTRODUCTION

Chemical studies carried out with the *Xylopia* genus showed the importance of to study the chemical profile of essential oils (EO). Geographic areas can affect the composition of secondary metabolites. This work deals with the chemical composition of EO from the leaves of *X. emarginata* and *X. frutescens* of the Municipality of Magalhães Barata, Pará, Brazil.

### METODOLOGY

The leaves were collected in the vicinity of Vila Nova, Municipality of Magalhães Barata, Pará, Brazil (1°42′30″S; 51°31′45″W), in December 2017, dried and submitted to hydrodistillation for 3h, using a Clevenger apparatus. Analysis of the chemical constituents were performed by GC/MS and the identification by comparison of mass spectra and retention index (RI) with those existing in system libraries and cited in the literature[1].

### RESULTS

The yield from *X. frutescens* EO was 1.50% and 0.27% for *X. emarginata*. A total of 57 compounds were indentified in *X. emarginata* EO and 73 in *X. frutescens* EO. Table 1 shows the compounds in the EO (≥2%). The major constituents of *X. emarginata* EO was spathulenol and caryophyllene oxide, while α and β-pinene were the main contituents of *X. frutescens* EO.

Table 1 – Chemical composition (≥2%) of essential oil of *Xylopia emarginata* and *Xylopia frutescens.*

| RI | Constituent | XE (%) | XF(%) |
|---|---|---|---|
| 924 | α-thujene | 4.89 | 4.89 |
| 932 | α-pinene | 3.14 | 20.84 |
| 946 | camphene | 2.72 | - |
| 974 | β-pinene | 2.01 | 25.95 |
| 1024 | limonene | - | 3.0 |
| 1025 | β-phellandrene | - | 2.6 |
| 1031 | 1,8-cineole | 3.36 | 1.0 |
| 1135 | trans-pinocarveol | 4.46 | 0.36 |
| 1160 | pinocarvone | 2.35 | 0.16 |
| 1195 | myrtenal | 3.24 | - |
| 1335 | δ-elemene | 2.32 | 4.19 |
| 1389 | β-elemene | 3.1 | 0.54 |
| 1474 | γ-muurolene | 3.06 | - |
| 1484 | germacrene D | 1.08 | 3.26 |
| 1500 | bicyclogermacrene | - | 7.85 |
| 1512 | γ-Cadinene | 2.67 | 0.13 |
| 1577 | spathulenol | 5.65 | 2.18 |
| 1582 | caryophyllene oxide | 5.63 | 0.18 |

XE: *X. emarginata* and XF: *X. frutescens*

### CONCLUSIONS

The sesquiterpenes spathulenol and caryophyllene oxide are considered chemotaxonomic markers to *Xylopia* genus. The chemical composition of *X. frutescens* EO could be considered a new chemotype characterized by the monoterpenes α and β-pinene.

### REFERENCES

[1]ADAMS, R. P. Book: Identification of essential oil components by gas chromatography/mass spectrometry. 4 ed, 2007, 804 p.

# Chemical Composition and biological activities of the essential oil from leaves of *Bauhinia cheilantha* Bong. Steud

**Ana Maria A. Silva (PG),[1*] Horlando C. da Silva (IC),[1] Aurelio O. Monteiro (PG),[1] Gilvandete M. P. Santiago (PQ),[1,2] Péricles B. Alves (PQ),[3] Gardênia C. G. Militão (PQ).[4]**

**gil@ufc.br; anamariaamaral@gmail.com**

*[1]Departamento de Química Orgânica e Inorgânica, UFC; [2]Departamento de Farmácia, UFC; [3]Departamento de Química, UFS; [4]Departamento de Fisiologia e Farmacologia, UFPE*

Palavras Chave: *Bauhinia cheilantha, Aedes aegypti, cytotoxic activity.*

## Highlights

*E*-caryophyllene and α-pinene were the major components identified in the essential oil. Larval bioassay against *Aedes aegypti* and cytotoxic activity showed favorable $LC_{50}$ and $IC_{50}$ values.

## Resumo/Abstract

The genus *Bauhinia* (Fabaceae) comprises about 500 species of shrubs and small trees distributed in tropical regions. Species of *Bauhinia* are popularly known as "cow's paw" or "cow's hoof" due to their leaf format and have been frequently used in folk medicine to treat diabetes. Other activities include antimalarial, anti-inflammatory, antioxidant and antimicrobial. This work describes the chemical composition of the essential oil from fresh leaves of *B. cheilantha* (EOBC), as well as the evaluation of their biological activity as larvicidal and cytotoxic agents. The chemical composition of EOBC, obtained by hydrodistillation, was determined and quantified by gas chromatography coupled to mass spectrometry (GC-MS) and flame ionization detector (CG-DIC). Forty five constituents were identified representing 97.84% of the total composition. The major components of this essential oil were identified as (*E*)-caryophyllene (21.65%) and α-pinene (11.74%). The monoterpene fraction amounts 18.51% of the oil, while the sesquiterpene fraction amounts 78.59%. The essential oil (EOBC) exhibited activity against instar III larvae of *Aedes aegypti*, showing $LC_{50}$ value of 40.84 ± 0.87 μg/mL. Additionally, EOBC was submitted to the MTT assay for the evaluation of their cytotoxic effects on HL-60 (pro-myelocytic leukemia), NCI-H292 (lung carcinoma) and MCF-7 (breast adenocarcinoma) human cancer cells lines (Table 1). Doxorubicin (DOX) was used as positive control. The essential oil was more active against HL-60 cell lines. The findings of the present study allow to indicate the essential oil (EOBC) as potential natural larvicidal and cytotoxic agent.

Figure 1 – Structures of (*E*)-caryophyllene (**1**) and α-pinene (**2**)

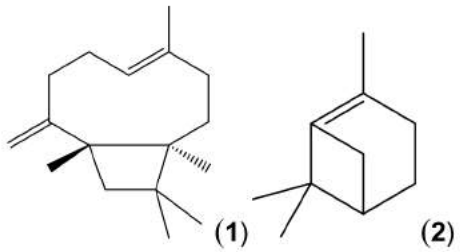

(**1**) (**2**)

Table 1 - $IC_{50}$ values (μg/mL) of EOBC and the respective 95% confidence intervals

| **SAMPLES** | $IC_{50}$ (μg/mL) | | |
|---|---|---|---|
| | HL-60 | NCI-H292 | MCF-7 |
| **EOBC** | 8.6 (5.9 - 12.6) | 33.08 (29.1 - 37.5) | 18.3 (16.0 - 21.0) |
| **DOX** | 0.03 (0.01 - 0.03) | 0.3 (0.1 - 0.4) | 0.3 (0.19 - 0.53) |

**Área: QPN** **Inscrição: 01164**

# Multivariate analysis of chemical composition and theoretical study on muscarinic receptors of essential oils from medicinal plants

**Giovanna N. da S. A. O. Rocha (IC),[1] Flávia C. R. Vilar (PQ),[1] Maria L. V. Camelo (PQ),[1] Vitor P. Lorenzo (PQ),[1] Laiana O. B. Silva (PQ).[1]***

**giovanna.nogueira@ifsertao-pe.edu.br; laianaobs@hotmail.com***

*[1]IF Sertão Pernambucano - Campus Petrolina Zona Rural*

Palavras Chave: *Molecular docking, Essential oil, Chemometric, PCA.*

## Highlights

Evaluation of the chemical similarity of essential oils using multivariate analysis. Molecular docking on muscarinic receptors M2, M3 and M4 seeking anti-inflammatory and antinociceptive activity.

## Abstract

Essential oils are a complex mixture of substances. Its chemical composition is determined by genetic factors and environmental stimulus. In this work, it was evaluate the essential oil of *Mentha spicata* (MS), *Ocimum basilicum* (OB), *Plectranthus barbatus Andrews* (PB), *Cymbopogon citratus* (CC) and *Lippia alba (Mill.) NE Brown (LA)* plants from IF Sertão-PE, in Petrolina city. The purpose of the investigation was to verify the chemical similarity of oils using Principal Component Analysis (PCA) and evaluate major compounds through molecular docking on muscarinic receptors (M2, M3 and M4). The essential oils were extracted by hydrodistillation using Clevenger apparatus and their chemical composition was determined by CG-MS. The diversity of chemical constituents varying between 69 and 126 compounds by essential oil, being the most relevants considered in PCA. PC1 (43.2%) and PC2 (31.0%) (Figure 1) allowed to chemically separate the samples into 3 groups. OB is segregated from the others in a region characterized by higher levels of eucalyptol, linalool and estragole. LA and CC were mainly grouped by presented the constituents neral and geraniol. PB and MS were the species that had the highest chemical similarity, showing relevant concentrations of 6 substances of the 12 evaluated. In molecular docking was observed that germacrene D, caryophyllene, geranial and neral presented lower interaction energy on the three evaluated targets (Table 1). These same substances, except neral, had significant weight on the grouping by similarity of PB and MS.

Figure 1. Plot of PC1 versus PC2 for the 5 plant species considering 12 chemical constituents.

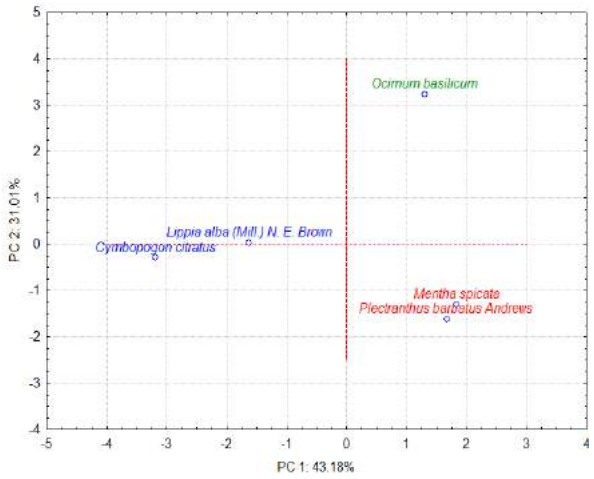


Tabel 1. MolDock Score energies of majoritary compounds of essential oil and original ligands on muscarinic receptors M2 (3UON), M3 (4DAJ) and M4 (5DSG).

| Compounds | 3UON | 4DAJ | 5DSG |
|---|---|---|---|
| Germacreme D | -99.53 | -101.95 | -106.15 |
| Caryophyllene | -98.62 | -98.44 | -102.37 |
| Geranial | -83.79 | -84.76 | -88.52 |
| Neral | -83.75 | -84.55 | -90.83 |
| QNB | -131.18 | -149.78 | -167,16 |

**Área: QPN** **Inscrição: 01192**

# CHEMICAL COMPOSITION AND BIOLOGICAL ACTIVITY OF ESSENTIAL OIL OF SPECIES *Nectandra lanceolata* (LAURACEAE)

**Érica R. Costa (PG),[1] Eduardo J. Coutinho (IC),[2] Gabriela M. Louro (PG),[1] Cleber L. Nicolau (PG),[1] Jaqueline C.M. da Silva (PG),[1] Euclésio Simionatto (PQ),[1] erica_rodrigues23@hotmail.com.**

[1]*Postgraduate Program in Natural Resources, State University of Mato Grosso do Sul*, PGRN/UEMS; [2]*Chemistry degree from the State University of Mato Grosso do Sul*, PIBIC/UEMS

Keywords: *Extraction, Hydrodistillation, Cancer cells, Antiproliferative activity, Acinetobacter baumanni.*

## Highlights

The essential oil extracted from the leaves and barks of the *Nectandra lanceolata* species was chemically characterized by chromatography and tested against *Acinetobacter baumanii* bacteria and nine cancer cell lines.

## Abstract

**Introduction:** The Lauraceae family consists of 52 genus and approximately 3,000 species.[1] The species of this family are rich in essential oils and considered medicinal, however there are few studies that prove the effectiveness of their oils against diseases. Therefore the work has as objective the chemical and biological study of the species *Nectandra lanceolata* collected in MS. **Results and Discussion:** After extraction the leaves and husks presented a yield of 0.04 and 0.09%, respectively, the extracted oils were submitted to chromatography (GC-MS) (Figure 1 and 2) and identification of the compounds [2]

**Figure 1.** Chromatographic profile of leaf oil

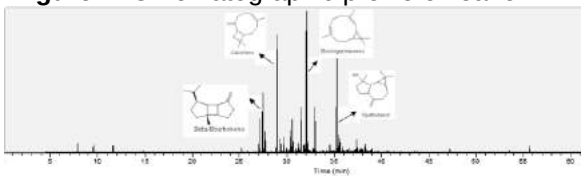

**Figure 2.** Chromatographic profile of bark oil

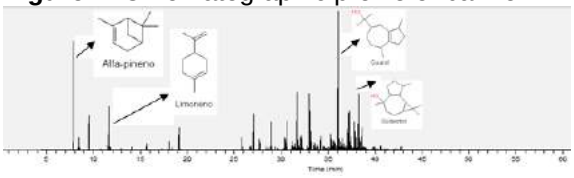


In the antimicrobial analyzes, a better activity was observed for the oil obtained from the bark of the species (Figure 3a and b), and the dilutions of the essential oil of the bark presented MIC of 1800 µg / mL.

**Figure 3.** Disk diffusion test (a) Minimum inhibitory concentration (MIC) test (b).

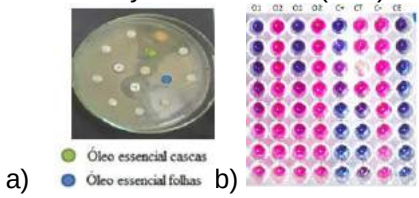


a) b)

Peel essential oil also showed better activity against two cancer cell lines (glioma and leukemia) as shown in Table 1.

**Table 1.** TGI * values of essential oils of leaves and bark of the species *Nectandra lanceolata*

| Cell lines | Stem bark oil | Leaf oil | Doxorrubicin |
|---|---|---|---|
| Glioma SNC | 37,3 | 75,8 | 0,83 |
| Breast | 77,0 | 89,0 | 9,8 |
| Drug resistant ovarian | 72,0 | 128,9 | >25 |
| Kidney | 67,5 | 102,8 | 13,1 |
| Lung | 70,1 | 85,6 | 12,9 |
| Prostate | 47,0 | >250 | 4,9 |
| Ovarian | 61,6 | 195,2 | 5,5 |
| Colon | 195,2 | 107,0 | >25 |
| Leukemia | 14,6 | 72,4 | 3,4 |

**Conclusion:** The chemical composition differed between the essential oils extracted from the leaf and the bark. The oil extracted from the bark showed a higher content of monoterpenes, and as a consequence this oil showed a better biological activity, both in antimicrobial and antitumor tests.

**References:** [1] Grecco, S.S., Lorenzi, H., Tempone, A.G., Lago, J.H.G. (2016). *Update: biological and chemical aspects of Nectandra genus (Lauraceae).* Tetrahedron: Asymmetry. 27: 793-810.

[2] Adams, R.P. *Identification of Essential Oil Components by Gas Chromatography / Mass Spectrometry*, 4th ed. *Carol Stream*, IL: *Allured Publishing Corp.*, 2007, 804p.

**Thanks:** PGRN, UEMS, FUNDECT.

**Área: QPN** **Inscrição: 01269**

# IDENTIFICAÇÃO DO COMPOSTO ANTIFÚNGICO NO ÓLEO ESSENCIAL DAS FOLHAS DE *Callistemon viminalis*

**Patrícia M. Valente (PG),[1]* Vânia M. M. Valente (PQ),[2] João A. M. Lima (IC)[2]**

**valente.moreira.patricia@gmail.com**

[1]*Centro de Ciências Agrárias UFES;* [2]*Instituto de ciências Exatas e Tecnológicas, UFVCRP;*

Palavras Chave: Bioprospecção, *Cladosporium herbarum*, fungicida, *Penicillium expansum*.

## Highlights

IDENTIFICATION OF THE ANTIFUNGAL COMPOUND IN THE ESSENTIAL OIL OF THE LEAVES OF *Callistemon viminalis*
The major compounds in the essential oil were: eucalyptol, α-terpineol and α-pinene.
CCD-bioautography indicated eucalyptol and α-terpineole as the antifungal agents of *C. viminalis* oil.

## Resumo/Abstract

Diversos fungos são responsáveis por injúrias na agricultura gerando grandes perdas econômicas desde o campo ao armazenamento. Os óleos essenciais destacam-se como alternativa mais sustentável no controle de doenças aumentando a busca por substâncias bioativas naturais. A espécie *Callistemom viminalis* (Myrtaceae) de origem australiana, é comumente encontrada no território brasileiro como ornamentação e apresenta atividade anti-helmíntica, antifúngica contra *Micobacterium tuberculosis* e fraca atividade antibacteriana. Neste trabalho o efeito fungicida do óleo essencial da *C. viminalis* foi investigado sobre os fungos *Aspergillus niger*, *Cladosporium herbarum e Penicillium expansum*.

O óleo essencial foi obtido por hidrodestilação em Clevenger a partir de folhas frescas com tempo ótimo de extração em 1h. A caracterização química foi realizada empregando cromatografia gasosa acoplada à espectrometria de massas e comparação dos espectros com a espectroteca NIST, associado ao cálculo do índice aritmético comparado à literatura. Os bioensaios foram realizados empregando as técnicas de poison food e CCD-bioautografia.

O óleo essencial apresentou um total de 12 compostos, conforme Figura 1, com rendimento médio de 0,9 mL por 100 g. A uma concentração de 0,2% o óleo causou inibição de crescimento sobre *P. expansum* (36,4%) e *C. herbarum* (43,7%), sendo observado que apesar de induzir o crescimento de *A. niger* houve inibição em sua esporulação. Os resultados da CCD-bioautografia indicaram eucaliptol e α-Terpineol como os agentes antifúngicos do óleo de *C. viminalis*, o eucaliptol ativo sobre o fungo *P. expansum* e α-Terpineol ativo sobre *C. herbarum*, conforme Figura 2.

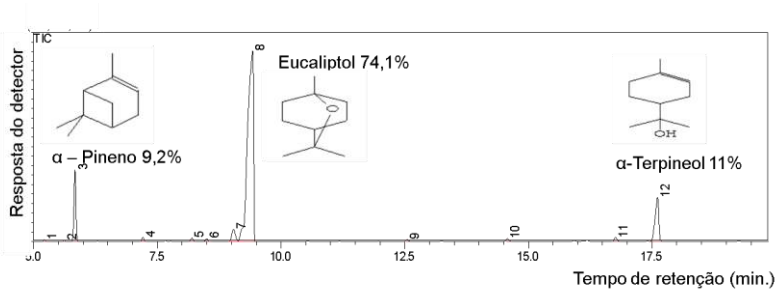


Figura 1. Composição química do óleo essencial de C. viminalis

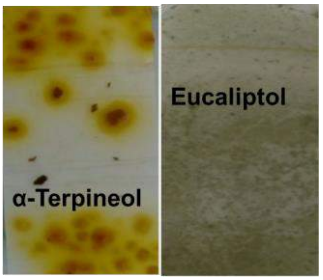


Figura 2. Resultado CCD-Bioautografia

**Área: QPN** **Inscrição:01286**

# Antimicrobial activity of essential oils of *Psidium salutare* var. sericeum e mucronatum (Myrtaceae) against *Candida albicans*

**Eduardo M. Ethur (PQ),[1*] Cassiana M. Bona (IC),[2] Bárbara Buhl (IC),[2] Talita Scheibel (IC),[2] Carla Kauffmann (PQ),[2] Lucélia Hoehne (PQ),[1] Elisete M. de Freitas (PQ),[2] Miriam I. Marchi (PQ)[1]**

**eduardome@univates.br**

*[1]Centro de Ciências Exatas e Tecnológicas, UNIVATES; [2]Centro de Ciências Biológicas e da Saúde, UNIVATES*

Palavras Chave: *Candidiasis, Antifungal activity, Pampa Biome, Psidium salutare, Essential oil, 1,8-Cineole*

## Highlights

The essential oils of *P. salutare* var. *sericeum* and var. *mucronatum* are formed predominantly by 1,8-cineole, terpinolene, limonene, α-terpinolene and linalool;
The MIC against *Candida albicans* is the same to the both essential oil of *P. salutare*.

## Resumo/Abstract

*Candida albicans* is an opportunistic pathogenic fungus that can cause superficial or systemic infections. The increasing prevalence of human pathogens resistant to antibiotics has stimulated studies for the discovery and development of new therapies. Essential oils (EO) represent one of the alternatives that have been studied in the search for active compounds with broad spectrum of action, low toxicity and low cost. The objective of this work was to identify the essential oil composition of *Psidium salutare* var. *sericeum* and mucronatum and to evaluate its antimicrobial activity against *C. albicans* (ATCC 10231). The essential oils were extracted using a modified Clevenger apparatus and the constituents were identified by GC-MS. The antifungal activity of the essential oil was evaluated the minimum inhibitory concentration (MIC) by broth microdilution method. The yield of OE from *P. salutare* var. *sericeum* was 1.78%, whereas the yield of var. *mucronatum* was 1.83%. In both species, the main constituents found were 1,8-cineol, linalool, terpinolene, α-terpineol and limonene (Table 1). Both species presented fungiostatic action of 2.5 $mg.mL^{-1}$ and fungicidal action of 10 $mg.mL^{-1}$. The results show that both essential oils present antifungal action at the same concentrations, even with qualitative and quantitative differences between the constituents.

Table 1 - Chemical composition of the major components (%area greater than 5%) of the essential oils of leaves of *Psidium salutare* var. *sericeum* e var. *mucronatum*

| Compound | KI | KI Adams | Area % | |
|---|---|---|---|---|
| | | | Var. sericeum | Var. mucronatum |
| Limonene | 1030 | 1029 | 9,39 | 3,69 |
| 1,8-Cineole | 1033 | 1031 | 22,65 | 19,66 |
| Terpinolene | 1091 | 1088 | 8,02 | 9,18 |
| Linalool | 1102 | 1096 | 7,84 | 10,68 |
| α-Terpineole | 1194 | 1188 | 9,67 | 7,11 |

KI = experimental Kovats index. KI Adams = Kovats index according Adams (2007).

Adams, R.P. (2007) *Identification of Essential Oils Components by Gas Chromatography/ Mass Spectroscopy*. Carol Stream Illinois: Allured Publishing Corporation.

**Área: QPN** **Inscrição:_0017**

# Flavonoids of *in situ* and *in vitro* culture from *Lomatozona artemisiifolia* Baker leaves.

**[1] Vinícius Galvão Wakui (PG),[2] Marlene Pires Moreira (PG), [1]Ana Paula Terezan (PQ), [2] Sérgio Tadeu Sibov (PQ), [3]Francis Julio F. Lopes (PQ),[1]Cecília Maria Alves de Oliveira (PQ),[1]Lucília Kato* (PQ)**

**luciakato@gmail.com; vgwakui@gmail.com**

*[1]Instituto de Química, Laboratório de Produtos Naturais e Síntese, UFG;*
*[2]Escola de Agronomia, Laboratório de Cultura de Tecidos, UFG;*
*[3]Instituto de Ciências Biológicas, UFG.*

Palavras Chave: *Asteraceae, conservation, LC-ESI (-)MS, micropropagation*

## Highlights

Evaluation and comparison of chemical profile (LC-MS/MS) of *in vitro (micropropagation)* and *in situ* (harvested) *L. artemisifolia* leaves. Four flavonoids were identified for first time in this genus.

## Resumo/Abstract

*Lomatozona artemisiifolia* Baker (Asteraceae), is unique specie of Lomatozoma genus and is endemic from Goiás Cerrado. There is no literature about its chemical composition and this work provides a chemical profile of the plants from micropropagation experiments and harvested plants. The aerial parts of *L. artemisiifolia* were collected on February 2016 in PESD, Mossamedes (GO). Seeds were submited to superficial disinfestation and in an optimum culture condition for germination, multiple shoots were generated and seedlings grew up in greenhouses under controlled conditions. These plants were called *in vitro L. artemisiifolia*. The fresh leaves of both plants were extracted with EtOAc to afford the EtOAc *in situ* and *in vitro* extract, which were analysed by HRLC-MS/MS experiments.

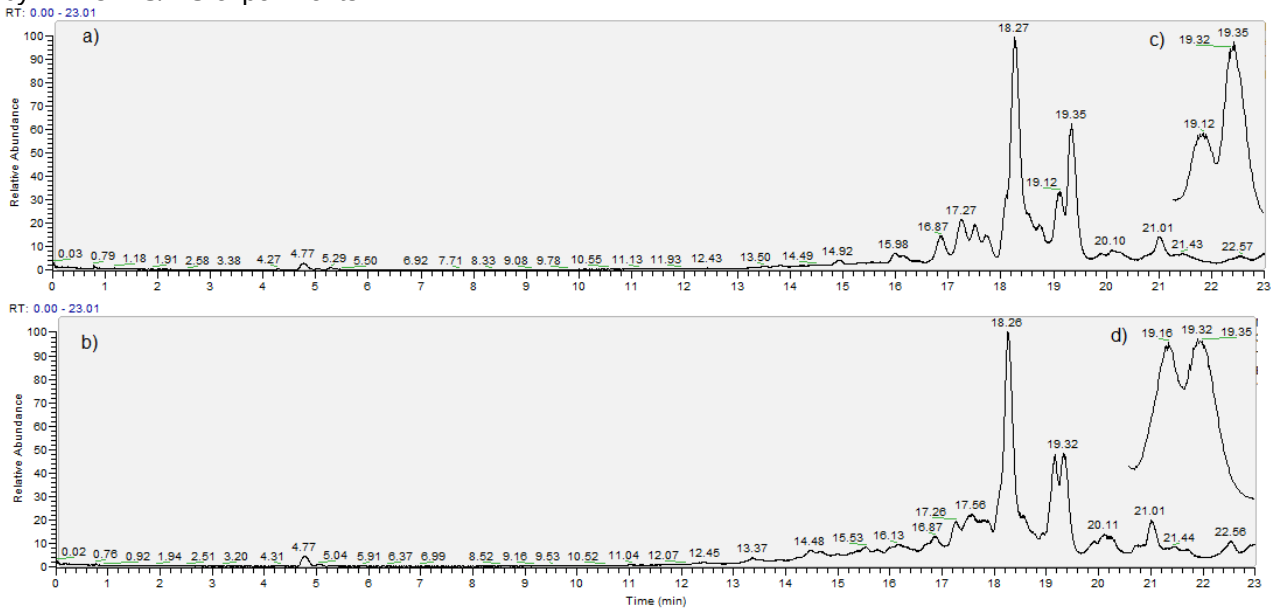


**Figure 1**. LC-ESI (-) MS of the **a**) EtOAc *in situ* and **b**) EtOAc *in vitro* extract; **c**) and **d**) expansion of the region between 19-20 min.

Identification of the compounds was based on the HRMS fragmentation pattern and comparison with Metlin database[2], showing the presence of the flavonoids, eupatorin: $C_{18}H_{16}O_7$, Rt 19.1 min, *m/z* 343.08249 ($[M-H]^-$), $MS^2$ main fragments 328.06, 313.04, 298.01, 285.04 and 270.02 and casticin: $C_{19}H_{18}O_8$, Rt 19.3 min, *m/z* 373.09320 ($[M-H]^-$), $MS^2$ main fragments 358.07, 343.05, 328.02, 300.03, 285.00, 272.03 and 256.04; jaceidin and quercetagetin-3,5,6,3´,4´-pentamethyl ether which were identified in a previous study[3]. Both chromatograms are similar but shows differences in the relative amounts of eupatorin and casticin. Further studies will be designed to clarify these observations.

[1.] Nakajima *et al*. Comparative analysis of red lists of the Brazilian flora: Asteraceae. Rodriguésia 63: 039-054. 2012; [2]. Smith, C.A. *et al*. METLIN: A metabolite mass spectral database. *Ther. Drug Monit.* 2005, 747–751. [3] Wakui *et al*. Flavonoides de *Lomatozona artemisiifolia* Baker (Asteraceae). II Workshop da Pós-graduação em Química. Goiânia, 2017

**Área: QPN** **Inscrição: 00052**

# *Pterodon pubescens* Benth. (Sucupira) Ethanol Extract Mouthwash Pharmaceutical Forms

**Natalia Alves (IC),[1] Mariana Cechetto Figueiredo (PG),[2] Mary Ann Foglio (PQ)[1]**

**maryann.foglio@fcf.unicamp.br; natalia.h.alves@hotmail.com**

*[1]Faculty of Pharmaceutical Science University at Campinas; [2]Faculty of Medical Science University at Campinas*

Key words:*Pterodon pubescens; Mouthwash; Gengivitis*

## Highlights

*Pterodon pubescens* Benth. (Sucupira) Ethanol Extract Mouthwash Pharmaceutical Forms

Parameters considered for the development of standardized herbal mouthwash formulations for gingivitis treatment.

## Abstract

**Introduction:** The search for natural therapies has increased the demand for herbal medicines for the treatment and prevention of diseases. In dentistry there has been an increase in research involving natural products due to the need for products with lower toxicity and greater pharmacological activity. Periodontal diseases are considered a public health issue and are characterized by inflammatory processes of infectious origin that reach the gingival tissues and supporting teeth tissue that can lead to alveolar bone damage. Mouthwashes are among the different products for treatment and prevention of these diseases. Rinses have a wide variety of active ingredients, with antibacterial activity. *Pterodon pubescens* (Sucupira) is popularly used for pain and inflammation.
**Scope:** development of a pharmaceutical mouthwash formulation using *Pterodon pubescens* ethanol extract.
**Experimental:** formulations were prepared according to ANVISA 2004 protocols.

**Results & Discussion:** The formulations, when evaluated on the 7$^{th}$ and 15$^{th}$ day showed macroscopic differences in color and odor when stored at -5$^0$C and +5$^o$C.. At room temperature, viscosity decrease was observed. After centrifugation process the formulations did not show phase separation under all conditions tested. A 12% decrease in the pH value of the formulation was observed at room temperature after 15 days.
**Conclusion:** Herein important parameters to be considered for the development of standardized herbal formulations are reported.

**Área: QPN** **Inscrição: 00070**

# Isolation in alginate microcapsules of the pathogen *Tritrichomonas foetus*, to evaluate the tricomonicidal activity of plant extracts.

**Maria R. Ramirez (PQ),[1]* Jorge A. Oyhenart (PQ) [2].**

**mr.ramirez@conicet.gov.ar**

*[1]Department of Biological Sciences, Faculty of Biochemistry and Cs. Biological-UNL-CONICET-Santa Fe; [2]Department Faculty of Exact and Natural Sciences-UNLPam-INCITAP - CONICET Santa Rosa, La Pampa, Argentina.*

Key words: Sodium *alginate, Bovine trichomonosis, Encapsulation, Plant extracts.*

## Highlights

The flagellated protozoan parasite *Tritrichomonas foetus* is a pathogen that causes bovine and feline trichomonosis. Bovine trichomonosis is a venereal disease that leads to reproductive failure in infected animals, resulting in economic loss in beef-producing areas where open range management and natural breeding are practiced. *T. foetus* has a simple life cycle that consists of a trophozoitic form, that under stress, the trophozoite takes on an endoflagellar form, called a pseudocyst. The pseudocyst is a reversible form and present a distinct mitotic mechanism, known as the budding. Despite its veterinary importance, the use of these microorganisms as a experimental model is restricted by the difficulty that their culture presents for the laboratory. On the other hand, the technique of encapsulation with sodium alginate allows the isolation of these microorganisms in an anaerobic environment, the recovery and the obtaining of colonies from a single cell. In this way, it allows direct use, in order to evaluate plant extracts, using the *Tritrichomonas fetus* parasite as an experimental model.

## Resumo/Abstract

*Tritrichomonas fetus* is a flagellated protozoan, agent of bovine trichomoniasis, a sexually transmitted disease. The vaccines developed against the parasite have only allowed to shorten this period of infection; that is why it is necessary to look for new therapeutic options. Alginate allows the release of living cells in an anaerobic environment and the obtaining of colonies from a single cell. Thus, they can be used directly in the laboratory as an experimental model to perform bioactivity tests on plant extracts. Therefore, our objective was to implement the encapsulation technique in pearls with alginate as a potential resource for the isolation, protection and recovery of these microorganisms. For the cell immobilization step, several solutions of sodium alginate were prepared and then *T. foetus* was added. These mixtures were dropped into the calcium chloride solution, thus forming the beads. Pearls with appropriate chemical and physical characteristics were obtained. The capsules were analyzed by means of the microscope, and later cultivated. By validating the results of the liberation of microorganism, was observed that the developed spheres, will be able to be used for the application of the proposal. In conclusion, this method represents a potential resource for the isolation and cultivation of the *T. foetus* so that it can be used as an experimental model in the laboratory, to look for new chemical compounds of pharmaceutical interest.

References: Oyhenart J et al., 2013 Veterinary Parasitology. 0304-4017.

**Área: QPN** **Inscrição: 00127**

# Estudo Químico de três espécies de *Chamaecrista* Moench nativas do Nordeste do Brasil

**Maria T.A. Costa (IC),[1*] Daniele R. Lima (PG),[1,2] Maria G.V. Silva (PQ). [1.2,3]**

**thiciane.a@outlook.com;**

*[1]Departamento de Química Orgânica e Inorgânica; [2]RENORBIO, [3]Departamento de Química Analítica e Físico-química-Universidade Federal do Ceará -UFC*

Palavras Chave: *Chamaecrista*, *Fenólicos, Flavonoides, HPLC, Produtos Naturais*

## Highlights

Chemical study of three native *Chamaecrista* Moench species from Northeastern Brazil

This study reports the chromatographic profile of *Chamaecrista* species.
Total phenolic and flavonoids were quantified by spectrophotometry.
Gallic acid and quercetin were identified by HPLC.

## Resumo

A bioprospecção de plantas permite o seu uso racional em diversas atividades, tal como na produção de novos fármacos, por meio do conhecimento empírico comprovado por dados científicos. *Chamaecrista* Moench (Leguminosae) é um dos gêneros da flora brasileira que apresenta raros estudos sobre sua composição química e potencial farmacológico. Um único artigo do século passado relata que em *Chamaecrista gregii*[1], foram identificados antraquinonas e triterpenos, que são classes de biocompostos ativos, com potencial aplicação na indústria de medicamentos, agroindústria e cosméticos. O presente estudo relata a prospecção química e o perfil cromatográfico de três espécies de *Chamaecrista* coletadas no Planalto da Ibiapaba-Ceará. O material botânico (folhas, flores e vagens) foi extraído utilizando-se a razão amostra/solvente de 100 mg/mL com etanol, álcool isopropílico e água (30:45:25), seguido por sonicação por 15 min[2]. A prospecção química realizada segundo Matos[3] permitiu identificar flavonoides, antraquinonas, triterpenos, xantonas, auronas e taninos nas espécies estudadas. Posteriormente, os fenólicos totais e flavonoides foram quantificados por espectrofotometria sendo os teores expressos em ácido gálico e quercetina respectivamente (tab. 1). A presença destes compostos foi confirmada por CLAE-DAD (fig. 1). Estes resultados permitem a seleção dos extratos com maior potencial para estudos mais completos, na busca de compostos bioativos para o desenvolvimento de fármacos e outros produtos úteis. (CNPQ/INCT–BioNat; CAPES)

**Tabela 1**- Teor de flavonoides e fenólicos totais em extratos de três espécies de *Chamaecrista* sp.

| | FENÓLICOS / FLAVONOIDES (µg/mg de extrato) | | |
|---|---|---|---|
| **PARTE BOTÂNICA** | I | II | III |
| **Folhas** | 112,57/112,9 | 12,8/117,9 | 125,4/142,5 |
| **Flores** | 115,5/100,0 | 129,6/125,9 | 159,3/139,8 |
| **Vagens** | 32,5/109,4 | 200,7/108,1 | 36,5/50,1 |

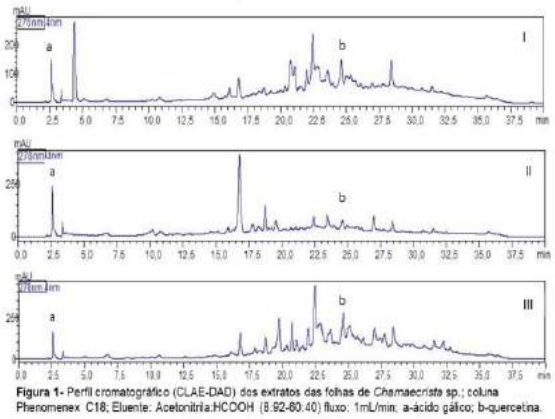


**Figura 1**- Perfil cromatográfico (CLAE-DAD) dos extratos das folhas de *Chamaecrista* sp.; coluna Phenomenex C18; Eluente: Acetonitrila:HCOOH (8:92-60:40) fluxo: 1mL/min; a-ácido gálico; b-quercetina.

I- *Chamaecrista* sp1; II- *Chamaecrista* sp2; III- *Chamaecrista* sp3.

1- Barba B *et al*. ***Phytochem.*** 1994, *37*, 3, 837.
2- Mazzi G.L *et al.* ***Anal. Methods,*** 2014*, 6,* 7781*.*
3- Matos F.J.A. ***Fitoquímica Experimental,*** Ed UFC, 2009.

**Área: QPN** **Inscrição: 00223**

# Comparative study of drying methods of *Vitis labrusca* grape peels: greenhouse or *Oshibana*?

**Jéssica B. Carra (PG),[1*] Ricardo L. N. de Matos (PG),[2] Ana P. Novelli (IC),[2] Rubia Casagrande (PQ),[2] Sandra R. Georgetti (PQ),[2] Nilton S. Arakawa (PQ),[2] Marcela M. Baracat (PQ).[2]**

**jessicabassettocarra@gmail.com; jessicabassettocarra@gmail.com**

*[1]Departamento de Química, UEL; [2]Departamento de Ciências Farmacêuticas, UEL*

Key words: *Anthocyanin content, Antioxidant activity, Phenolic compounds, Soluble solids content.*

## Highlights

There are several drying methods, the most common being the greenhouse. The drying method *Oshibana* preserves the different vegetal tissues with original characteristics of the moment of collection(1).

## Abstract

Herein we evaluated which drying processes preserve the bioactive compounds present in the grape peels (*Vitis labrusca*). The peels were dried by two methods: oven at 37±3 ºC and by the *Oshibana* method. The extracts were obtained by turbolysis followed by ultrasound using a hydroethanolic solution 50% (v/v) acidified, and after filtration both crude extract were concentrated by rotary evaporator at 80 °C and 150 rpm. The analysis of crude and concentrated extracts (triplicates) was: soluble solids(2), phenolic compounds(3), anthocyanin(4) and antioxidant activity(5) and statistical by Student T Test (p-valor < 0.05). The results presented statistical significance in the averages (Table); only the solids content of the crude extract did not present significant difference.

| | | Phenolic compounds* mgGAE $g^{-1}$ | % (m/m) | Anthocyanin content** mg $L^{-1}$ | % (m/m) | Antioxidant activity µg $mL^{-1}$ | Soluble solids content % |
|---|---|---|---|---|---|---|---|
| *Oshibana* extract | Crude | 191.76 | 19.20 | 145.51 | 0.02 | 173.643 | 0.57 |
| | Concentrated | 507.48 | 50.78 | 529.15 | 0.05 | 297.652 | 3.02 |
| Greenhouse extract | Crude | 224.15 | 22.42 | 125.67 | 0.01 | 166.581 | 0.56 |
| | Concentrated | 612.20 | 61.26 | 459.69 | 0.04 | 238.010 | 3.14 |

*expressed as mg equivalent of gallic acid
**expressed as equivalent of the monomeric pigment concentration of malvidin-3-glycoside

Phenolic compounds presented higher values for the extracts obtained with the oven drying, while the anthocyanin content was higher for the *Oshibana* method. Antioxidant activity had lower $IC_{50}$ values for oven drying, which suggests that the phenolic compounds significantly interfere in the antioxidant capacity. In both cases the soluble solids, anthocyanins and phenol contents increased from the crude extract to the concentrate, however, the antioxidant activity presented higher values of $IC_{50}$, which indicates that the heat exposure decreases the antioxidant activity. This suggests that the glycosidic bonds were being broken down in the concentration process, increasing the content, but destabilizing the molecule and reducing its activity. In conclusion, the drying method of the plant material should be chosen based on the bioactive compound of interest.

1. Carvalho JP, Carvalho PP, Pessoa AB. Editora Art press. 2016.
2. Farmacopéia Brasileira. 5th ed. Brasília; 2010;1:546 p.
3. Singleton VL, Orthofer R, Lamuela-Raventós RM. Methods Enzymol. 1999;299:152–78.
4. Giusti MM, Wrolstad RE. Curr Protoc Food Anal Chem. 2001;F1.2.1-F1.2.13.
5. Blois MS. Nature. 1958;181:1199–200.

**Área: QPN** **Inscrição: 00317**

# Ethnopharmacology of Medicinal Plants of the Cerrado Region (Goiás, Brazil)

**Yasmine F. Oliveira* (IC)[1], Núbia A. M. T. P. Gomides (PG)[2], Vanessa G. Pasqualotto Severino (PQ)[1]**

**yasminefernandes2012@gmail.com*; vanessa.pasqualotto@gmail.com**

*[1]Instituto de Química, Universidade Federal de Goiás, Goiânia, GO; [2]Instituto de Biociências, Universidade Federal de Mato Grosso, Cuiabá, MT.*

Palavras Chave: *Ethnobotanical Survey, Brazilian Cerrado, Coqueiros Community.*

## Highlights

Traditional knowledge is an important source of obtaining new bioactive compounds from plants.
This study provided information essential for guidance in bioprospecting for new drugs of plant.

## Resumo/Abstract

Traditional knowledge is an important source of obtaining bioactive compounds from plants. In this study, the ethnobotanical survey was conducted in Coqueiros Community, located in Catalão, Goiás, using structured interview and the observation participation. 109 species of plants belonging to 57 families were registered. The most representative families were Leguminosae, Lamiaceae, Myrtaceae, Annonaceae, Anacardiaceae, Rutaceae, Compositaea, Apocynaceae and Mimosaceae. The citations for therapeutic purposes were classified using the 13 categories of the CID[1]. The highest values of relative importance - index that reveals the relevance of a species based on number of uses mentioned by the interviewed - are presented in the table 1. In the table 2 are showed the values of Relative Frequency of Citation - index that reflects how much the population knows about each species, being an important indicator of which plants have more common medicinal uses - for the species most cited for various diseases, highlighting *K. coriacea* used to gum and tooth pains, cavity, among others. About problems that affect the mouth, scientific data confirms the potential of this species[2]. This antibacterial activity may be associated to the phenolic compounds, flavonoids and tannins, in synergism with other natural products[2]. However, there are other indications that need to be investigated for this plant and others. Therefore, this study provided information essential for guidance in bioprospecting for new drugs of plant.

[1]http://www.who.int/classifications/icd. Access on 02/02/18
[2]Martins, CM; et al. Evidence-Based Complementary and Alternative Medicine, 1-9, 2015.

Table 1. The great values of relative importance (RI) of species cited by Coqueiros Community

| ***Species*** | **RI** |
|---|---|
| *Kielmeyera coriacea* Mart. | 2.00 |
| *Pterodon emarginatus* Vogel | 1.20 |
| *Sechium edule* (Jacq.) Sw. | 1.00 |
| *Xanthosoma sagittifolium* (L.) Schott | 1.00 |
| *Caryocar brasiliense* Camb. | 0.85 |
| *Syzygium cumini* (L.) Skeels | 0.80 |
| *Cochlospermum regium* (Schrank) Pilg | 0.80 |
| *Strychnos pseudoquina* A. St. Hil | 0.80 |
| *Crocus sativus* L. | 0.80 |
| *Croton antisyphiliticus* Mart. | 0.80 |
| *Hancornia speciose* Gomez | 0.80 |
| *Petroselinum crispum* (Mill.) Fuss | 0.80 |

Table 2. Relative Frequency of Citation (FRC) values for the species most cited for various diseases

| ***Species*** | **FRC** |
|---|---|
| *Kielmeyera coriacea* Mart. | 1.00 |
| *Mentha* × *piperita* L. | 1.00 |
| *Cochlospermum regium* (Schrank) Pilg | 0.97 |
| *Sechium edule* (Jacq.) Sw. | 0.94 |
| *Caryocar brasiliense* Camb. | 0.94 |
| *Croton antisyphiliticus* Mart | 0.94 |
| *Bidens pilosa* L. | 0.94 |
| *P. emarginatus* | 0.84 |
| *Hymenaea stigonocarpa* Hayne | 0.81 |

**Área: QPN** **Inscrição: 00340**

# Phytochemical prospection and phytotoxic effect of plant species *Luehea candicans* stem bunch

**Marcos B.P. Câmara (PG),[1*] Antonio J.C. Filho (PQ),[1] Fernando J.C. Carneiro (PQ),[1] Edelson de J.S. Dias (PG),[1] Georgiana E. de C. Marques (PQ),[1] Sinval G. Pereira (PQ). [2]**

**prof.antoniofilho@ifma.edu.br; quimarcosbispo@hotmail.com**

[1]*Departamento Acadêmico de Química, IFMA; Departamento de Química UFMA*

Palavras Chave: *(Phytotoxic, Invasive plants, Seed germination).*

## Highlights

In phytochemical prospection of *Luehae candicans*, secondary metabolites classes with allelopathic effect were identified. Phytotoxicity bioassay for phytotoxicity was carried out on *M. pudica* and *S. obstusifolia* species.

## Abstract

Throughout history of mankind, invasive plants have been a major problem in agricultural ecosystems as they interfere on cultures' biological productivity. In order to investigate phytotoxic effect on pasture invasive plants (*Mimosa pudica* e *Senna obtusifolia*), *Luehea candicans* species, which belongs to Tiliaceae family, was chosen for phytochemical prospection and bioassays on seeds germination. Plant collecting happened in Contrato village, in Morros, MA. The material was dried and ground, and then extracted with hydroalcoholic solution. Phytochemical prospection was carried out, as well as determination of flavonoids, anthocyanin and total phenolic content. After hydroalcoholic extraction partition, hexane, ethyl acetate, n-butanol and methanol phases were obtained in order to carry out phytotoxicity bioassays. Phytochemical prospection analysis, as well as phenolic compounds content are shown in figures 1 and 2. Total phenol content detected was 1076.8 ± 3.86 mg. EAG. $g^{-1}$. In phytotoxic effect evaluation tests, the ethyl acetate and hexane phases were the most active when tested against *M. pudica*, inhibiting 44.3% and 64.0%, seed germination, respectively, as shown in figure 3. Investigation of preliminary prospection provided relevant information on secondary metabolites and significant levels as to phenolic compounds. Regarding bioassays, relevant results on seeds inhibition for invasive species may be related to secondary metabolites classes found present, whose phytotoxic activity was already reported in other studies.

**Figure 1:** Secondary metabolites classes present in hydroalcoholic extract.

| Constituents | Results |
|---|---|
| Phenols | – |
| Pyrogallic tannis | + + + |
| Flobabenic tannis | - |
| Flavonoids | + + + |
| Anthocyanidins | + + |
| Anthocyanins | + + + |
| Leucoanthocyanidins, | - |
| Catechins | + + |
| Flavonones | + + + |
| Flavonois | + + + |
| Flavananas | + + + |
| Flavanonols | + + + |
| Xantones | + + |
| Catechins (confirmation) | + + + |
| Free steroids | + |
| Saponis (heterosídeos saponínicos) | + + + |
| Saponis (confirmed) | + + + |
| Alkaloids | + + |

**Strong:** +++ **Average:** ++ **Baixo:** + **Suspect:** s **Insufficient:** -

**Figure 3:** Phytotoxic effect of organic phases on seeds germination.

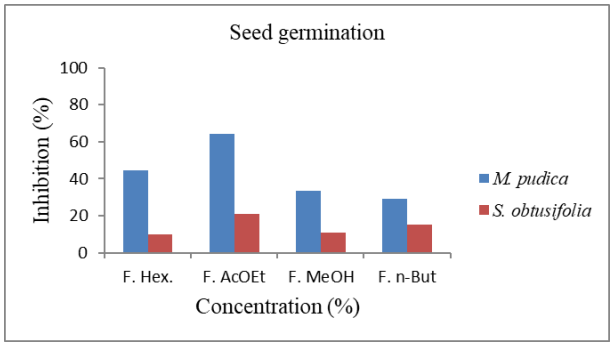


**Figure 2:** Anthocyanin and total flavonoid contents found in the hydroalcoholic extract

| Compounds/ λ( nm) | average (mg/100g) | Standard deviation | Concentration (mg/100g) |
|---|---|---|---|
| Anthocyanins / (535) | 0,409 | 0,003 | 8,330 |
| Flavonoids / (374) | 1,438 | 0,005 | 29,300 |

**Área: QPN** **Inscrição: 00342**

# Oxidative evaluation of blends of soy oil, chia oil and coconut oil in biodiesel

**Paulina Pedraça (IC), [1]* Marli A. Silva (IC),[1] Mikaelly L. De Souza (IC),[1] Alle P. Atala (TC),[1] Mayara C. Ávila (IC),[1] Isabel M. Fraga (PQ),[1] Demétrio A. Sousa (PQ).[2]**

**demetrio.sousa@cas.ifmt.edu.br; paulapedraca30@hotmail.com**

*[1] IFMT – Campus Cáceres; [2] IFMT – Campus Bela Vista*

Palavras Chave: *Blends, Biodiesel, Soy, Chia, Coconut, Oxidative Evaluation*

## Highlights

Blends with saturated and polyunsaturated oils can improve the oxidative stability of biodiesel. Natural antioxidants mixed with chia and coconut oils can increase the storage time

## Resumo/Abstract

Antioxidants and biodiesel blends can improve the biodiesel oxidative stability and its storage conditions. Chia oil has a high amount of polyunsaturated fatty acids and natural antioxidants, while coconut oil has a high amount of lauric acid and phenolic composts. Both of them are resistant to the oxidation process. The present research evaluated the oxidative stability efficiency of blends with soy oil, coconut oil and chia oil, used to produce methyl-biodiesel. The biodiesel production blends were defined by an experimental planning. 35 samples of biodiesel were produced by the transesterification process, trough basic catalysis. After washing and purification process, the biodiesel samples were storage in plastic containers, in ambient temperature and protected from light. The samples were characterized by acidity (IA), free fatty acids (AGL), specific mass (ME) and peroxide value (IP), from the production day, until 60 days. The blend with 90% of soy oil, 5% of coconut oil and 5% of chia oil presented characteristics according to the ANP parameters and the highest oxidative stability. This sample had the values for IA, AGL and ME constants, and IP changed after 45 days. This result shows that the lowest proportions for chia and coconut oil, rich in saturated and unsaturated fatty acids respectively, are promissory considering the oxidative stability of biodiesel

**Área: QPN** **Inscrição: 00388**

# Atividade antiproliferativa de frações ricas em biflavonoides de espécies de *Ouratea,* Ochnaceae.

**Queli C. Fidelis (PQ),[1,3] Renata T. Perdomo (PQ)[2], João V. de S. Teixeira (IC),[2] Mario G. de Carvalho (PQ)[3]**

**quelifidelis@gmail.com; renataperdomo@gmail.com**

*[1]Departamento de Ciência e Tecnologia, UFMA - Campus Balsas, MA; [2]Departamento de Farmácia, UFMS – Campo Grande, MS; [3]Departamento de Química, UFRRJ – Campus Seropédica, RJ.*

Palavras Chave: *Ouratea, biflavonoides, atividade antiproliferativa.*

## Highlights

**Antiproliferative activities of biflavonoids fractions from *Ouratea* species, Ochnaceae.**

Biflavonoids fractions were obtained from three *Ouratea* species.

Antiproliferative activities of fractions were evaluated *in vitro*.

The fractions exhibited inhibitory effects with IC>100 µg/ml.

## Resumo/Abstract

Três frações contendo biflavonoides foram obtidas de folhas das espécies *Ouratea hexasperma* (OHF), *O. ferrugínea* (OFF) e *O. semisserrata* (OSF). A composição química das frações foi determinada por cromatografia líquida de alta eficiência em comparação com padrões autênticos. Os biflavonoides identificados nas frações foram amentoflavona e sequoiaflavona em OFF, amentoflavona e agatisflavona em OHF, enquanto que apenas a amentoflavona e podocarpusflavona foram identificados dentre 11 biflavonoides presentes em OSF. A amentoflavona foi o constituinte majoritário nas três frações. Os ensaios antiproliferativos foram conduzidos com as frações, a amentoflavona e um quimioterápico de referência (doxorrubicina) frente as linhagens de câncer de mama humano (MCF-7), de próstata humano (PC), de cólon humano (HT), de rim humano (786), de fígado (HEPG2) e de células não neoplásicas (NIH/3T3). Os potenciais proliferativos foram expressos em valores de $CI_{50}$ (Concentração para inibir 50% do crescimento celular). Destaca-se a fração OHF que foi mais ativa contra a proliferação celular nos ensaios com linhagens de câncer de próstata humano (PC, $CI_{50}$ = 2,91 µg/ml), de cólon humano (HT, $CI_{50}$ = 5,52 µg/ml) e de rim humano (786, $CI_{50}$ = 8,11µg/ml) quando comparadas a atividade da amentoflavona (PC, $CI_{50}$ = 4,35 µg/ml; HT, $CI_{50}$ = 15,37 µg/ml; 786, $CI_{50}$ = 17,51 µg /ml). Esses resultados sugerem a ocorrência de um possível efeito sinérgico exercido pelos biflavonoides presentes nas frações, outros estudos com os constituintes isolados serão necessários para confirmar a ação sinérgica.

Agradecimentos: CNPq e FAPERJ pelo apoio financeiro.

**Área: QPN Inscrição: 00419**

# Phenolic composition of a propolis type from Ceará-Brazil: study of different extraction techniques

**Vanessa Moreira Frota (IC),[1] Francisco Matheus F. Dias (IC),[1] Hélcio Silva dos Santos (PQ),[1] Tigressa Helena S. Rodrigues (PQ),[1]* Paulo Nogueira Bandeira (PQ),[1] Jean Parcelli C. do Vale (PQ),[1]**

**Categorias: Pesquisador (PQ) e Estudante de graduação (IC).**

**Vanessa-frota1@hotmail.com; thelenasr@yahoo.com.br**

*[1]Curso de Química, Universidade Estadual Vale do Acaraú (UVA)*

Palavras Chave: *Propolis, Phenolic compounds, Extraction techniques, HPLC, Antioxidant activity.*

## Highlights

- Evaluation of propolis extraction tecnhiques (maceration, soxhlet and under reflux).
- Phenolic composition (p-coumaric, ferulic and trans-cinnamic acids) of a propolis type from Ceara-Brazil.

## Resumo/Abstract

Propolis is a complex mixture composed by secretions of bees and material collected by them from different part of plants, and its chemical composition varies according the habitat and season. In this study, ethanolic extraction of a propolis (EEP) type from Ceará-Brazil was performed using soxhlet, under reflux extraction and maceration at room temperature as extraction techniques. It was determinated the yield, total phenolic concentration, chromatography profile and antioxidant activity in all extracts obtained. According to the results, the extracts obtained from maceration showed the highest yields, 40.65 ± 0.21% when compared with obtained from soxhlet, 36.45 ± 1.39%, and under reflux, 24.03 ± 0.60%. Results revealed that the different extraction techniques did not affect the phenolic composition of EEP. It was obtained 41.33 ± 1.68; 41.65 ± 2.41 and 41.38 ± 4.32 mg/g of total phenolics from EEP by maceration, soxhlet and under reflux extraction, respectively. The EEP after liquid-liquid partition with hexane revealed a greater apolar composition (aprox. 80%) which explains the lower phenolic content. Besides this, liquid chromatography (HPLC) results showed the presence of p-coumaric, ferulic and trans-cinnamic acids as phenolic composition. Propolis extract exhibited 17% antiradical action against 1,1-diphenyl-2-picrylhydrazyl (DPPH) radicals at 20 ppm for all extracts. Based on this study, although the low antioxidant activity, it was possible to identify the main phenolic composition of a propolis from Ceará and tests to determinate other chemical compounds may be conducted in order to evaluate its potential.

**Área: QPN**
*(Inserir a sigla da seção científica para qual o resumo será submetido. Ex: ORG, BEA, CAT)*

**Inscrição: 01321**
*(Inserir o número de inscrição do autor que fez a submissão)*

# Evaluation of Syntetic Peptidomimetics as Cathepsin K Inhibitors

**Taynara L. Silva (PG)[1,2], Deborah A. dos Santos (PG)[1], Dieter Brömme (PQ)[2], Arlene G. Correia (PQ)[1], Paulo C. Vieira (PQ)[1]**

**taynara1203@gmail.com**

*[1]Departament of Chemistry, Federal University of São Carlos; [2]Department of Biochemistry and Molecular Biology, Faculty of Medicine, University of British Columbia.*

*Keywords: Cathepsin K inhibitors, Enzymatic assay, Peptidomimetics*

## Highlights

The cysteine proteases are involved in different physiological and pathologic processes, being recognized for decades as powerful therapeutic targets for the treatment of several diseases. Epoxide derivatives are described as potent cysteine proteases inhibitors.

## Abstract

Osteoporosis is a skeletal disease that causes low bone mass and microarchitectural deterioration of bone tissue[1]. Cathepsin K (CatK), papain-like family, is a lysosomal protease highly expressed in osteoclasts and responsible for the bulk degradation of the collagenous bone matrix thus an ideal target for antiosteoporotic drug development[2]. The cysteine proteases are involved in different physiological processes, in addition to be related to different pathologies, being recognized for decades as powerful therapeutic targets for the treatment of several diseases[3]. The use of enzymes as specific receptors through biochemical assays represents an excellent strategy in the search for bioactive compounds. They are considered attractive targets for pharmacological intervention for a large number of diseases[4]. Epoxide derivatives are described as potent cysteine proteases inhibitors[5]. We have been investigating the inhibitory activity of some synthetic compounds in CatK searching new inhibitor of this enzyme. In the present work we show the inhibitory activity of new peptidomimetics (epoxy-α-aciloxicarboxamidas) of CatK. Inhibition of CatK was determined in a spectro-fluorometric assay using the fluorogenic substrate Z-Phe-Arg-MCA, was recorded with a Fluorimeter (λex = 380 nm and λem = 450 nm). The $IC_{50}$ values of the compounds have been determined and are shown in figure 1. For compound 17 a mechanism of mixed inhibition and Ki 10.7 ± 3.0 were determined using Lineweaver burk and Dixon plots.

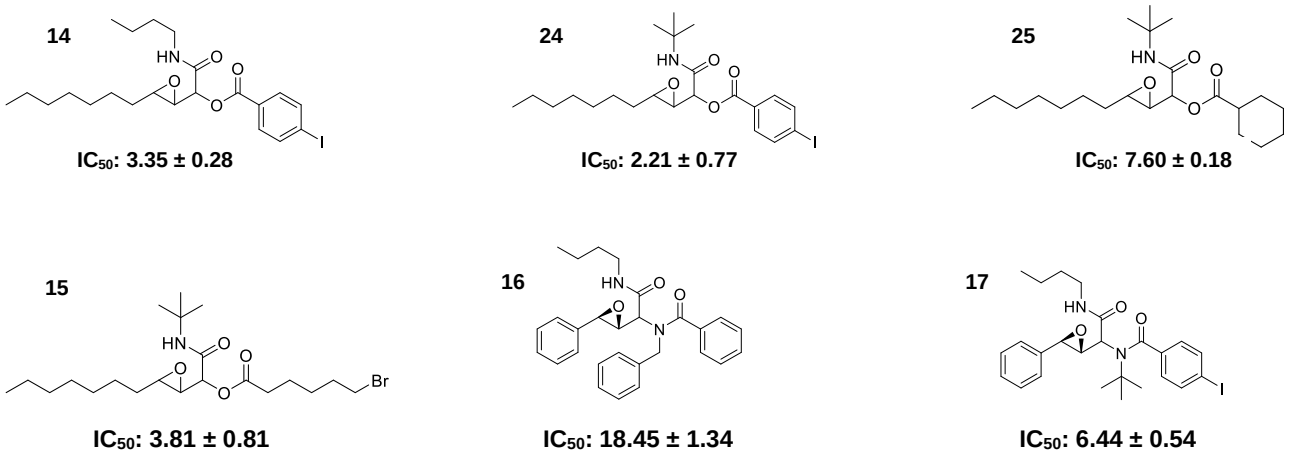


Figure 1: Peptidomimetic evaluated against CatK.

**References: 1-**Abdel-Magid, A. F., ACS Med. Chem. Lett, 6 (6): 628, 2015. **2-**Law, S.; Adrault, P. M.; Aguda, A. H.; Nguyen, N. T.; Kruglyak, N.; . Brayer, G. D.; Brömme, D. Biochemical Journal. 2017, 474, 851–864. **3-**Novinec, M.; Pavšič, M.; Lenarčič, B. Protein Expressi and Purific. 2012, 82, 1-5. **4-**Robertson, J. G. Biochem., 44 (15): 5561, 2005. **5-**Schiefer, I.T.; Tapadar, S.; Litosh, V.; Siklos, M.; Scism, R.; Wijewickrama, G. T.; Chandrasena, E. P.; Sinha, V.i; Tavassoli, E.; Brunsteiner, M. J. Med. Chem. 2013, 56, 6054.

**Área: QPN** **Inscription: 00470**

# Extraction of species Mimosa Tenuiflora (Willd.) front of different ethanolic concentrations and temperature

**Samara A. Morais (PG),1* Jaqueline dos Santos (IC),[2] Tatiane L. Balliano (PQ),[1] João I. Soletti (PQ).[2]**

**samaraaramorais@gmail.com; tlb@iqb.com.br**

*[1] Institute of chemistry and Biotechnology, UFAL; [2] Technology Centre – CTEC, UFAL.*

Keywords: *Mimosa tenuiflora; optimization; ethanol; extraction.*

## Highlights

Known as Jurema Preta, plant abundant in the caatinga of Brazil. Considering the potential taniferous of this species, assessed the ethanolic concentration point for your extraction.

## Resumo/Abstract

The *Mimosa tenuiflora* is a typical plant of the caatinga of Northeastern States of Brazil, with a height of 5 to 7 meters, belongs to the Fabaceae family. In folk medicine this species has demonstrated effectiveness in skin treatments, using the dust from the shells. Given the high bioavailability of jurema preta found in semi-arid, Paes *et. al.* (2006) evaluated this species and was considered a potential producer of tannins. However, the extraction process suffers the influence of some variables, such as temperature, solvent, solid-liquid, etc., so the extraction conditions should be optimized for industrial job.

With this, the work aimed at the extraction of *Mimosa Tenuiflora* rinds, varying ethanol-water concentrations and, later, the temperature of the system. The ratio by weight of solid solvent used was 1:35 (m/v) and extraction time 25 minutes. The analyzed moisture content of the bark was 9.93%. It was obtained the quantification of the total dry extract expressed in grams of dry extract per litre.

Figure 1 - Changes in the staining of the extracts made in different ethanolic concentrations.

Figure 2 - System point to ethanolic

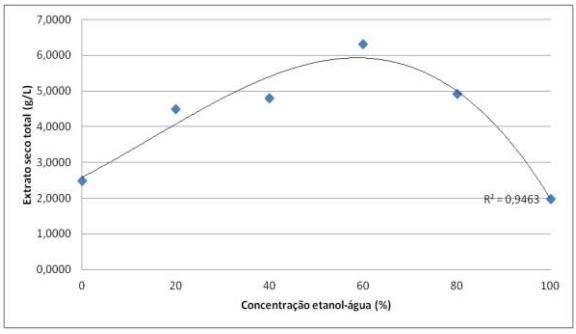


Figure 3 - Influence of temperature on the extraction of total solids.

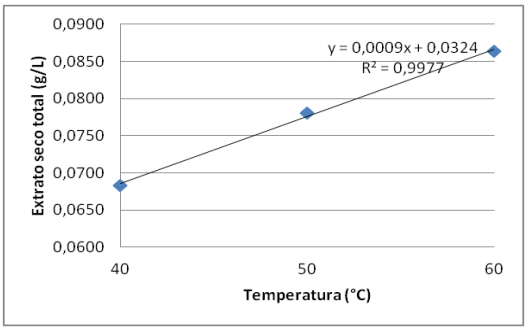


.

From Figures 1 and 2, it was possible to obtain the optimum solvent concentration point, 60% ethanol. With this, it was possible to evaluate this concentration under different temperatures. The temperature that obtained the highest concentration of total solids extracted was 60 ° C, according to Figure 3, due to the increased diffusivity.

**Área: QPN**
*(Inserir a sigla da seção científica para qual o resumo será submetido. Ex: ORG, BEA, CAT)*

**Inscrição: 00482**
*(Inserir o número de inscrição do autor que fez a submissão)*

# Chemical Characterization and Study of the Antibacterial Activities of the Extract of the Palm Tree *Acrocomia aculeata* (Jacq) Lodd ex Mart

**Adriana I. T. de Oliveira (PG),[1*] Raimundo F. Costa (PG),[2] Juliana F. M. da Silva (PQ),[2] Raphael S. Pimenta (PQ),[1] Talal S. Mahmoud (PQ),[3] Guilherme N. L. do Nascimento (PQ),[4] Paula B. de Morais (PQ).[1]**

**dritorcato@gmail.com**

*[1]Laboratório de Microbiologia Ambiental e Biotecnologia (LAMBIO), Universidade Federal do Tocantins, 77001-923 Palmas, TO, Brazil;[2]Laboratório de Microbiologia Geral e Aplicada (LMGA), Universidade Federal do Tocantins, 77001-923 Palmas, TO, Brazil; [3] Centro de Estudos do Mar (CEM), Universidade Federal do Paraná, 83255-976, Pontal do Paraná, PR, Brazil; [4]Laboratório de Ciências Básica e da Saúde, Universidade Federal do Tocantins, 77001-923 Palmas, TO, Brazil.*

Palavras Chave: *Palm Trees, Biological Activities, Microdilution, Chemical Compounds, Human Pathogens.*

## Highlights

The results this study demonstrates the potential of the extract of the Macaúba (*Acrocomia aculeata*) palm tree as an antimicrobial agent.

## Resumo/Abstract

In this research, the ethanolic extraction of chemicals from inflorescences and fruit pulp of *Acrocomia aculeate* was performed, in order to obtain the chemical characterization of their compounds and analyze their antibacterial potential against human pathogens. The presence of saturated and unsaturated fatty acids was reported in the chemical composition of inflorescence (EFM) and pulp (EPM) extracts detected by gas chromatographic analysis (GC-MS). The antimicrobial tests were carried out by the well diffusion and the microdilution methods. According to the well diffusion method, only the EFM extract displayed inhibition halo against the following bacteria: *Enterococcus faecalis, Staphylococcus aureus* and *Escherichia coli*, in concentration of 100 mg $mL^{-1}$. The minimum inhibitory concentration (MIC) has shown moderate (1.56 mg mL-1) inhibition for *S. aureus* and weak (3.13 mg $mL^{-1}$) inhibition for *E. coli*. The results indicate that the ethanolic extract obtained from the flowers of *A. aculeata* presents antibacterial activity against the strains tested, probably due to the presence of fatty acids, which highlights itself as a potential product for pharmaceutical purposes.

Table 1: Detected fatty acids (Area,%) and retention time (RT) of the ethanolic extracts of almond, pulp and flowers of *A. aculeata* by GC-MS analysis.

| Compounds | EAM | | EPM | | EFM | |
|---|---|---|---|---|---|---|
| | RT (min) | **Area %** | RT (min) | **Area %** | RT (min) | **Area %** |
| Caprylic Acid | 7.159 | **7.60** | nd | nd | nd | nd |
| Capric Acid | 10.158 | **3.74** | nd | nd | nd | nd |
| Myristic Acid | 12.930 | **63.79** | nd | nd | 25.411 | **1.27** |
| Palmitic Acid | 19.867 | **6.53** | 19.970 | **48.54** | 19.939 | **33.07** |
| Oleic acid | 24.665 | **14.36** | 24.718 | **43.70** | 24.667 | **28.84** |
| Lactic Acid | nd | nd | 29.171 | **1.31** | nd | nd |
| SFA | | **81.66** | | **49.85** | | **34.34** |
| UFA | | **14.36** | | **47,70** | | **28.84** |

SFA: saturated fatty acids, UFA: unsaturated fatty acids. RT: retention time in minutes, Area: proportional peak, nd: not detected.

**Área: QPN** **Inscrição: 00403**

# Dereplication Study by HPLC-MS-MS and activity against *Leishmania chagasi* of the leaf extract of *Trichilia emarginata*

**Flávia P. D. Viegas (PG),[1*] Patrícia F. Espuri (PG),[2] Juliano G. Amaral (PG),[3] Marcos J. Marques (PQ),[2] Norberto P. Lopes (PQ),[3] Marisi G. Soares (PQ),[1].**

**fpdviegas@gmail.com**

[1]Laboratório de Fitoquímica e Química Medicinal, Instituto de Química, UNIFAL-MG; [2]Laboratório de Parasitologia, Departamento de Patologia e Parasitologia, UNIFAL-MG; [3]Núcleo de Pesquisa em Produtos Naturais e Sintéticos, Departamento de Ciências Farmacêuticas, FCFRP-USP.

Keywords: HPLC-MS-MS, *Leishmania chagasi*, *Trichilia emarginata, dereplication, GNPS, chlorogenic acid*

## Highlights

The leaf extract of *Trichilia emarginata* was active against *Leishmania chagasi*. The bioactive leaf extract was dereplicated by HPLC-DAD-MS /MS assisted by the GNPS platform. 5-*O*-caffeoylquinic acid.

## Resumo/Abstract

The leaves extract of *T. emarginata* was evaluated for its activity against *Leishmania chagasi* and was studied by dereplication by HPLC-DAD-MS/MS analysis supported by the Global Natural Products and Social Molecular Networking (GNPS) platform[1]. The search for the chemical constituents of the crude extract and its fractions ethyl acetate (EAF) and hydroalcoholic (HAF) of de *T. emarginata* led to the identification of 5-*O*-caffeoylquinic acid (5-CQA), a substance already described in the *Trichilia* genus[2].However, other metabolites were identified for the first time in this genus, including the isomers 3 and 4-*O*-caffeoylquinic acids, aside from *p*-coumaroylquinic acid, di-O-caffeoylquinic acid and caffeoyl-dimethoxycinnamoylquinic acid. Due to the abundance of these acid metabolites in all samples of *T. emarginata*, it is believed to have a close relation with the leishmanicidal activity observed in the assays with *L. chagasi*. In addition, some flavonoids derived from quercetin and taxifolin were also identified. Among all tested samples, HAF showed to be the most potent with an $IC_{50}$ of 11.40 µg/m and its chromatographic profile showed that 5-CQA and its derivatives are the major constituents. The commercial 5-CQA was tested and showed higher leishmanicidal activity than HAF against *L. chagasi* ($IC_{50}$ = 7.38 µg/mL). In conclusion, our results strongly suggest that the leishmanicidal activity of HAF of *T. emarginata* is mainly due to the presence of 5-CQA and, possibly, of its other derivatives. The GNPS platform was of great value in the dereplication study, allowing for the identification of known metabolites.

### References

[1]WANG, M. *et al.* Sharing and community curation of mass spectrometry data with Global Natural Products Social Molecular Networking. *Nature Biotechnology*, v. 34, n. 8, p. 828–837, 20161

[2]*VIEIRA, I.* et al. *Secondary Metabolites of the Genus Trichilia:Contribution to the Chemistry of Meliaceae Family.* American journal of analytical chemistry*, v. 5, n. January, p. 91–121, 2014.*

**Acknowledgements**
The authors are grateful to CAPES and FAPEMIG for fellowship and financial support.

**Inscrição:** 00510

***Área:*** *QPN*

# Avaliação da composição química, toxicidade, atividades antioxidante e antimicrobiana de extratos das folhas de *Doliocarpus dentatus*

**Thalia A.F. Almeida (IC)[1], Luis Fernando Benitez Marcorini (PQ)[2], Claudia A.L. Cardoso (PQ)[1]**

**thalia.ta72@gmail.com; claudia@uems.br**

[1]Centro de Estudos em Recursos Naturais, Laboratório de Análise Instrumental, UEMS; [2]Centro Universitário da Grande Dourados,UNIGRAN.

Palavras Chave: *Flavonoides, Cipó-caboclo, Ácido Betulínico.*

## Highlights

Evaluation of the chemical composition, toxicity, antioxidant and antimicrobial activities of leaf extracts of *Doliocarpus dentatus*.
The leaves of *D. dentatus* presented antioxidant and antimicrobial activities.
The leaves showed the presence of betulin acid, betullin and sitosterol-3-O-β-D-glucopyranoside.

## Resumo/Abstract

A espécie *Doliocarpus dentatus* é vulgarmente demoninada de cipó-caboclo, sendo utilizada no tratamento de edemas e linfangites. Neste estudo foram realizados o isolamento e identificação de substancias e avaliações dos teores de flavonóides, compostos fenólicos, flavonol, taninos, atividade antioxidante, fator de proteção solar (FPS), toxicidade empregando *Artemia salina* e atividade antimicrobiana de extratos aquosos (EAF) e etanólicos (EEF) preparados com folhas de *D. dentatus*. Comparando os extratos aquoso e etanólico das folhas de *D.dentatus*, verificou-se que os extratos etanólicos possuem maior teor de compostos fenólicos, flavonoides, flavonol e taninos em relação aos extratos aquosos. No extrato etanólico foram isoladas e identificadas empregando ressonância magnética nuclear e espectrometria de massas as substancias: ácido betulinico, betulin e sitosterol-3-O-β-D-glucopiranosideo, sendo está última também isolada no extrato aquoso. O extrato etanólico também apresentou ação antioxidante tanto empregando o método de FRAP quanto de DPPH e também maior toxicidade em relação ao extrato aquoso. O FPS foi maior no extrato aquoso. Os extratos aquoso e etanólico apresentaram atividade antimicrobiana para *Staphylococcus aureus* e *Staphylococcus epidermidis.*

| | EAF M±DP | EEF M±DP | | EAF M±DP | EEF M±DP |
|---|---|---|---|---|---|
| **DPPH** | 732,31±13,95 | 247,39±6,14 | **FLAVONOL** | 0,15± 0,01 | 0,17±0,01 |
| **FRAP** | 390,79±1,38 | 217,77±2,13 | **TANINOS** | 4,82±0,10 | 4,96±0,12 |
| **FLAVONOIDES** | 14,21±0,21 | 43,20±0,19 | **FPS** | 4,55±0,05 | 3,19±0,10 |
| **FENÓIS** | 86,70±0,56 | 89,65±0,64 | | | |

M=média DP=desvio padrão

**Área: QPN** **Inscrição: 00527**

# Nutritional value, physicochemical and rheological parameters of pulp and by-products of buriti fruit (*Mauritia flexuosa*) after lyophilization

**Joilane A. P. Freire[1](PQ), Raiane O. Araújo[4,*] (IC), Jailane S. Aquino[2](PG), Ana R. N.Campos[3](PG), Vicente G. F. Viana[4](PQ), Joaquim S. Costa Júnior[4](PQ), Arkellau K. S. Moura[5](PG), Antônia Maria. G. L. Citó[5](PQ), Stella R. A. Medeiros[1](PQ), Ana Cristina S. de Lima[6] (PG), Maria D.A. Oliveira[5](PG); Paulo M.P. Ferreira[7](PQ).**

**joilane@hotmail.com; rayaneh_14@hotmail.com***

*[1] Federal University of Piauí, Department of Nutrition, Campus Senador Helvídio Nunes de Barros, Picos, Piauí, Brazil;*
*[2] Federal University of Paraíba, Department of Nutrition, Campus I, Castelo Branco, João Pessoa, Paraíba, Brazil.*
*[3] Federal University of Campina Grande, Department of Chemistry Campus Cuité, Olho d´agua da Bica, Cuité, Paraíba, Brazil.*
*[4] Federal Institute of Piauí, Department of Chemistry, Campus Central, Praça da Liberdade, Teresina, Piauí, Brazil;*
*[5] Federal University of Piauí, Department of Chemistry, Campus Ministro Petrônio Portela, Teresina, Piauí, Brazil.*
*[6]Federal University of Ceará, Fruit and vegetable Laboratory, Fortaleza, Ceará, Brazil.*
*[7] Federal University of Piauí, Department of Biophysics and Physiology, Campus Ministro Petrônio Portela, Teresina, Piauí, Brazil.*

**Keywords**: *Buriti, Fatty acids, Fiber, Morphology, Phytosterols, Rheology.*

## Highlights

The fruit of buriti (*Mauritia flexuosa* L.) belongs to the amazon and brazilian cerrado biomes. Its processing is important to expand production and availability, as the fresh product has limitations mainly due to the physicochemical characteristics related to high water loss and susceptibility to injury when stored in refrigerated environment[1]. The objective of this work was to evaluate the nutritional value and physicochemical parameters of buriti pulp, peel, and endocarp after lyophilization.

## Resumo/Abstract

The mineral profile was determined by X-ray fluorescence spectrometry (EDX), the fatty acids and phytosterols ware quantified by gas chromatography coupled to mass spectrometry (GC/MS), as well as the centesimal composition. Furthermore, another physicochemical parameters were evaluated (morphological by Scanning Electron Microscopy - SEM and X-ray Diffraction – DRx, thermal stability by Differential Scanning Calorimetry – DSC) and the rheologic properties in these samples. Pulp and its byproducts showed good yield (above 17.31%), and are rich in lipids (between 15.13 and 77.53%) and carbohydrates (between 11.54 and 51.67%). All samples analyzed are considered source of oleic acid, potassium and manganese. Buriti peel showed phytosterols (1.74%), mainly β-sitosterol and stigmasterol. The samples showed semi-crystalline profile in SEM and DRx. In the DSC curves the presence of exothermic degradation events was observed at 200 ºC in all samples, however, in the pulp these events were less intense, ie, less energy was required for the degradation of the components in this sample. Nutritional and physicochemical properties of the pulp and buriti fruit by-products are promising for industrial processing.

---

[1]FUJITA E, VIEITES R.L, DAIUTO É.R, & SMITH R.E. (2014). Refrigerated storage of the fruits of buriti (*Mauritia flexuosa L.*). Advances in Horticultural Science Journal, 28, 3-8.

| Área: QPN | Inscrição: 00538 |
|---|---|

# PHYTOCHEMICAL EVALUATION OF THE VEGETAL SPECIES *MANILKARA SUBSERICEA* (MART.) DUBARD

**Erika D. P. M. Gutierrez (PG),[1] Alexsandro Araujo da Silva (PQ),[1*] Carlos Alberto da Silva Riehl (PQ).[2]**

**professora_erika@yahoo.com.br; alexandro.araujos@gmail.com***

*[1]Instituto de Química, UERJ, Maracanã, RJ; [2]Instituto de Química, UFRJ, Ilha do Fundão, RJ.*

Palavras Chave: *Manilkara subsericea*, antioxidante, estresse oxidativo, triterpenos.

## Highlights

**PHYTOCHEMICAL EVALUATION OF THE VEGETAL SPECIES *MANILKARA SUBSERICEA* (MART.) DUBARD**

Compounds with antioxidant capacity extracted from plants are very important to combat the excess free radicals produced by the human organism due to oxidative stress.

## Resumo/Abstract

O estresse biológico produzido pelo aumento de radicais livres e espécies reativas de oxigênio (ERO) aumenta o risco de doenças e envelhecimento precoce, diminuindo assim a qualidade de vida[1]. O presente trabalho estuda a espécie vegetal, endêmica da Mata Atlântica Brasileira, *Manilkara subsericea,* da família *Sapotaceae*. Este estudo abrange a extração via Soxhlet com hexano e acetato de etila, seguida do fracionamento em coluna aberta de sílica, avaliação por CCF em escala analítica e separação em escala preparativa, além da identificação de compostos por CGAR-EM e RMN $^{1}H$ e $^{13}C$. A análise cromatográfica acoplada a espectrometria de massas das frações hexânica da *Manilkara* subsericea, aliada a estudos por RMN $^{1}H$ e $^{13}C$, forneceu dados que confirmam a presença dos seguintes compostos ainda não relatados na literatura para a espécie em estudo: esqualeno (Figura 1), importante precursor da rota biosintética dos triterpenos[2]; acetato de lupeol composto com atividade farmacológica[3]; α-Tocoferol, um dos oito isômeros que formam parte da vitamina E; uma série homóloga de hidrocarbonetos lineares saturados ($C_{19}$ a $C_{33}$), com predominância dos ímpares sobre os pares, comum em plantas terrestres superiores; e α-e β-ceto-amirina (Figura 2), além dos derivados de amirina já relatados na literatura.

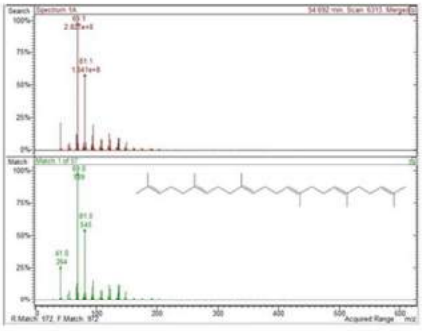

Figura 1. Comparação de espectros de massas do esqualeno (*NIST*) com o do composto obtido na fração hexânica da folha.

Tabela 1 – Comparação de deslocamentos químicos de RMN $^{13}C$ do esqualeno.

| Carbono | Deslocamento químico δ (ppm) | |
|---|---|---|
| # | Fração hexânica | Ref.: SDBS |
| 2 | 130,0 | 131,2 |
| 4 | 124,4 | 124,5 |
| 7 | 134,9 | 134,9 |
| 9 e 14 | 124,4 | 124,4 |
| 12 | 135,1 | 135,1 |

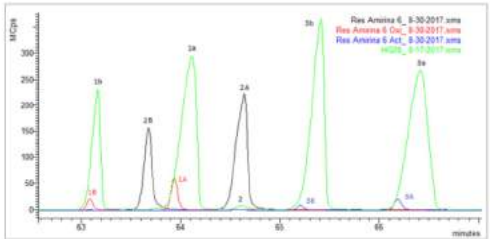

Figura 2. Sobreposição dos cromatogramas da fração hexânica HG28 e padrões de referências. 1A: α-amirina oxidada;1B: β-amirina oxidada; 2A: α-amirina; 2B: β-amirina; 3A: α-amirina acetilada 3B: β- amirina acetilada.

A presença de esqualeno, acetato de lupeol e derivados de amirina na fração hexânica da espécie *Manilkara subsericea* mostra uma provável capacidade antioxidante a ser determinada.

## Agradecimentos

CNPQ pela bolsa de mestrado. À Central Analítica Fernanda Coutinho (IQ/Uerj).

[1] FERREIRA, A.L.A.; MATSUBARA, 1997; [2] LOBO; LOURENÇO, 2007; [3] GALLO, M.B.C and SARACHINE, M.J.2009.

**Área: QPN** **Inscrição: 00542**

# Avaliação da atividade antioxidante e viabilidade celular de extratos do fruto de *Guazuma ulmifolia* Lam. (mutamba)

**[1]Mara Núbia Guimarães dos Santos*(PG), [2]Ana Paula Terezan (PQ), [1]Jaqueline Rodrigues da Silva (PQ), [1]Ricardo Bentes de Azevedo (PQ), [2]Denilson Rabelo (PQ), [2]Lucília Kato (PQ), [2]Cecília Maria Alves de Oliveira (PQ), [2]Patrícia Pommé Confessori Sartoratto (PQ)**

**santosmng@hotmail.com**

*[1] Instituto de Biologia, UnB, Brasília-DF, Brasil; [2] Instituto de Química, UFG, Goiânia-GO, Brasil*

Palavras Chave: *Guazuma ulmifolia, mutamba, compostos fenólicos, viabilidade celular*, atividade antioxidante.

## High lights

Evaluation of the antioxidant activity and cell viability of extracts of the fruits of *Guazuma ulmifolia* Lam. (mutamba). Antioxidant potentials correlate with the phenolic content. Ten phenolic compounds identified by HPLC/HRMS. Low to moderate cytotoxicity for four cell lines. Efficient inhibition of ROS production.

## Resumo/Abstract

A espécie *Guazuma ulmifolia* Lam. (Malvaceae) ocorre especialmente em formações de Cerrado, com extenso uso na medicina popular e propriedades antidiabetes, hipotensiva, antiviral, entre outras, já avaliadas (1). Este trabalho constitui-se no estudo inicial sobre a composição química e a atividade antioxidante e anti-inflamatória de extratos de frutos coletados no resquício da Mata Subcaducifólia Estacional, localizado no Campus da UFG, Goiânia/GO. O extrato metanólico (ExB) foi obtido por infusão a frio e as frações FP-D e FP-Ac foram obtidas a partir deste por partição líquido-líquido, empregando-se água/diclorometano e água/acetato de etila, respectivamente. Os extratos foram investigados quanto ao potencial antioxidante (DPPH), ao teor de compostos fenólicos (Folin-Ciocalteau) e analisados por HPLC/HRMS. Os resultados mostraram $EC_{50}$ de 323,6 e 86,2 µg/mL para ExB e FP-D, respectivamente, e 4,5 µg/mL para ácido ascórbico. O potencial antioxidante apresentou correlação positiva com o teor de fenólicos: 936,3±8,9 e 3090,7±21,6 mg ácido gálico/100g de ExB e FP-D, respectivamente. Foram identificados em FP-Ac, por comparação com padrões, os ácidos protocatequínico, gentísico, cafeico e p-cumárico, quercetina-3-O-β-glucosideo, rutina, quercetina, narigenina, luteolina e kaempferol. A viabilidade celular (MTT) e a produção de espécies reativas de oxigênio (EROs) para macrófagos de murinho (RAW 264.7), fibroblastos de camundongo (NIH-3T3), endotelial de aorta humana (EAHy926) e rim de cachorro (MDCK) foram avaliadas empregando-se ExB e FP-Ac. Um efeito citotóxico moderado foi observado para ambos os extratos a partir de 125 µg/mL, sendo mais pronunciado para macrófagos e fibroblastos (Figura 1). A produção de EROs foi significativamente inibida em toda faixa de concentração testada.

Figura 1: Viabilidade celular (A) e Produção EROs (B) em meio de cultura de macrófagos.

(1) Lopes, G. C; Rocha, J. C. B, Almeida, G. C.; Mello, J. C. P. J. Braz. Chem. Soc., 20 (6), 1103-1109, 2009.

Agradecimentos ao CNPQ e CAPES.

**Área: QPN** **Inscrição: 00710**

# Phytotoxic evaluation of agroindustrial vinasse residue in relation to *Lactuca sativa* and *Ipomoea purpurea*

**Dandara A. Luz* (PG),[1] Polianna S. Ferreira (IC)[1], Naomi K. Simas (PQ)[2], Anne Caroline C. Gomes (PQ),[3] Ricardo M. Kuster (PQ)[1]**

**dandara8806@hotmail.com**

*[1]Programa de pós-graduação em Química (PPGQUI) -UFES; [2]Faculdade de Farmácia, UFRJ; [3]Instituto Federal do Rio de Janeiro - IFRJ*

Palavras Chave: *Saccharum* ssp, Phytotoxicity, *Lactuca sativa, Ipomoea purpurea*, Fatty acids, Phenolic acids.

## Highlights

Phytotoxic potential of bioactive molecules (fatty acids and phenolic acids) present in agroindustrial waste vinasse against *Lactuca sativa* and *Ipomoea purpurea* (weed).

## Resumo/Abstract

The residue of sugarcane agroindustry, vinasse, is abundant in Brazil and in the world. The use of this waste solves problems related to waste and environmental pollution. The vinasse from the Paineiras sugar-ethanol plant was submitted to liquid / liquid partitions and tested for phytotoxic activity and analyzed by GC-MS to identify volatile compounds. Palmitic acid, 3,4 dimethoxybenzoic acid and 3,4,5-trimethoxybenzoic acid were present, in different relative concentrations, in the partitions. In the phytotoxicity bioassays against *Lactuca sativa* and *Ipomoea purpurea* (weed), the most active partition was dichloromethane (Figure 1A and 1B).

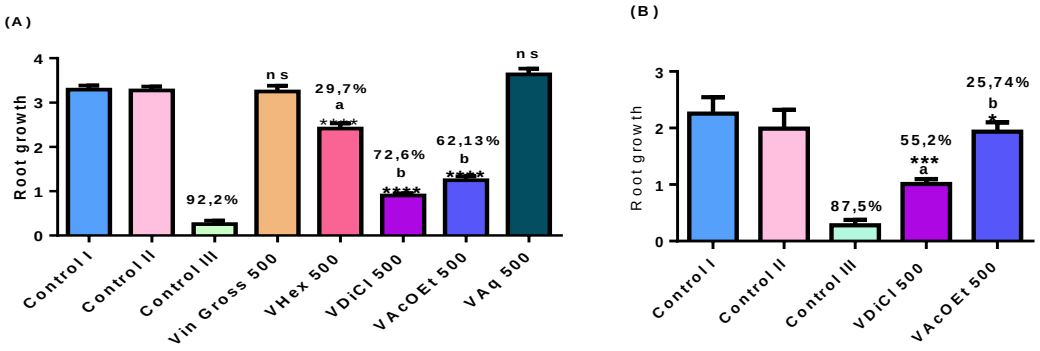


**Figure 1. Effect of vinasse partitions on root growth of *L. sativa* (A) and *I. purpurea* (B). [Control I = distilled water; Control II = 0.1% DMSO; Control III = Menadione (143 ppm)].**

In the GC-MS analysis, a similar proportionality was observed for the VDiCl sample in concentration for fatty acids (19.0%) and phenolic acids (23.0%). However, for the VAcOEt sample, a higher proportion of phenolic acids (70.0%) and lower fatty acids (2.6%) were observed. Fatty acids and phenolic acids are described as phytotoxic substances[1,2]. It is suggested that the interaction between these classes of substances, with different phytotoxic mechanisms, is important for a higher rate of inhibition, especially on herbicide resistant species, such as weeds. This work demonstrated the potential of bioactive molecules present in vinasse residue for phytotoxic activity, indicating that this residue can be used as raw material in the elaboration of innovation products for the control of weeds, reducing the risks of improper handling.

[1] Alamsjah, *et al* (2008). J Appl Phycol, 20,713–720.
[2.] Macías, *et al* (2007) J. C. Pest Manag Sci 63:327–348.

**Área: QPN** **Inscrição: 00800**

# Evaluation of three methodologies to optimization of phycobiliprotein extraction in aqueous fraction of *Arthrospira platensis*

**Laura P. de A. N. Cavalcanti (PG)[1,2], Cláudia M. L. L. Teixeira (PQ)[2], Roberto C. C. Martins (PQ)[1]**

**laurapatricionunes@gmail.com**

[1] *LAPEMESP, Instituto de Pesquisas de Produtos Naturais, UFRJ,* Av. Carlos Chagas Filho, 373, Prédio do CCS, Bloco H, Subsolo, Lab 18 SS, Ilha do Fundão, Cidade Universitária, Rio de Janeiro, RJ - CEP: 21944-97; [2] *Laboratório de Biotecnologia de Microalgas, Instituto Nacional de Tecnologia,* Av. Venezuela, 82 - Saúde, Rio de Janeiro - RJ, 20081-312

Palavras Chave: *Arthrospira platensis*, M*icroalgaa, Phycocyanin, Spectrophotometry, UV-Vis, Aqueous fraction extraction methods*

## Highlights

*A. platensis* is a microalga that has phycobiliproteins which have a broad spectrum of biological activities. This work evaluated the most effective extraction method for obtaining these substances.

## Abstract

**Introduction:** Phycobiliproteins are water pigment-proteins present in the microalga *Arthrospira platensis*, considering their biological activities it is very important to optimize their recovery [1,2]. **Objective:** to evaluate three methods for phycobiliproteins extraction in order to improve their recovery. **Methodology:** The three procedures are shown below (**Figure 1):**

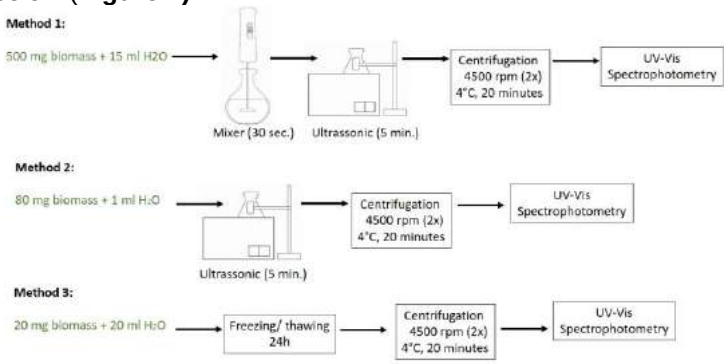


**Figure 1:** Methodologies applied to the extraction of the phycobiliproteins.

The quantification of the phycobiliproteins were carried out according to the equations of **Figure 2**.:

$$[PC] = \frac{DO_{615} - 0{,}474(DO_{652})}{5{,}34} * fator\ diluição = \alpha \quad [APC] = \frac{DO_{652} - 0{,}208(DO_{615})}{5{,}09} * fator\ diluição = \beta \quad [PE] = \left[\frac{(DO_{562} * fator\ diluição) - (2{,}41 * \alpha) - (0{,}849 * \beta)}{9{,}62}\right] = \gamma$$

**Figure 2:** Equations for quantification of the phycobiliproteins (mg/mL). [PC] = Phycocyanin, [APC] = Allophycocyanin, [PE] = Phycoerytrin.

**Results and Discussion:**

**Table 1:** Concentration (mg/mL) of phycobiliproteins in aqueous fraction (mean value ± standard deviation).

| | Method 1 | Method 2 | Method 3 |
|---|---|---|---|
| **Allophycocianin** | 0,0004 ± 0,0006 | 0,0255 ± 0,0081 | 0,0200 ± 0,0001 |
| **Phycocianin** | 0,0142 ± 0,0050 | 0,0368 ± 0,0090 | 0,0613 ± 0,0010 |
| **Phycoerytrin** | 0,0015 ± 0,0001 | 0,0005 ± 0,0001 | 0,0012 ± 0,0001 |

Based on the three procedures performed, it was possible to verify that the freezing / thawing extraction was the most efficient process, or it was the most efficient process to break the cells and exposure the proteins or the less aggressive process to these proteins, or even it might be a combination of these two possibilities.

**References:** [1]Hadiyanto *et al*. **Phyocyanin extraction from microalgae Spirulina platensis assisted by ultrasound irradiation: effect of time and temperature**, *Songklanakarin J. Sci. Technol.*, v.38, n.4, p.391-398, 2016 [2]Sivasankari, S. *et al.* **Comparison of Different Extraction methods for Phycocyanin Extraction and Yield from Spirulina platensis**, *Int.J.Curr.Microbiol.App.Sci*, v.3, n.8, p. 904-909, 2014.

**Área: QPN Inscrição: 01007**

# Chemical composition and biological activities of the leaves and stem of *Macrolobium rigidum* R.S. Cowan (Leguminosae).

**Bruna Oliveira do Nascimento (PG),[1] Jorge M. David (PQ),[1] Patrícia A. Santos (PG),[1] José Fernando A. Neto (PG),[1] Juceni P. David (PQ).[2]**

**b.oliveira.n@gmail.com**

*[1]Instituto de Química; [2]Faculdade de Farmácia, UFBA, Salvador - BA.*

Palavras Chave: *Macrolobium rigidum, Leguminosae, Antioxidant activities, chemical composition.*

## Highlights

This work describes the first chemical study of *Macrolobium rigidum* (Leguminosae). It was isolated lupeol and steroids. The antioxidant activities by DPPH quenching of extracts were determinated.

## Resumo/Abstract

*Macrolobium rigidum* R.S. Cowan is among the approximately 70–80 species from the subfamily Caesalpinioideae belonging to Leguminosae. The literature reports the presence of anthocyanin, catechin, condensed tannin and pyrogallic tannin in some species of this genus, but this genus is still little studied chemically and biologically. To date, there are not biological or phytochemical studies dealing with this species. In this work the biological activities and chemical composition of organic extracts of *M. rigidum* were studied. Dried leaves and stem were extracted with methanol through 48 hours obtaining the crude methanol extract of leaves (28.6526 g) and stem (21.1834 g). Both extracts were submitted to sequentially liquid-liquid partition between MeOH:$H_2O$ (7:3) and dichloromethane, ethyl acetate and butanol. The DCM soluble fraction of leaves (10.4 g) was subjected to successive chromatographic procedures employing silica gel as stationary phase and mixtures of DCM:MeOH in increasing polarity gradient as eluents. These procedures permitted to isolate lupeol (35,1mg), a mixture of $\beta$-sitosterol and stigmasterol (41.7mg) and one not identified compound (18,8mg). These compounds were identified through TLC comparison with the standards previously isolated on the group and by IR and melting point. The antioxidant activities of the organic extracts of leaves and stem were determined using radical DPPH quenching. Six concentrations (0.07 to 1mg/mL) of the different extracts were evaluated. The results are illustrated in Figures, which indicate the presence of antioxidant substances mainly in the EtOAc and MeOH extracts. (CNPq, FAPESB, CAPES)

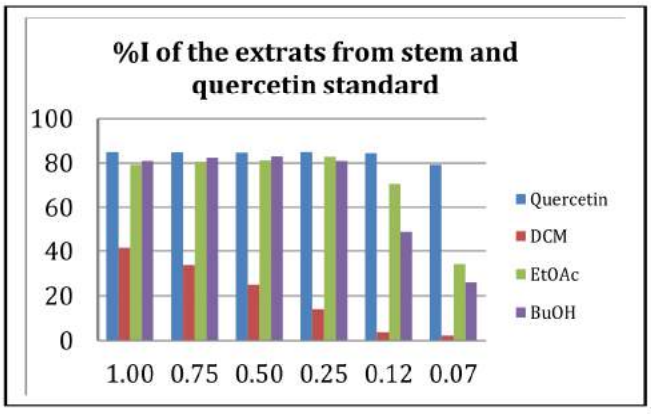


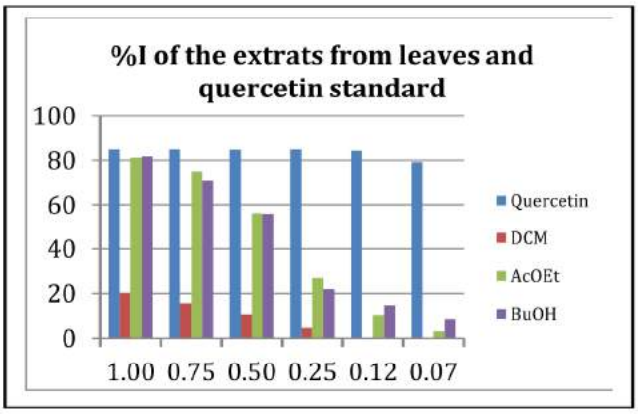

**Área: QPN** **Inscrição: 01047**

# Identification of alkaloids from the stem bunch of the plant species *Annona tomentosa* R. E. Fr. (Araticum-bravo)

**Aglaete de Araújo Pinheiro (IC),[1]* Cláudia Quintino da Rocha (PQ),[1] Marcos Bispo Pinheiro Camara (PG),[2] Gilvan de Oliveira Costa Dias (PQ),[1] Joselene Ribeiro de Jesus Santos (PQ),[1].**

**aglaete.araujo@yahoo.com.br***

*[1]Departamento de Química, UFMA; [2]Departamento de Química, IFMA*

Keywords: *Alkaloids, Annonaceae, Phytochemistry, Identification*

## Highlights

A FIA-ESI-IT-MSn assay was performed to identify the alkaloids from the stem carcass of the Annona tomentosa plant species.

## Resumo/Abstract

The Annonaceae family comprises approximately 180 to 129 genus and about 2.400 species, being the largest of the order Magnoliales. Known in Brazil as Araticum-bravo or Araticum of the shrub, Annona tomentosa R. E. Fr is a small tree found mainly in the coastal areas of the Brazilian territory. Folk medicine has used various parts of this plant to combat mainly diarrhea, headache, ulcer and eradication of lice. In tests with the crude extract a positive action against bacteria and fungi was evaluated. Based on the data collection of the phytochemical screening, the presence of alkaloids in the plant species was verified. Alkaloids present great pharmacological importance, as they present biological activities such as antitumor, anesthetic and antidepressant. For the identification of these compounds, the crude hydroethanolic extract was concentrated and lyophilized. The solid material was dissolved in water / methanol (8:2) in an acid medium. The partition was started with ethyl acetate, then the remaining aqueous phase was basified and chloroform was added to obtain the alkaloid phase. A FIA-ESI-IT-MSn assay was then performed for the identification of alkaloids.

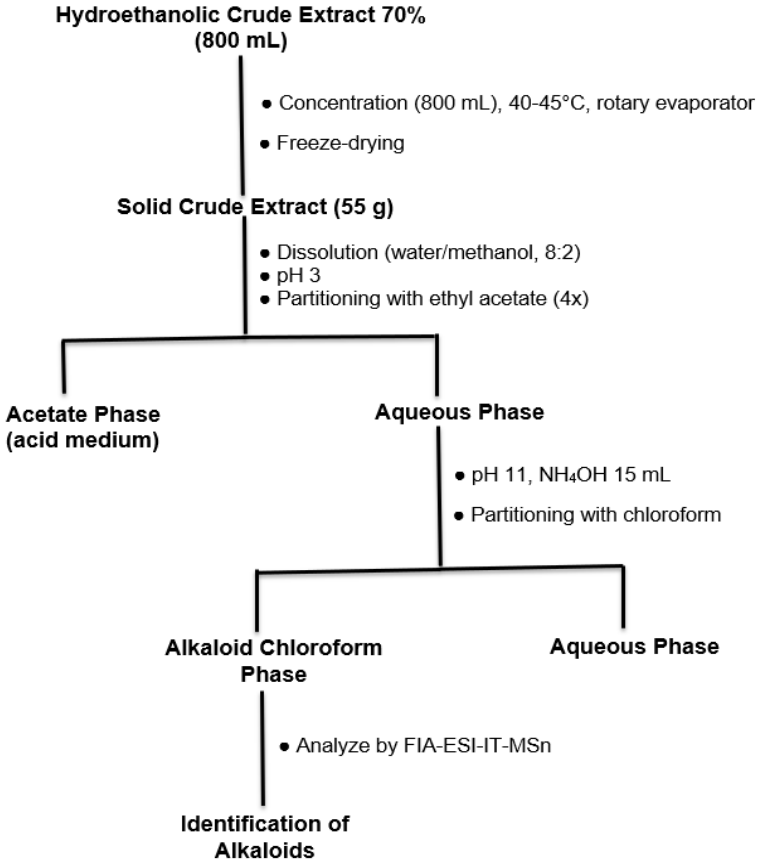

**Área: QPN** **Inscrição: 01050**

# Ocorrência de flavonoides e outros compostos fenólicos em folhas de *Casearia arborea* (Salicaceae)

**Augusto L. dos Santos (PG),[1]* Marcelo J. Pena Ferreira (PQ),[2] Marisi G. Soares (PQ),[3] João H.G. Lago (PQ),[4] Patrícia Sartorelli (PQ).[1]**

**aug.snt@gmail.com**

*[1]Instituto de Ciências Ambientais, Químicas e Farmacêuticas, UNIFESP; [2]Instituto de Biociências, USP; [3]Instituto de Química, UNIFAL; [4]Centro de Ciências Naturais e Humanas, UFABC.*

Palavras Chave: *Casearia arborea, Tricina, Ácido vanílico, Divaniloil Glicose, Fenólico.*

## Highlights

Phenolic compounds from leaves of *Casearia arborea* (Salicaceae). The *Casearia* genus is known by popular medicine in Asia, South America and Pacific Islands. The clerodane diterpenes are common in largery genus and phenylpropanoids as well, but few species shows flavonoids and among others phenolics. Have been related from *C. arborea* the presence of clerodane diterpenes and cucurbitacins from the root and vanillic acid, divanilloyl glucopiranoside and tricin from leaves. And this present study shows the majority of flavonoids and others phenolics from the DCM phase from the crude MeOH extract from leaves of *C. arborea*, by analyzing NMR $^1$H, but mainly UV-Vis spectras from HPLC-DAD analysis of the fractionation of DCM phase. In addition, the structure of 5,4'-dihydroxy-7,3',5'-trimethoxyflavone was determined by $^1$H NMR and by checking UV spectrum (Figure 1), but in admixture with other analogues.

## Resumo/Abstract

O gênero *Casearia* é conhecido pelo uso na medicina popular e por satisfazer uma diversidade farmacológica na ação anti-inflamatória e tratamento de doenças de pele, estômago, picada de cobra, diabetes, entre outras, bem como a avaliação biológica de seus metabólitos. Diterpenos clerodânicos e fenilpropanoides são comuns, porém poucas espécies apresentam flavonoides e outros fenólicos [1; 2]. De *C. arborea* ralata-se a presença de diterpenos clerodânicos e cucurbitacinas das raízes [3] e das folhas ácido vanílico, divaniloil glicose e tricina [4]. Adicionalmente, este trabalho apresenta a presença de flavonoides e fenólicos como majoritários da fase DCM do extrato bruto MeOH das folhas de *C. arborea*. O fracionamento desta fase em Sílica "flash" gerou 17 frações. Após o fracionamento em Sephadex LH-20 da fração 8 obteve-se a tricina e outras misturas de derivados desta flavona ($\lambda_{max}$: 210; 270; 350); da fração 9 obteve-se o ácido vanílico ($\lambda_{max}$: 205; 252; 286), bem como mistura de outros flavonoides ($\lambda_{max}$: 202; 270; 338). A fração 10 fracionada por sílica gel apresentou divaniloil glicose ($\lambda_{max}$: 206; 223; 265; 295) e ácido vanílico como majoritários. A fração 12 possui flavonoides ($\lambda_{max}$: 205; 260; 355) em mistura a divaniloil glicose e ácido vanílico. Adicionalmente, determinou-se a estrutura da 5,4'-dihidroxi-7,3',5'-trimetoxiflavona por RMN $^1$H e verificando espectro de UV (figura 1), porém em mistura a outros análogos.

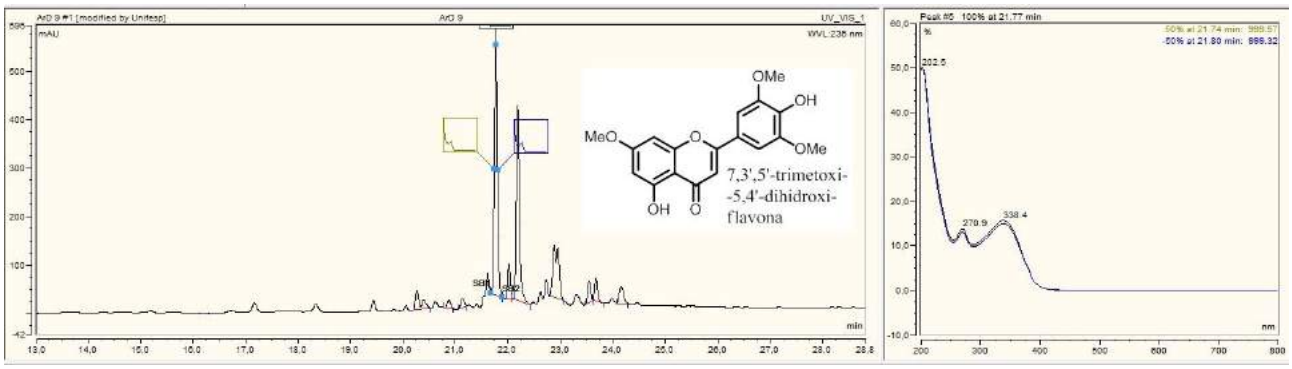


[1] Xia *et al*. (2015) *Phytochem. Rev.* 14, 99-135.
[2] Vieira Júnior *et al.* (2017) *Rev. Bras. Farmacogn.* 27, 785-787.
[3] Beutler *et al.* (2000) *J. Nat. Prod.* 63, 657-661.
[4] Santos *et al.* (2017) *Chem. Biodivers.* e1600458.

**Área: QPN**
*(Inserir a sigla da seção científica para qual o resumo será submetido. Ex: ORG, BEA, CAT)*

**Inscrição: 01054**
*(Inserir o número de inscrição do autor que fez a submissão)*

# Evaluation of Monoamine Oxidase Inhibitory Potential of *Erythrina verna* Alkaloids Using Zebrafish Model

**Douglas F. Rambo (PG),[1]* Renata Biegelmeyer (PQ),[2] Natally S. B Toson (IC),[1] Amélia T. Henriques (PQ).[1]***

**renata,biegel@gmail.com; douglasrambofar@hotmail.com**

*[1]Laboratório de Farmacognosia, Universidade Federal do Rio Grande do Sul, Porto Alegre/RS; [2]Departamento do Medicamento, Universidade Federal da Bahia, Salvador/BA*

Palavras Chave: *Erythrina verna, Alkaloids, Zebrafish, Neurodegenerative disorders, MAO.*

## Highlights

Zebrafish was employed as a source of Monoamine Oxidase enzyme (zMAO). *E. verna* fraction enriched in alkaloids (FEA) showed a potential inhibitory activity of zMAO.

## Resumo/Abstract

*Erythrina verna* Vell. is a well-known plant species due to their anxiolytic properties related to tetracyclic alkaloids. Neurodegenerative disorders (Parkinson and Alzheimer diseases) have a multifactorial etiology. So, the research area of compounds that interact with central nervous system targets, like cholinesterases (AChE and BChE) and monoamine oxidases (MAO-A and MAO-B), is a powerful tool in drug design. In this context, the present work aimed to evaluate the MAO inhibitory potential of *E. verna* trunk barks fraction enriched in alkaloids (FEA) using an alternative biological model. The MAO was isolated from zebrafish (zMAO) brain. Chemical analysis was performed by Gas Chromatography (GC-MS) and High-Resolution Mass Spectrometry (ESI-MS). The results were evaluated at ʎ = 492 nm after 60 min in a microplate reader. The chromogenic solution employed was: 1 mM of vanillic acid, 500 µM of 4-aminotipyrine and 4 U/ml of peroxidase radish tipe II in 0.2 M of potassium phosphate buffer. Chloroglyline, MAO-A inhibitor and Pargilin, MAO-B inhibitor were used as positive control at 10 µM. Chemical analysis revealed five alkaloids, being the major compound identified as 11-hydroxyerythratidinone. The inhibitory potential for chlorogyline and pargyline were 76,016 % and 96,964 %, respectively. We obtained significant values ($p$ <0.05) for *E. verna* FEA comparing with control in a concentration dependent manner. The inhibitory concentration of 50% ($IC_{50}$) of *E. verna* FEA was 0.8538 mg/mL ± 0.1806. In summary, the results showed the potential of *E. verna* alkaloids as MAO inhibitors.

**Área: QPN** **Inscrição: 01060**

# Composição química e atividade antiparasitária *in vitro* de *Nectandra barbellata* Coe-Teixeira (Lauraceae)

**Vinicius S. Londero (PG),[1*] Guilherme M. Antar (PG),[2] João B. Baitello (PQ),[3] Thais A. Costa-Silva (PG),[4] André G. Tempone (PQ),[5] João Henrique G. Lago (PQ).[4] [*]E-mail: viniciuslondero@gmail.com**

*[1]Instituto de Ciências Ambientais, Químicas e Farmacêuticas, Universidade Federal de São Paulo (UNIFESP); [2]Instituto de Biociências, Universidade de São Paulo (USP); [3]Instituto Florestal de São Paulo, Secretaria do Meio Ambiente do Estado de São Paulo (SMA-SP); [4]Centro de Ciências Naturais e Humanas, Universidade Federal do ABC (UFABC); [5]Centro de Parasitologia e Micologia, Instituto Adolfo Lutz (IAL).*

Palavras Chave: Nectandra barbellata*, Sesquiterpenos eudesmanos,* Leishmania infantum*,* Trypanosoma cruzi*.*

## Highlights

In the present work, was performed the chemical and biological analysis of the leaves and barks extracts from *Nectandra barbellata* Coe-Teixeira, endemic to the Atlantic Forest, in order to obtain metabolites with antiparasitic activity, more specifically against *Leishmania infantum* and *Trypanosoma cruzi*.

## Resumo

Um estudo recente publicado pela Organização Mundial da Saúde,[1] demonstrou que a Doença de Chagas e a Leishmaniose estão entre as principais parasitoses tropicais que acometem a população brasileira. Diante de um arsenal medicinal diminuto para essas moléstias, a flora brasileira pode se valer de sua grande biodiversidade na busca por moléculas bioativas. Estudos fitoquímicos realizados com espécies do gênero *Nectandr*a têm mostrado grande diversidade estrutural de metabólitos bioativos,[2] contudo, não há na literatura informações atreladas à composição química e/ou potencial biológico de *Nectandra barbellata*. Assim, com intuito de obter resultados iniciais no que tange a aspectos químicos e biológicos desta espécie, foi realizada uma coleta de galhos e folhas de *N. barbellata* (2 g de cada material) para a preparação dos extratos brutos. Após esse procedimento, os extratos foram avaliados quanto à atividade antiparasitária *in vitro*, em formas promastigotas de *L. infantum* e tripomastigotas de *T. cruzi*, cujos resultados estão expostos na Tabela 1.

**Tabela 1**. Avaliação da atividade antiparasitária *in vitro* dos extratos dos galhos e folhas de *N. barbellata,* testados à concentração máxima de 300 µg/mL.

| Amostra | % de morte do parasita | |
|---|---|---|
| | *L. infantum* | *T. cruzi* |
| Extrato galhos | 100 | 100 |
| Extrato folhas | 100 | 100 |

**Figura 1**. Estruturas químicas dos compostos **1** e **2**

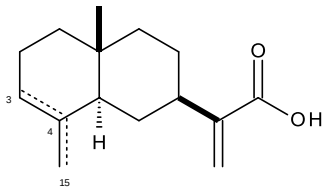


**1**: ácido cóstico ($\Delta^{4,15}$) e **2**: ácido isocóstico ($\Delta^{3,4}$)

Os dados revelam que os extratos são compostos por metabólitos com elevada atividade biológica para estes protozoários, os quais se tornaram inviáveis (100% de morte) na presença de ambos os extratos de *N. barbellata,* a 300 µg/mL. Estudos de desreplicação molecular empregando RMN de $^{1}$H e de $^{13}$C (500/125 MHz) indicaram a presença de sinais característicos de sesquiterpenos de esqueleto eudesmano. A comparação dos dados obtidos com aqueles descritos na literatura[3] permitiu inferir que os derivados majoritários são o ácido cóstico (**1**) e o ácido isocóstico (**2**) (Figura 1), metabólitos cujo potencial antiparasitário é ainda desconhecido. Assim, será dado prosseguimento aos procedimentos de extração em maior escala seguida do isolamento, identificação e caracterização dos demais compostos de modo a fornecer novos protótipos bioativos para o tratamento de doenças tropicais negligenciadas, especialmente Leishmaniose e Doença de Chagas, a partir de moléculas oriundas da biodiversidade brasileira.

**Referências:** [1]Martins-Melo, F.R. et al. *Bull World Health Organ*, **2016**, 94, 103-110. [2]Grecco, S.S. et al. *Tetrahedron: Asymmetry*, **2016**, 27, 793-810. [3]Garcez, F.R. et al. *Quim. Nova*, **2010**, 33, 1739-1742.

**Agradecimentos:** FAPESP (Projeto 2017/17044-1) e CNPq.

**Área: QPN** **Inscrição: 01070**

# Chemical composition of cuticular waxes of Bignonieae species (Bignoniaceae)

**Juliana C. S. Carvalho (PG)[1], Lúcia G. Lohmann (PQ)[1], Marcelo J. Pena Ferreira (PQ)[1]**

**jucajado@usp.br**

[1]*Instituto de Biociências, Universidade de São Paulo, 05508-090, São Paulo, Brazil.*

Keywords: cuticular waxes, n-alkanes, Bignonieae, Bignoniaceae

## Highlights

Chemical composition of cuticular waxes of Bignonieae species (Bignoniaceae)
- The first study of chemical composition of cuticular waxes from 19 species of Bignonieae
- n-Alkanes were the predominant chemical constituents observed in cuticular waxes of the tribe

## Abstract

Bignonieae, with 21 genera and 393 species[1], is the largest tribe in the Bignoniaceae and the main clade of lianas in the Neotropics. Despite its importance, only few studies to date have characterized the chemical composition of the tribe. This work aims to describe the chemical composition of cuticular waxes of 19 species from Bignonieae. Species were collected along the Rio Negro, Amazonas, Brazil. Air-dried leaves were separately extracted three times with dichloromethane for 30 seconds. For each species, extracts were grouped and the solid was subjected to recrystallization with methanol, after solvent removal. Derivatization of the insoluble material was carried out with pyridine and BSTFA (*N,O-bis-(trimethylsilyl)-trifluoroacetamide*) for GC/MS analysis. A total of 40 compounds were identified and the results are summarized in Table 1.

Table 1. Chemical class profiles (%) obtained from cuticular waxes of nineteen species of tribe Bignonieae

| | *Adenocalymma apurense* | *Adenocalymma schomburgkii* | *Amphilophium magnoliifolium* | *Amphilophium mansoanum* | *Anemopaegma foetidum* | *Anemopaegma paraense* | *Bignonia aequinoctialis* | *Bignonia sciuripabulum* | *Fridericia nigrescens* | *Fridericia triplinervia* | *Fridericia sp.* | *Martinella obovata* | *Pachyptera kerere* | *Pleonotoma sp. 1* | *Pleonotoma sp. 2* | *Pyrostegia cinerea* | *Tanaecium bilabiatum* | *Tanaecium jaroba* | *Tanaecium pyramidatum* |
|---|---|---|---|---|---|---|---|---|---|---|---|---|---|---|---|---|---|---|---|
| n-Alkanes | 68.50 | 54.53 | 75.75 | 50.41 | 87.36 | 66.70 | 15.25 | 88.69 | 46.69 | 7.63 | 97.68 | 55.06 | 43.45 | 59.69 | 98.31 | - | 90.97 | 47.01 | 45.18 |
| Alcohols | 0.15 | 11.70 | 1.10 | 4.89 | - | 0.70 | 4.85 | 3.06 | 0.72 | 7.36 | 0.19 | 2.44 | 4.04 | 1.26 | - | - | 1.01 | 1.34 | 1.83 |
| Fatty acids | 5.13 | 12.67 | 16.80 | 16.05 | 12.37 | 7.28 | 64.33 | 2.41 | 6.78 | 13.14 | 0.73 | 3.38 | 5.95 | 4.67 | - | 54.67 | 6.00 | 26.02 | 19.53 |
| Terpenoids | 0.23 | 12.18 | - | 0.62 | - | 0.56 | - | 0.15 | 0.45 | 0.22 | - | 3.72 | - | 0.11 | - | - | - | - | 0.09 |
| Total identified | 86.93 | 91.09 | 91.64 | 71.96 | 99.73 | 75.24 | 84.43 | 94.31 | 54.64 | 28.35 | 98.6 | 64.59 | 53.44 | 71.11 | 98.31 | 54.67 | 97.98 | 74.36 | 90.88 |

We found a predominance of n-alkanes, especially $C_{29}$, $C_{31}$ and $C_{33}$ homologous in cuticular waxes of most species of Bignonieae analyzed in this work. However, *Bignonia aequinoctialis, Fridericia triplinervia* and *Pyrostegia cinerea* showed a conspicuous predominance of fatty acids. Four species of the Bignoniaceae Paleotropical clade (*Kigelia africana*, *Markhamia acuminata*, *Newbouldia laevis* and *Spathodea campanulata*) had their chemical composition of cuticular waxes analysed previously[2]. Out of these four species, n-alkanes were observed as predominant components only in *K. africana* with $C_{31}$ and $C_{33}$ homologous representing the main constituents. Therefore, the chemical class of the n-alkanes seems to represent a chemotaxonomic marker of Bignonieae exclusively, although further studies are needed to confirm this hypothesis.

Acknowledgments: Fundação de Amparo à Pesquisa do Estado de São Paulo (FAPESP; Grant # 2012/50260-6) and Conselho Nacional de Desenvolvimento Científico e Tecnológico (CNPq).

References: [1]Lohmann, L.G.; Taylor, C.M. 2014. A new generic classification of tribe Bignonieae (Bignoniaceae). *Ann. Missouri Bot. Gard.* **99:** 348-489. [2]Gorgmann, R; Schreiber, L.; Kolodziej, H. 2004. Cuticular wax profiles of leaves of some traditionally used African Bignoniaceae. *Z. Naturforsch. C* **59**: 631-635.

**Inscrição: 01075**
*(Inserir o número de inscrição do autor que fez a submissão)*

***Área:***
***__QPN_____***

# Evaluation of Acaricidal Activity of Extracts of *Spilanthes acmella* (Jambu) against *Tetranychus urticae* and Isolation of Spilanthol

**Tainá M. Arrospide (IC)[1]* André P. Liesen (PQ)[1], Claudio A. Camara (PQ)[1], Marcílio M. Moraes (PQ)[1]**

**Milena M. Silva (PG)[1]**

**taina_arrospide@hotmail.com**

[1]*Departamento de Química, UFRPE.*

Keywords: *Spilanthes acmella; Spilanthol; Alkylamides; Acaricidal Activity.*

## Highlights

Acaricidal activity of *Spilantes acmella* extracts against *Tetranychus urticae;*
Quantification of *spilanthol* in extracts of *Spilantes acmella.*

## Resumo/Abstract

*Spilantes acmella* (L.) known as "jambu" is an herb that occurs most abundantly in the northern region of Brazil, in the state of Pará. Some alkylamides are present in this species, among of them spilanthol. This compound has been reported to possess various biological activities such as anesthetic activity, antibacterial activity and larvicidal activiy against *Aedes aegypti*. In this work, was performed the extraction of flowers and leaves from *S. acmella* (L) toward the spilanthol isolation and evaluation of the acaricidal activity against *Tetranychus urticae* of the obtained extracts. The ethanolic extraction of the different parts of S. acmella showed a higher concentration of spilanthol in the flowers (23.73%) than the leaf extract (16.72%). These ethanolic extracts were partitioned using n-hexane, chloroform and ethyl acetate. The presence of spilanthol in the hexanic extract of the flowers was confirmed by comparison of the mass spectra data found in the literature. The compound was carried out showing an isolation yield of 23.44% from the flower extract. On the other hand, the compound was not detected in the leaf extract. This result is in agreement with the literature. *T. urticae* was susceptible to flower extract, presenting LC50 of 1.63 mg/mL, but on the leaf extract did not present susceptibility. Structural modifications of the isolated spilanthol toward new analogues have been performed by our research group and the results of its biological activities evaluations will be reported in due course.

**Área: QPN** **Inscrição: 01143**

# Chemical study of *Myrcia sylvatica* (G. Meyer) DC. leaves

**Jéssica P. S. Delgado (PG)[1], Bárbara H. S. Duarte (PG)[1], Marcia M. Cascaes (PQ)[2], Giselle M. S. P. Guilhon (PQ)[1], Eloisa H. A. Andrade (PQ)[1,2], Lourivaldo S. Santos (PQ)[1].**

**jeproencia@hotmail.com; giselle@ufpa.br**

*[1]Programa de Pós-graduação em Química, ICEN, Universidade Federal do Pará; [2]COBOT, Museu Paraense Emílio Goeldi*

keywords: *Myrcia sylvatica, Triterpenes, Essential oils, Sesquiterpenes*

## Highlights

Volatile and non-volatile compounds from *Myrcia sylvatica* leaves. Essential oils rich on cariofilene (E), γ-elemene and germacrene–D. Isolation of common triterpenes and steroids.

## Abstract

Some Myrtaceae species have important uses by traditional Brazilian communities to treat many diseases. Among those species, there is one called *Myrcia sylvatica* included in the group of species known as “pedra-ume-caá” or vegetal insulin, which is used to treat diabetes[1]. Studies have shown the anesthetic and sedative effects of *M. sylvatica* essential oils on fish with preventing stress response and excess of reactive oxygen formation[2]. Considering the pharmacological potential of Myrtaceae species, the antioxidant activity of *Myrcia* species, the traditional use of *M. sylvatica* and the lack of published studies on the chemical composition of this species, the objective of this work was to investigate the volatile and non-volatile compounds from *M. sylvatica* leaves of a specimen collected in the city of Acará, state of Pará, Brazil. Dry leaves were extracted by maceration with methanol. Classical chromatographic and usual spectrometric methods (NMR and MS) led to the identification of the triterpenes α-amirin and β-amirin and glycosylated sitosterol from the methanolic extract. The essential oils were obtained by hydrodistillation and steam distillation and analyzed by GC/MS. The chemical composition of the essential oil shows the predominance of the sesquiterpene caryophyllene (E), γ-elemene and germacrene-D. The yield of these compounds varied depending on the extraction method. Extration by hydrodistillation resulted in higher contents of those three compounds.

[1] SILVA, F.K.S., et al. *Biota Amazon.* 2015, *5*, 7–15.
[2] SACCOL, E.M.H., et al. Aquaculture Research, 2017, 48, 2012–2031.

**Área: QPN** **Inscrição: 01151**

# Method for isolation of flavonoids from *Solanum paludosum* with activity on the enzyme human topoisomerase II-α

**Arthur V. T. Oliveira (IC)[1]*, Amanda F. F. da Silva (IC)[1], Girliane R. da Silva (PQ)[1] , Celso A. Camara (PQ)[1], Tania M.S. Silva (PQ)[1]**

**viniciusufrpe725@gmail.com**

[1]*Laboratório de Bioprospecção Fitoquímica, DQ-UFRPE*

Palavras Chave: *Solanum paludosum, Flavonoides, Topoisomerase II-α humana*

## Highlights

- Method for isolation of flavonoids from *Solanum paludosum* (Solananceae)
- Evaluation of the inhibition on the enzyme human topoisomerase II-α

## Resumo/Abstract

A espécie *Solanum paludosum* (Solanaceae) é popularmente conhecida como jurubeba, jurubeba-brava, jurubeba-roxa e todomaka. É uma espécie rica em flavonoides metoxilados. Neste trabalho um método foi desenvolvido para o isolamento de flavonoides bioativos da espécie *Solanum paludosum* (Figura 1), a partir do extrato etanólico bruto, obtido dos galhos da planta, utilizando técnicas de cromatografia clássica e moderna (analítica e preparativa). Foram isolados os flavonoides 3,4',7,8-tetra-*O*-metilgossipetina (1), 7-*O*-metilcanferol (ramnocintina, 2), 3,7-*O*-dimetilcanferol (kumatakenina, 3), 3,7,4',5'-tetra-*O*-metilmiricetina (4), 3,3',4',7,8-penta-*O*-metilgossipetina (5) e 3,3',4',7-tetra-*O*-metilquercetina (retusin, 7). A fração acetato de etila e os flavonoides isolados em maior quantidade foram testados para analisar o efeito sobre a ação da enzima topoisomerase II humana. O método desenvolvido para o isolamento dos flavonoides por HPLC permitiu obter uma fração rica só em flavonoides. Tanto a fração rica em flavonoides quanto os flavonoides isolados apresentaram atividade na inibição da enzima topoisomerase II-α humana.

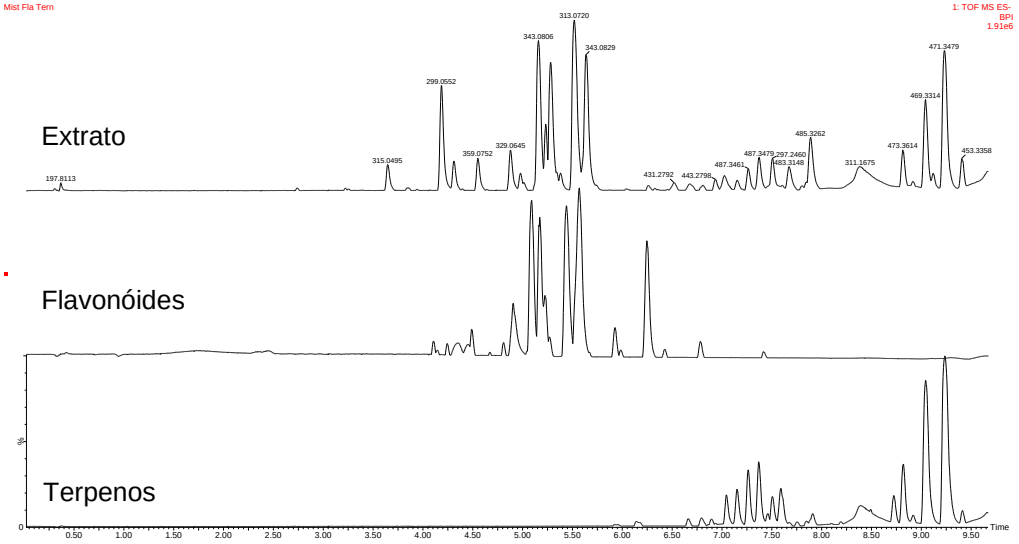


Figure 1. ESI base peak ion (BPI) chromatogram of the fractions from *Solanum paludosum* analyzed by UPLC-QTOF-MS/MS

Agradecimentos: CNPq e FACEP

**Área: QPN**
*(Inserir a sigla da seção científica para qual o resumo será submetido. Ex: ORG, BEA, CAT)*

**Inscrição: 01189**
*(Inserir o número de inscrição do autor que fez a submissão)*

# Antichemotactic activity of *Verbena montevidensis* and brasoside

**Angelica S. Vestena (PG),[1*] Krissie D. Soares (PG),[1] Gilsane L. von Poser (PQ),[1] José Angelo S. Zuanazzi (PQ),[1] Sergio A. L. Bordignon (PQ),[2] Miriam A. Apel (PQ).[1]**

**miriam.apel@ufrgs.br; angelica_signor@hotmail.com**

*[1] Programa de Pós-Graduação em Ciências Farmacêuticas, UFRGS; [2] Programa de Pós-Graduação em Avaliação de Impactos Ambientais, UNILASSALLE.*

Palavras Chave: *Verbena montevidensis, Verbenaceae, Brasoside, antichemotactic activity.*

## Highlights

Anti-inflammatory activity through the inhibition of the process of neutrophil migration of *Verbena montevidensis* and brasoside

## Resumo/Abstract

The genus *Verbena* (Verbenaceae) comprises about 44 species and this genus have been described in regions of South and North America. Many species of the genus *Verbena* are used in folk medicine for the treatment of inflammation, to relief pain and treat liver (intoxication). These effects are related to the secondary metabolites present in these plants, especially flavonoids, iridoids and phenylethanoids. This study aims to evaluate the antichemotactic activity of the methanolic extract of *V. montevidensis* and brasoside, isolated product of this extract, obtained from leaves. The plant material was collected in Quevedos-RS, dried, milled and macerated with methanol until exhaustion. The antichemotactic activity was carried out according to the modified Boyden chamber method. The leucocytes migration through the filter was measured using optical microscope. Samples were tested at concentrations from 0.1 to 10 µg/mL, using indomethacin as positive control and a neutrophil suspension without treatment as negative control. The results demonstrated inhibition of leukocyte migration 58% (10 µg/mL) and 100% (5 µg/mL) for *V. montevidensis* and brasoside, respectively. All samples in the different concentrations inhibited significantly leukocyte migration ($P < 0.05$) when compared to the negative control. It is observed that the isolated product showed higher activity in the lower concentration in comparison to extract, thus, the presented effect of the extract can be attributed to the isolated product. So, the samples tested could present antichemotatic activity through the inhibition of the process of neutrophil migration at the initial stage.

**Área: PQN** **Inscrição: 01194**

# Phytochemical screening of dried leaves of *Calea pinnatifida*(R. Br.) Less.

**Júlia Murozaki de Amorim (IC), Robson Miranda da Gama (PQ), José Armando Júnior[1] (PQ).**

**juliamurozaki@gmail.com; prof.armandojr@gmail.com**

*[1]Faculdade de Medicina da Fundação do ABC (FMABC), Laboratório Didático e de Pesquisa do Curso de Farmácia, CEP 09060-650, São Paulo, Brazil*

Key words: Medicinal Plants, Secondary metabolites, Phytochemical screening, *Calea pinnatifida* (R.Br) Less.

## Highlights

The present study describes a phytochemical screening, using qualitative assays, to determine the secondary metabolites and active principles of *Calea pinnatifida* (R. Br.) Less.

## Abstract

Phytochemicals occur naturally in medicinal plants and its main function is to act as an important defense mechanism and, consequently, to protect against several diseases[1]. The genus Calea is distributed essentially in tropical and subtropical regions of the America[2]. Some important biological activities (anti-inflammatory, antiplasmodal, antifungal, antimicrobial and anticancerigenic) were attributed to this genus[3].

The present study describes the phytochemical screening of *Calea pinnatifida* (R. Br.) Less (Fig. 1) cultivated and collected at FMABC Medicinal Botanical Garden. The collected leaves were dried, powdered and stored in glass dark flask. As there are few studies on the anatomical characteristics of this plant, histological sections to characterize it were performed, revealing the presence of anisocytic stomata (Fig 2) and nonglandular trichomes (Fig 3).

**Figure 1**

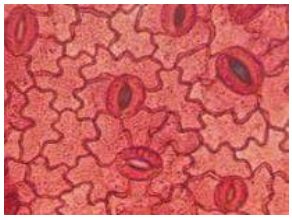

**Figure 2**

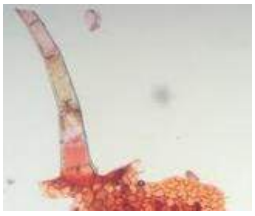

**Figure 3**

The phytochemical screening performed for triterpenes/steroids, alkaloids, anthraquinones, coumarins, flavonoids, saponins, and tannins were carried out according to the methods described in the literature. The color intensity of the solution or the precipitate formed were used as analytical responses of these assays[4] (Table 1).

The plant material also indicated the presence of secondary metabolites with potential biological activities, especially polyphenols (tannins and flavonoids) to which anti-inflammatory and antioxidant properties are strongly attributed.

Table 1. Phytochemical composition of *Calea pinnatifida* (R. Br.) Less

| Plant Constituents | Interference |
|---|---|
| Alkaloids | + |
| Anthraquinones | - |
| Coumarins | - |
| Flavonoids | + |
| Saponins | + |
| Tannins | + |
| Triterpenes/Steroids | - |

1] Krishnaiah, D.; Sarbatly, R.; Bono, A. *Biotechnology and Molecular Biology Review*, (2007), 1 (4), 97-104.
2] Roque, N.; Carvalho, V. C. *Rodriguésia*, (2011), 62 (3) 547-561.
3] Marchetti G. M. *et al*. *Journal of Experimental Pharmacology* (2012), 4157-4162.
4] Brasil. Farmacopeia Brasileira, Vol. 2. Brasília: Anvisa, 2010, 546p.

**Área: QPN Inscrição: 01264**

# Avaliação *in vitro* da atividade antifúngica e prospecção fitoquímica da *Lafoensia pacari* (Mangaba Brava)

**Anne K.M. Santos (IC),[1*] Fernando J.C. Carneiro (PQ),[1] Adriano S. Fonseca (IC),[1] Edelson J. S. Dias (P.G),[1] Marcos B.P. Câmara (PG),[1] Daniely V.V. Cardoso (PQ).[2]**

**E-mail: annemaiorana10@gmail.com**

*[1]Departamento Acadêmico de Química, IFMA; [2]Departamento de Biomedicina, UNESA*

Palavras Chave: *fitoquímica, metabólitos secundários, antifúngica.*

## Highlights

Antifungal activity evaluation *in vitro* and phytochemical prospection from of *Lafoensia pacari* (Mangaba Brava). The vegetal species *Lafoensia pacari* was collected in the village of Contrato, in the city of Morros-MA. Using the extracting solvent hydroalcoholic 70% in the proportion of 1:3 (m/v), was determined the phytochemical prospection of the species according to Matos(1997) and the antifungal activity was determined by drilling technique in Sabouraud medium and through serial microdilutions, demonstrating a fungicidal capacity in all strains of Candida genus.

## /Abstract

No Brasil, vem crescendo o número de estudos acerca de plantas que possuem potencial farmacológico, a partir da medicina popular. Contudo, é de suma importância conhecer os compostos químicos das espécies vegetais e avaliar sua presença nos mesmos, identificando grupos de metabólitos secundários relevantes (SIMÕES et al., 2004). Da mesma forma, os testes de sensibilidade in vitro, para fungos, têm importância na verificação de resistência de microrganismos, para o controle da terapêutica antimicótica e para pesquisa de novas substâncias alternativas para o tratamento, como por exemplo, a utilização de extratos vegetais (ALVES et al., 2006), onde destaca-se a *Lafoensia pacari*. Espécie esta, coletada no povoado Contrato, na cidade de Morros–MA, sob a localização S 02 ° 54 '47,6 "e W 043 ° 55' 30,1". Uma vez seca as cascas, o extrato foi obtido utilizando o solvente de extração hidroalcoólico 70% na proporção de 1: 3 (m / v) e seguindo-se de acordo com os procedimentos descritos por Francisco Matos(1997), foram realizados testes fitoquímicos para a identificação dos metabólitos contidos no extrato bruto hidroalcoólico da casca da planta, resultando-se conforme o (Quadro1).Posteriormente, o extrato foi submetido ao evaporador rotativo sob pressão reduzida, com temperatura controlada até 50 ° C, obtendo a concentração final de 2,9mg / mL. Utilizaram-se cepas padrão ATCC das seguintes leveduras: Candida albicans (ATCC 14053), Candida krusei (ATCC 6258) e Candida parapsilosis (ATCC 22019). A atividade antifúngica foi determinada pela técnica de perfuração em meio Sabouraud e através de microdiluições seriadas, evidenciando-se a capacidade fungicida em todas as cepas de gênero Candida, observadas nos seguintes resultados acerca do extrato bruto hidroalcoolico da casca da espécie *Lafoensia pacari*: MFC: 0,36 mg / mL, 0,18 mg / mL e 0,09 mg / mL a C. krusei, C . albicans e C. parapsilosis.

**Quadro1:** Resultados da prospecção fitoquímica do extrato bruto hidroalcoólico da espécie *Lafoensia p.*

| Metabólitos Secundários | Resultados | Metabólitos Secundários | Resultados |
|---|---|---|---|
| Fenóis | - | Flavononas | ++ |
| Taninos pirogálicos | +++ | Flavonóis, Flavononas, Flavanonas e/ou Xantonas, livre heterosideos | + |
| Taninos flobabênicos | - | Catequinas (confirmação) | - |
| Antocianinas e Antocianidinas | + | Esteróides (Livres) | ++ |
| Flavononas, Flavonóis e Xantonas | - | Triterpenoides Pentacíclico (Livre) | - |
| Chalconas e Auronas | + | Saponinas | +++ |
| Flavonóis | ++ | Confirmação de saponinas | +++ |
| Leocoantocianidinas | +++ | Alcalóides | +++ |
| Catequinas | - | **Legenda: forte(+++), médio(++), baixo(+) e insufic.(-)** | |

**Referências:**

ALVES, M. A. et al. Revista Brasileira de Farmacognosia. Atividade antifúngica do extrato de Psidium g. Linn. 16(2): 192-196, Abr./Jun. 2006.

SIMÕES, C.M.O. et al. Farmacognosia: da planta ao medicamento. 5. ed. Porto Alegre/Florianópolis: Editora da UFSC, 1102p. 2004.

**Área: QPN** **Inscrição: 01333**

# Semi-high resolution α-glucosidase and PTP1B inhibition profiling for investigation of antidiabetic constituents in *Picramnia bahiensis*

**Leila Gimenes (PG)[1,2], Maria F. G. F. da Silva (PQ)[1], Paulo C. Vieira (PQ)[1], João B. Fernandes (PQ)[1], Dan Staerk (PQ)[2]**

**leilagimenes@gmail.com**

[1] *Chemistry Department – Federal University of São Carlos, UFSCar, São Carlos, SP, Brazil*
[2] *Department of Drug Design and Pharmacology, University of Copenhagen, Copenhagen, Denmark*

Keywords: *Picramnia bahiensis, Anthrone, α-glucosidase, PTP1B*

## Highlights

Type 2 diabetes (T2D) is a chronic metabolic disorder that constitutes a global health problem. α-glucosidase is an enzyme involved in carbohydrate metabolism in the brush border of the small intestines. *Picramnia* shows high diversity of secondary metabolites, such as anthrones, oxanthrones, anthraquinones, coumarins, and triterpenes. Our on-going screening programme for antidiabetic compounds has evaluated the inhibitory profiling of *P. bahiensis.* The phytochemical investigation to this specie yielded in the isolation of two new C,O-diglycosides anthrones.

## Abstract

Type 2 diabetes (T2D) is a chronic metabolic disorder, and the incidence of T2D increases at an alarming rate and constitutes a global health problem[1]. The genus *Picramnia* shows high diversity of secondary metabolites, such as anthrones, oxanthrones, anthraquinones, coumarins, and triterpenes[2]. In this context, the use of plants as a source for inhibitors of α-glucosidase, an enzyme involved in carbohydrate metabolism in the brush border of the small intestines, seems as an attractive approach. In our on-going screening programme for antidiabetic compounds from plants, the methanolic extract from roots *P. bahiensis* showed an inhibitory concentration ($IC_{50}$) of 43.5 µg/mL towards α-glucosidase, and was therefore selected for further investigation. The extract was microfractionated in 176 wells of 96-well microplate, evaporated in a speed vacuum, and thus the α-glucosidase and PTP1B semi-high resolution inhibition assay was performed. Further analyses are being carried out for identification of the bioactive constituents. Besides the construction of the biochromatogram, the extract was also purified on reversed-phase $C_{18}$ by HPLC yielding in the isolation of two new C,O-diglycosides anthrones.These results are very promising and should contribute for chemosystematics of plants of genus *Picramnia*.

***Acknowledgements**:* FAPESP is acknowledged PhD scholarship to Leila Gimenes in Brazil and abroad (FAPESP Grants # 2013/20458-1, 2016/18024-1), as well CNPq and CAPES for the financial support received in Brazil. The Carlsberg Foundation, and the Danish Agency for Science, Technology and Innovation via the National Research Infrastructure funds for the Infrastructure used on this work.

**References:**

[1] Silva, E.L. *et al*., *Molecules*. **21**: 782-793 (2016).
[2] Rodríguez-Gamboa, T. *et al., J. Braz. Chem. Soc.* **12**: 386-390 (2001).

**Área: QPN** *(Inserir a sigla da seção científica para qual o resumo será submetido. Ex: ORG, BEA, CAT)*

**Inscrição:01385** *(Inserir o número de inscrição do autor que fez a submissão)*

# Estudo Químico do Extrato Acetato da Casca do Fruto da *Pithecoctenium crucigerum* Gentry (Bignoniaceae)

**Kelvin Gomes Picro (PG),[*1,2] Maísa Borges Costa (PQ),[1] Erika Thalyta Veras Pereira (PG),[2] Moacir Rossi Forim (PQ).[2]**

**[*]kelvinpicro@hotmail.com; maisabc@gmail.com**

*[1]-Laboratório de Síntese, Isolamento e Modificações de Compostos Orgânicos (LabSIMCO) – Campus de Ciências Exatas e Tecnológicas Henrique Santillo – Universidade Estadual de Goiás (UEG-CCET); Caixa Postal 459, Cep. 75132-400 – Anápolis-Go –Brasil*

*[2]-Departmento de Química, Universidade Federal de São Carlos (UFSCar), São Carlos, São Paulo*

Palavras Chave: *Pithecoctenium crucigerum, Amphilophium crucigerum, Bignoniaceae, CLAE, Metabólitos especiais.*

## Highlights

Chemical Study of the Acetate Extract of Fruit Bark of *Pithecoctenium crucigerum* Gentry (Bignoniaceae)
Acetate extract prepared from the fruit bark of *Pithecoctenium Crucigerum* was the most promising for the study.
The substance was isolated by HPLC with automatic collector and UV Vis detector

## Resumo/Abstract

*Pithecoctenium crucigerum* (sinônimo *Amphilophium crucigerum)* também conhecido como "pente-de-macaco" é uma espécie pertencente à família Bignoniaceae (CARNEIRO, 2010).

Este trabalho tem como objetivo a identificação, isolamento e a elucidação estrutural, de metabólitos especiais presentes na casca do fruto dessa espécie.

A partir da técnica de remaceração a frio, 150 g da casca triturada foi remacerada com solventes em ordem crescente de polaridade (hexano ⇒ diclorometano ⇒ acetato de etila ⇒ etanol) para a formação dos respectivos extratos brutos.

Inicialmente, optou-se pelo estudo com o extrato bruto acetato (EBAc) (164,6 mg). O EBAc foi cromatografado em coluna Sephadex LH-20 (h= 56cm e d= 6cm) com Metanol:Clorofórmio 1:1. Posteriormente, as amostras foram reunidas conforme sua semelhança. Através do equipamento de CLAE UV/Vis em 280 nm (Figura 1), com coletor automático acoplado, foi isolada a substância com o tempo de retenção em 34 minutos, sendo submetida às análises espectrométricas.

Figura 1 - Cromatograma da amostra proveniente da Sephadex

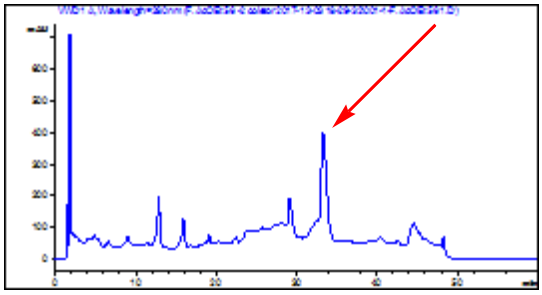

A análise estrutural em RMN $^{1}H$ unidimensional evidenciou hidrogênios aromáticos, olefínicos, e de grupos metoxila (3,9 ppm). O RMN de $^{13}C$ destaca a presença de C carbonílico de um éster cíclico (165 ppm), bem como o C ligado ao grupo $OCH_3$ (50,7 ppm). Estudos em RMN bidimensional estão sendo desenvolvidos para a elucidação estrutural desta provável lactona.

**Agradecimentos**

Os autores agradecem a CCET/UEG e DQ/UFSCar e aos órgãos de fomento a pesquisa como a CAPES e ao ProBIP/2016.

**Referências Bibliográficas**

CARNEIRO, E., Pente-de-macaco. Disponível em: <http://www.caliandradocerrado.com.br/2010/09/pente-de-macaco.html>. Acesso em 1 de fevereiro de 2018.

**Área: QPN** **Inscrição: 01394**

# Prospecção fitoquímica e atividade antifúngica da espécie vegetal *Humiria balsamifera* (Mirim).

**Juliane C. Marques (IC)[1*], Marcos B.P. Câmara (PG)[1], Georgiana E. C. Marques (PQ)[1], Antônio J.C. Filho (PQ)[1], Francyelle C. Moraes (PQ)[2], Andrey L.M. Melo (IC)[1], Edelson de J. S. Dias(PG)[1]**

**Email: jujucmarques@hotmail.com**

*[1]Departamento Acadêmico de Química, IFMA; [2]Departamento de Biomedicina, Estácio - MA*

Palavras Chave:*Fitoquímica, Metabolitos secundários, Antifúngica.*

## Highlights

Phytochemical prospection and antifungal activity of the plant species *Humiria balsamifera* (Mirim). In the phytochemical analysis of Humira balsamifera, it observed several types of classes of secondary metabolites identified with the potential of pharmacological action and antifungal activities.

## Resumo/Abstract

Candidiasis is a cunning fungal infection caused by the development of species of *Candida* in a variety of anatomical sites. The treatment of this disease employs various antifungal agents, which may cause undesirable side effects or may induce microbial resistance, especially in immunocompromised individuals. In this context, several studies have been conducted to look for plants of the Brazilian Cerrado that are empirically known for the antifungal properties, in which *Humiria balsamifera* is the most noticeable species. *Humira balsamifera* samples were collected in a village inside of the city of Morros – at location S 02 ° 33 '13.44 "and W 044 ° 13' 52.9". After drying, the extracts were obtained by using a 70% hydroalcoholic solvent in the ratio of 1: 3 (w / v). The extract was then subjected to a rotary evaporator under reduced pressure at a controlled temperature of up to 50°C, obtaining a final concentration of 30.8 mg / ml. Standard strains ATCC of the following yeasts were used: *Candida krusei* (6258), *Candida albicans* (14053), *Candida parapsilosis* (22019) and clinical isolates of *Candida glabrata* and *Candida albicans*. The antifungal activity was determined by the drilling technique in Sabouraud conditions and by serial microdilution. Only through the microdilution technique was it possible to verify the strong antifungal potential of the leaf extract of *Humiria balsamifera*. MIC and MBC of only 0.096 mg / mL were obtained before all yeast samples were tested, both the ATCC strains and the clinical specimens.

Figure 1: Kind of secondary metabolite classes present in the hydroalcoholic extract

| Constituinte | Resultados |
|---|---|
| Fenois | - |
| Taninos pirogálicos (taninos hidrolisáveis) | + |
| Taninos flobabênicos (taninos condensados ou catéquicos) | +++ |
| Antocianinas e Antocianidinas | S |
| Flavononas, Flavonóis e Xantonas | ++ |
| Chalconas e Auronas | S |
| Flavonois | - |
| Leocoantocianidinas | - |
| Catequinas (taninos catéquicos) | S |
| Flavononas | - |
| Flavonóis, Flavononas, Flavanonas e/ou Xantonas, livre heterosideos | - |
| Catequinas (confirmação) | S |
| Esteróides (Livres) | ++ |
| Triterpenoides Pentacíclico (Livre) | - |
| Saponinas (Heterosídeos saponínicos) | +++ |
| Confirmação de saponinas | +++ |
| Alcalóides | ++ |

**Forte:** +++ **Médio:** ++ **Baixo:** + **Suspeito:** S **Insuficiente:** -

**Área: QPN** *(Inserir a sigla da seção científica para qual o resumo será submetido. Ex: ORG, BEA, CAT)*

**Inscrição: 1398** *(Inserir o número de inscrição do autor que fez a submissão)*

# Atividade antioxidante por HPTLC-DPPH dos extratos de folhas, caule e raiz de *Pleonotoma jasminifolia* Kunth Miers. (Bignoniaceae)

**Cristiana Nunes Rodrigues (IC), Waldireny C. Rocha (PQ)*, Klenicy Kazumi de Lima Yamaguchi (PQ)**

**waldirenyrocha@ufam.edu.br; wal2002@gmail.com**

**Docentes e discente do Colegiado do Curso de Licenciatura em Ciências: Biologia e Química do Instituto de Saúde e Biotecnologia-ISB. Universidade Federal do Amazonas-UFAM;**

Palavras Chave: *cipó cacheado; Pleonotoma HPTLC; DPPH.*

## Highlights

- ✓ The chromatographic profile and antioxidant activity by HPTLC-DPPH of extracts from leaves, stems and roots of *Pleonotoma jasminifolia* Kunth Miers. (Bignoniaceae);
- ✓ A direct HPTLC assay was developed for the determination of ativity of the extratcs of the *Pleonotoma jasminifolia* Miers.) Bignoniaceae;
- ✓ The methanol extract by maceration of the root was the one that presented greater antioxidant activity and according to the Phytochemical prospecting carried this extract shows terpenes and phenols;

## Resumo

A espécie *Pleonotoma jasmonioides* pertence à família Bignoniaceae ocorre pela Amazônia. É utilizada como medicinal sendo as raízes úteis para tosse e as folhas em queimaduras e algumas vezes é cultivado pelo potencial paisagístico de suas folhagens[1]. Até o momento não foi encontrado, na literatura consultada, nenhum trabalho sobre as substâncias químicas presentes nesta espécie. As diferentes partes das plantas, folhas, caule e raiz, foram secas a temperatura ambiente e moídas em moinho de facas. A extração foi feita macerando 50 g de cada parte da planta em banho ultrassom com metanol por 10 minutos sem aquecimento. A extração foi realizada em triplicata. As amostras foram aplicadas em placas de sílica gel 60 F de alta resolução, com suporte de vidro (10x10 cm; Merck) com uma seringa de 100 mL (Hamilton, Suiça) usando o aplicador automático Linomat V (Camag, Suiça) em bandas de 6 mm. As placas foram desenvolvidas em cuba cromatográfica de vidro como sistema hexano e acetato de etila na proporção de 1:1 (UR=78% e T= 30 °C). Depois de desenvolvida as placas foram secas por 15 minutos e mergulhada em uma solução 0,05 mM de 1,1- difenil-2-picrilidrazil em metanol por 5 segundos [2]. As placas foram secas e envolvidas em papel alumínio a temperatura ambiente (33°C) for 90 s. O extrato em metanol por maceração da raiz foi o que apresentou maior atividade antioxidante e segundo a prospecção fitoquímica realizada apresenta terpenos e fenóis. A técnica de HPTLC-DPPH se apresentou como de uma metodologia rápida e reprodutível.

Agradecimento à UFAM pela bolsa de Iniciação científica e a estrutura dos laboratórios e regentes.

1.Gomes, Beatriz Machado. Revisão de *Pleonotoma* Miers (Bignoniaceae). Dissertação de Mestrado. Instituto de Ciências Biológicas, Universidade de Brasília, 96p., 2006.

2. Pozharitskaya, Olga N.; Ivanova, Svetlana A; Shikov, Alexander N.; Makarov, Valery G.: Curcuma longa using HPLC-DPPH method. Phytochemical Analysis, 19(3), pp.236-243, 2008.

3. Simões, Cláudia M. Oliveira. Farmacognosia da Planta ao Medicamento - 6 ª Ed. 2008.

**Área: ____QPN_____ Inscrição: __01145____**

# Obtenção de álcoois através de bioreduções de carbonilados utilizando células íntegras de *Phaseolus lunatus* (feijão-fava)

**Allana Kellen Lima Santos Pereira** (PQ),[1]* Maraylla Inácio de Moraes (PG),[2] Espedito de S. Saraiva (PG),[3] Edivan C. Vieira (PQ), [3] Franciglauber Silva Bezerra (PQ),[4] Luciana L. Machado (PQ), [5] Fátima Miranda Nunes (PQ),[6] Telma Leda Gomes de Lemos (PQ).[6]

*[1]Centro de Ciências e Tecnologia, UFCA; [2]Departamento de Química, IQ - UNESP; [3]Departamento de Química, UFPI; [4]CECITEC, UECE; [5]Departamento de Química, UFOB; [6]Departamento de Química, UFC.*

Palavras Chave:*Biotransformações, Enzimas, Aldeídos, Cetonas, Phaseolus lunatus*

## Highlights

Obtaining of alcohols through carbonylated bioreductions using whole cells of *Phaseolus lunatus* (fava beans)

Bioreduction of compunds carbonilic using whole cells; *Phaseolus lunatus* L used in biotranformation of carbonilic compounds; Obtaining alcohols from biotransformation reactions.

## Resumo/Abstract

As reações químicas envolvendo células inteiras têm sido estudadas em reações de biotransformação devido ao promissor potencial biotecnológico.[1,2,3] *Phaseolus lunatus L.* é uma planta herbácea, conhecida como feijão-fava, cultivada na Região Nordeste do Brasil. O objetivo foi identificar novas fontes biocatalíticas. Os substratos: acetofenona **(1)**, benzaldeído **(2)**, 4-(dimetilamino)benzaldeído **(3)**, 4-metoxibenzaldeído **(4),** cicloexanona **(5)**. Os produtos das reações foram analisados por GC/MS e RMN $^1$H. Em erlenmeyeres (250 mL) foram adicionados o biocatalisador (sementes de *P. lunatus,* 23 g), os substratos (200 mg) e 150 mL de água destilada, permanecendo em agitação por 72 h em um orbital shaker (150 rpm).[4] A mistura foi filtrada, submetida à extração líquido-líquido com AcOEt (3 x 50 mL), a fase orgânica foi seca com $Na_2SO_4$ anidro e concentrada em rota-evaporador, chegando ao extrato bruto da biorredução. Os bioprodutos: 1-feniletanol **(1a)**, álcool benzílico **(2a)**, álcool 4-(dimetilamino)benzílico **(3a)**, álcool 4-metóxibenzílico **(4a)**, cicloexanol **(5a)** foram purificados por coluna de gel de sílica. O substrato **(2)** foi reduzido a **(2a)** com conversão de 97%, enquanto que não houve reação com o **(3)**. O substrato **(4)** foi reduzido ao **(4a)** com conversão 86% além do ácido 4-metóxibenzóico. O *P. lunatus* apresentou uma baixa conversão, 5%, na biorredução de **(1)**, enquanto que **(5)** foi completamente reduzida a **(5a)**, >99%. Visto que as biorreduções de aldeídos e cetonas aos seus álcoois correspondentes apresentam conversões elevadas, com exceção de **(1)** e **(3)**, estamos no caminho certo.

Agradecimentos à FAPEPI, CNPq, UFPI, UFCA.

1. BERTINI, L.M.; LEMOS, T.L.G.; ALVES, L.A.; MONTE, F.J.Q.; de MATTOS, M.C.; de OLIVEIRA, M.C.F. Soybean (Glycine max) as a versatile biocatalyst for organic synthesis. **African Journal of Biotechnology**. 11, 7766-7770, 2012.

2. MACHADO, L. L.; MONTE, F. J. Q.; de OLIVEIRA, M. D. F.; de MATTOS, M. C.; LEMOS, T. L. G.; GOTOR- FERNANDEZ, V.; DE GONZALO, G.; GOTOR, V. Bioreduction of aromatic aldehydes and ketones by fruits- barks of Passiflora edulis. **Journal of Molecular Catalysis B: Enzymatic**, 54, 130-133, 2008.

3. ANDRADE, L. H.; UTSUNOMIYA, R. S.; OMORI, A. T.; PORTO, A. L. M.; COMASSETO, J. V. Edible catalysts for clean chemical reactions: Bioreduction of aromatic ketones and biooxidation of secondary alcohols using plants. **Journal of Molecular Catalysis B: Enzymatic**, 38, 84-90, 2006.

4. MACHADO, L. L.; SOUZA, J. S. N.; de MATTOS, M. C.; SAKATA, S. K.; CORDELL, G. A.; LEMOS, T. L. G. Bioreduction of aldehydes and ketones using Manihot species. **Phytochemistry**, 67, 1637-1643, 2006.

**Área: QPN**
*(Inserir a sigla da seção científica para qual o resumo será submetido. Ex: ORG, BEA, CAT)*

**Inscrição: 00230**
*(Inserir o número de inscrição do autor que fez a submissão)*

# SistematX, an online web-based cheminformatics tool for data management of secondary metabolites

**Marcus Tullius Scotti (PQ)[1]*, Chonny Herrera-Acevedo[1], Tiago Oliveira Branquinho (PQ)[2,3], Renan Paiva Oliveira Costa (IC)[1], Silas Yudi Konno de Oliveira Santos (PG)[1], Ricardo Pereira Rodrigues (PQ)[1], Luciana Scotti (PQ)[1], Fernando Batista Da-Costa (PQ)[3]**

**mtscotti@gmail.com;**

*[1]Postgraduate Program in Natural Products and Synthetic Bioactive, Federal University of Paraíba ; [2]Department of Pharmacy, Federal University of Sergipe (UFS-SE), [3]AsterBioChem research team, University of São Paulo (USP)*

Palavras Chave: *SistematX; secondary metabolites; data management; online web-based tool.*

## Highlights

http://sistematx.ufpb.br is an innovative web interface for the management of a secondary metabolite database and contains a wealth of useful information for the natural products scientific community.

## Resumo/Abstract

The traditional work of a natural products researcher consists in large part of time-consuming experimental work, collecting biota to prepare and analyze extracts and to identify innovative metabolites. However, along this long scientific path, much information is lost or restricted to a specific niche. The SistematX homepage is http://sistematx.ufpb.br, and the interface is implemented considering the following aspects: a) the ability to search by structure, SMILES (Simplified Molecular-Input Line-Entry System) code, compound name and species; b) the ability to save chemical structures found by searching; c) compound data results include important characteristics for natural products chemistry; and d) the user can find specific information for taxonomic rank (from family to species) of the plant from which the compound was isolated, the searched-for molecule, and the bibliographic reference and Global Positioning System (GPS) coordinates. The SistematX homepage allows the user to log into the data management area using a login name and password and gain access to administration pages. In this article, we introduced a modern and innovative web interface for the management of a secondary metabolite database. With its multiplatform design, it is able to be properly consulted via the internet and managed from any accredited computer. The interface provided by SistematX contains a wealth of useful information for the scientific community about natural products, highlighting the locations of species from which compounds are isolated.

**Área: QPN** **Inscrição: 00093**

# ANTIMICROBIAL ACTIVITY OF THE LICHEN *USNEA STEINERI* AND ISOLATED COMPOUNDS AGAINST PHYTOPATHOGENS

**Lucas S. Cintra (PG), Daiane F. Galvão Sampaio (IC), Maria Anita L. Vasconcelos (TC), Marcos G. Tozatti (PQ), Ana H. Januário (PQ), Patricia M. Pauletti (PQ), Márcio L. Andrade e Silva (PQ), Carlos H. G. Martins (PQ), Wilson R. Cunha*(PQ)**

**E-mail: wilson.cunha@unifran.edu.br**

*Universidade de Franca*

Keywords: *Antimicrobial activity, Difractaic acid, Usnea steineri, Usnic acid*

## Highlights

Four compounds were isolated from *Usnea steineri*, the antimicrobial activity was evaluated against phytopathogens, the compound usnic acid and difractaic acid were the most active.

## Resumo/Abstract

In the search for substitutes for synthetic compounds used to control diseases in agriculture, natural products are an alternative of economic and ecological interest very promising, where the use of compounds extracted of natural sources with a possible activity on phytopathogens inhibition could represent an option in the control of diseases in the field. In this study, we evaluated the antimicrobial activity of the extract and isolated compounds of *Usnea steineri* against six phytopathogens. A phytochemical study of the acetone extract of *U. steineri* was conducted and usnic acid, difractaic acid, norstictic acid and galbinic acid were isolated. The molecular identification was done through NMR $^{1}H$, NMR $^{13}C$ and mass spectrometry. The minimum inhibitory concentration (MIC) values were determined by using the broth microdilution method in 96-well microplates. The results showed that usnic acid and difractaic acid were the most effective against the microorganisms (Table 1). Although capable of inhibiting microbial growth, more studies are needed with these compounds to ensure the safe use. (Financial support: CNPq and FAPESP).

Table 1. Antimicrobial activity of the acetone extract of *Usnea steineri* and isolated compounds against phytopathogens

| Microorganisms | Minimum inhibitory concentration in µg.mL$^{-1}$ | | | | |
|---|---|---|---|---|---|
| | Samples | | | | |
| | 1 | 2 | 3 | 4 | 5 |
| *Macrophomina phaseolina* | 2000 | 500 | 500 | >2000 | >2000 |
| *Fusarium solani* | 2000 | 2000 | 250 | >2000 | >2000 |
| *Pestalotiopsis* sp | >2000 | 31.25 | 1000 | >2000 | >2000 |
| *Lasiodiplodia theobromae* | 2000 | 2000 | 500 | >2000 | >2000 |
| *Rhizoctonia solani* | >2000 | >2000 | 250 | >2000 | >2000 |
| *Colletotrichum gloesosporioides* | >2000 | 2000 | 1000 | >2000 | >2000 |

1. Acetone extract; 2. usnic acid; 3. difractaic acid, 4. norstictic acid; 5. galbinic acid

**Area: QPN** **Submission Number: 00143**

# *In vitro* cytotoxic potential of the crude extract of fungi derived from ascidians *Didemnum perlucidum* and *Botrylloides giganteum*

**Luis C. K. Filho (PG),[1*] Letícia P. Pimenta (PG),[1] Rita C. N. Pedroso (PG),[1] Rhenner N. A. Assis (IC),[1] Ester de O. dos Anjos (IC),[1] Wanderson Z. Cosme (TC),[1] Kátia. A. Siqueira (PG),[2] Marcos A. Soares (PQ),[2] Denise C. Tavares (PQ),[1] Ana H. Januário (PQ).[1] anahjanuario@gmail.com; luiskellner@gmail.com**

*[1]Natural Products Research Group, University of Franca, Franca, SP, 14404-600, Brazil; [2]Department of Botany and Ecology, University Federal of Mato Grosso, Cuiabá, MT, 78060-900, Brazil*

Keywords: *Ascidians, Marine fungi, Cytotoxicity*

## Highlights

Chemical study and cytotoxic potential of methanolic extracts from the marine-derived microorganisms *Alternaria solani, Penicillium citrinum, Pestalotiopsis sp, Hypocrea lixii*, and *Lasiodiplodia sp.*

## Abstract

Marine invertebrates have numerous bioactive metabolites and several associated microorganisms. The number of marine fungal species described in recent years (over 800) shows that researchers' interest in studying fungi associated with invertebrates has increased[1]. Studies have found that some microorganisms produce compounds that are the major components in host animals[2, 3]. In this study, the fungal species *Alternaria solani*-4A4, *Penicillium citrinum*-4A14, and *Pestalotiopsis sp.*-4A11 isolated from the ascidian *Didemnum perlucidum* and the fungal species *Hypocrea lixii*-5A7 and *Lasiodiplodia sp.*-5A12 associated with the ascidian *Botrylloides giganteum* were cultured in PDA medium and extracted by maceration in ethyl acetate/methanol (1:1), and their crude extracts were evaluated by means of *in vitro* cytotoxicity assays against the GM07492A cell line. *P. citrinum*-4A14, *A. solani*-4A4, and *Pestalotiopsis sp.*-4A11 derived from *D. perlucidum* presented distinct cytotoxicity against the tested cell; $IC_{50}$ values were 386.7; >2500.0, and 1440.0 µg/mL, respectively. The fungal strains isolated from *B. giganteum* presented $IC_{50}$ higher than 2500 µg/mL. A chemical study of the *P. citrinum*-4A14 extract was conducted by combining C-18 column and preparative HPLC, which led to the isolation of compound 1 (Rt 19.922 min, UV 248, 256, 315, and 328 nm) with ESI(+)MS $[M+H]^+$ 272.1501. The presence of methylene, methyl groups, and carbinolic carbons in the NMR spectra suggest that compound 1 has a terpenic nature. Further studies are underway to complete its structural elucidation.

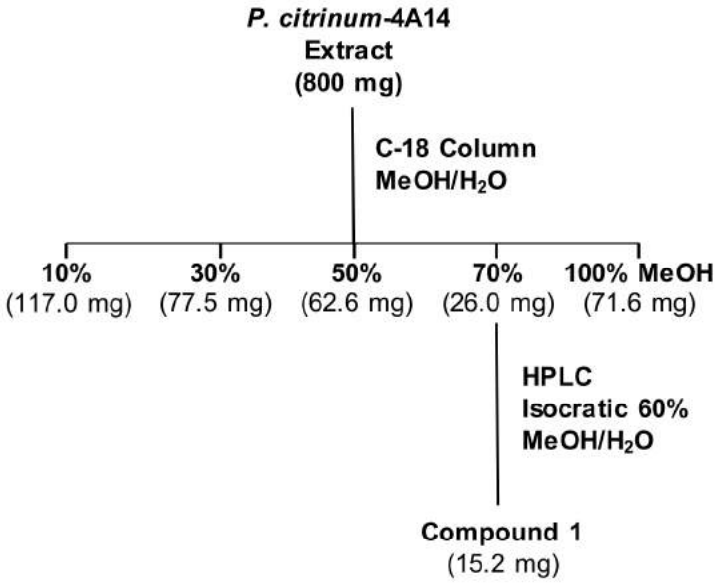


[1] Yarden, O. *Front Microbiol*.,5, 228, 2014.
[2] Radjasa, O. K.; Vaske, Y. M.; Navarro, G.; Vervoort, H. C.; Tenney, K.; Linington, R. G.; Crews, P. *Bioorg Med Chem.*, 19, 6658-74, 2011.
[3] Schmidt, E. W.; Donia, M. S.; Mcintosh, J.A.; Fricke, W.F.; Ravel, J. *J Nat Prod*., 75, 295-304. 2012.

**Área: QPN**
*(Inserir a sigla da seção científica para qual o resumo será submetido. Ex: ORG, BEA, CAT)*

**Inscrição: 459**
*(Inserir o número de inscrição do autor que fez a submissão)*

# Selective biotransformation of coumarins by *Cunninghamella elegans*

**Jainara Santos do Nascimento (PG)[1], João Carlos Silva Conceição (PG)[1], Wilson Elias Rozo Nuñez (PG)[1], Sílvio Cunha (PQ)[1], Eliane de Oliveira Silva (PQ)[1*]**

**elianeos@ufba.br**

[1]*Departamento de Química Orgânica, UFBA, Salvador, BA, Brasil*

Palavras Chave: Coumarin, Microbial transformation, Metabolites, Natural Products.

## Highlights

*Cunninghamella elegans* was able to selectively transform some coumarins.

Mono-hydroxylation and bulky group in the chemical structures are essential characteristics to coumarins biotransformation.

## Resumo/Abstract

Coumarins (1,2-benzopyrones) are ubiquitous in plants and comprising a vast array of biological properties. The great variety of applications of these compounds, combined to the difficulties in their isolation from natural sources, make them attractive for chemical synthesis and biotechnological studies. The biotransformation by microorganisms can generate chemical analogues with high selectivity, under mild and ecofriendly conditions. The aim of this study was to investigate the biotransformation of nine coumarins scaffolds (Figure 1) by the filamentous fungus *Cunninghamella elegans* ATCC 10028b. Firstly, the fungus was cultured in malt agar, for seven days, at 28°C. After this, *C. elegans* was transferred to 125 mL-Erlenmeyer flask containing 50 mL of Koch´s medium (glucose 0.18%; peptone 0.06%; yeast extract 0.04%) and 5 mg of each substrate separately dissolved in 200 μL of DMSO. All coumarins were previously synthetized through Pechmann reaction. The biotransfomation was carried out under agitation (120 rpm), at 28°C and during three days. Control flasks were incubated at the same conditions. Extraction using ethyl acetate yielded the crude extracts, which were analyzed by HPLC (reverse phase). *C. elegans* transformed the coumarins **4** and **7**, revealing the importance of only one hydroxyl group in the aromatic ring and a bulky group in the lactone ring to biotransformation of this compounds class. Taking into account that *C. elegans* is an important enzymatic system both for derivatives achievement and for mimic the mammalian metabolism, our results open new possibilities for the coumarins studies.

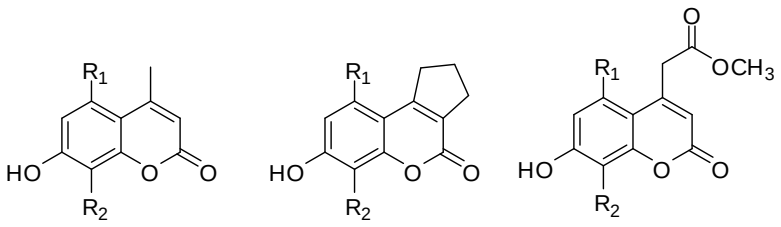


| | $R_1$ | $R_2$ |
|---|---|---|
| **1** | H | H |
| **2** | OH | H |
| **3** | H | OH |

| | $R_1$ | $R_2$ |
|---|---|---|
| **4** | H | H |
| **5** | OH | H |
| **6** | H | OH |

| | $R_1$ | $R_2$ |
|---|---|---|
| **7** | H | H |
| **8** | OH | H |
| **9** | H | OH |

**Figure 1:** Chemical structures of coumarins used in the biotransformation experiments.

**Área: QPN** **Inscrição: 00478**

# Dereplication of azaphilones from the Amazonian endophytic fungus *Penicillium sclerotium* by LC-QTOF-MS/MS and molecular networking

**Paulo A. L. Santiago (PG),[1,2] Danielle R. Guimarães (IC),[1] Mayane P. Souza (PG),[2] Célio F. F. Angolini (PQ),[3] Felipe M. A. da Silva, (PQ),[2] Emmanoel V. Costa (PQ),[2] Antonia Q. L. de Souza (PQ),[4] Afonso D. L. de Souza (PQ),[3] Hector H. F, Koolen (PQ).[1,*]**

***hkoolen@uea.edu.br**

*[1], Grupo de Metabolômica, Universidade do Estado do Amazonas – UEA; [2]Departamento de Química, Universidade Federal do Amazonas; [3]Instituto de Química, Universidade Estadual de Campinas – UNICAMP; [4]Faculdade de Ciências Agrárias – UFAM.*

Keywords: *Azaphilones, Dereplication, Endophytic fungus, Mass Spectrometry, Pigments*

## Highlights

1. From the fermented broth of *Penicillium sclerotium*, an antibacterial pigment rich fraction was obtained. 2. Untargeted metabolomics approach based on mass spectrometry was applied to investigate the chemical composition of this fraction. 3. By means of manual interpretation of product ion spectra with aid of molecular networking, chlorinated and hydrogenated azaphilones were identified. 4. New analogues were proposed to guide further fractionations of this fraction.

## Resumo/Abstract

The Amazon rainforest possesses the richest biodiversity of all the earth's ecosystems including an enormous diversity of microorganisms. From these, a vast range of fungi species play a vital role in the nutrient re-cycling, important for the maintenance of the rainforest, and one of the keys to sustain the Amazonian ecosystem. Among distinct types of fungi present in this environment, endophytes are receiving attention due to their ability to produce biologically active natural products. The endophyte *Penicillium sclerotium* was isolated from *Duguetia stelechantha* and cultivated in Petri dishes containing PDA medium. The metabolites were directly extracted from the medium with AcOEt/MeOH 1:1 (v:v). The obtained extract was fractionated over a micro-scale $C_{18}$ SPE cartridge, and the resulting fractions evaluated for their antimicrobial activity against a panel of human pathogens. Fraction 5 eluted with $H_2O$/MeOH 20:80 (v:v) was the main active one. Thus, this sample was selected for the mass spectrometry analysis. The main compound present in this fraction was the nitrogenated azaphilone sclerotioramine. Its characterization was performed by manual interpretation of the fragmentation pathway for the product ion spectrum. A common ethenone loss (-42 u), followed by water and carbon monoxide losses (-18 u and -28 u) was observed for most of the chromatographic peaks. Therefore, analysis of isotope patterns and molecular networking were employed to verify the correlations among the substances of this fraction. A total of 21 different compounds were detected, and at least 12 different azaphilones were identified, among them, new analogues were proposed based on the observed data. Our results will guide future fractionations for the isolation of the possibly undescribed compounds in the future.

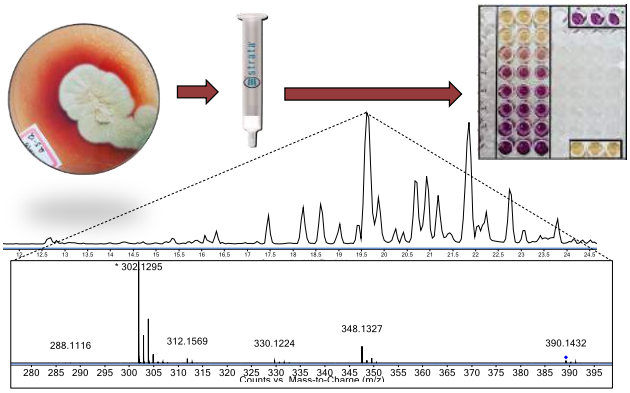


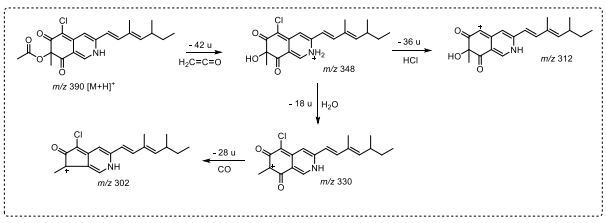

**Área: QPN** **Inscrição: 00548**

# Ion mobility spectrometry combined with ultra-performance liquid chromatography/mass spectrometry for the study of natural products

**Fausto Carnevale Neto (PQ),[1] Joseph Egan (PG),[2] Jason McFarlane (PG),[2] Letícia V. Costa-Lotufo (PQ),[3] Norberto P. Lopes (PQ),[1*] Roger G. Linington (PQ).[2*]**

**fausto_pos@yahoo.com; npelopes@gmail.com; rliningt@sfu.ca**

*[1]Departamento de Física e Química, Faculdade de Ciências Farmacêuticas de Ribeirão Preto da Universidade de São Paulo, Ribeirão Preto, SP, Brazil; [2]Department of Chemistry, Simon Fraser University, Burnaby, BC, Canada; [3]Departamento de Farmacologia, Instituto de Ciências Biomédicas, Universidade de São Paulo, São Paulo, SP, Brazil*

Keywords: Ion mobility-mass spectrometry, Natural products, CID fragmentation, Collisional cross section.

## Highlights

Liquid chromatography (LC) coupled with high-resolution tandem mass spectrometry (MS/MS) provides detailed, high-quality data for both the detection and structural elucidation. The enormous chemical diversity of natural extracts requires LC-MS-based workflows aiming to maximizing metabolome coverage and identity confirmation within a single analytical run. Ion mobility spectrometry-mass spectrometry (IMS-MS) is a powerful tool for analytical chemistry of natural products. IMS-MS adds an orthogonal separation in the gas-phase and provides coarse-grained structural information based on shape and collision cross section (CCS), allowing simultaneous analysis of isobaric and isomeric compounds.

## Resumo/Abstract

The major goal in natural products (NP) research is to interrogate complex extracts for the purposes of metabolic exploration and molecular discovery. In order to achieve this objective, NP studies rely on accurate and selective acquisition of all possible chemical information, which include the maximization of the number of detected metabolites and their correct molecular assignments. These requirements however, are intrinsically subordinate upon the employed analytical method and its capabilities considering chemical coverage and structural information. LC-MS has been recognized as the most powerful strategy to explore the chemical diversity of crude extracts. It is orders of magnitude more sensitive than nuclear magnetic resonance (NMR) and provides important chemical information in an extended selective analysis due to the pre-ionization chemical separation. Nonetheless, NP characterization by LC-MS is still a massive task, with two major drawbacks: the difficulty in achieve high chemical coverage due to the complex and convoluted nature of biological samples, and the limitations of MS in terms of structural assignment involving high dependence on the chemical behavior in the gas-phase, from ionization efficiency to distinct fragmentation expression. Here we demonstrate the value of combining UHPLC-MS/MS with ion mobility spectrometry (IMS) to separate and identify natural products. IMS-MS adds an orthogonal dimension of separation based on ion gas-phase conformation. Together with the UPLC separation and high-resolution MS/MS, it is possible to enhance peak capacity, spectral clarity and fragmentation specificity.

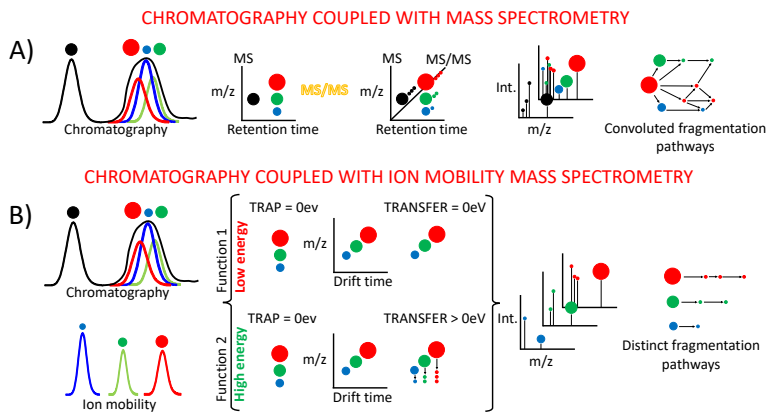


Schematic illustration of **(A)** data-independent MS/MS analysis (DIA) on conventional HPLC-MS/MS and **(B)** high-definition HD-DIA on UHPLC-IMS-Q-TOF instrument.

**Área:QPN** **Inscrição:00567**

# The role of secondary metabolites in structuring benthic communities in seaweeds of sandstone reefs on the coast of Pernambuco (Brazil)

**[1] José Souto Rosa Filho (PQ), [1] Pedro Henrique Leite Rebouças (IC), [1] Rodrigo Vinícius de Almeida Alves (IC), [2] Fausthon Fred da Silva (PQ), [3] Andréa Lopes Bandeira Delmiro Santana (PQ), [3] Talita Leão de Carvalho, [3] Victor Magno Santos do Nascimento, [3] Márcia Silva do Nascimento (PQ).**

**souto.rosa@ufpe.br**

*[1]Departamento de Oceanografia, UFPE; [2] Departamento de Química, UFPB; [3]Departamento de Antibióticos, UFPE*

Palavras Chave: *Phytochemical screening*, *Natural products, Macrofauna, Macrobenthos, Marine ecology.*

## Highlights

Secondary metabolites and benthic fauna were characterized in seaweeds. Most seaweed species had at least one tested metabolite class. More animals were in seaweeds without the metabolites tested.

## Abstract

Algal chemistry is known to have notable effects on mediating plant-animal interactions. In general, seaweeds produce secondary metabolites as a protection against predation by fishes and invertebrates. This study aimed to characterize secondary metabolites in nine species of seaweed on coastal sandstone reefs of Pernambuco State (Brazil), associating their presence with the benthic fauna associated with these algae. Samples were taken in Paiva and Enseada dos Corais in November 2017. Five samples of each seaweed species were taken (one sample for chemical analysis and four samples for faunal studies). Phytochemical screening was carried out according to the standard methods (Halborne 1998). Animals were identified at the phylum level and counted. Except alkaloids, all metabolites tested were recorded in at least one seaweed species. The absence of alkaloids is due to that seaweeds incorporate halogens into their secondary metabolites and do not produce the nitrogen containing alkaloids. *Palisada perforata* had three metabolite classes while *Chnoopora minima* and *Ochtodes secuniramea* did not present any. The macrofauna was dominated by crustaceans and molluscs, and the highest abundances were recorded in seaweeds without the tested secondary metabolites. In general, small mobile invertebrates like crustaceans (mainly amphipods) and molluscs (mainly gastropods) dominate benthic fauna in marine vegetated environments, and seaweeds with few secondary metabolites are more attractive to mesograzers that use algae as food.

Table 1 – Results of the phytochemical screening and characteristics of the macrobenthic communities.

| | Alkaloids | Flavonoids | Terpenes | Coumarins | Steroids | Tannins | Dominant phylum | Abundance (individuals.10 ml$^{-1}$) |
|---|---|---|---|---|---|---|---|---|
| *Ulva fasciata* | - | - | - | + | - | - | Crustacea | 1 |
| *Chnoospora minima* | - | - | - | - | - | - | Crustacea | 33.2 |
| *Sargassum* sp. | - | - | - | - | + | - | Crustacea | 5.4 |
| *Dictyota jamaicensis* | - | - | + | - | - | + | Crustacea | 16 |
| *Lobophora variegata* | - | - | + | - | - | - | Crustacea | 26.4 |
| *Padina* sp. | - | - | - | - | - | + | Mollusca | 7.1 |
| *Ochtodes secundiramea* | - | - | - | - | - | - | Crustacea | 63.9 |
| *Palisada perforata* | - | + | + | + | - | - | Mollusca | 20.3 |
| *Gracilaria caudata* | - | - | - | + | - | - | Crustacea | 5.6 |

HALBORNE, J.B. 1998. **Phytochemical Methods: A guide to moderntechniques of plant analysis**. 3rd ed. Chapman and Hall. 150 p.

**Área: QPN** **Inscrição: 00842**

# Bioprospecting anticancer metabolites from *Microsphaeropsis arundinis*, an endophytic fungi from *Paepalanthus planifolius*.

**[1]Weslei Bruno Botero (PG),[1] Marcelo Rodrigues Amorim (PG),[2] Marisa Campos Polesi Placeres (TC),[2] Iracilda Zeppone Carlos (PQ), [1]Lourdes Campaner dos Santos (PQ).**

**loursant@gmail.com; wesleibotero@gmail.com**

*[1]Department of Organic Chemistry, Institute of Chemistry, [2]Department of Biological Sciences, School of Pharmaceutical Sciences, Univ Estadual Paulista, 14800-900 Araraquara – SP,Brazil*

Keywords: *Microsphaeropsis arundinis, Paepalanthus planifolius, MTT assay, Polyketides, Eriocaulaceae.*

## Highlights

*Microsphaeropsis arundinis* is a endophytic from *P. planifolius.* This fungi are cultivate in 7 culture media and antitumor activity are evaluate by MTT assay. The active extract are fractionated resulting in 4 metabolites.

## Abstract

Eriocaulaceae family have 1200 species divided into 10 genera. This plants have chemical studies in literature that describe the presence of substances with biological potential, such as planifolin in *Paepalanthus planifolius*. Despite this, there are few data about the chemistry of the microorganisms associated with these species, such as endophytic fungi. In this study, we study chemically and biologically the endophytic fungus *Microsphaeropsis arundinis*, isolated from *P. planifolius* capitula. This endophyte are reported to have caused tissue infections in humans. The endophyte was cultivate in liquid culture media (Potato Dextrose Broth, YM Broth, Malt Extract, Nutrient Broth and Czapek-Dox Broth) and solid culture media (parboiled rice and corn) and the ethyl acetate extracts were biologically evaluated against adenocarcinoma cell lines LM3 (murine breast), LP07 (murine lung) and MCF-7 (human breast) (Table 1).

Table 1 - Cytotoxic values from ethyl acetate extracts from *M. arundinis* cultivate in different media

| Extracts | $IC_{50}$ ± (SD) [µg/mL] | | |
|---|---|---|---|
| | LM3 | LP07 | MCF-7 |
| PDB | 108.15 ± 1.36 | 266.12 ± 2.36 | 170.10 ± 5.56 |
| Czapek | 444.88 ± 52.37 | >1000 | 559.65 ± 39.72 |
| YM | 82.47 ± 7.67 | 793.84 ± 19.58 | 89.99 ± 23.20 |
| Malt | 63.21 ± 2.39 | 93.66 ± 6.33 | 66.60 ± 2.54 |
| Nutrient | 496.90 ± 9.24 | >1000 | 428.96 ± 34.40 |
| Rice | 39.91 ± 9.03 | 155.88 ± 3.28 | 51.93 ± 0.60 |
| Corn | 118.66 ± 7.62 | 180.37 ± 3.69 | 96.03 ± 14.38 |
| Cisplatin | 9.09 ± 1.11 | 1.3 ± 0.12 | 5.88 ± 1.38 |

The ethyl acetate extract cultivated in parboiled rice was the most active one against murine breast adenocarcinoma and human breast adenocarcinoma, being select to cultivated on an enlarged scale and fractionated result in the isolation of major substances. The use of spectroscopic and spectrometric techniques result in the identification of aromatic polyketides (**1**-**3**), with **1** (1-(2,5-dihydroxyphenyl)-3-hydroxybutanone) described for the first time as a natural product and a macrolide (**4**) described for the first time in the genus.

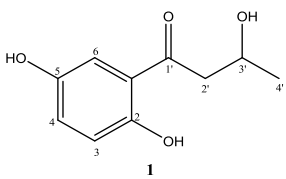


**1**

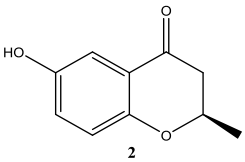


**2**

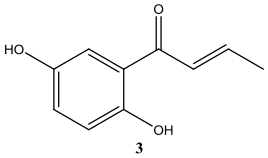


**3**

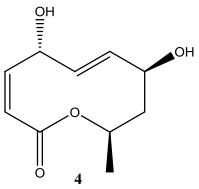


**4**

**Área: QPN** **Inscrição: 00891**

# Compounds identified by CG-MS in mycelium from *Cercospora brachiata* fungi

**John Kenedy R. P. Felisbino (PG)[1]*, Bruno Sérgio Vieira (PQ)[2], Neiliane Aparecida da Silva (PG)[3], Alberto de Oliveira (PQ)[1], Raquel M. F. Sousa (PQ)[1].**

**rsousa@ufu.br; johnkenedy7@hotmail.com**

*[1]Instituto de Química e [2]Instituto de Ciências Agrárias, Universidade Federal de Uberlândia, Uberlândia-MG, Brasil, [3]Instituto Federal do Triângulo Mineiro (IFTM), Uberaba-MG, Brasil*

Keywords: *Cercospora brachiata, mycelium, fatty acid, GC-MS.*

## Highlights

Secondary metabolites of the fungi were studied.

Compounds identified by GC-MS from the mycelia of the *Cercospora brachiata* fungi.

## Abstract

In 1863 Fresenius described the cercosporioides genus of fungi and, at the moment, there are numerous studies of species of this genus. Phytopathogens of these species promote some damage to their hosts, which are generally plants. The release of compounds produced by fungi results in stained leaves, fruits and seeds[2]. In this work, mycelia from *Cercospora brachiata* was macerated with methanol and dichloromethane. The solvent from extracts were removed and combined. The obtained extract was diluted in water and fractions in hexane and ethyl acetate were obtained by liquid-liquid partition. The hexane fraction was subjected to column chromatography using 60G silica gel as the stationary phase, and the gradient in hexane:ethyl acetate:methanol as the mobile phase. Fractions 3-7 were combined and refracted with the same stationary and mobile phases. Subfractions 6-12 and 14-20 were combined and analyzed in GC-MS using the Adams method[4]. The following compounds were identified by comparison with GC-MS libraries (NIST, SHIM and WILEY) using similarity index and arithmetic index (AI): palmitic acid (I) at 44.62 min (AI: 1938); oleic acid (II) at 50.68 min (AI: 2138) and ergost-7,22-dien-3-ol (III) at 93.23 (AI: 3092).

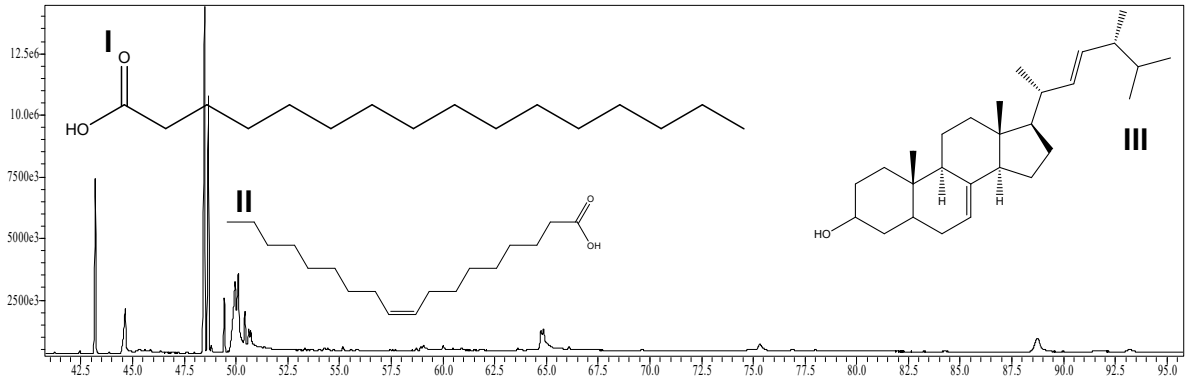


**Figure 1 -** GC-MS chromatogram of hexane fraction from micelium extract of *C. brachiata* fungi.

Acknowledgments: CAPES, FAPEMIG, CNPQ.

References: [1]FUCKEL, Hedwigia, **1863** (2), 1326. [2]GODOY et al., Manual de fitopatologia, 1997 (2), 184. [3]INTARAUDOM, Tetrahedron (2016 (72), 1415. [4]ADAMS, R. P. Identification of essential oil components by gas chromatography/mass spectrometry, 2007.

**Área:** QPN **Inscrição: 00919**

# Chemical study of *Aspergillus* sp. (FSF06), a soil fungus from the forest of the Serra de Carajás

**Luciano A. Watanabe (PG)[1]*, Arthur S. Rocha (IC)[2], Márcia Gleice S. Souza (PG)[3], Alberdan S. Santos (PQ)[1], André O. Feitosa (PG)[1], Josiwander M. Carvalho (PG)[1], Andrey M. R. Marinho (PQ)[1], Patrícia S. B. Marinho (PQ) [1].**

pat@ufpa.br; lucianowat@yahoo.com.br

*[1]Graduate Program in Chemistry - UFPA; [2]Amazon High School – ESAMAZ, [3]Faculty of Biotechnology – UFPA,*

Keywords: *Aspergillus* sp. *(FSF06), Chemical study, Antimicrobian activity, Pseurotin A, Bis(dethio)bis(methylthio)gliotoxin).*

## Highlights

The present work reports the isolation of the two alkaloids with antimicrobial activity from the chemical study of the fungus of *Aspergillus* sp. (FSF06), isolated from the forest soil of Serra de Carajás (PA).

## Resumo/Abstract

Most of the microorganisms producing antibiotics are commonly found in soil, among which are species of fungi of the genera *Penicillium* and *Cephalosporium*.[1] It is known that bacterial infection is a problem that attacks thousands of the people every day, which makes evident the need for new antimicrobials. Thus, the present work reports the preliminary chemical study of *Aspergillus* sp. (FSF06), isolated from the forest soil of Serra de Carajás (PA), in an attempt to search for antimicrobial substances. The fungus *Aspergillus* sp. (FSF06) was cultivated from czapek liquid medium with 2% yeast extract. After 09 days, the aqueous phase was filtered and partitioned liquid-liquid with ethyl acetate (3 x 2L), while the mycelium was added methanol (3 extractions). The organic solutions were filtered and concentrated to afford EtOAc (0.910 g) and MeOH (13.12 g) extracts. The EtOAc extract was fractionated through preparative CC and HPLC-DAD using as a stationary phase a C18 column and as a mobile phase $H_2O$/MeOH (50-100% B) gradient for 30 min, flow 13 mL/min., being obtained 7 sub-fractions. Sub-fractions 4 ($t_r$: 7.83 min., 65.0 mg) and 5 ($t_r$: 9.00 min., 10.8 mg) were shown to be pure for TLC and analyzed by $^1$H-NMR and MS. The $^1$H-NMR data of sub-fraction 4 were compared to the literature[2] and are described in Table 1. Its MS-ESI(-) spectrum showed the molecular ions peaks $[M-H]^-$ *m/z* 430.24 and $[M+2H_2O-H]^-$ *m/z* 466,25 suggesting a molecular mass of 431 Da, compatible with the molecular formula $C_{24}H_{23}NO_8$ of pseurotin A. $^1$H-NMR data of sub-fraction 5 and MS-ESI(+) were compared to literature[3] and showed that the compound is bis(dethio)bis(methylthio)gliotoxin. The two substances (Figure 1) are alkaloids and have antimicrobial activity.[2,4]

**Table 1:** $^1$H-NMR data of sub-fraction 4.

| | **Sub-fraction 4** H (δ, mult., *J* in Hz) | | **Sub-fraçao 4** H (δ, mult., *J* in Hz) |
|---|---|---|---|
| **1** | | **13** | 5.61 (*dd*, 10.3 e 7.5) |
| **2** | | **14** | 2.04-2.23 (*m*) |
| **3** | | **15** | 0.99 (*t*, 7.5) |
| **4** | | **16** | 1.68 (*s*) |
| **5** | | **17** | |
| **6** | | **18** | |
| **7** | 8.19 (*sl*) | **19** | 8.31 (*d*, 7.5) |
| **8OCH$_3$** | 3.43 (*s*) | **20** | 7.49 (*t*, 7.6) |
| **9** | 4.70 (*s*) | **21** | 7.65 (*t*, 7.5) |
| **10** | 4.58 (*d*, 5.1) | **22** | 7.49 (*t*, 7.6) |
| **11** | 4.75 (*dd*, 8.8 and 4.6) | **23** | 8.31 (*d*, 7.5) |
| **12** | 5.27 (*dd*, 10.3 and 8.8) | | |

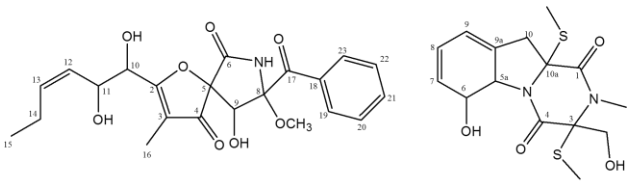


**Figure 1:** Alkaloids pseurotin A (left) and bis(dethio)bis(methylthio)gliotoxin (right).

**References:**
[1]STROBEL, G. A.; DAISY, B. **2003**, *Microbiol Mol Biol Rev.*, *67*, 4, 491-502.
[2]PINHEIRO, E. A. A. *et. al.* **2013**, *Nat. Prod. Res.*, *27*, 18, 1633-1638.
[3]LEE, H. J. *et. al.* **2001**, *Arch. Pharmacal Res.*, *24* (5), 397-401.
[4]LI, X. *et. al.* **200**6, Antibiot. (Tokyo), *59* (4), 248-250.

**Área: QPN** **Inscrição: 01093**

# Chemical prospection of *Humicola fuscoatra,* an endophyte of marine red alga *Asparagopsis taxiformis*.

**Iatã do C. Mendonça (PG)[1*], Alana E. Honório (PG)[1], Rebeca P. Medina (PD)[1], Dulce H. S. Silva (PQ)[1]**
iata.mendonca@hotmail.com
*[1]NuBBE - Núcleo de Bioensaios, Biossíntese e Ecofisiologia de Produtos Naturais Instituto de Química-UNESP, Araraquara, SP.*
Palavras Chave: *Marine, Endophytic fungi, Chemical prospection, Humicola fuscoatra*

## Highlights

Purification and elucidation of isocumarins and 2,5-diketopiperazine, obtained from the endophytic fungi *Humicola fuscoatra*, isolated from the marine red alga *Asparagopsis taxiformis.*

## Abstract

Marine ecosystems have provided several examples of useful compounds in the last decades. Their better understanding is essential for the improved exploration of their organisms as marine biome huge biodiversity is associated to an equally high chemodiversity. Marine red algae are known as the largest producers of halogenated compounds and may show, as many organisms, symbiotic relationships with endophytic fungi, which are also important sources of bioactive substances. This work aims to isolate and elucidate the structure of secondary metabolites of an endophyte strain, seeking for novel bioactive compounds.

A fungal strain of *Humicola fuscoatra* was isolated from the marine red alga *Asparagopsis taxiformis* and grown on Petri dishes containing PDA culture medium incubated for 10 days at 25ºC. Subsequent inoculation in Erlenmeyer flasks containing ultrapure water (200 ml) and malt growth medium (4 g) was held under 25ºC in static mode. Separation of mycelia from the fermented broth was carried out by vacuum filtration and the resulting solution was then subjected to liquid/liquid partition with EtOAc. After solvent evaporation the samples were analyzed by HPLC-DAD and fractioned on a Silica C-18 column, yielding 9 fractions with decreasing polarity. Fractions 3 and 5 were purified by semipreparative HPLC-DAD and afforded 11 compounds. From those, compounds **1, 2** and **3** were analyzed by 1D and 2D NMR and identified as 8,7-dihydroxy-3,4-dihydro-3-methyl-isocumarin, 8-hydroxy-3,4-dihydro-3,5-methyl-isocumarin and cyclo-Phe-Pro-diketopiperazine, respectively.

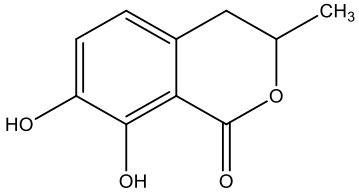


**1**

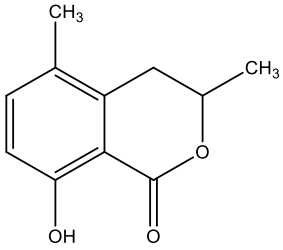


**2**

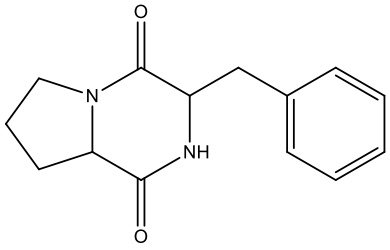


**3**

References:
BOLZANI, V. S., 2016. Biodiversidade, bioprospecção e inovação no Brasil. **Cien Cult,** vol. 68, no. 1, pp. 4-5.
PEREIRA, R. C.; TEIXEIRA, V. L., 1999. Sesquiterpenos das algas marinhas *Laurencia lamouroux* (Ceramiales, Rhodophyta). 1. Significado ecológico. Química Nova, vol. 22, pp. 369-374.
SPECIAN, V. et al, 2015. Metabólitos Secundários de Interesse Farmacêutico Produzidos por Fungos Endofíticos. J. Health Sci., vol. 16, no. 4, pp. 345-351.

**Área: QPN** **Inscrição: 01112**

# Metabolic production analysis of *Hypoxylon investiens*, an endophytic fungus isolated from the marine red algae *Asparagopsis taxiformis*

**Victor Hugo L. Rufino (PQ),[1*] Rebeca P. Medina (PD),[1] Dulce H. S. Silva (PQ).[1]**

Vh_lr@hotmail.com

[1]*NuBBE - Núcleo de Bioensaios, Biossíntese e Ecofisiologia de Produtos Naturais, Instituto de Química-UNESP, Araraquara, SP.*

keywords: *Endophytic fungi, Chemical prospection, Hypoxylon investiens, HPLC-DAD, [1]H NMR*

## Highlights

Growth medium variation on *Hypoxylon investiens* fungi isolated from the marine red algae *Asparagopsis taxiformis*. Metabolic production comparison seeking compounds such as binaphthalene tetrol derivatives.

## Resumo/Abstract

During recent decades bioprospection studies on marine microorganisms have increased exponentially due to their impressive chemodiversity and bioactivities. Among them, endophytic fungi have emerged as a promising source of novel and bioactive compounds, as *Hypoxylon investiens*, isolated from the marine red alga A*sparagopsis taxiformis*. Our recent studies on this species have revealed a high production of 3-nitropropionic acid in addition to several novel binaphtalene tetrols.

After inoculation of the fungal strain for 28 days at 25 ºC in Erlenmeyer flasks containing malt or potato-dextrose broth (PDB) dissolved in seawater (300 ml), the mycelium was vacuum filtrated and the fermented broth was partitioned with EtOAc. After solvent evaporation, each sample was analyzed by $^1$H NMR and HPLC-DAD and evidenced the metabolic variation between the extracts from both culture media. A marked decrease on the production of 3-nitropropionic acid was observed in the malt extract as shown on the $^1$H NMR spectra (Figure 1). Additionally, the HPLC and UV-Vis analyses evidenced the presence of compounds with $\lambda_{max}$ 226, 280 and 335 nm, consistent with the structure of binaphtalene tetrols previously isolated from this fungal strain. Such results confirm the importance of marine endophytes as an attractive source of novel metabolites and enable further steps in this study, which will include the isolation, structural elucidation and bioactivity evaluation of binaphthalene tetrol derivatives and additional chemical constituents.

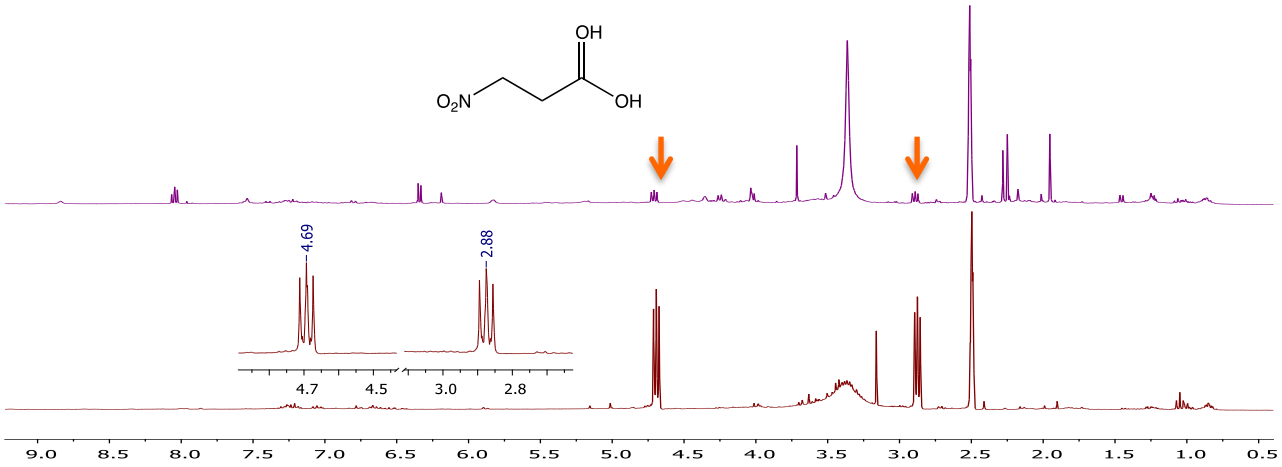


**Figure 1:** $^1$H NMR spectra (DMSO-*d6* 300 MHz) of malt (purple) and PDB (brown) extracts highlighting the triplets at δ4.69 and 2.88 assigned to nitropropionic acid.

**References:**

GERWICK, W. H.; MOORE, B. S. Lessons from the past and charting the future of marine natural products drug discovery and chemical biology. **Chemistry & Biology**, v. 19, n. 1, p. 85–98, Jan 2012.

CHANG, H. et al. Inhibitory Effects of Constituents of an Endophytic Fungus Hypoxylon investiens on Nitric Oxide and Interleukin-6 Production in RAW264.7 Macrophages. **Chemistry & Biodiversity**, v. 11, p. 949–961, 2014.

SILVA, A. D. **Bioprospecção do fungo endofítico Hypoxylon investiens associado à alga marinha Asparagopsis taxiformis: potencial antifúngico, anticolinesterásico e antitumoral.** 2016. 150 f. Dissertação (Mestrado em Química) - Instituto de Química, Universidade Estadual Paulista, Araraquara, 2016.

**Área: QPN**
*(Inserir a sigla da seção científica para qual o resumo será submetido. Ex: ORG, BEA, CAT)*

**Inscrição: 01272**
*(Inserir o número de inscrição do autor que fez a submissão)*

# Doxycycline biodegradation by symbiotic bacteria from *Diabrotica speciosa* (Coleoptera: Chrysomelidae)

**Karen S. Manjarrez Madera (IC)[1], Luis G. Cuadrado Durango (PG) [2], Eliane May de Lima (PG)[2], Orfa Contreras Martínez (PQ) [1], Moacir Rossi Forim (PQ) [2,*].**

***kmanjarrez12@gmail.com*; *mrforim@ufscar.br***

[1]*Department of Biology, University Nacional of Cordoba, St. 6 Nº 76-103, Nit. 891080031-3, CEP 230002, Montería-Cór, Colombia;* [2]*Chemistry Department, Federal University of São Carlos, Rod. Washington Luiz, Km 235, P.O. Box 676, CEP 13 565-905, São Carlos-SP, Brazil*

Keywords: Biodegradation, Tetracyclines, Symbiosis, Microorganisms, Insect pest, *Diabrotica speciosa*.

## Highlights

The main purpose of the present work was to evaluate the biodegradation capacity of the strains *Enterobacter cloacae* and *Stenotrophomonas maltophila* associated to the gut microbiota of the insect-pest *Diabrotica speciosa* to the antibiotic doxiclina. In this way, an analytical method was duly developed and validated for quantification of the antibiotic doxycycline presents in growth media. It was necessary to develop extraction, and purifcation approaches, as well as an analytical method by liquid chromatography coupled to mass spectrometry (LC-MS/MS). At the same time, this project highlights the fermentation process that made possible growth of bacterial strains together to the antibiotic. The results have showed a doxycycline biodegradation up to 40%.

## Abstract

Antibiotics constitute one of the most widely used groups within pharmaceuticals, being employed not only for the treatment and prevention of human diseases, but also in the promotion of animal growth and improvement[1,2]. However, improper use of these substances can lead to negative consequences, such as the acquisition of resistance and contamination of the environment, once an important part of antibiotics is not fully metabolized, being excreted by humans and animals in wastewater, which are soon spread in the agricultural soil fertilized with animal manure, generating contamination in the soil, water and the biomagnification of the trophic chains[3,4]. On the other hand, bacteria present in the gastrointestinal tract of pest insects are able to provide "new metabolic powers" resulting new behaviours and/or habilities to the host, such as promoting resistance mechanisms for xenobiotic substances through the biodegradation of these ones.[5] Two bacterial strains were selected after we evaluated the tolerance of the strains in the presence of the antibiotic and biodegradation potential, in a rich and deficient nutrient environment (growth media). We observed that the species *Enterobacter cloacae* and *Stenotrophomonas maltophila* could be grown in broth containing doxycycline. The degradation kinetics of the bacterial strains and their respective co-cultivos were evaluated, presenting a decrease in the doxycycline recovery in saline medium, suggesting the biodegradation of the antibiotic by the bacterium *E. cloacae* with recovery of 58.0±0.2% of analyte after 96 h. In rich medium, E. Cloacae presented a biodegradation rate of 23% in the period of 96 h. In its turn, *S. maltophila* showed an good cellular growth in both evaluated means, however, in both cases the recovery of doxycycline was almost total inside the period of evaluation.

**References**

1. Kebede, G. *et al,* (2014), *African Journal of Basic & Applied Sciences*, 6 (4), 87.
2. Alexandrino, D. A. *et al,* (2017), *Science of the Total Environment*, 581 359.
3. Sokolov, A. *et al,* (2018), *Chemical Engineering Journal*, 334 673.
4. Mboula, V. M. *et al,* (2012), *Journal of hazardous materials*, 209 355.
5. Pires, M., Chemistry Departament, University Federal of São Carlos, 2017.

**Área: QPN** **Inscrição: 01306**

# A Novel Strategy for Heterologous Production of the Depsipeptide Ionophore Valinomycin

**Renata Sigrist (PG), Bruno S. Paulo (PG), and Luciana G. de Oliveira (PQ)***

**luciana@iqm.unicamp.br; renata.sigrist@iqm.unicamp.br**

*Department of Organic Chemistry, University of Campinas, UNICAMP, Campinas, São Paulo, Brazil)*

Keywords*: valinomycin; ionophore; molecular networking; genome mining; heterologous expression.*

## Highlights

A gene cluster encoding the biosynthesis of valinomycin was annotated from *Streptomyces* sp. CBMAI 2042 genome sequencing. This BCG was successfully expressed in *S. coelicolor* M1146 host representing a unique platform for production of new derivatives.

## Resumo/Abstract

Genome analysis has helped to elect *Streptomyces* strains as one of the most prolific producers of secondary metabolites and a valuable source of natural products for drug discovery. Among the mostly useful natural products, those biosynthesized by nonribosomal peptides synthetases share both high molecular complexity and therapeutic activity. A gene cluster encoding the biosynthesis of valinomycin (VLM), a depsipeptide ionophore, was annotated from the whole genome sequencing of the endophytic strain *Streptomyces* sp. CBMAI 2042 isolated from *Citrus* ssp. Herein, we describe the association of genome mining, fermentation process and molecular networking to reveal the production of the cyclic depsipeptide antibiotic valinomycin (Fig. 1), the cyclooctadepsipeptide montanastatin (Fig. 1) and three unknown valinomycin derivatives by the endophytic strain. High accuracy MS/MS data acquired in an orbitrap mass spectrometer undoubtedly confirmed the production of VLM via the structurally diagnostic fragment ions (losses of CO (*m/z* 1083), Hiv-Val (*m/z* 884.52), Lac-Val (*m/z* 713.43), Hiv-Val (*m/z* 514.31), Lac-Val (*m/z* 343.22) and Hiv-Val (*m/z* 144.10)) and montanastatin (neutral losses of CO (*m/z* 735), Lac-Val (*m/z* 592.26), Hiv-Val (*m/z* 321) and Lac-Val (*m/z* 150.04)). Additionally, the heterologous expression of the entire valinomycin gene cluster in *S. coelicolor* M1146 host was successfully promoted supporting that all 5 metabolites share the same biosynthetic origin. The heterologous expression also represents an alternative and unique platform for production of new valinomycin derivatives in future studies.

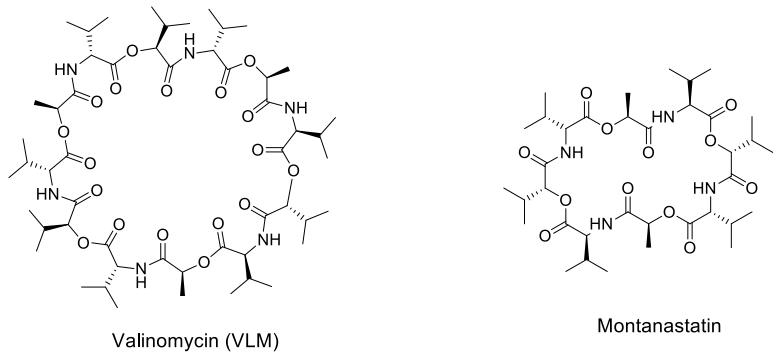


**Figure 1.** Chemical structures of valinomycin and montanastatin

**Área: QPN** **Inscrição: 01375**

# Interações Químicas de micro-organismos presentes no formigueiro das formigas cortadeiras: análise do metabolismo secundário do cocultivo do fungo mutualista, *Leucoagaricus gongylophorus*, com fungos negros

**Alana Kelyene Pereira[1] (PG), Dorai Periotto Zandonai[1] (PG), Eli Fernando Pimenta[1] (PQ), Fernando Carlos Pagnocca[2] (PQ), Maria Fátima das G. Fernandes da Silva[1] (PQ), Moacir Rossi Forim[1] (PQ), Paulo Cesar Vieira[1] (PQ), João Batista Fernandes[1] (PQ).**
**alanakelyene@gmail.com**

*[1]Departamento de Química, UFSCar; [2]UNESP Rio Claro*

Palavras Chave: formigas cortadeiras, interações, fungo mutualista, fungos negros, ecologia química

## Highlights

**Chemical interactions on micro-organisms in leaf-cutter ant's nest: study of secondary metabolism of coculture of mutualist fungi, *Leucoagaricus gongylophorus*, with black yeasts**. Inside of the nest there are attine ants that live with the fungi that they cultivate for food, cultivar-attacking microfungi in the genus *Escovopsis*, antibiotic-producing bacteria in the genus *Pseudonocardia*, and a black yeast parasitizing the ant-*Pseudonocardia* mutualism. All these interactions need more knowledge of different study areas. To evaluate the interactions with the mutualist fungi with black yeast, isolated recently over the garden, in co-culture. Co-culture systems are very important to understand the biological progress in the nature.

## Resumo/Abstract

A complexidade que envolve o ninho das formigas da tribo Attini intriga diversas áreas de pesquisa da ciência, como a Biologia, Ecologia Química e Microbiana, Genética e Química[1]. As formigas dessa tribo caracterizam por cultivar fungo mutualista, *Leucoagaricus gongylophorus,* conhecido como jardins de fungos, que possuem esse fungo e outros micro-organismos. A associação microbiana entre insetos é bastante complexa: actinobactérias ajudam a protege-las de parasitas, como fungos do gênero *Escovopsis*, que podem ameaçar o formigueiro. E fungos negros presentes no tegumento das formigas que podem ter correlação com as actinobactérias, mas precisam de estudos mais aprofundados[2] (figura 1). Esse trabalho teve o objetivo de compreender, através de cocultivos de fungos, quais as variações do perfil metabólico do fungo mutualista quando cultivado na presença dos fungos negros, a fim de entender a correlação química-ecológica entre organismos simbiontes. Foram realizados cultivos dos fungos negros e do fungo mutualista em meio sólido, em monoculturas, e coculturas desses fungos a fim de verificar as diferenças provocadas na presença de outro micro-organismo na mesma placa. Foi possível verificar alterações no perfil cromatográfico (figura 2), o que pode contribuir para estudos mais aprofundados, a fim de entender qual metabólito está sendo induzido na presença do segundo fungo. A estratégia de cocultivo parece bastante promissora para induzir metabolismo secundário de micro-organismos e podem ser uma fonte de produção de substâncias com atividades biológicas interessantes, como fungicida ou inseticida, a fim de controlar as formigas cortadeiras.

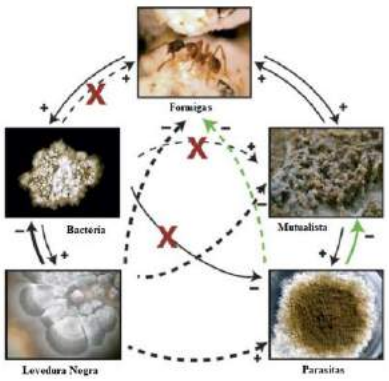


Figura 1: Inter-relações entre micro-organismos presentes no formigueiro

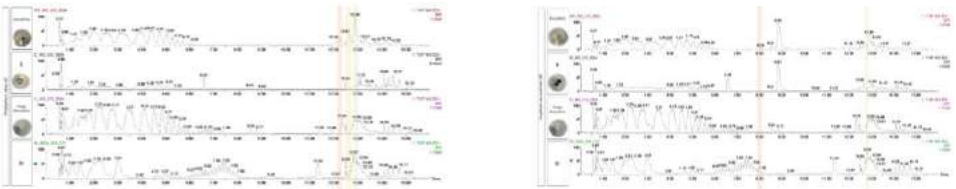

Figura 2: Alguns perfis cromatográficos das monoculturas e coculturas do fungo mutualista e de dois fungos

Referências:
[1] CALDERA, E. J., POULSEN, M., SUEN, G., CURRIE, C. R. Env. Entom. 38: 78-92, 2009.
[2] LITTLE, A. E. F.; CURRIE, C. R. Ecology, v. 89, n. 5, p. 1216-1222, 2008.
*Agradecimentos*: FAPESP proc. 2012/25299-6 e 2016/12304-2.

**Área: QPN** **Inscrição: 01388**

# Potencial fitotóxico do extrato e da citocalasina H produzidos pelo fungo endofítico *Diaporthe anacardii*.

**Juliana R. Lopes (IC),[1*] Carolina R. Biasetto (PQ), Vanderlan da S. Bolzani (PQ),[1] Angela Regina Araujo (PQ).[1]**

**angelarearaujo@gmail.com; jromanolopes@gmail.com**

[1]*Departamento de Química Orgânica, Instituto de Química da UNESP Araraquara.*

Palavras Chave: *Fungos endofíticos, Diaporthe anacardii, Citocalasina H.*

## Introdução

Os fungos endofíticos habitam assintomaticamente o interior de espécies vegetais e são prolíficos produtores de substâncias novas e bioativas, com uso potencial nas industrias de medicamento, alimentícia e na agricultura[1,2]. Este trabalho teve como motivação o estudo químico e biológico do fungo endofítico *Diaporthe anacardii*, isolado de *Eugenia brasiliensis*, devido aos resultados, preliminares, de atividade fitotóxica apresentada pelo extrato bruto obtido em extrato de malte (EM).

## Resultados e discussão

*D. anacardii* foi isolado dos ramos saudáveis de *Eugenia brasiliensis* de acordo com a metodologia descrita[2]. A linhagem pura foi inoculada em placas de Petri contendo BDA por sete dias a 25 ºC. Após esse período, pedaços do micélio foram inoculados no meio líquido de EM e cultivados por 28 dias a 25 ºC. O caldo fermentado foi separado do micélio por filtração à vácuo e submetido à partição líquido/líquido com acetato de etila (AcOEt), fornecendo o extrato bruto, após a evaporação do solvente. Este foi fracionado por CC de fase reversa (C18) e eluição em gradiente $H_2O$:$CH_3OH$, fornecendo cinco frações: Diap_Fr1-Diap_Fr5. As frações Diap_Fr3 e Diap_Fr4 foram submetidas a CLAE-DAD no modo preparativo, utilizando C18 e os eluentes $H_2O$:$CH_3CN$ em gradiente, conduzindo ao isolamento de várias substâncias. As análises dos dados de RMN de $^1H$ 1D e 2D, permitiram, até o momento, a caracterização da citocalasina H[3], além de outras substâncias que encontram-se em fase de determinação estrutural. A citocalasina H apresentou atividade fitotóxica frente aos coleóptilos de trigo, comparada ao herbicida comercial GOAL®.

**Figura 1**. Ensaio fitotóxico realizado para o extrato bruto (**a**) e para a citocalasina H (**b**) frente ao crescimento de coleóptilos de trigo.

(a) (b)

## Conclusões

Os resultados observados, até o momento, evidenciaram *D. anacardii* como um importante produtor de metabólitos secundários. O isolamento da citocalasina H e a significativa atividade herbicida, apresentada, reforçam a importância dos fungos endofíticos na produção de substâncias com potencial para aplicação na agricultura.

## Agradecimentos

A CNPq pelas bolsas concedidas, ao BIOTA/FAPESP e CEPID/CIBFar (Proc. N° 2013/07600-3) pelo suporte financeiro.

[1] Gunatilaka, A. A. L. *J. Nat. Prod.* **2006**, *69*, 509-526.
[2] Chapla, V. M.; Biasetto, C. R.; Araujo, A. R. *Rev. Virtual Quim.* **2013**, *5*, 421-437.
[3] Li, S. et al. *Chin. J. Nat. Prod.*, **2014**, *12*, 512-516.

**Área: ____QPN_____ Inscrição:___01384___**

# Bioreduções de aldeídos e cetonas utilizando *Cucurbita moschata* (abóbora) como biocatalisador para a produção de álcoois

**Fátima Miranda Nunes** (PQ),[1] Maraylla Inácio de Moraes (PG),[2] Espedito de S. Saraiva (PG),[3] Edivan C. Vieira (PQ), [3] Franciglauber Silva Bezerra (PQ).[4] Luciana L. Machado (PQ), [5] Telma Leda Gomes de Lemos (PQ),[1] Allana Kellen Lima Santos Pereira (PQ),[6]*

*[1]Departamento de Química, UFC; [2]Departamento de Química, IQ - UNESP; [3]Departamento de Química, UFPI; [4]CECITEC, UECE; [5]Departamento de Química, UFOB; [6]Centro de Ciências e Tecnologia, UFCA.*

Palavras Chave: *Biotransformações, Enzimas, Compostos carbonílicos, Cucurbita moschata.*

## Highlights

Bioreductions of aldehydes and ketones using *Cucurbita moschata* (pumpkin) as a biocatalyst for the production of alcohols

Preparation of alcohols through biotransformation reactions; *Cucurbita moschata* in biotransformation reactions of organic compounds; Use of *Cucurbita moschata* in the reduction of carbonyl compounds.

## Resumo/Abstract

O crescente interesse em biocatálise é devido ao grande potencial biotecnológico das reações enzimáticas, onde reportam uso de partes de plantas como agentes potenciais.[1,2,3] *Cucurbita moschata* (abóbora) é uma planta herbácea, rasteira ou trepadora utilizada na alimentação humana.[4] O objetivo era buscar novas fontes enzimáticas para uso em biotransformações. Acetofenona **(1)**, benzaldeído **(2)**, 4-(dimetilamino)benzaldeído **(3)**, 4-metoxibenzaldeído **(4)** e cicloexanona **(5)** foram utilizados como substratos. As análises dos bioprodutos foram realizadas por GC/MS e RMN $^1$H. O biocatalisador (sementes de *C. moschata,* 23 g), os substratos (200 mg) e 150 mL de água destilada foram acondicionados em erlenmeyeres (250 mL), permanecendo em agitação por 72 h em um orbital shaker (150 rpm).[3] A mistura, após filtração, foi submetida à extração líquido-líquido com AcOEt (3 x 50 mL). A fase orgânica foi seca com $Na_2SO_4$ anidro, concentrada em rota-evaporador, fornecendo extrato bruto. Os bioprodutos obtidos: 1-feniletanol **(1a)**, álcool benzílico **(2a)**, álcool 4-(dimetilamino)benzílico **(3a)**, álcool 4-metóxibenzílico **(4a)**, cicloexanol **(5a)** foram purificados por coluna de gel sílica. O substrato **(2)** foi reduzido a **(2a)** com conversão >99%, enquanto que a reação com o **(3)** resultou em conversões muito baixas. O substrato **(4)** foi reduzido ao **(4a)** com conversão 94%, ao passo que **(1)** não reagiu e **(5)** foi completamente reduzida a **(5a)**, >99%. Portanto, com exceção de **(1)** e **(3)**, o trabalho demostra um método biotecnológico adequado e simples para a preparação de vários álcoois de forma sustentável.

Agradecimentos à FAPEPI, CNPq, UFPI, UFCA.

1. ANDRADE, L. H.; UTSUNOMIYA, R. S.; OMORI, A. T.; PORTO, A. L. M.; COMASSETO, J. V. Edible catalysts for clean chemical reactions: Bioreduction of aromatic ketones and biooxidation of secondary alcohols using plants. **Journal of Molecular Catalysis B: Enzymatic**, 38, 84-90, 2006.

2. LUNA, H.; HERNÁNDEZ-VÁZQUEZ, L.; REYO, A.; ARIAS, L.; MANJARREZ, N.; NAVARRO-OCAÑA, A. Banana and maize leaf wastes as a green alternative for the preparation of benzyl alcohols used as starting materials for fra- grances. **Industrial Crops and Products**, 59, 105-108, 2004.

3. MACHADO, L. L.; SOUZA, J. S. N.; de MATTOS, M. C.; SAKATA, S. K.; CORDELL, G. A.; LEMOS, T. L. G. Bioreduction of aldehydes and ketones using Manihot species. **Phytochemistry**, 67, 1637-1643, 2006.

4. RESENDE, G. M. D.; BORGES, R. M. E.; GONÇALVES, N. P. S. Produtividade da cultura da abóbora em diferentes densidades de plantio no Vale do São Francisco. **Horticultura Brasileira**, 31, 504-508, 2013.

**Área: QPN** **Inscrição: 01085**

# Synthesis of artesunic acid and dihydroartemisinin acetate and studies of *in vitro* activity against *Schistosoma mansoni*, BH strain

**Sinésio Boaventura Júnior (PQ),[1]* Rosimeire Nunes de Oliveira (PQ),[2] Sheila de Andrade Penteado Corrêa (PG),[2] Silmara Marques Allegretti (PQ),[2] Vera Lúcia Garcia (PQ)[1]**

**sinesio@cpqba.unicamp.br**

*[1]Research Center for Chemical, Biological and Agricultural (CPQBA), State University of Campinas (UNICAMP); [2]Institute of Biology, Department of Animal Biology, State University of Campinas (UNICAMP)*

Keywords: *Schistosomiasis, Schistosoma mansoni, Artesunic acid, Dihydroartemisinin acetate*

## Highlights

Schistosomiasis is a parasitic disease with great social impact. Praziquantel is the reference drug against schistosomiasis. Derivatives of artemisinin showed high schistosomicide potential *in vitro*.

## Resumo/Abstract

Schistosomiasis is a neglected chronic disease caused by trematodes of *Schistosoma* genus. There are reports of resistance of Praziquantel, the reference drug to treat schistosomiasis. Thus, the synthesis of potentially antischistosomal compounds would help prevent resistance. Artesunic acid **2** and dihydroartemisinin acetate **3** are semisynthetic derivatives of artemisinin **1** (Figure A), a sesquiterpene lactone isolated from *Artemisia annua* L. (Asteraceae), that contains in its structure an endoperoxide function, which is attributed its activity. Therefore, this study aimed to synthesize and evaluate the *in vitro* activity of **2** and **3** on adult worms of *S. mansoni*, BH strain.

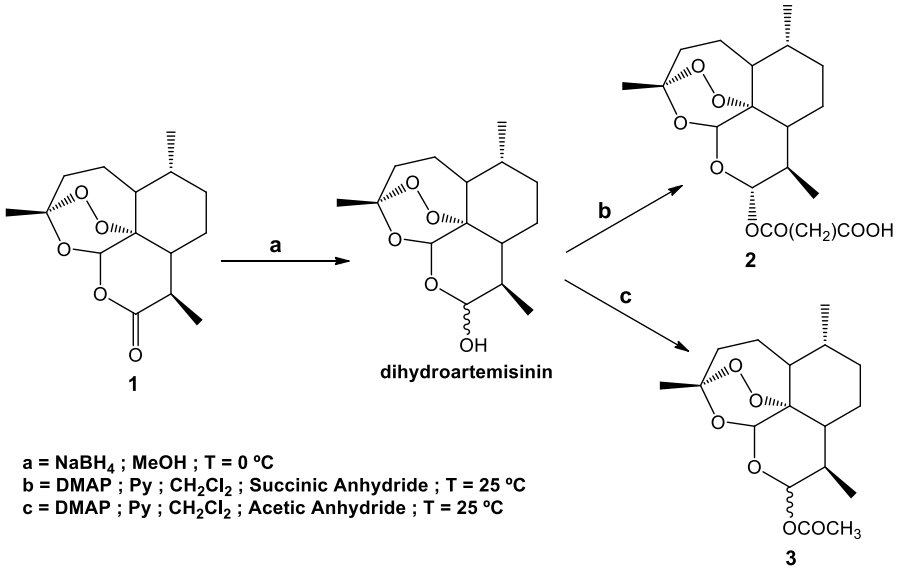


**Figure A:** Synthesis of artemisinin derivatives, artesunic acid (**2**) and dihydroartemisinin acetate (**3**)

The tests used female Swiss mice, infected with *S. mansoni*. Adult worms were recovered by perfusion and the samples were incorporated into polyvinylpyrrolidone and tested (25, 50, 100 and 200 µg/mL). We evaluated the motility, oviposition, skin and/or morphological alterations and mortality of worms. We observed that the motility for all samples tested decreased after the first 6 h of incubation. Regarding the mortality, we found that this parameter is directly dose and time dependent. In the treatment with **2**, 100% mortality of the worms was observed after 24 h incubation (200 µg/mL); whereas **3**, at concentration of 100 µg/mL, 100% mortality of the worms was observed at the same period. All male and female worms showed changes in the tegument and oral and acetabular suction cups and there was no oviposition. In conclusion, **2** and **3** presented high schistosomicide potential *in vitro*.

**Área: QPN** **Inscrição: 00541**

# Bergenin from *Peltophorum dubium*: isolation and cytotoxicity and antioxidant activities of its chemical derivatives

**Oscar C. Silva Neto (PG),[1*] Patrícia de A. Santos (PG),[1] Marla Thais F. Teodoro (PG),[1] Larissa S. Pinto (PG),[1] Juceni P. David (PQ),[2] Jorge M. David (PQ).[1]**

**oscarcaetano@hotmail.com;**

*[1]Instituto de Química, UFBA; [2]Faculdade de Farmácia UFBA*

Palavras Chave: *Bergenin, Peltophorum dubium, Antioxidant activity, Cytotoxicity, Derivatives.*

## Highlights

Method of bergenin isolation from methanol extract of *Peltophorium dubium* was developed. From the roots were obtained pure bergenin in good yield. Antioxidant and cytotoxic derivatives were prepared.

## Abstract

Bergenin (**1**) is a gallic acid derivative presenting *in vitro* and *in vivo* pharmacological and biochemical activities such as anti-inflammatory, anti-asthmatic, hepatoprotective besides others. It can be found in different plant families, especially Fabaceae. This work describes a methodology for isolation of this compound, chemical derivatization, the antioxidant and cytotoxicity of the isolated and prepared compounds. *Peltophorum dubium* (Spreng.) Taubert (Fabaceae) is a tree popularly known as “canisfítola”, “faveira”, “angico amarela” or “farinha-seca”. Bergenin was extracted from the dried root MeOH extracts of *P. dubium*; the hidro-alchoolic solution was partitionated between $CHCl_3$ furnishing crude bergenin precipitated. This preciptaded was purified by chromatographic techniques and the pure compound was identified by NMR analysis (3,48 % yield). In a sample were added DMF, $K_2CO_3$ and methyl iodide (SHAH, 2012) furnishing 5-methyl (**2)** and 5,7-dimethyl (**3**) bergenin. These derivatives were identified by NMR and MS data. These compounds were submitted to Brine Shrimp Test (*Artemia salina*) in different concentrations (MEYER et al., 1982). The dimethyl derivative presented higher mortality ($DL_{50}$ = 392.8 ppm) than the other compounds. The compounds were also submitted to radical DPPH quenching (BRAND-WILLIANS *et al*., 1995), the three compounds showed similar antioxidant activities, with a $CE_{50}$ ranging 155.62 to 178.48 µg/mL. (CNPq, CAPES, FAPESB)

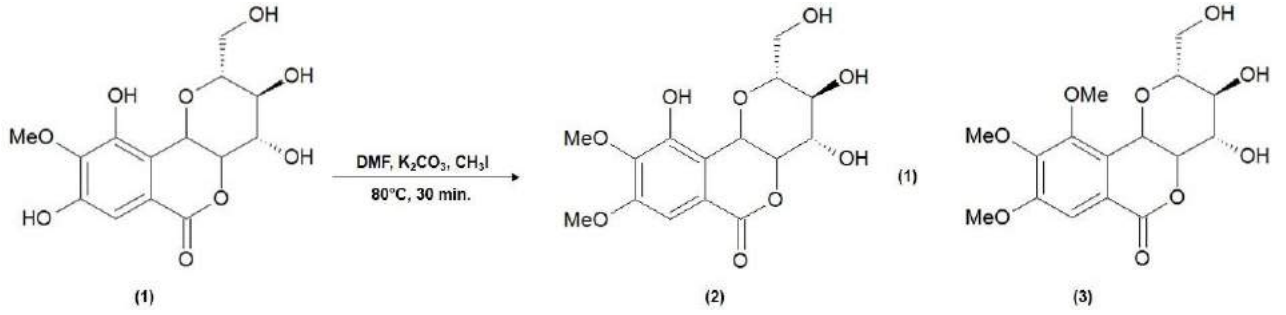

**Área: QPN** **Inscrição: 01319**

# Metabolomic analyses of *Strongylodon macrobotrys* (Leguminosae) and molluscicidal activity on *Achatina fulica*

**Lúcia Pinheiro Santos Pimenta (PQ),[1*] Bruna Aparecida de Souza (PG),[1,2] Nathália de Oliveira Melo (IC),[1] Flávia Maria Pereira da Costa (IC),[2] José D. de Souza Filho (PQ),[1] Alan R.T. Machado (PQ), [3,4]**

***lpimenta@qui.ufmg.br; lpimenta.qui@gmail.com***

*[1]CerQBio – Laboratório de Quimio e Bioprospecção de Plantas do Cerrado, Departamento de Química, UFMG; [2]Departamento de Zoologia, Instituto de Ciências Exatas, UFJF; [3] Departamento de Ciências Exatas Aplicadas e dos Materiais, Unidade João Monlevade, UEMG; [4] Instituto de Engenharia e Tecnologia, UniBH.*

Palavras Chave: Strongylodon macrobotrys, Achatina *fulica, metabolic profile, NMR, HPLC-ESI-MS/MS.*

## Highlights

*Strongylodon macrobotrys* was analysed by MS and NMR. Kaempferol, isovitexin and D-pinitol were identified and its flower polar extract showed great molluscicidal potential against the snail pest *A. fulica.*

## Resumo/Abstract

The African snail Achantina fulica has entailed problems within public health and affected agriculture, especially family farming. In order to lower the environmental impacts, the WHO recommends the use of vegetable origin molluscicides. Some of these constituents have been isolated from Leguminosae family which presents the species *Strongylodon macrobotrys,* popularly known as jade vine. However, little is known about the chemical composition of this plant. This study aimed to evaluate the metabolomic profile of *S. macrobotrys* flower hydromethanolic fractions through HPLC-ESI(+)-QTOF-MS/MS and 1D/2D NMR, as well as to verify the toxic effects against the *A. fulica* snail species. The crude flower extract of *S. macrobotrys* and its hydromethanolic fraction at 1000 and 1500 ppm showed significant molluscicidal activity on the snail *A. fulica*. Metabolomic analyses identified four carbohydrates, four amino acids, three organic acids, one alkaloid and ten flavonoids, mainly derived from apigenin and kaempferol. Eight of these flavonoids have been described here for the first time in this species. Mass spectrometry coupled with NMR were fundamental techniques for the unambiguous identification of 22 metabolites in the extract using few pre-purification steps. The hydromethanolic fraction at a concentration of 1000 ppm caused the highest mortality against *A. fulica* presenting itself as a promising molluscicidal agent.

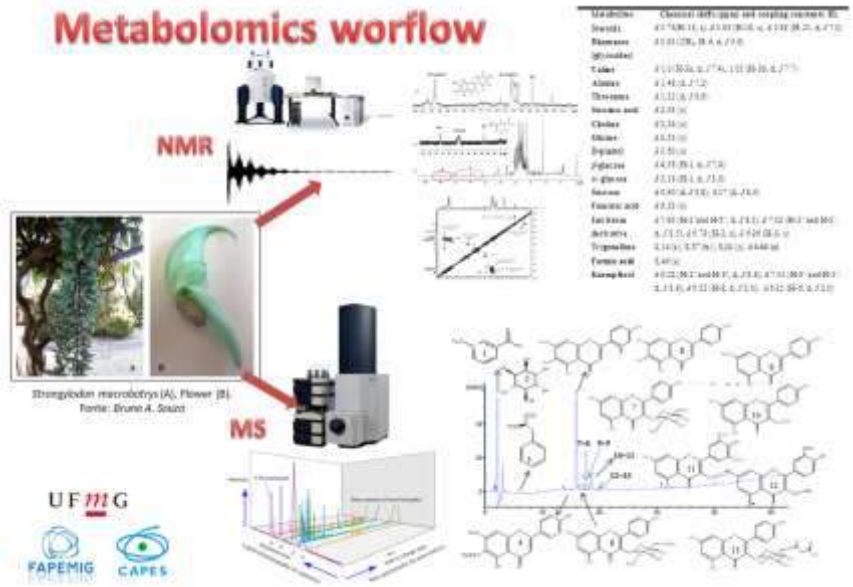


Acknowledgments: FAPEMIG, UFMG, Center Renné Rachou, FIOCRUZ MINAS.

**Área: QPN** **Inscrição: 01284**

# *Psychotria vellosiana* Benth: A cyclotide-rich species

**Meri Emili F. Pinto (PQ),[1]* Eduardo M. Cilli (PQ),[1] Vanderlan S. Bolzani (PQ).[1]**

**m.emili@iq.unesp.br, meriemily@hotmail.com**

[1]*Institute of Chemistry, São Paulo State University - UNESP, 14800-060, Araraquara, SP, Brazil.*

Keywords: Cyclotides, Cyclic peptides, Rubiaceae, *Psychotria.*

## Highlights

A novel bracelet cyclotide has been elucidated from stems of *Psychotria vellosiana* and a great diversity of possible cyclotides was identified.

## Abstract

Cyclic cystine knot proteins (cyclotides) are complex cyclic peptides that occur naturally in plants and have a peculiar cyclic structure, known as cyclic cystine motif (CCK). This topology confers them remarkable stability and wide range of biological and/or therapeutic applications, between them, anti-HIV,[1] anthelmintic,[2] insecticidal,[3] molluscicidal,[4] antimicrobial,[5] uterotonic,[6] cytotoxic,[7] hemolytic[8], trypsin inhibitory[9], and immunosuppressive activities.[10] In this context, both the scientific community and pharmaceutical industry have been a future view for using cyclotides in drug development. Thus, this work describes the diversity of this compound in stems and the identification of a novel cyclotide from *Psychotria vellosiana*.
Dried and pulverized stems were extracted with MeOH/$H_2O$ (60:40, v/v) at room temperature. The extract was partitioned with $CH_2Cl_2$:MeOH:$H_2O$ and the aqueous phases was concentrated and eluted through solid-phase extraction (SPE) cartridge. The fraction eluted with the mixture 80% buffer B (90% acetonitrile, 0.08% trifluoroacetic acid) in A (0.1% aqueous trifluoroacetic acid) was considered the peptide-rich fraction. This was submitted to MALDI-TOF mass spectrometry, to determine the molecular weight signals in the range between the 2500-4500 Da. It was observed the presence of many mass signals in this region, that indicate a great diversity of possible cyclotides. To separation and purification were employed HPLC chromatography that allowed to isolate a novel bracelet cyclotides from *P. vellosiana* with average mass m/z 2889. The cyclotide sequencing was performed by reduction, alkylation and enzymatic digest with endoproteinases Glu-C, trypsin, chymotrypsin and followed by MS/MS analysis.

## References

1. Hallock, Y. F.; Sowder, R. C.; Pannell, L. K.; Hughes, C. B.; Johnson, D. G.; Gulakowski, R.; Cardellina II, J. H.; Boyd, M. R. *J. Org. Chem*. **2000**, *65*, 124-128.
2. Colgrave, M. L.; Kotze, A. C.; Kopp, S.; McCarthy, J. S.; Coleman, G. T.; Craik, D. *J. Acta Trop*. **2009**, *109*, 163-166.
3. Barbeta, B.; Marshall, A.; Gillon, A.; Craiks, D.; Anderson, M. *Proc. Natl. Acad. Sci. U.S.A*. **2008**, *105*, 1221-1225.
4. Plan, M. R. R.; Saska, I.; Cagauan, A. G.; Craik, D. J. *J. Agric. Food Chem*. **2008**, *56*, 5237-5241.
5. Pranting, M.; Loov, C.; Burman, R.; Goransson, U.; Andersson, D. *J Antimicrob Chemother*. **2010**, *65*, 1964-1971.
6. Koehbach, J.; O'Brien, M.; Muttenthaler, M.; Miazzo, M.; Akcan, M.; Elliott, A. G.; Daly, N. L.; Harvey, P. J.; Arrowsmith, S.; Gunasekera, S.; Smith, T. J.; Wray, S.; Göransson, U.; Dawson, P. E.; Craik, D. J.; Freissmuth, M.; Gruber, C. W. Proc Natl Acad Sci U S A. 2013, 110, 21183-21188.
7. Herrmann, A.; Burman, R.; Mylne, J.; Karlsson, G.; Gullbo, J.; Craik, D.; Clark, R.; Goransson, U. Phytochemistry 2008, 69, 939-952.
8. Chen, B.; Colurave, M.; Wang, C.; Craik, D. J. Nat. Prod. 2006, 69, 23-28.
9. Hernandez, J. F.; Gagnon, J.; Chiche, L.; Nguyen, T. M.; Andrieu, J. P.; Heitz, A.; Trinh Hong, T.; Pham, T. T.; Le Nguyen, D. Biochemistry 2000, 39, 5722-5730.
10. Thell, K.; Hellinger, R.; Sahin, E.; Michenthaler, P.; Gold-Binder, M.; Haider, T.; Kuttke, M.; Liutkevičiūtė, Z.; Göransson, U.; Gründemann, C.; Schabbauer, G.; Gruber, C. W. *Proc Natl Acad Sci U S A*. **2016**, *113*, 3960-3965.

## Acknowledgements

The authors are grateful to Dr. Jacqueline Nakau Mendonça and Dr. Norberto P. Lopes (USP-Ribeirão Preto) for technical assistance during MALDI measurements, SISBIOTA-CNPq-FAPESP grant# 2010/52327-5, CEPID-FAPESP grant# 2013/07600-3, FAPESP grant# 2017/17098-4, CNPq grant# 162855/2015-0 and CAPES for scholarships and financial support.

**Área: QPN** **Inscrição: 01045**

# Ácidos aristolóquicos em chás de espécies de *Aristolochia*

**Tito da Silva (PQ),[1]* Ana Carolina Martins Pinto (IC),[2] Isabele R. Nascimento (PQ),[2] Lucia Maria Xavier Lopes (PQ).[2]**

**titodasilv@hotmail.com**

*[1]Coordenação do curso de Engenharia de Alimentos, CCSST- UFMA; [2]Departamento de Química Orgânica – Instituto de Química de Araraquara - Unesp*

Palavras Chave: *Aristolochia, Ácido aristolóquico, Chás, Quantificação.*

## Highlights

Aristolochic acids in teas from *Aristolochia* species. The aim of this work is the identification and quantification of aristolochic acids (AA I and AA II) in Brazilian *Aristolochia* species by modern chromatographic techniques (HPLC-DAD and HPLC- MS/MS). AA-containing herbs had been widely used as Chinese herbal medicines to treat tumors, rheumatism, snake bites, small pox, and pneumonia, however AAs were observed to be strong human carcinogens and nephrotoxins.

## Resumo/Abstract

Espécies da família Aristolochiaceae são utilizadas para o tratamento de várias doenças. Estudos químicos revelaram mais de 700 substâncias com ação farmacológica benéfica para o homem. Entretanto, tem-se observado há décadas ação maléfica crônica irreversível em indivíduos que consumem suplementos alimentares e/ou produtos medicinais, a exemplo de chás, contendo espécies de *Aristolochia*, acreditando-se que esta ação se deve a presença de ácidos aristolóquicos [2, 3].

O presente trabalho visou à identificação e à quantificação, por HPLC-DAD e HPLC- MS/MS, dos ácidos aristolóquicos AA-I e AA-II presentes em chás de dez espécies de *Aristolochia*. Os chás foram preparados por infusão, decocção e/ou maceração, de acordo com a recomendação da ANVISA [4]. Curvas de calibração dos padrões AA I e AA II foram criadas. Os coeficientes de regressão ($R^2$) para cada curva foram 0,9954 e 0,9997, respectivamente. Os intervalos de teste foram considerados adequados para a análise das dez espécies. Os resultados de linearidade, LD foi de 0,086 μg e 0,058 μg para o AA-I e AA-II, respectivamente, e o LQ foi de 0,216 μg e 0,195 μg para AA-I e AA-II, respectivamente. O resultado deste estudo demonstrou a presença do AA I em oito espécies, enquanto que o AA-II está presente em quatro espécies. Os dados analisados permitem afirmar que o AA I ocorre com abundância e maior frequência em raízes. A utilização de *Aristolochia* com fins etno-farmacólogico pelas populações brasileiras deveria ser limitada às partes aéreas, sobretudo às folhas das espécies que não apresentaram presença dos AAs.

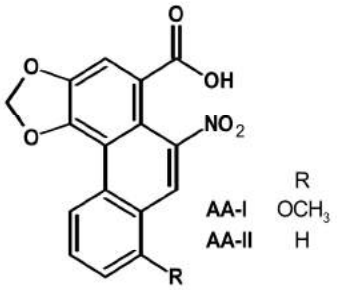


1. LOPES, L. M.X; NASCIMENTO, I. R; SILVA, T. Phytochemistry of the Aristolochiaceae family. *Research advances in phytochemistry*, v. 2, p. 19-108, 2001.
2. PEREIRA, M. D. P.; SILVA, T.; AGUIAR, A. C. C. LOPES, L. M.X. Chemical composition, antiprotozoal and cytotoxic activities of indole alkaloids and benzofuran neolignane of Aristolochia cordigera. Planta Med., v. 83, n. 11, p. 912-920, 2018.
3. BHATTACHARJEE, P.; BHATTACHARYYA, D. Characterization of the aqueous extract of the root of *Aristolochia indica*: Evaluation of its traditional use as anantidote for snake bites. Journal of Ethnopharmacology 145, p. 220–226, 2013.
4. ANVISA, Informe Técnico nº 45, de 28 de dezembro de 2010. Disponível em http://www.anfarmag.org.br/detalhes-da-legislacao/informe-tecnico-n-452010-regulamentacao-de-chas> Acesso em janeiro 2018.

**Área: QPN** **Inscrição: 00107**

# Chemical composition of bufonids toads from Legal Amazonia

**Jacqueline Kerkhoff (PG),[1]* Eloana B.R. Souza (PG),[1] Leonardo G. Vasconcelos (PG),[2] Domingos J. Rodrigues (PQ),[1] Evandro L. Dall'Oglio (PQ),[2] Adilson P. Sinhorin (PQ).[1]**

**jackerkhoff@gmail.com**

*[1]Institute of Natural, Humanities and Social Sciences, UFMT Sinop; [2] Department of Chemistry, UFMT Cuiabá.*

Palavras-Chave: *Bufonidae, Brazilian toads, Chemical profile, Argininyl bufadienolides.*

## Highlights

- Toads poison of three species of bufonidae family were collected in Legal Amazon.
- Methanolic extracts are mainly composed of alkaloids, bufadienolides and argininyl diacid derivatives.

## Abstract

The Bufonidae toad family contains about 52 genera and 607 species. These animals produce and store poison in their parotid glands. The poisons are composed mainly of steroids, biogenic amines and peptides, originated from the secondary metabolism of frogs [1]. These compounds have already presented, *in vitro*, different pharmacological effects, especially antiproliferative activity [2]. Thus, the objective of this work is to determine the chemical composition of venoms obtained from three different species of bufonids captured in the state of Mato Grosso. *Rhinella marina*, *Rhaebo guttatus* and *Rhinella schneideri* collected in the municipalities of Colniza, Nova Ubiratã and Poroxéu, respectively, were studied. The poisons were obtained by manual compression of the amphibian glands, dried and extracted with methanol. The extracts were analyzed by HPLC-MS-MS [3]. From the bufonids poisons, 31 compounds were identified or tentatively identified by spectrometric mass means. Among them, alkaloids, free bufadienolides and argininyl diacid derivatives of bufadienolides. The argininyl diacids included derivatives from bufalin, marinobufagin, telocinobufagin, hellebrigenin and resibufogenin. The poisons presented high chemical diversity in its constituents. These findings stimulate further work on the chemistry and bioactivity of Legal Amazonia toads.

References

[1] Sousa, L.Q. et al., 2017. Toxicon, 127, pp.63–76.
[2] Sciani, J.M. et al., 2013. Biomedicine and Preventive Nutrition, 3(1), pp.10–18.
[3] Schmeda-Hirschmann, G. et al., 2014. Journal of Ethnopharmacology, 155(2), pp.1076–1085.

**Área: QPN** **Inscrição: 01265**

# The citrus defense in response to phytopathogen *Xylella fastidiosa*

**Márcio S. Soares (PQ)[1], Jéssica C. Amaral (PG)[2], Danielle F. da Silva (PG)[2], Michelli M. da Silva (PG)[2], Maria Fátima das G. F. da Silva (PQ)[2*], João B. Fernandes (PQ)[2], Alessandra A. de Souza (PQ)[3].**

**jessica.amaral@yahoo.com.br; dmfs@ufscar.br**

*[1]Departamento de Ciências Exatas, Universidade Federal de Viçosa - Campus de Rio Paranaíba, 38810-000 Rio Paranaíba – MG, Brazil, [2]Departamento de Química, Universidade Federal de São Carlos, 13565-905 São Carlos - SP, Brazil; [3]Centro APTA Citros Sylvio Moreira, Instituto Agronômico 13490-970 Cordeirópolis, - SP, Brazil.*

Palavras Chave*: C. limonia, C. sinensis, Xylella fastidiosa, Xanthyletin, Seselin, HPLC-UV-MS.*

## Highlights

HPLC-UV method was developed for quantifying xanthyletin in Citrus with and without CVC symptoms after *X. fastidiosa* infection. Xanthyletin showed as a potential phytoanticipin against attack this pathogen.

## Resumo/Abstract

*Xylella fastidiosa* is a gram-negative bacterium that colonizes the xylem of plants, thereby causing diseases on several economically important crops, such as citrus variegated chlorosis (CVC) in sweet orange. The aims of this work were an investigation on the roots influence to CVC bacterium, as well as to verify whether compounds in the roots were associated with the citrus infection. To establish a representative chromatographic fingerprint for the roots of *C. sinensis* grafted on *C. limonia* cv. Pêra with and without CVC symptoms. Respective samples were individually analyzed using the established high performance liquid chromatography-diode array and liquid chromatography-ultraviolet-atmospheric pressure chemical ionization-mass spectrometric methods, and two peaks indicated the highest content among others with good resolution, and they were identified as xanthyletin and seselin, respectively. Thus, a HPLC-UV method was developed for quantifying both in roots, with a good linearity. The quantification method was applied to *Citrus* with and without CVC symptoms after *X. fastidiosa* infection (Figure 1). Xanthyletin showed a significant increase (44%) in its amount in symptomatic roots. Increased biosynthesis of this metabolite may represent a plant defense strategy in response to pathogen attack, since this compound showed antimicrobial activity on *X. fastidiosa* growth (MIC 34 nM). Our studies open up possibilities for engineering citrus enzymes to increase levels of xanthyletin and thereby enhance resistance against *X. fastidiosa*, and also show a model substance used by the plant itself as a defense mechanism, with the potential to become a bactericide.

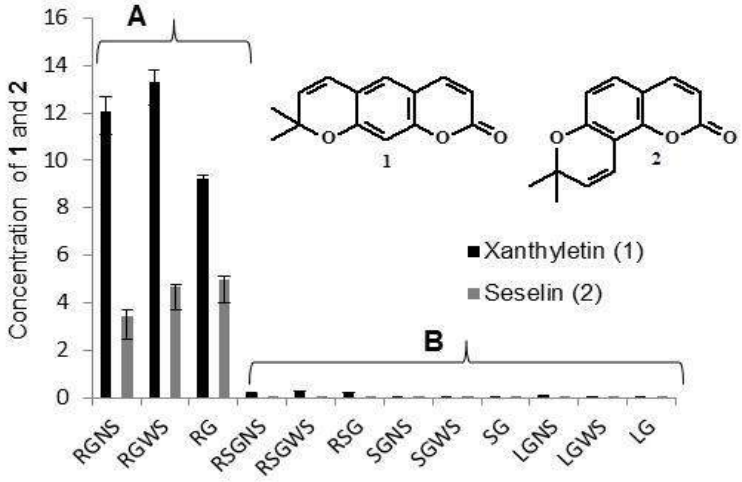


**Figure 1.** Variation in the contents of xanthyletin (1) and seselin (2) in diferent parts of C. sinensis grafted onto C. limonia with (WS) and without (NS) CVC symptoms. RG: negative control of roots of the graft; RSG: negative control of rootstock stem; SG: negative control of stem of the graft; LG: negative control of leaves of the graft. Results are expressed as the averages of three experiments and three individual analyses (mean ± S.D.; g $kg^{-1}$). A) Data from HPLC-UV experiments. B) Data from SRM experiments.

**Área: QPN** **Inscrição: 01222**

# Chemical composition and antiradicalar activity of pollen bee from *Melipona mandaçaia* Smith (Hymenoptera: Apidae)

**Amanda L. B. Monteiro (PG)[1,4], José F. Neto (PQ),[2] Eva M. S. Silva (PQ),[2] Rebert C Correia (PQ),[3] Celso A. Camara (PQ)[4], Tania M. S. Silva (PQ)[4]**

**amandalinsbmonteiro@gmail.com**

[1]Programa de Pós-Graduação em Biociência Animal, PPGBA-UFRPE *[2]Colegiado de Zootecnia, UNIVASF; [3]EMBRAPA-SEMI-ÁRIDO; [4]Laboratório de Bioprospecção Fitoquímica, DQ-UFRPE*

Palavras Chave: *Melipona mandaçaia, pólen, fenólicos, antiradicalar*

## Highlights

- Chemical composition of pollen from the stingless bee *Melipona mandacaia*
- Analysis by UPLC-PDA-qTOF-MS/MS
- Antiradical activity of pollen was evaluated

## Resumo/Abstract

A abelha mandaçaia (*Melipona mandacaia*) é uma das espécies sem ferrão endêmica do Nordeste Brasileiro. Além de sua importância como principal polinizador de inúmeras espécies nativas, os produtos obtidos desta espécie também podem ser fontes de compostos biologicamente ativos e desempenhar um papel importante na indústria nutricional. Duas amostras de pólen da mandaçaia foram coletadas no município de Remanso, Bahia. As amostras foram extraídas com Etanol. O extrato etanólico foi submetido a análise por UPLC-DAD-qTOF-MS/MS e atividade antiradicalar (DPPH). As duas amostras apresentaram semelhantes perfil químico (Figura 1), sendo identificados três flavonoides glicosilados: isorhamnetina-arabinopiranosídeo-ramnopiranosídeo (*m/z* 593.1506) isorhamnetina-rutinosideo-ramnopiranosídeo (*m/z* 769.2169) e isoramnetina-3-*O*-neohesperidosideo (*m/z* 623.1606) além de dois isômeros tipo amidas de ácidos cinâmicos com espemidina (*m/z* 762.3217). O teste antiradicalar apresentou valores de $CE_{50}$ (µg/mL): 204.8±7,1 para amostra 1 e 200.8±3,9 para amostra 2.

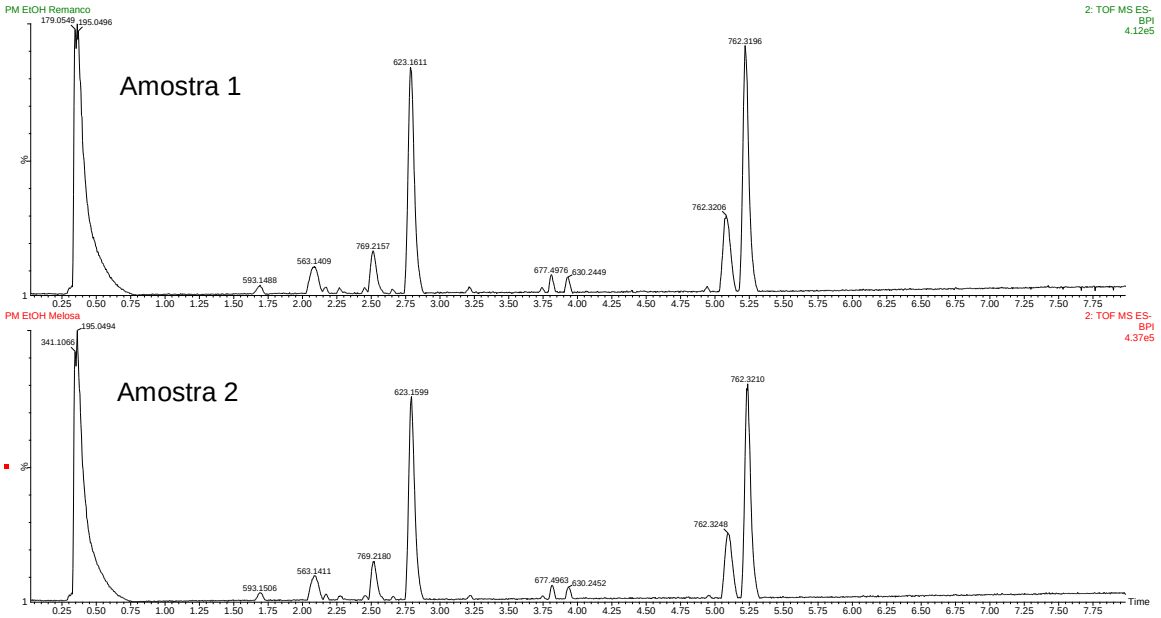


Figure 1. ESI base peak ion (BPI) chromatogram of the samples from *Melipona mandacaia* pollen analyzed by UPLC-QTOF-MS

Agradecimentos: CNPq (Projeto MeliApis) e FACEPE

**Área: QNP** **Inscrição: 01117**

# Analysis of geopropolis from the stingless bee *Melipona subnitida* (jandaira) by UHPLC-QTOF-MS/MS

**Hélter J.S. Souza (IC)[1*], Sonia P. Cabrera (PG)[1,2], Eva M. S. Silva (PQ)[3], Celso A. Camara (PQ)[1], Tania M.S. Silva (PQ)[1]**

**helter.ujr@gmail.com**

*[1]Laboratório de Bioprospecção Fitoquímica, DQ-UFRPE, [2]Programa de Pós-Graduação em Química, DQF- UFPE; [3]Colegiado de Zootecnia-UNIVASF*

*Keywords: Geopropolis, Melipona subnitida, UPLC-MS, Flavonoids*

## Highlights

- Chemical composition of Geopropolis from the stingless bee *Melipona subnitida* (jandaira)
- Presence of flavonoids identify by UPLC-PDA-qTOF-MS/MS

## Resumo/Abstract

*Melipona subnitida*, a stingless bee popularly known as “jandaira,” is native to northeastern Brazil. This species produces a variety of propolis popularly known as geopropolis, which consists of a mixture of resin, wax and soil. The objective of this study was to determine the chemical composition by ultra-high-pressure liquid chromatography along with quadrupole time-of-flight mass spectrometry (UHPLC-QTOF-MS/MS). The detected compounds in the sample (Table 1) were classified as aglycones flavonoids (flavonols, flavanonols, flavonones, flavones and chalcones). The mixture of flavonoids components may contribute to the activities related to geopropolis.

Table 1. Characterization of compounds from geopropolis collected by *Melipona subnitida*

| d | RT (min) | $\lambda_{max}$ (nm) | $[M-H]^-$ (*m/z*) | $[M-H]^-$ (*m/z*) Calculated | Tentative identification |
|---|---|---|---|---|---|
| 1 | 5.06 | 346 | 299.0546 | 299.0561 | Kaempferol methyl ether |
| 2 | 5.95 | 283 | 285.0757 | 285.0768 | Trimethoxy flavanone |
| 3* | 5.99 | 373 | 301.0356 | 301.0354 | Quercetin |
| 4 | 6.16 | 246 | 315.0500 | 315.0510 | Quercetin methyl ether |
| 5 | 6.21 | 287 | 301.0342 | 301.0717 | Trihydroxy-methoxy-flavanonol |
| 6 | 6.45 | 356 | 315.0500 | 315.0510 | Quercetin methyl ether |
| 7 | 6.60 | 356 | 345.0602 | 345.0616 | Myricetin dimethyl-ether |
| 8* | 6.82 | 288 | 271.0601 | 271.0611 | Naringenin |
| 9 | 6.97 | 364 | 285.0405 | 285.0404 | Fisetin |
| 10 | 7.04 | 343 | 299.0541 | 299.0561 | Kaempferol methyl ether |
| 11* | 7.11 | 361 | 315.0504 | 315.0510 | Isorhamnetin |
| 12 | 7.43 | 346 | 299.0545 | 299.0561 | Kaempferol methyl ether |
| 13 | 7.47 | 287 | 315.0500 | 315.0874 | Aromadendrin dimethyl ether |
| 14 | 7.61 | 345 | 329.0654 | 329.0667 | Quercetin dimethyl ether |
| 15 | 7.67 | 361 | 329.0657 | 329.0667 | Quercetin dimethyl ether |
| 16 | 7.85 | 369 | 285.0742 | 285.0404 | Trihydroxy-methoxy-chalcone |
| 17 | 8.10 | 296 | 301.0700 | 301.0717 | Trihydroxy-methoxy-flavanone |
| 18 | 8.22 | 275 | 269.0800 | 269.0819 | Hydroxy-methoxy-flavanone |
| 19 | 8.54 | 333 | 313.0703 | 313.0718 | Kaempferol dimethyl ether |
| 20 | 8.72 | 358 | 329.0642 | 329.0667 | Quercetin dimethyl ether |
| 21 | 8.91 | 341 | 343.0805 | 343.0823 | Quercetin trimethyl ether |
| 22* | 9.17 | 287 | 285.0741 | 285.0768 | 7-*O*-methyl naringenin (sakuranetin) |
| 23 | 9.33 | 339 | 283.0605 | 283.0612 | Dihydroxy methoxy flavone |
| 24 | 9.82 | 346 | 313.0703 | 313.0718 | Kaempferol dimethyl ether |
| 25 | 10.0 | 364 | 269.0814 | 269.0819 | Dihydroxy methoxy chalcone |
| 26 | 10.12 | 286 | 299.0914 | 299.0925 | Naringenin dimethyl ether |

Acknowledgments: CNPq (Grant no. 454249/2014-4), FACEPE (Grant no. PRONEM APQ-0741106/2014) and CAPES.

**Área:** QPN
*(Inserir a sigla da seção científica para qual o resumo será submetido. Ex: ORG, BEA, CAT)*

**Inscrição:** 01061
*(Inserir o número de inscrição do autor que fez a submissão)*

# Chemical composition and antioxidant potential of honey bee of abelha branca (*Frieseomelitta doederleini*)

**Rogelio M. Santisteban (PG),[1] José F. Neto (PQ),[2] Eva M. S. Silva (PQ),[2] Rebert C Correia (PQ),[3] Celso A. Camara (PQ)[4], Tania M. S. Silva (PQ)[4]**

**rogmoreno072@gmail.com**

*[1]Programa de Pós-Graduação em Química, DQF-UFPE; [2]Colegiado de Zootecnia, UNIVASF; [3]EMBRAPA-SEMI-ÁRIDO; Laboratório de Bioprospecção Fitoquímica, DQ-UFRPE*

Palavras Chave: *Frieseomelitta doederleini, Abelha branca, Mel, fenólicos, antioxidante*

## Highlights

- Chemical composition of honey from the stingless bee *Frieseomelitta doederleini*
- The antioxidant potential of honey was evaluated
- Presence of 24 phenolics by UPLC-PDA-qTOF-MS/MS

## Resumo/Abstract

A abelha-branca (*Frieseomelitta doederleini*) é uma abelha sem ferrão nativa da região semi-árida do Nordeste Brasileiro e produz um mel de aroma suave, além da capacidade de acumular grandes quantidades de resina e pólen. Não existe relato na literatura de estudos químicos com o mel desta abelha. Cinco amostras de mel foram coletadas no município de Remanso, Bahia. As amostras foram submetidas as análises físico-químicas, químicas (UPLC-PDA-qTOF-MS/MS) e potencial antioxidante (DPPH e ABTS). Os resultados dos testes físico-químicos mostraram-se dentro do padrão para os méis coletados por abelhas nativas. O perfil cromatográfico foi semelhante para as cinco amostras analisadas e foram identificados 24 fenólicos, sendo as flavanonas e os flavonols os componentes majoritários (Figura 1). Os testes antiradicalares com o mel puro mostrou resultados promissores com valores de $EC_{50}$ (mg/mL) variando entre 7,19±1,07-14,32±0,81 para o DPPH e 4,21±0,96-5,51±0,10. Os resultados obtidos com estas análises mostram que o mel de abelha branca pode apresentar potencial bioatividade.

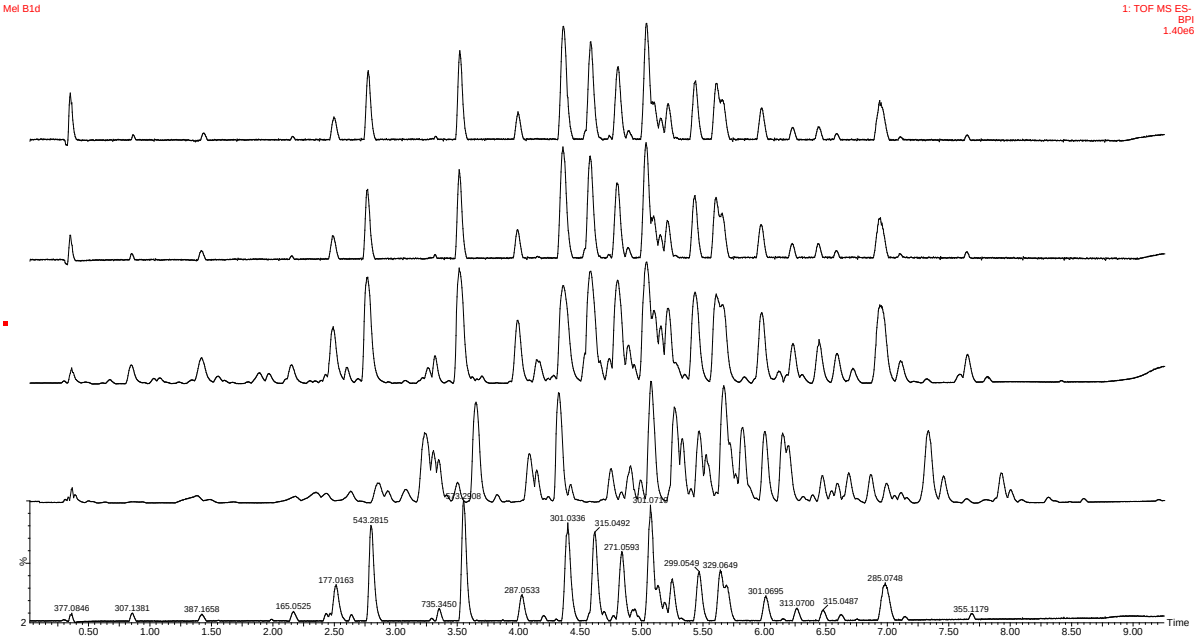


Figure 1. ESI base peak ion (BPI) chromatogram of the samples *Frieseomelitta doederleini* honeys (1-5) analyzed by UPLC-QTOF-MS

Agradecimentos: CNPq (Projeto MeliApis) e FACEPE

**Área: QPN** **Inscrição:00691**

# (*Z*)-octadec-9-enolide, a kairomone isolated from the Mediterranean flour moth (*Anagasta kuehniella)* frass

**Douglas J. de Melo (PG),[1] Arodi P. Favaris (PG),[2] Diogo M. Vidal (PQ),[3] José M. S. Bento (PQ),[2] Paulo H. G. Zarbin (PQ),[1*]**

**vidal@qui.ufmg.br; pzarbin@ufpr.br**

*[1]Departamento de Química, UFPR; [2]Departamento de Entomologia e Acarologia, ESALQ-USP; [3]Departamento de Química, UFMG.*

Palavras Chave: *chemical ecology, GC-FTIR, macrolide, frass volatiles.*

## Highlights

Frass produced by A. *kuehniella* are attractant to *Habrobracon hebetor females*. The lactone (*Z*)-octadec-9-enolide was identified (and synthesized) as the main candidate for the observed attractiveness.

## Resumo/Abstract

A*nagasta kuehniella* Zeller (Lepidoptera: Pyralidae) (Fig. 1A) is popularly known as Mediterranean flour moth. The eggs from this moth are among the most nutritious for mass-rearing of natural biological control agents, specially from the genus *Trichogramma* (Fig. 1B). One of the main problems on *A. kuhniella* mass-rearing is caused by the ectoparasitoid *Habrobracon hebetor* (Fig. 1C), which feeds on lepidoptera's larvae. Experimental data showed that *H. hebetor* are strongly attracted to *A. kuhniella* frass, suggesting the presence of a volatile kairomone. A possible solution for *H. hebetor* infestations would be the use of traps using the synthetic kairomone as lure. Based on the described observations, this study aims to extract, identify and synthesize the compound(s) which are bioactive in *H. hebetor* from the *A. kuehniella* frass. Natural samples were prepared by extracting fresh *A. kuehniella* frass with dichloromethane, followed by fractionation on silica flash. Bioassays showed that one fraction, which contained a major compound was attractive to *H. hebetor* females. GC-MS and GC-FTIR analyses suggested a structure related to a (*Z*)-octadecenolide. GC-MS analysis of a derivatization performed with DMDS suggested the double bond positioned at $C_9$-$C_{10}$. A synthetic route was proposed for (*Z*)-octadec-9-enolide (Scheme 1), starting by the mono-protection of 1,9-nonanediol (**2**) with THP, followed by oxidation of the remaining hydroxyl group with PCC, yielding **3**, in 56% global yield. The next step consisted on a Wittig reaction between 3 and the ylide from methyltriphenylphosphonium bromide, followed by the removal of the THP group and Jones oxidation, yielding 4 in 77% (3 steps). Compounds **4** and **5** were esterified by treatment with EDC and DMAP, yielding **6** in 80% yield. In the last step, a ring closing metathesis yelded the macrolide **1** in 21%.

MS and FTIR spectra, and retention indexes found for the synthetic **1** matched the data for the natural, confirming the proposed structure as (*Z*)-octadec-9-enolide. Laboratory and field bioassays using the synthetic compound are underwav.

**Figure 1.** The lepidopteran A*nagasta kuehniella* (**A**), and the parasitoids *Tricogramma spp.* (**B**) and *Habrobracon hebetor* (**C**). Credits: A- Stuart Marcus, B- John Rosenfeld, C- Sean McCann.

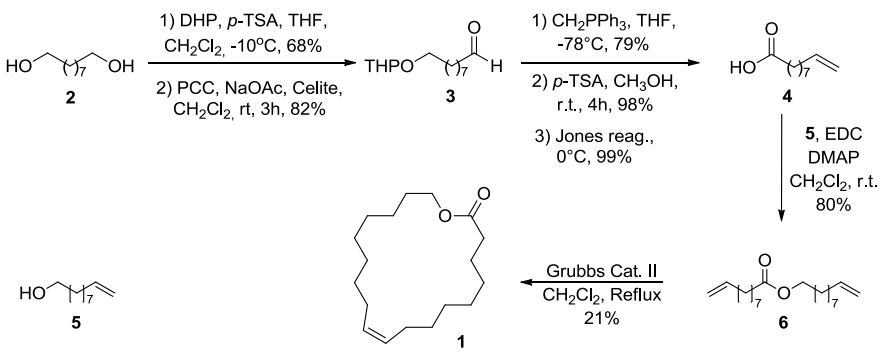


**Scheme 1.** Synthesis of (Z)-octedec-9-enolide (**1**).

**Acknowledgements:** INCT Semioquímicos na Agricultura and FAPEMIG.

**Área: QPN** **Inscrição: 01325**

# Amino-naphthoquinones and isatins of *Salinispora arenicola*, a Bacterium Recovered from the Marine Sediments of St. Peter and St. Paul, Brazil

**Alison B. da Silva (PG),[1] Edilberto R. Silveira (PQ),[1] Diego V. Wilke (PQ),[2] Leticia V. Costa-Lotufo (PQ),[3] Maria Conceição M. Torres (PQ)[4] and Otilia Deusdenia L.Pessoa (PQ).[1]**

**otilialoiola@gmail.com; alisonquimicaufc@hotmail.com**

*[1]Departamento de Química Orgânica e Inorgânica, Universidade Federal do Ceará, 60.021-970, Fortaleza-CE, Brazil; [2]Departamento de Fisiologia e Farmacologia, Universidade Federal do Ceará, Fortaleza, CE, 60.430–275, Brazil; [3]Departamento de Farmacologia, Universidade de São Paulo, 05508-900, São Paulo - SP, Brazil. [4]Departamento de Química, Universidade Estadual da Paraiba, 58429-500, Capina Grande-PB, Brazil.*

Palavras Chave: Marine microorganisms, *Salinispora arenicola*, Amino-naphothoquinones, isatins

## Highlights

-The chemical study of the marine bacteria *Salinispora arenicola*, recovered from sediments of St. Peter and St. Paul archipelago (Brazil) was investigated.
-Eight compounds, all previously unknown, were isolated.
-Amino-1,4-naphthoquinones, uncommon compounds, are important core for biologically active compounds.
-This is the first study of a Brazilian *S. arenicola* strain.

## Resumo/Abstract

Marine microorganisms, in particular the actinomycetes, are known as a prolific source of new active compounds. The taxon *Salinispora*, a group of actinomycetes exclusively marine, was formally described in 2005.[1] *Salinispora* spp. are most frequently reported from marine sediments, however, they have also been reported from an ascidian, seaweeds, and marine sponges.[2] *Salinispora* strains have been cultured from tropical and sub-tropical sites around the globe, and the primary interest has focused on its ability to produce biologically active secondary metabolites as the salinosporamides A-K, previously isolated of *S. tropica*.[3,4] Eight compounds (**1** – **8**), were isolated from the EtOAc extract obtained from the fermentation broth of a marine bacterial strain identified as *Salinispora arenicola*, which was isolated from sediments collected at the Brazilian Saint Peter and Saint Paul Archipelago. The structures of **1** - **8** were elucidated by interpretation of their spectroscopic data (IR, 1D and 2D NMR, and HRESIMS) and by comparison with published data of analogous compounds. Compounds **1** – **4** are 2- or 3-amino-1.4-naphtoquinones. Aminonaphthoquinones are found as the core of a number of commercially and biologically important natural products as rifabutin, a semisynthetic derivative of rifamycin S, currently used in the treatment of tuberculosis, and the natural product salinisporamycin, a promising antibacterial and anticancer agent.[5]

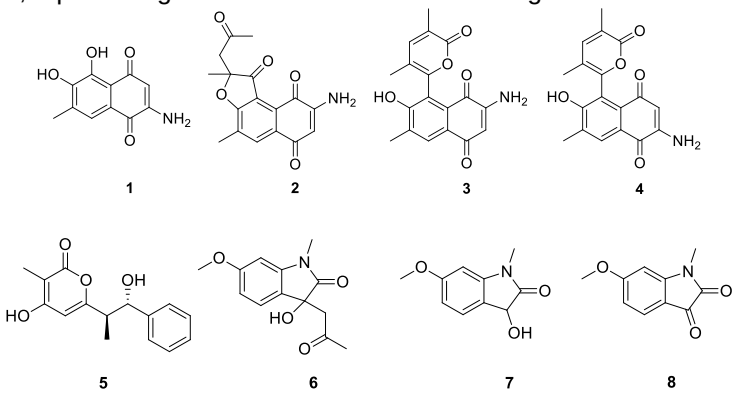


**Figure 1:** Structures of the new compounds **1** – **8**.

1**.** Luis A. Maldonado, L. A.; Fenical, W.; Jensen, P. R.; Christopher A. Kauffman, C. A.; Tracy J. Mincer, T. J.; Ward, A. C.; Bull, A. T.; Goodfellow, M. Int. J. Syst. Evol. Microbiol. 2005, 55, 1759–1766.
2. Jensen, P.R.; Moore, B. S.; Fenical, W. Nat. Prod. Rep. 2015, 32, 738-751
*3.* Gulder, T. A.; Moore, B. S. *Angew Chem Int Ed Engl. 2010, 49, 9346-9367.*
4. Feling, R. H.; Buchanan, G. O.; Mincer, T. J.; Kauffman, C. A.; Jensen P. R.; Fenical, W. *Angew Chem Int Ed Engl. 2003, 42, 355-357.*
5. Nawrat, C.C.; Lewis, W.; Moody, C. J. J. Org. Chem. 2011, 76, 7872–7881.

**Área: QPN** **Inscrição: 00969**
*(Inserir o número de inscrição do autor que fez a submissão)*

# Avaliação da atividade anti-*Trypanossoma cruzi* de alcalóides identificados em *Duguetia lanceolata*

**Erick P. Dantas (PG),[1] Lhaís Araújo Caldas* (PG),[1] João Henrique G. Lago (PQ),[2] Marisi G. Soares (PQ),[3] André G. Tempone (PQ),[4] Patricia Sartorelli (PQ).[1*]**

**dantaserick@hotmail.com; patty.sart@gmail.com**

[1] *Instituto de Ciências Ambientais, Químicas e Farmacêuticas, Universidade Federal de São Paulo, Diadema/SP.,* [2]*Centro de Ciências Naturais e Humanas, UFABC,* [3]*Instituto de Química, Universidade Federal de Alfenas/MG,* [4] *Centro de Parasitologia e Micologia, Instituto Adolfo Lutz, São Paulo/SP.*

Palavras Chave: *Duguetia lanceolata, Alcalóides, Atividade antiparasitária, T. cruzi.*

## Highlights

Evaluation of anti-*Trypanosoma cruzi* activity of alkaloids identified in *Duguetia lanceolata.* Alkaloids extraction of *Duguetia* lanceolata. Evaluation of the activity against *T. cruzi* from fractions of the alkaloid extract of *D. laceolata*. Identification of liriodenine, glaucine and anonaine from leaves of *D. lanceolata.*

## Resumo/Abstract

A família Annonaceae é composta por 135 gêneros e 2.500 espécies; 34 das quais encontradas na América do Sul, sendo 29 ocorrendo no Brazil, incluindo o gênero *Duguetia* [1, 2]. Os estudos de metabólitos secundários da família Annonaceae relatam vários metabólitos, como alcalóides, acetogeninas e ácido graxos, e demonstraram atividades biológicas, como, antitumoral, antimicrobiana, antiparasitária e inseticida [3]. Embora, exista um grande número de metabólitos bioativos isolados, os estudos com a espécie *Duguetia lanceolata* é bem pequeno, existindo relatos sobre os metabólitos fixos e voláteis, como também atividade inseticida e antiparasitária [4]. O presente trabalho teve por objetivo realizar a extração da fração alcaloídica das folhas de *Duguetia. lanceolata* e identificação de alcalóides biomonitorado pelo ensaio antiparasitário frente a tripomastigostas de *T. cruzi.* Desta forma o extrato bruto etanólico das folhas foi solubilizado com HCl 3% e então submetido à extração líquido-líquido com hexano. O pH da fase ácida foi ajustado para 10 com NaOH 25% e extraído com $CH_2Cl_2$, seguindo metodologia da literatura [1]. A fase orgânica foi então recolhida e concentrada em rotoevaporador produzindo 1,0 g de extrato alcaloídico (EA). Para a confirmação da presença dos alcalóides neste extrato, o mesmo foi submetido à CCD e revelado com solução de Draggendorff, confirmando a presença de alcaloides pelo tom alaranjado das manchas. O EA foi então submetido à CC em coluna de sílica flash com gradiente crescente de polaridade de MeOH:$CH_2Cl_2$. As frações EA9 e EA10 foram reveladas em Draggendorff sendo positivas para alcaloides. EA e estas frações foram então submetidas ao ensaio para detecção de atividade frente à tripomastigotas de *T. cruzi* eliminando 100% dos parasitas. A fração EA9 foi novamente submetida à CC em coluna de sílica flash, seguida por CC sephadex e CLAE gerando três sub-frações (EA9-3-6 P2, EA9-3-6-pico 3 e EA9-3-3-2) todas reveladas com Draggendorff. As analises dos dados de RMN de $^{1}H$ e de $^{13}C$ permitiram sugerir a presença dos alcaloides aporfínico anonaina e glaucina, além do alcaloide oxoaporfínico liriodenina, todos com ampla distribuição na familia Annonaceae [3].

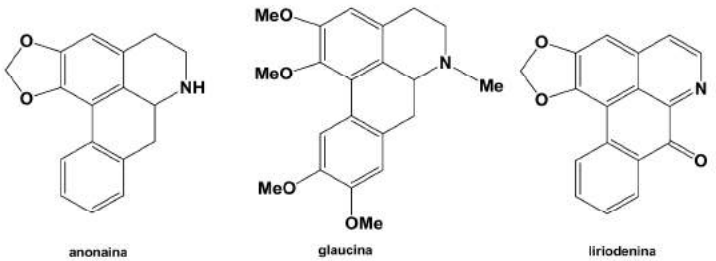


anonaina glaucina liriodenina

[1] CAROLLO, Carlos A. et al. Journal of Natural Products, v. 69, n. 8, p. 1222-1224, 2006.
[2]. KONG, Chuihua et al. Phytochemistry, v. 65, n. 8, p. 1123-1128, 2004.
[3] LEBOEUF, M. et al., Phytochemistry, v. 21, no. 12, pp. 2783-2813. 1982
[4] SOUSA, O.V. et al., Molecules. v. 17, p. 11056-11066. 2012.

**Área: ____QPN____ Inscrição:___00937___**

# Dereplication strategies for discovering cytotoxic compounds from *Swinglea glutinosa* (Rutaceae)

**Ana C. Carvalho (PG),[1] Alany I. Ribeiro (PG),[2] Maria Fátima das G. F. da Silva (PQ),[2] Lívia S. Medeiros (PQ),[1] Thiago A. M. Veiga (PQ),[1]**

**ana_c.carvalho@hotmail.com**

*[1]Departament of Chemistry, UNIFESP; [2]Departament of Chemistry, UFSCAR.*

Key words: *Swinglea glutinosa; Acridonic alkaloids; Leukemia assays.*

## Highlights

In this work three acridonic alkaloids were isolated from the steam hexane extract of *Swinglea glutinosa*. This extract presented cytotoxic effect against human leukemia cells (Kasumi-1 and Jurkat, 48 hrs).

## Resumo/Abstract

*Swinglea glutinosa* is a monotypic plant from Rutaceae family. It is a tropical plant originating from Southeast Asia. It can be found in Latin America, mainly in Colombia and Brazil[1]. *Swinglea* is widely used as ornamental plant, popularly called lemon swinglea[1]. There are already some studies concerning on metabolites isolated from *S. glutinosa* and its biological and biochemical activities[2,3,4]. The genus is characterized by the presence of acridonic alkaloids[2] and some biological activities were associated for acridones as herbicidal[2], cytotoxic[3] and antiparasitic[4]. In this work, the stem hexane extract of *S. glutinosa* presented cytotoxic effects against human leukemia cells (Kasumi-1 and Jurkat, 48 h) (Figure 1A). Based on the anti-cancer results, dereplication strategies[5] have been applied to guide the purification of the active fraction, which led to three prenylated acridones: 5-hydroxynoracronycine (**1**), pyranofoline (**2**) and 1,5-dihydroxy-4-methoxy-10-methyl-2-(3-methylbut-2-enyl)acridin-9(10H)-one (**3**) (Figure 1B). These compounds will be evaluated against the human leukemia cells (Jurkat, K-562, Kasumi-1 and Raji) to confirm the previous data observed for the crude-active sample.

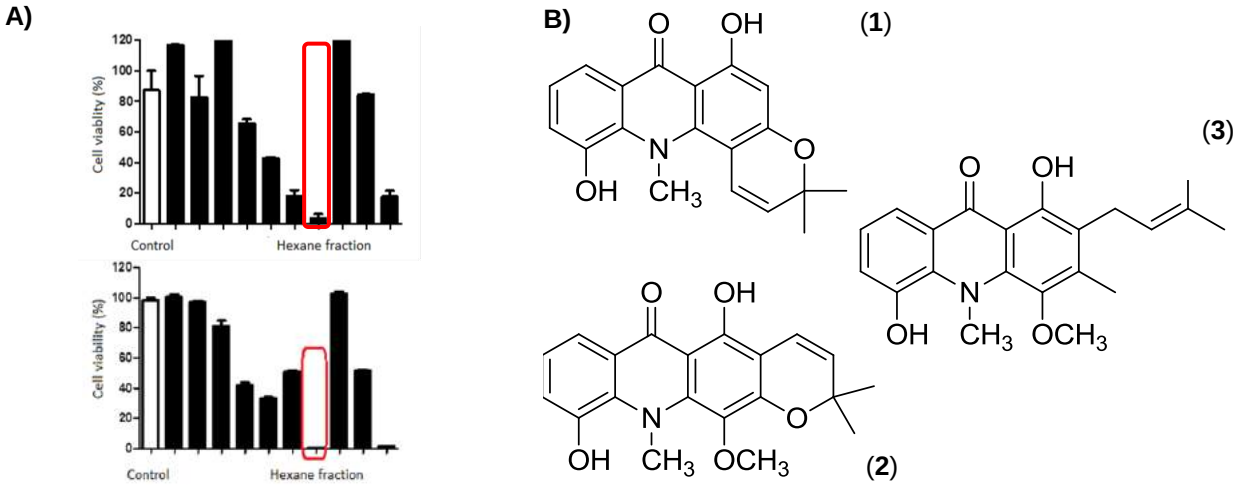


Figure 1: **A)** Cytotoxic activity against human leukemia cells (Kasumi-1 and Jurkat, 48 hrs). **B)** Acridonic alkaloids isolated from crude-active fraction of *S. glutinosa.*

**References**

[1] Weniger, B.; Um, B-H.; Valentin, A.; Estrada, A.; Lobstein, A.; Anton, R.; Maillé, M.; Sauvain, M.; J. Nat. Prod.v. 64, p. 1221, 2001.
[2] Arato Ferreira, P. H. et al. Biodiversity, v. 13, n. 1, p. 100–106, 2016.
[3] Braga, P. A. C. et al. Nat Prod Res, v. 21, n. 1, p. 47–55, 2007.
[4] Vieira, P. C.; Rattray, l.; Croft, S. L. J. Braz. Chem. Soc. v. 20, n. 4, p. 644–651, 2009.
[5] Carvalho, A.C. 6 th Brazilian Conference of Natural products. 2017.

**Área: QPN** **Inscrição: 00453**

# Duguetinine, an isoquinoline-derived alkaloid with an unprecedented skeleton from the bark of *Duguetia surinamensis* (Annonaceae)

**Rodolfo N. de Oliveira (PG),[1] Felipe M. A. da Silva (PQ),[1] Ingrid R. S. Baliza (IC),[2] Larissa M. Bomfim (IC),[2] Milena B. P. Soares (PQ),[2] Daniel P. Bezerra (PQ),[2] Jackson R. G. S. Almeida (PQ),[3] Hector H. F. Koolen (PQ),[4] Emmanoel Vilaça Costa (PQ).[1]***

*** emmanoelvc@gmail.com**

*[1]Department of Chemistry, Federal University of Amazonas – UFAM; [2]Gonçalo Moniz Institute, Oswaldo Cruz Foundation – IGM-FIOCRUZ/BA; [3]Center of Study and Research of Medicinal Plants, Federal University of Vale of São Francisco – UNIVASF; [4] Metabolomics and Mass Spectrometry Research Group, Amazonas State University – UEA.*

Keywords: *Duguetia surinamensis, Aporphine alkaloids, Oxahomoaporphine skeleton, Benzenoids, Cytotoxic activity.*

## Highlights

1. Eight alkaloids and two benzenoids were isolated and characterized for the first time in *Duguetia surinamensis*.
2. A new alkaloid named duguetinine with an unprecedented isoquinoline skeleton denominated as oxahomoaporphine is described herein.
3. A benzenoid isolated as natural product for the first known 1-(2,4,5-trimetoxyphenyl)-1,2-ethanediol was also described.
4. Cytotoxic activities were investigated for the isolated compounds.
5. Potent cytotoxicity was observed for 7-hydroxynordicentrine, dicentrine, duguetine, and duguetine-*N*-oxide.

## Abstract

*Duguetia surinamensis* (R.E. Fries) is a species of the Annonaceae family, unknown from both chemical and pharmacological points of view. It is endemic to the Amazon region found in Brazil, Colombia and Guianas. In this work, the phytochemical study through a bioactivity-guided approach was carried out by evaluating the *in vitro* cytotoxicity of *D. surinamensis*. By means of classical chromatography techniques, ten substances were isolated being eight alkaloids and two benzenoids. For the structural elucidations, mass spectrometry and nuclear magnetic resonance spectroscopy (1D/2D) were employed. The absolute stereochemistry was assigned by NOE NMR experiments, ECD spectroscopy, and theoretical calculations. The alkaloids were identified belonging to the subclasses: aporphine (duguetine-**1**, dicentrine-**2**, 7-hydroxynordicentrine-**3**, and duguetine-*N*-oxide-**4**), oxoaporphine (dicentrinone-**5**), tetrahydroprotoberberine, (tetrahydrojathrorrizine-**6**), and morphinan (pallidine-**7**). An alkaloid with an unprecedented isoquinoline skeleton, named duguetinine-**8**) was isolated. Benzenoids were identified as being 1,2,4-trimethoxybenzene-**9** and a new natural product 1-(2,4,5-trimetoxyphenyl)-1,2-ethanediol-**10**, described only as synthetic product. Among them, tetrahydrojathrorrizine, duguetine, duguetine-*N*-oxide, and dicentrinone were previously reported in *Duguetia*. Pallidine was the first alkaloid of the subclass morphinan isolated in *Duguetia*, and 7-hydroxydicentrine was isolated for the first time in Annonaceae. The methanolic extract presented moderate cytotoxic activity against HepG2 (human-hepatocellular-carcinoma) and K562 (human-chronic-myelocytic-leukemia) cell lines with $IC_{50}$ values equal to 46.86 and 35.58 µg/mL, respectively. The compounds 7-hydroxynordicentrine, dicentrine, duguetine, and duguetine-*N*-oxide alkaloids displayed promising cytotoxic activities against MCF7 (human-breast-adenocarcinoma), HCT116 (human-colon-carcinoma), HepG2, and HL-60 (human-promyelocytic-leukemia), with $IC_{50}$ below 8.0 µg/mL for all cells tested, except for the duguetine-*N*-oxide against HepG2 cell line, which had an $IC_{50}$ of 10.41 µg/mL. The results obtained in this reinforces the chemosystematics proposed for the Annonaceae family. Our findings also display *D. surinamensis* as a new reliable source of substances with potential cytotoxic activities.

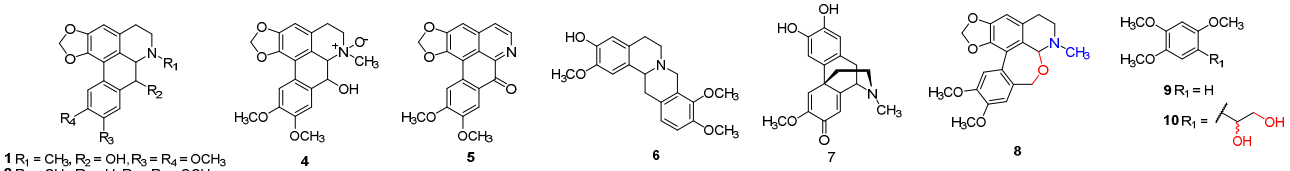

**1** $R_1 = CH_3$, $R_2 = OH$, $R_3 = R_4 = OCH_3$
**2** $R_1 = CH_3$, $R_2 = H$, $R_3 = R_4 = OCH_3$
**3** $R_1 = H$, $R_2 = OH$, $R_3 = R_4 = OCH_3$

**4** **5** **6** **7** **8**

**9** $R_1 = H$
**10** $R_1 =$

**Área: QPN** **Inscrição: 01030**

# Chemical, Cytotoxic and Antimalarial Study of *Dipteryx lacunifera*

**Leonardo S. Alexandre (IC),[1*] Mariana H. Chaves (PQ),[1] Gerardo Magela Vieira Jr. (PQ)[1]**

**leonardo.alexandre.ufpi@gmail.com**

[1]*Chemistry Department – Federal University of Piauí*

Keywords: Dipteryx lacunifera, *Flavonoids, Antimalarial, Cytotoxicity*

## Highlights

The chemical study of *D. lacunifera* led to the isolation of Isoliquiritigenin and 6,3',4'-trihydroxyflavone. Compounds are related for the first time in this species. The substances showed cytotoxic and antimalarial activities.

## Abstract

The *Dipteryx* genus has 14 species and accumulates in its chemical constitution coumarins, isoflavones and triterpenoids.[1] Previous studies with *D. lacunifera* has identified substances that have relevant radical scavenging activity and some of them related for the first time in this species.[2] Knowing its potential this work aims to isolate, identify and evaluate cytotoxic and antimalarial activity of the substances.

The ethereal phase of seed bark was submitted to chromatographic procedures in sephadex LH 20 and silica gel columns. Nuclear Magnetic Resonance and Mass Spectrometry were used to identify the fractions DFE-80-07 (**1**) and DFE-80-32 (**2**). The substances were submitted to cytotoxic and antimalarial activities.

The fractions DFE-80-07 and DFE-80-32 was identified, respectively, as Isoliquiritigenin (**1**) and 6,3',4'-trihydroxyflavone (**2**) (Figure 1). Table 1 shows values of medium Inhibitory Concentration capable of induce 50% of maximum effect, $IC_{50}$ by the MTT assay.

Figure 1 – Compounds **1** and **2** isolated from *D. lacunifera*

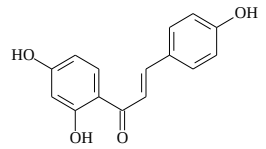


(**1**)

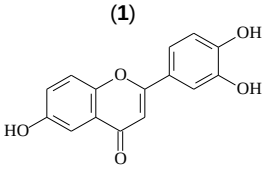


(**2**)

Table 1 – $IC_{50}$ of isolated compounds from *D. lacunifera*

| Compunds | Lines $IC_{50}$ (µg/mL) | | | | |
|---|---|---|---|---|---|
| | **HCT-116** (Colorectal) | **HL-60** (Leukemia) | **PC3** (Prostate) | **SNB19** (CNS) | **HEK-293** (Kidney – Non-tumor cell) |
| **1** | 13.06 | 2.47 | 7.04 | 12.11 | 8.00 |
| **2** | 21.13 | 5.18 | 20.17 | > 25 | > 25 |
| **Doxorrubicin** | 0.01 | 0.02 | 0.24 | 2.05 | 0.77 |

The substances showed cytotoxicity against all tested tumor cell lines, mainly in leukemia line, both showed cytotoxicity against human kidney, despite being a non-tumoral line it is an immortalized line.

The antimalarial activity of the substances was realized against *Plasmodium falciparum*. Compound **1** showed 81.25% and compound **2** 88.98% of reduction of parasitemia.

Through chromatographic and spectrographic techniques was possible to isolate and identify two flavonoids present in seed bark from *D. lacunifera*, for the first time in this species, which also showed good cytotoxic and antimalarial activities.

[1]MENDES, F. N. P., SILVEIRA, E. R. Fatty acids, sesqui- and diterpenoids from seed of *Dipteryx lacunifera*. **Phytochemistry**. v. 35, p. 1499-1503, 1994.

[2]VIEIRA JÚNIOR, G. M., SILVA, H. R., BITTENCOURT, T. C., CHAVES, M. H. Terpenos e ácidos graxos de *Dipteryx lacunifera* Ducke. **Química nova**. v. 30, n.7, p. 1658-1662, 2007.

[3]MARKHAM, K. R., TERNAI, B. 13C NMR of flavonoids–II: flavonoids other then flavone and a flavonol aglycones. **Tetrahedron.** Great Britain: Pergamon Press, vol. 32, p. 2607-2612, 1976.

**Área: QPN** **Inscrição: 01206**

# Elaboration of spectral library on HPLC-DAD and identification of chemical constituents in *Dipteryx lacunifera*

**João Paulo S. Gomes (IC),[1*] Mariana H. Chaves (PQ),[1] Gerardo Magela Vieira Jr. (PQ)[1]**

***pjoao523@gmail.com**

[1]*Department of Chemistry- UFPI*

Keywords: *Spectral Library, standards, HPLC-DAD, flavonoids, Dipteryx lacunifera*

## Highlights

Comparison by UV and retention time. Flavonoids dereplication database. Identification in extract from *Dipteryx lacunifera.*

## Abstract

Spectral libraries are important for the preliminary identification of compounds that is focus of research in the field of natural products.[1] Many parameters can be used to mount a comparative library, such as, retention time and spectra, which are used for dereplication of substances in different matrices.[2] The objective of this work is elaboration a flavonoid database in a HPLC-DAD and subsequent dereplication in extract from *D. lacunifera*.

The methodology used consists of the analysis of two compounds isolated plant patterns, being prepared in a ratio MeOH:$H_2O$ (7:3). The analysis was performed on a HPLC-DAD using as mobile phase MeOH:$H_2O$ with gradient programming of 5-100% (0-50 min) in a flow of 1 mL·min$^{-1}$, obtaining the UV spectrum and the retention time. The ethereal fraction of the *D. lacunifera* seeds was used for the comparation with standards.

The comparative analysis of the extract with the initial spectral library was possible to identify, in the ethereal fraction from seeds from *D. lacunifera*, two compounds, Isoliquiritigenin (**1**) and 6,3',4'-trihydroxyflavone (**2**) (Figure 1) with similarity of 99.61 and 99.93%, respectively. In conclusion, the initial spectral library performed, providing a fast identification of known substances in plants extracts.

Figure 1: Comparison spectral of chemical constituents (**1** and **2**) with the ethereal extract from *D. lacunifera*

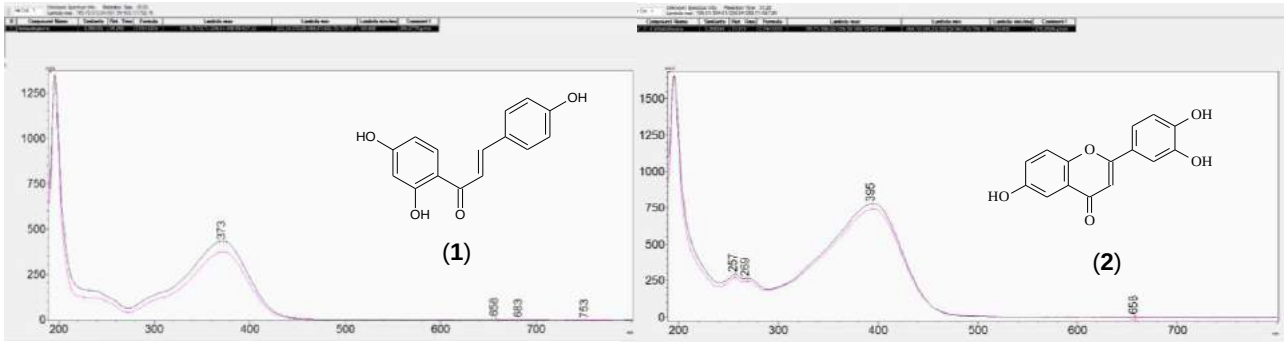


Similarity of (**1**) 99.61% and (**2**) of 99.93%

[1]FUNARI, C. S. CASTRO-GAMBOA, I; CAVALHEIRO, A. J.; BOLZANI, V. S. Química Nova. **2013**, 36, 1605.
[2]PAIVA, F.V.; SOUZA, N. C.; HAANDEL, A. C. V. Eng Sanit Ambient. **2011**, 16, 37.

**Área: QPN** **Inscrição: 1165**

# Phytochemical study of polar phases from *Richterago campestris* (Asteraceae)

**Victor F. Farinella (PG)[1]*, Cinthia I. Tamayose (PG)[2], Nádia Roque (PQ)[3], Marcelo J. P. Ferreira (PQ)[1]**

**marcelopena@ib.usp.br, victorffarinella@gmail.com**

*[1]Instituto de Biociências e [2]Instituto de Química - Universidade de São Paulo, 05508-090, São Paulo, Brazil; [3]Instituto de Biologia, Universidade Federal da Bahia, 40170-290, Salvador, Brazil*

Keywords: *Richterago campestris, Asteraceae, Flavonoids, chlorogenic acids derivatives*

## Highlights

Phytochemical study and antiradical activities of polar phases from *Richterago campestris* (Asteraceae).
- The first study of the chemical composition of polar phases from *Richterago campestris*;
- Five flavonoids, four chlorogenic acid derivatives and caffeic acid were identified

## Resumo/Abstract

Asteraceae, the second largest family of flowering plants, contains more than 25,000 species and 1700 genera distributed among 43 tribes. Gochnatieae tribe is the sister group of ~96% of the species in Asteraceae and shows 7 genera[1]. Among them, *Richterago* comprises 16 species, all endemic to Brazil. *Richterago campestris* Roque & J.N. Nakaj occurs only in Minas Gerais state[2] and no data about its chemical constituents are described in the literature. This work aims to report the first phytochemical study of polar phases from *R. campestris.* Extracts from aerial parts (68.46 g) of *R. compestris* were prepared with hexane and subsequently with methanol. Methanol extract was partitioned successively with hexane, dichloromethane, ethyl acetate (EtOAc) and buthanol (BuOH). These groups were analyzed with HPLC- UV-DAD. From the EtOAc and BuOH phases were identified through NMR and commercial standards five flavonoids [quercetin-3-O-galactoside **(1)**, quercetin-3-O-glucoside **(2)**, quercetin 3-O-β–(6”-O-E-caffeoyl)-galactoside **(3)**, tiliroside **(4)**, 3’-methoxy-helichrysoside **(5)**], four chlorogenic acids derivatives [5-O-(E)-caffeoylquinic acid **(6)**, 3,5-di-O-(E)-caffeoylquinic acid **(7)**, 4,5-di-O-(E)-caffeoylquinic acid **(8)**, 3,4-di-O-(E)-caffeoylquinic acid **(9)**], and the caffeic acid **(10)**. These compounds were reported for the first time in *R. campestris*.

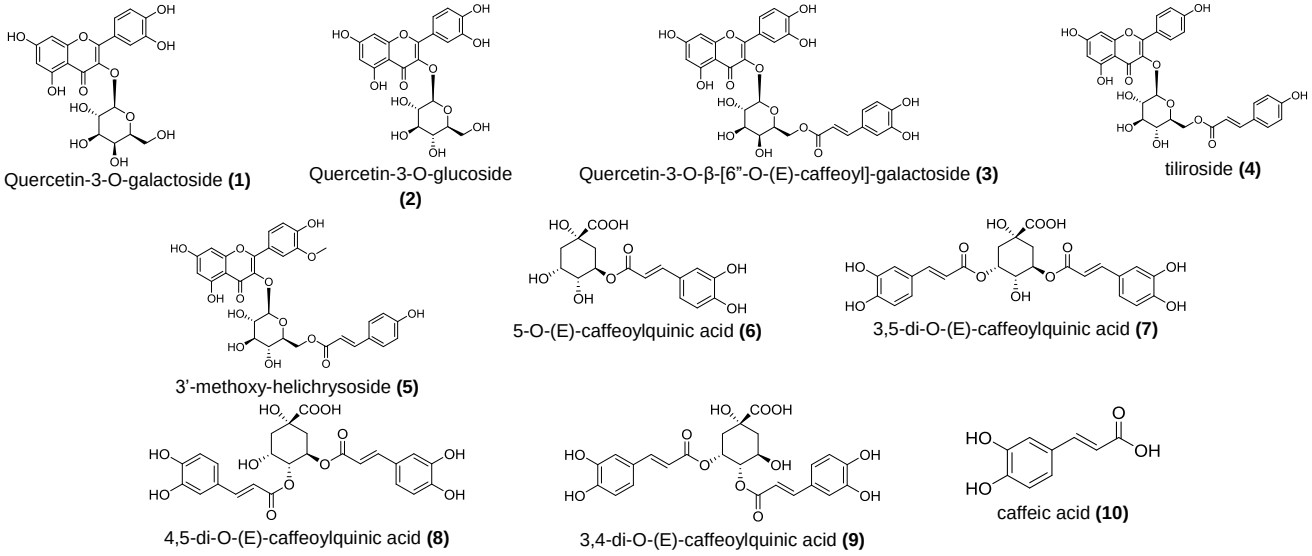


**Figure 1.** Chemical constituents identified from *R. campestris*.

**Acknowledgments**: Fundação de Amparo à Pesquisa do Estado de São Paulo (FAPESP; Grant # 2014/20932-8).

**References:**

[1]1Funk, V.A. et al. *Taxon* **63**: 859-882, 2014.
[2] Roque, N. & Pirani, J.R. *Syst. Bot.* **39**: 997-1026, 2014.

**Área: QPN** **Inscrição: 01058**

# Chemodiversity of exudates from foliar surfaces of *Richterago discoidea* (Asteraceae)

**Cinthia I. Tamayose (PG)[1]*, Nádia Roque (PQ)[2], Marcelo J. P. Ferreira (PQ)[3]**

**cinthiatamay@gmail.com**

*[1]Instituto de Química - Universidade de São Paulo, 05508-000, São Paulo, Brazil; [2]Instituto de Biologia, Universidade Federal da Bahia, 40170-290, Salvador, Brazil; [3]Instituto de Biociências - Universidade de São Paulo, 05508-090, São Paulo, Brazil.*

Keywords: *Richterago discoidea, Asteraceae, Flavone, Sesquiterpene Lactone*

## Highlights

Chemodiversity of exudates from foliar surfaces of Richterago discoidea (Asteraceae):
- In this work was reported for the first time the chemical composition of exudates from *Richterago discoidea*;
- Sesquiterpene lactones and flavones were characterized through $^{1}H$, $^{13}C$ and 2D NMR.

## Resumo/Abstract

Asteraceae is one the largest families of Eudicots comprising several species used for economic and medicinal purposes, and characterized by the production of various bioactive metabolites. Among the 1700 genera of the family, *Richterago* Kuntze comprises 16 species all endemic to Brazil[1]. The aim of this work is to report the phytochemical study of cuticular wax from *Richterago discoidea* (Less.) Kuntze. Leaves were air-dried and extracted three times with dichloromethane for 30 seconds. Extracts were grouped and after removal of solvent, the solid residue (1.76 g) was subjected to recrystallization with methanol. After cooling, the soluble and insoluble phases were separated by centrifugation (13,000 rpm; 5 min) and dried. Insoluble phase was submitted to a derivatization procedure with pyridine and BSTFA (N,O-bis-(trimethylsilyl)-trifluoroacetamide). Through GC-MS analysis and by comparison with fragmentation patterns of mass spectra, chemical constituents (Figure 1) were characterized as hexadecanoic (**1**) and octadecanoic acids (**2**) (fatty acids), heptacosane (**3**), nonacosane (**4**) and hentriacontane (**5**) (n-alkanes), hexacosanol (**6**), octacosanol (**7**), triacontanol (**8**), dotriacontanol (**9**) and tetratriacontanol (**10**) (long-chain primary alcohols) and tricosyl acetate (**11**) (Figure 1). Soluble phase was analyzed through HPLC-UV/DAD. The identification of compounds was made by comparison with commercial and previously isolated standards. Non-identified components were purified by preparative HPLC and their structures were elucidated by $^{1}H$ and $^{13}C$ NMR data. From this methodology, the flavone eupafolin (**12**), and five lactones artemisiifolin 6-O-(4-hydroxytiglate) (**13**), artemisiifolin 15-O-sarracinate (**14**), artemisiifolin 15-O-(4-hydroxytiglate) (**15**), 15-hydroxy-artemisiifolin 6-O-(4-hydroxytiglate) (**16**) and artemisiifolin 15-O-(5-acetylsarracinate) (**17**) (Figure 1) were identified from *R. discoidea*. Excepted for the sesquiterpene lactones already reported in literature[2], these compounds were reported for the first time in *R. discoidea*.

| $CH_3$-[$CH_2$]$_n$-R | | |
|---|---|---|
| Compound | n | R |
| Hexadecanoic acid (**1**) | 14 | $CO_2H$ |
| Octadecanoic acids (**2**) | 16 | $CO_2H$ |
| Heptacosane (**3**) | 25 | $CH_3$ |
| Nonacosane (**4**) | 27 | $CH_3$ |
| Hentriacontane (**5**) | 29 | $CH_3$ |
| Hexacosanol (**6**) | 25 | OH |
| Octacosanol (**7**) | 27 | OH |
| Triacontanol (**8**) | 29 | OH |
| Dotriacontanol (**9**) | 31 | OH |
| Tetratriacontanol (**10**) | 33 | OH |
| Tricosyl acetate (**11**) | 22 | $OCOCH_3$ |

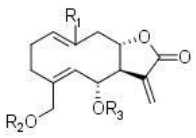


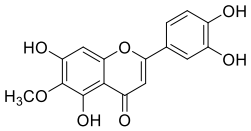


Eupafolin (**12**)

| Compound | $R_1$ | $R_2$ | $R_3$ |
|---|---|---|---|
| Artemisiifolin 6-O-(4-hidroxytiglate) (**13**) | $CH_3$ | H | 4-OH-Tig |
| Artemisiifolin 15-O-sarracinate (**14**) | $CH_3$ | Sar | H |
| Artemisiifolin 15-O-(4-hidroxytiglate) (**15**) | $CH_3$ | 4-OH-Tig | H |
| 15-hidroxy-artemisiifolin 6-O-(4-hidroxytiglate) (**16**) | $CH_2OH$ | H | 4-OH-Tig |
| Artemisiifolin 15-O-(5-acetylsarracinate) (**17**) | $CH_3$ | SarOAc | H |

**Figure 1.** Chemical structures of the compounds isolated exudates from foliar surfaces of *R. discoidea*.

**Acknowledgements:** Grant 2014 / 20932-8, São Paulo Research Foundation (FAPESP).

**References:**

[1]Roque, N.; Pirani, J.R. Taxonomic revision of *Richterago* (Asteraceae, Gochnatieae). *Syst. Bot. 39*: 997-1026, **2014**.

[2]Bohlmann, F.; Jakupovic, J.; Robison, H.; King, R. M. Five germacranolides from *Gochnatia discoidea. Phytochemistry 20:* 109-112, **1981**.

**Área: __QPN__** *(Inserir a sigla da seção científica para qual o resumo será submetido. Ex: ORG, BEA, CAT)*

**Inscrição: 00790** *(Inserir o número de inscrição do autor que fez a submissão)*

# Chemical characterization of antidiabetic active ethanolic extract from *Jatropha aethiopica* (Euphorbiaceae) leaves.

**Daylin Gamiotea-Turro (PG),[1,2*] Alexander B. Valerino-Diaz (PG),[1] Yarelis Ortiz-Nuñez (PQ),[2] Daniel Rinaldo (PQ),[3] José R. Bosqueiro (PQ),[4] Nathalia A.P. Camaforte (PQ),[4] Lourdes C. dos Santos (PQ).[1]**

**daylingamioteaturro@gmail.com**

*[1] UNESP -São Paulo State University, Chemistry Institute – Araraquara, SP, Brazil; [2] Institute of Fundamental Research in Tropical Agriculture "Alejandro de Humboldt" (INIFAT), Havana, Cuba; [3] UNESP - São Paulo State University, Department of Chemistry –Bauru, SP, Brazil; [4] UNESP - São Paulo State University, Department of Biological Sciences, Faculty of Sciences –Bauru, SP, Brazil.*

Keywords: *Jatropha aethiopica; medicinal plant; antidiabetic properties; flavonol triglycosides*

## Highlights

Chemical elucidation of the main metabolites (three flavonol triglycosides) present in the active ethanolic extract from *Jatropha aethiopica* leaves with antidiabetes properties was performed. The compounds were characterized by 1D and 2D NMR techniques as well as HRESIMS.

## Resumo/Abstract

*Jatropha aethiopica*, popularly known in Cuba as "mata diabetes", is used traditionally because its antidiabetic properties[1]. The aim of this work was chemical and biological characterize the ethanolic extract (**EE**) from *Jatropha aethiopica* leaves. The fractionation of the **EE** was performed by sephadex LH-20 yielding eighteen fractions purified by HPLC-PDA preparative. The structure of the compounds were elucidated using 1D and 2D NMR experiments as well as HRESIMS techniques. Three flavonol triglycoside compound were described, being one of them described as a new. The three flavonol triglycosides are quercetin 3-*O*-$\alpha$-L-rhamnopyranosyl-(1→2)-[$\alpha$-L-rhamnopyranolsyl-(1→6)]-$\beta$-D-galactopyranoside (**1**), kaempferol 3-*O*-$\alpha$-L-rhamnopyranosyl-(1→2)-[$\alpha$-L-rhamnopyranolsyl-(1→6)]-$\beta$-D-glucopyranoside (**2**) and, a new kaempferol 3-*O*-$\alpha$-L-rhamnopyranosyl-(1→4)-[$\alpha$-L-rhamnopyranolsyl-(1→6)]-$\beta$-D-galactopyranoside (**3**) (Figure 1). The antidiabetic property of the **EE** from *Jatropha aethiopica* leaves was previously demonstrated (Figure 2)[2].

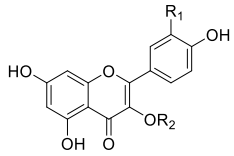


| Compound | $R_1$ | $R_2$ | $R_3$ |
|---|---|---|---|
| **1** | OH | 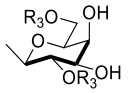 | 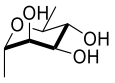 |
| **2** | H | 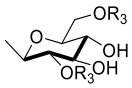 | 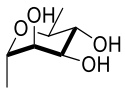 |
| **3** | H | 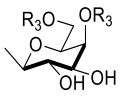 | 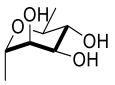 |

**Fig. 1**. Flavonol triglycosides isolated from *J. aethiopica*.

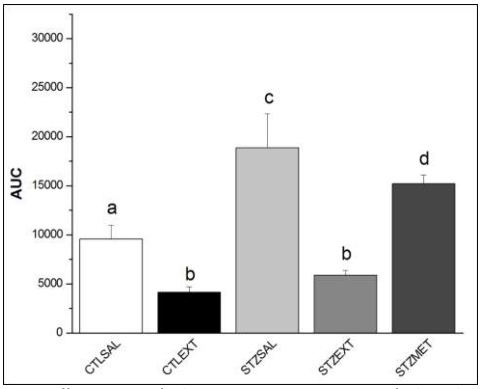


CTLSAL-saline control; CTLEXT-extract control; STZSAL-diabetic saline; STZEXT-diabetic extract; STZMET-diabetic metformin

**Fig. 2**. Effect of *J. aethiopica* treatment at the dose of 500 mg/kg on glucose tolerance.

[1] Roig y Mesa, J. T. Monografia de las plantas. *Plantas Medicinales, Aromáticas o Venenosas de Cuba*, 2th Edition; Mendoza, A., Ed.; Ediciones de Ciencia y Técnica, Instituto del Libro: La Habana, Cuba, 1974, pp. 554.

[2] Gamiotea-Turro, D; Camaforte, N.A.P.; Valerino-Diaz, A.B.; Ortiz Nuñez, Y; Rinaldo, D; Dokkedal, A.L.; Bosqueiro, J.R. and dos Santos L.C. Qualitative and quantitative analysis of ethanolic extract and phenolic fraction of *Jatropha aethiopica* (Euphorbiaceae) leaves and their hypoglycemic potential. JAFC, 2018. DOI: 10.1021/acs.jafc.7b05648.

**Área: QPN** **Inscrição: 00641**

# Acyl-glycosyl flavone from *Glandularia selloi* (Verbenaceae)

**[1]Angelica S. Vestena (PG), [1]Gilsane L. von Poser (PQ), [2]Marcia Vignoli-Silva (PQ), [3]Ian Castro-Gamboa (PQ), [1]José Angelo S. Zuanazzi (PQ)**

**zuanazzi@ufrgs.br; angelica_signor@hotmail.com**

*[1]Programa de Pós-Graduação em Ciências Farmacêuticas, UFRGS, [2]Departamento de Ciências Básicas da Saúde, UFCSPA, Departamento de Química Orgânica, UNESP.[3]*

Palavras Chave: *Glandularia selloi, Verbenaceae, Acyl- glycosyl flavone, Chrysoeriol, NMR*

## Highlights

New natural product from *Glandularia selloi* (Verbenaceae). Isolation and identification of a new acyl-glycosyl flavone determined by NMR.

## Resumo/Abstract

The genus *Glandularia* (Verbenaceae) is distributed in subtropical and temperate regions of South and North America and is represented by approximately 100 species. A previous study carried out with the species *Glandularia selloi*, native to southern Brazil, revealed the presence of compounds with profile of iridoids, phenylethanoids and flavones. This study aims to isolate and identify one of the major flavones present in the methanolic extract obtained from the leaves of *G. selloi*. The plant material was collected in Curumim, Capão da Canoa (RS), dried in room temperature, milled and macerated with methanol (48 h cycles) until exhaustion. The extract was submitted to column chromatography on silica gel using a gradient of ethyl acetate: methanol (100:0 → 0:100) as mobile phase, affording a main compound whose structure was determined by Nuclear Magnetic Resonance (Bruker 400 MHz Ascend), 1D (1H, 13C, APT) and 2D (COSY, HSQC, HMBC; TOCSY. As a result of the isolation, an acyl-glycosyl flavone has been identified. The compound was identified as Chrysoeriol-7-*O*-[β-D-glucopyranoside-(1→2)5‴-*O*-acetyl-β-D-apiofuranosyl, compound with unpublished structure, thus, a novel natural compound was elucidated. So, this study allowed the isolation and identification of a new natural product, an acyl-glycosyl flavone. The report of acetylated flavones is rare in this family. Subsequently, this product will be investigated for biological activities such as anti-inflammatory.

**Área: QPN** **Inscrição:_1017 ___**
*(Inserir o número de inscrição do autor que fez a submissão)*

# Phenolic compounds isolated from *Renealmia nicolaioides* rhizomes

**[1]* Kathlyn V. Gevú (PG), [2] Ilna G. Silva (PG), [3] Helena R. P. Lima (PQ), [1] Maura Da Cunha (PQ),[2] Mário G. de Carvalho (PQ).**

**mariogdecarvalho@gmail.com; kathlyn_vasconcelos@hotmail.com**

*[1]Centro de Biociências e Biotecnologia, UENF; [2]Departamento de Química, UFRRJ; [3]Departamento de Botânica, UFRRJ.*

Palavras Chave: *Zingiberaceae, Flavonoid, Diarylheptanoid.*

## Highlights

Three diarylheptanoids, including a new one, and one flavonoid were isolated.
These compounds are reported for the first time in *Renealmia*.

## Abstract

*Renealmia* L.f. comprises approximately 75 African and Neotropical species of herbaceous and rhizomatous plants from the family Zingiberaceae. Species from this genus have been used as food, and as medicinal plants. The chemical studies are scarce for the genus *Renealmia*. This study aims to identify special metabolites of the rhizome of *Renealmia nicolaioides* from the North Region of Brazil. The rhizomes were collected in June 2015, at the Catuaba Experimental Farm and the Humaitá Forest Reserve, both located in Rio Branco, state of Acre. The material was identified and a voucher 6646 was deposited in the herbarium of the Universidade Federal do Acre (UFACPZ). Air-dried powdered rhizomes were successively extracted with $CH_2Cl_2$ and $CH_3OH$ at room temperature and the residues of the extracts were partitioned with solvents. Chromatographic fractionation of fractions from the partition besides analyses of some fractions by $^{1}H$ and $^{13}C$ NMR, and mass spectra, $[\alpha]_D$, and CD allowed to identify four phenolic compounds. Three diarylheptanoids including a new compound (**3**), E-1,7-bis(4-hydroxyphenyl)-hept-1-en-3-one (**1**), 5*R*-1,7-bis(5-hydroxyphenyl)-(1*E*)-1-hepten-5-ol, (**2**), Rel-(1R,2R,5S)-2-hydroxy-1,7(p-hydroxyphenyl)-centrolobine (**3**), and one flavonoid, quercetin 3-methyl ether (**4**). The derivative **2a** was used to confirm the structure of **2**. All compounds are reported for the first time in this genus, and this is the first occurrence of compound **1** as a natural metabolite. Thus, the present study identifies *Renealmia* as a source of phenolic compounds and proposes new research for other species.

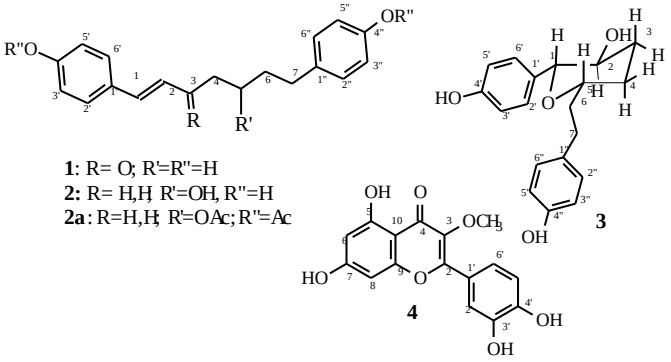


The authors thank to FAPERJ, CNPq, and CAPES for scholarship and financial support.

**Área: QPN** **Inscrição: 00902**

# Identificação de ácido elágico e derivados das folhas de *Terminalia actinophylla* por ESI-ITMS

**Renato P. Sousa (PG),[1] Bruno Q. Araújo (PQ),[1] Gerardo M. V. Júnior (PQ),[1] Mariana H. Chaves (PQ)[1]**

**renatopintto@hotmail.com;**

[1]*Departamento de Química - Universidade Federal do Piauí, 64049-550 Teresina-PI*

Palavras Chave: *Terminalia actinophylla, Taninos, Espectrometria de massas.*

## Highlights

Identification of ellagic acid and derivatives from *Terminalia actinophylla* leaves (Combretaceae) using ESI-ITMS. The etanolic extract from *T. actinophylla* leaves (EETa) is rich in phenolic acids and tannins. The investigation of EETa by ESI-ITMS showed a predominance of ellagic acid and derivatives.

## Resumo/Abstract

*Terminalia actinophylla* Mart. (Combretaceae), é uma espécie nativa do Brasil, conhecida popularmente por catinga de porca e chapada. Plantas do gênero *Terminalia* são ricas em polifenóis (flavonas, flavonois, fenilpropanoides e taninos)[1,2]. Este estudo, relata a investigação de constituintes do EETa por ESI(-)-ITMS.

O pó das folhas foi submetido à extração por maceração com EtOH 98%, obtendo-se o extrato EETa (57,9 g). Uma alíquota de 10 mg do EETa foi submetido a SPE C18 utilizando-se $H_2O$:MeOH (8:2; 1:1 e 2:8 v/v, respectivamente). As frações obtidas foram diluídas a 50 mg $L^{-1}$ e analisadas por inserção direta em espectrômetro de massas (Amazon X, Bruker Daltonis), nas seguintes condições: fonte de ionização ESI no modo negativo na faixa de *m/z* 100-1500, voltagem do capilar de 4,5 kV, gás nebulização a 8,0 L $min^{-1}$, com fluxo de 3,0 µL $min^{-1}$ e T = 220 °C. A identificação foi realizada pela aquisição de espectros $MS^n$ e comparação com a literatura[3].

O perfil (Fig. 1) da fração $H_2O$:MeOH (1:1) apresentou picos característicos de taninos, ácido gálico (*m/z* 169), galato de etila (*m/z* 197), ácido elágico (*m/z* 301) e derivados de hexahidroxidifenoila (HHDP), tais como galoil-HHDP-glicose (*m/z* 633), digaloil-HHDP-glicose (*m/z* 785) e um derivado de castalagina (*m/z* 965) (Fig. 2). Foi observado que os principais metabólicos secundários de *T. actinophylla* apresentam um fragmento $MS^2$: *m/z* 301, típico de lactonização de derivados de ácido gálico. A identificação desses constituintes químicos, em princípio, justifica a resposta antioxidante do EETa frente ao radical livre DPPH.

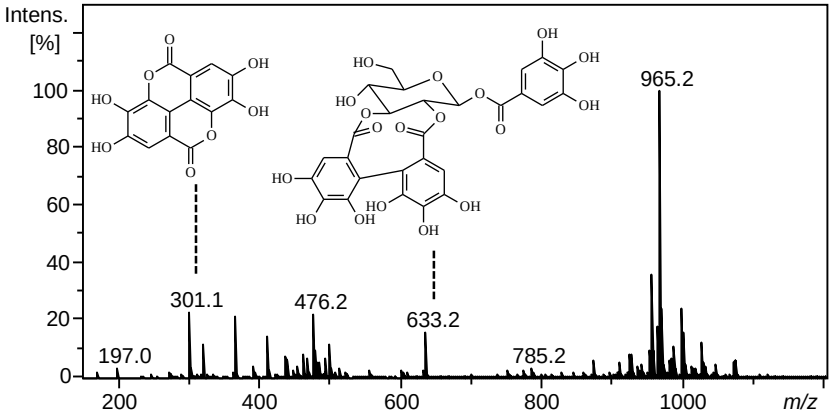


**Figura 1**. Perfil químico do EETa por ESI-ITMS

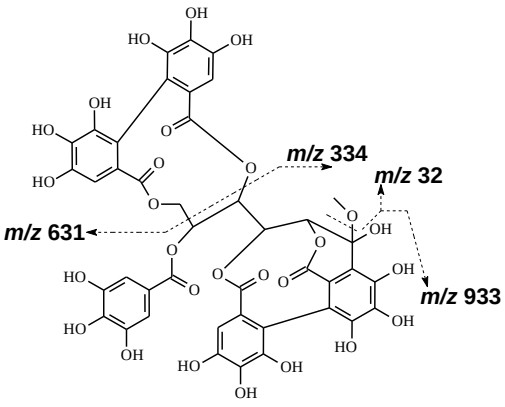


**Figura 2**. Fragmentos do $[M-H]^-$ 965

Agradecimentos: CAPES e CNPq pelas bolsas e apoio financeiro

[1]Farias, R. R. S. Tese de Doutorado; Universidade Federal do Piauí, Brasil 2016.
[2]Mendes, M. R. A.; Castro, A. A. J. F.; *CheckList* **2010**, *6*, 39.
[3]Fischer, V. A.; Carle, R.; Kammerer, D. R. *Food Chem.* **2011**, *127*, 807.; Wyrepkowski, C. C.; Costa, D. L. M. G.; Sinhorin, A. P; Vilegas, W.; Grandis, R. A.; Resende, F. A.; Varanda, E. A.; Santos, L. C; *Molecules* **2014**, *19*, 16039.

**Área: QPN**
*(Inserir a sigla da seção científica para qual o resumo será submetido. Ex: ORG, BEA, CAT)*

**Inscrição: 00883**
*(Inserir o número de inscrição do autor que fez a submissão)*

# Genotoxic and mutagenic assessment of neolignans isolated from *Nectandra leucantha* on human melanoma cells

**Fernanda S. de Sousa (PG),[1*] Emilene A. Nunes (PG),[2*] Simone dos S. Grecco (PQ)[3], Geanne A. Conserva (PG)[2], Giselle Cerchiaro (PQ),[2] João Henrique G. Lago (PQ)[2] Email: joaoghlago@gmail.com**

*Institute Environmental, Chemical and Pharmaceutical Sciences - UNIFESP; [2]Center of Natural Sciences and Humanities - UFABC; [3]Biotechnology and Innovation in Health Program, Anhanguera University of São Paulo.*

keywords: Nectandra leucantha*, neolignans, human melanoma, genotoxic, mutagenic*

## Highlights

The present study aimed to evaluate the genotoxic and mutagenic activity of dehydrodieugenol B and methyldehydrodieugenol B isolated from twigs of *Nectandra leucantha* (Lauraceae) through cytokinesis block micronucleus (CBMN) and Comet assay. Tested compounds showed to be deleterious for macromolecules like DNA, proteins and lipids. Additionally, was observed that these compounds are highly genotoxic to SKMEL-147 and SKMEL-29 cells.

## Abstract

Previously studies described the remarkable role in the induction of apoptosis played by dehydrodieugenol B (**1**) and methyldehydrodieugenol B (**2**), isolated from twigs of *Nectandra leucantha* (Lauraceae), accessed through DNA condensation and fragmentation, mitochondrial transmembrane potential and annexin V assay[1]. Furthermore, compound **1** may promote alkylation reactions in tumor cells, which could damage DNA or other nucleophiles in the cells. In continuation of our previous works, the present study aimed to evaluate the possible genotoxic and mutagenic activity of compounds **1** and **2** through cytokinesis block micronucleus (CBMN) and Comet assay.

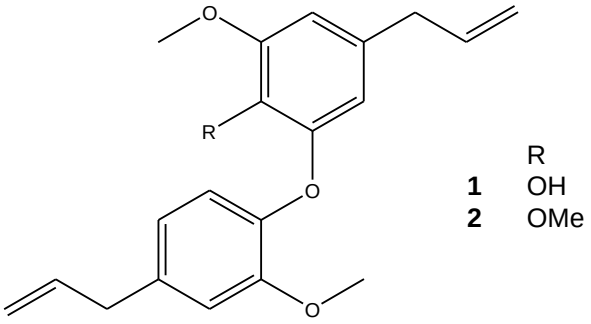


**Figure 1**: Dehydrodieugenol B (**1**) and methyldehydrodieugenol B (**2**) isolated from *Nectandra leucantha*

Compounds **1** and **2** displayed toxicity against human melanoma cell (SKMEL-147) with $IC_{50}$ values of 4.4 µg/mL and 43.6 µg/mL, respectively. The interaction of these compounds with the resistant cell line SKMEL-29 was also investigated[2]. The results showed the concentration-response relationship for DNA damage (DI and D%) for SKMEL-29 for compound **1** and a possible relation with the permeability of compound **2** to this cell line, observing the increase of DNA damage in its lower concentrations. Concerning the cytokinesis-block micronucleus cytome (CBMNCyt) assay, all treatments demonstrated increase in cytostatic and cytotoxic indexes in SKMEL-147 and SKMEL-29 cells. In micronucleus quantification (biomarker of mutagenicity), compound **1** displayed higher indices in comparison to negative control. Regarding necrotic and apoptotic cells, treatments with SKMEL-29 cells demonstrated 100% of the cell death induced by compound **1** at concentration of 25 µg/mL and compound **2** at 88 µg/mL. Additionally, was observed that apoptosis is prevalent in SKMEL-147 cells treated with compound **1** while necrotic cells were observed in SKMEL-29 cells in both compounds due to their location on the plasma membrane and cytoplasm. In conclusion, compounds **1** and **2** are promising as genotoxic and mutagenic agents against human melanoma resistant cells.

**Acknowledgments**: FAPESP and CNPq

**References:** [1]SOUSA et al. **2017**, *Phytochemistry*, 140, 108. [2]Fenech et al. **2007**, *Nature Protocols*, 2, 1084.

**Área: QPN** **Inscrição: 00788**

# Atividade antifúngica de quinoides isolados de *Pentacalia desiderabilis* (Vell.) Cuatrec. (Asteraceae)

**Kaio de S. Gomes (PG)[1], Cynthia Murakami[2], Maria Claudia M Young (PQ)[2], Guilherme M. Antar (PQ)[3], Marcelo J. Pena Ferreira[3], Patricia Sartorelli (PQ)[4], João Henrique G. Lago (PQ)[1]. E-mail: kaio.souza@ufabc.edu.br**

*[1]Centro de Ciências Naturais e Humanas, Universidade Federal do ABC - SP; [2]Núcleo de Pesquisa em Fisiologia e Bioquímica, Instituto de Botânica - SP; [3]Instituto de Biociências, Universidade de São Paulo – SP; [4]Instituto de Ciências Ambientais, Químicas e Farmacêuticas, Universidade Federal de São Paulo – SP.*

Palavras Chave: Pentacalia desiderabilis, *atividade antifúngica, quinoides.*

## Highlights

ANTIFUNGAL ACTIVITY OF QUINOIDS ISOLATED FROM *Pentacalia desiderabilis* (Vell.) Cuatrec. (Asteraceae). The present work reports the bioactivity-guided fractionation of MeOH extract from leaves of *Pentacalia desiderabilis.* After partition with n-hexane, $CH_2Cl_2$ and EtOAc, the $CH_2Cl_2$ phase displayed potential against *Cladosporium* sp. Several chromatographic procedures were performed to afford three quinoid related derivatives identified as jacaranone (**1**), quinolacetic acid (**2**) and methyl 1-hydroxy-4-oxo-cyclohexanacetate (**3**). All compounds were submitted to bioautography assay, **1** and **2** was active against *C. cladosporioides* (0.78 and 12.5 μg, respectively) and *C. sphaerospermum* (3.13 and 12.5 μg, respectively).

## Resumo/Abstract

Dentre os gêneros de Asteraceae encontrados no Brasil, um dos menores é o gênero *Pentacalia* com somente duas espécies: *P. tropicalis*, encontrada nos estados do Espírito Santo e Rio de Janeiro e *P. desiderabilis*, localizada nas regiões Sul e Sudeste. Conhecida como "catião-trepador", a *P. desiderabilis* é um cipó de copa amarelada comum nas bordas da Floresta Atlântica. No contexto fitoquímico, há descrição somente de dois compostos isolados desta planta, o sesquiterpeno germacreno D[1] e o quinoide jacaranona, o qual apresentou atividade antiparasitária e antitumoral *in vitro*.[2,3] A fim de contribuir com a busca de compostos ativos, especialmente antifúngicos, neste trabalho foi realizado o estudo fitoquímico biomonitorado de *P. desiderabilis* frente a *Cladosporium* sp. através do ensaio de bioautografia. O extrato MeOH das folhas foi submetido a partição com n-hexano, $CH_2Cl_2$ e AcOEt. A fase em $CH_2Cl_2$ foi aquela que mostrou maior potencial fungitóxico e, portanto, foi submetida a procedimentos cromatográficos, fornecendo os compostos: jacaranona (**1**), ácido quinolacético (**2**) e 1-hidroxi-4-oxo-ciclohexanoacetato de metila (**3**), cujas estruturas forma definidas através da análise dos espectros de RMN e EM (Figura 1). É digno de nota que essa é a primeira ocorrência dos compostos **2** e **3** no gênero *Pentacalia*.

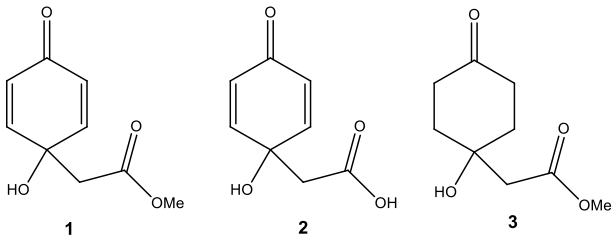


**Figura 1 -** Estrutura dos compostos **1 – 3** isolados de *P. desiderabilis*

Para avaliar o potencial antifúngico das substâncias isoladas, alíquotas de 50,00 a 0,78 μg dos compostos **1 – 3** foram dissolvidos em $CHCl_3$ ou MeOH, aplicadas em placas cromatográficas de sílica gel, nebulizadas com suspensão de esporos ($5x10^7$ esporos.$mL^{-1}$) dos fungos *Cladosporium sphaerospermum* e *C. cladosporioides* e incubadas em câmara úmida por 48h, tendo como controle positivo ácido cinâmico. O ensaio de bioautografia[4] mostrou que o composto **1** foi o mais ativo (Tabela 1) frente as linhagens testadas com limite de detecção similar ao controle positivo, ácido cinâmico (0,78 μg).

**Tabela 1**. Atividade antifúngica dos compostos **1 – 3** e controle positivo frente à *C. cladosporioides* e *C. sphaerospermum*

| | Atividade antifúngica (μg) | |
|---|---|---|
| **Composto** | *C. cladosporioides* | *C. sphaerospermum* |
| **1** | 0,78 | 3,13 |
| **2** | 12,50 | 12,50 |
| **3** | 50,00 | 50,00 |
| Ácido cinâmico | 0,78 | 0,78 |

Como observado acima, a esterificação do grupo carboxila observada no composto **1** tem influência positiva na atividade antifúngica, visto que o ácido precursor (composto **2**) apresenta reduzida bioatividade frente aos fungos testados. Além disso, a ausência das ligações duplas no anel quinônico (composto **3**) causa diminuição do potencial fungitóxico, quando comparado ao **1**, que possui o sistema carbonílico α,β-insaturado.

**Referências:** [1]DEUSCHLE, R. A. N. *et al. Rev. Bras. Farmacogn*, 17, 2, 220-223, **2007**. [2]. MORAIS, T. R. *et al*. *Parasitol. Res*. 110, 1, 95-101, **2012**. [3]. MASSAOKA, M. H. et al. *PLoS One*, 7, 6, **2012**. [4]. HOMANS, A. L. *et al. J. Chromatog.*, 51, 2, 327-329, **1970**

**Área: QPN**
*(Inserir a sigla da seção científica para qual o resumo será submetido. Ex: ORG, BEA, CAT)*

**Inscrição: 00727**
*(Inserir o número de inscrição do autor que fez a submissão)*

# Butenolídeos com atividade anti-*Leishmania* isolados de *Nectandra oppositifolia* Ness & Mart (Lauraceae)

**Geanne A. A. Conserva (PG)[1], Thais A. Costa-Silva (PG)[1], André G. Tempone (PQ)[2], Guilherme de M. Antar (PG)[3], João Henrique G. Lago (PQ)[1]**

*[1]Centro de Ciências Naturais e Humanas, Universidade Federal do ABC, Santo André, Brasil; [2]Instituto Adolfo Lutz, São Paulo, Brasil; [3]Departamento de Botânica, Instituto de Biociências, Universidade de São Paulo, São Paulo, Brasil. ** E-mail: geanneconserva@gmail.com*

Palavras Chave: *Lauraceae,* Nectandra oppositifolia*, Butenolídeos, Anti*-Leishmania*,* L. (L.) infantum*.*

## Highlights

The hexane extract from twigs of *Nectandra oppositifolia* (Lauraceae) displayed anti-*Leishmania* activity and was subjected to bioactivity-guided fractionation to give three bioactive butenolide derivatives (**1 – 3**).

## Resumo/Abstract

A Leishmaniose, pertencente ao grupo das Doenças Tropicais Negligenciadas (DTNs) é causada por diferentes parasitas do gênero *Leishmania* e encontra-se entre as cinco principais doenças infecto-parasitárias endêmicas de maior relevância, afetando em torno de 12 milhões de indivíduos [1]. O arsenal efetivo terapêutico disponível para o tratamento da leishmaniose é bastante reduzido e insatisfatório, devido aos graves efeitos colaterais indesejados e da longa duração do tratamento [2]. Assim, a busca por novos protótipos é indispensável, sendo os produtos naturais uma importante fonte desses compostos. Com base neste aspecto, o extrato hexânico dos galhos de *N. oppositifolia* exibiu atividade (100% da morte parasitária) contra formas promastigotas de *L. (L.) infantum* a 300 μg/mL. Assim, este extrato foi submetido a fracionamento guiado por bioatividade fornecendo três compostos bioativos: *seco*-subamolídio A (**1**) *iso*-linderanolideo *D* (**2**) e *iso*-linderanolideo *E* (**3**). As estruturas destes compostos foram definidas por diferentes métodos espectroscópicos/espectrométricos, incluindo RMN e EM.

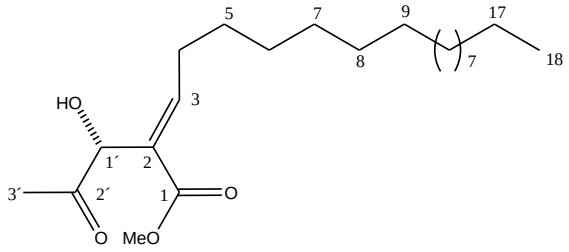


**1**

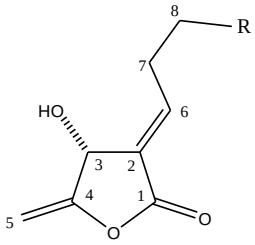


**2** R =

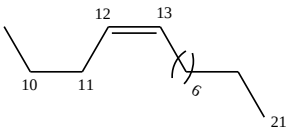


**3** R =

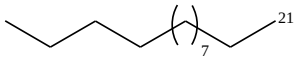


As formas promastigotas de *L. (L.) infantum* foram incubadas com os compostos **1 – 3** apresentando valores de $CE_{50}$ de 1,0, 47,0 e 26,9 μM, respectivamente. Para as formas amastigotas, apenas o composto **3** foi ativo, apresentando um valor de $CE_{50}$ de 10,5 μM. Com relação à citotoxicidade em células NCTC (fibroblasto de camundongo), apenas o composto **3** mostrou-se tóxico (42,3 μM), fornecendo índice de seletividade (IS) de 4,0. Por outro lado, o composto **1** mostrou atividade frente a formas promastigotas de *L. (L.) infatum* superior ao fármaco padrão miltefosina (17,8 μM) e com reduzida toxicidade. No que tange a estrutura química dos compostos isolados, **2** e **3** se diferem apenas pela presença de uma instauração na cadeia lateral de **2,** enquanto que o composto **1** apresenta-se como um éster metílico de cadeia aberta. Diante destas características estruturais, a atividade anti-*Leishmania* de **3** frente às formas amastigotas pode estar relacionada a presença do anel γ-lactônico, bem como sua cadeia lateral alifática saturada. Tal característica pode ter conferido essa atividade intracelular na infecção por *L. (L.) infantum,* sugerindo uma ativação do macrófago, o que poderia aumentar a sua capacidade microbicida [3].

**Agradecimentos:** FAPESP (projeto 2016/20633-6).

**Referências:** [1] World Health Organization, (2017). *Disponível em <http://www.who.int/leishmaniasis/en/* >(**2018**). [2] Menezes, J. P. B.,et al. (2015) *BioMed Res. Internal.* [3] Murray, H.W. et al., (**2005**) *Lancet* 366:1561-77.

**Área: PN** **Inscrição:** 00687

*(Inserir o número de inscrição do autor que fez a submissão)*

# Biological activities and identification of compounds of *Cordiera sessilis* Vell. (Kuntze)

**Francisco J.T. Aquino (PQ),[1] Alanna E. A. Ferreira (PG)[1*], Mario M. Martins, (PG)[1], Luís C. S. Cunha (PQ)[2], Carlos H. G. Martins (PQ)[3], Maria A. L. V. Ambrósio (PQ)[3], Sérgio A. L. Morais, (PQ)[1] Alberto de Oliveira(PQ)[1]**

**aquino@ufu.br; alannaevellin@hotmail.com**

*[1]Núcleo de Pesquisa em Produtos Naturais, Universidade Federal de Uberlândia, CEP 38400-902, Uberlândia/MG; [2]Núcleo de Estudos em Alimentos e Produtos Naturais, Instituto Federal de São Paulo, CEP 18707-150, Avaré/SP [3]Laboratório de Pesquisa em Microbiologia Aplicada, Universidade de Franca, CEP 14404-600, Franca/SP.*

Palavras Chave: *Cordiera sessilis, Cerrado biome, Biological activities, extract, HPLC-MS/MS.*

## Highlights

Ethanolic extract and fractions of the bark of *C. sessilis.*
The ethyl acetate fraction presented good activity against aerobic bacteria and against yeasts *Candida.* HPLC-MS/MS analisis identified geniposidic, coumaroylquinic, caffeoylquinic acid methyl esters, the lignan lyoniresinol glucopyranoside, and dicaffeoylquinic acid.

## Resumo/Abstract

*Cordiera sessilis* Vell. (Kuntze) is a synonym of *Alibertia sessilis*, known by the popular names "marmelinho do cerrado" or "marmelada de cachorro" belongs to the *Rubiaceae* family.[1] According to popular knowledge, its leaves are used in the form of baths or plasters to treat skin diseases.[2] This study aimed to verify the biological potential and identify biological compounds of the bark ethanolic extract and fractions. Approximately 1 kg of barks was collected in Morrinhos-GO. The barks were dried, crushed and macerated in ethanol to obtain the extract, at room temperature. The fractions were obtained by liquid-liquid partition with the solvent sequence: hexane, dichloromethane, ethyl acetate and *n*-butanol. The ethanolic extract and fractions were submitted to the evaluation of the antibacterial, antifungal, enzymatic inhibition and peroxyl radical scavanging activities. The ethyl acetate fraction presented good activity against aerobic bacteria *Streptococcus sanguinis* (MIC 100 µg $mL^{-1}$), moderate activity for anaerobic bacteria *Fusobacterium nucleatum* (MIC 200 µg $mL^{-1}$) and promising activity against yeasts *Candida albicans* (MIC 93.75 µg $mL^{-1}$) and *Candida tropicalis* (MIC 93.75 µg $mL^{-1}$). The ethyl acetate fraction also showed high scavenging capacity of the peroxyl radical (2415.5 ± 157.8 µmol Trolox eq $g^{-1}$). Additionally, the ethyl acetate fraction presented excellent ability to inhibit the action of the lipase enzyme (98.4%). Thus, the ethyl acetate fraction was selected for fractionation using C18 stationary phase and water with increasing additions of methanol as the mobile phase. As consequence,120 subfractions were monitored by TLC using the Liebermann-Burchard and aluminum chloride reagents and regrouped at 42 subfractions, designated '*n*A1'. The HPLC-MS/MS analisis (negative mode) of the subfraction 6A1 identified the following compounds: geniposidic, coumaroylquinic, and caffeoylquinic acid methyl esters, and lignan lyoniresinol glucopyranoside; the subfraction 12A1 presented the compound dicaffeoylquinic acid. The identification of compounds was performed by comparing the data obtained with those available in the literature.[3-7]

1. PERSSON, C. **Am. J. Bot.**, 87 (7), 1018-1028, 2000.
2. MATSUOKA, L. G. Morfo-anatomia dos ovários e dos frutos e sistemática de *Alibertia* e *Cordiera* (Rubiaceae, Gardenieae). Dissertação (Mestrado em Biologia) - UFG, Goiânia, 2008.
3. BENTES, A. de S. Compostos bioativos de jenipapo, laranja e manga: composição e desenvolvimento de métodos de extração. Tese (Doutorado em Engenharia de Alimentos) - UNESP, Campinas, 2014.
4. KREUTZMANN, S.; CHRISTENSEN, L. P.; EDELENBOS, M. **LWT - Food Sci. Technol.**, 41 (2), 193-205, 2008.
5. JAISWAL, R.; KUHNERT, N. **J. Mass Spectrom.**, 11 (2), 269-281, 2011.
6. JAISWAL, R.; KUHNERT, N. **J. Mass Spectrom.**, 11 (2), 269-281, 2011.
7. CLIFFORD, M. N.; KNIGHT, S.; KUHNERT, N. J. **Agric. Food Chem.**, 53, 3821-3832, 2005.

Acknowledgments: UFU, UNIFRAN, FAPEMIG.

**Área: QPN** **Inscrição:594**

# Constituintes químicos isolados das partes aéreas de *Serissa foetida* (Rubiaceae).

***Sebold, S. B. S. (PG)[1], José Guilherme de Souza Corrêa (IC)[1], Alexandre da Silva Avincola (PG) [1], Armando Mateus Pomini (PQ) [1], Silvana Maria de Oliveira Santin (PQ) [1].**

**monelotti@hotmail.com**

[1]*Departamento de Química, UEM*

Palavras Chave: *Rubiaceae, Serissa foetida, iridoide, cafeoil, ácido clorogênico, ácido paederosídico*

## Highlights

Chemical constituents isolated from the aerial parts of *Serissa foetida* (Rubiaceae). *Serissa foetida* is an ornamental plant of Asian origin used in the treatment of hepatitis, cirrhosis and various tumors such as liver, lung, pharynx, carcinoma, leukemia.

## Resumo

A partir do estudo químico da fração butanólica das partes aéreas da espécie vegetal *Serissa foetida* foi possível isolar e caracterizar o ácido clorogênico **4-O-cafeiolquínico** (**substância 1**) e o iridóide **ácido paederosídico** (**substância 2**). A **substância 1** foi isolada na forma de cristais amarelo claro solúveis em MeOH. A **substância 2** foi isolada na forma de um sólido viscoso, de coloração caramelo e aroma levemente adocicado, solúvel em MeOH e principalmente em água. Os dados espectrais foram comparados com a literatura e foram concordantes para o **ácido 4-*O*-cafeoil-quínico** e o **ácido paederosídico.** Os iridoides são marcadores quimiotaxionômicos da família Rubiaceae.

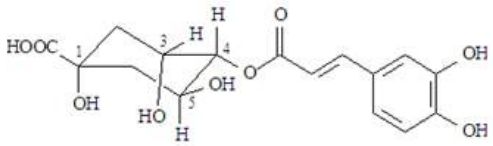


**4-O-cafeoil-quínico**

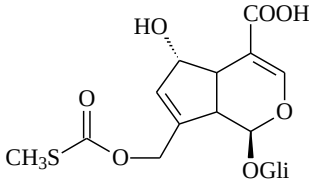


**ácido paederosídico**

**Tabela 01:** Dados de RMN $^{1}H$ e $^{13}C$ para o **ácido paederosídico (substância 2)** em $CD_3OD$.

| C | δ ($^{1}H$) | δ ($^{13}C$)/DEPT |
|---|---|---|
| 1 | 5,10 (*d;* 5,4Hz) | 103,1 (CH) |
| 3 | 7,74 (*d*; 1,2Hz) | 157,7 (C) |
| 4 | | 110,2 (C) |
| 5 | | 43,2 (CH) |
| 6 | | 75,8 (CH) |
| 7 | 6,18 (*d*; 1,8Hz) | 134,5 (CH) |
| 8 | | 146,7 (C) |
| 9 | 2,81 (*t*; 16,2 Hz) | 47,7 (CH) |
| 10 | 5,10 (*d*; 5,4Hz; Ha)<br>5,06 (*d*; 9,0Hz; Hb) | 68,4 ($CH_2$) |
| 11 | | 176,9 (C) |
| $\underline{C}OSCH_3$ | | 174,4 (C) |
| $COS\underline{C}H_3$ | 2,45 (*s*) | 15,8 ($CH_3$) |
| 1' | 4,91 (*d*; 7,8Hz) | 101,9 (CH) |
| 2' | | 77,0 (CH) |
| 3' | | 78,6 (CH) |
| 4' | | 72,4 (CH) |
| 5' | | 79,1 (CH) |
| 6' | | 63,7 ($CH_2$) |

**Área:** ***QPN*** *(Inserir a sigla da seção científica para qual o resumo será submetido. Ex: ORG, BEA, CAT)*

**Inscrição:** **00794** *(Inserir o número de inscrição do autor que fez a submissão)*

# New steroidal saponins from *Solanum paniculatum* L. (Solanaceae) leaves.

**Alexander B. Valerino-Díaz (PG),[1*] Daylin Gamiotea-Turro (PG),[1] Ana Caroline Zanatta (PG),[1] Wagner Vilegas (PQ),[2] Lourdes C. dos Santos (PQ).[1]**

alexandervalerinodiaz@gmail.com

*[1] UNESP -São Paulo State University, Chemistry Institute – Araraquara, SP, Brazil; [2]UNESP - São Paulo State University, Institute of Biosciences– São Vicente, Brazil.*

Keywords: *Solanum paniculatum, Spirostanic saponins, Steroidal saponins, Steroid glycoside, 22-α-O-spirostane, Medicinal plant.*

## Highlights

Three new steroidal saponins were isolated from the 70 % ethanolic extract from the *S. paniculatum* L. leaves. The compounds were characterized by 1D and 2D NMR tecniques as well as HRESIMS.

## Abstract

*Solanum paniculatum* L. known popularly as *jurubeba*[1] is a medicinal plant specie with a bitter taste widespread Tropical America especially in the Brazilian savana region used throughout in Brazil for culinary purposes and in folk medicine to treat gastric dysfunctions, as well as an antifever and a hangovers[2]. Due to the importance and the use of this plant in Brazil, the aim of our research group was to investigate chemically the 70 % ethanolic extract from the leaves of *S. paniculatum* L. The 70% ethanolic extract after fractionation using classical chromatographic techniques (liquid-liquid partition, Sephadex LH-20) resulting in a saponin fraction (**f26**), that after purification by HPLC-RI yielded three new spirostanic saponins 6-*O*-*α*-L-ramnopiranosil-(1''→3')-*β*-D-quinovopiranosil-(22*S*,23*R*,25*S*)-3*β*,6*α*,23-triidroxi-5*α*-espirostano (**1**), 6-*O*-*β*-D-xilopiranosil-(1''→3')-*β*-D-quinovopiranosil-(22*S*,23*R*,25*R*)-3*β*,6*α*,23-triidroxi-5*α*-espirostano (**2**) and 3-*O*-*α*-L-ramnopiranosil-(1''→3')-*β*-D-quinovopiranosil-(22*S*,23*S*,25*R*)-3*β*,6*α*,23-triidroxi-5*α*-espirostano (**3**). The structures of these compounds were elucidated using 1D and 2D NMR experiments along with HRESIMS.

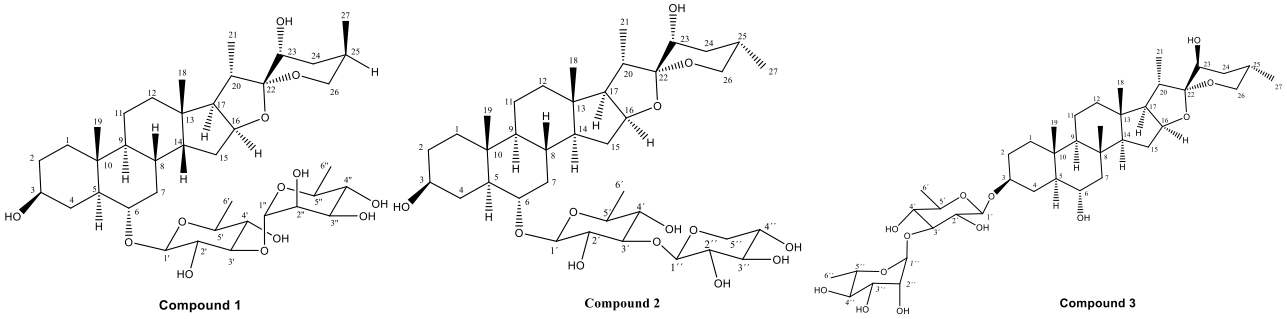

Compound 1 Compound 2 Compound 3

[1] Nee, M. Synopsis of *Solanum* the New World. In Solanaceae. Advances in Biology and Utilization, v. IV, p. 285–333, 1999.

[2] Vieira Júnior, G.M.; Quintino da Rocha, C.; Rodrigues, TdS.; Hakiko Hiruma-Lima, C.; Vilegas, W. New steroidal saponins and antiulcer activity from *Solanum paniculatum* L. Food Chemistry, <http://dx.doi.org/10.1016/j.foodchem>, 2014.

**Área: QPN** **Inscrição: 01274**

# Influence of the decoction time in the extraction of the bioactive terpenes of white sucupira`s seeds (*Pterodon emarginatus*) in alcoholic beverages

**Jhonatan B. de Oliveira (IC),[1] Barbara L. Ferreira (IC),[1] Ana Maria de R. Machado (PQ),[1] Esther Mª F. Lucas (PQ).[1]**

**jhonatanbo@hotmail.com*; esthermfl@cefetmg.br**

*[1]Departamento de Química, CEFET-MG - Centro Federal de Educação Tecnológica de Minas Gerais. Av. Amazonas, 5253 - Nova Suíssa, 30421-169, Belo Horizonte/MG, Brasil*

Palavras Chave: *Pterodron emarginatus, Sucupira, bioactive terpenes, phytoteraptics, .*

## Highlights

The extraction process determinates the chemical profile and the efficacy of herbal medicines. Extracts prepared by the decoction of sucupira seeds in alcoholic beverages are used in Brazil, to treat inflammatory diseases. This work describes how the presence and concentration of the bioactive metabolites of sucupira seeds are affected by varying the decoction time of beverages prepared with cachaças of different alcoholic contains. It was observed that all bioactive metabolites were present in beverage extracts of all the alchoholic concentration only whwn the decoction period was 60 days.

## Resumo/Abstract

**In Brazil it is very common to administer beverages (cachaça or wines) containing sucupira's seeds to treat inflammatory affections [1]. Pterodon species are recognized as white sucupira (P. emarginatus, P. polygaeflorus, P. abruptus, P. apparicioli) [1]. Some terpenes from sucupira oil´s that had their pharmacological activities proved are: spathulenol (I), germancrene-D (II), δ-cadinene (III) [2], β-elemene (IV) [3] and caryophyllene (V) [2]. In order to determinate the influence of decoction time on the extraction of these terpenes 10 g of grounded sucupira`s seed was immersed in** 100 mL of each one of five cachaças' **with different alcoholic content (44.5, 46.5, 48.5, 49,5 and 50.4%). Samples of each extract were collected after 15, 60 and 120 days and their chemical profiles was determined by using GC/MS. Decoction by 15 days promoted the extraction of the bioactive terpenes in all beverages except to the one of the lowest alcohol content. When the decoction was performed by 120 days, β-elemene was not observed in the extracts of the cahaças with alcoholic content of 46,5% and 50,4% and none of bioactive metabolites were present in beverage prepared with cachaça of 44,5% of alcohol. The decoction for 60 days promoted the extraction of all bioactive terpenes in cachaça´s of all alcohol content.**

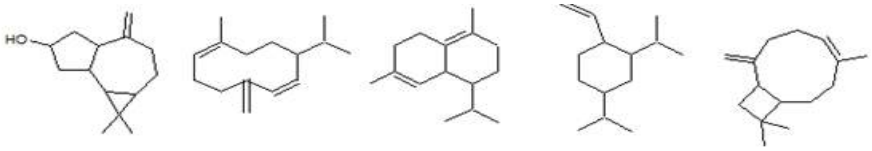


[1] HOSCHEID J.; CARDOSO M.LC. Arthritis, v. 2015.
[2] SANTOS A.P. et al; Brazilian Journal of Pharmacognosy, v. 20, p.891, 2010.
[3] SILVÉRIO M.S.et al. Molecules, v.18, p.9785, 2013.

**Área: QPN** **Inscrição: 01197**

# Triterpenoides do caule de *Tocoyena hispidula* Standl

**Elcilene Aves de Sousa (PG),[1*] Amauri Porto Ascenso Rosa (IC),[1] Gerardo Magela Vieira Júnior (PQ),[1] Mariana Helena Chaves (PQ),[1]**

***elcileneufpi@gmail.com**

[1]*Departamento de Química, Universidade Federal do Piauí, 64049-550 Teresina-PI.*

Palavras Chave: *Triterpenoides,* T. hispidula*, Rubiaceae.*

## Highlights

Triterpenoids from stem of *Tocoyena hispidula* Standl. Isolation and identification of triterpenoids of the $CHCl_3$ and EtOAc fractions obtained from the EtOH extract of the *Tocoyena hispidula* stem.

## Resumo/Abstract

*Tocoyena hispidula* (Rubiaceae) é conhecida popularmente como flor-do-cerrado e jenipapinho. É um arbusto encontrado nos estados do Pará, Piauí e Maranhão e utilizada na medicina popular no combate a dor de barriga e inflamação do útero[1]. A família Rubiaceae possui como marcadores quimiotaxonômicos iridoides, antraquinonas e alcaloides indólicos. O presente trabalho relata os triterpenoides isolados de *T. hispidula*. O extrato EtOH do caule (EE, 48 g, 3,5%) foi obtido por maceração a temperatura ambiente. Uma alíquota de 41 g do EE foi solubilizada em MeOH e submetida a cromatografia em coluna filtrante de gel de sílica utilizando hexano, $CHCl_3$, AcOEt e MeOH. A fração $CHCl_3$ (2,5 g) foi submetida à cromatografia em coluna de gel de silica eluída com Hex/AcOEt fornecendo 26 subfrações. As subfrações CC9, CC15 e CC24 foram purificados por cromatografia em coluna de Sephadex LH-20 fornecendo os compostos **1** (14,3 mg), uma mistura de **2+3** (17,7 mg) e **4** (25,9 mg) respectivamente. A fração AcOEt (2,5 g) foi aplicada em coluna Stracta (C18, 10 g) rendendo as frações MeOH/$H_2O$ 1:1, MeOH e $CHCl_3$. A fração MeOH foi submetida a cromatografia em coluna de Sephadex LH-20, fornecendo a subfração B10 que foi submetida a cromatografia em coluna de gel de silica, obtendo o composto **5** (2,6 mg). A determinação estrutural das substâncias **1**-**5** foi realizada por meio da análise dos espectros de RMN de $^1H$ e $^{13}C$ em comparação com a literatura. Os compostos **1**, **2, 4** e **5** são os triterpenos lupenona, lupeol, ácido acetil oleanólico e ácido oleanólico, respectivamente[2,3]. Esta classe de substâncias apresenta diversas atividades biológicas, tais como cardioprotetora, anti-inflamatória e antitumoral[4]. O composto **3** é o fitol, um diterpenóide que apresenta atividade neuroprotetora[5,6]. Todos os constituintes estão sendo relatados pela primeira vez no gênero *Tocoyena*.

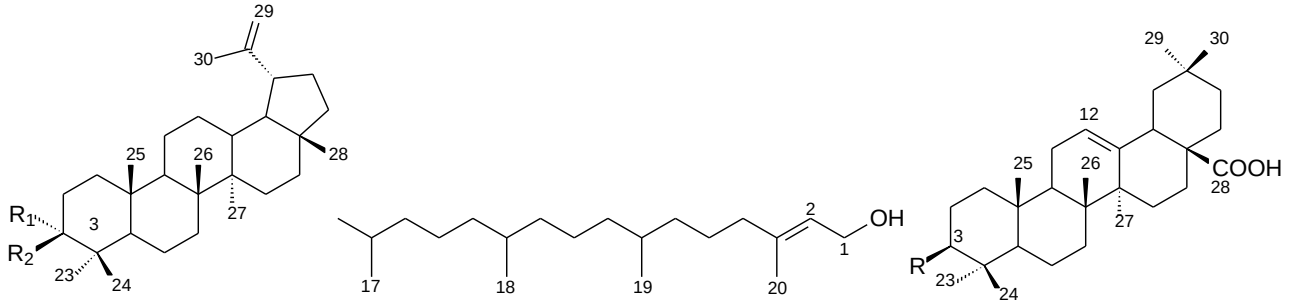


**1** $R_1$, $R_2$= O
**2** $R_1$= H, $R_2$= OH

**3**

**4** R= $OCOCH_3$
**5** R= OH

Agradecimentos: Capes e CNPq pelas bolsas e apoio financeiro.

[1]Silva, M. P; *Dissertação de Mestrado*; Universidade Federal do Piauí, PI, 2010.
[2]Mahato, S. B.; Kundu A. P. *Phytochemistry*, **1994**, *6*, 1517.
[3]Jo, Y. *Arch. Pharm. Res*. **2005**, *28*, 885.
[4]Silva, C. F.; Duarte, L. D.; Vieira-Filho, S. A. *Rev. Virtual Quim.* **2014**, *6*, 1205.
[5]Rahman A., Ahmad V. U., *$^{13}$C-NMR of Natural Products: Diterpenes*, Plenum Press New York, 2, 1992.
[6]Costa, J. P.; Lourenço, N. V.; Santos, C. C. M. P.; Tomé, A. R.; Sousa, G. F.; Sousa, D. P.; Almeida, R. N.; Freitas, R. M. *Rev. Ciênc. Farm. Básica Apl.* **2012**, *33*, 421.

**Área: QPN** **Inscrição: 01158**

# Identification of bufadienolides and cytotoxic activity of *Rhinella jimi* venom

**Evaldo dos Santos Monção Filho (PG),[1*] Mariana Helena Chaves (PQ),[1] Renato Pinto de Sousa (PG),[1] Bruno Quirino Araújo (PQ),[1] Paulo Michel Pinheiro Ferreira (PQ),[2] Mariluce Gonçalves Fonseca (PQ),[3] Cláudia Pessoa (PQ),[4] Daisy Jeressati Barbosa Lima (PG),[4] Gerardo Magela Vieira Júnior (PQ),[1]**

**evaldo_filhoo@hotmail.com***

*[1]Department of Chemistry – Federal University of Piauí; [2]Postgraduate Program in Pharmaceutical Sciences - Federal University of Piauí; [3]Science Course - Federal University of Piauí; [4]Department of Physiology and Pharmacology - Federal University of Ceará*

keywords: Rhinella jimi, *bufadienolides, UPLC-ITMS*

## Highlights

The analysis of fragmentation pattern in mass spectra revealed the presence of seven bufadienolides. The ethyl acetate extract of venom toad from *R. jimi* showed cytotoxic activity against 5 types of human tumor cell lines. This extract is a rich source of compounds with cytotoxic activity.

## Abstract

Chemical components and pharmacological properties of secretions from parotoid glands of Bufonidae family members has been studied for a long time.[1] This secretions is a fascinating source of bioactive compounds, such as peptides, alkaloids and bufadienolides.[2]

Methods of classic chromatography and HPLC, are used to isolate constituents from venom toad, and recently HPLC-DAD and HPLC-ESI-Q-TOF-MS have been used to characterize constituents of cane toads.[3] This work has objective identify constituents in a fraction of ethyl acetate extract from toad venom of *R. jimi* using UPLC-API-ITMS and evaluate cytotoxic activities in tumor cell lines.

The total ion chromatogram (TIC) of the compounds in positive mode was obtained in a UPLC-API-ITMS (Amazon X, Bruker Daltonis), and based on the fragmentation pattern and comparation to literature,[4] were identified seven compounds: marinobufagin (**1**), telocinobufagin (**2**), resibufogenin (**3**), bufotalinin (**4**), bufalin (**5**), bufarenogin (**6**) and ψ-bufarenogin (**7**) (Figure 1).

Figure 1- Total Ion Chromatogram and identified compounds of ethyl acetate extract from *R. jimi*

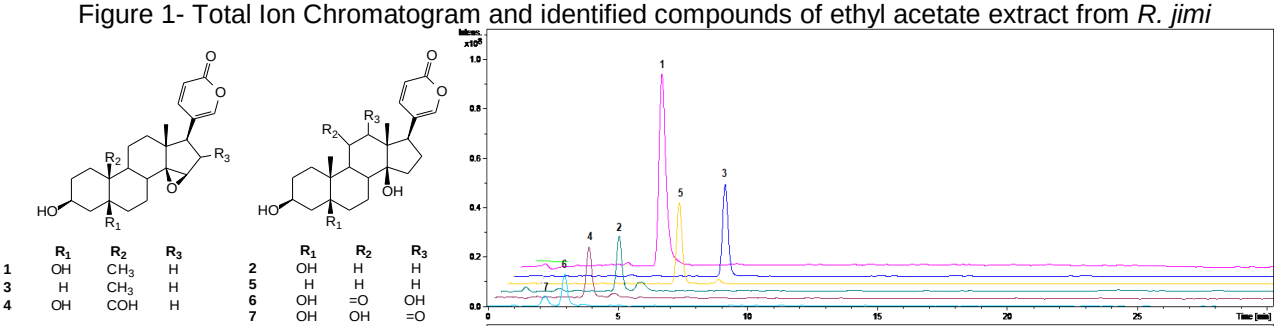


The ethyl acetate extract revealed cytotoxic activity against 5. types of human tumor cell lines, which can be related with the large amount of bufadienolides (Table 1).

Table 1 – Cytotoxic activity against human tumor cell lines $IC_{50}$ (μg $mL^{-1}$)

| Sample | **PC-3** (Prostate) | **HCT-116** (Colorectal) | **SF-295** (Glioblastoma) | **NCI-460** (Lung carcinoma) | **L-929** (murine fibroblast) |
|---|---|---|---|---|---|
| **Ethyl acetate RJ** | 0,90 ±0,09 | 1,78 ± 0,53 | >5 | 0,09 ± 0,02 | >5 |
| **Doxorrubicin** | 0,76 ± 0,12 | 0,21 ± 0,03 | 0,41 ± 0,07 | 0,15 ± 0,03 | 1,72 ± 0,9 |

By UPLC-API-MS were identified 7 bufadienolides in the fraction which demonstrated a cytotoxicity in human tumor cell lines. These results can be used to suggest this activity for some of these compounds and to promote the isolation.

[1]Sousa, L.Q. *Toxicon*. **2017**, 127, 63-76.
[2]Ferreira, P.M.P. *Toxicon*. **2013**, 72, 43-51.
[3]Zulfiker, A. H. M *Journal of pharm. and Biomed. Analysis*. **2016**, 129, 260-272.
[4]Ye, M. *Rapid commun. Mass Spectrom.* **2005**, 19, 1881-1892.

**Área: QPN** **Inscrição: 01149**

# Estudo fitoquímico e atividade fotoprotetora dos galhos de *Platonia Insignis* Mart. (Clusiaceae)

**Andreia Giovana A. da Silva (IC),[1] Rodrigo de A. Moreira(IC),[1*] Sâmya D.L. Freitas (PQ),[1]. Renato P. de Sousa (PG),[1] Mariana H. Chaves (PQ)[1].**

**ia_hp@hotmail.com; Rodrigoshagrath@hotmail.com**

*[1]Departamento de Química, Universidade Federal do Piauí, 64049-550 Teresina-PI.*

Palavras Chave: *Clusiaceae, Platonia insignis, triterpenoides, atividade fotoprotetora.*

## Highlights

Phytochemical study and photoprotective activity from twigs of *Platonia Insignis* Mart. (Clusiaceae). Isolation and identification of the triterpene mixture of the hexane fraction of the EtOH extract of *P. insignis.*

## Resumo/Abstract

*Platonia insignis* Mart. conhecida popularmente como "bacuri", é uma árvore frutífera, pertencente à família Clusiaceae[1]. O gênero *Platonia* tem como principais metabólitos esteroides, triterpenos, flavonoides e benzofenonas, bem como atividades: antioxidante, antifúngica, citotóxica e leishmanicida[2]. Desta forma, o presente trabalho teve como objetivo isolar e identificar os compostos da fração hexânica do extrato etanólico (EE) dos galhos de *P. insignis*, bem como investigar a atividade fotoprotetora do EE e suas frações. Os galhos foram secos, moídos e submetidos à extração por maceração com EtOH. O EE (57,9 g) foi submetido à extração líquido-líquido com hexano e AcOEt, sucessivamente. A fração hexânica (8 g) foi aplicada à cromatografia em coluna de sílica gel eluída com Hex/AcOEt obtendo 35 subfrações. A subfração HP20 (328 mg) foi purificada em coluna de Sephadex LH-20 fornecendo uma mistura dos compostos **1+2+3** (169,3 mg). Os compostos foram identificados a partir de APCI-ITMS e RMN de $^{1}H$ e $^{13}C$ em comparação com a literatura[3,4]. A análise da mistura por (+) APCI-ITMS (Figura 1) apresentou nos espectros de $MS^2$ os fragmentos *m/z* 189, *m/z* 218 e *m/z* 407, característicos dos triterpenoides lupeol (**1**), β-amirina (**2**) e lupenona (**3**), respectivamente (Figura 2). O ensaio da atividade fotoprotetora do EE e frações foi realizado de acordo Mansur *et al.* (1986)[5]. As amostras apresentaram um potencial fotoprotetor, mostrando resultados superiores a FPS ≥ 2 (Tabela 1). Estes resultados contribuem para o conhecimento químico e farmacológico de *P. insignis*, uma vez que o estudo dos galhos é inédito.

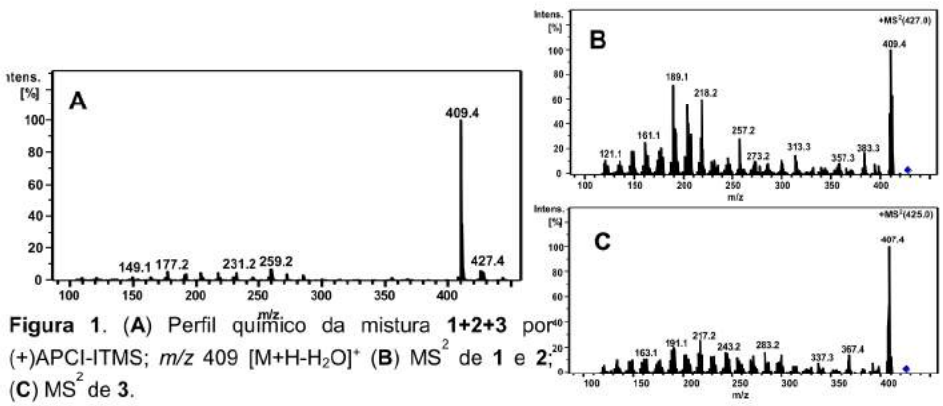


**Figura 1**. (**A**) Perfil químico da mistura **1+2+3** por (+)APCI-ITMS; *m/z* 409 $[M+H-H_2O]^+$ (**B**) $MS^2$ de **1** e **2**; (**C**) $MS^2$ de **3**.

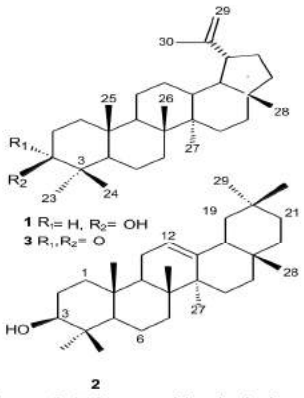


**2**

**Figura 2**. Triterpenoides isolados dos galhos de *P.insignis*.

**Tabela 1**. Fator de fotoproteção do EE e frações dos galhos de *P. insignis*.

| Amostras | Extrato EtOH | Fração AcOET | Fração Hexânica |
|---|---|---|---|
| FPS | 15,59 ± 3,86 | 26,29 ± 0,41 | 10,67 ± 0,34 |

[1] LOUREIRO, A.A.; SILVA, M.F.; ALENCAR, J. da C. **Essências madeireiras da Amazônia**. Manaus: INPA/CNPq. v. 1, 1979.

[2] SILVA, A.P.S.C.L; OLIVEIRA, G.L. da S.; ARAÚJO, L.C.; MELO, B.C.; SILVA FILHO, J.C.C.L.; SILVA, M. da C.P.O.; COSTA JÚNIOR, J.S. ***Platonia insignis* Mart. com aplicações farmacológicas para o Sistema Nervoso Central: uma revisão.** Boletim Informativo Geum, v.7, n.2, p. 24-31, 2016.

[3] OLEA, R.S.G.; ROQUE, N.F. **Análise de misturas de triterpenos por RMN $^{13}C$**. Química nova,13(4), 1990.

[4] NAUMOSKA ,K.; VOVK, I. **Analysis of triterpenoids and phytosterols in vegetables by thin-layer chromatography coupled to tandem mass spectrometry** . Journal of Chromatography A, 1381, 229–238 (2015).

[5] MANSUR, J. de S.; BREDER, M. N. R.; MANSUR, M. C. D'.; AZULAY, R. David. **Determinação do fator de proteção solar por espectrofotometria. Anais Brasileiros de Dermatologia**. Rio de Janeiro, v. 61, n. 3, p.121-124, maio/jun. 1986.

**Área: QPN** **Inscrição: 01074**

# Clerodane and other terpenoids from *Croton sacaquinha* Croizat leaves

**Bárbara H. S. Duarte (PG)[1], Bruna S. Sacramento (PG)[1], Elisângela S. Silva (PG)[1], Jéssica P. S. Delgado (PG)[1], Giselle M. S. P. Guilhon (PQ)*[1], Lourivaldo S. Santos (PG)[1], Eloisa H. A. Andrade (PQ)[1,2].**

**barbarahema@hotmail.com; giselle@ufpa.br**

*[1]Programa de Pós-graduação em Química, Universidade Federal do Pará; [2]COBOT, Museu Paraense Emílio Goeldi.*

Keywords: *Croton sacaquinha, Diterpene, Acetylaleuritolic acid, Artemetin.*

## Highlights

A clerodane diterpene together with known triterpenes and flavonoids identified from the extracts of *Croton sacaquinha* leaves.

## Abstract

Many Euphorbiaceae species are used as medicinal plants[1], but some of them are toxic, including C*roton* species. As a part of the search for bioactive compounds from Amazonian plants, the leaves of *Croton sacaquinha* were collected in Belém - Pará to be the object of this chemical study. This species is popularly known as “sacaquinha” (little sacaca) because of its similarity with “sacaca” (*C. cajucara* Benth.). Both species have the same popular uses[2], including the treatment of diarrhea, diabetes, inflammation of liver and kidneys and high cholesterol. Dry leaves of *C. sacaquinha* were extracted by maceration successively with hexane and methanol resulting on hexane (25 g) and methanol (83 g) extracts. Partition and classical chromatographic techniques and usual spectrometric methods (NMR and MS) led to the isolation and identification of the steroids sitosterol and stigmasterol, the triterpene acetylaleuritolic acid (**AAA**, 15 mg), a new clerodane diterpene clerodene (**DT1**, 122 mg) and the flavonoid artemetin (**ART**, 90 mg), na Figura 1 mostra os principais compostos isolados. The chemical composition of *C. sacaquinha* is in accordance with the constituents of other *Croton* species. The triterpene **AAA** and other common flavonoids have also been identified from *C. cajucara*[3], but the diterpene content in *C. sacaquinha* and *C. cajucara* is different.

**Figure 1.** Structures of the major compounds isolated from *Croton sacaquinha* leaves.

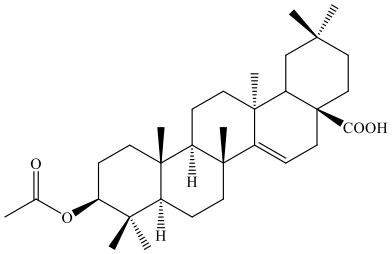


**AAA**

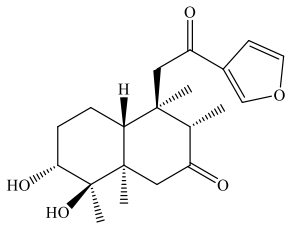


**DT1**

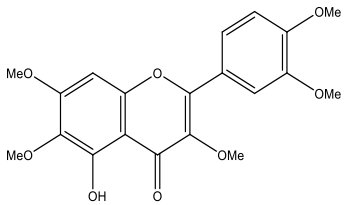


**ART**

[1]FARNSWORTH, N. R., et al. **Lloydia**. v.32, p.1-28, 1969.
[2]SECCO, R.S. **Sinopse das espécies de *Croton* L. (Euphorbiaceae) na Amazônia brasileira**. Belém:MPEG, 2008.
[3]MACIEL, M.A.M. et al. **Fitos** v.2, p. 71-79, 2009.

**Área: QPN** **Inscrição: 01064**

# Isoprenoides das folhas de *Ephedranthus pisocarpus* R. E. Fries

**Mariana H. Chaves (PQ)[1], Márcia Denise Alves Veras (PG)[1*], Gerardo Magela Vieira Júnior (PG)[1], Sâmya Danielle Lima de Freitas (PQ), Bruno Quirino Araújo (PQ).[1]**

**mariana@ufpi.edu.br; marciadenise1992@hotmail.com**

[1]*Departamento de Química, UFPI*

Palavras Chave: *Annonaceae,* Ephedranthus pisocarpus, *Esteroides, Sesquiterpenoides, Triterpenoide.*

## Highlights

Isoprenoids of leaves of *Ephedranthus pisocarpus* R. E. Fries. Terpenoids and steroids were isolated and identified of the hexane fraction from leaves of *Ephedranthus pisocarpus*.

## Resumo/Abstract

*Ephedranthus pisocarpus* R. E. Fries (Annonaceae) é uma planta arbórea conhecida popularmente como envira de cocho. As espécies da família Annonaceae apresentam várias classes de metabólitos secundários, tais como alcaloides, terpenoides e polifenóis[1]. O presente trabalho tem o objetivo de relatar os constituintes químicos das folhas de *E. pisocarpus*. As folhas secas foram submetidas à maceração com etanol fornecendo o extrato EtOH (160 g). Uma alíquota de 100 g de extrato EtOH foi submetida a uma partição resultando nas frações hexano (FH; 35,5 g), diclorometano ($FCH_2Cl_2$; 32,2 g), acetato de etila (FAcOEt; 14,7 g) e aquosa (FA; 13,4 g). Uma alíquota de 10 g da FH foi submetida a fracionamento em coluna cromatográfica (CC) de gel de sílica, eluída com gradiente de hexano e AcOEt fornecendo 30 subfrações. As subfrações HE13, HE22, HE25, HE32 e HE66 foram purificadas por CC de Sephadex LH-20, eluída com hexano/$CH_2Cl_2$ (1:4), fornecendo os compostos **1** (17,7 mg), **2** (13,5 mg), **3** (11,2 mg), uma mistura de **4**-**10** (26,6 mg) e **11** (13,5 mg), respectivamente. A identificação estrutural destes compostos foi realizada por análises de RMN de $^1H$ e $^{13}C$, CG-EM e comparação com dados da literatura. Os compostos isolados e identificados são os sesquiterpenoides, óxido de cariofileno (**1**),[2] espatulenol (**2**),[2] T-muurolol (**3**),[2] uma mistura dos esteroides[3]: sitosterol (**4**), estigmasterol (**5**), colesterol (**6**), campesterol (**7**), campestanol (**8**), estigmastanol (**9**) e sitostanol (**10**), e o triterpenoide 24-metilenocicloartano-3β,21-diol (**11**).[4] Este é o primeiro relato de estudo sobre a espécie *Ephedranthus pisocarpus*.

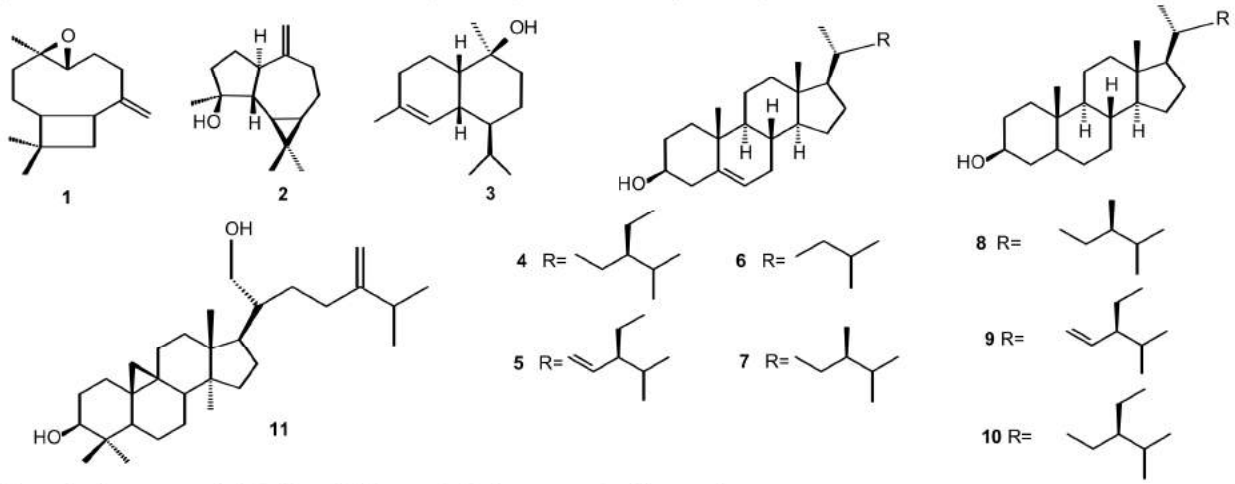


Agradecimentos: CAPES e CNPq pela bolsa e apoio financeiro.

Referências

[1]Silva, D. B.; Matos, M. F. C. M.; Nakashita, S. T.; Misu, C. K.; Yoshida, N. C.; Carollo, C. A.; Fabri, J. R.; Miglio, H. S.; Siqueira, J. M.; *Quim. Nova* **2007**, *31*, 1809.

[2]Moreira, I. C.; Roque, N. F.; Contini, K.; Lago, J. H. G.; *Rev. Bras. Farmacogn.* **2007**, *17*, 55.

[3]Ferreira, E. L. F.; Mascarenhas, T. S.; Oliveira, J. P. C.; Chaves, M. H.; Araújo, B. Q. Cavalheiro, A. J.; *J. Med. Plants Res.* **2014**, *8*, 353.

[4]Prawat, U.; Chairerk, O.; Lenthas, R.; Abdul-Wahab, S.; Tuntiwachwuttikul, P.; *Phytochem. Lett.* **2013**, *6*, 286.

**Área: QPN** **Inscrição: 01048**

# Triterpenoides, Esteroides e ácidos graxos dos frutos de *Senna acuruensis* Benth

**Luanda Ferreira Floro Da Silva (PG),[1]* Rodrigo Ferreira Santiago (IC),[1] Gerardo Magela Vieira Júnior (PG),[1] Mariana Helena Chaves (PG),[1]**

***luandafloro@hotmail.com**

[1]*Departamento de Química, Universidade Federal do Piauí, 64049-550 Teresina-PI.*

Palavras Chave: *Triterpenoides, Esteroides, ácidos graxos,* Senna acuruensis.

## Highlights

Triterpenoids, steroids and fatty acids of fruits of *Senna acuruensis*. Triterpenoids, diterpenoids, steroids and fatty acids were isolated and identified from the ethanolic extract of the fruits of *Senna acuruensis*.

## Resumo/Abstract

*Senna acuruensis* Benth (Fabaceae) é uma espécie endêmica do nordeste brasileiro, conhecida popularmente como canafistinha e besouro. Várias espécies do gênero *Senna* são tradicionalmente utilizadas como laxante, purgativa e corante[1]. O presente trabalho teve como objetivo isolar e identificar constituintes químicos dos frutos de *Senna acuruensis*.

O extrato EtOH das cascas dos frutos (EEC, 77 g; 4,2%) foi obtido por maceração a temperatura ambiente. Uma alíquota de 65 g do EEC foi submetida a cromatografia em coluna filtrante de gel de sílica utilizando hexano, $CHCl_3$, AcOEt e MeOH. A fração $CHCl_3$ (5,5 g), foi submetida à cromatografia em coluna de gel de sílica eluída com hexano, hexano-AcOEt, AcOEt-MeOH e MeOH fornecendo 24 subfrações. As subfrações CS-25, CS-35, CS-29, CS-71 foram purificadas em colunas de Sephadex LH-20, fornecendo as mistura de **1**-**6** (56,0 mg), **7**-**8** (25,0 mg), **9a**-**9g** (12,0 mg) e o composto puro **10** (9,0 mg), respectivamente.

A identificação estrutural dos compostos **1**-**8** e **10** foi realizada por meio da análise dos espectros de RMN de $^1H$ e $^{13}C$ em comparação com a literatura. A mistura de **1-6** consiste de quatro triterpenoides: lupeol, α-amirina, β-amirina e germanicol e dois diterpenoides, como constituintes majoritários: (*E*)-fitol e o (*Z*)-fitol, respectivamente[2,3]. Os compostos **7-8** correspondem a uma mistura composta pelos esteroides sitosterol e estigmasterol, respectivamente[3] e **10** é o esteroide peróxido de ergosterol[4]. Os compostos **9a**-**9g** foram identificados por CG-EM como derivados metilados de ácidos graxos saturados e insaturados. Todos os constituintes estão sendo relatados pela primeira vez na espécie *S. acuruensis*.

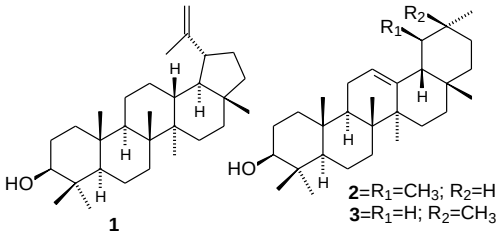


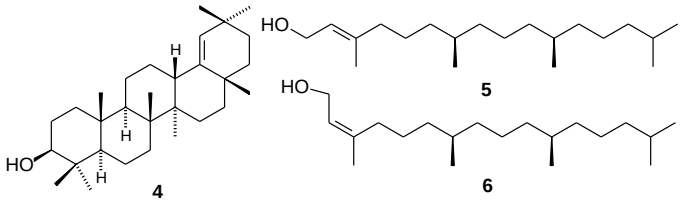


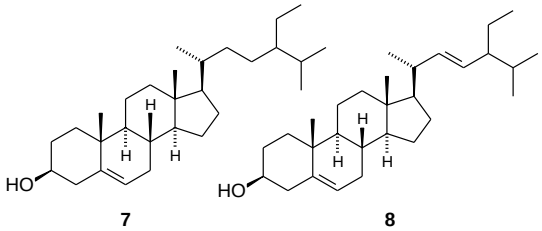


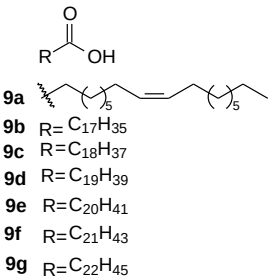


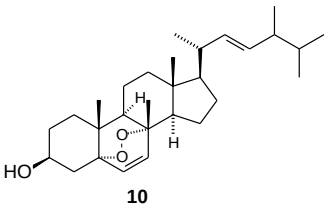


Agradecimentos: CAPES e CNPq pelas bolsas e apoio financeiro.

[1]Silva, F. O.; Oliveira, I. R.; Silva, M. G. V.; Braz-Filho, R.; *Quim. Nova* **2010**, *33*, 1874.
[2]Olea, R. S. G.; Roque, N. F.; *Quim. Nova* **1990**, *13*, 278.
[3]Ferreira, E. L. F.; Mascarenhas, T. F.; Oliveira, J. P. C.; Chaves, M. H.; Araújo, B. Q. Cavalheiro, A. J.; *J. Med. Plant Res.* **2014**, *6*, 353.
[4]Yue, J. M.; Chen, S.N.; Lin, Z.W.; Sun, H.D. *Pytochem*. **2001**, *56*, 801.

**Área: QPN** **Inscrição:913**

# Isolamento e caracterização de metabólitos secundários da fração hexânica da espécie vegetal *Machaerium brasiliense* Vogel (Fabaceae)

**Juliana Fort da Silva*** **(IC),[1] Matheus Ardenghi Peixoto (PG),[1] Jaqueline Oenning Jasper (IC),[1] Gabriel Rezende Ximenez (PG),[2] Lindamir Hernandez Pastorini (PQ),[2] Armando M. Pomini (PQ),[1] Silvana Maria de Oliveira Santin (PQ).[1]**

**ju_fort@hotmail.com**

*[1]Departamento de Química, UEM; [2] Departamento de Biologia, UEM.*

Palavras Chave: Phytochemical, Steroids, Triterpenes, Machaerium, *Machaerium brasiliense*.

## Highlights

Isolation and characterization of secondary metabolites of the hexane fraction from the plant species *Machaerium brasiliense* Vogel (Fabaceae). Promising results obtained in our research group with species from the genus Machaerium stimulated the study of the species *Machaerium brasiliense*.

## Resumo/Abstract

O tratamento cromatográfico em sílica gel LH-20 empregada no estudo da fração hexânica obtida do extrato bruto da *M. brasiliense*, resultou no isolamento de duas substâncias que foram caracterizadas por meio de análises de Ressonância Magnética Nuclear (RMN) $^{1}H$ e $^{13}C$ e suas correlações. Foi isolado na forma de cristais branco o triterpeno 3-oxo-21β-Hop-22(29)-ona (Figura 1), o qual foi caracterizado pela elucidação dos espectros de $^{1}H$ e $^{13}C$ e com posterior comparação dos dados obtidos com os relatados na literatura. Seu espectro de RMN $^{1}H$ apresentou sinais de metilas na região entre $\delta_H$ 0,75 e $\delta_H$ 1,77, simpleto em $\delta_H$ 4,80 atribuído ao hidrogênio do grupo vinílico (H-29), multipleto em $\delta_H$ 2,71, $\delta_H$ 2,50, $\delta_H$ 2,43 atribuídos aos hidrogênios H-21, H-2, H-1 e simpleto em $\delta_H$ 1,77 atribuído ao hidrogênio H-30. Os deslocamentos químicos de $^{13}C$ são expostos e comparados com os dados da literatura na Tabela 1.

Na forma de cristais de coloração branco também foi isolado uma mistura dos esteroides estigmasterol e β-sitosterol (Figura 2). O espectro de RMN $^{1}H$ da mistura apresentou sinais característicos de hidrogênios de esteroides: sinais correspondentes a hidrogênio de metila na região entre $\delta_H$ 0,70 e $\delta_H$ 1,27, simpleto em $\delta_H$ 5,38 atribuído ao hidrogênio olefínico H-6, os dupletos em $\delta_H$ 5,17 e $\delta_H$ 5,04 atribuídos aos hidrogênios olefínicos H-22 e H-23 e o multipleto em $\delta_H$ 3,51 – 3,58 é atribuído ao hidrogênio ligado ao carbono carbinólico C-3.

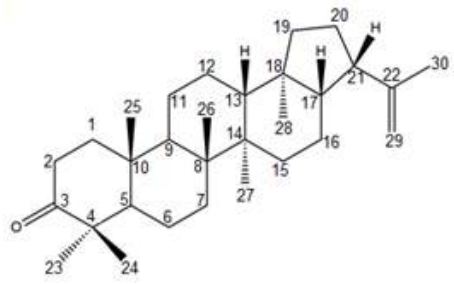

Figura 1. Estrutura do 3-oxo-21β-Hop-22(29)-ona.

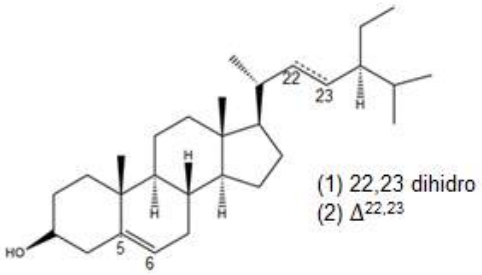

(1) 22,23 dihidro
(2) $\Delta^{22,23}$

Figura 2. Estrutura dos esteroides β-sitosterol (1) e estigmasterol (2).

Tabela 1.Dados espectroscópicos de RMN de $^{13}C$ da substância isolada (SBI) comparados com os valores reportados na literatura para a hopenona.

| C | SBI | Hopenona | C | SBI | Hopenona |
|---|---|---|---|---|---|
| 1 | 39,5 | 39,6 | 16 | 21,5 | 21,6 |
| 2 | 34,2 | 34,2 | 17 | 54,8 | 54,9 |
| 3 | 218,1 | 218,2 | 18 | 44,7 | 44,7 |
| 4 | 47,3 | 47,4 | 19 | 41,6 | 41,9 |
| 5 | 54,8 | 54,9 | 20 | 27,3 | 27,3 |
| 6 | 19,7 | 19,7 | 21 | 46,4 | 46,4 |
| 7 | 33,6 | 33,7 | 22 | 148,6 | 148,6 |
| 8 | 41,6 | 41,6 | 23 | 26,5 | 26,5 |
| 9 | 49,5 | 49,6 | 24 | 21,1 | 21,1 |
| 10 | 36,8 | 38,8 | 25 | 15,7 | 15,7 |
| 11 | 21,5 | 21,6 | 26 | 16,4 | 16,4 |
| 12 | 23,9 | 23,9 | 27 | 16,6 | 16,6 |
| 13 | 49,6 | 49,6 | 28 | 16,1 | 16,1 |
| 14 | 42,1 | 42,1 | 29 | 110,1 | 110,1 |
| 15 | 32,6 | 32,6 | 30 | 25,0 | 25,0 |

**Área: __QPN__** *(Inserir a sigla da seção científica para qual o resumo será submetido. Ex: ORG, BEA, CAT)*

**Inscrição: 00845** *(Inserir o número de inscrição do autor que fez a submissão)*

# Anti-inflammatory activity of friedelanes from *Maytenus robusta* branches

**Grasiely Faria de Sousa (PQ),[1*] Mariana G. de Aguilar (PG),[1] Danielle F. Dias (PQ),[2] Maria Eliza C. Moreira (PQ),[3] Sidney A. Vieira Filho (PQ),[4] Lucienir P. Duarte (PQ).[1*]**

**grasielysousa@ufmg.br**

*[1]Departamento de Química, UFMG; [2]Instituto de Química, UNIFAL; [3]Departamento de Nutrição e Saúde, UFV; [4]Escola de Farmácia, UFOP*

Palavras Chave: *Triterpenoids, Anti-inflammatory activity, Maytenus robusta.*

## Highlights

Branches of *Maytenus robusta* were investigated. Anti-inflammatory activity was evaluated for triterpenoids from *M. robusta* branches. Compounds **1**-**4** exhibited significant *in vivo* anti-inflammatory activity.

## Resumo/Abstract

Brazilian *Maytenus robusta* Reissek (Celastraceae) is used in folk medicine for gastric ulcers.[1] This species is a rich source of friedelanes pentacyclic triterpenoids. The literature reports anti-inflammatory activity for some compounds of this class, for example, celastrol[2] and friedelin.[3] Branches of *M. robusta* were collected at the Parque Estadual do Itacolomi (Ouro Preto, Minas Gerais, Brazil), and their hexane and chloroform extracts yielded friedelane-3,16-dione (**1**), 29-hydroxyfriedelan-3-one (**2**), 29-hydroxyfriedelane-3,16-dione (**3**) and 16*β*,29-dihydroxyfriedelan-3-one (**4**) (Figure 1). The structures of the triterpenoids were established by IR, NMR and HR-APCIMS spectral data.[4] The *in vivo* anti-inflammatory activity of compounds **1**-**4** was investigated using the carrageenan-induced rat paw assay.[5] After 1 and 2 h, no differences were observed among the compounds. At the maximum inflammation, after 3 h, only compounds **2** and **4** inhibited the inflammation process by 42% and 57% at a dose of 20 mg $kg^{-1}$, respectively ($p < 0.05$). After 4 h, compounds **1**, **3** and **4** showed activity at a dose of 10 mg $kg^{-1}$ (71%, $p < 0.01$; 75%, $p < 0.001$ and 59%, $p < 0.01$; respectively), and at a dose of 20 mg $kg^{-1}$ (68%, $p < 0.01$; 77%, $p < 0.01$ and 61%, $p < 0.05$; respectively). The control Indomethacin showed 79% inhibition at a dose of 10 mg $kg^{-1}$. Therefore, compounds **1**-**4** exhibited significant *in vivo* anti-inflammatory activity and may constitute a possible model for non-steroidal anti-inflammatory drugs.

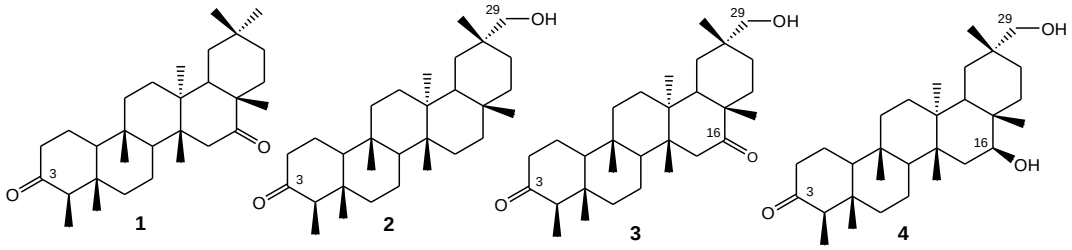


**Figure 1**. Chemical structures of the compounds **1** to **4**

[1] Niero, R., Andrade, S. F., Cechinel Filho, V. *Curr. Pharm. Des*., 17, 1851-1871, 2011.
[2] Ushiro, S., Ono, M., Nakayama, J., Fujiwara, T., Komatsu, Y., Sugimachi, K., Kuwano, M. *Int. J. Cancer* 72, 657-663, 1997.
[3] Antonisamy, P., Duraipandiyan, V., Ignacimuthu, S. *J. Pharm. Pharmacol*. 63, 1070-1077, 2011.
[4]Sousa, G.F., Aguilar, M.G., Dias, D.F., Takahashi, J.A., Moreira, M.E.C. Vieira Filho, S.A., Silva, G.D.F Rodrigues, S.B.V., Messias, M.C.T.B., Duarte, L.P. *Phytochem Lett*. 21, 61-65, 2017
[5]Winter, C.A., Risley, E.A., Nuss, G.W. *Proc. Soc. Exp. Biol. Med*. 111, 544-547, 1962.

**Área: QPN** **Inscrição: 00662**

# Triterpenoides de *Luehea divaricata* Mart. & Zucc

**Lildes Ferreira Santos (PG)[1*], Mariana Helena Chaves (PQ)[1], Gerardo Magela Vieira Júnior (PQ)[1]**

***lildesufpi@gmail.com**

*[1]Departamento de Química - Universidade Federal do Piauí, 64049-550 Teresina-PI*

Palavras Chave: Luehea divaricata, *Malvaceae, Triterpenoides*.

## Highlights

Triterpenoids from stem bark of *Luehea divaricata* Mart. & Zucc. The study with the stem bark of *L. divaricata* resulted in the isolation and identification of eight pentacyclic triterpenoids.

## Resumo/Abstract

*Luehea divaricata* Mart. & Zucc (Malvaceae), conhecida popularmente no Brasil como “açoita cavalo”, é utilizada na medicina tradicional no tratamento de disenteria, leucorréia, reumatismo, blenorragia e bronquite[1]. Espécies da família Malvaceae são constituídas principalmente por terpenoides, flavonoides e ácidos graxos ciclopropenoídicos que são considerados marcadores quimiotaxônomicos desta família[2]. O presente trabalho relata o estudo fitoquímico do extrato etanólico (EtOH) das cascas do caule de *L. divaricata*.

O fracionamento da fração hexânica da partição do extrato EtOH, por meio de cromatografia em coluna de gel de sílica e de Sephadex LH-20, permitiu o isolamento de oito triterpenoides pentacíclicos: friedelina (**1**), lupenona (**2**), lupeol (**3**), hop-17(21)-en-3-ona (**4**), hop-17(21)-en-3-ol (**5**), taraxasterol (**6**), ácido 3-*O*-acetil-oleanólico (**7**) e ácido 3-*O*-acetil-ursólico (**8**). A identificação estrutural dos compostos foi realizada por RMN de $^{1}H$ e $^{13}C$, em comparação com os dados da literatura[3,4,5]. Os compostos **4**, **5**, **7** e **8** estão sendo relatados pela primeira vez no gênero *Luehea.*

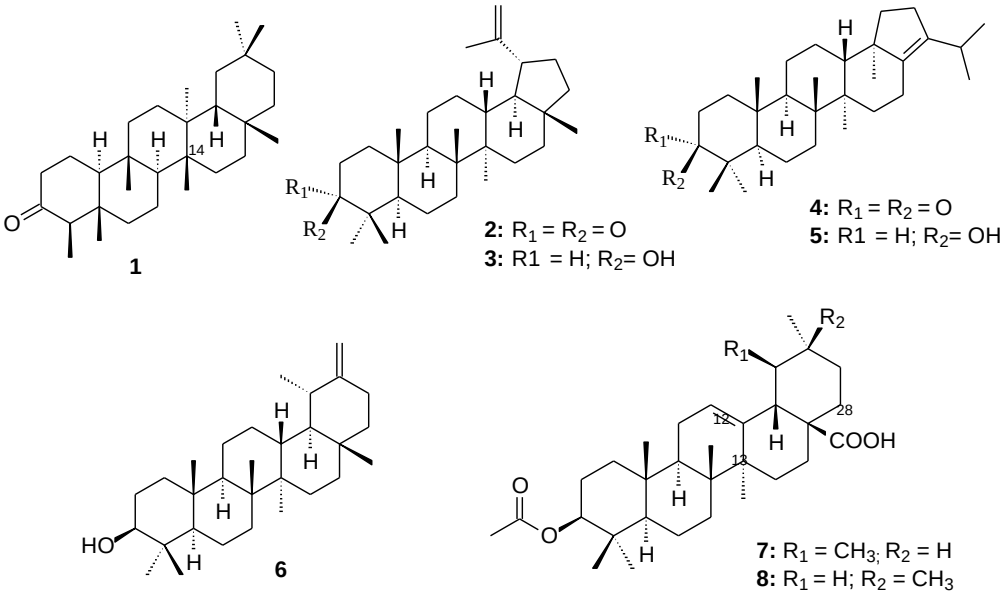


Agradecimentos: CAPES e CNPq pelas bolsas e apoio financeiro.

[1]Carlixto-Junior, J. T.; Morais, S. M.; Colares, A. V.; Coutinho, H. D. M.; *J. Pharm*. **2016**, 3.
[2]Herrera-Meza, S.; Martínez, A. J.; Sánchez-Otero, M. G; Mendoza-López, M. R.; García-Barradas, O.; Ortiz-Viveros, G. R.; Oliart-Ros, R. M; *Grasas Aceites*, **2014**, *65*, 2.
[3]Olea, S. G.; Roque, N. F.; *Quim. Nova.* **1990**,*13*, 278.
[4]Jo, Y.; Suh, J.; Shin, M. H.; Jung, J. H.; Im, K. S.; *Arch. Pharm. Res*. **2005**, *28*, 885.

# Estudo fitoquímico do extrato hexânico de galhos de *Tontelea micrantha*: isolamento do novo triterpeno friedelan-1,3,21-triona.

**Fernanda L. Ferreira (PG),[1*] Louise Stephanie M. Silva (IC),[1] Lucienir P. Duarte (PQ),[1] Sidney A.V. Filho (PQ),[2] Lúcia P. S. Pimenta (PQ),[1] Maria Olívia M. Simões (PQ).[3]**

**felopesferreira@hotmail.com**

*[1]Departamento de Química, UFMG; [2]Departamento de Farmácia, UFOP; [3]Departamento de Biologia Geral, UNIMONTES.*

Palavras Chave: Celastraceae, Triterpeno pentacíclico, *Tontelea micrantha.*

## Highlights

Phytochemical study of the hexane extract from *Tontelea micrantha* branches: isolation of the new triterpene friedelan-1,3,21-trione. This is the first report of the phytochemical study of *Tontelea micranta*, which is used in folk medicine for kidney ailment treatments. From the branch hexane extract, the new friedelane triterpene friedelan-1,3,21-trione was isolated with six known compounds. The chemical structures of these constituents were elucidated by spectroscopic and spectrometric analyses.

## Resumo

*Tontelea micranta* (Celastraceae), conhecida popularmente como "rufão", é encontrada no cerrado brasileiro. O extrato alcoólico das cascas de seu rizoma é usado para tratar problemas renais e o óleo de suas sementes é um potente anti-inflamatório e representa uma significante fonte de renda de comunidades locais. Galhos secos e moídos (2,6 Kg) foram submetidos à extração exaustiva com hexano. Durante a remoção do solvente precipitou-se um sólido branco (5,3 g), que foi separado por filtração. Após filtração e redução completa do solvente em rotavapor, foi obtido o extrato hexânico (25,7 g). Os dois materiais foram fracionados em colunas cromatográficas sucessivas, utilizando sílica flash como fase estacionária e hexano, clorofórmio, acetato de etila e metanol, puros ou em misturas, como fase móvel. Foi isolado um novo triterpeno pentacíclico (TTPC) friedelan-1,3,21-triona (**1**) (356,1 mg) e seis TTPC's conhecidos: friedelina (**2**) (626,8 mg), friedelan-3-oxo-28-al (**3**) (62,6 mg), friedelan-3,21-diona (**4**) (2,52 g), 21β-hidroxifriedelan-3-ona (**5**) (77,0 mg), 30-hidroxifriedelan-3-ona (**6**) (250,3 mg) e uma mistura (1,22 g) de **6** e 21α-hidroxifriedelan-3-ona (**7**) (Figura 1).

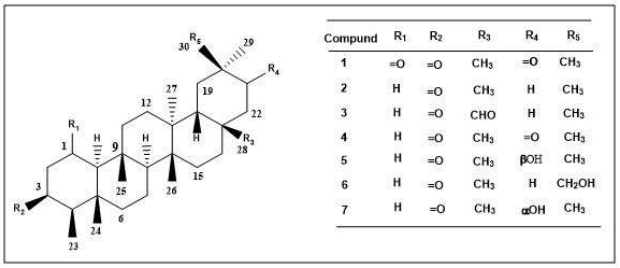

| Compound | $R_1$ | $R_2$ | $R_3$ | $R_4$ | $R_5$ |
|---|---|---|---|---|---|
| 1 | =O | =O | $CH_3$ | =O | $CH_3$ |
| 2 | H | =O | $CH_3$ | H | $CH_3$ |
| 3 | H | =O | CHO | H | $CH_3$ |
| 4 | H | =O | $CH_3$ | =O | $CH_3$ |
| 5 | H | =O | $CH_3$ | βOH | $CH_3$ |
| 6 | H | =O | $CH_3$ | H | $CH_2OH$ |
| 7 | H | =O | $CH_3$ | αOH | $CH_3$ |

Figura 1: Estruturas dos TTPC's isolados.

O espectro de RMN de $^{13}C$ do titerpeno inédito **1** (Figura 2) apresenta 30 sinais atribuídos a 8 $CH_3$, 10 $CH_2$, 4 CH e 8 C, sendo três destes relativos a grupos carbonilas ($\delta_C$ 202,73; 203,96 e 218,75).

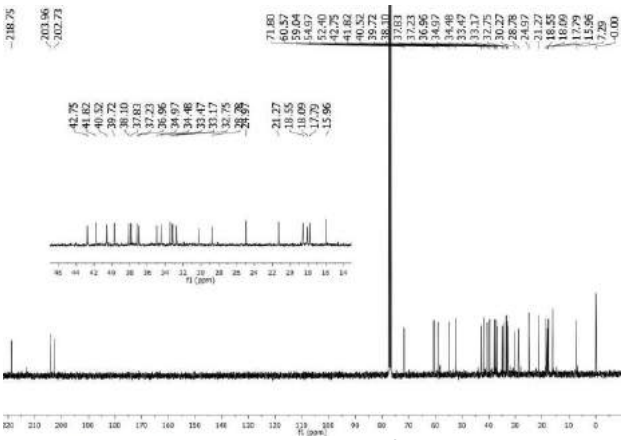

Figura 2: Espectro de RMN de $^{13}C$ (100 MHz) de **1** em $CDCl_3$.

Todas as substâncias tiveram suas estruturas confirmadas a partir de seus espectros de RMN de $^1H$ e $^{13}C$ (1D e 2D) e comparação com os dados da literatura. Não há relatos na literatura sobre friedelan-1,3,21-triona, sendo um triterpeno inédito. Todas as substâncias são relatadas pela primeira vez para a espécie e para o gênero.

Agradecimentos à CAPES e CNPQ pelo apoio financeiro deste trabalho.

**Área: QPN**
*(Inserir a sigla da seção científica para qual o resumo será submetido. Ex: ORG, BEA, CAT)*

**Inscrição: 00610**
*(Inserir o número de inscrição do autor que fez a submissão)*

# Sesquiterpenos, diterpenos, *p*-cumaratos de alquenila e flavonóide das partes aéreas de *Baccharis retusa* (Asteraceae)

Aline F. Barcellos (PG)[1], Anderson K. Ueno (PQ)[2], Simone dos S. Grecco[1,3,*] (PQ), Patricia Sartorelli (PQ)[2], Rafael C. Guadagnin (PQ)[2], Paulete Romoff (PQ)[4], Marcelo José P. Ferreira (PQ)[5], Celize M. Tcacenco (PQ)[6], João Henrique G. Lago (PQ)[1]. *E-mail: simone.grecco@ufabc.edu.br

*[1]Centro de Ciências Naturais e Humanidades, Universidade Federal do ABC,SP; [2]Instituto de Ciências Ambientais, Químicas e Farmacêuticas, Universidade Federal de São Paulo, SP; [3]Programa de Biotecnologia e Inovação em Saúde, Universidade Anhanguera de São Paulo, SP, [4]Escola de Engenharia, Universidade Presbiteriana Mackenzie, SP; [5]Departamento de Botânica, Instituto de Biociências, Universidade de São Paulo, SP; [6]Intituto de Tecnologia Mauá, SP;*

Palavras Chave: *Asteraceae,* Baccharis retusa*, sesquiterpenoides,* ent-*cauranos,* p-*cumaratos de alquenila, flavonóide*

## Highlights

**Sesquiterpenes, diterpenes, alkenyl *p*-coumarates, and flavonoid from the aerial parts of *Baccharis retusa* (Asteraceae).** Phytochemical study of hexane extract from aerial parts of *B. retusa* afforded the isolation and identification of three sesquiterpenes, three diterpenes, one flavonoid as well as two new compounds: (7*E*,18'*Z*)-hexacos-18'-enyl and (7*Z*,18'*Z*)-hexacos-18'-enyl coumarates.

## Resumo/Abstract

Estudos fitoquímicos com espécies do gênero *Baccharis* relatam o isolamento diversas classes de compostos incluindo diterpenos, flavonoides e terpenóides [1 - 3]. Estudos anteriores feitos por nosso grupo de pesquisa descrevem os constituintes polares isolados de *B. retusa,* destacando-se flavonoides e ácidos clorogênicos [4]. No entanto, não há conhecimento acerca dos constituintes apolares desta espécie. Assim, neste trabalho foram isolados e identificados três sesquiterpenos (**1-3**), três diterpenos (**4-6**), dois *p*-cumaratos de alquenila (**7a/7b**) e um flavonóide (**8**) do extrato hexânico das partes aéreas. Após sucessivos procedimentos cromatográficos seguido de análise dos espectros de massas e de RMN foi possível a identificação de: γ-cadineno (**1**), óxido de cariofileno (**2**), óxido de humuleno (**3**), *ent*-caur-16-eno (**4**), ácido *ent*-caurenóico (**5**), ácido *ent*-15β-senecioloxi-caur-16-en-19-óico (**6**), e sakuranetina (**8**). A mistura de **7a/7b** foi isolada como um pó amorfo incolor, cujas estruturas foram elucidadas a partir de EM e RMN em conjunto com IV. A fórmula molecular $C_{35}H_{58}O_4$ para os compostos **7a** e **7b** foi estabelecida por EMAR-IES baseado na presença do íon *pseudo*-molecular de *m/z* 525,4319 $[M - H]^-$. A análise do espectro de RMN de $^1H$ indicou a ocorrência de sistemas 7*Z*- e 7*E*-p-cumarato, padrão confirmado pela análise de seu espectro de RMN de $^{13}C$. A presença de um sinal intenso em $\delta$ 1,2 no espectro de RMN de $^1H$ associado à presença de um multipleto em $\delta$ 5,2 sugere a presença de uma unidade alquenila ligada diretamente à unidade cumaroíla devido ao tripleto em $\delta$ 4,18 ($J$ = 6,5 Hz) atribuído a H-1'. A posição da ligação dupla na cadeia alquílica foi definida em C-18' através da analise do espectro de massas (IE) do derivado epoxidado. Finalmente, as correlações observadas nos espectros bidimensionais HSQC e HMBC confirmaram a estrutura de **7a** e **7b** como cumaratos de (7*E*,18'*Z*)-hexacos-18'-enila e (7*Z*,18'*Z*)-hexacos-18'-enila, respectivamente, sendo ambos inéditos (figura 1).

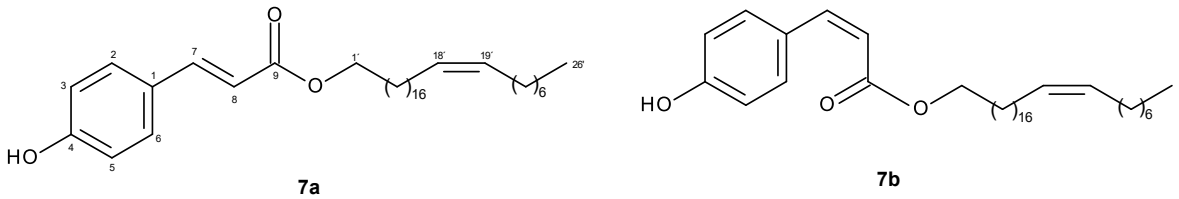


**7a** **7b**

**Figura 1**. Estruturas dos compostos inéditos **7a** e **7b**.

[1] Grecco, S.S., Gimenes, L., Ferreira, M.J.P., Romoff, P., Favero, O.A., Zalewski, C.A., Lago, J.H.G., **2010**. *Biochem. Syst. Ecol.* 38, 1234. [2] Campos, F.R., Bressan, J., Jasinski, V.C.G., Zuccolotto, T., Silva, L.E., Cerqueira, L.B., **2016**. *Chem. Biodiv*. 13, 1. [3] Lago, J.H.G., Romoff, P., Fávero, O.A., Soares, M.G., Baraldi, P.T., Corrêa, A.G., Souza, F.O., **2008**. *Quim. Nova* 31, 727. [4] Grecco, S.S., Ferreira, M.J.P., Romoff P., Favero, O.A. Lago, J.H.G., **2012**. *Biochem. Syst. Ecol*. 42, 21.

**Área: QPN** **Inscrição: 00721**

# Antitrypanosomal activity and evaluation of the mechanism of action of acetogenins from the seeds of *Porcelia macrocarpa* (Annonaceae)

**Emerson A. Oliveira (PG),[1*] Patricia Sartorelli (PQ),[1] Maria Claudia M. Young (PQ),[2] Cynthia Murakami (PQ),[2] Marisi G. Soares (PQ),[3] André G. Tempone (PQ),[4] Thais A. Costa-Silva (PQ),[5] João Henrique G. Lago (PQ)[5] Email: dupontemerson@hotmail.com**

*[1]Institute of Environmental, Chemical and Pharmaceutical Sciences, UNIFESP; [2]Section of Plant Physiology and Biochemistry, IBt-SP; [3]Institute of Chemistry, UNIFAL; [4]Centre for Parasitology and Mycology, Institute Adolfo Lutz; [5]Center of Natural and Human Sciences, UFABC.*

Key words: Annonaceae, *Porcelia macrocarpa*, *Trypanosoma cruzi*, Acetogenins.

## Highlights

These work reports the isolation of three acetogenins (**1 – 3**) from seeds of *Porcelia macrocarpa*. These compounds were evaluated against trypomastigote/amastigote forms of *Trypanosoma cruzi*. Compounds **1** and **2** displayed strong activity which could be caused by depolarization of mitochondrial membrane potential of trypomastigote forms of parasite.

## Abstract

*Porcelia macrocarpa* (Warming) R. E. Fries is Brazilian specie popularly known as “banana-de-macaco” and used in the folk medicine to treatment of several illnesses, including parasitic diseases. In the present work, dried seeds of *Porcelia macrocarpa* (479 g) were exhaustively extracted with *n*-hexane. After two weeks at refrigerator, was observed a precipitated (260 mg) which displayed antiparasitic activity (100% of parasite death at 300 µg/mL) against trypomastigotes and amastigotes forms of *T. cruz*i (Y strain). Therefore, part of this material (250 mg) was subjected to a bioactivity guided fractionation using column chromatography over silica gel eluted with increasing amounts of EtOAc in *n*-hexane to afford two actives acetogenins **1** (147 mg), **2** (24 mg) and a third inactive new acetogenin **3** (30 mg). The structures were elucidated by analysis of NMR and HRESIMS spectral data.

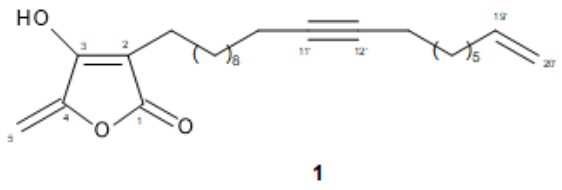


**1**

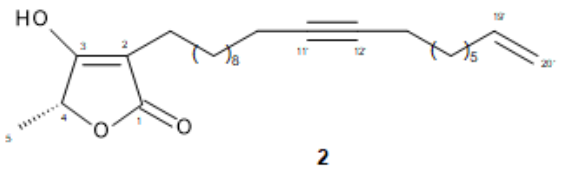


**2**

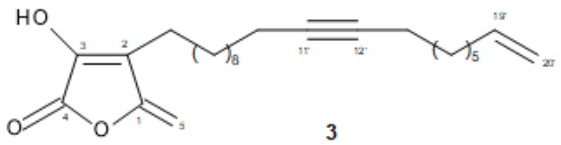


**3**

Acetogenins **1** and **2** displayed very strong activity against trypomastigotes and amastigotes forms of *T. cruzi* (Y strain) with $IC_{50}$ values of 0.4/23.0 µM and 3.6/27.7 µM respectively. The standard drug benznidazole displayed $IC_{50}$ values of 16.4/5.5 µM. Compound **2** and benznidazole induced no mammalian cytotoxicity (NCTC cells - clone L929) to the highest tested concentration (200 µM), while compound **1** displayed a $CC_{50}$ value of 80.0 µM. The selectivity index for trypomastigotes and amastigotes forms were 200.0/3.5 to compound **1**, 55.6/7.2 to compound **2** and 12.2/36.4 to benznidazole. Further studies demonstrated that compounds **1** and **2** were not able to induce an interference in the plasma membrane permeability and also were not effective to induce ROS production after 120 minutes of incubation. Otherwise, these compounds induce depolarization of the mitochondrial of the trypomastigotes after one hour of parasites incubation.

**Support**: FAPESP, CAPES and CNPq.

**Área: QPN** **Inscrição: 864**

# Potencial antiproliferativo em células tumorais humanas do alcaloide 4-*N*-óxido-harmano isolado da espécie *Psychotria schlechtendaliana*

**José Guilherme de Souza Corrêa* (IC)[1], Matheus Ardenghi Peixoto (PG)[1], Vagner Marques de Moura (PQ)[1], João Ernesto de Carvalho (PQ)[2], Ana Lúcia T. G. Ruiz (PQ)[2], Eduardo Cesar Meurer (PQ)[3], Armando M. Pomini (PQ)[1], Silvana Maria de Oliveira Santin (PQ)[1]**

**jguilhermedesouza22@gmail.com**

[1]*Departamento de Química, UEM;* [2]*Centro Pluridisciplinar de Pesquisas Química, Biológica e Agrárias, UNICAMP;* [3]*Universidade Federal do Paraná, UFPR*

Palavras Chave: *Rubiaceae, alkaloids, antiproliferative activity*

## Highlights

Antiproliferative potential in human tumor cells of the 4-N-oxide-harmano alkaloid isolated from the species *Psychotria schlechtendaliana*. The genus *Psychotria* is biosynthesizer of alkaloids and these compounds have a significant diversity of biological activities described in the literature, as well as anticancer potential.

## Resumo

A partir do tratamento em cromatografia em camada delgada preparativa da fração clorofórmica alcalina, obtida por extração ácido-base do extrato bruto metanólico das partes aéreas de *P. schlechtendaliana,* foi isolado um sólido amarelo, solúvel em metanol, em que mediante análises espectroscópicas de RMN tornou-se possível caracterizar o alcaloide indólico **4-*N*-óxido-3-metil-β-carbolínico** (4-*N*-óxido-harmano) (**Figura 1**).

No espectro de RMN $^{1}$H observou-se seis hidrogênios aromáticos em $\delta_H$ 8,34 (*d*; *J* = 6,1 Hz; H-6), 8,28 (*dt*; *J* = 8,1 e 1,0 Hz; H-9), 8,21 (*d*;*J* =6,2 Hz; H-5), 7,68 (*td*; *J* = 8,0 e 1,3 Hz; H-11), 7,66 (*m*; H-12) e 7,35 (*ddd*; *J* = 8,2 e 6,2 e 1,6 Hz; H-10) . O simpleto em $\delta_H$ 2,95 (*s*) integrado para três hidrogênios foi atribuído ao grupo metílico presente na estrutura.

Nos ensaios para atividade antiproliferativa em células tumorais humanas foram empregadas as linhagens U251 (glioma), MCF-7 (mama), NCI-ADR/RES (ovário resistente), 786-0 (rim), NCI-H460 (pulmão), PC-3 (próstata), OVCAR-3 (ovário), HT-29 (cólon), K-562 (leucemia) e uma linhagem não tumoral (HaCat, queratinócito humano). A proliferação celular foi determinada pelo método da Sulforrodamina B. Como resultado foi observado uma resposta citostática seletiva para a linhagem MCF-7 (mama) com $GI_{50}$ de 32,7 µg/mL. O isolamento do 4-*N*-óxido-harmano em *P. schlechtendaliana* é descrito pela primeira vez no gênero *Psychotria.*

**Figura 1:** Estrutura do alcaloide 4-*N*-óxido-3-metil-β-carbolínico

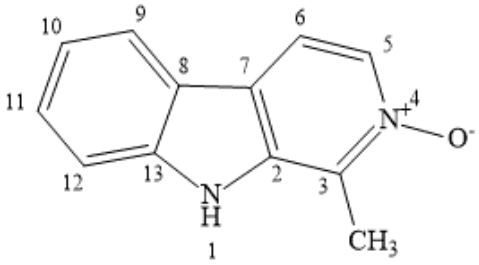

**Área: QPN** **Inscrição: 00938**

# Evaluation of the effect on the mitochondrial membrane potential in *L. amazonensis* caused by Calealactone C isolated from *Calea pinnatifida*

**Lhaís Araújo Caldas* (PG),[1] Meire L. Yoshinaga (IC),[1] Marcelo José P. Ferreira (PQ),[2] João Henrique G. Lago (PQ),[3] Luiz Felipe D. Passero (PQ),[4] Patrícia Sartorelli (PQ).[1]**

**lhais_araujo@hotmail.com***

*[1] Institute of Environmental, Chemical and Pharmaceutical Sciences, Federal University of São Paulo, São Paulo, Brazil; [2] Institute of Biosciences, University of São Paulo, Brazil; [3] Federal University of ABC, Santo André, São Paulo, Brazil; [4] Faculty of Medicine, University of São Paulo, São Paulo, Brazil.*

Keywords: *Calea pinnatifida, Asteraceae, Sesquiterpene lactones, Calealactone C, Antileishmanial activity, Mitochondrial membrane potential.*

## Highlights

Sesquiterpene lactones are a well-known class of compounds from Asteraceae species, with several biological activities reported in the literature[1]. Focusing on the genus *Calea*, mainly germacranolides are responsible for antimicrobial, antileishmanial and cytotoxic potential. In this research, three germacranolides were isolated from the leaves of *C. pinnatifida*: arucanolide, Calealactone B and Calealactone C. The last two of them were not reported for this species up until the present. From this point forward, Calealactone C was tested in promastigote forms of *L. amazonensis* in order to analyze the mitochondrial membrane potential of the compound. It was observed that the compound interfered with parasite mitochondria after incubation. Therefore, the loss of membrane potential leads to impairment of the physiological functions of the mitochondria and reduction of energy, which could cause, consequently, cell death[2].

## Abstract

*C. pinnatifida*, popularly known as "aruca" and “cipó-cruz”, has been encountered specially in Brazilian “cerrado” biome, and has been used in folk medicine to treat stomachaches, giardiasis and amebiasis[3]. Calealactone C, a germacranolide not reported previously for this species, isolated from the fractionation of the leaves of the crude methanolic extract of *C. pinnatifida,* displayed activity against promastigote forms of *L. amazonensis* with $EC_{50}$ of 4.6 μg $mL^{-1}$. The mitochondrial membrane potential was analyzed in promastigote forms using the probe rhodamine 123 (Rho). Oligomycin A was used as an inhibitor of mitochondrial membrane potential at 7,91 μg $mL^{-1}$. The compound demonstrated the same pattern of fluorescence intensity reduction over oligomycin A, a substance that acts as an inhibitor of ATP synthase, preventing the formation of ATP. Thus, to the best of our knowledge, this is the first study showing that calealactone C targets parasite mitochondria, leading to possible cell death. According to the results, this organella can be the first one to be impacted with the treatment.

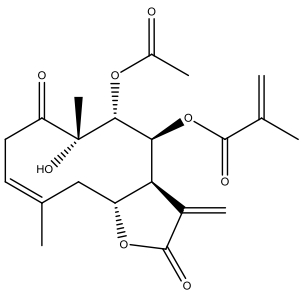


Calealactone C

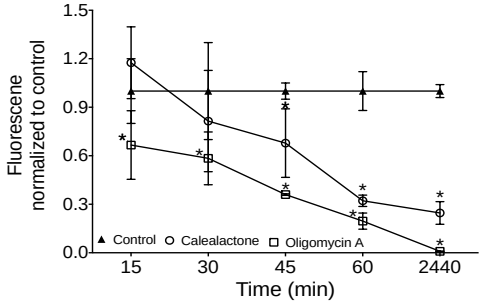


*L. amazonensis* treated with 4.6 μg $mL^{-1}$ of Calealactone C

**References:**

[1] SEAMAN, F. C. Sesquiterpene lactones as taxonomic characters in the Asteraceae. v. 48, n. 2, p. 121–592, 1982.

[2] P., SARTORELLI, et al. Evaluation of *in vitro* and ultrastructural changes in *Leishmania (L.) amazonensis* caused by sesquiterpene lactones from *Calea pinnatifida* (Asteraceae). Planta Med 2016; 82(S 01): S1-S381

[3] AMARAL, P.A., et al. The genus Calea L.: A review of isolated compounds and biological activities. Journal of Medicinal Plants Research, v. 11, n. 33, p. 518–537, 2017.

**Área: QPN** **Inscrição: 00643**

# A bioguided study of the *Tabernaemontana catharinensis*: the indole alkaloids in focus

**Pauline F. Rosales (PG),[1,2*] Yasmin T. Cusin (IC),[1] Bianca T. Canci (PG),[3] Mariana Roesch-Ely (PQ),[3] Adriana C.E. Gower (PQ),[1] Sidnei M. Silva (PQ).[1]**

**[*] pauline.quimica@gmail.com**

*[1]Laboratory of Biotechnology of Natural and Synthetic Products - University of Caxias do Sul, RS, Brazil; [2]Federal Institute of Education, Science and Technology of Rio Grande do Sul- Campus Bento Gonçalves, RS, Brazil,[3]Laboratory of Genomics, Proteomics and DNA Repair – Biotechnology Institute, University of Caxias do Sul, Brazil.*

Key words: Secondary metabolites, Ultrasound, Cytotoxicity, Apocynaceae, *MTT assay*

## Highlights

This work aim the *T.catharinensis* bioguided study searching indole alkaloids. The isolated and fractions enriched of these compounds were tested in tumor cells.

## Resumo/Abstract

The *Tabernaemontana catharinensis* L., belongs to the Apocynaceae family, which is known for the high content of indole alkaloids. This species has been extensively studied due to recurrent activity as analgesic, cytotoxic, antioxidant, and anticholinesterase [1]. Extracts containing indole alkaloids from *T. catharinensis* have already demonstrated antitumor activity. In this way, this study aimed the identification and the cytotoxic evaluation of these secondary's metabolites in a bioguided process. The stems were collected in city of Ijuí-RS. The triturated vegetal material underwent extraction with ultrasound using ethanol as extraction solvent (10mL/g) for 30 minutes at 40% amplitude. The alkaloids were extracted according to scheme 1.

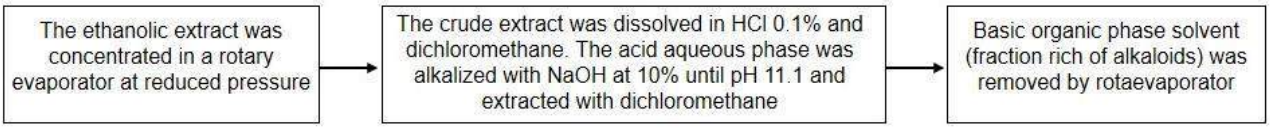


Scheme 1. Acid-base extraction.

The compounds were separated in an open column (25 cm with silicagel 60) which was eluted with a gradient of hexane, $CHCl_3$ and MeOH, with the polarity increasing gradually. The fractions were monitored by TLC, revealed with Dragendorff reagent, which has resulted in 33 fractions containing indole alkaloids. The High Resolution Mass Spectrometry - HRMS (Q-TOF QII Bruker daltonics) was used for compounds identification. The compounds affinisine, 16-epi-affinine, coronaridine, voachalotine, vobasine and 12-methoxy-nb-methyl-voachalotine were identified in different fractions, Figure 1.

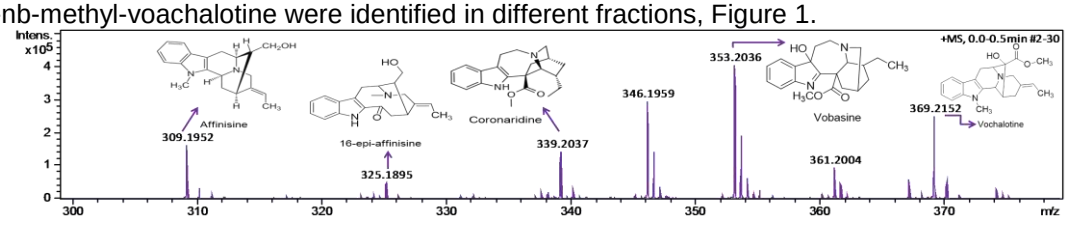


Figure 1. HRMS for the alkaloidal extract.

Five fractions containing the main indole alkaloids were chosen for the biological assay. The MTT assay was used to evaluate cytotoxicity against cell lines HEK 293, A549 and A375. The first results have indicated cytotoxicity ranging which demonstrated the high activity of this alkaloids. This work demonstrates the applicability of this plant to provide active compounds.

[1] Marinho, F. et. al., Fitoterapia, 114 (2016) 127-137.
[2] Nicola, C. et al., The Scientific World Journal, 1-10, 2013.

**Área: QPN** **Inscrição: 00608**

# Chemical composition and mineral content in monofloral bee pollen from *Elaeis guineensis*

**Ayala Nara P. Gomes (PG),[1,2]* Girliane R. da Silva (PQ),[2] Francisco de A. R. dos Santos (PQ),[3] Rodolfo de França Alves (PQ),[3] Celso A. Camara (PQ),[2] Tania M. S. Silva (PQ).[2]**

**ayalanara@gmail.com**

[1] *Programa de Pós-graduação em Desenvolvimento e Inovação Tecnológica em medicamentos - DQ UFRPE;*
[2] *Laboratório de Bioprospecção Fitoquímica - DQ UFRPE;*
[3] *Departamento de ciências Biológicas – UEFS.*

Palavras Chave: *Pólen apícola, Elaeis guineensis, monofloral, Minerais, Composição química.*

## Highlights

- •Chemical composition and mineral content in monofloral bee pollen from *Elaeis guineensis*.
- •Analysis by UPLC-PDA-qTOF-MS/MS
- Presence of flavonoids and *N*,*N*,*N*-tricaffeoylspermidine isomers as markers.

## Resumo/Abstract

A espécie *Elaeis guineensis* (dendê), possui grande importância econômica, principalmente no Nordeste brasileiro, sendo uma palmeira (Arecaceae) polinizada por abelhas. O pólen apícola é o resultado da aglutinação do pólen das flores, néctar e substâncias salivares das abelhas. Do ponto de vista econômico, nutricional e terapêutico o pólen apícola monofloral (predominância de pólen de uma espécie vegetal) apresenta vantagem por apresentar sempre as mesmas características físico-químicas e químicas, o que confere sempre as mesmas propriedades do produto. Oito amostras de pólen apícola de dendê coletadas na Bahia foram analisadas por UPLC-PDA-q-TOF-MS/MS e verificação do teor de minerais. O perfil cromatográfico mostrou a predominância de flavonoides glicosilados e amidas de ácidos cinâmicos com espermidina. Os compostos majoritários identificados foram: isoramnetina-3-*O*-neohesperidosideo e dois compostos isômeros tri-*N*,*N*,*N*-cafeil-espermidina. Quanto ao teor de minerais o elemento mais abundante encontrado foi o Mg (1159,4 ± 147,2 mg/100 g), seguido por K (475,7 ± 93,5 mg/100 g), Na (10,4 ± 3,8 mg/100 g), Mn (13,3 ± 3,0 mg/100 g), Ca (8,4 ± 3,0 mg/100 g), Zn (4,2 ± 0,2 mg/100 g), Fe (2,5 ± 0,4 mg/100 g), Cu (0,37 ± 0,1 mg/100 g) e Se (22,5 ± 5,2 µg/100 g). O pólen apícola de dendê é rico em minerais e apresenta como marcadores flavonoides glicosilados e amidas de ácidos cinâmicos com espermidina.

Agradecimentos: CNPq (Proc. 407659/2013-7) e FACEPE.

**Área: QPN**
*(Inserir a sigla da seção científica para qual o resumo será submetido. Ex: ORG, BEA, CAT)*

**Inscrição: 01404**
*(Inserir o número de inscrição do autor que fez a submissão)*

# Untargeted Metabolomics Analysis of Asteraceae Species, Targeting Glucose-Uptake enhancing Metabolites in C2C12 cells

**Olakunle A. Jaiyesimi[1] (PG); Igor H. Sampaio[1] (PG); Luciane C. Alberici[1] (FM); Carem G. Vargas-Rechia[1] (FM); Leonardo Gobbo-Neto[1*] (FM)**

**lakunlejaiyesimi@gmail.com; gobboneto@gmail.com**
[1]*Departamento de Física e Química, Faculdade de Ciências Farmacêuticas de Ribeirão Preto – Universidade de São Paulo – SP, Brazil*

*Keywords: Sesquiterpene Lactones, Flavonoids, Hyperglycaemia, Metabolomics, Asteraceae, Glucose Uptake*

## Highlights

Some Asteraceae species showed higher glucose-uptake activity in C2C12 compared to metformin
Metabolomics analysis showed flavonoids and sesquiterpene lactones to be responsible for this bioactivity.

## Resumo/Abstract

Prediabetes is characterized by persistent hyperglycaemia predisposing subjects to diabetes with attendant complications. Its high prevalence, with pronounced effects on manpower and countries' healthcare costs, warrants further search for phytoconstituents with potential to prevent, reduce or delay postprandial hyperglycaemia and development of diabetes. This study evaluated 73 Asteraceae species for their ability to improve glucose-uptake (GU) in C2C12 cells and applied metabolomics strategies to the bioactivity aiming to identify, *in silico*, the active metabolites. The GU activity was assessed with C2C12 exposed to extracts (10 μg/ml) or metformin (control; 10 μg/ml) with or without insulin (30 mU/ml). Amount of glucose-uptake by the cells was obtained by comparing the glucose levels in the tests against controls. The metabolic fingerprints of the plant extracts obtained using UHPLC-UV(DAD)-MS(Orbitrap) were processed in MzMine™, and the generated matrices analyzed in SIMCA using unsupervised (HCA and PCA) and supervised (PLS-DA) multivariate statistical analysis. The Hierarchical Clustering Analysis (HCA) validated the LC-MS fingerprints obtained by correctly clustering similar plants at genera and species levels. *Vernonia amygdalina, Spilanthes filicaulis* and *Baccharis genistelloides* significantly exhibited better glucose-uptake activities than controls in both Insulin-like and Insulin-sensitizing tests. By correlating the metabolic fingerprints with these bioactivities, the significant discriminant metabolites (VIP score > 1) for the Insulin-sensitizing activity were determined (Table 1) to include Flavonoids and Sesquiterpene Lactones. Results of our study showed that phytoconstituents may improve glucose-uptake in C2C12; hence, may have potential in preventing hyperglycaemia and development of diabetes.

**Table 1: Significant discriminant metabolites (VIP score > 1) for the Insulin-sensitizing activity**

| | RT | m/z $(M-H)^-$ | Calc. | Molecular Formulae | Compound Class |
|---|---|---|---|---|---|
| **1** | 12.91 | 315.0510 | 316.0588 | $C_{16}H_{12}O_7$ | Flavonol |
| **2** | 14.27 | 299.0561 | 300.0639 | $C_{16}H_{12}O_6$ | Flavone |
| **3** | 12.30 | 285.0404 | 286.0482 | $C_{15}H_{10}O_6$ | Flavone |
| **4** | 15.88 | 425.1816 | 426.1894 | $C_{21}H_{30}O_9$ | Sesquiterpene Lactone |
| | **RT** | **m/z $(M+H)^+$** | **Calc.** | **Molecular Formulae** | **Compound Class** |
| **1** | 14.43 | 367.1748 | 366.1670 | $C_{19}H_{26}O_7$ | Sesquiterpene Lactone |

**Área: QPN Inscrição: 00820**

# Estudo fitoquímico do extrato hexânico das folhas de *Maytenus quadrangulata* (Celastraceae)

**Mariana G. de Aguilar (PG),[1] Grasiely F. de Sousa (PQ),[1] Lucienir P. Duarte (PQ),[1] Sidney A. V. Filho (PQ),[2] Maria O. M. Simões (PQ).[3]**

**Marianag.a9@gmail.com**

*[1]Departamento de Química, UFMG; [2]Escola de Farmácia, UFOP; [3]Departamento de Biologia Geral, UNIMONTES*

*Maytenus quadrangulata, Celastraceae, Triterpeno pentacíclico, Esteroide*

## Highlights

Phytochemical study of the hexane extract from *Maytenus quadrangulata* (Celastraceae) leaves.
The study resulted in the isolation of five triterpenes: friedelan-3-one, friedelan-3*α*-ol, friedelane-3,7-dione, 3*β*-hydroxyfriedelan-7-one, 3,4-seco-friedelan-3,11*β*-olide and the steroid *β*-sitosterol.

## Resumo/Abstract

Várias espécies do gênero *Maytenus* são empregadas na medicina popular, principalmente para o tratamento de úlceras gástricas.[1] *Maytenus quadrangulata (Schrad.) L*oes é uma espécie endêmica encontrada na mata atlântica e na caatinga, popularmente conhecida como espinho-de-Deus.[2] Até o momento, não foi encontrado nenhum relato de estudo fitoquímico e avaliação da atividade biológica desta espécie. Neste trabalho, folhas de *M. quadrangulata* foram coletadas no distrito de Brejo do Amparo, município de Januária, norte de Minas Gerais. As folhas secas e moídas foram submetidas à extração utilizando hexano, clorofórmio, acetato de etila e metanol. Durante a remoção parcial do solvente do extrato hexânico ocorreu precipitação de um sólido que foi filtrado à pressão reduzida (SEH: 465,0 mg). Após remoção completa do solvente obteve-se o extrato hexânico (EH: 35,267 g). A partir de SEH, após purificação por cromatografia em coluna (CC), foi possível obter os triterpenos: friedelan-3-ona (**1:** 16,1 mg), friedelan-3*α*-ol (**2:** 87,4 mg), friedelano-3,7-diona (**3:** 6,9 mg) e 3*β*-hidroxifriedelan-7-ona (**4:** 11,0 mg). De EH, após a purificação por CC, foi possível isolar o triterpeno 3,4-*seco*-friedelan-3,11-*β*-olídeo (**5:** 707,4 mg) e o esteroide *β*-sitosterol (**6:** 222,8 mg) (Figura 1). As estruturas químicas foram determinadas por métodos espectroscópicos (IV, RMN de $^{1}H$,$^{13}C$ e DEPT-135) e comparação com dados da literatura. A continuidade dos estudos do extrato hexânico e dos demais extratos das folhas de *M. quadrangulata* apontam a possibilidade de identificar novos metabólitos secundários bioativos.

**Figura 1:** Estruturas químicas dos compostos 1-6.

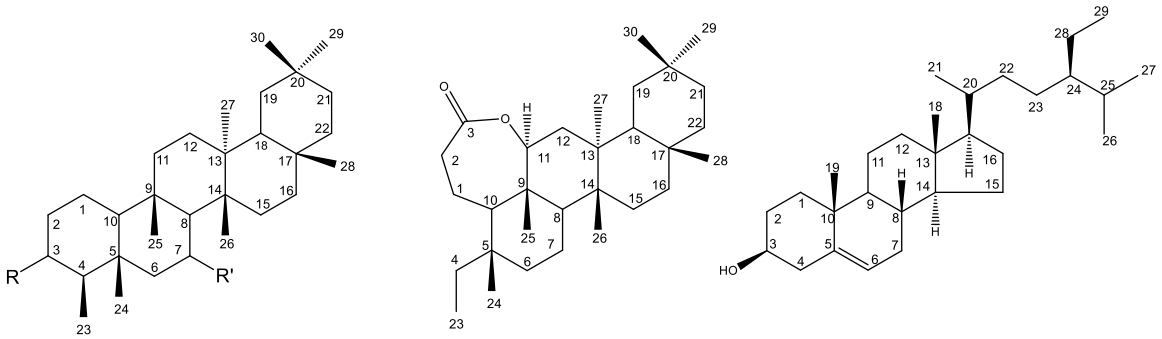


**1:** R: =O R': H **3:** R: =O R': =O
**2:** R: α–OH R': H **4:** R: β–OH R': =O

**5** **6**

[1] Niero, R.; Andrade, S. F.; Cechinel Filho, V. *Curr. Pharm. Des.*, 17, 1851-1871, **2011**.
[2] Carvalho-Okano, R. M. Tese de Doutorado. Instituto de Biologia. Universidade de Campinas. Campinas SP., **1992**.

**Agradecimentos:** CNPq, CAPES e FAPEMIG.

**Área: QPN** **Inscrição: 01193**

# Investigação das substâncias presentes nas frações apolares do extrato de uma amostra de própolis verde

**Lucas de Oliveira Pires (PG)[1], Rosane Nora Castro (PQ)[1]**

**luucasoliv@outlook.com; nora@ufrrj.br**

[1]*Departamento de Química, UFRRJ*

Palavras Chave: *Artepillin C, Metabólitos especiais, Capacidade Antioxidante.*

## Highlights

Investigation of metabolites in lipophilic fractions of one green propolis extract. Evaluation of different fractions of green propolis by GCMS showed that the chemical diversity is directly correlated to antioxidant properties.

## Resumo/Abstract

A própolis verde é elaborada pelas abelhas *Apis mellifera* a partir de espécies vegetais presentes na região sudeste do Brasil[1]. Suas propriedades biológicas estão relacionadas à diversidade química e à presença do marcador Artepillin C (ácido 3,5-diprenil-4-hidroxicinâmico), com elevado potencial antioxidante, anti-inflamatório e antimicrobiano[2].

Neste trabalho uma amostra de própolis verde (Paraíba do Sul, RJ) foi extraída por maceração dinâmica em etanol (48h, temperatura ambiente), e o extrato foi particionado sequencialmente com éter de petróleo e *n*-hexano. As frações obtidas foram analisadas por cromatografia gasosa, e as substâncias identificadas por espectrometria de massas através dos padrões da fragmentação comparados com a biblioteca (NIST) e a literatura[3].

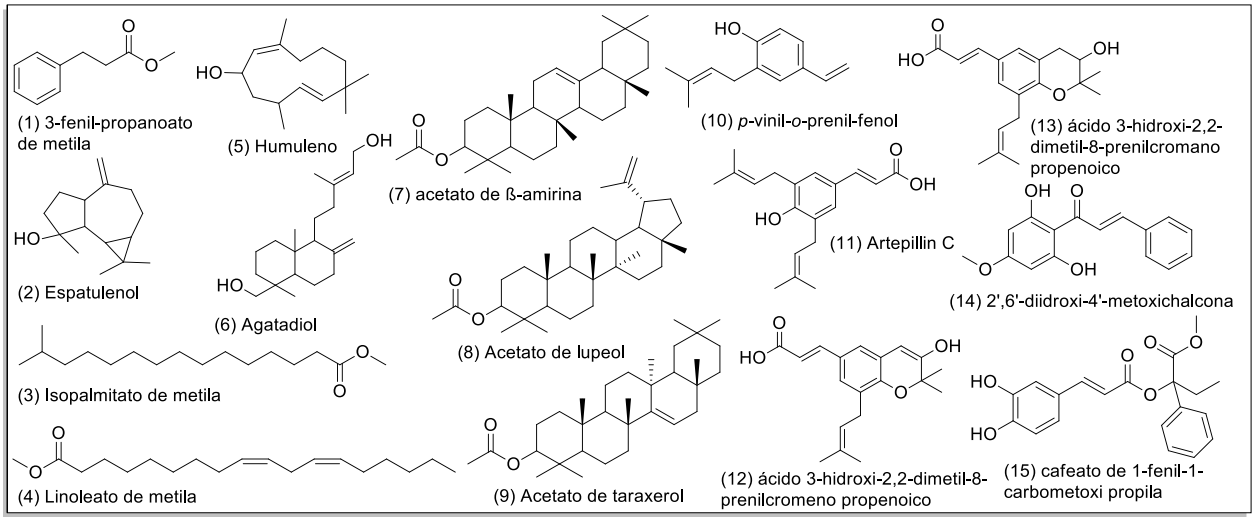


**Figura 1** – Algumas substâncias identificadas no extrato apolar de própolis verde.

Os extratos analisados se mostraram quimicamente diferentes: o éter de petróleo extraiu majoritariamente as substâncias mais lipofílicas (**Figura 1, 1-9**), enquanto o *n*-hexano foi seletivo para extrair os derivados prenilados, muito comuns em própolis verde (**Figura 1, 10-15**). A capacidade antioxidante frente ao radical 2,2-difenil-1-picrilhidrazil foi avaliada, sendo possível estabelecer uma correlação entre os $CE_{50}$ obtidos (14,75 ±1,64mg.ml$^{-1}$ fração hexânica e superior a 1000 mg.ml$^{-1}$ para a fração éter de petróleo) e o perfil químico dos extratos.

## Referências

[1]Salgueiro, F.B.; & Castro, R.N.; Quim. Nova**.** 2016, 10, 1192-1199;
[2]Shimizu, K.; Ashida, H.; Matsuura, Y.; Kanazawa, K.; A. Biochem. and Bioph**.** 2004, 404, 181-188;
[3]Righi, A. A.; Negri, G.; Salatino, A.; Evidence-Based Comple. Altern. Med. 2013.

**Área: PN**
*(Inserir a sigla da seção científica para qual o resumo será submetido. Ex: ORG, BEA, CAT)*

**Inscrição:01183**
*(Inserir o número de inscrição do autor que fez a submissão)*

# *Copaifera reticulata* and the antibacterial activity of the acidic diterpenes

**Claudia M. Rezende (PQ),[1]* Deiziane G. Santos (PG),[1] Thais M. Uekane (PQ),[1,2] Vinicius S. Castro (PG),[2] Carlos A. C. Junior (PQ)[2]**

**claudia.rezendeufrj@gmail.com; deizigomes08@gmail.com**

[1]*Programa de Pós-Graduação em Ciência de Alimentos, UFRJ;* [2]*Universidade Federal Fluminense, UFF.*

Palavras Chave: *Oil-resin, Copaifera reticulata, Acidic diterpenes, Antibacterial activity*.

## Highlights

- *Copaifera reticulata* is mainly composed by acidic diterpenes besides oxygenated and hydrocarbon sesquiterpenes..
- The acidic diterpenes showed relevant antibacterial activity for *Staphylococcus aureus.*

## Resumo/Abstract

The *Copaifera* L. trees have a wide range of pharmacological properties and the antibacterial activity has been one of the most studied. The aim of this study was to evaluate the antibacterial activity of *Copaifera reticulata* oil-resin. Fractions from the crude oil were obtained using a silica gel impregnated with potassium hydroxide column chromatography, with hexane, dichloromethane and methanol as eluents. Sesquiterpene hydrocarbons (SH), oxygenated sesquiterpenes (SO) and acidic diterpenes (AD) were observed in these fractions, respectively. The antibacterial activity of the fractions and the oil-resin were tested using the technique of minimum inhibitory concentration against the pathogens involved in cases of foodborne. The gram-positive bacteria tested were *Staphylococcus aureus* (ATCC-6538) and *Listeria monocytogenes* (ATCC-15313), while the gram-negative bacteria were *Salmonella typhimurium* (ATCC-14028) and *Escherichia coli* O157:H7 (ATCC-43895). The antibacterial activities in the crude oil-resin were 6.25 mg/ml for *S. aureus*, and 25 mg/ml for *Listeria, E. coli*, and *Salmonella*. In the fractions, SH showed 25 mg/ml for *S. aureus, Listeria* and *Salmonella* (*E. coli* negative). For SO, *S. aureus* showed 3.12 mg/ml, *Listeria* and *E. coli* 25 mg/ml, and *Salmonella* was negative. For AD, *S. aureus* showed 1.56 mg/ml, *E. coli*, 25 mg/ml, *Listeria*, and *Salmonella* were negative. The results demonstrated a major activity against *S. aureus* for AD and SO compared to the oil-resin. The nature of the acidic fraction chemical composition is in development.

**Referência:**
L.M. Leandro, F.S. Vargas, P.C.S. Barbosa, J.K.O. Neves, J.A. Silva, V.F. Veiga-Junior,Chemistry and biological activities of terpenoidsfromCopaiba (*Copaifera*spp.) oleoresins, Molecules 17 (2012) 3866e3889.

Área: QPN
*(Inserir a sigla da seção científica para qual o resumo será submetido. Ex: ORG, BEA, CAT)*

**Inscrição: 1442**
*(Inserir o número de inscrição do autor que fez a submissão)*

# PURIFICATION OF BIOACTIVE NATURAL PRODUCTS BY CENTRIFUGAL PARTITION CHROMATOGRAPHY (CPC)

**Tsvetelina Mandova (PG),[1,2] Grégoire Audo (TC),[2] Sylvie Michel (PQ),[2] Raphaël Grougnet (PQ),[2]**

**tmandova@gilson.com**

*[1]Laboratoire de Pharmacognosie, Université de Paris Descartes, Sorbonne Paris Cité, Faculté de Pharmacie de Paris, UMR-CNRS 8638 COMETE, 4 avenue de l'Observatoire, 75006 Paris, France; [2]Gilson Purification SAS, Application Laboratory, 22 rue Bourseul, F-56890 Saint-Avé, France*

## Highlights

The unique mechanism makes Centrifugal Partition Chromatography (CPC) a magical and powerful technique for the isolation of natural compounds from plants. In this work, three case studies emphasize its great potential for analytical, preparative or scale up applications.

## Resumo/Abstract

CPC is a continued liquid-to-liquid solvent partition where the target compounds are competitively distributed between the two-phase solvents due to their different partition coefficient. Using a centrifugal force, one phase is kept stationary while the other phase is pumped through the stationary one. There is no solid chromatographic support and the great advantage of this feature is that it allows higher yields of pure compounds when compared to other currently available preparative techniques. In this work, three case studies on the purification of natural products from plants will emphasize the great potential of the CPC technique. *Centaurium erythraea* Rafn. (Gentianaceae) is a widespread herbaceous plant used in the traditional medicine in more than 20 countries worldwide. The most abundant *seco*-iridoid glycosides, swertiamarin, sweroside and gentiopicrin, three structurally closely-related target natural products, were separated by CPC with swertiamarin purified from 8.72 mg/g in the crude extract until 770 mg/g (98.2%S) in enriched fractions. Experimental conditions were optimized in a different elution mode and different CPC devices coupled with MS detector allowed purification of the compounds for a shorter period of time and by using lower amounts of organic solvents. Cyclitols, indolizidine alkaloids, one *ent*-kaurane diterpene and its glycoside are some of the compounds isolated from two other species – an Argentinean spiny deciduous tree from *Prosopis* spp (Fabaceae) and the above ground parts of *Achillea clypeolata* Sibth. et Sim (Asteraceae), a Balkan endemic species. Therefore, we conclude that a suitable elution system using the CPC technology coupled to MS can afford good results in natural compound isolation and purification, with the great advantage of higher yields when compared to other separation techniques.

**Área: QPN_____** **Inscrição: 1467**
*(Inserir a sigla da seção científica para qual o resumo será submetido. Ex: ORG, BEA, CAT)* *(Inserir o número de inscrição do autor que fez a submissão)*

# Citrus phytopathogens battle: A nature'sæstory of chemical warfare and survival

**Jonas Henrique Costa[1](PG), Cristiane Izumi Wassano[1](IC), Célio Fernando Figueiredo Angolini[1] (PG), Marcos Eberlin[1] (PQ), Taícia Pacheco Fill,[1] (PQ)**

**taicia@iqm.unicamp.br**

[1]*Instituto de Química, UNICAMP- Universidade Estadual de Campinas*

Citrus phytopathogens, co-culture, natural products

## Resumo/Abstract

In nature, microorganisms co-exist within complex microbial communities involving different signaling and interactions, in which secondary metabolites play an important role. The survival in this competitive environment certainly requires strategies that are likely to culminate in the production of bioactive compounds[1]. Therefore, the strategy of mimicking nature and exploring such interactions, may lead to the discovery of new natural products with interesting bioactivities. Since Brazil is the largest producer and exporter of oranges in the world, the demand for techniques aimed at quality control is indispensable considering the losses caused by post-harvest fungal diseases[2]. Green and blue molds, caused by *Penicillium digitatum* and *P. italicum* respectively, are the main diseases that affect citrus fruits in the worldwide postharvest, resulting in great economic loss. Thus, due to the great economic impact that these fungi cause to Brazilian industry and to the greater control of food quality, we are looking for methods to control citrus infection. This research represents an approach of mimicking physiological conditions, interactions and chemical communications between *Penicillium digitatum* and *Penicillium italicum*, the two major post harvest pathogens of citrus fruits, through mixture cultures *in vivo* and *in vitro*. Imaging mass spectrometry (IMS) was demonstrated to be a powerful tool for surface screening at the molecular level leading to the detection of secondary metabolites that seem to play an important role in the fungus-fungus interaction.

[1]Brakhage, A. A. & Schroeckh, V. "Fungal secondary metabolites–strategies to activate silent gene clusters". Fungal Genetics and Biology, 48 (1): 15, 2011.

[2]Fischer, I. H.; Lourenço, S. A.; Amorim, L. Doenças pós colheita em citros e caracterização da população fúngica ambiental no mercado atacadista de São Paulo. Trop. Plant Pathol. v. 33, p. 219-226, 2008.

**Área: QPN** **Inscrição: 1459**
*(Inserir o número de inscrição do autor que fez a submissão)*

# Orbitides from *Jatropha mollissima* and their Synthetic Analogues as Inhibitors of Butyrylcholinesterase

**Suelem D. Ramalho[1*] (PQ), Meri Emili F. Pinto[1] (PQ), Juliana L. de Lima[2] (PG), Paulo R. S. Sanches[1] (PG), Eduardo M. Cilli[1] (PQ), Carmen L. Cardoso[2] (PQ), Vanderlan S. Bolzani[1] (PQ)**

**bolzaniv@iq.unesp.br; suelemd@hotmail.com**

*[1]Institute of Chemistry, São Paulo Estate University-UNESP, Araraquara-SP, 14800-060, Brazil. [2]São Paulo University - FFCLRP/USP, Ribeirão Preto-SP, 14040-901, Brazil.*

Palavras Chave: *Orbitides; Jatropha; Cyclic peptides; Butytylcholinesterase*

## Highlights

Among the plant species that contain orbitides, *Jatropha* genus (Euphorbiaceae) is one of the most promising sources of biologically active orbitides.
The biological activities of the peptides might be related to their amino acid sequences, charges and spatial arrangement.
Focus of this work is Investigating potential inhibitors of butyrylcholinesterase (BChE).

## Abstract

Orbitides are plant-derived cyclic peptides that have a range of relevant bioactivities. They present low molecular weight, comprise 5 to 12 *L*-amino acids residues, ribosomally synthesized and head-tail cyclization[1]. Among the species that contain orbitides, *Jatropha* genus is one of the most promising sources of biologically active orbitides[2]. In addition to the isolation from natural sources, peptides and their derivatives can be obtained by solid phase peptide synthesis (SPPS). This contributes to obtain analogues which can have a role in the development of drug-like compounds based. In this study we are investigating potential inhibitors of butyrylcholinesterase (BChE) which is an enzyme involved in the treatment of Alzheimer's disease. This assay use immobilized capillary enzyme reactors (ICERs) which is a ligand screening that has been adopted as a technique of high throughput screening (HTS)[3].
Latex obtainment was carried out by dropwise.The linear analogues were synthesized by SPPS using an insoluble resin[3] (Fmoc-Gly-Wang resin). All obtained compounds (natural and linear analogues) were evaluated against the enzyme BChE immobilized covalently in fused silica capillaries named ICER-$BChE_{hu}$.Three orbitides were isolated pohlianin A, B and C. Linear pohlianin A and C presented % of inhibition higher than 70%. Further assays of $IC_{50}$ and mechanism of action are under investigation. Results from this project can open new perspectives for the chemistry of natural products once only a limited number of orbitides have been isolated from plants, especially when involving the ones found in Brazilian plant species biodiversity.

## References

1. Arnison, P. G. et al. *Nat Prod Rep* 2013, *30*, 108.
2. Ramalho, S. D. et al. *Planta Medica* 2017. DOI: 10.1055/s-0043-122604
3. Vanzolini, K. L. et al. *Talanta* 2013, *15,* 116.

## Acknowledgements

The authors are grateful to FAPESP grant# 2015/09533-7, SISBIOTA-CNPq-FAPESP grant# 2010/52327-5, CEPID-FAPESP grant# 2013/07600-3, CNPq and CAPES for scholarships and financial support.

**Área: QVE** **Inscrição: 00013**

# Greem synthesis of Ag nanoparticles using quercetin flavonoid: Synthesis and characterization by UV/VIS and FTIR techniques

**Daiane R.F. Rodrigues (IC)[1]*, Verônica Ivachuck da Silva (IC)[1] Jefferson J. Soares (PQ)[1], Elton L.G. Denardin(PQ)[1]**

**edenardin@unipampa.edu.br; daianeraquel6@gmail.com**

[1]*LEFQPN/Campus Uruguaiana, Federal University of Pampa (UNIPAMPA)*

Keywords: Sil*ver nanoparticles, Green Synthesis, Quercitin, Characterization thecniques.*

## Highlights

- Silver nanoparticles are synthesized by Green Synthesis using quercetin flavonoid.
- The reduction of silver ion and formation of AgNPs have been assessed by UV/VIS and FTIR spectroscopy.
- UV/VIS spectroscopy shows resonance Plasmon band near to 375 nm
- FTIR spectroscopy shows disappearance of hydroxyl groups in quercetin structure.
- The method is simple, economic, efficient and nontoxic.

## Resumo/Abstract

The green synthesis of silver nanoparticles paved the way to improve and protect the environment by decreasing the use of toxic chemicals and eliminating biological risks in biomedical applications [1, 2]. Quercetin, a flavonoid, is present in several foods as vegetables fruit, wine and tea exerting beneficial effects on health as protection against various diseases such as cancer, cardiovascular diseases and aging [3].
Green synthesis of silver nanoparticles using 10 mM Quercetin flavonoid and 20 mM $AgNO_3$ in pH 10 are shown in Fig. 1. Fig. 1A shows the color of the reaction medium from yellow (quercetin) to gray (AgNPs). Fig. 1B shows de characteristic surface Plasmon absorption band at 375 nm. The structure of quercetin is shows in Fig. 1C. The Hydroxyl groups (3500 $cm^{-1}$) are not observed in FTIR spectra after AgNPs obtained indicating that the reduction process occurred and AgNPs were obtained. The method is simple, economic, efficient and nontoxic.

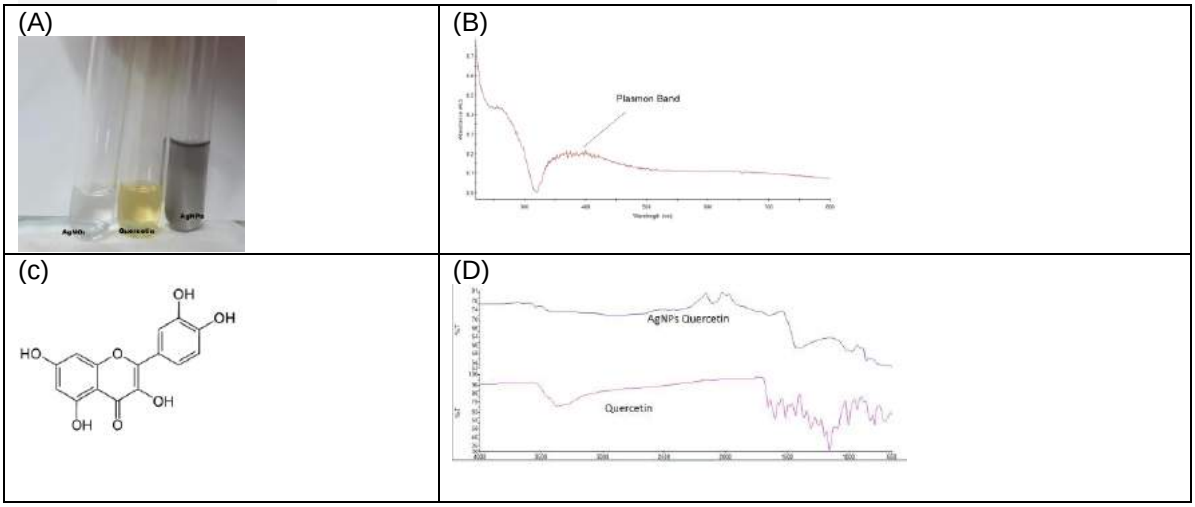


Fig. 1. A) $AgNO_3$, Quercetin and AgNPs images; B)UVVIS Analysis; C)Quercetin Structure; D) FTIR analysis

References:
1. Saxena A; Tripathi RM; Zafar F; Singh P; Mat.Let., 67 (2012), 91-94.
2. Bonnia NN; Kamaruddin MS; Nawawi MH; Ratim S; Azlina HN; Ali ES, Procedia Chem. 19 (2016), 594-602
3. Boots AW; Haenen GRMM; Bast A; Eur. J. Pharm. 585 (2-3) (2008) 325-337.

**Área: QVE** **Inscrição: 00077**

# Deep eutectic solvents as functional additives for Starch-based films.

**Rachel Azevedo Maia (IC),[1]* Ana Claudia de Lima Araújo (IC),[1] Isadora Maria Gouveia Andrade (IC),[1] Vanessa Freire de França (IC),[1] Whesley Silva de Morais (PG),[2] Tereziana Silva da Costa (TC),[1] Dayse das Neves Moreira (PQ).[1]**

**rachel-maia@hotmail.com**

*[1]Departamento de Química e Física, UFPB [2]Programa de Pós-Graduação em Ciência e Tecnologia de Alimentos, UFPB*

Keywords: *Biodegradable films, Starch, Deep Eutectic Solvents*

## Highlights

Starch based-films development. Biodegradable films. Deep eutectic solvents as alternative plasticizer agents. DES is a new alternative for the biofilms production.

## Resumo/Abstract

The interest in biofilms based on starch has grown in recent years, since it is an abundant biopolymer which forms resistant materials.[3] Starch-based biofilms are generally produced by the solubilization of the biopolymer in a solvent containing a plasticizer additive. The film-forming solution undergoes a drying operation to form the desired material. [1] As these films are brittle, the plasticizer addition is imperative to reduce the interactions between adjacent molecules and improve the film's flexibility.[4] Therefore, the objective of this work was to study the effect of the addition of ionic liquid (IL) and deep eutectic solvents (DES) as plasticizing agents. Additives were synthesized as described in the literature.[1] The film characterization was performed on a UV-vis spectrophotometer (wavelengh 700 nm) and the thickness was measured on a digital micrometer. Both additives were used in the film formulation which were prepared by the casting method. The plasticizers amount is shown in the Table 1. For comparison, we prepared a film containing only 1% glycerol as plasticizer. The data presented in Table 1 show a decrease in film thickness when DES was used as plasticizer as opposed to the data obtained with IL when compared to the standard film of glycerol. It was also observed that the addition of DES contributed to an increase in film transparency. In this way, DES is a new alternative for the biofilms production.

Table 1- Data[a] obtained from different formulations[b] to obtain the biofilms of starch.

| Plasticizer | Transmittance (%) | Thickness δ (μm) | Transparency (%) |
|---|---|---|---|
| Glicerol | 82,87 | 0,095 | 25,45 |
| [Ch]Asp IL | 71,67 | 0,123 | 22,73 |
| ChCl:Urea | 85,8 | 0,060 | 38,85 |

[a] All data were performed in triplicate and presented as the mean values.[b] heating a 2% aqueous solution of starch.

[1]Gontard, N.; Guilbert, S.; Cuq, J. L.; *J. of Food Sci*., **1992**, 53, 206-211.
[2]Ban, W.; Song, J.; Argyropoulos, D. S.; Lucia L. A. *Ind. Eng. Chem*. **2006**, 627-633.
[3] Mali, S.; Grossmann, M. V. e,; García, M. A.; et. al. *Carbohyd. Polym*. **2004**, 129-135, 56.
[4]Coupland, J. N.; Shaw, N.B.; et al. *J. Food Eng*. **2000**, 129-135,43.
[5]Madaleno, E.; Rosa, D. S.; Zawadzki, S. F.; Pedrozo, T. H. & Ramos, L. P.; *Polímeros*. **2009**, *19*, 263.

**Área: QVE**
*(Inserir a sigla da seção científica para qual o resumo será submetido. Ex: ORG, BEA, CAT)*

**Inscrição: 00190**
*(Inserir o número de inscrição do autor que fez a submissão)*

# Síntese de biodiesel metílico e de biodiesel etílico a partir do óleo de algodão

**Daniela Reolon (IC),[1] Grazieli Lazarotto (IC),[1] Paulo S.D. Lencina Filho (IC),[1] Caroline C. Schneid (PQ),[1] Renata Z. Osti (PQ),[1] Gustavo G. Shimamoto (PQ),[2] Matthieu Tubino (PQ),[2] Eva L.C. Silveira (PQ),[1*]**

**evaluciacs@gmail.com**

*[1]Instituto de Ciências Naturais, Humanas e Sociais, UFMT; [2]Instituto de Química, UNICAMP*
Palavras Chave: *Biodiesel, Óleo de algodão, Rota metílica, Rota etílica.*

## Highlights

Synthesis of cotton oil biodiesel. The synthesis de biofuel from vegetable oils is important because it contributes to the production of renovable energy.

## Resumo

O biodiesel é uma mistura de ésteres alquílicos de cadeia linear, obtida da transesterificação dos triacilgliceróis de óleos e gorduras com álcoois de cadeia curta. Neste trabalho, realizou-se a síntese de biodiesel a partir do óleo de algodão refinado empregando as rotas metílica e etílica visando a produção de um biocombustível amigável ao meio ambiente. A síntese foi realizada em duas etapas. Na primeira etapa adicionou-se 16 % (m/m) de metanol e 0,56 % (m/m) de metóxido de sódio 30 % m/m, calculados em relação à massa do óleo de algodão. O sistema foi aquecido à 60 °C por 1 hora, sob refluxo. Após a reação, os ésteres (fase superior) foram separados do glicerol e novamente submetidos à reação com adição de 4,0 % m/m de metanol e 0,14 % do catalisador. Após separação a fase superior foi lavada com água desionizada e filtrada em resina *Amberlite BD10 Dry*. Para a síntese do biodiesel etílico empregou-se o dobro da massa de álcool (40% m/m).

**Tabela 1. Características físico-químicas dos biodieseis de óleo de algodão sintetizados.**

| Característica | Óleo de Algodão | Biodiesel Metílico | Biodiesel Etílico | ANP nº 45/2014 |
|---|---|---|---|---|
| Densidade ($kg/m^3$) | 922 | 889 | 880 | 850-900 |
| Viscosidade ($mm^2/s$) | 32,46 ± 0,10 | 4,970 ± 0,005 | 4,631 ± 0,004 | 3,0-6,0 |
| Índice de acidez (mg KOH/g) | 0,516 ± 0,028 | 0,210 ± 0,005 | 0,190 ± 0,005 | <0,5 |
| Teor de fósforo (mg/kg) | < LD | < LD | < LD | Máx. 10 |

As análises por RMN $H^1$ confirmaram a formação de ésteres metílicos ou etílicos (96 %). Os parâmetros apresentados na Tabela 1 encontram-se em concordância com a ANP. Os resultados indicam a viabilidade do óleo de algodão, uma matéria prima de grande importância econômica no estado de Mato Grosso, para a produção de biodiesel.

**REFERÊNCIAS**

Boog, J.H.F; Silveira, E.L.C.; Caland, L.B.; Tubino, M. *Fuel*. **2011**, 90, 905.

**Área: QVE** **Inscrição: 00224**

# Sustainable catalysts for organophosphate degradation: rice husk functionalization with hydroxamic acid groups

**José G. L. Ferreira (PG), Willian H. Takarada (IC), Elisa S. Orth (PQ).**

**joseferreira@ufpr.br**

*Department of Chemistry, Universidade Federal do Paraná (UFPR), CP 19032, CEP 81531-980, Curitiba, PR, Brazil.*

Palavras Chave: *Organophosphates*, *Green Chemistry, Pesticides, Detoxification.*

## Highlights

Biocatalysts derived from rice husk waste comprising hydroxamic acid groups were obtained. They were highly effective in the chemical detoxification of organophosphates.

## Abstract

Rice feeds billions of people worldwide, but this crop produces a huge amount of residues: 22% weight of a rice grain is husk, besides other plant parts as straws. Also, rice crop is one of the biggest consumers of pesticides, mostly organophosphates (OP). OP are stable and toxic, which makes its degradation difficult. An approach is the utilization of alpha nucleophiles as hydroxamic acids, which are very reactive. Herein, rice husk (**RH**) was used to obtain sustainable catalysts for OP degradation. For that, the TEMPO/NaClO/NaBr method was used to enable carboxylic acid groups[1] that were further functionalized with hydroxamic acid groups by EDC/NHS/hydroxalamine hydrochloride method[2] (**SRHHDA** and **IRHHDA**). The samples obtained were characterized by x-ray diffraction, potentiometric and zeta titration, gel permeation chromatography, thermogravimetric analysis, fourier transform infrared spectroscopy and nuclear magnetic resonance proving the chemical modifications. Finally, **SRHHDA** and **IRHHDA** were evaluated as catalysts with the model substrate DEDNPP giving an increment of $1.6*10^7$-fold and $2.5*10^8$-fold, respectively, when compared to the spontaneous reaction (Figure 1). Regarding the pesticide Paraoxon, after 19 days, **SRHHDA** and **IRHHDA** degraded 48.28% and 48.12% of the initial concentration, respectively, an increment of $4.9*10^7$-fold over spontaneous reaction. To the best of our knowledge, it is the first reported polysaccharide material successfully functionalized with hydroxamic acid and the catalytic activities of **SRHHDA** and **IRHHDA** with organophosphates are between the highest reported in literature.

**Figure 1.** Scheme of synthesis and pH rate profile at 21 °C with DEDNPP.

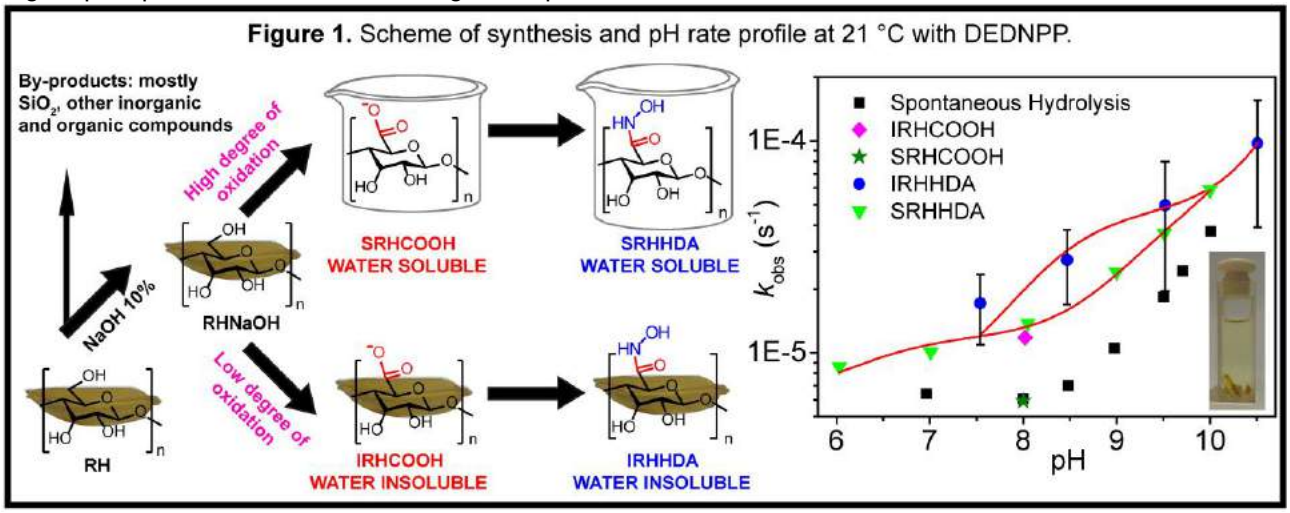


1. A. Isogai and Y. Kato, *Cellulose*, 1998, **5**, 153-164.
2. R. K. Shervedani and M. Bagherzadeh, *Electrochimica Acta*, 2008, **53**, 6293-6303.

Authors acknowledge the Financial support from UFPR, CNPq, CAPES, Fundação Araucária, FINEP, Centro de RMN da UFPR and L'Oréal-UNESCO-ABC.

**Área: QVE**
*(Inserir a sigla da seção científica para qual o resumo será submetido. Ex: ORG, BEA, CAT)*

**Inscrição:00282**
*(Inserir o número de inscrição do autor que fez a submissão)*

# Recuperação de solventes orgânicos. Alternativa sustentável já praticada na UFRGS

**Bruna C. Dias (IC),[1] Eduardo J. Leseux (IC),[1] Filipe W. Schwarz (PG),[1] Greice V. Oliveira (TC),[1] Silvio L. P. Dias (PQ),[1] Eduardo R. de Oliveira (PQ).[1]***

**eduardo.rolim@ufrgs.br**

[1]*Centro de Gestão e Tratamento de Resíduos Químicos, Instituto de Química, UFRGS*

Palavras Chave: *Recuperação de solventes, Resíduos químicos, sustentabilidade, Solventes*

## Highlights

Recovery of organic solvents. Sustainable alternative already practiced at UFRGS. The University receives approximately 15,000 L of organic solvents per year and has already recovered about 11 types of solvents, avoiding disposal, reducing costs and environmental impact

## Resumo/Abstract

A UFRGS em mais de 250 laboratórios produzem cerca de 15 mil litros de resíduos de solventes orgânicos. O descarte de forma adequada é feito por empresa licitada que os transporta para fora do RS, com todos os riscos daí advindos. Em 2016 gastou-se cerca de R$ 50.000,00 para envio de 15.7ton para incineração em SP. O CGTRQ é responsável pela coleta e tratamento dos resíduos químicos na UFRGSe e desenvolve trabalho de pesquisa e formação, mo estudo de metodologias para recuperação de resíduos de solventes orgânicos, inicialmente em pequena escala já estudou-se a purificação de AcOEt, (73% de rendimento após secagem -CG, IV e RMN) e etanol (90% - CG). Teores alcoólicos de 94 a 97%, (densidade). Hexano, $CHCl_3$ e MeOH, com apenas uma destilação. (94 a 96% - CG). Para xilol:e mistura de AcOEt e hexano ainda desenvolveu-se métodos de análise. De resíduos oriundos da graduação, recuperou-se hexano, $CH_2Cl_2$ e álcool amílico. E ainda estudou-se a recuperação de solventes de alto valor, como $CH_3CN$, $CH_2Cl_2$ e acetona. Em grande escala, em bateladas de 7 a 10 L, , como mostrado na tabela, foram obtidos, nos casos da acetona e do hexano, rendimentos de 76 a 96% (CG e índice de refração). No caso do xilol, é recuperada (60 a 88%) uma mistura dos 3 xilenos com etilbenzeno, em proporções que se mantém inalteradas em relação aos produtos comerciais originais. No caso da mistura de hexano e AcOEt os solventes foram recuperados na forma de soluções de AcOEt em hexano, em proporção média de 48 %, determinada por CG, com a utilização de uma curva de calibração construída com amostras padrão

| Custo por batelada | Xilol | Acetona | Hexano | Hexano/Acetato de Etila |
|---|---|---|---|---|
| **Sem destilação** | R$ 23,38 | R$ 22,45 | R$ 20,96 | R$ 20,89 |
| **Com destilação** | R$ 7,01 | R$ 4,72 | R$ 1,98 | R$ 1,65 |
| **Economia** | **R$ 16,37** | **R$17,73** | **R$ 18,98** | **R$ 19,24** |
| **Rendimento** | 74±14 | 87±9 | 84±8 | 73±3 |

Como pode ser observado na tabela, nos 4 casos observa-se que o custo da recuperação de cada um dos solventes, por batelada, é consideravelmente menor que o custo de descarte do mesmo, para incineração ou co-processamento, o que traz uma considerável economia de recursos para a Universidade. Mas ainda deve ser considerada, e certamente é o mais importante, a redução dos impactos ambientais advindos do descarte. Uma vez que não é permitida no RS a incineração, o CGTRQ tem que enviar os resíduos para SP, com todos os riscos de transbordo de grandes quantidades de resíduos no Centro e no destino, de transporte por rodovia em percurso de mais de 1.500 km. Alem de todos os problemas inerentes à incineração dos solventes, como a geração de subprodutos perigosos indesejados e gasto considerável de energia e água no processo. No CGTRQ todos os sistemas de refrigeração operam em circuito fechado, minimizando assim o consumo de água. Como perspectivas imediatas deste trabalho está-se incentivando iniciativas empreendedoras, com estudantes e a própria equipe do CGTRQ, para se aumentar a escala de produção dos solventes recuperados e implementação de logística de distribuição dos mesmos.

**Área: QV E** **Inscrição: 00294**

# Development of starch-based films using a biofriendly ionic liquid as plasticizer

**Ana Claudia de Lima Araújo (IC),[1*] Tereziana Silva da Costa (TC),[1] Alex Sandro Bezerra de Sousa[2] (PG), Silvanda de Melo Silva[1] (PQ), Dayse das Neves Moreira (PQ).[1]**

**anac.limaaraujo@gmail.com;**

*[1]Departamento de Química e Física, UFPB, Campus II, Areia-PB; [2]Departamento de Fitotecnia, Programa de Pós-Graduação em Agronomia, UFPB, Campus II, Areia-PB*

Keywords: *Ionic Liquids, Biodegradable Films, Starch.*

## Highlights

Starch based-films development. Biodegradable films. Ionic liquids as alternative plasticizer agents. New film formulations advantages. Great perspectives about the starch and ionic liquids synergy.

## Resumo/Abstract

Nowadays, starch has been used as matrix for biodegradable films, since in the presence of a plasticizer (water and polyols) and elevated temperature, a process known as "gelatinization" occurs, resulting in disruption of the granular semi-crystalline structure. In this context, Ionic Liquids (ILs) have been investigated as alternative plasticizers, due to their exceptional properties, such as negligible vapor pressure and plasticizing ability.[1-3] In this work, we present [Ch]Bz IL as a new plasticizer agent for the development of film formulations. The IL was obtained by a neutralization reaction between benzoic acid and cholinium chloride and, then, used in the film formulation through the casting method, which consists in the heating of an aqueous solution of starch 3%. For comparison, we prepared a film containing only glycerol 1% as plasticizer (Table 1). Films characterization were performed in a Minolta digital colorimeter and the data were used in the equation 1. Thickness was measured in a digital micrometer. The data showed a slight increase in the film thickness in both glycerol concentrations (0.5 and 1.0%), when 0.5% of IL was employed as plasticizer. Generally, the starch-based film formulations lead to a high opacity grade due to the plasticizer addition. However, we observed that the IL addition resulted on a lower opacity percentage when compared with the glycerol film, due to the compatibility between the IL and the starch polymeric chains. Thus, we presented herein a novel film formulation based on ionic liquids.

**Table 1.** Data from the different formulations used to obtain the starch based films.*

| Glycerol % (m/m) | IL [Ch]Bz % (m/m) | δ (μm) | White | | | Black | | | Opacity |
|---|---|---|---|---|---|---|---|---|---|
| | | | a* | b* | L* | a* | b* | L* | |
| 1.0 | - | 0.064 | 1.58 | 11.77 | 71.62 | 0.25 | 13.38 | 34.83 | 0.76 |
| 0.5 | 0.5 | 0.074 | 1.55 | 12.11 | 71.90 | 0.22 | 12.35 | 34.78 | 0.65 |
| 1.0 | 0.5 | 0.080 | 1.62 | 12.70 | 71.55 | 0.77 | 13.68 | 34.70 | 0.61 |

* All analyses were performed in triplicate and the data are referent to the media value.
%(m/m): plasticizer concentration; δ: thickness; a* (+red/-green), b* (+yellow/-blue): colorimetric coordinates; L*: luminosity

$$\text{Opacity} = \left[\frac{L^*_B / L^*_W}{\delta}\right] x\ 100 \quad \text{(eq. 1)}^4$$

[1] Tomé, L.C; Silva, N.H.C.S.; Soares, N.R; et al. *Green. Chem.* ***2015****, 17,* 4291.
[2]Zhang, B.; Xie, F.; Zhang, T.; et al. *Carbohydrate Polymers*. **2016,** 146, 67.
[3]Colomines, G.; Decaen, P.; Lourdin, D.; et al. *RSC Adv.* ***2016****, 6, 90331*
[4]Shirai, M.A.; Grossmann, M.V.E.; Mali, S. et al. *Carbohydrate Polymer.* **2013**, 92, 19.

**Área: QV E** **Inscrição: 00301**

# Effect of Deep Eutectic Solvents on the Heating Profile of Sonicated Organic Solvents

**Vanessa Freire de França (IC),[1]* Rachel Azevedo Maia (IC),[1] Isadora Maria Gouveia Andrade (IC),[1] Whesley Silva de Morais (PG),[2] Tereziana Silva da Costa (TC),[1] Dayse N. Moreira (PQ).[1]**

**vanessafreiree@live.com***

[1]*Departamento de Química e Física, UFPB* [2]*Programa de Pós-Graduação em Ciência e Tecnologia de Alimentos, UFPB*

Keywords: *Ultrasound irradiation, organic solvents, DES*

## Highlights

Effect of deep eutectic solvents was studied. Synergy of DES and ultrasound. Higher ultrasonic power promoted by the DES addition. Development of greener methodologies for organic synthesis.

## Abstract

Ultrasound (US) is considered a clean technology, allows less energy expenditure of chemicals and, consequently, less effluent generation, providing less processing time and reducing the need for heat application in several processes.[1] The ultrasound device with probe can emit the irradiation at higher frequencies and direct into the reaction mixture, being, therefore, an effective model for organic synthesis. However, there is still a great need to carry out methodological studies that evaluate the effects of the various reactional parameters related to this equipment. [2] The general objectives of this work are related to the influence of the deep eutectic solvent (DES) on the heating profile of different organic solvents when subjected to ultrasound irradiation. The heating profile of the ultrasonic solvents was determined on a Hielsher UP200Ht apparatus (1.25 mm probe, 90% amplitude). Ultrasonic power (Up) was determined using measurement data of the irradiated solvents, which were run in tubes containing 10 mL each for 15 minutes with and without the addition of DES (1 mmol) as shown in Table 1 (60.12 W), which was almost 3 and 6 times higher than acetonitrile and acetone, respectively. A great increase of Up (about 30%) was observed when DES was added to ethanol, demonstrating the ionic character of this substance. On the other hand, the presence of DES did not significantly alter Up. The data obtained for DES doped ethanol represent the promising environment to explore organic reactions.

Table 1. Data obtained from ultrasound irradiation for different organic solvents.

| Solvent | BP | $T_{(max)}$ | dT/dt | Cp | Up (W) |
|---|---|---|---|---|---|
| **Acetone** | 56°C | 38°C | 1,2727 | 2,18 | 10,97 |
| **Acetone + DES** | - | 40°C | 1,7182 | - | 14,81 |
| **Acetonitrile** | 82°C | 43°C | 2,3636 | 2,23 | 20,77 |
| **Acetonitrile + DES** | - | 44°C | 2,3273 | - | 20,45 |
| **Ethanol** | 78°C | 44°C | 2,0818 | 2,44 | 60,12 |
| **Ethanol + DES*** | - | 50°C | 3,0455 | - | 87,95 |

* DES synthesis was performed using choline chloride and urea (1:2), at 100 °C, for 2 h, under constant stirring.

[1]Paiva, A.; Craveiro, R.; Aroso, I.; *ACS Sustain. Chem. Eng.* **2014**, *2*, 1063−1071.
[2]Frizzo, C. P.; Bacim, C.; Moreira, D. N.; Rodrigues, L. V.; Zimmer, G. C.; Bonacorso, H. G.; Zanatta, N., Martinsa, M. A. P.; *Ultrason Sonochem.* **2016,** *32*, 2016.

**Área: QVE** **Inscrição: 00303**

# How green additives affect the water heating profile under ultrasound irradiation: a methodological study

**Isadora Maria Gouveia Andrade (IC),[1]* Rachel Azevedo Maia (IC),[1] Vanessa Freire de França (IC),[1] Whesley Silva de Morais (PG),[2] Tereziana Silva da Costa (TC),[1] Dayse N. Moreira (PQ).[1]**

**isagouveia18a@gmail.com***

[1]*Departamento de Química e Física, UFPB* [2]*Programa de Pós-Graduação em Ciência e Tecnologia de Alimentos, UFPB*

Keywords: *Ultrasound, Dissipated Ultrasonic Power, IL, DES*

## Highlights

Parameters effect of an ultrasound device was performed. A synergy study of ultrasound and green additives was investigated. DES influence on the dissipated acoustic power was evaluated.

## Abstract

The use of ultrasound irradiation (US) has grown up in the recent years, resulting in a significant number of researches. The US effect is dependent of different parameters, as the probe diameter, amplitude, frequency, kind of solvents, etc. When a solution is sonicated, the energy transferred, although induced by mechanical effects, is ultimately lost as heat. [1]Thus, ultrasonic processing usually results in a temperature increase, unless cooling is provided. The calorimetric method is generally used to measure the heat dissipated in a volume of liquid, which consider the heat capacity of this liquid (Cp) by which the acoustical energy is absorbed. [2] At the present work, we studied the behavior of sonicated water when two independent additives are employed, ionic liquids and deep eutectic solvents. The dissipated power was calculated by the calorimetric method, which involves the solvent heat capacity, mass and temperature variation: P (W) = CpMdT/dt. From the heating ramps were obtained from the slope, dT/dt and $R^2$. The graph 1 shows the variation of the dissipated power of the pure water and the water doped with the additives, as a function of the amplitude increase. These data show an interesting result when DES was employed, as the dissipated power increased considerably. On the other hand, when the IL was added no significant difference was observed. Thus, DES have enormous potential as additive, due to their tunable physicochemical properties.

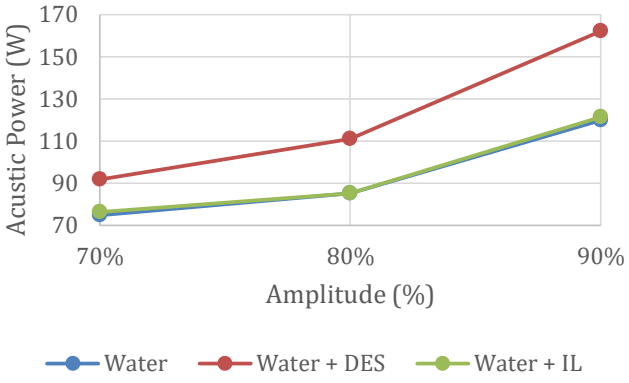


Graph 1 – Dissipated power for pure water, doped water with DES or IL

[1] Chatel, G.; MacFarlane, D. R. *Chem. Soc. Rev*. **2014,** *43*, 8132.
[2] Kentish, S.; Feng, H. *Annu Rev. Food Sci. Technol*. **2014,** *5*, 263.

**Área: _QVE_____ Inscrição:_00870_____**

# Synthesis of esters and ketals from levulinic acid and alcohols obtained by heterogeneous catalysis with a sulfonic acid resin

**Leina Soares Behenck (PG),[1] Fernando Henrique Maia de Paula (PG),[1] Adryena T. Teixeira (IC),[1] Laura Martins Pina de Almeida (IC),[1]Elizabeth Roditi Lachter (PQ)[1]***

**leinasoares@gmail.com; lachter@iq.ufrj.br**

*[1]Departamento de Química Orgânica, Instituto de Química, Universidade Federal do Rio de Janeiro, UFRJ*

Key words: *levulinic acid, glycerol 1-monoether, sulfonic resin, acetalization, esterification.*

## Highlights

The ketalization reaction of ethyl levulinate with diols catalyzed by ion exchange resin A70 lead to a high selectivity in the ketal product and with linear alcohols lead mainly to the transesterification product.
Ketal ethlyl levulinate obtained from a glycerol 1-monoether are attractive candidates as biolubricants.

## Resumo/Abstract

Currently, the increased demand for chemicals has led to the search for new sources of non-fossil feedstock [1]. The levulinic acid (4-oxopentanoic acid) and its esters are obtained from biomass and can be converted to chemicals such as plasticizers, biolubricants, solvents, surfactants and flavoring [1-3]. The reaction between ethyl levulinate and long chain diols leads to the formation of a ketal in the presence of an acid catalyst. The advantage of heterogeneous catalysis is the ease separation of the catalyst from the reaction mixture and possibility of its reuse [2]. The using of renewable raw material derivatives and heterogeneous catalysis are two of the twelve principles of green chemistry. The objective of this work is to study the ketalization reaction of ethyl levulinate with mono-alcohols (C8 and C12), 1,2 diol (C8, C10) and 1,2-diol obtained from glycerol (glycerol 1-monoether, C8 and C10) catalyzed by the sulfonic resin, Amberlyst 70. The solvent of the reaction was hexane, Dean Stark apparatus was used to remove water from the reaction and 1% of catalyst relative to the alcohol (limiting reagent) was employed. The products were identified by GC/MS. The formation of the ketals in the reactions with the diols was verified, having total conversion of the same ones after 2-4 hours of reaction. In the case of the mono-alcohols, the reaction were slower and after 24 hours, the main product was the transesterification product without the formation of the ketal.

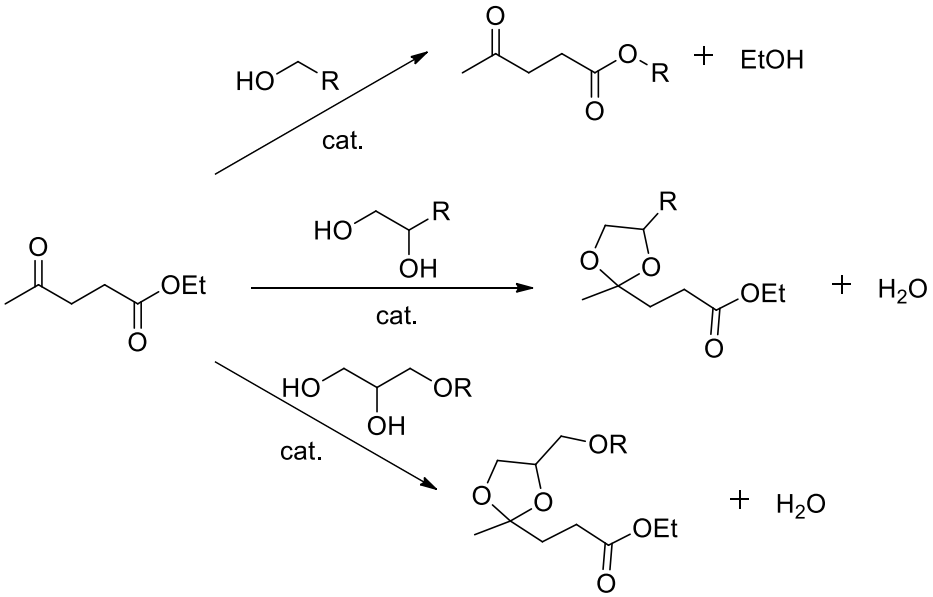


Referencias:
[1] A. Démolis; N. Essayem; F. Rataboul, ACS SustainableChem. Eng. 2 (2014) 1338−1352.
[2] K. Y. Nandiwale; S. K. Yadava; V.V. Bokade, Journal of Energy Chemistry vol. 23 no. 4 (2014).
[3] F.A.Freitas, D. Licursi, E.R.Lachter et al. Catalysis Communications 71 (2016) 84-87.

**Área: QVE** **Inscrição: 00914**

# A Green Chemistry Approach: Pectin Extraction of the Pinion Pell for Use in Synthesis of Silver Nanoparticles

**Marcelo Schram (IC),[1]* Neide Hiroko Takata (PQ),[1] Eryza Guimarães de Castro (PQ).[1]**

**E-mail: *marceloschram2013@gmail.com***

*[1] Universidade Estadual do Centro-Oeste, Rua Simeão Varela de Sá, 03 – Vila Carli, Guarapuava – PR, CEP 85040-080*

Palavras Chave: Casca de Pinhão, *Nanopartículas de Prata, Pectina, Síntese Verde.*

## Highlights

The use of biomolecules extracted from the pinion peel in the synthesis of silver nanoparticles, integrated the principles of green chemistry, performing an environmentally friendly synthesis process.

## Resumo/Abstract

A crescente expansão da nanotecnologia vem acompanhada da necessidade do desenvolvimento de métodos mais verdes para a síntese de nanopartículas. Desta forma, a integração dos princípios da química verde à síntese de nanopartículas é um dos caminhos a serem percorridos. Na síntese verde podem ser utilizados materiais de baixo custo e de baixa toxicidade, como extratos vegetais, por exemplo. As biomoléculas extraídas das plantas induzem a redução do íons $Ag^+$, proveniente do nitrato de prata ($AgNO_3$), aglomerando-as na forma de nanopartículas de prata (AgNP's). A pectina foi extraida da casca da semente da Araucária (Araucaria augustifólia) conforme o método de Bankar,[1] que consiste em ferver as cascas do pinhão em água destilada por 30 minutos a 90 ºC, seguida pela maceração, filtração e adição de volume equivalente de isopropanol. As AgNP's foram sintetizadas sob diferentes valores de pH, ajustando-o para 2, 4, 5, 6, 9 e 11. A influência da concentração de $Ag^+$ no meio foi estudada pela variação da concentração de $AgNO_3$, utilizando soluções 0,005, 0,010, 0,015 e 0,020 $molL^{-1}$ do sal. As AgNP's sintetizadas foram caracterizadas por técnicas de Espectroscopia UV-Visível, realizadas no Espectrofotômentro UV-Vis UV-1800 da Shimadzu. Os espectros obtidos constataram diferenças significativas entre as AgNP's sintetizadas em diferentes condições de pH (Fig. 1a), apresentando a banda mais bem definida entre o pH 5 e 6. Enquanto que em concentrações mais altas de $Ag^+$ as bandas estão melhor definidas (Fig. 1b). Os resultados foram condizentes com a literatura,[1,2] evidenciando o potencial da utilização da casca do pinhão na síntese de AgNP's.

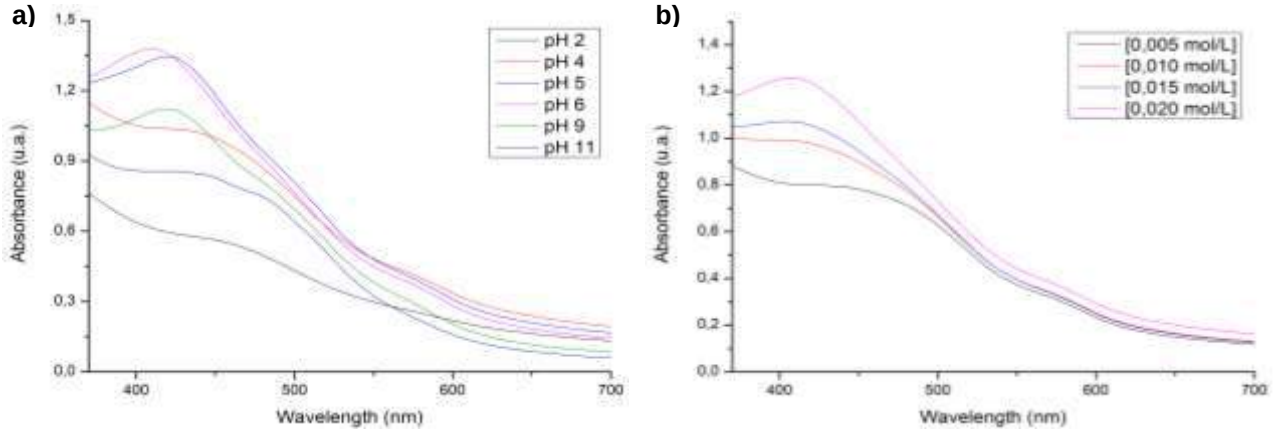


Fig 1 a. Espectros UV-Vis de AgNP's sintetizadas em diferentes valores de pH e concentração 0,002 $molL^{-1}$.
Fig 1b. Espectros UV-Vis de AgNP's em diferentes concentrações de $Ag^+$ e pH 5.

[1]Bankar, A., Joshi, B., Kumar, A.R., Zinjarde, S. Banana Peel Extract Mediated Novel Route For The Synthesis of Silver Nanoparticles. Colloids and Surfaces A: Physicochemical and Engineering Aspects, vol. 368, n. 1-3, pp. 58–63, 2010.
[2]Toma, H.E., Silva, D.G., Condomitti, U. Nanotecnologia Experimental. 1 ed. 167 p. São Paulo: Editora Blucher, 2016.

**Área: QVE** **Inscrição: 01330**

# An enzymatic catalysis for an enzymatic chemical: a gram scale conversion of furfural to furfuryl alcohol by carrots (*Daucus carota*)

**Daniela Yumia Yamamoto (IC),[a] Ronaldo Epifanio de Oliveira Filho (PG), Marina Gonçalves Capelletto (PG), Álvaro Takeo Omori (PQ)**

**daniela.yamamoto@aluno.ufabc.edu.br; alvaro.omori@ufabc.edu.br**

*Laboratório de Compostos Bioativos, Centro de Ciências Naturais e Humanas, UFABC - Santo André - SP*

Palavras Chave: *Biomass, Biocatalysis, Carrots, Furfural, Furfuryl alcohol, Hydrogenation.*

## Highlights

The bioconversion of furfural by means of carrot bits at room temperature and ambient pressure led to furfuryl alcohol in >99% conversion and >99% selectivity to the alcohol. This simple and "fully" green process is an alternative of classic hydrogenation processes.

## Abstract

Furfural (**1**) is one of the most promising renewable chemical derived from the lignocellulosic biomass. The number of the publications on furfural production or transformation is increasing exponentially.[1] In addition, the corresponding furfuryl alcohol (**2**) is considered the most important chemical derived from **1** and have a broad spectrum of applications in chemical industry. The hydrogenation process to convert **1** to **2** is already established but still depends on Cu/Cr (toxic) catalysts which require high temperatures and the use of hazardous and explosive hydrogen.[1] In this work, we present a very simple and environmentally friendly alternative to obtain furfuryl alcohol by bioreduction mediated by carrots (scheme 1). This presented method has been used in our group for synthetic purposes.

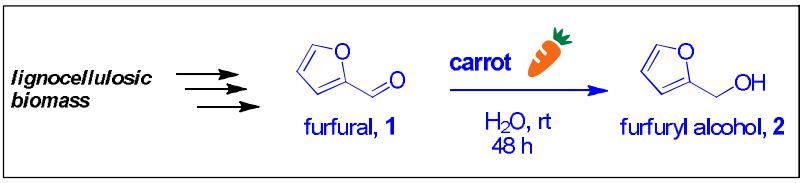


**SCHEME 1.** Bioreduction of furfural by carrots

***FACILE GREEN PROTOCOL***

1. Get a carrot in the local market
2. Cut into slices
3. Transfer to a Erlenmeyer flask containing water and the furfural
4. 48h orbital stirring
5. Liquid-liquid extraction
6. No purification needed!

Several parameters were investigated in order to optimize the reaction conditions. The reagent/catalyst/solvent ratio, the carrot source and the influence of the functional carbonyl group (aldehyde vs. ketone) were investigated. The preliminary results are summarized in tables 1-3.

**Table 1**. Preliminary results of furfural reduction with carrots at room temperature

| Factor | Reaction | 1 (mg) | Carrot (g) | $H_2O$ (mL) | Carrot/1 (g/L) | Conversion* 24h (%) | Conversion* 48h (%) | Selectivity (%) | Isolated yield** |
|---|---|---|---|---|---|---|---|---|---|
| Carrot source | #1 | 100 | 5 | 50 | 2 | 53 | **99** | **99** | **24%** |
| | #2 | 100 | 5 | 50 | 2 | 68 | **99** | **99** | **n.d.** |
| | #3 | 100 | 5 | 50 | 2 | 73 | **99** | **99** | **n.d.** |
| | #4 | 100 | 5 | 50 | 2 | 77 | **99** | **99** | **n.d.** |
| | #5 | 400 | 20 | 200 | 2 | 62 | **99** | **99** | **37%** |
| | #6 | 800 | 40 | 400 | 2 | 50 | **99** | **99** | **44%** |
| | #7 | 1600 | 80 | 200 | 8 | 14 | 40 | **99** | **n.d.** |
| | #8 | **1000** | **120** | **250** | **4** | **73** | **99** | **99** | **63%** |

According to the table 1, the best condition was achieved with 4 g/L of 1 with 63% isolated yield. This higher concentration is also attributed to the higher solubility of 1 in water in comparison of the corresponding ketone (methyl furyl ketone). Further studies are ongoing to establish better conditions.

**REFERENCES**

1. Mariscal, R.; MAireles-Torrs, P.; Ojeda, M.; Sádaba, I.; Granados, M. L. Energy Environ. Sci. 2016, 9, 1144.

**Área: QVE** **Inscrição: 01336**

# Avaliação do uso de óleo vegetal de Crambe (*Crambe abyssinica Hochst*) como fluído isolante para transformadores elétricos

**Ana Claudia C.S. Reis (PG),[1]* Carmen L.B. Guedes (PQ)[2].**

**anacquimica@gmail.com; carmen@uel.br**

*[1]Departamento de Química, UEL; [2]Departamento de Química UEL*

Palavras Chave: *óleos vegetais isolantes, óleo mineral, isolamento elétrico.*

## Highlights

Evaluation of the use of Crambe vegetable oil (*Crambe abyssinica Hochst*) as an insulating fluid for electrical transformers

Vegetable oils can be used as insulating fluids because they meet the principles of operational and environmental safety. Crambe is an option of insulating fluid due to its oxidative stability.

## Resumo/Abstract

Os óleos vegetais isolantes derivam de fontes renováveis e apresentam vantagens como, ser ambientalmente correto, biodegradável, renovável, barato, altamente disponível, não tóxico e mais seguro[1,2]. O óleo extraído do Crambe pode ser aproveitado para diversos fins e, esse projeto tem por objetivo seu uso como isolante elétrico.

O Óleo de Crambe foi caracterizado por testes físico-químicos antes e após o processo de refino, conforme descritos na Tabela 1. E o processo de refino seguiu as etapas de filtragem, degomagem, neutralização, branqueamento e aditivação.

Tabela 1 – Teste físico-químicos realizado com óleo de Crambe bruto e refinado

| Teste | Método | Unidade | Valor Obtido | | Valor de Referência |
|---|---|---|---|---|---|
| | | | Óleo Bruto | Óleo Refinado | |
| Teor de Sedimentos | ABNT NBR 10576 | % | 6,95 | 0,01 | - |
| Índice de Neutralização | ABNT NBR 14248 | mg de KOH/ g de óleo | 3,00 | 0,04 | 0,06 máx |
| Teor de água | ABNT NBR 10710 | ppm | 1515,3 | 128 | 200 máx |
| Densidade | ABNT NBR 7148 | g/cm$^3$ | 0,960 | 0,901 | 0,960 máx |
| Viscosidade a 100 °C | ABNT NBR 10441 | cSt | - | 8,95 | 15 máx |

Os testes de caracterização físico-química do óleo bruto são importantes para fins de comparações e certificação da eficiência do processo de refino. O óleo bruto apresentava resíduos sólidos e era altamente viscoso enquanto que o óleo refinado de Crambe atendeu os valores especificados na Norma ABNT NBR 15422 que estabelece valores limites para o uso de fluídos vegetais isolantes novos em transformadores, ressaltando, assim, a eficiência e importância do processo de refino do óleo.

Referências Bibliográficas

[1] *FANG, Yuan; LUO, Yunbai; YU, Ping. Determination of antioxidants in vegetable insulating oils by HPLC.* ***Journal of Renewable and Sustainable Energy,*** *Melville, NY, v. 8, p. 01-10, Junho 2016.*

[2] RAFIQ, M.; LV, Y. Z.; ZHOU, Y.; MA, K. B.; WANG, W.; LI, C. R.; WANG, Q. Use of vegetable oils as transformer oils – a review. **Renewable and sustainable energy reviews**, v. 52, p. 308-324, Agosto, 2015.

**Área: AMB** **Inscrição: 01002**

# CHEMICAL WASTE TREATMENT: importance of the academic community awareness about responsible disposal

**Karolynne C. Morais(IC)[1],Rafaela R. de Paula (IC)[1], Ray de S. Pereira (IC)[1],João Marcos S. R. dos Santos (IC)[1], Letícia D. F. de Siqueira (IC)[1], Iago S. Mesquita* (TM)[1], Aline M. S. Teixeira* (PQ)[1].**

**karolynne.campos@outlook.com; aline.santos@ifrj.edu.br**

[1]*Instituto Federal de Educação, Ciência e Tecnologia do Rio de Janeiro – IFRJ Campus Duque de Caxias*

Keywords: *Chemical Waste, Enviromental Awareness, Waste Treatment, Waste Disposal.*

## Highlights

Ambient awareness of the IFRJ Campus Duque de Caxias academic community at Science and Technological Week. Importance of storage and proper chemical waste treatment generated in teaching laboratories.

## Resumo/Abstract

This work highlights the importance of carrying out practical activities which promote the academic community awareness about the treatment and storage of chemical waste. During the IFRJ Science and Technological Week, a presentation was performed on the chemical waste definition[1,2], as well as demonstrative and practical activities focusing on environmental impact awareness and relevance of management and waste treatment. Before and after the project presentations, IFRJ students, teachers from different areas of expertise and other employees responded to the questionnaires in order to diagnose prior knowledge of the academic community and assess progress on the topic addressed. According to results of the research, before the presentation, 20% of participants had little or no information on appropriate chemical waste treatment and storage. The answers after the presentations demonstrated a substantial development of the knowledge on this topic (Figure 1a), evidencing the need to promote critical thinking and awareness about responsible disposal. Practical questions regarding the storage and treatment of waste commonly found in teaching laboratories was also applied. The comparison between the input and output questionnaires revealed the participants had developed the ability to apply the notions acquired in their laboratory everyday (Figure 1b). Furthermore, the project figured as an opportunity for a re-signification of the continuous process of student-school development, in an approach emphasized on the pillars of sustainability.

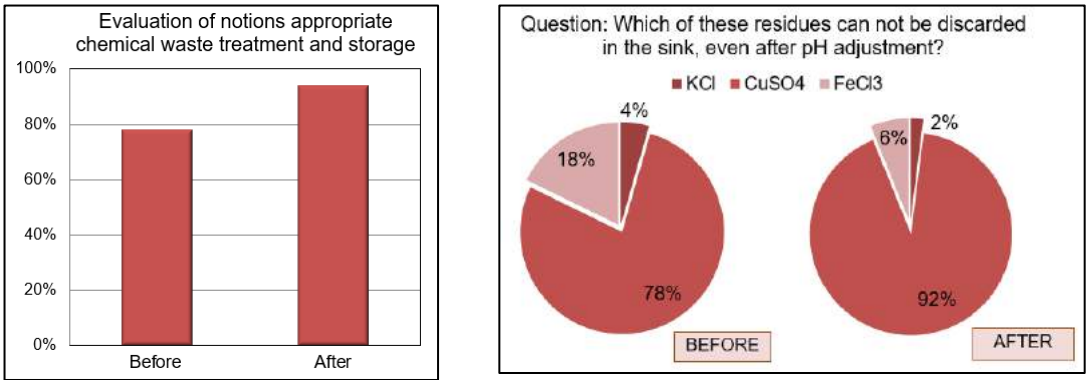


(a) (b)

**Figure 1.** Participants answers before and after presentation about(a)notions of chemical waste treatment and storage and (b)chemical waste disposal.

**REFERENCES:**

[1]ASSOCIAÇÃO BRASILEIRA DE NORMAS TÉCNICAS (ABNT). Resíduos Sólidos − Classificação**. Norma Técnica NBR 10004**. Rio de Janeiro: ABNT, 2004

[2]AFONSO, J. C.; NORONHA, L. A.; FELIPE, R. P.; FREIDINGER, N. **Gerenciamento de resíduoslaboratoriais: recuperação de elementos e preparo para descarte**, Quimica. Nova, Vol. 26, No. 4, 602-611, 2003.

**Área: TEC**
*(Inserir a sigla da seção científica para qual o resumo será submetido. Ex: ORG, BEA, CAT)*

**Inscrição: 00449**
*(Inserir o número de inscrição do autor que fez a submissão)*

# The Chemical Data Science by Scientific and Technological Knowledge in Big Data of the antiretrovirals patents

**Jorge L. Magalhães (PQ)[1,5]*, Flávia M. L. Mendes (PQ)[2,4], Adelaide M. S. Antunes (IC)[3,4], Zulmira Hartz (PQ)[5].**

**jorge.magalhaes@far.fiocruz.br ; jorge.magalhaes@far.fiocruz.br**

*[1]Center for Technological Innovation – NIT Farmanguinhos/FIOCRUZ; [2]Center for Strategic Studies – CEE/FIOCRUZ; [3]National Institute of Industrial Property – INPI; [4]Chemical School/UFRJ. RJ, Brazil; [5]University NOVA of Lisbon, IHMT – Global Health and Tropical Medicine (GHTM), Portugal.*

Palavras Chave: Big Data, Chemical Patents, Antiretroviral, Knowledge Management, Information Science.

## Highlights

Challenges & opportunities to manage 100 million patents growing 10% per year.
Knowledge management in technological information of new antiretroviral molecules – class A61K (chemical formulations).

## Resumo/Abstract

The magnitude of information science in the 21st century is undoubtedly true in all areas of science. The chemical science and technology sector advanced much more in the first decade than in the previous 50 years. The more than 100 million patents registered in the European Patent Office (EPO) provide an unprecedented source of scientific and technological information in the history of mankind. The technological management of this information is exploited to develop technological advances in scientific, technological and educational organizations and companies. New standards of product and process safety and effectiveness have been introduced across the world and public and private business strategies are under constant review to comply with the prevailing paradigm. The health sector releases more than 1 million papers a year on scientific progress, while technological (patents) advances 10%a.a. Thus, a case study in new chemical entities in antiretroviral will provide a contribution to reflection for the business in research, development and innovation in health. In 2017, 03 lists of strategic products for the Brazilian Health System were changed. Using new intelligence systems in intellectual property, the government has adopted new strategic partnerships with the private sector and were conceived in 2017 with budgets of more than US$ 2 billion. The 2017 list contemplates 56 strategic medicines, with 28 drugs to fight HIV - further 88 that are under development. Using SciFinder Scholar® and EPO database 4.554 HIV patents were extracted and processed in software vantage: 20 ARV used in BraziL: 06 are NRTI, 03 are NNRTI, 07 are PI, 02 are INI and 02 are FI. Dolutegravir more important key molecule 3,4,5-Piperidinetriol, 1-[(3-phenyl-2-propen-1-yl)oxy]-($C_{14}$ $H_{19}$ N $O_4$); second Raltegravir. Temporal evolution of the patent applications per priority year is shown beside.

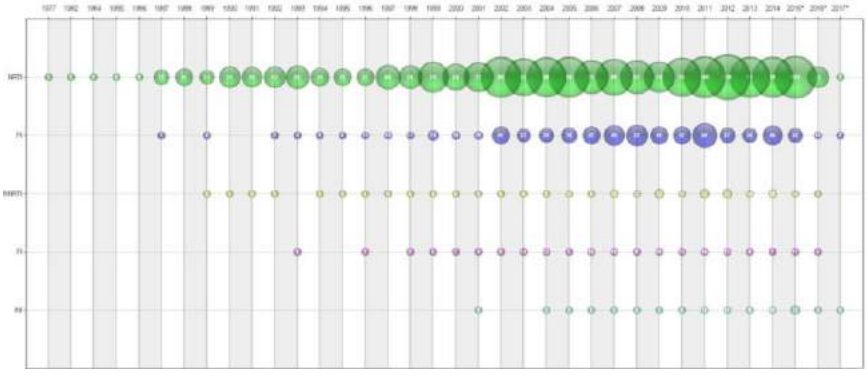

Knowledge management, using IT tools, could become a great ally in helping decision-makers in the private and public sectors alike. Technologies that are not protected in each country or which expire may then be produced generically and incremental innovations may be made, etc. Chemical patents documents can serve as a source of information. It was possible to identify common indicators in an analysis of patenting per class indicating emergence of new classes of drugs for HIV/Aids treatment. Major technological developments are EUA and China.

References: 1) CANADIAN INSTITUTES OF HEALTH RESEARCH. Knowledge Translation and Commercialiation. Disponível em: < http://www.cihr-irsc.gc.ca/e/29418.html#1 >.
2) PIERRET, J.-D. Methodologie et structuration d'un outil de decouverte de connaissances base sur la litterture biomedicale : une application basee sur le MeSH. [s.l.] Université du Sud Toulon Var, 28 fev. 2006.

**Área: TEC** **Inscrição:00475**

# Niobium oxide and calcium oxide catalyzing the transesterification reaction of *Acrocomia aculeate* and *Orbinya martiana* oils

**Diana C. Cubides-Román (PQ),[1*] André F. Constantino (PG),[1] Milena Castello de Araújo (IC),[1] Reginaldo Bezerra dos Santos (PQ),[1] Alvaro C. Neto (PQ),[1] Valdemar Lacerda Jr. (PQ).[1]**

**diana.roman@ufes.br**

*[1]Departamento de Química, UFES;*

Palavras Chave: *Biodiesel, Methyl fatty esters, heterogeneous catalyst.*

## Highlights

Mixtures of $Nb_2O_5$ and CaO catalyze the reaction to produce biodiesel. The reagents were methanol and Macauba and Babassu oil. The experimental design planned was a complete $2^3$ with 4 central points.

## Resumo/Abstract

Several niobium compounds (niobium ammonium oxalate, niobium oxide and niobium pentachloride) have been studied in the production of biodiesel, involving its application as Lewis acid [1-2]. As a basic catalyst, the calcium oxide (CaO) has been extensively studied [3]. Looking to improve the separation process, reuse the catalyst and decrease the reaction temperature in biodiesel production, there were investigated mixes of $Nb_2O_5$ and CaO as heterogeneous catalysts, as well as two oils from native Brazilian species, Macaúba (*Acrocomia aculeate*) and Babassu (*Orbinya martiana*). Using statistical methods to plan, analyze and optimize reactions, the biodiesel conversion was evaluated as a function of oil:methanol molar ratio (1:18, 1:27 and 1:36), mass of catalysts (1, 2 and 3%) and temperature (333, 343 and 353K) for both oils in individual experimental designs Table 1.

The results allowed us to conclude the interaction between the molar ratio and reaction temperature had a significant positive effect on biodiesel conversion, Figure 1. The reaction temperature by itself indicated a possibly significant positive effect. With both oils, biodiesel conversions obtained were above 79%, under optimized reaction conditions.

**Table 1**. Experimental planning (reaction conditions) and results of biodiesel conversion.

| | Experimental Variables | | | Conversion | |
|---|---|---|---|---|---|
| | A % Catalyst | B - molar ratio oil: methanol | C-Reaction temperature (°C) | Macaúba Biodiesel (%) | Babassu Biodiesel (%) |
| 1 | 1 | 1:36 | 60 | 23,1 | 45,0 |
| 2 | 3 | 1:36 | 60 | 23,9 | 58,5 |
| 3 | 1 | 1:18 | 60 | 15,1 | 26,1 |
| 4 | 3 | 1:18 | 60 | 79,3 | 88,7 |
| 5 | 1 | 1:36 | 80 | 76,7 | 85,7 |
| 6 | 3 | 1:36 | 80 | 63,5 | 52,9 |
| 7 | 1 | 1:18 | 80 | 64,7 | 77,0 |
| 8 | 3 | 1:18 | 80 | 68,2 | 80,7 |
| 9 | 2 | 1:27 | 70 | 41,0 | 59,0 |
| 10 | 2 | 1:27 | 70 | 43,0 | 60,0 |
| 11 | 2 | 1:27 | 70 | 43,3 | 64,2 |
| 12 | 2 | 1:27 | 70 | 45,6 | 67,4 |

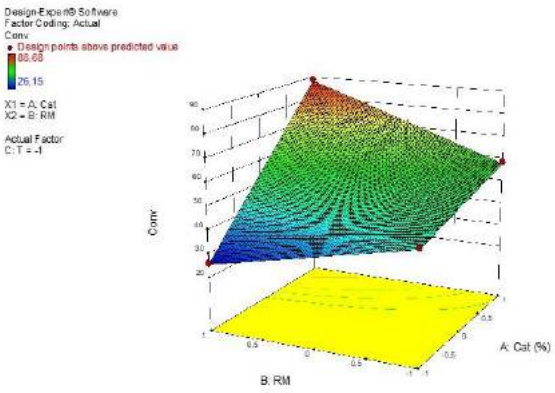


**Figure 1.** Response surface of transesterification yield as a function of catalyst %, and molar ratio methanol: oil for Babassu (at 60°C).

**References**.

**[1]** dos Santos, D.A.; *et a*l. *Mod. Res. Catal.* 2, 63–67, 2013.

**[2]** Lacerda Jr.,V.; *et a*l. *Aldrichimica Acta*, 45, 19–27, 2012.

**[3]** Marinković, D.M.; *et al*. *Renew. Sustain. Energy Rev*. 56, 1387–1408, 2016.

**Área: TEC** **Inscrição: 622**

# Incorporation of benzimidazoles and benzothiazoles to urea: Preparations and effects on ammonia loss from urea

**Breno G. F. Oliveira (PG),[1,*] Ângelo de Fátima (PQ),[1] Luzia V. Modolo (PQ),[2] Reinaldo B. Cantarutti (PQ).[3]**

*E-mails: brenogof@hotmail.com (BGFO) and adefatima@qui.ufmg.br (AF)

*[1]Departamento de Química, UFMG; [2]Departamento de Fisiologia Vegetal, UFMG; [3]Departamento de Solos, UFV.*

Keywords: *Urea, urease, enhanced efficincy fertilizer, benzimidazoles, benzothiazoles.*

## Highlights

►Urea is the most consumed nitrogenated (N) fertilizer in the world.►Up to 70% of urea is lost due to ammonia volatilization.►Benzimidazoles and Benzothiazoles reduced N loss when incorporated to urea.

## Resumo/Abstract

Due to its high nitrogen content and ease of handling, urea possesses a highlighted position in the world scenario. However, urea is susceptible to losses as volatilization of ammonia, caused by intense hydrolysis promoted by urease – a soil present enzyme and the main reason for this loss[1]. In this way the inhibition of urease constitutes a strategy aiming the minimization of urea hydrolysis. This work presents the synthesis of benzothiazoles and benzimidazoles and the evaluation on the effect of these on ammonia volatilization. The compounds were prepared with yields ranging between 80-90% (Scheme 1)[2].

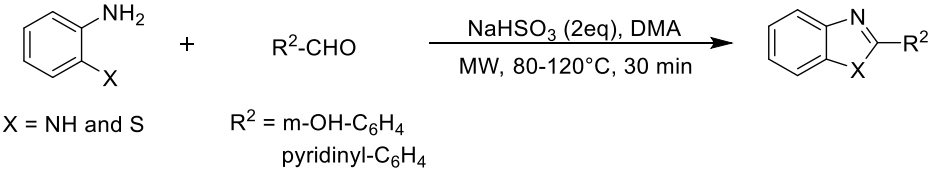


**Scheme 1:** Synthesis of benzimidazoles and benzothiazoles derivatives.

The compounds were incorporated to urea and the emission levels of ammonia – from the ground – were determined at a continuous air flow system[3]. The experimental design was completely randomized with four replications. The synthesized derivatives reduced ammonia's volatilization peak (27-42%), furthermore slowed by 6h the volatilization peak in comparison to urea. The accumulated volatilization in 144h was reduced by 35% compared to urea alone. The urea-incorporated inhibitors are an efficient way to reduce ammonia volatilization from urea, making itself a viable technology for fertilizer application in agriculture.

**Financial support:** CAPES, CNPq and FAPEMIG.

**References:**

[1] ANDA - Anuário Estatístico Setor de Fertilizantes **2016**.
[2] ARAÚJO, D. P. et al. RSC Advances, **2015**, *5*, 28814.
[3] SOARES, J.R. et al. Soil Biology & Biochemistry, **2012**, *52*, 82.

**Área: TEC** **Inscrição:T0627-1**

# Optimization of the transesterification reaction of soy oil catalyzed by sodium ethyleneglycoxide.

**Samuel José Santos (IC),[1,2*] Marluci Krever de Oliveira (IC),[1,2] Rodrigo Eckert Renner (IC),[1] Guilherme da Costa Espíndola (PG),[3] Guilherme de Souza (PQ),[1] Luiz Antonio Mazzini Fontoura (PQ),[1,2,4] Guilherme da Silva Priebe (PQ)[1]**

**samueljsantos@gmail.com**

*[1]Departamento de Engenharia de Processos, Fundação de Ciência e Tecnologia; [2]Curso de Química, Universidade Luterana do Brasil; [3]Programa de Pós-Graduação em Engenharia de Minas, Materiais e Metalurgia, Universidade Federal do Rio Grande do Sul, [4]Programa de Pós-Graduação em Engenharia de Materiais e Processos Sustentáveis, Universidade Luterana do Brasil.*

Palavras Chave: *Biodiesel, Transesterification, Sodium ethyleneglycoxide, Biofuel, Catalyst.*

## Highlight

Sodium ethyleneglycoxide can be used as homogeneous alkaline catalyst to produce biodiesel.

## Abstract

Biodiesel is constituted of a fatty esters mix, obtained by triglycerides transesterification or fatty esters esterification. The fatty esters low polarity and long chains make their proprieties similar to those exhibited by the hydrocarbons diesel is made from. By this reason, biodiesel has been employed as partial or total substitute to diesel fuel in compression ignition engines. Transesterification reaction rate is low. For this reason, a catalyst must be used. Sodium methoxide is the most used one, although its high cost and inflammability. Hydroxides are also used, but they produce water, when they are dissolved in the alcohol. Therefore, alternative catalysts have been subject of several studies. In this work, evaluate the use of sodium glyceroxide as catalyst for the transesterification reaction of soy oil with methanol. A Doehlert experimental design[1] was used. Methanol/triglyceride molar ratio and catalyst amount were investigated. All the reaction were carried out at 65 $^{o}$C im 30 min. The optimum conditions were found as 7.8:1 (methanol/triglyceride) molar ratio and 1.5 % (catalyst mass/triglyceride mass). When the catalyst amount is lower, the reaction conversion is higher, the higher is the molar ratio (Figure 1). When the catalyst is concentrated, the molar ratio is less important. When the optimized conditions are used, the bioidiesel is obtained with 97.5 % of purity.

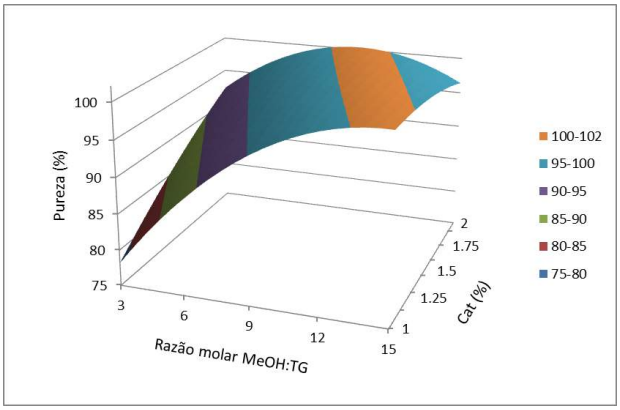


Figure 1 – Effect of the molar ratio (MeOH/TG) and the catalyst amount over transesterification conversion.

1. Teófilo, R. F.; Ferreira, M. M.; *Quim. Nova*, **2006**, *29*, 338.

**Área: TEC** **Inscrição: 00670**

# Determination of physicochemical properties of biodiesel and blends using low-field NMR and multivariate calibration

**André F. Constantino (PG),[1] Diana C. C. Román (PG),[1] Reginaldo B. dos Santos (PQ),[1] Álvaro C. Neto (PQ),[1] Lúcio L. Barbosa (PQ),[2] Paulo R. Filgueiras (PQ),[1] Valdemar L. Júnior (PQ).[1*]**

**andrefazoloc@gmail.com; vljuniorqui@gmail.com**

*[1]Departamento de Química, UFES; [2]Departamento de Ciências do Mar, UNIFESP.*

Keywords: *Biodiesel, Low-field NMR, PLS, Kinematic viscosity, Density, Refractive index*.

## Highlights

A new methodology to determine kinematic viscosity, density and refractive index in biodiesel is proposed. Low-field NMR associated with PLS is used. The methodology is rapid, nondestructive and low-cost.

## Abstract

The methods specify by regulatory agencies for determination of the physicochemical properties of biodiesel can be laborious and expensive, so that the development of alternative methodologies represent a major breakthrough. Thus, the low-field NMR (Nuclear Magnetic Resonance) is an advantageous option because is nondestructive and reduce the economic cost and time consumption.[1,2] In this study, Partial Least Squares (PLS) regression method was used to create models that correlated the decay curves of CPMG (Carr–Purcell–Meiboom–Gill) signal, obtained in an equipment of low-field NMR, with the kinematic viscosity, the density and the refractive index of biodiesel samples and their blends. Sixteen oilseeds were utilized to synthesize the biodiesel, diversifying between edible and inedible oils, which together with the binary blends totalize forty one samples. The Figure 1 exhibits the correlation between reference and predicted values by PLS. Table 1 shows the statistical parameters that characterize the resulting models. To perform the regressions were used four or five latent variables (LV) and the captured variance was greater than 99.4% in all cases. Furthermore, the strong coefficients of determination ($R^2$) for calibration sets demonstrate the high linearity of the models and the low values of Root Mean Square Error of Calibration (RMSEC) and prediction (RMSEP) indicate their accuracy. These results reveal the built models are very satisfactory and can predict the quality parameters of biodiesel and blends based in CPMG data with fairly efficacy.

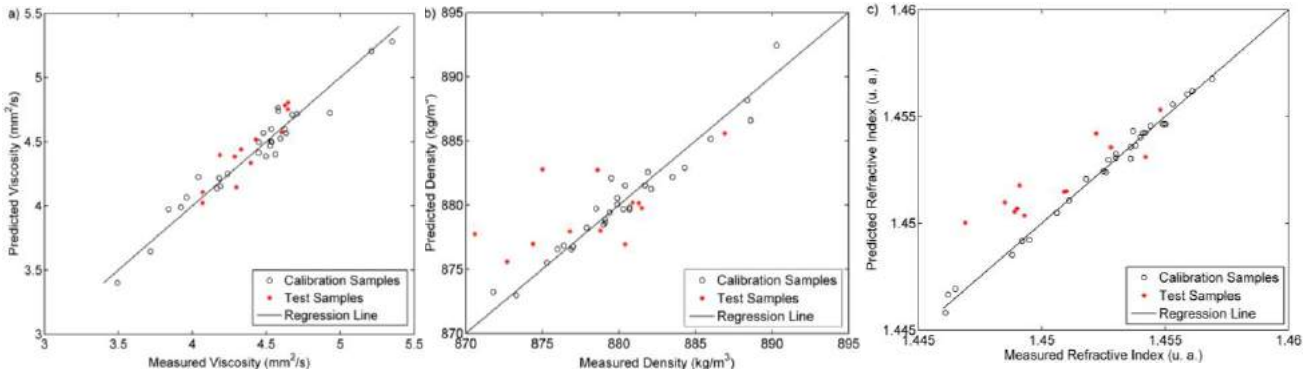


**Figure 1.** Predicted versus measured plot of PLS models for the properties: a) viscosity; b) density; and c) refractive index.

**Table 1.** Summary of the statistical parameters that describe the PLS model of each property.

| Property | Number of LV | Captured Variance (%) | $R^2$ | RMSEC | RMSEP |
|---|---|---|---|---|---|
| Viscosity | 4 | 99.45 | 0.9432 | 0.1 $mm^2/s$ | 0.1 $mm^2/s$ |
| Density | 4 | 99.45 | 0.9422 | 1.1 $kg/m^3$ | 3.7 $kg/m^3$ |
| Refractive Index | 5 | 99.47 | 0.9914 | 0.0003 | 0.002 |

### References

1. Santos, P. M. et al. *Energy Fuels*, **2015**, 29, 2299–2303.
2. Prestes, R. A. et al. *Anal. Chim. Acta,* **2007**, 596, 325–329.

**Área: TEC** **Inscrição:T0677-1**

# Evaluation of sodium glyceroxide as catalyst in the oils and fats transesterification reaction.

**Samuel José Santos (IC),[1,2*] Matheus Nunes Claro (IC),[1,2] Josué Azevedo da Silva (IC),[1,2] Rodrigo Eckert Renner (IC),[1] Evelin Monique Saibro de Castro (IC),[1,3] Guilherme de Souza (PQ),[1] Luiz Antonio Mazzini Fontoura (PQ),[1,2,4] Guilherme da Silva Priebe (PQ)[1]**

**samueljsantos@gmail.com**

*[1]Departamento de Engenharia de Processos, Fundação de Ciência e Tecnologia; [2]Curso de Química, Universidade Luterana do Brasil; [3]Curso de Engenharia Química, Universidade Luterana do Brasil; [4]Programa de Pós-Graduação em Engenharia de Materiais e Processos Sustentáveis, Universidade Luterana do Brasil.*

Palavras Chave: *Biodiesel, Transesterification, Sodium glyceroxide, Biofuel, Catalyst.*

## Highlights

Sodium glyceroxide can be used as homogeneous alkaline catalyst to produce biodiesel.
Canola, sunflower, tallow, lard, palm, palm kernel, babassu and coconut methyl biodiesel were obtained.

## Abstract

Biodiesel is a mixture of fatty esters, and has been employed as a biofuel in compression-ignition engines. It is obtained by triglycerides transesterification. Normally, methanol is the transesterification agent and sodium methoxide is the catalyst. Glycerol is the coproduct. This technology is well stablished, but the cost reduction is still a challenge. The use of glycerol conjugated base is a possibility. In this work, sodium glyceroxide was evaluated as catalyst in the transesterification of soy oil with methanol. Two Doehlert experimental design[1] were used. In the first set of experiments, methanol/triglyceride molar ratio and catalyst amount were investigated. The optimum conditions were found as 12:1 (methanol/triglyceride) molar ratio and 2 % (catalyst mass/triglyceride mass). Higher molar ratios produce a decrease in reaction conversion (Figure 1). In the second set of experiments, reaction temperature and time were studied. The best result was found when the reaction was carried out at 50 °C in 60 min (Figure 2). The catalyst was employed to other feedstock, including, canola, sunflower, tallow, lard, palm, palm kernel, babassu, and coconut. In all experiments, biodiesel purity was higher than 96.5 %.

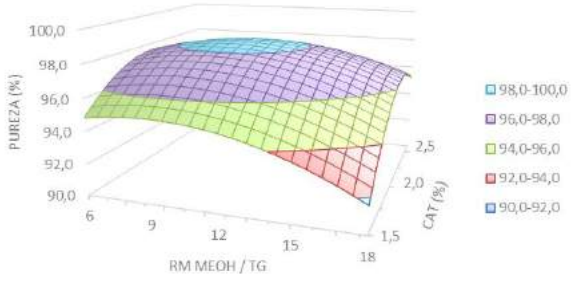


Figure 1 – Effect of the molar ratio (MeOH/TG) and the catalyst amount over transesterification conversion.

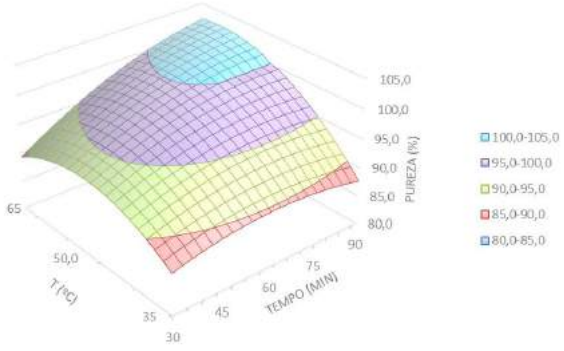


Figure 2 – Effect of the temperature and the reaction time over transesterification conversion.

1. Teófilo, R. F.; Ferreira, M. M.; *Quim. Nova*, **2006**, *29*, 338.

**Área: TEC** **Inscrição: 01231**

# Effect of acetic acid on the pyrolytic sugar yield during fast pyrolysis from several biomasses type

**Geraldo F. David (PQ),[1*] Victor H. Perez (PQ), [2] Sergio A. Fernandes (PQ),[3] Oselys R. Justo (PQ),[4] Valdemar Lacerda Jr. (PQ)[1]**

**geraldo_david@yahoo.com.br**

*[1]Departamento de Química UFES; [2]Departamento de Tecnologia em Alimentos UENF; [3]Departamento de Química UFV; [4]Estácio de Sá UESA.*

keywords: *1,6-anhydro-β-D-glucopiranose, Levoglucosan, Fast Pyrolysis, Pre-treatment, Biomass.*

## Highlights

Biomass from several sources were subjected to acetic acid treatment to improve levoglucosan production. Profiles of volatile pyrolytic compounds reveled high levels of pyrolytic sugar (levoglucosan).

## Resumo/Abstract

The aim of this work was to improve the levoglucosan production from several agro-industrial wastes such as: sugarcane bagasse, elephant grass, husk coffee, husk rice and husk peanut under during thermochemical biomass conversion (fast pyrolysis). Firstly, the biomasses were subjected to acetic acid treatment as an strategy to improve levoglucosan production (1,6-anhydro-β-D-glucopiranose) in the bio-oil. The biomasses were treated with 10% acetic acid solution for 10 min at 90°C, under constant stirring. Then, the biomass was washed with deionized water until neutral pH and subjected to pyrolysis at different temperatures (350°C to 600°C) using a Pyrolysis-Gas Chromatographic/Mass (Py-GC/MS)[1,2]. All biomasses had improved the sugar production compared with the control at different pyrolysis temperatures: sugarcane bagasse (9.33 fold at 400°C), elephant grass (7.5 fold at 400°C), husk coffee (9.5 fold at 400°C), husk rice (7.76 fold at 500°C) and husk peanut (8.21 fold at 550°C). Then, the best pyrolysis temperature to attain highest levoglucosan content was different for each type of biomass. Probably, the attained results can be explained by the removal alkali and alkaline earth metals from the biomass. These results are very attractive for technological applications since levoglucosan can be used as unconventional fermentation substrate to biofuels production like bioethanol.

**References**

[1] David, G.F., Perez, V.H., Justo, O.R., Garcia-Perez, M. (2017) Bioresource Technology 223, 74–83.
[2] Pecha, B., Arauzo, P., Garcia-Perez, M. (2015) Analytical and Applied Pyrolysis.

**Área: TEC** **Inscrição: 01252**

# Colorimetric Paper Indicator Associated with Smarthphone for Formaldehyde Detection in Milk Based and Personal Care Products

**Guilherme B.C. Martins (PG),[1]* Renata R. Sucupira (PG),[1] Paulo A.Z. Suarez (PQ).[1]**

**sucupirarr@gmail.com; guilherme.martins@docente.unip.br**

*1 INCT-CATÁLISE, Laboratório de Materiais e Combustíveis, Instituto de Química, Universidade de Brasília (IQ-UnB), Campus Universitário Darcy Ribeiro.*

Palavras Chave: *Formaldehyde, Colorimetrical indicator, Schiff's reagent, Milk, Cosmetics.*

## Highlights

- A simple way to detect formaldehyde in homemade productis through colors formation
- Low cost and portable detection technology
- The use of smartphones can associate with the detection technique
- The technique can be used in various cosmetics and food, mainly in milk and its derivatives
- Concentrations as low as 0.01 % (v/v) of formaldehyde in milk can be detected

## Resumo/Abstract

Due to its low cost, formaldehyde was used as conservative in hygienic and cosmetic products. However, formaldehyde is strongly reactive and toxic, so its use has been forbidden in several products. Recently, formaldehyde has been illegally added in milk, causing innumerous health problems. In this work we developed a colorimetric paper indicator based on Schiff's reagent, which can be associated with a smartphone application. The paper stabilizes the Schiff's reagent, avoiding its decomposition during short periods. The natural color of the paper indicator remains after the treatment with Schiff's reagent. The tests consist in apply a small amount of the test sample in the paper treated with Schiff's reagent, so that a new color will show up. If pink appears, the presence of formaldehyde is considered negative, whereas if the color purple shows the presence of formaldehyde in the sample can be considered positive. A smartphone application was developed to help people with difficulties or inability to distinguish those colors. The paper indicator successfully detected the presence of formaldehyde in commercial products such as detergents, shampoos and conditioners. Regarding milk-based products, the paper indicator is especially sensitive to detect formaldehyde, clearly identifying concentrations of 0.01% (v/v), as shown in Figure 1. The paper indicator has low cost and can help the supervision of milk and other products, as a trial test in regulatory agencies or for home consumers.

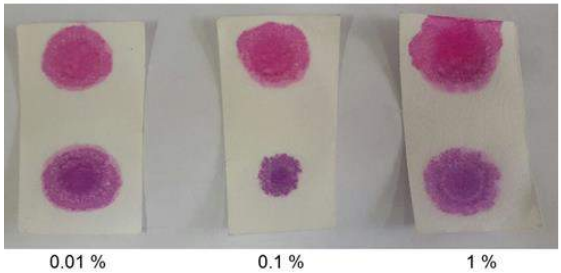


Figure 1. Colorimetric results of the paper indicator in milk. On the top of the paper there is milk without formaldehyde, and below the milk contaminated with formaldehyde in determinated concentrations (v/v).

**Área: TEC** **Inscrição: 01271**

# Ultrasound-assisted demineralization of sugar cane straw with hydrogen peroxide as pre-treatment for biofuel production

**Gustavo V. Motta (PG), Karen Giacobe (IC), Carolina M. Silva (IC), Daniel Santos (PG), Erico M. M. Flores (PQ) e Cezar A. Bizzi (PQ)*.**

***gustavoventtura@hotmail.com, *c_bizzi@yahoo.com.br***

*Departamento de Química, Universidade Federal de Santa Maria – UFSM*

Palavras Chave: *demineralization, sugar cane straw, ultrasound, hydrogen peroxide.*

## Highlights

The presence of metals may impair sugar cane straw fermentation due to catalyst poisoning and enzyme deactivation. Ultrasound-assisted pre-treatment is a promising alternative for biomass demineralization.

## Resumo/Abstract

Sugar cane straw is a by-product generated in large quantities by the alcohol industry. When properly treated and processed, sugar cane straw can produce biofuels (second generation ethanol)[1]. Its pre-treatment involves demineralization, which eliminates unwanted metals and contaminants that cause damages to equipment (clogging and corrosion)[2]. In this study, ultrasound-assisted demineralization (UAD) with $H_2O_2$ was evaluated for sugar cane straw demineralization. The efficiency of the proposed process was evaluated by Ca, K, Mg and Mn determination by ICP-OES. Sugar cane straw was cut into small fragments (5x5x2 mm). Several US systems (bath, probes and cup horn) with different frequencies and nominal power were evaluated (30 min reaction at 50ºC). For proving the US effect for demineralization of sugar cane straw, the process was investigated using mechanical agitation (100 rpm, silent condition) under the same experimental conditions. The total metal concentration was performed by sample digestion in a closed microwave system and further determination by ICP-OES. For the optimization of the UAD conditions a complete $2^4$ order factorial design was performed: time (10, 20 and 30 min); US amplitude (30, 50 and 70%);sample mass (150, 250 and 350 mg); and $H_2O_2$ concentration (5, 10 and 15%).

1. Santos, F., Colodette, J., Queiroz, J. H., Bioenergia e biorrefinaria, Editora UFV,2013.
2. Santos, D., Hidrólise ácida de biomassa assistida por ultrassom para obtenção de furfural.

**Área: TEC** **Inscrição: 01291**

# Extraction and characterization of passion fruit and guava oils from industrial residual seeds and their application as biofuels

**Osvaldo K. Ihara (PG)[1], Guilherme B. C. Martins (PG)[1], Erick Ehlert (IC)[1], Mateus de A. Montenegro (IC)[1], Renata R. Sucupira (IC)[1] and Paulo A. Z. Suarez (PQ).[1]***

**mdamontenegro@gmail.com; psuarez@unb.br**

[1]*LMC - Instituto de Química – Universidade de Brasília, Brasília - DF.*

Palavras Chave: Sustentabilidade, Resíduos, Biocombustíveis, Biodiesel, Bio-óleo.

## Highlights

- Analyses of passion fruit and guava oils from industry residues.
- Good oil content for passion fruit (25 mass%) and guava (9 mass%) residues.
- Both oils composed mainly by linoleic acid (50 %).
- Biodiesel produced from both oils match Brazilian specifications.
- The bio-oils obtained from both oils need further improvement.

## Resumo/Abstracta

The Brazilian legislation requires the addition of biodiesel in commercial diesel at a current content of 8%, tying the biodiesel production to diesel consumption. The food industry relies in a great diversity fruits to obtain different products such as juices, sauces and foods. However, the high quantities of fruits processed leads to tons of residues.[1] The aim of this work is the oil extraction and characterization from two popular industrial residues, guava seeds and passion fruit seeds. Another goal is to study their potential application as raw materials for biodiesel and bio-oil production. The oil content of passion fruit seeds and guava seeds were 25 % and 9 %, respectively. Both oils were predominantly composed of polyunsaturated fatty acids, as can be seen on Table 1. The biodiesel obtained by esterification/transesterification of both seed oils match most of the criteria adopted by Brazilian regulation. The bio-oils obtained by thermal cracking of the oils were mainly composed by hydrocarbons similar to those observed in petroleum diesel. We have shown that it is possible to extract oils from both residues and use them for biofuels production. The biodiesel obtained from both oils match the specified parameters for this biofuel in Brazil. However, the bio-oils from both seeds need a further upgrading process to remove oxygenated compounds and, thus, be used as diesel-like biofuel.

Table 1. Fatty acid composition of Passion Fruit and Guava oils.

| Fatty acid | Passion Fruit (%) | Guava (%) |
|---|---|---|
| C16:0 (palmitic) | 14 | 7 |
| C18:0 (stearic) | 7 | 16 |
| C18:1 (oleic) | 20 | 9 |
| C18:2 (linoleic) | 50 | 52 |
| C18:3 (linolenic) | 1 | <1 |
| Others | 8 | 16 |
| Saturated chains | 21 | 23 |
| Mono-unsaturated chains | 20 | 9 |
| Poly-unsaturated chains | 51 | 52 |

[1] Kobori, C. N., Jorge, N., Ciênc. Agrotec., 2005, 29, 1008-1014.

**Área: TEC** **Inscrição: 01300**

# Continuous ethanol production in an ideal mixing reactor

**Marcelo H. Armoa (PQ),[1] Suelen S. B. da Silva (IC)[1]*, Wagner R. Meyer (PQ)[1].**

**mharmoa@fatecjaboticabal.edu.br; suelen_borges2010@hotmail.com**

*[1]Faculdade de Tecnologia Nilo De Stéfani – FATEC de Jaboticabal - CEETEPS*

Palavras Chave: *Biocatalytic Membrane Reactor, Continuous Fermentation, Ceramic Membrane, Microfiltration, Ultrafiltration, Silica*

## Highlights

Only selected yeasts fermentation; *maintenance of substrate/product level;* high retention of colloids and chromogenic agentes; minimization of by-products (vinasse, fusel oil, higher alcohols); process in ideal mixing reactor.

## Resumo/Abstract

In alcoholic fermentation process, yeasts (Saccharomyces cerevisiae) are added to the wort, converting the substrate into ethanol and carbon dioxide. At high levels, bacterial contamination causes several operational problems. In order, to reduce the contaminating microbial, the sugarcane industries advocate the use of antibiotics and concentrated sulfuric acid in the traditional treatments, increasing costs and generating waste chemicals. The use of the membrane process can increase productivity, operating times, product uniformity and ease of automation, and reduce labor costs and sanitization of the reactors, eliminating the use of anitbiotics / sulfuric acid, as well as allow the removal of the impurities that come with the raw material, thus allowing the necessary nutrients the yeasts are not removed. In this search, the continuous process was carried out, adjusting inflow and outflow of substrate / product in the reactor and the (membrane area exposure/fill reactor) ratio, favoring the withdrawal of ethanol produced, thus in the ideal mixing reactor. The $SiO_2$ macroporous membranes were used to isolate microbiologically the reservoir and wine produced, allowing only the diffusion of substrate (sucrose) and final product (bioethanol). The characterization with refractometer, micro distiller, digital densimeter, optical microscope and gas chromatograph indicates promising results such level maintenance of substrate/product, reduction of secondary compounds, microbiological isolation of the must for fermentation, and fermentation yeasts to the must and wine, obtaining an alcoholic average content of 6,00%.

Figure 1. Biocatalict Membrane Reactor (ideal mixing reactor): a) viability of the fermentation process; b) Substrate (sugar) and product (etanol) contents.

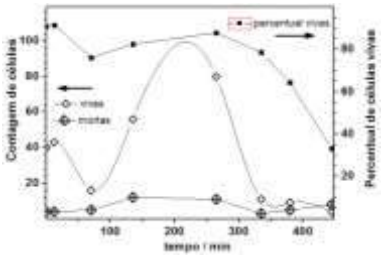


(a)

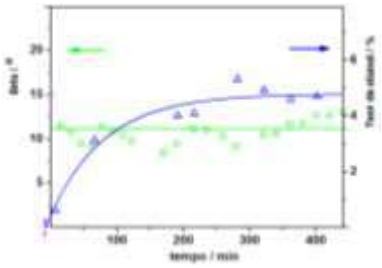


(b)

Table 1. Secundary componentes concentration analysed by gas chromatography (GC).

| Componente | Concentração / mg L$^{-1}$ | |
|---|---|---|
| | Reator de mistura não ideal | Reator de mistura ideal |
| Acetaldeído | 2,57 | 16,94 |
| Acetato de Etila | - | - |
| Metanol | 0,23 | - |
| n-Propanol | - | 1,00 |
| iso-Butanol | 24,32 | 10,63 |
| n-Butanol | 1,13 | - |
| iso-Amílico | 53,42 | 27,71 |
| Furfural | 2,85 | 0,51 |

**Área: TEO** **Inscrição:01036**

# Merging two coarse-grained force fields: Extension of the ELBA force field for dipeptides and lipopeptides through SIRAH force field.

**Rafael Maglia de Souza (PG),[1*] Luis Gustavo Dias (PQ).[1]**

**rafael.maglia.souza@usp.br; lgdias@ffclrp.usp.br**

*[1]Departamento de Química, Faculdade de Filosofia, Ciências e Letras de Ribeirão Preto - Universidade de São Paulo (FFCLRP);*

Palavras Chave: Coarse-grained, Molecular Dynamics, Peptides.

## Highlights

ELBA and SIRAH coarse-grained force field were merged together.
Molecular dynamics simulations of dipeptides and lipopeptides with a coarse-grained force field.

## Resumo/Abstract

The usefulness and importance of molecular simulations to investigate dynamic processes and interactions mechanisms at the molecular level were recognized in the 2013 Nobel Prize in Chemistry for the "development of multiscale models for complex chemical systems ".

Force fields in coarse-grained resolution stand out in molecular dynamics simulations by enabling the achievement of a larger space-time scale. Thus, the focus of this work was the development of a coarse-grained force field that allowed the simulation of self-assembled systems based on dipeptides and lipopeptides. In this sense, the ELBA coarse-grained force field developed for simulations of aqueous biomembranes, and SIRAH coarse-grained force developed for simulations of proteins were merged together into a new and consistent coarse-grained force field.

In ELBA, electrostatics is described by monopoles and dipoles with a shifted and truncated potential. In SIRAH, electrostatics is treated only with monopoles, including long-range corrections based on Ewald techniques. Thus, cross interactions between SIRAH amino acids's beads with ELBA water (a Lennard-Jones sphere with a point dipole) were reparametrized based on the electrostatic charging process through thermodynamic integration until the electrostatic free energy of solvation matches the underlying atomistic reference values. The dispersion-repulsion contribution to the free energy of solvation was also reparametrized adjusting the Lennard-Jones potential parameters.

The optimized parameters obtained with the calibration were applied in the simulation of dipeptides and lipopeptides and the results of these simulations were validated with experimental data and atomistic simulations.

**Área: __TEO_____**
*(Inserir a sigla da seção científica para qual o resumo será submetido. Ex: ORG, BEA, CAT)*

**Inscrição:___00785_____**
*(Inserir o número de inscrição do autor que fez a submissão)*

# Bonding Dissociation Energy of M-NO bonding on $[Ru(L_1)L_2NO]^n$ complexes

**Franciele B. Santos(IC)[1], Sebastião C. da Silva(PQ)[2*]**

**sebastião.claudino@gmail.com; franciele.ufv@outlook.com**

*[1]Instituto de Ciências Exatas e Tecnológicas,UFV; [2]Departamento de Química, UFMT*

Palavras Chave: NO release, DFT, ruthenium complexes

## Highlights

Bonding Dissociation Energy of M-NO bonding on $[ Ru(L_1)L_2NO]^n$ complexes. Theoretical DFT calculation BDE ( Bonding dissociation energy) for Ru-NO bonding were carried out for the complexes $[ Ru(L_1)L_2NO]^n$, where $L_1$ is $NH_3$ and $L_2$ is pyrazine, ammonia or $P(OEt)_3$.

## Resumo/Abstract

Nitric oxide (NO) is involved in a series of biologic process in the human organism, like antitumor activity, blood pressure control and neurotransmissor1. The maximization of that activity depends of the efficient carrier and the proper release rate. Ruthenium complexes of the type *trans*-[Ru (L1) 4 (L2) in] n + are known as efficient NO carriers. The release rate depends on the metal-NO bonding strength, that by your time and affected by intensity of metal link-L2 in the position trans to no. In this work are calculated by *ab initio* DFT method, the bonding dissociation energy (BDE) to three Ruthenium-NO *trans*-$[Ru(L_1)4(L_2)NO]^{n+}$, where L1 is NH3 for all complexes, and L2 is NH3, pyrazine or $P(OEt)_3$. The calculation were performed for both normal ($NO^+$) and reduced (new host.) species. There used the hybrid DFT B3LYP functional and DGDZVP basis for Ru and 6-31+g (d, p) for all the other atoms. The table below shows the results of the calculation for the reaction: $[Ru(L_1)4(L_2)NO] \rightarrow Ru(L_1)_4(L_2) + NO + \Delta E$ .
Values in ($\Delta E^*$ ) are corrected for Free Gibbs Energy

| Electronic energy(($E_h$)) | $\Delta$Ee ($E_h$) | $\Delta$Ee (kcal/mol) | $\Delta E_e$ (EG) | $\Delta E_G^*$ (kcal/mol) |
|---|---|---|---|---|
| $[Ru^{II}(NH_3)_4NH_3NO]^{3+}$ | 0,1162 | 72,9 | 0,0605 | 38,0 |
| $[Ru(NH_3)_4PzNO]^{3+}$ | 0,1013 | 63,6 | 0,0464 | 29,1 |
| $[Ru(NH_3)_4P(OEt)_3NO]^{3+}$ | 0,0883 | 55,3 | 0,0367 | 23,0 |
| $[Ru(NH_3)_4NH_3NO]^{2+}$ | 0,0442 | 27,7 | 0,0409 | 25,7 |
| $[Ru(NH_3)_4PzNO]^{2+}$ | 0,0363 | 22,8 | 0,0329 | 20,6 |
| $[Ru(NH_3)_4P(OEt)_3NO]^{2+}$ | 0,0181 | 11,4 | 0,022 | 13,8 |

Os resultados indicam que a taxa de liberação do ligante NO pode ser otimizada por uma substituição adequada ligante L *trans* ao NO.

1) Karpuzoglu, E.; Ahmed, S.A. Nitric Oxide – Biology and Chemistry 2006,15,117-186.
2) Gorevski, S et all. Electronic spectra of trans-$[Ru(NH3)4(L)NO]^{3+/2+}$ complexes. Inorganica Chimica Acta 300–302 (2000) 698–708.

**Área: TEO** **Inscrição: 00976**

# Directional search algorithm for electrochemical oscillating time-series in a multidimensional parameter space

**Renan C. C. de Miranda (PG) and Raphael Nagao (PQ)***

**renanchimie@gmail.com; nagao@iqm.unicamp.br**

*Institute of Chemistry – University of Campinas (UNICAMP)*

Keywords: *Electrochemical modeling, Numerical integration, Oscillatory behavior*

## Highlights

Development of a directional search algorithm for oscillating solutions through numeric integration; Parameter scanning methods in nonlinear dynamic systems; Recognition of oscillatory patterns;

## Abstract

Definitely, modeling complex electrochemical reactions is not a trivial task. The reaction kinetics, usually described by several independent variables, can be represented by an intricate combination of elementary steps through parallel and consecutive mechanisms. Because of this complexity, it is also extremely difficult to measure rate constants of the elementary steps experimentally which results in an incomplete knowledge of the parameters that drive the system. Therefore, a numerical integration of the model cannot be carried out since several unknown parameters values still have to be implemented. In order to overcome this restriction, we have developed a directional search algorithm for oscillating solutions in a multidimensional parameter space. Overall, the code identifies a set of parameters (rate constants, applied voltage, resistance and etc), where oscillatory behavior (potential or current oscillations) is found, by an adaptive scanning. Firstly, the algorithm integrates the differential equations, built from the kinetic rate laws, with a pre-determined set of parameters, then verifies if the output obeys the stablished criteria for a desired solution such as: characteristics of maximum and minimum points, and the convergence (see the flowchart); if not, the code modifies up to three chosen parameters randomically and iterates until the solution fills the selection criteria. If the criteria are satisfied, concomitantly, the solution is an oscillating behavior, the set of parameters is recorded. If not, the loop starts over. The algorithm is summarized in the following figure.

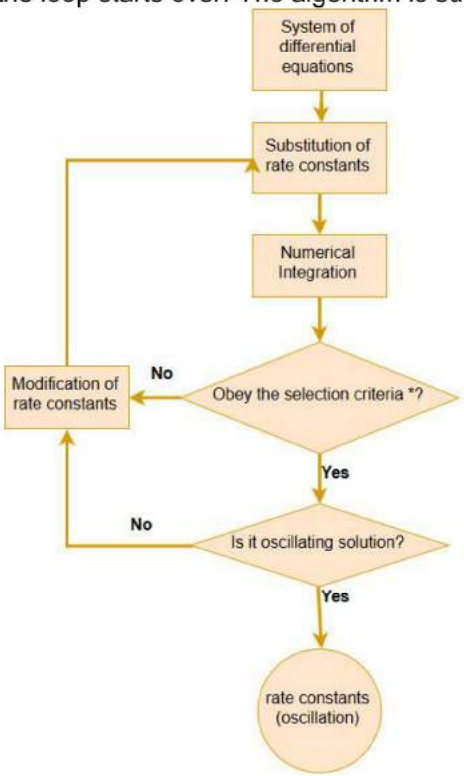


***Criteria that must obey:**

**-Characteristics of maximum and minimum points:**

Numbers;
Values;
Distance between the points;
etc.

**-Convergence:**

There must be no horizontal asymptotes: the time derivatives do not tend to zero when time tends to infinite.

**Área: TEO** **Inscrição: 00857**

# Evaluation of the Power Conversion Efficiencies of Organic Photovoltaic Devices – Theoretical Investigation

**Gabriela Martinez Miranda (PG),[1] Cristiano Zanlorenzi (PQ),[1] Leni Akcelrud (PQ),[1*].**

**gmartinezm92@gmail.com; akleniak@gmail.com**

[1]*Departamento de Química, UFPR.*

Palavras Chave: *Solar Cells, Organic photovoltaic, Power conversion efficiencies.*

## Highlights

Conjugated polymer and semiconductors for solar cells.
Theoretical investigation by methods of quantum chemistry for predicting of the power conversion efficiencies.

## Resumo/Abstract

The use of conjugated, semiconducting polymers as active layers in solar cells is a promising approach for the generation of clean and sustainable energy worldwide. Modifying the electron-withdrawing capability in donor-acceptor (DA) conjugated copolymers allows designing new polymers with better optical properties, being successfully applied in bulk heterojunction solar cell devices, with enhancement of conversion efficiencies (PCE). Recently, a work published by our group [1] reported a theoretical design rule to forecast the best polymer candidates, optimizing the band gap and orbital energy levels of the donor material simultaneously (Figure 1), in mode to obtain PCE values over 10%. This methodology was capable to predict theoretically the best efficiencies imparted by a group of 65 conjugated monomeric units selected from the literature, generating 2080 possible DA combinations. Thus, using the previous methodology, the rationale was to elaborate a methodology that would restrain the number of DA combinations with high probability of achieving enhanced performance, and ten DA pairs were chosen from those due their good correlation with the approach used previously. The DFT method using the B3LYP functional and 6-311g (d,p) basis set was applied to obtain the optimized oligomer's geometries, and the related frontier orbitals energies. Based on the results, it was possible predict the PCE of the copolymers, and the related results obtained showed PCE values between 8 – 9.6%.

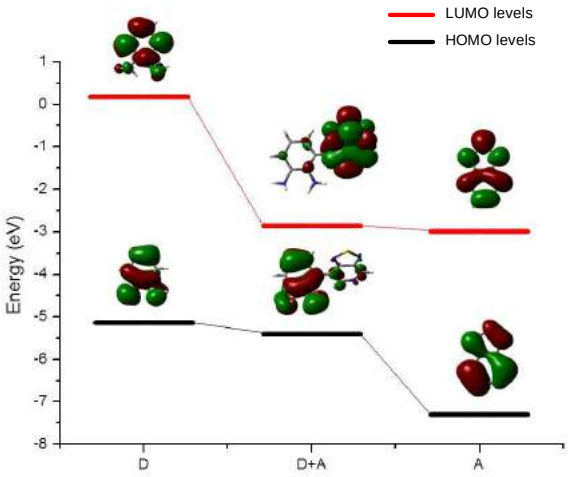


Figure 1: Frontier orbitals of the units DA.

[1] J. Polym. Sci. B Polym. Phys. 2017, 55, 919–927

**Area:** *TEO* **Register:** 01124

# Conformational analysis of chalcone 1-(4-nitrophenyl)-2-propen-3-(4-hydroxy-3-methoxyphenyl)-1-one

**Raphaela P. Guaringue (IC),[1*] Thiago C. Rozada (PQ),[1] Barbara C. Fiorin (PQ)[1].**

**raphaelaguaringue@outlook.com**

[1] *Chemistry Department, State University of Ponta Grossa, UEPG, PR, Brazil.*

Keywords: *Chalcone, Conformational analysis, Theoretical calculations, NBO*

## Highlights

The conformational analysis of chalcone was conducted by means of theoretical calculations in order to find the most stable conformation. By observing the interactions between ligand and anti-ligand orbitals, the *s-cis* conformations were seen to have a greater stabilizing effect (hyperconjugative).

## Abstract

Chalcones can be classified as α,β-unsaturaded ketones. They have been focus of attention due to the rich variety of biological activities they present as a function of their different substituents. Aiming to better understand and describe such structures, this work proposes the conformational analysis of chalcone represented in Figure 1 below. Theoretical calculations were employed to both determine the structures involved in the equilibrium and understand the stereoelectronic effects involved.

**Figure 1:** Chalcone (CHAL) structure, and its dihedral angles investigated.

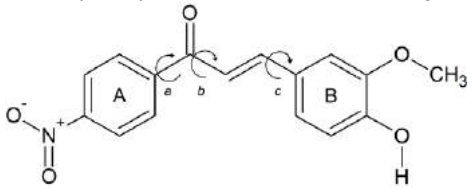


The chalcone was submitted to theoretical calculations using the GAUSSIAN 09 program and NBO 5.9 module for the calculations involving the natural bonding orbital theory. First, a selection of the most stable conformers was carried out through potential energy surface calculations as a function of the dihedral angles *a, b* and *c* (Figure 1) employing the HF/6-31G level of theory. From the six minimum energy points found, optimization and frequency calculations at M06-2X/6-311++G (2d, 2p) obtaining four different conformations.

Two conformers with carbonyl and double bond *s-cis* oriented, and another two conformers in *s-trans.* From this data, NBO calculations were carried out at the same level of theory of the optimizations to verify the influence of the hyperconjugative effect in the conformers stabilization. The interactions involving the ligand and anti-ligand orbitals were evaluated (Table 1).

**Table 1:** Relative energies, dihedral angles and the sum of orbital interaction energies ($\pi \rightarrow \pi^*$) of the conformers.

| Compound | ΔE (kcal/mol) | Dihedral angles a | b | c | Sum of orbital interactions (kcal/mol) |
|---|---|---|---|---|---|
| CHAL *s-cis* | 0.05 | 156.81 | 6.60 | 177.93 | 914.12 |
| CHAL *s-cis'* | 0.00 | 158.15 | 7.34 | 177.14 | 914.03 |
| CHAL *s-trans* | 0.45 | 139.59 | 158.40 | 177.91 | 901.89 |
| CHAL *s-trans'* | 1.24 | 140.58 | 156.06 | 170.09 | 899.58 |

Both *s-cis* conformations were more stable due to the planarity of the structure, which favored orbital interactions of the type $\pi \rightarrow \pi^*$, showing that this effect contributes more effectively to the stabilization of these structures.

**Área: TEO**
*(Inserir a sigla da seção científica para qual o resumo será submetido. Ex: ORG, BEA, CAT)*

**Inscrição: 793**
*(Inserir o número de inscrição do autor que fez a submissão)*

# Theoretical Study of Structural and Thermodynamic Properties for Ibuprofen Synthesis Mechanism

**Leonardo Viana das Chagas Lima (PG)[1] ; Nelson Henrique Morgon (PQ).[1]***

**morgon@iqm.unicamp.br**

[1]*Instituto de Química da UNICAMP*

Palavras Chave: *Ibuprofen, ECD, G4MP2, TDDFT.*

## Highlights

Ibuprofen ((R, S) -2- (4- (2-methylpropyl) phenyl) propanoic acid) is one of the most well known and used in its racemic form, in the treatment of fever, pain and inflammation. Ibuprofen Synthesis Mechanism. Until the early 1990's, industrial synthesis of the compound was almost exclusively by the Boots route. The Boots-Hoechst-Celanese (BHC) synthesis has been used as a model of green chemistry.

## Resumo/Abstract

Ibuprofen ((R,S)-2-(4- (2-methylpropyl) phenyl) propanoic acid), a non-steroid derived from 2-arylpropionic acid, is one of the most widely used (in its racemic form) in the treatment of fever, pain, and inflammation. Initially its synthesis, patented by Boots Pure Drug Company(known by BOOTS route), involved several steps, substantial formation of inorganic salts and low atomic efficiency. Subsequently, an alternative route was developed, by partnership between Boots and Hoechst Celanese (The BHC route). This route is characterized by three steps only, having a high atom economy and a low-waste production. The objective of this study was to evaluate the ibuprofen synthesis considering both routes. The mechanism was studied from the energetic point of view, in addition, the chirality of ibuprofen was analysed using of chiroptic methods. Thermodynamic properties were calculated using G4MP2 method. The energy profile of the BHC route (ΔG = -17,36 kcal/mol) was described by few steps in comparison with the BOOTS route. Time-dependent density functional theory (TDDFT) was employed for theoretical calculations of electronic circular dichroism (ECD). The chiral properties of the enantiomers were evaluated at the CAMB3LYP/GTLargeXP level of theory and quantitative agreement between the theoretical prediction and experiment was observed. All calculations were carried out with the GAUSSIAN 09 program.

**Área: TEO** **Inscrição:01010**

# Análise computacional dos isômeros do Espiropirano e suas possibilidades de formar complexos de Cobalto(II)

**Catarina Sampaio Furlani (IC)*** [1], **Izadora Fonseca Reis (PG)**[1], **Juliana Fedoce Lopes (PQ)**[1].

**furlanicat@gmail.com**

[1]*Laboratório de Química Computacional - LaQC, Instituto de Física e Química, UNIFEI.*

Palavras Chave: *Isomeria, TDDFT, NBO, Complexos de Coordenação.*

## Highlights

Computational analysis of Spyropiran isomers and their ligand possibilities to complex with cobalt(II). Spyropiran is a photochromic molecule under UV and temperature changes. This work presents a computational analysis of their isomers potential as ligand on coordination with cobalt(II).

## Resumo

O espiropirano é uma molécula fotocrômica que apresenta colorações diferentes e, consequentemente, propriedades diferentes de acordo com a forma isomérica. Agentes como a radiação UV, temperatura e até o meio solvente podem contribuir para deslocar o equilíbrio (KLAJN, 2014). Neste trabalho, a molécula de espiropirano é apresentada com um radical ácido propílico ligado ao nitrogênio da parte de indolina, como sintetizado pelos colaboradores experimentais.

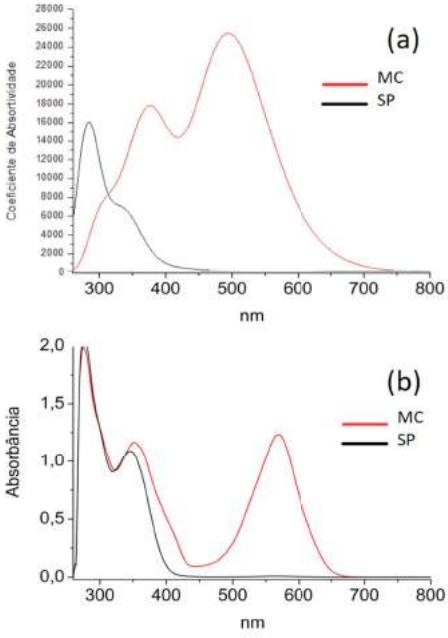


*Figura 1: Espectros de UV-Vis (a) por método computacional e (b) por método experimental do espiropirano- SP (preto) e da merocianina- MC (vermelho).*

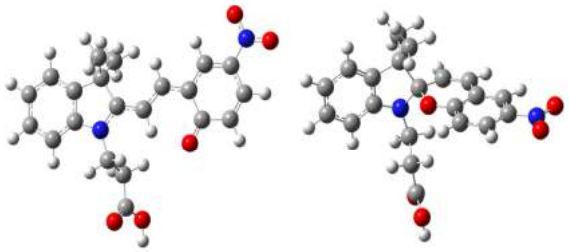

*Figura 2: Estrutura dos isômeros merocianina (à esquerda) e espiropirano (à direita).*

Com o objetivo de estudar as diferenças estruturais dos dois isômeros, espiropirano e merocianina, foram otimizadas as duas formas usando o conjunto de funções de base 6-31g(d,p) com o funcional DFT B3LYP. Para a obtenção do espectro teórico de UV-Vis foram calculadas 10 transições TDDFT, que posteriormente foram comparadas com o espectro obtido experimentalmente. Os dois apresentaram resultados muito similares, incluindo o desaparecimento da banda de maior λ para a merocianina (MC), que não aparece no espectro da forma espiropirano (SP)

Entretanto, para avaliar as possibilidades de coordenação com o Cobalto, foram obtidas as cargas atômicas pelo método NBO.

O esperado para poder se coordenar ao Cobalto são grupos doadores de densidade eletrônica. Portanto, a partir do cálculo de carga, pode-se inferir que o grupo nitro e os oxigênios da carboxila e da carbonila são os mais prováveis de se coordenar ao metal.

Para o estudo com Co(II) utilizou-se a função de base 6-31g(d,p) e o metal com geometria pentacoordenada, completando-se as valências com água. Contando com estes cálculos que ainda estão em andamento, até a data do evento em questão será apresentada a análise eletrônica pronta e os modos de coordenação mais estáveis.

**Agradecimentos:** FAPEMIG, CNPq, e DPI/UNIFEI.

KLAJN, Rafal. Spiropyran-based dynamic materials. **Chemical Society Reviews**, v.43, n.1, p.148-184, 2014.

**Área: TEO** **Inscrição:** 00102

# In silico methods applied in forensic science: simulated NMR spectra of new amphetamine- and cathinone-derived psychoactive substances.

**Caio Henrique Pinke Rodrigues (PG)[1], Victor Oliveira Assis (IC)[1], Jean Fernandes (IC)[1], Guilherme Dias (IC)[1], Aline Thaís Bruni (PQ)[1,2]***

**caio.pinke.rodrigues@usp.br; aline.bruni@usp.br**

[1]*Departamento de Química, FFCLRP – USP – RP*
[2]*Instituto Nacional de Ciência e Tecnologia Forense (INCT Forense), Ribeirão Preto/SP*

Keywords: *New Psychoactive Substances; Amphetamines; Cathinones; Forensic Science; Theoretical Calculations; NMR*

## Highlights

We simulate NMR spectra of amphetamine and cathinone NPS.
We use in silico methods to perform the study.
Theoretical spectra match experimental ones.
The simulated spectra are able to identify NPS.

## Abstract

New Psychoactive Substances (NSP) are synthetic compounds which mainly intend to mimic recreative effects of controlled substances and avoid their identification. There are many properties related to these drugs that are still unknown. Forensic Scientists have a great demand for information that are important for both law enforcement as for human rights guarantees. In silico methods present great potential to help to characterize these substances. The main goal of this work was use theoretical methods to foresee NMR spectra for pairs of similar amphetamines and cathinones. Structures were optimized by B3LYP/6-31G**. NMR spectra were generated by different in silico free softwares: ORCA 4.0.1 (B3LYP and PBE0, 6-31G**) and nmrdb.org. MestReLab, a commercial software, was also used. Available experimental data were compared by Principal Component Analysis (PCA). Results showed that both free and commercial softwares had good predictions. However, B3LYP/631G** ORCA calculations were more precise despite more time consuming.

**Área: TEO** **Inscrição:__646_____**

# Quantum mechanical molecular dynamics of liquid water – SCC-DFTB method reparametrized

**Maicon P. Lourenço (PQ),[1] Egon C. Dos Santos (PG),[2] Lars G. M. Pettersson (PQ),[3] Hélio A. Duarte (PQ)[2].**

**duarteh@ufmg.br; maiconpl01@gmail.com;**

*[1]Departamento de Química e Física -- CCENS, UFES; [2]Departamento de Química-ICEx, UFMG; [3]University of Stockholm, Suécia.*

PalavrasChave: SCC-DFTB, water, molecular dynamics, parameterization.

## Highlights

The FASP program was used, together with the Reverse Monte Carlo method (RMC), to obtain the SCC-DFTB repulsion energy ($E_{rep}$) for the O-X (X = H, O) in order to reproduce the experimental radial distribution function of liquid water. The method will permit to explore the water/solid interfaces using realistic molecular models.

## Resumo/Abstract

The SCC-DFTB is an approximate DFT method that permit to perform large scale calculations quantum-mechanically. Recently we have developed a method to automatize the parameterization of the SCC-DFTB. Born-Oppenheimer Molecular Dynamics (BOMD) at the SCC-DFTB potential energy surface has been envisaged to describe chemical systems that the water is a reactant such as water/metal oxides interfaces.
The SCC-DFTB parameters for water was initially obtained by the FASP[1] program and refined using the Reverse Monte Carlo approach[2] using the following thermal equation:

$$E_{rep}^{i+1} = E_{rep}^{i} - k_B T ln(\frac{g_{OX}^{i}(r)}{g_{OX}^{exp}(r)}); \quad (1)$$

where $g_{OH}^{i}(r)$ and $g_{OX}^{exp}$ are the Radial Distribution Function (RDF) of the O-X (X = H, O) from SCC-DFTB calculations and experiment, respectively; $E_{rep}^{i}$ is the *i*th SCC-DFTB repulsion energy, $k_B$ is the Boltzmann constant and $T$ is the temperature; $E_{rep}^{i+1}$ is the corrected repulsion. The RDFs for O-O and O-H are shown at Figure 1. The experimental O-H and O-O RDF were obtained from the RMC method and a O-O benchmark from references [3] and [4], respectively. The results are in very good agreement with the experimental data [3,4]. The geometrical and dynamic properties of the water in different temperatures will be presented and discussed in details. Preliminary results concerning the water/solid interface will be briefly presented.

(Acknowledgments: CNPq, FAPEMIG, CAPES).

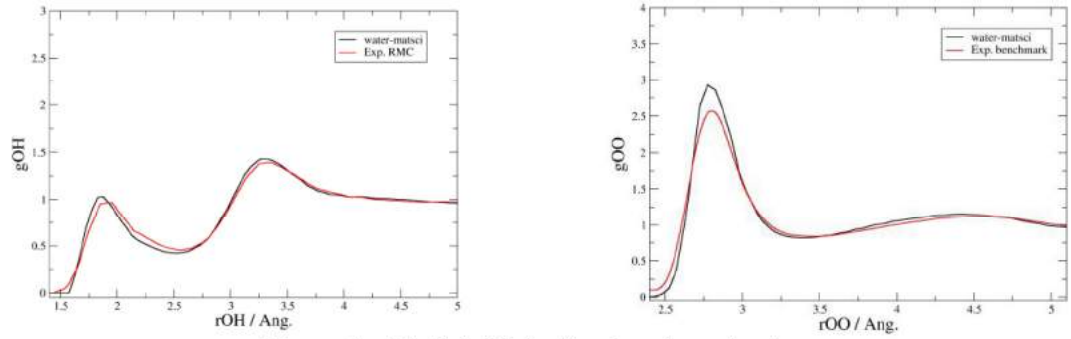


Figure 1 – Radial distribution function of water.

References:

1. Lourenço, M. P.; da Silva, M. C.; Oliveira, A. F.; Quintão, M. C.; Duarte, H. A., Theor. Chem. Acc., 135 (2016).
2. Goyal, P.; Qian, H. J.; Irle, S.; Lu, X. Y.; Roston, D.; Mori, T.; Elstner, M.; Cui, Q.; J. Phys. Chem. B., 118 (2014).
3. Wikfeldt, K. T.; Leetmaa, M.; Ljungberg, M. P.; Nilsson, A.; Pettersson, L. G. M.; J. Phys. Chem. B., 113 (2009).
4. Skinner, L. B.; Huang, C. C.; Schlesinger, D.; Pettersson, L. G. M.; Nilsson, A.; Benmore, C. J.; J. Chem. Phys., 138 (2013).

**Área: TEO** **Inscrição: 00905**

# Topological study of interactions between some inhibitors and ALK-5 using QTAIM methodology

**Michell de O. Almeida (PG),[1] Sergio H. D. M. Faria (PG),[2,3] Káthia Maria Honório (PQ),[4]**

*[1]Centro de Ciências Naturais e Humanas, UFABC; [2]Departamento de Química, UNICAMP; [3]Instituto de Ciências da Saúde, UNIP; [4]Escola de Artes, Ciências e Humanidades, USP*

Keywords: Cancer, ALK-5, Inhibitors, QTAIM.

## Highlights

Activin kinase type 5 (ALK-5) is a biological target related to some types of cancer. Inhibition of this target may be a form of cancer treatment. Six ALK-5 inhibitors were studied and the intermolecular interactions (hydrogen bonds) were evaluated using the QTAIM technique.

## Abstract

Activin kinase type 5 (ALK-5) is a biological target related to some types of cancer, such as breast cancer, being that the inhibition of this target is a strategy that has been studied as a way to treat cancer. Therefore, the objective of this work is to use the computational chemistry to evaluate the main interactions that occur between the main residues at the active site of ALK-5 (Lys232, Glu245, Tyr249, His283, Asp351 and one structural water) and six inhibitors of this biological target[1,2]. In this way, the intermolecular hydrogen bonds that occur between the six inhibitors and the active site of ALK-5 were evaluated using the QTAIM method (AIMALL software)[3,4]. Table 1 shows the values of electron density (ρ) and Laplacian of electron density ($\nabla^2\rho$) for bonds critical points (BCPs) for these interactions.

**Table 1.** Values of ρ and $\nabla^2\rho$ for the BCPs of interactions that occur between inhibitors and ALK-5

| Inhibitor Receptor | BCPs | ρ (a.u.) | $\nabla^2\rho$ (a.u.) | Inhibitor Receptor | BCPs | ρ (a.u.) | $\nabla^2\rho$ (a.u.) |
|---|---|---|---|---|---|---|---|
| Inhibitor 1 + $H_2O$ | N1 - H54 | 0.01 | 0.04 | Inhibitor 1 + Tyr249 | H18 - N27 | 0.02 | 0.07 |
| Inhibitor 1 + His283 | H10 - N31 | 0.01 | 0.04 | Inhibitor 2 + $H_2O$ | N9 - H54 | 0.02 | 0.05 |
| Inhibitor 2 + His283 | N30 - H72 | 0.02 | 0.04 | Inhibitor 3 + $H_2O$ | N16 - H60 | 0.01 | 0.03 |
| Inhibitor 3 + His283 | N28 - H65 | 0.01 | 0.04 | Inhibitor 4 + His283 | N15 - H68 | 0.01 | 0.03 |
| Inhibitor 5 + His283 | N16 - H68 | 0.01 | 0.03 | Inhibitor 6 + His283 | N16 - H60 | 0.01 | 0.03 |

Table 1 shows that ρ and ∇2ρ for both interactions are positive, confirming the electronic character of a hydrogen bond from the QTAIM theory. From QTAIM it is possible to evaluate the chemical interactions from an electronic point of view. Finally, the results also showed that the strongest binding between inhibitors and ALK-5 occurs between the inhibitor 1 (the most active, $IC_{50}$ = 0.57 nM) and Tyr249.

## References

[1] D. Kim, *et al.* Bioorg. Med. Chem. Lett. 21, 6049 (2011).
[2] D. Kim, *et al.* Bioorg. Med. Chem. Lett. 18, 4459 (2010).
[3] Richard. F. W. Bader, Acc. Chem. Res. 18, 9 (1985).
[4] AIMAll (Version 17.11.14), Todd A. Keith, TK Gristmill Software, Overland Park KS, USA, 2017.

## Acknowledgments

The authors would like to thank FAPESP, CAPES and UFABC for the financial support.

**Área: TEO** **Inscrição: 00462**

# LC-ωPBE: an appropriate DFT functional for a reliable description of transition energies in phthalocyanines

**Leonardo H. F. Silva (IC), Bruno P. Caixeta (PG), Antonio E. H. Machado (PQ)***

**aehmachado@gmail.com**

*Laboratório de Fotoquímica e Ciência de Materiais, Instituto de Química, UFU*

Keywords: *Transition energies, Q and B bands, Zn(II) phthalocyanines, DFT and TD-DFT, LC-ωPBE, CAM-B3LYP.*

## Highlights

Appropriate fit of the range separation parameter in LC-ωPBE; TD-DFT approach; Peak energies related with the Q and B bands of phthalocyanines; Minimum discrepancy compared to the experimental data.

## Resumo/Abstract

Phthalocyanine derivatives have been used in many fields as an important functional material[1-3]. Catalysis, optical disks, photodynamic therapy, are some applications of devices involving such compounds. Their useful properties are correlated to efficient electron transfer abilities[1], related to $^1(\pi\rightarrow\pi^*)$ transitions involving Q and B bands.[1]

In a previous study[4], in order to define a most appropriate TD-DFT methodology to study the photoinduced charge transfer from phthalocyanines to semiconductor oxides[5], the LC-ωPBE hybrid functional,[6] among a series of DFT functionals, showed to be the most suitable. Adjusting the range separation parameter (ω)[6] it was possible to estimate with minimum discrepancy compared to the experimental data, the energies of the highest intensity electronic transitions related to Q and B bands ($\mathbf{E_Q}$ and $\mathbf{E_B}$). In this communication, we present results on the implementation of this methodology to Zinc (II) phthalocyanine (ZnPc) and some tetrasubstituted derivatives. The solvated structures (DMSO)[7] were optimized using the M06[8] functional combined with the DZP-DKH atomic basis set[9]. For ZnPc the ω capable to give a good convergence for $\mathbf{E_Q}$ and $\mathbf{E_B}$ was estimated as being 0.17 bohr$^{-1}$. This value was then applied for the other phthalocyanines, **Table 1**. Similar estimates using the CAM-B3LYP[10] exchange-correlation hybrid functional resulted in high deviations for $\mathbf{E_B}$. All calculations were performed in Gaussian09[12].

The results suggests that LC-ωPBE with the proper fit of the ω parameter, furnishes with controlled discrepancy the energies of the highest intensity electronic transitions related to Q and B bands.

**Table 1.** Energies of the highest intensity transitions related to Q and B bands for Zn(II) phthalocyanine and some derivatives, calculated using LC-wPBE[6] and CAM-B3LYP,[10] and their deviations with respect to the experimental data.

| Compound | Functional[a] | Transition energy/eV (Deviation/%) | |
|---|---|---|---|
| | | Q band | B band |
| Zinc (II) phthalocyanine | LC-ωPBE | 1.968 (6.67) | 3.823 (6.70) |
| Zinc (II) phthalocyanine | CAM-B3LYP | 1.935 (4.88) | 4.108 (14.65) |
| 4-carboxi,13,22,31-triamino Zinc(II) phthalocyanine[b] | LC-ωPBE | **Qx**: 1.823 (2.65)<br>**Qy**: 1.924 (6.12) | 3.796 (7.78) |
| 4-carboxi,13,22,31-triamino Zinc(II) phthalocyanine[b] | CAM-B3LYP | **Qx**: 1.862 (4.84)<br>**Qy**: 1.964 (8.33) | 4.122 (17.04) |
| Tetra(*tert*-butyl) Zinc(II) phthalocyanine[c] | LC-ωPBE | 1.990 (8.80) | 3.876 (8.78) |

[a]ω=0.17 bohr$^{-1}$ for LC-ωPBE; [b]Synthesized in our laboratory; [c]Ref. 11.

**Acknowledgements:** To CNPq and FAPEMIG.

## References

[1]Kadish, K. M., Smith, K. M., Guilard, R. (Eds.), *The Porphyrin Handbook*, v. 17. Academic Press. San Diego, Ca, USA, **2017**; [2]Machado, A. E. H. et. al., *Int. J. Photoenerg.*, **2008**, Article ID 482373; [3]Tomazini, M. V. et. al., *An Bras Dermatol.* **2007**;82(6):535-541; [4]Silva, L. H. F., Machado, A. E. H., Souza, J. R., *XXXI ERSBQ MG*, **2017**; [5]Araújo, D. M. S. et al., *Proc. Quím.*, **2015**, 9:73-76; [6]Vydrov, O. A., Scuseria, G. E., *J. Chem. Phys.*, **2006**, 125:234109; [7] Scalmani, G., Frisch, M. J., *J. Chem. Phys.*, **2010**, 132:114110; [8] Y. Zhao, Y., Truhlar, D.G., *Theor Chem Acc.* **2006**, 120: 215–241; [9]Jorge, F. E., et. al., *J. Chem. Phys.*, **2009**, p.130, 064108; [10] Yanai, T., Tew, D. P., Handy, N. C., *Chem. Phys. Lett.*, **2004**, 393:51-57; [11]Isago, H. (Ed.), *Optical Spectra of Phthalocyanines and Related Compounds: A Guide for Beginners*. NIMS Monographs. Springer, Japan. **2015**; [12]Frisch, M. J. et al., Gaussian 09 rev. E.01, Gaussian, Inc., **2015**.

**Área:***TEO* **Inscrição:***00904*

# Inhibition Mechanism of Monoamine Oxidase B by Propargylamines: Molecular Docking and Quantum-Chemical Approaches

**Elaine F.F. da Cunha (PQ)**[1] **, Teodorico de Castro Ramalho (PQ)**[1]

**elaineffdacunha@gmail.com ou elaine_cunha@dqi.ufla.br; teodorico.ramalho@gmail.com**

[1]*Departamento de Química, UFLA, Lavras, MG*

Palavras Chave: *Monoamine oxidase B, Irreversible inhibition, Propargylamines, Theoretical calculation.*

## Highlights

MAO-B represents a target for the treatment of neurodegenerative disorders; Rasagiline analogs are irreversible MAO-B inhibitors; Theoretical tools were used to understand the inhibition mechanism.

## Resumo/Abstract

The flavin-containing monoamine oxidases B (MAO-B) is an outer mitochondrial membrane-bound enzyme that catalyzes the oxidative deamination of arylalkylamine neurotransmitters, such as serotonin and dopamine, and has been a target for a number of clinically used drug inhibitors. Rasagiline is a potent and selective inhibitor of MAO B and the inhibition of the enzyme results in the formation of a covalent N(5) flavin adduct [Bimda C. et al., *J. Med. Chem.* **2015**, 48, 8148-8154], as can be observed in the crystallographic structure of Rasagiline docked into the MAO-B cavity (PDB:1S2Q). In this work, theoretical techniques were used to study possible mechanisms of MAO-B inhibition (Scheme 1) by 12 propargylamines analogs [Huleatt P.B. et al., J. *Med. Chem.* **2015**, 58, 1400-1419], considering neutral, cationic, anionic, and radical complexes. The choice of these compounds can help us to answer questions about the *para*-substitution effect on inhibitors's reactivity. First, for the formation of covalent adducts between the co-factor and inhibitors, molecular docking was used. Second, all molecular geometries were optimized at the B3LYP/6–31G(d,p) level. Atomic charges were obtained by the NBO analyses. Frequencies and transition state structures were computed analytically at the same level of theory as the geometry optimizations to confirm whether the obtained structures were minima or transition states and to obtain zero-point energy corrections. The results show that the anionic mechanism is the most plausible.

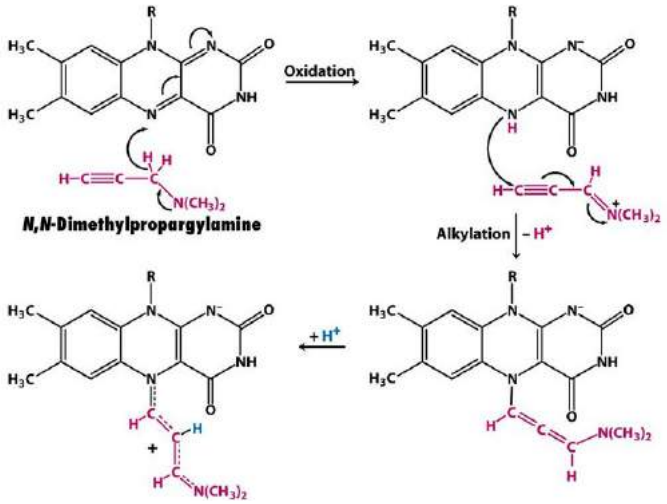


Scheme 1. Model of mechanism-based MAO-B inhibition.

**Área: ___TEO_____** *(Inserir a sigla da seção científica para qual o resumo será submetido. Ex: ORG, BEA, CAT)*

**Inscrição:___1227_____** *(Inserir o número de inscrição do autor que fez a submissão)*

# Free Energy Profile of Alkyl Mesylate Fluorination with CsF Promoted by BACCA in *tert*-butanol Solvent

**Josefredo R. Pliego Jr. (PQ).[1]***

***pliego@ufsj.edu.br**

[1]*Departamento de Ciências Naturais, UFSJ.*

Palavras Chave: *(nucleophilic fluorination, supramolecular catalysis, solvent effect, crown ether, bulk alcohols).*

## Highlights

- The BACCA solubilizes and activates the CsF salt for nucleophilic fluorination of alkyl mesylate.
- The two *tert*-alcohol units of BACCA interacts with the centers of charge of the $S_N2$ transition state via double hydrogen bonds.
- Theoretically predicted free energy barrier is in excellent agreement with the experimental data.

## Resumo/Abstract

The increased importance of organofluorine compounds has demanded the development of efficient catalyzed fluorination methods with cheap, available and nontoxic fluoride salts, such as potassium and cesium fluorides. Theoretical methods can play an important role in the design of catalysts, providing insights on how to solubilize and activate these fluoride salts for nucleophilic fluorination. In this work, the mechanism and free energy profile of nucleophilic fluorination of alkyl mesylate by the new bis *tert*-alcohol-functionalized crown-6-calix[4]arene (BACCA), reported by Jadhav *et al.*[1] was investigated by theoretical calculations at M06-2X/ma-def2-TZVPP//PBE/ma-def2-SVP level of theory, including solvent effect at SMD level. The present study shows that the BACCA is able to solubilize the CsF salt with a free energy of 8.9 kcal $mol^{-1}$. The transition state for nucleophilic fluorination has a calculated free energy barrier of 18.4 kcal $mol^{-1}$, resulting to an overall barrier of 27.3 kcal $mol^{-1}$. This theoretical value is in excellent agreement with the experimental value of 26.2 kcal $mol^{-1}$. The mechanism of activation involves the formation of two hydrogen bonds between the centers of charge of the $S_N2$ transition state and the *tert*-alcohol units in BACCA, as presented in the Figure below.

**References:**

(1) Jadhav, V. H.; Choi, W.; Lee, S.-S.; Lee, S.; Kim, D. W. *Chem. Eur. J.* **2016**, *22*, 4515

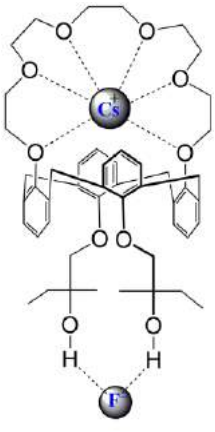


BACCA interacting with CsF

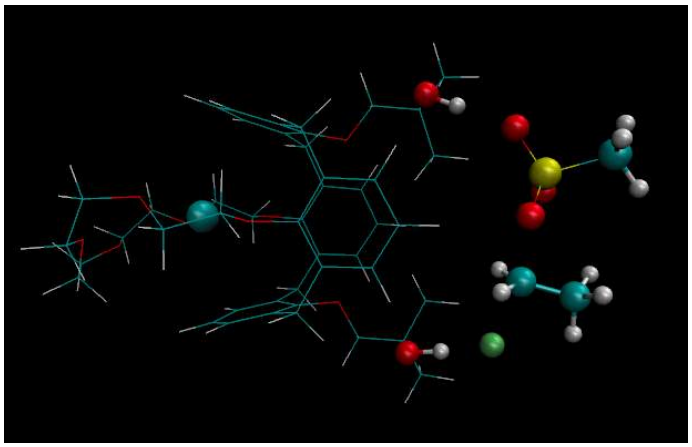

**Transition state**

**Área: TEO** **Inscrição: 01132**

# Computational evaluation of the effectiveness of Cu and Pt catalysts in the first steps of ethanol reforming

**Marcela M.L. Tormena (PG),[1] Rodrigo M. Pontes (PQ).[1*]**

**marcelamarta@icloud.com; rmpontes@uem.br**

[1]*Departamento de Química, UEM*

Palavras Chave: *Computational Chemistry, DFT, Ethanol Reforming, Catalysis, Metal clusters.*

## Highlights

The mechanism for the decomposition of ethanol over Cu and Pt has been investigated; Cu presents higher activation energy for a crucial step; the findings are coherent with the experimental observations.

## Resumo/Abstract

The production of hydrogen for fuel cells from ethanol is one of the most interesting processes for sustainable energy production in the near future. The availability of computational resources and the increasing capabilities of quantum mechanics methods have made possible to advance studies about chemical reactions without the need of an extended (and expensive) empirical investigation. In this work, the first steps for the mechanism for ethanol decomposition over Cu and Pt has been investigated. Catalysts nanoparticles were mimicked by the respective metal clusters (5 atoms of Cu or Pt). The ground states (GS) and transitions states (TS) of the reaction path were optimized using the GAMESS software [1]. Calculations ran with the B3LYP-D3 functional combined with the SBKJC ECP basis set for the metals and 6-31+G(d,p) for the remaining atoms. Figure 1 shows the relative energies, over the reaction path, for both catalyzers.

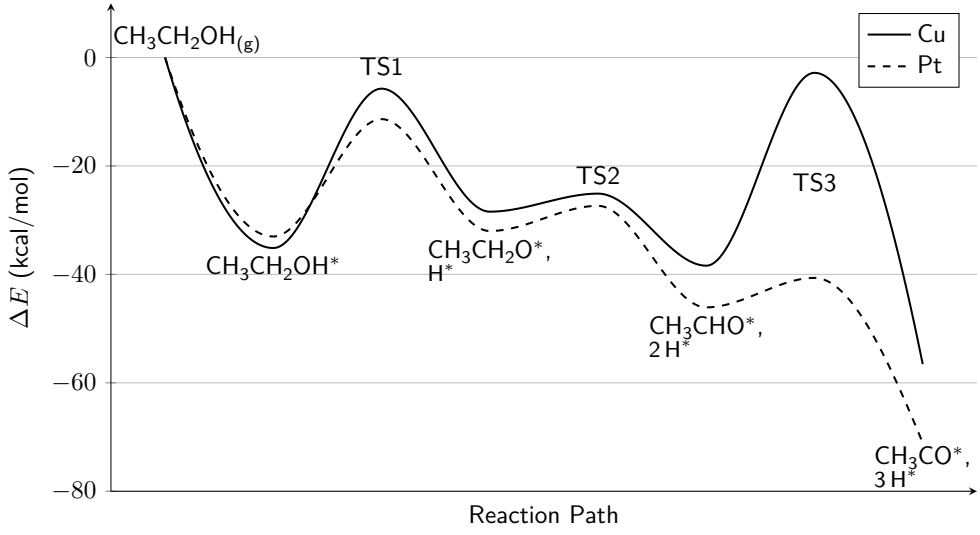


*Figure 1: Relative energies over reaction path. The '*' indicates that the molecule is attached to a metallic cluster.*

The first two steps, starting from the adsorbed ethanol molecule, are relatively similar for the two catalysts, with a small advantage in favor of Pt. However, the third step, the one responsible for acetaldehyde formation, clearly separates the two catalysts. Cu presents a substantially higher activation energy, and this justifies the well-known fact that Cu is much less efficient than Pt. A discussion about this difference will be presented.

References

[1] SCHMIDT, M.W. et al. The GAMESS program. **J. Comput. Chem.**, v. 14, p. 1347, 1993.

# A


Abdelraheem, W.; AMB-048
Abram, U.; INO-007, INO-038
Abreu Filho, P.; EDU-035
Abreu, D. S.; INO-004
Abreu, T. P.; AMB-038
Accioly, J. E. S.; AMB-070
Acevedo, M. S. M. S. F.; ANA-016
Adaime, M. B.; AMB-020
Adati, R. D.; INO-011, INO-037, INO-052
Afonso, B. A.; CAT-024
Agostinho, S. M. L.; EDU-053
Agouram, S.; INO-101
Agudelo, A. J. P.; COL-005
Aguiar De, V. M.; ORG-040
Aguiar, A. C. C.; MED-039
Aguiar, E. C.; MED-032
Aguiar, F. C. L.; FIS-033
Aguiar, L. M.; ANA-029
Aguiar, L. O.; ORG-035
Aguiar, L. P.; CAT-025
Aguilar, M. G.; QPN-110, QPN-120
Aguillón, A. R.; ORG-032, ORG-046
Akahoshi, L. H.; EDU-039
Akcelrud, L. C.; MAT-001, MAT-002, MAT-056, MAT-090, MAT-096
Akcelrud, L.; MAT-079, TEO-004
Akcelrud, Leni; MAT-117
Akiba, A. N.; AMB-045
Albano, R. L. B. S.; MAT-060
Alberici, L. C.; QPN-119
Albert, A. L. M.; ANA-093
Albino, J.; AMB-031
Albuquerque, G. Z. Q.; EDU-053
Albuquerque, JFC; MED-037
Albuquerque, M. G.; MED-053
Albuquerque, S.; INO-036
Alcantara, A. C.; ELE-010
Alcântara, G. P.; MED-054
Aldighieri Grigorovski Júnior, J. M.; INO-056
Alexandre, L. S.; QPN-088
Alexiou, A. D. P.; INO-083
Alhadas, R. D.; INO-050
Allegretti, S. M.; QPN-073
Almeida, C. A. P.; COL-013
Almeida, C. L. da C.; MAT-033
Almeida, F. A. F.; ANA-070
Almeida, F. G.; ELE-047
Almeida, G. A.; ANA-064
Almeida, G. B.; EDU-002
Almeida, G. C.; MAT-037, MAT-083
Almeida, I. A.; MED-057
Almeida, J. R. G. S.; QPN-087
Almeida, L. A.; MAT-112
Almeida, L. D.; AMB-068, EDU-002
Almeida, L. M. P.; QVE-009
Almeida, L. S.; ELE-032
Almeida, M. A. R.; CAT-026
Almeida, M. B; BEA-007
Almeida, M. B.; ANA-078, BEA-009
Almeida, M. D. S.; AMB-017, EDU-062
Almeida, M. O.; TEO-010
Almeida, M. T.; QPN-022
Almeida, M.; ORG-100, ORG-108
Almeida, P. S. V. B.; INO-024
Almeida, P. V. B.; ANA-012
Almeida, Q. A. R. de; ORG-109
Almeida, Q. A. R.; EDU-050, MAT-064
Almeida, R. M.; MAT-120
Almeida, S. H.; EDU-058
Almeida, T. A. F.; QPN-033
Almeida, V. A.; INO-093
Almeida, V. G. K.; ANA-008
Almeida, V. P.; AMB-055
Almeida, V. R. G.; CAT-025
Almerindo, G. I.; EDU-033
Alonso Freitas, G. A. F.; MAT-040
Alvarenga, E. S.; ORG-079
Alvarenga, G. M.; INO-073
Alvarez-Roca, R.; MAT-126
Alves Jr. , S.; INO-009
Alves, C. S.; MAT-122
Alves, C.; AMB-003
Alves, D. da P.; ANA-008
Alves, D. P; BEA-007
Alves, D. P.; ANA-078
Alves, G. F. S.; EDU-021
Alves, J. C.; AMB-010
Alves, L. A.; MAT-101
Alves, L. M. C.; AMB-058
Alves, N.; QPN-020
Alves, P. B.; MED-041, QPN-014
Alves, P. S.; ORG-089
Alves, R. B.; MED-058, ORG-028, ORG-061
Alves, R. F.; QPN-118
Alves, R. V. A.; QPN-062
Alves, V. A.; EDU-057
Alves, V. A.; EDU-061
Alves, V. N; ANA-046
Alves, W; FOT-013
Alves, W. A.; ELE-017, FOT-002, INO-095, MAT-051, MAT-118, MAT-120
Alves, W. A.; MAT-050
Alvim, T. R.; EDU-034
Alvino, A. C. B.; EDU-022
Amaral, B. S.; BIO-003
Amaral, J. C; QPN-079
Amaral, J. G.; QPN-032
Amaral, T. M.; FIS-003
Amarante, G. W.; CAT-015, ORG-019, ORG-093
Ambrosio, M. A. L. V.; QPN-006
Ambrósio, M. A. L. V.; QPN-008
Ameku, W. A. A.; ELE-030
Amim Jr. , J.; MAT-025
Amorim Camara, A. C.; QPN-012
Amorim, J. M.; QPN-049
Amorim, M. R.; QPN-063
Amorim, T. L.; ANA-003
Amoroso, H. C.; MAT-053
Amparo, S. Z. S.; MAT-083
Anaisse, F. J.; BEA-001
Andanson, J. M.; FIS-013
Andrade, C. B.; ORG-081
Andrade, C. H.; MED-002, MED-046
Andrade, D. C.; BEA-014
Andrade, D. F; ANA-069
Andrade, D. P. P.; FIS-002
Andrade, E. H. A.; QPN-013, QPN-046, QPN-106
Andrade, F. B. C.; ANA-075, ANA-079
Andrade, G. F. S.; FIS-018
Andrade, I. M. G.; QVE-002, QVE-007, QVE-008
Andrade, J. M. B.; COL-005
Andrade, S. N.; MED-022
Andrade, T. J. A. S.; EDU-048, ORG-063, ORG-089
Andrade, V. P.; AMB-081
Andricopulo, A. D.; MED-004, MED-027, MED-029, MED-048
Andricopulo, A. D.; MED-005
Andriolli, C. R.; COL-002
Angelucci, C. A.; ELE-026
Angnes, L.; ELE-022
Angolini, C. F. F.; QPN-060, QPN-124
Anjos Dos, V. E.; AMB-028
Anjos, D. S. C. dos A.; MAT-058
Anjos, D. S. C.; EDU-062
Anjos, J. P.; BEA-019
Anjos, N. S.; ORG-080
Anjos, T. O.; QPN-013
Antar, G. M.; QPN-043, QPN-097, QPN-098
Antonialli-Junior, W. A.; ANA-086
Antoniazzi, C.; MAT-110
Antunes, A. M. S.; TEC-001
Anunciação, D. S.; EDU-031
Apel, M. A.; QPN-048
Aquino Neto, F. R.; ANA-013
Aquino, C. B.; MAT-005
Aquino, F. J. T.; QPN-006, QPN-008
Aquino, J. S.; QPN-034
Aragão da Silva, A. G; QPN-105
Arakawa, N. S.; QPN-023
Araki, K.; ELE-013, MAT-063
Arantes, G. C. V.; EDU-055
Araújo De, M. C.; TEC-002
Araújo De, M. H.; ORG-055
Araújo Neto, J. F.; QPN-039
Araujo Silva, R.; ELE-009
Araujo, A R; QPN-071
Araújo, A. C. L.; QVE-002, QVE-006
Araújo, A. F.; ORG-097
Araújo, A.; ANA-072
Araújo, B. Q.; QPN-095, QPN-104, QPN-107
Araújo, D. M.; ORG-053
Araújo, E. S.; AMB-001
Araujo, M. H.; CAT-032
Araujo, M. H.; INO-039
Araújo, M. H.; INO-071
Araujo, M. H.; ORG-084
Araújo, M. L.; CAT-006
Araujo, M. S.; ELE-053
Araujo, N. S. de; FOT-012
Araujo, R. G. O.; AMB-010
Araújo, R. J.; CAT-011
Araújo, R. L. B.; BEA-015

Araújo, R. N. M.; BIO-011, BIO-014
Araújo, R. O.; QPN-034
Araújo, T. F.; QPN-003
Araujo, T. M. de R.; AMB-019
Araujo, W. R. de; ELE-013
Araujo, W. R.; ELE-046
Arbilla, G.; AMB-006, AMB-007
Ardisson, J. D.; ORG-084
Arenz, M.; ELE-015
Arenz, Matthias; ELE-036
Arguello, J.; INO-092
Armando Júnior, J.; QPN-049
Armoa, M. H.; TEC-011
Arrigo, V.; EDU-013
Arrospide, T. M.; QPN-045
Arruda, H. J.; INO-084
Arruda, T. F.; ANA-047
Arruda, V. M.; AMB-055
Artiushenko, O.; ANA-039
Ascari, J.; ORG-011
Asencios, Y. J. O.; CAT-004
Assis Felix, C. S.; ANA-041
Assis, L. R.; MED-034
Assis, O. B. G.; MAT-053, MAT-077
Assis, R. C.; AMB-064
Assis, R. N. A.; QPN-058
Assis, V. O.; TEO-008
Assuncao, N. A.; AMB-004
Ataide, V. N. de; ELE-013
Atala, A. P.; QPN-026
Atvars, T. D. Z.; MAT-001
Audo, G.; QPN-123
Augusti, R.; BEA-015
Aunque, R. F. O.; AMB-081
Aveiro, L. R.; ELE-016
Avelino, D. O. S.; EDU-021
Aversa, T. M.; EDU-019, MAT-064, MAT-112, ORG-109
Avila, J. N. L.; FIS-013
Ávila, M. C.; QPN-026
Ávila-Costa, M.; BIO-009
Avincola, A. S.; QPN-100
Ayala, A. H. F; BEA-007
Ayala, A. H.; ANA-078
Ayres, C.; EDU-007
Ayres-Pereira, T. I.; EDU-039
Azevedo, A. M. A.; QPN-003
Azevedo, F. R. P.; QPN-005
Azevedo, I. A. L.; INO-002
Azevedo, J. C. R.; AMB-024
Azevedo, R. B.; MAT-087
Azevedo, R. S. A.; ANA-018
Azevedo, R. S.; ANA-087
Azevedo, V. H. R.; ELE-062

## B

B. de Andrade, J; BEA-013
Bacil, R. P.; ELE-022
Back, D. F; INO-089
Back, D. F.; INO-019
Baev, A.; MAT-079
Bagatin, I. A.; INO-012, INO-059, INO-080, INO-086
Bagatin, M. C; BIO-012
Bail, A.; COL-002, COL-003, COL-012
Baitello, J. B.; QPN-043
Balbinot, F. P.; ANA-050
Baldassari, L. L.; ORG-034
Baldini, D. C.; INO-017, MAT-010
Balestrin, L. B. S.; FIS-027
Baliza, I. R. S.; QPN-087
Balliano, T. L.; QPN-030
Ballotin, F. C.; CAT-009
Ballotin, F. C.; CAT-031
Bandeira, P. N.; QPN-005, QPN-028
Baptista, Leonardo; FIS-002
Baptista, M. S.; MED-008
Baptista, V. S.; FIS-005
Bär, J.; MAT-014
Baracat, M. M.; QPN-023
Barbosa, D. B. A; ORG-072
Barbosa, D. B. A.; AMB-066, INO-050
Barbosa, D. B. A.; INO-063
Barbosa, E. C. M.; ELE-050
Barbosa, E. P; ORG-072
Barbosa, I. R.; ORG-012
Barbosa, J. L.; AMB-009
Barbosa, J. M. C.; MED-012, MED-054
Barbosa, J. R.; AMB-037, ANA-071
Barbosa, L. D.; MED-051
Barbosa, L. L.; TEC-005
Barbosa, L. M.; ANA-017
Barbosa, LRB; ORG-102
Barbosa, R. S.; INO-059
Barbosa, S. C.; MAT-042
Barbosa, S. L.; CAT-025, CAT-026
Barbosa, V. A.; MED-042, MED-052
Barbosa-Dekker, A. M.; MED-035, ORG-065
Barce, E. T.; MAT-015
Barcellos, A. F.; QPN-113
Barcellos, I. O.; FIS-028
Barcellos, P. S.; AMB-027
Barcelos, D. A.; AMB-026
Barcelos, V. H. T.; FIS-007
Barea, P.; MED-052
Bareño, V. D. O.; ORG-050
Bargieri, D. Y.; MED-002
Barin, J. S.; ANA-010, BEA-005
Barone, M.; CAT-036
Baroni, A . C. M.; ORG-081
Barreiro, E. J. B.; MED-015
Barreiros, A. L. B. S.; MED-041
Barreiros, B. S. B.; MED-041
Barreiros, M. L.; MED-041
Barrett Reina, L. Del C.; BEA-015
Barretto, F. A.; ORG-015
Barroco, C. V.; MAT-039
Barros, A.; MAT-014
Barros, M. F.; MAT-008
Barros, M. S. P.; EDU-060
Barros, O. S. R.; ORG-091
Barros, W. P.; INO-097
Barros, W. R. P.; ELE-027
Barud, H. S.; MAT-080
Basso, E. A.; ORG-031
Basso, L. A.; MED-060, ORG-075
Bastos, A. V.; ORG-050
Bastos, C. S.; EDU-065
Bastos, E. L.; FOT-015
Bastos, G. A.; ORG-007
Bastos, J. M. D.; MED-064
Bastos, M. A; EDU-022
Bastos, T. L.; EDU-055
Bataglion, G. A.; AMB-023
Batalha, P. N.; ORG-017
Batatinha, M. J. M.; MED-055
Batista, A. A; INO-100
Batista, A. A.; INO-034, INO-074
Batista, A. C. S.; MED-058, ORG-103
Batista, A. D; ANA-065
Batista, A. P. L.; MAT-105
Batista, B. L.; ELE-031
Batista, B.; EDU-035
Batista, G. F.; EDU-034
Batista, G. M. F.; ORG-093
Batista, J. C.; EDU-006
Batista, K. S.; ANA-049
Batista, R. B.; ORG-014
Batista, V. S; MED-044
Batista, V. S.; MED-063, MED-065
Batistela, V. R.; AMB-056, FIS-034, MAT-094
Batistuti, M. R.; ELE-048, ELE-060
Bautitz, I. R.; ANA-085
Bazito, R. C; CAT-021
Bazito, R. C.; CAT-036
Bazito, R.; BEA-017
Bazzi, C.; ANA-082
Beato, M. O.; ANA-033
Beatriz, AB; ORG-102
Bechara, E. J. H.; AMB-004
Bego, A. M.; EDU-009
Behenck, L. S.; QVE-009
Belgo, H. C.; COL-010
Beltrame, A. C. F.; EDU-037, INO-047
Benite, A. M. C; EDU-022
Benite, C. R. M; EDU-022
Benitez, L. B.; AMB-042
Bento, J. M. S.; QPN-083
Benvenho, A. R. V.; ELE-017
Bergamaschi, V. S.; CAT-014
Bergmann, B. R.; ORG-052
Bernardelli, J. K. B.; AMB-032
Bernardes, A.; MED-045
Bernardes, M. C.; AMB-011
Bernardes, T. M.; MED-035
Bernardino, A. M. R.; ORG-106
Berón, F.; INO-077
Bertacchi, J. P. F.; MAT-092
Bertoli, A. C.; CAT-031
Bertolino, L. C. B.; INO-102
Berton, G. H.; ORG-004
Bertotti, M.; ELE-003, ELE-008, ELE-043
Bertran, C. A.; COL-004, FIS-027, MAT-038, MAT-062
Beruski, O. B.; ELE-033
Bessa, I. A. A.; MAT-059

Bessa, R. A.; MAT-047
Bet, M. A.; EDU-047
Bezerra, D. P.; QPN-087
Bezerra, F. S.; QPN-055, QPN-072
Bezerra, L.; INO-089
Bezerra, M. A. M.; ORG-078
Bezerra, W. A.; INO-005
Bezerra, W. D.; INO-014
Bianchi, V. N.; AMB-054
Biasetto, C R; QPN-071
Bibi, N.; INO-013, INO-043, INO-077
Biegelmeyer, R.; QPN-042
Bielemann, N. J.; ANA-050, ANA-051
Bier, C. C.; ANA-058
Bilck, A. P.; MAT-065
Bilyuy, R.; MED-014
Bim, L. F. B.; INO-006, INO-010
Binatti, I; INO-069
Bioni, T. A.; ORG-002
Bisinoti, M. C.; AMB-030, AMB-078
Bispo, M. L. F.; MED-019
Bispo, V. M.; MAT-095, MAT-113
Bitencourt Oliveira, L. B. O.; ANA-036
Bitencourt, G. F.; AMB-074
Bitencourt, G. R.; ANA-052
Bitencourt, J.; ORG-100
Bittencourt, I.; AMB-014
Bittencourt, P. R. S.; MAT-022, MAT-074
Bizarro, C. V.; MED-060
Bizzi, C. A.; ANA-043, TEC-009
Bizzi, C. A.; ANA-052
Blanco, C.; ELE-058
Boaventura Jr. , S.; QPN-073
Boechat, F. C. S,; ORG-017
Boechat, F. C. S.; ORG-022, ORG-085, ORG-087, ORG-088
Boechat, N.; MED-008, MED-010, MED-030
Boechat-Roberty, H. M.; FIS-002
Bolzan, R. C.; ANA-044
Bolzani, V. S.; ANA-005, BEA-018, QPN-071, QPN-076, QPN-125
Bomfim, L. M.; QPN-087
Bona, C. M.; QPN-018
Bona, T. F.; EDU-033
Bonacin, J. A.; INO-096
Booth, S. G.; ELE-019
Bordignon, S. A. L.; QPN-048
Bordin, J. R.; MAT-009
Borges de Melo, E.; FIS-007
Borges, A. S. B.; INO-039
Borges, A.; MED-013
Borges, B. G. A. L.; MAT-100
Borges, C. B.; CAT-025
Borges, C. G.; AMB-019
Borges, C. P. F.; INO-031
Borges, E. M; EDU-054
Borges, J. C.; ORG-106
Borges, R. S.; MED-016
Borges, W. S.; QPN-002
Borissevitch, I. E.; FOT-011
Borsato, D.; ANA-029, ORG-065
Borsodi, M. P. G; ORG-052
Borsoi, A. F.; MED-060
Bortoleti, B. T. S.; MED-019
Bortolozi, G. G.; BEA-010
Bortoluzzi, A. J.; FIS-011
Bortoluzzi, J. H.; CAT-010
Boschen, N. L.; FIS-025
Bosqueiro, J. R.; QPN-092
Botelho, B. G.; BEA-008
Botero, W. B.; QPN-063
Botero, W. G.; AMB-036, AMB-062, FIS-030
Boto, S. M.; CAT-004
Bottoli, C. B. G.; ANA-074
Boza, I. A. F.; FIS-010
Braga, A.; AMB-007
Braga, R. C.; MED-002, MED-029
Braga, T. C.; MED-043
Bragaia, G. P.; ANA-028
Braibante, M. E. F.; EDU-012
Branco, A.; MED-055
Brandão, G. C.; ANA-081
Brandão, G. P.; AMB-031
Brandellero, M. V.; EDU-033
Brandt, J. V.; MAT-011
Branquinho, T. O.; QPN-056
Breitkreitz, M. C.; ANA-074
Brighente, I. M. C.; MED-003
Brillas, E.; FIS-012
Brito Júnior, G. A.; INO-055
Brito, A. V. S.; AMB-009
Brito, C. L.; ELE-040
Brito, E. B.; MAT-042
Brito, E. C. P.; EDU-061
Brito, H. A.; INO-061
Brito, H. F.; INO-085
Brito, J. F; ELE-029
Brito, P. V. N.; ANA-014, BEA-011
Brito, T. B.; MED-041
Brito, T. C.; CAT-022
Brito, T. O.; MED-019
Britto, D.; MAT-041
Broietti, F. C. D.; EDU-013
Brolo, A. G.; MAT-027
Brömme, D.; QPN-029
Brum, J. R.; ANA-051, BEA-016
Bruni, A. T.; MED-031, MED-066, TEO-008
Bruni, B. A.; MED-023
Bueno, E. A. S.; EDU-013
Bueno, M. C.; ANA-064
Buffon, E.; ELE-023
Bufon, C. C. B.; MAT-014
Buhl, B.; QPN-018
Burgo, T. A. L.; FIS-014, FIS-031
Burtoloso, A. C. B.; ORG-038
Busato, J. G.; AMB-034
Buzzá, H. H.; FOT-011

## C

Cabral, F. M.; INO-055
Cabral, M. F.; ELE-033
Cabral, M. R. P.; QPN-004
Cabral, P. F. O.; EDU-010
Cabrera, S. P.; QPN-081
Caetano, I. K.; AMB-033
Caetano, J.; MAT-016
Caixeta, B. P.; TEO-011
Calado, C. R.; MAT-107
Calado, H. D. R.; ELE-056
Caldas, L. A.; ANA-057, ANA-058, QPN-085, QPN-116
Calderon, E. R. D.; AMB-081
Cali, M. P.; FOT-005
Caliman, V.; MAT-043
Calisto, G. C. M.; INO-030
Calit, J.; MED-002
Camaforte, N. A. P.; QPN-092
Camara, A. C; QPN-082
Camara, C. A.; QPN-047
Camara, C. A.; QPN-080, QPN-081, QPN-118
Câmara, D. N.; ORG-046
Camara, M. B. P.; QPN-025, QPN-040
Câmara, M. B. P.; QPN-050
Câmara, M. B. P.; QPN-053
Camargo, D. H. S.; MAT-014
Camargo, L. P.; MAT-018
Camargo, M. R; EDU-022
Camargo, P. H. C.; CAT-012, ELE-050, MAT-005
Camargo, P. H. C.; MAT-105
Camelo, M. L. V.; QPN-015
Camilo, F. F.; ELE-045
Campos, A. R. N.; QPN-034
Campos, D. L.; MED-034
Campos, D. V. B.; AMB-029
Campos, E. C. G.; MAT-056
Campos, M. L. A. M.; AMB-012
Campos, N. R.; INO-029, INO-081
Campos, P. S.; FIS-032
Campos, R. B.; FIS-009
Campos, V. N. S.; INO-034
Campos, V. P.; AMB-009
Canan, C.; ANA-033
Canci, B. T.; QPN-117
Candido, E. G.; CAT-014
Cândido, E. G.; MAT-005
Candido, Geovany; EDU-027
Candido, J. M. B.; INO-048
Candido, L. V.; EDU-020
Canela, M. C.; AMB-027
Cangussu, D.; INO-005, INO-014, INO-053
Canisares, F. S. M.; MAT-088
Cantanhede Filho, A. J.; QPN-025
Cantarutti, R. B.; TEC-003
Capeletto, M. G; QVE-011
Caramori, G. F.; FIS-011
Cardoso, C. A. L; QPN-033
Cardoso, C. A. L.; ANA-086, QPN-007
Cardoso, C. L.; BIO-004, QPN-125
Cardoso, C. M.; ANA-090
Cardoso, D. V. V.; QPN-050
Cardoso, J. C; ELE-029
Cardoso, L. P.; INO-052
Cardoso, M. B; MAT-050
Cardoso, M. B.; FIS-027, MAT-030, MAT-080
Cardoso, M. F. C.; MED-025, ORG-045

Cardoso, R. M.; ANA-065, ELE-014, ELE-052
Cardoso, S. G.; MAT-020
Cardoso, S. H.; BIO-007
Cardoso, T. M. G.; ANA-067
Cardoso, V. A.; MAT-116
Cardozo Filho, L.; QPN-010
Caricatti, V.; CAT-036
Carlos, I. Z.; QPN-063
Carlos, R. M.; FOT-003, FOT-005, FOT-014
Carmignano, O.; CAT-031
Carmo, M.; EDU-036
Carmona, J. L. C.; EDU-059
Carneiro, C. E. A.; FIS-029
Carneiro, F. J. C.; QPN-025
Carneiro, F. J. C.; QPN-050
Carneiro, M. C.; ANA-038
Carneiro, M. T. W. D.; AMB-031
Carneiro, T. R. C; MED-015
Carneiro, Z. A.; INO-036
Carnevale Neto, F.; QPN-061
Carra, J. B.; QPN-023
Carvalho Andrade, H. M.; ANA-041
Carvalho Junior, E. J.; ELE-008
Carvalho, A. B.; INO-069
Carvalho, A. C.; QPN-086
Carvalho, A. E.; ELE-027, ELE-044
Carvalho, A. M. G.; MAT-020
Carvalho, A. N.; INO-070
Carvalho, A. S.; MED-010
Carvalho, C. M. de; ANA-093
Carvalho, C. M.; MAT-121
Carvalho, D. A.; FIS-029
Carvalho, D. B.; ORG-081
Carvalho, D. T.; MED-036
Carvalho, F. A. O.; BIO-013
Carvalho, F. F.; EDU-005
Carvalho, G. S. G.; CAT-015
Carvalho, G. S.; ANA-043
Carvalho, I. M.; COL-006, FIS-021
Carvalho, J. C. S; QPN-044
Carvalho, J. E.; QPN-115
Carvalho, J. M.; BIO-002, QPN-065
Carvalho, L. L.; MED-061
Carvalho, L. S.; CAT-001
Carvalho, M. G.; QPN-003, QPN-027
Carvalho, M. T. M.; ANA-061
Carvalho, P. L. G.; AMB-044, AMB-046
Carvalho, R. C.; ANA-069
Carvalho, R. D. E.; MAT-103
Carvalho, R. H.; MAT-103
Carvalho, S. A.; MED-012, MED-054
Carvalho, T. L.; QPN-062
Carvalho, V. S.; AMB-067
Carvalho, W. A.; CAT-006, MAT-111
Carvalho-Jr, V. P.; CAT-024, CAT-028, CAT-029, CAT-030
Casagrande, G. A.; INO-089
Casagrande, R.; QPN-023
Casanova Coltro, M. C. R.; MAT-052
Cascaes, M. M.; QPN-013, QPN-046
Casellato, A.; INO-067
Cass, Q. B.; BIO-003
Cassa, S. G. S.; EDU-064, ORG-109
Cassella, R. J.; ANA-040, ANA-042, ORG-086
Cassella, R. J.; ANA-047, ANA-055, ANA-056, ANA-084
Cassiano, G. C.; MED-002
Cassini, G. C.; EDU-064
Cassol, T. M.; ORG-004
Castel, D. K. A. D.; AMB-001
Castellano, E. E; INO-100
Castelo-Branco, F. S.; MED-008
Castiblanco, J. E.; ANA-060
Castilho, M. S.; MED-025
Castilho, Z. C.; INO-044
Castilhos, Z. C.; AMB-026
Castione, R. C. M. S.; EDU-028, EDU-047, EDU-059
Castro De, C. B.; INO-002
Castro De, P. R.; INO-006
Castro, A. A. N.; FIS-032
Castro, A. C.; ORG-075
Castro, A. L. P.; MAT-047
Castro, B. G.; ORG-058
Castro, C. J.; MED-023
Castro, E. G.; MAT-110, QVE-010
Castro, J. C.; MED-053
Castro, L. F.; AMB-057
Castro, L. M. F.; EDU-049
Castro, N; FIS-038
Castro, N. G.; MED-018
Castro, R. N.; QPN-121
Castro, S. V. F.; ELE-052
Castro, V. G.; FIS-003
Castro, V. S.; QPN-122
Castro-Gamboa, I.; QPN-093
Catalan, T. B. S.; QPN-007
Catalani, L. H; MAT-031
Catalani, L. H.; MAT-045
Catota Saénz, H. S.; ELE-008
Catunda Jr. , F. E. A.; QPN-003
Caumo, S.; AMB-003
Cavalcante, J. B. H.; AMB-005
Cavalcante, L. A.; EDU-049
Cavalcante, L. L.; AMB-071
Cavalcante, S. C. H.; MED-041
Cavalcanti, A. S.; MED-051
Cavalcanti, J. C. M.; FIS-030
Cavalcanti, L. P. A. N.; QPN-038
Cavaleiro, J. A. S.; ORG-088
Cavalieri, F.; INO-095, MAT-051
Cavallieri, M. C.; ELE-033
Cebim, M. A.; INO-006, INO-010, MAT-034, MAT-070
Cebrian, A. V. S.; MAT-080
Cechin, C. N.; INO-078
Celestino, G. G.; MAT-025
Cerchiaro, G.; QPN-096
Cerize, N. N. P.; COL-007
Cerqueira, G; ELE-055
Cerqueira, T.; AMB-021
Cesarino, I.; ELE-024
Cesarin-Sobrinho, D.; FOT-009
César-Oliveira, M. A. F.; MAT-046
Cesca, E. C.; INO-099
Chafran, L. S.; CAT-034
Chagas, F. O.; ANA-032, FIS-037
Chagas, F. O.; FIS-015
Chagas, J. O.; AMB-063
Chagas, R. P.; INO-005, ORG-091
Chang, R.; QPN-008
Chapadeiro, R. T.; ORG-028
Chaves, A R; ANA-020
Chaves, B. P.; ELE-033
Chaves, E. F. C. L.; MED-006
Chaves, F. A.; EDU-014
Chaves, M. C.; QPN-107
Chaves, M. H; QPN-111
Chaves, M. H.; QPN-088, QPN-089, QPN-095, QPN-103, QPN-104, QPN-108
Chaves, Mariana H. Chaves; QPN-105
Chern, M. S.; FIS-024
Chiapetta, S. C.; ANA-006
Chiapetta, S. C.; ANA-021, ANA-087, ANA-088, ANA-089
Chiaregato, C. G.; MAT-003
Chiarello, M.; ANA-077
Chiavassa, L. D.; ELE-032
Chiavassa, L. D.; ELE-045
Chinelate, B. M.; AMB-066
Chinelate, B. M.; INO-063
Chino, M. E. T. A.; MED-006
Chorro, T. H. D.; ORG-030
Christine Dutra da Silva, A. C. Dutra S.; ORG-074
Christoffolete, M. A.; ELE-017
Christovam, L. M.; ELE-021
Cicuto, C. A. T.; EDU-007
Cid, T. P.; EDU-025, EDU-029
Cid, Y. P.; ANA-011
Ciili, E. M.; QPN-076
Cilli, E. M.; QPN-125
Cintra, L. S.; QPN-057
Cipriano, T. C.; MAT-068
Cipriano, T.; ELE-017
Cistia, C. D. N.; MED-040
Cito, A. M. G. L.; ORG-063
Citó, A. M. G. L.; QPN-034
Ciuffi, K. J.; INO-017, INO-054, INO-098, MAT-010
Claro, M. N.; TEC-006
Clososki, G. C.; ORG-070
Cochran, K. H.; AMB-048
Codevilla, C. F.; ANA-010
Codognoto, L.; ELE-011
Coelho Junior, G. S.; BEA-016
Coffin, S.; AMB-048
Colares, R. P.; EDU-024, EDU-036, EDU-060
Coli, J. F. C.; INO-065
Colnago, L. A.; INO-016
Colombo, R. N. P.; ELE-055, MAT-082
Colombo, R.; AMB-067
Coltro, W. K. T.; ANA-066, ANA-067, ANA-068, ELE-028
Come, J. A. A. S. S.; MED-030
Comte Junior, C. A.; QPN-122

Conceição, J. C. S.; QPN-059
Conserva, G. A. A.; QPN-098
Conserva, G. A.; QPN-096
Consoli, R. A.; EDU-007
Constantino, A. F.; TEC-002, TEC-005
Constantino, I. C; AMB-078
Constantino, I. C.; AMB-030, AMB-078
Constantino, V. R. L.; MAT-025
Corazza, F. G.; INO-066
Corazza, M. Z.; ELE-044
Corbellini, V. A.; ANA-080
Cordeiro, M. E.; AMB-059
Cordeiro, P. S.; ORG-092
Córdoba de Torresi, S. I.; ELE-036
Coreixas de Sá, C. S.; ANA-063
Corio, P. C.; ELE-061
Corio, P.; INO-033
Cormanich, R. A.; ORG-068
Correa, B. G.; MAT-057
Corrêa, B. K.; ORG-020
Correa, C. P.; INO-063
Côrrea, J. G. S.; QPN-100
Corrêa, J. G. S.; QPN-115
Correa, L. A.; INO-039
Corrêa, L. B. M.; AMB-037
Corrêa, M. J. C.; BIO-014
Corrêa, R. S.; INO-034
Corrêa, S. A. P.; QPN-073
Corrêa, S. M.; AMB-006
Correia, A. G.; QPN-029
Correia, A. N.; ELE-020, ELE-059
Correia, C. R; QPN-082
Correia, C. R. D.; MED-039, ORG-023, ORG-030, ORG-098
Correia, R. C.; QPN-080
Corsi, W. L.; EDU-011
Cortez, M. V. M.; ORG-013
Cortón, E.; ANA-068
Cosme, W. Z.; QPN-058
Costa Cerqueira, B. C. C.; ORG-101
Costa Da, D. R. M.; EDU-006
Costa Da, G. L.; MED-020
Costa Ferreira, S. L.; ANA-041
Costa Júnior, J. S.; EDU-048, ORG-089, QPN-034
Costa, A. B.; BEA-005
Costa, A. C. S.; AMB-034
Costa, A. M.; MAT-024
Costa, A. R. P.; ORG-017, ORG-088
Costa, B. S.; AMB-060
Costa, C. L. S.; ANA-070
Costa, D. C. S; MED-025
Costa, É. R; QPN-016
Costa, E. R.; AMB-075
Costa, É. R.; QPN-004
Costa, E. V.; MED-041, QPN-060, QPN-087
Costa, F. M. P.; QPN-075
Costa, F. T. M.; MED-002
Costa, G. de S.; AMB-023
Costa, I. C.; MED-019
Costa, I. S.; EDU-064, MAT-112
Costa, J. H.; QPN-124
Costa, J. L.; ANA-017
Costa, J. M. de F.; ORG-100, ORG-108
Costa, J. M. S.; EDU-048, ORG-089
Costa, K. B. S.; MAT-058
Costa, K. R.; ANA-023
Costa, L. A. G.; FOT-016
Costa, L. A. S.; INO-048
Costa, L. A.; INO-042
Costa, L. M.; BEA-020
Costa, L. T.; ELE-018
Costa, M. B.; CAT-039, ORG-003, ORG-041, QPN-052
Costa, M. C. S.; EDU-018
Costa, M. F.; ELE-017
Costa, N. C.; ANA-064
Costa, P. R. A da; ORG-109
Costa, P. R. A.; EDU-064
Costa, R. F.; QPN-031
Costa, R. K. S.; MAT-075
Costa, R. N.; MAT-020
Costa, R. O.; AMB-027
Costa, R. P. O.; QPN-056
Costa, S. S. L.; AMB-010
Costa, T. S.; QVE-002, QVE-006
Costa, T. S.; QVE-007, QVE-008
Costa, V. A.; INO-040
Costa, V. G.; MAT-081
Costa, W. K. O. C.; ANA-037
Costa-Lotufo, L. V.; QPN-061, QPN-084
Costa-Silva, T. A.; QPN-043, QPN-098, QPN-114
Costódio, P. F. S.; EDU-033
Cotrim, B. A.; ELE-002
Cottet, L.; COL-013
Coutinho, E. J; QPN-016
Coutinho, E. J.; AMB-069, AMB-075, QPN-004
Couto, G. G.; EDU-056
Couto, G. H.; ORG-111
Couto, M. T.; ORG-086
Couto, T. R.; MED-032, ORG-037
Cravo, P. V. L.; MED-002
Crespo, L. T. C.; EDU-064
Crisóstomo, C. A. B.; CAT-003
Cristale, J.; AMB-018
Crocoli, L. C.; ANA-031
Cruz Júnior, J. W.; ORG-009
Cruz, G. C. S.; ANA-092
Cruz, G. F. B.; ANA-056
Cruz, N. C.; MAT-021
Cruz, R. P.; AMB-035, EDU-030
Cruz, T. R.; CAT-024
Cruz, V.; MED-051
Cubides-Román, D. C.; TEC-002
Cuendet, M.; BEA-018
Cuffini, S. L.; MAT-020
Cunha Da, E. F. F.; TEO-012
Cunha, A. C. C.; ELE-042
Cunha, B. S.; EDU-064
Cunha, E. M. S.; EDU-056
Cunha, L. C. S.; QPN-006, QPN-008
Cunha, M. F.; FIS-033
Cunha, O. M.; MAT-077
Cunha, S. D.; ORG-015, ORG-042, ORG-048, ORG-076, ORG-077
Cunha, S.; ORG-005, ORG-016, ORG-053, ORG-104, QPN-059
Cunha, T.; AMB-031
Cunha, W. R.; ORG-006, QPN-057
Cunha, W.; MAT-078
Cursino, A. C. T.; BEA-006
Curti, P. S.; MAT-004
Cusin, Y. T.; QPN-117
Custódio, D.; AMB-003
Custódio, T.; MAT-059

## D

D. Saint'pierre, T.; ANA-039
da Camara, C. A. G.; QPN-045
da Costa, W. F.; MED-052
da Cruz Jr, J. W.; INO-028, INO-060
da Cruz, G. N.; EDU-007
da Cruz, P. A. U.; ORG-067
da Cunha, M.; QPN-094
da Guarda, L. D. C.; AMB-013
da Paz, G. M.; CAT-031
da Rocha, D. R.; ORG-092
da Rocha, G. O.; AMB-010, ANA-009
da Rocha, R. G.; ELE-035
da Rosa, P. D.; BIO-008
da Silva Júnior, E. N.; ORG-029
da Silva, A. C.; MAT-028
da Silva, A. F. M; INO-068
da Silva, A. G. M.; MAT-105
da Silva, A. L. E. P.; MAT-054
da Silva, A. M.; ORG-052
da Silva, B. A.; AMB-023
da Silva, D. F; QPN-079
da Silva, E. C.; CAT-010
da Silva, E. F.; MED-012, MED-054
da Silva, E.; INO-054
da Silva, F. A. N. G. S.; INO-102
da Silva, F. D.; ELE-006
da Silva, F. M. A.; QPN-060, QPN-087
da Silva, G. A.; AMB-072
da Silva, G. O.; FIS-023
da Silva, H. C.; QPN-014
da Silva, J. A. F.; ANA-066
da Silva, J. A.; TEC-006
da Silva, J. D. S.; ANA-012
da Silva, J. L.; ELE-062
da Silva, J. R. N.; FIS-001
da Silva, J. R.; QPN-036
da Silva, J.; ORG-100
da Silva, K. N.; ELE-034
da Silva, L. A. L.; ELE-027
da Silva, L. H. M; FIS-015
da Silva, L. H. M.; ANA-032, COL-005, FIS-037
da Silva, M. F. Das G. F.; QPN-079
da Silva, M. F. G. F; QPN-051
da Silva, M. J.; CAT-009
da Silva, M. M; QPN-079
da Silva, M. V.; MAT-019
da Silva, R. C.; ELE-018

da Silva, R. P.; BIO-013
da Silva, V. H. M.; INO-076
da Silva, W. A.; ANA-004
da Silva, W. P.; ELE-035
da Silveira, E. F.; FIS-002
Dáas, A.; ANA-071
Da-Costa, F. B.; QPN-056
Dal Pozzo, D. M.; CAT-039, ORG-003
Dall'Oglio, E. L.; QPN-078
Dalla Vecchia, P.; ANA-054
Dall'Antonia, L. H; ELE-053
Dall'Antonia, L. H.; MAT-018
Damasceno, D.; MAT-052
Damasceno, F. D.; AMB-022
Damasceno, J. P. V.; MAT-109
Damasceno, R. N.; ANA-071
Damos, F. S.; ELE-049
Danczuck, M.; MAT-110
Dangui, A. Z.; FIS-026
Dantas, E. P.; QPN-085
Dantas, G.; AMB-007
Dantas, M. D. A.; BIO-005
Dantas, R. F.; AMB-050
Dantas, R. F.; MED-006, MED-026
Dantas, T. C.; AMB-006
Dantzger, D. R. C.; MED-062
Das Chagas, R. P.; INO-014, INO-053
David, G. F.; TEC-007
David, J. M.; ORG-013, QPN-039, QPN-074
David, J. P.; QPN-039, QPN-074
d'Avila, L. A.; ANA-069
Davolos, M. R.; MAT-034, MAT-070
de Abreu, H. A.; CAT-007
de Almeida, F. G.; ANA-045
de Almeida, R. M.; CAT-010
de Almeida, V. G.; FOT-009
de Andrade, A. R.; ELE-039
de Andrade, C. K.; AMB-028
de Andrade, F. H. P.; MAT-010
de Andrade, J. B.; ANA-009
de Andrade, J. K.; AMB-028
de Araujo, W. R.; ELE-012, ELE-022
de Avellar, M. G. B.; FIS-036
de Azevedo, R. B.; QPN-036
de Barros, W. A.; ORG-096
de Carvalho, M. G.; QPN-094
de Castro, E. M. S.; TEC-006
de Castro, M. R. C.; MED-045
de Castro, P. P.; ORG-093
de Castro, S. L.; MED-012, MED-054
de Faria, E. H; INO-054
de Faria, E. H.; MAT-010
de Fátima, A.; ORG-084, ORG-096, TEC-003
de França, I. V.; INO-060
de Freitas, E. M.; BIO-008
de Freitas, R. P.; ORG-028, ORG-029
de Godoi, K. T. S.; ELE-010
de Jesus, E. C.; ORG-066
de Jesus, P. C.; FIS-020
de La Cruz, A. R. H.; AMB-081
de La Cruz, J. K. H.; AMB-081
de La Cruz, M. N. S.; ANA-013
de La Fuente, M. S.; INO-101
de La Fuente-Nunez, C.; BIO-010
de Leo, T. C.; ELE-048
de Lima, E. C.; AMB-054
de Lima, Ednilza; ORG-100
de Lima, V. R. L.; AMB-023
de Lucas, N. C.; FOT-006, FOT-007
de Lucca Jr. , E. C.; ORG-023
de Macedo, W. P.; ORG-021
de Matos, C. F.; MAT-100
de Mattos, M. C. S.; ORG-007
de Melo, E. B.; MED-031
de Melo, L. N.; CAT-010
de Melo, L. S.; ORG-032
de Melo, M. G.; AMB-023
de Moura, A. F.; FIS-035
de Moura, E. M.; CAT-031
de Oliveira Almeida, C. M. de O. A.; ANA-036
de Oliveira Pedro, R.; FIS-016
de Oliveira Silva, M.; MAT-062
de Oliveira, B. S.; ORG-067
de Oliveira, C. H. C. S.; FOT-009
de Oliveira, C. M. A.; QPN-036
de Oliveira, E. R.; QVE-005
de Oliveira, H. F. M.; BIO-001
de Oliveira, K. C.; CAT-002
de Oliveira, L. G.; QPN-069
de Oliveira, L. L. G.; ANA-045
de Oliveira, M. K.; TEC-004
de Oliveira, M. T.; ANA-036
de Oliveira, P. R.; ORG-014
de Oliveira, R. N.; QPN-087
de Oliveira, V.; MED-050
de Oliveira-Filho, A. G. S.; MAT-105
de Paula, F. R.; ORG-073
de Paula, G. R.; ORG-045
de Paula, J. C.; MED-052
de Paula, R. D. P.; ORG-101
de Paulo, R. S.; CAT-018
de Sá, C. F.; AMB-013
de Sousa, D. N. R.; AMB-053
de Sousa, F. B.; INO-082
de Sousa, L. R. F.; MED-045
de Sousa, Renato P.; QPN-105
de Souza Mendes, P. R. S. M.; COL-008
de Souza, A. A.; QPN-079
de Souza, A. D. L.; QPN-060
de Souza, A. G.; ORG-088
de Souza, A. Q. L.; QPN-060
de Souza, A. R.; FIS-010
de Souza, G. E.; MED-039
de Souza, G.; TEC-004, TEC-006
de Souza, J. R.; ANA-012
de Souza, L. C.; ORG-032
de Souza, M. C. B. V.; ORG-088
de Souza, M. L.; MED-004
de Souza, M. P.; AMB-020
de Souza, R. M.; TEO-001
de Souza, R. O. M. A.; ORG-032
de Torresi, S. I. C.; ELE-009
de Torresi, S. I. C.; MAT-105
Decandio, C. C; MAT-050
Deflon, V. M.; INO-075
Dekker, A. M. B.; ELE-050
Dekker, R. F. H.; ELE-050, ORG-065
Del Cistia, C. D. N.; ORG-012
Del Colle, V.; FIS-030
Delgado, J. P. S.; QPN-046, QPN-106
Delgado-Silva, A. O.; MAT-021
Delolo, F. G.; CAT-002
Delpino, I. S.; ANA-044
Demicheli, C. P.; INO-016
Demuner, A. J.; ORG-079
Denardin, E. L. G.; QVE-001
Dessoy, M. A.; MED-004
Di Beneditto, A. P. M.; AMB-073
Di Vitta, C.; ORG-008
Dias, A. A.; ELE-028
Dias, A. O.; FIS-034
Dias, B. C.; QVE-005
Dias, C. S. B.; MAT-030
Dias, D. F.; MED-036, QPN-110
Dias, E. J. S.; QPN-025, QPN-053
Dias, E. J. S.; QPN-050
Dias, F. M. F.; QPN-005, QPN-028
Dias, F. S.; INO-032
Dias, G. O. C.; QPN-040
Dias, G. P.; ANA-069
Dias, G.; TEO-008
Dias, I. M.; INO-026, INO-061
Dias, J. A.; CAT-034
Dias, L. C.; MED-004
Dias, L. G.; TEO-001
Dias, M. R. G.; INO-052, ORG-111
Dias, R. F. C.; QPN-006
Dias, S. C. L.; CAT-034
Dias, S. L. P.; QVE-005
Dias, S. S.; EDU-014, MAT-086
Dias-Baruffi, M.; ELE-048
Dibo, V. S.; INO-004
Dillenburg Saint'pierre, T. D. S.; MAT-040
Diniz, B. P.; EDU-061
Diniz, C. F. S.; AMB-016
Diniz, G. A.; MAT-038
Diniz, M. M.; INO-067
Diniz, R.; CAT-007, INO-046
Diógenes, I. C. N.; INO-002, INO-004, INO-042
Diogo Junior, J. P.; AMB-050
Dionisio, E. R.; AMB-002
Dionysiou, D.; AMB-048
Dittz, D.; INO-016
do Lago, C. L.; ANA-066
do Nascimento, M. S. S.; MED-012
do Nascimento, V.; ORG-092
do Pim, W. D; MAT-091
do Pim, W. D.; EST-001, INO-029
do Prado, M. V.; INO-098
do Rego, E. L.; ANA-012
Dockal, E. R.; INO-028, INO-060, ORG-009
Dolabela, M. F.; BIO-002
Domakoski, A. C.; MAT-051
Domingos, J. D. S.; BEA-011
Domingues, H. P.; BEA-002
Domingues, J. T.; AMB-044

Domingues, M. P. P.; AMB-041
Domingues, R. A.; MAT-001
Domingues, S. H.; MAT-005, MAT-073, MAT-104
Dominutti, P. A.; AMB-008
Donagemma, R. A.; ANA-024
Donate, P. M.; ELE-060
Donato, F. F.; AMB-020
Donnici, C. L.; BIO-009, INO-039
Donnici, L. C.; MAT-024
Dorigon, L.; COL-002
Doriguetto, A. C.; EST-001, INO-029, INO-065, INO-081
Döring, T. H.; INO-028
Dornellas, R. M.; ELE-006
dos Anjos, E. O.; QPN-058
dos Anjos, J. P.; AMB-005
dos Anjos, J. P.; BEA-013
dos Santos, A. M. P.; ANA-081
dos Santos, C.; ORG-090
dos Santos, D. M.; ELE-047
dos Santos, E. C. M.; ANA-071
dos Santos, E. C.; TEO-009
dos Santos, E. F. S.; MED-039
dos Santos, E. N.; CAT-002, CAT-018
dos Santos, G. C.; ORG-026
dos Santos, H. F.; ORG-093
dos Santos, J.; MAT-123
dos Santos, L. C.; QPN-092, QPN-101
dos Santos, M. N. G.; QPN-036
dos Santos, M. R.; CAT-020
dos Santos, P. R.; INO-019
dos Santos, P. R.; ORG-073
dos Santos, R. V.; BIO-001, MED-001
dos Santos, W. N. L.; ANA-081
dos Santos, W. P. C.; ANA-081
Dourado, A. H. B.; ELE-015, ELE-036
Dourado, A. H. B.; MAT-105
Dourado, G. A. A.; ORG-016
Drabecki, A. B. A.; MAT-044
Dragunski, D. C.; MAT-016, MAT-074
Druzian, G. T.; ANA-044
Dryfe, R. A. W.; ELE-019
Duarte, A. P.; INO-089
Duarte, B. F.; ANA-086
Duarte, B. H. S.; QPN-046, QPN-106
Duarte, D. S.; MAT-041
Duarte, E A; EDU-027
Duarte, E. C.; INO-016
Duarte, F. A.; ANA-010, ANA-054, BEA-005
Duarte, H. A.; CAT-007, TEO-009
Duarte, J. P. P.; MAT-007
Duarte, L. C.; ANA-068, ELE-028
Duarte, L. G. T. A.; MAT-001
Duarte, L. P.; QPN-110, QPN-112, QPN-120
Duarte-Junior, G. F.; ANA-066
Dumych, T.; MED-014
Durango, L. G. C.; QPN-068
Durigon, M. C. S.; ORG-111
Dutra, A. J. B.; ANA-042
Dutra, B. N.; ORG-082
Dutra, G. S. V.; ANA-065
Dutra, J. P.; QPN-002
Dutra, R. C. Q.; INO-003
Dutra, R.; EDU-059

## E

e Silva, F. A.; CAT-014
e Souza, S. B.; ANA-024
Eberlin, M. N.; ANA-017, ANA-074, QPN-124
Echevarria, A.; MED-020, MED-051, ORG-012
Egan, J. M.; QPN-061
Egler, S. G.; AMB-025
Eguiluz, K. I. B.; ELE-059
Ehlert, E.; TEC-010
Ehrhardt, A.; EDU-033
El Seoud, O. A.; ORG-002
Espíndola, G. C.; TEC-004
Espuri, P. F.; MED-036, QPN-032
Estevão, A. P. S. S.; EDU-025, EDU-029
Esteves, H.; ORG-098
Esteves, I. O.; INO-025
Estimable, R.; EDU-059
Estrela, I. O.; MED-024
Ethur, E. M.; BIO-008
Ethur, E. M.; QPN-018
Evangelista, E. S.; ORG-005
Evangelista, F. C. G.; MED-022

## F

Fabris, M.; MED-019
Fadini, P. S.; AMB-053
Faez, R.; MAT-003, MAT-023, MAT-066, MAT-119
Fagnani, E.; AMB-018
Fagundes, N. V.; INO-078
Faiões, V. S.; ORG-087
Fajardo, A. R.; MAT-055
Falcão, A. C.; MED-007
Falcão, E. H. L.; INO-009
Falcão, J. S. A.; FOT-016, MAT-093
Falsetti, L. O. Z.; MAT-014
Faria, D. L. A.; MAT-082
Faria, E. H.; INO-017
Faria, M. L.; MAT-065
Faria, R. B; INO-045
Faria, R. B.; FIS-024
Faria, S. H. D. M.; TEO-010
Farias, I. F.; ORG-110
Farinella, V. F.; QPN-090
Faro, L. V.; ORG-085
Fatibelo-Filho, O.; ELE-001
Fátima De, A.; ORG-055
Fátima, A.; MED-043, MED-047
Faustino, G. A. A; EDU-022
Faustino, W. M.; INO-085
Favarin, L. R. V.; INO-089
Favaris, A. P.; QPN-083
Fávaro, S. L.; MAT-094
Féboli, A.; MED-013
Feijó, G. S.; EDU-023
Feiteira, F. N.; ANA-004
Feitosa, A. O.; QPN-065
Feitosa, L. M.; MED-030
Feitoza-Silva, M.; ANA-092, ANA-093, MAT-121, MAT-122
Feliciano, A. S.; ORG-041
Feliciano, J. M. O.; EDU-057
Felinto, M. C. F. C.; INO-085
Felippe Pacheco, F. P.; ANA-063
Felisbino, J. K. R. P.; QPN-064
Félix, A. M. A.; EDU-021
Felner, P. P.; ORG-032
Felsner, M. L.; AMB-028
Fengler, T. A. L.; ELE-056
Ferlin, S.; MAT-027
Fernandes, A R; ANA-020
Fernandes, A.; ANA-042
Fernandes, C. S.; ORG-031
Fernandes, F. O.; MAT-021
Fernandes, F. S; EDU-022
Fernandes, J. B; QPN-051
Fernandes, J. B.; FOT-014, QPN-070, QPN-079
Fernandes, J. M.; FIS-009
Fernandes, J. P. S.; MED-007
Fernandes, J.; TEO-008
Fernandes, L. S.; MAT-008
Fernandes, M. E. C.; ORG-067
Fernandes, M. S.; MED-056
Fernandes, P. D.; ORG-022
Fernandes, P. O.; MED-011, MED-058
Fernandes, S. A.; MED-047, ORG-068, TEC-007
Fernandes, S. S. L.; QPN-004
Fernandes, T. N. C.; ORG-049, ORG-051
Fernandes, T. S.; MAT-039
Fernandes, W. B. C.; BIO-011
Fernandez, C.; EDU-053
Ferraz, B. S. R.; BEA-008
Ferraz, F. A.; MAT-046
Ferraz, H. C.; AMB-038
Ferraz, W.; MED-017
Ferreira Júnior, J. C.; EDU-031
Ferreira Souza, A. L.; MED-064
Ferreira, A. C. L. N.; CAT-037
Ferreira, A. D.; ANA-002
Ferreira, A. H.; ANA-033
Ferreira, A. L. G.; COL-011
Ferreira, A. P.; ORG-097
Ferreira, A. S.; ORG-091
Ferreira, B. L.; QPN-102
Ferreira, E. A.; MAT-099
Ferreira, E. M.; ANA-038
Ferreira, F. F.; MAT-061
Ferreira, F. L.; QPN-112
Ferreira, G. B.; INO-015, INO-026, INO-061, INO-076
Ferreira, G. C. A.; ELE-051
Ferreira, G. M. D.; COL-005, COL-011, FIS-021
Ferreira, G. M. D.; FIS-022
Ferreira, G. M.; MED-017
Ferreira, H. B. P.; CAT-023, CAT-037
Ferreira, J. A.; ANA-074
Ferreira, J. G. L.; CAT-013, QVE-004

Ferreira, J. M. S.; ANA-074
Ferreira, K. C.; EDU-005
Ferreira, L. L. G.; MED-004, MED-029
Ferreira, L. L.; ELE-056
Ferreira, M. F.; MAT-010
Ferreira, M. G.; INO-022, INO-044
Ferreira, M. J. P.; QPN-041, QPN-113
Ferreira, M. J. P.; QPN-044, QPN-090, QPN-091, QPN-097, QPN-116
Ferreira, M. L. G.; MED-030
Ferreira, M. P.; MAT-103
Ferreira, N. S.; MAT-071
Ferreira, O. P.; MAT-060
Ferreira, P. M. P.; QPN-034, QPN-104
Ferreira, P. R.; AMB-014
Ferreira, P. S; QPN-037
Ferreira, P. S.; ANA-073
Ferreira, R. C.; FOT-009
Ferreira, R. G.; MAT-107
Ferreira, R. M. F.; AMB-077
Ferreira, R. S.; MED-004
Ferreira, T. P.; ANA-011
Ferreira, V. B.; AMB-072
Ferreira, V. F.; MED-025, ORG-045
Ferreira, V. F.; ORG-092
Ferreira, V. S.; EDU-044
Ferro, M. V.; ORG-060
Fidelis, Q. C.; QPN-027
Figueira, B. A. M.; AMB-060
Figueiredo Filho, A.; AMB-033
Figueiredo, E. C.; ANA-095
Figueiredo, E. R.; AMB-072
Figueiredo, F. C.; MAT-071
Figueiredo, I. M.; ANA-022, BIO-005, BIO-007, MED-042, MED-047
Figueiredo, M. C.; QPN-020
Figueiredo, M. K. K.; AMB-074
Figueiredo, N. G.; ANA-006
Figueiredo, N. G.; ANA-021
Figueredo, F.; ANA-068
Filgueiras, P. R.; ANA-073, TEC-005
Filho, A. J. C.; QPN-053
Filho, C. C. S.; QPN-004
Filho, F. M.; MAT-017
Filho, J. D. S; QPN-075
Filho, M. O. M.; ORG-110
Filho, P. F. A.; ORG-097
Filho, R. E. O; QVE-011
Filho, S. A. V.; QPN-120
Filippe, T. C.; AMB-024
Fill, T. P.; QPN-124
Finco, F. D. B. A.; AMB-072
Fiorentino, E. S. C.; ORG-080
Fiorin, B. C.; TEO-005
Fiorio, J. L.; CAT-016
Fiqueiredo, J. F. D.; ANA-037
Fischer, A. C. K.; EDU-033
Flor, J. B.; ELE-029
Flores, A. F. C.; ORG-050
Flores, D. C.; ORG-050
Flores, E. L. M.; AMB-013, ANA-033, ANA-044, ANA-082
Flores, E. M. M.; ANA-043, ANA-054, TEC-009
Flores, E. M. M.; ANA-052
Florez-Rodriguez, P. P.; CAT-017, CAT-033
Floriani, H. L.; FIS-020
Foglio, M. A.; QPN-020
Fokoue, H. H. F.; MED-015
Folquitto, L. R. S.; MED-036
Fonsaca, J. E. S.; MAT-073
Fonseca, A. M.; EDU-024, EDU-036, EDU-060
Fonseca, A. S.; ANA-075, ANA-079, EDU-062, EDU-066
Fonseca, A. S.; QPN-050
Fonseca, F. C.; CAT-014
Fonseca, K. C. J. L.; EDU-063
Fonseca, M. E.; CAT-038
Fonseca, M. G.; QPN-104
Fonseca, P. X.; MAT-067
Fontes, A.; FOT-016
Fontoura, B. M.; FIS-015
Fontoura, B. M.; FIS-037
Fontoura, L. A. M.; TEC-004, TEC-006
Forezi, L. M.; ORG-045
Forezi, L. S. M.; MED-025
Forezi, L. S. M.; ORG-092
Forim, M. R.; QPN-052, QPN-070
Forim, M. R.; QPN-068
Formiga, A. L. B.; INO-013, INO-043, INO-077, INO-096
Fornari Pereira, E.; MED-017
Fornaro, A.; AMB-008
Fortuna, A. C. B.; MED-007
Fostier, A. H.; MAT-027
Fraga, C. A. M.; MED-012, MED-054
Fraga, I. M.; QPN-026
Fraifeld, F.; AMB-014
França, D.; MAT-023
França, E. L.; ORG-013
França, I. A.; AMB-056
França, R. R. F.; MED-008
França, T. C. C.; MED-033
França, V. F.; QVE-002, QVE-007
França, V. F.; QVE-008
Francisco, C. B.; ORG-031
Francisco, J. E.; ANA-004
Franco, I. D.; MED-011
Franco, J. H.; ELE-039
Franco, M. P.; INO-091
Franco, P. C. I.; MAT-065
Frauches-Santos, C.; MED-051
Frediani, N. F; MED-044
Freire, A. S.; AMB-029
Freire, J. A. P.; QPN-034
Freire, R. S.; AMB-052
Freitas, A. L. M.; MAT-120
Freitas, A. S. M.; MAT-021
Freitas, E. M.; QPN-018
Freitas, H. F.; MED-024, MED-055
Freitas, L. G.; BEA-015
Freitas, M. P.; ORG-068
Freitas, M. S.; CAT-025
Freitas, R. P; MED-058
Freitas, R. P.; ORG-044, ORG-061, ORG-103
Freitas, S. D. L.; QPN-107
Freitas, S. S.; AMB-043
Freitas, Sâmya D. L; QPN-105
Freitas, T. R.; MED-022
Frem, R. C. G; ELE-029
Frezard, F.; INO-016
Friedrich, L. C.; ANA-085
Froes, T. Q.; MED-025
Frota, J. P. R. A.; COL-002
Frota, V. M.; QPN-028
Fryer, B.; AMB-048
Furlanetto, L.; EDU-033
Furlani, C. S.; TEO-007
Furlani, J. M. S.; EDU-020
Furnham, N.; MED-046
Furst, C. G.; BIO-009
Furtado, C. A.; MAT-049, MAT-103
Furtado, D. Z. S.; AMB-004
Furtado, P. R. P.; FIS-038
Furtado, R. A.; MAT-078
Fust, A. M. B. S.; ANA-092, ANA-094, MAT-121, MAT-122
Fust, A. M. B. S.; ANA-093

## G

Gaiola, L.; QPN-007
Galante, D.; FIS-036
Galdino, M. M.; FOT-010
Galembeck, F.; EDU-035, FIS-014, MAT-092
Galhardi, L. C. F.; MED-035
Galhardo, T. S.; CAT-027
Gálico, D. A.; MAT-089
Gallardo, H.; INO-099, MAT-106
Galvan, D.; ANA-029
Galvão, J. C. R.; ELE-053
Gama, E. M.; ANA-034, ANA-035
Gama, E. M.; BEA-020
Gama, M. R.; ANA-016
Gama, R. M.; QPN-049
Gamiotea-Turro, D.; QPN-092, QPN-101
Gandi, M. O.; MED-010
Garcia Osorio, D. S.; MAT-063
Garcia, A. D. P.; AMB-046
Garcia, C. A. B.; AMB-010
Garcia, C. R. S.; MED-039
Garcia, F.; MAT-030
Garcia, H.; BEA-004
Garcia, L. A.; QPN-008
Garcia, M. L.; MED-039
Garcia, M. N. U.; ANA-058
Garcia, V. L.; QPN-073
Garden, S. J.; FOT-006, FOT-007
Gariani, R. A.; ORG-107
Gariani, R. G.; FIS-038
Garoforo, E.; INO-049
Garrido, F. M. S.; INO-022, INO-044, INO-056
Garrido, F. M. S.; INO-067
Gato, F.; ORG-003
Gatti, F. M.; ELE-032

Gaubeur, G. I.; AMB-045
Gauze, G. F.; BIO-012
Gazolla, P. A. R.; ORG-052
Geglio, P. C.; EDU-045
Gemal, A. L.; MAT-121
Gentil, T. C.; ELE-005
Genú, A. M.; AMB-033
Geonmonond, R. S.; CAT-012
Georgetti, S. R.; QPN-023
Geris, R.; MAT-095, MAT-113
Gevú, K. V.; QPN-094
Giacobe, K.; TEC-009
Giareta, R.; ELE-041
Giertyas, C. J.; CAT-010
Giese, E. C.; AMB-025
Giese, S. O.; INO-041
Gil, C. C.; ORG-045
Gimenes, L.; QPN-051
Gioda, A. G.; MAT-040
Gioda, A.; AMB-002, AMB-081
Giona, R. M.; COL-002
Giona, R. M.; COL-003, COL-012
Giordan, M.; EDU-009
Girola, N.; MED-007
Giuntini, F; FOT-013
Giutinni, F.; FOT-002
Gobbo-Neto, L.; QPN-119
Godim, A. S.; INO-083
Godoy, A. A.; ELE-002, ELE-025
Godoy, I. M. W.; INO-020
Godoy, J. M.; AMB-014
Goes, L. F.; EDU-053
Goi, B. E.; CAT-024, CAT-028, CAT-029, CAT-030
Gois, P. D. S.; CAT-028
Goldani, L. Z.; BIO-008
Golembiouski, C.; ANA-007
Gomes, A. A.; ANA-072
Gomes, A. C. C; QPN-037
Gomes, A. K. S.; ANA-085
Gomes, A. N. P.; QPN-118
Gomes, A. T. P.; ORG-088
Gomes, A.; INO-031
Gomes, B. F.; MED-046
Gomes, C. B. S. M. R.; ORG-092
Gomes, C. L.; ANA-075, ANA-079
Gomes, D. C. C.; INO-087
Gomes, E. L.; INO-080
Gomes, I. F.; MAT-099
Gomes, I. S.; ANA-088
Gomes, J. P. S.; QPN-089
Gomes, K. S.; QPN-097
Gomes, M. F.; ELE-060
Gomes, M. S.; MAT-067
Gomes, O.; AMB-049
Gomes, P. O. M.; ELE-048, ELE-060
Gomes, S. F.; CAT-008
Gómez, J. A. G.; INO-068
Gomez, J. A. G.; INO-090
Gomides, N. A. M. T. P.; QPN-024
Gonçalves, A. D.; ANA-071
Gonçalves, C. B.; INO-065
Gonçalves, G. R. S.; FIS-021
Gonçalves, H.; AMB-021
Gonçalves, J. M.; ELE-003, ELE-013
Gonçalves, P. J.; FOT-011
Gonçalves, R. P.; BEA-002
Gonçalves, R. S. B.; ORG-040
Gonçalves, R. S.; MED-053
Gonçalves, R. V.; CAT-016, CAT-027
Gonçalves, T. R.; BEA-002
Gontijo, T. B.; ORG-044
Gontijo, V. S.; MED-018, MED-036
González-Borrero, P. P.; AMB-033
González-Moya, J. R.; MAT-102
Gotardo, L. E.; ORG-094
Gothe, M. L.; CAT-021
Gothe, M. L.; CAT-036
Goulart, M. O. F.; BIO-009, MED-058, ORG-029
Goulart, M. O. F.; ELE-049
Goveia, D.; AMB-036, AMB-062
Gower, A. C. E.; QPN-117
Gozzi, F.; FIS-012
Gracio, C. E. R.; AMB-054
Graeff, F.; BEA-002
Granato, A. S.; CAT-015
Granito, C. J.; MAT-010
Grawe, G. F.; INO-074
Grecco, S. S.; QPN-096
Grecco, S. S.; QPN-113
Green, W. H.; CAT-019
Gressler, P. D.; AMB-042
Grigorovski Júnior, J. M. A.; INO-044
Grillo, G. R.; BIO-001, MED-001
Grougnet, R.; QPN-123
Gruber, Jonas; ELE-024
Guadagnin, R. C.; QPN-113
Guade da Silva, G. S.; QPN-012
Guarieiro, L. L. N.; AMB-005, BEA-019
Guaringue, R. P; TEO-005
Guatimosim, S.; MED-043
Guedes, A. P. M.; INO-074
Guedes, C. L. B.; QVE-012
Guedes, G. P.; INO-024, INO-026, INO-061
Guedes, J. S.; ANA-021, ANA-089
Guedes, P. H. C.; ELE-037
Guerra, A. J. T.; AMB-035
Guerra, R. B.; INO-013, INO-043, INO-077
Guerra, W.; INO-036
Guerreiro, M. C.; CAT-005
Guha, S.; ELE-017
Guido, R. V. C.; MED-039
Guilhon, G. M. S. P.; BIO-011, BIO-014, QPN-013, QPN-046, QPN-106
Guimaraes, A. S.; BIO-007
Guimarães, A. S.; INO-018
Guimarães, D. R.; QPN-060
Guimarães, I. P. M.; AMB-037
Guinati, B. G. S.; ANA-067
Gulo, F; ELE-007
Gusevskaya, E. V.; CAT-002, CAT-018
Gutierrez, E. D. P. M.; QPN-035
Gutz, I. G. R. G.; ELE-030

## H

Haddad, P. S.; MAT-006
Hallwass, F; ORG-025
Handoko, C. T.; ELE-007
Hardt, J. C.; MAT-016
Hartz, Z.; TEC-001
Hashimoto, P. K.; CAT-030
Haun, U. G.; CAT-032
Hauser-Davis, R. A.; AMB-073
Hayashi, M.; INO-021
Heidelmann, G. P.; AMB-025
Heiden, G.; ORG-011
Heleno, F. F.; ANA-001
Helfer, G. A.; BEA-005
Hellinger, H. R.; FIS-006
Henn, A. S.; BEA-016
Henriques, A. T.; QPN-042
Henriques, R. R.; MAT-025
Henriques, R. R.; MED-061
Herbst, M. H.; ANA-090, INO-094
Hernández Saravia, L. P.; ELE-008
Herrera-Acevedo, C.; QPN-056
Hespanhol, M. C; FIS-015
Hespanhol, M. C.; ANA-032, FIS-037
Heying, R. S.; FIS-011
Higgins, M. J.; MAT-028
Higino, G. S. H.; ELE-004
Hilário, F. F.; MED-022
Hirata, F. T. H.; INO-033
Hoehne, L.; BIO-008, QPN-018
Hoeltz, M.; AMB-042
Hoelz, L. V. B.; MED-030
Holakoei, S.; MAT-100
Honorato, J.; INO-034
Honório, A. E.; QPN-066
Honorio, K. M.; MED-009
Honório, K. M.; MED-028, TEO-010
Hottes, E.; ANA-090, INO-094
Hottes, S.; INO-094
Hsieh, Y. L.; MAT-066
Huaman de La Cruz, A. R. H. L. C.; MAT-040
Huamaní, L. E. S. C.; INO-013, INO-043, INO-077
Huang, M. N.; ORG-097
Huang, Y; AMB-048
Huda, A.; ELE-007
Hughes, D. L; INO-041
Hughes, D. L.; INO-091
Humberto, J. L.; MED-022
Husmann, S.; ELE-019, MAT-108
Husson, P.; FIS-013

## I

Iamamoto, Y.; FOT-011
Idehara, A. H. S.; CAT-028
Idemori, Y. M.; INO-079
Ierick, I. F.; ANA-005
Iglesias, B. A.; INO-049
Ignácio, M. H.; INO-032
Iha, O. K.; TEC-010

Imbernon, R. A. L.; QPN-011
Immich, A. P. S.; MAT-045
Inagaki, C. S.; MAT-029
Inroga, F. A. D.; ELE-057
Iop, G. D.; ANA-010
Iorio, E. I. C.; MAT-032
Ishikawa, R. L; BEA-007
Ishiki, H. M.; MED-062
Islam, A.; INO-016
Itabaiana, I. Jr.; CAT-008
Itkes, M. P. M.; ELE-001

## J

Jafelicci Jr, M.; MAT-011
Jafelici Jr, M.; COL-001
Jaimes, R. F. V. V. J.; ELE-061
Jaiyesimi, O. A.; QPN-119
Jambo, R. B. A.; FIS-018
Janegitz, B. C.; ELE-001
Januário, A. H.; ORG-006, QPN-057
Januario, A. H.; QPN-058
Januário, G. O.; ORG-039
Jardim, G. A. M.; ORG-029
Jasper, J. O.; QPN-109
Jesus De, I. S.; ORG-077
Jesus, I. C. G.; MED-043
Jesus, N. A. M.; MAT-078
Jimenez, G. C.; INO-009
João, J. J.; AMB-040
Jorge, M. C. O.; AMB-035
Júdice, W. A. S.; MED-036
Junior, A. C.; EDU-001
Junior, A. M. M.; MAT-036
Júnior, A. M.; INO-089
Júnior, F. P. S.; MED-006
Junior, H. C. S.; INO-026, INO-061
Junior, I. I.; ORG-094
Junior, J. C. C. da S.; ORG-032
Junior, J. C. J.; MAT-112
Júnior, J. G. S.; FIS-030
Junior, J. S. C.; ORG-063
Junior, L. P.; ANA-049
Junior, M. G. O.; EDU-059
Junior, S. A.; ORG-004
Júnior, V. L.; TEC-005
Junqueira, C. M.; COL-006
Justo, O. R.; TEC-007

## K

Kadooca, L. N.; BIO-009
Kai, J. K.; MAT-040
Kai, J.; MAT-101
Kalinke, L. H. G.; INO-087
Kamogawa, M. Y; ANA-025
Kamogawa, M. Y.; ANA-082
Karas, L. J.; ORG-014
Kato, L.; MAT-087, QPN-019, QPN-036
Kattela, S.; ORG-023
Kauffmann, C.; QPN-018
Kehrig, H. A.; AMB-073
Keller, M.; AMB-056
Kellett, A.; INO-069
Kellner Filho, L. C.; QPN-058
Kerkhoff, J.; QPN-078
Khan, S.; ANA-091
Kich Severo, I.; FIS-008
Killner, M. H. M.; ANA-029
Kimura-Hara, S.; AMB-048
Kioshima, E. S.; BIO-012
Kist, L. T.; AMB-042
Kitagawa, R. R.; QPN-002
Klein, A. F. N. V.; AMB-069
Klimpovuz, C. R.; MAT-002, MAT-096
Klinkowski, B. H.; QPN-010
Koiti, A.; ELE-003
Komatsu, J. S.; MAT-111
Kool, J; BIO-004
Koolen, H. H. F.; AMB-023, QPN-060, QPN-087
Korn, M; ANA-083
Korn, M. Das G. A.; ANA-048
Korn, M. G. A.; ANA-083
Korn, M.; ANA-049, ANA-062
Kotov, N. A.; FIS-035
Krambrock, K.; FOT-002
Krause, M.; AMB-031
Krauser, M. O.; MAT-034, MAT-070
Krettlie, A. U.; MED-010
Kreutz, J. C.; COL-012
Krieger, N.; ORG-111
Krzyzaniak, S. R.; ANA-052
Kubota, L. T.; ELE-049
Kuca, K.; MED-033
Kuhn, D.; BIO-008
Kumar, A.; ELE-003
Kummerle, A. E.; FOT-008, INO-024, INO-084
Kunita, M. H.; MAT-114
Kürmmerle, A. E.; MED-040
Kuster, R. M; QPN-037
Kuster, R. M.; ANA-073
Kutz, M. S.; ORG-010

## L

La Scalea, M. A.; ELE-032
Labuto, G.; MAT-111
Lacerda Jr, V.; TEC-007
Lacerda Jr. , V.; TEC-002
Lacerda Junior, Vlj; ORG-102
Lacerda, I. C. A.; BEA-015
Lachter, E. R.; CAT-022
Lachter, E. R.; QVE-009
Lage, A. L. A.; INO-001, INO-018, INO-071, MAT-083
Lage, G. L. C.; CAT-026
Lage, T. C. A.; MED-047
Lago, J. H. G.; MED-007, QPN-043, QPN-085, QPN-096, QPN-097, QPN-098, QPN-114, QPN-116
Lago, J. H. G.; QPN-041, QPN-113
Lago, R. M.; CAT-009
Lago, R. M.; CAT-031, MAT-067
Lang, E. S.; INO-007, INO-038, INO-078
Lanznaster, M.; INO-023, INO-068, INO-090
Lara, L. R. S; MAT-091
Laranjeira, G. B.; INO-089
La-Scalea, M. A.; ELE-045
Laurentiz, R. S.; MED-013, MED-059, ORG-056, ORG-059
Lavall, R. L.; ELE-058, FIS-003
Lavayen, V. G.; ELE-057
Lavayen, V.; INO-092
Lazarotto, G.; QVE-003
Lazzarini, A. B.; INO-006
Leal, A. C.; MED-051
Leandro, K. C.; ANA-093, ANA-094, MAT-121, MAT-122
Leão, R. A. C.; ORG-032, ORG-046
Leão, R. A. C.; ORG-094
Ledesma, C. M; EDU-054
Leite, A. C. R.; BIO-005
Leite, C. M; INO-100
Leite, C. M.; INO-034, INO-074
Leite, D. S.; AMB-046
Leite, M. A. S.; EDU-032
Leite, M. M.; MAT-048
Leite, O. D.; AMB-013, ANA-033, ANA-082, BEA-002
Lelo, R. V.; CAT-005
Leme, L. B. P.; INO-091
Lemes, L. O.; AMB-051
Lemos, E. G. M.; AMB-058
Lemos, L. R.; AMB-064
Lemos, L. S.; AMB-073
Lemos, P. S.; MAT-126
Lemos, T. L. G.; ORG-110, QPN-055, QPN-072
Lencina Filho, P. S. D.; QVE-003
Lenz, G. F.; ANA-085
Leoncio, M. S.; MED-052
Leonel, T. F.; AMB-058
Lepri, F. G.; ANA-047
Leseux, E. J.; QVE-005
Lessa, E. F.; MAT-055
Li, Z.; FIS-017
Libardi, V. M; ANA-001
Liberato, M. S.; MAT-050
Liesen, A. P.; QPN-045
Lima da Silva, T. L. S.; ORG-074
Lima De, J. L.; QPN-125
Lima De, S. P.; CAT-001
Lima De, V. A.; BEA-001
Lima Junior, R. O.; MAT-071
Lima, A. C. S.; QPN-034
Lima, A. D. S.; ANA-022
Lima, A. M. F.; MAT-036, MAT-053, MAT-077
Lima, A. N.; MED-009
Lima, C. D.; CAT-025
Lima, C. H.; MED-053
Lima, D. J. B.; QPN-104
Lima, D. R.; QPN-022
Lima, E. M.; QPN-068
Lima, E. O.; ORG-097
Lima, G. C.; ANA-095
Lima, G. F.; ANA-064
Lima, G. L. M; EDU-022
Lima, H. G.; MED-055
Lima, H. R. P.; QPN-094

Lima, I. P.; ANA-011
Lima, J. A. M.; QPN-017
Lima, L. F.; MAT-029
Lima, L. F.; MAT-100
Lima, L. M. L.; MED-015
Lima, L. M.; INO-089
Lima, L. S.; FOT-010
Lima, L. V. C.; TEO-006
Lima, M. A.; INO-040, INO-075
Lima, M. C. A.; MED-032
Lima, M. F. O.; ORG-087
Lima, M. F.; INO-036, ORG-067
Lima, M. J. A; ANA-025
Lima, M. J. A.; ANA-026
Lima, M. N. N.; MED-002
Lima, MLL; MED-037
Lima, P. S. V.; ORG-097
Lima, R. S.; MED-045
Lima, S. A. M.; MAT-088
Lima, S. M; ORG-049
Lima, S. M.; ORG-051
Lima, S. P.; MAT-035
Lima, T. A.; FIS-017
Lima, T. R. Q.; EDU-030
Lima, T. S.; ELE-011, MED-032
Lima, W. P.; ORG-052
Lima-Neto, P.; ELE-020, ELE-059
Linardi, M.; CAT-014
Linck, Y. G; MAT-020
Linhares, G. T.; AMB-066
Linhares, R. E. C.; MED-035
Linington, R. G.; QPN-061
Lino, B.; MAT-009
Lins, P. M.; ANA-074
Lira, P. H. A.; EDU-021, FIS-001
Lira, R. K. S.; CAT-008
Lobato, C. C.; MED-016
Lobato, G. M. M.; MAT-031
Lobo, F. A.; AMB-063, AMB-072
Lobo-Junior, E. O.; ANA-066
Loh, W.; FIS-027
Lohmann, L. G.; QPN-044
Loiola, A. R.; MAT-047
Lombardi, K. C.; AMB-033
Londero, V. S.; QPN-043
Longo Jr. , L. S.; ORG-069, ORG-080
Longo, E.; MAT-126
Lopes Coriolano, D. L. C.; ANA-036
Lopes Jr. , M. A. A.; MED-061
Lopes Junior, M. L.; BIO-011, BIO-014
Lopes, B. H. S.; EDU-006
Lopes, C. T; BEA-007
Lopes, C. T.; ANA-078
Lopes, C. T.; BEA-009
Lopes, D. S.; INO-058
Lopes, F. J. F.; QPN-019
Lopes, J. C. D.; BIO-009
Lopes, J. F.; TEO-007
Lopes, L. C.; MAT-123
Lopes, L. G. F.; INO-088
Lopes, L. M. X.; QPN-077
Lopes, M. T. P.; INO-016
Lopes, N. P; QPN-032
Lopes, N. P.; QPN-061
Lopes, P. A. L.; FOT-004
Lopes, P. S.; INO-066
Lopes, R. P. M.; AMB-076
Lopez, N; CAT-016
Lorenzo, V. P.; QPN-015
Losito, D. W.; INO-066
Lougon, D. J. F.; ELE-002, ELE-025
Lourencetti, C.; EDU-051
Lourenço, M. P.; TEO-009
Lourenço, V. S.; CAT-004
Louro, G. M; QPN-016
Louro, G. M.; AMB-075, QPN-004
Lousa, P. H. F.; ORG-021
Lovera, D. C. V.; BEA-003
Lu, T. K.; BIO-010
Luber, J; QPN-002
Lucas, E. F.; MAT-064
Lucas, E. M. F.; QPN-102
Luccas, P. O.; ANA-064, ANA-095
Lucchetti, P.; INO-035
Lucena, G. N.; COL-001
Lucilha, A. C.; MAT-018
Lüdtke, D. S.; ORG-034
Ludwig, F. P.; ORG-050
Luna, M. A.; ANA-091
Lustosa, L. H.; AMB-033
Luz, D. A; QPN-037
Luz, D. A.; ANA-073
Luz, R. C.; ELE-049

## M

Macedo Jr. , F. C.; MED-019
Machado, A. B.; ANA-071
Machado, A. E. H.; FOT-009, TEO-011
Machado, A. M. R.; QPN-102
Machado, A. R. T.; QPN-075
Machado, B. A.; BEA-019
Machado, B. P.; INO-069
Machado, D.; INO-080
Machado, G. S.; INO-051
Machado, G.; MAT-102
Machado, L. A.; ORG-058
Machado, L. H. C.; ORG-001
Machado, L. L.; QPN-055, QPN-072
Machado, M. C.; EDU-003
Machado, M. M.; MAT-005
Machado, P.; MED-056, MED-060
Machado, S. P.; MAT-013
Machado, V. G.; FIS-011
Machado, W. T. V.; AMB-029
Machulek Jr. , A.; FIS-012
Maciel, C. A. O.; MED-025
Maciel, J. W. O.; INO-087
Maciel, T. M. S.; MED-047
Maciel, V. M. B.; MAT-033
Madalena, L. S.; EDU-061
Madari, B. E.; ANA-061
Madeira, T. B; BEA-007
Madeira, T. B.; ANA-078, BEA-009
Madera, K. S. M.; QPN-068
Madriaga, V. G. C.; MAT-039
Madureira, J.; INO-035
Magalhães, C. E. C.; MAT-116
Magalhães, J. L.; TEC-001
Magalhães, L. G.; MED-005
Magalhães, L. G.; MED-027, MED-048, MED-059
Magalhães, V. S.; ANA-011
Mageste, A. B.; AMB-064, COL-006, COL-011, FIS-021
Mageste, A. B.; FIS-022
Mahmoud, T. S.; QPN-031
Maia, C. E. B.; ORG-060
Maia, D J; EDU-027
Maia, F. L.; MED-053
Maia, G. A. R.; FIS-025
Maia, G.; INO-089
Maia, L. F. P. G.; AMB-002
Maia, R. A; QVE-007
Maia, R. A.; QVE-002, QVE-008
Maldaner, A. O.; ANA-032
Maldaner, L.; ANA-030
Malheiros, R. O.; INO-018
Malta, L. F. B.; MAT-007, MAT-057
Malta, M.; MAT-095, MAT-113
Malta, O. L.; INO-085
Malta, V. R. S.; FIS-001
Maltarollo, V. G.; MED-011, MED-049, MED-057
Malvestiti, J.; AMB-050
Mambrini, R. V.; CAT-038, MAT-091
Mandelli, D.; CAT-006
Mandova, T.; QPN-123
Manduca, B.; AMB-052
Mangrich, A. S.; MAT-044
Mantovani, A. C.; ORG-034
Marçal, L. L; ORG-036
Marcelo, C. R.; AMB-055, EDU-041
Marcelo, L. R.; AMB-055, AMB-068, EDU-002
Marchi, M. I.; QPN-018
Marchi, M. R. R.; ANA-019
Marchi, R. C.; FOT-003
Marchi, R. C.; FOT-014
Marciano, A. C.; INO-071
Março, P. H.; BEA-002
Marcondes, M. E. R.; EDU-039
Marcorini, L. F. B.; QPN-033
Maria, D. A.; ORG-108
Mariano Junior, D. R.; ANA-008
Mariano, L. S.; EST-001
Marinho, A. M. R.; BIO-002, QPN-065
Marinho, M. V.; EST-001, INO-029, INO-081
Marinho, O. R; ANA-026
Marinho, P. S. B.; BIO-002, QPN-065
Marinho, W.; ANA-072
Marques, A. L. B.; ELE-038
Marques, F. F. C.; ANA-024
Marques, G. E. C.; QPN-025, QPN-053
Marques, G. L.; ELE-047
Marques, J. A.; INO-031
Marques, J. C.; QPN-053
Marques, L.; CAT-036
Marques, M. F. V.; CAT-035, MAT-042

Marques, M. J.; MED-036, QPN-032
Marques, M. V.; ORG-062
Marques, R. F. C.; COL-001, EDU-005, MAT-011
Marson, G. A.; EDU-007
Martinelli, L. K. B.; ORG-075
Martínez, O. C.; QPN-068
Martini, F. A.; AMB-042
Martins, A. R.; CAT-001
Martins, A. R.; MAT-035
Martins, B. S.; ORG-038
Martins, C. H. G.; QPN-006, QPN-008, QPN-057
Martins, C. T.; MED-005
Martins, C. T.; MED-048
Martins, D. C. Da. S.; MAT-083
Martins, D. C. S.; INO-001, INO-005, INO-032, INO-071, INO-079
Martins, E. S.; EDU-024
Martins, F. T.; INO-029, INO-081, INO-087
Martins, G. B. C.; CAT-020, TEC-008, TEC-010
Martins, G. F. L.; ANA-095
Martins, G. O.; MAT-036
Martins, G. S.; INO-063
Martins, G. W.; INO-045
Martins, I. V.; MAT-008
Martins, J. B. L.; FIS-023
Martins, J. P. A.; FIS-007, MED-066
Martins, M. C. M. R.; MED-028
Martins, M. F.; EDU-019, MAT-064
Martins, P. L.; FIS-022
Martins, P. S.; MAT-067
Martins, R. C. C.; QPN-038
Martins, T. G.; ANA-055
Martins, T. S.; INO-066
Martins, V. E. P.; EDU-036
Martins, V. E. X.; QPN-008
Martins, V. G.; ANA-006
Martins, V. H. N.; MAT-076
Maruyama, J. A.; EDU-005
Maruyama, S. A.; BEA-006
Marzorati, L; ORG-008
Masia, C.; MED-047
Mass, E. B.; MED-005
Mass, E. B.; MED-048
Mateus, A. L.; EDU-026
Mathias, L. S.; MED-053
Matos, C. F.; MAT-009
Matos, C. R. M. O.; INO-027
Matos, G. F.; ORG-091
Matos, J. S.; ORG-042
Matos, R. L. N.; QPN-023
Matos, R. P.; ANA-034, ANA-035
Matos, R.; ELE-053
Matsushima, J. E.; ORG-095
Matsushita, M.; BEA-002
Mattos, G. J.; ELE-050
Mattos, R. R.; ORG-076
Maturi, F. E.; MAT-080
Maulide, N.; ORG-034
Mayumi, L.; AMB-024
Mazali, I. O.; ANA-053, INO-008, INO-055, MAT-014, MAT-027, MAT-030, MAT-089, MAT-097
Mazalli, A. V. G.; BEA-009
Mcfarlane, J.; QPN-061
Medeiros Junior, I.; ANA-066
Medeiros, A. R.; MED-029
Medeiros, F. C.; ELE-042
Medeiros, L. S.; QPN-086
Medeiros, M. E.; INO-022, INO-044, INO-056, MAT-007
Medeiros, M. E.; INO-067
Medeiros, R. A.; ELE-053
Medeiros, S. R. A.; QPN-034
Medeiros, T. A.; AMB-075
Medina, R. P.; QPN-066, QPN-067
Megid, J.; ELE-024
Meier, M. M.; EDU-016, FIS-038, FIS-039
Meira, A. C. R.; COL-012, MAT-074
Meira, V. N.; ELE-025
Meireles, A. M.; INO-005, INO-018, INO-079
Meireles, G. K. Q.; EDU-063
Melchert, W. R.; ANA-028
Mello, J. E.; ANA-051
Mello, L. S.; ORG-009
Mello, M. V. P.; INO-023
Mello, M. V. P.; INO-090
Mello, P. A.; ANA-010, ANA-054
Mello, P. A.; ANA-052
Melo Cardozo, I. M; BEA-013
Melo De, E. B.; MED-066
Melo, A. L. M.; QPN-053
Melo, B. C. L.; ORG-106
Melo, B. C.; MAT-098
Melo, B. C.; MAT-116
Melo, C. E. A.; FIS-011
Melo, D. J.; QPN-083
Melo, D. Q.; AMB-017, ANA-075, ANA-079
Melo, E. B.; MED-056
Melo, G. R.; AMB-001
Melo, I. K. L.; FIS-030
Melo, J. C. S.; EDU-056
Melo, J. O. F.; BEA-015
Melo, M. E.; MED-023
Melo, N. O.; QPN-075
Melo, U. Z.; ORG-031
Melo, V. F.; MAT-111
Mendes, A. L. G.; ANA-010
Mendes, A. P. S.; MAT-035
Mendes, B. H. M.; MED-021
Mendes, C.; COL-009
Mendes, F. M. L.; TEC-001
Mendes, L. C.; MED-045
Mendes, L. F.; ELE-013, ELE-022, ELE-046
Mendes, T P P; ANA-020
Mendivelso, E. A. C.; MAT-101
Mendonça, D. M. H.; ANA-065
Mendonça, F. G.; MAT-067
Mendonça, I. C.; QPN-066
Mendonça, J. G. P.; ORG-068
Mendonça, J. S.; MED-010
Mendonça, L. F. M.; ANA-095
Mendonça, M. L. T. G.; AMB-035, EDU-030
Mendonça, P. X; EDU-054
Meneghetti, L.; CAT-020
Meneghetti, M. R.; CAT-010
Menegon, E. A. S.; MAT-065
Menezes da Silva, V. H.; ORG-098
Menezes, E. A.; EDU-060
Menezes, G. da G.; AMB-019
Menezes, I. R. S.; MAT-067
Menezes, P. H.; ORG-024
Menna-Barreto, R. F. S.; ORG-029
Menozzi, C. A. C.; MED-008
Mercury, J. M. R.; AMB-060
Mesko, M. F.; ANA-050, ANA-051, BEA-016
Mesquita, B. M.; ORG-110
Mesquita, I. S.; AMB-065
Mesquita, I. S.; QVE-013
Mesquita, L. M.; EDU-030
Mesquita, N. A. S; EDU-040
Mesquita, N. A. S.; EDU-018, EDU-032
Mesquita, N. A.; EDU-044
Messa, L. L.; MAT-119
Metwally, K.; MED-038
Meurer, E. C.; QPN-115
Meurer, L.; INO-072
Meyer, W. R.; TEC-011
Mezalira, D. Z.; CAT-005
Michalik, D.; ORG-108
Michel, S.; QPN-123
Michelutti, K. B.; ANA-086
Miguel, E. L. M.; ORG-067
Miguel, T.; FIS-028
Mihos, F. C. S. S.; ELE-037
Mikhraliieva, A.; MAT-012
Milagre, C. D. F.; ORG-001
Milagre, H. M. S.; ORG-039
Milani, J. L. S.; INO-005, INO-014, INO-053
Milhomem, K. P.; AMB-043
Milinsk, M. C.; ANA-085
Militão, G. C. G.; QPN-014
Millan, R. D. S.; AMB-044
Millán, R. D. S.; AMB-046
Minatti, E.; COL-009
Miranda, A. C. G.; EDU-012
Miranda, F. da S.; FOT-012
Miranda, F. S.; FOT-008
Miranda, G. M.; TEO-004
Miranda, J. L.; AMB-038, CAT-023
Miranda, L. S. M.; ORG-032, ORG-040, ORG-046, ORG-078
Miranda, P. B.; FIS-016
Miranda, R. C. C.; ELE-034, TEO-003
Missina, J. M.; INO-091
Mittersteiner, M.; FIS-020
Moares, D. A.; MAT-061
Módenes, A. N.; MAT-074
Modesto, H.; MAT-111
Modolo, L.; MED-047
Mogili, V.; MAT-061
Mohallem, N. D. S.; MAT-083
Mohallen, N. D. S.; MAT-037
Moher, P.; MAT-027
Molin, F.; ORG-010, ORG-082
Molina, E. F.; MAT-078

Molinari, J.; MAT-117
Mombrini, L. M.; CAT-023
Monção Filho, E. S.; QPN-104
Monego, M. L. C. D.; AMB-024
Montagner, C. C.; AMB-048, AMB-080
Monte, J. P.; MAT-093
Monteiro, A. L. B.; QPN-080
Monteiro, A. L.; CAT-020
Monteiro, A. O.; QPN-014
Monteiro, F.; AMB-073
Monteiro, G. C.; ANA-005
Monteiro, M. I. C.; AMB-029
Monteiro, V. E. M. M.; MAT-043
Montenegro, M. A.; TEC-010
Montenegro, R. C.; ORG-092
Montero, P. J. E.; ELE-043
Monti, G. A.; MAT-020
Montini, A. C. S.; AMB-054
Mora, A.; FIS-020
Moraes, A. C.; EDU-023
Moraes, F. C.; ORG-079, QPN-053
Moraes, L. D.; AMB-076
Moraes, M. C.; ORG-075
Moraes, M. I.; QPN-055, QPN-072
Moraes, M. M.; QPN-045
Moraes, M. P.; EDU-037
Morais, A. A.; AMB-058
Morais, C. C.; INO-062
Morais, D. R.; ANA-017
Morais, K. C.; AMB-065
Morais, K. C.; QVE-013
Morais, N. K.; QPN-001
Morais, P. A. O.; ANA-061
Morais, P. B.; QPN-031
Morais, S. A. L.; QPN-006, QPN-008
Morais, S. A.; AMB-070, QPN-030
Morais, T. R.; MED-007
Morais, W. S.; QVE-002
Morais, W. S.; QVE-007, QVE-008
Moralles, V. A.; MAT-070
Mora-Seró, I.; INO-101
Moreira, A B; AMB-030
Moreira, A. B.; AMB-078
Moreira, A. F. S.; CAT-022
Moreira, B. C. T.; EDU-008, EDU-017, EDU-065
Moreira, C. S.; ORG-092
Moreira, D. de L.; ANA-015
Moreira, D. L.; QPN-009
Moreira, D. N.; EDU-045, QVE-002, QVE-006
Moreira, D. N.; QVE-007, QVE-008
Moreira, G. M.; INO-035
Moreira, I.; AMB-073
Moreira, K. S.; FIS-014, FIS-031
Moreira, L. F. P. P.; ELE-023
Moreira, M. E. C.; QPN-110
Moreira, M. P.; QPN-019
Moreira, R. A; QPN-105
Moreira, R. V.; MAT-082
Moretto, C.; AMB-058
Morgon, N. H.; FIS-010, TEO-006
Morro, F. G.; AMB-032
Mota, C. J. A. ,; CAT-022
Mota, F. D.; INO-040
Mota, Y. C. C.; MED-047
Motta, G. V.; TEC-009
Motta, H. B.; MAT-012
Mottin, M.; MED-002
Moura, A. K. S.; QPN-034
Moura, A. R; EDU-022
Moura, F. A.; ELE-049
Moura, F. S.; INO-067
Moura, I. M. R.; ORG-024
Moura, J. F.; AMB-073
Moura, L. C. M.; EDU-052
Moura, L. C.; AMB-038
Moura, R. A.; MAT-086
Moura, R. G.; ORG-008
Moura, S.; ANA-031, ANA-077, INO-019, ORG-073
Moura, V. M.; QPN-115
Moya, H. D.; ANA-059, BEA-010, BEA-012
Mozeto, A. A.; AMB-053
Munaro, A. P.; MAT-117
Munaro, M.; MAT-117
Munhos, R. L.; ELE-015
Muniz, A. S.; MAT-046
Muniz, E. C.; MAT-004, MAT-114
Munoz, R. A. A; ELE-052
Munoz, R. A. A.; ANA-065, ELE-014
Muñoz, R. A. A.; ELE-035
Muñoz-Sanjosé, V.; INO-101
Murakami, C.; QPN-097, QPN-114
Murie, V. E.; ORG-070
Murta, S. M. F.; MED-008
Mutti, A. M. G.; MAT-088

## N

Naal, Z.; ELE-048, ELE-060
Naccache, M. F. N.; COL-008
Nacif, J. E.; ANA-013
Nagao, R.; ELE-034, ELE-054, TEO-003
Nagaoka, D. A.; MAT-005, MAT-104
Nakabashi, M; MED-039
Nakagaki, S.; INO-051
Nakamura, C. V.; MED-052
Nakamura, T. C.; ANA-012, ANA-014, BEA-011
Nalepa, K. T.; EDU-033
Namikuchi, E. A.; ANA-053
Nandenha, J.; ELE-005, ELE-031
Naozuka, J.; AMB-004
Napoli Barbato, C. N. B.; INO-102
Nascentes, C. C.; AMB-016, ANA-034, ANA-035, ORG-096
Nascimento, B. N.; EDU-052
Nascimento, B. O.; QPN-039
Nascimento, E. A.; QPN-006, QPN-008
Nascimento, E. D.; BIO-013
Nascimento, G. N. L.; QPN-031
Nascimento, I. R; QPN-077
Nascimento, J. S.; QPN-059
Nascimento, L. A.; MAT-057
Nascimento, L. D; QPN-013
Nascimento, L. L. Q.; FIS-005, FIS-019
Nascimento, M. A.; ORG-094
Nascimento, M. M.; ANA-009
Nascimento, M. S.; QPN-062
Nascimento, N. F. C.; ANA-027
Nascimento, N. L.; MED-040
Nascimento, N. R. F.; INO-088
Nascimento, O. R.; INO-004
Nascimento, P. G. G.; ORG-110
Nascimento, R. S.; AMB-060
Nascimento, S. L. F.; MED-050
Nascimento, V.; MAT-039
Nascimento-Júnior, N. M; MED-044
Nascimento-Júnior, N. M.; MED-063, MED-065
Nascimentov, V. M. S.; QPN-062
Nassar, E. J.; INO-017, INO-054, MAT-010
Nasser, R. O.; MAT-112
Navarro-Vázquez, A; ORG-025
Nazarkovskyi, M.; MED-014
Neiva, E. G. C.; MAT-125
Nepovimova, E.; MED-033
Neres, M. E. S.; EDU-006
Neri, C. R.; FOT-011
Neri, J. A. M.; AMB-047
Neris, A. M.; ORG-097
Neto, A. C.; TEC-002, TEC-005
Neto, A. O.; ELE-005, ELE-031
Neto, ACN; ORG-102
Neto, F. J; QPN-082
Neto, J. F.; QPN-080
Neto, J. M. R.; MED-006
Neto, L. S.; ORG-096
Neto, P. R. C.; FIS-008
Netto-Ferreira, J. C.; FOT-009
Neves, A. A.; ANA-001
Neves, A. P.; INO-024, INO-084
Neves, B. J.; MED-002, MED-046
Neves, C. G.; ELE-027
Neves, M. F. F.; MAT-029
Neves, M. G. P. M. S.; ORG-088
Nhuyen, H. H.; INO-038
Nicacio, A. E.; ANA-030
Nicolau, C. L; QPN-016
Nicolau, C. L.; AMB-069, AMB-075, QPN-004
Nicoleti, C. R.; FIS-011
Nicolini, J.; AMB-059, FIS-026
Nicolini, K. P.; AMB-059, FIS-026
Nielsen, D. U.; ORG-019
Nishimura, R. H. V.; ORG-070
Nixdorf, S. L; BEA-007
Nixdorf, S. L.; ANA-078, BEA-009
Nóbrega, J. A.; ANA-037
Nogueira, H. P.; MAT-063
Nogueira, P. F.; MED-036
Nogueira, T. L C.; MED-064
Nogueira, T. L. C.; MED-061
Nogueira, T.; AMB-008
Nome, F.; ORG-067
Nonaka, L. H.; MAT-015
Nossol, A. B. S.; AMB-079
Nossol, E.; ELE-014

Nossol, Edson; ELE-052
Novacoski, E. J.; AMB-033
Novaes, A. B. S. V.; EDU-043
Novaes, L. F. T.; ORG-083
Novais de Abreu, A.; MAT-052
Novelli, A. P.; QPN-023
Novo, D. L. R.; ANA-051
Nowacki, B.; MAT-079
Nucci-Martins, C.; MED-003
Nuncira, J. A. V.; MAT-043
Nunes, A. V. J.; ORG-013
Nunes, C. da Silva; BIO-007
Nunes, C. R. de O.; AMB-019
Nunes, C. S.; MED-047
Nunes, D. S.; ORG-011
Nunes, E. A.; QPN-096
Nunes, F. M.; QPN-055, QPN-072
Nunes, G. G.; INO-091
Nunes, J. T. L.; AMB-017, ANA-075, ANA-079
Nunes, M. C.; FIS-019
Nunes, M. L.; MAT-055
Nunes, R. C.; EDU-015
Nunes, R. J.; COL-009, MED-003
Nunes, R. R.; MED-022
Nuñez, W. E. R.; QPN-059

## O

Ogava, L. E.; AMB-013
Oliboni, R. S.; FIS-011
Oliva, A. D.; EDU-028
Oliva, G.; MED-004, MED-027, MED-039
Oliveira De, C. M. A.; QPN-019
Oliveira De, D. F.; AMB-047
Oliveira De, M. S.; ORG-011
Oliveira De, S. J.; EDU-024
Oliveira Jr, V. X.; BIO-010
Oliveira, A. A.; INO-077
Oliveira, A. C. S.; ANA-024
Oliveira, A. F.; ANA-001, MED-056
Oliveira, A. H. B.; AMB-017
Oliveira, A. I. T.; QPN-031
Oliveira, A. L; BEA-017
Oliveira, A. R. M.; FIS-019
Oliveira, A. R. S.; MAT-046
Oliveira, A. S.; ANA-072, BEA-005
Oliveira, A. S.; MED-003
Oliveira, A. V. B.; MAT-094
Oliveira, A. V. T.; QPN-047
Oliveira, A.; QPN-006, QPN-064
Oliveira, B. G. F.; TEC-003
Oliveira, C. J.; ORG-058
Oliveira, C. M. A.; MAT-087
Oliveira, D. C. B; ORG-057
Oliveira, D. C. B.; EDU-042
Oliveira, D. H.; INO-037
Oliveira, E. A.; QPN-114
Oliveira, F. P. S.; AMB-017
Oliveira, G. G.; ELE-001
Oliveira, G. M.; INO-086
Oliveira, G. V.; QVE-005
Oliveira, H. F. S.; INO-064
Oliveira, I. N.; INO-062
Oliveira, I. R.; ORG-110
Oliveira, J. B.; QPN-102
Oliveira, J. F.; MED-032
Oliveira, J. M. D.; EDU-006
Oliveira, J.; QPN-013
Oliveira, K. M.; INO-034
Oliveira, K. T. DOS. S. DE; ANA-057
Oliveira, L. A; EDU-022
Oliveira, L. B.; ANA-059
Oliveira, L. C. de; AMB-062
Oliveira, L. C. S.; AMB-069
Oliveira, L. C.; AMB-036
Oliveira, L. H.; MAT-014
Oliveira, L. L.; INO-024
Oliveira, L. N.; MED-053
Oliveira, L. P.; INO-036
Oliveira, M. A. L.; ANA-003
Oliveira, M. B; EDU-020
Oliveira, M. D. A.; EDU-048, ORG-089
Oliveira, M. D. A.; QPN-034
Oliveira, M. D. D. A.; ORG-063
Oliveira, M. K. S.; INO-042
Oliveira, M. M.; MAT-002, MAT-029, MAT-072
Oliveira, M. M.; MAT-096
Oliveira, M. S.; EDU-025, EDU-029
Oliveira, P. C. O.; AMB-074
Oliveira, P. H. R.; ORG-022
Oliveira, P. M.; CAT-026
Oliveira, R. B.; MED-049
Oliveira, R. C.; ELE-020
Oliveira, R. F. de; ANA-062
Oliveira, R. F.; ORG-097
Oliveira, R. N.; QPN-073
Oliveira, S. C.; FIS-012
Oliveira, S. J.; EDU-036, EDU-060
Oliveira, T. C. C.; MED-064
Oliveira, T. S. A.; EDU-015
Oliveira, V. G.; ORG-087
Oliveira, V. H. A.; ELE-031
Oliveira, W. A.; ORG-064
Oliveira, W. V. O.; ELE-004
Oliveira, W. X. C.; INO-025
Oliveira, W. X. C.; ORG-029
Oliveira, Y. F.; QPN-024
Oliveira-Silva, D.; AMB-021
Omori, A. T; QVE-011
Orlandi, M. O.; ELE-007
Orlandin, G.; ANA-045
Orlando, B. H. S. L.; ORG-057
Orlando, R. M.; AMB-044, AMB-046, AMB-061, AMB-064
Orsato, A.; MED-035
Ortega, P. F. R.; ELE-058, FIS-003
Orth, E. S.; CAT-013, FIS-006, FIS-019, MAT-073, QVE-004
Ortiz, F. J. A.; EDU-059
Ortiz, R. S.; ANA-031
Ortiz-Nuñez, Y.; QPN-092
Osti, R. Z.; QVE-003
Otero, D. M.; INO-034
Ovalle, S.; MAT-106
Owens, R.; MED-046
Oyhenart, J. A.; QPN-021

## P

Pacheco, C. M.; INO-023
Pacheco, J. S.; ORG-087
Pacheco, W. F.; ANA-004
Pachel, B.; FOT-014
Padilla-Chavarría, H. I. P. C.; MAT-040
Padilla-Chavarría, H. I.; MAT-101
Paesano Júnior, A.; INO-077
Pagnocca, F. C.; QPN-070
Paim, A. P. S.; ANA-037
Paiva, F. F.; INO-016
Paiva, M. F.; CAT-034
Paiva, R. O.; MED-020
Paixão, D. A.; INO-036
Paixão, I. C. N. P.; ORG-085
Paixão, I. C. P.; ORG-106
Paixão, N. M.; INO-048
Paixão, T. R. L. C. da; ELE-013
Paixão, T. R. L. C. P.; ELE-030
Paixão, T. R. L. C.; ELE-022, ELE-046
Palanch, M. F.; ANA-058
Palma, D. Y. R.; ORG-008
Palomino-Salcedo, D. L.; MED-027
Pamphile-Adrian, A. J.; CAT-017
Pamphile-Adrián, A. J.; CAT-033
Panciera, M.; MED-039
Pantaleão, S. Q.; MED-009, MED-028
Papa, B. L.; ORG-027
Parente, T. P.; CAT-035
Parize, A. L.; COL-009
Parreira, L. S.; ELE-005, ELE-031
Paschoal, F. M. M.; AMB-030
Paschoalino, V. T.; ORG-031
Pascoalino, L. A.; MAT-004
Pasin, R. O.; EDU-059, ELE-041
Pasquini, C.; BEA-014
Passarelli, C.; ORG-100, ORG-108
Passero, L. F. D.; QPN-116
Passos, F. B.; CAT-017, CAT-033
Pastorini, L. H.; QPN-109
Pastre, J. C.; ORG-083
Pastrello, B.; ORG-026
Pastrián, F. A. C.; MAT-105
Patrício, P. R.; ANA-032
Paula De, E. L.; ORG-041
Paula, F. H. M.; QVE-009
Paula, F. R.; MED-056
Paula, R. C. M.; INO-042
Paula, R. R.; AMB-065
Paula, R. R.; QVE-013
Pauletti, P. M.; ORG-006, QPN-057
Pauli, I.; MED-004
Paulino, J. F.; ANA-038
Paulino-Lima, I. G.; AMB-071
Paulo, B. S.; QPN-069
Paulo, T. de F.; INO-002
Paumgartten, F. J. R.; ANA-015
Pavan, F. R.; INO-036, MED-034
Pavanelli, W. R.; MED-019

Paz, E. C.; ELE-011, ELE-016
Paz, I. A.; INO-088
Pazinato, J.; INO-095, INO-099
Pazinato, M. S.; EDU-012
Pazini, F.; MED-050
Pedraça, P.; QPN-026
Pedrosa, L. F.; MAT-099, ORG-058
Pedrosa, S. C. B. L.; MED-032
Pedroso, E. F.; INO-003, INO-025
Pedroso, N.; ORG-100
Pedroso, R. C. N.; ORG-006, QPN-058
Pedrotti, J. J. P.; ELE-004
Pedrotti, J. J. P.; MAT-032
Pedrozo, E. C.; EDU-052
Peixoto, B. S.; AMB-074
Peixoto, M. A.; QPN-109
Peixoto, M. A.; QPN-115
Pelin, J. N. B. D.; MAT-118
Pena, G. B. O; EDU-040
Penco, V. S. N.; EDU-025, EDU-029
Penido, J. A.; COL-006, COL-011, FIS-021
Penido, J. A.; FIS-022
Peralva, C. M. S.; MED-038
Peralva, V. N.; ANA-083
Perdigão, L. T.; CAT-009
Perdomo, R. T.; QPN-027
Perecim, G. P.; ORG-033
Perecin, C. J.; COL-007
Pereira Cabrera, P. C.; QPN-012
Pereira Netto, A. D.; AMB-011, ANA-004
Pereira, A. F.; MAT-072
Pereira, A. K. L. S.; QPN-055, QPN-072
Pereira, A. K.; QPN-070
Pereira, A. L. S.; MAT-047
Pereira, A. R. B.; AMB-005
Pereira, C. L. M.; INO-025
Pereira, C. M. P.; ORG-073
Pereira, E. T. V.; QPN-052
Pereira, G. M.; ORG-057
Pereira, H. K. M.; FOT-016
Pereira, H. S.; ORG-106
Pereira, K. T. O.; MED-042
Pereira, L. F.; AMB-068, EDU-002
Pereira, L. S. F.; ANA-052
Pereira, L. S. F.; ANA-054
Pereira, M. F.; EDU-064
Pereira, R. M.; ANA-050, ANA-051
Pereira, R. S.; AMB-065
Pereira, R. S.; QVE-013
Pereira, S. F. M.; QPN-013
Pereira, S. G.; QPN-025
Pereira, T. M.; EDU-038, EDU-046, FOT-008, INO-024
Pereira, W. S. G.; MAT-051
Pereira-Maia, E. C.; INO-069
Peres, R. L.; BEA-004
Perez, C. N.; MED-045
Perez, V. H.; TEC-007
Perini, J. A. L.; ELE-021
Peroni, L. A.; BIO-001, ELE-017
Pessoa, C.; QPN-104
Pessoa, O. D. L.; QPN-084
Pessoa, T. C. C.; EDU-064
Peterle, M. M.; ORG-062
Peternelli, L. A.; ANA-076
Petiot, L.; INO-008
Petizero, T. D.; INO-067
Petrônio, M. S.; MAT-036
Pettersson, L. G. M.; TEO-009
Philot, E. A.; MED-009
Piazza, R. D.; MAT-011
Picasso, G.; ANA-091
Pich, C. T.; INO-019
Picoloto, R. S.; ANA-033, ANA-043, ANA-044
Picro, K. G.; QPN-052
Pietezak, D. F.; EDU-016
Pietre De, M. K.; AMB-047
Pilissão, C.; INO-052, ORG-111
Pim, W. D. do; MAT-069
Pim, W. D.; INO-081
Pimenta, E. F.; QPN-070
Pimenta, L. P. S.; QPN-075, QPN-112
Pimenta, L. P.; ORG-006, QPN-058
Pimenta, L. T. G.; MAT-042
Pimenta, R. S.; QPN-031
Pimentel, J. V. P.; ORG-078
Pinheiro, A. A.; QPN-040
Pinheiro, A. F.; EDU-064
Pinheiro, C. B.; INO-097
Pinheiro, D. L. J.; ORG-019
Pinheiro, L. C. S.; MED-030
Pinheiro, M. V. B.; FOT-002
Pinheiro, V. S.; ELE-005, ELE-016, ELE-031
Pinke Rodrigues, C. H.; MED-066, TEO-008
Pinto, A. C. M.; QPN-077
Pinto, A. C.; MED-008
Pinto, C. O.; ANA-012
Pinto, L. M. C.; INO-089
Pinto, L. S.; QPN-074
Pinto, Licarion; ANA-072
Pinto, M. B.; CAT-007
Pinto, M. E. F.; QPN-076, QPN-125
Pinzón, A. D. G.; AMB-044
Pioker, F. C.; QPN-011
Piovezan, C E; AMB-030
Piovezan, C. E.; AMB-078
Pires, A. M.; MAT-088
Pires, B. M.; INO-096
Pires, I. C. B.; MAT-041, MAT-058
Pires, L. O.; QPN-121
Pires, N. J.; FIS-003
Pissinate, K.; MED-060
Pissurno, A. P. R.; MED-059, ORG-056
Pita, S. S. R.; MED-024, MED-055
Pita, S. S.; MED-038
Pivatto, M.; INO-036
Pizzuti, L.; INO-089
Pliego Jr. , J. R.; ORG-067
Pliego, J. R.; TEO-013
Pochapski, D. J.; COL-013
Polaquini, C. R.; ORG-067
Polesi, M. C.; QPN-063
Poli, C. T.; EDU-037
Polillo, G.; ORG-106
Politi, J. R. S.; FIS-023
Polo, E. C.; ORG-030
Pomini, A. M.; QPN-100, QPN-109
Pomini, A. M.; QPN-115
Ponquio, F. P.; ORG-047
Pontes, F. V. M.; AMB-026, ANA-038, ANA-069
Pontes, R. M.; TEO-014
Pontes, T. S.; ORG-058
Porcu, O. M.; BEA-001
Portella, R. B.; BEA-011
Porto, B. L. S.; BEA-008
Postal, K.; INO-091
Prasad, P. N.; MAT-079
Prestes, O. D.; AMB-020
Previdello, B. A. F.; FIS-004
Priebe, G. P. S.; TEC-004, TEC-006
Probst, L. F. D.; INO-072
Procópio, A. M. S.; MAT-017
Proença, G. S.; ORG-058
Pupin, R. R.; ANA-005

## Q

Queiroz, E. F.; BEA-018
Queiroz, M. E. L. R.; ANA-001
Queiroz, M. P.; ORG-096
Queiroz, S. F.; EDU-031
Queiroz, S. L.; EDU-010
Querino, A. L. de A.; INO-046
Quimas, J. V. F.; MED-061, MED-064
Quincoces, J.; ORG-100, ORG-108
Quinhones, R.; BEA-004
Quintão, M. C.; CAT-007
Quintino, M. P.; EDU-055, INO-057

## R

Rabelo, D.; MAT-087, QPN-036
Raimundo Jr, I. M.; ANA-053
Ramalho, S. D.; QPN-125
Ramalho, T. C.; MED-033, TEO-012
Rambo, D. F.; QPN-042
Raminelli, C.; ORG-020, ORG-033
Ramirez, M. R.; QPN-021
Ramos, A. I. B.; INO-004
Ramos, B. S.; AMB-022
Ramos, D. P.; ANA-070
Ramos, J. E. T.; EDU-014, MAT-086
Ramos, Y. J.; QPN-009
Rampon, D. da S.; ORG-099
Rangel, E. C.; MAT-021
Rangel, M. C.; MAT-035
Ratuchne, F.; MAT-110
Raul, L.; ORG-094
Rebouças, L. O.; MAT-045
Rebouças, P. H. L.; QPN-062
Receputi, C. C.; EDU-038, EDU-046
Regasini, L. O.; MED-034
Regina, C. A. C.; AMB-004
Rego, E. L.; ANA-014
Regufe, P. F.; ORG-087
Rehman, H. U.; INO-021
Reinaldo, A. C.; MAT-097
Reis, A. C. C. S.; QVE-012

Reis, A. K. C. A.; ORG-047, ORG-069
Reis, A. S.; EDU-023
Reis, B. F; ANA-025
Reis, B. F.; ANA-026
Reis, D. B.; ORG-043
Reis, D. M.; INO-041
Reis, G. R. L.; MAT-009
Reis, I. F.; INO-082, TEO-007
Reis, W. J.; ORG-061
Rengifo, A. F. C; COL-009
Renner, R. E.; TEC-004, TEC-006
Reolon, C. M. M.; COL-003
Reolon, D.; QVE-003
Requena, G. F.; MAT-070
Resende, G. O.; ELE-002
Resende, J. A. L. C.; MAT-020
Resende, M. V. B.; CAT-009
Resende, V. G.; MAT-049
Reviglio, L.; MAT-020
Rezende, C. R; QPN-122
Rezende, D. B.; EDU-038, EDU-046
Rezende, M. C.; FIS-011
Ribas, V. C.; INO-092
Ribeiro Filho, W. A.; ANA-057, ANA-058
Ribeiro, A. I; QPN-086
Ribeiro, A. O.; ORG-108
Ribeiro, C. M.; INO-036, MED-034
Ribeiro, E. S.; ANA-045
Ribeiro, E. S.; ELE-037
Ribeiro, G. M.; ORG-071
Ribeiro, G.; INO-070, MAT-099
Ribeiro, J. A. A.; AMB-047
Ribeiro, J. P. R.; AMB-002
Ribeiro, L. E. B.; ANA-068
Ribeiro, M. A.; EST-001
Ribeiro, M. C. C.; FIS-017
Ribeiro, M. S.; MAT-006, ORG-106
Ribeiro, R. P.; CAT-037
Ribeiro, S. J. L.; ELE-021, INO-039, MAT-080
Ribeiro, S.; MAT-099
Ribeiro, T. R.; MED-065
Ribeiro, V. S.; AMB-010
Ribeiro, W. S.; BIO-014
Richardson, S.; AMB-048
Richart, F. S.; MAT-117
Richter, A. R.; INO-042
Richter, E. M.; ANA-065, ELE-014, ELE-035, ELE-052
Riegel-Vidotti, I. C.; CAT-013
Riehl, C. A. S.; QPN-035
Rinaldo, D.; QPN-092
Rios, E. A. M.; ORG-099
Ripardo Filho, H. S.; BIO-011, BIO-014
Rittner Neto, R.; ORG-014
Rivero, E. A. I.; ORG-033
Rizzato, T. M.; AMB-056
Rizzo-Domingues, R. C. P.; FIS-008
Robaina, N. F.; ANA-056
Roberto, T. C.; ORG-090
Rocco, M. L. M.; MAT-013
Rocco, M. L. M.; MAT-100
Rocha, A. A.; ANA-071
Rocha, A. C. S.; EDU-025, EDU-029
Rocha, A. J. R.; MAT-116
Rocha, A. S.; CAT-025, QPN-065
Rocha, C. O.; COL-001, EDU-005
Rocha, C. Q.; QPN-040
Rocha, D. D.; ORG-110
Rocha, D. P.; ANA-065
Rocha, D. P.; ELE-052
Rocha, D. S.; ELE-028
Rocha, F. R. P.; ANA-016
Rocha, F. V.; INO-040, INO-064, INO-075
Rocha, G. F. S. R.; CAT-012
Rocha, G. N. S. A. O.; QPN-015
Rocha, H. V. A; MAT-020
Rocha, I. N. D. S.; MAT-124
Rocha, L. A.; INO-017, MAT-010
Rocha, L. D. S.; MAT-007, MAT-057
Rocha, L. R.; ELE-047
Rocha, M. G.; INO-051
Rocha, P. S. M.; ANA-084
Rocha, R. C. N.; ANA-057, ANA-058
Rocha, R. P. R. F.; ANA-027
Rocha, S. L.; FOT-001
Rocha, T. C. da; FOT-012
Rocha, W. C.; QPN-054
Rodrigues Gomes, M. R. R. G.; ANA-036
Rodrigues Pinto, M. R.; ELE-034
Rodrigues, A. C.; BEA-003
Rodrigues, A. T. G.; EDU-059
Rodrigues, A.; ORG-018, ORG-027, ORG-095
Rodrigues, C. A.; ANA-030
Rodrigues, C. C. S.; AMB-022
Rodrigues, C. N.; QPN-054
Rodrigues, D. J.; QPN-078
Rodrigues, D. R. F.; QVE-001
Rodrigues, E. A.; ANA-073
Rodrigues, E. M.; ELE-006
Rodrigues, F. A. V.; BIO-012
Rodrigues, F. H. A; MAT-116
Rodrigues, F. H. A.; MAT-098
Rodrigues, F.; AMB-039, AMB-071, FIS-036
Rodrigues, G. D.; AMB-044, AMB-046, AMB-061, AMB-064, ANA-034
Rodrigues, I. A.; ELE-038
Rodrigues, J. E. F. C; ORG-086
Rodrigues, L. C.; ANA-095
Rodrigues, L. M. S.; MED-032
Rodrigues, L. O.; MED-034
Rodrigues, L. S.; MAT-026
Rodrigues, M. K.; MAT-091
Rodrigues, M. N.; ANA-089
Rodrigues, M. V. R.; CAT-020
Rodrigues, M.; ELE-054
Rodrigues, N. M. C.; EDU-062, EDU-066
Rodrigues, P. R. P.; FIS-025
Rodrigues, R. C.; MED-023
Rodrigues, R. K. R.; COL-008
Rodrigues, R. P.; QPN-056
Rodrigues, T. H. S.; QPN-005, QPN-028
Rodrigues, T. S.; CAT-014
Roesch-Ely, M; QPN-117
Rohwedder, J. J. R.; ANA-029
Roiffé, R. R.; ANA-013
Rojas, J. E. U.; ELE-017
Roldão, T. M.; AMB-025
Román, D. C. C.; TEC-005
Roman, L. S. Roman; MAT-100
Roman, L. S.; MAT-029
Romanha, A. J.; MED-008
Romanhi, P.; ORG-058
Roman-Leshkov, Y.; CAT-019
Romano, J R; QPN-071
Romano, R. L.; FIS-004
Romeiro, G. A.; AMB-074
Romeiro, G. A.; ORG-060
Romeiro, N. C.; MED-061, MED-064
Roméro-Gonzalez, R.; ANA-077
Romoff, P.; INO-083, QPN-113
Ronconi, C. M.; INO-027, MAT-039, MAT-059
Rondan, F. S.; ANA-050, BEA-016
Roque, J. V.; ANA-076
Roque, N.; QPN-090, QPN-091
Roquetto, J. M.; ELE-026
Rosa Filho, J. S.; QPN-062
Rosa, A. P. A.; QPN-103
Rosa, F. A.; ORG-071
Rosa, I. M. L.; EST-001
Rosa, L. C. da; ANA-015
Rosa, L. N.; BEA-002
Rosa, M. C.; MED-018
Rosa, M. F.; MAT-047
Rosa, T. F.; MED-045
Rosales, P. F.; QPN-117
Rosenberger, A. G.; MAT-016
Rospendowiski, J.; ELE-054
Rosseto, R.; AMB-051, INO-062
Rossi, L. M.; CAT-016, CAT-021, CAT-027
Rossi, L. M.; CAT-036
Rozada, A. M. F.; BIO-012
Rozada, T. C.; TEO-005
Rozendo, J. D.; CAT-021
Rozo Nuñez, W. E.; ORG-104
Rubert, A.; AMB-042
Rubira, A. F.; MAT-114
Rufino, V. H. L.; QPN-067
Ruiz, A. L. T. G.; QPN-115
Ruiz, D.; CAT-001
Russo, H. M.; BEA-018
Russowsky, D.; MED-005, MED-048

## S

S. Filho, R. C.; BIO-005
S. Neto, M.; EDU-022
Sá Jr. , E. P.; QPN-003
Sá, A. C.; ELE-023
Sá, M. M.; ORG-062
Sá, N. R. L.; AMB-068
Sá, V. A.; AMB-070
Sabino, A. P.; MED-022
Sabino, J. R.; INO-057
Sacchelli, B. A. L.; MED-035
Sacramento, B. S.; QPN-106
Sáenz, H. S. C.; ELE-043

Sagrillo, F. S.; ORG-088
Saint'Pierre, T. D.; AMB-073
Sakukuma, M. C. K.; ORG-013
Salamoni, J.; QPN-010
Salazar-Banda, G. R.; ELE-059
Salcedo, W. J. S.; ELE-061
Sales-Júnior, P. A.; MED-008
Salgado, A. M.; ELE-037
Salgado, J. R. C.; EDU-028, EDU-047, EDU-059, ELE-041
Salomão, K.; MED-012, MED-054
Saltarelli, M.; INO-054
Salum, A. S.; MAT-117
Salviano, A. B.; MAT-067
Salzer, G.; ORG-072
Sampaio, D. F. G.; QPN-057
Sampaio, I. H.; QPN-119
Sanches, P. R. S.; QPN-125
Sandoval, W.; ANA-039
Sannomiya, M.; QPN-011
Sant'Ana, A. C; FIS-032
Sant'Ana, A. C.; COL-010
Sant'Anna, C. M. R.; MED-040
Santamaría, R.; ELE-058
Santana Soares de Araújo, L. S. S. de A.; ANA-036
Sant'Ana, A. C.; FIS-026
Santana, A. J.; MAT-001, MAT-090
Santana, A. L. B. D.; QPN-062
Santana, D. A. de; MAT-033
Santana, D. A.; ANA-018, EDU-017
Santana, F. O.; AMB-009
Santana, F. S.; INO-041, INO-091
Santana, K. S; ORG-036
Santana, L. H.; EDU-016
Santana, L. L. B.; ORG-016
Santana, M. H. P.; ELE-028
Santana, M. V. A.; ANA-018
Santana, S. M. F.; MAT-095
Sant'anna, C. M. R. S.; MED-015
Sant'Anna, C. M. R.; MED-021, ORG-012
Santelli, R. E.; AMB-029
Santiago, G. M. P.; QPN-014
Santiago, P. A. L.; QPN-060
Santiago, P. V. B.; ELE-026
Santiago, R. F.; QPN-108
Santiago, V. S.; ELE-025
Santin, M. O.; QPN-109
Santin, S. M. O; QPN-100
Santin, S. M. O.; QPN-115
Santisteban, M. R.; QPN-082
Santos Alves, G. F.; EDU-021
Santos Dos, F. S.; AMB-047
Santos Dos, G. R.; AMB-072
Santos Dos, J.; AMB-070, QPN-030
Santos Dos, K. R.; QPN-002
Santos Dos, L. C.; ORG-006
Santos Dos, R. B.; TEC-002
Santos Dos, S. S.; INO-038
Santos Junior, J. S; MAT-071
Santos, A. A. B.; AMB-005
Santos, A. C. F.; ELE-049
Santos, A. G. C.; BIO-006
Santos, A. H.; EDU-053
Santos, A. K. M.; QPN-050
Santos, A. L.; MED-006
Santos, A. L.; QPN-041
Santos, A. P. B.; EDU-064
Santos, A. P.; MAT-049, MAT-103
Santos, A. R. S.; MED-003
Santos, A. S; QPN-065
Santos, B. R. S.; ANA-081
Santos, B. R.; INO-047
Santos, B. S.; FOT-016, MAT-093
Santos, C. B. R.; MED-016
Santos, C. H.; INO-012
Santos, C. S.; ANA-058
Santos, D. A.; QPN-029
Santos, D. C. M. B.; ANA-083
Santos, D. C. P.; EDU-063
Santos, D. C.; MED-061, ORG-047
Santos, D. G.; QPN-122
Santos, D. J. S.; EDU-021
Santos, D. M. D.; EDU-052
Santos, D. P.; EDU-037, MAT-014
Santos, D. S.; ORG-075
Santos, D.; TEC-009
Santos, E. B. G. N.; ANA-049
Santos, E. B.; MAT-027
Santos, E. C. S; MAT-039
Santos, E. C. S.; MAT-059
Santos, E.; AMB-022
Santos, F B; TEO-002
Santos, F. A. R.; QPN-118
Santos, F. A.; ORG-059
Santos, F. K. O.; EDU-024
Santos, F. S.; ORG-103
Santos, G. A.; ORG-048
Santos, G. H. F.; COL-005
Santos, G. H. G.; MAT-115
Santos, G. J. S. R.; ORG-050
Santos, G. O.; ELE-058, FIS-003
Santos, H. S.; QPN-005, QPN-028
Santos, I. C.; AMB-072
Santos, I. da S. P.; AMB-068
Santos, I. M.; MAT-102
Santos, I. S. P.; EDU-002
Santos, J. A. O.; MAT-088
Santos, J. B.; EDU-064
Santos, J. C. C.; ANA-022, ANA-023, BIO-005, BIO-007, MED-042, MED-047
Santos, J. C.; EDU-001
Santos, J. de C.; FIS-002
Santos, J. L. O.; AMB-013, ANA-082
Santos, J. M. S. R.; AMB-065
Santos, J. M. S. R.; QVE-013
Santos, J. M.; ANA-017, ANA-060, ANA-074
Santos, J. R. J.; QPN-040
Santos, J. R. L; MAT-035
Santos, J. R. N.; INO-057
Santos, J. V. da S.; ANA-012
Santos, J. V.; BEA-011
Santos, J.; EDU-035
Santos, K. S.; FOT-004
Santos, L. A.; BIO-002
Santos, L. C.; QPN-063
Santos, L. F; QPN-111
Santos, L. P.; EDU-017
Santos, L. R.; ANA-083
Santos, L. S.; BIO-011, BIO-014, EDU-025, EDU-029, ORG-028, QPN-046, QPN-106
Santos, L. V. S.; AMB-037
Santos, M. A; EDU-022
Santos, M. C.; ELE-005, ELE-011, ELE-016, ELE-031
Santos, M. G. B.; AMB-079
Santos, M. K. S.; MED-006
Santos, M. M. dos; MAT-033
Santos, M. N. G.; MAT-087
Santos, M. R. D.; MAT-067
Santos, M. R.; BEA-003
Santos, M. S. F. S.; ELE-030
Santos, M. S.; MAT-111
Santos, P. A.; QPN-039, QPN-074
Santos, P. B.; FIS-018
Santos, P. R.; MED-056
Santos, P. V.; EDU-001
Santos, R. A.; EDU-042
Santos, R. B.; TEC-005
Santos, R. dos; ANA-015
Santos, R. F.; ANA-043, ANA-044
Santos, R. M. G. dos; MAT-033
Santos, R. M.; EDU-060
Santos, R. O.; QPN-011
Santos, R. P.; ANA-073
Santos, R. R. F.; BIO-007
Santos, R. R.; BEA-020
Santos, R. V.; MAT-057
Santos, S. A.; EDU-043
Santos, S. J.; TEC-004, TEC-006
Santos, S. S.; EDU-008
Santos, S. T; MAT-071
Santos, S. Y. K. O.; QPN-056
Santos, T. C.; AMB-008
Santos, T. S.; EDU-049, ORG-045
Santos, U. S.; FIS-035
Santos, V. de S.; ANA-048
Santos, V. F.; MAT-013
Santos, V. L; EDU-022
Santos, W. N. D.; ANA-018
Santos, W. P. C.; ANA-048
Saraiva, E. S.; QPN-055, QPN-072
Saraiva, M. F.; ORG-043
Saran, L. M.; AMB-058
Saravia, L. H.; ELE-043
Sardela, V. F.; ANA-013
Sarmento Silva, S. S.; QPN-012
Sarmento, J. P.; EDU-030
Sarragiotto, M. H.; MED-042, MED-052
Sartoratto, P. P. C.; MAT-087, QPN-036
Sartorelli, P.; MED-007, QPN-041, QPN-085, QPN-097, QPN-113, QPN-114, QPN-116
Sartori, E. R; ELE-050
Sauthier, M. C. S.; ANA-018
Savanhago, R. M.; FIS-039
Scaglioni, P. T.; ANA-050, BEA-016
Scapolan, M. I. X.; INO-011

Scaramboni, B; ORG-090
Scaramboni, C.; AMB-012
Scarpari, S. L.; INO-039
Scharf, D. R.; ORG-011, QPN-010
Scheibel, T.; QPN-018
Schiavon, M. A.; INO-101
Schirato, G. V.; MED-006
Schirmann, J. G.; ORG-065
Schlenk, D.; AMB-048
Schmidt, A.; MAT-108
Schmitz, F.; FIS-028, MAT-054
Schmoeller, L. A.; ORG-107
Schneid, C. C.; QVE-003
Schneider, L. A. E.; ANA-085
Schneider, R. C. S.; AMB-042
Schnitzler, D. C.; AMB-032
Schram, M.; QVE-010
Schroeder, P.; AMB-074
Schultz, J.; MAT-044
Schwarz, F. W.; QVE-005
Schwenck Brandão, V. S. B.; INO-102
Scorsin, L.; ORG-067
Scott, A. L.; MED-009
Scott, F. B.; ANA-011
Scotti, L.; MED-062, QPN-056
Scotti, M. T.; MED-062, QPN-056
Scremin, F. R.; MAT-022, ORG-003
Sebastião, R. C. O.; CAT-031
Sebold, S. B. S; QPN-100
Seckler, D. E. L.; MED-022
Seco, M. A.; EDU-024
Seeger, T. S.; ANA-054
Seixas, F. A. V.; BIO-012
Selva, J. S. G.; ELE-043
Semaan, F. S.; ELE-006
Semeano, A. T. S.; MAT-028
Sena, D. H. S.; BEA-009
Sena, KXFR; MED-037
Sena, M. M.; AMB-034
Sene, A. P.; FIS-034
Senger, M. R.; MED-006, MED-046
Senra, J. D.; MAT-057
Serodre, T.; MAT-049
Serra, O. A.; FOT-011
Serralbo, A. S.; ORG-069
Severino, R. P.; MED-045
Severino, V. G. P.; QPN-024
Severo, E. A.; ANA-082
Shetty, M.; CAT-019
Shiguemoto, C. Y. K.; ORG-081
Shiguihara, A. L.; MAT-025
Shimamoto, G. G; QVE-003
Shul'pin, G. B.; CAT-006
Sibov, S. T.; QPN-019
Siciliano, B.; AMB-007
Siciliano, S.; AMB-073
Siedler, S.; MAT-020
Signorelli, F.; COL-004
Sigoli, F. A.; INO-008, INO-055, MAT-014, MAT-089, MAT-097
Sigrist, R.; QPN-069
Silingardi, H. M. T.; QPN-008
Silva Da, A. R.; FOT-001
Silva Da, C. C.; MED-020
Silva Da, F. F.; INO-009
Silva Da, L. A. L.; ELE-044
Silva Da, L. C. D.; FOT-001
Silva Da, M. A. N.; INO-001
Silva Da, M. B. G.; AMB-041
SILVA Da, M. J. V.; ORG-071
Silva Júnior, E. N.; ORG-044
Silva Neto Da, J. F.; INO-009
Silva Neto, O. C.; QPN-074
Silva, A. A.; QPN-035
Silva, A. B.; QPN-084
Silva, A. C.; EDU-025, EDU-029, FIS-029
Silva, A. F. F.; QPN-047
Silva, A. G; EDU-022
Silva, A. L. N.; MAT-112
Silva, A. M. A.; QPN-014
Silva, A. N.; EDU-064
Silva, A. P.; CAT-005, MAT-043
Silva, A. R. S.; ELE-022
Silva, A. T.; ORG-024
Silva, B. A. E.; EDU-036
Silva, B. A.; MAT-101
Silva, B. B.; EDU-050
Silva, B. F.; AMB-015
Silva, C. A. S; ANA-046
Silva, C. C.; EDU-058
Silva, C. D. S.; INO-088
Silva, C. F.; MAT-099
Silva, C. H. T. P.; MED-016
Silva, C. M; ORG-036
Silva, C. M. de; AMB-006, AMB-007
Silva, C. M. F.; MAT-064
Silva, C. M.; TEC-009
Silva, C. R.; EDU-059
Silva, C. S.; AMB-040, ANA-037, EDU-004
Silva, D. A.; ORG-086
Silva, D. F.; FOT-014, ORG-097
Silva, D. G. B; ORG-025
Silva, D. G.; ANA-041
Silva, D. H. S.; ORG-063, QPN-066, QPN-067
Silva, D. O.; INO-021, ORG-033
Silva, E. E.; ORG-054
Silva, E. F. R.; ANA-081
Silva, E. M. G.; MED-005
Silva, E. M. G.; MED-048
Silva, E. M. S.; QPN-080, QPN-081
Silva, E. O.; QPN-059
Silva, E. R.; MED-030, ORG-066
Silva, E. S.; ANA-022, QPN-106
Silva, F. A. N. G.; AMB-026, INO-044
Silva, F. A.; ANA-043
Silva, F. C. A.; ELE-018
Silva, F. C.; MED-025, ORG-045, ORG-087
Silva, F. F.; QPN-062
Silva, F. I. C.; MAT-117
Silva, F. M.; FIS-033
Silva, F. S. Q.; ANA-092, MAT-121
Silva, G. A. L.; EDU-050
Silva, G. A.; AMB-063
Silva, G. B. A.; MAT-093
Silva, G. C.; ORG-060
Silva, G. F.; INO-018
Silva, G. G.; AMB-039, ELE-058, MAT-043
Silva, G. G.; FIS-003
Silva, G. L.; BEA-018
Silva, G. P. C.; AMB-024
Silva, G. R; QPN-047
Silva, G. R.; QPN-118
Silva, G. S.; AMB-080
Silva, G.; MAT-052
Silva, H. D. T.; AMB-004
Silva, H. M.; INO-085
Silva, H. V. C.; MAT-002, MAT-096
Silva, H.; INO-046, INO-073
Silva, I. C.; MAT-097, MED-034
Silva, I. F.; INO-097
Silva, I. G.; QPN-094
Silva, I. O.; EDU-030
Silva, J. A. D.; MAT-026, MAT-124
Silva, J. A. V.; MED-033
Silva, J. A.; ELE-057
Silva, J. B.; ANA-070
Silva, J. C. M; AMB-075, QPN-016
Silva, J. C. M.; AMB-069, QPN-004
Silva, J. D. S.; ANA-014
Silva, J. F. M.; QPN-031
Silva, J. F.; QPN-109
Silva, J. P; EDU-022
Silva, J. R; MAT-087
Silva, J. T.; INO-046, INO-073
Silva, J. V. S.; BIO-002
Silva, K. B. O.; AMB-002
Silva, K. K. S.; INO-062
Silva, K. M. S.; MED-019
Silva, L. A.; CAT-011, FOT-004, MED-032, ORG-049, ORG-051
Silva, L. A.; EDU-061
Silva, L. F. F.; QPN-108
Silva, L. H. F.; TEO-011
Silva, L. I.; AMB-014
Silva, L. L. da; AMB-006
Silva, L. L.; MED-061, MED-064
Silva, L. M. S.; ELE-038
Silva, L. M.; FIS-012
Silva, L. N.; AMB-060
Silva, L. O. B.; QPN-015
Silva, L. O.; EDU-042
Silva, L. P. S.; BIO-011
Silva, L. S. M.; QPN-112
Silva, L.; MAT-099
Silva, M. A. S.; INO-042
Silva, M. A.; QPN-026
Silva, M. B.; EDU-001
Silva, M. C; ORG-072
Silva, M. C. S; COL-009
Silva, M. C.; BEA-019, MAT-017
Silva, M. D. B.; EDU-023
Silva, M. F. G. F.; FOT-014, QPN-070
Silva, M. F. G. F.; QPN-086
Silva, M. G. A.; EDU-001
Silva, M. K. L.; ELE-024
Silva, M. L. A.; MAT-078, ORG-006, QPN-057
Silva, M. L. C.; ELE-037

Silva, M. M.; BIO-005, MED-042
Silva, M. M.; QPN-045
Silva, M. N. T.; ELE-052
Silva, M. P. A; BEA-007
Silva, M. P.; ANA-078
Silva, M. R.; BEA-015
Silva, M. V. L.; ANA-081
Silva, N. A.; QPN-064
Silva, P. G.; AMB-054
Silva, P. J. C.; ANA-062
Silva, P. S. G.; ELE-042
Silva, P. T.; QPN-005
Silva, R. A. C.; ORG-110
Silva, R. A.; ELE-036, MED-058, ORG-037
Silva, R. C.; FOT-011, ORG-017
Silva, R. E.; ORG-040
Silva, R. F.; ELE-012
Silva, R. M. A.; MAT-026
Silva, R. R.; MAT-080
Silva, R. V. S.; AMB-074
Silva, S C; TEO-002
Silva, S, S, B,; TEC-011
Silva, S. A.; EDU-043
Silva, S. C.; ELE-014
Silva, S. J. B.; COL-011
Silva, S. M. E; QPN-082
Silva, S. M. T; QPN-082
Silva, S. M.; MED-056, ORG-050, QVE-006
Silva, S. M.; QPN-117
Silva, S. R.; EDU-006, INO-016, INO-030, INO-058
Silva, S. V. F. N.; AMB-045
Silva, S. V.; FIS-006
Silva, S. W. D.; FIS-001
Silva, T; QPN-077
Silva, T. E. M.; INO-034, INO-074
Silva, T. F.; AMB-043
Silva, T. L.; ORG-029, QPN-029
Silva, T. M. R.; MAT-094
Silva, T. M. S; QPN-047
Silva, T. M. S.; QPN-080, QPN-081, QPN-118
Silva, T. O. B.; ORG-066
Silva, T. R. C.; ORG-020
Silva, V. B.; FIS-019
Silva, V. I.; QVE-001
Silva, V. P. R.; INO-044
Silva, V. R.; MAT-103
Silva, W. N.; ANA-083
Silva, W. P.; AMB-070
Silva, W. R.; ELE-060
Silva, Y. F.; CAT-029
Silva-Caldeira, P. P.; INO-069
Silva-Filho, L. C.; ORG-026
Silva-Jr, F. P.; MED-026
Silva-Junior, F. P.; MED-046
Silveira Da, C. H.; INO-049
Silveira, E. L. C.; QVE-003
Silveira, E. R.; QPN-084
Silveira, F. F.; MED-030
Silveira, G. P.; ORG-054
Silveira, R. G.; INO-064
Silveira, T. G. O.; MAT-043
Silveira-Lacerda, E. P.; INO-074
Simas, N. K; QPN-037
Simionatto, E; QPN-016
Simionatto, E. L.; ORG-011, QPN-010
Simionatto, E.; AMB-069, AMB-075, QPN-004
Simões, M. O. M.; QPN-112, QPN-120
Simões, Y. S.; BIO-013
Simosono, C. A.; INO-081
Singh, M. K.; MED-039
Sinhorin, A. P.; MED-050, QPN-078
Siqueira Júnior, J. M.; INO-015
Siqueira, C. T.; EDU-064
Siqueira, F. A; ORG-049
Siqueira, F. A.; ORG-051
Siqueira, K. A.; QPN-058
Siqueira, K. P. F.; MAT-019, MAT-075
Siqueira, L. D. F.; AMB-065
Siqueira, L. D. F.; QVE-013
Siqueira, M. C.; EDU-057
Siqueira, M. R. P.; ANA-015
Sirés, I.; FIS-012
Sisto, F.; MED-047
Sitta, E.; ELE-034
Skrydstrup, T.; ORG-019
Slafer, B. W.; MED-004
Smiderle, F.; INO-019
Soares Jr. , A. L.; CAT-007
Soares, B. G.; MAT-025
Soares, B. M.; INO-095
Soares, I. C.; INO-026, INO-061
Soares, J. F.; INO-041, INO-091
Soares, J. J.; QVE-001
Soares, K. D.; QPN-048
Soares, K. V.; MED-043
Soares, M. A.; ORG-006, QPN-058
Soares, M. B. P.; QPN-087
Soares, M. G.; QPN-032, QPN-085, QPN-114
Soares, M. G.; QPN-041
Soares, M. H. F. B.; EDU-018, EDU-032
Soares, M. S; QPN-079
Soares, O.; ORG-081
Soares, P. M. A.; ORG-018
Soares, R. R.; CAT-003
Soares, R.; AMB-029
Soares, S. S.; ANA-027
Soares, T. S.; ANA-032
Sobrinho, M. L.; AMB-011
Sodré, F. F.; AMB-034
Sofiatti, E.; MAT-038
Soletti, J. I.; QPN-030
Somensi, C. A; AMB-041
Sonsen, G. W.; BIO-004
Sotomayor, M. D. P. T.; ANA-091
Sotomayor, M. P. T.; ANA-005
Sousa De, L. M.; EDU-024
Sousa, A. S. B.; QVE-006
Sousa, C. P.; ELE-020, ELE-059
Sousa, E. A.; QPN-103
Sousa, E. H. S.; INO-088
Sousa, E. M.; QPN-013
Sousa, F. S.; QPN-096
Sousa, G. F.; QPN-110, QPN-120
Sousa, J. L. S.; CAT-001
Sousa, M. B.; EDU-060
Sousa, M. F. B.; COL-004, MAT-038
Sousa, N. C. O. S.; MAT-032
Sousa, N. G.; ELE-059
Sousa, N. M.; EDU-006
Sousa, R. M. F.; QPN-064
Sousa, R. P.; QPN-095, QPN-104
Sousa, S. C. B.; MAT-008
Sousa-Pereira, D.; MED-051
Souza De, D. H. F.; BIO-003
Souza De, D. M. B.; INO-009
Souza De, M. C. B. V.; ORG-085
Souza De, M. C.; ORG-085
Souza De, M. L.; QPN-026
Souza De, R. O. M. A.; ORG-046
Souza De, S. P.; ORG-046
Souza e Silva, J. M. S.; MAT-030
Souza Jr. , J. B.; MAT-061
Souza, A. G.; BEA-015
Souza, A. H. P.; BEA-003
Souza, A. L. F.; MED-061, MED-064
Souza, A. T.; EDU-064
Souza, B. A.; QPN-075
Souza, C. G.; ANA-069
Souza, D. A.; QPN-026
Souza, D. G.; ANA-085
Souza, D. L.; MED-030
Souza, D. M.; ANA-061
Souza, D. O.; INO-003, MAT-107
Souza, D. R.; FOT-010
Souza, E. A.; CAT-011
Souza, E. B. R.; QPN-078
Souza, E. M.; AMB-014
Souza, E. O.; FIS-005
Souza, F. A. M.; ORG-037
Souza, F. C.; ELE-002, ELE-025
Souza, F. L.; EDU-039, MAT-120
Souza, F. M.; ELE-005, ELE-031
Souza, G. B.; MED-041
Souza, G. C.; ORG-055
Souza, H. D. S.; ORG-097
Souza, H. J. S.; QPN-081
Souza, I. A.; ORG-105
Souza, I. P.; INO-069
Souza, J. C.; AMB-015
Souza, J. M.; ORG-086
Souza, J. M.; QPN-006
Souza, J. S.; INO-033, INO-093, MAT-120
Souza, K. R.; ANA-013
Souza, L. M.; MAT-022
Souza, M. C. B. V.; ORG-017, ORG-022, ORG-087
Souza, M. C. M.; EDU-060
Souza, M. C.; ORG-058
Souza, M. G. S; QPN-065
Souza, M. L.; MAT-099
Souza, M. O. G.; EDU-049
Souza, M. P.; AMB-042, QPN-060
Souza, M. V. N.; INO-036
Souza, P. B.; ANA-080
Souza, R. C.; ANA-012, BEA-011

Souza, R. M.; MAT-007
Souza, R. O. M. A.; ORG-078
Souza, R. O. M. A.; ORG-094
Souza, R. S.; MAT-081
Souza, S. P.; ORG-035
Souza, T. B.; MED-036
Souza, T. de C.; AMB-006
Souza, T. J.; ORG-004
Souza, T. M.; AMB-011
Souza, V. H. R.; MAT-015, MAT-076
Souza, W. F. L.; AMB-057
Souza, W. P.; ORG-006
Souza-Garcia, J.; ELE-026
Souza-Neto, L. R; MED-026
Staerk, D.; QPN-051
Stapelfeldt, D. M. A. S.; AMB-077
Stefanes, N. M; COL-009
Steinmacher, N. C.; BEA-003
Stevanato, A.; EDU-011, EDU-037, INO-047
Stevani, C. V.; ORG-063
Stocco, A. F.; INO-047
Stoeberl, B. J.; INO-041
Stradiotto, N. R.; ELE-023, ELE-062
Strohauer, S; INO-096
Stropa, J. M.; AMB-069, AMB-075
Stulp, S.; ELE-029
Stumpf, H. O.; EST-001, INO-029, INO-081, INO-097, MAT-069, MAT-091
Suagaura, L. E.; ANA-019
Suarez, P. A. Z.; CAT-020, FIS-033, TEC-008, TEC-010
Sucupira, R. R.; CAT-020, TEC-008, TEC-010
Suffedini, H. B.; ELE-010
Sukeri, A.; ELE-003
Sukeri, Anandhakumar; ELE-043
Suman, P. H.; ELE-007
Szpoganicz, B. P.; INO-072
Szpoganicz, B.; INO-072

## T

Takarada, W. H.; CAT-013, QVE-004
Takata, N. H.; QVE-010
Talero, A. G.; ORG-038
Tamayose, C. I.; QPN-090, QPN-091
Taranto, A. G.; MED-022
Tarley, C. R. T.; ANA-045, ELE-053
Tarley, C. R. T.; ELE-047
Tasic, L.; BIO-001, MED-001
Tavares, D. C.; MAT-078, ORG-006, QPN-058
Tavares, F. S. C.; EDU-013
Tavares, I. L. M.; ELE-042
Tavares, M. C.; FIS-030
Tavares, M. S.; INO-015
Tavella, T. A.; MED-002
Tcacenco, C. M.; QPN-113
Tecchio, C. M.; MAT-008
Teixeira, A. M. S.; AMB-065
Teixeira, A. M. S.; QVE-013
Teixeira, A. P. C.; CAT-009, CAT-031, CAT-032, INO-097
Teixeira, A. T.; QVE-009
Teixeira, B. S.; ANA-018
Teixeira, C. F. A.; INO-089
Teixeira, C. M. L. L.; QPN-038
Teixeira, I. F.; CAT-012, INO-097
Teixeira, I. N. S.; MED-049
Teixeira, J. V. S.; QPN-027
Teixeira, L. A.; ORG-045
Teixeira, L. R. S.; INO-036
Teixeira, R. I.; FOT-006, FOT-007
Teixeira, R. L.; MED-012
Teixeira, R. R.; ORG-052
Teixeira, S. F.; ELE-002, ELE-025
Teixeira, V. G.; AMB-057
Teixeira, W. S. R.; ELE-024
Teixeira-Neto, E.; CAT-016
Teles, S. C.; MAT-075
Telles, G. C.; AMB-060
Telmer, K.; MAT-027
Tempone, A. G.; MED-007, QPN-043, QPN-085, QPN-098, QPN-114
Teodoro, G. C.; AMB-030
Teodoro, M. T. F.; QPN-074
Teófilo, R. F.; ANA-076
Teotonio, E. E. S.; INO-085
Teotônio, G. L. E.; INO-010
Terezan, A. P.; MAT-087
Terezan, A. P.; QPN-019, QPN-036
Terra, F.; INO-053
Thiago, A.; FIS-036
Thomas, N.; ORG-003
Tiera, M. J.; MAT-036, MAT-053, MAT-077
Tiera, V. A. O.; MAT-036, MAT-053, MAT-077
Tirich, B. M.; COL-007
Tirloni, B.; INO-078
Tischer, B; BEA-005
Toigo, J.; COL-009
Toledo, S. P.; MAT-006
Toledo, T. A; ORG-072
Toledo, T. A.; AMB-066, INO-050
Toledo, T. A.; INO-063
Toledo, V. H.; MAT-006
Tolentino, N. M. C.; ORG-022
Tomaso, L. P. S.; ANA-090
Tomaz, K. C. P.; MED-002
Tondo, D. W.; COL-003
Tonin, M. D.; FOT-006
Tordato, E. A.; ORG-001
Tormena, C. F.; ORG-014
Tormena, M. M. L.; TEO-014
Tormin, T. F.; ELE-052
Torquato, A. S.; AMB-013, BEA-002
Torquato, L. D. M; ELE-021
Torquato, L. D. M.; ELE-007
Torres, J. P. M.; AMB-072
Torres, M. C. M.; QPN-084
Torres, M. D. T.; BIO-010
Torres, N. M. P. O.; MED-058
Torresi, R. M.; ELE-036, MAT-068
Torresi, S. I. C.; ELE-015, ELE-055, MAT-028, MAT-082
Torres-Santos, C.; ORG-087
Toschi, S. S.; AMB-078
Toson, N. S. B; QPN-042
Tostes, B. de V. A.; MAT-041, MAT-058
Tozatti, M. G.; QPN-057
Trevisan, J. T. T.; ELE-004
Trevisan, M. T. S.; ORG-110
Trindade, W. G.; AMB-030
Triolo, A.; FIS-013
Trossini, G. H. G.; ELE-032, MED-017
Trovo, A. G.; AMB-049
Trovó, A. G.; AMB-079
Tsang, E.; CAT-012
Tubino, M.; QVE-003
Turcheniuk, K.; MED-014
Turchetti, D. A.; MAT-001, MAT-002, MAT-056, MAT-090, MAT-096
Turci, C. C.; MAT-100

## U

Ucoski, G. M.; INO-051
Uekane, T.; QPN-122
Ueno, A. K.; QPN-113
Ueno, L. T.; FIS-034
Ulloa, J. E; FOT-013
Ulrich, A. H.; MAT-028
Urban, R. C.; AMB-001

## V

Vairolette, Lucas; EDU-053
Val, A. L.; AMB-023
Valderrama, P.; BEA-002
Valdo, A. K. S. M.; INO-029, INO-053, INO-081, INO-087
Vale, J. P. C; QPN-028
Vale, R. F. D.; ANA-092, ANA-094, MAT-121, MAT-122
Vale, R. F. D.; ANA-093
Vale, T. M.; ORG-022
Valenga, M. G. P.; FIS-025
Valente, L. J; BEA-007
Valente, P. M.; QPN-001, QPN-017
Valente, V. M. M.; QPN-001, QPN-017
Valente, W. C. G.; MED-006
Valerino-Diaz, A. B.; ORG-006, QPN-092, QPN-101
Vandresen, F.; INO-047
Vanzin, D.; FIS-034
Varanda, L. C.; COL-007, MAT-061
Varela, H.; ELE-015, ELE-051, FIS-004
Vargas, R. N; EDU-022
Vargas, S. J. R; FIS-015
Vargas, S. J. R.; FIS-037
Vargas, T. S.; ANA-087, ANA-088
Vargas-Rechia, C. G.; QPN-119
Varjão, T. A.; EDU-008
Varotti, F. P.; MED-022
Vasconcellos, P. C.; AMB-003
Vasconcelos, C. K. B.; MAT-008
Vasconcelos, L. G.; QPN-078
Vasconcelos, M. A. L.; QPN-057
Vasconcelos, M. G.; QPN-022
Vasconcelos, S. C.; ELE-006
Vassiliades, S. V.; FOT-002, MAT-051

Vaz, B G; ANA-020
Vaz, R. C. A.; INO-025
Veiga, T. A. M.; QPN-086
Velloso, M. C. C.; ORG-060
Veloso, M. C. C.; AMB-074
Venâncio, L. F.; ANA-092, ANA-094, MAT-121, MAT-122
Venâncio, L. F.; ANA-093
Veras, M. D. A.; QPN-107
Vestena, A. S.; QPN-048, QPN-093
Viana Rodrigues, P. V. R.; INO-102
Viana, A.; FIS-008
Viana, M. M.; MAT-008, MAT-037, MAT-083
Viana, T. K. F. P.; INO-025
Viana, V. G. F.; QPN-034
Viana, V. M.; ORG-079
Vicente, A.; AMB-003
Vichi, F. M.; MAT-048
Vicinguera, M. L. F.; EDU-028
Victor, M. M.; ORG-013
Vidal, D. M.; QPN-083
Vidinha, P.; BEA-017, CAT-021, CAT-036
Vidotti, I. C. R.; MAT-054
Viegas, C. V.; MED-018
Viégas, D. S. S.; ELE-038
Viegas, F. P. D.; QPN-032
Viegas, P. R.; ORG-058
Vieira Filho, S. A; QPN-110
Vieira Junior, G. M.; QPN-088, QPN-089
Vieira Júnior, G. M.; QPN-095, QPN-104, QPN-107, QPN-108
Vieira, A. A.; ORG-066
Vieira, A. V; ORG-035
Vieira, B. L. M.; AMB-066, INO-050
Vieira, B. S.; QPN-064
Vieira, C. D.; EDU-002
Vieira, D. F.; AMB-036, AMB-062
Vieira, E. C.; QPN-055, QPN-072
Vieira, E. G.; ANA-070
Vieira, F. S.; BEA-014
Vieira, G. A. B.; AMB-017, ANA-075, EDU-066
Vieira, G. M.; CAT-018
Vieira, J. C.; AMB-061
Vieira, J. L.; AMB-040
Vieira, J. S. C.; CAT-022
Vieira, K. C.; MAT-069
Vieira, L. V.; AMB-031
Vieira, P. C.; QPN-029, QPN-070
Vieira, P. C.; QPN-051
Vieira, S. S.; CAT-031, INO-071, ORG-084
Vieira-Filho, S. A.; QPN-112
Vieira-Júnior, G. M; QPN-111
Vieira-Júnior, G. M.; QPN-103
Viesser, R. V.; ORG-014
Vignoli-Silva, M.; QPN-093
Vilar, F. C. R.; QPN-015
Vilegas, W.; QPN-101
Vilela, G. A.; INO-014, INO-053
Villar, J. D. F.; FOT-012
Villegas, M. E; BEA-017
Vinhal, J. O.; ANA-040
Vinhato, E; ORG-105
Vinhato, E.; ORG-018, ORG-027
Virtuoso, L. S.; COL-006
Visconte, L. L.; MAT-081
Visentainer, J. V.; ANA-030
Vitoreti, A. B. F.; INO-101
Vitorino, L. S.; MAT-059
Vitório, F.; INO-084
Vogel, C.; ORG-108
Vogel, M.; EDU-038, EDU-046
Vollbrecht, C. P.; AMB-056
Volpe, P. L. O.; BIO-001
Von Poser, G. L.; QPN-048, QPN-093

## W

Wakui, V. G.; QPN-019
Waldman, W. R.; MAT-021
Wassano, C. I.; QPN-124
Watanabe, L. A.; QPN-065
Watanabe, L. S.; ANA-078
Weinert, P. L.; ANA-002, ANA-007
Werworn, L. F. M.; MED-050
Westphal, E.; INO-011, INO-020, INO-037, INO-095, INO-099, MAT-106, ORG-064
Wientage, G. H.; QPN-010
Wilke, D. V.; QPN-084
Winck, F. V.; MAT-031
Windmöller, C. C.; AMB-016, AMB-061, ANA-035
Winkler, M. E. G.; MAT-114
Winnischofer, H.; INO-020, INO-095, INO-099
Winnischofer, S. M. B.; INO-099
Wioppiold, T. A.; INO-007
Wisniewski, A.; ANA-060
Wisniewski, C.; ANA-064
Wodtke, F.; ORG-107
Wolfender, J. L.; BEA-018
Wyatt, N. L. P.; AMB-031

## X

Xavier, F. R.; ORG-107
Xavier, J. A.; BIO-009, MED-058
Ximenes, RM; MED-037
Ximenes, V. F.; FIS-010, ORG-026
Ximenes, V.; MAT-009
Ximenez, G. R.; QPN-109
Xing, Y.; MAT-101

## Y

Yamaguchi, K. K. Lima; QPN-054
Yamaguchi, L. F.; AMB-071
Yamamoto, D. Y; QVE-011
Yeom, J.; FIS-035
Yoshimura, T. M.; MAT-006
Yoshinaga, M. L.; QPN-116
Young, M. C. M.; QPN-097, QPN-114
Youssef, K.; BEA-012
Yunes, R. A.; MED-003

## Z

Zacchi, C. H. C.; ORG-055, ORG-084
Zafred, A. F. D; MAT-087
Zaitsev, V.; ANA-039, MAT-012, MAT-101, MED-014
Zanatta, A. C.; QPN-101
Zanatta, E. R.; CAT-039
Zanchet, D.; CAT-019
Zandonai, D. P.; QPN-070
Zanella, R.; AMB-020
Zanlorenzi, C.; MAT-056, MAT-079, TEO-004
Zanoni, M. V. B; ELE-029
Zanoni, M. V. B.; AMB-015, ELE-007, ELE-021
Zanotelli, N. C.; BEA-006
Zapata, M.; INO-065
Zapateiro, G. A.; EDU-037
Zarbin, A. J. G.; ELE-019, MAT-029, MAT-073, MAT-108, MAT-109, MAT-123, MAT-125
Zarbin, A. J. G.; MAT-100
Zarbin, P. H. G.; QPN-083
Zeraik, M. L.; BEA-018
Zhang, Y.; FIS-017
Zimmer, F. C.; BEA-003
Zimmermann, L. M.; MAT-054
Zuanazzi, J. A. S.; QPN-048, QPN-093

α-glucosidase; QPN-051
α-Pineno; QPN-003
α-Acylated β-thioenaminones; ORG-042
β-carboline; MED-052
β-carbolines; MED-042
β-diketonate; INO-006
β-diketone; INO-085
β-enaminodicetona; ORG-071
β-glucan; MED-035
η6-arenorutênio(II); INO-099
(N-aryl)phosphoramidic; ORG-021
(R)-1,2-propanediol; ORG-046
(Z)-thiobutenynes; ORG-081
[2+2]-cycloaddition; FOT-007
1,10-phenanthroline-5,6-dione; INO-059
1,2,3-triazoles; MED-018; ORG-061
1,3,4- oxadiazole; ORG-010
1,3,4-oxadiazol; INO-011
1,3,5,-triazine; MED-052
1,3,5-triazines; ORG-012
1,4-naphthoquinone; FOT-006
1,6-anhydro-β-D-glucopiranose; TEC-007
1,8-Cineole; QPN-018
1-Octanol; ANA-027
10-MDP; FIS-038
1H NMR; QPN-067
2,1,3-Benzotiadiazol; ORG-066
2,6-pyridinedicarboxylic acid; ANA-039
2-(4-hydroxiazobenzene)benzoic; INO-012
2-amino- 1,4-naphthoquinone; ORG-016
2-Aminonaphtoquinones; MED-020
2-Aminothiazoles; ORG-091
22-α-O-spirostane; QPN-101
25I-NBOH; ORG-096
25I-NBOMe; ORG-096
2H-Furo[3,2-b]benzopyran-2-one; ORG-104
3,4-dihydroisocoumarins; ORG-028
3-hydroxy-indole-2-one; ORG-048
3-Iodothiophenes; ORG-081
3D printer; EDU-027
3D printing; ANA-068
3D Similarity Chemical Model; MED-011
4-aminoantipyrine; INO-069
4-methoxy-1-naphthalene; BIO-012
4H hcp phase; MAT-061
5 amino-tetrazole; ORG-074
5-aminotetrazoles; ORG-077
7-MEOTA-4-PA; MED-033

# A

Ab initio molecular dynamics; FIS-035
abastecimento público; ANA-012
Abelha branca; QPN-082
Absorção plasmon; MAT-002; MAT-072
absorção plasmônica; AMB-076
Absorption; MED-057
ABTS; ORG-090
Academic Community Awareness; AMB-065
Acaricidal Activity; QPN-045
accessibility; EDU-027
acetalization; QVE-009
Acetaminophen; ANA-015
acetate; INO-012
Acetilcolinesterase; MED-064
Acetofenonas substituídas; ORG-032
Acetogenins; QPN-114
Acetophenone; MED-036
Acetylaleuritolic acid; QPN-106
acetylcholinesterase; AMB-027; MED-018; MED-024; MED-033; MED-055
Acetylene; CAT-005
acetylsalicylic acid; AMB-024
Achatina fulica; QPN-075
AChE; MED-061
Aciclonucleosídeo; ORG-085
Acid Chlorides; ORG-069
Acid oxidation; FIS-003
Acid Treatment; MAT-048
Acid violet 19; ANA-091
acidic diterpenes; QPN-122
Acidithiobacillus ferrooxidans; AMB-039
Acidity; CAT-034
ácido acetilsalicílico; INO-050
Ácido aristolóquico; QPN-077
ácido betulínico; QPN-033
ácido clorogênico; QPN-100
Ácido diluído; ANA-048; ANA-083
ácido paederosídico; QPN-100
ácido tânico; MAT-025
Ácido vanílico; QPN-041
ácidos clorogênicos; QPN-090
ácidos graxos; QPN-108
ácidos graxos metil ésteres; BEA-008
acids and Bases; EDU-006
Acilhidrazonas; MED-061
Aciltioureias; INO-100
Acinetobacter baumani; QPN-016
Acridonic alkaloids; QPN-086
acrylate copolymers; MAT-046
action mechanism; MED-042
activated carbon; MAT-092
Activated charcoal; CAT-025
active dressings; MAT-050
Actived carbon; MAT-074
açúcares; ANA-089
açúcares redutores; AMB-040
acyclic compounds; ORG-014
Acylhydrazones; ORG-064
Adamantane; INO-073
Adduct; MED-010
Adesivo; FIS-038
Aditivos; ANA-021
adsorção; AMB-034; AMB-043; AMB-077; FIS-028; INO-102; MAT-058; MAT-060
adsorção competitiva; AMB-034
adsorption; AMB-044; AMB-045; AMB-053; AMB-056; AMB-057; ANA-058; ANA-063; CAT-007; CAT-025; COL-003; COL-012; ELE-044; FIS-003; FIS-027; INO-054; INO-070; INO-083; INO-097; MAT-044; MAT-055; MAT-064; MAT-069; MAT-074
Adsorption isotherms; ANA-057
Adsorvente alternativo; FIS-028
adsorvente natural; AMB-043
aduct; INO-045
Adulterants; ANA-032; ANA-078
Adulteration; ANA-072
advanced oxidation process; AMB-049
Aedes aegypti; MED-041; ORG-089; QPN-014
Aeollanthus suaveolens; ORG-041
Aerogel; BEA-017
Aerogel de grafeno; ANA-095
África; EDU-022
Agonist activity; MED-044
Agregation; BIO-013
Agricultura; ANA-012
agrochemicals; AMB-032
agrodefensivos; ANA-012
agrotóxicos; AMB-017
água; ANA-012
Água de coco; ANA-014
Água do mar; FIS-029
água para consumo humano; AMB-055
águas; AMB-067
águas superficiais; AMB-011; AMB-028
air pollution; AMB-008
air quality; AMB-003
Airbrush; MAT-080
Albendazol; MED-013
Alcalóides; QPN-085
Alcanos; ANA-086
Alcohol oxidation; CAT-006; CAT-010; ELE-026
Alcoholic beverage; ANA-034
alcoholic beverages; BEA-005
Álcoois homoalílicos; ORG-037
Aldehyde; CAT-018
aldeídos; AMB-005; QPN-055
Aldoxime; MED-033
alfa arylation; ORG-019
algae; AMB-042
algae turf scrubber; AMB-042
Alilação; ORG-037
alimentos; BEA-011
ALK-5; TEO-010
alkaloids; MED-055; QPN-040; QPN-042; QPN-115
Alkylamides; QPN-045
Alkylation; ORG-026
alpha-hydroxy malonates; ORG-062
alpha-hydroxy-gamma-lactone; ORG-062
alpha-hydroxylation; ORG-062
Alternative green route; ORG-042
Aluminum; AMB-079
Alzheimer s disease; MED-018
Alzheimer's Disease; FOT-005
Alzheimer's disease; INO-095
Alzheimer´s disease; MED-044
Amazon; AMB-030
Amazon Basin; AMB-078
Amazon Region; AMB-060
Amazônia; AMB-023
amazonic aquatic systems; AMB-022
ambiental; EDU-049
Amide; ORG-007

Amides; FIS-009; ORG-047
Amido; BEA-017; MAT-065
Amiláceos; ANA-083
aminas quirais; ORG-051
Amine; ORG-007
amine oxidation; CAT-015
Amino acids; ORG-097
Amino-naphothoquinones; QPN-084
aminoácidos; INO-034
Ammonia; INO-097
Ammonium thiosulfate; FIS-015
Amostrador passivo; MAT-027
Amperometric; ELE-035
amphetamines; MED-066; TEO-008
Amphilophium crucigerum; QPN-052
Amphiphilic molecules; MAT-067
amphotericin B; MAT-059
Amyloid Beta Peptide; FOT-005
Amyloid-β; INO-095
Amyloids; MAT-118
análise conformacional; TEO-005
análise físico-química; AMB-035
Análise Multivariada; ANA-048
Analise por injeção em fluxo; ANA-095
análise térmica; AMB-075
análise termogravimétrica; ORG-003
Análises em fluxo; ANA-026
Análises por injeção em fluxo; ANA-028
Analytical standards; ORG-096
Anestésicos; ORG-078
anilines; ELE-025
anionic clays; AMB-051; INO-062
Annonaceae; QPN-013; QPN-040; QPN-107; QPN-114
anodization; MAT-102
ANP; ANA-087; ANA-088
Anthocyanin content; QPN-023
Anthrone; QPN-051
anthropogenic emissions; AMB-007
Anti helminthic; MED-006
anti-fouling; COL-004
Anti-helmínticos naturais; MED-013
Anti-inflammatory activity; QPN-110
Anti-Leishmania; QPN-098
Anti-Plasmodium falciparum; MED-010
anti-scaling; COL-004; MAT-038
Antiacetilcolinesterase; ORG-110
Antibacterial; ORG-054
Antibacterial Activity; MED-020
antibiótico; QPN-001
antibióticos; AMB-076; INO-071
anticancer activity; BIO-009
antichemotactic activity; QPN-048
Anticoagulant solution; ANA-092
anticonvulsant prototype; INO-019
antidiabetic properties; QPN-092
antifreeze; MAT-046
Antifungal activities; ORG-097
Antifungal activity; QPN-018
antifúngica; QPN-050; QPN-053
Antifúngico; ORG-036; QPN-001
antigen-antibody interaction; ELE-017
Antiglycation; MED-058
Antigungal activity; QPN-002
Antileishmanial activity; MED-019; MED-052; QPN-116
Antimalarial; MED-010; QPN-088
antimicrobial; MAT-053; MED-011; QPN-008
antimicrobial activity; INO-024; MED-037; QPN-057
Antimicrobial Peptides; BIO-010
Antimicrobian activity; QPN-065
Antimicrobianos; QPN-004
antimônio; INO-058
antineoplasico; ANA-006
antioxidant action; ORG-065
Antioxidant activities; QPN-039
Antioxidant activity; BEA-012; MED-003; QPN-023; QPN-028; QPN-074
Antioxidant capacity; BEA-010; BEA-018
Antioxidante; FOT-014; MED-061; QPN-035; QPN-082
antioxidantes; ANA-087; ANA-088
Antioxidants; BEA-002; FIS-025
antiparasitária; ORG-087
antiproliferative activity; MED-042; ORG-028; QPN-016; QPN-115
Antiproteolytic activity; MED-036
antiradicalar; QPN-080
Antiretrovirals; TEC-001
antitrypanosomal; MED-007
antitumor; INO-009; INO-016
Antitumor activities; INO-074
antitumoral; MED-007
antiviral activity; MED-035
Apdosperma; BIO-002
Apocynaceae; QPN-117
Aporphine alkaloids; QPN-087
Appropriation of Concepts; EDU-018
Aprendizagem; EDU-034; EDU-061
aqueous CO2 as a catalyst; MAT-114
aqueous dispersions; MAT-109
Aqueous fraction extraction; QPN-038
Aqueous medium; CAT-006
Aqueous two-phase system; FIS-015; FIS-037
aqueous two-phase systems; AMB-064; COL-011; FIS-021; FIS-022
Arduino; ANA-025
argila; MAT-025
arginase; MED-030
Argininyl bufadienolides; QPN-078
Aristolochia; QPN-077
aromas; CAT-008
Aromatizantes; ANA-021
Aroylbisthiourea; INO-007
arsênio; AMB-026
Arte e ensino; EDU-057
Artemetin; QPN-106
Artepillin C; QPN-121
Artesunic acid; QPN-073
Arthrospira platensis; QPN-038
Artigos científicos; EDU-010
Aryl ketones; ORG-038
Arylamides; ORG-069
Arylation; ORG-038
Aryldiazonium Salts; ORG-023
Arylpropanoids; QPN-009
Arynes; ORG-038
Ascidians; QPN-058
ASGM; MAT-027
ash; MAT-094
Aspergillus flavus; MAT-053
Aspergillus sp. (FSF06); QPN-065
asphaltene; FIS-027
Assigments; ORG-102
Assimetria; ORG-066
Asteraceae; QPN-019; QPN-090; QPN-091; QPN-113; QPN-116; QPN-119
astrobiologia; FIS-036
astrobiology; AMB-039; AMB-071
Astrochemistry; FIS-002
At-line-bioassay,; BIO-004
Atendimento Educacional Esp.; EDU-063
atividade anti-parasitária; QPN-085
Atividade antiangiogênica; FOT-011
Atividade Antifúngica; QPN-097
Atividade antimicrobiana; BIO-014; INO-066
atividade antipriônica; ORG-017
atividade antiproliferativa; QPN-027
atividade antixidante; QPN-036
Atividade citotóxica; ORG-110
Atividade Exper Investigativa; EDU-039
Atividade fotodinâmica; FOT-011
atividade fotoprotetora; QPN-105
atividade inibitória; BIO-008
Atividade tripanocida; MED-012
Atividades farmacológicas; ORG-041
Atmosfera; EDU-017
Atmospheric Biomonitoring; ANA-036
atmospheric chemistry; AMB-008
atmospheric contaminants; AMB-009
atmospheric deposition; AMB-013
atmospheric particulate matter; AMB-003
atmospheric pollution; AMB-002
atomic absorption spectrometry; ANA-045
Átomos; EDU-005
ATR; ANA-080
ATR-FTIR; ELE-036
Atrazina; AMB-080
atropisomers; ORG-012
ATRP; CAT-024; CAT-028
ATS; AMB-042
Au nanorods; MED-014
Au-S interaction; INO-002
Augmented; EDU-058
Aulas experimentais; EDU-056
Aulas práticas; EDU-060
AuNP; ELE-030
AuPd; MAT-095
AuPt; MAT-095
aurantricholide; ORG-104
auto-discharge; EDU-053
automação; ANA-064
Automated system; ANA-065
Azaphilones; QPN-060
Azlactone; ORG-093

azlactones; ORG-019
Azo dye; ELE-016
azo dyes; AMB-051
Azole; MED-008
Azul de Metileno; CAT-037; FIS-018; FOT-011

## B

BAμE; AMB-020
babaçu; AMB-075
Baccahris punctulata; ORG-011
Baccharis retusa; QPN-113
Bacteria detection; ANA-068
Bacterial cellulose; MAT-047
Bacterial infection; ELE-012
Bacterial infections; ORG-045
Bacterial Resistance; MED-025
bactericida; INO-030
bactericide; QPN-122
Bacuri; BIO-011
Bader Analysis; CAT-007
balanceamento; EDU-001
banana peels; AMB-056
Banisteriopsis; QPN-008
barigui rver; AMB-024
Barium; COL-003
Bark tree; ANA-036
Barley waste; FIS-025
base de Schiff; INO-067
baselines; AMB-022
Bases de Schiff; ORG-021
bases de Schiff tetradentadas; INO-060
Basic Catalysis; INO-080
Batch-injection analysis; ELE-052
Baterias; EDU-028; EDU-059
Bauhinia cheilantha; QPN-014
BDD; ELE-027
BDD electrode; ELE-010
beach; AMB-031
Bebidas adulteradas; ELE-028
Belousov-Zhabotinsky; FIS-024
Benzenoids; QPN-087
benzimidazol; FOT-012
benzimidazole; INO-014
benzimidazoles; TEC-003
Benzino; ORG-033
Benzophenone; MED-036
benzoquinona; ORG-017
benzothiazoles; TEC-003
Benzoylguanidines; MED-019
Benzyl alcohol; CAT-010
Berenil; ANA-022
bergenin; QPN-074
bernumidina; ORG-020
beta-dicetona; INO-011
beta-Hydroxy(amino)amides; ORG-001
beta-Zeolite; AMB-047
betalains; FOT-015
BIA; ELE-006
bifenil; FOT-012
biflavonoides; QPN-027
bifosfinas; INO-034
Big Data; TEC-001
Biginelli; ORG-107
Biginelli reaction; ORG-084
Bignoniaceae; QPN-044; QPN-052
Bignonieae; QPN-044
Bimetallic catalysts; CAT-017
BINANA-; MED-028
binary mixtures; FIS-026
Binding Affinity; MED-063
Bio-oil; CAT-009
bio-óleo; TEC-010
Bioaccumulation; AMB-058
bioactive terpenes; QPN-102
Bioavailability; ANA-035
Biocatalisador; MAT-124
biocatálise; CAT-008; ORG-040
biocatalysis; ORG-001; ORG-065; QVE-011
Biocatalyst; CAT-013
Biocatalytic Membrane Reactor; TEC-011
biocombustíveis; AMB-040; AMB-069; TEC-010
Biocompatible polymer; ELE-009
Biocromatografia; ORG-075
Biodegradable; MAT-028
Biodegradable films; QVE-002; QVE-006
Biodegradable polymer; ELE-009
Biodegradation; QPN-068
Biodiesel; ANA-029; ANA-087; ANA-088; CAT-009; EDU-010; EDU-036; EDU-051; FIS-025; FIS-033; MAT-046; ORG-109; QPN-026; QVE-003; TEC-002; TEC-004; TEC-005; TEC-006; TEC-010
bioenergia; AMB-041
Bioethanol; ELE-062
Biofilme; MAT-065
Biofuel; TEC-004; TEC-006
biogás; AMB-041
biogenic emissions; AMB-007
biogenic hydrocarbons; AMB-008
Bioglass; MAT-062
Biohíbrido; MAT-033
Bioindicador; AMB-081
Biological Activities; ORG-021; QPN-031; QPN-099
biological activity; INO-084; ORG-108; QPN-006
biological fluids; ELE-006
bioluminescent mushroom.; ORG-063
Biomarker; MAT-088
Biomarkers; ANA-020
biomass; AMB-042; AMB-059; AMB-074; CAT-019; CAT-038; QVE-011; TEC-007
biomassa; AMB-070; AMB-077; MAT-060
biomassa residual; AMB-040
Biomaterial; MAT-028; MAT-093
biomaterials; MAT-113
Biomonitoring; AMB-081
Biopolymer; MAT-042
Bioprospecção; QPN-017
bioreactors; ORG-039
Bioreductive Prodrugs; INO-068
bioremediation; AMB-042; AMB-058
biorreator a membrana; AMB-037
Biorremediation; AMB-054
biosensor; ELE-017; ELE-057
Biosensors; ELE-048
biosignature; AMB-039
biosignatures; AMB-071
biosorbent system; AMB-061
biosorption; AMB-025; ANA-057
biossensor; ELE-037
biossorvente; AMB-055
Biostimulant; ORG-057
biotemplates; MAT-113
Biothiols; ELE-049
Biotransformação; BIO-014; MAT-033
Biotransformações; QPN-055; QPN-072
Biotransformation; MED-050
Biphenylation; ORG-026
bipodal dicarboxylic ligand; INO-027
Bipy; BEA-010
Bis(dethio)bis(methylthio)glio; QPN-065
bis-benzoxazine; ORG-076
bis-hydrazones; BIO-009
Bis-trifluoromethylquinolines; MED-010
BisGMA; FIS-039
Bismuth; ANA-041; ORG-077
bismuto; INO-058
Bisperilenimidas; ORG-025
Bisphenol A; AMB-054; ANA-027
bistability; ELE-054
bixin; AMB-044; AMB-046; AMB-061
Black Mud; CAT-004
Black phosphorus; MAT-073
bleaching; MAT-119
bleaching catalysis; INO-051
Blendas; MAT-004
Blends; QPN-026
Blends of poly(lactic acid); CAT-034
Blind docking Study; MED-015
Block copolymers; MAT-090
Blood bag; ANA-093
Blood bags; ANA-092
blood brain barrier (BBB); MED-007
Boa noite cinderela; ELE-028
board game; EDU-019
Boehm titration; AMB-025
Bombix mori; MAT-022
Bone substitutes; MAT-093
Boold bags; ANA-094
Boro; ORG-086
Boron doped diamond; ELE-052
boron-doped diamond anode (BDD; FIS-012
boron-doped diamond electrode; ELE-049
borra de café; CAT-008
Boson Peak; FIS-017
Botryosphaeran; ELE-050; MED-035
Botryosphaeria rhodina MAMB--05; ORG-065
Bovine trichomonosis; QPN-021
BPA; ELE-057
Braille; EDU-027
Brasoside; QPN-048
Brazilian Cerrado; QPN-024

Brazilian Coast Fishes; AMB-072
Brazilian fruits; BEA-012
Brazilian toads; QPN-078
Bread; BEA-003
Breath-figure; MAT-082
brilliant green; AMB-044
Bromine; BEA-016
Bromoaminociclização; ORG-095
BSA; INO-049
BTEX; ANA-055; ANA-056; MAT-063
bufadienolides; QPN-104
Bufonidae; QPN-078
building blocks; INO-041
bulk alcohols; TEO-013
Bupivacaína; ORG-078
Buriti; QPN-034
Butenolídeos; QPN-098
Butytylcholinesterase; QPN-125
byproducts; AMB-027

## C

C sequestration; AMB-033
C-H activation; ORG-029
C. limonia; QPN-079
C. sinensis; QPN-079
C6-C4-derivatives; QPN-009
CA4; MED-015
Cabernet Sauvignon; BEA-007
Caesalpinia pulcherrima; QPN-003
cafeoil; QPN-100
caffeine; ANA-004; INO-054
Caffeine extraction; EDU-055
Calcium; CAT-001; MED-043
calcium alginate; ORG-039
Calcium carbonate; MAT-038
calcium channel; MED-043
Calcium polyphosphate; MAT-093
Cálculo; EDU-016
Cálculos teóricos; ORG-068; TEO-005
Calea pinnatifida; QPN-116
Calea pinnatifida (R.Br) Less.; QPN-049
Calealactone C; QPN-116
calixarene; INO-086
Calixarenes; INO-080; ORG-084
Calixarenos; ORG-055
calorimetry; BEA-005; COL-005
CAM-B3LYP; TEO-011
câmara de combustão; AMB-005
Camellia sinensis; ANA-018
camomila; BEA-004
cana-de-açúcar; AMB-012
câncer; FIS-001
Cancer; COL-007
Câncer; COL-009; INO-023; INO-032; INO-034
Cancer; INO-068; INO-075
Câncer; INO-090; INO-100
Cancer; MAT-101
Câncer; MED-005
Cancer; MED-015; MED-022
Câncer; MED-048
Cancer; MED-051; ORG-022; ORG-108; TEO-010
Cancer cells; QPN-016
Candidíase; ORG-036
Candidiasis; QPN-018
Candy; ANA-063
Capacidade Antioxidante; QPN-121
capillary zone electrophoresis; ANA-003
caracterização; INO-030
caracterização eletroquímica; ELE-053
Caracterização físico-química; FIS-030
Carbamatos alílicos; ORG-095
carbaril; AMB-043
Carbodiimidas; ORG-078
Carbohidrazonamidas; MED-012
carbohydrate synthesis; ORG-108
Carbohydrates; ANA-066
carbon black; INO-044; INO-056
carbon capture; AMB-006
carbon dioxide; AMB-006; CAT-033; INO-014
Carbon Dots; MAT-012
carbon fiber microelectrode; ELE-045
Carbon nanofibers; ELE-062
Carbon nanostructure; CAT-005
Carbon Nanotube; ELE-044; ELE-056; MAT-022; MAT-029
Carbon nanotubes; ANA-052; ELE-019; ELE-040; ELE-047; MAT-043; MAT-108
carbon nanotubes dispersions; MAT-109
Carbon nanotubes,; FIS-003
carbon steel; ELE-002
carbon structures; ELE-014
Carbon-based electrodes; ELE-033
Carbonatation; FIS-032
Carbonato de glicerila; ORG-094
carbonatos cíclicos; INO-005
carbonização hidrotérmica; MAT-060
carbonyl compounds; AMB-007; BEA-013
Carbonylation; ORG-019
Carboxilc acids; ORG-004
Carboxilic Acids; ORG-061
Carboxyl cellulose; CAT-020
carboydrazides; BIO-012
carcinogenic risk; AMB-029
Cardanol; ORG-102
cardiomyocyte; MED-043
Cardiovascular Diseases; INO-088
carotenoids; AMB-071; ANA-030
Carrapaticida; MAT-071
Carreadores de ânions; ORG-068
Carrots; QVE-011
Carvacrol; MED-003
Carvão ativado; MAT-058
casca de arroz; AMB-040
Casca de Pinhão; QVE-010
Casearia arborea; QPN-041
cashew gum; INO-042
Cassava; FOT-004; MAT-094
Catalisador; INO-079
catalisador biomimético; INO-018
catalisador heterogêneo; FIS-033
Catalisadores; MAT-035
catálise; INO-001; ORG-051
Catálise ácida; ORG-034
Catálise heterogênea; CAT-037; INO-071; ORG-055
Catálise híbrida; CAT-036
catálise homogênea; INO-005
Catálise orgânica; ORG-037
Catalysis; CAT-006; CAT-016; CAT-019; CAT-038; ORG-049; ORG-083; TEO-014
catalyst; CAT-035; MAT-057; TEC-004
Catalytic decomposition; CAT-005
Catechol; ELE-052; INO-063; INO-068
Catecholamines; ANA-020
Catecolaminas; ANA-013
Cathepsin D; MED-046
Cathepsin K inhibitors; ORG-044; QPN-029
cathinones; MED-066; TEO-008
cationic surfactant; COL-005
Cattle Tick; MED-024
CCR2; MAT-036
Cebola brava; BIO-011
Cédulas; ANA-008
Celastraceae; QPN-112; QPN-120
Cellulase immobilization; COL-001
Cellulose; MAT-042; MAT-066; MAT-080; MAT-092; ORG-002
Cellulose modification; CAT-020
Celular death; INO-074
CeO2; CAT-012
Ceramic Membrane; TEC-011
Cercospora brachiata; QPN-064
Ceria; ELE-005
céria; INO-015
cerium nanostructured; ELE-011
Cerium(IV) oxide; MAT-097
cerrado; QPN-008
Cerrado biome; QPN-099
cerveja; BEA-020
Cerveja artesanal; BEA-019
Cetonas; QPN-055
cevada; AMB-043
CG-MS; QPN-006
Chagas Disease; MED-004; MED-008; ORG-029
Chagas' disease; MED-017
chalcogenolate; INO-078
Chalcona; MED-053; TEO-005
Chalconas; BIO-014; MED-045
Chalconas sintéticas; ORG-110
Chalcone; MED-034
Chalcones; MED-041
Chamaecrista; QPN-022
Chamomilla recutita; BEA-004
CHAOTROPIC AGENTS; BIO-013
chaotropicity dependence; ELE-015
Characterization; MAT-023
Characterization of materials; FIS-008
Characterization thecniques.; QVE-001
Charge-Transfer; MAT-024
Chás; QPN-077
chelant agent; AMB-045
Chemical bonds; EDU-012

Chemical Circuit; EDU-064
Chemical composition; QPN-013; QPN-039
Chemical Compounds; QPN-031
chemical ecology; QPN-083
Chemical functionalization; ELE-040
Chemical Jury; EDU-018
Chemical Kinetics; EDU-013
Chemical patents; TEC-001
Chemical Polymerization; MAT-005
Chemical profile; QPN-078
Chemical prospection; QPN-066; QPN-067
Chemical recycling; CAT-035
Chemical study; QPN-065
Chemical synthesis of graphene; MAT-123
Chemical Waste; AMB-065; QVE-013
Chemiluminescent; ANA-025
Chemistry; EDU-042; EDU-058
Chemistry Education; EDU-013; EDU-033
Chemistry student; EDU-045
Chemistry teachers; EDU-040
Chemistry teaching; EDU-025; EDU-029; EDU-032; EDU-043; EDU-064
Chemistry Undergraduate; EDU-046
Chemometric; ORG-053; QPN-015
Chemometrics; ANA-070; ANA-072; ANA-073; BEA-002
Chemotherapy; MED-051
Chia; QPN-026
Chikungunya; ORG-085
Chiral amines; ORG-049
Chiral polymers; MAT-079
Chirality imprinting; FIS-035
Chirality parameter; MAT-079
Chitosan; FIS-016; MAT-023; MAT-036; MAT-053; MAT-055; MAT-071; MAT-077
Chitosan composites; MAT-055
Chitosan films; ANA-063
chlorination; AMB-027; ORG-053
Chlorine; ANA-050
chlorine dioxide; INO-045
chlorite; INO-045
chlorogenic acid; QPN-032
Choline Chloride; COL-011; FIS-021
chromatographic resolution; BIO-003
Chromatography; ANA-001; ANA-016
Chromium (VI); ANA-057; INO-083
chromium(III); INO-041
Chronic myeloid leukemia; MED-016
chumbo; AMB-034; ANA-042
cianetação; AMB-026
Ciclodextrina; FIS-039
ciclodextrinas; INO-048
CID fragmentation; QPN-061
Ciência e Arte; EDU-004
Cigarros; ANA-021
cinchona; ORG-018
cinética; EDU-049; FIS-020; INO-099
Cinnamomum verum; QPN-004
Cipó cacheado; QPN-054
cipó-caboclo; QPN-033
Ciprofibrate; ANA-007
Citocalasina H; QPN-071
Citotoxicidade; INO-066; MED-054
Citrate; ANA-092
Citric acid; MAT-012; MAT-018; MAT-067
Citrus phytopathogens; QPN-124
Cladosporium herbarum; QPN-017
CLAE; ANA-002; ANA-011; QPN-052
Classical analysis; ANA-085
Classificação textural; ANA-061
classroom; EDU-052
clay minerals; AMB-057
Click chemistry; MAT-011; MED-018; ORG-052
click reaction; MAT-051
clinical chemistry; ANA-080
cloração; AMB-067
clorexidina; AMB-067
cloroaminociclização; ORG-027
Clusia grandiflora; BIO-011
Clusiaceae; BIO-011; QPN-105
CNLS; ORG-102
CO Adsorption; FIS-008
Co nanoparticles; CAT-027
Co-crystals; MAT-020
co-culture; QPN-124
CO2; CAT-021
CO2 capture; AMB-038
CO2 reduction; ELE-021
CO2 supercrítico; BEA-017
CO2 utilization; MAT-114
CO2 valorization; CAT-027
Coarse-grained; TEO-001
coating; MAT-021
Coaxial fibers; MAT-045
cobalt catalysts; INO-053
Cobalt Complexes; INO-068
Cobalt oxide spinel; FIS-035
cobalt(II); EST-001; INO-029
Cobalt(II) Complexes; CAT-029
cobalto; INO-023
cobalto(II); INO-026; INO-091
Cobaltoceno; ORG-105
cobre; AMB-034; AMB-066; ANA-042; ORG-072
Cobre (I); INO-100
Cobre(II); INO-091
Cocaína; ANA-008
Cocaine; ANA-032
Coconut; QPN-026
coconut oil; ANA-074
cocoon; INO-035
cocos nucifera Linn.; ANA-074
Coffee grounds; ANA-058; MAT-055
Coffee quality control; ANA-078
Collisional cross section; QPN-061
colloidal stability; INO-042
Colloids; MAT-041
Color; AMB-079
Colorimeter; FIS-005
Colorimetria; ANA-090
Colorimetric transition; ANA-032
Colorimetrical indicator; TEC-008
column chromatography; ORG-101
Coluna de Pré-concentração; ORG-086
combustion method; INO-022
CoMFA; MED-009; MED-049
Comparative Modeling; MED-024
Compatibility; ANA-071
complex; INO-009; INO-076; MAT-088
Complex matrices; BIO-004
Complex Nitrosyls; INO-088
Complexação; EDU-021; FOT-011
Complexation capacity; ANA-025
complexes; INO-016; INO-055
Complexo; INO-082
Complexo de cobalto(III); INO-090
complexo de Mn(I); FOT-003
complexo de níquel (II); INO-067
Complexo Ru(II); FOT-014
complexos; INO-058
complexos binucleares; INO-060
complexos com amidas; INO-039
complexos de chumbo (II); INO-094
complexos de cobre(II); INO-047
Complexos de coordenação; TEO-007
complexos de inclusão; INO-048
Composição química; QPN-118
Composite; MAT-103; MAT-112
Composites; MAT-047
composto de coordenação; INO-011
Compostos carbonílicos; QPN-072
Compostos fenólicos; BEA-019; QPN-036
Comprimento de cadeia; ANA-086
Computacional Chemistry; INO-064
Computational Chemistry; TEO-014
Computer Aided Drug Design; MED-046
Computer-Aided prediction; BIO-009
CoMSIA; MED-049
Conceitos; EDU-005
Concentração ácida; ANA-062
conceptual profile; EDU-032
concreto; MAT-086
Condensation; CAT-026
condições sanitárias; AMB-068
Conducting; MAT-028
Conducting Polymer; MAT-110
conducting thin films; MAT-109
Conductive polymer; ELE-009
Conformational analysis; ORG-014
Conformations; ORG-031
Congo Red; ANA-058
conjugate rigid spacer; INO-027
Conjugated polymer; MAT-056
Conjugated polymers; MAT-090; MAT-096
connection mode; ANA-022
conservation; QPN-019
Consumo; EDU-015
Contacless detection; ANA-068
contagem microbiana; BEA-004
contaminantes ambientais; INO-071
contextualização; EDU-014; EDU-062
Continuous Fermentation; TEC-011
continuous flow; ORG-039
Continuous-flow; ORG-046
controle de qualidade de leite; ANA-067

Controlled drug delivery; MAT-045
Controlled release; BEA-006; MAT-003; MAT-078
Conventional heating; CAT-026
Conversão de $CO_2$; CAT-023
cooperative collectors; AMB-004
coordination chemistry; EST-001; INO-081
coordination complex; INO-029
coordination complexes; INO-059
coordination compound; INO-025; INO-037; INO-052
Coordination compounds; INO-002; INO-003; INO-040; INO-063
Coordination Polymer; INO-007
copaifera reticulata; QPN-122
copper (I) complexes; INO-089
Copper Complex; INO-004; INO-057
Copper Complexes; INO-064
Copper determination; ELE-062
coprostanol; AMB-023
Coqueiros Community; QPN-024
corante; AMB-077; EDU-049
Corante básico; FIS-028
Corante direto; FIS-028
Corantes têxteis; FIS-028
Cordiera sessilis; QPN-099
Core shell structures; INO-092
Core-hole clock method; MAT-100
Corn stalks (Zea Mays L.); ANA-057
corrosão; EDU-014; MAT-086; ORG-060
Corrosion; MAT-121
corrosion inhibitor; ELE-025
corrosion inhibitors; ELE-002
Cortisol; ELE-046
Cosmetics; ANA-037; BIO-006; TEC-008
coumarin; FOT-008; INO-024; MED-025; QPN-059
Coumarin derivatives; INO-084
Coupling reactions; CAT-020
Coupling Reagents; ORG-069
cozinha científica; EDU-060
Cr(III); AMB-028
Cr(VI); AMB-028
CRF; MAT-023
CRGO; ELE-006
Criminal Science; MED-023
Cristais líquidos; ORG-025; ORG-035; ORG-066
Cristais liquidos; ORG-082
Cristais liquidos ionicos; ORG-082
Cristal líquido iônico; MAT-106
cromaticidade; INO-015
Cromatografia; ANA-086; BEA-007; BEA-009; BEA-019
cromatografia à gás; BEA-008
Cromatografia em camada delgad; ANA-005
Cromatografia em camada fina; EDU-051
cromatografia gasosa; AMB-075; ANA-014; ANA-075; ANA-079
cromatografia iônica; AMB-019
Cromatografia Líquida; ANA-013; ORG-075
cross-β structure; MAT-050; MAT-051
crosslinked polymer; MAT-064
Croton; QPN-012
Croton sacaquinha; QPN-106
crown ether; TEO-013
Crude glycerol; CAT-025
Crude oil; ANA-054; FIS-027
Crude oils; ANA-060
Crumpled graphene balls; MAT-015
Cruzain; MED-004; MED-029
Crystal disorder; INO-008
crystal engineering; INO-081
Crystal nucleation; MAT-118
crystal size; MAT-057
crystal structure; INO-025
$CsPb_{1-x}Sn_xBr_3$; INO-101
$CsPbBr_3$; INO-101
CTAB; COL-006
Cu(II) complexes; INO-069
$Cu^{2+}$ ions; MAT-116
$Cu_2O$; MAT-105
$Cu_2V_2O_7$; MAT-018
Cucurbita moschata; QPN-072
Cupper ions; ANA-053
Cuprous oxide; INO-065
Curcumina; FOT-011
cuticular waxes; QPN-044
Cyanide; FOT-004
cyclic anhydrides,; ORG-004
cyclic carbonate; INO-014
cyclic carbonates; INO-053
cyclic peptides; QPN-125
Cyclic peptides; QPN-076
cyclic voltammetry; BIO-009; ELE-047; ELE-056; ELE-057; INO-059
cycloaddition; INO-014; ORG-016
Cyclohexylamine 2-substituted; ORG-031
Cyclopentane; COL-008
cyclopentene; ORG-030
Cyclotides; QPN-076
cytotoxic activity; INO-036; INO-069; MED-015; QPN-014; QPN-087
Cytotoxicity; INO-075; MAT-077; ORG-006; QPN-058; QPN-074; QPN-088; QPN-117

## D

D-mannitol; ORG-079
DAGL-alpha; MED-065
DAT; MED-031
data management; QPN-056
DBA/2 mice; ANA-015
DBP; AMB-048
DEA; AMB-080
Debris; FIS-003
Decavanadato; INO-091
Decolorization; ELE-016
Decoralin; BIO-010
Deep Eutectic Solvents; QVE-002
Defects; ANA-078
Deficiente Auditivo; EDU-063
degradação; ANA-089; CAT-037; FIS-020
degradação de poluentes; AMB-052
Dehydration; MAT-048
delineamento composto central; AMB-050
delta-decalactona; ORG-041
demineralization; TEC-009
Demolition timber; EDU-048
dengue fever; MED-035
Density; TEC-005
Density functional theory; FIS-010; INO-061; ORG-073; ORG-093
Dental; FIS-039
Deodorants; ANA-037
dephosphoryilation; FIS-005
Dephosphorylation; ORG-067
Dephosphorylation reactions; FIS-009
Deprived of liberty; EDU-042
dereplication; QPN-032; QPN-060
Derivado sulfonil-hidrazônico; ELE-032
Derivados de Pirazol; ORG-060
derivatives; QPN-074
DES; FIS-013; QVE-007; QVE-008
desalination; MAT-008; MAT-041
Descoloração; FIS-020
Desenvolvimento De Método; ANA-013
desinfecção; AMB-050
Desulfuriza; MAT-044
Detecção colorimétrica; ANA-067
detecção de fenol; ELE-037
Detecção eletroquímica; ELE-028
Determinação de metais; ANA-049
Detoxification; CAT-013; QVE-004
Dextran derivatizatiion; MAT-011
DFT; CAT-007; INO-048; MAT-013; ORG-012; TEO-002; TEO-014
DFT and TD-DFT; TEO-011
DFT Calculations; INO-064
DHPM; MED-064
DIA; AMB-080
Diabetes; MED-009; MED-028
Diabrotica speciosa; QPN-068
Diacylglycerols; ANA-069
diagnostic ratios; AMB-022
Dialkylphosphorylhydrazones; MED-021
diamine; ORG-076
diaminomaleonitrile; INO-028; ORG-009
Diaphorte anacardii; QPN-071
Diarylheptanoid; QPN-094
Diastereoseletividade; CAT-002
Didactic Material; EDU-029
Didática; EDU-031
Diels-Alder; ORG-079
Diels-Alder adducts; ORG-008
Dienone-amide; ORG-063
diesel; ANA-042
Diesel oil analysis; ANA-044
Diethylaminoethyl derivatives; MAT-077
Difractaic acid; QPN-057
Difusão; MAT-098
Digestão nítrica; ANA-083
Digital Image; EDU-054
Digital image analysis; ANA-063
Digital images; ANA-072
Dihidropirimidonas; ORG-107
Dihydroartemisinin acetate; QPN-073

dihydropyrimidinones; ORG-073
Diidrochalconas; BIO-014
diketopiperazine; INO-009
dinuclear; INO-046
Dióxido de Carbono; CAT-023; INO-005
Dipeptides; ORG-044
diphenylalanine; MAT-068
Diphosphine Ru complexes; INO-074
Dipteryx lacunifera; QPN-088; QPN-089
Direct analysis; ANA-037
Direct ethanol fuel cell; ELE-031
Direct Selenylation; ORG-099
diruthenium(II,III); INO-021
Disciplina Química; EDU-063
discoloration; MAT-018
Discóticos; ORG-082
disposable device; ELE-046
dispositivos analíticos; ANA-067
Dissipated Ultrasonic Power; QVE-008
Distal functionalisation; ORG-098
Disulfide; ORG-103
Diterpene; QPN-106
Divaniloil Glicose; QPN-041
DLLME; AMB-021
dmit; MAT-091
DMSO; FIS-013
DNA; INO-049
DNA and HSA interaction; INO-074
DNA binding; INO-069
DNA cleavage; INO-069
DNA interaction; ANA-022; BIO-007; INO-019; MED-042
DNMR; ORG-031
docetaxel; ANA-006
Docking; MED-009; MED-017; MED-028; MED-032; MED-038; MED-055; MED-062
Docking consensual; MED-013
docking molecular; BIO-007; MED-047
Doctor blade technique; MAT-076
Doehlert matrix; ANA-056
Doença de Alzheimer; MED-061
Doença de Chagas; ELE-032; MED-012
doenças; AMB-068
Doenças do Príon; ORG-017
dolphins; AMB-073
domestics wastes; AMB-074
domino reaction; ORG-056
Donor-acceptor systems; MAT-024
DOPAGEM; FIS-023
Dopamine; ELE-043; ELE-052
Doxiciclina; ANA-011
DPP-4; MED-009
DPP-IV Inhibitors; MED-028
DPPC; FIS-016
DPPG; FIS-016
DPPH; BIO-011; QPN-054
drinking water; AMB-048
Droplets; ANA-068
drug delivery system; MAT-059
Drug dependence; MED-031
Drug design; MED-016
Drug development; MED-006
Drug Discovery; MED-038; MED-046
drug sustained delivery; INO-062
drugs; AMB-024; AMB-064
DRUV; AMB-059
Duguetia lanceolata,; QPN-085
Duguetia surinamensis; QPN-087
dye; AMB-045
dye elimination; INO-056
dye photo degradation; INO-044
dye photodegradation; INO-022
dye-degradation; ELE-007
Dye-surfactant aggregates; COL-006
Dyes; FIS-022; MAT-083
dyes removal; MAT-069

# E

E-Cariofileno; QPN-003
EC50; ORG-090
ECD; TEO-006
ecologia química; QPN-070
economia circular; AMB-041
Ecovio®; MAT-004; MAT-074
EDC; ORG-078
EDCs; ANA-019
Edible gelatin; MAT-019
edible oil; ANA-033
EDLC; MAT-092
edta; INO-085
Educação Ambiental; EDU-015
educação do campo; EDU-041
Education; EDU-030
educational game; EDU-032
EDXRF; ANA-036
efeito fotoeletrocatalítico; ELE-053
Effect of the support; CAT-014
efficiency; AMB-053
effluent; AMB-044; AMB-045
EIEB; ANA-047
Eisenia andrei; BIO-008
Elaeis guineens; QPN-118
elaidic acid; ANA-003
electric arc furnac; CAT-038
electric double laye; FIS-014
Electric Double Layer (EDL); COL-013
electro-oxidation; ELE-051
electro-spining; AMB-046
Electroactive polymer; ELE-009
electroanalysis; ELE-022; ELE-049
electroanalytical sensor; ELE-024
Electrocatalysis; ELE-039; ELE-041; ELE-051; FIS-004; INO-004; INO-043; INO-096; MAT-110
electrocatalytic activity; ELE-011
Electrochemical biosensors; ELE-050
Electrochemical Capacitance; ELE-060
electrochemical cell; ELE-004
Electrochemical kinetics; ELE-033
electrochemical mechanism; ELE-022
Electrochemical modeling; TEO-003
Electrochemical oxidation; ELE-027; FIS-012
Electrochemical Polymerization; MAT-005
electrochemical sensor; ELE-022; ELE-023; ELE-040
Electrochemical Sensors; MAT-105
Electrochemistry; EDU-053; ELE-030; ELE-041; ELE-056
Electrode Modified; ELE-023
electrodeposition; ELE-003; ELE-054; ELE-055; MAT-082
electron-phonon; MAT-001
Electronic Circular Dichroism; FIS-010
electronic spectroscopy; INO-045
electronic waste electronic waste; AMB-004
electrooxidation; ELE-026; ELE-039
Electrophilic halogenation; ORG-007
Electrophoresis; ANA-066
Electrophoretic Mobility; COL-013
electropolymerization; ELE-024
Electroreduction; ELE-034
Electrospinning; MAT-045; MAT-074
electrostatic charging; FIS-014
Electrostatic interaction; MAT-096
Elementos; EDU-005
eletroanalítica; ELE-020
eletrocatálise; ELE-008
eletrodeposição; ELE-059
eletrodeposição NiFe; ELE-042
Eletrodo Grafite-SiO2-TiO2; ELE-037
Eletrodo de grafite; ELE-028
Eletrofiação; MAT-004; MAT-016
eletrônica flexível; EDU-035
Eletroquímica; EDU-028; EDU-035; EDU-047; EDU-059
Elipsometria; MAT-099
Elucidação estrutural; ORG-025
emerging contaminants; AMB-024; AMB-064; FOT-010; MAT-055
emerging organic pollutant; INO-098
Emerging Pollutants; AMB-054; ANA-027
emissões veiculares; AMB-012
emulsão; ANA-042
Emulsion Stability; COL-008
Enade reports; EDU-045
enaminones; ORG-005
Enantiomers; FIS-010
Enantioselective Catalysis; ORG-023; ORG-030
Enantioselective synthesis; ORG-079
Enantioseletividade; ORG-032
Enantiosseletividade; ORG-095
Encapsulation; QPN-021
Endophytic fungi; QPN-066; QPN-067
Endophytic fungus; QPN-060
endophytid fungi; BIO-002
energia renovável; AMB-070; EDU-036
Energy; ELE-039; INO-006
Energy Conversion; ELE-041
Energy harvesting; FIS-031
Energy recovery; CAT-011
energy transfer; FOT-007; MAT-010
Engaço uva; MAT-058
enhanced efficincy fertilizer; TEC-003
Ensaios Bioquímicos; MED-048

Ensaios celulares; MED-005
Ensino; EDU-016; EDU-028; EDU-047; EDU-059
Ensino de Química; EDU-002; EDU-022; EDU-031; EDU-037; EDU-039; EDU-041; EDU-044; EDU-060; EDU-062
Ensino de Química.; EDU-023
Ensino e Aprendizagem; EDU-037
Ensino Investigativo; EDU-039
Ensino superior; EDU-011
Ensino técnico; EDU-003
ensino-aprendizagem; EDU-014
ent-cauranos; QPN-113
enthalpimetry; BEA-005
Enthalpy of Formation; FIS-034
Entrega controlada de fármacos; INO-090
Enviromental Awareness; QVE-013
Environment; EDU-050
Environmental control; ANA-091
Environmental Education; EDU-050
Enzima; MAT-124
Enzimas; QPN-055; QPN-072
enzymatic assay; BIO-003; QPN-029
Enzymatic biofuel cell; ELE-039
Enzymatic Catalysis; ORG-111
enzymatic kinetic resolution; ORG-039
enzymes; ORG-001
Ephedranthus pisocarpus; QPN-107
epistemological obstacle; EDU-040
Epistemological obstacles; EDU-012
Epoxide; ORG-079
Epoxides; CAT-033
EPR; FOT-002; FOT-003; ORG-103
EPS; MAT-107
Equilíbrio; EDU-021
Equilíbrio Químico; EDU-016
Equilibrium; ORG-031
Equilibrium constant; EDU-054
Eriocaulaceae; QPN-063
Erythrina verna; QPN-042
Escherichia Coli; BIO-006
Escola; EDU-028; EDU-047; EDU-059
ESI-MS; ANA-074
ESKAPE pathogens; ORG-054
Espaço não-formal; EDU-003
especiação; BEA-020
especiação química; AMB-028
Espectrofotometria; ANA-028
Espectrometria De Massas; ANA-013; BEA-015; QPN-095
Espectroscopia Raman; MAT-099
Espiropirano; INO-082
essential oil; ORG-011; QPN-002; QPN-006; QPN-008; QPN-011; QPN-013; QPN-015; QPN-018
Essential oils; QPN-046
estabilidade; INO-099
Estabilidade Matabólica; MED-060
estabilidade térmica; AMB-069
estabilização de dejetos; AMB-041
estação de tratamento de água; AMB-080
estatística multivariada; AMB-035
Estequiometria; EDU-065
ésteres metílicos; ORG-003
esterificação; FIS-033
Esterification; CAT-009; CAT-022; QVE-009
Esteroide; QPN-120
Esteroides; QPN-107; QPN-108
Estresse oxidativo; MED-064; QPN-035
estrogen receptors,; FIS-007
Estrogens; ELE-047
estrôncio; INO-030
estrutura cristalina; INO-026
Estudantes de Química; EDU-038
Estudo de caso; EDU-066
estudo de estabilidade; ANA-089
Estudo químico; QPN-012
etanol; QPN-030
Ethanol; CAT-006; ELE-005; ELE-029; ELE-039; ORG-109
Ethanol oxidation reaction; ELE-031
Ethanol reforming; TEO-014
Ethanol steam reforming; CAT-014
Ethnobotanical Survey; QPN-024
ethylmercury; BIO-005
Eucaliptus grandi; INO-083
eucalyptus; AMB-070
Eugenia dysenterica; BEA-015
Eugenia uniflora; QPN-011
Eugenol; ORG-036; ORG-052; ORG-076
európio; INO-039
europium; MAT-001
Europium (III); MAT-034
Europium(III); MAT-070
eutrophication; AMB-057
evolução H2(g) e O2(g); FOT-003
ex vivo; MED-007
excitação acústica; AMB-005
Exfoliation; AMB-047
experiment; ORG-101
Experimentação; EDU-002; EDU-015; EDU-038; EDU-051
Experimentação no Ensino; EDU-039
Experimental Chemistry; EDU-050
Experimental class; EDU-055
Experimental design; ANA-007; ANA-071
Experimental evaluation; MED-002
experimental practice; EDU-006
Experimentation; EDU-064
Experimento; EDU-061
Extração; ANA-008; QPN-004; QPN-030
extração em fase sólida; ANA-095
Extração líquido-líquido; ANA-014
Extração on-line; ANA-028
extração por solvente; BEA-009
extração sequencial; AMB-026
Extração supercrítica; QPN-010
EXTRACELLULAR HEMOGLOBIN; BIO-013
Extracellular Matrix; MAT-031
extract; QPN-099
Extraction; ANA-040; ANA-045; QPN-016
Extraction techniques; QPN-028

## F

Factorial design; ANA-069; CAT-010
fármaco; INO-050; INO-079
fármacos; INO-001
Fases cromônicas; ORG-025
Fast Pyrolysis; TEC-007
fatty acid; QPN-064
Fatty acids; ANA-030; CAT-022; CAT-039; QPN-034; QPN-037
Fe(II); INO-087
Fe(II) complexes; INO-077
Fe(III); BEA-010
Fe(III)-4AA complex; FIS-012
FeCo alloy; INO-042
feijão carioca; ELE-037
feltro; EDU-001
fenitrothion; ELE-001
Fenólico; QPN-041
Fenólicos; QPN-022; QPN-080; QPN-082
Fentanyl; ANA-017
FEP; MED-027
Fermentação; EDU-060
Ferri/ferrocyanide; ELE-033
Ferrierite; AMB-047
ferro; BEA-020; MAT-035
ferrocene; INO-063
ferti-release; MAT-066
fertilizante; AMB-037
Fertilizer; MAT-023
few-walled carbon nanotubes; MAT-091
FIA; ANA-064
Fiber; QPN-034
Fibra; MAT-065
Fibras; MAT-004; MAT-016
Fibroin; FOT-013
Filamentous fungi; MED-050
filmes de biopolímeros; MAT-054
Fish scales; ANA-058
fitoquímica; QPN-050; QPN-053
fitossanitários; AMB-021
flame retardants; AMB-018
Flavin adenine dinucleotide; ELE-061
Flavone; QPN-091
Flavonoid; FIS-007; QPN-094
flavonoide; QPN-113
Flavonoides; QPN-012; QPN-022; QPN-033; QPN-047; QPN-090
flavonoids; ORG-090; QPN-081; QPN-088; QPN-089; QPN-093; QPN-119
flavonol triglycosides; QPN-092
Flavorizantes; ANA-021
flebotomíneos; INO-058
Flores; QPN-003; QPN-012
Flow analysis; ANA-025; ANA-027; ANA-082
Fluido Biológico; ANA-013
fluído biológico; BIO-008
fluorene; MAT-001
fluorescence; FOT-006; FOT-008; FOT-015; MAT-012; MAT-024
Fluorescência; INO-082
Fluorescent lamp phosphor; MAT-040
fluoride; INO-012

Fluoride ion; COL-012
fluoroquinolones; INO-036
Folin-Ciocalteau method; ANA-010
Folin-Ciocalteu method; ANA-024
Food; ANA-072
Food additives; ELE-010
Food analysis; BEA-001
Food packaging; FIS-031
foodborne; QPN-122
Forensic; ELE-052
forensic application; ELE-022
Forensic chemistry; ANA-032; MED-066
Forensic Science; TEO-008
Formação Continuada; EDU-039
Formação de Professores; EDU-004; EDU-008; EDU-039; EDU-057
Formação Docente; EDU-002
Formaldehyde; TEC-008
formigas cortadeiras; QPN-070
Forocromismo; INO-082
Fosfonato; ORG-085
Fotocatálise; EDU-049; INO-033
fotocatálise heterogênea; AMB-052
Fotocatálise Plasmônica; FIS-018
Fotocorrente; ELE-053
Fotografias; EDU-031
Fotólise por pulso de laser; FOT-009
fotoluminescência; INO-015; ORG-035
fotoquímica; AMB-012
fotossensibilizador; INO-032
Fotossíntese artificial; FOT-003
Foz; AMB-019
FPS; QPN-007
Fragment-based Lead Discovery; MED-026
Fragrâncias alérgena; ANA-079
frass volatiles; QPN-083
Free radical; ANA-059
Free solvent; CAT-026
Freundlich; AMB-034
Frieseomelitta doederleini; QPN-082
Frontside attack; ORG-067
Fructose; ELE-023
Fruit flour; BEA-001
Fruit Juices; ELE-023
frutas tropicais; BEA-009
Fuel Cell; ELE-005
Fuel cells; ELE-041
full characterization; INO-053
fumarprotocetraric acid; MED-047
functional nanocomposites; MED-014
Fundão dam; AMB-016
fungi; MAT-113
fungicida; QPN-017
Fungo endofítico; QPN-071
fungo mutualista; QPN-070
fungos; BIO-008
Fungos Filamentosos; MAT-033
fungos negros; QPN-070
Furfural; QVE-011
Furfuryl alcohol; QVE-011
Furosemide; ELE-006; ELE-013
Fused core columns; ANA-016

## G

G4; FIS-034
G4MP2; TEO-006
gadolínio; INO-039
Galectin-1; ELE-060
Gallic acid; ANA-024
galvanic cell; EDU-053
gas chromatography; AMB-032; ANA-060; QPN-005
Gas separation; MAT-115
Gasoline; ANA-040
Gastric emptying; ANA-015
gastrite; MED-045
GBB reaction; ORG-080
GC-FID; ANA-070; BEA-008
GC-FTIR; QPN-083
GC-MS; AMB-018; AMB-048; AMB-072; ANA-009; ANA-073; QPN-064
GC-MS-FID; ORG-011
GC/MS; QPN-008
Gelatinderivatization; MAT-011
Gels; FOT-016
general chemistry; EDU-052
genome mining; QPN-069
genotoxic; QPN-096
Geometria molecular; EDU-017
Geopropolis; QPN-081
Germagreno D; QPN-003
GF AAS; ANA-040
GGA; FIS-023
GIAO model; ORG-102
Gingivitis; QPN-020
Glandularia; QPN-093
Glass powder; MAT-112
Glass Transition; FIS-017
glassy carbon; ELE-040
Glifosato; ANA-090; INO-094; INO-102
global change; AMB-006
Glomerella cingulata; BIO-014
Glucose; ELE-030; ELE-051; MAT-105
Glucose Uptake; QPN-119
Glycation; MED-058
Glycerol; CAT-033; ELE-038; INO-080; MAT-067
glycerol 1-monoether; QVE-009
Glycerol hydrogenolysis; CAT-017
Glycerolysis; ANA-069
glycin; MAT-018
Glyphosate; ANA-077
GNPS; QPN-032
Goiás; AMB-001
Gold; CAT-012; CAT-016; MAT-014; MAT-082; MED-028
gold microelectrodes; ELE-004
gold mine sludge; INO-044
Gold nanocatalysts; CAT-010
gold nanoparticles; MAT-029; MAT-118
gold nanorods; MAT-061
Gold nanostructures; ELE-057
Gold Surface; ELE-061
grafite laminado; EDU-035
Gram-positive bacteria; ORG-045
Grape juice; ANA-024
grapefruit albedo; ORG-013
Graphene; MAT-049; MAT-103; MAT-125
graphene nanosheets; ELE-011
Graphene oxide; CAT-011; MAT-005; MAT-008; MAT-032; MAT-049; MAT-068; MAT-076
Graphite; ELE-030; MAT-092
Graphite exfoliation; MAT-104
greeenhouse gases; AMB-006
green chemistry; BEA-005; CAT-006; EDU-050; ORG-005; ORG-007; ORG-053; ORG-062; QVE-004
green solvents; FIS-013
Green Synthesis; QVE-001
Green- Coffee; MAT-042
greenhouse effect; AMB-033
groove; ANA-022
groundwater; AMB-014
Growth; MAT-118
GSH; AMB-073
guaiane; ORG-083
guavira; QPN-007
Guazuma ulmifolia; MAT-087; QPN-036
Gum Arabic; CAT-013

## H

H. pylori; MED-047
$H_2$ generation; ELE-015
$H_2O$; CAT-007; ORG-081
$H_2O_2$; CAT-006; CAT-007; ELE-030
Habilidade técnica; EDU-034
Habilidades Visuoespaciais; EDU-007
hair salon effluents; AMB-015
Halogênio; INO-079
Hammett theory; ORG-073
hazard quotient; AMB-029
HCA; ANA-081
HDAC; MED-022
HDO; CAT-019
Healt; ANA-093
Health Surveillance; MAT-121
Heavy metal; MAT-009
heavy metals; AMB-013; INO-076
Heck Reaction; ORG-023
Heck−Matsuda Reaction; ORG-030
Heck-Matsuda arylation; ORG-098
Helical polymers; MAT-079
Helicobacter pylori; MED-045
Hematite; MAT-030
Hemiacetalizaçao intramolecula; CAT-002
Hemoglobin; BIO-005
herbicida; INO-102
Herbicide; FIS-006
herpes; MED-035
Hesperetin; BIO-001
hesperidin; ORG-013
Hesperitin; MED-001
Heterocycle; INO-073; ORG-093
Heterocyclic Compounds; MED-051
Heterocyclics; ORG-016
heterodentate chelator; INO-038

Heterogeneous acid catalysts; CAT-009
heterogeneous catalysis; CAT-015; CAT-022; CAT-026; CAT-032; INO-098; ORG-084
heterogeneous catalyst; TEC-002
Heterogeneous Photocatalysis; CAT-004
heterologous expression; QPN-069
HG-AFS; ANA-041
Hidrocarbonetos; CAT-023
Hidrocarbonetos cuticulares; ANA-086
Hidrocloritiazida; ANA-002
Hidrodistillation; QPN-016
Hidrogel; MAT-098
hidrogenação enantiosseletiva; ORG-020
Hidróxido duplo lamelar; MAT-060
Hierarchically structured; MAT-047
High Purity Graphite; ANA-043
Hinoquinina; MED-013
Hipertension; INO-088
Hipóxia; INO-090
HIV-1; ORG-106
Hofmann degradation; ORG-007
hologramas; EDU-024
homogeneous catalysis; INO-014; INO-043
homogeneous redox catalysis; ELE-049
Honey; ANA-050
hopanes; AMB-003
Horizontes de leitura; EDU-010
HPA; AMB-001
HPA-S; ANA-038
HPAs; AMB-011
HPLC; AMB-043; ANA-007; ANA-008; ANA-018; QPN-022; QPN-028
HPLC-DAD; ANA-006; BEA-019; QPN-067; QPN-089
HPLC-DAD-UV; ANA-015
HPLC-ESI-MS/MS; QPN-075
HPLC-FLD; ANA-019
HPLC-MS-MS; QPN-032
HPLC-MS/MS; QPN-099
HPLC-PDA; ORG-089
HPLC-RI; ORG-006
HPLC-UV-MS; QPN-079
HPTLC; QPN-054
HQSAR; MED-049; MED-057
HRMS; QPN-019
HRTEM; MAT-061
human melanoma; QPN-096
Human Pathogens; QPN-031
Human serum albumin; FIS-010
Humic Substance; ORG-057
humic substances; AMB-078
Humicola fuscoatra; QPN-066
Hybrid; MAT-078
hybrid peptides; MAT-050
Hybrid Silicas; INO-080
Hydrate; COL-008
hydrazone; INO-024
Hydrocolloids; BEA-003
Hydrodeoxygenation; CAT-019
Hydrodynamic Size; COL-013
Hydroformylation; CAT-018
Hydrogel; FOT-002; FOT-013; MAT-011; MAT-031
Hydrogel composite; MAT-116
Hydrogen; CAT-001; CAT-011
hydrogen bond; ORG-014
hydrogen peroxide; TEC-009
Hydrogen Production; MAT-110
hydrogen sulfide; MED-043
hydrogenation; CAT-016; CAT-021; QVE-011
hydrolysis; CAT-003
Hydrophilic polymers; MAT-067
Hydrophobic papers; MAT-080
Hydrophobicity; COL-002; FIS-037; MAT-117
hydrothermal treatment; AMB-059; MAT-007
Hydroxylamine; ORG-067
hydroxyphenalene; INO-020
Hyperglycaemia; QPN-119
Hypericin; MAT-006
Hypodermic needles; MAT-121
Hypoxylon investiens; QPN-067

## I

i-optimal design; ORG-090
Ibuprofen; AMB-024; INO-021; TEO-006
IC; ANA-051
ICA; ANA-074
ICP OES; ANA-037
ICP-MS; AMB-016; ANA-052; BEA-016
ICP-OES; ANA-044; ANA-052; ANA-085
identificação; INO-050
Identification; QPN-040
Igarapés; AMB-023
IL; QVE-008
Image J; EDU-054
Imidas cíclicas; ORG-036
imidazo[2,1-b]thiazoles; ORG-080
imidazole; FIS-019
Imidazolina; ORG-105
imidazopyridine; INO-084
Immobilization; ORG-111
Immunoglobulins; BIO-001
Imobilização; ORG-094
Imobilização de enzima; CAT-036
impedance; ELE-017; ELE-056
impregnation; CAT-031
Improved Hummers Method; MAT-104
Impurities; ANA-044
In Silico Toxicity; MED-023
In situ electrochemical; ELE-061
In-line concentration; ANA-016
Inclusão; FIS-039
Inclusive education; EDU-025; EDU-029
Índice de seletividade; MED-059
Indigotine; ANA-063
Indole; ORG-054
Indoles; ORG-099
Induction period; FIS-024
Induction-Time; BEA-014
Industrial effluents; AMB-079
industrial waste; CAT-038
industrial wastes; AMB-074
Inflammatory diseases; MAT-036
inflorescences; ORG-011
Information Science; TEC-001
Infrared; ANA-072
infravermelho; INO-050
inhibition; MED-025
inhibitor; MED-039
Inhibitors; MAT-118; TEO-010
Inhibitory activity; MED-065
inhibitory concentration; AMB-059
Inibidores; ORG-060
Inorganic constituents; ANA-034
inorganic contaminants; AMB-061; ANA-052
inorganic oxides; MAT-113
Inorganic Spectroscopy; INO-064
Insect pest; QPN-068
inseticida; QPN-001
Instrumentação e automação; ANA-026
intensificação plasmônica; INO-033
Interação com DNA; MED-032
interações; QPN-070
interações não covalentes; INO-048
Interaction; FIS-022
interaction process; BIO-005
interactive tools; EDU-052
Intercalação; ORG-107
intercalation; MAT-007
Interdisciplinaridade; EDU-060
Interdisciplinarity; FIS-032
interfaces; FIS-014
Intermolecular interaction; FIS-037
Intumescimento; MAT-098
Invasive plants; QPN-025
inventário; AMB-017
Investigative experiments; EDU-013
Iodine; ANA-051; BEA-016
iodo; AMB-066
Iodocyclization; ORG-081
ion aqueous batteries; MAT-125
Ion Chromatography; ANA-050; ANA-092
Ion Exchange; AMB-047; MAT-007
Ion mobility-mass spectrometry; QPN-061
Ion-imprinted polymer; ANA-041
Ionic Gelling; MAT-041
Ionic Liquid; CAT-032; ELE-058; ORG-002
ionic liquids; ELE-045; FIS-017; ORG-004; QVE-006
ionogels; ORG-004
ionophore; QPN-069
íons; AMB-019
íons metálicos; AMB-036
Ipomoea purpurea; QPN-037
Iridium; CAT-017; MAT-088
iridoide; QPN-100
Iron; AMB-079; CAT-017
iron complexes; AMB-049
iron oxide; MAT-123
Iron thiocyanate; EDU-054
iron(II) acetylacetonates; INO-035
Iron(III) complexes; INO-028
ironporphyrin; INO-098

Irreversible inhibition; TEO-012
Isatin; ORG-048
isatins; QPN-084
Isocoumarins; ORG-028
isolamento elétrico; QVE-012
Isomer; FIS-010
Isomeria; TEO-007
Isopropylamine-TPD; CAT-003
Isoquinuclidines; ORG-008
isotope labeling; ORG-019
Itaconic Acid; ORG-050
ITIES; ELE-019
IUPAC nomenclature; EDU-019

## J

Jabuticaba; MAT-083
Jatropha; QPN-125
Jatropha aethiopica; QPN-092
Jogo Analógico; EDU-037
Jogo da velha; EDU-065
Jogo didático; EDU-008
Jogo Digital; EDU-037
Jogos didáticos; EDU-021
Jogos educativos; EDU-062
Jogos eletrônicos; EDU-056
Jogos Lúdicos; EDU-056
Jurema Preta; QPN-030

## K

Kallikrein inhibitors; BIO-004
ketoglutaric derivatives; MAT-053
ketoprofen; AMB-024
ketoreductase; ORG-001
kindler reaction; ORG-058
Kinect of degradation; MAT-103
Kinematic viscosity; TEC-005
KINETIC; BIO-013; FIS-027
kinetic parameters; BIO-003
Kinetic resolution; ORG-046
kinetics; CAT-003; ORG-002
Kit didático; EDU-035
kits didáticos; EDU-062
Klebesiella pneumae; BIO-006
Knowledge Management; TEC-001
Kohonen Neural Network; AMB-072

## L

L-Cysteine adsorption; ELE-036
L. (L.) infantum; QPN-098
Lab-made photoreactor; MAT-032
Label; ORG-103
Labil C; AMB-033
Laboratório escolar; EDU-034
laboratory glassware; EDU-019
Laboratory Instruction; EDU-048
Lacase; ORG-040
Laccase; AMB-054; ELE-050; ORG-065
Lactuca sativa; QPN-037
Langmir-Blodgett; INO-020
Langmuir monolayer; FIS-016
lantanídeos; INO-011
Lantânio; INO-082
lanthanide; AMB-025; INO-037; INO-052; INO-055; MAT-089
Lanthanide complexes; INO-085
Lanthanide organic frame-works; INO-008
lanthanides; MAT-010
Lanthanides salts; ORG-004
Larvicidal activity; MED-041
Lauraceae; QPN-098
Lawsone; ORG-045
layered double hydroxide; AMB-060
Layered hydroxide salt; BEA-006
layered hydroxide salts; INO-051
layered matrix; MAT-007
LBDD; MED-017
LC-ωPBE; TEO-011
LC-MS/MS; AMB-021; AMB-023; AMB-048; ANA-017
LCC; MAT-071
LCMS MS; EDU-048
LDB; EDU-044
LDH; COL-012; MAT-057
lead; AMB-047
lead contamination; AMB-004
Legumes; BEA-016
Leguminosae; QPN-039
Lei 10639; EDU-022
leishmania; ORG-087
Leishmania amazonensis; MED-019; MED-036; MED-052; MED-059
Leishmania chagasi; QPN-032
Leishmania infantum; QPN-043
leishmaniasis; MAT-059; MED-030
leishmanicidal activity; BIO-002; ORG-052
leishmaniose; INO-058
Leite; EDU-022
leite materno; BEA-011
Leitura; EDU-017
Leukemia; ORG-092
Leukemia assays; QPN-086
Levoglucosan; TEC-007
levulinic acid; QVE-009
LF-NMR; ANA-029
liberação controlada; AMB-063
LICENCIATURA; EDU-044
$LiFePO_4$; ELE-058
Liga NiFe; ELE-042
Ligações Químicas; EDU-023
ligand design; INO-077
ligante pirazólico; INO-026
Ligante Quiral; ORG-105
Limonene; MAT-080
limoneno; INO-047
Linear sweep anodic stripping; ELE-062
lipase; ORG-039; ORG-046; ORG-111
lipases; CAT-008; ORG-094
lipid; ANA-074
Lipoic acid; MED-058; ORG-103
Liquid chromatography; ANA-010; BEA-018
Liquid Crystals; ORG-010; ORG-064
Liquid-liquid Interface; ELE-019
Liquid-phase microextraction; ANA-027
Liquid/liquid interface; MAT-123
líquido iônico; ELE-059
lithium batteries; ELE-018
Living Cells; AMB-058
Lliberação tópica; MAT-098
Lobeline; MED-044
Losartano potássica; ANA-002
loss modulus; MAT-081
low-cost materials; ORG-101
Low-field NMR; TEC-005
LQTA-QSAR; FIS-007
LS-SVM; ANA-061
Lubricants; MAT-122
Ludic Activity; EDU-018
ludic learning; EDU-019
Luehea divaricata; QPN-111
Luminescence; INO-010; INO-017; INO-052; INO-055; INO-086; MAT-034; MAT-070; MAT-088; ORG-059
luminescência; FOT-012; FOT-014; INO-039; ORG-066
luminescent; MAT-010
luminescent copper compounds; INO-089
Luminescent Materials; ORG-010
Luminescent Probes; FOT-005
Luminomagnetic nanoparticles; ANA-053
Luz; INO-032

## M

Machaerium; QPN-109
Machaerium brasiliense; QPN-109
Macrobenthos; QPN-062
Macrofauna; QPN-062
macrolide; QPN-083
Macrolobium rigidum; QPN-039
Magnesium; CAT-001
magnetic; COL-003
Magnetic circular dichroism; FIS-035
Magnetic Hyperthermia; COL-007
Magnetic measurements; INO-077
Magnetic Nanoparticles; ANA-046; COL-001; INO-042
magnetic oxides; INO-022; INO-056
Magnetic particles; ORG-084
magnetic properties; INO-025
Magnetic reactors; COL-001
magnetic separation; INO-022; INO-056
Magnetic Solid Phase Extractio; ANA-046
Magnetite; COL-002; COL-007; COL-012; ELE-044; INO-092; MAT-026
magnetron sputtering depositio; CAT-027
maker culture; EDU-026
makerspace; EDU-026
Malaria; MAT-045; MED-002; MED-039
male and female specimens; ORG-011
Maleimides; ORG-015
malifolia; QPN-008
Maltose Binding Protein; ELE-060
Malvaceae; QPN-111
Manaus; AMB-023
Manilkara subsericea; QPN-035
Manipueira; FIS-030

MAO; QPN-042
Mariana disaster; AMB-016
Marine; QPN-066
Marine ecology; QPN-062
Marine fungi; QPN-058
Marine microorganisms; QPN-084
marinoquinoline; MED-039
mars; AMB-071
mass detector; AMB-032
Mass spectrometry; ANA-010; ANA-017; ANA-020; ANA-060; FIS-002; QPN-060
Mate tea beverages; ANA-010
Matemática; EDU-016
Materiais alternativos; EDU-023
materiais catalíticos; AMB-052
Materiais lenhosos; MAT-058
materiais multifuncionais; MAT-060
material didático; EDU-001; EDU-017; EDU-065
matrix effect; MAT-010
Matriz Doehlert; AMB-050
Matriz orgânica; ANA-083
Maytenus quadrangulata; QPN-120
Maytenus robusta; QPN-110
MBP-Gal-1; ELE-048
MCM-48; MAT-063
Mechanical and Thermal Propert; MAT-112
Mechanical Properties; MAT-077
Mechanism; ORG-067
Mechanized system; ANA-065
mechanochemistry; ORG-005; ORG-053
medicinal plant; QPN-092; QPN-101
Medicinal Plants; QPN-049
meio ambiente; AMB-017; AMB-026; EDU-047; FIS-030
Mel; QPN-082
Melatonin; ELE-033
Melipona mandaçaia; QPN-080
Melipona subnitida; QPN-081
Membranas semipermeáveis; ANA-055
membranes; MAT-008
mercerization; MAT-119
Mercúrio gasoso; MAT-027
mercury; AMB-061
Mesoionic; MED-051
Mesoporous carbon; ELE-058; MAT-111
Mesoporous Silica; CAT-032; MAT-026; MAT-063
mesoporous structures; CAT-035
Mesoporous-silica; COL-002
metabolic profile; QPN-075
Metabolites; QPN-059
Metabólitos; ANA-013
Metabólitos especiais; QPN-052; QPN-121
metabólitos secundários; QPN-050
Metabolitos secundários; QPN-053
metabolomic; AMB-071
Metabolomics; QPN-119
Metacrilato; FIS-039
metais; AMB-062; ANA-047; FIS-030
metal; AMB-045; ANA-085
Metal clusters; TEO-014
Metal complexes; INO-088
metal exposure; AMB-073
Metal ligand; CAT-020
metal organic frameworks; AMB-038; ELE-029
Metal Oxide; MAT-110
metal pollution; AMB-029
metal removal; AMB-046; AMB-061
metal traço; AMB-028
metal triflates; ORG-080
Metalation; ORG-070
Metallacrown; INO-007
metallic contaminants; ANA-033
metallic nanoparticle; MAT-096
metallodrug; INO-021
metallopolymer; MAT-001; MAT-056
metalloporphyrins; INO-049
metallothionein; AMB-073
Metalofármaco; INO-090
metalofármacos; INO-023
metaloporfirinas; INO-001
metals; AMB-016; AMB-030; ANA-037; ANA-040
metals alcalines íons; CAT-031
metanólise; FIS-033
metastability; MAT-126
meteorite; AMB-039
Metformin Hydrocloride; MAT-074
methacrylate copolymers; MAT-046
Methane; CAT-005
methanol; ELE-021; ELE-029
Methanol Electro-oxidation; FIS-004
Method validation; ANA-017
Methyl fatty esters; TEC-002
Methyl methacrylate; CAT-024; CAT-028
methyl orange; FIS-026
methylene blue; AMB-044; CAT-004; FIS-003; FOT-016; MAT-006; MAT-018
Método da Pipeta; ANA-061
Metodologia ativa; EDU-066
Metribuzin; ELE-044
Metrological certification; MAT-122
MIC; ANA-051; BEA-016
micelles; INO-016
Micro-ondas; ANA-049; ANA-083
Micro-ondas doméstico; ANA-014
micro/mesoporous silica; MAT-114
Microalga; QPN-038
microalgae; AMB-025
Microbial transformation; QPN-059
Microbiocidal; ORG-021
microcephaly; ORG-089
Microchip; ANA-066
Microdilution; QPN-031
Microdispositivos em papel; ANA-062
microeletrodos; ELE-008
Microemulsion; ANA-040
Microemulsion-assisted; ANA-053
Microesferas; MAT-098
microextração; ANA-042
microextraction; ANA-033
Microfiltration; TEC-011
Microfluidic; ANA-065
Microfluidics devices; ANA-068
Microorganisms; QPN-068
micropartículas; AMB-063
Microplastics; EDU-033
micropoluentes; AMB-067
micropropagation; QPN-019
microrganismos; AMB-040
Microsphaeropsis arundinis; QPN-063
Microtubule; MED-027
Microwave; EDU-050; ORG-059; ORG-109
Microwave Irradiation; MED-020
microwave irradiaton; ORG-047
Microwave-assisted; CAT-026
Microwave-assisted digestion; ANA-054
microwave-hydrothermal; ELE-007
Microwave-Induced Combustion; ANA-050
microwaves; ORG-056
Mieloperoxidase; MED-064
MIL-101(Cr); MAT-115
Milk; TEC-008
Mimosa tenuiflora; QPN-030
Minerais; QPN-118
mineral composition; AMB-010; ANA-081
Mineral Dietary Supplements; ANA-051
Mineral Water; BEA-013
Mineralization; ELE-016
Miniaturização; ANA-062
miniaturization; ELE-004
Miniaturized extraction; ANA-009
MIPs; ELE-047
MIR; ANA-061
Mistura; EDU-005
Mixed Esters; ORG-002
mixed matrix membranes; AMB-038; MAT-115
mixed oxide; ANA-045
mixed oxides; CAT-015
mixed Te(II)/Te(IV) derivative; INO-038
Mixed transition metal oxides; MAT-015
mixed-metal cation; INO-101
MMP; QPN-116
Mn(II); INO-087
Mn(II) and Fe(II) complexes; CAT-030
Mode of action; MED-022
modelagem; EDU-020
MODELAGEM MOLECULAR; MED-062
modelo cinético-molecular; EDU-020
modelos físicos; EDU-024
Modelos Moleculares; EDU-007
modificação no banho de watts; ELE-042
modified electrode; ELE-013; ELE-060
modos de representação; EDU-020
MOF; MAT-115
MOF's; INO-070
molar fraction; FIS-026
molecular aggregation; COL-005
Molecular docking; MED-016; MED-021; MED-027; MED-040; MED-044; MED-063; MED-065; QPN-015
molecular dynamics; ELE-018; MED-027; TEO-001; TEO-009
molecular fluorescence; ANA-022
Molecular imprinted polymer; ELE-024

molecular magnetism; INO-025
Molecular Modeling; FIS-034; MED-029; MED-033; MED-056
Molecular modeling kit; EDU-027
Molecular Modelling; MED-011
molecular models; EDU-026
molecular networking; QPN-069
molecular recognition; ELE-024; INO-007
molecular structure; INO-035
molecularly impressed polymers; ANA-004
Molecularly Imprinted Polymer; ELE-023
Molecularly imprinted polymers; ANA-091
Molybdates; MAT-075
Monastrol; MED-043
monitoramento; AMB-011
Monitoria; EDU-011
monitoring; AMB-002; AMB-031
Monoacylglycerols; ANA-069
Monoamine oxidase B; TEO-012
Monofloral; QPN-118
Monômero; FIS-038
monoterpenes; AMB-008; QPN-009
Moringa leaves; FIS-025
morphological; AMB-010
Morphology; MAT-100; QPN-034
Mössbauer Spectroscopy; INO-077
Mosto de Uva; ANA-048
Motivation; EDU-030
Mouthwash; QPN-020
MP; AMB-001
MPO; MED-061
MPPD•+; ANA-059
MRI applications; INO-016
MS-MS fragmentation; ORG-073
MTDLs; MED-018
MTT assay; ORG-108; QPN-063; QPN-117
Multi-component reactions; ORG-016
Multialvo; MED-064
Multiclass pesticides; ANA-009
Multicomponent reaction; ORG-015; ORG-058; ORG-059; ORG-080
Multicomponent synthesis; ORG-077
Multicomutação em análise em; ANA-026
Multidimensional; ORG-075
Multidrug-resistance; MED-034
Multifunctional material; MAT-075
multihierarchical electrode; MAT-120
Multivariate Exploratory Analy; AMB-072
multivariate optimization; AMB-018; ANA-041
Mustard seeds; ANA-030
mutagenic; QPN-096
mutamba; MAT-087; QPN-036
mycelium; QPN-064
Mycobacterium; MED-034
Mycobacterium tuberculosis; MED-060
Myrcia sylvatica; QPN-046

# N

n-Alkanes; AMB-003; QPN-044
N-alkyl-N-methylglucamine; INO-016
N-arilpirazol; ORG-071
N-doped carbon; CAT-016
N-ftalimidas; ORG-036
N-Halocompound; ORG-007
N-heterocycles; ORG-070
N-metilimidazólio; MAT-106
nAChRs α4β2; MED-063
nAChRs α7; MED-044
naftoquinonas; FIS-001
Naftoquinones; BIO-007
Nanocapsulas; COL-009
nanocomposite; ELE-014; MAT-030
Nanocomposites; MAT-049; MAT-108
nanocompósitos; MAT-054
Nanocubes; ELE-055
nanoencapsulação; MAT-087
nanoestruturas plasmônicas; INO-033
nanofibers; AMB-044; AMB-046; MAT-045
Nanofilters; MAT-009
Nanofluidic; ANA-065
nanohorn; ELE-001
Nanomateriais; INO-033
nanomaterial; AMB-036
Nanomaterials; MAT-049
Nanoparticle; MAT-030
Nanoparticles; CAT-012; CAT-016; COL-003; COL-007; ELE-055; FOT-001; MAT-006; MAT-036; MAT-052; MAT-082; MAT-095; MAT-097; MAT-101
nanopartícula de ouro; INO-033
Nanopartícula magnética; ANA-084
nanopartículas; AMB-062
Nanoparticulas; MAT-063
nanopartículas de BiVO4; ELE-053
Nanopartículas de ouro; MAT-002; MAT-072
Nanopartículas de Prata; FIS-018; MAT-072; QVE-010
Nanopartículas Magnéticas; MAT-039
nanopartículas metálicas mista; MAT-072
nanoporous gold; ELE-003
nanoporous gold microelectrode; ELE-043
nanorods; MAT-014
nanosondas fluorescentes; ANA-023
nanossensores; AMB-076
nanostructure; ELE-021; ELE-055
Nanostructured materials; ELE-050
Nanotechnology; BIO-006; MAT-008
Nanotube; MAT-030
Naphthoquinoline; ORG-059
naphthoquinone; ORG-029
naphthoquinones; EDU-048; ORG-045
Naphtoquinones; MED-020; ORG-092
naringin; ORG-013
native fruits; BEA-018
Natural dye; MAT-037
natural pigments; FOT-015
natural products; ORG-013; QPN-059; QPN-061; QPN-062; QPN-124
natural radioactivity; AMB-014
natural waters; ELE-006
NBO; TEO-005; TEO-007
Near-Infrared; BEA-014
near-infrared light absorbance; MAT-059
near-neutral conditions; AMB-049
Nectandra barbellata; QPN-043
Nectandra leucantha; QPN-096
Nectandra oppositifolia; QPN-098
Neglected Tropical Diseases; MED-046
neolignans; QPN-096
Neonothopanus gardneri; ORG-063
NET; MED-066
Neurodegenerative disorders; QPN-042
Neutron Scattering; FIS-017
Nevirapine; MAT-020
new phases; CAT-031
New Psychoactive Substances; MED-023; TEO-008
NEXAFS; MAT-100
Ni nanoparticles; CAT-027
nickel; MAT-091; ORG-049
nickel hexacyanoferrate; MAT-125
Nickel Hydroxide; ELE-055
Nickel molybdate; MAT-019
Nickel Niobate; CAT-001
Nicotine Addiction; MED-063
Niobia; CAT-007
niobium; CAT-015; ELE-031
Niobium Oxide; CAT-001
níquel; ANA-042; ORG-051
Niquel Hexacyanoferrate; ELE-038
Níquel(II); INO-091
NIR; ANA-029; ANA-078
nitric oxide; INO-055; INO-088
nitrile hydratases; ORG-001
nitro-anion radical; ELE-045
Nitroaldol; ORG-111
Nitrofural; ELE-040
nitrofurazone; ELE-045
Nitrogen doping; INO-093
Nitroheterocíclico; ELE-032
Nitroimidazol; MED-054
Nitrotriazole; MED-008
NMR; FIS-038; ORG-012; ORG-014; ORG-069; QPN-075; TEO-008
NMR calculations; ORG-102
NO release; TEO-002
Nociception; MED-003
non-linear optics; FOT-015
Nonlinear dynamics; ELE-034; ELE-054
nonofractionation; BIO-004
nonsteroidal anti-inflammatory; INO-062; ORG-047
Norbixin; COL-006
Norbornene; CAT-024; CAT-028
Normas Técnicas; EDU-015
Novozyme 435; ORG-032
Nuciferina; ORG-033
Núcleo Central; EDU-038
nucleophilic fluorination; TEO-013
number of theoretical plates; ANA-018
Numerical integration; TEO-003
Nutraceutical properties; BEA-006
nutrientes; AMB-037; AMB-063
Nutrients; ANA-035

## O

Obesity; MED-065
Ochterski; FIS-034
Ocotea catharinensis; QPN-004
octocrylene; INO-052
OEC; AMB-005
OHATZ; AMB-080
Oil/water interface; ELE-010
Oiti fruit; ANA-081
Oleate; MAT-067
Óleo de algodão; QVE-003
ÓLEO DE AZEITE; EDU-036
Óleo de coco; BEA-008
Óleo de peixe; ANA-047
Óleo essencial; QPN-003; QPN-004; QPN-010
óleo mineral; QVE-012
óleo vegetal; ANA-064
óleos vegetais; AMB-069
óleos vegetais isolantes; QVE-012
oleylamine-mediated route; MAT-061
OLIGOMERIC DISSOCIATION; BIO-013
Olimpíada de Química; EDU-005
Ômega-3; ANA-047
OMRP; CAT-030
On-line system; ANA-041
ONIOM; INO-048
online GCFID; AMB-008
online web-based tool; QPN-056
Open softwares; MED-031
Optical nanosensor; ANA-032
Oral bioavailability; MED-057
Oral History; EDU-046
orange albedo; ORG-013
Orange II; ELE-016
orbitides; QPN-125
Ordered Predictors Selection; ANA-076
organic chemistry; EDU-019; EDU-048; EDU-055; ORG-101
organic dye; INO-051
organic ligands; INO-006
Organic photovoltaic; TEO-004
organic pollutants; AMB-003
Organic solvents; ANA-070; QVE-007
organic synthesis; CAT-015; ORG-056; ORG-064; ORG-069; ORG-096; ORG-100
organocatálise; ORG-018; ORG-095
organoclay; INO-054
organoclorados; BEA-011
organofilização; INO-102
Organometallics; ORG-023
Organophosphate; FIS-006
Organophosphates; CAT-013; FIS-005; QVE-004
organophosphorus; AMB-018; FIS-019
Organoselenium; ORG-099
organosilicon; MAT-021
organoyl-thiolation; ORG-029
Organozinc; MED-056
Organozinc compounds; ORG-070
Oriented Immobilization; ELE-048
Origem da vida; FIS-029
Oscillating reaction; FIS-024
Oscillations; ELE-034; ELE-051
Oscillatory behavior; ELE-015; TEO-003
Osteoclastogenesis; ORG-061
Osteoporosis; ORG-044; ORG-061
Osteosarcoma; MED-051
otimização; QPN-030
Ouratea; QPN-027
ouro; AMB-026; ELE-008; ELE-059
Ouro nanométrico; MAT-027
overpotential; INO-013
oxadiazol; INO-046
Oxahomoaporphine skeleton; QPN-087
oxamate; EST-001; INO-097
oxamate ligands; INO-029
oxamato; INO-087
Oxazolidines; ORG-008
oxazolidinonas; ORG-027
oxidação; AMB-067; FIS-020
oxidação de cicloexano; INO-018
oxidation; INO-098
Oxidation products; BEA-002
oxidative addition; INO-078
Oxidative Evaluation; QPN-026
oxidative stress; AMB-073
oxides; ELE-026
óxido de cério (IV); INO-015
óxido de nióbio; MAT-035
óxido de zinco; MAT-054
oxigen reduction reaction; ELE-011
Oxisoil; AMB-033
oxone; ORG-062
oxygen evolution reaction; INO-096
Oxygen probe; MAT-089

## P

P-Aminophenol; AMB-015
p-cumaratos de alquenila; QPN-113
Paepalanthus planifolius; QPN-063
PAH; AMB-003; AMB-022
paládio; ORG-027
Palladium; ELE-031; INO-073; INO-075; INO-078; ORG-019; ORG-023; ORG-030
Palm Trees; QPN-031
Palygorskita; INO-102
PAMPA assay; MED-007
Pampa Biome; QPN-018
Papaína; INO-066
paper; ELE-046; MAT-092
Paper spray; BEA-015
Paper-based analytical devices; ELE-012
Paracoccidoides brasiliensis; BIO-012
Paramagnetic nanoparticles; FIS-035
parâmetros cinéticos; ORG-003
Paraoxon; ORG-067
parasitas; INO-058
parathion; FIS-019
Partial Least Squares; ANA-076
Particle size; ANA-037; MAT-064
particles; INO-021
Partículas magnéticas; ORG-055
partition coefficient; AMB-064
passive sampling; AMB-009; ANA-056
PBAT; MAT-016
PCA; ANA-073; ANA-074; ANA-081; QPN-015
PCL; MAT-016
PCL enzyme; MED-065
PDAH; INO-023; INO-090
pdms; MAT-089
PDT; INO-031
Peat; INO-072
Pectina; QVE-010
PEDOT; ELE-009
PEG-400; ORG-091
PEG-assisted solvothermal; ANA-053
pele; MAT-016
Peltophorum dubium; QPN-074
Penicillium expansum; QPN-017
Pentacalia desiderabilis; QPN-097
Pentacyclic triterpenes; ORG-006
Pentadecano; QPN-010
pentadienone derivative; ORG-108
Pentóxido de Nióbio; FIS-018
Peptide assemblies; MAT-118
Peptide copolymers; MAT-051
Peptides; INO-095; TEO-001
Peptidomimetics; QPN-029
Perfumes; ANA-075
Perfumes,; ANA-079
periphyton; AMB-042
permanent hair dyes; AMB-015
Permeability; MED-057
Perovskite; CAT-019
perovskite nanocrystals; INO-101
peroxidase; ELE-037
peróxido de hidrogênio; ELE-008; FIS-020
Peruvian Andes; AMB-081
perylene; INO-086
Pesticidas; ANA-014; BEA-011
pesticides; AMB-020; AMB-027; AMB-049; ANA-031; QVE-004
Petroleum; ANA-073
PFO-DBT; MAT-013
pH; INO-003
Pharmaceutical Forms; QPN-020
pharmaceutical formulations; ELE-022
pharmaceuticals; AMB-053
Pharmaceuticals contaminants; MAT-055
Pharmacokinetic Properties; MED-038
Pharmacokinetics; MED-007
Pharmacophore; MED-002
Phase diagram; FIS-015; FIS-037
Phase diagrams; COL-011; FIS-021
phase transition; FIS-014
Phaseolus lunatus; QPN-055
PHB; MAT-003
Phenol; CAT-004; INO-070
Phenolic acids; ANA-059; QPN-037
Phenolic compounds; ANA-010; ELE-050; ORG-090; QPN-023; QPN-028
Phenotypic Screening; MED-006

phenylenediamine; ANA-059; BEA-012
Phenylethylamine; ORG-096
Phlogopite; MAT-017
phosphate; AMB-057; ANA-092; INO-012
Phosphines; INO-075
Phospholipids; FIS-016
phosphonium salts; ORG-024
Phosphoramidates; ORG-021
Phosphoric Acid; FIS-004
Phosphorus; ANA-082
photo-oxidation; INO-031
Photocatalysis; CAT-011; CAT-012; FOT-004; FOT-007; INO-093; MAT-037; MAT-069
Photocathodes; INO-065
Photochemical reduction; MAT-032
Photodegradation; FOT-001; FOT-004; FOT-010; MAT-021; MAT-117
photodynamic efficiency; INO-031
Photodynamic inactivation; ORG-088
Photodynamic Therapy; MAT-101
photoelectrocatalysis; ELE-007; ELE-021; ELE-029; MAT-120
Photoelectrochemical; INO-065
photoelectrochemical oxidation; MAT-102
Photohaemolysis; FOT-001
Photoisomerization; ORG-064
photoluminescence; INO-008; INO-037; INO-085
photoluminescence spectroscopy; INO-006; INO-010
Photooxidation; CAT-012
photophysical properties; INO-027; MAT-056; ORG-026
Photophysics; MAT-090
photoprotection; BIO-007
Photosensitizer; FOT-002; FOT-016; INO-031
phototerapy; FOT-013
photovoltaic devices; MAT-029
Photovoltaics; MAT-100
Phthalocyanine; FOT-001
Phycocyanin; QPN-038
Physical-chemical treatment; AMB-079
Physicochemical Features; BIO-010
Physicochemical Properties; MAT-043; MED-056
Physisorption; COL-002
Phytochemical; QPN-109
Phytochemical screening; QPN-049; QPN-062
Phytochemistry; QPN-040
Phytosterols; ANA-030; QPN-034
phytoteraptics; QPN-102
Phytotoxic; QPN-025
Phytotoxicity; QPN-037
PIBID; EDU-004; EDU-008; EDU-009
PIBID-Chemistry; EDU-046
Picramnia bahiensis; QPN-051
pigments; AMB-071; QPN-060
Pilar[n]arenos; MAT-039
pilha a combustível; INO-067
Pilhas; EDU-028; EDU-047; EDU-059
Piper hispidinervum; QPN-010
pirazol; INO-061
pirazol polifuncionalizado; ORG-071
Pirazolina; COL-009
Pithecoctenium crucigerum; QPN-052
PKG; MED-002
planejamento; ANA-002; MED-060
Planejamento de fármacos; MED-005; MED-048
Planning of binary mixtures; BEA-003
Plant extracts; QPN-021
Plants; QPN-002
plasma; MAT-021
Plasma canino; ANA-011
Plasma sample; ANA-020
Plasmodium falciparum; MED-039
plasmonic; MAT-014
Plasmonic band; MAT-095
Plasmonic cancer therapy; MED-014
Plasmonic Catalysis; CAT-012
Plastic marine pollution; EDU-033
plastic waste; CAT-035
Plasticizers; ANA-093
Platinum; ELE-005; ELE-026; INO-046
platinum(II) complexes; INO-036
Platonia insignis; BIO-011; QPN-105
play activity; EDU-006
pleocarpanone; ORG-083
Pleonotoma; QPN-054
PLGA; MAT-087
PLGA-PEG; FOT-001
PLS; ANA-029; TEC-005
PLS-DA; ANA-080
Pluronic10R5; FIS-015
PM2.5; ANA-009
PNIPAAm; MAT-004
POAs; MAT-035
poder calórico; AMB-070
Point of Zero Charge; INO-072
Polaridade; EDU-017
pólen; QPN-080
Pólen apícola; QPN-118
polieletrólito; ELE-020
polietilenimina; MAT-025
polietilenoimina; ELE-020
Polímero; FIS-038; FIS-039
polímero de coordenação; ORG-072
Polímero luminescente; MAT-002
polímeros de coordenação; AMB-052; INO-061
Polímeros fluorescentes; ANA-005
políticas públicas; AMB-012
pollution; AMB-023; ANA-036
poluição; AMB-068
poluição ambiental; AMB-011
Poly(lactic acid); CAT-034
poly(vinyl alcohol); COL-005; MAT-103
polyaniline; COL-004; ELE-056; MAT-005; MAT-073; MAT-076; MAT-108
Polycatenar; ORG-064
Polycrystalline Platinum; FIS-004
Polydopamine; COL-007
Polyelectrolyte; MAT-041
polyethylene glycol (PEG); MAT-051
polyethylenimine; MAT-059
Polyfluorene derivatives; MAT-079
Polyheptazine; INO-093
Polyketides; QPN-063
polymer electrolytes; ELE-018
polymer membranes; AMB-038
polymeric additives; MAT-046
polymeric network; EST-001
Polymeric sponge; MAT-017
Polymerization; CAT-029
Polymers; FIS-031
polymorphism; MAT-126
polypropylene; MAT-021; MAT-081; MAT-112
Polystyrene; MAT-080
polythiophene; MAT-029
polyurethane foams; AMB-056
Ponto nuvem; ANA-028; BEA-020
pontos quântico; ANA-023
Pontos quânticos; MAT-054
população rural; AMB-055
Porcelia macrocarpa; QPN-114
porfirina; INO-032
porfirina de manganês; INO-018
porfirinas; INO-005
Porfirinas de manganês; INO-079
porosity; MAT-064
Porous ceramic; MAT-017
porous TiO2; MAT-069
porphyrin; INO-049; MAT-083
porphyrin derivatives; INO-031
Porphyrins; ORG-088
Portable and disposable sensor; ELE-012
portões; EDU-014
potássio; AMB-037
Potassium Nitrate; MAT-003; MAT-066
Potential Oscillations; FIS-004
Potentially Toxic Metals; AMB-058
pour point; MAT-046
Power conversion efficiencies; TEO-004
PPB; ELE-048
Pr-SO3H-SBA-15; CAT-022
praguicidas; AMB-021
prata; ELE-059
prática; EDU-049
Pré-concentração; ANA-084
Pre-service Teacher Preparat; EDU-009
Pre-treatment; CAT-039; TEC-007
Precipitação homogênea; ANA-049
precipitação química; AMB-037
Preclinical Research; MED-051
preconcentration; ANA-039; ANA-045
precursors; AMB-015
Preparo de amostra; ANA-084
Preparo de amostras; ANA-011
Printed electrodes; ANA-068
Pro-chiral; ORG-038
probe; ANA-022
Procedure validation; ANA-070
Processo Fenton; CAT-037

Processos Oxidativos Avançados; FIS-018
Product surveillance postmarke; MAT-122
Produto natural; FOT-014
PRODUTOS NATURAIS; MED-062; QPN-022
professional knowledge; EDU-040
prometazina; ELE-020
Promiscuity; ORG-111
Propargylamines; TEO-012
Propolis; QPN-028
Propoxur; ANA-028
propriedades físico-químicas; FIS-001
protamina; ANA-023
Protease Inhibitors; ORG-069
proteção; MAT-086
protein interaction; MED-047
proteínas catiônicas; ANA-023
Proteinases; BIO-001
protetor solar; QPN-007
Prussian blue; ELE-019; INO-096; MAT-108
prussian blue high stability; ELE-014
Pseudocapacitors; MAT-015
Pseudomonas aeruginosa; ELE-012
Pseudotitulação; ANA-062
Pseurotin A; QPN-065
Psidium Myrtoides O. Berg; QPN-006
Psidium salutare; QPN-018
PSiF-DBT; MAT-013
Psychotria; QPN-076
Pt surface oxidation; ELE-026
Pterodon pubescens; QPN-020
Pterodron emarginatus; QPN-102
PTP1B; QPN-051
PTS; AMB-002; AMB-072
public health; AMB-029
pulverolide; ORG-104
purification; BIO-003; CAT-025; ORG-101
Purina Nucleosídeo Fosforilase; ORG-075
push-pull compounds; ORG-100
Pyocyanin biosynthesis; MED-025
Pyrazoles; ORG-050
pyrazolines; INO-089
pyrazolopyrimidine; MED-030
Pyridazinones; ORG-048
Pyridinium salts; ORG-008
pyriproxifene; ORG-089
pyrite; INO-044
pyroaurite; AMB-060
pyrolysis; AMB-074; CAT-035
Pyrrolidines; ORG-050

## Q

Q and B bands; TEO-011
QCM; FIS-027
QCM-D; ELE-009; ELE-036
qNMR; ANA-031
QSAR; MED-002; MED-004; MED-031; MED-066
QSAR model; FIS-007
QTAIM; TEO-010
qualidade da água; AMB-068
Quality; ANA-085; ANA-094
Quantificação; ANA-090; QPN-077
Quantification; MAT-040
Quechers; ANA-019
queimaduras; MAT-016
Quelante; MED-061
Quercetin; QVE-001
Química Ambiental; AMB-052; AMB-076; EDU-002
Química Analítica; EDU-021
química forense; ANA-067; ELE-028
Química Inorgânica; EDU-011
Química limpa; ANA-028
Química Medicinal; MED-032
Química no cotidiano; EDU-060
Química prebiótica; FIS-029
química sustentável; FOT-003
Química verde; ANA-061; INO-005; INO-018; INO-071; INO-079
Quimiluminescência; ANA-026
quimiossíntese; FIS-036
Quinoides; QPN-097
quinoline; ORG-106
Quinoline Derivatives; ORG-026
quinolinyl lactones; ORG-056
quinolona; ORG-017; ORG-085; ORG-087
Quinolones; ORG-022; ORG-088
Quinoxalina; ORG-035
Quitosana; COL-009; MAT-065

## R

racemização; ORG-051
Racemization; ORG-093
radiação Gama; BEA-004
Radiation shielding; MAT-103
Radical Generation; INO-004
Radical polymerization; CAT-030
Radio-astronomy; FIS-002
radiólise; FIS-036
Radiopharmaceutical; ANA-070
Raman; ELE-019
Raman effect; COL-010
Raman Spectroscopy; FIS-017; MAT-097
Ramette; EDU-016
Rancimat; AMB-075
rare earth; INO-006; MAT-034
Rare earth elements; ANA-038; ANA-039; MAT-040
Rare earth metal; INO-010
Rare Earth Oxides; MAT-101
Rare earth oxysulfides; MAT-070
Rational Drug Design; MED-026
rational synthesis; INO-041
rCPB2.8; MED-036
rCPB3.0; MED-036
RDC; ORG-025
RDSE; AMB-020
Reação de Biginelli; MED-064
Reação multicomponentes; MED-059
reações de Michael; ORG-018
Reactive Oxygen Species; INO-004
Reactivity Assays; INO-068
realidade aumentada; EDU-024
Reality; EDU-058
Rearranjo [3,3] Sigmatrópico; ORG-034
reator de leito fixo; FIS-033
Recuperação de solventes; QVE-005
recyclable materials; AMB-004
Recycling; MAT-112
Redocking; MED-063
Redox-relay mechanism; ORG-098
reduced graphene oxide; ELE-013; ELE-023; ELE-038; MAT-059; MAT-104; MED-014
reductive; CAT-021
REELS; MAT-013
Refractive index; TEC-005
Regeneração de NADH; CAT-036
Regenerative Medicine; MAT-028
Regiospecific synthesis; ORG-092
Regulacion; MAT-122
Regulation; ANA-094
Relaxation Processes; FIS-017
Reline; FIS-013
Remazol Preto B; FIS-020
Representação Social; EDU-038
Residual Oil; ORG-109
Residue; MAT-042; MAT-094; MAT-119
residue analysis; ANA-001
residues; AMB-056
residues bauxite; AMB-060
resíduo; EDU-049
Resíduo industrial; FIS-028
resíduos; AMB-066; TEC-010
resíduos agropecuários; AMB-041
Resíduos químicos; QVE-005
resin oil; QPN-122
resistência Bacteriana; INO-001
Resolução cinética; ORG-032
resolução cinética dinâmica; ORG-020; ORG-051
resolution; ANA-018
Restrict Access Material; ANA-020
reuse of water; AMB-048
Reutilization; MAT-040
reverse transcriptase; ORG-106
reverse water gas shift; CAT-027
Reversibilidade; INO-082
Rheology; FOT-013; QPN-034
Rhinella jimi; QPN-104
Rhipicephalus microplus; MED-024; MED-055
Rhizobia; AMB-058
Rhodium Catalyst; CAT-018
Rhodium nanoparticles.; CAT-014
Rice husk ash; MAT-116
Richterago campestris; QPN-090
Richterago discoidea; QPN-091
Rio de Janeiro; AMB-014
Rio Doce basin; AMB-046
Rio Paraíba do Sul; AMB-019
rios; AMB-068
Risk Assessment; MED-023
river water; AMB-018
RMN; ORG-025; ORG-068
ROMP; CAT-024; CAT-028

Rota etílica; QVE-003
Rota metílica; QVE-003
rotational barrier; ORG-012
RP-DLLME; ANA-044
Ru polypyridyl complexes; INO-013
Ru terpyridine aquo complexes; INO-013
Ru(II) Complexes; FOT-005
Rubiaceae; QPN-076; QPN-100; QPN-103; QPN-115
rutenio (II); INO-034
ruthenium complex; INO-020; INO-095
Ruthenium complexes; CAT-024; CAT-028; INO-024; TEO-002
ruthenium(II) complexes; INO-043

# S

S. terebinthifolius genders; QPN-005
Saccharum ssp; QPN-037
safrol; QPN-010
Salen-type; ORG-009
Salicylic acid; MAT-020
salinidade; AMB-019
Salinispora arenicola; QPN-084
Saliva; ELE-035
Salmoura; ANA-049
salt bridge; EDU-053
sample preparation; AMB-020; ANA-004; ANA-010; ANA-033; ANA-052; ANA-054
SAP; ANA-073
SAR; MED-034
SAR Studies; BIO-010
SAR.; MED-025
SARA; ANA-060
SBA-15; INO-066
SBUs; ORG-072
Scaffold; MAT-062
Scale inhibitor; ANA-071
scanning electrochemical micro; ELE-043
SCC-DFTB; TEO-009
Schiff base; CAT-024; CAT-029; ORG-009
Schiff bases; CAT-030; INO-028
Schiff's reagent; TEC-008
Schistosoma mansoni; QPN-073
Schistosomiasis; MED-006; MED-046; QPN-073
Scientific Articles; EDU-030
Scintillation; MAT-034
Screen-printed electrode; ELE-062
Screening,; BIO-004
SDS; COL-006
seasonality; QPN-011
Seawater; ANA-041
SECM; ELE-043
Second generation ethanol; COL-001
Secondary ion emission; FIS-002
secondary metabolites; ORG-063; QPN-049; QPN-056; QPN-117
sediment; AMB-030; AMB-078
sediment quality guidelines; AMB-022
sediments; AMB-031
Seed germination; QPN-025
Selective functionalization; ORG-070
Selective Hydrogenation; CAT-032
selectivity; INO-012
Selenoacetilenos; ORG-034
Selenoésteres; ORG-034
Self-assembled films; MAT-076
Self-assembled monolayers; INO-002
self-assembly; MAT-014; MAT-113
self-neutralizing process; MAT-114
Semi-batch reactor.; CAT-033
Semiconductor Oxide; MAT-030
semiempirical method; MED-040
Semipermeable Membranes; ANA-056
Senna acuruensis; QPN-108
sensor; ELE-001; ELE-003; ELE-020; ELE-055; INO-012
Sensor Fotoeletroquímico; ELE-053
sensores ópticos; MAT-072
Sensores óticos; MAT-002
Sensorial analysis; ANA-078
Separação; ANA-049
separation; ANA-039; MAT-040
separation factor; ANA-018
sepiolite; INO-054
Sequential oscillations; FIS-024
sequiterpenes; QPN-122
Séries; EDU-016
Serine protease; MED-001; MED-021
Serissa foetida; QPN-100
Serotonin receptors; ORG-096
serpentinite; CAT-031
SERS; ELE-061; MAT-014; MAT-082; MAT-097
Seselin; QPN-079
Sesquiterpene Lactone; QPN-091
Sesquiterpene lactones; QPN-116; QPN-119
Sesquiterpenes; QPN-009; QPN-046
Sesquiterpenoid; QPN-006
Sesquiterpenoides; QPN-107; QPN-113
Sesquiterpenos eudesmanos; QPN-043
SFG spectroscopy; FIS-016
Shale; MAT-044
Show de Química; EDU-001
Signal separation; BEA-002
Silencing; MAT-036
silica; COL-003; MAT-006; MAT-088
Sílica; MAT-124
Silica; TEC-011
silica based adsorbent; ANA-039
Silica gel; MAT-012
Sílica gel; MAT-099
Sílica Mesoporosa Ordenada; INO-066
silica nanoparticles; MAT-050
sílicas funcionalizadas; ORG-086
Silicone oil; MAT-122
Silicone rubber; MAT-117
Silk; FOT-013
silk fibroin; ELE-017
Silver; MAT-037; MAT-052; ORG-099
Silver Nanoparticles; BIO-006; QVE-001
silver tungstate; MAT-126
Símbolos químicos; EDU-065
simulação computacional; EDU-020
Simvastatin; ANA-007
Single Extractions; ANA-035
single-molecule magnets; INO-041
Singlet Oxigen; FOT-013
Singlet oxygen; FOT-002; MAT-006
síntese; INO-030; INO-032
síntese e caracterização; INO-094
síntese em fluxo; INO-023
Síntese Enantiosseletiva; ORG-105
Síntese Orgânica; MED-053; ORG-018; ORG-040
Síntese Regiosseletiva; ORG-071
Síntese Verde; QVE-010
Sínteses totais; ORG-033
siRNA; MAT-036
Sirtuin 2; MED-017
Sistema Veiculador de Fármaco; MAT-039
sistemas aquáticos; AMB-036; AMB-062
sistemas biomiméticos; INO-001; INO-071
Sistemas de amostragem passiva; ANA-055
SistematX; QPN-056
slako-koster; TEO-009
SLE/LTP; ANA-001
slippery surface; COL-004
SLIPS; MAT-038
small experiments; EDU-052
SMILES; MED-031
SmTGR inhibitors; MED-026
Smuggling; ANA-031
Sn3O4/Ti; ELE-007
Snake venom; BIO-001; MED-001; MED-021
snakebites; MED-040
$SO_2$ oxidation; ELE-015
social behaviour; AMB-004
Socioeconomic profile; EDU-045
Sodium alginate; QPN-021
sodium diclofenac; FOT-010
Sodium ethyleneglycoxide; TEC-004
Sodium Glyceroxide; TEC-006
Soil; ANA-035
soil contamination; AMB-032
soil management; AMB-033
soil organic matter; AMB-033
Sol-gel method; MAT-019
Solanum lycopersicum; ORG-057
Solanum paludosum; QPN-047
Solanum paniculatum; QPN-101
solar cell; INO-017
solar cells; MAT-010; MAT-083; TEO-004
solar energy; INO-013
solid acid catalysts; CAT-003
solid phase extraction; ANA-039
solid phase synthesis; MAT-051
Solid Sampling; ANA-043
solo; AMB-035; EDU-047
solos; AMB-034
Solubilidade; FIS-029
Soluble solids content; QPN-023
Solute–solvent interactions; FIS-011
solution; INO-035

Solvatochromic dyes; FIS-011
Solvatochromic reversal; FIS-011
Solvatochromism; FIS-011; FOT-006
Solvent effect; ORG-014; TEO-013
Solvent-free; ORG-042
Solventes; QVE-005
Solventes orgânicos; MAT-107
Solventes Verdes; CAT-002
solvents; ORG-039
solvólise; INO-099
solvothermal syntheses; MAT-069
sorption; AMB-061; MAT-026
Soy; QPN-026
Soybean oil; ANA-077; CAT-003
Spacer; MED-033
SPE; ANA-019; BEA-007
speciation; ANA-045; FIS-022
Spectral Library; QPN-089
Spectrofluorimetry; ANA-024
Spectrophotometry; ANA-059; BEA-010; BEA-012; QPN-038
spectroscopic techniques; BIO-005; MED-042
Spectroscopy; BEA-014; INO-063; INO-076
spent fluorescent lamps; ANA-038
sphagnum subsecundum; AMB-013
Spilanthes acmella; QPN-045
Spilanthol; QPN-045
Spill; ANA-060
Spin; ORG-103
spin-coating; INO-017
Spirostanic saponins; QPN-101
Spray Dryer; MAT-023
SQ109; ORG-043
Square-wave voltammetry; ELE-035
ssDNA; ORG-107
Stability; INO-003; MAT-052; MAT-073
stacking fault; MAT-061
Stamps; ANA-017
Standards; QPN-089
Starch; QVE-002; QVE-006
stationary phase; ORG-101
Steam explosion; MAT-042
stearic acid; INO-020
STEM; EDU-026
Steroid glycoside; QPN-101
Steroidal saponins; QPN-101
Steroids; ELE-035; QPN-109
Stöber method; ANA-053
Stöber silica; INO-092
storage modulus; MAT-081
Strongylodon macrobotrys; QPN-075
Strontium; CAT-001
structure control; ELE-036
Structure determination; MAT-020
Submédio São Francisco; ANA-048
Substâncias; EDU-005
Substratos trissubstituídos; CAT-002
Sucupira; QPN-102
sugar cane straw; TEC-009
sugarcane; MAT-094
Sugarcane Bagasse; MAT-003; MAT-066
Sulfamida; ORG-068
sulfation; MED-035
sulfides; ORG-024
sulfonamides; ELE-025; MED-003
Sulfonation; CAT-009
Sulfone; ORG-054
sulfonic resin; QVE-009
Sulfoxide; ORG-054
Sulfoxonium ylides; ORG-038
Sulfur; ANA-050
sulfur-oxygen interactions; MED-015
Sunset Yellow dye; ELE-027
super capacitor; MAT-068
Superabsorbent hydrogel; MAT-116
Supercapacitor; MAT-005; MAT-092; MAT-123
Supercapatteries; ELE-058
Superfícies cerâmicas; MAT-107
Superheros; EDU-033
superhydrophobic surface; COL-004
Superparamagnetism; MAT-006
Supported catalysts; CAT-005
Supported heteropolyacid; CAT-034
Supported Ionic Liquid; CAT-032
supramolecular catalysis; TEO-013
supramolecular chemistry; INO-081; INO-095; INO-097
Surface Chemical Functionaliza; MAT-043
Surface Facets; MAT-105
Surface modification; FIS-031; MAT-050; MAT-088
Surface plasmon; COL-010
Surface roughness; MAT-117
Surfactant; COL-002; COL-006; FIS-022
susceptibilidade eletrofílica; INO-026
suspension polymerization; MAT-064
Sustainability; AMB-065; CAT-039
sustantability; MAT-094
sustentabilidade; QVE-005; TEC-010
Swinglea glutinosa; QPN-086
Swiss mice; ANA-015
Symbiosis; QPN-068
Symmetry; INO-010
synthesis; AMB-060; CAT-031; EDU-048; MAT-052; MAT-075; MED-041; ORG-047; ORG-049; ORG-074; ORG-091; ORG-097; ORG-106
synthesis of heterocycles; ORG-100
synthesis optimization; MAT-057
synthetic bitumen; MAT-081
Synthetic Cannabinoids; MED-023
Syringes; MAT-122
systemic mycoses; BIO-012

## T

T. cruzi; QPN-085
T. hispidula; QPN-103
Tabaco; ANA-021; ANA-089
Taninos; QPN-095
Tannery sludge; CAT-011
Tautomerism; FIS-009
Taxifolin; MED-050
TBHQ; ANA-088
TCCA; ORG-053; ORG-074
TDDFT; TEO-006; TEO-007
Teacher Education; EDU-046
teacher training; EDU-053
Teaching; EDU-058
Teaching and learning; EDU-012
teaching formation; EDU-040
Teaching Laboratory; AMB-065
Teaching performance; EDU-042
Teaching Sequences; EDU-009
Technical Course; EDU-043
Tecnol. Inf. e do Conhecimento; EDU-007
Tecnologhy; EDU-058
Temperatura; FIS-029
Temperature; FIS-015
Temperature probe; MAT-089
Template; MAT-082
TEMPO oxidation; CAT-020
teor de umidade; AMB-070
TEO-S hydrolysis; MAT-114
térbio; INO-039
Terbium complexes; MAT-056
Terminalia actinophylla; QPN-095
Terpene; CAT-018; ORG-083
Terpenes; QPN-005
Terpenóides; ORG-043
Tetracyclines; QPN-068
Tetrametilamônio; INO-091
Tetraporphyrin; FOT-002
Tetrazoles; ORG-022
Textured copper; MAT-038
texturometer; MAT-022
TFD; INO-032
Theoretical calculation; TEO-012
theoretical calculations; INO-035; MAT-079; TEO-008
theranostics; INO-016
thermal infrared; BEA-005
Thermal Processing; MAT-003
Thermal stability; BEA-006
Thermoanalytical profile; BEA-001
Thermochemistry; FIS-034
thermochromism; MAT-001; MAT-075
Thielaviopsis paradoxa; QPN-002
thimerosal; BIO-005
Thin film; INO-020; MAT-029; MAT-073; MAT-123
Thin films; INO-065; MAT-125
thioamides; ORG-058
thiol/disulfide; ELE-049
thiophene-imide; MAT-024
Thiosemicarbazide; MED-037
Thiosemicarbazone; INO-075; MED-037
thiosemicarbazones; INO-040; MED-021; MED-040
thiosulfonates; ORG-024
thiourea; INO-057; ORG-091
Three-dimensional graphene; MAT-009
Tibolone; ELE-035
TICs; EDU-031
Tijuca Forest; AMB-006; AMB-007

Time-dependent Density Functio; FIS-035
Timina; FIS-029
Tin; ELE-005
tin-substituted perovskite NC; INO-101
$TiO_2$; FIS-023; FOT-010
$TiO_2$ nanotubes; MAT-102
tiossemicarbazonas; INO-047
Tiramina; ORG-040
Tissue damage; MAT-062
Tissue Engineering; MAT-028; MAT-031
Titanate Nanostructures; MAT-048
Titanate nanotubes; INO-093
Titanium dioxide; MAT-037; MAT-083
titulação ácido-base; ANA-064
Tocopherols; ANA-030
Todos os Santos Bay; AMB-009
Tolano; MAT-106
Tomato; ORG-057
Tontelea micrantha; QPN-112
Topical Formulation; FOT-016
Topliss; MED-034
Topoisomerase; INO-075; MED-032
Topoisomerase I; INO-069
Topoisomerase II-α humana; QPN-047
Topological Model of Teaching; EDU-009
Total polyphenol; ANA-024
total suspended particles; AMB-010
total synthesis; ORG-083
Toxicity; ORG-054
toxicity assays; FOT-010
Trace Analysis; ANA-043; ANA-044
trace elements; AMB-010; AMB-031
Trace metals; AMB-081
Trametes versicolor; AMB-054
trans fatty acids; ANA-003
Transdermal device; MAT-045
Transest-Erificação; EDU-036; FIS-033; MAT-124
Transesterification; TEC-004; TEC-006
transformation products; AMB-048
Transient signal; ANA-082
Transition energies; TEO-011
tratamento resíduo; AMB-066
Tri-Ureasil; MAT-078
triângulo da corrosão; MAT-086
triazol; ORG-087
triazole; ORG-052
triazoles, corrosion inhibitor; ELE-002
Triboelectric generators; FIS-031
Trichilia emarginata; QPN-032
Tricina; QPN-041
Triclosan; MED-011
Triethylenetetramine; MAT-043
Trifenilfosfina; INO-100
Trifluoromethylquinolines; MED-010
trifluoromethylthiolation; ORG-029
Trihalomethanes; FIS-034
Trinitrotoluene; ELE-052
triplete; FOT-009
Tris(hidroximetil)aminometano; INO-091
Tristriazolotriazina; ORG-082
Tritepenoides; QPN-103
Triterpene; QPN-109
Triterpenes; QPN-046
Triterpeno pentacíclico; QPN-112; QPN-120
Triterpenoide; QPN-107
triterpenoides; QPN-105; QPN-108; QPN-111
Triterpenoids; QPN-110
Triterpenos; QPN-035
Triton-X100; COL-011; FIS-021
Tropical fruits; BEA-010
Trypanosoma; MED-054
Trypanosoma cruzi; MED-004; MED-008; MED-029; MED-038; QPN-043; QPN-114
Trypanothione Reductase; MED-038
Tuberculose; MED-053; ORG-043; ORG-075
tuberculosis; INO-036; MED-034
Tubulin; MED-015; MED-027
Tubulina; MED-048
Tungsten oxide nanowire; MAT-005
Turbidity; AMB-079
TXRF; ANA-034; ANA-035

## U

UFLC; BEA-013
UHPLC-MS/MS; ANA-077
UHPLC–MS/MS; AMB-020
Ultrafiltration; TEC-011
Ultrasound; QPN-117; QVE-008; TEC-009
Ultrasound irradiation; QVE-007
Ultrassom; ANA-008
upconversion; INO-017
UPLC-ITMS; QPN-104
UPLC-MS; QPN-081
uranium; AMB-014
urban area; AMB-010
urban forest; AMB-008
urea; MAT-018; TEC-003
urease; MED-045; MED-047; TEC-003
urinary tract infection; ANA-080
Usnea steineri; QPN-057
usnic acid; MED-047; QPN-057
UV radiation; MAT-032
UV-vis; BEA-020; QPN-038
UV-Vis Detection; FIS-006
UV-VIS-NIR spectroscopy; COL-010
UV-Visible SpectrophotometrY; ANA-057; ANA-058
UV/H2O2; AMB-050

## V

vaccenic acid; ANA-003
Valencene; CAT-018
Validation; ANA-031
valinomycin; QPN-069
Valorização de CO2; CAT-036
vanadato de bismuto; INO-033
vapor electricity; FIS-014
Variable Selection; ANA-076
variáveis; QPN-030
Vegetable Oils; BEA-014
Verbena montevidensis; QPN-048
Verbenaceae; QPN-048; QPN-093
Verubulin; ORG-070
viabilidade celular; QPN-036
Vibrational spectroscopy; FIS-032
Vídeo; EDU-034
Video digital; ANA-082
Vidro; MAT-099
Vidro poroso; MAT-027
vinhoto; AMB-037
Vinyl acetate; CAT-030
Vinyl Acetate CMRP.; CAT-029
Virtual screening; BIO-012; MED-002; MED-016
viscosity; MAT-081
visible light; FOT-007
visible-light; ELE-007
Visual impairment; EDU-025; EDU-029
Visualização; EDU-007
Vochysia divergens; ORG-006
Vochysiaceae; ORG-006
Volatile composition; QPN-005
Voltametria cíclica; ELE-032; INO-067
voltametria de onda quadrada; ELE-037
voltammetry; ELE-004; ELE-040
Vulcan-X; INO-044; INO-056

## W

waste; MAT-094
Waste Disposal; QVE-013
Waste Treatment; QVE-013
wastewater; FOT-004
Wastewater remediation; MAT-116
wastewater treatment; AMB-051
water; AMB-015; AMB-016; AMB-020; ORG-089; TEO-009
Water Concentration; FIS-004
water medium; ANA-045
water oxidation; INO-096
water oxidation catalysis; INO-043
water oxidation catalysts; INO-013
Water produced; ANA-056
Water radiolysis; FIS-002
water remediation; MAT-102
water splitting; INO-013; INO-043; INO-096; MAT-120
water treatment; AMB-027
water-soluble; INO-085
Webcam; ANA-082
Whisky; ANA-034
Wine; ANA-024; ANA-077
Wines; ANA-085; BEA-005
Wistar rats; ANA-015
Wittig reaction; ORG-015
WO2.72/Vulcan XC72; ELE-016

## X

X-ray analysis; BEA-001
X-ray crystallography; MED-026
X-ray diffraction; INO-029; INO-057; MAT-019; MAT-020
Xantenonas; ORG-055

Xanthate; INO-076
Xanthyletin; QPN-079
xantona; FOT-009
XEOL; MAT-070
XTT assay; MED-006
xylazine; ELE-022
Xylella fastidiosa; QPN-079
Xylopia; QPN-013

## Y

yeast biomass; MAT-111
yeast biomass from b-glucan; MAT-111
Young modulus; MAT-022

## Z

Zebrafish; QPN-042
zein; ELE-001
zeína; MAT-054
zeolite; AMB-053; MAT-047
Zeolite Imidazole Framework-8; ELE-029
Zeolite Synthesis NaY; FIS-008
zeolites; CAT-035
Zeta Potential; COL-013
zinc; AMB-047
Zinc (II); INO-019
zinc complexes; INO-014
Zingiberaceae; QPN-094
Zn(II); INO-087
Zn(II) complexes; INO-084
Zn(II) phthalocyanines; TEO-011
Zwitterionic Receptor; INO-007

Agência Brasileira do ISBN
ISBN 978-85-64099-21-0
9 788564 099210